U.S. Department
of Commerce

Volume 101
Number 1
January 2003

Fishery Bulletin

The *Fishery Bulletin* (ISSN 0090-0656) is published quarterly by the Scientific Publications Office, National Marine Fisheries Service, NOAA, 7600 Sand Point Way NE, BIN C15700, Seattle, WA 98115-0070. Periodicals postage is paid at Seattle, WA, and at additional mailing offices. POSTMASTER: Send address changes for subscriptions to Fishery Bulletin, Superintendent of Documents, Attn.: Chief, Mail List Branch, Mail Stop SSOM, Washington, DC 20402-9373.

The Secretary of Commerce has determined that the publication of this periodical is necessary according to law for the transaction of public business of this Department. Use of funds for printing of this periodical has been approved by the Director of the Office of Management and Budget.

For sale by the Superintendent of Documents, U.S. Government Printing Office, Washington, DC 20402. Subscription price per year: $45.00 domestic and $56.25 foreign. Cost per single issue: $28.00 domestic and $35.00 foreign. **See back for order form.**

Fishery Bulletin

***Fishery Bulletin* web site: fishbull.noaa.gov**

The *Fishery Bulletin* carries original research reports and technical notes on investigations in fishery science, engineering, and economics. It began as the Bulletin of the United States Fish Commission in 1881; it became the Bulletin of the Bureau of Fisheries in 1904 and the *Fishery Bulletin* of the Fish and Wildlife Service in 1941. Separates were issued as documents through volume 46; the last document was No. 1103. Beginning with volume 47 in 1931 and continuing through volume 62 in 1963, each separate appeared as a numbered bulletin. A new system began in 1963 with volume 63 in which papers are bound together in a single issue of the bulletin. Beginning with volume 70, number 1, January 1972, the *Fishery Bulletin* became a periodical, issued quarterly. In this form, it is available by subscription from the Superintendent of Documents, U.S. Government Printing Office, Washington, DC 20402. It is also available free in limited numbers to libraries, research institutions, State and Federal agencies, and in exchange for other scientific publications.

U.S. Department of Commerce
Seattle, Washington

Volume 101
Number 1
January 2003

Fishery Bulletin

Contents

The use of parasites in discriminating stocks of Pacific halibut (*Hippoglossus stenolepis*) in the northeast Pacific

Reginald B. Blaylock
Department of Biological Sciences
University of Alberta
Edmonton, AB T6G 2E9, Canada

and

Department of Fisheries and Oceans
Pacific Biological Station
Nanaimo, B.C. V9R 5K6, Canada
Present address: College of Marine Sciences
The University of Southern Mississippi
703 East Beach Blvd
P.O. Box 7000
Ocean Springs, Mississippi 39566-7000
E-mail address: reg.blaylock@usm.edu

Leo Margolis (deceased)
Department of Fisheries and Oceans
Pacific Biological Station
Nanaimo, B.C. V9R 5K6, Canada

John C. Holmes
Department of Biological Sciences
University of Alberta
Edmonton, AB T6G 2E9, Canada

Abstract—The use of parasites as indicators of the stock structure of Pacific halibut (*Hippoglossus stenolepis*) in the northeast Pacific was investigated by using 328 adult (>55 cm fork length) halibut from 15 composite localities ranging from northern California to the northern Bering Sea and 96 juvenile (10–55 cm) halibut from five localities ranging from the northern Queen Charlotte Islands to the Bering Sea. Counts of eight selected parasite species (the juvenile acanthocephalans *Corynosoma strumosum* and *C. villosum*, the metacestode *Nybelinia surmenicola*, the digenean metacercaria *Otodistomum* sp., and the larval nematodes *Anisakis simplex*, *Pseudoterranova decipiens*, *Contracaecum* sp., and Spirurid gen. sp.) that produce infections of long duration, do not multiply in the host, and that have a relatively high abundance in at least one geographic locality were subjected to discriminant function analysis. Juvenile Pacific halibut showed no separation and, even though they were not heavily infected with parasites, the analysis suggested that juveniles could be a mixed stock. Three groups of adults were identified: fish from California to the southern Queen Charlotte Islands, those from the northern Queen Charlotte Islands to the central Bering Sea, and those from the central and northern Bering Sea. These groups suggest that the single stock concept be more thoroughly evaluated.

Manuscript accepted 10 July 2002.
Fish. Bull. 101: 1–9 (2003).

The Pacific halibut (*Hippoglossus stenolepis*) is an Arctic–Boreal Pacific pleuronectid flatfish ranging throughout the North Pacific from southern California to northern Japan, but is most abundant in the Gulf of Alaska. The halibut supports one of the top five commercial fisheries in North America, with average annual landings of approximately 25,000 metric tons from 1991 to 1995 (IPHC, 1996), and is also widely sought in the sport fishery, thus contributing significantly to west coast economies. The International Pacific Halibut Commission (IPHC) is responsible for management of the resource. From the 1930s through the 1950s the IPHC recognized at least three stocks of halibut from tagging experiments, egg and larval drift, anatomical differences, and differences in growth rate: 1) those in the Bering Sea; 2) those from the Gulf of Alaska south to Cape Spencer, Alaska; and 3) those south of Cape Spencer (Skud, 1977). These boundaries roughly followed the zoogeographic zonation in the North Pacific. Skud (1977) re-analyzed the data and concluded that there was extensive intermingling of fish among areas and that there was no evidence to indicate that fish north and south of Cape Spencer, Alaska, constituted different stocks. Available biochemical evidence (Tsuyuki et al., 1969; Grant et al., 1984), although limited in scope and by sampling effort, suggests little genetic variation throughout the northeast Pacific. As a result, the IPHC manages halibut as a single population, but with statistical divisions for management of data.

Parasites have been used successfully to distinguish populations or stocks of fishes and, as a result, provide information useful in fisheries management (see

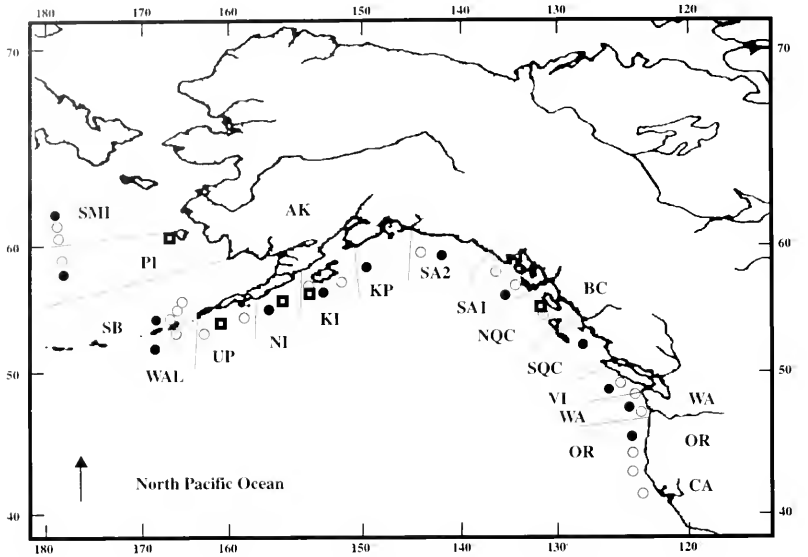

Figure 1

Sampling localities for 328 adult (circles) and 96 juvenile (squares) Pacific halibut, *Hippoglossus stenolepis*, in the northeast Pacific. OR = Oregon–northern California, WA = Washington, VI = Vancouver Island, SQC = southern Queen Charlotte Islands, NQC = northern Queen Charlotte Islands, SA1 = southeast Alaska site 1, SA2 = southeast Alaska site 2, KP = Kenai Peninsula, KI = Kodiak Island, NI = Nagai Island, UP = Unimak Pass, WAL = western Aleutian Islands, SB = southern Bering Sea, PI = Pribilof Island, SMI = St. Matthew Island. Individual hauls with at least 10 fish (for a total of 202 fish) are shown as solid circles. Other collection sites are shown as stippled circles. See Table 1 for sample sizes.

reviews by Lester, 1990; Moser, 1991; Williams et al., 1992). With respect to flatfish, Gibson (1972) used parasitological data to distinguish three groups of *Platichthys flesus* and Krzykawski and Wierzbicka (1982) used parasitological data and other information to distinguish between Barents Sea and Labrador stocks of Greenland halibut, *Reinhardtius hippoglossoides*. Khan et al. (1982) and Arthur and Albert (1993) used parasites to distinguish between Atlantic and Gulf of St. Lawrence stocks of *R. hippoglossoides*, and Boje et al. (1997) used parasites to indicate differences among Greenland stocks of Greenland halibut and stocks from the western Atlantic. No similar work on flatfishes has been done in the Pacific and, with the exception of Krzykawski and Wierzbicka (1982) and Boje et al. (1997), there has been no attempt to distinguish between stocks of a species across a significant portion of the species' range.

In this article, we use discriminant analysis on counts of some of the parasites from adult Pacific halibut to determine if they form discrete groups or stocks in the northeast Pacific. We do a similar analysis on the juvenile fish and compare the results to the adult analysis to determine when separation is likely to occur.

Materials and methods

A total of 328 adults (>55 cm fork length) from 15 composite localities, ranging from northern California to the vicinity of St. Matthew's Island in the Bering Sea and 96 juveniles (10–55 cm) from five localities ranging from the northern Queen Charlotte Islands to the Bering Sea (Fig. 1), were caught by staffs of the IPHC and the U.S. National Marine Fisheries Service during the summers of 1990–92 (using longlines and trawls). Most localities (for the adult samples) included fish taken from several hauls; however, 202 fish came from 13 individual hauls, each of which contained at least 10 fish. Fish were bagged individually and immediately frozen at sea for later examination.

Fish and parasites were processed by using standard parasitological techniques (see Blaylock et al., 1998a). We followed Bush et al.'s (1997) definitions for prevalence, abundance, and intensity. Parasites used in the analyses were chosen according to the guidelines of Arthur and Albert (1993). Only those species with infections of long duration, that do not multiply in the host, and that have a relatively high abundance in at least one geographic locality were used. Of the 59 parasite taxa identified from

Pacific halibut (Blaylock et al., 1998a), eight taxa met these criteria: the juvenile acanthocephalans *Corynosoma strumosum* (body cavity) and *C. villosum* (body cavity), the metacestode *Nybelinia surmenicola* (stomach wall), the digenean metacercaria *Otodistomum* sp. (stomach wall), and the larval nematodes *Anisakis simplex* (body cavity, organs, musculature), *Pseudoterranova decipiens* (body cavity, organs, musculature), *Contracaecum* sp.(body cavity), and Spirurid gen. sp. (stomach wall). A ninth taxon, the larval nematode *Hysterothylacium aduncum* (body cavity and organs) was included for the analysis of juveniles.

Because individual fish varied extensively in size (fork length), and the number of a parasite individuals was strongly correlated with fish size (Blaylock et al., 1998a), parasite numbers were corrected for differences in host size. Counts of individual parasites were first log-transformed ($\ln(x+1)$). To adjust for the effect of fish length, a regression of the transformed parasite numbers on fish length for each species in each locality (and haul) was calculated. This relationship was then used to adjust the number of parasite individuals within each fish in each locality (and haul) to that expected for the average-size fish in the overall sample (80.9 cm for adults, 39.2 cm for juveniles). These data were then used in discriminant function analyses. We applied the most widely used (and available) method of discriminant function analysis, in which the data were divided into training and test sets, and a discriminant function calculated on the training set was used to classify the test set. Interpretations were based on patterns in the test sets. To insure that any identified patterns were due to differences among localities rather than simply differences among individual hauls, we performed the same analysis on both the locality and the individual haul data.

Our training set consisted of six fish randomly selected from each haul ("haul" training set) or these fish plus four from the northern Queen Charlotte Islands and six from Unimak Pass ("locality" training set). Discriminant functions calculated from data on these "training" fish were used to classify each of the remaining fish from each haul ("haul" test set) or those fish plus all remaining fish ("locality" test set). The test set fish were first classified into one of the 13 hauls or 15 localities. Classification matrices were examined for the degree of misclassification. Hauls or localities were then grouped and regrouped into four and three groups based on patterns in the 13 or 15 category analyses and the zoogeographic zones from Blaylock et al. (1998b). Analyses were then repeated. Classifications were examined for misclassification, and boundaries adjusted for retesting. Results presented are those from the best fit "test" classifications. Statistical analyses were performed in SYSTAT for Windows version 5.05 (Wilkinson et al., 1992). The entire data set from which the data for this analysis came is available for purchase from the Depository of Unpublished Data, Document Delivery, CISTI, National Research Council of Canada, Ottawa, ON K1A 0S2, Canada.

Results

Of the taxa that met the Arthur and Albert (1993) criteria, *N. surmenicola* was most common and abundant in northern localities and fairly common and abundant in central localities. *Corynosoma strumosum*, although variable in prevalence and abundance, was much more common in the northernmost localities. *Corynosoma villosum*, although prevalent everywhere, was more abundant in northern fish. *Otodistomum* sp. and Spirurid gen. sp. were more common and abundant in southern localities. *Anisakis simplex*, although present in virtually every fish from every locality, was more abundant in southern fish. *Pseudoterranova decipiens* and *Contracaecum* sp. appeared to be more common in central areas (Table 1). In the juveniles, *A. simplex* and *P. decipiens* were more common in central localities, whereas *C. villosum*, *C. strumosum*, and *Hysterothylacium aduncum* were more common in northern localities (Table 2).

The haul analyses indicated that the majority of fish from some hauls (12/14 Vancouver Island [VI] fish, 3/4 Southeast Alaska 1 [SA1] fish, 3/5 from the Pribilof Islands [PI], and all 4 from St. Matthew's Island [SMI]) could be correctly classified but that fish from surrounding areas also were incorrectly classified to these hauls. Moreover, the percentage of fish correctly classified by the haul functions was, in all cases, within only a few percentage points of that correctly classified by the equivalent locality function. Thus, patterns do not appear to be associated with independent hauls. Therefore, we present only the results of the locality analyses.

Fifteen category discriminant analyses revealed severe misclassification in most areas. Only 39% were correctly classified to locality (Table 3). The functions did assign correctly the majority of test fish from two localities (19/26 from Vancouver Island [VI] and 14/22 from the southern Bering Sea [SB]). However, misclassification of fish from surrounding areas to these localities indicated less than accurate discrimination. The clearest indications from these analyses were that localities from the vicinity of the Queen Charlotte Islands south should be grouped together and that there is a suggestion that the two northern Bering Sea locations (PI and SMI) should be grouped.

Regrouping the localities into four categories by using boundaries from zoogeographic analyses (Blaylock et al., 1998b) plus the apparent northern Bering Sea grouping (PI–SMI), considerably improved the predictive ability of the functions. The "best fit" four-category grouping gave approximately 62% correct classification at the locality level (Table 4). The four-category functions were good predictors for the California–Oregon (OR) to southern Queen Charlotte Islands (SQC) fish; over 80% of these southern fish were correctly classified, and only about 6% of the other fish were misclassified to this group. Over 70% of the Pribilof–St. Matthew Island (PI–SMI) fish were correctly classified, and only 7% of the other fish were incorrectly classified to this group. There was much misclassification in the two central groups, and adjustment of the boundary between these two groups did not produce marked improvement (not shown).

Grouping into three categories by combining the two central groups resulted in substantial improvement in discrimination (83% correct) (Table 5). Shifting of the boundary between the northern and central group revealed that discrimination broke down when the southern

Table 1

Summary of parasites used for discrimination of stocks of adult Pacific halibut by locality. OR = Oregon–northern California, WA = SA1= southeast Alaska 1, SA2 = southeast Alaska 2, KP = Kenai Peninsula, KI = Kodiak Island, NI = Nagai Island, WAI = western bc = body cavity, o = organs, m = musculature, sw = stomach wall. Intensity = mean number of parasites per infected host.

			OR (n=23)		WA (n=14)	
Parasite	Site	Stage	%	Intensity	%	Intensity
Anisakis simplex	bc, o, m	larva	100	258.2 ±520.2	100	122.2 ±101.0
Corynosoma villosum	bc	juvenile	74	7.9 ±5.4	71	6.3 ±7.3
Corynosoma strumosum	bc	juvenile	52	5.6 ±6.4	50	6.3 ±5.2
Nybelinia surmenicola	sw	metacestode	17	2.8 ±2.9	14	4.0 ±4.2
Otodistomum sp.	sw	metacercaria	44	14.3 ±13.8	36	32 ±55.7
Pseudoterranova decipiens	bc, o, m	larva	44	2.5 ±2.1	21	2.3 ±1.5
Contracaecum sp.	bc	larva	0	0	0	0
Spirurid gen. sp.	sw	larva	22	1.4 ±0.5	50	11 ±24.7

	KP (n=21)		KI (n=26)		NI (n=13)	
Parasite	%	Intensity	%	Intensity	%	Intensity
Anisakis simplex	100	33.6 ±22.1	100	29.5 ±27.3	100	80.3 ±62.0
Corynosoma villosum	95	11.1 ±12.4	100	11.2 ±18.4	85	12.6 ±15.0
Corynosoma strumosum	19	1 ±0.0	27	1.3 ±0.5	8	2.0 ±0.0
Nybelinia surmenicola	43	4.2 ±3.9	65	29.5 ±106.6	39	42.2 ±89.0
Otodistomum sp.	14	2.0 ±1.7	4	1 ±0	8	1 ±0.0
Pseudoterranova decipiens	29	1.5 ±1.2	50	1.9 ±1.4	61	2.5 ±2.0
Contracaecum sp.	62	3.0 ±3.08	50	3.2 ±3.2	0	0
Spirurid gen. sp.	9	1.0 ±0	4	1 ±0.0	0	0

Table 2

Summary of parasites used for discrimination of stocks of juvenile Pacific halibut. NQC = northern Queen Charlotte Islands, NI = Nagai Island, UP = Unimak Pass, PI = Nunivak Island (central Bering Sea). bc = body cavity, o = organs, m = musculature, sw = stomach wall. Intensity = mean number of parasites per infected host.

			NQC (n=20)		KI (n=13)		NI (n=20)		UP (n=20)		PI (n=23)	
Parasite	Site	Stage	%	Intensity	%	Intensity	%	Intensity	%	Intensity	%	Intensity
Anisakis simplex	bc, o, m	larva	25	1.2	8	1.0 ±0	65	3.1 ±1.9	70	3.6 ±3.1	30	1.7 ±0.8
Corynosoma villosum	bc	juvenile	5	1 ±0.0	46	1.3 ±2.4	75	3.4 ±2.6	80	5.8 ±7.4	9	1.5 ±0.7
Corynosoma strumosum	bc	juvenile	0	0	8	1.0 ±0	0	0	5	1 ±0.0	48	1.2 ±0.4
Hysterothylacium aduncum	bc, o	juvenile	15	1 ±0.0	92	4 4 ±3.2	95	8 7 ±10.7	85	5.4 ±8.8	74	2.8 ±1.5
Nybelinia surmenicola	sw	metacestode	0	0	0	0	0	0	5	1 ±0.0	26	1.3 ±0.8
Pseudoterranova decipiens	bc, o, m	larva	0	0	8	1.0 ±0	25	1.4 ±0.9	15	1 ±0.0	4	6 ±0.0
Contracaecum sp.	bc	larva	0	0	15	1.0 ±0	10	5 ±5.7	0	0	0	0
Spirurid gen. sp.	sw	larva	0	0	0	0	5	2.0 ±0.0	0	0	0	0

Table 1

Washington, VI = southern Vancouver Island, SQC = southern Queen Charlotte Islands, NQC = northern Queen Charlotte Islands, Aleutian Islands, SB = southern Bering Sea, PI, Pribilof Island (central Bering Sea), SMI = St. Matthew Island (northern Bering Sea).

VI (n=32)		SQC (n=31)		NQC (n=8)		SA1 (n=20)		SA2 (n=29)	
%	Intensity	%	Intensity	%	Intensity	%	Intensity	%	Intensity
100	381.4 ±357.1	100	167.8 ±101.4	100	76.1 ±47.6	100	81.8 ±141.1	100	44.0 ±57.0
94	8.8 ±7.4	94	13.7 ±24.3	100	5.9 ±7.4	90	10.9 ±16.6	93	16.1 ±32.0
44	3.6 ±5.2	39	1.8 ±1.5	25	2.0 ±0.9	15	1.7 ±0.6	52	1.9 ±1.0
19	16.0 ±31.9	3	1.0 ±0.0	50	13.3 ±23.8	30	11.8 ±25.1	52	4.1 ±2.0
9.4	18.3 ±30.0	39	8.3 ±13.9	38	4.7 ±2.3	35	13.0 ±11.0	21	8.3 ±11.0
16	1.2 ±0.4	13	1.5 ±0.6	25	2.0 ±0.0	25	3.2 ±4.4	69	3.1 ±3.0
3	1.0 ±0	0	0	50	3.8 ±4.9	40	3.5 ±2.2	45	2.0 ±2.0
3	1.0 ±0	0	0	0	0	15	2.3 ±1.2	10	2.8 ±2.0
UP (n=20)		WAI (n=20)		SB (n=29)		PI (n=14)		SMI (n=28)	
%	Intensity	%	Intensity	%	Intensity	%	Intensity	%	Intensity
100	53.3 ±43.8	100	41.5 ±55.0	100	40.6 ±33.6	100	21.5 ±22.3	84	10.9 ±10.0
85	29.6 ±57.4	95	13.8 ±14.0	97	16.8 ±18.3	86	34.4 ±37.0	90	34.4 ±55.9
30	2.0 ±1.5	40	2.1 ±2.0	38	8.5 ±20.2	79	9.0 ±9.3	77	23.2 ±25.4
55	2.7 ±2.1	35	16.1 ±33.8	52	6.7 ±13.1	57	34.6 ±69.2	58	25.0 ±69.8
0	0	5	1 ±0	0	0	0	0	0	0
45	1.4 ±0.7	45	2.3 ±2.0	38	2.3 ±1.5	29	2.3 ±1.3	23	2.4 ±1.8
15	2.0 ±1.0	30	1.3 ±1.0	38	3.0 ±4.5	14	1.0 ±0	7	4.0 ±3.5
5	1.0 ±0.0	0	0	4	1 ±0.0	0	0	0	0

Bering Sea (SB) was included in the northern group (not shown). Inclusion of the northern Queen Charlotte Islands (NQC) in the southern group had little effect (81% correct classification) (not shown). These analyses indicated a southern (OR–SQC) group, a central (NQC–SB) group, and a northern (PI–SMI) group.

Classification into two categories (with SQC as the dividing line) provided no substantial improvement (87% correct) (not shown). Inclusion of NQC in the southern group had little effect (88% correct classification).

Discrimination of juveniles was poor with any organization of localities. The "best fit" classification correctly classified only 66% of the fish and there was substantial misclassification among the localities (Tables 6 and 7). Fish from the northern Queen Charlotte Islands (NQC) through Nagai Island (NI) separated reasonably well, but the majority of fish from the northernmost locality were also misclassified to this group. Note that parasite numbers and prevalences were low in the juveniles (Table 2).

Discussion

Our results show four things: 1) parasites clearly differentiate a group of southern adults; 2) parasites provide some evidence for a separation of the northernmost adults; 3) the differentiation is not always unequivocal; and 4) parasites do not differentiate groups of juvenile fish.

Skud (1977) concluded that southern and northern groups mixed extensively at all ages of their life history and that, although populations of adults may be largely discrete in the summer, any such discreteness was temporary because tagging evidence suggested more extensive winter migrations associated with spawning. Our data, on the other hand, suggest that there is some merit to the IPHC's early recognition of three stocks of adult halibut. Parasite data support the existence of two major groups of halibut and suggest the possibility of a third group in the central and northern Bering Sea. The high proportion of correct classifications based on parasites suggest that these differences are well established.

Recognition of three such groups is also supported by several of Skud's (1977) observations. He presented data suggesting that after fish home to spawning areas, southern and northern fish maintain reasonably separate migration circuits between feeding and spawning grounds. Data from Skud (1977) and more recent tagging data (Geernaert, 1996) also suggest that southern fish move less than their northern counterparts. Skud also recognized a resident population in the Bering Sea. These con-

Table 3

Cross validation results of a 15-category discriminant function classification of adult Pacific halibut in the northeast Pacific based on parasite data. Numbers of fish assigned to each locality and the corresponding percentage of the sample assigned to that category are shown. See Table 1 legend for key to abbreviations. Correct classifications are shown in bold (28% of 240).

True category	Assigned category														
	OR	WA	VI	SQC	NQC	SA1	SA2	KP	KI	NI	UP	WAL	SB	PI	SMI
OR	**4** **17%**	2 9%		1 4%	2 9%						2 9%		3 13%		
WA	2 25%	**2** **3%**			1 13%									1 13%	2 25%
VI		1 4%	**19** **73%**	2 8%	3 12%							1 4%			
SQC	1 4%	1 4%	10 40%	**11** **44%**							2 8%				
NQC					**2** **50%**	2 50%									
SA1		1 7%			1 7%	**4** **29%**		1 7%	1 7%	1 7%				3 21%	
SA2	1 4%				1 4%	2 9%	**1** **4%**	3 13%	3 13%	1 4%	1 4%		8 35%	1 4%	1 4%
KP						7 50%	1 7%	**1** **7%**	1 7%	1 7%	2 14%		1 7%		
KI						7 35%	2 10%	1 5%	**2** **10%**	1 5%	2 10%		3 15%	2 10%	
NI			1 14%		1 14%				2 29%	**1** **14%**	1 14%				
UP			2 14%			1 7%			2 14%	2 14%	**1** **7%**	2 14%	3 21%		1 7%
WAI						3 21%	1 7%	1 7%		2 14%	2 14%	**0**	5 36%		
SB		1 7%			1 7%	4 29%	3 21%	1 7%	2 14%	1 7%	2 14%	5 36%	**1** **7%**		2 14%
PI													1 13%	**3** **38%**	4 50%
SMI						**1** 5%			3 14%			3 14%		1 5%	**14** **64%**

clusions pose two questions. First, do fish from different groups mix extensively? Second, do such groups represent reproductive units or stocks?

Our analysis was based on a small set of larval parasites, all of which are known to be long-lived and do not multiply in the host. Other long-lived parasites such as the myxosporeans have been used in stock discrimination but were not included here because of a lack of abundance data. However, the decreased ability to detect differences because of the small data set was offset by an increased ability to detect the host's past activities. Most of these parasites live for at least several years; therefore, the presence and abundance of these parasites may indicate where the host has been over that time period. At least some of the individuals of each of the parasite species, however, were probably short-term acquisitions (lasting a few years); thus, there may be some bias in the data of the recent past.

Our data suggest less extensive movement of Pacific halibut in southern areas. Because parasites are generally more abundant in the south, southern fish may be more easily classified. Nevertheless, if the southern fish mingle extensively with more northern fish, there should be more similarity in the parasite faunas. In particular, central area fish should develop characteristics of southern fish. This did not happen, as is shown by the very low proportion of central fish misclassified as southern fish (Table 5). Our information cannot completely rule out the movement of southern fish to central areas during the spawning season, and then back to southern areas for the feeding season. Their long-lived parasite fauna, having been established in the distinct southern areas, would probably

Table 4

Cross validation results of a four-category discriminant function classification of adult Pacific halibut in the northeast Pacific based on parasite data. Numbers of fish assigned to a category and the corresponding percentage of the sample in that category are shown. Correct classifications are shown in bold (63% of 240). OR–SQC = Oregon–northern California to southern Queen Charlotte Islands, NQC–KP = northern Queen Charlotte Islands to Kenai Peninsula, KI–SB = Kodiak Island to southern Bering Sea, PI–SMI = Pribilof Islands to St. Matthew Island.

True category	Assigned category			
	OR–SQC	NQC–KP	KI–SB	PI–SMI
OR–SQC	**60**	3	7	6
	79%	4%	9%	8%
NQC–KP	3	**28**	21	4
	5%	**50%**	42%	7%
KI–SB	7	23	**41**	7
	9%	30%	**53%**	**9%**
PI–SMI		1	6	**23**
		3%	20%	**77%**

Table 5

Cross validation results of a three-category discriminant function classification for adult Pacific halibut in the northeast Pacific based on parasite data. Numbers of fish assigned to a category and the corresponding percentage of the sample in that category are shown. Correct classifications are shown in bold (83% of 240). OR–SQC = Oregon–northern California to southern Queen Charlotte Islands, NQC–SB = southeast Alaska to southern Bering Sea, PI–SMI = Pribilof Islands to St. Matthew Island.

True category	Assigned category		
	OR–SQC	NQC–SB	PI–SMI
OR–SQC	**63**	7	6
	83%	9%	8%
NQC–SB	10	**112**	12
	7%	**84%**	9%
PI–SMI		5	**25**
		17%	**83%**

Table 6

Cross validation results of five-category discriminant function classification for juvenile Pacific halibut in the northeast Pacific based on parasite data. Numbers of fish assigned to a category and the corresponding percentage of the sample in that category are shown. Correct classifications are shown in bold (44% of 62). NQC = northern Queen Charlotte Islands, NI = Nagai Island, UP = Unimak Pass, and PI = Nunivak Island (central Bering Sea).

True category	Assigned category				
	NQC	KI	NI	UP	PI
NQC	**9**	4			
	69%	31%			
KI	1	**5**	1		
	14%	**71%**	14%		
NGI	5	3	**3**	2	
	39%	23%	**23%**	15%	
UP	5		2	**5**	1
	39%		15%	**39%**	8%
PI	6	4		1	**5**
	38%	25%		6%	**31%**

Table 7

Cross validation results of a three-category discriminant function classification for juvenile Pacific halibut in the northeast Pacific based on parasite data. Numbers of fish assigned to a category and the corresponding percentage of the sample in that category are shown. Correct classifications are shown in bold (66% of 62). NQC = northern Queen Charlotte Islands, NI = Nagai Island, UP = Unimak Pass, PI = Nunivak Island (central Bering Sea).

True category	Assigned category		
	NQC–NI	UP	PI
NQC–NI	**30**	3	
	91%	9%	
UP	6	**6**	1
	46%	**46%**	8%
PI	10	1	**5**
	63%	6%	**31%**

not lose their southern character. Winter sampling could potentially determine if this is the case.

With respect to the Bering Sea, we suggest that the majority of the mixing occurs in the southern Bering Sea because classification breaks down when the southern Bering Sea is included in the northern region. This mixing is consistent with larval studies that show that larvae enter the Bering Sea through the Aleutian chain. Those fish may not disperse far into the Bering Sea. Rather, they either remain in the southern Bering Sea or migrate back to the Gulf of Alaska area (Skud [1977] believed that both occurred). A migration may explain why fish tagged in the Bering Sea tend to be recovered at greater distances from the tagging site than those tagged elsewhere (Geernaert, 1996). Migrations of the central and northern Bering Sea group appear to be in a more northerly direction (Skud,

1977), which would preclude mixing in the Aleutians and the Gulf of Alaska. Zoogeographic analysis with patterns of prevalence showed that Bering Sea parasites are rarely found outside the Bering Sea (Blaylock et al., 1998b).

The patterns identified in our analysis agree only in part with zoogeographic analyses (Blaylock et al., 1998b). The southern boundaries in both studies are in the vicinity of the Queen Charlotte Islands, providing additional support for the existence of a southern group of halibut. However, this analysis, unlike the zoogeographic analyses, indicated no sign of a division in the vicinity of Kodiak Island, suggesting that the division near Kodiak Island depends on short-lived species not included in this analysis. The evidence for the existence of a northern Bering Sea group is equivocal; it was supported by the clustering of localities by using prevalences and, to some degree, the clustering of individuals, but was not supported by any other analyses (Blaylock et al., 1998b).

With respect to juveniles, Skud's (1977) analysis clearly indicates compensatory movement from the Gulf of Alaska and southern Bering Sea to southern areas, and, as such, predicts that juveniles should have more similar parasite faunas among areas. Our data show this similarity, but there are significant caveats. First, our samples of juveniles came from areas that form a single group in the classification of adults. The sample from the northern Queen Charlottes is near the southern boundary of that group, and the sample from Nunivak Island is near the northern boundary. Samples of juveniles from other areas, particularly the southern area, should be examined to help clarify this issue. Second, and maybe more important, in these smaller fish, prevalences and intensities are low and perhaps hinder separation. However, because halibut at this stage are susceptible to bycatch in other fisheries (IPHC, 1996), management should probably consider juveniles a mixed stock to prevent impacts on future halibut populations in distant localities.

Overall, our analysis provides a less clear picture than that of Arthur and Albert (1993) for Greenland halibut in the northwest Atlantic. Part of the lack of clarity may be due to our use of the training and test set method rather than the bootstrapping method used by Arthur and Albert, which would increase the likelihood of correctly classifying similar fish. Also, Arthur and Albert were dealing with a very different system. Geological and oceanographic conditions around the Gulf of St. Lawrence are quite complex and create great potential for the isolation of stocks. The northeast Pacific is more open and has fewer isolating mechanisms than the northwest Atlantic. Further, the system is clinal (Blaylock et al., 1998b) and Pacific halibut are quite capable of migrating along the entire Pacific coast; therefore, less clear cut divisions are expected. Nevertheless, we successfully identified groups of fish, some with a high degree of accuracy.

Skud (1977) suggested that juveniles will, as adults, home to the areas in which they were spawned, making the existence of reproductive stocks at least possible. Modern molecular methods could address the issue. For example, molecular methods could potentially address the existence of separate stocks in the south and in the northern Bering Sea. The limited molecular studies done to date, however, have not elucidated any indentifiable stock structure because of limited sampling localities, the limited number of loci examined, and the use of juveniles only. Tsuyuki et al. (1969) examined a single serum hemoglobin transferrin locus in halibut from ten sites from Vancouver Island to the Bering Sea and found that only one southeast Alaska locality was different. Grant et al. (1984) found no differences between Gulf of Alaska and Bering Sea halibut at five loci but were able to distinguish northeast Pacific halibut from Japanese halibut. However, it is important to note that biochemical and genetic information measures differentiation at a different time scale than that reflected in parasite data (Lester et al., 1988). According to Grant (1984), movement of only a few Atlantic herring (*Clupea harengus*) may be sufficient to obscure true differences between different breeding stocks. Thus, even limited gene flow could obscure any differences in the loci examined.

Parasite or tagging information alone, however, can not determine whether or not the groups we identified are reproductive stocks. Therefore, all potential factors that might refine the halibut stock concept should be considered. The parasite data suggest a conservative approach to management that recognizes a mixed stock of juveniles and three potential stocks of adults—one in the south, another in the northern Bering Sea, and a third and largest centered in the Gulf of Alaska.

Acknowledgments

We thank the International Pacific Halibut Commission, Seattle, WA, for coordinating sampling and for financial support. Mark Higgins and John Quintero provided invaluable assistance in the laboratory. Tom McDonald and Dave Whitaker provided technical assistance. We also thank Al Shostak and Jeff Lotz for advice and comments.

Literature cited

Arthur, J. R., and E. Albert.
1993. Use of parasites for separating stocks of Greenland halibut (*Reinhardtius hippoglossoides*) in the Canadian northwest Atlantic. Can. J. Fish. Aquat. Sci. 50:2175–2181.

Blaylock, R. B., J. C. Holmes, and L. Margolis.
1998a. The parasites of Pacific halibut (*Hippoglossus stenolepis*) in the eastern North Pacific: host-level influences. Can. J. Zool. 76:536–547.

Blaylock, R. B., L. Margolis, and J. C. Holmes.
1998b. Zoogeography of the parasites of Pacific halibut (*Hippoglossus stenolepis*) in the northeast Pacific. Can. J. Zool. 76:2262–2273.

Boje, J., F. Riget, and M. Koie.
1997. Helminth parasites as biological tags in population studies of Greenland halibut (*Reinhardtius hippoglossoides* (Walbaum)), in the north-west Atlantic. ICES J. Mar. Sci. 54:886–895.

Bush, A. O., K. D. Lafferty, J. M. Lotz, and A. W. Shostak.
1997. Parasitology meets ecology on its own terms: Margolis et al. revisited. J. Parasitol. 83:575–583.

Geernaert, T.
1996. Tagging studies. *In* Report of assessment and research activities, 1995, p. 277–288. International Pacific Halibut Commission, Seattle, WA.
Gibson, D. I.
1972. Flounder parasites as biological tags. J. Fish Biol. 4:1–9.
Grant, W. S.
1984. Biochemical population genetics of Atlantic herring, *Clupea harengus*. Copeia 1984:357–364.
Grant, W. S., D. J. Teel, T. Kokayashi, and C. Schmitt.
1984. Biochemical population genetics of Pacific halibut (*Hippoglossus stenolepis*) and comparison with Atlantic halibut (*H. hippoglossus*). Can. J. Fish. Aquat. Sci. 41: 1083–1088.
IPHC (International Pacific Halibut Commission).
1996. Report of assessment and research activities, 1995, p. 121–172. IPHC, Seattle, WA.
Khan, R. A., M. Dawe, R. Bowering, and R. K. Misra.
1982. Blood protozoa as an aid for separating stocks of Greenland halibut, *Reinhardtius hippoglossoides*, in the northwest Atlantic. Can. J. Fish. Aquat. Sci. 39:1317–1322.
Krzykawski, S. and J. Wierzbicka.
1982. An attempt to determine the systematic position of Greenland halibut, *Reinhardtius hippoglossoides* (Walbaum, 1792), from Labrador region and Barents Sea on the basis of morphometric, biologic, and parasitological studies. Acta Ichthyol. Piscat. 22:59–75.
Lester, R. J. G.
1990. Reappraisal of the use of parasites for fish stock identification. Aust. J. Mar. Freshwater Res. 41:855–864.
Lester, R. J. G., K. B. Sewell, A. Barnes, and K. Evans.
1988. Stock discrimination of orange roughy, *Hoplostethus atlanticus*, by parasite analysis. Mar. Biol. 99:137–143.
Moser, M.
1991. Parasites as biological tags. Parasitol. Today 7:183–186.
Skud, B. E.
1977. Drift, migration, and intermingling of Pacific halibut stocks. International Pacific Halibut Commission, Scientific Rep. No. 63, 12 p. IPHC, Seattle, WA.
Tsuyuki, H., E. Roberts, and E. A. Best.
1969. Serum transferrin systems and the hemoglobins of the Pacific halibut (*Hippoglossus stenolepis*). J. Fish. Res. Board Can. 26:2351–2362.
Wilkinson, L., M. Hill, J. Welna, and G. Birkenbeuel.
1992. SYSTAT for Windows: statistics, version 5 edition, 750 p. SYSTAT Inc., Evanston, IL.
Williams, H. H., K. MacKenzie, and A. McCarthy.
1992. Parasites as biological indicators of the population biology, migrations, diet, and phylogenetics of fish. Rev. Fish Biol. Fish. 2:144–176.

Small-scale spatial and temporal variability in growth and mortality of fish larvae in the subtropical northcentral Gulf of Mexico: implications for assessing recruitment success

Bruce H. Comyns
Department of Coastal Sciences
College of Marine Sciences
The University of Southern Mississippi
703 East Beach Drive
Ocean Springs, Mississippi 39566
E-mail address: bruce.comyns@usm.edu

Richard F. Shaw
Department of Oceanography and Coastal Sciences
School of The Coast and Environment
Louisiana State University
Baton Rouge, Louisiana 70803

Joanne Lyczkowski-Shultz
Southeast Fisheries Science Center
National Marine Fisheries Service
P.O. Drawer 1207
Pascagoula, Mississippi 39568

Abstract—Extensive plankton collections were taken during seven September cruises (1990–93) along the inner continental shelf of the northcentral Gulf of Mexico (GOM). Despite the high productivity and availability of food during these cruises, significant small-scale spatial variability was found in larval growth rates for both Atlantic bumper (*Chloroscombrus chrysurus*, Carangidae) and vermilion snapper (*Rhomboplites aurorubens*, Lutjanidae). The observed variability in larval growth rates was not correlated with changes in water temperature or associated with conspicuous hydrographic features and suggested the existence of less-recognizable regions where conditions for growth vary. Cruise estimates of mortality coefficients (Z) for larval Atlantic bumper (n=32,241 larvae from six cruises) and vermilion snapper (n= 2581 larvae from four cruises) ranged from 0.20 to 0.37 and 0.19 to 0.29, respectively. Even in a subtropical climate like the GOM, where larval-stage durations may be as short as two weeks, observed variability in growth rates, particularly when combined with small changes in mortality rates, can cause order-of-magnitude differences in cumulative larval survival. To what extent the observed differences in growth rates at small spatial scales are fine-scale "noise" that ultimately is smoothed by larger-scale processes is not known. Future research is needed to further characterize the small-scale variability in growth rates of larvae, particularly with regard to microzooplankton patchiness and the temporal and spatial pattern of potential predators. Small-scale spatial variability in larval growth rates may in fact be the norm, and understanding the implications of this subtle mosaic may help us to better evaluate our ability to partition the causes of recruitment variability.

Manuscript accepted 11 July 2002.
Fish. Bull. 101(2):10–21 (2003).

For many marine fishes year-class strength undergoes large fluctuations because of the inherent variability in larval, postlarval, and juvenile survivorship (Hjort, 1914; Cushing, 1975; Lasker, 1975; Hunter, 1982; Houde, 1987; Goshorn and Epifanio, 1991; Pepin and Myers, 1991). Understanding and quantifying recruitment variability remains one of the greatest challenges in fisheries science today (Fritz et al., 1990; Cushing and Horwood, 1994; Leggett and Deblois, 1994; Mertz and Myers, 1995). Early survival rates are influenced not only by predation pressure but also by growth rate which can alter the duration of the larval stage when larvae are exposed to accumulative high mortality rates (Houde, 1987; Chambers and Leggett, 1987; Anderson, 1988; Bailey and Houde, 1989). Pepin (1991) formalized this concept by depicting the cumulative mortality (C) of a population from stage a to older stage b as the direct function of the instantaneous growth ($g[x]$) and mortality ($M[x]$) rates such that

$$C = \int_a^b \frac{M[x]}{g[x]}\,dx,$$

where x are factors that influence the vital rates (M and g) such as food availability, temperature, and abundance of potential predators.

Many questions remain concerning the causes of recruitment variability. Reasons for variability include the following: the inherent variability in growth and mortality rates and resulting survivorship; difficulties in estimating mortality rates with sufficient accuracy and precision; and the complex interrelationships among factors that affect survivorship of larvae (Parrish, 1973; Laurence, 1979; Houde, 1987; Beyer, 1989; Pepin, 1991). Houde (1989) hypothesized that cohort survivorship is more sensitive to small changes in vital rates in high latitude systems than in tropical or subtropical systems because the colder temperatures cause slower growth rates and longer larval stage durations, i.e. up to 100 days.

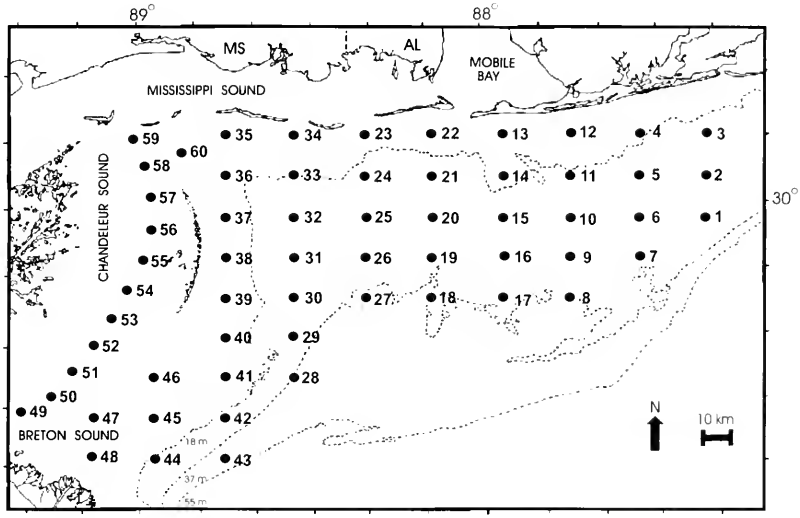

Figure 1

Station locations (•) of plankton collections in the northcentral Gulf of Mexico, September 1990 to 1993.

Pepin (1991) questioned this conclusion because he found no net effect of temperature on postlarval stage-specific mortality rates, although his study was based mainly on interspecific variation in mortality (Francis, 1994).

The objectives of our study were to determine if growth rates of Atlantic bumper (*Chloroscombrus chrysurus*, Carangidae) and vermilion snapper (*Rhomboplites aurorubens*, Lutjanidae) varied over small spatial scales in the northcentral Gulf of Mexico (GOM); determine the magnitude and variability of cruise estimates of larval mortality; and determine the potential influence of variability in these vital rates on cohort survivorship in a region where summer water temperatures approach 30°C and larval stage durations are as short as two to three weeks. Vermilion snapper is the most abundant species of snapper in the northern GOM (Goodyear and Schirripa[1]), and Atlantic bumper is the most abundant carangid.

Materials and methods

Sampling location and shipboard procedures

Seven, three-day cruises were conducted in inner-shelf waters of east Louisiana, Mississippi, and Alabama during September 1990–93 (Fig. 1). Cruise estimates of larval mortality were determined by using data from all cruises during the four-year period. Specimens used for age and growth analyses were collected during 14–16 September 1991 when larvae of both vermilion snapper and Atlantic bumper were abundant.

Larvae were collected with a 1 m × 1.4 m Tucker trawl fitted with a 333-μm mesh nitex net and a mechanical flowmeter. Oblique tows were taken from the surface to within a few meters of the bottom and back to the surface at a speed of approximately two knots (1.0 m/s). Samples were concentrated and stored in 95% ethanol. At each sampling location surface, midwater and bottom measurements of temperature and salinity were obtained with water-bottle casts.

Laboratory procedures

Lengths of larvae were measured to the nearest 0.1 mm by using a stereomicroscope (12× or 25×) fitted with an ocular micrometer and the larvae were sorted into 0.5-mm size classes. Measurements were taken from the tip of the snout to the end of the notochord in preflexion larvae (notochord length), and from the tip of the snout to the end of the urostyle or hypural plate (whichever was more distal) in flexion or postflexion larvae (standard length). Larval shrinkage was not accounted for because between-station and between-cruise comparisons of growth rates were made with larvae that were preserved in the same concentration of ethanol and stored for approximately the same length of time. Shrinkage of ethanol-preserved

[1] Goodyear, C. P., and M. J. Schirripa. 1991. A biological profile for vermilion snapper with a description of the fishery in the Gulf of Mexico. Unpublished report CRD 87/88-16, 53 p. Southeast Fisheries Science Center, National Marine Fisheries Service, 75 Virginia Beach Drive, Miami FL 33149.

larvae is not large, e.g. 0 to 7% (Theilacker, 1980; Fowler and Smith, 1983; Kruse and Dalley, 1990). It is unlikely that size-related shrinkage effects would have biased our estimates of growth rate because these estimates were based on larvae in similar size classes. Additionally, Theilacker (1980) found that preserving northern anchovy larvae after they had died during net capture caused additional shrinkage, but this shrinkage was at a constant rate that was proportional to fish length. Catches of larvae were standardized to account for sampling effort and expressed as number of larvae under 10 m^2 of sea surface. This method of expressing the abundance of larvae more accurately reflects station differences in abundance than a mean density (number/m^3) when fish larvae are not homogeneously distributed throughout the water column, as has been shown with other species from this area (Lyczkowski-Shultz and Steen, 1991), and when sampling (station) depths are variable, as they were in our study.

Dry weights of larvae were determined by rinsing specimens with distilled water, drying for 24 h at 60°C, and weighing to the nearest 0.1 µg. Both sagittal otoliths were removed following rehydration for 12 h. Otoliths were mounted convex side up on a glass microscope slide with a drop of Pro-Texx mounting medium and a cover slip. Otolith growth increments were counted in the sagittal plane under oil immersion (1250×).

A total of 140 Atlantic bumper larvae and 119 vermilion snapper larvae were selected for age analyses. Specimens were selected from stations where a wide size range of larvae were collected. Daily otolith increment formation has been validated for larval Atlantic bumper (Leffler and Shaw, 1992). Daily increment formation has not been validated for vermilion snapper; however, otolith increments observed in larval vermilion snapper were very similar in width and spacing to validated daily increments found in red snapper from this region (Szedlmayer, 1998; Lyczkowski-Shultz and Comyns[2]). Slopes of age-length regressions for larval vermilion snapper (n=11) and red snapper (n=25) collected during July 1992 in our study area were not significantly different, further indicating that vermilion snapper, like red snapper, form daily otolith growth increments.

Otolith growth increments were counted by using the sagitta (right or left) that provided the most distinct incremental zones. Paired t-test analyses showed no significant difference ($P \leq 0.05$) in diameters of left and right sagittae in both vermilion snapper (n=11) and Atlantic bumper (n=20). Daily increments were counted along the longest axis of the otolith from the core to the outer edge. Otoliths were read once by a single reader, and a random subsample of otoliths from vermilion snapper (n=30) and Atlantic bumper (n=30) was read a second time to examine within-reader variability. Otolith increment counts differed by one day for only two of the 30 otoliths during the second reading for both species.

Data analysis

Age-length and age-weight relationships were described by using the exponential equation

$$L \text{ or } W = \exp(a + bt),$$

where, in its linearized form, L = notochord or standard length in mm;
W = dry weight in mg;
a = Y-intercept;
b = slope of regression line (instantaneous growth rate); and
t = age of larvae in days.

Values of a and b were calculated from the linearized form of the growth equation after the length or weight data were transformed to their natural logarithms. The instantaneous growth rate (b), i.e. the slope of the log-transformed, age-length or age-weight relationship, is also referred to as the growth coefficient. Caution must be exercised when making dry-weight comparisons because of preservation-induced weight loss. Kristoffersen and Salvanes (1998) found that body weight loss was as high as 37–39% in small ethanol-preserved mesopelagic fishes. Dry weight data were used only to determine whether relative changes in weight tracked trends found in age-length relationships. Analysis of covariance (ANCOVA) was used to determine if differences existed among station estimates of instantaneous growth coefficients (Sokal and Rohlf, 1969; SigmaStat, 1995). If differences were found (α=0.05), the simultaneous test procedure (STP; Sokal and Rohlf, 1969) was used as an *a posteriori* test to determine station differences.

Cruise estimates of total larval abundance for each size class (catch curves) were developed for Atlantic bumper and vermilion snapper by summing the abundance estimates of each size class under 10 m^2 of sea surface from each station. Length-frequency distributions were converted to age-frequency distributions by assigning ages to mid-points of the 0.5-mm size classes with the age-length relationship previously described. Age-class abundances were corrected for stage duration by dividing the abundance estimate of each age class by their respective durations (Houde, 1977). It is necessary to correct for stage durations of age classes if growth rates are nonlinear. Stage durations of age classes were determined by assigning ages based on previously determined growth equations to end-points of the 0.5 mm size classes. This customary method for constructing catch curves relies on the rarely examined assumption that larvae at different sampling locations are growing at similar rates. The high r^2 values of the age-length relationships (0.92 for Atlantic bumper; 0.84 for vermilion snapper) that resulted when aged larvae from all stations were combined indicated that growth

[2] Lyczkowski-Shultz, J., and B. H. Comyns. 1992. Early life history of snappers in coastal and shelf waters of the north-central Gulf of Mexico late summer/fall months, 1983–1989. 12 p. + 9 tables, 17 figures. Technical Report submitted to the National Marine Fisheries Service, Southeast Regional Office, 9721 Executive Center Drive North, St. Petersberg, FL, 33702.

rates over the study area were similar enough to justify use of this technique.

Cruise estimates of larval mortality rates for Atlantic bumper and vermilion snapper larvae were estimated from catch curve analyses (e.g. Houde, 1977; Essig and Cole, 1986; Watanabe and Lo, 1988; Deegan, 1990; Comyns et al., 1991). The instantaneous mortality rate (Z) was estimated by the slope of the exponential function relating duration-corrected larval abundance and age (Ricker, 1975):

$$D_t = D_0 \exp(-Zt),$$

where D_t = total abundance of larvae at time t;
D_0 = total abundance of individuals at time 0;
Z = instantaneous mortality rate; and
t = age of size class in days since spawning.

Age and abundance of size classes were fitted to this exponential function with a nonlinear least squares routine, and only the descending limb of the regression was used to estimate mortality rates. To reduce potential biases associated with 1) any trend of increasing variance in the length-at-age distribution with increasing age, and 2) net avoidance by larger larvae, only Atlantic bumper and vermilion snapper larvae smaller than 6.1 mm and 6.0 mm, respectively, were used to estimate mortality rates. Kolmogorov-Smirnov two-sample tests showed no significant differences ($P<0.05$) between size-frequency distributions for day versus night catches within this size range for vermilion snapper and Atlantic bumper larvae.

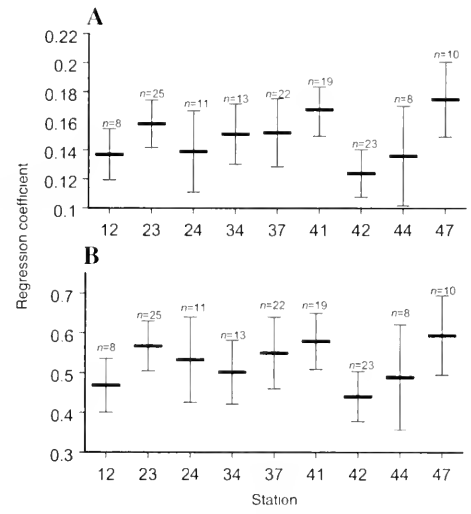

Figure 2

Growth coefficients (horizontal bars) for Atlantic bumper larvae collected at nine stations in the northcentral Gulf of Mexico, during 14–16 September 1991. Vertical lines represent 95% confidence intervals around the growth coefficients, and numbers above bars depict sample sizes; (**A**) shows age versus ln length growth coefficients and (**B**) shows age versus ln dry-weight growth coefficients.

Results

Age and growth

Atlantic bumper larvae, which were commonly found throughout the study area, ranged from 2 to 14 days old, 1.4 mm to 8.1 mm in length, and 0.003 mg to 1.446 mg in dry weight. Estimates of age versus length growth coefficients were not similar for all stations (ANCOVA; $P=0.001$). The STP revealed no overlap in 95% confidence intervals around growth coefficients for larvae collected at station 42 and larvae collected at stations 41, 23, and 47 (Figs. 2A and 3). According to their respective growth equations, Atlantic bumper larvae at station 42 grew at approximately 0.43 mm/d and reached a length of 6 mm in approximately 13.3 days. Larvae collected at adjacent station 41 grew faster, approximately 0.63 mm/d, and reached a length of 6 mm in 10.4 days.

Similarly significant differences in station estimates ($n=9$) of age–dry-weight growth coefficients were also found (ANCOVA; $P=0.01$), and growth coefficients for larvae collected at station 42 were significantly different from larvae collected at stations 41 and 23 (STP; Fig. 2B). By 11 days, the estimated dry weight of an Atlantic bumper larva at station 42 was 0.38 mg, whereas at station 41 larvae gained weight faster and the estimated dry weight of an 11-d-old larva was 0.58 mg. Adjacent stations 41 and 42 were 10 km apart, and water temperatures at these two locations were very similar. Surface temperatures varied by only 0.1°C (28.7°–28.8°C), and surface and midwater temperatures varied by only 0.5°C. Daily surface water temperatures recorded at a weather bouy within the study area showed that temperatures varied by less than 2°C during the 31-d period prior to our study.

Significant differences in station ($n=7$) growth rates of vermilion snapper larvae were also found in our 14–16 September 1991 cruise (ANCOVA; $P=0.03$). Vermilion snapper larvae ranged from 4 to 16 days old, 2.5 mm to 6.5 mm in length, and 0.014 mg to 0.696 mg in dry weight. Growth coefficients for larvae collected at stations 15 and 25 were significantly different (STP; Figs. 4A and 5). According to their respective growth equations, vermilion snapper larvae collected at station 15 reached a length of 5 mm in 10.7 days, whereas larvae collected at station 25 grew more slowly and did not reach a length of 5 mm until 12.6 days. Stations 15 and 25 were located 17 km apart on the inner shelf at water depths of 29–30 m. Surface water temperatures at these stations varied by 2.2°C, and both surface and midwater station temperatures differed by less than 2°C.

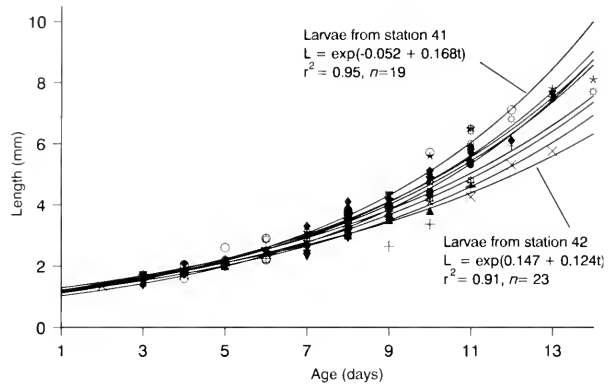

Figure 3

Age versus length data for Atlantic bumper larvae (n=140) collected at nine stations in the northcentral Gulf of Mexico during 14–16 September 1991. Highlighted are the age-length relationships at two adjacent stations where growth rates differed. L = notochord or standard length in mm; t = larval age in days.

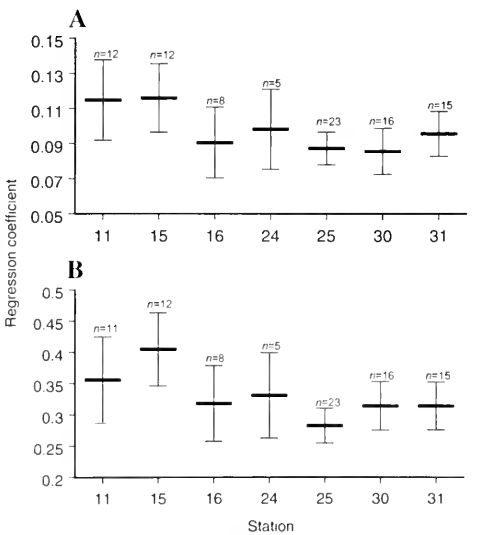

Figure 4

Growth coefficients (horizontal bars) for vermilion snapper larvae collected at seven stations in the northcentral Gulf of Mexico during 14–16 September 1991. Vertical lines represent 95% confidence intervals around the growth coefficients, and numbers above bars depict sample sizes. (**A**) shows age versus ln length growth coefficients, and (**B**) shows age versus ln dry-weight growth coefficients.

Differences in age versus dry-weight growth coefficients were also significantly different (ANCOVA; P=0.03) and once again stations 15 and 25 (Fig. 4B) were significantly different (STP). Vermilion snapper larvae gained weight faster at station 15 where an 11.0-d-old larva had an estimated dry weight of 0.28 mg. At station 25 the estimated dry weight of this same larva was only 0.17 mg. Although vermilion snapper larvae were collected at most of the stations within the study area (Fig. 1), abundances were low at shallow (12–14 m depth) stations immediately south of the Mississippi–Alabama coast, and larvae were never collected at stations within Chandeleur Sound. These stations were very shallow (4–9 m).

Although our study did not assess microzooplankton prey availability, macrozooplankton dry-weight estimates varied widely over space and time. At the 33 stations east of Chandeleur Sound where larvae of vermilion snapper and Atlantic bumper used in our study were captured, macrozooplankton dry-weight estimates at 20 stations exceeded 3g/100 m^3, and at eight of those stations values exceeded 5g/100 m^3. Seven days later only at five of the 33 stations were macrozooplankton dry-weight estimates >3g/100 m^3 and at no station did estimates exceed 5g/100 m^3.

Mortality estimates

Atlantic bumper was generally the most abundant species in plankton collections; 32,241 larvae were collected during six cruises conducted in September of 1990, 1991, and 1993. Mortality rates were not estimated for Atlantic bumper larvae collected during the two cruises conducted in September 1992 because abundances of larvae were very low. When station abundance data were pooled for each of the six cruises, size-frequency distributions gener-

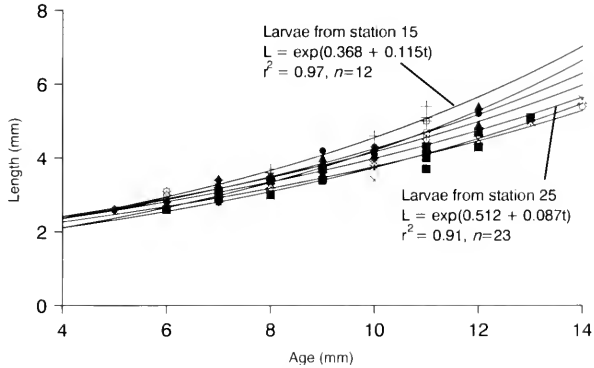

Figure 5

Age-length data for vermilion snapper larvae (n=89) collected at seven stations in the northcentral Gulf of Mexico during 14–15 September 1991. L = body length in mm; t = larval age in days. Highlighted are the age-length relationships at two stations where growth rates differed.

ally exhibited a similar decrease in abundance with successively larger size classes; however, the smallest size class (1.1–1.6 mm) was the most abundant in only three of the six cruises (Fig. 6, A, B, and F). This under representation of the smallest size class in several cruises was likely influenced by several potential factors, including a possible decrease in spawning prior to sampling and patchiness of eggs and newly hatched larvae caused by the aggregation of spawning adults. Cruise-estimates of mortality coefficients, which were derived by pooling data from all stations sampled during a cruise and omitting the smallest size class, ranged from 0.20 to 0.37 (Fig. 6). It is likely that mortality rates varied between stations, but as previously mentioned, an average cruise-estimate of mortality was determined to ascertain a realistic level about which the effects of small variations in growth rates could be assessed on the cumulative survival of larvae. Standard errors of Z estimates were low, ranging from 0.02 to 0.05.

Size-frequency distributions were derived for vermilion snapper larvae (n=2581) taken during two September 1991 cruises, and single late-September cruises in 1992 and 1993 (Fig. 7) when vermilion snapper larvae were abundant. Mortality estimates could not be estimated for five September cruises during the period 1990–93 because relatively few larvae were collected. Larvae collected during three of the four cruises when they were abundant showed a steady decrease in abundance of successively larger size classes (Fig. 7, A, C, and D). During the fourth cruise (late September 1991; Fig. 7B), the size-frequency distribution showed a distinct peak in abundance of intermediate-size larvae (4.0-mm size class). Mortality coefficients (Z) from the four cruises ranged from 0.19 to 0.30 and standard errors for the mortality coefficients were relatively low ranging from 0.02 to 0.05.

Discussion

Plankton collections taken in the northcentral GOM during September showed that growth and mortality rates did vary in time and space for Atlantic bumper and vermilion snapper larvae, and that these differences were great enough to significantly impact the cumulative survival of larvae in a subtropical climate where larval-stage durations are short (i.e. two weeks). Growth and mortality estimates of vermilion snapper larvae were previously unknown. Two previous studies of growth and mortality of Atlantic bumper larvae (Leffler and Shaw, 1992; Sánchez-Ramírez and Flores-Coto, 1998) provided no information on variability in growth rates at small spatial scales and no estimates of mortality during the period when our study was conducted.

Highly significant between-station differences in growth rates were observed for both Atlantic bumper and vermilion snapper larvae. The largest difference in age versus length growth coefficients for Atlantic bumper larvae was found at adjacent, inner-shelf stations located approximately 10 km apart. According to growth equations, the faster growing larvae grew to a length of 6 mm 2.9 days sooner than larvae at the adjacent station, and differences in larval weight gain as expressed by dry weight of 11-d-old larvae varied by over 30%. Water temperatures at these two stations were extremely similar; surface temperatures varied by only 0.1°C, midwater temperatures varied by 0.4°C, and surface and midwater temperatures varied by 0.5°C. It is likely that a similarly small temperature differential was present during the two-week period prior to this cruise, i.e. throughout the life of larvae used in our study because daily surface water temperatures recorded at a weather bouy within the study area during the previous month showed

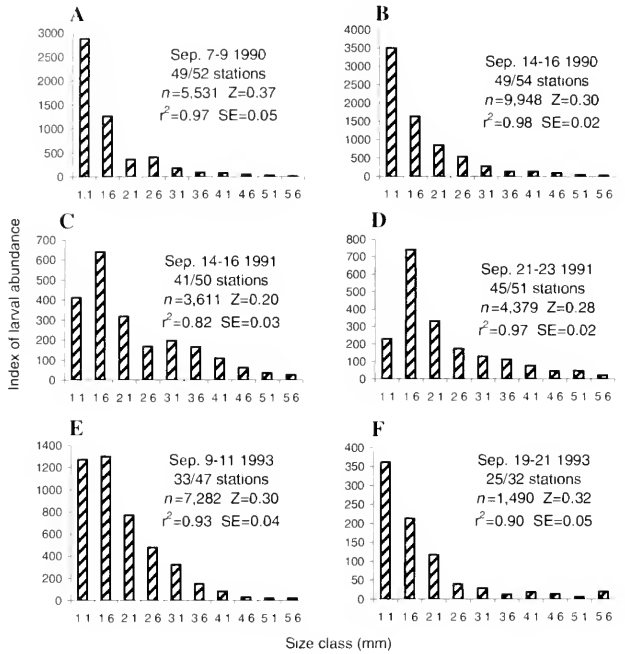

Figure 6

Size-frequency distributions of Atlantic bumper larvae collected during six cruises in the northcentral Gulf of Mexico during September 1990, 1991, and 1993. Values of Z, SE, and r^2 refer to mortality curves produced from the duration-corrected, age-frequency distributions (omitting the smallest size class). The fraction listed for each cruise refers to positive (larvae were collected) stations/total stations sampled. Abundance of each size class is pooled estimates of station abundances.

that temperatures varied by less than 2°C. Significant differences in both age versus length and age versus weight relationships were also found for vermilion snapper larvae collected at relatively close stations (i.e. 17 km apart). Water temperatures at these two stations were similar but differed by as much as 2°C. Faster growing larvae reached a length of 5 mm approximately 2 days sooner than larvae growing in nearby areas. Significant differences were also found in larval weight-gain; dry weight of 11-d-old larvae from different stations varyied by as much as 65%.

The variability in growth rates that we observed was likely caused by station differences in food availability and size-selective mortality, and to a lesser degree by water temperature. Unfortunately our data did not allow us to determine the individual effects of these factors on observed growth rates. At least for Atlantic bumper, the effects of temperature changes were probably minimal.

Larval survival is generally more influenced by factors other than temperature. Morse (1989) found a positive correlation between length-dependent mortality and surface water temperature for 26 larval fish taxa and attributed this to increased predator consumption rates (caused by increased metabolic rates) at higher temperatures. He also concluded that increased growth due to increases in temperature alone would generally impart no advantage to reduce larval mortality because of the concomitant increased predatory consumption rates. Increased larval-stage duration at cooler temperatures is not necessarily associated with increased cumulative larval mortality because predation rates decline with decreasing temperature (Pepin, 1991; Francis, 1994). Methot (1981) concluded that after correcting for the effect of temperature on growth rates, the mean growth rate of larval fish is an indicator of the degree to which larval growth, and presumably survival, is food limited.

We acknowledge that size-selective predation, i.e. "culling out" the slowest (or fastest) growing larvae, could have produced the differences in size-at-age structure among

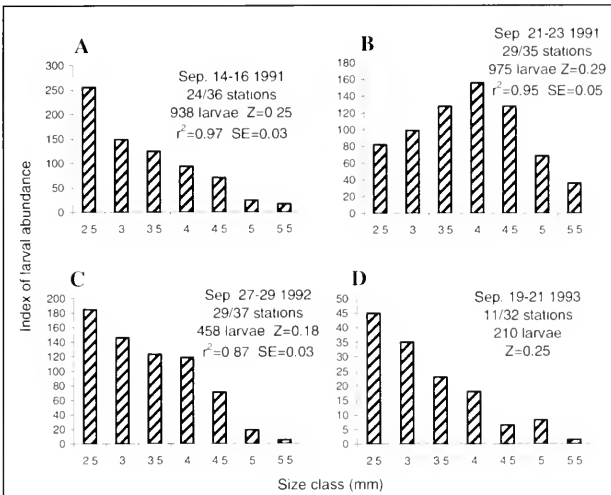

Figure 7

Size-frequency distributions of vermilion snapper larvae collected during four cruises conducted in the northcentral Gulf of Mexico during September 1991, 1992, and 1993. Estimates of Z, SE, and r^2 refer to mortality curves produced from duration-corrected age-frequency distributions. The fraction listed for each cruise refers to positive (larvae were collected) stations/total stations sampled. Abundance of each size class was pooled from estimates of station abundances.

stations that we observed. However, predation pressure seems unlikely to have been the primary cause of this variability. If among-station variability in size-selective mortality was largely responsible for the differences in larval growth rates, one would expect the variability in size-at-age at each station to be quite variable and this was not the case. Stations where the effects of size-selective mortality were minimal (or less) should have had both fast and slow growing larvae present; yet coefficients of determination (r^2) were ≥0.90 for age versus length regressions at all stations. Furthermore, there was no correlation between observed growth rates and r^2 values which would be expected if size selective predation was largely responsible for the variability in growth rates that we observed.

Many studies have shown that food availability has a large influence on growth rates of larvae (e.g. Houde and Schekter, 1981; Buckley et al., 1987; Pepin, 1991) and it is likely that station differences in food availability influenced our observed differences in larval growth rates. We did not collect the small size-fraction of prey eaten by fish larvae, but our data did reveal extensive spatial and temporal variability in the abundance of macrozooplankton. Macrozooplankton biomass at station 42, where relatively slow growth of Atlantic bumper occurred, was 2.6 mg/100 m^3 whereas at station 41, where larvae were growing faster, macrozooplankton dry weight (3.9 g/100 m^3) was 50% higher. When all stations were considered, there was no correlation between macrozooplankton dry weight and growth coefficients of larvae, but macrozooplankton biomass was certainly very patchily distributed. For most stations there was at least a 50% difference in macrozooplankton dry weight between one of the adjacent stations. It is equally likely that the smaller size fraction of zooplankton that fish larvae eat were also very patchily distributed. In addition, several other studies have shown that primary production in the northern GOM is dynamic and spatially heterogenous (Lohrenz et al., 1990, 1994; Redalje et al., 1994), although these studies have focused on regions influenced by discharge from the Mississippi and Atchafalaya rivers.

In many studies the significant spatial variability in growth rates of field-caught larvae cannot be explained by changes in water temperature. These reported differences in growth rates have often been associated with factors such as storm events (Lasker, 1975; Maillet and Checkley, 1991), different geographical locations (Mokness, 1992; Nixon and Jones, 1997; Allman and Grimes, 1998;), or distinct hydrographic features such as tidal fronts (Munk, 1993) and riverine discharge plumes (Govoni et al., 1985; DeVries et al., 1990; Lang et al., 1994). All studies in the GOM that have reported spatial differences in larval

growth rates have involved comparisons in the vicinity of the Mississippi River discharge plume (Govoni et al., 1985; DeVries et al., 1990; Lang et al., 1994; Allman and Grimes, 1998). The observed variability in larval Atlantic bumper and vermilion snapper growth rates reported in our study was not associated with conspicuous hydrographic features (e.g. hydrographic convergence zones) and suggests the existence of less-recognizable regions where conditions for growth vary.

Cruise estimates of mortality were determined to ascertain a realistic level about which the effects of small variations in growth rates on the cumulative survival of larvae could be assessed. In order to do this, data from all stations sampled during a cruise were pooled. This provided the most reliable general estimate of mortality for each cruise despite likely site-specific differences in mortality rates that are extremely difficult to measure. Such pooling of data is not unusual; in fact Morse (1989) suggested that samples should be summed over the larval production cycle. Essig and Cole (1986) estimated mortality rates of larval alewives (*Alosa pseudoharengus*) by using both converted length-frequency distributions, as we did, and actual age-frequency distributions. They found no statistical difference between the two methods. Pepin and Miller (1993), however, warned that because variability in observed length-at-age increases with larval age (Chambers et al., 1988), analyses that use size in older fish to represent age may yield biased estimates of mortality rates. Yet, Pepin and Miller (1993) observed that their mortality rates, which were estimated by using size as a proxy for age, were consistent with mortality rates reported from other environments and species. Ideally, all fish would be aged, but for our study this was not possible because of the large sample sizes, multiple cruises, and the labor-intensive nature of otolith preparation for age determination.

Atlantic bumper larvae were extremely abundant (n= 32,241 for six cruises), and cruise estimates of age-frequency distributions showed consistent, well-defined descending limbs. Estimates of mortality coefficients (Z) for Atlantic bumper larvae were similar for September cruises conducted in the same year. For example, in 1990 the two cruise estimates of Z were 0.37 and 0.30, in 1991 the two Z estimates were 0.20 and 0.28, and in 1993 estimates of Z were 0.30 and 0.32. These mortality rates are similar to estimates reported by Leffler and Shaw (1992) during four September cruises in the same area during 1986–87 (Z=0.17–0.35) and by Sánchez-Ramírez and Flores-Coto (1998) in the southern Gulf (0.15–0.30). In addition, standard errors of the mortality estimates from our study were low, ranging from 0.02 to 0.05.

Cruise estimates of mortality rates for vermilion snapper were determined during four cruises when larvae were relatively abundant (n=2581). The descending limbs of three of the size-frequency distributions uniformly spanned all seven size classes, but during one cruise the middle size class was most abundant and the descending limb of this size-frequency distribution was restricted to four size classes. However, mortality rates were quite similar during all cruises (Z=0.19 to 0.30) and each had a low standard error (SE=0.02 to 0.05).

Collections of Atlantic bumper and vermilion snapper larvae were taken when water temperatures ranged from 25° to 30°C, and the mortality coefficients estimated from these collections were similar to those reported for other species under similar temperature regimes. Houde (1989) summarized vital rates of six species of larval fish as reported in seven studies where the mid-points of water temperatures at the time of collection ranged from 26° to 28°C. Most of these studies generated a range of mortality estimates, and the mid-points of the ranges reported in six of these studies varied from 0.21 to 0.38, values that are consistent with the mortality estimates (0.19 to 0.39) that we observed.

Our primary reason for estimating mortality rates was to ascertain a realistic level about which small variations could be assessed for potential effects on the cumulative survival of larvae, particularly in conjunction with variability in larval growth rates. Our method assumes a constant birth rate, or recruitment rate into the population, and assumes that fish leave the population only through death. There is clearly some expected variability in the degree to which these assumptions were met; however, based on the similarity of mortality estimates, not only between cruises but also to previously published estimates, it is concluded that our mortality estimates are biologically meaningful.

The well-accepted fisheries paradigm holds that changes in year-class strength are determined by variability in mortality during early life stages (Sissenwine, 1984; Houde, 1987; Bailey and Houde, 1989; Cushing and Horwood, 1994). Despite extensive efforts to understand the causes of recruitment variability, significant questions remain because the operant factors are likely to be interrelated parts of the ecosystem dynamics that comprise a multidimensional system (Ellersten et al., 1995). For example, it is not the mortality or growth rate alone that determines survival during the early life-stages, but the ratio M/G, the stage-specific mortality rate (Pepin, 1991). Examining previously published information, Houde (1989) found an exponential increase in predicted larval-stage duration with decreasing water temperature for 26 species of larval fishes and surmised that when temperature is low, small changes in growth rates can induce large changes in larval-stage duration that may significantly affect the recruitment process.

To determine the potential effects that variability in vital rates might have on the cumulative survival of larvae, hypothetical numbers of newly hatched Atlantic bumper were projected to a size of 6 mm under the influence of the growth and mortality rates we observed in the study area (Table 1). According to these vital rates, and a hypothetical initial cohort size of 1×10^6 individuals, 124,930 larvae survive to a length of 6 mm under the scenario of relatively fast growth and low mortality (G=0.61 mm/d; Z=0.20). If the growth rate is slowed (G=0.45 mm/d) and it takes approximately three days longer to reach a length of 6 mm, the number of larvae that survive to this length is reduced by 44%. If the slower growing larvae are exposed to the higher mortality rate (Z=0.37), cumulative survival of larvae decreases by an order of magnitude, and only

Table 1

Hypothetical survival of Atlantic bumper larvae to a size of 6 mm under the influence of growth and mortality rates observed in the study area.

Initial number in cohort	Instantaneous mortality coefficient (per day)	Age of 6-mm larva (d)	Number of 6-mm larvae
1×10^6	0.20	10.4	124,930
1×10^6	0.20	13.3	69,948
1×10^6	0.30	10.4	44,157
1×10^6	0.30	13.3	18,499
1×10^6	0.37	10.4	21,322
1×10^6	0.37	13.3	7292

7292 larvae survive to a length of 6 mm. Houde (1987) published a projection on the mortality of larvae exposed to hypothetical levels of mortality and growth rates, but the theoretical exercise used relatively long larval-stage durations (45–56 days). Results of our study show that even in a subtropical climate where larval stage durations may be as short as two weeks, relatively small changes in observed larval growth rates, particularly when combined with small differences in mortality, can have a large impact on cumulative larval survival. To what extent the observed differences in growth rates at small spatial scales are fine-scale "noise" that is ultimately smoothed by larger-scale processes is not known. Future research is needed to further characterize the small-scale variability in growth rates of larvae, particularly with regard to microzooplankton patchiness and the temporal and spatial pattern of potential predators. Small-scale spatial variability in larval growth rates may in fact be the norm, and understanding the implications of this subtle mosaic may help us to better evaluate our ability to partition the causes of recruitment variability.

Acknowledgments

Collections serving as the basis of this research were supported by the SEAMAP program (Southeast Area Monitoring and Assessment Program) and the NOAA/NMFS MARFIN program (Marine Fisheries Initiative). Several cruises were also conducted by personnel from National Marine Fisheries Service in Pascagoula, Mississippi. Sorting of these plankton samples was made possible by funding provided by the U.S Fish and Wildlife Service through the Wallop Breaux program. This program is administered in Mississippi by the Department of Marine Resources (DMR) whose personnel must be thanked for providing support. Sorting of the plankton samples was made possible by the efforts of several people, including Mae Blake, Cindy Gavins, Pam Bond, Dianne Scott, Ngoc Bui, and Jean Bennett. We also thank Pam Bond for many contributions, including acting as field party leader during cruises, for larval identifications, much of the data entry and management, and for preparing otoliths. We are also grateful to Chet Rakocinski for providing help with statistical analyses.

Literature cited

Allman, R. J., and C. B. Grimes.
1998. Growth and mortality of little tunny (*Euthynnus alletteratus*) larvae off the Mississippi River plume and Panama City, Florida. Bull. Mar. Sci. 62:189–197.

Anderson, J. T.
1988. A review of size dependent survival during pre-recruit stages of fishes in relation to recruitment. J. Northwest Atl. Fish. Sci. 8:55–66.

Bailey, K. M., and E. D. Houde.
1989. Predation on eggs and larvae of marine fishes and the recruitment problem. Adv. Mar. Biol. 25 (ISBN 0-12-026125-1):1–83.

Beyer, J.
1989. Recruitment stability and survival: simple size-specific theory with examples from the early life dynamics of marine fish. Dana 7:45–147.

Buckley, L. J., T. A. Halavik, A. S. Smigielski, and G. C. Laurence.
1987. Growth and survival of the larvae of three species of temperate marine fishes reared at discrete prey densities. Trans. Am. Fish. Soc. Symp. 2:82–92.

Chambers, R. C., and W. C. Leggett.
1987. Size and age at metamorphosis in marine fishes: an analysis of laboratory-reared winter flounder (*Pseudopleuronectes americanus*) with a review of variation in other species. Can. J. Fish. Aquat. Sci. 44:1936–1947.

Chambers, R. C., W. C. Leggett, and J. A. Brown.
1988. Variation in and among life history traits of laboratory-reared winter flounder (*Pseudopleuronectes americanus*). Mar. Ecol. Prog. Ser. 47: 1–15.

Comyns, B. H., J. Lyczkowski-Shultz, D. L. Nieland, and C. A. Wilson.
1991. Reproduction of red drum in the north-central Gulf of Mexico: seasonality and spawner biomass. *In* Larval fish recruitment and research in the Americas; proceedings of the 13th annual larval fish Conference, Merida, Mexico, 21–26 May, 1989, p. 17–26. U.S. Dep. Commer., NOAA Tech. Rept. MNSS 95.

Cushing, D. H.
1975. Marine ecology and fisheries, 278 p. Cambridge Univ. Press, Cambridge.

Cushing, D. H., and J. W. Horwood.
1994. The growth and death of fish larvae. J. Plank. Res. 16:291–300.
Deegan, L. A.
1990. Effects of estuarine environmental conditions on population dynamics of young-of-the-year gulf menhaden. Mar. Ecol. Prog. Ser. 68:195–205.
De Vries, D. A., C. B. Grimes, K. L. Lang, and D. B. White.
1990. Age and growth of king and Spanish mackerel larvae and juveniles from the Gulf of Mexico and U.S. South Atlantic Bight. Environ. Biol. Fish. 29:135–143.
Ellersten, B., P. Fossum, P. Solemdal, and S. Sundby.
1995. The 'critical period' concept—a century of recruitment research. Mar. Ecol. Prog. Ser. 128:306–308.
Essig, R. J., and C. F. Cole
1986. Methods of estimating larval fish mortality from daily increments in otoliths. Trans. Am. Fish. Soc. 115:34–40.
Fowler, G. M., and S. J. Smith.
1983. Length changes in silver hake (*Merluccius bilinearis*) larvae: effects of formalin, ethanol and freezing. Can. J. Fish. Aquat. Sci. 40:866–870.
Francis, M. P.
1994. Duration of larval and spawning periods in *Pagrus auratus* (Sparidae) determined from otolith daily increments. Environ. Biol. Fish. 39:137–152.
Fritz, E. S., L. B. Crowder, and R.C. Francis.
1990. The National Oceanic and Atmospheric Administration plan for recruitment fisheries oceanography research. Fisheries 15:25–31.
Goshorn, D. M., and C. E. Epifanio.
1991. Development, survival, and growth of larval weakfish at different prey abundances. Trans. Am. Fish. Soc. 120: 693–700.
Govoni, J. J., A. J. Chester, D. E. Hoss, and P. B. Ortner.
1985. An observation of episodic feeding and growth of larval *Leiostomus xanthurus* in the northern Gulf of Mexico. J. Plank. Res. 7:137–146.
Hjort, J.
1914 Fluctuations in the great fisheries of northern Europe. Rapp. P.-V. Réun. Cons. Int. Explor. Mer 20:1–13.
Houde, E. D.
1977. Abundance and potential yield of the round herring, *Etrumeus teres*, and aspects of its early life history in the eastern Gulf of Mexico. Fish. Bull. 75:61–89.
1987. Fish early life dynamics and recruitment variability. Trans. Am. Fish. Soc. Symp. 2:17–29.
1989. Comparative growth, mortality, and energetics of marine fish larvae: temperature and implied latitudinal effects. Fish. Bull. 87:471–495
Houde, E. D., and R. C. Schecter.
1981. Growth rates, rations and cohort consumption of marine fish larvae in relation to prey concentrations. Rapp. P.-V. Reun. Cons. Int. Explor. Mer 178:441–453.
Hunter, J. R.
1982. Feeding ecology and predation of marine fish larvae. *In* Marine fish larvae: morphology, ecology, and relation to fisheries (R. Lasker, ed.), p. 34–77. Univ. Washington Press, Seattle, WA
Kristoffersen, J. B., and A. G. V. Salvanes.
1998. Effects of formaldehyde and ethanol preservation on body and otoliths of *Maurolicus Muelleri* and *Benthosema glaciale*. Sarsia 83:95–102.
Kruse, G. H., and E. L. Dalley.
1990. Length changes in capelin, *Mallotus villosus* (Muller), larvae due to preservation in formalin and anhydrous alcohol. J. Fish. Biol. 36:619–621
Lang, K. L., C. B. Grimes, and R. F. Shaw.
1994. Variations in age and growth of yellowfin tuna larvae, *Thunnus albacores*, collected about the Mississippi River plume. Environ. Biol. Fish 39:259–270.
Lasker, R.
1975. Field criteria for survival of anchovy larvae: the relation between inshore chlorophyll maximum layers and successful first feeding. Fish. Bull. 73:453–462.
Laurence, G. C.
1979. Larval length-weight relations for seven species of northwest Atlantic fishes reared in the laboratory. Fish. Bull. 76:890–895.
Leffler, D. L., and R. F. Shaw.
1992. Age validation, growth, and mortality of larval Atlantic bumper (Carangidae: *Chloroscombrus chrysurus*) in the northern Gulf of Mexico. Fish. Bull. 90:711–719.
Leggett, W. C., and E. Deblois.
1994. Recruitment in marine fishes: is it regulated by starvation and predation in the egg and larval stages? Neth. J. Sea Res. 32:119–134.
Lohrenz, S. E., M. J. Dagg, and T. E. Whitledge.
1990. Enhanced primary production at the plume/oceanic interface of the Mississippi River. Cont. Shelf Res. 10. 639–664.
Lohrenz, S. E., G. L. Fahnenstiel, and D. G. Redalje.
1994. Spatial and temporal variations of photosynthetic parameters in relation to environmental conditions in coastal waters of the northern Gulf of Mexico. Estuaries 17:779–795.
Lyczkowski-Shultz, J., and J. P. Steen Jr.
1991. Diel vertical distribution of red drum *Scioenops ocellatus* larvae in the northcentral Gulf of Mexico. Fish. Bull. 89:631–641.
Maillet, G., and D. M. Checkley Jr.
1991. Storm-related variation in the growth rate of otoliths of larval Atlantic menhaden *Brevoortia tyrannus*: a time series analysis of biological and physical variables and implications for larva growth and mortality. Mar. Ecol. Prog. Ser. 79:1–16.
Mertz, G., and R. A. Myers.
1995 Estimating the predictability of recruitment. Fish. Bull. 93:657–665.
Methot, R. D., Jr.
1981 Spatial covariation of daily growth rates of larval northern anchovy, *Engraulis mordax*, and northern lampfish, *Stenobrachius leucopsarus*. Rapp. P.-V. Reun. Cons. Int. Explor. Mer 178:424–431.
Morse, W. W.
1989. Catchability, growth, and mortality of larval fishes. Fish. Bull. 87:417–446.
Mokness, E.
1992. Differences in otolith microstructure and body growth rate of North Sea herring (*Clupea harengus* L.) larvae in the period 1987–1989. ICES J. Mar. Sci., 49:223–230
Munk, P.
1993. Differential growth of larval sprat *Sprattus sprattus* across a tidal front in the eastern North Sea. Mar. Ecol. Prog. Ser. 99 17–27.
Nixon, S. W., and C. M. Jones.
1997 Age and growth of larval and juvenile Atlantic croaker, *Micropogonias undulatus*, from the Middle Atlantic Bight and estuarine waters of Virginia. Fish. Bull. 95: 773–784
Parrish, B. B.
1973. Foreward, fish stocks and recruitment. Rapp. P.-V. Reun. Cons. Int. Explor. Mer 164:1–3

Pepin, P.
1991. Effect of temperature and size on development, mortality, and survival rates of the pelagic early life history stages of marine fish. Can. J. Fish. Aquat. Sci. 48:503–518
Pepin, P., and R. A. Myers.
1991. Significance of egg and larval size to recruitment variability of temperate marine fish Can. J Fish. Aquat. Sci. 48:1820–1828.
Pepin, P., and T. J. Miller.
1993. Potential use and abuse of general empirical models of early life history processes in fish. Can. J. Fish. Aquat. Sci. 50:1343–1345.
Redalje, D. G., S. E. Lohrenz, and G. L. Fahnensteil.
1994. The relationship between primary production and the vertical export of particulate organic matter in a river impacted coastal ecosystem. Estuaries 17:829–838.
Ricker, W. E.
1975. Computation and interpretation of biological statistics of fish populations. Bull. Fish. Res. Board Can. 191:382.
Sánchez-Ramírez, M., and C. Flores-Coto.
1998. Growth and mortality of larval Atlantic bumper *Chloroscombrus chrysurus* (Pisces: Carangidae) in the southern Gulf of Mexico. Bull. Mar. Sci. 63: 295–303.
SigmaStat.
1995. Statistical software version 2.0 for Windows 95, NT and 3.1. Jandel Scientific, San Rafael, CA.
Sissenwine, M. P.
1984. Why do fish populations vary? *In* Exploitation of marine communities (R. M. May, ed.), p. 59–94. Springer-Verlag, Berlin.
Sokal, R. R., and F. J. Rohlf.
1969. Biometry, 776 p. W.H. Freeman and Company, San Francisco, CA.
Szedlmayer, S. T.
1998. Comparison of growth rate and formation of otolith increments in age-0 red snapper. J. Fish. Biol. 53:58–65.
Theilacker, G. A.
1980. Changes in body measurements of larval northern anchovy, *Engraulis mordax*, and other fishes due to handling and preservation. Fish. Bull. 78:685–692.
Watanabe, Y., and N. C. H. Lo.
1988. Larval production and mortality of Pacific saury, *Cololabis saira*, in the northwestern Pacific ocean. Fish. Bull. 78:601–613.

Temporal changes in population density, fecundity, and egg size of the Hawaiian spiny lobster (*Panulirus marginatus*) at Necker Bank, Northwestern Hawaiian Islands

Edward E. DeMartini
Gerard T. DiNardo
Happy A. Williams

Honolulu Laboratory
Southwest Fisheries Science Center
National Marine Fisheries Service
2570 Dole Street
Honolulu, Hawaii 96822-2396
E-mail address (for E. E. DeMartini): Edward.DeMartini@noaa.gov

Abstract—Fecundity (F, number of brooded eggs) and egg size were estimated for Hawaiian spiny lobster (*Panulirus marginatus*) at Necker Bank, Northwestern Hawaiian Islands (NWHI), in June 1999, and compared with previous (1978–81, 1991) estimates. Fecundity in 1999 was best described by the power equations $F = 7.995\ CL^{2.4017}$, where CL is carapace length in mm (r^2=0.900), and $F = 5.174\ TW^{2.758}$, where TW is tail width in mm (r^2=0.889) (both n=40; $P<$ 0.001). Based on a log-linear model ANCOVA, size-specific fecundity in 1999 was 18% greater than in 1991, which in turn was 16% greater than during 1978–81. The additional increase in size-specific fecundity observed in 1999 is interpreted as evidence for further compensatory response to decreased lobster densities and increased per capita food resources that have resulted either from natural cyclic declines in productivity, high levels of harvest by the commercial lobster trap fishery, or both. The density decline is well-documented by a fivefold decrease in commercial catch-per-trap-haul (CPUE) during the late 1980s to early 1990s and by a similar decrease in research CPUE for all-sized (including juvenile) *P. marginatus* through the 1990s. Fecundity increases are consistent with decreases in median body size at sexual maturity, first described from comparisons of 1977–81 and 1986–87 specimens and consistently observed thereafter during the 1990s. Egg size covaried with fecundity; in 1999, individual eggs within broods had a 11% greater mass (15% greater volume) than eggs brooded in 1991. Implications of these observations are discussed in relation to possible future management measures for a commercial lobster fishery in the NWHI. More generally, our findings argue for the need to routinely reevaluate compensatory responses in exploited stocks of lobsters and other resources.

Manuscript accepted 20 September 2002.
Fish. Bull. 101:22–31 (2003).

The endemic Hawaiian spiny lobster (*Panulirus marginatus*) has been the principal target of the Northwestern Hawaiian Island (NWHI) commercial trap fishery since the mid- to late 1970s (Uchida and Tagami, 1984; Polovina, 2000). Landings and exvessel (wholesale) value have fluctuated greatly over the years, in part because of annual variations in trapping effort and a 1-yr fishery closure in 1993, but have been generally lower during the 1990s because of declines in oceanic productivity and recruitment and increased exploitation (Polovina and Moffitt, 1995; Polovina et al., 1995). The fishery was closed in 2000 because of increasing uncertainty in the population models used to assess stock status. In December 2000 President Clinton, through Executive Order (EO) 13178 and later through EO 13196, established the Northwestern Hawaiian Islands Coral Reef Ecosystem Reserve which may prohibit commercial lobster fishing in the NWHI for at least 10 years. Annual research surveys of the National Marine Fisheries Service (NMFS), Honolulu Laboratory, have demonstrated a decline (Fig. 1) in spiny lobster density (CPUE, catch-per-trap-haul) at Necker Bank, NWHI, one of the sites at which spiny lobsters have been consistently targeted since about the mid-1970s.

Polovina (1989) first described a density-dependent decrease in median body size at sexual maturity and an increase in asymptotic body size for spiny lobster at Necker Bank, based on a contrast between specimens collected during 1977–81 and 1986–87. DeMartini et al. (1993) observed an increase in size-specific fecundity for specimens collected in 1991, used to further characterize the Necker Bank population's status after-exploitation. Compensatory increases in juvenile growth and survival and increases in size at maturity as responses to decreased density following increased fishery exploitation have been observed for other spiny lobster stocks (e.g. see Pollock, 1995a, 1995b).

In this article, our objectives were to estimate recent (1999) berried female fecundity and egg size for the Hawaiian spiny lobster at Necker Bank and to relate these to prior, analogous estimates for lobsters collected in 1991 and 1978–81, analyzed by DeMartini et al. (1993). We then use the 1999 fecundity estimates and 1999 commercial catch data to characterize recent egg production by the Necker Bank population. We conclude with a brief discussion of the management implications of compensatory reproductive responses by the population.

Methods and materials

All specimens used in this study were trapped from Necker Bank surrounding Necker Island (23°34′N, 164°42′W), NWHI, during the species' mid-spring to mid-summer peak period of egg brooding at mid-archipelago latitudes (Uchida and Tagami, 1984). Specimens

for 1999 were collected on a cruise of the NOAA ship *Townsend Cromwell*. Details of specimen collection and processing of the 1978–81 and 1991 samples are described by DeMartini et al. (1993). The 1999 samples were collected during 9–22 June 1999 from the bank terrace at a median 27-m depth by using molded plastic ("Fathom Plus") traps baited with 1 kg of mackerel (*Scomber japonicus*) and fished with a standard (overnight) soak.

Shipboard processing

Specimens were processed identically to those collected in June 1991. All specimens were processed alive within minutes of trap retrieval. Both carapace length (CL: defined as the straight line distance between the anterior edge of the supraorbital ridge and the posterior edge of the carapace along the dorsal midline) and tail width (TW: defined as the straight line distance across the abdomen at the widest spot between the first and second abdominal segments) of each specimen were measured to 0.1 mm with dial calipers. TW is the present metric of choice for lobster management in the NWHI trap fishery. CL was the metric used to characterize body size in many prior research and management studies of the species, and its measurement was needed for comparison with results of studies made prior to the mid-1980s. Berried (ovigerous) females were scored for egg developmental stage by using a gross visual proxy (brooded eggs noted as either orange or brown in color to the unaided eye). Berried specimens were individually flash-frozen for laboratory evaluation ashore.

Laboratory analyses

Fecundity, here defined in the limited sense of a single brooded egg mass (see Chubb, 2000), was estimated for 5–10 females per 5-mm TW class in order to provide at least 40 total specimens spanning the entire size range for analyses. Except for sample sizes, procedures were identical to those used for the 1991 collection. Only females bearing orange egg clusters with embryos lacking visible melanin pigment (early embryonic development) were considered in order to minimize the probability of physical damage, egg loss, and fecundity underestimation during capture and handling, which is an apparent problem only for broods of heavily pigmented (brown), late-development eggs with soft capsules (DeMartini, unpubl. data). Frozen specimens were thawed overnight at 3°C. All four pairs of egg-bearing pleopods were then removed from the abdomen, gently blotted (damp-dry) on a paper towel, and weighed individually to 0.1 mg on an electric microbalance. Eggs were then carefully teased off pleopod setae with jeweler's forceps and stored after being wrapped in cool, damp paper towels to minimize evaporative weight loss. Individual pleopods were then reweighed and the weight of each pleopod's egg complement was calculated by difference. Three subsamples of 0.1–0.2 g, each comprising about 700–1000 eggs total (about 100 eggs per pleopod, pooled over all 8 pleopods), were next weighed to 0.1 mg, their component eggs counted, and relative fecundity (RF, number of eggs per gram of brooded eggs) was calculated as a simple ratio, with the three subsamples used to calculate a mean and standard error of RF. Fecundity (F, defined

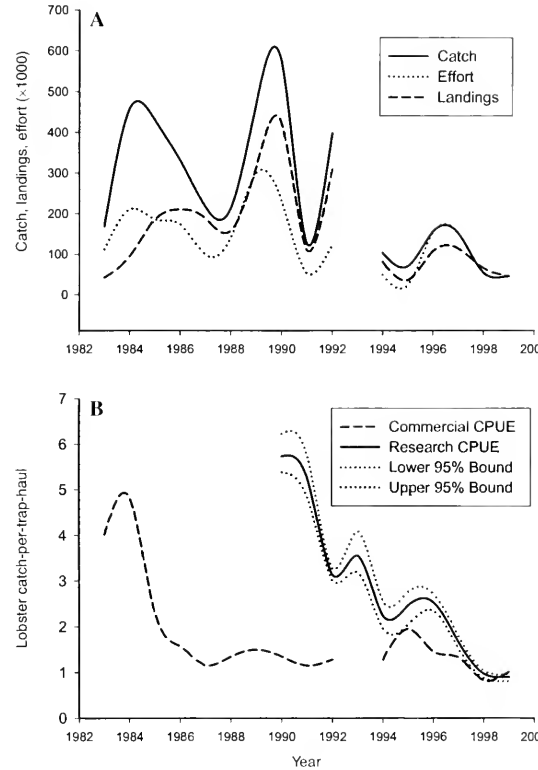

Figure 1

Time series plots of (**A**) the Northwestern Hawaiian Islands (NWHI) commercial trap catch and landings of *Panulirus marginatus* (no. of lobsters × 1000) and effort (no. of trap-hauls × 1000); and (**B**) total *P. marginatus* catch-per-trap-haul (CPUE) at Necker Bank, NWHI, during the 1983–99 commercial fishing seasons and as assessed on 1988–1999 lobster research cruises. (Research CPUE data are lacking for years prior to 1988.) Dashed lines framing the research CPUE curve in **B** represent bootstrapped 95% confidence intervals (DiNardo et al.[2]).

Table 1

(**A**) Summary catch statistics (*Townsend Cromwell* research cruise, Necker Bank, June 1999) and (**B–D**) fundamental linear-mass interrelationships for body and egg sizes of female Hawaiian spiny lobster (*Panulirus marginatus*) at Necker Bank, Northwestern Hawaiian Islands.

A Female catch statistics	Total		Berried		$TW_{all\ females}$		$TW_{berried}$	
	n	%	*n*	%	median	range	median	range
	834	54.6	350	42.0	50.1	24–72	51.1	38–72

B Relation of tail width to carapace length and vice versa; model: $Y = aX + b$

$$TW = 0.6087\ CL + 4.44 \text{ and } CL = 1.5772\ TW - 4.00,$$ [r^2=0.963, n=825, P<0.001]

where TW = tail width in mm, CL = carapace length in mm, and a and b are fitted constants.

C Relation of body weight to carapace length; model: $Y = aX^b$

$$BW = 0.00090\ CL^{2.9952},$$ [range: 51.9–114.7 mm CL, n= 197, P<0.001]

where BW = total body weight in g, and CL = carapace length in mm, for unberried females (source: Uchida and Tagami [1984]).

D Relation of egg weight to egg diameter; model: $Y = aX^b$

$$EW = 0.3985\ ED^{2.2472},$$ [r^2=0.833, n=40, P<0.001]

where EW = egg weight in 0.001 mg, and ED =egg diameter in mm.

as the total number of pleopod-brooded eggs) was calculated as the product of mean RF and total weight of the brooded egg mass. Pilot tests indicated that this procedure estimated F with coefficients of variation (CV, SD/mean × 100%) consistently <5%. Subsamples of 25 eggs were randomly taken from each female's total egg complement and the diameter of individual eggs were measured (random axis) at 500× magnification by using a dissecting microscope and an optical micrometer. Average individual egg weight was also independently derived as the ratio of the weight to numbers of eggs present in the parent sample.

Statistical analyses

Relations of female body size to fecundity and body size to egg size were evaluated for the 1999 samples by using both linear and nonlinear least squares procedures (proc REG, proc NLIN) of PC SAS for Windows v. 6.12 (SAS Institute, 1990a, 1990b). Analysis of covariance (ANCOVA; proc GLM; SAS Institute, 1990c; Chubb, 2000) was used to compare size-specific fecundity estimates of Necker Bank *P. marginatus* among the three exploitation periods: 1978–81, 1991, and 1999. Subseasonal variation within spawning seasons was controlled by the aforementioned restriction on month of specimen collection, and single collections were assumed to provide accurate characterizations within exploitation periods. Fecundity data used to characterize the 1978–81 and 1991 periods at Necker Bank are listed in Appendix A of DeMartini et al. (1993). Analogous comparisons of size-specific egg sizes were limited to the 1991 and 1999 periods because no data on variance of egg sizes were available for the 1978–81 samples (DeMartini et al., 1993). Body-size–fecundity relations were allometric, hence log-linear (see Somers, 1991); natural logarithms were used for ANCOVAs and regressions of log-linear relations.

An index of reproductive potential (IRP; Kanciruk and Herrnkind, 1976) was computed for the 1999 specimens in order to determine the size classes of females that contributed most to population egg production. The IRP was constructed by using data for female *P. marginatus* caught by the commercial fishery at Necker Bank during 1999, collected by several contracted fishery observers.

Results

Fecundity and egg size of lobsters in 1999

Fecundity A number of the female *Panulirus marginatus* trapped on the research cruise at Necker Bank during June 1999 were berried (Table 1). The estimated fecundity of 40 females, spanning 54.3 to 105.4 mm CL (39.3–67.4 mm TW, see CL-TW relation; Table 1), ranged more than fivefold, from 109,865 to 590,530 eggs (Appendix A). Fecundity was positively and nonlinearly related to TW (Fig. 2) and CL and best described by the power equations $F = a\ TW^b$ and $F = a\ CL^b$, respectively, as

$$F = 5.1743\ TW^{2.7580},$$ [r^2=0.889]

and

$$F = 7.9952\ CL^{2.4017}$$ [r^2=0.900, both n=40, P<0.001.]

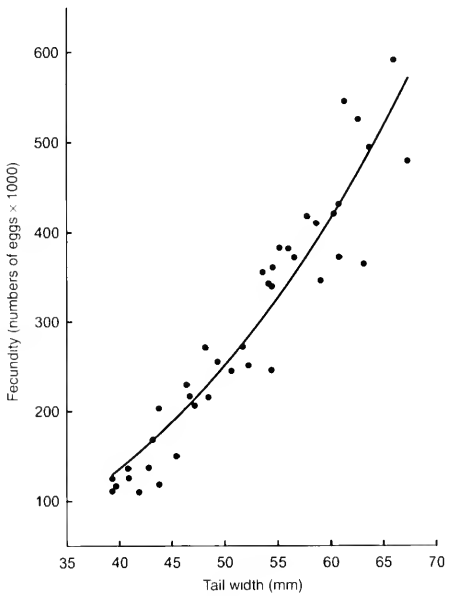

Figure 2

Scatterplot and fitted power curve describing the relation between fecundity (no. of brooded eggs×1000) and tail width (TW, in mm) for *Panulirus marginatus* collected at Necker Bank, 1999.

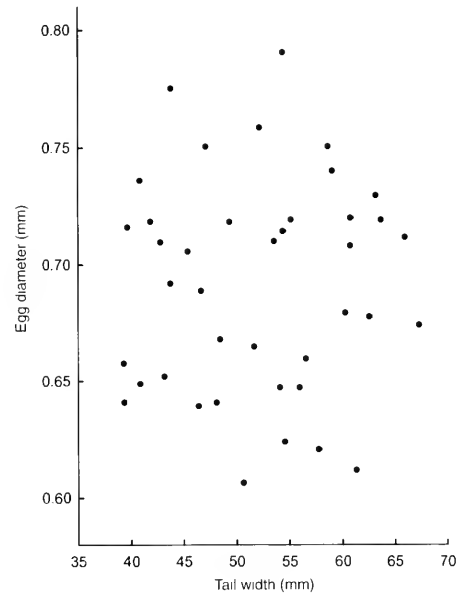

Figure 3

Scatterplot describing the relation between egg diameter (mm) and tail width (TW, in mm) for *Panulirus marginatus* collected at Necker Bank, 1999.

The standard errors of b were 0.1787 and 0.1472, respectively. A log-linear fit of the F-CL data ($\ln F$=2.5533 $\ln CL$ +1.3977) was nominally inferior (r^2=0.886) to the curvilinear fit but was required for the general linear model used in the ANCOVA comparisons that follow below. Fecundity subsamples averaged 1.5 ±0.14(SE)% of total brooded egg mass weight. Brooded egg masses weighed an average 51.4 g and ranged from 15.8 to 109.2 g. CVs of the three replicate estimates of RF averaged 1.2 ±0.11%. Mean RF was 5882 ±160(SE) eggs per g of brooded eggs and ranged nearly twofold from 4030 to 7930 eggs per g of eggs among the 40 females. Based on the aforedescribed nonlinear best fit, the fecundity of the median-size (53.8 mm TW, 80.9 mm CL) female caught at Necker Bank in 1999 by the commercial trap fishery was an estimated 306,400 ±90,200 (95% CI) eggs.

Egg size The mean (±SE) diameter of early-stage eggs carried by the 40 berried females was 0.69 ±0.007 mm, with a range of 0.61 to 0.79 mm. Analogous median (25th, 75th percentile) diameters were 0.70 (0.65, 0.72) mm. The corresponding egg weights were 0.17 ±0.005 and 0.18 (0.15, 0.20) mg (range: 0.13–0.25 mg). Individual egg size (diameter: Fig. 3; weight) was unrelated (both P>0.63) to female body size (TW). Individual egg weight was a power function of egg diameter (Table 1).

Temporal comparisons of fecundity and egg size

Fecundity Size-specific fecundities differed among the three periods, and body-size–adjusted means differed for each period (Table 2, Fig. 4). Size-adjusted mean fecundity in 1999 was 18% greater than in 1991, which in turn was 16% greater than during 1978–81. Lobster in 1999 thus exhibited a cumulative 36% increase in size-specific fecundity over that described for lobster collected during 1978–81. The statistical power (1 minus β, where β is the probability of making a type-II error) to detect an effect size equal in magnitude to the changes observed between 1978–81, 1991, and 1999 was estimated as >97% at α = 0.05.

Egg size Brooded eggs on average were about 5% greater in diameter (equivalent to 15% greater volume assuming the volume of a sphere, V=4/3 πr^3) and were 11% heavier in 1999 compared to 1991 (Table 3). The precision of our

Table 2

(**A**) ANCOVA and (**B**) component least squares regression statistics for log-linear ($\text{Ln}Y = \text{ln}a + b\text{Ln}X$) relations of fecundity (F) to carapace length (CL) for *P. marginatus* caught at Necker Bank during three periods: 1978–81, 1991, and 1999. Natural logs are used throughout. Underlines illustrate that the least-square means for each period differ from one another. MSE = mean square error.

A ANCOVA model: $\text{Ln}F = \text{Ln}CL$ + period (r^2=0.855; root MSE=0.1843)

Factor	df	MS	F	P
Model	3	6.82	199.6	0.0001
LnCL	1	17.16	502.1	0.0001
Period	2	0.87	25.5	0.0001
LnCL × period (P=0.27—ns; not included in final model)				
Error	105	0.03		
Total	108			

$$\underline{12.426 > 12.284} > \underline{12.119}$$
$$1999 > 1991 > 1978\text{–}81$$

B Regression models: $\text{Ln}Y = \text{Ln}a + b\text{Ln}X$

1978–81 $\text{Ln}F = 2.7994 + 2.1569\ \text{Ln}CL$,
r^2=0.708,
n=35,
P<0.001,
SE a=1.0367,
SE b=0.2412

1991 $\text{Ln}F = 1.5859 + 2.4778\ \text{Ln}CL$,
r^2=0.881,
n=34,
P<0.001,
SE a=0.6934,
SE b=0.1607

1999 $\text{Ln}F = 1.3977 + 2.5533\ \text{Ln}CL$,
r^2=0.886,
n=40,
P<0.001,
SE a=0.6452,
SE b=0.1485

measurements was sufficient for the observed change in egg diameter to have had an 87% chance of being detected at $\alpha = 0.05$.

Individual and population egg production

Based on the IRP of Kanciruk and Herrnkind (1976), most egg production by the Necker Bank population of *P. marginatus* in 1999 was by small adults (<60 mm TW) that now dominate the population (Table 4). Large adults (>60 mm TW), although highly fecund, are now too rare to contribute substantially to total population egg production (Table 4).

Table 3

(**A**) ANCOVA and (**B**) component least squares regression statistics for linear relations of egg diameter (ED, in eyepiece units, × 0.020=mm) to carapace length (CL, mm) of *P. marginatus* caught on research cruises to Necker Bank during 1991 and 1999. See Table 2 caption for additional details.

A ANCOVA model: $ED = CL$ + period (r^2=0.142; root MSE=2.193)

Factor	df	MS	F	P
Model	2	27.36	5.69	0.005
CL	1	3.33	0.69	0.41
Period	1	46.85	9.74	0.003
CL × period (P = 0.81—ns; not included in final model)				
Error	69	4.81		
Total	71			

$$\underline{0.691 > 0.658}$$
$$1999 > 1991$$

B Regression models: $ED = a + b\ CL$

1991 $ED = 31.1646 + 0.0230$ CL,
r^2=0.021,
n=32,
P<0.001,
SE a=2.1224,
SE b=0.0282

1999 $ED = 33.5760 + 0.0128$ CL,
r^2=0.006,
n=40,
P<0.001,
SE a=2.1768,
SE b=0.0274

Discussion

Size-specific fecundity and egg size

Fecundity The initial 16% increase in body size-specific fecundity between 1978–81 and 1991 occurred while commercial CPUE decreased fivefold. Unlike commercial data, research CPUE data were collected at fixed stations (including juvenile habitat), were uninfluenced by increased catchability (the targeting of larger adult lobster in more productive habitats by commercial fishermen), and continued to show a decline of similar magnitude during the 1991–99 period when size-specific fecundity increased an additional 18% (Fig. 1B). Thus both observed fecundity responses occurred simultaneously with declining lobster densities. The cumulative 36% increase in size-specific fecundity observed for Necker Bank *P. marginatus* over a >20-yr period of exploitation is not unreasonable given the evidence for concurrent, compensatory declines in body size at sexual maturity in this population (Polovina,

1989; DeMartini et al.[1]). Density-dependent changes in somatic growth, survival rates, and body sizes at sexual maturity have been described for numerous other palinurid species (Pollock, 1995a, 1995b). At least one case study provides further evidence for reproductive compensation. Chittleborough (1979) documented a decreased interval between broods as a response to increased exploitation in the Western Australian rock lobster, *P. cygnus*. Prior to the present study, the study of DeMartini et al. (1993) was the only published record of changes in size-specific fecundity in a spiny lobster, perhaps attributable to density declines resulting from exploitation, although perhaps only reflecting natural interannual variation independent of fishing (Pollock, 1995b).

The fecundity update for 1999 in this article further supports DeMartini et al.'s (1993) original interpretation of an increase in size-specific fecundity as a density-dependent response at lower population densities. Other data on body size at sexual maturity for the period 1988–99, to be reported elsewhere (DeMartini et al.[1]), extend the temporal pattern of smaller body size at sexual maturity first documented during 1986–87, after 10 years of exploitation, by Polovina (1989). The observed decrease in size at maturity could have been caused by slower growth (Pollock, 1995a) resulting from lower levels of oceanic productivity (Polovina et al., 1994, 1995). However, if smaller size at maturity has been a proximal response to decreased rather than increased per capita food availability, it is inconsistent with the simultaneous increases in size-specific fecundity and egg size which have occurred. Evidence for changes in the nutritional status of *P. marginatus* at Necker Bank during 1991–95 is equivocal (Parrish and Martinelli-Liedtke, 1999). Resolution of whether the lower densities of spiny lobsters at Necker Bank have resulted from natural declines in productivity, increased fishery exploitation (or both) would require comparative evaluations for lobsters collected from fished as well as unfished control areas at the bank; unfortunately, as of 1999 unfished lobster habitat at Necker Bank does not exist.

The observed increase in size-specific reproductive output of *P. marginatus* probably has been a phenotypic response to lower densities and higher per capita food availabilities at Necker Bank. It is unlikely, given the 3-yr generation time of *P. marginatus* (Uchida and Tagami, 1984) and relatively short (20+ yr) period over which the responses have occurred, that a genetic, rather than phenotypic, dynamic has been involved. More extensive comparisons of the egg productions of *P. marginatus* populations among Necker and other NWHI banks differing in natural and fishery-induced densities would be necessary to further distinguish natural variation from fishing effects. Complete resolution of this issue would require quantitative comparisons of growth rates and ages at maturity for a lengthy series of year classes of *P. marginatus* at Necker Bank and elsewhere.

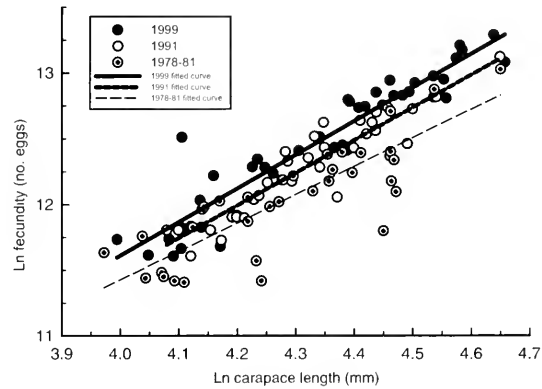

Figure 4

Log-linear scatterplot of fecundity (ln no. of brooded eggs) versus carapace length (ln CL, in mm) for *Panulirus marginatus* collected at Necker Bank during three periods (1978–81, 1991, and 1999).

Egg size Our data demonstrate that egg size can vary substantially among same-size *P. marginatus* collected during the midpoint of a single breeding season, as does fecundity among same-size females. It should not be surprising, then, that average population egg size has covaried with fecundity, even if egg size is body-size independent. The observed change in mean egg size between 1991 and 1999 could not have been due to either developmental or subseasonal changes because we evaluated egg size by consistent methods, using only early-development broods collected during the month of June. It is possible, although unlikely, that the larger eggs (hence larvae) produced in 1999 were somehow of inferior quality and had lower hatching success and poorer subsequent survival.

Intraspecific variation in egg size has rarely been described in spiny lobsters (Pollock, 1995a, 1997). Annala (1991) suggested that egg size increases with body size for a cold-temperate species, *Jasus edwardsii*, from mainland New Zealand. Egg size is unrelated to female body size in tropical *Panulirus argus* (Fonseca-Larios and Briones-Fourzan, 1998). In one particularly detailed study of the egg size dynamics of a small-bodied Caribbean palinurid, *P. guttatus*, Briones-Fourzan and Contreras-Ortiz (1999) detected no relation of egg size to female body size, even though egg size varied nearly twofold among females ranging over twofold in carapace length.

Few studies have documented temporal changes in egg size for palinurid lobsters. A seasonal decline in egg size

[1] DeMartini, E. E., R. B. Mofftt, and P. Kleiber. 2002. Unpubl. data. Honolulu Laboratory, Southwest Fish. Sci. Cent., Natl. Mar. Fish. Serv., NOAA, Honolulu, HI 96822-2396.

Table 4

Index of reproductive potential (IRP) calculated for female *Panulirus marginatus* caught by the Northwestern Hawaiian Islands commercial trap fishery at Necker Bank in 1999. IRP = $(A \times B \times C)/D$, where A= proportion of total females in each 1-mm TW class ($\times 100\%$), B = proportion of berried females per 1-mm class ($\times 100\%$), C = estimated brood size of the median-size female in each class ($\times 10^3$ eggs), and D = a constant (0.015788) used to standardize the most productive size class to 100% (Kanciruk and Herrnkind, 1976). E = % of total egg production; $F = E/A$, a class-specific measure of egg productivity.

TW class (mm)	Total no. of females	No. of berried females	A	B	C	IRP	E ($\times 10^3$)	F ($\times 10^3$)
<39	27	1	0.42	0.43	114	0.00	0.03	35.17
39–40	20	4	0.32	0.17	131	0.05	0.13	40.59
40–41	28	5	0.45	0.21	140	0.09	0.20	43.48
41–42	32	4	0.51	0.17	150	0.08	0.24	46.51
42–43	41	8	0.66	0.34	160	0.23	0.33	49.67
43–44	52	10	0.84	0.43	171	0.39	0.44	52.96
44–45	74	20	1.19	0.85	182	1.17	0.67	56.38
45–46	117	30	1.88	1.28	193	2.95	1.13	59.95
46–47	152	40	2.44	1.71	205	5.43	1.55	63.65
47–48	233	81	3.74	3.46	218	17.88	2.53	67.50
48–49	301	100	4.83	4.27	231	30.20	3.46	71.49
49–50	358	132	5.75	5.64	244	50.15	4.35	75.63
50–51	453	178	7.28	7.61	258	90.43	5.82	79.92
51–52	442	176	7.10	7.52	272	92.09	5.99	84.36
52–53	441	171	7.08	7.31	287	94.13	6.30	88.96
53–54	425	170	6.83	7.26	302	95.00	6.40	93.71
54–55	363	147	5.83	6.28	318	73.84	5.75	98.62
55–56	395	174	6.34	7.44	335	100.0	6.58	103.7
56–57	367	159	5.89	6.79	352	89.19	6.42	108.9
57–58	297	117	4.77	5.00	369	55.74	5.45	114.3
58–59	313	119	5.03	5.08	387	62.66	6.03	119.9
59–60	250	88	4.02	3.76	405	38.78	5.04	125.6
60–61	227	99	3.65	4.23	425	41.48	4.80	131.5
61–62	191	84	3.12	3.59	444	31.47	4.29	137.6
62–63	142	57	2.28	2.44	464	16.34	3.28	143.9
63–64	119	37	1.91	1.58	485	9.29	2.87	150.3
64–65	105	36	1.69	1.54	507	8.32	2.65	156.9
65–66	64	27	1.03	1.15	529	3.97	1.68	163.7
66–67	53	18	0.85	0.77	551	2.29	1.45	170.7
67–68	43	18	0.69	0.77	574	1.93	1.23	177.9
68–69	33	14	0.53	0.60	598	1.20	0.98	185.3
69–70	26	6	0.42	0.26	622	0.42	0.80	192.8
70–71	16	5	0.26	0.21	647	0.23	0.52	200.6
71–72	7	2	0.11	0.09	673	0.04	0.23	208.5
72–73	9	1	0.14	0.04	699	0.03	0.31	216.7
>73	7	2	0.11	0.09	782	0.01	0.08	242.3
Total	6226	2340	100.00	100.00		100.00		

for all-sized females has been observed in two Caribbean species, *Panulirus inflatus* (Gracia, 1985) and *P. argus* (Fonseca-Larios and Briones-Fourzan, 1998). Briones-Fourzan and Contreras-Ortiz (1999), however, could detect no difference in egg size among *P. guttatus* sampled during three consecutive years. Mean egg size declined within the spawning season, but this decline reflected a loss in mass caused by embryonic development within individual eggs rather than the production of smaller eggs later in the breeding season (Briones-Fourzan and Contreras-Ortiz,

1999). Pollock (1995c) noted that *P. guttatus* produces unusually few, but large eggs for a shallow-water tropical palinurid.

Using the CL-to-body-weight regression listed in Table 1, we estimated an inverse index of egg size (Pollock, 1997) for Necker Bank *P. marginatus* in 1999 that was 660 eggs per g total body weight. Such small eggs are typical within the derived lineage of shallow-water, subtropical and tropical members of the genus (Pollock, 1997).

We could find no other studies documenting changes in egg size as a response to density fluctuation in palinurid lobsters. Prior to the mid-1990s, information on temporal and size-related patterns of fecundity and egg size were largely restricted to cold- and warm-temperate members of the genus *Jasus* and *Panulirus* (Pollock, 1995c, 1997). Perhaps egg size, like size-specific fecundity, is phenotypically labile in tropical reef species of the genus *Panulirus* for which high and variable predation pressure makes such plastic responses adaptive. More research on size-specific, individual reproductive output is needed for *P. marginatus* and other tropical reef species of spiny lobsters.

It is unknown whether egg size lability in *P. marginatus* has a genetic or environmental basis. One could perhaps evaluate this for individual females by repetitively measuring egg subsamples from successively brooded egg masses of berried tagged and recaptured females. Fixed but differing egg sizes among individual females would be consistent with a genetic basis. On the other hand, changes in the size of eggs produced by the same individual female in successive broods would suggest that environmental factors are involved.

Management implications

One of our observations has major relevance to the management of *P. marginatus* in the NWHI lobster fishery. Based on the IRP of Kanciruk and Herrnkind (1976), egg production by the Necker Bank population of *P. marginatus* was dominated by the 50–57 mm TW classes in 1999, which together contributed >43% to population egg production (Table 4). Even though each large (>60 mm TW) individual produces a disproportionately great number of eggs, large females are now so poorly represented in the population that they no longer drive population egg production (Table 4). The eggs produced by smaller (50–57 mm TW) females are more important to the population now than before exploitation. In 1996 a "retain all" size policy was established for the commercial fishery, replacing a 50-mm-TW minimum size limit used previously, in part because of the high mortality of discarded lobsters (DiNardo et al., 2002). If a commercial lobster fishery with a minimum size limit were to be reinstated in the NWHI, a minimum size larger than the previous (50 mm TW) should be considered. Our findings on the size distribution of population egg production indicate that smaller adult females, which now produce most of the population's eggs, should be further protected, perhaps by using larger escape vents in traps. Doing so would increase total population egg production and might assist in countering recruitment overfishing (Botsford, 1991; Pollock, 1993). *Panulirus marginatus* production at Necker Bank historically and presently dominates archipelago-wide production by the species; this production is supported by empirical catch data (DiNardo et al.[2]) as well as modeling of its recruitment dynamics (Polovina et al., 1999). Augmenting egg production by the Necker Bank population might significantly bolster stock-wide productivity. The body size distribution of egg production by *P. marginatus* at other NWHI banks is presently unknown, however, and egg production by large females elsewhere possibly could partly offset the deficit in production at Necker. Our observations on the size distribution of egg production at Necker Bank nonetheless merit important consideration for setting size limits for spiny lobster management.

By necessity we calculated the IRP assuming that all size classes produced the same (single) brood per spawning period because data on size-specific spawning frequency were lacking. We caution that, if females >60 mm TW (whose size-specific egg production is greatest) produce broods more frequently than smaller females (Lipcius, 1985), we have proportionately underestimated the contribution of larger females to population egg production.

Individual *Panulirus marginatus* of all sizes likely produce multiple broods per individual spawning season, based on the protracted period during which females are berried (Uchida and Tagami, 1984; Polovina and Moffitt, 1995) and the occasional presence of new, intact (unused) spermatophore plates on spent females (unpubl. data, Honolulu Laboratory, NMFS). (The latter observation in fact suggests that Necker Bank *P. marginatus* can produce more than one brood per molt [like *P. argus*; Sutcliffe, 1953].) There are no time-series growth-rate data available with which to evaluate whether females of a given body size might now be producing larger broods at more frequent intervals than previously. If females are now growing faster, it is likely that the rates of both molting and brood production are now greater. Accurate estimates of individual spawning frequencies and how these might differ among females of varying body sizes, would be needed to fully describe the compensatory increase in reproduction which has occurred for the Necker Bank population of *P. marginatus*.

Acknowledgments

We thank several anonymous fishery observers for collection of invaluable commercial catch data and R. Moffitt, J. Polovina, and an anonymous reviewer for constructive criticisms of the manuscript.

[2] DiNardo, G. T., W. R. Haight, and J. A. Wetherall. 1998. Status of lobster stocks in the Northwestern Hawaiian Islands, 1995–97, and outlook for 1998. Southwest Fish. Sci. Cent. Admin. Rep. H-98-05, 35 p. Honolulu Laboratory, Southwest Fish.Sci. Cent., Natl. Mar. Fish. Serv., NOAA. Honolulu, HI 96822-2396.

Literature cited

Annala, J. H.
1991. Factors influencing fecundity and population egg production of *Jasus* species. *In* Crustacean egg production, Crustacean issues 7 (A. Wenner and A. Kuris, eds.), p. 301–315. Balkema, Rotterdam.

Botsford, L. W.
1991. Crustacean egg production and fisheries management. *In* Crustacean egg production, Crustacean issues 7 (A. Wenner and A. Kuris, eds.), p. 379–394. Balkema, Rotterdam.

Briones-Fourzan, P., and G. Contreras-Ortiz.
1999. Reproduction of the spiny lobster *Panulirus guttatus* (Decapoda: Palinuridae) on the Caribbean coast of Mexico. J. Crust. Biol. 19:171–179.

Chittleborough, R. G.
1979. Natural regulation of the population of *Panulirus longipes cygnus* George and responses to fishing pressure. Rapp. P-V. Reun. Cons. Perm. Int. Explor. Mer 175:217–221.

Chubb, C. F.
2000. Reproductive biology: issues for management. *In* Spiny lobsters: fisheries and culture, 2nd ed. (B. F. Phillips and J. Kittaka, eds.) p. 245–275. Fishing News Books, Blackwell Science Ltd., Oxford.

DeMartini, E. E., D. M. Ellis, and V. A. Honda.
1993. Comparisons of spiny lobster *Panulirus marginatus* fecundity, egg size, and spawning frequency before and after exploitation. Fish. Bull. 91:1–7.

DiNardo, G. T., E. E. DeMartini, and W. R. Haight.
2002. Estimates of lobster handling mortality associated with the Northwestern Hawaiian Islands lobster-trap fishery. Fish. Bull. 100:128–133.

Fonseca-Larios, M., and P. Briones-Fourzan.
1998. Fecundity of the spiny lobster *Panulirus argus* (Latreille, 1804) in the Caribbean coast of Mexico. Bull. Mar. Sci. 63:21–32.

Gracia, A.
1985. Variacion estacional en la fecundidad de la langosta *Panulirus inflatus* (Bouvier 1895) (Crustacea: Decapoda: Palinuridae). Ciencias Marinas 11:7–27. [In Spanish with Engl. abstract.]

Kanciruk, P., and W. F. Herrnkind.
1976. Autumnal production in *Panulirus argus* at Bimini, Bahamas. Bull. Mar. Sci. 26:417–432.

Lipcius, R. M
1985. Size-dependent reproduction and molting in spiny lobsters and other long-lived decapods. *In* Factors in adult growth, Crustacean issues 3 (A. Wenner, ed.), p. 129–148. Balkema, Rotterdam.

Parrish, F. A., and T. L. Martinelli-Liedtke.
1999. Some preliminary findings on the nutritional status of the Hawaiian spiny lobster (*Panulirus marginatus*). Pac. Sci. 53:361–366.

Pollock, D. E.
1993. Recruitment overfishing and resilience in spiny lobster populations. ICES J. Mar. Sci. 50:9–14.
1995a. Notes on phenotypic and genotypic variability in lobsters. Crustaceana 68:193–202.
1995b. Changes in maturation ages and sizes in crustacean and fish populations. S. Afr. J. Mar. Sci. 15:99–103.
1995c. Evolution of life-history patterns in three genera of spiny lobsters. Bull. Mar. Sci. 57:516–526.
1997. Egg production and life-history strategies in some clawed and spiny lobster populations. Bull. Mar. Sci. 61: 97–109.

Polovina, J. J.
1989. Density dependence in spiny lobster, *Panulirus marginatus*, in the Northwestern Hawaiian Islands. Can. J. Fish. Aquat. Sci. 46:660–665.
2000. The lobster fishery in the North-western Hawaiian Islands. *In* Spiny lobsters: fisheries and culture, 2nd ed. (B. F. Phillips and J. Kittaka, eds.), p. 98–104. Fishing News Books, Blackwell Science Ltd., Oxford.

Polovina, J. J., P. Kleiber, and D. R. Kobayashi.
1999. Application of TOPEX-POSEIDON satellite altimetry to simulate transport dynamics of larvae of spiny lobster, *Panulirus marginatus* in the Northwestern Hawaiian Islands, 1993–1996. Fish. Bull. 97:132–143.

Polovina, J. J., G. T. Mitchum, N. E. Graham, M. P. Craig, E. E. DeMartini, and E. N. Flint.
1994. Physical and biological consequences of a climate event in the central North Pacific. Fish. Oceanogr. 3:15–21.

Polovina, J. J., and R. B. Moffitt.
1995. Spatial and temporal distribution of the phyllosoma of the spiny lobster, *Panulirus marginatus*, in the Northwestern Hawaiian Islands. Bull. Mar. Sci. 56:406–417.

Polovina, J. J., W. R. Haight, R. B. Moffitt, and F. A. Parrish.
1995. The role of benthic habitat, oceanography, and fishing on the population dynamics of the spiny lobster, *Panulirus marginatus* (Decapoda, Palinuridae), in the Hawaiian Archipelago. Crustaceana 68:203–212.

SAS Institute.
1990a. Proc REG procedures. SAS/Stat user's guide, vol. 2, release 6, 4th ed., p. 1352–1456. SAS Institute, Inc., Cary, NC.
1990b. Proc NLIN procedures. SAS/Stat user's guide, vol. 2, release 6, 4th ed., p. 1135–1193. SAS Institute, Inc., Cary, NC.
1990c. Proc GLM procedures. SAS/Stat user's guide, vol. 2, release 6, 4th ed., p. 891–996. SAS Institute, Inc., Cary, NC.

Somers, K. M.
1991. Characterizing size-specific fecundity in crustaceans. *In* Crustacean egg production, Crustacean Issues 7 (A. Wenner and A. Kuris, eds.), p. 357–378. Balkema, Rotterdam.

Sutcliffe, W. H, Jr.
1953. Further observations on the breeding and migration of the Bermuda spiny lobster, *Panulirus argus*. J. Mar. Res. 12:173–183.

Uchida, R. N., and D. T. Tagami.
1984. Biology, distribution, population structure, and preexploitation abundance of spiny lobster, *Panulirus marginatus* (Quoy and Gaimard 1825), in the Northwestern Hawaiian Islands. *In* Proceedings of the second symposium on status of resource investigations in the Northwestern Hawaiian Islands (R. W. Grigg and K. Y. Tanoue, eds.), p. 157–198. Sea Grant Miscellaneous Report UNIHI-SEAGRANT-MR-84-01. Sea Grant Program, Univ. Hawaii, Honolulu, HI.

Appendix A

Two body size metrics (carapace length, CL; tail width, TW) and fecundity (F, number of brooded eggs) data for 40 individual spiny lobster (*Panulirius marginatus*) collected during 1999 at Necker Bank, Northwestern Hawaiian Islands. Data are ordered by increasing CL.

CL	*TW*	*F*
54.3	39.3	124,860
57.3	39.3	110,815
59.3	40.9	125,324
59.8	41.9	109,865
60.6	39.7	116,385
60.6	48.2	271,153
60.7	40.8	136,116
62.6	43.2	168,210
62.7	42.8	136,786
64.0	43.8	203,026
64.8	43.8	118,303
66.6	45.5	149,753
68.4	46.7	216,477
69.0	46.4	229,561
69.9	48.5	215,502
70.9	47.2	206,099
74.1	50.7	245,037
76.8	51.7	271,830
78.8	52.2	250,885
79.8	49.4	255,240
80.5	54.4	245,510
80.6	54.6	360,611
80.8	53.6	355,366
82.1	54.5	339,466
83.0	54.2	342,488
84.6	56.0	381,494
85.5	59.1	345,755
86.6	57.8	417,662
87.2	56.6	371,609
88.5	60.8	372,148
89.5	55.2	382,667
90.4	58.7	409,864
93.2	60.8	431,027
94.9	60.3	420,458
95.3	63.2	364,508
97.0	63.7	494,282
97.6	61.3	545,059
98.0	62.6	525,173
103.4	66.0	590,530
105.4	67.4	479,197

Impact of hatchery releases on the recreational fishery for Pacific threadfin (*Polydactylus sexfilis*) in Hawaii

Alan M. Friedlander
David A. Ziemann
The Oceanic Institute
Makapuu Point
Waimanalo, Hawaii 96795
E-mail address (for A. M. Friedlander): afriedlander@oceanicinstitute.org

Abstract—The Pacific threadfin (*Polydactylus sexfilis*) is considered one of the premier Hawaiian food fishes but even with catch limits, seasonal closures, and size limits, catches have declined dramatically since the 1960s. It was identified as the top candidate species for stock enhancement in Hawaii, based on the decline in stocks, high market value, and importance of the fishery.

In the stock enhancement program for Pacific threadfin, over 430,000 fingerlings of various sizes were implanted with coded wire tags and released in nursery habitats along the windward coast of Oahu between 1993 and 1998. Because few Pacific threadfin were present in creel surveys conducted between 1994 and 1998, Oahu fishermen were offered a $10 reward for each threadfin that was caught (for both hatchery-reared and wild fish). A total of 1882 Pacific threadfin were recovered from the reward program between March 1998 and May 1999, including 163 hatchery-reared fish, an overall contribution of 8.7% to the fishery. Hatchery-reared fish accounted for as high as 71% of returns in the release areas. Hatchery-reared fish were recovered on average 11.5 km (SD=9.8 km) from the release site, although some had moved as far away as 42 km. Average age for recovered hatchery-reared fish was 495 days; the oldest was 1021 days.

Cultured Pacific threadfin juveniles survived and recruited successfully to the recreational fishery, accounting for 10% of fishermen's catches on the windward side of Oahu. Recruitment to the fishery was highest for the 1997 release year; few juveniles from earlier releases were observed. Presence of a few large, fully developed females in the recreational fishery suggested that hatchery-reared fish can survive, grow, and reproductively contribute to the population. Implementation of an enhancement program that is focused on juveniles and perhaps large females, as part of an integrated fishery management strategy, could speed the recovery of this fish population.

Manuscript accepted 6 September 2002.
Fish. Bull. 101:32–43 (2003).

Declining marine fish stocks worldwide have led to an increased interest in marine fish stock enhancement (Blankenship and Leber, 1995; Schramm and Piper, 1995; Leber et al., 1996; Grimes, 1998; Howell et al., 1999). Stock enhancement of marine fishes has progressed since the late 1800s and several successful marine fish stock enhancement programs have been documented; however, nearly all have been directed toward temperate species such as chum salmon (Kaeriyama, 1996), Japanese flounder (Kitada et al., 1992), red sea bream (Imai et al., 1994; reviewed by Masuda and Tsukamoto, 1998), and red drum (McEachron and Daniels, 1995; McEachron et al., 1998). In one successful marine fish stock enhancement program in the tropics, hatchery-reared striped mullet (*Mugil cephalus*) successfully recruited to the fishery, accounting for 13% of the commercial mullet catch in Kaneohe Bay, Hawaii (Leber and Arce, 1996).

The Pacific threadfin (*Polydactylus sexfilis*), known locally as "moi," is the only representative of the threadfin family (Polynemidae) in Hawaii (Randall, 1996). The distribution of Pacific threadfin extends throughout the Indo-Pacific region from Madagascar (Bleeker, 1875) to the Ogasawara Islands of southern Japan, east to Hawaii and south to the Tuamotu Archipelago (Randall et al., 1990; Myers, 1991). In ancient Hawaiian culture, Pacific threadfin were reserved for the ruling chiefs and prohibited for consumption by commoners (Titcomb, 1972). Pacific threadfin were formerly harvested commercially, but commercial catches have declined steadily since the 1950s and have essentially ceased since 1968 when the daily catch limit was restricted to 15 fish per person. This decline in abundance, particularly around the more populated areas of the state, is likely the cumulative result of years of chronic overfishing (Shomura[1]). Current regulations comprise the following: a catch limit of 15 fish per person per day; a minimum fish size of 7 inch. TL (ca. 14.5 cm FL) for caught fish; and a closed season from 1 June to 30 September.

Pacific threadfin are typically found over shallow sand flats, along high wave-energy rocky shorelines, and in sandy beach wash zone habitats (Hosaka, 1990; Leber et al., 1998). They can also be found in turbid water near stream mouths and brackish mangrove estuaries (Randall et al., 1990; Myers, 1991). Local fishermen call areas where adult Pacific threadfin congregate "moi holes" (Hosaka, 1990); these usually occur in shoreline caves or sandy depressions and sand channels in the surf zone among boulders or reef areas.

Pacific threadfin are protandric hermaphrodites, initially maturing as males after a year at about 20–25 cm; they then undergo a sex reversal, passing through a hermaphroditic stage and becoming functional females between 30 and 40 cm FL at about three years of age (Santerre and May, 1977; Santerre et al., 1979; Szyper et al., 1991). Spawning occurs inshore

[1] Shomura, R. 1987. Hawaii's marine fishery resources: yesterday (1900) and today (1986). Admin. Rep. H-87-21, 14 p. U.S. Dep. Commer., NOAA, NMFS, Southwest Fisheries Science Center, Honolulu, Hawaii 96822.

Table 1

Summary of Pacific threadfin (*Polydactylus sexfilis*) releases on the windward side of Oahu Island, 1993–97. Release size is fork length in mm.

Release year	Release sites	No. of fish released	Adjusted no. of fish released	% tag retention	Release size range (mm)
1993	Kahana	10,020	9939	99.2	70–150
	Laniloa	9990	9858	98.7	
1994	Kahana	40,530	37,888	93.5	48–130
	Malaekahana	40,695	37,561	92.3	
1996	Kahana	31,258	30,164	96.5	85–130
	Kailua	14,952	14,223	95.1	
1997	Kahana	99,020	96,019	97.0	70–130
	Kailua	97,569	94,349	96.7	
1998	Kahana	75,687	71,672	94.7	70–130
	Kailua	11,273	10,827	96.1	
Totals		430,994	412,500		

and eggs are dispersed and hatched offshore (Lowell, 1971). Larvae and juveniles are pelagic up to about 6 cm FL, at which size they enter inshore habitats including surf zones, reefs, and stream entrances (Santerre and May, 1977; Santerre et al., 1979). Newly settled young Pacific threadfin, locally called "moi-lii" (Lowell, 1971; Tinker, 1982), appear in shallow waters in summer and fall where they are the dominant member of the nearshore surf zone fish assemblage (Ziemann et al.[2]).

Pacific threadfin is a popular and much sought-after sport fish that also supports a small subsistence fishery in Hawaii (Santerre et al., 1979; Leber et al., 1998). It is presently an important species in the Hawaii recreational fishery because of its reputation as one of the best tasting fishes in Hawaii (Hosaka, 1990) and its high market value (wholesale market price over US$3.00 per kilogram). A species prioritization study conducted early in the stock enhancement research program in Hawaii identified Pacific threadfin as the top candidate for stock enhancement, based partly on the decline of its stocks, its high market value, and importance in the recreational fishery (Oceanic Institute[3]). As part of the Stock Enhancement of Marine Fish in the State of Hawaii (SEMFISH) program funded by the National Marine Fisheries Service, juvenile Pacific threadfin were released in nursery habitats along the windward coast of Oahu between 1993 and 1997 to evaluate the contribution of hatchery-reared fish to the local fishery. Leber et al. (1998) demonstrated site-specific potential success in stocking programs for juveniles in 1993–94. The purpose of this article is to provide long-term tracking of catches to determine the contribution of hatchery-produced fish versus wild stocks in the recreational fishery on the windward side of Oahu.

Methods

The culture of Pacific threadfin at the Oceanic Institute (OI) is described by Ostrowski et al. (1996). Most fish were released into coastal waters between day 60 for small juveniles (70–85 mm FL) and day 90 for larger juveniles (130–150 mm FL).

During each of five release years, 10,000 to 100,000 juveniles (per release site) were sorted by size and released in multiple lots over 3–5 months; the total number released per release site usually varied between years (Table 1, Fig. 1). Over the five release years, a total of 430,994 Pacific threadfin fingerlings were released. Before release, all fish received coded wire tags (Northwest Marine Technology, Inc., Shaw Island, WA: Jefferts et al., 1963) in the snout area to identify release lots by release size, date, and location. Approximately 5% of each release lot was retained in culture at OI to determine tag retention rates. Fish were examined monthly from 1 to 6 months until tag loss rates stabilized (i.e. when the number lost had not increased since the previous month). Tag retention rates varied from 93% to 99%. All calculations of tag recovery rates were based on coded-wire-tag data adjusted for tag retention rates.

We conducted a roving creel survey, encompassing all release areas, intermittently from 1994 to 1998 on the windward side of Oahu 1) to determine if released Pacific threadfin were surviving and being caught in the fishery, 2) to estimate Pacific threadfin CPUE in the recreational fishery, and 3) to inform fishermen about the Pacific threadfin

[2] Ziemann, D. A., A. M. Friedlander, and P. Craig. 1998. Enhancement of Pacific threadfin *Polydactylus sexfilis* in Hawaii. I. Release optimization. Stock Enhancement of Marine Fish in the State of Hawaii (SEMFISH), Phase IX, 152 p. Oceanic Institute, 41-202 Kalanianaole highway, Waimanalo, HI 96795.

[3] Oceanic Institute. 1989. Selection of marine finfish species for stock enhancement in Hawaiian waters, 78 p. The Oceanic Institute, Makapuu Point, 41-202 Kalanianaole Highway, Waimanalo, HI 96795.

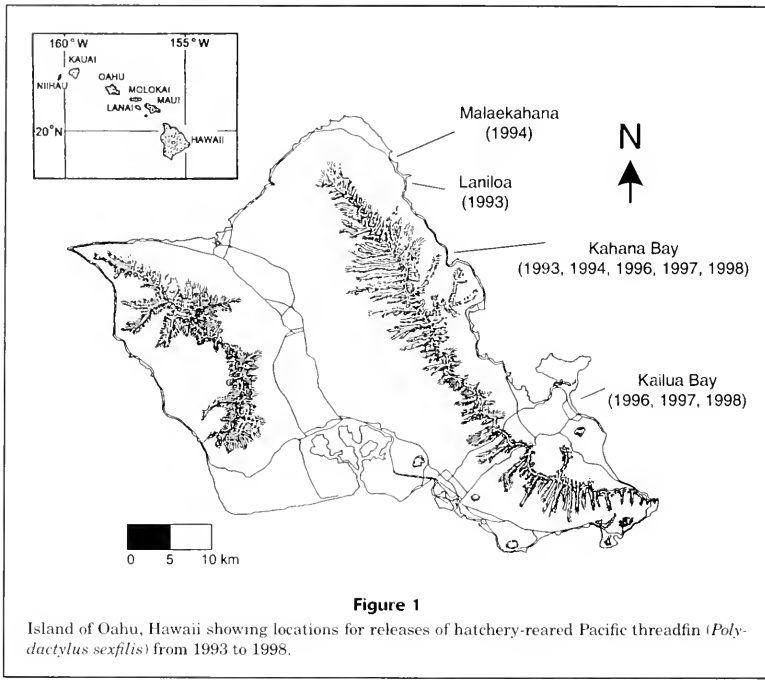

Figure 1

Island of Oahu, Hawaii showing locations for releases of hatchery-reared Pacific threadfin (*Polydactylus sexfilis*) from 1993 to 1998.

enhancement program. Fishermen were interviewed at boat docks and along the coastline to collect information about their catch and effort (species, lengths, number of hours fished per gear type). All Pacific threadfin in the catches were scanned for coded wire tags with a hand-held Northwest Marine Technologies cwt sensor ("wand").

Because Pacific threadfin were scarce in creel samples, we offered a $10 reward to Oahu fishermen for each Pacific threadfin (hatchery-reared and wild) caught in the open season between March 1998 and May 1999 (no retention is allowed from June to September). Posters, newspaper articles, and radio talk shows were used to publicize the reward program. We also informed participating fishermen that we were primarily interested in samples from the windward side of the island; thus, catches of Pacific threadfin from other parts of the island were underrepresented in our effort. To obtain the reward, fishermen provided date, location, gear used, fork length, and the head of each Pacific threadfin caught. Beginning in September 1998, fishermen had to return whole fish to obtain the $10 reward. This requirement allowed us to gather more accurate length information, as well as information on weight, sex, and gonadal condition. We obtained a relatively unbiased random sample from the fishery because fishermen were unable to determine visually whether a fish had a coded wire tag; this unbiased sample enabled us to calculate the contribution of hatchery-reared fish to the fishery.

A Mann-Whitney rank sum test (T-statistic) was used to compare distance traveled among sites and years for hatchery-reared fish. This test was also used to compare fork lengths of wild fish by sex between the 1999 and the 1962–68 sampling periods. We compared number of Pacific threadfin recovered in each size class in relation to the number of hatchery-reared fish released in that size class by using chi-square goodness of fit. Expected number of fish recaptured in each size class was calculated by taking the total number of recaptures for each year from each release site and multiplying it by the proportion of fish released in that size class at that site during that year.

A Kruskal-Wallis ANOVA on ranks with Dunn's multiple comparison procedure (Soko) and Rohlf, 1981) was used to identify pair-wise difference in CPUE among gear types; $\alpha = 0.05$. A two-way ANOVA (F) was conducted to compare fish length among gear types for wild and hatchery-reared Pacific threadfin during each reward year. Tukey multiple comparison procedures were conducted to determine pair-wise differences in fish length between gear types; $\alpha = 0.05$. Condition factor was calculated as

$$C = (W/L^3) \times 10{,}000,$$

where C = condition factor;
W = fish weight in grams; and
L = fork length in mm (Anderson and Neumann, 1996).

Table 2

Results of catch and effort from recreational creel surveys for Pacific threadfin conducted along the windward coast of Oahu between 1994 and 1998.

Gear type	Number of interviews	Total effort (h)	Number of threadfin	CPUE (number/h)	Number of hatchery-reared threadfin	Proportion hatchery-reared
Angling	464	3647	123	0.03	40	0.33
Gillnet	22	327	35	0.11	1	0.03
Throw net	42	93	3	0.03	0	0.00
Spear	23	81	0	0.00	0	0.00
Total	551	4148	161	0.04	41	0.25

Table 3

Summary of wild and tagged Pacific threadfin obtained from the recreational fishery from March 1998 to May 1999.

	1998				1999				Total			
Region	Hatchery-reared	Wild	Total	Proportion hatchery-reared	Hatchery-reared	Wild	Total	Proportion hatchery-reared	Hatchery-reared	Wild	Total	Proportion hatchery-reared
Ewa	0	18	18	0.00	0	0	0	0.00	0	18	18	0.00
Kahana	2	15	17	0.12	6	129	135	0.04	8	144	152	0.05
Kailua	35	14	49	0.71	4	6	10	0.40	39	20	59	0.66
Kaneohe	5	85	90	0.06	28	221	249	0.11	33	306	339	0.10
Laie	11	237	248	0.04	17	373	390	0.04	28	610	638	0.04
Mokapu	0	13	13	0.00	34	317	351	0.10	34	330	364	0.09
Mokuleia	0	8	8	0.00	0	0	0	0.00	0	8	8	0.00
North Shore	3	121	124	0.02	0	3	3	0.00	3	124	127	0.02
Sandy Beach	1	32	33	0.03	0	9	9	0.00	1	41	42	0.02
Waianae	0	18	18	0.00	0	0	0	0.00	0	18	18	0.00
Waimanalo	9	16	25	0.36	8	84	92	0.09	17	100	117	0.15
Total	66	577	643	0.10	97	1142	1239	0.08	163	1719	1882	0.09

Condition factors between sites and among release size classes were compared by using a two-way ANOVA (F); $\alpha = 0.05$. A Mann-Whitney rank sum test (T) was used to compare the gonadosomatic index (GSI=ovary weight/body weight×100) between hatchery-reared and wild Pacific threadfin recovered in the 1999 reward program.

Results

CPUE for Pacific threadfin from 551 creel survey interviews of recreational fishermen from 1994 to 1998 was very low (0.04 fish/h for all gear types combined) (Table 2): 1 per 33 hours by angling or 1 per 9 hours by gillnet. These values are probably low estimates because the creel survey was not directed at fishermen who targeted Pacific threadfin. Even though we saw a very small number of Pacific threadfin in the creel surveys, hatchery-reared fish made up 33% (40 of 123) of the angling catch and 25% (41 of 161) of the overall catch.

The voluntary reward program between March 1998 and May 1999 yielded 1882 Pacific threadfin (Table 3), of which 163 were hatchery-reared Pacific threadfin (8.7%). The period March–May 1998 provided 643 Pacific threadfin, compared to 1239 for the period September 1998–May 1999. Tag information was readable for 63 of 66 fish recovered in 1998 (3 damaged tags) and all 97 tags recovered in 1999. Of the total readable tags, fish released in 1997 made up 93.7% (n=59) of the 1998 reward fish and 95.9% (n=93) of the 1999 reward fish. Four fish from 1996 releases were recovered in each year. Although most fish recovered in the reward program were from the windward or eastern side of Oahu, 168 fish (26.1%), including 4 hatchery fish from the North Shore area, did come from other areas around the island in 1998 (Fig. 2). Three reward fish were returned from the North Shore in 1999. No hatchery-

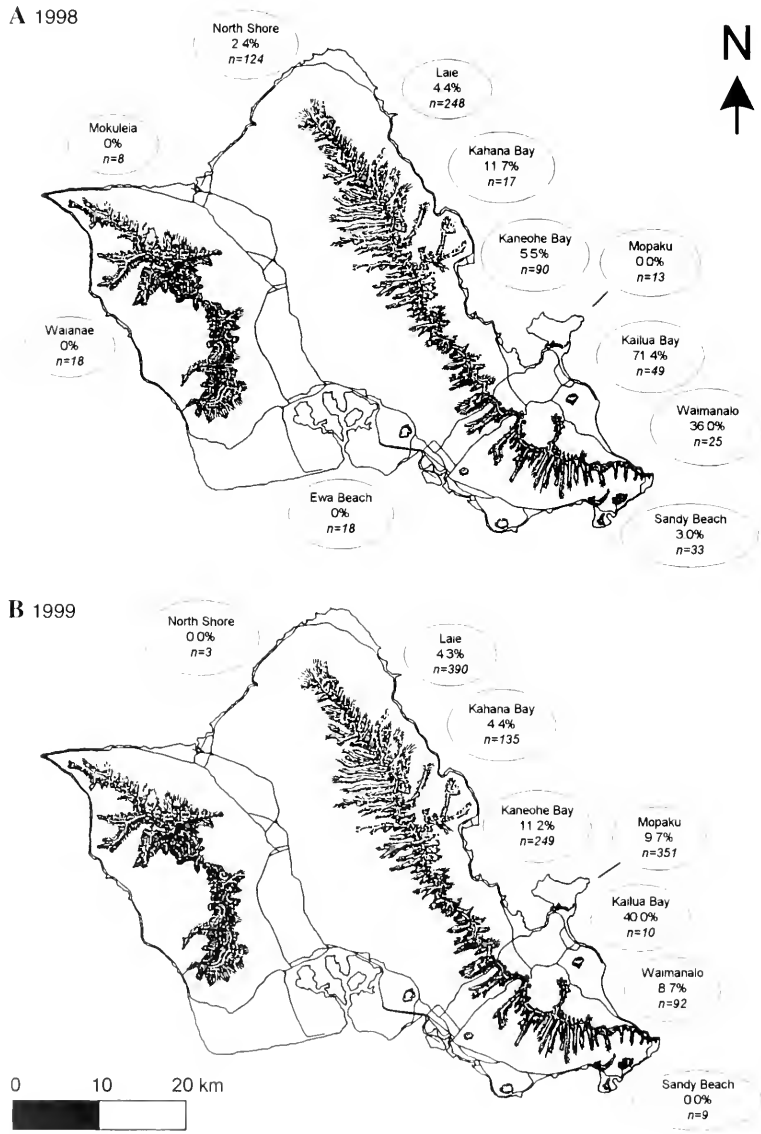

Figure 2

Percentage of hatchery-reared Pacific threadfin recovered from the recreational reward fishery program during the (**A**) 1998 and (**B**) 1999 fishing seasons. *n* = the total number of Pacific threadfin recovered at each site

Table 4

Number of 1997 released fish obtained from the reward fishery for the years 1998 and 1999. Expected values were derived from the total number of hatchery-reared fish returned during each reward year from each release site, multiplied by the proportion of fish released in each size class. No χ^2 value was significant at $P < 0.05$.

Release size (mm)	Adjusted no. of fish released	1998		1999	
		Hatchery-reared	Expected	Hatchery-reared	Expected
Kahana					
70–85	14,152	5	2.51	8	5.45
85–100	34,618	5	6.14	16	13.37
100–115	41,069	6	7.27	11	15.83
115–130	6,102	1	1.08	2	2.35
Total	96,019	17	17.00	37	37.00
χ^2			2.91		3.24
Kailua					
70–85	15,415	9	6.86	14	9.15
85–100	35,090	19	13.62	17	20.83
100–115	37,819	14	16.84	25	22.45
115–130	6,022	0	2.68	0	3.57
Total	94,349	42	42.00	56	56.00
χ^2			4.56		7.14

reared fish were recovered from the leeward coast or south shore areas. Highest proportions of hatchery-to-wild fish were found in Kailua Bay (71%) and at Waimanalo Beach (36%) during the 1998 season. For the Kahana Bay site, around 12% of the Pacific threadfin recovered in the 1998 reward program were hatchery-reared. For the 1999 reward program, Kailua Bay continued to have the highest percentage of hatchery-reared Pacific threadfin, 40%. Hatchery-reared Pacific threadfin were also recovered at Waimanalo Beach (8.7%), Mokapu Peninsula (9.7%), and Kaneohe Bay (11.2%); the latter two sites are north of the Kailua Bay release site.

Hatchery-reared Pacific threadfin released in Kahana Bay were recovered as far north as Kawela Bay (25 km) and south to Waimanalo Beach (33 km) (Fig. 3). Fish released in Kailua Bay were recovered 19 km to the south at Sandy Beach and 42 km to the north at Kahuku (Fig. 4). Fish were captured at significantly greater distances from the release sites in 1999 ($\bar{x}$=15.2 km, SD=10.2) than in 1998 ($\bar{x}$=11.0 km, SD=6.8) (T=2044.0, P=0.025). Fish released in Kahana Bay were recaptured at significantly greater distances from the release site ($\bar{x}$=14.6 km, SD=11.0) compared to the Kailua Bay releases ($\bar{x}$=9.6 km, SD=6.3; T=6129.0, P<0.001).

The proportion of fish recaptured in the reward program for 1998 and 1999 was lowest in the largest release size class (115–130 mm) and greatest in the middle two release size classes (85–100; 100–115 mm). Because the number of fish released in each size class in 1997 was different, it was necessary to compare the number of fish recovered in each size class in relation to the number released in that size class. Eight fish recaptured from the 1996 release were not included in our analyses. For both years and both locations, the catch of hatchery-reared Pacific threadfin divided by the adjusted release number was greatest in the smallest size class (70–85 mm) (Table 4).

Expected number of fish recaptured in each size class was calculated by taking the total number of recaptured fish for each year from each release site and multiplying it by the proportion of fish released in that size class at that site during that year (Table 4). There were no significant differences in number of fish recaptured in each size class in relation to expected recapture numbers for both years at the Kahana Bay release site (1998: χ^2=2.91, df=3, P>0.05; 1999: χ^2=3.24, df=3, P>0.05) and for Kailua Bay (1998: χ^2=5.74, df=3, P>0.05; 1999: χ^2=7.14, df=3, P>0.05).

Angling (pole and line fishing) accounted for the greatest number of hatchery-reared and wild Pacific threadfin acquired in the reward program but had the lowest CPUE among gear types (Table 5). Over both survey years, for wild and hatchery-reared fish combined, angling accounted for 63.0% of the total Pacific threadfin catch, followed by gillnets (19.2%), thrownets (13.9%), and surround nets (3.9%).

Length of Pacific threadfin caught varied among gear types, between years, and between hatchery-reared and wild Pacific threadfin. For 1998, mean size of Pacific threadfin captured was significantly different among gear types (F=6.378, df=3, 632, P<0.001) and between hatchery-reared and wild fish (F=11.833, df=1, 632, P<0.001). Gillnets tended to catch larger fish, and surround nets captured the smallest fish (Tukey multiple comparison test results—gillnets: 255.5 mm ≥ angling: 235.1 mm ≥ thrownet: 214.0 mm > surround nets: 193.7 mm). Mean length for hatchery-reared Pacific threadfin pooled over all gear types was 207.0 mm (SD=28.6) and mean length for wild Pacific threadfin was 242.2 mm (SD=52.7).

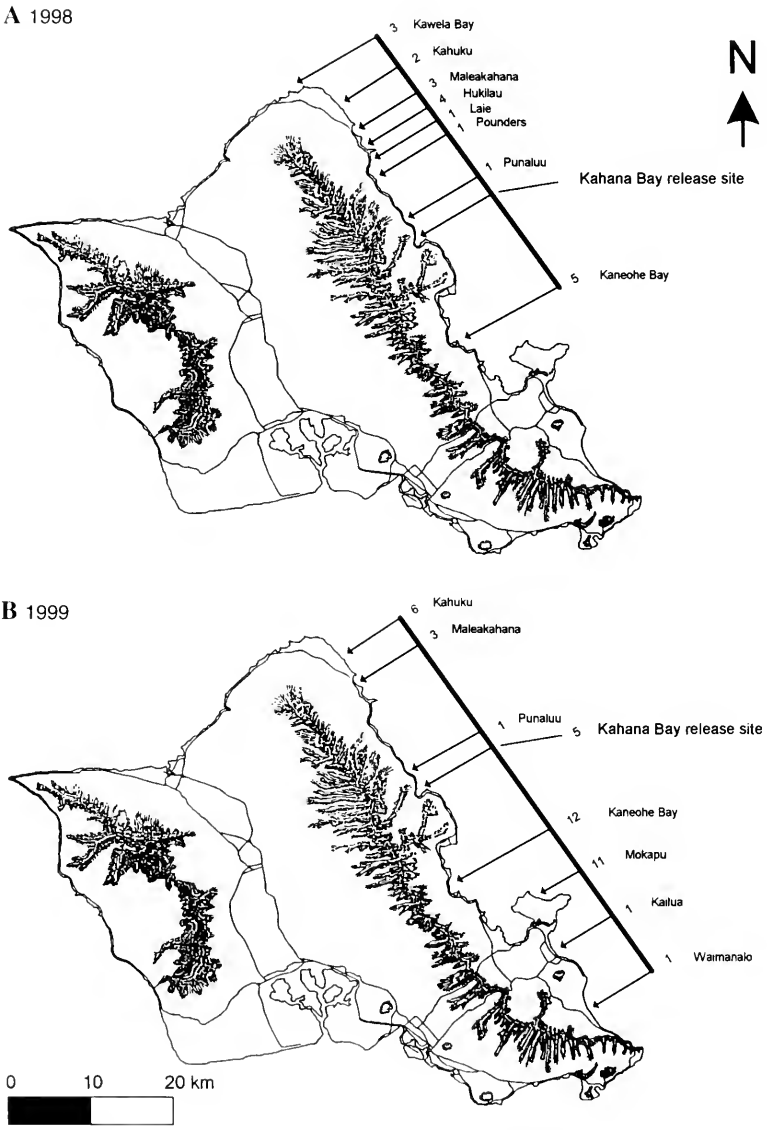

Figure 3

Movement patterns of hatchery-reared Pacific threadfin released in Kahana Bay from the reward fishery program during the (**A**) 1998, $n = 20$ and (**B**) 1999, $n = 40$ fishing seasons.

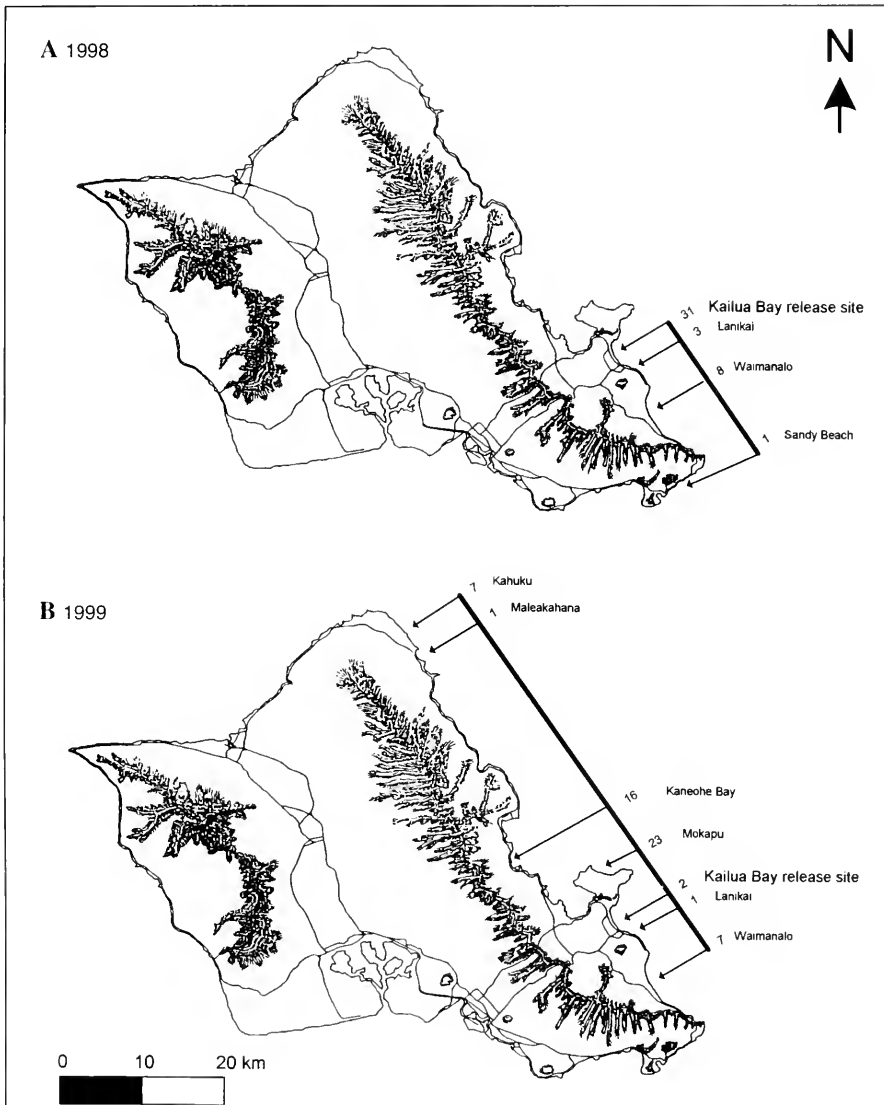

Figure 4

Movement patterns of hatchery-reared Pacific threadfin released in Kailua Bay from the reward fishery program during the (**A**) 1998, n = 43 and (**B**) 1999, n = 57 fishing seasons.

Information on sex of Pacific threadfin obtained in the reward program was available only during 1999 because whole fish were not acquired in 1998. The ratio of male to hermaphrodite to female was 56:17:27 for wild Pacific threadfin and 81:15:4 for hatchery-reared fish (Fig. 5). Three hatchery-reared fish that had changed from males

Table 5

Catch per unit of effort (CPUE) for Pacific threadfin caught by three different gear types used in the recreational-artisanal fishery. Mean rank computed for Kruskal-Wallis rank sum test (H=19.303, df=2, P<0.001). Results of Dunn's multiple comparison procedure. Gear types with the same letter (A, B) are not significantly different.

Gear type	n	Total hours	Total no. of threadfin	No hatchery-reared	Mean CPUE	SD CPUE	Dunn's multiple comparisons
Thrownet	16	55.0	166	7	5.49	9.34	A
Gillnet	31	83.5	221	20	3.52	4.89	A B
Angling	113	592.5	817	56	1.63	1.44	B
Grand total	160	731.0	1204	83	2.38	3.98	

Table 6

Comparison of size (mm FL) and sex for hatchery-reared and wild catch Pacific threadfin acquired from the reward fishery in 1999.

	Hatchery-reared				Wild			
Sex	Mean	Min.	Max.	n	Mean	Min.	Max.	n
Males	257.1	210	307	61	250.0	174	360	372
Hermaphrodites	267.2	220	323	11	275.0	200	380	112
Females	311.3	247	356	3	315.6	249	462	179

to females were recovered during 1999; one was released during summer 1996, the other two were released during summer 1997.

Mean size for males was 250.0 mm (SD=32.1) for wild fish and 257.1 mm (SD=24.8) for hatchery-reared fish; mean size for hermaphrodites was 275.0 mm (SD=27.5) for wild fish and 267.2 mm (SD=43.3) for hatchery-reared fish; mean size for females was 315.6 mm (SD=39.2) for wild Pacific threadfin and 311.3 mm (SD=57.1) for hatchery-reared threadfin (Table 6). The GSI for hatchery-reared males (x=0.629, SD=0.728) was not significantly different (T=6524, P=0.073) than the GSI for wild males (x=0.619, SD=0.842), likely because of the larger size of hatchery-reared males during 1999. Number of hatchery-reared females and hermaphrodites was too low for statistical comparisons.

Condition factor for hatchery-reared Pacific threadfin during 1999 was not significantly different between release sites (F=0.074, df=1, 79, P=0.786) or among release sizes (F=1.488, df=3, 79, P=0.224). Therefore, condition factors for all hatchery-reared fish were pooled and compared to condition factors for all wild fish recovered in 1999. No significant difference was found in condition factors between these two groups (T=47733.0, P=0.087).

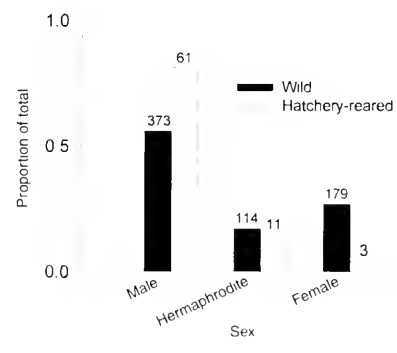

Figure 5

Sex ratio for wild and hatchery-reared Pacific threadfin returned for the 1999 reward fishing season. Values are total number of fish in each sex category.

Discussion

Cultured Pacific threadfin juveniles released into the ocean survived and recruited successfully into the recreational fishery, accounting for 10% and 8% of the catch on the windward side of the island of Oahu in two years (1998 and 1999, respectively). Hatchery fish from the 1997 release constituted the majority of the hatchery fish returns to the recreational fishery in 1998 (89.4%) and 1999 (95.9%). Few of the hatchery fish released in years prior to 1997 have been recovered from the recreational fishery. The large

Table 7

Comparisons of length of juveniles, males, hermaphrodites, and females for Pacific threadfin around Oahu from 1962 to 1968 and for wild fish from the 1999 reward fishery program. One standard deviation of mean fork length is shown in parentheses.

	1962–68, n=1651		1999 reward program, n=1105			
Sex	Fork length (mm)	Percentage of total	Fork length (mm)	Percentage of total	Mann Whitney T-value	P
Juveniles	227 (30)	6.4	191 (24)	39.7	44864	<0.001
Males	268 (29)	52.3	249 (35)	33.8	184831	<0.001
Hermaphrodites	317 (33)	17.8	275 (27)	10.3	11952	<0.001
Females	378 (45)	23.5	316 (39)	16.2	26200	<0.001

impact of a relatively small number of released fish on the recreational fishery shows that hatchery releases of limited numbers of fish have the potential to impact both the number of fish taken in the fishery and the rate at which the fishery can recover. The differences in contribution rates for different release years suggest that natural factors affecting the survival of juveniles, as well as early larval stages, vary between years.

Hatchery-reared and released fish collected in the recreational fishery showed growth rates, condition factors, and gonadosomal indices similar to those of wild fish, suggesting that hatchery-reared fish are able to adapt to the natural environment and integrate into the wild population. Our data (unpubl.) for wild and hatchery fish collected in nursery habitats showed no significant differences in growth rates. The mean size of hatchery-reared fish collected in 1998 was smaller than in 1999 (over 95% of the fish collected in 1998 and 1999 came from the same releases in 1997). Mean size for hatchery-reared fish in 1999 was not different from the mean size of wild fish for both years, which suggests that size of hatchery fish in 1999 represents the approximate size of 2–3 year-old threadfin and mean age of fish in the recreational fishery is also 2–3 years. The size-frequency distributions of hatchery and wild fish in 1998 and 1999 suggest that a significant portion of the wild fish in the fishery is younger than two years.

Small hatchery fish at release made a higher relative contribution to the recreational fishery than did the larger size group (but not significantly so, except for fish taken in Kailua Bay in 1999), and the nursery habitat sampling conducted after the 1997 releases showed the same (Leber et al., 1998; Ziemann et al.[2]). This pattern is in contrast to that observed for mullet in Hawaii (Leber, 1995) and Pacific threadfin for other years (Ziemann et al.[2])

Hatchery fish disperse slowly from the point of release along the windward coast of Oahu. In nursery habitats three months after release (Ziemann et al.[2]), hatchery fish represented in excess of 70% of the threadfin and they decreased within nine months to 10% or less. Some decrease is due to predation, but some is due to dispersal because in 1998, after 1 year at large, fish were caught in the recreational fishery a mean distance of 11.2 km from the release point, and after two years, mean distance had increased to 15.2 km. Dispersal from the two release sites differed: after one year mean distance for Kahana Bay releases was 14.6 km, whereas mean distance for fish releases in Kailua Bay was 9.6 km.

The 1999 reward sample contained 16% females, 44% males and hermaphrodites, and 40% immature fish. The life cycle of Pacific threadfin (protandric hermaphrodites) makes this skewed sex ratio even more problematic because individuals do not become functional females until about 30 cm FL and these larger fish are selectively removed from the population by fishing. For protogynous species, size-selective fishing mortality may result in differential loss of larger males (Sadovy, 1996; Beets and Friedlander, 1999). The percentage of juveniles in the catch was high. Mean size of Pacific threadfin in all sexual categories was significantly smaller than that reported by Kanayama[4] in 1962–68 (Table 7, Fig. 6); further, females constituted 23.5% of the catch in the 1960s, but only 16.2% of the catch in 1999. We demonstrated that cultured Pacific threadfin juveniles released in known nursery habitats survive and recruit successfully into the recreational fishery 1–2 years later. Our Pacific threadfin data indicate that recruitment of young fish to the population may be jeopardized because there are few mature females left in the population (recruitment overfishing), even with supplementation of hatchery-reared fish.

The underlying problem of the threadfin fishery on Oahu and the other Hawaiian Islands is primarily an intense local harvest by subsistence and recreational fishermen, as well as habitat loss from coastal and upland development. Current state regulations, as well as unregulated removal of larger individuals from the population, contribute to the male-biased sex ratios observed in our study. Stock recovery based on natural reproduction will be a long-term process. Implementation of an enhancement program for Pacific threadfin focused on juveniles and perhaps larger females could speed the rate of recovery of the local population.

[4] Kanayama, R. 1973. Life history aspects of the moi *Polydactylus sexfilis* in Hawaii, 50 p. State of Hawaii, Department of Lands and Natural Resources, Honolulu, Hawaii.

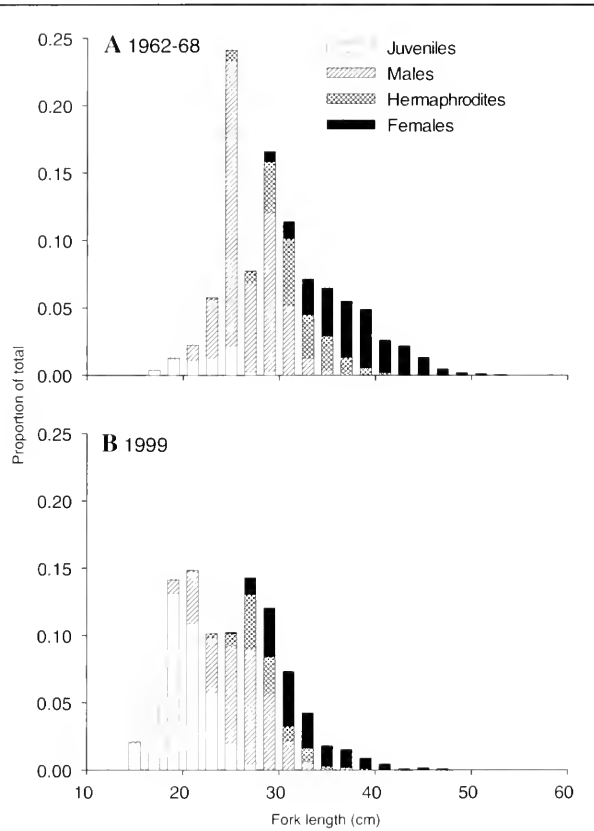

Figure 6

Proportion of juveniles, males, hermaphrodites, and females for Pacific threadfin from (**A**) 1962 to 1968 and (**B**) during the 1999 reward fishery program.

Acknowledgments

The authors acknowledge the contributions to this research made by Ken Leber, Peter Craig, Reiji Masuda, Robert Cantrell, Steve Arce, Scott Bloom, Tom Ogawa, Don Dela Pena, Rich Hall, Karl Keller and other members of the stock management staff at The Oceanic Institute, and of the culture support provided by Tony Ostrowski and the staff of The Oceanic Institute finfish program. Jim Parrish, Reiji Masuda, Ken Leber, two anonymous reviewers and editors provided valuable suggestions for the manuscript. This research was supported under NOAA grant NA76FY0059.

Literature cited

Anderson, R. O., and R. M. Neumann.
1996. Length, weight, and associated structural indices. *In* Fisheries techniques, 2nd ed. (B. R. Murphy and D.W. Willis, eds.), p. 447–482. Am. Fish. Soc., Bethesda, MD.

Blankenship, H. L., and K. M. Leber.
1995. A responsible approach to marine stock enhancement. Am. Fish. Soc. Symp. 15:165–175.

Beets, J., and A. Friedlander.
1999. Evaluation of a conservation strategy: a spawning aggregation closure for grouper in the Virgin Islands. Environ. Biol. Fish. 55:91–98.

Bleeker, P.
1875. Recherches sur la fauna de Madagascar et de ses dependances d'apres les descouvertes de Francois P. L. Pollen et D. C. van Dam. 4e Parte. Poissons de Madagascar et de l'le de la Reunion. Leiden, The Netherlands.

Grimes, C. B.
1998. Marine stock enhancement: sound management or techno-arrogance? Fisheries 23(9):18–23.

Howell, B. R., E. Moksness, and T. Svasand (eds.).
1999. Stock enhancement and sea ranching, 606 p. Fishing News Books. Oxford, England.

Hosaka, E. Y.
1990. Shore fishing in Hawaii, 175 p. Petroglyph Press, Ltd., Hilo, HI.

Imai, T, H. Takama, and I. Shibata.
1994. Estimates of the total amount of red sea bream caught by recreational party boats in Kanagawa Prefecture. Saibai Giken 23:77–83. [In Japanese.]

Jefferts, K. B., P. K. Bergman and H. F. Fiscus.
1963. A coded-wire identification system for macro-organisms. Nature (London) 198:460–462.

Kaeriyama, M.
1996. Population dynamics and stock management of hatchery-reared salmons in Japan. Bull. Natl. Res. Inst. Aquacult. Suppl. 2:11–15.

Kitada, S., Y. Taga, and H. Kishino.
1992. Effectiveness of a stock enhancement program evaluated by a two-stage sampling survey of commercial landings. Can. J. Fish. Aquat. Sci. 49:1573–1582.

Leber, K. M.
1995. Significance of fish size-at-release on enhancement of striped mullet fisheries in Hawaii. J. World. Aquacult. Soc., 26(2):143–153.

Leber, K. M. and S. M. Arce.
1996. Stock enhancement in a commercial mullet, *Mugil cephalus* L., fishery in Hawaii. Fish. Manage. Ecology 3: 261–278.

Leber, K. M, S. M. Arce, D. A. Sterritt, and N. P. Brennan.
1996. Marine stock-enhancement potential in nursery habitats of striped mullet, *Mugil cephalus*, in Hawaii. Fish. Bull. 94:452–471.

Leber, K. M., N. P. Brennan , and S. M. Arce.
1998. Recruitment patterns of cultured juvenile Pacific threadfin, *Polydactylus sexfilis* (Polynemidae), released along sandy marine shores in Hawaii. Bull. Mar. Sci. 62:389–408.

Lowell, N.
1971. Some aspects of the life history and spawning of the moi (*Polydactylus sexfilis*). M.A. thesis, 45 p. Univ. Hawaii, Honolulu, HI

Masuda, R., and K. Tsukamoto.
1998. Stock enhancement in Japan: review and perspective. Bull. Mar. Sci. 62:337–358.

McEachron, L. W., R. L. Colura, B. W. Bumguardner, and R. Ward.
1998. Survival of stocked red drum in Texas. Bull. Mar. Sci. 62:359–368.

McEachron, L. W., and K. Daniels.
1995. Red drum in Texas: a success story in partnership and commitment. Fisheries 20:6–8.

Myers, R. F.
1991. Micronesian reef fishes: a practical guide to the identification of the coral reef fishes of the tropical central and western Pacific, 298 p. Coral Graphics, Barrigada, Guam.

Ostrowski, A., T. Iwai, S. Monahan, S. Unger, D. Dagdagan, P. Murawaka, A. Schivell, and C. Pigao.
1996. Nursery production technology for Pacific threadfin (*Polydactylus sexfilis*). Aquaculture 139:19–29.

Randall. R. E.
1996. Shore fishes of Hawaii, 216 p. Natural World Press, Vida, OR.

Randall, J. E., G. R. Allen, and R. C. Steene.
1990. Fishes of the Great Barrier Reef and Coral Sea, 507 p. Univ. Hawaii Press, Honolulu, HI.

Sadovy, Y. J.
1996. Reproduction of reef fishery species. *In* Reef fisheries (N. V. C. Polunin and C. M. Roberts, eds.), p. 15–59. Chapman and Hall, London.

Santerre, M. J., G. S. Akiyama, and R. C. May.
1979. Lunar spawning of the threadfin, *Polydactylus sexfilis*, in Hawaii. Fish. Bull. 76:900–904.

Santerre, M. J., and R. C. May.
1977. Some effects of temperature and salinity on laboratory-reared eggs and larvae of *Polydactylus sexfilis* (Pisces: Polynemidae). Aquaculture 10:341–351.

Schramm, H. L., Jr., and R. G. Piper, eds.
1995. Uses and effects of cultured fishes in aquatic ecosystems, 608 p. Am. Fish. Soc. Symp. 15.

Sokol, R. R., and F. J. Rohlf.
1981. Biometry, 859 p. W.H. Freeman, San Francisco, CA.

Szyper, J. P, M. J. Anderson, and N. H. Richman.
1991. Preliminary aquaculture evaluation of moi (*Polydactylus sexfilis*). The Progressive Fish-Culturist 53:2025.

Tinker, S. W.
1982. Fishes of Hawaii, 532 p. Hawaiian Services, Inc., Honolulu, HI.

Titcomh, M.
1972. Native use of fish in Hawaii, 175 p. Univ. Hawaii Press. Honolulu, HI.

Yield- and biomass-per-recruit analysis for rotational fisheries, with an application to the Atlantic sea scallop (*Placopecten magellanicus*)

Deborah R. Hart
Northeast Fisheries Science Center
166 Water St.
Woods Hole, MA 02543
E-mail address: Deborah.Hart@noaa.gov

Abstract—A general model for yield-per-recruit analysis of rotational (periodic) fisheries is developed and applied to the sea scallop (*Placopecten magellanicus*) fishery of the northwest Atlantic. Rotational fishing slightly increases both yield- and biomass-per-recruit for sea scallops at F_{MAX}. These quantities decline less quickly when fishing mortality is increased beyond F_{MAX} than when fishing is at a constant rate. The improvement in biomass-per-recruit appears to be nearly independent of the selectivity pattern but increased size-at-entry can reduce or eliminate the yield-per-recruit advantage of rotation. Area closures and rotational fishing can cause difficulties with the use of standard spatially averaged fishing mortality metrics and reference points. The concept of temporally averaged fishing mortality is introduced as one that is more appropriate for sedentary resources when fishing mortality varies in time and space.

There has been growing interest in using rotational fishing to manage sessile or sedentary stocks (e.g. Caddy and Seijo, 1998). Under such a strategy, fishing mortality in a given area is varied periodically. Typically, the area is closed for a period of time, then fished, and then closed again. The openings of the different areas are timed so that at least one area is open to fishing each year. This approach has been proposed or is being used for abalone, corals, sea cucumbers, geoduck clams, sea urchins, and several species of scallops (Sluczanowski, 1984; Garcia, 1984; Botsford et al., 1993; Caddy, 1993; Heizer, 1993; Campbell et al., 1998; Caddy and Seijo, 1998; Lai and Bradbury, 1998).

Recently, area closures have been used to help manage the Atlantic sea scallop (*Placopecten magellanicus*) fishery off the northeastern United States. Three areas on Georges Bank were closed to scallop and groundfish fishing in December 1994 to help protect depleted groundfish resources. Subsequently, there have been substantial increases in scallop abundance, biomass, and mean size in these areas; mean scallop biomass in the closed areas, as measured by the Northeast Fisheries Science Center (NEFSC) sea scallop survey, rose from 0.6 kg/tow in 1994 to 15.8 kg/tow in 2000.[1] During limited openings of these areas to fishing in 1999 and 2000, nearly 5000 metric tons (t) of scallop meats (about 20% of the total landings during this period) were landed, while biomass levels remained high. In April 1998, two areas in the Mid-Atlantic Bight were closed to scallop fishing for three years in order to protect high concentrations of juvenile scallops. Scallop biomass has increased markedly since the closures in these areas as well, from 0.8 kg/tow in 1997 to 9.7 kg/tow in 2000[1] and about 3500 t of scallop meats have been landed in these areas in the year since they were reopened in May 2001. These data suggest that temporary or rotational closures can help increase scallop biomass and yield. For these reasons, a rotational management system for the U.S. Atlantic sea scallop fishery is currently under consideration.

Many common fisheries models may not be appropriate for sessile stocks because these models assume spatially uniform fishing mortality (Caddy, 1975). Such a "dynamic pool" assumption is strongly violated when a sessile stock is fished rotationally so that a portion of the stock is not fished in a given year. For this reason, many previous analyses of rotational fisheries have used either spatially explicit simulations (e.g. Caddy and Seijo, 1998), per-recruit analyses of pulse fishing, where all vulnerable individuals are removed from an area when the area is fished (e.g. Sluczanowski, 1984), or per-recruit analyses of a single cohort (e.g. Gribble and Dredge, 1994). Spatially explicit models suffer from their complexity, making it difficult to extract general principles from model

[1] NEFSC (Northeast Fisheries Science Center). 2001. Report of the 32nd northeast regional stock assessment workshop (32nd SAW). Stock Assessment Review Committee (SARC) consensus summary of assessments. NEFSC Ref. Doc. 01-05, 289 p. [Available from NEFSC, 166 Water St., Woods Hole MA 02543.]

Manuscript accepted 20 September 2002
Fish. Bull. 101:44–57 (2003).

simulations. Analysis of pulse fishing, although simple to apply and understand, is not applicable to those situations where only a portion of the available resource is removed when an area is opened periodically to fishing. Per-recruit analysis of a single cohort is not applicable to relatively nonselective multiple age-group fisheries.

Botsford et al. (1993) developed a mixed-age rotational yield-per-recruit model for red sea urchins. They showed that rotational fishing for these urchins would increase egg production considerably, while slightly decreasing yield-per-recruit. Recently, Myers et al. (2000) presented a mixed-age per-recruit analysis of a possible rotational fishery strategy for sea scallops. The emphasis of this study was on the effect of putative high levels of indirect (noncatch) fishing mortality on yield-per-recruit, and on a proposed rotational plan that Myers et al. suggested would help ameliorate this effect.

The purpose of the present article is to present a general theory for any type of periodic or rotational fishing strategy for a mixed-age sessile or sedentary stock. This work generalizes many of the above mentioned studies (in particular, that of Botsford et al., 1993) and does not require an assumption of constant recruitment or specific spatial configuration (or both). This theory is applied to the Atlantic sea scallop fishery of Georges Bank.

Measures of fishing mortality and overfishing definitions are usually based on models where fishing is assumed constant in space and time. In rotational fisheries, or in cases where part of a fishing ground has been closed indefinitely to fishing, these assumptions may be seriously violated, especially for stocks that are relatively immobile. Alternative measures of fishing effort and overfishing definitions are presented here that are more appropriate to fisheries of nonmobile stocks where rotational or indefinite closures are used.

Methods

The object of this analysis was to compute the expected yield-per-recruit and biomass-per-recruit of a cohort located in an area where fishing mortality may depend on the year and the variation in fishing mortality is periodic with time. Rotational fishing is usually thought of as a sequence of periodic closures and openings of different areas. The theory described here is more general, and can be applied to any situation where fishing mortality is varied periodically in a given area.

Suppose the fully recruited fishing mortality in an area during year k is F_k and that fishing mortality rates vary periodically with period p (where p is in years), so that $F_{p+k} = F_k$ for all k. Let F_{AVG} be the mean of $F_1, F_2, \ldots, F_p$. For simplicity, it is assumed that there is one recruitment event and one new cohort per year. However, extension of the theory to multiple cohorts per year is straightforward.

There are p possible patterns of fishing mortality experienced by a cohort, depending on the point of the cycle when it enters the fishery. The cohort that enters in the first year will experience fully recruited fishing mortality rates:

$$F_1, F_2, F_3, \ldots, F_p, F_1, F_2, F_3 \ldots \quad (1)$$

during successive years. The next cohort will experience the same fishing mortality rates, but in a different order:

$$F_2, F_3, F_4, \ldots, F_p, F_1, F_2, \ldots \quad (2)$$

and so on.

Two special cases are of particular interest: pulse rotation and symmetric rotation. Pulse rotation means that $F_k = 0$ for k=1,2,...,p–1 (the area is closed for p–1 years), then F_p>0 (the area is pulse fished for one year), and then F_k=0 for k=p+1, p+2,..., 2p–1 (the area is closed again), etc. Symmetric rotation, where p is even, means that $F_k = 0$ for $1 \le k \le p/2$, and $F_k = 2F_{\mathrm{AVG}}$ for $p/2 < k \le p$, i.e. the area is closed for p/2 years and then fished at a constant rate for the next p/2 years.

For each of the p patterns of fishing mortality, yield- and biomass-per-recruit can be calculated by using standard per-recruit techniques. Here, a method similar to the "generic per-recruit" model described in Quinn and Deriso (1999) is used (see Appendix). The only unusual aspect is that the mortality terms Z and F_c in Equations 11–13 (see Appendix) depend explicitly on time, i.e. on the year of the rotational cycle. Each of the p cohorts will have different yield-per-recruit $Y_1, Y_2, \ldots, Y_p$, and biomass-per-recruit $B_1, B_2, \ldots, B_p$ values because the ages at which they experience the fishing mortalities $F_1, F_2, \ldots, F_p$ are different.

Define Y_{AVG} and B_{AVG} to be the means of the p patterns of cohort yield- and biomass-per recruit, respectively. Y_{AVG} is the expected yield of a recruit chosen randomly with respect to cohort. In other words, Y_{AVG} is the long-term mean yield-per-recruit that can be expected from the rotational fishing strategy. Similarly, B_{AVG} is the expected long-term mean biomass-per-recruit. Note that unlike conventional per-recruit theory, yield- and biomass-per-recruit vary with cohort, so that the mean yield- and biomass-per-recruit obtained at any point in time may be different from Y_{AVG} and B_{AVG}.

Let $Y^{(1)}, Y^{(2)}, \ldots, Y^{(p)}$ be yield-per-recruit of the p cohorts, in decreasing order, so that $Y^{(1)}$ is the highest yield-per-recruit out of all the p cohorts and $Y^{(p)}$ the lowest. $Y^{(1)}$ is an upper bound on the yield-per-recruit that might be obtained with a rotational strategy if, for example, the closure pattern were timed to optimize yield-per-recruit from a large year class.

It is important when comparing rotational and constant fishing strategies to compare alternatives that have the same long-term survival rates, i.e the same natural mortalities and mean fishing mortality rates. If this is not done, then effects of rotation can be confounded with those due to variations in fishing mortalities. If there are initially N_0 fully recruited individuals in an area that are fished at a constant rate F_u, then there will be

$$N_p = N_0 \exp(-pM - pF_u) \quad (3)$$

of these individuals remaining alive after p years. If instead, fishing mortality was varied on a p year rotation, so that in each year of the cycle, fishing mortality in an

Table 1

Estimated life history parameters for Georges Bank sea scallops. Von Bertalanffy growth parameters are from Serchuk et al. (1979). Relations of shell height (SH) to meat weight (MW) (see Eq. 7) were obtained by combining the data of Serchuk and Rak[1] with that of NEFSC (Footnote 2 in the general text). The natural mortality estimate is from Merrill and Posgay (1964). The selectivity pattern is based on the current gear configuration of scallop dredges with 89-mm rings (NEFSC, Footnotes 1 and 2 in the general text).

	K (/yr) (growth)	L_∞ (mm) (growth)	M (/yr) (natural mortality)	a (ln g) (SH/MW parameter)	b (SH/MW parameter)	h_{min} (mm) (Min SH selected)	h_{full} (mm) (SH for full selectivity)	h_d (mm) (cull size)	d (discard mortality)
Value	0.3374	152.46	0.1	−11.6038	3.1221	65	88	75	0.2

[1] Serchuk, F. M., and R. S. Rak. 1983. Biological characteristics of offshore Gulf of Maine scallop populations: size distribution, relations of shell height to meat weight, and relative fecundity patterns. Reference document 83-07, 42 p. [Available from Northeast Fisheries Science Center, 166 Water St., Woods Hole, MA 02543.]

area is given by $F_1, F_2, , F_p$, respectively, then the number of individuals remaining alive after p years would be

$$N_p^* = N_0 \exp\left(-pM - \sum_{t=1}^{p} F_t\right). \quad (4)$$

In order for the long-term survivorship of the two strategies to be equal (i.e., N_p=N_p^*), the uniform fishing mortality F_u must equal the average fishing mortality

$$F_{AVG} = \frac{1}{p}\sum_{t=1}^{p} F_t \quad (5)$$

of the rotation plan. Therefore, F_{AVG} is used to scale all the graphs and per-recruit comparisons.

The model described above and in the Appendix was implemented as a Fortran-90 program where the integrals were numerically computed with a time step of 0.01 y. Parameters used in the model are given in Table 1 and represent estimates for growth and mortality of Atlantic sea scallops (*Placopecten magellanicus*), for which rotational management is currently under consideration.

Results

Yield-per-recruit curves for no rotation (continuous uniform fishing), three-year pulse rotation (i.e. the area is closed for two years and fished for one year), six-year pulse rotation, and nine-year pulse rotation are given in Figure 1. Note that the x axis in Figure 1 is the mean fishing mortality rate F_{AVG}, and the y axis is mean (i.e. expected) yield-per-recruit Y_{AVG}, averaged over cohorts. Because the mean fishing mortality rate is the same for all points at the same x coordinate, the three-year rotation has a fishing mortality rate during years when fishing occurs (F_p) that is three times as high, and the six-year rotation six times as high, as the constant F (no rotation) strategy with the same F_{AVG}.

Rotation affects the yield-per-recruit curve for sea scallop in three different ways (see Fig. 1). First, rotation modestly increases the maximum mean yield-per-recruit Y_{MAX}; the maximum mean yield-per-recruit for the nine-year rotation is about 9% greater than without rotation. Second, F_{MAX} (i.e. the value of F_{AVG} where Y_{MAX} is obtained) increases somewhat under rotation, especially for longer rotation periods. Third, there is less yield penalty in rotational management for exceeding F_{MAX}. For example, fishing at F = 1 results in a 38% loss of yield if there was no rotation, but only an 8% loss under a six-year pulse rotation. Although 6-yr pulse rotation results in only a 5% increase in yield-per-recruit over no rotation at their respective F_{MAX} values, the advantage of 6-yr pulse rotation at F = 1 is 43%.

Maximum yield-per-recruit for pulse fishing as a function of the rotation period p is shown in Figure 2. The best yield-per-recruit is obtained for long periods of 9 to 10 years. However, this type of strategy would imply that a number of years would pass before any yield would be obtained from most recruits and this strategy would only slightly increase maximum yield-per-recruit over that of steady fishing. Depending on management goals, it might be reasonable to discount future yields, so that the present value of yield taken t years into the future would be discounted by $\exp(-\delta t)$, where δ is the annual discount rate (assumed 10%/yr). The rotation period that maximizes discounted yield-per-recruit is 6 years (Fig. 2). If prices as a function of meat weight are known, it would also be possible to do a similar analysis to maximize discounted value-per-recruit.

Yield isopleths, commonly used to visualize yield-per-recruit analysis (Beverton and Holt, 1957), are given in Figure 3A (yield-per-recruit) and 3B (discounted yield-per-recruit). For rotational analyses, fishing mortality is placed on the x-axis and rotational period on the y-axis. Note again that for longer rotation times, the decline in yield for fishing mortalities greater than F_{MAX} is much less than without rotation. The value of F_{MAX} and maximum yield-per-recruit increases slightly with longer rotation periods.

Biomass-per-recruit for no rotation, 3-, 6- and 9-yr pulse rotation strategies is given in Figure 4. Compared to constant fishing, rotational fishing gives increased biomass-per-recruit; this increase is most evident for the longer

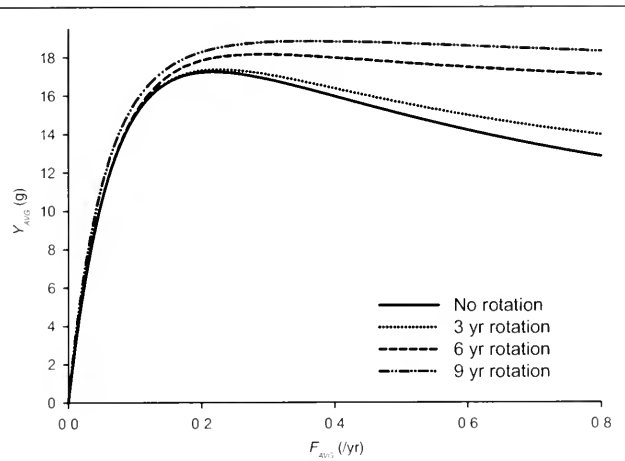

Figure 1

Yield-per-recruit curves for Georges Bank sea scallops with no rotation and with 3-, 6-, and 9-yr pulse rotations.

rotations and higher fishing mortalities. At F_{MAX}, the increase in biomass-per-recruit is slight, unless a very long (e.g. 9-yr) rotational period is employed.

The performance of rotation can be assessed as a function of selectivity at size. Figure 5A gives maximal yield-per-recruit for a number of pulse rotation strategies and a variety of values of h_{min}, the smallest size selected by the gear; the size of full selectivity, h_{full}, was taken as h_{min} + 23 mm (consistent with the assumed current gear selectivity pattern; see Table 1). Rotation can give substantial yield-per-recruit advantages when the gear selects animals of well below optimal size, especially for longer periods. However, long-period rotation actually gives less yield-per-recruit than constant fishing for larger values of h_{min}. Figure 5B gives a similar plot for biomass-per-recruit, where fully recruited fishing mortality is fixed at $F = 0.3$ in all cases. Unlike yield-per-recruit, rotational fishing increases biomass-per-recruit regardless of the selectivity pattern, especially when the rotational period is long.

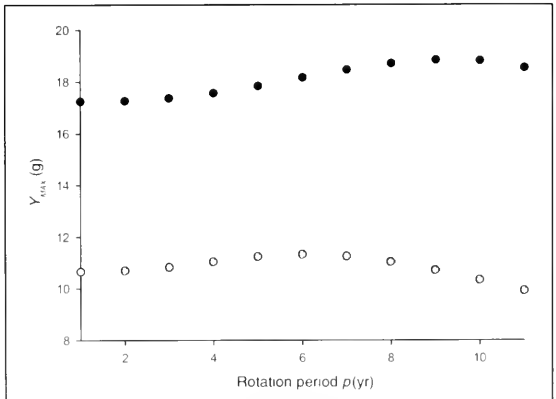

Figure 2

Maximum yield-per-recruit (solid circles) and discounted (10%) yield-per-recruit (open circles) for Georges Bank sea scallops with a pulse rotation of periods between 1 and 11 years.

Yield-per-recruit from different cohorts under a rotational system can vary considerably. The cohort which recruits into the fishery at about the time of the closure produces the highest yield-per-recruit, whereas the cohort that reaches exploitable size at about the time that the area is opened has the lowest. Figure 6 gives the mean yield-per-recruit together with that of the cohorts with the highest and lowest yield-per-recruit under six-year pulse rotational management (i.e. Y_{AVG}, $Y^{[1]}$, and $Y^{[6]}$, respectively). A 31% increase in maximal yield compared to constant fishing (and 25% increase over the average yield-per-recruit under rotation) can be obtained from the cohort whose yield-per-recruit is the highest under rotation. Note that, unlike conventional yield-per-recruit curves for sea scallops, yield-per-recruit from this cohort is almost completely insensitive to effort beyond a certain level.

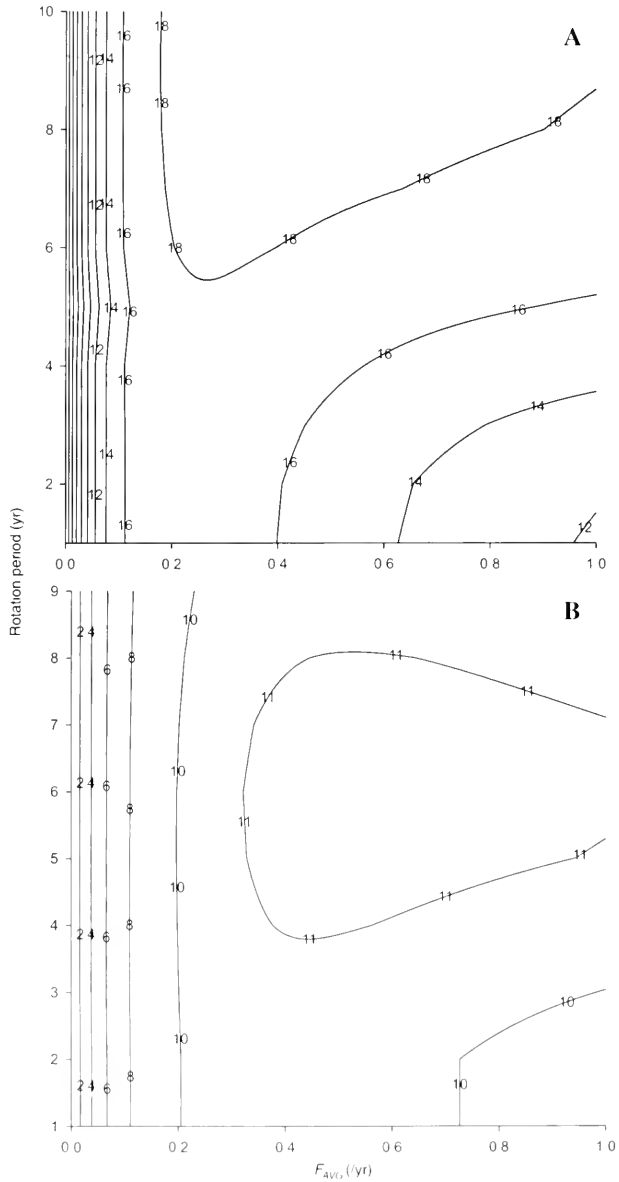

Figure 3

Yield-per-recruit (**A**) and discounted (10%) yield-per-recruit (**B**) isopleths for Georges Bank sea scallops with pulse rotation. Note that the *y* axes represent rotation period.

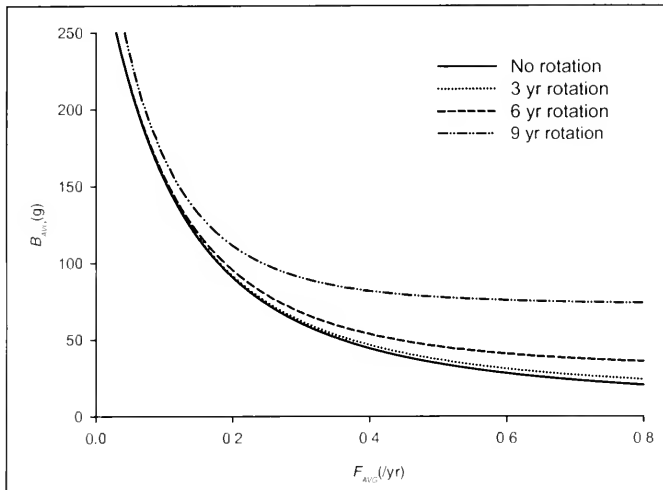

Figure 4

Biomass-per-recruit for Georges Bank sea scallops with no rotation and with 3-, 6-, and 9-yr pulse rotations.

Table 2

Calculated values of F_{MAX}, Y_{MAX}, B_{MAX}, and discounted (*Dsc*) Y_{MAX} (in grams, with a 10% discounting factor) for (**A**) pulse rotation with no incidental fishing mortality, (**B**) pulse rotation with 15% incidental fishing mortality, and (**C**) symmetric rotation with no incidental fishing mortality. p = period of rotation.

	p	F_{MAX}	Y_{MAX}	B_{MAX}	*Dsc* Y_{MAX}
A	1	0.217	17.25	84.0	10.66
	2	0.219	17.27	83.6	10.70
	3	0.225	17.38	82.4	10.83
	4	0.239	17.57	79.6	11.04
	5	0.259	17.84	76.8	11.24
	6	0.287	18.17	74.5	11.32
	7	0.324	18.47	73.8	11.25
	8	0.351	18.71	77.4	11.03
	9	0.363	18.84	84.2	10.71
	10	0.372	18.82	92.0	10.34
	11	0.374	18.69	100.6	9.93
B	1	0.192	14.62	91.9	8.79
	2	0.193	14.62	91.6	8.80
	3	0.197	14.68	90.5	8.88
B (cont.)	4	0.205	14.81	88.4	9.01
	5	0.219	14.99	85.4	9.16
	6	0.236	15.20	82.8	9.25
	7	0.257	15.43	81.2	9.25
	8	0.277	15.63	82.2	9.15
	9	0.292	15.75	86.0	8.96
	10	0.300	15.8	91.8	8.70
	11	0.302	15.75	99.0	8.4
C	2	0.219	17.27	83.6	10.70
	4	0.225	17.4	82.5	10.82
	6	0.235	17.56	81.0	10.90
	8	0.244	17.68	81.1	10.85
	10	0.248	17.73	83.5	10.68
	12	0.253	17.64	86.3	10.44

Yield-per-recruit curves for 6-yr symmetric rotation (i.e. closed for three years and then opened for three years), 10-yr symmetric rotation, 6-yr pulse rotation, and no rotation are given in Figure 7. Symmetric rotation gives yields-per-recruit that lie between that of pulse rotation and constant fishing. Maximum yield-per-recruit, together with the associated B_{MAX}, and maximal discounted yield for pulse rotation, with and without 15% incidental mortality, and for symmetric rotation without incidental mortality, are given for various rotation periods in Table 2.

Results from yield-per-recruit runs with incidental fishing mortality (Table 2B) show similar patterns to

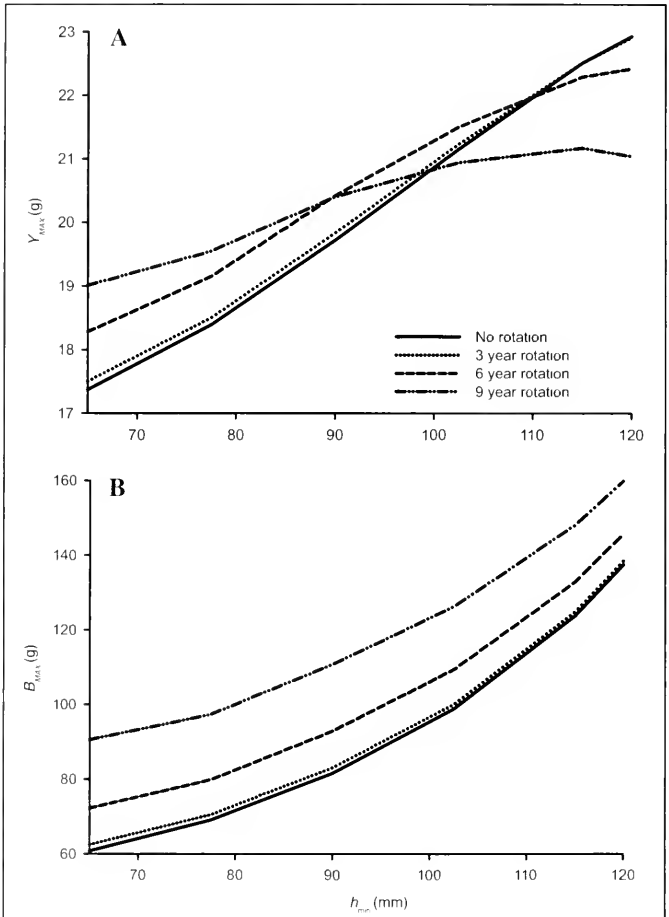

Figure 5

(**A**) Yield-per-recruit and (**B**) biomass-per-recruit for no rotation (solid line), 3-yr (dotted line), 6-yr (dashed line) and 9-yr (dot-dashed line) pulse rotations of sea scallops as a function of minimum selected shell height h_{min}. Scallops are assumed to be fully recruited to the fishery at shell height h_{min} + 23 mm.

results with no incidental fishing mortality (Table 2A). Note that both yields and the value of F_{MAX} are reduced if incidental fishing mortality exists and that the penalty for overfishing without rotation is somewhat higher (about 67% loss in yield-per-recruit for fishing at F=1 without rotation compared to 38% without incidental mortality). However, at F_{MAX}, the loss of yield due to incidental mortality is about the same for rotational fishing as for steady fishing.

Discussion

Rotational fishing can generate increased yield- and biomass-per-recruit for sea scallops compared to nonrotational fishing. The expected increase in maximum yield-per-recruit is modest (<10%) for a fixed rotational pattern. The over 30% gain in yield-per-recruit obtained from cohorts that reached exploitable size near the time of the closure is partially cancelled by the loss of yield-per-recruit

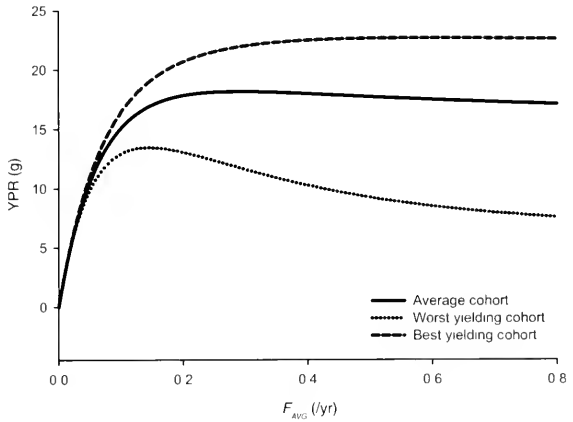

Figure 6

Yield-per-recruit for a 6-yr pulse rotation of Georges Bank sea scallops from an average cohort, and those that benefit the most and the least from rotation.

on those cohorts that reached exploitable size at about the time the area was reopened, thereby resulting in only a modest gain in yield-per-recruit. A more substantial gain in maximum yield-per-recruit (up to 30% greater than constant fishing) can be obtained if the closure is timed to optimally exploit an unusually large year class. These results are consistent with several studies that indicate that periodic fishing can often increase yields over constant fishing (Botsford, 1981; De Klerk and Gatto, 1981; McCallum, 1988; Clark, 1990; Myers et al., 2000).

A second, and perhaps more important, advantage of rotational fishing is that it alleviates the impact of both growth and recruitment overfishing. Growth overfishing (i.e. fishing at a level higher than F_{MAX}) under rotational management induces a substantially smaller reduction in yield-per-recruit than would occur with constant fishing. Rotation also increases biomass-per-recruit for sea scallops, especially for levels of F above F_{MAX}, thereby reducing the impact of possible recruitment overfishing. It might be argued that overfishing should not be occurring in any case. However, even when management measures are taken to eliminate overfishing, it can still occur, for example, if 1) reference points are incorrect because of uncertainty in life history parameters; 2) fishing mortality, or the effect of management measures on fishing mortality, has been underestimated; or 3) there is localized overfishing because of spatial variation in fishing intensities or life history parameters (or variation in both), even though when averaged spatially, $F_{AVG} \leq F_{MAX}$ (Caddy, 1975; Hart, 2001). Rotational fishing can thus be thought of as part of a precautionary strategy. In so much as it may increase maximum yield, rotational management is superior to many other precautionary measures that reduce yield. The only costs of rotational management are the costs of administrating and enforcing such a system, and socioeconomic costs from temporary closures of traditional fishing grounds. The latter might be significant if closures force fishermen to make long distance steams to unfamiliar areas. Because the optimal F_{AVG} under rotation is only slightly greater than the nonrotational F_{MAX}, the amount of effort and fleet capacity required to optimize yield-per-recruit under rotation is about the same as that needed under uniform fishing.

Rotation also imposes practical constraints on the level of average fishing effort, thereby limiting the extent to which stocks can be overfished. Fishing mortality rates for U.S. sea scallop stocks were estimated as exceeding 1.0/yr during the late 1980s and early 1990s.[1] This would correspond under a 6-yr pulse rotation to an unaveraged fishing mortality of over $F = 6$ in the area open to fishing. Such a high fishing morality rate, corresponding to about a 98% exploitation rate for fully recruited scallops, is likely to be impractical for both physical and economic reasons. Thus, F_{AVG} in a rotation plan would likely be considerably below the high levels seen in the late 80s and early 90s, even if there was no other restriction on fishing effort other than pulse rotation.

Myers et al. (2000) claimed that "near-optimal yields are achieved across a wide range of fishing mortalities" in their rotational scheme. However, much of their analysis was confounded by their use of unaveraged open area fishing mortality ($=pF_{AVG}$) on the x axis of their per-recruit curves. For example, in the case analyzed in Myers et al (2000), where one of p areas would be fished each year, the fishing mortality F applied in the area open to fishing in a 9-yr rotation (i.e. 1/9 of the area would be fished each

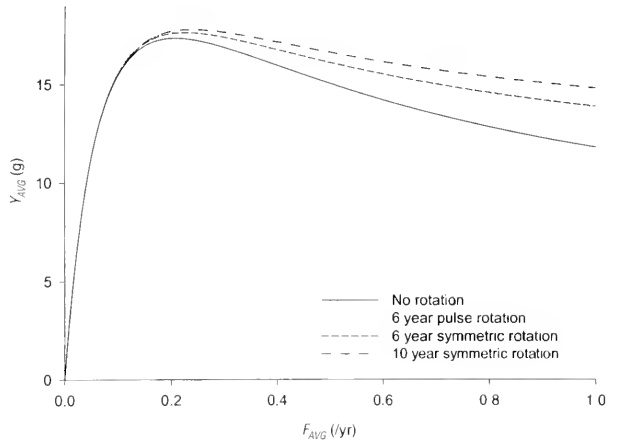

Figure 7

Comparison of yield-per-recruit for Georges Bank sea scallops with 6-year and 10-year symmetric rotations with that of a 6-yr pulse rotation or no rotation.

year and that $F = F_{AVG}/9$) would represent one ninth of the actual effort as the same F applied to the whole area under non-rotational fishing. Use of unaveraged fishing mortality has the effect of stretching the x axis by a factor of p, thereby making their graphs appear flatter than they actually are. F_{AVG} is representative of not only the true time-averaged fishing mortality but also in many cases would be proportional to spatially averaged fishing effort (as measured by, e.g., hours fished).

Myers et al. (2000) also suggested that rotational fishing would help lessen the impact of indirect (incidental) fishing mortality on yield-per-recruit. The analysis given in the present study indicates that incidental mortality lowers yield-per-recruit at F_{MAX} about the same amount regardless of whether or not rotational fishing is employed. At levels of fishing mortality well above F_{MAX}, rotational fishing does appear to modestly decrease the loss of yield-per-recruit due to incidental mortality. This decrease is due to the fact that incidental mortality, by somewhat lowering F_{MAX}, exacerbates the effects of overfishing, whereas rotation alleviates the loss of yield-per-recruit due to overfishing.

The effectiveness of sea scallop rotational fishing can be understood by examining fishing mortality at size for various rotational strategies. Figure 7 shows fishing mortality as a function of shell height for no rotation and for 3-, 6-, and 9-yr rotations for $F_{AVG} = 0.2$ (Fig. 8A), and $F_{AVG} = 0.6$ (Fig. 8B). Rotational fishing (especially for longer periods) tends to reduce the fishing mortality on small scallops and shift this effort onto larger individuals, thereby increasing yield-per-recruit, especially when overfishing is occurring. The periodic peaks in fishing mortality seen in the rotational strategies occur at the sizes where a new cohort begins to be fished (i.e. when the scallops are some integer number of years past their age at 40 mm). In practice, these peaks are likely to be much less pronounced because of variations in individual growth rates and settlement times. However, the qualitative pattern of increasing selectivity with size should not be affected by such variations.

Sea scallops are an ideal candidate for rotational management, combining fast growth and low natural mortality with a sedentary adult lifestyle. In addition, sea scallops are recruited into the fishery at a size that is well below optimal from a yield-per-recruit perspective. The increase in size-selectivity induced by rotation described above should therefore induce an increase in yield-per-recruit. However, in those fisheries where the size-at-entry to the fishery is much larger, rotation would not be expected to induce gains in maximal yield-per-recruit (see Fig. 5A). On the other hand, it appears that rotation increases biomass-per-recruit regardless of the size-selectivity of the fishery (Fig. 5B). Botsford et al. (1993) found that rotation increased biomass- but not yield-per-recruit for red sea urchins. These results are consistent with the above discussion because the minimum legal size for landing the urchins was already near-optimal.

Although the exact levels of yield- and biomass-per-recruit obtained with or without rotation are sensitive to such factors as natural mortality and growth rates, the relative gains of rotation over constant fishing are much less sensitive to these factors. Rotation will improve yield-per-recruit under a broad range of parameter choices provided that 1) the ratio of growth to mortality K/M is

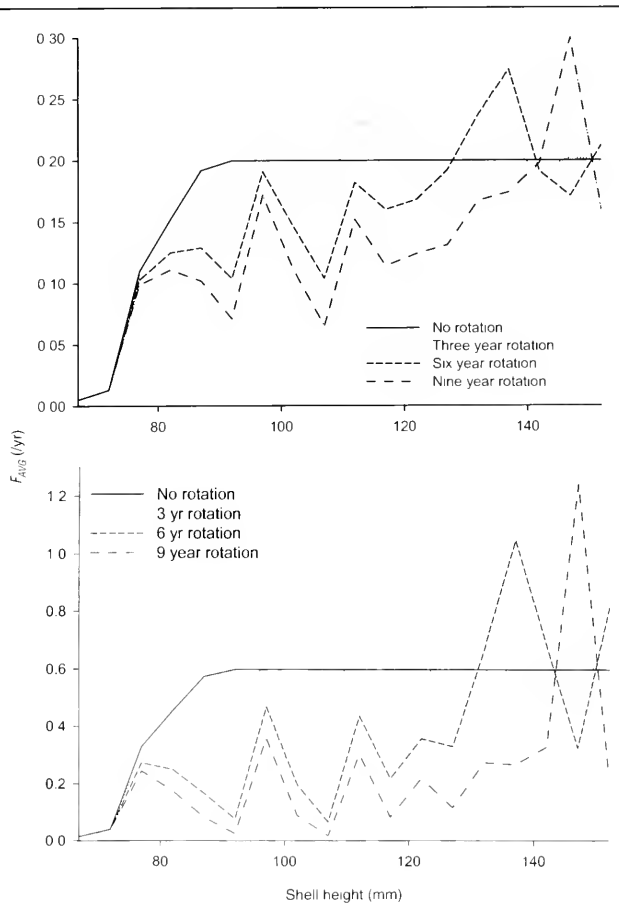

Figure 8

Mean fishing mortality at length for Georges Bank sea scallops with no rotation and with 3-, 6-, and 9-yr pulse rotations for (**A**) $F = 0.2$, and (**B**) $F = 0.6$.

sufficiently high (greater than about 0.5 with the other parameters in the model fixed as given in Table 1), and 2) size-selectivity is suboptimal. Rotation improves biomass-per-recruit under even a wider range of parameters.

Allee effects may occur in broadcast spawners such as urchins and scallops. Areas that are closed for several years may allow these animals to form dense aggregations (that would likely be heavily fished if not closed), thereby improving fertilization success (Botsford et al., 1993). Such an effect would mean that rotation could produce greater benefits in fecundity than would be suggested by biomass- or eggs-per-recruit curves.

Metapopulation structure might also be considered when designing a rotational strategy. If recruitment is limited by the supply of settling larva, an area that is a source of larva might be fished less than that required to maximize yield-per-recruit in order to increase larval supply (Tuck and Possingham, 1994).

The calculations that indicate long optimal rotational periods assume low constant natural mortality, independent of age or density, based on the study of Merrill and Posgay (1964). There is some evidence that the natural mortality rate of sea scallops may increase with age or size for shell heights greater than about 110 mm (Mac-

Donald and Thompson, 1986). If this is the case, optimal rotational periods would be shorter than calculated here, although the yield-per-recruit formalism would remain valid. More serious problems would be caused if there is density-dependent mortality of adults or if high adult densities inhibited recruitment because rotational closures can induce higher densities than would constant fishing. If either of these processes occur, shorter rotation periods would be advisable to minimize this problem. For sea scallops, however, observations of areas that have been closed to fishing for a number of years give no indication that such density-dependent processes are occurring (Fig. 2b in Hart 2001, and Table B5-8 in NEFSC[1]).

An extreme case of rotational fishing is true pulse fishing, where all exploitable individuals are removed at periodic intervals (see e.g. Sluczanowski, 1984). Thus, true pulse fishing corresponds to pulse rotation (as defined in the present study) with an infinite fishing mortality. Such pulse fishing is not optimal for sea scallops, as can be seen by the slight decline of yield-per-recruit at high fishing mortalities in Figure 1 because at very high fishing mortalities, the partial selectivity of the gear loses its effectiveness and all individuals that are even slightly selected to the gear (i.e. that are even slightly greater than $h_{\min}$) will be removed. To put it another way, at high fishing mortality rates, the additional (i.e. marginal) catch obtained from a further increase in F will disproportionately consist of small animals, thereby reducing yield-per-recruit. Pulse fishing would be optimal if knife-edge selectivity is assumed. For this reason, the assumption of knife-edge selectivity would lead to unrealistic results for cases such as sea scallops, where gear selectivity increases more gradually with size. Proper application of rotational theory therefore requires a careful examination of fishing selectivity with size.

Pulse fishing can be related to the classic Faustmann theory of forest rotation (see e.g. Reed, 1986; Clark, 1990). In this theory, if a stand of trees in an area that has last been harvested t years previously has value $V(t)$, then the optimal time to harvest the trees satisfies

$$V'(t) = \delta(V(t) - c) + \delta \frac{V(t) - c}{\exp(\delta t) - 1}, \qquad (6)$$

where δ = the discount rate; and
c = the cost of harvesting.

In the case of a fishery, $V(t)$ would represent the expected value of the exploitable stock (e.g. those of shell height greater than $h_{\min}$) at time t. (Note that in this context, unlike the original forest application, it is not necessary to assume that all exploitable individuals are the same age.) In the case of scallops, assuming all scallops command the same price per unit weight, $c = 0$, and $\delta = 0.1$, this formula would give an optimal rotation period of about 6.1 years (the optimal period would be moderately longer for realistic positive values of c). This value corresponds well to the rotation time of 6 years that optimizes discounted yield-per-recruit (see Fig. 2). However, the yield-per-recruit for 6-yr pulse fishing, $V(6)$, is less than 80% of the maximal yield-per-recruit obtained by fishing uniformly. Again, the reduced yield-per-recruit is due to the fact that pulse fishing induces knife-edge selectivity at $h_{\min}$, rather than the usual gradual increase in vulnerability to the gear.

Symmetric rotational strategies appear to give less benefit than does pulse rotation. However, optimal pulse rotation would require high, and possibly impractical, levels of effort in an area when it is opened (e.g. F of about 1.7 for a 6-yr pulse rotation). In addition, such a strategy would require that areas be closed most of the time, possibly inducing social-economic disruptions by closing traditional fishing grounds for long periods. Compared to pulse rotation, symmetric rotation requires less concentrated effort, allows areas to be open half the time, and is less sensitive to the assumption of constant natural mortality. One possible compromise between pulse and symmetric rotation is to close an area for half the time and then gradually increase effort during the opening. For example, an area might be closed for three years and then fished for the next three years at F_{MAX}, $2F_{MAX}$, and $3F_{MAX}$, respectively.

Questions have been raised regarding the appropriateness of the use of whole-stock fishing mortalities as targets or reference points for fisheries of sedentary stocks that include rotational or long-term closures (or both) (NEFSC[2]). The solid line in Figure 9 gives the whole stock (biomass-weighted) fishing mortality (assuming constant recruitment everywhere) for a pulse rotational system consisting of six areas, one of which is fished each year in turn. This whole-stock fishing mortality was obtained by simply dividing the yield-per-recruit for a 6-yr pulse rotation by the corresponding biomass-per-recruit. The x axis is F_{AVG}, which should be proportional to true effort. As can be seen, whole-stock fishing mortality is proportional to effort for low fishing mortalities, but then flattens to a maximum of just under 0.4.

A similar situation can happen even if an area is fished uniformly, except that a portion of the area is set aside as an indefinite closure. The dashed line in Figure 9 gives an example for the case when 10% of the area is permanently closed and is allowed to equilibrate to the biomass-per-recruit corresponding to zero fishing mortality. Whole-stock fishing mortality shows a relationship to the actual fishing effort (the fishing effort in the open area only) in the open areas that is similar to that of rotational fishing. In both cases, closed area biomass dominates the whole-stock fishing mortality calculation at high fishing effort. The yield at high fishing effort is essentially derived from incoming recruitment, which is not sensitive to fishing effort for very high effort levels. Therefore, the whole-stock fishing mortality becomes nearly constant when effort is high.

[2] NEFSC (Northeast Fisheries Science Center). 1999. Report of the 29th northeast regional stock assessment workshop (29th SAW). Stock Assessment Review Committee (SARC) consensus summary of assessments. NEFSC Ref. Doc. 99-14, 347 p. [Available from NEFSC, 166 Water St., Woods Hole, MA 02543.]

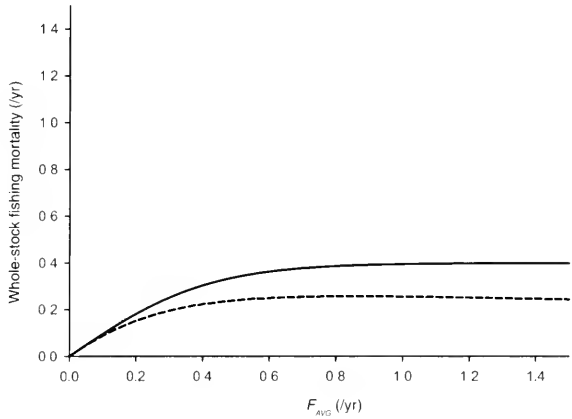

Figure 9

Whole-stock fishing mortality as a function of effort (F_{AVG}) for sea scallops with a 6-yr pulse rotation (solid line), and constant fishing with 10% of the area permanently closed (dashed line). The dotted line is the line $y = x$.

The current situation for sea scallops in Georges Bank gives an even more extreme example of this phenomenon. About 80% of the biomass lies in the groundfish areas that have been closed to scallop fishing for most of the time since December 1994. Because these areas will be closed to scalloping in 2002, the whole-stock fishing mortality in this year cannot exceed the F_{MAX} reference point of 0.24. Therefore, according to the current overfishing definition (the whole-stock F is below F_{MAX}), the stock cannot be overfished. Nonetheless, the fishing mortality in the open areas may exceed F_{MAX}, resulting in growth overfishing in these areas. Thus, the stock in the open areas could be overfished from a yield-per-recruit perspective even if the whole-stock F is below F_{MAX}.

The opposite situation could also occur. If scallops in the groundfish closed areas on Georges Bank were fished more than slightly above the F_{MAX} = 0.24 reference point, the whole-stock fishing mortality would also be above this reference point and overfishing would be considered to be occurring. However, an area that has been closed for a number of years should be fished harder, compared to an area that has never been closed, once the area is reopened in order to maximize yield-per-recruit. Thus, a strategy that would maximize yield-per-recruit might require a whole-stock F that would in some years be higher, and in some years lower, than the conventional overfishing reference point.

A whole-stock fishing mortality rate may therefore not be the most appropriate metric for overfishing definitions when some areas are temporarily or permanently closed to fishing. Its value may not be representative of the yield-per-recruit that could be obtained at that level of fishing mortality. Furthermore, when most of the biomass is in closed areas, estimated whole-stock fishing mortality may be more sensitive to variations in recruitment and measurement error than to actual changes in effort.

As an alternative to a whole-stock fishing mortality metric, the following considerations are suggested for a fishing effort measure that is compatible with yield-per-recruit calculations. (1) Stock from areas that are not fished in a given time period should not be included in the fishing mortality calculation for that time period. In a relatively sedentary stock, the amount of biomass in the closed areas is irrelevant in determining the yield-per-recruit that will be obtained from the stock in the open areas. (2) Time-averaging of fishing mortality in the open areas is required to take into account the previous fishing history of the area. An area that has been closed for a number of years needs to be fished harder once opened than an area that has been continuously fished in order to maximize yield-per-recruit.

Based on these considerations, the time-averaged fishing mortality computed from the open areas only, F_{AVG}, is an appropriate measure of fishing mortality in fisheries managed by using rotational or indefinite closures. It is natural to take the averaging period equal to the rotational period p. With this metric, F_{MAX} is only slightly sensitive to the rotational period p and completely insensitive to the level of closed area biomass. Indeed, even if no closures existed, but fishing effort varied with time, it may still be advisable to employ a time-averaged fishing mortality because the previous history of fishing mortalities strongly affects the level of effort required to maximize future yield-per-recruit. If an area has been fished harder than F_{MAX} for a number of years, so that the population

size-structure in this area is smaller than the equilibrium size-structure obtained by fishing at F_{MAX}, then fishing the next year at a level somewhat below F_{MAX} will improve long term yield-per-recruit. Similarly, if an area has been fished below F_{MAX}, so that its size structure is larger than what would occur when fishing at a constant rate of F_{MAX}, then it may be optimal to temporarily fish at a level higher than F_{MAX}.

In summary, rotational fishing can improve yield- and biomass-per-recruit for long-lived sedentary stocks such as sea scallops. Rotational management can be part of a precautionary strategy because it can help alleviate the effects of growth and recruitment overfishing. Rotational management will however require a rethinking of conventional yield-per-recruit reference points.

Acknowledgments

I would like to thank T. Kenchington for discussions regarding the equivalence of long-term survivorship under rotational and constant fishing. This paper also benefitted from discussions with and comments from P. Rago, L. Jacobson, S. Murawski, F. Serchuk, A. Applegate, and the reviewers.

Literature cited

Beverton, R. J. H., and S. J. Holt.
1957. On the dynamics of exploited fish populations, 533 p. Chapman and Hall, London, United Kingdom.

Botsford, L. W.
1981. Optimal fishery policy for size specific, density-dependent population models. J. Math. Biol. 12:265–293.

Botsford, L. W., J. F. Quinn, S. R. Wing, and J. G. Brittnacher.
1993. Rotating spatial harvest of a benthic invertebrate, the red sea urchin, *Strongylocentrotus franciscanus*. *In* Proceedings of the international symposium on management strategies for exploited fish populations. Alaska Sea Grant Report AK-SG-93-02, p. 409–428. Alaska Sea Grant Program, Anchorage, AK.

Caddy, J. F.
1973. Underwater observations on tracks of dredges and trawls and some effects of dredging on a scallop ground. J. Fish. Res. Board Can. 30:173–180.
1975. Spatial models for an exploited shellfish population, and its application to the Georges Bank scallop fishery. J. Fish. Res. Board Can. 32:1305–1328.
1993. Background concepts for a rotating harvesting strategy with particular reference to the Mediterranean red coral, *Corallium rubrum*. Mar. Fish. Rev. 55:10–18.

Caddy, J. F., and J. C. Seijo.
1998. Application of a spatial model to explore rotating harvest strategies for sedentary species. Can. Spec. Publ. Fish. Aquat. Sci. 125:359–365.

Campbell, A., R. M. Harbo, and C. M. Hand
1998. Harvesting and distribution of Pacific geoduck clams, *Panopea abrupta*, in British Columbia. Can. Spec. Publ. Fish. Aquat. Sci. 125:349–358.

Clark, C.W.
1990. Mathematical bioeconomics. The optimal management of renewable resources, 2nd ed., 386 p. Wiley, New York, NY.

De Klerk, P., and M. Gatto.
1981. Some remarks on periodic harvesting of a fish population. Math. Biosci. 56:47–69.

Garcia, S.
1984. Modèlisation et exploitation rationnelle des stocks de corail precieux: une première approche. FAO Fish. Rep. 306:109–121.

Gribble, N., and M. Dredge.
1994. Mixed-species yield-per-recruit simulations of the effect of seasonal closure on a Central Queensland coast prawn trawling ground. Can. J. Fish. Aquat. Sci. 51:998–1011.

Hart, D. R.
2001. Individual-based yield-per-recruit analysis, with an application to the Atlantic sea scallop, *Placopecten magellanicus*. Can. J. Fish. Aquat. Sci. 58:2351–2358.

Heizer, S.
1993. "Knob cod"-management of the commercial sea cucumber fishery in British Columbia. J. Shellfish Res. 12:144–145.

Lai, H., and A. Bradbury.
1998. A modified catch-at-size analysis model for a red sea urchin (*Strongylocentrotus franciscanus*) population. Can. Spec. Publ. Fish. Aquat. Sci. 125: 85–96.

MacDonald, B. A., and R. J. Thompson.
1986. Production, dynamics and energy partitioning in two populations of the giant scallop *Placopecten magellanicus* (Gmelin). J. Exp. Mar. Biol. Ecol. 101:285–299.

McCallum, H. I.
1988. Pulse fishing may be superior to selective fishing. Math. Biosci. 89:177–181.

Merrill, A. S., and J. A. Posgay.
1964. Estimating the natural mortality rate of sea scallop. Res. Bull. Int. Comm. N.W. Atlantic Fish. 1:88–106.

Myers, R. A., S. D. Fuller, and D. G. Kehler.
2000. A fisheries management strategy robust to ignorance: rotational harvest in the presence of indirect fishing mortality. Can. J. Fish. Aquat. Sci. 57:2357–2362.

Quinn, T. J., and R. B. Deriso.
1999. Quantitative fish dynamics, 542 p. Oxford U. Press. New York, NY, and Oxford, United Kingdom.

Reed, W. J.
1986. Optimal harvesting models in forest management—a survey. Natural Resource Modeling 1:55–79.

Serchuk, F. M., P. W. Wood, J. A. Posgay, and B. E. Brown.
1979. Assessment and status of sea scallop (*Placopecten magellanicus*) populations of the northeast coast of the United States. Proc. Natl. Shellfish. Assoc. 69:161–191.

Sluczanowski, P. R.
1984. A management oriented model of an abalone fishery whose substocks are subject to pulse fishing. Can. J. Fish. Aquat. Sci. 41:1008–1014.

Tuck, G. N., and H. P. Possingham.
1994. Optimal harvesting strategies for a metapopulation. Bull. Math. Biol. 56:107–127.

Appendix

Basic yield-per-recruit model

This appendix describes the basic yield-per-recruit model used for a cohort. In this model, recruits start at a specified shell height (or length) h_0. The shell height is converted into a starting age a_0 by using a von Bertalanffy growth equation. The shell height at time t is also obtained by using the von Bertalanffy growth curve. The shell height is converted into a meat weight by using a shell-height/meat weight formula:

$$w = \exp(a + b \ln(h)), \tag{7}$$

where w and h are in units of grams and millimeters, respectively.

Natural mortality occurs at a rate M, assumed for these simulations to be constant for all ages (M=0.1). The fishing mortality rate $F(h)$ on a scallop of shell height h is given by $F(h) = F_0 J(h)$, where F_0 is the fully recruited fishing mortality rate and $J(h)$ is the selectivity of the gear. $J(h)$ was taken to be 0 if h is less than a minimum shell height h_{min}, 1 if h is greater than a fully recruited threshold size h_{full}, and interpolated linearly as

$$J(h) = \frac{h - h_{\min}}{H_{\text{full}} - h_{\min}} \tag{8}$$

if $h_{\min} < h < h_{\text{full}}$. Individuals that are caught by the gear but are smaller than a maximum cull size h_d, are discarded and are subject to a discard mortality d. In these simulations, d is taken to be 0.2 (DuPaul[3]); however, the results are not very sensitive to the exact value of this parameter. All individuals caught at a size greater than h_d are assumed to be landed and are included in the total yield. $F_c(h)$ denotes the rate at which scallops of shell height h are caught and retained (i.e. not discarded).

The possibility has been raised that some scallops may be killed but not captured by the gear (Caddy, 1973; Myers et al. 2000). Caddy (1973) estimated that 15–20% of the scallops remaining on the bottom in the path of a scallop dredge are killed but not captured by the dredge. Murawski and Serchuk[4] estimated that less than 5% of the scallops remaining in the path of the dredge suffered incidental (noncatch) mortality. In order to use the above studies to estimate the relationship between incidental fishing mortality F_1 and the fully recruited capture fishing mortality rate F_0, it is necessary to know the efficiency e of the dredge on a fully recruited individual. Denote by i the fraction of scallops that suffer mortality among those that were in the path of the dredge but that were not caught, so that i is estimated at 0.15–0.2 by Caddy (1973), and less than 0.05 by Murawski and Serchuk.[3] The ratio R of fully recruited scallops in the path of the dredge that are caught to those killed but not caught is

$$R = e/[i(1-e)]. \tag{9}$$

If fully recruited scallops suffer capture fishing mortality at rate F_0, then the rate of incidental fishing mortality will be

$$F_1 = F_0 / R = F_0 i (1 - e)/e. \tag{10}$$

If e is taken as 50% (estimated as the average scallop dredge efficiency on Georges Bank[5]), then F_1 would be in the range 0.15 F_0 to 0.2 F_0 according to Caddy (1973) and less than 0.05 F_0 according to Murawski and Serchuk.[3] To ascertain the effects of incidental fishing mortality on the yield-per-recruit calculations, model runs were performed with no incidental mortality, and also when F_1 = 0.15 F_0; incidental fishing morality was applied to all size groups.

Let $Z(h)$ be the total mortality rate at shell height h (i.e. the sum of natural mortality, and discard, indirect, and landed fishing mortality). Then the fraction of recruits remaining t years after the beginning of the simulation is

$$S(t) = \exp\left(-\int_{a_0}^{t} Z(\tau)d\tau\right). \tag{11}$$

Total yield- and biomass-per-recruit are calculated by the formulas:

$$Y = \int_{a_0}^{a_f} S(t)F_c(h(t))w(h(t))dt \tag{12}$$

$$B = \int_{a_0}^{a_f} S(t)w(h(t))dt, \tag{13}$$

where a_f = the ending age of the simulation, taken to be $30 + a_0$.

For convenience in these simulations, a_0 is taken to be 2 years; this age is assumed to correspond to a shell height of precisely 40 mm. In the rotational simulations reported in this study, the fully recruited landed fishing mortalities $F_c(h)$ ($h > h_{\text{full}}$) are assumed to vary periodically and are given in year k by F_{j+k}, where j is the year that the cohort reaches the starting age a_0.

[3] DuPaul, W. D. 2000. Personal commun. Virginia Institute of Marine Science, P.O. Box 1346, Gloucester Point, VA 23062-1346.

[4] Murawski, S. A., and F. M. Serchuk. 1989. Environmental effects of offshore dredge fisheries for bivalves. ICES C.M. 1989/K:27.

[5] Rago, P. J. 2001. Personal commun. Northeast Fisheries Science Center, 166 Water St., Woods Hole, MA 02543

Estimating long-term growth-rate changes of southern bluefin tuna (*Thunnus maccoyii*) from two periods of tag-return data

William S. Hearn
CSIRO Marine Research
Private Bag No. 5
Wembley, Western Australia 6020
Australia
E-mail address: bill.hearn@marine.csiro.au

Thomas Polacheck
CSIRO Marine Research
GPO Box 1538
Hobart, Tasmania 7001
Australia

Abstract—Southern bluefin tuna (SBT) (*Thunnus maccoyii*) growth rates are estimated from tag-return data associated with two time periods, the 1960s and 1980s. The traditional von Bertalanffy growth model (VBG) and a two-phase VBG model were fitted to the data by maximum likelihood. The traditional VBG model did not provide an adequate representation of growth in SBT, and the two-phase VBG yielded a significantly better fit. The results indicated that significant change occurs in the pattern of growth in relation to a VBG curve during the juvenile stages of the SBT life cycle, which may be related to the transition from a tightly schooling fish that spends substantial time in near and surface shore waters to one that is found primarily in more offshore and deeper waters. The results suggest that more complex growth models should be considered for other tunas and for other species that show a marked change in habitat use with age. The likelihood surface for the two-phase VBG model was found to be bimodal and some implications of this are investigated.

Significant and substantial differences were found in the growth for fish spawned in the 1960s and in the 1980s, such that after age four there is a difference of about one year in the expected age of a fish of similar length which persists over the size range for which meaningful recapture data are available. This difference may be a density-dependent response as a consequence of the marked reduction in the SBT population. Given the key role that estimates of growth have in most stock assessments, the results indicate that there is a need both for the regular monitoring of growth rates and for provisions for changes in growth over time (possibly related to changes in abundance) in the stock assessment models used for SBT and other species.

Manuscript accepted 28 May 2002.
Fish. Bull. 101:58–74 (2003).

Estimating growth rates has been a major focus of fisheries research throughout the twentieth century, and a large body of literature exists on the topic (e.g. Lee, 1912; Ford, 1933; Walford, 1946; Manzer and Taylor, 1947; Allen, 1966; Yukinawa, 1970; Pitcher and MacDonald, 1973; Kimura, 1980; Fournier et al., 1990). This literature reflects, at least in part, the fundamental importance of information on growth rates in stock assessments and the subsequent provision of management advice for commercially harvested fish populations. For example, growth information is required for yield-per-recruit analyses and for the estimation of spawning stock biomass in the estimation of stock-recruitment relationships. In addition, for a number of species, estimates of growth rates have been the primary or only source of information that can be used to estimate the age of individual fish and the age distribution of commercial catches (particularly for tropical species and for tunas and billfish). Such information on age is a critical component required in the analyses and models used to assess and manage these fish stocks (Bayliff, 1991; Clay, 1991; Caton, 1991; Wild, 1994; Wild and Hampton, 1994; Polacheck et al.[1]).

Almost all the work on modeling growth has centered on modeling growth rate as a continuous, smooth, monotonically decreasing function of age, and the von Bertalanffy (1938) growth (VBG) equation, and its extensions, have been the most common approach used. In addition, the growth process has frequently been modeled as static. Temporal variations in average growth for fish of the same size, or age, (due, for example, to changes in the physical environment or population density) are often ignored or considered to be relatively minor (with some notable exceptions—e.g. Le Cren, 1958; Southward, 1967; de Veen, 1976; Toresen, 1990; Ross and Nelson, 1992; Kaeriyama, 1996; Sinclair and Swain, 1996).

For the large pelagic tunas and billfishes, the von Bertalanffy growth equation and extensions has been the standard used for modeling growth (Bayliff, 1980). For a variety of tuna species, numerous growth studies have been conducted, and generally a reasonable range of parameter values has been estimated (e.g. see the sets of parameter values estimates for the eight scrombrid species in Bayliff, 1980).

[1] Polacheck, T., A. Preece, A. Betlehem, and N. Klaer. 1998. Treatment of data and model uncertainties in the assessment of southern bluefin tuna stocks. *In* Fishery stock assessment models (F. Funk et al., eds.), p. 613–637. Alaska Sea Grant College Program Report AK-SG-98-01. Univ. Alaska, P.O. Box 755040, Fairbanks, AK 99775-5040.

Bayliff (1988) also investigated regional growth differences in Pacific skipjack and yellowfin tunas. Interpretation as to whether any differences found are merely an artifact of the data collection or procedures used or whether they reflect real temporal or spatial difference has generally not been possible because the basic data (e.g. tagging, hard parts, length-frequency data), data collection procedures, analytic approaches, and the areas and time periods from which the data were collected have varied greatly among studies.

For southern bluefin tuna (SBT) (*Thunnus maccoyii*), extensive juvenile tagging programs were conducted in the 1960s and 1980s, and a large number of returns with measured lengths were recovered. From both periods, some returns were received after times at liberty in excess of 10 years. These two sets of tagging experiments provide the basis for the direct comparison of growth over a time span of 30 years. Also, because of the large number of tags returned in these studies, a more detailed examination of the adequacy of the von Bertalanffy growth equation as a model of the growth process is possible than with many data sets. These tagging data (primarily those from the 1960s) have been used as a basis for a number of analyses of growth rates (Murphy, 1977; Kirkwood, 1983; Hearn, 1986; Hampton, 1991; Lucas[2]). In the present paper, we present results of the analyses of the growth increment data from these two sets of tagging experiments. We examine these data both in terms of 1) whether SBT growth differed between the tagging periods and 2) whether there was a change in the growth process between adult and juvenile SBT (i.e. whether a more complex model than the simple von Bertalanffy equation is required to provide an adequate description of SBT growth).

The results presented here incorporate and build upon the already cited published analyses of these tag-return data, unpublished reports, and discussions of SBT growth in scientific meetings on SBT (e.g. Hearn and Hampton[3]; Hearn and Polacheck[4]; Anonymous[5]).

[2] Lucas, C. 1974. Working paper on southern bluefin tuna population dynamics ICCAT (International Commission for the Conservation of Atlantic Tunas), SCRS/74/4. Collective Volume of Scientific Papers, vol. 111, p. 110–124. [Available from CSIRO Marine Laboratories, GPO Box 1538, Hobart, Tasmania 7001, Australia.]

[3] Hearn, W. S. and J. Hampton. 1990. SBT growth change. Ninth trilateral meeting on SBT, Hobart, Australia, September 1990, SBFWS/90/8, 19 p. [Available from CSIRO and the Commission for Conservation of Southern Bluefin Tuna, P.O. Box 37, Deakin West, ACT 2600, Australia.]

[4] Hearn, W. S., and T. Polacheck. 1993. Estimating SBT age-at-length relations for the 1960s and 1980/90s. Twelfth trilateral meeting on SBT, Hobart, Australia, October 1993. SBFWS/93/4, 21 p. [Available from CSIRO and the Commission for Conservation of Southern Bluefin Tuna, P.O. Box 37, Deakin West, ACT 2600, Australia.]

[5] Anonymous. 1994. Report of the southern bluefin tuna trilateral workshop; Hobart, Australia, January/February 1994, 161 p. [Available from CSIRO and the Commission for the Conservation of Southern Bluefin Tuna, P.O. Box 37, Deakin West, ACT 2600, Australia.]

Background: the SBT stock and fishery

SBT is a highly-migratory species that begins to spawn at about 10–12 years of age in waters south of Java during the southern summer, mainly from September to April (Farley and Davis, 1998). During the first year of life they tend to be transported south by the tropical Leeuwin Current to inshore waters between Perth and Esperance, Western Australia. From ages 1 to 4 years, they appear to mainly inhabit, at least in the summer months, the waters off the Great Australian Bight, southern New South Wales (NSW) and eastern Tasmania. Many move to oceanic waters during the winter months and apparently progressively so as they age. By five years of age almost all have migrated to oceanic waters between 30° and 50°S at all longitudes, but mostly in the Eastern Hemisphere.

Substantial surface fisheries operated off the south coast of Western Australia from 1969 to the mid 1980s, off the south coast of NSW from 1963 to the early 1980s, and off South Australia from 1964 to the present. Since 1959 a major Japanese longline fishery has operated in oceanic waters between 30° and 50°S, mainly from the mid-Atlantic and westwards to a few degrees west of New Zealand.

Materials and methods

Tagging programs

Description Large numbers of tagged fish were released by CSIRO staff in the period from 1959 to 1968 and again in the period from 1980 to 1984. The releases from these two periods are used in our present study. Most of the tagged fish were initially caught with pole-and-line gear with barbless hooks, although a relatively small number were caught with troll lines. After a fish was hooked, it was hauled aboard the vessel and placed on a measuring board (in the 1960s) or a vinyl cradle (in the 1980s), and its nose to caudal fork length was measured. The fish was then tagged by an operator who inserted a 12-cm plastic spaghetti dart tag into the fish about 4 cm to the rear of the second dorsal fin on either side of the fish and rereleased it into the water within about 30 seconds. After 1963 almost all fish were double tagged. The tag numbers and length of each fish were recorded, together with location and date of release. This information was later transferred to a computer database.

Tagging operations in both the 1960s and 1980s were concentrated in the nearshore, surface-water fisheries bordering the central and western southern coast of Australia and the southern coast of NSW. In the 1980s no tags were released from the NSW coast area because this component of the fishery had collapsed, and surface schools of juvenile SBT could no longer be found (Caton, 1991). The South Australian tagging took place in the Great Australian Bight or in the adjacent shelf waters generally between longitudes 128° and 136°E. Releases in Western Australia occurred in the Albany (between longitudes 112° and 119°E) and Esperance (between longitudes 119° and 125°E) areas. There were 33,309 juvenile SBT tagged by

CSIRO personnel during the 1960s (1959 to 1968) and 10,743 during the early 1980s (1980 to 1984). Of these fish, 1972 and 4280, respectively, were later recaptured.

On recapture, fishermen recovered the tags and recorded the fish's length (if measured), location, and date. The tags with the recorded information were returned to the scientific staff at CSIRO, who then provided a reward. Most of the recapture lengths were measured by fishermen or factory staff, but about 31% were measured by scientists. Those measured by scientists cannot be considered a representative sample. In particular, all of the measurements for longer-term recaptured fish come from fishermen aboard Japanese longline vessels. In addition to length, longliners often reported the dressed weight and sometimes the whole weight, or both, of recaptured fish. In the 1960s Australian fishermen seldom reported any weight measurements, but in the 1980s they commonly reported the whole weight of recaptured fish.

Data selection The tagging experiments were conducted mainly within a narrow range of months at each site; therefore returns within a few months would be most strongly influenced by the seasonal differences found in SBT growth (Hearn, 1986; Burgess et al., 1991; Leigh and Hearn 2000). A nine-month period at liberty coincides with a low frequency in the times at liberty for the experiments; therefore we excluded data from analyses with less than 270 days at liberty. We also excluded data for which fish were tagged by fishermen, or when the recovery length, year, or month were reported by the tag finder to be unknown or uncertain.

Previously reported weight-length relationships (Warashina and Hisada, 1970; Hampton, 1986; Robins[6]) were used to identify and screen out dubious recapture data. The details of the screening procedures are documented by Hearn[7] and Anonymous.[5] Longline recaptures were excluded if the expected weight of a recaptured fish for its reported length was either less than 2/3 of the reported weight or greater than 1.5 times the reported weight. Some of the major inconsistencies were thought to be due to measuring the length of a fish without its tail or without its head (Lucas[2]). For surface fish in the 1980s, a high proportion of the weight-length data for recaptured fish from four vessels was inconsistent with the weight-length relationships noted above. All tag-return data from these four vessels were excluded. Another 2.5% of the 1980 data were excluded because of highly unlikely values for the ratio of the reported weight to length of the recaptured fish.

For the screening methods used, no assumption was made about the underlying growth curve, and these methods were designed so that they would not induce a bias into the results. The selection process yielded data sets that were sufficiently large for valid analyses, being 730 and 1450 for the 1960s and 1980s data sets, respectively. Note that for other tuna species the selection process used in our study (particularly the deletion of recaptured fish with short times-at-liberty) may cause problems because of smaller data sets (e.g. skipjack and yellowfin tunas in Bayliff, 1988).

Experimental assumptions The use of the tag-return increment data for estimating growth rates requires the following assumptions about the tagging protocols and data collection procedures:

1 Tagging does not retard growth.
2 The tagged fish are uniquely and correctly recorded at release and recapture.
3 The lengths of fish are measured without bias at release and recapture.
4 A wide range of fish sizes are represented, in recaptures at least.
5 There are no significant size-selection processes for fish within similar age ranges.

With respect to tagging effects, Hampton (1986) and Hearn (1986) have shown that there can be a significant weight loss of 7–12% for tagged fish in the first month after release. However, tagged fish recover this weight loss within a year at liberty, and there is no apparent difference between tagged and untagged fish after this time (Hearn, 1986). (There is little information available on weight loss of tagged fish at liberty between one month and one year.) In terms of length, Hearn and Hampton[3] could not detect a reduction of growth from growth increment residuals in the tag-return data even within the first 30 days after release. Limited data from the effect of handling and tagging fish in commercial farm pens indicated no retardation in growth in length after 150 days. These farm fish did show a loss in weight when first caged, but the weight was regained over a period of a few months (Anonymous[5]); therefore we do not think that tagging had any substantial effect on the growth rate of tagged fished in our study. With respect to the other assumptions, all fish were tagged with uniquely numbered tags. During tagging operations, tags were arranged in blocks of sequential numbers to avoid confusion and the misrecording of tag numbers. Return of the physical tag was required for fishermen to obtain the reward, and the double tagging of almost all fish since 1963 has allowed cross verification of tagging numbers, which allows little scope for error in the recording of tag numbers. Approximately 23% of the length measurements for the selected recaptured fish were measured by scientists. Mainly due to the deletion of short-term recaptured fish (i.e. < 270 days), this is less than that for all data (31%). For the fishermen-measured lengths, there was no reason to suspect any consistent bias, and comparison of the residuals for fishermen- and scientist-

[6] Robins, J. P. 1963. Synopsis of biological data on southern bluefin tuna, *Thunnus thynnus maccoyii* (Castlenau) 1872. FAO Fisheries Report 6(2), p. 562–587. [Available from CSIRO Marine Laboratories, GPO Box 1538, Hobart, Tasmania 7001, Australia.]

Hearn, W. S. 1982. Fish tagging: data processing, editing and storage. *In* CSIRO data base for southern bluefin tuna (*Thunnus maccoyii* (Castlenau)) (J. Majkowski, ed.), p. 8–9. CSIRO Marine Laboratories, Rep. 142. [Available from CSIRO Marine Laboratories, GPO Box 1538, Hobart, Tasmania 7001, Australia.]

measured returns in the fitted models below did not indicate any systematic pattern. The recaptured fish used in our study ranged in size from 60 to 175 cm, although the number of fish in the larger size ranges was relatively small—less than 2% were larger than 140 cm. (The consequences of the small number of fish in the large-size category are discussed below.) Within both the surface and longline fishery, a range of sizes and age classes is harvested within a single operation. No indication exists that within the size range encompassed by a cohort at a given age, there existed significant gear or fishery size selectivity. Overall, the above basic assumptions seem reasonable in modeling growth from these SBT tagging data.

Analytical methods

Models Two basic models were used to analyze growth information from the tag-return data. The first was the simple VBG model:

$$l_t = L_\infty\left(1 - e^{-k(t-t_0)}\right), \tag{1}$$

where L_∞ = the length that fish grow to asymptotically;
l_t = the length of a fish at age (or time) t;
k = the exponential rate at which the growth rate slows; and
t_0 = the hypothetical age (or time) when a fish is of length zero.

When applied to tag-return data, this equation can be used to predict the growth increment as a function of the length at release and the time at liberty:

$$\delta l = (L_\infty - l)\left(1 - e^{-k\delta t}\right), \tag{2}$$

where δl = the growth increment;
δt = the time at liberty; and
l = the length of release.

Note, in this study we simplified the growth model by not accounting for seasonal growth. However, data on recaptured fish with short times at liberty were specifically deleted to ensure that our results were robust after this simplification.

Preliminary analyses of the tag-return data suggested that a simple and time invariant von Bertalanffy growth model may not provide an adequate description of the growth rate for SBT. These preliminary analyses suggested

1 Growth rates in the 1960s and the 1980s were not equal;
2 There were systematic deviations from a VBG curve, possibly corresponding to different growth processes or models for adults and juveniles.

Consequently, in the present study, we considered a more complex model than the simple VBG and conducted separate, as well as combined, analyses of the tag data from the two periods. The more complex model selected was the two-phase growth model developed by Bayliff et al. (1991). In this model, fish grow according to one model (or parameter set) up to a certain length and according to another thereafter. In our analyses, we assumed that fish have VBG throughout their lives but grow according to one set of VBG parameters ($L_{\infty 1}$ and k_1) up to length L^* and according to a second set ($L_{\infty 2}$ and k_2) at larger sizes, the two-phase VBG model. Thus, the predicted length as a function of time for this model is

$$l_t = \begin{cases} L_{\infty 1}\left(1 - e^{-k_1(t-t_0)}\right) & \text{for } t \le t^* \\ L^* + \left(L_{\infty 2} - L^*\right)\left(1 - e^{-k_2(t-t_{t_1})}\right) & \text{for } t > t^* \end{cases}, \tag{3}$$

where t^* = the predicted time for a fish to reach L^*.

Note that t^* can be solved for in terms of four of the parameters of the model (t_0, k_1, $L_{\infty 1}$, and L^*):

$$t^* = t_0 - \frac{1}{k_1}\log\left(1 - \frac{L^*}{L_{\infty 1}}\right), \tag{4}$$

where $$t_0 = t_1 + \frac{1}{k_1}\log\left(1 - \frac{l_{t_1}}{L_{\infty 1}}\right),$$

and l_{t1}= the length of a fish at the time of tagging, t_1.

As with this simple VBG model, Equation 3 can be solved to predict the growth increment as a function of the release length and the time of liberty $\delta t = t_2 - t_1$:

$$\delta l = \begin{cases} (L_{\infty 1} - l_{t1})\left(1 - e^{-k_1\delta t}\right) & \text{if } t_2 \le t^* \\ (L^* - l_{t1}) + & \\ (L_{\infty 2} - L^*)\left(1 - e^{-k_2(\delta t - (t^* - t_1))}\right) & \text{for } t_1 < t^* \text{ and } t_2 > t^* \\ (L_{\infty 2} - l_{t1})\left(1 - e^{-k_2\delta t}\right) & \text{if } t_1 \ge t^*. \end{cases} \tag{5}$$

It should be noted that in some of the analyses considered below, the estimate of $L_{\infty 1}$ did not converge (i.e. the estimate for $L_{\infty 1}$ was essentially infinite). In such cases, the estimated growth rate is linear, with growth rate R_1, and for the first phase we replaced the von Bertalanffy growth function with a simple linear one:

$$\delta l = R_1\delta t,$$

and $$t^* = t_1 - (L^* - l_{t_1})/R_1. \tag{6}$$

Model-fitting procedure A large body of literature exists on statistical approaches for estimating growth from tag-return data (e.g. Fabens, 1965; Sainsbury, 1980; Kirkwood and Somers, 1984; Francis, 1988; James, 1991; Hampton, 1991; Wang et al., 1995). The most appropriate approach depends on the error structure assumed for the model. We followed the maximum-likelihood approach and general error structure described by Hampton (1991). The measured growth increment of fish "i" is

$$\delta l_i = E[\delta l_i] + \varepsilon_i + e_i, \quad (7)$$

where ε_i is due to measurement error in the observed growth increment (i.e. the combined effect of any errors in measuring the lengths at the time of release and recapture) and e_i is due to process or model error. The latter may be a function of l_1, δt, δl, and the model parameters.

For the measurement error component, we allowed for different variances, depending upon whether the recaptured fish was measured by an independent and scientifically trained individual or by a fisherman. Scientifically trained individuals (i.e. scientists) included fishery observers, port samplers, and CSIRO staff. We assumed that the measurement error was normally distributed, with mean zero and variance σ_x^2, where x is one of f or s for recaptured fish measured by fishermen or scientists.

The choice of the functional form for the process error in growth models is a complex issue. One approach has been to consider that process error stems from variability among individuals in the expected value of the growth parameters (e.g. Sainsbury, 1980; Hampton, 1991; Wang et al., 1995). This approach in the case of the two-phase VBG model would result in many potential structures for the process error component because there could be individual variability in the expected value of any single or possible combination of parameters (of which there are 25 combinations). There is little theoretical basis for deciding which of these 25 combinations to use. As an alternative, we selected a more empirical approach. A function that increases with longer times at liberty seemed appropriate, and was also consistent with preliminary analyses. We explored both linear and quadratic functional relationships between the times at liberty and the process error component. The quadratic term was found to be insignificant, and therefore we chose to report only results for a simple linear functional relationship, namely $\sigma_m^2 \delta t$. Hence the corresponding variance of the expected growth increment of fish i is $V(\delta l_i) = \sigma_x^2 + \sigma_m^2 \delta t_i$. It should be noted that without independent data on measurement error any constant component in process error would be totally confounded with the measurement error term in the model. Therefore, σ_x^2 should be considered as a combined measurement and process error term. Both σ_s and σ_m were estimated empirically by maximum likelihood tag increment data.

Assuming a Gaussian error distribution, the likelihood function is

$$L = \prod_{i=1}^{n} \left\{2\pi V(\delta l_i)\right\}^{-\frac{1}{2}} \exp\left\{-\frac{\left\{\delta l_i - E[\delta l_i]\right\}^2}{2V(\delta l_i)}\right\}. \quad (8)$$

The estimates of the parameters are found by minimizing

$$\ln(L) = \frac{1}{2}\sum_{i=1}^{n}\left[\log\left\{2\pi V(\delta l_i)\right\} + \frac{\left\{\delta l_i - E[\delta l_i]\right\}^2}{V(\delta l_i)}\right]. \quad (9)$$

The minimum value was obtained for all models by using the minimizing subroutine MINIMD (programmed by D.E. Shaw, CSIRO Div. Maths. and Stats.), which uses the Nelder and Mead (1965) method.

Model selection The estimation of the full two-phase VBG models across both tagging periods contains 16 parameters (five model parameters plus three variance parameters for each time period). We examined a variety of alternative hypotheses to test whether the number of parameters could be reduced by eliminating some or equating them. For the model parameters, we considered whether the L_∞ or k terms were equal either between time periods or between the first and second phases within a time period. We also considered the simple VBG model, for which L^* doesn't exist.

For the L^* parameter, we considered whether the estimates were different between the two time periods. We also examined models in which the value of L^* was determined by assuming that the expected growth rate for a fish of length L^* was equal for both growth phases (i.e. by assuming that the changes in growth rates as a function of length is a continuous function). Under this assumption

$$L^* = \frac{L_{\infty 1}k_1 - L_{\infty 2}k_2}{k_1 - k_2}. \quad (10)$$

This model is referred to as the continuous rate two-phase model in the "Results" section. However, this model is not smooth because it has a discontinuity in the derivative of the growth rate at L^*. For the variance parameters, we considered whether any of them could be eliminated and also whether $\sigma_s = \sigma_f$. We used the log-ratio test and AIC criterion (Akaike, 1974) to identify the most parsimonious model.

Results

Best fits to the 1960s and 1980s data

Table 1 contains the maximum likelihood solutions for various assumptions when fitting growth models to either the 1960s or 1980s tag-return data separately. Using the AIC criteria, we found the best-fit model for the 1960s tag-return data was one with linear growth in the first phase and with the change between the two phases at approximately 74 cm (row 1, Table 1A). The fit to this model compared with all other parameter combinations yielded both the lowest AIC and negative log-likelihood values. The fit, however, was only marginally better then the fit (row 3, Table 1A) to the two-phase VBG curve with common k parameters (e.g. where the difference in the negative log-likelihood values is 1.21). Except for the first phase growth parameters, the estimates for the other parameters are nearly identical between these two models. This similarity reflects the fact that growth is nearly linear over the initial part of a VBG curve. Thus, by having a relatively high $L_{\infty 1}$ (271 cm), essentially similar growth rates can be achieved up through the 74 cm size range when $k_1 = k_2$, as compared with linear growth in the first phase. It should

Table 1

(**A**) Estimation of SBT growth parameters, and tests, from 1960s tag-return data with time at liberty of at least 270 days; (**B**) Estimation of SBT growth parameters, and tests, from 1980s tag-return data with time at liberty of at least 270 days. "na" = not applicable because this is the normal von Bertalanffy curve, i.e. with only one phase.

Common parameters	Number of parameters	$L_{\infty 1}$	k_1	$L_{\infty 2}$	k_2	L^*	σ_s	σ_f	σ_m	−Log likelihood	AIC
A											
none	6	22.23[1]	0.0000	210.90	0.1063	74.24	0.000	3.122	2.992	2055.53	4123.07[2]
$L_{\infty 1}=L_{\infty 2}$	6	212.73	0.1451	212.73	0.1044	75.75	0.000	3.134	2.999	2057.39	4126.77
$k_1=k_2$	6	271.35	0.1060	211.35	0.1060	74.71	0.000	3.130	2.997	2056.74	4125.49
$L_{\infty 1}=L_{\infty 2}$ $k_1=k_2$	5	172.67	0.1723	172.67	0.1723	na	2.201	3.782	2.855	2099.04	4208.08
continuous rate	6	114.14	0.4289	205.45	0.1128	81.55	0.000	3.203	3.021	2065.89	4143.78
$\sigma_m=0$	7	760.47	0.03425	191.33	0.1330	70.00	3.478	5.258	0.000	2088.19	4190.39
$\sigma_s=\sigma_f$	6	22.20	0.0000	209.65	0.1085	74.04	2.301	2.301	3.180	2068.33	4148.66
$\sigma_s=\sigma_f=0$	6	454.10	0.05660	214.26	0.1033	74.70	0.000	0.000	3.752	2071.57	4155.15
B											
none	8	226.70	0.1649	182.52	0.1841	84.90	2.305	4.501	3.018	4509.99	9035.97
$L_{\infty 1}=L_{\infty 2}$	7	183.09	0.2276	183.09	0.1832	85.65	2.266	4.497	3.031	4510.44	9034.88
$k_1=k_2$	7	210.24	0.1841	182.61	0.1841	84.99	2.276	4.492	3.030	4510.02	9034.03[3]
$L_{\infty 1}=L_{\infty 2}$ $k_1=k_2$	5	156.45	0.2884	156.45	0.2884	na	1.626	4.209	3.405	4530.88	9071.76
continuous rate	7	141.07	0.3590	182.25	0.1842	97.70	2.148	4.473	3.085	4514.54	9043.09
$\sigma_m=0$	6	206.71	0.1883	180.82	0.1883	84.85	4.149	5.920	0.000	4526.06	9064.11
$\sigma_s=\sigma_f$	6	210.74	0.1858	182.23	0.1858	85.36	3.948	3.948	3.183	4529.25	9070.49
$\sigma_s=\sigma_f=0$	5	209.46	0.1875	181.49	0.1875	85.30	0.000	0.000	4.737	4545.25	9100.49

[1] Here k_1 is zero,i.e. the growth rate is constant in the first phase; therefore we give the estimate of the growth rate instead of $L_{\infty 1}$.

[2] The least AIC value for estimates from the 1960s data Na= not applicable because this is the normal von Bertalanffy curve, i.e. with only one phase.

[3] The least AIC value for estimates from the 1980s data

also be noted that the two-phase VBG model with common L_∞ (row 2, Table 1A), was very similar to the common k parameterization, reflecting the high correlation between L_∞ and k in the VBG models. For the 1960s, the continuous two-phase VBG model was rejected, $P<0.005$ (row 5, Table 1A).

For the 1980s data, the best-fit model based on the AIC values was for the two-phase VBG model with a common value for the k parameter in both phases (row 3, Table 1B). The estimate of the size at which the change between the two phases occurs was 85 cm (compared to the estimate of 74 cm for the 1960s data). As with the results of the 1960s data, the common-k model, common-L_∞ model, and the full two-phase model yielded very similar values for both the likelihood and parameter estimates in the second phase, but not for those in the first phase. This similarity reflects the high correlation between k and L_∞ in the VBG model, so that over the limited size range below L^* nearly identical growth rates can be achieved in the common-k model by decreasing the value of $L_{\infty 1}$. For the 1980s (as with the 1960s), the continuous two-phase VBG model (7 parameters), was rejected, $P<0.005$ (row 5, Table 1B).

For both the 1960s and 1980s data, the two-phase model provided a substantially and significantly better fit to the tag return data than a simple VBG model. This can be seen in Table 1 (A and B) by comparing the negative log-likelihood and AIC values for the simple VBG model (row 4) with any that include a two-phase component, particularly the continuous rate two-phase VBG model. We also fitted a smooth Richards' (1959) growth model (a generalization of the VBG model) to the data, which fitted better than the simple VBG model, but worse than the two-phase VBG models.

Note, however, that the log-ratio test and AIC criterion may not be fully applicable for testing the differences between the simple and two-phase VBG models because the simple VBG model can arise in more than one way as a submodel of the two-phase model (e.g. with common L_∞ and k parameters or from L^* equaling zero or infinity) (Davies, 1977, 1987). Nevertheless, the large magnitude of the differences in the log-likelihood values indicates a significance difference.

For the 1960s data, it should be noted that the scientist measurement error (σ_s) was estimated to be essentially zero when it was included as an explicit term in several of the models. In these cases, we refitted the models excluding this parameter. Common sense dictates that measurement errors would not be zero. The most informative data

Table 2

Comparison of SBT growth parameter estimates for the 1960s and 1980s, between absolute maximum likelihood and local maxima likelihood.

Common parameters	Number of parameters	$L_{\infty 1}$	k_1	$L_{\infty 2}$	k_2	L^*	σ_s	σ_f	σ_m	−Log likelihood	AIC
1960s											
none	6	22.23[1]	0.0000	210.90	0.1063	74.24	0.000	3.122	2.992	2055.53	4123.07
none	8	118.08	0.3957	186.04	0.1500	91.23	1.061	3.398	2.855	2062.76	4141.51
1980s											
$k_1=k_2$	7	210.24	0.1841	182.61	0.1841	84.99	2.276	4.492	3.030	4510.02	9034.03
$k_1=k_2$	7	145.37	0.3371	169.03	0.3371	120.47	2.293	4.514	3.025	4512.98	9039.96

[1] Here k_1 is zero, i.e. the growth rate is constant in the first phase; therefore we give the estmate of the growth rate instead of $L_{\infty 1}$.

on measurement error would come from fish with short times at liberty because in these cases the amount of process error would be small. However, as explained above, fish with times at liberty of less than 270 days were excluded to eliminate seasonal effects. Process and measurement errors are partially confounded in the model. The estimation procedure could not distinguish an additional constant component to the linear, temporally increasing process error from the measurement error for recaptured fish measured by scientists. For the 1980s data, the estimation procedure was able to estimate a nonzero value for the scientist measurement error. The results for the 1980 returns suggest that the measurement error for the scientists was about 50% of that for fishermen.

For both the 1960s and 1980s data, the estimation procedure is able to distinguish between fishermen and scientist measurement error. The assumption that the measurement error of fishermen and scientists are the same is rejected by a statistical test (i.e. the second last line of both Table 1, A and B).

Examination of the residuals indicated no systematic lack of fit in either the 1960s or 1980s data (Fig. 1, A–D).

Shape of the likelihood function

It is worth noting that the likelihood function is bimodal with respect to the parameter determining the length at which growth changes between the two phases (L^*). Figure 2 shows the negative log-likelihood ($-LL$) values as a function of L^* for the 1960s and 1980s data for the best-fit model. For the 1960s data, the $-LL$ function has an absolute minimum at $L^* = 74$ cm and a second, local minimum at $L^* = 91$ cm. For the 1980 data, the absolute minimum occurs at $L^* = 85$ cm and the second, local minimum at $L^* = 120$ cm.

Monte Carlo and bootstrap simulations were conducted to evaluate the bimodal nature of the likelihood function. The Monte Carlo simulations were done by assuming the two-phase VBG growth model and were conditional on the SBT release lengths. Both types of simulations confirmed that the minima with the lowest absolute value for the negative log-likelihood function would switch between individual realizations within the simulations. Only the results of the bootstrap simulations are presented in this article. These were based on 1000 individual simulations for which the tag increment data were randomly sampled with replacement. For each individual simulation, the value of L^* that yielded the absolute minimum value for the negative log-likelihood function was determined. For the 1960s data, the best-fit estimate of L^* was near 74 cm in 930 of the simulations and 91 cm in 70. For the 1980 data, the absolute minimum in the negative log-likelihood function occurred 767 times when L^* was near 85 cm and 233 times when L^* was near 120 cm (Fig. 3). Thus, although the lower value for L^* was the most likely for both the 1960s and 1980s data, the 95% confidence intervals based on the bootstrap results would encompass both values. The estimated value of the other parameters determining the expected growth curve are correlated with that of L^*. Thus, the alternative minima in the log-likelihood function are associated with substantially different estimates for the k and L_∞ parameters (Table 2). This in turn has implications for possible biological interpretations of the parameter estimates (see below).

Joint analyses of the 1960s and 1980s data

Results of jointly modeling the 1960s and 1980s tag return data to test for common parameters are presented in Table 3. The model error (σ_m) was the only parameter found not to be significantly different in the combined analyses. Having a single parameter value for the model error component had virtually no effect on the parameters determining the expected growth rates, compared to those estimated in the separate analyses.

Comparison of 1960s and 1980s growth rates

The fact that all of the parameters that describe the expected growth rates significantly differ for the 1960s and 1980s data indicates that SBT growth rate changed between these two periods. For the best-fit solutions, the

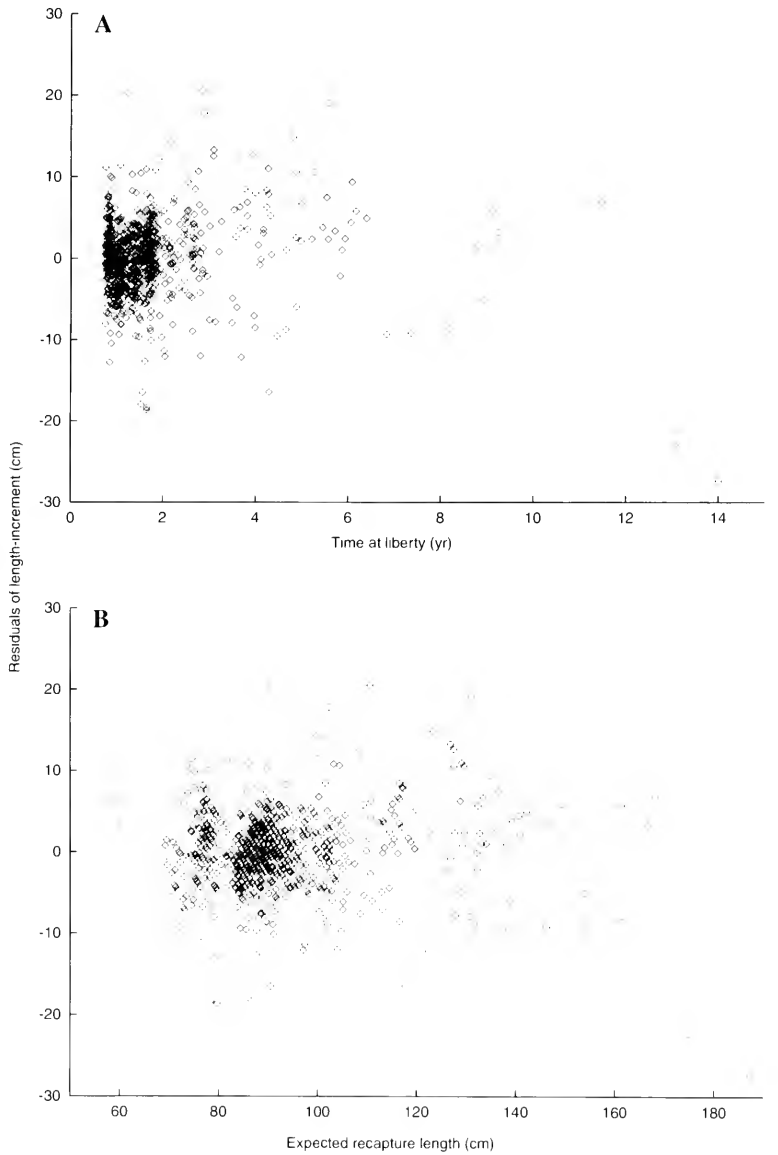

Figure 1

Residual plots from the best-fit models in Table 1 to the 1960s and 1980s tagging data: (**A**) residuals for time at liberty for the 1960s; (**B**) residuals for expected recapture lengths for the 1960s; (**C**) residuals for time at liberty for the 1980s; (**D**) residuals for expected recapture lengths for the 1980s.

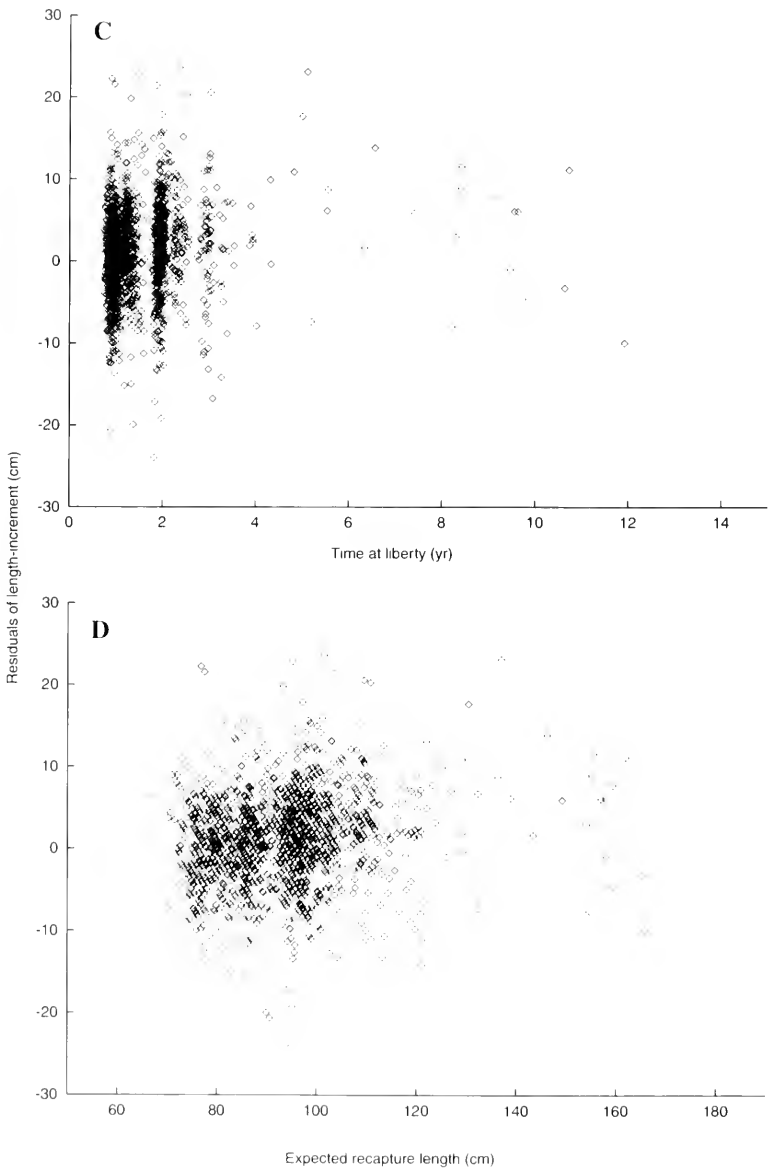

Figure 1 (continued)

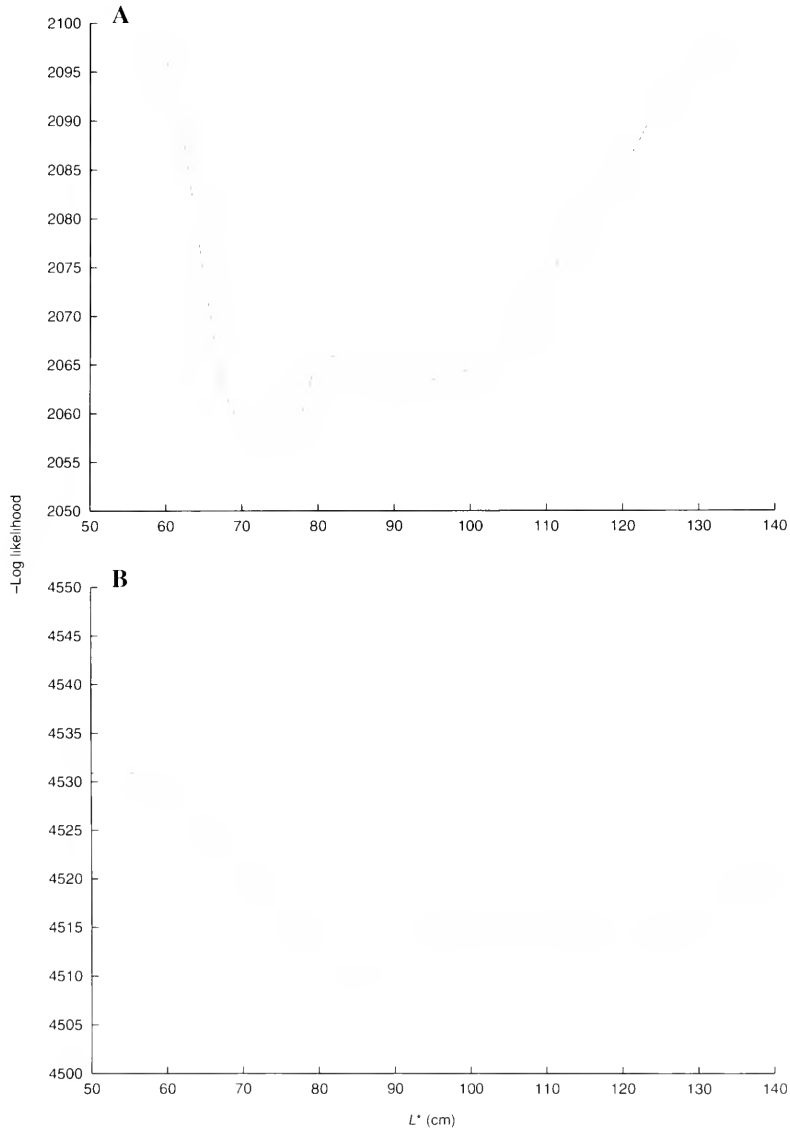

Figure 2

Negative log-likelihood value as a function of L^*: (**A**) for the 1960s; (**B**) for the 1980s.

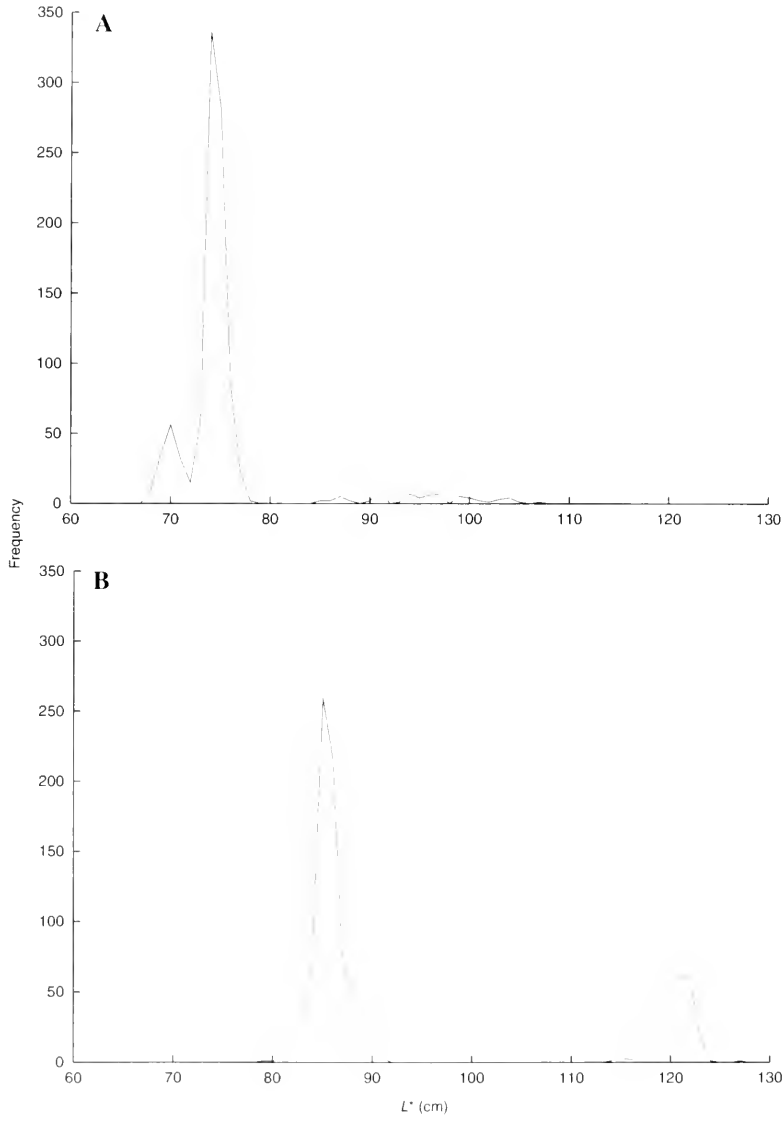

Figure 3

Frequency distribution for the estimates of L^* from 1000 bootstrap simulation results: (**A**) for the 1960s; (**B**) for the 1980s.

Table 3

Southern bluefin tuna growth parameters and tests, from jointly analyzing the 1960s and 1980s data.

Common parameters	Number of parameters	$L_{\sim 1}$	k_1	$L_{\sim 2}$	k_2	L^*	σ_s	σ_f	σ_m	−Log likelihood	AIC
none (60)	13	22.23[1]	0.0000	210.90	0.1063	74.24	0.000	3.122	2.992		
(80)		210.24	0.1841	182.61	0.1841	84.99	2.273	4.496	3.030	6565.55	13157.10
$\sigma_m 60 = \sigma_m 80$	12	22.23	0.0000	210.98	0.1062	74.25	0.000	3.115	2.998		
		210.31	0.1840	182.67	0.1840	85.00	2.309	4.514	2.998	6565.56	13155.11
$L60_{\sim 1} = L80_{\sim 1}$	12	213.29	0.1462	210.49	0.1069	75.03	0.000	3.133	3.001		
		213.29	0.1804	184.20	0.1804	85.00	2.323	4.518	3.001	6567.43	13158.85
$L60_{\sim 1} = L60_{\sim 2} = L80_{\sim 1}$	11	211.41	0.1480	211.41	0.1060	75.08	0.000	3.128	3.004		
		211.41	0.1827	183.24	0.1827	85.00	2.315	4.515	3.004	6567.44	13156.87
$k60_1 = k80_1$	12	185.24	0.1804	210.46	0.1069	75.11	0.000	3.119	3.008		
		213.26	0.1804	184.21	0.1804	85.01	2.325	4.510	3.008	6568.07	13160.15
$L60_{\sim 2} = L80_{\sim 2}$	11	22.20	0.0000	195.25	0.1232	73.74	0.000	3.120	3.010		
		233.55	0.1584	195.25	0.1584	85.22	2.302	4.516	3.010	6568.89	13159.78
$k60_2 = k80_2$	11	23.85	0.0000	186.76	0.1374	70.48	0.000	3.097	3.044		
		258.76	0.1374	207.04	0.1374	86.23	2.262	4.495	3.044	6575.52	13173.03
$L^*60 = L^*80$	12	110.51	0.4707	196.71	0.1269	85.45	0.000	3.196	3.014		
		211 13	0.1827	182.97	0.1827	85.45	2.306	4.505	3.014	6574.09	13172.19
$\sigma_s 60 = \sigma_s 80$	12	22.22	0.0000	210.59	0.1072	74.10	1.602	3.023	3.068		
		209.66	0.1842	182.49	0.1842	84.94	1.602	4.472	3.068	6570.46	13164.92
$\sigma_f 60 = \sigma_f 80$	11	22.28	0.0000	210.43	0.1064	74.23	0.000	4.174	2.975		
		210.40	0.1844	182.62	0.1844	85.02	2.394	4.174	2.975	6577.96	13177.91

[1] Here k_1 is zero, i.e. the growth rate is constant in the first phase, therefore we give the estimate of the growth rate instead of $L_{\sim 1}$.

SBT growth rates in the 1960s are estimated to be less than those in the 1980s up to 144 cm (Fig. 4). Comparison of the 1960s and 1980s expected growth curves over time for a 55-cm fish are presented in Figure 5. In making this comparison, we assumed that a 55-cm fish is approximately one year of age (Anonymous[5]) and that size at age one did not change between the 1960s and 1980s, as supported by length-frequency data from these two time periods (Leigh and Hearn, 2000; Anonymous[5]). Thus, Figure 5 can also be considered as an estimate of the expected length-at-age curve. Figure 5 indicates that the overall expected growth was significantly faster in the 1980s than in the 1960s, so that a fish of 55 cm or age 1 would take approximately four years in the 1960s to achieve the same length that would have been achieved in three years in the 1980s.

A feature of the best-fitted estimated growth parameters is that the expected growth curves intersect at ~170 cm, so that after age 13 a fish from the 1960s is estimated to be larger than a fish from the 1980s. This crossover is driven primarily by the difference in the estimates of $L_{\sim 2}$. The standard log-likelihood test indicates a low probability, P=0.01, that $L_{\sim 2}$ for the 1960s and 1980s are the same. However, the analyses of the bootstrap estimates of $L_{\sim 2}$ indicate that the estimates are bimodal, reflecting the bimodal distribution of L^*. Random sampling from the bootstrap distributions for $L_{\sim 2}$ showed that in 6.1% of cases the 1960s $L_{\sim 2}$ estimate was less than the 1980s estimate. For a two-sided test at the 5% significant level, at least 2.5% (and at most 97.5%) of the bootstrap samples would have been expected to have the 1960s $L_{\sim 2}$ less than that of the 1980s to justify the hypothesis that the two $L_{\sim 2}$ are equal. Thus, based on the bootstrap results, the hypothesis of equality cannot be rejected. Most of the 6.1% of cases are associated with the 1960s $L_{\sim 2}$ less than 180 cm, which are in turn associated with the upper mode of L^* in Figure 3A, i.e. near L^* = 91 cm. It is worth noting that only three recapture lengths were greater than 170 cm. There are, therefore, very minimal data for estimating growth rates beyond 170 cm and for precisely estimating $L_{\sim 2}$.

Discussion

The results in this study indicate that the traditional VBG model does not provide an adequate representation of growth in SBT. There appears to be a significant change in the pattern of growth in relation to a VBG curve during the juvenile stages of the SBT life cycle. This, in turn, may be related to the transition from a tightly schooling fish that spends substantial time in near and surface shore waters

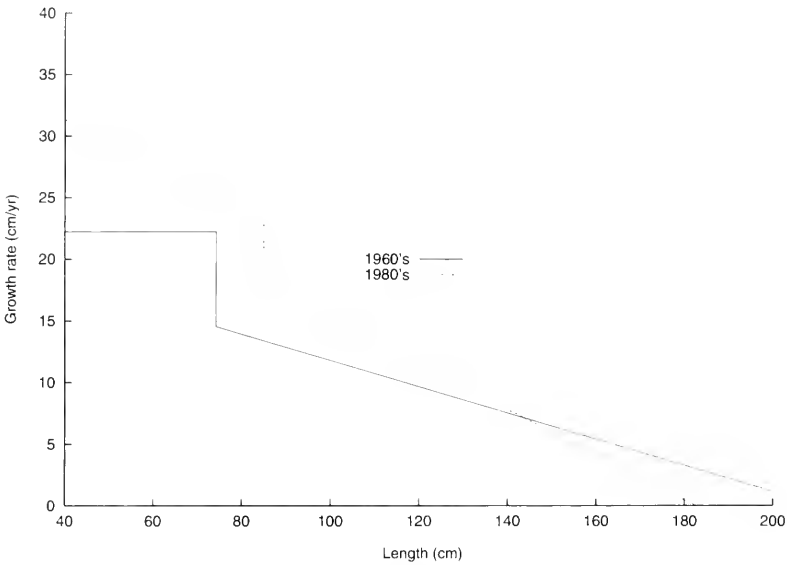

Figure 4

Comparison of the 1960s and 1980s best-fit estimates of southern bluefin tuna growth rates as a function of length.

to one that is found primarily in more offshore and deeper waters. In this regard, recent information from archival tags indicates that SBT between 80 and 90 cm (about two to three years old) commonly migrate during winter months to offshore oceanic waters in the Indian Ocean and the Tasman Sea and begin to feed at substantial depth (Gunn and Block, 2001). In contrast, catches and samples off Albany, Western Australia, show that many SBT less than 70 cm stay in nearshore Australian waters during winter (Hynd, 1965; Murphy[*]; and release data analyzed in this study). Thus, the growth changes estimated to be near $L^* = 80$ cm may correspond to a marked change in the SBT behavior during these winter months.

The von Bertalanffy growth equation and its modifications have been the standard for modeling tuna growth. The life history dynamics for most tuna species (e.g. north Pacific bluefin, albacore, bigeye, and yellowfin tuna) have a bimodal component analogous to that of SBT. Thus, juveniles are frequently found in densely packed surface schools, whereas at larger sizes individuals are rarely found near the surface and appear not to occur in densely packed schools (although there is little direct information on schooling for these larger fish). Moreover, mature tuna expend considerable energy in the spawning process, and in some cases swim thousands of kilometers and incur considerable weight losses during spawning (Warashina and Hisada, 1970). Bayliff et al. (1991) also found that growth models with a rate discontinuity at a certain size provided a better fit to Pacific northern bluefin tuna tag-return data than a simple continuous growth model. The extent to which this may be a general phenomenon in tuna or other fish species with marked changes in habitat use with age is not clear. However, the results from our study and those of Bayliff et al. (1991) suggest that a growth rate with a discontinuity at a certain size may be more common than existing modeling of growth may indicate. Complex growth models, which deviated from a simple continuous growth curve, have generally not been considered, and the available data, in many cases, may not have sufficient power to be able to statistically identify more complex growth processes if they exist.

Although the complex two-stage growth model used in our study clearly provided a substantial and significant improvement in fit to the growth-increment data, the model itself presents problems in terms of the biological interpretation of the parameter estimates for L^*. The bimodal nature of the likelihood function means that the size and

[*] Murphy, G. I. 1979. Southern bluefin tuna. Aust. CSIRO Div. Fish. Oceanogr. Fishery Situation Report 1, 10 p. [Available from CSIRO Marine Research, GPO Box 1538, Hobart 7000, Australia.]

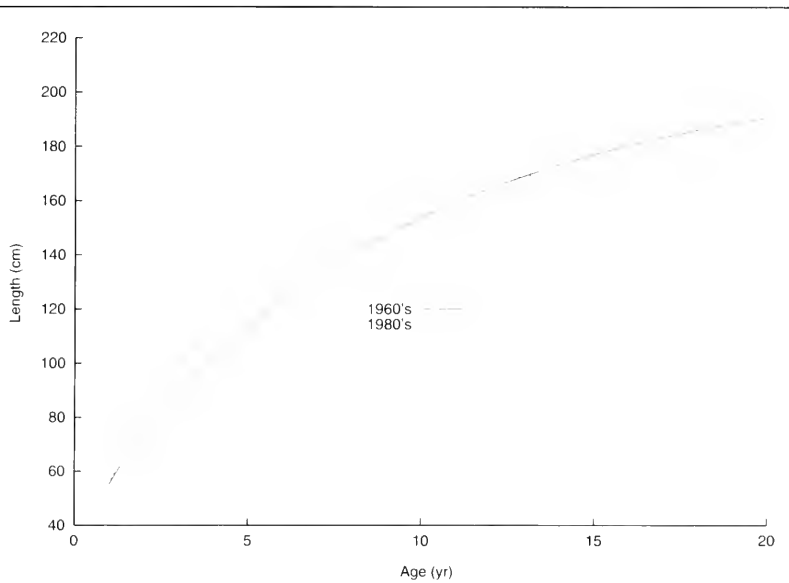

Figure 5

Comparison of the 1960s and 1980s best-fit estimates for the expected length of southern bluefin tuna as a function of age, assuming that the expected length of an age-1 fish is 55 cm.

age where the change in growth occurs is not well defined. This, in turn, confounds the evaluation of the plausibility of different specific possible biological hypotheses underlying the change. Moreover, although the change in growth patterns may be quite rapid, a large discontinuity in the growth rates at a specific length seems unrealistic. The continuous two-stage VBG model did not fit the 1960s and 1980s data as well as the discontinuous two-stage VBG models. However, the two-phase VBG models fitted the data better than the simple von Bertalanffy growth curve (Table 1, A and B) and its generalization—the simple Richards' (1959) curve (senior author, unpubl. results).

From both the statistical estimation and biological perspective, we think there is scope for the development of more appropriate complex growth models. In this context, there is also need for the development of estimation procedures for these complex models that can take into account alternative error structures that allow for individual variability in the growth rate parameters (e.g. Sainsbury, 1980; James, 1991; Wang et al., 1995).

In the joint analysis of the 1960s and 1980s data, σ_m was the only parameter found not to be significantly different between the two data sets. However, caution is warranted in any comparison and interpretation of growth curves determining parameter values because of the well-known negative correlation between k and L_∞ of the VBG growth model and the bimodal nature of the likelihood surface, as already noted. In particular, the differences in the estimates of $L_{\infty 2}$ should not be taken as strong evidence that the asymptotic growth of SBT decreased or that there was a crossover in the growth rates. These complex growth changes are difficult to explain from a biological perspective and, as noted above, the bootstrap results indicate that the hypothesis that the $L_{\infty 2}$ parameters are equal cannot be rejected. Moreover, we would note that there is a paucity of tag return data for larger fish. A total of only seven tags were recovered from fish with lengths exceeding 165 cm and only three for fish with lengths in excess of 170 cm. Fitting VBG models does not provide reliable estimates of growth when extrapolated beyond the range of the data because of the large negative correlation between k and L_∞. We, therefore, do not think that the current data are sufficient to determine whether, in fact, $L_{\infty 2}$ differed between the 1960s and 1980s.

One of the primary applications of the estimated SBT growth curves is to provide estimates of the age distribution of commercial catch in stock assessments based on catch-at-age analyses (e.g. Anonymous[5]). The predicted growth curves (assuming that an age-1 fish is 55 cm) indicate that the estimated ages of 165-cm fish have diverged by about a year for the curve based on a common $L_{\infty 2}$ compared with those for which $L_{\infty 2}$ is allowed to differ

between the 1960s and 1980s. For smaller sizes, the divergence is substantially less (e.g. for fish 140 cm or less the divergence is less than three months). In terms of using the growth rate data to estimate ages from lengths, these results indicate that for the older reproducing fish the results will be highly sensitive to assumptions about $L_{\infty 2}$.

The results from these tagging studies clearly show that growth rates for SBT hatched in the 1980s had increased in relation to those cohorts hatched in the 1960s. The increase in growth rates is substantial, so that a fish, on average, would have been expected to take four years to grow from 55 cm to 111 cm in the 1960s, but only three years to do so in the 1980s. In other words, after age 4 there is a difference of about one year in the expected age of a fish of similar length, and this difference persisted over the size range for which meaningful recapture data were available. The change in growth and its magnitude are consistent with the analyses in Leigh and Hearn (2000) of the modes in length-frequency distributions of juvenile fish captured in the Australian surface fishery. The underlying causes of the change in SBT growth rates are unknown. They could be associated with changes in environmental conditions, population size, or a combination of the two. The change in SBT growth rates between the 1960s and 1980s is associated with very substantial declines in both the adult and juvenile components of the SBT stock (Polacheck et al.[1]; Anonymous[9]).

There is an increasing number of examples in which growth rates have been reported to be inversely correlated to fish population numbers because of intraspecific competition. For example, Le Cren (1958) documented an increase in the growth rate of perch after a planned reduction of a lake population. In a converse case, Kaeriyama (1996) reported a decline in the growth rate of Japanese chum salmon following a many-fold increase in its population size because of a most successful hatchery enhancement scheme. Other accounts are published in Southward (1967), de Veen (1976), Toresen (1990), Ross and Nelson (1992), and Sinclair and Swain (1996). However, the reports are mainly on species for which direct aging data are reliable and regularly collected over a lengthy period, or the fish are hatchery reared.

The hypothesis that the increase in SBT growth rates was the result of the marked reduction in SBT population size would seem plausible, given the similar associations that have been found in a number of fisheries phenomena. As discussed in Leigh and Hearn (2000), changes in juvenile SBT growth rates based on analyses of length-frequency data are also consistent with the change having a density-dependent component. In this regard, it is worth noting that preliminary analyses of tag return data from the 1990s indicate that growth rates in the 1990s were similar to those in the 1980s (Polacheck and Preece[10]). Thus, these preliminary results are also consistent with the change in growth being a density-dependent response as both juvenile and adult SBT abundances remained at low levels during this period (e.g. Anonymous[9]; Polacheck and Preece[10]). Large uncertainty exists about possible recovery of the SBT stock in the near future (e.g. Anonymous[9]), but continued monitoring of SBT growth may provide one indicator of stock recovery.

To simplify our investigation we did not consider seasonal growth. We avoided possible bias, due to seasonal growth, by analyzing data only from fish with times at liberty more than or equal to 270 days. This restriction provided an efficient mechanism to focus on the long-term growth process and was effective because the resultant sets were large. Large numbers of recaptured fish with reliable information and times at liberty more than 9 months seem rare for other tunas, in which case the added complication of accounting for possible seasonable growth would be required to ensure the robustness of the results.

The analyses in this paper represent the first documented examples of substantial temporal changes in growth rates that persisted for an extended portion of the life span in a large pelagic tuna resource. For tuna stocks in general, estimates of growth rates play a major role in stock assessments and in the subsequent management advice derived from these assessments.

Acknowledgments

We thank the many crew and scientific staff who participated in the 1959–84 SBT tagging operations. We are especially grateful for Australian and Japanese fishermen who returned tags with information on recapture length. The 1983–84 tagging program was financially supported by an Australian Government grant.

Literature cited

Akaike, H.
1974. A new look at the statistical model identification. Institute of Electrical and Electronic Engineers Transactions on Automatic Control, AC-19, p. 716–723. IEEE Control Systems Society, New York, NY.

Allen, K. R.
1966. A method of fitting growth curves of the von Bertalanffy type to observed data. J. Fish. Res. Board Can. 23: 163–179.

Bayliff, W. H.
1980. Synopsis of biological data on eight species of scombrids. Inter-Am. Trop. Tuna Comm., Spec. Rep. 2 (W. H. Bayliff, ed.), 530 p. IATTC, San Diego, CA.
1988. Growth of skipjack, *Katsuwonus pelamis*, and yellowfin, *Thunnus albacares*, tunas in the eastern Pacific Ocean, as estimated from tagging data. Inter-Am. Trop. Tuna Comm. Bull. 19(4):311–385.

[9] Anonymous. 1998. Report of the 1998 Scientific Committee meeting 3–6 August 1998, Tokyo, Japan. [Available from the Commission for the Conservation of Southern Bluefin Tuna, PO Box 37, Deakin West, ACT 2600, Australia.]

[10] Polacheck, T., and A. Preece. 1998. Preliminary comparisons of the growth rates of southern bluefin tuna in the 1990s with those in the 1960s and 1980s. Tenth SBT recruitment monitoring workshop, 14–17th September 1998, Hobart, Australia. RMWS/98/5, 11 p. [Available from CSIRO and the Commission for the Conservation of Southern Bluefin Tuna, P.O. Box 37, Deakin West, ACT 2600, Australia.]

1991. Status of northern bluefin tuna in the Pacific Ocean. Inter-Am. Trop. Tuna Comm., Spec. Rep. 7:29–88.

Bayliff, W. H., I. Ishizuka, and R. B Deriso.
1991. Growth, movement, and attrition of northern bluefin tuna, *Thunnus thynnus*, in the Pacific Ocean, as determined by tagging. Inter-Am. Trop. Tuna Comm. Bull. 20(1): 1–94.

Burgess, D., A. Caton, J. Gunn, W. Hearn, T. Murray, and C. Proctor.
1991. Aging and growth of juveniles and adults. *In* Review of aspects of southern bluefin tuna: biology, population and fisheries (A. E. Caton, ed.), p. 210–224. Inter-Am. Trop. Tuna Comm., Spec. Rep. 7.

Caton, A. E.
1991 Review of aspects of southern bluefin tuna: biology, population and fisheries. Inter-Am. Trop. Tuna Comm., Spec. Rep. 7:181–357.

Clay, D.
1991. Atlantic bluefin tuna (*Thunnus thynnus thynnus* (L.)): a review. Inter-Am. Trop. Tuna Comm., Spec. Rep. 7:89–179.

Davies, R. B.
1977. Hypothesis testing when a nuisance parameter is present only under the alternative. Biometrics 64:247–254.
1987. Hypothesis testing when a parameter is present only under the alternative. Biometrics 74: 33–43.

de Veen, J. F.
1976. On changes in some biological parameters in the North Sea sole (*Solea solea* L.). J. Cons. Int. Explor. Mer 37:60–90.

Fabens, A. J.
1965. Properties and fitting of the von Bertalanffy growth curve. Growth 29:265–289.

Farley, J. H., and T. L. O. Davis.
1998. Reproductive dynamics of southern bluefin tuna, *Thunnus maccoyii*. Fish. Bull. 96: 223–236.

Ford, E.
1933. An account of the herring investigations conducted at Plymouth during the years from 1924 to 1933. J. Mar. Biol. Assoc. U.K. 19:305–384.

Fournier, D. A., J. R. Sibert, J. Majkowski, and J. Hampton.
1990. MULTIFAN a likelihood method for estimating growth parameters and age composition from multiple length frequency data sets illustrated using data from southern bluefin tuna (*Thunnus maccoyii*). Can. J. Fish. Aquat. Sci. 47:301–317.

Francis, R. I. C. C.
1988. Maximum likelihood estimation of growth and growth variability from tagging data. NZ J. Mar. Freshwater Res. 22:42–51.

Gunn, J. S. and B. A. Block.
2001. Advances in acoustic, archival and satellite tagging of tunas. *In* Tuna—physiological ecology and evolution (B. A. Block and E. D. Stevens, eds.), p. 167–224. Academic Press, New York, NY

Hampton, J
1986. Effect of tagging on the condition of southern bluefin tuna, *Thunnus maccoyii*, (Castlenau). Aust. J. Mar. Freshwater Res. 37:699–705.
1991. Estimation of southern bluefin tuna *Thunnus maccoyii* growth parameters from tagging data, using von Bertalanffy models incorporating individual variation. Fish. Bull. 89:577–590.

Hearn, W. S.
1986. Mathematical methods for evaluating marine fisheries. Ph.D. diss., 195 p. Univ. New South Wales, Sydney, New South Wales.

Hynd, J. S.
1965. Southern bluefun tuna populations in south-west Australia. Aust. J. Mar. Freshwater Res. 16: 25–32.

James, I. R.
1991. Estimation of von Bertalanffy growth curve parameters from recapture data. Biometrics 47: 1519–1530.

Kaeriyama, M.
1996. Population dynamics and stock management of hatchery-reared salmons in Japan. Bull. Natl. Res. Inst. Aquacult., Suppl. 2:11–15.

Kimura, D. K.
1980. Likelihood methods for the von Bertalanffy growth curve. Fish. Bull. 77:765–776.

Kirkwood, G. P.
1983. Estimation of von Bertalanffy growth curve parameters using both length increment and age-length data. Can. J. Fish. Aquat. Sci. 40:1405–1411.

Kirkwood, G. P., and I. F. Somers.
1984. Growth of two species of tiger prawn, *Penaeus esculentus* and *P. semisulcatus*, in the western Gulf of Carpentaria. Aust. J. Mar. Freshwater Res. 35:703–712.

Le Cren, E. D.
1958. Observations on the growth of perch (*perca fluviatilis* L.) over twenty two years with special reference to the effects of temperature and changes in population density. J. Anim. Ecol. 27: 287–334.

Lee, R. M.
1912. An investigation into the methods of growth determination in fishes. Publ. Circ. Cons. Explor. Mer 63:34.

Leigh, G. M., and W. S. Hearn.
2000. Changes in growth of juvenile southern bluefin tuna (*Thunnus maccoyii*): an analysis of length-frequency data from the Australian fishery. Mar. Freshwater Res. 51:143–154.

Manzer, J. I., and F. H. C. Taylor.
1947. The rate of growth of lemon sole in the Strait of Georgia. Fish. Res. Board Can. Prog. Rep. Pac. Coast Stns. 7224–27.

Murphy, G. I.
1977. New understanding of southern bluefin tuna. Aust. Fish. 36(1):2–6.

Nelder, J. A., and R. Mead.
1965. A simplex method for functional minimization. Comput. J. 7:308–313.

Pitcher, T. J., and P. D. M. MacDonald.
1973. Two models for seasonal growth in fishes. J. Appl. Ecol. 10:559–606.

Richards, F. J.
1959 A flexible growth function for empirical use. J. Exp. Bot. 10:290–300.

Ross, M. R., and G. A. Nelson.
1992. Influences of stock abundance and bottom-water temperature on growth dynamics of haddock and yellowtail flounder on Georges Bank. Trans. Am. Fish. Soc. 121: 578–587.

Sainsbury, K. J.
1980. Effect of individual variability on the von Bertalanffy growth equation. Can. J. Fish. Aquat. Sci. 37:241–247.

Sinclair, A. F., and D. P. Swain.
1996. Comment. Spatial implications of a temperature-based growth model for Atlantic cod *Gadus morhua* off the eastern coast of Canada Can. J. Fish. Aquat. Sci. 53:2909–2911.

Southward, G. M
1967. Growth of Pacific halibut. Rep. Int. Pac. Halibut Comm. 43, 40 p.

Toresen, R.
1990. Long-term changes in growth of Norwegian spring-spawning herring. J. Cons. Int. Explor. Mer 47:48–56.
von Bertalanffy, L.
1938. A quantitative theory of organic growth. (Inquiries on growth laws II). Hum. Biol., 10:181–213.
Walford, L. A.
1946. A new graphic method of describing the growth of animals. Biol. Bull. (Woods Hole, Mass.) 90:141–147.
Wang, Y. G., M. R. Thomas, and I. F. Somers.
1995. A maximum likelihood approach for estimating growth from tag-recapture data. Can. J. Fish. Aquat. Sci. 52:252–259.
Warashina, I., and K. Hisada.
1970. Spawning activity and discoloration of meat and loss of weight in the southern bluefin tuna. Bull. Far Seas Fish. Res. Lab. (Shimizu) 3:147–166. [In Japanese with English abstract.]
Wild, A.
1994. A review of the biology and fisheries for yellowfin tuna, *Thunnus albacares*, in the eastern Pacific Ocean. FAO Fish. Tech. Pap. 336/2:52–107.
Wild, A., and J. Hampton.
1994. A review of the biology and fisheries for skipjack tuna, *Katsuwonus pelamis*, in the Pacific Ocean. FAO Fish. Tech. Pap. 336/2:1–51.
Yukinawa, M.
1970. Age and growth of southern bluefin tuna, *Thunnus maccoyii* (Castlenau) by use of scale. Bull. Far Seas Fish. Res. Lab. (Shimizu) 3:229–257.

Life history of the Atlantic sharpnose shark (*Rhizoprionodon terraenovae*) (Richardson, 1836) off the southeastern United States

Joshua K. Loefer
South Carolina Department of Natural Resources
Marine Resources Research Institute
217 Fort Johnson Road
P.O. Box 12559
Charleston, South Carolina 29412-2559
E-mail address: loeferj@mrd.dnr.state.sc.us

George R. Sedberry
South Carolina Department of Natural Resources
Marine Resources Research Institute
217 Fort Johnson Road
P.O. Box 12559
Charleston, South Carolina 29412-2559

Abstract—The life history of the Atlantic sharpnose shark (*Rhizoprionodon terraenovae*) was described from 1093 specimens collected from Virginia to northern Florida between April 1997 and March 1999. Longitudinally sectioned vertebral centra were used to age each specimen, and the periodicity of circuli deposition was verified through marginal increment analysis and focus-to-increment frequency distributions. *Rhizoprionodon terraenovae* reached a maximum size of 828 mm precaudal length (PCL) and a maximum age of 11+ years. Mean back-calculated lengths-at-age ranged from 445 mm PCL at age one to 785 mm PCL at age ten for females, and 448 mm PCL at age one to 747 mm PCL at age nine for males. Observed length-at-age data (estimated to 0.1 year) yielded the following von Bertalanffy parameters estimates: L_∞ = 749 mm PCL (SE=4.60), K = 0.49 (SE=0.020), and t_0=−0.94 (SE=0.046) for females; and L_∞=745 mm PCL (SE=5.93), K=0.50 (SE=0.024), and t_0=−0.91 (SE=0.052) for males. Sexual maturity was reached at age three and 611 mm PCL for females, and age three and 615 mm PCL for males. *Rhizoprionodon terraenovae* reproduced annually and had a gestation period of approximately 11 months. Litter size ranged from one to eight (mean=3.85) embyros, and increased with female PCL.

Manuscript accepted 22 July 2002.
Fish. Bull. 101:75–88 (2003).

The Atlantic sharpnose shark (*Rhizoprionodon terraenovae*) is a small carcharhinid that inhabits the coastal waters of the western North Atlantic from the Bay of Fundy to the Yucatan (Castro, 1983). It is the most common small coastal species off the southeastern U.S. coast and the Gulf of Mexico (Branstetter, 1990). This species is frequently encountered by a variety of commercial fishing gear, including bottom longline, gill net, bandit reel (used by the snapper–grouper fishery), and shrimp trawl. *Rhizoprionodon terraenovae* is also a common catch in the recreational hook-and-line fishery.

The age and growth of this species has been described in the Gulf of Mexico by Parsons (1981, 1983a, 1985) and Branstetter (1981, 1986, 1987a). Although those studies provided significant information on the age and growth of *R. terraenovae*, data were collected from 1979 to 1984, a time in which fishing pressure on the *R. terraenovae* population was probably not as high as at present (Cortes, 1995). The previous studies dealt with fishes only from the northern Gulf of Mexico, and therefore may not represent the entire stock, although the stock structure for *R. terraenovae* in the northwestern Atlantic remains unclear (Heist et al., 1996). No published age and growth studies exist for specimens collected from the southeastern U.S. Atlantic coast. The reproductive biology of this species has been studied in both the Gulf of Mexico and off the southeastern U.S. coast (Parsons, 1983b; Castro, 1988, 1993; Castro and Wourms, 1993), but the lack of concurrent age and growth data off the southeastern United States limits the utility of these data for fishery management.

Considering the importance of accurate and timely age, growth, and reproductive information to fishery management, this study had two objectives: to describe age, growth, and reproduction in the southeastern U.S. population of *R. terraenovae*; and to compare these data to those of previous studies on the same species in the Gulf of Mexico.

Materials and methods

Rhizoprionodon terraenovae (n=1093) were collected throughout the year in coastal waters from April 1997 through March 1999. Collection sites ranged from Chesapeake Bay, Virginia, to Port Canaveral, Florida (Fig. 1). The majority of specimens were collected off the coast of South Carolina. A variety of sampling gears were employed for sample collection: bottom longline (47% of specimens), otter trawl (22%), port-sampling of commercial fishing

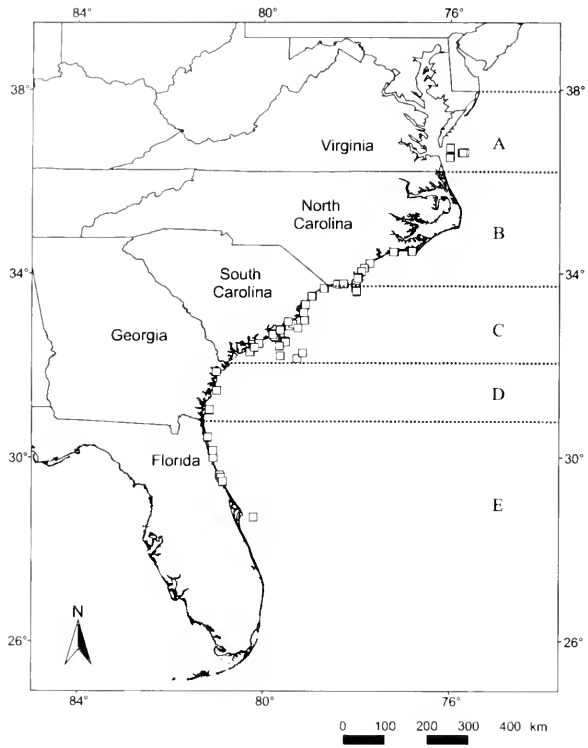

Figure 1

Sample collection sites and distribution by area (roughly equivalent to state borders) for *R. terraenovae* collected during this study, 1997–99. (□) represents locations where one or more *R. terraenovae* were captured. (**A**) = 13 males (694–793 mm PCL); (**B**) = 52 females (215–786 mm PCL), 51 males (200–765mm PCL); (**C**) = 497 females (197–813 mm PCL), 441 males (225–828 mm PCL); (**D**) = 8 females (302–763 mm PCL), 7 males (320–658 mm PCL); (**E**) = 6 females (335–738 mm PCL), 16 males (271–720 mm PCL).

vessels (16%), rod and reel (12%), gill net (3%), and other miscellaneous gear types (2%).

Following capture, the sex of each specimen was determined and the specimen was weighed (to the nearest 0.1 kg), evaluated for sexual maturity, and its body length was measured. Four body length measurements (to the nearest mm) were taken from each individual: precaudal length (PCL, measured from the tip of the snout to the anterior termination of the precaudal pit), fork length (FL), natural total length (NTL, measured with tail in a "natural" swimming position [Parsons, 1985]), and total length (TL, measured with dorsal portion of tail bent parallel to the body axis). Unless otherwise noted, precaudal lengths are used throughout this study. Regression relationships of TL, NTL, and FL on PCL were derived to facilitate comparison with other studies.

The claspers of males were measured from the clasper tip to the anterior termination of the vent. The siphon sac was measured from the base of the clasper fin (where the sac originates) to the anterior termination of the sac. The condition of the seminal vesicles was also recorded. Male maturity was indicated by calcification of the claspers and the presence of a fully formed siphon sac (Clark and von Schmidt, 1965; Parsons, 1983b). Gonadosomatic indices (GSIs, Parsons, 1983b) were calculated for male sharks with the formula

$$GSI = \textit{gonad weight}\ (g)/\textit{body weight}\ (g) \times 100.$$

The ovaries and uteri of females were examined macroscopically for indicators of maturity, such as yolking eggs, embryos, or placental scars. Vitellogenic oocytes were easily identified by their bright yellow coloration in contrast to the pale white coloration of nonvitellogenic oocytes. If vitellogenic oocytes were present, the diameter of all vitellogenic oocytes in the ovary was measured (to the nearest 0.1 mm) with dial calipers. If maturing oocytes were not present, the most differentiated nonvitellogenic oocytes (which were noticeably larger that the rest of the oocytes in the ovary) were measured. Any embryos were removed from the uteri, counted, their sex determined, and measured (TL). Female maturity was determined by the presence of embryos, umbilical scars in the uterus from previous pregnancy, or the presence of large vitellogenic oocytes (greater than 15 mm diameter) nearing ovulation (Parsons, 1983b).

A segment of the vertebral column extending from the cervical region (dorsal to the branchial chamber) to the origin of the first dorsal fin was removed from each specimen and frozen. Vertebrae from the cervical portion of the spinal column were used for aging because of the shallow concavity of the intermedalia and the size similarity between adjacent centra in this region. The shallow concavity of the vertebrae facilitated processing and measurement during aging (Branstetter and McEachran, 1986). Age determination was attempted on 890 of the 1093 specimens collected during the study. Vertebrae selected for aging were separated from the frozen segment, defrosted, and soaked in 5% sodium hypochlorite for 5–30 min (depending on size) and were removed from the solution as soon as all excess connective tissue had been dissolved. A longitudinal section approximately 500 µm thick was cut from the center of each vertebrae with a Mark-V wafering saw and allowed to air-dry for at least 24 h. Dried sections were then attached to glass slides with Accu-mount 60 mounting medium and hand polished with wet 600-grit sandpaper to a thickness of approximately 350 µm. Several staining or ring elucidation techniques (e.g. Parsons, 1983a; Branstetter, 1986; Brown and Gruber, 1988; Hoenig and Brown, 1988) failed to significantly increase increment visibility; therefore all aging was performed with unstained vertebral sections.

Vertebral sections were read on a dissecting microscope with transmitted light and a polarizing filter at 20× magnification. Increment radii and marginal increments were measured through the center of the corpus calcareum (Fig. 2) with OPTIMAS image analysis software (Media Cybernetics, 1999). Precaudal length was regressed on centrum radius (CR) for males and females to test for an isometric relationship.

The increments observed in vertebral sections were narrow circuli similar to those described by Simpfendorfer (1993), as opposed to the growth bands described by Branstetter (1987a). All increment counts were made without knowledge of the size, sex, or collection date of the specimen. The primary reader (senior author) counted increments on all samples twice; each reading was separated by at least two months. Increment counts that were not in agreement were counted a third time. If the third count did not agree with one of the first two counts, the specimen was excluded from the analysis. The secondary reader (coauthor) counted increments from all specimens not eliminated by the primary reader's analysis. Between-reader disagreements were re-examined by both observers simultaneously. All specimens for which a consensus could not be reached were discarded. The index of average percentage error (IAPE; Beamish and Fournier, 1981) was used to estimate precision between the final readings of the primary reader and the initial readings of the secondary reader

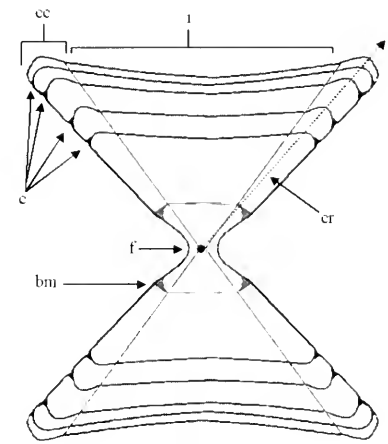

Figure 2

Diagrammatic representation of a vertebral section; bm = birth mark, c = circuli, cc = corpus calcareum, cr = line of centrum radii and annuli measurements, f = focus, i = intermedalia.

The annual periodicity of increment formation was verified through marginal increment analysis and focus-to-increment frequency distributions. Absolute marginal increment distances were converted to "relative" marginal increments by dividing the distance between the last increment and the edge of the centrum by the width of the last fully formed growth band (Skomal, 1990; Natanson, et al., 1995). This conversion compensated for differences in growth rates between age classes.

Back-calculated lengths at previous ages were estimated from vertebral measurements by using a modified Fraser-Lee equation proposed by Campana (1990):

$$L_a = L_c + [(C_a - C_c)(L_c - L_0)/(C_c - C_0)],$$

where L_a = length at age;
L_c = length at capture;
C_a = centrum radius from focus to increment a; and
C_c = centrum radius at capture.

L_0 and C_0 are biologically derived intercepts that represent the fish length and centrum radius, respectively, at which the proportionality between fish length and centrum growth are initiated. For the purposes of this study, mean body length and centrum radius at birth were used as the biologically derived constants (Sminkey and Musick, 1995).

The observed age-class data were used to estimate "actual ages" to 0.1 year. These were calculated by the number of circuli present plus growth since the formation of the last circulus. All specimens were given a 1 June birth date, which approximates the middle of the pupping season. This process corrected for growth since the last increment, preventing the potential overestimation of size-at-age that might result from analyzing the data by year class alone. All three types of length-at-age data (observed age class, observed actual age, and back-calculated age) were fitted to the von Bertalanffy growth equation (VBGE; von Bertalanffy, 1938):

$$L_t = L_\infty(1 - e^{-K(t - t_0)}),$$

where L_t = length at age t;
L_∞ = asymptotic length;
K = growth coefficient; and
T_0 = theoretical age at zero length.

Each of the three types were analyzed for sexes combined, as well as for each sex separately. The parameters for the VBGE were estimated through a stepwise Gauss-Newton iterative fitting process computed by JMP statistical analysis software (Anonymous, 1998).

Results

The sharpnose shark was abundant throughout the year in coastal waters within the sampling area. The ratio of males to females in the overall sample was not significantly different from a 1:1 ratio (chi-square test, n=1091, α=0.05, ν=1, χ^2=1.39, P=0.24).

Linear regression of TL, NTL, and FL on PCL resulted in the following equations:

$TL = 29.804 + 1.279PCL$ (n=1009, r^2=0.99, P<0.0001);
$NTL = 31.678 + 1.254PCL$ (n=493, r^2=0.99, P<0.0001);
$FL = 11.249 + 1.075PCL$ (n=1083, r^2=0.99, P<0.0001).

Reproduction and maturity

Size-at-maturity estimates were based on observations of 526 males and 564 females. The smallest fully mature male was 600 mm PCL, and the largest immature male was 615 mm PCL. All males greater than 615 mm PCL and 36% of males from 600 to 615 mm PCL were fully mature. The onset and completion of maturity in male *R. terraenovae* were demonstrated by the onset of development in the claspers and siphon sac (Fig. 3). Males began to mature at 500 mm PCL. The maturation of claspers and siphon sac reached completion approximately one year later, at 600 to 615 mm PCL.

The smallest maturing female was 509 mm PCL and contained one maturing oocyte five mm in diameter. The second smallest maturing female was 529 mm PCL. The smallest gravid female was 591 mm PCL. The largest immature female, based on lack of embryos or uterine scarring, was 611 mm PCL. Females from 591 to 611 mm PCL were either gravid (63%) or contained large (>10 mm diameter) maturing oocytes and were close to their first ovulation (37%). All females greater than 611 mm PCL were mature.

Mean GSI and mean ovarian egg diameter (MOD) both demonstrated prominent peaks during the calendar year. Male GSI values were highest in April and high values were also present in March and May (Fig. 4). However, the seminal vesicles remained turgid and full of semen for some time following the seasonal testicular degeneration which began in May. Female MOD values were highest in May and June. An increase in standard error along with a drop in mean value for the month of June (Fig. 4) demonstrated that ovulation began at that time. The extremely low MOD in July indicated the completion of ovulation.

Litter sizes ranged from one to eight, and generally increased with female PCL (Fig. 5). Mean litter size was 3.85 embryos, and significantly more embryos were found in the left uterus (mean=2.19) than in the right (mean=1.65; chi-square test, n=558, α=0.05, ν=4, χ^2=62.62, P<0.0001). Nonlinear regression of litter size on female PCL resulted in the following equation (n=278, r^2=0.51, P<0.0001):

$$Litter\ size = -11.07 + 0.021\ PCL + 1.37 \times 10^{-4}(PCL - 710.9)^2$$

Rhizoprionodon terraenovae were born at approximately 212 mm PCL. The smallest free-swimming neonate was 190 mm PCL, and the largest full-term embryo was 242 mm PCL. Most pupping occurred from mid-May to early June. However, a small number of neonates appeared as early as mid-April. Consequently, mean embryo total length was at a minimum in July and at a maximum in June (Fig. 6). The sexes of uterine embryos were not significantly different from the expected 1:1 ratio (chi-square test, n=844, α=0.05, ν=1, χ^2=0.076, P=0.78).

Age and growth

Separate linear regressions of PCL on centrum radius (CR) for males and females were not significantly different (ANCOVA, P=0.065) and were therefore combined (Fig. 7) to yield the following formula:

$PCL = 61.80 + 124.48CR$ (r^2=0.963, n=812, P<0.0001).

The regression line slightly overestimated centrum radius for the largest individuals (>700 mm PCL) of both sexes. Data transformation, as well as nonlinear regression, failed to increase the r^2 value, and only the largest specimens were affected.

Nonlinear regression of total body weight on length was significantly different between males and females (ANCOVA after log-transformation, P<0.001), and resulted in the following equations:

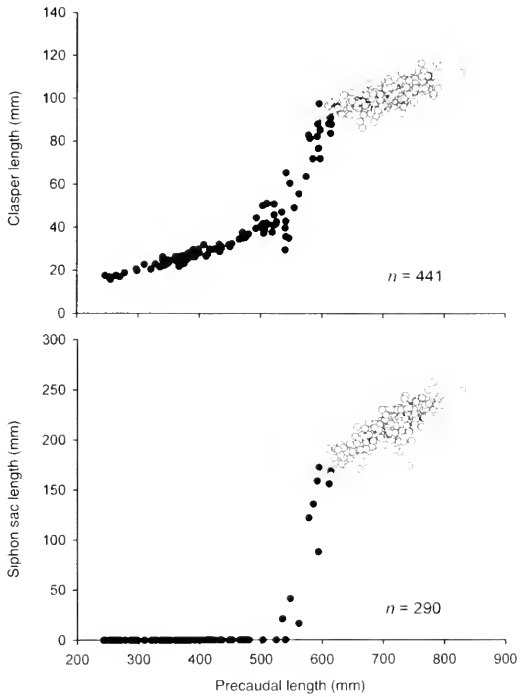

Figure 3

Relation of clasper and siphon sac length to precaudal length for male *R. terraenovae*; (●) represents individuals with uncalcified claspers; (○) represents individuals with fully calcified claspers.

Females: $W_t = e^{(-18.62)}PCL^{(3.04)}$
(r^2=0.99, P<0.0001, n=458);

Males: $W_t = e^{(-18.18)}PCL^{(2.96)}$
(r^2=0.99, P<0.0001, n=454),

where W_t = total body weight.

Aging was attempted on 890 specimens, 812 of which were aged without elimination. Agreement between the first and second counts conducted by the primary reader was 66%, with 91% within one increment, and 99% within two. Those sections that showed disagreement between the first and second reading (n=303) were counted a third time, and 96% agreed with one of the first two readings. The remaining 4% (12 specimens) were excluded from the analysis. Agreement between readers was 72%, with 95% within one increment and 99% within two. Vertebrae for which counts did not agree between readers (246 out of 878) were re-examined by both readers simultaneously. A concurrent age could not be reached on 66 vertebrae, which were eliminated from the study. The IAPE between the final readings of the primary reader and the initial readings of the secondary reader was 7.4%. Size-frequency distributions of the discarded individuals (data not shown) closely matched those of the raw data set and did not indicate the elimination of a large number of individuals from any age class during the aging process.

Mean relative marginal increments for age classes 1+ through 7+ combined demonstrated a minimum in July (Fig. 8). The 0+ age class was excluded from this analysis to ensure that growth from the birth mark did not affect the results. Frequency distributions of focus-to-increment measurements for ages 0+ through 7+ demonstrated single modes for all annuli in each age class for both males and females (Fig. 9).

Most *R. terraenovae* were found to have an increment in the intermedalia and an associated change in the angle of the corpus calcareum, which is similar to the birth mark

described by other authors (e.g. Casey et al., 1985; Branstetter, 1987b; Simpfendorfer, 1993). There were 239 young of the year *R. terraenovae* collected during this study, 88 of which contained no discernible birth mark. All young of the year lacking a birth mark were captured in June and July (Fig. 10), whereas all young of the year captured from August through April had a birth mark. Both marked and unmarked centra were noted in July and showed a readily apparent trend; individuals with a birth mark were significantly larger than those without a birthmark (*t*-test, df=96, t=–7.138, P<0.0001).

Back-calculated lengths-at-age were similar to observed lengths-at-age in all cases, although observed values were slightly higher for all age classes (Table 1). There was no evidence of Lee's phenomenon in the older age classes. Back-calculated size at the birth mark overestimated size at birth as determined by observations of neonates and full-term embryos.

The VBGE estimates calculated by age class, actual age, and back-calculated age demonstrated little variation either within or among data types (Table 2). The VBGE parameters from all data types corresponded well with known life history parameters for size at birth and maximum size. Unless otherwise noted, all comparisons throughout the remainder of this study were based on VBGE estimates derived from the "actual age" data type.

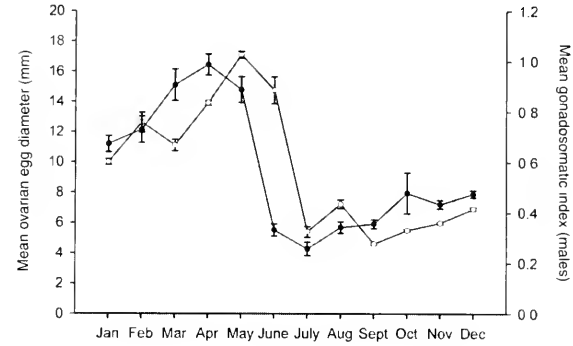

Figure 4

Mean gonadosomatic index and mean ovarian egg diameter by month for female *R. terraenovae*. Open circles indicate females (n=275), closed circles indicate males (n=214). Error bars represent mean ± one standard error.

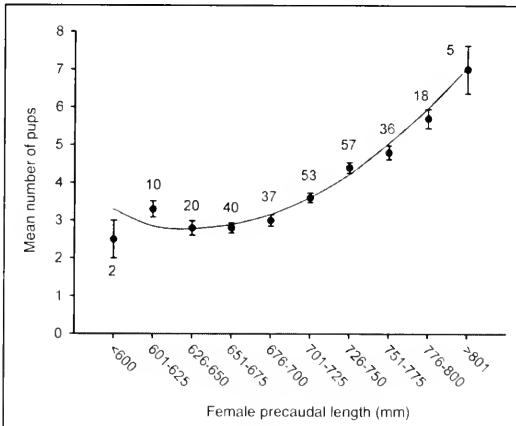

Figure 5

Mean litter size on female size class. Solid line represents best-fit quadratic equation. Numbers indicate sample size for each data point. Error bars represent mean ± one standard error.

Discussion

Reproduction

Length-at-maturity estimates for male *R. terraenovae* were similar among the three published studies. Parsons (1983b) estimated male maturity at ~610 to 653 mm PCL (lengths from other studies were converted to PCL by using the formulae derived from the current study) and Branstetter (1987a) estimated the same at 600 mm PCL. We determined that males reach full maturity at ~600 to 615 mm PCL. The three studies failed to agree on length at maturity for female *R. terraenovae*. Branstetter (1987a) and Parsons (1983b) approximated the size of females at maturity at 660 mm PCL and from 650 to 690 mm PCL, respectively. We found, however, that females mature at a smaller size, from 590 to 610 mm PCL.

The reproductive seasonality of *R. terraenovae* in our study appeared to lack synchrony; males reached their reproductive peak in April and females in May and June. Mature males dissected in late May and June had visibly atrophied testes compared to those collected in April and early May. However, their seminal vesicles were still highly swollen and contained large amounts of semen. This condition indicated that male *R. terraenovae* were still capable of mating during May and June, when female MOD values were highest. Therefore, the mating season of *R. terraenovae* off the southeastern U.S. coast appeared to last from mid May to early July. Simpfendorfer (1992) noted a similar misalignment of peaks in reproductive seasonality between the sexes in *R. taylori*.

The largest litters noted in our study contained eight pups (n=4). This increases the maximum litter size reported for *R. terraenovae* in the northwestern Atlantic

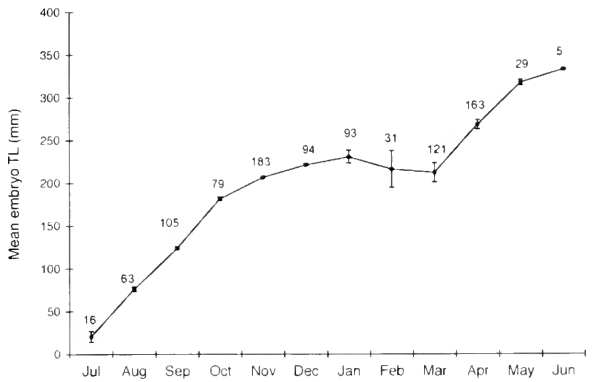

Figure 6

Mean total length by month for embryos collected from April 1997 through March 1999. Numbers indicate sample size for each data point. Error bars represent mean ± one standard error.

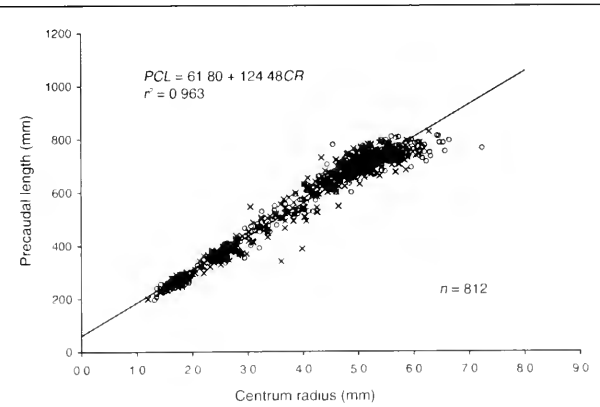

Figure 7

Linear regression of precaudal length (mm) on centrum radius (mm) for *R. terraenovae*; (X) represents males, (○) represents females.

(Parsons, 1983b; Castro and Wourms, 1993). Early reports of up to 12 pups in sharpnose sharks collected from Cuban waters (Bigelow and Schroeder, 1948) were likely the result of misidentification (Castro and Wourms, 1993).

Age and growth

The PCL-CR regression line slightly overestimated centrum radius for large individuals. This trend has also been noted in large female *Carcharhinus obscurus* (Natanson et al., 1995) and appears to result from a change in the slope of the linear relationship as growth becomes asymptotic near the maximum length of the species. This phenomenon was deemed to have a minimal effect on the linear regression formula used in this study. Although the linear relationship appears to undergo an immediate change in slope at about 700 mm PCL, there are not enough data following this change (that is, the animal does not increase substan-

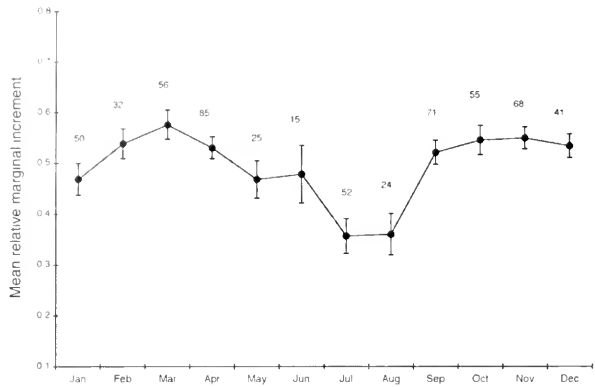

Figure 8

Mean relative marginal increment (mm) by month for age classes 1+ through 7+. Numbers indicate sample size for each data point. Error bars represent mean ± one standard error.

Table 1

Mean, minimum, and maximum lengths-at-age (mm) and statistics for observed actual and back-calculated ages (0–10+ years).

	0+	1+	2+	3+	4+	5+	6+	7+	8+	9+	10+
Females											
Back-calculated											
mean	249	452	556	619	665	698	722	740	754	775	777.9
minimum	189	307	422	521	563	600	627	673	711	754	
maximum	301	573	646	742	764	795	795	800	785	804	
SD	19	32	35	36	35	34	29	28	22	19	
n	379	305	273	232	186	137	90	42	13	5	1
Observed											
mean	320	513	629	676	700	717	741	755	762	788	787.0
minimum	197	391	469	606	615	345	663	688	726	764	
maximum	465	624	707	780	765	805	812	810	796	813	
SD	63	51	49	33	30	66	26	31	23	20	
n	123	32	42	46	50	47	48	29	8	4	1
Males											
Back-calculated											
mean	247	452	564	634	675	695	708	717	728	715	
minimum	191	310	372	519	582	625	651	690	706		
maximum	317	553	681	760	778	809	753	764	743		
SD	21	36	45	40	38	32	24	21	16		
n	337	260	225	191	159	102	49	15	4	1	
Observed											
mean	323	509	600	676	716	722	722	732	743	720	
minimum	200	340	387	578	623	653	661	699	729		
maximum	466	602	730	777	796	828	763	773	757		
SD	63	59	69	46	39	34	24	21	14		
n	116	35	34	32	57	53	35	10	3	1	

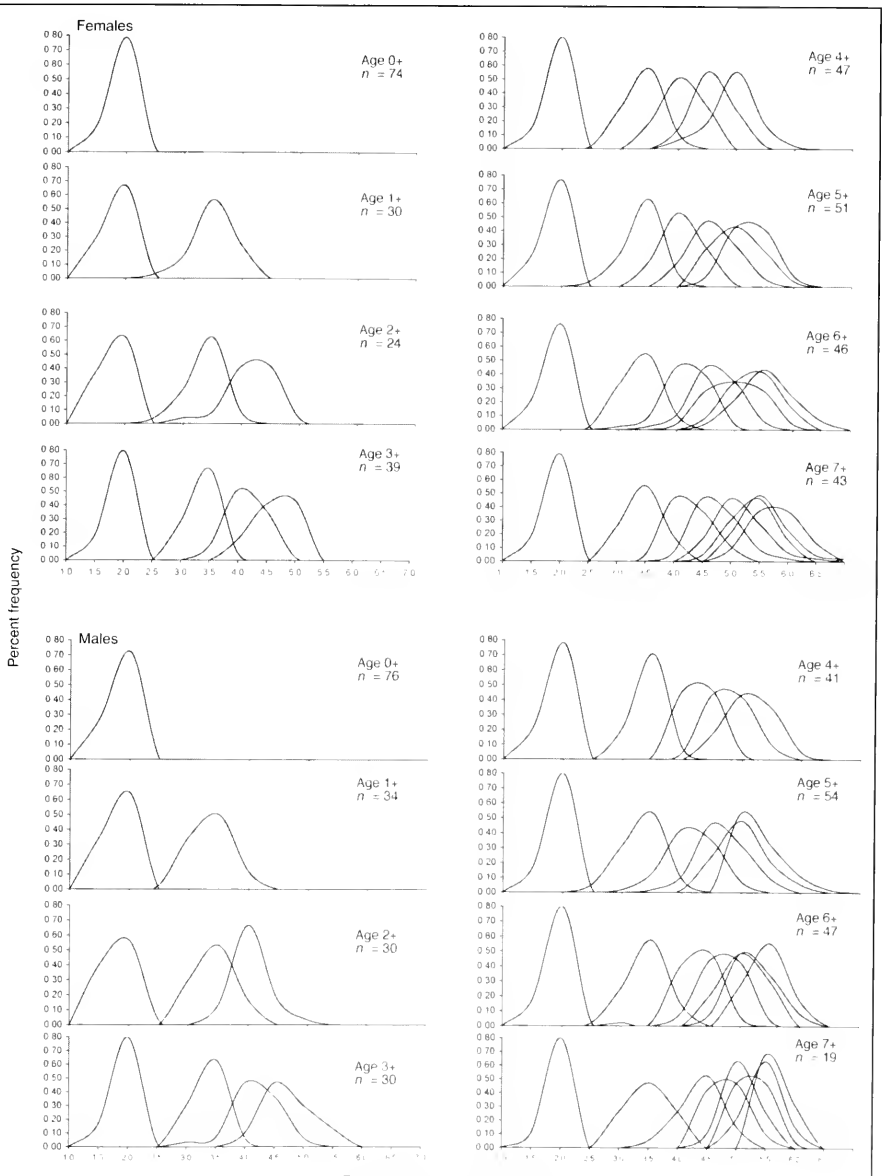

Figure 9

Focus to increment distance (mm) frequency distributions for males and females age 1+ to 7+. The first distribution represents the birth mark in all cases, subsequent distributions represent (from left to right) measurements to the first, second, third, fourth, fifth, sixth, and seventh increments, respectively.

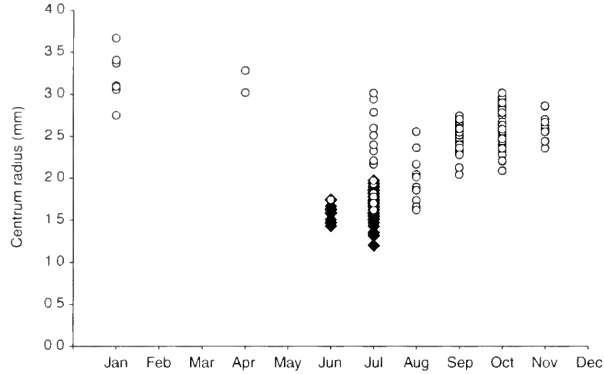

Figure 10

Centrum radius of age 0+ *R. terraenovae*, by month. (♦) represents individuals without a birth mark, (○) represents individuals with a birth mark.

Table 2

Von Bertalanffy growth parameters of *Rhizoprionodon terraenovae* from the southeastern coast of the United States. Von Bertalanffy growth parameters from previous studies in the northern Gulf of Mexico are included for comparison.

	Von Bertanalanffy growth parameters								
Sex	L_∞ (mm PCL)	K	t_0	SE of L_∞	SE of K	SE of t_0	n	Data type	Study
Females	752	0.52	−1.07	5.33	0.025	0.052	433	age class	current
Males	746	0.53	−1.07	6.83	0.030	0.059	379		
Sexes combined	750	0.52	−1.07	4.23	0.019	0.039	812		
Females	749	0.49	−0.94	4.60	0.020	0.046	433	estimated actual age	current
Males	745	0.50	−0.91	5.93	0.024	0.052	379		
Sexes combined	748	0.50	−0.92	3.65	0.015	0.034	812		
Females	738	0.46	−0.90	2.64	0.006	0.015	1856	back-calculation	current
Males	726	0.53	−0.79	3.14	0.009	0.016	1447		
Sexes combined	732	0.49	−0.85	2.02	0.006	0.011	3303		
Sexes combined	820	0.36	−0.99	—	—	—	20	estimated actual age	Branstetter (1987a)
Males	709	0.39 to 0.53	−2.01	—	—	—	15	age class	Parsons (1985)

tially in length following the shift) to reliably fit a second regression line. The back-calculation equation used in our study does not employ the linear regression in its calculations and was minimally affected by the negative bias that this phenomenon had on the slope of the regression.

Marginal increment analysis in the present study indicated that growth increments form in summer. This finding is contrary to that of earlier studies on *R. terraenovae*, which indicated winter deposition (Parsons, 1985; Branstetter and McEachran, 1986; Branstetter 1987a). However, other species in this genus have been shown to deposit increments during the summer months. Simpfendorfer (1993) demonstrated summer (February) increment deposition in *R. taylori* in Australian waters. He cited stress during the breeding season as a possible cause because hepatosomatic index and condition factor in both sexes were low during the mating season, an indication of probable stress. Furthermore, growth increments in elasmobranchs may reflect periods of slow calcareous accretion that have been compressed by increased growth (Gelsleichter, 1998). This pattern of deposition may result in increments from periods of slow growth not becoming

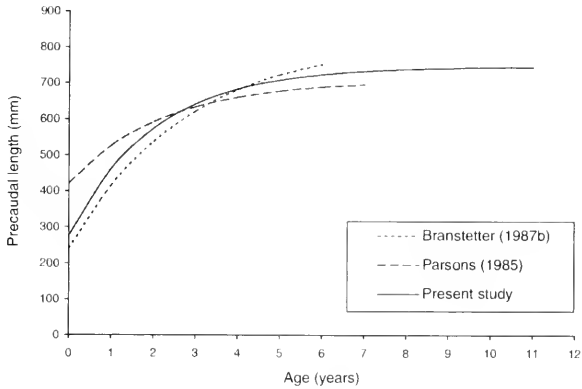

Figure 11

A comparison of growth curves for *R. terraenovae* from the present study with those from previous works by other authors. Growth curve from the present study is based on estimated actual ages for both sexes (parameter values are presented in Table 2).

visible for some time after their actual formation until enough new tissue has grown distally to provide the compression and contrast necessary for reliable identification. In other words, the increments observed in our study first became visible in July, but may have actually formed one to several months earlier. It should be noted that the methods of vertebrae processing and examination followed during our study were more similar to those of Simpfendorfer (1993) than to those of Parsons (1985) or Branstetter (1987a). These methods may have contributed to the close similarity found in both the physical appearance (i.e. that of "check marks" as opposed to pairs of growth bands) and temporal deposition of increments between our study and that of Simpfendorfer (1993).

We found young of the year *R. terraenovae* with and without a birth mark. This is unusual in that most studies that have documented the presence of a birth mark have found one present in all specimens examined (e.g. Casey et al., 1985; Branstetter, 1987b; Simpfendorfer, 1993). Simpfendorfer (1993) suggested that the "birth" mark in *R. taylori* was probably laid down sometime after birth because he observed the same overestimation of size at birth by back-calculations noted previously in our study. No temporal estimation of the lag between birth and the formation of a birth mark has been published. The young-of-the-year *R. terraenovae* examined during our study demonstrated a distinct temporal transition from the lack of a birth mark to the presence of a birth mark (Fig. 10). The data suggest that the birth mark is not actually laid down at birth in June, but approximately one month later in July. This time lag may explain the overestimation of size at birth by back-calculation. It is possible that the mechanism for the formation of the birth mark lies in the switch from embryonic to normal somatic growth, which may not occur immediately following parturition.

The von Bertalanffy growth parameters derived for our study demonstrated differences from those derived for previous studies (Fig. 11). Parsons (1985) estimated an L_∞ of 709 mm PCL, and Branstetter (1987a) 820 mm PCL. L_∞ for our study was 745 mm PCL for males, and 749 mm PCL for females. The t_0 value produced by Parsons was low at –2.01 yr, whereas the values produced by Branstetter (–0.99 yr) and our study (–0.90 yr for males and –0.94 yr for females) agreed well with the known gestation period of approximately 11 months. Parsons (1985) estimated K by several methods, resulting in values ranging from 0.39 to 0.53. The higher values agreed well with the estimates of our study (0.49 for females and 0.50 for males). Branstetter's (1987a) estimate of K was 0.36, lower than that of the current study.

Yearly growth rate estimates by Parsons (1983b) and Branstetter (1987a) revealed an increase of 133 to 211 mm PCL during the first year of life, 94 mm during the second year, 55 mm during the third year, and 16 to 32 mm growth after maturity. We found similar, though slightly higher growth rates: 198 to 202 mm PCL during the first year, 100 to 108 mm during the second, 63 to 69 mm during the third, and from 0 to 46 mm thereafter.

Parsons (1985) determined age at maturity by three methods: extrapolation of growth rates to size at maturity, the VBGE, and Holden's method (Holden, 1974). The estimates produced by these methods ranged from 2.0 to 3.5 for males, and 2.4 to 3.9 for females. Branstetter (1987a) compared his von Bertalanffy-derived estimates to those of Parsons (1985), and found his results in general agreement with Parsons' higher estimates. Branstetter (1987a)

thus concluded that males mature in three years and females in four. In our study, males reached full maturity at 2.4 to 2.6 years of age, making them functionally mature at the third breeding season following birth. Females were found to mature at 2.2 to 2.5 years, which would also result in full maturity just prior to the third postnatal breeding season. Although it was noted in both previously cited studies that males matured six months to one year earlier than females, no such discrepancy in age at maturity between the sexes was apparent in our study.

Differences between studies

The differences between this and previous studies on *R. terraenovae* are likely a combination of many contributing factors. These studies were conducted in different regions at separate times and may reflect clinal or temporal differences (or both) between Gulf of Mexico and northwestern Atlantic *R. terraenovae* populations. However, there are other contributing factors that must be considered as well, most notably differences in data collection and analysis techniques.

Parsons' (1985) growth curves were based on males and were grouped into age classes (not assigned actual ages). His von Bertalanffy parameters were then derived by using the Ford and Walford plot method (Parsons, 1985), requiring the use of mean lengths of each age class. This age class grouping does not take into account growth since the deposition of the last increment, and may therefore bias the Ford and Walford plot by pulling the data to a faster asymptote (Branstetter and McEachran, 1986; Branstetter, 1987a;). This bias produced a low L_{∞} (706 mm PCL) and t_0 (–2.01 years) in Parsons' estimates (Branstetter and McEachran, 1986; Branstetter, 1987a). This phenomenon was not evident in VBGE estimates based on age classes in our study, which were very similar to estimates based on actual ages (Table 2), and was probably due to the fact that iterative fitting of age data to the VBGE by computer software (an option unavailable to Parsons at the time of his study) is less sensitive to unaddressed growth than the graphically based Ford and Walford plot method.

Although the aging technique used by Branstetter (1987a) was similar to that of our study (counts on longitudinal sections of cervical centra), Parsons' (1985) aging technique took ring counts from the face of centra that had been removed from a more posterior region of the vertebral column than the region chosen in our study. It has been stated by several authors (Branstetter and McEachran, 1986; Martin and Cailliet, 1988; Kusher et al., 1992) that increment counts made from sections of vertebral centra are generally preferable to those taken from the face of unsectioned centra. Sectioned centra allow for better documentation of the increment structure near the edge because the increments become narrower and more difficult to delineate with increasing age (Branstetter and McEachran, 1986; Martin and Cailliet, 1988; Kusher et al., 1992). This distinction is critical when the potential consequences of age underestimation (including overestimation of K, growth rate, and maximum sustainable yield) are considered.

Based on comparison of our work to that of previous studies (Branstetter, 1981, 1987a; Parsons, 1983a, 1983b, 1985), there may be differences between the Gulf of Mexico and southeastern U.S. Atlantic populations of Atlantic sharpnose sharks. The question then becomes whether these differences are clinal or temporal in nature. Clinal variation, for instance, may explain the differences noted in size and age at maturity in female *R. terraenovae*. Simpfendorfer (1993) noted differences in size at maturity between populations of *R. taylori* in Australia, as did Parsons (1993) and Carlson et al. (1999) between populations of *Sphyrna tiburo* and *Carcharhinus acronotus*, respectively, off the Gulf coast of Florida. However, the extended time frame between the current and previous studies (15 to 20 years), also opens the possibility that the differences are related to a temporal change in population structure of the species across the entire Gulf and Western Atlantic region. In the earlier studies, data were collected during a time when fishing pressure (both directed and indirected) on *R. terraenovae* was lower than at present, and fisheries were shown to have dramatic effects on shark populations in less time (Anonymous[1]). The differences noted between the studies may thus be a manifestation of temporal changes in population structure of the species as a whole over the last two decades. A more current study on Gulf of Mexico *R. terraenovae* is needed to properly address these potential population differences.

Conclusion

Small shark species such as *R. terraenovae* tend to show rapid growth in the first few years of life and a dramatically slower growth rate once maturity is reached. This aspect of their growth complicates age estimation by vertebral increments because the most recent marks in older specimens are so closely spaced that accurate counting and measurement become problematic. The overlapping of increments in these older specimens or the lack of identifiable increment formation altogether due to asymptotic growth may lead to an underestimation of ages in large adults. Althhough the maximum age demonstrated in our study was 11+ years, the actual life span of *R. terraenovae* may be longer.

The life history parameter estimates that have been presented in our study are based on one of the largest short-term samples collected for any study of elasmobranch life history to date. The most significant aspect of this study is the documentation of differences in size and age at maturity between female *R. terraenovae* in the Gulf of Mexico and females off the southeastern U.S. coast. A difference in age of maturity of one year in an animal with a relatively short life span, such as *R. terraenovae,* can have a dramatic effect on the outcome of population models (see Cortes, 1995). Although the documentation of age at maturity differences by different researchers may be highly susceptible

[1] Anonymous. 1993. Fishery management plan for sharks of the Atlantic Ocean, 167 p. U.S. Dep. Commerce., NOAA, NMFS, Silver Spring, MD 20910.

to analytical bias during the aging process, the documentation of differences in size at maturity is unmistakable.

Acknowledgments

This project was funded by the University of Charleston (South Carolina), The Marine Resources Monitoring, Assessment and Prediction program (MARMAP), the Cooperative Atlantic States Shark Pupping and Nursery Survey (COASTSPAN), and the W. F. Pate Memorial fund. The authors would like to thank the following: MARMAP personnel; the Southeast Area Monitoring and Assessment Program (SEAMAP) personnel; Glenn Ulrich and the crew of the RV *Anita*; Dean Grubbs, Jack Musick, and the crew of the RV *Bay Eagle*; Bill Roumillat and the SCDNR Inshore Fisheries Project; Reese Hair and the crew of the FV *Malachi III*; Steve Johnson and the crew of the FV *Miss Gina*; and Gary Mckillop and the crew of the FV *Bonzai*, for assistance in sample collection. Patrick Harris, Charles Wenner, Steven Branstetter, Antony Harold, Glenn Parsons, Enric Cortes, Jim Gelsleichter, Colin Simpfendorfer, and Gregor Cailliet offered advice and constructive criticism.

Literature cited

Anonymous.
1998. JMP: Statistics and graphics guide, 593 p. SAS Institute, Inc., Cary, NC.

Beamish, R. J., and D. A. Fournier.
1981. A method for comparing the precision of a set of age determinations. Can. J. Fish. Aquat. Sci. 38:982–983.

Bigelow, H. B., and W. C. Schroeder.
1948. Sharks. *In* Fishes of the western North Atlantic, part one, vol.1 (J. Tee-Van, C. M. Breder, S. F. Hildebrand, A. E. Parr and W. C. Schroeder, eds.). p. 59–546. Mem. Sears Found. Mar. Res., Yale Univ.

Branstetter, S.
1981. Biological notes on the sharks of the North Central Gulf of Mexico. Contrib. Mar. Sci. 24:13–34.
1986. Biological parameters of the sharks of the Northwestern Gulf of Mexico in relation to their potential as a commercial fishery resource. Ph.D. diss., 138 p. Texas A&M University, TX.
1987a. Age and growth validation of newborn sharks held in laboratory aquaria, with comments on the life history of the Atlantic sharpnose shark, *Rhizoprionodon terraenovae*. Copeia 1987(2):291–300.
1987b. Age and growth estimates for blacktip, *Carcharhinus limbatus*, and spinner, *C. brevipinna*, sharks from the northwestern Gulf of Mexico. Copeia 1987(4):964–974.
1990. Early life-history implications of selected carcharhinid and lamnoid sharks of the northwest Atlantic. *In* Elasmobranchs as living resources: advances in the biology, ecology, systematics, and the status of the fisheries (H. L. Pratt Jr., S. H. Gruber, and T. Taniuchi, eds.), p. 17–28. U.S. Dep. Commer., NOAA Tech. Rep. NMFS 90.

Branstetter, S., and J. D. McEachran.
1986. Age and growth of four carcharhinid sharks common to the Gulf of Mexico: a summary paper. *In* Indo-Pacific fish biology, proceedings of the second international conference on Indo-Pacific fishes (T. Uyeno, R. Arai, T. Taniuchi, and K. Matsuura, (ds.), p. 361–371. Ichthyological Soc. of Japan, Tokyo.

Brown, C. A., and S. H. Gruber.
1988. Age assessment of the lemon shark, *Negaprion brevirostris*, using tetracycline validated vertebral centra. Copeia 1988(3):747–753.

Campana, S. E.
1990. How reliable are growth back-calculations based on otoliths? Can. J. Fish. Aquat. Sci. 47:2219–2227.

Carlson, J. K., E. Cortes, and A. G. Johnson.
1999. Age and growth of the blacknose shark, *Carcharhinus acronotus* in the Eastern Gulf of Mexico. Copeia 1999(3): 684–691.

Casey, J. G., H. L. Pratt Jr., and C. E. Stillwell.
1985. Age and growth of the sandbar shark (*Carcharhinus plumbeus*) from the western North Atlantic. Can. J. Fish. Aquat. Sci. 42:963–975.

Castro, J. I.
1983. The sharks of North American waters, 180 p. Texas A&M Univ. Press, College Station, TX.
1988. Investigations in the reproductive biology of sharks. Ph.D. diss., 110 p. Clemson Univ., SC.
1993. The shark nursery of Bulls Bay, South Carolina, with a review of the shark nurseries of the southeastern coast of the United States. Environ. Biol. Fishes 38:37–48.

Castro, J. I., and J. P. Wourms.
1993. Reproduction, placentation, and embryonic development of the Atlantic sharpnose shark, *Rhizoprionodon terraenovae*. J. Morph. 218:257–280.

Clark, E., and K. von Schmidt.
1965. Sharks of the central gulf coast of Florida. Bull. Mar. Sci. 15:13–83.

Cortes, E.
1995. Demographic analysis of the Atlantic sharpnose shark, *Rhizoprionodon terraenovae*, in the Gulf of Mexico. Fish. Bull. 93:57–66.

Gelsleichter, J.
1998. Vertebral cartilage of the clearnose skate, *Raja eglanteria*: development, structure, ageing, and hormonal regulation of growth. Ph.D diss., 215 p. College of William and Mary, Gloucester Point, VA

Heist, E. J., J. A. Musick, and J. E. Graves.
1996. Mitochondrial DNA diversity and divergence among sharpnose sharks, *Rhizoprionodon terroenovae*, from the Gulf of Mexico and Mid-Atlantic Bight. Fish. Bull. 94:664–668.

Hoenig, J. M., and C. A. Brown.
1988. A simple technique for staining growth bands in elasmobranch vertebrae. Bull. Mar. Sci. 42:334–337.

Holden, M. J.
1974. Problems in the rational exploitation of elasmobranch populations and some suggested solutions. *In* Sea fisheries research (F. R. Harden Jones, ed.), p. 117–137. Elek (Scientific books), London.

Kusher, D. I., S. E. Smith, and G. M. Cailliet.
1992. Validated age and growth of the leopard shark, *Triakis semifasciata*, with comments on reproduction. Environ. Biol. Fishes 35:187–203.

Martin, L. K., and G. M. Cailliet.
1988. Age and growth determination of the bat ray, *Myliobatis californica*, in central California. Copeia 1988(3): 762–773.

Media Cybernetics
1999. Optimas image analysis software, version 6.51. Media Cybernetics, L. P., Silver Spring, MD.

Natanson, L. J., J. G. Casey, and N. E. Kohler.
1995. Age and growth estimates for the dusky shark, *Carcharhinus obscurus*, in the western North Atlantic Ocean. Fish. Bull. 93:116–126.

Parsons, G. R.
1981. Growth and reproduction of the Atlantic sharpnose shark, *Rhizoprionodon terraenovae* (Richardson). M.S. thesis, 71 p. Univ. of South Alabama, Mobile, AL.
1983a. An examination of the vertebral rings of the Atlantic sharpnose shark, *Rhizoprionodon terraenovae*. Northeast Gulf Sci. 6:63–66.
1983b. The reproductive biology of the Atlantic sharpnose shark, *Rhizoprionodon terraenovae* (Richardson). Fish. Bull. 81:61–73.
1985. Growth and age estimation of the Atlantic sharpnose shark, *Rhizoprionodon terraenovae*: a comparison of techniques. Copeia 1985(1):80–85.
1993. Geographic variation in reproduction between two populations of the bonnethead shark, *Sphyrna tiburo*. Environ. Biol. Fishes 38:25–35.

Simpfendorfer, C. A.
1992. Reproductive strategy of the Australian sharpnose shark, *Rhizoprionodon taylori* (Elasmobranchii: Carcharhinidae), from Cleveland Bay, Northern Queensland. Aust. J. Mar. Freshwater Res. 43:67–75.
1993. Age and growth of the Australian sharpnose shark, *Rhizoprionodon taylori*, from North Queensland, Australia. Environ. Biol. Fishes 36:233–241.

Skomal, G. B.
1990. Age and growth of the blue shark, *Prionace glauca*, in the North Atlantic. M.S. thesis, 82 p. Univ. of Rhode Island, Kingston, RI.

Sminkey, T. R., and J. A. Musick.
1995. Age and growth of the sandbar shark, *Carcharhinus plumbeus*, before and after population depletion. Copeia 1995(4):871–883.

von Bertalanffy, L.
1938. A quantitative theory of organic growth (inquiries on growth laws II). Hum. Biol. 10:181–213.

A general framework for integrating environmental time series into stock assessment models: model description, simulation testing, and example

Mark N. Maunder
George M. Watters

Inter-American Tropical Tuna Commission
Scripps Institution of Oceanography
8604 La Jolla Shores Drive
La Jolla, California 92037-1508
E-mail address (for M. N. Maunder): mmaunder@iattc.org

Abstract—We present a method to integrate environmental time series into stock assessment models and to test the significance of correlations between population processes and the environmental time series. Parameters that relate the environmental time series to population processes are included in the stock assessment model, and likelihood ratio tests are used to determine if the parameters improve the fit to the data significantly. Two approaches are considered to integrate the environmental relationship. In the environmental model, the population dynamics process (e.g. recruitment) is proportional to the environmental variable, whereas in the environmental model with process error it is proportional to the environmental variable, but the model allows an additional temporal variation (process error) constrained by a log-normal distribution. The methods are tested by using simulation analysis and compared to the traditional method of correlating model estimates with environmental variables outside the estimation procedure. In the traditional method, the estimates of recruitment were provided by a model that allowed the recruitment only to have a temporal variation constrained by a log-normal distribution. We illustrate the methods by applying them to test the statistical significance of the correlation between sea-surface temperature (SST) and recruitment to the snapper (*Pagrus auratus*) stock in the Hauraki Gulf–Bay of Plenty, New Zealand. Simulation analyses indicated that the integrated approach with additional process error is superior to the traditional method of correlating model estimates with environmental variables outside the estimation procedure. The results suggest that, for the snapper stock, recruitment is positively correlated with SST at the time of spawning.

Manuscript accepted 20 September 2002.
Fish. Bull. 101:89–99 (2003).

Identifying a clear relationship between an environmental variable and processes in the dynamics of the population (recruitment, natural mortality, growth) or the fishery (catchability) would allow improved estimation and prediction of model parameters and derived quantities. It is well known that the environment plays a large role in the population dynamics and catchability of fish stocks. Many researchers (Green, 1967; Joseph and Miller, 1989; Hinton and Nakano, 1996; Lehodey et al., 1997; Shepherd et al., 1984) have identified correlations between population processes and environmental factors, and others (Hunter, 1983; Bertignac et al., 1998; Lehodey et al., 1998) have suggested hypotheses for the underlying causes of these correlations. Incorporation of environmental time series into stock assessment models may provide additional information to help estimate model parameters, particularly when fishing observations (catch, effort, length-frequencies) are missing. For the management of fish stocks, it can be advantageous to be able to predict future catch rates and population sizes. Because there is often a delay due to the propagation of the recruitment signal in the population structure or because statistical and numerical models can provide predictions for some environmental variables (e.g. temperature) (or for both reasons), the relationship can be used to predict future catch rates or population sizes.

Statistical catch-at-age analysis (e.g. Fournier and Archibald, 1982; Deriso et al., 1985; Methot, 1990) is more appropriate than cohort analysis (virtual population analysis) to include relationships between an environmental variable and processes in the dynamics of the population. In cohort analysis, if there are missing data, they are simply extrapolated without any statistical methods, which may cause bias in the parameter estimates. Also, the potential correlation with an environmental series is calculated outside of the estimation procedure, producing several disadvantages, including the loss of information and the difficulty of propagating uncertainty (Maunder, 1998a, 2001a, 2001b). However, in statistical catch-at-age analysis, there are robust statistical methods (maximum likelihood, with all the parameters estimated together by obtaining the best fit between predicted and observed data) that allow inclusion of multiple data sets and the integration of the environmental series into the stock assessment model. These methods automatically allow for missing data and provide confidence intervals, and the hypotheses can be easily incorporated and tested.

The methods used to integrate the environmental series into the stock assessment model can be applied to different processes in the population, but are illustrated here with the case of recruitment. Recruitment is the fundamental process in the population dynamic that is responsible for the fluctuations of the stock size. Many studies (e.g. Francis, 1993) show that environmental variables affect the recruitment. In statistical catch-at-age analysis, recruitment combines an average value with an annual deviate, constrained by using a

distributional assumption (e.g. Maunder and Starr, 2001). This constraint allows the estimation when there is no information (i.e. missing data). Traditional methods that relate recruitment to environmental factors use correlation analysis of an environmental time series with estimates of recruitment from a stock assessment model. For example, cohort analysis is first used to generate a time series of recruitment. Then the time series of recruitment is regressed against sea-surface temperature (SST). This two-step procedure has a number of disadvantages (Maunder, 1998a, 2001a, 2001b), including the loss of information and the difficulty of propagating uncertainty.

We introduce a method suggested by Maunder (1998a; see Maunder and Starr, 2001) that incorporates environmental time series into stock assessment models and tests the significance of the correlation between the population processes and the environmental time series. We test the model with simulated data and compare the results to correlating model estimates with environmental variables outside the estimation procedure. We illustrate this method with an application that investigates the correlation between SST and recruitment within the context of a statistical catch-at-age analyses used to assess snapper (*Pagrus auratus*) in the Hauraki Gulf–Bay of Plenty, New Zealand (Maunder and Starr, 2001).

Materials and methods

Integrating environmental indices into stock assessment models

Parameters that relate the environmental time series to population processes were included in the statistical catch-at-age stock assessment model. We added additional structure to the stock assessment model for each parameter of the stock assessment model (X) that was hypothesized to 1) have temporal variation, 2) be correlated with an environmental time series, and 3) have sufficient information in the data to be estimated for multiple time periods. This structure included a mean value for the stock assessment model parameter (μ), temporal deviations in the stock assessment model parameter (ε_t), a parameter that relates the environmental series to the stock assessment model parameter (β), and a scaling parameter (α) that ensures that μ is the mean value for the stock assessment model parameter over the time period used in the model.

$$X_t = \mu \exp(\alpha + \beta I_t + \varepsilon_t), \quad (1)$$

where t = time, and
I_t = the value of the environmental time series at time t.

The parameter α ensures that μ is equal to the mean over the whole time period (Gilbert[1]; see Maunder and Starr, 2001). Therefore, α removes the log normal bias and bias caused by an unnormalized environmental time series and is defined as

$$\alpha = \ln\left(\frac{n}{\sum \exp(\varepsilon_t + \beta I_t)}\right), \quad (2)$$

where n is the number of time periods.

The additional structure requires that a set of parameters (ε_t) that are constrained by a distributional assumption and two free parameters (μ, β) be estimated. The distributional assumption (referred to as a "prior" in the following description and represented by the negative logarithm of the prior probability, see Eq. 3) is a prior on the degree of temporal variation in the stock assessment model parameter. The default assumption is a normal distribution (assuming that the stock assessment model parameter is lognormally distributed) with mean zero and given standard deviation. Information about this distribution can be obtained from estimates for similar species (e.g. Myers et al., 1995). The prior

$$-\ln \text{ Prior}(\varepsilon \mid \sigma) = \sum_t \frac{(\varepsilon_t)^2}{2\sigma^2} \quad (3)$$

keeps the temporal deviations close to zero if there is no information in the data to the contrary. It is important to note that the prior is also needed to avoid making β a redundant parameter.

The parameters μ and β and the set of parameters ε, are estimated simultaneously with the other parameters of the stock assessment model, and the negative logarithm of the prior is added to the negative log-likelihood function of the stock assessment model. The parameter estimates are really the mode of the posterior distribution, but we treat them in a likelihood context. The influence of the environmental time series can be removed from the analysis by fixing β at zero. Therefore, likelihood ratio tests can be used to determine if the β parameter significantly improves the fit to the data. If the addition of β reduces the total negative log likelihood by more than about 1.92 units ($\chi^2_{1,\alpha=0.05}$), then the additional parameter significantly improves the fit to the data at the 0.05 level, and there is a statistically significant correlation between the population process and the environmental time series. Similar tests can be performed to test the significance of the set of temporal deviation parameters, ε_t, by taking into account the number of additional parameters. Hilborn and Mangel (1997) provided a simple description of the likelihood ratio test. (The Akaike information criterion or the Bayes information criterion could also be used.) Therefore, by fixing, or not, β or ε at zero we can define three types of statistical models:

1 Traditional model
β is fixed at zero, the parameter set ε_t is estimated, and a significant relationship is determined by testing if the correlation coefficient between ε_t and the environmental time series is significantly different from zero.

[1] Gilbert, D. J. 1999. Personal commun. National Institute of Water and Atmospheric Research Limited, P.O. Box 14-901, Wellington, New Zealand.

2 Environmental model
β is estimated, each value in the parameter set ε_t is fixed at zero, and a significant relationship is determined by testing if $\beta = 0$, using a likelihood ratio test.
3 Environmental model with process error
Both β and ε_t are estimated and a significant relationship is determined by testing if $\beta = 0$, with a likelihood ratio test.

Simulation testing

Simulation analysis was carried out to test the performance of the integrated approach and to compare this approach to the traditional model. A simple age-structured model (Appendix 1) was set up to simulate a population for 20 years, starting from an unexploited population and generating catch, effort, and catch-at-age data. The simulated recruitment was generated as having a component based on an environmental time series and a random component. Each component was given the same variance (0.6^2). The environmental time series was randomly generated with $\beta = 1$ for each simulation. The standard deviation of the observation error in the CPUE index, σ_{CPUE}, was set at 0.6, and the sample size of the catch-at-age data was set to 50. The same age-structured model was then fitted to the data to estimate the model parameters. The three models defined in the previous section (traditional model, environmental model, and environmental model with process error) were tested with the simulated data. In addition to the parameters outlined in the description of the three models, average recruitment, the catchability coefficient, and the standard deviation of the fit to the CPUE data were also estimated. We also used a model that had constant recruitment to provide likelihood values to use in testing the significance of the environmental model.

The simulation analysis was repeated 500 times for four scenarios: 1) using catch-at-age data for all years, 2) using catch-at-age data for the first 10 years, 3) using catch-at-age data for the last 10 years, 4) using catch-at-age data for all years, but using $\beta = 0$ when generating the simulated data. Scenario 4 was used to investigate the probability of type-I error of the models when used in combination with the statistical tests. For each set of simulated data and each model, we determine how often a significant relationship between the logarithm of annual recruitment and the environmental time series is detected, the estimate of the slope of the relationship between the logarithm of annual recruitment and the environmental time series, the estimates of average recruitment, and the depletion level (ratio of current to unexploited biomass). We also calculate minimum-width 95% confidence intervals for average recruitment, using the likelihood profile method for the simulated data sets with catch-at-age data for all years.

Application: relating recruitment in the Hauraki Gulf–Bay of Plenty snapper stock to SST

Recruitment to the Hauraki Gulf snapper (*Pagrus auratus*) stock is correlated with temperature (Paul, 1976). The abundance of 1+ snapper in the Hauraki Gulf estimated by trawl surveys has been shown to have a positive correlation with SST (Francis, 1993) and air temperature (Gilbert, 1994) around or just after the time of spawning in the previous year. This relationship has also been shown with catch-at-age analysis to continue to hold as snapper enter the fishery at ages 4 and older (Maunder and Starr, 1998).

We applied the integrated approach described in this study in combination with the age-structured statistical catch-at-age model described in Maunder and Starr (2001) to the Hauraki Gulf–Bay of Plenty snapper stock. The model was fitted to catch-at-age data and biomass estimates. The biomass estimates were available for 1985 and 1994 and were obtained from analysis of tagging data. The majority of the catch-at-age data were available from 1990 to 1997, but there were some catch-at-age data of dubious quality, small sample size, and high variability for 1970 to 1973. The annual recruitment at age 1 was estimated for the time period of the model (1970–98) and also for 18 age classes (ages 2 to 19) that comprised the initial conditions in 1970.

Results

Simulation analysis

For all four sets of simulated data the environmental model had the highest probability of detecting a relationship between recruitment and the environmental time series (Table 1). This model had a very high probability of detecting a relationship even when there was no relationship in the simulated data (Table 1D). This indicates that the likelihood ratio test is not appropriate for the environmental model (see Appendix III). For all data sets, except that with only catch-at-age data in the first 10 years, the traditional model had a higher probability of detecting a relationship between recruitment and the environmental time series than did the environmental model with process error. The environmental model with process error had a lower probability of detecting a true relationship than the traditional model, but also had a slightly lower probability of type-I error (the probability of incorrectly accepting a nonexistent relationship) than the traditional model. The probability of detecting a relationship was reduced as the number of catch-at-age data sets was reduced.

The environmental model with process error did not show any bias in the estimate of the slope of the relationship between the logarithm of annual recruitment and the environmental time series, β (Table 1). For this model, the variation in the estimates of β increased when fewer years with catch-at-age data were available. The environmental model showed a small negative bias and slightly more error in the estimates of β. The traditional model showed a large negative bias in the estimate of the slope of the relationship between the logarithm of annual recruitment and the environmental time series, and this bias increased as the amount of catch-at-age data was reduced. The traditional method also had larger error, which increased as less catch-at-age data were available.

The errors in the estimates of average recruitment and B_{cur}/B_0 increased slightly with less catch-at-age data

Table 1

(**A**) Results from the simulation analysis in which all the catch-at-age data were used. % = percentage of data sets that produced a significant relationship between the environmental time series and recruitment; β = average (average absolute relative error) of the estimates of the slope of the relationship between the environmental time series and recruitment; R_0 = average (average absolute relative error) of the estimates of the average recruitment; B_{cur}/B_0 = average error (average absolute relative error) in the estimate of the ratio of current to unexploited biomass. β was set to 1 when generating the simulated data. (**B**) Results from the simulation analysis using only the first 10 years of catch-at-age data. β was set to 1 when generating the simulated data. (**C**) Results from the simulation analysis using only the last 10 years of catch-at-age data. β was set to 1 when generating the simulated data. (**D**) Results from the simulation analysis using all the catch-at-age data, but setting $\beta = 0$ when generating the simulated data. (Absolute, rather than relative, error was used for β.) EMwPE = environmental model with process error.

	%	β	R_0	B_{cur}/B_0
A				
Traditional	92	0.86 (0.25)	996 (0.05)	−0.01 (0.15)
Environmental	99	0.95 (0.25)	1,024 (0.10)	0.03 (0.24)
EMwPE	83	1.01 (0.23)	988 (0.05)	−0.04 (0.14)
B				
Traditional	57	0.45 (0.55)	1,011 (0.07)	−0.03 (0.17)
Environmental	95	0.94 (0.33)	1,078 (0.17)	0.01 (0.27)
EMwPE	60	1.05 (0.30)	1,004 (0.07)	−0.03 (0.15)
C				
Traditional	81	0.68 (0.36)	1,022 (0.09)	0.04 (0.21)
Environmental	97	0.95 (0.32)	1,035 (0.10)	0.04 (0.25)
EMwPE	74	1.00 (0.26)	1,007 (0.08)	−0.02 (0.19)
D				
Traditional	3	−0.01 (0.20)	1,005 (0.04)	0.01 (0.10)
Environmental	61	−0.02 (0.22)	1,038 (0.09)	0.07 (0.21)
EMwPE	2	−0.01 (0.21)	1,003 (0.04)	0.01 (0.10)

Table 2

Results related to the confidence intervals for average recruitment from the simulation analysis obtained by using all the catch-at-age data. EMwPE = Environmental model with process error.

	Lower bound average	Upper bound average	Lower bound SD	Upper bound SD	True is within	True is below	True is above
Traditional	888	1,120	59	132	0.91	0.03	0.08
Environmental	963	1,117	94	176	0.44	0.32	0.24
EMwPE	887	1,118	56	120	0.92	0.01	0.07

(Table 1). The errors in these estimates were slightly greater for the environmental model (more bias and larger absolute error) than for the environmental model with process error and traditional model.

The confidence intervals on R_0 were, on average, greater for the traditional and environmental model with process error than for to the environmental model (Table 2), which greatly underestimated the width of the confidence intervals. However, the confidence intervals for the traditional and environmental model with process error showed the true value falling below the confidence interval less often than it fell above it.

As expected, an environmental relationship was more difficult to correctly detect with the traditional model in situations with missing data (e.g. when catch-at-age data were missing in the last few years of the series), and, as stated above, using the environmental model is inappropriate because it has a high probability of detecting a significant relationship when none exists. The environmental model also has a tendency to under estimate the width of the confidence interval for R_0 and the true value frequently falls outside of this confidence interval. Therefore, the environmental model with process error is the model of choice.

Application: relating recruitment in the Hauraki Gulf–Bay of Plenty snapper stock to SST

The environmental model with process error has the lowest negative log-likelihood, but this model has many more parameters than the environmental model (Table 3).

Table 3

Results from applying the three methods (traditional, environmental, and environmental with process error) to the snapper application. Constant = recruitment is constant each year and equal to the average recruitment. EMwPE = environmental model with process error. n/a = not applicable.

	Average recruitment	β	-ln(Likelihood)	Number of parameters
Constant	13,315 (11,381–15,381)	n/a	482.5	3
Traditional	11,406 (8,500–14,603)	0.20	466.8	50
Environmental	13,530 (11,527–15,569)	0.48	473.5	4
EMwPE	12,029 (9,147–15,328)	0.55	464.4	51

Using the likelihood ratio test at the 0.05 level and compensating for the difference in the number of parameters being estimated in each model, we consider the environmental model to be the model of choice. If the likelihood ratio test were used, the environmental model with process error would be chosen over the traditional model, indicating a statistically significant correlation between SST and recruitment. Due to the weaknesses of the environmental model discussed above, we concentrated on the results of the traditional model and the environmental model with process error.

The time series of estimated recruitments from the traditional model showed very little annual variation in recruitment for the first half of the time series and for the last few years of the time series (Fig. 1A). This indicates that there is very little information in the data (catch-at-age) about annual recruitment for these time periods and that the prior on the recruitment residuals constrains the estimated recruitment to be close to the average recruitment. This result is consistent with the catch-at-age data, which, ignoring the inconsistent data from the 1970s, started in 1990. The greatest age in the catch-at-age data that had individual information was age 19; therefore the 1971 cohort is the first for which there is information. However, at the current exploitation rates, very few snapper live to be more than 10 years of age, so that there is very little information about cohort size for any of the cohorts produced during the 1970s.

The environmental model with process error indicated high variation in recruitment for the whole time period (Fig. 1B). This is due to the formulation of the recruitment submodel, for which the annual anomalies are anomalies from the temperature-recruitment relationship; if there is no information in the data about recruitment for a particular year, the recruitment will follow the temperature-recruitment relationship.

The correlation of the estimated recruitment from the traditional model with SST had a low r-square (0.26), but it was statistically significant at the 0.05 level when a two-tailed test was used. In addition, the slope of the relationship between recruitment and SST was much less for the traditional model than for to the environmental model with process error (Table 3). The estimates of recruitment from the traditional model included a large number of estimates that were close to the mean because there was no information in the data about these recruitments. Therefore, it was inappropriate to use these recruitments to correlate with SST and, if used, they would result in a poor fit. However, a significant correlation, as obtained in this application, suggests that the correlation is probably stronger than apparent from the analysis, which should give confidence that a relationship exists and provide an incentive to apply the integrated models.

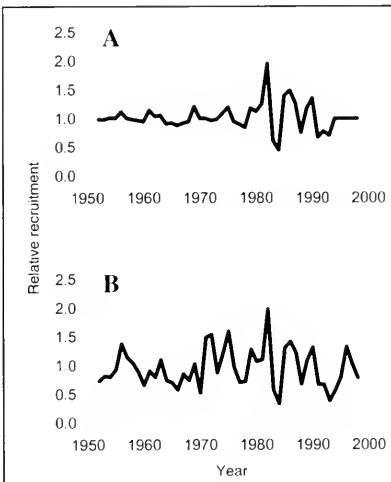

Figure 1

Annual estimates of relative recruitment strength at age 1 for the Hauraki Gulf–Bay of Plenty snapper stock from the traditional (**A**) and environmental model with process error (**B**) models

The environmental model with process error did not show a statistically significant improvement over the environmental model because, ignoring the 1970s data, the catch-at-age data were available only for the last part of the time period. The recruitment anomalies were estimated for the whole time period, as well as for the initial conditions. Many of these recruitment anomalies had very

little information associated with them and therefore did not add anything to the estimation procedure. However, they do add additional parameters, which reduce the possibility of accepting the model when using the likelihood ratio test. If the recruitment anomalies were estimated for only a limited number of years, it is likely that the environmental model with process error would be a statistically significant improvement over the environmental model. Statistical tests could be carried out to determine which annual recruitment anomalies should be estimated, but this would be very time consuming. Reducing the number of annual recruitment anomalies may also cause an underestimation of the confidence intervals. For the snapper example, removing the anomalies for the initial conditions may be a good compromise.

Discussion

We have developed a general framework for integrating environmental time series into stock assessment models that appears to perform better than traditional methods. The method is flexible and it can be used to model many different functional relationships between population or fishing processes and environmental time series and to include multiple environmental time series for any population model parameter (see Appendix II). Furthermore, it can be used with any statistical stock assessment model. The method can be used to test whether an environmental time series describes temporal variation in model parameters.

The traditional model, which estimates annual recruitment within the stock assessment model and subsequently correlates the recruitment with the environmental series outside the stock assessment model, performs poorly. It has a reasonable probability of detecting a relationship between recruitment and the environmental series, but this probability decreases rapidly as the number of years with missing catch-at-age data sets increases. The probability of incorrectly detecting a relationship when one is not present is low. This method has reasonable confidence-interval coverage for average recruitment and little bias or variance in the estimates of model parameters. The factor causing the poor performance of the traditional model is the large bias in the estimate of the slope of the relationship between recruitment and the environmental time series, which increases as the number of years with missing catch-at-age data increases. The bias occurs because the traditional model has a penalty on the absolute size of the annual recruitment deviations. This penalty constrains an annual recruitment anomaly to be close to the mean recruitment when there is little or no information about the recruitment in that year. Therefore, when the logarithm of the annual recruitment is correlated with the environmental time series, the estimated slope of the relationship is biased downward. Even in situations for which there is sufficient information for every recruitment anomaly, there will be a small tradeoff in the size of the anomaly, which reduces the contribution of the penalty to the objective function and the likelihood from the catch-at-age data. Unfortunately, if the penalty on the annual recruitment anomalies is removed, the estimation process can become unstable, particularly in data-poor situations for which the bias is greater. The amount of time that is required by the estimation algorithm also increases if the penalty is removed. When the penalty on the size of the recruitment anomalies is removed, the bias in estimates of the slope of the relationship between recruitment and the environmental time series is reduced when using all the catch-at-age data, but the variance in the estimates is greatly increased. In addition, when removing the penalty there was a large positive bias when using only the last 10 years of catch-at-age data and a large negative bias when using only the first 10 years of catch-at-age data. It is not known what results would be obtained if cohort analysis, which does not use a constraint on the annual recruitment anomalies, is used instead of the statistical catch-at-age analysis. It should be remembered that cohort analysis cannot be used or assumptions that are unlikely to be satisfied will have to be made when catch-at-age data are missing for some years.

The environmental model, which has a deterministic relationship between recruitment and the environmental time series that is integrated into the stock assessment model, also performs poorly. This method has poor confidence interval coverage for average recruitment because the size of the confidence intervals are greatly underestimated. The method has larger bias and variance in the estimates of model parameters compared to the other two methods. There is a small negative bias in the estimate of the slope of the relationship between recruitment and the environmental time series. The environmental model has a very high probability of detecting a relationship between recruitment and the environmental series, and this probability only decreases slightly as the number of missing years of catch-at-age data sets increases. However, this model has a very large probability of incorrectly detecting a relationship when one is not present. Therefore, when using the environmental model, the likelihood ratio test should not be used to determine if there is a significant relationship between recruitment and an environmental time series. The value used to compare to the χ^2 statistic in the likelihood ratio test for the environmental model is highly correlated with the catch-at-age sample size; therefore simulation analysis is needed to find the appropriate χ^2 statistic for the given sample size (see Appendix III). This is also important for calculating confidence intervals that are also based on the χ^2 statistic and is the reason for the poor coverage for R_0.

The environmental model with process error, which has a relationship between recruitment and the environmental time series that is integrated into the stock assessment model with additional process error, performs well. This model has a reasonable probability of detecting a relationship between recruitment and the environmental series, but this probability is lower than those of the other two models, and decreases as the amount of data is reduced. It has a low probability of incorrectly detecting a relationship when one is not present. These probabilities could be improved by using simulation analysis to find the appropriate χ^2 statistic (see Appendix III). This method has reasonable confidence interval coverage for average recruitment and has little bias or variance in the estimates of

model parameters. There is very little bias in the estimate of the slope of the relationship between recruitment and the environmental time series.

For the environmental model with process error, when there is little or no information in the data to estimate the recruitment for that year, the penalty on the annual recruitment anomalies causes recruitment to be estimated close to the recruitment predicted by the relationship between recruitment and the environmental time series. Therefore, if there is a relationship between recruitment and the environmental time series, this model should provide better estimates because additional information is included in the estimation procedure. This model has the favorable property that if there is no relationship between recruitment and the environmental time series, the model estimates β to be small, eliminating any influence of the relationship between recruitment and the environmental time series, and still estimates the annual recruitment anomalies to represent the variation in annual recruitment. The likelihood ratio test can be used to detect a relationship between recruitment and the environmental time series, and if a relationship does not exist, the results with β fixed at zero can be used. However, including β in the estimation procedure, even when there was no relationship between recruitment and the environmental time series, did not increase the error in the parameter estimates in relation to the model with β fixed at zero (see the results for the traditional model, Table 1D).

The method we describe can be used to integrate environmental time series for parameters of the stock assessment model other than recruitment. The influence of the environment on catchability of the fish would be an obvious choice because there are numerous publications on the topic. For example, Green (1967) suggested that thermocline data would improve estimation of tuna abundance from catch and effort data, by allowing for the differentiation between changes in tuna abundance and catchability due to vertical distribution of tunas influenced by temperature. We have used a method similar to the method that is presented in the present study to incorporate SST into the purse-seine catchability parameters for yellowfin and bigeye tuna (Maunder and Watters, 2001; Watters and Maunder, 2001). Maunder (2001a) presented a general method to integrate the standardization of CPUE data into stock assessment models, including the integration of environmental variables. Growth rates have been observed to have temporal variation, and this variation has been correlated with environmental factors. Several authors have presented growth curves that include temperature data (e.g. Mallet et al., 1999). Movement is another process that may be influenced by the environment. Lehodey et al. (1997) showed that spatial shifts in the western Pacific skipjack tuna population are linked to the movement of a large pool of warm water and that the movements of this large pool are related to El Niño-Southern Oscillation events.

Once a correlation between the environmental time series and the population process has been determined, this relationship can be used to improve the predictive ability of the model. For example, if a relationship between SST at the time of spawning and recruitment has been determined, and the age at recruitment to the fishery is 3 years, recruitment to the fishery can be estimated 3 years in advance. One should be cautious about assuming that these relationships are valid and will continue to hold into the future, however. Hilborn and Walters (1992) cautioned about using environmental data because there are many environmental indices that one can try, and if the data set has a few large and a few small observations, it is likely that one of the environmental data sets will correlate with the data. Myers (1998) reviewed a number of published correlations between recruitment and environmental factors and found that few of the correlations held when retested at later dates. Maunder and Starr (1998) also advised caution because they found that a strong cohort may not enter the fishery when expected because of variations in growth rates. We have found that, when applying this method to the bigeye tuna data, there is an inconsistency in the pre-1997 data and the data for 1997 and 1998 caused by much stronger than expected year classes entering the fishery in 1997 and 1998. There is also difficulty in deciding on the management strategy if environmental regime shifts are influencing the productivity of the stock (Maunder, 1998b). An advantage of the integrated approach, particularly the environmental model with process error, is that it more fully describes the uncertainty in the relationship between the population process and the environmental time series, and therefore this uncertainty can be included in any management advice based on the relationship.

Conclusions

Integrating environmental relationships in a statistical stock assessment model is an improvement over the traditional statistical model when there are large gaps in the data. However, it is important to include process error to avoid the high probability of detecting spurious correlations seen in the environmental model when using the likelihood ratio test. Therefore, the environmental model with process error is the model of choice because 1) there is no bias in the estimates, 2) when there is no relationship with the environmental series, it is equivalent to the traditional model, 3) when such a relationship exists, the recruitment estimates are improved, particularly if there are important gaps in the data, 4) it may be used for prediction, and 5) uncertainty about the relationship can be modeled.

Acknowledgments

We thank Dave Fournier for advice on using AD Model Builder and related software, and Bill Bayliff, Rick Deriso, Shelton Harley, and Ransom Myers for commenting on the manuscript.

Literature cited

Bertignac, M., P. Lehodey, and J. Hampton.
1998. A spatial population dynamics simulation model of

tropical tunas using a habitat index based on environmental parameters. Fish. Oceanogr. 7:326–334.

Beverton, R. J. H., and S. J. Holt.
1957 On the dynamics of exploited fish populations. Fish. Invest. Ser. II, Mar. Fish. G B. Minist. Agric. Fish. Food 19, 533 p.

Deriso, R. B., T. J. Quinn II, and P. R. Neal.
1985. Catch-age analysis with auxiliary information. Can. J. Fish. Aquat. Sci. 42:815–824.

Forsbergh, E. D.
1989. The influence of some environmental variables on the apparent abundance of skipjack tuna, *Katsuwonus pelamis*, in the eastern Pacific Ocean. Inter-Am. Trop. Tuna Comm. Bull. 19:433–569.

Fournier, D., and C. P. Archibald.
1982. A general theory for analyzing catch at age data. Can. J. Fish. Aquat. Sci. 39:1195–1207.

Francis, M. P.
1993. Does water temperature determine year class strength in New Zealand snapper (*Pagrus auratus*, Sparidae)? Fish. Oceanogr. 2:65–72.

Gilbert, D. J.
1994. A total catch history model for SNA 1. New Zealand Fisheries Research Document 94/24. 16 p. NIWA (National Institute of Water and Atmospheric Research), Wellington, New Zealand.

Granger, C. W. J.
1993. Forecasting in economics. *In* Time series prediction: forecasting the future and understanding the past (A. E. Weigend and N. A Gershenfeld, eds.), p. 529–538. SFI Studies in the Sciences of Complexity, Proc. Vol. XV. Addison-Wesley, Boston, MA

Green, R. E.
1967. Relationship of the thermocline to success of purse seining for tuna. Trans. Am. Fish. Soc. 96:126–130.

Hilborn, R., and M. Mangel.
1997. The ecological detective: confronting models with data, 315 p. Princeton Univ. Press, Princeton, NJ.

Hilborn, R., and C. J. Walters.
1992. Quantitative fisheries stock assessment: choice, dynamics and uncertainty, 570 p. Chapman and Hall, New York, NY

Hinton, M. G., and H. Nakano.
1996 Standardizing catch and effort statistics using physiological, ecological, or behavioral constraints and environmental data, with an application to blue marlin (*Makaira nigricans*) catch and effort data from Japanese longline fisheries in the Pacific. Inter-Am. Trop Tuna Comm. Bull. 21 171–200.

Hunter, J. R
1983 On the determinants of stock abundance. *In* From year to year (W. S. Wooster, ed.), p. 11–16. Washington Sea Grant Program, Univ. Wash., Seattle, WA.

Joseph, J., and F. R. Miller
1989 El Nino and the surface fishery for tunas in the eastern Pacific Japan Soc. Fish. Ocean., Bull. 53:77–80

Lehodey, P., J. Andre, M. Bertignac, J. Hampton, A. Stones, C. Menkes, L. Memery, and N. Grima
1998 Predicting skipjack tuna forage distributions in the equatorial Pacific using a coupled dynamical bio-geochemical model. Fish. Oceanogr. 7:317–325

Lehodey, P., M. Bertignac, J. Hampton, A. Lewis, and J. Picaut.
1997 El Nino Southern Oscillation and tuna in the western Pacific. Nature 389 715–718

Mallet, J. P., S. Charles, H. Persat, and P. Auger.
1999. Growth modelling in accordance with daily water temperature in European grayling (*Thymallus thymallus* L.). Can. J. Fish. Aquat. Sci. 56:994–1000.

Maunder, M. N.
1998a. Integration of tagging and population dynamics models in fisheries stock assessment. Ph.D. diss., 306 p. Univ. Washington, Seattle, WA.
1998b. Problems with using an environmental based recruitment index: examples from a New Zealand snapper (*Pagrus auratus*) assessment. *In* Fishery stock assessment models (F. Funk, T. J. Quinn II, J. Heifetz, J. N. Ianelli, J. E. Powers, J. J. Schweigert, P. J. Sullivan, and C. I. Zhang, eds.), p. 679–692. Alaska Sea Grant College Program Report No. AK-SG-98-01, Univ. Alaska, Fairbanks, AK.
2001a. A general framework for integrating the standardization of catch-per-unit-effort into stock assessment models. Can. J. Fish. Aquat. Sci. 58:795–803.
2001b. Integrated tagging and catch-at-age analysis (ITCAAN). *In* Spatial processes and management of fish populations (G. H. Kruse, N. Bez, A. Booth, M. W. Dorn, S. Hills, R. N. Lipcius, D. Pelletier, C. Roy, S. J. Smith, and D. Witherell, eds.), p. 123–146. Alaska Sea Grant College Program Report AK-SG-01-02. Univ. Alaska, Fairbanks, AK.

Maunder, M. N., and P. J. Starr.
1998. Validating the Hauraki Gulf snapper pre-recruit trawl surveys and temperature recruitment relationship using catch at age analysis with auxiliary information. New Zealand Fisheries Research Document 98/15, 23 p. NIWA (National Institute of Water and Atmospheric Research), Wellington, New Zealand.

Maunder, M. N., and P. J. Starr.
2001. Bayesian assessment of the SNA1 snapper (*Pagrus auratus*) stock on the northeast coast of New Zealand. N.Z. J. Mar. and Freshwater Res. 35:87–110.

Maunder, M. N., and G. M. Watters.
2001. Status of yellowfin tuna in the eastern Pacific Ocean. Inter-Am. Trop. Tuna Comm. Stock Assess. Rep. 1:5–86.

Methot, R. D.
1990. Synthesis model: an adaptable framework for analysis of diverse stock assessment data. Inter. North Pacif. Fish. Comm. Bull. 50:259–277.

Myers, R. A.
1998. When do environment-recruitment correlations work? Reviews in fish biology and fisheries 8:285–305.

Myers, R. A., J. Bridson, and N. J. Barrowman.
1995. Summary of worldwide spawner and recruitment data. Can. Tech. Rep. Fish. Aquat. Sci. 2020, iv + 327 p.

Paul, L. J
1976. A study on age, growth, and population structure of the snapper, *Chrysophrus auratus* (Forster), in the Hauraki Gulf, New Zealand. New Zealand Ministry of Fisheries and Agriculture, Fish. Bull. 13, 62 p.

Ricker, W. E.
1954 Stock and recuitment. J. Fish. Res. Board Can. 11: 559–623.

Shepherd, J. G., J. G. Pope, and R. D. Cousens.
1984 Variations in fish stocks and hypotheses concerning their links with climate. Rapp. P.-V. Reun., Cons. Int. Explor. Mer 185.255–267

Watters, G. M., and M. N. Maunder.
2001 Status of bigeye tuna in the eastern Pacific Ocean. Inter-Am. Trop. Tuna Comm. Stock Assess. Rep. 1:109–210

Appendix I: description of simulator and estimator

The following is a description of the model equations used for the data simulator and for the estimator. The model is run from an unexploited state at the start of the fishery for 20 years. The model includes 10 age classes, where the 10th age class is a plus group.

Dynamics

$$N_{y,1} = R_0 \exp(\beta I_y + \varepsilon_y^R + \alpha) \tag{I.1}$$

$$\alpha = \ln\left(\frac{n}{\sum \exp(\varepsilon_y^R + \beta I_y)}\right) \tag{I.2}$$

$$N_{y,a} = \left(N_{y-1,a-1}(1-u_{y-1}s_{a-1})\right)e^{-M_{a-1}} \text{ for } a < A \tag{I.3}$$

$$N_{y,A} = \left(N_{y-1,A-1}(1-u_{y-1}s_{A-1})\right)e^{-M_{A-1}} + \left(N_{y-1,A}(1-u_{y-1}s_A)\right)e^{-M_A} \tag{I.4}$$

$$u_y = \frac{C_y}{B_y} \tag{I.5}$$

$$B_y = \sum_a N_{y,a} s_a w_a \tag{I.6}$$

where $N_{y,a}$ = the numbers in age class a at the beginning of year y;
R_0 = the average recruitment;
ε_y^R = the recruitment anomaly for year y;
σ_R^2 = the standard deviations for the recruitment anomalies;
M_a = the age specific natural mortality rate;
A = the maximum age used in the analysis;
u_y = the exploitation rate in year y;
s_a = the selectivity to the fishing gear for age a individuals;
C_y = the total catch in weight for year y;
B_y = the exploitable biomass for year y; and
w_a = the weight for an individual of age a.

Initial conditions

$$N_{1,a} = R_0 e^{\sum_1^{a-1} M} \text{ for } 1 < a < A \tag{I.7}$$

$$N_{1,A} = \frac{N_{1,A-1} e^{-M_{A-1}}}{1 - e^{-M_A}} \tag{I.8}$$

Simulation

$$\varepsilon_y \sim N(0, \sigma_R^2) \tag{I.9}$$

$$I_a \sim N(0, \sigma_I^2) \tag{I.10}$$

$$\varepsilon_a^{CPUE} \sim N(0, \sigma_{CPUE}^2) \tag{I.11}$$

$$CPUE_y = qB_y \exp(\varepsilon_y^{CPUE} - 0.5\sigma_{CPUE}^2) \tag{I.12}$$

where q = the catchability coefficient for the CPUE index;
σ_I = the standard deviation for the variation in the recruitment index;
ε_a^{CPUE} = the observation error in the CPUE index; and
σ_{CPUE} = the standard deviation of the error in the CPUE index.

$$D_{y,a} \sim Multinomial\left(\frac{C_{y,a}^{numbers}}{\sum_a C_{y,a}^{numbers}}, n = 50\right) \tag{I.13}$$

$$C_{y,a}^{numbers} = N_a u_y s_a \tag{I.14}$$

where $D_{y,a}$ = the number of individuals of age a in the catch-at-age same in year y; and
n = the number in the catch-at-age sample; and
σ_{CPUE} = the catch in numbers of age a individuals in year y.

Estimation

The likelihood values can be calculated by using the following equations:

$$-\ln L(\theta \mid I) = \sum_y \left[\ln(\sigma_{CPUE}) + \frac{\left(\ln(CPUE_y) - \ln(qB_y)\right)^2}{2\sigma_{CPUE}^2}\right] \tag{I.15}$$

$$-\ln L(\theta \mid D) = -\sum_{y,a} D_{y,a} \ln(p_{y,a}) \tag{I.16}$$

$$p_{y,a} = \frac{C_{y,a}^{numbers}}{\sum_a C_{y,a}^{numbers}} \tag{I.17}$$

The penalities (priors) on the annual recruitment anomalies can be calculated by using the following equation:

$$-\ln \text{ Prior}(\varepsilon^R) = \sum_y \left[\frac{(\varepsilon_y^R)^2}{2\sigma_R^2}\right]. \tag{I.18}$$

The following values were used for the biological parameters:

$$w_a = l_a^3, \tag{I.19}$$

$$l_a = 1 - e^{-0.1}, \tag{I.20}$$

and $M = 0.2$ and $s = 1$, where the a for M and s are subscripted.

Appendix II: extensions

The recruitment-environmental submodel that we used to analyze the snapper stock is simple, and other submodels may improve the fit to the data and the explanatory ability of the environmental time series. A dome-shaped relationship has been observed between abundance of tuna larvae and SST (Forsbergh, 1989), indicating that a quadratic or higher-order polynomial submodel may be more appropriate.

$$R_t = \exp(\alpha + \beta_1 I_t + \beta_2 I_t^2 + \ldots \beta_n I_t^n + \varepsilon_t). \tag{II.1}$$

Regime-switching models (Granger, 1993) that have the ability to favor two levels of values may be more appropriate for species that are hypothesized to experience two environmental regimes.

$$X_t = \left\{ (ub - lb)\left[1 + \exp\left(-\ln(19)\frac{I_t - I_{50}}{I_{95} - I_{50}} \right) \right]^{-1} + lb \right\} \exp(\varepsilon_t), \tag{II.2}$$

where lb = the lower bound of the model parameter (low regime);
ub = the upper bound of the model parameter (high regime);
I_{50} = the environmental time series value that gives a 50% influence; and
I_{95} = the environmental time series value that gives a 95% influence.

If I_{95} is only slightly higher than I_{50}, the model will have two regimes. Therefore, the model can be simplified by setting I_{95} as a small fixed value above I_{50}, allowing for the use of a regime-shifting model that requires estimation of only the lower bound, upper bound, and the value of the environmental time series at the point of change.

The method can be easily extended to include multiple environmental factors,

$$X_t = \mu \exp\left(\varepsilon_t + \sum_i \beta_i I_{i,t} + \alpha \right), \tag{II.3}$$

where i indexes the environmental factor.

The method we have used assumes that recruitment is independent of spawner biomass (i.e. we penalize the deviation from a mean recruitment modified by the relationship with the environmental time series). Maunder (1998a) suggested applying the method to stock-recruitment relationships, and the models described by Hilborn and Walters (1992, p. 285–287) could be used to integrate spawner-recruitment models and environmental time series into the stock assessment model.

$$R_t = f(S_t) \exp(\beta I_t + \varepsilon_t + \alpha), \tag{II.4}$$

where $f(S_t)$ = the function for the stock-recruitment relationship and
S_t = the spawning biomass at time t.

The equation for the Ricker (1954) and Beverton and Holt (1957) models would be

$$R_t = S_t \exp(a - bS_t) \exp(\beta I_t + \varepsilon_t + \alpha). \quad \text{Ricker} \tag{II.5}$$

$$R_t = \frac{aS_t}{b + S_t} \exp(\beta I_t + \varepsilon_t + \alpha), \quad \text{Beverton-Holt} \tag{II.6}$$

where a and b are parameters of the stock recruitment models.

Appendix III: the hypothesis test problem for the environmental model

Let, $\hat{p}_j = \frac{n_j}{N}$

where $N = \sum_j n_j$

is the sample size and n_j is the number from category j in the sample. The negative log-likelihood (ignoring constant) is

$$-\ln L = N \sum_j -\hat{p}_j \ln(p_j).$$

$$\chi^2 = 2(\ln L_1 - \ln L_0) = 2N\left(\sum_j \hat{p}_j \ln(p_{1,j}) - \sum_j \hat{p}_j \ln(p_{0,j}) \right),$$

therefore χ^2 is proportional to N. LnL_1 (estimate β) has one more parameter than LnL_0 (β=0) and therefore will be at least slightly larger (two sets if independent random numbers always have a nonzero correlation). Therefore, there will be some value of N for which χ^2>3.84. Now, consider a simple example where

$$p_j = \frac{x_j}{\sum_j x_j} \text{ and } x_j = \mu \exp(\beta I_j + \varepsilon_j),$$

with the penalty $-\ln \text{ Prior}(\varepsilon \mid \sigma) = \sum_j \frac{(\varepsilon_j)^2}{2\sigma^2}$,

and σ is a constant. Consider two models: 1) $\varepsilon_j = 0$ and 2) estimate ε_j. For model 1, as N increases χ^2 increases in proportion to N, as explained above, because the penalty term is constant. However, for model 2, as N gets large, the

relative size of the penalty compared to $-\ln L_0$ gets smaller and therefore the estimates of ε_i change so that p_i gets closer to $\hat{p}_i$. Therefore, for model 2, χ^2 does not increase proportionally with N.

An appropriate test for the environmental model would be to produce sets of random environmental indices that have the same variance and auto-correlation as the actual environmental index to determine the appropriate value of χ^2 that would give the desired type-I error. This test would overcome the sample size effect. The method could also be used to refine the test for the environmental model with process error.

Seasonal distribution, abundance, and growth of young-of-the-year Atlantic croaker (*Micropogonias undulatus*) in Delaware Bay and adjacent marshes*

Michael J. Miller
David M. Nemerson
Kenneth W. Able

Marine Field Station
Institute of Marine and Coastal Sciences
Rutgers University
800 c/o 132 Great Bay Boulevard
Tuckerton, New Jersey 08087-2004
Email address (for K. W. Able, contact author): able@imcs.rutgers.edu

Abstract—We examined the spatial and temporal distribution, abundance, and growth of young-of-the-year (YOY) Atlantic croaker (*Micropogonias undulatus*) in Delaware Bay, one of the northernmost estuaries in which they consistently occur along the east coast of the United States. Sampling in Delaware Bay and in tidal creeks in salt marshes adjacent to the bay with otter trawls, plankton nets and weirs, between April and November 1996–99, collected approximately 85,000 YOY. Ingress of each year class into the bay and tidal creeks consistently occurred in the fall, and the first few YOY appeared in August. Larvae as small as 2–3 mm TL were collected in September and October 1996. Epibenthic individuals <25 mm TL were present each fall and again during spring of each year, but not in 1996 when low water temperatures in January and February apparently caused widespread mortality, resulting in their absence the following spring and summer. In 1998 and 1999, a second size class of smaller YOY entered the bay and tidal creeks in June. When YOY survived the winter, there was no evidence of growth until after April. Then the YOY grew rapidly through the summer in all habitats (0.8–1.4 mm/d from May through August). In the bay, they were most abundant from June to August over mud sediments in oligohaline waters. They were present in both subtidal and intertidal creeks in the marshes where they were most abundant from April to June in the mesohaline portion of the lower bay. The larger YOY began egressing out of the marshes in late summer, and the entire year class left the tidal creeks at lengths of 100–200 mm TL by October or November when the next year class was ingressing. These patterns of seasonal distribution and abundance in Delaware Bay and the adjacent marshes are similar to those observed in more southern estuaries along the east coast; however, growth is faster—in keeping with that in other northern estuaries.

Manuscript accepted 20 August 2002.
Fish. Bull. 101(1):100–115 (2003).

Atlantic croaker (*Micropogonias undulatus*) is a commercial and sport fishery species that inhabits demersal habitats in estuarine, coastal, and continental shelf systems along the Atlantic coast of North America and in the Gulf of Mexico (Joseph, 1972). They spawn primarily over the continental shelf during a protracted spawning season that, based on the presence of larvae along the Atlantic coast, may extend from early July through March (Lewis and Judy, 1983; Cowan and Birdsong, 1985; Warlen and Burke, 1990; Hettler et al., 1997; Nixon and Jones, 1997; Able and Fahay, 1998). The exact location of spawning in the Middle Atlantic Bight (MAB) may be related to the areal extent of favorable warm bottom waters for spawning (Norcross and Austin, 1988) and may sometimes occur within or close to the mouth of Chesapeake Bay (Barbieri et al., 1994b; Reiss and McConaugha, 1999). The larvae and postlarvae have been observed to be more abundant in deeper layers of water that may facilitate transport into and retention within estuarine nursery areas (Weinstein et al., 1980; Norcross, 1991). The young-of-the-year (YOY) usually begin to enter estuaries and tidal creeks along the Atlantic coast in September, or occasionally August, and they are often common components of the fish fauna in tidal creeks and estuaries until fall of the next year from New Jersey southward along the Atlantic coast and in the Gulf of Mexico (Chao and Musick, 1977; Knudsen and Herke, 1978; Weinstein, 1979; Currin et al., 1984; Ross, 1988; Able and Fahay, 1998). In some years there is a second pulse of small YOY that arrives in estuaries along the Atlantic coast in the spring or summer; this pulse may be the offspring from later spawning (Chao and Musick, 1977; Ross, 1988). In general, the YOY use estuarine habitats with salinities ranging from almost pure freshwater to seawater (Miglarese et al., 1982).

Although YOY Atlantic croaker are present in some Atlantic coast estuarine habitats during the winter (Haven, 1957; Bearden, 1964; Dahlberg, 1972; Chao and Musick, 1977; Shenker and Dean, 1979; Bozeman and Dean, 1980; Able and Fahay, 1998), they appear to experience winter mortality in the MAB in years with unusually cold winters (Massman and Pacheco, 1960; Joseph, 1972; Chao and Musick, 1977; Wojcik, 1978). Recent laboratory studies have found that YOY Atlantic croaker do not survive in sustained water temperatures of 3°C or lower (Lankford and Targett, 2001); therefore extended periods of low winter water temperatures may have drastic effects on their overwinter survival in some estuaries.

Previous studies have indicated that YOY Atlantic croaker reach about 107–187 mm TL after their first year

* Contribution 2002-22 from the Institute of Marine and Coastal Sciences, Rutgers University, New Brunswick, NJ 08901.

of growth in estuaries along the Atlantic coast and 102–250 mm TL in the Gulf of Mexico (Knudsen and Herke, 1978), but only a few studies have reported seasonal growth rates (Hansen, 1969; Knudsen and Herke, 1978). Length-frequency based growth rate estimates for the first year of growth for YOY along the Atlantic coast have ranged from 0.32 to 0.41 mm/d (Knudsen and Herke, 1978). However, these were based on the entire year, including the larval and early juvenile period when analysis of otolith daily growth rings indicates much slower growth rates of 0.18–0.41 mm/d during the fall and winter months (Nixon and Jones, 1997). Length-frequency data from estuarine nursery areas clearly indicate that most growth occurs during the spring and summer months (Haven, 1957; Chao and Musick, 1977; Ross, 1988; Able and Fahay, 1998).

Despite various studies of YOY Atlantic croaker in some areas of the Atlantic and Gulf coasts, there is relatively little known of their early life history near the northern part of their range in the MAB and this is especially true for Delaware Bay. Our four-year study used extensive collections in Delaware Bay and in adjacent tidal marsh creeks to describe the timing of Atlantic croaker ingress, their seasonal abundance and size, growth rates, and the timing of their egress out of the marshes.

Methods

Study sites

Delaware Bay is the estuary of the Delaware River and encompasses about 1878 km^2 of open water along the southern edge of New Jersey and the northern edge of Delaware (Fig. 1). It has a relatively deep area (10–30 m) in the middle of the lower bay, bordered by narrow shoals and flanked by extensive tidal flats and salt marshes, which contain an additional 85.5 km^2 of open water in tidal creeks bordered by approximately 640 km^2 of marsh-plain area. Depending on the amount of river discharge, salinities range from 30–31‰ at the mouth of the bay, to 1–10‰ in the lower Delaware River (Table 1; Cronin et al., 1962; Garvine et al., 1992).

Ichthyoplankton survey

Catch data from an ichthyoplankton survey (Table 2) was used to analyze the distribution, abundance, and size of larval Atlantic croaker in Delaware Bay and the lower Delaware River from April to October 1996. Sampling was performed during daylight hours once a month in April and October and twice a month from May to September. Each sampling period included one tow at 70 randomly selected stations distributed among eight designated sampling zones (Fig. 1). Samples were collected with a 1-m diameter plankton net (0.5-mm mesh) deployed with a depressor in single stepwise oblique tows from the surface to the bottom. Tows were made at a speed of 1.4–1.9 knots for four to six minutes in the direction of the tidal flow. Up to 50 individuals were measured to the nearest millimeter total length (TL) from each sample.

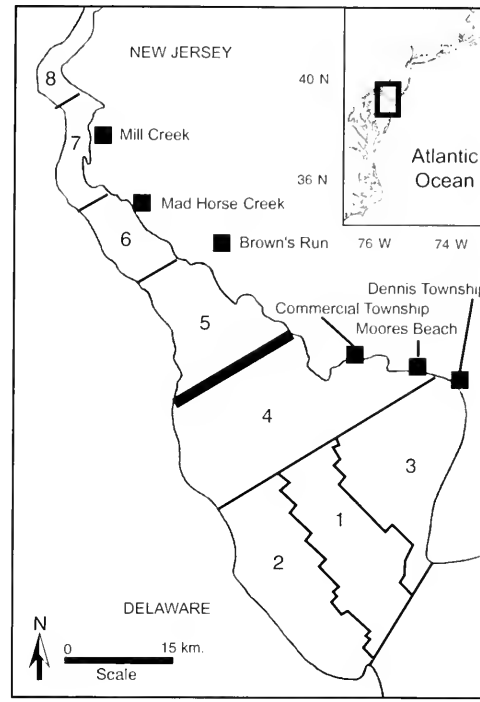

Figure 1

Locations of salt marsh tidal creek sampling sites (1996–99) and designated sampling zones (1–8) in the Delaware Bay and in the lower Delaware River for the ichthyoplankton (April–October 1996) survey and the otter trawl (April–October 1996–98) survey. The heavier line across the bay indicates the boundary between the upper (5–8) and lower (1–4) sampling zones and marsh sites.

Otter trawl survey

We used catch data from a three-year otter trawl survey (Table 2) to analyze the distribution, abundance, and growth of settled YOY Atlantic croaker in Delaware Bay and the lower Delaware River. Sampling was performed during daylight hours twice a month from April to October in 1996 and once a month in 1997 and 1998, at 40 stations divided up among the same eight sampling zones of the ichthyoplankton survey (Fig. 1). Station locations were selected by using a stratified random sampling design from a grid of 1002 stations, excluding the stations over the deepest water near the mouth of the bay in zone 1. There were eight stations sampled each month in zone 3, six in zone 4, and four in all the other zones. Trawling was done with 4.9-m otter trawls (6 mm stretched codend mesh), made against the prevailing direction of the tide at a speed of 1.8 m/sec for 10 minutes. Up to 100 individuals were measured from each sample. For presentation

Table 1

Physical characteristics of marsh and adjacent bay study sites located along the New Jersey shore of Delaware Bay, 1996–99. See Figure 1 for locations of individual sites.

Marsh site	Surface temp. range (°C)	Average surface temp. (°C)	Surface salinity range (‰)	Average surface salinity (‰)	Average surface dissolved oxygen (mg/L)
Upper bay					
Mill Creek	5.0–29.0	19.5	0–8.4	2.8	7.4
Mad Horse Creek	0–31.0	19.2	0.7–23.0	9.1	6.3
Browns Run	7.0–31.3	20.5	0.2–14.0	7.0	5.4
Bay	7.0–28.0	20.2	1.5–17.8	10.2	6.3
Lower bay					
Commercial Township	8.0–30.0	19.8	4.5–22.9	17.0	6.8
Upper Moores Beach	2.0–30.0	18.7	10.0–23.8	17.2	6.2
Lower Moores Beach	5.0–29.0	19.0	4.0–25.0	18.9	7.0
Dennis Township	6.0–32.0	20.4	6.2–24.7	17.0	5.7
Bay	6.0–29.1	19.6	11.1–24.7	17.8	7.3

Table 2

Yearly catch per unit of effort (CPUE=number of fish per tow or weir set) for the different types of gear in the marsh creeks or in Delaware Bay and the total number of Atlantic croaker collected by each type of gear. RUMFS = Rutgers University Marine Field Station; EEP = Public Service Enterprise Group Estuary Enhancement Program.

	1996 CPUE	1997 CPUE	1998 CPUE	1999 CPUE	Total number of tows/sets	Total number of fish	Source
Marsh creeks							
Otter trawl (creeks)	2.4	3.8	19.1	3.9	4,654	36,295	RUMFS
Otter trawl (bay)	164.6	15.3	29.3	49.5	336	12,755	RUMFS
Weir	1.1	41.6	46.8	98.7	443	20,714	RUMFS
Delaware Bay							
Otter trawl	4.6	2.8	19.7	—	1,438	13,497	EEP
1-m plankton net	1.7	—	—	—	957	1,638	EEP
Total fish	8,671	12,350	43,942	19,936	7,828	84,899	

and statistical analysis of some aspects of the data of the ichthyoplankton and otter trawl surveys in the bay, the upper four zones were combined into an upper bay region and the lower four combined into a lower bay region (Fig. 1).

Marsh creek survey

Tidal creek sampling was carried out at six salt marsh sites on the New Jersey side of Delaware Bay (Fig. 1, Table 1). Dennis Township, Commercial Township, and Moores Beach will be referred to collectively as the lower bay sites, and Browns Run, Mill Creek, and Mad Horse Creek will be referred to as the upper bay sites. The average depth of the trawling stations (1.3–2.6 m) and Secchi depth values (0.3–0.4 m) were similar at all sites. The upper bay sites in the mostly oligohaline region of the bay had average salinities of 2.8–9.1‰ and the lower bay sites were in the mesohaline region with average salinities of 17.0–18.9‰ (Table 1).

We sampled each of the marshes (Fig. 1) monthly from April through November 1996–99 (Table 2). Small intertidal marsh creeks were sampled with weirs set at high tide and hauled at low tide, approximately six hours later. Each weir (2.0 m × 1.5 m × 1.5 m, with 5.0 m × 1.5 m wings, 6.0-mm stretched mesh) consisted of a funnel-shaped net stretched across the channel with wings extended back onto the marsh surface from each end of the net. In cases when the creek did not drain completely the area in front of the weir was seined into the weir.

Trawling in larger intertidal to subtidal marsh creeks took place around high tide and consisted of four replicate two-minute tows per station, made against the current with a 4.9-m otter trawl (6-mm stretched codend mesh) towed at a constant engine RPM of 2500. Trawling station locations at each site were designed to sample fishes along

the mouth to upper creek gradients (see Able et al., 2000; 2001; Able et al.[1]). Thus, at each of the marshes there were six trawling locations. These locations included two large subtidal creeks and two smaller creeks with lower subtidal and upper subtidal or intertidal sections in each of the latter. Additional trawling locations were established in the bay immediately outside the mouth of the large creek at the Dennis Township, Moores Beach, Commercial Township, and Mad Horse Creek study sites (Fig. 1). The fish collected at these bay stations were used in the length-frequency figures for the bay (exclusive of November when there was no trawl survey sampling in the bay) and for the growth calculations, but not in the catch-per-unit-of-effort (CPUE) calculations for the bay. Atlantic croaker collected in each weir set and in each trawl were enumerated, and up to 50 individuals per weir set and 20 per trawl were measured to the nearest millimeter total length. Abundances (CPUE, number of fish per trawl) were compared between the upper and lower bay sites in Delaware Bay, among the six different marsh sites, and among years, by using the nonparametric Mann-Whitney *U*-test, or the Kruskal-Wallis ANOVA of ranks for multiple comparisons, and when differences were found, the Dunnís test was used (criteria for significance: $P<0.05$) to make pair-wise comparisons.

Physical variables were measured at the end of each weir and otter trawl sample in the marshes and in Delaware Bay (Table 1). Temperature, salinity, and dissolved oxygen concentrations were measured with a hand-held salinity, temperature, and oxygen meter (YSI Model 85), by lowering the probe into the water and recording surface values. Water transparency was measured by lowering a Secchi disc into the water column until it was no longer visible and recording the corresponding depth in 0.1-m increments.

Growth

Growth rates for YOY Atlantic croaker were calculated for samples collected during the late spring through fall in the upper and lower regions of the bay in 1997 and 1998 and in the upper and lower bay marsh sites during 1997, 1998, and 1999. We compared growth using the progression of the monthly median lengths in each area by computing the change in the median length of a cohort over a time period divided by the number of days in the period. This method was based on the following assumptions: 1) no new (small) recruits join the population during the calculation interval, and 2) no (large) individuals leave the population over the calculation interval. To best meet these assumptions, median growth rates were calculated by using the monthly length data from May to July when there was a minimum of movement of fish between different areas, and then for longer-term monthly comparisons, from May to August, September, and October when fish were moving out of the marshes into the bay. The smaller-size cohort present in the bay in June and July 1998 and in the marshes in 1999 was excluded from the growth calculations for those years. The linearity of the progression of median lengths was tested by using linear regression, and the resulting lines were compared between the upper and lower bay.

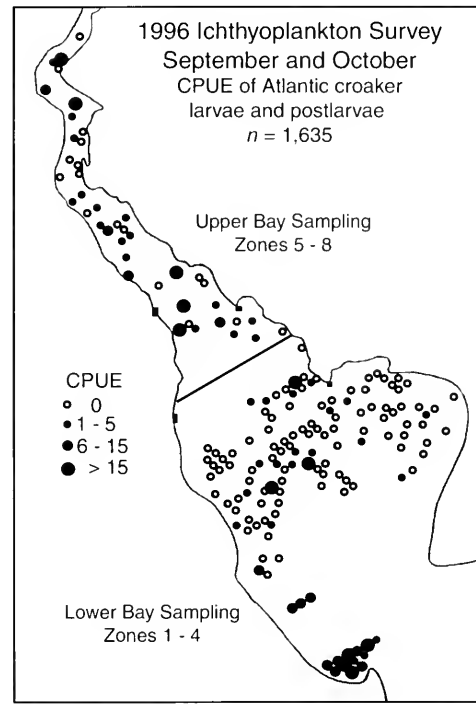

Figure 2

Catch per unit of effort (CPUE) of larval and postlarval Atlantic croaker (*Micropogonias undulatus*) collected in the ichthyoplankton survey in September and October 1996.

Results

Distribution, abundance, and size during fall ingress and settlement

Atlantic croaker larvae were collected only in the late summer and fall during the ichthyoplankton survey in Delaware Bay in 1996 (Figs. 2 and 3). A few individuals were first collected in August (n=3, CPUE=0.02 fish/tow), and then large numbers of larvae were collected through September (n=639, CPUE=3.6) and October (n=996, CPUE=9.0), but they were absent from April to July. The overall September–October CPUE was 9.0 fish/tow (range:

[1] Able, K. W., D. M. Nemerson, and T. M. Grothues. In review. Evaluating salt marsh restoration in Delaware Bay: continued analysis of fish response at former salt hay farms.

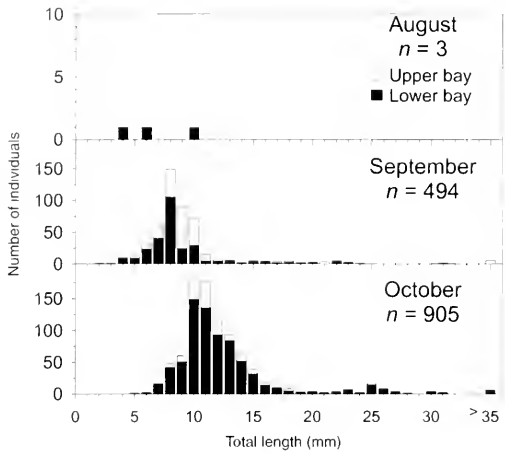

Figure 3

Length-frequency distributions of larval and postlarval Atlantic croaker (*Micropogonias undulatus*) collected in the upper and lower regions of Delaware Bay during the ichthyoplankton survey in 1996.

0–56) in the upper bay zones 5–8 and 4.9 (range: 0–36) in the lower bay zones 1–4 (Figs. 1 and 2), and these CPUE values were significantly different between zones (P=0.03). At least one individual was collected in each of the eight zones in both September and October; the highest two-month combined CPUE occurred in the uppermost zone 8 (CPUE=13.4), followed by zone 5 (CPUE=9.6), and the lowest occurred in zone 3 (CPUE=0.1). Larvae were 4–10 mm during August (all in zone 2), predominantly 2–24 mm in September, and 5–28 mm in October (Fig. 3)—the smallest individuals being caught in the lower bay.

Benthic YOY Atlantic croaker of a variety of sizes first appeared in substantial numbers in September in the otter trawl surveys in both the bay (Fig. 4) and marshes (Fig. 5) at lengths >5 mm, and with modes of 15–30 mm for the primary cohort. Exceptions occurred in the bay in 1997, when they were not collected by the trawl survey until October and when they were not collected during September at two of the three upper bay marsh sites each year.

The CPUE of benthic YOY Atlantic croaker was usually highest during October in the lower bay marshes (Fig. 6). This pattern of abundance is illustrated by the much higher four-year overall CPUE of recently ingressed YOY, especially at Dennis Township, Commercial Township, and Upper Moores Beach (Fig. 7). The combined four-year CPUE values were significantly different (P<0.001) at each of the six sites, and the CPUE values at the Dennis Township site were significantly greater than at all the sites except for Commercial Township. Similarly, Commercial Township was different from all sites except Dennis Township and Upper Moores Beach, and Upper Moores Beach also was different from Browns Run in the upper bay.

Recently settled YOY Atlantic croaker were also caught in the weirs in small intertidal marsh creeks during September, October, and November in all three years; the majority were collected at the Dennis Township marsh in the lower bay (Fig. 8). The monthly CPUE (fish per set) in the weirs at Dennis Township was greatest in October 1997 and November 1999 (the weirs were not in place until October 1996) and the largest total number was collected during 1999. The combined four-year CPUE values for 1996–99 at each of the six sites were significantly different (P<0.001), and the CPUE values at the Dennis Township site were significantly greater than those at all the sites, except Commercial Township.

The monthly CPUE values during ingress in the bay also were highest in October, but in contrast to the marsh sites were usually higher in the upper part of the bay (Fig. 6). The combined CPUE values for September and October were significantly different between the upper and lower bay regions in 1998 (P<0.001) and 1997 (P=0.048), but not in 1996 (P=0.51). The combined CPUE values for September and October for each year (1996–98) were significantly different among years (P<0.001) and were different between 1996 and 1997, and between 1996 and 1998.

A second, smaller cohort of YOY Atlantic croaker appeared in the bay in June and July 1998 and in the tidal

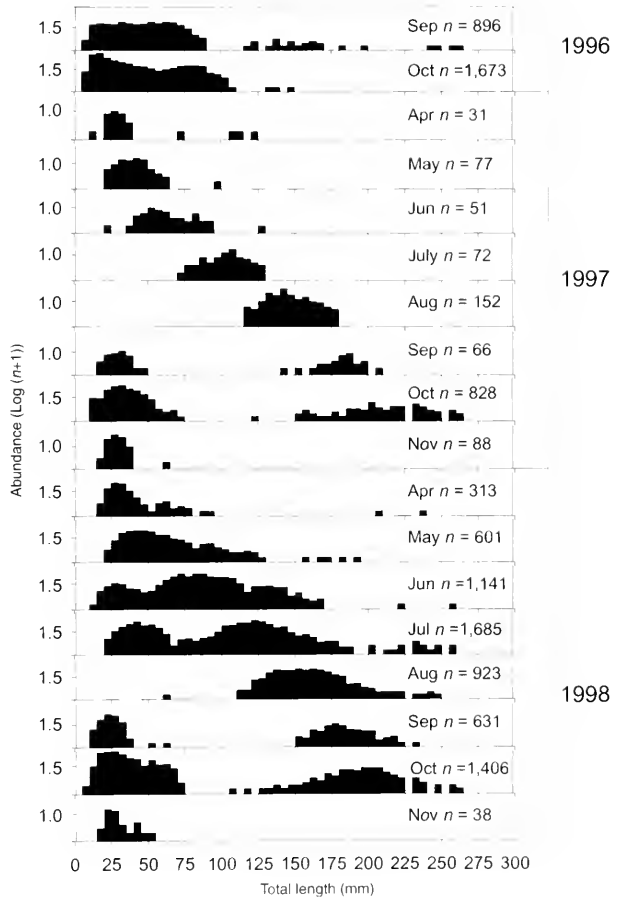

Figure 4

Length-frequency distributions of log $(n+1)$ transformed numbers of Atlantic croaker (*Micropogonias undulatus*) collected by otter trawl between April and November in Delaware Bay from 1996 to 1998. None were collected in the bay from April to August of 1996.

creeks in June 1999 (Fig 4). In the bay these were as small as 15 mm in June 1998 and had a mode of 26–30 mm. They were even more abundant in the bay during July 1998 and had a mode of 41–45 mm. Individuals of this cohort were collected at five of the eight zones in the bay during June and July but were rare in subsequent months (Fig. 4). A smaller size cohort of YOY (n=69 fish) also appeared in the marshes (Fig. 5) and in the associated bay stations in June 1999.

Distribution, abundance, and habitat use during summer residency

Young-of-the-year Atlantic croaker were abundant in Delaware Bay and in the adjacent marsh creeks from April through the fall egress of each year, except in 1996, when trawling in both the marshes and the bay caught no YOY until 26 individuals (115–200 mm) were collected in the bay in September and October (Fig. 4). In contrast, the

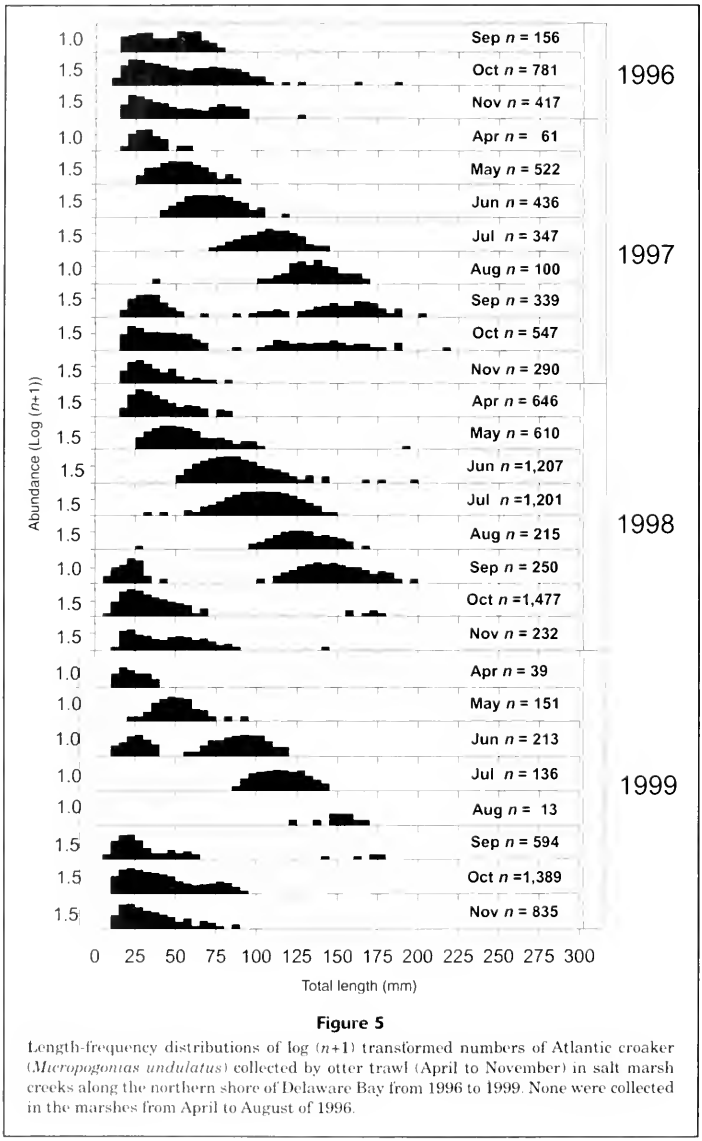

Figure 5

Length-frequency distributions of log (n+1) transformed numbers of Atlantic croaker (*Micropogonias undulatus*) collected by otter trawl (April to November) in salt marsh creeks along the northern shore of Delaware Bay from 1996 to 1999. None were collected in the marshes from April to August of 1996.

marsh creek surveys found YOY in both the large and small creeks from April to September during 1997, 1998, and 1999. Typically in the years after 1996, the CPUE was greatest from April to June at the lower bay marsh sites and then decreased after July to an almost total absence of fish toward the end of the fall egress out of the marshes in November (Fig. 6). The overall CPUE at each marsh site for all three year classes combined (April to November in 1997, 1998 and 1999) was highest at Dennis Township and Commercial Township and at Upper Moores Beach in the lower bay and lowest at Lower Moores Beach and at the upper bay sites (Fig. 7). As a result, the monthly

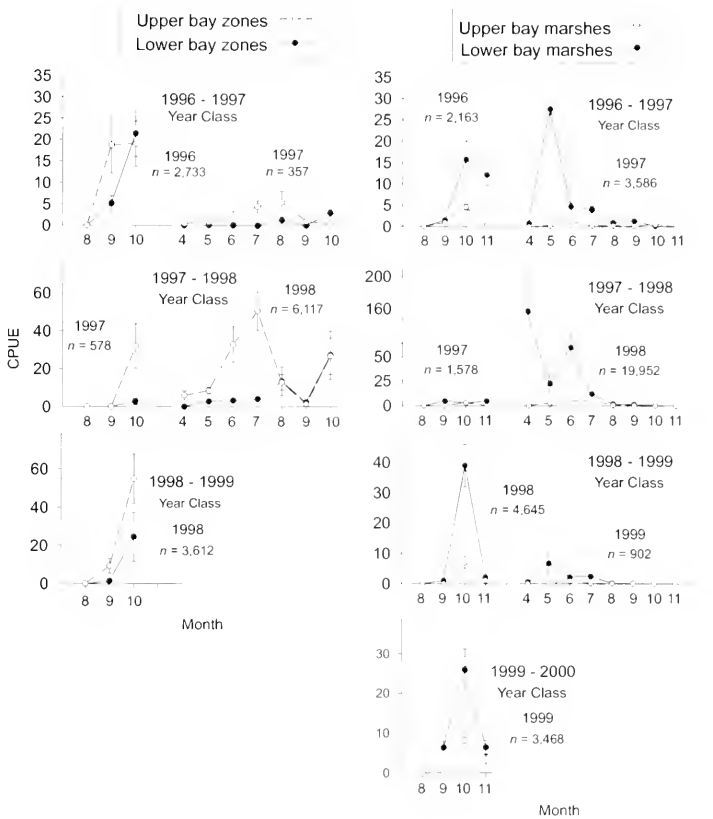

Figure 6

Monthly average catch per unit of effort (CPUE ±SEM) of young-of-the-year Atlantic croaker (*Micropogonias undulatus*) collected by otter trawl during the fall ingress and from April to November for three year classes in the upper and lower regions of Delaware Bay (left panels: CPUE=fish/10 min. tow) and of four year classes in tidal creeks at the upper and lower bay marsh sites (right panels: CPUE=fish/2 min. tow). No data are presented from April to July of 1996 because Atlantic croaker were absent from the bay and marshes until October.

CPUE at the lower bay marshes was consistently more than twice as high as that in the upper bay (Fig. 6). The combined four-year CPUE values for YOY caught during April–October 1997–99, at each of the six sites were significantly different ($P<0.001$), and the CPUE values at the Dennis Township site were significantly greater than at each of the other sites. The CPUE values at Commercial Township and Upper Moores Beach in the lower bay also were greater than those at all the upper bay sites.

Young-of-the-year Atlantic croaker also used small intertidal creeks in the marshes from April to August, where they were collected in weirs. They were most abundant at the Dennis Township site in the lower bay in all three years where they were present from May to July in 1997 and from April to August in 1998, 1999 (Fig. 8). The monthly CPUE (fish per set) in the weirs at Dennis Township was greatest in June of both 1997 and 1998. Compared to the total catch in the weirs at Dennis Township in all three years (n=3994), far fewer were caught in the weirs at the other sites in the lower bay during all three years (n=152) and fewer still at the sites in the upper bay (n=9). The CPUE of YOY Atlantic croaker in Delaware

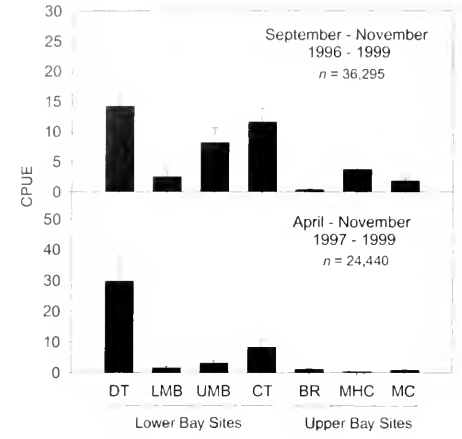

Figure 7

Combined overall average catch per unit of effort (CPUE= fish/2 min. tow [±SEM]) of young-of-the-year Atlantic croaker (*Micropogonias undulatus*) collected by otter trawl at the Dennis Township (DT), Lower Moores Beach (LMB), Upper Moores Beach (UMB), Commercial Township (CT), Browns Run (BR), Mad Horse Creek (MHC) and Mill Creek (MC) marsh sites during the fall ingress of four years (1996–99) and of post-ingress croaker (April to November 1997–99).

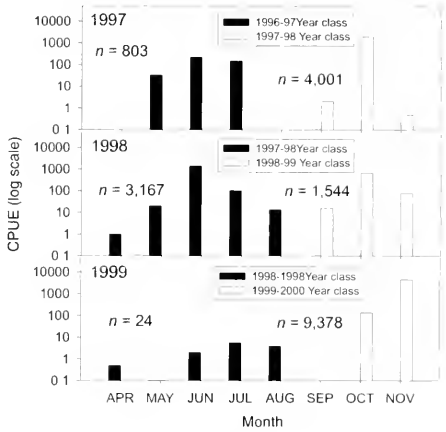

Figure 8

Catch per unit of effort (CPUE, fish/set) of four year classes of young-of-the-year Atlantic croaker (*Micropogonias undulatus*) caught each year in the two monthly weir sets across small intertidal creeks at the Dennis Township marsh site in the lower bay during the fall ingress (white bars) and during spring and summer of the following year (black bars).

Bay was higher in the upper bay, which has mud sediments in most areas, and was much higher in 1998 than in 1997. The monthly CPUE in the upper bay peaked in July or August, but in the lower bay it peaked in October of both years (Fig. 6). The combined CPUE values in the upper and lower bay zones were different between the two regions in both 1997 and 1998 ($P<0.001$) and the catches within each region were different between the two years ($P<0.001$).

During the summer most YOY were collected in areas of Delaware Bay that had muddy sediments (Fig. 9). In the upper bay zones 7 and 8, which likely have mostly pure mud sediments, YOY were collected at 82% of the stations. In contrast, they were absent in the deeper, large central area of the lower bay that has predominantly sandy and gravelly sediments. However, in the shallow portion of the lower bay, sandy mud, muddy sand, and gravelly mud sediments appear to be distributed on both sides of the bay, and YOY were almost exclusively collected over or near these substrates from April to August.

Growth

Although YOY Atlantic croaker showed rapid growth during the summer, there was no evidence of growth during the winter. The median growth rates for YOY Atlantic croaker calculated for two- to five-month periods beginning in May were fast and ranged from 0.5 to 1.5 mm/d (Table 3). They were slightly higher in the bay than in the marshes (avg.=1.2 mm/d in the bay and 0.9 mm/d in the marshes) and were lowest in 1998 when Atlantic croaker were most abundant. The growth rates dropped off in the marshes when calculated from May to September or October (Table 3). The lowest early summer growth rates occurred in the tidal creeks in the lower bay in 1998 when the CPUE was the highest. The growth rates in the upper and lower regions of Delaware Bay were similar in each year, but as in the lower bay marshes, the values were lower in 1998 when YOY were much more abundant. Linear regressions of the median lengths used to calculate these growth rates showed that median length was strongly correlated to date (P=0.02–0.001) and illustrated the slightly slower growth rates at the lower bay sites in both 1997 and 1998 (Fig. 10). These pairs of regression lines were not significantly different (ANCOVA) for upper and lower bay regions of either the marsh sites in 1997 (P=0.1), or in the bay in 1998 (P=0.6), except in 1998, when a lower growth rate was indicated at the lower bay marsh sites (P=0.03). In 1999, a similar linear progression of median lengths was observed in the lower bay marshes (r^2=0.98), but sample sizes were too small in the upper bay for growth-rate calculations. Although there was no sampling in the winter, the length-frequency distributions indicated that most fish collected in April in the bay and marshes were the same

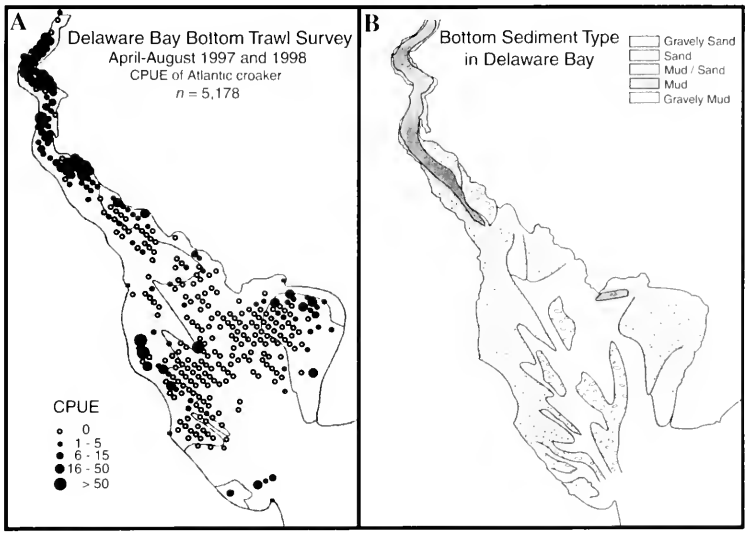

Figure 9

(**A**) Catch per unit of effort (CPUE=fish/10 min. tow) of young-of-the-year Atlantic croaker (*Micropogonias undulatus*) collected by otter trawl (April to August in 1997 and 1998). Sediments containing mud are indicated by shading. (**B**) The distribution of specific bottom sediment types in Delaware Bay is modified from Sharp (personal commun. [J. H. Sharp, Marine Studies, Univ. Delaware, Lewes, DE.]).

size or smaller than the ingressed fish collected during the previous fall of all three years (Figs. 4 and 5).

Consistent with the above fast growth rates, YOY Atlantic croaker reached lengths of about 70–140 mm by July and lengths ranging from 90 to 170 mm by August in the marshes and slightly larger in the bay (Figs. 4 and 5). As a result of these fast growth rates, the YOY attained a size of approximately 125–250 mm by September, approximately 12 months after ingress into the bay and adjacent marshes, and were distinctly larger than the next year class that began ingressing during September of each year.

Egress

Young-of-the-year Atlantic croaker showed a relatively consistent pattern of egress out of the marsh creeks in the late summer and fall of each year, and as a result, there was an increase in CPUE in the bay during October of both years. The monthly CPUE in both upper and lower bay marshes declined during the summer and were low by August in all three years (Fig. 6), but the number of fish present appeared to drop off more rapidly from August to October in 1999 than in other years (Figs. 5 and 6). In the bay, CPUE began to decrease somewhat later, after July or August, but then increased to the yearly maximum for the lower bay in October 1997 and 1998. By November of each year, almost all YOY appeared to move out of the marshes at sizes <200 mm, but in the bay there were large individuals >250 mm caught in October 1997 and 1998. The baywide trawling survey did not provide samples in November, so it was impossible to determine the timing of egress of the remaining YOY out of the bay, but very few age-1 fish were present in the bay or marshes by spring of the next year.

Discussion

Ingress and settlement

Young-of-the-year Atlantic croaker ingress into bay and marsh nursery areas starting in the fall of each year in Delaware Bay and in other estuaries along the Atlantic coast. The majority appeared in September, October, and November during our study and in previous collections in Delaware Bay (Able and Fahay, 1998), Chesapeake Bay (Haven, 1957; Chao and Musick, 1977), and North Carolina (Ross, 1988). However, the fall ingress of this cohort was not evident until October in Georgia (Dahlberg, 1972) and December in South Carolina (Bearden, 1964). The sudden appearance of significant numbers of larger fish (50–75 mm) in September 1996 in both the bay and marshes and to some extent in the marshes in 1999 suggests that individuals that experienced different growth rates or came from different spawning events sometimes occurred simultaneously in Delaware Bay.

Table 3

Estimated daily growth rates of young-of-the-year Atlantic croaker (*Micropogonias undulatus*) based on the monthly progression of median lengths in the upper and lower regions of Delaware Bay in 1997 and 1998 (see Fig. 1) and in tidal creeks in the marsh sites adjacent to the upper and lower bay in 1997, 1998, and 1999. Growth rate calculations were made for periods of two to five months, with each period starting in May. Calculations for locations with sample sizes <10 fish were excluded.

Habitat	Year	Location in bay	Average collection date	Sample size	Median length (mm TL)	Median growth rate (mm/d)
Delaware Bay	1997	Upper bay	17 May	25	33	—
			7 July	71	103	1.37
			5 Aug	88	143	1.38
			2 Sep	16	183	1.39
			2 Oct	10	190	1.14
		Lower bay	26 May	52	43	—
			16 Aug	64	154	1.35
			20 Sep	14	187	1.23
			4 Oct	96	218	1.34
	1998	Upper Bay	13 May	275	41	—
			15 Jul	873	121	1.27
			10 Aug	433	144	1.16
			6 Sep	45	177	1.17
		Lower Bay	15 May	326	57	—
			19 Jul	220	140	1.28
			16 Aug	490	164	1.15
			10 Sep	131	182	1.06
Marsh Creeks	1997	Upper Bay	21 May	17	46	—
			17 Jul	13	115	1.21
			20 Aug	16	154	1.19
			14 Oct	33	120	0.51
		Lower Bay	26 May	505	52	—
			23 Jul	334	110	1.00
			26 Aug	84	132	0.87
			21 Sep	99	161	0.92
			19 Oct	13	150	0.67
	1998	Upper Bay	8 May	142	41	—
			8 Jul	348	115	1.21
			5 Aug	41	143	1.15
			2 Sep	23	153	0.96
		Lower Bay	13 May	467	50	—
			14 Jul	851	100	0.81
			11 Aug	174	125	0.83
			9 Sep	126	142	0.77
	1999	Lower Bay	18 May	148	49	—
			18 Jul	128	114	1.07
			15 Aug	12	151	1.15

According to the sizes of individuals captured by plankton net in the water column, versus those collected by otter trawl on the bottom, settlement may occur over a broad size range, i.e. approximately 10–40 mm TL. Scale formation in Atlantic croaker begins at 14–16 mm SL and is completed at 31–38 mm SL during this time (Bridges, 1971) and is an indicator of transformation between larval and juvenile stages. Alternatively, collection of overlapping sizes in water column and bottom samples may imply frequent vertical movements as could occur during tidal stream transport (see Weinstein et al., 1980, for recent examples). These movements would provide an appropriate mechanism for small YOY to reach the bay and the lower Delaware River as has been suggested for larval Atlantic croaker in Chesapeake Bay (Norcross, 1991).

The length-frequency data from our study and from previous studies along the Atlantic coast indicate that a second, less-abundant cohort of YOY Atlantic croaker often

enter nursery areas during the spring and summer. This second cohort (between 10 and 45 mm) was observed in June 1998 and 1999 during our study and in May or August (20–30 mm) in the York River of the Chesapeake Bay (Chao and Musick, 1977). Similarly, a second mode was usually apparent from April through August during three years in North Carolina creeks and bays (Ross, 1988), and in May in Georgia (Dahlberg, 1972). In South Carolina, a second smaller cohort began appearing in March and subsequently became the dominant mode in June and July (Bearden, 1964). In addition, the larger-size individuals that have appeared during the fall months simultaneously with the ingressing fall cohort during our study and in the Chesapeake Bay (Haven, 1957; Chao and Musick, 1977), may be individuals of this late-arriving second cohort that did not enter the Chesapeake and Delaware bays until fall.

These late arrivals to nursery areas in the Chesapeake and Delaware bays may be individuals that were spawned close to or south of Cape Hatteras in late winter because there is no evidence of spawning in late winter or spring north of Cape Hatteras in the MAB. Atlantic croaker larvae were caught only from August to January 1977–1987 over the continental shelf in the MAB and while entering estuaries in central New Jersey (Able and Fahay, 1998), or from November to February in coastal Virginia (Cowan and Birdsong, 1985). In contrast, just south of Cape Hatteras, larvae as small as 5.2 mm SL were present in collections made from October through mid-April within and offshore of the Newport River estuary in North Carolina in both 1972–73 and 1973–74 (Lewis and Judy, 1983). Small larvae also were collected in the same estuary from November through mid-April in 1985–1986 (Warlen and Burke, 1990) and 1991–92 (Hettler et al., 1997) and in the Cape Fear estuary from mid-March to Mid-April in 1978 (Weinstein et al., 1980). Together, these studies indicate that late winter spawning occurs and suggests that it takes place south of Cape Hatteras. Analysis of otolith microstructure of larval and juvenile Atlantic croaker from the MAB indicates that later spawned larvae and juveniles have slower growth rates (Warlen, 1982; Nixon and Jones, 1997), which may account for the much smaller size of the later-arriving cohort when it enters the Chesapeake and Delaware bays during the late spring and early summer.

Ross (1988) suggested that there may be two groups of Atlantic croaker that overlap and mix in North Carolina. The first group, occurring from North Carolina southward through the northern Gulf of Mexico, with a tendency toward high mortality, lower longevity, early maturation, results from winter spawning (White and Chittenden, 1977; Barger, 1985) and mostly spring recruitment to estuaries. The second group ranges from North Carolina to about New Jersey and may exhibit lower mortality, higher longevity, greater size at age, late summer–fall spawning, mostly fall recruitment, and greater size at maturity (Wallace, 1940; Morse, 1980; Barbieri et al., 1994a). However, the group of larger, older Atlantic croaker observed by Ross (1988) apparently has been absent in Chesapeake Bay in recent years (Barbieri et al., 1994b). Lankford et al. (1999) did not find statistically significant genetic differences between fall-spawned YOY Atlantic croaker from north of Cape Hatteras and spring-spawned YOY from south of Cape Hatteras, but YOY from the Gulf of Mexico were genetically discrete from those from the Atlantic coast. This lack of marked genetic differences north and south of Cape Hatteras is not surprising if there is southward migration of adults from the MAB during winter as has been suggested (Haven, 1957). Although, spawning and recruitment to nursery areas does appear to occur later in the South Atlantic Bight (Bearden, 1964) and in the Gulf of Mexico (Pearson, 1929; Suttkus, 1955; Hansen, 1969), more research is needed to determine if there are significant biological differences between adults in these two areas and if the late arriving YOY in the north originate from spawning at or south of Cape Hatteras.

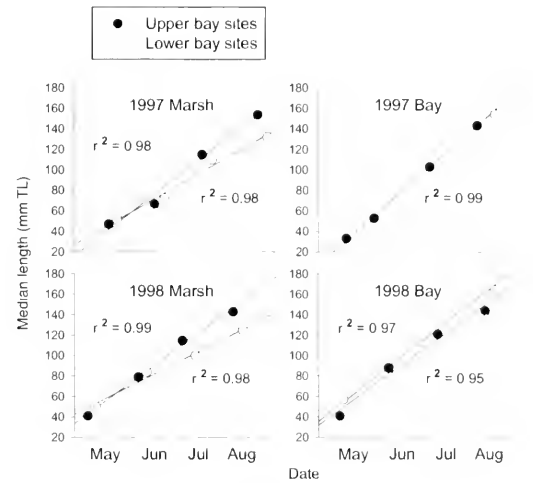

Figure 10

Linear regressions and goodness-of-fit measures of the monthly median total lengths of young-of-the-year Atlantic croaker (*Micropogonias undulatus*) caught at the upper bay (open circles) and lower bay (black circles) marsh sites and regions of Delaware Bay from May to August in 1997 and 1998 (see Table 3). The coefficient of determination is shown in the upper left for the upper bay regression lines and in the lower right for the lower bay. There is no regression for the lower bay because sample sizes in this region during June and July of 1997 were too small.

Habitat use

Young-of-the-year Atlantic croaker in this study used the entire range of marsh creek habitats, i.e. small intertidal

creeks and large subtidal creeks within the study area. Intensive tag and recapture studies in marsh creeks at the Dennis Township site found that YOY were resident for periods of up to 78 days from July through October 1998 (Miller and Able, 2002). As a result, our interpretations of habitat use and growth may be representative for much of the summer and fall in Delaware Bay marsh creeks.

In the deeper water of the bay, YOY were collected throughout the whole range of salinities but were most abundant over the predominantly pure mud sediments in the lower Delaware River and over areas with mud sediments elsewhere in the lower bay. This pattern is evident elsewhere because YOY have been reported to be most abundant over soft mud sediments in Apalachicola Bay in the Gulf of Mexico (Kobylinski and Sheridan, 1979). As in Delaware Bay, YOY have been collected over the full range of salinities in South Carolina (Bearden, 1964; Miglarese et al., 1982) and Georgia (Dahlberg, 1972). However, laboratory experiments suggest that lower salinities are metabolically less costly for YOY (Moser and Gerry, 1989; Peterson et al., 1999) and that in some areas of Chesapeake Bay, YOY are most abundant in regions with low salinities (<18‰) (Haven, 1957).

Habitat use and survival in the winter may vary between estuaries. Young-of-the-year Atlantic croaker appear to overwinter in estuaries in the Gulf of Mexico (Pearson, 1929; Suttkus, 1955; Hansen, 1969; Knudsen and Herke, 1978) and in the South Atlantic Bight (Bearden, 1964; Dahlberg, 1972; Bozeman and Dean, 1980), but in the MAB there is probably significant overwinter mortality in years with particularly cold winters. The YOY appear to overwinter in some estuarine habitats in the York River region of Chesapeake Bay in most years (Haven, 1957; Chao and Musick, 1977) and in deeper areas of the bay (Welsh and Breder, 1923), but in some years YOY have been observed to experience winter mortality based on their subsequent disappearance after a cold period (Massman and Pacheco, 1960) and on direct observations of mass mortalities and collections of dead YOY in years with unusually cold winters (Joseph, 1972; Chao and Musick, 1977, Wojcik, 1978). Further, analysis of long-term recruitment indices for Atlantic croaker from 1979 to 1993 indicates that the YOY of this species may have experienced winter mortality due to low water temperatures in 30% of the years in Chesapeake Bay and 74% of the years in Delaware Bay (Lankford and Targett, 2001).

Overwintering mortality apparently occurred in Delaware Bay in 1996 when water temperatures in the region dropped below 3°C and remained below 4°C for an extended period of time. The NOAA Buoy 4409, located in the ocean just south of the mouth of Delaware Bay, recorded water temperatures at about 2–4°C for 18 days during January and February 1996, which is at or below the approximate survival temperature of 3°C determined in laboratory experiments (Lankford and Targett, 2001). This apparently resulted in a total absence of YOY throughout the bay and in marsh creeks during the spring and summer, which is not surprising because temperatures in the estuary were likely cooler than in the ocean. In contrast, during the winters preceding the relatively high catch years of 1997 and 1998, water temperatures at the same location never dropped below 4.4°C during the winter of 1996–97 or below 5.6°C during 1997–98.

Growth

Growth rates that we calculated in both upper and lower regions of the Delaware Bay (two years) and in the marshes (three years) ranged from about 0.8 to 1.4 mm/d from May to July. The strong linear correlation between median length and date suggested that the average growth rates were relatively constant during the summer from May to August before egress from marshes. Seasonal growth rates of YOY Atlantic croaker in other estuaries along the Atlantic coast may be similar to those in Delaware Bay, but the way in which they were calculated influences the values. Knudsen and Herke (1978) reviewed the apparent growth rates of YOY Atlantic croaker from a variety of sources but presented growth rates only for the entire first year of growth, which were all less than 0.5 mm/d for studies along the Atlantic coast and in the Gulf of Mexico. However, these estimates included both larval and overwintering periods; therefore they probably underestimated the growth rates during the summer when growth rates are highest. Monthly modal progression in published lengths indicate relatively fast growth rates during the summer in estuarine areas south of Delaware Bay. Our calculation of modal progression in lengths from May to July in various parts of the York and Pamunkey rivers of Chesapeake Bay suggested growth rates of approximately 1.3 and 0.7 mm/d in 1952 and 1953, respectively (Haven, 1957) and of 0.9 mm/d in 1972 (Chao and Musick, 1977). Similarly, calculated values for May to July for fish from shallow creeks in North Carolina indicated growth rates of 0.6, 0.8, and 0.9 mm/d in 1979, 1980, and 1981, but the 1979 estimate is likely to be an underestimate because many of the larger fish appeared to be moving into deeper habitats during that time period (Ross, 1988). In our study, the growth rates remained relatively high when calculated through October (1.1–1.3 mm/d) in the bay but dropped off in the marshes (0.5–0.7 mm/d), potentially reflecting the egress of larger YOY out of the marshes into the bay.

Data from the Gulf of Mexico suggest slower growth rates of YOY Atlantic croaker in some areas but egress of larger fish out of the sampling area may also bias these estimates. Hansen (1969) used length-frequency data to determine growth rate estimates of 0.3 mm/d from January through August in the Pensacola Estuary on the Florida gulf coast in both 1964 and 1965 but noted the highest growth rates were in July (0.6 mm/d). Knudsen and Herke (1978) estimated growth of YOY in a semi-impounded marsh in Louisiana using recaptured individuals sprayed with fluorescent pigment during winter and spring and found rates of 0.4–0.5 mm/d for fish marked in late January and early February and recaptured into March. Rates for those marked mid-February to late March and recaptured into May were 0.8–0.92 mm/d. A previous study at the same location, using the same techniques, estimated that fish marked from December to March and recaptured into June grew at about 0.47 mm/d (Arnoldi et al., 1974). The monthly

length-frequency data from Lake Pontchartrain, Louisiana (Suttkus, 1955), indicated a constant but slow growth rate of 0.3 mm/d from February to September 1954, and no increase in growth rate during the summer. As a result of the above, it appears that growth rates may be faster, and thus countergradient in more northern populations, as suggested for *Menidia* (Conover and Present, 1990), but care should be taken in interpreting growth rates from the literature, especially those based on modal progression.

Egress

Young-of-the-year Atlantic croaker have a regular pattern of egress out of tidal creeks and estuaries in the MAB during the late summer and fall after reaching lengths of about 100–250 mm. As we observed in the Delaware Bay system, the majority left the marsh creeks from August to October at lengths <200 mm. The larger individuals appeared to leave the marshes first, as has been observed elsewhere (Haven, 1957; Yakupzack et al., 1977), and almost all had left by November. However, the CPUE increased in Delaware Bay in October of both years, and this may have been caused by fish egressing out of the marshes into the bay. Large individuals remained in Delaware Bay longer than in the marshes and substantial numbers of fish 150–300 mm were present in the bay in September and October. This finding suggests that egress from the tidal creeks caused the disappearance of Atlantic croaker there, and not gear avoidance, because large fish continued to be caught in the bay. The exact timing of egress of the majority of Atlantic croaker out of the bay is unclear due to lack of sampling throughout the bay after October. However, previous collections in Delaware Bay have shown no evidence of any individual >100 mm from November to March (Able and Fahay, 1998), suggesting that egress out of the bay is finished by November in some years. The same pattern of egress out of nursery habitats in the fall has been observed in Chesapeake Bay (Haven, 1957), but in some years there were substantial numbers of fish present into November (Chao and Musick, 1977). Very few of each year class reappear in collections during the spring and summer of the next year in either Chesapeake or Delaware bays (Haven, 1957; Chao and Musick, 1977; Able and Fahay, 1998) and therefore the fate of these individuals is unknown.

Fall egress also occurs out of estuaries in the South Atlantic Bight and the Gulf of Mexico, but in contrast to the Chesapeake and Delaware bays, more Atlantic croaker appear to either remain through the winter or re-enter these habitats in some areas in late winter or early spring. In North Carolina, egress out of tidal creeks was mostly completed by November, but this same year class was present again as age-1 fish in the bays in March, April, and May when sampling resumed (Ross, 1988). A similar pattern of egress from estuaries was observed in South Carolina, but the reappearance of age-1 fish in February was even more prominent and they continued to be collected until fall (Bearden, 1964). In the Gulf of Mexico, some age-1 fish have been observed to remain in estuarine habitats for an additional year in Lake Pontchartrain, Louisiana (Suttkus, 1955), or reappear from January to April after leaving the study area in December in coastal Texas (Pearson, 1929).

In summary, this study presents the first comprehensive examination of YOY Atlantic croaker seasonality and habitat use in Delaware Bay and the adjacent marshes. Although patterns of habitat use and seasonality are similar along the east coast, some divergence from the seasonal patterns in Delaware Bay are evident in estuaries in the South Atlantic Bight and the Gulf of Mexico. Growth estimates appear to be the most divergent of any characteristics examined—faster growth rates occurring in the more northern estuaries such as Delaware Bay.

Acknowledgments

Numerous individuals from the Rutgers University Marine Field Station participated in the field sampling or helped with data analysis. We would particularly like to thank Ralph Bush, Bertrand Lemasson, Steven Teo, and James Chitty. John Balletto and Ken Strait provided background information and logistical support. Jonathan Sharp provided data on sediments in Delaware Bay. Financial support was provided by the Estuary Enhancement Program of Public Service Enterprise Group.

Literature cited

Able, K. W., and M. P. Fahay.
1998. The first year in the life of estuarine fishes in the Middle Atlantic Bight, 342 p. Rutgers University Press, New Brunswick, NJ.

Able, K.W., D. Nemerson, R. Bush, and P. Light.
2001. Spatial variation in Delaware Bay (U.S.A.) marsh creek fish assemblages. Estuaries 24(3):441–452.

Able, K.W., D. M. Nemerson, P. R. Light, and R. O. Bush.
2000. Initial response of fishes to marsh restoration at a former salt hay farm bordering Delaware Bay. *In* Concepts and controversies in tidal marsh ecology (M. P. Weinstein and D. A. Kreeger eds.), p. 749–773. Kluwer Academic Publishers, The Netherlands.

Arnoldi, D. C., W. H. Herke, and E. J. Clairain Jr.
1974. Estimate of growth rate and length of stay in a marsh nursery of juvenile Atlantic croaker, *Micropogonias undulatus* (Linnaeus), "sandblasted" with fluorescent pigments. Gulf Caribb. Fish. Inst. 26:158–172.

Barbieri, L. R., M. E. Chittenden, Jr., and C. M. Jones.
1994a. Age, growth, and mortality of Atlantic croaker, *Micropogonias undulatus*, in the Chesapeake Bay region, with a discussion of apparent geographic changes in population dynamics. Fish. Bull. 92:1–12.

Barbieri, L. R., M. E. Chittenden Jr., and S. K. Lowerre-Barbieri.
1994b. Maturity, spawning, and ovarian cycle of Atlantic croaker, *Micropogonias undulatus*, in the Chesapeake Bay and adjacent coastal waters. Fish. Bull. 92:671–685.

Barger, L. Y.
1985. Age and growth of Atlantic croakers in the northern Gulf of Mexico, based on otolith sections. Trans. Am. Fish. Soc. 114:847–850.

Bearden, C. M.
1964. Distribution and abundance of Atlantic croaker, *Mi-*

cropogonias undulatus, in South Carolina. Contrib. Bears Bluff Lab., South Carolina 10:1–23.

Bozeman, E. L., Jr., and J. M. Dean.
1980. The abundance of estuarine larval and juvenile fish in a South Carolina intertidal creek. Estuaries 3:89–97.

Bridges, D.W.
1971. The pattern of scale development in juvenile Atlantic croaker (*Micropogonias undulatus*). Copeia 1971(2): 331–332.

Chao, L. N., and J. A. Musick.
1977. Life history, feeding habits, and functional morphology of juvenile sciaenid fishes in the York River Estuary, Virginia. Fish. Bull. 75:657–702.

Conover, D. O., and T. M. C. Present.
1990. Countergradient variation in growth rate: compensation for length of the growing season among Atlantic silversides from different latitudes. Oceologia 83:316–324.

Cowan, J. H., and R. S. Birdsong.
1985. Seasonal occurrence of larval and juvenile fishes in a Virginia Atlantic coast estuary with emphasis on drums (Family Sciaenidae). Estuaries 8:48–59.

Cronin, L. E., J. C. Daiber, and E. M. Hulbert.
1962. Quantitative seasonal aspects of zooplankton in the Delaware River estuary. Chesapeake Sci. 3(2):63–93.

Currin, B. M., J. P. Reed, and J. M. Miller.
1984. Growth, production, food consumption, and mortality of juvenile spot and croaker: a comparison of tidal and nontidal nursery areas. Estuaries 7:451–459.

Dahlberg, M. D.
1972. An ecological study of Georgia coastal fishes. Fish. Bull. 70:323–353.

Garvine, R. W., R. K. McCarthy, and K.-C. Wong.
1992. The axial salinity distribution in the Delaware Estuary and its weak response to river discharge. Estuar. Coast. Shelf Sci. 35:157–165.

Hansen, D. J.
1969. Food, growth, migration, reproduction, and abundance of pinfish, *Lagodon rhomboides*, and Atlantic croaker, *Micropogonias undulatus*, near Pensacola, Florida, 1963–65. Fish. Bull. 68:135–146.

Haven, D. S.
1957. Distribution, growth, and availability of juvenile croaker, *Micropogonias undulatus*, in Virginia. Ecology 38:88–97.
1959. Migration of the croaker, *Micropogonias undulatus*. Copeia 1959:25–30.

Hettler, W. F., D. S. Peters, D. R. Colby, and E. H. Laban.
1997. Daily variability in abundance of larval fishes inside Beaufort Inlet. Fish. Bull. 95:477–493.

Joseph, E. B.
1972. The status of the sciaenid stocks of the middle Atlantic coast. Chesapeake Sci. 13:87–100.

Knudsen, E. E., and W. H. Herke.
1978. Growth rate of marked juvenile Atlantic croakers, *Micropogonias undulatus*, and length of stay in a coastal marsh nursery in southwest Louisiana. Trans. Am. Fish. Soc. 107:12–20.

Kobylinski, G. J., and P. F. Sheridan.
1979. Distribution, abundance, feeding and long-term fluctuations of spot, *Leiostomus xanthurus*, and croaker, *Micropogonias undulatus*, in Apalachicola Bay, Florida, 1972–1977. Contrib. Mar. Sci. 22:149–161.

Lankford, T. E., Jr., and T. E. Targett.
2001. Low-temperature tolerance of age-0 Atlantic croakers: recruitment implications for U.S. Mid-Atlantic estuaries. Trans. Am. Fish. Soc. 130:236–249.

Lankford, T. E. Jr., T. E. Targett, and P. M. Gaffney.
1999. Mitochondrial DNA analysis of population structure in the Atlantic croaker, *Micropogonias undulatus*, (Perciformes: Sciaenidae). Fish. Bull. 97:884–890.

Lewis, R. M., and M. H. Judy.
1983. The occurrence of spot, *Leiostomus xanthurus*, and Atlantic croaker, *Micropogonias undulatus*, larvae in Onslow Bay and Newport River Estuary, North Carolina. Fish. Bull. 81:405–412.

Massman, W. H., and A. L. Pacheco.
1960. Disappearance of young Atlantic croakers from the York River, Virginia. Trans. Am. Fish. Soc. 89:154–159.

Miglarese, J. V., C. W. McMillan, and M. H. Sealy Jr.
1982. Seasonal abundance of Atlantic croaker (*Micropogonias undulatus*) in relation to bottom salinity and temperature in South Carolina estuaries. Estuaries 5:216–223.

Miller, M. J. and K.W. Able.
2002. Movements and growth of tagged young-of-the-year Atlantic croaker, *Micropogonias undulatus*, in restored and reference marsh creeks in Delaware Bay. J. Exp. Mar. Biol. Ecol. 267:15–38.

Morse, W. W.
1980. Maturity, spawning and fecundity of Atlantic croaker, *Micropogonias undulatus*, occurring north of Cape Hatteras, North Carolina. Fish. Bull. 78:190–195.

Moser, M. L., and L. R. Gerry.
1989. Differential effects of salinity changes on two estuarine fishes, *Leiostomus xanthurus* and *Micropogonias undulatus*. Estuaries 12:35–41.

Nixon, S. W., and C. M. Jones.
1997. Age and growth of larval and juvenile Atlantic croaker, *Micropogonias undulatus*, from the middle Atlantic Bight and estuarine waters of Virginia. Fish. Bull. 95:773–784.

Norcross B. L.
1991. Estuarine recruitment mechanisms of larval Atlantic croakers. Trans. Am. Fish. Soc. 120:673–683.

Norcross, B. L., and H. M. Austin.
1988. Middle Atlantic Bight meridional wind component effect on bottom water temperatures and spawning distribution of Atlantic croaker. Cont. Shelf Res. 8:69–88.

Pearson, J. C.
1929. Natural history and conservation of the redfish and other commercial sciaenids on the Texas coast. Bull. U. S. Bur. Fish. 44:129–214

Peterson, M. S., B. H. Comyns, C. F. Rakocinski, and G. L. Fulling.
1999. Does salinity affect somatic growth in early juvenile Atlantic croaker, *Micropogonias undulatus* (L.)? J. Exper. Mar. Biol. Ecol. 238:199–207.

Reiss, S. R., and J. R. McConaugha.
1999. Cross-frontal transport and distribution of ichthyoplankton associated with Chesapeake Bay plume dynamics. Cont. Shelf Res. 19:151–170.

Ross, S. W.
1988. Age, growth, and mortality of Atlantic croaker in North Carolina, with comments on population dynamics. Trans. Am. Fish. Soc. 117:461–473.

Shenker, J. M., and J. M. Dean.
1979. The utilization of an intertidal salt marsh creek by larval and juvenile fishes: abundance, diversity and temporal variation. Estuaries 2:154–163.

Suttkus, R. D.
1955. Seasonal movements and growth of the Atlantic croaker (*Micropogonias undulatus*) along the east Louisiana coast. Gulf Caribb. Fish. Inst. 7:151–158.

Wallace, D. H.
1940. Sexual development of the croaker, *Micropogonias undulatus*, and distribution of early stages in Chesapeake Bay. Trans. Am. Fish. Soc. 70:475–482.

Warlen, S. M.
1982. Age and growth of larvae and spawning time of Atlantic croaker in North Carolina. Proc. Annu. Conf., S.E. Assoc. Fish Wild. Agencies 34:204–214.

Warlen, S. M., and J. S. Burke.
1990. Immigration of larvae of fall/winter spawning marine fishes into a North Carolina estuary. Estuaries 13:453–461.

Weinstein, M. P.
1979. Shallow marsh habitats as primary nurseries for fishes and shellfish, Cape Fear River, North Carolina. Fish. Bull. 77:339–357.

Weinstein, M. P., S. L. Weiss, R. G. Hodson, and L. R. Gerry.
1980. Retention of three taxa of postlarval fishes in an intensively flushed tidal estuary, Cape Fear, North Carolina. Fish. Bull. 78:419–434.

Welsh, W. W., and C. M. Breder.
1923. Contributions to the life histories of Sciaenidae of the eastern United States coast. Bull. U.S. Bur. Fish. 39:141–201.

White, M. L., and M. E. Chittenden Jr.
1977. Age determination, reproduction, and population dynamics of the Atlantic croaker, *Micropogonias undulatus*. Fish. Bull. 75:109–123.

Wojcik, F. J.
1978. Temperature-induced croaker mortality. Coast. Oceanogr. Climatol. News 1:5.

Yakupzack, P. M., W. H. Herke, and W. G. Perry.
1977. Emigration of juvenile Atlantic croaker, *Micropogonias undulatus*, from a semi-impounded marsh in southwestern Louisiana. Trans. Am. Fish. Soc. 106:538–544.

Age validation, growth, mortality, and additional population parameters of the goldband snapper (*Pristipomoides multidens*) off the Kimberley coast of northwestern Australia

Stephen J. Newman
Iain J. Dunk
Western Australian Marine Research Laboratories
Department of Fisheries
Government of Western Australia
P.O. Box 20
North Beach, Western Australia 6920, Australia
E-mail address (for S. J. Newman): snewman@fish.wa.gov.au

Abstract—Goldband snapper (*Pristipomoides multidens*) collected from commercial trap and line fishermen off the Kimberley coast of northwestern Australia were aged by examination of sectioned otoliths (sagittae). A total of 3833 *P. multidens*, 80–701 mm fork length (98–805 mm total length), were examined from commercial catches from 1995 to 1999. The oldest fish was estimated to be age 30+ years. Validation of age estimates was achieved with marginal increment analysis. The opaque and translucent zones were each formed once per year and are considered valid annual growth increments (the translucent zone was formed once per year between January and May). A strong link between water temperature and translucent zone formation was evident in *P. multidens*. The von Bertalanffy growth function was used to describe growth from length-at-age data derived from sectioned otoliths. No significant differences in length-at-age were found between sexes and growth parameters were L_∞ = 598 mm, K = 0.187/yr, t_0 = –0.173 (r^2=0.76). Regression models of estimated age as a function of otolith and fish measurements indicated a significant relationship between estimated age and otolith weight (r^2=0.94). Total instantaneous mortality (Z) estimates generated from catch-at-age data of *P. multidens* from the northern demersal scalefish fishery (NDSF) were 0.65 for 1995–96, 0.87 for 1996–97, and 0.71 for 1997–98. Estimates of the annual instantaneous rate of natural mortality (M) were 0.10–0.14. The NDSF population of *P. multidens* is considered to be exploited above optimum levels on the basis of these mortality estimates. The protracted longevity, moderately slow growth and low natural mortality rates of *P. multidens* predispose this species as one vulnerable to overfishing, thus cautious management strategies will be required. Furthermore, capture of *P. multidens* from depths of 60 meters or greater results in a high mortality of fish because the physoclistous ruptures causing internal hemorrhaging and hence there is a low probability of survival of any fish returned to the sea. Thus traditional harvest strategies involving size limits will be inappropriate for these fish. Conversely, harvest strategies that include appropriately targeted spatial fishery closures may provide a useful additional means of preserving the spawning stock biomass of these fish and protect against recruitment overfishing.

Manuscript accepted 21 August 2002.
Fish. Bull. 116–128 (2003).

The goldband snapper (*Pristipomoides multidens*, Day), known also as goldbanded jobfish, Day's jobfish and large-scaled jobfish, is widely distributed throughout the tropical Indo-Pacific Ocean region from Samoa in the Central Pacific to the Red Sea in the Western Indian Ocean and from southern Japan south to Australia (Allen, 1985). Along Western Australia, *P. multidens* is found as far south as Cape Pasley (34°S) and is landed in commercial quantities from the Ningaloo Reef area (23°30′S) northwards (Kailola et al., 1993; Newman, unpubl. data). They inhabit hard bottom areas and areas of vertical relief and large epibenthos from depths of 60 to at least 245 m and are concentrated in depths from 80 to 150 m (Allen, 1985; Newman and Williams, 1996).

Pristipomoides multidens is a commercially important species throughout much of its range, forming an important part of the landed catch in both artisanal and developed fisheries (Dalzell and Preston, 1992; Newman, 2001). In Western Australia this highly valued resource is marketed whole, usually fresh on ice, and transported by road from regional ports to markets in most state capital cities. It is occasionally exported. In the Kimberley region, within the northern demersal scalefish fishery (NDSF), *P. multidens* has composed on average 37.7% of the landed catch from 1995 to 1999 (contributing on average 255 metric tons (t)/year). In terms of value to fishermen, it is second only to the red emperor snapper (*Lutjanus sebae*).

Information on the biology of *P. multidens* is limited. The juvenile habitats of *P. multidens* have not been identified, although Newman (unpubl. data) obtained juveniles from uniform sedimentary habitat with no relief. In previous studies, several age determination techniques were used to determine the age of *P. multidens* but there were limited attempts at age validation (Edwards, 1985; Mohsin and Ambak, 1996; Richards[1]). The accurate determination of fish age is the key to estimating growth rates and mortality. Errors in determining fish age can result in ambiguous demographic parameters and provide misleading impressions of the production potential of fish stocks (Newman et al., 2000a). There is a lack of reliable information on the longevity, growth parameters, mortality rates, and population characteristics of *P. multidens*, despite its ecological and commercial importance.

This work represents the first comprehensive study of age, growth, and mortality of a population of *P. multidens* based on age estimates from sectioned otoliths and contributes to the management of these stocks. The objectives of this study were to validate aging and to provide age, growth, mortality and population characteristics of *P. multidens* from the Kimberley region of Western Australia that are based on age estimates from sectioned otoliths.

[1] Richards, A. H. 1987. Aspects of the biology of some deep water bottomfish in Papua New Guinea with special reference to *Pristipomoides multidens* (Day). Report 87-01, 31p. Fisheries Research and Surveys Branch, Department of Primary Industry, Port Moresby, Papua New Guinea.

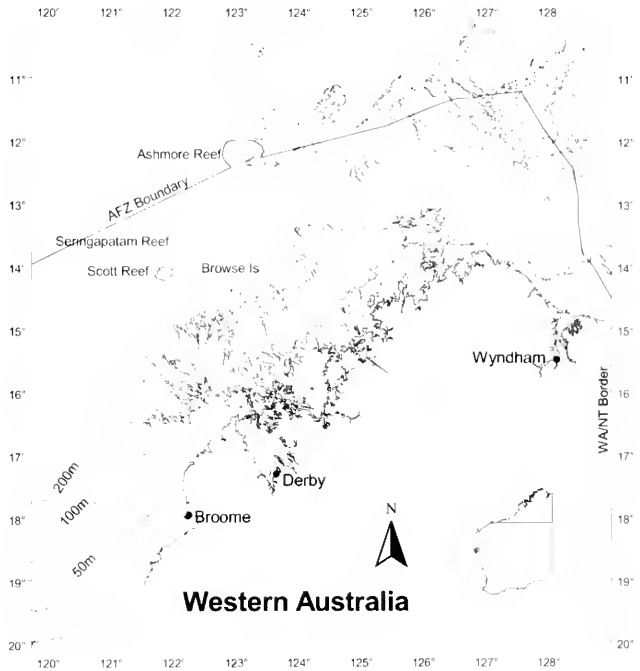

Figure 1

Location of the northern demersal scalefish fishery (NDSF) off the Kimberley coast of northwestern Australia showing the 50-m, 100-m, and 200-m depth contours. The NDSF is bounded in the west by the 120°E latitude line, to the north by the boundary of the Australian fishing zone (AFZ), and to the east by the border with the Northern Territory. Fishing primarily occurs in depths of 80–140 m.

A further objective was to investigate the relationship between estimated age and the measurements of both otolith and fish dimensions to assess the applicability of these measurements in predicting the age of this species.

Materials and methods

Commercial landings of *P. multidens* from the NDSF off the Kimberley coast of Western Australia were sampled from 1995 to 1999. Samples were acquired opportunistically from July 1995 to December 1996, whereas samples obtained from January 1997 to December 1999 were collected on a monthly basis among all vessels in the fleet. All specimens were captured with fish traps at depths of 60 to 200 m from 12°–20°S latitude (Fig. 1). Additional specimens were attained from research vessel cruises with fish traps.

All fish were measured to the nearest mm total length (TL), fork length (FL) and standard length (SL), weighed to the nearest g total weight (TW) and cleaned weight (CW), and where possible, sex was determined by examination of the gonads. Cleaned weight is defined as the TW after removal of the gills and viscera. Length measurements were used to derive conversion equations with linear regression models [$TL=a + b\,(FL)$, $FL=a + b\,(TL)$, $FL=a + b\,(SL)$ and $SL=a + b\,(FL)$].

Length-weight models

The relationships between FL and both TW and CW were described by the power function

$$W = aL^b,$$

where W = weight (TW or CW, g); and
L = FL (mm).

These relationships were fitted to log-transformed data and the parameters were back-transformed (with correction for bias) to the above form.

Analysis of covariance (α=0.05) was used to determine if there were significant differences in the weights-at-length (FL) relationships between sexes for *P. multidens*. Length and weight data were transformed to natural logarithms to satisfy assumptions of normality and homogeneity. Multiple comparisons were performed with Tukey's honestly significant difference (HSD) test. Trends in mean length and weight of fish over time were assessed by using analysis of variance (α=0.05).

Otolith preparation and analysis

Otolith removal, measurement, and preparation followed the procedures and protocols described in Newman et al. (1996), Newman et al. (2000b), and Newman and Dunk (2002). All age estimates were based on the analysis of thin transverse sections of otoliths. These thin sections were examined under a dissecting microscope at 10–30× magnification with reflected light on a black background.

The otoliths from eight juvenile *P. multidens* (80–140 mm FL) were examined for daily bands with a different technique. One sagitta per fish was embedded in epoxy resin and a thick transverse section (>500 µm) was cut. The section was then ground and polished from each side to a level near the core (perpendicular to the long axis of the otolith) by hand with ebony paper (1000 grade) and lapping film (9 and 3 µm). A polished thin transverse section approximately 100 µm thick was produced. The section was then examined with a compound microscope.

Age validation

Marginal increment analysis, routinely used to validate fish age, relies on the assumption that if a translucent zone is laid down once a year, there should be a clear pattern of periodic growth on the edge of the otolith during the year. Marginal increment analysis is appropriate only if all fish in the population lay down the translucent zone at the same time. Thus, an annulus consists of a single opaque and a single translucent cycle within a 12-month period. The opaque zone is believed to form during periods of slow growth.

Marginal increment analysis usually implies measurement of marginal growth and hence many researchers have measured the width of the edge of the otolith section over an annual cycle. This measurement approach has an advantage in that it should be possible to plot growth of the edge over time to validate that only a single translucent mark is laid down each year. However, in *P. multidens*, it can be difficult to determine a consistent location to measure on the otolith because of the inherent variability of their otoliths; hence this technique was not used in the present study.

Edge type analysis was adopted for the marginal increment analysis of *P. multidens* and edge types were classified according to Pearson (1996) as either translucent, narrow opaque (opaque area less than half of the previous opaque zone), or wide opaque (opaque area greater than half of the previous opaque zone). Sectioned otoliths of fish of all ages were examined under a dissecting microscope with reflected light on a black background.

Age determination

Because the peak spawning period of *P. multidens* occurs in late March, all fish were assigned a birth date of 1 April to assure proper year-class identification. Ages were assigned from counts of annual growth increments consisting of alternating opaque and translucent rings from sectioned otoliths (opaque rings were counted). Annual growth increments were counted in the ventral lobe of the otolith from the primordium to the proximal surface, as close as was practicable to the ventral margin of the sulcus acousticus. Annual growth increments were counted without reference to fish length or date of capture. Each otolith section was examined on four separate occasions. When the counts differed, otolith sections were re-examined. In most cases that required resolution, the fourth and final count was used for analysis of age and growth because by this time considerable experience had been gained in the interpretation of the otolith structure. Otoliths with structural irregularities (such as unusual calcification, deterioration of the ventral lobe, or poorly defined annual growth increments) were considered indecipherable and were excluded from analysis of fish age.

Counts were compared and the precision of age estimates were calculated with the average percent error (APE) of Beamish and Fournier (1981). Greater precision is achieved as the APE is minimized. The relationship between fish length (FL) and age and otolith dimensions was assessed with linear regression techniques.

Timing of translucent zone formation in *P. multidens* and mean sea surface temperatures (SST was assumed to reflect the temperature at depth) were compared by scaling values from the two data sets. The scaling process allowed direct comparison of each series and any time lags of one in relation to the other. Using the scaling score = 1 – ((maximum data value – data value) ÷ range), where (in the month of November) mean SST for the month was 29°C, the maximum for the year (data set) was 29.7 and the range of the data values was 3.7, we calculated the scaled SST = 1 – ((29.7–29) ÷ 3.7) = 0.81; in addition the scaled % frequency of otoliths with translucent edge types = 1 – ((67–20) ÷ 67) = 0.30.

Growth and mortality models

The von Bertalanffy growth function (VBGF) was fitted to estimates of length-at-age with nonlinear least squares estimation procedures. The VBGF is defined by the equation

$$L_t = L_\infty \left\{1 - \exp\left[-K(t - t_0)\right]\right\},$$

where L_t = mean length of fish of age t;
L_∞ = asymptotic mean length;
K = is a rate constant that determines the rate at which L_t approaches L_∞;
t = age of the fish; and
t_0 = the hypothetical age at which the mean length is zero if it had always grown in a manner described by the VBGF.

Table 1

Length-weight relationships for *P. multidens* off the Kimberley coast of northwestern Australia. Estimates were obtained for the parameters a and b of the relationship $W = aL^b$, the sample size (n), and the regression r^2 value (lengths used are fork length [FL] in mm and the weight is total weight [TW] or cleaned weight [CW] in g).

Group	a	b	n	r^2
P. multidens (all fish—TW)	2.483×10^{-5}	2.9501	3680	0.983
P. multidens (all fish—CW)	2.356×10^{-5}	2.9425	3073	0.983
P. multidens (male—TW)	2.156×10^{-5}	2.9737	1963	0.985
P. multidens (female—TW)	2.825×10^{-5}	2.9281	1671	0.987

The von Bertalanffy growth curves for both sexes were compared with the likelihood ratio test of Cerrato (1990).

Estimates of the instantaneous rate of total mortality (Z) were obtained from catch-at-age data from the NDSF. Annual catch in weight was converted to annual catch in numbers-at-age by the use of age-frequency data standardized by fishing effort to obtain catch-per-age class. Catch in weight was converted to catch in numbers based on the mean weight of *P. multidens* observed in the sampled catch each year. Mortality estimates were then derived between successive years by obtaining the natural logarithm of the catch per age class (e.g. age 7) in year t and subtracting the natural logarithm of the catch per age class (e.g. age 8) in year $t + 1$ for all fully recruited age classes. Mean total Z was then calculated across all fully recruited age classes. Instantaneous natural mortality rates (M) were derived by using the general regression equation of Hoenig (1983) for fish, where $\log_e Z = 1.46 - 1.01 \log_e t_{max}$ (t_{max}=the maximum age in years). The Hoenig equation has been shown to provide a reasonable approximation of M in tropical demersal fishes (Hart and Russ, 1996; Newman et al., 1996; 2000b).

The annual percentage removal was estimated by annual percentage = $[F/Z\ (1-e^{-Z})] \times 100\%$. Exploitation rates ($E$) were derived from the estimates of Z and F as defined by the equation $E = F/Z$ (F=the instantaneous rate of fishing mortality derived from the relationship $F=Z-M$). Reference points for target (optimal) and limit fishing mortality rates (F_{opt} and F_{lmit}) were calculated for *P. multidens* by using the estimate of natural mortality (M), because $F_{opt} = 0.5\ M$ (Walters, in press) and $F_{lmit} = 2/3\ M$ (Patterson, 1992).

Results

A total of 3833 *P. multidens* (ranging in size from 80 to 701 mm FL [10.6–5770 g TW]) were examined for age analysis. Of the fish collected, 2063 were males ranging from 245 to 671 mm FL and from 296 to 5195 g TW, and 1751 were females ranging from 284 to 701 mm FL and from 450 to 5770 g TW. Length conversion equations were derived for total length: $TL = (1.12 \cdot FL) + 21.84$ (n=2137, r^2=0.995); fork length: $FL = (0.89 \cdot TL) - 16.61$ (n=2137, r^2=0.995); $FL = (1.12 \cdot SL) + 6.44$ (n=2148, r^2=0.992); and standard length: $SL = (0.89 \cdot FL) - 2.14$ (n=2148, r^2=0.992).

Length-weight models

Length-weight relationships were calculated separately for males, females, and for both sexes combined (Table 1). The relationship between TW and FL is presented in Figure 2. ANCOVA of TW-at-FL and CW-at-FL were both significantly different between sexes (TW: F=42.56; df: 1, 3234; P<0.001; CW: F=94.29; df: 1, 2652; P<0.001); males were larger than females. The length-frequency distribution for male and female *P. multidens* is shown in Figure 3.

Temporal trends were evident in the mean length and weight of *P. multidens* over time. Mean FL was significantly different among years from 1995 to 1999 (ANOVA: F=31.29; df: 1, 4193, P<0.001), with (1995=1996=1997) > (1998=1999). Mean TW was also significantly different among years from 1995 to 1999 (ANOVA: F=89.33; df: 1, 3295, P<0.001), with 1995 > 1996 > 1997 > (1998=1999).

Age validation

Otoliths displayed alternating opaque and translucent zones. A consistent annual trend was evident; the translucent zone was laid down from January to May and the opaque zone formed from June to December. The trend in thin opaque zone formation in June and July was replicated in both 1997 and 1998. Figure 4 clearly demonstrates that the opaque and translucent zones are laid down once a year and represent valid annual growth increments. Because the marginal increment analysis involved random sampling across all age classes in the sampled population, the validation of annual growth increments can be expected to hold across all age classes. In addition, the formation of the translucent zone in the sagittal otoliths of *P. multidens* and the annual cycle of sea surface temperatures in the Kimberley region of northwestern Australia were found to be closely related (Fig. 5).

Otolith structure, analysis, and functionality

The sagittae of *P. multidens* are somewhat laterally compressed, elliptical structures. The distal surface is concave and the rostrum and postrostrum are somewhat pointed. The sagittae are characterized by variable growth reticulations along the dorsal edge from the postrostrum to

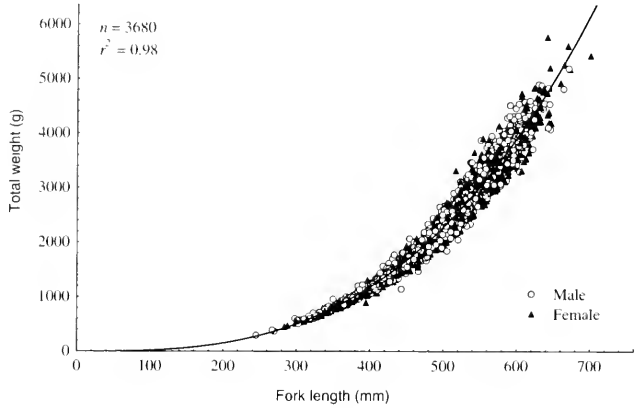

Figure 2

Relationship between fork length and total weight for *P. multidens* off the Kimberley coast of northwestern Australia.

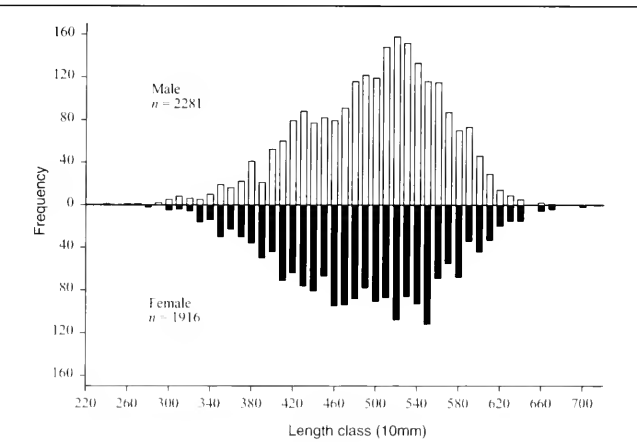

Figure 3

Length-frequency distribution (10-mm length classes) of male and female *P. multidens* sampled for age determination.

the antirostrum and along the ventral edge from the postrostrum to the rostrum. A curved sulcus crosses the proximal surface longitudinally, and the depth of the sulcal groove increases with fish age.

The precision of otolith readings of *P. multidens* was relatively high (APE of 10.4%). Given the variability encountered among otoliths, this APE reflects a moderately high level of precision among otolith readings and indicates that the aging protocol adopted is replicable.

Otolith length and breadth were useful predictors of fish length in *P. multidens*, accounting for more than 77% of the variability (Table 2). In contrast, otolith weight and, in particular, height were poor predictors of fish length (Table 2). Otolith weight was the best predictor of fish age for *P. multi-*

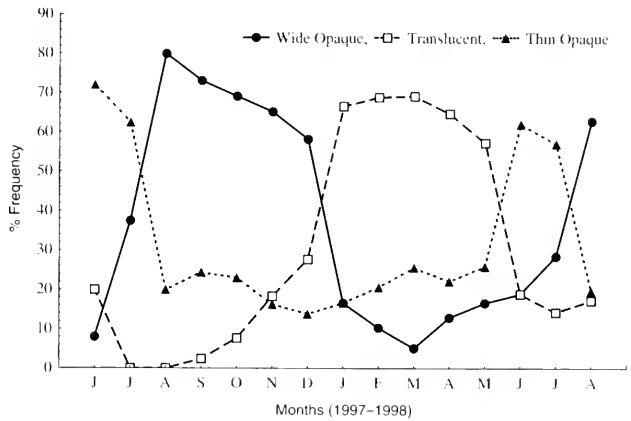

Figure 4

Marginal increment analysis of *P. multidens* sagittal otoliths using an edge type classification system (edge types: wide opaque, thin opaque, and translucent).

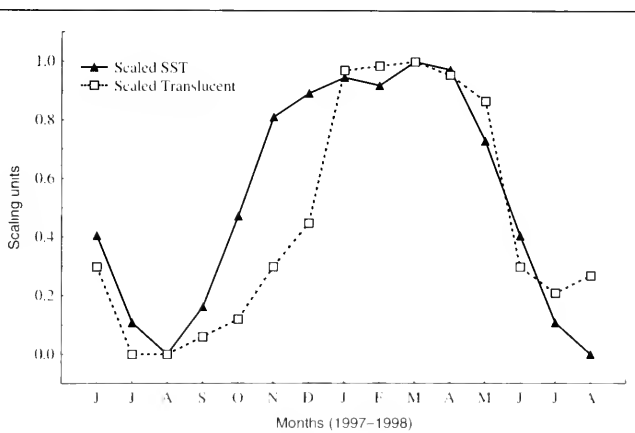

Figure 5

Comparison of the translucent zone formation on the sagittal otoliths of *P. multidens* with sea surface temperatures in the Kimberley region of northwestern Australia. Values are standardized to take into account any time lags and to allow comparison of each time series.

dens, accounting for 94.4% of the variability in age (Table 2, Fig. 6). Otolith height was also a useful predictor of fish age, accounting for 88% of the variability in age. In contrast, otolith length and breadth were poor predictors of age for *P. multidens* (Table 2).

Growth and mortality models

The von Bertalanffy growth curve was fitted to FL-at-age for all *P. multidens* (Fig. 7), and separately for each sex (Table 3). Growth in FL of *P. multidens* is relatively fast to

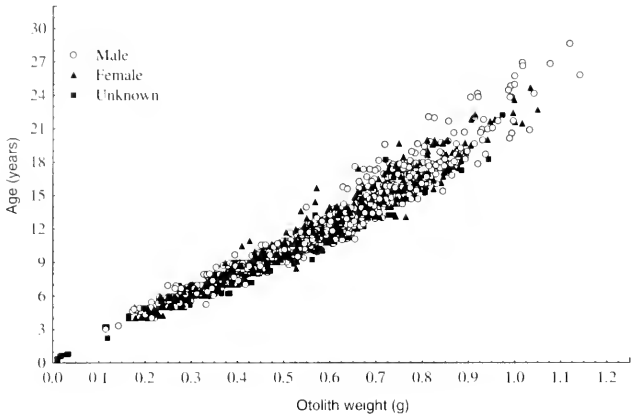

Figure 6

Relationship between otolith weight and age of *P. multidens* estimated from sectioned otoliths.

Table 2

Comparisons among otolith dimensions and length and age of *P. multidens*. The predictive equations are of the simple linear regression form $y = a + bx$ (OW=otolith weight; OL=otolith length; OB= otolith breadth; OH=otolith height). For regression analyses, fish length (FL) and age were used as the dependent variables (all regressions were significant at $P<0.001$). The standard error (SE) of the estimate is a measure of the dispersion of the observed values about the regression line.

Dependent variable	Independent variable	Sample size	Equation	r^2	SE of estimate
FL	*OW*	2590	$FL = (315.37 \times OW) + 339.46$	0.68	37.57
FL	*OL*	2493	$FL = (33.47 \times OL) - 111.43$	0.77	32.08
FL	*OB*	3745	$FL = (50.43 \times OB) - 124.36$	0.83	28.48
FL	*OH*	3988	$FL = (118.39 \times OH) + 175.14$	0.53	48.36
Age	*OW*	2408	$Age = (21.86 \times OW) - 0.68$	0.94	0.94
Age	*OL*	2305	$Age = (1.77 \times OL) - 21.68$	0.58	2.63
Age	*OB*	3469	$Age = (2.40 \times OB) - 19.14$	0.60	2.49
Age	*OH*	3652	$Age = (8.52 \times OH) - 12.81$	0.88	1.36

age 9 but is much reduced in age cohorts beyond 9 years of age. Parameters of the VBGF are listed in Table 3. FL-at-age of *P. multidens* was not significantly different between sexes (log-likelihood=0.9836, test statistic=1.001, $P>0.05$; no significant differences were found among parameters of the VBGF; see also Fig. 7). Generalized VBGFs of *P. multidens* from previous studies were compared to that derived from our study (Fig. 8).

The maximum observed age of *P. multidens* in the Kimberley region was 30 years. Given that the *P. multidens* resource in the Kimberley region has been exploited for over 20 years, it is possible that in an unfished population the longevity of *P. multidens* may be closer to 40 years. These two estimates of maximum age in *P. multidens* were applied to the Hoenig (1983) equation in order to derive an estimate of *M*. Consequently, *M* was considered to be in the range of 0.104–0.139, representing an annual survivorship of 87–90% for an unfished population. This range of *M* estimates for *P. multidens* is similar to that observed for other long-lived lutjanid species in the Indo-Pacific region (Newman et al., 1996, Newman et al., 2000a; Newman and Dunk, 2002).

The longevity of female and male *P. multidens* was somewhat similar at 27 and 30 years, respectively. The age structures of *P. multidens* in the commercial catch differed among years. The 1995 sample had a peak in year

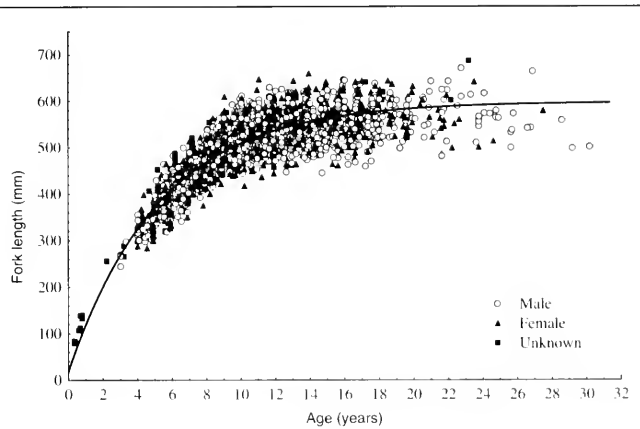

Figure 7

Length-at-age and von Bertalanffy growth curve for *P. multidens* off the Kimberley coast of northwestern Australia.

class 5 and relatively strong age classes 6, 8, and 10, but abundance per age class declined rapidly to age 20, after which few fish were found to be older (Fig. 9). The 1996 and 1997 samples were somewhat similar. In 1996 relatively strong year classes were present from age 5 through to age 11, and abundance per age class declined rapidly to age 26 (Fig. 9). One year later, the 1997 sample had relatively strong year classes present from age 6 through to age 12 (Fig. 9), providing further evidence of the annual formation of growth increments.

The 1998 sample had relatively strong 6, 7, and 8 age classes, and abundance per age class declined rapidly to age 24 (Fig. 9). The 1999 sample was similar to the 1998 sample with relatively strong 6, 7, and 8 age classes, and abundance per age class declined rapidly to age 20 (Fig. 9). Age classes 9 through 12 were somewhat eroded in the 1998 and 1999 samples in comparison to the 1996 and 1997 samples. In all years, abundance per age class declined rapidly to age 20, and fish older than 20 years were not well represented in the catch over the five years of catch sampling. In most years there was a strong mode of age-6 individuals present and this mode may reflect the age at full recruitment to the sampling gear (fish traps).

Pristipomoides multidens less than age 6 were in general not fully recruited to the sampled population and were therefore excluded from the mortality estimates derived from catch-at-age data. The year-specific total annual rate of mortality, Z, of *P. multidens* in the NDSF, was 0.65 for 1995–96 (fish aged 6–21 years), 0.87 for 1996–97 (fish aged 6–21 years), and 0.71 for 1997–98 (fish aged 6–21 years), representing an annual percentage removal of approximately 38%, 49%, and 41%, respectively, for each year (Table 4). In addition, exploitation rates were 0.79, 0.84, and 0.80, respectively.

Table 3

Growth parameters derived from the von Bertalanffy growth function and population characteristics of *P. multidens* off the Kimberley coast of northwestern Australia (n=sample size, FL is in mm, and age (t) is in years).

Parameters	Male	Female	Total
n	1879	1600	3479
L_∞	594.49	603.23	598.08
K	0.1868	0.1867	0.1873
t_0	–0.3601	0.0018	–0.1730
r^2	0.7394	0.7875	0.7630
n	2281	1916	4573
FL_{mean}	501.5	493.5	495.1
FL_{min}	245	284	80
FL_{max}	671	701	701
n	1872	1597	3833
t_{mean}	10.24	9.54	9.73
t_{min}	3	4	0.35
t_{max}	30	27	30

The optimum fishing mortality rate, F_{opt}, for *P. multidens* was estimated to be 0.052–0.069, and the limit reference point, F_{limit}, was estimated to be 0.069–0.092 (see Table 4). These results indicate that only approximately 6% of the

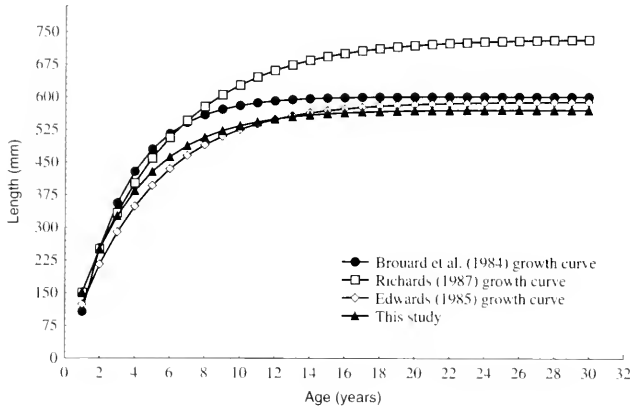

Figure 8

Comparison of generalized von Bertalanffy growth curves for *P. multidens* from previous studies with that derived from this study.

Table 4

Summary of total mortality (Z) estimates for *P. multidens* derived from catch-at-age data based on ages determined from sectioned otoliths. Estimates of fishing mortality (F) are derived by subtraction because $Z = F + M$ and are compared to estimates of optimum fishing mortality rates.

Year	Z	F	F_{opt}	F_{limit}
1995–96	0.649	0.510–0.545	0.052–0.069	0.069–0.092
1996–97	0.869	0.730–0.765	0.052–0.069	0.069–0.092
1997–98	0.710	0.571–0.606	0.052–0.069	0.069–0.092

available stock of *P. multidens* can be harvested on an annual basis in a sustainable manner and that annual harvest rates should not exceed 10% of the average stock size.

Discussion

Sagittal otoliths were determined to be valid structures for age determination in *P. multidens*. The edge-type classification system of three edge types used in this study is capable of indicating whether the opaque zone has just been formed or whether a new translucent zone is ready to form. The use of marginal increment analysis (MIA) of individuals of all ages exhibits a clear trend and demonstrates conclusively that annual growth increments are formed once per year. Annual growth increments were most conspicuous in the ventral lobe of the sagittal otoliths. However, we observed that experience is a critical factor in increasing the agreement and hence precision of successive counts of annual growth increments in *P. multidens*.

The spring–summer peak in opaque zone formation observed in our study is in accordance with the peak in opaque zone formation identified by Fowler (1995) and Beckman and Wilson (1995) for tropical fishes. The translucent zone (the period of fast growth in the otoliths) is formed in the summer months (January to May) and the opaque zone (the slow growth period) is formed in the winter-spring months (June to December). Translucent zones are relatively thin. Declining sea-surface temperature (which was assumed to reflect water temperature change at depth) was associated with the onset of opaque zone formation in the otoliths of *P. multidens*. Furthermore, reproduction is unlikely to play a significant role in the timing of translucent zone formation in *P. multidens* because spawning occurs primarily in the March–April period. These results indicate that water temperature, doubtless in association with other factors, provides a stimulus that influences the endolymph fluid

chemistry of these fish, culminating in the formation of annual growth increments.

Female and male fish older than 20 years of age were uncommon in the landed catch. Fish of both sexes between 5 and 12 years of age were common in the landed catch. The maximum age of *P. multidens* observed in our study was much greater than that recorded previously. Richards[1] reported a maximum age of 14 years in Papua New Guinea from counts of daily rings on otoliths, whereas Brouard et al. (1984) recorded a maximum age of only 8 years in Vanuatu with a similar method. Edwards (1985) analyzed vertebrae and scales of this species in the Timor Sea and reported a maximum age of 14 years. In contrast, Mohsin and Ambak (1996) estimated a maximum age of only 5 years from the east coast of peninsular Malaysia with length-frequency analysis. Variation in the longevity estimates of earlier works is related to the aging methods used and their biases. For example, growth increments in vertebrae are often difficult to detect despite the presence of numerous discontinuities in bone growth (Marriott and Cappo, 2000). Alternatively earlier longevity estimates may have been drawn from sample populations biased by gear selectivity or from populations with varying degrees of exploitation.

Otolith weight was a good predictor of age in *P. multidens*, accounting for 94% of the variability in age. The strong linear relationship between otolith weight and fish age from a very large sample size implies that otolith weight may be used as a proxy for age. The coefficient of determination of the regression model is affected by the degree of colinearity of the independent variables. The high r^2 value observed in our study provides the basis for a first-order age approximation. Thus, the potential exists for an age–otolith-weight key to be derived for *P. multidens*, as for an age-length key, whereby the age composition of the landed catch in future years may be obtained by weighing large numbers of otoliths. However, the accuracy and precision of adopting this monitoring strategy remains to be tested.

The fit of the regression model for the otolith weight-age relationship was much more precise than the fit of the fork-length–age relationship as described by the von Bertalanffy growth model. Considerable variation in length was observed within most age groups for both sexes. The large variation in length at a given age makes it difficult to accurately determine the age of *P. multidens* from length data alone. For example, fish ranging in length from 450 to 550 mm FL may vary in age from 5 to 30 years. This variability may explain the very low estimate of maximum age obtained by Mohsin and Ambak (1996), which was derived with length-frequency analysis.

Growth was most rapid through age 9 for both sexes. From age 9 onwards somatic growth slows with increasing age. The estimation of growth parameters is dependent upon adequate sampling across the length range of any species. The fish sampled in our study ranged in length from 80 to 701 mm FL, covering most of the length range of *P. multidens*. Therefore, it is unlikely that the growth parameters of *P. multidens* are biased because of inadequate sampling across the length range.

Despite methodological differences in age estimation, the estimates of K derived from the studies of Richards[1]

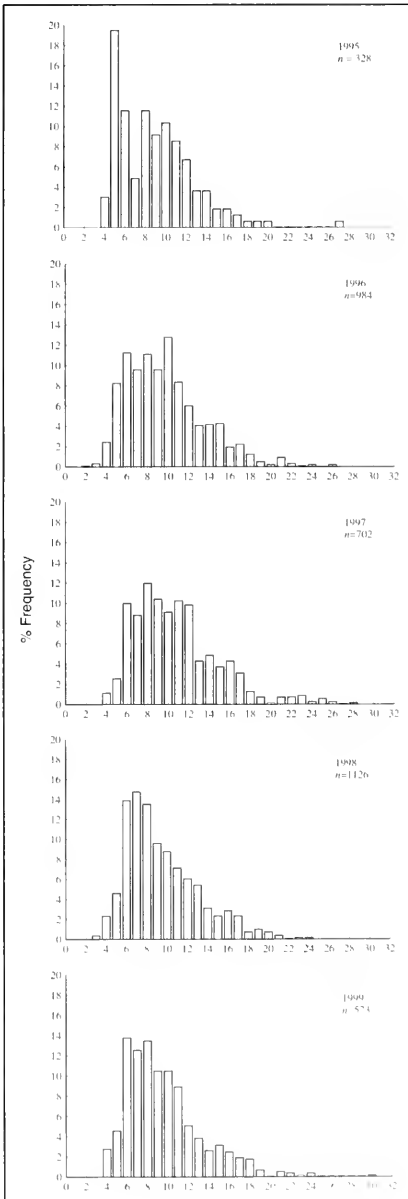

Figure 9

Age-frequency distributions of *P. multidens* in the northern demersal scalefish fishery from 1995 to 1999

(K=0.188), Ralston (1987; K=0.188), and Edwards (1985; K=0.219) were somewhat similar to that observed in this study (K=0.187). However, the asymptotic lengths reported by Richards[1] and Ralston (1987) were larger than our estimates, which were again similar to those of Edwards, 1985). In contrast, the estimates of K derived by Brouard et al. (1984), Brouard and Grandperrin (1985), and Mohsin and Ambak (1996), which ranged from 0.28 to 0.50, provided overestimates of the growth potential of *P. multidens* as observed in our study. Clearly, methodological differences in age estimation have the potential to unduly influence growth parameter estimation and may provide misleading impressions of the production potential of these fishes.

The similarity of growth in length-at-age between sexes indicates that there is little trade off in energetic investment into reproductive activity after sexual maturity at the expense of somatic growth as there is for some *Lutjanus* species (Newman et al., 1996, 2000b). Information on energy partitioning in the *Pristipomoides* is not known. However, females with a large body size would be reproductively "fitter" if they could accommodate a large mass of hydrated eggs prior to spawning, especially in a multiple male, multiple female spawning system.

The long life span of *P. multidens* and other lutjanid species (Loubens, 1980; Newman et al., 1996, 2000a; Newman and Dunk, 2002; Rocha-Olivares, 1998) may be an evolutionary adaptation that supports iteroparity. Many demersal reef fish are highly fecund, but egg and larval survivorship is low; therefore, spawning over numerous years may be necessary to maintain stable populations. In addition, numerous years of reproductive output may also be required to contend with environmental variability (e.g. the incidence of cyclones, El Niño–La Niña cycling), which may substantially influence recruitment success. Extended periods of high exploitation results in decreases in the spawning stock biomass and constriction of the age structure of fish populations, and thus diminishes the number of effective spawnings. Any reduction in the number of effective spawnings may result in a decrease in ecological fitness and hence limit the adaptive capacity of the species to combat environmental or anthropogenic induced stress.

Variation in life expectancy due to fishing pressure has the potential to bias estimates of M used in our study. To account for any M-associated difference, a range of M estimates have been considered in our study. *Pristipomoides multidens* were fully recruited to the commercial fishery in the NDSF by age 6. Catch-at-age data showed relatively consistent estimates of Z among years from 1995–96 through to 1997–98 and a relatively broad age structure in the landed catch.

Fishery management implications

Throughout much of its range *P. multidens* composes a significant proportion of the demersal catch of tropical multispecies fisheries. Within these multispecies fisheries *P. multidens* is taken as part of the directed target catch or as a part of the retained catch. In fish trawl-based fisheries, *P. multidens* can be harvested at all stages of their life history from juvenile to adult, making them especially vulnerable to overexploitation. In contrast, fisheries that use trap and line methods of capture (using bait to attract fish) only have the capacity to harvest fish in the subadult-to-adult phase of their life history. Hence, the method of capture and harvest strategy adopted has the capacity to influence the sustainable exploitation of the *P. multidens* resource.

Of particular relevance to fishery managers is the capacity that fish trawl-based fisheries have in being capable of continuing to function and to be economically viable (driven by the more productive, lower value species) while populations of higher valued species such as *P. multidens* become depleted. Thus, careful monitoring of the *P. multidens* resource will be required, particularly in trawl-based fisheries. Fishery managers need to be responsive to the intrinsic vulnerability of *P. multidens* to overharvesting as a corollary of its life history characteristics. Furthermore, fish such as *P. multidens*, which have low rates of natural mortality, low growth potential, extended longevity, mature relatively late in life and are either dead or moribund as a consequence of internal hemorrhaging when the physoclistous is ruptured during capture, are likely to be particularly sensitive to exploitation pressure. The apparent low survival rate for released fish in the fishing depths of the NDSF fleet indicates that the traditional use of legal minimum sizes to increase survival to spawning sizes and hence increase overall yields is not a practical option.

Populations of *P. multidens* have a low productive capacity and hence are vulnerable to overfishing as a consequence of slow growth, extended longevity, late maturity, and low rates of natural mortality. The demersal fish resources of the NDSF, of which *P. multidens* is a significant part, is currently being managed with an innovative total allowable effort system that allocates individually transferable effort units equitably to each licensee. However the highly mobile, efficient, and wide-ranging capacity of the NDSF fleet may require more complex management arrangements to maintain future breeding stock levels. The incorporation of appropriately targeted spatial or temporal (or both spatial and temporal) closures within the existing effort management framework is likely to provide an additional useful and robust mechanism to maintain spawning stock biomass and protect against recruitment overfishing. In the wider Indo-Pacific region, fishery managers should consider harvest strategies of low frequency or low intensity in conjunction with targeted spatial or temporal closures to protect the spawning stock biomass of these fishes.

Harvest strategies such as setting fishing mortality at or near natural mortality (F=M) were often prescribed prior to the 1990s (Gulland, 1970). Recently, the adoption of harvest strategies such as setting $F = F_{0.1}$ were thought to be quite conservative, but usually resulted in $F = M$ harvest strategies (Walters, in press). Following the meta-analysis of Myers et al. (1999), who examined stock-recruitment curve slopes expressed as maximum reproductive rates per spawner at low spawner biomass, Walters (in press) has reported that optimal fishing mortality rates are substantially lower than natural mortality rates for most species and stocks. Furthermore, Patterson

(1992) reported that fishing mortality rates above 2/3 M are often associated with stock declines, whereas fishing mortality rates below this level have resulted in stock recovery. Consequently, exploitation rates for long-lived reef fishes need to be very conservative.

The declines evident in the length and weight of fish in the landed catch over the duration of our study support the finding of the high levels of F. These data support the estimates of the annual percentage removals that indicate that the NDSF population of *P. multidens* is currently exploited above optimum levels. The age structure of the *P. multidens* stock within the NDSF currently consists of close to 30 age classes (ages 2 to 30 years). Therefore, depletion of the spawning stock biomass of these fishes will result in long population recovery times and the economic loss associated with recovering and rebuilding these fisheries may persist longer. A minimum of 30 years would be required for the fished population to recover in terms of both virgin spawner biomass and age structure. The results of our study provide the basis for a more detailed age-structured stock assessment for this species.

Acknowledgments

The authors gratefully acknowledge funding from the Fisheries Research and Development Corporation (FRDC) for this project. This work was undertaken as part of FRDC Project 97/136. The comments and suggestions of Rod Lenanton and Jim Penn and three anonymous reviewers contributed greatly to this manuscript. Logistical support was provided by the Department of Fisheries, Government of Western Australia. The authors are thankful to the fishermen of the NDSF for the provision of samples and to the fish wholesalers of Perth (Attadale Seafoods Pty. Ltd., Kailis Bros., New West Foods [W.A.] Pty. Ltd., Festival Fish Wholesalers) and Broome (Fortescue Seafoods) for access to specimens from northwestern Australia. Jerry Jenke provided invaluable support in all areas, Richard Steckis was responsible for maintaining the databases used for this project, and Peta Williamson assisted with the development of the figures.

Literature cited

Allen, G. R.
1985. FAO species catalogue. Snappers of the world. An annotated and illustrated catalogue of lutjanid species known to date. FAO Fisheries Synopsis 125, vol. 6, 208 p. FAO, Rome.

Beamish, R. J., and D. A. Fournier
1981. A method for comparing the precision of a set of age determinations. Can. J. Fish. Aquat. Sci. 38:982–983.

Beckman, D. W., and C. A. Wilson.
1995. Seasonal timing of opaque zone formation in fish otoliths. *In* Recent developments in fish otolith research (D. H. Secor, J. M. Dean, and S. E. Campana, eds.), p. 27–44 Univ. South Carolina Press, Columbia, SC.

Brouard, F., and R. Grandperrin.
1985. Deep-bottom fishes of the outer reef slope in Vanuatu. South Pacific Commission 17th regional technical meeting on fisheries (Noumea, New Caledonia, 5–19 August, 1985). SPC/Fisheries 17/WP.12, 127 p. [Original in French.]

Brouard, F., R. Grandperrin, M. Kulbicki, and J. Rivaton.
1984. Note on observations of daily rings on otoliths of deepwater snappers. ICLARM (International Centre for Living Aquatic Resources Management) Translations 3, 8 p. ICLARM, Manila, Philippines.

Cerrato, R. M.
1990. Interpretable statistical tests for growth comparisons using parameters in the von Bertalanffy equation. Can. J. Fish. Aquat. Sci. 47:1416–1426.

Dalzell, P., and G. L. Preston.
1992. Deep reef slope fishery resources of the South Pacific. A summary and analysis of the dropline fishing survey data generated by the activities of the SPC Fisheries Programme between 1974 and 1988. Inshore Fisheries Research Project Technical Document 2, 299 p. South Pacific Commission, Noumea, New Caledonia.

Edwards, R. C. C.
1985. Growth rates of Lutjanidae (snappers) in tropical Australian waters. J. Fish. Biol. 26:1–4.

Fowler, A. J.
1995. Annulus formation in otoliths of coral reef fish—a review. *In* Recent developments in fish otolith research (D. H. Secor, J. M. Dean, and S. E. Campana, eds.), p. 45–63. Univ. South Carolina Press, Columbia, SC.

Gulland, J. A.
1970. The fish resources of the ocean FAO Fisheries Technical Paper 97, 425 p.

Hart, A. M., and G. R. Russ.
1996. Response of herbivorous fish to crown of thorns starfish *Acanthaster planci* outbreaks. III. Age, growth, mortality and maturity indices of *Acanthurus nigrofuscus*. Mar. Ecol. Prog. Ser. 136:25–35.

Hoenig, J. M.
1983. Empirical use of longevity data to estimate mortality rates. Fish. Bull. 82:898–902.

Kailola, P. J., M. J. Williams, P. C. Stewart, R. E. Reichelt, A. McNee, and C. Grieve.
1993. Australian fisheries resources, 422 p. Bureau of Resource Sciences, Department of Primary Industries and Energy, and the Fisheries Research and Development Corporation, Canberra, Australia

Loubens, G.
1980. Biologie de quelques especes de poissons du lagon Neo-Caledonian. III. Croissance. Cahiers de l'Indo-Pacifique 2:101–153.

Marriott, R., and M. Cappo.
2000. Comparative precision and bias of five different ageing methods for the large tropical snapper *Lutjanus johnii*. Asian Fish. Sci. 13:149–160.

Mohsin, A. K. M., and M. A. Ambak.
1996. Marine fishes and fisheries of Malaysia and neighbouring countries, 744 p. Universiti Pertanian Malaysia Press, Serdang, Selangor Darul Ehsam, Malaysia.

Myers, R. A., K. G. Bowen, and N. J. Barrowman.
1999. Maximum reproductive rate of fish at low population sizes. Can. J. Fish. Aquat. Sci. 56:2404–2419.

Newman, S. J.
2001. Northern demersal scalefish interim managed fishery status report. *In* State of the Fisheries Report 1999–2000 (J. W. Penn, ed.), p. 61–64 Fisheries Western Australia, Perth, Western Australia.

Newman, S. J., and I. J. Dunk.
2002. Growth, age validation, mortality, and other popula-

tion characteristics of the red emperor snapper, *Lutjanus sebae* (Cuvier, 1828), off the Kimberley coast of North-Western Australia. Estuar. Coast. Shelf Sci. 55 (1):67–80.

Newman, S. J., and D. McB. Williams.
1996. Variation in reef associated assemblages of the Lutjanidae and Lethrinidae at different distances offshore in the central Great Barrier Reef. Environ. Biol. Fishes 46: 123–128.

Newman, S. J., M. Cappo, and D.McB. Williams.
2000a. Age, growth, mortality rates and corresponding yield estimates using otoliths of the tropical red snappers, *Lutjanus erythropterus*, *L. malabaricus* and *L. sebae*, from the central Great Barrier Reef. Fish. Res. 48 (1):1–14.
2000b. Age, growth and mortality of the stripey, *Lutjanus carponotatus* (Richardson) and the brown-stripe snapper, *L. vitta* (Quoy and Gaimard) from the central Great Barrier Reef, Australia. Fish. Res. 48 (3):263–275.

Newman, S. J., D. McB. Williams, and G. R. Russ.
1996. Age validation, growth and mortality rates of the tropical snappers (Pisces: Lutjanidae), *Lutjanus adetii* (Castelnau, 1873) and *L. quinquelineatus* (Bloch, 1790) from the central Great Barrier Reef, Australia. Mar. Freshwater Res. 47 (4):575–584.

Patterson, K.
1992. Fisheries for small pelagic species: an empirical approach to management targets. Rev. Fish Biol. Fish. 2(4): 321–338.

Pearson, D. E.
1996. Timing of hyaline-zone formation as related to sex, location, and year of capture in otoliths of widow rockfish, *Sebastes entomelas*. Fish. Bull. 94 (1):190–197.

Ralston, S.
1987. Mortality rates of snappers and groupers. *In* Tropical snappers and groupers: biology and fisheries management (J. J. Polovina, and S. Ralston, eds.), p. 375–404. Westview Press, Boulder, CO.

Rocha-Olivares, A.
1998. Age, growth, mortality and population characteristics of the Pacific red snapper, *Lutjanus peru*, off the southeast coast of Baja California, Mexico. Fish. Bull. 96:562–574.

Walters, C. J.
In press. Stock assessment needs for sustainable fisheries management. Bull. Mar. Sci.

An approach to estimating rockfish biomass based on larval production, with application to *Sebastes jordani**

Stephen Ralston
James R. Bence
Maxwell B. Eldridge
William H. Lenarz

Southwest Fisheries Science Center
National Marine Fisheries Service
110 Shaffer Road
Santa Cruz, California 95060

E-mail address (for S. Ralston, contact author): Steve.Ralston@noaa.gov

Abstract—An assessment of the total biomass of shortbelly rockfish (*Sebastes jordani*) off the central California coast is presented that is based on a spatially extensive but temporally restricted ichthyoplankton survey conducted during the 1991 spawning season. Contemporaneous samples of adults were obtained by trawl sampling in the study region. Daily larval production (7.56×10^{10} larvae/d) and the larval mortality rate (Z=0.11/d) during the cruise were estimated from a larval "catch curve," wherein the logarithm of total age-specific larval abundance was regressed against larval age. For this analysis, larval age compositions at each of the 150 sample sites were determined by examination of otolith microstructure from subsampled larvae (n=2203), which were weighted by the polygonal Sette-Ahlstrom area surrounding each station. Female population weight-specific fecundity was estimated through a life table analysis that incorporated sex-specific differences in adult growth rate, female maturity, fecundity, and natural mortality (M). The resulting statistic (102.17 larvae/g) was insensitive to errors in estimating M and to the pattern of recruitment. Together, the two analyses indicated that a total biomass equal to 1366 metric tons (t)/d of age-1+ shortbelly rockfish (sexes combined) was needed to account for the observed level of spawning output during the cruise. Given the long-term seasonal distribution of spawning activity in the study area, as elucidated from a retrospective examination of California Cooperative Oceanic Fisheries Investigation (CalCOFI) ichthyoplankton samples from 1952 to 1984, the "daily" total biomass was expanded to an annual total of 67,392 t. An attempt to account for all sources of error in the derivation of this estimate was made by application of the delta-method, which yielded a coefficient of variation of 19%. The relatively high precision of this larval production method, and the rapidity with which an absolute biomass estimate can be obtained, establishes that, for some species of rockfish (*Sebastes* spp.), it is an attractive alternative to traditional age-structured stock assessments.

Manuscript accepted 20 September 2002.
Fish. Bull. 101:129–146 (2003).

Shortbelly rockfish (*Sebastes jordani*) is an underutilized species that is distributed from Vancouver Island to northern Baja California (Eschmeyer, 1983), although it is especially abundant along the central California coast. Based on a swept-area bottom trawl survey of demersal rockfish, Gunderson and Sample (1980) estimated there were 24,000 metric tons (t) of shortbelly rockfish in the Monterey International North Pacific Fishery Commission (INPFC) area (35°30′N–40°30′N). This biomass estimate was far greater than that of any other species of rockfish in any area and, significantly, it did not include the midwater portion of the stock. Hydroacoustic estimates of shortbelly rockfish biomass in the shelf-slope area between Ascension Canyon and the Farallon Islands (37°00′–38°00′N), a distance of only 110 km, have ranged from 153,000 to 295,000 t (Nunnely[1]).

Although at present there is no directed fishery for this species (Low, 1991), much is known of its biology. Early work by Phillips (1964) provided basic information about the length-weight relationship, growth as estimated from scale annuli, spawning seasonality (i.e. parturition), fecundity, maturity, and the food habits of shortbelly rockfish. Lenarz (1980) later studied shortbelly rockfish growth using ages from whole otoliths and provided preliminary calculations of the effect of fishing on the stock. He also demonstrated marked spatial variation in age and length composition along both latitudinal and depth gradients. Growth was re-estimated by Pearson et al. (1991) using ages determined from broken and burnt otoliths. From the hydroacoustic biomass estimates cited above and an estimated range for the natural mortality rate (0.20–0.35 yr), they concluded that the maximum sustainable yield (MSY) of the shortbelly rockfish stock in the Ascension Canyon–Farallon Islands area was 13,400–23,500 t.

Shortbelly rockfish is one of the few *Sebastes* spp. that can be readily identified at all life history stages. Descriptions of the early life stages of shortbelly rockfish, from preflexion larvae through the pelagic juvenile stage, were provided by Moser et al. (1977). Extending that work, MacGregor (1986) provided a summary of the spatiotemporal distributions of shortbelly rockfish larvae taken in California Cooperative Oceanic Fisheries Investigation (CalCOFI) cruises conducted in five different years. His results showed that 99.1% of all shortbelly rockfish larvae (~4–10 mm) were captured within 90 km of shore and that 65.4% were sampled during the month of February. Moreover, a strong peak in larval abundance (i.e. 34.7% of the coastwide total) was concentrated in the vicin-

* Contribution 111 of the Santa Cruz Laboratory, Southwest Fisheries Science Center, National Marine Fisheries Service, Santa Cruz, CA 95060.

[1] Nunnely, E. 1989. Personal commun. Alaska Fisheries Science Center, 7600 Sand Point Way N.E., Bin C15700, Seattle, WA 98115-0070.

ity of Pioneer Canyon (CalCOFI line 63). Later research by Laidig et al. (1991) resulted in the development of a detailed growth model for young-of-the-year shortbelly rockfish, from extrusion through the late pelagic juvenile stage (~180 d), and verified the feasibility of a daily aging protocol by validating a one-to-one correspondence between counts of daily increments and elapsed time in days. More recent work by Ralston et al. (1996) showed that larval shortbelly rockfish can be accurately aged by using optical microscopy.

For the year 2000 the Pacific Fishery Management Council (PFMC) revised the shortbelly rockfish acceptable biological catch (ABC) downwards from 23,500 to 13,900 t/yr (PFMC[2]). The new ABC is based on the low end of the estimated MSY range presented in Pearson et al. (1991); it was reduced due to a probable natural decline in standing stock during the 1990s arising from poor ocean conditions (MacCall, 1996). The original range, however, was derived by using quite variable data from unpublished hydroacoustic surveys and Pearson et al. (1991) considered it a strictly preliminary estimate. Given that the biomass of shortbelly rockfish along the central California coast was once thought to be very large (Gunderson and Sample, 1980; MacGregor, 1986), and that the species is still probably the single largest rockfish contribution available to the west coast groundfish fishery, data are needed to estimate the size of the stock more precisely than results available from these previous investigations.

The goal of this study was to develop an analytical approach to estimate the total biomass of shortbelly rockfish in the region of Pioneer and Ascension Canyons and to gather field data to evaluate the method. Successful application of the method to shortbelly rockfish would provide to the PFMC information useful for management. On a more fundamental level, it would also assist in developing fishery-independent survey techniques capable of assessing other, more highly exploited, species of rockfish.

The assessment approach

The basic premise of egg and larval surveys is that it is easier to estimate the absolute abundance of ichthyoplankton than it is to estimate that of adults (Saville, 1964; Gunderson, 1993). This is especially true when the spatial distribution of adults exhibits some type of size- or age-specific pattern. Shortbelly rockfish is one such species (Lenarz, 1980) and obtaining a representative sample of the adult population is challenging (Lenarz and Adams, 1980). Conversely, early life history stages (i.e. eggs and preflexion larvae) can be sampled effectively with standard plankton nets (Smith and Richardson, 1977). Due to the direct coupling between egg production and spawning biomass, mediated through population weight-specific fecundity(Φ[eggs/g]), egg and larval surveys have proven successful for estimating spawning biomass in many applications (e.g. Houde, 1977; Parker, 1980; Richardson, 1981; Lasker, 1985; Armstrong et al., 1988; Hunter et al., 1993).

Members of the scorpionfish genus *Sebastes* are distinctive because they are primitive viviparous livebearers (Wourms, 1991), resulting in parturition of advanced yolksac larvae (Bowers, 1992). This reproductive strategy lends itself to a larval production stock assessment because the age of all spawning products can be accurately determined from otolith microstructure (Laidig et al., 1991; Ralston et al., 1996). In contrast, in egg surveys, egg age is back-calculated to the time of spawning by 1) defining a series of developmental stages, 2) estimating the relationship between stage-specific developmental rates and temperature, 3) assigning a thermal history to each egg, and 4) determining the time required to account for embryo development from spawning to the observed stage (see for example Lo, 1985; Moser and Ahlstrom, 1985). Because a distinctive extrusion check forms on the otoliths of *Sebastes* larvae at the time of parturition (Ralston et al., 1996), a rockfish larval production estimate does not require information on temperature-dependent developmental rates and the ambient thermal history of egg samples.

In the approach presented in the present study, a spatially extensive but temporally restricted ichthyoplankton survey was conducted. The age composition of larvae in each plankton tow was determined by subsampling the catch, aging the subsample, and expanding the subsample age composition back to that of the tow total. The total age-specific abundance of larvae in the study region was calculated by weighting the larval catch-at-age in each plankton sample by the polygonal area around it (see Sette and Ahlstrom, 1948). Characterization of the declining trend in total larval abundance at age with an exponential mortality model allowed estimation of the production rate of day-0 larvae and the larval mortality rate at the time the ichthyoplankton cruise was conducted.

Information on adult reproduction was obtained from contemporaneous data collected during two separate cruises conducted during the spawning season. In particular, the following functional relationships were estimated from the data collected: 1) weight as a function of total length, 2) sex-specific weight at age (i.e. male and female von Bertalanffy growth equations), 3) fecundity as a function of total weight, 4) maturity as a function of age, and 5) the population sex ratio. From these relationships, a life table was constructed, based on an estimate of natural mortality (/yr), that yielded estimates of population weight-specific fecundity (Φ). As defined here, population weight-specific fecundity includes the biomass contributions to total population size from males and immature females.

Together, these estimates (daily larval production and population weight-specific fecundity) can be used to calculate the "daily" total biomass of fish in the population required to produce the observed abundance of larvae. The long-term mean seasonal distribution of shortbelly

[2] PFMC (Pacific Fishery Management Council). 1999. Status of the Pacific coast groundfish fishery through 1999 and recommended acceptable biological catches for 2000, 4-t p. + 5-t tables and 5 figs. Pacific Fishery Management Council, 2130 SW Fifth Ave., Portland, OR 97201

rockfish larvae and spawning activity was then determined by a retrospective analysis of all CalCOFI ichthyoplankton samples collected in the vicinity of Pioneer Canyon. Based upon the timing of our larval survey with respect to the long-term mean distribution of spawning activity, total "annual" biomass was calculated by expansion. Finally, the robustness of the total biomass estimate was evaluated through a simulation study and sensitivity analyses.

Methods

Trawl sampling of adults

Specimens of adult shortbelly rockfish were collected during February–March 1991 by the FV *New Janet Ann* and the RV *Novodrutsk* (Table 1). Shortbelly rockfish aggregations in and around Ascension and Pioneer Canyons (Fig. 1) were targeted from acoustic surveys. A total of 28 trawls (12 bottom and 16 midwater) were conducted over bottom depths ranging from 115 to 384 m, at an average net depth of 126 m (range: 18–210 m). The bottom trawl codend mesh size was 3.8 cm and the midwater trawl mesh was 5.1 cm. Duration of the trawls ranged from 3 to 73 min ($\bar{x}$=26 min). All landings were either fully weighed or subsampled, depending on the size of the catch. Landings were highly variable, ranging from 23 to 36,300 kg.

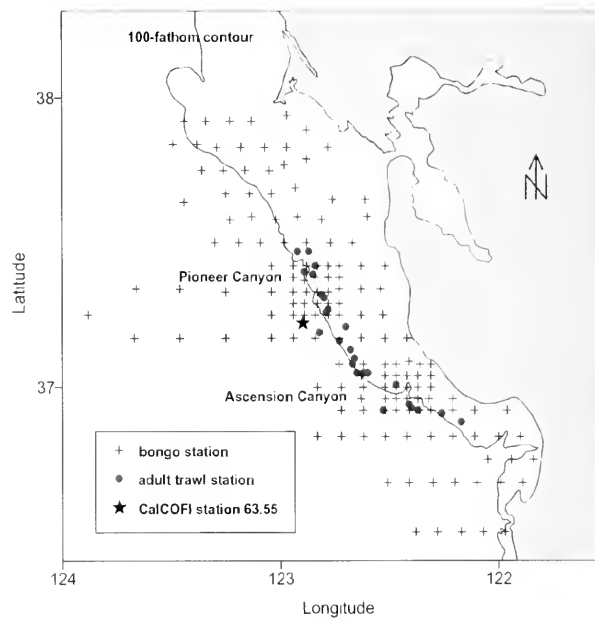

Figure 1

Map of the central California study region showing bongo net and adult trawl sampling locations. The annual spawning season was estimated by the long-term seasonal distribution of shortbelly rockfish larvae at CalCOFI station 63.55.

Two subsamples were taken from each trawl landing. The first was used to determine the overall age, size, sex, and maturity composition of the catch; it was obtained by randomly selecting and examining 100–300 individuals from each trawl, depending on the availability of both time and fish. For these specimens, total lengths (TL) were measured to the nearest mm, gonads were examined to determine sex and to assign gross maturity stages (see below), and otoliths were removed for later age determination by the break-and-burn method (Pearson et al., 1991). A second smaller subsample of 25–50 specimens was also taken to estimate length-weight and fecundity relationships. For each of these fish, TL was measured, weight was determined to the nearest mg, the otoliths were extracted, and late vitellogenic ovaries were dissected from females and fixed in Gilson's fluid.

We rated females in terms of maturity based on gross gonadal condition. A summary of the scale we used is the following: 1.0 = immature; 2.0–2.9 = vitellogenic oocytes (yolk deposition with associated oocyte and ovary enlargement); 3.0–3.9 = fertilized eggs (embryos to hatched larvae); 4.0 = spent; and 5.0 = reorganization and recovery.

Fecundity of female shortbelly rockfish was estimated gravimetrically from vitellogenic ovaries after 2–4 months fixation with periodic stirring. Entire fixed ovaries from each female were blotted dry and weighed to the nearest 1.0 mg. Duplicate subsamples of both ovaries were weighed

Table 1

Summary information of trawl collections for adults. Trawl locations are shown as closed circles in Figure 1. NJA = RV *New Janet Ann*; NOV = RV *Novodrutsk*.

Date	Vessel	Trawl type	
		Bottom	Midwater
14 Feb 1991	NJA	3	1
15 Feb 1991	NJA	2	1
22 Feb 1991	NJA	4	1
23 Feb 1991	NJA	3	1
15 Mar 1991	NOV	0	3
16 Mar 1991	NOV	0	3
17 Mar 1991	NOV	0	2
18 Mar 1991	NOV	0	2
19 Mar 1991	NOV	0	2

to the nearest 0.1 mg and their egg contents counted with the aid of a dissecting microscope. The mean number of eggs per gram from each fish was then expanded to the total ovary weight to estimate annual fecundity (total eggs per individual female).

To estimate population weight-specific fecundity, first the length and weight data were fitted to the power function and the bias-corrected regression equation was used to estimate the weight of every fish that was aged. Next, for each sex, growth equations were obtained by fitting the weight and age "data" to the von Bertalanffy growth model (Ricker, 1975). Maturity was quantified by fitting the logistic equation to the proportion of females that were mature within 5-mm-TL intervals, and fecundity was estimated by fitting fecundity and female weight data to the power function, with appropriate bias-correction. These various functional relationships were then combined in a life table analysis to determine the expected biomass per female recruit and the expected lifetime larval production per female recruit. The ratio of these quantities is the estimated equilibrium cohort weight-specific fecundity (i.e. Φ[larvae/g]) of female shortbelly rockfish. Given an estimate of total age-0 larvae (N_0), the female biomass responsible for the observed larval production can be estimated as $N_0\Phi^{-1}$. Finally, the combined sex biomass can be determined by expanding female biomass using weight-based cohort sex ratio estimates from the life table analysis.

Ichthyoplankton sampling

The primary set of ichthyoplankton samples used in our study was obtained by using bongo nets during a cruise of the NOAA RV *David Starr Jordan* (DSJ-9102) conducted in the winter of 1991. Sampling began at 1500 h on 8 February and ended at 0230 h on 15 February. During that 6½-day period 150 stations were occupied in the region bounded from lat. 36°30′N to lat. 38°00′N and offshore to a maximum distance of 130 km (Fig. 1). The study area included Pioneer and Ascension Canyons—two features in the continental slope known to harbor large numbers of adults (Lenarz, 1980; MacGregor, 1986; Chess et al., 1988). At these sites the sampling density was increased.

Field and laboratory processing of the bongo net samples followed prescribed CalCOFI guidelines (i.e. Kramer et al., 1972; Smith and Richardson, 1977), with minor modification. For example, at every fifth sampling station, the bongo frame was deployed with 333-µm and 505-µm mesh nets to determine the extent of extrusion of small larvae in the standard 505-µm mesh (Lenarz, 1972; Somerton and Kobayashi, 1989). After the nets were washed down, samples from both mesh sizes were preserved in 80% EtOH. At all other stations, the net frame was deployed with two 505-µm mesh nets; one sample was preserved in 80% EtOH (to allow later age determinations from larval otoliths), and the other was preserved in 10% buffered formalin. In addition, because *Sebastes* larvae were believed to occur only in the upper mixed layer (Ahlstrom, 1959), the maximum amount of wire deployed was 200 m, resulting in a maximum depth fished equal to 140 m. Following splitting, sorting, identification, and enumeration of the larvae in the laboratory, abundance was expressed as the number of shortbelly rockfish per 10 m^2 of sea surface.

To estimate the age composition of the larval population, the sorted shortbelly rockfish larvae from each of the 150 EtOH-preserved bongo hauls were randomly subsampled for otolith microstructure examination. To determine the size of an age subsample (N_s), based upon the total number of larvae occurring in a haul (N_h), we applied the following rule: 1) for N_h less than or equal to 10, $N_s = N_h$, 2); for N_h greater than 10 but less than or equal to 410, $N_s = 10 + 0.10[N_h - 10]$; and 3) for N_h greater than 410, $N_s = 50$. Otoliths were extracted from each specimen in the haul subsample and individual ages determined by methods outlined in Laidig et al. (1991) and Ralston et al. (1996).

The age composition of the larvae in each bongo sample was then estimated by expanding the percent age-frequency obtained from the subsample to the haul total (N_h). The estimated numbers-at-age of larvae in each haul were standardized to the number per 10 m^2 of sea surface (n_{Ti} for age T and haul i) by application of standard haul factors (Kramer et al., 1972; Smith and Richardson, 1977).

We expanded the n_{Ti} to the entire survey area by using the method of Sette and Ahlstrom (1948). The Sette-Ahlstrom estimate is calculated by the following equation (see Kendall and Picquelle, 1990):

$$\hat{N}_T = \sum_{i=1}^{k} A_i \times n_{Ti},$$

where for each of k hauls A_i = the area that haul i represents (units of 10 m^2); and
N_T = the total abundance of larvae of age T in the entire survey area.

The area for a haul (A_i) is defined as the area circumscribed by a polygon containing all points in space closer to a haul's location than to the location of any other haul. With this definition, we were able to write a simple computer program to calculate Sette-Ahlstrom weights by dividing the study area into a fine grid and assigning each grid point to a haul. Note that this definition and procedure for obtaining Sette-Ahlstrom areas is equivalent to constructing polygons manually using perpendicular bisectors and measuring their areas (Sette and Ahlstrom, 1948).

The mean daily larval production rate during the cruise was estimated as the bias-corrected antilogarithm of the y-intercept of the ordinary least-squares linear regression of $\log_e[N_i]$ against larval age. Moreover, the regression slope provides an estimate of the total instantaneous mortality rate of the larvae (Z [/d]). This calculation implicitly assumes that the age distribution of larvae was stationary throughout the 6½-day period of the cruise.

To determine if shortbelly rockfish larvae occur deeper in the water column than 140 m, a series of 1-m^2 multiple-opening-closing-net with environmental sensing system (MOCNESS) tows was conducted aboard the RV *David Starr Jordan* (cruise DSJ-9203) during the 1992 spawning season. At that time, 21 tows were made in the area of

Pioneer and Ascension Canyons from 1800 h on 21 February to 0600 h on 23 February. Where bottom depth permitted, discrete depth samples were gathered using 505-µm mesh nets, sampling obliquely in the 0–40, 40–80, 80–120, 120–160, 160–200, 200–300, and 300–400 m depth intervals. Sampling was arrayed along seven onshore–offshore transects, each composed of three tows conducted at different bottom depths, i.e. mid-continental shelf (110 m), the shelf-break (183 m), and well off the shelf (550 m). All samples were preserved in EtOH and after sorting, identifying, and enumerating the larvae in the laboratory, we expressed abundances as the number of shortbelly rockfish larvae per 1000 m^3 water sampled.

Spawning seasonality

At its inception, this assessment was intended to be an application of the fecundity reduction method described by Lo et al. (1992, 1993). However, samples from the February and March adult trawl surveys showed that a higher proportion of females had completed spawning in the earlier cruise in comparison with the later cruise, an indication that sampling was not representative during one or both of the cruises. Consequently, the fecundity reduction method was abandoned and an alternative approach was devised. Instead, we estimated the seasonal distribution of spawning activity based on the temporal distribution of preflexion shortbelly rockfish larvae in samples collected as part of the CalCOFI program from December to April from 1952 to 1984 (see Ahlstrom et al., 1978). We then used this seasonal spawning pattern to expand our estimate of the daily spawning biomass from the short period represented by our 1991 plankton samples to the entire year.

To estimate the seasonal spawning distribution, we first identified the appropriate samples from CALCOFI station 63.55 in the vicinity of Pioneer Canyon by using results from MacGregor (1986) as a guide. Plankton samples at this location (Fig. 1) were re-examined and the total number of preflexion shortbelly rockfish larvae were enumerated from *Sebastes* subsets. These samples amounted to 41 plankton tows (bongo and ring nets) taken in 21 different years.

Next, we calculated the mean density of preflexion larvae for each month, assigned these densities to the midpoint day of the month, and used nonlinear least-squares regression to fit the normal curve to approximate the seasonal spawning pattern, i.e.

$$\hat{N}_p(t) = \frac{\psi}{\hat{\sigma}_p\sqrt{2\pi}} e^{-\frac{(t-\hat{\mu}_p)^2}{2\hat{\sigma}_p^2}},$$

where $\hat{N}_{p(t)}$ = the estimated density of preflexion larvae on calendar day t (for December t is negative);

$\hat{\mu}_p$ = the expected value of the seasonal distribution of preflexion larvae;

$\hat{\sigma}_p$ = the standard deviation of the distribution; and

Ψ = a "nuisance" scaling constant.

To determine the seasonal distribution of age-0 larval production that generates the seasonal distribution of preflexion larvae, we assumed that the preflexion larval period has a duration of 15 days (Laidig et al., 1991) and that larvae experience the estimated preflexion mortality rate (see above). As with preflexion larvae, we approximated the seasonal distribution of age-0 larval production with a normal curve, with mean μ_0 and standard deviation σ_0. Given particular values for μ_0 and σ_0 we calculated the corresponding relative numbers of age-0 larvae produced during each day of the spawning season, and the integrated seasonal distribution of preflexion larvae, i.e.

$$N^*_p(t) = \sum_{i=0}^{15} N_0(t-i)e^{-iZ}$$

We started the estimation with trial values of μ_0 and σ_0 and then recursively adjusted the parameter estimates until the mean and standard deviation of the inferred seasonal distribution of preflexion larvae ($N^*_{p(t)}$) converged on the empirical estimates of $\hat{\mu}_p$ and $\hat{\sigma}_p$.

Lastly, based on the timing of the larval survey within the long-term mean spawning distribution, total biomass was calculated by simple expansion. Specifically, the midpoint of the 1991 bongo survey was 11 February (i.e. calendar day 42). Consequently we calculated λ, which is the proportion of annual spawning under the age-0 larval production curve that occurs from day 41.5 to 42.5. Total population biomass was then estimated by multiplying the estimate of "daily" biomass by $1/\lambda$. This calculation implicitly assumes that the seasonal progression of spawning has been stable over years. Therefore, the sensitivity of the biomass estimate to a violation of this assumption was evaluated by profiling over a range of values for the mean date of spawning (μ_0), which has a substantial effect on λ.

Precision of the biomass estimate

The determination of total biomass requires the estimation of numerous statistical relationships, each with its own parameter set. The results of fitting these functions were then combined algebraically to produce the final biomass estimate. We calculated the precision of the final biomass estimate by using the delta method (Seber, 1982, p. 8), i.e.

$$V[g(\theta)] = \sum_i V[\theta_i]\left(\frac{\partial B}{\partial \theta_i}\right)^2 + 2\sum_{i<j}\sum \mathrm{cov}[\theta_i,\theta_j]\frac{\partial B}{\partial \theta_i}\frac{\partial B}{\partial \theta_j},$$

where $g(\theta)$ = the algebraic combination of functions used to produce the final biomass estimates; and

θ = the full set of estimated parameters.

Application of this method requires estimates of variances for each parameter, covariances among parameters, and partial derivatives of estimated biomass with respect to each parameter ($\partial B/\partial\theta$). Partial derivatives of the final biomass estimate with respect to the parameters were calculated numerically by using central differencing by per-

turbing each parameter ±1% and calculating the resulting effect on biomass.

In some instances, variance estimates (i.e. squared standard errors) and covariances were extracted directly from computer output produced by the SAS (1987) procedures PROC REG and PROC NLIN. In the case of linear regressions, these are the usual estimates of these quantities (e.g. Draper and Smith, 1981), whereas for nonlinear regression, these are asymptotic variances and covariances (e.g. Seber and Wild, 1992). In addition, following the assumptions of normal-based regression, the residual error parameter estimates ($\hat{\sigma}^2_{mse}$) used in bias adjustments are independent of other regression parameters (i.e. covariances are zero) and $n\hat{\sigma}^2_{mse}/\sigma^2_{mse}$ has a chi-square distribution with k degrees of freedom, where k is the degrees of freedom associated with $\hat{\sigma}^2_{mse}$ (e.g. for a linear regression $k=n-2$). This chi-square distributed random variable, i.e.

$$\mathrm{var}\left(\frac{n\hat{\sigma}^2_{mse}}{\sigma^2_{mse}}\right) = 2k,$$

was then used to estimate the variance of the mean square errors (Larsen and Marx, 1981)

$$\mathrm{var}\left(\hat{\sigma}^2_{mse}\right) = \left(\frac{\hat{\sigma}^4_{mse}}{n^2}\right) \times 2k.$$

This straightforward approach to obtaining variances and covariances is appropriate when a suite of parameters estimated by a regression procedure is based on a data set that could reasonably be expected to be independent of data sets used to estimate other parameters, and when values of other estimated parameters were not used as "known" constants during a regression or estimation procedure. In two cases, however, estimates of other parameters were treated as known constants during a regression or estimation procedure. These cases were 1) estimation of the mean and standard deviation of the seasonal distribution of age-0 larvae, and 2) estimation of von Bertalanffy growth equation parameters. In the case of the seasonal distribution of age-0 larvae, parameter estimates depended upon the natural mortality rate estimated for larvae (Z). Hence, variances for these parameters calculated directly from the regression procedure are conditional on the estimated mortality rate. Imprecision associated with estimating this rate adds to variances of these parameters, and influences their covariance. Likewise, for von Bertalanffy growth, the weight "data" used were calculated on the basis of the estimated relationship between weight and length. Hence regression estimates of variance and covariances for the von Bertalanffy parameters are conditional on the parameters for the weight-length relationship. Uncertainty associated with the estimates of the weight-length parameters influences the unconditional variances and covariances of the von Bertalanffy parameters, sets up covariances between the two suites of parameters, and because the same weight-length relationship was used for both sexes, also sets up covariances among the von Bertalanffy parameters for males and females.

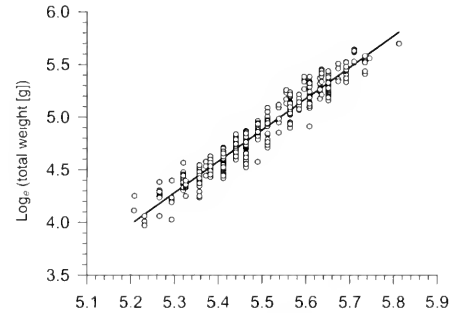

Figure 2

Fit of ordinary least-squares regression to $\log_e$-transformed weight and length data from shortbelly rockfish sampled by trawl in February–March 1991.

For these cases, a generalized version of the delta method was used to estimate covariances (and variances):

$$\mathrm{cov}\left[g(x,y),h(x,z)\right] = \sum_{ij}\sum \mathrm{cov}\left[x_i,x_j\right]\frac{\partial g}{\partial x_i}\frac{\partial h}{\partial x_j}$$

(Seber, 1982, p. 9). Here g and h represent regression procedures by which two specified parameters are estimated, x represents a set of shared values (assumed known parameters and data) used by the two regression procedures, y and z represent distinct data or parameters with no covariance among them, and partial derivatives are calculated as described above.

Results

Population weight-specific fecundity and sex ratio

The weight (W) of a fish is equated to its length (TL) by use of the power function, i.e.

$$W = \alpha TL^{\beta},$$

where α and β are fitted parameters (Ricker, 1975).

In our study, weight (gm) and TL (mm) data were collected from 352 fish sampled during the two adult trawl cruises. The data from these fish were $\log_e$-transformed and fitted by linear regression (Fig. 2, Table 2). The fit was good, as indicated by a high r^2 value (0.94), and the distribution of residuals did not deviate from normality (P=0.109). To predict weight at length on the untransformed scale, a

Table 2

Functional relationships, estimated parameters, statistical results, and sensitivity analyses of shortbelly rockfish larval production biomass estimate.

Function	Parameter	Estimate	Standard error	% Effect on biomass −1 SE	% Effect on biomass +1 SE
Length-weight relationship	$\log_e(\alpha)$	−11.512	0.2225	0.00%	0.00%
$\log_e(W) = \log_e(\alpha) + \beta(\log_e[TL])$	β	2.980	0.0405	0.09%	−0.08%
	σ^2_{MSE}	0.008820	0.000667	0.00%	0.00%
Female von Bertalanffy growth	$W_{\infty,\varphi}$	248.1	2.6245	0.64%	−0.63%
$W_\varphi = W_{\infty,\varphi}[1 - \exp[-K_\varphi(T-t_{0,\varphi})]]^\beta$	K_φ	0.2843	0.00917	1.73%	−1.58%
	$t_{0,\varphi}$	−0.78	0.11026	−0.91%	0.96%
Male von Bertalanffy growth	$W_{\infty,\sigma}$	209.9	3.0872	−0.67%	0.67%
$W_\sigma = W_{\infty,\sigma}[1-\exp[-K_\sigma(T-t_{0,\sigma})]]^\beta$	K_σ	0.2432	0.00984	−2.05%	2.01%
	$t_{0,\sigma}$	−1.48	0.15183	1.55%	−1.54%
Adult survival	$\log_e(\eta_0)$	3.194	0.30662	0.00%	0.00%
$\log_e(N_T) = \log_e(\eta_0) - MT$	M	0.2616	0.02656	−1.46%	1.53%
Fecundity at weight	$\log_e(\phi)$	3.8155	0.1732	18.91%	−15.90%
$\log_e(F) = \log_e(\phi) + \delta(\log_e[W])$	δ	1.1416	0.0366	19.88%	−16.61%
	σ^2_{MSE}	0.2972	0.01827	0.92%	−0.91%
Maturity at length	v	2.888	0.0237	0.00%	0.00%
$S = 1 + v/\{1+\exp[-\rho(TL - TL')]\}$	ρ	0.6046	0.10318	0.00%	0.00%
	TL'	135.05	0.85515	−0.15%	0.00%
Larval production and survival	$\log_e(N_0)$	−0.3775	0.1737	−15.97%	19.01%
$\log_e(N_T) = \log_e(N_0) - Z(T)$	Z	0.1107	0.01157	0.70%	−0.67%
	σ^2_{MSE}	0.1960	0.05659	−2.79%	2.87%
Spawning seasonality	Ψ	$5.2 \cdot 10^4$	$2.36 \cdot 10^3$	0.00%	0.00%
$N_p(t) = (\Psi/\sigma_p\sqrt{2\pi})\exp[-(t-\mu_p)^2/2\sigma_p^2]$	μ_p	37.88	1.1250	4.02%	−3.45%
	σ_p	17.39	1.1042	−4.58%	4.78%

bias-correction term ($\hat{\sigma}^2_{mse}/2$) was applied prior to exponentiation (Miller, 1984). However, because σ^2_{mse} was small (0.00882), the correction had little effect on predictions of weight at TL. Moreover, predicted values of weight at length did not differ materially from those given in Phillips (1964) and Lenarz (1980).

A total of 586 female shortbelly rockfish were aged from trawl samples. The weights (g) of these fish were individually estimated from measurements of TL (mm) by using the regression results described above. The derived weight-at-age (yr) data were then fitted to the von Bertalanffy growth equation by using a nonlinear regression routine (SAS, 1987). The specific form of the fitted model was

$$W_\varphi = W_{\infty,\varphi}[1 - e^{-K_\varphi(T - t_{0,\varphi})}]^\beta,$$

where W_φ = female weight (g)
$W_{\infty,\varphi}$ = the asymptotic mean weight of females at a hypothetically infinite age (g);
K_φ = the instantaneous growth coefficient specific to females (/yr);
T = age (yr);
$t_{0,\varphi}$ = the x-intercept of the growth curve (yr); and
β = the allometric growth parameter estimated from the regression of weight on length (Ricker, 1975).

The β parameter is often set equal to 3.0, implying isometric growth, although β was fixed at 2.980 in this application (see above). Likewise, 535 adult male fish were aged, their weights estimated from measurements of TL, and the data fitted to the weight-based von Bertalanffy growth model. Regression results for both sexes are presented in Figure 3 and Table 2.

A simple exponential mortality model is used to describe the observed pattern of shortbelly rockfish abundance with age. The model is of the form

$$N_T = \eta_0 e^{-MT},$$

where N_T = the number of individuals alive at age T (yr);
η_0 = the extrapolated number at age T=0; and
M = the instantaneous rate of natural mortality (/yr).

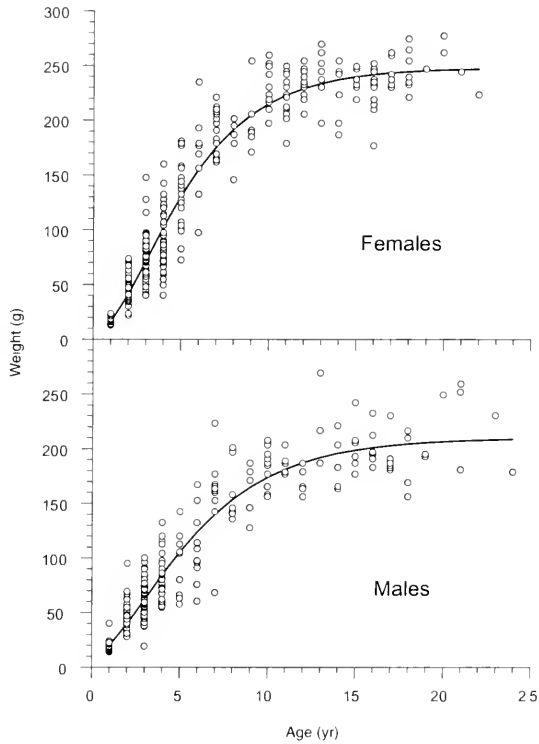

Figure 3

Weight-based von Bertalanffy growth curves fitted to shortbelly rockfish data collected by trawling during February–March 1991.

In this application a term for fishing mortality is assumed to be unnecessary because there is no commercial or recreational harvest of shortbelly rockfish. The model was fitted by a weighted linear regression of $\log_e(N_T)$ on T, where the statistical weights were derived from expansions of the aged subsamples to the full trawl catches. Results showed a declining trend in abundance with age (Table 2, Fig. 4), and an estimated adult natural mortality rate of 0.26/yr.

Like the weight-length relationship, fecundity is typically related to fish size with the power function (Bagenal and Braum, 1968), which is linearized by logarithmic transformation, i.e.

$$F = \phi W^{\delta},$$

$$\log_e(F) = \log_e(\phi) + \delta \cdot \log_e(W),$$

where F = individual annual fecundity (larvae/female);

W = female weight (g); and

$\log_e[\phi]$ and δ = fitted parameters.

In our study fecundity estimates were gathered from 531 females taken during the trawl surveys and the transformed data were fitted by simple regression (Fig. 5, Table 2). There was considerable residual variability in the fecundity at weight relationship (r^2=0.65; $\hat{\sigma}^2_{mse}$ =0.29715) and, in this instance, the addition of a bias-correction term had a noticeable effect on back-transformed predictions of fecundity at weight on the arithmetic scale. Although the distribution of regression residuals deviated significantly from normal (P=0.0001), due in large part to negative skewness, the overall fit was deemed adequate. Predictions of fecundity at weight were ~25–35% less than the results presented in Lenarz (1980), although his equation is based on only the 10 data points provided in Phillips (1964).

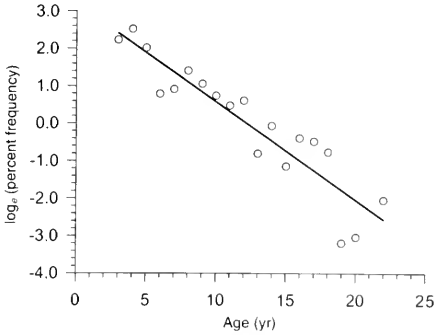

Figure 4

Weighted linear regression of $\log_e$-transformed shortbelly rockfish abundance on age (statistical weights based on expansions of aged subsamples to full trawl catches; all samples collected by trawling during February–March 1991).

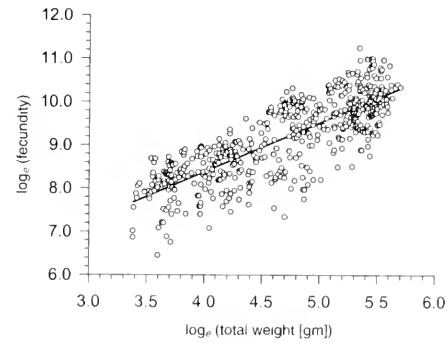

Figure 5

Fit of ordinary least-squares regression to $\log_e$-transformed fecundity and weight data from shortbelly rockfish sampled by trawling during February–March 1991.

There was no evidence that the sex ratio of the fish sampled during the 1991 spawning season (n=1121 from February and March cruises combined) varied with age. A two-way test for independence of age and sex yielded χ^2=27.55, df=23, P=0.23. Moreover, there was no evidence that the overall population sex ratio was other than 50:50 (N_{φ}=586, N_{σ}=535; χ^2=2.32, df=1, P=0.14). From these results, we concluded that females and males both enter the population at approximately the same rate and thereafter they experience a similar natural mortality rate.

The maturity stage data were used to establish a maturity schedule for female shortbelly rockfish collected during the 1991 winter spawning season. Fish were first stratified by size class (5-mm-TL intervals), and for each size group, the mean coded ovarian stage was computed. The data were then fitted by nonlinear regression (SAS, 1987) to a logistic model of the form

$$S = 1 + \frac{\nu}{1 + e^{-\rho(TL - TL')}},$$

where S = the mean coded maturity stage;
TL = total length (mm); and
ν, ρ, and TL' = fitted parameters.

Results show (Fig. 6, Table 2) an abrupt change in ovarian condition at a length of 135 mm. At the time of sampling (February–March), virtually all fish above that size were gestating or had already released their larvae, whereas fish smaller than that cutoff size were almost exclusively immature. All females were therefore assumed to be reproductively mature if TL was greater than 135 mm. The proportion of fish in each age class that exceeded 135 mm TL was used to define an empirical age-based

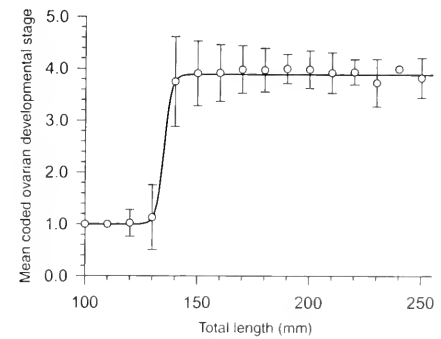

Figure 6

Fit of the logistic maturity function to coded ovarian developmental stage data. Circles are means, which are bracketed by ±1.0 standard deviation (all samples collected by trawling during February–March, 1991).

maturity ogive. Results indicated that 7.9% of 1-yr-old fish spawned, whereas 99.0% of 2-yr-old females reproduced.

When coupled with some type of recruitment model, the four functional relationships given in Figures 3–6 can be used to estimate population weight-specific fecundity and a weight-based population sex ratio. These latter two variables are presented in Table 3 as part of a life table projection for shortbelly rockfish. In the table, age is incremented discretely in one year steps to a maximum life span of 30 yr, which extends well beyond the maximum observed age of 22 years (Pearson et al., 1991). All calculations were

Table 3

Life table for shortbelly rockfish (*Sebastes jordani*) based upon samples of adults obtained during the 1991 spawning season (February–March).

Age (yr)	♀ or ♂ numbers	♀ Wt (g)	♀ Cohort Wt (g)	Fecundity (larvae/♀)	Weight-specific fecundity (no. of larvae/g of female)	Proportion mature	Cohort fecundity (larvae)	♂ Wt (g)	♂ cohort Wt (g)
1	1.0000	15.9	15.85	1235	77.90	0.079	98	19.9	19.89
2	0.7698	41.0	31.54	3651	89.11	0.990	2783	39.6	30.50
3	0.5926	71.5	42.37	6893	96.42	1.000	4085	62.0	36.72
4	0.4562	102.4	46.72	10,390	101.45	1.000	4740	84.4	38.50
5	0.3512	130.8	45.93	13,736	105.03	1.000	4824	105.3	36.99
6	0.2704	155.3	41.98	16,710	107.61	1.000	4518	124.0	33.52
7	0.2081	175.6	36.55	19,227	109.50	1.000	4002	140.0	29.14
8	0.1602	192.0	30.76	21,291	110.89	1.000	3411	153.6	24.60
9	0.1233	205.0	25.28	22,943	111.93	1.000	2830	164.7	20.32
10	0.0950	215.1	20.43	24,245	112.70	1.000	2302	173.9	16.51
11	0 0731	223.0	16.30	25,258	113.27	1.000	1846	181.3	13.25
12	0.0563	229.0	12.89	26,040	113.70	1.000	1465	187.2	10.54
13	0.0433	233.6	10.12	26,640	114.02	1.000	1154	192.0	8.32
14	0.0333	237.2	7.91	27,098	114.26	1.000	904	195.8	6.53
15	0 0257	239.8	6.16	27,446	114.44	1.000	705	198.8	5.10
16	0.0198	241.8	4.78	27,710	114.58	1.000	548	201.1	3.98
17	0.0152	243.4	3.70	27,910	114.68	1.000	425	203.0	3.09
18	0.0117	244.5	2.86	28,061	114.76	1.000	329	204.5	2.39
19	0.0090	245.4	2.21	28,175	114.82	1.000	254	205.7	1.85
20	0.0069	246.1	1.71	28,261	114.86	1.000	196	206.6	1.43
21	0.0053	246.5	1.32	28,326	114.89	1.000	151	207.3	1.11
22	0.0041	246.9	1.02	28,375	111.92	1.000	117	207.9	0.85
23	0.0032	247.2	0.78	28,412	114.94	1.000	90	208.3	0.66
24	0.0024	247.4	0 60	28,440	114.95	1.000	69	208.7	0.51
25	0.0019	247.6	0.46	28,461	114.96	1.000	53	208.9	0.39
26	0.0014	247.7	0.36	28,476	114.97	1.000	41	209.1	0.30
27	0.0011	247.8	0.28	28,488	114.97	1.000	32	209.3	0.23
28	0.0009	247.8	0.21	28,497	114.98	1.000	24	209.4	0.18
29	0.0007	247.9	0.16	28,504	114 98	1.000	19	209.6	0.14
30	0.0005	247.9	0 13	28,509	114 98	1.000	14	209 6	0.11
Total		411.37					42,028		347.65

based on a discrete time origin that was centered in the spawning season and it was assumed that samples were obtained at that time.

For simplicity, constant annual recruitment to the population at age 1 is assumed, although this particular assumption is later relaxed and its specific effect on estimates of population weight-specific fecundity is evaluated. To start the simulated population, recruitment was arbitrarily set equal to N_1 = 1.0/yr for both females and males. Then, given female weight at age (Fig. 3) and female numbers at age (Fig. 4), one can calculate age-specific female cohort biomass as the product of numbers and individual weights (Table 3), which when summed over all ages yields the total equilibrium female biomass (411.37 g/female recruit). Likewise, age-specific cohort fecundity is calculated as female numbers at age, multiplied by estimates of individual female fecundity (Fig. 5), multiplied by the proportion of females that are mature (Fig. 6), which when summed over all ages classes yields the expected lifetime larval production of a cohort (42,028 larvae). The ratio of these two quantities (Φ=102.17 larvae/g of female) estimates the population weight-specific fecundity of female shortbelly rockfish. This population statistic can be compared with individual age-specific estimates presented in Table 3. These weight-specific fecundities range from 77.90 larvae/g of female for the mature 1-yr-old females, to 114.98 larvae/g of female for the oldest fish.

It is also revealing to compare predicted weight-specific fecundity at age from the life table analysis (Table 3) with the observed data calculated directly from individual fish (Fig. 7). Results show a great deal of variability in the observed data, which is consistent with the extensive residual variability in fecundity (see Fig. 5, Table 2). Life table predictions were generally similar to, but slightly higher than, the observed data. This slight difference is

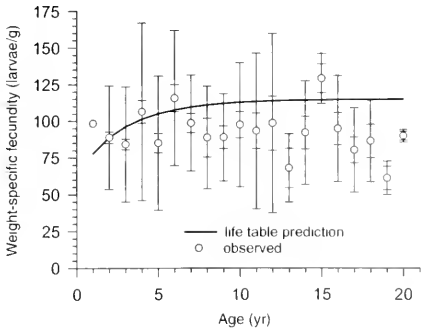

Figure 7

Weight-specific fecundity and its dependency on age. Observed values are means of measured females, bracketed by ±1.0 standard error and ±1.0 standard deviation (all samples collected by trawl during February–March, 1991). The solid line, which is not fitted to the "observed" points, is the predicted relationship from the life table analysis presented in Table 3.

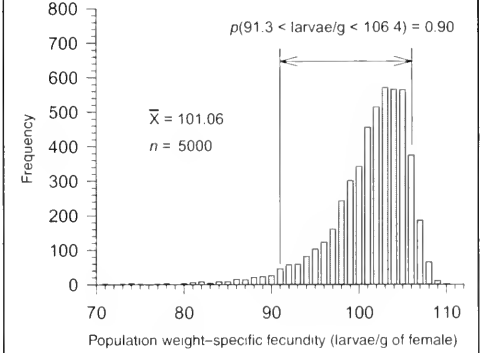

Figure 8

Results of Monte Carlo simulation evaluating the effect of recruitment stochasticity on calculations of shortbelly rockfish population weight-specific fecundity.

due to the bias correction that occurs when the fecundity relationship, which was fitted on the log-scale, is back-transformed to the arithmetic scale. Irrespective of the type of data, however, it is evident that weight-specific fecundity is only weakly dependent on age. This finding implies that changing the equilibrium age structure of the population, as mediated through an alteration in the natural mortality rate (M), will have little effect on the population's weight-specific fecundity.

The assumption that recruitment is constant and uniform does not appear to appreciably bias the estimate of population weight-specific fecundity derived from the life table analysis (102.17 larvae/g of female). Population weight-specific fecundity was also estimated in a Monte Carlo life table simulation that used a more realistic lognormal recruitment model (Fogarty, 1993). Annual recruitments in that simulation were determined as $N_1 = \exp(\mu + \sigma X)$, where N_1 is the number of recruits at age 1, $\mu = \log_e[10{,}000]$, $\sigma = 0.921$, and X is a standard normal deviate (i.e. $X \sim N[0,1]$). This level of variability in lognormal recruitment is comparable to that observed in the widow rockfish fishery (Bence et al., 1993; Hightower and Lenarz[3]), where 20-fold differences in recruitment have been observed in a 10-yr time period. Results of the simulation showed that fluctuating, lognormal recruitment can produce values of population weight-specific fecundity that range from 71 to 110 larvae/g of female, depending on the exact sequence of year classes and their resulting affect on age structure (Fig. 8). Even so, the mean of the sample distribution ($\bar{x}$=101.06 larvae/g of female, n=5000) did not differ significantly from the life table calculation that had no recruitment variability. In addition, 90% of all the lognormal recruitment realizations were within ±10% of the constant recruitment result.

By definition, population weight-specific fecundity represents the number of larvae produced by one gram of female biomass (including immature 1-yr-olds). We expanded female biomass to total biomass including males. Results presented in Table 3 show that age-specific male cohort biomass, like that of females, is calculated as the product of numbers-at-age and individual weights-at-age, which when summed over all ages yields the total equilibrium male biomass (347.64 g/male recruit). Total population biomass (i.e. females+males) is then 759.01 g, of which females comprise 54.2% by weight. Thus, the total biomass is estimated by applying a 1.845 expansion factor to female biomass.

Larval production

Sampling with different mesh-size bongo nets (333 and 505 µm) allowed an assessment of whether a portion of smaller larvae retained by the smaller mesh was lost with the standard 505-µm mesh. Although shortbelly rockfish are relatively large and stout at parturition (~5.0 mm, Moser et al., 1977), undersampling of small, young larvae could seriously bias larval production estimates. Results presented in Figure 9 show, however, that the standardized catches of larvae (number/[10 m^2]) in the two net sizes were quite similar. A paired t-test of catches (333 minus

[3] Hightower, J. E., and W. H. Lenarz. 1990. Status of the widow rockfish fishery in 1990. *In* Status of the Pacific coast groundfish fishery through 1990 and recommended acceptable biological catches for 1991. Stock assessment and fishery evaluation, appendix vol. 2, 48 p. Pacific Fishery Management Council, Portland, OR.

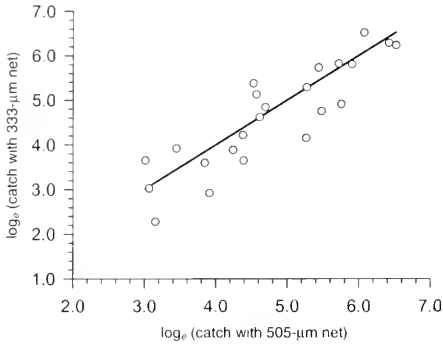

Figure 9

Paired comparison of log$_e$-transformed larval shortbelly rockfish catches taken in bongo nets with different mesh sizes (all samples collected during February 1991). Also shown is the line of equality.

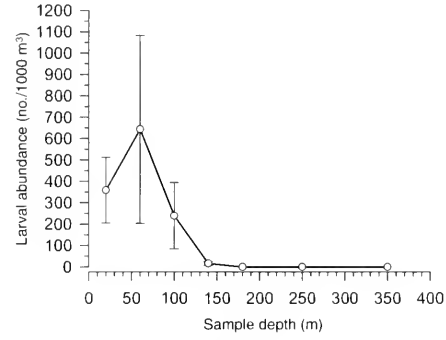

Figure 10

Mean catch rate of shortbelly rockfish larvae in seven depth strata taken by a MOCNESS sampler during March 1992. Means are bracketed by ±1.0 standard error.

505) resulted in $\bar{x} = -0.1458$, $n = 23$, $t = -1.24$, and $P = 0.23$, indicating no difference in the catch of the larger mesh net in relation to the smaller net. We conclude that the 505-µm net was an effective sampler of rockfish larvae.

Examination of the standardized catches from the MOCNESS tows conducted in 1992 revealed that shortbelly rockfish larvae were not caught in depths below the 120–160 m interval (Fig. 10). The mean catch rate in that depth range was 16.8 larvae/1000 m^3, which amounted to only 1.3% of the combined average catch at all depths, i.e. 98.7% of all larvae were captured at depths < 120 m. Because the bongo net was deployed to a maximum depth of 140 m in 1991, and because the mixed layer depth was depressed during MOCNESS sampling in 1992 due to strong El Niño conditions (Lynn et al., 1995), we concluded that the 1991 bongo net survey sampled the entire depth range where shortbelly rockfish larvae occurred.

For this assessment, a total of 2203 shortbelly rockfish larvae were subsampled from the 505-µm bongo net catches and were aged by using optical microscopy (see Ralston et al., 1996). Results from that work indicated that the ages were quite precise (84% agreement among three readers to within ±1 d) and there were, moreover, no increment interpretation differences between optical observations and those made with a scanning electron microscope (SEM).

The horizontal distribution of very young (0–2 d) shortbelly rockfish larvae was strongly associated with the continental shelf break (Fig. 11) and, latitudinally, with the Pioneer Canyon area. Due to the coincidence of this distribution with the locus of adult sampling sites (Fig. 1), we concluded that the trawl survey sampled the adults that produced the larvae captured in the ichthyoplankton survey. This finding supports the coupling of our population weight-specific fecundity statistic (102.17 larvae/g of female) with larval production to estimate the total biomass of shortbelly rockfish in the Pioneer Canyon region. Although not shown, older age classes of larvae tended to be more dispersed and to occur increasingly to the northwest—a pattern consistent with hydrographic conditions at the time of the survey (Sakuma et al., 1995).

When Sette-Ahlstrom weights were used to expand age-specific standardized bongo net catches to the entire study region, the composite age-frequency distribution of shortbelly rockfish larvae appeared to support a log$_e$-linear model with constant exponential mortality (Z [/d]), i.e.

$$N_T = N_0 e^{-ZT},\ \log_e(N_T) = \log_e(N_0) - ZT,$$

where N_T = the total abundance of larvae of age T (d);
Z = the instantaneous larval mortality rate (/d); and
N_0 = the larval renewal rate (i.e. daily production of larvae).

The model was fitted over the first 25 days of life, which largely represents the preflexion stage. In addition, the N_T were first coded by scaling all observations to 1×10^{11} and 0.5 was added to all larval ages as a continuity correction (see Ralston et al., 1996). Results show (Fig. 12, Table 2) a satisfactory fit, although there is some suggestion of an aberrant, serially correlated pattern in the residuals from age 0–9 d. The y-intercept term ($\log_e[N_0] = -0.3775$), when back-transformed (with bias-correction) yields $N_0 = 7.562\times10^{10}$ age-0 larvae.

Given estimates of daily larval production (7.562×10^{10} larvae) and population weight-specific fecundity (Φ= 102.17 larvae/g of female), we calculated from the ratio of these two quantities that 740 t of female shortbelly rockfish spawned each day during the bongo net cruise (DSJ-9102), which is equivalent to a daily biomass of 1366 t/d (sexes combined).

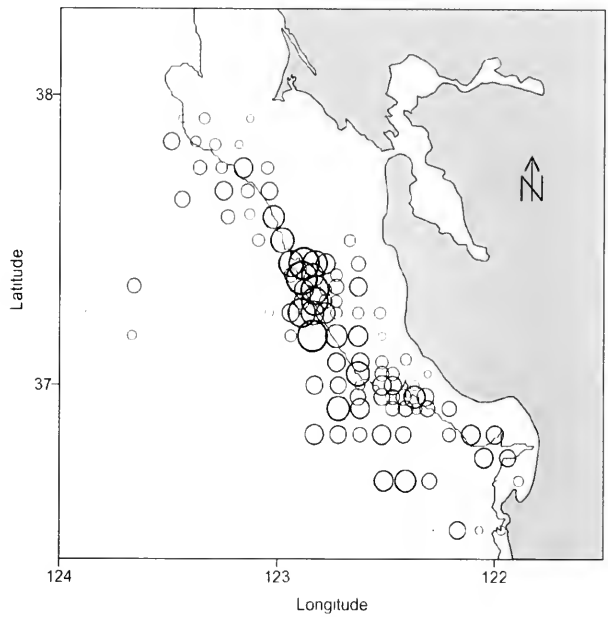

Figure 11

Map showing the spatial distribution of very young (0–2 d) shortbelly rockfish larvae sampled during February 1991. The size of the circles is proportional to $\log_e$(catch+1).

Historical data from CalCOFI station 63.55 (Fig. 1) showed that in the vicinity of Pioneer Canyon the seasonal availability of preflexion shortbelly rockfish larvae peaks during January–March (see "observed" in Fig. 13). These data were fitted to a normal curve (see "predicted" in Fig. 13) and indicated that the distribution of preflexion larvae is centered on 7 February (calendar date $\hat{\mu}_p$= 37.88) and the spawning season typically lasts ~70 d ($\hat{\sigma}_p$=17.39). Assuming that preflexion larvae represent a pool of fish 1–15 d old (Laidig et al., 1991) that experience a daily instantaneous mortality rate of $Z = 0.11$/d (Table 2), the distribution of age-0 larval production is centered earlier in the spawning season, i.e. 2 February (calendar date $\hat{\mu}_0$ =32.62) and the spawning season is slightly less protracted ($\hat{\sigma}_0$=16.86). The estimated long-term mean distribution of age-0 larval shortbelly rockfish production at CalCOFI station 63.55 (Fig. 1) is depicted in Figure 13 as a solid line.

The midpoint of the 1991 bongo-net survey (DSJ-9102) was 11 February (calendar date 42). If larval production were normally distributed and centered at $\hat{\mu}_0$ = 32.62, with $\hat{\sigma}_0$ = 16.86, we calculated that the area under the curve from 41.5 to 42.5 is 0.02026. This represents the estimated fraction of the total annual larval production that occurred per day at the midpoint of the cruise and is the area under the curve between the two vertical lines shown in Figure 13. Thus, we expanded by 49.35 spawning d/yr (1/0.02026) the estimated daily biomass (1366 t/d) to 67,392 t/yr, which is the estimated total stock biomass of shortbelly rockfish in the study area. The standard error of this estimate, based upon delta-method computations, is 12,900 t/yr, yielding a coefficient of variation of 19%.

Sensitivity of the biomass estimate

Presented in Table 2 is a simple sensitivity analysis of all parameters estimated in the larval production spawning stock biomass assessment of shortbelly rockfish. For each of the 23 parameters, the coefficient of variation (expressed as a percentage) is given. In addition, the effects of individual parameter perturbations on the final estimate of spawning stock biomass are shown. In each case, a parameter (Θ) was altered by plus or minus one standard error of the estimate (s_Θ) and the resulting overall effect on the assessment was expressed as the percentage change of the perturbed biomass estimate in relation to the unperturbed value, i.e.

$$\Delta_i = 100\left[\frac{B_i - B_0}{B_0}\right],$$

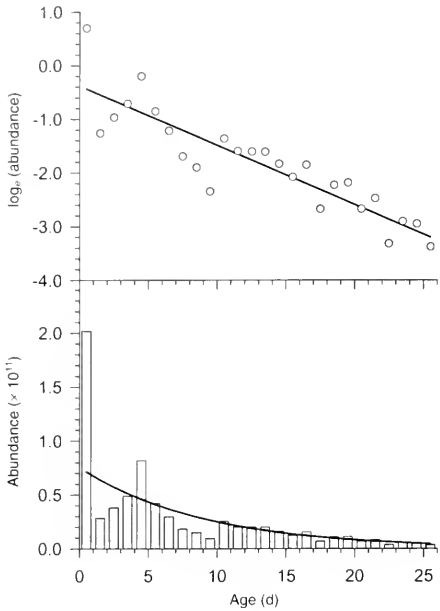

Figure 12

Fit of ordinary least-squares regression of $\log_e$-transformed coded larval abundance ($\hat{n} \times 10^{-11}$) on corrected larval age (T+0.5) (upper panel). The lower panel shows the back-transformation of the $\log_e$-linear model (with bias correction) superimposed on the original abundance data.

where Λ_Θ = the relative sensitivity of the assessment to parameter "Θ";
B_Θ = the resulting biomass after altering parameter "Θ" by $\pm s_\Theta$; and
B_0 = the original unperturbed biomass estimate (67,392 t/yr).

Perturbations equal to $\pm 1\ s_\Theta$ were selected to reflect the level of statistical uncertainty in the parameters themselves. Results showed that within this range of uncertainty, certain parameters had essentially no effect on the final estimate of spawning stock biomass (e.g. $\log_e|\eta_0|$, ν, ρ, Ψ), and others had a more substantial effect. In particular, the assessment was most sensitive to estimates of the two fecundity parameters ($\log_e|\phi|$ and δ) and to the intercept term of the larval production and survival model ($\log_e|N_0|$); both of these findings are consistent with intuition.

Also note that the estimate of adult natural mortality rate (M) has only a minor influence on projected biomass. Low sensitvity to this parameter is important because M alone governs the adult age-structure, implying that variation in age-structure has little effect on the overall stock assessment. This conclusion was portended by results presented in Figures 7 and 8, which illustrate the relative insensitivity of weight-specific fecundity to age. Fundamentally, this conclusion is due to the nearly linear relationship between individual female fecundity and specimen weight (δ=1.14, Table 2, Fig. 5); that is, a fixed mass of mature females produces roughly the same larval output, irrespective of its age composition.

This property is quite useful because it suggests that an accurate estimate of M is not required to make useful projections of total biomass. As discussed previously, obtaining a representative sample of adult rockfish is difficult (Lenarz and Adams, 1980); yet such a sample is usually needed to estimate mortality. Pearson et al. (1991) also highlighted the problem of estimating the natural mortality rate of shortbelly rockfish. Using empirical longevity estimates ($T_{max,\varphi}$=22 yr, $T_{max,\sigma}$=20 yr) as inputs to Hoenig's (1983) regression equation and sample size model, they concluded that for shortbelly rockfish $0.20 \leq M \leq 0.35$/yr. Even over this rather broad range of plausible natural mortality values, our results indicate that biomass estimates vary by only ~9% (Fig. 14).

In contrast, mis-specification of the temporal progression of spawning could have a very large effect on the total biomass estimate. Results presented in Figure 15 show the sensitivity of the total biomass estimate to a range of values for μ_0. Because this parameter depends directly on μ_p and σ_p, which were estimated with good precision (Table 2), the expected effect on the total biomass estimate is relatively minor. Even so, if the mean of the spawning distribution actually occurred two weeks earlier (i.e. 18 January instead of 2 February), the biomass estimate would be grossly in error.

Discussion

It is widely recognized that most age-structured stock assessments depend critically on the availability of auxiliary information to adequately constrain solutions to these complex models (Deriso et al., 1985; Hilborn and Walters, 1992; NRC 1998; Quinn and Deriso, 1999). However, even with lengthy time series of landings, discards, age compositions, length compositions, survey CPUE data, and logbook effort statistics, it is by no means certain that complex stock assessment models will precisely or accurately estimate total stock biomass (NRC, 1998). Faced with this dilemma, simple procedures like the one presented here become far more attractive, particularly because the coefficient of variation on the final biomass estimate from this pilot study was relatively precise (i.e. 19%). Moreover, the estimate of absolute biomass does not depend on the development of a long time series of data and it can be obtained rather quickly.

We note that in comparison with previous hydroacoustic assessments, which ranged from 153,000–295,000 t,[1] our estimate of the total biomass of shortbelly rockfish in the vicinity of Pioneer and Ascension Canyons (67,400 t) is substantially lower. Because one of the primary goals of our study was to obtain a more precise biomass estimate than the hydroacoustic estimates, it is important to care-

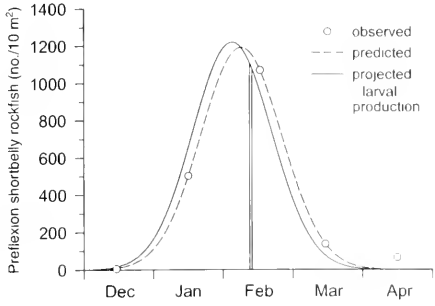

Figure 13

Seasonal pattern in the catch of preflexion shortbelly rockfish larvae at CalCOFI station 63.55 (Pioneer Canyon; see Fig. 1). Observed data were fitted with a normal curve; projected larval production assumes $M = 0.11$/d.

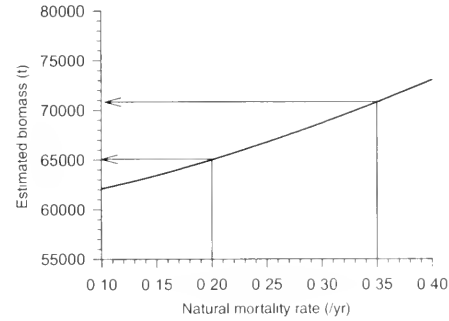

Figure 14

Sensitivity of the larval production estimate of shortbelly rockfish total biomass to the estimated natural morality rate. Vertical dashed lines extending up from the abscissa encompass the likely range of shortbelly rockfish natural mortality (Pearson et al., 1991).

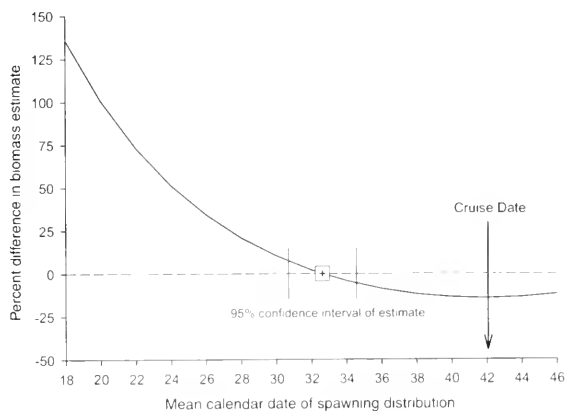

Figure 15

Sensitivity of the total biomass estimate to the mean of the seasonal distribution of shortbelly rockfish larval production, based on CalCOFI samples collected at station 63.55. The estimated mean (μ_0=32.62) is represented by the square, which is bounded by its 95% confidence interval. The effect of misspecifying μ_0 over a broader range (i.e. ±2 weeks) is also shown.

fully consider sources of error and uncertainty in the larval production estimate.

Results presented in Table 2 show that errors in estimating the six growth curve parameters had negligible effects on the biomass estimate, ranging at most from −2.05% to +2.01%. However, estimation errors in the logarithmically transformed power function regression of fecundity on weight had a considerably greater effect. Parameter perturbations in this function altered biomass estimates by ~15–20%. In contrast, errors in estimating the parameters of the logistic maturity ogive had virtually no effect.

We have shown that weight-specific fecundity was only weakly dependent on age (Fig. 7). If these variables were independent, the age structure of the stock would have no influence on population fecundity; that is, a ton of 5-yr-old fish would have the same reproductive output as a ton of 20-yr-old fish. Thus, if age and weight-specific fecundity are independent, the natural mortality rate (M) has no influence on the estimation of biomass, which agrees with the relative insensitivity of the total biomass estimate to estimated natural mortality rate (Table 2, Fig. 14). This a highly desirable characteristic of the assessment methods proposed here. Unlike stock assessments that are predicated on measuring the abundance of ichthyoplankton, results from standard age-structured stock assessment models often depend critically on what is almost always an assumed value of M (e.g. Ralston and Pearson[4]). This can have the effect of reducing an entire stock assessment modeling exercise to guesswork.

Daily larval production ($\log_e[N_0]$) is the other estimated parameter that most strongly influences the calculation of biomass, with parameter perturbations of ±1.0 standard error that result in a 16–19% effect on estimated stock biomass (Table 2). This parameter was determined by assuming a constant mortality rate model, which yielded Z = 0.11/d. However, we view the selection of a specific mortality model to be of considerable importance and wish to emphasize that other alternatives to the exponential survivorship case are available, including the Pareto model (Lo et al., 1989). Researchers who wish to apply the method that we outline here would be well-advised to examine this particular issue carefully because the estimate of daily larval production (N_0) will depend critically on the mortality model used.

Another underlying assumption of the larval production method is that over the period represented by the data, the larval production rate and the mortality rate remained constant. Violations of this assumption could cause patterns like those evidenced in Figure 12. However, we conclude that the existing data do not allow us to distinguish between explanations based on correlated estimation errors and those based on time-varying larval production rates. Also, the ichthyoplankton survey took place over a 6½-day period and samples close together in space were also close together in time, which further complicates the issue. Possible future approaches might consist of sampling designs that include spatial and temporal replication.

Another major source of uncertainty in our assessment lies in the expansion of "daily" total biomass to "annual" total biomass. Based upon the long-term mean distribution of spawning activity (Fig. 12), we calculated that the annual biomass was ~50 times larger than the daily biomass on 11 February. Use of the long-term mean distribution has obvious limitations, however, if the spawning season varies interannually (see Fig. 15).

Results presented in MacGregor (1986) can be used to examine the assumption that spawning seasonality is the same every year. He sorted all shortbelly rockfish larvae from all plankton samples that were collected as part of CalCOFI surveys conducted in 1956, 1966, 1969, 1972, and 1975. In each of these years, cruises were conducted in every month and he presented monthly total larval abundances by year in tabular form. His findings showed that, within the region bounded by CalCOFI lines 60–137 (i.e. San Francisco, CA, to Magdalena Bay, Mexico), the mean date of preflexion larval abundance (μ_p) encompassed only four days among those five years, which together spanned two decades. Similarly, with the exception of 1972 (an El Niño year) the standard deviation of the preflexion larval distribution (σ_p) varied by only five days. These results are consistent with other studies that have shown a remarkable consistency in the timing of fish reproduction (Cushing, 1969; Anderson, 1984; Pedersen, 1984; Picquelle and Megrey, 1993; Gillet et al., 1995; but see Hutchings and Myers, 1994). Thus, although misspecification of the mean time of spawning has the potential to seriously impact the biomass estimate, the observed data suggest that in this application the effect is negligible.

Perhaps a more important structural assumption we have made is that the spawning season can be represented by a normal distribution. Although Saville (1956, 1964) advocated use of the normal distribution for this purpose, we question the generality and accuracy of this symmetric function when used to model spawning seasonality. In the case of shortbelly rockfish, the fit of the five data points to the distribution was reasonably good (dashed line in Fig. 13). Even so, we note that the observed data were monthly means and the April value did not conform well to expectation. Therefore, in future applications of the larval production method we recommend strongly that a well-defined year-specific estimate of the seasonal distribution of spawning activity (i.e. the production rate of age-0 larvae) be obtained. In principle these data could be gathered by high-frequency sampling of either the larval or adult portions of the stock, and even through monitoring the maturity of females in commercial landings.

It is also true that the entire spatial distribution of early larvae must be surveyed in order for the larval production estimate (N_0) to represent the complete spawning stock. This concern is not unique to this assessment, however; it is a requirement that must be satisfied whenever egg and larval surveys are used to estimate the absolute biomass of a fish stock. Nonetheless, in this application it is not likely to have been fully met (Fig. 11). Although the primary spawning concentration of shortbelly rockfish along the central California seems to have been largely encompassed, there is evidence that the offshore extent of very young larvae was not fully captured

Acknowledgments

We would like to thank all the current and former members of the Groundfish Analysis and Physiological Ecol-

[4] Ralston, S., and D. Pearson. 1997. Status of the widow rockfish stock in 1997. *In* Status of the Pacific coast groundfish fishery through 1997 and recommended acceptable biological catches for 1998. Stock assessment and fishery evaluation, appendix, 54 p. Pacific Fishery Management Council, Portland, OR

ogy Investigations at the SWFSC Santa Cruz/Tiburon Laboratory who worked on this project for their dedicated efforts—Cheryl Callahan, Joe Hightower, Brian Jarvis, Anne McBride, Don Pearson, Cathy Preston, Dale Roberts, Keith Sakuma, and David Woodbury. In addition, we credit Geoff Moser and co-workers at the SWFSC La Jolla Laboratory, especially Elaine Acuña, Dave Ambrose, Sherrie Charter, and Bill Watson, for their most helpful assistance in enumerating all the preflexion shortbelly rockfish larvae that occurred in plankton samples taken at CalCOFI Station 63.55 from 1952 to 1984. We are also grateful for the assistance provided by Gary Stauffer of the AFSC Sand Point Laboratory in securing shiptime aboard the Soviet RV *Novodrutsk* for the second survey of adult shortbelly rockfish. Furthermore, a number of thoughtful comments and suggestions were received from reviewers of this manuscript, particularly from Paul Crone, Gareth Penn, and Erik Williams. Lastly, we would like to express our gratitude and appreciation to Alec MacCall for his continued encouragement and support for this work.

Literature cited

Ahlstrom, E. H.
1959. Vertical distribution of pelagic fish eggs and larvae off California and Baja California. Fish. Bull. 60:107–146.

Ahlstrom, E. H., H. G. Moser, and E. M. Sandknop.
1978. Distributional atlas of fish larvae in the California Current region: rockfishes, *Sebastes* spp., 1950–1975. CalCOFI (California Cooperative Oceanic Fisheries Investigations) Atlas 26.

Anderson, J. T.
1984. Early life history of redfish (*Sebastes* spp.) on Flemish Cap. Can. J. Fish. Aquat. Sci. 41:1106–1116.

Armstrong, M., P. Shelton, I. Hampton, G. Jolly, and Y. Melo.
1988. Egg production estimates of anchovy biomass in the southern Benguela system. Calif. Coop. Oceanic Fish. Invest. Rep. 29:137–157.

Bagenal, T. B., and E. Braum.
1968. Eggs and early life history. *In* Methods for assessment of fish production in fresh waters (T. B. Bagenal, ed.), p. 165–201. IBP Handbook 3. J. B. Lippincott Co., Philadelphia, PA.

Bence, J. R., A. Gordoa, and J. E. Hightower.
1993. Influence of age-selective surveys on the reliability of stock synthesis assessments. Can. J. Fish. Aquat. Sci. 50: 827–840.

Bowers, M. J.
1992. Annual reproductive cycle of oocytes and embryos of yellowtail rockfish *Sebastes flavidus* (Family Scorpaenidae). Fish. Bull. 90:231–242.

Chess, J. R., S. E. Smith, and P. C. Fischer.
1988. Trophic relationships of the shortbelly rockfish, *Sebastes jordani*, off central California. Calif. Coop. Oceanic Fish. Invest. Rep. 29:129–136.

Cushing, D. H.
1969. The regularity of the spawning season of some fishes. J. Cons. Int. Explor. Mer 33:81–97.

Deriso, R. B., T. J. Quinn, and P. R. Neal.
1985. Catch-age analysis with auxiliary information. Can. J. Fish. Aquat. Sci. 42:815–824.

Draper, N. R., and H. Smith.
1981. Applied regression analysis, 407 p. John Wiley & Sons, Inc., New York, NY.

Eschmeyer, W. N.
1983. A field guide to Pacific coast fishes of North America, 336 p. Houghton Mifflin Co., Boston, MA.

Fogarty, M. J.
1993. Recruitment in randomly varying environments. ICES J. Mar. Sci. 50:247–260.

Gillet, C., J. P. Dubois, and S. Bonnet.
1995. Influence of temperature and size of females on the timing of spawning of perch, *Perca fluviatilis*, in Lake Geneva from 1984 to 1993. Environ. Biol. Fishes 42:355–363.

Gunderson, D. R.
1993. Surveys of fisheries resources, 248 p. John Wiley & Sons, Inc., New York, NY.

Gunderson, D. R., and T. M. Sample.
1980. Distribution and abundance of rockfish off Washington, Oregon, and California during 1977. Mar. Fish. Rev. 42(3–4):2–16.

Hilborn, R., and C. J. Walters.
1992. Quantitative fisheries stock assessment, 570 p. Chapman and Hall, New York, NY.

Hoenig, J. M.
1983. Empirical use of longevity data to estimate mortality rate. Fish. Bull. 81:898–903.

Houde, E. D.
1977. Abundance and potential yield of the round herring, *Etrumeus teres*, and aspects of its early life history in the eastern Gulf of Mexico. Fish. Bull. 75:61–89.

Hunter, J. R., N. C.-H. Lo, and L. A. Fuiman (eds.).
1993. Advances in the early life history of fishes; Part 2, Ichthyoplankton methods for estimating fish biomass. Bull. Mar. Sci. 53:723–935.

Hutchings, J. A., and R. A. Myers.
1994. Timing of cod reproduction: interannual variability and the influence of temperature. Mar. Ecol. Prog. Ser. 108:21–31.

Kendall, A. W., Jr., and S. J. Picquelle.
1990. Egg and larval distributions of walleye pollock *Theragra chalcogramma* in Shelikof Strait, Gulf of Alaska. Fish. Bull. 88:133–154.

Kramer, D., M. J. Kalin, E. G. Stevens, J. R. Thrailkill, and J. R. Zweifel.
1972. Collecting and processing data on fish eggs and larvae in the California Current region. U.S. Dep. Commer., NOAA Tech. Rep. NMFS Circ. 370, 38 p.

Laidig, T. E., S. Ralston, and J. R. Bence.
1991. Dynamics of growth in the early life history of shortbelly rockfish *Sebastes jordani*. Fish. Bull. 89:611–621.

Larsen, R. J., and M. L. Marx.
1981. An introduction to mathematical statistics and its applications, 536 p. Prentice Hall, Inc., Englewood Cliffs, NJ.

Lasker, R. (editor).
1985. An egg production method for estimating spawning biomass of pelagic fish: application to the northern anchovy, *Engraulis mordax*. U.S. Dep. Commer., NOAA Tech. Rep. NMFS 36, 99 p.

Lenarz, W. H.
1972. Mesh retention of larvae of *Sardinops caerulea* and *Engraulis mordax* by plankton nets. Fish. Bull. 70: 789–798.
1980. Shortbelly rockfish, *Sebastes jordani*: a large unfished resource in waters off California. Mar. Fish. Rev. 42(3–4): 34–40.

Lenarz, W. H., and P. B. Adams.
1980. Some statistical considerations of the design of trawl surveys for rockfish (Scorpaenidae). Fish. Bull. 78:659–674.

Lo, N. C.-H.
1985. A model for temperature-dependent northern anchovy egg development and an automated procedure for the assignment of age to staged eggs. *In* An egg production method for estimating spawning biomass of pelagic fish: application to the northern anchovy, *Engraulis mordax* (R. Lasker, ed.), p. 43–50. U.S. Dep. Commer., NOAA Tech. Rep. NMFS 36.

Lo, N. C.-H., J. R. Hunter, and R. P. Hewitt.
1989. Precision and bias of estimates of larval mortality. Fish. Bull. 87:399–416.

Lo, N. C.-H., J. R. Hunter, H. G. Moser, and P. E. Smith.
1992. The daily fecundity reduction method: a new procedure for estimating adult fish biomass. ICES J. Mar. Sci. 49:209–215.

Lo, N. C.-H., J. R. Hunter, H. G. Moser, and P. E. Smith.
1993. A daily fecundity reduction method of biomass estimation with application to Dover sole *Microstomus pacificus*. Bull. Mar. Sci. 53:842–863.

Low, L.-L. (ed.).
1991. Status of living marine resources off the Pacific Coast of the United States as assessed in 1991. U.S. Dep. Commer., NOAA Tech. Memo. NMFS F/NWC-210, 69 p.

Lynn, R. J., F. B. Schwing, and T. L. Hayward.
1995. The effect of the 1991–1993 ENSO on the California Current System. Calif. Coop. Oceanic Fish. Invest. Rep. 36:57–71.

MacCall, A. D.
1996. Patterns of low-frequency variability in fish populations of the California Current. Calif. Coop. Oceanic Fish. Invest. Rep. 37:100–110.

MacGregor, J. S.
1986. Relative abundance of four species of *Sebastes* off California and Baja California. Calif. Coop. Oceanic Fish. Invest. Rep. 27:121–135.

Miller, D. M.
1984. Reducing transformation bias in curve fitting. Am. Statistician 38(2):124–126.

Moser, H. G., and E. H. Ahlstrom.
1985. Staging anchovy eggs. *In* An egg production method for estimating spawning biomass of pelagic fish: application to the northern anchovy, *Engraulis mordax* (R. Lasker, ed.), p. 37–41. U.S. Dep. Commer., NOAA Tech. Rep. NMFS 36.

Moser, H. G., E. H. Ahlstrom, and E. M. Sandknop.
1977. Guide to the identification of scorpionfish larvae (Family Scorpaenidae) in the eastern Pacific with comparative notes on species of *Sebastes* and *Helicolenus* from other oceans. U.S. Dep. Commer., NOAA Tech. Rep. NMFS Circ. 402, 71 p.

NRC (National Research Council).
1998. Improving fish stock assessments, 177 p. Committee on Fish Stock Assessment Methods, National Research Council, National Academy Press, Washington D.C.

Parker, K.
1980. A direct method for estimating northern anchovy, *Engraulis mordax*, spawning biomass. Fish. Bull. 78:541–544.

Pearson, D. E., J. E. Hightower, and J. T. H. Chan.
1991. Age, growth, and potential yield for shortbelly rockfish *Sebastes jordani*. Fish. Bull. 89:403–409.

Pedersen, T.
1984. Variation of peak spawning of Arcto-Norwegian cod (*Gadus morhua* L.) during the time period 1929–1982 based on indices estimated from fishery statistics. *In* The propagation of cod *Gadus morhua* L. (E. Dahl, D. S. Danielssen, E. Moksness, and P. Solemdal, eds.), p. 301–316. Flodevigen rapportser, 1, Arendal.

Phillips, J. B.
1964. Life history studies on ten species of rockfish (genus *Sebastodes*). Calif. Dept. Fish and Game, Fish. Bull. 126, 70 p.

Picquelle, S. J., and B. A. Megrey.
1993. A preliminary spawning biomass estimate of walleye pollock, *Theragra chalcogramma*, in the Shelikof Strait, Alaska, based on the annual egg production method. Bull. Mar. Sci. 53:728–749.

Quinn, T. J., II., and R. B. Deriso.
1999. Quantitative fish dynamics, 542 p. Oxford Univ. Press, New York, NY.

Ralston, S., E. B. Brothers, D. A. Roberts, and K. M. Sakuma.
1996. Accuracy of age estimates for larval *Sebastes jordani*. Fish. Bull. 94:89–97.

Richardson, S. L.
1981. Spawning biomass and early life of northern anchovy, *Engraulis mordax*, in the northern subpopulation off Oregon and Washington. Fish. Bull. 78:855–876.

Ricker, W. E.
1975. Computation and interpretation of biological statistics of fish populations. Fisheries Research Board of Canada Bulletin 191, 382 p.

Sakuma, K. M., F. B. Schwing, H. A. Parker, and S. Ralston.
1995. The physical oceanography off the central California coast during February and May–June, 1991: a summary of CTD data from larval and pelagic juvenile rockfish surveys. U.S. Dep. Commer, NOAA Tech. Memo., NOAA-TM-NMFS-SWFSC-220, 156 p.

SAS Institute Inc.
1987. SAS/STAT™ guide for personal computers, version 6 edition, 1028 p. SAS Institute, Inc., Cary, NC.

Saville, A.
1956. Eggs and larvae of haddock (*Gadus aeglefinus* L.) at Faroe. Mar. Res. Scot. 4, 27 p.
1964. Estimation of the abundance of a fish stock from egg and larval surveys. Rapp. P.-V. Reun. Cons. Int. Explor. Mer 155:164–173.

Seber, G. A. F.
1982. The estimation of animal abundance and related parameters, 654 p. MacMillan Publishing Co., Inc., New York, NY.

Seber, G. A. F, and C. J. Wild.
1992. Nonlinear regression, 768 p. John Wiley & Sons, New York, NY.

Sette, O. E., and E. H. Ahlstrom.
1948. Estimations of abundance of the eggs of the Pacific pilchard (*Sardinops caerulea*) off southern California during 1940 and 1941. J. Mar. Res. 7(3):511–542.

Smith, P. E., and S. L. Richardson.
1977. Standard techniques for pelagic fish egg and larva surveys. FAO Fish. Tech. Paper 175, 100 p.

Somerton, D. A., and D. R. Koyabashi.
1989. A method for correcting catches of fish larvae for the size selection of plankton nets. Fish. Bull. 87:447–455.

Wourms, J. P.
1991. Reproduction and development of *Sebastes* in the context of the evolution of piscine viviparity. Environ. Biol. Fishes 30:111–126.

Prey consumption of Steller sea lions (*Eumetopias jubatus*) off Alaska: How much prey do they require?

Arliss J. Winship
Andrew W. Trites

Department of Zoology and Marine Mammal Research Unit
Fisheries Center, Room 18, Hut B-3
University of British Columbia
6248 Biological Sciences Road
Vancouver, British Columbia, Canada, V6T 1Z4
E-mail address (for A. J. Winship): winship@zoology.ubc.ca

Abstract—The effects of seasonal and regional differences in diet composition on the food requirements of Steller sea lions (*Eumetopias jubatus*) were estimated by using a bioenergetic model. The model considered differences in the energy density of the prey, and differences in digestive efficiency and the heat increment of feeding of different diets. The model predicted that Steller sea lions in southeast Alaska required 45–60% more food per day in early spring (March) than after the breeding season in late summer (August) because of seasonal changes in the energy density of the diets (along with seasonal changes in energy requirements). The southeast Alaska population, at 23,000 (±1660 SD) animals (all ages), consumed an estimated 140,000 (±27,800) t of prey in 1998. In contrast, we estimated that the 51,000 (±3680) animals making up the western Alaska population in the Gulf of Alaska and Aleutian Islands consumed just over twice this amount (303,000 [±57,500] t). In terms of biomass removed in 1998 from Alaskan waters, we estimated that Steller sea lions accounted for about 5% of the natural mortality of gadids (pollock and cod) and up to 75% of the natural mortality of hexagrammids (adult Atka mackerel). These two groups of species were consumed in higher amounts than any other. The predicted average daily food requirement per individual ranged from 16 (±2.8) to 20 (±3.6) kg (all ages combined). Per capita food requirements differed by as much as 24% between regions of Alaska depending on the relative amounts of low-energy-density prey (e.g. gadids) versus high-energy-density prey (e.g. forage fish and salmon) consumed. Estimated requirements were highest in regions where Steller sea lions consumed higher proportions of low-energy-density prey and experienced the highest rates of population decline.

Manuscript accepted 20 September 2002
Fish. Bull. 101:147–167 (2003).

Nutritional stress may account for the decline of Steller sea lions (*Eumetopias jubatus*) in Alaska (Alverson, 1992), which have declined by over 70% in the last 20–25 years (Loughlin et al., 1992; Trites and Larkin, 1996). Merrick et al. (1997) found a negative correlation between Steller sea lion diet diversity and the rate of population change among six regions of Alaska in the early 1990s. The greatest rates of population decline occurred in areas with low diet diversity, where Steller sea lions predominantly preyed on either walleye pollock or Atka mackerel. Steller sea lions from areas that did not experience a decline, or experienced a lower rate of decline, preyed on both walleye pollock and Atka mackerel along with several other groups of prey species.

Merrick et al. (1997) suggested that the relationship between diet diversity and the rate of population decline reflected differences in the efficiency with which Steller sea lions could find, capture, and handle different numbers of prey categories. However, the energy content of the diet may also have a substantial effect on the foraging efficiency of Steller sea lions. Steller sea lions consuming a low diversity diet of primarily low-energy-density species (e.g. gadids) need to consume more prey biomass than Steller sea lions eating a more diverse diet including high-energy-density species (e.g. forage fish, salmon) to obtain the same amount of energy. Thus, it may be more difficult for Steller sea lions consuming a diet of low-energy content to meet their energy requirements or to forage efficiently than it would be for animals consuming prey of high-energy content.

The overall goal of our study was to estimate the amount of prey required by Steller sea lions in Alaska during the 1990s using a previously developed bioenergetic model (Winship et al., 2002). Our first objective was to examine how daily food biomass requirements were affected by seasonal differences in the energy density of the diet of Steller sea lions in southeast Alaska. Our second objective was to use the same model to compare the food requirements of Steller sea lions among seven regions of Alaska during the 1990s (regions based on Merrick et al., 1997, and Sease and Loughlin, 1999; Fig. 1). Our third objective was to use data from 1998 to compare estimates of Steller sea lion prey consumption with fisheries catches and estimates of prey stock sizes (and natural mortality rates).

Methods

Model structure

The bioenergetic model that we used is described in detail by Winship et al. (2002). In brief, gross energy requirements were calculated for individuals of each age, sex, reproductive status (immature, mature, pregnant), and day of the year by using information on Steller sea lion energetics (basal metabolic rates, active metabolic rates, activity budgets, body growth and composition, digestive efficiency and the

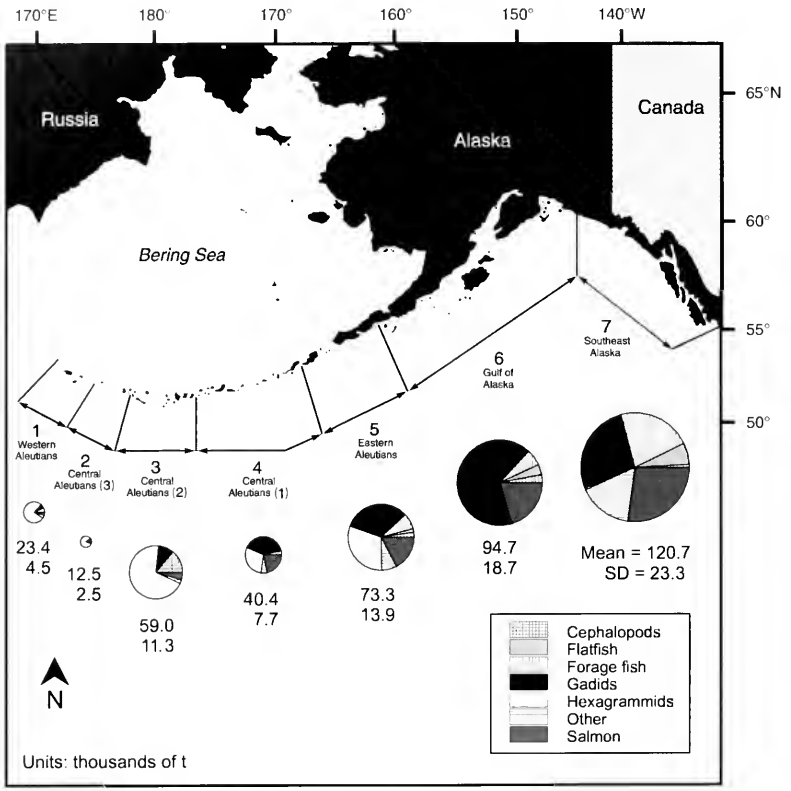

Figure 1

Estimated annual food biomass requirements (thousands of t) for Steller sea lions in 1998 in seven study areas of Alaska assuming that the summer diets were consumed all year long. SDs were obtained by using Monte Carlo simulations (1000 runs). Pie charts represent the proportions of diet biomass that each prey species category represents (defined in text). Diameters of the pie charts are proportional to their respective mean food requirement estimates. The map and study areas were adapted from Merrick et al. (1997) and Sease and Loughlin (1999). Numbers in parentheses in the central Aleutians (areas 2–4) are subarea numbers.

heat increment of feeding or the efficiency of using metabolizable energy). Metabolizable energy requirements of individuals were assumed to be the same in all regions of Alaska. Gross energy requirements of individuals were expected to vary among regions of Alaska because digestive efficiency and the heat increment of feeding are dependent upon the energy density of the diet, which varied among regions. Next, population size and composition were calculated by using pup count data from 1998, and a life table for Steller sea lions in Alaska. Population size varied by region of Alaska, but we assumed that population composition (i.e. sex and age structure) was the same for all regions. Finally, food requirements were calculated by assuming a given diet composition (percent contribution of each prey category to diet biomass) and by using information on the energy density of prey. Diet composition varied by region of Alaska, but we assumed the energy density of individual prey categories did not.

The model incorporated a Monte Carlo random sampling routine which allowed us to estimate the error in the model predictions based on the assumed uncertainty in each parameter value. Three types of parameter sampling distributions were used: uniform (defined by upper and lower limits; e.g. 0.1–0.3), triangular (defined by a median, an upper limit and a lower limit; e.g. 0.2, 0.1–0.3), and normal (defined by a mean and SD; e.g. 0.2 ±0.05).

It is important to note that the model estimates of daily food requirements are not estimates of daily food consumption (Winship et al., 2002). Steller sea lions do not necessarily feed on a daily basis and breeding adults fast for periods during the breeding season. For example, the food required by a breeding male during the breeding season fast (to meet its energy requirement) would have been consumed before or after the breeding season (i.e. outside the breeding season). On an annual basis, however, the model estimates of food requirements are equal to food consumption if animals are consuming enough food to meet their energy requirements. We assumed that the amount of food consumed by the Steller sea lion population in Alaska in 1998 equaled the food requirement of the population.

Bioenergetic parameters

We used sampling distributions for bioenergetic parameters that were identical to those used by Winship et al. (2002) with the exception of fecal digestive efficiency and the heat increment of feeding for maintenance (for nonpups). Winship et al. (2002) defined fecal digestive efficiency as 1 minus the proportion of gross energy lost in feces, and assumed that its value ranged from 0.90–0.96 for Steller sea lions (i.e. fecal digestive efficiency was sampled from a uniform distribution). However, several studies have shown that the digestive efficiency of pinnipeds is positively correlated with the energy density of their prey (Keiver et al., 1984; Mårtensson et al., 1994; Lawson et al., 1997). In contrast, two other studies found that the digestive efficiencies of pinnipeds did not differ significantly among diets of different energy densities, although in both studies the average digestive efficiency was highest for the diet with the highest energy density (Fisher et al., 1992; Fadely et al.[1]). Rosen and Trites (2000a) found that the fecal digestive efficiency of captive Steller sea lions fed herring, pollock, salmon, and squid was positively correlated with the energy density of their diet. We therefore fitted a logistic equation to the data in Rosen and Trites (2000a; their Tables 1 and 2) using nonlinear least-squares regression (Nonlin; SYSTAT, Inc., 1992) and used this fitted equation (n=20, r^2=0.75) to calculate fecal digestive efficiency as a function of the energy density of prey:

$$DE_i = \frac{A}{1 + e^{-k(ED_i - ED_0)}},$$

where DE_i = fecal digestive efficiency for prey category i;
A = 0.951 (±0.0039 SE);
k = 1.86 (±0.016);
ED_i = energy density of prey category i (kJ/g wet mass); and
ED_0 = 2.10 (±0.089).

The fitted parameters (A, k, and ED_0) were randomly sampled from normal distributions with the previously described means and SEs (in each run of the model).

Winship et al. (2002) defined the heat increment of feeding for maintenance as the proportion of metabolizable energy used for maintenance that is lost due to the metabolic cost of digesting and processing food energy, and used a uniform sampling distribution of 0.10–0.15. However, there is evidence that the heat increment of feeding in Steller sea lions, like fecal digestive efficiency, varies with the energy density of prey (Rosen and Trites, 1997; 1999; 2000b). We fitted a linear equation to the data from Rosen and Trites (1997; their Table 1, including data for both meal sizes) and the raw data (Rosen[2]) from Rosen and Trites (1999) and Rosen and Trites (2000b) using linear least-squares regression and used this equation (n=22, P<0.0001, r^2=0.60) to calculate heat increment of feeding as a function of the energy density of prey:

$$HIF_i = a \times ED_i + b,$$

where HIF_i = heat increment of feeding for prey category i (as proportion of gross energy);
a = –0.013 (±0.0023 SE); and
b = 0.229 (±0.0173).

The fitted parameters (a and b) were randomly sampled from normal distributions with the previously described means and SEs (in each run of the model). HIF was then divided by fecal and urinary digestive efficiency to obtain the heat increment of feeding as a proportion of metabolizable energy (Winship et al., 2002).

Population parameters

We used the same sampling distributions for population composition parameters (survival, maturity, and reproductive rates) as outlined in Winship et al. (2002). The sampling distributions for population composition parameters used by Winship et al. (2002) were based on life tables developed for Steller sea lions (York, 1994, Trites and Larkin[3]) that were based on collections done in the 1970s in Alaska (Calkins and Pitcher, 1982). Those life tables were developed on the assumption of a stable population size. However, since the 1970s the sizes of Steller sea lion populations in some regions of Alaska

[1] Fadely, B. S., J. A. Zeligs, and D. P. Costa. 1994. Assimilation efficiencies and maintenance requirements of California sea lions (*Zalophus californianus*) fed walleye pollock (*Theragra chalcogramma*) and herring (*Clupea harengus*). Final report to the National Marine Mammal Laboratory (NMML), 28 p. NMML, NOAA, 7600 Sand Point Way N. E., Seattle, WA 98115.

[2] Rosen, D. A. S. 2001. Personal commun. Marine Mammal Research Unit, Fisheries Center, University of British Columbia Room 18, Hut B-3, 6248 Biological Sciences Road, Vancouver, B.C., Canada, V6T 1Z4

[3] Trites, A. W., and P. A. Larkin. 1992. The status of Steller sea lion populations and the development of fisheries in the Gulf of Alaska and Aleutian Islands. Unpubl rep., 134 p. Marine Mammal Research Unit, Fisheries Center, University of British Columbia, Room 18, Hut B-3, 6248 Biological Sciences Road, Vancouver, B.C., Canada, V6T 1Z4

Table 1

Number of Steller sea lion pups counted on rookeries in Alaska in 1998 (Sease and Loughlin, 1999) and minimum total breeding season population size estimates (including pups), assuming pups represent 20.5% of the population (Winship et al., 2002). Areas are defined in Figure 1.

Area	Number of rookeries	Geographic range	Pup count	Population size
Southeast Alaska	3	Forrester–White Sisters	4234	20,669
Gulf of Alaska	9	Seal Rocks–Chernabura	2971	14,503
Eastern Aleutian Islands	6	Pinnacle Rock–Akutan	2340	11,423
Central Aleutian Islands (subarea 1)	8	Bogoslof–Kasatochi	1297	6332
Central Aleutian Islands (subarea 2)	8	Adak–Ayugadak	1729	8440
Central Aleutian Islands (subarea 3)	3	Kiska–Buldir	355	1733
Western Aleutian Islands	3	Agattu–Attu	681	3324
All	40	Forrester–Attu	13,607	66,425

have declined dramatically (Loughlin et al., 1992; Trites and Larkin, 1996). Thus, it is unlikely that population structure was the same in the 1990s as it was in the 1970s and that population structure was the same in all regions of Alaska. Unfortunately, there are very few data available with which to determine the relationship between the structure and the rate of change in size of a population of Steller sea lions. To account for this uncertainty Winship et al. (2002) used sampling distributions for survival, maturity, and reproductive rates that approximated the uncertainty in population structure (ranges of sampling distributions were about 10–20%).

The population size during the breeding season in each region of Alaska was estimated by using pup count data from the U.S. National Marine Fisheries Service and Alaska Department of Fish and Game surveys done in June and July 1998 (Table 1; Sease and Loughlin, 1999). We assumed that the actual number of pups born could have been as much as 20% greater than the number counted because of pups that were hidden during the surveys, pup mortality before the survey dates, and births after the survey dates (Trites and Larkin, 1996). The number of pups in each region was therefore assumed to range from the values in Table 1 to 1.2 × these values (uniform sampling distributions). Total population size was estimated by dividing the number of pups by the proportion of the total population size that they represented as described by Winship et al. (2002).

Diet parameters

Prey species were grouped into seven prey categories as defined by Merrick et al. (1997): 1) cephalopods: squid and octopus; 2) flatfish: Pleuronectidae; 3) forage fish: Pacific herring (*Clupea pallasi*), Pacific sandlance (*Ammodytes hexapterus*), eulachon (*Thaleichthys pacificus*), and capelin (*Mallotus villosus*); 4) gadids: walleye pollock (*Theragra chalcogramma*), Pacific cod (*Gadus macrocephalus*), and other Gadidae; 5) hexagrammids: Atka mackerel (*Pleurogrammus monopterygius*) and other Hexagrammidae; 6) salmon: Pacific salmon (*Oncorhynchus* spp.); and 7) other: rockfish (*Sebastes* spp.), sculpins (Cottidae), pricklebacks (Stichaeidae), skates (*Raja* spp.), lamprey (*Lampetra* spp.), sharks, and other demersal fish.

The diet composition of Steller sea lions in southeast Alaska was estimated from data reported by Trites and Calkins[4] for scat collected in the 1990s on rookeries during the summer breeding season and on nonbreeding haulouts (in inside waters) during the rest of the year (Table 2). Split-sample frequencies of occurrence (Olesiuk et al., 1990) of prey categories were used as the median percent contributions of each prey category to diet biomass. Four seasonal diet compositions were used: a "winter" diet commencing on 1 December, a "spring" diet commencing on 1 March, a "summer" diet commencing on 1 June, and an "autumn" diet commencing on 1 September. In order to make the modeled transitions between seasonal diets more gradual, the season dates were sampled from uniform distributions with upper and lower limits equal to ±1 week. It was assumed that all ages and both sexes had the same diet composition.

Diet compositions for Steller sea lions in all other regions of Alaska (Gulf of Alaska–western Aleutian Islands) were estimated from data reported by Merrick et al. (1997) for scats collected mainly on breeding rookeries during the summers of the early 1990s (Table 2). As with southeast Alaska, split-sample frequencies of occurrence were used as the median percent contributions of each prey category to diet biomass. We assumed the same diet composition for all ages and both sexes year-round in these regions. The only area not covered by Trites and Calkins[4] and Merrick et al. (1997) was the eastern Gulf of Alaska. We assumed that the diet composition of Steller sea lions in the eastern Gulf of Alaska was the same as the diet of Steller sea lions in the Gulf of Alaska region from Merrick et al. (1997).

We randomly sampled the diet from triangular distributions to incorporate uncertainty in the diet composition

[4] Trites, A. W., and D. G. Calkins. 2002. Unpubl data. Department of Zoology and Marine Mammal Research Unit, Fisheries Center, Univ. British Columbia, Room 18, Hut B-3, 6248 Biological Sciences Road, Vancouver, B.C., Canada, V6T 1Z4.

Table 2

Diet composition (median percent biomass contribution of each prey species category in the diet) of Steller sea lions in Alaska. Values for southeast Alaska are based on split-sample frequency of occurrence data from Trites and Calkins,[4] and values for the Gulf of Alaska through the western Aleutian Islands are based on split-sample frequency of occurrence data from Merrick et al. (1997). Prey categories are defined in the text and areas are defined in Figure 1.

	Prey category						
Area	Cephalopods	Flatfish	Forage fish	Gadids	Hexagrammids	Other	Salmon
Southeast Alaska							
Winter (Dec–Feb)	8.1	7.6	13.5	49.1	0.0	20.4	1.2
Spring (Mar–May)	5.0	7.6	21.0	52.5	0.0	12.5	1.4
Summer (Jun–Aug)	0.8	6.4	21.9	27.3	0.4	16.0	27.3
Autumn (Sep–Nov)	7.0	6.2	12.5	62.2	0.1	8.8	3.3
Gulf of Alaska	2.9	3.9	6.1	66.5	0.3	0 0	20.3
Eastern Aleutian Islands	2.3	1.8	7.7	32.9	30.7	7.3	17.3
Central Aleutian Islands (subarea 1)	0.0	0.0	3.3	40.2	29.4	5.4	21.8
Central Aleutian Islands (subarea 2)	13.7	0.0	0.0	9.7	69.7	2.2	4.7
Central Aleutian Islands (subarea 3)	7.1	0.0	0.0	3.2	84.2	4.9	0.5
Western Aleutian Islands	6.7	0.0	0.0	6.9	77.3	4.6	4.6

(percentage of biomass that each prey category represented in the diet). These distributions had medians from Table 2 and upper and lower limits equal to ±45% of medians ≥10%, or ±98% of medians <10%. These percentages were then standardized so that all prey categories were summed to 100% for a given diet. The ranges of the assumed errors in diet composition were determined by using estimates of the minimum and maximum split-sample frequencies of occurrence of prey categories (Olesiuk et al., 1990; Olesiuk, 1993; see "Discussion" section).

The energy density of fish is a function of their chemical composition, especially their lipid content (Stansby, 1976; Hartman and Brandt, 1995). Thus, the energy density of fish can vary with age (older fish tend to store more lipid; Brett, 1983; Harris et al., 1986; Paul et al., 1998a), season (lipid content can vary with foraging conditions; Paul et al., 1993; Paul et al., 1998a; Robards et al., 1999), reproductive status (lipid content of spawning fish can be different from nonspawning fish; Dygert, 1990; Smith et al., 1990; Hendry and Berg, 1999), and geographic location (feeding conditions can vary with location; Paul and Willette, 1997; Lawson et al., 1998; Paul et al., 1998b). The quantity and resolution of data on the energy density of prey of Steller sea lions varied depending on the prey species (Appendix 1). When detailed season-specific energy-density data were available for prey species, we generally incorporated seasonal changes in energy density. Unfortunately, no detailed geographic-specific energy density data were available for any prey species; therefore we assumed that the energy density of prey did not vary among regions of Alaska. We used relatively wide ranges of possible energy-density values for all prey in order to incorporate the uncertainty in how energy density varies with season and geographic location.

Many data were available on the energy density of forage fish (Appendix 1). The energy densities of forage fish species are relatively high, but vary seasonally in relation to spawning periods, the over-winter fast, and spring and autumn phytoplankton blooms (Anthony et al., 2000). For example, eulachon had a very high energy density (7.5–11.1 kJ/g wet mass) and its energy density was slightly higher in the summer than in late winter (Payne et al., 1999). The energy density of capelin was lower, ranging from 3.5 to 7.0 kJ/g wet mass. In the Gulf of Alaska, the energy density of capelin was high in June (start of spawning) after the spring phytoplankton bloom and decreased through the summer with advancing reproductive stage (Anthony et al., 2000). The energy density of capelin increases again in the fall and early winter as the fish feed on the autumn phytoplankton bloom (Lawson et al., 1998; Payne et al., 1999; Anthony et al., 2000).

Pacific herring and Pacific sandlance were the two main forage fish species consumed by Steller sea lions in Alaska in the 1990s (Merrick et al., 1997, Trites and Calkins[4]). The energy density of Pacific herring increased with age, and the energy density of adults (age >0) ranged from 4.4–11.7 kJ/g wet mass (Appendix 1). In the Gulf of Alaska, Pacific herring were highest in energy content in the autumn and lowest in energy content in the spring (after the overwinter fast; Paul et al., 1998a), but the exact timing of these seasonal changes varied depending on the region of Alaska (Perez, 1994). Pacific sandlance (age >0) ranged in energy density from about 3.2 to 6.1 kJ/g wet mass. Pacific sandlance from the Gulf of Alaska was highest in energy content in June (after the spring bloom), and its energy content decreased through autumn (spawn mid-autumn) and remained low throughout the winter fasting period (Robards et al., 1999; Anthony et al., 2000). We assumed

the energy density of the forage fish prey category was 4.9–11.7 kJ/g in the summer and autumn, and 3.2–6.3 kJ/g in the winter and spring.

Gadids consumed by Steller sea lions in Alaska in the 1990s were primarily walleye pollock, but Pacific cod was also an important prey species (Merrick et al., 1997, Trites and Calkins[4]). The energy density of walleye pollock increases with age, and the energy density of pollock in the size range primarily consumed by Steller sea lions (age>0, range 5–65 cm; Pitcher, 1981, Calkins 1998, Calkins and Goodwin[5]) ranged from about 3.2 to 5.9 kJ/g (Appendix 1). The data in Appendix 1 do not suggest that walleye pollock undergo marked seasonal changes in energy density in Alaska. Pacific cod (age>0) was similar in energy density to walleye pollock and ranged from about 3.3 to 4.5 kJ/g (Appendix 1). However, Smith et al. (1990) found that adult Pacific cod had a relatively high energy density in early spring (ripe, prespawning), declined to a low energy density in the summer (postspawning), and then increased to a high energy density again by early winter. Because the energy density of Pacific cod throughout the year was within the range of the energy density of walleye pollock, we assumed that the energy density of the gadid prey category was constant year-round and equal to 3.2–5.9 kJ/g.

Flatfish species from the northeast Pacific Ocean had energy densities ranging from approximately 2.9 to 6.0 kJ/g (Appendix 1). Two species, English sole (*Parophrys vetulus*) and yellowfin sole (*Pleuronectes asper*), exhibited seasonal changes in energy density. The energy density of adult female English sole increased from spring through mid-autumn (feeding and energy storage period) and decreased thereafter (Dygert, 1990). Juvenile and adult yellowfin sole increased rapidly in energy density at the beginning of summer (June, spawning period), and energy density then decreased through the following spring (Paul et al., 1993). Dygert (1990) and Paul et al. (1993) have suggested that these seasonal patterns of energy density are common for most northern flatfish species. We assumed the energy density of the flatfish prey category was 4.0–6.0 kJ/g in the summer and autumn and 2.9–4.9 kJ/g in the winter and spring.

The primary factors affecting the energy density of Pacific salmon are size and age (Appendix 1). The data in Appendix 1 do not indicate substantial seasonal variability in the energy density of Pacific salmon. Energy density increases with size until salmon return to freshwater and spawn—at which point energy density drops drastically (Brett, 1983; Hendry and Berg, 1999). Steller sea lions in Alaska consumed salmon approximately 25–60 cm in length (Trites and Calkins[4]), which we assumed corresponded to a range in mass of approximately 0.3–3 kg, and an energy density ranging from about 6.1 to 8.7 kJ/g.

Hexagrammids were a major component of the diet of Steller sea lions in the western regions of Alaska during the 1990s (Table 2). The main hexagrammid species consumed was Atka mackerel (Merrick et al., 1997). Unfortunately, very few data are available on the energy density of Atka mackerel. Juvenile hexagrammids (≤12 cm), including Atka mackerel, have energy densities ranging from about 3.5 to 4.7 kJ/g (Appendix 1). However, Steller sea lions likely consume fish longer than 12 cm, which may have higher energy densities. We therefore assumed the energy density of the hexagrammid prey category was 3.5–6.0.

Detailed seasonal and size-specific data on the energy density of cephalopods and other fish species were not available. We assumed (from the data in Appendix 1) that the energy densities of the cephalopod and "other" prey categories were 3.8–6.5 kJ/g and 3.1–6.9 kJ/g, respectively.

Results

Seasonal food requirements (southeast Alaska)

Predicted seasonal changes in gross energy requirements of Steller sea lions in southeast Alaska (per individual) were largely driven by changes in activity budgets (Fig. 2; Winship et al., 2002). Immature animals and mature males were assumed to have relatively constant activity budgets and therefore had relatively constant daily energy requirements. The exception was a drop in the energy requirements of mature males during the breeding season. Energy requirements of mature females were also lowest during the breeding season and generally increased from summer through the following spring, especially if females were pregnant. The energy required to nurse a pup increased steadily throughout the pup's first year of life.

A small part of the seasonal change in gross energy requirements of all animals other than pups can be attributed to variation in the energy density of prey and associated differences in digestive efficiency and the heat increment of feeding. The summer diet had the largest proportions of prey species with high energy densities (forage fish and salmon), and therefore had a higher overall energy density than the autumn, winter, and spring diets (Table 2). Thus, digestive efficiency was highest and the heat increment of feeding was lowest in the summer. The winter and spring diets in southeast Alaska had a lower energy density due to the higher proportions of species with low energy densities and because flatfish and forage fish were assumed to have a lower energy density during winter and spring. As a result, digestive efficiency was lower and the heat increment of feeding was higher during the winter and spring than during the summer. The energy density of the autumn diet (and digestive efficiency and the heat increment of feeding) was intermediate between the energy densities of the summer diet and the winter and spring diets. These seasonal changes in efficiency resulted in up to 4% increases in gross energy requirements during the autumn, winter, and spring in

Calkins, D. G., and E. Goodwin. 1988. Investigation of the declining sea lion population in the Gulf of Alaska. Unpubl. rep., 76 p. Alaska Department of Fish and Game, Division of Wildlife Conservation, 333 Raspberry Road, Anchorage, AK 99518-1599.

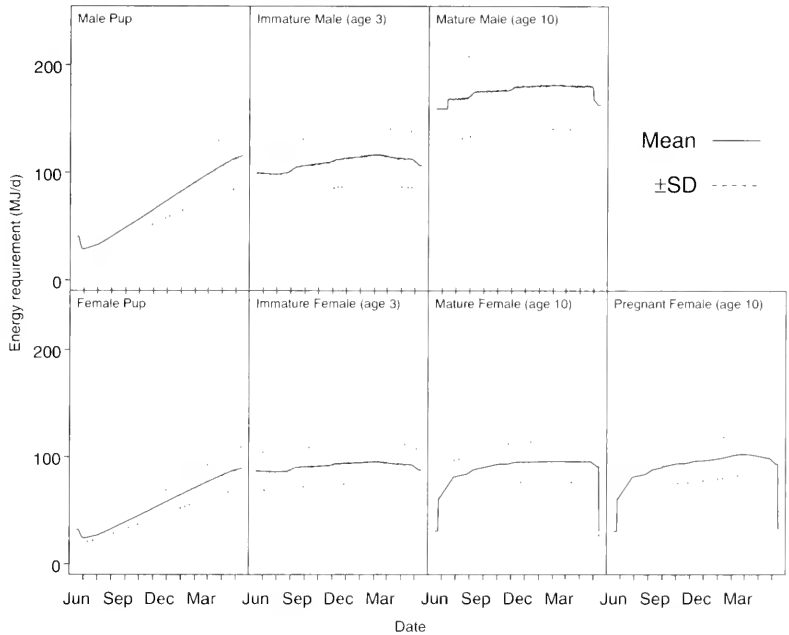

Figure 2

Gross energy requirements of individual Steller sea lions by day of the year. Pup energy requirements represent the amount of energy a female would require to support an entirely dependent pup (i.e. they include energy lost by the mother as waste and the inefficiency of milk synthesis). SDs were obtained by using Monte Carlo simulations (1000 runs). We assumed the date of birth was 15 June. Note that these are plots of energy requirements, not energy consumption. For example, mature males do not consume energy during the breeding season fast (late May–early July).

relation to summer (independent of seasonal changes in metabolizable energy requirements).

Estimated seasonal changes in food requirements in southeast Alaska during the 1990s (Fig. 3) were more pronounced than seasonal changes in energy requirements (Fig. 2) because seasonal changes in the energy density of the diet resulted in large seasonal changes in the amount of food biomass required per unit of gross energy. In general, food requirements were highest in the winter and spring when the energy density of the diet was lowest. Food requirements were lowest in the summer when the energy density of the diet was highest, and food requirements in the autumn were intermediate between those of summer and winter–spring. The maximum daily food requirements in southeast Alaska occurred in March when immature 3-year-old males and females required 25 (±6.9 SD) kg and 21 (±5.2) kg respectively, and mature 10-year-old males and nonpregnant females required 39 (±10.4) kg and 21 (±5.0) kg, respectively. The maximum daily food requirement for a pregnant 10-year-old female nursing a pup averaged 40–46 kg (mid-May). In comparison, daily food requirements in summer, just after the breeding season (1 August), were only 62–69% of these maximum food requirements (immature 3-year-old male: 16 [±4.0] kg, immature 3-year-old female: 14 [±3.1] kg, mature 10-year-old male: 27 [±6.7] kg, mature nonpregnant 10-year-old female: 13 [±2.8] kg). A mature female nursing a pup required only an average of 17–18 kg of food per day at this time of year (39–43% of her maximum daily food requirement).

Regional food requirements

Total annual population food requirements in 1998 varied among regions, as expected because of differences in diet and population size (Fig. 1). When annual food requirements were estimated with diet information from summer only, the model predicted that the southeast Alaska popu-

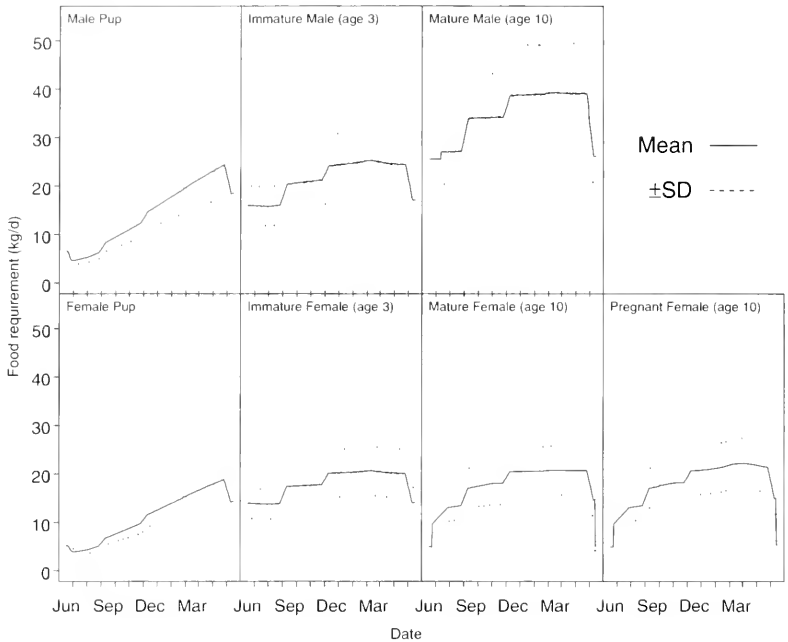

Figure 3

Food biomass requirements for individual Steller sea lions in southeast Alaska by day of the year. Pup food requirements represent the amount of food a female would require to support an entirely dependent pup. SDs were obtained by using Monte Carlo simulations (1000 runs). We assumed the date of birth was 15 June. Note that these are plots of food requirements, not food consumption. For example, mature males do not consume food during the breeding season fast (late May–early July).

lation consumed the most prey biomass on an annual basis (121,000 [±23,300] t) and the central Aleutian Islands 3 population consumed the least (12,500 [±2470] t). The large difference in total consumption primarily reflects the large difference in population size between regions. For southeast Alaska, the only region where diet information was available for all four seasons, the estimated prey biomass consumed on an annual basis increased from 121,000 (±23,300) t (assuming a summer diet all year) to 140,000 (±27,800) t (when diet changed seasonally) because of higher proportions of low-energy-density prey in the diet (and therefore lower energy density of the diet) in autumn, winter, and spring (Table 2). The CVs of total annual population food biomass consumption were 19–20%.

Based on summer diets, the predicted average daily food requirement per individual (all ages) ranged from 16 (±2.8) kg (southeast Alaska) to 20 (±3.6) kg (central Aleutian Islands [subarea 3]) – a 24% difference (Fig. 4). The average daily per capita food requirement for southeast Alaska increased by 3 kg (to 19 [±3.4] kg) when the diets for all four seasons were considered. In general, per capita food requirements were lowest in regions where Steller sea lions consumed high proportions of high-energy-density prey (forage fish and salmon), as in the eastern Aleutian Islands and central Aleutian Islands (subarea 1), and were highest in regions where the diet contained larger proportions of low-energy-density prey (gadids and hexagrammids), as in the western Aleutian Islands and central Aleutian Islands (subareas 2 and 3).

The greatest estimated consumption of a single prey species category in a region in 1998 was 68,600 (±14,400) t of gadids in southeast Alaska (using diet information for all seasons; Fig. 5). Gadids were consumed in a similar amount in the Gulf of Alaska (62,700 [±12,800] t). Alaska-wide, the top two prey categories in terms of biomass consumption were gadids and hexagrammids (gadids – 179,000 [±36,700] t, hexagrammids – 104,000 [±20,600] t). The Steller sea lion population in the central Aleutian Islands (subarea 2) (Fig. 1) consumed the most hexagram-

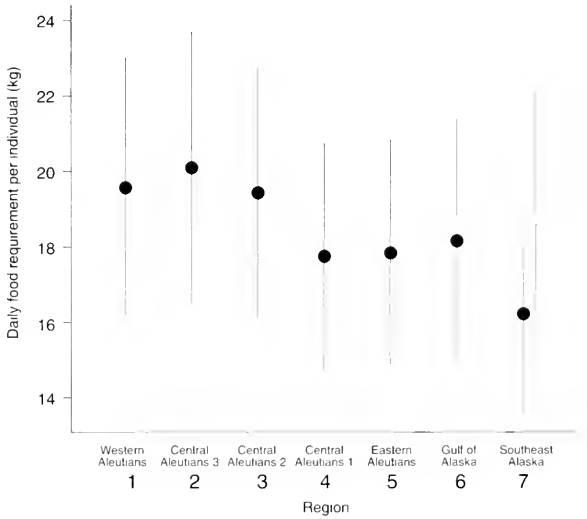

Figure 4

Estimated average daily food biomass requirements per individual Steller sea lion (all ages combined) from seven regions of Alaska based on summer diet information (filled circles). For southeast Alaska, the estimated per capita food requirement based on diet information for all four seasons is also shown (unfilled circle). Error bars represent ±1 SD (obtained by using Monte Carlo simulations–1000 runs).

mid biomass of any region (41,000 [±8070] t). CVs of individual prey category consumption ranged from 20 to 39%.

Discussion

Uncertainty in model predictions

An important aspect of our model is that it produces distributions of predicted food requirements rather than point estimates (Winship et al., 2002). This allowed us not only to estimate mean predicted food requirements but also to estimate the potential error in these mean predictions by using either SD or CV (SD as a percentage of the mean). We found that the CVs of mean predicted food requirements at the population level (both total biomass and individual prey categories) were approximately 20–40%. The ranges of food requirements predicted by the model were of course much wider than ±1 CV. For instance, 5% of the predicted values lie beyond ±1.96 CV if the normal distribution is used to approximate the distribution of model predictions. The minimum and maximum food requirement estimates predicted by the model were generally <40% of the mean and >160% of the mean, respectively, if the CV of the mean predicted food requirement was 30%. Thus, the ranges of predictions produced by our model reflect considerable uncertainty in the food requirements of Steller sea lions because of the assumed errors that we attributed to certain bioenergetic parameters (e.g. metabolic rate at sea), population parameters (e.g. age- and sex-specific survival rates), and diet parameters (e.g. diet composition). Future research on key parameters in our model will help to refine the predictions of this model and improve the accuracy of estimates of the food requirements of this species.

Biases in diet composition

The diet compositions that we used were estimated from the hard parts of prey found in scats collected on haul-outs and rookeries and were limited by incomplete sampling coverage by time of the year and by sex- and age-class. Diet data from the western Aleutian Islands through the Gulf of Alaska came mainly from mature females on breeding rookeries during late June, early July, and early August in the early 1990s (Merrick et al., 1997). Thus, these data reflect a specific segment of the population during a short period of the year.

We applied the diets reported by Merrick et al. (1997) to all age- and sex-classes of Steller sea lions in 1998 and assumed that those diets did not change seasonally. Data

reported by Sinclair and Zeppelin (2002) suggest that the dominant prey in more recently collected samples from the Gulf of Alaska and Aleutian Islands in summer (breeding females on rookeries) and winter (juvenile and adult males and females on nonbreeding haul-outs) were similar to those reported by Merrick et al. (1997). Sinclair and Zeppelin (2002) found walleye pollock more frequently than any other prey species in Steller sea lion scats from the Gulf of Alaska and eastern Aleutian Islands during the summer and winter, whereas Atka mackerel was the second most frequently occurring prey species in the eastern Aleutian Islands, and the most frequently occurring prey species in the central and western Aleutian Islands during summer and winter. However, Sinclair and Zeppelin (2002) did find significant seasonal changes in the frequency of certain prey species in the diets of Steller sea lions at specific sites in Alaska. For example, Pacific cod occurred more frequently in scats collected on haul-outs during the winter than in scats collected on rookeries during the summer in all regions (Gulf of Alaska through western Aleutian Islands). Pacific salmon occurred more frequently in the summer than in the winter in the Gulf of Alaska and the eastern Aleutian Islands, while this seasonal difference was reversed in the central and western Aleutian Islands. A seasonal change in the proportion of the diet comprising high-energy prey species like salmon can have a substantial effect on the total and per capita amount of food biomass required by Steller sea lions (e.g. our results for southeast Alaska). Nevertheless, given the similarities between the two summer and winter data sets (from Sinclair and Zeppelin, 2002, and Merrick et al., 1997), and given the level of uncertainty that we incorporated in our diet compositions, we feel that the diet compositions that we assumed for Steller sea lions in the western Aleutian Islands through Gulf of Alaska regions in 1998 were reasonable approximations.

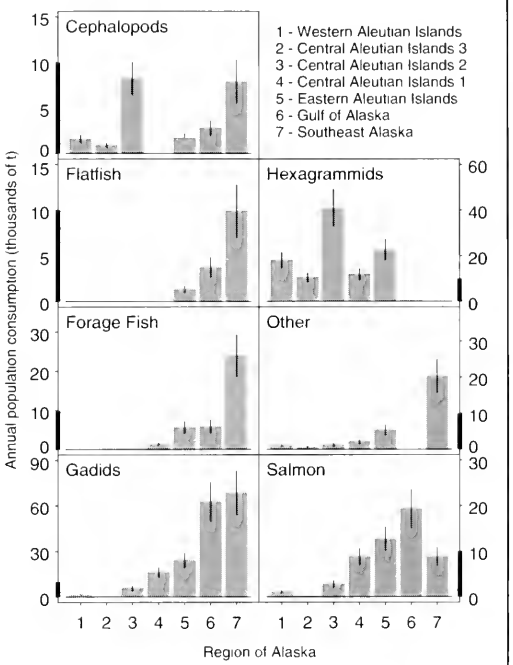

Figure 5

Annual prey biomass consumption for Steller sea lions in 1998 in the seven study areas of Alaska. Values for southeast Alaska were estimated by using diet information for all four seasons. Error bars represent ±1 SD (obtained by using Monte Carlo simulations–1000 runs).

The scat data we used to estimate the diet of Steller sea lions in southeast Alaska had better temporal and demographic coverage. Trites and Calkins[4] reported data from scats collected in every month except September. Although the scat data from the summer months were again from breeding females on rookeries, the scat data from the rest of the year were from nonbreeding animals on haul-outs. Animals using these haul-outs included adult and juvenile males and females. Thus, those scats were more representative of the average diet of the population than scats collected on rookeries during the breeding season. There is evidence that the diet of mature females on rookeries differs from the diet of nonbreeding animals on haul-outs during the summer (Trites and Calkins[4]), but it is difficult to translate this difference into sex- or age-specific dietary differences.

In addition to sampling limitations, there are at least two other potential biases associated with using scat data to assess diet composition. The first potential bias is the possibility that some of the consumed prey species were not represented in the scat samples (Bowen, 2000). Although the identification of prey hard parts other than otoliths in scats increases the probability of detection of prey species, cartilaginous fish or fish with small or fragile bony structures may be completely digested and not evident in scat (Olesiuk et al., 1990). For example, in captive Steller sea lion feeding trials, the average number of hard parts recovered in scat was 31.2 per pollock, but only 7.9 per herring (Cottrell and Trites, 2002). Thus, there was a greater chance of an individual herring being missed compared to an individual pollock. However, small fish are likely consumed in larger numbers, which would increase the likelihood of detecting their presence in scat.

The second potential source of dietary bias arises from using the "split-sample frequency of occurrence" technique to estimate the percentage of biomass that different prey represent in the diet. This technique assumes that the prey identified in a scat sample represent all the prey consumed in a meal, and that all prey species of a meal are consumed in equal biomasses (Olesiuk et al., 1990). This

method may overestimate the contribution of small prey and underestimate the contribution of large prey to diet biomass. However, as previously mentioned, such a bias would be reduced if small prey are consumed in greater numbers than large prey in a given meal. A potentially better technique than split-sample frequency of occurrence is volumetric or biomass reconstruction analysis (i.e. the estimation of the actual size of each prey in a scat from the size of otoliths or other hard parts), but otoliths are usually not available from Steller sea lion scat (Merrick et al., 1997) and digestion correction factors (Tollit et al., 1997) and regressions of hard-part size on body size are currently not available for prey of Steller sea lions.

Olesiuk et al. (1990) and Olesiuk (1993) estimated the error associated with a key assumption of the split-sample frequency of occurrence technique (all prey categories in a scat are consumed in equal quantities) by calculating the minimum and maximum split-sample frequencies of occurrence of prey. For example, the minimum split-sample frequency of occurrence of a prey category was calculated by assuming that when the prey category was found in a scat with another prey category, it represented a negligible proportion of the biomass of the meal represented by that scat. We considered their estimates of the minimum and maximum split-sample frequencies of occurrence of prey to approximate the total potential errors in the diet compositions we used. Thus, the assumed errors in diet were based only on the potential error in estimating diet from scats and not on the potential error due to sampling limitations.

Our assumed errors in diet composition were relatively large. For example, if a prey category was assumed to comprise a median of 50% of the diet, the proportion of the diet represented by that prey category in any one run of the model ranged from 27.5% to 72.5% (before the diet was standardized to 100%). Nevertheless there is still the possibility of sampling biases in the diet compositions that we assumed for Steller sea lions in Alaska. Future studies of the diet of Steller sea lions will allow us to obtain better estimates of the regional, seasonal, and intrapopulation variability in diet. Also, studies of captive Steller sea lions will assist in determining the biases and variability associated with the estimation of diet from scats (Cottrell and Trites, 2002).

Effect of diet on food requirements

We found that changes in the energy density of the diet can have large effects on the amount of food that Steller sea lions need to consume. In southeast Alaska, seasonal changes in the energy density of the diet resulted in large seasonal changes in daily food requirements, even when daily energy requirements were relatively constant. Immature and mature animals (excluding lactating females) required approximately 45–60% more food per day in early spring than in late summer (Fig. 3). Regional differences in the energy density of the diet resulted in smaller, but still substantial differences in food requirements among Steller sea lions in different regions of Alaska (up to a 24% difference based on summer diets).

The effect of diet on food requirements, can be further illustrated by considering two diets: one of entirely gadids (walleye pollock, Pacific cod) and one of entirely small schooling fish (herring, sandlance). Based on caloric differences between prey types and differences in digestive efficiency and the heat increment of feeding, a 10-year-old male would require an average of 30 (±7.7) kg of small schooling fish per day (5% of body mass), but would require 41 (±9.7) kg of gadids (6% of body mass): a 37% increase in prey biomass requirements. A 10-year-old female's (pregnant, no pup) average daily food requirement would increase by a similar percentage with a diet shift from small schooling fish to gadids (15 [±3.7] kg to 21 [±4.7] kg or 6% to 8% of body mass).

A large animal may be able to compensate for changes in prey biomass requirements, but immature or recently weaned animals may be more susceptible to changes in prey biomass requirements because they need to consume more food per unit body mass than adult animals (Winship et al., 2002). A 1-year-old male would require an average of 16 (±4.2) kg of small schooling fish per day (12% of body mass), but would require an average of 22 ±5.4 kg of gadids (16% of body mass). Similarly, a 1-year-old female would need 14 (±3.2) kg of small schooling fish (13% of body mass) or 18 (±4.1) kg of gadids (17% of body mass). The difference in energy density between the gadid and forage fish categories was greater in the summer and autumn than in the winter and spring; thus the difference between the daily food requirement of a sea lion consuming only gadids and the food requirement of a sea lion consuming only forage fish was greatest in the summer and autumn. Although animals prey on more than one species category in nature, which would buffer the effects of changes in diet composition, differences in the energy density and digestibility of prey can have large effects on prey biomass requirements, especially for young animals.

Merrick et al. (1997) found a significant relationship between the diversities of Steller sea lion diets and the rates of change in the numbers of adult and juvenile Steller sea lions counted on rookeries between 1990 and 1994 in different regions of Alaska (Gulf of Alaska through the western Aleutian Islands). Sea lions in regions with high rates of population decline had low dietary diversity. Plotting the rates of population decline against the amount of prey required in each region (using summer diets), we found a significant (α=0.05) relationship (Spearman rank correlation coefficient r_s=–0.929, P=0.02; Fig. 6), indicating that sea lions in areas with high rates of decline had higher per capita food requirements. This finding suggests that the energy density of the diet may have had a role in the population decline in some regions of Alaska during the early 1990s.

The correlation we report between food requirements and population change (Fig. 6) is based on summer diets and limited data on the energy density of sea lion prey categories such as hexagrammids. When seasonal diet information for southeast Alaska was considered, our model predicted a substantially greater per capita food requirement in that region (Fig. 4). Seasonal data are required from all regions of Alaska to describe diet composition

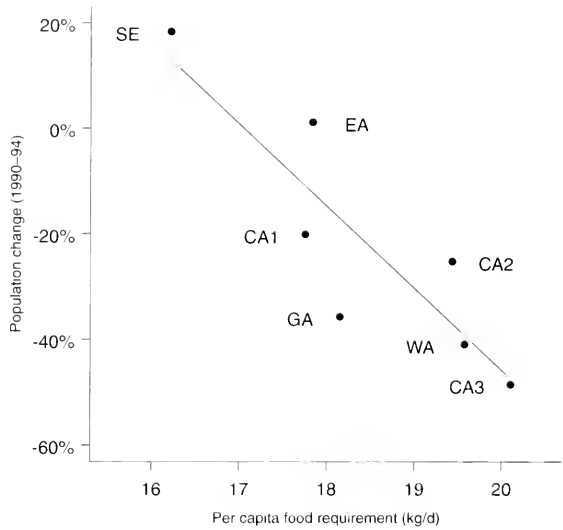

Figure 6

Per capita daily food biomass requirement predicted by our model (based on summer diets) versus rate of change in the number of adult and juvenile Steller sea lions counted on rookeries between 1990 and 1994 by region of Alaska (SE=Southeast Alaska, GA=Gulf of Alaska, EA=Eastern Aleutians, CA=Central Aleutians, WA=Western Aleutians). The Spearman rank correlation coefficient (r_s) for the data is –0.929 (P=0.02). The line represents a linear least-squares regression (r^2=0.77). Data on population change are from Merrick et al. (1997), except the value for southeast Alaska (18.3%) which we calculated from data reported by Strick et al. (1997) for three rookeries (Forrester, Hazy, and White Sisters islands).

and energy density, so that the potential relationship between rates of population change and per capita food requirements can be fully explored. Nevertheless, the data that are currently available are intriguing and suggest a possible mechanism for the original relationship reported by Merrick et al. (1997) between diet diversity and population decline.

Steller sea lions may use a couple of strategies to respond to increases in food requirements. The first and obvious strategy is to increase the rate of food intake. Many studies have found that animals increase their food intake on low-energy diets (Hammond and Wunder, 1991; Veloso and Bozinovic, 1993; Brekke and Gabrielsen, 1994; Weber and Thompson, 1998). Fadely et al.[1] found that the intake rates of captive California sea lions (*Zalophus californianus*) eating walleye pollock were approximately 1.4 times greater than when consuming herring. In order to increase their rate of food intake, Steller sea lions would likely have to increase the amount of time spent foraging or their activity level while foraging (or would have to do both). An increase in foraging time would likely result in increased pup mortality because mothers would be absent from haul-outs for longer periods of time (Trillmich and Dellinger, 1991; Boyd et al., 1994) or in increased susceptibility of these mothers to predation by killer whales (*Orcinus orca*) or sharks. An increase in foraging intensity may result in an increase in the energy cost of foraging, and therefore additional increases in food requirements (Costa and Gentry, 1986).

A second strategy Steller sea lions may employ to respond to decreases in the energy content of their diet is to reduce energy expenditures and thereby prevent an increase in food biomass requirements. For example, Veloso and Bozinovic (1993) found that degus (*Octodon degus*) eating low-quality forage, had lower basal metabolic rates than degus eating high-quality forage. A similar metabolic depression was observed in captive Steller sea lions eating low-energy squid and walleye pollock (Rosen and Trites, 1999; Rosen and Trites, 2000b). Steller sea lions may also reduce energy expenditures by decreasing their activity levels. Studies of the rifleman (*Acanthisitta chloris*; Lill, 1991) and white-footed sportive lemur (*Lepilemur leuco-*

pus; Nash, 1998) found that animals conserved energy by reducing the time they spent active and by increasing the time they spent resting when energy requirements for thermoregulation increased during cold periods. Mature female Steller sea lions may also have an additional option of reducing energy investment in reproduction by aborting fetuses to conserve energy during periods of nutritional stress (Pitcher et al., 1998).

Steller sea lions consuming very low–energy-density diets may be unable to consume enough food biomass to meet even reduced energy requirements. This situation could result from prey handling and digestion-time constraints or from an inability to capture enough prey. Juvenile animals would likely be the most susceptible to both situations. As discussed, juvenile animals have much higher mass-specific food requirements, and young animals may not be able to process 16–17% of their body weight in food per day (mean daily food requirements of 1-year-olds on a strictly gadid diet). Juvenile animals may also experience diving constraints (e.g. dive depth; Merrick and Loughlin, 1997) that adults do not, and may have more difficulty capturing sufficient quantities of low-energy prey.

An important consideration regarding the effect of diet composition on food requirements is the energetic cost of foraging on different prey species. Differences in the size and behavior of individual prey items may reduce differences in food biomass requirements resulting from differences in the energy density of prey. For example, consider a situation where a Steller sea lion can consume either small herring of high energy density or large pollock of low energy density. To obtain a given amount of prey biomass the sea lion can consume either several small herring or one large pollock. Based on the energy density of the prey, the sea lion would acquire a greater absolute amount of energy from the herring than from the pollock. However, if the energetic cost of pursuing and capturing several herring was greater than the cost of pursuing and capturing one pollock, then the net amount of energy obtained (energy consumed minus energy spent) per unit of prey biomass may not differ between the herring and the pollock diets. In other words, the sea lion's food requirement would be similar whether it was foraging on the small herring or the large pollock.

We did not incorporate differential costs associated with foraging on different prey categories in our model. We also did not consider the size of individual prey items consumed by Steller sea lions. Data on foraging costs for Steller sea lions in relation to prey species and prey size are currently limited and should be incorporated into bioenergetic models as they become available, in the form of functional relationships between diet composition and the energetic cost of foraging.

Prey consumption by Steller sea lions in Alaska in 1998

Regional variation in the amount of prey consumed by Steller sea lions in Alaska in 1998 (Figs. 1 and 5) was mainly due to differences in population size, as well as differences in diet composition (previous section). Gadids and hexagrammids were the top two prey categories in terms of biomass consumed. Gadids dominated the diet in the eastern areas (Gulf of Alaska), whereas hexagrammids dominated the diet in the western areas (central Aleutians 2 to western Aleutians). Gadids also dominated the diet in southeast Alaska when considered on an annual basis.

The mean model estimate of gadid consumption by Steller sea lions in all study regions of Alaska in 1998 was 179,000 (±36,700) t per year. This represents about 7% of the total estimated walleye pollock biomass, 20% of the total estimated Pacific cod biomass, or 5% of combined pollock and cod biomass dying naturally in 1998 in the Gulf of Alaska, Aleutian Islands, Bogoslof area, and eastern Bering Sea (Table 3). Steller sea lion consumption of gadids also represents 12% of the total gadid biomass removed in 1998 by commercial fisheries. Thus, estimated total gadid biomass consumption by Steller sea lions in Alaska is less than that taken by the fishery, and is small in relation to total gadid natural mortality. Livingston (1993) also estimated that the pollock biomass taken by sea lions in the eastern Bering sea in 1985 was small in relation to that taken by the fishery and remarked that cannibalism of adults on juveniles was the greatest source of mortality for walleye pollock.

We estimated that Steller sea lions in all areas of Alaska consumed a total of 104,000 (±20,600) t of hexagrammid biomass in 1998 (75% of estimated exploitable Atka mackerel biomass dying naturally in the Aleutian Islands, and 181% of fishery catches in the Aleutian Islands and the Gulf of Alaska in 1998; Table 3). Thus, Steller sea lions removed more Atka mackerel biomass than the fishery in 1998, and Steller sea lion predation accounted for a large proportion of natural Atka mackerel mortality. However, this proportion would be lower if Steller sea lions also prey on juvenile Atka mackerel. As with gadids, other fish species (e.g. Pacific cod) are also important predators on Atka mackerel (Yang, 1997).

Inferences about prey availability and competition for prey between fisheries and Steller sea lions should be made with caution given that we did not explicitly consider the size of prey in our study. For example, Steller sea lions have been shown to generally prey on juvenile pollock and not consume pollock longer than about 60 cm (Pitcher, 1981; Calkins, 1998; Calkins and Goodwin[5]). Thus, with respect to prey availability it may be more appropriate to compare our estimate of the gadid biomass consumed by Steller sea lions to the biomass of juvenile gadids dying naturally rather than to the total gadid biomass dying naturally. Our estimate of the biomass of gadids consumed by Steller sea lions in Alaska in 1998 represented 18% of the natural mortality of juvenile pollock and cod combined (23% of juvenile pollock alone or 80% of juvenile cod alone), which was more than triple the value (5%) when total pollock and cod biomass was considered (Table 3). The impact of Steller sea lions on specific segments of their prey populations (e.g. juvenile Pacific cod) may then be much greater than the impact that is suggested when only total biomass is considered. With respect to competition with fisheries, the pollock and cod fisheries generally target fish ≥3 years old. Thus,

Table 3

Biomass (t), natural mortality, fishery catches (t), and predicted Steller sea lion consumption of gadids (walleye pollock and Pacific cod) and hexagrammids (Atka mackerel) in Alaska in 1998.

	Walleye pollock	Pacific cod	Gadid (pollock+cod)	Hexagrammid (Atka mackerel)
Adult (age 3+)				
biomass [1]	7,362,000	2,125,000	9,487,000	536,000
M	0.30[2]	0.37[3]		0.30[4]
biomass dying naturally[5]	1,908,096	657,190	2,565,286	138,921
Juveniles				
biomass	1,616,049[6]	466,463[6]	2,082,512	no data
M	0.65[7]	0.65[7]		no data
biomass dying naturally	772,397	222,948	995,345	no data
Total				
biomass	8,978,049	2,591,463	11,569,512	
biomass dying naturally	2,680,493	880,138	3,560,631	
fishery catches[8]	1,250,594	267,968	1,518,562	57,493
Steller sea lion population consumption			179,000 ±36,700	104,000 ±20,600
% total biomass dying naturally	6.7	20.3	5.0	
% adult biomass dying naturally	9.4	27.2	7.0	74.9
% juvenile biomass dying naturally	23.2	80.3	18.0	
% fishery catches	14.3	66.8	11.8	180.9

[1] Sum of estimated exploitable biomass from Gulf of Alaska (pollock and cod only) (Plan Team for the Groundfish Fisheries of the Gulf of Alaska. 1999. Summary. *In* Stock assessment and fishery evaluation report for the groundfish resources of the Gulf of Alaska, p. 1–31. North Pacific Fishery Management Council, P.O. Box 103136, Anchorage, AK 99510), Aleutian Islands, Bogoslof (pollock only), and eastern Bering Sea (pollock and cod only) regions (Plan Team for the Groundfish Fisheries of the Bering Sea and Aleutian Islands. 1999. Summary. *In* Stock assessment and fishery evaluation report for the groundfish resources of the Bering Sea/Aleutian Islands regions, p. 1–36. North Pacific Fishery Management Council, P.O. Box 103136, Anchorage, AK 99510). Estimate of exploitable biomass of Atka mackerel in the Gulf of Alaska not available, but the population was much smaller than the Aleutian Islands population.

[2] Dorn, M. W., A. B. Hollowed, E. Brown, B. Megrey, C. Wilson, and J. Blackburn. 1999. Walleye pollock *In* Stock assessment and fishery evaluation report for the groundfish resources of the Gulf of Alaska, p. 33–104. North Pacific Fishery Management Council, P.O. Box 103136, Anchorage, AK 99510.

[3] Thompson, G. G., H. H. Zenger, and M. W. Dorn. 1999. Assessment of the Pacific cod stock in the Gulf of Alaska. *In* Stock assessment and fishery evaluation report for the groundfish resources of the Gulf of Alaska, p. 105–184. North Pacific Fishery Management Council, P.O. Box 103136, Anchorage, AK 99510.

[4] Lowe, S. A., and L. W. Fritz. 1999. Assessment of Bering Sea/Aleutian Islands Atka mackerel. *In* Stock assessment and fishery evaluation report for the groundfish resources of the Bering Sea/Aleutian Islands regions, p. 569–638. North Pacific Fishery Management Council, P.O. Box 103136, Anchorage, AK 99510.

[5] Annual mortality rate = $1 - e^{-M}$.

[6] Assumed to be 18% of total biomass based on value used by Trites et al. (1999) for pollock.

[7] Assumed to be the median M reported by Wespestad and Terry (1984) for 1- and 2-year-old pollock (range=0.45–0.85).

[8] Sum of catches from Gulf of Alaska (Plan Team for the Groundfish Fisheries of the Gulf of Alaska, see Footnote 1 above), Aleutian Islands, Bogoslof (pollock only), and eastern Bering Sea (pollock and cod only) regions (Plan Team for the Groundfish Fisheries of the Bering Sea and Aleutian Islands, see Footnote 1 above).

there may only be minor overlap between the fish taken by humans and the fish taken by Steller sea lions even though our estimate of the gadid biomass consumed by Steller sea lions in Alaska in 1998 was 12% of the combined pollock and cod catch (Table 3).

Caution should also be used when making inferences about competition and prey availability even when estimates of prey biomass and catch are size-specific. Spatial and temporal distributions of prey (and fishing) at the local scale determine the availability of food resources for Steller sea lions. Estimates of total prey abundance are not enough to make inferences about the food that is available to Steller sea lions. For example, if estimates of the amount of food that Steller sea lions require were less than the estimated available prey biomass (minus the prey taken by fisheries), it would not necessarily mean that Steller sea lions had enough to eat. Sea lions may not have access to all of the prey due to local differences between their foraging space and time and the spatial and temporal distribution of the fish. Local prey densities encountered by Steller sea lions are more relevant than absolute abundance when assessing prey availability.

Our study provides the first estimates of the biomass of prey consumed by Steller sea lions in different regions of Alaska. However, our estimates of prey consumption are neither species-specific nor size-specific and have con-

siderable uncertainty associated with them. Thus, the management applications of our findings are limited by the quality of data currently available for Steller sea lions. Nevertheless, our estimates of consumption shed light on the trophic relationships between Steller sea lions and their prey and provide insights into possible relationships between food consumption and differential rates of population decline in different regions of Alaska. As more detailed diet information becomes available for Steller sea lions in Alaska, our model can be used to provide more refined estimates of prey consumption that can be incorporated in prey stock assessments and management decisions (e.g. Hollowed et al., 2000).

Acknowledgments

We thank D. A. S. Rosen for sharing his data on digestive efficiency and heat increment of feeding with us. We also thank I. L. Boyd, V. Christensen, S. Cox, W. K. Milsom, D. Pauly, D. A. S. Rosen, D. J. Tollit, and C. J. Walters for helpful comments and criticism on the study and earlier drafts of this manuscript. We appreciate the constructive comments and suggestions of M. K. Alonso and an anonymous journal reviewer which improved our manuscript. We are also grateful for the administrative support of Pamela Rosenbaum. Financial support was provided to the North Pacific Universities Marine Mammal Research Consortium by the U.S. National Oceanographic and Atmospheric Administration through the North Pacific Marine Science Foundation. Financial support also was provided by the Natural Sciences and Engineering Research Council (Canada) in the form of a postgraduate scholarship to AJW.

Literature cited

Alverson, D. L.
1992. A review of commercial fisheries and the Steller sea lion (*Eumetopias jubatus*): the conflict arena. Rev. Aquat. Sci. 6:203–256.

Anthony, J. A., D. D. Roby, and K. R. Turco.
2000. Lipid content and energy density of forage fishes from the northern Gulf of Alaska. J. Exp. Mar. Biol. Ecol. 248: 53–78.

Bowen, W. D.
2000. Reconstruction of pinniped diets: accounting for complete digestion of otoliths and cephalopod beaks. Can. J. Fish. Aquat. Sci. 57:898–905.

Boyd, I. L., J. P. Y. Arnould, T. Barton, and J. P. Croxall.
1994. Foraging behaviour of Antarctic fur seals during periods of contrasting prey abundance. J. Anim. Ecol. 63: 703–713.

Brekke, B., and G. W. Gabrielsen.
1994. Assimilation efficiency of adult Kittiwakes and Brunnich's Guillemots fed Capelin and Arctic Cod. Polar Biol. 14:279–284.

Brett, J. R.
1983. Life energetics of sockeye salmon, *Oncorhynchus nerka*. *In* Behavioral energetics: the cost of survival in vertebrates (W. P. Aspey and S. I. Lustick, eds.), p. 29–63. Ohio State Univ. Press, Columbus, OH.

Calkins, D. G.
1998. Prey of Steller sea lions in the Bering Sea. Biosphere Conserv. 1:33–44.

Calkins, D. G., and K. W. Pitcher.
1982. Population assessment, ecology and trophic relationships of Steller sea lions in the Gulf of Alaska. *In* Environmental assessment of the Alaskan continental shelf: final reports of principal investigators, vol. 19, p. 445–546. U.S. Dep. Commer., N.O.A.A., Juneau, AK.

Costa, D. P., and R. L. Gentry.
1986. Free-ranging energetics of northern fur seals. *In* Fur seals: maternal strategies on land and at sea (R. L. Gentry and G. L. Kooyman, eds.), p. 79–101. Princeton Univ. Press, Princeton, NJ.

Cottrell, P. E., and A. W. Trites.
2002. Classifying prey hard part structures recovered from fecal remains of captive Steller sea lions (*Eumetopias jubatus*). Mar. Mamm. Sci. 18:525–539.

Dygert, P. H.
1990. Seasonal changes in energy content and proximate composition associated with somatic growth and reproduction in a representative age-class of female English sole. Trans. Am. Fish. Soc. 119:791–801.

Fisher, K. I., R. E. A. Stewart, R. A. Kastelein, and L. D. Campbell.
1992. Apparent digestive efficiency in walruses (*Odobenus rosmarus*) fed herring (*Clupea harengus*) and clams (*Spisula* sp.). Can. J. Zool. 70:30–36.

Hammond, K. A., and B. A. Wunder.
1991. The role of diet quality and energy need in the nutritional ecology of a small herbivore, *Microtus ochrogaster*. Physiol. Zool. 64:541–567.

Harris, R. K., T. Nishiyama, and A. J. Paul.
1986. Carbon, nitrogen and caloric content of eggs, larvae, and juveniles of the walleye pollock, *Theragra chalcogramma*. J. Fish Biol. 29:87–98.

Hartman, K. J., and S. B. Brandt.
1995. Estimating energy density of fish. Trans. Am. Fish. Soc. 124:347–355.

Hendry, A. P., and O. K. Berg.
1999. Secondary sexual characters, energy use, senescence, and the cost of reproduction in sockeye salmon. Can. J. Zool. 77:1663–1675.

Hollowed, A. B., J. N. Ianelli, and P. A. Livingston.
2000. Including predation mortality in stock assessments: a case study for Gulf of Alaska walleye pollock. ICES J. Mar. Sci. 57:279–273.

Keiver, K. M., K. Ronald, and F. W. H. Beamish.
1984. Metabolizable energy requirements for maintenance and faecal and urinary losses of juvenile harp seals (*Phoca groenlandica*). Can. J. Zool. 62:769–776.

Lawson, J. W., A. M. Magalhães, and E. H. Miller.
1998. Important prey species of marine vertebrate predators in the northwest Atlantic: proximate composition and energy density. Mar. Ecol. Prog. Ser. 164:13–20.

Lawson, J. W., E. H. Miller, and E. Noseworthy.
1997. Variation in assimilation efficiency and digestive efficiency of captive harp seals (*Phoca groenlandica*) on different diets. Can. J. Zool. 75:1285–1291.

Lill, A.
1991. Behavioural energetics of overwintering in the rifleman, *Acanthisitta chloris*. Aust. J. Zool. 39.643–654

Livingston, P. A.
1993. Importance of predation by groundfish, marine mammals and birds on walleye pollock *Theragra chalcogramma* and Pacific herring *Clupea pallasi* in the eastern Bering Sea. Mar. Ecol. Prog. Ser. 102:205–215.

Loughlin, T. R., A. S. Perlov, and V. A. Vladimirov.
1992. Range-wide survey and estimation of total number of Steller sea lions in 1989. Mar. Mamm. Sci. 8:220–239.
Martensson, P.-E., E. S. Nordoy, and A. S. Blix.
1994. Digestibility of crustaceans and capelin in harp seals (*Phoca groenlandica*). Mar. Mamm. Sci. 10:325–331.
Merrick, R. L., M. K. Chumbley, and G. V. Byrd.
1997. Diet diversity of Steller sea lions (*Eumetopias jubatus*) and their population decline in Alaska: a potential relationship. Can. J. Fish. Aquat. Sci. 54:1342–1348.
Merrick, R. L., and T. R. Loughlin.
1997. Foraging behavior of adult female and young-of-the-year Steller sea lions in Alaskan waters. Can. J. Zool. 75: 776–786.
Nash, L. T.
1998. Vertical clingers and sleepers: seasonal influences on the activities and substrate use of *Lepilemur leucopus* at Beza Mahafaly Special Reserve, Madagascar. Folia Primatol. 69 (suppl. 1):204–217.
Olesiuk, P. F.
1993. Annual prey consumption by harbor seals (*Phoca vitulina*) in the Strait of Georgia, British Columbia. Fish. Bull. 91:491–515.
Olesiuk, P. F., M. A. Bigg, G. M. Ellis, S. J. Crockford, and R. J. Wigen.
1990. An assessment of the feeding habits of harbour seals (*Phoca vitulina*) in the Strait of Georgia, British Columbia, based on scat analysis. Department of Fisheries and Oceans, Fisheries Research Branch, Pacific Biological Station, Nanaimo, B.C., Canada, Can. Tech. Rep. Fish. Aquat. Sci. 1730.
Paul, A. J., and J. M. Paul.
1998. Comparisons of whole body energy content of captive fasting age zero Alaskan Pacific herring (*Clupea pallasi* Valenciennes) and cohorts over-wintering in nature. J. Exp. Mar. Biol. Ecol. 226:75–86.
Paul, A. J., J. M. Paul, and E. D. Brown.
1998a. Fall and spring somatic energy content for Alaskan Pacific herring (*Clupea pallasi* Valenciennes 1847) relative to age, size and sex. J. Exp. Mar. Biol. Ecol. 223:133–142.
Paul, A. J., J. M. Paul, and R. L. Smith.
1993. The seasonal changes somatic energy content of Gulf of Alaska yellowfin sole, *Pleuronectes asper*. J. Fish Biol. 43:131–138.
1998b. Seasonal changes in whole-body energy content and estimated consumption rates of age 0 walleye pollock from Prince William Sound, Alaska. Estuar. Coast. Shelf Sci. 47:251–259.
Paul, A. J., and M. Willette.
1997. Geographical variation in somatic energy content of migrating pink salmon fry from Prince William Sound: a tool to measure nutritional status. *In* Forage fishes in marine ecosystems, p. 707–720. Univ. Alaska Sea Grant College Program Report 97-01, Fairbanks, AK.
Payne, S. A., B. A. Johnson, and R. S. Otto.
1999. Proximate composition of some north-eastern Pacific forage fish species. Fish. Oceanogr. 8:159–177.
Perez, M. A.
1994. Calorimetry measurements of energy value of some Alaskan fishes and squids. U.S. Dep. Commer., N.O.A.A. Tech. Memo. NMFS-AFSC-32, 32 p.
Pitcher, K. W.
1981. Prey of the Steller sea lion, *Eumetopias jubatus*, in the Gulf of Alaska. Fish. Bull. 79:467–472.
Pitcher, K. W., D. G. Calkins, and G. W. Pendleton.
1998. Reproductive performance of female Steller sea lions: an energetics based reproductive strategy? Can. J. Zool. 76:2075–2083.
Robards, M. D., J. A. Anthony, G. A. Rose, and J. F. Piatt.
1999. Changes in proximate composition and somatic energy content for Pacific sand lance (*Ammodytes hexapterus*) from Kachemak Bay, Alaska relative to maturity and season. J. Exp. Mar. Biol. Ecol. 242:245–258.
Rosen, D. A. S., and A. W. Trites.
1997. Heat increment of feeding in Steller sea lions, *Eumetopias jubatus*. Comp. Biochem. Physiol. A118:877–881.
1999. Metabolic effects of low-energy diet on Steller sea lions, *Eumetopias jubatus*. Physiol. Biochem. Zool. 72:723–731.
2000a. Digestive efficiency and dry matter digestibility of Steller sea lions fed herring, pollock, squid, and salmon. Can. J. Zool. 78:1–6.
2000b. Pollock and the decline of Steller sea lions: testing the junk-food hypothesis. Can. J. Zool. 78:1243–1250.
Sease, J. L., and T. R. Loughlin.
1999. Aerial and land-based surveys of Steller sea lions (*Eumetopias jubatus*) in Alaska, June and July 1997 and 1998. U.S. Dep. Commer., NOAA Tech. Memo. NMFS-AFSC-100, 61 p.
Sinclair, E. H., and T. K. Zeppelin.
2002. Seasonal and spatial differences in diet in the western stock of Steller sea lions (*Eumetopias jubatus*). J. Mammal. 83:973–990.
Smith, R. L., A. J. Paul, and J. M. Paul.
1988. Aspects of energetics of adult walleye pollock, *Theragra chalcogramma* (Pallas), from Alaska. J. Fish Biol. 33:445–454.
1990. Seasonal changes in energy and the energy cost of spawning in Gulf of Alaska Pacific cod. J. Fish Biol. 36: 307–316.
Stansby, M. E.
1976. Chemical characteristics of fish caught in the northeast Pacific Ocean. Mar. Fish. Rev. 38:1–11.
Stewart, D. J., and M. Ibarra.
1991. Predation and production by salmonine fishes in Lake Michigan, 1978–88. Can. J. Fish. Aquat. Sci. 48:909–922.
Strick, M., L. Fritz, J. P. Lewis, and D. C. McAllister.
1997. Aerial and ship-based surveys of Steller sea lions (*Eumetopias jubatus*) in Southeast Alaska, the Gulf of Alaska, and Aleutian Islands during June and July 1994. U.S. Dep. Commer., NOAA Tech. Memo. NMFS-AFSC-71, 55 p.
SYSTAT, Inc.
1992. SYSTAT for Windows: Statistics, version 5, 750 p. SYSTAT, Inc., Evanston, IL.
Tollit, D. J., M. J. Steward, P. M. Thompson, G. J. Pierce, M. B. Santos, and S. Hughes.
1997. Species and size differences in the digestion of otoliths and beaks: implications for estimates of pinniped diet composition. Can. J. Fish. Aquat. Sci. 54:105–119.
Trillmich, F., and T. Dellinger.
1991. The effects of El Niño on Galapagos pinnipeds. *In* Pinnipeds and El Niño: responses to environmental stress (F. Trillmich and K. A. Ono, eds.), p. 66–74. Springer-Verlag, Berlin, Germany.
Trites, A. W., and P. A. Larkin.
1996. Changes in the abundance of Steller sea lions (*Eumetopias jubatus*) in Alaska from 1956 to 1992: how many were there? Aquat. Mamm. 22:153–166.
Trites, A. W., P. A. Livingston, M. C. Vasconcellos, S. Mackinson, A. M. Springer, and D. Pauly.
1999. Ecosystem change and the decline of marine mam-

mals in the Eastern Bering Sea: testing the ecosystem shift and commercial whaling hypotheses. Fisheries Centre Research Reports, vol. 7(1), 106 p. Univ. British Columbia, Vancouver, B.C., Canada.

Van Pelt, T. I., J. F. Piatt, B. K. Lance, and D. D. Roby.
1997. Proximate composition and energy density of some North Pacific forage fishes. Comp. Biochem. Physiol. A118: 1393–1398.

Veloso, C., and F. Bozinovic.
1993. Dietary and digestive constraints on basal energy metabolism in a small herbivorous rodent. Ecology 74: 2003–2010.

Weber, M. L., and J. M. Thompson.
1998. Seasonal patterns in food intake, live mass, and body composition of mature female fallow deer (*Dama dama*). Can. J. Zool. 76:1141–1152.

Wespestad, V. G., and J. M. Terry.
1984. Biological and economic yields for eastern Bering Sea walleye pollock under differing fishing regimes. N. Am. J. Fish. Manage. 4:204–215.

Winship, A. J., A. W. Trites, and D. A. S. Rosen.
2002. A bioenergetic model for estimating the food requirements of Steller sea lions *Eumetopias jubatus* in Alaska, USA. Mar. Ecol. Prog. Ser. 229:291–312.

Yang, M.-S.
1997. Trophic role of Atka Mackerel (*Pleurogrammus monopterygius*) in the Aleutian Islands. *In* Forage fishes in marine ecosystems, p. 277–279. Univ. Alaska Sea Grant College Program Report 97-01, Fairbanks, AK.

York, A. E.
1994. The population dynamics of northern sea lions, 1975–1985. Mar. Mamm. Sci. 10:38–51

Appendix I

Energy density of prey of Steller sea lions in Alaska. Length and energy-density data are ranges, means, or ranges of means depending [BC=bomb calorimetry].

Species	Location	Time of year
Cephalopods		
squid	Gulf of Alaska, Eastern Aleutian Islands	Jul, Aug
squid (5 spp.)	Gulf of Alaska, Bering Sea, north Pacific Ocean	Feb, Jun, Jul
Flatfish		
arrowtooth flounder	Gulf of Alaska, Bering Sea	Feb, Jul, Aug
English sole	Washington	Jan–Mar, Jun, Jul, Sep–Dec
Pleuronectidae (≥2 spp.)	Gulf of Alaska	May–Sep
yellowfin sole	Gulf of Alaska	Jan–Nov
Forage fish		
capelin	Gulf of Alaska, Bering Sea	Jul, Aug
	Gulf of Alaska, Eastern Aleutian Islands	Jul, Aug
	Bering Sea	
	Gulf of Alaska	May–Sep
	Gulf of Alaska, Bering Sea	Feb, Jun–Sep
eulachon	Gulf of Alaska	Mar, Aug
	Gulf of Alaska	May–Sep
	Gulf of Alaska, Bering Sea	Feb, Mar, Jun–Sep
Pacific herring	Gulf of Alaska, Bering Sea	Jul, Aug
	Gulf of Alaska	May–Sep
	Gulf of Alaska	Aug
	Gulf of Alaska	spring, fall
	Gulf of Alaska	Mar, Dec
	Gulf of Alaska, Southeast Alaska, British Columbia	
Pacific sandlance	Gulf of Alaska, Eastern Aleutian Islands	Jul, Aug
	Gulf of Alaska	May–Sep
	Gulf of Alaska, Bering Sea	Apr–Sep, Nov

Appendix I

on the data that were available. Method is the technique used to obtain the energy density value (PC=proximate composition analysis,

Age or length (or both)	Energy density (kJ/g wet mass)	Method	Source
7–13 cm	3.81	PC	Van Pelt et al. (1997)
	3.85–6.53	BC	Perez (1994)
	5.15	BC	Perez (1994)
adult, 39–40 cm	4.90 (Mar)	BC	Dygert (1990)
	5.95 (Oct)		
7–15 cm	2.86–3.95	PC	Anthony et al. (2000)
juvenile, 18–21 cm	3.3–3.5 (May)	BC	Paul et al. (1993)
adult, 24–29 cm	4.4 (Jun)		
	7.03	BC	Perez (1994)
age 1, 8–9 cm	4.84 (age 1)	PC	Van Pelt et al. (1997)
age 2, 10–12 cm	3.54–4.67 (age 2)		
	5.50	BC	Miller[1]
age 1, 5–8 cm	4.17 (age 1)	PC	Anthony et al. (2000)
age >1, 8–13 cm	6.7 (age >1, Jun)		
	3.7 (age >1, Sep)		
8–13 cm (Gulf)	5.26 (Gulf)	PC	Payne et al. (1999)
13–15 cm (BS)	6.48 (BS)		
	11.05 (August)	BC	Perez (1994)
	10.96 (March)		
age >0, 14–20 cm	7.49	PC	Anthony et al. (2000)
10–23 cm	10.10 (Feb–Mar)	PC	Payne et al. (1999)
	10.62–10.86 (Jun–Sep)		
	5.44 (BS)	BC	Perez (1994)
	11.72 (Gulf)		
age 0, <10 cm	3.69 (age 0)	PC	Anthony et al. (2000)
age >0, 10–19 cm	5.84 (age >0)		
6 cm	3.43	PC	Payne et al. (1999)
ages 0–7	5.7 (age 0, fall)	BC	Paul et al. (1998a)
	8.0 (age 1, fall)		
	9.4–10.2 (age 2, fall)		
	4.4 (age 0–1, spring)		
	5.2–6.3 (ages ≥2, spring)		
age 0, 8–9 cm	5.2 (Dec)	BC	Paul and Paul (1998)
	3.4–3.8 (Mar)		
	7.95	PC[2]	Stansby (1976)
age 0, 8–9 cm	4.95 (age 1)	PC	Van Pelt et al. (1997)
age 1, 11–13 cm	3.18 (age 0)		
age ≥2, 15–19 cm	5.67 (age ≥2)		
age 0, 7–10 cm	6.5 (age 0, Jun)	PC	Anthony et al. (2000)
age >0, 10–19 cm	4.8 (age 0, Jul)		
	5.3 (age 0, Aug)		
	5.6 (age >0, Jun)		
	4.9 (age >0, Sep)		
7–15 cm	5.20 (Gulf)	PC	Payne et al. (1999)
	6.11 (BS)		

continued

Appendix 1 (continued)

Species	Location	Time of year
Pacific sandlance (cont.)	Gulf of Alaska	Feb, Jun–Nov
Gadids		
Pacific cod	Gulf of Alaska, Bering Sea	Jul, Aug
	Gulf of Alaska, Eastern Aleutian Islands	Jul, Aug
	Gulf of Alaska	May–Sep
	Gulf of Alaska	Mar–May, Jul, Oct–Dec
walleye pollock	Gulf of Alaska, Bering Sea	Mar, Jul, Aug
	Gulf of Alaska, Eastern Aleutian Islands	Jul, Aug
	Bering Sea	
	Gulf of Alaska	May–Sep
	Gulf of Alaska	Aug
	Gulf of Alaska	Mar, May, Jun, Aug, Oct
	Gulf of Alaska	Mar–Apr
	Gulf of Alaska	
Hexagrammids		
Atka mackerel	Gulf of Alaska, Eastern Aleutian Islands	Jul, Aug
	Gulf of Alaska	Aug
greenling	Gulf of Alaska, Eastern Aleutian Islands	Jul, Aug
lingcod	Gulf of Alaska	May–Sep
Salmon		
chinook		
coho		
pink	Gulf of Alaska	May–Sep
	Gulf of Alaska	May–Jun
sockeye	Gulf of Alaska	May–Sep
	northeast Pacific Ocean	entire life cycle
	southeast Bering Sea	Jul (prior to river entry)
Other		
pricklebacks	Gulf of Alaska	Jun, Aug
pricklebacks (6 spp.)	Gulf of Alaska	May–Sep
rockfish (*Sebastes* spp.)	Gulf of Alaska, Eastern Aleutian Islands	Jul, Aug
rockfish (≥3 *Sebastes* spp.)	Gulf of Alaska, Bering Sea	Feb, Jul, Aug
sculpins (4 spp.)	Gulf of Alaska, Bering Sea	Feb, Jul, Aug
sculpins (12 spp.)	Gulf of Alaska	May–Sep

[1] Miller, L. K. 1978. Energetics of the northern fur seal in relation to climate and food resources of the Bering Sea. Rep. MMC-75/08, 27 p. U.S. Marine Mammal Commission, Washington, D.C.

[2] We assumed lipid = 39.3 kJ/g and protein = 17.8 kJ/g (Anthony et al. 2000).

Appendix I (continued)

Age or length (or both)	Energy density (kJ/g wet mass)	Method	Source
age 0, 6–9 cm	3.40–3.55 (age 0, 6 cm)	PC	Robards et al. (1999)
age 1 12–14 cm	4.62–4.86 (age 0, 9 cm)		
	3.22–3.32 (age ≥1, Nov)		
	3.23–3.25 (age ≥1, Feb)		
	5.46–5.75 (age ≥1, Jun–Jul)		
	3.93	BC	Perez (1994)
7–10 cm	2.94	PC	Van Pelt et al. (1997)
age 0, 6–9 cm	3.65 (age 0)	PC	Anthony et al. (2000)
age >0, 11–14 cm	3.54 (age >0)		
56–74 cm	4.00–4.30 (Mar)	BC	Smith et al. (1990)
	3.33–3.38 (Jul)		
	4.13–4.49 (Dec)		
43–53 cm	4.64	BC	Perez (1994)
age 0, 5–9 cm	2.73	PC	Van Pelt et al. (1997)
	5.89	BC	Miller[1]
age 0, 5–6 cm	3.47 (age 0)	PC	Anthony et al. (2000)
age >0, 12–18 cm	3.24 (age >0)		
7–8 cm	3.93	PC	Payne et al. (1999)
3–11 cm	2.7 (Jun)	BC	Paul et al. (1998b)
	3.4 (Aug)		
	3.6 (Oct)		
	3.4–4.0 (Mar)		
	4.0 (May)		
adult	3.68–4.03 (ripe)	BC	Smith et al. (1988)
	3.26–3.41 (spent)		
juvenile, <34 cm	5.45	BC	Harris et al. (1986)
7 cm	4.02	PC	Van Pelt et al. (1997)
12 cm	4.66	PC	Payne et al. (1999)
6–7 cm	3.45	PC	Van Pelt et al. (1997)
7–9 cm	3.98	PC	Anthony et al. (2000)
equation relating energy density to weight	6.06 (300 g)		Stewart and Ibarra (1991)
	8.72 (3 kg)		
equation relating energy density to weight	6.06 (300 g)		Stewart and Ibarra (1991)
	8.72 (3 kg)		
age 0, 6–10 cm	3.41 (age 0)	PC	Anthony et al. (2000)
age >0, 10–14 cm	3.73 (age >0)		
fry, 3–6 cm	3.2–4.4	BC	Paul and Willette (1997)
age 0, 7–8 cm	4.35	PC	Anthony et al. (2000)
entire life cycle	6.68 (300 g)		Brett (1983)
	7.77 (2.1 kg)		
adult, 49 cm	6.89–7.69	PC	Hendry and Berg (1999)
9–24 cm	5.40	PC	Payne et al. (1999)
8–30 cm	4.11–4.90	PC	Anthony et al. (2000)
4–6 cm	2.97	PC	Van Pelt et al. (1997)
	5.77–6.23	BC	Perez (1994)
	5.56 (northern rockfish, BS, Jul)		
	6.85 (northern rockfish, Gulf, Feb)		
	3.51–5.19	BC	Perez (1994)
4–22 cm	3.05–5.26	PC	Anthony et al. (2000)

A Monte Carlo demographic analysis of the silky shark (*Carcharhinus falciformis*): implications of gear selectivity

Lawrence Beerkircher
Mahmood Shivji
Guy Harvey Research Institute
Oceanographic Center
Nova Southeastern University
8000 N. Ocean Drive
Dania Beach, Florida 33004
E-mail address (for L. Beerkircher): beerkirc@ocean.nova.edu

Enric Cortés
National Marine Fisheries Service
3500 Delwood Beach Road
Panama City, Florida 32408

Demographic analysis has recently been used as a tool to approximate the dynamics of shark populations (Cailliet, 1992; Sminkey and Musick, 1996; Au and Smith, 1997; Cortés, 1999). The widespread use of demographic models for shark species, however, is hampered by a paucity of information on vital rates, which are required as input parameters for the models. A vital rate of special importance is natural mortality, which remains unknown for most shark species and many other marine taxa. Demographic models thus must often rely on indirect methods of natural mortality estimation rather than empirically observed values specific to a given population. Several methods to estimate natural mortality have shown promise for shark demographic analysis (Cortés, 1998). Other vital rates such as fecundity, although often strongly influenced by size and age, likely also vary independently of time over the lifespan of individuals within a population. Incorporation of Monte Carlo simulation in demographic models has been used to account for some of this uncertainty in vital rate estimates and construct confidence intervals for model output (Cortés, 1999, 2002).

One of the most valuable aspects of demographic modeling is the ability to examine how populations might respond to various levels of fishing mortality (Au and Smith, 1997; Cortés, 1998; Smith et al., 1998; Simpfendorfer, 1999). To date, most authors have used empirical estimates of fishing mortality (F) and either applied them uniformly to all age groups or have produced various scenarios with F applied starting at a particular age to simulate various fisheries management schemes (Sminkey and Musick, 1996; Au and Smith, 1997; Liu and Chen, 1999). Gear selectivity and its effect on F at various ages, however, has not been incorporated into demographic models even though it is very likely that some selection occurs. Here, we produce a demographic analysis of the silky shark (*Carcharhinus falciformis*) off the southeastern United States. Monte Carlo methods are used to simulate variability in model input parameters, and multiple scenarios are considered, incorporating natural mortality only, and added fishing mortality components. We include in our analysis scenarios that reflect possible longline gear selectivity for silky sharks, using catch-at-age information estimated from length-frequency data provided by the U.S. pelagic longline observer program for the southeastern U.S. coast. Finally, we compare scenarios that incorporate the same mean value of fishing mortality, but with different assumptions of selectivity patterns. The results of the demographic analysis are discussed in the context of the robustness of model assumptions.

Materials and methods

Life history parameters for the silky shark demography were obtained from the best available literature sources. Von Bertalanffy parameters of L_∞ = 311 cm total length, K = 0.101/yr, and t_0 = –2.718 yr were taken from Bonfil et al. (1993). To account for some of the uncertainty in the estimate of age-at-maturity (t_{mat}) of 12 years given by Bonfil et al. (1993), values for t_{mat} were drawn at random from a discrete probability distribution of P = 0.25, 0.5, and 0.25 for ages 11, 12, and 13, respectively. Longevity (t_{max}) was similarly varied by assigning the estimate of Bonfil et al. (1993) of 22 years a P = 0.5 and linearly decreasing P by 50% for each subsequent year.

Estimates of natural mortality (M) were selected by using three methods: Peterson and Wroblewski (1984), Chen and Watanabe (1989), and Jensen (1996) (Table 1). For the Peterson and Wroblewski method, weights-at-age were determined by calculating total length-at-age from the von Bertalanffy growth function, and then converting these values to fork length and weight (in grams) by using the relationships given by Kohler et al. (1995) for the silky shark. Wet weight was used instead of dry weight to generate values of M. Annual survival (S_x; $S=e^{-M}$, x=age) values were randomly drawn from a distribution in which the three methods of calculating mortality rates had equal probability.

Fecundity (m_x), the number of female pups produced per each year of life, was calculated by combining the data of Fourmanoir (1961), Bane (1966), Gilbert and Schlernitzauer (1966), Branstetter (1987), and Bonfil et al. (1993), which yielded a mean of 10.3 (SD=2.213, n=16) pups per litter. Observations in the literature of litter sizes lower than five pups were not included because of the possibility that females might have aborted pups from one uterus during capture

Manuscript accepted 10 July 2002.
Fish. Bull. 101:168–174 (2003).

Table 1

Natural mortality (M) estimation methods used in demographic models for silky sharks (*Carcharhinus falciformis*). W = body weight in grams, K, t_0 = von Bertalanffy growth parameters, and t_{max} = maximum age.

Citation	Method
Peterson and Wroblewski (1984)	$M = 1.92\,W^{-0.25}$
Jensen (1996)	$M = 1.6K$
Chen and Watanabe (1989)	$M(t) = K/[1 - e^{-K(t-t_0)}]$, for $t = 0$ through 11
	$M(t, t_{max}) = [1/(t_{max} - t)]\ \ln\ [(e^{Kt_{max}} - e^{Kt_0})/(e^{Kt} - e^{Kt_0})]$

(Branstetter, 1987; Bonfil et al., 1993). Pups-per-litter estimates were then converted into female pups per year (m_x) by using the embryo sex ratio of 1:1.17 (male:female) given by Bonfil et al. (1993) and a reproductive cycle of two years suggested by Branstetter (1987). All females were assumed to enter the breeding population after first age-at-maturity, and reproductive senescence was assumed to occur at age (t_{max}+1). Actual values of fecundity (m_x) used as model input were drawn at random from a normal distribution with a mean of 10.3 and a standard deviation of 2.213 calculated as described above, and then scaled to represent female pups per year.

The parameters estimated above were used to construct life tables by using standard methods, but incorporating Monte Carlo simulation for output parameter estimation. Output parameters (net reproductive rate, R_0; mean generation length, G; and intrinsic rate of population increase, r) were calculated by standard demographic methods (Wilson and Bossert, 1971; Krebs, 1985), and r was solved iteratively with the Euler equation.

Various scenarios, each of which varied vital rates as described above, were analyzed. A base scenario incorporated natural mortality only. To attempt to incorporate gear selectivity, we compared a model that incorporated total mortality only (Z, scenario 1) estimated from a traditional catch curve with a model incorporating Z estimated from a modified catch curve method. To produce a catch curve estimate of Z, length-frequency data for silky sharks observed on longlines off the southeastern United States during 1992–98 (NMFS[1]) were used with an age-length key derived from the length-at-age data of Bonfil et al. (1993). The assumptions in this method are that in all years 1) recruitment is constant, 2) fishing mortality is constant, and 3) catchability is equal (there is no gear selectivity). The decrease in population over time is

$$N_t = N_{t-1}\, e^{-Za},$$

where N_t = population in numbers at time t; and
a = age.

An assumption of gear selectivity was then used to modify the standard catch equation. If one assumes that gear selectivity exists, then Z can no longer be constant and Z can be estimated at each age:

$$-Z = \ln(N_t / N_{t-1}) / a.$$

To avoid positive values of Z at some ages (due to those ages not being present in the catch as predicted by the age-length key) an exponential curve was fitted to the catch-at-age data to produce the values of N_t. Because the value of Z cannot be calculated for age 0 with this method, we assumed that total mortality was the same for ages 0 and 1. The values of Z-at-age produced by this method were used in a demographic model (scenario 2) and compared with scenario 1. For ages where estimates of Z were not reasonable (Z<M), the natural mortality estimate was used for that age.

To examine the effect of various patterns of selectivity, we also compared scenarios with the same average value of fishing mortality, but with various assumptions of selectivity patterns. These scenarios added a fishing mortality component into the base scenario. Scenario 3 incorporated the 1997 instantaneous fishing mortality (F) value of 0.093 estimated for Atlantic large coastal sharks (Anonymous[2]) applied uniformly to all age groups. An exponential function of the form $y=be^{(-ax)}$, where $y = F$, x = age, and the mean $F = 0.093$, was fitted to the catch-at-age data assuming zero fishing mortality after age 13 (scenario 4) and a positive level of fishing mortality through all age groups (scenario 5). Scenario 6 applied an F value of 0.034, calculated to produce maximum sustainable yield (MSY) for large coastal sharks (Anonymous[2]), uniformly to all age groups. Scenarios 7 and 8 were constructed in the same manner as scenarios 4 and 5, respectively, but with the mean value of $F = 0.034$.

Each of the scenarios were run 1000 times with vital rates (first age-at-maturity, fecundity, longevity, and natural mortality where appropriate) varying as described above. The 2.5th and 97.5th percentiles of the ranked output were used as approximate percentile confidence

[1] NMFS (National Marine Fisheries Service). 2000. Unpubl. data. Southeast Fisheries Science Center Pelagic Observer Program, 75 Virginia Beach Drive, Miami, FL 33149.

[2] Anonymous. 1998. Report of the shark evaluation workshop, 109 p. Panama City Laboratory, National Marine Fisheries Service, 3500 Delwood Beach Rd., Panama City, FL 32408.

intervals for the parameters R_0, G, and r. Finite rates of population increase or decrease (e^r) and approximate percentile confidence intervals were then calculated based on the r value output. All simulations were run by using Microsoft Excel spreadsheet software.

Results

The three methods used to estimate natural mortality yielded annual survivorship (S) values ranging from 0.657 to 0.904 (Table 2). The method of Peterson and Wroblewski produced S values of 0.760 (age 0) to 0.904 (age 22), slightly higher than the values produced by the method of Chen and Watanabe (0.657 to 0.874, ages 0–11; 0.890, ages 12+). The method of Jensen produced the lowest S value (0.851) for ages 7 and above, and the highest survivorship in the first 4 years of life.

The catch-at-age histogram indicated that few silky sharks over the age of 7 years were caught in the southeastern pelagic longline fishery (Fig. 1). The catch curve estimated a Z value of 0.329 (r^2=0.838, Fig. 2). The Z-at-age values calculated from the modified catch curve method predicted values of $Z = 0$ for ages 12 and above (scenario 2; Table 3). Values of F-at-age used in scenarios 3–8 (Table 3) were as high as 0.287 (scenario 4, age 0).

The results of the base scenario (Table 4) indicated that the silky shark population, in absence of fishing mortality, would increase at a median rate of 4.9 %/yr. The approximate percentile lower confidence limit also showed positive population growth (e^r=1.027). Incorporating the Z obtained from the catch curve into the model (scenario 1) resulted in the greatest rate of population decline of any of the scenarios considered (e^r=0.895). However, the use of the Z-at-age values from the modified catch curve method (scenario 2) produced a positive population increase of 1.8 %/yr.

With estimated F for large coastal sharks in 1997 applied to all age groups (scenario 3), the population would decline at a rate of 4.4 %/yr. Application of exponentially decreasing fishing mortality resulted in a more optimistic median e^r value when the mean F was confined to ages 0–12 (scenario 4), but when mean F was applied to all ages (scenario 5), the output was more pessimistic than that for the constant F = 0.093 model. With F estimated for maximum sustainable yield (scenario 6), the silky shark population would slowly increase at a rate of 1.5 %/yr. Incorporation of variable F-at-age in scenarios 7 and 8 resulted in e^r values slightly higher and lower, respectively, than the constant F scenario.

Figure 1

Estimated silky shark (*Carcharhinus falciformis*) catch-at-age from pelagic longlines off the southeastern U.S. coast, 1992–98.

Table 2

Annual survivorship (S) estimates calculated from three studies based on best available life history information for the silky shark (*Carcharhinus falciformis*).

Age (yr)	Peterson and Wroblewski	Chen and Watanabe	Jensen
0	0.760	0.657	0.851
1	0.799	0.724	0.851
2	0.824	0.766	0.851
3	0.840	0.794	0.851
4	0.853	0.815	0.851
5	0.862	0.830	0.851
6	0.869	0.842	0.851
7	0.875	0.851	0.851
8	0.880	0.858	0.851
9	0.884	0.865	0.851
10	0.887	0.870	0.851
11	0.890	0.874	0.851
12	0.892	0.890	0.851
13	0.894	0.890	0.851
14	0.896	0.890	0.851
15	0.898	0.890	0.851
16	0.899	0.890	0.851
17	0.900	0.890	0.851
18	0.901	0.890	0.851
19	0.902	0.890	0.851
20	0.903	0.890	0.851
21	0.904	0.890	0.851
22	0.904	0.890	0.851

Discussion

The base scenario results given in our study match well those from other demographic models for silky sharks. Using a demographic model that incorporated density-dependence, Smith et al. (1998) found an r value of 0.043 for silky sharks. Cortés (2002) found an average r value of 0.055 for silky sharks from the southern Gulf of Mexico

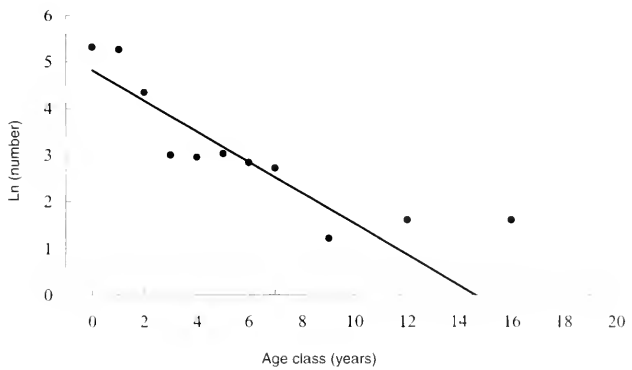

Figure 2

Catch curve for silky sharks (*Carcharhinus falciformis*) from pelagic longlines off the southeastern U.S. coast 1992–98.

using density-independent matrix simulation models. These r values place the silky shark toward the middle of the range of productivity values calculated for a mix of species (Smith et al., 1998; Cortés, 2002).

The pessimistic results of the model that incorporated Z calculated from the catch curve are consistent with the stock assessments that indicate large coastal sharks are overfished and suggest, in particular, that exploitation rates in the pelagic longline fishery may not be sustainable for silky sharks. However, incorporating gear selectivity with the modified catch curve method altered the results, yielding one of the highest rates of population growth of any of the scenarios. If the assumptions about the relationship between the catch curve and selectivity are reasonable, the results indicate that incorporation of gear selectivity into demographic analysis is important.

The importance of considering selectivity as explored by the fishing mortality scenarios was less clear. Scenario 3 indicated that a recently estimated level of fishing mortality would produce declines in the population, whereas scenario 6 indicated that the fishing mortality level producing maximum sustainable yield would result in a slightly increasing population. When exponentially decreasing F-at-age was incorporated (scenarios 4, 5, 7, and 8), the results differed—but much less so than those of scenarios 1 and 2—from those obtained in the constant F scenarios (3 and 6). All the fishing mortality scenarios (3–8) used mean values of F estimated through density-dependent modeling and were used here only as comparative base values.

Stock assessments of northwestern Atlantic shark stocks are based on species groups rather than individual species. These assessments use data from fisheries of various gear types, which may not correctly represent the life history or the pattern of exploitation of an individual species. In that respect, *Carcharhinus falciformis* may be an excellent example. Off the coast of the southeastern United States, pelagic longlines may be the dominant cause of silky shark fishing mortality, whereas bottom longlines rarely capture, and drift gillnets do not capture, this species (Parrack et al., 1993; Trent et al., 1997). Examination of length frequencies from the pelagic longline fishery observer database suggests that age 8+ silky sharks are rarely caught. Therefore, the assumption of constant fishing mortality throughout all age groups for this species is probably invalid, at least for the pelagic fishery off the southeastern United States. If individual species management of silky sharks is ever to become a reality, the patterns of selectivity of longline gear are very important.

It seems logical that the larger the shark, the higher the probability it can bite through the monofilament gangions used by U.S. pelagic longliners and escape. Because size is correlated with age, there must be a functional relationship that describes the probability of retention and capture for a given age. Accurate elucidation of such gear selectivity patterns requires knowledge of the actual size-at-age characteristics of the population that can only be derived from sampling studies in which methods that are not size-selective are used, or that are at least less size-selective than longline gear. These types of comparative data are almost wholly lacking for sharks in the pelagic environment. Indirect methods of estimating selectivity for shark species by comparing catches from gillnets of various mesh sizes have shown promise (Kirkwood and Walker, 1986; Simpfendorfer and Unsworth, 1998). Previous indirect studies of selectivity in hook and line gear (Cortez-Zaragoza et al., 1989; Ralston, 1990) cannot be applied in this case because selectivity in those studies was described as a function of hook size rather than the actual breaking strength of the line, which is the speculated mechanism of selection in the present study. Walker

Table 3

Values of total mortality (Z) or fishing mortality (F) used in demographic models for the silky shark (*Carcharhinus falciformis*). For scenario 1, Z was used instead of estimates of natural mortality (M). In scenario 2, Z was used only when $Z>M$. In scenarios 3–8, F was added to natural mortality.

	Scenario							
Age (yr)	1 Z	2 Z	3 F	4 F	5 F	6 F	7 F	8 F
0	0.329	0.486	0.093	0.287	0.276	0.034	0.105	0.068
1	0.329	0.486	0.093	0.210	0.225	0.034	0.077	0.058
2	0.329	0.243	0.093	0.164	0.195	0.034	0.060	0.053
3	0.329	0.162	0.093	0.132	0.174	0.034	0.048	0.049
4	0.329	0.121	0.093	0.107	0.158	0.034	0.039	0.046
5	0.329	0.097	0.093	0.087	0.144	0.034	0.032	0.043
6	0.329	0.081	0.093	0.069	0.133	0.034	0.025	0.041
7	0.329	0.069	0.093	0.054	0.123	0.034	0.020	0.040
8	0.329	0.061	0.093	0.041	0.114	0.034	0.015	0.038
9	0.329	0.054	0.093	0.029	0.107	0.034	0.011	0.037
10	0.329	0.049	0.093	0.019	0.100	0.034	0.007	0.035
11	0.329	0.044	0.093	0.009	0.093	0.034	0.003	0.034
12	0.329	0.000	0.093	0.09×10^{-5}	0.087	0.034	0.09×10^{-5}	0.033
13	0.329	0.000	0.093	0.000	0.082	0.034	0.000	0.032
14	0.329	0.000	0.093	0.000	0.077	0.034	0.000	0.031
15	0.329	0.000	0.093	0.000	0.072	0.034	0.000	0.030
16	0.329	0.000	0.093	0.000	0.068	0.034	0.000	0.029
17	0.329	0.000	0.093	0.000	0.063	0.034	0.000	0.029
18	0.329	0.000	0.093	0.000	0.059	0.034	0.000	0.028
19	0.329	0.000	0.093	0.000	0.056	0.034	0.000	0.027
20	0.329	0.000	0.093	0.000	0.052	0.034	0.000	0.026
21	0.329	0.000	0.093	0.000	0.049	0.034	0.000	0.026
22	0.329	0.000	0.093	0.000	0.045	0.034	0.000	0.025
23	0.329	0.000	0.093	0.000	0.042	0.034	0.000	0.025
24	0.329	0.000	0.093	0.000	0.039	0.034	0.000	0.024
25	0.329	0.000	0.093	0.000	0.036	0.034	0.000	0.024
26	0.329	0.000	0.093	0.000	0.034	0.034	0.000	0.023
27	0.329	0.000	0.093	0.000	0.031	0.034	0.000	0.023
28	0.329	0.000	0.093	0.000	0.028	0.034	0.000	0.022
29	0.329	0.000	0.093	0.000	0.026	0.034	0.000	0.022

(1992) incorporated hook selectivity into an age-structured model, but he assumed that all recruited members of a stock had an equal value of catchability with longline gear. We believe that an assumption of equal catchability is incorrect for silky sharks, and sharks in general, hooked on monofilament pelagic longline gear.

Determining actual patterns of selectivity and resulting estimates of fishing mortality-at-age, however, was beyond the scope of our analysis, which was to suggest that patterns of gear selectivity can affect results from demographic models. We chose a simple modification of a traditional catch curve and an intuitive, although arbitrary, assumption of selectivity patterns for silky sharks on pelagic longlines to explore this effect. Arbitrarily derived selectivity schedules were employed previously to examine the potential effects of gear selection in yield-per-recruit models (Goodyear, 1996). Clearly this approach, as applied here, has limitations. For example, the curve fitted to catch-at-age data used to calculate Z values estimated zero total mortality at ages 12+, whereas the catch-at-age data showed a few captures of ages 12+ (Fig. 1). No mortality is assumed for individual animals that escape the gear, although it is possible that some animals may die. Despite shortcomings in the methods to estimate F-at-age values used in our study, better estimates of fishing mortality will require more robust, comparative selectivity data.

Like many other studies of shark populations, the results reported in our study must be considered preliminary

Table 4

Demographic output (R_0=net reproductive rate; G=mean generation length; r=intrinsic rate of population growth; e^r=finite rate of population growth) and lower (LCL) and upper (UCL) approximate confidence limits for the silky shark (*Carcharhinus falciformis*) off the southeastern U.S. coast. The base scenario incorporated natural mortality (M) only; scenario 1 incorporated a constant value of total mortality (Z), scenario 2 incorporated various values of Z-at-age, and scenarios 3–8 incorporated the mean value of fishing mortality (F) shown in the second column.

Scenario	Mean F (or Z)	R_0	LCL	UCL	G	LCL	UCL	r	LCL	UCL	e^r	LCL	UCL
base	none	2.161	1.547	2.959	16.115	14.942	17.570	0.048	0.027	0.071	1.049	1.027	1.074
1	0.329	0.195	0.127	0.284	14.380	13.266	15.484	−0.111	−0.130	−0.091	0.895	0.878	0.913
2	0.065	2.615	2.083	3.158	16.091	14.965	17.582	0.018	0.001	0.032	1.018	1.001	1.033
3	0.093	0.508	0.345	0.724	15.190	14.042	16.544	−0.044	−0.066	−0.022	0.957	0.936	0.978
4	0.093	0.652	0.477	0.886	16.113	14.946	17.546	−0.026	−0.045	−0.008	0.974	0.956	0.992
5	0.093	0.262	0.175	0.375	15.427	14.235	16.857	−0.084	−0.105	−0.066	0.919	0.900	0.936
6	0.034	1.266	0.898	1.747	15.755	14.605	17.176	0.015	−0.006	0.037	1.015	0.994	1.038
7	0.034	1.392	0.991	1.920	16.105	14.937	17.565	0.021	−0.001	0.043	1.021	0.999	1.044
8	0.034	1.130	0.783	1.539	15.815	14.623	17.261	0.008	−0.015	0.029	1.008	0.985	1.029

because of the lack of validated age and growth information and the uncertainty in the estimates of longevity and fecundity for the silky shark. It is difficult to determine how representative the von Bertalanffy parameters (Bonfil et al., 1993), which were derived from silky sharks in the Campeche Bank in the southern Gulf of Mexico, are for silky shark populations from the entire southeastern U.S. Atlantic. Although tagging data (Kohler et al., 1998) indicate movement of silky sharks between the Gulf of Mexico and the U.S. Atlantic coast, the small number of tagged and recaptured individuals makes firm conclusions about whether these are the same or separate stocks very difficult. The age and growth results of Bonfil et al. (1993) from the southern Gulf of Mexico differed from a study on silky sharks by Branstetter (1987) in the northern Gulf. It is possible, however, that these variations may be a result of methodological or sampling differences because Branstetter's (1987) data came from pelagic longline operations and had fewer specimens over 250 cm TL, compared to Bonfil et al.'s (1993) data which came mainly from specimens caught in gillnet fisheries. Even if migration of silky sharks occurs between the northern Gulf of Mexico, southern Gulf of Mexico, and southeastern U.S. Atlantic coastal region, the populations of sharks in these areas might have significant life history differences. Given the absence of age and growth studies from Atlantic silky sharks, the Gulf of Mexico studies must be regarded as the best available age and growth information for this species. Similarly, fecundity and longevity estimates are relatively uncertain. Especially important in fecundity estimates is information regarding age-specific birth rate and the possibility of reproductive senescence, which can affect demographic results.

As with other demographic analyses, theoretical estimates of natural mortality (M) were used in our study. It has been shown that the output of demographic models of shark populations is particularly sensitive to changes in M, especially during the first few years of life (Sminkey and Musick, 1996; Liu and Chen, 1999; Cortés, 2002). Moreover, results may vary considerably in analyses that use different methods of M estimation (Simpfendorfer, 1999). In recognition of these limitations, three different methods were used here to estimate M. The methods of Chen and Watanabe (1989) and Jensen (1996) are based on a relationship between M and growth rates. Because the age and growth information for silky sharks is unvalidated, the von Bertalanffy growth parameters used in our study may not adequately describe individuals from the population analyzed. Finally, the method of Peterson and Wroblewski (1984) involves the assumption that M is due primarily to predation. Although this may be true for the younger ages of large coastal sharks like the silky shark, it may not be true for the larger, older sharks. Additionally, wet weight was used instead of dry weight, as prescribed in the original equation of Peterson and Wroblewski (1984), because the estimates of M obtained by using wet weight seem more believable for sharks (Cortés, 2002). Despite the difficulties associated with all three methods of estimating natural mortality, these methods, together with catch curves and tag-recapture studies, are the only methods available for estimating M. The use of Monte Carlo simulation to randomly vary the estimates of natural mortality can account for some of the uncertainty associated with these methods (Cortés, 1999; 2002).

Conclusions from this analysis of the silky shark population off the southeastern U.S. coast are similar to those for other large shark species. Even under scenarios assuming natural mortality only, the population would grow at a fairly slow rate, and even moderate levels of fishing mortality might produce population declines. Inclusion of age-dependent patterns of fishing mortality into the analyses, however, appear to substantially affect model results. Several key elements that need to be clarified to obtain a more conclusive analysis for silky sharks include validated age and growth information, life history param-

eters such as longevity, fecundity, and natural mortality, and estimates of age-dependent fishing mortality.

Acknowledgments

We thank Ramón Bonfil for providing his silky shark length and age data. We also thank Dennis Lee and Cheryl Brown of the National Marine Fisheries Service Pelagic Observer Program for catch-at-length data. The comments of three anonymous reviewers greatly improved this paper.

Literature cited

Au, D. W., and S. E. Smith.
1997. A demographic method with population density compensation for estimating productivity and yield per recruit of the leopard shark (*Triakis semifasciata*). Can. J. Fish. Aquat. Sci. 54:415–420.

Bane, G. W.
1966. Observations on the silky shark, *Carcharhinus falciformis*, in the Gulf of Guinea. Copeia 1966:354–357.

Bonfil, R., R. Mena, and D. de Anda.
1993. Biological parameters of commercially exploited silky sharks, *Carcharhinus falciformis*, from the Campeche Bank, Mexico. U.S. Dep. Commer., NOAA Tech. Rep. NMFS 115:73–86.

Branstetter, S.
1987. Age, growth, and reproductive biology of the silky shark, *Carcharhinus falciformis*, and the scalloped hammerhead, *Sphyrna lewini*, from the northwestern Gulf of Mexico. Environ. Biol. Fishes 19(3):161–173.

Cailliet, G. M.
1992. Demography of the Central California population of the leopard shark (*Triakis semifasciata*). Aust. J. Mar. Freshwater Res. 43:183–193.

Chen, S., and S. Watanabe.
1989. Age dependence of natural mortality coefficient in fish population dynamics. Nippon Suisan Gakkaishi 55(2): 205–208.

Cortés, E.
1998. Demographic analysis as an aid in shark stock assessment and management. Fish. Res. 39:199–208.
1999. A stochastic stage-based population model of the sandbar shark in the western North Atlantic. *In* Life in the slow lane: ecology and conservation of long-lived marine animals (J. A. Musick, ed.), p. 115–136. Am. Fish. Soc. Bethesda, MD.
2002. Incorporating uncertainty into demographic modeling: application to shark populations and their conservation. Conserv. Biol. 16(4):1048–1062.

Cortez-Zaragoza, E., P. Dazell, and D. Pauly.
1989. Hook selectivity of yellowfin tuna (*Thunnus albacares*) caught off Darigayos Cove, La Union, Philippines. J. Appl. Ichthyol. 1:12–17.

Fourmanoir, P.
1961. Requins de la côte ouest de Madagascar. Ser. Oceanog. 4:3–81.

Gilbert, P., and D. A. Schlernitzauer.
1966. The placenta and gravid uterus of *Carcharhinus falciformis*. Copeia 1966:451–457.

Goodyear, C. P.
1996. Variability of fishing mortality by age: consequences for maximum sustainable yield. N. Am. J. Fish. Manage. 16:8–13.

Jensen, A. L.
1996. Beverton and Holt life history invariants result from optimal trade-off of reproduction and survival. Can. J. Fish. Aquat. Sci. 53:820–822.

Kirkwood, G. P., and T. I. Walker.
1986. Gill net mesh selectivities for gummy shark *Mustelus antarcticus* Gunther, taken in south-eastern Australian waters. Aust. J. Mar. Freshwater Res. 37:689–697.

Kohler, N. E, J. G. Casey, and P. A. Turner.
1995. Length-weight relationships for 13 species of sharks from the western North Atlantic. Fish. Bull. 93:412–418.
1998. NMFS cooperative shark tagging program, 1962–93: an atlas of shark tag and recapture data. Mar. Fish. Rev. 60(2):1–79.

Krebs, C. J.
1985. Ecology: the experimental analysis of distribution and abundance, 800 p. Harper and Row, New York, NY.

Liu, K. M., and C. T. Chen.
1999. Demographic analysis of the scalloped hammerhead, *Sphyrna lewini*, in the Northwestern Pacific. Fish. Sci. 65(2):218–223.

Parrack, M. L., J. I. Castro, and J. E. Powers.
1993. The United States Atlantic coastal shark fishery. Int. Comm.Conserv. Atl. Tuna, Collect. Vol. Sci. Pap. 126: 406–408.

Peterson, I., and J. S. Wroblewski.
1984. Mortality rate of fishes in the pelagic ecosystem. Can. J. Fish. Aquat. Sci. 41:1117–1120.

Ralston, S.
1990. Size selection of snappers (*Lutjanidae*) by hook and line gear. Can. J. Fish. Aquat. Sci. 47:696–700.

Simpfendorfer, C. A.
1999. Mortality estimates and demographic analysis for the Australian sharpnose shark, *Rhizoprionodon taylori*, from northern Australia. Fish. Bull. 97:978–986.

Simpfendorfer, C. A., and P. Unsworth.
1998. Gill-net mesh selectivity of dusky sharks (*Carcharhinus obscurus*) and whiskery sharks (*Furgaleus macki*) from south-western Australia. Aust. J. Mar. Freshwater Res. 49:713–718.

Sminkey, T.R., and J.A. Musick.
1996. Demographic analysis of the sandbar shark, *Carcharhinus plumbeus*, in the western North Atlantic. Fish. Bull. 94:341–347.

Smith, S. E., D. W. Au, and C. Snow.
1998. Intrinsic rebound potentials of 26 species of Pacific sharks. Aust. J. Mar. Freshwater Res. 49:663–678.

Trent, L., D. E. Parshley, and J. K. Carlson.
1997. Catch and bycatch in the shark drift gillnet fishery off Georgia and East Florida. Mar. Fish. Rev. 59(1):19–28.

Walker, T. I.
1992. Fishery simulation model for sharks applied to the gummy shark, *Mustelus antarcticus* Guenther, from southern Australian waters. Aust. J. Mar. Freshwater Res. 43: 195–212.

Wilson, E. O., and W. H. Bossert.
1971. A primer of population biology, 192 p. Sinauer Associates, Sunderland, MA

Indirect estimates of natural mortality rate for arrowtooth flounder (*Atheresthes stomias*) and darkblotched rockfish (*Sebastes crameri*)

Donald R. Gunderson
School of Aquatic and Fishery Sciences
Box 355020
University of Washington
Seattle, Washington 98195
E-mail address (for D. R. Gunderson): dgun@u.washington.edu

Mark Zimmermann
Daniel G. Nichol
Alaska Fisheries Science Center,
National Marine Fisheries Service
7600 Sand Point Way N.E.
Seattle, Washington 98115-0070

Katherine Pearson
School of Aquatic and Fishery Sciences
Box 355020
University of Washington
Seattle, Washington 98195

Indirect estimates of instantaneous natural mortality rate (M) are widely used in stock assessment and fisheries management. They are essentially a form of meta-analysis, in which prior information on M and key life history parameters from a variety of stocks is used to estimate M for the stock in question.

In this study we report indirect estimates of M for arrowtooth flounder (*Atheresthes stomias*) and darkblotched rockfish (*Sebastes crameri*) obtained by the methods described in Gunderson (1997), and a modification of Pauly's method (1980), and compare them with estimates previously derived by Hoenig's (1983) method. Pauly's original method was based on the correlation of M with von Bertalanffy growth parameters (K and L_∞) and temperature. The modification we used was indicated by a number of reviews of Pauly's data (Charnov, 1993; Pascual and Iribarne, 1993; Jensen, 1996) and relies only on the correlation between M and K. The high correlation between these variables has been observed in a number of taxa and is the basis for the M–K "invariant" used widely in life history theory (Beverton, 1992; Charnov, 1993).

Gunderson's method is based on the high correlation between reproductive effort and natural mortality rate and has a well-established basis in experimental ecology and life history theory (Reznick, 1996). Increases in reproductive effort often come at a cost, and trade-offs between reproductive effort and adult growth or survival have been reported in a wide range of field studies and manipulation experiments (Roff, 1992; Stearns, 1992). Gunderson (1997) found a linear relationship (r^2=0.75) between M and reproductive effort as measured by the gonadosomatic index (GSI=ovary weight/somatic body weight) for 28 stocks of fish, and theoretical analysis (Charnov et al., 2001; Charnov, 2002) has shown that this equation can be a predictable result when maximizing the lifetime production of young.

Pascual and Iribarne (1993) noted that one shortcoming of indirect methods of estimating natural mortality is that no variance estimate is usually associated with the predicted value of M. In this study, we used the delta method (Seber, 1982) to derive estimates of the variance of predicted values of M using Gunderson's technique and Jensen's (1996) modification of Pauly's technique. In the case of the method developed by Hoenig, where natural mortality is estimated from longevity, no comparable variance estimator could be obtained because the results depend on the sample size used to estimate longevity (Hoenig, 1983).

Materials and methods

Data on darkblotched rockfish were collected in 1986 and 1987 during research surveys conducted off the Oregon coast (43°10′–45°50′) aboard commercial groundfish and shrimp trawlers. Fish were weighed to the nearest gram, and fork length was measured to the nearest millimeter. Gonads were removed and weighed to the nearest 0.01 g. Gonad color, size, and structure were recorded for each specimen, and macroscopic observations were made at sea for the presence of fertilized eggs, eyed larvae, and residual larvae in the ovaries. Gonads were preserved in 10% phosphate-buffered formalin and histological analysis was conducted later in the laboratory for selected specimens. It was assumed that the ovaries collected during November–January were fully mature because oocyte fertilization occurs during December–February (Nichol, 1990). Only mature females (36.7 cm or greater) classified as being in the "vitellogenesis" stage (Nichol and Pikitch, 1994) during November–January (n=28) were used to estimate the parameters for the length–ovary-weight relationship, and fish collected during August–November were added when estimating the length–somatic-weight relationship (total n=86).

Data on arrowtooth flounder were collected from research trawls made during September 1993 on Portlock Bank near the eastern end of Kodiak Island, Alaska (Zimmermann, 1997). Fish (less stomach contents) were weighed (+/–2 g) and fork length (cm)

Manuscript accepted 10 July 2002.
Fish. Bull. 101:175–182 (2003).

was obtained. Gonads were assigned a macroscopic maturity stage based on external appearance, and were removed and preserved in 10% formalin buffered with sodium acetate. Gonads were subsequently removed from formalin, weighed (+/–0.001 g) in the laboratory, and classified histologically to maturity stage. Only mature females (47 cm and greater) with ovaries in the "migratory nucleus" stage (Zimmermann, 1997) were used in estimating the length–ovary-weight relation (n=19), and fish in the "late vitellogenesis" stage were added when estimating the length–somatic-weight relation (total n=59).

A fresh-weight to formalin-weight conversion equation for gonads was obtained by collecting 22 females during a research cruise conducted during late October and early November 1999 off Oregon and northern California. Gonads for these specimens were weighed fresh at sea (+/–2 g) and again after being stored for 1–4 months in 10% formalin buffered with sodium bicarbonate (+/–0.001 g). Fresh ovary weights for these specimens ranged from 2 to 500 g. The equation for conversion of fresh weight to formalin weight obtained by linear regression was

$$\textit{Fresh weight} = 1.04305\,(\textit{formalin weight}) + 1.82277 \quad (P<0.001)$$

and was used to correct all arrowtooth flounder ovary weights to fresh weights.

The length–somatic-weight (where somatic weight=total weight minus gonad weight) and length–ovary-weight relationships for both species followed allometric ($y=aX^b$) relationships and were fitted by using nonlinear regression (EXCEL SOLVER, Microsoft Corp., 1998). The relation of length to GSI (gonadosomatic index=ovary weight/somatic weight) was fitted to an allometric relationship because the ratio of two allometric relationships will also be an allometric relationship. The length-GSI relationship was then used to predict the GSI for a mature female of average size in the population.

The average size of a mature darkblotched rockfish was estimated to be 42.7 cm, based on the size composition of females greater than 36.5 cm (the size at 50% maturity, Nichol and Pikitch, 1994) during the 1977 NMFS triennial trawl survey (Rogers[1]). There is no directed fishery for arrowtooth flounder, and they have been exploited only lightly. As a result, the average size of a mature (47 cm or greater; Zimmermann, 1997) arrowtooth flounder was estimated to be 55.5 cm, based on the size composition in the 1999 NMFS trawl survey, which covered their entire size range with a single gear type (Brown[2]).

The instantaneous rate of natural mortality was estimated from the equation M=1.79 GSI developed by Gunderson (1997). The variance of this estimate was estimated using the delta method to obtain

$$\mathrm{Var}(\hat{M}) = \mathrm{Var}(\hat{k}\,\hat{GSI}) = (\hat{GSI})^2\,\mathrm{Var}(\hat{k}) + \hat{k}^2\,\mathrm{Var}(\hat{GSI}),$$

$$\mathrm{Var}(\hat{GSI}) = \left[ef(\bar{L}_m)^{f-1}\right]^2 \mathrm{Var}(\bar{L}_m) + (\bar{L}_m^{2f})\mathrm{Var}(e) + \left[e\,\bar{L}_m^f \ln(\bar{L}_m)\right]^2 \mathrm{Var}(f) + (2\bar{L}_m^f)\left[e\bar{L}_m^f \ln(\bar{L}_m)\mathrm{Cov}(e,f)\right];$$

$$\mathrm{Var}(\hat{k}) = \frac{s^2}{\sum (GSI_i - \overline{GSI})^2} \quad \text{(Draper and Smith, 1981) = 0.03389)}$$

where L_m = mean length of a mature female in the unexploited population;

e,f = coefficients in the length-GSI relationship (GSI=eL^f);

s^2 = residual mean square from GSI-M regression equation (Gunderson, 1997);

$\hat{GSI}$ = mean value of GSI used to predict M in this study;

$\overline{GSI}$ = mean value of GSI in regression sample (Gunderson, 1997);

GSI_i = GSI value for i^{th} species in the regression sample; and

$\hat{k}$ = constant from the GSI-M regression = 1.79.

The Var (e), Var (f), and Cov (e,f) terms in Var ($\hat{GSI}$) were estimated from the variance-covariance matrix of a nonlinear regression algorithm for the length-GSI relationship by using S-PLUS (Venables and Ripley, 1997). The Var($\bar{L}_m$) term was estimated from the length-frequency data used to estimate $\bar{L}_m$.

Indirect estimates of M were also obtained using a modification of Pauly's (1980) method. Jensen (1996) showed that in terms of either the standard error or proportion of variation in predicted M, the simple linear regression of M on the von Bertalanffy growth parameter K is as good as a multiple linear regression model that includes asymptotic size and temperature. The correlation between M and K is a predictable result from life history theory when optimizing the trade-off between survival and fecundity (Jensen, 1996), and has been shown to occur in a wide variety of invertebrate and vertebrate groups (Beverton, 1992; Charnov, 1993).

Pauly's (1980) data for 175 stocks of fish were used to estimate the coefficient ($\hat{g}$=1.598; r^2=0.72) in the equation $M=\hat{g}K$. Estimates of K were obtained by fitting age-length data (sexes combined) for 3930 darkblotched rockfish and 706 arrowtooth flounder to the Von Bertalanffy growth model (Ricker, 1975) by using a nonlinear regression algorithm in AD Model Builder (Fornier, 2001;Wilderbuer[3]). The variance of the estimates was estimated with the delta method to be

$$\mathrm{Var}(M) = \hat{g}^2\mathrm{Var}(K) + K^2\mathrm{Var}(\hat{g}).$$

The Var(K) term was estimated by using AD Model Builder, and Var($\hat{g}$) was estimated by using Pauly's data, and the same method used above to estimate Var($\hat{k}$) (Draper and Smith, 1981).

[1] Rogers, J. B. 2001. Personal commun. Northwest Fisheries Science Center, 2030 SE Marine Science Dr., Newport OR 97365.

[2] Brown, E. S. 2002. Personal commun. Alaska Fisheries Science Center, 7600 Sand Point Way NE, Seattle, WA 98115.

[3] Wilderbuer, T. K. 2002. Personal commun. Alaska Fisheries Science Center, 7600 Sand Point Way NE, Seattle, WA 98115.

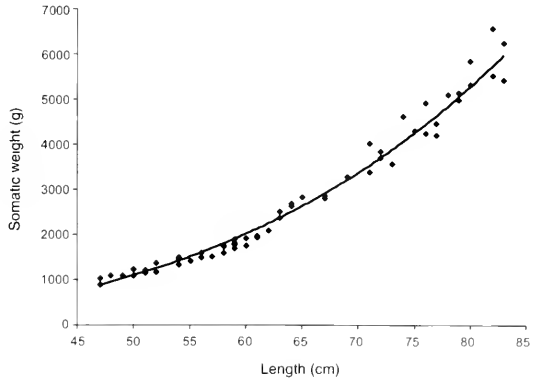

Figure 1

Length–somatic-weight relationship for arrowtooth flounder (*Atheresthes stomias*).

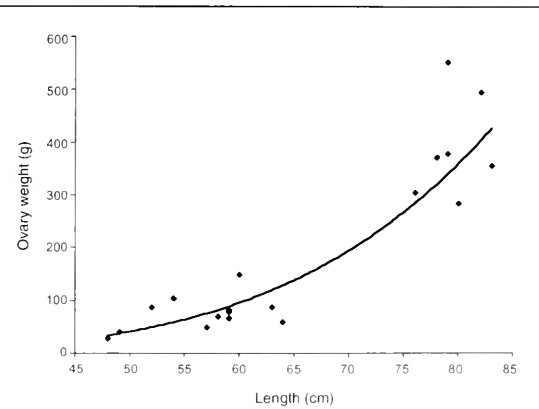

Figure 2

Length–ovary-weight relationship for arrowtooth flounder (*Atheresthes stomias*).

Results

The length–somatic-weight and length–ovary-weight data for arrowtooth flounder (Figs. 1 and 2) and darkblotched rockfish (Figs. 3 and 4) both conformed to allometric relationships. Length–somatic-weight data for both species conformed closely to the model fitted to them (r^2=0.90–0.98, Table 1). The data for the length–ovary-weight relationship conformed to the fitted line reasonably well for arrowtooth flounder (r^2=0.85) and only moderately well for darkblotched rockfish (r^2=0.65). Although sample sizes for ovary weight data were low for both species (n=19–28), the histological classifications available for arrowtooth flounder helped to assure that all fish collected were fully mature and to minimize the scatter about the length–ovary-weight relationship. The scatter about the length-GSI relationships for both species (Figs. 5 and 6) was relatively high (r^2=0.32 for arrowtooth and 0.36 for

darkblotched rockfish). The GSI estimates for both species were at the lower end of the distribution of the GSI and M values used to develop the original predictive relationship (Fig. 7).

Indirect estimates of the instantaneous rate of natural mortality were estimated to be M = 0.08 for arrowtooth flounder with the gonadosomatic index and 0.11 with the growth coefficient K (Table 1). Corresponding estimates for darkblotched rockfish differed more substantially (M=0.11 with the gonadosomatic index and 0.30 with K). Precision for the estimates of M was higher for the estimates based on K (CV=5 to 12%) than for those based on the gonadosomatic index (CV=17%).

Table 1

Estimates of instantaneous natural mortality rate (M) using the gonadosomatic index (GSI), von Bertalanffy growth coefficient (K), and maximum age. Allometric coefficients are shown for length–ovary-weight ($y=aL^b$), length–somatic-weight ($y=eL^d$), and length-GSI ($y=eL^f$) relationships. CI = approximate 95% confidence interval.

	Arrowtooth flounder	Darkblotched rockfish
Mean length (cm)	55.5	42.7
a	0.000000591	1.33E-09
b	4.62	6.57
r^2	0.85	0.65
n	19	28
c	0.0022	0.0322
d	3.35	2.82
r^2	0.98	0.90
n	59	86
e	0.000422	0.00000154
f	1.16	2.82
r^2	0.32	0.36
n	19	28
GSI	0.045	0.0598
VAR (GSI)	0.0000344	0.0000705
M (Gunderson)	0.081	0.107
VAR (M)	0.00018	0.00035
SE (M)	0.0134	0.0186
CI	0.054–0.108	0.07–0.144
K	0.0701	0.1852
Var (K)	0.000060	0.0000085
M (Jensen)	0.112	0.296
Var (M)	0.000175	0.000175
SE (M)	0.0132	0.0132
CI	0.09–0.14	0.27–0.32
Max. age (yr)	23	105
M (Hoenig)	0.18	0.05

Discussion

An estimate of Z=0.18 was previously obtained for arrowtooth flounder by using Hoenig's (1983) relationship between total instantaneous mortality rate (Z) and maximum age in 84 stocks of fish, and an estimated maximum age of 23 years (Turnock et al.[4]). Because this stock has been exploited only lightly, it was assumed that the resulting estimate of Z was equivalent to M. The resulting estimate was somewhat higher than the value obtained from reproductive effort (M=0.08) or K (M=0.11) and outside the approximate 95% confidence limits (±2SE) for both estimates (Table 1).

A range of maximum ages (60 to 105 years) was previously used to obtain estimates of Z (assumed to be approximately equal to M) = 0.025–0.05 for darkblotched rockfish based on Hoenig's method, due to uncertainties in age determination (Rogers et al.[5]). An estimate of M=0.05 provided the best fit to a population dynamics model, although it is somewhat lower than the estimate of M=0.11 obtained in this study with the gonadosomatic index and substantially lower than the estimate of M=0.30 with the growth coefficient K. The estimate obtained with Hoenig's method was once again outside the approximate 95% confidence limits for the other indirect estimates.

Although none of the data on somatic and ovary weights were collected with the specific aim of estimating natural mortality, they served to provide a reasonable estimate of M for arrowtooth flounder and a first approximation of this parameter for darkblotched rockfish. More detailed histological data on the ovaries used in the darkblotched rockfish analysis would have improved the reliability of this estimate and a larger sample size of mature ovaries for both species would have been preferable.

The estimates of M derived from the growth coefficient K (Table 1) were obtained by using age-length data for sexes combined because most of the original data (Pauly, 1980) was in this format. However, because of sexual dimorphism in growth, estimates of M would have differed if males and females had been treated as separate "stocks" as was done for 33 of the observations in Pauly's database. Sexual dimorphism was substantial for arrowtooth flounder, where K was 0.194 (corresponding to an estimated M=0.31) for males and 0.065 (M=0.10) for females and was less pronounced in darkblotched rockfish, where K was 0.211 (M=0.34) for males and 0.164 (M=0.26) for females. Averaging these sex-specific estimates would not change

[4] Turnock, B. J., T. K. Wilderbuer, and E. S. Brown. 1999. Arrowtooth flounder. *In* Stock assessment and fishery evaluation report for the groundfish resources of the Gulf of Alaska, p. 226–253. North Pacific Fishery Management Council, Anchorage, AK.

[5] Rogers, J. B., R. D. Methot, T. L. Builder, K. Piner, and M. Wilkins. 2000. Status of the darkblotched rockfish (*Sebastes crameri*) resource in 2000. *In* Stock assessment and fishery evaluation: appendix to the status of the Pacific Coast groundfish fishery through 2000 and recommended acceptable biological catches for 2001, 71 p. Pacific Fishery Management Council, Portland, OR.

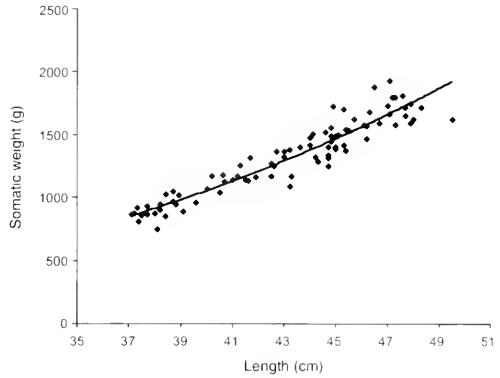

Figure 3

Length–somatic-weight relationship for darkblotched rockfish (*Sebastes crameri*).

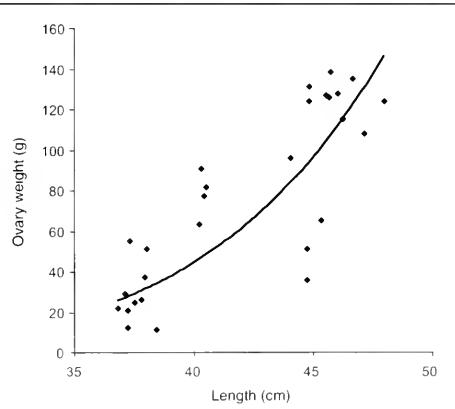

Figure 4

Length–ovary-weight relationship for darkblotched rockfish (*Sebastes crameri*).

the darkblotched estimate of M appreciably from what was obtained by pooling the age-length data to estimate a common K, but the estimate for arrowtooth flounder would increase from 0.11 to 0.21.

All indirect methods of estimating M rely on the correlation established in their basic data set (28 fish stocks for Gunderson, 175 for Pauly, and 84 for Hoenig). As a result these methods are subject to bias in the estimates of M, K, maximum age, and reproductive effort in the original correlation data, and in the estimates of these parameters being used to extrapolate the correlations to new species. Although Pauly's database is the most extensive (in terms of the number of stocks available), age determination and stock assessment methods have improved in the years since it was initially compiled, and estimates of M have tended to decline. An updated database would probably reduce the estimates of M based on K.

The estimate of maximum age required by Hoenig's method assumes that the age determination technique being employed is unbiased. Validating this assumption is of-

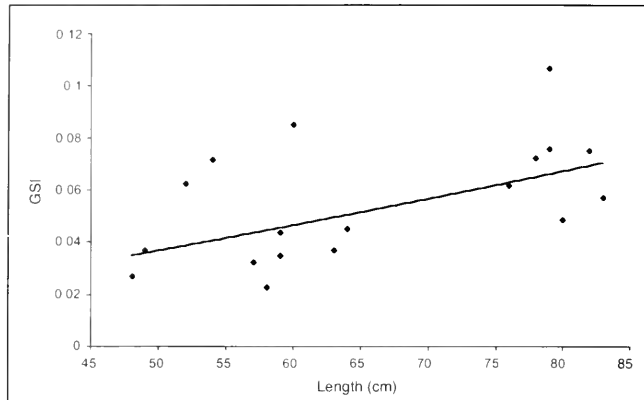

Figure 5

Length-gonadosomatic index (GSI) relationship for arrowtooth flounder (*Atheresthes stomias*).

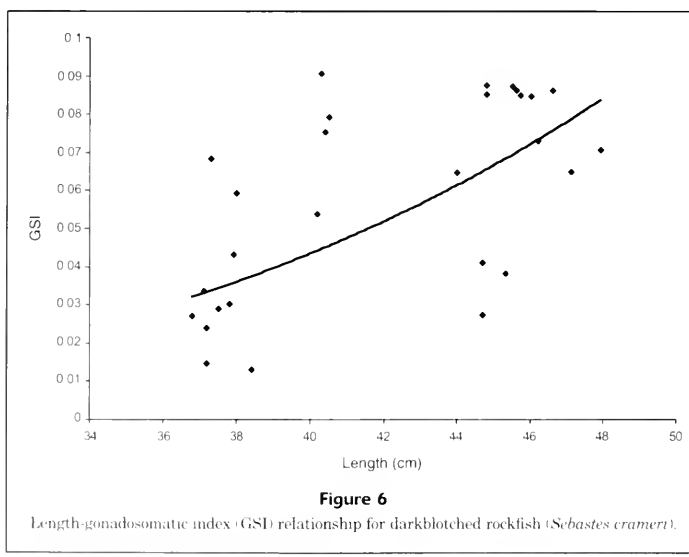

Figure 6

Length-gonadosomatic index (GSI) relationship for darkblotched rockfish (*Sebastes crameri*).

ten difficult for the older, more difficult-to-age individuals but can be accomplished by using a variety of techniques ranging from marking to analysis of radioactive isotopes (Lai et al., 1996). The estimate of longevity is also dependent on sample size and previous fishing history. Hoenig (1983) showed that maximum age tends to increase slowly with increasing sample size after about 200 individuals have been examined, but longevity has probably declined from historical levels because of fishing, particularly in the case of the darkblotched rockfish. A small sample size for age determination, underaging, and previous exploitation would all result in an overestimate of M with Hoenig's method and might explain some of the difference between the estimate of arrowtooth flounder mortality based on reproductive effort or K (M=0.08–0.11) and the previous estimate (M=0.18).

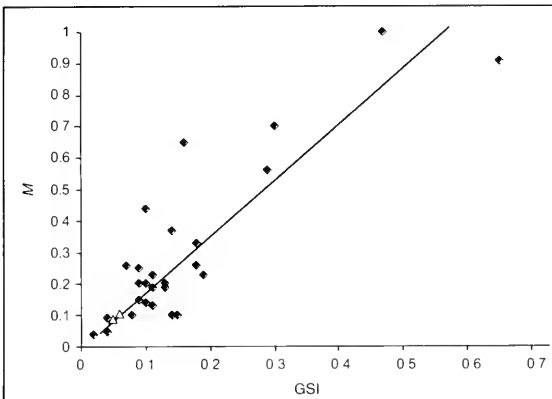

Figure 7

Location of arrowtooth flounder *Atheresthes stomias*) and darkblotched rockfish (*Sebastes crameri*) (open triangles) in relation to the data set for gonadosomatic index (GSI) and natural mortality rate (M) used to obtain the predictive relation between them (Gunderson, 1997).

In the case of darkblotched rockfish, the estimate of mortality based on reproductive effort (M=0.11) was actually higher than the estimate based on longevity (M=0.05), and neither undersampling nor underaging would explain the differences. Overestimation of the gonadosomatic index (and the estimated M) by using macroscopic rather than histological criteria to classify maturation stage may explain the higher estimate but seems less likely than underestimating it because several oocyte size classes that might be included in the "vitellogenesis" stage are not fully developed. Underestimation of the mean length of a mature female could also lead to an estimate of GSI (and M) that is too low, but estimates of GSI are relatively insensitive to length. For darkblotched rockfish, the mean length of a mature female would have to be 32.4 cm (below the size at maturity) in order for M to equal 0.05.

Indirect estimates of M offer access to a meta-analysis that can be used to explore consistency of natural mortality estimates with prior knowledge on a variety of stocks and put these estimates in the broader context of life history theory. The use of several alternative indirect techniques can minimize bias in stock assessment and expose any misconceptions or errors regarding reproductive biology or age determination at an early stage in a stock assessment program.

Bias is clearly a more important problem than precision when using indirect methods to estimate M. Each of the methods used in our study has a firm basis in life history theory (the M–K and M–GSI "invariants") or population dynamics (Z≈1/maximum age), and when derived from a database for a large number of species, they can be relatively precise (CV=5–17% for the estimates made in this paper). Nevertheless, many of the original data points on which these relationships are based have become outdated as improved methods of age determination and stock assessment have come into wide usage and ignoring these outdated data points can lead to significant bias when using them to estimate M. Indirect methods are widely used, and it is important that the databases from which they are derived be continually updated and expanded as new information becomes available.

Acknowledgments

We thank Dan Kimura and Saang-Yoon Hyun for their invaluable statistical advice and assistance, and Jean Rogers, Tom Wilderbuer, and Eric Brown for providing age and length data. This research was supported by the Joint Institute for the Study of the Atmosphere and Ocean (JISAO) under NOAA Cooperative Agreement No. NA67RJ0155 (contribution 814).

Literature cited

Beverton, R. J. H.
1992. Patterns of reproductive strategy parameters in some marine teleost fishes. J. Fish Biol. 41 (suppl. B):137–160.

Charnov, E. L.
1993. Life history invariants: some explorations of symmetry in evolutionary ecology. 167 p. Oxford Univ. Press, Oxford.
2002. Reproductive effort, offspring size and benefit—cost ratios in the classification of life histories. Evol. Ecol. Res. 4:1–10.

Charnov, E. L., T. F. Turner, and K. O. Winemiller.
2001. Reproductive constraints and the evolution of life histories with indeterminate growth. Proc. Natl. Acad. Sci. 98:9460–9464.
Draper, N. R., and H. Smith.
1981. Applied regression analysis, 2nd ed., 709 p. John Wiley, New York, NY.
Fornier, D.
2001. An introduction to AD Model Builder version 6.0.2 for use in nonlinear modeling and statistics, 202 p. Otter Research Ltd., Sydney, British Columbia, Canada.
Gunderson, D. R.
1997. Trade-off between reproductive effort and adult survival in oviparous and viviparous fishes. Can. J. Aquat. Sci. 54:990–998.
Hoenig, J. M.
1983. Empirical use of longevity data to estimate mortality rates. Fish Bull. 81:893–903.
Jensen, A. L.
1996. Beverton and Holt life history invariants result from optimal trade-off of reproduction and survival. Can. J. Fish. Aquat. Sci. 53:820–822.
Lai, H. L., V. F. Gallucci, and D. R. Gunderson.
1996. Age determination in fisheries: methods and applications to stock assessment. *In* Stock assessment: quantitative methods and applications for small-scale fisheries (V. F. Gallucci, S. B. Saila, D. J. Gustafson, and B. J. Rothschild, eds.), p. 82–178. CRC Press, Lewis Publishers, Boca Raton, New York, London, Tokyo.
Microsoft Corporation.
1998. EXCEL SOLVER. Microsoft Corporation, Redmond, WA.
Nichol, D. G.
1990. Life history examination of darkblotched rockfish (*Sebastes crameri*) off the Oregon coast. M.S. thesis, 124 p. Oregon State Univ., Corvallis, OR.
Nichol, D. G. and E. K. Pikitch.
1994. Reproduction of darkblotched rockfish off the Oregon coast. Trans. Am. Fish. Soc. 123:469–481.
Pascual, M. A., and O. O. Iribarne.
1993. How good are empirical predictions of natural mortality? Fish. Res. 16:17–24
Pauly, D.
1980. On the interrelationships between natural mortality, growth parameters, and mean environmental temperature in 175 fish stocks. J. Cons. Int. Explor. Mer 39 175–192.
Reznick, D.
1996. Life history evolution in guppies: a model system for the empirical study of adaptation. Neth. J. Zool. 46(3–4): 172–190.
Ricker, W. E.
1975. Computation and interpretation of biological statistics of fish populations. Bull. Fish. Res. Board Can. 191, 382 p.
Roff, D. A.
1992. The evolution of life histories: theory and analysis, 535 p. Chapman and Hall, New York, NY.
Seber, G. A. F.
1982. The estimation of animal abundance and related parameters, 2nd ed., 654 p. Macmillan Publ. Co., Inc., New York, NY
Stearns, S. C.
1992. The evolution of life histories, 249 p. Oxford Univ. Press, Oxford.
Venables, W. N., and B. D. Ripley.
1997. Modern applied statistics with S-Plus, 2nd ed., 548 p. Springer-Verlag, New York, NY.
Zimmermann, M.
1997. Maturity and fecundity of arrowtooth flounder, *Atheresthes stomias*, from the Gulf of Alaska. Fish. Bull. 95: 598–611.

Use of parasites in stock identification of the deepwater redfish (*Sebastes mentella*) in the Northwest Atlantic

David J. Marcogliese
St. Lawrence Centre
Environment Canada
105 McGill, 7th Floor
Montreal, Québec H2Y 2E7, Canada
E-mail address: david.marcogliese@ec.gc.ca

Elaine Albert
Department of Fisheries and Oceans
Maurice Lamontagne Institute
P.O. Box 1000
Mont-Joli, Québec G5H 3Z4, Canada

Pierre Gagnon
St. Lawrence Centre
Environment Canada
105 McGill, 7th Floor
Montreal, Québec H2Y 2E7, Canada

Jean-Marie Sévigny
Department of Fisheries and Oceans
Maurice Lamontagne Institute
P.O. Box 1000
Mont-Joli, Québec G5H 3Z4, Canada

An important aspect of fisheries management is the correct delineation of boundaries between fish stocks. With the recent collapse of the groundfish fishery in eastern Canada, redfish (*Sebastes* spp.) has become an increasingly important resource. Currently, the two most economically important redfish species (*S. fasciatus* and *S. mentella*) are partitioned into eight management areas in the Northwest Atlantic (Fig. 1). In this study, we examined the parasite fauna of the deepwater redfish *S. mentella*, collected from different areas in the Northwest Atlantic, to determine if the distribution and abundance of the parasite fauna can aid in stock discrimination of this species and focused on differentiating fish from the Gulf of St. Lawrence (unit 1) from those from the Cabot Strait and Laurentian Channel (unit 2). The deepwater redfish is the most common redfish species in the Gulf of St. Lawrence and is considered to have a more northerly range and deeper distribution than its congeners (Atkinson, 1987; Scott and Scott, 1988).

In eastern Canada, parasites have been successfully employed to discriminate among stocks of another deepwater fish, the Greenland halibut (*Reinhardtius hippoglossoides*) (Arthur and Albert, 1993), as well as Atlantic cod (*Gadus morhua*) (McClelland and Marcogliese, 1994). Moles et al. (1998) suggested that parasites could be used to discriminate among stocks of rockfishes (*Sebastes* spp.) in the Gulf of Alaska, and Stanley et al. (1992) used the monogenean *Microcotyle sebastis* to confirm that the yellowtail rockfish *Sebastes flavidus* was distributed in discrete groups along the Pacific coast of North America. However, there is not much information on *Sebastes* spp. from the Northwest Atlantic because studies of redfish parasites prior to that of Bourgeois and Ni (1984) must be treated with caution because of the possible confusion in identification of redfish species (Moran et al., 1996).

Materials and methods

Host and parasite collections

A total of 170 deepwater redfish of size >22 cm were sampled by bottom trawl from five areas representing four management units off the Atlantic coast of Canada between August 1996 and January 1997. Summer and winter samples were available only in unit 2 (Fig. 1, Table 1). Fish were measured on board, individually bagged, and deep frozen immediately after capture for later examination. Because fish from southwestern Labrador Sea and Flemish Cap were not measured on board, estimates of fresh length were made for these fish by using a regression of fresh length on frozen length obtained from the other fishes.

Fish were thawed in the laboratory, measured (total length), and weighed. Prior to parasitological examination, species of redfish were identified by the number of soft anal-fin rays. Only those that had 8 or more soft rays at the anal fin were retained for the analyses (Ni, 1981). Examinations for metazoan parasites were performed with a stereomicroscope using standard parasitological methods. The external surface was examined and scars from previous infestations of *S. lumpi* were noted. The gills were removed, rinsed, and their arches were detached and examined separately. Because of the pressure changes when redfish were hauled out from the deep water most of the stomachs were everted. The internal organs (heart, liver, spleen, gall bladder, swim bladder, digestive tract, gonads, kidney, urinary bladder) were inspected for parasites (lying free or encapsulated on the exterior),

Manuscript accepted 21 August 2002.
Fish. Bull. 101:183–188 (2003).

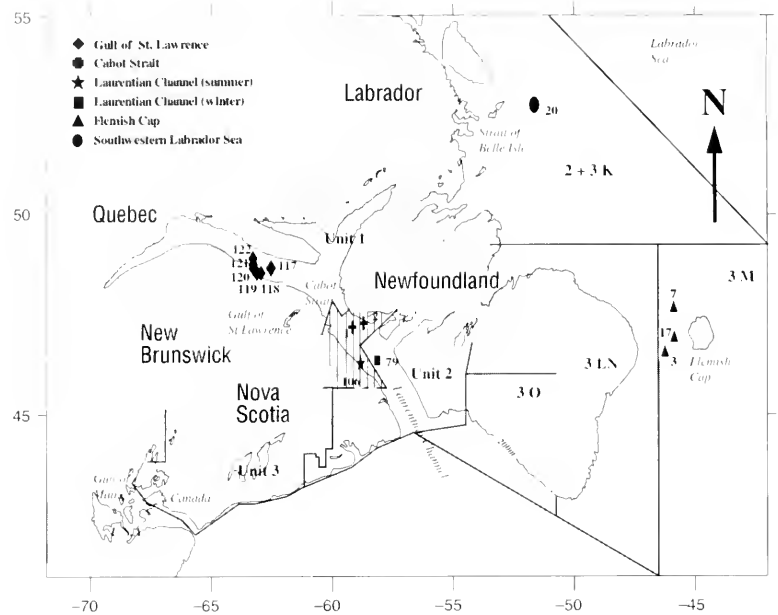

Figure 1

Map of redfish (*Sebastes mentella*) collection sites (various symbols) in the northwestern Atlantic Ocean in 1996 and 1997. The eight areas currently used for redfish management are delineated: 1) subarea 2 and division 3K (southwestern Labrador Sea), 2) divisions 3LN (northern and western Grand Banks); 3) division 3M (Flemish Cap); 4) division 3O (southwestern Grand Banks); 5) unit 1 (Gulf of St. Lawrence); 6) unit 2 (Laurentian Channel); 7) unit 3 (Scotian Shelf); and 8) the Gulf of Maine. The hatched area (Cabot Strait) is part of unit 1 from January to May and unit 2 from June to December. Numbers near collection sites represent set numbers. Jagged line indicates the 200-m depth contour.

separated, and then examined individually. The stomach, pyloric ceaca, and intestine were separated, opened longitudinally, and their contents rinsed into beakers where they were mixed with sodium bicarbonate and allowed to settle to remove endoparasitic helminths. The wall of the stomach, pyloric ceaca, and intestine, and the liver, spleen, kidney, and heart were compressed between glass plates and examined for parasites. The body musculature was removed from the vertebral column, the skin was removed from the fillets, and flaps were thinly sliced and all were inspected for helminths and dead neck stalks or sores caused by old infestations by *Sphyrion lumpi*.

All parasites were sorted into major taxonomic groups, cleaned, and counted for each organ. Nematoda and Copepoda were identified fresh to the lowest taxon and then fixed in 70% ethanol with 10% glycerin. Old cephalothoraces and sores caused by *Sphyrion lumpi* were identified and counted. Digenea and Cestoda were fixed in alcohol-formalin-acetic acid (AFA) and stained in acetocarmine for later identification.

Statistical analyses

Results of analyses may be influenced by variations in factors such as size and sex. In our study, there were no significant differences in mean size of fish sampled from the various regions (Table 1). Males were smaller than females from all regions, except those from the Labrador Sea, where the size difference was reversed. However, none of the parasites retained for multiple parametric analyses differed between the sexes (ANOVA, $P>0.05$).

Because parasite counts for all areas were not normally distributed and normality could not be reached by using various transformations, multiple nonparametric analyses (SAS version 8.0, SAS Institute, Inc., 1999) were used to investigate the usefulness of parasites in discriminating host collections. All parasites used in this analysis were relatively long lived and thus accumulated with host age (length). However, the relationship between size and intensity of certain parasites (*Anisakis simplex*) was not linear, thus rendering covariant analyses inappropriate.

Table 1

Summary of collection data for redfish (*Sebastes mentella*) in the Northwest Atlantic Ocean, 1996–97.

Geographic region	NAFO management area	Latitude-longitude	Date	Number of fish	Mean length (mm) ±SD (range)
Gulf of St. Lawrence	unit 1 (4T)	48.91°N, 63.29°W to 48.66°N, 62.55°W	August 1966	30	330.0±37.4 (220–400)
Cabot Strait	unit 2 (3Pn)	47.19°N, 59.18°W to 47.26°N, 58.72°W	August 1996	49	318.0 ±30.5 (220–390)
Laurentian Channel	unit 2 (4Vn)	46.28°N, 58.84°W	August 1996	31	315.2 ±22.3 (250–350)
Southwestern Labrador Sea	2J	52.74°N, 51.65°W	Autumn 1996	13	321.5 ±59.6 (250–440)
Flemish Cap	3M	47.64°N, 45.89°W to 48.08°N, 44.55°W	Autumn 1996	16	317.0 ±53.6 (228–443)
Laurentian Channel	unit 2 (3Ps)	46.36°N, 58.15°W	January 1997	31	324.5 ±27.5 (260–390)

Table 2

Number of fish involved in redfish (*Sebastes mentella*) statistical comparisons of parasite mean abundance between management units. Winter and summer samples from unit 2 were pooled for these analyses.

	Length class (mm)														
Comparison	220	260	280	290	300	310	320	330	340	350	360	380	390	440	All
FlemishCap—Labrador Sea		2	2	2	2	3	3		3		3			2	22
Flemish Cap—unit 2		3	7	5	12	24	25		14		4	4			98
Labrador Sea—unit 1				2	3		8	5	4		5				27
unit 1 and unit 2	2			5	13		30	18	15	10	6		3		102

The following analyses were performed. For each pair of geographically adjacent management units, that is, across the four stock boundaries encountered around Newfoundland (See Fig. 1), fish were divided into 1-cm length classes. For a given comparison, only length classes containing fish from both units involved were retained. Within each class, the parasite infection intensities were attributed standard normal ranks. The ranks from all length classes were then combined to perform a *t*-test. This test corrects for the effects of host size on parasite mean abundance and for variance heterogeneity while preventing outlying observations from having too much influence. The multiplicity of the statistical tests (many pairs of stocks multiplied by many parasites) was accounted for by a bootstrap procedure (PROC MULTTEST, SAS, version 8, SAS Institute, Inc., 1999). The numbers of fish from each length class involved in the comparisons are detailed in Table 2.

Intensity refers to the number of parasites of a given species in an infected individual fish and mean intensity refers to the mean number of parasites of a given species per infected fish in a sample. Mean abundance is defined as the mean number of parasites of a given species per host, infected and uninfected, in a sample. Prevalence is the proportion of fish infected with a given parasite in a sample, expressed as a percentage (Bush et al., 1997).

Results

Sixteen taxa were found to infect *S. mentella* in eastern Canada in this survey. These included one myxozoan (*Ceratomyxa* sp.), eight digeneans (*Anomalotrema koiae*, *Derogenes varicus*, *Hemiuris levinseni*, *Lecithaster gibbosus*, *Lecithophyllum botryophorum*, *Olssonium turneri*, *Podocotyle reflexa*, and *Progonus muelleri*), two cestodes (*Bothriocephalus scorpii*, and *Scolex pleuronectis* plerocercoids), three nematodes (*Anisakis simplex*, Contracaecinea, and *Hysterothylacium aduncum*), and two copepods (*Chondracanthus nodosus* and *Sphyrion lumpi*). This is the first report of *O. turneri* and *P. muelleri* from *Sebastes* spp.

Preliminary analyses demonstrated that only larvae of *Anisakis simplex* and *Hysterothylacium aduncum*, both anisakid nematodes occurring on the viscera of fish, and the copepod ectoparasite *Sphyrion lumpi* could be used

Table 3

Prevalence (%), mean intensity (no. of parasites, ±SD), and range of intensity of infections of redfish (*Sebastes mentella*) with parasites used as biological tags in the Northwest Atlantic. *n* = sample size.

Region	*n*	Parasite	Prevalence (%)	Intensity (mean ±SD)	Range of intensity
Gulf of St. Lawrence (unit 1-4T)	30	*Anisakis simplex*	53.3	2.8 ±3.1	1–13
		Hysterothylacium aduncum	20.0	1.2 ±0.4	1–2
		Sphyrion lumpi	23.3	1.7 ±0.8	1–3
Cabot Strait (unit 2-3Pn)	49	*Anisakis simplex*	26.5	2.0±1.2	1–4
		Hysterothylacium aduncum	44.9	1.6 ±0.7	1–3
		Sphyrion lumpi	51.0	1.9 ±1.4	1–7
Laurentian Channel–summer (unit 2–4Vn)	31	*Anisakis simplex*	16.1	1.0 ±0.0	1
		Hysterothylacium aduncum	32.3	1.5 ±1.0	1–4
		Sphyrion lumpi	67.7	1.7 ±0.9	1–4
Laurentian Channel–winter (unit 2–3Ps)	31	*Anisakis simplex*	29.0	1.1±0.3	1–2
		Hysterothylacium aduncum	29.0	1.4 ±0.7	1–3
		Sphyrion lumpi	41.9	2.2 ±2.2	1–9
Labrador Sea (2J)	13	*Anisakis simplex*	46.2	25.2 ±35.5	1–92
		Hysterothylacium aduncum	30.8	7.0 ±6.8	2–17
		Sphyrion lumpi	7.7	2.0	2
Flemish Cap (3M)	16	*Anisakis simplex*	56.3	2.7 ±3.5	1–12
		Hysterothylacium aduncum	93.8	93.8 ±92.4	1–259
		Sphyrion lumpi	6.3	10.0	10

to discriminate among redfish stocks (SAS GLM procedure, SAS, 2001). Gastrointestinal digeneans were not used because differences were not noted among regions (SAS GLM procedure). Furthermore, evagination of most of the redfish stomachs during collection caused losses of gastrointestinal parasites and rendered the worm counts unreliable. Myxozoans and *C. nodosus* were not common enough to be used as tags for deepwater redfish (1% and 2% prevalence overall, respectively). *Sphyrion lumpi* use redfish as its definitive host but only adult females are embedded permanently in the flesh, and sores of previous infections were taken into account in our study.

Larvae of *A. simplex* were common at almost all sites, but were particularly abundant off Labrador, on the Flemish Cap, and in the Gulf of St. Lawrence. The most prevalent and abundant parasite encountered was *H. aduncum* in redfish from the Flemish Cap. The copepod *S. lumpi* was most prevalent in the Gulf of St. Lawrence and the Laurentian Channel. Prevalence and mean intensity of these parasites are shown in Table 3.

Results of multiple nonparametric analyses demonstrated that at least one of the three parasite species differed in mean abundance between all adjacent areas, with the exception of the Labrador Sea and the Gulf of St. Lawrence. Mean abundance of both *H. aduncum* and *S. lumpi* in redfish from the Flemish Cap and the Cabot Strait–Laurentian Channel were significantly different (bootstrap adjusted $P<0.0001$ and 0.01, respectively). Mean abundance of *H. aduncum* also differed between fish from the Flemish Cap and the Labrador Sea (bootstrap adjusted $P<0.05$). Lastly, mean abundance of *A. simplex* differed between fish from the Gulf of St. Lawrence and those from the Cabot Strait–Laurentian Channel (bootstrap adjusted $P<0.01$) (Table 4).

Given that the Gulf of St. Lawrence (unit 1) and the Cabot Strait–Laurentian Channel (unit 2) populations are currently managed as separate stocks, we wished to validate our results. Analyses demonstrate that for *A. simplex*, mean abundance is significantly different in fish from unit 2 collected in winter and those from the Gulf of St. Lawrence (unit 1) collected in summer (bootstrap adjusted $P<0.05$), but no difference could be shown between those collected in winter versus summer from unit 2, nor between those collected in the summer compared to winter within the Cabot Strait–Laurentian Channel (Table 5).

Discussion

Criteria for the use of parasites as biological markers of fish populations have been reviewed by Williams et al. (1992). In this study, we employed the following four criteria for biological markers: geographic variation in prevalence or abundance, longevity of infection, absence of reproduction directly in or on the host, and ease of detection and enumeration. First, geographic variation in prevalence and abundance was observed in the various parasites. Second, the parasites or their remains have a

Table 4

Nonparametric length-stratified comparison of parasite mean abundance in redfish (*Sebastes mentella*) between management units. Winter and summer samples from unit 2 were pooled for these analyses. Overall test multiplicity is corrected for by bootstrap.

Parasite	Comparison	Raw *P*-value	Bootstrap *P*-value
Anisakis simplex	Flemish Cap and Labrador Sea	0.4941	0.9997
	Flemish Cap and unit 2	0.0083	0.0900
	Labrador Sea and unit 1	0.0184	0.1932
	unit 1 and unit 2	0.0008	0.0090*
Hysterothylacium aduncum	Flemish Cap and Labrador Sea	0.0014	0.0151*
	Flemish Cap and unit 2	<.0001	<0.0001*
	Labrador Sea and unit 1	0.1794	0.9039
	unit 1 and unit 2	0.1546	0.8629
Sphyrion lumpi	Flemish Cap and Labrador Sea	0.7774	1.0000
	Flemish Cap and unit 2	0.0006	0.0077*
	Labrador Sea and unit 1	0.3077	0.9872
	unit 1 and unit 2	0.0308	0.3065

Table 5

Nonparametric, length stratified comparison of parasite mean abundance in redfish (*Sebastes mentella*) between unit 1 (Gulf of St. Lawrence) and unit 2 (Cabot Strait–Laurentian Channel). Overall test multiplicity is corrected for by bootstrap.

Parasite	Comparison	Raw *P*-value	Bootstrap *P*-value
Anisakis simplex	unit 1(summer) and unit 2 (winter)	0.0042	0.0238*
	unit 2 (summer) and unit 2 (winter)	0.9150	1.0000
Hysterothylacium aduncum	unit 1(summer) and unit 2 (winter)	0.9050	1.0000
	unit 2 (summer) and unit 2 (winter)	0.1613	0.6454
Sphyrion lumpi	unit 1(summer) and unit 2 (winter)	0.4326	0.9653
	unit 2 (summer) and tunit 2 (winter)	0.4018	0.9517

long life span in their hosts. Larval anisakid nematodes can survive for a number of years in the fish host; McClelland and Marcogliese (1994) provided a detailed discussion of the use of anisakid parasites as biological tags for fish stocks. They pointed out that although prevalence and abundance of anisakids may vary over longer time scales, they are stable over the time frame (a few years) of a given survey, rendering them suitable for a stock discrimination study. Remarkably, of the 24 studies on biological tags reviewed by Arthur (1997) between 1990 and 1997, eight of them employed anisakid nematodes. Although the copepod *S. lumpi* has a limited life span, the cepahlothorax and scar tissue from previous infections persist for many years (Templeman and Squires, 1960; Sindermann, 1961; Reimer and Szuks, 1989; Bakay, 1988[1]). Third, none of these parasites multiply directly on the host and thus augment their abundance, as in the case of some protozoans and monogeneans. The anisakids are larval stages, and the copepod produces free-swimming larvae. Lastly, the parasites chosen are easily detected and counted.

We have shown that the parasite fauna of the deepwater redfish (*S. mentella*) can provide useful information on stock discrimination and definition of stock boundaries, as has been demonstrated for other fishes (see Williams et al. 1992; Arthur, 1997). Indeed, fish from all adjacent zones, with the exception of the Labrador Sea and Gulf of St. Lawrence, could be separated on the basis of abundance of at least one species of parasite. Distinction between redfish from the Gulf of St. Lawrence (unit 1) and the Cabot Strait–Laurentian Channel (unit 2) is reinforced by analyses demonstrating differences between the mean abundance of *A. simplex* in fish collected from the Gulf in summer and those in unit 2 in winter or summer. Furthermore, there were no differences in abundance of *A. simplex* detected in fish from unit 2 between winter and summer. Our results also support those of previous studies that demonstrated differences between redfish from the Flem-

[1] Bakay, Y. I. 1988. Application of results from parasitological investigations in redfish (*Sebastes mentella* Travin) populational structure studies. Int. Coun. Explor. Sea C.M. 1988/G: 35, 14 p.

ish Cap and the Labrador Sea according to their parasite fauna (Templeman and Squires, 1960; Bourgeois and Ni, 1984). All areas sampled in our study are currently managed as separate stocks, and our results do not suggest that management strategies should change. However, the inclusion of Cabot Strait in unit 1 in the winter should be re-evaluated with further sampling.

Our parasite results are in contrast with results using microsatellite DNA markers (Roques et al., 2002), in which *S. mentella* from the Gulf of St. Lawrence could not be differentiated from those of the Laurentian Channel. For this species, only three divergent populations were defined across the North Atlantic: 1) a western population in the Gulf of St. Lawrence and offshore Newfoundland; 2) a panoceanic population; and 3) an eastern population in Norway and the Barents Sea. Thus redfish from unit 1 could not be differentiated from those of unit 2. Similar results were reported for *S. fasciatus* sampled in units 1 and 2 (Roques et al., 2001). Redfish populations in both units are characterized by the presence of hybrid and introgressed individuals between *S. fasciatus* and *S. mentella* (Roques et al., 2001). Stock distinction does not preclude genetic exchange between stocks, but managers must be aware of the size and spatial boundaries of stocks, as well as the level of gene flow between the stocks.

Acknowledgments

We thank Johanne Guérin, Hélène Dionne, and Yves Desdevises for technical assistance in the laboratory. The map was prepared by Eric Parent. Lastly, we appreciate the assistance of the officers and crew of the research vessels C.S.S. *Alfred Needler*, C.S.S. *Teleost*, and C.S.S. *Wilfred Templeman* for assistance with the sampling.

Literature cited

Arthur, J. R.
1997. Recent advances in the use of parasites as biological tags for marine fish. *In* Diseases in Asian aquaculture III (T. W. Flegel and I. H. MacRae, eds.) p. 141–154. Fish Health Section, Asian Fisheries Society, Manila, Philippines.

Arthur, J. R., and E. Albert.
1993. Use of parasites for separating stocks of Greenland halibut (*Reinhardtius hippoglossoides*) in the Canadian Northwest Atlantic. Can. J. Fish. Aquat. Sci. 50:2175–2181.

Atkinson, D. B.
1987. The redfish resources off Canada's east coast. *In* Proceedings of the international rockfish symposium, Anchorage, Alaska, October 1986, report 87-2, p. 15–33. Lowell Wakefield Fisheries Symposium Series, Alaska Sea Grant College Program, Fairbanks, AK.

Bourgeois, C. E., and I. H. Ni.
1984. Metazoan parasites of Northwest Atlantic redfishes (*Sebastes* spp.). Can. J. Zool. 62:1879–1885.

Bush, A. O., K. D. Lafferty, J. M. Lotz, and A. W. Shostak.
1997. Parasitology meets ecology on its own terms: Margolis et al. revisited. J. Parasitol. 83:575–583.

McClelland, G., and D. J. Marcogliese.
1994. Larval anisakine nematodes as biological indicators of cod (*Gadus morhua*) populations in the southern Gulf of St. Lawrence and on the Breton Shelf, Canada. Bull. Scan. Soc. Parasitol. 4: 97–116.

Moles, A., J. Heifetz, and D. C. Love.
1998. Metazoan parasites as potential markers for selected Gulf of Alaska rockfishes. Fish. Bull. 96:912–916.

Moran, J. D. W., J. R. Arthur, and M. D. B. Burt.
1996. Parasites of sharp-beaked redfishes (*Sebastes fasciatus* and *Sebastes mentella*) collected from the Gulf of St. Lawrence, Canada. Can. J. Fish. Aquat. Sci. 53:1821–1826.

Ni, I.-H.
1981. Numerical classification of sharp-beaked redfishes, *Sebastes mentella* and *S. fasciatus*, from the Northeastern Grand Bank. Can. J. Fish. Aquat. Sci. 38:873–879.

Reimer, L.W., and H. Szuks.
1989. Differences of infestation in the redfish *Sebastes mentella* by *Sphyrion lumpi* in the North Atlantic. *In* Proceedings of the international workshop on *Sphyrion lumpi*. Gustrow, 3–5 October, 1989 (L.W. Reimer, ed.), p. 41–46. Padagogische Hochschule, Gustrow, Federal Republic of Germany.

Roques, S., J.-M. Sevigny, and L. Bernatchez.
2001. Evidence for broadscale introgressive hybridization between two redfish (genus *Sebastes*) in the Northwest Atlantic: a rare marine example. Mol. Ecol. 10:149–165.

Roques, S., J.-M. Sévigny, and L. Bernatchez.
2002. Weak genetic structuring in the deep-water redfish, *Sebastes mentella*, across the North Atlantic evidenced by microsatellite variation. Mar. Biol. 140:297–307.

SAS Institute Inc.
1999. SAS OnlineDoc®, version 8. SAS Institute, Inc., Cary, NC.
2001. SAS system for Windows, release 8.02. SAS Institute, Inc., Cary, NC.

Scott, W. B., and M. G. Scott.
1988. Atlantic fishes of Canada. Can. Bull. Fish. Aquat. Sci. 219, 731 p.

Sindermann, C. J.
1961. Parasitological tags for redfish of the western North Atlantic. Special publication 3, ICES/ICNAF Redfish Symposium, p. 111–117. A. F. Host, Copengagen.

Stanley, R. D., D. L. Lee, and D. J. Whitaker.
1992. Parasites of yellowtail rockfish, *Sebastes flavidus* (Ayres, 1862) (Pisces: Teleostei), from the Pacific coast of North America as potential biological tags for stock identification. Can. J. Zool. 70:1086–1096.

Templeman, W., and H. J. Squires.
1960. Incidence and distribution of infestation by *Sphyrion lumpi* (Kroyer) on the redfish, *Sebastes marinus* (L.), of the western North Atlantic. J. Fish. Res. Board Can. 17:5–31.

Wilhams, H. H., K. MacKenzie, and A. M. McCarthy.
1992. Parasites as biological indicators of the population biology, migrations, diet, and phylogenetics of fish. Rev. Fish. Fish Biol. 2:144–176.

Dive-depth distribution of loggerhead (*Carretta carretta*) and olive ridley (*Lepidochelys olivacea*) sea turtles in the central North Pacific: Might deep longline sets catch fewer turtles?

Jeffrey J. Polovina

Honolulu Laboratory
Southwest Fisheries Science Center
National Marine Fisheries Service, NOAA
2570 Dole Street
Honolulu, Hawaii 96822-2396
E-mail address: Jeffrey.Polovina@noaa.gov

Evan Howell

Denise M. Parker

Joint Institute for Marine and Atmospheric Research
University of Hawaii
1000 Pope Road
Honolulu, Hawaii 96822

George H. Balazs

Honolulu Laboratory
Southwest Fisheries Science Center
National Marine Fisheries Service, NOAA
2570 Dole Street
Honolulu, Hawaii 96822-2396

The Hawaii-based longline fishery operates over a large area in the central North Pacific, from the equator to latitude 45°N, between longitudes 130°W and 180°W. In 2000, 125 vessels were active in the fishery, producing total landings estimated at 24 million pounds and exvessel (wholesale) revenues of $50 million. The target species include bigeye tuna (*Thunnus obesus*), yellowfin tuna (*T. albacares*), and albacore tuna (*T. alalunga*), and swordfish (*Xiphias gladius*).

Caught incidentally with these target species are leatherback (*Dermochelys coriacea*), loggerhead (*Carretta carretta*), olive ridley (*Lepidochelys olivacea*), and green (*Chelonia mydas*) sea turtles.

Over the period 1994–99, it was estimated that an annual average of 418 loggerhead, 112 leatherback, 146 olive ridley, and 40 green sea turtles were caught in the Hawaii-based longline fishery (McCracken[1]).

Historically, the Hawaii longline fishery has set longlines considerably shallower than 100 m to target swordfish (*Xiphias gladius*) or substantially deeper than 100 m to target bigeye tuna. Incidental hookings of loggerhead turtles have been reported in the Hawaii longline fishery observer data, which cover about 5% of the total annual effort. Analyses of these data found that loggerhead turtles were caught only when gear was set shallow enough to target swordfish, primarily in the northern portion of the fishing ground. No loggerhead sea turtles were caught when longline gear was set deep to target bigeye tuna, primarily in the southern portion of the fishing ground. These analyses suggest that a ban of shallow sets in the fishery since 1 April 2001 may reduce future incidental catches of loggerhead sea turtles. However, analyses based only on observer data suffer from the limited observer coverage and the dependence between depth of setting and area fished. For example, swordfish are targeted at night in the north, whereas tuna are targeted during the day in the south. To better understand the depths inhabited by sea turtles, we used diving depth distributions collected from satellite-linked dive recorders attached to two loggerhead and two olive ridley sea turtles caught and released in the Hawaii-based longline fishery. Although other studies on the dive depths of olive ridley and loggerhead sea turtles have been conducted in the Pacific, these have been conducted with sea turtles in coastal areas rather than in the oceanic central Pacific (Sakamoto et al., 1993; Beavers and Cassano, 1996).

Materials and methods

We attached Wildlife Computer Argos satellite-linked depth recorders (SDR-T10) to two loggerhead and two olive ridley sea turtles that had been caught with commercial longline fishing gear. One loggerhead and one olive ridley were hooked in the mouth and were released after the hook and line had been removed. The other loggerhead and olive ridley sea turtle had deeply ingested hooks, and for both of these turtles the fishing line was cut close to the mouth but the hook was not removed. Trained observers on the fishing vessel attached transmitters to the carapace of each of the four sea turtles, using fiberglass cloth strips and polyester resin patterned after the method presented in Balazs et al. (1996). The observers noted that all four sea turtles swam vigorously away after release.

[1] McCracken, M. L. 2000. Estimation of sea turtle take and mortality in the Hawaiian longline fisheries. Southwest Fish. Sci. Cent. Admin. Rep. H-00-06. 29 p. Southwest Fish. Sci. Cent., Honolulu Lab., Natl. Mar. Fish. Serv., NOAA, Honolulu, HI 96822-2396.

Manuscript accepted 20 September 2002.
Fish. Bull. 101 (1):189–193 (2003).

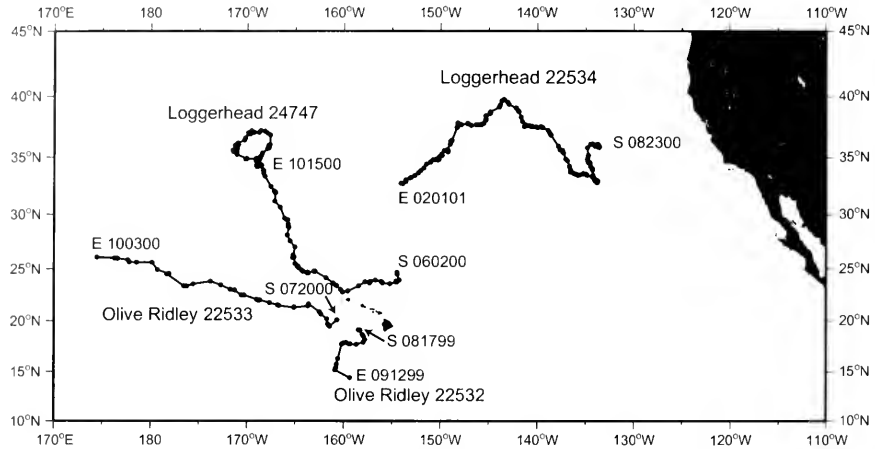

Figure 1

The start (S) and end (E) dates and track lines for the four turtles with satellite-linked dive recorders.

Data on daily location of the turtles were estimated from the signals received by the Argos receiver on a NOAA satellite. The position data were edited, and only the single most accurate daily position was plotted. The accuracy of each position was estimated by Argos as a function of the number and configuration of satellites and the number of transmissions received. Data on the dive behavior transmitted by the Argos receiver were not individual dive profiles but rather frequency distributions of time at depth, dive duration, and maximum dive depth, aggregated over four 6-hour periods and binned in specific depth or time intervals. The lower range of the depth bins (in meters) for the time-at-depth distributions were 1, 3, 5, 10, 15, 25, 35, 50, 60, 75, 100, 125, 150, 150+. Each time the turtle descended below 2 m, it was recorded as a dive. The lower range of the depth bins (in meters) for the dive-depth distributions were 5, 10, 15, 20, 25, 30, 40, 50, 60, 70, 80, 100, 150, 150+. The 6-hour periods over which the time-at-depth and dive-depth data were pooled were programed in Hawaii standard time as 2100–0300, 0300–0900, 0900–1500, and 1500–2100 h. One period was night, another mid-day; one included dawn, the other dusk. Mean time-at-depth and dive-depth distributions for each turtle in each of the four time periods were computed as the average of all frequency distributions for each 6-hour period. Mean time-at-depth and dive-depth distribution for the combined four time periods for each species were computed as the average of the four mean time-at-depth and dive depth distributions for each turtle, then averaged by species.

Finally, after every 20 transmissions a special status message that contained technical data about the operation of the transmitter and the maximum dive depth of that day was transmitted. Both the loggerhead and the olive ridley sea turtles made some dives below 150 m; however, the histogram data did not indicate how much deeper than 150 m these animals dived. The maximum dives sent in the status messages were used to obtain some data on the deep dives.

Results

The positions of the four turtles showed that the turtles were occupying the characteristic habitats for each species: the loggerhead sea turtles were found in the northern portion of the subtropical gyre, and the olive ridley sea turtles were found farther south, well within the center of the subtropical gyre (Fig. 1). Loggerhead no. 24747, which was released with the hook removed, measured 83 cm (straight carapace length (SCL)) and transmitted data for 5.4 months. Loggerhead no. 22534, released with the hook deeply ingested, measured 61 cm SCL and transmitted data for 5.2 months. Olive ridley no. 22533, released with the hook deeply ingested, measured 57 cm SCL and transmitted data for 3.4 months. Olive ridley no. 22532, which was released after a hook was removed, measured 58 cm SCL and transmitted data for 0.8 months.

The time-at-depth frequency distributions for day and night periods for each of the sea turtles showed consistent diurnal and species differences in their dive-depth distributions (Fig. 2). The turtles spent more time at the surface during the day than at night and also dived deeper during the day (Fig. 2). We do not show the dive-depth distribution for the dawn and dusk periods, but these frequency distributions fell between the distribution for day and night periods.

Because it can often take as long as 20 hours to completely set and retrieve a longline, we examined time-at-

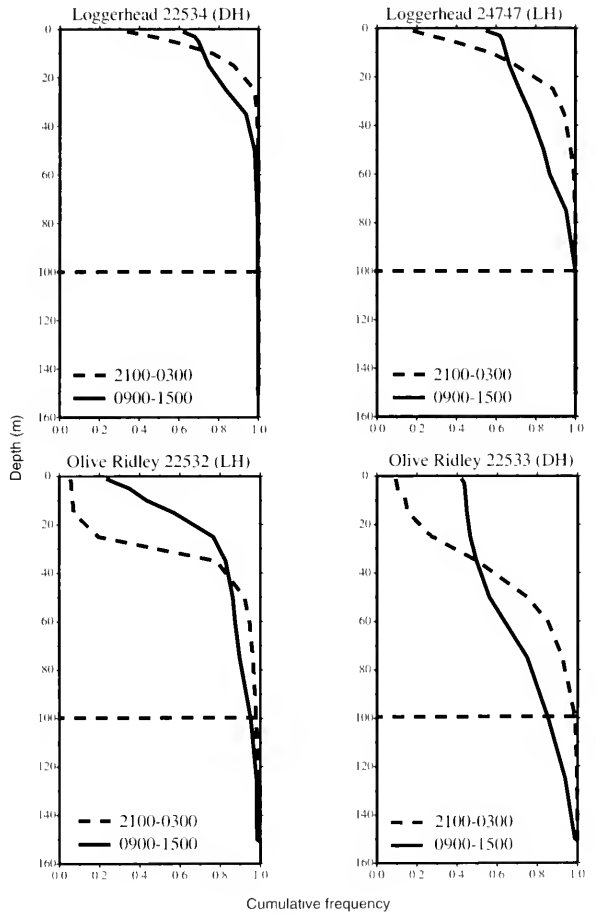

Figure 2

Time-at-depth cumulative frequency distributions for day (0900–1500 h) and night (2100–0300 h) periods for each of the four turtles. The 100 m reference depth is noted with a dashed line. DH indicates that the turtle was released with the hook deeply ingested, LH indicates that the turtle was lightly hooked and released with the hook removed.

depth and dive-depth distributions pooled over the four 6-hour time periods by species. The time-at-depth frequency distribution showed that the loggerhead sea turtles spent about 40% of their time in the top meter and virtually all their time shallower than 100 m (Fig. 3). We also examined the frequency distribution of the maximum depth of each dive and the deepest dive in a 24-hour period. The cumulative distribution of maximum depth of each dive indicated that most dives were very shallow: 70% of the dives were no deeper than 5 m (Fig. 3). The cumulative distribution of the maximum dive depth achieved over a 24-hour period indicated that for approximately 5% of the days, a dive exceeded 100 m (Fig. 3). Status messages reported that the deepest daily dive recorded was 178 m.

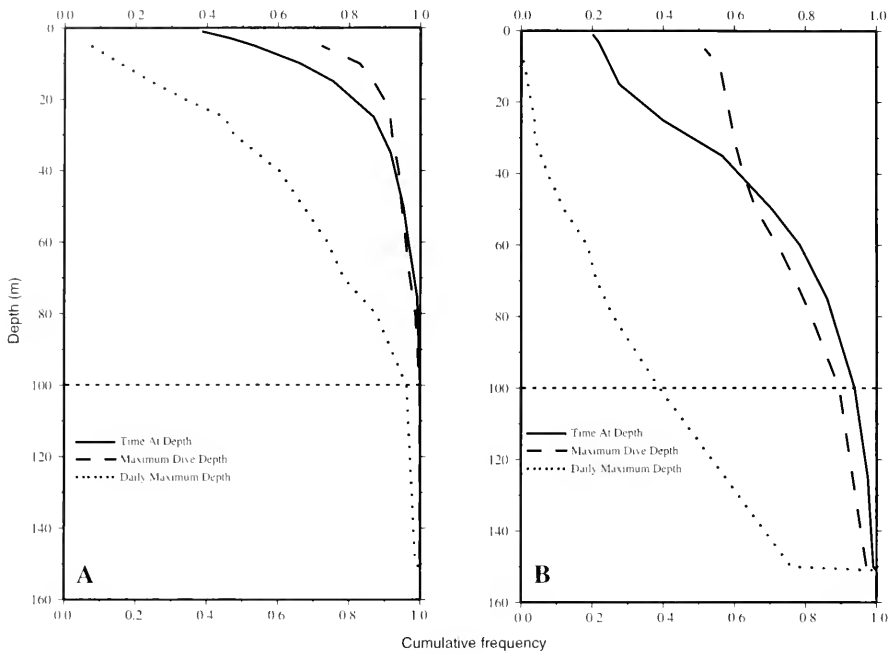

Figure 3

The time-at-depth, maximum dive depth, and daily maximum dive-depth cumulative frequency distributions for all periods combined: (**A**) the two loggerhead sea turtles combined; (**B**) the two olive ridley sea turtles combined.

By comparison, the time-at-depth and maximum depth-frequency distributions of the two olive ridley sea turtles showed considerably deeper depth distribution (Fig. 3). These sea turtles spent only about 20% of their time in the top meter and about 10% of their time deeper than 100 m (Fig. 3). Their daily maximum depth exceeded 150 m at least once in 20% of the days (Fig. 3). Status messages reported that daily dives of 200 m occurred—one dive recorded at 254 m.

Discussion

The loggerhead dive-depth distributions indicated that these animals tended to remain at shallower depths than that of 100 m. If shallow longline sets were replaced with deep longline sets, the incidental takes of loggerhead sea turtles should be reduced substantially. Further, even though olive ridley sea turtles dived deeper than loggerhead sea turtles, only about 10% of their time was spent deeper than 100 m. Therefore, their incidental catches should also be substantially reduced with the elimination of shallow longline sets. However, when deep sets are being made or retrieved or when current shear prevents the gear from sinking to its expected depth, hooks will be present in relatively shallow depths and could result in incidental catches of turtles.

Results to date in the fishery confirm the reduction in incidental catches of turtles that can be achieved from the elimination of shallow sets. Beginning in April 2001, shallow sets were prohibited in the Hawaii-based longline fishery. Data from the onboard observers in the longline fleet, which now comprise 20% of the fishing effort, showed that no loggerhead and only two olive ridley sea turtles were caught from April through December 2001.

The relatively shallow dive-depth distribution for loggerhead sea turtles in the central North Pacific is consistent with our understanding of their ecology; they forage and migrate along convergent fronts where they encounter a shallow aggregation of forage (Polovina et al., 2000). Although oceanic loggerhead sea turtles have a shallower dive behavior than that of olive ridley sea turtles, they appear to dive deeper in oceanic habitat than loggerhead sea turtles in coastal habitat. For example, the dive dis-

tribution of two loggerhead sea turtles between nesting periods off Japan indicated that virtually all their dives were shallower than 30 m (Sakamoto et al., 1993). The deeper-dive distribution of olive ridley sea turtles is also consistent with their oceanic habitat, which is south of the loggerhead habitat in the central portion of the subtropical gyre. The oceanography of this region is characterized by a warm surface layer, a deep thermocline depth, and an absence of strong horizontal temperature gradients and physical or biological fronts. It is likely that the deeper diving seen in the olive ridley sea turtles results from foraging at depths associated with the deep scattering layer.

Acknowledgments

We wish to acknowledge the NMFS observers who attached the transmitters to the turtles; we also wish to thank Shawn K. K. Murakawa and Shandell Eames who assisted in observer training and logistics.

Literature cited

Balazs, G. H., R. K. Miya, and S. C. Beavers.
1996. Procedures to attach a satellite transmitter to the carapace of an adult green turtle (*Chelonia mydas*). *In* Proc. 15th annual symposium on sea turtle biology and conservation (J. A. Keinath, D. E. Bernard, J. A. Mubick, J. A., and B. A. Bell, comps.), p. 21–26. U.S. Dep. of Commer., NOAA Tech. Memo. NMFS/SWFSC-37.

Beavers, S. C., and E. R. Cassano.
1996. Movement and dive behavior of a male sea turtle (*Lepidochelys olivacea*) in the eastern tropical Pacific. J. Herpetol. 30(1):97–104.

Polovina, J. J., D. R. Kobayashi, D. M. Parker, M. P. Seki, and G. H. Balazs.
2000. Turtles on the edge: movement of loggerhead turtles (*Caretta caretta*) along oceanic fronts, spanning fishing grounds in the central North Pacific, 1997–1998. Fish. Oceanogr. 9:71–82.

Sakamoto, W., K. Sato, H. Tanaka, and Y. Naito.
1993. Diving patterns and swimming environment of two loggerhead turtles during internesting. Nippon Suisan Gakkaishi 59(7):1129–1137.

Age-validation of a leopard shark (*Triakis semifasciata*) recaptured after 20 years

Susan E. Smith
Southwest Fisheries Science Center
National Marine Fisheries Service, NOAA
8604 La Jolla Shores Drive
La Jolla, California 92037
E-mail address: susan.smith@noaa.gov

Robert A. Mitchell
26530 Grant Street
St. Clair Shores, Michigan 48081

Dan Fuller
Inter-American Tropical Tuna Commission
8604 La Jolla Shores Drive
La Jolla, California 92037

On 10 July 1999, vertebrae bearing an oxytetracycline (OTC) time mark were retrieved from a tagged leopard shark (*Triakis semifasciata*) recaptured in San Francisco Bay, CA, after being at liberty for almost 20 years. An additional long-term leopard shark tag return was received in June 2001, for which growth information (but not vertebrae) was obtained. The first recapture is significant in that it represents the longest at-liberty period for an age-validated (OTC-injected) shark, extends and completes age validation for this species, spanning all age classes up to its estimated average maximum age, and provides an example of the persistence of the OTC time mark in an elasmobranch at liberty for almost 20 years. The recaptured leopard shark made in 2001 also provides valuable information on long-term growth from time of release to time of recapture. Findings are documented here so that other researchers are aware that validation is complete for this species, to present pertinent evidence of considerable interannual variability in growth in this species, and to report observations on processing difficulties relating to the ephemeral nature of the 20-yr-old OTC mark.

Earlier results from the tagging study that led to these recaptures were published by Smith (1984), Smith and Abramson (1990), and Kusher et al. (1992). These authors concluded that one pair of vertebral growth bands (one opaque, one translucent) is produced each year in this species for the age classes they examined (up to 17 years). Opaque bands are deposited primarily in late spring and summer (mainly in August in the San Francisco Bay area); translucent bands, presumably representing minimum growth periods, are deposited primarily in late fall and winter (Kusher et al., 1992). Average annual growth of recaptured leopard sharks examined in these studies ranged from 0.0 cm per year to 4.0 cm per yr (mean of 2.14 cm per yr); centra grew proportionately to shark length over all size classes sampled.

The leopard shark occurs from Baja California, Mexico, to Oregon; maximum confirmed size is 180 cm TL (Kato et al., 1967), but fish over 146 cm TL are uncommon off central California (Herald et al., 1960; Kusher et al., 1992). Age and size at which females first reach maturity have been estimated at approximately 13 yr and 110 cm TL, respectively; the gestation period is estimated at 10–12 months; and parturition takes place in spring (April–May peak) in San Francisco Bay (Smith and Abramson 1990; Kusher et al. 1992).

Methods

The recaptured sharks were from a group of 948 leopard sharks tagged and released off Hunters Point (37°44′N lat., 122°21′W long.) in South San Francisco Bay between 26 July and 13 September 1979. All were injected with oxytetracycline hydrochloride (OTC), tagged on the dorsal fin with yellow plastic livestock rototags, and released as described by Smith (1984).

The shark returned in 1999 was caught on 10 July off Oakland Airport in San Francisco Bay by a recreational angler fishing ~8 km east of the original release point. The fish was measured and the vertebrae removed and later frozen. In the laboratory, the vertebrae were sectioned and mounted as described by Smith (1984). Various vertebral section widths (from 0.4 mm to 1.3 mm wide) were tested to determine the best thickness for interpreting narrow band patterns near the centrum edge. The transverse sections were viewed illuminated alternately by ultraviolet UV (365 nm) and transmitted light. Micrographs were taken with a Leica DMLB microscope with a Diagnostic Instruments SPOT CCD (charged coupled device) digital camera coupled through a 0.6× phototube, multiplied by the ocular magnifications of 1, 5, and 10× to obtain a total magnification of 0.6, 3, and 6×. The three magnifications were evaluated for the best possible counting path. The images were then analyzed with Media Cybernetics Image Pro Plus image analysis software (Media Cybernetics, 1998), with which increments were enhanced with an edge-sharpening filter. After the application of the filter the images were evaluated and counts from the OTC mark to the margin were made. An annulus was defined as the distal edge of each translucent band in the corpus calcareum, at the distal edge of each band pair (e.g. Kusher et al. 1992; Branstetter and Stiles 1987 and

Manuscript accepted 19 August 2002.
Fish. Bull. 101:194–198 (2003).

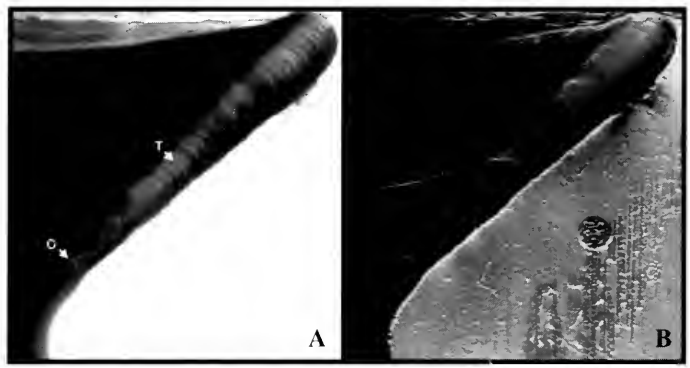

Figure 1

Photomicrographs of a transverse section of a vertebral centrum from a leopard shark (*Triakis semifasciata*) recaptured 10 July 1999 after ~20 years at liberty. (**A**) Transverse section viewed with transmitted white light showing broad dark opaque and narrow light translucent growth zones and ages up to year of tagging; and (**B**) the same section viewed with reflected ultraviolet light showing the OTC mark. 0 = first winter annulus, T = tagging and OTC injection of late summer 1979.

others). The first translucent band was interpreted as the first winter growth after parturition (year 0); the subsequent annulus interpreted as year 1. Band pairs distal to the tetracycline mark were compared with the number of years that the fish had been at liberty. For publication, digital photomicrographs were further enhanced to improve contrast and definition with Jasc Paintshop Pro software (Jasc Software, Inc., 1999).

Growth information for the other tagged fish (male, tag no. 337, recaptured in South San Francisco Bay on 9 June 2001) was obtained by comparing tagging and recapture size. Age and growth information for both recaptured sharks was compared with Kusher et al.'s (1992) von Bertanlanffy growth curves (their Figs. 4, 9, and 10) based on aged vertebrae from 1) fishery and market samples, and 2) earlier recaptures from the same 1979 tagging experiment.

Results

The shark recaptured in July 1999 was a mature female measuring 124 cm TL at recapture. At liberty growth and exact time at liberty could not be calculated because the tag number had worn away, preventing referral back to original tagging length and day. Because the one-time tagging experiment took place 26 July–13 September 1979, the fish had been at liberty from 19.8 to 19.9 years. The tetracycline mark was visible as a thin yellow line in all vertebral sections examined (Fig. 1). In less than a minute, the fluorescence began to decay rapidly, much more rapidly than tetracycline marks observed by the senior author in previous recaptured sharks (sharks at liberty 7 years or less). This fast decay made viewing of actual samples brief; most time was dedicated to setting up and taking digital photomicrographs of the sections.

Twenty annuli up to winter 1998 (including the 1979–80 winter annulus deposited after tagging) were visible distal to the time mark (Fig. 2), including a partially formed opaque band interpreted as the 1998 summer band (Fig. 3). We could not determine with any certainty whether the narrow opaque edge represented the beginning of the summer 1999 band (Fig. 3). On all sections examined, the last band pair at the centrum edge (i.e. the most recently deposited) was very narrow and faint, or incomplete and difficult to differentiate, especially on vertebral sections that were sliced too thick or too thin (best thickness was 0.6 mm). Proximal to the OTC mark were five annuli, indicating that the fish was 4+ yr old at tagging and was probably born in spring of 1974. The fish was aged as 24+ or in its 25th year. Width of the opaque bands indicative of annual summer growth was highly variable, although it generally tended to decrease with increasing age. Greatest relative growth in centrum diameter occurred in the first few years of life, and also in 1985, 1986, and 1987, judging from the width of the corresponding opaque zones (ages 11, 12, and 13). The recapture size (124 cm TL) was 11 cm smaller than that predicted for an age-25 female with the von Bertalanffy growth function (VBGF) generated by Kusher et al. (1992, their Fig. 4) for 162 untagged leopard sharks. But it was close to that predicted by their FISHPARM VBGF generated from band counts and lengths of tag recaptures from this same 1979 experiment (Kusher et al. 1992, their Fig. 10).

The other recaptured leopard shark (a male, no. 337) was caught 9 June 2001 in South San Francisco Bay off

San Mateo, CA, making a total of 120 recaptured leopard sharks from the original 1979 tagging. The tag number was readable and traceable back to the tagging date (23 August 1979) and length (87 cm TL), which was compared with the recapture length (119.4 cm TL) and date. This individual exhibited an average annual growth of only 1.47 cm/yr, but its recapture length for its presumed age (30) was also close to that predicted by the Kusher et al. (1992) asymptotic FISHPARM VBGF for tagged and recaptured leopard sharks.

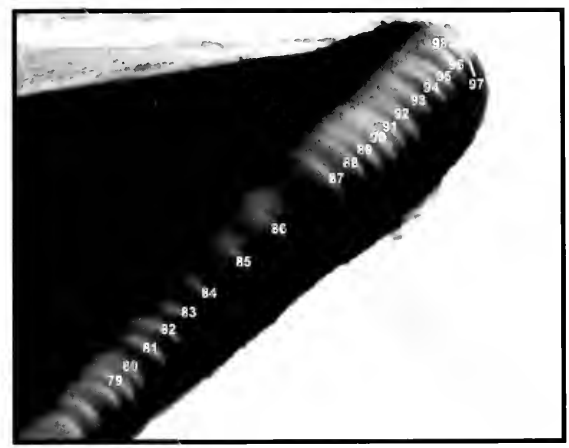

Figure 2

Enlargement of photomicrograph of a transverse vertebral section of a leopard shark (*Triakis semifasciata*) showing years (abbreviated in figure) that correspond to annuli distal to the tetracycline mark at year 1979 on the corpus calcareum.

Discussion

The tagging and recapture of fish whose calcified structures have been marked with the calcium-labeling fluorophor OTC offer a simple and conclusive method for establishing the timing of growth zone formation in these structures. Validating the timing of centrum or spine band formation is especially important for elasmobranchs as a group because, unlike teleosts, the assumption of annual deposition of band pairs has not been confirmed for many species and has been challenged for some. It has been suggested that two band pairs are deposited annually in the basking shark, *Cetorhinus maximus* (Parker and Stott, 1965) and the shortfin mako shark, *Isurus oxyrinchus* (Pratt and Casey, 1983), although validation is still pending for these species. Furthermore, Natanson (1984) and Natanson and Cailliet (1990), working with OTC-injected Pacific angel sharks, *Squatina californica*, found no correlation between centrum band deposition and any temporal cycle and concluded that bands were deposited in response to somatic growth. Nevertheless, elasmobranchs for which the deposition of one band pair per year has been established and validated with OTC (for at least selected size and age classes) include the thornback ray, *Raja clavata*, (Holden and Vince, 1973; Ryland and Ajayi, 1984); *R. microocellata* and *R. montagui* (Ryland and Ajayi, 1984); *Raja erinacea* (Natanson, 1993); *Bathyraja* sp. (Gallagher and Nolan, 1999); lemon shark, *Negaprion brevirostris* (Gruber and Stout, 1983; Brown and Gruber, 1988); spiny dogfish, *Squalus acanthias* (Beamish and McFarlane, 1985; Tucker 1985) leopard shark, *Triakis semifasciata* (Smith, 1984; Kusher et al., 1992); neonate sharpnose, *Rhizoprionodon terraenovae*, and sandbar, *C. plumbeus*, sharks (Branstetter 1987); and bonnethead shark, *Sphyrna tiburo* (Parsons 1993).

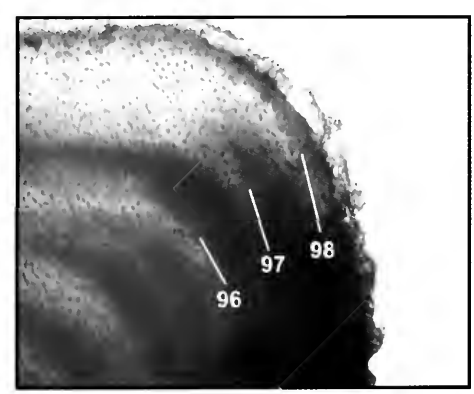

Figure 3

Enlarged view of the edge of the corpus calcareum of a transverse section of a leopard shark (*Triakis semifasciata*) vertebra, showing partially complete annuli at the centrum edge.

By demonstrating the persistence of OTC in the mineralized tissue of a cartilaginous fish at liberty for nearly two decades, our study confirms the long-term effectiveness of this age validation tool. The number of band pairs conformed to the number of years at liberty, although bands near the centrum periphery appeared in some sections to be absent or incompletely formed, even after careful embedding and sectioning. This emphasizes the importance of interpreting bands nearest the growing margin

with extreme care, especially when examining band patterns in older, slow-growing sharks. For these fish, less precise preparation methods (such as examining whole centrum faces) are probably inadequate for interpreting narrow growth bands that form later in life. Additionally, in species like the leopard shark, the most recently deposited band pair may only become clearly defined or fully differentiated as new tissue after the accretion of subsequent bands. Thus, although most band pairs seem to be relatively well defined in this species (even in older specimens such as this one), the peripheral bands can be indistinct or incomplete. Beamish and McFarlane (2000), who recently reported on a sablefish (*Anoplopoma fimbria*) recaptured up to 20 years after being injected with OTC, also warned that the aging structures of long-lived fish require very careful preparation and interpretation.

In the vertebrae of the 1999 recaptured leopard shark, substantial centrum growth occurred in the late 1980s, e.g. the width of the 1987 growth zone (at 13 yr old) was over twice that of annual growth zones adjacent to it. We cannot explain why this period may have been so favorable for this shark over previous and subsequent years, but it does suggest that this species is capable of great interannual variability in growth, even at a relatively advanced age. Lenarz et al. (1995) described mild El Niño conditions off central California in 1987–88, although temperatures were less elevated than during other El Niño events, and only short periods of unusually high sea-level anomalies were observed. Moser et al. (2002) classified 1985–87 as a "normal" oceanographic period off California, between the warm 1982–83 El Niño episode and a cool-water 1988 La Niña episode.

OTC fluorescence is known to fade with exposure to UV light; therefore samples are traditionally stored in darkness and processed in dim light (Weber and Ridgeway 1962). The OTC mark in the leopard shark at liberty for 20 years was especially light-sensitive, disappearing after a few minutes exposure, much more quickly than tetracycline marks observed previously by one of the authors in earlier recaptures from this study. This may be due to diminishment of the phosphorescent properties of the chemical, combined with compression of the mark within the cartilage matrix over time. Therefore, when working with cartilaginous fishes (especially those at liberty for many years), it may be extremely important to obtain as many vertebrae as possible, to keep OTC-labeled centra away from light, to preplan microscope viewing sessions carefully, and to process and photograph samples quickly.

Previous studies have validated annual periodicity in leopard sharks up through age 17 (Smith 1984; Kusher et al. 1992). Beamish and McFarlane (1983) pointed out that band periodicity must be established for a full range of age classes to fully meet the requirement of age validation in fishes. This requirement is seldom met and has not yet been achieved for any elasmobranch. The OTC-labeled fish recaptured in 1999 measured 2 cm longer but was 8 years older than the oldest age-validated leopard shark of Kusher et al. (1992). This latter fish, also a female, measured 122 cm TL and was estimated to be 17 yr of age. It had been at liberty for 7.3 years—the longest duration recorded in that study. Results of the present study extend age validation for this species to fish at liberty for up to 19+ years, up to 124 cm TL, and up to 25 yr old. Longevity of this species has been estimated at 25–30 years (Smith, 1984); thus full validation for this species spanning ages 0 through 25 is now complete.

Acknowledgments

We thank David Au, John Butler, Sandy McFarlane, and anonymous reviewers for helpful comments on drafts of this manuscript. We are also grateful to the anglers who recaptured and returned to us the vertebrae of the fish recaptured in 1999 (Jeff King of Fairfield, California, and Howard Arnold, a cooperating volunteer for the California Department of Fish and Game Shark Tagging Program), and to Bretta Larson (Romberg Tiburon Center, SFSU) and Bay Van To for return of tag recapture no. 337.

Literature cited

Beamish, R. J., and G. A. McFarlane.
1983. The forgotten requirement for age validation in fisheries biology. Trans. Am. Fish. Soc. 112:735–743.
1985. Annulus development on the dorsal spine of the spiny dogfish (*Squalus acanthias*) and its validity for age determination. Can. J. Fish. Aquat. Sci. 42:1799–1805.
2000. Reevaluation of the interpretation of annuli from otoliths of a long-lived fish, *Anoplopoma fimbria*. Fish. Res. 46 (2000):105–111.

Branstetter, S.
1987. Age and growth validation of newborn sharks held in laboratory aquaria, with comments on the life history of the Atlantic sharpnose shark, *Rhizoprionodon terraenovae*. Copeia 1987(2):291–300.

Branstetter, S., and R. Stiles.
1987. Age and growth of the bull shark, *Carcharhinus leucas*, from the northern Gulf of Mexico. Environ. Biol. Fishes 20: 169–181.

Brown, C. A., and S. H. Gruber.
1988. Age assessment of the lemon shark, *Negaprion brevirostris*, using tetracycline validated vertebral centra. Copeia 3:747–753.

Gallagher, M., and C. P. Nolan.
1999. A novel method for the estimation of age and growth in rajids using caudal thorns. Can. J. Fish. Aquat. Sci. 56(9):1590–1599.

Gruber, S. H., and R. G. Stout.
1983. Biological materials for the study of age and growth in a tropical marine elasmobranch, the lemon shark, *Negaprion brevirostris* (Poey). U.S. Dep. Commer., NOAA Tech. Rep. NMFS 8, p. 193–205.

Herald, E. S., W. S. Schneebeli, N. Green, and K. Innes.
1960. Catch records for seventeen shark derbies held at Elkhorn Slough, Monterey, California. Calif. Fish. Game 46(1):59–67.

Holden, M. J., and M. R. Vince.
1973. Age validation studies on the centra of *Raja clavata* using tetracycline. J. Cons. Int. Explor. Mer 35(1):13–17.

Jasc Software, Inc.
1999. Jasc Paint Shop Pro version 5.03. Jasc Software, Inc., Eden Prarie, MN.

Kato, S., S. Springer, and M. Wagner
1967. Field guide to eastern Pacific and Hawaiian sharks. U.S. Fish Wildl. Serv., Circ. 271, 47 p.
Kusher, D. I., S. E. Smith and G. M. Cailliet.
1992. Validated age and growth of the leopard shark, *Triakis semifasciata*, with comments on reproduction. Environ. Biol. Fishes 35(2):187–203.
Lenarz, W. H., F.B. Schwing, D.A. Ventresca, F. Chavez, and W. M. Graham.
1995. Explorations of El Nino events and associated biological population dynamics off central California. CalCOFI (California Cooperative Oceanic and Fisheries Investigations) Rep., vol. 36, p. 106–119.
Media Cybernetics, Inc.
1998. Image-Pro Plus software version 4.0. Media Cybernetics, Silver Spring, MD.
Moser, H. G., R. L. Charter, P. E. Smith, D. A. Ambrose, W. Watson, S. R. Charter, and E. M. Sandknop.
2002. Distributional atlas of fish larvae and eggs from Manta (surface) samples collected from CalCOFI surveys from 1977 to 2000. CalCOFI Atlas 35, 97 p.
Natanson, L. J.
1984. Aspects of the age, growth and reproduction of the Pacific angel shark, *Squatina californica*, off Santa Barbara, California. M.S. thesis, 71 p. San Jose State University, San Jose, CA.
1993. Effect of temperature on band deposition in the little skate, *Raja erinacea*. Copeia 1993(1):199–206.
Natanson, L. J., and G. M. Cailliet.
1990. Vertebral growth zone deposition in Pacific angel sharks. Copeia 1990:1133–1145.
Parker, H. W., and F. C. Stott.
1965. Age, size and vertebral calcification in the basking shark, *Cetorhinus maximus* (Gunnerus). Zool. Meded. 40 (34):305–319.
Parsons, G. R.
1993. Age determination and growth of the bonnethead shark *Sphyrna tiburo*: a comparison of two populations. Mar. Biol. 117(1):23–31.
Pratt, H. L., Jr., and J. G. Casey.
1983. Age and growth of the shortfin mako, *Isurus oxyrinchus*, using four methods. Can. J. Fish. Aquat. Sci. 40:1944–1957.
Ryland, J. S., and T. O. Ajayi.
1984. Growth and population dynamics of three Raja species (Batoidei) in Carmarthen Bay, British Isles. J. Cons. Int. Explor. Mer 41:111–120.
Smith, S. E.
1984. Timing of vertebral band deposition in tetracycline-injected leopard sharks. Trans. Am. Fish. Soc. 113 (3):308–313.
Smith, S. E., and N. J. Abramson.
1990. Leopard shark (*Triakis semifasciata*) distribution, mortality rate, yield, and stock replenishment estimates based on a tagging study in San Francisco Bay. Fish. Bull. 88:371–381.
Tucker, R.
1985. Age validation studies on the spines of the spurdog (*Squalus acanthias*) using tetracycline. J. Mar. Biol. Assoc. U.K. 65:641–651.
Weber, D. D., and G. J. Ridgeway.
1962. The deposition of tetracycline drugs in bones and scales of fish and its possible use for marking. Progressive Fish-Culturist 24:150–155.

Superintendent of Documents **Publications** Order Form

*5178

☐ YES, please send me the following publications:

____ Subscriptions to *Fishery Bulletin*
for $55.00 per year ($68.75 foreign)

The total cost of my order is $ _____ . Prices include regular domestic postage and handling and are subject to change.

_____
(Company or Personal Name) (Please type or print)

_____
(Additional address/attention line)

_____
(Street address)

_____
(City, State, ZIP Code)

_____
(Daytime phone including area code)

_____
(Purchase Order No.)

Charge your order. IT'S EASY!

VISA

MasterCard

Please Choose Method of Payment:

☐ Check Payable to the Superintendent of Documents

☐ GPO Deposit Account ☐☐☐☐☐☐☐–☐

☐ VISA or MasterCard Account

☐☐☐☐☐☐☐☐☐☐☐☐☐☐☐☐

☐☐☐☐ (Credit card expiration date)

To fax your orders (202) 512-2250

_____
(Authorizing Signature)

Mail To: Superintendent of Documents
P.O. Box 371954, Pittsburgh, PA 15250-7954

Thank you for your order!

Fishery Bulletin

Guidelines for contributors

Content of papers

Articles

Articles are reports of 10 to 30 pages (double spaced) that describe original research in one or a combination of the following fields of marine science: taxonomy, biology, genetics, mathematics (including modeling), statistics, engineering, economics, and ecology.

Notes

Notes are reports of 5 to 10 pages without an abstract that describe methods and results not supported by a large body of data. Although all contributions are subject to peer review, responsibility for the contents of articles and notes rests upon the authors and not upon the editor or the publisher. It is therefore important that authors consider the contents of their manuscripts carefully. Submission of an article is understood to imply that the article is original and is not being considered for publication elsewhere. Manuscripts must be written in English. Authors whose native language is not English are strongly advised to have their manuscripts checked for fluency by English-speaking colleagues prior to submission.

Preparation of papers

Text

Title page should include authors' full names and mailing addresses (street address required) and the senior author's telephone, fax number, e-mail address, as well as a list of key words to describe the contents of the manuscript. **Abstract** must be less than one typed page (double spaced) and must not contain any citations. It should state the main scope of the research but emphasize the author's conclusions and relevant findings. Because abstracts are circulated by abstracting agencies, it is important that they represent the research clearly and concisely. **General text** must be typed in double-spaced format. A brief introduction should state the broad significance of the paper; the remainder of the paper should be divided into the following sections: Materials and methods, Results, Discussion (or Conclusions), and Acknowledgments. Headings within each section must be short, reflect a logical sequence, and follow the rules of multiple subdivision (i.e. there can be no subdivision without at least two subheadings). The entire text should be intelligible to interdisciplinary readers; therefore, all acronyms and abbreviations should be written out and all lesser-known technical terms should be defined the first time they are mentioned. The scientific names of species must be written out the first time they are mentioned; subsequent mention of scientific names may be abbreviated. Follow *Scientific style and format: CBE manual for authors, editors, and publishers* (6th ed.) for editorial style and the most current issue of the *American Fisheries Society's common and scientific names of fishes from the United States and Canada* for fish nomenclature. Dates should be written as follows: 11 November 1991. Measurements should be expressed in metric units, e.g. metric tons (t). The numeral one (1) should be typed as a one, not as a lower-case el (l).

Footnotes

Use footnotes to add editorial comments regarding claims made in the text and to document unpublished works or works with local circulation. Footnotes should be numbered with Arabic numerals and inserted in 10-point font at the bottom of the first page on which they are cited. Footnotes should be formatted in the same manner as citations. If a manuscript is unpublished, in the process of review, or if the information provided in the footnote has been conveyed verbally, please state this information as "unpubl. data," "manuscript in review," and "personal commun.," respectively. Authors are advised wherever possible to avoid references to nonstandard literature (unpublished literature that is difficult to obtain, such as internal reports, processed reports, administrative reports, ICES council minutes, IWC minutes or working papers, any "research" or "working" documents, laboratory reports, contract reports, and manuscripts in review). If these references are used, please indicate whether they are available from NTIS (National Technical Information Service) or from some other public depository. Footnote format: author (last name, followed by first-name initials); year; title of report or manuscript; type of report and its administrative or serial number; name and address of agency or institution where the report is filed.

Literature cited

The literature cited section comprises works that have been published and those accepted for publication (works in press) in peer-reviewed journals and books. Follow the name and year system for citation format. In the text, write "Smith and Jones (1977) reported" but if the citation takes the form of parenthetical matter, write "(Smith and Jones, 1977)." In the literature cited section, list citations alphabetically by last name of senior author: For example, Alston, 1952; Mannly, 1988; Smith, 1932; Smith, 1947; Stalinsky and Jones, 1985. Abbreviations of journals should conform to the abbreviations given in the *Serial sources for the BIOSIS previews database*. Authors are responsible for the accuracy and completeness of all citations. Literature citation format: author (last name, followed by first-name initials); year; title of report or article; abbreviated title of the journal in which the article was published, volume number, page numbers. For books, please provide publisher, city, and state.

Tables

Tables should not be excessive in size and must be cited in numerical order in the text. Headings in tables should be short but ample enough to allow the table to be intelligible on its own. All unusual symbols must be explained in the table legend. Other incidental comments may be footnoted (use italic arabic numerals for footnote markers). Use asterisks only to indicate probability in statistical data. Place table legends on the same page as the table data. We accept tables saved in most spreadsheet software programs (e.g. Microsoft Excel). Please note the following:

- Use a comma in numbers of five digits or more (e.g. 13,000 but 3000).
- Use zeros before all decimal points for values less than one (e.g. 0.31).

Figures

Figures include line illustrations, computer-generated line graphs, and photographs (or slides). They must be cited in numerical order in the text. Line illustrations are best submitted as original drawings. Computer-generated line graphs should be printed on laser-quality paper. Photographs should be submitted on glossy paper with good contrast. All figures are to be labeled with senior author's name and the number of the figure (e.g. Smith, Fig. 4). Use Helvetica or Arial font to label anatomical parts (line drawings) or variables (graphs) within figures; use Times Roman bold font to label the different sections of a figure (e.g. **A**, **B**, **C**). Figure legends should explain all symbols and abbreviations seen within the figure and should be typed in double-spaced format on a separate page at the end of the manuscript. We advise authors to peruse a recent issue of *Fishery Bulletin* for standard formats. Please note the following:

- Capitalize the first letter of the first word of axis labels.
- Do not use overly large font sizes to label axes or parts within figures.
- Do not use boldface fonts within figures.
- Do not create outline rules around graphs.
- Do not use horizontal lines through graphs.
- Do not use large font sizes to label degrees of longitude and latitude on maps.
- Indicate direction of degrees longitude and latitude on maps (e.g. 170°E).
- Avoid placing labels on a vertical plane (except on y axis).
- Avoid odd (nonstandard) patterns to mark sections of bar graphs and pie charts.

Copyright law

Fishery Bulletin, a U.S. government publication, is not subject to copyright law. If an author wishes to reproduce any part of *Fishery Bulletin* in his or her work, he or she is obliged, however, to acknowledge the source of the extracted literature.

Submission of papers

Send four printed copies (one original plus three copies)—clipped, *not stapled*—to the Scientific Editor, at the address shown below. Send photocopies of figures with initial submission of manuscript. Original figures will be requested later when the manuscript has been accepted for publication. Do not send your manuscript on diskette until requested to do so.

Dr. Norman Bartoo
National Marine Fisheries Service, NOAA
8604 La Jolla Shores Drive
La Jolla, CA 92037

Once the manuscript has been accepted for publication, you will be asked to submit a software copy of your manuscript. The software copy should be submitted in WordPerfect or Word format (in Word, save as Rich Text Format). Please note that we do not accept ASCII text files.

Reprints

Copies of published articles and notes are available free of charge to the senior author (50 copies) and to his or her laboratory (50 copies). Additional copies may be purchased in lots of 100 when the author receives page proofs.

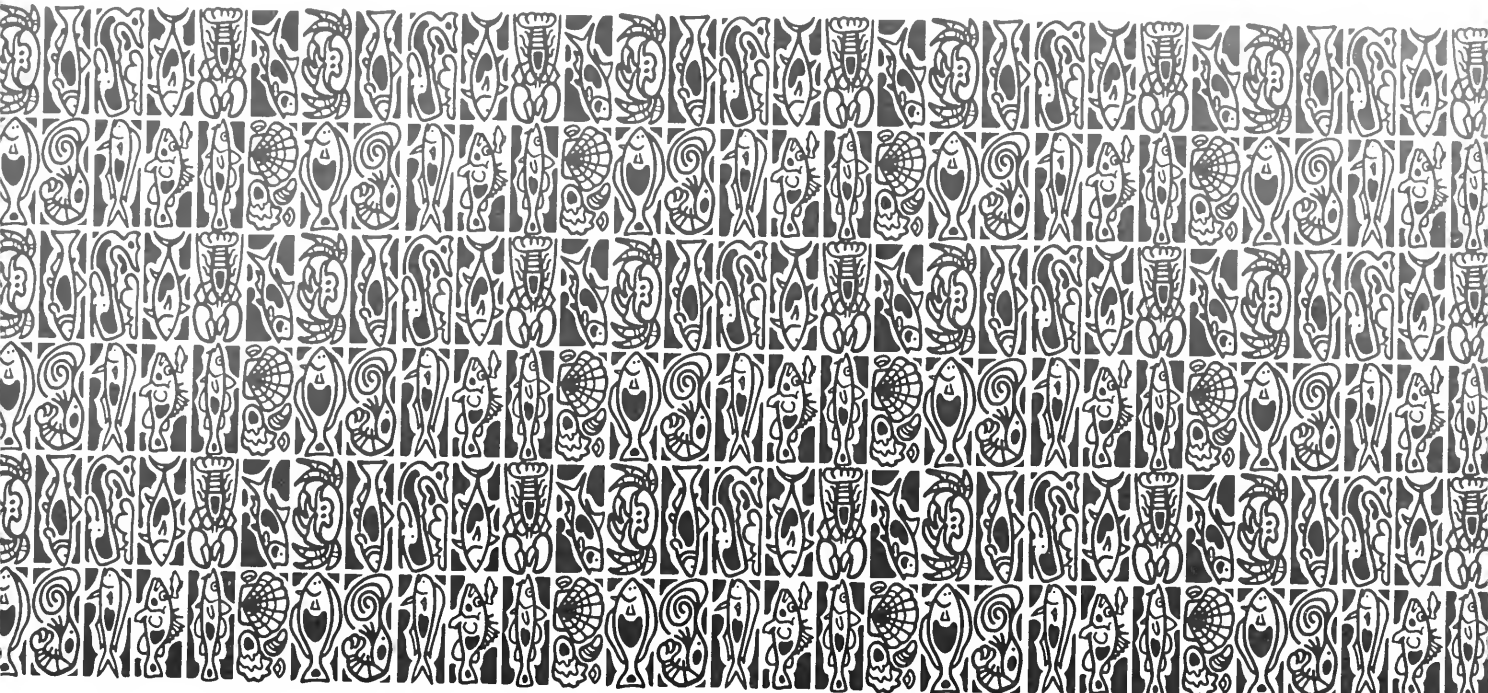

U.S. Department
of Commerce

Volume 101
Number 2
April 2003

Fishery Bulletin

The *Fishery Bulletin* (ISSN 0090-0656) is published quarterly by the Scientific Publications Office, National Marine Fisheries Service, NOAA, 7600 Sand Point Way NE, BIN C15700, Seattle, WA 98115-0070. Periodicals postage is paid at Seattle, WA, and at additional mailing offices. POSTMASTER: Send address changes for subscriptions to Fishery Bulletin, Superintendent of Documents, Attn.: Chief, Mail List Branch, Mail Stop SSOM, Washington, DC 20402-9373

The Secretary of Commerce has determined that the publication of this periodical is necessary according to law for the transaction of public business of this Department. Use of funds for printing of this periodical has been approved by the Director of the Office of Management and Budget.

For sale by the Superintendent of Documents, U.S. Government Printing Office, Washington, DC 20402. Subscription price per year $45.00 domestic and $56.25 foreign. Cost per single issue $28.00 domestic and $35.00 foreign. **See back for order form.**

Fishery Bulletin

***Fishery Bulletin* web site: fishbull.noaa.gov**

The *Fishery Bulletin* carries original research reports and technical notes on investigations in fishery science, engineering, and economics. It began as the Bulletin of the United States Fish Commission in 1881, it became the Bulletin of the Bureau of Fisheries in 1904 and the *Fishery Bulletin* of the Fish and Wildlife Service in 1941. Separates were issued as documents through volume 46; the last document was No. 1103. Beginning with volume 47 in 1931 and continuing through volume 62 in 1963, each separate appeared as a numbered bulletin. A new system began in 1963 with volume 63 in which papers are bound together in a single issue of the bulletin. Beginning with volume 70, number 1, January 1972, the *Fishery Bulletin* became a periodical, issued quarterly. In this form, it is available by subscription from the Superintendent of Documents, U.S. Government Printing Office, Washington, DC 20402. It is also available free in limited numbers to libraries, research institutions, State and Federal agencies, and in exchange for other scientific publications.

U.S. Department of Commerce
Seattle, Washington

Volume 101
Number 2
April 2003

Fishery Bulletin

Contents

Use of ocean and estuarine habitats by young-of-year bluefish (*Pomatomus saltatrix*) in the New York Bight*

Kenneth W. Able
Peter Rowe
Marine Field Station
Institute of Marine and Coastal Sciences
Rutgers University
800 c/o 132 Great Bay Blvd.
Tuckerton, New Jersey 08087-2004
E-mail address (for K. W. Able): able@imcs.rutgers.edu

Mark Burlas
U.S. Army Corps of Engineers
Project Biological Monitoring Program, CENAN-PL-EA
26 Federal Plaza
New York, New York 10278-0090

Don Byrne
New Jersey Department of Environmental Protection
Nacote Creek Research Station
P.O. Box 418
Port Republic, New Jersey 08241

Abstract—Young-of-year (YOY) bluefish (*Pomatomus saltatrix*) along the U.S. east coast are often assumed to use estuaries almost exclusively during the summer. Here we present data from 1995 to 1998 indicating that YOY (30–260 mm FL) also use ocean habitats along the coast of New Jersey. An analysis of historical and recent data on northern and southern ocean beaches (0.1–2 m) and the inner continental shelf (5–27 m) during extensive sampling in New Jersey waters from 1995 to 1998 indicated that multiple cohorts occurred (June–August) in every year. When comparable collections of YOY were made in the ocean and in an adjacent estuary, the abundance was 1–2 orders of magnitude greater on ocean beaches during the summer. The YOY were even more abundant in ocean habitats in the fall (September–October), presumably as a result of YOY leaving estuaries to join the coastal migration south. During 1999 and 2000, YOY bluefish were tagged with internal sequential coded wire microtags in order to refine our understanding of habitat use and movement. Few (0.04%) of the fish tagged on ocean beaches were recaptured; however, 2.2% of the fish tagged in the estuary were recaptured from 2 to 27 days after tagging. Recaptured fish grew quickly (average 1.37 mm FL/d). On ocean beaches YOY fed on a variety of invertebrates and fishes but their diet changed with size. By approximately 80–100 mm FL, they were piscivorous and fed primarily on engraulids, a pattern similar to that reported in estuaries. Based on distribution, abundance, and feeding, both spring- and summer-spawned cohorts of YOY bluefish commonly use ocean habitats. Therefore, attempts to determine factors affecting recruitment success based solely on estuarine sampling may be inadequate and further examination, especially of the contribution of the summer-spawned cohort in ocean habitats, appears warranted.

Manuscript accepted 3 September 2002.
Manuscript received 31 December 2002 at NMFS Scientific Publications Office.
Fish. Bull. 101:201–214 (2003).

Bluefish (*Pomatomus saltatrix*) are an important component of recreational, and to a lesser degree, commercial fisheries along the east coast of the U.S. Catches of this species peaked in the late 1970s and early 1980s and have declined consistently since then (Klein-MacPhee, 2002). As a result, the Atlantic States Marine Fisheries Commission has established priority research needs for this species, including studies of recruitment (Kline[1]).

The available literature indicates that there are multiple cohorts of young-of-year (YOY) bluefish, which result from spring spawning in the South Atlantic Bight (south of Cape Hatteras) and summer spawning in the Middle Atlantic Bight (between Cape Hatteras and Cape Cod), but their relative contribution is variable and still under discussion (see review by Juanes et al., 1996; McBride et al., 1993; Smith et al., 1994; Hare and Cowen, 1996; Able and Fahay, 1998; Munch and Conover, 2000). The YOY are assumed to be estuarine-dependent (McHugh, 1966) and a worldwide review also indicates that estuaries are important for this widely distributed species (Juanes et al., 1996) although little is known of their movements within estuaries and between estuaries and the adjacent ocean (Lund and Maltezas, 1970; Morton et al., 1993). Along the east coast of the U.S., numerous studies have demonstrated that YOY of spring- and summer-spawned cohorts use estuaries as habitat, including those from Rhode Island (McBride et al., 1995), Long Island (Nyman and Conover, 1988; McBride and Conover, 1991), New Jersey (McBride and Conover, 1991; Rountree and Able, 1992a, 1992b, 1993; Able and Fahay, 1998), and North Carolina and South Carolina (McBride et al., 1993), and that size at estuarine ingress is at approximately 40–100 mm FL. However, one of the most comprehensive treatments of

* Contribution 2003-05 of the Rutgers University Institute of Marine and Coastal Sciences, New Brunswick, NJ 08901.

[1] Kline, L. L. 1997. Atlantic State Marine Fisheries Commission prioritized research needs in support of interjurisdictional fisheries management, 189 p. Atlantic States Marine Fisheries Commission, Washington, D.C.

bluefish suggests that those spawned during the summer might remain at sea and never enter estuaries (Kendall and Walford, 1979). Thus, it is useful to assess whether YOY bluefish use ocean habitats. To this end, the purpose of this paper is to summarize data from extensive collections and multiple sources for YOY bluefish along the coast of New Jersey in order to help determine the relative contributions of oceanic habitats by comparing them with an adjacent estuary. Further, we conducted tag and recapture studies to begin to further assess habitat use and movements.

Materials and methods

Study sites

The study area encompassed four distinct regions along the New Jersey coast (Fig. 1). First, the inner continental shelf (5–27 m), from the northern coast of New Jersey to the mouth of Delaware Bay (Fig. 1). Much of this area slopes gently offshore; however, the surface has a complex topography, as evidenced by convoluted isobaths (Uchupi, 1970). At the margins of the study area are two major shelf valleys, Hudson and Delaware. In between are numerous linear sand ridges (McBride and Moslow, 1991). Bottom salinities and temperatures in this region during the study period ranged from 27.1‰ to 33.4‰ and from 7.7° to 25.4°C, respectively. The second region was located in northern New Jersey along a 25-km stretch of ocean beach between Deal and Manasquan Inlet (Fig. 1). These beaches are divided at frequent intervals by groins. The third region consisted of sampling sites located in southern New Jersey on relatively undeveloped (few groins) beaches in the vicinity of Little Egg Inlet and more developed (abundant groins) beaches on the central portion of Long Beach Island (Fig. 1). The sandy beaches in both of these areas are steeply sloping and exposed to high wave energy (wave heights of 0.3–1.2 m and durations of 5–9 seconds and tidal range is approximately 1.4 m, Nordstrom et al., 1977). Salinities on these beaches during the study period were 26–32‰, and temperatures ranged from 13° to 27°C. A fourth region comprised estuarine beach sites in Great Bay and Little Egg Harbor (Fig. 1). These sites had sandy bottoms, a shallow profile with sandy fringing beaches, and a 1.1-m tidal range typical of these bays (Able et al., 1999). Salinities were 22–32‰ and temperatures were 10.5–30°C during the sampling period.

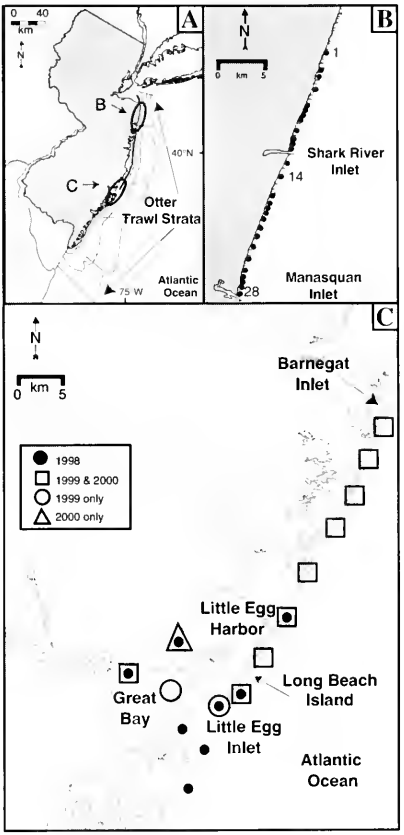

Figure 1

Study area along the Atlantic Ocean coast of New Jersey (**A**). Strata (5–10, 11–20, 21–27 m) for inner continental shelf collections, and location of ocean and estuarine beach sampling sites are indicated, including northern New Jersey ocean beaches (sites numbered 1–28 from north to south) (**B**) and southern New Jersey ocean and estuarine beaches (**C**) for 1998–2000. Additional information concerning these sites can be found in Table 1.

Sampling techniques

Young-of-year bluefish were sampled as part of several programs off the coast of New Jersey during 1995–98 (Fig. 1, Table 1). In all surveys, YOY were defined by characteristic lengths (<200 mm FL) from earlier studies in the region (see Able and Fahay, 1998). Individuals from inner continental shelf waters were collected by the New Jersey Department of Environmental Protection with 20-min duration otter trawl (30-m head rope, 6-mm codend) tows during daylight in stratified random sampling over an area of 4600 km^2 from the entrance to New York Harbor to the entrance of Delaware Bay in depths from 5 to 27 m (Byrne[2]). This sampling occurred seasonally and bluefish were available during the June, August, and October cruises.

[2] Byrne, D. 1994. Stock assessment of New Jersey's nearshore recreational fisheries resources. *In* Proceedings of the workshop on the collection and use of trawl survey data for fisheries management (T. Berger, ed.), p. 36–42. Atlantic States Marine Fisheries Commission, 1444 Eye St. NW, 6th Floor, Washington D.C. 20005.

Table 1

Summary of available data used to evaluate habitat use for young-of-year bluefish. NJDEP = New Jersey Department of Environmental Protection, Division of Fish and Wildlife; ACE = Army Corps of Engineers; RUMFS = Rutgers University Marine Field Station.

Sampling location	Habitat	Depths sampled (m)	Sampling duration	Sampling frequency	Gear	Number of samples	Source
Off New Jersey	inner continental shelf	5–27	1995–98	five times per year	otter trawl	480	NJDEP
Northern New Jersey	ocean beaches	0–2	1995–98	bimonthly (June–October)	seine	1926	ACE
Southern New Jersey	ocean and estuarine beaches	0–2	1998	weekly (May–Nov)	seine	387	RUMFS

On ocean beaches along northern New Jersey, sampling was conducted biweekly by the U.S. Army Corps of Engineers at 28 stations with a 15.2 × 1.8 m beach seine with a 1.8-m^2 bag (6-mm mesh) during one-week periods from August through October 1995–98 (Fig. 1, Table 1). At each location three seine hauls were completed during daylight, two near the groins bordering each site and one between the groins. Comparisons between ocean and estuarine beaches (Fig. 1) were conducted during 1998 with seasonal sampling in the Great Bay–Little Egg Harbor estuary and adjacent ocean by the Rutgers University Marine Field Station. All of these samples were collected with a 30 × 1.8 m bag seine with 6-mm mesh in the wings and 2-mm mesh in the bag.

For all of these sampling programs bluefish were enumerated and measured to either total length, standard length, or fork length, but for purposes of consistency, all lengths were converted to fork length (FL) for ease of comparison with earlier studies by using the regressions in Able and Fahay (1998).

Tag and recapture

The spatial and temporal components of this study were part of a larger sampling program to compare habitat use of YOY fishes on ocean and estuarine beaches. During this program, YOY bluefish were sampled during daylight hours with beach seines (30 m × 1.8 m, 2-mm mesh bag, 6-mm mesh wings) from 18 May to 28 October 1999 and from 22 May to 9 October 2000. The beach seines were deployed in depths <1.5 m, 10–40 m from shore depending on beach slope, tidal stage, wave and current conditions, and spread parallel to the beach, and then pulled back to shore. Seining on ocean beaches—Tuckers Island and Seven Islands (Fig. 1)—typically occurred between the two hours before and after low tide, whereas seining at Graveling Point occurred at various times in the tidal cycle, but mostly during the 4-hour window around high tide. At ocean sites, sampling at all but two sites (Barnegat Light and Holgate) occurred up to about 50 m from each side of groins that were present at most sites. At Graveling Point, hauls were made down the length of the beach. Regular, biweekly sampling across all 11 sites consisted of three standardized tows at each site. Additional sampling at these same sites used the same techniques but consisted of 1–20 seine hauls per site to collect YOY bluefish for tagging and recapture. Data from the regular sampling are presented as catch per unit of effort (CPUE) and data from both sampling programs were used for construction of length-frequency distributions that are available elsewhere (Rowe et al.[3]).

Young-of-year fish were tagged as they became available. Individuals caught in the seines were transported in buckets of water to shallow, 112-cm diameter circular tanks filled to a depth of 10–15 cm with aerated seawater and held at ambient conditions, typically below 25°C with bottles of ice used to maintain water temperature. Then they were anesthetized in a 65 mg/L solution of MS-222 (3-aminobenzoic acid ethyl ester methanesulfonate salt, Sigma Inc., St. Louis, MO), measured to the nearest millimeter and a sequential coded wire tag (1×0.25 mm) was injected dorsolaterally behind the head and anterior to the dorsal fin by using a hand-held multishot injector (Northwest Marine Technology, Shaw Island, WA). Each fish was checked for the presence of the tag with a hand-held "wand" tag detector before being released. Tagged fish were allowed to recover for 1–4 hours in holding tanks and were then released within the area of capture.

This approach yielded a high rate of tag retention and low mortality. In 1998, we tagged 25 fish (115–170 mm FL) and had 10 fish (130–188 mm FL) as controls, which were all held in 930 liter containers with ambient flow-through water from Great Bay. One mortality occurred in a tagged fish on the first day after tagging and the remainder (96%) survived for 30 days. Tag retention during this period was 100%. In 1999, we tagged 16 fish (16–92 mm FL) and had 6 control (77–101 mm) fish. There was no mortality after 45 days, in either group, and tag retention was 100%. At this time a power failure in the seawater system caused some mortality. The surviving 8 fish had 100% tag retention to 65 days when the experiment was terminated.

[3] Rowe, P. M., K. W. Able and M. J. Miller. In review. Distribution, abundance and size of young-of-the-year bluefish (*Pomatomus saltatrix*) in ocean and estuarine habitats in southern New Jersey during 1999–2000.

All YOY fish caught after tagging began were checked for tags with the hand-held "wand" detector during all sampling events. Recaptured fish were measured to the nearest mm FL and then preserved in 95% ETOH in the field. Tags were dissected out of each recaptured fish in the laboratory and read with a dissecting scope to identify each individual. The growth of each recapture was then calculated by dividing the difference in length at recapture and at tagging by the number of days between tagging and recapture.

Food habits

Young-of-year bluefish collected by seine in 1998 from northern (n=581 stomachs with prey) and southern (n=667) New Jersey ocean beaches and from the Great Bay–Little Egg Harbor estuaries (n=72) were analyzed for food habits. Emphasis was placed on food habits on ocean beaches because little is known about this aspect of their life history. Samples were immediately preserved in 10% formalin and, in the laboratory, were measured and divided into 10-mm FL size classes, and the analysis was performed on up to 12 individuals in each size class from 30–39 mm FL to ≥150 mm FL. The gastro-intestinal tract was dissected from each fish and all contents removed from the esophagus to the pylorus. Prey items were identified to the lowest possible taxon and their relative contribution based on percent frequency of occurrence.

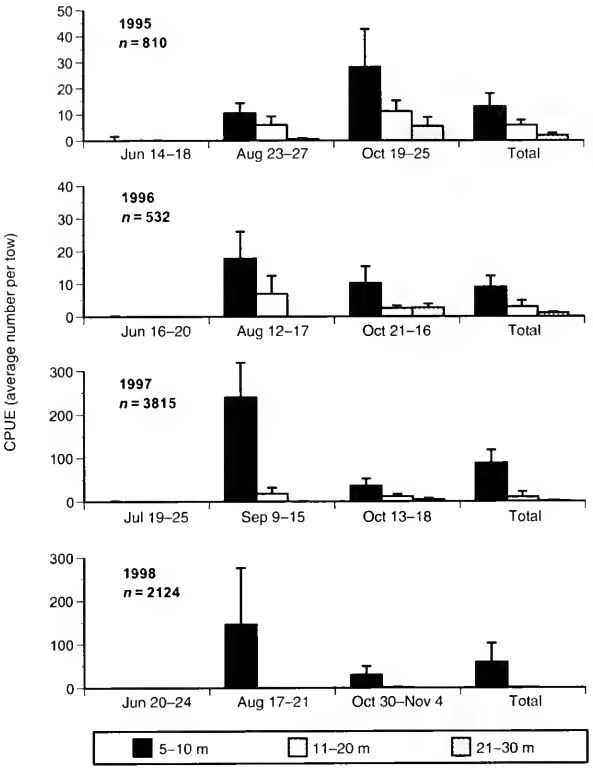

Figure 2

Abundance (CPUE) by depth of young-of-year bluefish on the inner continental shelf off New Jersey during 1995–98. None were collected during other periods of the year. Note differences in y-axes. See Figure 1 for sampling strata.

Results

Seasonal occurrence and abundance

Young-of-year bluefish were consistently collected in the ocean during summer and early fall from inner continental shelf waters to beaches along the New Jersey coast. On the inner shelf, in depths between 5 and 27 m, YOY were collected from June through October; greatest abundance occurred in August, September, and October during 1995–98 (Fig. 2). Abundance varied between years and average CPUE was an order of magnitude lower in 1995–96 than in 1997 and 1998. During the periods of peak abundance, catches averaged greater than 100–200 individuals/tow. The seasonal pattern of abundance varied between years and the peaks occurred in October in 1995 and in August–September in 1996–98. In every year the greatest abundance typically occurred in the shallowest nearshore stations (5–10 m), and the lowest value were at the deepest stations (21–27 m).

The YOY were consistently present on ocean beaches in northern New Jersey during the summer and fall sampling period in 1995–98 (Fig. 3). Interestingly, the pattern of annual abundance was consistent with the otter trawl sampling, i.e. peak CPUE was lower in 1995–96 and an order of magnitude higher in 1997–98. Seasonal abundance on these beaches varied between these high and low abundance periods and peaks in from late July through early August in 1995–96 and in late August–September in 1997–98. In all four years abundance was very low by mid-October. On smaller spatial scales on ocean beaches the pattern of occurrence was quite variable, regardless of year (Fig. 4); thus there were no sampling locations where catches were consistently high and instead peaks in abundance continually shifted.

The seasonal pattern of abundance on ocean beaches in southern New Jersey in 1998 differed from those elsewhere

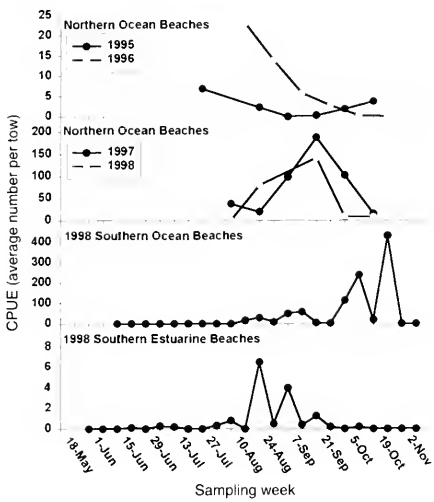

Figure 3

Abundance (CPUE) of young-of-year bluefish on northern New Jersey ocean beaches during 1995–98 and southern New Jersey ocean beaches and estuarine beaches during 1998. See Figure 1 for sampling locations.

(Fig. 3). Peaks occurred much later in October in relation to northern beaches in all years and, compared to the estuary, relative abundance was much higher than in the adjacent estuary during the entire sampling period, with peak abundance reaching approximately 400 individuals/tow (in the estuary only 6 individuals/tow were collected). Both ocean and estuarine beaches had very small numbers in late June and July, and abundance peaks in August and early September. Although estuarine catches declined by late September, with zero catches continuing through the end of the sampling period, catches on ocean beaches were highest in late September and early October and did not decline until October or early November.

Size composition

Young-of-year bluefish were represented by different size classes or cohorts and these varied between years and locations (Figs. 5–7). The size at first occurrence in the ocean was as small as approximately 20 mm FL in some years and around 50 mm FL in other years. Largest YOY were collected in otter trawl collections on the inner continental shelf where individuals >19 cm were common (Fig. 5). In 1995 several size classes were evident in August and three in October; the largest, in the latter, was approximately 17–26 cm FL, the smallest was 6–9 cm FL, and an intermediate group was 10–16 cm FL (Fig. 5). In 1996, only one size class was represented in August and only two in October. The larger mode in October approximated the size of the larger mode in October 1995, and the smaller mode resembled that of the intermediate mode during the same month. In September 1997 there was a single size mode, and perhaps two in October, and the latter were similar in size to the largest and intermediate modes in 1995. In 1998 the YOY were represented by a small size mode similar to that in August 1995 and the dominant size class in October was similar to the intermediate group in October 1995; thus the larger mode, that was present in other years was not present in 1998. Over the same time period, there appeared to be some relationship between distance offshore, depth, and size (Fig. 5). When fish occurred in the deepest strata sampled they were often the largest individuals and this was especially evident in 1995 and 1996.

Young-of-year on northern New Jersey beaches had similar mean sizes but fewer large and small fish than in inner continental shelf collections (Fig. 6). Often two modes were represented but these did not occur consistently in all collections. In early fall one mode often consisted of very small fish (<4–7 cm FL). This was obvious in early October 1995, September and October 1996, October 1997 and 28 September–1 October 1998. Large fish (>17 cm FL) were also represented in the fall, especially in October 1995 and 1998.

The average size of YOY on ocean beaches in southern New Jersey in 1998 was similar to those collected on the inner continental shelf, on northern New Jersey beaches, and in the estuary (Fig. 7). In most instances a single mode was evident, with the exception of October when few larger fish were present.

Residency and movements

The results from the tag and recapture experiments differed markedly between the estuary and the ocean and in no instance were fish from the estuary or the ocean captured in the other area (Fig. 8). Of the fish tagged in the ocean during 1999 (n=4987, 50–202 mm FL) only two (0.04%) were recaptured, whereas in 2000 (n=649, 55–241 mm FL) none were recaptured. The number of tag returns was much higher in the estuary during 1999 (n=856, 59–250 mm FL) with 29 (3.4%) recaptured; whereas in 2000 (n=661, 55–244 mm FL) only five (0.8%) were recaptured. In the ocean, the two fish recaptured were both at liberty for 15 days. In fact, they were tagged on the same day at the same location and recaptured together on the same day and at the same location, suggesting that they were traveling together. Over that period they traveled a minimum of 17 km from the tagging location at Surf City south to the recapture location at Holgate (Fig. 1). In the estuary the number of days at liberty ranged from 2 to 18 days in 1999 and 5–27 days in 2000 (Fig. 8). All of the fish tagged in the estuary at Graveling Point in both years were captured at the same location, indicating a much higher period of residency than could be demonstrated in the ocean.

Growth

Maximum growth rates for bluefish are among the highest recorded for the YOY of any fish species. Values for tagged and

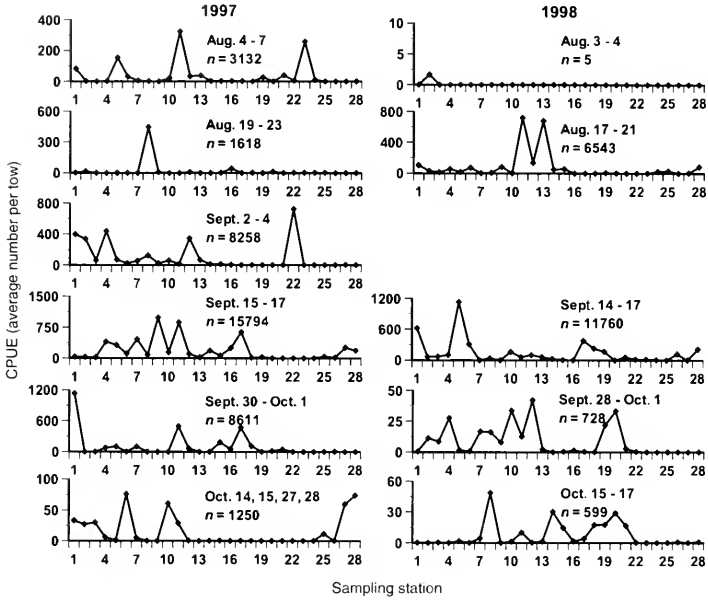

Figure 4

Spatial variation in abundance (CPUE) of young-of-year bluefish by sampling period on northern New Jersey beaches by collection date during 1997 and 1998. See Figure 1 for sampling locations.

recaptured individuals ranged from 0.1 to 2.2 mm FL/day with a mean value of 1.4 mm FL/day across all habitats (Fig. 9). The differences between years in the estuary and between the estuary and the ocean were not significantly different. Growth rates, in length, did decline slightly over the summer with the highest individual growth occurring in July and August and lower values in late August or September through October regardless of how the growth is expressed (Fig. 9).

Food habits

Fish dominated the stomach contents of YOY bluefish from ocean beaches in northern and southern New Jersey and in the estuary, occurring in more than 60% of the stomachs in both areas (Table 2). Prey fish species in the ocean included bay anchovy (*Anchoa mitchilli*, 27.6% and 24.7% frequency of occurrence on northern and southern beaches, respectively), silversides (*Menidia* spp., <2%), northern kingfish (*Menticirrhus saxatilis*, <0.5%), and northern pipefish (*Syngnathus fuscus*, <0.2%), with about 40% of the fish in both areas unidentified. Evidence of cannibalism was rare, with only 2.3% (northern) and 0.3% (southern) incidence. Other important prey categories (>10% frequency of occurrence) included gammarid amphipods and a variety of decapod crustaceans. The occurrence of empty stomachs was infrequent. In the estuary, stomach contents were somewhat different: the dominant prey fish species consisted of *Menidia* spp. (22.0% frequency of occurrence), smaller numbers of *Fundulus majalis* less frequently (5.1%), and a large proportion of unidentified fish (55.9%). *Anchoa* spp. were notable by their absence in relation to diets in the ocean. Other important categories included decapod crustaceans, which were mostly unidentified shrimp. Empty stomachs represented 18% of the total examined, as a result of this and the relatively small number examined, the effective sample size was much smaller than those from ocean beaches.

The relative contribution of fish and invertebrates in the diet changed with size and to some degree location (Fig. 10). Fish from the ocean beaches were consumed by virtually all size classes of YOY bluefish, including some of the smallest individuals in our collections (<40 mm FL), but fish occurrence in the diet became more frequent beginning at sizes of approximately 80–100 mm FL, depending on area. In northern New Jersey beaches, invertebrates dominated the diet at sizes of 30–>70 mm FL, whereas fish occurred in >70% of stomachs at sizes >80 mm FL, which increased to >80% in sizes >90 mm FL. In southern New Jersey beaches, where smaller bluefish (<50 mm FL) were not captured, invertebrates dominated the diets of bluefish up to 80–90 mm,

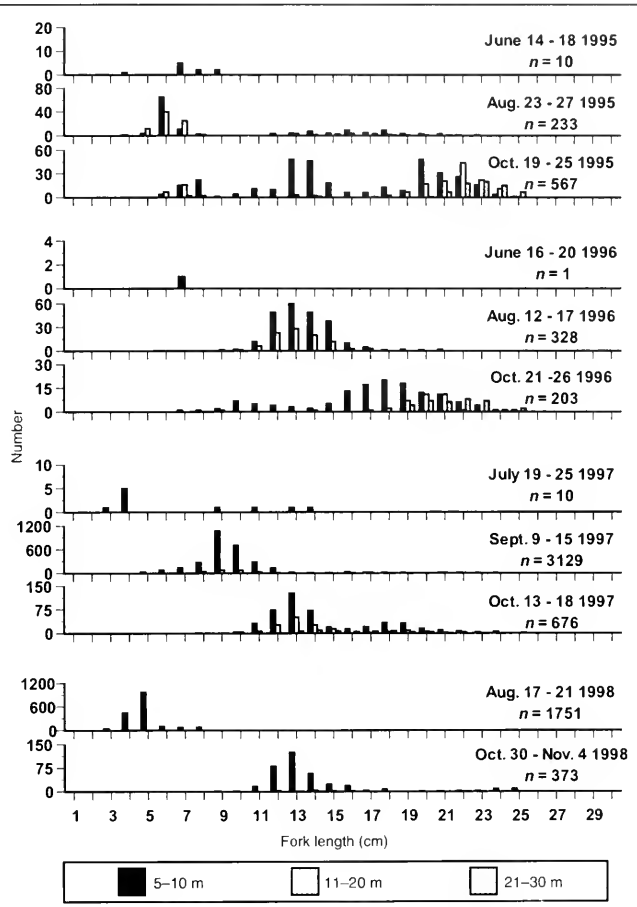

Figure 5

Size composition of young-of-year bluefish from inner continental shelf collections by collection date during 1995–98.

and fish occurred in over 70% of the diet at larger sizes. In the estuary, fish were consumed at smaller sizes, 50–60 mm FL, where they made up 100% of the diet. At larger sizes they continued to be of considerable importance.

Discussion

Habitat use in the ocean

Our results indicated that YOY bluefish use the inner continental shelf and ocean beaches in the New York Bight during summer and fall. They occurred consistently and abundantly in these habitats during July through mid-September during 1995–98, at a period when bluefish populations were at very low levels. In addition, an extensive analysis of bluefish from the Middle Atlantic Bight from 1973 through 1995 indicated that YOY were consistently collected in the summer in nearshore waters (Munch and Conover, 2000). Young-of-year have also been found on ocean beaches in the summer on the south shore of Long Island (Schaefer, 1967) and southern New Jersey (McDermott, 1983). These should be distinguished from the collections on ocean beaches in the fall when other

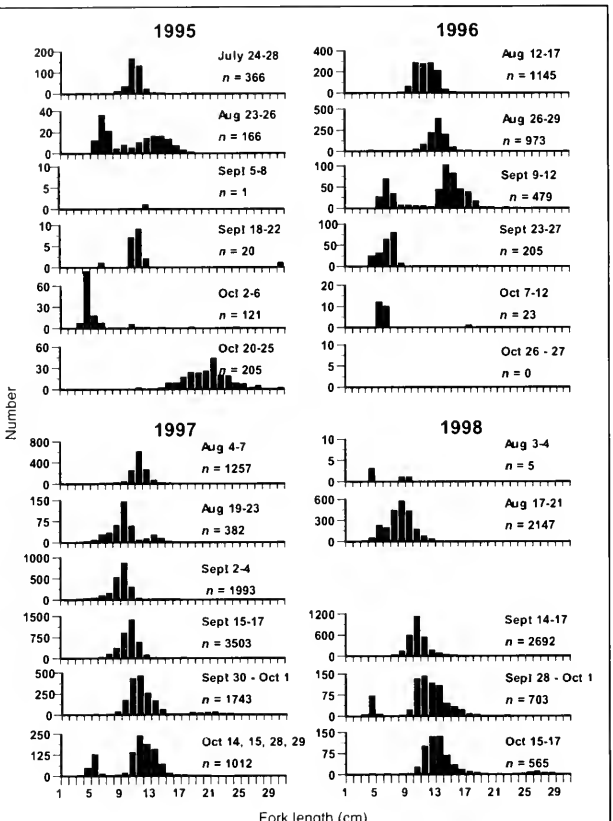

Figure 6

Size composition of young-of-year bluefish by collection date during 1995–98 from northern New Jersey ocean beaches.

YOY leave estuaries and join those in the ocean and make a southerly migration to overwintering habitats (Kendall and Walford, 1979; and see Able and Fahay, 1998) as water temperatures decline to below 15°C (Lund and Maltezos, 1970; Olla and Studholme, 1971). The occurrence of YOY in ocean waters in the fall has been reported elsewhere (Chiarella and Conover, 1990; McBride and Conover, 1991; McBride et al., 1993; Creaser and Perkins, 1994; Able and Fahay, 1998).

It is clear that YOY bluefish in the New York Bight use estuaries extensively (Kendall and Walford, 1979) and this use has been reported for a number of locations including Rhode Island (McBride et al., 1995), Long Island (Nyman and Conover, 1988; McBride and Conover, 1991), New Jersey (Fig. 3 in this paper; McBride and Conover, 1991; Rountree and Able, 1992a, 1992b, 1993; Able and Fahay, 1998) and North and South Carolina (McBride et al., 1993). As a result, YOY bluefish have been considered estuarine dependent (McHugh, 1966). However, it is not surprising that they also occupy other habitats such as ocean beaches because bluefish are widely distributed (Juanes et al., 1996), and YOY elsewhere have been found in the surf (Bennett, 1989; Ayvazian and Hyndes, 1995), along exposed coasts (van der Elst, 1976; Smale, 1984; McBride et al., 1993; Lenanton et al., 1996; Young et al., 1999) and shallow reefs (Bennett, 1989) in the South Atlantic Bight of the United States, Australia, and South Africa.

This annual pattern of abundance in the ocean in the study area could be dependent on the relative contribution of different cohorts. Although there has been much discussion of the importance of spring- versus summer-spawned individuals to the YOY population in estuaries in the

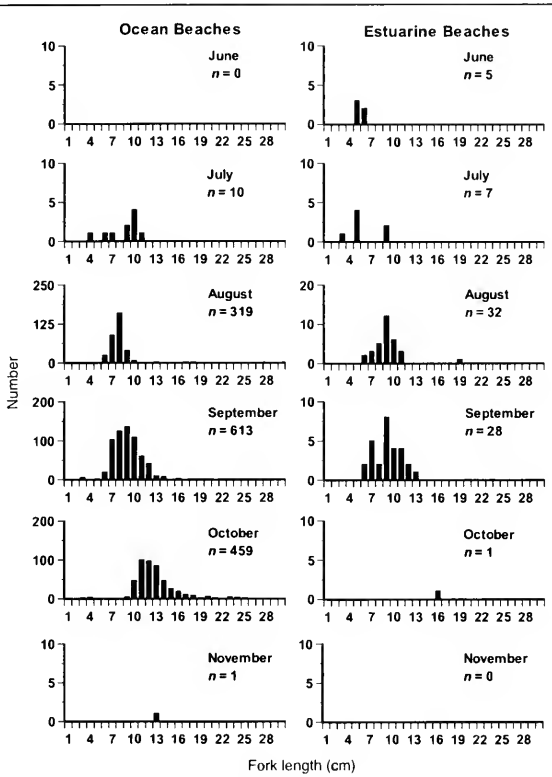

Figure 7

Size composition of young-of-year bluefish from southern New Jersey ocean beaches and the adjacent Great Bay estuary by month during 1998.

Middle Atlantic Bight (McBride et al., 1993; Hare and Cowen, 1996; Juanes et al., 1996; Able and Fahay, 1998), it appears that multiple cohorts occur in ocean habitats as well, based on the occurrence of the appropriate-size individuals in inner continental shelf (Fig. 5) and ocean beach (Figs. 6 and 7) sampling sites and in many of the same sites in the study area based on further extensive collections in 1999 and 2000 (Rowe et al.[3]).

In most years the smaller individuals of the presumed summer-spawned cohort were more abundant in ocean habitats. Others have suggested that summer-spawned individuals may be more abundant in the ocean (Kendall and Walford, 1979; Wilk, 1982) than in the estuary. Gear biases could influence the size of the YOY collected, as indicated by McBride and Conover (1991) for beach seines; therefore it is difficult to separate the effects of gear versus habitat to determine what is responsible for the average larger YOY collected in the ocean by otter trawl from the smaller average-size individuals collected on ocean beaches with seines. However, the occurrence of the largest fish in the deepest waters (21–27 m) suggests that habitat preference may be involved. A similar pattern was observed by Munch and Conover (2000), who found that the larger spring-spawned individuals were usually found in deeper waters than those for smaller summer-spawned individuals.

The contribution of the smaller bluefish cohort(s) to the population dynamics of the species in the Middle Atlantic Bight is unknown. The occurrence of very small (<50 mm) YOY bluefish in late summer occurred in a number of years during the study and subsequently (Rowe et al.[3]). These fish may represent late spawning or slow growth. They, along with the relatively small pelagic juveniles present in the water column in inner continental shelf waters in the study area at the same time (Rowe and Able, unpubl. data), may not contribute to the adult population because they enter the fall at relatively small sizes and may not survive

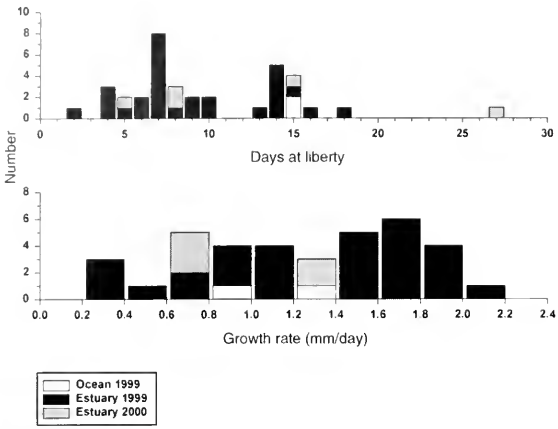

Figure 8

Summary of tag-recapture data from YOY bluefish during 1999 and 2000 at southern New Jersey estuarine and ocean beaches, including days at liberty and growth rate.

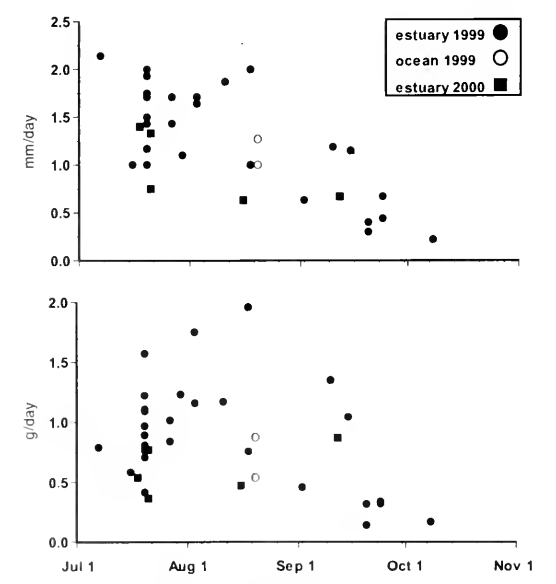

Figure 9

Growth rate by length and weight of tag-recapture fish during 1999 and 2000 at southern New Jersey estuarine and ocean beaches.

the overwinter period because of size-selective mortality (see Sogard, 1997; Hales and Able, 2001). Alternatively, the relatively large numbers of presumed summer-spawned YOY in collections implies that they could contribute substantially to the adult population. The only prior analysis, that we are aware of, suggested that the spring-spawned contingent was the principal contributor to the adult population (Chiarella and Conover, 1990). Regardless of the habitats used, the relative contribution by the summer-spawned individuals to the adult population could vary over annual or decadal scales. More attention to broad geographical responses over longer temporal periods is probably necessary to resolve the relative contribution issue of the different cohorts.

Residency and movements

Our understanding of the importance of ocean habitats to YOY bluefish is confounded by a lack of information about the movements of these fast-swimming fishes. Collections at northern New Jersey beaches suggests their occurrence and abundance may be sporadic based on the lack of consistent catches over time at the sites sampled (Fig. 4). The same pattern was observed in the study area during 1999 and 2000 (Rowe et al.[3]). This sporadic abundance could be due to several factors including inshore-offshore movements from the beaches to deeper water beyond the reach of seine samples, as appears to occur on estuarine beaches on a diel period (Buckel and Conover, 1997), or movements along the beach. A similarly variable pattern of occurrence has also been noted for beaches in South Africa (van der Elst, 1976).

The results of the tag and recapture efforts indicated that at least some of the YOY were resident on an estuarine beach for a considerable portion of the summer. Perhaps the number of recaptures (0.76–3.4%) would have been higher if not for the three hurricanes that occurred in the region during September 1999 that could have contributed to movement from shallow beaches into deeper waters of the estuary or into the ocean. The only other tag-recapture study of YOY (<270 mm FL) bluefish, of which we are aware, occurred in Moreton Bay, Queensland, Australia (Morton et al., 1993). The high rate of returns (11%) from the externally tagged fish in that study was attributed to the intensive fishery for this species and the fact that sheltered estuaries within the study area presumably provided

Table 2

Diet composition for young-of-year bluefish (*Pomatomus saltotrix*) collected on ocean beaches in southern and northern New Jersey during 1998. Percent frequency of occurrence based on number of stomachs with prey. The miscellaneous category includes macroalgae, detritus, shell fragments, and sand. See Figure 1 for sampling locations.

	Southern beaches		Northern beaches		Estuary	
Prey category	Total number of prey	Percent frequency of occurrence	Total number of prey	Percent frequency of occurrence	Total number of prey	Percent frequency of occurrence
Annelida (Polychaeta)	14	1.8	7	1.0	0	0
Crustacea	3560	45.7	8463	42.5	46	33.9
Amphipoda (Gammaroidea)	938	16.9	513	18.6	2	1.7
Cladocera	151	0.3	3961	6.9	0	0.0
Copepoda	447	3.8	3449	15.7	15	3.4
Calanoida	268	2.3	2165	8.2	0	0.0
Harpacticoida	0	0.0	12	0.5	0	0.0
Unidentified	179	1.5	2417	8.9	0	0.0
Decapoda	1830	27.9	296	10.1	29	28.8
Megalopa	476	11.4	35	3.0	0	0.0
Zoea	406	4.1	83	3.2	0	0.0
Emerita talpoida	251	7.2	160	2.2	0	0.0
Ovalipes ocellatus	5	0.7	6	1.0	0	0.0
Pagurus spp.	1	0.1	0	0.0	0	0.0
Unidentified crabs	9	0.7	1	0.2	2	3.4
Crangon spp.	13	1.3	1	0.2	0	0.0
Palaemonetes spp.	588	6.3	6	0.5	0	0.0
Thalassinoidea	18	1.2	0	0.0	0	0.0
Unidentified shrimps	63	3.5	4	0.5	27	25.4
Mysidacea	47	1.9	210	4.7	0	0.0
Stomatopoda	14	0.6	1	0.2	0	0.0
Unidentified	133	7.2	33	3.9	0	0.0
Larvacea	91	0.6	287	1.2	0	0
Mollusca	96	4.5	10	1.2	0	0.0
Bivalvia	95	4.4	5	0.5	0	0.0
Cephalopoda	1	0.1	5	0.7	0	0.0
Pisces	786	64.1	533	70.0	57	83.0
Anchoa spp.	414	25.1	248	27.6	0	0.0
Clupeidae	3	0.4	0	0.0	0	0.0
Fundulus majalis	0	0	0	0	3	5.1
Menidia spp.	15	1.6	11	0.5	17	22.0
Menticirrhus soxatilis	3	0.4	0	0.0	0	0.0
Pomatomus saltatrix	2	0.3	14	2.3	0	0.0
Syngnathus fuscus	6	0.1	0	0.0	0	0.0
Unidentified	343	39.7	260	39.7	37	55.9
Unidentified	134	12.3	65	6.4	14	23.7
Miscellaneous	160	21.5	61	9.7	—	—

optimal habitats where YOY bluefish may choose to remain resident for longer periods of time. The lower rates of recapture in both years and areas (estuary and ocean) in our study may in part be attributable to the fact that coded wire tags are not detectable by fishermen.

The very low level of tag returns from the ocean in our study (0.04%) makes it difficult to discern patterns of habitat use with this approach. This may be due to the fact that sampling with seines in the ocean was largely limited to the relatively shallow portions of the surf zone and it appears that YOY bluefish also use deeper portions of the coastal ocean (Fig. 2). In addition, the lack of returns could be due to more extensive movements on ocean beaches in relation to the estuary—a point supported by the fact that the sporadic nature of bluefish captures during the intensive sampling in 1997 and 1998 (Fig. 4) and in subsequent years (Rowe et al., in review). In addition, the same pattern of reasonable recapture rates in this estuary and low or no recaptures in

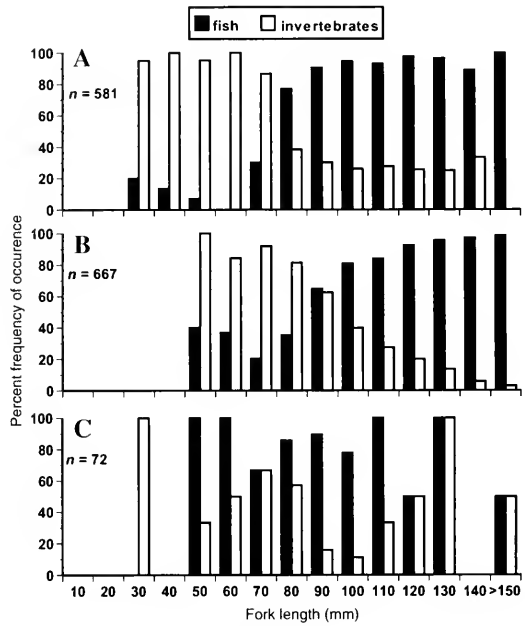

Figure 10

Ontogenetic changes in diet of YOY bluefish based on percent frequency of occurrence of fish and invertebrate prey for individuals collected on ocean beaches in northern (**A**) and southern (**B**) New Jersey and on estuarine beaches (**C**) in southern New Jersey during summer and fall 1998. See Figure 1 for location of beaches.

the ocean also occurred for another species, *Menticirrhus saxatilis*, during the same period with exactly the same tag and recapture techniques (Miller et al., 2002).

Growth

Earlier estimates for the same and other estuarine systems indicated an average growth rate of 0.9–2.1 mm/day for YOY bluefish (McBride and Conover,1991; McBride et al., 1995; Juanes et al., 1993, 1996). Another species, *Menticirrhus saxatilis*, that occurred in the same estuarine habitat, had slightly higher growth rates (Mean 1.8 mm/day, range 0.7–2.8 mm/day) (Miller et al., 2002). These estimates of growth for bluefish average greater than that for YOY of most other estuarine fish, at least in the Middle Atlantic Bight, where most nonresident, i.e. the fastest-growing species, range from 0.3 to 1.1 mm/day (Able and Fahay, 1998).

Food habits

Just as an understanding of YOY bluefish distribution and abundance in the New York Bight has been largely based on estuarine collections, so has the knowledge of their food habits. The ontogenetic shift reported in the diet of YOY bluefish during the transition from pelagic juveniles in the ocean to larger juveniles in estuarine habitats (Marks and Conover, 1993) also occurs on ocean beaches. Observations on northern and southern New Jersey beaches indicate that this transition, from invertebrates to fishes, occurs at approximately the same sizes (80–100 mm FL) as reported elsewhere (Marks and Conover, 1993; Juanes and Conover, 1994a, 1994b; Creaser and Perkins, 1994).

The diet of YOY bluefish in the coastal ocean is similar to that reported elsewhere in the world. The selection of engraulids and atherinids, as occurs on New Jersey beaches, is similar to that for other populations (Juanes et al., 1996), except that atherinids made up a much smaller percentage of the diet (Table 2). This difference is not easily explained because atherinids are a large component of the surf zone fish assemblage on New Jersey beaches during the summer and fall (Rowe and Able, unpubl. data).

In summary, ocean beaches and deeper waters of the inner continental shelf are used continuously by YOY bluefish from summer through the fall migration. Bluefish in

these habitats appear to share some characteristics with estuarine bluefish, such as monthly occurrence in the summer, size composition, growth, and food habits. The exception is that the smaller, summer-spawned cohort may be relatively more abundant in ocean habitats. This possible distinction should be considered when assessing the importance of different cohorts to recruitment. Another exception is that the degree of residency varied between the estuary and the ocean with higher recapture rates on at least one estuarine beach. Further study is necessary, however, to resolve the degree to which ocean bluefish are resident there. The available data suggest that their movements may be much more dynamic in the ocean.

Although YOY bluefish are clearly not obligate estuarine users because of the large numbers found in coastal waters, it will take more detailed studies of bluefish and other "estuarine-dependent" species to determine if their use of estuarine or ocean habitats is facultative, varies annually or varies with different cohorts. This view is in keeping with the "basin model" of MacCall (1990), which recognizes a variety of factors that may influence habitat use.

Acknowledgments

A number of individuals assisted with the northern New Jersey ocean beaches sampling, especially Howard Rubin and Bob Will from the U. S. Army Corps of Engineers and Keith Brewer from Barry Vittor and Associates. Collections on southern New Jersey beaches were assisted by Geoff Bell, David Bottinelli, Ryan Nichols, Christian Jeitner, Kara Della Torre, and Brian Rokeach. Geoff Bell also assisted in the analysis of the food habits. David Bottinelli, Ryan Nichols, Christian Jeitner, Kara Della Torre, and Robert Rinaldi assisted in the tagging experiment. Lindy Barry and Stacy Hagan prepared the figures. Funding from U.S. Fish and Wildlife Service provided for the New Jersey Department of Environmental Protection sampling. The sampling program by the Rutgers University Marine Field Station was funded through a collaborative program with Rutgers University and the National Marine Fisheries Service. We are grateful to all of the above.

Literature cited

Able, K. W., and M. P. Fahay.
1998. The first year in the life of estuarine fishes in the Middle Atlantic Bight, 342 p. Rutgers Univ. Press, New Brunswick, NJ.

Able, K. W., R. L. Lathrop and M. P. De Luca.
1999. Compendium of research and monitoring in the Jacques Cousteau National Estuarine Research Reserve at Mullica River-Great Bay, 67 p. Institute of Marine and Coastal Sciences Technical Report 99-21, Rutgers Univ., New Brunswick, NJ.

Ayvazian, S. G., and G. A. Hyndes.
1995. Surf-zone fish assemblages in south-western Australia: do adjacent nearshore habitats and the warm Leeuwin Current influence the characteristics of the fish fauna? Mar. Biol. (Berlin) 122:527–536.

Bennett, B. A.
1989. The fish community of a moderately exposed beach on the southwestern Cape coast of South Africa and an assessment of this habitat as a nursery for juvenile fish. Est. Coast. Shelf Sci. 28:293–305.

Buckel, J. A., and D. O. Conover.
1997. Movements, feeding periods, and daily ration of piscivorous young-of-the-year bluefish, *Pomatomus saltatrix*, in the Hudson River estuary. Fish. Bull. 95:665–679.

Chiarella, L. A., and D. O. Conover.
1990. Spawning season and first-year growth of adult bluefish from the New York Bight. Trans. Am. Fish. Soc. 119: 455–462.

Creaser, E. P., and H. C. Perkins.
1994. The distribution, food, and age of juvenile bluefish, *Pomatomus saltatrix*, in Maine. Fish. Bull 92: 494–508.

Hales, L. S., Jr., and K. W. Able.
2001. Winter mortality, growth, and behavior of young-of-the-year of four coastal marine fishes in New Jersey (USA) waters. Mar. Biol. 139:45–54.

Hare, J. A., and R. K. Cowen.
1996. Transport mechanisms of larval and pelagic juvenile bluefish (*Pomatomus saltatrix*) from South Atlantic Bight spawning grounds to Middle Atlantic Bight nursery habitats. Limnol. Oceanogr. 41(6):1264–1280.

Juanes, F., and D. O. Conover.
1994a. Rapid growth, high feeding rates, and early piscivory in the young-of-the-year bluefish (*Pomatomus saltatrix*). Can. J. Fish. Aquat. Sci. 51:1752–1761.
1994b. Piscivory and prey size selection by young-of-the-year bluefish: predator preference or size-dependent capture success? Mar. Ecol. Prog. Ser. 114:59–69.

Juanes, F., J. A. Hare, and A. G. Miskiewicz.
1996. Comparing early life history strategies of *Pomatomus saltatrix*: a global approach. Mar. Freshwater Res. 47: 365–379.

Juanes, F., R.E. Marks, K. A. McKown and D. O. Conover.
1993. Predation of age-0 bluefish on age-0 anadromous fishes in the Hudson River estuary. Trans. Am. Fish. Soc. 122: 348–356.

Kendall, A. W., Jr., and L. A. Walford.
1979. Sources and distribution of bluefish, *Pomatomus saltatrix*, larvae and juveniles off the east coast of the United States. Fish. Bull. 77:213–227.

Klein-MacPhee, G.
2002. Bluefish: family Pomatomidae. *In* Bigelow and Schroeder's fishes of the Gulf of Maine (B. B. Collette and G. Klein-MacPhee, eds.), p. 400–406. Smithsonian Institution Press, Washington, D.C.

Lenanton, R. C., S. G. Ayvazian, A. F. Pearce, R. A. Steckis and G. C. Young.
1996. Tailor (*Pomatomus saltatrix*) off western Australia: where does it spawn and how are the larvae distributed? Mar. Freshwater Res. 47:337–346.

Lund, W. A., and G. C. Maltezos.
1970. Movements and migrations of the bluefish, *Pomatomus saltatrix*, tagged in waters of New York and southern New England. Trans. Am. Fish. Soc. 99. 719–725.

MacCall, A. D.
1990. Dynamic geography of marine fish populations, 153 p. Washington Sea Grant Program, Univ. Washington Press, Seattle, WA.

Marks, R. E., and D. O. Conover.
1993. Ontogenetic shift in the diet of young-of-the-year bluefish, *Pomatomus saltatrix*, during the oceanic phase of the early life history. Fish. Bull. 91:97–106.

McBride, R. A., and T. F. Moslow.
1991. Origin, evolution, and distribution of shoreface sand ridges, Atlantic inner shelf, U.S.A. Mar. Geol. 97:57–85.
McBride, R. S., and D. O. Conover.
1991. Recruitment of young-of-the-year bluefish (*Pomatomus saltatrix*) to the New York Bight: variation in abundance and growth of spring and summer-spawned cohorts. Mar. Ecol. Prog. Ser. 78:205– 216.
McBride, R. S., J. L. Ross, and D. O. Conover.
1993. Recruitment of bluefish (*Pomatomus saltatrix*) to estuaries of the South Atlantic Bight, U.S.A. Fish. Bull. 91: 389–395.
McBride, R. S., M. D. Scherer, J. C. Powell.
1995. Correlated variations in abundance, size, growth, and loss rates of age-0 bluefish in a southern New Jersey estuary. Trans. Am. Fish. Soc. 124:898–910.
McDermott, J. J.
1983. Food web in the surf zone of an exposed sandy beach along the Mid-Atlantic coast of the United States. *In* Sandy beaches as ecosystems (A. McLachlan and T. Erasmus, eds.), p. 529–538. W. Junk, The Hague.
McHugh, J. L.
1966. Management of estuarine fishes. Am. Fish. Soc. Spec. Publ. 3:133–154.
Miller, M. J., P. M. Rowe and K.W. Able.
2002. Occurrence and growth rates of young-of-year northern kingfish, *Menticirrhus saxatilis*, on ocean and estuarine beaches in southern New Jersey. Copeia 2002(3):815–823.
Morton, R. M., l. Halliday, and D. Cameron.
1993. Movement of tagged juvenile Tailor (*Pomatomus saltatrix*) in Moreton Bay, Queensland. Aust. J. Mar. Freshwater Res. 44:811–816.
Munch, S., and D. Conover.
2000. Recruitment dynamics of bluefish, *Pomatomus saltatrix*, on the continental shelf from Cape Hatteras to Cape Cod, 1973–1995. ICES J Mar. Sci. 57:393–402.
Nordstrom, K. F., S. F. Fisher, M. A. Barr, E. L. Frankel, T. C. Buckalew, and G. A. Kucma.
1977. Coast geomorphology of New Jersey. Vol. II: Basis and background for management strategies. (T.R.-77-1), 130 p. CCES Rutgers, New Brunswick, NJ.
Nyman, R. M., and D. O. Conover.
1988. The relation between spawning season and the recruitment of young-of-the-year bluefish, *Pomatomus saltatrix*, to New York. Fish. Bull. 86:237–250.
Olla, B. L., and A. L. Studholme.
1971. The effect of temperature on the activity of bluefish, *Pomatomus saltatrix* L. Biol.Bull. 141:337–349.
Rountree, R. A., and K. W. Able.
1992a. Fauna of polyhaline subtidal marsh creeks in southern New Jersey: composition, abundance and biomass. Estuaries 15(21):171–185.
1992b. Foraging habits, growth, and temporal patterns of salt-marsh creek habitat use by young-of-year summer flounder in New Jersey. Trans. Am. Fish. Soc. 121:765–776.
1993. Diel variation in decapod crustacean and fish assemblages in New Jersey polyhaline marsh creeks. Estuar. Coast. Shelf Sci. 37:181–201.
Schaefer, R. H.
1967. Species composition, size and seasonal abundance of fish in the surf waters of Long Island. NY Fish Game J. 14:1–46.
Smale, M.J.
1984. Inshore small-mesh trawling survey of the Cape south coast. 3. The occurrence and feeding of *Argyrosomus hololepidotus*, *Pomatomus saltatrix* and *Merluccius capensis*. S. Afr. J. Zool. 19: 170–179.
Smith, W. G., P. Berrien, and T. Potthoff.
1994. Spawning patterns of bluefish, *Pomatomus saltatrix*, in the northeastern continental shelf ecosystem. Bull. Mar. Sci. 54:8–16.
Sogard, S. M.
1997. Size-selected mortality in the juvenile stages of teleost fishes: a review. Bull. Mar. Sci. 60:1129–1157.
Uchupi, E.
1970. Atlantic continental shelf and slope of the US–shallow structure. U.S. Geol. Surv. Prof. Paper 529I.
van der Elst, R.
1976. Game fish of the east coast of southern Africa. I. The biology of elf, *Pomatomus saltatrix* (Linnaeus), in the coastal waters of Natal. Oceanographic Research Institute (Durban, South Africa) Investigational Report 44.
Wilk, S. J.
1982. Bluefish, *Pomatomus saltatrix*. MESA (Mar. Ecosyst. Anal.). N.Y. Bight Atlas, Monogr. 15:86–89.
Young, G. C., B. S. Wise and S. G. Ayvazian.
1999. A tagging study on tailor (*Pomatomus saltatrix*) in western Australian waters: their movement, exploitation, growth and mortality. Mar. Freshwater Res. 50:633–642.

Dynamics of bigeye (*Thunnus obesus*) and yellowfin (*T. albacares*) tuna in Hawaii's pelagic fisheries: analysis of tagging data with a bulk transfer model incorporating size-specific attrition

M. Shiham Adam
John Sibert
David Itano

Pelagic Fisheries Research Program
Joint Institute of Marine and Atmospheric Research
University of Hawaii at Manoa
1000 Pope Road, Marine Sciences Bldg. #313
Honolulu, Hawaii 96822
E-mail address (for M. S. Adam): msadam@hawaii.edu

Kim Holland

Hawaii Institute of Marine Biology
University of Hawaii
Kaneohe, Hawaii 96744

Abstract—Tag release and recapture data of bigeye (*Thunnus obesus*) and yellowfin tuna (*T. albacares*) from the Hawaii Tuna Tagging Project (HTTP) were analyzed with a bulk transfer model incorporating size-specific attrition to infer population dynamics and transfer rates between various fishery components. For both species, the transfer rate estimates from the offshore handline fishery areas to the longline fishery area were higher than the estimates of transfer from those same areas into the inshore fishery areas. Natural and fishing mortality rates were estimated over three size classes: yellowfin 20–45, 46–55, and ≥56 cm and bigeye 29–55, 56–70, and ≥71 cm. For both species, the estimates of natural mortality were highest in the smallest size class. For bigeye tuna, the estimates decreased with increasing size and for yellowfin tuna there was a slight increase in the largest size class. In the Cross Seamount fishery, the fishing mortality rate of bigeye tuna was similar for all three size classes and represented roughly 12% of the gross attrition rate (includes fishing and natural mortality and emigration rates). For yellowfin tuna, fishing mortality ranged between 7% and 30%, the highest being in the medium size class. For both species, the overall attrition rate from the entire fishery area was nearly the same. However, in the specific case of the Cross Seamount fishery, the attrition rate for yellowfin tuna was roughly twice that for bigeye. This result indicates that bigeye tuna are more resident at the Seamount than yellowfin tuna, and larger bigeye tunas tend to reside longer than smaller individuals. This may result in larger fish being more vulnerable to capture in the Seamount fishery. The relatively low level of exchange between the Seamount and the inshore and longline fisheries suggests that the fishing activity at the Seamount need not be of great management concern for either species. However, given that the current exploitation rates are considered moderate (10–30%), and that Seamount aggregations of yellowfin and bigeye tuna are highly vulnerable to low-cost gear types, it is recommended that further increases in fishing effort for these species be monitored at Cross Seamount.

Manuscript accepted 28 October 2002.
Manuscript received 31 December 2002 at NMFS Scientific Publications Office.
Fish. Bull. 101:215–228 (2003).

Around the Hawaiian Islands, a variety of small and medium-scale fisheries target bigeye (*Thunnus obsesus*) and yellowfin tuna (*T. albacares*) associated with offshore seamounts, weather monitoring buoys, an inshore network of fish aggregating devices (FADs), and natural aggregation sites (Itano and Holland, 2000). These fisheries, conducted from longline, troll, and handline (and to a lesser extent pole-and-line) vessels provide an important source of revenue for the state of Hawaii (Boggs and Ito, 1993; Ito and Machado[1]). The small-gear fleet (essentially trolling and the handline vessels) supports recreational and subsistence fisheries for both residents and the tourist industry (Pooley, 1993; Hamilton and Huffman, 1997).

An important sector of the small-scale commercial fisheries is the offshore handline fishery, which targets mixed species aggregations found in association with offshore NOAA weather-monitoring buoys and seamounts (Itano and Holland, 2000). Most of the catch and effort in this fishery, which currently lands roughly 500 t per year, concentrates on the Cross Seamount and takes mostly juvenile and subadult yellowfin and bigeye tunas. Concerns have been raised as to whether the seamount fishery intercepts too many juveniles that might otherwise recruit to inshore fisheries or to the offshore longline fishery (Holland et al., 1999). There is also concern among the handline fishermen exploiting the seamount that further increases in fishing effort could overexploit offshore tuna resources and reduce the economic viability of their fishery. Moreover, yellowfin and bigeye tuna around Hawaii are part of the wider Pacific Ocean stock that are being exploited by the various coastal and high seas fisheries (Hampton and Fournier, 2001; Hampton and Fournier[2]) and therefore the overall health of the Pacific-wide stock is important for the viability of the local fisheries. In these concerns, the Hawaiian Cross Seamount fishery exemplifies resource

[1] Ito, R. Y., and W. Machado. 1999. Annual report of the Hawaii-based longline fishery for 1998. Honolulu Laboratory Admin Report. H-99-06, 62 p. National Marine Fisheries Service, NOAA, SWFSC, 2570 Dole St., Honolulu, HI-96822-2396.

[2] Hampton, J., and D. Fournier. 2001. A preliminary stock assessment model for bigeye tuna in the Pacific Ocean. Working Paper submitted to the Fourteenth Meeting of the Standing Committee on Tuna and Billfish, 9–16 August 2001. Secretariat of Pacific Community, BP D5, 98848 Noumea Cedex, New Caledonia

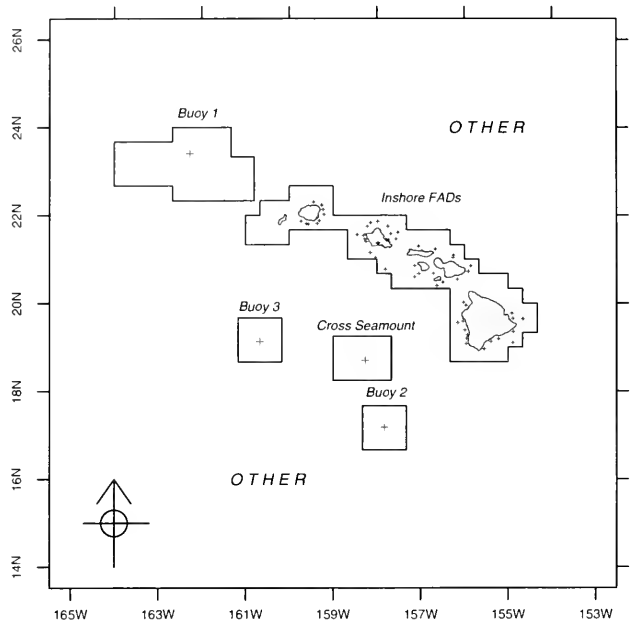

Figure 1

The study area around the Hawaiian archipelago showing the boundaries of the sites used in the model. Individual crosses indicate the geographic location of the FADs.

allocation and sustainability issues that are increasingly frequent in all oceans.

Conventional tagging of bigeye and yellowfin tuna was initiated in 1995 in order to advance understanding of the dynamics of tuna aggregations in the Hawaiian fishery and to provide management guidance. Although initially concentrating on the Cross Seamount, the Hawaii Tuna Tagging Project (HTTP) expanded its scope to tag fish throughout the archipelago and has tagged and released more than 17,000 bigeye and yellowfin tuna of roughly equal numbers during a five-and-half year period.

Previous analyses of the data suggested that recruitment (transfer) rates from the Cross Seamount to the inshore areas were low and concluded that fishing effort on the Cross Seamount was not having an adverse impact on other components (inshore trolling and handlining, offshore longlining) of the local tuna fisheries (Sibert et al., 2000). It was also suggested that bigeye tuna on the Cross Seamount had a higher mean residence time than yellowfin tuna (Holland et al., 1999; Sibert et al., 2000).

However, those previous analyses were made while tagging was still in progress, using a small set of recapture data. Since that time, many more tag releases and recoveries have been made which permit a more complete view of movement and residence times. The work presented here includes releases and recoveries up to June 2001. A size and site-specific tag attrition model was developed to analyze the data and provides information on transfer and exploitation rates that are important for management of the resource and for subsequent fishery assessments. The approach used in this research may prove useful in other areas where resource allocation issues need to be addressed.

Materials and analytical method

Data and tag attrition model

The analysis includes recaptures of tagged bigeye and yellowfin tuna released between August 1995 through November 2000 in the Hawaiian pelagic fishery in the geographic region 165°W to 153°W and 14°N to 26°N (Fig. 1). A total of 12,848 tag releases from within the area are examined here of which 7541 (59%) were bigeye and 5307 (41%) were yellowfin tuna. Releases were made primarily at the Cross Seamount which is located about 290 km south of Oahu at approximately 18°42′N, 158°16′W. Releases were also made at NOAA data buoys 51001, 51002, and 51003 (identified as buoy 1, buoy 2, and buoy 3 in this paper, see Fig. 1) and at inshore areas immediately surrounding the main Hawai-

Table 1

Summary of tag releases and recaptures by site and species with usable information. Geographic areas of the sites are given in Figure 1.

Site	Release	Recapture
Bigeye tuna		
Buoy 2	1493	317
Buoy 3	326	29
Cross Seamount	5371	653
Inshore areas	160	50
Other	0	48
Total	7350	1097
Yellowfin tuna		
Buoy 1	247	20
Buoy 2	260	40
Buoy 3	59	9
Cross Seamount	3423	635
Inshore areas	1239	254
Other	0	12
Total	5228	970
Grand total	12578	2067

ian Islands. Additional details on the tagging program and the fisheries are given in Itano and Holland (2000). As of June 2001, 1131 (14.9%) bigeye and 983 (18.5%) yellowfin tuna were recovered. A summary of releases and recaptures with usable information given in Table 1.

The method used to analyze the data is an extension of a tag attrition model commonly used in the analysis of tuna tagging data (e.g., Kleiber et al., 1987, Hampton, 1991a). We developed a site- and size-specific model to describe the dynamics of the tagged population in the study area by combining Sibert et al.'s (2000) site-specific model with Hampton's (2000) size-specific model. This size- and site-specific tag attrition model can be written as

$$\frac{dN_{kt}}{dt} = -\left(F_{i,I(l_k,\bar{t})} + M_{I(l_k,\bar{t})} + \lambda \sum_{j=1}^{n} T_{ij} \right) N_{kt} + \sum_{j=1}^{n} (T_{ji} N_{kt}), \tag{1.1}$$

where $T_{ii} = T_{jj} = 0$; and at t=0, $N_{k1} = \alpha N_{k1}^{0}$.

$$L(l_k,\bar{t}) = \left[\bar{L}_{\infty} - l_k\right] + \left[1 - e^{\left(-K(\bar{t}-t_0)\right)}\right] + l_k \tag{1.2}$$

$$\frac{dC_{kt}}{dt} = F_{i,I(l_k,\bar{t})} N_{kt} \quad \text{at } t = 0;\ C_{kt} = 0. \tag{1.3}$$

The subscripts i and j (i, j=1,2..,n) indicate release and recapture sites and k is the release cohort stratified over three size classes (see below). Note "site" is used in this paper to refer to a release or recapture "compartment" from the modeling perspective. Equation (1.1) partitions the rate of attrition (loss of tags) into fishing mortality F, natural mortality M, tag shedding λ, and the transfer rates T_{ij} (emigration from site i to j). It may also include immigration of returnees that occurred in previous time step(s). Note that T_{ii} are not defined in the model and are set to zero. Tag shedding parameters λ and α were estimated by an independent tag-shedding analysis (see below). F and M are defined as functions of release size l_k and time-elapsed since release up to the middle of the current time interval $\bar{t}$. Because there is no direct way of observing the size of released cohorts as they grow in the model, we used a growth model to track their growth in the model. We assumed that individuals in tagged population grow according to the von Bertlanffy growth model (Eg. 1.2), which has the parameters t_0, K, and $\bar{L}_{\infty}$. The parameters of the growth model (K, and $\bar{L}_{\infty}$) may be estimated from the same data set by using the growth increment and time-at-liberty data (Hampton, 1991b). We attempted estimating the model parameters using our data set from various approaches (James, 1991; Kirkwood and Somers, 1984; Wang and Thomas, 1995). Regrettably none of the approaches provided satisfactory estimates of the growth parameters to cover the full size range of the fish that would be required for the attrition model. The usable growth data and the size range available in the data set were simply not sufficient for estimating the growth parameters. Instead we used the parameter estimates for bigeye and yellowfin tuna from the tropical Central Pacific estimated by (Hampton, 2000). The third part of the model (Eq. 1.3) describes the recapture rate of the tagged fish (C_{kt}), which is assumed to be proportional to the numbers available (N_{kt}) in the time period—the proportionality constant being the fishing mortality rate.

For the purposes of this model, a release cohort is defined as the number of releases of a given size class stratified by site. One-centimeter initial size classes were used resulting in 252 cohorts (29–133 cm fork length, [FL]) for bigeye and 247 cohorts (20–140 cm FL) for yellowfin tuna for all the sites. The recoveries from each cohort were stratified by the recovery sites over 10-day time-at-liberty intervals. Further stratification of releases by calendar date was not practical because of the small numbers of releases and subsequent recaptures in each 1 cm × date × site stratum. Instead, we assumed that all releases occurred at time zero. This assumption in tag releases inevitably led us to assume that fishing effort was constant during the recovery period (1995–2000). This is a common assumption (e.g. Hampton, 2000) and justified if the fishery operated at a more or less constant level during the recovery period. Although the crude catch and effort (fishing days) data that we have show seasonality in the catch rates, we felt it was reasonable to assume the fishing effort exerted on the fishery remained constant throughout the experiment

We assumed zero tagging-induced mortality and that nearly all (95%) recoveries were reported, at least from the local fisheries. Close communication and a high level of cooperation between the fishing and fish processing

community of Hawaii and the HTTP were maintained to ensure high levels of reporting. There were 191 releases of bigeye (2.5% of release) lacking size of fish or geographic position of released fish (or both), which are necessary information for the analysis. For yellowfin tuna this figure was 79 (1.5% of release). The number of tag returns with no usable information, i.e. accurate recapture fork length or recapture position (or both) were few (2.9% for bigeye and 1.1% for yellowfin tuna). We had to assume a value for α, because this parameter cannot be estimated accurately from tagging data. The components included in α were the proportions recoveries with no useful information, proportion of tags lost immediately following release (the so called type-I shedding, see below) and the nonreporting of recoveries. Using the proportions in these categories, we obtained values of α as 0.85 for bigeye and 0.87 for yellowfin tuna, which were fixed in the model fits.

In order to reduce the number of parameters, attrition was estimated over size classes instead of the one-centimeter release cohorts. First a vector indexed from the smallest to the largest possible size was used to assign the one-centimeter size classes of the cohort as it "grew" in the model over time. A second vector with the same number of elements indexed with the desired size-class numbers can then be mapped onto the previous vector to estimate attrition over size classes. The attrition rates were estimated over three size classes for each species. For yellowfin tuna the size classes were 20–45, 46–55, and ≥56 cm FL and for bigeye tuna the size classes were 29–55, 56–70, and ≥71 cm FL. There was no reason for selecting these size classes but these ranges produced strata with sufficient numbers of recaptures to give model stability and convergence.

The number of parameters to be estimated can be further reduced by only estimating transfer coefficients for empirically observed transfers. It is possible to estimate coefficients for all possible transfers. However, we found that estimated coefficients for nonobserved transfers are not well determined by the data. Therefore in the interest of parsimony and model stability, we estimated transfer coefficients for the observed transfers only and assumed transfer coefficients for unobserved transfers to be zero.

Attrition from cohorts was followed independently for 140 ten-day time periods (approximately 47 months). A semi-implicit finite difference approximation was used to obtain numerical solutions of Equation 1.1. The estimates of the parameters were the values, which maximized the Poisson likelihood function:

$$L = P(C_{kit} \mid \hat{C}_{kit}) = \prod_{k} \prod_{i} \prod_{t} \left[\frac{\hat{C}_{kit}^{\,C_{kit}} e^{-\hat{C}_{kit}}}{C_{kit}!} \right], \qquad (2)$$

where C_{kit} = the observed recoveries; and
$\hat{C}_{kit}$ = the predicted recoveries from the model.

The maximum likelihood estimates of the parameters were obtained by minimizing the negative log of the likelihood function (Eq. 2) with ADModel Builder nonlinear optimization package (Otter Research Ltd., 2000).

Tag shedding

Tag shedding was estimated independently from a double tagging experiment conducted simultaneously with the main experiment with identical methods and procedures. The first tag was inserted on the left side and the second tag on the right side. Of the total 200 fish (bigeye and yellowfin tuna) double tagged and released, 57 were recovered; 49 with two tags and eight with one tag. The model used to estimate tag shedding was a simple exponential decay model with constant type-II shedding rate (Kirkwood and Walker, 1984; Hampton, 1997). The probability of retaining a tag $Q(t)$ over time is given by

$$Q(t) = \alpha e^{-\lambda t} \text{ where } 0 < \alpha \leq 1, \qquad (3)$$

where α = the type-I retention proportion; and
λ = the constant type-II shedding rate.

Using the assumptions and method described in Adam and Kirkwood (2001), we obtained the maximum likelihood estimates of the parameters by comparing the observed and predicted returns using exact dates of recovery.

Site selection

One of the primary goals of conducting the HTTP was to estimate the transfer rates between various fishery components, such as the Cross Seamount and the inshore fishing areas, and the Cross Seamount and offshore longline fishery. For the type of "bulk transfer" model described here, a site can be any arbitrary area with reasonable numbers of releases or recoveries (or both). The sites used in our study were carefully selected to represent individual fishery components from a management perspective. A total of six such compartments were identified and are shown in Figure 1. There were no releases of bigeye tuna from buoy 1 and only two recoveries of bigeye tuna were made from buoy 1 from the releases made elsewhere. For these reasons, these two recoveries were assigned to "other" area. This protocol resulted in five sites for bigeye and six sites for yellowfin tuna (see Table 1).

The NOAA weather-monitoring buoys 1, 2, and 3, act as *de facto* fish aggregating devices that concentrate large schools of bigeye and yellowfin tuna, making them highly vulnerable to the handline fishery (Itano and Holland, 2000). From a management point of view, the fishery around these offshore FADs is essentially similar to the Cross Seamount fishery and is exploited by the same vessels. The primary method of fishing at these areas is handlining. The inshore fishing areas contain a network of some 50 moored FADs that, when combined, can be considered one of the most frequently visited inshore fishing areas used by a diverse small-boat fleet (Itano and Holland, 2000). Fishing methods around inshore FADs include surface trolling, live baiting, jigging, and handline. The "other" area specified in the model is essentially the longline fishing ground more than 50 nmi offshore from the inshore sites. From the model's perspective, this area,

Table 2

Bigeye tuna: Observed and predicted tag transfers from the full model $M_3F_{3,5}T_{13}$, $n = 31$. The rows are release sites and columns are recapture sites.

	Recapture sites					
Tag release sites	All	Buoy 2	Buoy 3	Cross Seamount	Inshore	Other
Observed						
All	1097	317	29	653	50	48
Buoy 2	321	294	5	18	3	1
Buoy 3	40	2	19	11	1	7
Cross Seamount	711	21	5	623	22	40
Inshore	25	0	0	1	24	0
Other	0	0	0	0	0	0
Predicted						
All	1115.8	332.0	29.7	652.7	50.9	50.5
Buoy 2	342.4	296.2	5.2	22.6	7.9	10.6
Buoy 3	36.8	0.7	18.5	12.6	2.0	3.1
Cross Seamount	715.3	34.3	5.9	604.7	34.1	36.1
Inshore	21.3	0.7	0.1	12.8	6.9	0.8
Other	0.0	0.0	0.0	0.0	0.0	0.0

which is the area other than the bounded compartments, would represent the entire Pacific-wide fishery.

Results

The maximum likelihood method of estimating parameters allows one to statistically select among nested models those models that best fit the data on the basis of the likelihood ratio test (Brownlee, 1965; Hilborn and Mangel, 1997). The size-specific attrition model is a special case and is nested within the general model with constant mortality rates. By setting the size-specific attrition to be the same for all the sizes, the model reverts to the general case. Thus, with only a minor change, the model can be made to estimate attrition over a single size class or a single F for more than one site by describing alternative models of the data.

The parameters of the tag shedding model were estimated at $\alpha = 0.94 \pm 0.035$ and $\lambda = 0.000243 \pm 0.000452$ per day. Because the standard deviation of the estimate of λ was greater than the estimate, λ was assumed to be zero in the analysis. Estimates of α and the point estimate of λ were consistent with what has been estimated elsewhere with the same methods of tag release (Table 2, Adam and Kirkwood, 2001).

Several variants of the attrition model were evaluated including attrition estimated over a single size class and common fishing mortality rates among the offshore sites, (buoy 1, buoy 2, buoy 3, and Cross Seamount). The number of parameters to be estimated may be conveniently used to identify these structurally different models. For example, $M_3F_{3,5}T_{13}$ is the model in which M is estimated over three size classes, F over three size class and by five sites and with 13 transfer coefficients for the observed exchanges.

For both species, the model in which the attrition is partitioned over size classes demonstrated significant improvement ($P>0.999$ using a likelihood ratio test) over the reduced models: $M_3F_{3,5}T_{13}$ versus $M_1F_{1,5}T_{13}$ for bigeye tuna and $M_3F_{3,6}T_{17}$ versus $M_1F_{1,6}T_{17}$ for yellowfin tuna. Similarly, the models with site-specific fishing mortalities described the data significantly better ($P>0.999$) than models where a common fishing mortality was estimated for all offshore sites. The observed and predicted tag returns by time-at-liberty and by initial size classes of releases provide good descriptions of the data. The graphs for the Cross Seamount fishery are shown in Figures 2 and 3. Agreement between observed and predicted number of tags by site is reasonably good, particularly for sites where large numbers of recoveries were made (Tables 2 and 3).

The transfer coefficient estimates for movements between the various sites ranged from virtually zero to 0.05/day (Tables 4 and 5). For bigeye tuna, the transfer rate estimates from buoy 2, buoy 3, and the Cross Seamount to the longline fishery were higher than the transfer rates from those same sites to inshore areas (Tables 3 and 4). For yellowfin tuna, the pattern was similar except for the additional high transfer estimate from buoy 1 to the longline area. These differences between the transfer rates (from offshore sites to inshore site versus offshore sites to longline area) in both species were statistically significant (taken to mean that the 95% CI ranges did not overlap) showing the importance of emigration into the longline fishery compared with emigration into the inshore area. Yellowfin tuna transfer rate from inshore to the Cross Seamount was virtually zero but transfer from inshore to the longline area was very low (0.00703/day). There was no observed transfer of bigeye tuna to the longline fishery from the inshore areas and a very low transfer rate was estimated to the Cross Seamount (0.00375/day).

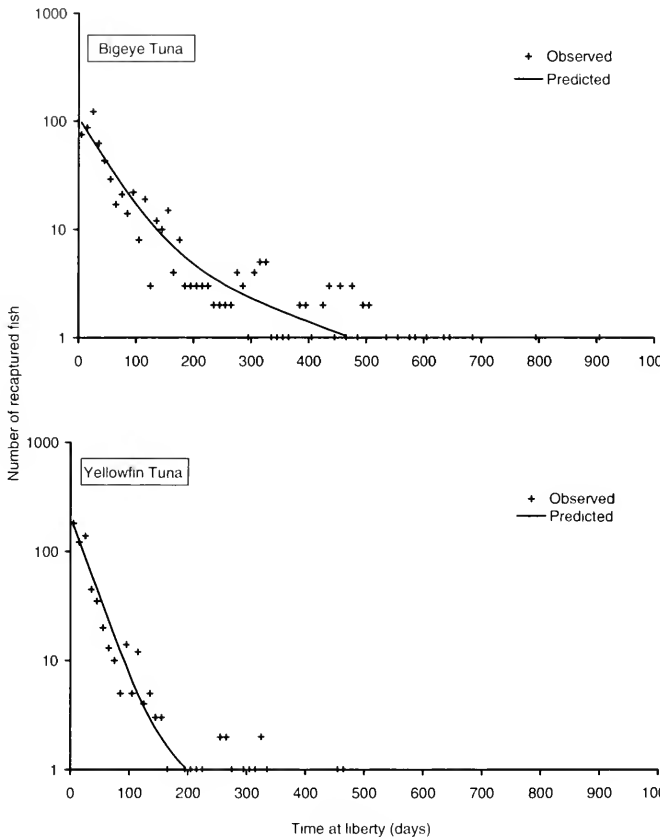

Figure 2

Observed (crosses) and predicted (continuous lines) tag returns by time at liberty from the Cross Seamount for bigeye and yellowfin tuna.

The estimates of natural mortality rate for both species were highest in the smallest size class. The estimates decreased gradually for both species, but for yellowfin tuna there was a slight increase in the largest size class, yielding a "U" shaped curve (Fig. 4). The estimates for bigeye tuna were 0.00576, 0.00372, and 0.00181/day (2.102, 1.356, and 0.660/yr) for 29–55, 56–70, and >71 cm, respectively, and for yellowfin tuna they were 0.01425, 0.00221, and 0.00361/day (5.203, 0.806, and 1.316/yr) for 20–45, 46–55, and ≥56 cm, respectively (Fig. 4 and Table 6). These estimates are within the range of the values estimated by Hampton (2000) from analyses conducted for fisheries in other regions of the Pacific.

Fishing mortality estimates are highly variable both within the three size classes and between the sites (Fig. 5). For the Cross Seamount, F was nearly the same for bigeye tuna over the three size classes (≈0.0026/day) Yellowfin tuna F, estimated for Cross Seamount, was higher for the medium size than for the smaller and large size class (i.e. 0.0027, 0.0115, and 0.0067/day).

The total attrition rate by size k and by site i can be calculated from $Z_{ik} = M_k + F_{ik} + \lambda + \Sigma T_{ij}$, from which the averages for the size class or site may be obtained. Alternatively these could be estimated from a model in which Z is kept constant over the size classes. Although there were large variations in the estimates for different sites, the estimates were not appreciably different for each of the three size classes at any particular site. At the Cross Seamount, the gross attrition rate for yellowfin of 0.038/day was roughly twice that for bigeye tuna (0.022/day). However, the

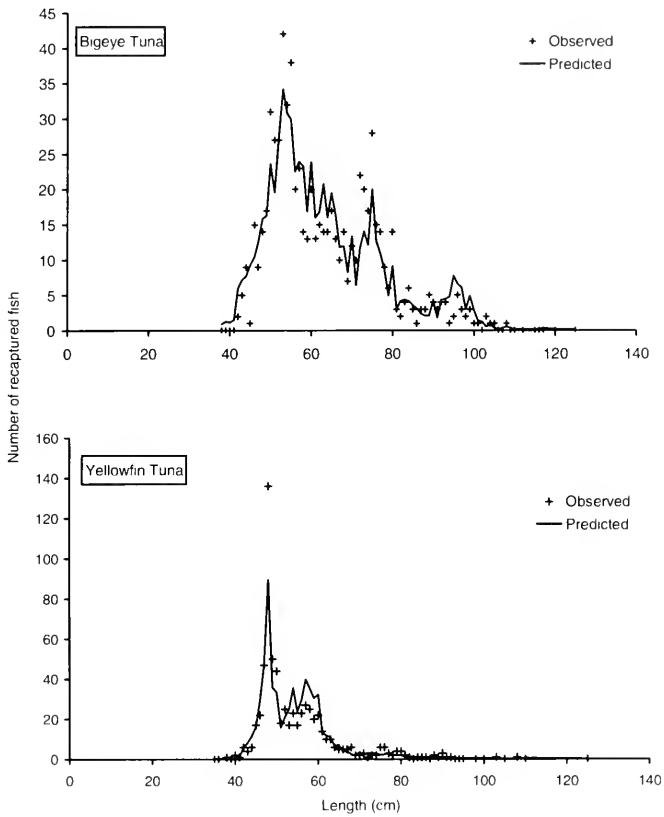

Figure 3

Observed (crosses) and predicted (continuous lines) tag returns by initial release length from the Cross Seamount for bigeye and yellowfin tuna.

average gross attrition for the entire geographic range of the model area was not very different for the two species (0.033/day for bigeye and 0.034/day for yellowfin tuna). Similar results were obtained in a preliminary analysis of the early recaptures (Holland et al., 1999). In other words, there are consistent indications that yellowfin and bigeye tuna behave differently at Cross Seamount.

The attrition rate measures the rate of loss from the system. A more intuitive measure may be calculated from "half-life" ($\ln(2)/Z_{ik}$) which is a proxy for population residence (Holland et al., 1999). Essentially, half-life is the time required to reduce an existing size of the population by half. The half-life of about 18 days for yellowfin tuna at Cross Seamount was roughly one half that of bigeye tuna (31 days). Although the half-life across the size classes for yellowfin tuna was similar, the half-life for the large size classes of bigeye tuna were significantly longer than those for the smallest size class (Table 6).

Table 7 shows the ratios of the attrition components to the total gross attrition for both species on the Cross Seamount. Roughly 70% of the total loss is due to emigration. Fishing mortality accounted for about 12% for each of the three size classes of bigeye tuna whereas yellowfin tuna F estimates were 7%, 30%, and 20%, respectively. The contribution of natural mortality to overall attrition in the smaller size classes was substantial. This was 24% for bigeye and 35% for yellowfin tuna. In the larger size classes, the contributions were in the range 6–16%.

Table 3

Yellowfin tuna: Observed and predicted tag transfers from the full model $M_3F_{3,6}T_{17}$, n = 38. The rows are tag release sites and columns are recapture sites.

	Recapture sites						
Tag release sites	All	Buoy 1	Buoy 2	Buoy 3	Cross Seamount	Inshore	Other
Observed							
All	970	20	40	9	635	254	12
Buoy 1	36	19	0	0	5	9	13
Buoy 2	47	0	32	1	7	6	1
Buoy 3	13	0	2	8	2	1	0
Cross Seamount	667	0	5	0	618	38	6
Inshore	207	1	1	0	3	200	2
Other	0	0	0	0	0	0	0
Predicted							
All	978.9	20.2	40.6	8.7	634.5	258.8	16.1
Buoy 1	33.5	18.6	0.5	0.0	5.0	8.1	1.3
Buoy 2	46.4	0.1	17.4	4.0	16.9	7.7	0.4
Buoy 3	7.8	0.0	0.6	1.1	3.9	2.0	0.1
Cross Seamount	677.1	0.4	20.7	3.2	606.5	34.3	11.9
Inshore	214.1	1.0	1.4	0.4	2.3	206.6	2.4
Other	0.0	0.0	0.0	0.0	0.0	0.0	0.0

Table 4

Bigeye tuna: Estimated transfer coefficients (per day) from the full model $M_3F_{3,5}T_{13}$, n = 31. Elements with asterisks indicate transfers that were not observed. The diagonal elements (dashed) were not defined in the model.

	Recapture sites				
Tag release sites	Buoy 2	Buoy 3	Cross Seamount	Inshore	Other
Buoy 2	—	0.00245	0.00113	0.00752	0.02707
Buoy 3	0.00000	—	0.01111	0.01073	0.03927
Cross Seamount	0.00045	0.00026	—	0.00464	0.01057
Inshore	**	**	0.00375	—	**
Other	**	**	**	**	—

Table 5

Yellowfin tuna: Estimated transfer coefficients (per day) from the full model $M_3F_{3,6}T_{17}$, n = 38. Elements with asterisks indicate transfers that were not observed. The diagonal elements (dashed) were not defined in the model.

	Recapture sites					
Tag release sites	Buoy 1	Buoy 2	Buoy 3	Cross Seamount	Inshore	Other
Buoy 1	—	**	**	0.00648	0.01055	0.04935
Buoy 2	**	—	0.04301	0.00217	0.00000	0.00024
Buoy 3	**	0.00036	—	0.00205	0.00101	**
Cross Seamount	**	0.00226	**	—	0.00136	0.02051
Inshore	0.00042	0.00069	**	0.00000	—	0.00703
Other	**	**	**	**	**	—

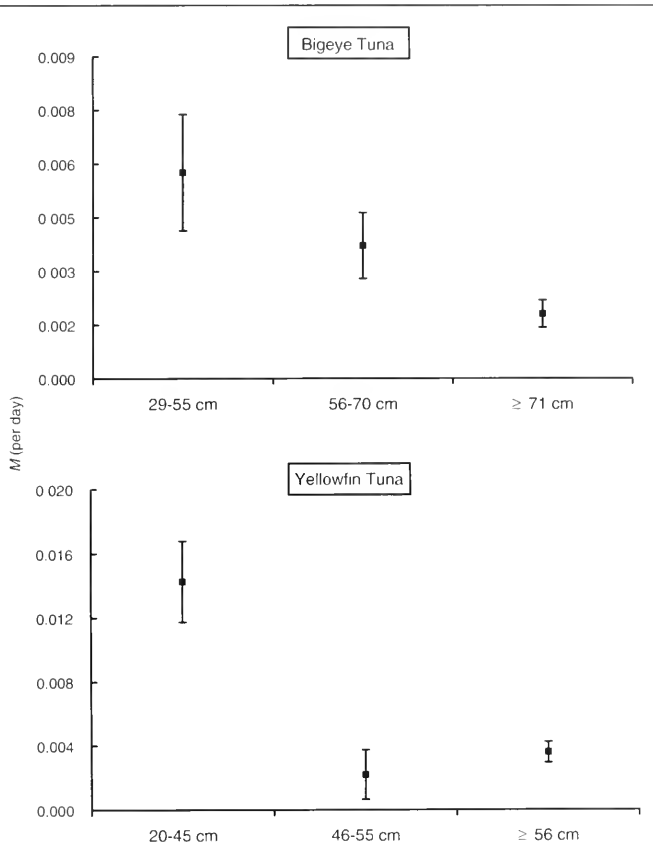

Figure 4

Estimates of natural mortality rates (M) by size classes for bigeye and yellowfin tuna. Error bars are one standard deviation across the mean value.

Discussion

The size- and site-specific attrition model described in this study is new and potentially applicable to other fish species where release and recapture data meet the model requirements. What is required are the size and geographic position of releases and recaptures. One difficulty encountered related to the quantity of release data that was available for analysis. Because releases were stratified over 1-cm size class cohorts to reliably track their growth over time, larger numbers of releases would be required to have reasonable numbers in the cohorts. Thus we assumed that all tags were released at some arbitrary time zero.

Attempts to estimate size-specific transfer rates were unsuccessful because of poor convergence of the numerical estimation procedure. Size-specific transfer rates were poorly defined in the data sets because of the low number of recaptures in the relevant strata. It is, however, trivial to incorporate size-specific transfer rates in the model and use the same procedure to estimate the transfer rates by the size classes under consideration.

The growth of yellowfin and bigeye tuna in our model is assumed to follow the von Bertalanffy growth function for the entire lifetime of the cohort. However, Lehodey and Leroy,[4]

[4] Lehodey, P., and B. Leroy. 1998. Age and growth of yellowfin tuna (*Thunnus alabcares*) from the western and central Pacific Ocean as indicated by daily growth increments and tagging data. Working paper 12. Eleventh Standing Committee on Tunas and Billfish, Secretariat of Pacific Community, BP D5, 98848 Noumea Cedex, New Caledonia

Table 6

Estimates of size specific attrition components (per day) and residence times (half-life [days]) at the Cross Seamount with standard deviations of the estimates (in parentheses). Note: The different size classes for the two species; size classes. Also note that the size-independent transfer rates makes the emigration component constant for all the size classes. M is natural mortality rate; F is fishing mortality rate.

		Bigeye tuna		
Component	From	29–55 cm	56–70 cm	≥71 cm
M	All	0.0058 (0.0016)	0.0037 (0.0009)	0.0018 (0.0004)
F	Cross	0.0023 (0.0003)	0.0029 (0.0003)	0.0026 (0.0003)
Emigration rate	Cross	0.0159 (0.0017)	0.0159 (0.0017)	0.0159 (0.0017)
Residence time	Cross	28.9 (2.6)	30.7 (206)	34.0 (3.1)
		Yellowfin tuna		
	From	20–45 cm	46–55 cm	≥56 cm
M	All	0.0143 (0.0025)	0.0022 (0.0016)	0.0036 (0.0006)
F	Cross	0.0027 (0.0009)	0.0115 (0.0019)	0.0067 (0.0007)
Emigration rate	Cross	0.0241 (0.0019)	0.0241 (0.0019)	0.0241 (0.0019)
Residence time	Cross	16.9 (1.3)	18.3 (1.1)	20.1 (1.4)

Hampton and Fournier (2001) and Hampton and Fournier[2] have shown that growth of smaller-size fish does not conform to the von Bertalanffy function. They estimated a more linear and an increased growth rate for smaller sizes (<120 cm FL for yellowfin and <80 cm FL for bigeye tuna) than could be accounted from the von Bertalanffy function for the entire size range. Although this could, in principal, bias our size-based estimates of F and M, considering the growth variability and the large size ranges we have considered, we feel departure from von Bertalanffy growth is of little importance.

One of the primary objectives of the HTTP was to improve understanding of the dynamics of tuna aggregations at the Cross Seamount and to determine the importance of Cross Seamount associated fish to domestic longline and inshore fisheries. This discussion will therefore focus on the Cross Seamount fishery and its potential interaction with other fisheries. Previous analyses (using fewer data) have estimated gross attrition rates and residence times (Holland et al., 1999) and transfer and attrition rates (Sibert et al., 2000). Using the more recent and complete data set and including size specific attrition to improve the tag-attrition model, we have been able to extend the analysis to provide a more detailed picture of fishery dynamics and interactions.

The natural mortality rate is a critical parameter in stock assessment models, and size- (or age-) specific estimates would greatly improve stock assessment efforts. Unfortunately, natural mortality is not linked to a well-defined *in situ* process, and M is always estimated indirectly (e.g. Fournier et al., 1998). In tag attrition models, M is the "residual attrition" that cannot be accounted for by processes specified in the model. In our model, M would also include permanent emigration beyond the model area. Hampton (2000) estimated natural mortality rates from tagging data for a large number of size classes from a "single fishery" model. We have shown here that the attrition component can also be partitioned into size classes in a bulk transfer model. The relatively low number of recoveries from most of the sites did not allow us to estimate attrition over a larger number of size classes. However, our estimates of M are consistent with Hampton's (2000) estimates for both species within the size ranges considered.

Table 7

Attrition component ratio (scaled by the total attrition) by size classes at Cross Seamount for bigeye and yellowfin tuna. E is the emigration rate.

Size class (cm)	M/Z	F/Z	E/Z
Bigeye tuna			
29–55	0.24	0.10	0.66
56–70	0.16	0.13	0.71
≥71	0.09	0.13	0.78
Yellowfin tuna			
20–45	0.35	0.07	0.59
46–55	0.06	0.30	0.64
≥56	0.10	0.20	0.70

The relatively low transfer rate estimates for both species from the Cross Seamount to the inshore areas supports earlier findings (Sibert et al., 2000). However, the relatively high transfer rates estimated for both species from the Cross Seamount and the offshore buoys to the longline fishery (and by inference to the Pacific-wide fishery)

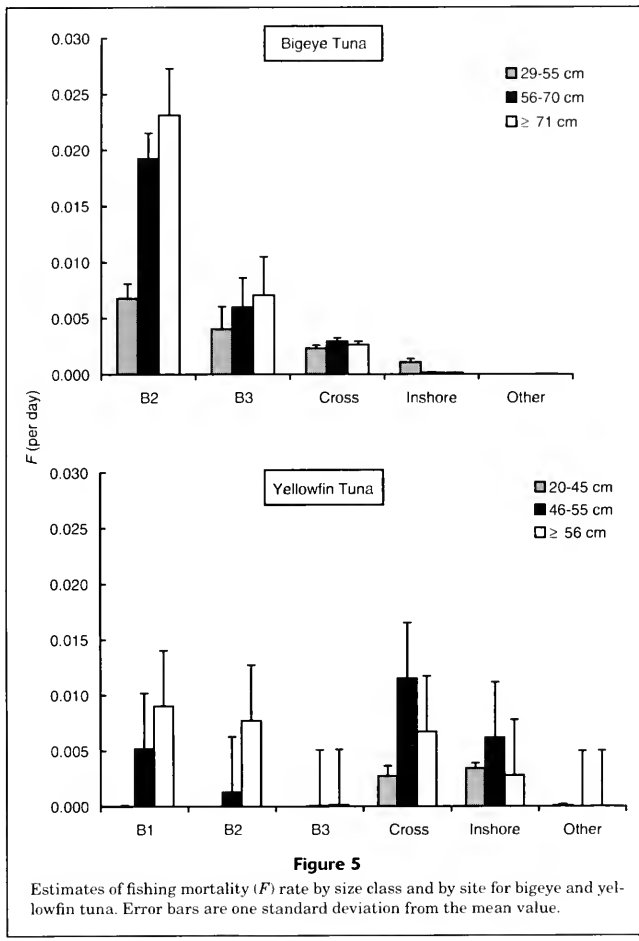

Figure 5

Estimates of fishing mortality (F) rate by size class and by site for bigeye and yellowfin tuna. Error bars are one standard deviation from the mean value.

suggests that fish associated with these structures contribute substantially to the longline catch. Furthermore, the longline fishery considered in our model is an open compartment with no boundaries. Any recoveries outside the bounded compartments will be considered as an emigrant from inshore and offshore fisheries' perspective. In the likely scenario of higher underreporting of recoveries from non-Hawaii-based fisheries, our estimate of transfer rates from inshore and offshore sites to the longline fishery will be lower.

At first glance the higher transfer rates to the longline fishery could be explained by the fact that these offshore locations are contained within the geographical areas of operation of the longline fishery. However, analysis of the time-at-liberty of fish released at Cross Seamount indicates that they first become vulnerable within the inshore FAD areas before recruiting to the longline fishery. For instance, bigeye tuna released at Cross Seamount were caught after 238 ±156 (median 254) days in the inshore fisheries but in the longline fishery they were caught after 542 ±297 (median 509) days. For yellowfin tuna however, there was little difference; 154 ±134 (median 88) days in the inshore fisheries and 157 ±112 (median 89) days in the longline fishery. These interspecific differences could be due in part to the different vulnerability of the two species to the gears used in the inshore and longline fisheries. Inshore fisheries generally target surface swimming fish, thereby favoring the exploitation of smaller-size yellowfin tuna, whereas the longline gear targets deep swimming adults. Implicit in these results are size-specific vulnerabilities in the inshore

and longline fishery. Similar to the inshore fisheries, the Seamount fishery targets surface swimming fish favoring small- to medium-size classes.

Because of the way in which cohorts were aggregated to maximize the number released per cohort, time varying fishing effort could not be used to reparameterize F with a catchability coefficient (e.g. Hampton, 2000). Instead, F was estimated as a constant proportion of the numbers available at a given time period. This was considered reasonable because there was no reason to believe that the fishery underwent notable change during the period of the tagging experiment. Under this assumption, F is similar to a catchability coefficient. Because both species are targeted with the same suite of gears (Itano and Holland, 2000), the differences in F would reflect their vulnerability to the gears. Higher overall F (vulnerability) at the Cross Seamount for yellowfin compared to bigeye tuna indicates that yellowfin tuna are more vulnerable there.

The gross attrition rate for any given spatial component Z_i in our model includes size-dependent M and F and size-independent T (emigration rate). At the Cross Seamount, the actual estimates of all three components were generally lower for bigeye than for yellowfin tuna, thereby making the estimated residence times for bigeye tuna roughly twice as high as those for yellowfin tuna (Table 6). Our estimate of residence time for bigeye tuna agree closely with earlier estimates (Holland et al., 1999; Sibert et al., 2000). More recently Musyl et al. (2003) found similar results from archival tagging data based on geolocation and vertical movement patterns. They estimated bigeye tuna residence time of 25 ±12 days at the Cross Seamount area—a value consistent with the estimates derived here using conventional tagging data.

Putting aside M, we do know why yellowfin tuna emigration rate from the Cross Seamount is higher while they appear to be more vulnerable in the fishery than bigeye tuna. Their higher vulnerability could in part be explained by their shallower swimming depths that bring them into more frequent contact with handline and troll gear. However, bigeye tuna contribute greatest to the commercial catches by weight from the Seamount (Itano and Holland, 2000). Sibert et al. (2000) suggested that this apparent discrepancy could be due to a much higher biomass of bigeye tuna on the Seamount compared to biomass of yellowfin tuna, coupled with longer residence times.

The apparent longer residence times for bigeye tuna at the Seamount could be due to longer periods of continuous residence or a greater tendency to revisit over time (or to both factors). It is possible that bigeye tuna may gain a trophic advantage by extended association with seamounts (Fonteneau, 1991; Brill and Lutcavage, 2001). Behavior of bigeye tuna associated with Cross Seamount, inferred from archival tag data (Musyl et al., 2003), indicates that their vertical movements are akin to the characteristic open water behavior. That is, they move within the surface mixed layer at night but remain deep during the day except for brief upward excursions (Holland et al., 1990; Dagorn and Josse, 2000). However, Musyl et al. (2003) note the irregular and sometimes more extended day-night transitions of the putative Cross Seamount associated bigeye tuna. This modified behavior at Cross Seamount, during day and night, could indicate that bigeye tuna are exploiting a food source that may not be available to or not preferred by sympatric yellowfin tuna. Unfortunately, similar vertical movement observations for yellowfin tuna at Cross Seamount are not currently available. Preliminary investigation on the food habits of bigeye and yellowfin tuna at Cross Seamount and offshore weather buoys suggest feeding ecology is very different between the two species even at immature sizes (Grubbs et al.[4]). They suggest that separation in vertical distribution may be maintained during feeding. Bigeye tuna may target the deep-scattering-layer prey while yellowfin tuna feed primarily on mixed-layer prey.

Estimates of horizontal movement patterns of bigeye tuna equipped with archival tags suggest that almost all bigeye tuna released from the Seamount stayed within close proximity of the seamount and around the Main Hawaiian Island chain (Sibert et al., 2003). The relatively high transfer rates between the Cross Seamount and the NOAA weather buoys and the similar magnitude of transfer rates between Cross Seamount and inshore areas suggests that the apparently lower emigration rate of bigeye tuna is due to returnees contributing to the recapture attrition curve. Given the estimated F at the Seamount for the two species in this study, the number of bigeye tuna residing at Cross Seamount has to be at least an order of magnitude greater than that for yellowfin tuna to match the catch observed in fishery statistics.

The overall picture emerging from the analysis is similar to the earlier findings of Sibert et al. (2000). At any given time the resident population (or standing stock) of yellowfin on the Cross Seamount is considerably smaller than the bigeye tuna population. However, during their brief stopovers on the Cross Seamount, yellowfin tuna are highly vulnerable to the offshore handline-troll fishery that occurs there. They associate with the Cross Seamount but leave quite rapidly, and most of them never return. In contrast, the longer apparent residency, or persistence, of bigeye tuna at the Cross Seamount may be due to longer periods of association and a tendency to return to the Seamount over time. Even though they tend to leave the Seamount (perhaps permanently when they grow to larger sizes), they appear to remain in the Hawaii area, at least for two to three years. Some of them become vulnerable in the inshore area but, if not captured, they are later caught by the longline fishery. This situation is very similar to the aggregation of bigeye tuna in the Coral Sea in northwestern Australia (Hampton and Gunn, 1998) where bigeye tuna appear to have a lower attrition rate than yellowfin tuna. Hampton and Gunn (1998) argued that although both species gradually disperse from the Coral Sea area, large numbers of bigeye tuna remain resident in the area for some

[4] Grubbs, R. D., K. Holland, and D. Itano. 2001. Food habits and trophic dynamics of structure-associated aggregations of yellowfin and bigeye tuna (*Thunnus albacares*, and *T. obesus*) in the Hawaiian Islands. Project description, rationale and preliminary results. Presented at the Fourteenth Standing Committee on Billfish and Tunas; Yellowfin Research Group, 9–16 August 2001. Secretariat of Pacific Community, BP D5, 98848 Noumea Cedex, New Caledonia.

time and become vulnerable in the fishery. More recently, archival tagging on drifting FADs in the eastern Pacific Ocean have shown that bigeye tuna remain resident in the general area of release for at least about an year (Schaefer and Fuller, 2002). In our study virtually all (99.4%) of bigeye tuna recoveries were made within the model area. These observations suggest some degree of regional fidelity in the exploited phase (medium size) of bigeye tuna and a low level of mixing with the central western Pacific region for these immature size classes. However, it appears that larger size bigeye tuna are not resident in Hawaiian waters because spawning condition adults do not recruit to the local longline or handline fisheries. It is likely that as these fish mature they move to warmer waters to the south of Hawaii where bigeye tuna spawning is known to occur (Nikaido et al., 1991).

The extent of catch interaction between the Cross Seamount fishery and the domestic inshore and longline fisheries does not appear to be of great management concern at current levels of exploitation. However, given that current exploitation rates are considered moderate (10–30%) and the seamount aggregations are highly vulnerable to low cost gear types, it was recommended that further increases in fishing effort for yellowfin and bigeye tuna be monitored at Cross Seamount. This note of caution is reinforced by the increased concern over recent bigeye and yellowfin tuna stock assessments from the western and central Pacific (Hampton and Fournier, [2001]; Hampton and Fournier[2]). These assessments suggest declining adult biomass, declining recruitment, and greatly increased fishing mortality on juveniles in the equatorial region, which is probably the main source of recruitment to the Cross Seamount and Hawaii-based fisheries.

Additional strategic tagging experiments involving the release of tuna should represent the full geographic and size range landed in the fisheries to adequately refine our estimates of fishery interaction and transfer rates. Comparative studies of yellowfin and bigeye tuna using electronic tags would also help to understand differences in how the two species partition their habitat. However, the current size-based estimates of natural and fishing mortality rates, together with transfer rates and other ancillary information, still remain useful to conduct a yield-per-recruit analysis to investigate various scenarios arising from an increase or decrease in fishing effort and its effects on the fishery components. The results of this analysis will also be useful in refining stock assessment models that are currently being developed for the species.

Acknowledgments

The research was funded under Cooperative Agreement No. NA67RJ0154 from National Oceanographic Atmospheric Administration and administered by the Pelagic Fisheries Research Program, Joint Institute of Marine and Atmospheric Research of the University of Hawaii. We are grateful to Pierre Kleiber for his advice in the data analysis. Comments from two anonymous reviewers greatly improved the manuscript.

Literature cited

Adam, M. S., and G. P. Kirkwood.
2001. Estimating tag-shedding rates for skipjack tuna, *Katsuwonus pelamis*, off the Maldives. Fish. Bull. 99: 193–196.

Boggs, C. H., and R. Y. Ito.
1993. Hawaii's pelagic fisheries. Mar. Fish. Rev. 55(2): 69–82.

Brownlee, K. A.
1965. Statistical theory and methodology, 590 p. John Wiley & Sons, New York, NY.

Brill, R. W., and M. E. Lutcavage.
2001. Understanding environmental influences on movements and depth distributions of tunas and billfishes can significantly improve population assessments. Am. Fish. Soc. Symp. 25:179–198.

Dagorn, L., P. Bach, and E. Josse.
2000. Movement patterns of large bigeye tuna (*Thunnus albacares*) in the open ocean determined using ultrasonic telemetry. Mar Biol. 136:361–371.

Fonteneau, A.
1991. Seamounts and tuna in the Tropical Eastern Pacific. Aquat. Living Res. 4:13–25.

Fournier, D., J. Hampton, and J. R. Sibert.
1998. MULTIFAN-CL: a length-based, age-structured model for fisheries stock assessment, with application to south Pacific albacore, *Thunnus alalunga*. Can. J. Fish. Aquat. Sci. 55:2105–2116.

Hamilton, M. S., and S. W. Huffman.
1997. Cost-earnings study of Hawaii's small boat fishery, 1995–1996, 104 p. University of Hawaii, Joint Institute for Marine and Atmospheric Research, Honolulu, HI.

Hampton, J.
1991a. Estimation of southern bluefin tuna *Thunnus maccoyii* natural mortality and movement rates from tagging experiments. Fish. Bull. 89:591–610.
1991b. Estimation of southern bluefin tuna *Thunnus maccoyii* growth parameters from tagging data, using von Bertallanffy models incorporating individual variation. Fish. Bull. 89:577–590.
1997. Estimation tag reporting and tag-shedding rates in a large-scale tuna tagging experiment in the western tropical Pacific Ocean. Fish. Bull. 95:68–79.
2000. Natural mortality rates in tropical tunas: size really does matter. Can. J. Fish. Aquat. Sci. 57:1002–1010.

Hampton, J., and D. Fournier.
2001. A spatially-disaggregated, length-based, age-structured population model of yellowfin tuna (*Thunnus albacares*) in the western and central Pacific Ocean. Mar. and Freshwater Res. 52:937–963.

Hampton, J., and J. Gunn.
1998. Exploitation and movements of yellowfin tuna (*Thunnus albacares*) and bigeye tuna (*T. obesus*) tagged in the north-western Coral Sea. Mar. Freshwater Res. 49:475–89

Hilborn, R., and M. Mangel.
1997. The ecological detective: confronting models with data Monographs in population biology series, no. 28, 136 p. Princeton Univ. Press, Princeton, NJ.

Holland, K., R. W. Brill, and R. K. C. Chang.
1990. Horizontal and vertical movements of yellowfin and bigeye tuna associated with fish aggregating devices. Fish. Bull. 88:493–507.

Holland, K. N., P. Kleiber, and S. M. Kajiura.
1999. Different residence times of yellowfin tuna, *Thunnus*

albacares, and bigeye tuna, *T. obesus*, found in mixed aggregations over a seamount. Fish. Bull. 97:392–395.

Itano, D., and K. Holland.
2000. Movement and vulnerability of bigeye (*Thunnus obesus*) and yellowfin tuna (*T. albacares*) in relation to FADs and natural aggregation points. Aquat. Living Resour. 13: 213–223.

Kirkwood, G. P., and M. H. Walker.
1984. A new method for estimating tag shedding rates, with application to data for Australian Salmon, *Arripis trutta esper*, Whitely. Aust. J. Mar. Freshwater Res. 35:601–606.

Kirkwood, G. P., and I. F. Somers.
1984. Growth of two species of tiger prawn, *Panoeus esculentus* and *P. semisculatus*, in the western Gulf of Carpentria. Aust. J. Mar. Freshwater Res. 35:703–712.

James, I. R.
1991. Estimation of von Bertalanffy growth curve parameters from recapture data. Biometrics 47:1519–1530.

Kleiber, P., A. W. Argue, and R. E. Kearney.
1987. Assessment of Pacific skipjack tuna (*Katsuwonus pelamis*) resources by estimating standing stock and components of population turnover from tagging data. Can. J. Fish. Aquat. Sci. 44:1122–1134.

Musyl, M. K., R. W. Brill, C. H. Boggs, D. S. Curran, T K. Kazama, and M P. Seki.
2003. Vertical movements of bigeye (*Thunnus obesus*) associated with islands, buoys, and seamounts near the main Hawaiian Islands from archival tagging data. Fish. Oceanogr. 12(2):1–18.

Nikaido, H., N. Miyabe, and S. Ueyanagi.
1991. Spawning time and frequency of bigeye tuna, *Thunnus obesus*. Nat. Res. Inst. Far. Seas Fish. Bull. 28:47–73.

Otter Research Ltd.
2000. AD model builder documentation. Otter Research Ltd. [URL: http://otter-rsch.com/admodel.htm>], accessed November 2002.

Pooley, S. G.
1993. Economics and Hawaii's marine fisheries. Mar. Fish. Rev. 55(2):93–101.

Schaefer, K. M., and D.W. Fuller.
2002. Movements, behavior, and habitat selection of bigeye tuna (*Thunnus obesus*) in the eastern equatorial Pacific, ascertained through archival tags. Fish. Bull. 100(4): 765–788.

Sibert, J. R., K. Holland, and D. Itano.
2000. Exchange rates of yellowfin and bigeye tunas and fishery interaction between Cross seamount and near-shore FADs in Hawaii. Aquat. Living Resour. 13:225–232.

Sibert, J. R., M. K. Musyl, and R. W. Brill.
2003. Horizontal movements of bigeye tuna (*Thunnus obesus*) near Hawaii determined by Kalaman filter analysis of archival tagging data. Fish. Oceanogr. 12(3):1–11.

Wang, Y.-G., and M. R. Thomas.
1995. Accounting for individual variability in the von Bertalanffy growth model. Can. J. Fish. Aquat. Sci. 52:1368–1375.

The geographic basis for population structure in Fraser River chinook salmon (*Oncorhynchus tshawytscha*)

Terry D. Beacham
K. Janine Supernault
Michael Wetklo
Bruce Deagle
Karen Labaree
James R. Irvine
John R. Candy
Kristina M. Miller
R. John Nelson
Ruth E. Withler

Department of Fisheries and Oceans
Pacific Biological Station
3190 Hammond Bay Road
Nanaimo, British Columbia, Canada V9T 6N7
E-mail address (for T. D. Beacham): Beachamt@pac.dfo-mpo.gc.ca

Abstract—We surveyed variation at 13 microsatellite loci in approximately 7400 chinook salmon sampled from 52 spawning sites in the Fraser River drainage during 1988–98 to examine the spatial and temporal basis of population structure in the watershed. Genetically discrete chinook salmon populations were associated with almost all spawning sites, although gene flow within some tributaries prevented or limited differentiation among spawning groups. The mean F_{ST} value over 52 samples and 13 loci surveyed was 0.039. Geographic structuring of populations was apparent: distinct groups were identified in the upper, middle, and lower Fraser River regions, and the north, south, and lower Thompson River regions. The geographically and temporally isolated Birkenhead River population of the lower Fraser region was sufficiently genetically distinctive to be treated as a separate region in a hierarchial analysis of gene diversity. Approximately 95% of genetic variation was contained within populations, and the remainder was accounted for by differentiation among regions (3.1%), among populations within regions (1.3%), and among years within populations (0.5%). Analysis of allelic diversity and private alleles did not support the suggestion that genetically distinctive populations of chinook salmon in the south Thompson were the result of postglacial hybridization of ocean-type and stream-type chinook in the Fraser River drainage. However, the relatively small amount of differentiation among Fraser River chinook salmon populations supports the suggestion that gene flow among genetically distinct groups of postglacial colonizing groups of chinook salmon has occurred, possibly prior to colonization of the Fraser River drainage.

Manuscript accepted 22 October 2002.
Manuscript received 31 December 2002 at NMFS Scientific Publications Office.
Fish. Bull. 101(2):229–242 (2003).

The Fraser River drainage supports the largest group of chinook salmon (*Oncorhynchus tshawytscha*) populations in North America, and the most abundant individual chinook salmon population in British Columbia (the Harrison River in the lower Fraser River drainage). Chinook salmon are distributed throughout the entire Fraser River drainage, and spawning populations exist in approximately 65 tributaries (Fraser et al., 1982). There is substantial variation among and within populations for life history traits such as length of juvenile freshwater residence, size and age at maturity, and timing of adult migration and spawning. Juveniles (largely from the Harrison River population) can migrate to the marine environment immediately after fry emerge in the spring, or during the first summer after developing in fresh water for several months ("ocean-type"), or they can remain in fresh water for a year or longer ("stream-type") before migrating to the ocean (Fraser et al., 1982; Healey, 1983, 1991).

Migrating adult chinook salmon returning to spawn in Fraser River tributaries enter the drainage from April to October—individual populations having characteristic migration times (Fraser et al., 1982). Spring or "early run" populations are designated as those in which at least 50% of the fish pass through the lower Fraser by 15 July and include populations of the mid and upper Fraser areas, the lower Thompson area, and a small lower Fraser population that spawns in the upper reaches of the Harrison drainage (Birkenhead River). Summer or "mid run" populations are those in which the majority of the fish pass through the lower Fraser after 15 July, but before 31 August, and include populations of the mid Fraser area, and the north and south Thompson areas. Chinook salmon of the large Harrison River population are fall or "late run" fish and enter the lower Fraser in September and October. Thus, in the Fraser drainage, it is the late-run Harrison population of the lower Fraser that is characterized by ocean-type juveniles, whereas the earlier migrating spring and summer populations of the interior Fraser drainage are characterized by stream-type juveniles. Exceptions are

several interior populations of the South Thompson River system, which produce substantial proportions of both stream- and ocean-type juveniles (DFO[1]).

Variability in chinook salmon flesh pigmentation levels exceeds that of other Pacific salmonids, resulting from a phenotypic dichotomy of "red-fleshed" and "white-fleshed" forms that is under relatively simple genetic control (Withler, 1986; McCallum et al., 1987). Chinook salmon that return to spawn in the Fraser River are mixtures of red- and white-fleshed fish (Godfrey, 1975). The large Harrison River population is considered to be entirely white-fleshed; whereas red-fleshed fish predominate in populations of the upper Fraser and Thompson drainages. Red-fleshed chinook salmon are also abundant in mid-Fraser tributaries, but a number of populations are polymorphic for flesh color (e.g. the Quesnel River population consists of approximately equal proportions of the two flesh colors).

Similar variation in migration timing and juvenile fresh water residence times is observed in chinook salmon of the Columbia River drainage (Myers et al., 1998). In that system, adult migration time is not simply correlated with juvenile life history type; spring-, summer-, and fall-run populations in the lower and mid Columbia regions can all be characterized by ocean-type juveniles. Genetic analysis has indicated that, in the Columbia drainage, juvenile life history type is a better indicator of genetic relationships among populations than is adult migration time and supports the suggestion that the juvenile life history types might represent separate "races" in that area (Myers et al., 1998). In British Columbia, which has been recolonized by chinook and other salmon species in the last 10,000 years since the Wisconsin glacial period from as many as four possible refugial areas (Gharrett et al., 1987; Wilson et al., 1987; Utter et al., 1989; Cronin et al., 1993), the phylogenetic relationships of ocean- and stream-type populations have yet to be determined and may vary on a geographic basis dependent on both adaptation and the history of colonization.

In the Fraser River, a genetic demarcation between fish of the lower and interior Fraser watersheds observed in coho and sockeye salmon and attributed to independent postglacial colonization of the two regions (Wehrhahn and Powell, 1987; Wood et al., 1994; Small et al., 1998; Withler et al., 2000), is also evident in chinook salmon (Beacham et al., 1996; Teel et al., 2000; Nelson et al., 2001). Factors underlying the substantial genetic differentiation among chinook salmon occupying different areas of the interior Fraser watershed, a region postulated to have been colonized from the Columbia River refuge (Utter et al., 1989), are less clear (Teel et al., 2000; Nelson et al., 2001).

Differentiation among areas within the Thompson drainage, and between the interior Fraser and Thompson drainages, has also been observed in coho and sockeye salmon. Of the three species, the chinook salmon is the most extensively and continuously distributed throughout the interior Fraser region. The variability in age of maturity, both within and among populations, is greater in chinook salmon than in coho or sockeye salmon—a factor that may increase the effective number of spawning fish each year and reduce genetic variability due to drift both within and among populations of chinook salmon. On the other hand, the development of population-specific anatomical structures and life history traits indicate that recent gene flow has been sufficiently restricted among populations to enable strong adaptation (Taylor, 1991).

The presence of ocean-type juveniles in the Eagle and Shuswap River populations of the relatively warm and productive South Thompson River drainage may represent a relatively recent adaptive response to environmental conditions enabling attainment of sufficient size in the first spring of freshwater residence for juveniles to undertake seaward migration. Conversely, Teel et al. (2000) suggested that chinook salmon of the south Thompson region were genetically intermediate to those of the mid–upper and lower Fraser areas and might represent hybridization of stream- and ocean-type races that independently colonized the lower and interior portions of the Fraser drainage.

Conservation of chinook salmon genetic diversity within the Fraser River requires delineation of the phylogenetically and adaptively distinct groups within the drainage, an understanding of their origins and the evolutionary processes promoting and maintaining their differentiation, and the ability to manage them on an independent basis. Similar zoogeographic factors will have influenced the coho, chinook, and sockeye populations recolonizing the Fraser drainage, although the differing utilization of glacial refugia, environmental requirements, and propensities for homing and straying may have resulted in quite different evolutionary responses among them.

The objective of the present study was to analyze variation at 13 microsatellite loci in 52 samples of chinook salmon from the Fraser and Thompson River drainages to determine population structure. By detecting differentiation in allelic frequencies, levels of allelic diversity, and the presence of unique alleles, we were able to use the high levels of polymorphism and heterozygosity at the microsatellite loci to indicate the relationships among chinook salmon occupying different regions of the Fraser drainage. The distribution of genetic diversity in the Fraser River drainage among regions, populations, and sampling years is estimated, as well as the stability of population structure within major tributaries of the Fraser River. We also examined the patterns of divergence within the drainage with respect to ocean- and stream-type life histories.

Materials and methods

Collection of baseline DNA samples and laboratory analysis

Genomic DNA was extracted from either liver, scales, operculum punches, or fin clips from chinook salmon sampled between 1987 and 1998 by using the phenol-chloroform

[1] DFO (Department of Fisheries and Oceans). 1995. Fraser River chinook salmon. Fraser River Action Plan, Fishery Management Group, Vancouver, British Columbia, Canada, 24 p. [Available from Fisheries and Oceans, 555 West Hasting St., Suite 1220, Vancouver, British Columbia, Canada V6B 5G3.]

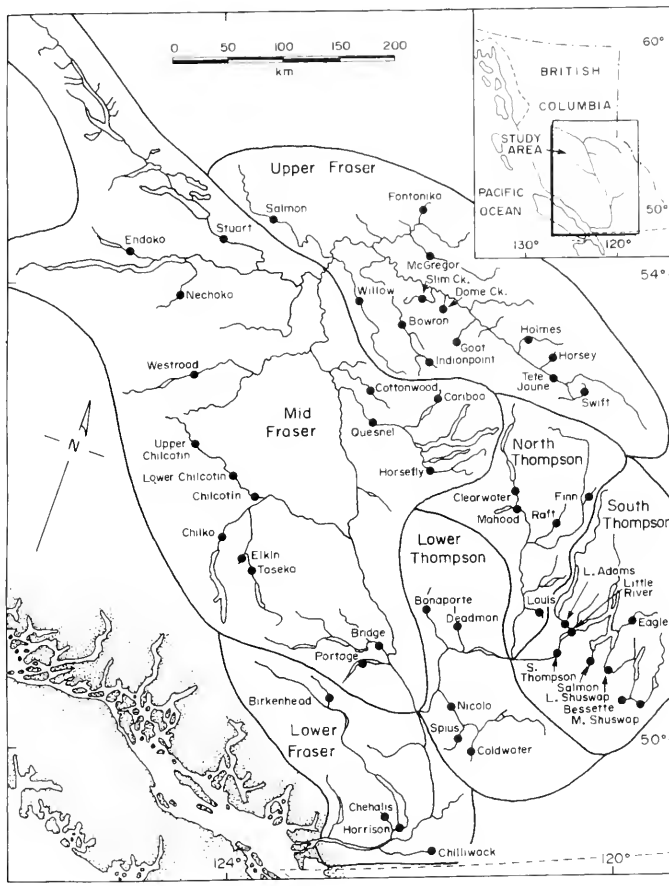

Figure 1

Locations in the Fraser River drainage where 52 chinook salmon spawning aggregates were sampled at least once during 1988–98.

protocol of Miller et al. (1996) (early extractions) or the chelex resin protocol of Small et al. (1998) (later extractions). Samples were derived from adults in all areas except the McGregor River where, because of the difficulty of obtaining adults, juveniles were sampled (Fig. 1). Samples of adults were obtained from hatcheries during egg collections, from wild spawning fish or carcasses on the spawning grounds, or in the case of the Chilcotin River sample, from a mixed sample of angled fish from the river.

For the survey of baseline populations, PCR products at six microsatellite loci—*Ots100*, *Ots101*, *Ots102*, *Ots104*, *Ots107* (primers outlined by Nelson and Beacham, 1999) and *Ssa197* (O'Reilly et al., 1996)—were size-fractionated on nondenaturing polyacrylamide gels by staining with 0.5 mg/mL ethidium bromide in water and illuminating with ultraviolet light. Nelson et al. (1998, 2001) have provided a more complete description of gel electrophoretic conditions. Three 20-bp marker lanes (Gensura Labs Inc., Del Mar, CA), 24 population samples, and one standard fish were run on each gel. The size of the amplified alleles were determined from the molecular size grid created with the 20-bp markers. Digital images of the resulting gels were analyzed by using BioImage Whole Band software (Millipore Corp. Imaging Systems, Ann Arbor, MI). Beacham and Wood (1999) provided a more complete description of the methods used to identify alleles with this technology. Precision of estimation of allele size with this technology has been outlined for *Ots100*, *Ots101*, and *Ots102* by Nel-

son et al. (2001), and for loci in other species by Beacham and Wood (1999) and Beacham et al. (2000). Precision of estimation of allele size for *Ots104*, *Ots107*, and *Ssa197* was similar to that for other loci with alleles spanning a similar size range. For example, estimated allele size for a standard fish analyzed 515 times at *Ots107* was within a 4-bp interval 98% of the time for an estimated allele size of 171 bp, and 85% of the time for an allele size of 300 bp. As outlined by Nelson et al. (2001), bin widths were expanded at larger allele sizes to account for less precise estimation of allele size as determined from the standard fish, and alleles were defined on the basis of bin width.

With the acquisition of an automated DNA sequencer (the ABI Prism 377) in our laboratory, PCR products at seven additional loci—*Ogo2*, *Ogo4* (Olsen et al., 1998), *Oke4* (Buchholz et al., 1999), *Omy325* (O'Connell et al., 1997), *Oki100* (K. M. Miller, unpubl. data), and *Ots2*, *Ots9* (Banks et al., 1999)—were size fractionated (96 samples on a gel) on 4.5% denaturing polyacrylamide gels run at 3000 V for 2.25 h at a gel temperature of 51°C. PCR products at *Ots2* and *Ots9* were amplified with a single PCR reaction, as were *Ogo4* and *Omy325*, and *Ogo2* and *Oke4*. Primer concentrations in the multiplex PCR reactions were adjusted to ensure equal amplification of both loci. Allele sizes were determined with Genescan 3.1 and Genotyper 2.5 software (PE Biosystems, Foster City, CA). Allele frequencies for all location samples surveyed in this study are available at http://www-sci.pac.dfo-mpo.gc.ca/aqua/pages/bgsid.htm.

Conversion of allele sizes between manual and automated sizing systems

With the acquisition of an automated DNA sequencer, we switched the survey of variation at *Ots100*, *Ots101*, *Ots102*, *Ots104*, *Ots107*, and *Ssa197* from the previous manual gel method to the automated sequencer, although most of the alleles surveyed in this study at these loci would have been analyzed on manual gels. Estimated allele sizes at these loci differed between those derived from nondenaturing gels stained with ethidium bromide and those derived from the denaturing gels and flourescent tags on the automated sequencer. In order to convert allele sizes between the two systems, we analyzed approximately 600 fish on both systems and determined the distributions of allele frequencies. By inspection of the allele frequencies, we were able to match specific allele sizes obtained from the sequencer to specific allele sizes from the manual gels and then convert the sizing in the automated sequencer data set to match that obtained from the manual gels. Estimated allele sizes from both systems were very highly correlated (r^2>0.987 for all loci). In general, sizes for the same allele from the sequencer were larger than those estimated from manual gels, with the differential increasing with allele size.

Data analysis

Each population at each locus was tested for departure from Hardy-Weinberg equilibrium (HWE) by using GENEPOP (Raymond and Rousset, 1995). The dememorization number was set at 1000, and 50 batches were run for each test with 1000 iterations/batch (Raymond and Rousset, 1995). Annual samples within populations were tested separately, and 106 tests were conducted at each locus (Table 1). Linkage disequilibrium between loci in each population was also evaluated by using GENEPOP; 106 tests were conducted for each two-locus combination. With 13 loci, there were 78 different two-locus combinations to evaluate. Critical significance levels for simultaneous tests were evaluated by using sequential Bonferroni adjustment (Rice, 1989). F_{ST} estimates for each locus were calculated with FSTAT (Goudet, 1995), and the standard deviation of the estimate for an individual locus was determined by jackknifing over populations and for all loci combined by bootstrapping over loci. All annual samples available for a location were combined to estimate population allele frequencies, as was recommended by Waples (1989). Computation of allelic diversity (the average number of alleles observed per locus), and identification of unique alleles was carried out with genetic data analysis (GDA) (Lewis and Zaykin, 2001). To minimize the effects of varying sample sizes on estimates of allelic diversity, values were reported only for population samples consisting of at least 50 fish. The number of unique alleles observed per region was standardized by calculating the number observed for each one-hundred fish sampled within each region. A neighbor-joining analysis illustrating genetic relationships among populations was also conducted with GDA incorporating TreeView (http://taxonomy.zoology.gla.ac.uk/rod/treeview.html) presentation.

Estimation of variance components of regional differences, population differences within regions, and annual variation within populations was determined with GDA. Six regions were defined based upon observed population structure: lower, middle, and upper Fraser River, south, north, and lower Thompson River. One highly distinctive population, the Birkenhead River, was handled in two ways. It was either included in the analysis as a separate (seventh) region, or excluded from the analysis of regional structure. Balanced experimental designs were required for variance component analysis, and thus two or more populations in each region were required (each population sampled in at least two years). When the Birkenhead River was treated as a region, two populations were defined from the four annual samples available for the regional analysis. The 1993 and 1996 samples were treated as one population, and the 1997 and 1998 samples as the second population. Samples included in the variance components analysis were the 28 locations from which at least two annual samples were available and at least 25 fish in total were sampled (Table 1, Horsey and Goat excluded). Population structure within tributaries of the Fraser River and Thompson River was evaluated with variance components analysis for seven tributaries. These were major tributaries of either the Fraser River or Thompson River for which we had surveyed populations in the tributary for two or more years and included the Harrison, Chilcotin, Quesnel, Nechako rivers in the Fraser River drainage and the Nicola and Shuswap rivers in the Thompson River drainage (Fig. 1). Variance components due to sampling locations within tributaries were compared with variance components due to sampling

Table 1

Population sample, collection years, number of fish sampled per year, total number of fish sampled, expected heterozygosity (H_e), observed heterozygosity (H_o), and percentage of tests significant for pairwise linkage disequilibrium (n=106 tests per locus pair combination) for 52 samples of Fraser River chinook salmon in seven regions of the Fraser River drainage.

Population	Years	Annual n	Total n	H_e	H_o	Linkage
Birkenhead						
Birkenhead River[1,3]	1993, 1996, 1997,1 998	43, 31, 20, 27	121	0.75	0.68	0.6
Lower Fraser						
Harrison (white)[2,3]	1988, 1992, 1994	134, 99, 100	333	0.86	0.83	25.6
Chehalis (red)[2,3]	1994	25	25	0.82	0.78	1.3
Chilliwack (white)[2,3]	1994, 1995	83,89	172	0.85	0.81	3.2
Chilliwack (red)[2,3]	1994	28	28	0.83	0.81	0.0
Mid Fraser						
Cottonwood[1]	1995	53	53	0.81	0.78	0.0
Quesnel[1,3]	1990, 1994, 1995, 1996, 1997	14, 69, 91, 226, 73	473	0.83	0.78	2.8
Cariboo[1]	1996	12	12	0.77	0.74	0.0
Stuart[1]	1991, 1992, 1994, 1995, 1996	58, 56, 73, 99, 172	458	0.83	0.81	1.3
Nechako[1]	1991, 1992, 1994, 1995, 1996	58, 63, 61, 69, 137	388	0.84	0.78	3.1
Horsefly[1]	1996, 1997	14, 15	29	0.82	0.76	0.0
Westroad[1]	1997	31	31	0.85	0.83	5.1
Chilko[1]	1994, 1995	43, 79	122	0.82	0.78	0.6
Upper Chilcotin[1]	1995, 1998	22, 21	43	0.82	0.77	1.3
Lower Chilcotin[1]	1996	74	74	0.83	0.76	0.0
Chilcotin[1]	1997	47	47	0.85	0.80	0.0
Taseko[1]	1997, 1998	37, 27	64	0.79	0.75	0.0
Endako[1]	1997, 1998	25, 32	57	0.83	0.81	9.6
Elkin[1]	1995, 1996	19, 216	235	0.83	0.77	3.8
Portage[1]	1996	27	27	0.84	0.80	0.0
Bridge[1,3]	1994, 1995, 1996	23, 35, 326	384	0.84	0.78	0.0
Upper Fraser						
Tete Jaune[1]	1993, 1994, 1995	66, 94, 88	248	0.83	0.80	18.8
Dome Creek[1,3]	1991, 1994, 1995, 1996	34, 51, 94, 148	327	0.83	0.80	5.8
Horsey[1]	1995, 1997	13, 11	24	0.83	0.76	0.0
Goat[1]	1995, 1997	12, 12	24	0.84	0.81	0.0
Holmes[1]	1995, 1996	43, 54	97	0.84	0.79	1.3
Swift[1]	1995, 1996	63, 164	227	0.82	0.78	2.6
Slim Creek[1]	1995	65	65	0.82	0.80	0.0

continued

years within locations. In the Harrison River–Lillooet River drainage, the Birkenhead River was treated as a single population with four years of samples in this analysis.

Results

Variation within populations

The number of alleles observed per locus ranged from 12 to 54, and fewer alleles were observed at the loci with dinucleotide repeats (*Ogo2*, *Ogo4*, *Oke4*, *Omy325*, *Ots2*, and *Ots9*) than at the loci with tetranucleotide repeats. Heterozygosities were generally lower for the loci with dinucleotide repeats (mean H_e=0.71) than for the other loci (mean H_e=0.91) (Table 2). Genotypic frequencies at each locus within sampling location and year generally conformed to Hardy-Weinberg equilibrium expectations, with the notable exception of *Ots102*. At this locus, 57% of the HWE tests were statistically significant, and in all cases there was an excess of observed homozygotes. One or more nonamplifying allele(s) was likely present at this locus in many of the Fraser River populations surveyed. Observed heterozygosities were less than expected heterozygosities for all loci analyzed on the manual gels. Unequal amplification of alleles (Wattier et al., 1998) may have resulted in the failure to detect large alleles in some heterozygous individuals with ethidium bromide staining. There was no evidence of linkage between any of the microsatellite loci used in this study, but four of the 52 samples surveyed in the study exhibited significant linkage disequilibrium in more than 10% of the pairwise comparisons between loci (Table 1). These sample locations were Harrison River, Tete Jaune, Fontoniko, and Bessette Creek.

Table 1 (continued)

Population	Years	Annual *n*	Total *n*	H_e	H_o	Linkage
Upper Fraser (cont.)						
Indianpoint[1]	1995	42	42	0.82	0.81	1.3
Willow[1]	1995, 1996	53, 16	69	0.83	0.75	0.0
Fontoniko[1]	1996	57	57	0.80	0.77	19.7
McGregor[1]	1997	119	119	0.81	0.80	2.6
Salmon River[1]	1996, 1997	95, 131	226	0.82	0.76	3.8
Bowron[1]	1995, 1997, 1998	54, 16, 39	109	0.82	0.78	6.4
Lower Thompson						
Nicola[1,3]	1992, 1994, 1995, 1997	54, 73, 75, 49	251	0.81	0.77	1.0
Coldwater[1,3]	1994, 1995, 1996, 1997	27, 31, 75, 43	176	0.82	0.77	0.0
Spius[1,3]	1996	58	58	0.80	0.80	2.6
Deadman[1]	1996, 1997	132, 61	193	0.82	0.77	1.9
Bonaparte[1]	1996	306	306	0.82	0.79	5.1
North Thompson						
Mahood[1]	1995	17	17	0.82	0.74	0.0
Raft[1]	1995, 1996	14, 115	129	0.83	0.80	0.6
Finn[1]	1996	101	101	0.80	0.74	0.0
Louis[1]	1996, 1997	32, 107	139	0.78	0.74	1.9
Clearwater[1]	1997	169	169	0.82	0.76	5.1
South Thompson						
Little River[2]	1996	53	53	0.83	0.73	0.0
Lower Shuswap[2]	1994, 1995, 1996, 1997	130, 73, 90, 42	335	0.82	0.77	2.6
Middle Shuswap[2]	1994, 1995, 1997	109, 86, 118	313	0.81	0.76	0.9
Salmon[1]	1996, 1997	72, 56	128	0.82	0.77	1.3
Eagle[1,2]	1995	36	36	0.80	0.69	1.3
Lower Adams[2,3]	1996	103	103	0.83	0.78	3.8
South Thompson[2]	1996	157	157	0.84	0.80	5.1
Bessette[1]	1998	17	17	0.81	0.79	17.9

[1] Stream-type population.
[2] Ocean-type population.
[3] Hatchery-enhanced population.

Population structure

The mean F_{ST} value over 52 samples and 13 loci surveyed was 0.039 (0.040 with *Ots102* excluded), and the dinucleotide loci had higher mean F_{ST} values (0.067) than the other loci (mean=0.026) (Table 2). With the exception of several sampling locations within tributaries affected by transplantation (discussed below), the geographically distinct sampling sites of this study possessed individual spawning populations of chinook salmon. Neighbor-joining clustering based on F_{ST} values for the 12 loci in HWE indicated a regional population structure which corresponded broadly to six groups: lower, middle, and upper Fraser River, and south, north, and lower Thompson River. An exception was the Birkenhead River population of the lower Fraser region, which was distinct from all other populations (Fig. 2). Thompson River populations were well differentiated from those of the Fraser River, and within the Thompson River drainage, the populations of the south, north, and lower regions were distinctive. Only the Louis Creek population of the north Thompson failed to cluster geographically, instead grouping rather distantly with the lower Thompson populations. The mid and upper Fraser River populations each formed distinctive groups, although the Portage Creek and Bridge River populations of the mid Fraser showed similarities to lower Fraser and lower Thompson populations, respectively. The transplanted red-fleshed "Chilliwack" and "Chehalis" River populations in the lower Fraser drainage clustered with source populations Slim Creek and Bowron River from the upper Fraser drainage. Mean F_{ST} values both within and among regions were statistically significant (all $P<0.05$) (Table 3).

The distinctive lower Fraser region, providing the Harrison and Chilliwack River samples, was differentiated from all other regions, although F_{ST} values indicated a somewhat closer relationship of lower Fraser with mid Fraser populations than with populations of other regions (Table 3). The distinctiveness of the Birkenhead River population was apparent in the F_{ST} values obtained in comparisons with all regional groups. The upper Fraser

and north Thompson regions were both closely related to mid Fraser populations, but less similar to each other. The lower and south Thompson regions were distinctive from other regions (with the exception of the Louis Creek population from the north Thompson which resembled lower Thompson populations), and from each other. Removal of the Louis Creek population from the analysis resulted in the F_{ST} value among the North Thompson populations decreasing from 0.043 to 0.026 and the F_{ST} value between the north and lower Thompson regions increasing from 0.047 to 0.058 (Table 3).

Heterozygosity was highest in the lower Fraser region but similar among all interior Fraser regions (Table 4). Allelic diversity was also high in the lower Fraser samples, but on a regional basis, allelic diversity was highest in the mid Fraser region followed by the south Thompson and lower Fraser regions. More unique alleles were observed per hundred fish sampled in the Birkenhead and Lower Fraser region than elsewhere in the drainage (Table 4). Among the interior regions, the mid Fraser and south Thompson regions each had more than one unique allele recorded per hundred fish sampled, whereas the remaining regions had less than one.

Table 2

Number of alleles, expected heterozygosity (H_e), observed heterozygosity (H_o), percent significant Hardy-Weinberg equilibrium tests (HWE, n=106 tests), and F_{ST} among 52 chinook salmon spawning locations (standard deviation in parentheses) for 13 microsatellite loci.

Locus	Alleles	H_e	H_o	HWE	F_{ST}
Ogo2	18	0.71	0.70	1.9	0.077 (0.011)
Ogo4	20	0.80	0.80	3.7	0.076 (0.014)
Oke4	14	0.66	0.63	1.9	0.074 (0.014)
Oki100	39	0.92	0.92	7.4	0.026 (0.003)
Omy325	31	0.77	0.75	8.4	0.081 (0.012)
Ots2	18	0.71	0.71	6.5	0.042 (0.009)
Ots9	12	0.58	0.58	0.0	0.051 (0.009)
Ots100	34	0.91	0.87	10.3	0.022 (0.002)
Ots101	33	0.91	0.86	13.1	0.016 (0.003)
Ots102	54	0.89	0.61	57.0	0.036 (0.003)
Ots104	33	0.92	0.89	8.4	0.022 (0.003)
Ots107	47	0.90	0.86	13.1	0.036 (0.004)
Ssa197	33	0.92	0.90	4.7	0.024 (0.003)
All loci					0.039 (0.006)

Distribution of genetic variation

Gene diversity analysis of the 12 microsatellite loci in HWE was used to determine the magnitudes of variation among annual samples within populations and of variation among chinook salmon populations of seven regions (Birkenhead treated as a region) or six regions (the Birkenhead River population excluded). For seven regions, the hierarchical analysis indicated that 95.0% of the variation occurred within populations (Table 5). Variation among regions was the greatest source of the remaining variation (3.1%), followed by variation among populations within regions (1.3%), and variation among years within populations (0.5%). With the Birkenhead population excluded, regional variation accounted for 2.6% of the total, whereas the variation attributed to populations and sampling year was unchanged. The differences observed among regions, among populations within regions, and among years within populations were significant (all P<0.01). On average, differences among populations (includes regional and population components) were about 8.5 times greater than annual variation within populations.

Structure within major tributaries

In many cases, samples from separate locations within tributary systems clustered together (Fig. 2), indicating that a higher rate of gene flow may occur among chinook salmon spawning aggregates within tributaries. Gene diversity analysis confirmed that chinook salmon sampled from separate spawning locations within tributaries tended

Table 3

Mean pairwise F_{ST} averaged over 12 loci for 50 locations of chinook salmon for seven regional groups in the Fraser River and Thompson River drainages. Comparisons were conducted between individual populations in each region (the numbers of populations in each region are listed in Table 1). The transplanted red Chehalis and red Chilliwack populations were not included in the analysis. Standard deviation is shown in parentheses. Boldface font indicates the diagonal.

	Lower Fraser	Middle Fraser	Upper Fraser	North Thompson	South Thompson	Lower Thompson
Birkenhead	0.107 (0.023)	0.125 (0.014)	0.132 (0.007)	0.137 (0.017)	0.111 (0.017)	0.138 (0.008)
Lower Fraser	**0.005 (—)**	0.067 (0.022)	0.069 (0.021)	0.080 (0.023)	0.068 (0.021)	0.073 (0.027)
Middle Fraser		**0.025 (0.012)**	0.028 (0.013)	0.043 (0.018)	0.049 (0.011)	0.047 (0.013)
Upper Fraser			**0.017 (0.008)**	0.048 (0.016)	0.045 (0.009)	0.042 (0.008)
North Thompson				**0.043 (0.021)**	0.052 (0.014)	0.047 (0.011)
South Thompson					**0.022 (0.009)**	0.051 (0.008)
Lower Thompson						**0.011 (0.005)**

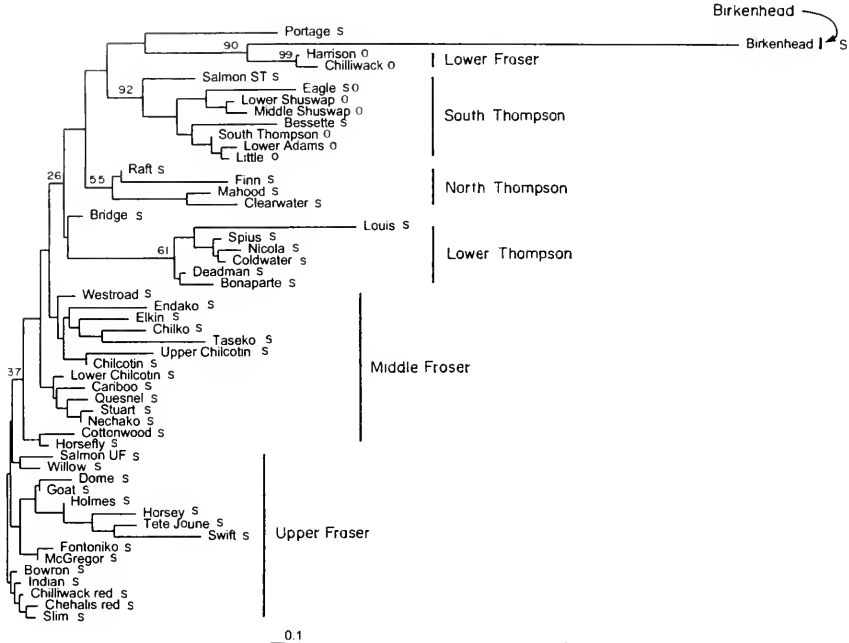

Figure 2

Neighbor-joining dendrogram of F_{ST} differences for 52 spawning groups of Fraser River chinook salmon surveyed at 12 microsatellite loci in Hardy-Weinberg equilibrium. Bootstrap values at the tree nodes indicate the percentage of 100 trees where populations beyond the node occurred together. Populations have been designated as ocean type (O) or stream type (S) after the name of the population.

to be more similar to each other but that the degree of differentiation among populations within tributaries varied among tributary systems (Table 6). For example, in the Nicola River drainage, temporal variation in allele frequencies within the Nicola and Coldwater samples was about three times larger than differences between them (Table 6). There was no significant difference in allele frequencies at any locus between the two locations in relation to annual variation within location (all 13 $P>0.10$). Thus it seems likely that there is sufficient gene flow between these two sites (and likely the Spius Creek site) that the Nicola River drainage can be considered to contain a single chinook salmon population. Significant differentiation was observed between the lower and middle Shuswap River samples at *Ogo2* ($F=7.82$, $P<0.05$), indicating that there has been some restriction of gene flow between the two spawning locations. Structure was observed among the three sites sampled from the Nechako River system, with significant differences observed at *Oke4*, *Ogo2*, and *Ots9* (all $F>6.0$, $P<0.05$). Similarly, after accounting for annual variation, significant differentiation between the Quesnel and Horsefly sites in the Quesnel River drainage was observed at *Ogo2* ($F=6.63$, $P<0.05$), and among four Chilko River sites at *Ots107*, *Ogo4*, *Ots9*, and *Omy325* (all >6.6, all $P<0.05$). The most pronounced allele frequency differentiation was observed between the Harrison and Birkenhead River populations in the Harrison River–Lillooet River drainage. Interpopulation differentiation was 24 times greater than intrapopulation variation; the two populations differed in allele frequencies at all loci except *Ssa197* and *Ots101* (all $F>6.6$, all $P<0.05$).

Discussion

Population structure

The genetic structure of Fraser drainage chinook salmon populations has a strong geographic basis, indicating that isolation by distance is a major component of population structure. Regional differentiation accounts for approximately twice the variation in allele frequencies as does

Table 4

Regional and population level allelic diversity (mean number of alleles per locus) and expected heterozygosity (H_e) at microsatellite loci for Fraser River chinook salmon. *n* indicates the sample number of fish included for regional values and the number of populations included for population values. The number of unique alleles observed per hundred fish sampled is shown for each region; the total number of unique alleles is shown in parentheses.

	n	Allelic diversity	H_e	Unique alleles
Birkenhead	1 (52 fish)	13.3	74.0	3.85 (2)
Lower Fraser				1.95 (5)
population	2	22.2	85.2	
region	256	24.2	85.5	
Mid Fraser				1.16 (16)
population	5	19.2	82.3	
region	1380	27.2	83.5	
Upper Fraser				0.75 (5)
population	5	16.7	82.2	
region	670	23.1	83.4	
Lower Thompson				0.21 (1)
population	4	17.4	81.0	
region	480	21.3	81.7	
South Thompson				1.79 (10)
population	5	18.7	81.5	
region	558	24.8	82.2	
North Thompson				0.98 (2)
population[1]	2	19.2	82.1	
region	204	22.5	82.7	
Louis Creek	68	14.6	76.7	

[1] Louis Creek population excluded

Table 5

Hierarchical gene diversity analysis for 28 populations (pops) of Fraser River chinook salmon for the 12 microsatellite loci in HWE; only populations sampled for at least two years were included in the analysis. Regions, populations within regions, and years within populations are outlined in Table 1.

	Absolute diversity		Relative diversity			
Locus	Total	Within populations	Within populations	Among years within populations	Among populations within regions	Among regions
Ogo2	0.7465	0.7007	0.9386	0.0023	0.0155	0.0436
Ogo4	0.8788	0.8071	0.9184	0.0089	0.0109	0.0618
Oke4	0.7288	0.6822	0.9360	0.0042	0.0128	0.0470
Oki100	0.9513	0.9259	0.9733	0.0017	0.0140	0.0110
Omy325	0.8477	0.7770	0.9166	0.0047	0.0181	0.0606
Ots2	0.7364	0.7083	0.9619	0.0032	0.0133	0.0216
Ots9	0 6139	0.5962	0.9712	0.0008	0.0146	0.0134
Ots100	0.9492	0.9279	0.9776	0.0053	0.0075	0.0096
Ots101	0.9364	0.9173	0.9796	0.0073	0.0058	0.0073
Ots104	0.9475	0.9240	0.9751	0.0054	0.0083	0.0112
Ots107	0.9423	0.9053	0.9607	0.0042	0.0098	0 0253
Ssa197	0.9456	0.9216	0.9746	0.0060	0.0079	0.0115
All			0.9499	0.0053[1]	0.0134[1]	0.0314[1]

[1] $P<0.01$

Table 6

Hierarchical gene-diversity analysis of spawning aggregations within six tributaries of the Fraser River for 12 microsatellite loci. sites within the tributary divided by the variance component of sampling years within sites.

	Nicola, Coldwater (Lower Thompson)		Lower, Middle Shuswap (South Thompson)		Harrison, Birkenhead (Lower Fraser)	
Locus	Among years within sites	Between sites within tributary	Among years within sites	Between sites within tributary	Among years within sites	Between sites within tributary
Ogo2	0.0000	0.0000	0.0002	0.0063	0.0000	0.1171
Ogo4	0.0147	0.0000	0.0017	0.0040	0.0003	0.0559
Oke4	0.0093	0.0030	0.0055	0.0000	0.0064	0.0559
Oki100	0.0003	0.0062	0.0017	0.0062	0.0025	0.0289
Omy325	0.0260	0.0006	0.0008	0.0020	0.0000	0.2452
Ots2	0.0042	0.0000	0.0053	0.0000	0.0034	0.0814
Ots9	0.0004	0.0000	0.0010	0.0004	0.0002	0.0153
Ots100	0.0080	0.0034	0.0048	0.0044	0.0033	0.0423
Ots101	0.0042	0.0033	0.0082	0.0000	0.0090	0.0291
Ots104	0.0030	0.0000	0.0094	0.0000	0.0018	0.0182
Ots107	0.0036	0.0045	0.0037	0.0030	0.0086	0.0550
Ssa197	0.0056	0.0080	0.0101	0.0117	0.0026	0.0135
All	0.0090	0.0026	0.0057	0.0040	0.0040	0.0939
Sites/Years	0.29		0.70		23.5	

intraregional variation among populations, and spawning sites within a tributary system may or may not support genetically discrete populations. Time of adult migration also appears to promote genetic differentiation.

The Birkenhead River population, the most distinctive of the 52 individual chinook salmon spawning aggregates surveyed, occupies the upper portion of the Harrison River–Lillooet River drainage and is characterized by a very early adult migration time. Historical recreational fisheries on this population occurred in the Birkenhead River during April and May (Fraser et al., 1982). Conversely, the Harrison River population in the lower reaches of the same drainage is a late run, entering the Harrison River just prior to spawning in October and November. The Birkenhead River population has low levels of polymorphism and heterozygosity at both allozyme loci (Teel et al., 2000) and microsatellite loci, likely reflecting small population size at least in recent history and low levels of gene flow because of its spatial and temporal isolation from other populations. Another example of a spawning population isolated temporally from neighboring sites is the Louis Creek population of the north Thompson region. The migration time of Louis Creek chinook salmon is early or "spring run," whereas other north Thompson populations are later "summer run" migrants. The distant clustering of the Louis Creek chinook salmon with the lower Thompson populations may reflect either a common origin or more recent gene flow due to common migration times. The low level of allelic diversity observed in the Louis Creek population and its distinction from the lower Thompson populations indicate that current levels of gene flow are low, and the genetic similarity may be due to common ancestry.

Significant linkage disequilibrium was detected in samples from four populations: Harrison River, Tete Jaune (main stem Fraser River), Fontoniko Creek, and Bessette Creek. Linkage disequilibrium may reflect sample admixture (Waples and Smouse, 1990) in the Harrison River and Tete Jaune samples. The Harrison River samples were obtained from broodstock collections at a hatchery on the Chehalis River, a tributary of the Harrison River. Initial broodstock for the hatchery was derived from chinook salmon collected from the Harrison River, and over time broodstock has been developed from fish returning to the hatchery. Chinook salmon returning to the Chehalis hatchery were also used to found the Chilliwack River population, which is maintained by production in the Chilliwack hatchery and spawning in the Chilliwack River. During the 1990s, chinook salmon were transplanted back from the Chilliwack hatchery to the Chehalis hatchery. Thus, the samples examined in our study, collected between 1988 and 1994, may reflect some mixing of genetically related but heterogeneous groups of fish from the Harrison, Chehalis, and Chilliwack rivers in the Chehalis hatchery broodstock. The Tete Jaune samples were obtained at Tete Jaune Cache in the extreme headwaters of the Fraser River. Because the samples were collected from the mainstem Fraser River, there is potential for admixture of populations, although it is thought that there are few chinook salmon spawning sites upstream from this location. Significant linkage disequilibrium was detected in single-year samples from Fontoniko Creek (a tributary of the McGregor River) and Bessette Creek (a tributary of the Shuswap River). Population admixtures would not typically be expected in such terminal locations, and the cause of the disequilibrium is unknown.

Table 6

Spawning sites within each tributary are indicated in the first row of the table. "Sites/Years" is the ratio of the variance components of

Nechako, Stuart, Endako (Mid Fraser)		Quesnel, Horsefly (Mid Fraser)		Chilko, Upper Chilcotin, Elkin, Taseko (Mid Fraser)	
Among years within sites	Between sites within tributary	Among years within sites	Between sites within tributary	Among years within sites	Between sites within tributary
0.0005	0.0073	0.0019	0.0411	0.0014	0.0080
0.0111	0.0000	0.0064	0.0233	0.0028	0.0418
0.0031	0.0127	0.0000	0.0031	0.0147	0.0211
0.0008	0.0041	0.0000	0.0094	0.0013	0.0197
0.0042	0.0016	0.0041	0.0146	0.0046	0.0319
0.0023	0.0057	0.0000	0.0177	0.0000	0.0122
0.0000	0.0041	0.0027	0.0396	0.0000	0.0224
0.0030	0.0026	0.0028	0.0068	0.0070	0.0174
0.0030	0.0027	0.0020	0.0009	0.0117	0.0000
0.0030	0.0025	0.0014	0.0019	0.0052	0.0156
0.0022	0.0043	0.0020	0.0111	0.0000	0.0244
0.0046	0.0047	0.0017	0.0025	0.0085	0.0102
0.0039	0.0049	0.0232	0.0170	0.0057	0.0232
1.25		7.40		4.07	

The disequilibrium observed in the Bessette Creek sample may simply reflect small sample size (17 fish).

Samples of Fraser River chinook salmon of the Harrison and Chilliwack rivers were little differentiated (F_{ST}=0.004), in accordance with their common origin from the Harrison River system. In addition, eggs from early migrating red-fleshed chinook salmon from Bowron River and Slim Creek in the upper Fraser and from the Quesnel and Chilko rivers of the mid Fraser were transplanted to the lower Fraser hatcheries between 1985 and 1988. Fish from these transplants returned to the lower Fraser hatcheries, maintaining an early migration time and red flesh coloration that distinguishes them from the native fall-run population. Fish returning from the initial releases were chosen as brood stock for succeeding generations only if they carried a coded wire tag indicating that they were of Slim Creek or Bowron River origin. Transplantation from the Chilliwack to the Chehalis hatchery of the red-fleshed fish occurred during years in which returns to the Chehalis hatchery were low. The observed strong genetic affinity of the Chehalis and Chilliwack red-fleshed fish to each other and to upper Fraser chinook salmon reflects this transplantation record.

Although the lower Fraser was the most genetically distinct of the six geographic regions examined, the genetic distinctiveness of the upper Fraser, lower Thompson, and south Thompson populations from each other was almost as great as their differentiation from the lower Fraser populations. Differentiation among regions within the smaller Thompson drainage was greater than that between the mid and upper Fraser regions of the larger interior Fraser drainage. The mean pairwise F_{ST} value within the Thompson drainage was 0.050, whereas within the interior Fraser drainage it was 0.028. Relatively strong differentiation among salmonids of the north, south, and lower Thompson regions has been noted previously not only for chinook salmon (Teel et al., 2000), but also coho (Small et al., 1998) and sockeye (Withler et al., 2000) salmon. The consistent population structure of the region across species, with quite distinct patterns of spatial variability (Myers et al., 1998), indicates that colonization of the Thompson and interior Fraser drainages may have been episodic, rather than a single event. If this is the case, the current affinities among the interior Fraser and Thompson regions may represent some combination of related but distinct founding populations and subsequent gene flow.

Origin of chinook salmon in the Fraser River

During the Wisconsin glaciation, ice-free refugia existed to the south of British Columbia in the Columbia River drainage and Pacific coastal regions. Extant chinook salmon populations in these areas display a genetic dichotomy that is well correlated with juvenile life history type (Myers et al., 1998). The presence of genetically distinct chinook salmon in the lower and interior Fraser River drainages has led to the suggestion that the drainage was colonized independently by stream-type chinook salmon from the Columbia refuge and ocean-type chinook salmon from a Pacific coastal (Teel et al., 2001) or northern Beringial (Utter et al., 1989) refuge. In a large survey of chinook salmon populations, including those of ocean- and stream-type populations from nonglaciated southern regions, Utter et al. (1989) found that 87% of genetic variation was contained within populations, and the remainder was partitioned among populations. In

five genetically distinct groups of chinook salmon in the Sacramento and San Joaquin rivers of California, 8.2% of genetic variation determined from a microsatellite survey was not contained within populations (Banks et al., 2000). In our present study of Fraser River chinook salmon, 95% of genetic variation was present within populations, where 3.0% was due to differences among regions (including the lower Fraser, putatively colonized independently) and 1.3% was due to differences among populations within regions.

Pairwise F_{ST} values between geographic regions of the Fraser drainage (Birkenhead excluded) did not exceed 0.080. Thus, if indeed Fraser River chinook salmon are descendants of genetically distinct chinook salmon "races" from two (or more) glacial refugia, the observed relatively low levels of differentiation suggest that introgression has occurred among the races before or since their colonization of the Fraser drainage. Support for the idea of the Fraser drainage as a chinook salmon "melting pot" comes from allozyme data (Fig. 19 in Myers et al., 1998) which indicate that chinook salmon of the both the lower and interior Fraser drainages are genetically intermediate to chinook salmon sampled from three postulated glacial refugia (the Columbia drainage, the Pacific coast and Beringia, the northern refuge). Minisatellite DNA variation has also indicated that Fraser River chinook salmon are genetically intermediate to populations in southern and northern British Columbia, groups putatively derived from southern and northern refugial areas (Beacham et al., 1996).

Teel et al. (2000) suggested that the presence of populations in the south Thompson region that have high proportions of ocean-type juveniles, and the genetic distinctiveness of the region, indicate that hybridization of ocean- and stream-type chinook salmon occurred within this region of the Fraser drainage. However, our study revealed that chinook salmon of the lower Thompson and south Thompson regions are the most genetically distinct of the interior chinook salmon groups, apparently strongly isolated from each other as well as from chinook salmon from all other regions. The south Thompson populations were not more closely related to the ocean-type chinook salmon of the lower Fraser than were the predominantly stream-type populations in other interior regions. Moreover, whereas the high level of allelic diversity observed in the south Thompson region may support the idea of historical hybridization, the presence in the south Thompson samples of a relatively large number of unique alleles (i.e. alleles not observed in other Fraser regions) does not support the idea that the hybridization occurred between the ocean-type chinook salmon that colonized the lower Fraser and the stream-type populations elsewhere in the drainage. The genetic distinction of the south Thompson chinook salmon seems more likely due to a unique colonization history than to recent gene flow within the Fraser drainage. South Thompson chinook salmon may have resulted from a historical admixture of refugial ocean- and stream-type races, but their genetic similarity to other interior Fraser chinook salmon groups, and the intermediate genetic position of all Fraser River chinook populations, indicate that all groups of Fraser chinook salmon may possess similar racial admixture. The ocean-type chinook salmon populations of the south Thompson may have originated from stream-type fish and thus reflect adaptation to environmental conditions conducive to the production of large juveniles capable of smolting in their first year of life.

Our data provide some evidence of gene flow among chinook salmon in different regions of the Fraser. Mid Fraser chinook salmon were characterized by a high level of allelic diversity but were notable in their low level of differentiation from chinook salmon of both the upper Fraser and north Thompson regions. Mid Fraser fish were also the most closely related of all the interior groups to lower Fraser chinook salmon. As for the south Thompson region, a high number of unique alleles in the mid Fraser region indicated that the high level of diversity was unlikely to result solely from hybridization of postglacial founding populations from the lower and upper Fraser regions.

Further genetic analysis of chinook salmon in British Columbia and refugial areas will reveal the nature of genetic variation in the Fraser River and other regions of southern British Columbia that likely represent "contact zones" of postglacial recolonization. Although extensive introgression may complicate the identification of conservation units based on "important phylogeographic subdivisions within species, those based on historical separations or fluctuations that are still evident in the gene pool" (Moritz, 1994), it may also have endowed the chinook salmon of southern British Columbia with a high level of adaptive diversity and evolutionary potential. It is thus important to determine if the regional structure evident within the Fraser drainage represents an intermediate step in the erosion of genetic differentiation among refugial groups by ongoing gene flow, or in the differentiation of introgressed founding groups adapting to environmental variability. Comparison of the distribution of variation at neutral and adaptive loci, such as that conducted for sockeye salmon of the Fraser River drainage (Miller et al., 2001), may help determine the geographic scale of adaptation for Fraser River chinook salmon.

Acknowledgments

We would like to acknowledge all those people involved in spawning ground sample collections. Numerous people from various groups were involved, including regional staff R. Bailey and B. Rosenberger, and many staff of salmon enhancement facilities throughout the drainage. Scale samples from selected populations were provided to us by D. Gillespie of the Ageing Laboratory at the Pacific Biological Station. The manuscript was improved by constructive comments from two referees. Funding was provided by several sources from the Fisheries and Oceans Canada.

Literature cited

Banks, M. A., M. S. Blouin, B. A. Baldwin, V. K. Rashbrook, H. A. Fitzgerald, S. M. Blankenship, and D. Hedgecock.
1999. Isolation and inheritance of novel microsatellites in chinook salmon (*Oncorhynchus tshawytscha*). J. Hered. 90: 281–288.

Banks, M. A., V. K. Rashbrook, M. J. Calavetta, C. A. Dean, and D. Hedgecock.
2000. Analysis of microsatellite DNA resolves genetic structure and diversity of chinook salmon (*Oncorhynchus tshawytscha*) in California's Central Valley. Can. J. Fish. Aquat. Sci. 57: 915–927.

Beacham, T. D., R. E. Withler, and T. A. Stevens.
1996. Stock identification of chinook salmon (*Oncorhynchus tshawytscha*) using minisatellite DNA variation. Can. J. Fish. Aquat. Sci. 53:380–394.

Beacham, T. D, and C. C Wood.
1999. Application of microsatellite DNA variation to estimation of stock composition and escapement of Nass River sockeye salmon (*Oncorhynchus nerka*). Can. J. Fish. Aquat. Sci. 56:1–14.

Beacham, T. D, K. D. Le, M. R. Raap, K. Hyatt, W. Luedke, and R. E. Wither.
2000. Microsatellite DNA variation and estimation of stock composition of Barkley Sound, British Columbia sockeye salmon. Fish. Bull. 98:14–24.

Buchholz, W., S. J. Miller, and W. J. Spearman.
1999. Summary of PCR primers for salmonid genetic studies. U.S. Fish. Wild. Serv. Alaska Fish. Prog. Rep. 99-1.

Cronin, M. A., W. J. Spearman, R. L. Wilmot, J. C. Patton, and J. W. Bickham.
1993. Mitochondrial DNA variation in chinook (*Oncorhynchus tshawytscha*) and chum salmon (*O. keta*) detected by restriction enzyme analysis of polymerase chain reaction (PCR) products. Can. J. Fish. Aquat. Sci. 50:708–715.

Fraser, F. J., P. J. Starr, and A. Y. Federenko.
1982. A review of the chinook and coho salmon of the Fraser River. Can. Tech. Rep. Fish. Aquat. Sci. 1126.

Gharrett, A. J., S. M. Shirley, and G. R. Tromble.
1987. Genetic relationships among populations of Alaskan chinook salmon (*Oncorhynchus tshawytscha*). Can. J. Fish. Aquat. Sci. 44:765–774.

Godfrey, H.
1975. Review of the occurrence of red- and white-fleshed chinook salmon in British Columbia with particular reference to Fraser River fish present off the west coast of Vancouver Island. Fish. Res. Board Canada Man. Rep. 1359, 49 p.

Goudet, J.
1995. FSTAT A program for IBM PC compatibles to calculate Weir and Cockerham's (1984) estimators of F-statistics (version 1.2). J. Heredity 86:485–486.

Healey, M. C.
1983. Coastwide distribution and ocean migration patterns of stream- and ocean-type chinook salmon, *Oncorhynchus tshawytscha*. Can. Field-Nat. 97:427–433.
1991. The life history of chinook salmon (*Oncorhynchus tshawytscha*). *In* Life history of Pacific salmon (C. Groot and L. Margolis, eds.), p. 311–393. U.B.C. Press, Vancouver, B.C.

Lewis, P. O., and D. Zaykin.
2001. Genetic data analysis: computer program for the analysis of allelic data, version 1.0 (d16c). Free program distributed by the authors over the internet from http://lewis.eeb.uconn.edu/lewishome/software.html.

McCallum, I. M., K. M. Cheng, and B. E. March.
1987. Carotenoid pigmentation in two strains of chinook salmon (*Oncorhynchus tshawytscha*) and their crosses. Aquaculture 67:291–300.

Miller, K. M., K. H Kaukinen, T. D. Beacham, and R. E. Withler.
2001. Geographic heterogeneity in natural selection on an MHC locus in sockeye salmon. Genetica 111:237–257.

Miller, K. M., R. E. Withler, and T. D. Beacham.
1996. Stock identification of coho salmon (*Oncorhynchus kisutch*) using minisatellite DNA variation. Can. J. Fish. Aquat. Sci. 53:181–195.

Moritz, C.
1994. Defining "evlutionarily significant units" for conservation. TREE 9:373–375.

Myers, J. M., R. G. Kope, G. J. Bryant, D. Teel, L. J. Lierheimer, T. C. Wainwright, W. S. Grant, F. W. Waknitz, K. Neely, S. T. Lindley, and R. S. Waples.
1998. Status review of chinook salmon from Washington, Idaho, Oregon, and California. U.S. Dep. Commer., NOAA Tech. Memo. NMFS-NWFSC-35, 443 p.

Nelson, R. J., and T. D. Beacham.
1999. Isolation and cross species amplification of microsatellite loci useful for study of Pacific salmon. Anim. Genet. 30:228–229.

Nelson, R. J, T. D. Beacham, and M. P. Small.
1998. Microsatellite analysis of the population structure of a Vancouver Island sockeye salmon (*Oncorhynchus nerka*) stock complex using non-denaturing gel electrophoresis. Mol. Mar. Biotech. 7:312–319.

Nelson, R. J., M. P. Small, T. D. Beacham, and K. J. Supernault.
2001. Population structure of Fraser River chinook salmon (*Oncorhynchus tshawytscha*): an analysis using microsatellite DNA markers. Fish. Bull. 99:94–107.

Olsen, J. B., P. Bentzen, and J. E. Seeb.
1998. Characterization of seven microsatellite loci derived from pink salmon. Mol. Ecol. 7: 1083–1090.

O'Connell, M., R. G. Danzmann, J. M. Cornuet, J.M. Wright, and M. M. Ferguson.
1997. Differentiation of rainbow trout populations in Lake Ontario and the evaluation of the stepwise mutation and infinite allele mutation models using microsatellite variability. Can. J. Fish. Aquat. Sci. 54:1391–1399.

O'Reilly, P. T., L. C. Hamilton, S. K. McConnell, and J. M. Wright.
1996. Rapid analysis of genetic variation in Atlantic salmon (*Salmo salar*) by PCR multiplexing of dinucleotide and tetranucleotide microsatellites. Can. J. Fish. Aquat. Sci. 53: 2292–2298.

Raymond, M., and F. Rousset.
1995. GENEPOP (version 1.2): population genetics software for exact tests and ecumenism. Heredity 86:248–249.

Rice, W. R.
1989. Analyzing tables of statistical tests. Evolution 43: 223–225.

Small, M. P., T. D. Beacham, R. E. Withler, and R. J. Nelson.
1998. Discriminating coho salmon (*Oncorhynchus kisutch*) populations within the Fraser River, British Columbia using microsatellite markers. Mol. Ecol. 7:141–155.

Taylor, E. B.
1991. A review of local adaptation in Salmonidae, with particular reference to Pacific and Atlantic salmon. Aquaculture 98:185–207.

Teel, D. J., G. B. Milner, G. A. Winans, and W. S. Grant.
2000. Genetic population structure and origin of life history types in chinook salmon in British Columbia, Canada. Trans. Am. Fish. Soc. 129:194–209.

Utter, F., G. Milner, G. Stahl, and D. Teel.
1989. Genetic population structure of chinook salmon, *Oncorhynchus tshawytscha*, in the Pacific Northwest. Fish. Bull. 87:239–264

Waples, R. S.
1989. Temporal variaiton in allele frequencies: testing the right hypothesis. Evolution 43: 1236–1251.

Waples, R. S., and P. E. Smouse.
1990. Gametic disequilibrium analysis as a means of identifying mixtures of salmon populations. Am. Fish. Soc. Symp. 7:439–458.

Wattier, R., C. R. Engel, P. Saumitou-LaPrade, and M. Valero.
1998. Short allele dominance as a source of heterozygote deficiency at microsatellite loci: experimental evidence at the dinucleotide locus Gv1CT in *Gracilaria gracilis* (Rhodophyta). Mol. Ecol. 7:1569–1573.

Wehrhahn, C. F., and R. Powell.
1987. Electrophoretic variation, regional differences, and gene flow in the coho salmon (*Oncorhynchus kisutch*) of southern British Columbia. Can. J. Fish. Aquat. Sci. 44:822–831.

Wilson, G. M., W. K. Thomas, and A. T. Beckenbach.
1987. Mitochondrial DNA analysis of Pacific Northwest populations of *Oncorhynchus tshawytscha*. Can. J. Fish. Aquat. Sci. 44:1301–1305.

Withler, R. E.
1986. Genetic variation in carotenoid pigment deposition in the red-fleshed and white-fleshed chinook salmon (*Oncorhynchus tshawytscha*) of Quesnel River, British Columbia. Can. J. Gen. Cytol. 28:587–594.

Withler, R. E., K. D. Le, R. J. Nelson, K. M. Miller, and T. D. Beacham.
2000. Intact genetic structure and high levels of genetic diversity in bottlenecked sockeye salmon, *Oncorhynchus nerka*, populations of the Fraser River, British Columbia, Canada. Can. J. Fish. Aquat. Sci. 57:1985–1998.

Wood, C. C., B. E. Riddell, D. T. Rutherford, and R. E. Withler.
1994. Biochemical genetic survey of sockeye salmon (*Oncorhynchus nerka*) in Canada. Can. J. Fish. Aquat. Sci. 51 (suppl. 1):114–131.

Evaluation and application of microsatellites for population identification of Fraser River chinook salmon (*Oncorhynchus tshawytscha*)

Terry D. Beacham
John R. Candy
K. Janine Supernault
Michael Wetklo
Bruce Deagle
Karen Labaree
James R. Irvine
Kristina M. Miller
R. John Nelson
Ruth E. Withler

Department of Fisheries and Oceans
Pacific Biological Station
3190 Hammond Bay Road
Nanaimo, British Columbia, Canada V9T 6N7
E-mail address (for T. D. Beacham): Beachamt@pac.dfo-mpo.gc.ca

Abstract—Variation at 13 microsatellite loci was previously surveyed in approximately 7400 chinook salmon (*Oncorhynchus tshawytscha*) sampled from 50 localities in the Fraser River drainage in southern British Columbia. Evaluation of the utility of the microsatellite variation for population-specific stock identification applications indicated that the accuracy of the stock composition estimates generally improved with an increasing number of loci used in the estimation procedure, but an increase in accuracy was generally marginal after eight loci were used. With 10–14 populations in a simulated fishery sample, the mean error in population-specific estimated stock composition with a 50-population baseline was <1.4%. Identification of individuals to specific populations was highest for lower Fraser River and lower and North Thompson River populations; an average of 70% of the individual fish were correctly assigned to specific populations. The average error of the estimated percentage for the seven populations present in a coded-wire tag sample was 2% per population. Estimation of stock composition in the lower river commercial net fishery prior to June is of key local fishery management interest. Chinook salmon from the Chilcotin River and Nicola River drainages were important contributors to the early commercial fishery in the lower river because they comprised approximately 50% of the samples from the net fishery prior to mid April. Mid Fraser River populations were the dominant group of chinook salmon in the catch in April and comprised at least 30% of the catch until late May. Upper Fraser River populations did not occur in any significant proportions in the fishery until the last week of April. By late May, they were the dominant contributors to the lower river fishery, and by June generally comprised approximately 70% of the weekly catch. Microsatellite variation allows accurate estimation of population-specific contributions to lower river fisheries.

Manuscript accepted 22 October 2002.
Manuscript received 31 December 2002 at NMFS Scientific Publications Office.
Fish. Bull. 101(2):243–259 (2003).

Chinook salmon (*Oncorhynchus tshawytscha*) are widely distributed within the Fraser River drainage, spawning in tributaries ranging from the headwaters to near the mouth of the river. There is substantial variation in life history features among populations within the drainage; populations vary in size at maturity, timing of spawning, and juvenile freshwater residence. Juveniles (largely from the Harrison River population) can migrate directly to the marine environment after fry emerge in the spring or perhaps develop in nonnatal tributaries in the lower river (Murray and Rosenau, 1989). Juveniles from some populations migrate to the ocean during the first summer of rearing ("ocean-type"), whereas in other populations juveniles remain in fresh water for a year or longer ("stream-type") before migrating to the ocean (Fraser et al., 1982). Management for conservation of genetic diversity within the drainage requires knowledge of genetic variation among populations, as well as population-specific information from fisheries.

Effective management of fisheries within major drainages like the Fraser River generally requires information on timing of return of specific populations, should managers wish to change exploitation rates on specific populations for conservation purposes. To acquire this information is a particularly daunting task within the Fraser River because chinook salmon spawn in approximately 65 tributaries of the Fraser River (Fraser et al., 1982). Maturing adults from these populations return annually to the Fraser River throughout the year—the majority of fish returning from February through November. For management purposes, Fraser River chinook salmon are currently divided into three groups based on their migration timing into the lower river: the spring run consists of all populations where at least 50% of the individuals are estimated to migrate through the lower river before 15 July; the summer run consists of populations that migrate through the lower river from 15 July to 31 August; and the fall run consists of populations that migrate through the lower river primarily in

September and October (DFO[1,2]). However, the adequacy of managing Fraser River chinook salmon based upon run timing is currently under review (Candy et al.[3]), and changes in management objectives are likely. During their migration through the lower river, chinook salmon are exploited by several distinct fisheries, among them commercial net fisheries, and the recreational fishery.

Conservation concerns for specific populations requires more information on timing of returns beyond the present designations of "spring," "summer," and "fall." Timing of some specific populations through the lower river can be inferred from their arrival on the spawning grounds. For example, chinook from the Birkenhead River (about 300 km from the Fraser River mouth) have historically supported a local recreational fishery on that river in April and early May (Fraser et al., 1982), indicating a very early timing of passage through the lower Fraser River. Coded-wire tagging (CWT) has been conducted on some enhanced populations, but these populations have been limited in scope given the size of the drainage, and coded-wire tag returns within the Fraser River have provided limited information on the timing of population returns.

Stock or population identification of chinook salmon migrating through the lower river is a continuing issue of management concern, and until recently there has been no effective way to provide estimates of population composition in the detail required by fishery managers. Although allozyme-based methods of stock identication have proven useful in estimation of chinook salmon stock composition in mixed-stock fisheries (Shaklee et al., 1999), the level of population discrimination available in the Fraser River was not sufficient for population-specific applications. Chinook salmon returning to spawn in specific rivers were considered as populations in our analysis, whereas stocks were a collection of populations from a particular geographic area or management unit. Minisatellite variation has been very effective in discriminating among individual Fraser River populations (Beacham et al., 1996), but we considered this technology not practical because of the cost and the time required for laboratory analysis. Any new technology employed had to meet these criteria: rapidity of analysis, moderate cost, and ability to discriminate among populations. Because variation in microsatellite loci meets these criteria and has been applied to other species requiring discrimination among salmonid populations within watersheds (Small et al., 1998; Beacham and Wood, 1999; Beacham et al., 2000), and has been shown to be useful in stock discrimination in chinook salmon (Banks et al., 2000), we chose to survey variation at microsatellite loci for Fraser River chinook salmon (Beacham et al., 2003) and evaluate and apply the variation to practical problems of stock identification.

In the current study, we surveyed variation at 13 microsatellite loci and evaluated the utility of using microsatellite variation for stock identification of Fraser River chinook salmon. These procedures were accomplished by analysis of simulated mixtures and application to a sample of chinook salmon that had previously been marked with coded-wire tags. We evaluate the accuracy of identifying individuals to population and region of origin. We also estimate stock compositions from fisheries in the lower river to determine the timing and relative abundance of specific populations through the fishery.

Materials and methods

Collection of baseline DNA samples and laboratory analysis

Genomic DNA was extracted from either liver, scales, operculum punches, or fin clips from chinook salmon sampled between 1987 and 1998 by using the phenol-chloroform protocol of Miller et al. (1996) (early extractions) or the chelex resin protocol of Small et al. (1998) (later extractions) (Table 1, Fig. 1). Samples were derived from adults in all areas except the McGregor River, where because of the difficulty of obtaining adults, juveniles were sampled. For the survey of baseline populations, PCR products at six microsatellite loci—*Ots100, Ots101, Ots102, Ots104, Ots107* (primers outlined by Nelson and Beacham, 1999) and *Ssa197* (O'Reilly et al., 1996)—were initially size-fractionated on nondenaturing polyacrylamide gels by staining with 0.5 mg/mL ethidium bromide in water and illuminating with ultraviolet light. Nelson et al. (1998) have provided a more complete description of gel electrophoretic conditions. Three 20-bp marker lanes were run on each gel, and the size of the amplified alleles was determined from the molecular size grid created with the 20-bp markers. Beacham and Wood (1999) have provided a more complete description of the methods used to identify alleles with this technology. With the acquistion of an automated sequencer (the ABI 377) in our laboratory, PCR products at seven additional loci—*Ogo2*, *Ogo4* (Olsen et al., 1998), *Oke4* (Buchholz et al., 1999), *Omy325* (O'Connell et al., 1997), *Oki100* (K. M. Miller, unpubl. data), and *Ots2*, *Ots9* (Banks et al., 1999)—were size-fractionated on denaturing polyacrylamide gels and allele sizes were determined with Genescan software (PE Brosystems, Foster City, CA). The six loci previously analyzed on nondenaturing polyacrylamide gels stained with ethidium bromide were subsequently analyzed on the automated sequencer when it became available.

Collection of fishery samples

In 1995, samples were collected from a daily gillnet test fishery at Albion in the lower Fraser River in southern

[1] DFO (Department of Fisheries and Oceans). 1995. Fraser River chinook salmon. Fraser River Action Plan, Fishery Management Group, Vancouver, British Columbia, Canada, 24 p. [Available from Fisheries and Oceans, 555 West Hasting St., Suite 1220, Vancouver, British Columbia, Canada V6B 5G3.

[2] DFO (Department of Fisheries and Oceans). 1999. Fraser River chinook salmon. DFO Science Stock Status Report D6-11, 7 p. [Available from Fisheries and Oceans, 555 West Hasting St., Suite 1220, Vancouver, British Columbia, Canada V6B 5G3.]

[3] Candy, J. R., J. R. Irvine, C. K. Parken, S. L. Lemke, R. E. Bailey, M. Wetklo, and K. Johsen. 2002. A discussion paper on possible new stock groupings (conservation units) for Fraser River chinook salmon. Can. Stock Assessment Secretariat. Res. Doc. 2002/85, 57 p. [Available from http://www.dfo-mpo.gc.ca/Csas/English/Index_e.htm.]

Table 1

Regions and populations within regions included in the survey of variation at 13 microsatellite loci in Fraser River chinook salmon and used in estimation of stock composition in mixed-stock samples. Numbers of fish surveyed in each population are shown in parentheses.

Region	Number of populations	Populations
Lower Fraser	2	Harrison (333),[2] Chilliwack (172)[1,2]
Birkenhead	1	Birkenhead (121)[2]
Middle Fraser	16	Cottonwood (53), Quesnel (473),[2] Cariboo (12), Horsefly (29), Stuart (458), Nechako (388), Endako (57), Westroad (31), Chilko (122), Upper Chilcotin (43), Lower Chilcotin (74), Chilcotin (47), Taseko (64), Elkin (235), Portage (27), Bridge (384)[2]
Upper Fraser	13	McGregor (119), Salmon (226), Bowron (109), Fontoniko (57), Willow (69), Indianpoint (42), Slim (65), Swift (227), Holmes (97), Goat (24), Horsey (24), Dome (327),[2] Tete Jaune (248)
Lower Thompson	5	Nicola (251),[2] Coldwater (176),[2] Spius (58),[2] Bonaparte (306), Deadman (193)
North Thompson	5	Raft (129), Finn (101), Louis (139), Clearwater (169), Mahood (17)
South Thompson	8	Lower Adams (103),[2] Lower Shuswap (335),[2] Middle Shuswap (313),[2] Little (53), Eagle (36),[2] Salmon (128), Bessette (17), South Thompson (157)

[1] Fall-run population.
[2] Hatchery population.

British Columbia (Dempson et al.[4]) (Fig. 1). The test fishery is conducted from April to October annually and operates daily (two sets of 30-min duration are made consecutively) except during commercial gillnet fishery openings. In 1995, a single mesh size of 20.3 cm (8.0 inch) was used to capture chinook salmon, and samples were collected from all chinook salmon caught in the fishery and surveyed for variation at five microsatellite loci. Further details of the test fishery have been outlined by Shubert et al. (1988). During 1997–99, operculum punches preserved in 90% ethanol were obtained from commercial fisheries in the lower Fraser River and mid Fraser. We were also able to obtain operculum punches from chinook salmon caught in marine fisheries in British Columbia that had previously been marked with coded-wire tags (CWTs) and for which the CWT had been recovered and decoded to determine marking location. We subsequently used this sample of 83 Fraser River fish to evaluate the accuracy of estimated stock compositions using a sample of known origin.

Conversion of allele sizes between manual and automated sizing systems

In the 1998 and subsequent fishery samples, we surveyed variation at *Ots100*, *Ots101*, *Ots102*, *Ots104*, *Ots107*, and *Ssa197* on the automated sequencer. However, estimated allele sizes at these loci differed between those derived from nondenaturing gels stained with ethidium bromide and those derived from the denaturing gels and flourescent tags on the automated sequencer. In order to convert allele sizes between the two systems, we analyzed approximately 600 fish on both systems and determined the distributions of allele frequencies. By inspection of the allele frequencies, we were able to match specific allele sizes obtained from the sequencer to specific allele sizes from the manual gels, and then convert the sizing in the automated sequencer data set to match that obtained from the manual gels. Estimated allele sizes from both systems were very highly correlated (r^2>0.987 for all loci). In general, sizes for the same allele from the sequencer were larger than those estimated from manual gels, with the differential increasing with allele size.

Population structure

Regional structure was observed in the baseline populations; the Birkenhead River, the lower Fraser River, mid Fraser River, upper Fraser River, lower Thompson River, North Thompson River, and South Thompson River populations comprised seven geographically based groups or "stocks" (Beacham et al., 2003). The populations surveyed in each of these regions are summarized in Table 1.

Identification of individuals

Identification of individuals to specific populations was done with the program GENECLASS 1.0 (Cornuet et al.,

[4] Dempson, J. B., J. R. Irvine, and R. E. Bailey. 1998. Relative abundance and migration timing of chinook salmon (*Oncorhynchus tshawytscha*) from the Fraser River, British Columbia, Albion test fishery, 1981–1995. Can. Man. Rep. Fish. Aquat. Sci. 2459, 25 p.

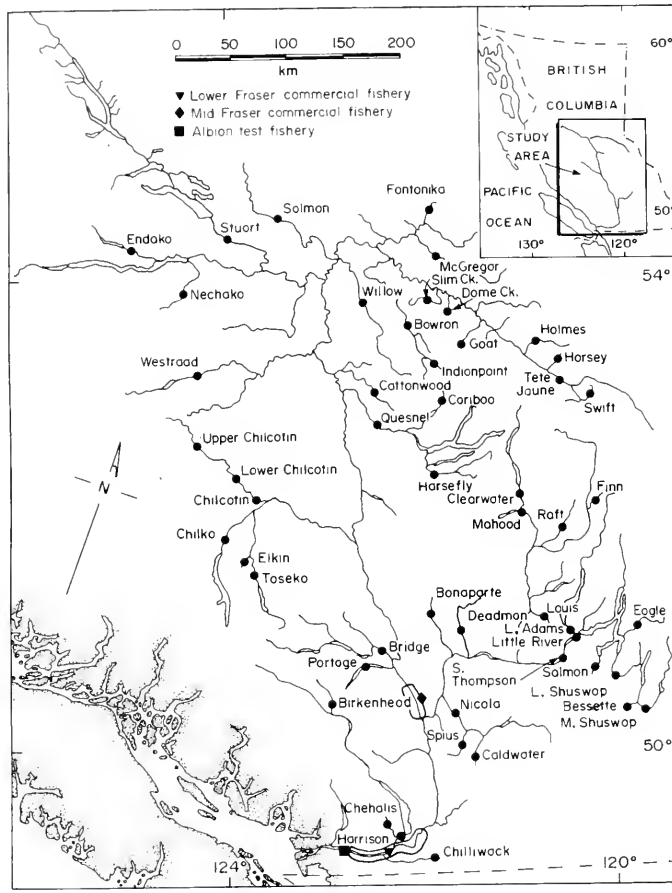

Figure 1

Locations in the Fraser River drainage where chinook salmon spawning aggregates were sampled at least once during 1988–98, as well as locations of the commercial and test fisheries in the lower river and commercial fishery in the mid Fraser.

1999). The probabilities of individuals belonging to all populations were calculated by using a Bayesian approach and each individual was assigned to the population in which it had the highest marginal probability.

Estimation of stock composition

Genotypic frequencies were determined at each locus in each population and the statistical package for the analysis of mixtures software program (SPAM) (Debevec et al., 2000) was used to estimate stock composition of each mixture. More alleles were present at the microsatellite loci than was practical for stock identification applications. We combined low frequency (frequency generally <0.02 in all populations) adjacent alleles to reduce the number of genotypic frequencies to be estimated with the available samples with the pooling strategy for each locus outlined in Table 2. This was done to minimize and hopefully eliminate the occurrence of fish in the mixed sample from a specific population having an allele not observed in the baseline samples. Expected genotypic frequencies under Hardy-Weinberg equilibrium were determined from the observed allele frequencies and were used as model inputs. Genotypic frequencies at *Ots102* were not in Hardy-Weinberg equilibrium in approximately 50% of the populations surveyed (Beacham et al., 2003), but increased accuracy in estimated stock compositions was

Table 2

Method of pooling low-frequency alleles if they should occur in any population to reduce the number of genotypic frequencies to be estimated in baseline populations for mixed stock analysis. Not all allele bins considered for pooling may contain observed alleles for Fraser River chinook salmon.

Pooled alleles, renumbered	Micosatellite allele numbers pooled for each locus												
	*Ogo*2	*Ogo*4	*Oke*4	*Oki*100	*Ots*100	*Ots*101	*Ots*102	*Ots*104	*Ots*107	*Ots*2	*Ots*9	*Omy*325	*Ssa*197
1	1–8	1–3	19	1–11	1–4	1–9	1–8	1–5	1–3	1–9	1–7	1–4	1–7
2	9	4–5	10	12–14	5–8	10–11	9–10	6–7	4–5	10	8	5	8–11
3	10–11	6–7	11	15–16	9–12	12	11–12	8–11	6–7	11	9	6	12–13
4	12	8–9	12	17–18	13–15	13	13–16	12–13	8–9	12	10	7	14
5	13	10–11	13	19–19	16–18	14–15	17–18	14–15	10–11	13–15	11	8	15
6	14–15	12–13	14–19	20	19	16–18	19–20	16	12	16	12–15	9	16–17
7	16–17	14		21	20–22	19–20	21–22	17–18	13	17		10	18
8	18	15		22	23–24	21	23–25	19–20	14–15	18		11	19
9	19–21	16		23–24	25–26	22–23	26–28	21–22	16–18	19		12	20
10	22–30	17		25–26	27–28	24–25	29–30	23–24	19–20	20		13–14	21–22
11		18		27–28	29–30	26–27	31–33	25–26	21–22	21		15–16	23
12		19–21		29–30	31–32	28–29	34–35	27–28	23–24	22–24		17–18	24–25
13		22–24		31–32	33–34	30–31	36–37	29–30	25–26	25		19–24	26–27
14				33–36	35–36	32–50	38–40	31–34	27–28	26		25–32	28–29
15				37–40	37–41		41–44	35–36	29–31	27		33–44	30–31
16				41–54	42–45		45–52	37–45	32–36	28–32			32–33
17					46–54		53–60		37–47				34–36
18													37–40
19													41–45
Number of observed alleles	18	20	14	39	34	33	54	33	47	18	12	31	43

obtained by using expected genotypic frequencies for all loci. A comparison of estimated stock composition of a CWT sample with all loci in expected genotypic frequencies in the baseline populations compared with observed genotypic frequencies at *Ots102* resulted in more accurate estimates with expected genotypic frequencies at all loci. Similar results were observed by Beacham et al. (2001) in mixed-stock analysis of coho salmon. Stock compositions from the 1995 test fishery at Albion were estimated with five loci (*Ots100, Ots101, Ots102, Ots104*, and *Ssa197*), those from the 1997 net fisheries with six loci (previous five loci plus *Ots107*), and those from 1998 and 1999 fisheries with 13 loci. The change in the number of loci used in estimation of stock composition over time was reflected in the number of loci available in the baseline populations. The initial analysis of baseline populations started in 1994 and three loci were included the population survey (Nelson et al., 2001). By early 1996, at the time of analysis of the first test fishery samples, five loci were routinely scored in the baseline populations and mixed-stock fishery samples, and by 1997 six loci were routinely scored for both baseline and mixed-stock fishery samples. With the acquistion of an automated sequencer in our laboratory in 1998, an additional seven loci were added to the routine survey of baseline population and mixed-stock fishery samples.

Reported stock compositions for the CWT and actual fishery samples are the point estimate of each mixture analyzed, with variance estimates derived from 100 bootstrap simulations. Each baseline population and fishery sample was sampled with replacement in order to simulate random variation involved in the collection of the baseline and fishery samples. Reported stock composition for simulated mixtures was the bootstrap mean, along with the standard deviation of the mean.

Results

Comparison of individual loci

Determination of the relative power of individual loci for either population or regional discrimination is of prime significance for practical stock identification applications. In simulations comparing the relative power of the microsatellite loci to estimate stock compositions of representative single-population samples, there were only minor differences in the relative power of the best nine loci, with "best" defined as those loci resulting in the minimum bias in the estimated stock compositions. The mean error of the estimates ranged between 20% and 31% (Table 3). The power of

Table 3

Mean bias (%) in estimated stock compositions for nine representative populations of chinook salmon calculated with individual loci and with combinations of four loci (*Omy325, Oki100, Ogo4, Ots107*), eight (previous four plus *Ots102, Ots104, Ots100, Ots101*), and all 13 microsatellite loci. Simulations were conducted using a 50-population baseline, 200 fish in the mixture sample, and 500 resamplings in the mixture sample, and baseline samples, with each mixture sample composed solely of chinook salmon from one population. Standard deviations are shown in parentheses.

Locus	Birkenhead	Harrison	Elkin	Quesnel	Stuart-Nechako	Tete Jaune	Nicola drainage	Lower Shuswap	Clearwater	Mean
Omy325	1.9 (1.9)	26.7 (20.8)	12.7 (7.3)	31.9 (15.6)	29.5 (15.3)	26.2 (15.4)	13.0 (9.6)	24.3 (16.6)	12.7 (7.3)	20.7
Oki 100	3.3 (3.3)	34.1 (11.9)	21.8 (9.5)	35.5 (13.2)	55.7 (18.4)	19.0 (9.3)	11.0 (6.6)	15.0 (8.0)	21.8 (9.5)	23.4
Ogo4	0.7 (1.0)	23.9 (12.3)	21.3 (13.4)	40.3 (15.1)	33.2 (14.7)	29.1 (18.1)	28.6 (15.9)	25.4 (15.0)	21.3 (13.4)	26.0
Ots107	2.6 (2.7)	32.5 (17.9)	32.5 (17.9)	28.0 (14.8)	66.5 (20.0)	4.6 (2.5)	24.3 (14.3)	35.3 (16.2)	32.5 (17.9)	26.8
Ots102	18.8 (99.8)	18.3 (11.9)	34.0 (15.2)	67.2 (23.8)	34.0 (14.7)	8.2 (6.9)	24.8 (14.3)	15.6 (9.7)	34.0 (15.2)	28.2
Ots104	6.8 (5.9)	27.6 (13.1)	9.7 (6.4)	34.3 (16.3)	73.8 (20.8)	43.7 (21.9)	21.3 (14.3)	21.3 (14.3)	9.7 (6.4)	29.8
Ots100	9.7 (6.5)	26.8 (15.5)	20.0 (11.0)	32.5 (14.5)	46.0 (19.9)	47.5 (21.4)	25.7 (16.4)	25.2 (19.6)	20.0 (11.0)	30.2
Ots101	8.3 (7.1)	37.1 (17.6)	22.4 (11.7)	35.4 (13.8)	50.4 (18.7)	32.1 (14.1)	36.7 (16.5)	22.9 (12.4)	22.4 (11.7)	31.6
Ogo2	7.0 (5.6)	25.4 (14.9)	19.2 (13.4)	32.8 (23.5)	78.3 (21.2)	51.7 (29.1)	27.0 (16.7)	14.9 (12.6)	19.2 (13.4)	31.6
Ots2	6.2 (7.1)	39.2 (24.6)	28.4 (17.3)	45.6 (27.1)	43.4 (23.6)	27.0 (17.4)	29.4 (18.2)	45.7 (22.3)	28.4 (17.3)	36.3
Ssa197	10.1 (6.7)	34.7 (17.5)	35.0 (16.4)	55.9 (22.7)	60.6 (22.2)	61.2 (24.8)	41.1 (20.4)	23.5 (13.1)	35.0 (16.4)	38.4
Oke4	12.5 (9.0)	20.9 (19.4)	79.8 (22.2)	86.9 (19.1)	78.5 (21.9)	16.3 (11.3)	32.6 (19.2)	69.8 (27.9)	79.8 (22.2)	52.7
Ots9	15.5 (15.4)	64.6 (27.9)	32.2 (27.2)	96.5 (9.4)	92.0 (14.9)	82.1 (23.9)	14.7 (13.3)	69.4 (27.0)	32.2 (27.2)	60.8
Best four	2.4 (1.9)	9.2 (5.9)	7.1 (3.8)	14.3 (5.9)	12.2 (6.3)	9.4 (4.5)	6.9 (4.5)	9.2 (5.0)	7.1 (3.8)	8.5
Best eight	5.0 (2.5)	6.6 (4.4)	5.3 (3.0)	7.2 (4.1)	12.2 (3.5)	5.3 (2.9)	6.6 (3.6)	6.2 (3.9)	5.3 (3.0)	6.7
All thirteen	5.6 (3.4)	5.4 (3.2)	5.0 (2.9)	4.5 (2.9)	12.2 (3.0)	4.6 (2.5)	6.7 (3.7)	6.1 (3.4)	5.0 (2.9)	6.3

a single locus to provide accurate estimates of stock composition varied considerably among loci and among populations. For example, the mean error in estimation of stock composition of a sample of pure Birkenhead River chinook salmon was less than 1% when only *Ogo4* was used to estimate stock compositions but ranged as high as 40% when a sample of pure Quesnel River chinook salmon was evaluated. Clearly, not all loci were equally effective in stock identification, and the usefulness of the loci varied among populations. The accuracy of the estimates generally improved with an increasing number of loci used in the estimation procedure, but the increase in accuracy was generally marginal after eight loci were used to estimate stock compositions. In the case of the Birkenhead River, additional loci did not increase the accuracy over that observed with only *Ogo4*. The precision of the estimates generally increased with an increasing number of loci used, but the increase in precision was marginal when the least effective five loci were added to the estimation procedure.

On average, the number of alleles present at a locus was related to the power of the locus to provide accurate estimation of stock composition. For example, the mean bias of estimated stock composition for loci with fewer than 20 observed alleles (*Ogo2, Oke4, Ots2, Ots9*) was 45% per locus, whereas the mean bias for loci with 20 or more alleles was 26% per locus (Table 3). Loci with fewer than 20 observed were generally less valuable for stock identification applications than loci with greater numbers of alleles.

Population estimation of stock composition

We evaluated whether the degree of genetic differentiation observed among Fraser River populations included in the baseline was sufficient for mixed-stock analysis in which the objective was estimation of specific population contributions to fishery samples. Three simulated fishery mixture samples were developed, representing an early, middle, and late-timing return to the lower Fraser River. With 14 populations present in a simulated spring fishery sample, the mean error in population specific estimated stock composition with a 50-population baseline was 1.4% (Table 4). Similar mean population-specific error rates were observed in the simulated summer fishery sample containing fish from 10 populations (1.2%), and in the simulated fall sample containing fish from seven populations (1.1%). Regional estimates of stock contributions were all within 2% of the actual value. We concluded that accurate

Table 4

Estimated percentage composition of three simulated mixtures of Fraser River chinook salmon incorporating variation at 13 microsatellite loci and estimated with a 50-population baseline. Each mixture of 150 fish was generated 500 times with replacement, and stock compositions of the mixtures were estimated by resampling each baseline population with replacement to obtain a new distribution of allele frequencies. "Regional sum" is the regional sum of all populations in the region. The appearance of each population in each of the simulated mixtures is indicated in parentheses after the population name. Standard deviations are given in parentheses.

	Spring		Summer		Fall	
Population and sum for region	Actual	Estimated	Actual	Estimated	Actual	Estimated
Birkenhead (spring)	2.4	2.2 (1.7)	0.0	0.0 (0.1)	0.0	0.0 (0.0)
Harrison (fall)	0.0	0.1 (0.3)	0.0	0.2 (0.5)	60.0	59.8 (6.7)
Chilliwack (fall)[1]	0.0	0.0 (0.2)	0.0	0.0 (0.1)	20.0	18.4 (5.6)
Sum for Lower Fraser region	0.0	0.2 (0.4)	0.0	0.2 (0.5)	80.0	78.9 (4.3)
Westroad (spring)	11.8	5.8 (2.4)	0.0	0.1 (0.3)	0.0	0.0 (0.1)
Bridge (summer)	0.0	1.6 (1.9)	10.0	8.8 (3.8)	0.0	0.2 (0.4)
Cottonwood (spring)	5.9	4.2 (2.1)	0.0	0.1 (0.3)	0.0	0.0 (0.1)
Elkin (spring)	11.8	11.0 (3.4)	0.0	0.2 (0.4)	0.0	0.1 (0.2)
L.Chilcotin (spring)	11.8	8.5 (3.1)	0.0	0.2 (0.4)	0.0	0.1 (0.4)
Quesnel (summer, fall)	0.0	1.4 (1.8)	10.0	10.2 (3.9)	5.0	4.7 (2.8)
Stuart–Nechako (summer, fall)	0.0	4.0 (3.2)	10.0	10.7 (4.4)	5.0	6.0 (2.8)
Sum for Mid Fraser region	41.2	39.2 (5.6)	30.0	30.5 (4.9)	10.0	11.5 (3.4)
Slim (spring)	11.8	7.8 (3.0)	0.0	0.1 (0.3)	0.0	0.0 (0.2)
Swift (summer)	0.0	0.2 (0.4)	2.0	1.8 (1.3)	0.0	0.0 (0.2)
Bowron (spring)	11.8	11.7 (4.2)	0.0	0.1 (0.4)	0.0	0.2 (0.6)
Willow (spring)	5.9	5.0 (2.6)	0.0	0.1 (0.3)	0.0	0.1 (0.2)
Holmes (spring, summer)	11.8	11.1 (3.9)	3.0	2.2 (2.1)	0.0	0.0 (0.2)
MacGregor (spring)	3.5	4.2 (3.5)	0.0	0.2 (0.5)	0.0	0.1 (0.3)
Sum for Upper Fraser region	44.7	46.0 (5.7)	5.0	5.4 (2.6)	0.0	0.6 (0.9)
Clearwater (summer)	0.0	0.1 (0.4)	10.0	9.4 (3.0)	0.0	1.0 (1.1)
Finn (summer)	2.4	2.1 (1.8)	5.0	4.5 (2.4)	0.0	0.0 (0.2)
Louis	0.0	0.0 (0.1)	0.0	0.0 (0.0)	0.0	0.0 (0.1)
Mahood (fall)	0.0	0.0 (0.1)	0.0	0.0 (0.1)	5.0	1.4 (1.5)
Raft (spring, summer)	3.5	3.5 (2.3)	5.0	5.1 (2.7)	0.0	1.4 (1.3)
Sum for North Thompson region	5.9	5.8 (2.9)	20.0	19.1 (4.3)	5.0	3.8 (1.9)
Eagle (summer, fall)	0.0	0.1 (0.2)	10.0	5.9 (2.6)	2.0	1.1 (1.2)
L Shuswap (spring, summer)	2.4	2.2 (1.6)	20.0	21.7 (5.0)	0.0	0.4 (0.7)
M Shuswap (spring, summer)	3.5	3.7 (2.0)	5.0	5.9 (3.0)	0.0	0.1 (0.5)
South Thompson (summer, fall)	0.0	0.3 (0.6)	10.0	9.9 (3.5)	3.0	2.8 (2.0)
Sum for South Thompson region	5.9	6.4 (2.5)	45.0	44.7 (4.9)	5.0	5.0 (2.4)
Sum for Lower Thompson region	0.0	0.2 (0.4)	0.0	0.2 (0.4)	0.0	0.1 (0.3)

[1] White-fleshed population.

estimation of regional stock compositions should be available when the genetic data outlined in our study is applied to actual mixed-fishery samples.

Identification of individuals

Individuals were classified with respect to origin for 50 populations in the Fraser River drainage. Success rate of classification of individuals varied considerably among populations and to some extent was reflective of sample size of individual populations. For example, success rate of identication of individual Goat Creek and Horsey River chinook salmon was about 5%, but approximately only 20 fish from each population were included in the analysis used to characterize the populations (Table 5). Success rate of classification of other upper Fraser River populations was higher, but more fish were available to quantify the variation in the populations. Success rate was partially attributable to sample size but was also markedly influenced by genetic differentiation in the population. For example, all individual Birkenhead River fish were correctly assigned to the population of origin in a 50-population baseline—indicative of the genetic distinctiveness of this population. Overall, highest rates of classification to individual populations were observed for lower Fraser River and lower and North Thompson River populations, with an average

Table 5

Percent correct classification of individual chinook salmon to population and region of origin for 50 populations in the Fraser River drainage. Individuals must have been scored for at least 10 loci in order to be included in the analysis. n = number of fish in sample.

Population	n	Population	Region	Population	n	Population	Region
Sum for Birkenhead region	117	100.0	100.0	Indianpoint	41	4.9	80.5
Harrison	317	74.4	97.5	Willow	68	25.0	80.9
Chilliwack	170	60.6	95.3	Fontoniko	57	42.1[4]	93.0
Sum for Lower Fraser region	487	69.7	96.8	McGregor	118	27.1[5]	85.6
Cottonwood	49	57.1	73.5	Salmon River	226	58.4	80.1
Quesnel	423	52.2	84.2	Bowron	79	30.3	81.0
Cariboo	2	0.0	50.0	Sum for Upper Fraser region	1594	50.9	80.5
Horsefly	15	13.3	46.2	Nicola[6]	251	84.4	93.6
Stuart	430	47.7[1]	89.3	Coldwater[6]	162	86.4	96.3
Nechako	309	30.1[2]	77.7	Spius[6]	57	66.6	86.0
Endako	59	54.2	81.3	Deadman	193	49.7	91.7
Westroad	27	29.6	77.8	Bonaparte	306	69.3	95.6
Upper Chilcotin[3]	42	61.9	88.1	Sum for Lower Thompson region	969	72.0	93.6
Lower Chilcotin[3]	69	47.8	73.9	Mahood	17	11.8	64.7
Chilcotin[3]	47	51.1	83.0	Raft	122	44.3	59.8
Chilko	122	61.5	91.0	Finn	101	81.2	92.1
Elkin	211	68.2	84.8	Louis	139	92.8	97.8
Taseko	51	60.8	88.2	Clearwater	165	82.4	92.1
Bridge	384	53.9	75.8	Sum for North Thompson region	544	74.1	85.5
Portage	23	78.3	87.0	Little River	42	28.6	88.1
Sum for Mid Fraser region	2263	50.7	80.5	Lower Shuswap	335	68.1[7]	96.1
Tete Jaune	248	68.5	89.9	Middle Shuswap	313	73.2[8]	95.8
Dome Creek	327	62.7	93.9	Salmon	128	76.6	91.4
Horsey	22	27.3	90.1	Eagle	36	58.3	86.1
Goat	19	5.2	73.7	Lower Adams	96	46.9	89.6
Holmes	97	18.6	82.5	South Thompson	144	48.6	91.7
Swift	227	78.4	94.3	Bessette	16	31.3	100.0
Slim Creek	65	43.0	92.3	Sum for South Thompson region	1110	63.8	93.8

[1] 64.4% correct to Stuart–Nechako complex.

[2] 46.9% correct to Stuart–Nechako complex.

[3] Upper Chilcotin, Lower Chilcotin, and Chilcotin considered as a single population in the analysis. The Chilcotin sample was a mixed-population sample collected in the Chilcotin River.

[4] 68.4% correct to McGregor River watershed

[5] 38.1% correct to McGregor River watershed.

[6] Coldwater, Spius, and Nicola considered as single population in the analysis.

[7] 81.2% correct to Shuswap River watershed.

[8] 86.6% correct to Shuswap River watershed.

of 70% of the individual fish correctly assigned to specific populations. Correct assignment to region of origin was achieved for at least 80% of the chinook salmon from all regions; the highest rates were for the Birkenhead River and three Thompson River regions, and the lowest rates for the middle and upper Fraser regions.

Application to a coded-wire tag (CWT) sample

CWTs were available from seven Fraser River populations caught in marine fisheries. The average error of the estimated percentage for the seven populations present was 2% per population for the 83-fish sample estimated with a 50-population baseline (Table 6). Tags recovered from the upper Adams River population were combined with the lower Shuswap River because the Upper Adams fish were recent transplants from the Lower Shuswap River population. Similarly, tags recovered from the Stave River population were combined with the Harrision River population because the Stave River fish were recent transplants from the Harrison River. The average error of the estimated percentage for the five regions present was 1.4%. The accuracy of estimated stock compositions obtained from analysis of the CWT sample were within the range expected based upon the analysis of the simulated mixtures.

Lower Fraser commercial net fishery

Estimation of stock composition in the lower river commercial net fishery is of key local fishery management interest,

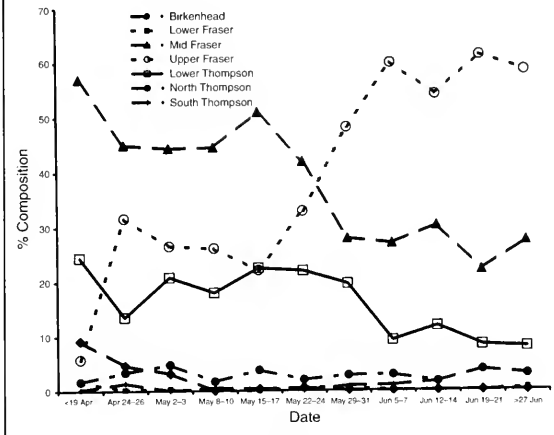

Figure 2

Average percentage of Birkenhead, Lower Fraser, Mid Fraser, Upper Fraser, Lower Thompson, North Thompson, and South Thompson stocks at specific time intervals in samples from the lower Fraser River commercial gillnet fishery, 1997–99.

particularly prior to June. For the fishery samples from 1997 to 1999 collected in April of each year, chinook salmon from the Chilcotin River and Nicola River drainage were important contributors to the fishery, as they, combined, comprised approximately 50% of the samples from the net fishery prior to 19 April (Appendix Table 1). By late April, the Chilcotin River population constituted on average approximately 20% of the fishery samples, and the Nicola drainage populations about 10%. The Birkenhead River population was also identified as contributing 5% to 10% of the catch in the early lower river fishery but was virtually absent from the fishery after 3 May. The Stuart and Nechako river drainage populations were identifed as contributing significantly to the early catches, with estimates as high as 20% in some weeks in some years. Upper Fraser River populations contributed more to the fishery in May, and the significant populations were from the Holmes River, the Fraser River mainstem at Tete Jaune, the Salmon River, and the McGregor River (Appendix Table 1).

On a regional basis, mid Fraser River populations were the dominant group of chinook salmon in the catch in April, and comprised at least 30% of the catch until late May (Fig. 2). Upper Fraser River populations did not occur in any significant proportions in the fishery until the last week of April. By late May, they were the dominant contributors to the lower river fishery and by June could comprise approximately 70% of the weekly catch. South Thompson River and North Thompson River populations comprised only trace proportions of the fishery samples from April through to the end of June. In fact, the contributions of populations in the entire Thompson River drainage were dominated by the tributary Nicola River drainage populations, and these populations were present from the beginning of sampling in early April to the end of sampling in late June. Lower Fraser River popula-

Table 6

Percentage composition of a sample of 83 coded-wire tagged (CWT) Fraser River chinook salmon obtained from fisheries in British Columbia in 1997 and estimated using 13 microsatellite loci with a 50-population Fraser River baseline. Because all fish in the sample were marked with CWTs, the actual composition of the sample is known. Standard deviations are shown in parentheses.

Population and sum for region	Actual %	Estimated %
Dome Creek	1.2	1.2 (1.0)
Sum for Upper Fraser region	1.2	1.2 (1.0)
Nechako–Stuart	4.9	4.1 (3.3)
Quesnel	17.1	12.7 (4.0)
Sum for Mid Fraser region	22.0	22.5 (4.4)
Chilliwack	25.6	25.5 (6.5)
Harrison–Stave	19.5	20.6 (6.5)
Sum for Lower Fraser region	45.1	46.1 (4.5)
Sum for Birkenhead region	0.0	0.0 (0.0)
Sum for North Thompson region	0.0	0.0 (0.9)
Lower Shuswap–Upper Adams	13.4	13.0 (5.9)
Middle Shuswap	15.9	12.7 (4.0)
Sum for South Thompson region	29.3	28.9 (5.2)
Sum for Lower Thompson region	2.4	1.4 (1.4)

tions virtually did not contribute to the fishery from April through June.

Mid Fraser commercial net fishery

Samples from the net fishery in the mainstem Fraser River were obtained from areas largely upstream of the confluence of the Thompson and Fraser rivers. Thus, the estimated percentage of Thompson River chinook salmon was <2% in this fishery (Appendix Table 2). Mid-Fraser populations were estimated to comprise 63% of the samples from late June and early July in 1998 in this fishery, and the Chilcotin River population was the dominant population. By mid July, the majority of the fish sampled originated from upper Fraser populations, and chinook salmon from Salmon River, Bowron River, McGregor River, and the mainstem Fraser River at Tete Jaune were the dominant contributors to the catch (Appendix Table 2).

Lower Fraser test fishery

As was observed in the commercial gillnet fishery in the lower Fraser River, chinook salmon from mid-Fraser populations dominated the catch in April and May, comprising over 50% of the fish sampled (Appendix Table 3). The Chilcotin River and Stuart/Nechako rivers populations were the main populations from the mid-Fraser region. However, unlike the commercial gillnet fishery, salmon from the lower Thompson River comprised 5% or less of the catch in April and May. North and South Thompson River populations comprised <5% of the catch as well, as was observed in the commercial gillnet fishery. Upper Fraser River populations had largely passed through the test fishery by the end of July. Chinook salmon from the North and South Thompson rivers dominated the samples in August, and the mainstem-spawning South Thompson population was the dominant population in the fishery. By September chinook salmon from the lower Fraser River were the main group of fish sampled in the test fishery, and they comprised 45% of the catch. By October, they dominated the test fishery, comprising more than 80% of the chinook salmon sampled.

Discussion

Evaluation of microsatellites

The survey of microsatellite variation of Fraser River chinook salmon was initiated to determine genetic structure of chinook salmon populations within the Fraser River drainage and to provide population-specific estimates of stock composition in mixed-stock fisheries in the drainage for management purposes. Analysis of simulated mixtures has generally indicated that the estimates of stock composition are sufficiently accurate such that reliable estimates of population-specific composition should be obtained when applied to mixed-stock fisheries. Application to a CWT sample indicated that the average error of the estimated percentage for the seven populations present was 2% per population and for the five regions present was 1.4%. These levels of accuracy were judged to be sufficient for management applications. Indeed, there is no other technique currently available that can provide current levels of accuracy in estimation of stock composition for Fraser River chinook salmon.

The 13 microsatellite loci evaluated in our survey clearly differed in their ability to provide accurate estimates of stock composition. Generally, loci with fewer numbers of alleles (<20) were less effective for population identification than were loci with greater numbers of alleles. Theoretical studies of locus characteristics to guide selection for individual identification suggested that a modest number of independent loci was best, where each locus would have a modest number of alleles and where each allele had a modest frequency (Smouse and Chevillon, 1998). For chinook salmon, loci with greater than 20 observed alleles would likely be more effective for stock or individual identification than loci with fewer allleles. With respect to number of loci to include in stock identification applications, analysis of the simulated samples indicated that bias was minimized when all 13 loci surveyed were included in the analysis, but the least effective loci provided only a modest increase in accuracy of estimated stock compositions. Increasing the number of loci included in the stock identification applications would be the preferred option, provided that the number of loci included in the analysis provided a cost-effective method for fishery management applications.

Estimation of stock composition and classification of individuals to specific populations are two goals for stock identification, but estimation of stock composition is the more practical goal for fisheries management. In stock composition analysis, the characteristics of the whole sample are used to provide the most likely estimate. For classification of individuals, only the characteristics of the individual to be identified are used. Because more information is available from a stock mixture rather than from a single individual, and misallocations between individual populations will cancel, estimates of stock composition will generally be more accurate than classifications of individual fish. For example, individual Chilliwack River fish were correctly identified to river of origin approximately 61% of the time, but in the 83-fish CWT sample, the estimate of the Chilliwack River component was within 4% of the true estimate, equivalent to estimating about 25 Chilliwack River fish present instead of 21 fish. Although more difficult, identication of individual fish to specific river of origin does have some management applications for Fraser River chinook salmon. Because the Birkenhead River population is very distinct genetically, it is possible to identify specific individuals as originating from the Birkenhead River with a high degree of accuracy in fisheries both within and outside of the Fraser River drainage. Given current conservation concerns for the Birkenhead River population and with the appropriate level of sampling, it is possible to identify all areas and periods in which chinook salmon from this population are present.

Given the large number of chinook salmon populations spawning in the Fraser River drainage, the area of the drainage, and the cost of both obtaining representative samples from spawning populations and their analysis,

it is necessary that the annual variation in population-discriminating characters within populations be substantially less than the differences among populations. If the annual variation in population-discriminating characters within populations is less, then annual baseline sampling of populations would not be necessary, and samples from individual populations could be pooled over time to increase the reliability of observed allele frequencies. This procedure is required in order that a stock identification method be feasible from both technical and financial perspectives. For Fraser River chinook salmon, the genetic variation attributable to population differentiation was about eight times the variation attributable to annual variation within populations (Beacham et al., 2003), rendering annual variation in allele frequencies of little practical significance in estimation of stock composition for fisheries in the drainage. In particular, annual estimation of microsatellite allele frequencies in baseline populations would not be required for practical applications, although some level of monitoring of allele frequencies over time would clearly be desirable. The annual stability of microsatellite allele frequencies for Fraser River chinook salmon in relation to population differentiation is very similar to that reported for other salmonids (Beacham et al., 1999; Tessier and Bernatchez, 1999).

The two major fall-return populations in the lower Fraser River are from the Harrision River and Chilliwack River. Analysis of simulated mixtures and the CWT sample suggested that discrimination between the Harrision River and Chilliwack River populations was possible. Transplants have occurred between these two populations (Candy and Beacham, 2000), but the level of transplantation has not been sufficient to homogenize genetic differentiation between the populations.

Application to commercial and test fisheries

Analysis of estimated stock compositions of the 1997–99 lower river commercial gillnet fishery and the 1995 lower river test gillnet fishery indicated a discrepancy between the relative abundance of lower Thompson River populations, particularly the Nicola River drainage populations. In the commercial gillnet fishery, Nicola River drainage populations comprised 10–30% of the samples in April and May, but only 0–5% of the test fishery samples. Absolute population abundance may have differed between the two time periods, but a more likely explanation was the fact that the 1995 test fishery was conducted with a single mesh gillnet of 20.3 cm, a mesh size selective for larger-bodied chinook salmon. Lower Thompson River chinook salmon populations are substantially smaller in body size than other chinook salmon populations in the Fraser River drainage (Beacham and Murray, 1993), and thus were not likely to have been sampled in proportion to their abundance by the gear used in the test fishery. Multipanel, multimesh gillnets have been used in the test fishery since 1997 in order to obtain more representative sampling of migrating chinook salmon.

Timing of return of specific populations through the lower Fraser River has been outlined by DFO.[1] The designation of populations as "spring run," "summer run," or "fall run" is based upon a number of factors, of which peaks of occurrence of CWTs in the test fishery in the lower river and peak of arrival on the spawning grounds are key factors. Recoveries of CWTs are largely restricted to tagged, enhanced populations because little CWT marking has been conducted for wild populations. There was, in general, good correspondence between run timing determined by CWTs or other factors and those observed in our analyses of the lower river commercial fishery. For example, the Birkenhead River population is known to return very early through the lower Fraser River (Fraser et al., 1982). Highest proportions of Birkenhead River chinook salmon were consistently observed in the lower Fraser River commercial fishery prior to 19 April, indicative of an early passage through the lower Fraser River. The Coldwater River, Spius Creek, and Nicola River populations are all found in the Nicola River drainage, and all are classified as spring-run populations (DFO[1]). The Nicola River drainage aggregrate was a major contributor to catch in the commercial fishery from April to early June. The other lower Thompson River populations, the Deadman River and Bonaparte River, were classified as spring-run populations, and they were detected in the lower river commercial fishery. The Chilcotin River stock aggregrate (upper and lower Chilcotin populations) was classified as spring run (DFO[1]), and again this stock was a dominant contributor to the lower river commercial fishery in April and May. In the upper Fraser River, the mainstem spawning population at Tete Jaune and the Bowron River population are thought to be spring run, and this timing was observed in both the commercial fishery and the test fishery.

The summer-run populations migrate through the lower Fraser River mainly after 15 July and originate primarily from the North and South Thompson River watersheds (a few major populations come from the middle Fraser River (DFO[1]). Analysis of the lower Fraser River test fishery supports this conclusion, with 60–75% of the fish sampled in the test fishery in August of North and South Thompson River origin. Populations contributing significantly to the test fishery included the Clearwater River, Adams River, and Shuswap River, and these have been defined as summer-run populations. Fall-run populations occur after 1 September and are thought to be largely restricted to the lower Fraser River (DFO[1]). Lower Fraser River populations certainly dominated the test fishery catch in October, but lower Fraser populations were estimated to have comprised only 45% of the catch in September. Summer-run populations were clearly present in the lower river in September, and in fact comprised the majority of the catch.

There was one significant discrepancy between the previous designation of timing of return (DFO[1]) and that observed in the fishery sampling in our study. The populations in the Nechako River and Stuart River in the mid Fraser region have been defined as summer run, based largely on the timing of recoveries of CWTs from Stuart River chinook salmon in the lower river test fishery. However, in the analysis of the lower river commercial and test fisheries, the Stuart-Nechako population was estimated to have comprised up to 20% of the catch in a period prior to 15 July. The Stuart-Nechako drainage is large, and there

are some spawning populations that we have not yet analyzed. These populations include those in the Driftwood River and Middle River in the Stuart River drainage, and the Chilako River and Nadina River in the Nechako River drainage. These populations are likely most similar to the Stuart River and Nechako River populations with respect to microsatellite variation, and the Stuart-Nechako stock in the baseline may be a proxy for the occurrence of one or more of these populations in the fishery samples.

The application of microsatellite variation to estimation of stock composition of chinook salmon in Fraser River mixed-stock fisheries was conducted as a result of conservation concerns, particularly for early-migrating populations. The mixed-stock analysis enabled accurate estimates of stock composition in mixed-stock fishery samples and can even be applied to nonretention fisheries because the fish can be released alive after sampling. The applications developed for Fraser River chinook salmon is an example of the power of microsatellite variation that will likely be applied to an increasing number of species and fisheries for which the management concerns of identifying population structure and detecting specific populations in mixed-stock fisheries arise.

Acknowledgments

We would like to acknowledge all those people involved in sampling the commercial fisheries in the Fraser River, with most of the sampling coordinated by Melanie Sullivan and Terry Robertson. The test fishery was conducted and sampled by Alan Baker. Improvements to the manuscript were suggested by an anonymous referee. Funding was provided by the Department of Fisheries and Oceans.

Literature cited

Banks, M. A., M. S. Blouin, B. A. Baldwin, V. K. Rashbrook, H. A. Fitzgerald, S. M. Blakenship, and D. Hedgecock.
1999. Isolation and inheritance of novel microsatellites in chinook salmon (*Oncorhynchus tschawytscha*). J. Hered. 90:281–288.

Banks, M. A., V. K. Rashbrook, M. J. Calavetta, C. A. Dean, and D. Hedgecock.
2000. Analysis of microsatellite DNA resolves genetic structure and diversity of chinook salmon (*Oncorhynchus tshawytscha*) in California's Central Valley. Can. J. Fish. Aquat. Sci. 57 915–927.

Beacham, T. D., J. R. Candy, K. J. Supernault, T. Ming, B. Deagle, A. Schulze, D. Tuck, K. H. Kaukinen, J. R. Irvine, K. M. Miller, and R. E. Withler.
2001. Evaluation and application of microsatellite and major histocompatibility complex variation for stock identification of coho salmon in British Columbia. Trans. Am. Fish. Soc. 130:1116–1149

Beacham, T. D, K. D. Le, M. R. Raap, K. Hyatt, W. Luedke, and R. E. Withler.
2000. Microsatellite DNA variation and estimation of stock composition of Barkley Sound, British Columbia sockeye salmon. Fish. Bull. 98:14–24

Beacham, T. D., and C. B. Murray.
1993. Fecundity and egg size variation in North American Pacific salmon (*Oncorhynchus*). J. Fish Biol. 42:485–508.

Beacham, T. D., S. Pollard, and K. D. Le.
1999. Population structure and stock identification of steelhead in southern British Columbia, Washington, and the Columbia River based on microsatellite DNA variation. Trans. Am. Fish. Soc. 128:1068–1084.

Beacham, T. D., K. J. Supernault, M. Wetklo, B. Deagle, K. Labaree, J. Irvine, J. R. Candy, K. M. Miller, R. J. Nelson, and R. E. Withler.
2003. The geographic basis of population structure of Fraser River chinook salmon (*Oncorhynchus tshawytscha*). Fish. Bull. 101:229–242.

Beacham, T. D., R. E. Withler, and T. A. Stevens.
1996. Stock identification of chinook salmon (*Oncorhynchus tshawytscha*) using minisatellite DNA variation. Can. J. Fish. Aquat. Sci. 53:380–394.

Beacham, T. D, and C. C. Wood.
1999. Application of microsatellite DNA variation to estimation of stock composition and escapement of Nass River sockeye salmon (*Oncorhynchus nerka*). Can. J. Fish. Aquat. Sci. 56:1–14.

Buchholz, W., S. J. Miller, and W. J. Spearman.
1999. Summary of PCR primers for salmonid genetic studies. U.S. Fish. Wild. Serv. Alaska Fish. Prog. Rep. 99-1, 30 p.

Candy, J. R, and T. D. Beacham.
2000. Patterns of homing and straying in southern British Columbia coded-wire tagged chinook salmon (*Oncorhynchus tshawytscha*) populations. Fish. Res. 47:41–56.

Cornuet, J. M., S. Piry, G. Luikart, A. Estoup, M. Solignac.
1999. Comparison of methods employing multilocus genotypes to select or exclude populations as origins of individuals. Genetics 153:1989–2000.

Debevec, E.M., R. B. Gates, M. Masuda, J. Pella, J. Reynolds, and L. W. Seeb.
2000. SPAM (version 3.2): Statistics program for analyzing mixtures. J. Hered. 91:509–510.

Fraser, F. J., P. J. Starr, and A. Y. Federenko.
1982. A review of the chinook and coho salmon of the Fraser River. Can. Tech. Rep. Fish. Aquat. Sci. 1126, 130 p.

Miller, K. M., R. E. Withler, and T. D. Beacham.
1996. Stock identification of coho salmon (*Oncorhynchus kisutch*) using minisatellite DNA variation. Can. J. Fish. Aquat. Sci. 53:181–195.

Murray, C. B., and M. L. Rosenau.
1989. Rearing of juvenile chinook salmon in nonnatal tributaries of the lower Fraser River, British Columbia. Trans. Am. Fish. Soc. 118:284–289.

Nelson, R. J., and T. D. Beacham.
1999. Isolation and cross species amplification of microsatellite loci useful for study of Pacific salmon. Anim. Genet. 30:228–229.

Nelson, R. J., T. D. Beacham, and M. P. Small.
1998. Microsatellite analysis of the population structure of a Vancouver Island sockeye salmon (*Oncorhynchus nerka*) stock complex using non-denaturing gel electrophoresis. Mol. Mar. Biotech 7: 312–319.

Nelson, R. J., M. P. Small, T. D. Beacham, and K. J. Supernault.
2001. Population structure of Fraser River chinook salmon (*Oncorhynchus tshawytscha*): an analysis using microsatellite DNA markers. Fish. Bull. 99:94–107.

Olsen, J. B., P. Bentzen, and J. E. Seeb.
1998. Characterization of seven microsatellite loci derived from pink salmon. Mol. Ecol. 7: 1083–1090.

O'Connell, M., R. G. Danzmann, J. M. Cornuet, J.M. Wright, and M. M. Ferguson.
1997. Differentiation of rainbow trout populations in Lake Ontario and the evaluation of the stepwise mutation and infinite allele mutation models using microsatellite variability. Can. J. Fish. Aquat. Sci. 54:1391–1399.

O'Reilly, P. T., L. C. Hamilton, S. K. McConnell, and J. M. Wright.
1996. Rapid analysis of genetic variation in Atlantic salmon (*Salmo salar*) by PCR multiplexing of dinucleotide and tetranucleotide microsatelllites. Can. J. Fish. Aquat. Sci. 53:2292–2298.

Shaklee, J. B., T. D. Beacham, L. Seeb, and B. A. White.
1999. Managing fisheries using genetic data: case studies from four species of Pacific salmon. Fish. Res. 43:45–78.

Shubert, N. D., P. G. Paterson, and C. M. McNair.
1988. The Fraser River chinook salmon test fishery: data summary, 1980–87. Can. Data Rep. Fish. Aquat. Sci. 709, 193 p.

Small, M. P., T. D. Beacham, R. E. Withler, and R. J. Nelson.
1998. Discriminating coho salmon (*Oncorhynchus kisutch*) populations within the Fraser River, British Columbia using microsatellite markers. Mol. Ecol. 7: 141–155.

Smouse, P.E., and Chevillon, C.
1998. Analytical aspects of population-specific DNA fingerprinting for individuals. J. Hered. 89: 143–150.

Tessier, N., and L. Bernatchez.
1999. Stability of population structure and genetic diversity across generations assessed by microsatellites among sympatric populations of landlocked Atlantic salmon (*Salmo salar* L.). Mol. Ecol. 8:169–179.

Appendix Table 1

Estimated percentage stock compositions of chinook salmon from lower Fraser River commercial fisheries in 1997–99. Stock compositions were estimated with a 50-population Fraser baseline by using six loci for the 1997 samples and 13 loci for the 1998 and 1999 samples. Main populations identified within regions are listed, and populations within regions having minor allocations grouped as "Other Mid Fraser," etc. *n* is the number of fish sampled in each period. Standard deviations are shown in parentheses and were estimated from 100 resamplings of both the baseline and mixtures.

		Prior to 19 April			24–26 April		
	Population	1997	1998	1999	1997	1998	1999
n		115	114	142	29	30	191
Birkenhead	Birkenhead	7.2 (2.9)	8.4 (2.5)	12.1 (2.7)	4.0 (4.2)	8.6 (5.7)	1.6 (0.8)
Lower Fraser	All populations	4.8 (2.2)	0.0 (0.4)	0.0 (0.4)	0.0 (3.0)	0.0 (0.0)	0.7 (0.7)
Mid Fraser	Nechako–Stuart	20.1 (6.5)	16.0 (5.8)	8.6 (4.4)	0.0 (5.6)	0.0 (6.7)	12.7 (4.1)
	Endako	1.5 (2.1)	2.7 (2.4)	0.0 (0.0)	0.0 (3.3)	0.0 (5.7)	3.8 (1.5)
	Up.–Lower Chilcotin	32.3 (6.2)	30.3 (6.2)	34.8 (6.0)	18.5 (10.3)	26.2 (11.3)	13.4 (2.8)
	Bridge	0.0 (4.2)	4.0 (6.5)	2.5 (2.5)	9.6 (7.3)	0.1 (8.5)	7.4 (4.2)
	Cottonwood	4.4 (2.3)	3.2 (2.1)	0.0 (1.4)	20.8 (10.0)	8.2 (6.5)	9.4 (2.2)
	Chilko	0.0 (0.3)	0.0 (0.2)	1.3 (1.2)	0.0 (2.1)	0.0 (1.1)	0.7 (0.8)
	Elkin	0.0 (0.0)	0.0 (0.2)	0.0 (0.2)	0.0 (2.2)	0.0 (0.0)	0.0 (0.0)
	Westroad	0.0 (1.3)	3.8 (3.4)	0.0 (2.9)	0.0 (0.9)	0.0 (1.8)	4.1 (1.5)
	Other Mid Fraser	0.0 (1.3)	0.0 (0.7)	5.6 (3.0)	0.0 (2.2)	0.0 (1.1)	0.0 (0.9)
Upper Fraser	Tete Jaune	0.0 (0.0)	0.0 (0.2)	0.0 (0.0)	0.0 (2.0)	0.0 (2.4)	0.0 (1.0)
	Willow	0.0 (1.0)	0.0 (1.1)	0.0 (2.1)	0.0 (5.7)	0.0 (4.6)	5.1 (2.2)
	Holmes	0.0 (0.5)	0.4 (1.2)	0.0 (1.0)	0.0 (6.2)	11.6 (7.1)	5.8 (3.5)
	Salmon	3.2 (2.9)	1.7 (3.4)	1.3 (3.1)	0.0 (4.6)	10.6 (10.4)	6.8 (2.9)
	Bowron	0.0 (2.9)	0.0 (0.3)	0.0 (3.5)	1.4 (11.0)	6.2 (9.8)	1.5 (2.4)
	McGregor	0.0 (0.4)	0.0 (0.0)	0.0 (0.0)	0.5 (7.2)	10.3 (8.7)	0.0 (0.7)
	Dome	2.4 (1.7)	0.0 (0.8)	0.0 (1.4)	0.0 (3.8)	0.0 (2.2)	2.0 (1.7)
	Goat	2.5 (1.4)	0.0 (0.9)	0.0 (1.1)	9.6 (6.9)	0.3 (4.9)	3.4 (1.5)
	Other Upper Fraser	0.0 (1.6)	0.5 (1.0)	5.3 (3.0)	18.3 (9.0)	0.0 (2.1)	1.6 (1.2)
Lower Thompson	Cold–Spius–Nicola	11.1 (5.6)	24.6 (5.3)	26.0 (5.2)	9.4 (5.9)	13.5 (7.6)	13.8 (2.6)
	Deadman	8.5 (4.9)	2.5 (3.4)	0.0 (1.4)	0.0 (2.5)	0.0 (2.8)	0.0 (0.9)
	Bonaparte	0.1 (3.1)	0.8 (3.3)	0.0 (0.9)	0.0 (4.0)	0.0 (0.1)	4.2 (1.8)
North Thompson	All populations	1.7 (1.9)	1.2 (1.1)	2.3 (1.6)	3.6 (4.5)	4.4 (4.1)	2.3 (1.2)
South Thompson	All populations	0.2 (1.2)	0.1 (0.9)	0.2 (1.0)	4.3 (3.7)	0.0 (1.1)	0.0 (0.1)

Continued

Appendix Table 1 (continued)

Region	Population	2–3 May 1997	2–3 May 1998	2–3 May 1999	8–10 May 1998	8–10 May 1999	15–17 May 1998	15–17 May 1999
n		51	50	62	119	137	164	126
Birkenhead	Birkenhead	5.3 (3.1)	4.4 (2.7)	0.0 (0.0)	0.0 (0.0)	0.0 (0.0)	0.6 (1.1)	0.0 (0.0)
Lower Fraser	All populations	0.8 (4.6)	0.0 (0.6)	0.0 (0.2)	0.0 (0.0)	0.0 (0.3)	0.0 (0.5)	0.0 (0.1)
Mid Fraser	Nechako–Stuart	6.9 (6.4)	5.4 (7.9)	21.1 (7.6)	9.0 (4.8)	13.6 (5.0)	5.8 (6.7)	9.0 (4.4)
	Endako	0.9 (4.2)	3.7 (3.9)	0.0 (1.6)	2.7 (3.0)	0.0 (1.1)	1.5 (3.2)	0.0 (0.8)
	Up.–Lower Chilcotin	13.9 (7.7)	9.7 (5.7)	18.1 (6.2)	10.7 (4.0)	23.3 (4.6)	19.6 (4.5)	18.6 (4.4)
	Bridge	5.9 (7.2)	0.0 (8.8)	2.6 (4.4)	1.7 (5.6)	6.8 (5.5)	6.3 (5.3)	1.6 (5.0)
	Cottonwood	8.9 (5.4)	20.2 (8.4)	1.4 (2.7)	10.5 (5.1)	1.9 (1.4)	17.5 (4.5)	14.9 (4.0)
	Chilko	9.0 (5.6)	0.0 (2.6)	0.0 (0.4)	2.6 (3.3)	0.0 (1.3)	0.0 (0.2)	0.0 (0.8)
	Elkin	0.0 (3.1)	0.0 (0.0)	0.0 (0.3)	0.0 (0.2)	0.0 (0.3)	0.0 (0.0)	0.0 (0.1)
	Westroad	0.0 (1.7)	0.0 (3.4)	5.5 (2.6)	0.0 (0.6)	4.3 (1.9)	1.7 (1.9)	3.4 (1.5)
	Other Mid Fraser	0.0 (1.0)	0.0 (1.2)	0.0 (1.1)	0.1 (1.2)	2.0 (0.9)	1.3 (1.3)	0.8 (0.8)
Upper Fraser	Tete Jaune	0.0 (1.3)	2.5 (3.3)	0.0 (2.1)	0.0 (1.3)	0.0 (0.3)	8.7 (4.1)	0.0 (0.9)
	Willow	2.5 (4.7)	8.8 (5.5)	0.0 (2.1)	9.2 (4.4)	2.5 (2.3)	1.6 (2.3)	2.7 (1.9)
	Holmes	0.0 (0.8)	0.0 (2.4)	10.3 (4.6)	11.3 (7.2)	4.6 (2.9)	3.0 (5.1)	5.5 (3.5)
	Salmon	12.8 (7.9)	7.5 (9.3)	0.1 (4.4)	14.2 (7.5)	4.9 (3.5)	8.9 (4.9)	4.7 (3.4)
	Bowron	0.3 (6.6)	3.0 (6.0)	0.3 (2.3)	0.0 (3.4)	0.0 (1.8)	0.0 (3.6)	0.0 (1.8)
	McGregor	0.0 (2.5)	0.0 (2.8)	0.0 (1.4)	0.0 (0.9)	0.0 (0.6)	1.9 (2.2)	1.0 (2.1)
	Dome	6.9 (6.6)	0.0 (3.6)	0.0 (0.0)	1.3 (5.9)	1.1 (1.7)	0.0 (2.9)	0.0 (0.8)
	Goat	0.0 (3.4)	3.3 (3.8)	1.8 (1.1)	0.1 (2.4)	0.0 (0.5)	0.3 (2.2)	1.1 (1.0)
	Other Upper Fraser	9.2 (5.9)	6.3 (5.3)	4.2 (3.0)	3.2 (2.5)	0.0 (1.0)	3.2 (2.9)	1.8 (1.6)
Lower Thompson	Cold-Spius-Nicola	7.3 (5.4)	6.0 (7.0)	15.6 (6.1)	15.0 (5.8)	28.4 (4.8)	13.5 (4.0)	25.1 (4.7)
	Deadman	9.5 (5.1)	0.2 (2.2)	5.5 (4.5)	7.7 (4.3)	3.3 (2.8)	0.0 (1.4)	3.0 (3.0)
	Bonaparte	.0 (2.9)	0.0 (0.0)	8.7 (5.5)	0.0 (3.4)	0.0 (2.5)	0.0 (1.6)	3.5 (2.5)
North Thompson	All populations	0.0 (1.1)	9.1 (6.4)	5.2 (4.5)	0.0 (0.8)	3.4 (2.4)	4.7 (3.2)	2.8 (2.5)
South Thompson	All populations	0.0 (0.1)	0.0 (0.2)	0.0 (0.0)	1.0 (1.0)	0.0 (0.3)	0.0 (0.3)	0.7 (0.8)

Continued

Appendix Table 1 (continued)

Region	Population	May 22–24		May 29–31		June 5–7	
		1998	1999	1998	1999	1998	1999
	n	234	99	201	37	245	85
Birkenhead	Birkenhead	0.0 (0.8)	1.0 (1.5)	0.0 (0.0)	0.0 (0.0)	0.0 (0.0)	0.0 (0.0)
Lower Fraser	All populations	1.2 (1.1)	0.0 (0.2)	1.0 (1.0)	0.0 (0.0)	0.0 (0.2)	0.0 (0.0)
Mid Fraser	Nechako–Stuart	9.7 (4.7)	15.4 (5.5)	3.6 (3.7)	2.8 (5.6)	4.8 (3.3)	9.3 (5.6)
	Endako	8.1 (3.6)	2.3 (2.0)	7.5 (3.0)	0.0 (0.0)	4.9 (2.6)	0.0 (0.8)
	Up.–Lower Chilcot	12.2 (3.7)	13.3 (4.3)	4.8 (2.5)	4.7 (5.5)	3.2 (1.9)	2.5 (1.8)
	Bridge	0.3 (3.7)	0.6 (2.6)	4.0 (5.0)	4.1 (4.8)	3.0 (3.5)	10.2 (5.2)
	Cottonwood	7.0 (3.5)	8.0 (2.9)	6.6 (2.8)	5.0 (3.3)	5.5 (2.5)	6.8 (3.4)
	Chilko	0.0 (1.4)	0.0 (0.0)	0.0 (1.0)	3.6 (2.9)	0.0 (0.4)	0.0 (0.4)
	Elkin	0.0 (0.1)	0.0 (0.0)	0.0 (0.5)	0.0 (0.0)	0.0 (0.2)	0.0 (0.4)
	Westroad	3.9 (1.5)	0.0 (1.2)	1.6 (1.4)	0.0 (1.4)	0.0 (0.4)	0.0 (0.5)
	Other mid Fraser	0.4 (1.2)	2.8 (2.0)	0.0 (0.9)	7.6 (5.3)	1.4 (1.5)	2.6 (4.1)
Upper Fraser	Tete Jaune	1.7 (1.8)	0.0 (2.7)	6.9 (4.2)	0.0 (1.0)	1.7 (2.7)	10.2 (4.2)
	Willow	1.2 (2.3)	4.6 (2.7)	8.1 (4.1)	0.3 (5.3)	7.0 (3.5)	1.6 (2.3)
	Holmes	14.0 (5.4)	9.9 (4.9)	8.3 (6.1)	9.5 (5.8)	10.5 (6.1)	19.9 (6.4)
	Salmon	11.1 (4.7)	1.7 (3.0)	5.2 (4.0)	17.7 (11.6)	12.2 (4.8)	3.8 (3.7)
	Bowron	5.9 (3.9)	3.0 (3.1)	0.0 (2.7)	10.0 (9.2)	1.1 (3.3)	0.0 (2.6)
	MacGregor	1.7 (1.8)	0.0 (2.4)	2.9 (3.5)	0.0 (3.8)	13.5 (4.4)	0.0 (2.0)
	Dome	5.9 (4.5)	0.0 (2.4)	8.6 (5.6)	0.0 (2.4)	7.2 (4.4)	9.1 (4.7)
	Goat	1.3 (2.1)	0.0 (0.7)	7.8 (3.0)	0.0 (0.6)	11.9 (3.8)	0.0 (0.7)
	Other Upper Fraser	0.6 (1.7)	3.4 (2.2)	4.1 (3.5)	7.1 (5.2)	1.6 (1.7)	8.7 (4.2)
Lower Thompson	Cold–Spius–Nicola	9.7 (2.8)	30.7 (4.9)	9.8 (3.6)	27.6 (9.4)	4.2 (2.6)	13.2 (3.5)
	Deadman	0.0 (0.6)	0.0 (2.9)	0.0 (0.7)	0.0 (2.3)	1.1 (1.2)	0.0 (1.0)
	Bonaparte	1.2 (1.7)	2.5 (2.2)	1.9 (2.5)	0.0 (2.0)	0.0 (0.6)	0.0 (0.5)
North Thompson	All populations	3.0 (2.1)	0.9 (0.8)	5.5 (3.7)	0.0 (1.1)	3.5 (2.6)	2.3 (2.7)
South Thompson	All populations	0.0 (0.3)	0.0 (0.0)	1.8 (1.2)	0.0 (0.3)	1.9 (1.0)	0.0 (0.3)

Continued

Appendix Table 1 (continued)

Region	Population	12–15 June		19–June		After 27 June	
		1998	1999	1998	1999	1998	1999
n		258	172	322	203	63	113
Birkenhead	Birkenhead	0.0 (0.0)	0.0 (0.0)	0.0 (0.0)	0.0 (0.0)	0.0 (0.7)	0.0 (0.0)
Lower Fraser	All populations	0.0 (0.0)	0.0 (0.0)	0.0 (0.0)	0.0 (0.0)	0.8 (1.9)	0.0 (0.0)
Mid Fraser	Nechako–Stuart	0.0 (0.0)	14.2 (3.9)	0.0 (2.6)	4.6 (3.4)	6.0 (5.1)	7.2 (4.9)
	Endako	2.1 (1.6)	3.1 (1.7)	0.6 (1.6)	0.0 (0.9)	6.6 (4.6)	2.0 (1.6)
	Up.–Lower Chilcotin	0.8 (1.8)	8.4 (2.2)	3.2 (2.6)	10.4 (3.0)	6.5 (4.6)	12.1 (4.2)
	Bridge	16.3 (4.3)	2.6 (3.5)	8.5 (4.1)	4.2 (3.3)	0.0 (2.4)	0.0 (0.0)
	Cottonwood	2.7 (1.8)	2.5 (1.5)	0.0 (1.0)	6.0 (1.9)	0.0 (1.1)	3.9 (2.4)
	Chilko	0.0 (1.1)	0.0 (1.0)	3.4 (2.0)	0.5 (0.8)	0.0 (0.8)	1.9 (1.3)
	Elkin	0.2 (1.2)	0.0 (1.0)	0.0 (0.4)	0.0 (0.0)	0.0 (0.4)	1.6 (1.3)
	Westroad	0.3 (1.2)	1.6 (1.1)	0.0 (0.2)	0.3 (0.6)	3.4 (2.8)	0.9 (1.0)
	Other Mid Fraser	1.0 (1.1)	4.8 (3.2)	0.9 (1.5)	1.7 (1.9)	0.2 (6.3)	2.6 (5.1)
Upper Fraser	Tete Jaune	3.4 (4.1)	0.0 (0.9)	12.0 (3.8)	3.4 (2.5)	6.6 (8.9)	1.7 (2.3)
	Willow	3.4 (2.9)	6.9 (3.0)	0.1 (2.1)	0.9 (1.6)	0.0 (2.5)	1.1 (1.9)
	Holmes	16.2 (5.6)	12.5 (4.3)	18.0 (5.0)	17.8 (4.4)	16.6 (10.0)	8.7 (3.6)
	Salmon	4.2 (3.3)	2.8 (2.8)	4.7 (3.1)	12.9 (4.0)	0.0 (3.9)	15.0 (4.9)
	Bowron	1.8 (4.2)	0.9 (2.6)	1.1 (3.1)	0.5 (1.8)	9.1 (6.5)	6.5 (4.1)
	McGregor	15.1 (6.2)	8.8 (3.4)	8.1 (3.8)	6.3 (3.5)	0.0 (3.9)	5.3 (4.3)
	Dome	0.0 (3.2)	10.1 (4.0)	10.1 (3.7)	10.4 (3.9)	11.0 (7.0)	6.7 (4.1)
	Goat	13.7 (3.3)	0.7 (0.5)	6.2 (2.6)	0.0 (1.0)	16.5 (6.6)	1.9 (0.8)
	Other Upper Fraser	5.6 (3.8)	2.3 (1.9)	7.8 (4.6)	2.5 (2.5)	5.0 (5.2)	5.4 (2.9)
Lower Thompson	Cold–Spius–Nicola	8.2 (2.5)	12.4 (3.2)	3.0 (1.5)	8.2 (2.3)	6.0 (5.1)	6.6 (2.7)
	Deadman	0.0 (0.7)	0.9 (1.7)	0.0 (0.8)	2.7 (1.8)	0.0 (0.0)	0.0 (0.6)
	Bonaparte	0.4 (1.1)	2.7 (2.1)	0.3 (0.8)	2.6 (1.6)	0.0 (0.0)	3.5 (2.3)
North Thompson	All populations	2.2 (1.3)	1.0 (1.6)	5.2 (2.9)	3.5 (3.4)	2.9 (2.8)	2.3 (1.8)
South Thompson	All populations	2.4 (2.3)	0.8 (0.7)	7.0 (3.1)	0.6 (0.7)	2.8 (2.2)	3.2 (2.4)

Appendix Table 2

Estimated percentage stock compositions of chinook salmon from a mid-Fraser River commercial fishery in 1998. Main populations identified within regions are listed, and populations within regions having minor allocations are grouped as "Other Mid Fraser," etc. *n* is the number of fish sampled in each period. Standard deviations are shown in parentheses and were estimated from 100 bootstrap resamplings of both the baseline and mixtures.

Region	Population	21 Jun–4 July	5–13 July
n		59	101
Mid Fraser	Upper-Lower Chilcotin	35.6 (8.6)	4.9 (2.6)
	Stuart-Nechako	13.1 (8.3)	7.9 (6.1)
	Cottonwood	5.3 (3.9)	5.4 (3.6)
	Horsefly	8.7 (3.5)	3.2 (3.2)
	Other Mid Fraser	0.0 (2.0)	9.9 (4.6)
	All Mid Fraser	62.7 (11.3)	31.3 (8.3)
Upper Fraser	Salmon	30.3 (10.4)	5.6 (5.1)
	Bowron	0.0 (6.0)	14.1 (8.1)
	McGregor	0.0 (1.1)	13.5 (7.9)
	Tete Jeune	0.0 (1.4)	13.3 (6.2)
	Goat	2.9 (2.7)	13.6 (5.6)
	Other Upper Fraser	2.1 (3.3)	7.5 (4.9)
	All Upper Fraser	35.3 (11.7)	67.6 (9.0)
Lower Thompson	All populations	2.0 (2.2)	0.0 (0.3)
South Thompson	All populations	0.0 (0.5)	1.1 (1.4)

Appendix Table 3

Estimated percentage stock compositions of chinook salmon from a lower Fraser River test fishery at Albion in 1995. Stock compositions were estimated with a 50-population Fraser baseline and five microsatellite loci. Main populations identified within regions are listed. *n* is the number of fish sampled in each period. Standard deviations are shown in parentheses and were estimated from 100 bootstrap resamplings of both the baseline and mixtures.

Region	Population	14–30 Apr	1–31 May	1–15 Jun	16–30 Jun	1–15 Jul
n		44	94	128	415	251
Birkenhead	Birkenhead	2.3 (2.0)	0.0 (0.0)	1.1 (1.2)	0.0 (0.2)	0.0 (0.2)
Lower Fraser	All populations	1.8 (2.4)	0.0 (0.0)	0.0 (0.6)	0.0 (0.8)	0.0 (1.1)
Mid Fraser	Chilcotin	38.0 (8.8)	10.9 (3.0)	9.9 (3.7)	4.4 (1.9)	2.2 (2.2)
	Stuart–Nechako	10.6 (8.2)	22.2 (6.6)	1.9 (2.4)	4.1 (3.4)	4.6 (3.8)
	Quesnel	3.1 (5.5)	0.8 (4.4)	0.0 (3.4)	2.8 (2.4)	4.0 (3.6)
	Chilko	0.0 (2.2)	0.0 (1.4)	5.9 (4.3)	9.6 (3.2)	11.0 (3.5)
	All populations	64.6 (9.6)	51.2 (6.2)	40.1 (7.8)	31.1 (4.4)	34.3 (5.5)
Upper Fraser	Tete Jaune	2.4 (3.9)	2.9 (2.5)	0.0 (2.4)	2.9 (2.3)	10.8 (3.8)
	McGregor	0.0 (1.1)	14.3 (5.0)	11.8 (5.3)	11.1 (3.3)	0.0 (2.7)
	Salmon	10.3 (6.0)	3.8 (3.8)	7.3 (5.3)	0.0 (1.5)	2.3 (2.8)
	Goat	0.0 (0.5)	0.3 (1.0)	7.0 (3.8)	1.8 (1.6)	6.0 (2.9)
	Holmes	9.8 (5.2)	2.8 (3.7)	0.0 (2.2)	3.6 (3.1)	0.0 (2.3)
	All populations	22.5 (8.3)	43.3 (6.4)	44.4 (7.4)	51.6 (4.0)	38.6 (4.9)
Lower Thompson	Cold–Spius–Nicola	5.2 (3.5)	0.0 (1.3)	5.5 (3.7)	2.5 (1.67)	4.5 (2.1)
	All populations	5.2 (3.5)	2.5 (1.7)	5.6 (3.5)	5.1 (1.7)	5.0 (2.3)
North Thompson	Clearwater	0.0 (0.9)	0.0 (0.2)	3.0 (2.4)	0.0 (0.8)	4.7 (2.4)
	Raft	3.6 (4.3)	0.0 (0.0)	0.0 (1.6)	1.8 (1.8)	0.0 (0.9)
	All populations	3.6 (4.4)	2.0 (0.9)	3.0 (2.9)	2.1 (2.0)	6.2 (3.3)
South Thompson	South Thompson	0.0 (0.0)	0.0 (0.0)	0.0 (0.4)	1.6 (1.4)	1.0 (1.4)
	Lower Adams	0.0 (0.6)	0.0 (0.0)	1.5 (1.6)	0.0 (0.5)	2.5 (1.7)
	Lower Shuswap	0.0 (0.0)	1.1 (0.9)	2.2 (1.8)	3.3 (1.8)	5.1 (2.5)
	All populations	0.0 (0.8)	1.1 (0.9)	5.9 (2.7)	10.0 (2.2)	16.0 (2.8)

Region	Population	16–31 Jul	1–15 Aug	16–31 Aug	1–30 Sep	1–25 Oct
n		292	302	180	83	61
Birkenhead	Birkenhead	0.0 (0.1)	0.0 (0.0)	0.0 (0.2)	0.0 (1.2)	3.8 (2.7)
Lower Fraser	All populations	1.6 (1.5)	0.4 (1.0)	3.1 (2.3)	44.8 (7.5)	80.7 (6.2)
Mid Fraser	Chilcotin	1.9 (1.4)	0.8 (1.4)	3.6 (2.4)	6.1 (5.1)	2.2 (2.1)
	Stuart–Nechako	10.9 (4.2)	6.8 (3.0)	2.8 (2.7)	1.8 (3.7)	2.5 (3.4)
	Quesnel	5.0 (3.5)	10.8 (3.7)	12.1 (4.4)	3.0 (4.5)	0.0 (0.8)
	Chilko	8.1 (3.0)	5.9 (2.8)	0.2 (1.5)	2.4 (3.1)	2.4 (2.9)
	All populations	31.5 (4.6)	29.2 (4.2)	22.0 (4.2)	23.6 (7.4)	7.1 (4.9)
Upper Fraser	Tete Jaune	3.7 (2.1)	1.9 (1.5)	0.0 (0.0)	0.6 (2.6)	0.0 (0.4)
	McGregor	1.7 (2.0)	0.0 (0.5)	0.0 (0.0)	0.0 (0.3)	0.0 (0.0)
	Salmon	1.6 (1.8)	1.1 (1.2)	0.0 (0.0)	0.0 (0.4)	0.4 (1.4)
	Goat	0.8 (1.1)	0.0 (1.1)	0.1 (0.7)	0.0 (1.3)	0.0 (0.0)
	Holmes	1.1 (2.9)	0.0 (0.9)	0.0 (0.0)	0.0 (2.3)	0.0 (0.4)
	All populations	20.7 (4.6)	7.2 (2.7)	0.8 (1.6)	7.3 (5.1)	0.4 (1.9)
Lower Thompson	Cold–Spius–Nicola	2.5 (1.2)	0.0 (0.4)	0.0 (0.8)	0.0 (0.9)	0.0 (1.3)
	All populations	2.5 (1.5)	0.0 (0.5)	0.0 (1.4)	0.0 (1.8)	0.0 (1.4)
North Thompson	Clearwater	18.5 (3.7)	7.9 (2.9)	14.0 (3.9)	4.9 (3.5)	0.0 (1.6)
	Raft	4.2 (3.4)	7.5 (3.3)	0.0 (1.7)	0.0 (2.5)	3.5 (5.0)
	All populations	26.2 (4.6)	18.7 (3.4)	16.3 (4.3)	4.9 (4.2)	5.8 (5.7)
South Thompson	South Thompson	6.0 (3.4)	24.7 (5.9)	24.6 (6.4)	14.7 (7.1)	2.2 (1.8)
	Lower Adams	5.7 (2.6)	2.3 (3.5)	10.1 (5.2)	0.0 (3.6)	0.0 (0.0)
	Lower Shuswap	2.6 (1.8)	14.4 (3.9)	7.6 (5.2)	0.0 (2.7)	0.0 (0.0)
	All populations	17.6 (3.7)	44.4 (4.2)	57.7 (4.8)	19.4 (6.3)	2.2 (2.4)

Biology and population dynamics of cowcod (*Sebastes levis*) in the southern California Bight

John L. Butler
National Marine Fisheries Service
Southwest Fisheries Science Center
P. O. Box 271
La Jolla, California 92038
E-mail address: John.Butler@noaa.gov

Larry D. Jacobson
National Marine Fisheries Service
Northeast Fisheries Science Center
166 Water Street
Woods Hole, Massachusetts 02543

J. Thomas Barnes
California Department of Fish and Game
Southwest Fisheries Science Center
P. O. Box 271
La Jolla, California 92038

H. Geoffrey Moser
National Marine Fisheries Service
Southwest Fisheries Science Center
P. O. Box 271
La Jolla, California 92038

Abstract–Cowcod (*Sebastes levis*) is a large (100-cm-FL), long-lived (maximum observed age 55 yr) demersal rockfish taken in multispecies commercial and recreational fisheries off southern and central California. It lives at 20–500 m depth: adults (>44 cm TL) inhabit rocky areas at 90–300 m and juveniles inhabit fine sand and clay at 40–100 m. Both sexes have similar growth and maturity. Both sexes recruit to the fishery before reaching full maturity. Based on age and growth data, the natural mortality rate is about M =0.055/yr, but the estimate is uncertain. Biomass, recruitment, and mortality during 1951–98 were estimated in a delay-difference model with catch data and abundance indices. The same model gave less precise estimates for 1916–50 based on catch data and assumptions about virgin biomass and recruitment such as used in stock reduction analysis. Abundance indices, based on rare event data, included a habitat-area–weighted index of recreational catch per unit of fishing effort (CPUE index values were 0.003–0.07 fish per angler hour), a standardized index of proportion of positive tows in CalCOFI ichthyoplankton survey data (binomial errors, 0–13% positive tows/yr), and proportion of positive tows for juveniles in bottom trawl surveys (binomial errors, 0–30% positive tows/yr). Cowcod are overfished in the southern California Bight; biomass during the 1998 season was about 7% of the virgin level and recent catches have been near 20 metric tons (t)/yr. Projections based on recent recruitment levels indicate that biomass will decline at catch levels > 5 t/yr. Trend data indicate that recruitment will be poor in the near future. Recreational fishing effort in deep water has increased and has become more effective for catching cowcod. Areas with relatively high catch rates for cowcod are fewer and are farther offshore. Cowcod die after capture and cannot be released alive. Two areas recently closed to bottom fishing will

Manuscript accepted 13 September 2002.
Manuscript received 31 December 2002 at NMFS Scientific Publications Office.
Fish. Bull. 101:260–280 (2003).

Cowcod (*Sebastes levis*) are a large (up to 100 cm fork length, FL) laterally compressed rockfish with large head and large jaws that equip it for life as an ambush predator in the deep continental shelf and upper slope waters off the west coast of North America (Miller and Lea, 1972; Eschmeyer et al., 1983). Cowcod are found from central Oregon to central Baja California and Guadalupe Island, Mexico (Eschmeyer et al., 1983). Like many rockfishes (genus *Sebastes*), cowcod have been the object of commercial and recreational fisheries since at least the beginning of the 20th century (Lenarz, 1987).

The southern California Bight (SCB, Fig. 1) is located off southern California between Point Conception in the north and the Mexico-U.S. border in the south. It is the center of the cowcod's geographical distribution and they were "abundant" there during the 1890s (Eigenmann and Beeson, 1894). They are rare off Oregon and northern California and were taken in only 13 of 3245 tows north of Cape Mendocino, California (40°28′N. lat.), during National Marine Fisheries Service (NMFS) triennial bottom trawl surveys on the continental shelf during 1976–98 (Wilkins[1] and see "Discussion" section). The NMFS survey tends to avoid rocky ground, however, where cowcod are most common.

As with other rockfishes, fertilization is internal and female cowcod give birth to first-feeding stage planktonic larvae (Moser, 1967; Boehlert and Yoklavich, 1984). Gonadosomatic indices of females are highest during November–April when embryos are maturing. Peak abundance of cowcod larvae in California Cooperative Oceanic Fisheries Investigation (CalCOFI)

[1] Wilkins, M. 1999. Personal commun. Alaska Fisheries Science Center, National Marine Fisheries Service, 7600 Sand Point Way, BIN C15700, Seattle, WA 98115-0070.

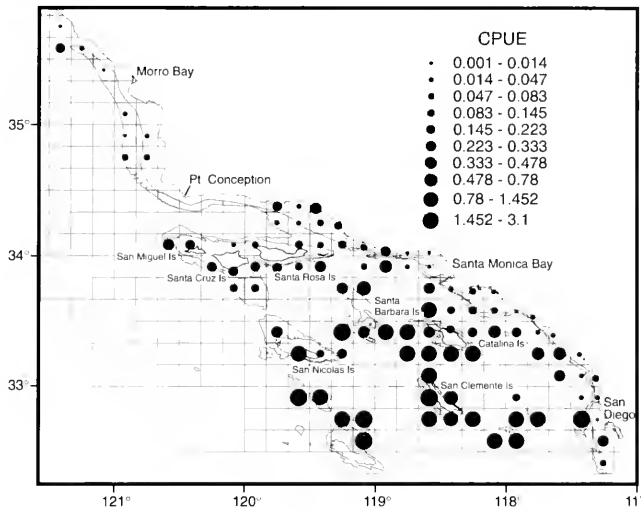

Figure 1

Cowcod habitat in central and southern California. The southern California Bight (SCB) between Pt. Conception and the Mexico–U.S. border is the center of the cowcod population's distribution. Assumed habitat areas for adult cowcod at 100–300 m are shaded light gray. Square outlines identify California Department of Fish and Game fishing blocks (generally 10′×10′) used to analyze commercial passenger fishing vessel (CPFV) logbook data. Dots show CPFV mean catch rates (cowcod per angler day) for each fishing block during the 1964–74 seasons (no dot means zero CPUE).

ichthyoplankton surveys is during January–April, and some larvae are present during November–August (Moser et al., 1994). Cowcod larvae spend about 100 days in the plankton and settle to the bottom as juveniles at about 50–60 mm FL (Johnson, 1997).

Cowcod are found at depths of 20–500 m. Juveniles (50% maturity at about 44 cm FL [Love et al., 1990]) generally inhabit relatively shallow water (<100 m) on relatively sandy bottom and adults generally inhabit deeper water (>100 m) on rocky bottom (Miller and Lea, 1972; Eschmeyer et al., 1983; Butler et al., 1999). Average length of cowcod increases with depth (Love et al. 1990) as is the case with many other species along the west coast of North America (Jacobson et al., 2001). Adult cowcod habitat off Southern California comprises a series of basins and ridges that form islands and offshore banks (Emery, 1960). Juveniles in Monterey Bay recruit to fine sand and clay sediments at depths of 40–100 m during the months of March–September (Johnson, 1997). In submersible surveys at the northern end of the SCB, juvenile cowcod (<40 cm TL) were most common at 90–149 m and adults were most common at depths of 120–209 m (Butler et al., 1999). California commercial bottom trawl fishermen take cowcod at depths of 120–500 m, but mainly at 120–300 m (Fig. 2). We used total bottom area at 100–300 m (measured using a geographic information system and depth data) as a crude estimate of habitat area for cowcod (Fig. 1, see "Discussion" section).

Cowcod are an important part of multispecies commercial and recreational fisheries off central and southern California. Fishermen target cowcod, particularly in the recreational fishery, because of their large body size. Close association with rocky bottom features makes adult cowcod relatively easy to catch with stationary gear (e.g. hook-and-line and set nets) in both the recreational and commercial fisheries. Prior to 1983, the recreational fishery accounted for most of the annual catch, but the commercial fishery was usually dominant during subsequent years.

Commercial fishery

Cowcod have been landed in fifteen different California Department of Fish and Game market categories. Likewise, fourteen species of *Sebastes* have been landed in the cowcod market category. Of these, the bronzespotted rockfish, *S. gilli*, is most common. Exvessel (wholesale) prices (adjusted for inflation to 1998) paid by processors for landings in the cowcod market category rose from $1.02/lb in 1981 to $1.56/lb in 1998 and peaked at $1.85/lb in 1990 (Butler et al.,1999).

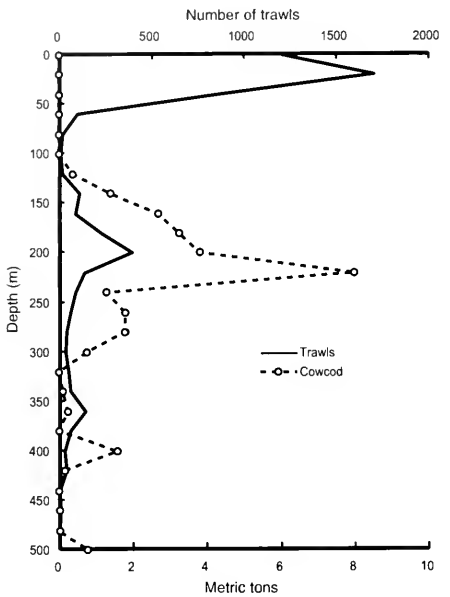

Figure 2

Distribution of cowcod landings by depth from 224 commercial bottom trawl tows during trips off southern California during 1981–97. Also shown is the distribution of total fishing effort (number bottom trawl tows) from all logbook data for trips in the same area and during the same years.

Commercial fishermen use hook-and-line, set nets, and trawl gear to catch cowcod, typically while targeting a group of species. Set nets accounted for 48%, trawls 27%, and hook-and-line 25% of cowcod landings in California during 1980–96 (Butler et al., 1999). Trawling accounted for 80% of landings north of 36°N, whereas hook-and-line and set nets accounted for 92% of landings south of 36°N (Butler et al., 1999). Differences in principal fishing gear north and south of 36°N are due to bottom topography in southern areas that makes bottom trawling impractical.

Recreational fishery

Due to their large size, and despite low catch rates (about 0.1 fish per angler day in recent years), cowcod are a highly prized trophy fish in the recreational fishery. Recreational fishing effort is undertaken from the commercial passenger fishing vessel (CPFV) fleet (Young, 1969; Golden, 1992) and private fishing boats. CPFV vessels include charter boats (contracted by a group of anglers), and party boats (open to the general public without reservations). Anglers take cowcod with hook-and-line gear using multiple baited hooks per rod, or single treble hooks. The official California record for cowcod in the recreational fishery is about 10 kg, but specimens as large as about 15 kg have been confirmed in recent years (Wertz[2]).

CPFV fishing effort targeting multiple rockfish species was probably the most important recreational fishery component for cowcod prior to new restrictions on rockfish during 2000, although anglers on private vessels were also important. Marine Recreational Fisheries Statistical Survey (MRFSS, http://www.psmfc.org/recfin) results in the RecFIN (PSMFC[3]) database indicate that CPFV vessels accounted for approximately 60% of recreational fishing effort in southern California during 1980–89 and 1993–97. Young's (1969) list of preferred species in the southern California CPFV fleet during 1963 did not include rockfish, but they were listed as an important part of the catch. By 1974 attitudes had apparently changed, probably in response to declining catch rates for traditional sportfish, and fishing effort for rockfish increased (MacCall et al.[4]).

Although actively sought by anglers during recent decades, cowcod comprised less than 1% of the CPFV total rockfish catch in number during 1961 (Miller and Gotshall, 1965), 0.4% of the total during the 1970s, (Collins[5]), and 0.3% of the total during 1985–87 (Young, 1969; Golden, 1992). Limited data for 211 cowcod (Fig. 3) sampled during MRFSS creel surveys (PSFMC[3]) indicate that the southern California CPFV fishery takes cowcod that are mostly 30–80 cm FL.

Less is known about cowcod catch taken by private fishing vessels, but MRFSS survey data indicate that trends in catch and effort are similar to those in the CPFV fishery. Cowcod catch rates were low in the private boat fishery during 1975–76 when cowcod accounted for only 179 out of 140,296 fish sampled by the California Department of Fish and Game in a survey of private boats in the southern California sport fishery (Wine and Hoban[6]).

Fishery management

The Pacific Fishery Management Council manages cowcod and other rockfish under its fishery management plan (FMP) for groundfish (PFMC, 1982). The California

[2] Wertz, S. 1999. Personal commun. California Department of Fish and Game, 4665 Lampson Ave., Suite C. Los Alamitos, CA, 90720.

[3] PSMFC (Pacific States Marine Fishery Commission), 45 SE 82 Drive, Suite 100, Gladstone, OR 97027-2522.

[4] MacCall, A. D., G. D. Stauffer, and J-P. Troadec. 1975. Report on CDF&G–NMFS cooperative stock assessment, fishery evaluation, and fishery management of southern California recreational and commercial fisheries. Admin. Rep. LJ-74-24, 144 p. Southwest Fisheries Center, NMFS, La Jolla, CA.

[5] Collins, R. 1999. Personal commun. California Department of Fish and Game, 20 Lower Ragsdale Rd., Suite 100, Monterey, CA 93940.

[6] Wine, V., and T. Hoban. 1976. Southern California independent sportfish sampling survey annual report—July 1, 1975–June 30, 1976. Calif. Dept. Fish and Game, Mar. Res. Div. Admin. Rep. No. 76-14, 299 p. [Available from: California Department of Fish and Game, Marine Region Library, 4665 Lampson Ave., Suite C, Los Alamitos, CA 90720.]

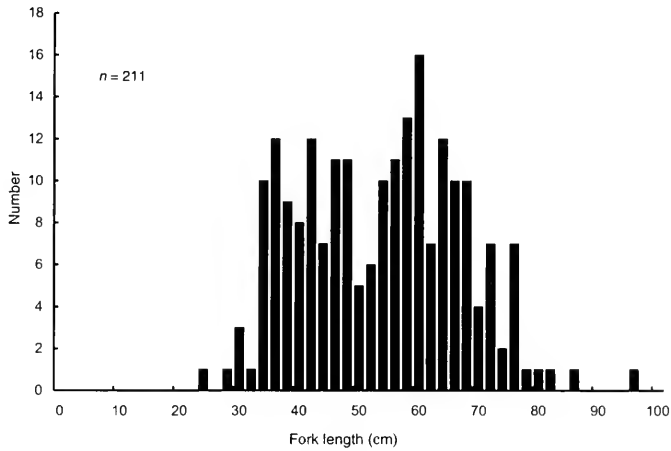

Figure 3

Length composition data for 211 cowcod taken by anglers during commercial passenger fishing vessel (CPFV) trips during 1980–98.

Department of Fish and Game plays a key role because cowcod are caught primarily off southern California. Cowcod received relatively little attention from managers until Butler et al.'s (1999) stock assessment indicated that the SCB stock was "overfished" and that "overfishing" was occurring. The Magnuson-Stevens Fishery Conservation and Management Act and National Standard Guidelines (DOC, 1998) require each FMP to specify a minimum stock size threshold ($B_{Threshold}$), and a maximum fishing mortality rate threshold ($F_{Threshold}$). According to Council guidelines (PFMC, 1999), $B_{Threshold}$ for cowcod is 25% of virgin biomass. $F_{Threshold}$=$F_{40\%}$ (the fishing mortality rate that reduces spawning biomass per recruit to 40% of the unfished level; Clark, 1991) when stock biomass is at or above 40% virgin biomass. $F_{Threshold}$ is reduced at lower biomass levels. According to the National Standard Guidelines, a stock is overfished when stock size falls below $B_{Threshold}$ and overfishing occurs when fishing mortality rates exceed $F_{Threshold}$ for a period of one year or more. The goal for most rebuilding plans is to achieve the target biomass level (usually B_{MSY}, the stock biomass for maximum sustained yield) in ten years or less. However, even with zero fishing mortality, ten years may not be sufficient to rebuild some overfished stocks, and this is the case for cowcod. In such situations, the National Standard Guidelines allow for a rebuilding time no longer than one mean generation time plus the expected time to recovery in the absence of fishing mortality.

In this paper, we summarize existing and new information (Butler et al., 1999) about cowcod; develop an extended time series of catch and abundance index data; estimate biomass, fishing mortality, and recruitment since 1951 (with crude but plausible estimates for 1916–50); describe current status of the stock and effects due to fishing and environmental changes; and discuss problems and opportunities in rebuilding the stock to higher abundance levels. In addition, we show how standardized abundance indices can be derived from rare event and presence-absence data. Finally, we demonstrate techniques for tuning stock assessment models to presence-absence indices with binomial distributions, low expected values, and zero values.

Materials and methods

We estimated annual commercial landings for cowcod during 1951–97 from two different types of information. Commercial landings estimates during 1980–97 were from the PacFIN (PSMFC[3]) database based on exvessel sales receipts (total landings by market category) and port samples (used to estimate proportions of each species by market category). During the period of 1980–97, cowcod comprised 0.5% of total commercial rockfish landings in California. The time series of annual ratios for cowcod and total rockfish landings was variable and showed no clear trend over time.

Direct estimates of cowcod landings were not available for years prior to 1980 because no port sampling was conducted to partition the catch for rockfish market categories into species-specific components. Consequently, we used the ratio estimate (0.00479, CV=26%) to reconstruct historic annual cowcod landings from 1916 to 1981 based on total reported rockfish landings in California in CMASTER records (California Commercial Fisheries Data Base,

Eres[7]). Total landings estimates for 1980–81 from PacFIN were imprecise because of inadequate port sampling, so we used the ratio estimates of cowcod landings for 1980–81 in further analysis.

Recreational landings

We developed a time series of annual recreational cowcod catch from three sources including MRFSS surveys (PSMFC[3]) for 1980–89 and 1993–97, California CPFV logbooks for 1964–98 (Hill and Barnes[8]) and *Los Angeles Times* newspaper reports for 1959–97 (Butler et al., 1999). The *Los Angeles Times* reports daily CPFV catches in California by species (including cowcod since 1959 and rockfish since 1939) and port. Small cowcod (<2 kg) in catches may not be identified to species and were likely counted as "rockfish" in logbooks and *Los Angeles Times* reports.

From 1964 through 1979, we estimated recreational catch of cowcod by expanding annual catch from CPFV logbooks and annual catch in *Los Angeles Times* reports. Expansions used ratio estimators based on MRFSS estimates of total recreational cowcod catch during years (1980–89 and 1993–97) when the MRFSS survey was conducted in California. Expanded estimates based on CPFV logbook and *Los Angeles Times* records were similar. Therefore, expanded CPFV and *Los Angeles Times* estimates were averaged to obtain a single time series of recreational cowcod catch estimates for 1965–97. For 1951–64, recreational cowcod catches were estimated by using the ratio of cowcod and total rockfish catch from CPFV logbooks during 1965–97, and CPFV logbook estimates of total rockfish catch in earlier years.

Age, growth, and reproductive biology

We used otoliths to estimate age and growth for 129 cowcod sampled from the recreational fishery during April 1975–June 1981 and 131 cowcod sampled from the commercial fishery during February 1982–January 1986. Four juveniles sampled from bycatch in the spot prawn pot fishery during 1996 were used as well. Otoliths were sectioned and read independently by three readers (four readers for some specimens). Individual age estimates for each fish were averaged and rounded to the nearest integer to obtain a single age estimate for each specimen. Von Bertalanffy growth curves were fitted to size-at-age data for male and female cowcod. The hypothesis of sexual dimorphism in growth was evaluated with a likelihood ratio test (Kimura, 1980).

Maturity at age was estimated by converting maturity-at-length estimates in Love et al. (1990) to maturity at age based on a von Bertalanffy curve. Body weights (in grams) were calculated from fork lengths by using $W=0.0101\,L^{3.09}$, where L was fork length in cm (Love et al., 1990). The relationship between body size and fecundity for 27 female cowcod (46–80 cm FL) was $E=0.170\,L^{3.15}$, where E was fecundity in millions of eggs (Love et al., 1990).

Natural mortality

Four methods based on age data (i.e. catch curves, Heincke, 1913; Robson and Chapman, 1961; Ricker, 1975; and Hoenig, 1983) were used to estimate average total annual mortality rates (Z) for cowcod during 1975–86. The purpose in estimating Z from age composition data was primarily to find bounds for estimates of the annual natural mortality rate (M) in cowcod. In addition, we used Jensen's (1997) method based on von Bertalanffy growth parameters to estimate M. Age data for cowcod used in our study were for an exploited stock; so total mortality estimates included natural mortality (M) and fishing mortality (F).

Biological reference points

We calculated biological reference points (Thompson and Bell, 1934; Clark, 1991) for cowcod based on yield-per-recruit (F_{MAX} and $F_{0.1}$) and spawning biomass-per-recruit ($F_{40\%}$). Managers use $F_{40\%}$ as a proxy for $F_{Threshold}$ and F_{MSY} (the fishing mortality rate for maximum sustained yield) in managing rockfish (PFMC, 1982). Fishery selectivity assumptions in reference point calculations were based on catch curve results and fishery length composition data (Butler et al., 1999). Female body mass was used to measure reproductive output in reference point calculations.

CalCOFI ichthyoplankton data

We used CalCOFI ichthyoplankton survey data to construct an index of larval presence-absence for cowcod (Mangel and Smith, 1990; Smith, 1990). The CalCOFI index gives the probability of a positive tow (i.e. catching one or more cowcod larvae) under standard conditions. CalCOFI ichthyoplankton data are used routinely to track spawning biomass of pelagic fish (Jacobson et al., 1994; Deriso et al., 1996; Hill et al.[9]) but are seldom used for rockfish because of difficulties in identifying the species of rockfish larvae and lack of overlap between the area surveyed and distribution of many groundfish stocks. However, cowcod are one of several rockfish species readily identifiable as larvae (MacGregor, 1986; Moser, 1996; Jacobson et al.[10]).

[7] Eres, J. 1999. Personal commun. California Department of Fish and Game, 4665 Lampson Ave., Suite C, Los Alamitos, CA 90720.

[8] Hill, K. T., and J. T. Barnes. 1998. Historical catch data from California's commercial passenger fishing vessel fleet: status and comparisons of two sources. Calif. Dept. Fish and Game, Marine Region Tech. Rep. 60, 44 p. [Available from California Department of Fish and Game, Marine Region Library, 4665 Lampson Ave., Suite C, Los Alamitos, CA 90720.]

[9] Hill, K. T., M. Yaremko, and L. D. Jacobson. 1999. Status of the Pacific mackerel resource and fishery in 1998. Calif. Dep. Fish Game, Marine Region Admin. Rep. 99-3, 57 p. [Available from: California Department of Fish and Game, Marine Region Library, 4665 Lampson Ave., Suite C, Los Alamitos, CA 90720.]

[10] Jacobson, L.D., S. Ralston, and A.D. MacCall. 1996. Historical larval abundance indices for bocaccio rockfish (*Sebastes paucispinis*) from CalCOFI data. Southwest Fisheries Science Center, Admin. Report LJ-96-06, 30 p. [Available from: Southwest Fisheries Science Center, P.O. Box 271, La Jolla, CA 92038.]

Moreover, the geographic area of the CalCOFI survey and cowcod stock are both centered in the SCB.

Sampling gear, sampling procedures, and standardization of numbers of larvae caught in CalCOFI tows are described by Moser et al. (1993) and Ohman and Smith (1995). Our analysis used data from all tows within the "current" sampling area in the SCB during calendar years 1951–98 because it was the largest region sampled consistently since 1951 (Hewitt, 1988; Moser et al., 1993; 1994), and because cowcod larvae are most common there (Moser et al., 1994). CalCOFI data from the current sampling pattern included a total of 46 "seasons" used in modeling (e.g. the 1951 season was July 1951–June 1952) and 12,274 bongo or ring net tows of which 120 (0.98%) contained at least one cowcod larva. Almost all positive tows (116 or 97%) were inshore of CalCOFI station 67.5 (Moser et al., 1994). Almost all positive tows (117 or 98%) were made during January–June (Moser et al., 1994). Numbers of positive tows ranged from 5 to 32 per month between January and June and only 1 to 2 per month otherwise. Based on these preliminary results, we used data for all tows (n=5003) collected inshore of CalCOFI station 67.5 during January–June for the remainder of our analysis.

We used a logistic model to derive a standardized index of larval presence for cowcod from CalCOFI data. The logistic model was a generalized linear approach (McCullagh and Nelder, 1989) that accommodates zeroes (tows catching no cowcod larvae). It was fitted to tow-by-tow CalCOFI data by logistic regression (assuming a binomial distribution for statistical errors). The dependent variable was 0 (if no cowcod larvae were observed in a tow) or 1 (if larvae were observed). Independent variables included years, months, and a dummy variable that was 1 if the tow was in the "inshore" area (Butler et al., 1999) and 0 otherwise. The best model for cowcod CalCOFI data was identified by using a step-wise procedure and Mallow's C_p statistic. The index of abundance was the expected probability that a CalCOFI tow is positive for cowcod larvae in each year for an arbitrary reference month and arbitrary reference location.

Trawl surveys

Two sets of trawl survey data were available for cowcod. Trawl survey data collected by the Los Angeles City Sanitation District and Orange County Sanitation District (LAOCSD) off southern California were used as an index of presence for juvenile cowcod. Beginning in 1973, the Los Angeles City Sanitation District sampled twelve stations along four cross-shelf transects and at three depths (23 m, 61 m, and 137 m) twice each year (Stull, 1995; Stull and Tang, 1996). Beginning in November 1970, the Orange County Sanitation District sampled a fixed grid of 8 stations at 20–170 m quarterly (Mearns, 1979). Juvenile cowcod in these trawls ranged from 3 to 38 cm in length. Catch rates were highly variable; therefore we used a simple average of the proportion of positive tows in both surveys as a single index (LAOCSD) of juvenile cowcod presence-absence in the SCB during the 1972–94 seasons (Mangel and Smith, 1990).

CPFV catch per unit of effort (CPUE)

We calculated a habitat-area–weighted (Hilborn and Walters, 1992) average recreational catch per unit of fishing effort (CPUE) index for cowcod from CPFV logbook data for trips in the SCB during 1963–97. As described in the discussion section, the index measured catch rates while accounting for important changes in the spatial distribution of fishing effort over time and spatial differences in abundance trends. Data for trips before 1964 were not available because cowcod catches were combined with rockfish in early years. Each record contained total number of rockfish caught, number of cowcod caught, and total angler hours from logbooks for one month and one "block" (10′×10′ area, Fig. 1).

We assumed total angler hours reported on CPFV logs for sampling blocks with rockfish catches during November–April was a measure of relative fishing effort for cowcod. CPUE was in units of numbers of fish per angler hour (fish/h).

We used CPFV logbook records for November–April to model trends because the CPFV fishery tends to target rockfish during the winter when migratory game fish are seldom caught. Data from blocks in U.S. waters south of Point Conception (blocks 651–897, Butler et al., 1999) were used in the analysis so that CPUE was measured for the entire SCB. Logbooks for 1979 were not summarized by month in logbook records and were therefore excluded. We excluded records for blocks 600, 699, 700, 799, 800, and 899 because these codes are used for data of uncertain origin. We excluded a few records that reported cowcod catches larger than total rockfish catches, and records with high catches from blocks with no cowcod habitat as likely database errors. We also excluded data for the 1979 and 1998 seasons because data for some months were missing and the number of blocks with logbook reports was low (<150).

It was necessary to have at least one logbook record for each spatial stratum during each season, but many blocks had missing data for some seasons. We therefore stratified CPFV logbook data based on "pseudo-blocks." In some cases, pseudo-blocks were the same as fishing blocks. In other cases, pseudo-blocks were composed of many fishing blocks with similar average catch rates.

The first step in stratifying the data was to delete data for blocks with mean CPUE (over the entire time series) that was zero or in the first quartile (<0.05 cowcod per angler day). Blocks with zero CPUE values were from areas where cowcod had never been reported and where there was probably no habitat. Blocks with very low mean CPUE provided little information about trends in cowcod abundance. Of 190 blocks (covering 19,000 nmi^2), there were 102 blocks with mean cowcod CPUE greater than the first quartile.

In the second step, we calculated the number of seasons with rockfish catch and effort data for each block. Twenty-seven blocks had complete time series and were assigned to a pseudo-block that was the same as the original fishing block.

The third step was to assign blocks with incomplete time series to pseudo-blocks based on mean CPUE. Specifically,

blocks with incomplete time series and mean CPUE in the second quartile were assigned to pseudo-block 2. Blocks with mean CPUE in the third quartile were assigned to pseudo-block 3. Blocks with mean CPUE in the fourth quartile were assigned to pseudo-block 4.

We fitted a "Poisson" generalized linear model to CPFV logbook data and used it to compute CPUE indices for cowcod in each pseudo-block and year. The model was fitted by quasilikelihood assuming the Poisson distribution for statistical errors (McCullagh and Nelder, 1989). This approach accommodated zeroes in the data (no cowcod in some blocks during some months) and the generally rare and random nature of cowcod catches. Quasilikelihood estimation (McCullagh and Nelder, 1989) assumes that the variance of CPUE data increases in proportion to the mean (i.e. $\sigma^2=\phi\mu$, ϕ not necessarily equal to one) and is appropriate for CPUE data that typically show this pattern (Hilborn and Walters, 1992). CPUE was the dependent variable. Independent variables were pseudo-blocks, years, and months, and interactions occurred between pseudo-blocks and years. The interaction between psuedo-blocks and years allowed the model to estimate different trends in each psuedo-block. Other interactions were not included because of data and computer limitations. The best Poisson model for cowcod CPUE data was identified by using a step-wise procedure with Mallow's C_p statistic.

The CPUE index for the whole stock in each season was computed as the habitat-area–weighted average of CPUE in each pseudo-block. Variance estimates for the Poisson CPUE index were from standard formulas for weighted means and Poisson model estimates of variances. Variance estimates were biased low because the poststratification scheme (pseudo-blocks) was based on block means.

Population dynamics modeling

The assessment model for cowcod in the SCB (Butler et al., 1999) was a biomass dynamic approach based on Schnute's (1985) delay difference equation implemented in C++ using AD-Model Builder (Otter Software, Ltd.[11]). It estimated "fishable" biomass of cowcod about 40+ cm FL (roughly age 10+), fishing mortality, and recruitment to the fishable biomass. Fishable biomass is less than total biomass because it includes only the portion of the stock available to the fishery. The assumed natural mortality rate M=0.055/yr was the same for all ages and years.

The assessment model for cowcod included "virgin" (prior to any fishing), "historical" (1917–50) and "recent" (1951–98) seasons, as well as deterministic projections for the 1999–2009 seasons (Butler et al., 1999). Virgin and historical periods were linked in the model by stock biomass calculations, an assumed level of constant mean recruitment during the historical period, and an assumed low level of fishing mortality (F=0.001/yr) prior to the 1917 season. The historical and recent periods were linked by stock biomass calculations and assumptions about mean recruitment during the historical period. Similar to stock reduction analysis (Kimura and Tagart, 1982; Kimura et al., 1984; Kimura, 1985), virgin and historical calculations were used to estimate the maximum size of the cowcod stock, and recent data and calculations were used to estimate trends as the cowcod stock was fished down from maximum size. Only catch data were available for the historical period. Both abundance index and catch data were available for the recent period.

Abundance index data for the recent period used to tune the cowcod assessment model included the Poisson CPUE index from CPFV logbooks, the logistic index from CalCOFI survey data, and proportion of positive tows from LAOCSD bottom trawl tows. Probability of a positive tow in CalCOFI and LAOCSD indices is almost proportional to abundance when positive tows are rare (Mangel and Smith, 1990). At higher levels, the probability of a positive tow is a nonlinear function of larval abundance. Goodness of fit for proportions (CalCOFI and LAOCSD data) assumed binomial measurement errors with adjustments for effective sample size (Appendix).

LAOCSD bottom trawl data for cowcod were used to track recruitment because the LAOCSD survey takes cowcod about three years old. In tuning the model, we compared recruitment of three-year-old cowcod in 1980 as measured by LAOCSD data, for example, with model estimates of recruitment at about age 10 during 1987.

In modeling, CalCOFI presence-absence data were used as an index of fishable stock abundance (Appendix). CalCOFI data were not used as an index of recruitment because the link between spawning adults and the presence of larvae is shorter and more direct than the link between presence of larvae and numbers of recruits to the fishable stock at about age 10 yr. The latter would be more variable due to variability in larval, juvenile, and adult survival and growth rates.

CPFV index data were assumed proportional to abundance in the fishable stock and goodness-of-fit was computed by assuming lognormal measurement errors. The original logbook data were assumed to follow a Poisson-like distribution in calculation of the index (see "Material and methods" section). However, the index, like a log normally distributed random variable, had no zero values (Butler et al., 1999).

Yearly catch data were assumed accurate in modeling although cowcod catch data, particularly for early years, were imprecise. Recruitments were assumed to follow a random walk process with relatively small changes from year to year.

Results

Estimated commercial landings (Table 1 and Fig. 4) were less than 20 t/yr during 1916–44, and ranged from 18 to 39 t/yr during 1951–72. Commercial landings increased during the 1970s and early 1980s, peaked during 1984 at about 108 t and then declined rapidly to 8 t in 1991. During 1993–97 commercial landings averaged 20 t/yr. Estimated recreational catch peaked in 1973–74 at about 228 t (Table 1 and Fig. 4) and declined steadily to only 6 t

[11] Otter Research Ltd., Box 2040, Sidney, British Columbia, V8L 3S3, Canada.

Table 1

Catch, fishable biomass, recruitment (in metric tons [t]), and fishing mortality estimates for cowcod during the 1951–97 seasons. Seasons start in July and end in June. The 1951 season, for example, started 1 June 1951.

Season	Recreational landings (t)	Commercial landings (t)	Total landings (t)	Biomass (t)	CV	Recruitment (t)	CV	Fishing mortality (/yr)	CV
1951	7	18	24	3198	0.09	31	0.36	0.008	0.09
1952	9	24	33	3181	0.09	34	0.45	0.011	0.09
1953	10	23	34	3156	0.09	38	0.50	0.011	0.09
1954	24	27	50	3133	0.10	42	0.53	0.017	0.10
1955	42	27	69	3096	0.10	46	0.55	0.023	0.10
1956	49	28	76	3044	0.11	50	0.55	0.026	0.11
1957	37	32	69	2989	0.12	54	0.55	0.024	0.12
1958	33	35	68	2946	0.13	57	0.55	0.024	0.13
1959	22	39	61	2907	0.14	58	0.54	0.022	0.14
1960	36	30	66	2878	0.15	59	0.53	0.024	0.15
1961	33	24	57	2846	0.16	59	0.53	0.021	0.16
1962	35	21	56	2824	0.17	58	0.53	0.021	0.17
1963	51	26	76	2802	0.18	56	0.53	0.021	0.18
1964	70	18	88	2778	0.18	53	0.53	0.019	0.18
1965	95	20	115	2756	0.19	50	0.54	0.024	0.19
1966	218	22	240	2719	0.19	47	0.54	0.041	0.20
1967	199	21	220	2633	0.20	43	0.54	0.052	0.21
1968	190	21	210	2519	0.22	39	0.53	0.041	0.22
1969	130	20	150	2436	0.22	36	0.52	0.031	0.23
1970	190	23	213	2377	0.23	34	0.51	0.045	0.23
1971	143	24	167	2285	0.24	33	0.50	0.039	0.24
1972	221	36	257	2210	0.24	33	0.49	0.060	0.25
1973	228	48	276	2096	0.25	33	0.49	0.074	0.26
1974	228	47	275	1963	0.27	35	0.48	0.097	0.28
1975	206	51	258	1803	0.28	37	0.47	0.096	0.30
1976	223	53	277	1665	0.30	41	0.46	0.127	0.32
1977	172	45	218	1501	0.32	46	0.46	0.104	0.33
1978	136	45	181	1399	0.32	54	0.47	0.090	0.33
1979	193	62	255	1341	0.30	66	0.52	0.120	0.32
1980	133	31	165	1255	0.28	65	0.56	0.092	0.30
1981	135	49	184	1192	0.27	42	0.58	0.107	0.28
1982	143	41	184	1123	0.25	47	0.59	0.108	0.26
1983	64	71	135	1040	0.24	25	0.62	0.104	0.25
1984	65	108	173	963	0.23	20	0.64	0.170	0.25
1985	61	81	142	830	0.24	15	0.66	0.142	0.26
1986	55	100	155	735	0.25	13	0.67	0.181	0.27
1987	47	75	122	626	0.27	12	0.68	0.161	0.29
1988	42	62	104	543	0.29	10	0.69	0.172	0.31
1989	39	22	61	465	0.31	8	0.70	0.087	0.32
1990	27	16	43	433	0.31	8	0.70	0.070	0.32
1991	32	8	40	412	0.30	8	0.70	0.061	0.31
1992	35	35	70	395	0.29	9	0.71	0.144	0.31
1993	24	19	43	350	0.30	9	0.69	0.088	0.32
1994	37	24	61	328	0.30	8	0.69	0.143	0.32
1995	6	27	32	292	0.31	8	0.72	0.114	0.33
1996	23	16	39	268	0.32	8	0.77	0.099	0.34
1997	10	13	23	250	0.33	7	0.80	0.080	0.34

in 1995. During 1993–97 recreational landings averaged 20 t. Total landings were relatively high during 1986–88, peaked at 277 t in 1976, but fell to 23 t in 1997 (Table 1 and Fig. 4).

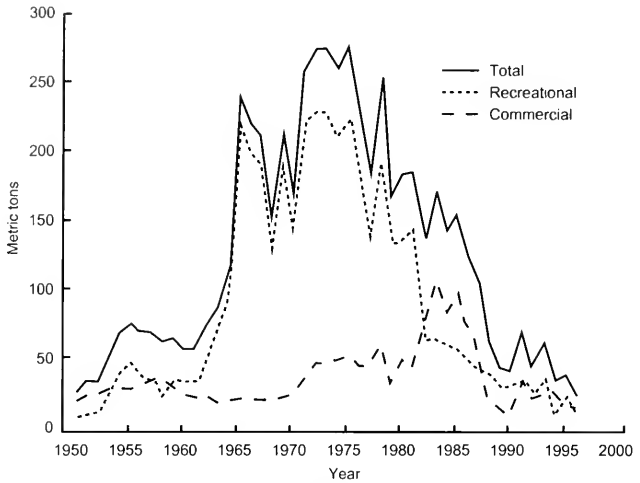

Figure 4
Estimated recreational, commercial, and total cowcod landings during 1951–97.

Age, growth, and maturity

The youngest fish in the 263 cowcod sampled for age determination was age 1, and the oldest was age 55. Average percent error (Beamish and Fournier, 1981) for readings by three (or four) readers was 0.09 and the index of precision (Chang, 1982) was 0.08.

Von Bertalanffy parameter estimates for male and female cowcod size at age were L_∞ = 91.5 and 91.8 cm FL, k = 0.0459 and 0.0447, and t_0 = –2.41 and –1.88/yr. Growth parameters were not significantly different; therefore we combined data from both sexes and included specimens for which sex was not determined. Von Bertalanffy parameter estimates for growth in length with sexes combined were L_∞ = 86.9 cm FL, k = 0.0524, and t_0 = –1.94/yr (Fig. 5). The corresponding von Bertalanffy parameter estimates for growth in weight were W_∞ = 35.1 kg, K = 0.00605, t_0 = 4.78 (Fig. 6). The estimate W_∞ = 35.1 kg appears to be an imprecise estimate of maximum body mass because the largest cowcod reported in the recreational fishery are about 10–15 kg (Wertz[2]). Male and female cowcod appear to reach sexual maturity at about the same ages and lengths (Table 2).

Natural mortality

Slopes of catch curve regressions were similar for male and female cowcod and for samples from the commercial and recreational fisheries (Butler et al., 1999). We therefore combined data for males, females, and unsexed samples to increase sample size and reduce variance. The best choice for age at full recruitment in catch curve analysis was not clear, but the age at full recruitment appeared to fall somewhere between age 10 and age 20. Age 17 was used in the catch curve analysis because it gave the highest coefficient of determination (r^2) in catch curve regressions. The mean of four estimates of mortality based on age data (Table 3) was Z=0.071/yr.

The natural mortality rate (M) for cowcod by Jensen's (1997) method was 0.069/yr. In modeling and reference point calculations for cowcod, we used the lowest estimate (Z=0.055/y) to approximate M. This estimate is crude, imprecise, and may be biased high because total mortality Z includes both natural mortality (M) and fishing mortality (F).

Yield per recuit and spawning biomass per recruit

Biological reference points for cowcod rockfish from yield-per-recruit and spawning-biomass-per-recruit calculations were relatively low because of low natural mortality, prolonged growth, and recruitment to the fishery prior to full maturity. In particular, with M=0.055/yr, F_{MAX}=0.11, $F_{0.1}$=0.048, and $F_{40\%}$=0.039/yr.

Abundance index data

The best logistic model for CalCOFI data included terms for season, month, line, and station effects and all 2- and 3-way interactions. Residual plots showed no evidence of lack of fit. Larval presence for cowcod in the SCB (Table 4 and Fig. 7) varied without trend during 1950–67, was elevated during 1968–74, and was then low beginning in

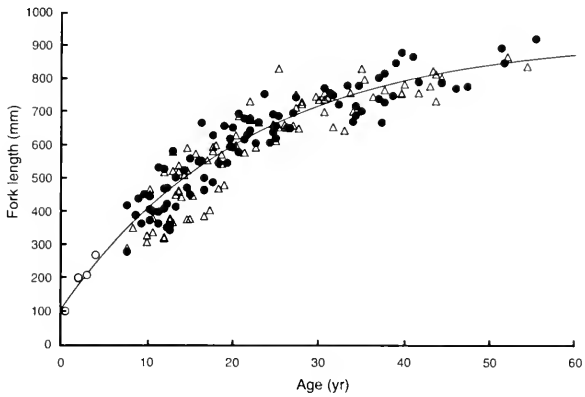

Figure 5

Length-at-age data for cowcod (n=264) with a von Bertalanffy curve for males and females combined (open circles for unknown sex, open triangles for females, solid circles for males).

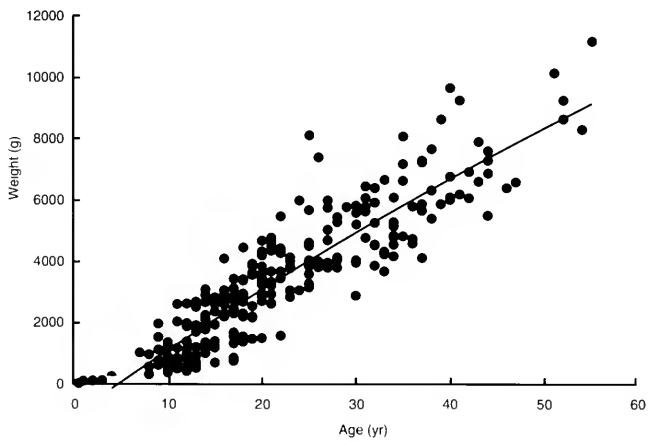

Figure 6

Weight-at-age data for cowcod (n=264) with a von Bertalanffy curve for males and females combined.

1977, with the exception of the period 1989–91. The proportion of LAOCSD survey bottom trawls with juvenile cowcod declined from about 30% in 1974 to near zero levels in the late 1990s (Table 4 and Fig. 8).

The "best" Poisson model for CPFV logbook data included pseudo-block, year, and months as main effects and interactions between pseudo-blocks and years. CPFV results suggest declining trends in catch rates in most pseudo-blocks (Fig. 9) and for the SCB as a whole (Table 4 and Fig. 10). Love et al. (1998) found similar trends in CPUE for cowcod and five other species of rockfish during 1980–96 based on MRFSS data.

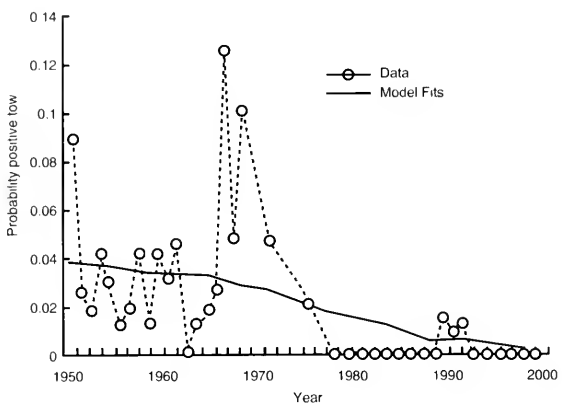

Figure 7

Probability of positive tows (at least one cowcod larvae, an index of larval presence used to track spawning biomass) in California Cooperative Oceanic Fishery Investigation (CalCOFI) ichthyoplankton surveys. "Data" are from the logistic model for larval presence. "Model fits" are predicted values from the stock assessment model fitted to the data.

Table 2

Length and age at first, 50%, and 100% sexual maturity for cowcod (first and 100% maturity as defined by Love et al., 1990).

	Males		Females	
Maturity	Fork length (cm)	Age (yr)	Fork length (cm)	Age (yr)
First	34	8	42	11
50%	44	12	43	11
100%	48	14	52	16

Table 3

Estimates of total mortality (Z) using age composition data for cowcod sampled in commercial and recreational fisheries during 1975–86.

Method	Z (/yr)	Method	Z (/yr)
Catch curve (Ricker, 1975)	0.055	Heincke (1913)	0.065
Robson-Chapman (1961)	0.087	Hoenig (1983)	0.075

Effective sample sizes (Appendix) based on goodness of fit in preliminary assessment model runs were less than actual sample sizes. This discrepancy often occurs when binomial or multinomial proportions are used to track biological characteristics of fish stocks (e.g. age composition of catches) and sample size is large (Fournier and Archibald, 1982). Geometric mean effective sample sizes for cowcod were about 75 bongo net tows per year for CalCOFI index data and about 50 bottom trawl tows per year for LAOCSD index data. The number of actual CalCOFI tows during 1987–98 was about one-third of the number during 1951–86 because sampling intensity was reduced beginning in 1987 (Hewitt, 1988). For simplicity and to avoid placing too much emphasis in fitting our assessment model to LAOCSD and noisy CalCOFI indices, goodness-of-fit calculations in subsequent assessment model runs assumed sample sizes of 75 tows per year for CalCOFI data during 1951–86, 25 tows per year for CalCOFI data during the 1987–98 seasons, and 50 tows per year for LAOCSD index data. Use of smaller effective sample size values in model calculations helped us avoid placing too much weight on the noisy CalCOFI data when fitting our model.

Population dynamics modeling

Like the abundance data, preliminary model runs indicated that cowcod biomass declined during the 1951–98 seasons and that recruitment declined after the 1980 season. Catches were relatively low during the historical period prior to 1951, particularly during earlier years. Therefore, biomass was likely high prior to the 1951 season due to good recruitment and low catches. Based on these consid-

Table 4

Abundance data for cowcod in the southern California Bight including catch per unit of effort for anglers on commercial passenger fishing vessels (CPFV), probability of a positive tow for cowcod larvae in CalCOFI ichthyoplankton survey tows, and probability of a positive tow for juvenile cowcod in Los Angeles and Orange County Sanitation District (LAOCSD) bottom trawl survey tows. Seasons start in July and end in June. The 1951 season, for example, started 1 June 1951.

Season	CalCOFI (probability of positive tow)	CV (%)	LAOCSD (probability of positive tow)	CV (%)	CPFV (fish/h)	CV (%)
1951	0.0238	0.58				
1952	0.0165	0.53				
1953	0.0403	0.47				
1954	0.0271	0.55				
1955	0.0121	0.65				
1956	0.0184	0.59				
1957	0.0425	0.49				
1958	0.0143	0.59				
1959	0.0403	0.48				
1960	0.0309	0.60				
1961	0.0441	0.56				
1962	0.0000	7.02				
1963	0.0122	0.60			0.051	0.18
1964	0.0152	0.67			0.056	0.15
1965	0.0247	0.53			0.046	0.15
1966	0.1255	0.83			0.066	0.11
1967	0.0474	0.60			0.055	0.11
1968	0.1014	0.42			0.036	0.14
1969					0.057	0.12
1970					0.042	0.16
1971	0.0466	0.50			0.041	0.12
1972			0.281	0.28	0.023	0.14
1973			0.300	0.20	0.035	0.11
1974	0.0266	0.48	0.088	0.43	0.034	0.14
1975			0.271	0.21	0.052	0.09
1976			0.036	0.69	0.025	0.13
1977	0.0000	4.37	0.091	0.39	0.026	0.12
1978	0.0000	5.19	0.018	0.99	0.027	0.21
1979	0.0000	6.67	0.051	0.49	0.018	0.15
1980	0.0000	5.73	0.049	0.49	0.014	0.15
1981	0.0000	9.01	0.025	0.70	0.028	0.11
1982	0.0000	8.98	0.012	0.99	0.009	0.2
1983	0.0000	6.10	0.013	0.99	0.015	0.15
1984	0.0000	6.03	0.024	0.70	0.012	0.16
1985	<0.0001	4.99	0.000		0.006	0.27
1986	<0.0001	8.15	0.061	0.43	0.010	0.22
1987	<0.0001	7.71	0.013	0.99	0 006	0.31
1988	<0.0001	8.65	0.038	0.57	0.010	0.18
1989	0.0149	0.83	0.000		0.011	0.19
1990	0.0095	0.83	0.013	0.99	0.011	0.19
1991	0.0124	0.83	0.000		0.008	0.2
1992	<0.0001	8.73	0.000		0.008	0.25
1993	<0.0001	7.23	0.009	1.00	0.008	0.23
1994	<0.0001	9.01	0.020	0.70	0.005	0.3
1995	<0.0001	9.13			0.003	0.38
1996	<0.0001	9.04			0.003	0.33
1997	<0.0001	8.85			0.012	0.43

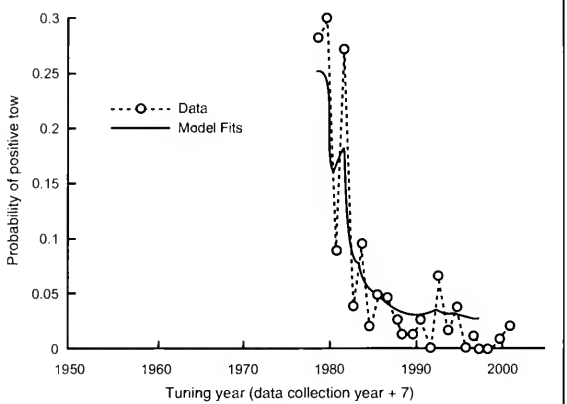

Figure 8

Observed and predicted probability of positive tows (at least one juvenile cowcod, an index of juvenile presence used to track recruitment) for Los Angeles City and Orange County Sanitation Districts (LAOCSD) bottom trawl surveys. "Data" are trawl survey data. "Model fits" are predicted values from the stock assessment model fitted to the data.

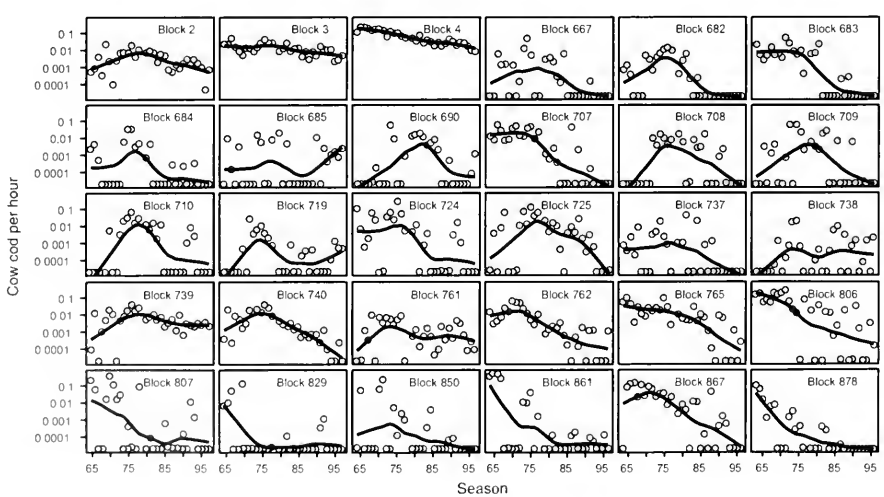

Figure 9

Log scale mean catch per unit of effort (CPUE) for cowcod from the Poisson model for commercial passenger fishing vessel logbook data. Smooth lines were fitted by LOESS (locally weighted regression smoothing) (Cleveland et al., 1988) to show trends.

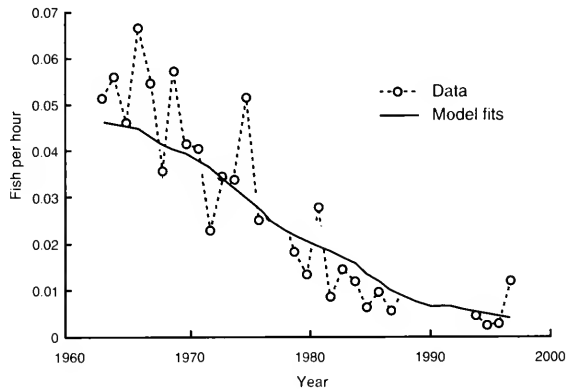

Figure 10

Area-weighted catch per unit of effort (CPUE) for cowcod in the commercial passenger fishing vessel fleet during 1964–96. "Observed" values are habitat-area-weighted means. "Model fits" are predicted values from the stock assessment model fitted to the data.

erations, we used average estimated recruitment during the 1951–80 seasons as the assumed level of constant recruitment during the virgin and historical periods in the final model run used to estimate biomass, recruitment, and fishing mortality for management purposes.

Trends in historical estimates indicate that cowcod biomass was near the virgin level in 1916 and remained relatively stable throughout the historical period (prior to 1951), whereas catches were low and recruitment was assumed relatively high (Table 1 and Fig. 11). Biomass began to decline slowly in the 1950s, and the decline accelerated through the 1970s because catch increased while recruitment remained relatively constant. Recruitment, biomass, and catches all declined dramatically after the early 1980s. Reduced catches from the mid-1980s to 1990s were not enough to offset continuous reductions in biomass and recruitment; fishing mortality rates increased and usually exceeded 0.1/yr. SCB cowcod biomass during the 1998 season (about 238 t, CV 33%) was 7.4% (CV 28%) of the level in the 1951 season (3198 t) and 6.5% of the virgin level (3472 t). During the most recent decade (1989–98 seasons), recruitment biomass averaged 8 t/yr and catches averaged 52 t/ yr.

Discussion

We used the best available information to estimate total cowcod catch but the data and our estimates were imprecise. It is possible, for example, that CPFV captains overreport cowcod catches as a means of attracting business, although cowcod are a small part of the catch on most CPFV vessels, but we are not aware of such a practice. Uncertainty about catch affects the magnitude of F and biomass estimates, but had little effect on estimated biomass trends after 1951 or the ratio of current and virgin biomass (Butler et al., 1999).

Our estimates of habitat area for cowcod (Fig. 1) were crude because depth preferences are uncertain and because we were not able to distinguish rocky areas that are preferred by adult cowcod. Fortunately, our analysis of CPUE in the CPFV fishery was robust to errors in estimating total potential habitat because habitat areas were used as relative (rather than absolute) weights in computing average CPUE.

Biomass, recruitment, and fishing mortality estimates from the stock assessment model for cowcod were less precise for seasons prior to 1951 because historical estimates were based on catch data and no abundance data and because they involved assumptions about virgin biomass and an educated guess about average recruitment during 1916–51 (Kimura and Tagart, 1982; Kimura et al., 1984; Kimura, 1985). Despite these caveats, the estimates for seasons prior to 1951 were plausible and based on all available data.

Rare-event data

Our experience with cowcod suggests that rare-event data for fish stock assessment work is an important topic for future research. Rare events may be particularly important in understanding the population dynamics of naturally rare, severely overexploited or difficult to sample organisms, particularly if long-term data from intensive sampling programs are unavailable. The underlying theory is understood (Mangel and Smith, 1990), statistical tools are

available (McCullagh and Nelder, 1989), and applications have been described (e.g. Smith, 1990; Newman, 1997), but more research and experience are required.

Zero observations ("zeroes") can be expected to be common in rare-event data and frequently encountered in fishery survey data for many species (Lo et al., 1992; Syrjala, 2000). They are usually considered a problem in stock assessment work because conventional assessment models assume lognormal measurement errors for abundance indices and the lognormal distribution does not include the possibility of zero values. However, our experience with CalCOFI and LAOCSD data for cowcod demonstrates the tractability of maximum likelihood estimation using the binomial distribution for proportion positive data with zeroes. Effective sample size calculations can be used with binomial data (e.g. for cowcod) in the same way that Fournier and Archibald (1982) and Methot (1990) used effective sample size techniques to gauge the information content of multinomial age- and length-composition data.

CPFV data

CPFV logbook data present a bleak time series for cowcod. Because this series was critical to the analysis, it is important to consider factors other than abundance that may affect CPUE in the CPFV fishery. For example, changes over time in targeting and identification of cowcod in catches would affect reporting and CPUE, but we are not aware of any changes in catch reporting since 1964.

Trends in CPUE tend to be optimistic (biased towards high biomass in recent years) if fishing effort becomes more effective over time. Changes in angler's gear likely had little effect on catch rates for cowcod because gear used on CPFV vessels has changed little since the early 1960s. Ability of the CPFV fleet to identify, locate, and return to fishing grounds with high catch rates have improved over the last three decades as electronics, including depth finders and global positioning systems, became available and were improved. Effort in later years was likely more effective because CPFV operators were better able to locate and return to locations where rockfish and cowcod were abundant.

Logbook data indicate that recreational fishing effort for rockfish moved from inshore areas (where cowcod are less abundant) to offshore areas during the 1960s to 1980s. Thus, the proportion of total angler hours in the CPFV fishery that could potentially catch cowcod in relatively deep water increased over time as the proportion of anglers fishing offshore and in deep water increased.

Robustness of area-weighted CPUE index

The area-weighted CPUE index for cowcod is robust to interannual changes in the spatial distribution of fishing effort among blocks. This is an important point because CPUE computed as the sum of total catch divided by total fishing effort would be biased high, for example, if the amount of relative fishing effort in a stratum with high catch rates increased. Blocks and pseudo-blocks are strata, in statistical terms, that are sampled during each year. Our area-weighted CPUE index for cowcod is a weighted average of mean CPUE in each stratum during one year. The weights used in computing the index are proportional to the amount of potential cowcod habitat in each stratum.

Thus, the contribution of each stratum to the overall index is proportional to the amount of cowcod habitat in each stratum, not the amount of fishing effort. Increases or decreases in the amount of fishing effort in a stratum with high catch rates will change the precision of the stratum mean and the precision of the index as a whole but would not change the expected value of the area weighted index as a whole. In statistical terms, the expected value of the area-weighted CPUE index should be similar to the expected value of mean CPUE computed from anglers distributed randomly across the entire area of potential habitat. Of course, our area-weighted approach does not accommodate interannual changes in the distribution of fishing effort within strata, and movement of fishing effort within strata towards areas of high catch rate would tend to inflate the index as a whole.

CalCOFI presence-absence data

CalCOFI data were not used in the assessment model as a recruitment index (see "Materials and methods" section). However, considering the time lag between cowcod larvae and juveniles at about age 3, the qualitative trend in CalCOFI ichthyoplankton data appears to match the trend in LAOCSD bottom trawl survey data. In particular, CalCOFI and LAOCSD data both suggest that cowcod recruitment is likely to be poor in the coming years.

Climate change

Declines in cowcod abundance over the last several decades may have been due to reductions in spawning biomass from fishing or to the environmental regime shift (Lluch-Belda et al., 1989) in the SCB and California current towards warmer water during the late-1970s (Barnes et al., 1992, Moser et al., 2000), or to both factors (Jacobson and MacCall, 1995). CalCOFI data show that the probability of occurrence for cowcod larvae in CalCOFI tows declined during the mid- to late-1970s (Fig. 7) and that estimated recruitment to the fishable stock, predictably, declined a decade later (Table 1 and Fig. 11). Catches, recruitment, and abundance for other stocks in the California current changed at about the same time (Beamish, 1995).

Environmental effects on recruitment estimates during 1917–50 are a source of uncertainty in calculating virgin biomass. Historical calculations for cowcod assumed recruitment at average levels during 1951–80, which was a relatively cold-water period in the SCB (as measured by sea surface temperatures at Scripps Pier in San Diego, California; Barnes et al., 1992). However, sea surface temperatures in the SCB were moderately warm during 1917–50 (Barnes et al. 1992). If warm sea surface temperatures are correlated with poor cowcod recruitment, then we may have overestimated historical recruitment and virgin biomass, so that the ratio of biomass in 1998 and virgin biomass (6.5%) was underestimated. However, this

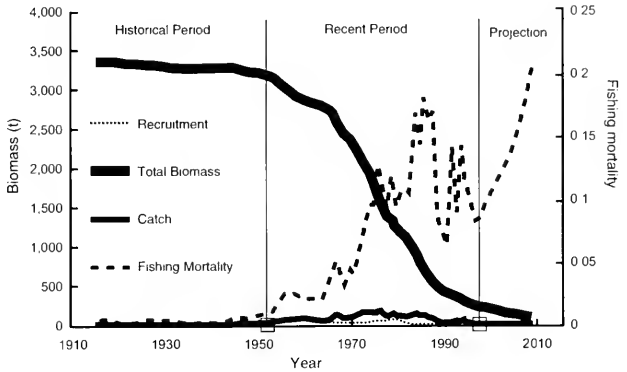

Figure 11

Trends in estimated biomass, recruitment, landings, and fishing mortality during 1916–97 from the stock assessment model for cowcod. Projections starting in 1999 were determined from average catch during 1990–97 (20 t/year) and recruitment equal to the mean (8 t) during the 1990–97 seasons.

uncertainty has little affect on our estimate of the ratio of biomass in 1998 and biomass in 1951 (7.4%) or on the general conclusion that cowcod biomass was low in 1998.

Offshore fishing grounds

Over time, the total number of blocks with rockfish effort in the SCB increased (Fig. 12) as the fishery expanded offshore. Catch rates in blocks nearest to shore have decreased to levels that are low in relation to earlier years (Figs. 1 and 13). Thus fishing grounds in the SCB nearest to shore have been most heavily exploited. Areas of highest cowcod abundance and catch rates are now offshore (Figs. 1 and 13).

Northern areas

Our analysis focused on the SCB where cowcod abundance is highest. However, Butler et al. (1999) examined presence-absence data and CPUE for cowcod in triennial bottom trawl surveys on the continental shelf during 1977–98 (Wilkins[1]). Cowcod were rare in trawl catches north of the SCB and CPUE was generally zero off Oregon and Washington. However, changes in the spatial distribution of positive tows over time indicated that cowcod became more abundant north of the SCB or colonized northern areas after 1986.

Rebuilding

Recent recruitment levels are probably not sufficient to sustain or rebuild the SCB cowcod stock at recent or substantially reduced catches levels. Short-term projections (Fig.11), assuming recruitment at the estimated average for the 1990–98 seasons, indicate that cowcod biomass will continue to decline and that fishing mortality rates will continue to increase over the next ten years at constant catch levels > 5 t/yr (Butler et al., 1999).

Estimates of rebuilding time for cowcod are much longer than the ten-year default time frame used by managers (DOC, 1998). Jacobson and Cadrin (2002) used cowcod as an example in calculating rebuilding times of 30–50 yr for cowcod with F=0, based on a simple logistic surplus production model, but stressed that their "calculations are examples only and not for use by managers." Refined calculations with better models, additional information, and more realistic assumptions about incidental mortality and recruitment (DeVore[12]) give estimated rebuilding times that are generally longer than those of Jacobson and Cadrin (2002). Mean generation time (Restrepo et al., 1998) for cowcod is approximately 37 years. Thus, managers' estimates of the time frame for rebuilding SCB cowcod (one generation time plus expected time to rebuild with F=0) may be greater than 87 yr.

Recreational fishing effort in the SCB directed at rockfish, and likely to encounter cowcod, remains relatively high. Logbook records indicate that CPFV vessels alone generate 400–600 thousand angler hours of rockfish effort each year (Fig. 12). MRFSS data indicate that CPFV vessels constitute about half of the recreational fishing effort during each year off California. Thus, total recreational fishing effort likely to impact cowcod rockfish might be as high as 800–1200 thousand angler hours/yr.

[12] DeVore, J. 2002. Personal commun. Pacific Fishery Management Council, 7700 Northeast Ambassador Place, Suite 200, Portland, OR 97220-1384.

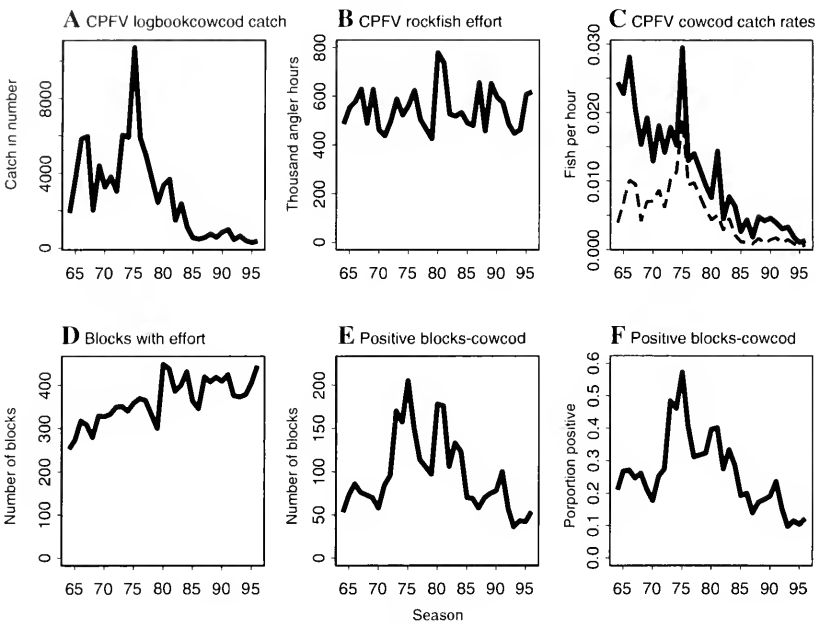

Figure 12

Commercial passenger fishing vessel (CPFV) log book data during the 1964–97 seasons including: CPFV cowcod catch (**A**); fishing effort for rockfish (**B**); catch per unit of effort (CPUE) from cowcod catch and rockfish effort (**C**); number of California Department of Fish and Game (CDFG) fishing blocks with rockfish effort (**D**); number of blocks with cowcod catch > zero (**E**); and proportion of blocks positive (catch > zero) for cowcod (**F**). In Panel C, the solid line shows trends in CPUE computed as the mean of catch divided by effort for each logbook record during each season. The broken line shows trends in CPUE computed as total catch divided by total effort during each season.

Managers may develop harvest limits to discourage targeting and catch of cowcod but effectiveness will likely be undermined by discard mortality. Cowcod are part of a multispecies commercial and recreational fishery and are harvested along with a large number of other species. As shown above, an increasing fraction of recreational fishing effort occurs offshore where cowcod are most common. Adult cowcod are associated with rocky bottom features that attract other species of recreational and commercial fishing interest and are easy to find with modern navigational equipment. Adult cowcod are strictly demersal, are generally found in waters deeper than 90 m, and cannot be released alive because they have swimbladders that rupture when these fish are caught and brought to the surface during commercial and recreational fishing.

In response to the challenging problems in rebuilding cowcod, the Pacific Fishery Management Council and California Department of Fish and Game established new management measures, effective January 2001. New measures for cowcod include two cowcod conservation areas (CCAs) in the SCB, which encompass about 14,750 km^2 of surface area and include prime offshore cowcod habitat (Fig. 13). Regulations prohibit most bottom-fishing activities in waters deeper than 37 m within the CCAs, no retention of cowcod taken anywhere along the coasts of California, Oregon, and Washington, and reductions in the number of hooks per rod in the California recreational fishery (from five to two per rod). In planning, a 1% harvest rate is used to account for unavoidable mortality due to contact with fishing gear directed at other species.

Cowcod is just one example of a long-lived, relatively sedentary apex predator closely associated with bottom structure that has been exploited by commercial and recreational fisheries. Data for cowcod, including long time series of catch estimates, recreational CPUE, and ichthyoplankton data, are sufficient to describe the stock's decline in the SCB. The cowcod conservation areas were the first large no-take marine protected areas on the West Coast and may be important in rebuilding rockfish populations off southern California. However, managers have

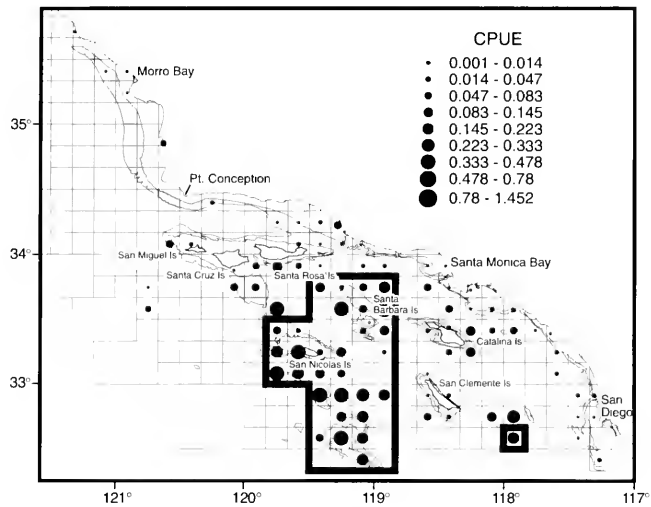

Figure 13

Commercial passenger fishing vessel (CPFV) mean catch rates (cowcod per angler day) for each fishing block during the 1990–98 seasons (no dot means zero CPUE). Heavy black lines surround two cowcod conservation areas.

little experience managing cowcod to increase abundance. Long time series do not exist for many species of groupers and snappers that have similar life histories and similar abundance declines in the Caribbean (Huntsman et al., 1997, Coleman et al., 2000). No-take marine protected areas in the Caribbean Sea have greater numbers and more biomass of large grouper species than adjacent areas where fishing takes place (Chiappone et al., 2000). Thus, comparative studies may be useful in understanding the population dynamics of similar species with little data and in rebuilding species with little management history.

Acknowledgments

We appreciate and acknowledge the work of many people at the National Marine Fisheries Service (NMFS) Southwest Fisheries Science Center (SWFSC), Northwest Fisheries Science Center (NWFSC), Alaska Fisheries Science Center (AFSC), and California Department of Fish and Game (CDFG) who contributed to this project. Elaine Acuna, Dave Ambrose, Sherri Charter, and Bill Watson (SWFSC) carefully checked all identifications of cowcod larvae in the CalCOFI collection. Rich Charter (SWFSC) provided CalCOFI station data. Kevin Hill (CDFG) provided data on cowcod catch rates in the commercial passenger fishing vessel fleet. Jim Allen and Shelly Moore, Southern California Coastal Water Resource Project (SCCWRP), provided data on cowcod juveniles in otter trawl surveys. Rich Cosgrove (SWFSC) analyzed bathymetric data and provided GIS maps. Robson Collins and Bob Lea, (CDFG) provided otoliths. Dan Fuller (SWFSC) prepared and read sections of otoliths. Don Pearson (SWFSC) provided data on commercial catches of cowcod. Mark Wilkins (AFSC) provided data from the triennial survey. J. DeVore (Pacific Fishery Management Council) provided advice and information about current management. Milton Love (University of California, Santa Barbara) provided cowcod data from submersible observations. Henry Orr (SWFSC) prepared illustrations. Sam Herrick (SWFSC) provided economic information about cowcod landings. Richard Methot (NWFSC), Ray Conser (SWFSC), Robert Mohn (Department of Fisheries and Oceans, Canada), Sam Herrick (SWFSC), and Tom Ghio (Moss Landing, CA) carefully reviewed the stock assessment upon which this paper is based. Three anonymous reviewers made suggestions that helped us improve the paper substantially.

Literature cited

Barnes, J. T., L. D. Jacobson, A. D. MacCall, and P. Wolf.
1992. Recent population trends and abundance estimates for the Pacific sardine (*Sardinops sagax*). Calif. Coop. Oceanic Fish. Invest. Rep. 33:60–75.

Beamish, R. J. (ed.).
1995. Climate change and northern fish populations. Can. Spec. Publ. Fish. Aquat. Sci. 121, 739 p.

Beamish, R. J., and D. A. Fournier.
1981. A method for comparing the precision of a set of age determinations. Can. J. Fish. Aquat. Sci. 38:982–983.

Boehlert, G. W., and M. M. Yoklavich.
1984. Reproduction, embryonic energetics, and the maternal-fetal relationship in viviparous genus *Sebastes* (Pisces: Scorpaenidae). Biol. Bull. 167:354–370.

Butler, J. L., L. D. Jacobson, J. T. Barnes, H. G. Moser, and R. Collins.
1999. Stock assessment of cowcod. *In* Pacific Fishery Management Council. Appendix: status of the Pacific coast groundfish fishery through 1998 and recommended biological catches for 1999: stock assessment and fishery evaluation. [Available from Pacific Fishery Management Council, 2130 SW Fifth Avenue, Suite 224, Portland, OR 97220-1384.]

Chang, W. Y. B.
1982. A statistical method of evaluating the reproducibility of age determination. Can. J. Fish. Aquat. Sci. 39: 1208–1210.

Chiappone, M., R. Sluka, and K. M. S. Sealey.
2000. Groupers (Pisces:Serranidae) in fished and protected areas of the Florida Keys, Bahamas and northern Caribbean. Mar. Ecol. Prog. Ser. 198: 261–272.

Clark, W. G.
1991. Groundfish exploitation rates based on life history parameters. Can. J. Fish. Aquat. Sci. 48:734–750.

Cleveland, W. S., S. J. Devlin, and E. Grosse.
1988. Regression by local fitting: methods, properties and computational algorithms. J. Econometrics 37:87–114.

Coleman, F. C., C. C. Koenig, G. R. Huntsman, J. A. Musick, A. M. Eklund, J. C. McGovern, R. W. Chapman, G. R. Sedberry, and C. B. Grimes.
2000. Long-lived reef fishes: the grouper-snapper complex. Fisheries 25:14–21.

DOC (Department of Commerce).
1998. Magnuson Stevens Act Provisions, National Standard Guidelines. Federal Register 63(84): 24212–24237.

Deriso, R. B., J. T. Barnes, L. D. Jacobson and P. J. Arenas.
1996. Catch-at-age analysis for Pacific sardine (*Sardinops sagax*), 1983–1995. Calif. Coop. Oceanic Fish. Invest. Rep. 37:175–187.

Eigenmann, C. H., and C. H. Beeson.
1894. A revision of the fishes of the subfamily *Sebastinae* of the Pacific Coast. Proc. U. S. Nat. Mus. 17: 375–407.

Emery, K. O.
1960. The sea off southern California, 366 p. John Wiley and Sons, New York, NY.

Eschmeyer, W. N., E. S. Herald, and H. Hammann.
1983. A field guide to Pacific Coast fishes of North America: from the Gulf of Alaska to Baja, California. Houghton Mifflin, Boston, MA.

Fournier, D., and C. P. Archibald.
1982. A general theory for analyzing catch at age data. Can. J. Fish. Aquat. Sci. 39 1195–1207.

Golden, M. F.
1992. Marine recreational fisheries. *In* California's living marine resources and their utilization (W. S. Leet, C. M. Dewees, and C. W. Haugen, eds.), p. 204–207. Calif. Sea Grant Ext. Publ. UCSGEP-92-14.

Heincke, F.
1913. Investigations on the plance. General report. I. Plaice fishery and protective regulations. Part I. Rapp. P.-V. Reun. Cons. Perm. Int. Explor. Mer 17A:1–153.

Hewitt, R. P.
1988. Historical review of the oceanographic approach to fishery research. Calif. Coop. Oceanic Fish. Invest. Rep. 22 111–125.

Hilborn, R., and C. Walters.
1992. Quantitative fisheries stock assessment: choice, dynamics and uncertainty, 570 p. Chapman and Hall, New York, NY.

Hoenig, J. M.
1983. Empirical use of longevity data to estimate mortality rates. Fish. Bull. 82:898–903.

Huntsman, G. R., J. Potts, R. W. Mays, and D. Vaughn.
1997. Groupers (Serranidae, Epinephalinae): Endangered apex predators of reef communities. *In* Life in the slow lane: ecology of long-lived marine animals (J. A. Musick, ed.), p. 217–231. Am. Fish. Soc. Symp., vol. 23.

Jacobson, L. D., J. Brodziak, and J. Rogers.
2001. Depth distributions and time-varying bottom trawl selectivities for Dover sole (*Microstomus pacificus*), sablefish (*Anoplopoma fimbia*) and thornyheads (*Sebastolobus alascanus* and *S. oltivelis*) in a commercial fishery. Fish. Bull. 99: 309–327.

Jacobson, L. D., and S. X. Cadrin.
2002. Stock-rebuilding time isopleths and constant-*F* stock-rebuilding plans for overfished stocks. Fish. Bull. 100. 519–536.

Jacobson, L. D., N. C. H. Lo, and J. T. Barnes.
1994. A biomass based assessment model for northern anchovy, *Engraulis mordax*. Fish. Bull. 92:711–724.

Jacobson, L. D., and A. D. MacCall.
1995. Stock-recruitment models for Pacific sardine (*Sardinops sagax*). Can. J. Fish. Aquat. Sci. 52:566–577.

Jensen, A. L.
1997. Origin of the relation between K and L_{inf} and synthesis of relations among life history parameters. Can. J. Fish. Aquat. Sci. 54:987–989.

Johnson, K. A.
1997. Rockfish (*Sebastes* spp.) recruitment to soft bottom habitats in Monterey Bay, CA. M.S. thesis, 70 p. Moss Landing Marine Laboratories, California State University, Stanislaus, CA.

Kimura, D. K.
1980. Likelihood methods for the von Bertalanffy growth curve. Fish. Bull. 77:765–776.
1985. Changes to stock reduction analysis indicated by Schnute's general theory. Can. J. Fish. Aquat. Sci. 42. 2059–2060.

Kimura, D. K., J. W. Balsiger, and D. H. Ito.
1984. Generalized stock reduction analyses. Can. J. Fish. Aquat. Sci. 41:1325–1333.

Kimura, D. K., and J. V. Tagart.
1982. Stock reduction analysis, another solution to the catch equations. Can. J. Fish. Aquat. Sci. 39:1467–1472.

Lenarz, W. H.
1987. A history of California rockfish fisheries. *In* Proceedings of the international rockfish symposium (B. R. Melteff, ed.), p. 35–41. Alaska Sea Grant Rep. 87-2, Univ. Alaska, Fairbanks, AK.

Lluch-Belda, D., R. J. M. Crawford, T. Kawasaki, A. D. MacCall, R. H. Parrish, R. A. Schwartzlose, and P. E. Smith.
1989. World-wide fluctuations of sardine and anchovy stocks: the regime problem. S. Afr. J. Mar. Sci. 8: 195–205.

Lo, N. C. H., L. D. Jacobson, and J. L. Squire.
1992. Indices of relative abundance from fish spotter data based on delta-lognormal models. Can. J. Fish. Aquat. Sci. 49 2515–2526.

Love, M. S., J. E. Caselle, and W. V. Buskirk.
1998. A severe decline in the commercial passenger fishing vessel rockfish (*Sebastes* spp.) catch in the Southern Cali-

fornia Bight, 1980–1996. Calif. Coop. Oceanic Fish. Invest. Rep. 39:180–195.

Love, M. S., P. Morris, M. McCrae, and R. Collins.
1990. Life history aspects of 19 rockfish species (Scorpaenidae: *Sebastes*) from the Southern California Bight. Dep. Commer., NOAA Tech. Rep. NMFS 87, 38 p.

MacGregor, J. S.
1986. Relative abundance of four species of *Sebastes* off California and Baja California. Calif. Coop. Oceanic Fish. Invest. Rep. 27:121–135.

McCullagh, P., and J. A. Nelder.
1989. Generalized linear models (2nd ed.), 335 p. Chapman and Hall, New York, NY.

Mangel, M., and P. E. Smith.
1990. Presence-absence sampling for fisheries management. Can. J. Fish. Aquat. Sci. 47: 1875–1887.

Mearns, A. J.
1979. Abundance, composition and recruitment of nearshore fish assemblages on the Southern California mainland shelf. Calif. Coop. Oceanic Fish. Invest. Rep. 20:111–119.

Methot, R. D.
1990. Synthesis model: an adaptable framework for analysis of diverse stock assessment data. Int. N. Pac. Fish. Comm. Bull. 50:259–277.

Miller, D. J., and D. Gotshall.
1965. Ocean sportfish catch and effort from Oregon to Point Arguello, California. Calif. Dep. Fish Game Fish Bull. 130: 1–135.

Miller, D. J., and R. N. Lea.
1972. Guide to the coastal marine fishes of California. Calif. Dep. Fish Game, Fish Bull. 157:1–235.

Moser, H. G.
1967. Reproduction and development of *Sebastodes paucispinis* and comparison with other rockfishes off Southern California. Copeia 1967:773–797.
1996. Scorpaenidae. *In* The early stages of the fishes of the California Current region (H. G. Moser, ed.), p. 733–796. Calif. Coop. Oceanic Fish. Invest. Atlas 33.

Moser, H. G., R. L. Charter, P. E. Smith, D. A. Ambrose, S. R. Charter, C. A. Meyer, E. M. Sandknop, and W. Watson.
1993. Distributional atlas of fish larvae and eggs in the California Current region: taxa with 1000 or more total larvae, 1951 through 1984. Calif. Coop. Oceanic Fish. Invest. Atlas 31, 233 p.

Moser, H. G., R. L. Charter, P. E. Smith, D. A. Ambrose, S. R. Charter, C. A. Meyer, E. M. Sandknop, and W. Watson.
1994. Distributional atlas of fish larvae and eggs in the California Current region: taxa with less than 1000 total larvae, 1951 through 1984. Calif. Coop. Oceanic Fish. Invest. Atlas 32, 181 p.

Moser, H. G., R. L. Charter, W. Watson, D. A. Ambrose, J. L. Butler, S. R. Charter, and E. M. Sandknop.
2000. Abundance and distribution of rockfish in the Southern California Bight in relation to environmental conditions and fishery exploitation. Calif. Coop. Oceanic Fish. Invest. Rep. 41:132–147.

Newman, K.
1997. Bayesian averaging of generalized linear models for passive integrated transponder tag recoveries from salmonids in the Snake River. N. Am. J. Fish. Manage. 17: 362–377.

Ohman, M. D., and P. E. Smith.
1995. A comparison of zooplankton sampling methods in the CalCOFI time series. Calif. Coop. Oceanic Fish. Invest. Rep. 36:153–158.

PFMC (Pacific Fishery Management Council).
1982. Fishery management plans for the California, Oregon and Washington groundfish fishery. [As amended through 2000, available from Pacific Fishery Management Council, 7700 Northeast Ambassador Place, Suite 200, Portland, Oregon 97220-1384.]
1999. Status of the Pacific Coast groundfish fishery through 1998 and recommended catches for 2000: stock assessment and fishery evaluation. [Available from Pacific Fishery Management Council, 7700 Northeast Ambassador Place, Suite 200, Portland, OR 97220-1384.]

Restrepo, V. R., G. G. Thompson, P. M. Mace, W. L. Gabriel, L. L. Low, A. D. MacCall, R. D. Methot, J. E. Powers, B. L. Taylor, P. R. Wade, and J. F. Witzig.
1998. Technical guidance on the use of precautionary approaches to implementing National Standard 1 of the Magnuson-Stevens Fishery Conservation and Management Act. U.S. Dep. Commer., NOAA Tech. Memo. NMFS-F/SPO-31, 54 p.

Ricker, W. E.
1975. Computation and interpretation of biological statistics of fish populations. Bull. Fish. Res. Board Can. 191, 382 p.

Robson, D. S., and D. G. Chapman.
1961. Catch curves and mortality rates. Trans. Am. Fish. Soc. 90:181–189.

Schnute, J.
1985. A general theory for analysis of catch and effort data. Can. J. Fish. Aquat. Sci. 42:414–429.

Smith, P. E.
1990. Monitoring interannual changes in spawning area of Pacific sardine. Calif. Coop. Oceanic Fish. Invest. Rep. 31: 145–151.

Stull, J. K.
1995. Two decades of marine biological monitoring, Palos Verdes, California, 1972 to 1992. Bull. Southern California Acad. Sci. 94(1):21–45.

Stull, J. K., and C. L. Tang.
1996. Demersal fish trawls off Palos Verdes, Southern California, 1973–1993. Calif. Coop. Oceanic Fish. Invest. Rep. 37:211–240.

Syrjala, S. E.
2000. Critique on the use of the delta distribution for the analysis of trawl survey data. ICES J. Mar. Sci. 57: 831–842.

Thompson, W. F., and F. H. Bell.
1934. Biological statistics of the Pacific halibut fishery. 2. Effect of changes in intensity upon total yield and yield per unit of gear. Rep. Int. Fish (Pacific halibut) Comm. 6, 108 p.

Young, P. H.
1969. The California partyboat fishery 1947–1967. Calif. Dep. Fish Game, Fish Bull. 145, 91 p.

Appendix

Modeling abundance based on presence absence data and effective sample size

The negative log-likelihood used to measure goodness of fit for CalCOFI and LAOCSD data in the cowcod assessment model was

$$L = -\lambda\left\{\sum_{t=1}^{N}\left[I_t \ln(\hat{I}_t) + (1-I_t)\ln(1-\hat{I}_t)\right] - A\right\},$$

where A is a constant;

N = the number of years with data; λ was the effective sample size (tows/yr); and observed I_t and predicted $\hat{I}_t$ index values are proportions.

The constant A has no effect on model estimates but makes the log-likelihood easier to interpret, plot, and understand. Following Methot (1990), it was calculated with the following equation:

$$A = \sum_{t=1}^{N} D_t\left[I_t \ln(I_t) + (1-I_t)\ln(1-I_t)\right],$$

where the dummy variable D_t was one if $0 < I_t < 1$ and zero otherwise.

The constant depends only on the data (not the fit) and is the minimum possible log likelihood (if observed and predicted values match exactly).

Effective sample size calculations were based on the variance of residuals in preliminary model runs (Methot, 1990). This manual "iterative re-weighting" approach was repeated several times until assumed and calculated variances were roughly equal. The expected variance of an index value based on standard formulas for proportions and n tows is

$$Var(\hat{p}) = \frac{\hat{p}(1-\hat{p})}{n},$$

so that

$$\lambda = \frac{\hat{p}(1-\hat{p})}{Var(p)},$$

with λ instead of n for the effective sample size. The variance $Var(p)$ of residuals in one year was calculated by using another standard formula:

$$Var(p) = \frac{\left\{(p-\hat{p})^2 + \left[(1-p)-(1-\hat{p})\right]^2\right\}}{n-1} = 2(p-\hat{p})^2.$$

To estimate an effective sample size for the time series as a whole, we calculated the geometric mean of the effective sample sizes for each year.

Life history and population dynamics of the finetooth shark (*Carcharhinus isodon*) in the northeastern Gulf of Mexico

John K. Carlson
Enric Cortés

Southeast Fisheries Science Center
National Marine Fisheries Service, NOAA
3500 Delwood Beach Road
Panama City, Florida 32408
E-mail address: john.carlson@noaa.gov

Dana M. Bethea

Center for Marine Sciences and Technology
North Carolina State University
Department of Zoology
303 College Circle
Morehead City, NC 28557

Abstract—The life history and population dynamics of the finetooth shark (*Carcharhinus isodon*) in the northeastern Gulf of Mexico were studied by determining age, growth, size-at-maturity, natural mortality, productivity, and elasticity of vital rates of the population. The von Bertalanffy growth model was estimated as L_t=1559 mm TL $(1-e^{-0.24\,(t+2.07)})$ for females and L_t= 1337 mm TL $(1-e^{-0.41\,(t+1.39)})$ for males. For comparison, the Fabens growth equation was also fitted separately to observed size-at-age data, and the fits to the data were found to be similar. The oldest aged specimens were 8.0 and 8.1 yr, and theoretical longevity estimates were 14.4 and 8.5 yr for females and males, respectively. Median length at maturity was 1187 and 1230 mm TL, equivalent to 3.9 and 4.3 yr for males and females, respectively. Two scenarios, based on the results of the two equations used to describe growth, were considered for population modeling and the results were similar. Annual rates of survivorship estimated through five methods ranged from 0.850/yr to 0.607/yr for scenario 1 and from 0.840/yr to 0.590/yr for scenario 2. Productivities were 0.041/yr for scenario 1 and 0.038/yr for scenario 2 when the population level that produces maximum sustainable yield is assumed to occur at an instantaneous total mortality rate (Z) equaling 1.5 M, and were 0.071/yr and 0.067/yr, when Z=2 M for scenario 1 and 2, respectively. Mean generation time was 6.96 yr and 6.34 yr for scenarios 1 and 2, respectively. Elasticities calculated through simulation of Leslie matrices averaged 12.6% (12.1% for scenario 2) for fertility, 47.7% (46.2% for scenario 2) for juvenile survival, and 39.7% (41.6% for scenario 2) for adult survival. In all, the finetooth shark exhibits life-history and population characteristics intermediate to those of sharks in the small coastal complex and those from some large coastal species, such as the blacktip shark (*Carcharhinus limbatus*).

Manuscript accepted 31 May 2002.
Manuscript received 23 January 2003 at NMFS Scientific Publications Office.
Fish. Bull. 101:281–292 (2003).

In 1993, a fishery management plan for sharks (NMFS, 1993) was developed for the management of shark populations in waters of the U.S. Atlantic and Gulf of Mexico. Because species-specific catch and life history information was limited, sharks were grouped and managed under three categories: large coastal, small coastal, and pelagic, based on known life history, habitat, market value, and fishery characteristics (NMFS, 1993). Sharks in the large coastal grouping included relatively large, slow-growing, and long-lived species, whereas the small coastal complex included relatively small, fast-growing, and short-lived species of sharks.

Generally, commercial fishermen target and harvest sharks in the large coastal complex (e.g. blacktip shark (*Carcharhinus limbatus*) and sandbar shark (*Carcharhinus plumbeus*)). Small coastal sharks are usually taken incidentally in numerous commercial fisheries and are commonly discarded or used for bait. More recently, with the reductions in commercial quotas for large coastal species since 1993 (NMFS, 1999), fishermen have been increasingly targeting small coastal sharks. Estimated commercial landings of small coastal sharks increased from 7 metric tons (t) dressed weight in 1994 to 305 t dressed weight in 1999. Estimated recreational catches of small coastal sharks reached a peak of 170,000 animals in 1998 (Cortés[1]). Given the importance of small coastal sharks as bycatch and their increasing value in directed commercial and recreational fisheries, it is important to obtain current and accurate information on their life history. This information can then be used in population models incorporating variation and uncertainty in estimates of life-history traits to predict the productivity of the stocks and ensure that they are harvested at sustainable levels.

The finetooth shark (*Carcharhinus isodon*) is a moderate-size species of the small coastal shark group found in coastal waters of the northwestern Atlantic Ocean from North Carolina to Florida, throughout the Caribbean Sea, and the Gulf of Mexico (Compagno, 1984; Castro, 1993). This species makes up a significant portion of a directed drift gillnet fishery operating off the southeast U.S. coast (Trent et al., 1997;

[1] Cortés, E. 2000. 2000 shark evaluation annual report. Sustainable Fisheries Division contribution no. SFD-00/01-119, 23 p. Southeast Fisheries Center, National Marine Fisheries Service, 3500 Delwood Beach Rd., Panama City, FL 32408.

Carlson[2]), with estimated commercial landings peaking at about 129.4 t dressed weight in 1999 (Cortes, unpubl. data). However, life-history information for this species is mostly restricted to some aspects of its reproduction and general biology (Branstetter, 1981; Castro, 1993). The purpose of the present study is to investigate the life history and population dynamics of the finetooth shark from the northeastern Gulf of Mexico. Specifically, we wish 1) to estimate age, growth, and natural mortality, 2) to determine size-at-maturity, and 3) to assess productivity and identify the vital rates to which population growth rates are most sensitive.

Materials and methods

Collection and laboratory processing

Finetooth sharks were collected from fishery-independent surveys in the northeastern Gulf of Mexico, from St. Andrew Bay to Apalachicola Bay, FL, during April–October from 1995 to 1999 (Carlson and Brusher, 1999). A 186-m long gill net consisting of panels of six different mesh sizes was used for sampling. Stretched mesh sizes ranged from 8.9 cm to 14.0 cm in steps of 1.27 cm, and an additional mesh size of 20.3 cm was used. Panel depths when fishing were 3.1 m. Webbing for all panels, except for that with 20.3-cm mesh size, was clear monofilament, double-knotted and double-selvaged. The 20.3-cm webbing was made of no. 28 multifilament nylon, single-knotted, and double-selvaged. When set, the nets were anchored at both ends. Generally, soak time ranged from 1.0 to 2.0 hours.

Precaudal (PC), fork (FL), total (TL), and stretched total (STL) length (mm), sex, and maturity state were determined for each shark. We developed several morphometric relationships to convert length measurements. Linear regression formulae were determined as FL=1.10(PC)+0.60; TL=1.23(FL)+20.34; and STL=1.10(TL)+11.25. All equations were highly significant (P<0.0001) and had coefficients of determination (r^2) between 0.97 and 0.99. Because most previous studies on small coastal species have summarized information in total length, i.e. the straight line from the tip of the snout to the tip of the tail in a natural position, our results are reported in natural TL to provide a direct comparison.

Maturity was assessed according to the guidelines of Castro (1993). Males were deemed mature if they possessed hardened claspers and the rhipidion opened freely. Females were considered mature if they were gravid, had oocytes larger than 26 mm in diameter, or if nidamental gland width was greater than 20 mm.

Vertebrae for age determination were collected from the column between the origin and termination of the first dorsal fin. Vertebral sections were placed on ice after collection and were frozen upon arrival at the laboratory. Thawed vertebrae were cleaned of excess tissue and soaked in a 5% sodium hypochlorite solution for 5–30 min to remove remaining tissue. After cleaning, the vertebrae were soaked in distilled water for 30 min and stored in 95% isopropanol alcohol. Prior to examination, vertebrae were removed from alcohol, dried, and measured (length and width in mm).

Visual enhancement of growth bands

Various methods were tested to enhance visibility of growth bands. Sagittal sections were cut from the vertebral centrum at different thicknesses and stained with 0.01% crystal violet (Johnson, 1979; Schwartz, 1983), alizarin red (Gruber and Stout, 1983), or left unstained. Each section was mounted on a glass microscope slide with clear resin and examined under a dissecting microscope with transmitted light. Growth bands were found to be most apparent with the crystal violet stain on sagittal sections with a thickness of 0.35 mm (Fig. 1).

The distances from the centrum origin to the distal edge of each growth band and from the centrum origin to the centrum edge were measured by using the Image Tools, version 2 software package (UTHSCSA Image Tool, 1997). Each growth band included a broad light mark representing summer growth and a thin dark mark representing winter growth (Branstetter and Stiles, 1987). All three authors aged each specimen without knowledge of its length or sex. Two sets of independent age readings were made, the second set after consultation among the authors. The index of average percent error (APE; Beamish and Fournier, 1981) and the percentage of disagreements by $\pm i$ rings among authors were computed for the first set of age readings.

Determination of growth curves

Sex-specific relationships between total length (TL) and vertebral radius (VR) were calculated to determine the most appropriate method for back-calculation. Because no difference was found between sexes (ANCOVA: F=0.40, df=1, P≥0.05), they were combined to generate a linear relationship: TL= 153.75(VR) + 305.68 (P<0.0001; r^2=0.90; n=239). Because the intercept of the relationship did not pass through the origin, we applied a method proposed by Campana (1990), which is a modified Fraser-Lee equation that uses a biologically derived intercept:

$$L_a = L_0 + \left((O_a - O_0) \times (L_c - L_0)\right) / (O_c - O_0),$$

where L_a = length at age a;
O_a = otolith distance from focus to annulus a;
O_c = otolith radius at capture;
L_c = length at capture;
L_0 = length at birth; and
O_0 = otolith radius at birth.

The biologically derived intercept corresponds to the size of the otolith (or analogous aging structure, i.e. vertebra)

[2] Carlson, J. K. 2000. Progress report on the directed shark gillnet fishery right whale season, 2000. Sustainable Fisheries Division contribution no. SFD-99/00-90, 12 p. Southeast Fisheries Center, National Marine Fisheries Service, 3500 Delwood Beach Rd., Panama City, FL 32408

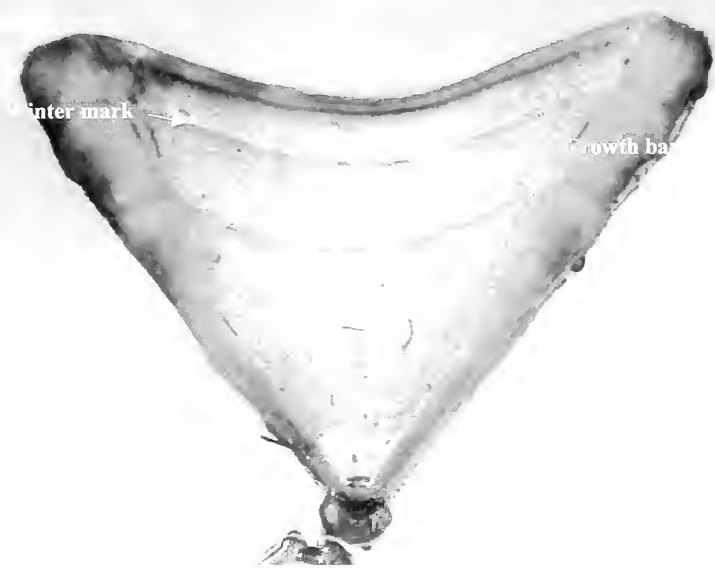

Figure 1

Sagittal section from a finetooth shark (*Carcharhinus isodon*) vertebra used for age determination. Winter marks correspond to thin dark areas under transmitted light, whereas summer marks correspond to wide light zones. Each growth band includes a dark zone and a light zone.

and fish at the time of hatching (Campana, 1990). For the finetooth shark, we used the estimated size at birth in the northeastern Gulf of Mexico (520 mm TL; Carlson, unpubl. data).

In developing theoretical growth models, we assumed that 1) the birth mark is the band associated with a pronounced change in angle in the intermedialia and is formed on an arbitrary birth date of 1 June, 2) growth bands are formed once a year, and 3) the narrow dark marks are deposited in winter on an arbitrary date of 1 January. Ages were calculated by using the algorithm: *age = the birth mark + number of winter marks* −1.5, *+ the proportion of the year from winter mark deposition to the date of capture.* If only the birth mark was present, age was calculated as the time between birth and date of capture.

The von Bertalanffy growth model (Eq. 1; von Bertalanffy, 1938) was fitted separately to observed and back-calculated size-at-age data using the equation

$$L_t = L_\infty(1-e^{-K(t-t_0)}),$$

where L_t = predicted length at time t;
L_∞ = theoretical asymptotic length;
K = growth coefficient; and
t_0 = theoretical age at zero length.

Growth model parameters were estimated by using least-squares nonlinear regression (SAS PROC NLIN; SAS, 1988).

For comparison, an alternate equation of the von Bertalanffy growth model (Eq. 2; Fabens, 1965) was also fitted separately to observed size at age data. This equation is described as

$$L_t = L_\infty(1-be^{-Kt}) = L_\infty-(L_\infty-L_0)e^{-Kt},$$
$$b = (L_\infty-L_0)/L_\infty = e^{Kt_0},$$

where L_t = predicted length at time t;
L_∞ = theoretical asymptotic length;
K = growth coefficient; and
L_0 = the length at birth.

Verification of the annual period of band formation was attempted by using the relative marginal increment analysis (Natanson et al., 1995):

$$MIR = (VR-R_n)/(R_n-R_{n-1}),$$

where MIR = the marginal increment ratio;
VR = the vertebral radius;

R_n = the last complete band; and
R_{n-1} = the next-to-last complete band.

Mean MIR was plotted against month to determine trends in band formation. A single factor analysis of variance was used to test for differences in MIR among months.

Chi-square tests of likelihood ratios (Kimura, 1980; Cerrato, 1990) implemented by using SAS code were used to determine whether there were differences between sexes. Theoretical longevity was estimated as the age at which 95% of L_∞ is reached ($5(\ln 2)/K$; Fabens, 1965; Cailliet et al., 1992).

Estimation of size at maturity

Median total length at maturity for male and female sharks was determined by fitting a logistic model, $Y=1/(1+e^{-(a+bX)})$, where Y=the binomial maturity data (immature=0, mature=1; Mollet et al., 2000) and X=total length (mm). Median total length at maturity was expressed as $MTL=-a/b$. The model was fitted using least squares nonlinear regression (S-Plus 2000, 2000).

Estimation of natural mortality, productivity, and elasticity

The instantaneous rate of natural mortality (M) was estimated by five indirect life-history methods described extensively elsewhere (see Cortés, 2002, and references therein). Four of the five methods (Pauly, 1980; Chen and Watanabe, 1989; and two methods by Jensen, 1996) use parameters estimated through the von Bertalanffy growth model. The fifth method (Peterson and Wroblewski, 1984) estimates M based on body mass. All required parameter estimates (age at maturity, maximum age, L_∞, K, t_0) were taken from the aging section of the present study. Mean annual water temperature (21.8°C), which is needed in the Pauly method, was taken from Brusher and Ogren (1976). Body mass of finetooth sharks at age was estimated by converting age into length through the growth model derived in the present study, and length into weight through the power relationship given in Castro (1993).

Population growth rates and productivity were estimated by two methods that complement each other. Productivity (i.e. rebound potential as defined in Smith et al., 1998) was calculated by a modified demographic technique that incorporates concepts of density dependence (Smith et al., 1998). In this method, rebound potentials or productivities (r_Z) are calculated at the population level producing maximum sustainable yield (MSY), which is assumed to occur at $Z = 1.5\,M$ or, alternatively, at $Z = 2\,M$ (Z=total instantaneous mortality rate).

Two methods that assume density independence also were used. Life tables allowed calculation of mean generation times (A), and Leslie matrix population models were used to estimate population growth rates ($\lambda=e^r$) and to calculate elasticities (proportional sensitivities; Caswell, 2001). Elasticities for fertility, juvenile survival, and adult survival were obtained by summation of matrix element elasticities across relevant age classes (e.g. fertility elasticity is the sum of all first-row elasticities) and sum to 1. The fertility term in matrix methodology includes survival to age-1 (see Cortés, 2002, for details).

Probability density functions (pdfs) were developed to describe age at maturity, maximum age, M, survivorship at age ($S_x=e^{-M}$), and fecundity at age (m_x) for females, following in part the method and rationale in Cortés (2002). Two scenarios, based on the results of the two equations used to describe growth, were considered.

Scenario 1 Age at maturity was represented by a triangular distribution with 4.3 yr as the likeliest value and ±1 yr (3.3, 5.3 yr) as lower and upper bounds. Maximum age was represented by a linearly decreasing distribution scaled to a total relative probability of 1. The likeliest value corresponded to the age of the oldest animal aged in the age and growth study (8 yr) and the lower bound was the theoretical estimate of longevity (14.4 yr).

Natural mortality (M) for adults for the Smith et al. (1998) method was represented by a uniform distribution ranging from 0.162 (minimum) to 0.499 (maximum). Conversely, annual survivorship at age in the density-independent model was represented by a uniform distribution that ranged from the minimum estimate ($0.607=e^{-0.499}$) to a maximum, generally corresponding to the estimate derived through the weight-based method (which ranged from 0.722/yr at age 0 to 0.850/yr at age 15). Fecundity at age was assumed to follow a normal distribution with a mean of 4.036 and SD=0.793, with the lower and upper bounds of 2 and 6 reflecting the range of litter sizes reported for this species (Castro, 1993). We assumed a 1:1 male-to-female ratio, that 100% of females were reproductively active after reaching maturity, and a reproductive cycle of 2 yr. The percentage of mature females at age was estimated from the logistic model.

Scenario 2 The age-at-maturity and fecundity-at-age distributions were identical to those in scenario 1. The only difference in the pdf describing maximum age in this scenario compared to that used in scenario 1 was that the theoretical estimate of longevity (9.9 yr) was lower. Natural mortality for adults for the Smith et al. (1998) method was also represented by a uniform distribution ranging from a minimum of 0.174 to a maximum of 0.528. Survivorship at age in the density-independent model was represented by a uniform distribution that ranged from the minimum estimate ($0.590=e^{-0.528}$) to a maximum, generally corresponding to the estimate derived through the weight-based method (which ranged from 0.689/yr at age 0 to 0.840/yr at age 10).

The simulation and projection process involved randomly selecting a set of life-history traits from the pdfs describing each individual trait and calculating productivity (r_Z) in the modified demographic technique and population growth rates (λ), generation times (A), and fertility, juvenile survival, and adult survival elasticities in the life table and matrix population model approach. This process was repeated 10,000 times, yielding frequency distributions, means, medians, and confidence intervals (calculated as the 2.5th and 97.5th percentiles) for parameter estimates. All

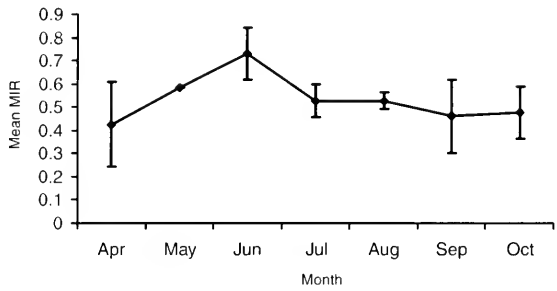

Figure 2

Mean marginal increment analysis (MIR) by month for combined sexes of finetooth sharks. Vertical bars are ±1 standard deviation.

simulations were run with Microsoft Excel spreadsheet software (Math Tools, Ltd., 1999) equipped with risk analysis and matrix algebra software and Microsoft Visual Basic for Applications (Crystal Ball, 2000).

Results

Age, growth, and maturity

The precision of band counts was high among the readers (authors). The first set of readings resulted in two or three out of three band count estimates agreeing in 97.7% of the cases, and an APE of 6.8%. Percent disagreement in band counts among the three readers was 42.9% within ±1 band, 5.6% within ±2 bands, and 0.4% within ±3 bands. After consultation, we reached agreement in 239 out of 247 (97%) vertebrae. Samples where counts had differed among the readers were discarded.

Although monthly changes in marginal increment analysis were found, peaks were not statistically different (single factor ANOVA; df=6, P=0.371). An increase in increment growth occurred from April until June, followed by a slow decrease and leveling until October (Fig. 2). The decrease in incremental growth from June through October was not large enough to indicate a double band formation (Natanson et al., 1995); thus bands were assumed to form once a year. A similar trend of increment growth was also reported for the blacknose shark (*Carcharhinus acronotus*) by Carlson et al. (1999).

The values of K (0.24/yr versus 0.35/yr for females, and 0.41/yr versus 0.49/yr for males) and L_∞ (1560 mm versus 1442/mm for females, and 1338/mm versus 1309/mm for males) obtained with the original von Bertalanffy (1938) growth equation (Eq. 1) and the modified equation of Fabens (1965) (Eq. 2) were somewhat different, but the fits to the observed data were similar (Table 1; Fig. 3). Because of the similarity between the models and the general and ubiquitous use of equation 1 (von Bertalanffy, 1938), we present and compare further age and growth results using only the von Bertalanffy (1938) model.

Observed and back-calculated von Bertalanffy parameters and growth rates differed between males and females (Table 1 and Table 2). For both sexes, growth was rapid until age 4–5, slowing down for males thereafter, whereas the reduction in growth rate for females was not so accentuated (Fig. 3). Females had a lower growth coefficient (K=0.24/yr) than males (K=0.41/yr), and a higher theoretical maximum size (L_∞=1560 mm for females versus 1338 mm for males). Significant differences (log-likelihood ratio=14.46; P<0.001) between von Bertalanffy growth curves of males and females were found. Theoretical longevity estimates were 14.4 and 8.5 yr for scenario 1, and 9.9 and 7.2 yr for scenario 2, and the oldest aged sharks were 8.0 and 8.1 yr for females and males, respectively.

We found no significant differences (Kruskal-Wallis χ^2=0.101, P=0.751) in age distribution between sexes (Fig. 4). The most frequently occurring age classes were ages 4+, 3+, and 2+ for males, and ages 2+ and 3+ for females, each comprising between 19–22% and 18–24% of the samples for each sex, respectively. Young-of-the-year sharks (age 0+) made up 7.3% of all males and 11.1% of all females, whereas adults (ages 5–8) constituted 17.1% and 22.2%, respectively.

Back-calculated size at birth was estimated at 538 mm TL for both male and female sharks and matched well the known size at birth in the northeastern Gulf of Mexico (480–530 mm TL; Carlson, unpubl. data) (Table 2). Back-calculated mean lengths were smaller than observed lengths and when these were compared among older-aged sharks, Lee's phenomenon (Ricker, 1992) was apparent.

Median total length at maturity differed between males and females (Fig. 5). For males, the size at which 50% of the population reached maturity was 1187 mm TL, which corresponds to an age at maturity of ~3.9 yr. The smallest mature male found was 1000 mm TL and the largest

Table 1

Parameters of the von Bertalanffy growth models for male and female finetooth sharks. Estimates are provided for models developed with observed and back-calculated size at age. Equation 1 is the original von Bertalanffy growth model (von Bertalanffy, 1938) and Equation 2 is the modified von Bertalanffy growth model (Fabens, 1965). n = number of sharks in sample.

	Male	Asymptotic standard error	Lower 95% confidence limit	Upper 95% confidence limit	Female	Asymptotic standard error	Lower 95% confidence limit	Upper 95% confidence limit
Observed (Eq. 1)								
L_∞ (mm)	1337.8	27.9	1282.5	1393.2	1559.6	69.7	1421.6	1697.6
K (/yr)	0.412	0.043	0.327	0.496	0.244	0.036	0.173	0.315
t_0 (yr)	−1.390	0.178	−1.744	−1.037	−2.067	0.274	−2.610	−1.524
n	123				117			
Observed (Eq. 2)								
L_∞ (mm)	1309.3	20.657	1268.4	1350.2	1441.6	36.4	1369.5	1513.7
K (/yr)	0.487	0.033	0.422	0.551	0.352	0.029	0.295	0.409
n	123				117			
Back-calculated								
L_∞ (mm)	1347.1	19.3	1309.2	1385.0	1519.1	35.0	1450.3	1588.0
K (/yr)	0.383	0.019	0.347	0.419	0.282	0.018	0.247	0.318
t_0 (yr)	−1.135	0.054	−1.243	−1.209	−1.348	0.081	−1.490	−1.205
n	493				457			

Table 2

Back-calculated mean total length (mm) and observed mean total length (mm) at band formation for male (n=123) and female (n=117) finetooth sharks.

Band number	Birth	1	2	3	4	5	6	7	8
Male									
Back-calculated	538	758	963	1090	1173	1229	1252	1256	1220
SD	54.6	54.3	70.2	81.8	78.6	81.4	78.6	97.6	183.7
n	122	113	94	71	48	21	15	7	2
Observed	629	872	1006	1115	1201	1273	1307	1287	1230
SD	84.8	56.7	67.3	72.2	74.4	97.7	40.3	59.6	183.8
n	9	19	23	24	27	6	8	5	2
Female									
Back-calculated	538	751	950	1097	1199	1258	1317	1401	1445
SD	60.0	71.4	88.1	80.1	78.0	82.0	80.4	55.0	0.1
n	117	104	89	61	40	26	13	5	2
Observed	651	852	994	1109	1223	1287	1322	1434	1461
SD	53.9	79.3	96.7	62.7	63.1	82.6	85.8	30.4	21.3
n	13	15	28	21	14	13	8	3	2

immature male was 1298 mm TL. For females, the size at which 50% of the population was mature was 1230 mm TL, which is about 4.3 yr of age. The smallest mature female was 1187 mm TL and the largest immature female was 1240 mm TL.

Natural mortality, productivity, and elasticity

Scenario 1 Estimates of instantaneous rates of natural mortality for adults ranged from a minimum of 0.162 obtained through the Peterson and Wroblewski (1984) method to a maximum of 0.499 obtained through the Jensen (1996) method for an age at maturity of 3.3 yr or, when expressed as survivorship, from 0.850/yr to 0.607/yr. All other annual survivorship estimates for adults fell within that range: 0.671/yr for the Pauly (1980) method, 0.732/yr for the Jensen (1996) method based on an age at maturity of 5.3 yr, 0.694/yr for the Jensen (1996) method based on K, and 0.745–0.762/yr for the Chen and Watanabe (1989) method. Estimates of survivorship at age from the

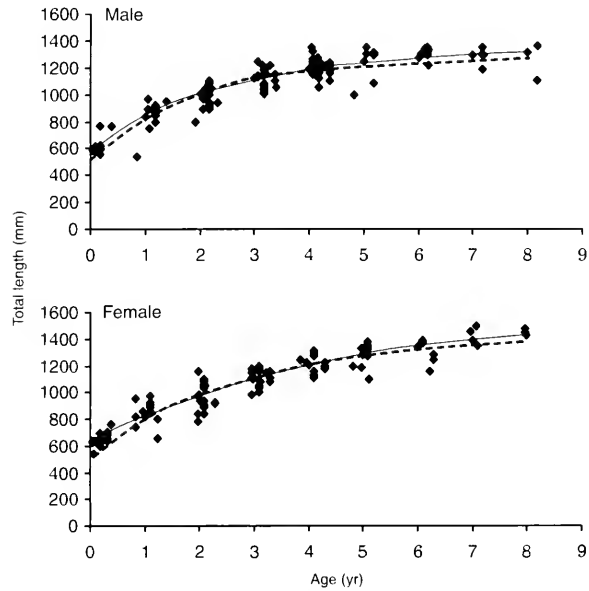

Figure 3

Growth functions fitted to observed size-at-age data for male and female finetooth sharks from the northeastern Gulf of Mexico. The equation of von Bertalanffy (1938), $L_t=L_\infty(1-e^{-K(t-t_0)})$, is represented by the solid line and the equation of Fabens (1965), $L_t = L_\infty-(L_\infty-L_0)e^{-Kt}$, is represented by the dashed line.

Peterson and Wroblewski (1984) method ranged from 0.722/yr for age-0 sharks to 0.850 for age-15 sharks.

Productivities obtained through the density-dependent method averaged 0.041/yr, (median 0.042, 95% confidence limits: 0.024–0.054) for Z=1.5 M and 0.071/yr (0.073, 0.045–0.091) for Z=2 M (Fig. 6). Generation times obtained through life table simulation averaged 6.96 yr (6.90, 6.13–8.01). Expressed as a percentage, fertility elasticities averaged 12.6% (12.6, 11.1–14.0), elasticities of juvenile survival were 47.7% (48.9, 37.4–56.9), and those of adult survival totaled 39.7% (38.9, 31.5–50.2).

Scenario 2 Estimates of M for adults ranged from a minimum of 0.174 obtained through the Peterson and Wroblewski (1984) method to a maximum of 0.528 obtained through the Jensen (1996) method based on K or, when expressed as survivorship, from 0.840/yr to 0.590/yr. All other annual survivorship estimates for adults fell within that range: 0.596/yr for the Pauly (1980) method, and 0.607 and 0.732/yr for the Jensen (1996) method based on ages at maturity of 3.3 and 5.3 yr, respectively. Estimates of survivorship at age from the Peterson and Wroblewski (1984) method ranged from 0.689/yr for age-0 sharks to 0.840/yr for age-10 sharks.

Productivities from the density-dependent method averaged 0.038/yr (0.038, 0.023–0.052) for Z=1.5 M and 0.067/yr (0.068, 0.043–0.088) for Z=2 M (Fig. 6). Mean generation lengths from life tables averaged 6.34 yr (6.32, 5.75–7.04), fertility elasticities averaged 12.1% (12.3, 4.3–12.8), juvenile survival elasticities were 46.2% (48.9, 35.1–59.4), and adult survival elasticities totaled 41.6% (38.8, 28.6–53.2).

Discussion

Finetooth sharks exhibit age and growth characteristics intermediate to those of sharks in the small coastal complex (e.g. Atlantic sharpnose, blacknose, and bonnethead shark) and those of some large coastal sharks, such as the blacktip shark. For example, the bonnethead shark (*Sphyrna tiburo*) has been reported to have K values of 0.28–0.69/yr, age at maturity of 2.0–2.4 yr, and longevity of 6–12 yr (Parsons, 1993a; Carlson and Parsons, 1997). Finetooth sharks displayed lower K values (0.24–0.41/yr), and higher age at maturity (3.9–4.3 yr) and longevity (8–14 yr) estimates. These growth characteristics are closer to those exhibited by the blacktip shark (Branstetter, 1987;

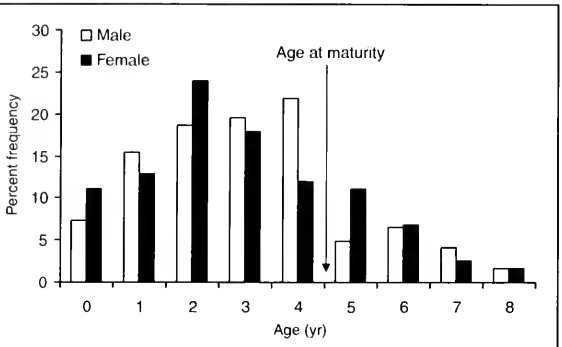

Figure 4

Estimated age composition for male and female finetooth sharks collected in the northeastern Gulf of Mexico.

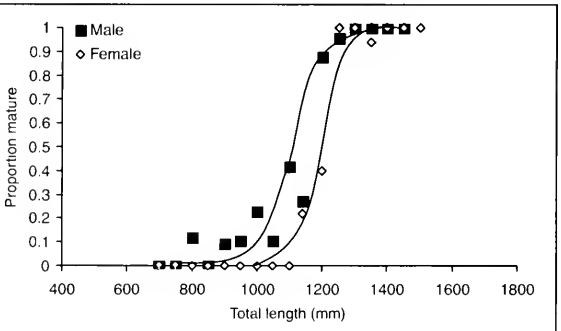

Figure 5

The relationship between maturity and total length for male and female finetooth sharks. Mean total length and proportion mature were plotted in lieu of the binomial data for clarity. Size class intervals are 50 mm TL.

Killam and Parsons, 1989) than to those from other small coastal species (Table 3).

The von Bertalanffy age and growth model based on observed data appears to provide a sound estimate for this population of finetooth sharks. The model was checked by comparing parameters from the observed model with those estimated by back calculation (Cailliet et al., 1986; Cailliet, 1990). For both methods, theoretical maximum length and growth coefficients (K) were similar. Theoretical maximum length (1587 mm TL for females and 1352 mm TL for males) matched well the empirical size of the largest sharks in the study area (1498 mm TL and 1360 mm for females and males, respectively). In addition, the average percent error in aging (APE=6.8%) was low and within the range of estimates provided in other studies that also used sagittal sections for aging (ranging from 3.0% for the oceanic whitetip shark, *Carcharhinus longimanus* [Lessa et al., 1999] to 8.1% for the blacktip shark [Wintner and Cliff, 1995]). The fairly high precision is probably a result of good band readability and reader experience.

All age estimates from growth band counts were based on the hypothesis of annual growth band deposition. Although attempts were made to verify annual band deposition through marginal increment analysis, the pattern was inconclusive because of the lack of samples from November to March. However, the decrease in incremental growth from June through October was not large enough to indicate a double band formation (Natanson et al., 1995). Annual winter mark formation has also been assumed in other studies of subtropical species (Branstetter and Stiles, 1987; Natanson et al., 1995; Carlson et al., 1999) where the marginal increment analysis showed a pattern similar

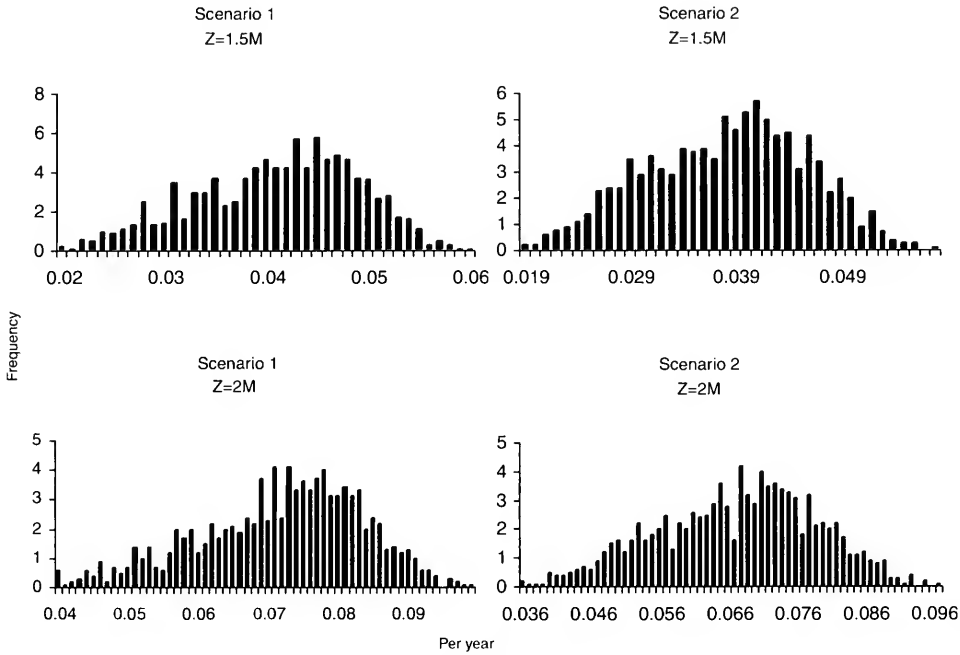

Figure 6

Frequency distributions of the results of 10,000 productivity simulations. Histograms are presented for runs simulating information from scenario 1 and scenario 2, at Z=1.5 M and Z=2.0 M.

Table 3

A comparison of life-history characteristics and population parameter estimates for the finetooth shark with three other small and one large coastal shark species. Values reported are for females.

	Size at birth (cm) TL[1]	Maximum size (cm) TL[1]	K (/yr)[1]	Longevity (yr)[1,2]	Age at maturity (yr)[1]	Fecundity (/yr)[1]	$R_{Z=2M}$[3]	Generation time ($\bar{A}$; yr)[4]
Atlantic sharpnose	32	107	0.36–0.45	7 (10)	3	5	0.084	4.9
Bonnethead	30	104–124	0.28–0.69	7 (12)	2.2	9	0.105	3.9
Blacknose	42	130–154	0.21–0.48	5 (17)	3.5	2.5	—	4.2
Finetooth	53	160	0.24–0.41[5]	8 (14)[5]	4.3[5]	2	0.071[5]	6.9[5]
Blacktip	58	191–200	0.20–0.27	10 (18)	7	2.5	0.054	10

[1] From Appendix in Cortés (2000).
[2] Values in parentheses indicate theoretical estimates.
[3] From Smith et al. (1998).
[4] From Cortés (2002).
[5] From the present study, scenario 1.

to that found in the present study for the finetooth shark. However, future validation studies through chemical marking, tag-recapture, or bomb dating are needed to determine that growth bands are deposited annually for the finetooth shark as well as numerous other species.

Very few studies have applied the method of Fabens (1965) for estimating growth in sharks, but some have suggested that using an estimate of size at birth (L_0) rather than t_0 is a more robust technique (Goosen and Smale, 1997). In the present study, the estimates of K obtained with the Fabens (1965) method were slightly higher than those estimated with the original von Bertalanffy (1938) equation, probably because the former method forces the model through the y-intercept, making the initial part of the curve steeper (Fig. 3). Beyond age 1, both models were very similar for both sexes and in some cases overlapped in size at age. In addition, the estimates of productivity, generation time, and elasticities, where results from either model were used, were very close. The similarities in growth models with both techniques (Fabens and von Bertalanffy) are likely a reflection of adequate samples throughout all ages. The application of the Fabens (1965) method may be appropiate when there is an inadequate sample of very small individuals.

Differences in reproduction may exist between finetooth sharks from the Gulf of Mexico and northwestern Atlantic Ocean. Although not subjected to a quantitative analysis, Castro (1993) reported size at maturity to be about 1300 mm STL (1271 mm TL) for males and 1350 mm STL (1320 mm TL) for females off South Carolina. This is approximately 80–90 mm TL greater than the median size at maturity estimated for finetooth sharks from the Gulf of Mexico. There is growing evidence that differences in life-history traits between geographically separated populations of sharks are not unusual. To cite a few examples, Parsons (1993a, 1993b) and Carlson and Parsons (1997) found a clinal variation in reproduction and age and growth among populations of bonnethead sharks from the eastern Gulf of Mexico; Wintner and Cliff (1995) found that size at maturity differed greatly between blacktip sharks from South Africa and the Gulf of Mexico; and Mollet et al. (2000) found that the median length at maturity for female mako sharks (*Isurus oxyrinchus*) is greater in the western north Atlantic Ocean than in the southern hemisphere. Whether these deviations in life-history parameters are the result of phenotypic plasticity or genotype is yet to be determined.

Despite no known directed or indirect fishing mortality on the population of finetooth sharks from the northeastern Gulf of Mexico, younger age classes (ages 0 and 1) were not very important. Our sampling design incorporated a multiple-mesh gill net that was thought to capture all sizes of juvenile sharks (Carlson and Brusher, 1999). However, because selectivity functions have not been calculated for this species, we cannot ascertain whether these age groups are indeed naturally low in abundance in the areas sampled or whether this finding is an artifact due to sampling bias.

In addition to age and growth characteristics, the finetooth shark exhibits other life-history traits and population parameters that fall between those of the blacktip shark and those of other small coastal species (Table 3). Indeed, this species can be placed between the blacktip shark and the Atlantic sharpnose shark and bonnethead along the continuum of productivity estimates (r_2, with Z=2 M) of Smith et al. (1998), and also between the blacktip shark and the Atlantic sharpnose shark, bonnethead, and blacknose shark in the "fast-slow" continuum of life-history traits and population parameters identified by Cortés (see his Fig. 2, 2002). Thus, the finetooth shark appears to be the "slowest" of the small coastal sharks studied so far, and to have moderate rebound potential and intermediate generation time. In addition, the probabilistic elasticity analysis indicated that population growth rates of finetooth sharks are much more sensitive to survival of the juvenile and adult stages than to survival of age-0 individuals or fecundity, as recently found for a suite of shark species (Cortés, 2002). This finding suggests that management actions should focus on protection of juveniles and adults rather than age-0 individuals, a recommendation that generally applies to sharks located towards the "fast" end of the life-history continuum. Minimum size limits could thus be effective measures to enhance juvenile survival and time-area closures could protect reproductive females, adult survival, and reproductive potential, should stocks of this species become overfished and management actions be required. Moreover, this study suggests that, when feasible, sharks should be managed on a species-specific basis, rather than by groupings of multiple species that may ignore marked differences in life-history traits.

Acknowledgments

We thank the staff of the National Marine Fisheries Service, Panama City, FL, for their help throughout this study. Special thanks go to Karen Hanson for cleaning and sectioning all the vertebrae. Henry Mollet provided guidance with determining size at maturity. We also thank Lee Trent, and the many interns who provided assistance with collection of sharks. All animals were collected under the Florida Department of Environmental Protection Special Permit no. 96S-075.

Literature cited

Beamish, R. J., and D. A. Fournier.
1981. A method for comparing the precision of a set of age determinations. Can. J. Fish. Aquat. Sci. 38:982–983.

Branstetter, S.
1981. Biological notes on the sharks of the north central Gulf of Mexico. Contrib. Mar. Sci. 24:13–34.
1987. Age and growth estimates for blacktip, *Carcharhinus limbatus*, and spinner, *C. brevipinna*, sharks from the northwestern Gulf of Mexico. Copeia 1987:964–974.

Branstetter, S., and R. Stiles.
1987. Age and growth estimates of the bull shark, *Carcharhinus leucas*, from the northern Gulf of Mexico. Environ. Biol. Fishes 20:169–181.

Brusher, H. A., and L. H. Ogren.
1976. Distribution, abundance, and size of penaeid shrimps in the St. Andrew Bay system, Florida. Fish. Bull. 74:158–166.

Cailliet, G. M.
1990. Elasmobranch age determination and verification: an updated review. *In* Elasmobranchs as living resources: advances in biology, ecology, systematic and the status of the fisheries (H. L. Pratt Jr., S. H. Gruber, and T. Taniuchi, eds.), p. 157–165. U.S. Dep. Commer., NOAA Tech. Rep. NMFS 90.
Cailliet, G. M., H. F. Mollet, G. P. Pittenger, D. Bedford, and L. J. Natanson.
1992. Growth and demography of the Pacific angel shark (*Squatina californica*) based upon tag returns off California. Aust. J. Mar. Freshwater Res. 43:1313–1330.
Cailliet, G. M., R. L. Radtke, and B. A. Weldon.
1986. Elasmobranch age determination and verification: a review. *In* Indo-Pacific fish biology: proceedings of the second international conference on Indo-Pacific fishes (T. Uyeno, R. Arai, T. Taniuchi, and K. Matsuura, eds.), p. 345–360. Ichthyol. Soc. Jpn., Tokyo.
Campana, S. E.
1990. How reliable are growth back calculations based on otoliths? Can. J. Fish. Aquat. Sci. 47:2219–2227.
Carlson, J. K., and J. H. Brusher.
1999. An index of abundance for coastal species of juvenile sharks from the northeast Gulf of Mexico. Mar. Fish. Rev. 61(3):37–45.
Carlson, J. K., E. Cortés, A. G. Johnson.
1999. Age and growth of the blacknose shark, *Carcharhinus acronotus*, in the eastern Gulf of Mexico. Copeia 1999: 684–691
Carlson, J. K., and G. R. Parsons.
1997. Age and growth of the bonnethead shark, *Sphyrna tiburo*, from northwest Florida, with comments on clinal variation. Environ. Biol. Fishes 50:331–341.
Castro, J. I.
1993. The biology of the finetooth shark, *Carcharhinus isodon*. Environ. Biol. Fishes 36:219–232.
Caswell, H.
2001. Matrix population models: construction, analysis, and interpretation, 2nd ed., 722 p. Sinauer, Sunderland, MA.
Cerrato, R. M.
1990. Interpretable statistical tests for growth comparisons using parameters in the von Bertalanffy growth equation. Can. J. Fish. Aquat. Sci. 47:1416–1426.
Chen, S. B., and S. Watanabe.
1989. Age dependence of natural mortality coefficient in fish population dynamics. Nippon Suisan Gakkaishi 55:205–208.
Compagno, L. J. V.
1984. FAO species catalogue: sharks of the world. An annotated and illustrated catalogue of shark species known to date. FAO Fisheries Synopsis (125), vol. 4, part 1: Hexanchiformes to Lamniformes, 249 p. FAO, Rome.
Cortés, E.
2000. Life history patterns and correlations in sharks. Rev. Fish. Sci. 8:299–344.
2002. Incorporating uncertainty into demographic modeling: application to shark populations and their conservation. Conserv. Biol. 16(4):1–15.
Crystal Ball 2000.
2000. Decisioneering, 1515 Arapahoe St., Suite 1311, Denver, CO.
Fabens, A. J.
1965. Properties and fitting of the von Bertalanffy growth curve. Growth 29:265–289.
Goosen, A.J.J., and M.J. Smale.
1997. A preliminary study of the age and growth of the smoothhound shark *Mustelus mustelus* (Triakidae). S. Afr. J. Mar. Sci. 18:85–91.
Gruber, S. H., and R. G. Stout.
1983. Biological materials for the study of age and growth in tropical marine elasmobranch, the lemon shark, *Negaprion brevirostris* (Poey). *In* Proceedings of the international workshop on age determination of oceanic pelagic fishes; tunas, billfishes, and sharks (E. D. Prince and L. M. Pulos, eds.), p. 193–205. U.S. Dep. Commer., NOAA Tech. Rep. NMFS 8.
Jensen, A. L.
1996. Beverton and Holt life history invariants result from optimal trade-off of reproduction and survival. Can. J. Fish. Aquat. Sci. 53:820–822.
Johnson, A. G.
1979. A simple method for staining the centra of teleost vertebrae. Northeast Gulf Sci. 3:113–115.
Killam, K. A., and G. R. Parsons.
1989. Age and growth of the blacktip shark, *Carcharhinus limbatus*, near Tampa Bay, Florida. Fish. Bull. 87:845–857.
Kimura, D. K.
1980. Likelihood methods for the von Bertalanffy growth curve. Fish. Bull. 77:765–776.
Lessa, R., F. M. Santana, and R. Paglerani.
1999. Age, growth, and stock structure of the oceanic whitetip, *Carcharhinus longimanus*, from the southwestern equatorial Atlantic. Fish. Res. 42:21–30.
Mathsoft Inc.
2000. SPLUS 2000. Mathsoft, Inc., Cambridge, MA.
Math Tools, Ltd.
1999. MatriXL, version 4.5. Math Tools, Ltd., Ft. Washington, PA.
Mollet, H. F., G. Cliff, H. L. Pratt Jr., and J. D. Stevens.
2000. Reproductive biology of the female shortfin mako, *Isurus oxyrinchus* Rafinesque, 1810, with comments on the embryonic development of lamnoids. Fish. Bull. 98: 299–318.
NMFS (National Marine Fisheries Service).
1993. Fishery management plan for sharks of the Atlantic Ocean, 167 p. U.S. Dep. Commer., Washington, D.C. National Oceanic and Atmospheric Administration, Silver Spring, MD.
1999. Fishery management plan of the Atlantic Tunas, swordfish and sharks, vol. 1, 321 p. U.S. Dep. Commer., Washington, D.C., National Oceanic and Atmospheric Administration. Silver Spring, MD.
Natanson, L. J., J. G. Casey, and N. E. Kohler.
1995. Age and growth estimates for the dusky shark, *Carcharhinus obscurus*, in the western North Atlantic Ocean. Fish. Bull. 193:116–126.
Parsons, G. R.
1993a. Age determination and growth of the bonnethead shark *Sphyrna tiburo*: a comparison of two populations. Mar. Biol. 117:23–31.
1993b. Geographic variation in reproduction between two populations of the bonnethead shark, *Sphyrna tiburo*. Environ. Biol. Fishes 38:25–35.
Pauly, D.
1980. On the interrelationships between natural mortality, growth parameters, and mean environmental temperature in 175 fish stocks. J. Cons. Int. Explor. Mer 39:175–192.
Peterson, I., and J. S. Wroblewski.
1984. Mortality rate of fishes in the pelagic ecosystem. Can. J. Fish. Aquat. Sci. 38:1117–1120.
Ricker, W. E.
1992. Back-calculation of fish lengths based on proportionality between scale and length increments. Can. J. Fish. Aquat. Sci. 49:1018–1026.

SAS Institute, Inc.
1988. SAS/STAT, release 6.03 edition. SAS Institute, Inc., Cary, NC.
Schwartz, F. J.
1983. Shark aging methods and age estimation of scalloped hammerhead, *Sphyrna lewini* and dusky, *Carcharhinus obscurus*, sharks based on vertebral ring counts. *In* Proceedings of the international workshop on age determination of oceanic pelagic fishes: tunas, billfishes, and sharks (E. D. Prince and L. M. Pulos, eds), p. 167–174. U.S. Dep. Commer., NOAA Tech. Rep. NMFS 8.
Smith, S. E., D. W. Au, and C. Show.
1998. Intrinsic rebound potentials of 26 species of Pacific sharks. Mar. Freshwater Res. 49:663–678.
Trent, L., Parshley, D. E., and J. K. Carlson.
1997. Catch and bycatch in the shark drift gillnet fishery off Georgia and Florida. Mar. Fish. Rev. 59(1):19–28.
UTHSCSA.
1997. Image Tool, IT version 2.0. Department of Dental Diagnostics Science, University of Texas Health Center, Austin, TX.
von Bertalanffy, L.
1938. A quantitative theory of organic growth (inquires on growth laws. II). Human Biology 10:181–213.
Wintner, S. P., and G. Cliff.
1995. Age and growth determination of the blacktip shark, *Carcharhinus limbatus*, from the east coast of South Africa. Fish. Bull. 94:135–144.

Quantifying annual variation in catchability for commercial and research fishing

R.I.C. Chris Francis
Rosemary J. Hurst
James A. Renwick

National Institute of Water and Atmospheric Research
P.O. Box 14901
Wellington, New Zealand
E-mail address (for R.I.C.C. Francis): c.francis@niwa.cri.nz

Abstract—Biomass indices, from commercial catch per unit of effort (CPUE) or random trawl surveys, are commonly used in fisheries stock assessments. Uncertainty in such indices, often expressed as a coefficient of variation (CV), has two components: observation error, and annual variation in catchability. Only the former can be estimated directly. As a result, the CVs used for these indices either ignore the annual-variation component or assume a value for it (often implicitly). Two types of data for New Zealand stocks were examined: 48 sets of residuals and catchability estimates from stock assessments using either CPUE or trawl survey indices; and biomass estimates from 17 time series of trawl surveys with between 4 and 25 species per time series. These data show clear evidence of significant annual variation in catchability. With the trawl survey data, catchability was detectably extreme for many species in about one year in six. The assessment data suggest that this annual variability typically has a CV of about 0.2. For commercial CPUE the variability is slightly less, and a typical total CV (including both components) of 0.15 to 0.2. This is much less than the values of 0.3 to 0.35 that have commonly been assumed in New Zealand. Some estimates of catchability are shown to be implausible.

Manuscript accepted 17 December 2002.
Manuscript received 31 December 2002 at NMFS Scientific Publications Office.
Fish. Bull. 101: 293–304 (2003).

Catchability is a key parameter that is estimated in many fish stock assessments (Arreguín-Sánchez, 1996). It is the constant of proportionality between biomass indices (either from commercial catch per unit of effort (CPUE) or random trawl surveys) and absolute biomass. Despite its importance it is usually thought of as a "nuisance" parameter: one that is not of intrinsic interest but which needs to be estimated so that other quantities, which are of interest (e.g. biomass), can be estimated. For this reason estimates of catchability are not often reported.

Uncertainty in biomass indices, often expressed as a coefficient of variation (CV), has two components: observation error and annual variation in catchability. Only the former can be estimated directly. As a result, the CVs used for these indices either ignore the annual-variation component or assume a value for it (often implicitly). Our objectives in this study were to estimate the extent to which catchability varies from year to year for New Zealand stocks. We used all available data, including residuals and catchability estimates from stock assessments and biomass estimates from time series of trawl surveys. We show that standard New Zealand practice typically overestimates catchability variation for trawl survey indices and underestimates it for CPUE, and suggest that some catchability estimates are clearly implausible. More details concerning the data and analyses below are given by Francis et al. (2001).

We assume throughout that catchability does not vary systematically with abundance. There is much controversy surrounding this assumption, particularly for CPUE. Since Paloheimo and Dickie (1964) gave theoretical reasons to expect that catchability would increase as biomass declined, many authors have presented confirmatory data (e.g. Schaaf, 1975; Pope, 1980; Winters and Wheeler, 1985; Quinn and Collie, 1990). Nevertheless, many stock assessments are based on the assumption that catchability is independent of abundance. It is data from such assessments that we examine here. We also assume, of necessity, that the role of CVs in stock assessments is to describe the precision of biomass indices, rather than their quality. This issue is discussed further in the final paragraph of this paper. To begin with, we describe more precisely what we mean by catchability.

Definitions

"Catchability" is used in several slightly different ways in the fisheries literature. The use we are concerned with is as a parameter (conventionally denoted by q) in a stock assessment model, defined by the equations

$$I_i = qB_i\varepsilon_i \text{ or } \log(I_i) = \log(qB_i)\varepsilon'_i \quad (1)$$

where I_i = the index in year i;
B_i = the corresponding true biomass; and
the error terms, ε_i and ε'_i are random variables with expectation 1 and CV (coefficient of variation) c_i.

The interpretation of q in (Eq. 1) depends on whether the I_i are from CPUE or trawl surveys (other types of biomass index—e.g. from acoustic surveys—are possible but not considered here). In

the former case, q may be interpreted as the proportion of the population biomass that is caught by one unit of effort. Often the CPUE is standardized (using methods akin to those of Punt et al., 2000), so that the unit of effort is a standard one (e.g. if nationality and area are factors in the CPUE standardization, then the standard unit of effort will be that for a vessel from the reference nation in the reference area). However, the unit of effort is changed when, as is common in New Zealand, CPUE indices are standardized to have value 1 in a reference year. If the I_t are from a trawl survey series, the interpretation of q is slightly different. Here, it is the product of the survey area and the proportion of the biomass that is caught per unit of area swept (because trawl survey indices are usually scaled up by the survey area, whereas no such scaling is done for CPUE indices).

Trawl survey catchability may also be interpreted as the product of three components: vulnerability, v, vertical availability, u_v, and areal availability, u_a (Francis[1]). These components are defined in the framework of a conceptual model in which the trawl gear is thought of as sweeping a volume of water in the shape of a cuboid of width equal to the distance between the trawl doors, height equal to the headline height, and length equal to the distance trawled. Vulnerability is the average proportion of fish in the swept volume that are caught. Vertical availability is the proportion of fish in the survey area that could be encountered by the trawl gear (i.e. that are close enough to the bottom to be below the trawl headline but not so close as to pass under the footrope). Areal availability is the proportion of fish in the population being surveyed that are in the survey area at the time of the survey (this is important in stock assessment when the full range of the stock being assessed is not covered by a survey).

These three components are usually of more theoretical than practical use. That is, they help us to think about the relationship between a trawl survey biomass index and the actual biomass. In New Zealand the common practice is to calculate survey biomass indices as if all three constants had value 1. This means that the catchability associated with these indices is the product of the three components, i.e. $q = vu_v u_a$. This interpretation restricts the range of plausible values for a trawl survey q. Because all three catchability components are defined as proportions their product should be less than (or equal to) 1. (It is technically possible for v to exceed 1 [if, for instance, fish that are initially above the headline, and thus unavailable to the net, are herded downwards] but it is most unlikely that vu_v would be greater than 1; u_a cannot exceed 1.) Thus, if the default values of the catchability components have been used, we would expect q to be less than 1. Also, very small values of q are implausible for any species that is assessed by using trawl survey biomasses. Although there are species that are not well caught by trawls (e.g. because they are fast-swimming, high above the bottom, or because they burrow in the substrate) and thus have very low values of v or u_v (or both), such species are not, for that reason, assessed with trawl survey indices. Similarly, a very low areal availability (implying that most of a fish stock is outside the survey area) would rule out the use of trawl surveys in assessing a stock.

There is also a limit to how much we would expect values of q for the same species to vary between surveys. For a given fishing vessel and trawl net, the components v and u_v are determined by fish behavior (e.g. swimming speed, typical height above the bottom, reaction to an approaching net). This means that if the same vessel and gear are used in surveys in different areas we would expect the product vu_v not to vary very much for the same species (except, perhaps, between spawning and nonspawning periods, when there may be substantial behavioral differences). If different vessels, or gear, are used, we might obtain larger differences in vu_v.

Materials and methods

Data

Two types of New Zealand data were examined: those from stock assessments and those from random trawl surveys.

Assessment data We gathered data from all recent stock assessments that used biomass indices from either trawl surveys or CPUE. One data set was constructed for each separate series of biomass indices (so that an assessment using two different series provided two data sets). Each data set consisted of the following variables:

- the biomass indices input to the assessment;
- the years associated with these indices;
- the CV(s) assumed for these indices;
- a description of the assumed error distribution type;
- the model estimates of (absolute) biomass that correspond to each biomass index; and
- the model estimate of catchability, q, for the indices.

For each stock the latest available assessment (usually carried out in 2000) was used. Data sets with fewer than four annual indices were discarded.

A total of 48 such data sets was constructed (30 with CPUE indices and 18 with trawl survey indices), ranging in length from 4 to 40 indices, with CVs between 0.02 and 0.61 (Fig. 1A) (details of the individual assessments are given in Francis et al., 2001). In most data sets (43 of 48) a single CV was assumed for all indices. Two rock lobster assessments used a time step of six months; all other assessments used a one-year time step. Amongst these data sets there were three different error-distribution assumptions; these determine how standardized residuals are calculated (Table 1).

We refer to the CVs for the assessment data sets as "assumed," rather than "estimated," because we can estimate only one component of these CVs, that due to observation

[1] Francis, R. I. C. C. 1989. A standard approach to biomass estimation from bottom trawl surveys. N.Z. Fish. Assess. Res. Doc. 89/3, 4 p. National Institute of Water and Atmospheric Research, P.O. Box 14901, Wellington, New Zealand.

error. By setting a value for one of these CVs we are implicitly making an assumption about the other component: annual variation in catchability. We did not solicit information on how these CVs were set for individual assessments. However, the most common way is based on a subjective assessment of the "reliability" of the associated biomass indices: the less reliable the indices are judged to be, the higher the assumed CV (by "reliability" we mean the combination of two very different properties of an index, its precision, and its "quality"—the extent to which it is likely to be proportional to biomass). This is why almost half of the CPUE series (13 out of 30) have assumed CVs of 0.35, and many of the trawl survey series (13 of 18) have CVs of 0.25. In most cases, the CVs assumed for trawl survey indices differ from the observation error CVs calculated from the trawl survey data (Fig. 1B).

Trawl survey data Data from all New Zealand random trawl surveys were considered. The surveys were grouped into series, each of which contained surveys covering (approximately) the same area at about the same time of year and using the same (or similar) vessel(s) and gear. Some series were split into two, by area, because they were deemed to survey two distinct fish communities. Series with fewer than four surveys were rejected. This left 17 series, with between four and 11 surveys per series.

For each trawl survey series a list of "suitable" species was generated by listing all species caught in the series and then excluding species deemed to be "unsuitable" for any of the following reasons:

- species caught in only a small percentage of tows;
- species caught in small quantities (low mean catch per tow);
- species not well caught by the net because they are too small, too large, too close to the sea floor, or too high in the water column;
- species for which identification was poor, or inconsistent over time;
- species whose range was poorly covered by the surveys (e.g. those occurring mostly on rough ground, or mostly in water shallower or deeper than that covered by the series).

The idea was to include as many species as possible for each series. In considering a particular species in a specific trawl survey series, the following question was useful: "If this were a valuable commercial species would it be appropriate to use this series of trawl surveys to generate biomass indices to put into a stock assessment?" An answer of "yes" (or even "maybe") was a good reason to include this species. The CVs of biomass estimates were not considered in making this decision. For each series the list of suitable species was compiled by people with an intimate knowledge of that series and the associated species. No attempt was made to derive consistent objective criteria (e.g. exclude all species that occurred in fewer than 30% of tows) for all series. The exclusion of a species from one series was no barrier to its inclusion in another. The number of acceptable species in a series varied between 4 and 25.

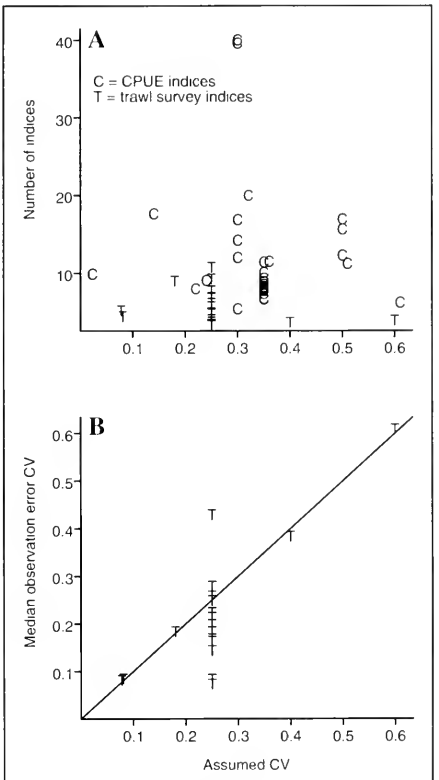

Figure 1

Descriptive statistics for the assessment data sets: assumed CV plotted against (**A**) the number of indices (all data sets) and (**B**) the median observation error CV (data sets with trawl survey indices only). Each point represents one data set; in A the points are jittered slightly to separate coincident points; where different indices in a data set had different assumed CVs the median of these is plotted.

Biomass indices, and CVs, were calculated for each suitable species in each survey. In all series but two, vulnerability, areal availability, and vertical availability were set to 1. There was a wide range of estimated CVs. Even when the CVs for each species in a series were averaged over all surveys, these averaged values spanned an order of magnitude, from 0.07 to 0.70 (Fig. 2).

Analyses

Our analyses addressed a series of questions, which are given as subheadings in this section.

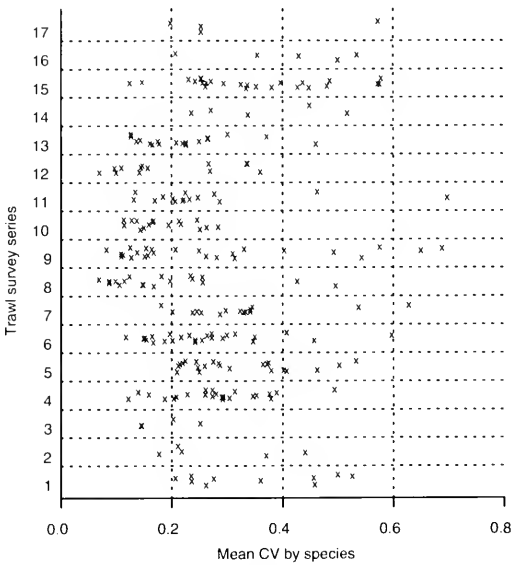

Figure 2

Mean CVs, by species, of biomass indices in the trawl survey data sets. Each plotted point relates to one species in a trawl survey series, and indicates the mean of all estimated CVs for that species in that series. Points are jittered vertically to avoid overlap.

Table 1

Three alternative error-distribution assumptions for biomass indices in stock assessments, and the associated form of the standardized residuals. Notation: I_i is the ith biomass index and B_i is the corresponding model estimate of (absolute) biomass; for assumption lnorm, $\sigma_i^2 = \log(c_i^2 + 1)$.

Label	Description	Standardized residual
norm	I_i is normally distributed with mean qB_i and assumed CV c_i	$\frac{1}{c_i}\left(\frac{I_i}{qB_i} - 1\right)$
lnorm	I_i is lognormally distributed with mean qB_i and assumed CV c_i	$\frac{1}{\sigma_i}\left[\log\left(\frac{I_i}{qB_i}\right) + 0.5\sigma_i^2\right]$
lognorm	$\log(I_i)$ is normally distributed with mean $\log(qB_i)$ and s.d. c_i	$\frac{1}{c_i}\log\left(\frac{I_i}{qB_i}\right)$

Are the assessment CVs the right size?

We constructed a residual statistic, κ, that was designed to indicate whether the CVs assumed in the stock assessment (the c_i) were too small or too large in each data set. A positive (or negative) value of κ suggests that the residuals were too large (too small), and thus CVs were too small (too large). The statistic is based on the median absolute standardized residual (MASR), rather than the residual variance, because the latter is not very robust (it is easily inflated by outliers). We defined

$$\kappa = \begin{cases} 2(\mu - \mu_{0.5})/(\mu_{0.5} - \mu_{0.025}) & \text{if } \mu < \mu_{0.5} \\ 2(\mu - \mu_{0.5})/(\mu_{0.975} - \mu_{0.5}) & \text{if } \mu > \mu_{0.5} \end{cases},$$

where μ = the MASR from the assessment data; and
μ_r = the rth quantile of the sampling distribution of μ.

To calculate the μ_r we assumed that the standardized residuals follow a Student's t-distribution with $n-2$ degrees of freedom, where n is the number of indices in the data set. [We assumed $n-2$ degrees of freedom because, in an assessment with only a single series of relative biomass indices, only two parameters can be estimated, e.g. initial biomass and q (Francis, 1992). When there are many data inputs there may be many more than two parameters estimated.] For each value of the sample size n, the μ_r were estimated by simulating 1000 data sets of size n from a t-distribution with $n-2$ degrees of freedom, calculating the median absolute value for each simulated data set, and taking the rth quantile of this set of 1000 medians.

We used the κ statistics in two ways. We tested the null hypothesis that the CVs were, on average, of the correct size by using a simple signs test (under this hypothesis we would expect about 50% of the κ's to be of each sign). If significantly more than half are positive (or negative) this shows a tendency to use CVs that are too large (or too small). This test considers all the CVs at once. We also tested each CV separately; a value of κ greater than 2 (less than −2) is statistically significant.

Next, we investigated how much, if at all, we should change the assumed CVs to make their size appropriate. This was done by changing the assumed CVs, recalculating the residual statistic and checking to see whether the new values of κ were evenly distributed about zero. We did this separately for the CPUE and trawl survey indices. For the former we simply set them all to a single default value and searched for the default value that produced an even distribution. For the latter, we assumed that the CV associated with annual variation in catchability was the same for all stocks and "added" this CV to the observation error CVs to obtain assumed CVs for the stock assessments. Note that CVs are "added" as squares, so that when we "add" CVs of 0.2 and 0.3 we get 0.36 [$= (0.2^2+0.3^2)^{0.5}$]. Here we were searching for the value of the catchability CV that produced an even distribution of κ.

Strictly speaking we should rerun each assessment each time we change a CV. However, it is not practical to do this for so many assessments. Thus we have to assume that changing a CV will not change the model estimates too much. Our experience is that this is true for assessments with only one series of biomass indices. It is least likely when there are more than one series and these show markedly different trends.

Can we detect years of extreme trawl survey catchability?

First, as an informal procedure to identify possible years of extreme trawl survey catchability, the trawl survey biomass indices were standardized (by dividing each time series for a particular species by its mean) and plotted by survey. Next, the following more formal procedure was used to identify extreme years. For each species in a trawl survey data set, the survey years were ranked in order of increasing biomass index, and then these ranks were averaged across species to obtain a mean rank for each year. Then the rank deviations, $d_i = |r_i - 0.5(n+1)|$, were calculated, where r_i is the mean rank for year i, n = the number of survey years, and $0.5(n+1)$ is the overall mean of the mean ranks (Table 2).

Table 2

Example, using trawl survey series-3 data, of the stages in the procedure for calculating a mean rank and rank deviation for each survey year in a trawl survey data set.

		Survey year					
	Species	1983	1985	1990	1992	1996	1999
Biomass indices	A	125	482	1565	1141	969	1644
	B	355	47	413	272	320	365
	C	63	48	131	257	118	89
	D	113	111	157	236	191	176
Ranks	A	1	2	5	4	3	6
	B	4	1	6	2	3	5
	C	2	1	5	6	4	3
	D	2	1	3	6	5	4
Mean ranks, r_i		2.25	1.25	4.75	4.5	3.75	4.5
Rank deviations, d_i		1.25	2.25	1.25	1.00	0.25	1.00

The following simulation procedure was used, for each series, to determine which years should be labeled as extreme (i.e. how large the d_i's need to be to be statistically significant).

1 The actual biomass indices were replaced by randomly generated indices (by using a uniform distribution [because our statistic is based on ranks it does not matter what distribution is used to generate the biomass indices]);
2 Mean ranks, and rank deviations, were calculated for each survey year by using these simulated biomass indices;
3 The largest of these rank deviations, $d_{\max,1}$, was stored;
4 Steps 1 to 3 were repeated 999 times, generating $d_{\max,j}$, for $j = 2,...,1000$;
5 Year i was labeled as extreme if d_i was greater than or equal to at least 95% of the $d_{\max,j}$.

In other words we asked, for each rank deviation d_i, how likely we would be to observe a deviation at least as large as this if there were no between-species correlations. If the probability were less than or equal to 0.05, we would label the year as extreme.

As a diagnostic tool, to examine possible reasons for these extreme years, we calculated between-year changes

in biomass indices, expressed as ratios. This was done for all species and for each pair of consecutive surveys that included one extreme year.

Are there consistencies between data sets?

Three types of consistency were sought in the data. First, is the range of estimated trawl survey catchabilities plausible? Second, is there any consistency, between trawl survey series, in the years that are labeled as having high or low catchability? Third, is there consistency between the extreme years in the trawl survey data and the CPUE indices in the assessment data? To address the latter question, each person who provided CPUE data was asked, for each series, which, if any, of the trawl survey data sets were "comparable" in that they related to similar areas, depths, and seasons. For "comparability" it was not necessary that the CPUE species be a target for the trawl survey. We were interested in knowing whether the person thought that the fact that the catchability seemed to be extreme for many species in the trawl survey in some year would be reasonable grounds to believe that this would affect their CPUE index in a similar way (but this person was not told which trawl survey years were considered extreme). For each match that was found between a CPUE index and a trawl survey extreme year we asked whether the two were consistent: that is, whether high (or low) trawl survey catchability corresponded to a positive (or negative) CPUE residual.

Results

Are the assessment CVs the right size?

Results were different for the two types of assessment data (Fig. 3). For those with CPUE indices, there was a tendency for CVs to be too large: κ was negative for 21 of the 30 data sets (this is significantly more than half, P=0.02) and was less than –2 for 9 of them. In contrast, κ was positive for 13 out of the 18 data sets with trawl survey indices (again, significantly more than half, P=0.02) and was greater than 2 for 2 of them. Median CVs for data sets for which the CVs were found to be significantly too large ranged from 0.3 to 0.5; where CVs were significantly too small the median CVs were between 0.02 and 0.24.

If a default CV is to be used for all CPUE series, the best value lies between 0.15 and 0.2; values in this range give approximately equal numbers of positive and negative values of κ (Table 3). The best default value for a trawl survey annual variation CV appears to be about 0.2; this gives approximately equal numbers of positive and negative values of κ (Table 4).

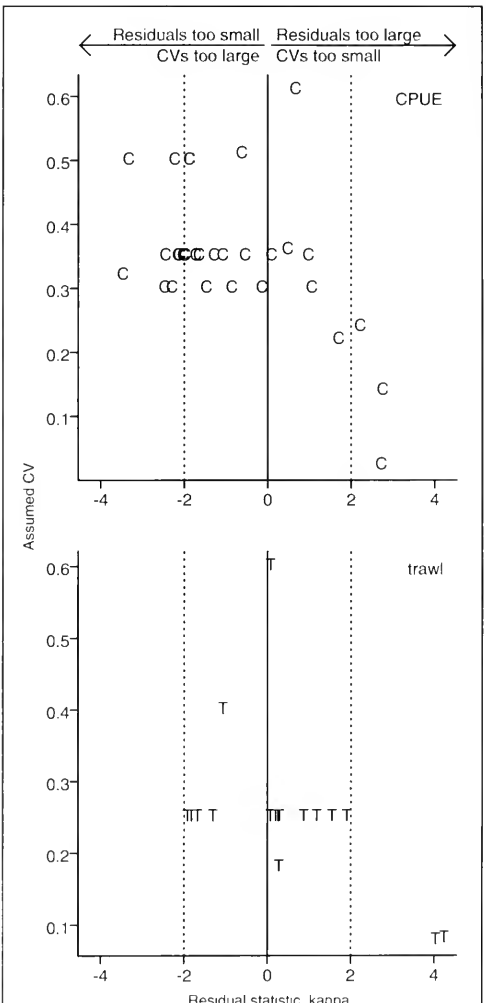

Figure 3

The residual statistic, κ, plotted against assumed CV for each of the assessment data sets: those with CPUE indices in the upper panel, those with trawl survey indices in the lower panel. Each point represents one data set; where different indices in a data set had different assumed CVs, the median of these is plotted.

Can we detect years of extreme trawl survey catchability?

Our informal graphical procedure showed that, for some trawl survey series, the biomass indices for many species fluctuate synchronously, which suggests annual variation in catchability. Two clear examples are shown in Figure 4: for series 5, the biomass indices for many species follow the same up-down-up pattern; for series 6, the opposite pattern (down-up-down) is followed by many species (but not

Table 3

Effect of using different default CVs for the 19 assessment data sets with CPUE indices and assumed CVs of either 0.3 or 0.35. Each line of the table gives the number of these data sets for which κ falls in the given range for the given default CV.

	Number of data sets			
Default CV	$\kappa < -2$	$-2 < \kappa < 0$	$0 < \kappa < 2$	$2 < \kappa$
0.1	0	1	9	9
0.15	0	8	6	5
0.2	0	11	5	3
0.25	3	10	5	1
0.3	6	10	3	0
0.35	7	9	3	0

Table 4

Effect of using different default annual variation CVs for the 18 assessment data sets with trawl survey indices. Each line of the table gives the number of these data sets for which κ falls in the given range when the assumed CV in the assessment is calculated by "adding" the given default CV to the observation error CVs.

Default CV for annual variation	Number of data sets			
	$\kappa < -2$	$-2 < \kappa < 0$	$0 < \kappa < 2$	$2 < \kappa$
0	0	4	10	4
0.1	0	6	9	3
0.15	0	6	11	1
0.2	0	9	8	1
0.25	1	9	8	0
0.3	1	11	6	0

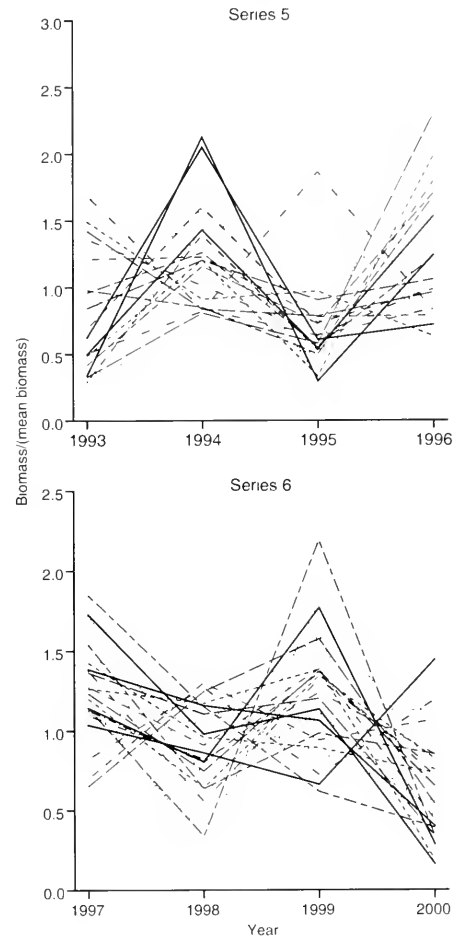

Figure 4

Standardized biomass indices, plotted against year, for trawl survey series 5 and 6. For each species in a series, the biomass indices were standardized by dividing by the mean index for that species.

in the same years). These patterns would be very unlikely to occur by chance alone if there were no between-species correlations. For series 5, 14 of the 22 species had their two highest biomass indices in the same years (1994 and 1996). The probability that an outcome as extreme as this would occur by chance alone (assuming no correlations) is only 6.4×10^{-6}. For series 6, the probability is 9.8×10^{-8} (here 17 of 25 species had their two highest years in 1996 and 1998). These very low probabilities are clear evidence that there are sometimes strong between-species correlations in a survey series. We will argue below that the main cause of these correlations is that catchability was extreme (for many species) in some years.

In our more formal analysis, 16 of a total of 94 survey years were found to be significantly extreme (nine with high catchability, and seven with low), and there were eight survey series for which no years were extreme (Fig. 5). (Note that the vertical distance between the broken lines in Figure 5, which indicates how extreme a mean rank needs to be to be judged significant, decreases with increasing number of species and with decreasing number of survey years.) We also investigated three modifications to the above procedure for identifying extreme years to see whether they might be useful. None was (see Appendix for details).

For some extreme years the biomass ratio statistics (Table 5) are so large that it is unlikely that actual bio-

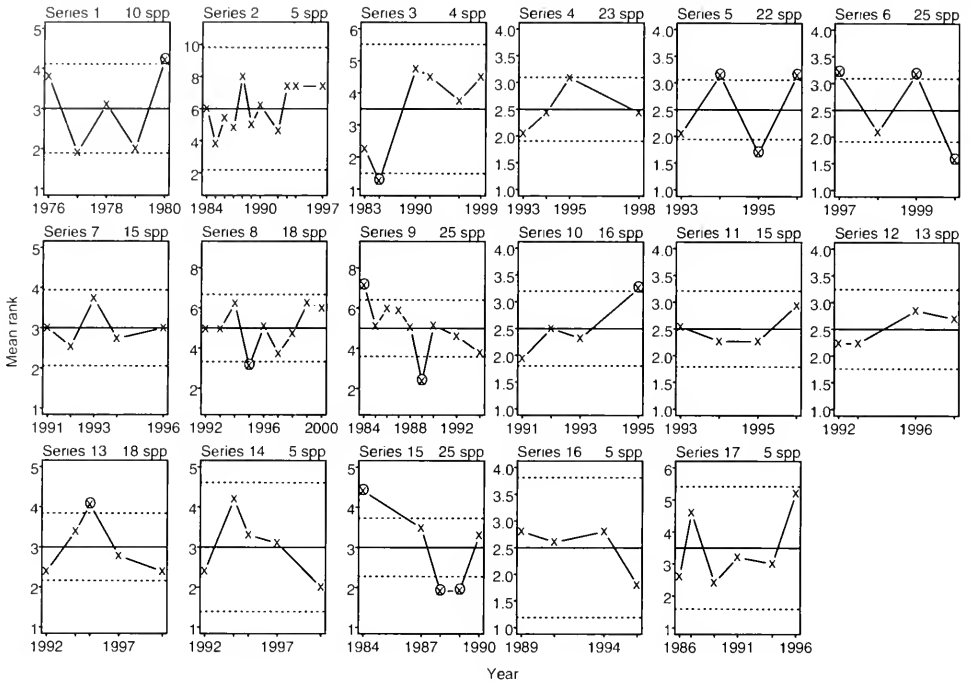

Figure 5

Mean ranks (calculated as illustrated in Table 2) for each trawl survey data set. The solid horizontal line in each panel indicates the overall mean rank; mean ranks outside the broken lines (circled points) indicate extreme survey years.

masses changed by so much. For example, for series 1 the median change in biomass index between 1979 and 1980 (calculated over 10 species) was a factor of 3.4. It is not plausible to say that the biomass of so many species changed by that much in just one year. A second example is years 1988 to 1990 for series 9. Here the median change (over 25 species) was a halving, from 1988 to 1999, followed by a doubling, from 1989 to 1990. Again, it is not plausible to say that the actual biomasses changed by this much.

Are there consistencies between data sets?

The range of estimated trawl survey catchabilities is very wide, covering more than two orders of magnitude, from 0.0035 to 1.6 (Fig. 6). Although the theoretical maximum value for a trawl survey q is 1, the two values that exceed this may not be of concern if we allow for estimation error. However, the lowest values *are* of concern. If these are accurate, then it would seem inappropriate to use trawl surveys to assess these stocks. For example, a q that is less than 0.01 means that more than 99% of the stock is, in some sense, not available to the trawl survey—either because it is outside the survey area (low areal availability), does not encounter the trawl (low vertical availability), or easily avoids it (low vulnerability). For two species the range of values was implausibly wide: for species F the four estimates varied by a factor of 79 (0.0039 to 0.31); for species E the factor was 49 (0.0035 to 0.17) (the next widest range was for species C, a factor of just 2.8).

There is only limited scope for between-series comparisons because the years or seasons covered by different series may not overlap and, in any case, only about one in six years is labeled as extreme. There are three years which were labeled as extreme for more than one series: 1984, 1989, and 1995. In two of these three, the labels are consistent: series 9 and 15 (both of which were deepwater surveys targeting orange roughy, *Hoplostethus atlanticus*, in different areas) agree in finding catchability to be high in winter 1984 and low in winter 1989. For 1995, two surveys found low catchability (series 5 in depths 20–400 m in February and March, and series 8 in 200–800 m in January) and two found high (series 10 in 750–1500 m in October and November, and series 13 in depths 20–400 m in March and April). Given the differences in depth ranges

Table 5

Biomass ratio statistics for "extreme" years (as identified in Fig. 5) in the trawl survey data. For each series, the table has one row for each pair of consecutive surveys that includes one extreme year (extreme years are underlined). A biomass ratio for the two years is calculated for each species; the table presents the median of these ratios, as well as the number of species for which this ratio exceeds 1.5. In each row, the order of the years is such that the expected biomass ratio is greater than 1.

Series	Years	Median ratio	Number of species where ratio exceeds 1.5
1	1980/1979	3.4	8/10
3	1983/1985	1.2	1/4
	1990/1985	3.0	3/4
5	1994/1993	1.8	12/22
	1994/1995	1.6	14/22
	1996/1995	1.9	13/22
6	1997/1998	1.4	11/25
	1999/1998	1.5	14/25
	1999/2000	1.9	18/25
8	1994/1995	1.4	8/18
	1996/1995	1.6	10/18
9	1984/1985	1.7	15/25
	1988/1989	2.0	16/25
	1990/1989	2.1	19/25
10	1995/1993	1.4	7/16
13	1995/1994	1.1	1/18
	1995/1997	1.4	8/18
15	1984/1987	1.4	11/25
	1987/1988	2.3	16/25
	1990/1989	1.9	13/25

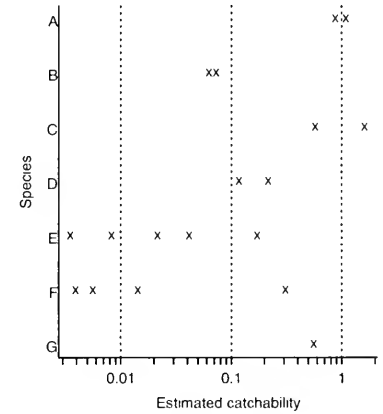

Figure 6

Estimates of trawl survey catchability by species. Each point corresponds to an assessment data set; estimates for different stocks of the same species are plotted in the same horizontal line.

and months for these series, it is unclear how much consistency in catchability could be expected.

In comparing the trawl survey and CPUE series, we found only 12 matches, and the data were consistent at 8 of these (67%). This is not significantly different from the value of 50% that we would expect if the data were uncorrelated (P=0.39). Another place one might look for consistency is between biomass trends for the same species in different survey series. We made plots of biomass trends for every instance where there were at least three survey series with that species and at least three years in common. A few of the 16 such plots showed strong consistency but it was difficult to judge the significance of this because of the possibility of obtaining agreement by chance.

Discussion

It is difficult to make inferences about catchability because we cannot measure it directly. Instead, we must estimate it indirectly with stock assessment models. These estimates are compromised by the weakness of our models, which provide only crude representations of population dynamics (because the data to develop more complex models are not available). With trawl survey data alone we cannot estimate catchability; we can only detect years when catchability was extreme for many species. Nevertheless, the large data sets we have assembled do allow us to draw some conclusions about New Zealand catchabilities.

Are the assessment CVs the right size?

Our results imply that, on average, the CVs used for CPUE in New Zealand are too large, and those used for trawl surveys are too small. For CPUE, the common (but usually tacit) assumption that catchability varies from year to year is supported. It is clear from Figure 3 and Table 3 that, had the CPUE CVs been set equal to the observational error (typically less than 0.1, Francis[2]), the associated stock assessment residuals would have been much too large. However, too much allowance for annual variability seems to have been made: the CVs that are used in stock assessments are, more often that not, too large. In other words, the annual variability in CPUE catchability is not as large as is implied by these CVs. Where the use of a default CV is appropriate, it would seem that values around 0.15–0.2 would be better than the values of 0.3–0.35 that are currently used. This implies that annual variability in CPUE catchability is less that 0.2. For trawl survey indices, the

[2] Francis, R. I. C. C. 1999. The impact of correlations in standardised CPUE indices. N.Z. Fish. Assess. Res. Doc. 99/42, 30 p. National Institute of Water and Atmospheric Research, P.O. Box 14901, Wellington, New Zealand.

results of Table 4 suggest that 0.2 is a reasonable default CV for annual variability in survey catchability. This CV should be "added" to the observation error CVs to obtain a CV for use in stock assessments.

The blanket use of default CVs is clearly undesirable. It is obviously wrong to assume that all CPUE indices have the same CV, regardless of which species or fishery they describe, or the quality and quantity of data from which they are calculated. Similarly, we should expect that annual variability in trawl survey catchability will vary from stock to stock. However, we have little choice in this matter. In most stock assessments we do not have the information to depart from a default value (although there is sometimes evidence that CPUE data sets were unusually weak, Doonan et al.[3]). The above default values imply smaller CVs for CPUE than for trawl surveys. This is surprising and contrary to the prevailing view that trawl surveys are more "reliable" than the CPUE (in the sense defined in the above section on the assessment data). Nevertheless, it is clearly indicated by the data sets examined here.

Can we detect years of extreme trawl survey catchability?

There is clear evidence of extreme years in New Zealand trawl surveys, i.e. years in which the biomass indices for many species are extreme (all low, or all high). However, can we be confident that these extreme years are caused by extremes in catchability? There are two other factors that could cause these extremes.

The first is sampling error, which is associated with the element of chance involved in whether there happen to be many fish at a randomly chosen location at the time it is sampled by the trawl. Because some pairs of species co-occur, we can expect that if we are "lucky" with one species (i.e. we happen to hit dense concentrations of it), then we will tend to be "lucky" with its co-occurring species. Thus, the sampling errors of co-occurring species will be correlated. It seems unlikely that the extreme mean ranks shown in Figure 5 (or the biomass ratios in Table 5) were caused solely by correlated sampling errors. In principle, we should be able to quantify this likelihood. From the survey tow-by-tow data we could infer the extent of between-species correlations at the level of individual stations, from which we could calculate correlations for whole surveys (we would expect more correlations in surveys covering a wider range of species). This information could then be used to calculate the probability of generating biomass ratios as large as those in Table 5. However, to do so would be a major multilevel simulation exercise which is beyond the scope of the present work. What we do know, from other studies, is that between-species correlations, when they exist, are not large. Values of 0.2 to 0.4 seem to be typical (for square-root–transformed catch rates in the same depth stratum, Bull[4]). It does not seem at all likely that such small correlations would cause the very substantial synchronous fluctuations we see in Figure 5 and Table 5.

A second interpretation of the extreme years is that they occur because changes in abundance of co-occurring species are correlated (because fishing that reduces the abundance of one species is likely to do the same for co-occurring species). Table 5 allows a subjective evaluation of the likelihood that biomasses in the extreme years changed by as much as the survey biomass indices suggest. This evaluation is complex because the likelihood depends on the magnitude of the ratios, the number of years between surveys, the number of species involved, and any "adjacent" changes (e.g. for series 9, a large drop in biomass in 1989 is less plausible because it appears to be followed by a large rise in the next year). Thus it is not easy to provide a threshold and say that some changes are plausible but others are not; but there is a clear range of plausibility. At one extreme are the changes associated with 1980 in series 1 and 1989 in series 9; we have argued above that these changes are clearly implausible. At the other extreme the changes for 1995 in series 13 are not as implausible, but it is a matter of judgment as to whether one could call them plausible.

Another point to bear in mind is that if we use observation error CVs (as routinely calculated from trawl survey data) in stock assessments, we obtain residuals that are, more often than not, larger than they ought to be.

We are left with the conclusion that the trawl survey data contain clear evidence that research-vessel catchability does vary significantly from year to year. In most, if not all, of the circled years in Figure 5 the catchability of many species appears to have been either much higher or much lower than normal. This finding is consistent with those of Myers and Cadigan (1995), who expressed this variation in terms of between-age within-year correlations in trawl-survey estimates of numbers at age. Also, Millar and Methot (2002) found evidence of significant departures from mean catchability in four of eight years in the triennial series of trawl surveys carried out on the Pacific coast of the United States. This variation in catchability may be environmentally driven. It would not be difficult to find plausible environmental variables that were extreme in the right years. However, because most of our trawl-survey time series were short we could have little confidence that this correlation was indicative of causation. Another possible cause of variation in catchability is between-survey changes in gear and fishing practice (although care is taken to avoid such changes).

Are there consistencies between data sets?

Our only important result under this heading is that some estimates of trawl survey catchability are not credible. For two species, we found that some estimates were implausi-

[3] Doonan, I. J., P. J. McMillan, R. P. Coburn, and A. C. Hart. 1999. Assessment of OEO 3A black oreo for 1999–2000. N.Z. Fish. Assess. Res. Doc. 99/52, 30 p. National Institute of Water and Atmospheric Research, P.O. Box 14901, Wellington, New Zealand.

[4] Bull, B. 2000. Personal commun. National Institute of Water and Atmospheric Research, P.O. Box 14901, Wellington, New Zealand.

bly low and the variation amongst stocks of the same species was implausibly high. Where possible, this variability should also be examined for CPUE catchabilities (as long as they are comparable—note that we should not compare trawl and long-line catchabilities). We did not make this comparison in our study because it involves adjusting for different reference units of of effort in different CPUE series, which requires specialist knowledge about the individual fisheries and data sets.

Concluding comment

Our analyses have not been able to take account of the practice, in some stock assessments, of using CVs as a measure of the "quality" of a biomass index, rather than its precision. This practice happens when a high CV is assigned to a series (often of CPUE) that is believed not to index biomass well. The intention is to lessen the contribution of the series to the assessment. A problem with this practice is that the judgment of quality is subjective, as is the decision as to how high a CV to assign to represent poor quality. It would be very rare that we had sufficient information to determine whether the judgment of poor quality was justified, and whether the assigned CVs were appropriate. It may be that some of the assessments analyzed above produced a biomass trajectory that was a very good fit to a CPUE series (suggesting that a low CV should have been used) but that the trajectory was wrong because, in this case, CPUE was not proportional to abundance. We cannot distinguish such an outcome from one in which a precise CPUE series indexed abundance well. The practice of assigning CVs subjectively is not desirable. Ideally, we should change the model assumption of proportionality between biomass and index rather than inflate CVs. However, we acknowledge that stock assessment is a very pragmatic discipline in which many compromises are necessary, and we hope that the above results will provide practitioners with empirical evidence to support some of their subjective decisions.

Acknowledgments

We are indebted to the many people who provided trawl survey and assessment data for this work. Dave Gilbert, Larry Paul, Paul Breen, and Stuart Hanchet offered useful comments on an earlier version of this paper, and Richard O'Driscoll detected what would have been an embarrassing data error. We are grateful to Steve Cadrin and an anonymous referee for useful suggestions. This project was partially funded by the New Zealand Ministry of Fisheries under project SAM1999/01.

Literature cited

Arreguin-Sánchez, F.
1996. Catchability: a key parameter for fish stock assessment. Rev. Fish Biol. Fisheries 6(2):221–242.

Francis, R. I. C. C.
1992. Use of risk analysis to assess fishery management strategies: a case study using orange roughy (*Hoplostethus atlanticus*) on the Chatham Rise, New Zealand. Can. J. Fish. Aquat. Sci. 49:922–930.

Francis, R. I. C. C., R. J. Hurst, and J. A. Renwick.
2001. An evaluation of catchability assumptions in New Zealand stock assessments. N.Z. Fish. Assess. Rep. 2001/1, 37 p.

Millar, R. B., and R. D. Methot.
2002. Age-structured meta-analysis of U.S. West Coast rockfish (Scorpaenidae) populations and hierarchical modeling of trawl survey catchabilities. Can. J. Fish. Aquat. Sci. 59:383–392.

Myers, R. A., and N. G. Cadigan.
1995. Statistical analysis of catch-at-age data with correlated errors. Can. J. Fish. Aquat. Sci. 52:1265–1273.

Paloheimo, J. E., and L. M. Dickie.
1964. Abundance and fishing success. Rapp. P-V. Réun. Cons. int. Explor. Mer 155:152–163.

Pope, J. G.
1980. Some consequences for fisheries management of aspects of the behaviour of pelagic fish. Rapp. P-V. Réun. Cons. Int. Explor. Mer 177:466–476.

Punt, A.E., T. I. Walker, B. L. Taylor, and F. Pribac.
2000. Standardization of catch and effort data in a spatially-structured shark fishery. Fish. Res. 45:129–145.

Quinn, T. J., II, and J. S. Collie.
1990. Alternative population models for eastern Bering Sea pollock. Int. North Pac. Fish. Comm. Bull. 50:243–257.

Schaaf, W. E.
1975. Fish population models: potential and actual links to ecological models. *In* Ecological modeling in a resource management framework (C. S. Russell, ed.), p. 211–239. Resources for the Future, Inc., Washington, D.C.

Winters, G. H., and J. P. Wheeler.
1985. Interaction between stock area, stock abundance, and catchability coefficient. Can. J. Fish. Aquat. Sci. 42(5): 989–998.

Appendix

Alternative mean rank calculations

In this Appendix we describe some alternative (but unfruitful) mean rank calculations referred to in the "Results" section under the subheading "Can we detect years of extreme trawl survey catchability?"

We tried three variations on the above procedure for identifying extreme years. In each case we were evaluating an alternative hypothesis about the nature of between-species correlations. Each hypothesis leads to a different method of calculating mean ranks (or alternative statistics), and we applied the new method to both the survey data, and to simulated data (to calculate threshold values for the new statistics). If the hypothesis were true we would expect to see more extreme years. In fact, we saw fewer extreme years for all of these alternatives.

First, we repeated the above calculations after omitting species for which the mean CV (see Fig. 2) exceeded 0.4. The idea here is that, for species with high CVs, there is little information in the year-to-year changes in their biomass

indices. Thus these indices may mask the synchronous fluctuations in the other species, so that omitting them would produce more extreme years. In some cases it did make the most extreme rank deviations more extreme. However, it also had the effect of increasing the threshold (because the number of species decreased). The net effect was to produce slightly fewer extreme years. There was one additional extreme year—1993 for series 7. However, the following years were no longer deemed extreme: 1980 for series 1; 1994 and 1996 for series 5; and 1988 for series 15.

Our second alternative was based on the idea that environmental changes may affect different species differently. That is, an environmental extreme produces extreme catchability, but this may be high for some species and low for others. To test this we calculated rank deviations for each species and then averaged the rank deviations (rather than averaging the ranks and then calculating deviations). This method identified only four extreme years—three were as in Figure 5 (1984 and 1989 for series 9 and 1995 for series 10) and one was new (1979 for series 1).

The third alternative was a variant on the second. We assumed that the species for each series fall into two groups: one group whose catchabilities are all affected in the same way by environmental changes, and a second group for which the effect is opposite. That is, when catchability is high for the first group it will be low for the second, and vice versa. We calculated the mean ranks as above and then determined, for each species, the Euclidean distance between these mean ranks and 1) the species ranks, and 2) the "inverse" of the species ranks (if a species ranks are, say, 1, 4, 2, 3, then the inverse ranks are 4, 1, 3, 2). When the latter distance was smaller, the species was said to fall into the second group. The ranks for all group-two species were replaced by their inverse ranks and the mean ranks (and thus rank deviations) were recalculated. With this method only two extreme years were found, both of which are extreme in Figure 5 (1984 and 1989 for series 9). Often there was no clear separation between groups one and two. Sometimes (but only when there were few species) group two was empty. We also tried a cluster analysis approach to the identification of groups one and two but this produced no better results.

The effect of intensive line fishing on the virgin biomass of a tropical deepwater snapper, the crimson jobfish (*Pristipomoides filamentosus*)

Edwin M. Grandcourt

Marine Environmental Research Centre
Environmental Research and Wildlife Development Agency
Corniche Road
P.O. Box 45553
Abu Dhabi, United Arab Emirates
E-mail address: egrandcourt@erwda.gov.ae

Abstract—An intensive commercial hook-and-line fishing operation targeted the demersal fisheries resources at Saya de Malha Bank in the Southwest Indian Ocean. Fishing was conducted with 12 dories that were equipped with echo sounders and electric fishing reels and supported by a refrigerated mothership. Over a 13-day period in the 55–130 m depth range, a total of 74.3 metric tons (t) of fish were caught, of which the crimson jobfish (*Pristipomoides filamentosus*) represented 80%. Catch rates decreased with time and could not be attributed to changes in location, climatic conditions, fishing depth, fishing method, or bait type. The initial virgin biomass of *P. filamentosus* available to a line fishery at the North Western promontory of Saya de Malha Bank was estimated at 72.6 t through application of the Leslie model to daily catch and effort data. Biomass densities of 2364 kg/km^2 and 1206 kg/km were obtained by applying the initial biomass estimates to the surface area and to the length of the dropoff that was fished. The potential sustainable yield prior to exploitation was estimated at 567 kg/km^2 per year. The quantity of *P. filomentosus* caught by the mothership-dory fishing operation represented 82% of the initial biomass available to a hook-and-line fishery, equivalent to more that three times the estimated maximum sustainable yield. The results of the study are important to fisheries managers because they demonstrate that intensive line fishing operations have the potential to rapidly deplete demersal fisheries resources.

Manuscript accepted 23 October 2002.
Manuscript received 9 January 2003 at NMFS Scientific Publications Office.
Fish. Bull. 101:305–311 (2003).

The crimson jobfish, *Pristipomoides filamentosus* (Valenciennes, 1830), occurs throughout the tropical Indo-Pacific from the Red Sea in the west to Hawaii in the east and has a latitudinal distribution in the western Pacific ranging from southern Japan to New Caledonia (Randall et al., 1997). It is discontinuously distributed in the western Indian Ocean and has been recorded from Madagascar, Réunion, the east coast of Africa, the west coast of India, and the Chagos archipelago (Allen, 1985), and tends to aggregate in shoals in upcurrent localities and near underwater promontories and headlands (Ralston et al., 1986). The habitat occupied is characterized by deep waters from 90 to 360 m over rocky bottoms, along the edge of the continental shelf, and around isolated oceanic islands and banks (Randall et al., 1997).

Juveniles inhabit flat, featureless shallow banks and sediment bottoms close to sources of drainage, moving into deeper waters as they mature (Haight et al., 1993a; Parrish et al., 1997). Nevertheless, for adult fish there has been no correlation found between size and depth (Ralston and Williams, 1988).

Studies from Hawaii showed that *P. filamentosus* is primarily a zooplanktivore, although fish, crustaceans, and mollusks also feature in the diet (Ralston et al., 1986; Haight et al., 1993b). Reproductive studies of *P. filamentosus* in the Seychelles suggest that spawning is protracted and peaks between February and April, and in November (Mees, 1993). The size at which 50% of females reach sexual maturity (Lm_{50}) on banks in the South West Indian Ocean is approximately 52 cm fork length (Mees, 1993).

Pristipomoides filamentosus is a commercially important tropical snapper that is caught with handlines, electric fishing reels, and deepwater gill nets (Hardman-Mountford et al., 1996). Because lutjanid species are favored for consumption or sale, they are commonly targeted by fishermen (Munro, 1983; Koslow et al., 1988) and their aggressive nature and relatively large size makes them more vulnerable to fishing gears (Munro and Williams, 1985). Furthermore, low rates of growth, recruitment, and natural mortality, combined with a prolongation in the attainment of sexual maturity, make lutjanids particularly vulnerable to overfishing (Russ, 1991). Owing to the steeply shelving substratum over which *P. filamentosus* is found, the stock density for this fish has been estimated to be 10 times greater than that of other lutjanids in adjacent shelf areas (Mees, 1993). The concentration of the stock in a narrow depth band makes targeting easy and consequently the potential for overfishing is great (Mees, 1993).

Intensive fishing, over a period that is sufficiently short to permit the assumption that a population is closed, can produce data suitable for estimating the initial population size (e.g. Mees, 1993; Polovina, 1986). Where a population is exploited for the first time, knowing the initial biomass is often useful in determining whether overexploitation has occurred during the development of the fishery (Hilborn and Walters, 1992). The practicality of using daily catch-and-effort data from commercial

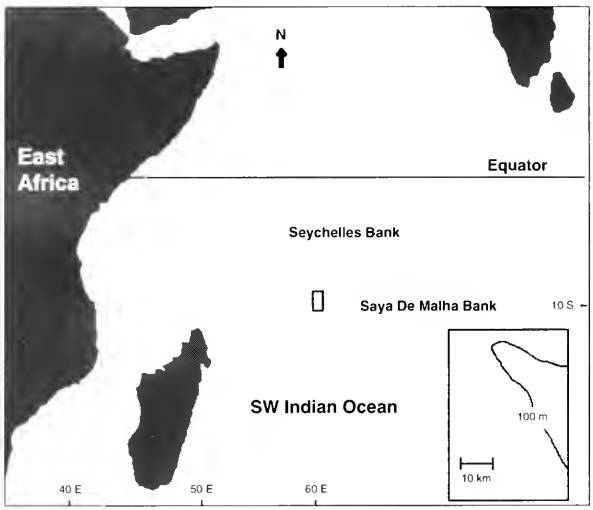

Figure 1

The position of Saya de Malha Bank in the SW Indian Ocean and the location of the hook-and-line fishing ground for demersal fishes (see small rectangular box in map and enlarged inset).

fishing operations may be limited because of confounding effects from changes in target species, fishing depth, and other factors that would normally be controlled within the experimental design of a research cruise. Despite these constraints, valuable management information may be obtained from commercial fisheries data at a much lower cost in cases where these factors have remained constant or have not influenced catch rates of the target species (e.g. Mees, 1996a).

An intensive line fishing operation, consisting of a refrigerated cargo mothership and 12 catcher boats (dories), targeted *P. filamentosus* on the dropoff at Saya de Malha Bank in the southwest Indian Ocean during March 1993. The operation had previously fished at locations in the Seychelles archipelago and had been shown to rapidly deplete reef fisheries resources (Mees[1]).

The mode of operation was characteristic of a "hit and run" fishery, where fishing would be conducted at a location until catch rates dropped to a level where it was not longer viable to continue. Daily catch and effort data are used in the present study to determine the effect of intensive line fishing on the initial virgin biomass of *P. filamentosus* at Saya de Malha Bank in the southwest Indian Ocean.

[1] Mees, C. C. 1992. *Pecheur Breton*: an analysis of data relating to a mothership dory fishing operation in Seychelles waters from March 1991 -June 1992. Seychelles Fishing Authority Technical Report (SFA/R&D/023), 38 p. Seychelles Fishing Authority, Government of Seychelles, P.O. Box 449, Victoria, Mahe, Seychelles.

Materials and methods

Study area

Saya de Malha Bank is located on the Mascarene Plateau in the southwest Indian Ocean (Fig. 1). The bank consists of three plateau areas, the periphery of which ranges in depth from 15 to 200 m. The specific study area was 60.2 km of the dropoff in the 55–130 m depth range between latitude 9°53′S, longitude 59°45′E and latitude 94°3′S, longitude 59°50′E. The area corresponds to the grounds fished by the mothership-dory fishing operation over a 13-day period.

The region has a tropical humid climate modified by the NW monsoon from December to March and the SE trade winds from May until October. Intermonsoon periods of light, variable winds and frequent calms occur during April and November when equatorial troughs affect the region (Walsh, 1984).

Data collection

During March 1993, 12 fiber glass dories equipped with echo sounders and electric fishing reels were deployed at Saya de Malha Bank from an 88-m refrigerated cargo ship. Fishing was conducted during the day and catches were landed to the mothership each evening. A daily log of the activities of individual catcher boats per fishing trip was maintained, which included the total weight by species, fishing trip duration, fishing method, bait type, depth range fished, number of men, and the number of lines used. In

addition, the weather condition and current strength were recorded on a subjective scale from 1 (good) to 5 (poor).

Data analysis

Daily catch and effort data were analyzed by fishing trip duration, depth, gear type, bait type, and climatic conditions to determine the effect on catch rates. The catchability coefficient (q) of the Leslie constant catchability model (Leslie and Davis, 1939) and intercept parameter (a) were determined by using least squares linear regression, where "q" is the value of the regression coefficient. The adjusted cumulative catch (x)—the cumulative catch to interval i plus one half of the catch during interval i—was used as the independent variable; this adjustment proposed by Chapman (1961) compensates for the decline in catchability during each time interval (King, 1995). The daily catch per unit of effort was used as the dependent variable. Data from the first day of fishing were excluded from the analyses because *P. filamentosus* was not being fully targeted. The Leslie constant catchability model was used to derive an estimate of the initial population biomass of *P. filamentosus* accessible to a line fishery within the study area. Polovina (1986) described the Leslie model as the catch per unit of effort during a time interval (t), and because ($CPUE_{(t)}$) is defined as the product of catchability (q) and the mean population biomass present during the period t ($B_{(t)}$), the model can be expressed as

$$CPUE_{(t)} = qB_{(t)}. \quad (1)$$

Suppose that up to the beginning of period t, $K_{(t)}$ fish have been caught and removed. If the period t is relatively short, the population of fish closed or isolated, and the fishing pressure heavy enough so that it can be assumed that mortality from other factors is negligible, then $B_{(t)}$ can be expressed as

$$B_{(t)} = B_{(0)} - K_{(t)}.$$

Where $B_{(0)}$ is the initial population biomass at the beginning of the experiment (t=0), inserting this expression for $B_{(t)}$ in Equation 1 produces the Leslie constant catchability model:

$$CPUE_{(t)} = qB_{(0)} - qK_{(t)}.$$

For the initial population biomass estimate, bootstrapping was used to determine 95% confidence intervals. 100 runs were made. Daily estimates of the remaining biomass size were calculated by subtracting the cumulative catch from the initial biomass estimate i.e: $B_{(t)} = B_{(0)} - K_{(t)}$, where $B_{(t)}$ is the biomass present at the beginning of time (t); $B_{(0)}$ is the initial virgin biomass prior to fishing at t = 0; and $K_{(t)}$ is the cumulative catch to the beginning of time period (t).

The length of the 100-m contour, mean width of the 55–130 m depth band, and surface area of the fishing ground were determined from chart data. Stock density was calculated by applying the initial biomass estimate to the length and surface area of the grounds fished. The annual maximum sustainable yield (MSY) was determined by using the results of Mees (1993), where the MSY was estimated as 24% of the initial virgin biomass of *P. filamentosus* on the edge of the Seychelles Bank, situated 400 km north west of the study site. Potential yield estimates were calculated per km and km^2 on a yearly and daily basis by applying the maximum sustainable yield as a proportion to the respective biomass densities.

Table 1

Species composition of the catch from the dropoff at Saya de Malha Bank.

Species	Weight (kg)	Proportion of total (%)
Aprion virescens	784	1.1
Carangoides gymnostethus	171	0.2
Carangoides sp.	147	0.2
Coryphaena hippurus	44	0.1
Epinephelus chlorostigmo	1846	2.5
Epinephelus morrhua	1847	2.5
Epinephelus multinotatus	5337	7.2
Epinephelus sp.	432	0.6
Gymnosarda unicolor	128	0.2
Lethrinus olivaceus	6	0.0
Lutjanus sp.	118	0.2
Lethrinus sp.	116	0.2
Pristipomoides filamentosus	59,522	80.1
Seriola rivoliana	3646	4.9
Thunnus albacares	57	0.1
Variola louti	83	0.1

Results

A total of 173 dory fishing trips with a mean trip length of 7.7 hours were made over a period of 13 days. There were two fishermen in each of the 12 dories; all used electric fishing reels, the hooks of which were baited with skipjack tuna (*Katsuwonus pelamis*). The mean catch rate for all species was 28.5 kg/man hour, equivalent to 429.4 kg per dory trip. The crimson jobfish represented 80.1% of the total catch of 74.3 t. The Serranidae were the second most abundant family, and of this family *Epinephelus multinotatus* formed 7.2%, *Epinephelus chlorostigma* 2.5%, and *Epinephelus morrhua* 2.5% of the total catch from the dropoff at Saya de Malha Bank (Table 1). The mean depth fished was 88.8 m and ranged from 55 m to 130 m. The length of the 100-m contour was 60.2 km, mean width of the 55–130 m depth band was 510 m, and the surface area of the grounds fished was 30.7 km^2.

There was an overall reduction of the catch rate over the 13-day period (Fig. 2 and Table 2). This could not be

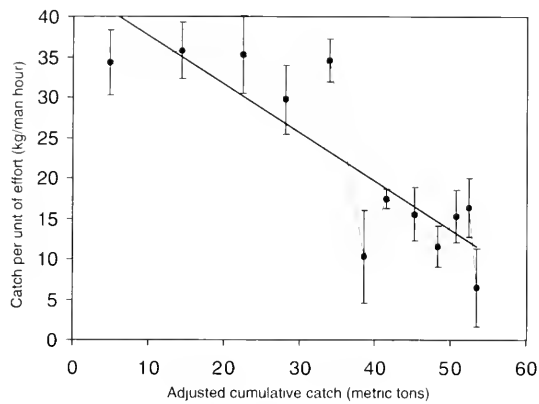

Figure 2

The relationship between mean daily catch per unit of effort (±SE) and the adjusted cumulative catch for *Pristipomoides filamentosus* on the dropoff at Saya de Malha Bank. Straight line shows the Leslie plot; $CPUE_{(t)} = q(B_{(0)} - K_{(t)})$, fitted by least squares linear regression (r^2=0.729).

Table 2

Daily effort, catch, catch per unit of effort, cumulative catch, and adjusted cumulative catch for the deepwater snapper *Pristipomoides filamentosus* at Saya de Malha Bank.

Day	Effort (man/hours)	Catch (kg)	Catch per unit of effort (kg/man hour)	Cumulative catch (kg)	Adjusted cumulative catch (kg)
1	264.6	5623	21.3	0	2812
2	286.4	9817	34.3	5623	10,532
3	253.4	9077	35.8	15,440	19,979
4	202.8	7158	35.3	24,517	28,096
5	143	4252	29.7	31,675	33,801
6	207.2	7163	34.6	35,927	39,509
7	199.4	2061	10.3	43,090	44,121
8	223.4	3899	17.5	45,151	47,101
9	233.6	3634	15.6	49,050	50,867
10	221	2554	11.6	52,684	53,961
11	151.6	2318	15.3	55,238	56,397
12	57.4	939	16.4	57,556	58,026
13	158.2	1027	6.5	58,495	59,009

attributed to changes in fishing method, bait type, or current strength, all of which remained constant. In addition, weather condition, depth fished, and trip duration did not have a significant effect on the catch rate (P>0.05).

The reduction in the daily catch per unit of effort with increasing cumulative catch was significant (P<0.05, 12 df, F=9.729). The results of the regression analysis, with the adjusted cumulative catch as the independent variable and the daily catch per unit of effort as the dependent variable was

$$y = 43.633 + 0.0006x \qquad (r^2=0.729).$$

Application of the Leslie model with the catchability coefficient (q) = 0.0006 (±0.0001 SE) and intercept parameter (a)

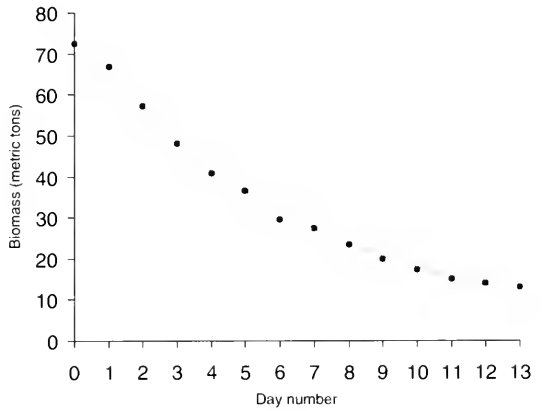

Figure 3

Reduction in the biomass of *Pristipomoides filamentosus* over the fishing period at Saya de Malha Bank. Line shows the exponential model; $y = 72.972\,e^{-1397x}$ fitted to the data (r^2=0.994).

of 43.633 (±4.538 SE) kg/man hour gave an initial biomass estimate of 72,582 kg for *P. filamentosus* accessible to a line fishery at the study site. Bootstrapped upper and lower 95% confidence limits for the initial biomass estimate were 62,750 and 91,376 kg, respectively. Analysis of the daily estimates showed that there was an exponential decrease in remaining biomass over the fishing period (Fig. 3). The biomass densities, potential yield estimates, and respective 95% confidence intervals are given in Table 3.

Mees (1993) derived a maximum sustainable yield estimate of 24% for the virgin biomass of *P. filamentosus* on the edge of the Seychelles Bank using the method of Beddington and Cooke (1983).

Applying this proportion to the initial biomass for *P. filamentosus* on the north western promontory of Saya de Malha Bank gives an annual maximum sustainable yield estimate of 17.4 t. The quantity of *P. filamentosus* caught by the mothership-dory fishing operation represented 82% of the initial virgin biomass available to a hook-and-line fishery. The amount removed was equivalent to more than three times the estimated annual maximum sustainable yield.

Table 3

Initial biomass density and the potential yield prior to exploitation for *Pristipomoides filamentosus* at Saya de Malha Bank.

	Estimate	95% CI
Biomass density (kg/km^2)	2364	2044–2976
Biomass density (kg/km)	1206	1042–1518
Potential yield (kg/km^2 per day)	1.6	1.3–2.0
Potential yield (kg/km^2 per year)	567	490–714
Potential yield (kg/km per day)	0.8	0.7–1.0
Potential yield (kg/km per year)	289	250–364

Discussion

The fisheries resources of Saya de Malha Bank have been exploited by Mauritian mothership-dory fishing operations since the late 1960s.

However, the fisheries operate only to a maximum depth of 50 m, and a single species (*Lethrinus mahsena*) constitutes 80–90% of the catch (Mees[2]). The exploitation of *P. filamentosus* had not occurred prior to the present study because of the belief that the fish were ciguatoxic (Samboo and Mauree, 1987), and consequently the population remained in a virgin state.

The Leslie constant catchability model assumes that the population is completely closed, i.e. there is no recruitment, growth, natural mortality, immigration or emigration during the time frame of the data to which it is applied. Natural mortality, recruitment, and growth can be assumed to

[2] Mees, C. C. 1996. Management of multi-species tropical fisheries, 193 p. Marine Resources Assessment Group Ltd., 47 Princes Gate, London SW7 2QA, UK.

be negligible over the fishing period. However, the initial population biomass, stock density, and potential yield could have been overestimated if there was immigration into the study area from adjacent habitats. Although the study site is characteristic of the habitat in which *P. filamentosus* aggregates (Ralston et al., 1986), the data relate to the peak spawning period of this species on the nearby Seychelles Bank. If there was an inward flux of fish to a spawning site during the time that fishing was conducted, the biomass would have been overestimated. Conversely, it would have been underestimated if there was emigration out of the area. Because of the short time frame over which fishing took place, it is assumed in the present study that the population was closed and any such flux was insubstantial.

Inconstant catchability is perhaps the greatest potential source of error in applying methods of estimation based on secular change in catch per unit of effort (Ricker, 1975). The Leslie model assumes that catchability (q) is constant over the fishing period. However, it is often found that the first few units of effort cause a rapid depletion of more vulnerable, faster, and more aggressive fish, and an accompanying rapid change in catch per unit of effort or other abundance indices. After this initial removal, the remaining fish have effectively lower q values, so that q declines progressively as depletion proceeds. There may even be a large pool of fish with $q = 0$ for some reason, and this pool will not be sampled by the depletion process. Thus, the general effect of varying catchability among individuals is that the estimate of q is biased upwards (and consequently the initial biomass estimate is biased downwards), so that underestimates of biomass in the order of 30% to 50% are not unlikely (Hilborn and Walters, 1992). The use of an adjusted cumulative catch is intended to compensate for the decline in catchability during each time interval (Chapman, 1961). Nonetheless, as suggested by Cowx (1983), estimates should be treated with care.

In commercial fishing operations, fishermen may maintain their catch rates as abundance drops by targeting the remaining high concentrations of fish. As a result, catchability can be underestimated and the initial stock size overestimated. The data used in the present study showed a relatively constant catch rate for the first six days of fishing, followed by a dramatic reduction for the remaining seven days. This pattern may be result of an overall shift in location of the fishing units. However, because the individual dories were not equipped with position-fixing equipment, there were no data collected on the precise location of individual catches. Furthermore, the phenomena could equally have been caused by a change in the behavioral characteristics of the fish. A sudden drop in water temperature, caused by localized upwelling or an increase in planktonic prey abundance (or by both), could have contributed to the decline in catch per unit of effort. The patterns observed in the data suggest that they do not conform well to the assumptions of a depletion model and therefore limit the integrity of the biomass estimates. Position-fixing capability on each of the dories and an independent means of determining behavioral characteristics, such as an underwater video system, would have helped to elucidate the cause of the irregular decline in catch per unit of effort.

A problem with the use of depletion estimators in the case of multispecies applications is that the catchability of each of the component species may not remain constant in relation to each other over the period that fishing is conducted. Interactions between species, such as the competition for baits, can alter catchability, e.g. Rothschild (1967). An increase in the catchability of a subordinate species may occur as a result of the removal of a more competitive species, as shown to be the case with the deepwater snappers *Pristipomoides auricilla* and *Pristipomoides zonatus* (Polovina, 1986). *Pristipomoides filamentosus* comprised 80.1% of the total catch from the fishing grounds on Saya de Malha Bank. Of the remaining species in the catch, there was none that was considered abundant enough to bias the catchability estimate through species interactions, such as competition for bait.

Polovina (1986) showed that after over half of the initial biomass of the deepwater snapper *Pristipomoides zonatus* had been removed, there was very little change in size composition with cumulative catch. Despite this finding, size-specific behavior has been considered to affect catchability and could be a potential source of error in the estimate of "q" determined in the present study. Given the need for studies of the effects of fishing on commercially important tropical species (Russ, 1991) and recent developments in aging *Pristipomoides filamentosus* (Hardman-Mountford et al., 1996), future studies should examine the implications of intensive line fishing on the age structure of snapper populations.

The major reproductive peak for *P. filamentosus* on the edge of the Seychelles Bank, 400 km to the northwest of Saya de Malha Bank, was found to occur between February and April (Mees, 1993). If the reproductive peak for the stock at Saya de Malha Bank occurred at the same time, then the catcher boats may have been targeting spawning aggregations. If this was the case, the population biomass and subsequently stock density at the study site would be lower during periods of the year when there is a reduction in spawning activity. Furthermore, *P. filamentosus* tends to aggregate in shoals in upcurrent localities and near underwater headlands and promontories (Ralston et al., 1986). In addition to being the possible behavior of spawning aggregations, this behavioral characteristic explains why *P. filamentosus* comprised 80.1% of the total catch of what is basically a multispecies fishery.

Errors may have occurred in the calculation of the width of the 55–130 m depth band. If the gradient of the seabed in this depth range was steeper than that estimated, the biomass density would be greater and *vice versa*. A bathymetric survey would have improved the precision of the surface area calculations and biomass density estimates.

Nevertheless, the biomass density obtained in the present study (2364 kg/km^2) is of the right order compared to that of Mees (1993), where the mean initial biomass density of *P. filamentosus* on three banks in the Seychelles was 2987 kg/km^2 for populations that had not previously been exploited. Likewise, the estimated potential yield of 567 kg/km^2 per year derived in the present study compared well to the maximum sustainable yield of 717 kg/km^2 per

year (Mees, 1993) for *P. filamentosus* in the Seychelles. The proportion (82%) of the initial biomass of *P. filamentosus* removed is not dissimilar to that estimated by Polovina (1986) for *P. zonatus* (68%) in the Mariana Archipelago over the same number of fishing days.

The results of this study are relevant to fisheries managers because they demonstrate that although intensive line fishing operations are efficient at harvesting offshore demersal fisheries resources, they have the potential to heavily overexploit populations in a short time frame.

Acknowledgments

I thank Kerlson Gonzales for enduring the difficult living conditions aboard the mothership during the trip to Saya de Malha Bank and for the high quality of data collected, Cecile Botsoie for entering the log book information into the database, Chris Mees for instruction in the use of the programme PBRETON used in the analysis of the daily catch records, and Francis Marsac for providing constructive comments and discussion.

Literature cited

Allen, G. R.
1985. FAO species catalogue. Vol. 6: Snappers of the world: an annotated and illustrated catalogue of Lutjanid species known to date. FAO Fish Synopses 125, 208 p. FAO, Rome.

Beddington, J. R., and J. G. Cooke.
1983. The potential yield of fish stocks. FAO Fisheries Technical Paper 242, 47 p. FAO, Rome.

Chapman, D. G.
1961. Statistical problems in dynamics of exploited fisheries populations. Proc. Berkeley Symp. Math. Stat. Probab. 4: 153–168.

Cowx, I. G.
1983. Review of the methods for estimating fish population size from survey removal data. Fish. Manag. 14:67–82.

Haight, W. R., D. R. Kobayashi and K. E. Kawamoto.
1993a. Biology and management of deepwater snappers of the Hawaiian archipelago. Mar. Fish. Rev. 55(2):17–24.

Hardman-Mountford, N. J., N. V. C. Polunin and D. B. Boulle.
1996. Can the age of tropical species be determined by otolith measurement? A study using *Pristipomoides filamentosus* (Pisces: Lutjanidae) from the Mahé Plateau, Seychelles. NAGA. The ICLARM Quarterly 20(2):27–31.

Haight, W. R., J. D. Parrish and T. A. Hayes.
1993b. Feeding ecology of deepwater lutjanid snappers at Penguin Bank, Hawaii. Trans. Am. Fish. Soc. 122: 328–347.

Hilborn, R., and C. J. Walters.
1992. Quantitative fisheries stock assessment. Choice, dynamics and uncertainty, 570 p. Chapman and Hall, New York, NY.

King, M.
1995. Fisheries biology, assessment and management, 341 p. Fishing News Books, Blackwell Science, Oxford.

Koslow, J. A., F. Hanley, and R. Wicklund.
1988. Effects of fishing on reef fish communities at Pedro Bank and Port Royal Cays, Jamaica. Mar. Ecol. Prog. Ser. 43:201–212.

Leslie, P. H., and D. H. S. Davis.
1939. An attempt to determine the absolute number of rats on a given area. J. Anim. Ecol. 8:94–113.

Mees, C. C.
1993. Population biology and stock assessment of *Pristipomoides filamentosus* on the Mahé Plateau, Seychelles. J. Fish Biol. 43:695–708.
1996. Demersal fish stock assessment in Seychelles: An analysis of a mothership/catcher boat fishery. *In* Biology, fisheries and culture of tropical groupers and snappers (F. Arreguin-Sánchez, J. L. Munro, M. C. Balgos, and D. Pauly, eds.), 449 p. ICLARM Conf. Proc. 48.

Munro, J. L.
1983. Epilogue: progress in coral reef fisheries research, 1973–1982. *In* Caribbean reef fishery resources, vol 7, p. 249–265. International Centre for Living Aquatic Resources Management, Manila, Philippines.

Munro, J. L., and D. M. Williams.
1985. Assessment and management of coral reef fisheries: biological, environmental and socio-economic aspects. Proc. Int. Coral Reef Cong., 5th, 4:545–581.

Parrish, F. A., E. E. DeMartini, and D. M. Ellis.
1997. Nursery habitat in relation to production of juvenile pink snapper, *Pristipomoides filamentosus*, in the Hawaiian archipelago. Fish. Bull. 95:137–148.

Polovina, J. R.
1986. A variable catchability version of the Leslie model with application to an intensive fishing experiment on a multispecies stock. Fish. Bull. 84(2):423–428.

Randall, J. E. G. R. Allen, and R. C. Steene.
1997. Fishes of the Great Barrier Reef and Coral Sea, 557 p. Univ. Hawaii Press, Honolulu, HI.

Ralston, S., R. M. Gooding, and G. M. Ludwig.
1986. An ecological survey and comparison of bottom fish resources assessments (submersible versus handline fishing) at Johnston atoll. Fish. Bull. 84:141–155.

Ralston, S., and H. A. Williams.
1988. Depth distributions, growth and mortality of deep slope fishes from the Marianas archipelago. U.S. Dep. Commer., NOAA Tech. Memo. SWFC113, 47 p.

Ricker, W. E.
1975. Computation and interpretation of biological statistics for fish populations. Fish. Res. Board Can. Bull. 191, 382 p.

Rothschild, B. J.
1967. Competition for gear in a multiple-species fishery. J. Cons. 31:102–110.

Russ, G. R.
1991. Coral reef fisheries: effects and yields. *In* The ecology of fishes on coral reefs (P. F. Sale, ed.), p. 601–635. Academic Press, London.

Samboo, C. R., and D. Mauree.
1987. Summary of fisheries and resources information for Mauritius. *In* Proceedings of the workshop on the assessment of the fishery resources in the Southwest Indian Ocean (M. J. Sanders, P. Sparre and S. C. Venema, eds.), p. 62–79. FAO/UNDP: RAF/79/065/WP/41/88/E. Food and Agricultural Organization of the United Nations, Viale delle Terme di Caracalla 00100, Rome.

Walsh, R. P. D.
1984. Climate of the Seychelles. *In* Biogeography and ecology of the Seychelles Islands (D. R. Stoddard, ed.), p. 39–62. DR W. Junk Publishers, The Hague.

Demographic assessment of the blue crab (*Callinectes sapidus*) in Chesapeake Bay using extractable lipofuscins as age markers*

Se-Jong Ju
David H. Secor
H. Rodger Harvey

Chesapeake Biological Laboratory
University of Maryland Center for Environmental Science
Box 38
Solomons, Maryland 20688
E-mail address (for H. Rodger Harvey, contact author): harvey@cbl.umces.edu

Abstract—The blue crab (*Callinectes sapidus*) plays an important economic and ecological role in estuaries and coastal habitats from the Gulf of Mexico to the east coast of North America, but demographic assessments are limited by length-based methods. We applied an alternative aging method using biochemical measures of metabolic byproducts (lipofuscins) sequestered in the neural tissue of eyestalks to examine population age structure. From Chesapeake Bay, subsamples of animals collected from the 1998–99 (n=769) and 1999–2000 (n=367) winter dredge surveys were collected and lipofuscin was measured. Modal analysis of the lipofuscin index provided separation into three modes, whereas carapace-width data collected among the same individuals showed two broad modes. Lipofuscin modal analysis indicated that most adults (carapace width >120 mm) were <2 years old. The results indicate that use of extractable lipofuscin can provide a more accurate and better resolved estimation of demographic structure of blue crab populations in the field than size alone.

Manuscript accepted 21 October 2002.
Manuscript received 31 December 2002 at NMFS Scientific Publications Office.
Fish. Bull. 101:312–320 (2003).

In fisheries management, age-structured models are the most common method for estimating optimal yields and determining the effect of fishing on population dynamics (Gulland, 1983). For some species of commercial marine fish, age can be determined by using otoliths or other hard parts (Secor et al., 1995). This is not possible for crustaceans, including the blue crab (*Callinectus sapidus*), which periodically molts its calcareous exoskeleton to accommodate future growth and thereby abandons any external evidence of age or previous size. As a consequence, modal analysis of length-frequency data has often been used as an alternative to direct aging methods (e.g. Rothschild et al., 1992). Unfortunately, this approach has proven difficult to validate because 1) growth is characterized by strong interannual and seasonal variability and 2) the spawning season is protracted, which leads to a wide, and sometimes multimodal distribution of sizes per year class (Prager et al., 1990; Ju et al., 2001). The critical need for understanding the demographic structure of crab populations led us to investigate an alternative method for age determination. Age pigments known as lipofuscins accumulate as stable mixtures in postmitotic tissue as a consequence of peroxidation reactions during normal metabolism (see review by Gutteridge, 1987). These biochemical measures have been applied to determine age in crustaceans (Ettershank and George, 1984; Belchier et al., 1994; Sheehy et al., 1995; Sheehy et al., 1996; Wahle et al., 1996). Recently, a modified approach that relies on the concentration of these products normalized to tissue protein has been developed and validated for the blue crab (Ju et al., 1999).

We hypothesize that lipofuscin can provide a more robust measure of age than current size-based measures. For example, variance in size among individuals within the same year class, and declining growth rate with increasing age, can result in significant overlap of sizes among adjacent age classes and can reduce the accuracy of age determinations with length-frequency analysis. Additionally, the blue crab's natural longevity is an important factor and one still disputed by scientists because of the lack of reliable long-term tag returns and absence of age information. If blue crabs reach maturity quickly and live to age three to four as has been suggested (Ju et al., 1999; Van Engel et al., 1958, 1999; Helser and Kahn, 1999), then higher fishing rates may be sustained than those for crabs that mature more slowly and live to age six or older (Rugolo et al., 1998; Miller, 2001). In the present study, we conducted a large-scale application of the lipofuscin aging method using subsamples from fishery-independent winter dredge surveys (1998–99 and 1999–2000). The goal of this study was

* Contribution 3626 of the University of Maryland Center for Environmental Science, Solomons, MD 20688.

to assess the age structure of the blue crab population in the Chesapeake Bay through measurement of lipofuscin and to compare the demographics with those determined by the more traditional size-based approach.

Materials and methods

Sample collections

Winter bottom-dredge surveys (WDS) are conducted annually in the Chesapeake Bay system to monitor blue crab recruitment and size. Surveys were conducted according to a stratified random design, and sampling intensity was apportioned according to depth and site area (for details, see Volstad et al., 2000). Although collections target all sizes of crabs, juvenile crabs (<15 mm carapace width [CW]) are not fully susceptible to the dredge gear and are underestimated in abundance (Rothschild et al., 1992). Further, lipofuscin (LF) index in small crabs (<40 mm CW) cannot be determined because of analytical limitations (Ju et al., 1999). Only juvenile crabs >40 mm CW were selected for our study. The elimination of crabs smaller than 40 mm CW in our lipofuscin sample should result in under-representation by juvenile crabs spawned late during the previous spawning season (i.e. August–September) and by other slow growing juveniles. Subsamples were collected from three different regions of Chesapeake Bay: the eastern shore (Fishing Bay and Honga River), western shore (Potomac River), and lower bay (James River) from December through February in 1998–99 and 1999–2000. A portion of juveniles <70 mm CW (n=58) from the 1998–99 survey was excluded for use in a growth and calibration study as recently reported in Ju et al. (2001).

Analysis of lipofuscin index

Crabs were anesthetized on ice prior to being sacrificed. Carapace width (mm) was measured and eyestalk tissues were carefully dissected. Each collected tissue was transferred to a 4-mL amber vial for extraction of lipofuscins with a solvent. Measurement of fluorescence intensity was modified slightly from Ju et al. (1999) to improve sensitivity and accommodate larger sample numbers by switching from individual sample detection to a scanning fluorescence spectrophotometer (Waters 474) equipped with a flow cell. Volumes of 10 μL from each extract were injected by an auto-sampler with methanol (MeOH) as the carrier solvent (1 mL/min). Fluorescence intensity was measured at a maximum emission wavelength of 405 nm by using a maximum excitation at 340 nm at constant temperature (10°C).

To provide a quantitative measure of lipofuscin, fluorescence intensities of extracted lipofuscin were calibrated by using quinine sulfate (in 0.1N H_2SO_4) and normalized to protein content of extracted tissue measured by the modified bicinchoninic acid assay (Nguyen and Harvey, 1994). Although fluorescence intensity can be accurately calibrated against external standards, the lipofuscin amount per unit tissue volume (wet or dry weight) has often been measured either before or after extraction (e.g. Ettershank and George, 1984). Such measures are inherently variable and subject to differences among tissue types and processing methods. The use of cellular protein as a basis for measurement of extractable lipofuscin concentrations eliminates many previously encountered difficulties. Protein-normalized lipofuscin content is expressed as the lipofuscin index or normalized-lipofuscin (μg-LF/mg-protein).

Statistical analysis

The lipofuscin index (μg-LF-content/mg-protein) of samples were natural-log-transformed before statistical analyses to satisfy assumptions of homogeneity of variances and normality of residuals. In order to determine whether the lipofuscin index varied between sexes in each sampling year, analysis of covariance (ANCOVA) with CW as a covariate was performed. Regression analysis also was performed to compare the relationship between size (CW) and lipofuscin index for each sex in each sampling year. Statistical analysis was done with SAS (SAS, Inc., 1996).

The frequency distribution of CW and lipofuscin index frequencies were analyzed for modal separation. We specified that modal means should be separated by more than two standard deviations (SD) (Gulland and Rosenberg, 1992). Lipofuscin index frequency distributions, which showed more than two modes, were analyzed by using ENORMSEP (FiSAT; Gayanilo et al., 1996), which is a maximum likelihood method for identifying modes. A chi-squared analysis was used to test the assumption that frequencies were normally distributed for each mode. Class interval was specified at 10 mm and 0.04 ug lipofuscin-content/mg-protein for CW and lipofuscin index, respectively. Although this exceeded the precision of the lipofuscin measurement, it provided class size ranges between 5 and 25 individuals to facilitate the analysis of distribution modes. The age class of each mode was then assigned based on the lipofuscin index accumulation rate determined through rearing experiments (Ju et al., 2001). The formula for this age assignment is

$$Age\,(\mathrm{yr}) = 0.824 \times \exp^{(1.133 \cdot LF\,index)}. \quad (1)$$

Age classes were defined as 0, 1, and 2 and consisted of individuals 0 to <1, 1 to <2, and ≥2 yr old, respectively. The chronological "age" in this study is related to hatching dates of animals, i.e. the release of the first stage zoea. The age class of each mode identified from modal analysis was assigned according to the lipofuscin index accumulation rate (Eq. 1). Size (CW)-based age classification of 0, 1, 2+ age individuals corresponded to crabs of CW < 60, 60 ≤ CW < 120, and CW ≥ 120 mm, respectively, according to a recent Chesapeake Bay blue crab demographic assessments (Rugolo et al., 1998). In our study, age 2+ references all crabs ≥2 years of age. All crabs of CW > 60 mm (n=217 and 208 for 1998–99 and 1999–2000 WDS, respectively) were included to estimate the relative abundance of each age class determined by either lipofuscin or CW. Although some juveniles (<80 mm CW) were not measured, they were assumed to be <1 yr old (age-0 class).

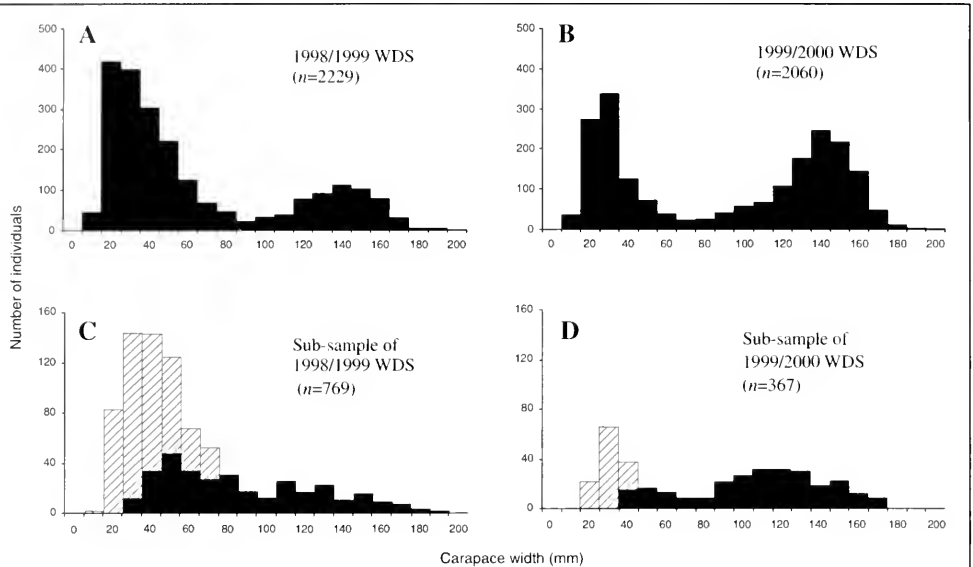

Figure 1

Size-frequency distributions for blue crabs collected in 1998–99 (**A**) and 1999–2000 (**B**) winter dredge surveys and size-frequency distributions (**C** and **D**) of subsamples used in this study. Hatched bars in C and D indicate samples excluded from lipofuscin analysis.

Results

Size frequencies of blue crabs collected in the winter dredge survey differed significantly between the two sampling years (chi-square test; α=0.05; Fig. 1, A and B). Although the total number of crabs collected from 1998–99 and 1999–2000 winter surveys were equivalent, a greater proportion of crabs >80 mm CW occurred in the second year. For both years, frequency distributions of CW data supported the fit of two modes (Fig. 1) and juveniles were clearly distinguishable from adult crabs as individuals <80 mm CW (or 90 mm CW for 1998–99). For 1998–99 WDS, males and females subsets of crabs had mean CW of 56.4 ±2.0 mm (mean ±SD; n=165) and 52.2 ±2.0 mm (n=152), respectively. For 1999–2000 WDS, CW for males and females was 91.5 ±2.7 mm (n=162) and 72.0 ±3.0 mm (n=97), respectively. The number of crabs sampled for lipofuscin analysis was halved (from n=769 to 367) in the second year because of a much more restricted analysis of juveniles <80 mm CW that were assumed to be <1 year of age. In both years, the subsamples examined for lipofuscin were skewed towards crabs >60 mm CW (Fig. 1, C and D), reflecting our analytical criteria and objective to include all adults in the analysis of age structure.

Lipofuscin index varied positively with CW (Table 1, Fig. 2) but there was high variability in lipofuscin index for a given size. All subcategories (sex and year) supported significant regressions of lipofuscin on CW, but coefficients of determination were quite low, ranging as low as 0.04 for females in the first sampling year. ANCOVA analysis showed that lipofuscin adjusted for CW effects was significantly different only between sexes for the first sampling year (Table 2). We had expected that the lipofuscin index in mature females (CW >120 mm) would be higher at a given CW than in males because females discontinue molting following their first mating (Millikin and Williams, 1984). As a result, females living beyond their final molt would be predicted to accumulate lipofuscin independently of size. Results were scattered, however, and there was no statistical evidence for higher lipofuscin index in mature females. The lack of compelling evidence for differences in overall lipofuscin levels among sexes allowed males and females to be combined in the subsequent age structure analysis.

Frequency distributions for the lipofuscin index were fitted by multiple modes in both years (Fig. 3, A and B). Intervals between modal means were greater than two standard deviations for the first three modes in each sample (Table 3) and lipofuscin index-based modal distributions were not significantly different from expected normal distributions (chi-square test; α=0.05). Modes were consistent with the presence of 0, 1, and 2 age classes in each collection. Ages derived from lipofuscin index values (Eq. 1) for the first mode in each year were higher (ages 0.8–1.0 yr) than those expected for juveniles produced during the previous spawn-

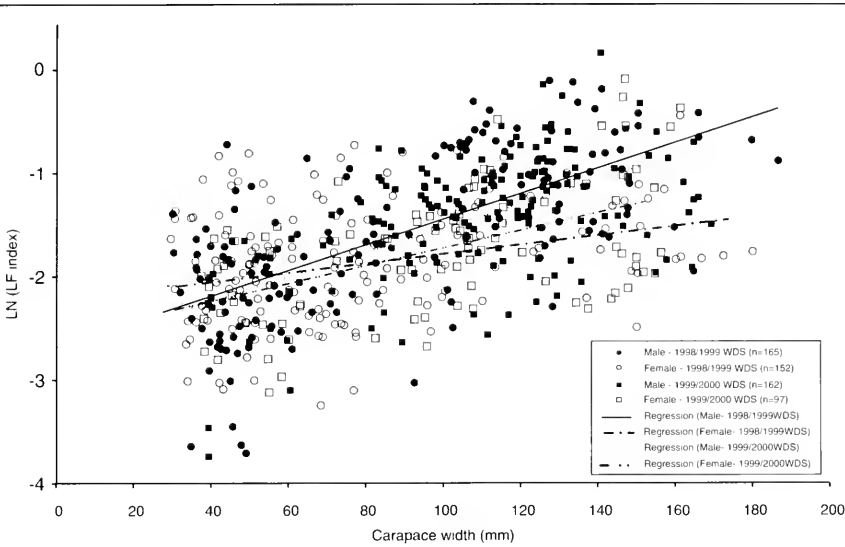

Figure 2

Plot of natural log (lipofuscin index) versus carapace width (mm) of subsampled crabs collected from 1998–99 and 1999–2000 in winter dredge surveys in Chesapeake Bay. Each regression line represents one sex during one year as described in Table 1.

Table 1

Lipofuscin index ($\log_e$-transformed) and size (CW) relationship for each sex in each sampling year as determined in the regression analysis. The slope (±95% CL), intercept (±95% CL), adjusted coefficient of determination (adj. r^2), and probability of type-I error (P) are shown. WDS = winter bottom-dredge survey.

	Slope (±95% CL)	Intercept (±95% CL)	Adj. r^2	P
1998–99 WDS				
Male	0.012 ±0.002	−2.684 ±0.218	0.41	<0.001
Female	0.004 ±0.003	−2.118 ±0.218	0.04	<0.005
1999–2000 WDS				
Male	0.012 ±0.003	−2.709 ± 0.283	0.34	<0.001
Female	0.009 ±0.003	−2.581 ±0.290	0.28	<0.001

ing seasons (ages 0.4–0.6 yr) (Fig. 4). It seems likely that juvenile modes were skewed towards older juvenile ages because small crabs (40 mm CW) were excluded from analysis. In the 1999–2000 WDS sample, modal analysis supported a second subannual mode for age-1 crabs, which infers a bimodal recruitment pattern during the summer and fall of 1998 and may not have occurred in 1997 (i.e. 1998–99 WDS samples). Several lipofuscin values actually exceeded the third dominant mode (the fourth mode for 1999–2000 WDS samples), which suggests that several crabs attained ages ≥3 years. Nevertheless, these individuals could not be statistically distinguished from the last dominant mode.

There was a large discrepancy between the individuals assigned age classes by lipofuscin index and those assigned by CW criteria. Lipofuscin measures suggested that most crabs could attain 120 mm CW in less than two complete years of life (Table 4). Conversely, the index predicted that some individuals could grow quite slowly, remaining <60 mm CW into their second year of life (Fig. 3A). Although the samples analyzed did not include every animal from the WDS, the age structure suggested a pattern of declining

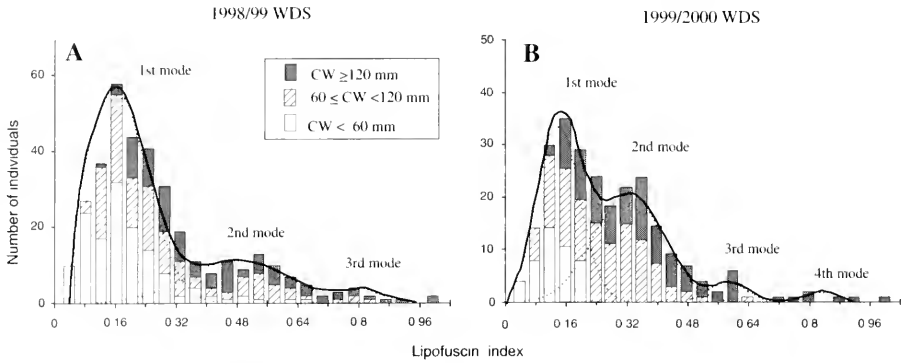

Figure 3

Frequency histograms of lipofuscin index (**A** and **B**) in eyestalks of crabs collected in 1998–99 (n=317) and 1999–2000 (n=259). Solid lines are derived from a predicted frequency distribution and dashed lines show normally distributed components of each mode. Age assignments of each mode in lipofuscin index histograms and size classification are shown in Table 3 and Figure 4.

abundance with the lipofuscin index, consistent with a predominate pattern of mortality among age classes. Based on lipofuscin analysis, the relative abundance between age classes (age 1 and 2+ classes) was not significantly different between two sampling years (t-test; P>0.05).

Discussion

Size-specific patterns of crab abundance in the Chesapeake Bay exhibit significant interannual variation; a significant decline in juveniles was seen during the second year (1999–2000) of the study (Fig. 1, A and B). Such variations have been observed previously in Chesapeake Bay (Abbe, 1983; Hines et al., 1987; Lipcius and Van Engel, 1990), and may result from interannual variation in recruitment of larvae, postlarvae, and juveniles (related to the spawning stock), physicochemical conditions, and food availability (Holland et al., 1987; McConaugha, 1988). Density-dependent processes such as cannibalism and predation may also regulate juvenile abundance and dampen recruitment variation, particularly when stock levels are high (Lipcius et al., 1995; Kahn et al., 1998).

Age estimates based upon lipofuscin index were more highly resolved than those based on CW, and there were at least three age modes (ages 0, 1, and 2) apparent in both sampling years. Perhaps more importantly, individuals were classified differently with lipofuscin than with CW, which indicated that age estimates based upon CW could lead to substantial errors in determination of growth, mortality, and fishery yield estimates. Recent growth-rate measures have indicated that Chesapeake Bay blue crabs may grow substantially faster than previously recognized, but also that some crabs may grow at very slow rates under unfavorable environmental conditions (Ju et al., 2001). In other words, lipofuscin-based age determinations indicate highly variable individual growth rates. We speculate that such variability is the result of the discontinuous nature of crab growth combined with the protracted spawning season and strong seasonal pattern in growth (driven by temperature), which together amplify relatively small differences in hatching dates and early growth rates into large differences in carapace sizes. Spatial heterogeneity in habitat would also be a contributor to high variability in crab growth rates. Alternatively, the degree with which lipofuscin reflects true chronological age may have contributed to the high variation seen in CW-based ages versus

Table 2

The results of analysis of covariance with CW (carapace width) as a covariate to determine effects between sex and the lipofuscin index ($\log_e$-transformed) of crabs collected from winter dredge surveys. NS = not significant at P=0.05. WDS = winter bottom-dredge survey.

Source	df	F	P
1998–99 WDS			
CW	1	85.12	<0.001
sex	1	13.23	<0.001
sex (CW)	1	25.86	<0.001
1999–2000WDS			
CW	1	114.71	<0.001
sex	1	0.39	0.532^{NS}
sex (CW)	1	2.74	0.100^{NS}

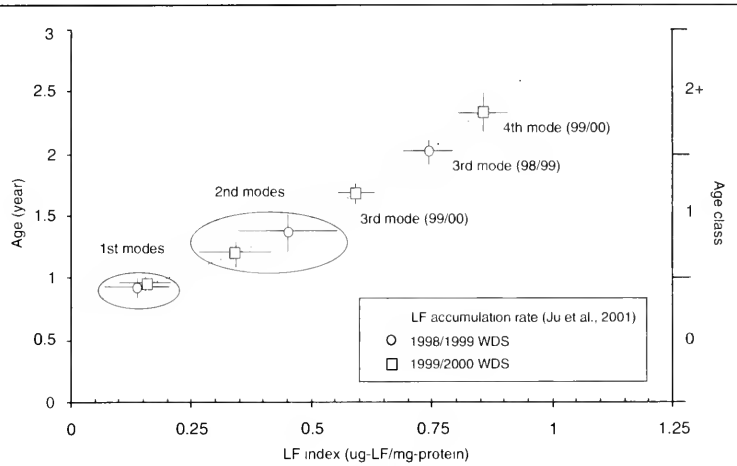

Figure 4

Mean (circle and square) ± standard deviation (error bar) of each mode estimated from modal analyses of the lipofuscin index (see Table 3). Circles and squares represent 1998–99 and 1999–2000 winters, respectively. Age was calibrated by using the empirical lipofuscin index accumulation rate ($Age\ (yr)=0.824 \times \exp^{(1.133 \times LF\ index)}$) from Ju et al. (2001) and shown as a dotted line.

Table 3

Modal frequency analysis of lipofuscin (LF) index for crabs from 1998–99 and 1999–2000 winter bottom-dredge surveys (WDS). χ^2, chi-square test; df, degree of freedom.

	1998–99 WDS		1999–2000 WDS	
Group	Mean LF ±SD	No. of ind./mode	Mean LF ±SD	No. of ind./mode
1st mode	0.146 ±0.076	219	0.150 ±0.053	119
2nd mode	0.440 ±0.120	86	0.330 ±0.088	119
3rd mode	0.734 ±0.060	12	0.590 ±0.046	12
4th mode			0.860 ±0.066	9
Total		317		259
χ^2	21.04		18.83	
df	19		22	

lipofuscin-based ages. In past studies on crustaceans (e.g. O'Donovan and Tully, 1996), lipofuscin has been shown to be significantly influenced by metabolism, leading some authors to conclude that lipofuscin is a closer measure of physiological than chronological age. Recent work on laboratory- and pond-reared crabs, however, has shown that LF accumulation is relatively constant and that average winter and summer rates differ by 27% (Ju et al., 2001). During winter months LF continued to accumulate in the eyestalks of pond-reared crabs, even though growth in CW ceased on account of winter temperatures. Further, the lipofuscin-index versus age relationship in these rearing studies (coefficient of determination: r^2=78%) was substantially less variable than the CW versus age relationship (r^2=59%). Nevertheless, variance in the lipofuscin index versus age relationship is sufficient to cause misclassification of individuals, and it is important to obtain sufficient samples to permit age modes among cohorts to be resolved.

The protracted spawning season for Chesapeake Bay blue crabs (mid-May through mid-September; Van Engel, 1999) has important implications for subsequent size and

Table 4

Lipofuscin (LF)-based age composition and relative abundance (in parentheses) of each age group in subadult (60 ≤ carapace width <120 mm) and adult (≥120 mm) size classes for crabs from 1998–99 and 1999–2000 winter bottom-dredge surveys (WDS). Crabs <60 mm were excluded due to gear selectivity and our exclusion of crabs ≤40 mm (see "Materials and methods" section).

Age group (LF based)	1998–99 WDS Size class		1999–2000 WDS Size class	
	60 ≤ CW < 120 mm	CW ≥ 120 mm	60 ≤ CW < 120 mm	CW ≥ 120 mm
0	80 (0.63)	31 (0.34)	67 (0.57)	30 (0.33)
1	44 (0.35)	50 (0.56)	60 (0.51)	54 (0.59)
2+	3 (0.02)	9 (0.10)	0 (0.00)	7 (0.08)
Total number	127	90	117	91

age structure. Crabs that spawn early may grow rapidly and attain "subadult"size (>60 mm) by the end of the first growth season (Ju et al., 2001). If this is the case, then a significant fraction of subadults (defined as ≥60 mm CW) may have been misclassified on the basis of past CW criteria as being 1-yr-old subadults. We would argue that crabs spawned late in the season (late summer–early fall) may overwinter at small sizes but will emerge the next spring and experience rapid growth in warm temperatures to reach maturity within their first year of life. In support of this view, Ju et al. (2001) have shown in growth studies that pond-reared crabs from late-spawning cohorts overwinter and undergo extremely rapid growth during the following summer months. Most of these crabs attained 127 mm CW (size of entry into the hard crab fishery) before their second winter. Occasionally such a protracted period of spawning may result in multimodal patterns in recruitment. As reported by van Montfrans et al. (1990, 1995), we observed two subannual cohorts of age-1 blue crabs in 1999–2000; therefore it is likely that these crabs were recruited from a bimodal pattern of juvenile production during 1998. These subannual cohorts were statistically separated into modes (Fig. 3) based on known lipofuscin accumulation rate in blue crabs (Fig. 4). Modal analysis of lipofuscin index for 1998–99 did not show evidence of multimodal recruitment (Fig. 3A). The inconsistent appearance of "subannual" cohorts between sampling years may result from the interannual variation of settlement and spawning patterns, which in turn is related to yearly spawning stock conditions and physicochemical conditions in the Chesapeake Bay region (McConaugha et al., 1983; van Montfrans et al., 1990, 1995).

According to lipofuscin modal analysis, crabs <2 yr old are a significant fraction of the harvestable (>127 mm CW) stock in Chesapeake Bay. This finding argues that size (CW) criteria, on which past assumptions of greater ages in the Chesapeake Bay blue crab stocks are based, is insufficient for assessing blue crab demographics. It appears that size may be more reflective of interannual differences in growth rates than age structure alone.

Given that lipofuscin-based age distributions show that >2 year old crabs are a minor contributor to the harvestable stock, we speculate that the population dynamics of crabs available for harvest is strongly influenced by numbers of juveniles produced in each year and that growth conditions experienced by these juvenile cohorts during their first full year is a dominant determinant of the reproductive potential of the blue crab. It also suggests that seasonal yield patterns in commercial fisheries are strongly influenced by seasonal patterns in time of spawning and subsequent juvenile growth. If relatively older (>2 yr) crabs are minor contributors to the adult stock, then the Chesapeake Bay fishery may essentially depend on an annual crop of crabs, produced over a protracted spawning season. The consequence of this pattern is that landings will be more tightly coupled with juvenile production levels (e.g. settlement rates of postlarvae) and environmental conditions (e.g. winter duration) that affect their growth into the adult stock, not unlike the dynamics observed in penaeid shrimp fisheries (e.g. Haas et al., 2001). Other attributes including sex ratio and size- and age-specific reproductive rates are other important considerations in assessing the reproductive condition of the Chesapeake Bay blue crab stock (Jivoff and Hines, 1998; Rugolo et al., 1998).

Uncertainties remain in applying these results to the assessment of the Chesapeake Bay. We note that samples used in our study did not cover the entire Chesapeake system and that the abundance and size distributions of blue crabs are expected to vary locally. Nevertheless, these results strongly suggest that for moderately large sample sizes, crabs can be assigned to annual or subannual cohorts on the basis of lipofuscin measures, thereby significantly improving our knowledge of population dynamics and life history. Natural longevity in Chesapeake Bay blue crabs remains an open question, particularly because crabs (≥3 yr old) are likely to be very rare because of the combined effects of high exploitation and natural mortality (Miller, 2001).

Acknowledgments

The authors thank the Maryland Department of Natural Resources (DNR) and the Virginia Institute of Marine Science winter dredge survey and vessel operations staff for kindly providing subsamples from 1998–99 and 1999–2000

surveys. We also thank T. Gunderson and S. Larsen for technical assistance and B. Yates for manuscript preparation. Reviewers provided many helpful comments on earlier versions of the manuscript. This study was funded by NOAA grant NA76FU0560 through the Chesapeake Bay Program.

Literature cited

Abbe, G. R.
1983. Blue crab (*Callinectes sapidus* Rathbun) populations in mid-Chesapeake Bay in the vicinity of the Calvert Cliffs nuclear power plant, 1968–1981. J. Shellfish Res. 3: 183–193.

Belchier, M., P. M. Shelton, and C. J. Chapman.
1994. The identification and measurement of fluorescent age-pigment abundance in the brain of a crustacean (*Nephrops norvegicus*) by confocal microscopy. Comp. Biochem. Physiol. 108B:157–164.

Ettershank, G., and R. Y. George.
1984. A new approach to the assessment of longevity in the Antarctic krill *Euphausis superba*. J. Crust. Biol. 4: 295–305.

Gayanilo, F. C., Jr., P. Sparre, and P. Pauly.
1996. FAO/ICLARM stock assessment tools (FiSAT). FAO, Rome.

Gulland, J. A.
1983. Fish stock assessments: a manual of basic methods. FAO/Wiley series on food and agriculture, vol. 1, 100 p. Wiley, New York, NY.

Gulland, J. A., and A. A. Rosenberg.
1992. A review of length-based approaches to assessing fish stocks. FAO Fisheries Technical Paper 323, 100 p. FAO, Rome.

Gutteridge, J. M. C.
1987. Oxygen radicals, transition metals and aging. Advances in the biosciences 64:1–22.

Haas, H. L., E. C. Lamon, K. A. Rose, and R. F. Shaw.
2001. Environmental and biological factors associated with the stage-specific abundance of brown shrimp (*Paneus aztecus*) in Louisiana: applying a new combination of statistical techniques to long-term monitoring data. Can. J. Fish. Aquat. Sci. 58:2258–2270.

Helser, T. E., and D. M. Kahn.
1999. Stock assessment of Delaware Bay blue crab (*Callinectes sapidus*) for 1999, 100 p. Delaware Division of fish and wildlife, Dover, DE.

Hines, A. H., R. N. Lipcius, and A. M. Haddon.
1987. Population dynamics and habitat partitioning by size, sex, and molt stage of blue crabs *Callinectes sapidus* in a subestuary of central Chesapeake Bay. Mar. Ecol. Prog. Ser. 36:55–64.

Holland A. F., A. T. Shaughnessy, and M. H. Hiegel.
1987. Long-term variation in mesohaline Chesapeake Bay macrobenthos: spatial and temporal patterns. Estuaries 10:227–245.

Jivoff P., and A. H. Hines.
1998. Female behaviour, sexual competition and mate guarding in the blue crab, *Callinectes sapidus*. Anim. Behav. 55(3):589–603.

Ju, S.- J., D. Secor, and H. R. Harvey.
1999. The use of extractable lipofuscin for age determination of the blue crab, *Callinectes sapidus*. Mar. Ecol. Prog. Ser. 185:171–179.
2001. Growth rate variability and lipofuscin accumulation rates in the blue crab, *Callinectes sapidus*. Mar. Ecol. Prog. Ser. 224:197–205.

Kahn, D. M., R. W. Cole, S. F. Michels, and W. H. Whitmore.
1998. Development of life-stage-specific indices of relative abundance and stock-recruitment relationships for the Delaware Bay blue crab stock. J. Shellfish Res. 17(2): 529–541.

Lipcius, R. N., and W. A. Van Engel.
1990. Blue crab population dynamics in Chesapeake Bay: variation in abundance (York River, 1972–1988) and stock-recruit functions. Bull. Mar. Sci. 46(1):180–194.

Lipcius, R. N., J. van Montfrans, and A. H. Hines.
1995. Population dynamics and fishery ecology of the blue crab. Bull. Mar. Sci. 57(3):918–919.

McConaugha, J. R.
1988. Export and reinvasion of larvae as regulators of estuarine decapod populations. Am. Fish. Soc. Symp. 3:90–103.

McConaugha, J. R, D. F. Johnson, A. J. Provenzano, and R. C. Maris.
1983. Seasonal distribution of larvae of *Callinectes sapidus* (Crustacea: Decapoda) in the waters adjacent to Chesapeake Bay. J. Crust. Biol. 3(4):582–591.

Miller, T. J.
2001. Matrix-based modeling of blue crab population dynamics with applications to the Chesapeake Bay. Estuaries 24: 535–544.

Millikin, M. R., and A. B. Williams.
1984. Synopsis of biological data on the blue crab, *Callinectes sapidus* Rathbun. U.S. Dep. Commer., NOAA Technical Report NMFS1:1–39.

Nguyen, R. T., and H. R. Harvey.
1994. A rapid micro-scale method for the extraction and analysis of protein in marine particulates. Mar. Chem. 45:1–14.

O'Donovan V., and O. Tully.
1996. Lipofuscin (age pigment) as an index of crustacean age: correlation with age, temperature and body size in cultured juvenile *Homarus gammarus*. J. Exp. Mar. Biol. Ecol. 207:1–14.

Prager, M. H., J. R. McConaugha, C. M. Jones, and P. J. Greer.
1990. Fecundity of blue crab, *Calinectes sapidus*, in Chesapeake Bay. Biological, statistical, and management considerations. Bull. Mar. Sci. 46:170–179.

Rothschild, B., J. Ault, E. Patrick, S. Smith, H. Li, T. Maurer, B. Daugherty, G. Davis, C. Zhang, and R. McGarvey.
1992. Assessment of the Chesapeake Bay blue crab stock. Chesapeake Bay Biological Lab. Rep. CB92-003-036, CEES 07-4-30307, 60 p. Univ. Maryland, Solomons, MD.

Rugolo, L., K. S. Knotts, A. M. Lange, and V. A. Crecco.
1998. Stock Assessment of Chesapeake Bay Blue Crab (*Callinectes sapidus* Rathbun). J. Shellfish Res. 17(2): 493–517.

Secor, D. H., J. M. Dean, and S. E. Campana [eds.].
1995. Recent Developments in fish otolith research, 732 p. Belle W. Baruch Library in Marine Sciences Number 19. Univ. South Carolina Press, Colombia, SC.

Sheehy, M. R., E. Cameron, G. Marsden, and J. McGrath.
1995. Age structure of female giant tiger prawns *Penaeus monodon* as indicated by neuronal lipofuscin concentration. Mar. Ecol. Prog. Ser. 117:59–63.

Sheehy, M. R. J., P. M. J. Shelton, J. F. Wickins, M. Belchier, and E. Gaten.
1996. Ageing the European lobster *Homorus gammarus* by lipofuscin in its eyestalk ganglia. Mar. Ecol. Prog. Ser. 143:99–111

Van Engel, W. A.
1958. The blue crab and its fishery in Chesapeake Bay. Part 1. Reproduction, early development, growth, and migration. Commer. Fish. Rev. 20(6):6–17.
1999. Laws, regulations, and environmental factors and their potential effects on the stocks and fisheries for the blue crab, *Callinectes sapidus*, in the Chesapeake Bay region, 1880–1940, 88 p. Virginia Institute of Marine Science, Gloucester Point, VA.

Van Montfrans, J., C. E. Epifanio, D. M. Knott, R. N. Lipcius, D. J. Mense, K. S. Metcalf, E. J. Olmi 3, R. J. Orth, M. H. Posey, E. L. Wenner, and T. L. West.
1995. Settlement of blue crab postlarvae in western north Atlantic estuaries. Bull. Mar. Sci. 57(3):834–854.

Van Montfrans J., C. A. Peery, and R. J. Orth.
1990. Daily, monthly and annual settlement patterns by *Callinectes sapidus* and *Neopanope sayi megalopae* on artificial collectors deployed in the York river, Virginia: 1985–1988. Bull. Mar. Sci. 46(1):214–229.

Volstad, J. H., A. F. Sharov, G. Davis, and B. Davis.
2000. A method for estimating dredge catching efficiency for blue crabs, *Callinectes sapidus*, in Chesapeake Bay. Fish. Bull. 98(2):410–420.

Wahle, R. A., O. Tully, and V. O'Donovan.
1996. Lipofuscin as an indicator of age in crustaceans: analysis of the pigment in the American lobster *Homarus americanus*. Mar. Ecol. Prog. Ser. 138:117–123.

Abstract—We estimated the impact of striped bass (*Morone saxatilis*) predation on winter-run chinook salmon (*Oncorhynchus tshawytscha*) with a Bayesian population dynamics model using striped bass and winter-run chinook salmon population abundance data. Winter-run chinook salmon extinction and recovery probabilities under different future striped bass abundance levels were estimated by simulating from the posterior distribution of model parameters. The model predicts that if the striped bass population declines to 512,000 adults as expected in the absence of stocking, winter-run chinook salmon will have about a 28% chance of quasi-extinction (defined as three consecutive spawning runs of fewer than 200 adults) within 50 years. If stocking stabilizes the striped bass population at 700,000 adults, the predicted quasi-extinction probability is 30%. A more ambitious stocking program that maintains a population of 3 million adult striped bass would increase the predicted quasi-extinction probability to 55%. Extinction probability, but not recovery probability, was fairly insensitive to assumptions about density dependence. We conclude that winter-run chinook salmon face a serious extinction risk without augmentation of the striped bass population and that substantial increases in striped bass abundance could significantly increase the threat to winter-run chinook salmon if not mitigated by increasing winter chinook salmon survival in some other way.

Manuscript accepted 23 October 2002.
Manuscript received 31 December 2003 at NMFS Scientific Publications Office.
Fish. Bull. 101:321–331 (2003).

Modeling the effect of striped bass (*Morone saxatilis*) on the population viability of Sacramento River winter-run chinook salmon (*Oncorhynchus tshawytscha*)

Steven T. Lindley
Michael S. Mohr
Santa Cruz Laboratory
National Marine Fisheries Service
110 Shaffer Road
Santa Cruz, California 95060
E-mail address (for S. T. Lindley): Steve.Lindley@noaa.gov

Predation is a factor in the decline of many Pacific salmon populations (Nehlsen et al., 1991), and fisheries managers may need to evaluate the potential benefits of predator control or the possible impacts of predator augmentation. Such evaluations require estimates of the current predation rate, how the predation rate would change with changes in predator abundance, and how changes in predation rate affect the prey population viability. Predation rate can be estimated in at least three ways. Coordinated studies of predator and prey distribution and abundance, combined with predator diet studies, can provide direct estimates of predation rate (e.g. Rieman et al., 1991). This approach, however, is time-consuming, labor-intensive, and difficult because of the typically patchy distribution of predators and prey in space and time. Another approach is to build highly detailed, spatially explicit simulation models of predator and prey populations (e.g. Jager et al., 1997; Petersen and DeAngelis, 2000). Such models, although biologically realistic, are data-intensive, have many parameters, and have outputs that can be sensitive to parameter values that are not well constrained by data. An alternative modeling approach is to use simple models of predator and prey population dynamics and estimate the unknown parameters from time series of predator and prey abundance within a statistical framework (Walters et al., 1986; Berryman, 1991; Carpenter et al., 1994). This approach is based on readily available data and is relatively quick to implement, making it suitable for initial assessments of predation effects. The model, once its unknown parameters have been estimated, can also be used to assess the impact of predator population size changes on the prey population.

We took this statistical modeling approach to investigate how the proposed augmentation of the Sacramento River striped bass (*Morone saxatilis*) population might increase the risk of extinction faced by the endangered winter-run chinook salmon (*Oncorhynchus tshawytscha*). Striped bass prey on juvenile chinook salmon in the Sacramento River system (Stevens, 1966; Thomas, 1967), as well as in other west-coast rivers (Shapovalov, 1936), and striped bass prey upon juvenile Atlantic salmon in east-coast rivers were they co-occur (Blackwell and Juanes, 1998). Although winter-run chinook salmon juveniles are not the primary prey of striped bass and striped bass predation is only one of many mortality sources affecting winter-run chinook salmon, an increase in striped bass abundance has the potential to negatively impact winter-run chinook salmon. This potential must be assessed before the striped bass population can be augmented because winter-run chinook salmon are listed as endangered under the U. S. Endangered Species Act.

Because few data are available on the details of the interaction between winter-run chinook salmon and striped bass (e.g. functional response, role of alternate prey), we explored the simplest models that can capture the predation effect to assess the effect of striped bass population manipulations.

The ultimate goal is to assess whether the proposed plan might pose a significant increase in risk of extinction. We took a Bayesian approach in order that uncertainty in parameter estimates could be incorporated into extinction risk predictions (Ludwig, 1996). If significant risk cannot be ruled out, managers might reduce the scope of proposed striped bass stocking and collect data to better constrain the predation rate so that appropriate mitigation can be implemented. Although not the primary focus of this paper, our results also serve as a population viability assessment (PVA) for winter-run chinook salmon that can be compared to the recent winter-run chinook salmon PVA reported by Botsford and Brittnacher (1998).

Methods

Background and data

Winter-run chinook salmon Sacramento River winter-run chinook salmon are genetically distinct from other chinook salmon populations (Kim et al., 1999; Banks et al., 2000) and have a unique life history pattern that is a blend of the stream- and ocean-type life histories. Spawning fish leave the ocean in winter, mature in freshwater, and spawn in headwater areas from April through September (Healey, 1991). Juveniles enter the ocean the following spring. Up to 200,000 winter-run chinook salmon may have once spawned in the Sacramento River headwaters (Fisher, 1994). The completion of Shasta Dam in 1944 blocked access to the entire historic winter-run chinook salmon spawning range but created suitable spawning conditions for some distance (≈100 km) downstream of the dam (Moffett, 1949) (Fig. 1). In 1967, Red Bluff Diversion Dam (RBDD) was installed about 110 km downstream from Shasta Dam. Installation of RBDD apparently created passage problems for both adult and juvenile chinook salmon and the winter-run chinook salmon population has declined dramatically since completion of RBDD; fewer than 100 adults returned to spawn in 1980 (Fig. 2). Additional factors contributing to the decline of winter-run chinook salmon include high summer water temperatures, water diversions, habitat modification and degradation, fishing, hydropower operations, toxic spills, and predation by native and introduced animals, including striped bass (NMFS[1]). Winter-run chinook salmon were listed as threatened under the U.S. Endangered Species Act (ESA) in 1989 and as endangered in 1994.

The California Department of Fish and Game counts returning winter-run chinook salmon as they pass over fish ladders on RBDD, counts have been reported by Myers et al. (1998). Fish are determined to be adult (age 3 or 4) or "jack" (age 2, usually male), but are not otherwise routinely aged or sexed. From 1967 to 1985, nearly complete counts of winter-run chinook salmon were made. Since 1985, the dam flashboards have been removed for much of the year to improve passage of juvenile and adult winter-run chinook salmon. During this period, winter-run chinook salmon spawning escapement (spawning population size) has been estimated by expanding fish ladder counts made when the flashboards are in place. It is estimated that about 15% of the run is now counted, but the actual fraction observed in any given year is unknown. Population estimates made since 1985 therefore contain measurement error.

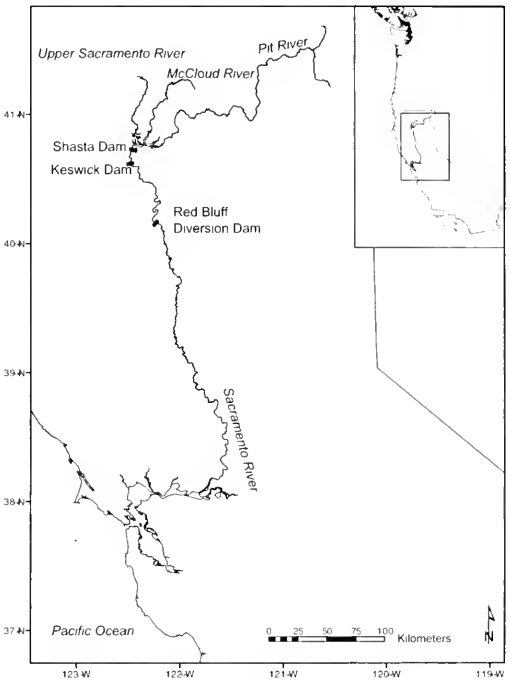

Figure 1

Sacramento River, tributaries, and dams. Current spawning range of winter chinook salmon spawning is between Keswick Dam and Red Bluff Diversion Dam.

Striped bass Striped bass were intentionally introduced to the Sacramento River in 1879, supported a commercial fishery in the early twentieth century, and now support a popular sport fishery (Kohlhorst, 1999). Over the last 30 years, the striped bass population has declined from around 2.2 million adults to fewer than 1 million adults (Fig. 3). The striped bass decline has been attributed to entrainment of striped bass larvae by the large State and Federal water diversion facilities in the Sacramento River delta (Stevens et al., 1985) and ecosystem changes that have reduced the carrying capacity for subyearling striped bass (Kimmerer et al., 2000). The State of California has a legal obligation to mitigate the negative effects of State water diversions on striped bass, but striped bass

[1] NMFS (National Marine Fisheries Service). 1997. NMFS proposed recovery plan for the Sacramento River winter-run chinook. Southwest Region, 501 West Ocean Blvd, Long Beach, CA 90802-4213.

augmentation is constrained by the ESA because of the potential impact on winter-run chinook salmon. Striped bass prey upon a wide variety of invertebrates and fish and are predominately piscivorous from age 2. In the Sacramento River system, juvenile chinook salmon compose a variable portion of the diet depending on season and location (Stevens, 1966; Thomas, 1967). By rearing juvenile striped bass captured at the water diversion fish screens in net pens and releasing them after one or two years, it is thought that the adult striped bass population could be stabilized at 3 million adults. Without augmentation, the population is expected to decline to about 500,000 adults. For a striped bass augmentation program to be in compliance with the ESA, the level of mortality on winter-run chinook salmon must be specified and the impact of this mortality must not appreciably reduce the likelihood of winter-run chinook salmon survival and recovery.

The California Department of Fish and Game estimates annually the abundance of striped bass; estimates have been reported by Kohlhorst (1999). Adult striped bass are captured with gill and fyke nets during the spring spawning migration and tagged with disc tags. Tags are recovered in summer and fall creel surveys and in subsequent springtime tagging operations. The field methods and estimation procedure, based on the Peterson estimator, are described by Stevens (1977). The estimate includes animals that are 3 or more years old, although striped bass begin feeding on juvenile salmon during their second year of life. We assume that the adult striped bass abundance estimate is a reasonable index of the total striped bass population capable of preying on juvenile chinook salmon. Note that an abundance index is sufficient because the predation parameter estimate will scale accordingly, i.e. the product of the striped bass abundance index and the predation rate parameter is unitless, as explained below.

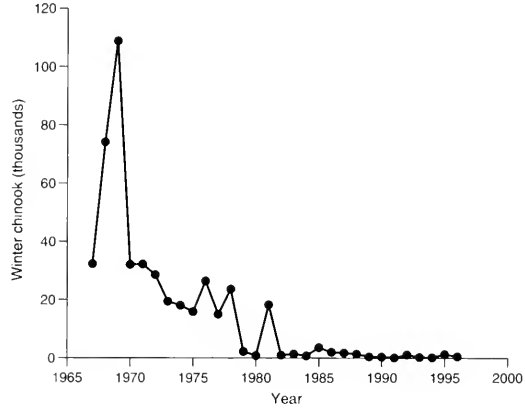

Figure 2

Estimated number of winter-run adult spawning chinook salmon passing the Red Bluff Diversion Dam.

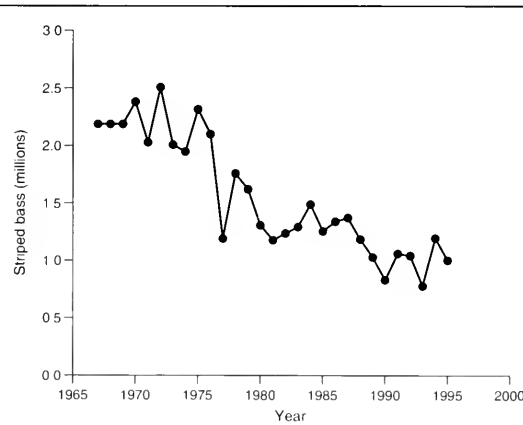

Figure 3

Peterson mark-recapture estimates of adult striped bass population size in the Sacramento-San Joaquin rivers and estuary.

Winter-run chinook salmon population model

In this section, we develop a probability model for winter-run chinook salmon spawning escapement. The model includes several potentially important factors influencing winter-run chinook salmon population growth: predation by striped bass, initiation of conservation measures in 1989, possibly density-dependent reproduction, and lognormal variability in reproduction (so-called process variation). Because winter-run chinook salmon juveniles are a minor prey item in the striped bass diet, owing to the rarity of winter-run chinook salmon in relation to other chinook populations, we do not model the striped bass population dynamics but rather treat the striped bass population-size observations as an input to the winter-run chinook salmon population model.

Winter-run chinook salmon adults spawn mostly at age 3 and to a lesser extent at age 4 (some males return at age 2, but we did not include them in the analysis on the presumption that 2-year-old males contribute little to population growth). The number of adult spawning fish in year t is the sum of 3- and 4-year-old spawning fish:

$$W_t = W_{t,3} + W_{t,4}. \quad (1)$$

The number of age a spawning fish in year t depends on the number of spawning fish a years before, the productivity (g) of these fish, and the propensity to spawn at age a (π_a) given survival to spawning:

$$W_{t,a} = W_{t-a} g_{t-a} \pi_a. \quad (2)$$

For winter-run chinook salmon, $a \in \{3,4\}$ and we set $\pi_3 = 1-\pi_4 = 0.89$ (Botsford and Brittnacher, 1998), assuming that the maturation rate of age-3 fish and the annual mortality rate of age-4 fish is constant across years. We modeled $\log(g_t)$ as the sum of several effects,

$$\log(g_t) = \mu + \Delta I_t - \alpha S_{t+1} - \beta W_t + \varepsilon_t, \varepsilon_t \sim \text{Normal}(0,\sigma^2), \quad (3)$$

including a mean population growth rate in the absence of striped bass and density dependence (μ); a possible change (Δ) in the mean population growth rate resulting from conservation measures initiated in 1989 (Williams and Williams, 1991) (I_t=0 for t<1989; I_t=1 for $t \geq 1989$); an effect due to variations in the abundance of striped bass (αS_{t+1}, where S_{t+1} is the abundance of adult striped bass in year t+1 and α is the per-bass predation rate); a density dependence effect (βW_t); and a normally distributed process error (ε_t) having mean = 0 and variance = σ^2. We ignored the measurement error in $\{W_t, t>1985\}$ for simplicity; the main effect of including measurement error would be to increase the uncertainty in Δ. Together, Equations 2 and 3 imply that $W_{t,a}$ is a lognormal random variable, and that W_t (see Eq. 1) is distributed as the sum of two lognormal random variables.

Density dependence in this formulation is equivalent to the Ricker model of stock-recruitment (Ricker, 1954): as stock size increases to infinity, per-capita productivity declines exponentially to zero. Because population viability analysis (PVA) model predictions can be sensitive to density dependence, we also considered Equation 3 with β set to zero.

Equation 3 states that predation by an individual striped bass is a linear function of winter-run chinook salmon abundance, ignoring the possibility of satiation or a minimum prey abundance to initiate feeding. Although the actual functional response of striped bass to winter-run chinook salmon is probably more complex, it is unlikely that satiation is a major issue for a rare prey species such as winter-run chinook salmon. We use S_{t+1} rather than S_t because striped bass population size is estimated in the spring, and the juvenile winter-run chinook salmon born in year t are vulnerable to striped bass predation as they develop and migrate to sea the following winter and spring (year t+1).

Parameter estimation

In this section, we couple the time series data and the winter-run chinook salmon population dynamics model with a prior distribution of the model's parameters to yield a Bayes posterior distribution for those parameters. For convenience, we denote the vector of model parameters as $\theta = (\mu, \Delta, \alpha, \beta, \sigma)$, and the data vectors as $W = (W_{1967}, W_{1968}, \ldots)$, $S = (S_{1967}, S_{1968}, \ldots)$, and $I = (I_{1967}, I_{1968}, \ldots)$. We denote a probability density as $p(\cdot)$ and a conditional probability density as $p(\cdot \mid \cdot)$. The unnormalized Bayes posterior distribution of the model parameters is given by

$$p(\theta \mid W, I, S) \propto p(\theta) p(W \mid I, S, \theta), \quad (4)$$

where $p(\theta)$ is the prior distribution of θ, and $p(W \mid I, S, \theta)$ is the model probability density function of W conditional on I, S, and θ, given by

$$p(W \mid I, S, \theta) = \prod_t P(W_t \mid W_{t-3}, W_{t-4}, I_{t-3}, I_{t-4}, S_{t-2}, S_{t-3}, \theta). \quad (5)$$

From the previous subsection, $p(W_t \mid \cdot)$ on the right hand side of Equation 5 is the probability density for a sum of two lognormal random variables. We evaluated $p(W_t \mid \cdot)$ using the analytic expression provided in Johnson et al. (1994, Eq. 14.20), solving the integral contained therein by adaptive quadrature.

The prior density $p(\theta)$ is the joint probability of the components of θ: $p(\theta) = \prod_i p(\theta_i)$. Because we have little information about θ that is independent of the data used in our analysis, we desired a prior that would have little influence on the posterior. There are many ways such a noninformative prior could be specified. In the results presented here, we set $p(\mu, \Delta, \alpha, \beta) \propto 1$ over the range of the parameters (α and β are restricted to positive values) and $p(\sigma) \propto \sigma^{-1}$, following the recommendations of Lee (1989) and Gelman et al. (1995) based on the work of Jeffreys (1961). We also examined the effects of using other reference priors, such as normal and exponential distributions with very large variances, and found there to be little difference in the results (not shown).

We did not attempt to derive a closed-form analytical expression for the posterior distribution of θ. Instead, we used the Metropolis-Hastings algorithm (Metropolis et al., 1953; Hastings, 1970; Gilks et al., 1996), a Markov chain Monte Carlo method. The Metropolis-Hastings algorithm produces a Markov chain with a stationary distribution equivalent to the posterior of θ. Estimates of parameter means, medians, and credible intervals were obtained from samples of the stationary Markov chain. We used a multivariate normal distribution centered on the current value of θ for the algorithm's proposal distribution. The variance-covariance matrix of the proposal distribution was adjusted by trial and error until the resulting Markov chain was well-mixed and the probability of accepting candidates fell in the range of (0.15, 0.50) (Gilks et al., 1996). Note that the proposal distribution form does not presume anything about the distribution of the unknown parameters, and as long as certain criteria are met (see Gilks et al. [1996]), only the convergence speed and mixing are affected, not the stationary distribution of the chain. To assess convergence, we initiated chains from many widely varying starting places and observed convergence to the same distribution. We found that 50,000 iterations following an initialization of 10,000 iterations provided stable parameter estimates. For an additional convergence

check, we compared the modes of θ to maximum likelihood estimates of θ obtained using a quasi-Newton method for minimization of a multivariate function with simple bounds (IMSL Fortran Numeric Library subroutine BCONF, Visual Numerics, Inc., Houston, TX).

Extinction and recovery probabilities

Given our winter-run chinook salmon population dynamics model, alternative striped bass population levels, and the posterior distribution of θ, we used Monte Carlo methods to determine the probability distribution of winter-run chinook salmon abundance in each of the next 100 years. From these distributions, the probability (P) that winter-run chinook salmon abundance is below a quasi-extinction threshold or above a recovery benchmark can be estimated directly. It was assumed, for simplicity, that striped bass abundance over the next 100 years will be held constant (S_t=S) at a level depending on the intensity of striped bass stocking. We considered three levels of striped bass abundance of interest to fishery managers, corresponding to no stocking (S=512,000 adults), moderate stocking (S=700,000 adults), and heavy stocking (S=3,000,000 adults). For comparative purposes, we also examined the effect of removing all striped bass (S=0 adults). Of particular interest is the increase in extinction probability due to striped bass stocking in relation to the no-stocking alternative. We denote this increase in extinction risk as δ. We generated the distribution of extinction and recovery probabilities and δ under the four striped bass population levels as follows:

1 Initialize the model by setting $\{W_t, t=-3, -2, -1, 0\}$ equal to the four most recent observations of spawning escapement.
2 Randomly select a value for θ according to its posterior density using the Metropolis algorithm.
3 For each striped bass abundance level S, $\{W_t, t=-3, -2, -1, 0\}$, and the particular value of θ, simulate 1000 100-year trajectories of winter-run chinook salmon spawning escapement according to Equations 1, 2, and 3.
4 For year t, the fraction of simulations in which spawning escapement was below the quasi-extinction threshold or above the recovery benchmark (levels specified below) approximates $P_t(\text{quasi-extinction} \mid S,\theta)$ and $P_t(\text{recovery} \mid S,\theta)$, respectively, for t=1,2,...,100.
5 For year t=50 and each level of striped bass abundance S, the increase in extinction probability in relation to that for the no-stocking level is approximated by $\delta(S, \theta) = P_{t=50}(\text{quasi-extinction} \mid S,\theta) - P_{t=50}(\text{quasi-extinction} \mid S=512{,}000, \theta)$.
6 Repeat steps 2–5 10,000 times. For each year t and striped bass abundance level S, the average values of $P_t(\text{quasi-extinction} \mid S,\theta)$ and $P_t(\text{recovery} \mid S,\theta)$ over these repetitions approximates their expected values with respect to θ given S. For brevity, in the "Results" and "Discussion" sections, we refer to these values as simply the probabilities of quasi-extinction and recovery in year t given striped bass abundance S.

We focused on quasi-extinction to avoid the problems of modeling depensatory effects, such as demographic stochasticity, inbreeding depression, and Allee effects (Allee, 1931). Estimates of absolute extinction risk are very sensitive to how these processes are modeled and parameterized, and relevant data are lacking. Quasi-extinction is less sensitive to these processes and is more likely to occur over short time horizons; therefore it is a more useful management benchmark than absolute extinction (Beissinger and Westphal, 1998). The draft recovery plan for winter-run chinook salmon (NMFS[1]) defines the quasi-extinction level as 100 females and the recovery level as 10,000 adult females; therefore we set the quasi-extinction threshold at 200 adults and the recovery threshold at 20,000 adults on the working assumption that the sex ratio is approximately 1.

Results

Parameter estimates and model fit

Table 1 lists summary statistics for parameter estimates for both the density-dependent and density-independent models; Figure 4 shows posterior marginal distributions and pairwise bivariate density contour plots for the winter-run chinook salmon density-dependent population dynamics model. The posterior median of μ was –0.69 per generation and the 0.90 credible interval (CI lower and upper endpoints of the posterior distribution equal to the 0.05 and 0.95 percentiles, respectively) for μ was (–1.2, –0.046), which indicates that the decline of winter-run chinook salmon most probably reflects a real trend rather than solely a series of random events. The median of the posterior distribution of the listing effect parameter Δ was positive, which suggests that the winter-run chinook salmon population growth rate has increased since initiation of conservation measures in 1989. The present-day realized growth rate, $\log(g)$, as determined from the joint posterior distribution and current winter-run chinook salmon and striped bass abundance according to Equation 3, has a median of –0.19 (0.90 CI=(–1.08, 0.66)), which indicates that the winter-run chinook salmon population may still be in decline in spite of the conservation measures and the decline in striped bass abundance.

At current striped bass abundance, the median estimate of α translates into about a 9% chance of an individual juvenile chinook salmon being consumed by a striped bass. Because $\log(g_t)$ is highly variable (median of σ estimate was 1.18), only fairly large values of α are inconsistent with the data. Furthermore, there was positive correlation between the estimates of α and μ (correlation coefficient=0.77), meaning that fairly high predation rates are consistent with the data if the underlying population growth rate was also high. The negative correlation of Δ with μ and α indicates that the potential improvement in winter-run chinook salmon population growth rate could have been due to either conservation measures or reduced predation.

At recent population sizes, there is little reduction in winter-run chinook salmon population growth due to density-dependent effects: the median of β translates into a

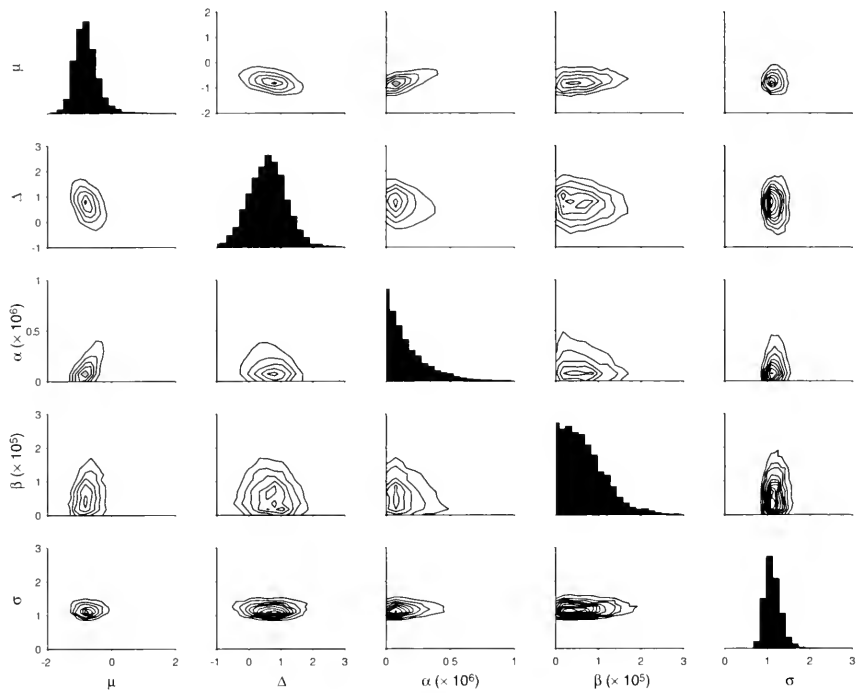

Figure 4

Posterior marginal distributions (histograms along the diagonal) and bivariate densities (off-diagonal contour plots) for the density-dependent winter chinook salmon population dynamics model parameters.

Table 1

Summary of posterior distributions under alternative model formulations. DD refers to density-dependent model, DI refers to density-independent model.

Model	Parameter	Mean	Median	0.90 CI
DD	μ (growth rate)	−0.694	−0.735	(−1.20, −0.046)
	Δ (growth rate change)	0.683	0.692	(−0.275, 1.64)
	α^1 (predation rate)	1.86	1.29	(0.100, 5.44)
	β^2 (density dependence)	7.16	6.26	(0.507, 16.9)
	σ (process error SD)	1.20	1.18	(0.936, 1.53)
DI	μ (growth rate)	−0.777	−0.825	(−1.34, −0.051)
	δ (growth rate change)	0.823	0.829	(−0.118, 1.77)
	α^1 (predation rate)	2.19	1.63	(0.116, 6.29)
	β (process error SD)	1.18	1.16	(0.921, 1.50)

[1] Values multiplied by 10^6 to increase legibility.
[2] Values multiplied by 10^5 to increase legibility.

$\log(g_t)$ of only 2.6×10^{-3} per generation less than that at a stock size near zero. At the recovery target population size of 20,000 adult winter-run chinook salmon, in contrast, the median estimate of β corresponds to a population growth rate reduction of 0.13 per generation.

The fit of the model was assessed by comparing the observed spawning escapement data series to the posterior predictive distribution of W (Gelman et al., 1995), which was estimated by drawing 10,000 samples from $p(\theta|\cdot)$ and a normal$(0,\sigma^2)$ and applying Equations 1–3. Figure 5 shows the observed data and boxplots of the posterior predictive distributions for the data points. Observed escapement in 1980 and 1991 was below the fifth percentile of the distribution for predicted escapement for those years. Winter-run chinook salmon returning in 1980 and 1991 were born during the drought years of 1976–77 and 1987–88. The 1976–77 drought was particularly severe; there were very low river flows and water temperatures exceeded 21°C during the winter-run chinook salmon egg incubation period, well above the 50% mortality temperature of 16°C reported for chinook salmon (Alderice and Velsen, 1978). The association between these outliers and droughts suggests that the model does not accurately handle an important source of risk. The estimate of σ was influenced by the 1980 and 1991 escapements, but because critically dry years appear to reduce survival more than wet years increase it (as suggested by the lack of large positive deviations in Fig. 5), estimates of absolute extinction risk may be optimistic. Our focus, however, is on the relative risk of extinction under different management scenarios.

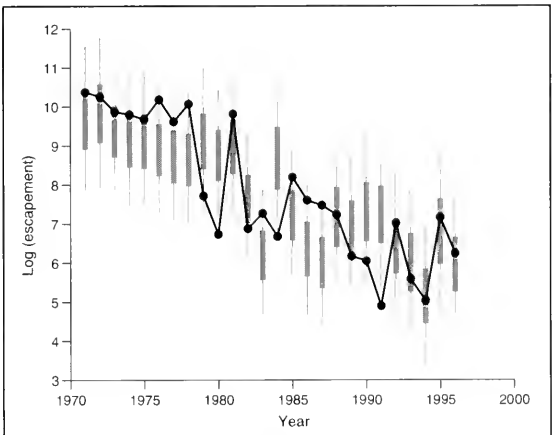

Figure 5

Posterior predictive distributions (gray boxes and whiskers) and observed winter chinook salmon spawning escapement (circles). Gray boxes cover the middle 0.50 percentile interval, and whiskers represent the middle 0.90 percentile interval.

Extinction risk estimation and stocking plan analysis

Figure 6 shows the cumulative distributions of quasi-extinction and recovery probabilities under the three striped bass stocking levels predicted by the density-dependent model. Winter-run chinook salmon have a 28% chance of becoming quasi-extinct and a 11% chance of recovering to more than 20,000 adults in 50 years, if no striped bass stocking were to occur (Table 2). If a striped bass stocking program were to stabilize the striped bass population at 700,000 adults, the probability of quasi-extinction in 50 years would rise from 28% to 30% (δ=1.9%, 0.9 CI=[1.2%, 2.6%]), and the probability of recovery would decline from 11% to 10%. A future adult bass population of 3.0×10^6 would raise the chance of winter-run chinook salmon quasi-extinction to 55% (δ= 27.7%, 0.9 CI=[25.4%, 30.1%]) and lower the recovery probability to 3.8%. If, on the other hand, striped bass predation could be eliminated completely, the probability of quasi-extinction would decline to 23% (δ=–4.5%, 0.9 CI=[–5.6%, –3.4%]) and the probability of recovery within 50 years would rise to 14%.

The probability of quasi-extinction according to the density-independent model is quite similar to that of the density-dependent model, but the predicted probability of recovery is substantially higher with density independence

Table 2

Expected probabilities of quasi-extinction and recovery within 50 years under alternative model formulations. DD refers to density-dependent model, DI refers to density-independent model.

Probability	Striped bass abundance	Model	
		DD	DI
Extinction	0	0.231	0.198
	512,000	0.276	0.246
	700,000	0.295	0.268
	3,000,000	0.554	0.582
Recovery	0	0.135	0.405
	512,000	0.107	0.328
	700,000	0.097	0.302
	3,000,000	0.038	0.116

(Table 2). Extinction probability is somewhat more sensitive to striped bass predation in the density-independent model. This greater sensitivity to striped bass abundance results from the higher estimate for the bass predation rate parameter and the lack of compensation in the density-independent model.

The density-dependent model indicates that without further population growth rate increases, winter-run chinook salmon are unlikely to reach the recovery benchmark: recovery will not occur within 20 years, and there is less than an 11% chance of reaching the 20,000 adult

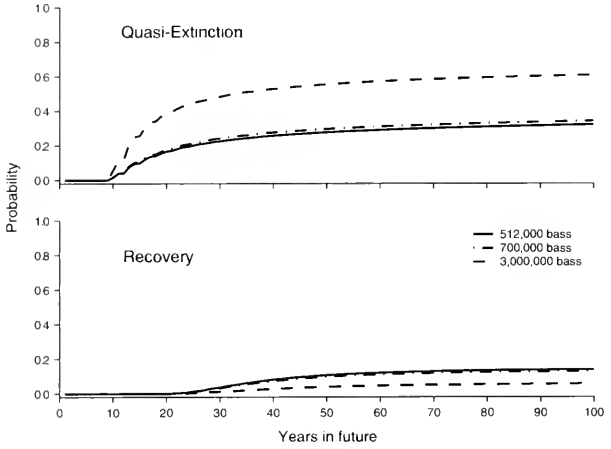

Figure 6

Probabilities of winter chinook salmon quasi-extinction and recovery under different adult striped bass population sizes.

winter-run chinook salmon level within 50 years. The low probability of recovery predicted by the density-dependent model is due in part to reductions in productivity at moderate population sizes. The median equilibrium winter-run chinook salmon population size, given by $(\mu+\Delta-\alpha S)/\beta$ with S = 512,000, is 18,100, which is below the recovery target of 20000.

Discussion

Predation by striped bass and effect of stocking

The results presented here indicate that striped bass predation may be a nontrivial source of mortality for winter-run chinook salmon. According to our analysis, the current striped bass population of roughly 1×10^6 adults consumes about 9% of winter-run chinook salmon outmigrants. By comparison, 85,000 northern squawfish consume about 11% of juvenile salmonids passing through the John Day Reservoir on the Columbia River (Rieman et al., 1991), based on prey consumption rates and predator and prey abundances. Jager et al. (1997), using a spatially explicit individual based model, estimated that between 13% and 57% of fall-run chinook fry were consumed by piscivorous fish in the Tuolumne River, California. The predation rate by striped bass on winter-run chinook salmon juveniles inferred from the time series of their abundances appears plausible in light of these comparisons. If striped bass predation is truly in this range, a significant increase in striped bass abundance could substantially increase the risk of winter-run chinook salmon extinction and reduce the likelihood of recovery. A limited program aimed at stabilizing the striped bass population at its recent size might pose an acceptably small risk: the model indicates with 95% certainty that the stabilization program would add less than 3.1% to the baseline extinction risk of 28%. Although this analysis suggests that striped bass predation may be a significant risk factor for winter-run chinook salmon, striped bass eradication would not be enough to ensure recovery of winter-run chinook salmon. In the following two subsections, we discuss how data limitations and model uncertainty influence the results and our interpretation of them.

Model uncertainty

Model uncertainty arises from our ignorance of the exact processes driving population dynamics. Although there is a well-developed statistical basis for model identification and selection (Burnham and Anderson, 1998), different models may fit the data equally well yet make quite different predictions (Pascual et al., 1996). In such cases, one should consider a variety of models and ensure that important conclusions are upheld by all of them (Beissinger and Westphal, 1998).

Population dynamics and PVA models can be very sensitive to the presence and form of density dependence in the model. Because the work presented here was concerned primarily with the change in extinction risk posed by a change in striped bass abundance, it is encouraging that the probability of quasi-extinction was not sensitive to assumptions about density dependence. We presented results of both a Ricker-type density dependent model and a density-

independent model; we also analyzed a Beverton-Holt type model (where per-capita productivity reaches an asymptote instead of declining to zero as population size increases to infinity) and found that it gave similar predictions to the Ricker model (results not shown). The insensitivity of extinction risk to the form of density dependence is perhaps not surprising because density dependence is considered to have little influence on the extinction process if populations are well below carrying capacity (Emlen, 1995), although it has the potential to create both compensatory population growth that can increase population persistence and oscillatory or chaotic dynamics that can reduce population persistence (Ginzburg et al., 1990; Mills et al., 1996; Belovsky et al., 1999). The probability of recovery, however, was strongly dependent on whether density dependence was included: regardless of striped bass stocking level, the recovery probability predicted by the density-independent model was about threefold higher than that predicted by the density-dependent model. Although the density dependence parameter was not well-identified by the data, winter-run chinook salmon are currently restricted to a limited portion of the Sacramento River and it is certainly possible that there is not enough habitat to support a spawning run of 20000 adults. Further study of the Sacramento River's carrying capacity for winter-run chinook salmon is warranted.

The dynamics of food web and predator-prey models can also be sensitive to the form of the predator's functional response to prey abundance (Overholtz et al., 1991; Beryman, 1992). The models presented here assumed that the predation-related per-capita mortality of winter-run chinook salmon is a linear function of striped bass abundance only. It is possible, however, that this mortality rate depends on winter-run chinook salmon abundance as well, through the feeding response of individual striped bass to winter-run chinook salmon abundance. In deterministic models, the form of the functional response (as well as predator abundance and prey productivity) determines the equilibrium prey population size. In particular, whether a prey population can persist may depend on whether the predator's functional response is sigmoidal or increases monotonically to an asymptote with increasing prey abundance (Sinclair et al., 1998). In cases where the prey is the major food source of the predator, it can be possible to detect a nonlinear functional response from the time series themselves (Jost and Arditi, 2000), especially if the system is perturbed (Carpenter et al., 1994). Winter-run chinook salmon are not the main prey of striped bass, and any possible depensatory effect of predation may be reduced by alternate prey, including juvenile chinook salmon of other races. Juvenile fall chinook salmon, in particular, are abundant, and often co-occur with winter-run chinook salmon (Healey, 1991). If the abundance of fall chinook salmon is uncorrelated with, and high in relation to, winter-run chinook salmon, then the striped bass predation rate may be related to fall chinook salmon abundance and unrelated to winter-run chinook salmon abundance. In the absence of relevant data, further consideration of nonlinear feeding responses and effects of alternate prey (e.g. Spencer and Collie, 1995), is beyond the scope of this paper.

Another aspect of model uncertainty is the assumption that the future will be like the present. The future will probably include increased conservation efforts, changing ocean productivity, and perhaps further habitat degradation. Although the level of absolute risk would change substantially if these processes were included in the simulations, the relative risks posed by the different striped bass stocking schemes would change much less. The main goal of this work was to compare these relative risks; a secondary goal was to predict what would happen if things continued in the future as they are now. We therefore feel confident in stating that a large striped bass stocking program would be risky and that further winter-run chinook salmon restoration actions are needed.

Data uncertainties

Imprecise estimates of predator and prey abundance limit the precision of parameter estimates and can bias parameter estimates if not accounted for (Seber and Wild, 1989; Carpenter et al., 1994). For the bulk of the winter-run chinook salmon series, observation error is probably quite low because all fish were counted directly; the CV for the striped bass population estimates is thought to be about 25% (Stevens, 1977). We ignored measurement error in both the striped bass and winter-run chinook salmon population abundance data. Further work is required to assess how much of an influence these errors might have on parameter estimates for the model presented here.

Informative priors

A major advantage of the Bayesian approach is the ability to include informative prior probability distributions for model parameters. Informative priors can greatly improve the precision of posterior parameter estimates and model predictions. In the example presented here, the estimate of the striped bass predation rate could be improved, and uncertainty in stocking impacts reduced, by incorporating direct information on the rate of striped bass predation on winter-run chinook salmon into an informative prior on α. Such information would include estimates of the number of salmon that striped bass eat per day (obtainable from food habits and metabolic studies), and the number of juvenile salmon that are vulnerable to striped bass predation. Some information on these quantities is available for the Sacramento system (Stevens, 1966; Thomas, 1967).

A Bayesian meta-analysis of the available food habits data was performed to estimate the number of salmon that striped bass eat per day, and the number of juvenile salmon passing through the Sacramento River system was estimated from ocean catches, spawning escapements, and considerations of smolt-to-adult survival rates. Unfortunately, including the informative prior did not substantially improve the precision of the posterior distribution of α, nor did it significantly alter the central tendency. Given the number of necessary assumptions, the complexity of the meta-analysis, and the minimal impact of including the informative prior on the posterior distribution of α, we opted to retain a noninformative prior on α. Should better

data become available, it could be worthwhile to include them in the prior for α, although there is no practical value in including the data currently available.

Status of winter-run chinook salmon

Although not the primary purpose of this study, our model does provide an assessment of the present status of winter-run chinook salmon: the quasi-extinction probability of 28% within 50 years indicates that winter-run chinook salmon face a substantial extinction risk, in spite of the probable improved survival since the ESA listing. The ESA does not specify quantitative risk levels corresponding to threatened or endangered status, but under the World Conservation Union's Red List extinction risk criteria (IUCN, 1994), winter-run chinook salmon would be classified as "vulnerable" (>10% extinction probability in 100 years). Winter-run chinook salmon extinction risk is higher than the 10% probability of extinction in 50 years specified as "safe" by Botsford and Brittnacher (1998). Furthermore, the true quasi-extinction risk is probably higher than indicated by our analysis because we have neglected some sources of risk that could be significant at population levels in excess of the quasi-extinction threshold, such as catastrophic events.

Botsford and Brittnacher (1998) developed a somewhat similar model of winter-run chinook salmon spawning escapement that predicts almost certain extinction for winter-run chinook salmon in the absence of increased survival. The differences between the results presented here and those of Botsford and Brittnacher (1998) illustrate the importance of including parameter uncertainty and allowing for time-varying population growth rate. Their model assumed constant mean population growth rate, whereas ours allowed for a change (Δ) in the population growth rate following the conservation measures initiated in 1989. The more optimistic prediction in this paper derives mostly from the substantial probability that population growth rate increased following implementation of conservation measures. This can be illustrated by setting Δ to zero and refitting our model. The quasi-extinction probability with $\Delta = 0$ is 69%. Much of the remaining discrepancy between our results and those of Botsford and Brittnacher (1998) arises from including parameter uncertainty, which allows for the possibility that population growth might be higher than its maximum likelihood estimate. The predicted decline of the adult striped bass population from 700,000 to 512,000 contributes a smaller effect to increased survival probability than does the effect of conservation measures. Both analyses are similar, however, in that they indicate winter-run chinook salmon face significant extinction risk and require further conservation action.

Acknowledgments

This work benefited from participation by STL in the Predicting Extinction Working Group supported by the National Center for Ecological Analysis and Synthesis, a Center funded by NSF (grant no. DEB-94-21535), the University of California at Santa Barbara, and the State of California. The authors thank L. Goldwasser and E. Bjorkstedt for comments on an earlier version of this manuscript, and J. Emlen and M. Prager for critical reviews of the final version. Any remaining errors are the responsibility of the authors.

Literature cited

Alderice, D. F., and F. P. J. Velsen.
1978. Relation between temperature and incubation time for eggs of chinook salmon (*Oncorhynchus tshawytscha*). J. Fish. Res. Board Can. 35:69–75.

Allee, W. C.
1931. Animal aggregations, 431 p. Univ. Chicago Press, Chicago, IL.

Banks, M. A., V. K. Rashbrook, M. J. Calavetta, C. A. Dean, and D. Hedgecock.
2000. Analysis of microsatellite DNA resolves genetic structure and diversity of chinook salmon (*Oncorhynchus tshawytscha*) in California's Central Valley. Can. J. Fish. Aquat. Sci. 57:915–927.

Beissinger, S. R., and M. I. Westphal.
1998. On the use of demographic models of population viability analysis in endangered species management. J. Wildl. Manage. 62:821–841.

Belovsky, G. E., C. Mellison, and P. A. van Zandt.
1999. Experimental studies of extinction dynamics. Science 286:1175–1177.

Berryman, A. A.
1991. Population theory: an essential ingredient in pest prediction, management, and policy making. Am. Entomol. 37:138–142.
1992. The origins and evolution of predator-prey theory. Ecology 73:1530–1535.

Blackwell, B. F., and F. Juanes.
1998. Predation on Atlantic salmon smolts by striped bass after dam passage. N. Am. J. Fish. Manage. 18:936–939.

Botsford, L. W., and J. G. Brittnacher.
1998. Viability of Sacramento River winter-run chinook salmon. Conserv. Biol. 12:65–79.

Burnham, K. P., and D. R. Anderson.
1998. Model selection and inference: a practical information-theoretic approach, 353 p. Springer, New York, NY.

Carpenter, S. R., K. L. Cottingham, and C. A. Stow.
1994. Fitting predator-prey models to time series with observation errors. Ecology 75:1254–1264.

Emlen, J. M.
1995. Population viability of the Snake River chinook salmon *Oncorhynchus tshawytscha*. Can. J. Fish. Aquat. Sci. 52:1442–1448.

Fisher, F. W.
1994. Past and present status of Central Valley chinook salmon. Conserv. Biol. 8:870–873.

Gelman, A., J. B. Carlin, H. S. Stern, and D. B. Rubin.
1995. Bayesian data analysis, 526 p. Chapman & Hall, London.

Gilks, W. R., S. Richardson, and D. J. Spiegelhalter.
1996. Introducing Markov chain Monte Carlo. *In* Markov chain Monte Carlo in practice (W. R. Gilks, S. Richardson, and D. J. Spiegelhalter, eds.), p. 1–19. Chapman & Hall, London.

Ginzburg, L. R., S. Ferson, and H. R. Akçakaya.
1990. Reconstructibility of density dependence and the con-

servative assessment of extinction risks. Conserv. Biol. 4: 63–70.

Hastings, W. K.
1970. Monte Carlo sampling methods using Markov chains and their applications. Biometrika 57:97–109.

Healey, M. C.
1991. Life history of chinook salmon (*Oncorhynchus tshawytscha*). *In* Pacific salmon life histories (C. Groot and L. Margolis, eds.), p. 311–394. UBC Press, Vancouver, BC.

IUCN (International Union for the Conservation of Nature and Natural Resources).
1994. IUCN red list categories. IUCN, Gland, Switzerland.

Jager, H. I., H. E. Cardwell, M. J. Sale, M. S. Bevelhimer, C. C. Coutant, and W. Van Winkle.
1997. Modelling the linkages between flow management and salmon recruitment in rivers. Ecol. Mod. 103:171–191.

Jeffreys, H.
1961. Theory of probability, 3rd ed., 447 p. Oxford Univ. Press, London.

Johnson, N. L., S. Kotz, and N. Balakrishnan.
1994. Continuous univariate distributions, vol. 1, 2nd ed., 756 p. John Wiley & Sons, New York, NY.

Jost, C., and R. Arditi.
2000. Identifying predator-prey processes from time-series. Theor. Popul. Biol. 57:435–337.

Kim, T. J., K. M. Parker, and P. W. Hedrick.
1999. Major histocompatibility complex differentiation in Sacramento River chinook salmon. Genetics 151:1115–1122.

Kimmerer, W. J., J. H. Cowan, L. W. Miller, and K. A. Rose.
2000. Analysis of an estuarine striped bass (*Morone saxatilis*) population: influence of density-dependent mortality between metamorphosis and recruitment. Can. J. Fish. Aquat. Sci. 57:478–486.

Kohlhorst, D. W.
1999. Status of striped bass in the Sacramento-San Joaquin estuary. Cal. Fish Game 85:31–36.

Lee, P. M.
1989. Bayesian statistics: an introduction, 294 p. Oxford Univ. Press, New York, NY.

Ludwig, D.
1996. Uncertainty and the assessment of extinction probabilities. Ecol. Appl. 6:1067–1076.

Metropolis, N., A. W. Rosenbluth, M. N. Rosenbluth, A. H. Teller, and E. Teller.
1953. Equations of state calculations by fast computing machine. J. Chem. Phys. 21:1087–1091.

Mills, L. S., S. G. Hayes, C. Baldwin, M. J. Wisdom, J. Citta, D. J. Mattson, and K. Murphy.
1996. Factors leading to different viability predictions for a grizzly bear data set. Conserv. Biol. 10:863–873.

Moffett, J. W.
1949. The first four years of king salmon maintenance below Shasta Dam, Sacramento River, California. Cal. Fish Game 35:77–102.

Myers, J. M., R. G. Kope, G. J. Bryant, D. Teel, L. J. Lierheimer, T. C. Wainwright, W. S. Grant, F. W. Waknitz, K. Neely, S. T. Lindley, and R. S. Waples.
1998. Status review of chinook salmon from Washington, Idaho, Oregon, and California. U.S. Dep. Commer., NOAA Tech. Memo. NMFS-NWFSC-35, 443 p.

Nehlsen, W., J. E. Williams, and J. A. Lichatowich.
1991. Pacific salmon at the crossroads: stocks at risk from California, Oregon, Idaho, and Washington. Fisheries 16: 4–21.

Overholtz, W. J., S. A. Murawski, and K. L. Foster.
1991. Impact of predatory fish, marine mammals, and seabirds on the pelagic fish ecosystem of the northwestern USA. ICES Mar. Sci. Symp. 193:198–208.

Pascual, M. A., P. Kareiva, and R. Hilborn.
1996. The influence of model structure on conclusions about viability and harvesting of Serengeti wildebeest. Conserv. Biol. 11:966–976.

Petersen, J. H., and D. L. DeAngelis.
2000. Dynamics of prey moving through a predator field: a model of migrating juvenile salmon. Math. Biosci. 165: 97–114.

Ricker, W. E.
1954. Stock and recruitment. J. Fish. Res. Board Can. 11: 559–623.

Rieman, B. E., R. C. Beamesderfer, S. Vigg, and T. P. Poe.
1991. Estimated loss of juvenile salmonids to predation by northern squawfish, walleyes, and smallmouth bass in John Day Reservoir, Columbia River. Trans. Am. Fish. Soc. 120: 448–458.

Seber, G. A. F., and C. J. Wild.
1989. Nonlinear regression, 768 p. Wiley, New York, NY.

Shapovalov, L.
1936. Food of the striped bass. Cal. Fish Game 22:261–271.

Sinclair, A. R. E., R. P. Pech, C. R. Dickman, D. Hik, P. Mahon, and A. E. Newsome.
1998. Predicting effects of predation on conservation of endangered prey. Conserv. Biol. 12:564–575.

Spencer, P. D., and J. S. Collie.
1995. A simple predator-prey model of exploited marine fish populations incorporating alternative prey. ICES J. Mar. Sci. 53:615–628.

Stevens, D. E.
1966. Food habits of striped bass, *Roccus saxatilis*, in the Sacramento-San Joaquin delta. *In* Ecological studies of the Sacramento-San Joaquin delta (J. L. Turner and D. W. Kelly, eds.), p. 68–96. Calif. Dep. Fish Game, Fish Bull. 136.
1977. Striped bass (*Morone saxatilis*) monitoring techniques in the Sacramento-San Joaquin estuary. *In* Proceedings of the conference on assessing the effects of power-plant-induced mortality on fish populations, Gatlinburg, Tennessee, May 3–6, 1977 (W. Van Winkle, ed.), p. 91–109. Pergamon Press, New York, NY.

Stevens, D. E., D. W. Kohlhorst, and L. W. Miller.
1985. The decline of striped bass in the Sacramento-San Joaquin estuary, California. Trans. Am. Fish. Soc. 114:12–30.

Thomas, J. L.
1967. The diet of juvenile and adult striped bass, *Roccus saxatilis*, in the Sacramento-San Joaquin river system. Cal. Fish Game 53:49–62.

Walters, C. J., M. Stocker, A. V. Tyler, and S. J. Westrheim.
1986. Interaction between Pacific cod (*Gadus macrocephalus*) and herring (*Clupea harengus pallasi*) in the Hecate Strait, British Columbia. Can. J. Fish. Aquat. Sci. 43:830–837.

Williams, J. E., and C. D. Williams.
1991. The Sacramento River winter chinook salmon. *In* California's salmon and steelhead: the struggle to restore an imperiled resource (A. Lufkin, ed.), p. 105–115. Univ. California Press, Berkeley, CA.

Seasonal egg production of whitemouth croaker (*Micropogonias furnieri*) in the Río de la Plata estuary, Argentina-Uruguay

Gustavo J. Macchi
Consejo Nacional de Investigaciones Científicas y Técnicas (CONICET)
Rivadavia 1917
(1033) Buenos Aires, Argentina
Present address: Instituto Nacional de Investigación y Desarrollo Pesquero (INIDEP)
Paseo Victoria Ocampo
N°1 CC. 175
Mar del Plata (7600), Argentina
E-mail address: gmacchi@inidep.edu.ar

Eduardo M. Acha
María I. Militelli
Instituto Nacional de Investigación y Desarrollo Pesquero (INIDEP)
Paseo Victoria Ocampo
N°1 CC. 175
Mar del Plata (7600), Argentina

Abstract—The reproductive biology of the whitemouth croaker (*Micropogonias furnieri*) inhabiting the estuarine waters of the Río de la Plata (Argentina-Uruguay) was studied by using histological analysis of the ovaries. Samples were collected during the spawning peak and the end of two breeding seasons (November 1995–February 1996 and November 1997–March 1998). *Micropogonias furnieri* is a multiple spawner with indeterminate annual fecundity. Spawning frequency, determined by using the percentage of females with postovulatory follicles, was about 31% in November 1995 and 25% in February 1996. At these frequencies, a female on average spawned a new batch of eggs every 3–4 days during the spawning season. Batch fecundity was fitted to a power function of length and a linear function of ovary-free female weight. The number of hydrated oocytes decreased at the end of the breeding season, coinciding with an increase of atresia. Annual egg production for a 40-cm-TL female was estimated to be between 3,300,000 and 7,300,000 eggs. In addition to the seasonal decrease in fecundity and spawning activity, a decline in egg size and weight toward the end of the breeding season was also observed.

Manuscript accepted 17 December 2002.
Manuscript received 31 December 2002 at NMFS Scientific Publications Office.
Fish. Bull. 101:332–342 (2003).

The whitemouth croaker, *Micropogonias furnieri* (Sciaenidae), is a demersal coastal species distributed along the eastern coast of Central and South America, from the Yucatán Peninsula to south of Buenos Aires Province (41°S), Argentina (Isaac-Nahum, 1988). It is an economically important resource in the Río de la Plata area and the most heavily exploited coastal species in the commercial fisheries of Argentina and Uruguay (Lasta and Acha, 1996).

The reproductive biology of *M. furnieri* has been extensively studied off Brazil, Uruguay, and Argentina (Vazzoler, 1970; Haimovici, 1977; Isaac-Nahum and Vazzoler, 1983; Castello, 1986; Macchi and Christiansen, 1992a; Acuña et al., 1992; Macchi et al., 1996; Lasta and Acha, 1996). Spawning in the Río de la Plata area extends over a protracted period, from early November to March, and peaks during November–December (Macchi and Christiansen, 1996). In this area, spawning takes place in the inner zone of the Río de la Plata estuary, where the river and the oceanic waters form a bottom salinity front (Macchi et al., 1996; Macchi, 1997; Acha et al., 1999).

Whitemouth croaker is a multiple spawner with an indeterminate annual fecundity; in other words, unyolked oocytes continuously mature and are spawned throughout the reproductive season (Macchi, 1997). Previously, fecundity estimates for *M. furnieri* were made by counting the number of yolked oocytes in ripe ovaries (Vazzoler, 1970; Macchi and Christiansen, 1992b; Pravia et al., 1995). This method does not account for the multiple spawning pattern of this species; therefore, estimates may be incorrect by as much as an order of magnitude (DeMartini and Fountain, 1981; Conover, 1985, Brown-Peterson et al., 1988, Lowerre-Barbieri et al., 1996). Spawning frequency and batch fecundity in the whitemouth croaker of the Río de la Plata area has been estimated only during the spawning peak (November) and is, therefore, considered to be a preliminary estimate for this species (Macchi et al., 1996).

In this paper, we examine ovaries histologically and analyze planktonic eggs of *M. furnieri* from the Río de la Plata estuary, collected during the spawning peak and near the end of the breeding season. We also determine the time of day when this species spawns and compare the spawning frequency, batch fecundity, and egg sizes obtained during the spawning peak and the end of the reproductive season.

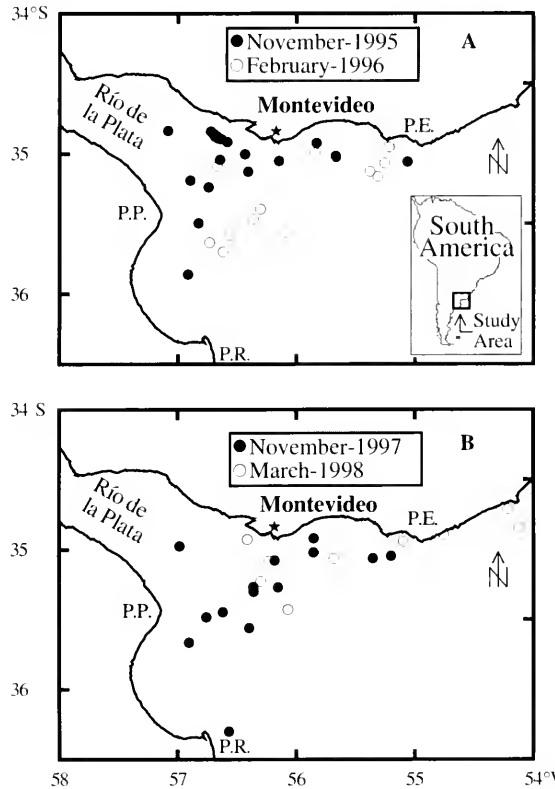

Figure 1

Study area and samples location for the 1995–96 (**A**) and 1997–98 (**B**) spawning seasons. November samples correspond to the main spawning peak and February–March to the end of the breeding season of *M. furnieri*. PE = Punta del Este, Uruguay; PP = Punta Piedras; and PR = Punta Rasa, Argentina.

Material and methods

Sampling

Whitemouth croaker females were collected in the Río de la Plata estuary during four research surveys (Fig. 1), namely during the peak of spawning and at the end of the breeding season for the two spawning seasons (November 1995–February 1996 and November 1997–March 1998). Fish were collected with bottom trawls by using a net with a mouth width of about 20 m, a height of about 4 m, and with a 20-mm mesh at the inner cover of the codend. Total length (TL, cm) and total wet weight (TW, g) were recorded for each fish sampled. Only adult females larger than 30 cm TL were analyzed (Table 1) because *M. furnieri* mature at approximately 33 cm TL (Macchi and Acha, 1998).

During the 1995–96 spawning season, oceanographic sampling was performed with a Sea-Bird 19 CTD (conductivity–temperature–depth profiler), with a lowering speed of 0.5 m/s. Data were processed to achieve a 1-m vertical resolution (precision of ±0.03°C in temperature and ±0.05 units in salinity).

Whitemouth croaker eggs were taken from the plankton samples during the spawning peak and late reproductive season only in the 1995–1996 breeding period. Ichthyoplankton were collected with a Nackthai sampler (Nellen and Hempel, 1969) equipped with a single net with a 20-cm diameter mouth opening and 405-µm mesh (Acha et al.,

Table 1

Statistic data from the seasonal samples of *M. furnieri* females collected in the Rio de la Plata estuary. TL = total length; SD = standard deviation.

Date	*n*	Length range (cm)	Average TL (cm)	SD
November 1995	359	31–72	44.6	7.8
February 1996	206	32–67	41.9	6.4
November 1997	159	33–62	44.3	3.9
March 1998	154	32–58	42.6	4.2

1999). Eggs of *M. furnieri* were identified on the basis of the descriptions reported by Weiss (1981).

Laboratory processing

Ovaries were removed immediately after capture of the fish and fixed in 10% buffered formalin for two weeks. The ovaries were weighed (GW) to the nearest 0.1 g and a sample of about 2.0 g was removed from each ovary, dehydrated in methanol, cleared in benzol, and embedded in paraffin. Sections were cut at 4 µm and stained with Harris' hematoxylin and eosin Y. Ovaries were classified histologically into seven categories: developing early (1), developing late (2), fully developed (3), gravid (4), partially spent (5), spent (6) and resting (7). This classification is a modification of that given by Mayer et al. (1988) and has previously been employed to describe the ovarian development in *Cynoscion guatucupa* (Macchi, 1998). The criteria for identifying the different atresia stages and the atretic condition of the ovary were adopted from Hunter and Macewicz (1985).

One hundred planktonic eggs collected during the main spawning peak and during the end of the breeding season were measured (±0.01 mm) by using a microscope equipped with a calibrated eyepiece. Two diameters at right angles to each other were measured per egg and an average was taken. Egg weights were estimated for each portion of the spawning period from two samples of 100 eggs each. The eggs were rinsed in distilled water, dried for 20 hours at 60°C, and weighed (±0.1 mg). The diameter and weight of the eggs collected during the spawning peak and the end of the breeding season were compared by analysis of variance (Draper and Smith, 1981).

Estimation of spawning frequency

Spawning frequency was estimated by the incidence of females with postovulatory follicles (POF), following the method described by Hunter and Goldberg (1980). The description of the stages of POF degeneration was based on six females that spawned in captivity during the research cruise carried out in March 1998. Two fish were sampled at the time of spawning and the others were sacrificed 6, 12, 24, and 36 hours after spawning. The ovaries of these fish were preserved in 10% buffered formalin and used to establish histological criteria for the aging of POFs of the sea-caught females.

Postovulatory follicle degradation in *M. furnieri* was faster than that reported by Hunter and Goldberg (1980) for northern anchovy (*Engraulis mordax*). A 24-h-old POF showed advanced signs of degeneration similar to those observed in *E. mordax* 48 h after spawning. Therefore, daily percentage of spawning females (spawning frequency) was estimated by taking the total of females with POFs less than 24 h old (Hunter et al., 1986). Mean and variance of this parameter were calculated according to the equation developed by Picquelle and Stauffer (1985), which allows weighing of each station according to the subsample size.

Fecundity estimation

Batch fecundity (BF; number of oocytes released per spawning) was estimated gravimetrically with the hydrated oocyte method on fixed ovarian samples (Hunter et al., 1985). Ovaries used showed no evidence of recent spawning (i.e. no new POFs). Batch fecundity was determined for 87 females (57 from November 1995, 16 from February 1996, three from November 1997, and 11 from March 1998). Three pieces, approximately 0.1 g each, were removed from the anterior, middle, and posterior part of each ovary, weighed (±0.1 mg), and the number of hydrated oocytes were counted. Batch fecundity for each female was the product of the mean number of hydrated oocytes per unit of ovarian weight and the total ovarian weight. Relative fecundity (RF) was defined as the number of hydrated oocytes per gram of ovary-free body weight. Fecundity values obtained for the different months within the spawning season were compared with a test of equality of means (Draper and Smith, 1981). The relationships of batch fecundity to total length and to total weight (ovary free) were described with standard linear regressions. Comparisons between the different months were based on overlapping length ranges of the samples, and an analysis of covariance with log-transformed data was applied (Draper and Smith, 1981).

Results

Spawning season

During November 1995, in the Rio de la Plata estuary, 93% of the sampled females were found to be in a reproductive state, with ovaries being either in a developing phase or partially spent (maturity stages 2 to 5). Gravid females (with hydrated oocytes) accounted for about 20% and spent ovaries were scarce (Fig. 2). Near the end of this spawning season (February 1996), 98% of the females had apparently spawned at least once and the proportion of spent ovaries was about 15%. During November 1997, females were mainly undergoing ovarian development and only a few individuals with hydrated oocytes were observed (Fig. 2). In March 1998, the proportion of spent ovaries was about 20% and the proportion of those in the resting stage was

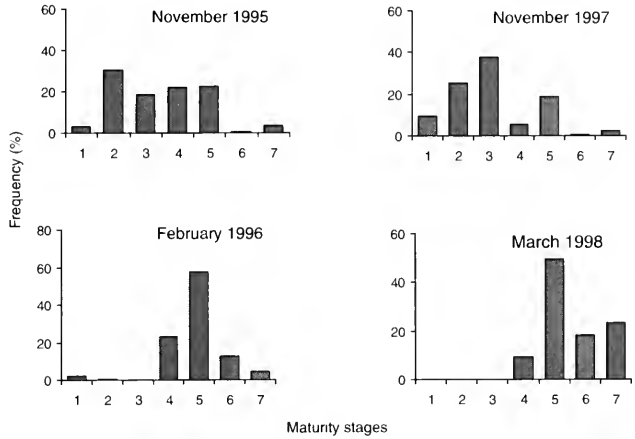

Figure 2

Maturity-stage frequency of *M furnieri* during the spawning peak (November 1995 and 1997) and the end of the reproductive season (February 1996 and March 1998). Stages: 1 = developing early; 2 = developing late; 3 = fully developed; 4 = gravid; 5 = partially spent; 6 = spent; 7 = resting; modified after Mayer et al. (1988).

higher than in February 1996 (3% vs. 25%, respectively). In general, we noted an increase in the presence of atretic oocytes as the spawning season progressed (Fig. 3). Furthermore, the incidence of atresia was higher in 1997–98 than in 1995–96 (Fig. 3); during the last season about 60% of females were classified as in atretic state 1, whereas in 1995–96 about 20% of females were in this state.

Spawning site and oceanographic variables

Bottom salinity at the estuary ranged between 0 and 30 psu. Maximum upriver penetration of salt water during November 1995 and February 1996 was similar, reaching a line between Montevideo and Punta Piedras (Fig. 4). The Argentine coast of the estuary showed a similar salinity pattern during both months, whereas the salt water intrusion along the Uruguayan coast showed more upriver penetration during November 1995, which generated a stronger horizontal salinity gradient (Fig. 4A). In contrast, the salinity pattern along the Uruguayan coast during February 1996 showed a weaker horizontal salinity gradient (Fig. 4B).

Bottom temperature in the estuary ranged from 13.8 to 20.2°C during November 1995, and from 20.1° to 25.0°C during February 1996. In the spawning area, bottom temperatures ranged from 20.0°C to 20.2°C during the main reproductive period and from 21.5°C to 25.0°C at the end of the breeding season.

Whitemouth croaker of the Río de la Plata estuary spawn in the region of high salinity gradients. During November 1995, spawning took place near Montevideo, coinciding with the bottom salinity front (Fig. 4A). During February

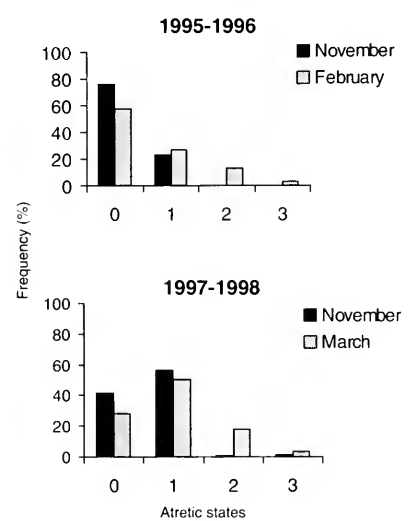

Figure 3

Atretic-state frequency of *M furnieri* during two spawning seasons (1995–96 and 1997–98), according to the Hunter and Macewicz (1985) scale.

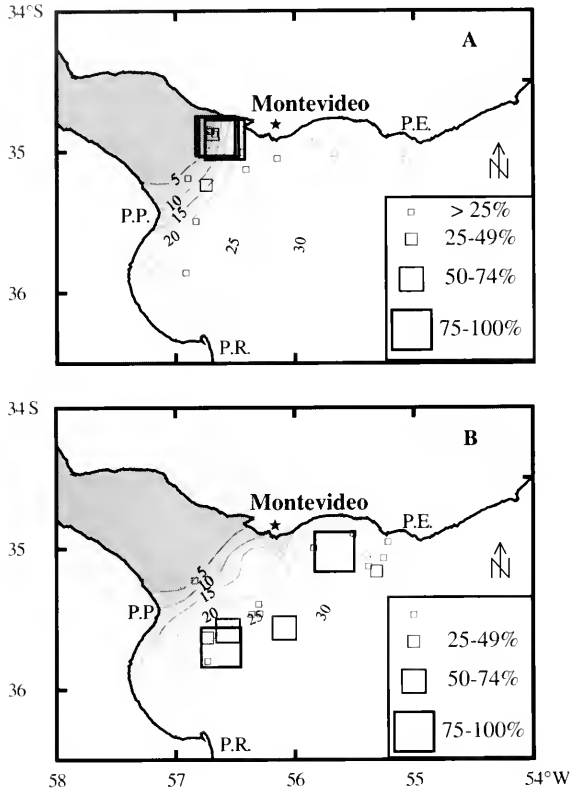

Figure 4

Spatial location of the *M furnieri* spawning area during November 1995 (**A**) and February 1996 (**B**). The size of the squares is proportional to the percentage of gravid females (with hydrated oocytes). In both maps, the isohalines expressed as psu) represent the bottom salinity field. PE = Punta del Este, Uruguay; PP = Punta Piedras; and PR = Punta Rasa, Argentina.

1996, spawning occurred in the outer part of the estuary, and gravid females were more scattered compared to November 1995 (Fig. 4B).

Postovulatory follicles and spawning frequency

The new POFs (between 0 and 6 h after spawning) have an irregular shape with many folds; the granulosa cells are aligned with a prominent nucleus, and the lumen is clearly visible (Fig. 5, A–B). A 12-h-old POF shows degenerative processes with fewer convolutions, the walls of the granulosa cells are not well defined, and the lumen becomes reduced (Fig. 5C). A 24-h-old POF shows pronounced signs of degeneration and forms a compact structure much smaller than that at age-12-h. The granulosa layer is still evident but consists of a few cells (Fig. 5D). Postovulatory follicles older than 24 h are difficult to distinguish and may be confused with atresia stages.

Only females collected during the season 1995–96 were used to estimate spawning frequency of *M. furnieri* because during 1997–98 spawning females (with POF or hydrated oocytes) were scarce. For the samples taken in November 1995 (Table 2), the mean percentage of mature females with postovulatory follicles was 31.51% (CV=0.18), equivalent to a spawning interval of about 3 days. During February 1996, the percentage of mature females with postovulatory follicles was 25.35% (CV=0.27), which would indicate that each female spawned about every 4 days (Table 3).

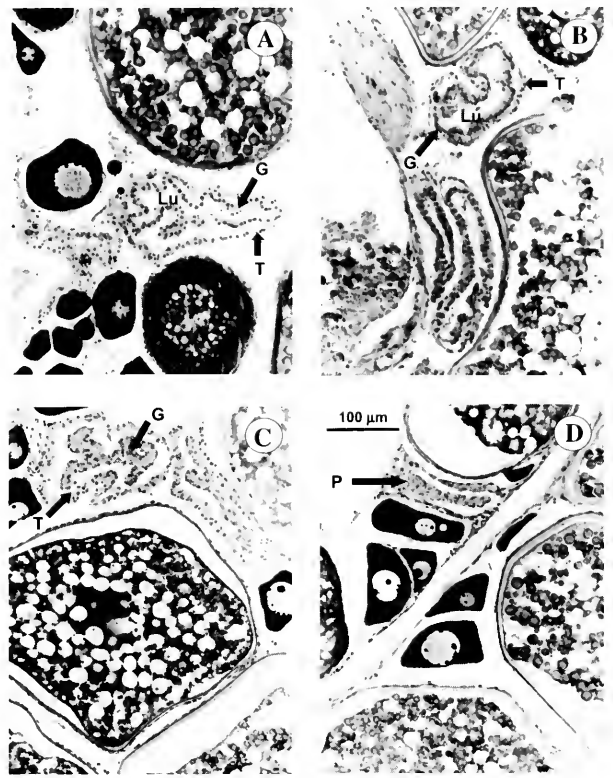

Figure 5

Degeneration of postovulatory follicles of *M. furnieri* at different times after spawning: (**A** and **B**) 0–6 h after spawning (no evidences of degeneration); (**C**) 12 h after spawning (with signs of degradation); (**D**) 24 h after spawning (with advanced signs of degeneration). T = thecal layer; G = granulosa layer; Lu = lumen; P = postovulatory follicle. Magnification is shown in (**D**).

Daily cycle of spawning

Percentages of females with hydrated oocytes and with POFs collected at different times during the spawning peak in November 1995 can be observed in Figure 6. Hydrated ovaries were observed mainly in the morning and in the afternoon. At dusk, females with hydrated oocytes were not observed, and ovaries showing age-0-h POFs increased sharply to about 40%, declining to about 5% at midnight. Postovulatory follicles older than 6 hours (POF stages 1 and 2) were observed at different times during the day and night. These observations indicate that some spawning of whitemouth croaker apparently took place early in the afternoon, when many females had hydrated oocytes. However, the vast majority of spawning occurred at dusk (near 20:00 h), when the frequency of hydrated oocytes decreased to 0% and the incidence of females with new postovulatory follicles reached a maximum.

Fecundity

Batch fecundity estimates for females sampled during 1995–96 revealed significant differences ($P<0.01$) between the spawning peak and the end of the reproductive season, being significantly greater in November (216,700 ±151,700 oocytes) than in February (96,900 ±52,000 oocytes). During 1997–98, females with hydrated eggs were scarce, but fecundity values obtained in March were

Table 2

Number of reproductively active females of *M. furnieri* sampled during November 1995 in the Río de la Plata estuary. H = hydrated oocytes without POF; POF-0 = elapsed time from spawning ≤ 6 h; POF-1 = elapsed time from spawning ≅ 12 h; . POF-2 = elapsed time from spawning ≅ 24 h.

Day of month	H	POF-0	POF-1	POF-2	Total mature females
16	0	0	0	0	5
16	0	7	2	5	37
17	0	0	0	0	16
18	0	0	1	0	20
18	1	1	2	0	6
18	0	0	1	0	10
19	0	0	0	0	10
19	0	0	0	0	7
19	0	0	0	0	10
21	1	0	2	0	9
21	17	0	10	5	36
21	1	1	4	3	29
21	0	1	1	2	20
22	7	0	2	3	25
22	0	11	5	5	26
22	1	1	5	3	13
23	0	0	2	4	9
23	9	0	3	9	30
23	2	7	2	2	13
23	0	4	0	2	11
Total	39	33	42	43	342

Table 3

Number of reproductively active females of *M. furnieri* sampled during February 1996 in the Río de la Plata estuary. H = hydrated oocytes without POF; POF-0 = elapsed time from spawning ≤ 6 h; POF-1 = elapsed time from spawning ≅ 12 h; . POF-2 = elapsed time from spawning ≅ 24 h.

Day of month	H	POF-0	POF-1	POF-2	Total mature females
10	0	1	0	3	5
11	0	0	0	0	6
11	0	0	0	1	26
11	0	5	4	4	21
12	0	0	0	1	13
14	2	1	2	2	26
14	6	4	2	1	14
15	6	5	1	1	21
15	0	2	0	0	28
17	3	0	0	0	6
17	0	0	1	0	9
18	5	0	1	2	10
Total	22	18	11	15	185

lower than in November, similar to that observed in the 1995–96 season. The relationship between batch fecundity and total length, for females taken during the spawning peak (combining November 1995 and 1997 data) and near the end of the season (combining February 1996 and March 1998 data), was curvilinear in both cases (Fig. 7A) and described by the equations

$$BF = 0.676TL^{3.282} \quad (r^2=0.82, n=60)$$

(spawning peak)

$BF = 0.028TL^{4.009}$ (r^2=0.69, n=27) (end of reproductive season).

Analysis of covariance indicated that the regression slopes did not differ between months (P>0.05), but the intercepts were significantly different (P<0.01).

The relationship between batch fecundity and ovary-free body weight was linear (Fig. 7B):

$BF = 223.15TW - 23{,}693$ (r^2=0.81, n=60) (spawning peak)

$BF = 231.82TW - 82{,}325$ (r^2=0.81, n=27) (end of reproductive season).

Relative fecundity ranged from 52 to 305 hydrated oocytes per gram of female (ovary-free). Mean values obtained from the spawning peak (196 ±55 oocytes) and the end of the reproductive season (139 ±50 oocytes) for females of the same average length (45 cm TL) were significantly different (P<0.01).

Egg production

The spawning season of *M. furnieri* lasted about six months. Taking into account the above estimations, a female would spawn between 60 and 45 times during this period, assuming a spawning interval of three or four days. On the other hand, batch fecundity appears to vary within the reproductive season, declining toward the end of the spawning period. With the minimum and maximum values of batch fecundity and spawning frequency, it is possible to obtain an approximate range of the annual oocyte production. We estimated that a 40-cm-TL female could produce annually between 3,300,000 and 7,300,000 eggs, depending on whether batch fecundity and spawning frequency were estimated during the end of reproductive season or the spawning peak, respectively.

Because batch fecundity is proportional to female body size, larger females (>50 cm TL) showed relatively high egg production than the most abundant size classes (35–45 cm TL) at least during the spawning peak (Fig. 8).

Egg size

Egg size in plankton samples declined as the spawning season progressed. Mean egg diameter for November 1995 was 970.4 µm (SD=34.1 µm) and 865.6 m (SD=35.0 µm) for February 1996. Mean dry weight of 100 eggs was 2.60 mg (SD=0.1 10^{-4} mg) for the first period and 1.92 mg (SD=1.16 10^{-4} mg) for the second. Analysis of variance indicated significant differences (P<0.01) in egg diameters and in egg dry weights (P<0.05) from samples collected during early and late spawning season.

Discussion

In the Río de la Plata estuary, reproductive investment of *Micropogonias furnieri* varied both within the spawn-

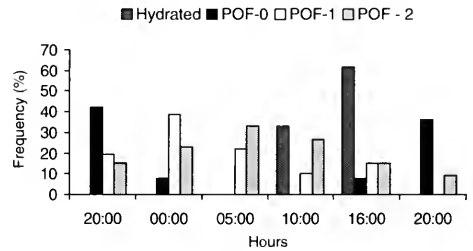

Figure 6

Hourly incidence of ovaries with hydrated oocytes (hydrated) and with postovulatory follicles in POF-0 (elapsed time from spawning ≤6 h), POF-1 (elapsed time from spawning ≅12 h) and POF-2 (elapsed time from spawning ≅24 h) stages, sampled within the spawning area during November 1995.

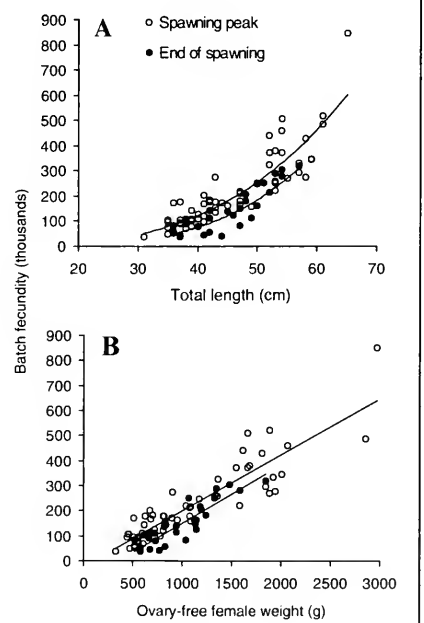

Figure 7

Batch fecundity as a function of total length (**A**) and ovary-free female wet weight (**B**) for data obtained during the spawning peak (November 1995 and 1997) and the end of the reproductive season (February 1996 and March 1998).

ing season and between years. In the 1995–96 season, a higher percentage of gravid females (with hydrated oocytes) was observed than in 1997–98. In both cases, we found that near the end of the season (February–March) the number of reproductively active females decreased when compared to the main spawning peak (November), and at the same time increased rates of atresia were observed. High levels of atresia have been used to identify regressing ovaries and to establish the cessation of spawning in other species (Hunter and Macewicz, 1985; Hunter et al., 1986; Dickerson et al., 1992; Barbieri et al., 1994).

Whitemouth croaker spawn in the estuarine waters of the Río de la Plata. During November, spawning occurs in the innermost part of the estuary, coinciding with the bottom salinity front (Macchi et al., 1996; Macchi, 1997; Acha et al., 1999). In the outer sector of the estuary, the females remain in recovering stage, eventually returning to the inner part where they complete maturation and spawn (Macchi et al., 1996). During February 1996, at the end of the reproductive season, the salinity front shows a more seaward position and a weaker horizontal salinity gradient than during November 1995, especially on the Uruguayan coast. Thus gravid females show a more scattered distribution, and the spawning area seems to be located in more coastal waters (25–30 psu). This may indicate that oceanographic conditions take priority over salinity in spawning-site selection, as had been suggested by Acha et al. (1999).

We observed a diel spawning periodicity in whitemouth croaker at Río de la Plata estuary, which may allow fish in spawning condition to concentrate at the same time and maximize fertilization (Holt et al., 1985). The estimated time of spawning peak for *M. furnieri* was near dusk, based on the incidence of females with new postovulatory follicles (less than 6 h after spawning). Spawning at dusk is a general reproductive pattern for different sciaenids, which are not dependent on light for courtship behavior because they use sound to locate mates (Holt et al., 1985). Maximum sound production for different sciaenids occurs during spawning, generally between 17:00 and 22:00 h (Saucier and Baltz, 1993). Spawning in darkness may reduce predation on eggs by visual feeders and may minimize the deleterious effects of sunlight on eggs (Saucier and Baltz, 1993). In the highly turbid waters of the Río de la Plata estuary, however, these advantages may not be as important.

Postovulatory follicle degradation in *M. furnieri* of the Río de la Plata was faster than that observed for *E. mordax* (Hunter and Goldberg, 1980). This more rapid degeneration may be a reflection of water temperature in the spawning area of whitemouth croaker, which is higher (20–25°C) than that recorded for the northern anchovy (Hunter et al., 1985). This result is coincident with that reported by Fitzhugh and Hettler (1995), who analyzed the effect of temperature on POF degeneration in Atlantic menhaden (*Brevoortia tyrannus*).

Spawning frequency estimated during the main reproductive peak in November 1995 (31.51%) was slightly higher than that estimated at the end of the spawning season in February 1996 (25.3%). These percentages indicate that the spawning interval of *M. furnieri* in the Río de la Plata estuary, ranged between three and four days during the season 1995–96. Daily spawning fraction estimated for this species was similar to that reported for *Pogonias cromis* from the Gulf of Mexico (Fitzhugh et al., 1993), but higher than those estimated for other sciaenids, such as *Seriphus politus* (DeMartini and Fountain, 1981), *Genyonemus lineatus* (Love et al., 1984), *Cynoscion nebulosus* (Brown-Peterson et al., 1988) and *Cynoscion guatucupa* (Macchi, 1998). There is only one previous report of spawning frequency for *M. furnieri* of the Río de la Plata area (Macchi et al., 1996). However, this estimate is not definitive because at that time the duration of the POF was unknown, and the authors used only a fraction of the females with postovulatory follicles to estimate this parameter.

Analysis of covariance applied to the batch fecundity and length data from November (1995–97) and February 1996–March 1998 showed similar slopes. However, the regression intercept for November was significantly greater than the intercept estimate for February–March. This result indicates that batch fecundity of *M. furnieri* decreases at the end of the breeding season, coinciding with an increase of atresia. The number of oocytes per female weight showed the same pattern, decreasing in February–March. The mean relative fecundity for whitemouth croaker during the reproductive peak (196 ±55 oocytes) was less than that obtained for other sciaenids, such as *Cynoscion nebulosus* (451 ±43 oocytes); (Brown-Peterson et al., 1988), *Cynoscion regalis* (200–750 oocytes); (Lowerre-Barbieri et al., 1996) and *Cynoscion guatucupa* (210 ±53 oocytes); (Macchi, 1998). Nevertheless, this variable varies among years, depending on environmental or nutritional factors (Nieland and Wilson, 1993).

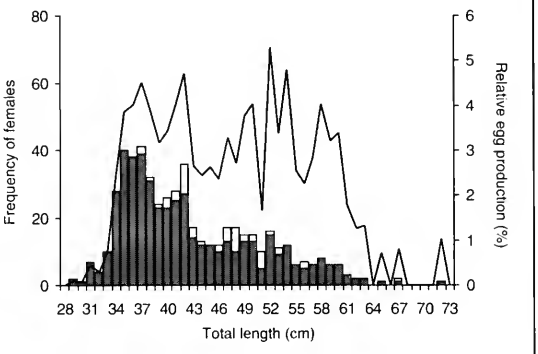

Figure 8

Relative egg production of *M furnieri* by length class (line), during the spawning peak (November 1995). Solid bars represent females in reproductive state (maturity stages 2 to 5), white bars correspond to inactive females.

From the duration of the breeding season, batch fecundity, and spawning frequency, it is possible to get a rough estimate of the annual egg production for whitemouth croaker of the Río de la Plata. Therefore, assuming a spawning season of about six months, we estimated that a 40-cm-TL female could produce between 3,300,000 and 7,300,000 eggs, depending on whether batch fecundity and spawning frequency were estimated near the end of the season or during the spawning peak, respectively. This annual egg production is within the range of that estimated for *M. furnieri* from the West Indies (from 2.4 to 13.5 million eggs); (Manickchand-Heileman and Ehrhardt, 1996).

During February–March, the percentage of whitemouth croaker females with active ovaries decreased significantly and oocyte production was half of that estimated for the spawning peak. Furthermore, the plankton data showed that *M. furnieri* egg diameters and dry weights decreased at the end of the breeding season. The seasonal decrease in egg size has been reported for other species (Ware, 1975; DeMartini and Fountain, 1981; Kjesbu et al., 1996). Explanations for this change in marine batch spawners include variations in temperature or nutritional state of the female (Hinckley, 1990; McEvoy and McEvoy, 1991). Some authors have suggested that larger eggs are advantageous because they result in larger hatchlings that are able to avoid predators more effectively (Hinckley, 1990; Wootton, 1994). In this case, in addition to the decrease in fecundity and spawning activity observed during the end of breeding season, the quality of the eggs produced for the last batches could be lower than in the spawning peak. These results suggest that the annual recruitment of *M. furnieri* in the Río de la Plata area depends to a great extent on females spawning during November.

Acknowledgments

This work is part of the INIDEP's Coastal Project. We thank Teresa Carlé and Haraldo E. Christiansen for the preparation of histological sections and Marcela Tobio for the photographic procedures. We would also like to thank Olav S. Kjesbu for a critical reading of our manuscript.

Literature cited

Acha, E. M., H. Mianzan, C. A. Lasta, and R. Guerrero.
1999. Estuarine spawning of the whitemouth croaker *Micropogonias furnieri* in the Rio de la Plata, Argentina. Mar. Freshwater Res. 50(1):57–65.

Acuña, A. A., J. Verocai, and S. Márquez.
1992. Aspectos biológicos de *Micropogonias furnieri* (Desmarest 1823) durante dos zafras en una pesquería artesanal al oeste de Montevideo. Rev. Biol. Mar. 27:113–132.

Barbieri, L. R., M. E. Chittenden Jr., and S. K. Lowerre-Barbieri.
1994. Maturity, spawning, and ovarian cycle of Atlantic croaker, *Micropogonias undulatus*, in the Chesapeake Bay and adjacent coastal waters. Fish. Bull. 92:671–685.

Brown-Peterson, N., P. Thomas, and C. R. Arnold.
1988. Reproductive biology of the spotted seatrout, *Cynoscion nebulosus*, in south Texas. Fish. Bull. 86:373–388.

Castello, J. P.
1986. Distribucion, crecimiento y maduración sexual de la corvina juvenil (*Micropogonias furnieri*) en el estuario de la "Lagoa Dos Patos," Brasil. Physis (Sec. A) 44(106):21–36.

Conover, D. O.
1985. Field and laboratory assesment of pattern in fecundity of a multiple spawning fish: the Atlantic silverside, *Menidia menidia*. Fish. Bull. 83:331–341.

DeMartini, E. E., and R. K. Fountain.
1981. Ovarian cycling frequency and batch fecundity in the queenfish, *Seriphus politus*: attributes representative of serial spawning fishes. Fish. Bull. 79:547–560.

Dickerson, T. L., B. J. Macewicz, and J. R. Hunter.
1992. Spawning frequency and batch fecundity of chub mackerel, *Scomber japonicus*, during 1985. Calif. Coop. Oceanic Fish. Invest. Rep. 33:130–140.

Draper, N., and H. Smith.
1981. Applied regression analysis, 2nd edition, 709 p. J. Wiley & Sons, New York, NY.

Fitzhugh, G. R., and W. F. Hettler.
1995. Temperature influence on postovulatory follicle degeneration in Atlantic menhaden, *Brevoortia tyrannus*. Fish. Bull. 93:568–572.

Fitzhugh, G. R., B. A. Thompson, and T. G. Snider III.
1993. Ovarian development, fecundity, and spawning frequency of black drum *Pogonia cromis* in Louisiana. Fish. Bull. 91:244–253.

Haimovici, M.
1977. Idade, crescimento e aspectos gerais da biologia da corvina *Micropogon opercularis* (Quoy e Gaimard, 1824) (Pisces Sciaenidae). Atlantica 2(1):21–49.

Hinckley, S.
1990. Variation of egg size of walleye pollack *Theragra chalcogramma* with a preliminary examination of the effect of egg size on larval size. Fish. Bull. 88:471–483.

Holt, G. J., S. A. Holt, and C. R. Arnold.
1985. Diel periodicity of spawning in sciaenids. Mar. Ecol. Prog. Ser. 27:1–7.

Hunter, J. R., and S. R. Goldberg.
1980. Spawning incidence and batch fecundity in northern anchovy, *Engraulis mordax*. Fish. Bull. 77:641–652.

Hunter, J. R., and B. J. Macewicz.
1985. Rates of atresia in the ovary of captive and wild northern anchovy, *Engraulis mordax*. Fish. Bull. 83:119–136.

Hunter, J. R., N. C. H. Lo, and R. J. H. Leong.
1985. Batch fecundity in multiple spawning fishes. *In* An egg production method for estimating spawning biomass of pelagics fish: application to the northern anchovy, *Engraulis mordax* (R. M. Lasker, ed.), p. 67–77. U.S. Dep. Commer., NOAA Tech.Rep.NMFS 36.

Hunter, J. R., B. J. Macewicz, and J. R. Sibert.
1986. The spawning frequency of Skipjack Tuna, *Katsuwonus pelamis*, from the South Pacific. Fish. Bull. 84:895–903.

Isaac-Nahum, V. J.
1988. Synopsis of biological data on the whitemouth croaker, *Micropogonias furnieri* (Desmarest, 1823). FAO Fisheries Synopsis 150, 35 p. FAO, Rome.

Isaac-Nahum, V. J., and A. E. A. De M. Vazzoler.
1983. Biologia reprodutiva de *Micropogonias furnieri*, (Desmarest, 1823) (Teleostei, Sciaenidae). Factor de condiçao como indicador do periodo de desova. Bol. Inst. Oceanogr. Sao Paulo 32(1):63–69.

Kjesbu, O. S., P. Solemdal, P. Bratland, and M. Fonn.
1996. Variation in annual egg production in individual captive atlantic cod (*Gadus morhua*). Can. J. Fish and Aquat. Sci. 53:610–620.

Lasta, C. A., and E. M. Acha.
1996. Cabo San Antonio: su importancia en el patrón reproductivo de peces marinos. Frente Maritimo 16:39–45.

Love, M. S., G. E. McGowen, W. Westphal, R. J. Lavenberg, and L. Martin.
1984. Aspects of the life history and fishery of the white croaker, *Genyonemus lineatus* (Sciaenidae), off California. Fish. Bull. 82:179–198.

Lowerre-Barbieri, S. K., M. E. Chittenden Jr., and L. R. Barbieri.
1996. Variable spawning activity and annual fecundity of weakfish in Chesapeake Bay. Trans. Am. Fish. Soc. 125: 532–545.

Macchi, G. J.
1997. Reproducción de la corvina rubia (*Micropogonias furnieri*) del sector rioplatense. Su relación con los gradientes horizontales de salinidad. Rev. Invest. y Des. Pesq. 11:19–38.
1998. Preliminary estimate of spawning frequency and batch fecundity of striped weakfish, *Cynoscion striatus*, in coastal waters off Buenos Aires province. Fish. Bull. 96: 375–381.

Macchi, G. J., and E. M. Acha.
1998. Aspectos reproductivos de las principales especies de peces muestreadas durante la campaña costera H-13/94. INIDEP Inf. Téc. 21:67–89

Macchi, G. J., and H. E. Christiansen.
1992a. Estudio histológico del ciclo reproductivo en hembras de la corvina rubia (*Micropogonias furnieri*). Análisis de la estructura madurativa en distintas localidades del área bonaerense. Frente Marítimo 11:47–56.
1992b. Estimación de la fecundidad de la corvina rubia (*Micropogonias furnieri*) mediante la aplicación del método estereométrico. Frente Maritimo 12:17–22.
1996. Análisis temporal del proceso de maduración y determinación de la incidencia de atresias en la corvina rubia (*Micropogonias furnieri*). Frente Marítimo 16:93–101.

Macchi, G. J., E. M. Acha, and C. A. Lasta.
1996. Desove y fecundidad de la corvina rubia (*Micropogonias furnieri* Desmarest, 1823) del estuario del Río de la Plata, Argentina. Bol. Inst. Esp. Ocean. 12(2):99–113.

Manickchand-Heileman, S. C., and N. M. Ehrhardt.
1996. Spawning frequency, fecundity and spawning potential of the whitemouth croaker, *Micropogonios furnieri* in Trinidad, West Indies. Bull. Mar. Sci. 58(1):156–164.

Mayer, I, S. E. Shackley, and J. S. Ryland.
1988. Aspects of the reproductive biology of the bass, *Dicentrarchus labrax* L.I. An histological and histochemical study of oocyte development. J. Fish Biol. 33:609–622.

McEvoy, L. A., and J. McEvoy.
1991. Size fluctuations in the eggs and newly hatched larvae of captive turbot *Scophthalmus maximus*. J. Mar. Biol. Assoc. 71:679–690.

Nellen, W., and G. Hempel.
1969. Versuche zur Fängigkeit des "Hai" und des modifizierten Gulf-V-Plankton-Samplers "Nackthai." Berichte der Deutschen Wissenschaftlichen Kommision für Meeresforschung 20:141–154.

Nieland D. L., and C. A. Wilson.
1993. Reproductive biology and annual variation of reproductive variables of black drum in the northern Gulf of mexico. Trans. Am. Fish. Soc. 122:318–327.

Picquelle, S. J., and G. Stauffer.
1985. Parameters estimation for an egg production method of northern anchovy biomass assessment. *In* An egg production method for estimating spawning biomass of pelagics fish: application to the northern anchovy, *Engraulis mordax* (R. M. Lasker, ed.), p. 7–16. U.S. Dep. Commer., NOAA Tech.Rep.NMFS 36.

Pravia, M. A., C. Garcia, L. Ares, and N. Berois.
1995. Estimación de la fecundidad y determinación del tipo de desove de la corvina blanca (*Micropogonias furnieri*) (Teleostei: Sciaenidae). Rev. Bras. Biol. 55(1):13–25.

Saucier, M. H., and D. M. Baltz.
1993. Spawning site selection by spotted seatrout, *Cynoscion nebulosus*, and black drum, *Pogonias cromis*, in Louisiana. Environ. Biol. Fishes 36:257–272.

Vazzoler, A. E. A. de M.
1970. *Micropogon furnieri*. Fecundidade e tipo de desova. Bolm. Inst. Oceanogr. S. Paulo, 18(1):27–32.

Ware, D. M.
1975. Relation between egg size, growth and natural mortality of larval size. J. Fish Res. Board. Can. 32:2503–2512.

Weiss, G.
1981. Ictioplancton del estuario de Lagoa dos Patos, Brasil. Ph.D., diss. 164 p. Universidad Nacional de La Plata, Facultad de Ciencias Naturales y Museo, La Plata, Argentina.

Wootton, R. J.
1994. Life histories as sampling devices: optimum egg size in pelagic fishes. J. Fish Biol. 45:1067–1077.

Abstract—Growth, recruitment, and abundance of young-of-the-year (YOY) striped mullet (*Mugil cephalus L.*) in estuarine habitats in South Carolina from 1998 to 2000 were examined and compared to historical data (1986–91) of growth, recruitment, and abundance. Daily growth increments from the sagittal otoliths of juvenile striped mullet were validated by using fish immersed in oxytetracycline hydrochloride (OTC) for five hours from the Charleston Harbor Estuary system. The distribution of back-calculated birthdates indicated that striped mullet spawn from October to late April and estuarine recruitment occurs from January through May. Juveniles were more abundant in mesohaline and polyhaline salinity regimes but were found throughout the estuary. Juvenile growth after recruitment into the estuary can be described by the relationship *Total length* (mm) = 0.341 $(Age)^{1.04}$ (r^2=0.741, P=0.001). Growth of juveniles according to the analysis of size-frequency data from historical surveys (1986 to 1991) in the same estuaries gave the relationship *Total length* (mm) = 8.77 $(month)^{1.12}$ (r^2=0.950, P=0.001). The similarity in the growth curves for both groups of fish suggests that juvenile striped mullet in South Carolina have consistent annual growth during the first year of life.

Manuscript accepted 12 December 2002.
Manuscript received 31 December 2002 at NMFS Scientific Publications Office.
Fish. Bull. 101:343–357 (2003).

Growth, recruitment, and abundance of juvenile striped mullet (*Mugil cephalus*) in South Carolina estuaries*

Christopher J. McDonough
Charles A. Wenner
Marine Resources Research Institute
South Carolina Department of Natural Resources
217 Fort Johnson Rd.
Charleston, South Carolina 29422-2559
E-mail address (for C. J. McDonough, contact author): mcdonoughc@mrd.dnr.state.sc.us

The striped mullet (*Mugil cephalus*) is distributed circumglobally in tropical and semitropical waters between latitudes 42°N and 42°S (Thomson, 1963; Rossi et al., 1998). The species can be found year round throughout the full range of estuarine salinities (including freshwater) in the southeastern United States (Jacot, 1920; Anderson, 1958). Striped mullet are harvested commercially throughout the world and used in aquaculture. Along the southeastern coast of the United States there are significant commercial fisheries in North Carolina and Florida. South Carolina and Georgia have smaller landings (Statistics and Economic Division[1]). The species is also harvested in the Gulf Coast states.

Fishing for striped mullet (for "roe fish") is most intense during the fall spawning migration. Throughout the rest of the year striped mullet are fished commercially for bait, if they are fished at all (Anderson, 1958). Landings of this species in the areas where it is heavily fished were significant and yielded an economic value of 38.2 million dollars from 1994 to 1998 (Statistics and Economic Division[1]). Striped mullet are also one of the most important forage fishes in the estuaries of the southeast and represent a significant food source for upper-level piscivores (Wenner et al.[2]).

Striped mullet spawn from October through February along the southeast coast of the United States (Jacot,1920; Broadhead, 1956; Anderson, 1958; Arnold and Thompson, 1958; Stenger, 1959; Dindo and MacGregor, 1981; Greeley et al., 1987; Render et al., 1995; and Hettler et al., 1997) and are considered isochronal spawning fishes (Greeley et al., 1987; Render et al., 1995) (i.e. they have synchronous gamete development and spawn all their reproductive material at once or in batches over a very short period of time). There have been few observations of spawning activity (Arnold and Thompson, 1958) and eggs and yolk-sac larvae have rarely been collected offshore (Anderson, 1958; Finucane et al., 1978; Collins and Stender, 1989).

Juvenile striped mullet recruit to the estuarine nursery habitat in South Carolina as early as December (Cain and Dean, 1976); this movement continues into June, peaking in February and March (Jacot, 1920; McGovern and Wenner, 1990). Juveniles are 18–30 mm total length (TL) at recruitment and have the silvery sheen of the pelagic stage. They are more laterally compressed than older juveniles and adults and hence are more streamline in shape. This shape is lost after they reach inshore waters at 32 mm TL (Eggold and Motta, 1992).

* Contribution 507 of the Marine Resources Research Institute, South Carolina Department of Natural Resources, Charleston, SC 29412.

[1] Statistics and Economics Division. 2000. Personal commun. Statistics and Economic Division, National Marine Fisheries Service, 1315 East-West Hwy., Silver Spring, MD 20910. http://www.st.nmfs.gov/st1/index.html.

[2] Wenner, C. A., W. A. Roumillat, J. E. Moran, M. B. Maddox, L. B. Daniel, and J. W. Smith. 1990. Investigations on the life history and population dynamics of marine recreational fishes in South Carolina, part 1, p. 6–35. South Carolina Marine Resources Research Institute, Completion reports, Project F-37, Charleston and Project F-31, Brunswick. Marine Resources Research Institute, P.O. Box 12559, Charleston, SC 29422-2559.

The size range of striped mullet at the time of estuarine recruitment is well documented; however, the ages of these juveniles are not well known (Chang, et al., 2000). These data are most easily obtained by examining the sagittal otoliths for daily growth increments. The importance of daily growth increments to estimate age in juvenile and larval fish for life history characteristics such as growth, recruitment, and determining spawning season is well documented (Brothers et al., 1976; Ralston and Miyamoto, 1983; Jones, 1986; Ralston and Williams, 1988; Campana and Moksness, 1991; Campana et al., 1994; Sponaugle and Cowen, 1997; Gillanders and Kingsford, 1996).

Several authors (Jones, 1986; Campana and Moksness, 1991; Campana et al., 1994) have concluded that daily growth increments should be validated for each species individually because of the variability in the time of deposition of the first daily increment, consistency of their formation, and their legibility with time. Radtke (1984) validated daily growth increments in cultured larval striped mullet in Hawaii and showed that daily growth increments were deposited well into the juvenile stage. Daily growth increments in juvenile striped mullet caught in the wild from Taiwan have also been validated (Chang et al., 2000).

The periodicity of increment deposition can be determined by either of two methods. Rings on otoliths from fish of known age (hatched in the laboratory) can be counted back to the core at specified times to check the increments. This method is accurate because factors affecting the fish (environmental, behavioral, and biological) can be more tightly controlled or manipulated in the laboratory (Jones, 1986). However, cultured conditions, at best, can only closely approximate conditions in the wild. In the second method, the otoliths of wild fishes are chemically marked. Fishes are sampled at various times and the increments deposited after this reference point are counted to estimate daily age (Jones, 1986).

The purposes of our study were 1) to demonstrate that juvenile striped mullet in South Carolina deposit daily growth increments on the sagittae; 2) to validate these marks as daily; 3) to use these validated ages and length data to model growth during the first year. Accurate age determinations through daily aging would provide important life history information, such as age at recruitment and the length of the spawning season through back-calculation of the spawning date. In addition, comparisons of the growth, spawning season, and occurrence of juvenile striped mullet from our study were made with historical data of abundance and length frequencies in South Carolina (1986 to 1991).

Materials and methods

Data collection and processing

The juvenile aging study was conducted from April of 1998 to December of 2000. A minimum of 20 juvenile striped mullet were collected monthly with a 7-m seine with 6-mm stretch mesh from the mudflats located in Grice Cove near Fort Johnson, South Carolina (Fig. 1). Additional samples came from the South Carolina Department of Health and Environmental Control (DHEC) and were caught from an electroshock boat in the freshwater portions of the Santee River, Cooper River, Ashley River, and Combahee River. Also, the Tidal Creek Project workgroup of the South Carolina Department of Natural Resources (SCDNR) used cast nets (1.87-m diameter with 6-mm mesh) in the tidal creeks of the lower Ashley River to catch juvenile striped mullet. A total of 2800 juvenile striped mullet were collected during the study; the number of these fish that were aged was 335.

Hydrographic data (water temperature and salinity) were recorded after sampling. Each specimen was measured in millimeters (mm) for total length (TL), fork length (FL), and standard length (SL). Sagittal otoliths were removed from the fish, and the right otolith was mounted on a microscope slide with Cytoseal mounting medium. Otoliths were polished with a felt polishing wheel loaded with tin oxide polishing compound (10 micron grit) by using a Crystalite lapidary polisher along the sagittal axis until the core was clearly discernible with increments visible to the outer edge. Age was determined at 1000× magnification under visible light as the mean of two independent readings of the counts of increments from the core to the outer edge. A third reading was made if the counts of the two previous readers differed by more than 10%.

Age validation

For the age validation experiment, 275 juvenile striped mullet were collected on 29 February 2000 from Fort Johnson Creek, a tributary of Parrot Point Creek in the Charleston Harbor estuary (Fig. 1), by seining. Specimens were transported to the laboratory and placed in a 1.3-m diameter tank, and acclimated overnight in well water at 15 parts per thousand (ppt) and 20°C. After transferral to a 38.7-L aquarium (15 ppt; 20°C) for marking, fish were immersed in oxytetracycline hydrochloride (OTC) at a concentration of 10 parts per million for five hours (Hettler, 1984). There were no mortalities during the treatment process. Marked specimens were placed in an outdoor 1.8-m diameter tank filled with (15 ppt, 20°C) well water. Water in the tank was replaced over a twenty-four hour period with ambient water from Charleston Harbor. These juveniles remained in the outside tank for the duration of the experiment to approximate as closely as possible the natural conditions of the local creek habitats. The fish were fed a daily ration of Tetramin floating commercial flakes (Tetramin, Blacksburg, VA) and were observed feeding one day after the OTC treatment. Salinity and water temperature, as well as dissolved oxygen concentration, were monitored daily.

Ten specimens were collected weekly for the next three weeks. Sagittal otoliths were removed and subjected to the same process as that given the otoliths used in the juvenile aging study. Each otolith was checked for the OTC mark under ultraviolet (UV) light at 1000× magnification by using a Nikon labophot compound microscope. The OTC mark appeared as a fluorescent mark when exposed to UV light (Fig. 2). Once the OTC mark was identified and its position marked, counts of increments after the OTC mark were made under visible light and recorded. This count was compared to the known number of days that had passed since marking with OTC.

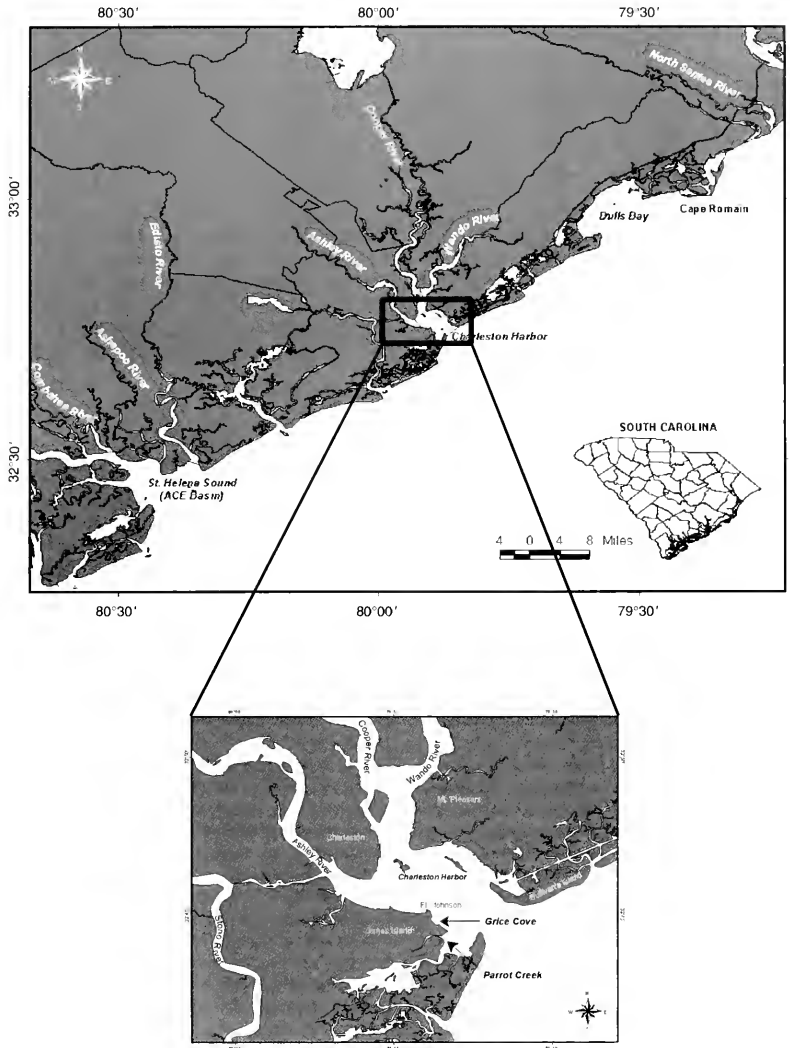

Figure 1

The major estuaries sampled during the juvenile aging study. Locations of collection sites for aging (Grice Cove) and increment validation (Parrot Creek) in the Charleston Harbor estuary are indicated in the inset.

Data analysis

The null hypothesis for the validation study was that the number of increments counted after the OTC mark equaled the number of days since marking. If these two numbers did not differ significantly, we could accept the hypothesis that the increments were deposited daily. The null hypothesis was tested by using a linear regression and a parametric paired *t*-test.

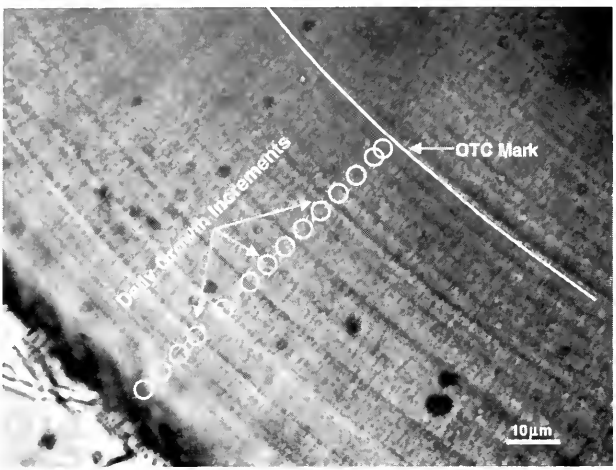

Figure 2

Photomicrograph of daily growth increments from the otolith of a striped mullet at 1000× magnification 14 days after OTC marking. The OTC mark is indicated and each subsequent daily growth increment is marked.

We also estimated the accuracy of the assigned ages of the fish. At the end of the study, 69 previously aged specimens were chosen at random and re-aged without knowledge of the prior assigned age. The percent agreement between the two sets of age readings was examined, and an age-bias plot was constructed for comparisons of the coefficients of variation between the two sets of ages for the same specimens (Campana et al., 1995).

The growth of juvenile striped mullet and the relationship of size at age once they recruit into the estuarine nursery habitats were described by using a least squares regression:

$$Y = aX^b \pm \varepsilon,$$

where Y = total length;
X = age;
a = the y-intercept;
b = the regression coefficient (slope); and
ε = the error term.

This would give a basic growth model from the juvenile aging study.

The distribution of the birthdates for the juveniles aged was backcalculated by subtracting the daily age of the fish from the date of capture. For the historical-survey fish (captured with rotenone), age was predicted from the application of the growth equation (least squares regression of size at age) to the observed lengths. We assumed in using the predicted age to estimate birthdates for the historical-survey fish that both groups (i.e. historical and current survey) had equal variances and similar growth patterns.

The historic data analyzed in our study were obtained from rotenone and plankton-net surveys in South Carolina from 1986 to 1991. The sampling technique for these surveys has been described (see Wenner et al.[2]). These data included length and hydrographic data similar to the data collected during our juvenile aging study and represented an additional 5498 fishes. The historical data were collected from three different salinity zones (oligohaline, mesohaline, and polyhaline) primarily within the Charleston Harbor estuary. The growth of juvenile striped mullet for the historical data was calculated from changes in mean total length per month by using a least squares regression. For fishes collected with rotenone, month of capture was substituted for age in the model. Mean size per month for each year of the rotenone survey (1986 to 1991) was determined separately. The growth from the juvenile aging study and from the historical data were then compared by using an analysis of covariance (ANCOVA) to compare the differences in the slopes and intercepts.

The different salinity regimes within the estuaries were defined by using the Venice scale of estuarine salinities (Anonymous, 1959). This scale provides five distinct salinity regimes within an estuary: freshwater (0 ppt), oligohaline (0.1 to 5 ppt), mesohaline (5.1 to 18 ppt), polyhaline (18.1 to 30 ppt), and euhaline (>30.1 ppt). Growth was compared between the different salinity regimes and significance was tested by comparing the changes in mean size per month within each salinity regime against the others by using an ANCOVA.

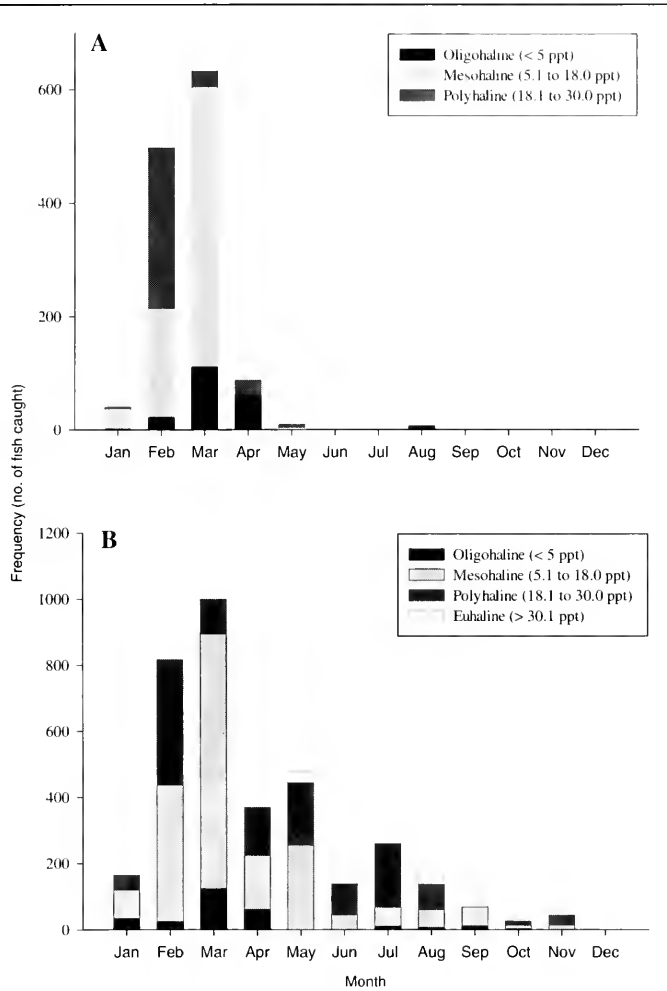

Figure 3

Total catch frequency for juvenile striped mullet stratified by salinity regime from plankton net tows (**A**) (n=1252) and rotenone surveys (**B**) (n=4246).

Results

Abundance and recruitment

Plankton tows from 1986 and 1987 showed that the highest abundance of striped mullet in the Charleston Harbor Estuary occurred in February and March (Fig. 3A). The majority of these young-of-the-year were captured in mesohaline (65% of the total) and polyhaline salinities (28% of the total).

The historical rotenone surveys indicated that numerical abundance of juvenile striped mullet was highest in February and March (Fig. 3B). The earliest captures of young-of-the-year striped mullet in the rotenone survey were 19 specimens in November of 1986 and a single specimen in December of 1986. Abundances for the different salinity

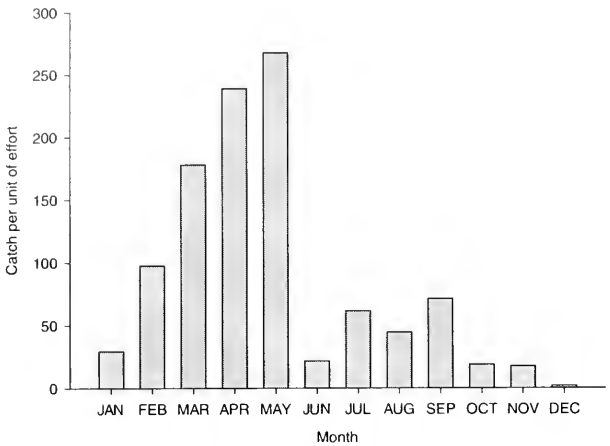

Figure 4

Catch per unit of effort for juvenile striped mullet in South Carolina estuaries from rotenone surveys, 1986 to 1991. n = 4246.

regimes showed that most of these fish were recruiting into mesohaline and polyhaline salinities. One difference in the rotenone data was that few juveniles were caught at oligohaline sites during the recruitment time period. Young-of-the-year striped mullet were caught at euhaline sites starting in May when the mean size was greater than 40 mm. Specimens captured by plankton net in freshwater and oligohaline salinities had very low abundances. The plankton net did not catch any juveniles in euhaline salinities. Catch per unit of effort (CPUE) for the rotenone surveys also demonstrated increasing abundance from February to May (Fig. 4).

Size frequencies in the different salinity regimes for the juvenile aging study (Fig. 5) showed young-of-the-year striped mullet (fish less than 200 mm) were found mostly at mesohaline and polyhaline salinities. The earliest occurrence of a young-of-the-year specimen in the juvenile aging study was a 25-mm specimen captured in December of 2000.

Age validation

The variability in the physical parameters during the age validation experiment approximated the diurnal variations in tidal creek habitats. Temperature and salinity ranged from 14.2° to 19.0°C and 21.3 ppt to 29.0 ppt. Dissolved oxygen ranged from 6.2 mg/L to 8.1 mg/L during the experiment.

There was no detectable growth during the experiment—probably a result of the short duration of the experiment. Age ranged from 57 to 121 days and mean age was 83 ±17.4 days. The mean age did increase over the course of the experiment with each collection (65.3 ±1.45 days, 82.2 ±2.47 days, and 102.5 ±3.59 days, respectively).

The OTC mark was visible under UV fluorescence on all the specimens examined. A paired t-test between the number of days after OTC marking and the number of increments counted after the OTC mark showed that the two variables were not significantly different (P=0.000, t=0.000, df=29, F=1648.0). Regression analysis (Fig. 6) indicated that the slope of the line running through these points did not differ significantly from 1.0 (r^2=0.998). These analyses allow the acceptance of the null hypothesis that the increments counted were deposited daily.

There was an 84.5% agreement between the original age and the second age read for the subsample of 69 specimens that were re-aged. An age bias plot (Fig. 7) showed the difference between the two ages for each specimen and the original age assigned to that specimen showed no detectable age bias. In addition, the coefficients of variance for each set of ages were similar (originally assigned age CV=0.434 and the second blind read age CV=0.429). An ANOVA comparing the mean ages for each group (original age=170.7 ±8.93 and blind read second age mean=170.6 ±8.80) also showed no significant differences (P=0.00, df=68, F=6878.8).

Growth

Growth of striped mullet from the juvenile aging study was described by the equation

$$Total\ length = 0.342\ (Age)^{1.039} \pm 19.4$$
$$(r^2=0.741 \text{ at } P=0.001).$$

Size at age was more variable in fish larger than 90 mm TL (Fig. 8); however, there was still clearly a strong relationship.

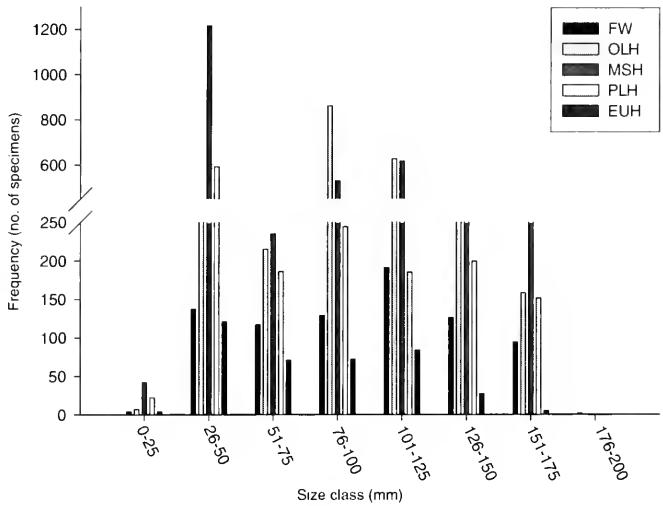

Figure 5

Striped mullet abundance stratified by size class and salinity regime for young-of-the-year (< 200 mm) for all years and gear types combined. Salinity zones: FW = freshwater, OLH = oligohaline, MSH = mesohaline, PLH = polyhaline, and EUH = euhaline. n = 8714.

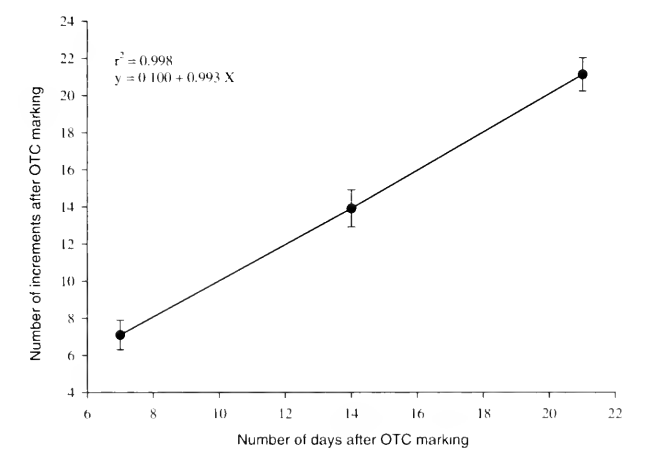

Figure 6

Regression analysis of striped mullet daily growth increments and number of days after oxytetracycline (OTC) marking. Each data point represents the mean number of daily growth increments for ten specimens taken each week of the experiment and error bars represent standard errors of the mean.

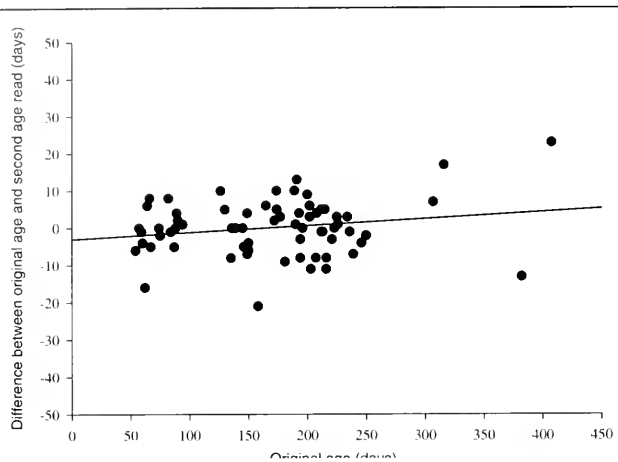

Figure 7

Age bias plot for juvenile striped mullet showing differences between blind read ages and the originally assigned ages. n = 69.

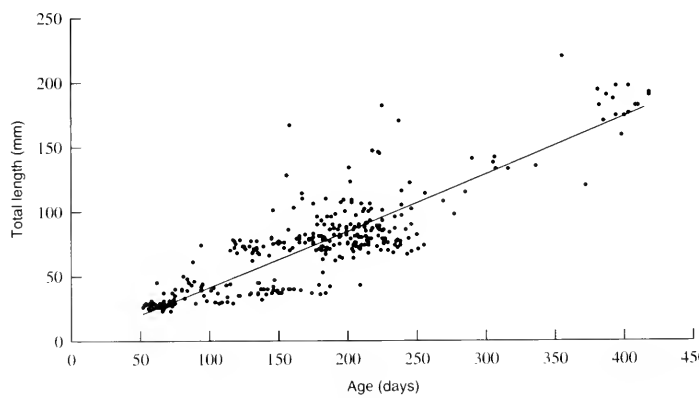

Figure 8

Size at age regression for young-of-the-year striped mullet. r^2 = 0.992 at P = 0.001, n = 335.

Mean size and age per month for these juveniles (Fig. 9, A and B) indicated steady growth throughout the year. One particular problem occurred in the month of April for fish in the juvenile aging study. For the first year when juveniles were collected, the size range was 130 to 180 mm and for the second year of the study, an April collection was not made because of equipment problems. The mean size and age for the fish collected in April indicated that these fish were one-year-old juveniles, not young of the year. Therefore, these fish were removed from the data set in subsequent analyses.

Specimens were not present for every month of every year for the rotenone survey, except for 1990 and 1991, because of differing sampling strategies employed. Therefore, all the rotenone data were pooled and collections for every month were represented in one data set. The resulting

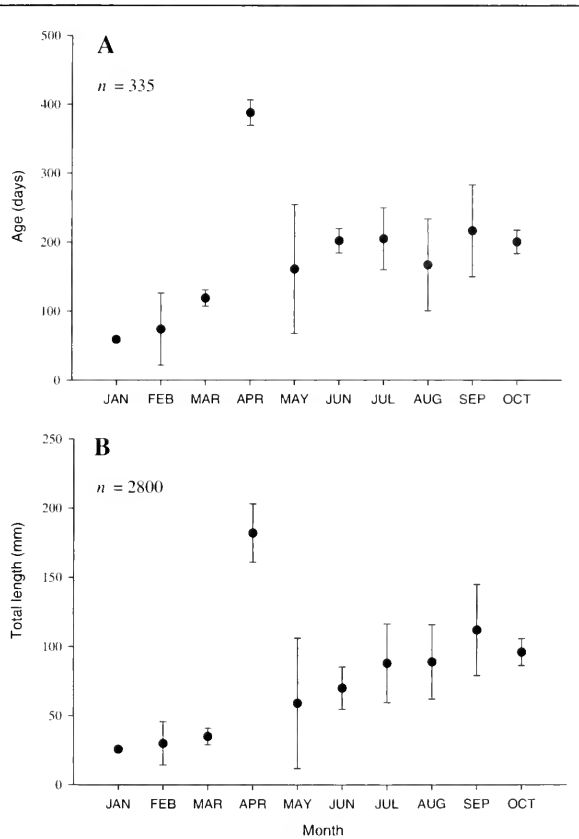

Figure 9

Mean age (**A**) and total length (**B**) at capture by month for young-of-the-year striped mullet from the juvenile aging study, 1998 to 2000.

growth curve (Fig. 10) for the rotenone study was described by the equation

$$Total\ length = 8.77\ (month\ of\ capture)^{1.13} \pm 9.20$$
$$(r^2=0.950 \text{ and } =235.0 \text{ at } P=0.001).$$

Month of capture was a good approximation of age because January represented the approximate middle of the spawning season (October to April) and it provided a measurable time frame in which to make both statistical comparisons and calculate growth rates.

The ANCOVA indicated that there was no significant difference between the slopes of our juvenile aging study and the rotenone studies (P=0.001); the coefficients of variation were not significantly different, and the residuals were normally distributed. However, there was a difference in the y-intercepts (0.346 for the juvenile aging study and 8.77 for the rotenone study). This difference was due to the age factor used in the separate regressions. Days were the units and in our juvenile aging study, whereas month of capture was used for age in the rotenone study. The higher r^2 for size at age in the rotenone survey reflected the use of changes in mean size per month for a larger sample (n=2576) than the actual size at age used for the juvenile aging study data (n=335).

The distribution of back-calculated birth dates for striped mullet from the juvenile aging study shows that the main spawning period ranges from October through April (Fig. 11A). The birthdate distribution for the rotenone fish defines the main spawning period from October to Febru-

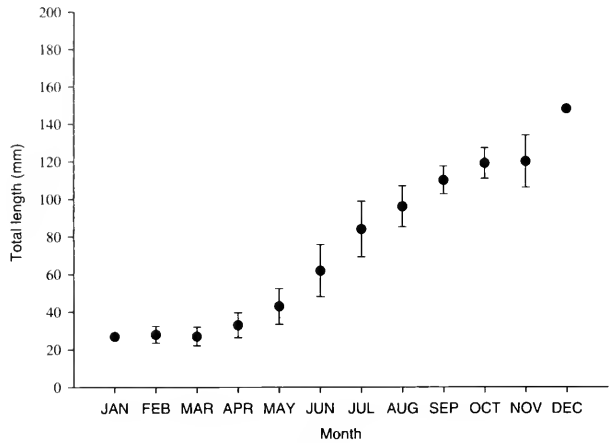

Figure 10

Mean total length per month for young-of-the-year striped mullet from historical rotenone and plankton net collections, 1986 to 1991. n = 5498.

ary with much less spawning activity in March and April (Fig. 11B). Both groups of striped mullet had peak spawning in December. The distribution of birthdates from fish in the juvenile aging study indicated a more protracted spawning season. A few individuals had birthdates outside the October–April time period, but the percentage of these fish was extremely low and within the margin of error for the back-calculated birthdates.

There was no significant difference in the mean size per month of juveniles captured at different salinity regimes (P=0.05) (Fig. 12). The initial growth rates for fish in all salinity regimes were very similar and fairly flat from January through April, and the mean size was still less than 40 mm. Growth increased noticeably in May and continued at a higher rate through the end of the year.

Discussion

Recruitment

The backcalculated birthdates from the juvenile aging study indicated that the spawning season extended from October to April. The earliest recruitment for fish in the rotenone surveys occurred in November and in December for the juvenile aging study. However, these were not standard samples and the early recruits represented a very small percentage of the young-of-the-year. Given that the youngest fish in the juvenile aging study were the most recent recruits, this was direct evidence that fish spawned in October were recruiting to South Carolina estuaries as early as November. Other studies have also found early recruits occurring prior to January in other estuaries from South Carolina (Cain and Dean, 1976), North Carolina (Hettler et al., 1997), Georgia (Anderson, 1958; Rogers et al., 1984), and Florida (Kilby, 1949). One of the earliest reported occurrences of young-of-the-year striped mullet was 19 November (Anderson, 1958) in Georgia. Offshore studies of ichthyoplankton in the South Atlantic Bight have indicated that the major spawning period occurs from December to February (Anderson, 1958; Collins and Stender, 1989). The smallest identifiable larvae caught in these studies were in the 3–5 mm range, and according to our growth model would have been approximately two to six days old. No studies to date have documented actual striped mullet spawning areas in the South Atlantic Bight. However, there is some evidence that striped mullet spawn near the edge of the continental shelf (Collins and Stender, 1989).

The peak abundances in our study for young-of-the-year striped mullet in South Carolina (February to May) agreed with available published data (Jacot, 1920; Anderson, 1958; McGovern and Wenner, 1990). In North Carolina, larval abundance has been shown to be highest from January through March and peaks in February (Hettler et al., 1997). The lack of substantial change in length and weight of striped mullet over the recruitment season suggested continued recruitment of new individuals from offshore (Hettler et al., 1997). Juveniles already recruited had dispersed throughout the estuary and were not abundant in catches afterwards. The recruitment of these juvenile striped mullet into North Carolina estuaries in pulses approximately three to four weeks apart was possibly related to the lunar cycle (Hettler et al., 1997). This type of pulse of new recruits into South Carolina was not seen in our study. In Georgia,

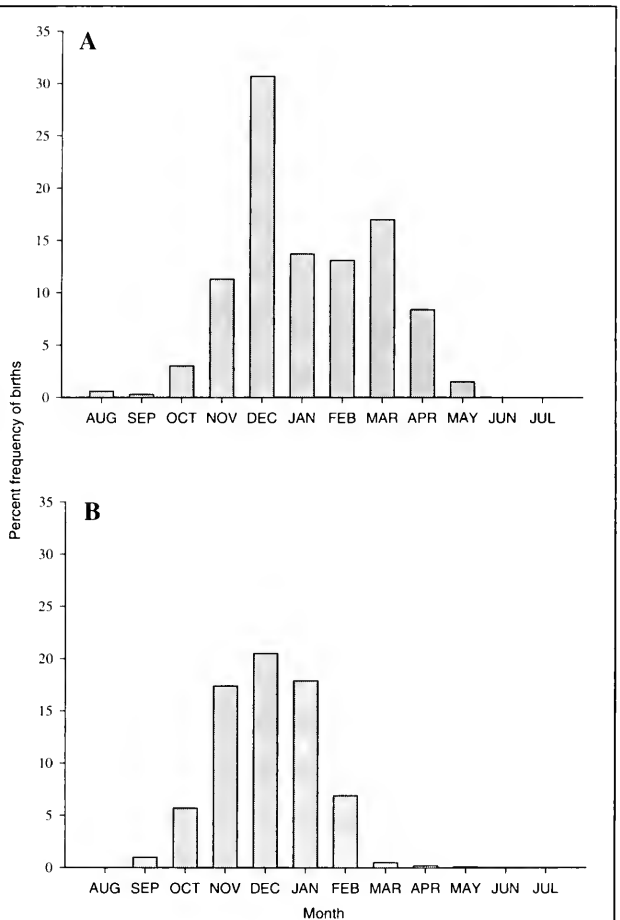

Figure 11

Percent frequency of births per month for striped mullet from the juvenile aging study (**A**) (n= 335) and the historical surveys (**B**) (n=5498).

mean lengths of young-of-the-year striped mullet also remained relatively constant from December to June, indicating an even more protracted period of juvenile recruitment than in either North or South Carolina (Rogers et al., 1984). Recruitment in Florida also appeared to occur over a much broader time scale than that for the Carolinas; newly recruited juveniles occurred from December to June (Kilby, 1949; Anderson, 1958). The longer recruitment season seen in the southern portion of the South Atlantic Bight may be due to faster onshore transport of striped mullet larvae and juveniles, proximity to the spawning grounds, i.e. the continental shelf, or a longer spawning season resulting from warmer temperatures.

Age validation

Otoliths form a permanent record of growth in juvenile fishes and can be an important "barometer" of growth and the conditions under which it occurred. Radtke (1984) validated daily growth increments in striped mullet juveniles from Hawaii using hatchery-reared fish. The primary difference in our study was the use of wild-caught juveniles

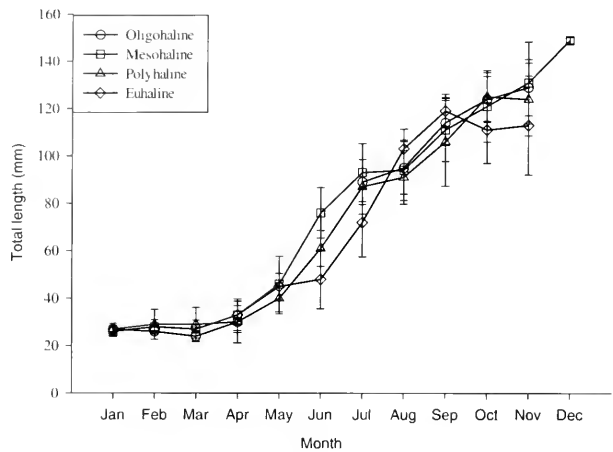

Figure 12

Mean size per month for young-of-the-year striped mullet stratified by salinity regime for pooled data from 1986 to 2000. n = 8714.

to validate daily growth increments. Another more recent study by Chang et al. (2000), using wild-caught striped mullet marked with OTC, also validated daily growth increments in Taiwanese estuaries.

The variation in physical parameters of temperature, salinity, and dissolved oxygen throughout the validation experiment approximated the existing conditions found in the harbor during this time period. Food sources may have differed between the tank and the tidal creeks; however, the fish were observed feeding on the growth on the sides of the tank in addition to ingesting the floating commercial food during most of the experiment. Because the mullet were observed actively feeding during this experiment, starvation stress probably did not affect increment deposition. In addition, concurrent collections of wild striped mullet for the juvenile aging study revealed size and age distributions similar to those for specimens used in the age validation part of our experiment.

Validation of daily growth increments is an important step in providing estimates of growth and age for larval and juvenile fishes. Accurate age and growth information enables better examinations of recruitment, population dynamics, and other important aspects of the life histories of juvenile fishes. Validation of daily growth increments in striped mullet allows for more accurate estimates of age in adults and juveniles, in particular, and thus this process helps to determine the first growth increment. Validation also helps determine different aspects of size at age in juvenile striped mullet, sexual differentiation, and development, and a more precise determination of spawning time periods in adult striped mullet through back calculation of birthdates.

Growth

Growth of newly recruited fish during the January–April time period was relatively low when compared to the rest of the year. This time period also coincided with the time of heaviest recruitment of these juvenile mullet. However, when we look at mean size per month for all of the juveniles pooled together, we find a similar growth curve in both the historical and current data. It was not until May, when the juvenile striped mullet reach a mean size of greater than 40 mm, that growth increased markedly. The results of the growth curves from our study appeared to support this. The greatest increase in growth came after a mean size of 40 mm was reached and during the months when mean monthly temperatures were higher. However, the differences in growth between different salinity regimes examined in our study were not found to be significant.

Growth for juvenile striped mullet was similar in both the rotenone study (1986 to 1991) and the juvenile aging study (1998 to 2000). This was evident from the nonsignificant differences in the slopes of the two curvilinear regressions. The coefficient of variation was also similar between the two groups. Because the growth rate for the rotenone study specimens was calculated from pooled data over a six-year period, it provided a fairly good estimate of growth over a range of environmental and biological conditions. As with the fish from the juvenile aging study, growth in the rotenone mullet study was fairly flat from January until May when mean size reached 40 mm or larger. After May the growth rate increased dramatically until it slowed again in the fall. The increase in growth rate from May to

October also coincided with seasonal increases in photoperiod and temperature.

The mean size at one year of age has been found to vary from 140 mm to 222 mm (TL, FL, SL) in striped mullet (Broadhead, 1956; Anderson, 1958; Thomson, 1966; Chubb et al., 1981). This wide range is most likely due to differences in methods of measurement. Previous studies have used length frequencies or ages determined from scales to calculate size at one year of age. These techniques are not as accurate in determining age as methods where otoliths are used (Campana et al., 1995). Our estimates of size at one year of age were 157 ±9.20 mm total length for the rotenone-caught fish and 157 ±19.4 mm for the fish in the juvenile aging study. Again, these sizes (in this case, mean size at one year of age) are consistent between the two studies, despite the different time scales used to calculate the growth curves. The ability to estimate size at age is important in the determination of the first annulus; however, the first annular growth increment for striped mullet in South Carolina was deposited in July at 15 to 23 months of age (McDonough, unpubl. data). Therefore, at 12 months of age the first annular increment would not have been deposited yet. The time lag between 12 months in age and the actual time of annual increment deposition probably also contributed to the wide range in sizes at one year of age in the literature.

The wide range of size at age of both juveniles and adult striped mullet is probably due to a range of environmental and biological factors that affect their growth. Kuo et al. (1973) found the greatest mortality in striped mullet during the first ten days of life. The end of this period coincided with the onset of intensive feeding behavior, which was approximately five days after complete yolksac depletion. The differences in the size range of these striped mullet during the 42-day larval period indicated differential growth. In Kuo et al.'s (1973) experiment, food was not a limiting factor and all the fish were hatched at the same time. A similar wide range in size at age was observed in the fish from the juvenile aging study. If food was not a growth-limiting factor for these fish, the only biological processes that could account for the differences would be either differing specific metabolic rates or intraspecific competition among larvae. These fish could have come from a wide range of geographic areas (where spawning occurred) at different times of the spawning season and food resources offshore could have been better for some groups of larvae than for others. Environmental factors that may have affected growth could include temperature and photoperiod, which could vary for larvae spawned at different times of the spawning season. Fish spawned in the mid-part of the spawning season (December to February) may have some advantage over fish spawned either earlier or later in the season. Rooker and Holt (1997) found cohort-specific growth rates to be higher in larval red drum (*Sciaenops ocellatus*) that were spawned during mid-season versus fish spawned at the beginning and end of the season. Fish that arrived earlier would spend more time in cold water and have slower growth. In addition, resources at spawning locations probably vary and these differences may show up as differential growth in comparably aged fish. We have found that variability in size at age is even more apparent in adult fish (McDonough, unpubl. data). The wide range of size at age found in the adults may be due to the same factor that causes differential growth in larval and juvenile striped mullet. This would not be uncommon because processes that occur during the larval phases of oceanic spawning fishes have been found to affect many characteristics of the adult population, namely recruitment, abundance, and growth (Houde, 1987, 1997; Bradford, 1992; Mertz and Myers, 1995; Comyns, 1998; Levin, 1998).

In summary, striped mullet in South Carolina deposit daily growth increments on the sagittal otoliths. The spawning season for these fish, as determined through birthdate back-calculation, was from October though April and subsequent recruitment occurred from January through May. However, there was evidence that young-of-the-year striped mullet can recruit as early as November. After recruitment, juvenile striped mullet were found most frequently at mesohaline and polyhaline salinities within the estuaries of South Carolina. Growth during the first year appears to be relatively consistent over time for juvenile striped mullet as indicated by the similarities in growth between fish collected in our study (1998 to 2000) and those collected in the rotenone study (1986 to 1991).

Acknowledgments

A great debt of gratitude is owed to all of those who assisted in this study. We thank Ted Smith, Wallace Jenkins, and Charlie Bridgham of the Marine Resources Research Institute (MRRI) for providing the facilities used to conduct the validation experiment, as well as expert advice and assistance in oxytetracycline marking. We also thank J. Archambault, H. Von Kolnitz, W. Hegler, L. Goss, G. Riekerk, C. Johnson at the MRRI for assistance in collections and sampling, and C. Altman from the S.C. Department of Health and Environmental Control for additional freshwater samples of juvenile striped mullet. Lastly, we thank B. Roumillat and M. Brouwer, as well as the anonymous reviewers, for careful and helpful suggestions for this manuscript. This research was made possible through National Marine Fisheries Service MARFIN Grant no. NA77FF0550 and National Marine Fisheries Service Grant no. NA97FL0359.

Literature cited

Anderson, W. W.
1958. Larval development, growth, and spawning of striped mullet (*Mugil cephalus*) along the south Atlantic coast of the United States. Fish. Bull. 58:501–519.

Anonymous.
1959. Symposium on the classification of brackish waters, Venice. Archives for Oceanography and Limonology 2 (suppl. 1):1–24.

Arnold, E. L., and J. R. Thompson.
1958. Offshore spawning of the striped mullet, *Mugil cephalus*, in the Gulf of Mexico. Copeia 1958:130–132.

Bradford, M. J.
1992. Precision of recruitment predictions from early life history stages of marine fishes. Fish. Bull. 90:439–453.
Broadhead, G. C.
1956. Growth of the black mullet, *Mugil cephalus*, in west and northwest Florida. Mar. Lab Tech. Series, Mar. Lab Tech. Serv. 25:1–29.
Brothers, E. B., C. P. Mathews, and R. Lasker.
1976. Daily growth increments in otoliths from larval and adult fishes. Fish. Bull. 74:1–8.
Cain, R. L., and J. M. Dean.
1976. Annual occurrence, abundance, and diversity of fish in a South Carolina inter-tidal creek. Mar. Biol. 36:369–379.
Campana, S. E., M. C. Annand, and J. I. McMillan.
1995. Graphical and statistical methods for determining the consistency of age determinations. Trans. Am. Fish. Soc. 124:131–138.
Campana, S. E., A. J. Fowler, and C. M. Jones.
1994. Otolith elemental fingerprinting for stock identification on Atlantic cod (*Gadus morhua*) using laser ablation ICPMS. Can. J. Fish. Aquat. Sci. 51:1942–1950.
Campana, S. E., and E. Moksness.
1991. Accuracy and precision of age and hatch date estimates from otolith microstructure examination. ICES J. Mar. Sci. 48:303–316.
Chang, C.W., W. N. Tzeng, and Y. C. Lee.
2000. Recruitment and hatching dates of grey mullet (*Mugil cephalus L.*) juveniles in the Tanshui estuary of Northwest Taiwan. Zool. Studies 39:99–106.
Chubb, C. F., I. C. Potter, C. J. Grant, R. C. J. Lenanton, and J. Wallace.
1981. Age, structure, growth rates, and movements of sea mullet, *Mugil cephalus* L., and yellow eye mullet, *Aldrichetta forsteri* (Valenciennes), in the Swan-Avon river system, Western Australia. Aust. J. Mar. Freshwater Res. 32:605–628.
Collins, M. R., and B. W. Stender.
1989. Larval striped mullet (*Mugil cephalus*) and white mullet (*Mugil curema*) off the southeastern United States. Bull. Mar. Sci. 45:580–589.
Comyns, B. H.
1998. Growth and mortality of fish larvae in the North-central Gulf of Mexico and implications to recruitment. Dissertation abstracts international, part B: science and engineering 58(10), p. 4651.
Dindo, J. J., and R. MacGregor.
1981. Annual cycle of serum gonadal steroids and serum lipids in striped mullet. Trans. Am. Fish. Soc. 110:403–409.
Eggold, B. T., and P. J. Motta
1992. Otogenetic dietary shifts and morphological correlates in striped mullet, *Mugil cephalus*. Environ. Biol. Fish. 34: 139–158.
Finucane, J. H., L. A. Collins, and L. E. Barger.
1978. Spawning of the striped mullet, *Mugil cephalus*, in the northwestern Gulf of Mexico. Northeast. Gulf. Sci. 2: 148–150.
Gillanders, B. M., and M. J. Kingsford.
1996. Elements in otoliths may elucidate the contribution of estuarine recruitment to sustaining coastal reef populations of a temperate reef fish. Mar. Ecol. Prog. Ser. 141(1–3):13–20.
Greeley, M. S., D. R. Calder, and R. A. Wallace.
1987. Oocyte growth and development in the striped mullet, *Mugil cephalus*, during sesonal ovarian recrudescence: relationship to fecundity and size at maturity. Fish. Bull. 85: 187–200.
Hettler, W. F.
1984. Marking otoliths by immersion of marine fish larvae in tetracycline. Trans. Am. Fish. Soc. 113:370–373.
Hettler, W. F., D. S. Peters, D. R. Colby, and E. H. Laban.
1997. Daily variability in abundance of larval fishes inside Beaufort Inlet. Fish. Bull. 95:477–493.
Houde, E. D.
1987. Fish early life history dynamics and recruitment variability. 10th annual larval fish conference. Proceedings of a conference held in Miami, Florida, USA, May 18-23, 1986. Am. Fish. Soc. Symp. ser. vol. 2L:17–29.
1997. Patterns and trends in larval stage growth and mortality in teleost fish. Ichthyolplankton Ecology, Fish. Soc. Brit. Isle., 22 p.
Jacot, A. P.
1920. Age, growth, and scale characters of the mullets, *Mugil cephalus* and *Mugil curema*. Trans. Am. Fish. Soc. 39(3): 199–229.
Jones, C.
1986. Determining age of larval fish with otolith increment technique. Fish. Bull. 84:91–103.
Kilby, J. D.
1949. A preliminary report on the young striped mullet (*Mugil cephalus* Linnaeus) in two gulf coastal areas of Florida. Quart. J. Fl. Acad. Sci. 11(1)7–23.
Kuo, C. M., Z. H. Shehaheh, and K. K. Milisen.
1973. A preliminary report on the development, growth and survival of laboratory reared larvae of the grey mullet, *Mugil cephalus* L. J. Fish Biol. 5:459–470.
Levin, P. S.
1998. The significance of variable and density-independent post-recruitment mortality in local populations of reef fishes. Aust. J. Ecol. 23(3):246–251.
McGovern, J. C., and C. A. Wenner.
1990. Seasonal recruitment of larval and juvenile fishes into impounded and non-impounded marshes. Wetlands 10(2):203–221.
Mertz, G., and R. A. Myers.
1995. Estimating the predictability of recruitment. Fish. Bull. 93:657–665.
Radtke, R.
1984. Formation and structural composition of larval striped mullet otoliths. Trans. Am. Fish. Soc. 113:186–191.
Ralston, S., and G. T. Miyamoto.
1983. Analyzing the width of daily otolith increments to age the Hawaiian snapper, *Pristipomoides filamentosus*. Fish. Bull. 81:523–535.
Ralston, S., and H. A. Williams.
1988. Numerical integration of daily growth increments: an efficient means of ageing tropical fishes for stock assessment. Fish. Bull. 87:1–16.
Render, J. H., B. A. Thompson, and R. L. Allen.
1995. Reproductive development of striped mullet in Louisiana estuarine waters with notes on the applicability of reproductive assessment methods for isochronal species. Trans. Am. Fish. Soc. 124(1):26–36.
Rogers, S. G., T. E. Targett, and S. B. Van Sant.
1984. Fish-nursery use in Georgia salt marsh estuaries: The influence of springtime freshwater conditions. Trans. Am. Fish. Soc. 113:595–606.
Rooker, J. R., and S. A. Holt.
1997. Utilization of subtropical seagrass meadows by newly settled red drum *Sciaenops ocellatus*: patterns of distribution and growth. Mar. Ecol. Prog. Ser. 158:139–149.

Rossi, A. R., M. Capula, D. Crosetti, D. E. Campton, and L. Sola.
1998. Genetic divergence and phylogenetic inferences in five species of Mugilidae (Pisces: Perciformes). Mar. Biol. 131: 213–218.
Sponaugle, S., and R. K. Cowen.
1997. Early life history traits and recruitment patterns of Carribbean wrasses (Labridae). Ecol. Mono. 67(2)177–202.
Stenger, A. H.
1959. A study of the structure and development of certain reproductive tissues of *Mugil cephalus* Linnaeus. Zoologica 44(2):53–70.
Thomson, J. M.
1963. Mullet life history strategies. Aust. J. Sci. 25:414–416.
1966. The grey mullets. Oceanogr. Mar. Biol. Ann. Rev. 4: 301–335.

Migration patterns of spiny dogfish (*Squalus acanthias*) in the North Pacific Ocean

Gordon A. McFarlane
Jacquelynne R. King
Pacific Biological Station
Fisheries and Oceans Canada
Nanaimo, British Columbia, Canada V9R 5K6
E-mail address (for G. A. McFarlane, contact author): McFarlaneS@pac.dfo-mpo.gc.ca

Abstract—From 1978 to 1988, approximately 71,000 spiny dogfish (*Squalus acanthias*) were tagged off the west coast of Canada. This program is the most extensive tagging study conducted for a shark species. Twelve years after the last year of tagging, recaptured tagged spiny dogfish are still being reported. As of December 2000, 2940 tagged fish (4.1%) have been recaptured. Spiny dogfish were tagged in three major areas: Strait of Georgia, west coast Vancouver Island, and northern British Columbia waters. Generally, spiny dogfish were recaptured close to their release site; however, extensive migrations (up to 7000 km) did occur. Migration rates varied across release areas. Spiny dogfish tagged in the Strait of Georgia underwent the least extensive movement; only 10–14% of the recaptures occurred outside the strait. Spiny dogfish tagged off the west coast of Vancouver Island or in northern British Columbia waters underwent more extensive movement; approximately 49–80% of the tagged spiny dogfish recaptured outside of the release areas. Spiny dogfish from all three release areas were recaptured off the west coast of United States and Alaska. Most impressive are the recaptures of tagged spiny dogfish off the coast of Japan. Over 30 spiny dogfish were recaptured near Japan, most of which originated off the west coast of Vancouver Island or from northern British Columbia waters.

Manuscript accepted 23 October 2002.
Manuscript received 31 December 2002 at NMFS Scientific Publications Office.
Fish. Bull. 101:358–367 (2003).

Interest in sharks, particularly the spiny dogfish (*Squalus acanthias*), is not new. Off the west coast of British Columbia dorsal spines from spiny dogfish have been found in shell midden sites dating as far back as 4000 years (Ketchen, 1986). Aside from a source of food, the skin of the spiny dogfish was used for polishing, the spines as perforation awls, and the liver oil for various domestic purposes. Dogfish even played a role culturally, for native peoples took the dogfish as a symbol of their families. More recently, commercial fisheries for spiny dogfish were dominant from the late-1800s to the mid-1900s as a source of oil for lubrication, lighting, and vitamin A, and as a source of fishmeal, in addition to or in place of fertilizer. In addition, since the mid-1970s spiny dogfish have been used exclusively as a source of food for human consumption.

Spiny dogfish biology is equally as fascinating as their cultural history. They are long lived and slow growing, attaining ages in the North Pacific in excess of 80 years, and sizes in excess of 130 cm (McFarlane and Beamish, 1987). Females in the North Pacific mature at 35 years (Saunders and McFarlane, 1993). One very unique aspect of dogfish biology is their long gestation period (fertilization to birth)—22 months (Holden, 1977)—which is longer than their closest rival for longest gestation, the Asiatic elephant (*Elephas maximus*).

Despite their unique position both economically and culturally, spiny dogfish have been the recipients of considerable disdain, from commercial and sport fishermen alike. The species has been used as a "poster child" for trash fish and has been accused of preying upon other valuable fish such as salmon, herring, and crabs, and of destroying fishing gear. Reports of dogfish being released minus their snouts, fins, and tails; of two fish being tied together (tail to tail), and other ghastly stories are common. Despite all this, spiny dogfish are ubiquitous and abundant throughout the North Pacific Ocean.

Spiny dogfish are distributed from California to Alaska, along the Aleutian chain to the Asian coast, south to Japan. Ketchen (1986) pointed out that knowledge of the movements of spiny dogfish and the interrelationships of spiny dogfish from different areas is at best incomplete. In this report, we present the results of the spiny dogfish tagging program conducted off the west coast of Canada between 1978 and 1988. To date, it is the most comprehensive tagging program for spiny dogfish or for any shark species.

Methods

Tagging occurred in three major areas off the west coast of Canada: Strait of Georgia (SOG) from Johnstone Strait through to, and including, the Juan de Fuca Strait; the west coast of Vancouver Island (WCVI); and northern British Columbia (NBC) from Queen Charlotte Sound through Hecate Strait into Dixon Entrance (Fig. 1).

One of the impediments to studying spiny dogfish movements has been the availability of a suitable, durable tag. The use of Floy anchor tags was inappropriate because dogfish placoid scales wore through the plastic. Initially (in 1978 and 1979), a Petersen disc tag was used to tag spiny dogfish in the Strait of Georgia. However, based on observed severe wounding caused by the

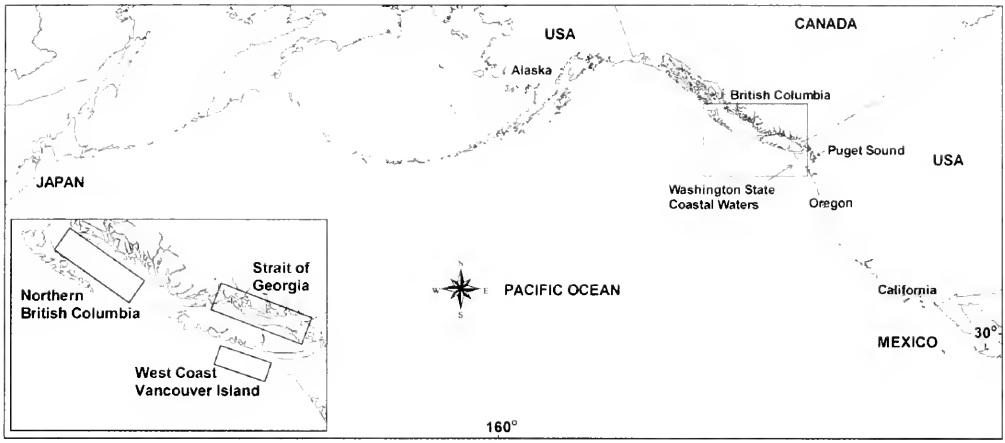

Figure 1

Tagged spiny dogfish were recaptured along the North American coast from Mexico to Alaska through to the eastern Pacific (Japan) and grouped by the areas indicated. The inset shows the west coast of Canada, and release areas for tagged spiny dogfish are denoted by rectangular boxes. Tagging occurred in the Strait of Georgia, northern British Columbia, and the west coast of Vancouver Island.

Petersen disc tag, a modified elongated tag was developed (McFarlane and Beamish, 1986). In 1979, approximately 30% of the tags deployed were modified elongated disc tags. Since then, only the modified elongated tag has been deployed. The tag consists of two elongated plastic discs with rounded ends (Fig. 2A). The application of the tag is similar to that of a Petersen disc tag (Wydoski and Emery, 1983). Each disc is attached to the fish by two pins, which are inserted through holes drilled in each disc 2.5 mm from each end. The disc is fastened to the fin of a dogfish with titanium pins made specifically for this study from grade 4, commercially pure (Ti70A) titanium wire (Fig. 2, A and B). Each pin is 7.6 cm long and 0.99 mm in diameter.

The applicator consists of a pair of hypodermic needles attached to a plexiglas handle (Fig. 2C) in a way that allows for the insertion of the pins with the exact spacing required (McFarlane and Beamish, 1986). The discs, on each side of the fish, are attached just below the anterior base of the first dorsal fin. During the tagging operation, the hypodermic needles are pushed through the base of the fin, the two pins are inserted through one disc and into the hypodermic needles, and the applicator is withdrawn, leaving the pins and disc attached to the fish. The second disc is placed over the pins and secured by bending the end of each pin 180° to form a small circle, with the free end of the pin resting under the bent portion of the pin that projected from the hole in the disc. The discs are loosely affixed and bent outwards to follow the contour of the fish. In 1988, another modification to the tag was initiated in the Strait of Georgia. A more flexible plastic was used as the tag material in one third of the tags used that year.

Barbless hooks were used to capture most fish; however, barbed hooks and bottom trawls also were used. In most cases fish were held in tanks on the vessel and only fish that appeared healthy were tagged. Fish were anaesthetized with MS 222 (tricaine methane sulfonate) prior to tagging and were measured for total length (nearest mm) from the tip of the snout to the tip of the upper lobe of the caudal fin when held in a horizontal position. Most tagged fish also were held in shipboard tanks to ensure recovery prior to release. A reward was paid for recaptured fish. Capture locations were recorded for major areas (Fig. 1). All returned fish were measured for length (nearest mm) and their sex was determined.

Movement between major areas was described as the percentage of recaptured fish originating from each release area. Because the number of fish recaptured will decline with time at liberty, we initially assessed the proportion of total fish recaptured (by release area) as a function of time at liberty to select an appropriate timeframe to use as a focus for reporting the percentage of recaptured fish.

It is important to note that these percentages do not reflect differences in fishing effort between major areas. In order to compare long-term movements between areas, it was necessary to standardize tag returns to effort, exploitation rate, or catch. Accurate effort data and estimates of exploitation rates are unavailable for the areas of tag returns. Catch (metric tons [t]) data for spiny dogfish were available for the areas in which the majority ot tagged fish were recaptured (Table 1). The use of catch to standardize recoveries between areas is valid only if population abundances are approximately equal between areas. This is true only for the Strait of Georgia and Puget Sound and west coast of Vancouver Island (Saunders, 1989; Ware and McFarlane, 1995). It is likely that the abundance off the Washington State coast is similar to that off the lower west coast of

Vancouver Island (Ketchen, 1986). For these four areas of tag recapture, annual catch (excluding discards) was used to estimate relative effort. Because catches are reported for the whole year, tag recaptures in the year of release were not standardized. We standardized tag recaptures in each area as the number of recaptured fish per 1000 t.

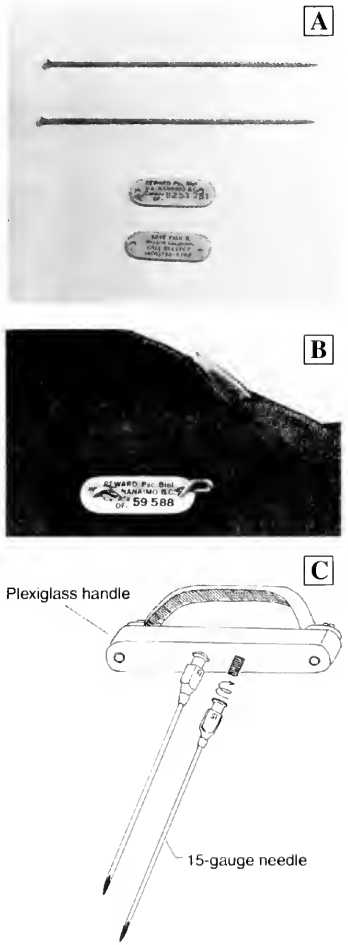

Figure 2

(**A**) Titanium pins and modified elongated disc tags developed for spiny dogfish. (**B**) Modified tag attached to spiny dogfish showing position of attachment, label of tag, and wire pins holding label in position. (**C**) Diagram of plexiglass tag applicator.

In order to elucidate differences in movement due to size at release or sex, the following categories were used: males ≤70 cm (M1); males >70 cm (M2); females ≤70 cm (F1); females 71–85 cm (F2); females ≥86 cm (F3). Size categories were based on approximate size at maturity and habitat use. Males mature at about 70 cm, which coincides with their movement from a mainly pelagic habitat to a deeper mid-water and demersal habitat. Females undergo a similar habitat change at 70 cm; however, their size at maturity is approximately 85 cm. Recoveries by the categories were then examined by area of recapture.

Results

Suitability of tag

McFarlane and Beamish (1986) reported preliminary results for the modified tag used in the present study compared to Petersen disc tags and Floy anchor tags. In contrast to the Petersen disc tag, the Floy anchor tag was quickly abraded and lost. Of 1688 fish receiving both tags, 49 were recovered from 1978 to 1982. All recovered fish had a Petersen disc tag; however only 11 fish had both tags, and 9 of these were recaptured during the first 18 months. McFarlane and Beamish also compared the modified Petersen disc tag to Petersen disc tags (McFarlane and Beamish, 1986). Petersen discs attached to spiny dogfish in 1978 and 1979 and recaptured from 1978 to 1980 were compared to modified Petersen disc tags applied from 1979 to 1982 and standardized for catch. The standardized recovery percentage (3.9%) for the modified Petersen disc tag compared to the Petersen disc tag (2.4%) was significantly higher (P=0.01).

Because the materials used in the tags were similar and none of the modified tags were returned with one pin missing, the decrease in percentage of recoveries of Petersen tags probably was due to mortality caused by tag wounds and not to disc or pin loss. For a description of the tag wounds see McFarlane and Beamish (1986). Both titanium pins remained in the tag in all recovered fish. A metallurgical stress test indicated that the pins were durable in salt water and might be expected to last more than 20 years (McFarlane and Beamish, 1986). In the present study we report that fish with the modified Petersen disc tag were recaptured with tags intact 20 years after release. After correcting for differences between years in catch (t) for tagged fish recaptured in the Strait of Georgia in 1988–90, a chi-square test on the ratios of the numbers released to the numbers returned indicated no significant level of difference in return percentages between the standard hard plastic tag and the more flexible plastic tag used in 1988 (P=0.304).

Tag return rates

Within the Strait of Georgia, tagging took place every year from 1978 to 1988 with the exception of 1986 (Table 2). Off the west coast of Vancouver Island, tagging was conducted in 1984, 1985, and 1987 (Table 2). Tagging was conducted in northern British Columbia waters in 1980, 1982, and 1987 (Table 2). In total, 70,770 fish were tagged throughout all

Table 1

Catch (in metric tons) from 1978 to 2000 of spiny dogfish (*Squalus acanthias*) for areas in which targeted fisheries operate.

Year	Strait of Georgia	West coast of Vancouver Island	Puget Sound	Washington State coastal waters
1978	2366	271	2647	42
1979	4469	303	3882	129
1980	2133	1874	3004	57
1981	781	312	1808	79
1982	1297	973	1944	38
1983	1281	596	1291	26
1984	1991	460	1445	318
1985	962	1499	971	274
1986	610	1935	746	113
1987	1247	2110	1429	984
1988	1200	3724	1396	200
1989	852	1847	1098	319
1990	820	2353	904	488
1991	667	1958	1303	853
1992	575	1426	931	1044
1993	135	111	758	1245
1994	941	876	958	1392
1995	1494	1076	929	367
1996	3019	938	818	251
1997	1584	531	214	425
1998	1831	953	115	462
1999	1062	1787	111	515
2000	610	2951	62	627

areas: 51,063 fish tagged in the Strait of Georgia, 10,087 fish tagged off the west coast of Vancouver Island, and 9620 fish tagged in northern British Columbia waters (Table 2). As of 31 December 2000, the total number of tagged fish recaptured were 2454 (4.8%) for Strait of Georgia released fish; 297 (2.9%) for the west coast of Vancouver Island fish; and 190 (2.0%) for fish in northern British Columbia waters (Table 2).

Recoveries over time

Approximately 93%, 96%, and 93% of the fish released in the Strait of Georgia, west coast of Vancouver Island, and northern British Columbia waters, respectively, were recaptured in the first 10 years at liberty (Fig. 3). Most recoveries (>70%) were made within ≤5 years after release (Fig. 3). In the Strait of Georgia, 81% were recovered ≤5 years; for the west coast of Vancouver Island 88% were recovered ≤4 years; and for northern British Columbia waters 71% were recovered ≤5 years. The maximum time at liberty was 19, 15, and 20 years for the Strait of Georgia, west coast of Vancouver Island, and northern British Columbia waters, respectively (Table 2).

Movement of tagged fish outside of release areas

Tagged spiny dogfish were recaptured throughout the North Pacific, from Japan, through Alaska, south to Mexico (Fig. 4). A large number of recaptured fish were reported from Puget Sound and Washington State coast (Table 3). For fish released in the Strait of Georgia, only three fish were recaptured outside of Canadian or Washington State waters (Table 3). For fish released in coastal waters (west coast of Vancouver Island and northern British Columbia), a large number of fish were recaptured in Japan (n=18+11) and United States waters, excluding Washington State (n=17+5). Two fish tagged off the west coast of Vancouver Island were recaptured in Mexico (Table 3).

Movement between release areas

Approximately 98% of the total number of recaptured fish were recaptured in Canadian waters or Washington State waters (coastal and Puget Sound). Because at least 70% of the recoveries occurred within the first 5 years at liberty (Fig. 3), we compared movement between release areas by examining the proportion of recaptured fish (percentage) at liberty for 5 years or less. For fish released in the Strait of Georgia, the majority (91%) were recaptured in the Strait of Georgia and another 5% off the west coast of Vancouver Island (Table 4). Only 2% were recaptured in northern British Columbia waters and 1% were recaptured in Puget Sound or in Washington State coastal waters (Table 4). For fish released off the west coast of Vancouver Island, again the majority of recaptures (62%) were in the area of release. A large percentage were recaptured in the

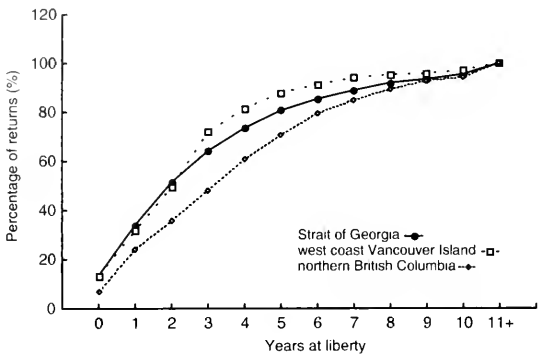

Figure 3

The cumulative percentage of recoveries standardized to catch by release area and years at liberty.

Table 2

Summary of the number of released and recaptured spiny dogfish by release year and release area.

Year of release	Released	Recaptured	Max. years at liberty
Strait of Georgia			
1978	1692	56	12
1979	4563	320	17
1980	7522	478	19
1981	7054	426	17
1982	10646	569	18
1983	1630	61	16
1984	7333	332	17
1985	4124	108	14
1987	3124	39	11
1988	3375	65	12
Total	51063	2454	
West coast of Vancouver Island			
1984	2066	77	14
1985	7124	198	15
1987	897	22	11
Total	10087	297	
Northern British Columbia			
1980	1075	34	20
1982	4873	120	16
1987	3672	36	11
Total	9620	190	

Strait of Georgia (13%) and in other areas (11%) including Japan, Alaska, Oregon, California, and Mexico (Fig. 4B). Only half of the recaptured fish from northern Bristish Columbia releases were recaptured in northern British Columbia (Table 4). Approximately 13% were recaptured in the Strait of Georgia, and another 28% off the west coast of Vancouver Island. As with west coast Vancouver Island releases, a large proportion (7%) of recaptured fish were found in other areas, namely in waters off Japan, Alaska, Oregon, and California (Fig. 4C).

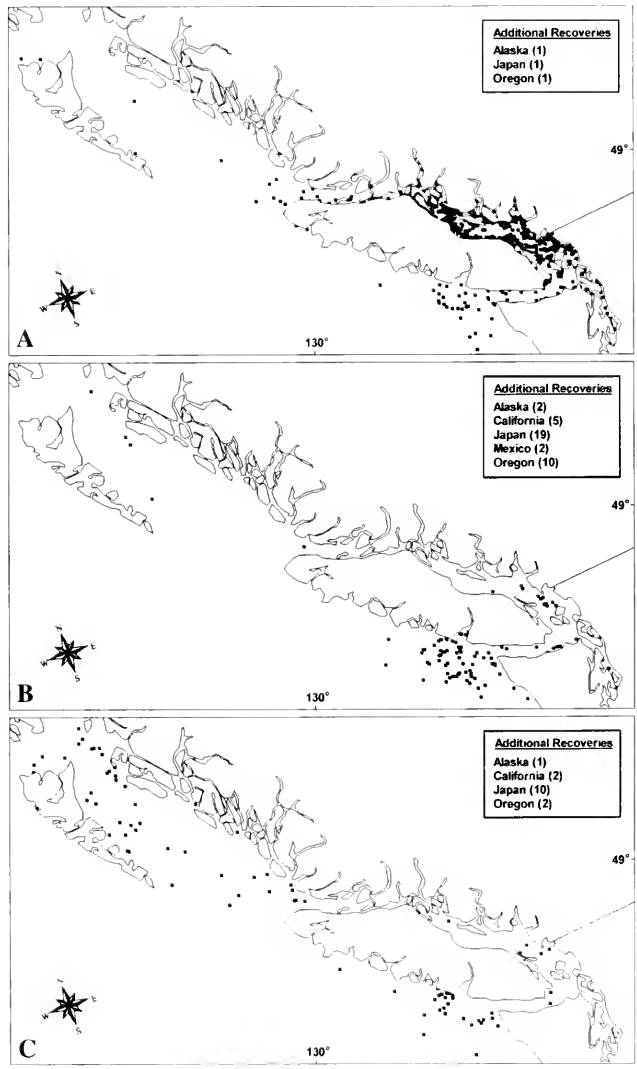

Figure 4

Recapture locations of tagged spiny dogfish released in (**A**) the Strait of Georgia; (**B**) west coast of Vancouver Island; and (**C**) northern British Columbia. The number of additional recoveries of spiny dogfish (by recapture area) that are not plotted on each figure are listed in the upper right key.

Table 3

The number of tagged dogfish recaptured from outside Canadian waters. SOG = Strait of Georgia; WCVI = west coast of Vancouver Island; NBC = northern British Columbia.

Area of release	Area of recapture							
	Japan	Alaska	Puget Sound	Washington	Oregon	California	Mexico	Total
SOG	1	1	28	18	1	0	0	49
WCVI	18	2	11	13	10	5	2	61
NBC	11	1	0	2	2	2	0	18
Total	30	4	39	33	13	7	2	128

Similar to the results for nonstandardized recoveries, the standardized recaptures for Strait of Georgia, Puget Sound, west coast of Vancouver Island, and Washington State coastal waters were based on recaptured fish at liberty for 5 years or less. For fish released in the Strait of Georgia, the majority (86%) were recaptured in the Strait of Georgia (Table 4). A further 7% were recaptured off the west coast of Vancouver Island, 6% in Washington State coastal waters, and only 1% in Puget Sound (Table 4). For fish released off the west coast of Vancouver Island, the majority of standardized recoveries (73%) occurred in Washington State coastal waters (Table 4). Only 20% were recaptured in the area of release.

Table 4

Mean percentage (%) of recaptured fish (at liberty ≤5 years) by area of release and known area of recapture including Puget Sound (PS), Washington State coastal waters (WS), and other areas. Standardized percentages could be calculated for only Strait of Georgia (SOG), west coast Vancouver Island (WCVI), Puget Sound, and Washington State coastal waters and are based on total standardized recaptures for these areas only. Standardized percentages could not be calculated for northern British Columbia (NBC).

Release area	Recapture area	Percentage of recaptures	
		Non-standardized	Standardized
SOG	SOG	91	86
	WCVI	5	7
	NBC	2	
	PS	1	1
	WS	1	6
	Other	0	
WCVI	WCVI	62	20
	SOG	13	5
	NBC	4	
	PS	5	2
	WS	5	73
	Other	11	
NBC	NBC	51	
	SOG	13	
	WCVI	28	
	PS	0	
	WS	1	
	Other	7	

Movement by sex and size

In general, small-size females (<70 cm) released in the Strait of Georgia and northern British Columbia were of the sex-size category (F1) of spiny dogfish that were recaptured in the highest proportion in other areas (Table 5). All sex-size categories of spiny dogfish (except M1, small males <70 cm) released off the west coast of Vancouver Island were recaptured in other areas in high proportions (Table 5).

Discussion

The low recovery percentage in this study is probably related to a low reporting rate. Until recently spiny dogfish catches in Canadian waters were discarded without being examined. However, this low recovery percentage also reflects the high abundance of spiny dogfish off the west coast of North America. Ketchen (1986) reported abundance estimates of 300 000 t for the whole North American coast and Saunders (1989) estimated 210,000–260,000 t in Canadian waters. It is clear that spiny dogfish are common and relatively abundant from northern Oregon to southeastern Alaska. Knowledge of the movements of spiny dogfish within eastern waters and between eastern and western waters is still limited but indicates that this shark is a key species in these coastal ecosystems. The use of the more durable modified Petersen tag in other areas would add to our knowledge of dogfish movement between these ecosystems.

Holland (1957), reporting on tagging studies conducted in the 1940s, concluded that Puget Sound and the Strait of Georgia supported indigenous populations. However, Ketchen (1986) reviewing studies by Foerster (1942), Fujioka et al. (1974), and McFarlane et al. (1982) suggested more movement between the inside populations than reported in

Table 5

Percentage (%) of tagged dogfish by size at release and sex-size category across recapture areas. (M1=males ≤70 cm; M2=males >70 cm. F1=females ≤70 cm; F2=females 71–85 cm; F3=females ≥86 cm.)

		Recapture area		
Release area	Sex-size category	Strait of Georgia	West coast Vancouver Island	Northern British Columbia
Strait of Georgia	M1	90	6	4
	M2	85	6	9
	F1	53	2	45
	F2	94	6	0
	F3	86	8	6
West coast of Vancouver Island	M1	0	100	0
	M2	37	63	0
	F1	17	61	22
	F2	0	23	77
	F3	39	50	11
Northern British Columbia	M1	0	0	100
	M2	9	9	82
	F1	9	21	70
	F2	0	6	94
	F3	6	8	86

earlier studies. Ketchen (1986) concluded that populations in inside waters (i.e. Strait of Georgia and Puget Sound) are largely independent of those off the open coast. Our study supports the idea that the majority of spiny dogfish in the Strait of Georgia remain in the Strait of Georgia. However, the low proportion of standardized recoveries in Puget Sound suggests very little movement between these two areas. In fact, a higher proportion of standardized recoveries of spiny dogfish from the Strait of Georgia were reported for coastal waters of Washington State than for Puget Sound.

Until this present study, little tagging had been conducted in open waters off the west coast of North America (Bonham et al., 1949; Holland, 1957; Ketchen, 1986). Holland (1957) observed a tendency for fish tagged off Washington and Vancouver Island to move south in the fall and winter, and north in spring and summer. The distance travelled (with a few exceptions) was generally small. Ketchen (1986) reported a similar pattern (based on seasonal fishery catches during the liver fishery of the 1940s) but noted that fishing did occur year round from northern British Columbia to Oregon. He concluded that some individuals may traverse the full commercial range of the species (Oregon to northern British Columbia) between summer and winter, but these instances are more the exception than the rule.

Seasonal movement aside, it is clear from our study that male and female spiny dogfish of all size categories in open coastal areas migrate considerably farther than previous studies suggest. For example, in the recapture areas where abundance estimates are similar and standardization to catch is possible (Strait of Georgia, Puget Sound, west coast Vancouver Island, Washington State coastal waters), the percentage of recaptures for west coast Vancouver Island releases indicates substantial movement south to Washington State coastal waters. This movement is greatly underestimated with nonstandardized data. Unfortunately it is not possible to standardize recapture data for all releases because of the paucity of fishing data or abundance estimates. Outside of Canadian waters, excluding Washington State (Puget Sound and coastal waters), there are no targeted spiny dogfish fisheries (i.e. landings are typically less than 10 t) and therefore the proportion of recaptured spiny dogfish in these areas would be expected to be small. However, it is possible to comment on the long-range movements (up to 7000 km) of these open coastal dogfish.

Tagged spiny dogfish released between 1980 and 1987 in open coastal waters (west coast of Vancouver Island and northern British Columbia) underwent extensive migrations and approximately 16% of recaptured fish came from outside Canada waters. From earlier studies, a few recaptured fish indicated that some spiny dogfish at least are highly mobile. In the early 1940s a large male dogfish tagged in northern British Columbia waters was recovered off California 171 days later (Manzer, 1946). Holland (1957) reported that a fish tagged off the west coast of Vancouver Island was recaptured off Baja California. One trans-Pacific migration (Washington State to Japan) was reported by Kauffman (1955). In our study, the 30 fish captured off Japan were all (with one exception) tagged in outside waters. These recaptures represented 6% of the recaptures from these release areas. Similarly, nine fish were captured off

California and Mexico, all from outside tag release areas. These rather remarkable recaptures do provide evidence for the trans-Pacific connection of spiny dogfish stocks but pose the question of the significance of such east to west exchanges. One possible significance would be the transfer of genetic material. The fact that these recaptures occurred regularly from 1982 to 2001 suggests ongoing migration between areas. Two recent recoveries off Japan support this hypothesis. One fish, a 69-cm female was released off the west coast of Vancouver Island in 1984, and the other, also a female (72-cm) was released in the Strait of Georgia in 1988. Both fish were recovered in May 2001 off Hokkaido. Although the evidence is limited, and the magnitude of the exchange between eastern and western Pacific stock, and indeed northern Canadian fish and those off southern California and Mexico, is small, it is clear that the interrelationships between these areas needs to be examined if ecosystem management incorporating these apex predators is to be developed.

In the eastern North Pacific, the management of spiny dogfish was recently identified as a priority by the American Fisheries Society (Musick et al., 2000). In addition, the global decline in many shark populations, and in particular spiny dogfish in the Atlantic ocean (Stevens et al., 2000), raises the question: What are the effects of the removal of large numbers of sharks (spiny dogfish) on marine ecosystems? A recent attempt (Stevens et al., 2000) to examine this question (albeit a somewhat simplistic one) identified a number of significant ecological and economic impacts. The study illustrated that under differing conditions, the consequences of depleting sharks in certain ecosystems are complex and could lead to unforeseen consequences that extend beyond the fished ecosystem. The highly migratory nature of many shark species complicates management efforts (Musick et al., 2000), and adding to the complexity are relationships between distribution, migration, and environmental conditions, such as those documented for blue, salmon, and thresher sharks in the northern Pacific (Holts, 1988; McKinnell and Seki, 1998; Bigelow et al., 1999). The development of effective ecosystem-based management hinges on understanding the implications of indirect and direct impacts on ecosystem structure and function (Fogarty and Murawski, 1998) and will require improved understanding of 1) species interactions, i.e. what, when, and where dogfish eat, and what eats dogfish, 2) migration patterns (both seasonal and long term) from and between all ecosystems within the range for dogfish (identified in this report), and 3) changes in migration and distribution in relation to changing climate and ocean conditions. To date, the effects of the removal of large numbers of spiny dogfish remain essentially unexamined, in part because of the limited information in each of these three areas.

Acknowledgments

We thank Bill Andrews, Brad Beaith, Mark Saunders, Mike Smith, and Maria Surry for conducting field work, maintaining databases, and preliminary production of tables and figures.

Literature cited

Bigelow, K. A., C. H. Biggs, and X. He.
1999. Environmental effects on swordfish and blue shark catches in the US North Pacific longline fishery. Fish. Ocean. 8:178–198.

Bonham, K., F. B. Sanford, W. Clegg and G. C. Brucker.
1949. Biological and vitamin A studies of dogfish (*Squalus acanthias*) landed in the State of Washington. Wash. Dep. Fish. Biol. Rep 49A:83–114.

Foerster, R. E.
1942. Dogfish tagging—preliminary results. Fish. Res. Board Can., Pac. Progr. Rep. 53:12–13.

Fogarty, M. J., and S. A. Murawski.
1998. Large-scale disturbance and the structure of marine systems: fishing impacts on Georges Bank. Ecol. Appl. 8 (suppl. 1):56–522.

Fujioka, B. P., and G. DiDonato.
1974. Dogfish tagging studies in Washington waters. *In* Puget Sound dogfish (*Squalus acanthias*) studies, 85 p. Wash. Dep. Fish, Mar. Fish. Invest., Suppl. Progr. Rep. 74-01.

Holden, M. J.
1977. Elasmobranchs. *In* Fish population dynamics (A. Gulland, ed.), p. 187–215. J. Wiley and Sons, New York, NY.

Holland, G. A.
1957. Migration and growth of the dogfish shark, *Squalus acanthias* (Linnaeus) of the eastern North Pacific. Wash. Dep. Fish. Res. Pap. 2(1):43–59.

Holts, D. B.
1988. Review of US west coast commercial shark fisheries. Mar. Fish. Rev. 50(1):1–8.

Kauffman, D. E.
1955. Noteworthy recoveries of tagged dogfish. Wash. Dep. Fish. Res. Pap. 1(3):39–40.

Ketchen, K. S.
1986. The spiny dogfish (*Squalus acanthias*) in the northeast Pacific and a history of its utilization. Can. Spec. Publ. Fish. Aquat. Sci. 88, 78 p.

McFarlane, G. A., and R. J. Beamish.
1986. A tag suitable for assessing long-term movements of spiny dogfish and preliminary results from use of this tag. N. Am. J. Fish. Manage. 6: 69–76.
1982. Validation of the dorsal spine method of age determination for spiny dogfish. *In* Age and growth of fish (R. C. Summerfelt and G. E. Hall, eds.), p. 287–300. Iowa State Univ. Press, Ames, IA.

McFarlane, G. A., R. J. Beamish, M. S. Smith, V. Egan, and D. Brown.
1982. Results of spiny dogfish (*Squalus acanthias*) tagging in the Strait of Georgia, Queen Charlotte Sound, Hecate Strait and Dixon Entrance, during 1980. Can. Man. Rep. Fish. Aquat. Sci. 1646, 123 p.

McKinnell, S., and M. P. Seki.
1998. Shark bycatch in the Japanese high seas squid driftnet fishery in the North Pacific ocean. Fish. Res. 39: 127–138.

Manzer, J. I.
1946. Interesting movements as shown by the recovery of certain species of tagged fish. Fish. Res. Board Can. Pac. Progr. Rep. 67, 31 p.

Musick, J. A., G. Burgess, G. Cailliet, M. Camhi, and S. Fordham.
2000. Management of sharks and their relatives (Elasmobranchii). Fisheries 25(3):9–13.

Saunders, M. W.
1989. Dogfish. *In* Groundfish stock assessments for the West Coast of Canada in 1988 and recommended yield options for 1989 (J. Fargo and A.V. Tyler, eds.), p. 169–176. Can. Tech. Rep. Fish. Aquat. Sci. 1646.
Saunders, M. W., and G. A. McFarlane.
1993. Age and length at maturity of the female spiny dogfish (*Squalus acanthias*) in the Strait of Georgia, British Columbia, Canada. Environ. Biol. Fishes 38:49–57.
Stevens, J. D., R. Bonfil, N. K. Duluy, and P. A. Walker.
2000. The effects of fishing on sharks, rays, and chimaeras (chondrichthyans) and implications for marine ecosystems. ICES J. Mar. Sci. 57:476–494.
Ware, D. M., and G. A. McFarlane.
1995. Climate-induced changes in Packific hake (*Merluccius productus*) abundance and pelagic community interactions in the Vancouver Island upwelling system. *In* Climate change and northern fish populations (R. J. Beamish, ed.), p. 509–521. Can. Spec. Pub. Fish. Aquat. Sci. 121.
Wydoski, R., and L. Emery.
1983. Tagging and marking. *In* Fisheries techniques (L. A. Nielson and D. L. Johnson, eds.), p. 215–237. Am. Fish. Soc., Bethsuda, MD.

Larval development of the southern sea garfish (*Hyporhamphus melanochir*) and the river garfish (*H. regularis*) (Beloniformes: Hemiramphidae) from South Australian waters

Craig J. Noell

Department of Environmental Biology
Adelaide University
South Australia 5005
Present address: SARDI Aquatic Sciences
PO Box 120
Henley Beach
South Australia 5022
E-mail address: noell.craig@saugov.sa.au

Abstract—Larval development of the southern sea garfish (*Hyporhamphus melanochir*) and the river garfish (*H. regularis*) is described from specimens from South Australian waters. Larvae of *H. melanochir* and *H. regularis* have completed notochord flexion at hatching and are characterized by an elongate body with distinct rows of melanophores along the dorsal, lateral, and ventral surfaces; a small to moderate head; a heavily pigmented and long straight gut; a persistent preanal finfold; and an extended lower jaw. Fin formation occurs in the following sequence: caudal, dorsal and anal (almost simultaneously), pectoral, and pelvic. Despite the similarities between both species and among hemiramphid larvae in general, *H. melanochir* larvae are distinguishable from *H. regularis* by 1) having 58–61 vertebrae (vs. 51–54 for *H. regularis*); 2) having 12–15 melanophore pairs in longitudinal rows along the dorsal margin between the head and origin of the dorsal fin (vs. 19–22 for *H. regularis*); and 3) the absence of a large ventral pigment blotch anteriorly on the gut and isthmus (present in *H. regularis*). Both species can be distinguished from similar larvae of southern Australia (other hemiramphids and a scomberosocid) by differences in meristic counts and pigmentation.

Manuscript accepted 25 October 2002.
Manuscript received 31 December 2002 at NMFS Scientific Publications Office.
Fish. Bull. 101:368–376 (2003).

The beloniform family Hemiramphidae (garfishes or halfbeaks) are small to medium-size surface-dwelling marine, estuarine, and freshwater fishes. The family contains 12 genera and 101 species worldwide, and more than one-third of the species belong to the genus *Hyporhamphus* (Froese and Pauly[1]). The Hemiramphidae are related to the Exocoetidae (flyingfishes) and, more distantly, to the Scomberosocidae (sauries), Belonidae (needlefishes), and Adrianichthyidae (ricefishes) (Collette et al., 1984). Six genera and 17 species of hemiramphids occur in Australian waters, where garfishes have long been considered valuable food and bait fish (Collette, 1974; Kailola et al., 1993).

Two hemiramphid species inhabit the waters of South Australia (S.A.), namely the southern sea garfish *Hyporhamphus melanochir* (Valenciennes, 1846) and the river garfish *H. regularis* (Günther, 1866). Adults of both are widely distributed along southern Australia from Western Australia (W.A.) to New South Wales, although *H. regularis* have not been recorded in Tasmania (Tas.). They support important commercial and recreational fisheries, particularly in S.A. (Kailola et al., 1993). *H. melanochir* are commonly found in sheltered coastal waters, whereas *H. regularis* are confined to estuaries (Jones et al., 1996). Juveniles and adults of both species co-occur in some estuaries of southern Australia, e.g. Port River-Barker Inlet of S.A. (34°45′S, 138°31′E) (Jones et al., 1996) and Peel-Harvey Estuary of W.A. (32°32′S, 115°43′E) (Noell, unpubl. data).

Despite their widespread distribution and economic importance, the early life history of *H. melanochir* is only partially described (i.e. reproductive biology [Ling, 1958]; egg development [Jordan et al., 1998], and there is no published information for *H. regularis*. Furthermore, although adults are easily identified with keys and descriptions provided by Collette (1974), no such information exists for the larvae. A fundamental prerequisite for any larval fish study is, undoubtedly, their accurate identification (Neira et al., 1998).

Thus far, at least some larval stages have been described for 19 hemiramphids worldwide (Sudarsan, 1966; Talwar, 1967; Hardy, 1978; Chen, 1988; Watson, 1996; Prince Jeyaseelan, 1998), eight of which belong to *Hyporhamphus*. The purposes of this paper are to describe the larval development of *H. melanochir* and *H. regularis* and to document distinguishing characters between larvae of these species.

[1] Froese, R., and D. Pauly. 2001. FishBase. World Wide Web electronic publication. Accessed 28 Nov 2001. Web site: www.fishbase.org.

Materials and methods

Most larvae were collected with a neuston net in Gulf St. Vincent (34°29′S, 138°15′E) and the Bay of Shoals (35°37′S, 137°37′E) of South Australia. The neuston net was a square-framed bongo net with a mouth area of 0.5 m^2 fitted with 500-µm mesh, to which a 30-cm diameter pneumatic float was attached to both sides of the frame. This attachment ensured that, while being towed, the top of the frame rode steadily above the water surface and that ~0.4 m^2 of the mouth area was submerged. The net was towed from the stern of the vessel inside a circular direction for 5 min at speeds of 2–4 knots. Additional larvae were collected by hand from beneath a wharf in Barker Inlet where they often school during daylight at mid-flood tide. Transforming larvae and juveniles were collected at night with a dip net and spotlight at Outer Harbor (34°46′S, 138°28′E) and Barker Inlet. The term "transforming" is used here to describe the stage between the end of the larval phase and the start of the juvenile phase, i.e. after the attainment of all fin rays and before the formation of scales. All specimens examined in this study were collected between November and March. Larvae were sorted from plankton samples immediately after collection based on reference larval specimens from the South Australian Museum fish collection that were identified to family. Larvae were fixed in 10% formalin buffered with sodium β-glycerophosphate (1 g/L) and later preserved in 70% ethanol.

A total of 47 *H. melanochir* (6.4–48.3 mm body length, BL) and 49 *H. regularis* (7.0–46.9 mm BL) larvae through juveniles were used to describe morphometrics, meristics, and pigmentation. Larvae were identified as hemiramphids based on larval and adult characters reported in the literature (Collette, 1974; Hardy, 1978; Collette et al., 1984; Chen, 1988; Watson, 1996; Trnski et al., 2000). Developmental series were assembled by using the series method (Neira et al., 1998), the accuracy of which was verified by a molecular technique (Noell et al., 2001). Terminology of early life history stages follows that of Kendall et al. (1984). Representative series for both species are deposited with the I.S.R. Munro Fish Collection (CSIRO, Hobart, Tas.). (Registration numbers: *H. melanochir* (n=13), CSIRO L 3072-01, 3073-01 to -08, 3074-01 to -02, 3075-01 to -02; *H. regularis* (n=12), CSIRO L 3076-01 to -07, 3077-01 to -02, 3078-01 to -03.)

Larvae were examined with a Wild M3Z stereomicroscope at 6.5–40× magnifications by using various combinations of incident and transmitted light. Body measurements were taken with SigmaScan Pro® 4.01 image measurement software (SPSS Inc., 1999) and are accurate to less than 0.05 mm. This method was particularly useful for measuring cumulative distances of bent larvae. Abbreviations and definitions of routinely taken body measurements follow Leis and Carson-Ewart (2000). Lower jaw length (LJ) is defined as the horizontal distance from the tip of the lower jaw to the anterior margin of the pigmented region of the eye. Lower jaw extension (LJx) is defined as the horizontal distance from the tip of the lower jaw to the tip of the snout. Eye diameter was measured along both horizontal (EDh) and vertical midlines (EDv) of its pigmented region. Body depth was measured at two points: at the pectoral base (BDp) and at the anus (BDa). Other measurements taken were snout length (SnL), head length (HL), pre dorsal-fin length (PDL) and preanal length (PAL). All measurements are expressed as a percentage of BL. Pigment refers to melanin. Drawings were prepared with the aid of a camera lucida.

Selected specimens were cleared and stained with alcian blue and alizarin red-S, following the method of Potthoff (1984), in order to count fin rays and vertebrae. Myomeres were difficult to count reliably at either end and thus vertebral counts (which include the urostyle) of stained larvae were taken instead. For small larvae that had unformed centra, corresponding neural or haemal spines were counted to obtain the number of vertebrae.

Results

Southern sea garfish (*Hyporhamphus melanochir* Valenciennes, 1846) (Fig. 1)

Description of larvae The smallest *H. melanochir* larva examined was a 6.4-mm newly hatched, laboratory-reared, postflexion-stage specimen. Some yolk remained, although yolk absorption was complete in the smallest field-collected larva (6.9 mm).

Larvae are elongate to very elongate (BDp=7–13% BL), and have a body depth slightly tapered towards the anus (BDa= 7–9% BL). Relative body depth at the pectoral base decreases slightly during larval development (Table 1). Larvae have 58–61 vertebrae (Table 2). The gut is relatively thick, long, straight, and nonstriated. PDL and PAL remain in the ranges of 70–75% and 71–76% BL, respectively (except for the 17.0-mm larva, which had a PDL and PAL of 62% BL). The first dorsal-fin ray is slightly anterior to or directly above the corresponding anal-fin ray. There is no gap between the anus and the anal fin. A long preanal finfold, initially the same length as the gut, persists through to the transformation stage before it disappears. There is no head spination. The small to moderate head (HL=16–24% BL) decreases in size in relation to BL with larval growth (Table 1). The longer lower jaw protrudes beyond the snout (LJx) by 4% BL at 11.0–11.5 mm, increasing to a maximum of 34% BL in the 29.3-mm juvenile. The mouth is oblique and reaches to the level of the center of the eye in newly hatched larvae. The maxilla subsequently moves forward in relation to the eye and by 12.1–14.4 mm it does not reach the eye. Very small villiform teeth are present on both the premaxilla and dentary in newly hatched larvae. The moderate to large eye (EDh=6–10% BL or 33–42% HL) is elongate (EDv=78–88% EDh) and decreases in size in relation to BL. A single rudimentary nasal papilla first appears as a small fleshy lump in the olfactory pit by 17.0 mm. Scales first appear between 20.4 and 29.3 mm laterally on the tail, anterior to the caudal peduncle.

Development of fins Completion of fin development in *H. melanochir* occurs in the following sequence: C → D → A → P_1, P_2 (Table 2). All principal rays of the caudal fin (7+8)

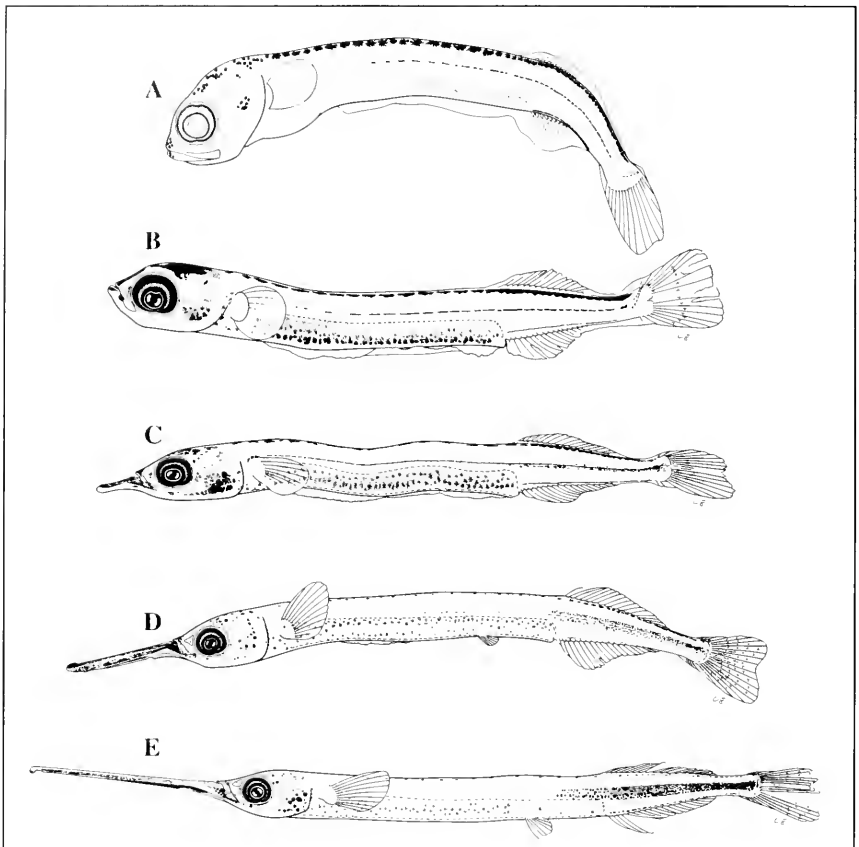

Figure 1

Larval, transforming larval, and juvenile *Hyporhamphus melanochir*. (**A**) 6.4-mm reared yolksac larva; newly hatched (redrawn from Jordan et al., 1998) (L 3072-01). (**B**) 9.3-mm larva (L 3073-01). (**C**) 13.3-mm larva (composite drawing of two damaged larvae of same BL) (L 3073-02 and -03). (**D**) 20.4-mm transforming larva (L 3074-01). (**E**) 29.3-mm juvenile (L 3074-02). Myomeres omitted in (D) and (E).

and several incipient dorsal- and anal-fin rays are present in newly hatched larvae. A full complement of 15–18 dorsal-fin and 17–20 anal-fin rays is attained at 11.4 and 12.1 mm, respectively. The pectoral base and finfold form prior to hatching, and incipient rays appear shortly after (by 7.2 mm); all 11–13 rays are formed by 19.6 mm. The pelvic fin buds appear by 13.3 mm, and all six pelvic-fin rays are formed by 19.6 mm.

Pigmentation *Hyporphamphus melanochir* larvae are moderately to heavily pigmented. Head pigmentation consists of melanophores on the tip of the lower jaw, snout, olfactory pit, and opercula, and a patch of several large melanophores on the midbrain. The extended lower jaw is heavily pigmented throughout development and melanophores extend laterally along the dentary. The eye is partially pigmented in the newly hatched larva, but fully pigmented by 6.9 mm. The gut is heavily and uniformly pigmented dorsally and laterally along the entire length, and melanophores are often coalesced, but pigmentation becomes obscured as the overlying musculature develops. Dorsal pigmentation initially consists of 12–15 large melanophore pairs in longitudinal rows between the head and origin of the dorsal fin (Fig. 2A), and a continuous band along either side of the dorsal-fin base. Dorsal pigmentation gradually decreases in intensity thereafter. Three

Table 1

Morphometrics of larval, transforming larval, and juvenile *Hyporhamphus melanochir* (expressed as % of BL). Mean ±SD is given when sample size n >1. Dashed lines differentiate larvae, transforming larvae, and juveniles in descending order.

BL (mm)	n	SnL	LJ	LJx	EDh	EDv	HL	PDL	PAL	BDp	BDa
6.4[1]	1	2.1	2.7	0.6	9.9	8.7	24.4	74.6	75.5	16.3[2]	8.0
6.9	1	3.0	4.0	1.0	9.2	7.5	23.5	69.7	71.9	12.7	8.6
7.0–7.5	9	2.8 ±0.8	3.9 ±1.1	1.1 ±0.4	9.1 ±0.3	7.3 ±0.3	22.0 ±0.8	70.8 ±0.9	72.6 ±1.0	11.9 ±0.3	8.9 ±0.3
7.5–8.0	7	3.6 ±0.9	4.6 ±1.2	1.0 ±0.4	9.1 ±0.5	7.1 ±0.3	22.8 ±1.6	71.3 ±1.3	73.0 ±0.9	11.8 ±0.6	8.9 ±0.7
8.0–8.5	9	3.6 ±0.5	4.9 ±0.8	1.3 ±0.4	8.8 ±0.3	7.1 ±0.3	21.9 ±1.0	70.9 ±0.7	72.7 ±0.9	11.7 ±0.7	8.9 ±0.7
8.5–9.0	3	3.5 ±0.8	5.0 ±1.1	1.5 ±0.3	8.6 ±0.2	7.0 ±0.3	21.1 ±0.2	71.5 ±0.2	72.5 ±0.4	11.3 ±0.5	9.1 ±0.5
9.0–9.5	4	3.4 ±0.5	5.0 ±0.7	1.6 ±0.3	8.0 ±0.3	6.5 ±0.2	20.9 ±0.8	71.7 ±0.7	72.8 ±0.6	11.4 ±0.7	8.4 ±0.3
11.0–11.5	4	3.7 ±0.7	7.2 ±1.5	3.5 ±1.2	7.5 ±0.4	6.3 ±0.2	20.3 ±1.3	71.6 ±0.6	72.3 ±0.5	10.6 ±0.7	8.5 ±0.6
12.1	1	4.1	9.0	4.9	7.6	6.4	19.7	72.6	72.6	10.2	8.6
14.4	1	3.7	12.3	8.6	6.9	5.8	19.2	70.2	71.4	9.4	7.8
17.0	1	2.9	10.3	7.4	5.6	4.7	15.9	61.7	61.7	7.3	6.6
19.6	1	4.9	28.7	23.8	6.0	4.9	18.6	70.4	71.2	8.2	7.4
20.4	1	4.0	24.2	20.2	5.7	5.0	17.5	72.5	71.6	8.9	7.6
29.3	1	4.4	38.4	34.0	5.3	4.8	17.0	69.9	71.0	8.2	7.2
33.3	1	4.9	38.3	33.4	5.3	4.6	17.9	71.7	72.7	8.5	7.6
41.3	1	5.2	36.2	31.1	5.5	5.1	18.6	74.1	74.1	9.2	7.8
48.3	1	5.6	36.9	31.3	5.2	4.8	17.8	74.0	74.0	9.7	8.1

[1] Yolksac larva.
[2] Includes yolk sac.

Table 2

Meristic counts of larval, transforming larval, and juvenile *Hyporhamphus melanochir*. Numbers in bold indicate the BL at which a full complement of rays is first attained. Dashed lines differentiate larvae, transforming larvae, and juveniles in descending order. D = dorsal; A = anal; P_1 = pectoral; P_2 = pelvic; C = caudal.

	Fin rays						
BL (mm)	D	A	P_1	P_2	C	Branchiostegal rays	Vertebrae
6.4[1]	8	9	base		0+**7**+**8**+0	3	38+21
7.2	8	8	1		0+7+8+0	3	39+20
7.3	9	10	1		0+7+8+0	3	39+19
7.6	11	11	1		0+7+8+0	3	38+20
7.9	10	11	1		0+7+8+0	3	40+20
8.3	11	11	2		0+7+8+0	4	39+20
8.4	13	14	2		1+7+8+1	5	39+21
9.4	14	16	4		1+7+8+1	5	40+21
11.4	**15**	16	6		2+7+8+1	7	38+20
12.1	16	**17**	7		2+7+8+2	7	39+20
14.4	16	19	9	bud	2+7+8+2	9	39+20
19.6	17	19	**11**	**6**	**4**+7+8+**4**	**12**	38+20
20.4	16	17	12	6	4+7+8+4	12	39+19
29.3	17	18	11	6	4+7+8+4	13	38+20
33.3	17	18	12	6	5+7+8+5	12	38+20
41.3	16	19	11	6	4+7+8+5	12	40+19
48.3	16	19	11	6	4+7+8+5	12	39+19

[1] Yolksac larva.

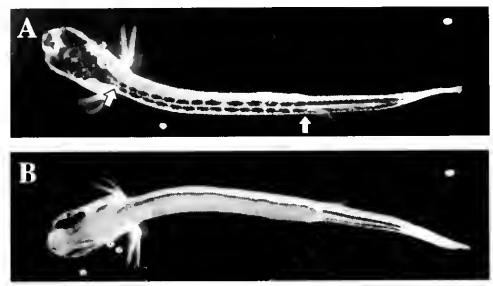

Figure 2

Pigmentation of an 8.5-mm *Hyporhamphus melanochir* larva. (**A**) Dorsal view; arrows indicate the margins of the 12–15 melanophore pairs in longitudinal rows. (**B**) Ventral view.

Table 3

Morphometrics of larval, transforming larval, and juvenile *Hyporhamphus regularis* (expressed as % of BL). Mean ±SD is given when sample size $n > 1$. Dashed lines differentiate larvae, a transforming larva, and juveniles in descending order.

BL (mm)	*n*	SnL	LJ	LJx	EDh	EDv	HL	PDL	PAL	BDp	BDa
7.0[1]	1	3.2	4.4	1.2	8.2	6.5	20.4	73.2	71.6	11.6[2]	7.4
7.5–8.0	9	2.8 ±0.3	4.4 ±0.4	1.7 ±0.3	7.6 ±0.1	6.3 ±0.1	19.9 ±0.6	73.1 ±0.6	71.8 ±0.4	11.2 ±0.2	8.2 ±1.2
8.0–8.5	12	2.8 ±0.4	4.3 ±0.5	1.5 ±0.3	7.5 ±0.3	6.2 ±0.2	19.6 ±0.9	72.8 ±0.7	71.6 ±0.6	11.0 ±0.5	7.7 ±0.3
8.5–9.0	10	2.8 ±0.2	4.2 ±0.2	1.5 ±0.2	7.2 ±0.2	5.9 ±0.1	19.2 ±0.3	72.9 ±0.9	71.8 ±0.9	10.6 ±0.2	7.4 ±0.3
9.0–9.5	5	2.8 ±0.1	4.4 ±0.4	1.6 ±0.4	7.0 ±0.1	6.0 ±0.2	19.1 ±0.4	72.3 ±0.7	71.5 ±0.6	10.6 ±0.2	7.6 ±0.3
9.5–10.0	3	2.8 ±0.1	4.4 ±0.3	1.7 ±0.2	6.9 ±0.4	5.8 ±0.2	18.7 ±0.5	72.1 ±1.6	71.2 ±1.7	10.6 ±0.4	7.3 ±0.2
10.0–10.5	3	3.0 ±0.3	4.8 ±0.9	1.8 ±0.6	6.8 ±0.2	5.8 ±0.2	18.9 ±0.6	72.2 ±0.6	71.3 ±0.6	10.2 ±0.3	7.6 ±0.3
13.1	1	4.0	7.6	3.7	6.9	5.4	19.6	73.2	71.9	9.1	7.8
18.1	1	4.5	18.6	14.1	6.3	5.4	19.9	73.8	72.6	9.5	8.1
24.7	1	5.6	27.7	22.1	6.3	5.5	20.8	72.9	73.6	9.7	8.1
31.5	1	6.2	30.0	23.9	6.0	5.5	21.0	74.4	75.5	10.7	8.5
33.8	1	6.4	27.7	21.3	6.1	5.6	21.6	74.3	74.3	10.9	8.9
46.9	1	7.3	damaged	damaged	5.6	4.7	21.8	75.4	75.4	11.2	9.8

[1] Yolksac larva

[2] Includes yolk sac.

distinct lines of pigment appear along the dorsal margin in juveniles (by 29.3 mm) and remain to adult stage. A series of melanophores form a dashed, sometimes continuous, midlateral line. Melanophores appear laterally on the caudal peduncle by 14.4 mm and then proliferate anteriorly to form a broad medial stripe that remains, forming a silver stripe from the caudal peduncle to the operculum of adults. Ventral pigmentation consists of continuous bands of melanophores either side of the anal-fin base (Fig. 2B). Fins are unpigmented, except the caudal fin, which has small melanophores on the ray bases.

River garfish (*Hyporhamphus regularis* Günther, 1886) (Fig. 3)

Description of larvae The smallest *H. regularis* larva examined (7.0 mm) had completed notochord flexion and had a yolk sac. Yolk absorption was complete by 7.6 mm.

Larval *H. regularis* closely resemble larval *H. melanochir* morphologically (see Tables 1 and 3), but differ somewhat in relative length of the lower jaw, relative positions of the dorsal- and anal-fin origins, and in number of vertebrae. The longer lower jaw protrudes beyond the snout (LJx) by

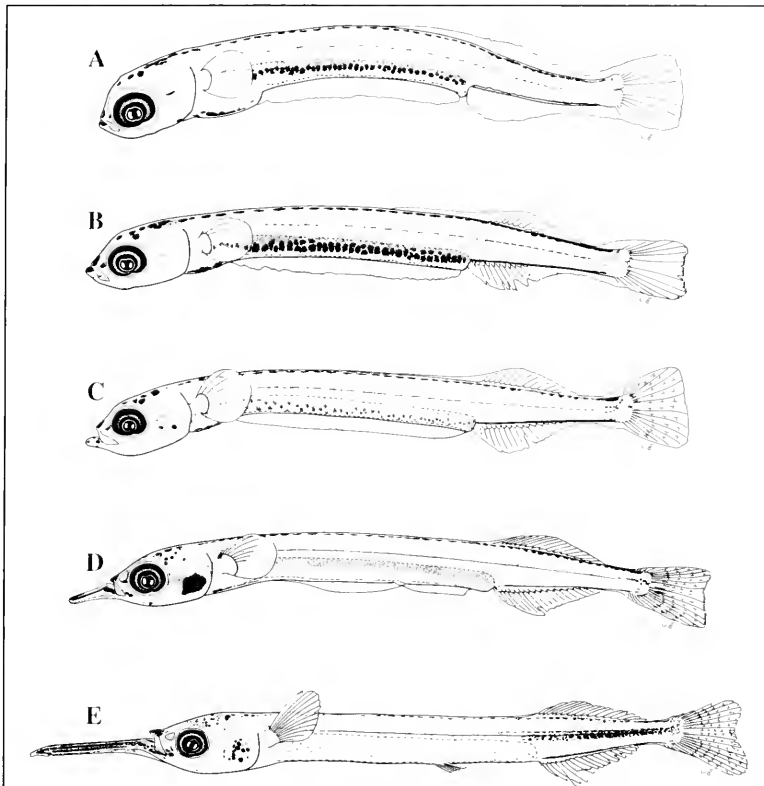

Figure 3

Larval and juvenile *Hyporhomphus regularis*. (**A**) 7.1-mm yolksac larva (L 3076-01). (**B**) 9.4-mm larva (L 3076-02). (**C**) 12.3-mm larva (L 3076-03). (**D**) 15.5-mm larva (L 3076-04). (**E**) 24.7-mm juvenile (L 3077-01). Myomeres omitted in (D).

4% BL at 13.1 mm and increases to a maximum of 24% BL in the 31.5 mm juvenile. The first dorsal-fin ray is slightly posterior to or directly above the corresponding anal-fin ray. Larvae have 51–54 vertebrae. Scales first appear between 18.1 and 24.7 mm laterally on the tail, anterior to the caudal peduncle.

Development of fins Completion of fin development in *H. regularis* occurs in the following sequence: C → D → A → P_1, P_2 (Table 4). Development of the caudal fin is incomplete at birth; 6 + 7 principal rays are present in the 7.0-mm yolksac larva, and the full complement (7+8) shortly after, by 7.7 mm. Distinct anal-fin bases are visible at 7.0 mm. A full complement of 14–17 dorsal and 15–19 anal-fin rays is attained at 10.1 and 10.5 mm, respectively. The pectoral base and finfold are present at birth, and incipient rays first appear by 8.1 mm; all 11–12 rays are formed by 18.1 mm. The pelvic fin buds appear by 13.1 mm, and all six pelvic-fin rays are formed by 18.1 mm.

Pigmentation Pigmentation of *H. regularis* larvae is similar to that of *H. melanochir* larvae except along the dorsal and ventral margins. Dorsal pigmentation consists of 19–22 melanophore pairs in longitudinal rows between the head and dorsal fin origin (Fig. 4A). A large pigment blotch is present ventrally on the isthmus and anteriorly on the gut.

Discussion

This study provides the first descriptions of larval development of hemiramphids endemic to marine (*H. melanochir*) and estuarine (*H. regularis*) waters of Australia.

Table 4

Meristic counts of larval, transforming larval, and juvenile *Hyporhamphus regularis*. Numbers in bold indicate the BL at which a full complement of rays is first attained. Dashed lines differentiate larvae, a transforming larva, and juveniles in descending order. D = dorsal; A = anal; P_1 = pectoral; P_2 = pelvic; C = caudal.

	Fin rays						
BL (mm)	D	A	P_1	P_2	C	Branchiostegal rays	Vertebrae
7.0[1]	anlage	bases	base		0+6+7+0	2	35+19
7.7	4	6	base		0+**7**+8+0	3	34+19
7.8	6	7	base		0+7+8+0	4	34+18
8.1	5	7	1		0+7+8+0	4	34+19
8.3	8	9	2		0+7+8+0	4	33+20
8.6	9	11	2		0+7+8+0	5	34+19
8.9	11	11	2		0+7+8+1	5	34+20
9.3	11	12	3		1+7+8+1	5	33+18
9.6	10	11	3		0+7+8+1	5	35+19
10.1	**14**	14	4		1+7+8+1	6	33+20
10.5	13	**15**	5		1+7+8+1	6	35+19
13.1	14	16	7	bud	2+7+8+2	8	35+19
18.1	14	17	**11**	**6**	**4**+7+8+**4**	**12**	35+18
24.7	16	17	12	6	4+7+8+4	11	34+19
31.5	15	17	12	6	4+7+8+4	11	34+18
33.8	15	18	11	6	4+7+8+4	11	33+19
46.9	16	17	11	6	4+7+8+4	11	35+18

[1] Yolksac larva.

Both *H. melanochir* and *H. regularis* share characters common to other described hemiramphid larvae. They are generally characterized by their lack of head or fin spines; elongate body; long straight gut; extended lower jaw; a main pigmentation pattern consisting of rows of melanophores on the dorsal, lateral, and ventral surfaces of the body; and advanced state of development at hatching (Collette et al., 1984; Watson, 1996; Trnski et al., 2000). Although the size at which fins develop varies slightly between *H. melanochir* and *H. regularis*, the sequence of development for both species is the same as that for most hemiramphids, i.e. C → D, A → P_1 → P_2 (Collette et al., 1984).

Hyporhamphus melanochir larvae are distinguishable from *H. regularis* by 1) having 58–61 vertebrae (vs. 51–54 for *H. regularis*); 2) having 12–15 melanophore pairs in longitudinal rows along the dorsal margin between the head and origin of the dorsal fin (vs. 19–22 for *H. regularis*); and 3) the absence of a large ventral pigment blotch anteriorly on the gut and isthmus which is present in *H. regularis*. Despite the difficulty in counting myomeres, either the number of vertebrae in cleared and stained specimens or the number of myomeres between the pectoral-fin base and anus (usually three less than the number of precaudal vertebrae; see Tables 2 and 4) revealed a consistent difference between both species.

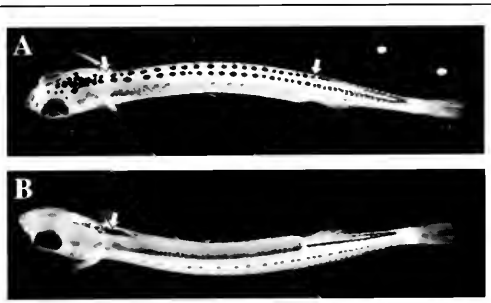

Figure 4

Pigmentation of an 8.7-mm *Hyporhamphus regularis* larva. (**A**) Dorsal view; arrows indicate the margins of the 19–22 melanophore pairs in longitudinal rows. (**B**) Ventral view; arrow indicates the ventral pigment blotch.

The geographic distributions of larval *H. melanochir* and *H. regularis* were separate in most samples; only three *H. melanochir* were found among *H. regularis* from Barker Inlet, whereas no *H. regularis* were among *H. melanochir* from the Bay of Shoals or Gulf St. Vincent. Larvae of other

hemiramphid species may overlap in distribution with those of *H. melanochir* and *H. regularis* outside South Australian waters. Meristic characters (summarized in Table 5) can often distinguish *H. melanochir* and *H. regularis* from the other species, except the eastern sea garfish (*H. australis*), which has overlapping meristic counts and currently undescribed larvae. The storm garfish (*Hemiramphus robustus*) has fewer anal-fin rays (11–14) and develops both a dark blotch below the dorsal fin and a pigmented pelvic fin in the juvenile stage (Collette, 1974; Collette et al., 1984). The long-finned garfish (*Euleptorhamphus viridis*), an oceanic species that rarely frequents nearshore waters, is strikingly different from other hemiramphids, being much more elongate and slender, and having divergent meristic counts, including more dorsal- and anal-fin rays (21–25 and 20–24, respectively), more vertebrae (69–73), fewer pectoral-fin rays (7–9), and fewer gill rakers (25–33) (Collette, 1974; Hardy, 1978; Chen, 1988; Trnski et al., 2000).

Larvae of the saury (*Scomberosox saurus*) (family Scomberosocidae) also occur in southern Australia and are the only other species that could be confused with hemiramphids. These are distinguishable from hemiramphid larvae by their higher myomere count (62–70), greater number of principal caudal-fin rays (16–17), presence of dorsal and anal finlets, and much heavier pigmentation (Bruce and Sutton, 1998; Trnski et al., 2000).

Acknowledgments

I am grateful to D. Short, L. Triantafillos, and the crew of the RV *Ngerin* for assisting in the field collection of specimens. The South Australian Museum allowed access to catalogued hemiramphid specimens, and A. Jordan donated a newly hatched *H. melanochir* larva and assisted with the examination of distinguishing characters. B. Bruce and F. J. Neira provided tips on larval drawing techniques. I also thank B. Bruce, S. Donnellan, A. Fowler, A. Jordan, F. J. Neira, T. Trnski, and T. Ward for kindly reviewing the manuscript. This project was supported by a Fisheries Research and Development Corporation grant 97/133 and was undertaken while receiving an Australian Postgraduate Award (Industry) at Adelaide University.

Table 5

Meristic counts of adult hemiramphids found in southern Australia. Data collated from Collette (1974) except where footnoted. A second range from another source is given if not in total agreement with Collette (1974). The distinguishing vertebral counts for *H. melanochir* and *H. regularis* in this study are also included. Vertebrae are given as precaudal + caudal; gill rakers are given as upper + lower. ? = no information available. D = dorsal; A = anal; P_1 = pectoral; P_2 = pelvic; C = caudal.

Species	Fin rays					Branchiostegal rays	Vertebrae	Gill rakers
	D	A	P_1	P_2	C			
Euleptorhamphus viridis	21–25	21–24 20–24[2]	8–9 7–9[2]	6[2]	?+7+8+?[4]	?	69 – 73 (44 – 46) + (26 – 29) = 70 – 75[4]	(5 – 9) + (18 – 23) = 25 – 33
Hemiramphus robustus	13–15	11–14	12–13	6[5]	4+7+8+5[5]	13[5]	(35 – 37) + (17 – 19) = 52–55 (33 –34) + (16 – 17) = 49-50[1]	(27 – 33) + (20 – 25) = ?
Hyporhamphus australis	15–17	17–20	11–13 10–13[1]	6[5]	4+7+8+4[5]	12–13[5]	(37 – 39) + (18 – 20) = 56–58 (38 – 40) + ?[1]	(31 – 39) + (23 – 33) = ?
Hyporhamphus melanochir	15–18	17–20	11–13	6[3]	4–5+7+8+4–5[5,6]	12–13[5,6]	(36 – 41) + (18 – 21) = 55-61 (38 – 40) + (19 – 21) = 58–61[6]	(27 – 35) + (21 – 29) = ?
Hyporhamphus regularis	14–17	15–19	11–12	6[3]	4+7+8+4[5,6]	10–12[5,6]	(33 – 38) + (18 – 20) = 51 – 58 (33 – 35) + (18 – 20) = 51 – 54[6]	(30 – 36) + (21 – 27) = 52 – 61

[1] Parin et al. (1980).
[2] Chen (1988).
[3] Gomon et al. (1994).
[4] Trnski et al. (2000).
[5] Noell (unpubl. data).
[6] This study.

Literature cited

Bruce, B. D., and C. A. Sutton.
1998. Scomberosocidae: sauries. *In* Larvae of temperate Australian fishes: laboratory guide for larval fish identification (F. J. Neira, A. G. Miskiewicz, and T. Trnski, eds.), p. 98–101. Univ. Western Australia Press, Perth, Western Australia.

Chen, C. H.
1988. Hemiramphidae. *In* An atlas of the early stage fishes in Japan (M. Okiyama, ed.), p. 265–275. Tokai Univ. Press, Tokyo. [In Japanese.]

Collette, B. B.
1974. The garfishes (Hemiramphidae) of Australia and New Zealand. Rec. Aust. Mus. 29:11–105.

Collette, B. B., G. E. McGowen, N. V. Parin, and S. Mito.
1984. Beloniformes: development and relationships. *In* Ontogeny and systematics of fishes (H. G. Moser, W. J. Richards, D. M. Cohen, M. P. Fahay, A. W. Kendall Jr., and S. L. Richardson, eds.), p. 335–354. Am. Soc. Ichthyol. Herpetol., Spec. Publ. 1.

Gomon, M. F., C. J. M. Glover, and R. H. Kuiter.
1994. The fishes of Australia's south coast, 992 p. State Print, Adelaide, Australia.

Hardy, Jr., J. D.
1978. Development of fishes of the mid-Atlantic Bight: an atlas of egg, larval and juvenile stages. Vol. II. Anguillidae through Syngnathidae. U.S. Fish Wildl. Serv. FWS/OBS-78/12, 458 p.

Jones, G. K., J. L. Baker, K. Edyvane, and G. J. Wright.
1996. Nearshore fish community of the Port River-Barker Inlet Estuary, South Australia. I. Effect of thermal effluent on the fish community structure, and distribution and growth of economically important fish species. Mar. Freshwater Res. 47:785–800.

Jordan, A. R., D. M. Mills, G. Ewing, and J. M. Lyle.
1998. Assessment of inshore habitats around Tasmania for life-history stages of commercial finfish species. Fishing Research and Development Corporation, Final Report Project 94/037, 176 p.

Kailola, P. J., M. J. Williams, P. C. Stewart, R. E. Reichelt, A. McNee, and C. Grieve.
1993. Australian fisheries resources, 422 p. Bureau of Resource Sciences and the Fisheries Research and Development Corporation, Canberra, Australia.

Kendall, A. W., Jr., E. H. Ahlstrom, and H. G. Moser.
1984. Early life history stages of fishes and their characters. *In* Ontogeny and systematics of fishes (H. G. Moser, W. J. Richards, D. M. Cohen, M. P. Fahay, A. W. Kendall Jr., and S. L. Richardson, eds.), p. 11–22. Am. Soc. Ichthyol. Herpetol., Spec. Publ. 1.

Leis, J. M., and B. M. Carson-Ewart.
2000. The larvae of Indo-Pacific coastal fishes: an identification guide to marine fish larvae. Fauna Malesiana Handbooks, 2, 850 p. Brill, Leiden.

Ling, J. K.
1958. The sea garfish, *Reporhamphus melanochir* (Cuvier and Valenciennes) (Hemiramphidae), in South Australia: breeding, age determination, and growth rate. Aust. J. Mar. Freshwater Res. 9:60–110.

Neira, F. J., A. G. Miskiewicz, and T. Trnski.
1998. Larvae of temperate Australian fishes: laboratory guide for larval fish identification, 474 p. Univ. Western Australia Press, Perth, Western Australia.

Noell, C. J., S. Donnellan, R. Foster, and L. Haigh.
2001. Molecular discrimination of garfish *Hyporhamphus* (Beloniformes) larvae in southern Australian waters. Mar. Biotechnol. 3:509–514.

Parin, N. V., B. B. Collette, and Y. N. Shcherbachev.
1980. Preliminary review of the marine halfbeaks (Hemiramphidae, Beloniformes) of the tropical Indo-West-Pacific. Trudy Inst. Okeanol. Akad. NAUK SSSR 97:7–173. [In Russian.]

Potthoff, T.
1984. Clearing and staining techniques. *In* Ontogeny and systematics of fishes (H. G. Moser, W. J. Richards, D. M. Cohen, M. P. Fahay, A. W. Kendall Jr., and S. L. Richardson, eds.), p. 35–37. Am. Soc. Ichthyol. Herpetol., Spec. Publ. 1.

Prince Jeyaseelan, M. J.
1998. Manual of fish eggs and larvae from Asian mangrove waters, 193 p. UNESCO, Paris.

SPSS Inc.
1999. SigmaScan® Pro 5.0. Chicago, Il.

Sudarsan, D.
1966. Eggs and larvae of a hemirhamphid fish from Mandapam. J. Mar. Biol. Assoc. India 8:342–346.

Talwar, P. K.
1967. Studies on the biology of *Hemiramphus marginatus* (Forsskål) (Hemirhamphidae-Pisces). J. Mar. Biol. Assoc. India 9:61–69.

Trnski, T., J. M. Leis, and B. M. Carson-Ewart.
2000. Hemiramphidae. *In* The larvae of Indo-Pacific coastal fishes: an identification guide to marine fish larvae (J. M. Leis, and B. M. Carson-Ewart, eds.), p. 154–158. Fauna Malesiana Handbooks, 2. Brill, Leiden.

Watson, W.
1996. Hemiramphidae: halfbeaks. *In* The early stages of fishes in the California Current region (H. G. Moser, ed.), p. 634–641. Calif. Coop. Oceanic Fish. Invest. Atlas 33.

Age and growth of the estuarine dolphin (*Sotalia guianensis*) (Cetacea, Delphinidae) on the Paraná coast, southern Brazil

Fernando César Weber Rosas
Instituto Nacional de Pesquisas da Amazônia (INPA)
Laboratório de Mamíferos Aquáticos
Caixa Postal 478
Manaus, AM, 69011-970, Brazil
E-mail address: frosas@inpa.gov.br

André Silva Barreto
Universidade do Vale do Itajaí (UNIVALI)
CTTMar, Caixa Postal 360
Itajaí, SC, 88302-202, Brazil

Emygdio Leite de Araujo Monteiro-Filho
Universidade Federal do Paraná (UFPR)
Departamento de Zoologia
Caixa Postal 19020
Curitiba, PR, 81531-970, Brazil

and

Instituto de Pesquisas Cananéia (IPeC)
Rua João Salim, Lote 26-Quadra Y
Parque Xangrilá
13098-106, Campinas, São Paulo, Brazil

Abstract—Teeth of 71 estuarine dolphins (*Sotalia guianensis*) incidentally caught on the coast of Paraná State, southern Brazil, were used to estimate age. The oldest male and female dolphins were 29 and 30 years, respectively. The mean distance from the neonatal line to the end of the first growth layer group (GLG) was 622.4 ±19.1 µm (n=48). One or two accessory layers were observed between the neonatal line and the end of the first GLG. One of the accessory layers, which was not always present, was located at a mean of 248.9 ±32.6 µm (n=25) from the neonatal line, and its interpretation remains uncertain. The other layer, located at a mean of 419.6 ±44.6 µm (n=54) from the neonatal line, was always present and was first observed between 6.7 and 10.3 months of age. This accessory layer could be a record of weaning in this dolphin. Although no differences in age estimates were observed between teeth sectioned in the anterior-posterior and buccal-lingual planes, we recommend sectioning the teeth in the buccal-lingual plane in order to obtain on-center sections more easily. We also recommend not using teeth from the most anterior part of the mandibles for age estimation. The number of GLGs counted in those teeth was 50% less than the number of GLGs counted in the teeth from the median part of the mandible of the same animal. Although no significant difference (P>0.05) was found between the total lengths of adult male and female estuarine dolphins, we observed that males exhibited a second growth spurt around five years of age. This growth spurt would require that separate growth curves be calculated for the sexes. The asymptotic length (TL_∞), k, and t_0 obtained by the von Bertalanffy growth model were 177.3 cm, 0.66, and −1.23, respectively, for females and 159.6 cm, 2.02, and −0.38, respectively, for males up to five years, and 186.4 cm, 0.53 and −1.40, respectively, for males older than five years. The total weight (TW)/total length (TL) equations obtained for male and female estuarine dolphins were $TW = 3.156 \times 10^{-6} \times TL^{3.2836}$ (r=0.96), and $TW = 8.974 \times 10^{-5} \times TL^{2.6182}$ (r=0.95), respectively.

Manuscript accepted 28 October 2002.
Manuscript received 31 December 2002 at NMFS Scientific Publicaitions Office.
Fish. Bull. 101:377–383 (2003).

Until recently the genus *Sotalia* was monospecific (*S. fluviatilis*) and had a marine and a riverine ecotype (da Silva and Best, 1996). Using tridimensional morphometric analyses, Monteiro-Filho et al. (2002) were able to separate it into two distinct species: *Sotalia fluviatilis*, which lives in freshwater, and *Sotalia guianensis*, which lives in the marine environment. Because tucuxi is the vernacular name used for the freshwater species, Rosas and Monteiro-Filho (2002) suggested "estuarine dolphin" as the vernacular name for *S. guianensis*, as previously mentioned by Watson (1988).

Age is important in characterizing population dynamics of mammals. Growth layer groups (GLGs) observed in teeth of mammals have been used to estimate ages, and the greatest progress in this area has occurred with studies carried out on marine mammals (Klevezal, 1980; Hohn et al., 1989). The method consists of counting GLGs found in the dentine and cement of the animals' teeth, which are deposited every year in most species (Klevezal, 1996). Calibrating age estimates and identifying accessory layers (not annual) are essential for reliable age determination (Hohn, 1990). Some population parameters are extremely sensitive to errors and age estimate deviations, and the absence of or an inadequate calibration, could lead to incorrect interpretations (Hohn et al., 1989).

Because there is no sexual dimorphism in the body proportions of adult *Sotalia guianensis*, all previous growth studies analyzed both sexes together (Borobia, 1989; Schmiegelow, 1990; Ramos et al., 2000). However, there is evidence of differentiated growth between male and female estuarine dolphins around puberty (Rosas and Monteiro-Filho, 2002), thereby making it necessary to analyze growth separately for the sexes.

The objectives of this paper were 1) to estimate the ages of *S. guianensis*

caught incidentally or stranded on the Paraná coast, Brazil; 2) to give some guidelines to promote reliable age estimates in this species; 3) to describe the growth in body length (cm) according to the ages (years) of male and female estuarine dolphins, by using classical mathematical growth models; and 4) to describe the body-weight–body-length relationship for both sexes of this dolphin.

Materials and methods

Teeth from 71 individuals of *S. guianensis* (34 males, 28 females and 9 of undetermined sex), incidentally caught or found stranded on the Paraná coast, southern Brazil (25°18′S; 48°05′W–25°5′S8; 48°35′W), from January 1997 to July 1999, were used to estimate age. The total body weight (kg) and standard measurements of individuals were made in accordance to Norris (1961). Total length (cm) was measured in a straight line from the tip of the beak to the central notch of the tail, in an axial projection. The skulls and teeth were collected, prepared, and deposited in the collection of the Instituto de Pesquisas Cananéia (IPeC).

Preparation of the teeth, from the decalcification to the mounting of the slides, was carried out in the Laboratory of Marine Mammals and Marine Turtles of the Department of Oceanography of the Fundação Universidade do Rio Grande (FURG). The method of Hohn et al. (1989) was used, with the following adaptations: 1) decalcification time varied from one hour for newborn or young individuals, up to a maximum of 12.5 hours for old adults, 2) Harris's hematoxilin was used for staining, according to Molina and Oporto (1993), and immersion times of the sections varied from three to six minutes.

Because the absence of a pre-established age estimation model for *S. guianensis*, we tested both anterior-posterior and buccal-lingual planes for cutting teeth. Age estimation was performed by counting GLGs in the dentine. GLGs were defined as being the sequence of a thin nonstained layer, a thick stained layer, and a very thin layer that is strongly stained (very dark). Each complete GLG was assumed to represent one year (Ramos et al., 2000).

Teeth were selected from the middle of the tooth rows. However, to check for differences in age estimation among those positioned along the tooth row, we compared the number of GLGs in teeth from the middle of the tooth row with the number of GLGs in those from the most anterior part of the tooth row of the same animal.

The senior author read teeth slides at least three times during a minimum period of three weeks. Estimated age was taken as the last reading, assuming that reading accuracy improves with practice (Pinedo and Hohn, 2000). Age was estimated without access to biometric and biological data, thereby avoiding reader bias.

By using only central sections or those close by, in which at least 80% of the pulp cavity was exposed (Fig. 1), we obtained the following measurements with an ocular micrometer in a compound microscope: 1) distance (in μm) from the neonatal line up to the end of the first GLG in the dentine; 2) distance from the neonatal line to the first accessory layer in the dentine; and 3) distance from the neonatal line to the second accessory layer in the dentine, if present. All measurements were made perpendicular to the external margin and at the neck of the tooth (an area located between the crown and root of the tooth).

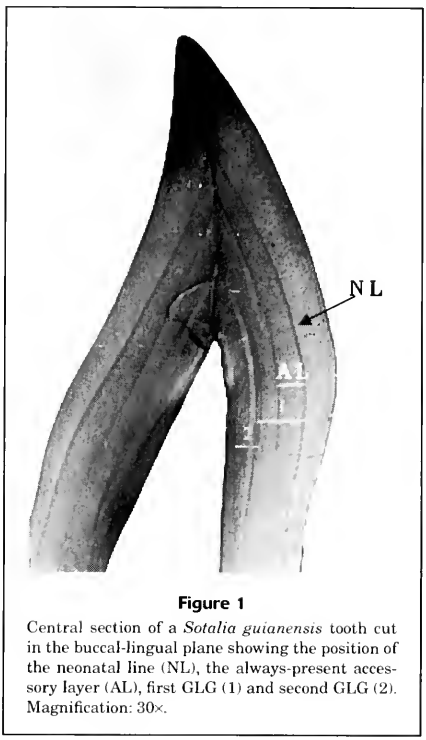

Figure 1

Central section of a *Sotalia guianensis* tooth cut in the buccal-lingual plane showing the position of the neonatal line (NL), the always-present accessory layer (AL), first GLG (1) and second GLG (2). Magnification: 30×.

Ages of individuals less than one year were estimated in months, by using as a base the percentage proportion of the mean distance between the neonatal line and the end of the GLG of the first year (Ramos, 1997).

Several models have been created over the years to describe growth, including the von Bertalanffy, Gompertz, logistical, and Richards models. Schnute's generic growth model helps to choose the model which is best adapted to the length and age data of the species studied. Schnute's model (1981) is defined as:

$$Y(t)=\left[y_1^b+(y_2^b-y_1^b)\frac{1-e^{-a(t-\tau_1)}}{1-e^{-a(\tau_2-\tau_1)}}\right]^{\frac{1}{b}},$$

where $Y(t)$ represents a measurement (length, weight, volume) at age t; variables τ_1 and τ_2 are ages of young and old specimens, respectively, and y_1 and y_2 are sizes at these ages. These sizes, together with a and b, are the parameters

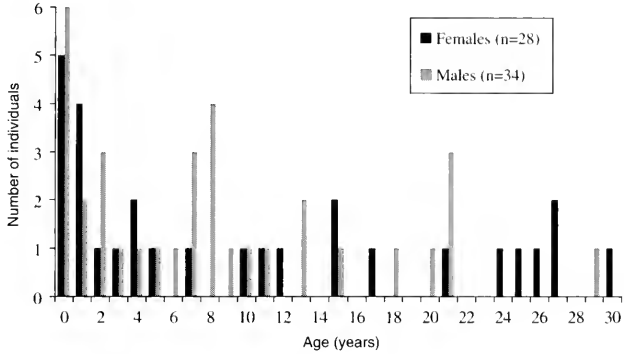

Figure 2

Age distribution of female and male *Sotalia guianensis* on the Paraná coast, southern Brazil, recorded between 1997 and 1999.

to be estimated. To define the growth model that would best fit the length and age data of *S. guianensis*, the Schnute model was applied to the length-at-age data.

Growth equations were calculated separately for the sexes, with 34 males and 28 females. Growth model adjustment to the data was made by using the nonlinear iterative Quasi-Newton method, minimizing the residual sum of squares.

Total-weight to total-length relationships were established by using 42 individuals of *S. guianensis* (23 males and 19 females) with the equation

$$TW = \phi \times TL^{\theta} \quad \text{(Santos, 1978)},$$

where TW = total weight in kg;
TL = total length in cm;
$\phi = e^{a}$ (e=base of the natural logarithm);
$\theta = b$ (θ is the length exponent); and finally
a and b = correlation parameters between the weight and length, obtained by the method of the least square by adjusting the logarithm data of TW and TL.

Results

Age estimation

The mean distance from the neonatal line to the end of the first GLG was 622.4 ±19.1 µm (n=48). There is one accessory layer, sometimes two, between the neonatal line and the end of the GLG of the first year. One of them, located at a mean distance of 248.9 ±32.6 µm (n=25) from the neonatal line, is not always present. The other, which is sometimes very conspicuous at the tip of the tooth, is always present, located at a mean distance of 419.6 ±44.6 µm (n=54) from the neonatal line, and is first observed between 6.7 and 10.3 months of age.

No difference was observed in age estimates of teeth sections orientated in the anterior-posterior and buccal-lingual planes. However, the buccal-lingual orientation made it easier to obtain on-center sections.

The number of GLGs counted in the small teeth from the most anterior part of the tooth row was 50% less than those counted in the teeth from the median part of the mandibles of the same animal.

The proportion of sexes in the sample studied was not significantly different (χ_c^2=1.39; df=1; P>0.05). However, among the animals with an age equal to or greater than 24 years (n=7), 85.7% were females. The oldest male was 29 years old and the oldest female was 30 years old (Fig. 2).

Age estimates for *S. guianensis* individuals varied from 0 to 30 years. Although the age mode was in the 0 and 1 year classes (Fig. 2), 53.5% of all animals whose ages were estimated were seven years or more. This proportion remained relatively constant between the sexes; 55% of the males and 50% of the females were equal to or greater than seven years.

Growth

When applied to the present data, Schnute's model indicated that the von Bertalanffy growth equation fitted the length and age data of *S. guianensis* better (Table 1, a>0 and b>1; Schnute, 1981). Even though the predictive power of Schnute's model is greater than von Bertalanffy's (see "Explained variance" in Tables 1 and 2), the latter is justified by its historical use, and therefore has a greater value for populational comparison, and incorporates a better understanding of the biological meaning of its variables.

Comparing the total lengths (TL) of the estuarine dolphins of six years or more, we found no significant differ-

ence between the sexes (t-test, $P>0.05$). However, it was observed that males possibly exhibit a discontinuity in growth around five years. The existence of a secondary growth spurt around this age was considered to be due to the onset of puberty in this species (Rosas and Monteiro-Filho, 2002), and necessitated the calculation of separate growth curves for each sex. It should be noted that sexual maturity of the dolphins here analyzed was determined by Rosas and Monteiro-Filho (2002) to occur at seven years in males. In order to estimate the fit of a two-step model, the sample was divided into two groups: 1) up to five years (prepuberty) and 2) older than five years (subadult and adults).

The growth parameters obtained for males and females are given in Table 2. The results obtained by Borobia (1989) and Schmiegelow (1990) using the von Bertalanffy growth model are also indicated in Table 2 for comparison. The growth parameters obtained by the analyses of males up to five years of age and those older than five are presented in Table 3. By dividing the sample in two, the fit of the von Bertalanffy model improved considerably (Tables 2 and 3). The growth curves of *S. guianensis* males and females obtained by the von Bertalanffy model are presented in Figure 3.

The t-test applied to parameters a and b of the weight/length regression equations for males and females revealed a significant difference (t=2,25; df=38; $P<0.05$). Therefore, this relationship was analyzed for the sexes separately and the equations obtained were

$$TW = 3.156 \times 10^{-6} \times TL^{3.2836} \quad \text{(males) } (r=0.96)$$
$$TW = 8.974 \times 10^{-5} \times TL^{2.6182} \quad \text{(females) } (r=0.95).$$

Table 1

Schnute growth model parameters applied to *Sotalia guianensis* on the Paraná coast, southern Brazil. "τ_1" and "τ_2" are predetermined ages in years; "y_1" and "y_2" are estimated sizes at ages τ_1 and τ_2, in cm; "a" and "b" are adimensional parameters. "SQ" represents the residual sum of squares, and "Expl. var." represents the variance of the data explained by the model.

Parameters	Females	Males	All
τ_1	0	0	0
y_1	93.11	86.04	89.53
τ_2	28	28	28
y_2	181.72	190.45	185.70
a	0.14	0.07	0.13
b	7.64	9.45	7.86
SQ	1242.35	1898.75	4375.56
Expl. var. (%)	93.47	92.17	92.47
n	28	34	71

Discussion

Age estimation

Although there was no difference in the age estimation between teeth orientated in the buccal-lingual and anterior-posterior planes, we recommend the buccal-lingual plane to obtain easier on-center or close-to-center sections, which are essential for accurate age estimates.

The differences found in counting GLGs in teeth from the anterior extremity and the median region of the tooth row of the same animal corroborate the results obtained by Hui (1980) for *Tursiops truncatus*. Therefore, we also do not recommend using teeth from the most anterior part of the mandible for age estimation in *S. guianensis*.

The mean distance between the neonatal line and the end of the first GLG obtained in the present study (622.4 µm) was approximately double that obtained by Ramos (1997) (297.8 µm) for estuarine dolphins on the coast of Rio de Janeiro. The differences, however, must be analyzed carefully: the measurements carried out in our study were always made in the neck of the teeth, whereas those made by Ramos (1997) were from the base of the neonatal line. However, the differences may be related to the interpretation of the position of the first annual layer. The accessory layers (nonannual), observed between the neonatal line and the end

Table 2

Von Bertalanffy growth model parameters applied to *Sotalia guianensis* on the Paraná coast, southern Brazil, and parameters from the literature. "TL_∞"= asymptotic length (cm), "k"= growth constant and "t_0"= theoretical age at which the length of the animal is zero. "SQ" represents the residual sum of squares, and "Expl. var." represents the variance of the data explained by the model.

	Our study				
Parameters	Females	Males	All	Borobia (1989)	Schmiegelow (1990)
TL_∞	177.31	179.10	179.53	187.21	182.6
k	0.66	1.00	0.79	0.20	0.41
t_0	−1.23	0.72	0.95	−4.05	−1.57
SQ	1944.25	3732.30	6942.93	—	—
Expl. var. (%)	89.78	84.61	88.06	—	—
n	28	34	71	24	22

of the GLG of the first year, frequently appear in a very conspicuous manner, especially in the tip of the tooth, and can be easily confused with annual layers. The assumption that accessory layers are annual could result in a duplication of the real age of young animals up to two years old, with significant consequences in the interpretations of populational biological parameters (Hohn, 1990). The ideal situation would be that a GLG deposition model already existed for the species being studied, thereby avoiding counting accessory layers as being annual (Hohn et al., 1989). In most odontocete species, including *S. guianensis*, accessory layers do not continue up to the end of the root of the tooth, in contrast to annual layers, which can be seen from the tip to the base of the root of the tooth. However, to identify accessory layers it is necessary that the sections selected for age determination are central, or close to the center of the pulp cavity (Pinedo and Hohn, 2000). Off-center sections can be used for age estimation, but reading errors increase markedly and consequently induce unreliable age estimates (Pinedo and Hohn, 2000).

The reasons for GLG deposition in teeth are unknown (Hohn et al., 1989). However, several reasons have been suggested, including seasonal variations in growth rate, genetic physiological cycles, dietary changes, hormonal influences, and intrinsic factors on the metabolism in general (Boyde, 1980; Klevezal, 1980; Scheffer and Myrick, 1980). Although all these factors could be influential, variations in the diet certainly play a significant role. According to Klevezal (1996), a descriptive record of the dietary changes of an animal during the year should initially be looked for in structures that have a large degree of sensitivity, such as teeth. It is known that dentine reacts to the introduction of fluoride, calciferol and a series of other components in the organism, forming layers with different degrees of mineralization (Klevezal, 1996), which is known as a calcium-traumatic reaction of dentine. Therefore, it is possible to find a record of dietary changes in the dentine, starting from weaning (Klevezal, 1996).

We believe that the accessory layer in the dentine found at approximately 419.6 µm from the neonatal line, could be a record of the end of weaning in the estuarine dolphin. It was observed in all the teeth of individuals older than 6.7 months and could be a hypomineralized layer caused by a reduction of calcium in the body due to the absence of milk in the diet (Klevezal, 1996). The other accessory layer found closer to the neonatal line (mean of 248.9 µm) was not observed in all animals and the interpretation of this layer remains uncertain. It may be related to the beginning of weaning, as has been suggested for the bottlenose dolphin

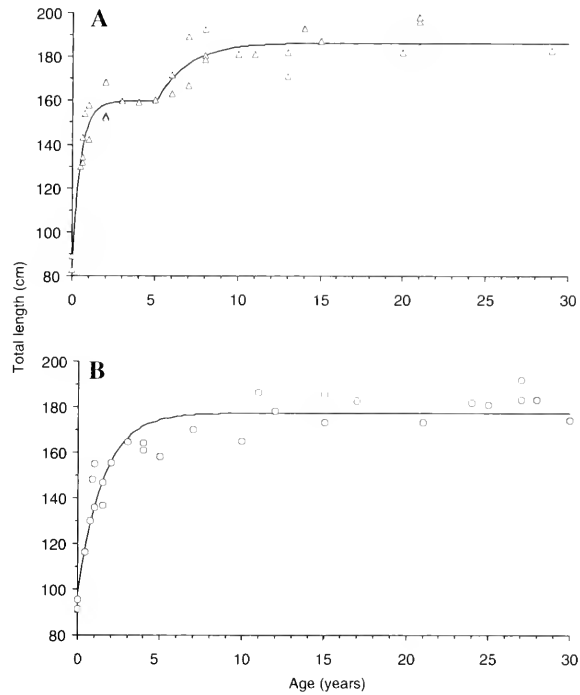

Figure 3

Growth curve of male (**A**) and female (**B**) *Sotalia guianensis* on the Paraná coast, southern Brazil.

Table 3

Von Bertalanffy growth model parameters for male *Sotalia guianensis* on the Paraná coast, southern Brazil. "TL_∞"= asymptotic length (cm), "k"= growth constant and "t_0"= theoretical age at which the length of the animal is zero. "SQ" represents the residual sum of squares, and "Expl. var." represents the variance of the data explained by the model.

Parameters	Up to 5 years	More than 5 years
TL_∞	159.64	186.41
k	2.02	0.53
t_0	−0.38	−1.40
SQ	510.99	1013.98
Expl.var. (%)	94.20	50.90
n	15	19

(*T. truncatus*) (Hohn[1]). This hypothesis still needs to be confirmed. However, all the *S. guianensis* individuals that were still nursing, but which already had remains of solid food in their stomachs (n=5), had only an accessory layer that is closer to the neonatal line—they did not have the layer that we are assuming marks the end of weaning.

According to Rosas (2000), there was no significant difference in incidental catches between mature and immature individuals of *S. guianensis* caught on the coast of Paraná, suggesting a similar vulnerability of young and adult estuarine dolphins to fisheries. Because the animals analyzed in our study were the same ones used by Rosas (2000), this lack of significant difference between mature and immature individuals can suggest a representative age distribution of the individuals analyzed.

Because the maximum estimated age in our study was 30 years, and because the dolphins here analyzed were incidentally caught in fishing nets, it seems reasonable to assume that the longevity of the estuarine dolphin may be 30–35 years. This hypothesis is also corroborated by the study carried out by Ramos (1997) with *S. guianensis* on the coast of Rio de Janeiro State (southeastern Brazil). Although the age of the oldest male observed in our study was 29 years, the frequency of males older than 21 years was less than 3%, which is extremely low when compared with the frequency of 21.5% for females older than 21 years. These results suggest a greater life expectancy for females, which is also corroborated by a study carried out by Ramos (1997) in Rio de Janeiro.

Growth

The use of Schnute's model is helpful in deciding which growth model should be used. Even though the researcher can usually decide which model is most appropriate by looking at the data, subtle differences in data distribution could cause one or another model to be more adequate. Use of a generic model allows this choice without intervention of the researcher and avoids any unconscious bias towards or against any model.

The discontinuity of growth in male *S. guianensis* in our study could have been due to the small sample size or may have been due to a second growth spurt, which has already been observed in the total length of *Stenella attenuata* (Perrin et al., 1976), *Lissodelphis borealis* (Ferrero and Walker, 1993), and *Phocoenoides dalli* (Ferrero and Walker, 1999), and in the weight of male *Tursiops truncatus* (Cockroft and Ross, 1990). The k value obtained for male *S.guianensis* up to five years was very high, meaning that asymptotic length in this phase of life was reached quickly. The cessation of growth exhibited by the model for males up to 5 years probably is not true in the biological sense but could be an artifact created by the model and the small sample size. Most probably there is a marked reduction in growth with the start of sexual maturation and a greater investment in the weight or reproductive apparatus (or both). The hypothesis of a greater investment in weight is supported by the observed difference in the weight-length coefficient between males and females. Additionally, sexual investment of male estuarine dolphins is very high—testes of adult males can reach up to 32 cm in length and weigh up to 3.3% of the total body weight (Rosas and Monteiro-Filho, 2002).

After the secondary growth spurt in males, the final asymptotic length did not differ very much from that in females. Previous growth studies carried out by Borobia (1989), Schmiegelow (1990), and Ramos et al. (2000) with the estuarine dolphin did not mention the existence of a second growth spurt in males, possibly because the authors did not analyze the growth of males and females separately. According to Ramos et al. (2000), male and female data were combined because of the absence of sexual dimorphism in the body size of adults of this species.

Borobia (1989) and Schmiegelow (1990), who also used the von Bertalanffy model, obtained different values for the growth equation parameters (Table 1). The sample used by Borobia (1989) did not have many individuals in ages 1 and 2, and none in the 0 age class. The absence of animals that "anchor" the beginning of the curve could result in low estimates of k and t_0. Additionally, Borobia (1989) examined individuals from different locations along the distribution of the species and thus did not take into consideration possible geographical variations. The results obtained by Schmiegelow (1990) are similar to those of our study, probably because both of them used animals from the same region.

Ramos et al. (2000) analyzed the growth of *S. guianensis* using the Gompertz growth model and obtained an asymptotic length (191.7 cm) which was much greater than that obtained in our study and in previous studies (Borobia, 1989; Schmiegelow, 1990) (Table 1). This difference could be due to 1) the small number of individuals older than 12 years (n=3) in their sample; or 2) a difference in asymptotic lengths between southeastern and southern Brazil populations. Similar differences have been observed between asymptotic lengths of *Pontoporia blainvillei* from Rio de Janeiro (southeastern Brazil) and São Paulo and Paraná (same area of the present study), where larger individuals were found in Rio de Janeiro (Ramos et al., 2000; Rosas, 2000). Therefore, it is possible that environmental variables could be responsible for larger sizes in the area studied by Ramos et al. (2000), both for *S. guianensis* and for *P. blainvillei*.

Although no significant difference was observed in the asymptotic length between adult males and females, the differentiated growth in time between the two sexes is probably responsible for the difference observed in the weight-length relationship.

In most species, the length exponent (θ) of the weight-length relationship is usually close to 3 (Santos, 1978). The estimated values of this exponent for the estuarine dolphin (3.2 for males and 2.6 for females) suggest that the longitudinal and transversal body growth in this species follows a similar pattern.

Our results suggest that it is important to study growth by analyzing the sexes separately, because there may be differential growth between the sexes before the adult age.

[1] Hohn, A. A. 1999. Personal commun. Beaufort Laboratory, Southeast Fisheries Science Center, National Marine Fisheries Service, 101 Privers Island Road, Beaufort, NC 28516-9722.

Acknowledgments

We sincerely thank the fishermen of Vila da Barra do Superagüi and Ilha das Peças (Paraná coast) for the information they provided and their help in collecting the incidentally caught dolphins. We thank Fundação O Boticário de Proteção à Natureza and the MacArthur Foundation for financial support, and IBAMA/PR, especially Guadalupe Vivekananda, head of the National Park of Superagüi. We also thank Maria Cristina Pinedo, who allowed us to use her laboratory and equipment for the age estimations, and Kesä K. Lehti, who translated the manuscript from Portuguese into English. Renata Ramos and an anonymous referee provided critical and insightful comments on the manuscript. Coordenação de Pessoal de Nível Superior (CAPES) provided a fellowship to the senior author. This study is part of a dissertation presented by Fernando C. Weber Rosas, submitted in partial fulfillment for a Ph.D. degree in Zoology at the Universidade Federal do Paraná, Curitiba, Brazil.

Literature cited

Borobia, M.
1989. Distribution and morphometrics of South American dolphins of the genus *Sotalia*. MSc. thesis, 81 p. McDonald College, McGill University. Montreal, Quebec, Canada.

Boyde, A.
1980. Histological studies of dental tissues of Odontocetes. *In* Age determination of toothed whales and sirenians (W. F. Perrin and A. C. Myrick, eds.), p. 65–87 Rep. Int. Whal. Comm., Special Issue 3.

Cockcroft, V. G., and G. J. Ross.
1990. Age, growth, and reproduction of bottlenose dolphins *Tursiops truncatus* from the east coast of Southern Africa. Fish. Bull. 88:289–302.

da Silva, V. M. F., and R. C. Best.
1996. *Sotalia fluviatilis*. Mammalian Species 527:1–7.

Ferrero, R. C., and W. A. Walker.
1993. Growth and reproduction of the northern right whale dolphin, *Lissodelphis borealis*, in the offshore water of the North Pacific Ocean. Can. J. Zool. 71:2335–2344.
1999. Age, growth and reproductive patterns of Dall's porpoise (*Phocoenoides dalli*) in the Central North Pacific Ocean. Mar. Mamm. Sci. 15(2):273–313.

Hohn, A. A.
1990. Reading between the lines: Analysis of age estimation in dolphins. *In* The Bottlenose dolphin (S. Leatherwood and R. R. Reeves, eds.), p. 575–585. Academic Press, New York, NY.

Hohn, A. A.; M. D. Scott, R. S. Wells, J. C. Sweeney, and A. B. Irvine.
1989. Growth layers in teeth from known-age, free-ranging bottlenose dolphins. Mar. Mamm. Sci. 5 (4):315–342.

Hui, C. A.
1980. Variability of dentine deposition in *Tursiops truncatus*. Can. J. Fish. Aquat. Sci. 37:712–716.

Klevezal, G. A.
1980. Layers in the hard tissues of mammals as a record of growth rhythms of individuals. *In* Age determination of toothed whales and sirenians (W. F. Perrin and A. C. Myrick, eds.), p. 89–94. Rep. Int. Whal. Comm. Special Issue 3.
1996. Recording structures of mammals. Determination of age and reconstruction of life history, 274 p. A.A. Balkema, Rotterdam, Netherlands.

Molina, D. M., and J. A. Oporto.
1993. Comparative study of dentine staining techniques to estimate age in the Chilean Dolphin, *Cephalorhynchus eutropia* (Gray, 1846). Aquat. Mamm. 19 (1):45–48.

Monteiro-Filho, E. L. A., L. R. Monteiro, and S. F. dos Reis.
2002. Skull shape and size divergence in the dolphins of the genus *Sotalia*: a tridimensional morphometric analysis. J. Mamm. 83 (1):125–134.

Norris, K. S.
1961. Standardized methods for measuring and recording data on the smaller cetaceans. J. Mamm. 42 (4):471–476.

Perrin, W. F., J. M. Coe, and J. R. Zweifel.
1976. Growth and reproduction of the spotted porpoise, *Stenella attenuata*, in the offshore eastern tropical Pacific. Fish. Bull. 74(2):229–269.

Pinedo, M. C., and A. A. Hohn.
2000. Growth layer patterns in teeth from the franciscana, *Pontoporia blainvillei*: developing a model for precision in age estimation. Mar. Mamm. Sci. 16 (1):1–27.

Ramos, R. M. A.
1997. Determinação de idade e biologia reprodutiva de *Pontoporia blainvillei* e da forma marinha de *Sotalia fluviatilis* (Cetacea:Pontoporiidae e Delphinidae) no norte do Rio de Janeiro. M.Sc. thesis, 95 p. Universidade Estadual do Norte Fluminense. Campos dos Goytacazes, Rio de Janeiro, Brasil.

Ramos, R. M. A., A. P. M. Di Beneditto, and N. R. W. Lima.
2000. Growth parameters of *Pontoporia blainvillei* and *Sotalia fluviatilis* (Cetacea) in northern Rio de Janeiro, Brazil. Aquat. Mamm. 26 (1):65–75.

Rosas, F. C. W.
2000. Interações com a pesca, mortalidade, idade, reprodução e crescimento de *Sotalia guianensis* e *Pontoporia blainvillei* (Cetacea, Delphinidae e Pontoporiidae) no litoral sul do Estado de São Paulo e litoral do Estado do Paraná, Brasil. Ph.D. diss., 145 p. Universidade Federal do Paraná. Curitiba, PR, Brasil.

Rosas, F. C. W., and E. L. A. Monteiro-Filho.
2002. Reproduction of the estuarine dolphin (*Sotalia guianensis*) on the coast of Paraná, southern Brazil. J. Mamm. 83(2):507–515.

Santos, E. P.
1978. Dinâmica de populações aplicada à pesca e piscicultura, 129 p. Editora de Humanismo, Ciência e Tecnologia "HUCITEC" Ltda, São Paulo.

Scheffer, V. B., and A. C. Myrick.
1980. A review of studies to 1970 of growth layers in the teeth of marine mammals. *In* Age determination of toothed whales and sirenians (W. F. Perrin and A. C.Myrick, eds.), p. 51–63. Rep. Int. Whal. Comm., Special Issue 3.

Schmiegelow, J. M. M.
1990. Estudo sobre cetáceos odontocetes encontrados em praias da região entre Iguape (SP) e Baía de Paranaguá (PR) (24°42'S–25°28'S) com especial referência a *Sotalia fluviatilis* (Gervais, 1853) (Delphinidae). M.Sc. thesis, 149 p. Universidade de São Paulo, Instituto Oceanográfico, São Paulo.

Schnute, J.
1981. A versatile growth model with statistically stable parameters. Can. J. Fish. Aquat. Sci. 38:1128–1140.

Watson, L.
1988. Whales of the world. A handbook and field guide to all the living species of whales, dolphins and porpoises, 302 p. Hutchinson, London.

The relative value of different estuarine nursery areas in North Carolina for transient juvenile marine fishes

Steve W. Ross

NC National Estuarine Research Reserve
5600 Marvin Moss Ln.
Wilmington, North Carolina 28409
E-mail address: rosss@uncwil.edu

Abstract—Offshore winter-spawned fishes dominate the nekton of southeastern United States estuaries. Their juveniles reside for several months in shallow, soft bottom estuarine creeks and bays called primary nursery areas. Despite similarity in many nursery characteristics, there is, between and within species, variability in the occupation of these habitats. Whether all occupied habitats are equally valuable to individuals of the same species or whether most recruiting juveniles end up in the best habitats is not known. If nursery quality varies, then factors controlling variation in pre-settlement fish distribution are important to year-class success. If nursery areas have similar values, interannual variation in distribution across nursery creeks should have less effect on population sizes or production. I used early nursery period age-specific growth and mortality rates of spot (*Leiostomus xanthurus*) and Atlantic croaker (*Micropogonias undulatus*)—two dominant estuarine fishes—to assess relative habitat quality across a wide variety of nursery conditions, assuming that fish growth and mortality rates were direct reflections of overall physical and biological conditions in the nurseries. I tested the hypothesis that habitat quality varies for these fishes by comparing growth and mortality rates and distribution patterns across a wide range of typical nursery habitats at extreme ends of two systems. Juvenile spot and Atlantic croaker were collected from 10 creeks in the Cape Fear River estuary and from 18 creeks in the Pamlico Sound system, North Carolina, during the 1987 recruitment season (mid-March–mid-June). Sampled creeks were similar in size, depth, and substrates but varied in salinities, tidal regimes, and distances from inlets. Spot was widely distributed among all the estuarine creeks, but was least abundant in the creeks in middle reaches of both systems. Atlantic croaker occurred in the greatest abundance in oligohaline creeks of both systems. Instantaneous growth rates derived from daily otolith ages were generally similar for all creeks and for both species, except that spot exhibited a short-term growth depression in the upriver Pamlico system creeks—perhaps the result of the long migration distance of this species to this area. Spot and Atlantic croaker from upriver oligohaline creeks exhibited lower mortality rates than fish from downstream polyhaline creeks. These results indicated that even though growth was similar at the ends of the estuaries, the upstream habitats provided conditions that may optimize fitness through improved survival.

Manuscript accepted 25 October 2002.
Manusript received 31 December 2002 at NMFS Scientific Publications Office.
Fish. Bull. 101:384–404 (2003).

Offshore winter-spawned (OWS) fishes are a major component of the nekton of southeastern United States and Gulf of Mexico estuaries. Their larvae migrate across the shelf, enter estuaries, and the majority of juveniles reside for several months in shallow, soft bottom estuarine creeks and bays called primary nursery areas (PNAs). Very high concentrations of fishes in these PNAs suggest that they are valuable habitats, perhaps because they are good sources of food and shelter (Boesch and Turner, 1984; McIvor and Odum, 1988; Miltner et al., 1995). Despite similarity in some PNA physical characteristics, there is variability in habitats occupied (between and within species), especially with regard to salinity, tidal influence, accessibility (i.e. distance from inlets), and, perhaps, food and predator regimes (Weinstein, 1979; Ross and Epperly, 1985). Assessing the relative value of all PNA habitats to individuals of the same species is increasingly important (Weinstein, 1982; Sogard, 1992; Guindon and Miller, 1995; Beck et al., 2001). If PNA value varies, do most of the recruiting juveniles end up in the best habitats (Thresher, 1985)? Understanding variation in habitat quality during a major early life history phase should yield insight into causes of variability in year-class strength, particularly if juvenile fish distributions vary interannually. If PNA quality varies, then factors controlling variation in presettlement distribution are important to year class success because animals could be transported to habitats of unpredictable quality. If nursery areas have similar value, interannual variations in distribution across nursery creeks should have less effect on ultimate population sizes or production.

General estuarine distributions of two dominant OWS fishes, spot (*Leiostomus xanthurus*) and Atlantic croaker (*Micropogonias undulatus*), exhibit consistent patterns throughout their ranges. Juvenile Atlantic croaker routinely concentrate in oligohaline creeks or bays (Weinstein, 1979; Mercer, 1987a) —a pattern that suggests that the upstream regions are most valuable to this species. Spot, however, are more ubiquitously and variably distributed through the shallow PNAs (Ross and Epperly, 1985; Mercer, 1987b), perhaps indicating less dependence on a particular estuarine region. Despite these generalities, both species can be present in large numbers in almost any estuarine creek or bay over the full salinity range (e.g. Nelson et al., 1991). In general, juveniles of both species seem to avoid (or are unsuccessful in) more open water areas of estuaries during the early part of the nursery period.

The main purpose of this paper is to assess relative habitat value for two dominant members of the OWS fish group, spot and Atlantic croaker, across a wide variety of North Carolina PNA conditions. I assumed that fish growth and mortality rates were direct reflections (integrators) of overall physical and biological conditions in PNA habitats. Therefore, I used early nursery period age-specific growth and mortality rates of spot and Atlantic croaker, in addition to distribution data, to assess relative habitat quality, testing the hypothesis that habitat quality varies for these fishes across a broad range of typical PNAs in two very different estuarine systems. Growth and mortality can be influenced by fish density; however, Ross (1992) found similar growth and mortality rates for spot and Atlantic

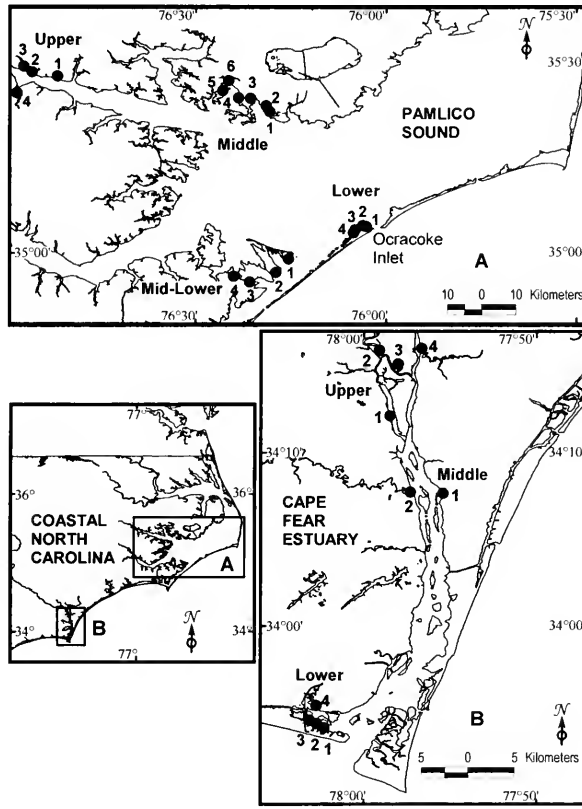

Figure 1

Pamlico Sound (**A**) and Cape Fear Estuary (**B**) in coastal North Carolina. General areas (e.g. upper, middle, lower) and sampling locations during March–June 1987 (solid dots) are labeled in the enlargements. Numbers correspond to station descriptions in Table 1.

croaker across wide ranges of densities in these systems. The similarity in these rates imply that PNAs were below carrying capacities. Thus, I did not consider density as a variable affecting growth or mortality for the following comparisons of PNA quality.

Methods

Study area

To encompass the greatest variability possible in estuarine habitats, I sampled nursery creeks in two widely separated, geophysically different North Carolina estuarine systems: 1) Pamlico Sound and River and 2) the Cape Fear River (Fig. 1). Each system was partitioned into general areas (e.g. upper, middle, lower) and stations were selected to represent these areas. Stations were located in creeks throughout both systems that previous sampling (Weinstein, 1979; Ross and Epperly, 1985; NC Division of Marine Fisheries[1]) indicated were consistently productive for juvenile marine fishes during the spring-summer season. All creeks were similar in depth, size, and sediment type. The greatest physical differences between stations were the salinities, tidal regimes, and distances from the nearest inlets (Table 1).

Pamlico Sound is a shallow lagoon estuary whose hydrography is controlled by wind (Giese et al., 1979; Pietrafesa et al., 1986a; Pietrafesa and Janowitz, 1988).

[1] NC (North Carolina) Division of Marine Fisheries. Unpubl. data. Program 120 Nursery Area Survey, P.O. Box 769, Morehead City, NC 28557.

Table 1

Distances to nearest inlets (D in km), salinity (‰) ranges and means, mean depths (m), and sediments of stations sampled from mid-March through mid-June 1987 in the Pamlico Sound and Cape Fear systems. Sediment symbols are m = mud, fs = fine sand, g = grass, and fs-m = fine sand and mud.

Area	D	Salinity range (mean)	Mean depth	Sediment
Pamlico Sound				
Lower				
"Coastguard" Creek	3	15.5–23.0 (18.9)	0.9	m
"Doctors" Creek	4	15.0–24.5 (18.6)	0.7	m
"Tom Bragg Slough"	7	13.0–22.0 (17.4)	0.9	fs-m
Royal Point Bay	8	17.0–20.4 (18.6)	0.7	fs
Mid–Lower				
Oyster Creek	26	11.0–15.0 (13.5)	0.9	m
Southwest Prong	33	13.5–23.0 (17.8)	1.0	m [1]
Merkle Hammock Creek	41	11.0–14.5 (15.1)	0.9	fs-g[1]
Codduggen Creek	46	9.0–14.5 (12.3)	0.9	fs-m[1]
Middle				
Caffee Creek	46	10.8–18.5 (13.4)	1.8	m
Oyster Creek	48	10.8–17.8 (13.2)	1.2	m[1]
unnamed Creek	51	10.9–18.0 (13.7)	1.6	fs-m
"Swan" Creek	60	10.0–15.9 (12.4)	1.1	m
Tooley Cr	61	10.2–17.1 (12.5)	1.3	m[1]
Head Rose Bay	64	10.0–13.3 (11.1)	2.5	m
Upper				
Mallard Creek	92	1.3–7.2 (3.5)	1.2	m
Flatty Creek	99	0.9–4.0 (2.6)	1.0	m
Broad Creek	101	0.3–8.7 (2.4)	1.4	m
Little Creek	104	0.6–3.9 (2.3)	1.0	m
Cape Fear estuary				
Lower				
Molasses Creek	4	15.4–29.0 (21.5)	1.0	m
Piney Pt. Creek	6	15.0–29.9 (22.5)	0.6	m
Dennis Creek	7	11.8–31.0 (21.7)	1.0	m-fs
Dutchman Creek	7	12.6–24.6 (17.7)	0.6	m
Middle				
Town Creek	29	0.0–10.2 (3.7)	2.0	m
Mott Creek	29	0.0–13.4 (5.6)	1.0	m
Upper				
Jackeys Creek	36	0.0–6.9 (1.7)	0.5	m
Toomers Creek	44	0.0–2.3 (0.3)	3.0	m
Horseshoe Bend	43	0.0–2.3 (0.4)	0.6	m
Smith Creek	44	0.0–4.8 (1.5)	1.3	m

[1] See Ross and Epperly (1985) for additional sediment data.

Eighteen stations were located in creeks in four areas along an approximately 100-km transect from Ocracoke Inlet to the upper Pamlico River (Fig. 1). Four polyhaline stations were located on Portsmouth Island (lower area). Water depths there were largely controlled by semidiurnal lunar tides (range usually <0.7 m, Giese et al., 1979); however, on one occasion I observed that northerly winds (≥37 km/h) moved large quantities of water into these creeks. The mid-lower area consisted of four stations on Cedar Island, which exhibited less depth variation (dampened lunar tides) than creeks on Portsmouth Island. Six creeks were sampled in the middle area: three each in Rose and Swanquarter bays. Tidal influence was negligible here (Pietrafesa et al., 1986a). The creeks in the above three areas were largely surrounded by *Spartina* and *Juncus* marsh grasses. The upper area was represented by four creeks (oligohaline or freshwater) surrounded by a mixture of woodlands and patches of marsh. Water levels and currents here were almost entirely controlled by winds or river flow (or both) (Hobbie, 1970; Pietrafesa et al., 1986a).

The Cape Fear River is more typical (compared to the Pamlico Sound system) of United States East and Gulf

coasts estuaries (i.e. a drowned river valley). Diurnal lunar tides (average range about 1.5 m) were a dominant feature throughout the study area (Welch and Parker, 1979; Pietrafesa and Janowitz, 1988). Ten stations were located along a 50-km transect of the Cape Fear system (Fig. 1). In the lower estuary, four polyhaline creeks were sampled on the west side of the inlet (Oak Island). Two creeks were sampled on opposite sides of the middle of the estuary and four oligohaline creeks were sampled in the upper estuary near Wilmington. All stations in this system were surrounded by *Spartina* marshes.

Field sampling

All stations were sampled during daylight with two one-minute tows (68.6 m each) of a small-mesh trawl (3.2-m headrope length, 6.4-mm bar mesh wings and body, 3.2-mm tail bag mesh). Catches from the two tows were combined for the station sample. Surface and bottom salinities (nearest ‰) and water temperatures (nearest °C) were recorded after each sample. Mean salinities and temperatures for each area were analyzed for differences by using *t*-tests for all possible combinations of area pairs.

Sampling was designed to provide biological data during the time of early residency in the nursery creeks, but before significant emigration. Most recruitment of young juvenile fishes into these creeks has ended by late-April, and some fishes begin to emigrate by June–July (Weinstein, 1979; Ross and Epperly, 1985; author's pers. obs.). To minimize the influence of emigration on the calculation of growth and mortality rates, sampling occurred during seven periods, every other week from mid-March through mid-June 1987 (about 14 d between samples). Synoptic samples over this large region were generated by assigning areas to four crews for trawling during the same period of each sample week.

Newly recruiting OWS juvenile fishes of the 1987 year class were sorted from the catches and preserved in the field in 100% ethyl alcohol. About one month after collection the fishes were identified, counted, and standard lengths (SL) were measured to the nearest mm. Analyses were limited to spot and Atlantic croaker, the two most abundant species. Catch per unit of effort (CPUE) was calculated by dividing the total number of individuals of a species captured by the number of trawl tows in a time period or area. Subsamples of these fishes representing several collection dates and all areas were measured for SL, blotted, and weighed to the nearest 0.01 g and were used to develop a weight-length relationship using linear regression. Differences in weight-length relationships between areas were assessed by using analysis of covariance (covariate=log*SL*) in a general linear model procedure (SAS Institute, 1988).

Otolith aging

Subsamples for aging were randomly selected from early (early and mid-April) and late (mid and late May) dates and from downstream (lower) and upstream (upper) areas in each system. Sagittae were removed from these fishes, mounted on microscope slides with thermoplastic cement, and polished (often on both sides) until thin sections were obtained. Otoliths were viewed with oil immersion and transmitted polarized light at magnifications between 500 and 625×, and images were projected through a video system to a screen. Rings, presumed to be daily, were counted. The formation of daily rings has either been validated (Peters et al., 1978; Baldevarona, 1987; Siegfried and Weinstein, 1989) or assumed (Warlen and Chester, 1985; Cowan, 1988) for the two species in the size ranges used here. Even so, the counted rings need not be deposited daily for growth rate comparisons, nor is it necessary to know their periodicity. It is required that groups of fish being compared exhibit the same ring formation periodicity over the time and space of the comparison. Spot and Atlantic croaker do not form growth rings until after yolksac absorption, about four to five days after spawning (Peters et al., 1978; Warlen, 1980). Therefore, to estimate actual ages for mortality calculations, five days were added to the ring counts.

Although it seems reasonable to assume that juvenile spot and Atlantic croaker form daily sagittae rings, the precision (repeatability) of ring counts and the ability to identify daily rings needs addressing. Before aging the samples used in this study, I examined several hundred spot and Atlantic croaker otoliths. Counts by myself and 2–3 other otolith readers were compared. Our ring identifications were compared to samples of known age spot and Atlantic croaker provided by the National Marine Fisheries Service (Warlen[2]). These preliminary samples were used as a training device to ensure that daily rings were accurately identified and were not confused with shadows or subdaily rings. Subdaily rings may not even be resolvable at the magnifications (≤625×) used in the present study (Campana et al., 1987; Isely[3]). After aging the samples used in this study, I re-aged a random selection of spot (without knowledge of previous age assignments) and obtained a mean difference in counts of 2.85 (SD=2.03, n=27). Because Atlantic croaker otolith rings were usually easier to count, I assumed that the above count difference was generally similar for this species. I assumed that the ages reported here had a count precision of ±3 days. I also assumed that any aging errors were randomly distributed throughout the samples and were not spatially or temporally biased.

Growth and mortality

Linear regression of the form $\text{Log}_{10}SL = b + m(age)$ was used to model growth. The slope of this line, m, is the instantaneous daily growth rate. Differences in growth rates between areas were assessed by using analysis of covariance (covariate=age) in a general linear model procedure (SAS Institute, 1988). Absolute and relative daily growth rates were calculated by using values predicted with the age-SL regression equation (Ricker, 1975). For each sampling date, mean SLs were compared between all

[2] Warlen, S. M. 1989. Personal commun. National Marine Fisheries Service Beaufort Lab, Beaufort, NC 28516.

[3] Isely, J. 1989. Personal commun. Zoology Dept., NC State Univ., Raleigh, NC 27695.

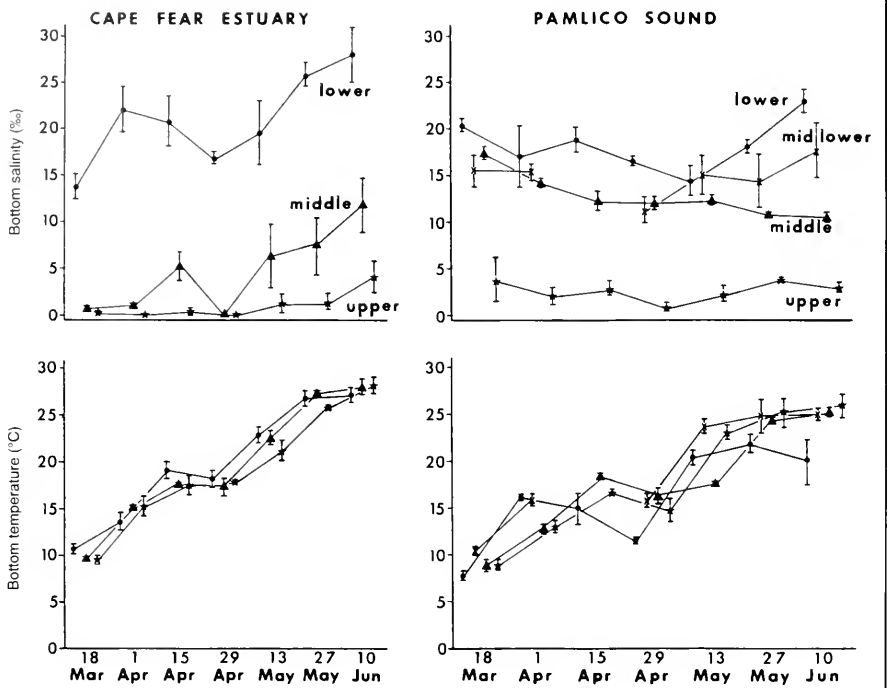

Figure 2

Mean bottom water temperature and salinity for general areas (circle=lower, triangle= middle, x=mid-lower, star=upper) of the Cape Fear and Pamlico Sound, NC, estuaries by sampling week, March–June 1987. Vertical bars represent 95 percent confidence intervals around the means.

areas and systems by using pairwise *t*-tests for all possible pair combinations as an option in the general linear models procedure (SAS Institute, 1988).

Instantaneous and daily mortality rates were calculated for spot and Atlantic croaker by using methods similar to Crecco et al. (1983) and Essig and Cole (1986). Inverse regression (Zar, 1984) of the relationship between age and SL was used to estimate age from SL. Ages were then calculated for all fish sampled, and the natural logarithm of the slope of the descending limb of the catch curve was the instantaneous natural mortality rate (Z). Analysis of covariance (covariate=age) in a general lineal model procedure was used to test for differences in mortality rates between areas (SAS Institute, 1988). The daily mortality rate (M, %/d) for the whole time period was calculated as $M = 1-e^{Z}$ (Ricker, 1975).

Because null hypotheses of no differences in growth or mortality rates between areas were accepted in many cases, probabilities of type-II errors (B, H_0 actually false) existed. Calculations of power ($1-B$), the probability of correctly rejecting H_0, are difficult with ANOVA or ANCOVA (Zar, 1984; Neter et al., 1985). A power analysis was probably unnecessary for spot and Atlantic croaker age-SL regressions because the precisions of the slope estimates were good (i.e. proportional SEs of the estimates were 2–4% of the slopes).

Results

Hydrographic data

Only bottom hydrographic data are presented because the waters of these shallow stations were well mixed. Bottom water temperatures in all areas of both systems were similar on a given sampling date (Fig. 2). In the Cape Fear estuary, mean water temperatures were not significantly different (*t*-test, $P>0.05$) between areas. Mean temperatures throughout the Pamlico system were not significantly different ($P>0.05$), except that the lower area was cooler than the others ($P<0.05$). Comparisons between systems revealed no significant differences ($P>0.05$) between middle or upper area temperatures. Lower Cape Fear creeks were

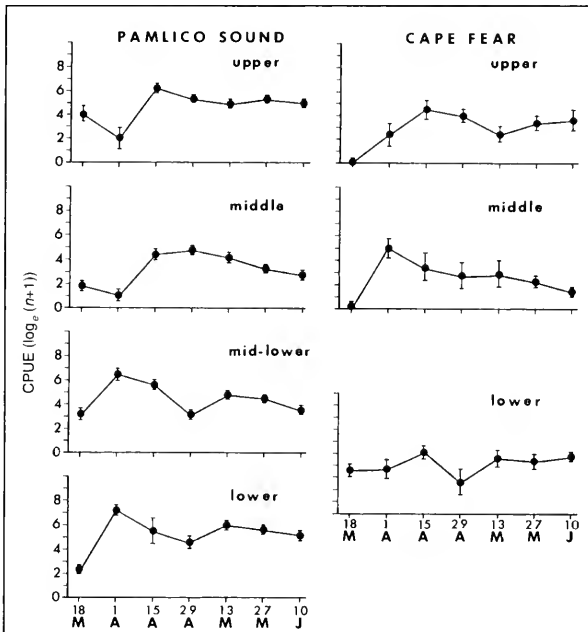

Figure 3

Mean catch per unit of effort for spot in general areas of the Cape Fear and Pamlico Sound, NC, estuaries by sampling week, March–June 1987. Vertical bars represent plus and minus one standard error of the mean. The *x*-axis abbreviations (from left to right) stand for March, April, April, April, May, May, June.

significantly ($P<0.05$) warmer than those of the lower Pamlico. The cooler temperatures in the lower Pamlico may have resulted from sampling there at earlier times of the day or on different days of the sampling week.

Salinity was more variable than temperature, particularly within the mesohaline and polyhaline areas (Fig. 2). Within both the Pamlico and Cape Fear systems all areas exhibited significantly different (*t*-test, $P<0.05$) bottom salinities from each other. As expected, the Cape Fear estuary, with its larger, more channeled river flow and obvious tidal effects, was a more variable system than the Pamlico system. During this study mean salinities within the lower and middle areas of the Cape Fear system varied over a range of 11.8‰ and 14.2‰, respectively, whereas mean salinities in all other areas (including the Pamlico) varied over a range less than 9‰. The lower Cape Fear creeks had significantly higher ($P<0.05$) salinities than those of the lower Pamlico; however, the middle and upper Pamlico areas had significantly higher ($P<0.05$) salinities than their counterparts in the Cape Fear, even though the upper Pamlico area was twice as far from an inlet as the upper Cape Fear. Salinities declined rapidly in the Cape Fear with increasing distance from the inlet; however, this relationship was more variable in the Pamlico System (Fig. 2). In both systems, overall mean salinity (S) was accurately predicted by distance (D, in km) from the inlet: Cape Fear: $S=23.5 - 0.55(D)$, $r^2=0.95$, $n=10$ and Pamlico: $S=20.4 - 0.17(D)$, $r^2=0.92$, $n=18$.

Leiostomus xanthurus

Distribution Spot was the more widely distributed of the two species (Figs. 3–5). At the earliest sample date, small numbers of spot had accumulated in all areas of the Pamlico system (Fig. 3). Peak abundance was observed in the lower and mid-lower areas by the second sample date and in the middle and upper areas by the third sample date. Although more spot were collected in the lower Pamlico, numerical differences between areas were not extreme (Figs. 3 and 4). Overall, the least numbers of spot occurred in the middle region (Figs. 3 and 4).

In the Cape Fear system, overall spot abundance was similar between the upper and lower regions, and, as in the Pamlico, the least numbers were collected from the middle

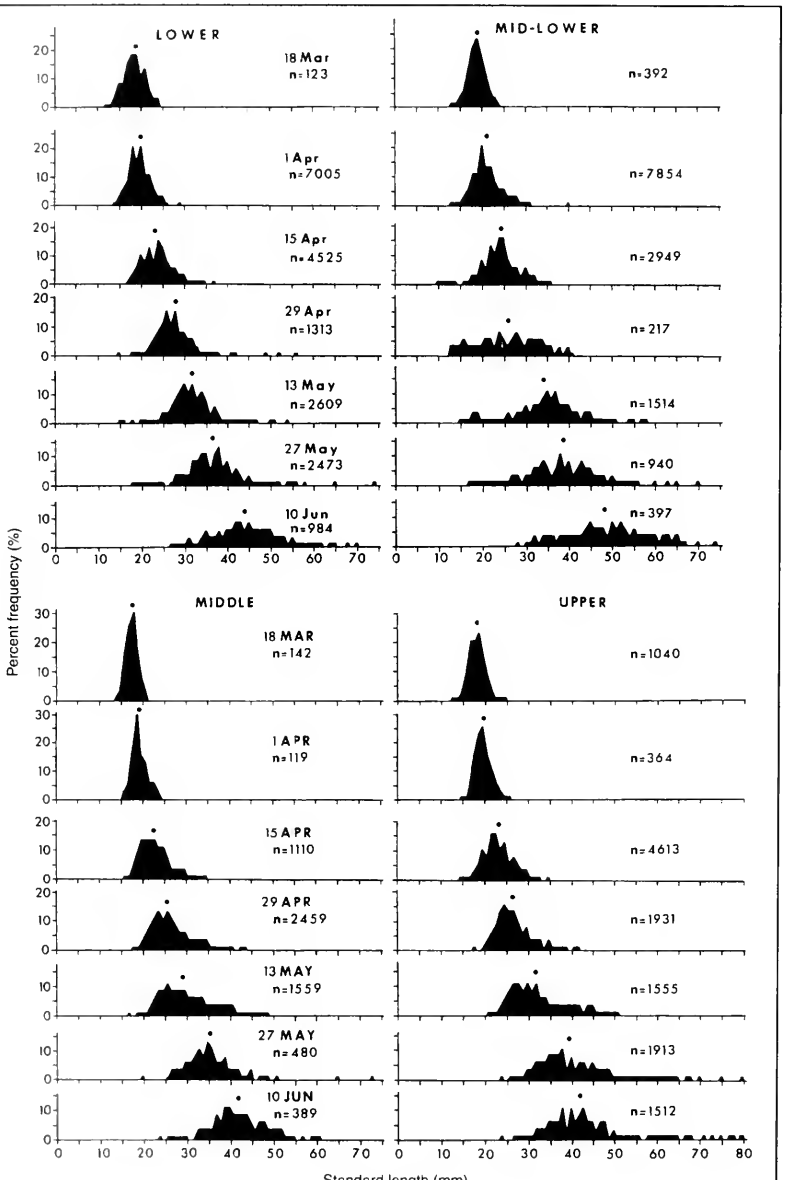

Figure 4

Spot length frequencies in general areas of the Pamlico Sound, NC, estuary by sampling week, March–June 1987. Solid dots represent mean SL.

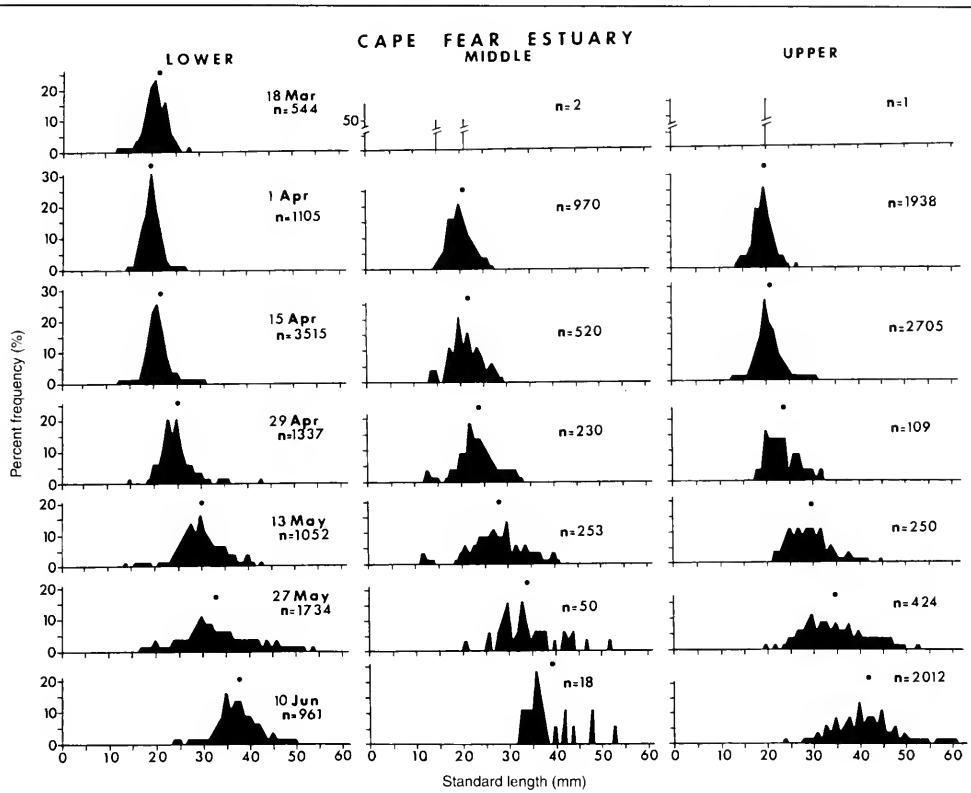

Figure 5

Spot length frequencies in general areas of the Cape Fear, NC, estuary by sampling week, March–June 1987. Solid dots represent mean SL.

area creeks (Figs. 3 and 5). Initial recruitment was high in the lower Cape Fear area, whereas it lagged behind in the middle and upper areas (Fig. 3). Nevertheless, all Cape Fear areas reached peak numbers by the second or third sampling dates (Fig. 3).

Size distributions The bulk of the spot year class recruited to all creeks from mid-March to early April; however, some small fish (≤25 mm) continued to enter the creeks through the end of May (Figs. 4 and 5). The smallest spot captured in both systems were always between 13 and15 mm SL (Figs. 4 and 5). Because the trawl can collect spot and Atlantic croaker at least to 10 mm SL , 13–15 mm probably represented the smallest recruitment sizes of spot to nursery habitats.

Differences in mean spot SLs between areas steadily increased during the study from <1 mm (through mid-April) to 4.3 mm in the Cape Fear and from 1 to 6.2 mm in the Pamlico. Although mean spot SLs exhibited the smallest variations between areas in the Cape Fear system (Fig. 5), they were significantly different (paired t-tests, $P<0.05$) between areas on most sampling dates. No area in the Cape Fear had consistently larger or smaller mean spot SLs. After mid-April mean SLs of spot from all four Pamlico areas were larger than those from the Cape Fear. Within the Pamlico system (Fig. 4) spot in the mid-lower area had significantly larger ($P<0.05$) mean SL (except sampling weeks four and six), and fish in the middle area were always significantly smaller ($P<0.05$) than those in the other three areas.

Growth Estimated spot ages ranged from 61 to 157 days (17–35 mm SL, $n=379$). All of the age-SL relationships used to assess growth rates (Fig. 6) were highly significant ($P<0.0001$). Regression residuals were evenly distributed around zero, indicating that the exponential growth model

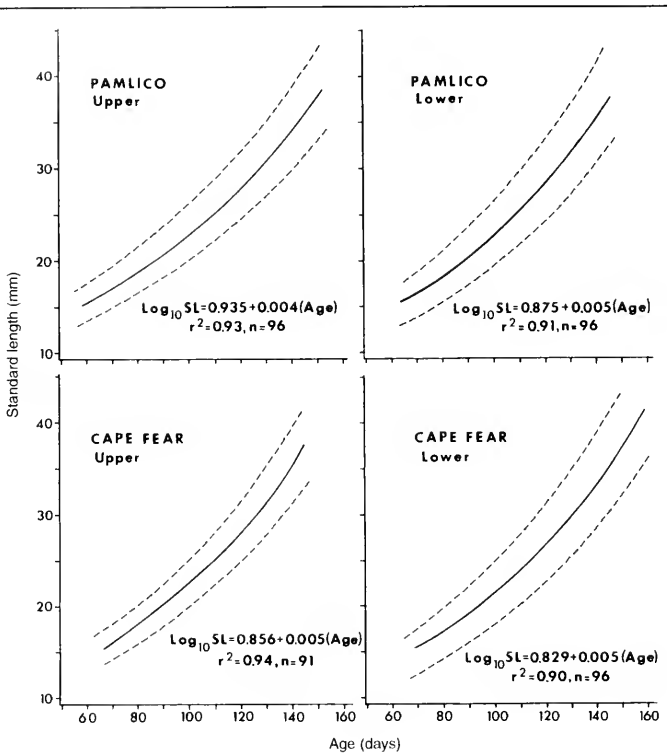

Figure 6

Spot growth rate curves (solid lines) based on otolith daily ages for upper and lower areas of the Pamlico Sound and Cape Fear, NC estuaries. Dotted lines represent 95 percent confidence intervals.

($\log_{10}SL = b + m(age)$) was appropriate. Instantaneous daily growth rates (slopes of the regressions) were similar (analysis of covariance, $P>0.05$) between upper and lower areas in the Cape Fear and the lower Pamlico (Fig. 6). Therefore, a combined age-*SL* regression for all spot in the upper and lower Cape Fear estuary and the lower Pamlico area was developed: $\log_{10}SL = 0.861 + 0.0048(age)$, r^2=0.90, n=283. Analysis of covariance indicated that spot from the upper Pamlico region exhibited significantly slower ($P>0.05$) overall growth rates (Fig. 6) than fish from the other three areas.

Age-specific absolute and relative growth of spot was predicted from the age-SL regression for the upper and lower Cape Fear and lower Pamlico combined and the upper Pamlico (Table 2). Predicted absolute growth rates in the Cape Fear and lower Pamlico areas increased from 0.16 mm/d between 60 and 65 days of age to 0.43 mm/d between ages 150 and 155 days of age, and the largest increase in absolute growth occurred between ages 95 and 105 days of age (Table 2). Relative growth remained constant around 1.13–1.14 %/d SL over the whole age range examined (Table 2). Although predicted sizes at ages were larger in the upper Pamlico area than those of the other three areas, the absolute growth rates were lower, increasing from 0.16 mm/d between ages 60 and 65 d to 0.39 mm/d between ages 150 and 155 d (Table 2). Absolute growth rates in this area also exhibited the largest increases around 100–105 days. Relative growth rates in the upper Pamlico were lower than in the other areas and averaged 1.01 %/d SL (Table 2). The ages when absolute growth in all areas was greatest (95–105 d) translated to SL ranges around 21–23 mm. This SL range dominated the length frequencies in all areas during the first two weeks of April (Figs. 4 and 5). Water temperatures were steadily increasing in all areas prior to mid-April (Fig. 2).

Growth was also compared by using weight-length relationships. These relationships for spot were highly significant (analysis of covariance, $P<0.0001$) and took the usual

Table 2

Predicted age-specific mean standard lengths (SL), absolute (mm/d), and relative (%/d SL) growth rates for spot from the upper and lower Cape Fear and lower Pamlico combined (CFR + LPAM) and the upper Pamlico area (UPPAM).

	CFR + LPAM			UPPAM		
Age (days)	Mean SL	Absolute growth rate	Relative growth rate	Mean SL	Absolute growth rate	Relative growth rate
60	14.09			15.60		
65	14.89	0.16	1.14	16.39	0.16	1.01
70	15.74			17.22		
75	16.63	0.18	1.13	18.09	0.17	1.01
80	17.58			19.01		
85	18.58	0.20	1.14	19.98	0.19	0.99
90	19.63			20.99		
95	20.75	0.22	1.14	22.05	0.21	1.00
100	21.93			23.17		
105	23.17	0.25	1.13	24.35	0.24	1.04
110	24.49			25.59		
115	25.88	0.28	1.14	26.88	0.26	1.02
120	27.35			28.24		
125	28.91	0.31	1.13	29.68	0.29	1.03
130	30.55			31.19		
135	32.28	0.35	1.15	32.77	0.32	0.99
140	34.12			34.43		
145	36.06	0.39	1.14	36.18	0.35	1.02
150	38.11			38.02		
155	40.27	0.43	1.13	39.95	0.39	1.03

Table 3

Weight-standard length (W-SL) relationships for spot and Atlantic croaker from all areas of the Cape Fear and Pamlico systems, March–June 1987.

Area	Formula	r^2	n
Spot			
Cape Fear Upper	$W = 10^{-6.25}(SL^{4.02})$	0.96	100
Cape Fear Middle	$W = 10^{-4.90}(SL^{3.05})$	0.97	134
Cape Fear Lower	$W = 10^{-5.00}(SL^{3.12})$	0.97	212
Pamlico Upper	$W = 10^{-6.09}(SL^{3.87})$	0.98	456
Pamlico Middle	$W = 10^{-5.73}(SL^{3.62})$	0.97	252
Pamlico Mid-Lower	$W = 10^{-6.12}(SL^{3.89})$	0.98	246
Pamlico Lower	$W = 10^{-6.22}(SL^{3.95})$	0.97	250
Atlantic croaker			
Cape Fear Upper	$W = 10^{-5.80}(SL^{3.64})$	0.97	138
Cape Fear Middle	$W = 10^{-5.30}(SL^{3.31})$	0.86	118
Cape Fear Lower	$W = 10^{-5.64}(SL^{3.48})$	0.93	98
Pamlico Upper	$W = 10^{-5.55}(SL^{3.43})$	0.96	188
Pamlico Lower	$W = 10^{-4.85}(SL^{2.98})$	0.88	46

curvilinear form (Table 3, Fig. 7). In the Pamlico system differences between areas were not large; however, middle area spot had significantly ($P<0.05$) lower weights per length, especially in larger individuals (Fig. 7). In the Cape Fear system, spot in the upper area had significantly ($P<0.05$) larger weights per length than those from the other two areas.

Mortality Spot mortality rates were based on individuals aged ≥85 days. All regression slopes describing the declining numbers of spot with increasing ages were significantly different from zero ($P<0.0001$). Instantaneous mortality rates over this time period ranged from 0.037 to 0.066 (Fig. 8). Analysis of covariance indicated that within each

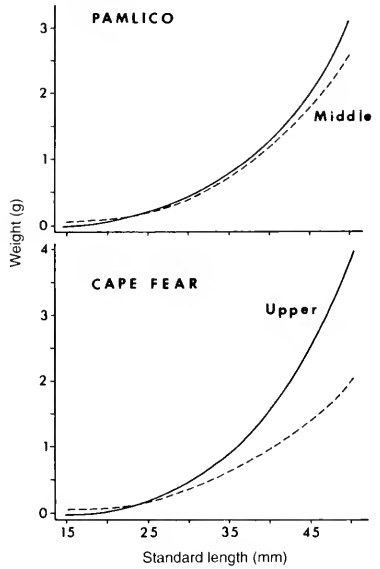

Figure 7

Spot weight-length relationships for the Pamlico and Cape Fear, NC, estuaries, March–June 1987. The line for the area that exhibited a significant difference was labeled (i.e. Pamlico Middle area, dashed line, was different and Cape Fear Upper area, solid line was different); the remaining line in each panel represented the relationship for all other areas combined.

system, upper area spot displayed significantly ($P<0.05$) lower instantaneous mortality rates than did fish from the lower estuaries, especially in Cape Fear. Lower Cape Fear spot exhibited a statistically similar ($P>0.05$) instantaneous mortality rate to those in the lower and upper Pamlico creeks. Daily mortality rates during the present study were 4.97 %/d in the upper Pamlico, 6.39 %/d in the lower Pamlico, 3.63 %/d in the upper Cape Fear, and 6.01 %/d in the lower Cape Fear.

Micropogonias undulatus

Distribution Atlantic croaker distributions in both systems were skewed toward upstream, oligohaline creeks (Fig. 9–11). In the Pamlico system almost no Atlantic croaker were collected in the lower or middle areas (Fig. 9). Atlantic croaker recruitment in the Pamlico lagged behind the Cape Fear in abundance and timing (Fig. 9), and peak densities occurred throughout the Pamlico near the end of the sampling.

Patterns of Atlantic croaker recruitment were like those of spot in the upper and middle Cape Fear. Like spot, most of the Atlantic croaker year class had recruited to these areas by mid-April, although small Atlantic croaker (≤20 mm) continued to colonize these creeks through mid-late May (Fig. 10). Also, peak abundance was reached in the middle and upper Cape Fear during the same weeks as those for spot (2nd and 3rd, respectively) (Fig. 9). Except for the larger CPUE in mid-March, Atlantic croaker recruitment in the lower Cape Fear was similar to that of most Pamlico system creeks (Fig. 9).

Atlantic croaker entering PNAs from mid-March through late April in both systems appeared to bypass lower and middle area nursery creeks (unlike spot) to a greater extent than fish recruiting after April (Fig. 9). Late recruitment of small Atlantic croaker was especially apparent in the mid-lower Pamlico (Fig. 11).

Size distribution Atlantic croaker initially collected in the Cape Fear creeks through the first week of April spanned a size range of 11–23 mm (Fig. 10, 15.4 mm SL mean), and mean sizes were not significantly different (paired t-test, $P>0.05$) between areas in the first or second sampling week. After this time, Atlantic croaker from the middle

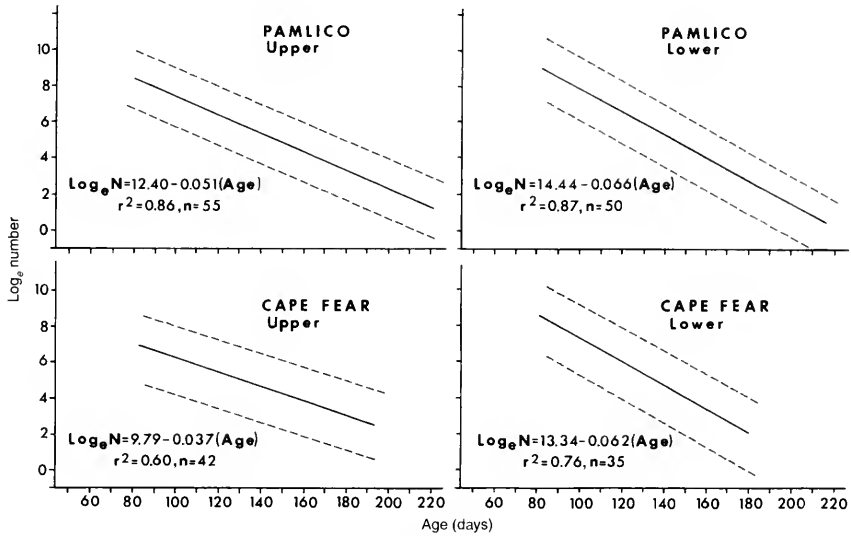

Figure 8

Spot mortality rate curves (solid lines) based on otolith daily ages for upper and lower areas of the Pamlico and Cape Fear, NC, estuaries. Dotted lines represent 95 percent confidence intervals.

Cape Fear area were usually significantly shorter ($P<0.05$) than those from other areas, and Atlantic croaker from the lower Cape Fear were significantly longer ($P<0.05$) than those of other areas.

Atlantic croaker collected from the upper Pamlico creeks were significantly larger ($P<0.05$) on all sample dates than those occupying any area of the Cape Fear during the same weeks. Within the Pamlico, upper and mid-lower mean SLs were the same ($P>0.05$) except in the last week when mid-lower mean SL was significantly larger ($P<0.05$).

Growth Atlantic croaker (12–35 mm SL, $n=383$) ages estimated from otoliths ranged from 62 to 234 days, and all age-SL relationships (Fig. 12) were significant ($P<0.0001$). Residuals of these regressions exhibited no pattern; therefore, the growth models appeared to be appropriate. The instantaneous daily growth rates within each system were not significantly different (analysis of covariance, $P<0.05$) between upper and lower areas (Fig. 12). Between systems, upper Pamlico Atlantic croaker grew more slowly than those from the upper Cape Fear ($P<0.05$). Overall age-length relationships for upper and lower Cape Fear combined and for the upper and lower Pamlico Atlantic croaker combined were the following: for Cape Fear—$\log_{10}SL = 0.915 + 0.0027(age)$, $r^2=0.87$, $n=229$; for Pamlico—$\log_{10}SL = 0.970 + 0.0024(age)$, $r^2=0.87$, $n=158$.

The above combined equations for each system were used to calculate age-specific absolute and relative Atlantic croaker growth rates (Table 4). Early absolute Atlantic croaker growth rates in the Cape Fear system increased most rapidly in ages <105 days, averaging 0.085 mm/d (Table 4). After this age, Cape Fear growth rates increased at a steady, slow rate, reaching 0.19 mm/d by age 215 days. Relative Atlantic croaker growth rates in the Cape Fear were constant over the whole age range at about 0.63 %/d SL. The larger Pamlico system Atlantic croaker exhibited similar absolute growth rates to Cape Fear fish and these increased rapidly from 0.077 mm/d between ages 60 and 65 d to 0.106 mm/d between ages 120 and 125 d to 0.175 mm/d between ages 210 and 215 d (Table 4). Relative growth rates were less than those from the Cape Fear and were constant around 0.56 %/d SL.

Weight-length relationships for Atlantic croaker were highly significant in all areas ($P<0.0001$) (Table 3). In both systems fish from upper area creeks exhibited significantly larger ($P<0.05$) weights per length than those from other areas, particularly at the larger sizes (Fig. 13). Slopes of middle and lower Cape Fear weight-length relationships were not significantly different from each other ($P>0.05$).

Mortality Catch curves used to estimate Atlantic croaker mortality rates were calculated by using ages ≥125 days. All regression slopes were significantly different from zero ($P<0.0001$), although the relationship was more variable for the mid-lower Pamlico area because of the small sample size. Instantaneous mortality rates for Atlantic croaker in the nursery creeks ranged from 0.008 to 0.038 (Fig. 14). Atlantic croaker in the upper and mid-lower Pamlico

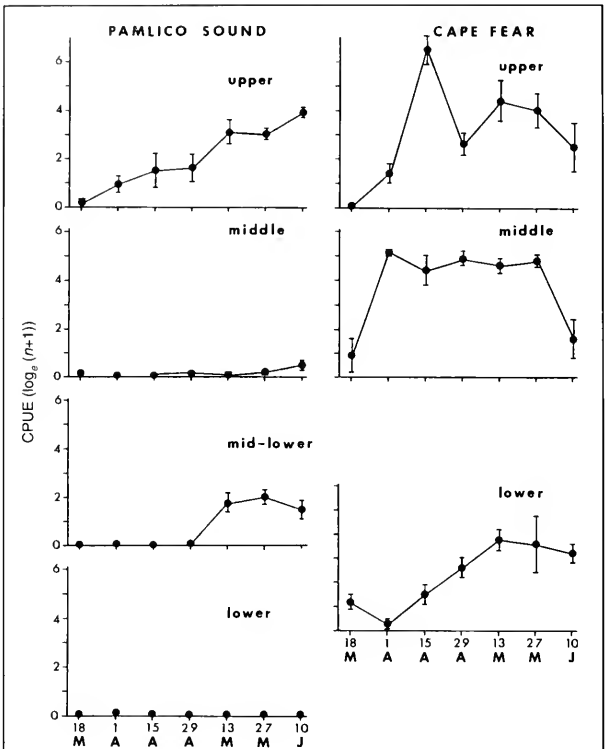

Figure 9

Mean catch per unit of effort for Atlantic croaker in general areas of the Cape Fear and Pamlico Sound, NC, estuaries by sampling week, March–June 1987. Vertical bars represent plus and minus one standard error of the mean. The *x*-axis labels (from left to right) stand for March, April, April, April, May, May, June.

areas had similar instantaneous mortality rates (analysis of covariance, $P>0.05$). Upper Cape Fear Atlantic croaker exhibited significantly lower mortality rates than those in the lower Cape Fear ($P<0.05$). All Atlantic croaker mortality rates in the Cape Fear were significantly higher than those in the Pamlico. Daily mortality rates for Atlantic croaker in the upper and lower Cape Fear were 2.96 %/d and 3.73 %/d, respectively and in the upper and mid-lower Pamlico were 0.90 and 0.80 %/d, respectively.

Discussion

Primary nursery area habitats in two different estuaries were not equally valuable for spot and Atlantic croaker. Considered together, growth, mortality, and distribution data indicated that upstream oligohaline creeks provided the best environment, followed closely by downstream polyhaline areas. In all regards, the middle reaches of the estuary appeared to be less valuable (or at least less used). These consistent results for both species in the two separate estuarine systems lend support to their general applicability. Other studies were marginally useful in evaluating these results because of their lack of synoptic comparisons across a wide variety of habitats and because of limitations in or lack of growth and mortality data for estuarine juveniles of these species.

The main evidence that oligohaline habitats provided better environments than polyhaline areas was that spot (both systems) and Atlantic croaker (in Cape Fear) exhibited significantly lower mortality in the freshwater PNAs. Miller et al. (1985) reported lower mortality for these species in mesohaline areas compared to high salinity areas of Pamlico Sound. In the Cape Fear River, Weinstein and

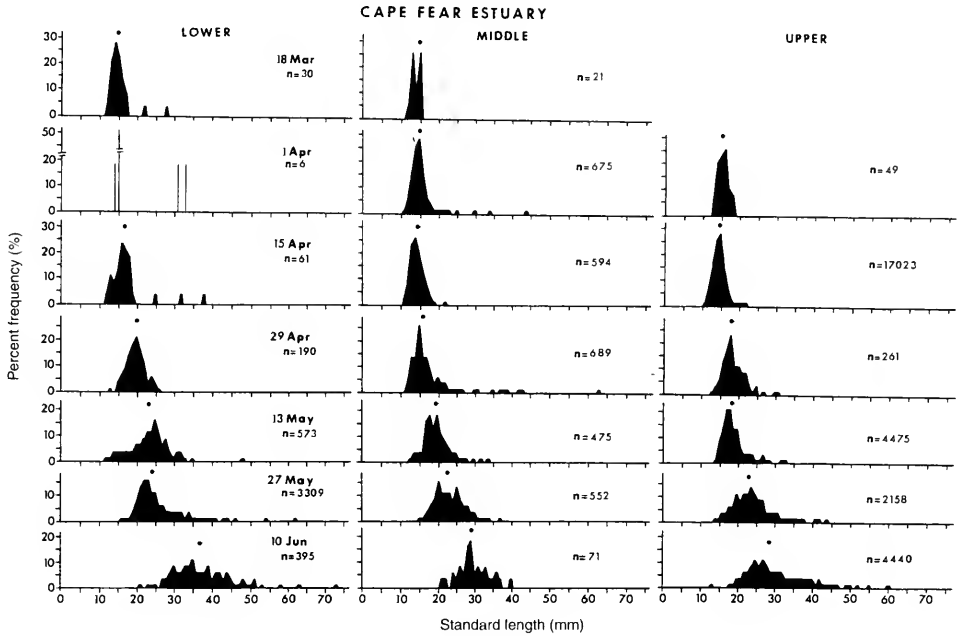

Figure 10

Atlantic croaker length frequencies in general areas of the Cape Fear, NC, estuary by sampling week, March–June 1987. Solid dots represent mean SL.

Walters (1981) found consistently high mortality for spot in polyhaline creeks during two years, but variable mortality between years (one year higher, one year lower) in low salinity regions. Mortality rates reported in the present study may not be affected by fish density (Ross, 1992), and it is unlikely that starvation (Currin et al., 1984) played a major mortality role. Predation may cause most of the PNA natural mortality; it was previously proposed that predation rates were lowest in oligohaline habitats because these areas contained relatively fewer predators (Weinstein and Walters, 1981; Currin et al., 1984; Miller et al., 1985). This hypothesis continues to lack direct, convincing evidence. Predators in oligohaline habitats (e.g. southern flounder, catfishes, gar, striped bass, etc.) may, in fact, be just as numerous near the upriver nurseries (author's pers. obs.; Patrick and Moser, 2001; Moser[4]) as marine predators are around polyhaline creeks. Also, because water levels in the upriver creeks, especially in the Pamlico, do not vary as much as in polyhaline areas, predators may have more opportunity to use these creeks (Currin et al., 1984).

One alternative explanation for lower mortality estimates in upriver PNAs is that mortality could be related, perhaps indirectly, to ambient salinity. Although freshwater conditions probably do not increase mortalities of these fishes (Moser and Hettler, 1989), there may be negative effects of high salinity on survival that have not been investigated. Moser and Hettler (1989) reported that spot exhibited the highest respiration rates in high salinity conditions, which suggest increased stress.

Another potential explanation is that fishes may leave high salinity areas more rapidly than freshwater areas. Although I attempted to minimize effects of emigration on mortality estimates by limiting the analyses to the period before mid-June, the mortality rates I calculated could have contained an unknown effect of emigration. Other studies (Weinstein, 1983; Weinstein and O'Neil, 1986; Miller and Able, 2002; author's pers. obs.) supported my assumption that emigration of spot and Atlantic croaker from PNAs was negligible at least through June. Such early habitat fidelity seems to be a common trait among juvenile fishes (Rountree and Able, 1992; Ross and Lancaster, 2002). Many individuals of OWS juvenile fishes leave PNAs by July (Ross, 1988; NC Division of Marine Fisheries[1]); therefore,

[4] Moser, M. L. 1998. Personal commun. NW Fisheries Science Center, NMFS, 2725 Montlake Blvd., Seattle, WA 98112.

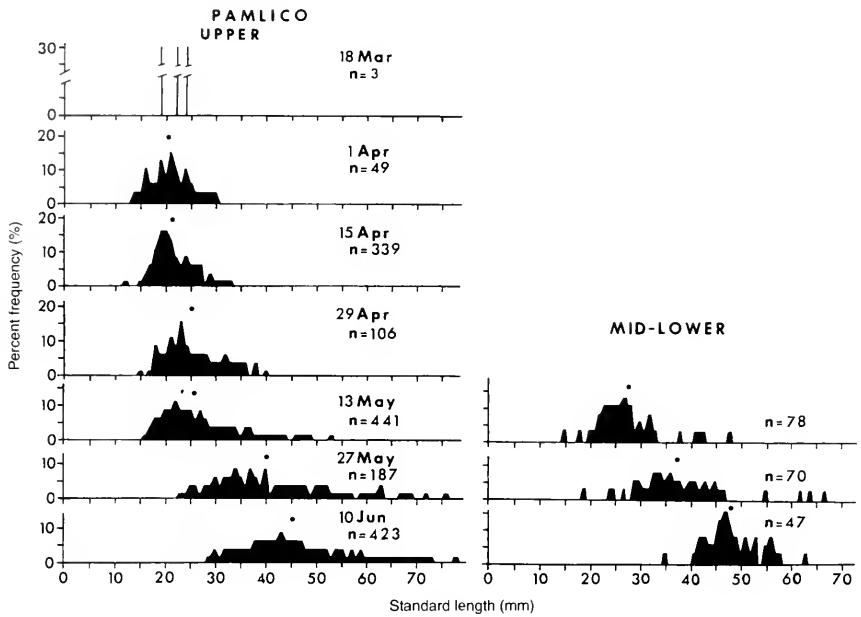

Figure 11

Atlantic croaker length frequencies in general areas of the Pamlico Sound, NC, estuary by sampling week, March–June 1987. Solid dots represent mean SL.

previous mortality estimates are likely confounded by emigration because measures of declining fish numbers were extended longer into the nursery season (through August, Weinstein and Walters, 1981; through October, Currin et al., 1984; through July, Miller et al., 1985).

Growth in weight (weight-length relationships) also indicated advantages of oligohaline habitats for these fishes. Higher weights per length have been equated with greater fitness (Friedland et al., 1988; Bolger and Connolly, 1989). Improved fitness was suggested by a consistent trend for individuals of both spot and Atlantic croaker in both systems to be heavier per length in the oligohaline creeks. Laboratory experiments on spot (Moser, 1987) resulted in heavier fish per length in freshwater, and the weight difference was attributed to a higher feeding rate in freshwater, rather than water absorption because of osmotic imbalance. Spot from oligohaline areas of the James River, VA, were heavier per length compared to those from several other estuaries (McCambridge and Alden, 1984), but the role of salinity in these differences was unclear. Peterson et al. (1999) indicated that reduced salinity itself caused higher growth rates (in weight) for Atlantic croaker in oligohaline conditions.

Growth (in length) rates and size distributions indicated that PNA habitats at extreme ends of estuaries were equally valuable to both species (with one exception). The exception—depressed spot growth rates in the upper Pamlico area—did not appear to be correlated with lower salinities or temperatures because spot from other areas with low salinity and similar or lower temperatures exhibited higher growth rates. The most obvious difference between upper Pamlico creeks and all other areas was the extremely long (often >100 km) estuarine migration required to reach them. Potential costs involved in such migrations should be examined as should the degree to which the lower spot growth rates persisted into later life. General lack of growth rate variation between oligohaline and polyhaline habitats suggested that salinity (and probably tidal influence) did not affect growth to a degree detectable in the present study. This conclusion is supported by previous studies (Moser and Gerry, 1989; Moser and Hettler, 1989; Miller et al., 2000) despite a general prediction that fish growth rates should be higher in brackish waters (Boeuf and Payan, 2001). The lack of evidence for negative effects of fish density on growth (Ross, 1992) indicated that resources in oligohaline or polyhaline PNAs may not limit these fishes. Currin et al. (1984) also suggested that food resources did not limit spot production in middle areas of Pamlico Sound.

Lack of spatial variation in early estuarine growth rates was also found in the few relevant studies available. Wein-

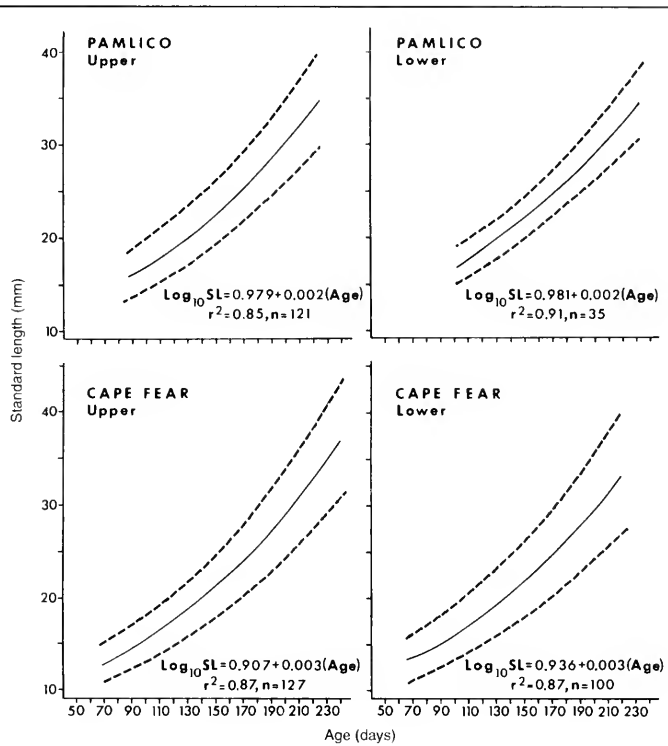

Figure 12

Atlantic croaker growth rate curves (solid lines) based on otolith daily ages for upper and lower areas of the Cape Fear and Pamlico Sound, NC, estuaries. Dotted lines represent 95 percent confidence intervals.

stein and Walters (1981) and O'Neil and Weinstein (1987) reported no consistent differences in spot growth rates between oligohaline and polyhaline creeks in the Cape Fear River and York River, VA, estuaries, respectively. Miller et al. (1985) indicated that spot and Atlantic croaker growth rates were probably not different between Pamlico Sound mesohaline and polyhaline areas. Similarly, Beckman and Dean (1984) found no significant differences in spot growth rates among localities in a small, polyhaline South Carolina estuary. Necaise (2000) failed to find growth differences among juvenile summer flounder caged (and fed *ad libitum*) over a wide range of abiotic habitats in southern North Carolina. Guindon and Miller (1995), however, did find growth rate differences among caged (not fed) southern flounder across abiotically similar oligohaline habitats in the Pamlico River. Differences in fish growth rates among estuarine habitats (e.g. Sogard, 1992) indicate that there are different species-specific responses to habitats, responses related to zoogeography, or responses related to habitat structure or food availability. My data and most of the above studies, covering different years and a variety of estuaries, suggest that variation in growth rates, especially for spot, between PNAs is generally lacking or at least difficult to detect. Such results are consistent with the view that these fishes are hardy, omnivorous, opportunistic colonizers of an undersaturated environment.

Increasing evidence suggests that oligohaline or freshwater habitats in the southeastern United States are important nurseries for the OWS juvenile fishes (Rogers et al., 1984; Rozas and Hackney, 1984; Moser and Gerry, 1989; Moser and Hettler, 1989; Peterson and Ross, 1991). In fact, they may be the most valuable habitats, particularly for maximizing survival of some species. The nursery creeks I sampled supported similar growth rates for two species; however, fitness may be most improved upriver, where both growth (in weight) and survival are optimized. Anderson (1988) predicted that juvenile temperate fishes generally choose to maximize growth over reducing mortality,

Table 4

Predicted age-specific mean standard lengths (SL), absolute (mm/d), and relative (%/d SL) growth rates for Atlantic croaker from the upper and lower Cape Fear combined (CFR) and the upper and mid-lower Pamlico combined (PAM).

	CFR			PAM		
Age (days)	Mean SL	Absolute growth rate	Relative growth rate	Mean SL	Absolute growth rate	Relative growth rate
60	11.94			13.61		
65	12.32	0.08	0.63	14.00	0.08	0.57
70	12.71			14.39		
75	13.11	0.08	0.62	14.79	0.08	0.56
80	13.52			15.21		
85	13.95	0.09	0.63	15.63	0.08	0.55
90	14.39			16.07		
95	14.84	0.09	0.63	16.52	0.09	0.56
100	15.31			16.98		
105	15.79	0.10	0.63	17.45	0.10	0.56
110	16.29			17.95		
115	16.81	0.01	0.64	18.45	0.10	0.56
120	17.34			18.97		
125	17.89	0.11	0.63	19.50	0.11	0.56
130	18.45			20.04		
135	19.03	0.12	0.63	20.61	0.11	0.57
140	19.63			21.18		
145	20.25	0.12	0.64	21.78	0.12	0.56
150	20.89			22.39		
155	21.55	0.13	0.63	23.01	0.13	0.56
160	22.23			23.66		
165	22.94	0.14	0.63	24.32	0.13	0.56
170	23.66			25.00		
175	24.41	0.15	0.63	27.70	0.14	0.56
180	25.18			26.42		
185	25.97	0.16	0.63	27.16	0.15	0.56
190	26.79			27.93		
195	27.64	0.17	0.63	28.71	0.16	0.56
200	28.51			29.51		
205	29.41	0.18	0.63	30.34	0.17	0.56
210	30.34			31.19		
215	31.30	0.19	0.63	32.06	0.18	0.56

although the two are intimately related (Werner and Gilliam, 1984). Selecting for optimized growth, however, appears not to be an issue for these two estuarine generalists. If upstream PNAs are better nurseries (i.e. provide better conditions for survival and perhaps growth), delayed PNA recruitment (longer estuarine migrations), especially for Atlantic croaker, may maximize ultimate fitness (Miller et al., 1985; Shapiro, 1987). Factors affecting transport of young to upstream areas may, therefore, be an important determinant of population fitness.

Unexpected patterns of recruitment into middle region creeks suggested that their function or recruitment potential as fish nursery areas may differ significantly from other regions. Even though these creeks were physically similar to creeks on either end of the estuarine transects, lower abundances of spot and Atlantic croaker in middle areas suggested that they either avoided (bypassed) middle areas or endured higher initial mortalities there. Higher initial mortality in middle regions seems unlikely because catches were generally low throughout the sampling period. Relatively poor habitat quality could explain the low densities of fishes in these creeks. This hypothesis was supported by the fact that most fishes settling in middle regions of both systems exhibited significantly smaller mean lengths and were lighter per length. The same pattern was observed for Atlantic menhaden in these systems (Ross, 1992). Szedlmeyer (1991) also found lower abundances and species richness in middle reaches of a Florida estuary and suggested that either less diverse habitat or greater salinity variation (or both) influenced this result. Ross and Epperly (1985) found stations close to the periphery of Pamlico Sound (including the middle area of this study)

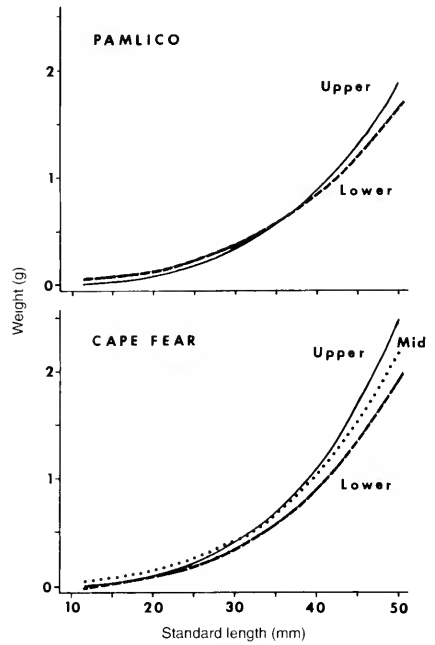

Figure 13

Atlantic croaker weight-length relationships by area in the Pamlico and Cape Fear, NC, estuaries, March–June 1987.

to be the most productive, but their study lacked stations near the inlets and in freshwater areas. Weinstein et al.'s (1980) uppermost Cape Fear stations were the same as my middle area and generally produced lower densities of spot than polyhaline areas, but lacking upriver stations, the meaning of this in the present context is inconclusive. These fishes seem to opt either for rapid settlement in polyhaline environments or delayed settlement in oligohaline areas—mesohaline settlement being less "preferred."

The conclusion that PNAs were not equally valuable and the observation that spot were not most abundant in the best habitats, indicated that variation in estuarine distribution could control or at least regulate (fine tune) year-class strength. If movement to general regions of the estuary is largely passive (Pietrafesa et al., 1986b; Pietrafesa and Janowitz, 1988), then my results predict that year-class strength of these species would be decreased when transport conditions force the majority of the recruits toward middle or lower region PNAs. Alternatively, year class strength would be enhanced by conditions favoring greater upstream transport, assuming carrying capacities of the habitats were not exceeded. Ross (1992) proposed that these systems were recruitment limited, that post-settlement mortality was less important in controlling year-class strength than early life history events prior to settlement. If true, factors affecting variation in estuarine distribution may indirectly adjust year-class strength, not control it. Additional data on mortality rate variation in relation to density during the estuarine and oceanic early life history is required to validate this hypothesis.

Acknowledgments

I thank John M. Miller, G. T. Barthalmus, L. B. Crowder, and L. J. Pietrafesa for their support during this study. I thank K. H. Pollock for statistical advise. Field sampling required the efforts of many people. The NC Division of Marine Fisheries (Washington and Wilmington offices) played a large role in sampling, and I especially thank Fred Rohde, John Schoolfield, Otto Rutten, Morris Allison, Greg Judy, Lele Tison, and Jess Hawkins of that organization. B. M. "Mac" Currin was important throughout the study, and I thank him for his contributions in the field, laboratory, and in reviewing manuscripts. John S. Burke also provided help in the field. I thank the Beaufort Labo-

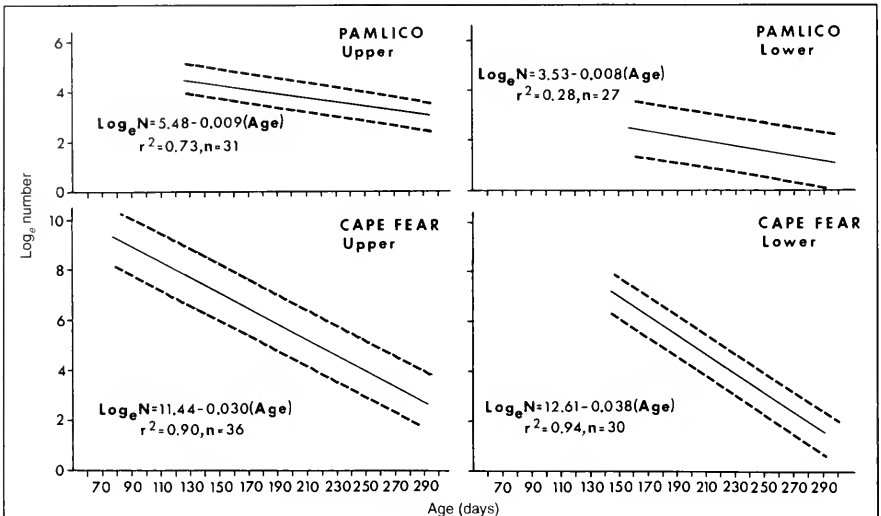

Figure 14

Atlantic croaker mortality rate curves (solid lines) based on otolith daily ages for upper and lower areas of the Pamlico and Cape Fear, NC, estuaries. Dotted lines represent 95 percent confidence intervals.

ratory (National Marine Fisheries Service) and the Biology Laboratory of Carolina Power and Light Company for providing space. David Colby made valuable contributions to this research. I appreciate Jeff Isely's advice and help in analyzing fish otoliths. I thank Ernie Aschenbach for sorting samples and mounting otoliths. And lastly I thank Mary L. Moser for help and support during all stages of this work from field sampling to reading numerous manuscript drafts.

Literature cited

Anderson, J. T.
1988. A review of size dependent survival during pre-recruit stages of fishes in relation to recruitment. J. Northwest Atl. Fish. Sci. 8:55–66.

Baldevarona, R. B.
1987. Effects of feeding and stocking density on growth and survival of spot, *Leiostomus xanthurus*. Ph D. diss., 117 p. Univ. South Carolina, Columbia, SC.

Beck, M. W., K. L. Heck Jr., K. W. Able, D. L. Childers, D. B. Eggleston, B. M. Gillanders, B., Halpern, C. G. Hays, K. Hoshino, T. J. Minello, R. J. Orth, P. F. Sheridan, M. P. Weinstein.
2001 The identification, conservation, and management of estuarine and marine nurseries for fish and invertebrates. Bioscience 51 633–641.

Beckman, D. W., and J. M. Dean.
1984 The age and growth of young-of-the-year spot, *Leiostomus xanthurus* Lacepede, in South Carolina. Estuaries 7:487–496.

Boeuf, G., and P. Payan.
2001. How should salinity influence fish growth? Comp. Biochem. Physiol. (part C) 130:411–423.

Boesch, D. F., and R. E. Turner.
1984. Dependence of fishery species on salt marshes: the role of food and refuge. Estuaries 7:460– 468.

Bolger, T., and P. L. Connolly.
1989. The selection of suitable indices for the measurement and analysis of fish condition. J. Fish. Biol. 34:171– 182.

Campana, S. E., J. A. Gagn, and J. Munro.
1987. Otolith microstructure of larval herring (*Clupea harengus*): image or reality? Can. J. Fish. Aquat. Sci. 44: 1922–1929.

Cowan, J. H., Jr.
1988. Age and growth of Atlantic croaker, *Micropogonias undulatus*, larvae collected in the coastal waters of the northern Gulf of Mexico as determined by increments in saccular otoliths. Bull. Mar. Sci. 42:349–357.

Crecco, V., T. Savoy, and L. Gunn.
1983. Daily mortality rates of larval and juvenile American shad (*Alosa sapidissima*) in the Connecticut River with changes in year-class strength. Can. J. Fish. Aquat. Sci. 40:1719–1728.

Currin, B. M., J. P. Reed, and J. M. Miller.
1984 Growth, production, food consumption and mortality of juvenile spot and croaker: a comparison of tidal and non-tidal nursery areas. Estuaries 7:451–459.

Essig, R. J., and C. F. Cole.
1986. Methods of estimating larval fish mortality from daily increments in otoliths. Trans. Am. Fish. Soc. 115:34–40.

Friedland, K. D., G. C. Garman, A. J. Bejda, A. L. Studholme, and B. Olla.
1988. Interannual variation in diet and condition in juvenile

bluefish during estuarine residency. Trans. Am. Fish. Soc. 117:474–479.

Giese, G. L., H. B. Wilder, and G. G. Parker Jr.
1979. Hydrology of major estuaries and sounds of North Carolina. U.S. Geological Survey Water Resources Invest. 79-46, 175 p.

Guindon, K. Y., and J. M. Miller.
1995. Growth potential of juvenile southern flounder, *Paralichthys lethostigma*, in low salinity nursery areas of Pamlico Sound, North Carolina, USA. Netherlands J. Sea Res. 34: 89–100.

Hobbie, J. E.
1970. Hydrography of the Pamlico River Estuary, N.C. Water Resources Res. Inst. Rep. 39, 69 p. Water Resources Research Institute, Raleigh, NC.

McCambridge, J. T., Jr., and R. W. Alden III.
1984. Growth of juvenile spot, *Leiostomus xanthurus* Lacepede, in the nursery region of the James River, Virginia. Estuaries 7:478–486.

McIvor, C. C., and W. E. Odum.
1988. Food, predation risk, and microhabitat selection in a marsh fish assemblage. Ecol. 69: 1341–1351.

Mercer, L. P.
1987a. Fishery management plan for Atlantic croaker (*Micropogonias undualtus*). Atlantic States Mar. Fish. Comm. Fish. Management Rep. 10, 90 p. Atlantic States Marine Fisheries Commission, Washington, DC.
1987b. Fishery management plan for spot (*Leiostomus xanthurus*). Atlantic States Mar. Fish. Comm. Fish. Management Rep. 11, 81 p. Atlantic States Marine Fisheries Commission, Washington, DC.

Miller, J. M., L. B. Crowder, and M. L. Moser.
1985. Migration and utilization of estuarine nurseries by juvenile fishes: an evolutionary perspective. *In* Migration: mechanisms and adaptive significance (M. A. Rankin, ed.), p. 338–352. Contrib. Mar. Sci. (suppl. 27.

Miller, J. M., W. H. Neill, K. A. Duchon, and S.W. Ross.
2000. Ecophysiological determinants of secondary production in salt marshes: a simulation study. *In* Concepts and controversies in tidal marsh ecology (M. P. Weinstein and D. A. Kreeger, eds.), p. 315–331. Kluwer Academic Press, Dordrecht, NL.

Miller, M. J. and K. W. Able.
2002. Movements and growth of tagged young-of-the-year Atlantic croaker (*Micropogonias undulatus* L.) in restored and reference marsh creeks in Delaware Bay, USA. J. Exp. Mar. Biol. Ecol. 267:15–33.

Miltner, R. J., S. W. Ross, and M. H. Posey.
1995. Influence of food and predation on the depth distribution of juvenile spot (*Leiostomus xanthurus*) in tidal nurseries. Can. J. Fish. Aquat. Sci. 52:971–982.

Moser, M. L.
1987. Effects of salinity fluctuation on juvenile estuarine fish. Ph.D. diss., 150 p. North Carolina State Univ., Raleigh, NC.

Moser, M. L., and L. R. Gerry.
1989. Differential effects of salinity changes on two estuarine fishes, *Leiostomus xanthurus* and *Micropogonias undulatus*. Estuaries 12:35–41.

Moser, M. L., and W. F. Hettler.
1989. Routine metabolism of juvenile spot, *Leiostomus xanthurus* (Lacepede), as a function of temperature, salinity and weight. J. Fish Biol. 35:703–707.

Necaise, A. M.
2000. Habitat evaluation as measured through the growth of juvenile red drum, *Sciaenops ocellatus*, and summer flounder, *Paralichthys dentatus*. M.S. thesis, 49 p. North Carolina State Univ. Raleigh, NC.

Nelson, D..M., M..E. Monaco, E..A. Irlandi, L..R. Settle, and L. Coston-Clements.
1991. Distribution and abundance of fishes and invertebrates in southeast estuaries. ELMR (Estuarine Living Marine Resources) Rep. 9, 167 p. NOAA/NOS Strategic Environmental Assessment Division, Rockville, MD.

Neter, J., W. Wasserman, and M. H. Kutner.
1985. Applied linear statistical models. Regression, analysis of variance, and experimental design, 1127 p. Irwin. Homewood, IL.

O'Neil, S. P., and M. P. Weinstein.
1987. Feeding habitats of spot, *Leiostomus xanthurus*, in polyhaline versus meso-oligohaline tidal creeks and shoals. Fish. Bull. 85:785–796.

Patrick, W. S., and M. L. Moser.
2001. Potential competition between hybrid striped bass (*Morone saxatilis* x *M. americana*) and striped bass (*M. saxatilis*) in the Cape Fear River estuary, North Carolina. Estuaries 24:425–429.

Peters, D. S., J. C. DeVane Jr., M. T. Boyd, L. C. Clements, and A. B. Powell.
1978. Preliminary observations on feeding, growth, and energy budget of larval spot (*Leiostomus xanthurus*). *In* Ann. Rep. Southeast Fish. Cent., Beaufort Lab. to U.S. Dep. Energy, p. 377–379. Beaufort Laboratory, National Marine Fisheries Service, Beaufort, NC.

Peterson, M. S., and S. T. Ross.
1991. Dynamics of littoral fishes and decapods along a coastal river-estuarine gradient. Est. Coast. Shelf Sci. 33: 467–483.

Peterson, M. S., B. H. Comyns, C. F. Rakocinski, and G. L. Fulling.
1999. Does salinity affect somatic growth in early juvenile Atlantic croaker, *Micropogonias undulatus* (L.)? J. Exp. Mar. Biol. Ecol. 238:199–207.

Pietrafesa, P. J., and G. S. Janowitz.
1988. Physical oceanographic processes affecting larval transport around and through North Carolina inlets. Am. Fish. Soc. Symp. 3:34–50.

Pietrafesa, L. J., G. S. Janowitz, T. Chao, R. H. Wiesberg, F. Askari and E. Noble.
1986a. The physical oceanography of Pamlico Sound. Univ. North Carolina Sea Grant Publ. UNC-WP-86-5, 125 p. Univ. North Carolina Sea Grant Program, Raleigh, NC.

Pietrafesa, L. J., G. S. Janowitz, J. M. Miller, E. B. Noble, S. W. Ross, and S. P. Epperly.
1986b. Abiotic factors influencing the spatial and temporal variability of juvenile fish in Pamlico Sound, North Carolina. *In* Estuarine variability (D. A. Wolfe, ed.), p. 341–353. Academic Press, New York, NY.

Ricker, W. E.
1975. Computation and interpretation of biological statistics of fish populations. Bull. Fish. Res. Board Can. 191, 382 p.

Rogers, S. G., T. E. Targett, and S. B. Van Sant.
1984. Fish-nursery use in Georgia salt-marsh estuaries: the influence of springtime freshwater conditions. Trans. Am. Fish. Soc. 113:595–606.

Ross, S. W.
1988. Age, growth and mortality of Atlantic croaker in North Carolina, with comments on population dynamics. Trans. Am. Fish. Soc. 117:461–473.
1992. Comparisons of population dynamics of juvenile spot (*Leiostomus xanthurus*), Atlantic croaker (*Micropogonias*

undulatus), and Atlantic menhaden (*Brevoortia tyrannus*) among diverse North Carolina estuarine nursery areas. Ph.D. diss., 144 p. North Carolina State Univ., Raleigh, NC.

Ross, S. W., and S. P. Epperly.
1985. Utilization of shallow estuarine nursery areas by fishes in Pamlico Sound and adjacent tributaries, North Carolina. *In* Fish community ecology in estuaries and coastal lagoons (A. Yanez-Arancibia, ed.), Ch. 10, 207–232. UNAM (Universidad National Autonoma de Mexico) Press, Mexico.

Ross, S. W., and J. E . Lancaster.
2002. Movements and site fidelity of two juvenile fish species using surf zone nursery habitats along the southeastern North Carolina coast. Environ. Biol. Fishes 63:161–172.

Rountree, R. A., and K. W. Able.
1992. Foraging habitats, growth, and temporal patterns of salt-marsh creek habitat use by young-of-the-year summer flounder in New Jersey. Trans. Am. Fish. Soc. 121:765–776.

Rozas, L. P. and C. T. Hackney.
1984. Use of oligohaline marshes by fishes and macrofaunal crustaceans in North Carolina. Estuaries 7: 213–224.

SAS Institute, Inc.
1988. SAS/STAT user's guide, release 6.03 edition. SAS Inst., Inc. Cary, NC.

Shapiro, D. Y.
1987. Inferring larval recruitment strategies from the distributional ecology of settled individuals of a coral reef fish. Bull. Mar. Sci. 41:289–295.

Siegfried, R. C., II, and M. P. Weinstein.
1989. Validation of daily increment deposition in the otoliths of spot (*Leiostomus xanthurus*). Estuaries 12:180–185.

Sogard, S. M.
1992. Variability in growth rates of juvenile fishes in different estuarine habitats. Mar. Ecol. Prog. Ser. 85:35–53.

Szedlmayer, S. T.
1991. Distribution and abundance of nearshore fishes in the Anclote River estuary, west-central Florida. Northeast Gulf Sci. 12:75–82.

Thresher, R. E.
1985. Distribution, abundance, and reproductive success in the coral reef fish *Acanthochromis polyacanthus*. Ecol. 66: 1139–1150.

Warlen, S. M.
1980. Age and growth of larvae and spawning time of Atlantic croaker in North Carolina. Proc. Ann. Conf. Southeast Assoc. Fish. Wildl. Agencies 34:204–214.

Warlen, S. M., and A. J. Chester.
1985. Age, growth, and distribution of larval spot, *Leiostomus xanthurus*, off North Carolina. Fish. Bull. 83:587–599.

Weinstein, M. P.
1979. Shallow marsh habitats as primary nurseries for fishes and shellfish, Cape Fear River, North Carolina. Fish. Bull. 77:339–357.
1982. Commentary: a need for more experimental work in estuarine fisheries ecology. Northeast Gulf Sci. 5:59–64.
1983. Population dynamics of an estuarine-dependent fish, the spot (*Leiostomus xanthurus*), along a tidal creek-seagrass meadow coenocline. Can. J. Fish. Aquat. Sci. 40: 1633–1638.

Weinstein, M. P., and S. P. O'Neil.
1986. Exchange of marked juvenile spots between adjacent tidal creeks in the York river estuary, Virginia. Trans. Am. Fish. Soc. 115:93–97.

Weinstein, M. P., and M. P. Walters.
1981. Growth, survival and production in young-of-the-year populations of *Leiostomus xanthurus* Lacepede residing in tidal creeks. Estuaries 4:185–197.

Weinstein, M. P., S. L. Weiss, and M. F. Walters.
1980. Multiple determinants of community structure in shallow marsh habitats, Cape Fear River estuary, North Carolina, USA. Mar. Biol. 58:227–243.

Welch, J. M., and B. B. Parker.
1979. Circulation and hydrodynamics of the lower Cape Fear River, North Carolina. U.S. Dep. Commer., NOAA Tech. Rep. NOS 80, 108 p.

Werner, E. E., and J. F. Gilliam.
1984. The ontogenetic niche and species interactions in size-structured populations. Ann. Rev. Ecol. Syst. 15:393–425.

Zar, J. H.
1984. Biostatistical analysis, 2nd ed., 718 p. Prentice Hall, Inc., Englewood Cliffs, NJ.

Abstract—Age and growth estimates for the winter skate (*Leucoraja ocellata*) were estimated from vertebral band counts on 209 fish ranging in size from 145 to 940 mm total length (TL). An index of average percent error (IAPE) of 5.8% suggests that our aging method represents a precise approach to the age assessment of *L. ocellata*. Marginal increments were significantly different between months (Kruskal-Wallis $P<0.001$) and a distinct trend of increasing monthly increment growth began in July. Estimates of von Bertalanffy growth parameters suggest that females attain a slightly larger asymptotic TL (L_∞=1374 mm) than males (L_∞=1218 mm) and grow more slowly (k=0.059 and 0.074, respectively). The oldest ages obtained for the winter skate were 19 years for males and 18 years for females, which corresponded to total lengths of 932 mm and 940 mm, respectively. The results indicate that the winter skate exhibits the characteristics that have made other elasmobranch populations highly susceptible to exploitation by commercial fisheries.

Age and growth estimates of the winter skate (*Leucoraja ocellata*) in the western Gulf of Maine

James A. Sulikowski
Michael D. Morin
Seung H. Suk
W. Huntting Howell

Zoology Department, Spaulding Hall
University of New Hampshire
46 College Road
Durham, New Hampshire 03824
E-mail address (for J. A. Sulikowski): jsulikow@hotmail.com

Little is known about the biology of many elasmobranchs, including important parameters such as validated age, growth, age at maturity, reproductive cycles and annual fecundity (Frisk et al., 2001). Difficulty in obtaining samples, the large size of specimens, their high mobility, and minor commercial value are just a few of the problems that make such studies complicated and in some respects impractical (Cailliet et al., 1983; Cailliet et al., 1986). The recent intensification in commercial fishing of elasmobranchs (Cailliet et al., 1983; Brown and Gruber, 1988; Kusher et al., 1992; Dulvey et al., 2000) has made the collection of their life history information essential to the realistic management of their populations (Cailliet et al., 1983; Ryland and Ajayi, 1984; Dulvey et al., 2000). Historically, batoids have been of minimal commercial value (Otwell and Lanier, 1979; Sosebee, 1998); hence the majority of research on elasmobranchs has focused on commercially valuable sharks (e.g. Holden, 1977; Natanson et al., 1995; Walmsley-Hart et al., 1999). According to the characteristics outlined by Winemiller and Rose (1992) and the comparative analyses of Frisk et al. (2001), skates, like other elasmobranchs, fall into the category of equilibrium strategists and as such reach sexual maturity at a late age, have a low fecundity, and are relatively long-lived. These characteristics, coupled with fisheries that select for the removal of large individuals (especially those over 100 cm total length), make these particular fish highly susceptible to overfishing (Hoenig and Gruber, 1990; Dulvey et al., 2000; Frisk et al., 2001).

Traditionally, skates caught by ground fishing operations were discarded (Martin and Zorzi, 1993; Junquera and Paz, 1998; Sosebee, 1998). New and expanding markets for skate wings have made retention of these fish commercially more lucrative in recent years (Sosebee, 1998; New England Fishery Management Council[1]). Skate harvests in the U.S. portion of the western North Atlantic are currently unregulated. Moreover, biological information on skate life histories is almost nonexistent (Frisk, 2000). This combination of factors is believed to have led to a depletion of common skates (*Raja batis*) in the Irish sea (Brander, 1981).

The winter skate (*Leucoraja ocellata*) is a large species (total length over 100 cm) of skate of the family Rajidae (Bigelow and Schroeder, 1953; Robins and Ray, 1986; New England Fishery Management Council[1]). It is endemic to the inshore waters of the western Atlantic, from the Newfoundland Banks and the southern Gulf of St. Lawrence in Canada to North Carolina in the United States (Bigelow and Schroeder, 1953). Despite this wide range, little direct biological data is available for this species (Simon and Frank, 1996; Casey and

[1] New England Fishery Management Council. 2001. 2000 Stock assessment and fishery evaluation (SAFE) report for the northeast skate complex, 179 p. New England Fishery Management Council, 50 Water Street, Mill 2 Newburyport, MA 01950.

Manuscript accepted 17 December 2002.
Manuscript received 31 December 2002 at NMFS Scientific Publications Office.
Fish. Bull. 101:405–413 (2003).

Myers, 1998, Frisk, 2000). Recent assessment studies in the northeast U.S. (Northeast Fisheries Science Center[2]), suggest that the biomass of the winter skate may be below threshold levels mandated by the Sustainable Fisheries Act (SFA). To add insight into the life history of this species and the status of the stock (Simpfendorfer, 1993; Frisk et al., 2001), we estimated age and growth rates of *L. ocellata* by interpreting annular counts and marginal increments on vertebral centra from specimens collected in the western Gulf of Maine.

Materials and methods

Sampling

A total of 304 winter skates were captured by otter trawl between November 1999 and May 2001 at locations that ranged from 1.6 to 32 km off the coast of New Hampshire. Approximate depths at these locations ranged between 9 and 107 m. Skates were maintained alive on board the vessel until transport to the University of New Hampshire's Coastal Marine Laboratory (CML). There, individual fish were euthanized (0.05g/L bath of MS222). We measured total length (TL in mm) as a straight line distance from the tip of the rostrum to the end of the tail, and disc width (DW in mm) as a straight line distance between the tips of the widest portion of pectoral fins. Total wet weight (kg) was also recorded. In order to differentiate between the small, immature specimens of little skates (*Leucoraja erinacea*, a congener species also found in the Gulf of Maine) and winter skates, rows of teeth in the upper jaw were counted. Skates whose number of teeth ranged between 72 and 110 per row were identified as *L. ocellata* and skates whose number of teeth ranged between 38 and 64 per row were identified as *L. erinacea* (Bigelow and Schroeder, 1953). To reduce any uncertainty in species identification, skates having between 38 and 71 teeth per row were not used in this study.

Preparation of vertebral samples

Vertebral samples, taken from above the abdominal cavity, were removed from 132 females and 98 males, labeled, and stored frozen. After defrosting, three centra from each specimen were freed from the vertebral column, stripped of excess tissue and air dried. Large centra were cut sagittally, while held within a vise, with a Dremel™ tool fitted with a mini-saw attachment. Smaller centra were sanded with a Dremel™ tool to replicate a sagittal cut. Processed vertebrae were mounted horizontally on glass microscope slides and ground with successively finer grits (#180, #400, #600), of wet-dry sandpaper. Each vertebra was then remounted and the other side ground to produce a thin (300 micrometer) "hourglass" section.

[2] Northeast Fisheries Science Center. 1999. 30th northeast regional stock assessment workshop, 477 p. Northeast Fisheries Science Center, 166 Water Street Woods Hole, MA 02543-1026.

Counts of annuli

Vertebral sections were viewed through a compound microscope (25–40×) with reflected light (Fig. 1). A growth ring (annulus) was defined as an opaque and translucent band pair that traversed the intermedialia and that clearly extended into the corpus calcareum (Casey et al., 1985; Brown and Gruber, 1988). The birth mark (age zero) was defined as the first distinct mark distal to the focus that coincided with a change in the angle of the corpus calcareum (Casey et al., 1985; Wintner and Cliff, 1996).

Three nonconsecutive counts of annuli were made for the three vertebral sections from each specimen without prior knowledge of the length of the skate or previous counts. If the variability between readings was more than two years, that particular specimen was eliminated from further analyses. Count reproducibility was estimated by using the index of average percent error (IAPE) described by Beamish and Fournier (1981):

$$IAPE = 1/N \sum \left(1/R \sum \left(\left| X_{ij} - X_j \right| / X_j \right) \right) \times 100,$$

where N = the number of skates aged;
R = the number of readings;
X_{ij} = the ith age determination of the jth fish; and
X_j = the average calculated for the jth fish.

An upper limit for the IAPE was arbitrarily set at 15% for each vertebra. Vertebrae with statistically acceptable IAPE indexes were used for estimation of asymptotic growth rates (Brown and Gruber, 1988; Cailliet and Tanaka, 1990). The average of the mean counts for all three centra defined the age estimate for each specimen (Casey et al., 1985; Wintner and Cliff, 1996).

A von Bertalanffy growth function (VBGF) was fitted to the data with the following equation (von Bertalanffy, 1938):

$$L_t = L_\infty \left(1 - e^{-K(t - t_0)} \right),$$

where L_t = total length at time t (age in years);
L_∞ = theoretical asymptotic length;
K = Brody growth constant; and
t_0 = theoretical age at zero length.

Growth in length data were analyzed by using FISHPARM, a computer program for parameter estimation of nonlinear models with Marquardt's (1963) algorithm for least-square estimation of nonlinear parameters (Prager et al., 1987).

Marginal increment analyses

The annual periodicity of band pair formation was investigated by using marginal increment analyses (MIA). Because the annuli in older specimens were closer together, marginal increments were calculated from five specimens per month whose centra contained either four or five annuli. For MIA determination, the distance of the final opaque band and the penultimate opaque band from the centrum edge were measured with an ocular micrometer.

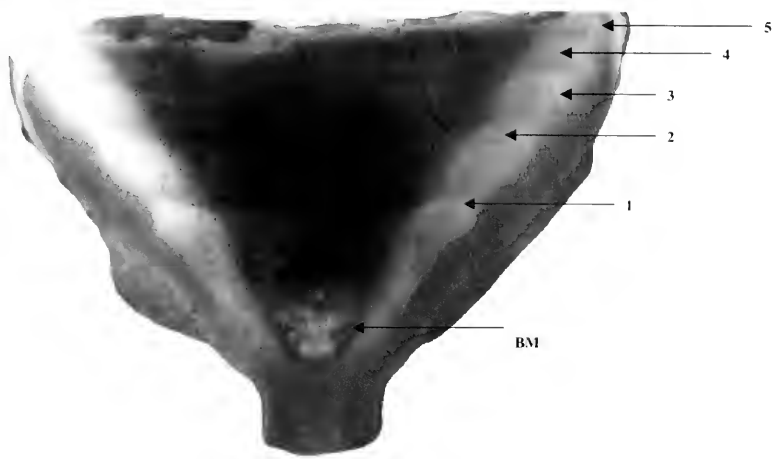

Figure 1

Longitudinal cross-section of a vertebral centrum from a 422-mm-TL male caught in July and estimated to be 5 years. BM= birth mark; Arrows represent age in years.

The marginal increment was calculated as the ratio of the distance between the last and penultimate bands (Branstetter and Musick, 1994; Cailliet, 1990; Simpfendorfer, 1993; Simpfendorfer, 2000). Mean average increments by month of capture were plotted to identify trends in band formation by using a Kruskal-Wallis one-way analysis of variance on ranks. (Simpfendorfer, 1993; 2000).

Results

Morphological measurements

A total of 230 specimens were used for this study. Males (n=98) ranged between 147–932 mm TL, 82–601 mm DW, and 0.015–6.2 kg. Females (n=132) ranged between 145–940 mm TL, 82–635 mm DW, and 0.015–7.5 kg. A linear relationship existed between the total length, disk width, and mass relationships for male, female, and the sexes combined (all r^2 values were greater than 0.85). Two skates (one male: TL=147 mm, DW=82 mm, weight=0.015 kg; and one female TL=145 mm, DW=82 mm, weight=0.015 kg) hatched from egg cases during May 2001 in the CML after gestating 18 months. One wild male specimen (age-0, TL=175 mm, DW=100 mm, weight=0.027 kg) was also captured and incorporated into the results of this study.

Vertebral analyses

No difficulty was encountered in estimating the age of *L. ocellata*. False bands (bands that do not completely encircle the centra) were easily distinguished from complete bands. Of the 230 processed vertebrae, 209 (91%) were readable. These 209 vertebrae (males=88; females=121) had annular count estimates that agreed within two years, resulting in an IAPE of 5.8%. Mean total length and disk width at age for male, female, and sexes combined are given in Table 1. The relationship between TL and centrum diameter was linear (r^2=0.92; P<0.05; Fig. 2) and there were no significant differences (ANCOVA, P<0.05) between males and females. Because no significant difference existed for TL and centrum diameter between the sexes, the data were combined (Fig. 2).

Marginal increments were averaged from five specimens for each month, except June when skates belonging to the 4 and 5 year age classes were unavailable. Marginal increments were significantly different between months (Kruskal-Wallis P<0.001) and a distinct trend of increasing monthly increment growth began in July (Fig. 3). Maximum marginal increment measurement occurred in May. Minimum marginal increment measurement occurred in July. Two recently hatched males (one from the laboratory (147 mm TL) and one from field collections (175 mm TL)) had opaque zones on the distal edge of their vertebral centra. Reviewing this information, we suspect that a single opaque band may be formed annually on the vertebral centra during June–July in the winter skate.

Age and growth estimates

We assumed that opaque-translucent band pairs were formed annually, and we fitted von Bertalanffy growth

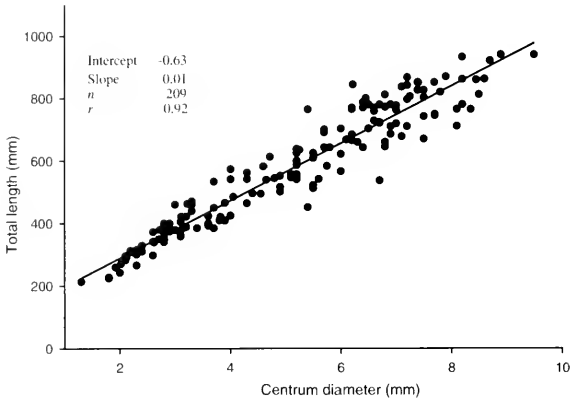

Figure 2

The relationship of total length (mm) to centrum diameter (mm) for combined sexes of winter skate.

Table 1

Average total length, TL, and disc width, DW, at age for winter skates (*L. ocellata*) by sex and combined sexes. Mean ±1 SEM; sample sizes (no. of fish in sample) are given in parentheses.

Age	Male TL	Female TL	Sexes combined	Male DW	Female DW	Sexes combined
0	161 (2) ±14	145 (1)	156 (3) ±10	93 ±7	81	89 ±7
1	228 (1)	—	228 (1)	139	—	139
2	264 (5) ±14	268 (4) ±21	266 (9) ±11	153 ±5	158 ±8	155 ±5
3	340 (4) ±20	317 (9) ±9	324 (13) ±9	198 ±6	188 ±6	191 ±6
4	379 (12) ±8	392 (25) ±8	388 (37) ±6	223 ±8	233 ±5	230 ±4
5	435 (4) ±19	429 (16) ±13	430 (20) ±6	264 ±11	259 ±13	260 ±6
6	536 (5) ±13	501 (7) ±16	516 (12) ±12	338 ±8	310 ±15	322 ±11
7	609 (1)	551 (12) ±6	556 (13) ±7	392	342 ±6	346 ±6
8	651 (1)	565 (11) ±13	570 (12) ±13	401	352 ±10	356 ±10
9	658 (9) ±24	632 (9) ±20	645 (18) ±15	420 ±18	403 ±16	411 ±11
10	690 (12) ±20	704 (8) ±18	696 (20) ±14	441 ±22	447 ±17	444 ±11
11	735 (10) ±17	761 (5) ±22	744 (15) ±14	479 ±24	498 ±20	485 ±14
12	743 (5) ±24	763 (5) ±19	753 (10) ±15	488 ±12	501 ±15	494 ±8
13	830 (3) ±7	772 (3) ±16	801 (6) ±15	495 ±6	506 ±8	500 ±5
14	838 (4) ±10	803 (3) ±23	821 (7) ±13	530 ±9	527 ±24	529 ±10
15	841 (4) ±12	—	841 (4) ±12	541 ±19	—	541 ±13
16	860 (4) ±4	842 (1) ±0	857 (5) ±5	565 ±16	542	560 ±10
17	921 (1)	—	921 (1)	579	—	579
18	—	940 (2) ±0	940 (2) ±0	—	623 ±13	623 ±13
19	932 (1)	—	932 (1)	601	—	601

curves (VBGC) to total length-at-age data (Fig. 4). The VBGC provided a good fit with a low standard error for males, females, and both sexes combined (Table 2). The t_0 values (−1.4 to −1.6) compared favorably with gestation rates for the two skates hatched in captivity (1.5 years) (Table 2). The von Bertalanffy growth parameters for males, females, and the sexes combined were similar but k values were higher for males and sexes combined, than for females.

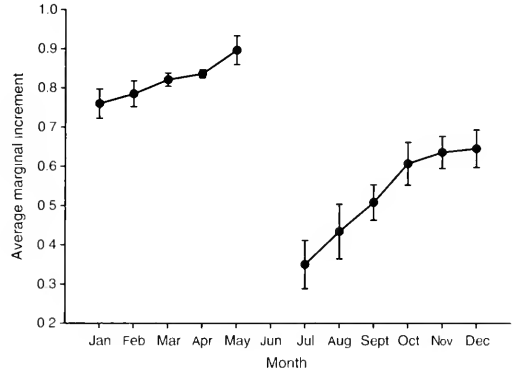

Figure 3

Mean monthly marginal increments of opaque bands for *L. ocellata* from the Gulf of Maine. Marginal increments were calculated from five specimens per month whose centra contained either 4 or 5 annuli. Error bars represent ±1 SEM.

Discussion

The relationship between TL and centrum diameter was linear and significant, indicating that the centra grew proportionally to skate length for all size classes, and thus this structure was useful for age analyses (Kusher et al., 1992). The 5.8% IAPE index suggests that our aging method represents a precise approach to the age assessment of *L. ocellata*. Minimal width of the marginal increment for winter skates captured in May supports the hypothesis of annual band formation in this species. Moreover, these results compare favorably to growth cycles in marginal increments for other skates found in temperate waters whose vertebral bands are formed annually (Holden and Vince, 1973; Waring, 1984; Natanson, 1993).

Von Bertalanffy parameters, as determined by our study, suggest that females attain a slightly larger asymptotic TL_∞ (1374 mm) than males (1218 mm) and grow more slowly (k=0.059 and 0.074, respectively). This trend follows a common pattern in batiods. Holden (1977), Waring (1984), Ryland and Ajayi (1984), Brander (1981), and Walmsley-Hart et al. (1999) found similar tendencies in several species of skates, and Martin and Cailliet (1988) found comparable results in the bat ray (*Myliobatis californica*).

Our estimates of L_∞ exceeded those of the largest specimens in our field collections (940 mm for females and 932 mm for males). Nevertheless, data from extensive trawl surveys in the western Gulf of Maine and the Mid-Atlantic offshore region spring and autumn bottom trawl surveys from 1967 to 2000 (Northeast Fisheries Science Center[2]) indicated that mean TL did not exceed 1000 mm. Thus, we suspect that our von Bertalanffy equation produces an accurate estimation of L_∞ for winter skate. Walmsley-Hart et al. (1999) overestimated L_∞ for *R. pullopunctata* and suggested that small sample size and rareness of large individuals were most likely responsible. Because fishing gear was not biased towards a specific marketable skate size and because all size classes of *L. ocellata* were represented, it is quite possible that the rareness of large individuals led to the augmented L_∞ in combined and individual sexes in our study. Possibly, a larger sample size of winter skates would produce significant and divergent results with regard to von Bertalanffy parameters. However, the close fit of the data to the VBGC for *L. ocellata* indicates the VBGC is an appropriate model for this species.

Preliminary estimates of age and growth parameters are available for winter skate in Canadian waters (eastern Scotian Shelf) from Simon and Frank (1996), who reported the results of a study conducted at St. Mary's University by R. Nearing. Combined sexes of winter skates (n=242) with TL

Table 2

Calculated von Bertalanffy parameters for male, female, and combined sexes of *L. ocellata*. r^2 is the coefficient of determination.

Parameter	Male	Female	Combined sexes
L_∞ (mm TL)	1218	1374	1314
k (/year)	0.074	0.059	0.064
t_0 (year)	−1.418	−1.609	−1.531
r^2	0.946	0.939	0.946
SE	0.01	0.01	0.001
n	88	121	209

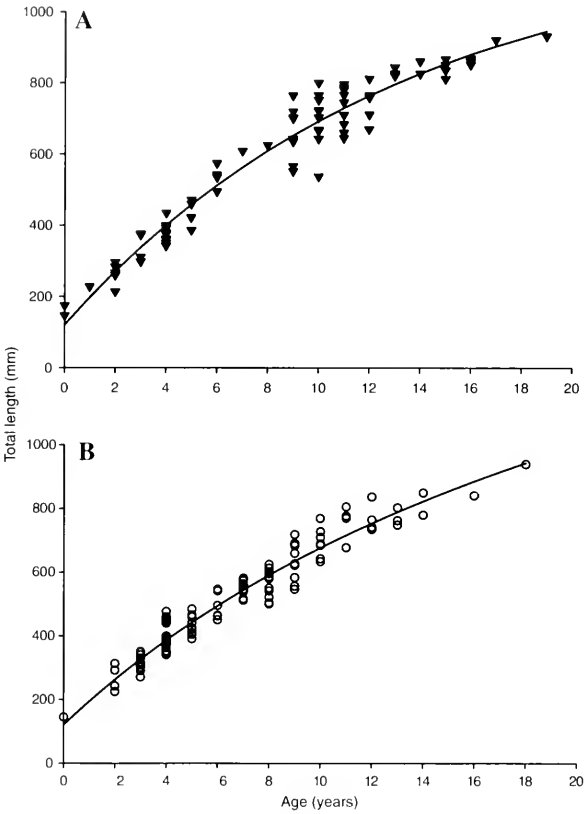

Figures 4

Von Bertalanffy growth curves generated from vertebral data for (**A**) male, (**B**) female, and (**C**) combined sexes of winter skate (*L. ocellata*) from the western Gulf of Maine. Individual VBGC parameters are given in Table 3.

ranging from 120 to 1060 mm and ages from 0 to 16 years provided von Bertalanffy parameters of L_∞ = 114.1 cm, k = 0.14405, and t_0 = 0.00315. However, these data should be viewed with caution because no IAPE values nor validation of the annual nature exist for these estimates, and it is likely that the older specimens had been under-aged by four or more years (Simon[3]).

K values (an estimation of how quickly an animal grows to L_∞) were similar for both sexes of winter skate. These growth rates are commensurate with other skate species of similar size, but slower than skate species of smaller size (Table 3). The oldest ages obtained for the winter skate were 19 and 18 years for males and females, respectively. These data are in agreement with the assumption that larger batoids, such as *L. ocellata* and *R. pullopunctata* (Walmsley-Hart et al., 1999) are longer lived and grow more slowly than smaller species, such as *R. erinacea*, which has been aged to 8 years with a k value of 0.352 (Johnson, 1979; Waring, 1984).

Accurate stock assessment data for skates is difficult to collect in the northeast United States because species are rarely differentiated in landings information (New England Fishery Management Council[1]). Because of this lack of differentiation of species in landings, fluctuations in stock size

[3] Simon, J. 2001. Personal commun. Bedford Institute of Oceanography, P.O. Box 1006, Dartmouth, Nova Scotia, Canada B2Y 4A2.

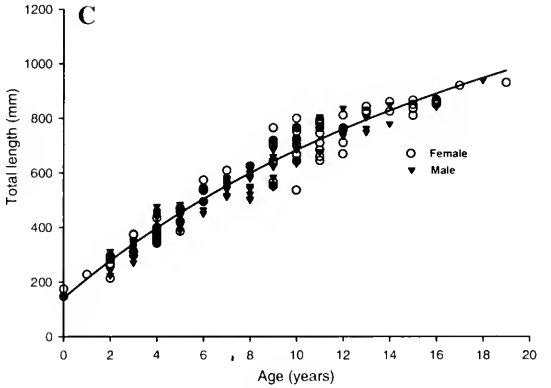

Figures 4 (continued)

Table 3

Comparison of von Bertalanffy growth parameters for several skate species.

Scientific name	Sex	L_∞ (mm)	k	t_0 (years)	Max age (yr)	Source
Raja rhina	♀♂	1047 (TL)	0.17	−0.16	13	Zeiner and Wolf, 1993
Raja microocellata	♀♂	1370 (TL)	0.086	−3.009	9	Ryland and Ajayi, 1984
Raja montagui	♀♂	978 (TL)	0.152	−1.719	7	Ryland and Ajayi, 1984
Raja erinacea	♀♂	527 (TL)	0.352	−0.449	8	Waring, 1984
Raja wallacei	♀♂	422 (DW)	0.26	−0.17	15	Walmsley-Hart et al., 1999
Raja clavata	♀♂	1050 (TL)	0.215	0.045	10	Brander and Palmer 1985
Raja pullopunctata	♂	771 (DW)	0.05	−2.20	18	Walmsley-Hart et al., 1999
Raja pullopunctata	♀	1327 (DW)	0.08	−1.95	14	Walmsley-Hart et al., 1999
Leucoraja ocellata	♀♂	1314 (TL)	0.064	−1.531	19	This study

will be difficult to detect and successful implementation of fisheries management plans will remain problematic. Our study provides some basic age and growth parameters for the winter skate and it supports the hypothesis that *L. ocellata*, like other elasmobranchs, require conservative management because they grow slowly and are susceptible to overexploitation (Brander, 1981; Kusher et al., 1992; Zeiner and Wolf, 1993; Frisk et al., 2001).

Acknowledgments

We thank Captain Joe Jurek of the FV *Mystique Lady* for the collection of skates. We also thank Noel Carlson for maintenance of the fish at the U.N.H. Coastal Marine Laboratory and Charles Walker for use of his equipment. This project was supported by a University of New Hampshire Hubbard Endowment Fund and the U.N.H. Center for Marine Biology.

Literature cited

Beamish, R. J., and D. A. Fournier.
1981. A method for comparing the precision of a set of age determinations. Can. J. Fish. Aquat. Sci. 38:982–983.

Bigelow, H. B., and W. C. Schroeder.
1953. Fishes of the Gulf of Maine. Fish. Bull. 53:63–65.

Brander, K.
1981. Disappearance of common skate *Raia batis* from Irish Sea. Nature 290 (5801):48–49.

Brander, K., and D. Palmer.
1985. Growth rate of *Raja clavata* in the Northeast Irish Sea. J. Cons. Ciem. 42(2):125–128.

Branstetter, S., and J. A. Musick.
1984. Age and growth estimates for the sand tiger in the northwestern Atlantic ocean. Trans. Am. Fish. Soc. 123:242–254.

Brown, C. B., and S. H. Gruber.
1988. Age assessment of the lemon shark, *Negaprion brevirostris*, using tetracycline validated vertebral centra. Copeia 3:747–753.

Cailliet, G. M.
1990. Elasmobranch age determination and verification: an updated review. *In* Elasmobranchs as living resources: advances in the biology, ecology, systematics and the status of the fisheries (H. L. Pratt Jr, S. H. Gruber, and T. Tanuichi eds), p. 157–165. U.S. Dep. Commer., NOAA Technical Report, NMFS 90.

Cailliet, G. M., L. K. Martin, D. Kusher, P. Wolf, and B. A. Weldon.
1983. Techniques for enhancing vertebral bands in age estimation of California elasmobranchs. U.S. Dep. Commer., NOAA Tech. Report NMFS 8:157–165.

Cailliet, G. M., R. L. Radtke and B. A. Weldon.
1986. Elasmobranch age determination and verification. *In* Indo-Pacific fish biology: proceedings of the second international conference on Indo-Pacific fishes (T. Uyeno, R. Arai, T. Taniuchi and K. Matsuura, eds.), p. 345–360. Ichtyol. Soc. Jpn., Tokyo.

Cailliet, G. M., and S. Tanaka.
1990. Recommendations for research needed to better understand the age and growth of elasmobranches. *In* Elasmobranchs as living resources: advances in the biology, ecology, systematics and the status of the fisheries (H. L. Pratt Jr., S. H. Gruber and T. Tanuichi, eds), p. 505–508. U.S. Dep. Commer., NOAA Technical Report NMFS 90.

Casey, J. G., H. L. Pratt, and C. E. Stillwell.
1985. Age and growth of the sandbar shark (*Carcharhinus plumbeus*) from the western North Atlantic. Can. J. Fish. Aquat. Sci. 42(5):963–975.

Casey, J. M., and R. A. Myers.
1998. Near extinction of a large widely distributed fish. Science 28:690–692.

Dulvey, N. K., J. D. MetCalfe, J. Glanville, M. G. Pawson, and J. D. Reynolds.
2000. Fishery stability, local extinctions, and shifts in community structure in skates. Cons. Biol. 14(1):283–293

Frisk, M. G.
2000. Estimation and analysis of biological parameters in elasmobranch fishes and the population dynamics of the little skate *Raja erinacea*, winter skate *R. ocellata* and Barndoor skate *R. laevis*. Masters thesis, 167 p. Center for Environmental Science, Univ. Maryland, College Park, MD.

Frisk, M. G., T. J. Miller, and M. J. Fogarty.
2001. Estimation and analysis of biological parameters in elasmobranch fishes: a comparative life history study. Can. J. Fish. Aquat. Sci. 58(5):969–981.

Hoenig, J. M., and S. H. Gruber.
1990. Life history patterns in the elasmobranchs: implications for fisheries management. *In* Elasmobranchs as living resources: advances in the biology, ecology, systematics and the status of the fisheries (H. L. Pratt Jr, S. H Gruber and T. Tanuichi eds), p. 1–16. U.S. Dep. Commer., NOAA Technical Report, NMFS 90.

Holden, M. J., and M. R. Vince.
1973. Age validation studies on the centra of *Raja clavata* using tetracycline. J. Cons. Int. Explor. Mer 35:13–17.

Holden, M. J.
1977. Elasmobranchs. *In* Fish population dynamics (J. A. Gulland, ed.), p. 187–214 J. Wiley and Sons, London.

Johnson, G. F.
1979 The biology of the little skate, *Raja erinacea*, in Block Island Sound, Rhode Island. Masters thesis, 119 p. Univ. Rhode Island, Kingston, RI.

Junquera, S., and X. Paz.
1998 Non-traditional resources: skate fishery and survey results in Division 3 NO. Sci. Counc. Res. Doc. NAFO, no. 98/26, 6 p. Northwest Atlantic Fisheries Organization, Dartmouth, Nova Scotia [Canada].

Kusher, D. I., S. E. Smith, and G. M. Cailliet.
1992. Validated age and growth of the leopard shark, *Triakis semifasciata*, with comments on reproduction. Environ. Biol. Fish. 35:187–203.

Martin L. K., and G. M. Cailliet.
1988. Age and growth determination of the bat ray, *Myliobatis californico*, in central California. Copeia 3:762–763.

Martin, L., and G. D. Zorzi.
1993. Status and review of the California skate fishery. *In* Conservation biology of elasmobranchs (S. Branstetter, ed.), p. 39–52. U.S. Dep. Commer., NOAA Tech. Report NMFS 115.

Marquardt, D. W.
1963. An algorithm for the least squares estimation of nonlinear parameters. J. Soc. Ind. Appl. Math. 2:431–441.

Natanson, L. J.
1993. Effect of temperature on band deposition in the little skate, *Raja erinacea*. Copeia 1993(1):199–206.

Natanson, L. J., G. C. Casey, and N. E. Kohler.
1995. Age and growth estimates for the dusky shark, *Carcharhinus obscurus*, in the western North Atlantic Ocean. Fish. Bull. 93(1):116–126.

Otwell, W. S., and T. C. Lanier.
1979. Utilization of North Carolina skates and rays. Compl. Rep. N.C. Div. Mar. Fish. February, 49 p. North Carolina Department of Natural Resources and Community Development, Morehead City, NC.

Prager, M. H., S. B. Saila, and C. W. Recksiek.
1987. Fishparm: a microcomputer program for parameter estimation of nonlinear models in fishery science. Tech. Rep. (87-10):1–37. Old Dominion University, Norfolk VA,

Robins, C. R., and G. C. Ray.
1986. A field guide to Atlantic coast fishes of North America, 354 p. Houghton Mifflin Company, Boston, MA.

Ryland, J. S., and T. O Ajayi.
1984. Growth and population dynamics of three *Raja* species (Batoidei) in Carmarthen Bay, British Isles. J. Cons. Int. Explor. Mer 41:111–120.

Simon, J. E., and K. T. Frank.
1996. Assessment of the Division 4VsW Skate Fishery. DFO Atl. Fish. Res. Doc. 96/105, 6 p. Department of Fisheries and Oceans, Dartmouth, Canada.

Simpfendorfer, C. A.
1993. Age and growth of the Australian sharpnose shark, *Rhizoprionodon taylori*, from north Queensland, Australia. Environ. Biol. Fish. 36(3):233–241.
2000. Age and growth of the whiskery shark, *Furgaleus macki*, from southwestern Australia. Environ. Biol. Fish. 58:335–343.

Sosebee, K.
1998. Skates. Status of fishery resources off the northeastern United States. U.S. Dep. Commer., NOAA Tech. Memo. NMFS-NE. 115:114–115.

von Bertalanffy, L.
1938. A quantitative theory of organic growth (inquires of growth laws II). Human Biology 10:181–183.

Walmsley-Hart, S. A., W. H. H. Sauer, and C. D. Buxton.
1999. The biology of the skates *Raja wallacei* and *R. pullopunctata* (Batnidea: Rajidae) on the Agulhas Bank, South Africa. S. Afr. J. Mar. Sci. 21:165–179.

Waring, G. T.
1984. Age, growth and mortality of the little skate off the northeast coast of the United States. Trans. Am. Fish. Soc. 113:314–321.

Winemiller, K. O., and K. A. Rose.
1992. Patterns of life history diversification in North American fishes: implication for population regulation. Can. J. Fish. Aquat. Sci. 49:2196–2218.

Wintner, S. P. and G. Cliff.
1996. Age and growth determination of the blacktip shark, *Carcharhinus limbatus*, from the east coast of South Africa. Fish. Bull. 94:135–144.

Zeiner, S. J., and P. G. Wolf.
1993. Growth characteristics and estimates of age at maturity of two species of skates (*Raja binoculata* and *Raja rhina*) from Monterey Bay, California. *In* Conservation biology of elasmobranches (S. Branstetter, ed.) p. 87–90. U.S. Dep. Commer., NOAA Technical Report NMFS 115.

Abstract—Large (>458 mm) striped bass (*Morone saxatilis*) are dominant predators in Chesapeake Bay. In recent years, the Chesapeake Bay stock of striped bass has increased dramatically, raising concerns about their predatory impact and their forage requirements. In response to these concerns and the need for more recent ecological studies, this investigation was conducted to characterize feeding habits of large striped bass in Chesapeake Bay. Stomach contents from 1225 striped bass from 458 to 1151 mm TL were examined in the spring and fall of 1997 and 1998. Striped bass consumed 52 different species of vertebrates and invertebrates; however, only a few species of clupeoid and sciaenid fishes dominated diets across both the seasons and size ranges of striped bass examined. Of finfish species, menhaden (*Brevoortia tyrannus*) was the dominant prey in most areas and gizzard shad (*Dorosoma cepedianum*) replaced menhaden in importance in lower salinity waters. Spot (*Leiostomus xanthurus*) and other sciaenid fishes and anadromous herrings (*Alosa* spp.) also contibuted large percentages of striped bass diet. Although pelagic schooling fishes formed the majority of the diet, benthic fishes contributed a higher percentage to the diet than in previous studies of striped bass diet composition.

Manuscript accepted 22 October 2002.
Manuscript received 9 January 2003 at NMFS Scientific Publications Office.
Fish. Bull. 101:414–423 (2003).

Diet composition of large striped bass (*Morone saxatilis*) in Chesapeake Bay*

John F. Walter III
Herbert M. Austin
Virginia Institute of Marine Science
School of Marine Science
The College of William and Mary
PO Box 1346, Gloucester Point, Virginia 23062
E-mail address (for J. F. Walter): jfwalter@vims.edu

Along the Atlantic coast of North America, the striped bass is one of the most important commercial and recreational fishes (Richards and Rago, 1999). In the face of intense overfishing, the Atlantic Coast population of striped bass experienced drastic declines in the 1970s (Field, 1997; Richards and Rago, 1999). During these periods of intense harvesting, smaller fish dominated the stock composition and the fishery (Koo, 1970). With the relaxation of fishing pressure and the implementation of regulations designed to protect older age classes, populations rebounded to the point where, currently, large, older fish comprise a high percentage of the population (Richards and Rago, 1999). The increased abundance of large striped bass has raised concerns over both the predatory impact and prey needs of this large population of seasonally abundant species in Chesapeake Bay.

Within Chesapeake Bay, historically a center of striped bass abundance and one of the largest sources of juvenile production for the Atlantic coast (Merriman, 1941; Berggren and Lieberman, 1978; Kohlenstein, 1981), striped bass are seasonally abundant upper trophic level predators. Chesapeake Bay striped bass are partitioned into a resident, primarily male or juvenile, group of fish found year-round and a migratory group consisting of older, larger (>711 mm total length) and often primarily female fish found in the spring and fall (Chapman, 1987). The Atlantic States Marine Fisheries Commission manages fish greater than 711 mm (28 inches) total length as migratory (ASMFC[1]) because the majority of these fish leave Chesapeake Bay and migrate throughout the Atlantic coast. Striped bass within Chesapeake Bay migrate during the spring when mature fish ascend tidal freshwater tributaries to spawn (Chapoton and Sykes, 1961; Dorazio et al., 1994). After spawning, these fish leave Chesapeake Bay and migrate northward along the Atlantic coast, returning to Chesapeake Bay in large numbers during the fall. With a major peak in March–April and a minor peak in October–November, the historical landings data reflect the migratory behavior and seasonal abundance of larger fish (Koo, 1970).

Diet studies represent the first step in determining the magnitude and direction of trophic interactions and are essential data for the management of both predators and prey (Livingston, 1985). For the management of multispecies fisheries, detailed information on fish food habits is required in order to account for the temporal, spatial, and ontogenetical nature of trophic interactions (Walters et al., 1999; Hollowed et al., 2000; Whipple et al, 2000). Although the feeding habits of resident juvenile and early adult striped bass have received considerable study in Chesapeake Bay (Hollis, 1952; Markle

* Contribution 2507 of the Virginia Institute of Marine Science, School of Marine Science, The College of William and Mary, Gloucester Point, VA 23062.

[1] ASMFC (Atlantic States Marine Fisheries Commission). 2000. Public information document for Amendment 6 to the Interstate Fishery Management Plan for striped bass, 17 p. ASMFC, 1444 Eye Street NW, Washington, DC 20005. http://www.jcaa.org/PID.htm (March 2001).

and Grant, 1970; Setzler et al., 1980; Boynton et al., 1981; Limburg et al., 1997; Hartman and Brandt, 1995a) and in other locations (Schaefer, 1970; Manooch, 1973; Rulifson and McKenna, 1987), no studies have included enough specimens larger than 600 mm total length to adequately characterize the diet of migratory fish. The absence of dietary information for these larger striped bass may have been due to the difficulty in sampling larger striped bass and also to the relative scarcity of large striped bass in Chesapeake Bay during times of severe overfishing (Koo, 1970). Nevertheless, the absence of diet data represents a gap in our knowledge of the trophic dynamics of large striped bass that form the major portion of the spawning stock, are prized fisheries targets and, through successful fisheries management, have emerged as a significant seasonal predatory force within Chesapeake Bay. We specifically address the diet composition of large (458–1151 mm) striped bass in Chesapeake Bay to determine the important species in their diet during the spring and fall periods of abundance.

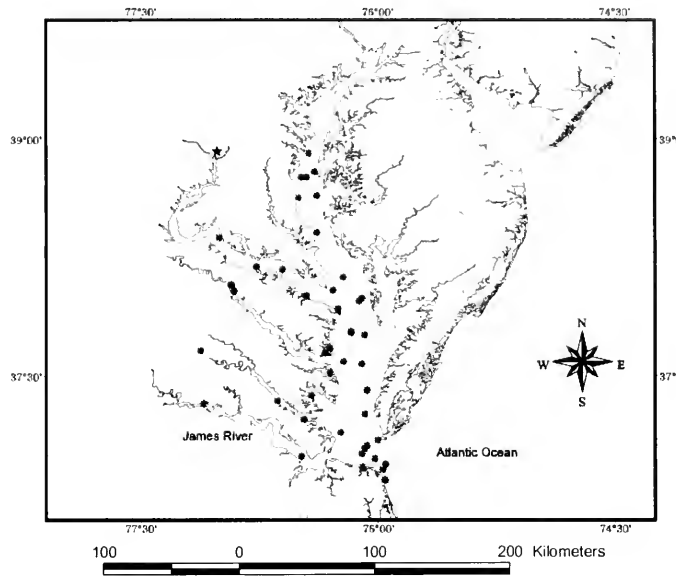

Figure 1

Map of Chesapeake Bay showing spatial distribution of striped bass samples from March 1997 to May 1998.

Methods

From March 1997 to May 1998, 1225 striped bass were collected from various localities in Chesapeake Bay, its Virginia tributaries, and the Chesapeake Bay mouth (Fig. 1). Fish were collected from recreational fishermen, charterboat captains, and seafood dealers, as well as from scientific monitoring programs in the spring (48.5%) and fall (51.5%), corresponding to seasonal migration patterns and fishing seasons. Fish ranged in size from 458 to 1151 mm TL (mean 653.7mm) and were 0.91–17.6 kg in weight (mean 3.69 kg). Hook-and-line gear, gill nets, fyke nets, and otter trawls were used to capture fish. Fish captured in pound nets were excluded from this analysis because of complications introduced by the confinement of the fish in pound nets. Fish captured by hook and line were recorded as such in order that the bait and chum used with this gear could be excluded from the diet analyses. Total length (±1.0 mm), sex, and weight (±0.001 kg wet weight) were recorded for each fish, as well as location, date, and method of capture. Stomachs were removed by cutting the alimentary canal anterior to the stomach and posterior to the pylorus and the contents were frozen until processed. In some cases, stomachs of fish donated by charterboat captains and recreational fishermen were removed by the fisherman.

Fish stomachs were thawed and emptied, and their contents were blotted dry and weighed. Contents were sorted and identified to the lowest possible taxon, weighed, counted, and measured. Diet composition was analyzed by using three measures described in Hyslop (1980): percent frequency of occurrence, percent weight, and percent number. These values were combined to give an index of relative importance (Pinkas et al., 1971). The index of relative importance for a particular prey category i (IRI_i) is expressed as

$$IRI_i = (\%N + \%W) \times \%F,$$

where $\%N$ = the percentage of a prey species by number;
$\%W$ = the percentage of a prey species by weight; and
$\%FO$ = the percent frequency of occurrence of a prey species.

IRI values were calculated as percent IRI values (Cortes, 1997). In calculating IRI values, we excluded several items appearing in the stomachs, such as chum (ground menhaden), bait, trash and plant material because they were deemed to be non-naturally occurring food items. Several prey species were combined either because of difficulties in identification of partially digested prey to species or because of ecological or taxonomic similarity. Both bay anchovy (*Anchoa mitchilli*) and striped anchovy (*Anchoa*

hepsetus) were combined into a single-prey category. In addition, gizzard and threadfin shad (*Dorosoma cepedianum* and *D. petenense*), and blueback and alewife herring (*Alosa aestivalis* and *A. pseudoharengus*) were treated as single-prey categories. Unidentified prey consisted primarily of unidentified fish remains and were recorded as such.

Striped bass were categorized by fish length and month of capture. Fish were partitioned into two size classes corresponding to mixed resident and migratory fish (458–710 mm total length) and coastal migrant fish (711–1255 mm total length) based on the Atlantic States Marine Fisheries Service classification of fish 711 mm and above as fully recruited to the coastal migratory stock. For spatial analysis of feeding habits, each fish was placed into one of two salinity regimes: tidal freshwater (0–5 ppt) or mesohaline waters (6–28 ppt). Tidal freshwater-waters include the upper reaches of the James, York, Rappahannock, and Potomac rivers. Mesohaline waters include the open waters of Chesapeake Bay and the lower reaches of most rivers. No fish were collected in the fall from tidal freshwater. For both monthly and spatial analyses, diet was quantified by weight only.

To measure intensity of feeding, a stomach fullness index (SFI) was calculated according to Hureau (1969):

$$SFI = \frac{Stomach\ content\ weight}{Fish\ weight} \times 10.$$

SFI values were calculated for all fish regardless of the presence or absence of stomach contents.

A regression of striped bass total length versus prey total length was fitted by least-squares linear regression of the untransformed values. Prey lengths were reconstructed from partially digested backbones by using regressions of backbone length on total length obtained from samples collected in 1998 by the authors and those given by Hartman and Brandt (1995a).

Results

Of the 1225 striped bass examined, 688 (56%) contained items in the stomachs (Table 1). Thirty-four different species of fish and 18 species of invertebrates were observed in the diet. Overall, clupeid fishes dominated the diet and menhaden, in particular, accounted for 44% of the weight and occurred in 18% of all stomachs (Table 2). Menhaden ranged in length from 103 to 360 mm total length. A % IRI value of 58.3 for menhaden was higher than that for all other species combined. Anchovies were numerically the most abundant (22%) of all prey items and were equal to spot (*Leiostomus xanthurus*) in % IRI, both sharing a value of 12.3. Other prey in order of decreasing %IRI were gizzard shad (genus *Dorosoma*) with a % IRI of 6.7, and blue crab (*Callinectes sapidus*) with %IRI values of 3.4. Atlantic croaker (*Micropogonius undulatus*) and summer flounder (*Paralichthys dentatus*) had %IRI values of 1.1 and 1.0, respectively.

All other prey categories had %IRI values <1 and appeared relatively unimportant in the overall diet of striped bass, although some increased in relative importance at certain times and locations. Invertebrates were relatively minor constituents of the overall diet of large striped bass, providing only 4.4% of the total IRI. In contrast, clupeid fishes contributed 65% of the IRI and both sciaenid and engraulid fishes combined contributed over 25% of the total IRI.

Clear seasonal and spatial patterns in diet corresponded with the migratory behavior of large striped bass. Striped bass in both sizes classes, 458–710 mm and 711 mm and above, migrated into tidal freshwater to spawn in the months of March, April, and May. Striped bass fed in the tidal freshwater region, although at a reduced intensity as evidenced by the lower stomach fullness values and the lower percentages of nonempty stomachs compared to those at other times and locations (Table 1). Gizzard shad, white perch (*Morone americana*), and anadromous herrings (*Alosa pseudoharengus* and *Alosa aestivalis*) were the main constituents of the diet of both sizes of striped bass in the tidal freshwater region (Table 3, Fig. 2).

During spring, striped bass also pass through the mesohaline waters of Chesapeake Bay prior to and after spawning, during which time they feed fairly heavily as indicated by higher than average stomach fullness values and percentages of nonempty stomachs (Table 1). Approximately 83% of the striped bass sampled from mesohaline waters during this time had food in the stomachs indicating active feeding during the pre- and postspawning migration. Menhaden dominated the diets by weight of both size classes of striped bass from mesohaline waters in the spring. Striped bass of both size classes also consumed croaker, blue crab, and white perch (Table 3, Fig. 2); however, the size classes differed in that smaller fish consumed bay anchovy and juvenile spotted hake (*Urophycis regia*) and larger striped bass consumed anadromous herrings.

Large striped bass are generally absent from Chesapeake Bay in significant numbers in the summer and return in the fall to mesohaline waters of Chesapeake Bay and its lower tributaries. The fall return is essentially a feeding migration and the high stomach fullness values and high percentages of nonempty stomachs (Table 1) indicate active feeding. Striped bass of both size classes fed predominantly upon menhaden, which had percent weight values between 53% and 58 % (Fig. 3). Sciaenid fishes, including spot, Atlantic croaker, and weakfish (*Cynoscion regalis*) combined provided between 23% and 31% of the diet by weight for both size classes of fish. Notable differences occurred in the high percentage of summer flounder (*Paralichthys dentatus*) found in the diets of larger striped bass (15% by weight) and in the high percentage of both butterfish (*Peprilus triacanthus*, 4%) and gizzard shad (11%) found in the diets of smaller fish (Fig. 3). The only invertebrates found in abundance in the diets during this time were blue crabs, which contributed 70% of the diet by weight for the smaller size class of striped bass in September (Table 3). The greatest number of species occurred in the diet in fall with forty-four different species of prey items observed, although many were isolated occurrences of rare prey and only a few species contributed to the overall diet at this time.

Table 1

Distribution of striped bass collections by month with location, capture method, percentage of nonempty (% full) stomachs, and stomach fullness index.

Month	Location	Method	Total	% full	Stomach fullness index	Standard deviation
Striped bass, 458–710 mm total length						
Feb	Potomac River	gill net	14	64.3%	1.13	1.73
Mar	York,Rappahannock, James River	gill net, fyke net	116	47.4%	0.36	0.79
Apr	York, Rappahannock, James River	gill net, fyke net	159	25.2%	0.38	1.52
May	Upper York River	electroshock	28	71.4%	1.15	1.80
Jun	Middle Bay	gill net, hook and line	77	93.5%	4.85	3.87
Sep	Middle Bay	hook and line, gill net	74	27.0%	0.30	0.62
Oct	Lower Bay	hook and line, gill net	245	58.4%	1.06	1.93
Nov	Lower Bay	hook and line, gill net	114	74.6%	2.08	3.08
Dec	Lower Bay	hook and line, gill net, trawl	12	91.7%	1.48	1.24
Striped bass 711–1255 mm total length						
Mar	York, Rappahannock, James River	gill net, fyke net	12	50.0%	0.31	0.69
Apr	York, Rappahannock, James River	gill net, fyke net	85	31.8%	0.60	1.44
May	Upper York River	electroshock	7	85.7%	0.82	1.74
Jun	Middle Bay	hook and line	66	81.8%	2.75	2.14
Sep	Middle Bay	hook and line, gill net	20	25.0%	0.21	0.24
Oct	Lower Bay	hook and line, gill net	45	42.2%	0.71	1.52
Nov	Lower Bay	hook and line, gill net	95	74.7%	1.69	2.80
Dec	Lower Bay	hook and line, gill net	56	80.4%	1.23	1.66
Total	all	all	1225	56.1%	1.00	2.03

Table 2

Stomach contents of striped bass from Chesapeake Bay, 1997–98 (n=688, total number of stomachs with quantified contents).

Prey	Occurrences	% frequency of occurrence	Number	% by number	Weight in grams	% by mass	%IRI
Class Osteichthyes							
Clupeidae							
Brevoortia tyrannus	132	20.63	319	18.11	14757.03	44.40	58.34
Alosa spp.	7	1.09	20	1.14	977.38	2.94	0.20
Dorosoma spp.	43	6.72	142	8.06	4623.73	13.91	6.68
Unknown clupeid	18	2.81	21	1.19	134.56	0.40	0.20
Moronidae							
Morone saxatilis	1	0.16	1	0.06	19.46	0.06	0.00
Morone americana	19	2.97	24	1.36	750.09	2.26	0.49
Sciaenidae							
Leiostomus xanthurus	86	13.44	179	10.16	3315.84	9.98	12.25
Bairdiella chrysoura	13	2.03	17	0.97	244.61	0.74	0 16
Cynoscion regalis	15	2.34	19	1.08	835.62	2.51	0.38
Micropogonias undulotus	20	3.13	21	1.19	2123.82	6.39	1.07
Unknown sciaenid	14	2.19	21	1.19	61.41	0.18	0.14

continued

A significant relationship between striped bass total length and prey total length (P<0.05, r^2=0.26) was observed which indicated that larger and older striped bass ate larger prey (Fig. 4). The fit of the regression was poor, indicating that, although larger striped bass did consume larger prey, they also consumed smaller prey.

Table 2 (continued)

Prey	Occurrences	% frequency of occurrence	Number	% by number	Weight in grams	% by mass	%IRI
Engraulidae							
Anchoa spp.	74	11.56	399	22.66	256.29	0.77	12.26
Other fish							
Paralichthys dentatus	17	2.66	30	1.70	2256.59	6.79	1.02
Membras martinica	1	0.16	15	0.85	26.17	0.08	0.01
Menidia menidia	12	1.88	25	1.42	27.00	0.08	0.13
Anguilla rostrata	10	1.56	21	1.19	544.48	1.64	0.20
Symphurus plagiusa	9	1.41	40	2.27	111.59	0.34	0.17
Peprilus triacanthus	6	0.94	12	0.68	385.88	1.16	0.08
Urophycis regia	3	0.47	26	1.48	400.00	1.20	0.06
Notropis spp.	3	0.47	5	0.28	8.45	0.03	0.01
Trinectes maculatus	5	0.78	5	0.28	23.56	0.07	0.01
Pomatomus saltatrix	3	0.47	3	0.17	184.21	0.55	0.02
Eucinostomus argenteus	3	0.47	3	0.17	39.92	0.12	0.01
Gobiosoma bosc	1	0.16	1	0.06	0.10	0.00	0.00
Synodus foetens	2	0.31	2	0.11	68.54	0.21	0.00
Strongylura marina	1	0.16	3	0.17	67.96	0.20	0.00
Scophthalmus aquosus	1	0.16	1	0.06	14.42	0.04	0.00
Mugil curema	1	0.16	1	0.06	36.08	0.11	0.00
Sphoeroides maculatus	1	0.16	1	0.06	4.80	0.01	0.00
Hypsoblennius hentzi	1	0.16	1	0.06	4.15	0.01	0.00
Fundulus heteroclitus	1	0.16	1	0.06	3.39	0.01	0.00
Unidentified fish remains	56	8.75	71	4.03	128.37	0.39	1.75
Class Crustacea							
Callinectes sapidus	55	8.59	129	7.33	439.81	1.32	3.36
Neomysis americana	13	2.03	90	5.11	11.09	0.03	0.47
Squilla empusa	23	3.59	35	1.99	174.26	0.52	0.41
Ovalipes ocellatus	13	2.03	15	0.85	103.68	0.31	0.11
Lironeca ovalis	6	0.94	6	0.34	0.54	0.00	0.01
Callinectes spp.	4	0.63	7	0.40	28.83	0.09	0.01
Penaeus setiferus	5	0.78	5	0.28	13.00	0.04	0.01
Crangon septemspinosa	3	0.47	5	0.28	1.34	0.00	0.01
Puleamonetes pugio	4	0.63	9	0.51	2.24	0.01	0.01
Cancer irroratus	1	0.16	1	0.06	7.73	0.02	0.00
Upogebia affinis	1	0.16	1	0.06	0.59	0.00	0.00
Class Bivalvia	*	*	*	*	2.00	*	**
Mytilus edulis	*	*	*	*	2.00	*	**
Crossostrea virginica							
Class Gastropoda							
All gastropods	1	0.16	1	0.06	0.39	0.00	0.00
Class Polychaeta							
All polychaetes	4	0.63	4	0.23	7.92	0.02	0.01
Class Hydrozoa							
All hydroids	2	0.31	2	0.11	0.00	0.00	0.00
Phylum Porifera							
All sponges	1	0.16	1	0.06	2.29	0.01	0.00
Miscellaneous items							
Chum (ground menhaden)	159	*	*	*	*	*	**
Bait (menhaden, spot, etc)	28	*	*	*	*	*	**

continued

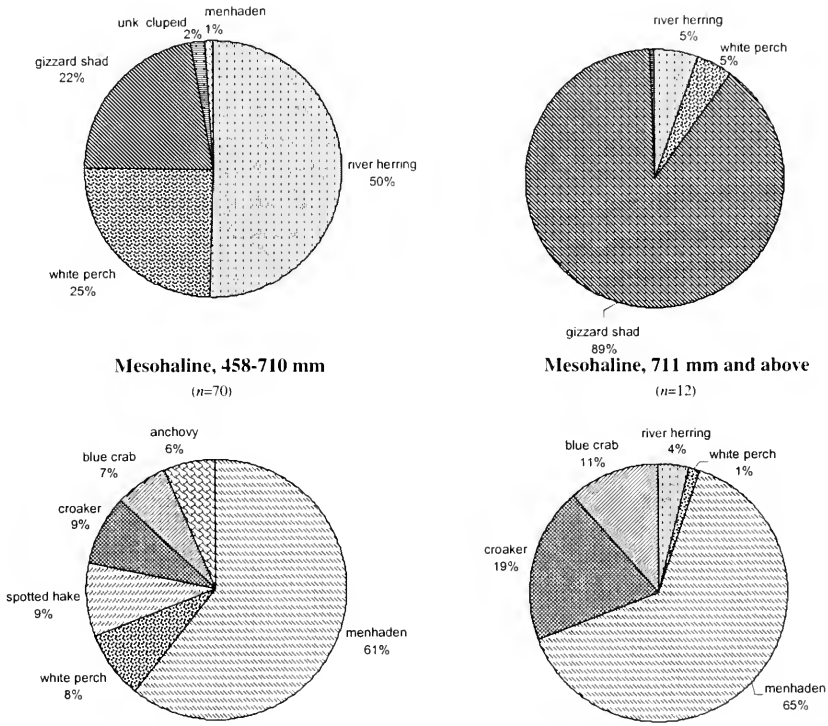

Figure 2

Percentage by weight of prey in the diets of striped bass captured in the spring (February–June). Note that only stomachs with contents other than bait were used in the construction of these figures.

Table 2 (continued)

Prey	Occurrences	% frequency of occurrence	Number	% by number	Weight in grams	% by mass	%IRI
Miscellaneous items (cont.)							
Plant material	11	*	*	*	*	*	**
Woody material	6	*	*	*	*	*	**
Plastic trash	1	*	*	*	*	*	**
Cigarette butts	2	*	*	*	*	*	**
Stones, gravel	2	*	*	*	*	*	**
Feathers	2	*	*	*	*	*	**

* Not quantified.
** Not included in IRI calculations.

Table 3

Seasonal diet composition by percent weight for striped bass from Chesapeake Bay, 1997–98. Sample sizes are listed in parentheses.

Month	Menhaden	*Dorosoma* spp.	White perch	*Alosa* spp.	*Callinectes* spp.	Spot	Other fish	Other invertebrates	Croaker	*Anchoa* spp.	Silversides
Striped bass 458–710 mm total length											
Feb (9)	0.0	43.1	56.9	0.0	0.0	0.0	0.0	0.0	0.0	0.0	0.0
Mar (55)	2.1	37.3	13.9	0.0	1.0	1.6	14.3	2.4	0.0	27.5	0.0
Apr (40)	0.0	23.4	27.4	18.9	1.6	0.0	25.1	2.0	1.0	0.5	0.0
May (20)	0.9	0.0	0.0	73.7	11.4	0.0	2.0	0.0	12.0	0.0	0.0
Jun (72)	78.2	0.0	10.6	0.0	4.4	0.0	0.0	0.0	6.8	0.0	0.0
Sep (20)	16.4	0.0	0.4	0.0	69.5	0.0	0.0	1.9	0.0	6.8	5.0
Oct (143)	38.0	22.0	0.1	0.0	2.7	21.0	14.2	0.6	0.0	0.9	0.5
Nov (85)	55.9	1.6	0.0	0.0	0.0	27.4	8.5	2.0	3.8	0.1	0.7
Dec (11)	44.1	0.0	0.0	0.0	0.0	33.7	1.0	0.0	0.0	20.7	0.4
Striped bass 711–1151 mm total length											
Mar (6)	0.0	96.5	0.1	0.0	0.1	0.0	3.3	0.0	0.0	0.0	0.0
Apr (27)	0.0	90.4	5.1	3.5	0.0	0.0	0.9	0.0	0.0	0.0	0.0
May (6)	0.0	22.2	0.0	77.1	0.0	0.0	0.6	0.0	0.0	0.0	0.0
Jun (54)	61.9	0.0	1.1	3.9	14.3	0.0	0.0	0.0	18.7	0.0	0.0
Sep (5)	76.5	0.0	23.2	0.0	0.3	0.0	0.0	0.0	0.0	0.0	0.0
Oct (19)	24.7	0.0	0.0	0.0	2.9	5.7	10.3	6.3	0.0	35.7	14.3
Nov (71)	43.1	2.2	0.0	0.0	0.2	6.8	5.9	1.2	14.6	3.8	22.1
Dec (45)	73.3	0.0	0.0	0.0	0.0	10.8	12.5	0.1	2.6	0.3	0.4

Discussion

Our study addresses the diet of striped bass above 458 mm total length in Chesapeake Bay. In previous studies of striped bass diet (Hollis, 1952; Hartman and Brandt, 1995a) in Chesapeake Bay and adjacent waters (Manooch, 1973), few fish above 458 mm were sampled. The comprehensive work by Hartman and Brandt (1995a) did not include fish above age 6. The current study focuses specifically on the diet of larger striped bass that previously were undersampled or were rare during periods of severe overfishing (Koo, 1970).

Throughout the two size ranges of striped bass sampled and in both seasons and locations, schooling fishes dominated the diets in Chesapeake Bay. In particular, clupeid fishes (menhaden, gizzard shad) and the closely related anchovies exceeded all other prey species in frequency of occurrence, number, and biomass. Among other fishes, only spot rivaled the clupeids and anchovies in overall importance; however, white perch, croaker, weakfish, and summer flounder contributed important percentages of the diet in certain seasons. Hollis (1952), Manooch (1973) and Hartman and Brandt (1995a) and Overton (2002) also found that schooling clupeoid fishes formed the majority of the diets of striped bass from Chesapeake Bay and nearby Albemarle Sound.

There was a shift in the relative importance of smaller schooling fishes (anchovies) in striped bass 458–710 mm to larger schooling fishes (menhaden, gizzard shad) in striped bass 711–1151 mm. Although there was a tendency for larger striped bass to consume larger prey, this relationship should more accurately be described as one where larger striped bass have a greater size range of prey to consume (Fig. 4). The largest striped bass consumed prey ranging from several millimeters up to 400 mm in total length, corresponding to 40% of their total length and equaling the ratio of mean maximum forage length to striped bass length found by Manooch (1973). Similarly, smaller striped bass consumed prey that approached 40% of their total length; however, most prey consumed by all sizes of striped bass were smaller, young-of-the-year fishes—a finding corroborated by Overton (2002), who predicted an optimal prey size to be 21% of the striped bass length.

The predominance of fish in adult striped bass diets attests to the piscivorous nature of larger striped bass and corroborates the findings of other studies (Hollis, 1952; Manooch, 1973; Overton, 2002). Hartman and Brandt (1995a) and Gardinier and Hoff (1982) observed an ontogenetic shift at 200 mm TL

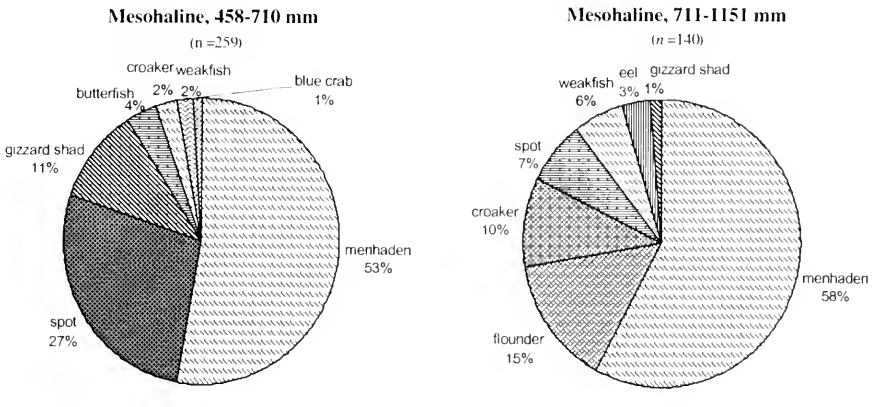

Figure 3

Percent by weight of prey in the diet of striped bass captured in the fall (September–December). Note that only stomachs with contents other than bait were used in the construction of these figures.

from invertebrate to vertebrate prey in the diet of smaller striped bass. In the present study, we sampled size ranges above 458 mm and found no clear ontogenetic dietary shift between vertebrate and invertebrate prey. Invertebrates, primarily blue crab, constituted a minor percentage of the overall diet and were significant in the diet only in May and September in mesohaline waters of Chesapeake Bay. This is in contrast to the high percentages of invertebrates found in the diets of large striped bass in New England waters and likely represents latitudinal differences in the availability of fish prey (Nelson et al.[2]).

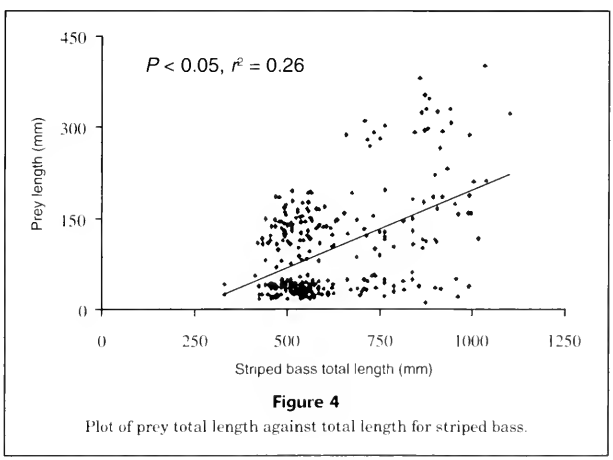

Figure 4

Plot of prey total length against total length for striped bass.

The seasonal and spatial differences in the diet of striped bass correspond to the behavioral and seasonal migration patterns of the fish and reflect changes in the community composition at the location and time of capture. The major seasonal trend is spring feeding on gizzard shad, anadromous herrings, and white perch, corresponding to spawning migrations of both striped bass and their prey into tidal freshwater. Many spring samples came from upper river sites where gizzard shad and white perch are year-round residents and herrings are anadromous migrants (Murdy et al., 1997). This pattern of spring feeding on anadromous herrings and gizzard shads was also found by Trent and Hassler, 1966) in the Roanoke River, NC.

Striped bass captured in spring from the lower, more saline sections of the rivers exhibited high levels of feeding intensity and consumed primarily menhaden, sciaenids, anchovies, and blue (VIMS[3]) crabs. In the spring, Manooch

[2] Nelson, G. A., B. C. Chase and J. Stockwell. 2002. Feeding habits of striped bass (*Morone saxotilis*) from coastal waters of Massachusetts, 29 p. Massachusetts Department of Marine Fisheries Annisquam River Marine Fisheries Field Station 30 Emerson Ave. Gloucester, MA 01930.

[3] VIMS (Virginia Institute of Marine Science). 2002. Juvenile fish and blue crab trawl survey. VIMS, P. O. Box 1346 Gloucester Point, VA 23062. http://www.fisheries.vims.edu/vimstrawl data/. (March 2001)

(1973) found menhaden and anadromous herrings to be predominant (Homer and Boynton[4]) foods in brackish waters of Albemarle Sound and Hollis (1952) found menhaden as well as anchovies and blue crabs to be predominant food of striped bass in brackish waters of Chesapeake Bay. The predatory impact of migratory striped bass depends upon their residence time in these waters, as well as on striped bass population size and feeding rates. Carmichael et al. (1998) estimated that striped bass spend approximately one week in their upstream and one week in their downstream transit of the Roanoke River. There are no estimates of residence time in the open waters of Chesapeake Bay or Albemarle Sound; however, striped bass larger than 711 mm are captured in recreational fisheries in Chesapeake Bay into June, suggesting that they are present in Chesapeake Bay from March through June.

After leaving Chesapeake Bay and summering in New England waters, large striped bass return to the bay in fall (Dorazio et al., 1994) and fed primarily upon menhaden, spot, and anchovies. At this time, most fish were taken from open waters of Chesapeake Bay. In the lower bay during fall, large numbers of transient young-of-the-year (YOY) marine fishes (menhaden, spot, croaker, flounder, and weakfish) congregate in open waters of Chesapeake Bay prior to the fall out-migration, thus making them accessible prey for returning striped bass. Striped bass exhibited higher stomach fullness values and higher percentages of nonempty stomachs in November and December than in all other months, with the exception of June. This finding, in conjunction with observations of striped bass aggressively pursuing baitfishes in surface waters during the fall (Hollis, 1952, this study), indicates high feeding intensity. In bioenergetic simulations, striped bass growth potential and prey density peaked in October (Brandt and Kirsch, 1993). Because much of the annual growth (Hartman and Brandt, 1995a, 1995b) and gonadal development (Berlinsky and Specker, 1991) occur in the fall, this period is of primary importance both for the accumulation of body mass for overwintering and for the initial development of gonadal products.

Although pelagic fishes, notably anchovy and menhaden, provided the bulk of the diet for large striped bass, this study differs from the diet study of Hartman and Brandt (1995a) and the network analysis of Baird and Ulanowicz (1989) in that benthic fishes also contributed significantly to the diets. Baird and Ulanowicz (1989) estimated that striped bass obtained 91–100% of their diet from pelagic trophic pathways and Hartman and Brandt (1995a) estimated that 68–75% of the diet of age-2 to age-6 striped bass came from pelagic sources. These estimates contrast with the high percentages of benthic spot, croaker, summer flounder, and gizzard shad observed in this study and indicate that larger striped bass either prey to a greater extent upon benthic fishes or the overall diet has shifted towards benthic prey. Menhaden and bay anchovy juvenile abundance indices have declined over the past 10 years (VIMS[3]) suggesting that a dietary shift towards benthic prey may have occurred since the collections of Hartman and Brandt (1995a) and the studies cited in the Baird and Ulanowicz (1989) model. Without comprehensive and systematic annual diet sampling, it is difficult to separate dietary shifts from differences in the sizes of fish sampled or the sampling locations. Baird and Ulanowicz (1989) incorporated diet composition data from Hollis (1952), Gardinier and Hoff (1982), Manooch (1973), and Homer and Boynton[4] that included very few striped bass larger than >600 mm and their model included no linkages between striped bass and gizzard shad, spot, croaker, or summer flounder. Furthermore, the absence of gizzard shad in the Baird and Ulanowicz (1989) model represents a missing pathway that might link benthic detritus directly to piscivore production as occurs in freshwater impoundments where gizzard shad are the major prey of striped bass (Mathews et al., 1988) and play a pivotal role in the freshwater ecosystem (Stein et al., 1995).

[4] Homer, M., and W. R. Boynton. 1978. Stomach analysis of fish collected in the Calvert Cliffs region, Chesapeake Bay—1977. Rep. UMCEES 78-154 CBL, 363 p. Chesapeake Biological Laboratory, Univ. Maryland, Solomons, MD.

Acknowledgments

This work represents part of a thesis presented to the College of William and Mary (School of Marine Science) by the first author. We would like to thank the first author's committee members, David Evans, Robert Diaz, John Hoenig, and Thomas Munroe, for reviewing the thesis and this manuscript. We would like to acknowledge the many seafood dealers and recreational and commercial fisherman who provided fish samples. This research was funded by the Virginia Recreational Fishing Advisory Board and the Virginia Commercial Advisory Board (grant numbers RF-97-08 and CF-97-08).

Literature cited

Baird, D., and R. E. Ulanowicz.
1989. The seasonal dynamics of the Chesapeake Bay ecosystem. Ecol. Mono. 59(4):329–364.

Berggren, T. J., and J. T. Lieberman.
1978. Relative contribution of Hudson, Chesapeake and Roanoke striped bass, *Morone saxatilis*, stocks to the Atlantic Coast fishery. Fish. Bull.76:335–342.

Berlinsky, D. L. ,and J. L. Specker.
1991. Changes in gonadal hormones during oocyte development in the striped bass, *Morone saxatilis*. Fish Phys. Biochem. 9:51–62.

Boynton, W. R., T. T. Polgar, and H. H. Zion.
1981. Importance of juvenile striped bass food habits in the Potomac estuary. Trans. Am. Fish. Soc. 110:56–63.

Brandt, S. B., and J. Kirsch.
1993. Spatially explicit models of striped bass growth potential in Chesapeake Bay. Trans. Am. Fish. Soc. 122: 845–869.

Carmichael, J. T., S. L. Haeseker, and J. E. Hightower,
1998. Spawning migration of telemetered striped bass in the Roanoke River, North Carolina. Trans. Am. Fish. Soc. 127:286–297.

Chapman, R. W.
1987. Changes in the population structure of male striped

bass spawning in three areas of the Chesapeake Bay from 1984 to 1986. Fish. Bull. 85:167–170.

Chapoton, R. B., and J. E. Sykes.
1961. Atlantic coast migration of large striped bass as evidenced by fisheries and tagging. Trans. Am. Fish. Soc. 90: 13–20.

Cortes, E.
1997. A critical review of methods of studying fish feeding based on analysis of stomach contents: an application to elasmobranch fishes. Can. J. Fish Aquat. Sci. 54: 726–738.

Dorazio R. M., K. A. Hattala, C. B. McCollough, and J. E. Skjeveland.
1994. Tag recovery estimates of migration of striped bass from spawning areas of the Chesapeake Bay. Trans. Am. Fish. Soc. 123:950–963.

Field, J. D.
1997. Atlantic striped bass management: Where did we go right? Fisheries 22:6–9.

Gardinier, M., and T. Hoff.
1982. Diet of striped bass in the Hudson River Estuary. N.Y. Fish Game J. 29:152–165.

Hartman, K. and S. Brandt.
1995a. Trophic resource partitioning, diets and growth of sympatric estuarine predators. Trans. Am. Fish. Soc. 124: 520–537.
1995b. Predatory demand and impact of striped bass, bluefish and weakfish in the Chesapeake Bay: applications of bioenergetics models. Can. J. Fish. Aquat. Sci. 52: 1667–1687.

Hollis, E. H.
1952. Variations in the feeding habits of the striped bass, *Roccus saxotilis*, in Chesapeake Bay. Bull. Bingh. Ocean. Coll. 14(1):111–131.

Hollowed, A. B., N. Bax, R. Beamish, J. Collie, M. Fogarty, P. Livingston, J. Pope, and J. C. Rice.
2000. Application of multispecies models in assessment of impacts of commercial fishing. Symposium proceedings in the ecosystem effects of fishing. ICES J. Mar. Sci. 57: 707–719.

Hureau, J. C.
1969. Biologie comparée de quelques poissons anarctiques (Nototheniidae). Bull. Inst. Oceangr. Monaco 68:1–44.

Hyslop. E. J.
1980. Stomach content analysis- a review of methods and their application. J. Fish Biol. 17:411–429.

Kohlenstein, L. C.
1981. On the proportion of the Chesapeake Bay stock of striped bass that migrates in the coastal fishery. Trans. Am. Fish. Soc. 110:168–179.

Koo, T. S. Y.
1970. The striped bass fishery in the Atlantic states. Ches. Sci. 11:73–93.

Livingston, P. A.
1985. An ecosystem model evaluation: the importance of fish food habits data. Mar. Fish. Rev. 47:9–12.

Limburg, K. E., M. L Pace, and D. Fischer.
1997. Consumption, selectivity and use of zooplankton by larval striped bass and white perch in a seasonally pulsed estuary. Trans. Am. Fish. Soc. 126:607–621.

Manooch, C. S., III.
1973. Food habits of yearling and adult striped bass, *Morone saxatilis*, from Albemarle Sound, North Carolina. Ches. Sci. 14:73–86.

Markle, D., and G. Grant.
1970. The summer food habits of young-of-the-year striped bass in three Virginia rivers. Ches. Sci. 11:50–54.

Mathews, W. J., L. G. Hill, D. R. Edds, J. J. Hoover, and T. G. Heger.
1988. Trophic ecology of striped bass, *Morone saxatilis*, in a freshwater reservoir (Lake Texoma, USA). J. Fish Biol.: 33:273–288.

Merriman, D.
1941. Studies on the striped bass (*Roccus saxatilis*) of the Atlantic Coast. Fish. Bull. 50:1–77.

Murdy, E. O., R. Birdsong, and J. A. Musick.
1997. Fishes of the Chesapeake Bay, 324 p. Smithsonian Institute Press, Washington, DC.

Overton, A. S.
2002. Striped bass predator-prey interactions in Chesapeake Bay and along the Atlantic Coast. Ph.D. diss., 226 p. Univ. Maryland Eastern Shore, Princess Anne, MD.

Pinkas, L.
1971. Food habits study. *In* Food habits of albacore, bluefin tuna and bonita in California waters (L. Pinkas, M. S. Oliphant, and I. L. K. Iverson, eds.), p. 47–63. Calif. Dep. Fish Game, Fish. Bull. 152.

Richards, R. A., and P. J. Rago.
1999. A case history of effective fishery management: Chesapeake Bay striped bass. N. Am. J. Fish. Manage. 19:356–375.

Rulifson, R. A., and S. A. McKenna.
1987. Food of striped bass in the upper Bay of Fundy, Canada. Trans. Am. Fish. Soc. 116:119–122.

Schaefer. R.
1970. Feeding habits of striped bass from the surf waters of Long Island. N.Y. Fish Game J. 17:1–17.

Setzler, E. M., W. R. Boynton, K. V. Wood, H. H Zion, L Lubbers, N. K. Mountford, P. Frere. L. Tucker, J. A. Mihursky.
1980. Synopsis of biological data on striped bass, *Morone saxatilis* (Walbaum). U.S. Dep. Commer., NOAA Technical Report NMFS Circ. 433, 69 p.

Stein, R. A., D. V. DeVries, and J. M. Dettmers.
1995. Food-web regulation by a planktivore: exploring the generality of the trophic cascade hypothesis. Can. J. Fish Aquat. Sci. 52: 2518–2526.

Trent, L., and W. Hassler.
1966. Feeding habits of adult striped bass, *Roccus saxatilis*, in relation to stages of sexual maturity. Ches. Sci. 7: 189–192.

Walters, C., D. Pauly, and V. Christensen.
1999. Ecospace: prediction of mesoscale spatial patterns in trophic relationships of exploited ecosystems, with emphasis on the impacts of marine protected areas. Ecosystems 2:539–554.

Whipple, S. J., J. S. Link, L. P. Garrison, and M. J. Fogarty.
2000. Models of predation and fishing mortality in aquatic ecosystems. Fish Fisheries 1(1):22–40.

Abstract—The tautog, *Tautoga onitis* (Linnaeus), ranges from Nova Scotia to South Carolina and has become a popular target for recreational and commercial fisheries. Although tautog are a multiple spawning species, reproductive potential, measured as annual fecundity, has not been estimated previously with methods (batch fecundity, spawning frequency) necessary for a species with indeterminate annual fecundity. A total of 960 tautog were collected from the mouth of the Rappahannock River in the lower Chesapeake Bay to 45 km offshore of Virginia's coastline to investigate tautog reproductive biology in the southern portion of the species range. Tautog did not exhibit a 1:1 sex ratio; 56% were females. Male tautog reached 50% maturity at 218 mm TL, females at 224 mm TL. Tautog spawned from 7 April 1995 to 15 June 1995, at locations from the York River to 45 km offshore. Batch fecundity estimates ranged from 2800 to 181,200 eggs per spawning for female tautog age 3–9, total length 259–516 mm. Mean batch fecundity ±SEM for female tautog ages 4–6 was 54,243 ±2472 eggs and 106,256 ±3837 eggs for females ages 7–9. Spawning frequency was estimated at 1.2 days, resulting in 58 spawning days per female in 1995. Estimates of potential annual fecundity for tautog ages 3–9 ranged from 160,000 to 10,510,000 eggs.

Reproductive seasonality, fecundity, and spawning frequency of tautog (*Tautoga onitis*) in the lower Chesapeake Bay and coastal waters of Virginia*

Geoffrey G. White
School of Marine Science
Virginia Institute of Marine Science
College of William and Mary
P.O. Box 1346
Gloucester Point, Virginia 23062
Present address: Atlantic States Marine Fisheries Commission
1444 Eye Street, NW, 6th Floor
Washington, D.C. 20005
E-mail address: gwhite@asmfc.org

Thomas A. Munroe
National Marine Fisheries Service
National Systematics Laboratory, NMFS/NOAA
Smithsonian Institution
Post Office Box 37012
NHB, WC 57, MRC-153
Washington, D.C. 20013-7012

Herbert M. Austin
School of Marine Science
Virginia Institute of Marine Science
College of William and Mary
P.O. Box 1346
Gloucester Point, Virginia 23062

Manuscript accepted 22 October 2002.
Manuscript received 31 December at NMFS Scientific Publications Office.
Fish. Bull. 424–424 (2003).

The tautog, *Tautoga onitis* (Linnaeus), ranges from Nova Scotia (Bleakney, 1963; Scott and Scott, 1988) to South Carolina (Sedberry and Beatty, 1989; Bearden[1]), although it is most abundant between Cape Cod and New Jersey (Bigelow and Schroeder, 1953). In Virginia, tautog occur within the Chesapeake Bay from Gwynn's Island (mouth of Rappahannock River) and Sandy Point (Eastern Shore) southward to the mouth of the bay (Hildebrand and Schroeder, 1928), and in coastal Atlantic waters out to 65 km offshore (Richards and Castagna, 1970; Musick, 1972; Hostetter and Munroe, 1993). The major habitat requirement for this species is hard-bottom structure that fish can remain under, within, or alongside (Olla et al., 1974). Adult tautog inhabit hard-bottom environments including natural reefs and rock outcroppings, as well as man-made structures such as jetties, bridge-tunnel networks, artificial reefs, and shipwrecks. Near the southern terminus of the species range suitable hard-bottom habitat to support tautog populations becomes less abundant and may limit population size (Eklund and Targett, 1990; Hostetter and Munroe, 1993).

Tautog are a long-lived, slow-growing species with a maximum recorded age of 34 years in Rhode Island (Cooper, 1967)

* Contribution 2505 of the Virginia Institute of Marine Science, Gloucester Point, VA 23062.

[1] Bearden, C. M. 1961. Common marine fishes of South Carolina. Bears Bluff Lab. Contr., vol 34, 47 p. [Deposited at South Carolina Department of Natural Resources, Marine Resources Library, 217 Fort Johnson Road, P.O. Box 12559, Charleston, SC 29422.]

and 31 years in Virginia (White, 1996). Growth parameters of fish between northern and southern regions (Hostetter and Munroe, 1993) are comparable, except that Virginia tautog have exhibited almost twice the growth increments in young-of-the-year and age 13+ fish. Likewise, growth relationships are similar for tautog from New York (Briggs, 1977) and Virginia (Hostetter and Munroe, 1993).

Within preferred habitats, juvenile and adult tautog develop home sites (Olla et al., 1979). Tagging studies indicate seasonal movements between inshore and offshore habitats, but minimal north-south movement (Cooper, 1966; Briggs, 1977; Lynch[2]; Bain and Lucy[3]). During winter, adult tautog located offshore of Virginia are active at temperatures above 6.1°C (Adams, 1993). Likewise, tautog at inshore locations within Chesapeake Bay (Arendt et al., 2001a, 2001b) remain active at water temperatures of 5°C or above. In northern parts of its range, adult tautog move inshore and spawn when water temperatures increase in the springtime (Chenoweth, 1963; Cooper, 1966; Stolgitis, 1970; Olla et al., 1974, 1979), although some portion of the population remains offshore year-round (Olla and Samet, 1977; Hostetter and Munroe, 1993). Very little is known about the reproductive biology of tautog in Virginia. Tautog begin spawning when water temperatures reach about 11°C (Chenoweth, 1963; Olla et al., 1974, 1980; Eklund and Targett, 1990; Hostetter and Munroe, 1993); thus the spawning season begins later in the spring at higher latitudes. Spawning season extends from mid-April through June in Virginia (Hostetter and Munroe, 1993), mid-May through early August in Massachusetts (Stolgitis, 1970), and from late May to early June in Rhode Island (Chenoweth, 1963). Macroscopic gonad analyses and gonadosomatic indices have indicated that male tautog mature by age 3 and females by age 3–4 throughout the species range (Chenoweth, 1963; Cooper, 1967; Stolgitis, 1970; Briggs, 1977; Hostetter and Munroe, 1993); however, sample sizes of young (age 2–3) fish were small in these studies, and earlier maturation has been noted (Olla and Samet, 1977; Hostetter and Munroe, 1993). To date there has been no histological examination of the reproductive biology of this species in Virginia, or elsewhere.

In laboratory aquaria, tautog have been observed to be a multiple spawning species, spawning as discrete pairs and as groups (Olla and Samet, 1977; Olla et al., 1977). Although hermaphroditism is common among labrids (Warner and Robertson, 1978), tautog are thought to be strictly gonochoristic (Olla and Samet, 1977). However, two color patterns of males exist in samples from Virginia waters; approximately 85% of males exhibit strong dimorphism and 15% of smaller males (<550 mm) show external coloration similar to females (Hostetter and Monroe, 1993, this study). Further, histological analysis of 379 male tautog revealed no evidence of hermaphroditism (Munroe and White, unpubl. data)

The reproductive potential of tautog, measured as annual fecundity, has not been addressed to date. To accurately estimate potential annual fecundity for multiple spawning species, batch fecundity must be multiplied by the number of spawnings per year, i.e. spawning frequency multiplied by spawning season length (Hunter and Macewicz, 1985). Chenoweth (1963) and Stolgitis (1970) estimated batch fecundity and length of spawning season but did not measure spawning frequency. The only estimate of number of spawnings per female per year were those of Olla et al. (1977), who observed tautog spawning daily for 68–96 consecutive days in laboratory aquaria; however, results obtained in aquaria studies may not directly apply to natural habitats and have not been used to estimate potential annual fecundity.

Our study, the first to investigate cellular aspects of the reproductive biology of tautog in natural habitats of the lower Chesapeake Bay, was necessary 1) to describe this species as a determinate or indeterminate spawner; 2) to describe annual and spawning season ovarian cycles at the cellular level; 3) to assess age at maturity based on histological sections of gonad tissue; 4) to estimate batch fecundity for females from the southern portion of the species range; 5) to estimate spawning frequency; and 6) to estimate potential annual fecundity.

Materials and methods

A total of 960 tautog (>150 mm total length [TL]) were collected opportunistically between April 1994 and September 1995 from commercial and recreational fishermen (ca. 90%) as well as from research projects (ca. 10%) at Virginia Institute of Marine Science (VIMS). A minimum size of 150 mm TL was selected based on maturity information presented in Hostetter and Munroe (1993). Collection locations ranged from Gwynn's Island at the mouth of the Rappahannock River to 45 km offshore of Virginia's coastline, at depths of 1–35 m (Fig. 1). Approximately one quarter of the fish were taken from within the Chesapeake Bay, one quarter from the Chesapeake Bay Bridge Tunnel (CBBT, depth=5–15 m), and one half from around the Chesapeake Bay Light Tower (24 km offshore, depth=17–20 m).

For each fish, total length (mm) and total weight (TW, g) were measured. Sex was assessed externally from several dimorphic characters previously described by Cooper (1967), Olla and Samet (1977), and Hostetter and Munroe (1993). Males were distinguished by their pronounced white chin, blunt forehead, solid black or gray coloration on the upper half of the body and white underneath, and a small white spot (about 15 mm diameter) mid-laterally, below the middle of the dorsal fin. Female tautog have a less pronounced chin, sloped forehead, and a mottled brown coloration. After determination of sex (external examination), gonads were excised, staged macroscopically, and

[2] Lynch, T. R. 1996. Marine finfish investigation, sport fish population survey in Rhode Island marine waters: tautog studies, 1987–1993. Rhode Island Division of Fish and Wildlife performance report project: F-54-R-1, study I-I, reference document TT-396, 55 p. Rhode Island Division of Fish and Wildlife, Marine Fisheries Section, 3 Fort Wetherill Road, Jamestown, RI 02835.

[3] Bain, C. M., and J. A. Lucy. 1996. Virginia Game Fish Tagging Program annual report, 1995. Virginia Mar. Res. Rep. 96-2, 10 p. Virginia Marine Resources Commission, 2600 Washington Ave, Newport News, VA 23067.

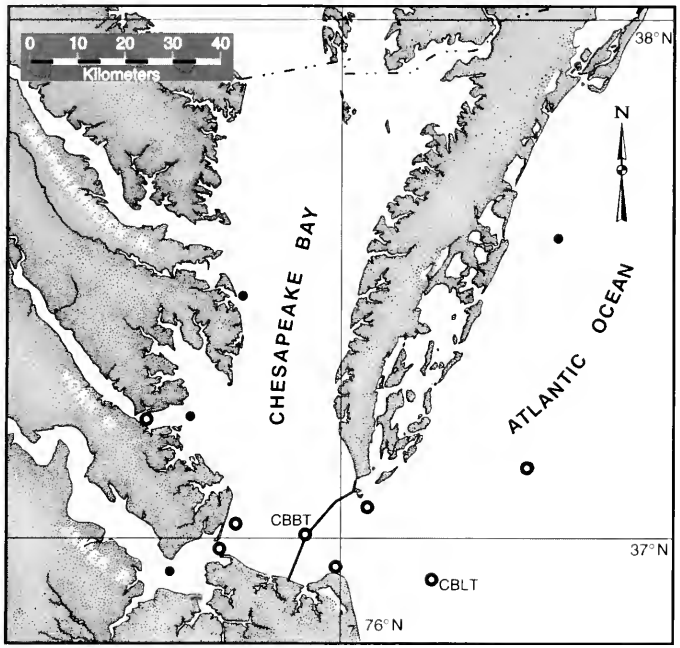

Figure 1

Map of lower Chesapeake Bay and nearby coastal waters of Virginia. Closed circles indicate sites where tautog were collected; open circles indicate collection sites of tautog in spawning condition. CBBT = Chesapeake Bay Bridge Tunnel. CBLT = Chesapeake Bay Light Tower.

weighed to the nearest 0.01 g (GW). Maturity classification was assigned as outlined in Table 1, based on eight macroscopic stages, modified from Lowerre-Barbieri et al. (1996) for multiple spawning species. One gonad was randomly chosen by coin toss for histological processing and placed in Davidson's fixative. For females staged macroscopically as spawning females, the remaining ovary was placed in 10% neutrally buffered formalin for batch fecundity counts.

Whole unsectioned opercle bones are the accepted method to age tautog (Cooper, 1967; Simpson, 1989; Hostetter and Munroe, 1993). Opercle bones were removed and processed to examine age at maturity and age-related fecundity. Opercles were boiled for 1–3 minutes to remove flesh, scrubbed under warm flowing water, dried for two days, and read with transmitted light. Age of each fish was determined from two readings of both opercles (when possible). An annulus was defined as the transition from a translucent zone to an opaque zone. Annulus formation was previously validated by Hostetter and Munroe (1993). 1 April was used as a birth date to allow maximum growth within the biological year (April to March), and to avoid overlap with fish in the next year class.

Gonads selected for histological processing were placed in Davidson's fixative for two days before transverse sections of anterior, middle, and posterior ovarian tissue (or anterior and posterior sections of testes) were taken and placed in tissue cassettes. Variation between left and right gonads was accounted for by random selection of one gonad for fixation. Tissue samples were then rinsed overnight with flowing tap water and placed in 70% EtOH. Standard histological processing (tissue embedded in paraffin, sectioned at 5–7 µm, and stained with Harris's hematoxylin and eosin-Y) (Luna, 1968) was performed for all samples. Male gonads were classified microscopically into two stages: sexually mature or immature. Female microscopic gonad stages were assigned based on the occurrence and relative abundance of seven oocyte developmental stages (Wallace and Selman, 1981; West, 1990; Hunter et al., 1992): primary growth, cortical alveoli, partially yolked, advanced yolked, germinal vesicle migration, germinal vesicle breakdown, and hydrated oocytes. Final oocyte maturation (FOM) comprises germinal vesicle migration, germinal vesicle breakdown, and hydrated oocyte stages (Wallace and Selman, 1981; West, 1990). Fully developed ovaries were distinguished from partially spent/redeveloping ovaries by the presence of postovulatory follicles (POFs). Microscopic gonad stages are described in "Description of microscopic gonad stages," ("Results" section), summarized

Table 1

Description of macroscopic and microscopic gonad stages (modified from Lowerre-Barbieri et al.,1996) for female tautog. Macroscopic criteria refer to whole fresh ovaries. Gonad stages 4, 5, and 3a comprise the inner spawning cycle. FOM = final oocyte maturation. GSI = gonadosomatic index. GVBD = germinal vesicle breakdown. POF = postovulatory follicle. MA = macrophage aggregate.

Gonad stage	Macroscopic criteria	Microscopic criteria
1 Immature	Ovaries very small, tubular in shape, white to light pink in color; no oocytes visible (mean GSI=0.50)	Oogonia and primary growth oocytes present; high proportion of connective tissue, no atresia or MAs, ovarian membrane thinner than in resting stage.
2 Developing	Ovaries small to medium, tubular shape, dark yellow to light orange in color; yolked (opaque) oocytes begin to appear (mean GSI=2.25)	Primary growth, cortical alveoli, and some partially yolked oocytes present.
3 Fully developed	Ovaries medium to large, appear slightly grainy, pale mustard in color; yolked oocytes are abundant (mean GSI=3.25)	Primary growth to advanced yolked oocytes present; no FOM stages, POFs, or remnant HOs.
4 Hydrated	Ovaries large to very large, pink to orange in color; firm, yolked oocytes interspersed with large transparent (hydrated) oocytes (mean GSI=11.74)	Primary growth to germinal vesicle migration (GVM) and hydrated oocytes present, hydrated oocytes are unovulated; 1-day POFs may be present.
5 Running ripe	Ovaries large to very large; few transparent oocytes in ovarian tissue, transparent oocytes have been ovulated into expanded lumen, and are easily extruded when gonad is excised (mean GSI=10.12)	Primary growth through GVM, and ovulated hydrated oocytes and fresh POFs present; lumen usually seen as separation of ovigerous folds.
3a Partially spent/ redeveloping	Ovaries somewhat flaccid, large, slightly more pink than in hydrated stage; lumen has collapsed, occasionally a few remnant hydrated oocytes extruded from excised ovary (mean GSI=8.84); similar to stage 3.	Primary growth through GVBD oocytes present, no unovulated hydrated oocytes, few remnant ovulated hydrated oocytes; lumen collapsed, POFs abundant.
6 Spent/ regressing	Ovaries flaccid, small to medium, red to purple; some tissue devoid of yolked oocytes at anterior end of ovary, yolked oocytes visible but less abundant (mean GSI=1.37)	Primary growth through advanced yolked oocytes present; major atresia of all stages except primary growth oocytes.
7 Resting	Ovaries small, purple-opaque to maroon in color; few or no yolked (opaque) oocytes visible (mean GSI=1.50)	Primary growth and cortical alveoli oocytes present, occasional atretic oocytes; MAs abundant, more oogonia tissue, less connective tissue, and thicker ovarian membrane than in immature stage.

in Table 1, and shown in Figure 2, A–H. Percent agreement between macroscopic and microscopic female gonad stages was calculated to evaluate the accuracy of macroscopic staging (used in all previous studies of tautog reproductive biology). Microscopic stages were assumed to be more accurate because histologic examination provides evidence of differences in cellular development.

Chi-square analysis (n=489 fish) was used to test for significant deviations from an expected 1:1 sex ratio for all fish. Deviations from a 1:1 sex ratio among 100-mm length intervals were also analyzed by chi-square to determine if size or age had a significant effect on sex ratio.

Length and age at maturity were analyzed for fish collected from April to mid-June to reduce the possibility of classifying resting, mature fish as immature. Females were considered mature if classified into microscopic stages 2–7 (Table 1). Males were considered mature if spermatocytes or spermatozoa were present in histological sections. Length at maturity was based on 110 females and 79 males (150–350 mm TL). A logistic regression curve was fitted to the data, to estimate length at 50% maturity (L_{50}). Age at maturity was based on 135 females and 104 males (ages 1–6).

To determine the annual spawning season, a gonadosomatic index (GSI=(*gonad weight*/*somatic weight*) × 100) was calculated by using somatic weight (SW=TW–GW) for each sex. A more precise estimate of tautog spawning season was determined from microscopic gonad stages. The spawning season was defined by the first and last day that female tautog were collected with ovaries staged as either hydrated, running ripe, or partially spent/redeveloping. Spawning locations were detected by the presence of hy-

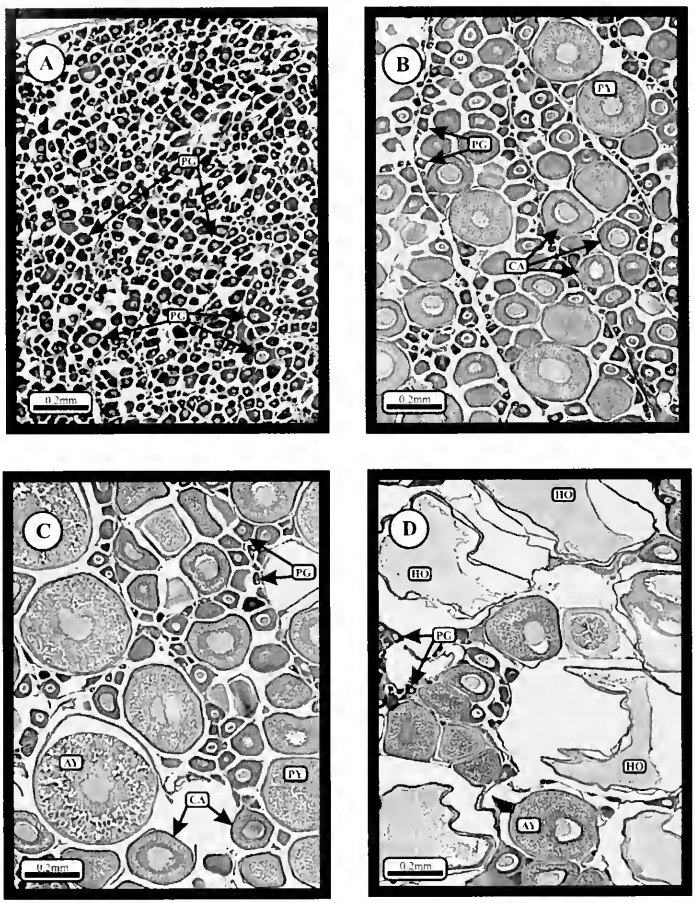

Figure 2, A–D.

Histologic stages of tautog ovaries. (**A**) immature (stage 1). (**B**) developing (stage 2). (**C**) fully developed (stage 3). (**D**) hydrated (stage 4). PG = primary growth oocyte. CA = cortical alveoli oocyte. PY = partially yolked oocyte. AY = advanced yolked oocyte. HO = hydrated oocytes. Magnification = 50×.

drated and running ripe fish because those stages have high abundances of hydrated oocytes and fresh POFs, which indicate either imminent or recent spawning activity (Hunter and Macewicz, 1985).

Oocyte development patterns (synchronous, group synchronous, or asynchronous) and type of annual fecundity (indeterminate or determinate) were assessed by oocyte size-frequency distributions (Hunter and Macewicz, 1985) and histology (Hunter and Macewicz, 1985; West, 1990). Six fish were selected for analysis of oocyte size-frequency distributions; three fish (TL=300, 400, 450 mm [±10 mm]) in April and another three in June, representing gonad development early and late in the spawning season. For each fish, oocytes were hydraulically separated from the ovarian membrane and each other, collected in a 0.1-mm sieve, and preserved in 2% formalin following the method of Lowerre-Barbieri and Barbieri (1993). Preserved samples were stirred to reduce bias due to differential settling of different

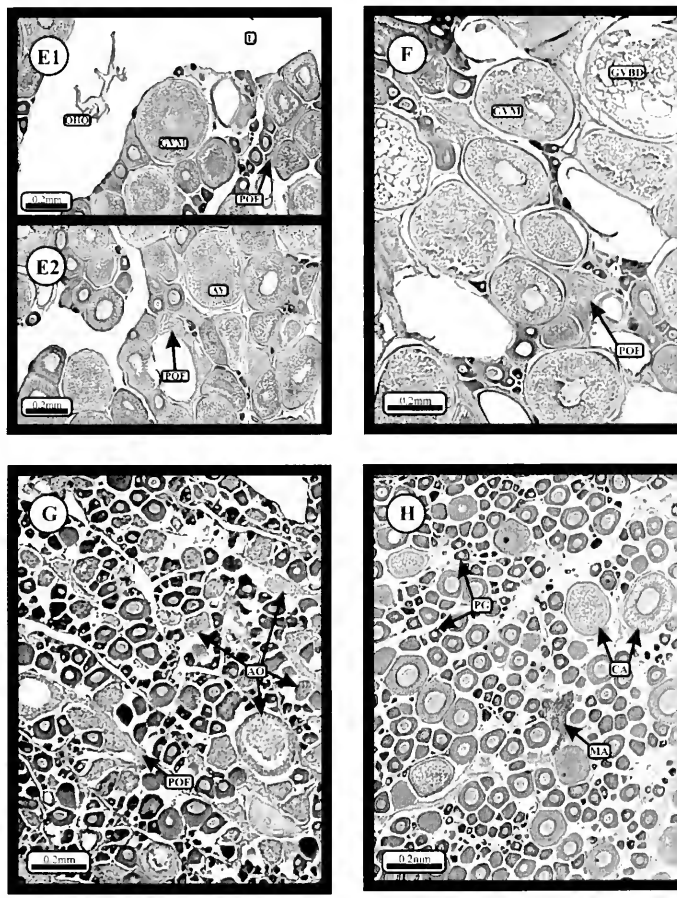

Figure 2, E–H.

Histological stages of tautog ovaries (continued). (**E**) running ripe (stage 5), frame 1 shows obvious lumen as distinguishing character, frame 2 shows typical field of view without lumen. Hydrated oocytes have been ovulated (OHO) and now reside in the lumen (L). (**F**) partially spent/redeveloping (stage 3a). (**G**) spent (stage 6). (**H**) resting (stage 7). PG = primary growth oocyte. CA = cortical alveoli oocyte. AY = advanced yolked oocyte. GVM = germinal vesicle migration oocyte. GVBD = germinal vesicle breakdown oocyte. POF = postovulatory follicle. AO = atretic oocyte. MA = macrophage aggregate. Magnification = 50×.

stage oocytes, and a 5-mL aliquot was removed and placed in a gridded petri dish. Grids were selected for counting by using a random number table, and maximum diameters of the first 500 oocytes encountered were measured to the nearest 0.001 mm with a Biosonic Optical Pattern Recognition System.® Data were grouped in 0.05-mm size classes for presentation (0.1 mm group=0.075 to 0.124 mm oocytes).

Batch fecundity was determined gravimetrically by using a modification of the hydrated oocyte method (Hunter et al., 1985). The method calls for both ovaries to be fixed in 10% formalin, but we had a formalin wet weight for only

one ovarian lobe. Therefore, we conducted a calibration experiment to determine the percent change in ovarian weight between fresh- and formalin-fixed ovaries. On 25 April 1996, 18 female tautog were collected, fresh ovarian weight was measured to the nearest 0.01 g, and both ovaries were placed in 10% neutrally buffered formalin. Formalin-fixed wet weight was measured to the nearest 0.01 g six times over 30 days to determine when weight stabilized after fixation. Percent change in weight was calculated for each specimen, and regressed against fresh weight of the ovary, thus percent change in weight between formalin-fixed wet weight and fresh ovary weight was calculated with the negative exponential relationship:

$$Percent\ weight\ change = 21.452\ e^{(-0.0163GW)} \quad [r^2=0.67];$$

where GW = fresh gonad weight.

Calibrated (formalin fixed) gonad weight (CGW) was calculated as

$$CGW = percent\ weight\ change \times GW.$$

Then, batch fecundity was estimated by using the formula

$$Y = (y/x)\,CGW,$$

where Y = batch fecundity;
y = number of hydrated oocytes in the tissue sample;
x = formalin wet weight of tissue sample; and
CGW = calibrated formalin-fixed wet weight of ovaries.

Assumptions of the hydrated oocyte method which must be met include 1) all eggs in the most advanced mode are spawned; 2) fecundity is directly proportional to ovary weight; and 3) no bias exists in the estimation of egg abundance within the most advanced mode, in the selection of mature females for analysis, or in the position within and between ovaries from which subsamples were taken (Hunter and Goldberg, 1980; Hunter et al., 1985). The use of hydrated oocytes, which are much larger than the next largest cell size class and are formed only when spawning is imminent, supported acceptance of these assumptions. Following the methods of Hunter et al. (1985), we selected ovaries from 29 females for batch fecundity analysis. These were the only females that had stage-4 (hydrated, Table 1) ovaries without postovulatory follicles as confirmed through histological analysis. If postovulatory follicles were found in histological sections, then that fish was excluded from fecundity analysis.

To test for differential oocyte development between anterior, middle, and posterior sections of ovarian tissue, point counting analyses (Weibel et. al., 1966) were performed on histological sections to determine the relative volume of seven cell types and POFs in the ovary. The relative volume of each cell type was calculated by using the number of points within a grid (121 points/grid) overlying each cell type:

$$V_v = P_n / P_{tot},$$

where V_v = relative volume of one cell type;
P_n = number of points overlying a specific cell type; and
P_{tot} = number of points in grid.

To ensure that fields of view were chosen randomly, each ovarian section was divided into 5×5 mm areas with an overlay grid. Three areas per section were chosen with a random number table to ensure that counting fields of view did not overlap. Within each 5×5 mm area, point counts were made through a gridded reticule (121 points) at 4× magnification. Average relative volume of each cell class was calculated from the three areas as $P_n/363$, and compared between anterior, middle, and posterior ovarian sections with multiple analysis of variance (MANOVA) (Minitab, 1995). Response variables (8) were the average relative volume of each cell class. Differences between fish (10) were removed by blocking on fish. After no positional effects were detected (Wilk's test value 0.25, F=1.35, df=16,22, P=0.25), it was concluded that oocyte development was evenly distributed throughout the ovaries of tautog. Blocking by fish proved beneficial and effective in removing any artifact caused by differences in kill time between fish, and in increasing the quality of the test by increasing sample size. Nonsignificant positional effects in ovarian development allowed estimation of batch fecundity from only the middle ovarian section. All hydrated oocytes were counted from three subsamples of approximately 0.3 g from the middle of the formalin-fixed ovary.

Simple linear regressions were used to describe relationships between batch fecundity and TL, TW, and age. Relative fecundity was calculated as batch fecundity divided by GW, and regressed against TL, TW, and age.

Diel spawning periodicity estimates for tautog at the mouth of the Chesapeake Bay indicated that spawning occurs during daylight hours but that spawning windows shift with ebb tidal currents (White, unpubl. data). To estimate spawning frequency by the hydrated oocyte method (DeMartini and Fountain, 1981; Hunter and Macewicz, 1985), samples with known kill times must be collected just prior to, and during, the spawning window. Most samples were collected at dockside; thus kill time for individual fish was unknown, and the hydrated oocyte method could not be performed. Therefore, spawning frequency was estimated by the POF method (Hunter and Goldberg, 1980; Hunter and Macewicz, 1985) by using descriptions of fresh (day 0, 0–12 h) and degenerating (day 1, 12–24 h) POFs of tautog (White, unpubl. data). Fresh POFs in tautog ovaries can be identified as a clearly defined, loosely folded ribbons of thecal and granulosa cells that contain visible lumina, similar to "0 day" POFs in anchovies (Hunter and Macewicz, 1985). One-day-old tautog POFs have deteriorated such that individual cell walls are no longer apparent in thecal and granulosa cells, and the structure appears less organized and has a small or indistinguishable lumen similar to that of 24–48 h anchovy POFs (Hunter and Macewicz, 1985). A full description of POF degeneration in tautog ovaries is presented elsewhere (White, unpubl. manscr.).

Annual fecundity was estimated as the number of spawnings per female multiplied by batch fecundity for

Table 2

Percent agreement between microscopic and macroscopic ovarian stages assigned to tautog (n=484) captured from June 1994 through September 1995. See Table 1 for gonad stage descriptions. Data are expressed as number of ovaries staged.

Microscopic stage	Macroscopic gonad stage							
	1	2	3	4	5	3a	6	7
1	34	—	—	—	—	—	3	—
2	3	15	—	—	—	—	—	40
3	3	18	11	3	—	2	—	5
4	—	—	—	31	1	—	—	—
5	—	—	1	38	8	—	—	—
3a	1	—	4	55	3	11	1	—
6	1	—	—	—	—	1	6	—
7	12	3	—	—	—	—	38	132
Agreement	63%	42%	69%	24%	67%	79%	13%	75%

each fish. Number of spawnings per female was calculated by dividing the number of days in the spawning season by estimated annual spawning frequency. The relationship between mean annual fecundity per 50-mm length interval and total length was analyzed with both linear and exponential regression.

Results

Description of microscopic gonad stages

Tautog ovarian development was described by eight microscopic gonad stages (Table 1) characteristic of multiple spawning species. Each stage can be differentiated by a unique suite of histological characteristics. Immature ovaries (Fig. 2A) are characterized by the presence of only oogonia and primary growth oocytes within a thin ovarian membrane and a relatively high volume of connective tissue. Developing stage ovaries (Fig. 2B) are characterized by the presence of primary growth, cortical alveoli, and partially yolked oocytes. The fully developed ovary (Fig. 2C) is characterized by the presence of primary growth to advanced yolked oocytes and the absence of oocytes in final oocyte maturation (FOM) classes, POFs, or remnant HOs. Hydrated ovaries (Fig. 2D) are distinguished by the prominence of hydrated oocytes still inside the ovarian follicles and may also contain degenerating POFs from an earlier spawning, but they noticeably lack oocytes in the germinal vesicle breakdown state (GVBD). The running ripe stage (Fig. 2E) is classified by the presence of an expanded ovarian lumen, ovulated hydrated oocytes free in the lumen (although hydrated oocytes are frequently washed out of the sample during the staining procedure), a large number of fresh POFs, and germinal vessicle migration (GVM) oocytes that tend to be the most advanced stage present within ovigerous folds. Partially spent/redeveloping ovaries (Fig. 2F) are classified by the lack of an ovarian lumen and presence of occasional remnant hydrated oocytes, primary growth to GVBD oocytes, and an abundance of POFs. The spent stage (Fig. 2G) is characterized by resorption of yolked oocytes (atresia), and sometimes the presence of macrophage aggregates (MAs), which are groups of cells containing the pigments lipofuscin, ceroid, and melanin (Wolke, 1992). These cells appear to be a collection of scavenging cells that remove cellular debris and foreign substances by phagocytosis when stimulated by excessive degenerating tissue (Wolke, 1992). In tautog ovaries, MAs are assumed to be associated with the resorption of yolked oocytes after the spawning season. Resting stage ovaries (Fig. 2H) contain primary growth and cortical alveoli oocytes, and atresia may be present. Resting ovaries can be distinguished from immature stage ovaries by a thickened ovarian membrane, relatively more oogonia than connective tissue and the presence of MAs.

The reliability of macroscopic staging to predict actual reproductive stage as detected by microscopic analysis was examined for 484 females. We considered any level of agreement above 80% to be acceptable. The ability of macroscopic staging to predict actual microscopic stage varied considerably, from 13% to 79% agreement for individual stages (Table 2), indicating that macroscopic staging was generally unreliable for estimating actual reproductive stage for many ovarian stages. Percent agreement between macroscopic and microscopic staging was only 51% overall. The best agreement was for the fully developed, partially spent/redeveloping, and resting ovarian stages (agreement 69%, 79%, 75%, respectively). Intermediate values were obtained for immature, and running ripe stages, (agreement 63% and 67%, respectively). The poorest agreement occurred in assigning developing and spent stages (42%, 13%, respectively).

Sex ratios

Of the 938 tautog sexed, 522 (56%) were females and 416 were males. Overall, sex ratios varied significantly from an expected 1:1 ratio, with more females than males (1.25:1, χ^2=11.98, P<0.01). At lengths ≤400 mm, females were

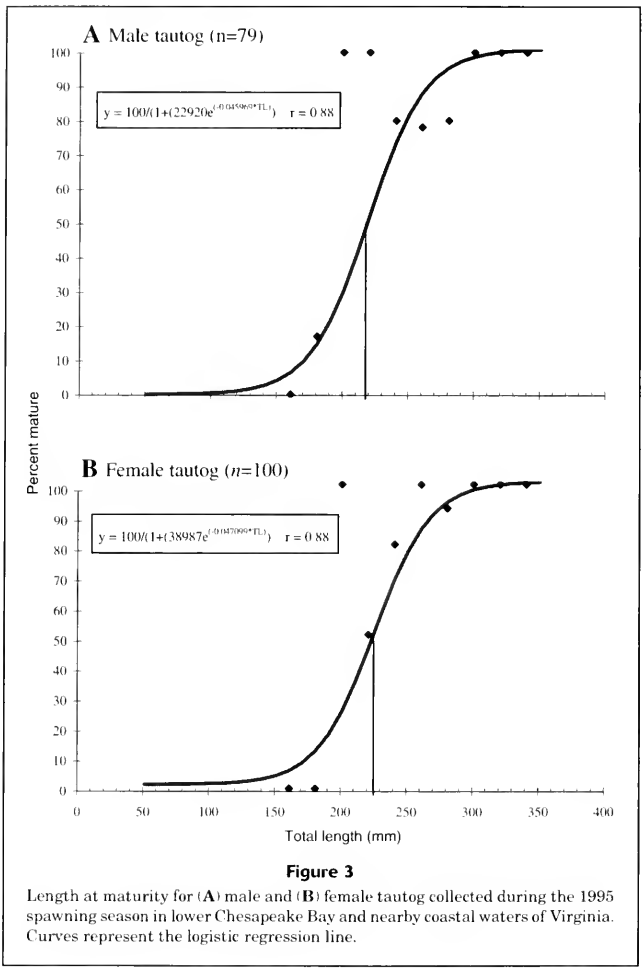

Figure 3

Length at maturity for (**A**) male and (**B**) female tautog collected during the 1995 spawning season in lower Chesapeake Bay and nearby coastal waters of Virginia. Curves represent the logistic regression line.

more abundant than males, whereas the sex ratios were not significantly different from 1:1 at fish lengths >400 mm (Table 3).

Length and age at maturity

Tautog length at 50% maturity (L_{50}) was 218 mm for males (n=79) and 224 mm for females (n=110, Fig. 3). All males and females were mature at 300 mm. No females less than 227 mm had hydrated oocytes or POFs that would have indicated spawning activity.

Age at first maturity was defined as the age at which at least 50% of the fish are mature. Mature gonads were present in 0% of males at age 1, 38% at age 2, and 93% at age 3. Zero percent of females were mature at age 2, 78% at age 3, and >97% at age 4.

Spawning season and location

GSI values indicated that tautog spawned from April through June and that peak values occurred in April for the 1995 spawning season (Fig. 4). The 1995 spawning season was more precisely defined as 7 April–15 June based on the presence of females in spawning condition (i.e. staged histologically as hydrated, running ripe). At the beginning of the spawning season, females progressed into spawning condition over approximately two weeks. The end of the spawning season was determined conservatively, based

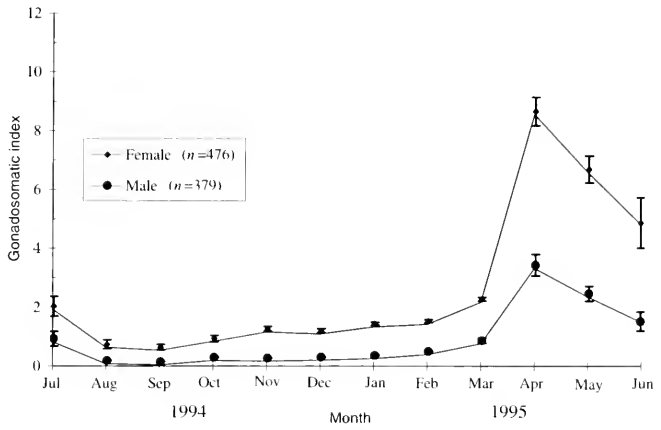

Figure 4

Gonadosomatic index based on somatic weight (total weight–gonad weight) for tautog collected in lower Chesapeake Bay during 1994–95. *n*=sample size; error bars indicate sample standard deviation.

Table 3

Sex ratio of tautog by 100-mm length intervals and chi-square values of tests for a 1:1 ratio. *Significance at P=0.05. **Significance at P=0.01. NS = nonsignificant.

Total length (mm)	No. of males	No. of females	No. expected (50%)	% Females	Chi-square
101–00	12	24	18	67	4.00*
201–300	57	88	73	61	6.63*
301–400	147	216	182	60	13.12**
401–00	140	125	133	47	0.85 NS
501–600	38	53	46	58	2.47 NS
601–700	11	14	13	56	0.36 NS
Total	405	520			

on the last day female tautog were collected in spawning condition (15 June) instead of the first collection date of a spent female (27 June).

Tautog were collected (Fig. 1) in spawning condition within the Chesapeake Bay (York River, Buckroe Beach), at the mouth of the Chesapeake Bay (Chesapeake Bay Bridge Tunnel, Cape Henry wrecks, Anglo-African wreck), and at offshore locations (Chesapeake Bay Light Tower, one site 45 km offshore) and there was no apparent trend in spawning season by location.

Ovarian developmental pattern and type of fecundity

Ovarian stages defined for tautog (Table 1) are typical of multiple spawning species. Tautog hydrate and spawn only a small fraction of the yolked oocytes in the ovary for any one spawning event. Macroscopically, hydrated ovaries appear speckled because of the intermittent occurrence of large, clear hydrated oocytes among the dominant numbers of opaque, yolked oocytes. Further, the lumen of running ripe ovaries was full of ovulated hydrated oocytes, yet there was still a large volume of tissue with maturing yolked oocytes. The occurrence of spawning stage ovaries over a protracted period also suggested a multiple spawning pattern. Tautog were collected in spawning condition (hydrated and running ripe stages) and the partially spent/redeveloping stage throughout the April–June spawning period, but no spent or resting fish were collected until late June, suggesting that individual females were spawning repeatedly during the spawning season.

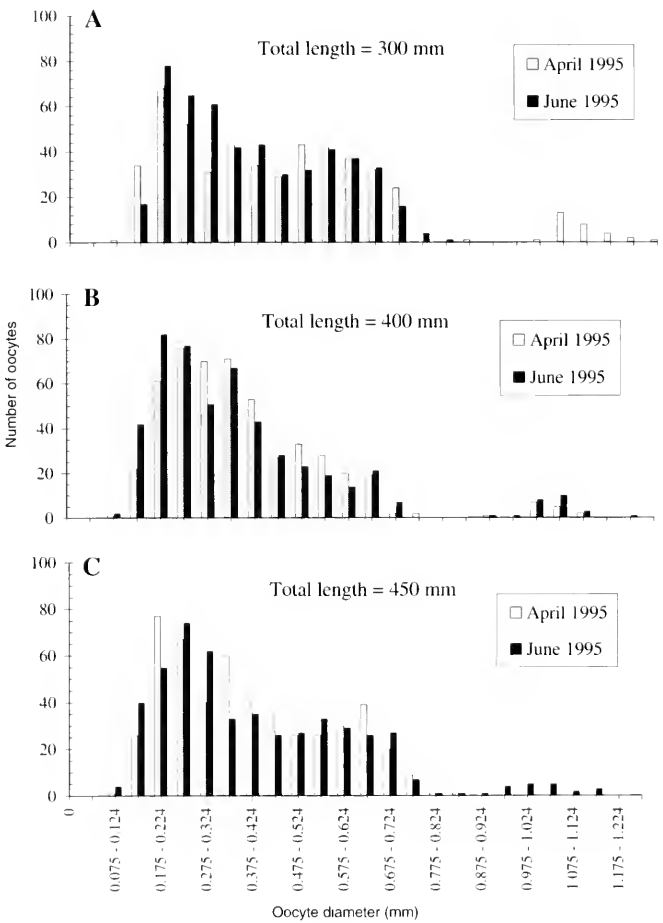

Figure 5

Oocyte size frequency distributions (0.05-mm intervals) in tautog ovaries. Six fish are represented, two in each length class: (**A**) 300 mm, (**B**) 400 mm, (**C**) 450 mm. Collection dates were 26 April 1995 and 2 June 1995. Fish were staged macroscopically as hydrated or running ripe, and oocytes were hydraulically separated and the diameter of 500 oocytes was measured to the nearest 0.001 mm.

Oocyte size-frequency distributions measured at the beginning and end of the spawning season were also used to classify tautog annual fecundity as determinate or indeterminate. Primary growth and cortical alveoli oocytes were continuously yolked, matured, and spawned throughout the spawning season, evidenced by 1) lack of hiatus between advanced yolked oocytes and less mature oocytes, and 2) abundance of yolked oocytes (size range 0.30–0.55 mm) not decreasing over the spawning season (Fig. 5). This type of development defines tautog as having indeterminate fecundity.

Two patterns of oocyte development are common among multiple spawning fishes: group synchronous and asynchronous oocyte development. Tautog oocyte size-frequency distributions (Fig. 5) show no distinct gaps in develop-

ment, or modes of oocytes, except for hydrated oocytes (0.95 to 1.25 mm)—a finding that indicates asynchronous oocyte development. The presence of primary growth through advanced yolked oocytes, as well as oocytes in FOM and POFs in histologic sections of fully developed and partially spent ovaries (Fig. 2, C and F), is evidence that tautog exhibit a multiple spawning pattern.

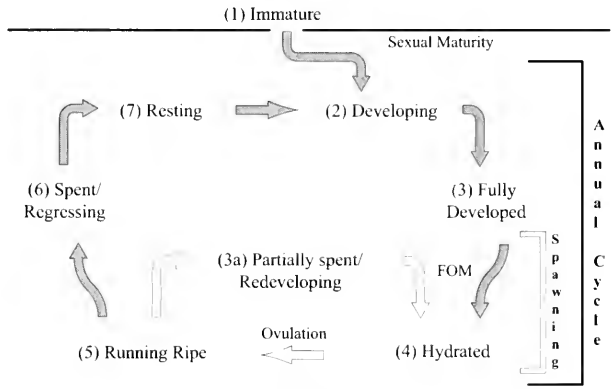

Figure 6

Annual and spawning season cycles of ovarian development in tautog. FOM = final oocyte maturation.

Ovarian cycle

Egg maturation in tautog is a complex process comprising both seasonal and annual components. This complex pattern of multiple spawning exhibited by an inner spawning cycle (made up of hydration, ovulation, spawning, and redevelopment) within the annual ovarian developmental cycle, is summarized for tautog in Virginia in Figure 6. In the spring, fully developed ovaries contain primary growth to advanced yolked oocytes, but lack POFs. Fish enter the spawning cycle by hydration and ovulation of the first batch of oocytes. After the first spawning event, partially spent/redeveloping ovaries contain fresh POFs (indicating recent spawning during the previous 24 hours) and another batch of oocytes in FOM in preparation for the next spawning event. Thereafter, the inner spawning cycle is repeated throughout the spawning season. Histological examination of hydrated ovaries during the spawning season revealed the co-occurrence of hydrated oocytes (indicating an imminent spawn) and degenerating POFs, suggesting that some tautog are capable of repeating the inner spawning cycle on a daily basis. At the end of the spawning season, ovaries progress to the spent-regressing stage, where, through the process of oocyte atresia, the remaining stock of yolked oocytes are resorbed before the ovary enters the resting stage.

Batch fecundity

Batch fecundity was determined for 29 female tautog ranging in total length from 260 to 520 mm, total weight 475 to 3,500 g, and ages 3–9 (Fig. 7). Although there was a high degree of variation in batch fecundity between individual fish, significant relationships were found between batch fecundity and fish length, weight, and age. Batch fecundity was more closely related to total length and total weight than to age. Batch fecundity (BF) increased significantly with total length (ANOVA, n=29, F=16.92, P<0.0005, power=0.97), following the regression equation (Fig. 7A)

$$BF = 425.76(TL) - 84{,}534 \qquad [r^2=0.39].$$

Batch fecundity increased significantly with total weight (ANOVA, n=29, F=16.80, P<0.0005, power=0.99), the regression equation being (Fig. 7B)

$$BF = 56{,}066\ \mathrm{Ln}(TW) - 322{,}091 \qquad [r^2=0.50].$$

Batch fecundity also increased significantly with age (ANOVA, n=29, F=10.22, P<0.004, power=0.88), following the regression equation (Fig. 7C)

$$BF = 15{,}731(AGE) - 20{,}599 \qquad [r^2=0.27].$$

Tautog relative fecundity (BF/GW) did not increase significantly with fish length (ANOVA, n=29, F=1.98, P=0.17) or age (ANOVA, n=29, F=1.72, P=0.20), but there was a significant increase in relative fecundity with total fish weight (ANOVA, n=29, F=4.46, P=0.044).

Spawning frequency

Histological examination of 169 tautog collected from 7 April 1995 to 15 June 1995 revealed some variation in the abundance of three reproductive states that were indicative of imminent or recent spawning. Forty-four percent of female tautog had HOs, 32% had fresh POFs without any HOs, and 84% of females collected had 1-day-old POFs (Table 4). Tautog spawning frequency was calculated as 1.2 days based on the percentage of fish with 1-day-old POFs following the methods of Hunter and Goldberg (1980). Number of spawnings per female tautog in 1995 was calculated as the spawning season (70 days) divided by spawning frequency (1.2 days/spawning), yielding 58 spawnings per female.

Individual tautog in natural habitats were capable of spawning daily after entering the spawning season. Evidence of daily spawning was provided by the rapid ovarian development observed in histological sections: 1) 70 fish with HOs and degenerating POFs; 2) 90 fish with both fresh and degenerating POFs; and 3) partially spent/

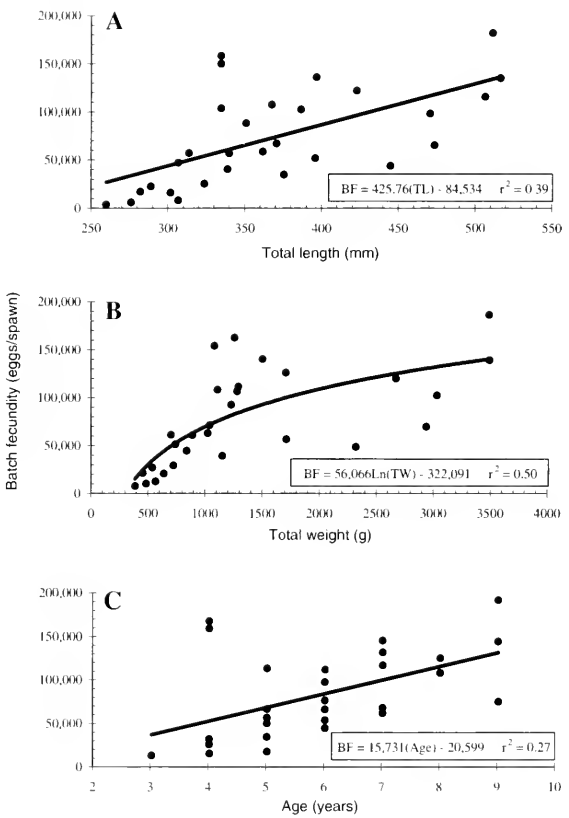

Figure 7

Tautog batch fecundity (no. of eggs) versus (**A**) total length (mm), (**B**) total weight (g) and (**C**) age (years) for 29 tautog collected in lower Chesapeake Bay and nearby coastal waters of Virginia in 1995. (Complete data for individual fish are available in White, 1996).

redeveloping females with both GVBD oocytes and fresh POFs (Fig. 2F).

Potential annual fecundity

Annual fecundity was calculated as 58 spawnings/female multiplied by batch fecundity. Annual fecundity varied from 160,000 eggs (259 mm, age-3 fish), to 10,510,000 eggs (511 mm, age-9 fish). Mean annual fecundity increased significantly (ANOVA, n=5, F=16.69, P=0.015) with fish size. A linear regression of mean annual fecundity on fish length (50 mm size classes, Fig. 8), was described by the following relationship:

$$\text{Mean } AF = 23{,}480(TL) - (5\times10^6) \qquad [r^2 = 0.81].$$

Discussion

Macroscopic and microscopic gonad staging

Macroscopic ovarian staging of multiple spawning fishes can be difficult because subtle differences at the cellular level may not be detectable macroscopically (Parrish et al., 1986). However, macroscopic analysis does provide a rapid estimate of maturity and results in a general description of spawning seasons at a reduced cost compared to

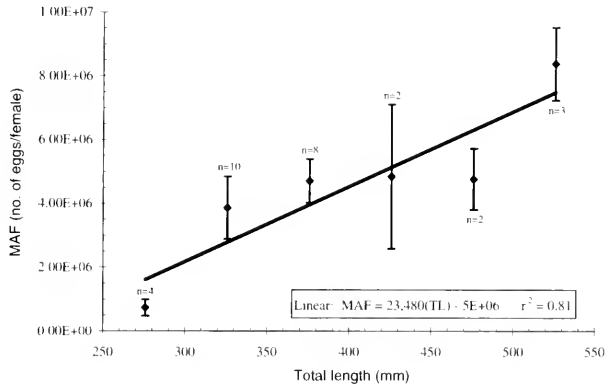

Figure 8

Linear relationship between mean annual fecundity (MAF) and body length in 50-mm length classes for tautog. Sample sizes are noted above each data point. Error bars indicate standard error of the mean.

Table 4

Reproductive state of female tautog collected during 1995 spawning season. HO = hydrated oocyte. POF = postovulatory follicle.

Date (1995)	No. with HOs	No. with fresh POFs, no HOs	No. with 1-day POFs	No. mature, not spawning	Total no. of mature females
7 April	11	0	11	1	13
8 April	11	4	12	13	29
15 April	1	0	1	0	1
22 April	9	2	10	4	14
26 April	12	23	47	1	49
9 May	15	16	33	2	35
24 May	0	0	1	0	1
31 May	5	6	11	0	11
1 June	10	33	14	0	14
2 June	1	0	1	0	1
15 June	0	0	1	0	1
Total	75	54	142	21	169
Total %	44.4	32.0	84.0	—	—

time-consuming histological methods. West (1990) noted that there have been few attempts to assess the accuracy of macroscopic gonad staging with histological analysis. Most scientists attempting to assess reproductive stage of female tautog will most likely use macroscopic criteria. Given that all eight microscopic stages cannot be identified in a macroscopic context, a revised macroscopic gonad staging was developed (Table 5) with validated agreement against microscopic analysis. The validated stages (Table 5) generally agree with previous studies of tautog reproductive biology (Chenoweth, 1963; Stolgitis, 1970; Hostetter and Munroe, 1993). However, even with this revised, simplified staging criteria, we caution others that agreement between the new criteria and microscopic staging is still low for some ovarian stages, rendering this method less reliable than microscopic analysis.

Despite these limitations, macroscopic staging errors were usually off by only one developmental stage (Table 2). Errors in macroscopic staging were most likely due to the rapid development of ovarian tissue required to sustain daily spawning events. The low percent agreement (51% overall) between macroscopic and microscopic classifications of tautog ovar-

Table 5

Revised macroscopic gonad stages for future research on tautog. These revised macroscopic stages are based on the gonad stages seen in Table 1.

Gonad stage (Table 1)	Revised gonad stage	Macroscopic appearance
Immature	Immature	Ovaries very small, tubular in shape, white to light pink in color, no oocytes visible. (Same as "immature stage" from Table 1.)
Developing and Fully developed	Developing	Ovaries medium to large with slightly grainy appearance, pale mustard in color, yolked (opaque) oocytes present, no hydrated (transparent) oocytes visible through ovarian membrane. (This stage is a combination of "developing" and "fully developed" stages from Table 1.)
Hydrated and Partially spent/ redeveloping	Spawning	Ovaries large to very large, pink to orange in color, may be dotted with transparent oocytes, yolked oocytes interspersed with large transparent (hydrated) oocytes, occasionally a few remnant hydrated oocytes. (This stage is a combination of "hydrated" and "partially spent/redeveloping" stages from Table 1.)
Running ripe	Running ripe	Ovaries large to very large, pink to orange in color, hydrated oocytes have been ovulated, expand lumen of ovary and are easily extruded from excised ovary; few hydrated oocytes in ovarian tissue. (Same as "running ripe" stage from Table 1.)
Spent and Resting	Spent	Ovaries flaccid, small to medium, red to purple in color, few yolked (opaque) oocytes visible, some or all of ovary having no oocytes visible. (This stage is a combination of "spent" and "resting" stages from Table 1.)

ian stages is similar to that of studies on *Lutjanus vittus*, which found the accuracy of macroscopic staging for ripe gonads to be only 61% (CSIRO data, cited in West, 1990).

Macroscopic staging of tautog ovaries functioned to describe the annual gonad cycle, yet it did not separate the fully developed (stage-3) and partially spent (stage-3a) ovaries. Macroscopic analysis does not yield proof of POFs, atretic oocytes, and macrophage aggregates—cellular structures that help distinguish fully developed, partially spent/redeveloping, spent, and resting females. Thus, macroscopic analysis could not provide evidence of multiple spawning in tautog. Histological techniques used in this study were necessary to accurately describe the annual cycle and the inner (multiple spawning) spawning cycle of ovarian development for tautog. Histological staging also permitted identification of fully hydrated ovaries that could then be used for batch fecundity estimation. Further, histology slides were used for point-counting analyses to test for positional differences in development between anterior, middle, and posterior regions within the ovary.

Sex ratios

Sex ratios vary greatly among published studies on tautog life history. This variability may be due to true differences in the composition of local populations, or it may be an artifact of sampling strategies rooted in collection seasons or gear biases. In our study, sex ratios were skewed towards females for fish under 400 mm and did not differ significantly from a 1:1 ratio for tautog greater than 400 mm. Collections were primarily made by hook-and-line angling throughout the year, although sample sizes were low between July and September. Hostetter and Munroe (1993) found no significant difference in sex ratios for fish less than 200 mm, but significantly more males than females for fish between 201–500 mm in Virginia. Their sampling occurred over a period of seven years, and fish were collected primarily with fish traps and hook and line. Eklund and Targett (1990) found a female-to-male sex ratio of 0.86:1 in the trap fishery between April and December 1987. Chenoweth (1963) collected more females than males with an otter trawl at three stations in Narragansett Bay, RI, between May and September 1961. Factors that affect sex ratios of tautog from fishery-dependent collections are still unknown and provide an opportunity for further research into the sex ratios and reproductive success of this species.

Length and age at maturity

Published reports of tautog length and age at maturity (from studies with macroscopic techniques and GSI) are similar for the entire species range. Estimates of tautog lengths and ages at maturity in our study were similar to results reported by Hostetter and Munroe (1993) for tautog captured off Virginia. Hostetter and Munroe (1993) reported that both sexes show evidence of gonadal maturation at age 3 in Virginia. Likewise, age and length at maturity for tautog collected in Massachusetts (Stolgitis, 1970) are also similar; 40% of age-2 (149–175 mm) males and 87% of age-3 (171–239 mm) males were mature, and females attained 71% maturity at age 3 (187–206 mm) and 100% maturity at age 4. In Rhode Island, Cooper (1966)

found that males matured at 200 mm (age 3) and females at 190 mm (age 3).

For a small number of fish sampled in northern areas, Hostetter and Munroe (1993) suggested that precocious development may be occurring in tautog as a response to fishing pressure. The smallest females collected in spawning condition have been 227 mm in Virginia (this study), 261 mm in Massachusetts (Stolgitis, 1970), 216 mm (Chenoweth, 1963) and 180 mm (Hostetter and Munroe, 1993), in Rhode Island. A definitive answer on precocious development is not possible at this time because data on small fish are limited in all studies. Detailed histological analysis should be performed on tautog from 100 to 250 mm TL to discern maturity schedules for specimens in this size range.

Spawning season and location

Tautog spawn over at least a two-month period throughout the species range, and the initiation of spawning activity occurs later in the spring to early summer in more northern regions (Chenoweth, 1963; Stolgitis, 1970; Briggs, 1977; Hostetter and Munroe, 1993). In our study, spawning occurred from 7 April through 15 June 1995 (70 days), similar to the time interval reported by Hostetter and Munroe (1993) for tautog in Virginia. In New York waters, tautog have been recorded to spawn for four months (early May through early September; Austin, 1973). In Rhode Island, tautog spawn from early June through late July (Chenoweth, 1963), and spawning seasons as long as three months (mid-May through early August) have been reported for fish in Massachusetts (Stolgitis, 1970). Abundance of tautog eggs in plankton collections also shows that the spawning season occurs progressively later in more northern regions (Sogard et al., 1992). The earlier spawning season in Virginia has been attributed to differences in water temperature (Hostetter and Munroe, 1993). Increasing water temperature during springtime is a major cue to initiate spawning, but termination of spawning activity has not been related to environmental cues. However, Austin (1973) suggested that the effective spawning season may be shorter than the season of egg release for this species, based on a decrease in larval abundance as water temperature exceeded 21.0°C in Long Island Sound.

Tautog were collected in spawning condition within the Chesapeake Bay and as far as 56 km offshore in this study and by Hostetter and Munroe (1993). Eklund and Targett (1990) sampled tautog in spawning condition 22–37 km off the coast of Maryland and Virginia. Field observations of daily movements showed that tautog exhibit fidelity to a home site which they return to each night (Olla et al., 1974, 1975), suggesting that tautog remain at one location throughout the spawning season. Arendt et al. (2001b) found that tautog tended to move between sites during the winter and early spring as the spawning season began and remained at a single site throughout the summer. Tagging studies indicate that discrete spawning groups exist at sites in Narragansett Bay (Cooper, 1966); however, movements between sites were not quantified. Sufficient data are not available to determine if tautog exhibit spawning-site fidelity throughout the spawning season, or if multiple spawning sites are used within general inshore and offshore classifications. It is generally believed that most tautog migrate inshore in the spring to spawn (Cooper, 1966) and some portion of the population remains offshore year round (Eklund and Targett, 1990; Hostetter and Munroe, 1993). Although we have documented adult spawning activity at both inshore and offshore locations, spawning success in these areas, as well as larval drift and recruitment patterns, are unknown at this time.

Spawning pattern and type of fecundity

Histological analysis of ovarian tissue supports the classification of tautog as a multiple spawning species with a complex reproductive cycle. The complexity of ovarian maturation (Fig. 6) in this species has not been recognized in previous studies on its reproductive biology. The typical cycle of female development for multiple spawning species is defined by eight microscopic gonad stages (Lowerre-Barbieri et al., 1996) which include an annual cycle (5 stages) and an inner spawning cycle (3 stages). Although tautog have been observed to be multiple spawners in laboratory aquaria (Olla and Samet, 1977; Olla et al., 1977), we define oocyte development and type of fecundity using recently improved methods (Lowerre-Barbieri and Barbieri, 1993) and histological techniques on fish taken from natural environments; therefore, they are directly comparable to other studies of reproductive biology without artifacts associated with aquarium conditions. Analysis of oocyte size-frequency distributions and histological sections of ovarian tissue indicates that tautog have asynchronous oocyte development and indeterminate annual fecundity. Therefore, counting the number of oocytes in the ovary prior to the spawning season is inadequate to measure potential annual fecundity because new batches of eggs continuously mature from primary growth oocytes through hydrated oocytes and are released during spawning events (Hunter et al., 1985). Chenoweth (1963) analyzed oocyte size-frequency distributions of three tautog collected over the course of the spawning season in Rhode Island and noted that the number of mature yolked oocytes did not decline through the spawning season. He suggested that not all yolked oocytes were spawned and that some portion remained in the ovary and were resorbed after the spawning season. This observation is consistent with asynchronous oocyte development.

Fecundity

This is the first study on tautog reproduction for which potential annual fecundity has been estimated by multiplying batch fecundity by spawning frequency. Batch fecundity was more closely related to total length and total weight than to age. This result makes sense when one considers the extreme variability in length at age exhibited by tautog (Cooper, 1967; Hostetter and Munroe, 1993). Batch fecundity ranged from 2800 eggs to 181,200 eggs in 29 females age 3–9 (Fig. 7). The oldest tautogs collected in this study were a 31-year-old male and a 17-year-old female. After reaching maturity, individual females may spawn up to 58 times a year for at least 14 years.

Table 6

Comparison of batch fecundity estimates for tautog from three different studies. Mean batch fecundity was calculated for two age groups, 4–6 and 7–9, because all females were mature by age 4 and over 90% of all tautog sampled in White (1996) were less than 10 years old.

	Mean batch fecundity ±SEM			
Study	Age 4–6	*n*	Age 7–9	*n*
Chenoweth (1963)[1] Rhode Island	49,967 ±1032	29	103,214 ±4005	14
Stolgitis (1970)[1] Massachusetts	46,833 ±4500	6	117,478 ±2488	23
White (1996)[1] Virginia	54,243 ±2472	18	106,256 ±3837	10

[1] Mean batch fecundity for age groups 4–6 and 7–9 was calculated from the raw data presented in the reference.

Previous estimates of tautog fecundity by Chenoweth (1963) and Stolgitis (1970) were not annual fecundity estimates (Table 6). They counted mature, transparent eggs in the ovary, currently referred to as hydrated oocytes, but they did not distinguish tautog as having indeterminate annual fecundity and had no measure of spawning frequency. By counting only the hydrated oocytes, these investigators actually estimated batch fecundity. However, it is interesting to note the similarity of batch fecundity estimates (Table 6) over the period of 30 years between studies and wide geographic areas, i.e. from Chesapeake Bay to Narragansett Bay (550 km).

Spawning frequency had not been previously calculated for tautog with methods developed by Hunter and Macewicz (1985). Although the hydrated oocyte method is less expensive, it requires collection of females just prior to spawning. With the hook-and-line collection method, it is difficult to collect sufficient samples in a short period of time. Therefore spawning frequency was estimated in our study by using the POF method to read histologic preparations of ovarian tissue. A female spawning every 1.2 days over the 70-day spawning window would spawn on an estimated 58 days in 1995. Under artificial conditions, Olla et al. (1977) observed tautog spawning on 68–96 consecutive days in laboratory aquaria. Therefore, an estimate of 58 spawning days in natural habitats is not unrealistic. Chenoweth (1963) raised, but could not answer, the question of whether individual tautog spawn throughout the entire spawning season. The spawning-frequency estimate presented here, and observations of tautog spawning on 68–96 consecutive days in laboratory aquaria (Olla et al., 1977), indicate that tautog are capable of spawning daily throughout the spawning season in natural habitats under appropriate environmental conditions (temperature, day length, etc.).

Estimates of potential annual fecundity for Virginia tautog age 3–9 ranged from 160,000 to 10,510,000 eggs. However, net annual fecundity may be lower because of remnant hydrated oocytes, atresia, nutritional status of adult females, or environmental conditions (McEvoy and McEvoy, 1992). Based on our samples (females age 3–9), a linear regression provided the most predictive power (r^2=0.81) to estimate mean annual fecundity (Fig. 8). Although female tautog live to be 17+ years old, it is estimated that 90% of tautog in Virginia waters are age 10 or younger (Hostetter and Munroe, 1993). Therefore, as the data range in this study is similar to the age structure of the resource, we suggest that the regression equation ($Mean\ AF$=23,480(TL) – (5×10^6)) is the most appropriate formula for use by fishery managers for estimating annual fecundity of tautog in the southern portion of its range.

We have made a theoretical comparison of potential annual fecundity for tautog (ages 4–9) between the northern and southern areas by combining results from several studies in the northern range of tautog. Although commonly cited as representing annual fecundity estimates, the methods of Chenoweth (1963) and Stolgitis (1970) clearly show that their results are batch fecundity estimates. For our comparison, we selected the lowest value for age-4 and the highest for age-9 tautog as the sampled range of batch fecundity estimates. We averaged northern data from Chenoweth (1963: age 4, 265 mm TL, 6000 BF and age 9, 401 mm TL, 224,000 BF) and Stolgitis (1970: age 4, 261 mm TL, 7000 BF and age 9, 486 mm TL, 260,000 BF) to create a batch fecundity range of 6500–242,000 eggs. This range was multiplied by the 68-day "spawning season" observed in laboratory aquaria by Olla et al. (1977) to calculate a range for potential annual fecundity of 442,000 to 16,456,000 eggs per female in northern areas. Our samples from the southern range (age 4: 275 mm TL, 5000 BF and age 9: 511 mm TL, 181,200 BF) multiplied by 58 spawning events in 1995 results in potential annual fecundity of 290,000 to 10,510,000 eggs per female. Differences in these estimates of potential annual fecundity are primarily due to the number of spawnings per year and are questionable because the spawning frequency estimate based on aquarium studies may not apply for naturally spawning fish. This comparison indicates that we still lack adequate information on the spawning frequency and annual fecundity for fish from the northern part of the species range.

Although batch fecundity estimates appear similar between southern and northern portions of the tautog's range, previous batch fecundity estimates from northern populations are 30 years old. Reported spawning seasons between areas also vary in length from two to four months, which could greatly affect potential annual fecundity estimates with this method. Estimates of annual fecundity in

the northern regions of the species range should be pursued to determine if tautog annual fecundity varies with latitude. Evidence of different growth rates (Cooper, 1965, 1966, 1967; Stolgitis, 1970; Hostetter and Munroe,1993; White, 1996), seasonality of occurrence in coastal waters, and winter activity cycles between tautog in southern versus northern regions (Olla et al., 1974; Hostetter and Munroe, 1993; Arendt et al., 2001a, 2001b) strongly point to considering latitudinal effects when analyzing and comparing any biological features of this species. Even if batch fecundity and spawning frequency remain relatively constant over latitude, size structure of the stock will dictate estimates of total egg production: thus continued research is necessary to monitor size structure and abundance of tautog resources throughout the species range. Additional data on larger, older females is necessary to evaluate the relative contribution of older females to population fecundity and egg production. Because many aspects of tautog life history affect recruitment, further investigation is required on egg dispersal, egg mortality, larval drift, larval mortality, hatching success, first feeding success, pre- and postsettlement mortality, juvenile mortality, recruitment, stock structure, and spawning stock biomass (ASMFC[4]).

Historically, tautog have supported a predominantly (90%) recreational fishery throughout their range (ASMFC[4]). Over the past 15 years, this popular food and sport fish has increased substantially in value as a commercially targeted species. As popularity and fishing effort increased, landings peaked in 1993 but have declined more recently, prompting the Atlantic States Marine Fisheries Commission (ASMFC[4]) to pass a coastwide management plan for tautog in April 1996.

Tautog annual fecundity is a key piece of data necessary for egg production models and estimates of spawning stock biomass, and there are no reliable estimates of tautog spawning stock biomass to date (ASMFC[4]). In April 1998, the ASMFC imposed a 14-inch (350-mm) minimum size limit, effective for tautog caught from Massachusetts to Virginia. The benefits of instituting a size limit for tautog are well supported by data from this study. A minimum size limit allows tautog in the southern regions of the species' distribution to have at least one spawning season, and most likely two, thereby affording the opportunity for each female to contribute on average 3.22 million eggs (calculated from the linear regression equation, Fig. 8) towards the annual population fecundity.

Acknowledgments

The authors gratefully acknowledge suggestions and criticisms of three anonymous reviewers that greatly improved the manuscript. We thank all of those who made this research possible. This study represents part of a M.S. thesis (by G. G. White) School of Marine Science, Virginia Institute of Marine Science (VIMS), College of William and Mary. VIMS volunteers who assisted with our sampling efforts included D. Estes, R. Holmquist, D. Seaver, and M. Wagner, members of the Juvenile Finfish Trawl Survey, and T. Holden, who collected specimens. We appreciate the interest and cooperation of recreational and commercial fishermen, especially "Old Joe," Clark and Chester Stultz, who provided fish, For help processing samples, we thank J. Brust, W. Coles, C. Cooksey, S. Gaichas, J. Harding, and M. Wagner (taug circles). We thank C. Bonzek and R. Harris for computing assistance, D. Evans, R. Diaz, and L. Garrison for statistical help, and J. Harding for critical editorial reviews of an earlier draft of the manuscript. We also thank P. Blake for training in histology procedures, and W. Vogelbein for aid with interpretation of histology sections. Finally G. White thanks his parents, who had the foresight to get him "hooked on" life in, on, or under water while very young. This project was funded by grant numbers RF-94-5 and RF-95-3 from the Virginia Marine Resources Commission, Recreational Saltwater License Fees.

Literature cited

Adams, A. J.
1993. Dynamics of fish assemblages associated with an offshore artificial reef in the Southern Mid-Atlantic Bight. Unpubl. M.S. thesis, 97 p. College of William and Mary, Williamsburg, VA.

Arendt, M. D., J. A. Lucy, and D. A. Evans.
2001a. Diel and seasonal activity patterns of adult tautog, *Tautoga onitis*, in lower Chesapeake Bay, inferred from ultrasonic telemetry. Environ. Biol. Fishes 62: 379–391.

Arendt, M. D., J. A. Lucy, and T. A. Munroe.
2001b. Seasonal occurrence and site utilization patterns of adult tautog, *Tautoga onitis*, (Labridae), at manmade and natural structures in lower Chesapeake Bay. Fish. Bull. 99:519–527.

Austin, H. M.
1973. Distribution and abundance of ichthyoplankton in the New York Bight during the fall in 1971. N.Y. Fish Game J. 23:58–72.

Bigelow, H. B., and W. C. Schroeder.
1953. Fishes of the Gulf of Maine. U.S. Fish Wildl. Serv., Fish. Bull. 53:1–577.

Bleakney, J. S.
1963. Notes on the distribution and reproduction of the fish *Toutogo onitis* in Nova Scotia. Can. Field-Nat. 77:64–65.

Briggs, P. T.
1977. Status of tautog populations at artificial reefs in New York waters and effect of fishing. N.Y. Fish Game J. 24: 154–167.

Chenoweth, S. B.
1963. Spawning and fecundity of tautog, *Tautoga onitis* (L.). Unpubl. M.S. thesis, 60 p. Univ. Rhode Island, N. Kingston, RI.

Cooper, R. A.
1965. Life history of the tautog, *Toutoga onitis* (Linnaeus), from Rhode Island. Unpubl. Ph.D. diss., 153 p. Univ. Rhode Island, N. Kingston, RI.
1966. Migration and population estimation of the tautog, *Tautoga onitis* (Linneaus), from Rhode Island. Trans. Am. Fish. Soc. 95:239–247.

[4] ASMFC (Atlantic States Marine Fisheries Commission). 1996. Fishery management plan for tautog. Fish. Manage. Rep. 25, 56 p. Atlantic States Marine Fisheries Commission, 1444 Eye Street, NW, 6th Floor, Washington, DC 20005.

1967. Age and growth of the tautog, *Tautoga onitis* (Linnaeus), from Rhode Island. Trans. Am. Fish. Soc. 96:134–142.

DeMartini, E. E., and R. K. Fountain.
1981. Ovarian cycling frequency and batch fecundity in the queenfish, *Seriphus politus*: attributes representative of serial spawning fishes. Fish. Bull. 79:547–60.

Eklund, A. M., and T. E. Targett.
1990. Reproductive seasonality of fishes inhabiting hard bottom areas in the Middle Atlantic Bight. Copeia 1990: 1180–1184.

Hildebrand, S. F., and W. C. Schroeder.
1928. Fishes of the Chesapeake Bay. Bull. U.S. Bur. Fish. 43 (part 1):1–366.

Hostetter, E. B., and T. A. Munroe.
1993. Age, growth, and reproduction of tautog *Tautoga onitis* (Labridae: Perciformes) from coastal waters of Virginia. Fish. Bull. 91:45–64.

Hunter, J. R., and S. R. Goldberg.
1980. Spawning incidence and batch fecundity in northern anchovy, *Engraulis mordax*. Fish. Bull. 77:641–652.

Hunter, J. R., and B. J. Macewicz.
1985. Measurement of spawning frequency in multiple spawning fishes. *In* An egg production method for estimating spawning biomass of pelagic fish: application to the northern anchovy, *Engraulis mordax* (R. Lasker, ed.), p. 79–94. U.S. Dep. Commer., NOAA Tech. Rep. NMFS 36.

Hunter, J. R., N. C. H. Lo, and R. J. H. Leong.
1985. Batch fecundity in multiple spawning fishes. *In* An egg production method for estimating spawning biomass of pelagic fish: application to the northern anchovy, *Engraulis mordax* (R. Lasker, ed.), p. 67–77. Dep. Commer., NOAA Tech. Rep. NMFS 36.

Hunter, J. R., B. J. Macewicz, N. C. H. Lo, and C. A. Kimbrell.
1992. Fecundity, spawning, and maturity of female Dover sole *Microstomus pacificus*, with an evaluation of assumptions and precision. Fish. Bull. 90:101–128.

Lowerre-Barbieri, S. K., and L. R. Barbieri.
1993. A new method of oocyte separation and preservation for fish reproduction studies. Fish. Bull. 91: 165–170.

Lowerre-Barbieri, S. K., M. E. Chittenden Jr., and L. R. Barbieri.
1996. The multiple spawning pattern of weakfish in the Chesapeake Bay and Middle Atlantic Bight. J. Fish Biol. 48:1139–1163.

Luna, L. G. (ed.)
1968. Manual of histologic staining methods of the Armed Forces Institute of Pathology. American Registry of Pathology, 3rd ed., 258 p. McGraw-Hill Book Co., New York, NY.

McEvoy, L. A., and J. McEvoy.
1992. Multiple spawning in several commercial fish species and its consequences for fisheries management, cultivation and experimentation. J. Fish Biol. 41(suppl. B):125–136.

Minitab.
1995. Minitab reference manual, release v10Xtra, 542 p. Minitab Inc., State College, PA.

Musick, J. A.
1972. Fishes of Chesapeake Bay and the adjacent coastal plain. *In* A checklist of the biota of the lower Chesapeake Bay (M. L. Wass, ed.), p. 175–212. Virg. Inst. Mar. Sci. Spec. Sci. Rep. 65.

Olla, B. L., A. J. Bejda, and A. D. Martin.
1974. Daily activity, movements, feeding, and seasonal occurrence in the tautog, *Tautoga onitis*. Fish. Bull. 72:27–35.
1975. Activity, movements, and feeding behavior of the cunner, *Tautogolabrus adspersus*, and comparison of food habits with young tautog, *Tautoga onitis*, off Long Island, New York. Fish. Bull. 73:895–900.
1979. Seasonal dispersal and habitat selection of cunner, *Tautogolabrus adspersus*, and young tautog, *Tautoga onitis*, in Fire Island Inlet, Long Island, New York. Fish. Bull. 77:255–261.

Olla, B. L., A. J. Bejda, and A. L. Studholme.
1977. Social behavior as related to environmental factors in the tautog, *Tautoga onitis*. *In* The behavior of marine organisms: social behavior and communication; navigation; and development of behavior, p. 47–99. Proc. Annu. Northeast Reg. Meet. Animal Behav. Soc. Plenary Papers. Mar. Sci. Res. Lab. Tech. Rep. 20, Memorial Univ., St. John's, Nfld.

Olla, B. L., and C. Samet.
1977. Courtship and spawning behavior of the tautog, *Tautoga onitis* (Pisces: Labridae), under laboratory conditions. Fish. Bull. 75:585–599.

Olla, B. L., A. L. Studholme, A. J. Bejda, and C. Samet.
1980. Role of temperature in triggering migratory behavior of the adult tautog *Tautoga onitis* under laboratory conditions. Mar. Biol. (Berl.) 59:23–30.

Parrish, R. H., D. L. Mallicoate, and R. A. Klingbeil.
1986. Age dependent fecundity, number of spawnings per year, sex ratio, and maturation stages in northern anchovy, *Engraulis mordax*. Fish. Bull. 84:503–517.

Richards, C. E., and M. Castagna.
1970. Marine fishes of Virginia's Eastern Shore (inlet, marsh, and seaside waters). Chesapeake Sci. 11:235–248.

Scott, W. B., and M. G. Scott.
1988. Atlantic fishes of Canada. Can. Bull. Fish. Aquat. Sci. 219:1–731.

Sedberry, G. R., and H. R. Beatty.
1989. A visual census of fishes on a jetty at Murrells Inlet, South Carolina. J. Elisha Mitchell Sci. Soc. 105:59–74.

Simpson, D. G.
1989. Population dynamics of the tautog, *Tautoga onitis*, in Long Island Sound. Unpubl. M.S. thesis, 65 p. Southern Connecticut State Univ., New Haven, CT.

Sogard, S. M., K. W. Able, and M. P. Fahay.
1992. Early life history of the tautog *Tautoga onitis* in the Mid-Atlantic Bight. Fish. Bull. 90:529–539.

Stolgitis, J. A.
1970. Some aspects of the biology of the tautog, *Tautoga onitis* (Linnaeus), from the Weweantic River Estuary, Massachusetts, 1966. Unpubl. M.S. thesis, 48 p. Univ. Mass., Amherst, MA.

Wallace, R. A., and K. Selman.
1981. Cellular and dynamic aspects of oocyte growth in teleosts. Am. Zool. 21:325–343.

Warner, R. R., and D. R. Robertson.
1978. Sexual patterns in the labroid fishes of the Western Caribbean, I: the wrasses (Labridae). Smithson. Contrib. Zool. 254:1–27.

Weibel, E. R., G. S. Kistler, and W. F. Scherle.
1966. Practical stereological methods for morphometric cytology. J. Cell Biol. 30:23–28.

West, G.
1990. Methods of assessing ovarian development in fishes: a review. Aust. J. Mar. Freshwater Res. 41: 199–222.

White, G. G.
1996. Reproductive biology of tautog, *Tautoga onitis*, in the lower Chesapeake Bay and coastal waters of Virginia. Unpubl. M.S. thesis, 100 p. College of William and Mary, Williamsburg, VA.

Wolke, R. E.
1992. Piscine macrophage aggregates: a review. Ann. Rev. Fish Dis. 1992:91–108.

Investigation of congeneric hybridization in and stock structure of weakfish (*Cynoscion regalis*) inferred from analyses of nuclear and mitochondrial DNA loci*

Jan F. Cordes
John E. Graves

School of Marine Science
Virginia Institute of Marine Science
College of William and Mary
Gloucester Point, Virginia 23062
Present address (for J. F. Cordes): Department of Animal Science
University of California
Davis, California 95616
E-mail address (for J. F. Cordes): jfcordes@ucdavis.edu

The weakfish (*Cynoscion regalis*) is distributed along the east coast of the United States from Massachusetts to eastern Florida and is most abundant from New York to North Carolina (Bigelow and Schroeder, 1953). Historically there has been some question as to the taxonomic relationship between weakfish and sand seatrout (*Cynoscion arenarius*); some suggest they may be separate populations of a single species (Moshin, 1973; Weinstein and Yerger, 1976; Cowan, 1985; Ditty, 1989), and others treat them as separate species (Schlossman and Chittenden, 1981).

Weakfish support substantial commercial and recreational fisheries throughout their range. Precipitous drops in total annual catches between 1980 and 1994 led to a temporary ban on commercial fishing in federal waters in 1995 (Anonymous, 1995), and there is concern that bycatch of juvenile weakfish by shrimp trawlers at the southern end of the species' range is adversely impacting abundance (Vaughan et al.[1]).

As water temperatures warm in the spring, weakfish move north and inshore into estuaries to spawn. When inshore temperatures cool in the fall, juveniles move south to overwinter off the coast of North Carolina, and older fish are thought to migrate south and offshore (Wilk[2]). Traditional studies based on tag and recapture data (Nesbit, 1954), scale structure (Perlmutter et al., 1956), morphometric data (Scoles, 1990), and various life history characters (Shepherd and Grimes, 1983, 1984) suggest two or more independent stocks of weakfish. These characters may be influenced by environmental differences, however (Shepherd and Grimes, 1983), and may not reflect genetically distinct (reproductively isolated) stocks. Genetic analyses of weakfish stock structure in the mid Atlantic Bight employing allozyme analysis (Crawford et al., 1989) and restriction fragment length polymorphism (RFLP) analysis of whole molecule mitochondrial (mt) DNA (Graves et al., 1992) were unable to reject the null hypothesis that weakfish along the U.S. east coast comprise a single, genetically homogeneous stock. However, the power of both the analyses was limited by low overall genetic variation.

Recent analyses of new molecular markers, including microsatellite DNA loci and nuclear gene intron regions, have revealed elevated levels of genetic variation in relation to traditional methods, such as allozymes or RFLP analysis of mtDNA (Miller and Kapuscinski, 1996; Brunner et al., 1998). Although higher levels of genetic variation do not necessarily provide greater stock resolution (Seeb et al., 1998), microsatellite loci have revealed stock structure for some species, where more traditional molecular markers have not (Bentzen et al., 1996; Ruzzante et al., 1996; Patton et al., 1997). Similarly, analyses of variable gene intron regions have revealed stock structure within several marine fishes (Palumbi and Baker, 1994; Moran et al., 1997; Leclerc et al., 1996; Chow and Takeyama, 2000). In this study we employed analyses of nuclear and mtDNA markers to evaluate stock structure in weakfish along the east coast of the United States and to investigate possible hybridization between weakfish and other *Cynoscion* species.

Materials and methods

Sample collections were restricted to young-of-the-year (YOY) fish (less than 140 mm SL) that are reported to remain in their natal estuaries during the first several months of growth (Rowe and Epifanio, 1994). YOY were collected in the summers of 1996 and 1997 from five sites along the east coast of the United States (Fig. 1), maintained on ice after capture, transported to the laboratory, and frozen at –80°C. Muscle tissue was excised from each sample and either stored at –80°C or placed in DMSO buffer (25 mM EDTA, 20% DMSO, saturated NaCl) and stored at room temperature. Genomic DNA was isolated by following the protocol of Sambrook et al. (1989), as modified in Cordes (2000).

Specific identification of individuals was determined by using a molecular key for 16 species of Chesapeake Bay

* Contribution 2532 of the Virginia Institute of Marine Science, College of William and Mary, Gloucester Point, VA 23062.

[1] Vaughan, D. S., R. J. Seagraves, and K. West. 1991. An assessment of the Atlantic weakfish stock, 1982–1988. Atl. States Mar. Fish. Comm. Spec. Rep. 21. 29 p. + tables. Atlantic States Marine Fisheries Commission, 1444 Eye St., NW 6th Floor, Washington, D.C. 20005.

[2] Wilk, S. J. 1976. The weakfish—a wide ranging species. Atl. States Mar. Fish. Comm, Mar. Resourc. Atl. Coast Fish. Leaflet 18, 4 p. Atlantic States Marine Fisheries Commission, 1444 Eye St., NW 6th Floor, Washington, D.C. 20005.

Manuscript accepted 21 October 2002.
Manuscript received 9 January 2003 at NMFS Scientific Publications Office.
Fish. Bull. 101:443–450 (2003).

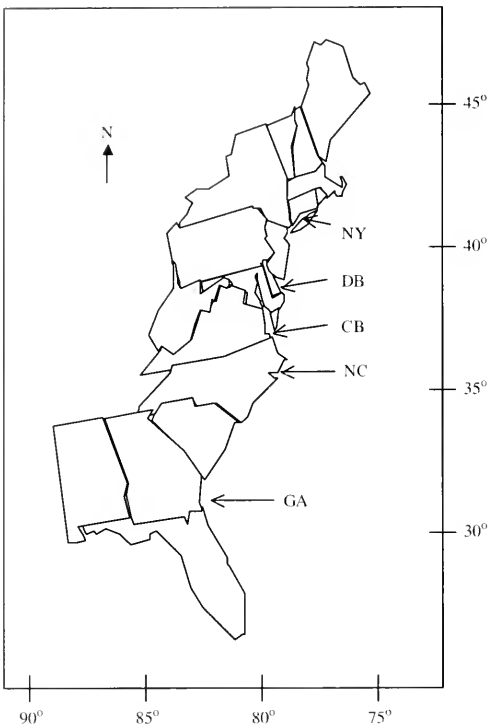

Figure 1

Sampling locations for young-of-the-year (YOY) weakfish (*Cynoscion regalis*) in the summers of 1996 and 1997. Sites are Peconic Bay, New York (NY); Delaware Bay, Delaware (DB); Chesapeake Bay, Virginia (CB); Pamlico Sound, North Carolina (NC); and Doboy Sound, Georgia (GA).

sportfishes (including eight species of sciaenids) based on a 12S/16S mtDNA gene region digested with *Rsa* I (Cordes et al., 2001). Additional 12S/16S mtDNA/*Rsa* I patterns were generated for silver seatrout (*Cynsoscion nothus*) and sand seatrout (*C. arenarius*) from the Gulf of Mexico, as well as for banded drum (*Larimus fasciatus*), gulf kingfish (*Menticirrhus littoralis*), and star drum (*Stellifer lanceolatus*) from the South Atlantic Bight following procedures in Cordes et al. (2001).

The following microsatellite primers (Table 1) developed for red drum (*Sciaenops ocellatus*) and spotted seatrout (*Cynoscion nebulosus*) loci were used to amplify weakfish DNA: SOC050 and SOC044 (Turner et al., 1998), SOC014 (Chapman[3]), and CNE612 (Chapman et al., 1999). Amplifications of all microsatellite loci were carried out in 10 µL reactions containing 8.30 µL sterile dH_2O, 1.0 µL 10× PCR buffer with 15 mM $MgCl_2$, 0.20 µL 10 mM dNTP mixture, 0.05 µL forward primer (100 pm/µL) labeled with a fluorescent dye (Licor), 0.20 µL reverse primer (100 pm/µL), 0.05 µL *Taq* I polymerase (5 U/µL), and 0.20 µL weakfish DNA. Samples were first denatured for 4 min at 95°C, followed by 32 cycles of PCR amplification performed under the following conditions: 1 min. at 94°C, 1 min. at 50°C, and 1 min. at 72°C. Reactions were given a final 7 min. extension at 72°C. PCR product alleles were separated electrophoretically on a 6% Long Ranger™ polyacrylamide gel with a model 4000 automated DNA infrared sequencer from Li-Cor (Lincoln, NE).

Universal actin gene primers developed by G. Warr and M. Wilson (cited in Reece et al., 1997) were used to identify and refine an approximately 800-bp actin intron region locus (CRESIA1) in weakfish (Cordes, 2000). Weakfish PCR amplification products obtained with S7 ribosomal protein intron 2 (RP2) primers originally developed from swordfish *Xiphius gladius* (Chow and Hazama, 1998) were cloned and sequenced as described in Cordes (2000) and checked against sequences published in Genbank to confirm their identity. The original RP2 primers were then used without modification for amplification of all samples. Both the CRESIA1 and RP2 amplifications were carried out under the same conditions outlined above for the microsatellite loci, with the exception that the annealing temperature was lowered to 45°C. CRESIA1 and RP2 amplification products from a subset of each weakfish collection were screened for polymorphisms with a panel of restriction endonucleases and the resulting digestions were separated on 2.5% agarose gels with 1% NuSieve and 1.5% agarose in 1×TBE buffer (Cordes, 2000). Gels were stained in 1×TBE buffer containing 30 µL (5 mg/mL) ethidium bromide (EtBr), visualized on a Spectroline model TR-302 transilluminator, and photographed with a Polaroid CU-5 land camera. *Dra* I was the only enzyme that revealed polymorphic restriction sites within CRESIA1, and only *Hinf* I revealed reliably scored polymorphisms in RP2. All YOY weakfish samples were subsequently screened for variation at CRESIA1/*Dra* I and RP2/*Hinf* I.

Microsatellite gel images and restriction enzyme digestion patterns for CRESIA1 and RP2 were analyzed by using the software program RFLPScan Plus 3.0 (CSPI-Scanalytics, 1996). Statistical analyses for all loci were performed with the Arlequin 1.1 software program of Schneider et al. (1997). Nonparametric, exact-significance tests (exact θ significance tests and exact probability tests) were used to evaluate sample genotype distributions for departures from Hardy-Weinberg expectations. Unbiased estimators of exact significance probabilities for the Hardy-Weinberg equilibrium tests were calculated by using the Markov chain algorithm of Guo and Thompson (1992) with a Markov chain length of 100,000 steps. Patterns of genetic diversity and divergence within and between populations were evaluated by using the analysis of molecular variance (AMOVA) of Excoffier et al. (1992), which generates F-statistics analogous to the θ values of Weir and Cockerham (1984). Significance of F-statistics was evaluated with exact F permutation procedures (Excoffier et al.,

[3] Chapman, R. W. 1998. Unpubl. data. Marine Resources Research Institute, Department of Natural Resources, Charleston, SC 29422.

1992). Type-I error was controlled for all multiple testing with the sequential Bonferroni method of Rice (1989).

Results and discussion

Inclusion of nontarget species in weakfish samples

Initial analysis of the SOC050 microsatellite data revealed a significant departure of genotypic frequencies from expectations of Hardy-Weinberg equilibrium for the Georgia 1997 sample, even after correction for multiple tests (α=0.005). Similarly, initial SOC050 AMOVA results indicated a significant within-population variance (P=0.031), and exact F permutation tests of population pairwise F_{ST} values resulted in a number of near-significant corrected P values, all involving the Georgia 1997 sample. Inspection of the Georgia 1997 SOC050 alleles revealed a bimodal size distribution due to the presence of several unusually small alleles less than 187 bp in size. It was suspected that alleles in the smaller mode might be the result of misidentified individuals, hybridization, or introgression.

Analysis of putative weakfish with small SOC050 alleles with the 12S/16S marker of Cordes et al. (2001) resulted in three distinct restriction digestion patterns. One pattern matched that reported for weakfish, and the other two did not match any of the 16 species surveyed by Cordes et al. (2001). To determine the identity of the unknown patterns, voucher samples of five additional sciaenid species (listed in the "Materials and methods" section above) were analyzed with the 12S/16S mitochondrial marker. The two unknown patterns matched those of silver seatrout (*Cynoscion nothus*) and sand seatrout (*C. arenarius*) (Table 2). The SOC050 locus was subsequently amplified for all silver seatrout (n=13) and sand seatrout (n=15) samples, produ-

Table 1

Primer sequences for amplifying microsatellite, actin gene intron, and ribosomal protein 2 gene intron loci in weakfish (*Cynoscion regalis*).

Locus	Primer sequence (5'–3')	Length (bp)	Repeat motif in weakfish	Annealing temperature	Original reference
Microsatellites					
CRE66	CRE66F: TGGTCTGTTAGTCCACAGTGTTG CRE66R: CGTTGCCTTCATTACAGGAGAC	251	$[GATA]_{25}$	40°C	This study
CRE80	CRE80F: ACAGCATGTGAGGGTTAAGGAT CRE80R: TACAGCTCTCTGACTGATGTAGTTGA	136	$[GATA]_9$	40°C	This study
SOC050	SOC050F: CCCGTGATTTTAGGCTCATCAGATA SOC050R: CCTTTAGACGTGCAGTAAGTGATTT	193	$[GT]_4n_9[GT]_{10}$ $n_7[GT]_9$	50°C	(Turner et al., 1998)
SOC044	SOC044F: GAGGGTGACGCTAACAGTTGA SOC044R: CACAGCTCCACTCTGATATG	202	$[CA]_3n_{39}[GT]_3$ $n_5[GT]_2n_2[GT]_2$	50°C	(Turner et al., 1998)
SOC014	SOC014F: GTATGTATTAAGGGCACAAGGTG SOC014R: GATTGCTGCTGGACAGACTG	114	$[CA]_{15}$	50°C	(Chapman[1])
CNE612	CNE612F: CAAGTGCACGGTATGTGATG CNE612R: AGGAACCTGACCAATCCAAA	131	$[GT]_{15}n_{10}[GT]_{11}$		(Chapman et al., 1999)
Introns					
CRESIA1	CRESIA1F: ATGCCTCTGGTCGTACCACTGG CRESIA1R: CAGGTCCTTACGGATGTCG	545	—		This study
RP2	RP2F: AGCGCCAAAATAGTGAAGCC RP2R: GCCTTCAGGTCAGAGTTCAT	731	—		(Chow and Hazama, 1998)

[1] Chapman, R. W. 1998. Unpubl. data. Marine Resources Research Institute, Department of Natural Resources, Charleston, SC 29422.

Table 2

Restriction digestion patterns of the 12S/16S mitochondrial DNA region for putative weakfish (*Cynoscion regalis*) individuals in the Georgia 1997 sample, sand seatrout (*C. arenarius*) and silver seatrout (*C. nothus*) digested with the enzyme *Rsa* I. *n* = number of individuals exhibiting the adjacent pattern. Apparent total size differences may be gel artifacts due to unresolved bands <100 bp in one or more of the species.

Species	*n*	Restriction	Fragment	Sizes	(bp)	Total size (bp)
Georgia 1997 Sample						
weakfish	3	461	300	200	167	1128
unknown A	7	413	300	200	167	1080
unknown B	5	461	300	256	167	1184
Known standards						
Cynoscion arenarius	15	461	300	256	167	1184
Cynoscion nothus	13	413	300	200	167	1080

cing allele sizes of 175–181 bp for silver seatrout and 175–193 bp for sand seatrout. Amplification of the silver seatrout and sand seatrout samples with the remaining three microsatellite and two intron loci did not provide further evidence of hybridization. SOC044 and CNE612 allele size ranges for both species fell within the range exhibited by the weakfish samples, and the SOC014 and both intron loci did not amplify in either the silver seatrout or sand seatrout samples.

Individuals with unusually small SOC050 alleles from the Georgia 1997 sample fell into one of four general classes. Seven individuals had silver seatrout mtDNA and two small SOC050 alleles and were presumably pure silver seatrout. The inclusion of these individuals in the collection may not be surprising because both weakfish and silver seatrout are common in the South Atlantic Bight (Bigelow and Schroeder, 1953; Hildebrand, 1955) and are difficult to distinguish during their early life history stages. Although the latter species is known to inhabit deeper waters as adults (Ginsburg, 1931), both species are inshore summer spawners (Devries and Chittenden, 1982; Shepherd and Grimes, 1984).

Three individuals possessed sand seatrout mtDNA and two small SOC050 alleles and were presumably pure sand seatrout. Some researchers have suggested that weakfish and sand seatrout represent separate populations of a single species (Moshin, 1973; Weinstein and Yerger, 1976; Cowan, 1985; Ditty, 1989), and others treat them as separate species (Schlossman and Chittenden, 1981) with distributions confined to the western Atlantic (weakfish) and the Gulf of Mexico (sand seatrout). Paschall (1986) was unable to distinguish between the two species using allozyme electrophoresis. In contrast, results presented here are consistent with the existence of two distinct species, with weakfish and sand seatrout co-occurring off the east coast of the United States at least as far north as Doboy Sound, Georgia. This distribution pattern is consistent with the phylogeographic patterns of 19 freshwater, coastal, and marine species distributed along the U.S. East Coast and the Gulf of Mexico that exhibited geographically concordant forks in their intra- or interspecific mtDNA phylogenies (or in both phylogenies) (Avise, 1992). In the present situation, apparently distinct Gulf (sand seatrout) and Atlantic (weakfish) species may have reestablished contact in a hybrid zone (see below) through movement of the Gulf species into the Atlantic.

Three individuals had weakfish mtDNA and a single small SOC050 allele and were presumably hybrids of weakfish and sand seatrout or silver seatrout (with female weakfish parentage). In addition, two individuals possessed sand seatrout mtDNA and a single small SOC050 allele and were presumably hybrids of weakfish and sand seatrout with female sand seatrout parentage. These data suggest that hybridization occurs between weakfish and sand seatrout and that the genetic exchange is not gender restricted. Because of the overlap in microsatellite allele sizes seen between silver seatrout and sand seatrout, hybridization between weakfish and silver seatrout could not be excluded. The lack of suspected hybrids with silver seatrout mtDNA, however, suggests that hybridization did not involve this species. The possibility exists that the putative hybrids are in fact weakfish with rare mtDNA haplotypes common to the three *Cynoscion* species studied here. This seems unlikely because only one 12S/16S mtDNA/*Rsa* I pattern was noted among 40 weakfish in the species identification study of Cordes et al. (2001). Furthermore, analysis of 20 weakfish taken from each of the four locations outside of Georgia with the 12S/16S marker revealed no new mtDNA patterns. Also, the mtDNA haplotypes seen in sand seatrout and silver seatrout seem to vary in size and can not be clearly related to the weakfish haplotype by the addition or deletion of presumed restriction sites. This condition is more in keeping with mtDNA of different species, although the apparent size differences may be gel artifacts due to unresolved bands <100 bp in one or more of the species.

Re-evaluation of the remaining 1996-97 SOC050 data revealed occasional occurrences of small alleles in individual fish in all but the New York samples (Table 3). Examination of the 12S/16S mtDNA region of these individuals identified a single silver perch (*Bairdiella chrysoura*) in the Chesapeake Bay 1997 sample (silver perch mtDNA

Table 3

Frequencies of unusual alleles in four geographical samples of weakfish (*Cynoscion regalis*) taken in 1996 and 1997. The number of individuals with anomalous alleles that were subsequently eliminated from the population structure analysis is given in parentheses after the sample names.

Sample	Allele (bp)	Frequency
Georgia 1996 (4)	175	0.018
	177	0.009
	179	0.009
North Carolina 1996 (1)	177	0.010
Chesapeake Bay 1996 (1)	177	
Delaware Bay 1996 (2)	179	0.011
	181	0.011
Georgia 1997 (15)	171	0.021
	173	0.010
	175	0.125
	177	0.094
	179	0.010
North Carolina 1997 (1)	177	0.009
Chesapeake Bay 1997 (3)	171	0.009
	177	0.009
	179	0.009
Delaware Bay 1997 (5)	177	0.023
	181	0.034

and two alleles 171 bp in size). All other individuals were putative hybrids with weakfish mtDNA and a single small SOC050 allele characteristic of silver and sand seatrout. As mentioned previously, subsequent analysis of 20 weakfish taken from each of the four locations outside of Georgia with the 12S/16S marker revealed only weakfish mtDNA. If the small SOC050 alleles found in the more northern populations are not simply rare weakfish alleles shared in common with the other two *Cynoscion* species, they may indicate that introgressive hybridization is responsible for the migration of the smaller alleles into northern waters (although the northward movement of hybrid fish out of the contact zone cannot be excluded). As a result of these findings, all individuals in the 1996 and 1997 collections exhibiting at least one small SOC050 allele less than 183 bp in length were eliminated from the population structure analyses.

Stock structure analysis

All four microsatellite loci were polymorphic in all sampled locations in both years. Allele frequency distributions for each locus are available from the authors upon request. Sample sizes (n), number of alleles (N), expected heterozygosities (gene diversities), and significance test results for Hardy-Weinberg equilibrium are provided in Table 4. Levels of variation differed greatly among the four microsatellite loci. The number of alleles ranged from two (SOC014) to 37 (CNE612), and average expected heterozygosities ranged from 0.085 (SOC014) to 0.928 (CNE612). These values are consistent with heterozygosity ranges reported in other multilocus microsatellite studies on species including Atlantic cod (Bentzen et al., 1996), northern pike (Miller and Kapuscinski, 1996), pink and sockeye salmon (Seeb et al., 1998), and Arctic char (Brunner at al., 1998). In contrast, Crawford et al. (1989) and Graves et al. (1992) found very low levels of genetic variation in an analysis of weakfish populations using allozymes and mtDNA restriction fragment-length polymorphism (RFLP) analyses, respectively. None of the genotypic distributions for any of the four microsatellite loci at any of the collection locations in either year differed significantly from Hardy-Weinberg expectations after correcting for multiple tests (Table 4).

Digestion of actin intron (CRESIA1) amplifications with the restriction endonuclease *Rsa* I revealed a single polymorphic restriction site that produced two alleles. Expected heterozygosities ranged from 0.000 for the monomorphic Georgia 1997 sample to 0.096 for the Chesapeake Bay 1996 sample. Digestion of the RP2 amplifications with the restriction endonuclease *Hinf* I also resulted in two alleles. Expected heterozygosities ranged from 0.194 in the Delaware Bay 1997 sample to 0.370 in the Georgia 1997 sample. Levels of genetic variation within the two nuclear gene intron regions were low in relation to three of the four microsatellite loci and were more similar to those found in the polymorphic allozyme loci of Crawford et al. (1989). In another study where nuclear intron RFLP analysis was used, similar levels of heterozygosity in Pacific salmon were found (Moran et al., 1997), as in RFLP studies of anonymous single copy nuclear (ascn) DNA loci in Atlantic cod (*Gadus morhua*) (Pogson et al., 1995) and blue marlin (*Makaira nigricans*) (Buonaccorsi et al., 1999). In contrast, higher heterozygosities (44–58%) were reported in an ascnDNA/RFLP analysis of striped bass (*Morone saxatilis*) by Leclerc et al. (1996). None of the sample genotype distributions for either locus differed significantly from Hardy-Weinberg expectations after correcting for multiple tests (Table 4).

To test for population structure, microsatellite loci were analyzed individually and as a combined data set. AMOVA results did not reveal significant differences between sample locations or years for any of the four loci or for the combined data (all $P>0.05$). Single-locus population pairwise F_{ST} values were relatively low, and mean F_{ST} values ranged from 0.002 (SOC050 and CNE612) to 0.018 (SOC044). Exact F permutation tests were not significant for any of the four loci or the combined data set after correction for multiple testing.

AMOVA results for both the actin and RP2 loci indicated no significant differences between sample locations or years (all $P>0.05$). Single-locus population pairwise F_{ST} values for the actin locus were consistently low (mean=0.005), ranging from $F_{ST} < 0.000$ for most of the comparisons to an F_{ST} of 0.035 between Georgia 1996 and Georgia 1997 and between Chesapeake Bay 1996 and Georgia 1997. A single exact F permutation test, between Delaware 1996

Table 4

Sample sizes (n), number of alleles (N), expected heterozygosities (H_{exp}), and P values for tests of Hardy-Weinberg equilibrium for four microsatellite loci, the actin intron (CRESIA1), and the ribosomal protein 2 intron (RP2) gene regions. GA = Georgia, NC = North Carolina, CB = Chesapeake Bay, DB = Delaware Bay, NY = New York. NT = monomorphic sample not tested.

	GA 1996	NC 1996	CB 1996	DB 1996	NY 1996	GA 1997	NC 1997	CB 1997	DB 1997	NY 1997
SOC050										
n	51	49	64	46	46	33	52	55	42	54
N	7	6	6	5	7	6	6	6	8	7
H_{exp}	0.741	0.702	0.694	0.731	0.724	0.758	0.712	0.740	0.737	0.722
P[1]	0.067	0.542	0.507	0.130	0.959	0.566	0.577	0.721	0.349	0.174
SOC044										
n	47	46	63	55	55	36	60	56	52	56
N	2	3	2	2	2	2	2	2	2	2
H_{exp}	0.362	0.434	0.374	0.251	0.416	0.407	0.302	0.350	0.203	0.419
P[1]	1.000	0.019	0.496	0.303	0.512	0.010	0.669	0.116	0.0.512	0.198
SOC014										
n	43	48	64	52	54	39	56	55	52	57
N	2	2	2	2	2	2	2	2	2	2
H_{exp}	0.090	0.081	0.046	0.075	0.170	0.144	0.053	0.088	0.038	0.068
P[1]	1.000	1.000	1.000	1.000	1.000	1.000	0.027	1.000	1.000	1.000
CNE612										
n	39	43	62	50	46	33	54	52	50	56
N	17	23	20	20	22	19	25	23	22	23
H_{exp}	0.916	0.943	0.928	0.912	0.916	0.935	0.934	0.934	0.923	0.936
P[1]	0.050	0.113	0.898	0.530	0.238	0.752	0.522	0.419	0.060	0.290
CRESIA1										
n	40	42	40	42	40	36	51	54	45	55
N	2	2	2	2	2	1	2	2	2	2
H_{exp}	0.096	0.089	0.031	0.055	0.096	0.000	0.025	0.053	0.047	0.020
P[1]	0.076	0.091	1.000	0.036	0.078	NT	1.000	1.000	1.000	1.000
RP2										
n	48	45	45	42	41	29	48	49	42	41
N	2	2	2	2	2	2	2	2	2	2
H_{exp}	0.237	0.200	0.217	0.230	0.253	0.373	0.237	0.201	0.194	0.253
P[1]	0.184	0.432	0.104	0.120	0.180	0.298	0.189	0.465	0.052	0.179

[1] None of the samples differed significantly from Hardy-Weinberg expectations after sequential Bonferroni corrections (α=0.005).

and Georgia 1997, was significant after correction for multiple testing (α<0.001). Single-locus population pairwise F_{ST} values for the RP2 locus were also low (mean=0.006), ranging from $F_{ST} < 0.000$ for most of the comparisons to a high of 0.050 between Georgia 1997 and Delaware Bay 1997. None of the exact F permutation tests were significant after correction for multiple testing.

From our results we were unable to reject the null hypothesis that weakfish comprise a single, genetically homogeneous stock. These results are consistent with those based on allozymes (Crawford et al., 1989) and RFLP analysis of mtDNA (Graves et al., 1992) and illustrate the point that increased genetic variability in microsatellites in relation to more traditional markers will not always provide greater stock resolution (Seeb et al., 1998). The amount of genetic exchange necessary to prevent the accumulation of significant genetic divergence between fish from different locations may be as little as a few individuals per generation (Allendorf and Phelps, 1981). Weakfish tagging data indicate that low levels of exchange occur between geographically distant populations of weakfish (Bain et al., 1998). Estimates of natal homing in yearling weakfish, calculated by Thorrold et al. (2001) using geochemical signatures in the otoliths of the same weakfish used in the present study, indicated spawning-site fidelity ranging from 61% to 81%, suggesting exchange rates sufficient to prohibit genetic divergence between locations.

The inclusion of nontarget species in our weakfish samples illustrates the advantages in using multiple marker systems. If only a single microsatellite locus had been used, or if the study had been restricted to nuclear intron markers alone, it is very likely that the sand seatrout and

silver seatrout specimens would have gone unnoticed. This could easily have resulted in a type-II error. Likewise, if nongenetic markers such as otolith microchemistry had been used exclusively, the analyses of Thorrold et al. (2001) would have been based on a mixed-species sample. Instead, it was possible not only to recognize the individuals as anomalous but also to identify them to species and provide evidence of hybridization between at least two of the *Cynoscion* congeners. It is hoped that further refinement of the inter- and intraspecific molecular markers developed here and in other studies will eventually be helpful in further clarifying the taxonomic status, population structure, and possible hybridization within the genus *Cynoscion*.

Acknowledgments

We would like to thank all those who supplied us with weakfish samples, including Louis Barbieri, Susan Lowerre-Barbieri, Christina Grahn, Patrick Geer, Mike Greene, and Simon Thorrold. We also appreciate the samples of banded drum, gulf kingfish, and star drum provided by Trey Knott and the silver seatrout and sand seatrout specimens provided by Bill Karel. We gratefully acknowledge Kim Reece, John Gold, Linda Richardson, and Robert Chapman for generously providing us with their published and unpublished primer sequences. Funding for this study was provided through the Virginia Marine Resources Commission.

Literature cited

Allendorf, F. W., and S. R. Phelps.
1981. Use of allelic frequencies to describe population structure. Can. J. Fish. Aquat. Sci. 38(12):1507–1514.

Anonymous.
1995. Overfished weakfish stock forces closure of federal waters. Fisheries 21:46–47.

Avise, J. C.
1992. Molecular population structure and the biogeographic history of a regional fauna: a case history with lessons for conservation biology. Oikos 63:62–76.

Bain C., J. Lucy, and M. Arendt.
1998. Virginia game fish tagging program annual report 1997. Virginia Marine Resource Report 98-3 (VSG-98-01), 22 p. Virginia Institute of Marine Science, Virginia Sea Grant Marine Advisory Program, College of William and Mary, Gloucester Point, VA.

Bentzen P., C. T. Taggart, D. E. Ruzzante, and D. Cook.
1996. Microsatellite polymorphism and the population structure of Atlantic cod (*Gadus morhua*) in the northwest Atlantic. Can. J. Fish. Aquat. Sci. 53 (12):2706–2721.

Bigelow H., and W. Schroeder.
1953. Fishes of the Gulf of Maine. U.S. Fish and Wildlife Service Fish. Bull. 53, 577 p.

Brunner P. C., M. R. Douglas, and L. Bernatchez.
1998. Microsatellite and mitochondrial DNA assessment of population structure and stocking effects in Arctic charr *Salvelinus alpinus* (Teleostei: Salmonidae) from central Alpine lakes. Mol. Ecol. 7 (2): 209–223.

Buonaccorsi V. P., K. S. Reece, L. W. Morgan, and J. E. Graves.
1999. Geographic distribution of molecular variance within the blue marlin (*Makaira nigricans*): a hierarchical analysis of allozyme, single-copy nuclear DNA, and mitochondrial DNA markers. Evolution 53 (2):568–579.

Chapman R. W., G. R. Sedberry, J. C. McGovern, B. A. Wiley, and J. A. Musick.
1999. The genetic consequences of reproductive variance: studies of species with different longevities. *In* Life in the slow lane: ecology and conservation of long-lived marine animals. Am. Fish. Soc. Symp. 23:169–181.

Chow S., and K. Hazama.
1998. Universal PCR primers for S7 ribosomal protein gene introns in fish. Mol. Ecol. 7:1247–1263.

Chow, S., and H. Takeyama.
2000. Intron length variation observed in the creatine kinase and ribosomal protein genes of the swordfish *Xiphias gladius*. Fish. Sci. 64(3):397–402.

Cordes, J. F.
2000. Application of genetic markers to provide species identification and define stock structure: analyses of selected marine fishes of the mid-Atlantic bight. Ph.D. diss., 142 p. Virginia Institute of Marine Science, College of William and Mary, Gloucester Point, VA.

Cordes, J. F., S. L. Armknecht, E. A. Starkey, and J. E. Graves.
2001. Forensic identification of sixteen species of Chesapeake Bay sportfishes using mitochondrial DNA restriction fragment-length polymorphism (RFLP) analysis. Estuaries 24(1):49–58.

Cowan, J. H., Jr.
1985. The distribution, transport and age structure of drums (family Sciaenidae) spawned in the winter and early spring in the continental shelf waters off west Louisiana. Ph.D. diss., 182 p. Louisiana State University, Baton Rouge, LA.

Crawford, M. K., C. B. Grimes, and N. E. Buroker.
1989. Stock identification of weakfish, *Cynoscion regalis*, in the middle Atlantic region. Fish. Bull. 87: 205–211.

CSPI-Scanalytics.
1996. RFLPScan Plus, version 3.0. SCPI-Scanalytics, Billerica, MA.

DeVries, D. A., and M. E. Chittenden Jr.
1982. Spawning, age determination, longevity, and mortality of the silver seatrout, *Cynoscion nothus*, in the Gulf of Mexico. Fish. Bull. 80:487–500.

Ditty, J. G.
1989. Separating early larvae of sciaenids from the western North Atlantic: a review and comparison of larvae from the northern Gulf of Mexico off Louisiana and Atlantic coast of the U.S. Bull. Mar. Sci. 44:1083–1105.

Excoffier, L., P. Smouse, and J. Quattro.
1992. Analysis of molecular variance inferred from metric distances among DNA haplotypes: application to human mitochondrial DNA restriction data. Genetics 131:479–491.

Ginsburg, I.
1931. On the differences in the habitat and size of *Cynoscion arenarius* and *Cynoscion nothus*. Copeia 1931:144.

Guo, S., and E. Thompson.
1992. Performing the exact test of Hardy-Weinberg proportion for multiple alleles. Biometrics 48:361–372.

Graves, J. E., J. R. McDowell, and M. L. Jones.
1992. A genetic analysis of weakfish *Cynoscion regalis* stock structure along the mid-Atlantic coast. Fish. Bull. 90:469–475.

Hildebrand, H. H
1955. A study of the fauna of the pink shrimp (*Penaeus duorarum* Burkenroad) grounds in the Gulf of Campeche. Publ. Inst. Mar. Sci. 4:169–232.

Leclerc, G. M., M. Diaz, and B. Ely.
1996. Use of PCR-RFLP assays to detect genetic variation at

single-copy nuclear loci in striped bass (*Morone saxatilis*). Mol. Mar. Biol. Biotechnol. 5:138–144.

Miller, L. M., and A. R. Kapuscinski.
1996. Microsatellite DNA markers reveal new levels of genetic variation in northern pike. Trans. Am. Fish. Soc. 125(6):971–977.

Moran, P., D. A. Dightman, R. S. Waples, and L. K. Park.
1997. PCR-RFLP analysis reveals substantial population-level variation in the introns of Pacific salmon (*Oncorhynchus* spp.). Mol. Mar. Biol. Biotechnol. 6(4):315–327.

Moshin, A. K. Mohammad.
1973. Comparative osteology of the weakfishes (*Cynoscion*) of the Atlantic and Gulf coasts of the United States (Pisces-Sciaenidae). Ph.D. diss., 148 p. Texas A&M Univ., College Station, TX.

Nesbit, R. A.
1954. Weakfish migration in relation to its conservation. U.S. Fish Wildl. Serv., Spec. Sci. Rep. Fish. 115:81.

Palumbi, S. R., and C. S. Baker.
1994. Contrasting population structure from nuclear intron sequences and mtDNA of humpback whales. Mol. Biol. Evol. 11:426–435.

Paschall, R. L.
1986. Biochemical systematics of the seatrouts of the western Atlantic genus *Cynoscion*. Master's thesis, 100 p. Univ. New Orleans, New Orleans, LA.

Patton, J. C., B. J. Galloway, R. G. Fechhelm, and M. A. Cronin.
1997. Genetic variation of microsatellite and mitochondrial DNA markers in broad whitefish (*Coregonus nasus*) in the Colville and Sagavanirktok rivers in northern Alaska. Can. J. Fish. Aquat. Sci. 54:1548–1556.

Perlmutter, A., S. W. Miller, and J. C. Poole.
1956. The weakfish (*Cynoscion regalis*) in New York waters. N.Y. Fish Game 3:1–43.

Pogson, G. H., K. A. Mesa, and R. G. Boutilier.
1995. Genetic population structure and gene flow in the Atlantic cod *gadus morhua*: a comparison of allozyme and nuclear RFLP loci. Genetics 139:375–385.

Reece, K. S., M. E. Siddall, E. M. Burreson, and J. E. Graves.
1997. Phylogenetic analysis of *Perkinsus* based on actin gene sequences. J. Parasitol. 83(3):417–423.

Rice, W. R.
1989. Analyzing tables of statistical tests. Evolution 43: 223–225.

Rowe, P. M., and C. E. Epifanio.
1994. Tidal stream transport of weakfish larvae in Delaware Bay, USA. Mar. Ecol. Prog. Ser. 110:105–114.

Ruzzante, D. E., C. T. Taggart, and D. Cook.
1996. Spatial and temporal variation in the genetic composition of a larval cod (*Gadus morhua*) aggregation: cohort contribution and genetic stability. Can. J. Fish. Aquat. Sci. 53:2695–2705.

Sambrook, J., E. F. Fritsch, and T. Maniatis.
1989. Molecular cloning: a laboratory manual, 3 vols. Cold Spring Harbor Laboratory Press, Cold Spring Harbor, NY.

Schlossman, P. A., and M. E. Chittenden Jr.
1981. Reproduction, movements, and population dynamics of the sand seatrout, *Cynoscion arenarius*. Fish. Bull. 79: 649–669.

Schneider, S., J.-M. Kueffer, D. Roessli, and L. Excoffier.
1997. Arlequin: a software for population genetics data analysis (vers. 2.0), 111 p. Univ. Geneva, Switzerland.

Scoles, D. R.
1990. Stock identification of weakfish, *Cynoscion regalis*, by discriminant function analysis of morphometric characters. Masters thesis, 55 p. Virginia Institute of Marine Science, College of William and Mary, Gloucester Point, VA.

Seeb, J. E., C. Habicht, J. B. Olsen, P. Bentzen, J. B. Shaklee, and L. W. Seeb.
1998. Allozyme, mtDNA, and microsatellite variants describe structure of populations of pink and sockeye salmon in Alaska. Bull. NPAFC 1:300–319.

Shepherd, G. R., and C. B. Grimes.
1983. Geographic and historic variations in growth of weakfish, *Cynoscion regalis*, in the middle Atlantic Bight. Fish. Bull. 81:803–813.
1984. Reproduction of weakfish, *Cynoscion regalis*, in the New York Bight and evidence for geographically specific life history characteristics. Fish. Bull. 82:501–511.

Thorrold, S. R., C. L. Latkoczy, P. K. Swart, and C. M. Jones.
2001. Natal homing in a marine fish metapopulation. Science 291:297–299.

Turner, T. F., L. R. Richardson, and J. R. Gold.
1998. Polymorphic microsatellite DNA markers in red drum (*Sciaenops ocellatus*). Mol. Ecol. 7(12):1771–1788.

Weinstein, M. P., and R. W. Yerger.
1976. Protein taxonomy of the Gulf of Mexico and Atlantic Ocean seatrouts, genus *Cynoscion*. Fish. Bull. 74:599–607.

Weir, B. S., and C. C. Cockerham.
1984. Estimating *F*-statistics for the analysis of population structure. Evolution 38:1358–1370.

Dynamic age-length keys

Are Salthaug
Institute of Marine Research
Nordnesgaten 50
P.O. Box 1870
N-5817 Bergen, Norway
E-mail address: ares@imr.no

Information about age composition is important when analyzing fish population dynamics. Age determination of individual fish is more difficult and time consuming than the recording of length measurements but by using age-length keys, age distributions can be estimated without much difficulty from length distributions (Fridrikson, 1934). Knowledge of the age-length composition in the population or in a given subgroup of the population is required for constructing adequate age-length keys. Various methods for construction and evaluation of age-length keys are described in the literature (see e.g. Fridrikson, 1934; Macdonald and Pitcher, 1979; Schnute and Fournier, 1980; Kimura and Chikuni, 1987; Hayes, 1993; Terceiro and Ross, 1993; Goodyear, 1997). Because of individual variation in growth rates and the variation in mortality rates at different ages and sizes, the age and length composition of a fish stock are constantly changing. With sufficient information about a fish stock, the change in the age-length composition can be modeled and theoretical age-length keys can be constructed for specific time periods. Age distributions can then be estimated from length distributions taken at different times of the season. In this work, a simple but useful modeling approach for constructing dynamic age-length keys is described and applied to data from the Atlantic cod (*Gadus morhua*) stock in the Barents Sea.

Material and methods

The model is based on principles described by Schnute and Fournier (1980) and Fournier et al. (1990). In an age-structured fish population, the probability of an individual being a certain length (l) within an age group (a) at a given time is assumed to follow a normal probability density function (Fig. 1A), $N(\mu_a, \mu_a)$, with expectation s_a and standard deviation σ_a. When lengths of individual fish are recorded, they are normally classified as discrete length groups (e.g. 1-cm or 5-cm length intervals). The probability (P) for an individual in age group a to belong in a discrete length group, s, at a given time is then given by

$$P_{as} \int_{l_{\min,s}}^{l_{\max,s}} N(\mu_a, \sigma_a) dl, \qquad (1)$$

where $l_{\max,s}$ and $l_{\min,s}$ are the upper and lower length limits of length group s, respectively.

Because the normal distribution is defined on the interval $(-\infty,\infty)$, it has mass below zero which may not be negligible for distributions centered near zero or with large variance. Thus, the P_{as}'s should be normalized across length groups for each age, i.e.

$$P_{as} \rightarrow P_{as} \Big/ \sum_{s} P_{as},$$

so that

$$\sum_{s} P_{as} = 1.$$

The theoretical number of individuals in age group a and length group s, N_{as}, can then be found (Fig. 1B):

$$N_{as} = P_{as} N_a, \qquad (2)$$

where N_a = the number of individuals in age group a.

The proportion of individuals from age group a in length group s, Q_{as}, is consequently found by dividing the number of individuals in age group a and length group s by the total number of individuals in the length group (Fig. 1C):

$$Q_{as} = \frac{N_{as}}{\sum_{a'} N_{a's}}. \qquad (3)$$

The total number of individuals in length group s (denominator) is found by summarizing the individuals from all age groups (a') in the length group. Note that an index of abundance (i.e. a relative measure) can be used as the estimated number of individuals in an age group (N_a). The expectation (μ_a) and standard deviation (σ_a) increase with time as the individuals grow larger at different growth rates. By analyzing age and length data from a fish stock, μ_a and σ_a can be estimated from observed data or models.

The method was applied to data on the Atlantic cod (*Gadus morhua*) stock in the Barents Sea from the period 1981 to 2000. Data from the annual bottom trawl surveys in the Barents Sea, which is conducted by the Institute of Marine Research in Bergen (Norway) around February (see e.g. Jakobsen et al.[1]), was used to estimate the parameters in the model (N_a, μ_a, and σ_a) for each month by interpolating between annual estimates (described later). Monthly age-length keys (Q_{as}) from the model were then tested by comparing predicted and observed age distributions in samples from commercial catches where the individual fish were both age and size measured. Note that the data used to estimate parameters and the data used to test the model were from different sources.

Equation 1 and 4 in Pennington et al. (2002) were used to estimate the average length (μ_a) in February and

[1] Jakobsen, T., K. Korsbrekke, S. Mehl, and O. Nakken. 1997. Norwegian combined acoustic and bottom trawl surveys for demersal fish in the Barents Sea during winter. ICES CM 1997/Y:17, 26 p.

Manuscript accepted 22 October 2002.
Manuscript received 9 January 2003 at NMFS Scientific Publications Office.
Fish. Bull. 101:451–456 (2003).

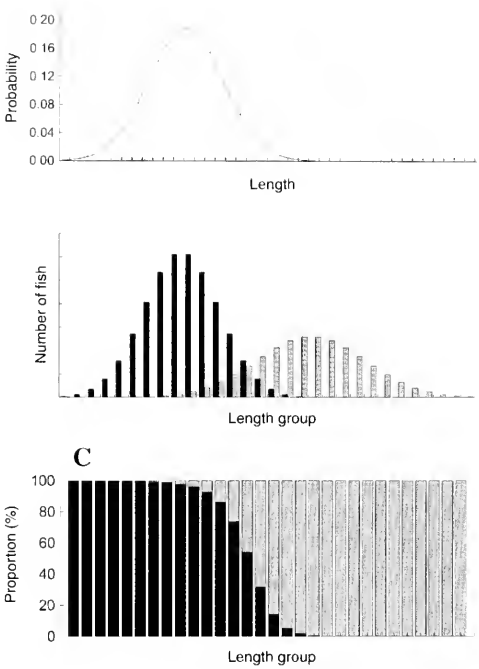

Figure 1

Graphs of Equations 1–3 (A=Eq. 1; B=Eq. 2; C=Eq. 3) showing two different age groups with overlapping length distributions. Sections A, B, and C are referred to in the description of the model in the "Materials and methods" section of the paper.

the standard deviation of length in February (σ_a), respectively. A linear length increment between surveys was assumed for individuals in a cohort, and the average length in a given month was estimated by interpolating from the linear growth curve (i.e. the length corresponding to the mid-point of the month). Although the μ_a's were estimated from mean lengths specific to a given year, the standard deviation of length at age was assumed constant and to increase linearly with time (or age) for a cohort. A regression analyzis of age and average standard deviation of length at age gave the fitted line in Figure 2. The equation from this regression was used to calculate σ_a for a given age (where age is measured in months). Abundance indices (estimate of N_a) from the Norwegian bottom trawl survey in the Barents Sea were taken from ICES,[2] and the relative number of individuals in each age group was assumed constant in the rest of the year. The size of the length group intervals ($l_{\min,s} - l_{\max,s}$ in Eq. 1) was 5 cm, and the number of length groups in the model was set to 30.

All recorded individuals of Northeast Arctic cod that were sampled randomly from commercial catches were pooled over each month (these data are available from 1985 onwards). Monthly length distributions (5-cm length groups) and corresponding (observed) age distributions were then constructed. The predicted proportion of each age group in a given month (based on the length distribution) was

$$\left(\sum_s Q_{as} N_s\right) \Big/ N,$$

where Q_{as} = the theoretical age-length key (from Eq. 3);
N_s = the observed number of individuals in length group s; and
N = the number of sampled individuals.

[2] ICES. 2001. Report of the Arctic Fisheries Working Group, Bergen, Norway, 24 April–3 May 2001. ICES CM 2001/ACFM:19, 380 p. ICES, Palægade 2-4 DK-1261, Copenhagen K, Denmark.

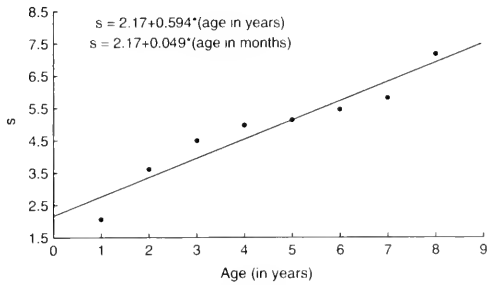

Figure 2

Average standard deviation (s) in length (measured in cm) at age of Northeast Arctic cod (from surveys in February in the period 1981–2001). The fitted regression line is shown (r^2=0.91) and corresponding equations are given. In the equation where age is measured in months, the cod individuals are assumed to be born around February.

The corresponding observed proportion of each age group was N_a/N, where N_a is the observed number of individuals in age group a. Only months with more than 300 sampled individuals were used in the testing of the age-length keys.

Results

The predicted age distributions from the model (based on monthly length distributions) were generally quite similar to the observed age distributions, although they varied between the investigated years (Fig. 3). Deviations from the observed age distributions were especially large in the years 1992–94. The commercial catches were dominated by the age groups 4–6, and there was a slight tendency that the model underestimated proportions. It is also worth noting that points from the same age group within years often seemed to form a line with a slightly different slope or intercept from the diagonal.

Discussion

The application and testing of the theoretical age-length keys is only an indication of the quality and usefulness of the method. An important assumption about the samples from the commercial catches is that individuals are sampled randomly within the 5-cm size groups from the population. If some age groups are over- or under-represented within size groups in the catches, in relation to the true population, there will be deviations in the proportion of age groups seen in Figure 3. Catches (and thereby the samples) are often taken from a restricted area within the total distributional area of the cod stock, where the length-at-age of individuals may differ from the rest of the population or where particular age groups dominate. In addition, errors in the age readings may occur.

The model's potential inability to capture the true age-size structure in the population may also lead to deviations in Figure 3. The estimates of the parameter values may suffer from sampling error, and simplifying assumptions may lead to errors (e.g. linear length increment between years and equal mortality rates for all age groups within years). Monthly growth rates for gadoids in temperate areas often vary seasonally (Jørgensen, 1992; Hayes, 1993). In addition, both the fishing mortality and the natural mortality are expected to vary for different ages and sizes because of ecological factors, fishermen's strategy, and the selection properties of commercial fishing gears.

By reading the age of a limited number of individuals at different times during the season, the resulting average lengths at age can be used to estimate the current value of μ_a. Another solution is to model the dynamics in average length more exactly (see e.g Schnute and Fournier, 1980). The seasonal change in the (relative) number of fish in each age group can be estimated by using available information about the fishing mortality. More complex modeling of structured populations than the approach described here, which is quite simple, can of course be used (see e.g. Tuljapurkar and Caswell, 1997). However, the main point is to use a method that gives a fairly accurate estimate of the age-length distribution in the population at a given time, and a complex model is not necessarily a better one in this respect.

Acknowledgments

I thank the Research Council of Norway for financial support. Ulf Dieckmann and Mikko Heino are thanked for assistance with aspects of the theoretical model.

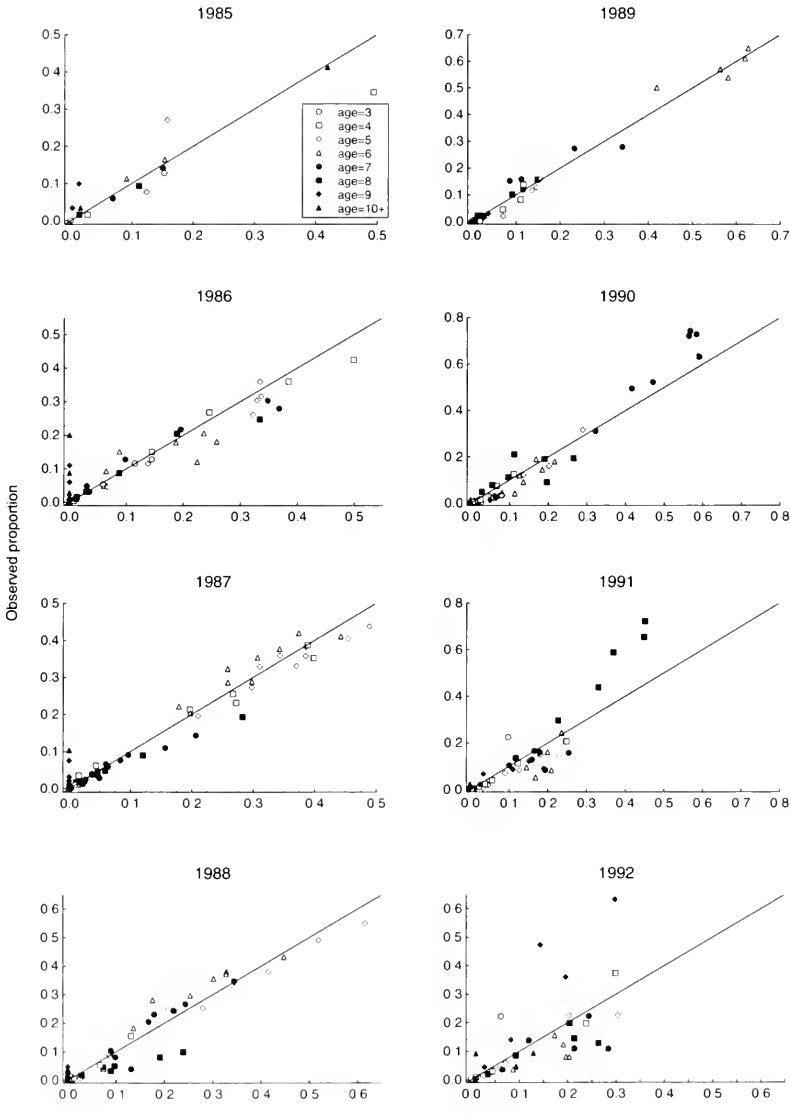

Figure 3

Observed and predicted proportions of different age groups in monthly samples (n>300) from commercial catches in the period 1985–2000. Each age group has its own symbol (see plot for 1985 and 1993). The diagonal is shown, which is where the points should lie. Note that the range on the axes varies between years according to the maximum values.

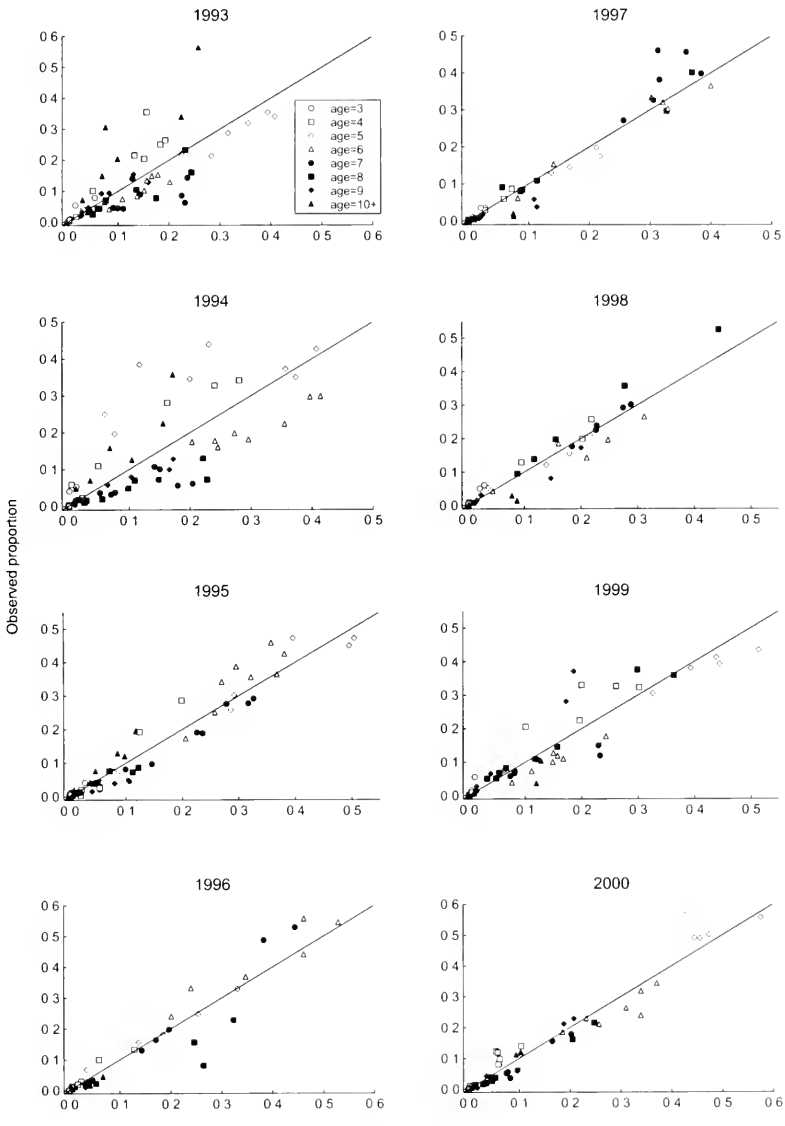

Figure 3 (continued)

Literature cited

Fournier, D. A., J. R. Sibert, J. Majkowski, and J. Hampton.
1990. MULTIFAN a likelihood-based method for estimating growth-parameters and age composition from multiple length frequency data sets illustrated using data for southern bluefin tuna (*Thunnus maccoyii*). Can. J. Fish. Aquat. Sci. 47:301–317.

Fridrikson, A.
1934. On the calculation of age distribution within a stock of cod by means of relatively few age determinations as a key to measurements on a large scale. Rapp. P. V. Réun. Cons. Int. Explor. Mer 86:1–14.

Goodyear, C. P.
1997. Fish age determined from length: an evaluation of three methods using simulated red snapper data. Fish. Bull. 95:39–46.

Hayes, B.
1993. A statistical method for evaluating differences between age-length keys with application to Georges Bank haddock, *Melanogrammus aeglefinus*. Fish. Bull. 91:550–557.

Jørgensen, T.
1992. Long-term changes in growth of North-east Arctic cod (*Gadus morhua*) and some environmental influences. ICES J. Mar. Sci. 49:263–277.

Kimura, D. K., and S. Chikuni.
1987. Mixtures of empirical distributions: an iterative application of the age-length key. Biometrics 43:23–35.

Macdonald, P. D. M., and T. J. Pitcher.
1979. Age-groups from length-frequency data: a versatile and efficient method of analyzing distribution mixtures. J. Fish. Res. Board Can. 36:987–1001.

Pennington, M., L-M. Burmeister, and V. Hjellvik.
2002. Assessing trawl-survey estimates of frequency distributions. Fish. Bull. 100:74–80.

Schnute, J., and D. Fournier.
1980. A new approach to length-frequency analysis: growth structure. Can. J. Fish. Aquat. Sci. 37:1337–1351.

Terceiro, M., and J. L. Ross.
1993. A comparison of alternative methods for the estimation of age from length data for Atlantic coast bluefish (*Pomatomus saltatrix*). Fish. Bull. 91:534–549.

Tuljapurkar, S., and H. Caswell.
1997. Structured-population models in marine, terrestrial, and freshwater systems, 570 p. Chapman & Hall, London.

Effects of blood extraction on horseshoe crabs (*Limulus polyphemus*)

Elizabeth A. Walls

Department of Fisheries and Wildlife Sciences
Virginia Polytechnic Institute and State University
Blacksburg, Virginia 24061-0321
Present address: Center for Environmental Studies
Virginia Commonwealth University
1000 West Cary Street, Box 843050
Richmond, Virginia, 23284

Jim Berkson

Department of Fisheries and Wildlife Sciences
Virginia Polytechnic Institute and State University
Blacksburg, Virginia 24061-0321
E-mail address (for J. Berkson, contact author): jberkson@vt.edu

Horseshoe crabs (*Limulus polyphemus*) are caught by commercial fishermen for use as bait in eel and whelk fisheries (Berkson and Shuster, 1999)—fisheries with an annual economic value of $13 to $17 million (Manion et al.[1]). Horseshoe crabs are ecologically important, as well (Walls et al., 2002). Migratory shorebirds rely on horseshoe crab eggs for food as they journey from South American wintering grounds to Arctic breeding grounds (Clark, 1996). Horseshoe crabs are also essential for public health (Berkson and Shuster, 1999). Biomedical companies bleed horseshoe crabs to extract a chemical used to detect the presence of endotoxins pathogenic to humans in injectable and implantable medical devices (Novitsky, 1984; Mikkelsen, 1988). Bled horseshoe crabs are returned to the wild, subject to the possibility of postbleeding mortality. Recent concerns of overharvesting have led to conflicts among commercial fishermen, environmentalists acting on behalf of the shorebirds, and biomedical companies (Berkson and Shuster, 1999; Walls et al., 2002).

In order to create an effective, sustainable management policy for the horseshoe crab resource, the completion of a stock assessment that incorporates human-induced mortalities is necessary. A stock assessment is not currently available because of a lack of critical information on the horseshoe crab population (Berkson and Shuster, 1999). One critical piece of information needed is an estimate of the mortalities involved in the biomedical bleeding process. With an estimated 260,000 horseshoe crabs bled in 1997 (HCTC[2]), the last year with data available, mortalities may not be negligible.

Five biomedical companies on the Atlantic coast of the United States bleed horseshoe crabs in the laboratory for the production of Limulus Ameobocyte Lysate (LAL). The horseshoe crabs are caught by fishermen under contract to biomedical companies, bled, then returned to their point of capture.

The LAL test used to detect endotoxins in humans is derived from the blue, copper-based blood of the horseshoe crab. Although alternate tests exist for the detection of endotoxin, the LAL test is the most effective because it is capable of detecting as little as one millionth of a billionth of a gram of endotoxin (Mikkelsen, 1988). The LAL test is now a standard test used to protect human health around the world, and horseshoe crabs are the sole source of LAL.

Each biomedical company maintains its own procedures for harvesting horseshoe crabs, extracting the horseshoe crabs' blood, releasing the bled horseshoe crabs, and developing the LAL substance. In 1998, the Atlantic States Marine Fisheries Commission (ASMFC), the Commission responsible for horseshoe crab management in the United States, mandated that all biomedical companies actively bleeding horseshoe crabs estimate mortality rates resulting from their bleeding process (Schrading et al.[3]). Because of the unique methods of the different biomedical companies, each company was required to quantify its own rate of mortality.

BioWhittaker, a CAMBREX company, is the largest producer of LAL. In response to the ASMFC mandate, BioWhittaker requested that Virginia Tech conduct the mortality study for their company. Our objective was to determine horseshoe crab mortality for a two-week period following the bleeding process.

Methods

We compared mortality rates between horseshoe crabs that underwent the bleeding process (bled) and horseshoe crabs that were suitable to undergo the bleeding process but were not bled (unbled). Throughout the 1999, 2000, and 2001 bleeding seasons (June through August), BioWhittaker obtained horseshoe crabs by trawling in the Atlantic Ocean off the coasts of Chincoteague, Virginia, or Ocean City, Maryland (or off both coasts). After capture, the horseshoe crabs were brought to BioWhittaker's bleeding

[1] Manion, M. M., R. A. West, and R. E. Unsworth. 2000. Economic assessment of the Atlantic coast horseshoe crab fishery, 71 p. Division of Economics, U.S. Fish and Wildlife Service, Arlington, VA.

[2] HCTC (Horseshoe Crab Technical Committee). 1998. Status of the horseshoe crab (*Limulus polyphemus*) population of the Atlantic coast, 9 p + figures and tables. Horseshoe Crab Technical Committee, Atlantic States Marine Fisheries Commission. Washington, D.C.

[3] Schrading, E., T. O'Connell, S. Michels, and P. Perra. 1998. Interstate management plan for horseshoe crab, 59 p. Atlantic States Marine Fisheries Commission, Washington D.C.

Manuscript accepted 6 November 2002.
Manuscript received 9 January 2003 at NMFS Scientific Publications Office.
Fish. Bull. 101:457–459 (2003).

Table 1

Comparison of mortality rates between bled and unbled groups of horseshoe crabs captured near Chincoteague, Virginia, and Ocean City, Maryland, 1999–2001.

	Unbled horseshoe crabs			Bled horseshoe crabs		
Dates monitored	No. of crabs monitored	No. of crabs that died	% dead at study end	No. of crabs monitored	No. of crabs that died	% dead at study end
8–22 Jul 99	10	0	0%	10	0	0%
22 Jul 99–5 Aug 99	10	0	0%	10	3	30%
19 Jun 00–3 Jul 00	30	0	0%	30	0	0%
7–21 Jul 00	30	0	0%	30	0	0%
1–15 Aug 00	30	1	3.3%	30	6	20%
6–20 Jun 01	30	0	0%	30	0	0%
20 Jun 01–04 Jul 01	30	0	0%	30	2	6.7%
15–29 Aug 01	30	0	0%	30	5	16.7%
Total	200	1	0.5%	200	16	8%

facility in Chincoteague, Virginia. At the bleeding facility, we randomly selected a predetermined number (10 in 1999, 30 in 2000 and 2001) of newly matured male horseshoe crabs (identified by pristine shell condition and the presence of boxing-glove lower claws [Shuster[1]]) from all of the horseshoe crabs obtained in that day's trawls. We selected newly matured male horseshoe crabs to minimize covariance in our study. These horseshoe crabs were not bled and served as a control in the experiment. They were packed in coolers labeled "unbled," and set aside. The same number of newly matured male horseshoe crabs were then randomly selected from the remaining horseshoe crabs and underwent BioWhittaker's normal bleeding process. Upon completion of the bleeding process, the horseshoe crabs were packed in coolers labeled "bled."

All coolers containing horseshoe crabs, both bled and unbled, were immediately packed in an air-conditioned vehicle and transported to the Virginia Seafood Agricultural Research and Extension Center in Hampton, Virginia. The horseshoe crabs were removed from the coolers and the unbled horseshoe crabs were marked with external tags to distinguish them from the bled horseshoe crabs. These markings were unobtrusive and did not cause any undue stress to the unbled horseshoe crabs. All of the horseshoe crabs were placed in four replicated, flow-through holding tanks, and equal numbers of bled and unbled horseshoe crabs were held in each tank. The horseshoe crabs remained in the tank system at Hampton for two weeks. Horseshoe crabs were maintained in appropriate conditions (Brown and Clapper, 1981), and monitored daily. Horseshoe crabs that died during the two-week period were removed and returned to the ocean at the time of their death.

At the conclusion of each two-week period, the status of each horseshoe crab (dead or alive) was recorded. All surviving horseshoe crabs were removed from the tank, placed in coolers, packed in an air-conditioned vehicle, returned to BioWhittaker's bleeding facility in Chincoteague, Virginia, and returned to the Atlantic Ocean in accordance with BioWhittaker's standard operating procedures. This procedure was repeated eight times during summers 1999, 2000, and 2001. The results from each of the replicates were combined, and the overall percentage mortality was calculated for the bled and unbled groups.

Using Fisher's exact test, we evaluated statistical significance of differences in mortality between the bled and unbled horseshoe crabs (Mehta and Patel, 1999). We then calculated a 95% confidence interval for average differential mortality using the common odds ratio in the statistical program StatXact (Mehta and Patel, 1999).

Results

A Fisher's exact test for statistical significance showed differences between mortality rates in bled and unbled horseshoe crabs (P=2.085E-04). Bled horseshoe crabs (n=200) had an overall mortality rate of 8% compared to the 0.5% mortality rate of the unbled horseshoe crabs (n=200; P<0.001) (Table 1). Thus, this study estimates average differential mortality between bled and unbled horseshoe crabs to be 7.5%. The 95% confidence interval for this average differential mortality ranges from 0.14% to 38.1% as calculated with the common odds ratio (Mehta and Patel, 1999).

Discussion

Our results indicate that horseshoe crab mortality due to bleeding is relatively low. Two small-scale studies had previously estimated postbleeding mortality. Rudloe (1983), observing bled and unbled horseshoe crabs in a penned cove in Florida, found that bleeding increased mortality by

[1] Shuster, C. N., Jr. 1999. Managing the horseshoe crab resource: it's the adult age that counts, 32 p. Virginia Institute of Marine Science, College of William and Mary, Gloucester Point, VA.

10% during the first year after bleeding, and 11% during the second year. Thompson (1998) estimated that mortality associated with LAL processing was 15% during the first week following blood extraction by observing bled and unbled horseshoe crabs in tanks in South Carolina.

Each LAL producer has a unique bleeding method, method of capture, distance and method of travel to the bleeding laboratory, a different holding time and conditions, and method of return of the bled crab that is most appropriate to that company's setting and situation. The results found in this study reflect those of BioWhittaker and may not be reflective of other companies' procedures.

We examined the survival of the horseshoe crabs in a controlled environment (tank), as opposed to their natural environment. Our survival rate for horseshoe crabs may not reflect the survival rate of horseshoe crabs returned to the wild. Transfer and holding processes induce stress on the horseshoe crabs. Thus, the survival of the bled horseshoe crabs could be compromised by translocation and confinement in tanks. However, the tank environment may provide protection for horseshoe crabs when they are in a weakened state and are more susceptible to predation following blood-extraction.

Further, this study looked only at newly matured male horseshoe crabs in an attempt to minimize variation of external influences, so that the only difference between the two groups was whether or not they underwent the blood extraction process. Additional studies should examine differences in mortality in other age and sex classes.

The Food and Drug Administration estimates that 260,000 horseshoe crabs were caught, bled, and returned by biomedical companies when last reported in 1997 (HCTC[5]). Assuming the 7.5% mortality rate found in our study is applicable to each biomedical company, and assuming that the number harvested for the biomedical companies has stayed relatively constant, we estimate that approximately 18,750 horseshoe crabs die yearly as a result of the biomedical procedure. In comparison, the commercial fishery reported landings of 5,543,000 pounds in 1999 and 3,756,000 pounds reported in 2000, all with a 100% mortality rate (NMFS, 2002). In the overall picture of the magnitude of horseshoe crabs caught and the associated mortality rates, it is evident that the bleeding process has a substantially smaller impact than the commercial fishery on the horseshoe crab population. However, information on both biomedical and commercial fishery-induced mortality are necessary to determine the total harvest mortality of horseshoe crabs.

The information presented in this study provides an estimate of the postbleeding mortality rate, an element of human-induced mortality on horseshoe crabs. This is one critical piece of information required to conduct a stock assessment and to develop an effective management strategy.

[5] HCTC (Horseshoe Crab Technical Committee). 1998. Status of the horseshoe crab (*Limulus polyphemus*) population of the Atlantic coast, 9 p. + figures and tables. Horseshoe Crab Technical Committee, Atlantic States Marine Fisheries Commission. Washington, D.C.

Acknowledgments

The authors wish to thank Carl N. Shuster Jr. and William McCormick for their helpful advice on the design of this study. Michael Schwarz, Ryan Cool, and Michael Jahnke of the Virginia Seafood Agricultural Research and Extension Center, a unit of Virginia Tech, provided the facilities for holding the horseshoe crabs and maintained them. Funding for this study was provided by BioWhittaker, a CAMBREX company. We especially thank Tammy Newcomb and Michael Vaughan for their helpful advice throughout all stages of this study.

Literature cited

Berkson, J., and C. N. Shuster Jr.
1999. The horseshoe crab: the battle over a true multiple use resource. Fisheries 24:6–10.

Brown, G. G., and D. L. Clapper.
1981. Procedures for maintaining adults, collecting gametes, and culturing embryos and juveniles of the horseshoe crab, *Limulus polyphemus*. *In* Laboratory animal management: marine invertebrates, p. 268–290. National Academy Press, Washington, D.C.

Clark, K.
1996. Horseshoe crabs and the shorebird connection. *In* Proceedings of the horseshoe crab forum: status of the resource. (J. Farrell and C. Martin, eds.), p. 23–25. Univ. Delaware Sea Grant College Program, Lewes, DE.

Mehta, C., and N. Patel.
1999. StatXact 4 Windows. CYTEL Software Corporation, Cambridge, MA.

Mikkelsen, T.
1988. The secret in the blue blood, 125 p. Science Press, Beijing, China.

NMFS (National Marine Fisheries Service).
2002. Annual commercial landing statistics. Available online at www.nmfs.gov. Accessed 03/01/02.

Novitsky, T. J.
1984. Discovery to commercialization: the blood of the horseshoe crab. Oceanus 27:13–18.

Rudloe, A.
1983. The effect of heavy bleeding on mortality of the horseshoe crab, *Limulus polyphemus*, in the natural environment. J. Invert. Path. 42:167–176.

Thompson, M.
1998. Assessments of the population biology and critical habitat for the horseshoe crab, *Limulus polyphemus*, in the South Atlantic Bight. M.Sc. thesis, 50 p. Univ. Charleston, Charleston, SC.

Walls, E. A., J. Berkson, and S. A. Smith.
2002. The horseshoe crab, *Limulus polyphemus*: 200 million years of existence, 100 years of study. Rev. Fish. Sci. 10(1): 39–73.

Erratum

Fishery Bulletin **98(1):127–138 (2000).**

Seyoum, Seifu, Michael D. Tringali, Theresa M. Bert, Doug McElroy, and Rod Stokes

An analysis of genetic population structure in red drum (*Sciaenops ocellatus*) based on mtDNA control region sequences

On page 128 (right column, second paragraph) the authors wrote ". . . state agencies in Alabama, Florida, South Carolina, and Texas studied the feasibility of stock enhancement as a means of supplementing wild populations." Later in the same paragraph, they also stated that ". . . because broodstock for large-scale enhancement programs along the Atlantic seaboard have been obtained from Mosquito Lagoon and nearby esturaries, there is a potential for artificial genetic exchange between putatively separate gene pools (e.g. those of Mosquito Lagoon and the Carolinas)."

The authors would like to clarify that the South Carolina Department of Natural Resources uses only locally obtained red drum for broodstock in its stocking programs. It was culturists for private facilities in South Carolina who used broodstock from Florida Mosquito Lagoon to produce red drum for worldwide distribution. The risk posited in our Introduction, as it related to the Carolinas, pertained to escapement or mishandling of the imported broodstock and their progeny.

Fishery Bulletin

Guidelines for contributors

Content of papers

Articles

Articles are reports of 10 to 30 pages (double spaced) that describe original research in one or a combination of the following fields of marine science: taxonomy, biology, genetics, mathematics (including modeling), statistics, engineering, economics, and ecology.

Notes

Notes are reports of 5 to 10 pages without an abstract that describe methods and results not supported by a large body of data. Although all contributions are subject to peer review, responsibility for the contents of articles and notes rests upon the authors and not upon the editor or the publisher. It is therefore important that authors consider the contents of their manuscripts carefully. Submission of an article is un-derstood to imply that the article is original and is not being considered for publication elsewhere. Manuscripts must be written in English. Authors whose native language is not English are strongly advised to have their manuscripts checked for fluency by English-speaking colleagues prior to submission.

Preparation of papers

Text

Title page should include authors' full names and mailing addresses (street address required) and the senior author's telephone, fax number, e-mail address, as well as a list of key words to describe the contents of the manuscript. **Abstract** must be less than one typed page (double spaced) and must not contain any citations. It should state the main scope of the research but emphasize the author's conclusions and relevant findings. Because abstracts are circulated by abstracting agencies, it is important that they represent the research clearly and concisely. **General text** must be typed in double-spaced format. A brief introduction should state the broad significance of the paper; the remainder of the paper should be divided into the following sections: Materials and methods, Results, Discussion (or Conclusions), and Acknowledgments. Headings within each section must be short, reflect a logical sequence, and follow the rules of multiple subdivision (i.e. there can be no subdivision without at least two subheadings). The entire text should be intelligible to interdisciplinary readers; therefore, all acronyms and abbreviations should be written out and all lesser-known technical terms should be defined the first time they are mentioned. The scientific names of species must be written out the first time they are mentioned; subsequent mention of scientific names may be abbreviated. Follow *Scientific style and format: CBE manual for authors, editors, and publishers* (6th ed.) for editorial style and the most current issue of the *American Fisheries Society's common and scientific names of fishes from the United States and Canada* for fish nomenclature. Dates should be written as follows: 11 November 1991. Measurements should be expressed in metric units, e.g. metric tons (t). The numeral one (1) should be typed as a one, not as a lower-case el (l).

Footnotes

Use footnotes to add editorial comments regarding claims made in the text and to document unpublished works or works with local circulation. Footnotes should be numbered with Arabic numerals and inserted in 10-point font at the bottom of the first page on which they are cited. Footnotes should be formatted in the same manner as citations. If a manuscript is unpublished, in the process of review, or if the information provided in the footnote has been conveyed verbally, please state this information as "unpubl. data," "manuscript in review," and "personal commun.," respectively. Authors are advised wherever possible to avoid references to nonstandard literature (unpublished literature that is difficult to obtain, such as internal reports, processed reports, administrative reports, ICES council minutes, IWC minutes or working papers, any "research" or "working" documents, laboratory reports, contract reports, and manuscripts in review). If these references are used, please indicate whether they are available from NTIS (National Technical Information Service) or from some other public depository. Footnote format: author (last name, followed by first-name initials); year; title of report or manuscript; type of report and its administrative or serial number; name and address of agency or institution where the report is filed.

Literature cited

The literature cited section comprises works that have been published and those accepted for publication (works in press) in peer-reviewed journals and books. Follow the name and year system for citation format. In the text, write "Smith and Jones (1977) reported" but if the citation takes the form of parenthetical matter, write "(Smith and Jones, 1977)." In the literature cited section, list citations alphabetically by last name of senior author. For example, Alston, 1952; Mannly, 1988; Smith, 1932; Smith, 1947; Stalinsky and Jones, 1985. Abbreviations of journals should conform to the abbreviations given in the *Serial sources for the BIOSIS previews database*. Authors are responsible for the accuracy and completeness of all citations. Literature citation format: author (last name, followed by first-name initials); year; title of report or article; abbreviated title of the journal in which the article was published, volume number, page numbers. For books, please provide publisher, city, and state.

Tables

Tables should not be excessive in size and must be cited in numerical order in the text. Headings in tables should be short but ample enough to allow the table to be intelligible on its own. All unusual symbols must be explained in the table legend. Other incidental comments may be footnoted (use italic arabic numerals for footnote markers). Use asterisks only to indicate probability in statistical data. Place table legends on the same page as the table data. We accept tables saved in most spreadsheet software programs (e.g. Microsoft Excel). Please note the following:

- Use a comma in numbers of five digits or more (e.g. 13,000 but 3000).
- Use zeros before all decimal points for values less than one (e.g. 0.31).

Figures

Figures include line illustrations, computer-generated line graphs, and photographs (or slides). They must be cited in numerical order in the text. Line illustrations are best submitted as original drawings. Computer-generated line graphs should be printed on laser-quality paper. Photographs should be submitted on glossy paper with good contrast. All figures are to be labeled with senior author's name and the number of the figure (e.g. Smith, Fig. 4). Use Helvetica or Arial font to label anatomical parts (line drawings) or variables (graphs) within figures; use Times Roman bold font to label the different sections of a figure (e.g. **A**, **B**, **C**). Figure legends should explain all symbols and abbreviations seen within the figure and should be typed in double-spaced format on a separate page at the end of the manuscript. We advise authors to peruse a recent issue of *Fishery Bulletin* for standard formats. Please note the following:

- Capitalize the first letter of the first word of axis labels.
- Do not use overly large font sizes to label axes or parts within figures.
- Do not use boldface fonts within figures.
- Do not create outline rules around graphs.
- Do not use horizontal lines through graphs.
- Do not use large font sizes to label degrees of longitude and latitude on maps.
- Indicate direction of degrees longitude and latitude on maps (e.g. 170°E).
- Avoid placing labels on a vertical plane (except on *y* axis).
- Avoid odd (nonstandard) patterns to mark sections of bar graphs and pie charts.

Copyright law

Fishery Bulletin, a U.S. government publication, is not subject to copyright law. If an author wishes to reproduce any part of *Fishery Bulletin* in his or her work, he or she is obliged, however, to acknowledge the source of the extracted literature.

Submission of papers

Send four printed copies (one original plus three copies)—clipped, *not stapled*—to the Scientific Editor, at the address shown below. Send photocopies of figures with initial submission of manuscript. Original figures will be requested later when the manuscript has been accepted for publication. Do not send your manuscript on diskette until requested to do so.

Dr. Norman Bartoo
National Marine Fisheries Service, NOAA
8604 La Jolla Shores Drive
La Jolla, CA 92037

Once the manuscript has been accepted for publication, you will be asked to submit a software copy of your manuscript. The software copy should be submitted in WordPerfect or Word format (in Word, save as Rich Text Format). Please note that we do not accept ASCII text files.

Reprints

Copies of published articles and notes are available free of charge to the senior author (50 copies) and to his or her laboratory (50 copies). Additional copies may be purchased in lots of 100 when the author receives page proofs.

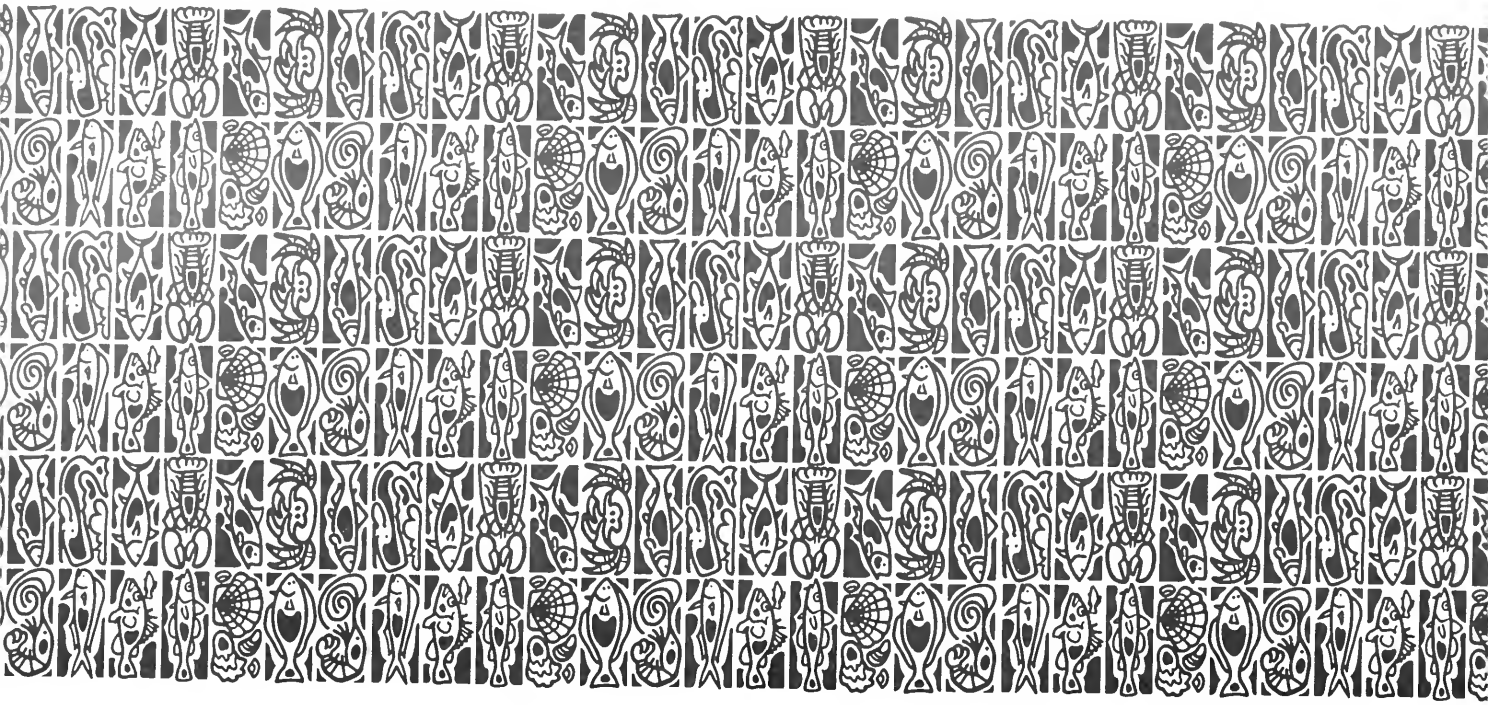

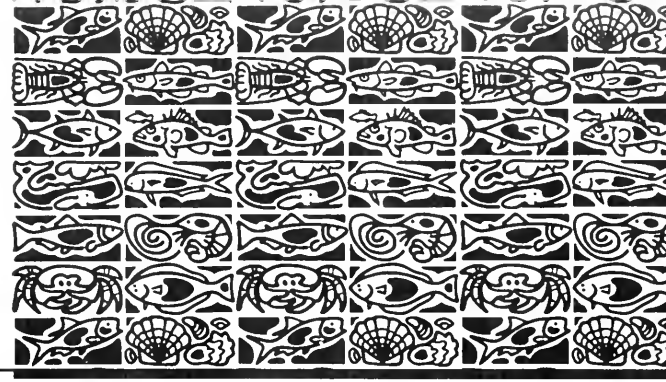

U.S. Department
of Commerce

Volume 101
Number 3
July 2003

Fishery Bulletin

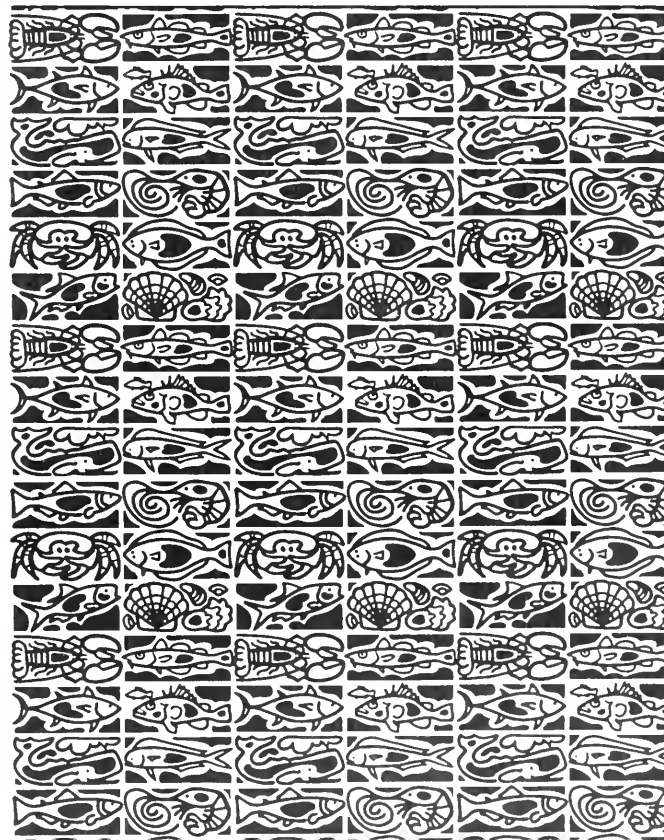

The *Fishery Bulletin* (ISSN 0090-0656) is published quarterly by the Scientific Publications Office, National Marine Fisheries Service, NOAA, 7600 Sand Point Way NE, BIN C15700, Seattle, WA 98115-0070. Periodicals postage is paid at Seattle, WA, and at additional mailing offices. POSTMASTER: Send address changes for subscriptions to Fishery Bulletin, Superintendent of Documents, Attn.: Chief, Mail List Branch, Mail Stop SSOM, Washington, DC 20402-9373.

The Secretary of Commerce has determined that the publication of this periodical is necessary according to law for the transaction of public business of this Department. Use of funds for printing of this periodical has been approved by the Director of the Office of Management and Budget.

For sale by the Superintendent of Documents, U.S. Government Printing Office, Washington, DC 20402. Subscription price per year: $45.00 domestic and $56.25 foreign. Cost per single issue: $28.00 domestic and $35.00 foreign. **See back for order form.**

Fishery Bulletin

***Fishery Bulletin* web site: fishbull.noaa.gov**

The *Fishery Bulletin* carries original research reports and technical notes on investigations in fishery science, engineering, and economics. It began as the Bulletin of the United States Fish Commission in 1881; it became the Bulletin of the Bureau of Fisheries in 1904 and the *Fishery Bulletin* of the Fish and Wildlife Service in 1941. Separates were issued as documents through volume 46; the last document was No. 1103. Beginning with volume 47 in 1931 and continuing through volume 62 in 1963, each separate appeared as a numbered bulletin. A new system began in 1963 with volume 63 in which papers are bound together in a single issue of the bulletin. Beginning with volume 70, number 1, January 1972, the *Fishery Bulletin* became a periodical, issued quarterly. In this form, it is available by subscription from the Superintendent of Documents, U.S. Government Printing Office, Washington, DC 20402. It is also available free in limited numbers to libraries, research institutions, State and Federal agencies, and in exchange for other scientific publications.

U.S. Department of Commerce
Seattle, Washington

Volume 101
Number 3
July 2003

Fishery Bulletin

Contents

Reproduction in the protogynous black grouper (*Mycteroperca bonaci* (Poey)) from the southern Gulf of Mexico

Thierry Brulé
Ximena Renán
Teresa Colás-Marrufo
Yazmin Hauyon
Armin N.Tuz-Sulub

Centro de Investigación y de Estudios Avanzados del IPN Unidad Mérida
Antigua Carretera a Progreso km.6
Apartado postal 73 Cordemex
Código Postal 97310 Mérida
Yucatán, México
E-mail address (for T. Brulé): tbrule@mda.cinvestav.mx

Christian Déniel

Institut Universitaire Européen de la Mer, Ressources Halieutiques-Poissons Marins
Université de Bretagne Occidentale
Place Nicolas Copernic
Technopôle Brest Iroise
29820 Plouzané, France

Abstract—An analysis was made of sexual pattern, spawning season, sizes at sexual maturation, and sex change in black grouper (*Mycteroperca bonaci*) from the southern Gulf of Mexico. Samples were taken between 1996 and 2000, from industrial and small-craft commercial fisheries, in offshore and inshore waters of the continental shelf of the Yucatan Peninsula (Campeche Bank), including the shallow waters of National Marine Park Alacranes Reef. For all collected specimens (n=1229), sex and maturation condition were determined by histological analysis of the gonads. The offshore sample consisted of 75.1% females, 24.3% males, and 0.6% transitional-stage fish. All individuals collected from inshore waters were females. Gonadal structure and population structure characteristics for Campeche Bank black grouper were consistent with the characteristics of monandric protogynous hermaphrodism for a serranid fish. Sexually active males and females were observed year-round, although ripening females, with stage-III, -IV, and -V vitellogenic oocytes in the ovaries, dominated in samples taken between December and March. In addition, peak occurrence of ripe-running females with hyaline oocytes or postovulatory follicles (or both) in the ovaries was recorded in January and February. A few precocious females began spawning in October and November, and others were still in spawning condition in May and June. Fifty percent maturity of females was attained at 72.1 cm fork length (FL). Median size at sexual inversion was 103.3 cm FL, and 50% of the females measuring 111.4 cm FL had transformed into males. The southern Gulf of Mexico grouper fishery was considered deteriorated and lacked a well-defined management strategy. Results of the present study provide helpful information on black grouper reproduction in this area and could help Mexican authorities choose appropriate management strategies for this fishery, such as minimum size limit, closed fishing season, and protection of spawning aggregations.

Manuscript approved for publication 11 February 2003 by Scientific Editor.
Manuscript received 4 April 2003 at NMFS Scientific Publications Office.
Fish. Bull. 101:463–475 (2003).

The black grouper (*Mycteroperca bonaci*) is one of the 20 most commonly sought serranid fishes in the tropical western Atlantic region (Sadovy, 1994). The species ranges from Massachusetts and Bermuda to southeastern Brazil (Böhlke and Chaplin, 1993; Fischer, 1978; Bullock and Smith, 1991; Begossi and Figueiredo, 1995). It is found on irregular bottoms such as coral reefs, drop-off walls, and rocky ledges, in depths from 10 to at least 100 m (Roe, 1977; Manooch and Mason, 1987; Bullock and Smith, 1991; Heemstra and Randall, 1993; Huntsman et al., 1994).

According to Shapiro (1987), the salient feature of grouper reproduction is protogynous hermaphroditism. The first reasonable evidence of protogyny in *M. bonaci* was published by Smith (1959), although there have been other occasional reports on black grouper reproduction (Erdman, 1956; Smith, 1961, 1971, 1972; Naranjo in García-Cagide et al., 1994). Systematic study of sexual pattern and sexual maturation in the species has only been carried out by García-Cagide and García (1996) in Cuban waters and by Crabtree and Bullock (1998) in Florida waters. This grouper has been reported to form spawning aggregations in the Gulf of Mexico and Caribbean Sea (Fine, 1990; Carter and Perrine, 1994; Domeier and Colin, 1997; Eklund et al., 2000).

Black grouper is an important commercial and recreational fin fish resource in Bermuda, southern Florida, Cuba, the southern Gulf of Mexico, and Venezuela (Manooch and Mason, 1987; Cervigon, 1991; Heemstra and Randall, 1993; Claro et al., 1994). In the southern Gulf of Mexico between 1989 and 1999, groupers accounted for 18–30% of the total offshore commercial marine resources harvested from the Campeche Bank (the continental shelf surrounding the northern coast of the Yucatan Peninsula) and resources landed in inshore waters off the state of Yucatán (SEMARNAP, 2000a). At least 18 grouper species are commercially exploited in this region—the most important of these by catch number and weight are red grouper (*Epinephelus morio*), followed by black grouper and gag (*Mycteroperca microlepis*) (Colás-Marrufo et al., 1998). Because grouper landings in

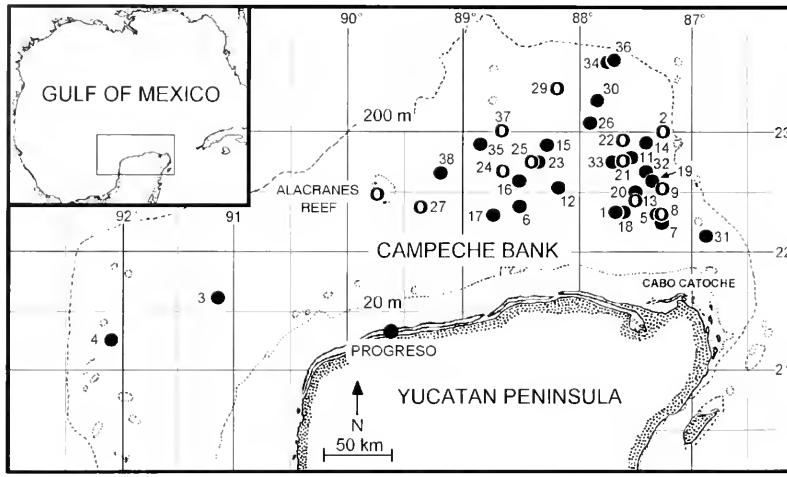

Figure 1

Map of the Campeche Bank, Mexico, showing the geographic distribution of sampling locations (●) for black grouper (*Mycteroperca bonaci*) observed during the period 1996–2000. Samping locations marked (O) are where ripe-running female black grouper were caught. Sample locations: 1 = April 1996; 2 = April and May 1996; 3,4 = May 1996; 5 = November 1996; 6, 7 = December 1996; 8 = January 1997; 9 = January and February 1997; 11 = February 1997; 12 = May 1997; 13 = June 1997; 14 = June and July 1997; 15 = July 1997; 16 = July and August 1997; 17, 18 = August 1997; 19 = September 1997; 20 = September and October 1997; 21 = October and November 1997; 22 = November 1997; 23 = December 1997; 24,25 = January 1998; 26 = January and February 1998; 27 = February and March 1998; 29 = March 1998; 30,31 = June 1998; 32 = July 1998; 33 = August 1998; 34 = August and September 1998; 35 = September 1998; 36 = April 1999; 37,38 = May 1999; Alacranes Reef was sampled November and December 1999, January, February, and August to November 2000. No black grouper were caught in sample locations 10 (22°33′–88°24′W; February 1997) and 28 (22°30′N–89°30′W; March 1998).

the Campeche Bank decreased between 1991 and 1997, the Mexican government proposed management measures to protect the grouper resource, but without considering the biological characteristics and fishery aspects of each exploited species (SEMARNAP, 2000a, 2000b). Given that sustainable resource management is founded on stock assessments and knowledge of the biology of exploited species (Sadovy, 1997), more information on the biology of the most abundant groupers from the southern Gulf of Mexico in general, including Campeche Bank, is necessary to implement and refine management strategies.

This lack of knowledge is especially acute for Campeche Bank black grouper. For example, although growth, feeding, and reproduction of the Yucatan red grouper are well documented, none of this information is available for the black grouper in this region (Brulé and Déniel, 1994; Brulé et al., 1994, 1999). This lack of information is alarming because *M. bonaci* can account for 40% of the grouper catch by weight for some commercial vessels, and if this species is not included in stock monitoring and reproduction studies, effective overall management of the southern Gulf of Mexico grouper fishery could be seriously undermined (Colás-Marrufo et al., 1998).

With the final aim of defining more accurate and efficient management practices for the Campeche Bank grouper fishery, we present analyses of sexual status, sexual cycle, spawning season, size at sexual maturation, and sex change for black grouper from the southern Gulf of Mexico.

Materials and methods

Black grouper were collected from commercial catches taken from rocky bottoms in both offshore and inshore waters of the Campeche Bank and in the shallow waters of the Alacranes Reef complex. Alacranes Reef is the most important complex of coral reefs located on the Yucatan continental shelf. Because of its high scientific and economic potential, the Mexican government declared this reef a National Marine Park in June 1994 (Fig. 1). In offshore waters, black grouper (n=880) were caught by the long-line industrial fleet from 38 locations mainly situated in the northeastern part of the Campeche Bank, at depths ranging from 40 to 210 m, between April 1996 and May 1999. In inshore waters, some specimens (n=39) were obtained

from the small craft-fleet, whose crew captured them using spear guns at depths ranging from 4 to 20 m, in areas close to the port of Progreso, between November 1998 and May 1999. On Alacranes Reef, black groupers (n=206) were captured with spear guns by small-craft fishermen at depths of 10–12 m between November 1999 and February 2000.

Fork and standard lengths (FL, SL), whole and gutted weights (WW, GW), and weight of gonads (gW), were recorded for all collected fish. All lengths reported in the present study are fork length and all weights are gutted weight. In discussion, total length data for Cuba (García-Cagide and García, 1996) and Florida (Crabtree and Bullock, 1998) populations were converted to fork lengths by using the fork-length to total-length relationship calculated by Crabtree and Bullock (1998).

Criteria presented by Sadovy and Shapiro (1987) were used to diagnose sequential hermaphroditism in black grouper of Campeche Bank. Sex by size-frequency distributions for black groupers were compared by using the Kolmogorov-Smirnov nonparametric test, and differences between male and female mean fork lengths were analyzed by using a one-tailed z-test (if n>30) or a one–tailed t-test (if n<30). The male-to-female ratio (M:F), excluding transitional-stage fish (referred to as "transitional fish" in this article), was calculated and Pearson chi-square or Yates's corrected chi-square goodness-of-fit tests were carried out to determine if sex ratio differed significantly from unity (Scherrer, 1984). Significance level, α, was 0.05 in all instances.

Sex-dependent change in fin pigmentation, as described by Crabtree and Bullock (1998), was examined in a subset of fish (n=104) caught from Alacranes Reef between August and November 2000. The colors of the pectoral, anal, dorsal, and caudal fins were recorded and histological sections of the gonads were prepared and assessed for sex identification.

For all the fish sampled in all locations, sex and sexual development were determined by examination of the microscopic structure of the gonads. These were preserved in Bouin's fluid, embedded in Paraplast and sectioned to 6 μm thickness. Ovaries and testes sections were stained in Gabe and Martoja's triple stain for light microscopy (Gabe, 1968). Fish were identified as female, male, or as transitional. Based on red grouper microscopic features for oogenesis (Brulé et al., 1999) and for spermatogenesis (Moe, 1969), six descriptive stages were recognized in black grouper ovaries and five in the testes. Histological sections of the ovaries were also scanned for the presence of postovulatory follicles and atretic oocytes in alpha or beta stages (Lambert, 1970). Using the criteria defined by Smith (1959) and Sadovy and Shapiro (1987), we considered individuals with gonads containing primarily ovarian tissue, degenerating or not, with few clusters of spermatocytes, spermatids, or spermatozoa to be undergoing sexual inversion. According to the sexual classes defined by Brulé et al. (1999) for red grouper, female and male black grouper were classified as resting, ripening, ripe-running, or spent, and fish in the process of sexual inversion were classified as transitional. Using the histological features considered by Shapiro et al. (1993) as sign of prior spawning activity for the red hind (*Epinephelus guttatus*) we were able to distinguish resting mature females from immature (virgin) females that had never spawned.

Reproduction periodicity was evaluated for both sexes by examining seasonal variations in the gonadosomatic index (GSI=100×gW/GW) and in the relative proportion of individuals in each sexual class. Specimens from offshore waters taken during different years were pooled by month, and mean GSI values and percent frequencies of sexual classes were generated monthly for a single year. Immature individuals were discarded from this analysis.

Size at which 50% of females were sexually mature (L_{50}) was determined by using a binary logistic regression (SYSTAT statistical computer package for Windows, version 8.0, SPSS Inc., Chicago, IL). For our analysis, resting mature, ripening, ripe-running, and spent females were considered as sexually mature individuals. Moreover, the minimum size at which females become sexually mature (L_{min}) was recorded, and the percentage of females of maximum length at first maturity, L_{min}/L_{max} with L_{max} = maximum length of females recorded in samples, was determined (Grimes, 1987). Sexual transition was analyzed by using a binary logistic regression to estimate the length at which 50% of the females transformed to males (P_{50}) according to Crabtree and Bullock (1998). The size range and median size at which sex inversion occurs were estimated by following the procedures of Shapiro (1984). Furthermore, the variation in size at sex change was analyzed by using two ratios defined by Shapiro (1987): ratio 1, size range of transitional fish divided by maximum size of fish in samples; and ratio 2, range of overlap in size of males and females divided by maximum size of fish in samples.

Results

Size-frequency distributions

All individuals collected from inshore waters were females ranging from 25.6 to 58.0 cm in length (Fig. 2). The offshore fish sample, which did not include the Alacranes Reef sample, was composed of 75.1% females, 24.3% males, and 0.6% transitional fish. Females ranged in size from 57.0 to 123.5 cm, males from 86.0 to 132.0 cm, and transitional fish from 99.0 to 121.5 cm. The Alacranes Reef sample was composed of 95% females ranging in size from 46.0 to 100.0 cm and 5% males from 97.0 to 135.0 cm. In the offshore sample, the male size range differed significantly from that of the females (Kolmogorov-Smirnov; n=875; P<0.05), and male mean fork length (114.6 ±7.1 cm; mean ±SD) was greater than female mean fork length (96.6 ±12.1 cm; one-tailed z-test, n=875; P<0.05). Similar results for male and female size ranges (Kolmogorov-Smirnov; n=206; P<0.05) and male (115.7 ±12.9 cm) and female (67.6 ±11.2 cm) mean fork lengths (one-tailed t-test, n=206; P<0.05) were observed for black grouper from the Alacranes Reef sample.

Sex ratio

The male-to-female ratios were calculated for each 5-cm size class from 25.1 to 135.0 cm length (Table 1). The

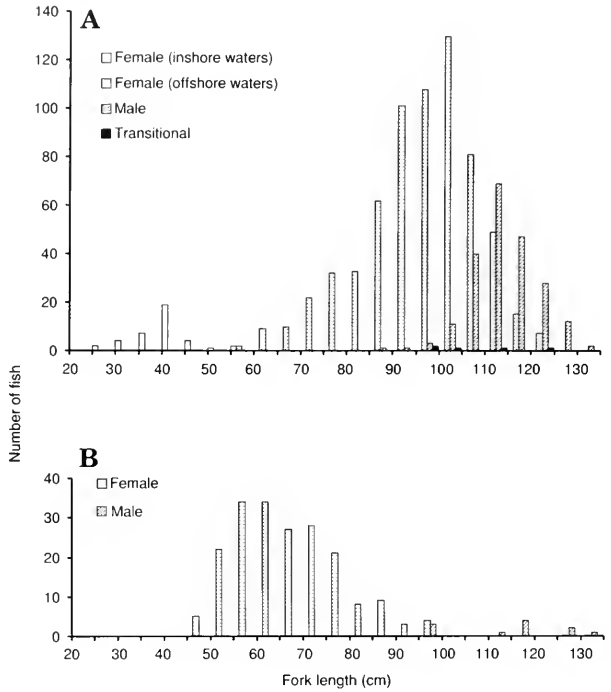

Figure 2

Size-frequency distribution for females, transitional individuals, and males for black grouper (*Mycteroperca bonaci*) caught between April 1996 and February 2000 in offshore and inshore waters of the Campeche Bank (**A**), and in shallow waters of Alacranes Reef (**B**), Mexico.

sex ratios were female-biased in size classes less than 110.1 cm, did not differ significantly from a 1:1 sex ratio in the 110.1–115.0 cm size class, and were male-biased in size classes larger than 115.0 cm. The overall black grouper sex ratio was 1:4, which differed significantly from unity (χ_1^2 =400.8, P<0.05).

Fin pigmentation

Of the 104 black grouper analyzed to detect gender-associated color changes, 98 were females (size range 47.0–99.0 cm), five were males (99.0–115.0 cm), and one, which presented previtellogenic oocytes and nests of spermatocytes and spermatozoa in its gonads, was classified as transitional (99 cm). All males, as well as the transitional specimen, displayed the male color phase with jet black pigmentation on pectoral, anal, and caudal fins. Only 5% of the females (size range 50.0–100.0 cm, n=5) had jet black pigments on their fins.

Gonadal structure

All ovaries presented a central cavity with a germinal epithelium forming the surface layer of a series of projecting ovigerous folds or lamellae of the tunica albuginea.

Of the 225 males assessed histologically, 76% (n=170) presented a membrane-lined central cavity in the testes. This lumen remained unused in the transport of spermatozoa, and sperm ducts or sinuses within the gonadal capsule were observed in 37% of the specimens (n=84) (Fig. 3, A and B). Previtellogenic oocytes (stages I and II) remained in the testes of 13% of the males (n=30), and only one of these (107.0 cm) presented previtellogenic oocytes in degeneration within lamellae in a fully developed testis dominated by crypts of spermatocytes, spermatids, and spermatozoa. Yellow bodies were observed in the testes of 96% of the males.

Internal gonadal structure for the five black groupers classified as transitional was very similar to that of im-

Table 1

Number of sampled fish; proportion of females, males, and transitional-stage fish (transitional fish); and sex ratio by length class for black grouper (*Mycteroperca bonaci*) collected in the inshore and offshore waters of the Campeche Bank and shallow waters of Alacranes Reef, México, between April 1996 and February 2000. Alacranes collection = collection at the Alacranes Reef.

	Females			Total collected		Transitional fish: Offshore collection		Males				Sex ratio (male: female)
Fork length class (cm)	Inshore collection	Offshore collection	Alacranes collection	*n*	(%)	*n*	(%)	Offshore collection	Alacranes collection	*n*	(%)	for total collected
25.1–30.0	2	0	0	2	100.0	0		0	0	0		
30.1–35.0	4	0	0	4	100.0	0		0	0	0		
35.1–40.0	7	0	0	7	100.0	0		0	0	0		
40.1–45.0	19	0	0	19	100.0	0		0	0	0		
45.1–50.0	4	0	5	9	100.0	0		0	0	0		
50.1–55.0	1	0	22	23	100.0	0		0	0	0		
55.1–60.0	2	2	34	38	100.0	0		0	0	0		
60.1–65.0	0	9	34	43	100.0	0		0	0	0		
65.1–70.0	0	10	27	37	100.0	0		0	0	0		
70.1–75.0	0	22	28	50	100.0	0		0	0	0		
75.1–80.0	0	32	21	53	100.0	0		0	0	0		
80.1–85.0	0	33	8	41	100.0	0		0	0	0		
85.1–90.0	0	62	9	71	98.6	0		1	0	1	1.4	1:71
90.1–95.0	0	101	3	104	99.0	0		1	0	1	1.0	1:104
95.1–100.0	0	108	4	112	93.3	2	1.7	3	3	6	5.0	1:18.67
100.1–105.0	0	130	0	130	91.5	1	0.7	11	0	11	7.7	1:11.82
105.1–110.0	0	81	0	81	66.9	0		40	0	40	33.1	1:2.03
110.1–115.0	0	49	0	49	40.8	1	0.8	69	1	70	58.3	1:0.70*
115.1–120.0	0	15	0	15	22.7	0		47	4	51	77.3	1:0.29
120.1–125.0	0	7	0	7	19.4	1	2.8	28	0	28	77.8	1:0.25
125.1–130.0	0	0	0	0		0		12	2	14	100.0	
130.1–135.0	0	0	0	0		0		2	1	3	100.0	
Total	39	661	195	895	79.6	5	0.4	214	11	225	20.0	1:3.98

* Value did not differs significantly from 1:1 sex ratio (χ_1^2; $P>0.05$).

mature or resting females. Stage-I and -II oocytes, yellow bodies, and sometimes bundles of muscle and connective tissue were present within the lamellae. Intermixed with the female tissue, these gonads contained a few nests of spermatogonia, spermatocytes, or spermatozoa, although degeneration of female germinal tissue was not observed (Fig. 3C). These transitional specimens were captured in September, November, and December 1997 and in January and March 1998.

Sexual cycle

Females captured from inshore waters during January, February, March, May, November, and December were immature and had low individual GSI values (GSI range 0.01–0.18%), and only oogonia and previtellogenic oocytes were observed in their ovaries.

Mean GSI for mature females caught in offshore waters began to increase in December (0.5%), reached a maximum value in February (2.2%), and declined to a near minimum level in March (0.7%) and April (0.6%) (Fig. 4). Highest individual GSI values for females were observed in October (4.9%), December (6.0%), January (6.7%), and February (9.6%). Mean GSI for males caught in offshore waters increased in December (0.13%) and January (0.14%)—reaching a maximum value in February (0.22%) and declining from March (0.12%) to August (0.11%) (Fig. 4). Highest individual GSI values for males were observed in September (0.43%) and February (0.39%).

Ripening females, with stage-III, -IV, and -V vitellogenic oocytes in their ovaries, were observed year-round, but dominated in collections made between December and March (42–56% of females) (Fig. 5). Advanced vitellogenic oocytes undergoing final oocyte maturation were noted only for some females captured between January and March (Fig. 6A). Ripe-running females, with hyaline oocytes or postovulatory follicles (or with both) in their ovaries, were recorded between October and June, and peaked in occur-

rence in January (28%) and February (52%)(Fig. 6B). The gonads of 50 ripe-running females caught between January and April, and during June and November, contained both postovulatory follicles and stages III–V vitellogenic oocytes without sign of degeneration (Fig. 6C). Spent females, with atretic and remaining vitellogenic oocytes in their gonads, were caught between January and August (3–29%). Resting mature females, with stages -I and -II oocytes, bundles of muscle, and yellow bodies in their ovaries were abundant in samples taken from May to November (54–98%). Ripening or ripe-running males were recorded year-round and spent males were observed in November (4%), from January to March (10–40%), and from May to July (8–22%).

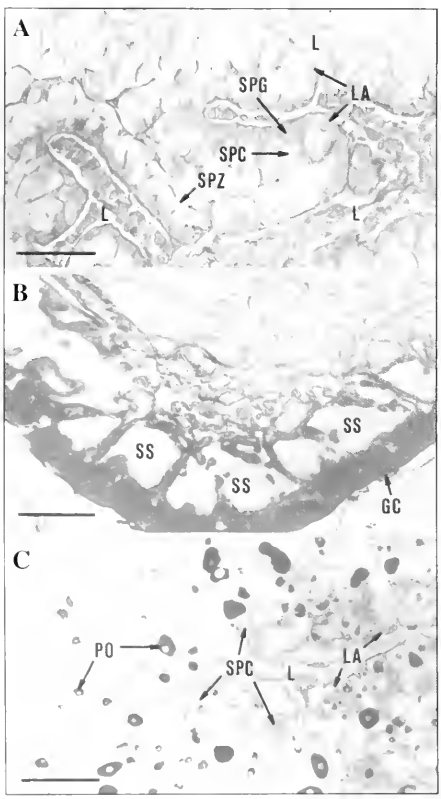

Figure 3

Photomicrographs of histological sections from male and transitional black grouper (*Mycteroperca bonaci*) gonads collected from Campeche Bank, Mexico. (**A**) Section from a 114-cm-FL ripening male captured in July 1997, showing lamellae, lumina, spermatogonia, and spermatocyte cysts, and lamellae sinuses full of spermatozoa. (**B**) Section from a 122-cm-FL ripe-running male captured in September 1997, with sperm sinus full of spermatozoa in gonadal capsule. (**C**) Section from a 113-cm-FL transitional fish captured in January 1998, showing previtellogenic oocytes (stages I) and scattered spermatocyte cysts. GC = gonadal capsule; L = lumen; LA = lamellae; PO = previtellogenic oocyte; SPC = spermatocyte; SPG = spermatogonia; SPZ = spermatozoa; SS = sperm sinus. Scale bars = 200 microns.

Various females from the Alacranes Reef were ripening in November (GSI range: 0.03–4.44%, n=12), December (GSI range: 0.22–7.18%, n=9) and February (GSI range: 0.10–6.61%, n=25). In February, some of them were ripe-running, with postovulatory follicles in ovaries (GSI=1.77% and 1.91%, n=2) and others were spent (GSI=0.74% and 0.88%, n=2). Alacranes Reef males were ripening or ripe-running in November, December, and February (GSI range: 0.03–0.44%, n=11).

Location and timing of spawning

Between April 1996 and February 2000, 61 ripe-running females were caught at 11 offshore fishing locations situated in the northeastern part of the Campeche Bank (depth range: 51–68 m), and from shallow waters of the Alacranes Reef (8–10 m) (Fig. 1). All had vitellogenic oocytes (stages-III–V) with hyaline oocytes or postovulatory follicles (or with both) in their ovaries. Most of these females were caught during, or close to, the new moon phase (Table 2).

Sizes at maturity and at sexual transition

The smallest mature female (L_{min}=58.0 cm) was caught in shallow waters of the Alacranes Reef and had stage-III oocytes in its ovaries. Fifty-percent maturity of females was attained at 72.1 cm in size and all females larger than 95.1 cm were mature (Fig. 7). Because the largest female observed in samples was 123.5 cm (L_{max}), the percentage of females at maximum length at first maturity was L_{min}/L_{max}= 47%.

Females changed sex between 85.5 and 125.0 cm in length (the overlap zone between male and female sizes) and the median size of sexual inversion was 103.3 cm. By the time they attained a length of 111.4 cm, 50% of the females in the sample had transformed into males (Fig. 8). Size range of transitional fish (99.0–121.5 cm) was 17% of maximum fish size (135.0 cm) (ratio 1, see "Materials and methods"section), and sex change occurred over 29% of the maximum size observed for the species (ratio 2). Immature males were not observed during the study.

Discussion

Sexual pattern

Previous research strongly suggests that sex reversal occurs in *M. bonaci* (Smith, 1959, 1961; Garcia-Cagide and Garcia, 1996; Crabtree and Bullock, 1998). Observations on gonadal and population structure characteristics for black

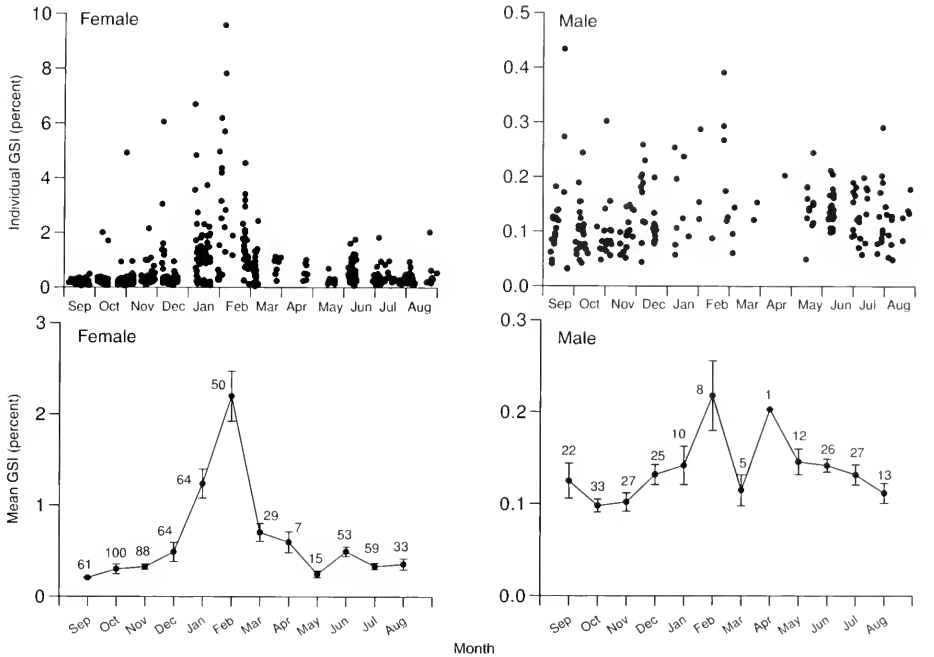

Figure 4

Individual and mean gonadosomatic index (GSI) values for female and male black grouper, (*Mycteroperca bonaci*) collected in offshore waters of the Campeche Bank, Mexico, between April 1996 and May 1999. All calculated GSI for this study were grouped to show monthly variations over a single year. Vertical bars denote standard error. Numbers above the bars denote the sample sizes.

grouper from the Campeche Bank are consistent with the description of monandric protogynous hermaphroditism previously used for this species. During the present study, three of the five criteria suggested by Sadovy and Shapiro (1987) for identifying protogyny in hermaphroditic fishes were identified in black grouper: membrane-lined central cavities in testes; sperm sinuses in the gonadal wall; and transitional individuals. The five black grouper specimens considered as transitional individuals (0.6% of sampled offshore fish) did not have degenerating ovarian tissue in their gonads. For protogynous species, the degeneration of ovarian tissue should logically accompany proliferation of testicular tissue for the specimen to be termed "transitional." However, according to Sadovy and Shapiro (1987), the paucity of reported cases providing such descriptions raises doubts as to whether transitional gonads display this kind of histological profile. These observations also may be a function of the fact that the incidence of transitional fish in field collections is generally relatively low, as shown by the single transitional specimen (0.1% of fish collection) identified by Crabtree and Bullock (1998) in a sample of the Florida black grouper population. Precocious spermatocyte or sperm cysts in immature or functional ovaries as observed by Smith (1964; 1965) and Bullock et al. (1996) in coney (*Cephalopholis fulva*), graysby (*Cephalopholis cruentata*), and yellowedge grouper (*Epinephelus flavolimbatus*) were not found in black groupers ovaries during our study.

Other aspects of population structure indicating monandric protogynous hermaphrodism were also seen in *M. bonaci* from the Campeche Bank. These included bimodal size-frequency distributions, where males were larger than females, female-biased sex ratios in size classes less than 110.1 cm, and male-biased ratios in size classes larger than 115.0 cm. No male smaller than 86.0 cm was identified in any of the samples. Despite these biases, the overall male-to-female sex ratio calculated in our study (1:4) was less skewed towards females than those reported by Garcia-Cagide and Garcia (1996) (1:30.3) and Crabtree and Bullock (1998) (1:15.4). Notwithstanding, the sex ratio for black

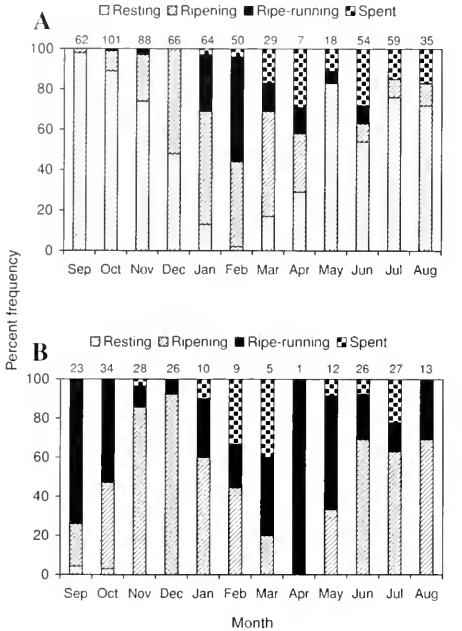

Figure 5

Monthly percent frequencies of female (**A**) and male (**B**) black grouper (*Mycteroperca bonaci*) collected in offshore waters of the Campeche Bank, Mexico (April 1996–May 1999), sorted according to sexual classes over one year. Number of fish sampled is given for each month.

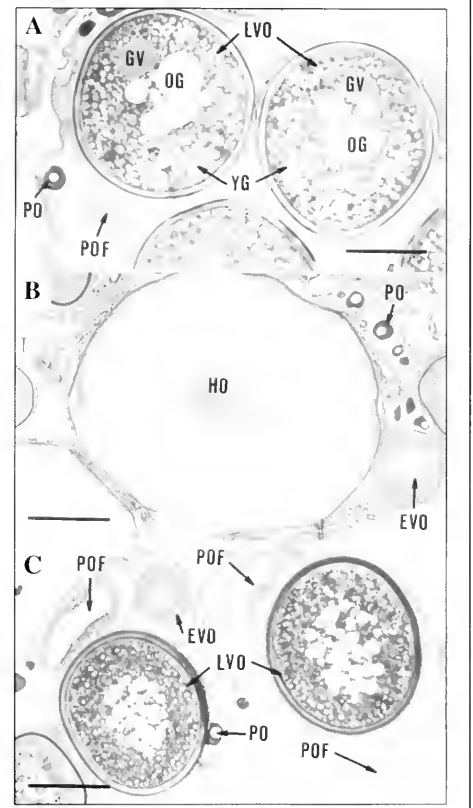

Figure 6

Photomicrographs of histological sections from female black grouper (*Mycteroperca bonaci*) gonads collected from Campeche Bank, Mexico. (**A**) Section from a 97-cm-FL ripe-running female captured in January 1998, showing late vitellogenic oocytes (stage V) undergoing final oocyte maturation, showing yolk and oil globule fusion and germinal vesicle migration; note presence of postovulatory follicle. (**B**) Section from a 79-cm-FL ripe-running female captured in February 1998, with hyaline oocyte (stage VI) and some early and late vitellogenic oocytes (stages III and IV). (**C**) Section from a 92-cm-FL ripe-running female captured in November 1997, with early and late vitellogenic oocytes (stages III and V) and postovulatory follicles. EVO = early vitellogenic oocyte; GV = germinal vesicle; HO = hyaline oocyte; LVO = late vitellogenic oocyte; OG = oil globule; PO = previtellogenic oocyte; POF = postovulatory follicle; YG = yolk globule. Scale bars = 200 microns.

grouper sampled from Florida waters may not resemble that for the entire population. Crabtree and Bullock (1998) stated that they probably underestimated the number of males in their sample because the large black grouper examined were eviscerated and could not be sexed. .

As observed for the first time by Crabtree and Bullock (1998) for black grouper from Florida waters, sexual dimorphism was displayed by the Campeche Bank population. Notwithstanding, a low proportion of females possessed fin pigmentation. Furthermore, it is also possible that individuals undergoing transition from female to male display the male color phase. However, conclusions based on differences in fin pigmentation in male, female, and transitional black grouper from the Campeche Bank are limited by the small number of specimens examined for this purpose.

Spawning season

Sexually active black groupers from the Campeche Bank (ripening females and ripening or ripe-running males) were observed year-round. The monthly relative proportion of individuals in each sex class and mean gonadosomatic indices showed a more consistent annual cycle for

Table 2

Description of samples of ripe-running female black grouper (*Mycteroperca bonaci*) collected in the offshore waters of the Campeche Bank and shallow waters of Alacranes Reef, México, between April 1996 and February 2000. Numbers refer to map locations in Figure 1. HO = hyaline oocyte; POF = postovulatory follicle. WW = whole weight.

Sampling dates	Fishing location	Depth of capture (m)	Date of full and new moon	*n*	Histological feature of ovaries	Size range of females	
						FL (cm)	WW (kg)
31 Oct 1997	21	51–55	15 1, 31 Oct	1	HO	101.0	17.2
21, 22, 27 Nov 1997	22	68	14 29 Nov	3	POF	75.0–91.5	5.3–11.2
6–12 Jan 1997	8	—	23 8 Jan	6	HO or POF	85.0–108.5	8.6–16.5
8–21 Jan 1998	24	59	12 28 Jan	10	POF or HO and POF	91.0–105.5	11.8–17.3
29, 30 Jan 1998	25	59	12 28 Jan	2	POF	94.0; 101.0	12.4;14.8
1–5 Feb 1997	9	—	22 7 Feb	9	HO or POF	88.0–110.0	11.0–20.2
22–28 Feb 1998	27	55	11 26 Feb	17	HO and POF	76.0–117.0	6.4–25.1
3, 6 Feb 2000	Alacranes reef	8–10	19 5 Feb	2	HO and/or POF	89.0; 88.0	8.0; 10.0
2, 8 Mar 1998	27	55	12 27 Mar	2	POF	76.0; 84.0	6.2; 8.0
25 Mar 1998	29	—	12 27 Mar	2	POF	78.0; 94.0	5.4; 9.1
24 Apr 1996	2	55	17 3 Apr	1	POF	75.0	6.3
16 May 1999	37	67	30 15 May	1	POF	90.0	10.2
4–11 Jun 1997	13	64	20 5 Jun	5	OH or POF	69.5–97.0	4.7–13.9

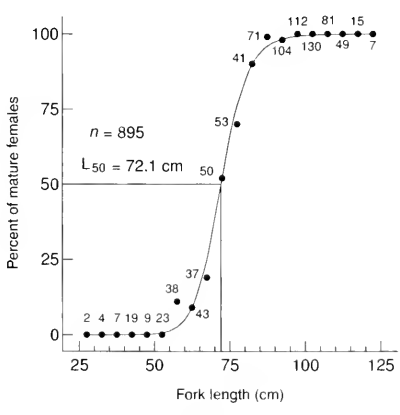

Figure 7

Percent of mature females at length for black grouper (*Mycteroperca bonaci*) from inshore and offshore waters of the Campeche Bank and shallow waters of Alacranes Reef, Mexico (April 1996–February 2000). Proportion of sexually mature females within each size class is plotted with a binary logistic regression. Line indicates length at 50% maturity (L_{50}). Number of fish sampled is given for each size class.

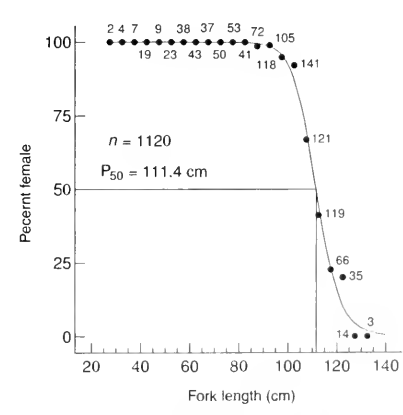

Figure 8

Percentage of female black grouper (*Mycteroperca bonaci*) as a function of fork length. Samples were taken between April 1996 and February 2000 in inshore and offshore waters of the Campeche Bank and shallow waters of Alacranes Reef, Mexico. P_{50} is the length predicted by binary logistic regression at which 50% of the sampled black grouper are female. Number of fish sampled is given for each size class.

females than for males. According to Sadovy (1996), ovaries best reflect duration of fish spawning activity. Under this assumption, the length of the black grouper spawning season was evaluated by using Sadovy's criteria (1996) as defined to assess the duration of annual spawning in reef fish species. Spawning season for black grouper from the Campeche Bank was shown to extend from December to March—a spawning month being defined as one in which

50% or more of the sampled females have yolked oocytes. Peak spawning occurred in February when 50% or more of the sampled females had hyaline oocytes or postovulatory follicles (or both) in their ovaries. In the case of spawning seasonality evaluated by GSI data, peak spawning activity was assigned to the months of January and February in which the mean GSI of female attained was 50% or more of the maximum mean female GSI recorded during the study (2.20% in February). A very few precocious females started to spawn in October (1% of sampled fish) and November (3%) and some were still in spawning condition during May (4%) and June (8%). These results are consistent with previous reports of the *M. bonaci* spawning season in Puerto Rico, the Bahamas, Cuba, and Florida (Erdman, 1956; Smith, 1961, 1971, 1972; García-Gagide et. al., 1994; García-Gagide and García, 1996; Crabtree and Bullock, 1998). Spawning in Bermuda appears to be anomalous, with reproductive activity extending from about early May to early August (Smith, 1971).

Spawning pattern

The authors did not observe spawning aggregations for black grouper from the Campeche Bank as defined by Domeier and Colin (1997) for tropical reef fishes. Black grouper is reported to form spawning aggregations between January and February in Belize, Honduras, and Florida (Carter, 1989; Fine, 1990; Carter and Perrine, 1994; Eklund et al., 2000). Only indirect methods of establishing spawning occurrence, based on female gonadal condition, were used in the present study. Ripe-running females were caught at 11 offshore locations on the Campeche Bank and in the shallow waters of National Marine Park Alacranes Reef, during eight months of the year. The species seemed to spawn preferentially at or around the new moon phase. However, more information, such as direct observations of spawning behavior and data on fish densities at aggregation sites during nonreproductive and reproductive periods, is necessary to know precisely where and when adult *M. bonaci* gather for spawning in the southern Gulf of Mexico. The presence of oocytes at various stages of vitellogenesis in the ovaries of ripening females and the co-existence of postovulatory follicles and vitellogenic oocytes in those of ripe-running females suggest that some individuals may spawn more than once during the spawning season.

Sexual maturity and sex change

The size at which 50% of females were sexually mature (L_{50}) was lower for black grouper from the Campeche Bank (72.1 cm) than for those from Florida (82.6 cm) or Cuban (84.4–108.7 cm) waters. The L_{min}/L_{max} ratio indicated that the females from the Campeche Bank reached first maturity at a higher proportion of maximum length (47%) than those from Florida waters (40%). This spatial variation in size at first sexual maturity has also been observed in female red grouper from southern and eastern Gulf of Mexico (Brulé et al., 1999).

The size at which 50% of the females transformed to males (P_{50}) was lower for black grouper from the Campeche Bank (111.4 cm) than for those from Florida (119.9 cm). Notwithstanding, the size range in which males overlapped with females and the ratio-2 results were almost identical for black grouper from Campeche Bank (39.5 cm and 29%) and south Florida (39 cm and 26%) waters (Crabtree and Bullock, 1998). According to Shapiro (1987), these data are more consistent with a mechanism for behavioral induction of sex change than with the idea that this process occurs at a characteristic size or age for all members of a population.

Fishery characteristics and fishery management

As members of the warm-temperate and tropical reef fish complexes, groupers have consistently proven highly vulnerable to anything other than light levels of fishing pressure (Sadovy, 1997). Because of their biological characteristics, these species must be conservatively managed to avoid rapid overfishing and stock collapse (Sadovy, 1997; Coleman et al., 2000). Some groupers from the western Atlantic are even considered endangered and threatened species (IUCN/SSC[1]). Assessment of Morris et al. (2000) and Musick et al. (2000) led to the classification of black grouper as a vulnerable species, that is, not critically endangered, endangered, or threatened severely, but facing a high risk of extinction in the wild in the medium-term future.

The trend in grouper catches in the state of Yucatán has been one of progressive decline from an historical maximum of 13,993 metric tons (t) in 1991, to 8556 t in 1997, followed by an increase to 11,045 metric tons in 2000 (SAGARPA, 2001). According to Monroy-García et al. (2001), catch increase reflects an increase in fishing effort during the last three years. Recent assessments of red grouper population from the Campeche Bank indicate that the current biomass of exploited stock is well below that of maximum biological productivity and that the fishery is considered deteriorated (SEMARNAP, 2000a, 2000b). In response to the multiple threats facing groupers in the Gulf of Mexico, the U.S. and Mexican governments have implemented regulations designed to either reduce or contain effective fishing effort (input controls), or to restrict total catch (output controls) to predefined limits. Notwithstanding, grouper fishery regulations used in Mexican waters are less restrictive than those imposed in U.S. waters. The U.S. regulations currently consist of the following: an annual commercial quota of 4445 t for the shallow-water grouper complex, which includes the black grouper; commercial and recreational minimum size limits of 61.0 cm TL and 55.9 cm TL, respectively; a seasonal closure on commercial harvest and prohibition on sale of this species from 15 February to 15 March; and a recreational aggregate daily bag limit of five groupers per person (Gulf of Mexico Fishery Management Council[2]). The Mexican regulations include license limita-

[1] 2001. IUCN/SSC (International Union for the Conservation of Nature and Natural Resources/Species Survival Commission). SSC Red List Programme IUCN/SSC UK Office, 219c, Huntingdon Road, Cambridge CB3 ODL, United Kingdom. Web page: http://www.redlist.org

[2] 2001. Gulf of Mexico Fishery Management Council. The Commons at Rivergate, 3018 U.S. Hwy. 301 N., Suite 1000 Tampa, Florida 33619-2266. Web page: http://www.gulfcouncil.org

tion and a minimum legal total length of 30 cm for the Mexican fleet, and an annual catch quota of 3900 t for the Cuban fleet (SEMARNAP, 2000b). As can be seen, commercial and recreational exploitation of the Campeche Bank grouper resource still lacks a well-defined management strategy. Many of the obstacles noted by Huntsman and Waters (1987) in developing snapper-grouper management plans for the Gulf of Mexico and U.S. South Atlantic are seen in the southern Gulf of Mexico. For instance, grouper landings are not identified to the species level in Mexican fisheries statistic, but all species are reported in the "mero" (grouper) category, which includes eighteen species of the genera *Cephalopholis*, *Epinephelus*, and *Mycteroperca* (Colás-Marrufo et al., 1998). Information on grouper recreational catches is lacking, and biological data on the Campeche Bank species, especially on reproduction, are either scarce or nonexistent. Moreover, the 30-cm-TL minimum size limit was applied to prevent the marketing of fish considered too small and was only related to the growth overfishing problem.

Although landing trends by species for the southern Gulf of Mexico grouper fishery remain undetermined, black grouper along with red grouper and gag appear to be the most abundant serranid fishes off the northern coast of the Yucatán Peninsula. Colás-Marrufo et al. (1998) reported black grouper to be second to red grouper in total number (12%) and weight (40%) of grouper catches taken from the Campeche Bank by some commercial fishing boats between 1996 and 1998. If a decrease in commercial grouper landings from Mexican waters is confirmed in the near future, protection measures such as regulation of specific catch will be required for each of these three grouper species.

Results from the present study may aid in better estimating and thus maintaining reproductive output in the black grouper population from the Campeche Bank. With these data, fishing regulations can be based on reproductive aspects. This information will make it possible to propose a minimum size limit for this species near the size at which 50% of females are sexually mature (72 cm FL) (output control) and a closed season during peak spawning in February (input control)—both of which would help prevent recruitment overfishing. Furthermore, if it is confirmed that black grouper from the Campeche Bank spawn in the shallow waters of the Alacranes Reef complex, it should be easy to temporarily ban fishing in the spawning area(s) through enforcement of the regulations protecting this National Marine Park.

Acknowledgments

This research was supported by grant 2184P-B9507 from the Consejo Nacional de Ciencia y Tecnología (CONACYT); grant C-1-99/062 from the Fondo Mexicano para la Conservación de la Naturaleza (FMCN); and the SEMARNAP/S.S.S. "24 de Febrero"/CINVESTAV agreement for use of the fishing vessel *Unicap VII*. For their assistance during this study, we would like to thank R. Robles de Benito, V. Alcantar-Cárdenas, and M. Garduño-Andrade from SEMARNAP/IPN-CRIPY (Mérida/Yucalpetén); J. Peraza-Menéndez and M. Castillo-Martínez from CECADESU/CREDES (Yucalpetén); J. Rodríguez-Felix from S.S.S. "24 de Febrero" (Progreso); A.M. Pech from CONYUC fish house (Progreso); J.L. Carrillo-Galaz and F. Alvarez-Carrillo from the fishing cooperative SCPP "Pescadores de Sisal" (Progreso); and L. Contreras-García, Port Captain of Progreso. For their assistance in all aspects of the field collection, we are grateful to M. Sánchez-Crespo; V. Durarte-Gracía, S. Mena-González, C. Ureña-Chio, J. Hernández-Viguegas, T. Ramírez-Hernández, and P. Mina-Coello. We also wish to thank L. Gus-Peltinovich for assistance with photography.

Literature cited

Begossi, A., and J. L. de Figueiredo.
1995. Ethnoichthyology of southern coastal fishermen: cases from Búzios island and Sepetiba bay (Brazil). Bull. Mar. Sci. 56:710–717.

Bohlke, J. E., and C. G. H. Chaplin.
1993. Fishes of the Bahamas and adjacent tropical waters, 2nd ed., 771 p. Univ. Texas Press, Austin, TX.

Brulé, T., and C. Déniel.
1994. Exposé synoptique des données biologiques sur le mérou rouge *Epinephelus morio* (Valenciennes, 1828) du golfe du Mexique. FAO Synopsis sur les pêches 155, 39 p. FAO, Rome.

Brulé, T., C. Déniel, T. Colás-Marrufo, and M. Sánchez-Crespo.
1999. Red grouper reproduction in the southern Gulf of Mexico. Trans. Am. Fish. Soc. 128:385–402.

Brulé, T., D. Ordaz Avila, M. Sánchez Crespo, and C. Déniel.
1994. Seasonal and diel changes in diet composition of juvenile red grouper (*Epinephelus morio*) from Campeche Bank. Bull. Mar. Sci. 55:255–262.

Bullock, L. H., M. F. Godcharles, and R. E. Crabtree.
1996. Reproduction of yellowedge grouper, *Epinephelus flavolimbatus*, from the eastern Gulf of Mexico. Bull. Mar. Sci. 59:216–224.

Bullock, L. H., and G. B. Smith.
1991. Seabasses (Pisces: Serranidae). Mem. Hourglass Cruises, vol..8, part 2, 243 p.

Carter, J.
1989. Grouper sex in Belize. Nat. Hist. 10:61–68.

Carter, J., and D. Perrine.
1994. A spawning aggregation of dog snapper, *Lutjanus jocu* (Pisces: Lutjanidae) in Belize, Central America. Bull. Mar. Sci. 55:228–234.

Cervigon, F.
1991. Los peces marinos de Venezuela, vol. 1, 2nd ed., 423 p. Fundación Científica Los Roques, Caracas.

Claro, R., J. Baisre, and J. P. García-Arteaga.
1994. Evolución y manejo de los recursos pesqueros. *In* Ecología de los peces marinos de Cuba (R. Claro, ed.), p. 435–456. Centro de Investigaciones de Quintana Roo (CIQRO), Chetumal, Quintana Roo.

Colas-Marrufo, T., T. Brulé, and C. Déniel.
1998. Análisis preliminar de las capturas de meros realizadas a través de unidades de la flota mayor en el sureste del Golfo de México. Proc. Gulf Caribb. Fish. Inst. 50:780–803.

Coleman, F. C., C. C. Koenig, G. R. Huntsman, J. A. Musick, A. M. Eklund, J. C. McGovern, R. W. Chapman, G. R. Sedberry, and C. B. Grimes.
2000. Long-lived reef fishes: the grouper-snapper complex. Fisheries 25 (3):14–21.

Crabtree, R. E., and L. H. Bullock.
1998. Age, growth, and reproduction of black grouper, *Mycteroperca bonaci*, in Florida waters. Fish. Bull. 96:735–753.
Domeier, M. L., and P. L. Colin.
1997. Tropical reef fish spawning aggregations: defined and reviewed. Bull. Mar. Sci. 60:698–726.
Eklund, A. M., D. B. McClellan, and D. E. Harper.
2000. Black grouper aggregation in relation to protected areas within the Florida Keys National Marine Sanctuary. Bull. Mar. Sci. 66:721–728.
Erdman, D. S.
1956. Recent fish records from Puerto Rico. Bull. Mar. Sci. Gulf Caribb. 6:315–340.
Fine, J. C.
1990. Groupers in love: spawning aggregations of Nassau grouper in Honduras. The Explorers Journal, Fall 1990, 131–134.
Fischer, W.
1978. FAO species identification sheets for fisheries purposes. Western Central Atlantic (fishing area 31), vols. 1–7, var. pag. FAO, Rome.
Gabe, M.
1968. Techniques histologiques, 1113 p. Masson, Paris.
García-Cagide, A., R. Claro, and B. V. Koshelev.
1994. Reproducción. *In* Ecologia de los peces marinos de Cuba (R. Claro, ed.), p. 187–261. Centro de Investigaciones de Quintana Roo (CIQRO), Chetumal, Quintana Roo.
García-Cagide, A., and T. García.
1996. Reproducción de *Mycteroperca bonaci* y *Mycteroperca venenosa* (Pisces: Serranidae) en la plataforma cubana. Rev. Biol. Trop. 44:771–780.
Grimes, C. B.
1987. Reproductive biology of the Lutjanidae: a review. *In* Tropical snappers and groupers: biology and fisheries management (J. J. Polovina and S. Ralston, eds.), p. 239–294. Westview Press, Boulder, CO.
Heemstra, P. C., and J. E. Randall.
1993. FAO species catalogue, vol. 16: Groupers of the world (Family Serranidae, Subfamily Epinephelinae). An annotated and illustrated catalogue of the grouper, rockcod, hind, coral grouper and lyretail species known to date. FAO Fisheries Synopsis 125, 382 p. FAO, Rome.
Huntsman, G. R., J. Potts, and R. W. Mays.
1994. A preliminary assessment of the populations of seven species of grouper (Serranidae, Epinephelinae) in the Western Atlantic Ocean from Cape Hatteras, North Carolina to the Dry Tortugas, Florida. Proc. Gulf Caribb. Fish. Instit. 43: 193–213.
Huntsman, G. R., and J. R. Waters.
1987. Development of management plans for reef fishes-Gulf of Mexico and U.S. South Atlantic. *In* Tropical snappers and groupers: biology and fisheries management (J. J. Polovina and S. Ralston, eds.), p. 533–560. Westview Press, Boulder, CO.
Lambert, J. G. D.
1970. The ovary of the guppy, *Poecilia reticulata*. The atretic follicle, a corpus atreticum or a corpus luteum praeovulationis. Z. Zellforsch. Mikrosk. Anat. 107:54–67.
Manooch, C. S., and D. L. Mason.
1987. Age and growth of the Warsaw grouper and black grouper from the southeast region of the United States. Northeast Gulf Sci. 9:65–75.
Moe, M. A.
1969. Biology of the red grouper *Epinephelus morio* (Valenciennes) from the eastern Gulf of Mexico. Fla. Dep. Nat. Resour. Mar. Res. Lab. Prof. Pap. Ser. 10, 95 p.
Monroy-García, C., R. Burgos-Rosas, V. Moreno-García, and E. Gimenez-Hurtado.
2001. Informe de investigaciones conjuntas México-Cuba sobre el mero (*Epinephelus morio*, Valenciennes, 1828) en el Banco de Campeche. Convenio de pesca Mxico-Cuba, 42 p. Secretaria de Agricultura, Ganadería, Desarrollo Rural, Pesca y Alimentación (México) y Ministerio de la Industria Pesquera (Cuba). Instituto Nacional de la Pesca, Progreso, Yucatán.
Morris, A. V., C. M. Roberts, and J. P. Hawkins.
2000. The threatened status of groupers (Epinephelinae). Biodivers. Conserv. 9:919–942.
Musick, J. A., M. M. Harbin, S. A. Berkeley, G. H. Burgess, A. M. Eklund, L. Findley, R. G. Gilmore, J. T. Golden, D. S. Ha, G. R. Huntsman, J. C. McGovern, S. J. Parker, S. G. Poss, E. Sala, T. W. Schmidt, G. R. Sedberry, H. Weeks, and S. G. Wright.
2000. Endangered Species-Marine, estuarine, and diadromous fish stocks at risk of extinction in North america (exclusive of pacific salmonids). Fisheries (Bethesda) 25(11): 6–30.
Roe, R. B.
1977. Distribution of snappers and groupers in the Gulf of Mexico and Caribbean Sea as determined from exploratory fishing data. *In* Proceedings of the Colloquim on snapper-grouper fisheries ressources of the western Central Atlantic Ocean (H. R. Bullis and A. C. Jones, eds.), p. 129–164. Florida Sea Grant Program, Report 17, State University System of Florida Sea Grant Program, Gainesville, FL.
Sadovy, Y.
1994. Grouper stocks of the western central Atlantic: the need for management and management needs. Proc. Gulf Caribb. Fish. Inst. 43:43–64.
1996. Reproduction of reef fishery species. *In* Reef fisheries (N. V. C. Polunin and C. M. Roberts, eds.), p. 15–59. Chapman and Hall, London.
1997. Problems of sustainability in grouper fisheries. Proc. Fourth Asian Fish. Forum, p. 321–324. China Ocean Press, Beijing.
Sadovy, Y., and D. Y. Shapiro.
1987. Criteria for the diagnosis of hermaphroditism in fishes. Copeia 1987:136–156.
Scherrer, B.
1984. Biostatistique, 850 p. Gaëtan Morin Editeur, Boucherville, Québec.
SAGARPA (Secretaria de Agricultura, Ganadería, Desarrollo Rural, Pesca y Alimentación).
2001. Anuario estadistico de pesca 2000, 268 p. SAGARPA, México.
SEMARNAP (Secretaria de Medio Ambiente, Recursos Naturales y Pesca).
2000a. Anuario estadistico de pesca 1999, 271 p. SEMARNAP, México.
2000b. Sustentablilidad y pesca responsable en México. Evaluación y manejo 1997–1998, 691 p. SEMARNAP-IPN, México.
Shapiro, D. Y.
1984. Sex reversal and sociodemografic processes in coral reef fishes. *In* Fish reproduction: strategies and tactics, 3rd ed. (G. W. Potts and R. J. Wootton, eds.), p. 103–118. Academic Press, London.
1987. Reproduction in groupers. *In* Tropical snappers and groupers: biology and fisheries management (J. J. Polovina and S. Ralston, eds.), p. 295–327. Westview Press, Boulder, CO.

Shapiro, D. Y., Y. Sadovy, and M. A. McGehee.
1993. Periodicity of sex change and reproduction in the red hind, *Epinephelus guttatus*, a protogynous grouper. Bull. Mar. Sci. 53:1151–1162.
Smith, C. L.
1959. Hermaphroditism in some serranid fishes from Bermuda. Pap. Mich. Acad. Sci. 44:111–119.
1961. Synopsis of biological data on groupers (*Epinephelus* and allied genera) of the Western North Atlantic. FAO Fisheries Biology Synopsis 23, 61 p. FAO, Rome.
1964. Hermaphroditism in Bahamas groupers. Bull. Mus. Nat. Hist., N.W. 73:42–47.
1965. The patterns of sexuality and the classification of serranid fishes. Am. Mus. Novit. 2207:1–20.
1971. A revision of the American groupers: *Epinephelus* and allied genera. Bull. Am. Mus. Nat. Hist. 146:67–242.
1972. A spawning aggregation of Nassau grouper, *Epinephelus striatus* (Bloch). Trans. Am. Fish. Soc. 101:257–261.

The effect of timing of tagging on streamer-tag recapture rates for American lobster (*Homarus americanus*)

Michel Comeau
Manon Mallet
Department of Fisheries and Oceans
343 University Ave
Moncton, New Brunswick, Canada E1C 9B6
E-mail address (for M. Comeau): comeaum@dfo-mpo.gc.ca

Abstract—Streamer tags are commonly used to study the ecology and population biology of the American lobster (*Homarus americanus*). Aquarium observations suggest that streamer tag loss, either through tag-induced mortality or tag shedding, is related to the molt stage of the lobster at the time of tagging, and the molting event itself. Tag-induced mortality, where lobsters did not molt, occurred within eleven and sixteen days following tagging for lobsters tagged in postmolt (4%) and late premolt (10%) stages, respectively; whereas no lobsters tagged in early premolt or intermolt stages died. Tag-induced mortality at time of molting was observed for lobsters tagged in late premolt stage (11%), and tag shedding was observed for lobsters tagged both in early (25%) and late premolt (11%) stages, but was significantly higher (P=0.014) for lobsters tagged in early premolt stages. Autopsies revealed that lobsters died mainly of organ perforations (hepato-pancreas and pericardial sac) following the tagging process, and rupture of the dorsal thoraco-abdominal membrane during the molting process. The total tag loss was estimated at 4% for lobsters tagged after molting, and 27% and 31% for lobsters tagged in early and late premolt stages, respectively. There was no tag loss for lobsters tagged in the intermolt stage during four months of laboratory observations (July–October). To minimize streamer tag loss, lobsters should be tagged during the intermolt or postmolt stage. Based on field studies, recapture rates for lobsters tagged in premolt stage are always lower than those of lobsters tagged in postmolt stage. Furthermore, recapture rates during the second year, for lobsters that molt in the year following tagging, were drastically reduced, and no lobster was recaptured after four years at large. Finally, to account for tag loss during the first year at large, a minimal adjustment of 24.9% (SD 2.9%) and 4.4% (SD 1.6%) for the recapture rate of lobsters tagged immediately before and after the molting season, respectively, is recommended. Adjustments beyond one year at large are not recommended for the American lobster at this time.

Manuscript approved for publication 19 February 2003 by Scientific Editor.
Manuscript received 4 April 2003 at NMFS Scientific Publications Office.
Fish. Bull. 101:476-483 (2003).

Tagging methods to study the movement, growth, and exploitation rate for the American lobster (*Homarus americanus*) have improved over the last 70 years. One major improvement in the mid 1960s was the introduction of an insertion tag called the "sphyrion tag" that is anchored to muscle tissue (Scarratt and Elson, 1965), instead of body tags (Templeman, 1935) or carapace-piercing tags (Wilder, 1953) used earlier. By the late 1980s, the sphyrion tag was replaced by another insertion tag called the polyethylene "streamer tag" (Landsburg, 1991; Moriyasu et al., 1995) initially developed for shrimps (*Penaeus* spp.; Marullo et al., 1976). Insertion tags have the advantage of being retained through a series of molts, thus providing information on long-term movement and more accurate data on growth.

Tag loss could greatly bias the estimate of population characteristics and fishery parameters (Ricker, 1975). For obtaining population estimates from mark-recapture data, tag loss generally refers to the reduction of the initial number of tagged animals by means other than fishing. In a series of tagging studies, Comeau et al. (1999) noticed a constant pattern of lower tag recovery rates for lobsters tagged in the premolt stage than for lobsters tagged in the postmolt stage. They indicated that the level of fishermen participation (recovery rate) could be a possible cause of tag loss because they noticed a steady decline of recapture rates where multiyear tagging studies were conducted. However, because the same type of streamer tag was used and each lobster was handled individually, the fishermen participation could not explain the difference between recapture rates for lobsters tagged in premolt and postmolt stages for a given year; hence possible tag loss at molting was suspected as the cause of the lower recapture rates (Comeau et al., 1999). Furthermore, in an attempt to estimate mortality rates, Comeau and Mallet (2001) used a mark-recapture model and simulations to evaluate the best estimator. They concluded that the level of tag loss is high and could be a serious problem for estimating fishery parameters for the American lobster if information on tag loss is not available.

Moriyasu et al. (1995) showed that sphyrion tag loss for lobsters held in aquaria varies between 3% and 23% depending on the molt stage at tagging. They also mentioned that lobsters tagged with sphyrion tags showed a significantly lower return rate (19%) than lobsters tagged with streamer tags (44%) in a recapture study in the field and suggested a possible lower level of tag loss among lobsters tagged with streamer tags. However, they did not estimate the tag loss for streamer-tagged lobsters. Recently, Rowe and Haedrich (2001) showed that the shedding rate for streamer tags in the field could reach 18% (40% for molted animals and 11% for nonmolting animals) after 8–12 months based on double tagging with a secondary carapace marking. They also found that streamer tag shedding was not related to sex or size, but they did not study the level of tag-induced mortality.

Various causes can reduce the initial number of tagged animals, mainly tag shedding, tag-induced mortality, and

death from natural causes (Beverton and Holt, 1957). In the present article, "tag shedding" refers to the physical detachment of the tag from a lobster and "tag-induced mortality" refers to the actual death of a lobster caused by the tagging process.

In the southwestern Gulf of St. Lawrence, lobsters are harvested either in the spring prior to the July–August molting season, or in late summer and early fall (early-August to early October, partially during and shortly after molting) (Comeau and Savoie, 2001). The purpose of our study was to estimate the level of streamer tag loss for the American lobster tagged before and after the summer (July–August) molting season by using aquarium observations. From the results of our aquarium study, we determined adjustments of the recapture rate in relation to the molt stage at the time of tagging.

Materials and methods

Aquarium observations

Two experiments were carried out at the "Aquarium et centre marin" (New Brunswick Department of Agriculture, Fisheries and Aquaculture) in Shippagan, New Brunswick, with lobsters captured in Baie des Chaleurs (47°52'N; 64°52'W). Because the main focus of our study was to investigate tag loss in relation to the molting stage, only males were considered because they have a higher probability of molting annually compared to sexually mature females (Comeau and Savoie, 2001). All lobsters caught were brought to the laboratory where carapace length (CL) and shell rigidity were recorded (the latter with a durometer) (Comeau and Savoie, 2001). In both experiments, lobsters were tagged by the same person to avoid variability in tagging procedure following the technique described by Moriyasu et al. (1995). Streamer tags manufactured by Hallprint Pty. Ltd. (15 Crozier Rd, Victor Harbor, South Australia, 5211 Australia) were used. As is routinely done in our tagging studies in the field (Comeau et al., 1998, 1999), tagged lobsters were kept in a holding tank for a minimum of 30 min following tagging, and dead lobsters were removed from the experiment. Tagged lobsters were then transferred to large tanks partitioned with 25×25 cm individual compartments. These tanks were supplied with running seawater at ambient temperature. Lobsters were fed rainbow smelt (*Osmerus mordax*) twice a week. Lobsters were examined three times a day in July and August, and on a daily basis for the rest of the experiment. The date of tag shedding, of molting, or of death was recorded for each lobster.

Limited aquarium space prevented the use of a control group of untagged lobsters. However, autopsies were performed on all lobsters that died in the course of the experiments in order to identify the cause of death. The following tagging traumas, causing death, were identified (Krouse and Nutting, 1990): 1) perforation of vital organs, such as the pericardial sac and the hepato-pancreas; 2) rupture of the thoraco-abdominal membrane; and 3) necrosis or infection of lobster tissue at both the point of entry and exit of the tag.

The first experiment began on 23 June 1998 before the summer molting season with the tagging of 229 hard-shell male lobsters ranging between 66 and 78 mm CL. To avoid unnecessary manipulation of the lobsters, the molt stage at tagging was estimated by the number of days between tagging and molting. Individuals that molted within 30 days of and 30 days after tagging were considered lobsters tagged in late premolt and early premolt stages (Aiken, 1980), respectively. The molt stage of lobsters that died during the experiment was determined by observations of the pleopods (Aiken, 1980). A total of 191 male lobsters were tagged in premolt stage (56 in early and 135 in late premolt stage) and 38 in the intermolt stage (lobsters that did not molt over the entire experiments). Observations of premolt tagged lobsters that molted in June and July ended on 8 September 1998. Observations of the remaining lobsters tagged on 23 June 1998 ended on 30 October 1998. Before releasing the lobsters in the water, their wounds from the tag insertion were examined for infection.

The second experiment began 9 September 1998 with the tagging of 187 soft-shell male lobsters in the postmolt stage based on shell condition criteria (Aiken, 1980; Comeau and Savoie, 2001). They ranged in size between 66 and 83 mm CL. Observations of postmolt tagged lobsters ended on 30 October 1998.

Field studies

Comparison of recapture rates from field studies Six tagging studies were carried out after the fishing season (May–June) in Caraquet, New Brunswick, between 1994 and 1996. Male and female lobsters were captured, tagged, and released on the commercial fishing grounds. For each year, tagging was done before (in early July with hard-shell lobsters) and after (in mid-September with soft-shell lobsters) the molting season. In 1995, the July tagging was delayed one week because the lobster fishing season ended on 7 July instead of 30 June. In 1996, tagging was carried out in early October instead of mid-September because of bad weather. As with the aquarium experiments, the same person performed the tagging procedure. Tagged lobsters were kept in a holding tank for a minimum of 30 min following tagging and any dead lobsters were removed. Finally, an awareness campaign described in Comeau et al. (1998) was conducted to maximize the participation of fishermen in reporting tagged lobsters as tag recovery took place during the fishing seasons following the year of tagging.

Adjustment of the recapture rate Recapture rates observed during the fishing season following tagging were adjusted by using the information from the aquarium observations. In contrast to tag misreporting that biases the estimated number of recaptured lobsters, tag loss affects the number of tagged animals (N) in the population available to the fishery. To account for possible tag loss in our field studies, N was adjusted as follows. Let p represent the tag-retention rate parameter estimate based on aquarium observations with variance $p(1-p)n^{-1}$, where n is the total number of animals observed in each aquarium experiment.

Table 1

Number and rate (in percentage) of tag shedding and tag induced mortality for American lobsters (*Homarus americanus*) tagged in postmolt, intermolt, and premolt stages in the aquarium experiments. Lobsters tagged in the premolt stage have been separated into early and late premolt divisions, and n is the number of lobster used to calculate the adjusted recapture rate.

	Premolt				
	Early	Late	Total	Intermolt	Postmolt
Initial number[1] (n)	56	135	191	38	183
Tag loss without molting					
Tag-induced mortality	0	13 (10%)	13 (7%)	0	7 (4%)
Shedding	0	0	0	0	1 (<1%)
Total	0	13 (10%)	13 (7%)	0	8 (4%)
Tag loss during or after molting					
Tag-induced mortality	1 (2%)	14 (10%)	15 (8%)		
Shedding	14 (25%)	15 (11%)	29 (15%)		
Total	15 (27%)	29 (21%)	44 (23%)		
Total tag loss	15 (27%)	42 (31%)	57 (30%)	0 (0%)	8 (4%)

[1] Number used in the experiment after accounting for lobsters that died within 30 minutes of tagging.

The adjusted number of tagged animals released during the field studies effectively available to the fishery is equal to

$$N_{adj} = Np, \tag{1}$$

with variance

$$V(N_{adj}) = Np(1-p). \tag{2}$$

The field study recapture rate (t) is defined as

$$t = m(N_{adj})^{-1}, \tag{3}$$

where m = the number of tags returned.

The variance of t can be calculated by using conditional theory and an approximate variance of $(N_{adj})^{-1}$ (Seber, 1982). In this study, we used Monte-Carlo simulations to obtain the 90% confidence interval (CI) for t. The simulations were carried out in two steps to include variability associated with tag loss from the initial N animals tagged and released, and variability in recapture rate. First, assuming that the number of tags retained (N_{adj}) follows a binomial distribution with parameters N and p, a random number ($\tilde{N}_{adj}$) was selected from a *Binomial*(N,p), where N was set equal to the number of animal tagged during a particular study, and p equal to the proportion of tag retention estimated from the aquarium study. With this simulated $\tilde{N}_{adj}$ a conditional value of t was derived as

$$t_c = m_o(\tilde{N}_{adj})^{-1}, \tag{4}$$

where "~" = the simulated value; and
m_o = the observed number of recaptures in a field study.

Secondly, a value for $\tilde{m}$ was obtained from a binomial distribution with parameters $\tilde{N}_{adj}$ and a conditional recapture rate t_c. A simulated recapture rate was calculated as

$$\tilde{t} = m\,(\tilde{N}_{adj})^{-1}. \tag{5}$$

The process was repeated 1000 times and the 90% CI for $\tilde{t}$ was defined as the 5% and 95% quantiles of the resulting 1000 Monte-Carlo values of $\tilde{t}$.

Results

Aquarium observations

Tag-induced mortality was observed within 30 min of tagging for two lobsters tagged in the late premolt stage (1.5%) and for four in postmolt stage (2.1%) but not for lobsters tagged in early premolt and intermolt stages. The autopsies revealed that all of these lobsters died from perforation of the pericardial sac and these lobsters were not used in our experiments.

Tag loss of premolt lobsters was associated solely with tag-induced mortality and this was restricted to 10% (13) of the late premolt lobsters (Table 1). Autopsies revealed that six lobsters died within three days of tagging from the rupture of the dorsal thoraco-abdominal membrane, one died after one day from the perforation of the pericardial sac, and six died between three to sixteen days after tagging from a perforated hepato-pancreas (Table 2). In contrast, only 4% (7) of postmolt lobsters died from tag-induced mortality (Table 1). Autopsies revealed that all deaths were associated with the rupture of the dorsal thoraco-abdominal membrane. Another death was not related to tagging (Table 2).

Table 2

Number of lobsters (*Homarus americanus*) that died during the aquarium experiments from different traumas identified by autopsies. The number of days between tagging and death, and between molting and death, are indicated in parentheses in the "Before molting" and "During or after molting" categories, respectively.

	Premolt stage		
	Early	Late	Postmolt stage
Total number of lobster in the experiments	56	133	183
Before molting			
Perforation of the pericardial sac	0	1 (1)	0
Rupture of the dorsal thoraco-abdominal membrane	0	6 (1–3)	7 (1–11)[1]
Perforation of the hepato-pancreas	0	6 (3–16)	0
No sign of trauma (death not related to tagging)	0	0	1 (5)
During or after molting			
Rupture of the dorsal thoraco-abdominal membrane	0	11 (<1–1)	—
Poor healing of the entry and exit wounds revealing a punctured dorsal thoraco-abdominal membrane	1 (1)	3 (5–57)[2]	—
No sign of trauma (death not related to tagging)	0	1 (<1)	—

[1] Five lobsters died within four days, and two more died after nine and eleven days.

[2] Two lobsters died five and ten days after molting, and one lobster died 57 days after molting from severe infections at the tag-insertions sites.

A total of 70% (134) of the lobsters tagged in the premolt stage molted between 30 June and 8 September (between 7 and 77 days after tagging) without any tag loss (Table 1). Tag-induced mortality represented 8% (15) of the tag loss (Table 1). Autopsies revealed that the majority (11) of the lobsters tagged in late premolt stage died from the rupture of the dorsal thoraco-abdominal membrane (Table 2); the tag was still attached to the old membrane and had caused the rupture of the new one. The four remaining lobsters died from poor healing of the tissue at the point of entry and exit of the tag, revealing a punctured dorsal thoraco-abdominal membrane (Table 2). For all lobsters that healed poorly and later died, one side of the tag had been pulled inside the body cavity during molting. One death was not related to tagging but was caused by the crusher claw becoming wedged within the old carapace, thus preventing the animal from successfully completing the molting process. Furthermore, the autopsy for this lobster did not reveal any sign of tagging trauma.

Tag shedding was observed during molting for 21% (29) of the lobsters tagged in the premolt stage (Table 1). Tag shedding was observed for lobsters tagged in both early and late premolt stages (Table 1) but was significantly higher (χ^2=5.9; P=0.014) for lobsters tagged in the early premolt stage. Twenty-one percent (28) of lobsters tagged in the premolt stage that molted had a misaligned tag (pulled to one side).

Only 4% (8) of the lobsters tagged in the postmolt stage died during the second experiment, and only one individual (<1%) shed a tag (Table 1). The autopsies revealed that tags were not well embedded in the muscle tissue and large scars were observed on the dorsal thoraco-abdominal membrane of seven individuals (Table 2). These lobsters died within 11 days of tagging. The death of the other individual was not related to tagging for there was no sign of tagging trauma. Three percent (5) of the lobsters had a misaligned tag at the end of the experiment.

From a total of 229 lobsters initially tagged for the first experiment, 17% (38) were in the intermolt stage. Although the sample number was small, none of these lobsters shed their tag, died from the tagging procedure, or molted. This finding indicates that these small male lobsters (67–78 mm CL) skipped an entire molting season (July–August) in 1998 and retained their tags without risk. Only one (3%) lobster had a misaligned tag at the end of the experiment. No lobster that was returned to the sea after the experiments had infected wounds from the tag insertion procedure.

Field studies

Tag-induced mortality was observed within 30 min in every tagging study conducted between 1994 and 1996, varying in rate between 0.4% to 3.5%. The majority of the lobsters tagged in early July 1994, 1995, and 1996 were in the premolt stage because 94% to 99% had molted before being recaptured the following fishing season. Except for two lobsters (1.1%) tagged in 1994 that were recaptured the following fishing season with a size increase, all of lobsters tagged in September–October were in the postmolt stage. Recapture rates based on the first recapture period for lobsters tagged in early July (premolt) were significantly lower than the recapture rates for lobsters tagged in September–October (postmolt) for the 1994 (χ^2=10.6; P=0.001) and 1995 (χ^2=11.4.; P=0.0007) tagging, but not for the 1996 (χ^2=2.0; P=0.156) tagging (Table 3). Although

Table 3

Numbers and percentage (in parentheses) of lobsters (*Homarus americanus*) tagged and recaptured during the field tagging studies. Lobsters were tagged before (July) and after (September–October) the molting season between 1994 and 1996, and recaptured the following fishing seasons (May–June). The recapture rates during the first fishing season were adjusted on the basis of the tag loss observed in aquarium observations, and Monte-Carlo simulations were used to calculate the confidence interval. The recapture is based only on the number of legal-size (LS=66.7 mm) lobsters released for the experiment (n). No lobster was recaptured during its fourth year at liberty.

Dates of tagging	Number of LS lobsters released (n)	Number recaptured (1st fishing season)	Number recaptured (2nd fishing season)	Number recaptured (3rd fishing season)	Adjusted recapture rate (1st fishing season)	90% confidence interval
6–7 Jul 1994	476	153 (32.1%)	8 (1.6%)	0 (0.0%)	42.7%	(39.0, 48.0)
14–15 Sep 1994	427	182 (42.6%)	10 (2.3%)	4 (0.9%)	44.6%	(40.7, 48.9)
11–13 Jul 1995	320	79 (24.7%)	5 (1.6%)	2 (0.6%)	32.9%	(28.0, 38.7)
19–20 Sep 1995	442	160 (36.2%)	15 (3.4%)	3 (0.7%)	37.9%	(34.3, 42.1)
3–5 Jul 1996	111	31 (27.9%)	3 (2.7%)	0 (0.0%)	37.2%	(28.7, 48.1)
2–3 Oct 1996	355	125 (35.2%)	22 (6.2%)	3 (0.8%)	36.8%	(32.5, 41.6)

lobsters were recaptured for up to three years following their tagging, the recapture rate was drastically reduced between the first and second recapture period (Table 3). No lobsters were recaptured after four years.

Based on the information from our aquarium observations, the adjusted recapture rates of the field tagging studies showed no difference between lobsters tagged in the premolt and postmolt stages (Table 3). Because the 1995 July tagging was carried out one week later and the molting season was early that year (Comeau and Savoie, 2001), the adjusted recapture rate, based only on late premolt lobsters, was 35.2% (CI 30.8, 42.1). The confidence intervals calculated from Monte-Carlo simulations were always wider for lobsters tagged in the premolt stage (Table 3).

Discussion

Our results suggest that streamer tag loss for the American lobster depended upon the molt stage of the lobster at the time of tagging. Tag-induced mortality without molting was observed mainly within four days of tagging for lobsters tagged in late premolt and postmolt stages; whereas lobsters tagged in early premolt and intermolt stages seemed to be less affected by tagging trauma because none died following the tagging process. Autopsies revealed that the length of time between tagging and death was related to a specific tagging trauma and depended upon the molt stage. Perforation of the pericardial sac caused massive bleeding and resulted in death within 30 min of tagging. The rupture of the dorsal thoraco-abdominal membrane, which also caused bleeding, killed the lobsters within days. Perforation of the hepato-pancreas killed the lobsters within weeks. These types of tagging trauma that caused death were reported by Krouse and Nutting (1990) for American lobsters tagged with Australian western rock lobster (*Panulirus longipes cygnus*) insertion tags. With more careful tagging manipulations, these types of trauma could possibly be reduced. However, even with extreme care during tagging manipulations, the rupture of the dorsal thoraco-abdominal membrane for lobsters tagged in the postmolt stage might be difficult to avoid. Tagging postmolt lobsters was sometimes difficult because the abdominal muscles of some lobsters were thin, and insuring the insertion of the tag through these muscles was a delicate operation. Thus, streamer tags not completely embedded into well-developed abdominal muscles could be a serious problem for tag retention. Tag shedding without molting was observed only for one lobster tagged in the postmolt stage. In general, lobsters tagged with streamer tags during intermolt and postmolt stages had a lower level of tag loss than lobsters tagged in the premolt stage. The level of streamer tag loss was the highest for lobsters tagged in the late premolt stage.

Tag-induced mortality observed during or shortly after molting was almost exclusively observed for lobsters tagged in the late premolt stage. Although lobsters tagged in the early premolt stage did not die from tagging trauma, they shed proportionately more tags during molting than lobsters tagged in the late premolt stage. Unlike tag loss for lobsters that did not molt, tag loss at molting was not the result of the perforation of internal organs or a questionable tag insertion during tagging but was caused by the tag being firmly attached to the old thoraco-abdominal membrane and being shed, still attached to the exuvia. For tagged lobsters that died during molting, which were almost exclusively lobsters tagged in the late premolt stage, tag loss was caused by massive bleeding resulting from the rupture of the entire new thoraco-abdominal membrance by the tag that was still firmly attached to the old thoraco-abdominal membrane. In addition, we observed a high level (21%) of tag misalignment due to the partial attachment of the tag to the old carapace for lobsters that did not have tag loss during molting. For these lobsters, incorrect insertion of the streamer tag was not an issue. Hence, firm tag attachment of the tag to the dorsal thoraco-abdominal membrane of the old carapace (which causes tag-induced mortality or tag shedding) is a serious problem.

The level of streamer tag shedding in nature seems to be higher than that observed in our aquarium observations and could provide additional information for adjusting streamer-tag recapture rates. From a field study, Rowe and Haedrich (2001) observed that 11% of nonmolted lobsters shed their tags in a one-year period. If we assumed that these lobsters were tagged in the intermolt and postmolt stages, their estimate for streamer-tag shedding is higher than our estimate of less than 1%. Different tagging techniques could explain this difference because Rowe and Haedrich (2001) tagged larger lobsters (>100 mm) differently (with the tag inserted in only one abdominal muscle) than did Moriyasu et al. (1995) for smaller lobsters. The difference could also be explained by the artificial conditions of our aquarium experiment. Under natural conditions tagged lobsters could shed their tags through interspecific interactions (Rowe and Haedrich, 2001), intraspecific interactions, and by being dislodged by obstacles in their habitat (Ennis, 1986; Krouse and Nutting, 1990). Streamer tag loss related to inter- and intraspecific interactions and the habitat has already been reported for the brown shrimp (Howe and Hoyt, 1982; *P. aztecus*) and the tiger prawn (Hill and Wassenberg, 1985; *P. esculentus*). However, more research would be needed to identify the cause of tag shedding in nature and assess its variability in relation to different lobster habitat before the recapture rate could be adjusted based on inter- and intraspecific interactions and the habitat.

The overall level of streamer tag loss compared to sphyrion tag loss seems to be lower, but also depends upon the molt stage of the lobster at tagging and molting. In their study, Moriyasu et al. (1995), suggested that sphyrion tag loss mainly occurs within days after tagging or during molting and is related to the lobster molt stage at tagging. We observed lower levels of tag loss compared to those of Moriyasu et al. (1995), except for the tag shedding during molting for early premolt lobsters and tag-induced mortality for lobsters tagged in late premolt. They observed 3% and 11% of tag shedding without molting for lobsters tagged in early and late premolt stages, respectively, compared to none in our study. Furthermore, the most striking difference is the level of tag loss that reached 10% and 30% for lobsters tagged in intermolt and postmolt stages compared to 0% and <1%, respectively, in our study. The difference in tag loss for lobsters tagged in the postmolt stage could be explained by the physical nature of the tags themselves and the tagging techniques. Compared to the streamer tag that is threaded through two abdominal muscles, the sphyrion tag is anchored to only one muscle by means of a hypodermic needle (Moriyasu et al., 1995). Because the muscles of postmolt lobsters (in the early stages) are not well formed, it is difficult to firmly embed an object, such as a tag, and the probability of tag loss for a tag embedded into only one thin muscle is greater than that for a tag treaded through two muscles. Hence, it seems that streamer tags are more effective in terms of tag retention compared to sphyrion tags for lobsters tagged in intermolt and postmolt stages, but equally so for lobsters tagged in the premolt stage.

In field tagging studies, streamer tags yielded a good recapture rate within the first year following tagging for lobsters tagged immediately before or after the molting season. The efficiency of streamer tags compared to sphyrion tags had already been established (Moriyasu et al., 1995; Comeau et al., 1999). Moriyasu et al. (1995) reported that there was a significantly greater recapture rate for lobsters tagged with streamer tags (44%) compared to those tagged with sphyrion tags (19%). Based on the results of Comeau et al. (1999), the recapture rate of lobsters tagged with sphyrion tags is 22% and 16% for lobsters tagged in premolt and postmolt stages, respectively, compared to 33% and 45% for lobsters tagged with streamer tags. These recapture rates corroborate aquarium observations by Moriyasu et al. (1995) on the tag retention of sphyrion tags and ours on the tag retention of streamer tags for lobster tagged at various molt stages.

Knowledge of the level of tag loss is paramount for adjusting the recovery rate to estimate population characteristics and fishery parameters for the American lobster. We observed that the recapture rate dropped significantly in the second and third years at large; this finding suggests a high level of tag loss. A similar multiple-years recapture rate pattern was observed for six other sites within the southwestern Gulf of St. Lawrence (Comeau and Savoie, 2002). Rowe and Haedrich (2001) indicated that the streamer tag shedding level for lobsters that molted almost a year later reached 40%. This high level of tag shedding, probably related to the streamer tag remaining firmly attached to the old dorsal thoraco-abdominal membrane during molting, might explain the drastic decrease of tag recaptures observed between the first and the second tag-recapture periods in our field study. We believe that the adjustment of the recapture rate due to tag loss should be limited to lobsters recaptured within the first year at large and prior to the molting season for lobsters tagged in intermolt and postmolt stages.

The multiple-years recapture pattern of a high recapture rate within the first year at large followed by low recapture rates in subsequent years could have a significant impact on multiyear tagging models. These models that were proposed by Seber (1970) could be used to estimate population characteristics and fishery parameters if underlying assumptions are followed. Based on these multiyear models originally developed for birds (Seber, 1970; Brownie et al., 1985), a suite of models adapted for fishery data and adjustments, mainly by reparameterization, were proposed to address underlying assumption violations (Pollock et al., 1991, 2001; Hearn et al., 1998, 1999; Hoenig et al., 1998a, 1998b; Frusher and Hoenig, 2001; Latour et al., 2001a, 2001b). Some of these models were developed to take into account fishing effort, incomplete mixing, and tag recovery rate. The latter is a composite parameter involving tag retention and tag-induced mortality (tag loss), exploitation rate, and tag reporting rate. There is no argument that the participation of fishermen in returning tags (tag reporting rate) is very important; however, for crustacean fisheries, underlying assumptions dealing with tag loss (see assumptions 2 and 3 in Pollock, 1991, 2001) are equally important and have to be addressed. In general, Pollock et al. (2001) indicated that the assumptions of no tag loss could be violated in two ways: by tag loss in the first

few days after tagging or by chronic tag loss spread over an extended period of time, the latter being more difficult to model. Furthermore, Seber (1970) mentioned that the usefulness of the multiyear models depends not only on the validity of the underlying assumptions but also on the number of recaptures (i.e. parameter estimates based on a small number of tag recaptures would be biased). From our aquarium observations and field studies that show a small number of lobsters caught during the second and third recapture periods, we conclude that a significant chronic tag loss does occur for the American lobster due to molting (i.e. the molt stage of the lobster at tagging and molting itself). Chronic tag loss impedes the effectiveness of multiyear recapture models currently used (Hearn et al, 1998; Hoenig et al., 1998a; Frusher and Hoenig, 2001) because it is not taken into account. We believe that assuming only a constant short-term tag loss for lobsters tagged with streamer tags is inadequate and can only bias estimates of survival and exploitation rate. Correcting for chronic tag loss after the first year at large for the American lobster, however, requires further knowledge, and more studies would be required to fully understand long-term tag loss.

In conclusion, a high level of streamer tag loss is a major obstacle for using tagging studies to estimate natural mortality or to apply multiyear models for the American lobster. Because streamer tag loss is related to molting, adjustment is difficult because the molting frequency is size, sex, and environment dependent (Comeau and Savoie, 2001). In our attempt to estimate mortality at molt, it was found that differences in recapture rates of lobsters tagged in premolt and postmolt stages for a given molting period were not statistically significant, thus suggesting a low level of natural mortality during the molt. The recapture rate for the 1996 tagging, for instance, was even higher for lobsters tagged in the premolt stage. Hence, tagging with streamer tags to establish the level of natural mortality during the molt, or any other mortality that could be low, for the American lobster is not recommended. The alternative would be to develop another insertion tag with better retention through the molting process. Nevertheless, the streamer tag remains an adequate choice for studying lobster ecology and population biology. Streamer tags could be used to tag intermolt and postmolt lobsters during single recapture tagging studies to estimate the exploitation rate (Xiao et al., 1999). Based on our observations, a minimum adjustment of 24.9% (SD 2.9%) and 4.4% (SD 1.6%) is suggested for lobsters tagged in premolt and inter- or postmolt stages, respectively, and recaptured during the first recovery period.

Acknowledgments

The authors wish to thank all fishermen from Caraquet and the adjacent wharves that returned lobster tags and T. Brideau, B. Comeau, J. Roussel, and F. Savoie for their technical assistance in the field and during the tag collection. We especially thank A. Godin and his staff at the Aquarium et centre marin in Shippagan, New Brunswick, for their professional help during the aquarium experiment. We also want to thank J. M. Hanson and M. Moriyasu for critically reviewing the manuscript, and three anonymous reviews for thoughtful suggestions that improved the quality of this manuscript.

Literature cited

Aiken, D. E.
1980. Molting and growth. *In* The biology and management of lobsters. Vol. I: Physiology and behavior (J. S. Cobb and B. F. Phillips, eds.), p. 91–163. Academic Press, New York, NY.

Beverton, R. J. H., and S. H. Holt.
1957. On the dynamics of exploited fish populations. U.K. Minist. Agric. Fish., Fish. Invest. 19:1–533.

Brownie, C., D. R. Anderson, K. P. Burhnam, and D. S. Robson.
1985. Statistical inference from band recovery data: a handbook, 2nd ed. U.S. Fish Wildl. Serv. Resour. Publ. 156, 305 p.

Comeau, M., W. Landsburg, M. Lanteigne, M. Mallet, P. Mallet, G. Robichaud, and F. Savoie.
1998. Lobster (*Homarus americanus*) tagging project in Caraquet (1993)—tag return from 1994 to 1997. Can. Tech. Rep. Fish. Aquat. Sci. 2216, 35 p.

Comeau, M., M. Lanteigne, G. Robichaud, and F. Savoie.
1999. Lobster (*Homarus americanus*) movement in the southern Gulf of St. Lawrence—summary sheets of tagging projects conducted between 1980 and 1997. Can. Ind. Rep. Fish. Aquat. Sci. 249, 111 p.

Comeau, M., and M. Mallet.
2001. Estimating mortality rates by capture-recapture, catch-effort and change-in-ratio models for a spring American lobster (*Homarus americanus*) fishery (LFA 23). Can. Tech. Rep. Fish. Aquat. Sci. 2373, 20 p.

Comeau, M., and F. Savoie.
2001. Growth increment and molt frequency of the American lobster (*Homarus americanus*) in the southwestern Gulf of St. Lawrence. J. Crust. Biol. 21:923–936.
2002. Movement of American lobster (*Homarus americanus*) in the southwestern Gulf of St. Lawrence. Fish. Bull. 100: 181–192.

Ennis, G. P.
1986. Sphyrion tag loss from the American lobster *Homarus americanus*. Trans. Am. Fish. Soc. 115:914–917.

Frusher, S. D., and J. M. Hoenig.
2001. Estimating natural and fishing mortality and tag reporting rate of southern rock lobster (*Jasus edwardsii*) from a multiyear tagging model. Can. J. Fish. Aquat. Sci. 58:2490–2501.

Hearn, W. S., K. M. Pollock, and E. N. Brooks.
1998. Pre- and post-season tagging models: estimation of reporting rate and fishing and natural mortality rates. Can. J. Fish. Aquat. Sci. 55:199–205.

Hearn, W. S., T. Polacheck, K. H. Pollock, and W. Whitelaw.
1999. Estimation of tag reporting rates in age-structured multicomponent fisheries where one component has observers. Can. J. Fish. Aquat. Sci. 56:1255–1265.

Hoenig, J. M., N. J. Barrowman, W. S. Hearn, and K. H. Pollock.
1998a. Multiyear tagging studies incorporating fishing effort data. Can. J. Fish. Aquat. Sci. 55:1466–1476.

Hoenig, J. M., N. J. Barrowman, K. H. Pollock, E. N. Brooks, and W. S. Hearn.
1998b. Models for tagging data that allow for incomplete mixing of newly tagged animals. Can. J. Fish. Aquat. Sci. 55:1477–1483.

Hill, B. J., and T. J. Wassenberg.
1985. A laboratory study of the effect of streamer tags on mortality, growth, moulting and duration of nocturnal emergence of the tiger prawn *Penaeus esculentus* (Haswell). Fish. Res. 3:223–235.
Howe, N. R., and P. R. Hoyt.
1982. Mortality of juvenile brown shrimp *Penaeus aztecus* associated with streamer tags. Trans. Am. Fish. Soc. 111: 317–325.
Krouse, J. S., and G. E. Nutting.
1990. Effectiveness of the Australian western rock lobster tag for marking juvenile American lobsters along the Maine coast. Am. Fish. Soc. Symp. 7:94–100.
Landsburg, A. W.
1991. A field comparison of recapture rates of polyethylene streamer and modified sphyrion tags through molting of lobster (*Homarus americanus*). J. Shellfish. Res. 10, 225 p.
Latour, R. J., J. M. Hoenig, J. E. Olney, and K. H. Pollock.
2001a. Diagnostics for multiyear tagging models with application to Atlantic striped bass (*Morone saxatilis*). Can. J. Fish. Aquat. Sci. 58:1716–1726.
2001b. A simple test for nonmixing in multi-year tagging studies: application to striped bass tagged in the Rappahannock River. Trans. Am. Fish. Soc. 130:848–856.
Marullo, F., D. A. Emiiani, C. W. Caillouet, and S. H. Clark.
1976. A vinyl tag for shrimp (*Panaeus* spp.). Trans. Am. Fish. Soc. 105:658–663.
Moriyasu M., W. Landsburg, and G.Y. Conan.
1995. Sphyrion tag shedding and tag induced mortality of the American lobster, *Homarus americanus* H. Milne Edwards, 1837 (Decapoda, Nephropidae). Crustaceana 68:184–192.
Pollock, K. H., J. M. Hoenig, W. S. Hearn, and B. Calingaert.
2001. Tag reporting estimation: an evaluation of the reward tagging method. N. Am. J. Fish. Manage. 21:521–532.
Pollock, K.H., J. M. Hoenig, and C. M. Jones.
1991. Estimating of fishing and natural mortality when a tagging study is combined with a creel survey or port sampling. Am. Fish. Soc. Symp. 12:423–434.
Ricker, W. E.
1975. Computation and interpretation of biological statistics of fish populations. Bull. Res. Board Can. 191, 382 p.
Rowe, S., and R. L. Haedrich.
2001. Streamer tag loss from American lobsters. Trans. Am. Fish. Soc. 130:516–518.
Scarratt, D. J., and P. F. Elson.
1965. Preliminary trials of a tag for salmon and lobsters. J. Fish. Res. Board Can. 22:421–423.
Seber, G. A. F.
1970. Estimating time-specific survival and reporting rates for adult birds from band returns. Biometrika 57: 313–318
1982. The estimation of animal abundance and related parameters, 2nd ed., 654 p. Griffin, London.
Templeman, W.
1935. Lobster tagging in the Gulf of St. Lawrence. J. Biol. Board Can. 1:269–278.
Wilder, D. G.
1953. The growth of the American lobster (*Homarus americanus*). J. Fish. Res. Board Can. 10:371–403.
Xiao, Y., J. D. Stevens, and G. J. West.
1999. Estimation of fishing and natural mortalities from tag experiments with exact or grouped times at liberty. Can. J. Fish. Aquat. Sci. 56:868–874.

Estimation of bycatch in shrimp trawl fisheries: a comparison of estimation methods using field data and simulated data

Sandra L. Diamond
Department of Biology
Box 3131
Texas Tech University
Lubbock, Texas 79409
E-mail address: Sandra.Diamond@ttu.edu

Abstract—Bycatch, or the incidental catch of nontarget organisms during fishing operations, is a major issue in U.S. shrimp trawl fisheries. Because bycatch is typically discarded at sea, total bycatch is usually estimated by extrapolating from an observed bycatch sample to the entire fleet with either mean-per-unit or ratio estimators. Using both field observations of commercial shrimp trawlers and computer simulations, I compared five methods for generating bycatch estimates that were used in past studies, a mean-per-unit estimator and four forms of the ratio estimator, respectively: 1) the mean fish catch per unit of effort, where unit effort was a proxy for sample size, 2) the mean of the individual fish to shrimp ratios, 3) the ratio of mean fish catch to mean shrimp catch, 4) the mean of the ratios of fish catch per time fished (a variable measure of effort), and 5) the ratio of mean fish catch per mean time fished. For field data, different methods used to estimate bycatch of Atlantic croaker, spot, and weakfish yielded extremely different results, with no discernible pattern in the estimates by method, geographic region, or species. Simulated fishing fleets were used to compare bycatch estimated by the five methods with "actual" (simulated) bycatch. Simulations were conducted by using both normal and delta lognormal distributions of fish and shrimp and employed a range of values for several parameters, including mean catches of fish and shrimp, variability in the catches of fish and shrimp, variability in fishing effort, number of observations, and correlations between fish and shrimp catches. Results indicated that only the mean per unit estimators provided statistically unbiased estimates, while all other methods overestimated bycatch. The mean of the individual fish to shrimp ratios, the method used in the South Atlantic Bight before the 1990s, gave the most biased estimates. Because of the statistically significant two- and 3-way interactions among parameters, it is unlikely that estimates generated by one method can be converted or corrected to estimates made by another method: therefore bycatch estimates obtained with different methods should not be compared directly.

Manuscript approved for publication 17 December 2002 by Scientific Editor.
Manuscript received 3 April 2003 at NMFS Scientific Publications Office.
Fish. Bull. 101:484–500 (2003).

Bycatch, as used in the present study, is the incidental catch of nontarget organisms that occurs to some extent in almost all commercial fisheries (Alverson, 1994). Some of these incidentally caught organisms may be protected species—such as marine mammals, marine turtles, and seabirds—or they may be fish or invertebrates that are either harvested as target species by other fisheries, or species that fishermen call "trash fish" because they have little or no economic value. Bycatch in most commercial fisheries has only been a major issue since the 1980s—primarily because individuals caught as bycatch have historically been discarded at sea, leaving fishery managers and the general public unaware of the extent of bycatch mortality. For many organisms, bycatch may be a significant source of mortality, and inclusion of bycatch mortality in stock assessments or management plans may be critical for effective management.

Because bycatch species are not usually landed, quantifying bycatch poses a very different problem from that of quantifying the catch of a target species. Several methods of quantifying bycatch have been tried, including the requirement that fishermen record catch and bycatch in logbooks (Walsh and Kleiber, 2001), use of research vessel surveys to model commercial fishing (Nichols et al.[1]), and the placement of observers aboard fishing vessels (Julian and Beeson, 1998). Although direct observation is the most accurate method, unless observer coverage of the fleet is complete, estimation of bycatch from observation data requires sampling of the fleet and then extrapolating from the samples (the observations) to the entire fleet using statistical estimators. Two types of statistical estimators are used: mean-per-unit estimators and ratio estimators. In both types of estimators, the observed catch of the bycatch species (y) is linked to an auxiliary variable (x) for which the population total is known (Cochran, 1977). In mean-per-unit estimators, the auxiliary variable is a measure of fishing effort such as tow, day, trip, etc., where each unit of effort is the same as one observation. In ratio estimators, the auxiliary variable is a variable that is correlated with the catch of the bycatch species, such as the catch of the target species or the number of hours fished (Cochran, 1977). The major difference between these two types of estimators is that the auxiliary variable in the mean-per-unit estimator is a substitute for the number of observations rather than a mean value with a variance, while the auxiliary variable in the ratio estimator is the mean value of a quantity that varies from sample to sample. Although the statistical properties of these two types of estimators are well known, the choice of which estimator to use in bycatch research is often based on the ease of collecting fleet information on the auxiliary variable, and not on any inherent properties of the estimators themselves or on any specific information about the relationship between the catch of bycatch species and the auxiliary variable.

[1] Nichols, S., A. Shah, G. Pellegrin Jr., and K. Mullin. 1990. Updated estimates of shrimp fleet bycatch in the offshore waters of the US Gulf of Mexico, 22 p. Pascagoula Laboratory, Southeast Fisheries Science Center, NMFS, PO Drawer 1207, Pascagoula, MS 39568-1207.

Bycatch is a major issue in the shrimp trawl fisheries of the Gulf of Mexico and the South Atlantic Bight. These fisheries are the most valuable fisheries in the southeastern United States; almost 136,000 metric tons of shrimp, worth over $700 million, were landed in 2000 (NMFS[2]). It is estimated that 60–80% of the catch by weight in these fisheries is bycatch. Over 150 species have been reported in shrimp trawl bycatch, including marine turtles (Crouse et al., 1987) and juveniles of species that are highly valued as adults in other fisheries, such as weakfish (*Cynoscion regalis* [Vaughan et al.[3]]) and red snapper (*Lutjanus campechanus* [Goodyear[4]]).

Both types of statistical estimators have been used to estimate bycatch in shrimp trawl fisheries. In the South Atlantic, biologists have periodically participated as observers aboard commercial shrimp trawlers since at least the 1950s to characterize bycatch and estimate its magnitude (Fahy, 1966; Latham,[5] Lunz et al.,[6] Fahy,[7] Fahy,[8] Fahy,[9] Wolff,[10] Keiser,[11] Knowlton[12]). For most of the studies conducted between the 1950s and the 1980s, fisheries bycatch was estimated by using a ratio estimator, that is to say by calculating the observed ratio of fish (F) bycatch to shrimp (S) by weight and then multiplying by the total pounds of shrimp landed by the fleet (the F:S ratio estimator). The catch of shrimp was used as the auxiliary variable primarily because better records were kept of shrimp landings than of any measure of fleet effort. By the late 1980s, the problem of shrimp trawl bycatch in the United States was considered to be of such magnitude that in 1990 the Magnuson Fishery Conservation and Management Act (Magnuson Act) was amended to include bycatch research. Beginning in 1992, observers trained by the National Marine Fisheries Service (NMFS) to use a standardized sampling protocol (NMFS[13]) rode aboard paid volunteer commercial vessels in the South Atlantic and Gulf of Mexico. The 1992–94 observation data collected in the South Atlantic were used to estimate bycatch by species with a mean-per-unit estimator, which was the weight or number of fish caught per observed trip multiplied by the total number of trips taken by the fleet (the CPUE-mean-per-unit estimator). Trips were used as the auxiliary variable because fleet effort data were available at the trip level and this method was thought to be less variable than the F:S ratio method (SEAMAP[14]).

To date, there have been no detailed studies on how these different techniques compare to each other, or how accurately they estimate bycatch. Vaughan and Nance[15] in a draft paper compared the estimated bycatch of mackerels (*Scomberomorus* spp.) and cobia (*Rachycentron canadum*) using both methods and found much higher estimates with the F:S ratio estimator than with the CPUE-mean-per-unit estimator. Because of the wide range of estimation methods used over the years, the discrepancy in the estimates generated by the different methods, and the increasing importance of bycatch estimation for shrimp trawl fisheries

[2] NMFS (National Marine Fisheries Service). 2002. Unpubl. data Website: http://www.st.nmfs.gov/st1/commercial/index.html.

[3] Vaughan, D. S., R. J. Seagraves, and K. West. 1991. As assessment of the status of the Atlantic weakfish stock, 1982–1988. Special Report 21, 29 p. Atlantic States Marine Fisheries Commission, 1444 Eye Street, N.W., Sixth Floor, Washington, DC 20005.

[4] Goodyear, C. P. 1995. Red snapper in US waters of the Gulf of Mexico. Contribution MIA-95/96-05, 171 p. Miami Laboratory, Southeast Fisheries Science Center, NMFS,75 Virginia Beach Drive, Miami, Florida 33149-1099.

[5] Latham, F. F. 1951. Evidence of fish loss due to shrimping in Pamlico Sound. Appendix B *in* The destruction of small fish by the shrimp trawlers in Pamlico Sound, North Carolina (G. R. Lunz, J. L.,McHugh, E. W. Roclofs, R. E. Tiller, and C. E. Atkinson), p. 17–24. Committee Report to the Atlantic States Marine Fisheries Commission, 1 November 1951. Atlantic States Marine Fisheries Commission, 1444 Eye Street, N.W., Sixth Floor, Washington, DC 20005.

[6] Lunz, G. R., J. L. McHugh, E. W. Roclofs, R. E. Tiller, and C. E. Atkinson. 1951. The destruction of small fish by the shrimp trawlers in Pamlico Sound, North Carolina. Committee Report to Atlantic States Marine Fisheries Commission, 1 November 1951, 34 p. Atlantic States Marine Fisheries Commission, 1444 Eye Street, N.W., Sixth Floor, Washington, DC 20005.

[7] Fahy, W. E. 1965a. Report of trash fish study in North Carolina in 1962. Division of Commercial and Sports Fisheries, NC Department of Conservation and Development, Special Scientific Report 5, 20 p. NC Division of Marine Fisheries, 3441 Arendell St., Morehead City, NC 28557.

[8] Fahy, W. E. 1965b. Report of trash fish study in North Carolina in 1964. Division of Commercial and Sports Fisheries, NC Department of Conservation and Development, Special Scientific Report 7, 13 p. NC Division of Marine Fisheries, 3441 Arendell St., Morehead City, NC 28557.

[9] Fahy, W. E. Unpubl. data cited in Brown, J., and E. McCoy. 1969. A review of the North Carolina scrap fishery. Division of Commercial and Sports Fisheries, NC Department of Conservation and Development, Information Series 1, 12 p. NC Division of Marine Fisheries, 3441 Arendell St., Morehead City, NC 28557.

[10] Wolff, M. 1972. A study of North Carolina scrap fishery. NC Department of Natural and Economic Resources, Special Scientific Report 20, 29 p. NC Division of Marine Fisheries, 3441 Arendell St., Morehead City, NC 28557.

[11] Keiser, R. K. 1977. The incidental catch from commercial shrimp trawlers of the South Atlantic states. Technical Report 26, 38 p. South Carolina Wildlife and Marine Resources Department, South Carolina Department of Natural Resources, Rembert C. Dennis Building, 1000 Assembly Street, Columbia, SC 29201.

[12] Knowlton, C. J. 1972. Fishes taken during commercial shrimping in Georgia's close inshore ocean waters. Contributed Series 21, 42 p. Georgia Department of Natural Resources, Coastal Resources Division, One Conservation Way, Suite 300, Brunswick, GA 31520.

[13] NMFS (National Marine Fisheries Service). 1992. Shrimp trawl bycatch characterization. Sampling Protocol Manual for Data Collection, 62 p. Galveston Laboratory, Southeast Fisheries Science Center, NMFS, 4700 Avenue U, Galveston, TX 77551-5997.

[14] SEAMAP (Southeast Area Monitoring and Assessment Program). 1996. Estimates of finfish bycatch in the South Atlantic Shrimp Fishery, July 24, 1995 (R. Peuser, ed.), 64 p. Final report of the Southeast Area Monitoring and Assessment Program (SEAMAP), SEAMAP-South Atlantic Committee, Shrimp Bycatch Work Group. Atlantic States Marine Fisheries Commission, 1444 Eye Street, N.W., Sixth Floor, Washington, DC 20005.

[15] Vaughan, D. and J. Nance. 1998. Estimates of bycatch of mackerel and cobia in US South Atlantic shrimp trawls. Report for Gulf of Mexico and South Atlantic Fishery Management Councils, February 16, 1998, 26 p. NMFS –SEFSC, Beaufort Laboratory, 101 Pivers Island Road, Beaufort NC 28516.

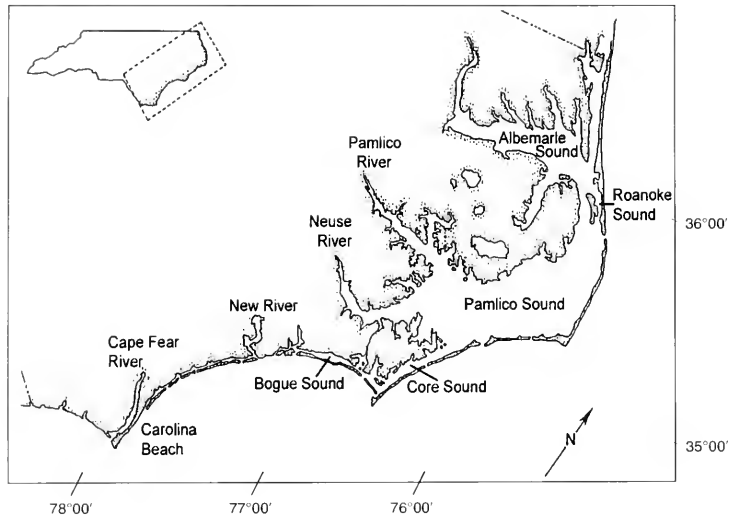

Figure 1

Map of North Carolina waters. Shrimping operations were observed in northern Pamlico Sound (between the mouth of the Pamlico River and southern Roanoke Sound) and the lower third of the Cape Fear River. For total bycatch, fleet shrimp landings and fleet shrimp effort, the northern region includes Pamlico Sound and its tributaries, and the southern region includes from the Cape Fear River to the New River.

and other fisheries, fishery biologists need clear guidance on which method to use to estimate bycatch and they need a definitive knowledge of which methods are best under the varying conditions that might be found in a field observer study.

In this article, I use both field data and computer simulations to compare the methods of bycatch estimation used in past studies. First, using field observations of Atlantic croaker (*Micropogonias undulatus*), spot (*Leiostomas xanthurus*), and weakfish bycatch from shrimp trawlers in North Carolina, I compare bycatch estimates generated by the CPUE-mean-per-unit estimator with two different forms of the F:S ratio estimator, the mean of the individual fish to shrimp ratios and the ratio of the mean catch of fish to the mean catch of shrimp. I then simulate fishing fleets with different catches of fish and shrimp, and estimate bycatch using the following five different estimators, a mean-per-unit estimator and four forms of the ratio estimator, respectively: 1) the mean fish catch per unit of effort, where unit effort is a proxy for sample size, 2) the mean of the individual fish to shrimp ratios, 3) the ratio of mean fish catch to mean shrimp catch, 4) the mean of the ratios of fish catch per time fished (a variable measure of effort), and 5) the ratio of mean fish catch per mean time fished. The simulations employ different mean catches of fish and shrimp, different levels of variability around the catches of fish and shrimp and around the variable measure of effort in the ratio estimator, and different levels of observer coverage, or the number of observations. I also investigate the effects on the bycatch estimates of different underlying distributions of fish and shrimp, including normal distributions of fish and shrimp with different levels of correlation between the catches of fish and shrimp, and delta lognormal distributions of both fish and shrimp, with differing probabilities of catching fish or shrimp.

Materials and methods

Field sampling

To compare the methods described in the literature using field data, I observed shrimping operations aboard commercial shrimp boats from July through October 1995 in Pamlico Sound, North Carolina, and from August through October 1995, in the Cape Fear River, North Carolina (Fig. 1). These two areas have different levels of fishing effort, different fish-to-shrimp ratios, and different probabilities of catching fish and shrimp. All fishermen cooperators were unpaid volunteers, and I did not direct them in any way regarding where or how to fish. Although sampled boats were not randomly chosen, the fishermen appeared to use gear and fishing methods similar to those of other shrimpers, and other shrimpers were often seen fishing in the area near the sampled boats.

Sampled shrimp boats towed one or two nets, and all nets contained some form of turtle excluder device (TED) and bycatch reduction device (BRD) required by regulation.

To sample the catch, I used the NMFS bycatch sampling protocol as described below. If the boat carried two nets and no try net (the small net towed in front of the main nets which is used to survey the catch at short time intervals), I randomly picked one net (the "selected net") by flipping a coin. If the boat had a try net, I picked the opposite net. I weighed the total catch of the selected net on a flat agricultural scale by emptying the net into a plastic tub placed on a scale. After having been weighed, the catch of the selected net was dumped onto the deck or into a culling tray that was divided so that the catch of the selected net was separated from the catch of the unselected net. Following the NMFS protocol, I mixed the selected net contents thoroughly with a shovel, then took a random sample and set it aside until after the rest of the net contents had been sorted. To sort the net contents, marketable shrimp, which are pink shrimp (*Farfantepenaeus duorarum*), brown shrimp (*Farfantepenaeus aztecus*), and white shrimp (*Litopenaeus setiferus*) larger than would comprise about a 70–80 count (i.e. 70–80 shrimp per pound) were separated from the rest of the contents of the selected net, weighed, and then returned to the fisherman. The unsampled bycatch from the selected net was discarded overboard. The random sample taken from the selected net was then weighed. Market shrimp in the sample were taken out, weighed and counted by species, and returned to the fisherman. The bycatch portion of the sample, including undersized market shrimp, mantis shrimp, and all other fish and invertebrates, was packaged in plastic bags and placed on ice for the remainder of the trip. Bycatch samples were brought back to the laboratory and frozen. Samples, including market shrimp, averaged 12% by weight of the total catch of the selected net, and ranged from 5% to 37% by weight.

Expansion of observed bycatch to the entire tow In the laboratory, I thawed and rehydrated the bycatch sample in water. I sorted each sample by species and weighed each species as a group. All individuals of each species were then weighed and measured separately. To account for differences between the scales used on the boat and those used in the laboratory, and for weight loss due to freezing, I corrected the weight of the total catch of each net measured on the boat by the ratio of the sample weight from the laboratory to the sample weight from the boat as follows:

$$\textit{Corrected total weight}_j = \textit{boat total weight}_j \times \frac{\textit{lab sample weight}_j}{\textit{boat sample weight}_j}, \quad (1)$$

where $\textit{corrected total weight}_j$ = the corrected weight of the j^{th} selected net;
$\textit{boat total weight}_j$ = the weight of the entire catch of the j^{th} selected net measured on the boat;
$\textit{lab sample weight}_j$ = the weight of the bycatch sample of the j^{th} net measured in the laboratory plus the shrimp sample weight from the boat; and
$\textit{boat sample weight}_j$ = the weight of the entire sample (including shrimp) from the j^{th} net weighed on the boat.

This correction averaged less than 5% across all selected nets. To expand the catch in weight of each bycatch species from the sample to the entire selected net (called the "species net weight"), the total corrected weight of each selected net was multiplied by the fraction of the sample from the selected net that consisted of the bycatch species, as follows:

$$\textit{Species net weight}_{i,j} = \textit{corrected total weight}_j \times \frac{\textit{species sample weight}_{i,j}}{\textit{total sample weight}_j}, \quad (2)$$

where $\textit{species net weight}_{i,j}$ = the estimated catch in weight of the i^{th} species in the j^{th} net;
$\textit{corrected total weight}_j$ = the corrected weight of the total catch of the j^{th} net from Equation 1;
$\textit{species sample weight}_{i,j}$ = the weight of the i^{th} species in the sample from the j^{th} net; and
$\textit{total sample weight}_j$ = the weight of the bycatch sample from the j^{th} net measured in the laboratory plus the weight of the market shrimp in that sample measured on the boat.

Because the net contents were thoroughly mixed before sampling, I assumed, following the NMFS protocol, that there would be minimal variance among samples if more than one were taken.

Expanding the catch in numbers of each bycatch species from the sample to the entire selected net (called the "species net number") could not be done in the same way as the expansion for the species net weight because there were often organisms like sea lettuce or pieces of fish or crabs that were weighed but that could not be counted. The species net number was therefore calculated by dividing the species net weight by the average weight per whole individual:

$$\textit{Species net number}_{i,j} = \textit{species net weight}_{i,j} \div \frac{\textit{species sample weight}_{i,j}}{\textit{species sample number}_{i,j}}, \quad (3)$$

where $\textit{species net number}_{i,j}$ = the estimated number of individuals of the i^{th} species in the j^{th} net;
$\textit{species net weight}_{i,j}$ = the estimated total weight of the i^{th} species in the j^{th} net from Equation 2;

$species\ sample\ weight_{i,j}$ = the weight of the i^{th} species in the bycatch sample from the j^{th} net; and

$species\ sample\ number_{i,j}$ = the number of whole individuals of the i^{th} species in the bycatch sample from the j^{th} net.

To expand the observed bycatch from selected net to the entire tow, I multiplied either the species net weight or the species net number from each net by the number of nets towed concurrently.

Bycatch estimation To compare the methods of bycatch estimation used in past studies, I estimated the bycatch of Atlantic croaker, spot, and weakfish (three of the most commonly caught bycatch species) using two categories of statistical estimators: a mean-per-unit estimator using the mean observed bycatch per day expanded by the total number of days fished (the CPUE-mean-per-unit method) and a ratio estimator using the observed ratio of fish to shrimp expanded by the total shrimp landings (the F:S ratio method). Because my purpose was to compare bycatch estimation methods and not to generate bycatch estimates that could be used for management purposes, I estimated total bycatch of these three species only for certain months and geographic regions within North Carolina corresponding to the times and areas that I observed shrimp trawling. The term "shrimp fleet" in the following paragraphs therefore refers only to shrimpers operating in those times and areas. In the calculations, I used bycatch per day instead of the bycatch per tow or bycatch per trip. I could not use tow as the unit of effort because there was no information on the number of tows made by the fleet to use as an expansion factor. Although information on the number of trips made by the fleet was available, I could not use trip as the unit of effort because, although trips can last several days, all of the trips that I sampled were one-day trips. If my observations had also included a random sample of multiday trips, the unit of effort would have been trips instead of days.

The CPUE mean per unit method was based on the following equations:

$$\frac{Mean\ observed\ bycatch_i}{day} = \frac{1}{n}\sum_{d=1}^{n} F_{i,d}, \tag{4}$$

where $mean\ observed\ bycatch_i\ per\ day$ = the observed average bycatch in weight or number of the i^{th} species on the d^{th} day;

n = the number of days observed; and

$F_{i,d}$ = the sum of the expanded weight or number of the i^{th} bycatch species observed in all tows made on the d^{th} day; and

$$Total\ bycatch_{i,CPUE} = \frac{mean\ observed\ bycatch_i}{day} \times total\ trips \times \frac{mean\ days}{trip}, \tag{5}$$

where $total\ bycatch_{i,CPUE}$ = the total fleet bycatch of the i^{th} species estimated by the CPUE method;

$mean\ observed\ bycatch_i\ per\ day$ = the observed average bycatch of the i^{th} species per day from Equation 4;

$total\ trips$ = the total number of trips taken by the shrimp fleet; and

$mean\ days\ per\ trip$ = the average number of days that each fishing trip lasted based on the fleet.

The total trips and mean days per trip were calculated from the North Carolina Division of Marine Fisheries (NCDMF) trip ticket database, as follows. To obtain the total number of trips, I first collapsed the trip ticket database so that each fisherman could have only one ticket for shrimp on a single day. In the database, each trip ticket does not represent one trip, but the sale to one dealer. Fishermen could obtain more than one trip ticket per day by selling different size categories of shrimp (each size category commands a different price, and generates a separate trip ticket), or by selling their catch to more than one dealer. I then calculated the time (in days) between the first and last trips for each fisherman whose trips occurred between 1 July and 31 October in Pamlico Sound and its tributaries (called the northern region) and between 1 August and 31 October in the Cape Fear River and nearby waters (the southern region). Because inshore waters were closed to shrimping on weekends, I multiplied all time spans greater than 7 days by 5/7 (0.714) to obtain the number of days fished. The number of days fished was summed and then divided by the number of trips for each region to obtain the mean days per trip.

The F:S ratio estimator method was initially undertaken in two ways: by using the mean of the fish to shrimp ratios, called the mean of the ratios or the "basic" F:S ratio estimator method (Equation 6), and by using the ratio of the average catch of fish to the average catch of shrimp, called the ratio of the means or the "grand" F:S ratio estimator method (Equation 7). The two methods are shown mathematically as follows:

$$Total\ bycatch_{i,FSB} = \frac{1}{n}\sum_{d=1}^{n}\frac{F_{i,d}}{S_d} \times total\ shrimp\ landed, \tag{6}$$

$$Total\ bycatch_{i,FSG} = \frac{\sum_{d=1}^{n} F_{i,d}}{\sum_{d=1}^{n} S_d} \times total\ shrimp\ landed, \tag{7}$$

where $total\ bycatch_{i,FSB}$ = the total fleet bycatch of the i^{th} species estimated by the basic F:S method;

$total\ bycatch_{i,FSG}$ = the total fleet bycatch of the i^{th} species estimated by the grand F:S method;

$F_{i,d}$ = the sum of the expanded weight or number of the i^{th} species observed in all tows made on the d^{th} day;
S_d = the sum of the expanded weight of market shrimp observed in all tows made on the d^{th} day; and
n = the number of days observed.

Because of the small number of days observed in each area, I also used the basic F:S ratio estimator with the Hartley-Ross correction for biases caused by small sample size (Cochran, 1977):

$$Total\ bycatch_{i,HR} = total\ bycatch_{i,FSB} + \frac{n(N-1)}{n-1}(\bar{y}_i - \bar{r}\bar{x}), \quad (8)$$

where $total\ bycatch_{i,HR}$ = the total fleet bycatch of the i^{th} species estimated by the bias-corrected F:S ratio estimator;
$total\ bycatch_{i,FSB}$ = the total fleet bycatch of the i^{th} species estimated by the basic F:S ratio using Equation 6;
n = the number of days observed;
N = the total number of days fished from the trip ticket database;
$\bar{y}_i$ = the mean bycatch of of the i^{th} species observed per day in weight or numbers from Equation 4;
$\bar{r}$ = the mean of the F:S ratios from Equation 6; and
$\bar{x}$ = the mean catch of market shrimp observed per day in weight or numbers.

Total shrimp landings used in Equations 6 and 7 were obtained from the NCDMF trip ticket database for the northern region from July to October and for the southern region from August to October. In the trip ticket database, some shrimp weights were reported as "heads-on" and others as "heads-off"; therefore I converted heads-off weight to heads-on weight with a conversion factor of 1.583, taken from the average of pink, brown, and white shrimp conversion information used by the National Marine Fisheries Service (Fisheries Statistics of the United States, 1977).

Bycatch simulations

For the bycatch simulations, I created different fishing fleets of 1000 "boats" in Matlab 5.0 (The Mathworks, Natick, MA). For the normally distributed catch data, the catch of fish, the catch of shrimp, and the hours fished for each boat in a fleet were generated by using multivariate random normal distributions with a mean and variance that was specific to that fleet. I simulated observer data for each fleet by taking a random sample of boats from the fleet, resampling the sample 1000 times, then using the mean of the bootstrapped observer data in the equations described below to estimate fleet bycatch. In the different fleets, the mean catches of fish and shrimp ranged from 0.01 to 1000, giving fish to shrimp ratios of 0.001 to 100,000. In some fleets, the catches of fish and shrimp were correlated, with correlation coefficients ranging from 0.5 to –0.5 (Table 1). Coefficients of variation (CVs) for fish catch and hours fished ranged from 20% to 80%, CVs for shrimp catch ranged from 20% to 120%, and the number of observations ranged from 20 to 500, giving observer coverages of 2% to 50% of the fleet. Although the range of mean catches I used in the simulations may seem fairly broad, they are within the range of the field data, depending on whether these were the mean catches per tow, per day, or per trip. The ranges of CVs for fish and shrimp catches were fairly narrow compared to those from the field data because CVs vary up to several hundred percent, particularly for patchy species. Observer coverage in the field is usually much less than 50%, but I picked 50% as the upper limit of the range to see if greater observer coverage (i.e., a greater sample size of observations per fleet) increased the accuracy of the bycatch estimates.

Bycatch estimates were calculated by using a mean per unit estimator and four forms of the ratio estimator, as described below. The CPUE mean per unit estimator was calculated by using the following equations, which are more general versions of Equations 4 and 5:

$$\frac{Mean\ observed\ bycatch_i}{UE} = \frac{1}{n}\sum_{UE=1}^{n} F_{i,UE} \quad (9)$$

$$Total\ bycatch_{i,CPUE} = \frac{Mean\ bycatch_i}{UE} \times total\ fleet\ effort. \quad (10)$$

where $mean\ observed\ bycatch_i\ per\ UE$ = the observed average bycatch of the i^{th} species per unit of effort (tow, day, or trip);
n = the number of observed tows, days, or trips;
$F_{i,UE}$ = the expanded weight or number of the i^{th} bycatch species observed on the UE^{th} tow, day, or trip;
$total\ bycatch_{i,CPUE}$ = the total fleet bycatch estimated by the CPUE method; and
$total\ fleet\ effort$ = the total number of tows, days, or trips fished by the fleet.

The four ratio estimators were as follows: 1) the mean of the individual F:S ratios, called the "basic F:S" ratio estimator (Eq. 11), 2) the ratio of the F:S means, called the "grand F:S" ratio estimator (Eq. 12), 3) the mean of the individual catch per effort ratios using a variable measure of effort such as hours fished as the auxiliary variable, called the "basic CPE" ratio estimator (Eq. 13), and 4) the ratio of the mean catch per mean effort using a variable measure of effort such as hours fished as the auxiliary variable, called the "grand CPE" ratio estimator (Eq. 14). Both F:S ratio estimators (Eqs. 11 and 12) are similar to the ones used in the field study (Eqs. 6 and 7), except that the observations could be from a tow, day, trip, or other measure of unit effort, rather than one day, as used in the field study.

$$Total\ bycatch_{i,FSB} = \frac{1}{n}\sum_{e=1}^{n}\frac{F_{i,e}}{S_e} \times total\ shrimp\ landed \qquad (11)$$

$$Total\ bycatch_{i,FSG} = \frac{\sum_{e=1}^{n} F_{i,e}}{\sum_{e=1}^{n} S_e} \times total\ shrimp\ landed \qquad (12)$$

where $total\ bycatch_{i,FSB}$ = the total fleet bycatch of the i^{th} species estimated by the basic F:S ratio estimator;

$total\ bycatch_{i,FSG}$ = the total fleet bycatch of the i^{th} species estimated by the grand F:S ratio estimator;

$F_{i,e}$ = the expanded weight or number of the i^{th} bycatch species observed in the e^{th} tow, day, or trip;

S_e = the expanded weight of market shrimp observed in the e^{th} tow, day, or trip;

n = the number of tows, days, or trips observed; and

$total\ shrimp\ landed$ = the sum of the total weight of shrimp landed by the fleet.

$$Total\ bycatch_{i,CPEB} = \frac{1}{n}\sum_{e=1}^{n}\frac{F_{i,e}}{H_{i,e}} \times total\ hours\ fished \qquad (13)$$

$$Total\ bycatch_{i,CPEG} = \frac{\sum_{e=1}^{n} F_{i,e}}{\sum_{e=1}^{n} H_e} \times total\ hours\ fished \qquad (14)$$

where $total\ bycatch_{i,CPEB}$ = the total fleet bycatch of the i^{th} species estimated by the basic CPE ratio estimator;

$total\ bycatch_{i,CPEG}$ = the total fleet bycatch of the i^{th} species estimated by the grand CPE ratio estimator;

$F_{i,e}$ = the expanded weight or number of the i^{th} bycatch species observed in the e^{th} tow, day, or trip;

H_e = the hours fished in the e^{th} tow, day, or trip;

n = the number of observed tows, days, or trips; and

$total\ hours\ fished$ = the sum of all hours fished by the fleet.

To avoid confusion, it is important to note how fishing effort is used in the five estimators. All five estimators use a unit measure of fishing effort, such as a tow, day, or trip, as one sample, and the sample size for a fleet is the number of tows, days, or trips observed. In the CPUE mean-per-unit estimator, the estimate of total bycatch is a simple expansion of the observed bycatch per sample to the whole fleet. In the F:S ratio estimators, the unit effort appears in the calculations because the ratios of fish to shrimp are the amounts caught per tow, day, or trip (i.e. per sample). In the CPE ratio estimators, two measures of effort are used. As before, one measure of effort is the unit effort, such as a tow, day, or trip, that is equivalent to a sample, and the second measure of effort is the variable measure of effort, such as the hours fished, the distance towed, or the area covered, that is used as the auxiliary variable. The CPE ratio estimator is thus based on the amount of fish caught per hour fished (for example) in each tow, day, or trip.

The delta lognormal simulations were very similar to the normal simulations, except that I simulated the catch of fish and shrimp by using probabilities of catching fish or shrimp ranging from 0.05 to 0.95, multiplied by average catches of fish or shrimp generated from random lognormal distributions with means ranging from 0.01 to 1000. Lognormal functions have parameters of μ and σ^2, which are the mean and variance of the normally distributed variable before logarithmic transformation. To obtain values of μ and σ^2 from a lognormal distribution with a given mean and variance, I used an iterative procedure (the Solver procedure in Microsoft Excel, vers. 2000, Microsoft Corporation, Redmond, WA) to estimate μ and σ^2 based on the following equations:

$$mean = e^{\left(\mu+\frac{\sigma^2}{2}\right)} \qquad (15)$$

$$\mathrm{var} = e^{(2\mu+2\sigma^2)} - e^{(2\mu+\sigma^2)}, \qquad (16)$$

where $mean$ = the mean of the lognormal distribution of the catch of fish or shrimp;

var = the variance of the lognormal distribution of the catch of fish or shrimp;

μ = the mean of the normally distributed catch of fish or shrimp before logarithmic transformation; and

σ^2 = the variance of the normally distributed catch of fish or shrimp before logarithmic transformation.

Levels of observer coverage and CVs for fish catch, shrimp catch, and effort and were the same as in the normally distributed data. In these simulations, sampled shrimp catch could be zero if the probability of catching shrimp was low and the number of observations was small, leading to F:S ratios of infinity. In these cases, for the basic F:S ratio estimator, the fish-to-shrimp ratio was the catch of fish divided by the expected catch of shrimp (probability of catching shrimp times the mean catch). For the grand F:S ratio estimator, if the average bootstrapped sample catch of shrimp was zero, Matlab substituted a value of 65535 to avoid division by zero. To avoid biases, these grand F:S simulations were left out of the subsequent analyses. In field sampling, tows that caught no shrimp at all were rare, but tows that caught only small unmarketable shrimp that were discarded as bycatch occurred occasionally early in the season and after big rainstorms.

Table 1

Parameters and their values used in the bycatch simulations for normal and delta lognormal distributions of fish and shrimp. Abbreviations for the parameters are shown in parentheses.

Distribution	Parameter	Values
Normal	Mean fish catch (AvgF)	0.01, 0.1, 1, 10, 100, 1000, 10,000
	Fish CV (FCV)	20%, 50%, 80%, 120%
	Mean shrimp catch (AvgS)	0.01, 0.1, 1, 10, 100, 1000, 10,000
	Shrimp CV (SCV)	20%, 50%, 80%
	Mean hours fished	1.0
	Hours fished CV (ECV)	20%, 50%, 80%
	F:S ratio	0.001, 0.01, 0.1, 1, 10, 100, 1000, 10,000, 100,000
	Correlation coefficient (r)	−0.5, −0.25, 0, 0.25, 0.5
	Number of observations (n)	20,50,100,500
	Observer coverage	2%, 5%, 10%, 50%
Delta lognormal	Probability of catching fish (P(F))	0.05, 0.2, 0.5, 0.8, 0.95
	Mean fish catch (AvgF)	0.01, 0.1, 1, 10, 100, 1000, 10,000
	Fish CV (FCV)	20%, 50%, 80%
	Probability of catching shrimp (P(S))	0.05, 0.2, 0.5, 0.8, 0.95
	Mean shrimp catch (AvgS)	0.01, 0.1, 1, 10, 100, 1000, 10,000
	Shrimp CV (SCV)	20%, 50%, 80%, 120%
	Mean hours fished	1.0
	Hours fished CV (ECV)	20%, 50%, 80%
	F:S ratio	0.001, 0.01, 0.1, 1, 10, 100, 1000, 10,000, 100,000
	Number of observations (n)	20,50,100,500
	Observer coverage	2%, 5%, 10%, 50%

To statistically analyze the overall biases shown by each estimator regardless of fishing conditions (i.e. mean catches of fish or shrimp, CV, etc.), I first used paired sample t-tests (SAS v. 8, The SAS Institute, Cary, NC) to separately compare each of the five estimates of fleet bycatch with the "actual" bycatch for that fleet, based on the following equation:

$$\%\ bias_{m,b} = \frac{estimated\ bycatch_{i,m,b} - \text{"}actual\text{"}\ bycatch_{i,b} \times 100}{\text{"}actual\text{"}\ bycatch_{i,b}} \quad (17)$$

where $\%\ bias_{m,b}$ = the bias in the m^{th} estimator for the b^{th} fleet;

$estimated\ bycatch_{i,m,b}$ = the bycatch of the i^{th} species by the m^{th} estimator for the b^{th} fleet; and

$\text{"}actual\text{"}\ bycatch_{i,b}$ = the simulated actual bycatch of the i^{th} species by the b^{th} fleet.

For these statistical tests, all fleets with normal distributions of fish and shrimp were combined and analyzed separately from the fleets with delta lognormal distributions of fish and shrimp, giving sample sizes of 21,600 fleets for the normal distribution and 118,810 fleets for the delta lognormal distribution (Table 1). To look for significant factors influencing the bycatch estimates for each of the five estimation methods, I used ANOVAs on all main effects and all 2-way and 3-way interactions of the main effects for each estimator. Although 7-way interactions were possible in the normally distributed simulations and 8-way interactions were possible in the delta lognormal simulations (Table 1), I stopped the analysis at 3-way interactions because of the difficulty in interpreting higher level interactions. Main effects were the following: mean catches of fish and shrimp, CVs of fish catches, CVs of shrimp catches, CVs of hours fished, number of observations or observer coverage, correlation coefficient in the normally distributed simulations, and the probabilities of catching fish and shrimp in the delta lognormal simulations. In these ANOVAs, the response variable was the percent bias for each method, as calculated above.

Results

Field sampling

I observed 16 tows from five trips in Pamlico Sound between July and October 1995 and 24 tows from five trips in the Cape Fear River between August and October 1995 (Table 2). According to the 1995 trip tickets, these months comprised the peak of the summer brown shrimp and fall white-pink shrimp seasons; 77% of the total shrimp catch and 75% of the total trips in the northern region and 63% of the total shrimp catch and 54% of the total trips in the southern region occurred during those months. All observed tows were daytime tows, which is when fishing generally occurs in these areas. All nets sampled in July were 2-seam or 4-seam flat trawls, designed to catch brown shrimp, and

Table 2

Characteristics of boats and fishing operations observed in North Carolina waters in 1995. All boats were commercial shrimp trawlers operating using their standard operating procedures. Each entry represents one observed fishing trip. Each observed fishing trip lasted one day. Avg. h/tow = mean hours per tow.

Area	Month	Boat name	Boat length (m)	No. of tows	No. of nets	Headrope length (m)	Avg. h/tow
Pamlico Sound	Jul	*Last Toy*	8.3	5	2	9.8	1.2
	Aug	*Islander*	8.9	2	1	18.4	1.1
	Aug	*Last Toy*	8.3	2	1	13.1	1.3
	Sep	*Islander*	8.9	5	1	18.4	1.1
	Oct	*Islander*	8.9	2	1	18.4	1.2
Average			8.7	3.2	1.2	15.6	1.2
Cape Fear River	Aug	*Cajun Lady*	16.0	9	2	18.0	0.9
	Aug	*Cajun Lady*	16.0	2	2	18.0	0.7
	Sep	*Sea Mullet*	14.2	4	2	14.8	1.3
	Sep	*Cajun Lady*	16.0	5	2	18.0	1.0
	Oct	*Dorothy Glen*	11.4	4	1	19.7	1.9
Average			14.7	5	1.8	17.7	1.2

Table 3

Landed and observed shrimp catch (heads-on kg landed), effort (total number of trips and days/trip), and catch per unit of effort (CPUE, kg /trip and kg/day) for regions within North Carolina. Information on fleet totals was obtained from the North Carolina Department of Marine Fisheries trip ticket database for vessels fishing during July through October 1995 in the Northern region (Pamlico Sound and tributaries), and during August through October 1995 in the Southern region (the Cape Fear River and nearby waters). Observations were conducted during these same months in Pamlico Sound and the Cape Fear River.

Region or location	Shrimp catch (kg landed)	No. of trips	Mean days/trip	CPUE (kg/trip)	Days fished[1]	CPUE (kg/day)
Fleet totals						
Northern	2,018,612	3196	3.64	631.6	11,633	173.5
Southern	122,893	1716	3.48	71.5	5972	20.6
Observations						
Pamlico Sound	278	5	1	55.6	5	55.6
Cape Fear River	867	5	1	173.4	5	173.4

[1] This value represents the maximum days fished because the calculations are based on the assumption that fishing takes place every allowable day between landings.

both tongue trawls and flat trawls were sampled in August through October. Tongue trawls are modified mongoose trawls that have a higher vertical profile for catching white shrimp. In addition, the tongue trawls had a greater headrope length than the flat trawls; therefore many of the fishermen switched from pulling two flat trawls to pulling one larger tongue trawl. Tows typically lasted around one hour. The observed catch of shrimp per day in the Cape Fear River was almost three times higher than the observed catch of shrimp per day in Pamlico Sound (Table 3).

Total shrimp landings and total shrimp trips during the observed months from the 1995 trip ticket database were used as the expansion factors in the estimates. Over half of the total shrimp landings, or 2,018,622 kg, were caught in the northern region between July and October and only 122,893 kg came from the southern region between August and October, the months that corresponded to the observations. Although there were about twice the number of trips and days fished the northern region, the average catch per trip (kg/trip) from the northern region was almost nine times higher than the catch per trip from the southern region (Table 3).

The different estimation methods made a tremendous difference in the estimates of bycatch, but the differences were exactly opposite in the two geographic regions and varied somewhat by species. Total bycatch estimates derived with the basic F:S ratio estimator (mean of the ratios) by both weight and number were two to seven times higher than those based on the CPUE-mean-per-unit method for all species in the northern region, and about two to five times lower by both weight and number for all species in the southern region (Table 4). For Atlantic croaker and

Table 4

Total bycatch in weight and numbers estimated from observation data using different estimation methods. The CPUE-mean-per-unit estimator (CPUE=catch per unit of effort), which is based on the catch per day, uses day as a proxy for sample size. The basic F:S ratio estimator is the mean of individual fish (F) to shrimp (S) ratios, and the grand F:S ratio estimator is the ratio of the mean catch of fish to the mean catch of shrimp. The Hartley-Ross method is the basic F:S ratio estimator corrected for small sample sizes. AC = Atlantic croaker, SP = spot, and WF = weakfish. The northern region includes Pamlico Sound and its tributaries, and the southern region includes from the Cape Fear River to the New River. Estimates are for July through October 1995 in the northern region and August through October 1995 in the southern region. See text for calculations. Equations for the 95% CL are from Cochran (1977), Equations 2.24, 6.12, and 6.14.

	Bycatch estimate by weight (millions of kg)							
	CPUE-mean-per-unit estimator		F:S ratio estimator					
			Basic		Grand		Hartley-Ross	
Region and species	Total wt.	±95% CL	Total wt.	±95% CL	Total wt.	±95% CL	Total wt.	±95% CL
Northern								
AC	0.6	0.5	2.1	4.1	1.7	0.1	2.6	0.1
SP	0.5	0.8	2.9	5.6	1.5	0.3	2.3	0.3
WF	0.6	1.2	1.5	1.5	1.9	0.4	1.7	0.4
Southern								
AC	0.1	0.2	0.03	0.05	0.02	0.09	N/A[1]	N/A
SP	0.02	0.05	0.006	0.01	0.003	0.03	N/A	N/A
WF	0.2	0.2	0.03	0.04	0.2	0.1	N/A	N/A

	Bycatch estimate by number (millions)							
	CPUE-mean-per-unit estimator		F:S ratio estimator					
			Basic		Grand		Hartley-Ross	
Region and species	Total no.	±95% CL	Total no.	±95% CL	Total no.	±95% CL	Total no.	±95% CL
Northern								
AC	28.1	23.7	186.0	263.8	84.8	8.4	144.1	8.4
SP	18.7	27.2	146.5	305.5	56.5	11.7	109.2	11.7
WF	11.8	20.8	36.2	34.8	35.7	6.4	35.9	6.4
Southern								
AC	13.7	20.9	4.1	7.1	1.7	12.7	N/A	N/A
SP	1.5	3.4	0.4	0.6	0.2	1.8	N/A	N/A
WF	19.1	29.2	3.5	4.9	2.3	16.3	N/A	N/A

[1] The estimator gave negative estimates for bycatch.

spot, the grand F:S ratio estimate (ratio of the means) was intermediate between the basic F:S ratio estimate and the CPUE-mean-per-unit estimate in the northern region, but was lower than either of the other estimates in the southern region. The grand F:S ratio estimate for weakfish was larger by both weight and number than either of the other two estimates in the northern region and was the smallest in the southern region. The Hartley-Ross bias-corrected F:S ratio estimator gave estimates for the northern region that fell between the basic and grand F:S methods but gave negative estimates for the southern region (Table 4). CVs of the catch rates were generally larger for the basic F:S ratio estimator method than for CPUE-mean-per-unit estimator for spot in the northern region and Atlantic croaker in both regions, and smaller for spot in the southern region and weakfish in both regions. CVs estimated by the grand F:S ratio method were much smaller than those for either of the other methods for the northern region and much larger than the others for the southern region (Table 5). The variance of the catch rates with both methods was usually much larger than the mean (sometimes by an order of magnitude), indicating that catches were aggregated (Table 5). The confidence intervals around the bycatch estimates were huge regardless of method because of the small number of observed fishing days and the large variability in catch rates (Table 4).

Table 5

Observed catch rates in weight and numbers for selected species obtained with different estimation methods from field data. Observations in Pamlico Sound took place in July through October 1995 and observations in the Cape Fear River took place in August through October 1995. The CPUE-mean-per-unit estimator (CPUE=catch per unit of effort), which is based on the catch per day, uses day as a substitute for sample size. The basic F:S ratio estimator is the mean of the individual fish (F) to shrimp (S) ratios, and the grand F:S ratio estimator is the ratio of the mean catch of fish to mean catch of shrimp. AC = Atlantic croaker, SP = spot, and WF = weakfish. See text for calculations. Equations for the standard deviations are taken from Cochran (1977), Equations 2.20 and 2.45.

	Observed catch rate by weight								
				F:S ratio estimator					
				Basic			Grand		
	CPUE-mean-per-unit estimator								
Location and species	Avg. kg/day	SD	CV (%)	kg fish/kg shrimp	SD	CV (%)	kg fish/kg shrimp	SD	CV (%)
Pamlico Sound									
AC	49.64	34.79	70	1.62	1.05	154	0.86	0.05	6
SP	41.57	52.40	126	1.46	2.21	152	0.72	0.17	16
WF	53.04	79.90	151	0.75	0.60	80	0.92	0.15	16
Cape Fear River									
AC	24.01	21.56	90	0.27	0.31	116	0.14	0.61	438
SP	4.14	6.71	162	0.05	0.06	129	0.02	0.18	757
WF	31.80	30.10	95	0.25	0.24	94	0.18	0.81	443

	Observed catch rate by number								
				F:S ratio estimator					
				Basic			Grand		
	CPUE-mean-per-unit estimator								
Location and species	Avg. no./day	SD	CV (%)	no. fish/kg shrimp	SD	CV (%)	no. fish/kg shrimp	SD	CV (%)
Pamlico Sound									
AC	2418	1639	68	92.15	105.29	114	42.02	3.37	8
SP	1610	1885	117	72.56	121.92	168	27.97	4.69	17
WF	1014	1438	142	17.92	13.89	77	17.62	2.54	14
Cape Fear River									
AC	2287	2826	124	33.70	46.90	139	13.20	83.35	632
SP	257	464	181	3.05	4.16	136	1.48	12.10	816
WF	3198	3941	123	28.09	32.14	114	18.45	106.75	579

Bycatch simulations

For the normally distributed data, the CPUE-mean-per-unit estimator was the only estimator whose estimated bycatch was not significantly different than the actual simulated bycatch (% bias=0.006, P=0.94). All four of the ratio estimators significantly overestimated bycatch (Table 6), although the average bias was less than a 1% overestimate for the grand F:S and grand CPE ratio estimators. The basic F:S ratio estimator and the basic CPE ratio estimator both overestimated bycatch by 300–400% (Table 6). Using a model that included all main effects and all 2-way and 3-way interactions in the ANOVA, I found that the CV of the auxiliary variable (either shrimp catch or hours fished) was a significant main effect for all four of the ratio estimators, but there were no significant main effects for the CPUE mean-per-unit estimator (Table 7). Observer coverage was also a significant main effect for the F:S and CPE grand ratio estimators, but was not significant for the basic F:S or CPE ratio methods. The grand F:S ratio estimator, the grand CPE ratio estimator, and the basic F:S ratio estimator all showed several significant 2-way and 3-way interactions (Fig. 2), whereas the basic CPE ratio estimator had no significant 2-way or 3-way interactions. The CPUE-mean-per-unit estimator showed only two significant 3-way interactions among variables, and observer coverage occurred in both. The correlation between fish catches and shrimp catches was a significant main effect for the basic

Table 6

Mean percent bias of each of the estimators with normal and delta lognormal distributions of fish (F) and shrimp (S) from simulated data. Percent bias (Eq. 17) was calculated separately for each simulated fleet. N = the number of fleets in each analysis. The * indicates that the mean estimated bycatch is significantly different than the mean actual bycatch in a paired sample t-test ($P<0.05$). The CPUE-mean-per-unit estimator (CPUE=catch per unit of effort) uses unit effort as a proxy for sample size. The basic F:S ratio estimator is the mean of the individual fish to shrimp ratios, and the grand F:S ratio estimator is the ratio of the mean catch of fish to the mean catch of shrimp. The basic CPE ratio estimator is the mean of the ratios of catch per effort, where effort is a variable measure such as hours fished, and the grand CPE estimator is the ratio of the mean catch of fish to the mean estimate of effort.

	Mean % bias	
Estimator	Normal distribution N = 21,600	Delta lognormal distribution N = 118,810
CPUE mean-per-unit	0.006	0.09
Basic F:S ratio	427.80*	9.98*
Grand F:S ratio	0.65*	12.23*
Basic CPE ratio	336.13*	30.75*
Grand CPE ratio	0.46*	0.47*

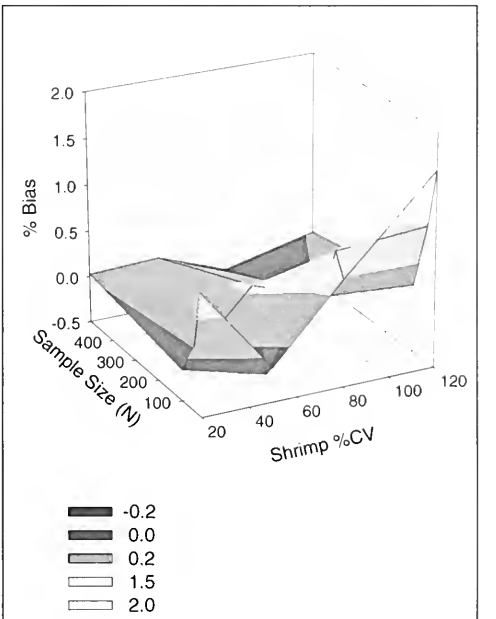

Figure 2

An example of a significant 3-way interaction among parameters in the bycatch simulations. This interaction is between shrimp CV and observer coverage (n) for the grand F:S ratio estimator with a correlation coefficient (r) of 0.5 between the catches of fish and shrimp. The simulated fish and shrimp catches were normally distributed. The lack of pattern in the % bias due to the interactions among various parameters was a common feature of all the estimators.

F:S estimator, and showed significant interactions with other parameters in both the grand F:S and grand CPE ratio estimators.

For the delta lognormally distributed data, the CPUE-mean-per-unit estimator was the only estimator whose estimated bycatch was not significantly different than the actual simulated bycatch (% bias=0.087%, P=0.64). All four of the ratio estimators significantly overestimated bycatch (Table 6), with estimates ranging from a less than 1% overestimate using the grand CPE ratio estimator to a 30% overestimate with the basic CPE ratio estimator (Table 6). Using all 2-way and 3-way interactions in the ANOVA, I found that significant main effects for both the basic and grand F:S ratio estimators were the probability of catching shrimp and the CV of the shrimp catch. The CV of the fish catch and observer coverage were also main effects in the grand F:S ratio method. The probability of catching fish was an additional main effect in the basic F:S ratio method. The only significant main effect in both CPE ratio estimators was the CV of effort, and the only significant main effect in the CPUE-mean-per-unit method was the CV of the fish catch. All five methods exhibited several statistically significant 2-way and 3-way interactions (Table 7).

Discussion

The differences in bycatch estimates generated from the field data show how confusing bycatch estimation can be and how difficult it is to compare bycatch estimates from past and recent studies. There was tremendous variability in the bycatch estimates generated by the different methods in the field study; for example, the estimate of Atlantic croaker bycatch in the northern region of North Carolina was either 28 million (±24 million), 84 million (±264 million), 144 million (±8.4 million), or 186 million (±8.4 million) fish depending on the estimator used. In addition, each method could give estimates that were higher or lower than the other methods without any consistent pattern by region or species; for example, in the northern region, the basic F:S ratio estimate was the highest estimate for spot, but it was one of the lowest for weakfish.

Based on the simulation results, the CPUE-mean-per-unit estimator was the best estimator, both because it showed less bias than the ratio estimators and because it was less influenced than the ratio estimators by parameters such as the mean or variance of the catch, observer coverage, or the correlation between the catches of fish and

Table 7

Significant parameters and interactions among parameters influencing bycatch estimates from simulated data. Significance was tested by using ANOVAs. *** = $P < 0.001$, ** = $0.001 \leq P < 0.02$, * = $0.02 \leq P \leq 0.05$. AvgF = the mean catch of fish; AvgS = the mean catch of shrimp; FCV = fish CV; SCV = shrimp CV; ECV = Effort CV; r = the correlation coefficient between the catch of fish and the catch of shrimp, n = observer coverage; P(S) = probability of catching shrimp; and P(F) = probability of catching fish. The ranges of values for all parameters are shown in Table 1. The CPUE-mean-per-unit estimator (CPUE=catch per unit of effort) uses unit effort as a proxy for sample size. The basic F:S ratio estimator is the mean of the individual fish to shrimp ratios, and the grand F:S ratio estimator is the ratio of the mean catches of fish and shrimp. The basic CPE ratio estimator is the mean of the ratios of catch per effort, where effort is a variable measure of effort, and the grand CPE estimator is the ratio of the mean catch of fish to the mean estimate of effort.

	CPUE	Ratio estimators			
Normal distribution	Mean-per-unit	Basic F:S	Grand F:S	Basic CPE	Grand CPE
Main effects					
SCV		***	***		
ECV		**		***	***
r		**			
n			***		***
Two-way interactions					
AvgS × AvgF			**		
SCV × n			***		
FCV × n			**		
ECV × n					***
ECV × r		**			
Three-way interactions					
AvgS × AvgF × FCV		**			
AvgS × FCV × n	**				
AvgS × n × r			*		
AvgF × SCV × ECV					*
AvgF × FCV × n					**
AvgF × ECV × n					**
SCV × FCV × ECV		**			
SCV × n × r	**				
FCV × ECV × r			**		
FCV × n × r					*

continued

shrimp. In fact, only the mean-per-unit estimators gave overall bycatch estimates that were statistically unbiased for both the normally distributed and delta lognormally distributed data. Three other estimators, the grand F:S and the grand CPE ratio estimators for the normally distributed data and the grand CPE ratio estimator for the delta lognormally distributed data, gave bycatch estimates that differed by less than 1% on average from the actual simulated bycatch, although these differences were statistically significant. In these simulations, the reason that a bias of less than 1% was statistically significant was probably due to the large number of fleets included in the paired-sample t-tests for each distribution, which made the standard errors and confidence intervals very small. Both the F:S and CPE basic ratio estimators (mean of the ratios) performed poorly in terms of bias in both normally distributed and delta lognormally distributed data, overestimating bycatch by between 10% and 427%, regardless of whether shrimp catch or hours fished was used as the auxiliary variable.

The ANOVAs performed on the simulated data indicated why the different estimates are so variable, and showed the complexities of the interactions among the parameters. The CPUE-mean-per-unit estimators displayed the fewest main effects and showed the fewest higher-level interactions among parameters. In the normally distributed data, there were no significant main effects or 2-way interactions for the CPUE-mean-per-unit estimator although observer coverage, (the sample size for each fleet) was a factor in both significant 3-way interactions. For the delta lognormally distributed data, the CV of the catch of fish was a significant main effect for the CPUE-mean-per-unit estimator, and observer coverage was a factor in three of the four significant 3-way interactions. The probability of catching fish and the CV of the fish catch were also fac-

Table 7 (continued)

Delta lognormal distribution	CPUE Mean-per-unit	Ratio estimators Basic F:S	Grand F:S	Basic CPE	Grand CPE
Main effects					
P(S)		***	***		
P(F)		*			
SCV		***	***		
FCV	**		*		
ECV				***	***
n			***		
Two-way interactions					
P(S)×SCV		***	***		
P(S)×FCV			***		
P(S)×n			***		
P(F)×FCV	***				
P(F)×n			**		*
Avg(S)×FCV			*		
Avg(S)×ECV					*
Avg(F)×ECV					**
SCV×n			***		
ECV×n					***
Three-way interactions					
P(S)×AvgS×SCV		*			
P(S)×AvgS×ECV			**		
P(S)×AvgS×n	*				
P(S)×SCV×ECV		**			
P(S)×SCV×n			***		
P(F)×AvgS×AvgF		**	*		
P(F)×AvgS×SCV		**			
P(F)×AvgS×ECV				**	**
P(F)×AvgF×ECV					*
P(F)×SCV×n	**				
P(F)×FCV×ECV				***	
P(F)×FCV×n	**	**			**
AvgS×SCV×FCV	*				
AvgS×FCV×ECV			**		
SCV×FCV×n				***	**
FCV×ECV×n				**	

tors in several significant 2-way and 3-way interactions for the CPUE mean-per-unit estimator with delta lognormally distributed catches of fish and shrimp. All four of the ratio estimators were extremely sensitive to variance in the auxiliary variable, which was either shrimp catch or a variable measure of effort such as hours fished. Often in field data, the variance in the catch of shrimp will be much greater than the variance in the measure of effort; therefore the basic F:S ratio method has both the greatest bias and the highest variance in the auxiliary variable, making it the least desirable of the five methods tested. Both of the grand ratio methods were very sensitive to observer coverage for normally distributed data, although because of interactions with other parameters, it was hard to discern how increasing the number of observations changed the bias of the estimates (Fig. 2). Surprisingly, the correlation between the catch of shrimp and the catch of fish in the normally distributed simulations was only a significant main effect for the basic F:S ratio estimator, and even for that estimator the CV of shrimp catch had a much more profound effect. In the grand F:S ratio estimator, there were two 3-way interactions between the correlation coefficient and other parameters, but the other variables seemed to exert much more influence on the bycatch estimate than the correlation between the catches of fish and shrimp.

Comparisons of bycatch estimators between the normally distributed data and delta lognormally distributed data

suggested that the basic ratio methods (mean of the ratios) might actually be less biased for lognormally distributed data than for normally distributed data. Both the CPE and F:S basic ratio estimators showed only about 10% of the bias with the delta lognormal data that they had with normally distributed data. The change in underlying distribution made very little difference to the bias shown by the grand CPE ratio method and increased the bias in the grand F:S method. For the CPUE-mean-per-unit method, the normally distributed data had less bias by an order of magnitude than the delta lognormal data, but neither of the biases was statistically significant, and both were much less than a 1% overestimate.

Cochran (1977) stated that the ratio estimator is the best linear unbiased estimate if the relationship between y_i, which is the catch of the bycatch species, and x_i, which is the auxiliary variable, is a straight line through the origin (indicating that the ratio of bycatch to shrimp or the catch of bycatch per hour fished is constant over all observations) and if the variance of y_i about this line is proportional to x_i. In practice, these conditions rarely hold true. The ratio of fish to shrimp catches and the bycatch per hour fished from field data often vary considerably among observations because of the patchy spatial distributions of fish and shrimp, seasonal differences in the relative abundances of fish and shrimp, movements associated with development through different life stages, and environmental factors. In addition, the bias of a ratio estimator is on the order of $1/n$, indicating that the bias will be small if n is large (Cochran, 1977). In practice, n, or the number of onboard bycatch observations, is often very small, particularly if the data are stratified by season or area, leading to large biases in ratio estimators.

The Hartley-Ross ratio estimator, which is a form of the basic ratio estimator method, may in some cases be an unbiased or less biased ratio estimator for small samples (Cochran, 1977). However, the Hartley-Ross method was not effective for the field data in the present study, giving nonsensical negative estimates of bycatch for all species in the southern region, although the estimates in the northern region were generally (but not always) somewhere between the basic and grand F:S ratio methods. The problems with the Hartley-Ross ratio estimator in the southern region may have been due to two factors: 1) the very low value for total shrimp landings from trip tickets in the southern region, and 2) discrepancies between the observed average catch of shrimp per day and the fleet shrimp catch per day from the trip ticket database. The Hartley-Ross equation starts with the mean of the individual fish to shrimp ratios expanded by the total shrimp landings (the basic F:S ratio estimator) and corrects the estimate based on the sampling fraction multiplied by a quantity that includes the average observed catch of shrimp per day (Eq. 8). The total shrimp landings recorded on trip tickets for the southern region were extremely low, about 16 times lower than the total shrimp landings in the northern region, although the number of days fished was about half as many in the southern region. In addition, the average shrimp catch per day on vessels that I observed in the southern region was much greater than the average reported on trip tickets (173.4 kg per day observed vs. 20.6 kg per day from trip tickets), whereas the average shrimp catch per day of shrimp that I observed in the northern region was much lower than the catch per day shown on trip tickets (55.6 kg per day observed vs. 173.5 kg per day from trip tickets). The result of this combination of factors was that the estimated total bycatch before correction in the southern region was very small due to the low amount of total shrimp landings, whereas the correction factor was very large because of the high observed average catch of shrimp, leading to negative estimates of total bycatch. These problems did not occur in the northern region. Low shrimp landings in the southern region compared to the northern region may have been due to an actual difference in the abundance of shrimp or differences in fishing habits such as a smaller number of nets per boat, tows per day, or tow times per tow in the southern region. However, it is also possible that more fishermen in the southern region than the northern region keep their catch or sell part of their catch independently without generating a trip ticket, which would reduce the total landings of shrimp in the trip ticket database. The differences in the average observed catch of shrimp per day were probably due to a combination of factors, most of them based on the problem of nonrandom or nonrepresentative sampling of boats. Because I depended on volunteer fishermen, the observed shrimp boats and captains were not randomly selected. In addition, because no records are kept of the boat size, gear used, fishing habits, or effort history of fishermen in the fleet, sampled boats could not be compared to unsampled boats for these factors. However, most of the fishermen whose boats I observed in the Cape Fear River (the southern region) owned large boats and made an average of 5 tows per day, whereas the fishermen I observed in Pamlico Sound (the northern region) generally had smaller boats and made an average of 3.2 tows per day. If the fishermen whose boats I observed in the Cape Fear River fished more than the average number of tows per day and the observed fishermen in Pamlico Sound fished fewer than the average number of tows per day, then the catch per day values would show these discrepancies. Other factors could have been differences between observed boats and average boats in the number of nets per boat, or tow times.

All of the methods that I used for bycatch estimation for the field data were based on the summed catches over all tows on a single day, because in this study the variance of catches among tows within days was much less than the variance among days. The use of tows as the basic unit of effort would therefore have underestimated the total variance. Sampling only day-trips probably contributed to the covariance among tows because tows spread over several days (and probably several locations) in a multiday trip would probably vary more among tows within a trip than tows in a single day. For randomly sampled multiday trips, estimation methods based on tows rather than days or trips may be preferred to those based on a trip as the unit of effort because the sample size of tows increases faster than the sample size of days or trips, which would tighten the confidence intervals around the estimates. However, the use of tows as the unit of effort could be considered pseu-

doreplication (Hurlbert, 1984) and could lead to erroneous variance estimates if the tows in a trip are not independent samples (Cochran, 1977). The choice of whether to use trips or tows as the unit of effort is dependent on two factors: 1) whether there is a high degree of covariance among tows in a trip, and 2) whether there is an independent estimate of the average number of tows per trip to use as an expansion factor.

Confidence intervals around the bycatch estimates are not symmetrical, although they are shown in Table 4 as symmetrical to allow for easier comparisons between the methods in the field study. Because of the small numbers of observations, most of the confidence intervals in the field study were larger than the means, with the general exceptions of the grand ratio estimators for all species in the northern region, which were surprisingly small. Most grand ratio estimators underestimate the true catch rate and are positively skewed unless the sample size is greater than 30 and the CVs of both the observed fish catch and the auxiliary variable are less than 10% (Cochran, 1977). As seen in Table 5, CVs of the observed fish catch from field data are rarely as low as 10%, and many are over 100%. The very small confidence intervals for all species in the northern region, and the very large confidence intervals for all species in the southern region generated by the grand ratio estimators are due to the nonrandom sampling of boats for the average catch of shrimp in both areas. This nonrandom sampling affects the confidence intervals because the average catch per day is a term in the denominator of the equation used to estimate the variance of the grand ratio estimator (Eq. 2.45 in Cochran, 1977). A very large value for the average catch per day from trip tickets compared to the value from observations as in the northern region causes an underestimate in the variance and reduces the confidence intervals, whereas a small value for the average catch per day from trip tickets compared to the value from observations as in the southern region causes an overestimate in the variance and increases the confidence intervals.

The field data shown here indicate some of the problems that are peculiar to observing and estimating bycatch in shrimp trawl fisheries in comparison to other fisheries. First, there are several hierarchical levels of variability that are ignored because of the logistical difficulties of sampling shrimp trawls. If the National Marine Fisheries Service (NMFS) protocol for shrimp trawl bycatch is followed, only one sample of the catch is taken from a net because of the large numbers of organisms caught in a typical tow. The NMFS protocol depends on the observer thoroughly mixing the catch so that a single sample characterizes the entire catch without variance, but mixing the catch to obtain a random sample is sometimes difficult because of the weight of the catch, the position of the culling tray, the size of the boat, or weather conditions. In addition, some species such as crabs may redistribute themselves after the catch is mixed by simply walking away. Stender and Barans (1994) found differences in fish-to-shrimp ratios when sampling the net compared with enumerating everything in the net. However this source of variability is not measured when following the NMFS protocol and not included in the bycatch estimates. Second, only one net is generally sampled per tow, although the boat may tow two, four, or more nets. There is therefore an expansion from the sampled net to the number of nets per tow so that variance among nets is ignored, and this process also adds error. Third, the expansion term, regardless of whether the total shrimp landings or the total shrimp effort is used, is assumed known without error. To include the error in the expansion term further widens the confidence intervals around the final estimates (Diamond and Hanan[16]).

One of the most interesting findings from the simulations was that all the methods tended to overestimate bycatch. None of the overall bycatch estimates, and relatively few of the individual fleet simulations, generated underestimates of the actual values. Although the mean-per-unit and grand ratio estimates overestimated bycatch by less than 1%, if the bycatch is large enough, these estimators could erroneously add hundreds of thousands of fish to the catch-at-age matrices used in stock assessments. Inaccurate stock assessments could have consequences for the management of fisheries, particularly for species like red snapper that are managed by quotas on the directed fisheries that are based on the level of bycatch or that have target levels set for rebuilding fish stocks. One method that might be used to "correct" bycatch estimates for the mean-per-unit estimator would be to use the estimator to calculate the catch of the target species from the observations, and then to compare the estimated target species catch with the total landings. Although this correction method assumes that the total landings of the target species are accurate (which is rarely a valid assumption), comparison of the estimated total catch of the target species to the actual landed catch might help to pinpoint biases and to adjust the estimated bycatch.

Because of the differences in estimates generated by the different methods of estimating bycatch, interpretations of bycatch estimates and comparisons of bycatch studies should be made very cautiously. It is often difficult to tell in past studies whether estimates were generated by basic F:S or grand F:S methods, but basic F:S methods overestimate bycatch to a much greater degree. Because of the statistically significant 2-way and 3-way interactions among parameters, it is unlikely that estimates generated by one method can be converted or corrected to other methods, so bycatch estimates made over time using different methods should not be directly compared. In addition, any bycatch estimate should include some indication of the variance around either the estimate or the catch rate, although variance estimates can be misleading if samples are not random. Finally, estimates of the weight or number of species taken as bycatch, no matter how large or small, are meaningless without an estimate of population abundance. Small populations could be harmed by relatively small amounts of bycatch, whereas large populations

[16] Diamond, S. L., and D. Hanan. 1986. An estimate of harbor porpoise mortality in California set net fisheries April 1, 1983 through March 31, 1984. National Marine Fisheries Service Admin. Report SWR-86-15, 40 p.

could be able to withstand even large amounts of bycatch. For this reason, the consequences of bycatch can only be evaluated if examined in conjunction with some estimate of stock size.

Acknowledgments

My sincerest gratitude goes to the fishermen who allowed me on their boats: Allan Hines, Bud George, Pete Dixon, Ben Ingraham, H.O. Golden, Tommy Peters, Al Gillikin, and Brad Styron. Bud George also provided many helpful suggestions on how to weigh the catch. I also appreciate the help given to me by Oliver and Tina Lewis, Bimbo Melton, Tony Cahoun, Gracie Golden, Jim Bahen, John Schoolfield, Beth Burns, Bob Hines, and Jim Murray. Trish Murphey, Mike Street, and Dee Lupton from NCDMF provided the shrimp trip ticket data. Peter Lamb, Tyler Stanton, Sue Zwicker, Pam Robinson, Walter Mayo, Amy Makepeace, Martin Gallagher, Dawn O'Harra, and Jim Armstrong helped to sort and identify the bycatch species. Jim Rice, Larry Crowder, Joe Hightower, Ken Pollock, and Doug Vaughan provided valuable input on earlier drafts of this manuscript. Thanks also to Rich Strauss and Richard Stevens for their help in using Matlab software. This manuscript was significantly improved by the comments of Scott Nichols and two anonymous reviewers. This research was supported by a National Science Foundation Pre-doctoral Fellowship, the J. Francis Allen Scholarship from the American Fisheries Society, the Joseph L. Fisher Dissertation Award from Resources for the Future, and MARFIN Grant no. NA57FF0299.

Literature cited

Alverson, D. L. 1994.
1994. A global assessment of fisheries bycatch and discards, 233 p. FAO (Food and Agriculture Organization) of the United Nations, Rome, Italy. [ISBN 92-5-103555-5.]

Cochran, W. G.
1977. Sampling techniques, 428 p. John Wiley and Sons, New York, NY.

Crouse, D. T., L. B. Crowder, and H. Caswell.
1987. A stage-based population model for loggerhead sea turtles and implications for conservation. Ecology 68(5): 1412–1423.

Fahy, W. E.
1966. Species composition of the North Carolina industrial fish fishery. Comm. Fish. Rev. 28(7):1–8.

Fisheries Statistics of the United States.
1977. U.S. Fish and Wildlife Service, Bureau of Commercial Fisheries, Statistical Digest 71, 407 p.

Hurlbert, S. H.
1984. Pseudoreplication and the design of ecological field studies. Ecol. Monogr. 54 (2):187–211.

Julian, F., and M. Beeson.
1998. Estimates of marine mammal, turtle, and seabird mortality for two California gillnet fisheries: 1990–1995. Fish Bull. 96:271–284.

Stender, B. W., and C. A. Barans.
1994. Comparison of the catch from tongue and two-seam shrimp nets off South Carolina. North Am. J. Fish. Manage. 14:178–195.

Walsh, W.A., and P. Kleiber.
2001. Generalized additive model and regression tree analysis of blue shark (*Prionace glauca*) catch rates by the Hawaii-based commercial longline fishery. Fish. Res. 52(2):115–131.

Applications in adaptive cluster sampling of Gulf of Alaska rockfish

Dana H. Hanselman
Terrance J. Quinn II
School of Fisheries and Ocean Sciences
University of Alaska Fairbanks
11275 Glacier Hwy.
Juneau, Alaska 99801
E-mail address (for D. H. Hanselman): ftdhh@uaf.edu

Chris Lunsford
Jonathan Heifetz
David Clausen
Auke Bay Laboratory
Alaska Fisheries Science Center
National Marine Fisheries Service
11305 Glacier Hwy.
Juneau, Alaska 99801

Abstract—Adaptive cluster sampling (ACS) has been the subject of many publications about sampling aggregated populations. Choosing the criterion value that invokes ACS remains problematic. We address this problem using data from a June 1999 ACS survey for rockfish, specifically for Pacific ocean perch (*Sebastes alutus*), and for shortraker (*S. borealis*) and rougheye (*S. aleutianus*) rockfish combined. Our hypotheses were that ACS would outperform simple random sampling (SRS) for *S. alutus* and would be more applicable for *S. alutus* than for *S. borealis* and *S. aleutianus* combined because populations of *S. alutus* are thought to be more aggregated. Three alternatives for choosing a criterion value were investigated. We chose the strategy that yielded the lowest criterion value and simulated the higher criterion values with the data after the survey. Systematic random sampling was conducted across the whole area to determine the lowest criterion value, and then a new systematic random sample was taken with adaptive sampling around each tow that exceeded the fixed criterion value. ACS yielded gains in precision (SE) over SRS. Bootstrapping showed that the distribution of an ACS estimator is approximately normal, whereas the SRS sampling distribution is skewed and bimodal. Simulation showed that a higher criterion value results in substantially less adaptive sampling with little tradeoff in precision. When time-efficiency was examined, ACS quickly added more samples, but sampling edge units caused this efficiency to be lessened, and the gain in efficiency did not measurably affect our conclusions. ACS for *S. alutus* should be incorporated with a fixed criterion value equal to the top quartile of previously collected survey data. The second hypothesis was confirmed because ACS did not prove to be more effective for *S. borealis*-*S. aleutianus*. Overall, our ACS results were not as optimistic as those previously published in the literature, and indicate the need for further study of this sampling method.

Manuscript approved for publication 30 January 2003 by Scientific Editor.
Manuscript received 4 April 2003 at NMFS Scientific Publications Office.
Fish. Bull. 101:501–513 (2003).

In nature, populations are sometimes distributed in a patchy, rare, or aggregated manner. Conventional sampling designs such as simple random sampling (SRS) do not take advantage of this spatial differentiation. Thompson (1990) introduced a sampling design called adaptive cluster sampling (ACS) to survey these types of distributions.

Adaptive cluster sampling, in theory, can be much more precise for a given amount of effort than conventional sampling designs (Thompson, 1990). In practice, however, this is not always the case. In some cases, the variance is greatly reduced, but bias is induced from stopping rules and criterion values that are sometimes changed mid-survey (Lo et al., 1997). In 1998, we conducted a survey on Gulf of Alaska rockfish in which ACS was efficient and successful, but the gains in precision, if any, were small compared to those of a SRS of the same size (Quinn et al., 1999; Hanselman et al., 2001).

Recently papers about ACS have included efficiency comparisons (Christman, 1997), restricted ACSs (Lo et al., 1997; Brown and Manly, 1998), bootstrap confidence intervals (Christman and Pontius, 2000), and bias estimates (Su and Quinn, 2003). However, little work has been done on determining the criterion value that, when exceeded, invokes additional sampling. In the following study, we examine the details for choosing this criterion value by using data from a 1999 field survey for Gulf of Alaska rockfish. We then simulate the outcome of the experiment with different criterion values after the survey. We also compare the efficiency of ACS to SRS.

In the basic adaptive cluster sampling (ACS) design, a simple random sample (SRS) of size n is taken; if y (the variable of interest) exceeds c (a criterion value), then neighborhood units are added (e.g. units above, below, left, and right in a cross pattern, Fig. 1) to the sample. These are called network units. If any network unit has $y>c$, then its neighborhood is added. Units that do not exceed the criterion are called edge units, and sampling does not continue around them. This process continues until no units are added or until the boundary of the area is reached (Thompson and Seber, 1996). Neighborhoods can be defined in any general way. The only condition is that if unit i is in the neighborhood of j, then unit j is in the neighborhood of i. The "unbiasedness" of the estimators relies on all neighborhood units of $y>c$ being sampled. If logistics cause the sampling to be curtailed before the sampling is complete, then biased estimators can

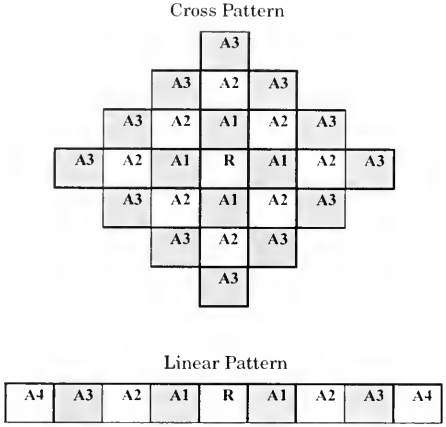

Figure 1

Diagram of a basic cluster sampling design, showing the maximum possible number of adaptive hauls for the cross (S=3) and the linear (S=4) patterns with the imposition of a stopping rule. The initial random tow is denoted as "R," and the adaptive tows as "A" and their respective level number.

result. For our study, all samples were called "tows" because our study was a trawl survey.

When little information is available to preset a fixed criterion value, order statistics are often used to choose a criterion value (Thompson and Seber, 1996). The basic idea is that an initial random sample is conducted. Next, the values of the random tows are ordered, and ACS is conducted around the top r stations. The variable r is decided by the experimenter and depends on the amount of resources available and the suspected aggregation of the population. The criterion value is then set at the value of the next highest tow (r+1). This was the design used in the 1998 adaptive cluster sampling survey for rockfish (Quinn et al., 1999, Hanselman et al., 2001). The use of order statistics has several limitations, however. First, initial random samples must be taken before the adaptive phase can begin. This procedure can be inefficient, because the experiment may have to move a large distance back to the previous tows that exceeded the criterion, by which time the aggregation may have moved or dispersed. In some cases, this procedure may result in a very small criterion value that leads to an overwhelming amount of adaptive sampling around some tows. Second, the process of achieving simple unbiased estimates of abundance is more complicated with order statistics because the criterion value is dependent on the sampling.

In our study, we address methods to avoid these limitations and illustrate these methods with a 1999 ACS survey for Gulf of Alaska rockfish. The primary target of the survey was Pacific ocean perch (*Sebastes alutus* [POP]). These fish have extremely uncertain biomass estimates in the Gulf of Alaska (Heifetz et al.[1]). The estimates are based in part on a standardized stratified random survey conducted by the National Marine Fisheries Service every three years (every two since 2000). This uncertainty is likely due to their highly clustered distribution (Lunsford, 1999) and has led to two independent surveys (1998, 1999) to test the benefits of ACS in sampling POP. Shortraker (*S. borealis*) and rougheye (*S. aleutianus*) rockfish combined (SR-RE) are also tested to compare the results of a population that is considered highly clustered (POP) versus one that is considered more uniformly distributed (SR-RE). SR-RE are combined because they co-occur in identical habitat and are managed as a complex.

Materials and methods

In June 1999, ACS was carried out between 140° and 144° west longitude near Yakutat in the Gulf of Alaska (Fig. 2). Approximately 75% of sampling was directed toward the POP depth stratum (180–300 m) and 25% directed toward SR-RE depths (300–450 m). A 182-ft. factory trawler, the *Unimak*, was chartered to conduct trawl samples. Fishing and field operations are described in Clausen et al.[2] Duration of all trawl hauls was 15 (POP) and 30 (SR-RE) minutes on the bottom. SR-RE tows were made parallel to the depth contours in a linear pattern (Fig. 1) because the slope that SR-RE inhabit is too steep for perpendicular tows. Travel time between all tows was recorded to examine time efficiency.

Initially, a set of systematic random tows was conducted from west to east across the entire study area to determine the criterion value. Samples were chosen systematically by longitude and distributed randomly by depth within each longitudinal strip. This procedure was a necessary proxy for simple random sampling because of poorly known bathymetry in the area. The use of simple random latitudes and longitudes often results in the selection of sites that are well out of the sampling depth interval. After random sampling was completed, we compiled and examined the data to set the criterion value. Criterion values were chosen based on a hierarchy of three alternatives described below. Next, we conducted a new set of random tows from east to west across the area, in which any tows exceeding the criterion value were adaptively sampled. A distance of 0.19 km (0.1 nmi) was used between all adaptive tows and the initial random tow to avoid depletion effects on the catches.

[1] Heifetz, J., D. L. Courtney, D. M. Clausen, J. T. Fujioka, and J. N. Ianelli. 2001. Slope rockfish. *In* Stock assessment and fishery evaluation for the groundfish resources of the Gulf of Alaska, 72 p. North Pacific Fishery Management Council, 605 W. 4th Ave, Suite 306, Anchorage, AK 99501.

[2] Clausen, D. M., D. H. Hanselman, C. Lunsford, T. Quinn II, and J. Heifetz. 1999. *Unimak* enterprise cruise 98-01 rockfish adaptive sampling experiment in the central Gulf of Alaska 1998, 49 p. Auke Bay Lab, NMFS, NOAA, 11305 Glacier Hwy, Auke Bay, Alaska, 99801.

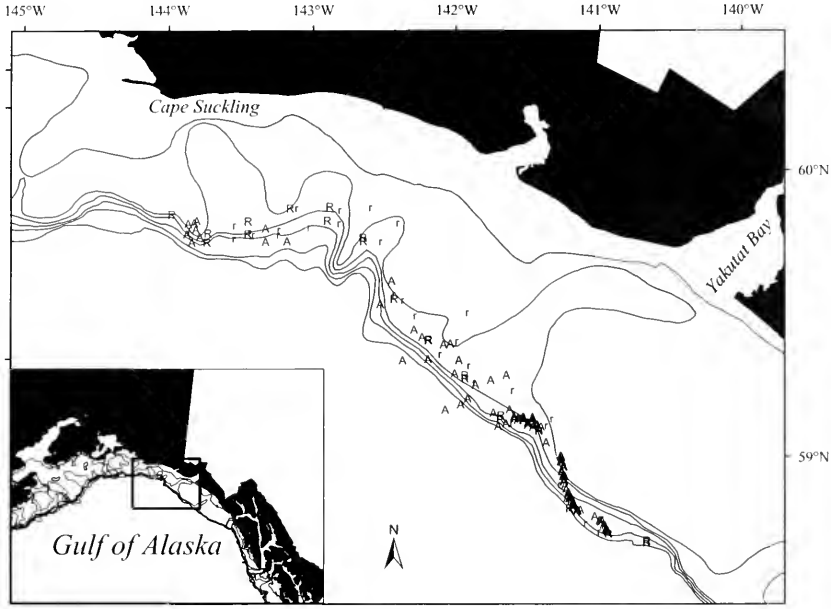

Figure 2

Map of sampling area in the Gulf of Alaska on the *Unimak* 99-01 adaptive sampling cruise. "R" symbols are the initial random tows for the criterion phase, "r" symbols are random stations in the survey phase, "A" symbols are adaptive cluster samples.

Three methods were formulated for determining a fixed criterion value c of POP catch-per-unit-of-effort (CPUE). (1) We combined and calibrated past survey and fishing data to provide the anticipated distribution of CPUE in the 1999 survey. Then we calculated the 80th percentile of that distribution as the criterion value. Our rationale was that this value would correspond to that obtained from order statistics. (Three networks were sampled in 1998; therefore the criterion value was set to the 4th highest of the ordered 15 initial tows, which corresponded approximately to the 80th percentile.) (2) We used the mean CPUE of past survey and fishery data because when we compared the 80th percentile criterion against the 1998 ACS survey's data, the sampling would have resulted in primarily edge units. (3) After a representative random sample was taken across the entire area in 1999, we would use the initial mean CPUE for the criterion value for the return trip. The rationale for using mean CPUE above is that in an aggregated population, the majority of the tows would be less than the mean. The actual values of the criterion chosen under each alternative are described in the results.

We chose the SR-RE criterion to be the mean CPUE of initial tows. We assumed this was a reasonable criterion value because if the population of SR-RE were somewhat uniform, a lower value would result in too much ACS, but mean CPUE would still be low enough to allow higher criterion values to be examined. Although we concentrated on evaluating criterion alternatives for POP, we present the SR-RE data to illustrate that different levels of aggregation could affect how much can be gained with ACS in terms of precision and efficiency.

A major problem in applying adaptive sampling is that sampling may continue indefinitely because of a low criterion value. To limit the amount of adaptive sampling, an arbitrary stopping rule of S levels was imposed. For those strata where the cross pattern of adaptive sampling was used (POP), the stopping rule was $S = 3$ levels, allowing for a maximum of 24 adaptive tows around each high-CPUE random tow (Fig. 1). For the strata with the linear pattern of adaptive sampling (SR-RE), the stopping rule was $S = 4$ levels, for a maximum of eight adaptive tows around each high-CPUE random tow. This stopping rule differs from that of the previous year in which we used a stopping rule of six because we believed that the possible 30-km difference between the ends of the networks was too large for efficient sampling (Clausen[2]). In addition, no adaptive sampling extended beyond a stratum boundary. The result of adaptive sampling around each high-CPUE tow was a network of tows that extended over and, in some cases, delineated the geographic boundaries of a rockfish aggregation.

Statistical analysis of the results was based on adaptive cluster sampling (Thompson and Seber, 1996). First, we estimated the abundance (kg/km) for the targeted rockfish species from the n initial random tows using the standard simple random sampling (SRS) estimator. Then, two adaptive estimators of abundance, a Hansen-Hurwitz estimator (HH) and a Horvitz-Thompson estimator (HT), were calculated. We computed standard error (SE) as a measure of precision. The unbiased HH estimator for the ACS mean is

$$\hat{\mu}_{HH} = \frac{1}{n}\sum_{i=1}^{n} w_i = \frac{1}{n}\sum_{i=1}^{n} \frac{y_i^*}{x_i}, \quad (1)$$

where w_i and y_i^* = the mean and total (respectively) of the x_i observations in the network that intersects sample unit i.

The HH estimator essentially replaces tows around which adaptive sampling occurred with the mean of the network of adaptive tows that exceeded the criterion CPUE.

The unbiased HT estimator for the ACS mean is

$$\hat{\mu}_{HT} = \frac{1}{N}\sum_{k=1}^{\kappa} \frac{y_k^*}{\alpha_k}, \quad (2)$$

where y_k^* = the sum of the y-values for the kth network;
κ = the number of distinct networks in a sample;
α_k = the probability that network k is included in the sample; and
N = the total number of sampling units.

If there are x_k units in the kth network, then

$$\alpha_k = 1 - \binom{N - x_k}{n} \Big/ \binom{N}{n}, \quad (3)$$

where N = the total number of sampling units;
n = the initial random sample; and
x_k = the number of units in the network.

The HT estimator is based on the probability of sampling a network given the initial tows sampled and involves the number of distinct networks sampled (in contrast to the HH estimator which is based only on the initial tows). The HT estimator often outperforms other estimators as seen in simulation studies (Su and Quinn, 2003). Both estimators use the network samples and initial random samples, but not the edge units. This sample size is referred to as v' (convention established by Thompson (1990) and used in Thompson and Seber (1996)). To include edge units into the estimates Thompson and Seber (1996) and Salehi (1999) used the Rao-Blackwell theorem, which is a complex method that could theoretically result in more precise estimates. However, it had little effect for the 1998 survey data (<1% improvement, Hanselman, 2000); therefore these calculations were not used in our study.

When a stopping rule is used, the theoretical basis for the adaptive sampling design changes. It may result in incomplete networks that overlap and are not fixed in relation to a specified criterion—changing with the pattern of the population. In contrast, the nonstopping-rule scheme has disjoint networks that form a unique partition of the population for a specified criterion. This partitioning is the theoretical basis for the unbiasedness of $\hat{\mu}_{HH}$ and $\hat{\mu}_{HT}$. Thus with a stopping rule, some bias may be introduced.

Recent simulation studies (Su and Quinn, 2003) have estimated the bias induced by using a stopping rule on each estimator with order statistics, but not with a fixed criterion. Because the use of a fixed criterion is design unbiased, its estimate should be less biased by the stopping rule than a sample with order statistics. Therefore, we can use the Su-Quinn simulation results to approximate the maximum bias induced by the stopping rule. With a stopping rule of three and the HH estimator, the maximum positive bias is 17% for a highly aggregated simulated population. With a stopping rule of three and the HT estimator, the maximum bias is approximately 12%. Considering our design, we accepted the tradeoff of relatively small bias for gains in precision and logistical efficiency.

Additionally, nonparametric bootstrap methods were adapted from Christman and Pontius (2000) and we used the HH version of the estimates to examine bias from our survey. Five thousand resamples were performed by using n for the SRS bootstrap, and the sample size from the original criterion value of 220 kg/km (v') was used for the ACS bootstrap. Bootstrap distributions of the data were examined for SRS and ACS designs to examine the capability of each design to clearly demonstrate a central tendency.

We evaluated two hypotheses: 1) Adaptive sampling would be more effective in providing precise estimates of POP biomass than would a simple random survey design; and 2) Assessment of POP abundance would benefit more from an adaptive sampling design than would SR-RE because POP are believed to be more clustered in their distribution than SR-RE. SRS estimates were obtained from the initial random tows, and variance estimates were calculated for the initial sample size (n) and for the equivalent sample size that included the adaptive tows but not the edge units (v'). This procedure makes the theoretical comparison fair because each estimate is based on the same number of samples. Total sample size including edge units (v) was not used in the theoretical precision comparison but was considered when efficiency issues were examined later. These hypotheses were assessed by comparing the standard errors (SEs) of ACS to those of SRS. Substantial reductions in SE with ACS for POP would support the first hypothesis, whereas no reductions of SE using ACS for SR-RE would support the second hypothesis. This comparison is qualitative because relevant significance tests are unavailable and the two methods are different in terms of efficiency.

To evaluate different alternatives and criterion values, each network was reconstructed as if the higher criterion values had been used in the field. We also examined the tradeoff between amounts of additional sampling compared with the gains in precision. A comparison was made of the SRS results by using sample sizes constructed with the number of possible samples with the time-per-sample

Table 1

Data used to determine criterion values c for the 1999 adaptive cluster sampling (ACS) survey. Data from a 1998 ACS survey from a different area is divided by the National Marine Fisheries Service triennial survey data and fishery data from the same area to obtain gear efficiency values. The mean of these gear efficiencies are then multiplied against triennial and fishery data from the new area to yield gear-calibrated CPUEs for the new area. Only numbers in bold were used in calculations. n = the number of observations of that data set; 80% = the 80th percentile catch of that data set.

Data source	Year	Mean CPUE (kg/km)	80%	n
ACS results from different area and year	1998	**284.94**	**223.92**	57
(divided by)			÷	
CPUEs of corresponding previous area from triennial and fishery data	Triennial 1993	**38.36**	**7.89**	50
	1996	**46.64**	**27.33**	51
	1993–96	**42.54**	**18.79**	101
	Fishery 1996–98	**30.64**	**14.03**	434
(equals)			=	
Gear efficiency of the *Unimak*	1993	7.44	28.18	
	1996	6.12	8.14	
	1993–96	6.71	11.84	
	1996–98	9.32	15.85	
	Mean	**7.63**	**17.39**	
(multiplied by)			×	
Prior CPUE data from area for 1999 ACS survey	Triennial 1993	**40.32**	**46.74**	29
	1996	**26.50**	**33.50**	25
	1993–96	**33.92**	**38.85**	54
	Fishery 1996–98	**19.61**	**30.47**	190
(equals)			=	
Calibrated CPUE data for 1999 ACS survey	Triennial 1993	**307.52**	**812.67**	29
	1996	**202.06**	**582.52**	25
	1993–96	**258.69**	**675.63**	54
	Fishery 1996–98	**149.57**	**529.90**	137
Criterion value c	Mean	**219.71**	**641.69**	

data we collected. In this comparison we used three new sample sizes: 1) v_t, the number of samples that could have been taken in the same amount of time as that for a SRS if sampling time for edge units was negligible; 2) v_e, in which the edge units had taken the same amount of time as non-edge units; and 3) v_d, in which the average distance between each tow type was used as effort instead of time (with edge units included).

Results

Formulation of criterion alternatives

A total of 164 tows were conducted for the ACS experiment. Nearly all tows were made successfully; only a few exceptions were deemed untrawlable and moved to the nearest trawlable bottom. We determined the POP criterion value for alternatives 1 and 2 (see below) before the survey by looking at the 1998 ACS results from a different geographic area, as well as prior survey and fishery data in our study area. We obtained the criterion value by calculating a gear efficiency coefficient for the 1998 survey by using NMFS survey data (1993, 1996) and fishery data (1996–98) from the observer program for the same area. This gear coefficient was then multiplied by the same data for the new area to establish the expected catches. The data used and the calculations are shown in Table 1. To implement alternative 3, we conducted 13 initial POP and 10 initial SR-RE random tows across the entire area. Catches from these initial tows gave us the following results for each criterion alternative:

Alternative 1 For alternative 1, the mean of the 80th percentile of the data from Table 1 is 641.69 kg/km. We rounded this downward to c = 540 kg/km (1000 kg/nmi) for ease of operation in the field (the design was originally in kg/nmi units).

Alternative 2 The mean calibrated CPUE for the area from Table 1 yielded a criterion value c of 220 kg/km (rounded).

Alternative 3 In this alternative, the mean CPUEs from the initial sample in 1999 yielded criterion values of c = 250 kg/km for POP and c = 418 kg/km for SR-RE.

Table 2

Summary of density estimates ($\hat{\mu}$) and standard errors (SE) for the 1999 adaptive cluster sampling experiment for the *Sebastes alutus* and the *S. borealis-S. aleutianus* complex. c is the criterion value, r is the number of adaptive networks, n is the initial sample size, v' is the adaptive sampling size (excluding edge units). SRS = simple random sampling estimator, HH = Hansen-Hurwitz adaptive estimator, and HT = Horvitz-Thompson adaptive estimator. Alt. = criterion alternative.

	Sebastes alutus				*Sebastes borealis* and *S. aleutianus*	
	Alt. 2	Alt. 3	Alt. 1	—	Alt. 3	—
c (kg/km)	>220	>250	>540	>1080	>418	>540
r	6	6	5	3	5	3
n	25	25	25	25	9	9
v'	74	73	55	48	30	14
$\hat{\mu}_{SRS}$	904	904	904	904	447	447
SE_n	496	496	496	496	115	115
SE_v'	288	290	334	358	63	92
$\hat{\mu}_{HH}$	498	501	566	526	511	486
SE	166	167	192	197	128	141
$\hat{\mu}_{HT}$	471	472	567	527	511	486
SE	167	167	192	197	128	141

The second phase of the experiment began with random tows in an east to west direction. Complete location and CPUE data for both species are located in Appendix I. In order to analyze all alternatives, the lowest alternative was used in the field for adaptive sampling during the second phase, which resulted in the 220 kg/km criterion value for POP from alternative 2. For SR-RE, the criterion value was the mean CPUE of 418 kg/km from alternative 3. The remaining alternatives were simulated following the completion of the survey.

POP results

After the initial tows, 25 random tows were selected for the return trip across the area. All 25 were completed, of which six became networks of more than one unit. A total of 106 tows were completed in the POP stratum. At one of the tows that exceeded the criterion value, the captain deemed that further adaptive sampling was not feasible because of the presence of coral. Of the six networks, two overlapped, resulting in five distinct networks. In these networks, 81 adaptive samples were taken, of which 49 exceeded the criterion and 32 did not and were therefore edge units and not included in the sample estimates.

We compared the results of the original adaptive sample (alternative 2) with the simulated results of higher criterion values (Table 2). The precision of simple random sample estimates with both n (number of random samples) and v' (number of random samples plus the number of adaptive network samples, not edge units) was contrasted with that of the adaptive estimators described above. As the criterion value increased, n remained the same, whereas v' and r (the number of networks) decreased. At the 220 kg/km criterion value (alt. 2), there were substantial reductions in SE over the SRS estimators by using ACS estimators for both the n and v' sample sizes. The 250 kg/km criterion value (alt. 3) resulted in a nearly identical sample to that of the 220 kg/km (alt. 2) criterion value and the loss of only one network sample. Hence, the estimates were nearly identical. The HT mean estimates were slightly lower than the HH estimates for the two lowest criterion values (alts. 2 and 3) because two networks overlapped. These networks became separate at the next higher criterion value, which aligned the estimators. The next highest criterion value of 540 kg/km (alt. 1) showed that even though the sample size was reduced by 19 tows from the original criterion value, the ACS estimators performed nearly as well, yielding just slightly larger SEs. When the criterion was arbitrarily doubled to 1080 kg/km, the sample size was further reduced by seven, and had similar SEs to the 540 kg/km criterion value.

The SRS and ACS bootstraps for POP resulted in very different distributions. Five thousand replications showed that the SRS distribution was bimodal and right skewed (Fig. 3). The SRS mean fell on the second mode, which is more than twice the ACS mean. This bimodal distribution is driven by the presence of the very large random catch (tow no. 60). If that haul is present in a bootstrap replicate, then the SRS estimate tends to be high, leading to the second mode in the bootstrap distribution. The ACS bootstrap distribution was symmetric and closely resembled a normal distribution (Fig. 3). The average estimates of bias showed that the bias of HH was +4% and the bias of HT was −1%. The standard error had an estimated bias of +3% for HH and HT.

The results from this POP study and the previous 1998 study were both greatly affected by one or two very large catches, as we expected for a highly clustered population. Of interest is what happened when the largest catch was changed to a nominal catch that still exceeded the criterion value. Appendix II shows the results of changing haul no. 60 from 12,000 kg/km to 540 kg/km. In the comparison at v', SRS outperforms ACS in terms of SE. However, it also

Table 3

Comparisons of time per travel (TPT) and time per sample (TPS) of adaptive sampling against simple random sampling for Pacific ocean perch (*S. alutus*) and for shortraker (*Sebastes borealis*) and rougheye (*S. aleutianus*) rockfish combined, on a 1999 adaptive sampling cruise. TPT is the travel time between tows in hours; TPS is the travel time plus haul time in hours. "Distance between" is the average travel distance (km) between two adaptive stations and between two random stations. "Adjusted distance" is the distance if the random sample size was increased to 106.

	S. alutus		*S. borealis* and *S. aleutianus*	
	Random	Adaptive	Random	Adaptive
Time (h)	10.4	11.4	4.4	12.0
No. of hauls	23	72	9	24
TPT	0.45	0.16	0.49	0.50
TPS	0.95	0.66	1.49	1.50
Distance between	20.2	3.22		
Adjusted distance	4.73	3.22		

shows that the mean of ACS is stable because it changes little by removing a high catch, whereas the SRS mean is reduced by half.

SR-RE results

At every third POP random tow, a tow was made in the SR-RE depth stratum. A total of 35 tows were made in the SR-RE stratum. Nine random tows yielded five distinct networks with 21 network tows and five edge units. The stopping rule was invoked for three of the five networks.

At the mean CPUE criterion (418 kg/km, alt. 3), the adaptive estimators performed approximately the same in terms of SE compared to the SRS estimator using n (Table 2). With v', the SRS estimator yielded a lower SE than both adaptive estimators. When the criterion value increased to an arbitrarily higher value (540 kg/km), the adaptive estimators performed worse than SRS estimates for both n and v'.

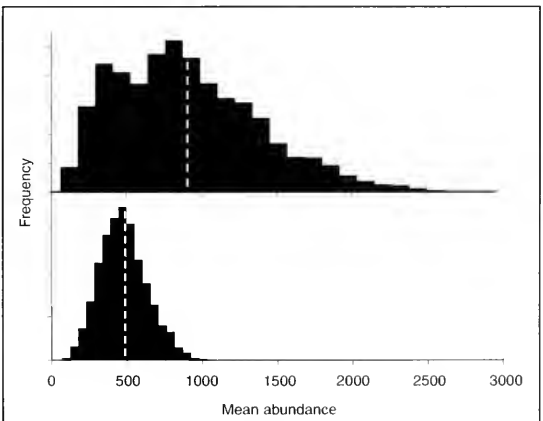

Figure 3

Bootstrap distributions for the 1999 adaptive sampling survey (25,000 replicates). Dotted line is the sampling estimate of mean abundance (kg/km) from the survey. Top graph is the distribution of mean abundance estimates for simple random sampling. Bottom graph is the distribution of mean abundance estimates for adaptive cluster sampling (obtained with the Hansen-Hurwitz estimator).

Time efficiency

We recorded and compared travel time between adaptive tows and simple random tows for 149 of the tows (Table 3). Not all the tows were used because of mechanical failure or because the factory capacity was reached. In the survey, 38 hours out of 10 days were spent in transit between sampling tows, which for a short survey was a substantial amount of the available time. For POP, substantial gains in travel-time efficiency were achieved with ACS. Average travel time for simple random tows (0.45 h) was nearly triple that of adaptive tows (0.16 h) for POP, which indicated that ACS can maximize sampling tows for POP when time is limited. In the SR-RE sampling, travel time for adaptive sampling (0.5 h) was about the same as simple random sampling (0.49 h), which was due to long linear samples that are not as close together as POP tows (Fig. 1). Also, determination of CPUE required processing of the catch, which took various amounts of time after the completion of the tow. Because of this delay, we went to the opposite tow on the other side of the random tow when sampling SR-RE with the linear pattern, whereas there were many nearby tows when sampling POP with the cross pattern.

The travel time was added to the average tow time from gear deployment to full retrieval of 0.5 h for POP and 1.0 h for SR-RE to obtain total sampling time (per sample). Travel time was reduced by 31% with adaptive sampling (0.66 h/sample) in relation to simple random sampling

(0.95 h/sample) for POP. Sampling time efficiency for SR-RE was approximately the same for adaptive sampling (1.5 h/sample) and simple random sampling (1.49 h/sample) for SR-RE. These results are confounded by the fact that the random tows are spread apart because of the lesser effort applied to them. The average distance between random tows (20.2 km) was adjusted to a distance of 4.73 km as if there were 106 random tows distributed throughout the area. This distance is still larger than the average distance between tows in adaptive sampling (3.22 km).

From these time and distance data, we re-estimated the precision of SRS under three new sample sizes in order to further compare the relative efficiency of ACS. We denoted the sample size that could have been taken under SRS, using the same amount of time as was used during the adaptive sampling including edge units, as v_e. An alternative sample size v_t was the equivalent SRS sample size if the amount of time to sample edge units in ACS was negligible. This statistic would be useful if edge units could be determined (i.e. hydroacoustically or visually [presence or absence]) without actually trawling them. A third alternative was to find the equivalent SRS sample size v_d that would result from applying the total distance traveled in the ACS design on random stations instead. For v_e, more random POP samples would have been taken than were included in the adaptive estimators (Table 4). The SEs of ACS were still much lower across all criterion values (Table 2). When we used v_t (Table 4), SRS was much less precise than ACS (Table 2). Finally, when we used distance instead of time (v_d), the results were almost exactly the same as those for v_e (Table 4).

Table 4

Comparison of simple random sampling (SRS) precision estimates with the inclusion of time and distance information. c is the criterion value. v' is the original adaptive cluster sampling adjusted sample size. v_e is the time-adjusted sample size, including edge units. v_t is the time-adjusted sample size with edge unit cost set to zero. v_d is the distance-adjusted sample size including edge units. $\hat{\mu}$ is the mean SRS density estimate, SE is the standard error for that sample size.

	c (kg/km)			
	>220	>250	>540	>1080
$\hat{\mu}$	904	904	904	904
v'	74	73	55	48
SE	294	296	341	365
v_e	81	80	67	55
SE	281	283	309	341
v_t	59	58	46	41
SE	329	332	373	395
v_d	80	79	67	54
SE	283	285	309	344

Discussion

Our two hypotheses were that ACS would be more precise than SRS for POP and no more precise for SR-RE combined. The results from the 1999 field study showed that the SEs for the adaptive POP estimates were smaller than both SRS estimates, with n and v', and thus support the first hypothesis. One curious result is that in both 1998 and 1999, the SRS estimate of density was substantially larger than the ACS estimate, even though, on average, they were both essentially unbiased. We attributed this curiosity to the more variable and skewed SRS distribution in which large sampling error on the high side is possible more often than in the ACS estimation. Of course we fully expected that both estimates would average to be the same value if the experiment could be repeated many times. ACS reduced the influence of one large CPUE in the relatively small initial sample, as illustrated by the symmetric and near-normal shape of the ACS bootstrap distribution. Consequently, we concluded that ACS is a more robust estimator of density than SRS for aggregated populations. One caveat is that the precision of the estimates, if measured in terms of coefficient of variation, is similar between the two methods because of the much larger mean estimate for the SRS estimate. Monte Carlo simulations would be useful to examine the properties of the estimators under different criterion values and population densities along the lines of Su and Quinn (2003).

The SR-RE adaptive estimates all have higher SEs than the SRS estimates, and this finding supports the second hypothesis. More than twice as many samples were directed toward POP than SR-RE, yet the POP density estimates are much more variable than those for SR-RE. This much larger variability for POP was indicative of the clustering that we expected.

This experiment showed that for POP, ACS with a fixed criterion has some distinct advantages over simple random sampling and over adaptive cluster sampling with order statistics, which was used in the previous 1998 survey. Lower SEs were obtained, at one third less effort than if we just added an equivalent number of random samples. Sampling over a broader area yielded better results than the tightly stratified 1998 design. Our study also assumed stationary aggregations of fish. This assumption may have been better satisfied with a fixed criterion because the adaptive sampling was conducted immediately after a sample exceeded the criterion value.

Although the fixed criterion eliminates bias induced by a variable criterion value, we still used stopping rules. If bootstrapping is a good indicator of bias, then the bias induced by stopping rules is negligible. Additionally, we have shown that a relatively high criterion value could be used to help minimize the use of these stopping rules.

Our study showed that ACS is a fast and efficient way to gain a large number of samples. However, if edge units do not contribute to a better estimate and they have a similar cost or time expense as included samples, then little is gained. This deficiency shows the need for some method of determining edge units without actually sampling them. In fisheries surveys, this use might be a double sampling design with hydroacoustics as an auxiliary variable

(Fujioka[3]) or a design called TAPAS that hydroacoustically delineates clusters (Everson et al., 1996). In other surveys, it might be possible to detect the presence of the item of interest without actually surveying the unit (as in aerial surveys.)

An ACS design should not be attempted without some prior knowledge of the population distribution. Populations for which the design would be useful should have an aggregated distribution that can be described by correlated variation with distance, not just a large variance in relation to the mean. One way to examine the data is to fit variograms to examine spatial autocorrelation (Hanselman et al., 2001). If no prior data exist, it would not make sense to attempt ACS as an initial sampling design. We have shown that a wide range of criterion values can be used without considerable differences in the results. Therefore, only enough prior data are needed so that an adequate range of population density can be estimated. If the criterion value chosen resulted in too many or too few samples, the criterion could be adjusted, and then the design stratified into two different areas.

Most commercial fish species have survey data that can be used to determine a fixed criterion. If possible, criterion values should be determined prior to the survey, so that maximum efficiency can be attained. We have shown that it may be appropriate to choose a relatively high sampling criterion such as the 80th percentile of past CPUE without sacrificing estimation capabilities. This high sampling criterion has several practical advantages. First, the design is attractive for commercial boats to perform the adaptive phase at no-cost because only large catches are sampled. The current design does not use the fish sampled during the survey, which, in the case of deepwater rockfish, would cause certain mortality. Under an adaptive design, a commercial boat would take the larger catches and could put them to use. Second, fewer overall networks would be sampled because the higher criterion would evoke less adaptive sampling, which may mean less overall sampling in the survey. Finally, precision would be gained at a minimal cost and effort. Stopping rules would be unnecessary, ensuring an unbiased estimate. However, cluster sampling is most effective when the cluster samples are as heterogeneous as possible. Therefore, caution is required not to set the criterion too high, or the resulting clusters will be either too homogeneous or contain only edge units, leading to no improvement in the estimators. Similarly, if there are large changes in density from year to year, a fixed criterion may not be appropriate. In conclusion, adaptive cluster sampling is appropriate for surveys of highly clustered species with low temporal fluctuations, for which a fixed criterion can be determined beforehand.

Acknowledgments

We thank the crew of the FV *Unimak*, in particular Captain Paul Ison and Production Manager Rob Elzig, for their excellent cooperation in this study. We also acknowledge the hard work of the scientists that participated in the cruise and the NMFS personnel who prepared for the charter. We greatly appreciate the helpful comments from three anonymous reviewers that helped us refine the paper.

This publication is the result of research sponsored by Alaska Sea Grant with funds from the National Oceanic and Atmospheric Administration, Office of Sea Grant, Department of Commerce, under grant no. NA90AA-D-SG066, project number R/31-04N, from the University of Alaska with funds appropriated by the state. Further support was provided by the Auke Bay Laboratory, Alaska Fisheries Science Center, National Marine Fisheries Service and by a Population Dynamics Fellowship to Hanselman through a cooperative program funded by Sea Grant and NMFS.

Literature cited

Brown, J. A., and B. J. F. Manly.
1998. Restricted adaptive cluster sampling. Environ. Ecol. Stat. 5:49–63.

Christman, M. C.
1997. Efficiency of some sampling designs for spatially clustered populations. Environmetrics 8:145–166.

Christman, M. C., and J. S. Pontius.
2000. Bootstrap confidence intervals for adaptive cluster sampling. Biometrics 56:503–510.

Everson, I., M. Bravington, and C. Goss.
1996. A combined acoustic and trawl survey for efficiently estimating fish abundance. Fish. Res. 26:75–91.

Hanselman, D. H.
2000. Adaptive sampling of Gulf of Alaska rockfish. M.S. thesis, 72 p. Univ. Alaska, Fairbanks, AK.

Hanselman, D. H., T. J. Quinn, C. Lunsford, J. Heifetz, and D. M. Clausen.
2001. Spatial inferences of adaptive cluster sampling on Gulf of Alaska rockfish. *In* Proceedings of the 17th Lowell-Wakefield symposium: spatial processes and management of marine populations, p. 303–325. Univ. Alaska Sea Grant Program, Fairbanks, AK.

Lo, N., D. Griffith, and J. R. Hunter.
1997. Using a restricted adaptive cluster sampling to estimate Pacific hake larval abundance. Calif. Coop. Oceanic Fish. Invest. Rep. 38:103–113.

Lunsford, C.
1999. Distribution patterns and reproductive aspects of Pacific ocean perch (*Sebastes alutus*) in the Gulf of Alaska. M.S. thesis, 154 p. Univ. of Alaska Fairbanks, Fairbanks, AK.

Quinn II, T. J., D. H. Hanselman, D. M. Clausen, J. Heifetz, and C. Lunsford.
1999. Adaptive cluster sampling of rockfish populations. Proceedings of the American Statistical Association 1999 Joint Statistical Meetings, Biometrics Section, 11-20. Am. Statist. Assoc., Baltimore, MD.

Salehi, M. M.
1999. Rao-Blackwell versions of the Horvitz-Thompson and Hansen-Hurwitz in adaptive cluster sampling. Environ. Ecol. Stat. 6:83–195.

Su, Z., and Quinn, T. J., II.
2003. Estimator bias and efficiency for adaptive cluster sampling with order statistics and a stopping rule. Environ. Ecol. Stat. 10, pp. 17–41.

[3] Fujioka, J. 2001. Unpubl. manuscr. Using hydroacoustics and double sampling to improve rockfish abundance estimation, 8 p. Auke Bay Laboratory, National Marine Fisheries Service, NOAA, 11305 Glacier Hwy, Auke Bay, AK 99801.

Thompson, S. K.
1990. Adaptive cluster sampling. J. Am. Stat. Assoc. 412: 1050–1059.

Thompson, S. K., and G. A. F. Seber.
1996. Adaptive sampling, 265 p. Wiley, New York, NY.

Appendix I

CPUE (kg/km) data from the 1999 adaptive cluster sampling survey. CPUE is given in kg/km. The format of "Adaptive 26-1" corresponds to the first adaptive tow around haul no. 26. POP = Pacific ocean perch; SR-RE = shortraker and rougheye rockfish combined.

Summary table

Tow type	Initial random	2nd phase random	Adaptive network	Adaptive edge unit	Total[1]
POP	13	25	49	32	106 (119)
SR-RE	10	9	21	5	35 (45)
Total	23	34	70	37	141 (164)

[1] Values in parenthesis include initial random tows that are not included in estimation results.

Criterion determining random tows

Tow	Latitude	Longitude	Tow type	POP CPUE	SR-RE CPUE
3	59.59	−143.81	POP random	39.3	43.7
4	59.54	−143.55	POP random	49.2	13.7
5	59.51	−143.55	SR-RE random	3.4	870.9
6	59.58	−143.28	POP random	174.8	112.0
7	59.56	−143.28	SR-RE random	17.7	582.3
8	59.67	−143.01	POP random	72.7	21.0
9	59.69	−142.75	POP random	21.3	6.1
10	59.64	−142.75	SR–RE random	6.3	6.3
11	59.60	−142.49	POP random	9.6	36.2
12	59.59	−142.48	SR–RE random	3.8	608.0
13	59.40	−142.22	POP random	20.7	113.0
14	59.28	−141.96	POP random	25.3	394.4
15	59.27	−141.96	SR–RE random	19.1	713.1
16	59.17	−141.68	POP random	185.4	68.5
17	59.16	−141.68	SR–RE random	24.9	48.5
18	59.04	−141.41	SR–RE random	1.7	450.4
19	59.03	−141.41	POP random	196.5	21.9
20	59.01	−141.14	SR–RE random	30.0	676.9
21	58.78	−140.88	POP random	2271.6	0.0
22	58.75	−140.88	SR–RE random	65.9	80.6
23	58.67	−140.61	POP random	80.6	101.1
24	58.66	−140.35	POP random	98.2	55.0
25	58.66	−140.35	SR–RE random	21.2	140.5
			Beginning of adaptive random tows		
26	58.70	−140.64	POP random	576.7	0.0
27	58.68	−140.65	SR–RE random	16.3	115.8
28	58.73	−140.71	POP adaptive 26-1	138.1	12.0
29	58.72	−140.65	POP adaptive 26-2	138.4	9.7
30	58.69	−140.62	POP adaptive 26-3	2294.2	0.0
31	58.70	−140.64	POP adaptive 26-4	290.1	0.4
32	58.70	−140.63	POP adaptive 26-8	334.8	0.0
33	58.69	−140.62	POP adaptive 26-9	56.5	21.2
34	58.69	−140.63	POP adaptive 26-10	16.4	1.9
35	58.71	−140.67	POP adaptive 26-11	20.7	3.7
36	58.72	−140.67	POP adaptive 26-12	30.2	1.0

continued

Appendix I (continued)

Criterion determining random tows

Tow	Latitude	Longitude	Tow type	POP CPUE	SR-RE CPUE
37	58.69	−140.61	POP adaptive 26-18	1299.4	1.2
38	58.69	−140.61	POP adaptive 26-17	965.0	55.9
39	58.70	−140.75	POP random	62.0	148.0
40	58.76	−140.85	POP Random	3591.0	58.4
41	58.79	−140.89	POP adaptive 40-1	5934.1	0.0
42	58.77	−140.86	POP adaptive 40-2	4521.0	0.0
43	58.74	−140.83	POP adaptive 40-3	515.7	9.1
44	58.76	−140.86	POP adaptive 40-4	4453.7	37.3
45	58.79	−140.90	POP adaptive 40-5	1338.8	0.0
46	58.79	−140.88	POP adaptive 40-6	393.9	0.0
47	58.77	−140.86	POP adaptive 40-7	109.4	0.0
48	58.75	−140.82	POP adaptive 40-8	85.0	0.0
49	58.73	−140.80	POP adaptive 40-9	67.9	0.1
50	58.74	−140.83	POP adaptive 40-10	128.0	17.6
51	58.76	−140.86	POP adaptive 40-11	1597.3	0.0
52	58.78	−140.89	POP adaptive 40-12	268.5	3.8
53	58.80	−140.90	POP adaptive 40-24	1282.9	0.0
54	58.81	−140.92	POP adaptive 40-13	2304.4	0.0
55	58.80	−140.90	POP adaptive 40-14	776.2	0.0
56	58.79	−140.88	POP adaptive 40-15	882.6	0.0
57	58.75	−140.86	POP adaptive 40-22	168.1	2.7
58	58.78	−140.89	POP Adaptive 40-23	253.9	0.2
59	58.83	−140.95	SR-RE random	24.1	290.2
60	58.88	−140.95	POP random	12001.5	0.0
61	58.87	−140.96	POP adaptive 60-4	10659.3	0.0
62	58.91	−140.97	POP adaptive 60-1	1179.0	0.0
63	58.89	−140.95	POP adaptive 60-2	3050.4	0.0
64	58.86	−140.95	POP adaptive 60-3	2984.7	0.0
65	58.86	−140.95	POP adaptive 60-10	3590.4	0.0
66	58.88	−140.96	POP adaptive 60-11	1086.9	0.0
67	58.91	−140.98	POP adaptive 60-12	1311.7	8.7
68	58.92	−140.98	POP adaptive 60-5	1581.0	0.0
69	58.91	−140.96	POP adaptive 60-6	4148.4	0.0
70	58.89	−140.95	POP adaptive 60-7	1297.4	0.0
71	58.86	−140.94	POP adaptive 60-8	214.1	0.0
72	58.84	−140.94	POP adaptive 60-9	2190.3	0.0
73	58.84	−140.94	POP adaptive 60-20	1502.2	0.0
74	58.83	−140.93	POP adaptive 60-19	2828.9	0.0
75	58.84	−140.93	POP adaptive 60-18	102.9	0.0
76	58.86	−140.94	POP adaptive 60-17	46.6	0.0
77	58.89	−140.95	POP adaptive 60-16	27.8	0.0
78	58.89	−140.95	POP adaptive 60-15	53.4	0.0
79	58.92	−140.97	POP adaptive 60-14	495.7	0.0
80	58.93	−140.98	POP adaptive 60-13	1323.4	0.0
81	59.05	−141.05	POP random	1448.8	0.4
82			Coral encountered	N/A	N/A
83	59.03	−141.08	POP random	560.6	102.8
84	59.03	−141.19	POP random	283.6	298.5
85	59.04	−141.19	POP adaptive 83-1	1119.7	101.3
86	59.04	−141.26	POP adaptive 83-2	1407.0	21.7
87	59.02	−141.22	POP adaptive 83-3	398.1	29.2

continued

Appendix I (continued)

Criterion determining random tows

Tow	Latitude	Longitude	Tow type	POP CPUE	SR-RE CPUE
88	59.03	−141.16	POP adaptive 83-4	264.6	87.0
89	59.05	−141.20	POP adaptive 83-5	416.6	47.3
90	59.04	−141.29	POP adaptive 83-6	2186.1	7.0
91	59.04	−141.25	POP adaptive 83-7	482.0	8.7
92	59.03	−141.22	POP adaptive 83-8	115.2	36.6
93	59.02	−141.19	POP adaptive 83-9	182.5	36.4
94	59.02	−141.13	POP adaptive 83-10	41.4	45.5
95	59.02	−141.16	POP adaptive 83-11	29.2	41.1
96	59.04	−141.20	POP adaptive 83-12	261.4	80.6
97	59.04	−141.25	POP adaptive 83-24	109.3	32.0
98	59.04	−141.29	POP adaptive 83-23	62.0	69.4
99	59.05	−141.26	POP adaptive 83-13	186.4	56.2
100	59.05	−141.32	POP adaptive 83-14	443.8	4.5
101	59.04	−141.29	POP adaptive 83-15	1497.1	5.4
102	59.04	−141.25	POP adaptive 83-16	892.0	21.4
103	59.03	−141.22	POP adaptive 83-17	604.8	26.1
104	59.03	−141.16	POP adaptive 84-3	123.5	91.4
105	59.03	−141.22	POP adaptive 84-4	129.3	285.3
106	59.04	−141.26	POP adaptive 84-1	231.2	602.5
107	59.02	−141.32	SR-RE random	49.3	721.9
108	59.05	−141.26	POP adaptive 84-5	214.6	1408.9
109	59.04	−141.35	POP adaptive 84-6	215.0	123.6
110	59.04	−141.31	POP adaptive 84-12	61.5	664.5
111	59.04	−141.32	SR-RE adaptive 107-1	57.5	758.1
112	59.02	−141.37	SR-RE adaptive 107-2	0.0	490.7
113	59.05	−141.20	SR-RE adaptive 107-3	0.0	408.6
114	59.01	−141.42	SR-RE adaptive 107-4	0.0	669.1
115	59.00	−141.14	SR-RE adaptive 107-6	0.0	760.8
116	58.97	−141.09	SR-RE adaptive 107-8	0.0	1540.6
117	58.11	−141.06	SR-RE random	0.0	443.2
118	59.14	−141.60	SR-RE adaptive 117-1	0.0	1052.8
119	59.09	−141.64	SR-RE adaptive 117-2	0.0	1042.0
120	59.16	−141.50	SR-RE adaptive 117-3	51.3	621.6
121	59.07	−141.69	SR-RE adaptive 117-4	25.7	2096.7
122	59.05	−141.46	SR-RE adaptive 117-6	68.4	480.5
123	59.19	−141.40	SR-RE adaptive 117-5	41.2	924.3
124	59.21	−141.73	SR-RE adaptive 117-7	189.0	731.9
125	59.04	−141.78	SR-RE adaptive 117-8	82.3	772.2
126	59.14	−141.34	POP random	61.9	4.8
127	59.15	−141.60	POP random	82.6	55.8
128	59.21	−141.65	POP random	68.5	8.1
129	59.29	−141.75	POP random	84.6	0.0
130	59.23	−141.85	SR-RE random	6.1	1024.1
131	59.27	−141.85	SR-RE adaptive 130-1	2.6	626.9
132	59.21	−141.94	SR-RE adaptive 130-2	1.5	451.9
133	59.27	−141.81	SR-RE adaptive 130-3	4.2	2208.3
134	59.28	−142.00	SR-RE adaptive 130-5	7.4	1605.6
135	59.31	−142.06	SR-RE adaptive 130-7	5.0	1305.2
136	59.19	−142.11	SR-RE adaptive 130-4	0.0	432.4
137	59.17	−141.75	SR-RE adaptive 130-6	1.6	457.4
138	59.39	−141.70	POP random	181.8	25.9
139	59.36	−142.05	POP random	62.9	12.2

continued

Appendix I (continued)

Criterion determining random tows

Tow	Latitude	Longitude	Tow type	POP CPUE	SR-RE CPUE
140	59.40	−142.15	SR-RE random	3.7	772.3
141	59.45	−142.25	SRRE adaptive 140-1	1.1	222.7
142	59.38	−142.31	SRRE adaptive 140-2	0.0	209.0
143	59.42	−142.22	POP random	177.2	36.0
144	59.67	−142.25	POP random	45.4	33.5
145	59.60	−142.35	POP random	8.3	117.8
146	59.71	−142.45	POP random	4.3	32.0
147	59.67	−142.65	SR-RE random	2.0	47.0
148	59.64	−142.65	POP random	18.0	50.8
149	59.67	−142.95	POP random	34.2	3.4
150	59.61	−142.85	POP random	125.0	18.8
151	59.57	−143.05	SR-RE random	3.6	530.5
152	59.59	−143.05	POP random	139.0	39.7
153	59.56	−143.15	SR-RE adaptive 151-1	5.1	555.2
154	59.59	−143.16	SR-RE adaptive 151-2	2.6	255.5
155	59.55	−143.00	SR-RE adaptive 151-3	0.0	314.5
156	59.56	−143.22	POP random	23.5	567.4
157	59.57	−143.25	POP random	43.3	399.3
158	59.54	−143.35	SR-RE random	9.3	82.2
159	59.58	−143.36	POP random	74.9	493.0
160	59.55	−143.45	POP random	2838.5	1.8
161	59.57	−143.65	POP adaptive 160-1	1674.5	54.5
162	59.53	−143.69	POP adaptive 160-2	2912.8	1.8
163	59.55	−143.63	POP adaptive 160-3	196.5	0.0
164	59.52	−143.65	POP adaptive 160-4	148.2	0.5
165	59.52	−143.60	POP adaptive 160-5	75.6	21.0
166	59.58	−143.63	POP adaptive 160-6	863.1	9.4
167	59.56	−143.69	POP adaptive 160-7	41.3	0.0

Appendix II

Results of estimation with haul no. 60 changed from 12000 kg/km to 540 kg/km. c is the criterion value (kg/km), $\hat{\mu}$ is the mean Pacific ocean perch density (kg/km) for each estimator, n is the random sample size, v' is the adaptive sample size without edge units. SE is the standard error of the mean.

	c (kg/km)					c (kg/km)			
	>220	>250	>540	>1080		>220	>250	>540	>1080
$\hat{\mu}_{srs}(n)$	445	445	445	445	SE	148	149	175	158
SE	179	179	179	179	$\hat{\mu}_{HT}$	442	443	536	413
SE (v')	104	104	104	104	SE	149	149	175	158
$\hat{\mu}_{HH}$	470	473	535	412					

Migration patterns of young Pacific bluefin tuna (*Thunnus orientalis*) determined with archival tags

Tomoyuki Itoh
Sachiko Tsuji
National Research Institute of Far Seas Fisheries
5-7-1 Shimizu-Orido, Shizuoka
Shizuoka, 424-8633, Japan
E-mail address (for T. Itoh): itou@fra.affrc.go.jp

Akira Nitta
Japan NUS Co., Ltd.
Loop-X Bldg., 3-9-15 Kaigan, Minato
Tokyo, 108-0022, Japan

Abstract—We investigated the migration and behavior of young Pacific bluefin tuna (*Thunnus orientalis*) using archival tags that measure environmental variables, record them in memory, and estimate daily geographical locations using measured light levels. Swimming depth, ambient water temperature, and feeding are described in a companion paper. Errors of the tag location estimates that could be checked were −0.54° ±0.75° (mean ±SD) in longitude and −0.12° ±3.06° in latitude. Latitude, estimated automatically by the tag, was problematic, but latitude, estimated by comparing recorded sea-surface temperatures with a map of sea-surface temperature, was satisfactory. We concluded that the archival tag is a reliable tool for estimating location on a scale of about one degree, which is sufficient for a bluefin tuna migration study. After release, tagged fish showed a normal swimming behavioral pattern within one day and normal feeding frequency within one month. In addition, fish with an archival tag maintained weight-at-length similar to that of wild fish; however, their growth rate was less than that of wild fish. Of 166 fish released in the East China Sea with implanted archival tags, 30 were recovered, including one that migrated across the Pacific Ocean. Migration of young Pacific bluefin tuna appears to consist of two phases: a residency phase comprising more than 80% of all days, and a traveling phase. An individual young Pacific bluefin tuna was observed to cover 7600 km in one traveling phase that lasted more than two months (part of this phase was a trans-Pacific migration completed within two months). Many features of behavior in the traveling phase were similar to those in the residency phase; however the temperature difference between viscera and ambient temperature was larger, feeding was slightly more frequent, and dives to deeper water were more frequent.

Manuscript approved for publication 22 October 2002 by Scientific Editor.
Manuscript received 3 January 2003 at NMFS Scientific Publications Office.
Fish. Bull. 101:514–534 (2003).

Pacific bluefin tuna (*Thunnus orientalis*), a highly migratory species, is mainly distributed in the temperate zone of the northern Pacific Ocean (Yamanaka, 1982; Bayliff, 1994) in contrast to *T. thynnus*, which inhabits the Atlantic Ocean (Collette, 1999).

Current knowledge on the migration of Pacific bluefin tuna is summarized in the following studies: Aikawa (1949); Bell (1963a); Okachi (1963); Orange and Fink (1963); Nakamura (1965); Clemens and Flittner (1969); Shingu et al. (1974); Yorita (1976); Bayliff (1980); Yamanaka (1982); Yonemori (1989); and Bayliff et al. (1991). The majority of bluefin tuna spawn in the northwest Pacific Ocean in an area from the Philippines past Taiwan to Okinawa from April to June, and small numbers spawn off southern Honshu in the Pacific Ocean in July and in the Sea of Japan in August (Yabe et al., 1966; Ueyanagi, 1969; Okiyama, 1974; Yonemori, 1989; Kitagawa et al., 1995). Carried by the Kuroshio Current, juveniles arrive near the coast of Japan, move northward during summer and early autumn, and then most turn around and move back southward during late autumn and winter along the Japanese coast. During the first few years of their lives, the majority of young fish repeat a similar north–south seasonal migration. However a small fraction, increasing each year, moves away from the Japanese coast and often reaches the eastern side of the Pacific Ocean, off the United States and Mexico. These fish stay in the eastern Pacific Ocean for 1–3 years. Some time later, as mature fish, they gather in the northwest Pacific Ocean to spawn and then disperse after the spawning season.

This information on Pacific bluefin tuna movements has been accumulated through analyses of fishery catch data and tag-recapture data. Fishery catch data are based on different individuals from limited areas where, and particular seasons when, fishing took place. Conventional tagging data provide migration information regarding only two points: release and recapture. Acoustic tracking, another method used for investigating behavior and migration of individuals, can collect detailed information on fish movements and behavior on a time scale of seconds, but the duration of the tracking period of each individual has usually been less than several days in studies of Pacific bluefin tuna (Marcinek et al., 2001; Hisada et al.[1]) as well as in other studies of *Thunnus* species (e.g. Carey and Olson, 1982; Holland et al., 1990; Cayré, 1991; Cayré and Marsac, 1993; Block

[1] Hisada, K., H. Kono, and T. Nagai. 1984. Behavior of young bluefin tuna during migration. *In* Progress report of the marine ranching project 4, p. 1–7. Nat. Res. Inst. Far Seas Fish. Pelagic Fish Resource Division, 5-7-1 Shimizu-Orido, Shizuoka, Shizuoka, 424-8633, Japan. [In Japanese, the title was translated by authors.]

et al., 1997). These methods have not yielded detailed information regarding migration, behavior, and their relation to environmental factors for Pacific bluefin tuna over a long period.

An archival tag is an electronic device that measures environmental variables and records data in its memory. When attached to an animal, it allows direct examination of the relationship between an animal's behavior and physiological condition, or the ambient environment. One type of "archival" tag merely stores data; however, another type not only stores data but also provides daily geographical locations of the fish by processing the measured environmental data. This type of archival tag was anticipated since the 1980s as a tool that could collect detailed information on individual fish behavior (Hunter et al., 1986; Anonymous, 1994). Metcalfe and Arnold (1997) estimated the geographical locations and tracks of plaice, a demersal species, by comparing tidal depth variations with the time series depth data recorded by archival tags attached to the fish. However, this method is not suitable for pelagic fish, which change swimming depth freely. A type of archival tag that can estimate geographical locations based on change of light levels during a day—a method more suitable for pelagic species—has been commercially available since the early 1990s. So far, archival tags of this type have been used in several tagging projects (Arnold and Dewar, 2001). The results published in a few reports on southern bluefin tuna (*T. maccoyii*) (Gunn and Block, 2001), and Atlantic bluefin tuna (*T. thynnus*) (Block et al., 2001), show the remarkable value of archival tag data.

As archival tags have come into wide use, results of several experiments conducted to evaluate the reliability of its geolocation estimates have been published (Welch and Eveson, 1999; Musyl et al., 2001; Gunn et al.[2]). However, several points remain to be tested: tag reliability when a number of tags are deployed for long duration, reliability of sensors for variables other than light, and the effects of attaching the tag to fish.

After two preliminary experiments with tags in 1994, the first with tags placed at a known outdoor location on land and in air, and the second with tags attached to young Pacific bluefin tuna held in pens, we applied archival tags to wild young Pacific bluefin tuna to investigate their behavior and migration. In the present study we report the characteristics of migration for this species based on data on daily geographical location, as well as the reliability of archival tag data and the effect of attachment of the tag to fish. Analyses for swimming depth, ambient water temperature, and feeding frequency of the species are undertaken in other papers (Kitagawa et al., 2000; Itoh et al., 2003).

[2] Gunn, J., T. Polacheck, T. Davis, M. Sherlock and A. Betlehem. 1994. The development and use of archival tags for studying the migration, behavior and physiology of southern bluefin tuna with an assessment of the potential for transfer of the technology to groundfish research. Proc. ICES mini-symposium on migration, St. Johns, Newfoundland. ICES C.M. Mini:2.1, 23 p. International Council for the Exploration of the Sea, Palægade 2-4, DK-1261 Copenhagen K, Denmark.

Materials and methods

Outline of the archival tag used in this study

The archival tag used in this study (Northwest Marine Technology, Inc. Shaw Island, WA) had a cylindrical stainless-steel body (16 mm in diameter and 100 mm long, and weighing 52 g) that was implanted in the animal. A flexible sensor stalk 2.2 mm in diameter and 150 mm long extended from the tag through the skin of the animal into the water. The end of the stalk housed an external temperature sensor and a light capture region. Light was led from the capture region by optical fiber to a photodiode sensor in the body of the tag, which also housed sensors for pressure, internal temperature, and light. Response times for the temperature sensor were three seconds for the external sensor and 20 seconds for the internal sensor, and temperature resolution was 0.2°C for both sensors. Resolution of the pressure sensor record was 1 m at shallow depths up to 126 m, then changed to 3 m from that depth to the scale limit of 510 m. Clock drift was less than 30 seconds per year. The tag had a data measurement interval of 128 seconds, a 256-kByte data memory, and an operating life exceeding seven years. Data were downloaded from recovered tags by using a personal computer and a fiber-optic connector.

Two types of data files were created within the tag memory. One data file stored daily records containing date, estimated times of sunrise and sunset, water temperatures at 0 m plus two other selectable depths (we selected 60 m and 120 m), and other information required for, or produced in, the course of location estimates for each day. This file is referred as the "summary file" in the "Results" section, and it stored data for all days after the memory was last cleared. The times of sunrise and sunset were estimated within the tag from sea-surface light intensities, which were inferred from measured depth and measured light intensity at depth and a water opacity factor determined from the measured data each Universal Time (UT) day. The time of midday was determined as the midpoint between sunrise and sunset times, and longitude was calculated from the difference between the midday time and 1200h UT, at a rate of 15 degrees longitude per hour, corrected for astronomical effects. Latitude was estimated from the duration of daylight (Hill, 1994).

The second data file contained unprocessed time series data records taken at 128-second intervals. The tag could record at any integer multiple of its 128-second measurement interval and a multiple of one was chosen. Each record consisted of external temperature, internal temperature, pressure, and light intensity, and corresponded to a known time. This is referred to as the "detail file" in the "Results" section. It could hold about 54,000 records, or about 80 days of steady recording at the high data rate chosen—a small fraction of the tag's overall lifetime. The time-series memory was divided into two sections, and the size allocations for the two sections were determined by the user. The first section filled first and did not change thereafter. The second section filled next, but once full, it was continually overwritten by new data. Thus the first section always contained the earliest data retrieved from a tag; the

second always contained the latest data. We divided the file into two 40-day sections for releases in 1995 and 1996, and into 20- and 60-day sections for releases in 1997.

Reliability and calibration of archival tags in air

To examine the reliability of location estimates made by archival tags, 117 archival tags were left outdoors (34°59′N; 138°59′E) where they were not affected by artificial light during July–September 1996 (55 days, five tags), May–August 1997 (86 days, 14 tags), and October 1997 (five days, 100 tags). Two of the tags were used in two of the experiments.

Calibration tests of internal and external temperature sensors were conducted for all tags before being implanted in fish that were released, and the sensors were recalibrated for nine tags after they were recovered. Temperature calibration was done by immersing tags into a series of water tanks that were set to temperatures ranging from 5.0° to 30.0°C by 5°C intervals. Calibration tests of pressure sensors were also conducted for all tags before release and on 27 tags after being recovered. Tags were placed in a pressure chamber with a resolution of 0.1 bar and examined up to 20 bar. The tags were left at least five minutes at each temperature or pressure to obtain at least two measurements at the 128-second recording interval.

Experiment with pen-held fish

Archival tags were attached to three pen-held young Pacific bluefin tuna of 93–97 cm fork length (FL) at Kasasa in Kagoshima Prefecture (31°25′N; 130°11′E) in November 1994. The fish had been reared in a net pen (40 m × 25 m with 12 m depth) for more than two years and were acclimated to the environment at the time of the experiment. Archival tags were inserted into the abdominal cavities of two of the three fish by the following method. A fish caught by hook and line was put into a styrofoam box, and its eyes were covered with a black polyethylene bag. The belly of the fish was cut with a scalpel about 4 cm anterior to the anus, 3–4 mL of antibiotic (artificial penicillin, Doil, Tanabe Seiyaku Co., Ltd., Osaka, Japan) was injected into abdominal cavity of the fish, and an archival tag was inserted there with the stalk extending through the incision. A stitch was made in the middle of the incision with an absorbable suture (Coated Vicryl, type J583G, Ethicon Inc., Cornelia, GA), and the fish was released back into the pen. All tools and tags were disinfected with 100% ethanol. No anesthetic was used because with their eyes covered, the fish remained quiet during the surgery. This simplified procedure (from making the incision to releasing the fish) could be completed in less than 90 seconds, thus minimizing total stress on the animal and, in later experiments on wild fish, providing the best chance for the animal to rejoin its original school. In this pen study, the third fish was tagged externally instead of internally, the tag being connected by a thin wire rope to a small metal arrowhead inserted in a muscle near the second dorsal fin base.

During the pen-held fish experiment, none of the fish were observed to die as a result of tagging. The tag that had been attached externally came loose from the fish and was retrieved from the bottom of the pen four days after tagging. One tagged fish escaped when the pen was broken. The remaining tag was recovered 453 days later when the fish was caught from the pen as part of a commercial catch.

Experiments with wild fish

Tag and release experiments on wild young Pacific bluefin tuna were conducted near Tsushima, at the northeastern end of the East China Sea, by using chartered commercial trolling vessels, every November and December from 1995 to 1997. A total of 166 fish, ranging from 43 to 78 cm FL (age 0 or 1), were internally tagged as described above and released immediately. Two dart-type conventional tags were also attached to the second dorsal-fin base of each fish in the 1997 experiment as visual markers in an attempt to improve the recovery rate.

Thirty archival tags (18.1%) were recovered. The durations at sea were 50 days or less for 13 fish, 96–211 days for 13 fish, and 359–375 days for three fish, all recaptured around Japan. One additional fish was recaptured off the west coast of Mexico, on the east side of the Pacific Ocean, at 610 days after release. Data could not be downloaded from one archival tag released in 1995 and recovered 30 days after release; all other tags returned data.

Results

Reliability of location estimates

The tag recovered from a fish penned in a known location for 453 days yielded a record of positions automatically estimated during that time. Figure 1 plots the errors in those estimates and the date when each was made. This tag provided the only position sequence of long duration obtained from a captive fish. Unfortunately it was discovered later, after the experiment was completed and after this particular tag was no longer available for further testing, that the light sensitivity of this tag, as well as that of the tag that yielded data for four days in the captive fish experiment, was at least a factor of ten lower than that of other tags. This discrepancy in light sensitivity could be seen in the daily noon-light intensity data in the summary file, both during the in-water experiment (when compared with typical values for tags in wild fish) and when tested in air (compared with other tags of the group tested in air). On dark days there was an unusual pattern of early sunset times and late sunrise times that the tag manufacturer interpreted as being associated with the low light sensitivity. Thus, although the general trends of error size with season can be expected to be representative, the absolute size of the errors was likely inflated in this, the only long-term record obtained from a captive fish.

Longitude error showed no change with season, but latitude error increased dramatically near the equinoxes as expected because day length does not vary significantly with latitude at that time, and therefore carries little in-

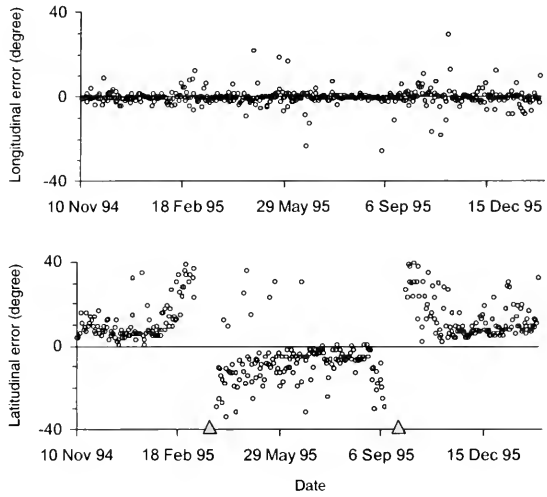

Figure 1

Seasonal change of errors in location estimate. Upper and lower panels show longitudinal and latitudinal errors, respectively. Triangles show equinoxes. Data are from an archival tag implanted in a fish held in a pen for 453 days.

formation about latitude. The tag did not provide a latitude estimate for 18 days around and at the vernal (autumn) equinox and had large errors for one month before (or after) as well as 10 days after (or before) that period, respectively. The same pattern was observed in the test with archival tags that were left in air. In addition, the latitude estimates were biased toward south in summer and toward north in winter, that is, toward erroneously short day lengths.

Occasional large deviations were observed in both latitude and longitude estimates. These were easily identified as outliers in our analyses of data obtained from wild fish by comparing them with estimated locations for adjacent days. When evaluating the accuracy of location estimates for practical use in analyses of wild fish movements, we excluded longitude or latitude estimates that differed more than 10° from the real location and the latitude estimates not provided by the tag near the equinoxes. These accounted for 2.8% of longitude estimates and 8.9% of latitude estimates obtained in the tests in air, as well as 4.8% of longitude data and 47.5% of latitude data obtained in the tests of pen-held fish.

Figure 2 shows the position estimates and error bars corresponding to one standard deviation for 117 tags tested in air—most of them for a 5-day period, five for 82 days, and twelve others for various intermediate durations. The aggregate of all observations in air yields an error estimate (mean ±standard deviation) of −0.54° ±0.75° for longitude, and −0.12° ±3.06° for latitude.

When individual tags tested in air were examined separately, 96% of tags (112/117) showed average position errors within a range of ±1.5° in longitude. Among these 112 tags with small longitude errors, 95 had been manufactured within the last half year and had an average and standard deviation of position error equal to −0.50° ±0.19°, and the other 17 tags were more than one year old and had an average position error of −0.51 ±0.75°. The average is not significantly different (ANOVA F=0.01, P>0.05) and the younger tags had a smaller standard deviation (F=412, P<0.01). No significant difference of accuracy was observed among the 17 older tags that could be related to their history, i.e. among four tags kept in air without release and 13 tags released with fish and recovered (F=1.01 for average and F=2.81 for standard deviation, both P>0.05).

For the two tags attached to fish in pens, one tag measured only five positions with a resulting error estimate of −2.38 ±0.39 for longitude, and −1.82° ±1.58° for latitude. The other measured 432 positions, with a resulting error estimate of −0.53° ±2.46° for longitude and 1.26° ±5.33° for latitude. This is the data series presented earlier in Figure 1. The large standard deviation in longitude error—much larger than that obtained in other tests—initially raised questions regarding the effect of water on the positioning techniques. However as mentioned earlier, the low light sensitivity of both tags used in captive fish was identified as the likely cause of these large errors.

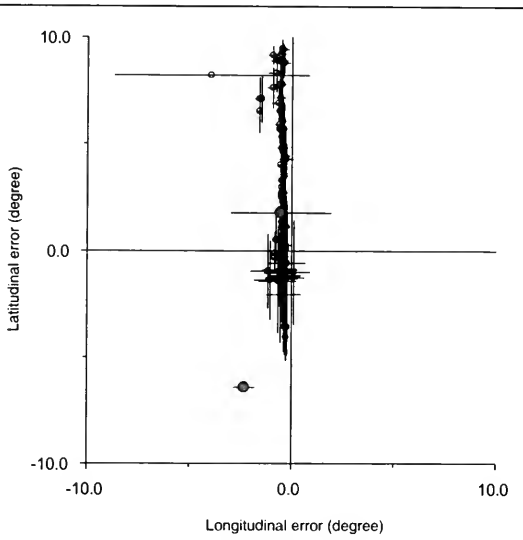

Figure 2

Average errors of location estimates from each archival tag in the benchmark tests. Smaller circles are the average errors of the tags tested in air and the larger circles are the average errors for archival tags implanted in pen-held fish. Bar shows a standard deviation.

A more useful measure of in-water accuracy was provided by comparison between actual recapture locations of 18 tags and the locations that those tags estimated one or two days prior to capture (thus avoiding the disturbed light data on the final day). Average differences of the 18 tags were –0.1 ±0.8° (range: –2.0 ±1.7°) in longitude and –1.6 ±1.8° (range: –5.7 ±0.6°) in latitude.

Because the tag's latitude estimate based on day length was found to have limited reliability, we estimated latitude using sea-surface temperature (SST) as recorded in the summary file for each day. The temperature reference field used was the SST map published by Japan Fisheries Information Service Center, which gave average SST weekly for the western Pacific Ocean (west of 160°E), and every 10 days for the eastern Pacific Ocean (east of 160°E). The longitude value determined automatically by the tag was used to choose a longitude on the SST map. Along that longitude line a point was sought where the map SST matched the SST value recorded by the tag. If multiple points were found to satisfy this criterion, the point that gave the most plausible movement was selected, based on fish locations on several adjacent days. If a location still could not be determined, it was interpolated as a midpoint between the adjacent two days' locations.

One example of location re-estimation is shown in Figure 3. After consulting with the SST maps, we used 1.4% of the locations estimated automatically from 29 recaptured tags, and 79.7% of latitudes were changed by +0.3 (±2.8°) on average with the SST method. The remaining 18.9% of days did not provide any reasonable location estimates for various reasons, including anomalous longitudinal estimates, no match points of SST along the estimated longitudinal line, or the existence of a wide latitudinal area showing the same SST.

Reliability of temperature and pressure sensors

One hundred tags calibrated within half a year of manufacture showed average errors of 0.1 ±0.1°C for both internal and external temperature sensors. Nine tags recovered from fish and tested more than one year after manufacture showed average errors of 0.0 ±0.1°C for both sensors. It thus appears that no deterioration of the temperature sensors occurred because of release-recapture or the passage of time.

No large error in pressure sensors was observed during calibration of tags before release. However, 20 of 27 tags recovered from tagged and released fish were found on recalibration to record substantially lower than actual pressure. One example is shown in Figure 4. No further deterioration of pressure sensors was observed when these tags were kept in air for an additional half year. There was no way to know exactly when the sensor deterioration had occurred during the time the fish were in water. However, the frequency of records showing swimming at 0 m depth was remarkably higher in the second part of

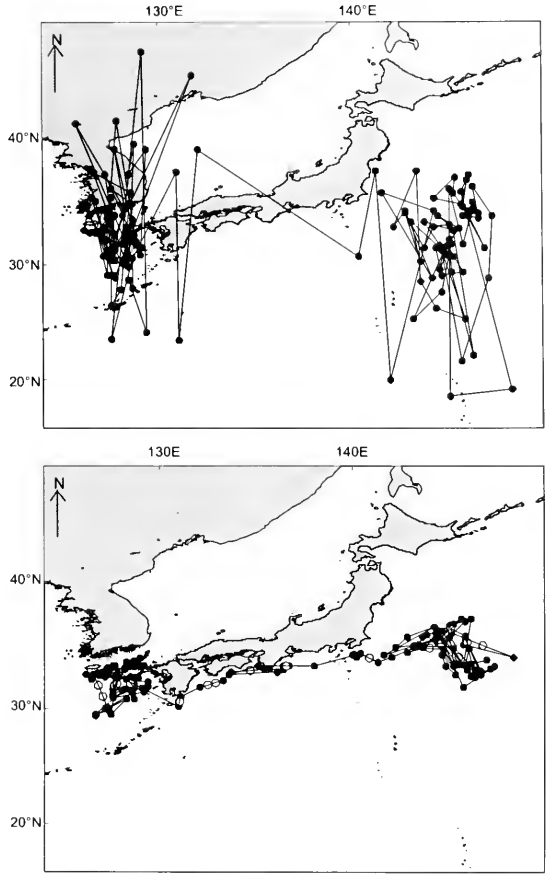

Figure 3

Locations estimated by an archival tag with a young Pacific bluefin tuna before (upper panel) and after (lower panel) replacement of the original latitudinal estimate based on day length by one using sea-surface temperature. Locations out of the range of the figure and those for which latitude was not estimated were not drawn in the upper panel. Estimated locations for all days are shown in the lower panel. Open circles in the lower panel are interpolated locations.

the detailed file (i.e. just before recapture) when compared to the first part of the detailed file (i.e. just after release). The tag manufacturer analyzed this deterioration in the pressure sensors, and expected the sensor characteristics to remain constant after an initial change (if one occurred), and agreed that the early and late pressure data should be treated separately. We assumed that the deterioration occurred sometime during the middle period of the time the fish was free, when no record was being kept in the detail file. Recorded depths in the second part of the detail file for eight tags with relatively large deterioration detected were corrected by using two regression lines joined at around 30 m in real depth for each tag (Fig. 4).

Effect of the archival tag on fish

The effect of both the implantation process and the presence of the implanted tag in the fish was investigated by macroscopic observation of recovered fish. Further information was obtained by comparing the weight at length

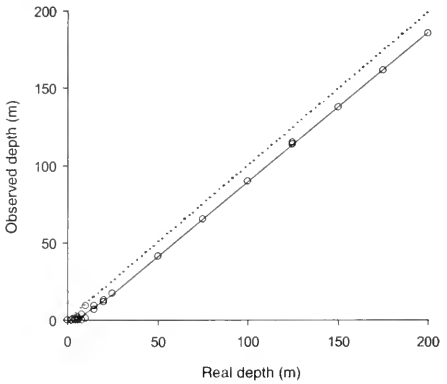

Figure 4

An example of observed deterioration in a pressure sensor of an archival tag in a postdeployment recalibration. The horizontal axis shows the test pressure, vertical axis is pressure recorded by the tag. Dots are observed data. The solid line bent at 25 m of real depth is formed from two regression lines, one fitted to data below and one to data above 25 m depth. This approximation to the deteriorated sensor characteristic was used to correct pressure data for this tag. Pressure values are converted to depth in meters. A broken line is that of observed depth equal to real depth.

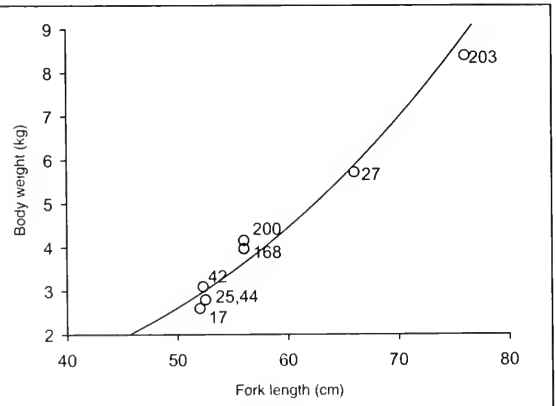

Figure 5

Comparison of weight at length of young Pacific bluefin tuna between recaptured fish tagged with archival tags and wild (untagged) fish. Numerals show days at liberty. An average (thick solid line) and upper and lower 95% confidence limits (thin solid lines) are derived from 11,777 wild fish from 40 to 80 cm in fork length caught in 1995 and 1996 around Japan. Equations for average is $W=2.844\times10^{-5}\times L^{2.918}$, upper 95% limit is $W=3.028\times10^{-5}\times L^{2.930}$, and lower 95% limit is $W=2.745\times10^{-5}\times L^{2.906}$, where L = fork length in cm and W = body weight in kg.

and the monthly average growth rates of tagged fish with wild fish, and also by evidence of feeding to be found in the records returned in the tags.

The bodies of two fish among 30 recoveries were available for observation. One fish recaptured 27 days after release still had a scar on its skin but no trace of the tag insertion surgery was found in its belly muscle. Another fish recaptured 200 days after release had no trace of surgery either on its skin or in its belly muscle. Surface skin around tag stalks was ulcerated in both fish. The stalks were immobilized in the belly muscle. The cylindrical bodies of both tags were covered with membrane and located between the stomach and the pyloric caeca. No infection or necrosis was observed in the visceral organs around tag bodies or in the muscle around tag stalks.

Body weights of all recaptured fish that were measured (n=8, 17–203 days after release) were within the range of those of wild fish of the same fork length (Fig. 5). An average growth rate of recaptured fish was 1.4 ±0.5 cm per month (n=6, three fish recaptured at short durations of liberty that showed no or negative growth were excluded). A subgroup of four fish recaptured after more than 5 months from release, i.e. fish at liberty during the summer when growth might be expected to be faster, had an average growth rate of 1.3 ±0.6 cm—similar to that from all durations.

The average number of daily feeding events, which were found by specific changes of visceral temperature (Itoh et al., 2003), increased linearly from no feeding on the day of release up to a steady rate beginning about 30 days after release. Thus, it appeared that fish did not feed normally during this initial period (Fig. 6).

Horizontal movement

Estimated tracks of all fish that traveled out of the East China Sea along with one fish that remained in the East China Sea are shown in Figure 7 and Figure 8. All of these fish were released off Tsushima in November or December and remained in the East China Sea at least 90 days. After that, four fish entered the Sea of Japan and moved northward from April to July (Fig. 7, A–D). Two of them moved southward in November one year after release (Fig. 7, C and D), and one of the two fish returned to the region off Tsushima where the fish were released (Fig. 7C). One fish remained and was recaptured within the East China Sea in November, one year after release, although it had moved to the east coast of the Korea Peninsula for a period in August and September (Fig. 7E). Ten fish remained within the East China Sea for more than five months and were recaptured from May to June, five to seven months after release (Fig. 7F).

Two fish moved to the Pacific Ocean (Fig. 7G and Fig. 8). One of these fish entered the Pacific Ocean on 7 March 1996, and then traveled eastward straight from a position off the south coast of Kyushu (31°N, 131°E) to one off the east coast of Choshi (36°N, 142°E), then stayed for a while

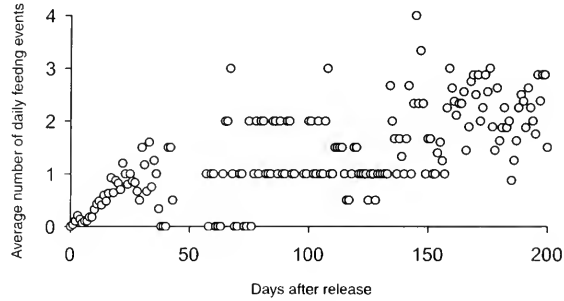

Figure 6
The average number of daily feeding events plotted against days after release.

in an area of 32–37°N, 143–147°E (Fig. 7G). This fish was recaptured by purse seine on 7 June 1996.

The other fish traveled from the western Pacific Ocean to the eastern Pacific Ocean as follows (Fig. 8). It was released off Tsushima on 29 November 1996 at 55 cm FL and remained for a period within the East China Sea. It moved to the Pacific Ocean on 1 May 1997 and then traveled eastward straight from a position off the south coast of Kyushu to one off the east coast of Choshi then stayed for a while in an area of 34–39°N, 143–150°E. It moved northeastward from 30 July to 18 August 1997, then stayed in the area 40–44°N, 152–163°E. It began the trans-Pacific migration on 11 November 1997 at 41°N, 163°E, and traveled straight to northern California, U.S.A. (36°N, 127°W) arriving on 15 January 1998.

After arriving in the eastern Pacific Ocean, this fish initially stayed in an area of 33–40°N, 122–128°W, then moved southward from 25 February to 3 March, then again stayed in an area of 25–29°N, 116–119°W. It started moving northward on 9 May and reached 40°N, 127°W on 25 May, but without staying there moved again southward and reached an area of 25–29°N, 116–120°W on 12 June, close to the place from which it had departed. The fish was recaptured by a recreational fishing vessel on 1 August 1998, 610 days after release, off Baja California, Mexico (31°48′N, 117°18′W), at 87.6 cm FL

The track of this fish consisted of apparently separable segments, five traveling periods and six resident ones. All of the fish that moved out of the East China Sea showed the same type of pattern, staying resident in an area for a relatively long period and then traveling continuously for at least several days in a stable direction.

The terms "traveling phase" and "residency phase" are used in the following description. If a fish moved continuously for more than three days in a stable direction covering more than 700 km in total distance, it was considered to be in a traveling phase—at all other times in a residency phase. A few movements for short periods or short distances (or both) were also observed during periods of a residency phase: a fish resident off the east coast of Hokkaido (40–44°N, 152–163°E) shifted eastward gradually within the area during a period of two months (Fig. 8). Another fish resident in the northern area of the East China Sea moved rapidly to the southern area of the East China Sea at the end of December and came back rapidly to the northern area in early May (Fig. 9). Individual movements were completed within a few days and the total distances moved were far shorter (380 and 310 km, respectively) than those seen in traveling phases.

A total of 12 traveling phases were identified in records of six fish (Table 1). The direction of travel stayed constant within each phase, except in one case where a fish completely turned around in the middle of traveling (in the eastern Pacific Ocean in May and June 1998). Daily distances moved during those traveling phases were calculated. To reduce the influence of scatter in the estimated locations, three-day running averages of latitude and longitude were used for calculation. Excluding the one trans-Pacific migration phase of exceptional length, 7636 km (66 days), the total distance per traveling phase ranged from about 730 to 3406 km (average: 1430 km). The duration of a traveling phase was four to 35 days (average: 17 days) and the distance traveled ranged from 59 to 182 km (average: 104 km). Six residency phases which occurred between two clearly identified traveling phases lasted from 40 to 125 days (average: 81 days). In total, 83% of days were in a residency phase and 17% of days were in a traveling phase. If residency phases for which the beginning or end could not be defined because of fish release or recapture were also included, the average duration of residency phases increased to 110 days, and the proportion days belonging to each phase became 87% in residency and 13% in traveling phases.

Comparison of fish behavior and ambient water temperature between traveling and residency phases

Several points regarding fish behavior, described in detail in Itoh et al. (2003), were compared between all days in a traveling phase and ten days in the residency phase that for four fish immediately preceded the traveling phase. In the case of one fish (no. 241) where data for preceding

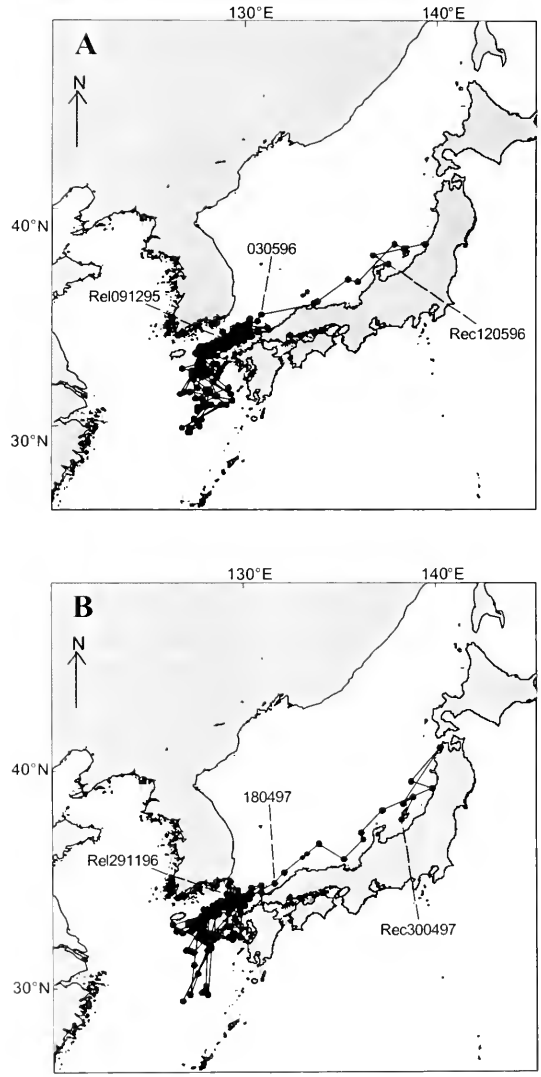

Figure 7

Tracks of young Pacific bluefin tuna estimated by archival tags. "Rel" and "Rec" mean release and recapture, respectively. Numerals are dates in ddmmyy. Each panel shows the track of one fish with an archival tag.

days were not available, ten days from the residency phase immediately following were used instead. Because errors in determining geographical positions introduced scatter in the sequence of estimated positions, the onset (or end) of a traveling phase was not always easy to define. In response to this situation, three days of the residency phase nearest

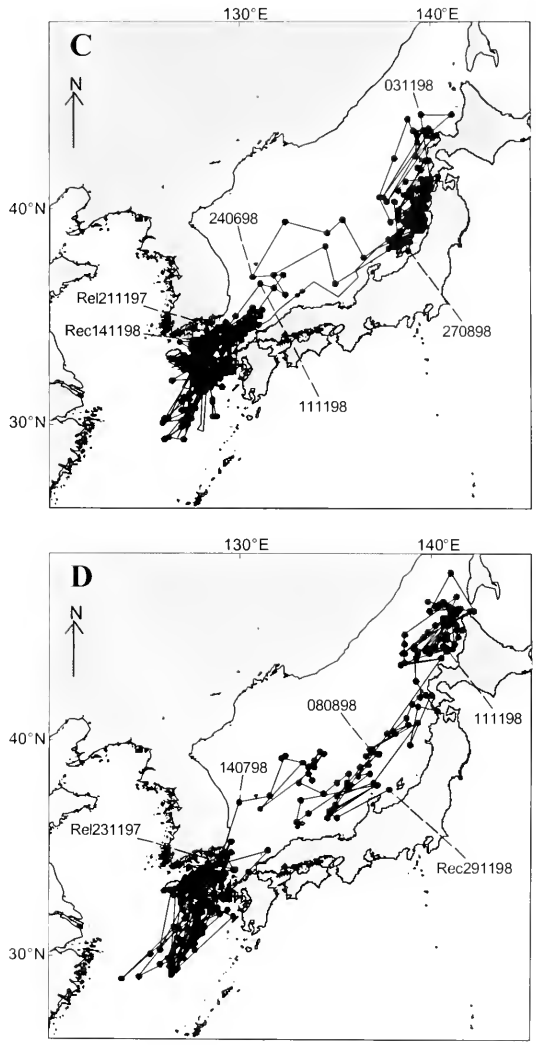

Figure 7 (continued)

to the traveling phase were not included, that is to say, ten days between the fourth and thirteenth days preceding (or following) the onset (or end) of a traveling phase were used.

Among 12 features investigated, three differed between the two phases (Table 2). The temperature difference between fish viscera and ambient water (thermal excess) was more than 1.0°C higher during the traveling phase for four out of five fish. In the one remaining fish (no. 241), data used for analysis were those from days at the end of the traveling phase. The larger thermal excess during a traveling phase was observed at both daytime and nighttime (Fig. 10). The second significant feature was that all fish dived to water deeper than 150 m more frequently during the traveling phase. Except for one fish (no. 241), which spent a long time in water deeper than 150 m, almost all

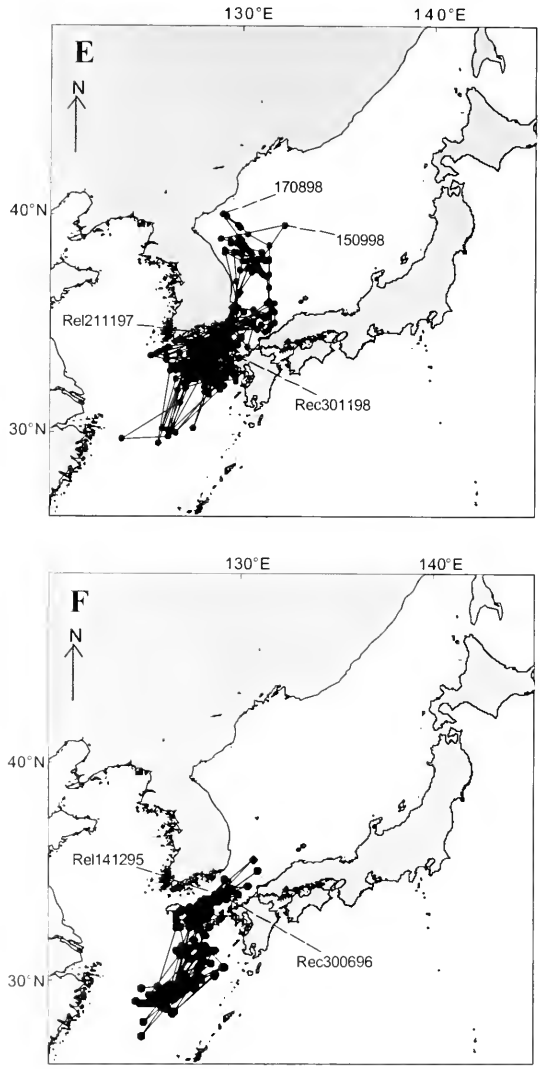

Figure 7 (continued)

records of excursions below 150 m were due to spikes of deep diving of short duration, less than 10 minutes. Finally the frequency of daily feeding events, detected by a change of visceral temperature, was slightly higher during a traveling phase (1.6 ±0.6) than a residency phase (1.1 ±0.4).

Records of surface temperature from the summary file were examined to answer three questions regarding the relation of water temperature to traveling. The first question was whether any water temperature change, an increase in spring and summer or a decrease in winter, was observed several days prior to the onset of the traveling phase. Such a temperature change was observed in 10 out of 12 cases (Table 3, Fig. 11). In those 10 cases, the water temperature increased in spring and summer to 19–26°C (average of 22°C), and decreased in winter to 15–17°C (16°C).

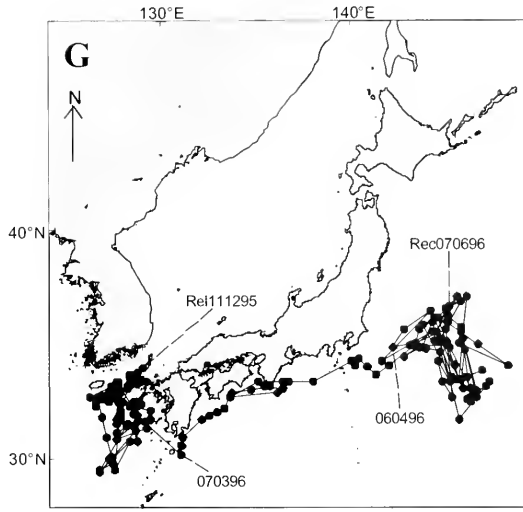

Figure 7 (continued)

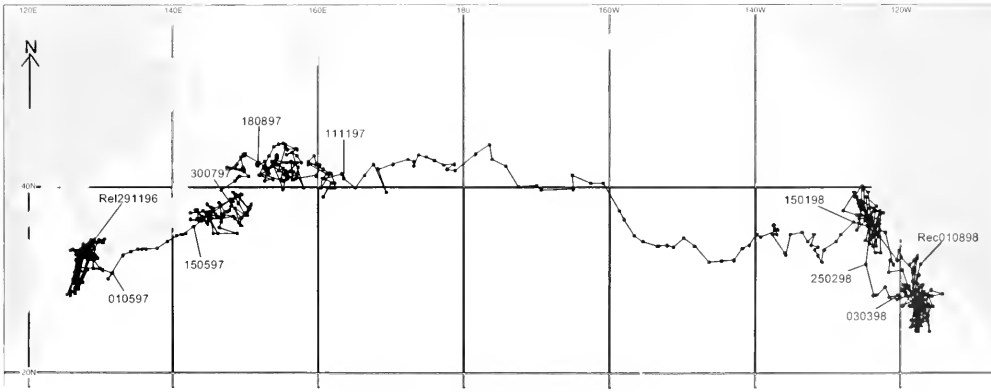

Figure 8

Track of a young Pacific bluefin tuna that traversed the Pacific Ocean, estimated with an archival tag. "Rel" and "Rec" mean release and recapture, respectively. Numerals are dates in ddmmyy.

The second question is whether the water temperature at the onset or end of traveling was within the temperature range of 14–20°C, considered to be in the temperature range preferred by young Pacific bluefin tuna (Itoh et al., 2003). If the act of traveling was simply a reaction to the water temperature, fish would be expected to travel from water with a temperature out of that range to one within that range. However that was observed in only two of 12 cases (Table 3).

The third question was whether the temperature at the end of traveling was a temperature that the fish encountered for the first time since the onset of traveling. We found, however, that there was no specific trend in water temperatures during traveling phases (Fig. 11). Six of 12 temperatures at the ends of traveling phases were not the first one that the fish had experienced during the phase (Table 3).

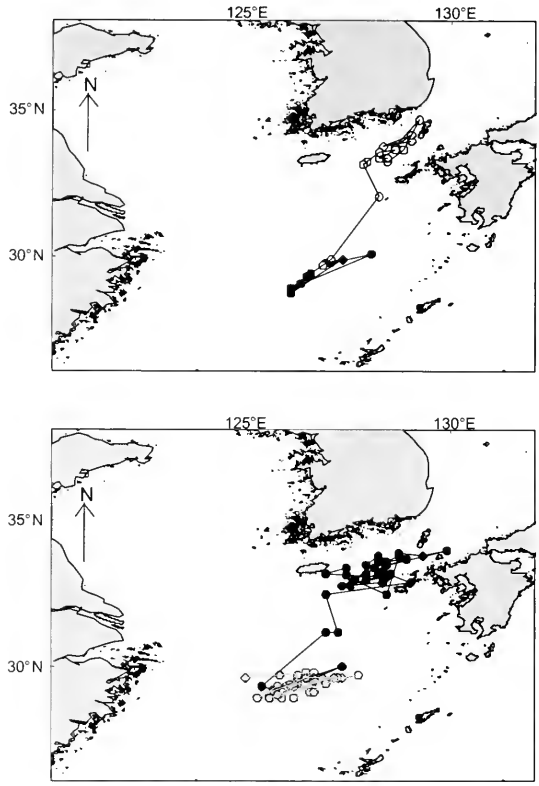

Figure 9

Rapid movements of a fish with an archival tag in the residency phase in the East China Sea. The fish moved rapidly south (upper panel; open circles are in December 1995 and solid circles are in January 1996) and north (lower panel; open circles are in April 1996 and solid circles are in May 1996).

Discussion

Reliability of archival tag data

The reliability of archival tag data for geolocation estimates based on measured light intensity has been examined by implanting the tags in pen-held fish or attaching the tags to a stationary subsurface mooring (Welch and Eveson, 1999; Musyl et al., 2001; Gunn et al.[2]). About one degree of reliability for both longitude and latitude were the results. Our study included further tests: for a large number of tags; for sensors other than light sensors; for reliability of tags over time; for tags manufactured by Northwest Marine Technology that were applied to wild young bluefin tuna and not fully examined in previous studies; and finally for the effect of tag attachment on Pacific bluefin tuna.

The benchmark test in this study showed that longitude estimated by archival tags had an error (mean ±standard deviation) of −0.54° ±0.75°, which differed by only −0.1° ±0.8° from a comparison of in-water tag position results with actual recapture locations. In the on-land benchmark test, the mean error did not change with tag age, although the standard deviation slightly increased. Ninety-six percent of all tags tested were considered to have sufficient reliability in longitudinal estimation. We concluded, therefore, that the archival tag is a reliable tool to estimate longitude on a scale of about one degree.

Latitudes estimated automatically from day length carried larger errors than estimations of longitude, and the accuracy of estimation changed with season as well as with the latitude itself (Hill, 1994; Hill and Braun, 2001). Smith and Goodman (1986) recommended estimating latitude by

Table 1

Information on traveling phases of young bluefin tuna as recorded by archival tags. Daily travel distances were estimated from a three-day running average of latitude and longitude.

ID of fish and number (e.g. M1) of traveling phase	Area	Onset of traveling phase		End of traveling phase		Duration of traveling phase (days)	Total distance traveled (km)	Daily distance traveled (km/day)
		Date	Location	Date	Location			
241 M1	western Pacific	1 May 1997	31N 132E	15 May 1997	36N 143E	15	1,341	89.4
241 M2	western Pacific	30 Jul 1997	40N 147E	18 Aug 1997	42N 152E	20	1,161	58.1
241 M3[1]	central Pacific	11 Nov 1997	41N 163E	15 Jan 1998	36N 127W	66	7,636	115.7
241 M4	eastern Pacific	25 Feb 1998	32N 126W	3 Mar 1998	29N 121W	7	1,043	148.9
241 M5[2]	eastern Pacific	9 May 1998	29N 119W	12 Jun 1998	27N 120W	35	3,406	97.3
209 M1	western Pacific	7 Mar 1996	30N 131E	6 Apr 1996	35N 142E	31	1,860	60.0
164 M1[2]	Sea of Japan	4 May 1996	36N 134E	12 May 1996	38N 138E	9	770	85.6
319 M1[2]	Sea of Japan	18 Apr 1997	35N 132E	30 Apr 1997	38N 138E	13	1,346	103.5
688 M1	Sea of Japan	23 Jun 1998	37N 132E	30 Jun 1998	39N 138E	8	877	109.7
688 M2[2]	Sea of Japan	3 Nov 1998	44N 140E	14 Nov 1998	34N 128E	12	1,611	134.2
760 M1	Sea of Japan	13 Jul 1998	35N 129E	8 Aug 1998	40N 137E	27	1,590	58.9
760 M2[2]	Sea of Japan	11 Nov 1998	44N 141E	14 Nov 1998	38N 136E	4	727	181.7
Average						16.5[3]	1430[3]	103.6

[1] Trans-Pacific migration.

[2] Detail file during the traveling phase exists and was used for analyses in Table 2.

[3] The trans-Pacific migration, which was too long in time and distance, was not included in the calculation.

comparing measured water temperatures at three depths to the water temperature maps at each depth. However, it is quite difficult to obtain water temperature maps for the whole range of times and areas where tuna migrate other than those for SST. Therefore we decided for the latitudinal estimation to rely on the SST maps and on longitude estimated by the tags. One difficulty with the SST method for latitude is that water of the observed surface temperature might occur at two different latitudes, thus not implying a single unique position. However because the latitude of about 80% of all days could be uniquely determined from SST, we considered the adjustment method taken here to be acceptable for the purpose of the present study. Although it was not possible to check the accuracy of the latitudinal estimation independently, judging from the accuracy of the longitude values we used to locate the appropriate North-South stripe on the SST maps and from the rapidity of temperature variations found along those stripes, which in most cases tightly constrained our estimates, we expected the accuracy of latitudinal estimation to be around one degree, which would be sufficient for a study of Pacific bluefin tuna migration.

Some deterioration was observed in pressure sensors. The need for recalibration of sensors after recovery should be emphasized.

Effect of the tag on fish

Fish in this study were much smaller than those in other archival tag studies of southern bluefin tuna and Atlantic bluefin tuna (Block et al., 2001; Gunn and Block, 2001). The tagging success achieved confirms that the type of archival tag we used can be applied to fish at least down to 43 cm FL. No fish died because of the attachment of the tag during the experiment on pen-held fish. The recovery rate (18.1%) for fish tagged with archival tags was similar to the rate (19.1%) for those in the conventional tagging experiment conducted in the 1980s off Nagasaki Prefecture, including Tsushima, for the same size fish of the species (Bayliff et al., 1991). This comparison should be made cautiously for the following reasons. The unusual appearance of an archival tag body would attract the attention of the finder who gutted the fish and might lead to a higher reporting rate. Increased fishing effort for young Pacific bluefin tuna in the northern part of the East China Sea in the 1990s compared to that in the 1980s might lead to a higher recapture rate. The inconspicuous stalk of an archival tag which was the only externally detectable sign of its existence might lead to a low discovery rate. Indeed, because many recoveries of archival tags were made by consumers while gutting the fish, archival tags implanted in the body of the fish must have been overlooked by fishermen and by sellers at fish markets. However, judging not only by the similar but also high recovery rates, it seems that damage and stress of handling at implantation and that due to the archival tags being carried by the fish did not have much more effect on fish survival than did the conventional tags.

Macroscopic observations of two wild fish recovered with archival tags showed that the surgical injuries that occurred during archival tag implantations healed after one month

Table 2

Comparison of various averaged environmental, physiological, and behavioral values between a traveling phase and a residency phase for young Pacific bluefin tuna.

Subject	Phase	ID of fish 164	241	319	688	760	Average of difference
Number of days	Traveling	9	2	13	12	4	
	Residency	10	10	10	10	10	
Swimming depth (m)	Traveling	8.7	22.7	12.0	22.8	7.5	
	Residency	14.0	15.0	45.3	10.2	17.4	
	Difference	−5.3	7.7	−33.3	12.5	−9.9	−5.6
Ambient water temperature (°C)	Traveling	12.9	17.4	12.8	19.8	16.3	
	Residency	17.2	17.9	15.6	18.7	15.3	
	Difference	−4.3	0.5	2.8	1.1	0.9	−1.1
Temperature of viscera (°C)	Traveling	17.8	21.1	17.5	25.9	22.7	
	Residency	20.7	21.8	19.1	23.2	20.8	
	Difference	−2.9	−0.7	−1.6	2.7	1.9	−0.1
Temperature difference between ambient water and fish viscera (°C)	Traveling	4.9	3.7	4.7	6.1	6.4	
	Residency	3.6	3.9	3.6	4.5	5.5	
	Difference	1.4	−0.2	1.2	1.6	1.0	1.0
The number of depth records deeper than 150 m per day	Traveling	5.4	36.0	1.6	3.7	4.3	
	Residency	1.3	13.7	0.0	0.3	0.2	
	Difference	4.1	22.3	1.6	3.4	4.1	7.1
The number of feeding events per day	Traveling	2.6	1.0	1.6	1.7	1.3	
	Residency	1.7	0.6	1.2	0.9	1.3	
	Difference	0.9	0.4	0.4	0.8	0.1	0.5
Percentage of days when a rapid ascent at dawn was observed	Traveling	11%	100%	8%	67%	0%	
	Residency	70%	70%	50%	40%	0%	
	Difference	−59%	30%	−42%	27%	0%	−9%
Percentage of days when a rapid descent at dusk was observed	Traveling	11%	50%	8%	27%	50%	
	Residency	80%	100%	50%	10%	40%	
	Difference	−69%	50%	−42%	17%	10%	−27%
Percentage of days when swimming depth was significantly deeper during daytime than at nighttime	Traveling	89%	100%	50%	75%	25%	
	Residency	80%	70%	90%	80%	100%	
	Difference	9%	30%	−40%	−5%	−75%	−16%
Percentage of days when ambient water temperature was significantly lower during daytime than at nighttime	Traveling	56%	100%	58%	67%	50%	
	Residency	70%	100%	30%	60%	70%	
	Difference	−14%	0%	28%	7%	−20%	0%
Percentage of days when temperature of fish viscera was significantly higher during daytime than at nighttime	Traveling	89%	0%	92%	75%	100%	
	Residency	80%	20%	100%	90%	100%	
	Difference	9%	20%	−8%	−15%	0%	−7%
Accumulated swimming depth change per day (m)	Traveling	5097	6031	6224	7884	4576	
	Residency	5639	4533	6123	5266	6386	
	Difference	−542	1498	101	2618	−1810	373

and there was no scar after a half year. No damage to visceral organs was observed for the two fish. The finding is consistent with that for southern bluefin tuna (Gunn et al.[2]).

Fish tagged with archival tags usually showed similar behavioral patterns, such as diurnal change of swimming depth and vertical excursions at dawn and dusk (Itoh et al.,

Table 3

Water temperature changes associated with the traveling phase of Pacific bluefin tuna.

Test 1: Circles mark the occurrence of a sea-surface temperature change before the onset of a traveling phase (increasing in spring-summer, decreasing in autumn-winter). T-change (temperature change) shows the maximum (in spring–summer) and minimum (in autumn-winter) water temperature (in the temperature change before traveling.

Test 2: Comparison of temperatures at the onset and end of traveling to a temperature range of 14–20°C, which is thought to be a preferred temperature range for young Pacific bluefin tuna. Temperature values within the range of 14–20°C are underlined.

Test 3: Circles mark cases where the temperature at the end of the traveling was a temperature that the fish encountered for the first time since the onset of the traveling Pacific.

			Test 1		Test 2		
Season	ID of fish	Traveling phase number	T-change		T-onset	T-end	Test 3
Spring	209	M1	○	20	20.7	17.0	—
	164	M1	○	19	14.7	12.4	○
	319	M1	—	16	15.6	13.0	—
	241	M1	○	23	21.7	19.1	○
Summer	241	M2	○	23	21.9	17.4	○
	241	M5	○	20	18.2	19.3	—
	688	M1	○	21	19.5	20.7	—
	760	M1	○	26	24.0	23.6	—
Autumn–winter	241	M3	○	15	14.7	14.3	—
	241	M4	—	13	16.0	17.4	○
	688	M2	○	17	19.9	22.3	○
	760	M2	○	15	14.5	20.1	○

2003) from the second day after release, and their feeding frequency reached a constant level one month after release. Also, the fish maintained weight-at-length similar to that of wild fish. The average growth rate of fish tagged with archival tags observed in our study (1.3 cm/month) was less than the growth rate of wild fish observed between ages one and two in previous studies (1.7–3.3 cm/month, Aikawa and Kato, 1938; Yokota et al., 1961; Yukinawa and Yabuta, 1967; Bayliff et al., 1991; Bayliff, 1993; Foreman, 1996), except for the result of Bell (1963b) (1.3 cm/month). Because similar growth rates were observed for fish recaptured more than a half year after release that spent the summer at large, it appears that the lesser growth rate in the present study is not due to the fact that some fish spent only winter at liberty, when the growth rate is less than that in summer (Yukinawa and Yabuta, 1967; Bayliff, 1993). Judging from these facts, we suggest that the effect of archival tags on fish behavior and physiology seems to be minor, although there is a possibility that carrying an archival tag caused a reduction in growth rate of the fish.

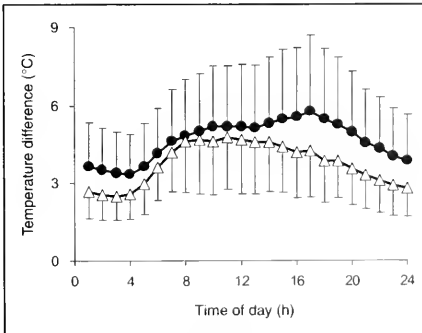

Figure 10

Hourly averages of temperature difference between ambient water and fish viscera in both traveling (circle) and residency phase (triangle) of young Pacific bluefin tuna with archival tags. Data from five individuals are all combined. Bar indicates the standard deviation.

Horizontal movement

Archival tags revealed the movement pattern of young Pacific bluefin tuna individuals, which could be divided into the two clearly-separable phases of traveling and residency. These two phases were observed for all individuals that moved out from the East China Sea.

The residency phase is considered a normal condition for young bluefin tuna, comprising 83–87% of their time. Fish with archival tags tended to stay in the areas of the East

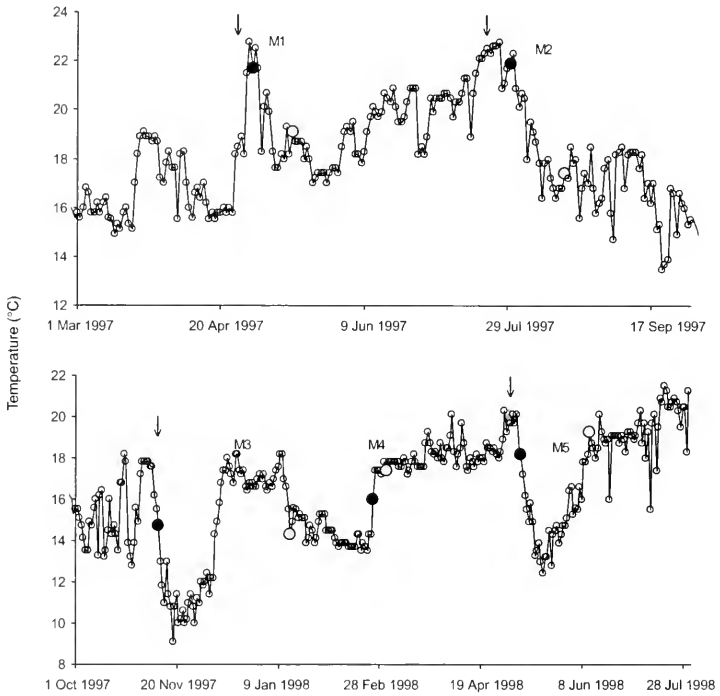

Figure 11

Changes in ambient water temperature recorded by an archival tag in a young Pacific bluefin tuna. Data are for the fish that traversed the Pacific Ocean. The symbols from M1 to M5 designate from the first to fifth traveling phase of the fish. Each dot is an ambient water temperature at 0 m depth recorded in the summary file of the archival tag each day. Large black and brighter circles are temperatures at the onset and end of traveling, respectively. Arrows indicate the observed ambient water temperature changes several days before the onset of the travel phase.

China Sea, off the east coast of Choshi, off the east coast of Hokkaido in the western Pacific Ocean, off Southern California and Baja California, off northern California in the eastern Pacific Ocean, and off the west coast between Akita and Hokkaido in the northern Sea of Japan. The first four areas correspond to the major known fishing grounds of young Pacific bluefin tuna.

The last two areas do not correspond to previously known fishing areas for young Pacific bluefin tuna. In the eastern Pacific, young bluefin tuna are usually caught in an area from 23 to 34°N, off California to Baja California, from May to October by purse seine (Calkins, 1982). Catch records in the northern area around 40°N were scarce, and all of them were for catches from summer to autumn (Radovich, 1961; Bayliff, 1994). It was not expected that young Pacific bluefin tuna were to be found around 40°N in winter, but the archival tag records showed fish staying in an area of 33–40°N, off northern California, from winter to spring. In the northern Sea of Japan, young Pacific bluefin tuna are usually caught by set nets in coastal areas, and are not caught in the offshore area. The archival tag records again showed fish staying in this area in summer and moving southward without being captured. These cases clearly indicate the ability and advantage of archival tags to provide information on fish distribution and migration when and where fishing has not been conducted.

An archival tag demonstrated that an individual young Pacific bluefin tuna was able to travel more than 7000 km without pause and to travel for more than two months. The daily moving distance during the traveling phase ranged from 59 to 182 km, and averaged 104 km. Assuming a constant swimming speed, the daily average swimming speed was estimated as a range from 1.3 to 4.1 knots (average of 2.3 knots).

These horizontal swimming speeds (1–4 knots) are comparable to those of larger young Pacific bluefin tuna and same-size fish of other *Thunnus* species, namely yellowfin tuna (*T. albacares*), bigeye tuna (*T. obesus*), and albacore (*T. alalunga*), determined from acoustic tracking experiments (Laurs et al., 1977; Carey and Olson, 1982; Holland et al., 1990; Block et al., 1997; Marcinek et al., 2001). Sustainable swimming speeds based on oxygen demand and supply for yellowfin tuna and skipjack tuna (*Katsuwonus pelamis*) of 1.5–2 kg in body weight were estimated to be 2–4 times FL per second (Brill, 1996; Korsmeyer et al., 1996), corresponding to 2.3–4.7 knots for fish of 60 cm FL. Applying to young bluefin tuna the same rule (2 –4 times FL) used by those workers as a summary of their data, the expected range of sustainable swimming speeds that do not accumulate an oxygen debt would cover the range of estimated average swimming speeds during traveling phases. Of course, the swimming speed of young Pacific bluefin tuna based on a constant moving speed between two successive daily locations obviously carries some errors. First, a fish might not maintain a constant swimming speed all day long. For example, the daytime swimming speed of albacore observed in an acoustic tracking experiment was reported to be 1.3–2.1 times as great as that at night (Laurs et al., 1977). Second, the influence of water current which should be taken into consideration (Brill, 1996) was completely ignored. Third, assuming straight-line travel between two daily positions would lead to underestimation of actual daily distances traveled, even though the direction during traveling phases could be approximated as a straight line. Even if these errors had been large and the true swimming speed had been twice as large as that which was estimated, these estimated average swimming speeds were still within the range of sustainable speeds.

Although the horizontal movement clearly differed, many features regarding vertical movement were the same for both residency and traveling phases. One parameter that did differ was that of temperature, where the difference between water and fish viscera was 1.0°C larger during the traveling phase than during the residency phase. Feeding causes an increase of visceral temperature in tuna (Carey et al., 1984; Gunn et al., 2001; Itoh et al., 2003). However, the slightly more frequent feeding in traveling phases was not enough to explain the large thermal excess. In addition, the larger temperature difference was observed not only at daytime when the visceral temperature was usually higher because of more frequent feeding, but also at night when the visceral temperature was usually lower (Itoh et al., 2003). The visceral temperature seemed to be raised by high muscle temperature during traveling phases. If this is indeed the case, this would lead to an increase in the delivery rate of oxygen to muscle, which would make the fish less tired and more able to travel (Stevens and Carey, 1981; Brill, 1996). The distinct traveling phase might be one of the tactics adopted by young Pacific bluefin tuna to use energy most efficiently for long distance travel.

During the traveling phase, the frequency of feeding increased slightly and the fish dived to water deeper than 150 m depth more frequently. The fish would feed and seek food at least as aggressively as in the residency phase.

Ambient water temperature is one of the most important environmental factors for young Pacific bluefin tuna (Sund et al., 1981; Koido and Mizuno, 1989; Ogawa and Ishida, 1989; Itoh et al., 2003). The onset of most traveling phases were preceded by specific water temperature changes that reached the upper or lower limit of the preferable water temperature of 14–20°C for young Pacific bluefin tuna (Itoh et al., 2003). Changes in ambient water temperature appears to be a possible trigger for a fish to move. Because no remarkable change in frequency of feeding was observed within several days before or after traveling began, the possibility that shortage of prey is a trigger for migration does not seem to be plausible.

If the impulse to travel in young Pacific bluefin tuna is regulated only by the search for the preferred water temperature range and the aim of traveling is to reach the preferred water temperature range, the ambient temperature would be expected to be out of the preferred range at the onset of travel and within that range at the end. However this did not occur in the fish studied. In addition, half of the observed traveling phases were continued after the fish encountered along the way the same temperature that was present at the end of traveling. According to these results, it appears that the preferred water temperature is neither the sole regulator of traveling in young Pacific bluefin tuna nor is it the sole aim of traveling.

Data from tagged fish released around Japan in the 1980s revealed that some fish released from Nagasaki prefecture migrated to the Sea of Japan and others to the Pacific Ocean (Bayliff et al., 1991). Archival tag data showed that fish released in the same season and same area migrated in various patterns involving different onset times and different destinations when traveling from the East China Sea. In addition, some fish continued to remain in the East China Sea. The migration scenario seems not to be fixed or limited for age 0–1 fish distributed around the East China Sea. A detailed examination of fish behaviors relating to the water temperature has suggested that although young Pacific bluefin tuna prefer a specific temperature range, they can still tolerate temperatures outside of this range (Itoh et al., 2003). This temperature tolerance would contribute to the diversity of migration scenarios for the species.

The trans-Pacific migration

The trans-Pacific migration of Pacific bluefin tuna was originally validated by tagging tuna both from the western Pacific Ocean to the eastern Pacific Ocean and from the eastern Pacific Ocean to the western Pacific Ocean (Orange and Fink, 1963; Clemens and Flittner, 1969). The duration required for trans-Pacific migration was estimated as 215 days from the shortest interval between the release of fish from one side of the Ocean to the recovery of fish on the other side (Bayliff et al., 1991). The present study obtained a full record of daily locations during a trans-Pacific migration of one fish. The fish took two months to traverse the whole Pacific Ocean, which was much shorter than expected from previous records. The starting time for trans-Pacific migration was estimated by Yamanaka (1982) as May–

August based on fishery information and as autumn and winter by Bayliff et al. (1991) based on tagging data. The fish observed in our study started its trans-Pacific migration in late autumn. Although data concerning distribution of young Pacific bluefin tuna in the central Pacific Ocean is limited, a record of young Pacific bluefin tuna catch (age 1–3, age 1 mainly) in the area of 35–45°N, 150°E–140°W from April to November has been reported (Saito et al.[3]). Moreover, two tagged fish were recaptured in the central Pacific Ocean at 38°N, 172°E in June and 39°N, 162°W in June, respectively (Bayliff et al., 1991). Although the seasons differ, the path of the fish tagged with an archival tag passed near these locations. The limited data available at present suggest that the trans-Pacific migration route lies in this area. Together with data which would be obtained from future recovery of additional fish tagged with archival tags, we expect that the overall features of trans-Pacific migration to be revealed in the near future.

Acknowledgments

We thank the staff of the Marino Forum 21 and the Kagoshima Fisheries Experimental Station for their cooperation in the pen-held fish experiment. We also thank troll fishermen, staff in the Kamiagata Fisheries Cooperative Association, the Tsushima Fisheries Extension Service, and the Nagasaki Fisheries Experimental Station for their cooperation with tag and release procedures. We acknowledge fishermen, consumers, and staff of the Inter-American Tropical Tuna Commission for their kindness in returning archival tags along with pertinent information about the recapture. We especially thank J. Gunn in CSIRO for giving us valuable information about implanting the archival tag in fish. We are grateful to Northwest Marine Technology Inc. and Tanaka Sanjiro Co., Ltd., for providing us with archival tags. We would like to thank P. Ekstrom of Northwest Marine Technology Inc. for his critical review and help with the English text. We thank our staff in Japan NUS Co., Ltd., the Suidosya Co., Ltd., and the National Research Institute of Far Seas Fisheries, and also T. Kitagawa in the Ocean Research Institute of the University of Tokyo, for their help in implanting the tags in fish. We gratefully acknowledge S. Kume of Japan NUS Co., Ltd., N. Baba of Fishery Research Agency, and Z. Suzuki and Y. Uozumi of National Research Institute of Far Seas Fisheries for their critical review.

Literature cited

Aikawa, H.
1949. Fisheries population ecology. Sangyo Tosho Co. Ltd., Tokyo, 545 p. [In Japanese.]

[3] Saito, S., K. Shimazaki, and T. Sato. 1981. Distribution of bluefin tuna around the area of polar front in the north Pacific Ocean. *In* Report of the Maguro Gyogyo Kenkyu Kyogikai, in 1980, p. 247–252. Nat. Res. Inst. Far Seas Fish. Pelagic Fish Resource Division, 5-7-1 Shimizu-Orido, Shizuoka, Shizuoka, 424-8633, Japan. [In Japanese, the title was translated by authors.]

Aikawa, H., and M. Kato.
1938. Age determination of fish. I. Bull. Japan. Soc. Sci. Fish. 7:79–88. [In Japanese.]

Anonymous.
1994. Archival tags 1994: present and future. U.S. Dep. Commer., NOAA Tech. Memo. NMFS-SEFSC-357, 42 p.

Arnold, G., and H. Dewar.
2001. Electronic tags in marine fisheries research: a 30-year perspective. *In* Electronic tagging and tracking in marine fisheries (J. R. Sibert and J. L. Nielsen, eds.), p. 7–64. Kluwer Academic Publisher, Netherlands.

Bayliff, W. H.
1980. Synopsis of biological data on the northern bluefin tuna, *Thunnus thynnus* (Linnaeus, 1758), in the Pacific Ocean. Spec. Rep. IATTC 2:261–293.
1993. Growth and age composition of northern bluefin tuna, *Thunnus thynnus*, caught in the eastern Pacific Ocean, as estimated from length-frequency data, with comments on trans-pacific migrations. Bull. IATTC, 20:503–540.
1994. A review of the biology and fisheries for northern bluefin tuna, *Thunnus thynnus*, in the Pacific Ocean. FAO Fish. Tech. Pap. 336/2:244–295.

Bayliff, W. H., Y. Ishizuka, and R. B. Deriso.
1991. Growth, movement, and attrition of northern bluefin tuna, *Thunnus thynnus*, in the Pacific Ocean, as determined by tagging. Bull. IATTC 20:1–94.

Bell, R. R.
1963a. Synopsis of biological data on California bluefin tuna *Thunnus saliens* Jordan and Everman 1962. FAO Fish. Rep. 6(2):380–421.
1963b. Preliminary age determination of bluefin tuna, *Thunnus thynnus*. Calif. Fish. Game 49:307.

Block, B. A., H. Dewar, S. B. Blackwell, T. D. Williams, E. D. Prince, C. J. Farwell, A. Boustany, S. L. H. Teo, A. Seitz, A. Walli, and D. Fudge.
2001. Migratory movements, depth preferences, and thermal biology of Atlantic bluefin tuna. Science 293:1310–1314.

Block, B. A., J. E. Keen, B. Castillo, H. Dewar, E. V. Freund, D. J. Marcinek, R. W. Brill, and C. Farwell.
1997. Environmental preferences of yellowfin tuna (*Thunnus albacares*) at the northern extent of its range. Mar. Biol. 130:119–132.

Brill, R. W.
1996. Selective advantages conferred by the high performance physiology of tunas, billfishes, and dolphin fish. Comp. Biochem. Physiol. 113A:3–15.

Calkins, T. P.
1982. Observations on the purse-seine fishery for bluefin tuna (*Thunnus thynnus*) in the eastern Pacific Ocean. Bull. IATTC 18:123–225.

Carey, F. G., J. W. Kanwisher, and E. D. Stevens.
1984. Bluefin tuna warm their viscera during digestion. J. Exp. Biol. 109:1–20.

Carey, F. G., and R. J. Olson.
1982. Sonic tracking experiments with tunas. ICCAT Coll. Vol. Sci. Papers XVII. 2:458–466.

Cayré, P.
1991. Behavior of yellowfin tuna (*Thunnus albacares*) and skipjack tuna (*Katsuwonus pelamis*) around fish aggregating devices (FADs) in the Comoros Islands as determined by ultrasonic tagging. Aquat. Living. Resour. 4:1–12.

Cayré, P., and F. Marsac
1993. Modeling the yellowfin tuna (*Thunnus albacares*) vertical distribution using sonic tagging results and local environmental parameters. Aquat. Living Resours. 6:1–14.

Clemens, H. B., and G. A. Flittner.
1969. Bluefin tuna migrate across the Pacific Ocean. Calif. Fish Game 55:132–135.
Collette, B. B.
1999. Mackerels, molecules, and morphology. Soc. Fr. Ichthyol. 25:149–164.
Foreman, T.
1996. Estimates of age and growth, and an assessment of ageing techniques for northern bluefin tuna, *Thunnus thynnus*, in the Pacific Ocean. Bull. IATTC 21:75–123.
Gunn, J., and B. Block.
2001. Advances in acoustic, archival, and satellite tagging of tunas. *In* Tuna: physiology, ecology, and evolution (B. A. Block and E. D. Stevens, eds.), p.167–224. Academic Press, San Diego, CA.
Gunn, J., J. Hartog, and K. Rough
2001. The relationship between food intake and visceral warming in southern bluefin tuna (*Thunnus maccoyii*). Can we predict from archival tag data how much a tuna has eaten? *In* Electronic tagging and tracking in marine fisheries (J. R. Sibert and J. L. Nielsen, eds.), p. 109–130. Kluwer Academic Publisher, Netherlands.
Hill, R. D.
1994. Theory of geolocation by light levels. *In* Elephant seals, population ecology, behavior and physiology (B. J. LeBoeuf and R. M. Laws, eds.), p. 227–236. Univ California Press, Berkeley, CA.
Hill, R. D.,and M. J. Braun
2001. Geolocation by light level. The next step: latitude. *In* Electronic tagging and tracking in marine fisheries (J. R. Sibert and J. L. Nielsen, eds.), p. 315–330. Kluwer Academic Publisher, Netherlands.
Holland, K. N., R. W. Brill, and R. K. C. Chang.
1990. Horizontal and vertical movements of yellowfin and bigeye tuna associated with fish aggregating devices. Fish. Bull. 88:493–507.
Hunter, J. R., A. W. Argue, W. H. Bayliff, A. E. Dizon, A. Fonteneau, D. Goodman, and G. R. Sekel.
1986. The dynamics of tuna movements: an evaluation of past and future research. FAO, Fish. Tech. Pap. 277:vi, 78 p.
Itoh, T., S. Tsuji, and A. Nitta.
2003. Swimming depth, ambient water temperature preference, and feeding frequency of young Pacific bluefin tuna (*Thunnus orientalis*) determined with archival tags. Fish. Bull. 101:535–544.
Kitagawa, Y., Y. Nishikawa, T. Kubota, and M. Okiyama.
1995. Distribution of ichthyoplanktons in the Japan Sea during summer, 1984, with special reference to scombroid fishes. Bull. Jpn. Soc. Fish. Oceanogr. 59(2):107–114. [In Japanese.]
Kitagawa, T., H. Nakata, S. Kimura, T. Itoh, S. Tsuji, and A. Nitta.
2000. Effect of ambient temperature on the vertical distribution and movement of Pacific bluefin tuna *Thunnus thynnus orientalis*. Mar. Ecol. Prog. Ser. 206:251–260.
Koido, T., and K. Mizuno.
1989. Fluctuation of catch for bluefin tuna (*Thunnus thynnus*) by trap nets in Sanriku coast with reference to hydrographic condition. Bull. Jpn. Soc. Fish. Oceanogr. 53: 138–152. [In Japanese.]
Korsmeyer, K. E., H. Dewar, N. C. Lai, and J. B. Graham.
1996. The aerobic capacity of tunas: adaptation for multiple metabolic demands. Comp. Biochem. Physiol. 113A:17–24.
Laurs, R. M., H. S. H. Yuen, and J. H. Johnson.
1977. Small-scale movements of albacore, *Thunnus alalunga*, in relation to ocean features as indicated by ultrasonic tracking and oceanographic sampling. Fish. Bull. 75:347–355.
Marcinek, D. J., S. B. Blackwell, H. Dewar, E. V. Freund, C. Farwell, D. Dau, A. C. Seitz, and B. A. Block.
2001. Depth and muscle temperature of Pacific bluefin tuna examined with acoustic and pop-up satellite archival tags. Mar. Biol. 138:869–885.
Metcalfe, J. D. and G. P. Arnold
1997. Tracking fish with electronic tags. Nature 387:665–666.
Musyl, M. K., R. W. Brill, D. S. Curran, J. Gunn, J. R. Hartog, R. D. Hill, D. W. Welch, J. P. Eveson, C. H. Boggs, and R. E. Brainard.
2001. Ability of archival tags to provide estimates of geographical position based on light intensity. *In* Electronic tagging and tracking in marine fisheries (J. R. Sibert and J. L. Nielsen, eds.), p. 343–367. Kluwer Academic Publisher, Netherlands.
Nakamura, H.
1965. Tuna resources of the world (II), 52 p. Japan Fisheries Resources Conservation Association, Tokyo, Japan. [In Japanese.]
Ogawa, Y., and T. Ishida
1989. Hydrographic conditions governing fluctuations in the catch of *Thunnus thynnus* by set-nets along the Sanriku coast. Bull. Tohoku Reg. Fish. Res. Lab. 51:23–39. [In Japanese.]
Okachi, I.
1963. Studies on the distribution and structure of the fish fauna in the Japan Sea by—catch statistics. II. Supplement of seasonal distribution and fishing condition of the bluefin tuna. Bull. Jap. Sea Reg. Fish. Res. Lab. 11:9–21. [In Japanese.]
Okiyama, M.
1974. Occurrence of the postlarvae of bluefin tuna, *Thunnus thynnus*, in the Japan Sea. Bull. Japan Sea Reg. Fish. Res. Lab. 25:89–97. [In Japanese.]
Orange, C. J., and B. D. Fink.
1963. Migration of a tagged bluefin tuna across the Pacific Ocean. Calif. Fish Game, 49:307–309.
Radovich, J.
1961. Relationships of some marine organisms of the northwest Pacific to water temperatures particularly during 1957 through 1959. Fish Bull. Calif. Dep. Fish Game 112: 1–62.
Shingu, C., I. Warashina, and N. Matsuzaki.
1974. Distribution of bluefin tuna exploited by longline fishery in the western Pacific Ocean. Bull. Far Seas Fish. Res. Lab. 10:109–140. [In Japanese.]
Smith, P. and D. Goodman.
1986. Determining fish movements from an "Archival" tag: precision of geographical positions made from a time series of swimming temperature and depth. U.S. Dep. Commer., NOAA-TM-NMFS-SWFC-60, 13 p.
Stevens, E. D., and F. G. Carey
1981. One why of the warmth of warm-bodied fish. Am. J. Physiol. 240:R151–R155.
Sund, P. N., M. Blackburn, and F. Williams.
1981. Tunas and their environment in the Pacific Ocean: a review. Oceanogr. Mar. Biol. 19:443–512.
Ueyanagi, S.
1969. Observations on the distribution of tuna larvae in the Indo-Pacific Ocean with emphasis on the delineation of the spawning areas of albacore, *Thunnus alalunga*. Bull. Far Seas Fish. Res. Lab. 2:177–256. [In Japanese.]

Welch, D. W., and J. P. Eveson
1999. An assessment of light-based geoposition estimates from archival tags. Can. J. Fish. Aquat. Sci. 56:1317–1327.
Yabe, H., S. Ueyanagi, and H. Watanabe.
1966. Studies on the early life history of bluefin tuna *Thunnus thynnus* and on the larvae of the southern bluefin tuna *T. maccoyii*. Rep. Nankai Reg. Fish. Res. Lab. 23:95–129. [In Japanese.]
Yamanaka, H.,
1982. Fishery biology of the bluefin tuna resource in the Pacific Ocean, 140 p. Japan Fisheries Resources Conservation Association, Tokyo, Japan. [In Japanese.]
Yokota, T., M. Toriyama, F. Kanai, and S. Nomura.
1961. Studies on feeding habit of fishes. Rep. Nankai Reg. Fish. Res. Lab. 14:1–234. [In Japanese.]
Yonemori, T.
1989. To increase the stock level of the highly migrated pelagic fish. *In* Marine ranching (Agriculture, Forestry and Fisheries Research Council secretariat, eds.), p. 9–59. Koseisha-Koseikaku, Tokyo, Japan. [In Japanese, the title was translated by authors.]
Yorita, T.
1976. Bluefin tuna in the Sea of Japan in Hokkaido. Monthly report of Hokkaido Fishery Experimental Station, 33(3): 2–11. [In Japanese.]
Yukinawa, M., and Y. Yabuta.
1967. Age and growth of bluefin tuna, *Thunnus thynnus* (Linnaeus), in the north Pacific Ocean. Rep. Nankai Reg. Fish. Res. Lab. 25:1–18. [In Japanese.]

Swimming depth, ambient water temperature preference, and feeding frequency of young Pacific bluefin tuna (*Thunnus orientalis*) determined with archival tags

Tomoyuki Itoh
Sachiko Tsuji

National Research Institute of Far Seas Fisheries
5-7-1 Shimizu-Orido, Shizuoka
Shizuoka, 424-8633, Japan
Email address (for T. Itoh): itou@fra affrc.go jp

Akira Nitta

Japan NUS Co., Ltd.
Loop-X Bldg.
3-9-15 Kaigan, Minato
Tokyo, 108-0022, Japan

Abstract—We investigated the migration and behavior of young Pacific bluefin tuna (*Thunnus orientalis*) using archival tags. The archival tag measures environmental variables, records them in its memory, and estimates daily geographical locations based on measured light levels. Of 166 archival tags implanted in Pacific bluefin tuna that were released at the northeastern end of the East China Sea from 1995 to 1997, 30 tags were recovered, including one from a fish that migrated across the Pacific. This article describes swimming depth, ambient water temperature, and feeding frequency of young Pacific bluefin tuna based on retrieved data. Tag performance, effect of the tag on the fish, and horizontal movements of the species are described in another paper.

Young Pacific bluefin tuna swim mainly in the mixed layer, usually near the sea surface, and swim in deeper water in daytime than at nighttime. They also exhibit a pattern of depth changes, corresponding to sunrise and sunset, apparently to avoid a specific low light level. The archival tags recorded temperature changes in viscera that appear to be caused by feeding, and those changes indicate that young Pacific bluefin tuna commonly feed at dawn and in the daytime, but rarely at dusk or at night. Water temperature restricts their distribution, as indicated by changes in their vertical distribution with the seasonal change in depth of the thermocline and by the fact that their horizontal distribution is in most cases confined to water in the temperature range of 14–20°C.

Manuscript approved for publication 22 October 2002 by Scientific Editor.
Manuscript received 3 January 2003 at NMFS Scientific Publications Office.
Fish Bull. 101:535–544 (2003).

Swimming behavior of *Thunnus* species and its relation to various environmental factors have been examined mainly by acoustic tracking (e.g. Carey and Lawson, 1973; Laurs et al., 1977; Carey and Olson, 1982; Holland et al., 1990b; Cayré, 1991; Cayré and Marsac, 1993; Block et al., 1997). Acoustic tracking has also been applied to young Pacific bluefin tuna (*T. orientalis*): to one fish tracked for three hours around Japan (Hisada et al.[1]), and to six fish tracked for several days each in the eastern Pacific Ocean (Marcinek et al., 2001). Acoustic tracking can monitor fish movement, behavior, and even physiological conditions on a time scale of seconds. However, the duration of monitoring any one fish is generally limited to several days at most because of the short life of the tracking transmitter. This limitation, together with the high cost of adequate ship-time, generally makes it difficult to monitor the behavior of a large number of fish over a long period of time.

An archival tag is an electronic device that measures environmental variables and records raw or processed data in its memory. The archival tag can monitor animal behavior, its physiological conditions, and the several environmental factors that the animal is actually experiencing, simultaneously. Data can be collected for a much longer period than with acoustic tracking, if the tags are successfully retrieved. Recently, a type of archival tag that can estimate geographical locations has been developed. This type of tag has been applied to southern bluefin tuna *T. maccoyii* (Gunn and Block, 2001) and Atlantic bluefin tuna *T. thynnus* (Block et al., 1998a, 1998b). These reports show the remarkable value of the archival tag data for investigating fish migration and behavior.

We have implanted archival tags in young Pacific bluefin tuna since 1994 to investigate their migration and behavior. This article describes the results obtained from recovered tags and places special emphasis on vertical swimming behavior, preferred water temperature, and feeding frequency. Some insights regarding vertical swimming depth have already been reported in Kitagawa et al. (2000) who used some of the same data. We have described in another paper (Itoh et al., 2003) the performance of the archival tag used in the present study and the characteristics of young Pacific bluefin tuna migration based on data from these same tags.

[1] Hisada, K., H. Kono, and T. Nagai. 1984. Behavior of young bluefin tuna during migration. *In* Progress report of the marine ranching project 4, p. 1–7. Nat. Res. Inst. Far Seas Fish. Pelagic Fish Resource Division, 5-7-1 Shimizu-Orido, Shizuoka, 424-8633, Japan. [In Japanese, the title is translated by the authors.]

Materials and methods

The archival tag used in the present study (Northwest Marine Technology, Inc., Shaw Island, WA) had four sensors—for external temperature, internal temperature, pressure, and light intensity. The external and internal temperature sensors had a 0.2°C resolution and response times of three seconds and 20 seconds, respectively. Resolution of the pressure sensor was 1 m of depth between the surface and 126 m, then 3 m down to the scale limit of 510 m. The tags measured data every 128 seconds.

Two types of data files were created within the tag memory. One data file stored daily records containing date, estimated times of sunrise and sunset, water temperatures at 0 m, plus two other selectable depths (we selected 60 m and 120 m), and other information required or produced in the course of location estimates for each day. This file is referred to as the "summary file" in this article, and it stored daily data from the time the memory was last cleared.

The second data file contained unprocessed time series data records taken at 128-second intervals. The tag could record at any integer multiple of its measurement interval and a multiple of one was chosen. Each record consisted of external temperature, internal temperature, pressure, and light intensity, and corresponded to a known time. This file is referred to as the "detail file" in this article. It can hold about 54,000 records, or about 80 days of steady data at the high rate chosen—a small fraction of the tag's lifetime. The time-series memory was divided into two sections, and the size allocation between the two sections was determined by the user. The first section filled first and did not change thereafter. The second section filled next, but once full, it is then continually overwrote old data. Thus the first section always contained the earliest data seen in a tag deployment and the second always contained the latest data. We divided the detail file into two 40-day sections for releases in 1995 and 1996, and into 20- and 60-day sections for releases in 1997. Most of the analyses in this study were conducted with the detail file.

Prior to experiments on wild fish, we applied archival tags to three pen-held Pacific bluefin tuna from 93 to 97 cm in fork length (FL) at Kasasa in Kagoshima Prefecture (31°25'N, 130°11'E) in November 1994 to observe the effect of archival tag attachment and implantation on fish. One of the fish that had an archival tag inserted in its abdominal cavity was recovered 453 days after tag implantation, when the fish was caught for sale in the market.

Experiments on wild young bluefin tuna were conducted near Tsushima at the northeastern end of the East China Sea every November and December from 1995 to 1997. A total of 166 fish, ranging from 43 to 78 cm FL (age 0 or 1), were caught by chartered trolling vessels, tagged on the vessel by inserting archival tags into their abdominal cavities, and released immediately. Details of the tag, its performance, and the manner of tagging are described in Itoh et al. (2003).

Thirty of the 166 archival tags (18.1%) were recovered. The durations of the tags at sea were 50 days or less for 13 fish, 96–211 days for 13 fish, and 359–375 days for three fish, all recaptured around Japan. One additional fish was recaptured off the west coast of Mexico, on the east side of the Pacific Ocean, 610 days after release. Data could not be downloaded from one archival tag released in 1995 and recovered 30 days after release; all other tags yielded data.

Results

Sample records of swimming depth, water temperature, and temperature of fish viscera as recorded in the detail file are shown in Figure 1 for three days in winter and three days in summer. The fish changed swimming depth frequently with rapid dives and ascents. The water temperature changed little in winter, but it changed frequently and substantially corresponding to dives in summer. Visceral temperature changed gradually.

Diurnal and seasonal change of swimming depth

Differences between daytime and nighttime swimming depth, water temperature, visceral temperature, and the temperature difference between water and fish viscera (thermal excess) were examined by using the Mann-Whitney U test (P=0.05) with data in the detail file. Data taken during the hour before and the hour after both dawn and dusk (four hours in all) were excluded from the test in order to distinguish clearly between daytime and nighttime. For this purpose, dawn and dusk were taken as the times the tag sensed the first or final light of the day. The average swimming depth was significantly deeper during daytime for 70% of all recorded days, which accounts for the additional observation that the water temperature was significantly lower during daytime for 66% of the days. The visceral temperature was significantly higher during daytime for 71% of the days, and thermal excess was significantly larger during daytime for 85% of the days.

Fish spent about 40% of their time within a 0–9 m depth range and the time spent within each depth interval decreased as depth increased. This concentration in the 0–9 m depth range was observed at both daytime and nighttime, but was more pronounced at night (Fig. 2).

The vertical thermal profiles (Fig. 2) show the change of depth range of the surface mixed layer, the ocean layer that lies above the seasonal thermocline, for one year. Although young Pacific bluefin tuna aggregated in the 0–9 m depth range for almost all months, swimming depth was more broadly distributed in winter when the depth range of the mixed layer was greater (e.g. January and March). When the depth range of the mixed layer became less in summer (e.g. May and July), fish tended to concentrate near the sea surface. Then as the depth range of the mixed layer became greater in autumn (e.g. September and November), the vertical distribution of the tuna gradually expanded toward deeper water.

Vertical swimming behavior at dawn and dusk

The fish commonly showed a distinctive vertical movement at dawn and dusk. At dawn, after a slow and steady descent for about 40 minutes to reach to a maximum depth of 82 ±28 m (average ±SD), fish suddenly and rapidly ascended

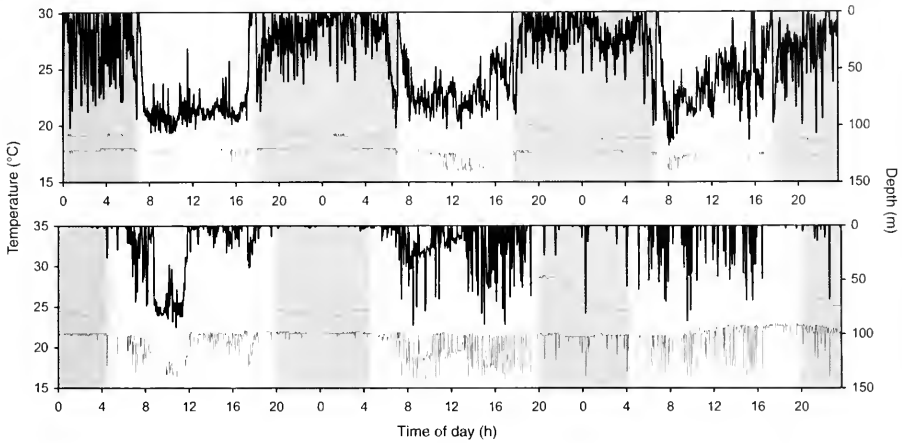

Figure 1

Sample records of swimming depth (thick solid line), water temperature (lower thin solid line), and temperature of viscera (upper thin solid line) for Pacific bluefin tuna from the detail files of two archival tags. Upper panel: records of a fish from 23 to 25 December 1995 in the East China Sea. Lower panel: records of another fish from 15 to 17 June 1997 in the East China Sea. Shadows indicate nighttime.

to near the sea surface (upper panel in Fig. 1, and Fig. 3). At dusk, after a rapid descent from near the sea surface to the maximum depth of 89 ±34 m, fish slowly and steadily ascended for about 40 minutes. The time that maximum depth was recorded was most frequently at four minutes before (or after) the time when the archival tag sensed the first (or final) light at dawn (dusk) for 29% (37%) of cases where this behavior was observed. The end (onset) of rapid ascents (descents) occurred most frequently at the time when the tag sensed the first (final) light, that is to say for 68% (49%) of all cases. The light detection threshold for the tags used in our study corresponded to an intensity in the blue-green transmission window of seawater (470 nanometers (nm) center, 60 nm width of the filter) of about 3×10^{-6} times the surface noon solar intensity on a clear day in that same spectral band. Because the light-sensitive region of the measurement stalk was located below the animal's body, we assumed that the eyes encountered a somewhat higher intensity than did the light sensor. Quick examination of tags in air in the early October revealed that the time when the archival tag sensed the first light at dawn or the final light at dusk was about 40 minutes before sunrise or about 40 minutes after sunset, respectively. Some combination of these vertical swimming behaviors was observed in 1081 of 1452 days (74%) during which the detail file data were available for both dawn and dusk. They occurred at both dawn and dusk in 679 days (47%), only at dawn in 77 days (5%), and only at dusk in 325 days (22%).

Occurrences of these behaviors differed by area and season (Table 1). The area was determined by using fish locations estimated as described in Itoh et al. (2003). The average occurrence of these depth excursions at dawn and dusk was as high as 87–88% in the East China Sea from November to January but decreased to 15–49% from February to June and October. In the Sea of Japan, the average occurrence was 4–39% in April, May, and September to November. In the Pacific Ocean, the behaviors were observed in 75–90% of days from May to July, in contrast to the relatively low occurrences within the East China Sea in the same season.

Water temperature

Water temperatures recorded in archival tags ranged from 8.3° to 28.4°C at 0 m depth, and 1.4° to 28.4°C when all depths were combined. A range of water temperatures that appeared to be preferred by young Pacific bluefin tuna was estimated. A simple frequency distribution of recorded water temperatures was inappropriate because fish could be forced to tolerate water out of their preferred temperature range because of a lack of water with a more favorable temperature within the geographical range accessible to the fish. Instead we compared the range of water temperature within the geographical area accessible to the fish with the frequency distribution of actual recorded water temperatures, grouped by year, month, and sea. We assumed that the accessible areas in each sea were those areas that a tag reported as its position. These include areas along the Japanese coast between 35° and 45°N in the Sea of Japan, 30–45°N in the western Pacific Ocean west of 160°E, and 25–45°N in the eastern Pacific Ocean east of 160°E. In

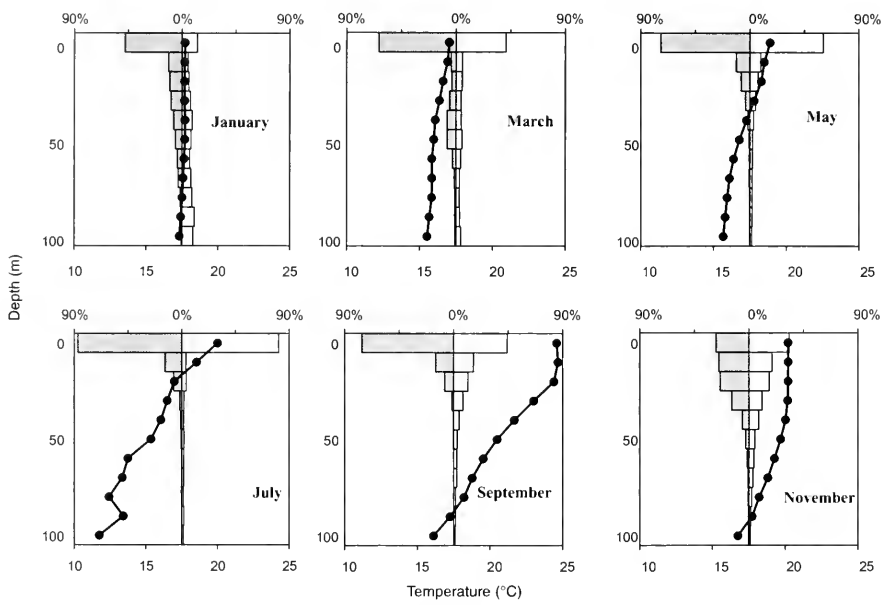

Figure 2

Vertical occurrence frequencies of young Pacific bluefin tuna in daytime (clear bar) and nighttime (shaded bar) and vertical thermal profile (line with dots) by month.

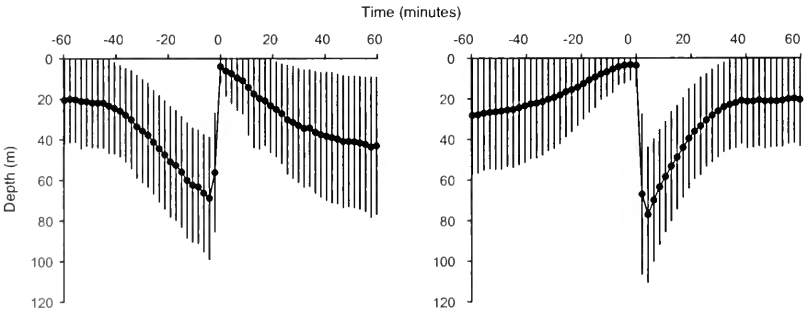

Figure 3

Average swimming depth of young Pacific bluefin tuna recorded by archival tags at dawn (left panel) and dusk (right panel). Times marked as 0 are the time just after the end of rapid ascent at dawn and just before the onset of rapid descent at dusk. All of records in which a rapid ascent or rapid descent occurred were averaged. Bar shows standard deviation.

the East China Sea, the area considered was enclosed by four points of 29°N–126°E, 29°N–128°E, 35°N–130°E, and 33°N–126°E, where the majority of estimated tag locations occurred. The temperature range in each area was derived from the sea-surface temperature maps published by the Japan Fisheries Information Service Center.

Table 1

The number of days during which swimming behaviors with rapid ascent at dawn and rapid descent at dusk were observed by area and month.

			Dawn			Dusk			
Area	Month	Number of fish	Total days	Observed days	Observed rate	Total days	Observed days	Observed rate	Average observed rate
East China Sea	1	7	87	73	84%	86	77	90%	87%
	2	1	23	6	26%	22	16	73%	49%
	3	2	36	11	31%	37	12	32%	31%
	4	7	66	24	36%	67	41	61%	49%
	5	10	220	51	23%	221	128	58%	41%
	6	8	182	17	9%	176	37	21%	15%
	10	1	24	4	17%	24	6	25%	21%
	11	23	132	109	83%	153	142	93%	88%
	12	29	487	388	80%	489	457	93%	87%
Sea of Japan	4	1	13		0%	12	1	8%	4%
	5	1	9	1	11%	9	1	11%	11%
	9	1	12		0%	12	4	33%	17%
	10	2	61	10	16%	61	22	36%	26%
	11	2	43	15	35%	42	18	43%	39%
Pacific Ocean	5	1	16	11	69%	16	13	81%	75%
	6	2	26	19	73%	26	25	96%	85%
	7	1	31	25	81%	31	31	100%	90%
Total			1468	764	52%	1484	1031	69%	61%

The tag temperature used in our comparison was the temperature at 0 m depth recorded in the summary file because that file contained a much larger number of days than that of the detail file. In support of this, we confirmed that the average water temperature over all depths for a day in the detail file had only slight differences of −0.1 ±0.7°C in average (range: −4.0–+4.3°C) from the temperature at 0 m recorded for the day in the summary file. Because the fish swam near the surface, the temperature recorded to represent 0 m depth also represented well the temperature at all depths where the fish actually swam. Frequencies of days were summed from the data for all individuals in one-degree temperature bins separated by year, by month, and by area, such as the East China Sea, the Sea of Japan, and the Pacific Ocean.

The water temperature recorded by archival tags commonly ranged from 14° to 20°C (Fig. 4). When water of this temperature range was located within an accessible area (e.g. many months in the East China Sea and the Pacific Ocean, and November in the Sea of Japan), almost all fish were found in such water. Where water temperature was higher (e.g. June 1996, June 1997, and between June and October 1998 in the East China Sea) or lower (e.g. May 1996 and April 1997 in the Sea of Japan), fish tended to choose water that was close to this range. However there were a few cases in which fish stayed in water with a temperature outside of this range (e.g. between July and September 1998 in the Sea of Japan) even when water of the 14–20°C range was accessible to them.

Visceral temperature and feeding events

Temperature of the fish viscera ranged from 13.0° to 30.9°C. It was usually higher than the water temperature and the thermal excess for a given individual ranged from 1.3° to 4.6°C, and averaged 3.0° ±1.0°C. The visceral temperature changed in parallel with the water temperature all year (Fig. 5).

In preliminary experiments, pen-held fish were fed completely thawed mackerel of 20–30 cm FL twice a day at approximately 900 h and 1500 h. The following changes in visceral temperature before and after feeding were generally observed (Fig. 6). All figures given below regarding thermal excess and timing after feeding are average values. The visceral temperature in a stable state just before feeding (n=5) was 3.7°C higher than ambient water temperature. This thermal excess decreased to 2.3°C at 22 minutes after feeding, and then increased to 7.6°C at 7.7 hours after feeding. Then it slowly decreased again and reached a stable thermal excess of 3.1°C at 21.0 hours after feeding. When the fish fed again before the visceral temperature stabilized (n=7), with the thermal excess still as high as 6.8°C, the thermal excess reached a high of 8.5°C but the increase after feeding was 1.7°C, much smaller than that observed in the previous case (3.9°C). The time required to reach the highest visceral temperature and the time to change back to a stable state were similar to the previous case. When the fish were not fed, because of rough sea conditions, the visceral temperature stayed stable all day (e.g. 16 January on Fig. 6).

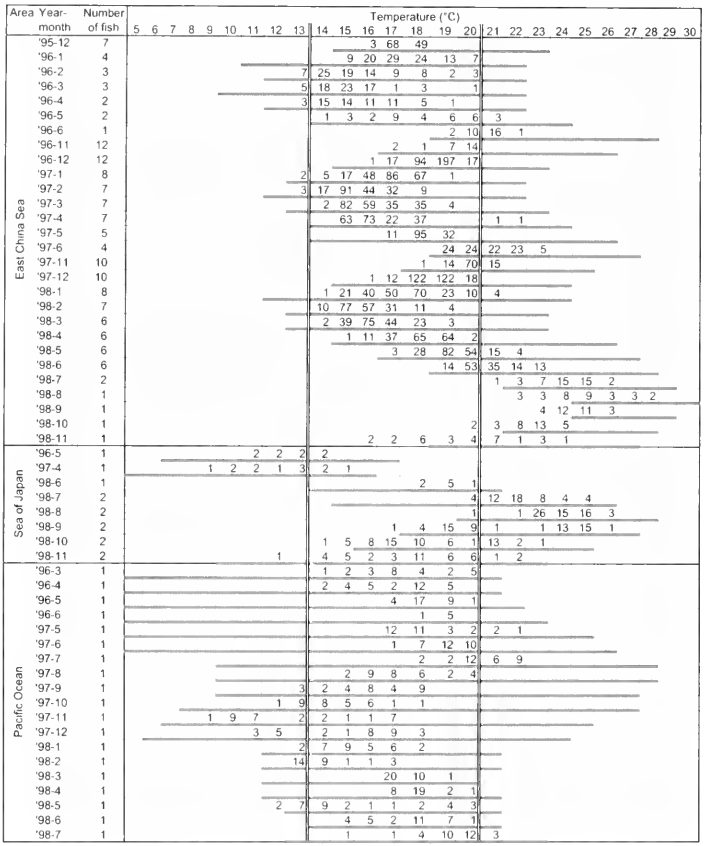

Figure 4

Frequencies of sea-surface water temperatures for young Pacific bluefin tuna with archival tags. The number given is the sum (over all individuals) of days in the category based on temperature at 0 m depth from the summary files. Gray, thick bars indicate the sea-surface temperature range that appeared to be accessible to the fish in each month.

In the detail files obtained from wild fish, the following three types of visceral temperature changes were identified as indicators of feeding (Fig. 7). Type A: a sharp decrease of 1–2°C followed by an increase above the initial temperature. Type B: an increase above the initial temperature, preceded by either no decrease or a slow decrease. Type C: a sharp decrease of 1–2°C followed by a return to the initial temperature. In addition, in only cases where the visceral temperature changes could not be explained by water temperature changes were they counted as being caused by feeding. For example, a slow decrease of visceral temperature when the fish dived into cold water was not counted as a feeding event. Cases where the water temperature changed frequently were also excluded as too difficult to interpret.

Feeding events were observed in 942 days out of 1494 total recorded days (63%). Because it was found that fish did not feed normally for approximately the first 30 days after release (Itoh et al., 2003), data from the first 60 days after release were excluded in the following description. After exclusion of data for the first 60 days, feeding events were observed in 726 out of the remaining 807 recorded days (90%). The number of daily feeding events ranged from zero to ten, with an average of 1.8 ±1.4. Feeding events occurred most frequently in the daytime (69% of all observed feeding events more than 60 days after release), followed by dawn with 27% (Fig. 8). Feeding events rarely occurred at dusk and at night, accounting for only 1% and 3% of the total feeding events, respectively. For this analysis, dawn

and dusk were defined as explained above, a one-hour period centered on the time of first or last detected daylight. Changes in visceral temperature of "type B" (increase only) were observed most frequently (51.4% of total observed feedings), followed by "type C" (decrease only, 45.2%). Bipolar events (type A) were as few as 3.5%.

When averaged over individual months, the number of feeding events per day per individual ranged from 0.9 in January to 2.2 in June and averaged 1.5. Feeding events were observed all year, although they were slightly more frequent in May and June than in other months (Fig. 9).

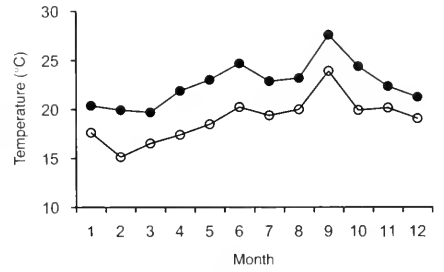

Figure 5

Monthly change of average water temperature (○) and average visceral temperature (●) in young Pacific bluefin tuna with archival tags. Average values of each individual were averaged.

Discussion

Diurnal and seasonal change of swimming depth

Young Pacific bluefin tuna were previously assumed to swim near the sea surface based on the fact that most of the catch was made by surface fishing gear and fish schools were observed at the sea surface (Yabe et al., 1953). However, details of their vertical swimming behavior and relationships between their behaviors and oceanic structures have not been well investigated. Recently, Marcinek et al. (2001) observed during an acoustic tracking experiment over several days that Pacific bluefin tuna in the eastern Pacific Ocean spent the majority of their time in the top portion of the water column. Our archival tag data showed that young bluefin tuna in the western Pacific Ocean also ordinarily stayed within the surface mixed layer and most frequently near sea surface, regardless of the time of day or the season. The vertical distribution of fish changed according to the seasonal change in depth range of the surface mixed layer and appeared to be controlled by the depth of the thermocline. Restriction by the thermocline was also observed for yellowfin tuna (*T. albacares*) and bigeye tuna (*T. obesus*) (Carey and Olson, 1982; Holland et al., 1990b; Cayré and Marsac, 1993; Block et al., 1997). Occasionally young Pacific bluefin tuna dived through the thermocline into deep, cooler water, but they returned to the surface mixed layer after a short period.

Diurnal change in swimming depth, i.e. deeper swimming depth during daytime, was reported by acoustic tracking studies not only for *Thunnus* species, such as yellowfin tuna (Carey and Olson, 1982; Holland et al., 1990b; Cayré, 1991; Yonemori[2]) and bigeye tuna (Holland et al., 1990b), but also for other large pelagic species, such as skipjack tuna, *Katsuwonus pelamis* (Yuen, 1970; Dizon et al., 1978); swordfish, *Xiphias gladius* (Carey and

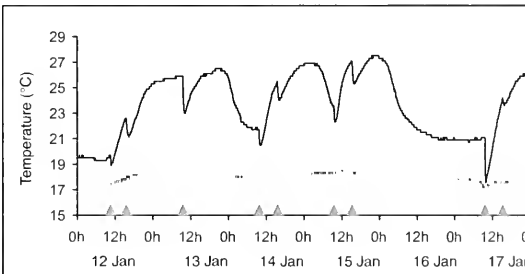

Figure 6

Visceral temperature (thick line) and water temperature (thin line) of a pen-held young Pacific bluefin tuna recorded by an archival tag. Triangles indicate the time of feeding.

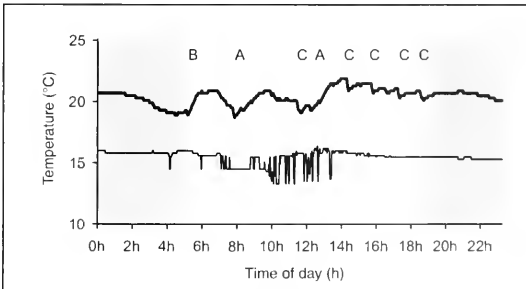

Figure 7

An example of visceral temperature change in a wild young Pacific bluefin tuna recorded by an archival tag. Visceral temperature (thick line) and water temperature (thin line) are shown. Shadows indicate nighttime. Data are from a fish in the Sea of Japan on 2 May 1996. A, B, and C indicate the types of visceral temperature changes described on page 540.

[2] Yonemori, T. 1982. Swimming behavior of tunas by the use of sonic tags—a study particularly of swimming depth. Far Seas Fish. Res.Lab. Newsletter 44:1–5. Pelagic Fish Resource Division, 5-7-1 Shimizu-Orido, Shizuoka, Shizuoka, 424-8633, Japan. [In Japanese.]

Robison, 1981); blue marlin, *Makaira nigricans* (Holland et al., 1990a); mako shark, *Isurus oxyrinchus*; and blue shark, *Prionace glauca* (Carey and Scharold, 1990). However some reports did not note any difference in swimming depth between day and night, such as that of Block et al. (1997) for yellowfin tuna, Cayré (1991) for skipjack tuna, and Brill et al. (1993) for striped marlin, *Tetrapturus audax*. The swimming depth of young bluefin tuna recorded by the archival tags in the present study was deeper during the day for 70% of recorded days. This finding agrees with the speculation made by Carey and Olson (1982) that a deeper swimming depth in the daytime is a common feature for large pelagic fish.

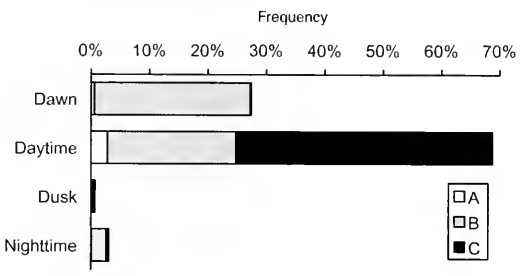

Figure 8

Frequency of feeding events of young Pacific bluefin tuna by period within a day. Only data taken more than 60 days after release were used. A, B, and C indicate the types of temperature changes of viscera described on page 540.

Vertical swimming behavior at dawn and dusk

A characteristic vertical movement pattern was found in young Pacific bluefin tuna. They dived gradually and constantly for about 40 minutes and then rapidly ascended to the sea surface at dawn. Inverse behavior were observed at dusk. The same behavior was reported in larger size Pacific bluefin tuna in the eastern Pacific Ocean and in yellowfin tuna (Block et al., 1997; Marcinek et al., 2001). The percentage of days when this behavior was observed varied according to the season and area. This variation was commonly observed in individuals as well as in the group as a whole.

Two potential reasons for this behavior were considered. The first one was avoidance of a specific range of light intensities. The times of onset and end of the behavior are apparently related to the time of sunrise and sunset. Assuming that young Pacific bluefin tuna dislike a specific light intensity range, we describe their vertical movements at dawn and at dusk as follows. About 80 minutes before sunrise when the light intensity at the sea surface reaches a specific value near the lower boundary of the avoided range, fish begin descending into water with lower light intensity. About 40 minutes before sunrise when the light intensity in deep water reaches that avoided range, the fish rapidly ascend almost to sea surface, and as the light brightens further, gradually expand into their normal distribution pattern while staying within the range of water depths where light intensities exceed the avoided low-intensity range. A possible reason for avoiding a specific intensity range might be an increased risk of predation at intensities where tuna see less well than some predator that hunts visually.

The other potential reason for the characteristic vertical movements is feeding. It is well known that some small animals show diurnal vertical migration, i.e. they descend gradually as the light level increases toward dawn and rise again at dusk. Young Pacific bluefin tuna following these species to feed on them would show similar behavior. However, young Pacific bluefin tuna were observed to feed only at dawn, not at dusk, although the characteristic vertical behavior was observed at both dawn and dusk. In addition, rapid ascents and descents at a specific time with respect to sunrise and sunset could not be explained by the vertical migration behavior of bait species. Therefore, feeding seems not to be a primary cause of the vertical migration in young Pacific bluefin tuna.

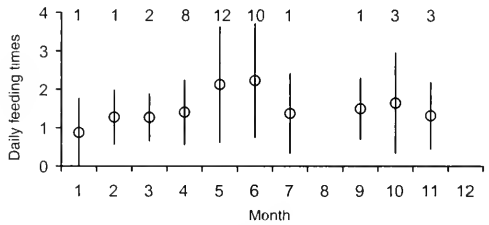

Figure 9

Average frequency of feeding events by month for young Pacific bluefin tuna. Only data taken more than 60 days after release were used. The number above each point indicates the number of individuals contributing to the average. Bars show standard deviations.

Generally speaking, fishermen consider dawn and dusk to be good times for catching Pacific bluefin tuna. The archival tag records showed that young Pacific bluefin tuna did not usually feed at dusk, although tag records showed that fish aggregated very close to the sea surface after their rapid ascent at dawn and before their rapid descent at dusk. Judging from this behavior, good fishing seemed to be caused by a concentration of fish near the sea surface rather than by the feeding activities. Moreover, the low light level at these times would make it difficult for fish to distinguish between artificial bait with a hook and live prey.

Preferred water temperature

Water temperature is thought to be one of the most important environmental factors controlling the distribution of young Pacific bluefin tuna (Sund et al., 1981; Koido and Mizuno, 1989; Ogawa and Ishida, 1989). Kitagawa et al. (2000) attached importance to the gradient of water temperature; however Uda (1957) emphasized the absolute value of temperature, although his study was presumably for large-size fish. Data from the archival tags indicated that young Pacific bluefin tuna seemed to prefer to remain in water of 14–20°C. When there was no accessible water within this temperature range, the fish tended to stay in water of a temperature as close as possible to this range. In addition, archival tags showed that the vertical distribution of young Pacific bluefin tuna was restricted by the thermocline, even when the temperature below the thermocline was in the tuna's preferred temperature range (14–20°C). These observations support the importance of water temperature as shown in previous studies and suggest that both the absolute value and the gradient of water temperature are important as environmental factors controlling the distribution of young Pacific bluefin tuna.

Feeding

Visceral temperature of pen-held Pacific bluefin tuna with archival tags changed in a specific way during feeding. Stomach temperature changes have also been observed in pen-held giant bluefin tuna in the Atlantic and in pen-held southern bluefin tuna (Carey et al., 1984; Gunn et al., 2001). The cycle of visceral temperature change for young Pacific bluefin tuna was completed in 21 hours (shorter than that observed in previous studies of 1.5 to 2 days) probably due to the smaller size of the fish. Similar visceral temperature changes were also noted in the records of archival tags recovered from wild fish, ranging from a distinct pattern the same as that observed in pen-held fish (type A) to less distinct ones such as type B or type C, which were observed more frequently. All of these changes could be distinguished quite easily from gradual decreases of visceral temperature when fish dived into cold water. Therefore, we assumed that these three types of temperature changes were caused by feeding. Temperature changes of type A could be expected if fish consumed a large amount of food at one time as they do when fed in a pen. However, wild fish may seldom have an opportunity for such large meals, and the apparently more frequent small meals would be expected to cause the less dramatic visceral temperature changes of types B or C.

In the present study, a visceral temperature change was taken to indicate feeding only when that change could not be explained by a change in water temperature. Also, when the water temperature changed very frequently, it was difficult to decide whether water temperature could account for a feeding event and it was not counted as such. Finally it is possible that feeding might not cause a recognizable change in visceral temperature. As a result of these three factors the feeding frequency estimated in our study might have been underestimated.

Frequencies of feeding events did not change much over the year, although there was a slightly higher frequency in early summer. Growth in length of young Pacific bluefin tuna is known to become slow in winter (Yukinawa and Yabuta, 1967; Bayliff, 1993). Because fish weight at a length was constant throughout the year for wild young Pacific bluefin tuna (Itoh, 2001), food consumption in winter appears not to be used for increasing weight at a length. We did not reach a conclusion on this question and further investigation of seasonal change in food items and of the physiology of tuna is needed.

Acknowledgments

We thank the staff of Marino Forum 21 and the Kagoshima Fisheries Experimental Station for their cooperation in the pe-held fish experiment. We also thank troll fishermen, staff in the Kamiagata Fisheries Cooperative Association, the Tsushima Fisheries Extension Service, and the Nagasaki Fisheries Experimental Station for their cooperation with the experiment on wild fish. We greatly acknowledge fishermen, consumers, and staff at the Inter-American Tropical Tuna Commission for their kindness in returning recovered archival tags bearing the information necessary for our study. We especially thank J. Gunn at CSIRO for giving us valuable information about implanting the archival tag in fish. We are also grateful to the staff of Northwest Marine Technology Inc. and Tanaka Sanjiro Co., Ltd., for providing us with tags. We would like to thank P. Ekstrom of Northwest Marine Technology Inc. for his critical review and help with the English text. We thank our staff in Japan NUS Co., Ltd., the Suidosya Co., Ltd., and the National Research Institute of Far Seas Fisheries, and also T. Kitagawa in the Ocean Research Institute of the University of Tokyo, for their efforts in regard to implantation of the tags in fish. We gratefully acknowledge S. Kume of Japan NUS Co., Ltd., N. Baba of Fishery Research Agency, Z. Suzuki, and Y. Uozumi of National Research Institute of Far Seas Fisheries for their critical review.

Literature cited

Bayliff, W. H.
1993. Growth and age composition of northern bluefin tuna, *Thunnus thynnus*, caught in the eastern Pacific Ocean, as estimated from length-frequency data, with comments on trans-pacific migrations. Bull. IATTC 20:503–540.

Block, B. A., H. Dewar, E. V. Freund, C. Farwell, and E. D. Prince.
1998a. A new satellite technology for tracking the movements of Atlantic bluefin tuna. Proc. Natl. Acad. Sci. USA 95:9384–9389.

Block, B. A., H. Dewar, T. Williams, E. D. Prince, C. Farwell, and D. Fudge.
1998b. Archival tagging of Atlantic bluefin tuna (*Thunnus thynnus thynnus*). Mar. Tech. Soc. J. 32: 37–46.

Block, B. A., J. E. Keen, B. Castillo, H. Dewar, E. V. Freund, D. J. Marcinek, R. W. Brill, and C. Farwell.
1997. Environmental preferences of yellowfin tuna (*Thunnus albacares*) at the northern extent of its range. Mar. Biol. 130:119–132.

Brill, R. W., D. B. Holts, R. K. C. Chang, S. Sullivan, H. Dewar, and F. G. Carey.
1993. Vertical and horizontal movements of striped marlin (*Tetrapturus audax*) near the Hawaiian Islands, determined by ultrasonic telemetry, with simultaneous measurement of oceanic currents. Mar. Biol. 117:567–574.

Carey, F. G., J. W. Kanwisher, and E. D. Stevens.
1984. Bluefin tuna warm their viscera during digestion. J. Exp. Biol. 109:1–20.

Carey, F. G., and K. D. Lawson.
1973. Temperature regulation in free-swimming bluefin tuna. Comp. Biochem. Physiol. 44A:375–392.

Carey, F. G., and R. J. Olson
1982. Sonic tracking experiments with tunas. ICCAT Collective Volume of Scientific Papers XVII. 2:458–466.

Carey, F. G., and B. H. Robison
1981. Daily patterns in the activities of swordfish, *Xiphias gladius*, observed by acoustic telemetry. Fish. Bull. 79: 277–292.

Carey, F. G., and J. V. Scharold
1990. Movements of blue sharks (*Prionace glauca*) in depth and course. Mar. Biol. 106:329–342.

Cayré, P.
1991. Behavior of yellowfin tuna (*Thunnus albacares*) and skipjack tuna (*Katsuwonus pelamis*) around fish aggregating devices (FADs) in the Comoros Islands as determined by ultrasonic tagging. Aquat. Living. Resour. 4:1–12.

Cayré, P. and F. Marsac.
1993. Modeling the yellowfin tuna (*Thunnus albacares*) vertical distribution using sonic tagging results and local environmental parameters. Aquat. Living Resours. 6:1–14.

Dizon, A. E., R. W. Brill, and H. S. H. Yuen.
1978. Correlations between environment, physiology, and activity and the effects on thermoregulation in skipjack tuna. *In* The pysiological ecology of tunas (G. D. Sharp and A. E. Dizon, eds.), p. 233–259. Academic Press, New York, NY.

Gunn, J., and B. Block.
2001. Advances in acoustic, archival, and satellite tagging of tunas. *In* Tuna: physiology, ecology, and evolution (B. A. Block and E. D. Stevens, eds.), p. 167–224. Academic Press, San Diego, CA.

Gunn, J., J. Hartog, and K. Rough.
2001. The relationship between food intake and visceral warming in southern bluefin tuna (*Thunnus maccoyii*). Can we predict from archival tag data how much a tuna has eaten? *In* Electronic tagging and tracking in marine fisheries (J. R. Sibert and J. L. Nielsen, eds.), p. 109–130. Kluwer Academic Publisher, Netherlands.

Holland, K. N., R. W. Brill, and R. K. C. Chang.
1990a. Horizontal and vertical movements of Pacific blue marlin captured and released using sportfishing gear. Fish. Bull. 88:397–402.
1990b. Horizontal and vertical movements of yellowfin and bigeye tuna associated with fish aggregating devices. Fish. Bull. 88:493–507.

Itoh, T.
2001. Estimation of total catch in weight and catch-at-age in number of bluefin tuna *Thunnus orientalis* in the whole Pacific Ocean. Bull. Nat. Res. Inst. Far Seas Fish. 38: 83–111. [In Japanese.]

Itoh, T., S. Tsuji, and A. Nitta.
2003. Migration patterns of young Pacific bluefin tuna (*Thunnus orientalis*) determined with archival tags. Fish. Bull. 101: 514–534.

Kitagawa, T., H. Nakata, S. Kimura, T. Itoh, S. Tsuji, and A. Nitta.
2000. Effect of ambient temperature on the vertical distribution and movement of Pacific bluefin tuna *Thunnus thynnus orientalis*. Mar. Ecol. Prog. Ser. 206:251–260.

Koido, T., and K. Mizuno.
1989. Fluctuation of catch for bluefin tuna (*Thunnus thynnus*) by trap nets in Sanriku coast with reference to hydrographic condition. Bull. Jpn. Soc. Fish. Oceanogr. 53: 138–152. [In Japanese.]

Laurs, R. M., H. S. H. Yuen, and J. H. Johnson
1977. Small-scale movements of albacore, *Thunnus alalunga*, in relation to ocean features as indicated by ultrasonic tracking and oceanographic sampling. Fish. Bull. 75: 347–355.

Marcinek, D. J., S. B. Blackwell, H. Dewar, E. V. Freund, C. Farwell, D. Dau, A. C. Seitz and B. A. Block.
2001. Depth and muscle temperature of Pacific bluefin tuna examined with acoustic and pop-up satellite archival tags. Mar. Biol. 138:869–885.

Ogawa, Y., and T. Ishida.
1989. Hydrographic conditions governing fluctuations in the catch of *Thunnus thynnus* by set-nets along the Sanriku coast. Bull. Tohoku Reg. Fish. Res. Lab. 51:23–39. [In Japanese.]

Sund, P. N., M. Blackburn and F. Williams.
1981. Tunas and their environment in the Pacific Ocean: a review. Oceanogr. Mar. Biol. 19:443–512.

Uda, M.
1957. A consideration of the long years trend of the fisheries fluctuation in relation to sea condition. Bull. Jap. Soc. Sci. Fish. 23:368–372

Yabe, H., N. Anraku, and T. Mori.
1953. Scombroid youngs found in the coastal seas of Aburatu, Kyusyu, in summer. Contribution of Nankai Reg. Fish. Res. Lab. 1:1–10. [In Japanese.]

Yuen, H. S. H.
1970. Behavior of skipjack tuna, *Katsuwonus pelamis*, as determined by tracking with ultrasonic devices. J. Fish. Res. Board Canada 27:2071–2079.

Yukinawa, M., and Y. Yabuta.
1967. Age and growth of bluefin tuna, *Thunnus thynnus* (Linnaeus), in the north Pacific Ocean. Rep. Nankai Reg. Fish. Res. Lab. 25:1–18. [In Japanese.]

Demersal groundfish densities in trawlable and untrawlable habitats off Washington: implications for the estimation of habitat bias in trawl surveys

Thomas Jagielo
Annette Hoffmann
Jack Tagart
Washington Department of Fish and Wildlife
600 Capitol Way N
Olympia, Washington 98501-1091
E-mail address (for T. Jagielo): jagieth|@dfw.wa.gov

Mark Zimmermann
National Marine Fisheries Service
7600 Sandpoint Way NE
Seattle, Washington 98115-0070

Abstract—Demersal groundfish densities were estimated by conducting a visual strip-transect survey via manned submersible on the continental shelf off Cape Flattery, Washington. The purpose of this study was to evaluate the statistical sampling power of the submersible survey as a tool to discriminate density differences between trawlable and untrawlable habitats.

A geophysical map of the study area was prepared with side-scan sonar imagery, multibeam bathymetry data, and known locations of historical NMFS trawl survey events. Submersible transects were completed at randomly selected dive sites located in each habitat type. Significant differences in density between habitats were observed for lingcod (*Ophiodon elongatus*), yelloweye rockfish (*Sebastes ruberrimus*), and tiger rockfish (*S. nigrocinctus*) individually, and for "all rockfish" and "all flatfish" in the aggregate. Flatfish were more than ten times as abundant in the trawlable habitat samples than in the untrawlable samples, whereas rockfish as a group were over three times as abundant in the untrawlable habitat samples.

Guidelines for sample sizes and implications for the estimation of the continental shelf trawl-survey habitat-bias are considered. We demonstrate an approach that can be used to establish sample size guidelines for future work by illustrating the interplay between statistical sampling power and 1) habitat specific-density differences, 2) variance of density differences, and 3) the proportion of untrawlable area in a habitat.

Manuscript approved for publication 12 February 2003 by Scientific Editor.
Manuscript received 4 April 2003 at NMFS Scientific Publications Office.
Fish Bull. 101:545–565 (2003).

Despite their utility, trawl surveys cannot obtain quantitative samples from rough, rocky habitats, and thus have a limited ability to sample all habitats representatively (Uzmann et al., 1977; Kulbicki and Wantiez, 1990; Krieger, 1993; Gregory et al., 1997). Since 1977, triennial bottom trawl surveys have been used to estimate the abundance of commercially and recreationally exploited groundfish species in the continental shelf waters off Washington, Oregon, and California (Shaw et al., 2000). The data generated from these NMFS surveys are often a key component of groundfish stock assessments which are used to set levels of acceptable biological catch (ABC) for selected species (PFMC, 2001). Clearly, proper interpretation of these survey data with respect to fish habitat preferences is an important part of developing unbiased stock assessments for fisheries management.

In trawl survey methodology, population biomass is related to *CPUE* by the following equation (Dark and Wilkins, 1994):

$$B_i = \frac{A_i}{a_i}\left(\overline{CPUE}_i \times \frac{1}{q}\right),$$

where i = area-depth stratum;
B_i = estimated biomass in the ith area-depth stratum;
A_i = total area in the ith stratum;
a_i = total area swept during a standard trawl haul in stratum i;
$\overline{CPUE}_i$ = mean catch per unit of effort in the ith stratum; and
q = the catchability coefficient of the sampling trawl.

For this model to be an unbiased estimator of abundance, it is necessary to assume that the area sampled by the trawl is representative of the entire area-depth stratum of interest (i.e. a_i is representative of A_i). Validating this assumption becomes particularly important where untrawlable habitat comprises a significant proportion of the total area assessed, and where species composition and density vary between habitats. We shall refer to error in trawl survey estimates of abundance due to differences in groundfish density between habitat types as the trawl-survey habitat-bias.

The trawl-survey habitat-bias may be substantial on the west coast continental shelf because of the considerable spatial extent of untrawlable habitat in some management regions (Shaw et al., 2000). It is also widely recognized that demersal groundfish species composition and density can vary considerably by bottom type (Richards, 1986;

Matthews and Richards, 1991; Stein et al.,1992; O'Connell and Carlile, 1993; Gregory et al., 1997; Krieger and Ito, 1999; Nasby, 2000; Yoklavich et al., 2000). Thus, there is considerable interest in evaluating alternative survey tools.

One alternative to trawl surveys that has gained increased attention in recent years is the method of direct observation of the seafloor, typically conducted with a remotely operated vehicle (ROV) or with an occupied submersible (Auster et al., 1989; Krieger, 1993; Caimi et al., 1993; Adams et al., 1995; Gregory et al., 1997; Nasby, 2000). We evaluated the sampling power of the benthic video-strip transect method, using videotapes of the sea floor collected *in situ* with an occupied submersible. Our goal was to judge the feasibility of using this approach to provide meaningful comparisons of demersal groundfish densities between trawlable and untrawlable habitats on spatial scales large enough to be useful for west coast fisheries management.

We prepared a geophysical map of the bottom and conducted a submersible survey at a study site located on the continental shelf off Cape Flattery, Washington. Our objective was to provide guidelines on sample sizes (number of submersible transects) that would be needed to characterize differences in density between the two habitat types, and specifically, sample sizes that would be needed to estimate the trawl survey habitat bias in subsequent studies designed to cover wider geographic areas. The study was structured to answer the following questions: 1) what species occupy trawlable and untrawlable habitats off Washington; 2) what magnitude of density differences can be expected between trawlable and untrawlable habitats; 3) what is the variability of fish density within each habitat type; and 4) what sample sizes are required to estimate density differences between habitats, and the trawl survey habitat bias, in a statistically reliable manner. Our focus was on the benthic species and species groups that could be assessed reliably with our submersible survey method; primarily rockfish (*Sebastes* spp.), lingcod (*Ophiodon elongatus*), and flatfish (Pleuronectiformes).

Materials and methods

Study site

Selection of the study site was aided by examination of historical NMFS trawl survey records and Washington Department of Fish and Wildlife (WDFW) trawl fishery logbook data. We chose a rectangular area west of the Point of Arches, Washington, which extends from the Juan de Fuca Canyon in the east (125°17′W) to Nitinat Canyon in the west (125°37′W) and ranges from 48°13′ in the south to 48°16′ in the north (Fig. 1). We selected this area because 1) this portion of the Washington coast has been the site of a productive groundfish fishery since the 1940s (Alverson 1951), 2) this location has been surveyed tri-annually since 1977 as part of the NMFS west coast shelf survey, 3) the area has demersal groundfish species of interest, and 4) the area contains both trawlable and untrawlable habitats. The seafloor of this area was sculpted and shaped by ice movements during the late Pleistocene period (approximately 18–20 thousand years ago) and is characterized by boulder fields resulting from glacial deposition that cover substantial portions of the area (Goldfinger[1]). Planning for the submersible survey required geodetically precise knowledge of the seafloor characteristics of the study area. This was facilitated by conducting geophysical surveys and by preparing a detailed map, which was instrumental to the submersible survey design.

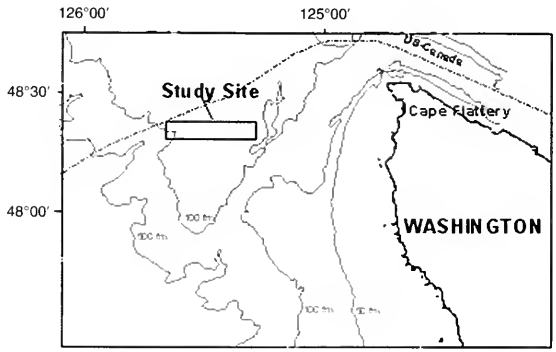

Figure 1

Location of the study area (marked "study site" on map) on the continental shelf off Washington State.

Geophysical surveys and map preparation

Geophysical surveys of the study site were conducted by collecting side-scan sonar and multibeam bathymetry data simultaneously during a five-day effort on board the USN *Agate Passage* (YP-697) in May 1998. Slant-range-corrected side scan sonar data were collected by using a Waverly widescan 100-kHz system, with a swath width of 800 m. Eighteen parallel track lines were conducted with 100% overlap. The resulting imagery was assembled into a mosaic map of the bottom relief for a rectangular area measuring approximately 5.6 by 24.8 km (13,888 hectares). Bathymetric data, with resolution on the order of ±0.4 m were collected with a Reson Model 8101 multibeam bathymetry system. The multibeam bathymetry data were processed to produce a detailed map of the bottom topography with 1-m depth contour intervals.

Map overlays were prepared that showed the locations of trawl survey events and trawl fishery tows. Detailed NMFS records were used to identify the location of various events associated with historical surveys of the area. The NMFS survey event types included good hauls, bad hauls, short hauls (tows ended early because of rough bottom),

[1] Goldfinger, C. 2001. Personal commun. Department of Geology, Oregon State University, Corvalis, OR 97331.

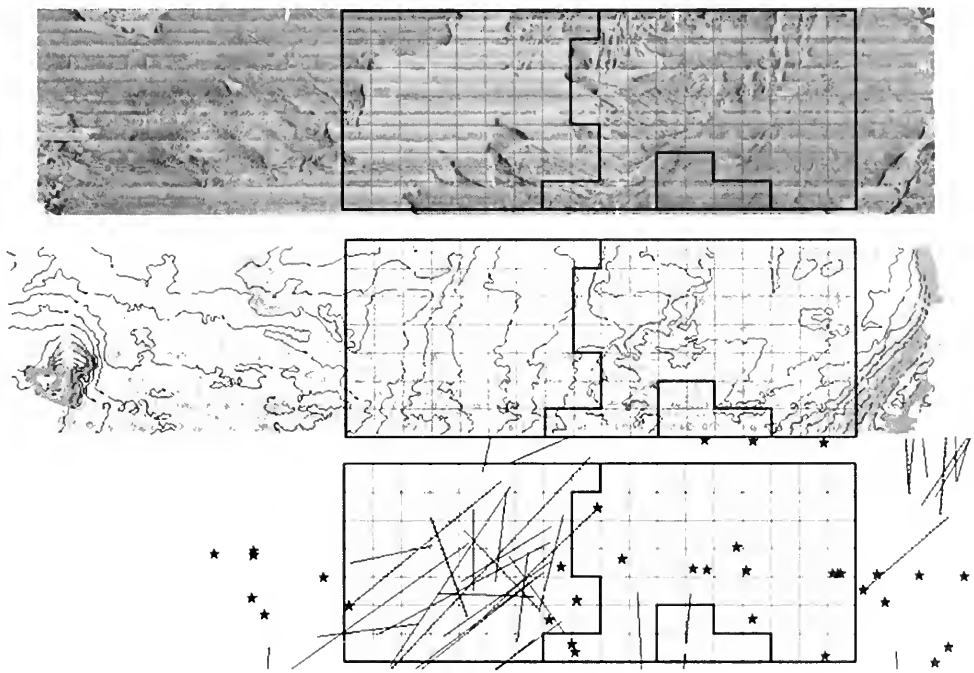

Figure 2

Geophysical map of the study area with associated overlays. Area outlined in bold is the submersible survey area. The grid squares are 800 by 800 m sample units. (**Top**): Mosaic of side-scan imagery of the seafloor. (**Middle**): Depth contours (1-m isobaths) obtained from multibeam bathymetry. (**Bottom**): Locations of historical NMFS shelf trawl survey events. Hatched lines = chain drags, stars = chain snags, unhatched lines = successful tows.

skipped hauls, chain drags, and chain snags. Interviews with knowledgeable fishermen were also conducted to establish the locations of known trawling sites within the area. The resulting geophysical map, with overlays, provided a geographically accurate reference of the study area that allowed *a priori* classification of the bottom into trawlable and untrawlable habitat types (Fig. 2). The final map consisted of the following layers: 1) a mosaic of side-scan imagery of the bottom (Fig. 2, top); high-resolution depth contours (1-m isobaths) obtained from multibeam bathymetry (Fig. 2, middle); and 3) locations of historical NMFS trawl survey events (Fig. 2, bottom).

Experimental design

Our survey design process made use of the detailed map of the study area for 1) definition of the sampling unit, 2) classification of all sampling units as trawlable or untrawlable habitats, and 3) specification of the *in situ* survey area. A sample of units to be surveyed by submersible was selected from each habitat type by using computer-generated pseudo-random numbers.

In defining the size of the sampling unit, we sought to strike a balance between a spatial scale that was small enough to have homogeneity but large enough to have meaning as a trawlable or untrawlable space. We chose square sample units of 800 by 800 m in size. This size was smaller than the standard NMFS tow length of about 3,000 m and was well within the order of resolution of the multibeam bathymetry and side-scan imagery used for discerning rock outcrops. A grid consisting of the 800 by 800 m sampling units was prepared and overlaid onto the map of the study area (Fig. 2).

Classification of the sampling units into "trawlable" and "untrawlable" habitats was facilitated by examination of the geophysical map of habitat features, together with an evaluation of historical NMFS trawl survey records. The survey map layer helped us to interpret the appearance of trawlable and untrawlable habitat on the bathymetric and side-scan geophysical map layers. Trawlable bottom

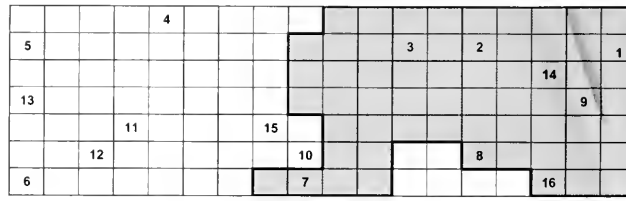

Figure 3

Schematic diagram of the study area divided into 800 m by 800 m sample units and classified *a priori* as untrawlable (shaded) and trawlable (unshaded) habitat types. The numbered sites represent the eight sample units selected at random from each habitat type, which were numbered sequentially for the cruise plan.

was inferred from locations with good hauls and uneventful chain drags; untrawlable bottom was inferred from bad hauls, short hauls, skipped hauls, and chain snags. On the side-scan mosaic layer, untrawlable locations were typically darker than surrounding areas, indicating boulder fields or hard, rocky bottom. Such areas often showed high bottom relief, as evidenced by shadows on the mosaic, and bathymetric contours that indicated abrupt topographic features, such as sharp ridges or pinnacles. A sample unit was classified as untrawlable habitat when 1) NMFS survey events within the unit indicated rough bottom, or 2) the mosaic or bathymetric layers of the unit resembled other units that were classified as untrawlable, or 3) a sample unit of unknown habitat type was completely surrounded by untrawlable habitat. A sample unit was classified as trawlable habitat when 1) NMFS survey events indicated successful trawl tows in the unit or 2) when the mosaic or bathymetric layers of the unit resembled other units that were classified as trawlable. Our trawlable and untrawlable habitat assignments agreed well with information obtained from knowledgeable fishermen. Each sampling unit in the entire mapped area was examined visually in detail according to the above procedure and was classified accordingly as trawlable or untrawlable habitat.

We selected the eastern portion of the mapped area for the submersible survey (Figs. 2 and 3). Our focus was restricted to this section to minimize the difference in bottom depths between the trawlable and untrawlable areas as a factor, and for logistical convenience to complete the most submersible dives possible within our survey budget. Because the 800 m by 800 m sampling units were too large to be surveyed in their entirety, we sampled using the strip transect method at each location. Logistically, this was accomplished by conducting 2–3 nonoverlapping passes across the sampling unit and by pooling these segments together to form a single transect for analysis.

Submersible survey

We used the submersible *Delta* to conduct the fish survey with the support vessel FV *Auriga* in July of 1998. The *Delta* is 4.7 m long, accommodates one observer and one pilot, and has a maximum operating depth of 365 m. An acoustic Trak-Point system was used with differential GPS and WinFrog navigational software (Thales GeoSolutions (Pacific), San Diego, CA) to track and log the position of the submersible from the support vessel. The *Delta* was equipped with halogen lights, external video cameras, an external Photosea 35-mm camera with strobe, and a Pisces Box data-logging system that recorded 1) the time of day, 2) depth of the submersible, 3) its distance from the bottom, and 4) sea temperature at 5-second intervals. Strip transects were conducted 1–2 m off bottom at a cruising speed of approximately 2.5 km/h. All dives were made during daylight hours.

To quantify fish density, each strip transect was documented with a high 8-mm video camera mounted externally on the bow of the *Delta*, and pointed forward. The camera was equipped with two parallel lasers, spaced 20 cm apart, which were used for estimating the area that was swept. The scientific observer onboard the *Delta* verbally annotated the videotape record with observations taken through the submersible viewing ports, to help identify fish and interpret the videotapes during subsequent analysis. The high 8-mm tapes were copied to S-VHS format to facilitate videotape analysis. The transect area that was swept (m^2) was estimated as the product of average area swept per second (m^2/min) and the total transect duration in minutes (see Appendix 1 for details). The average area that was swept per second (m^2/min) was determined from a set of 30-second samples randomly selected from the transect. On average, approximately 29% of each transect was subsampled in this manner. Bottom habitat type was also visually characterized for the transect subsamples. Following the method of Stein et al. (1992) and using the classification criteria developed by Greene et al. (1999), we categorized bottom microhabitat type (mud, pebble, cobble, boulders, and rock ridge) as primary (at least 50% of the area viewed) or as secondary (>20% of the area viewed). The bottom-type measurements observed directly in the transect subsamples were expanded to estimate microhabitat coverage for each transect.

Fish were enumerated by identifying and counting only those fish observed in the lower portion of the video monitor screen (counting area), below the imaginary line connecting the laser spots. Lighting and visibility was greatest in this zone, and we assumed that the probability of observing and counting fish in this portion of the video image was 100% (i.e. q=1). A fish was counted if any portion of the fish was visible in the counting area. The distance observed between the two laser spots was used as a reference to classify fish into two size categories: large (>20 cm) and small (<20 cm). Fish were identified to the lowest taxonomic level possible. We recognized that fish detection and identification were subject to observer error. The variability describing that error was obtained by conducting a repeat counting of a sample of transects by the same observer. Additional validation checks were made between multiple observers.

Analytical methods

Fish density estimates (number/10^3 m^2) were computed by dividing the total number of fish counted by the total estimated area-swept at each sample-unit site. Statistical comparisons of fish density estimates between the trawlable and untrawlable habitat types were limited to the level of classification (e.g. species or species group) where identifications were considered to be reliable. Estimates of the sample variance of fish density for the trawlable and untrawlable habitats (s_t^2 and s_u^2, respectively) were estimated as the sample variance of the fish density estimates among sites within each habitat type.

We used a power analysis for detecting differences in fish density between habitat types to generate sample size requirements to describe the sampling power of the submersible survey. The greater the sampling power, the fewer samples needed. Statistical power (i.e. the probability of correctly rejecting a false null hypothesis) is inversely related to the significance criterion (α) and is positively correlated with sample size and effect size (Peterman, 1990). The significance criterion is the rate of rejecting a true null hypothesis (the probability of type-1 error) and was fixed at 0.05 for our analysis. Effect size can be thought of as the degree to which a phenomenon exists (Cohen, 1988). In our study, the effect size was the hypothesized true difference in fish densities between trawlable and untrawlable habitats. Given a significance level and effect size, power is a function of sample size. Because the effect size is the quantity being tested, it is unknown. Therefore a power analysis is a theoretical "what if" exercise, which asks the question: "If the effect is this big, would the test be likely to detect it with this sample size?" Although the choice of effect size values used for a power analysis are arbitrary, they should be set at some meaningful threshold level, such that if the true effect is less than this threshold, it would not be important to detect it.

In our power analysis we used the approximation

$$Z_{1-b} = \frac{d(n-1)\sqrt{2n}}{2(n-1)+1.2\,1(Z_{1-\alpha}-1.06)} - Z_{1-\alpha} \qquad (1)$$

(Dixon and Massey, 1957; Cohen, 1988),

where Z_{1-b} = the percentile of the unit normal which gives power;

$Z_{1-\alpha}$ = the percentile of the unit normal for the significance criterion; for a two-tailed test, $\alpha = \alpha_{(2)}/2$;

d = the standardized effect size index for the two-tailed t-test calculated as

$$d = \frac{|m_t - m_u|}{s_p}, \qquad (2)$$

where m_t and m_u = the true densities in trawlable and untrawlable habitat, respectively; and

s_p^2 = the true pooled variance of the submersible survey density estimator.

By design, our study drew independent samples of equal size from each of the two habitat types, and $s_p^2=(s_t^2+s_u^2)$.

The power approximation procedure was convenient to use, in lieu of an exact method, because it was dependent only on the effect size-index (d) and sample size. Note from Equation 2 that d is unitless, so that statistical power and sample size could easily be compared across a range of species groups, where the absolute density differences between trawlable and untrawlable habitats can vary considerably (Cohen, 1988).

For the analysis, we derived a standardized effect size-index for the density comparison (d_b). The derivation was based on the relationship between density, abundance, and an effect size-threshold selected for abundance (Appendix II). The effect size-threshold for the abundance estimator was arbitrarily chosen to be equal to its standard error under the assumption that a lesser effect size would be difficult to detect. Under this assumption, the standardized effect size index is given by

$$d_b = \left[\frac{A}{A_u} SD(\hat{D}_t)/s_p\right], \qquad (3)$$

where A_u = the area of untrawlable habitat;

A = the total area;

$SD(\hat{D}_t)$ = the standard deviation of the trawl survey abundance estimator; and

s_p = the pooled standard deviation of the submersible survey density estimates.

The standardized effect size index (d_b) depends on 1) the proportion of untrawlable habitat in the total area (A_u/A), and 2) the variability in the trawl survey density estimator in relation to the variability in the submersible survey density estimator ($SD(\hat{D}_t)/s_p$) (Eq. 3). One can see that as A_u/A increases, d_b decreases; conversely, as $SD(\hat{D}_t)/s_p$ increases, d_b increases.

The relationship between the standard deviations ($SD(\hat{D}_t)/s_p$) and d_b creates an apparent paradox. Greater uncertainty in the trawl survey estimator ($SD(\hat{D}_t)$) in relation to the submersible survey estimator (s_p) causes d_b to increase, and thus the power of the submersible survey. Because

Table 1

Summary of the depth range in meters (m) and estimates of the area-swept (10^3 m^2) for randomly chosen sample units. Site type: T = trawlable, U = untrawlable.

Site	Site type	Depth (m)	Transect duration (minutes)	Surveyed area (10^3 m^2)	CV (%)	SE
4	T	130–135	53.0	5.08	24	0.22
5	T	130–135	46.5	5.77	9	0.10
6	T	145–148	49.5	4.68	19	0.15
10	T	106–110	54.5	6.06	12	0.14
11	T	132–140	48.5	4.46	13	0.11
12	T	137–141	49.5	5.40	14	0.14
13	T	136–141	50.5	5.17	13	0.12
15	T	117–119	54.0	4.77	18	0.14
1	U	95–102	52.8	4.59	21	0.21
2	U	95–100	53.5	4.73	13	0.11
3	U	105–109	43.5	5.57	11	0.11
7	U	110–118	55.0	5.66	16	0.17
8	U	102–105	55.0	6.93	16	0.21
9	U	90–98	53.5	5.90	24	0.26
14	U	96–100	39.0	4.67	21	0.21
16	U	105–105	53.5	6.45	11	0.12

greater power results in lesser sample size requirements, it appears that species with higher trawl survey uncertainty require fewer submersible survey samples. The reason fewer samples are required is that the effect size-index threshold has been increased and, generally, fewer samples are needed to detect larger effects. The key to understanding this relationship is that effect size is related to $SD(\hat{D}_t)$, but power is a function of that effect size in relation to the uncertainty in the data (s_p). Essentially, the greater the effect size in relation to the uncertainty in the data, the greater the power. As $SD(\hat{D}_t)/s_p$ increases, the level of resolution that can be detected by the trawl survey decreases. Thus, our choice to set the effect size-threshold (the level of bias we need to be able to detect) equal to the uncertainty of the trawl survey estimator (Appendix II) created a tradeoff between the level of resolution of the hypothesis test and the power to detect that level. This criterion was an arbitrary choice; a different relationship to describe this tradeoff would yield different results. In practice, the relative level of acceptable bias versus precision will depend on particular management objectives.

To obtain sample size guidelines for estimating the trawl survey habitat bias, we calculated d_b using estimated values for $SD(\hat{D}_t)$, s_p, and a range of assumed values for A_u/A for selected groundfish groups. We used information from our submersible survey to characterize the variability of density estimates within trawlable and untrawlable habitats (s_p), and information from past trawl surveys to characterize the variability in trawl survey estimates of abundance ($SD(\hat{D}_t)$). The trawl survey statistics used were derived from the 1998 survey estimates available for the US-Vancouver International North Pacific Fisheries Commission (INPFC) area shallow stratum (55–183 m) (Shaw et al., 2000), which encompasses the study area location. By substituting the calculated d_b for d in Equation 1, we solved iteratively for sample size (n) using Excel Solver (Excel 2000 vers. 9.0.2720, Microsoft Corp., Redmond, WA). The sample sizes obtained provide guidelines so that a similarly designed study will have an x% chance (e.g. power of 0.80=80% chance) of detecting a difference in mean density at least as large as the random noise inherent in the trawl survey density estimator.

Results

Submersible survey

Sixteen dive sites were sampled—eight in each habitat type (trawlable and untrawlable) (Table 1). In total, an estimated 85,900 m^2 was covered across all sites. The untrawlable sites (90–118 m) tended to be somewhat shallower than the trawlable sites (106–148 m); however, we assumed that this difference had little effect on fish density and species composition within the study area. In general, we were not successful in obtaining useful transect plots or reliable distance-traveled information with the WinFrog navigational software package; however, we found the Trak-Point acoustic tracking system to be useful for obtaining the location of the submersible with respect to the ship's position. We used this information, together with the subsea communication system, to guide the submersible along the predesignated transect segments at each dive site.

Our video survey largely confirmed our *a priori* assignments of trawlable and untrawlable habitat (Table 2). At

the dive sites designated trawlable prior to the video transect survey, mud bottom predominated (78.5%), followed by pebble (11.5%), mud-pebble (3.7%), and pebble-cobble (3.3%). At the sites designated *a priori* to be untrawlable, pebble bottom was most common (62.0%) followed by pebble-boulder (14.6%), mud (7.8%), boulder-pebble (6.3%), and boulder-cobble (6.0%). Microhabitat classifications unique to untrawlable habitat comprised 14.5% of the total and included cobble-pebble, cobble, boulder-pebble, boulder-cobble, rock-ridge, boulder, and cobble-boulder. The mud-pebble microhabitat was observed at trawlable sites but not at untrawlable sites. Bottom perturbations, which we presumed were trawl-door tracks, were observed at 6 of 8 *a priori* trawlable locations (sites 4, 5, 10, 12, 13, and 15), and at 2 of 8 *a priori* untrawlable locations (sites 3 and 14).

We counted 3647 fishes representing 26 species or generic group classifications (Table 3). Some fishes were readily identifiable to species; for example, lingcod, ratfish (*Hydrolagus colliei*), canary rockfish (*Sebastes pinniger*), and wolf-eel (*Anarrhichthys ocellatus*) were very distinctive. Other fishes could not always be identified to species level. In such cases, fish were assigned to the generic groups of "unidentified" rockfish, flatfish, or roundfish. It is likely that greenstriped (*S. elongatus*), redstripe (*S. proriger*), rosethorn (*S. helvomaculatus*), silvergray (*S. brevispinis*), and yellowtail rockfish (*S. flavidus*) were sometimes classed as unidentified rockfish; more rarely, large quillback (*S. maliger*), tiger (*S. nigrocinctus*), and yelloweye rockfish (*S. ruberrimus*) may have been assigned to this category. Flatfish were very difficult to identify to species; it is very likely that arrowtooth (*Atheresthes stomias*), Dover sole (*Microstomus pacificus*) and Pacific halibut (*Hippoglossus stenolepis*) were sometimes classed as unidentified flatfish.

The reliability of our fish counts was in part a function of fish size.

Table 2

Characterization of bottom type at sites classified *a priori* as trawlable (T) and untrawlable (U) habitat. Microhabitat type classifications include a primary (at least 50% of the area viewed) and a secondary (over 20% of the area viewed) component; M = mud, P = pebble, C = cobble, B = boulder, R = rock ridge.

		Estimated coverage (10^3 m^2)																
		Low relief						High relief										
Site	Site type	M-M	M-P	P-P	P-C	C-P	C-C	Total	M-B	P-B	C-B	B-P	B-C	B-B	R-R	Total	Station total
4	T	5.08	0.00	0.00	0.00	0.00	0.00	5.08	0.00	0.00	0.00	0.00	0.00	0.00	0.00	0.00	5.08
5	T	0.00	0.00	4.42	1.35	0.00	0.00	5.77	0.00	0.00	0.00	0.00	0.00	0.00	0.00	0.00	5.77
6	T	4.68	0.00	0.00	0.00	0.00	0.00	4.68	0.00	0.00	0.00	0.00	0.00	0.00	0.00	0.00	4.68
10	T	6.04	0.00	0.00	0.00	0.00	0.00	6.04	0.02	0.00	0.00	0.00	0.00	0.00	0.00	0.02	6.06
11	T	4.46	0.00	0.00	0.00	0.00	0.00	4.46	0.00	0.00	0.00	0.00	0.00	0.00	0.00	0.00	4.46
12	T	5.40	0.00	0.00	0.00	0.00	0.00	5.40	0.00	0.00	0.00	0.00	0.00	0.00	0.00	0.00	5.40
13	T	2.07	1.51	0.33	0.00	0.00	0.00	3.91	0.46	0.80	0.00	0.00	0.00	0.00	0.00	1.26	5.17
15	T	4.77	0.00	0.00	0.00	0.00	0.00	4.77	0.00	0.00	0.00	0.00	0.00	0.00	0.00	0.00	4.77
1	U	0.00	0.00	3.04	0.04	0.00	0.01	3.09	0.00	1.05	0.08	0.05	0.31	0.00	0.00	1.49	4.59
2	U	0.00	0.00	2.66	0.00	0.00	0.00	2.66	0.00	0.44	0.00	0.63	1.00	0.00	0.00	2.07	4.73
3	U	0.00	0.00	4.65	0.30	0.30	0.00	5.24	0.00	0.33	0.00	0.00	0.00	0.00	0.00	0.33	5.57
7	U	3.48	0.00	1.51	0.00	0.00	0.00	4.99	0.17	0.50	0.00	0.00	0.00	0.00	0.00	0.67	5.66
8	U	0.00	0.00	6.36	0.00	0.00	0.00	6.36	0.00	0.45	0.00	0.00	0.00	0.05	0.07	0.57	6.93
9	U	0.00	0.00	1.71	0.00	0.00	0.00	1.71	0.00	1.95	0.00	0.84	1.36	0.04	0.00	4.19	5.90
14	U	0.00	0.00	3.47	0.00	0.00	0.00	3.47	0.00	0.56	0.00	0.26	0.01	0.07	0.29	1.19	4.67
16	U	0.00	0.00	4.17	0.00	0.00	0.00	4.17	0.00	1.23	0.00	1.01	0.00	0.05	0.00	2.28	6.45
Totals	T	32.50	1.51	4.75	1.35	0.00	0.00	40.11	0.48	0.80	0.00	0.00	0.00	0.00	0.00	1.28	41.39
	U	3.48	0.00	27.57	0.34	0.30	0.01	31.69	0.17	6.51	0.08	2.80	2.69	0.20	0.36	12.80	44.50
Percent	T	78.5%	3.7%	11.5%	3.3%	0.0%	0.0%	96.9%	1.2%	1.9%	0.0%	0.0%	0.0%	0.0%	0.0%	3.1%	100.0%

A summary of counts for large (>20 cm) and small (<20 cm) fish is shown in Table 4. Small flatfish and rockfish were very difficult to count, often becoming indistinguishable from the background when the videotape was paused, and their counts are most likely underestimated. Among the large fish, "total rockfish" as a group was the most abundant numerically followed by "total flatfish" as a group. Of the large rockfish identified to species (Table 5), rosethorn rockfish were the most abundant followed in order by yellowtail, greenstriped, yelloweye, tiger, and redstripe rockfish. Unidentified rockfish represented 30% of the total large rockfish enumerated. Of the large flatfish identified to species (Table 6), Dover sole were most abundant followed in order by arrowtooth flounder and Pacific halibut. Unidentified flatfish represented 78% of the total large flatfish counted. Other individual fish species and groups identified below the generic classification level were dominated by eelpout (Zoarcidae), ratfish , skates and rays (*Raja*), and greenling (*Hexagrammos* spp.) (Table 7).

Species composition differed considerably between habitats. The number of individually identified species was 15 in the trawlable habitat, and 18 in the untrawlable habitat (Table 8). Flatfish dominated in the trawlable habitat, and rockfish in the untrawlable habitat. Yelloweye, redstripe, silvergray, and quillback rockfish, as well as greenling and wolf-eel were observed in the untrawlable habitat but not in the trawlable habitat. Spiny dogfish (*Squalus acanthias*), Pacific cod (*Gadus macrocephalus*), and salmon (*Oncorhynchus* spp) were observed in the trawlable habitat but not in the untrawlable habitat.

Comparisons of fish densities and variances between habitat types were made only for fish >20 cm in length and in taxonomic units where reliable identification and enumeration could be assured (Table 9). Thus, density comparisons were performed at the species level for distinctive species (i.e. lingcod, yelloweye rockfish, and tiger rockfish), but were made at the group level for "all rockfish" and "all flatfish" because of the presence of fish that could not be identified to individual species within each of these groups. For all comparisions, tests of homogeneity of variance of fish density between habitats (H_0: $s^2_t = s^2_u$) were rejected using Cochran's test (Winer, 1971) (α=0.05, k=2, df=7), indicating heteroscedastisity (Table 9). Significant differences in densities between habitats were found for each of the species and group comparisons using the Mann-Whitney two-sample test on ranks (Winer, 1971) (α=0.05, 2) (Table 9). Densities were higher in the untrawlable habitat for the "all rockfish" group, tiger rockfish, yelloweye rockfish, and lingcod; densities were higher in the trawlable habitat for the "all flatfish" group.

Table 3

Common and scientific names of fishes observed at 16 submersible dive sites off Cape Flattery, Washington.

Common name	Scientific name
Canary rockfish	*Sebastes pinniger*
Greenstriped rockfish	*Sebastes elongatus*
Quillback rockfish	*Sebastes maliger*
Redstripe rockfish	*Sebastes proriger*
Rosethorn rockfish	*Sebastes helvomaculatus*
Silvergray rockfish	*Sebastes brevispinis*
Tiger rockfish	*Sebastes nigrocinctus*
Yelloweye rockfish	*Sebastes ruberrimus*
Yellowtail rockfish	*Sebastes flavidus*
Greenling	*Hexagrammos* spp.
Lingcod	*Ophiodon elongatus*
Pacific cod	*Gadus macrocephalus*
Arrowtooth flounder	*Atheresthes stomias*
Dover sole	*Microstomus pacificus*
Pacific halibut	*Hippoglossus stenolepis*
Spotted ratfish	*Hydrolagus colliei*
Spiny dogfish	*Squalus acanthias*
Longnose skate	*Raja rhina*
Big skate	*Raja binoculata*
Salmon	*Oncorhynchus* spp.
Wolf-eel	*Anarrhichthys ocellatus*
Eelpout	Zoarcidae
Poacher	Agonidae
Generic group classifications	
Unidentified rockfish	*Sebastes* spp.
Unidentified flatfish	Pleuronectiformes
Unidentified roundfish	Osteichthyes

Statistical power analysis

The validity of our approach for analyzing the statistical sampling power of the submersible survey depends upon, among other things, fidelity to the assumptions of the two-sample t-test of means. The t-test requires that 1) the two sample means are estimated from random samples drawn from normally distributed populations, and that 2) the variance of the two populations are equal. Because our estimates of variance differed considerably between habitats (Table 9), we examined the properties of our data in more detail to confirm the reliability of using the t-test for our statistical power analysis. We conducted a bootstrap simulation experiment, in which we compared estimates of empirical power derived from our study (n=8) with the estimates of power obtained with Equation 1, under the assumption of asymptotic normality. The results of this comparison indicated that estimates of statistical power obtained from Equation 1 were generally conservative (indicated lower power) in relation to the empirical estimates of power for simulated known differences in density (Fig. 4). Given this result, we proceeded with our power analysis based on the t-test, under the assumption that, based on our observations, this approach will tend to err in the conservative direction; that is, it will tend to understate statistical power.

It is evident that, as it becomes necessary to detect smaller effect sizes, the required sample size increases accordingly. The relationship between sample size (n=the number of sample units [submersible dive sites] in each habitat type) and the effect size-index (d) for density comparisons

Table 4

Summary of fish counts for large (>20 cm) and small (<20 cm) fish for major fish groups. Site type: T = trawlable, U = untrawlable.

		Number of large fish (> 20 cm)					Number of small fish (< 20 cm)			
Site	Site type	Rockfish	Lingcod	Flatfish	Other	Total	Rockfish	Flatfish	Other	Total
4	T	0	1	77	8	86	0	95	48	143
5	T	8	0	54	17	79	0	94	15	109
6	T	2	0	76	12	90	0	68	63	131
10	T	7	3	29	5	44	0	26	107	133
11	T	0	1	35	10	46	0	8	101	109
12	T	0	0	46	5	51	0	6	63	69
13	T	39	1	119	19	178	0	77	37	114
15	T	0	0	31	2	33	0	70	64	134
1	U	115	1	6	16	138	43	0	10	53
2	U	128	14	12	28	182	348	3	52	403
3	U	9	2	28	10	49	41	9	58	108
7	U	43	9	13	22	87	0	21	46	67
8	U	32	3	4	9	48	40	2	12	54
9	U	206	5	6	14	231	339	0	11	350
14	U	30	3	8	11	52	38	7	27	72
16	U	111	5	30	9	155	28	4	17	49
Totals	T	56	6	467	78	607	0	444	498	942
	U	674	42	107	119	942	877	46	233	1156
	All	730	48	574	197	1549	877	490	731	2098

Table 5

Summary of fish counts by site for large rockfish (>20 cm). Site type: T = trawlable, U = untrawlable.

		Number of fish (>20 cm)										
Site	Site type	Rose-thorn	Yellow-tail	Silver-gray	Green-striped	Canary	Quill-back	Red-stripe	Tiger	Yellow eye	Unidentified	Total
4	T	0	0	0	0	0	0	0	0	0	0	0
5	T	0	0	0	8	0	0	0	0	0	0	8
6	T	0	0	0	2	0	0	0	0	0	0	2
10	T	0	0	0	0	2	0	0	0	0	5	7
11	T	0	0	0	0	0	0	0	0	0	0	0
12	T	0	0	0	0	0	0	0	0	0	0	0
13	T	2	1	0	14	0	0	0	1	0	21	39
15	T	0	0	0	0	0	0	0	0	0	0	0
1	U	31	1	0	9	0	1	0	0	8	65	115
2	U	88	3	0	0	0	0	0	7	12	18	128
3	U	8	0	0	0	0	0	0	0	1	0	9
7	U	16	14	0	1	0	0	0	2	3	7	43
8	U	25	2	0	1	2	0	0	1	0	1	32
9	U	121	1	1	3	0	0	16	6	5	53	206
14	U	15	10	0	1	0	0	0	1	0	3	30
16	U	34	17	3	0	0	0	0	2	7	48	111
Totals	T	2	1	0	24	2	0	0	1	0	26	56
	U	338	48	4	15	2	1	16	19	36	195	674
	All	340	49	4	39	4	1	16	20	36	221	730

Table 6

Summary of fish counts by site for large flatfish (>20 cm). Site type: T = trawlable, U = untrawlable.

Site	Site type	Number of fish (>20 cm)				
		Arrowtooth flounder	Dover sole	Pacific halibut	Unidentified	Total
4	T	3	6	2	66	77
5	T	3	8	1	42	54
6	T	15	2	6	53	76
10	T	0	3	3	23	29
11	T	1	3	3	28	35
12	T	5	2	5	34	46
13	T	10	13	7	89	119
15	T	0	2	1	28	31
1	U	0	4	0	2	6
2	U	0	2	0	10	12
3	U	0	4	2	22	28
7	U	0	0	5	8	13
8	U	0	0	0	4	4
9	U	0	1	1	4	6
14	U	0	1	0	7	8
16	U	1	0	0	29	30
Totals	T	37	39	28	363	467
	All	38	51	36	449	574

Table 7

Summary of fish counts by site for other large (>20 cm) fish. Site type: T = trawlable, U = untrawlable.

Site	Site type	Number of fish (>20 cm)								
		Greenling	Pacific cod	Ratfish	Spiny dogfish	Skates/Rays	Eelpout	Salmon	Unidentified	Total
4	T	0	0	0	0	0	8	0	0	8
5	T	0	0	6	1	0	10	0	0	17
6	T	0	0	0	0	1	11	0	0	12
10	T	0	0	0	0	4	1	0	0	5
11	T	0	0	0	0	1	8	1	0	10
12	T	0	2	0	0	1	2	0	0	5
13	T	0	1	1	6	5	5	0	1	19
15	T	0	0	0	0	0	1	0	1	2
1	U	2	0	1	0	0	12	0	1	16
2	U	1	0	1	0	0	26	0	0	28
3	U	1	0	1	0	1	6	0	1	10
7	U	3	0	0	0	4	15	0	0	22
8	U	2	0	2	0	0	5	0	0	9
9	U	2	0	6	0	0	5	0	1	14
14	U	0	0	2	0	0	9	0	0	11
16	U	1	0	5	0	0	3	0	0	9
Totals	T	0	3	7	7	12	46	1	2	78
	U	12	0	18	0	5	81	0	3	119
	All	12	3	25	7	17	127	1	5	197

between trawlable and untrawlable habitats is shown in Figure 5. To achieve power of 80% (α=0.05), the required number of dives ranges from n = 5 (d=2.0) to n = 17 (d=1.0); similarly, to obtain 90% power would require 8 to 27 dives. Empirical estimates of d from our study ranged from 1.1 for tiger rockfish to 2.0 for flatfish. This result suggests

Table 8

Composition of fish densities in trawlable and untrawlable sites by species (>20 cm), ranked in descending order of observed abundance (avg. no./hectare). Italicized species were not found in the other habitat type.

Trawlable sites		Untrawlable sites	
Species or group	Avg. no./hectare	Species or group	Avg. no./hectare
Eelpout	11.46	Rosethorn rockfish	77.78
Dover sole	9.33	Eelpout	19.26
Arrowtooth flounder	9.25	Yellowtail rockfish	10.70
Pacific halibut	6.88	Lingcod	9.78
Greenstriped rockfish	5.65	*Yelloweye rockfish*	8.65
Skate	2.81	Tiger rockfish	4.40
Spiny dogfish	1.67	Spotted ratfish	3.90
Spotted ratfish	1.54	Greenstriped rockfish	3.76
Lingcod	1.39	*Redstripe rockfish*	3.39
Pacific cod	0.70	Dover sole	3.00
Rosethorn rockfish	0.48	*Greenling*	2.67
Canary rockfish	0.41	Pacific halibut	1.77
Salmon	0.28	Skate	1.11
Yellowtail rockfish	0.24	*Silvergray rockfish*	0.79
Tiger rockfish	0.24	*Wolf-eel*	0.49
		Canary rockfish	0.36
		Quillback rockfish	0.27
		Arrowtooth flounder	0.19
Generic group			
All flatfish	114.29	All flatfish	23.90
All rockfish	13.14	All rockfish	155.63
All fish	146.65	All fish	211.70

that it is relatively more difficult (i.e. more dive sites are required) to detect density differences between habitats for tiger rockfish, as compared to flatfish. The associated power curves for these two values of d are illustrated in Figure 6. Figure 6 suggests that, given our observations (for values of d as low as 1.1), a sample size guideline of approximately 15 submersible dive sites in each habitat type would yield approximately an 80% chance of detecting a difference in mean density at least as large as the random noise estimated in the data for a similarly designed study.

Our statistical power analysis also indicated that, when the relative proportions of untrawlable and trawlable habitat, as well as the variability in the trawl survey estimates of abundance, are taken into consideration, the problem of estimating the trawl survey habitat bias can require substantially more samples than would be required simply to compare the density differences between two habitat types. Values of the trawl-survey habitat-bias effect size-index (d_b), calculated for a range of untrawlable habitat proportions with empirical trawl and submersible survey data, are given in Table 10 and are plotted for rockfish and flatfish in Figure 7. Using the calculated values of d_b from Table 10, we derived sample size guidelines for rockfish and flatfish (at power=0.80, α=0.05). The resulting relationship between the sample size required to estimate the trawl survey habitat bias (the n=number of submersible dive sites in each habitat type) and the proportion of untrawlable habitat in a management area (A_u/A) is illustrated in Figure 8. If, for example, the area of untrawlable habitat represented 20% of a management unit, Figure 8 indicates that the sample size required to estimate the trawl survey habitat bias would be n = 31 for rockfish (d_b=0.73), and n = 9 for flatfish (d_b=1.41). Sample sizes for lingcod were much higher (n>100), owing to the comparatively small detectible effect size required (d_b=0.13).

Discussion

Our study successfully obtained a first look at the variability in groundfish densities in trawlable and untrawlable habitats for a study area off Washington. We also developed a framework to use these types of observations to derive sample size guidelines for designing larger-scale studies to estimate the trawl survey habitat bias. The limited geographic scope of our study precludes extrapolation of our specific results to the west coast at large. However, we demonstrated an approach that can be used to establish sample size guidelines for future work by illustrating the interplay between statistical sampling power and 1) habitat-specific density differences, 2) variance of density estimates, and 3) the proportion of untrawlable area in a habitat.

In our study area, we observed striking differences in species composition and fish density between the traw-

Table 9

Summary of estimated fish densities (no./hectare) and summary statistics for selected fish groups (>20 cm). Site type: T = trawlable, U = untrawlable.

		Estimated fish density (number/10^3 m^2)									
		Rockfish		Flatfish		Lingcod		Yelloweye rockfish		Tiger rockfish	
Site	Site type	Mean	SE	Mean	SE	Mean	SE	Mean	SE	Mean	SE
4	T	0.00	0.00	15.16	8.55	0.20	0.28	0.00	0.00	0.00	0.00
5	T	1.39	0.10	9.36	1.26	0.00	0.00	0.00	0.00	0.00	0.00
6	T	0.43	0.63	16.26	3.70	0.00	0.00	0.00	0.00	0.00	0.00
10	T	1.15	1.96	4.78	0.45	0.49	0.02	0.00	0.00	0.00	0.00
11	T	0.00	0.00	7.84	3.54	0.22	0.36	0.00	0.00	0.00	0.00
12	T	0.00	0.00	8.52	1.12	0.00	0.00	0.00	0.00	0.00	0.00
13	T	7.54	9.23	23.01	8.97	0.19	0.40	0.00	0.00	0.19	0.40
15	T	0.00	0.00	6.49	3.13	0.00	0.00	0.00	0.00	0.00	0.00
1	U	25.07	29.36	1.31	0.54	0.22	0.34	1.74	1.79	0.00	0.00
2	U	27.05	19.23	2.54	1.61	2.96	2.49	2.54	2.00	1.48	1.24
3	U	1.61	2.68	5.02	4.63	0.36	0.28	0.18	0.30	0.00	0.00
7	U	7.60	8.83	2.30	1.29	1.59	2.65	0.53	0.88	0.35	0.59
8	U	4.62	0.97	0.58	0.55	0.43	0.06	0.00	0.00	0.14	0.27
9	U	34.92	15.63	1.02	0.12	0.85	0.47	0.85	0.93	1.02	1.19
14	U	6.43	7.41	1.71	1.62	0.64	0.80	0.00	0.00	0.21	0.27
16	U	17.20	7.37	4.65	2.58	0.77	0.51	1.08	0.93	0.31	0.28
Summary statistics											
	m_t	1.31		11.43		0.14		0.00		0.02	
	s^2_t	6.64		37.92		0.03		0.00		0.00	
	m_u	15.56		2.39		0.98		0.87		0.44	
	s^2_u	151.58		2.69		0.82		0.81		0.28	
Cochran's test for homogeneity of variance (Winer 1971); $C_{crit} = 0.83$											
	C	0.96		0.93		0.96		1.00		0.98	
Mann Whitney test for equality of fish densities (Winer 1971); $U_{crit} = 51$											
	U	61		63		60		56		51	
Statistics to calculate effect size index (d) for submersible survey power analysis											
	$\lvert m_t - m_u \rvert$	14.25		9.04		0.84		0.87		0.42	
	s_p	8.894		4.51		0.65		0.64		0.38	
	d	1.6		2.0		1.3		1.4		1.1	

lable and untrawlable habitats. Flatfish were more than ten times as abundant in the trawlable habitat samples, whereas rockfish as a group were over three times as abundant in the untrawlable habitat samples. Silvergray, quillback, redstripe, and yelloweye rockfish were observed in the untrawlable habitat but not in any of the trawlable habitat samples.

We know of no visual-transect data comparable to that presented here for fish abundances off Washington. However, previous habitat specific studies in other areas have also reported differences in species composition and fish densities between low relief (trawlable) and highly rugose (untrawlable) habitats. Richards (1986) conducted a submersible study in the Strait of Georgia, British Columbia (21–140 m), and observed that the distribution of greenstriped, quillback, and yelloweye rockfish varied by depth and bottom type. Greenstriped rockfish were most abundant in fine sediment habitats, such as mud and cobble terrain. Quillback rockfish were most abundant in complex habitats, and yelloweye rockfish had higher densities in wall and complex habitats than in fine sediment habitats. In the coastal fjord of Saanich Inlet, British Columbia (21–150 m), Murie et al. (1994) also reported that quillback rockfish density was higher in areas of complex or wall habitat, compared to areas of sand-mud habitat. Additionally, tiger, copper (*S. caurinus*), yellowtail, and yelloweye rockfish were observed only over complex or wall habitats, and greenstriped rockfish were seen mostly over sand-mud habitat. Using sunken gill nets to sample trawlable and untrawlable habitats off Vancouver Island, B.C. (198–311 m in depth), Matthews and Richards (1991) reported differences in species composition between trawlable and untrawlable areas and higher species diversity in trawlable habitat. Major species on trawlable bottom

were Pacific ocean perch (*S. alutus*), splitnose rockfish (*S. diploproa*), greenstriped rockfish, and bocaccio (*S. paucispinis*). Major species on untrawlable bottom were sharpchin (*S. zacentrus*) and redbanded rockfish (*S. babcocki*). In a submersible study conducted off Southeastern Alaska (188–290 m), Krieger (1993) compared the fish densities of 4 untrawlable sites with 16 trawlable or marginally trawlable sites, and reported that densities of large (>25 cm) rockfish (a category that included Pacific ocean perch, sharpchin rockfish, redstripe rockfish, and harlequin rockfish (*S. variegatus*) were highest at trawlable sites. In a study of shortraker (*S. borealis*) and rougheye (*S. alcutianus*) rockfish conducted on the upper continental slope off southeastern Alaska (262–365 m), Krieger and Ito (1999) reported that soft substrates of sand or mud usually had the greatest densities; hard substrates of bedrock, cobble, or pebble had the least densities; and habitats containing steep slopes and numerous boulders had greater densities of rockfish than habitats with gradual slopes and few boulders. O'Connell and Carlile (1993) conducted a submersible survey off southeastern Alaska in two depth strata; shallow (<108 m) and deep (≥108 m). Yelloweye rockfish were observed in cobble, continuous rock, broken rock and boulder habitats but were most abundant in broken rock and boulder habitats of the deep stratum. Habitat-specific studies in Oregon and California have used finer scales of habitat classification to characterize fish-habitat associations than our comparatively coarse trawlable or untrawlable classification. In Oregon waters, Stein et al. (1992) reported estimates of fish density by habitat-type from a submersible study of six stations at Heceta Bank in waters ranging from 60 to 340 m in depth. Rockfishes, particularly pygmy (*S. wilsoni*), sharpchin, rosethorn, and yellowtail, dominated all substrates except mud, where Dover sole and blackbelly eelpouts (*Lycodes pacificus*) were most abundant. In California waters, Yoklavich et al. (2000) conducted a submersible study at Soquel canyon (94–305 m) in Monterey Bay. Cluster analysis grouped fish densities into six habitat guilds; most distinct were 1) guild I (fish associated with uniform mud bottom of flat or low relief, dominated by stripetail rockfish (*S. saxicola*)) and guild VI (fish associated with rock-boulder habitat of low to high relief, dominated by pygmy rockfish).

To contrast our results in Washington with findings from Oregon and California, we summarized the fish density estimates reported by Stein et al. (1992) and Yoklavich et al. (2000) into a format roughly comparable to our data. Differences in the objectives and methods of their studies precluded a rigorous quantitative comparison with our results, particularly because of differences in habitat classification and survey design (random sampling in our study, purposive sampling in the other two studies). However, some interesting similarities are apparent if the most highly rugose habitats of these two studies are treated as a proxy for untrawlable habitat and if the low bottom relief habitats are treated as a proxy for trawlable habitat (Table 11). Seven species (italicized in Table 11) co-occurred in all three studies. For all three studies, greenstriped rockfish and Dover sole densities were higher in the trawlable habitat, and rosethorn, yelloweye and yellowtail rockfish densites were higher in the untrawlable habitat. Results were mixed for canary rockfish (more abundant in trawlable habitat in Washington but more abundant in untrawlable habitat in the Oregon and California studies) and lingcod (more abundant in trawlable habitat in Oregon but more abundant in untrawlable habitat in the Washington and California studies).

The most striking contrast among the three studies was the much lower overall magnitude of the fish densities in Washington compared to Oregon and California. One possible explanation for this difference could be due to the

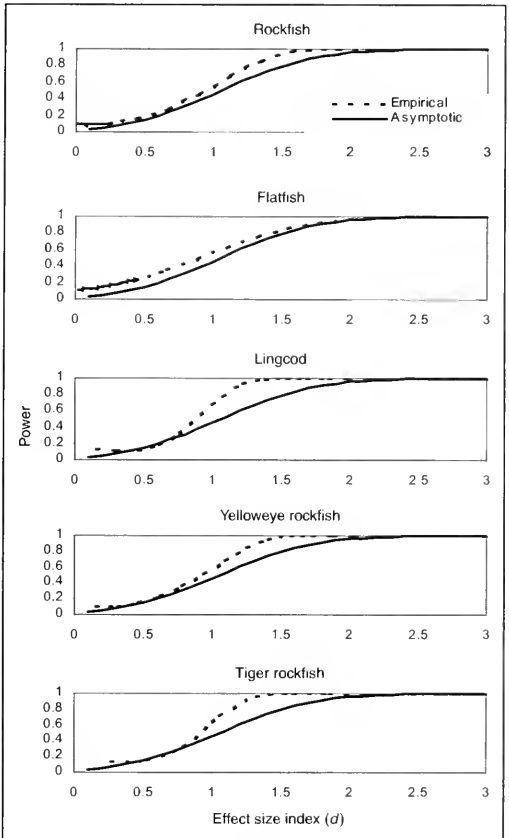

Figure 4

Comparison of empirical power (from bootstrap simulation results) with power calculated by using Equation 1 under the assumption of asymptotic normality (α=0.05, n=8) for rockfish and flatfish in the aggregate and for lingcod, yelloweye rockfish, and tiger rockfish individually.

nature of the respective study designs. The Oregon and California studies both targeted particular substrate types to characterize fish assemblages and fish habitat associations. Our study in Washington was structured to conduct random sampling within each of the two broad habitat classifications and thus did not focus purposively on particular local features (e.g. individual rock outcrops) which could serve as areas of more concentrated fish density. Another factor could be the nature of the fishing history of the study areas; the Washington site has long been subjected to heavy fishing pressure, whereas the other sites, particularly portions of the Soquel canyon site, may have received relatively less fishing pressure (Yoklavich[2]). It is also possible that zoogeographic differences, interannual variability, and the relatively small spatial scales of the sampled areas could also explain the differences in densities observed between the studies.

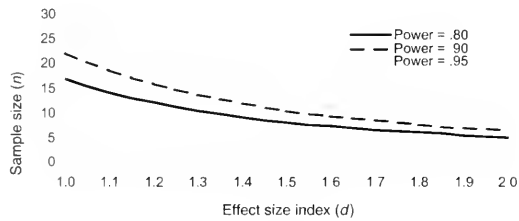

Figure 5

Sample size (n=number of submersible dives in each habitat type) as a function of the effect size index (d) for comparisons of fish density between trawlable and untrawlable habitats (α=0.05).

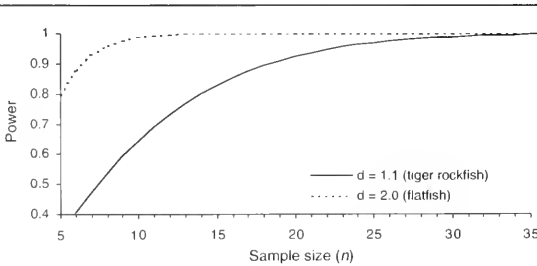

Figure 6

Statistical Power as a function of sample size (n=number of submersible dives in each habitat type) for the lowest (d=1.1) and highest (d=2.0) values of the effect size index observed in the present study (α=0.05).

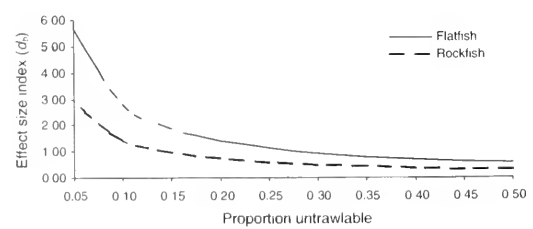

Figure 7

Trawl-survey habitat-bias effect size-index (d_b) as a function of the proportion of untrawlable habitat (A_u/A) in a management area for two categories of fish.

The level of concordance among the habitat-specific studies reviewed in the present study suggests that the potential exists for differences in fish density between trawlable and untrawlable habitats. These differences can be of great importance in the interpretation of trawl survey results for groundfish stock assessments. The presently available data are insufficient, however, to accurately quantify the magnitude of the trawl-survey habitat bias for west coast groundfish stock assessment and management. First, the absolute magnitude of such a bias will depend largely on the amount of untrawlable habitat present, which is not well estimated at this time. Modern benthic mapping technology and geographic information systems are capable of yielding detailed habitat maps over large spatial scales for habitat area quantification, but such maps are not yet available for most of the west coast (Nasby, 2000). Second, although many of the habitat-specific studies conducted to date tend to support the notion of significant fish density differences between trawlable and untrawlable habitats on small scales, studies with larger geographic scope are needed in order to be relevant to the assessment and management of west coast benthic fishery stocks. In particular, studies structured *a priori* with stratified random sampling designs can afford improved statistical inference by providing representative observations and unbiased parameter estimates across a spectrum of habitat types.

Estimation of the trawl-survey habitat-bias may not be the preferred solution to address habitat-specific density differences for all groundfish species. The approach is likely to work best for situations where 1) variability in the density estimates obtained from the survey used to sample both habitats (in our case, visual transects collected by submersible) is relatively small compared to the variability in the trawl survey, and 2) untrawlable habitat does

[2] Yoklavich, M. 2001. Personal commun. NMFS, Santa Cruz, California 95060.

Table 10

Statistics used to calculate the trawl-survey habitat-bias effect size-index (d_b) derived from observations of the present study.

Species or group	Trawl survey density (D_t) (no./hectare)	Trawl survey $SD(D_t)$	Submersible survey s_p (no./hectare)
Rockfish	58.94	12.97	88.94
Flatfish	141.38	12.72	45.07
Lingcod	0.85	0.17	6.52

Proportion untrawlable A_u/A	Trawls-survey habitats-bias effect size-index (d_b)		
	Rockfish	Flatfish	Lingcod
0.50	0.29	0.56	0.05
0.45	0.32	0.63	0.06
0.40	0.36	0.71	0.07
0.35	0.42	0.81	0.07
0.30	0.49	0.94	0.09
0.25	0.58	1.13	0.10
0.20	0.73	1.41	0.13
0.15	0.97	1.88	0.17
0.10	1.46	2.82	0.26
0.05	2.92	5.65	0.52

not comprise a large portion of the area to be assessed. Our data suggest, for instance, that it would probably be unfeasible to estimate a trawl survey bias correction factor for lingcod. It appears that lingcod density can be estimated with relatively good precision in trawlable areas by the trawl survey (CV=0.20, Table 10). However, our submersible survey found high variability across both habitat types (CV=1.17, Table 9), which resulted in a relatively low-effect size-index threshold values for lingcod (e.g. A_u/A d_b=0.52, Table 10). The required sample size rapidly exceeded n = 100 submersible dive sites as the proportion of the management area that was untrawlable increased above 5% (P=80%, α=0.05; Fig. 8). In cases requiring such large sample sizes, estimation of a trawl-survey bias correction factor would probably not be an acceptable alternative to direct, synoptic surveys structured to obtain unbiased estimates of abundance in untrawlable habitats. By contrast, the trawl survey bias correction factor approach may be more feasible for species where the ratio between the trawl survey and submersible survey variation is smaller. Our data suggest that flatfish may fall into this category. The trawl survey precision (CV=0 .09, Table 10) in relation to the submersible survey precision (CV=0.65, Table 9) resulted in a relatively high-effect size-index threshold value for flatfish at the proportion level of 5% for area that was untrawlable (d_b=5.65, Table 10). The required sample size was less than n = 25 submersible dive sites, even as the ratio of A_u/A (the proportion of the management area that is untrawlable area) exceeded 30% (P=80%, α=0.05; Fig. 8). However, because our analysis aggregated flatfish as a group, these results do not address the estimation of a bias correction factor for individual species, which is a requirement for any correction factor to be useful for stock assessment purposes.

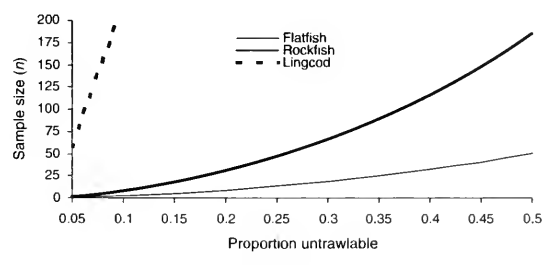

Figure 8

Sample size guidelines for estimating the trawl survey habitat bias (n=the number of submersible dives in each habitat type) as a function of the proportion of untrawlable habitat (A_u/A) in a management area, for power = 80% and α=0.05 for three categories of fish.

As for any survey method, the visual transect survey method has an array of advantages and disadvantages, which have been well chronicled elsewhere (Uzmann et al., 1977; Ralston et al., 1986; Butler et al., 1991; Adams et al.,1995; Starr et al., 1996; Cailliet et al., 1999). Some of the disadvantages include 1) difficulties in fish identification, particularly for small fish or fish with subtle coloration, 2) the potential for attraction or repulsion of fish from the

Table 11

Comparison of fish density estimates (average number of fish/hectare) in trawlable (D_t) and untrawlable (D_u) habitats from submersible studies in Washington, Oregon, and California. Densities for italicized species were reported in all three studies.

	Washington (present study)		Oregon[1]		California[2]	
Species	D_t	D_u	D_t	D_u	D_t	D_u
Rockfish						
Bank rockfish					0.00	105.00
Bocaccio					6.33	586.00
Canary rockfish	*0.41*	*0.36*		*120.00*	*0.00*	*148.00*
Cowcod				4.33	152.67	
Darkblotched rockfish					86.33	52.00
Greenblotched rockfish					1.33	36.33
Greenspotted rockfish					162.33	237.67
Greenspotted and greenblotched rockfish					1.67	16.33
Greenstriped rockfish	*5.65*	*3.76*	*165.00*	*39.50*	*218.67*	*46.00*
Halfbanded rockfish					220.00	85.67
Pygmy rockfish			510.00	892.50	126.33	734.33
Quillback rockfish		0.27				
Redstripe rockfish		3.39				
Rosethorn rockfish	*0.48*	*77.78*	*479.50*	*574.50*	*40.33*	*175.33*
Sharpchin rockfish					96.50	138.50
Shortspine thornyhead			119.50		41.33	5.33
Stripetail rockfish				304.67	63.67	
Tiger rockfish	0.24	4.40				
Widow rockfish					0.33	33.67
Yelloweye rockfish		*8.65*		*13.50*	*0.67*	*78.67*
Yellowtail rockfish	*0.24*	*10.70*	*33.50*	*95.50*	*2.67*	*28.00*
Flatfish						
Arrowtooth flounder	9.25	0.19				
Dover sole	9.33	3.00	249.50	7.50	58.00	3.00
Pacific halibut	6.88	1.77				
Other Fish						
Eelpout	11.46	19.26				
Greenling		2.67				
Lingcod	*1.39*	*9.78*	*33.50*	*15.00*	*43.67*	*91.67*
Pacific cod	0.70					
Pacific hagfish					25.67	4.00
Pacific hake					14.67	14.00
Poachers			93.00	9.00	138.00	22.67
Spotted ratfish	1.54	3.90				
Salmon	0.28					
Skate	2.81	1.11				
Spiny dogfish	1.67					
Wolf-eel		0.49				

[1] Oregon data source: Table 3 of Stein et al. (1992). Categories "mud" and mud-cobble" were averaged and used as a proxy for trawlable habitat; categories "flat rock" and "rock ridge" were averaged and used as a proxy for untrawlable habitat.

[2] California data source: Table 2 of Yoklavich et al. (2000). Categories "mud," "cobble-mud" and "mud-pebble" were averaged and used as a proxy for trawlable habitat; categories "rock-mud," "rock ridge," and "rock boulder" were averaged and used as a proxy for untrawlable habitat.

submersible, 3) variation in countability due to habitat type; for example, due to reduced visibility when the submersible maneuvered off bottom to avoid large boulders, or the failure to detect fish hiding behind boulders, and 4) the limitation of the technique to quantifying the density of benthic species found in close proximity to the bottom. The advantages of the visual transect survey method include the ability to 1) sample in habitats that are inaccessible to other survey methods, 2) observe *in situ* fish behavior, and 3) observe the distribution of fish and fish-habitat associations on a fine

scale. Although our study was subject to the limitations of the visual transect method, we assumed that the method could reliably estimate (with a catchability of $q=1.0$) the true density of selected demersal bottomfish in both trawlable and untrawlable habitats for evaluation of the habitat bias present in the trawl-survey approach (which does not allow for sampling in untrawlable habitat). We do not feel that this assumption was severely violated, although we have no objective measure of the potential biases of the method, and thus we cannot estimate the consequences of assumption failure. We did recognize clearly that difficulties in fish identification limited the number of species that we could quantitatively sample with this technique. Technological improvements in underwater videography and image recognition software are likely to enhance the capabilities of the visual transect survey technique in the future.

In conclusion, it is clear that relatively large-scale surveys are needed to assess bottomfish densities in habitats that are not accessible to trawl survey gear. For some species, it may be possible to derive an area-specific trawl-survey bias correction factor, but for many other species it is likely that there will be no substitute for direct estimation of densities in untrawlable habitat on a routine and synoptic basis. In either case, stratified random sampling designs should be employed with sample sizes sufficient to ensure acceptable levels of statistical power. At present, the *in situ* visual transect submersible survey method appears to be a useful tool for this purpose, and the utility of this method will likely improve further with technological advances.

Acknowledgments

We would like to thank Farron Wallace and Brian Culver for help during the submersible dive survey and with fish identification on the videotapes; Cindy Knudsen for videotape area-swept data collection; Kevin Redman and Colin Stewart (Williamson and Associates) for geophysical data analysis and mapping, and Mike Farnam, and Brian Bunge (USN) for geophysical data acquisition; the captains and crews of the USN *Agate Passage* and FV *Auriga* for excellent support vessel services; D. Slater, C. Ijames, and J. Lilly of Delta Oceanographics for safe and efficient use of the *Delta* submersible; Victoria O'Connell and Waldo Wakefield for advice on field logistics and data collection; and Marion Larkin (FV *Larkin*), for his insights regarding trawlable and untrawlable habitat obtained from many years of fishing experience in the study area. This study was supported by the NOAA National Undersea Research Program, West Coast and Polar Regions Undersea Research Center, University of Alaska Fairbanks (grant no. UAF 98-0045), the Washington Department of Fish and Wildlife, and the National Marine Fisheries Service.

Literature cited

Adams, P. B., J. L. Butler, C. H. Baxter, T. E. Laidig, K. A. Dahlin, and W. W. Wakefield.
1995. Population estimates of Pacific coast groundfishes from video transects and swept-area trawls. Fish. Bull. 93:446–455.

Alverson, D. L.
1951. Deep water trawling survey off the coast of Washington (August 27–October 19, 1951) Commercial Fisheries Review 13:11. U.S. Dep. Fish. Wild. Serv., Sep. 292.

Auster, P. J., L. L. Stewart, and H. Sprunk.
1989. Scientific imaging with ROVs: tools and techniques. Mar. Technol. Soc. J. 23(3):16–20.

Butler, J. L., W. W. Wakefield, P. B. Adams, B. H. Robison, and C. H. Baxter.
1991. Application of line transect methods to surveying demersal communities with ROV's and manned submersibles. Proceedings of the Oceans 91 Conference, Honolulu, Hawaii, 1–3 October 1991, p. 689–696. Marine Technology Soc., Columbia, MD.

Cailliet, G. M., A. H. Andrews, W. W. Wakefield, G. Moreno, and K. L. Rhodes.
1999. Fish faunal and habitat analyses using trawls, camera sleds and submersibles in benthic deep-sea habitats off central California. Oceanol. Acta 22(6):579–592.

Caimi, F. M., J. H. Blatt, B. G. Grossman, D. Smith, J. Hooker, D. M. Kocak, and F. Gonzalez.
1993. Advanced underwater laser systems for ranging, size estimation, and profiling. Mar. Technol. Soc. J. 27(1):31–41.

Cohen, J.
1988. Statistical power analysis for the behavioral sciences, 2nd ed., 567 p. L. Erlbaum Associates, Hillsdale, NJ.

Dark, T. A., and M. E. Wilkins.
1994. Distribution, abundance, and biological characteristics of groundfish off the coast of Washington, Oregon, and California, 1977–1986. U.S. Dep. Commer. Nat. Mar. Fish. Serv., NOAA Tech. Rep. NMFS 117, 73 p.

Davis, D. L., and R. F. Tusting.
1991. Quantitative benthic photography using laser calibrations, 5 p. Undersea World, San Diego, CA.

Dixon, W. F., and F. J. Massey.
1957. Introduction to statistical analysis, 2nd ed., p. 244–255. McGraw-Hill, New York, NY.

Greene, H. G., M. M. Yoklavich, R. M. Starr, V. M. O'Connell, W. W. Wakefield, D. E. Sullivan, J. E. McRea, Jr., and G. M. Cailliet.
1999. A classification scheme for deep seafloor habitats. Oceanol. Acta 22(6):663–678.

Gregory, R. S., J. T. Anderson, and E.L. Dalley.
1997. Distribution of juvenile Atlantic cod *Gadus morhua* relative to available habitat in Placentia Bay, Newfoundland. Northwest Atl. Fish. Organ. Sci. Counc. Stud. 29:3–12.

Krieger, K. J.
1993. Distribution and abundance of rockfish determined from a submersible and by bottom trawling. Fish. Bull. 91:87–96.

Krieger, K. J., and D. H. Ito.
1999. Distribution and abundance of shortraker rockfish, Sebastes borealis, and rougheye rockfish, *S. aleutianus*, determined from a manned submersible. Fish. Bull. 97: 264–272.

Kulbicki, M., and L. Wantiez.
1990. Comparison between fish bycatch from shrimp trawl-net and visual censuses in St.Vincent Bay, New Caledonia. Fish. Bull. 88:667–675.

Matthews, K. R., and L. J. Richards.
1991. Rockfish (Scorpaenidae) assemblages of trawlable and untrawlable habitats off Vancouver Island, British Columbia. N. Am. J. Fish. Manage. 11:312–318.

Murie, D. J., D. C. Parkyn, B. G. Clapp, and G. G. Krause.
1994. Observations on the distribution and activities of rockfish, *Sebastes* spp., in Sannich Inlet, British Columbia, from the Pisces IV submersible. Fish. Bull. 92:313–323.
Nasby, N. M.
2000. Integration of submersible transect data and high-resolution sonar imagery for a habitat-based groundfish assessment of Heceta Bank, Oregon. M.S. thesis, 50 p. Marine Resource Management Program, College of Oceanic and Atmospheric Science, Oregon State Univ., Corvallis, OR.
O'Connell, V. M., and D. W. Carlile.
1993. Habitat-specific density of adult yelloweye rockfish *Sebastes ruberrimus* in the eastern Gulf of Alaska. Fish. Bull. 91:304–309.
PFMC (Pacific Fishery Management Council).
2001. Status of the Pacific Coast groundfish fishery through 2001 and recommended biological catches for 2002: stock assessment and fishery evaluation, 26 p. [Document prepared for the Council and its advisory entities]. Pacific Fishery Management Council, Portland, OR.
Peterman, R. M.
1990. Statistical power analysis can improve fisheries research and management. Can. J. Fish. Aquat. Sci. 47:2–15.
Ralston, S., R. M. Gooding, and G. M. Ludwig.
1986. An ecological survey and comparison of bottom fish resources assessments (submersible versus handline fishing) at Johnston Atoll. Fish. Bull. 84:141–155.
Richards, L. J.
1986. Depth and habitat distributions of three species of rockfish (*Sebastes*) in British Columbia: observations from the submersible Pisces IV. Environ. Biol. Fish. 17(1): 13–21.
Shaw, F. R., M. E. Wilkins, K. L. Weinberg, M. Zimmermann, and R. R. Lauth.
2000. The 1998 Pacific West Coast bottom trawl survey of groundfish resources: estimates of distribution, abundance, and length and age composition. NOAA Technical Memorandum NMFS-AFSC-114, 138 p.
Starr, R. M., D. S. Fox, M. A. Hixon, B. N. Tissot, G. E. Johnson, and W. H. Barss.
1996. Comparison of submersible-survey and hydroacoustic-survey estimates of fish density on a rocky bank. Fish. Bull. 94:113–123.
Stein, D. L., B. N. Tissot, M. A. Hixon, and W. Barss.
1992. Fish-habitat associations on a deep reef at the edge of the Oregon continental shelf. Fish. Bull. 90:540–551.
Uzmann, J. R., R. A. Cooper, R. B. Theroux, and R. L. Wigley.
1977. Synoptic comparison of three sampling techniques for estimating abundance and distribution of selected megafauna: submersible vs. camera sled vs. otter trawl. Mar. Fish. Rev. 39(12):11–19.
Winer, B. J.
1971. Statistical principles in experimental design, 2nd ed., 907 p. McGraw Hill, New York, NY.
Yoklavich, M. M., H. G. Greene, G. M. Cailliet, D. E. Sullivan, R. N. Lea, and M. S. Love.
2000. Habitat associations of deep-water rockfishes in a submarine canyon: an example of a natural refuge. Fish. Bull. 98:625–641.

Appendix I: Procedure used for estimating the swept transect area

At each sample unit (submersible dive site), we estimated the total swept transect area, where the swept area (m^2) = (average area swept per second [m^2/sec]) × (total elapsed time [seconds]). The average area swept per second (m^2/sec) was computed for a set of randomly selected thirty second portions of each transect. Conceptually, we determined the average area swept per second for the subsampled areas from a series of adjacent trapezoids (Fig. 1).

For each trapezoid, we determined swept area (A_t) by measuring the width that was swept (l_t) and distance that was swept (T_t), where

$$A_t = \frac{1}{2}(l_t + l_{t+1})T_t.$$

The process involved a frame-by-frame analysis of the video image, which required tracking an object from the center of the video monitor display to the bottom edge of the video display for a known time interval (Fig. 2). The elapsed time for this interval was obtained from the video frame count, and was used to calculate area swept per second.

Width-swept estimates (l_t) were calculated from 1) the distance between the laser spots on the video monitor display (w_t), 2) the width of the video monitor display (V), and 3) the known distance between the lasers (W) (20 cm), where

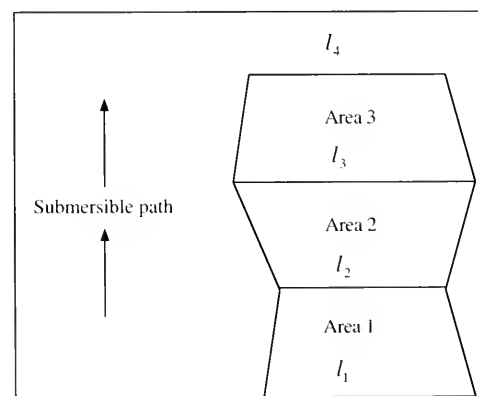

Figure 1
Schematic representation of adjacent trapezoids.

$$l_t = \frac{VW}{w_t}. \quad (1)$$

Because the width that was swept varied as the submersible distance off bottom varied, it was measured for each block. The following procedure was performed in sequence:

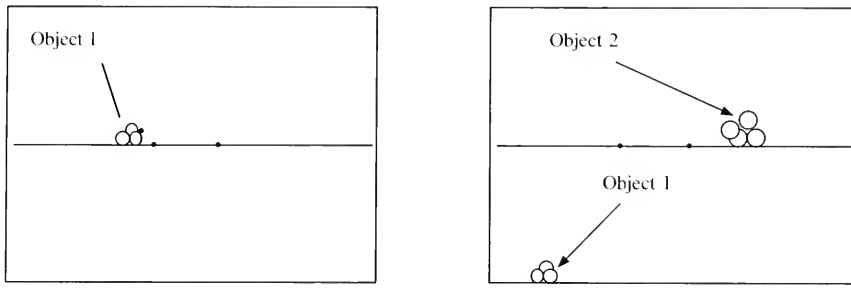

Screen 1: Distance between laser spots, w_1, is measured and object adjacent to lasers is identified.

Screen 2: Frame by frame advance until object adjacent to lasers in screen 1 rests at bottom of video screen; then, distance between laser spots, w_2, is measured, and the process repeats.

Figure 2

Illustration of the video-monitor display showing the frame-by-frame screen advance procedure used to determine the area swept per second.

1) w_1 was measured to the nearest millimeter, 2) an object on the seafloor adjacent to the laser spots was identified, 3) the videotape was advanced until the object appeared at the bottom of the video monitor display, and 4) w_2 was measured again (Fig. 2). The distance that was swept during this interval (T) is calculated trigonometrically by using the angle of the camera and constants estimated with the following procedures of Davis and Tusting (1991). The process is illustrated in Figures 3 and 4.

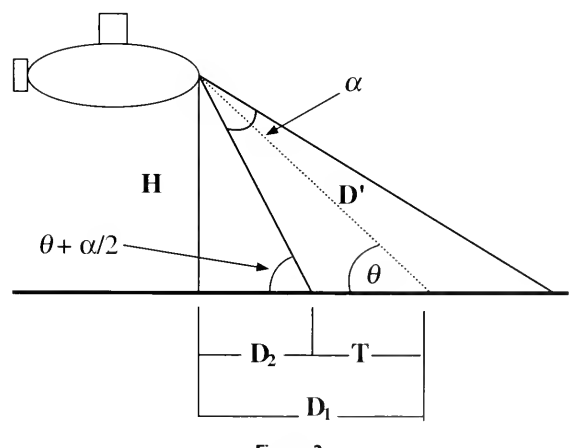

Figure 3

Schematic representation of the submarine and camera orientation to the bottom (the line labeled D' represents the center line of the camera). Definitions for the variables are provided in the left column of text on this page.

The variables of interest are

T = the geodetic distance between the location of the laser spots on the seafloor and the bottom edge of the camera's field of view (distance swept);
H = the height of the video camera above the sea floor;
α = the angle of the camera lens;
θ = the tilt angle of the camera;
D = the distance between the focal point of the camera and the reflection of the laser spots on the seafloor;
D_1 = the horizontal distance from the camera to a point on the sea floor at the center of the camera's field of view;
D_2 = the horizontal distance from the camera to a point on the sea floor at the bottom edge of the field of view; and
D' = the distance from the camera lens to the reflection of the laser spots on the seafloor;
w = the distance measured between the laser spots as they appear on the video monitor display;
W = the known distance (20 cm) between the lasers mounted in parallel on the camera housing.

Note the following relationships:

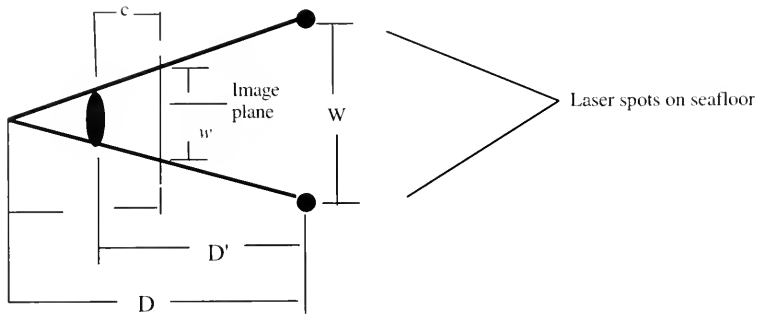

Figure 4

Schematic representation of the relationship between the camera lens, image plane, and laser spots on the seafloor.

$$D_1 = D' \cos\theta, \text{ and } H = D' \sin\theta \quad (2)$$

$$D_2 = \frac{H}{\tan\left(\theta + \frac{\alpha}{2}\right)} = \frac{D' \sin\theta}{\tan\left(\theta + \frac{\alpha}{2}\right)}, \quad (3)$$

In Equation 3, estimation of D_2 requires the height of the camera above the seafloor (H); however, the need for a direct measurement of H can be eliminated by using camera parameters that provide an independent estimate of D' (Fig. 4).

Figure 4 shows the relationships between the camera lens, image plane, and laser spots, where d is a constant representing the distance from the focal point to the image plane, and c is a constant representing the distance from the camera lens to the image plane (note that c may be positive or negative),

Note that both d and c are specific to the video display monitor employed, W, θ, and α are fixed, and w is observed.

$$D' = D - d - c, \text{ and } D = d\frac{W}{w}. \quad (4)$$

Therefore,

$$D' = d\left(\frac{W}{w} - 1\right) - c, \quad (5)$$

Underwater tests were conducted and the constants c and d were estimated for *Delta's* video camera and laser set-up by following the procedures of Davis and Tusting (1991). The distance traveled (T) for each area-swept trapezoid (from the center of the image to the lower edge of camera field of view), then, is

$$T = D_1 - D_2 = D'\left(\cos\left(\frac{\pi}{180}\theta\right) - \frac{\sin\left(\frac{\pi}{180}\theta\right)}{\tan\left(\frac{\pi}{180}\left(\theta + \frac{\alpha}{2}\right)\right)}\right). \quad (6)$$

Appendix II: Derivation of the trawl-survey habitat-bias estimator, and the trawl-survey habitat-bias effect size-index (d_b)

To estimate the trawl survey habitat bias, we contrasted 1) the traditional abundance estimator, which does not discriminate between fish density differences in trawlable and untrawlable habitats (habitat-biased), with 2) an unbiased abundance estimator that explicitly allows for density differences between trawlable and untrawlable habitats.

Let D_t = the true density in the trawlable habitat;
A_t = the area of trawlable habitat;
D_u = the true density in the trawlable habitat;
A_u = the area of untrawlable habitat;
A = the total area = $A_t + A_u$;
N = total abundance; and
Δ = the difference in true densities = $D_t - D_u$.

Then, for the unbiased estimator,

$$N = D_t A_t + D_u A_u.$$

and for the biased estimator,

$$N = D_t A = D_t A_t + D_t A_u.$$

The habitat bias, then, is the difference of the two estimators, or

$$Bias = (D_t A_t + D_t A_u) - (D_t A_t + D_u A_u) = (D_t - D_u) A_u = \Delta A_u. \quad (1)$$

The total error in the abundance estimator is a function of both the bias and the variance $V(\hat{D}_t)$ of the fish density estimator

$$MSE = Bias^2 + (A^2)V(\hat{D}_t), \quad (2)$$

where $V(\hat{D}_t)$ describes the uncertainty in the abundance estimator. If the bias is much less than this uncertainty, then its impact will be minimal. Therefore, we arbitrarily set

$$Bias^2 = (A^2)V(\hat{D}_t), \tag{3}$$

and substituting ΔA_u for bias from Equation 1 into Equation 3 gives

$$A_u{}^2\Delta^2 = (A^2)V(\hat{D}_t). \tag{4}$$

Solving for Δ gives

$$\Delta = \frac{A}{A_u} SD(\hat{D}_t), \tag{5}$$

where $SD(\hat{D}_t)$ = the standard deviation of the trawl survey density estimator in the trawlable habitat.

Thus, the effect size threshold used for detecting differences in mean density in the power analysis is a product of the arbitrary decision for the bias in the abundance estimator to be equal to its standard error.

For the statistical power analysis, we expressed Δ (the difference in densities between habitats) as the standardized effect size index (d_b) for a two-sample t-test (Cohen, 1988); dividing (Eq. 5) by an estimate of the population standard deviation, which yields

$$d_b = \left[\frac{A}{A_u} SD(\hat{D}_t) / s_p \right].$$

Diving behavior of immature Steller sea lions (*Eumetopias jubatus*)

Thomas R. Loughlin
Jeremy T. Sterling
National Marine Mammal Laboratory
Alaska Fisheries Science Center, NMFS
7600 Sand Point Way, NE
Seattle, Washington 98115
E-mail address (for T. R. Loughlin): tom.loughlin@noaa.gov

Richard L. Merrick,
Northeast Fisheries Science Center, NMFS
166 Water Street
Woods Hole, Massachusetts 02543

John L. Sease
Anne E. York
National Marine Mammal Laboratory
Alaska Fisheries Science Center, NMFS
7600 Sand Point Way, NE
Seattle, Washington 98115

Abstract—Understanding the ontogenetic relationship between juvenile Steller sea lions (*Eumetopias jubatus*) and their foraging habitat is key to understanding their relationship to available prey and ultimately their survival. We summarize dive and movement data from 13 young-of-the-year (YOY) and 12 yearling Steller sea lions equipped with satellite dive recorders in the Gulf of Alaska and Aleutian Islands (n=18), and Washington (n=7) from 1994 to 2000. A total of 1413 d of transmission ($\bar{x}$=56.5 d, range: 14.5–104.1 d) were received. We recorded 222,073 dives, which had a mean depth of 18.4 m (range of means: 5.8–67.9 m; SD=16.4). Alaska YOY dived for shorter periods and at shallower depths (mean depth=7.7 m, mean duration=0.8 min, mean maximum depth=25.7 m, and maximum depth=252 m) than Alaska yearlings ($\bar{x}$=16.6 m, 0=1.1 min, $\bar{x}$=63.4 m, 288 m), whereas Washington yearlings dived the longest and deepest (mean depth=39.4 m, mean duration=1.8 min, mean maximum depth=144.5 m, and maximum depth=328 m). Mean distance for 564 measured trips was 16.6 km; for sea lions ≤10 months of age, trip distance (7.0 km) was significantly less than for those >10 months of age (24.6 km). Mean trip duration for 10 of the 25 sea lions was 12.1 h; for sea lions ≤10 months of age, trip duration was 7.5 h and 18.1 h for those >10 months of age.

We identified three movements types: long-range trips (>15 km and >20 h), short-range trips (<15 km and <20 h) during which the animals left and returned to the same site, and transits to other haul-out sites. Long-range trips started around 9 months of age and occurred most frequently around the assumed time of weaning, whereas short-range trips happened almost daily (0.9 trips/day, n=426 trips). Transits began as early as 7 months of age, occurred more often after 9 months of age, and ranged between 6.5 and 454 km. The change in dive characteristics coincided with the assumed onset of weaning. These yearling sea lion movement patterns and dive characteristics suggest that immature Steller sea lions are as capable of making the same types of movements as adults.

Manuscript approved for publication 29 October 2002 by Scientific Editor.
Manuscript received 4 April 2003 at NMFS Scientific Publications Office.
Fish Bull 101:566–582 (2003).

Steller sea lions range throughout the North Pacific Ocean rim and are declining in numbers in most of Alaska and Russia (Loughlin et al., 1992; Loughlin and York 2000). Studies of mitochondrial DNA suggest that at least two stocks exist: an eastern stock (California through southeast Alaska) and a western stock (Prince William Sound and areas west) (Bickham et al., 1996; Loughlin, 1997). For the western U.S. stock (west of 144°W), counts of adults and juveniles have fallen from about 110,000 individuals in the late 1970s to about 25,000 individuals in 2000—a decline of almost 80%. Although the numbers of sea lions that died were greater from the late 1970s to the early 1990s than at present, the rate of decline has remained high. As a result of this decline the U.S. government designated the western stock as "endangered" in 1997 under the U.S. Endangered Species Act; the eastern stock is designated as "threatened." Reasons for the decline in numbers are unknown but may be linked to reduced availability of prey caused indirectly by environmental changes or commercial fishing activities, or both (Loughlin and Merrick, 1989; Merrick, 1995). Severe environmental perturbations and commercial fishing, both resulting in changes in the abundance or availability of prey, have been implicated in the alteration of pinniped foraging behavior and declines in pinniped abundance (e.g. Trillmich and Ono, 1991; Melin, 2002). One method for studying the effect of reduced prey availability on pinnipeds is to measure diving behavior and foraging ecology by using either a time-depth-recorder (Kooyman et al., 1983; Gentry and Kooyman, 1986) from which dive data are retrieved after the animal returns from a feeding trip (e.g. Goebel et al., 1991; Boyd et al., 1994; Werner and Campagna, 1995), or by using a satellite-linked time-depth recorder (SLTDR; the newer version is called a "satellite dive recorder" SDR), which transmits dive and transmitter-status information to orbiting satellites and thus eliminates the need to recapture the animal (e.g. Merrick et al., 1994).

Few data are available concerning the foraging ecology of Steller sea lions. Merrick et al. (1994) and Merrick and Loughlin (1997) presented information on the dive characteristics and foraging

Table 1

Satellite transmitter number (PTT number), deployment location, age, sex, and morphometric measures of 25 Steller sea lions studied for diving behavior in Alaska and Washington, 1994–2000. The ten ST-10 and ST-16 SDRs we deployed that transmitted time-line messages are shown with **. 1 = Washington State area; 2 = Kodiak area; 3 = Shumagin Islands; 4 = Unimak Pass area; 5 = Sequam area. n/d = no data obtained. PTT number is the satellite transmitter identification number. Est. = estimated.

PTT number	Location code (regional)	Age (months)	Sex	Deployment date	Length of transmission (d)	Mass (kg)	Girth (cm)	Length (cm)
14073	1	12	M	6/8/95	51.67	86.26	n/d	151
14084	1	11	F	5/5/99	50.22	77.18	102	159
14085	1	19	M	1/5/00	14.50	154.36	133	193
14087	1	16	F	10/3/97	68.99	122.45	113	171
14089	1	16	F	10/3/97	55.58	111.11	122	173
21103**	1	22	M	3/30/00	63.80	139.23	128	192
21106**	1	22	M	3/30/00	83.28	143.31	119	192
14071	2	6	M	12/2/94	19.61	92.00	n/d	n/d
14074	2	6	M	12/6/94	53.13	79.80	n/d	n/d
14077	2	18	M	12/9/94	39.63	n/d	n/d	n/d
14078	2	18	F	12/7/94	57.99	n/d	n/d	n/d
14079	2	7	F	1/14/96	27.11	94.90	115	155
14080	2	7	M	1/16/96	79.04	106.20	115	156
14170**	2	21	M	3/12/00	93.99	Est. 95–105	n/d	150
21094**	2	9	M	3/12/00	66.40	62.20	90	145
14076	3	21	F	3/1/96	52.21	103.70	111	n/d
14081	3	9	M	3/2/96	45.02	n/d	144	n/d
14072	4	22	F	4/13/95	56.35	116.10	n/d	n/d
14075	4	8	F	2/25/96	31.76	104.00	123	140
14164**	4	9	M	3/8/00	97.61	79.60	n/d	n/d
14167**	4	9	F	3/9/00	29.67	100.20	n/d	155
14111**	5	9	F	2/29/00	61.71	87.00	108.5	151
14114**	5	9	F	2/29/00	52.53	85.80	108	157
14116**	5	9	F	2/29/00	56.61	76.20	102.5	148
14163**	5	9	M	2/29/00	104.14	109.00	113	156

behavior of a small sample of Steller sea lions in Alaska; Loughlin et al. (1998) provided similar information for Steller sea lions off the Kuril Islands, Russia. Merrick et al. (1990) and Brandon (2000) presented information on female pup-attendance behavior of sea lions with VHF radio-transmitters off the Kuril Islands and Alaska, respectively. These studies showed that during the breeding season, adult female Steller sea lions generally spent about half their time at sea on relatively brief (18–20 h) foraging trips. Dives tended to be shallow ($\bar{x}$=21 m), brief ($\bar{x}$=1.4 min), and frequent (about 13/h). Observations during winter showed that females with suckling yearlings (17–22 months of age) had feeding trips of about 2.3 days, whereas those with young-of-the-year (5–10 months of age) had trips lasting 0.9 of a day; time on shore for lactating females of both groups averaged 14.2 hours (Porter, 1997). Baba et al. (2000) were able to follow a yearling Steller sea lion for 5 months using two location-only satellite transmitters; one was attached to the top of the head and the other on the back. This animal traveled from Hokkaido to Sakhalin Island and throughout the southern Okhotsk Sea. No dive data were obtained.

Our objective is to present a description of the diving behavior of juvenile Steller sea lions for the western stock of Steller sea lions in Alaska and the eastern stock in Washington state. We deployed SDRs on juvenile Steller sea lions over a broader geographical range in Alaska and over a wider range of dates, providing a more comprehensive picture of the diving behavior of young Steller sea lions. Additionally, SDRs are now smaller and of higher quality, so that more detailed information on diving behavior is available. We then provide in the "Discussion" section a comparison of the accounts in the present study to those we published earlier on adult female diving behavior (e.g. Merrick and Loughlin, 1997).

Materials and methods

We captured 25 free-ranging Steller sea lions of both sexes from approximately 6–22 months of age at rookeries and haul-out sites in the Aleutian Islands and Gulf of Alaska (Table 1, Fig. 1) throughout the year from 1994 to 2000, and during 1995–2000 at Shilshole Marina in Puget Sound, near Seattle, Washington. Animal age was estimated by using

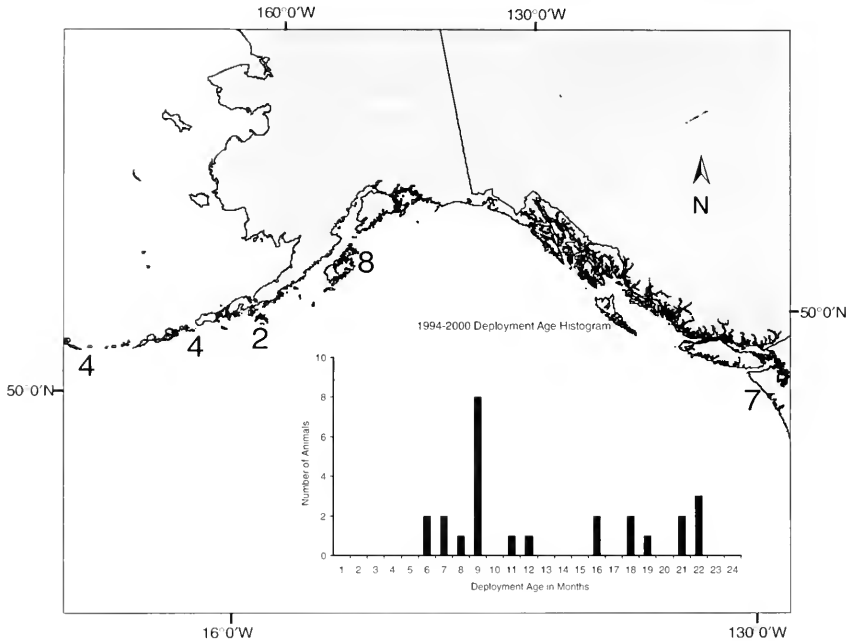

Figure 1

Locations where satellite dive recorders (SDRs) were deployed on 25 Steller sea lions in Alaska and Washington between 1994–2000. "Deployment age" is the age of the sea lions when satellite transmitters were attached.

mid-June as the presumed birth date (Pitcher and Calkins, 1981) and published accounts of mass, standard length, and girth at age (Calkins et al., 1998). Some juveniles before 1996 were chemically immobilized with Telazol[tm] injected intramuscularly by a dart fired from a pneumatic gun (Loughlin and Spraker, 1989). Those animals were not weighed; therefore exact dosage levels were not determined. However, dosages were most likely between 1.5 and 2.5 mg/kg. Once a sea lion was immobilized, intramuscular injection of 3–10 cc of Dopram was administered to stimulate respiration and facilitate recovery. After 1996, young sea lions were captured on land with a hoop net and physically restrained. During all years a SLTDR or SDR was glued to the pelage on the animal's back with fast-setting epoxy resin (Loughlin et al., 1987), and two plastic cattle ear tags with the same identification numbers were attached, one to each front flipper. The instruments were not recovered and were expected to be shed during or before molt.

Instrument description and programming

We used 0.5-watt ST-6 SLTDRs (packaged by Wildlife Computers, Redmond, WA), which provide dive depth, dive duration, and transmitter status. Further development by Wildlife Computers resulted in 0.25-watt ST-10 and ST-16 SDRs which could provide five messages: 1) dive depth, 2) dive duration, 3) transmitter status, 4) proportion of time at depth, and 5) a time line. Messages are sent at prescribed intervals; transmission interval at sea is every 43 sec and on land it is every 1 min 28 sec. The number of transmissions (and thus messages received) while the sea lion is at sea depends on the length of exposure of the instrument's salt-water switch at the surface. Location data are not sent by the transmitter but are calculated by Service-Argos, Inc. from the received message. Additional information on these instruments and their capabilities can be found in Merrick et al. (1994). The satellite tracking system (Argos) is described in detail in Fancy et al. (1988) and Stewart et al. (1989). Additional information can be obtained from the manufacturer at their web site (www.wildlifecomputers.com).

The ST-6 SLTDR stored, summarized, and transmitted dive data as histograms. Individual dives and surface intervals were not provided; therefore sampling frequency for measuring dive behavior was not a consideration (e.g. Boyd, 1993). Software programming of the SLTDR subdivided each day into four 6-h periods (2100–0300 h, 0300–0900 h, 0900–1500 h, and 1500–2100 h local time). Frequency histo-

grams were summarized separately for dive depth and dive duration for each of the four time periods. The SLTDRs recorded dive depth information in six separate "bins": 4–10 m, 10–20 m, 20–50 m, 50–100 m, 100–250 m, and >250 m. We used 4 m as the minimum depth for a dive based on earlier studies in Alaska (Merrick et al., 1994). Dive-duration bins were 0–60 sec, 60–120 sec, 120–180 sec, 180–240 sec, 240–360 sec, and >360 sec.

The ST-10 and ST-16 units used the same 6-h periods as the ST-6. However, the ST-10 and ST-16 SDRs subdivided dive depth information into 14 bins: 4 m; 4–6 m, 6–10 m, 10–20 m, 20–34 m, 34–50 m, 50–74 m, 74–100 m, 100–124 m, 124–150 m, 150–174 m, 174–200 m, 200–250 m, and >250 m. Dive duration also contained 14 bins at one-minute intervals (e.g. 1–2 min, 2–3 min, 3–4 min, etc.). The 14 time-at-depth bins coincided with dive-depth bins (e.g. 0, 4, 4–6, 6–10, etc. and the last was >200). However, the first bin was set to zero to determine if an animal was on land based on the proportion of dry readings of the salt-water switch during a 6-hour period. Time-at-depth was calculated as the proportion of time that dives occurred within a particular depth bin of a 6-h period while the sea lion was at sea (e.g. if an animal was at sea for 3 hours during a 6-h period and spent half its dive time in bin 50–74, the value in bin 50–74 would be 25%).

We deployed ten ST-10 and ST-16 SDRs (Table 1) which transmitted time-line messages in bins of 20-min periods (there are 72 periods of 20-min each in a 24-h day). These messages provide information on whether the instrument was wet or dry >10 min of a 20-min period for each of the 72 periods. Time-line messages thus allow calculation of time spent at sea and on land.

Maximum dive depth in a 24-h period, from midnight GMT to midnight GMT, was provided in the status message. This is a separate message that provides information on transmitter status, including a pressure offset, battery status, number of transmissions to date, at-surface data, date, time, ID of message, and a saltwater conductivity reading. All 25 transmitters that we deployed transmitted a status message.

The ST-6 SLTDRs were on 24 h/day and transmitted a maximum of 400 transmissions/day. To save battery power the instrument had a 6-h haul-out period; that is, it would turn off only if the transmitter was "dry" for 6 hours, indicating that the animal was on land. The ST-10 and ST-16 SDRs had 3-h haul-out periods; the ST-10 had a maximum of 250 transmissions/day, and the ST-16 had a maximum of 325/day. Both the ST-10 and ST-16 had duty cycles of 4 h on and 2 h off during a 24-h period to distribute transmissions during different times of the day and to ensure recording of information in all bins. All duty cycles started at midnight, with an offset of +13 h from GMT for Alaska.

Location data

Locations were estimated by the Service-Argos, Inc. classification scheme, where location class (LC) 3 is accurate to <150 m, LC 2 is accurate 150 m–≤350 m, LC 1 is accurate 350 m–1000 m, and LC 0 is accurate >1000 m. LCs A and B have no assigned accuracy range (Service-Argos, 1984; Keating, 1994). However, after our analysis, Vincent et al. (2002) used an algorithm published by McConnell et al. (1992) to filter satellite locations and found that both filtered and unfiltered LC A locations were of a similar accuracy to LC 1 locations for four gray seals (*Halichoerus grypus*). Because of the large variance in our samples associated with LC A locations, we excluded them (and the LC Bs) from our analyses. We sorted location data by date and time line to determine the locations for each trip.

Data analysis

Data analysis followed that of Merrick et al. (1994) and Merrick and Loughlin (1997). Analysis of the number of dives was prepared by summing counts of dives from the histograms. Median depths and durations of dives were calculated by using the range midpoint of a bin (e.g. 7 m for a 4–10 m bin) as the depth for all dives in the bin. We recognize that this approach invokes a possible error for dive profiles in large increment bins (e.g. 50–100 m) where the mean dive depth is the same, 75 m, regardless of whether the animal made most of its dives between 51 and 60 m or if it made most of its dives between 90 and 100 m. This error is inherent in the data collection process and could not be eliminated with the instruments used in our study. We also recognize that more locations will be recorded when the animals are at the surface for long periods or when transiting to different locations. However, because of the repetitive transmission of the histogram data and the usual short duration of short-range trips, there should be no inherent behavior-based bias in the dive data reported. Differences in dive depth and duration between locations were tested by using the Pearson chi-square tests or analysis of variance (ANOVA) (F-statistic), and P-value differences less than 0.05 were considered significant. Analysis of trip distance and duration were analyzed by using a repeated measures ANOVA, and because the distances were skewed, they were log-transformed to examine differences among groups.

Trips were defined and measured for distance by using an integrated process of the SDR data. For animals deployed with ST6 SDRs, which did not contain time line data sets (n=15), trip distances were extracted by using a combination of the dive histogram, duration histogram, and land or sea data sets to estimate arrival and departure times as well as locations calculated at sea or on land. Once arrival and departure times were estimated, the location data were examined to confirm that all locations calculated during that trip were wet locations. We then had all locations for an individual trip and from those locations we filtered out all A and B locations and imposed a swim speed filter (3 m/s). Finally, we reported the maximum straight-line distance from the departure site. For animals with ST10/16 SDRs, we were able to extract arrival and departure times from the time-line messages. However, if a day of time-line data was not received, we referenced the time-at-depth data, depth, and duration histograms to reconstruct the missing day of data. Once arrival and departure times were calculated we then followed the protocol stated above.

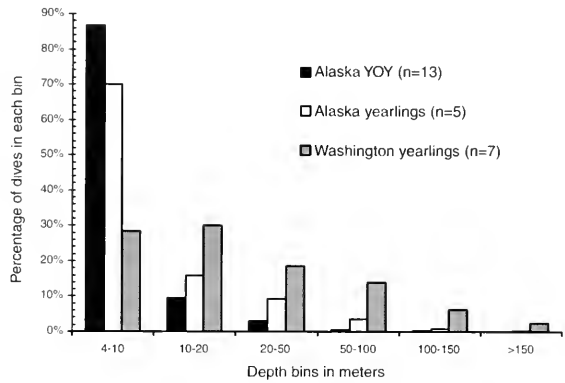

Figure 2

Percentage of dives occurring in each dive-depth bin for Alaska young-of-the-year (YOY), Alaska yearling, and Washington yearling Steller sea lions. Twenty-five animals are represented from 1994 to 2000 and a total of 222,073 dives.

Results

We report on SDR data obtained from 25 (13 male, 12 female) young-of-the-year and juvenile (estimated ages of <2 yr) Steller sea lions from Washington state, Gulf of Alaska, and Aleutian Islands, Alaska (Table 1). Most (22 of 25) were caught during October–March 1995–2000 and the remainder during May–July (Table 1). Mean number of days of transmission received from the SDRs was 56.8 d (range 14.5–104.1 d).

Dive characteristics

We recorded over 222,073 dives for young-of-the-year and juvenile Steller sea lions which had a mean dive depth of 18.4 m (range of means: 6.1–67.0 m; SD=16.23). Alaska young-of-the-year dived to shallower depths and for shorter periods (mean depth=7.7 m, SD=1.7; mean duration=0.8 min, SD=0.1; mean maximum depth=25.7 m, SD=16.9; and maximum depth=252 m) than did Alaska yearlings (mean depth=16.6 m, SD=10.9; mean duration=1.1 min, SD=0.4; mean maximum depth=63.4 m, SD=37.7; and maximum depth=288 m), whereas Washington yearlings dived the deepest and the longest (mean depth=39.4 m, SD=14.9; mean duration=1.8 min, SD=0.6; mean maximum depth=144.5 m, SD=32.6; and maximum depth=328 m). Alaska animals dived to much shallower depths (mean depth=10.3 m) than animals from Shilshole, WA. There was no significant difference in the mean dive depths among locations in Alaska (P=0.8). Alaska animals, in comparison to the Washington animals, had a significantly greater proportion of dives in the 4–10 m depth bin (70%, P<0.001) than in the deeper depth bins.

We compared the proportion of dives in the shallowest bin (depth bin 4–10 m) for animals captured in Washington state versus Alaska using a generalized linear model with a binomial link function (McCullagh and Nelder, 1989). The proportion of shallow dives was significantly greater (P<0.001) among the Alaskan animals (81.4%) than among the Washington state animals (43.8%). Among the Washington state animals, the proportions of dives in the 1020 m depth bin (20.4%) and the 20–50 m depth bin (19.4%) were similar; proportions of dives in the deeper depth bins were progressively fewer (Fig. 2). Maximum and mean-maximum dive depth were also greater for young sea lions from Washington that dived to 141.5 m (SE=11.4) mean-maximum depth versus 33.8 m (SE=7.2) for Alaska sea lions (F=63.4, 23 and 24 df; P<0.001) (Table 2). We plotted the maximum depth for each 24-h period by the number of days in which the Argos satellite received a status message (which contains maximum depth for 24 hours) and found that with one exception (PTT 14078), Washington yearlings consistently dived deeper than their Alaska counterparts (Fig. 3, A and B). Two of three Alaska young-of-the-year were shallow divers and the third dived to 250 m once and beyond 100 m on numerous occasions late in the tracking period (Fig. 3C). The maximum depth for all sea lions that we studied was 328 m for a juvenile sea lion that was equipped with a SDR at Shilshole, WA (PTT 21106); the deepest dive for a yearling Alaska sea lion was 288 m (PTT 14078) (Fig. 3).

Mean dive duration was 1.1 min for all young sea lions (n=226,497 dives). Dive duration was significantly longer for Shilshole sea lions ($\bar{x}$=1.75 min; range: 0.95–3.10) compared to Alaska sea lions ($\bar{x}$=0.85 min; range: 0.61–1.86; F=24.5, 23 and 24 df; P<0.001). Few dives were greater

Table 2

Summary of dive parameters from satellite dive recorders (SDRs) deployed on Steller sea lions in Washington and Alaska, 1994–2000. "PTT" is the satellite transmitter identification number.

	PTT	Mean max. dive depth (m)	Mean max. dive depth (*n*)	Max. depth (m)	Mean depth (m)	Mean depth (*n*)	Mean duration (min)	Mean duration (*n*)
Washington	14073	77.68	38	168	31.99	10,746	0.96	11,241
	14084	154.12	34	288	47.29	5183	1.69	5047
	14085	187.67	12	280	67.94	1991	3.10	2025
	14087	164.37	53	256	33.21	14,287	1.69	14,572
	14089	144.00	46	200	44.76	9682	1.82	9659
	21103	124.22	18	256	23.59	6920	1.40	5431
	21106	159.09	44	328	26.92	11,839	1.61	11,647
Alaska	14071	10.44	18	12	7.20	1541	0.61	1732
	14074	11.07	30	20	7.24	3044	0.72	2954
	14077	28.57	21	144	9.67	4745	0.81	5146
	14078	125.74	23	288	35.00	4186	1.82	3657
	14079	12.80	20	44	7.13	7546	0.71	8482
	14080	15.80	59	24	7.60	17,236	0.96	18,056
	14170	41.87	47	180	10.23	17,741	0.91	19,447
	21094	48.90	31	152	11.67	9745	0.79	9388
	14076	51.69	26	144	9.29	11,593	0.86	12,739
	14081	11.76	34	20	7.25	8717	0.70	9013
	14072	68.98	49	100	18.69	12,597	1.06	11,931
	14075	8.00	15	12	7.01	5424	0.67	4869
	14164	26.09	44	60	9.46	16,352	0.96	16,426
	14167	20.73	11	60	7.01	2985	0.81	3022
	14111	17.76	25	40	6.44	10,919	0.72	10,903
	14114	13.75	16	16	5.84	5846	0.68	6256
	14116	24.24	17	40	6.70	7359	0.73	7739
	14163	65.55	49	252	10.94	13,849	0.82	15,204
Mean		62.42		135.36	18.42		1.10	
SE		11.50		3.23	3.23		0.11	

than 6 min (Fig. 4). There was a significant positive linear relationship between dive duration and dive depth (r^2=0.89, F=7.06, 1 and 23 df, P<0.001), and a significant positive relationship between sea lion mass at the time of capture and mean dive duration (r^2=0.46, F=3.86, 1 and 20 df, P<0.001) but not girth (r^2=0.10, F=1.62, 1 and 14 df, P=0.22). The relationship between dive duration and dive depth for males was not different from that for females (F=1.16, 2 and 21 df, P=0.33). The positive relationship between dive duration and mass was likely driven by the greater mass of the male sea lions because the relationship was not statistically significant when the analysis was restricted to females.

Dive depth and duration showed an interesting ontogenetic trend. Alaska animals 7–10 months old typically had a mean dive duration of <1 min and a mean dive depth of about 10 m; by 11–12 months of age both increased, almost doubling in most cases (Fig. 5). Although sample size was small, this ontogeny of diving to deeper depths for longer periods at about 11–12 months of age was evident in the percentage of time at depth (Fig. 6). There was a higher proportion of time spent in the deeper depth bins during May and June (at age 11 and 12 months, respectively) than when younger, and the proportion of time hauled out was reduced for the older animals. Interestingly, the decrease in dive depth and dive duration for two Washington animals at 23 months of age (Fig. 5) corresponded with movement from inside Puget Sound to deeper waters off the Washington coast.

The greatest proportion of all diving (37%) occurred during 2100–0300 h; the least (about 16%) during 0900–1500 h (Fig. 7). There were no periods when young-of-the-year or juvenile sea lions from any location did not dive. The frequency distribution of dives was similar in all time periods for all age groups from Alaska and Washington (Fig. 7).

Distance and duration of trips at sea

Mean distance of trips at sea for 564 measured trips of the 25 study animals was 16.6 km (SD=44.9 km; range:

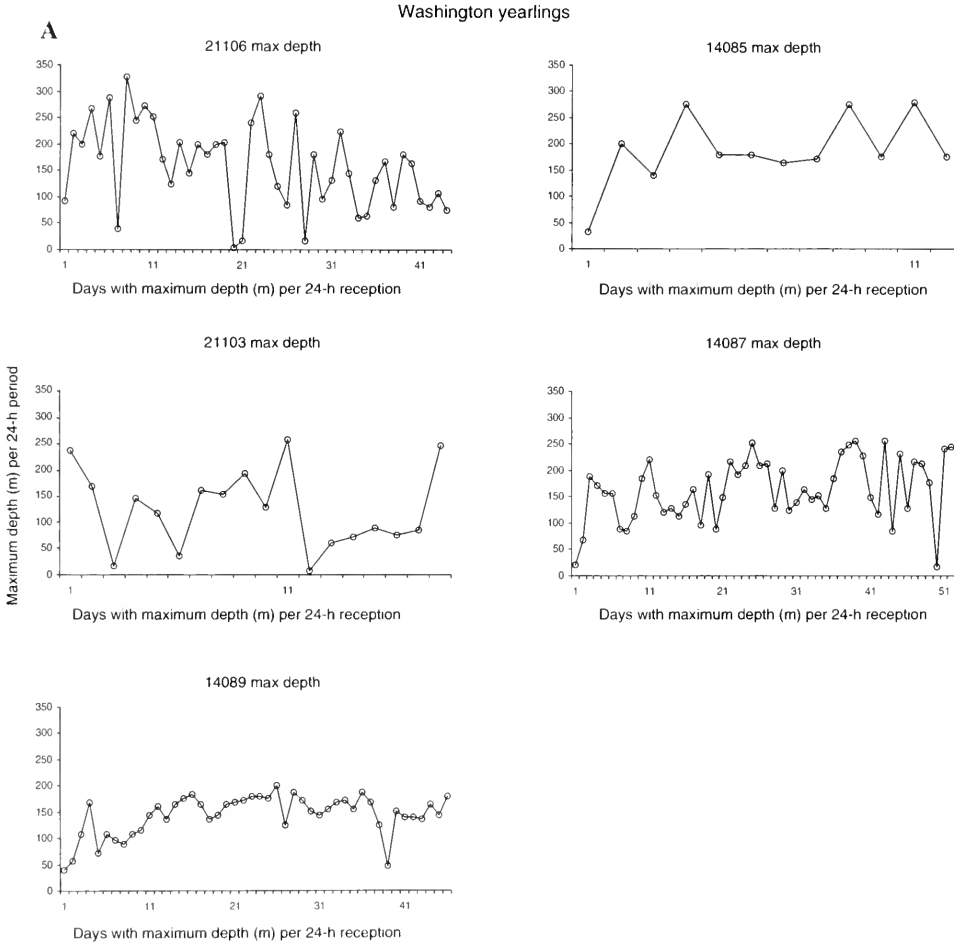

Figure 3

Summaries of the maximum depth (m) for each 24-h period (O) in which a status message containing maximum depth information was received by the Argos satellite for 13 of the 25 SDR-equipped Steller sea lions. For example, the Argos satellite received a status message from SDR 21106 for about 44 days, yet the SDR was operational for a total of 83 days (A; see Table 1). These 13 were chosen to compare yearlings of comparable age in Washington (**A**), and Alaska (**B**), and to provide typical examples of Alaska young-of-the-year (**C**).

<1–447.3 km; median=4.2 km). For sea lions ≤10 months of age, the mean distance of all trips was 7.0 km (n=257 trips; range=0.1–260.7 km; SD=19.0 km; median=2.7 km) (Fig. 8); for sea lions >10 months of age, the mean distance of all trips was 24.6 km (n=307; range: <1–447.3 km; SD=57.2 km; median=5.6 km) (Fig. 8). Averaged across individual animals, the mean distance of trips at sea ranged between 2.3 and 55.6 km; for the younger animals this range was 4–17 km and 2–55 km for the older animals. The repeated-measures ANOVA on the logarithm of trip distance showed that the older sea lions traveled significantly farther (P<0.001) than younger animals and that there were neither signifi-

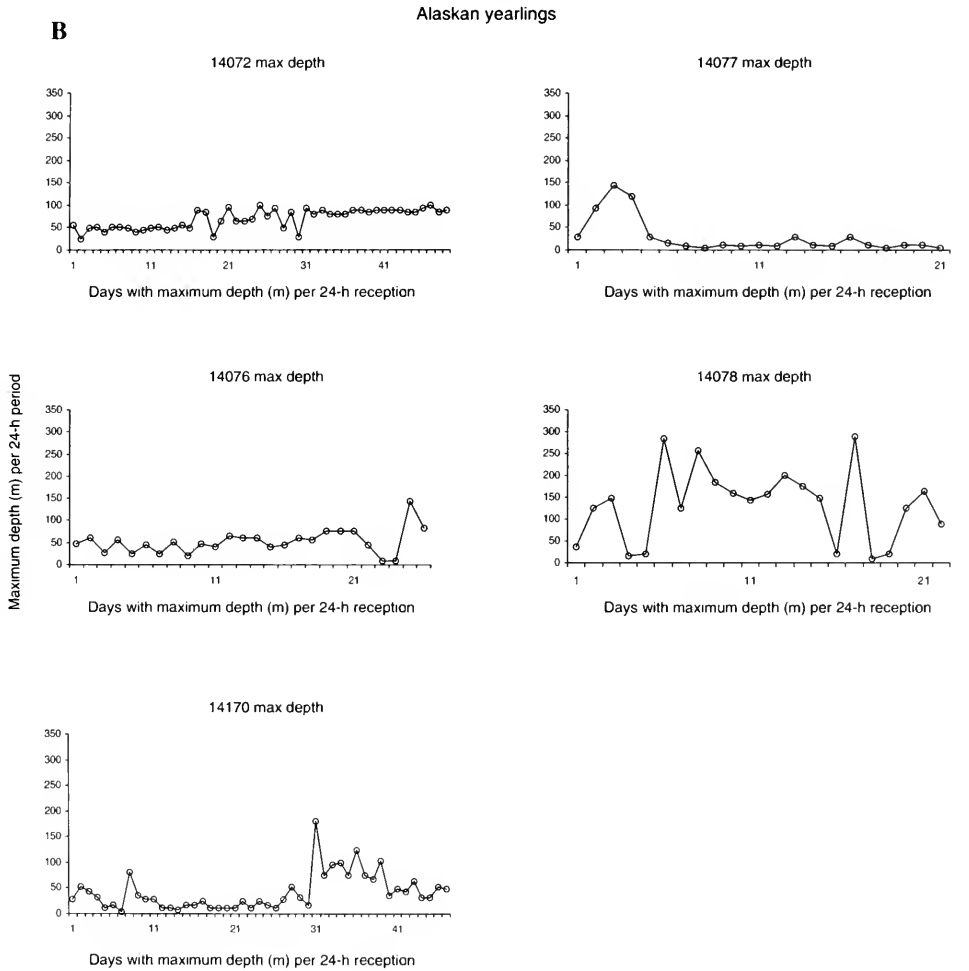

Figure 3 (continued)

cant gender (P = 0.6) nor gender×age interaction effects (P=0.19).

Trip distance increased with age. For example, we captured a 9-month-old male sea lion (bearing transmitter identification number PTT 21094, Table 1) near Kodiak Island in March 200. It had short trip distances (<10 km) which tended to concentrate near the capture site and nearshore (Fig. 8). As the animal matured through April and May, trip distance progressively increased until the sea lion was swimming over 50 km offshore beyond the 100-m depth contour and had a maximum dive depth >150 m (Table 2; Fig. 8).

Trip duration was measured for 10 of 25 animals with SDRs containing time-line data (it was not possible to calculate trip duration for 15 SDRs with the earlier SLTDRs that did not transmit time-line data). Mean trip duration for these 10 animals was 12.1 hours (n=544; SD=23.83 h; range: 1–344 h; median=7.3 h). For animals ≤10 months

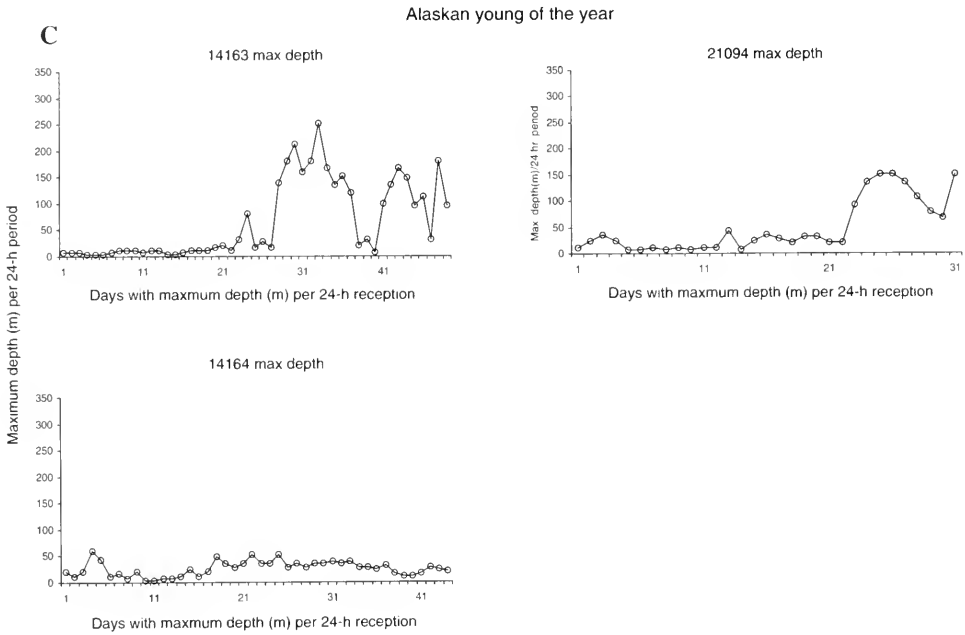

Figure 3 (continued)

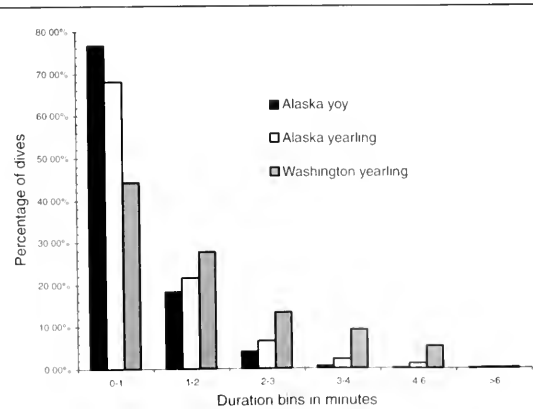

Figure 4

Percentage of dives occurring in each duration bin for Alaska young-of-the-year (YOY), Alaska yearling, and Washington yearling Steller sea lions. Twenty-five animals are represented from 1994 to 2000 with a total of 226,497 dives.

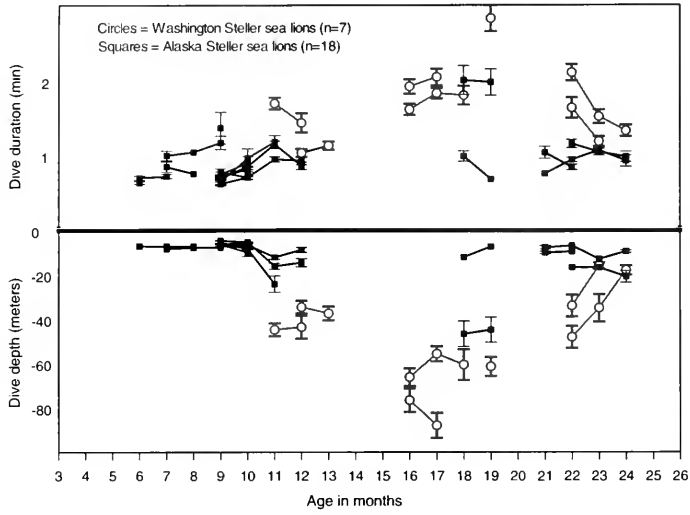

Figure 5

Mean dive depth and duration as a function of age in months for Washington and Alaska Steller sea lions. Error bars represent the standard error. Each connected symbol represents one individual sea lion monitored over several months.

of age, the mean trip duration was 7.5 hours (n=307; SD=7.5 h; range: 1–81.3 h; median=6 h) and for sea lions >10 months of age, the mean duration of all trips was 18.1 hours (n=237; SD=34.2 h; range: 1–344 h; median=10.3 h). Averaged across individual animals, the mean duration of trips at sea ranged between 6.2 to 21.4 hours; this range was 6.2 to 17.2 hours for the younger animals and 10.3 and 21.4 hours for the older animals. The analysis of the repeated-measures ANOVA on the logarithm of trip duration showed that the older sea lions had longer trip durations (P<0.001). We could not test for gender and gender×age effects because there were no measured trip durations for females >10 months. Among the younger animals, there was no gender difference in mean trip duration (P=0.11).

Types of movement

We identified three types of movements for the sea lions at sea: long-range trips (>15 km and >20 h), short-range trips (<15 km and <20 h), and transits to other haul-out sites (Fig. 9). Long-range trips most likely were foraging trips and began around 9 months of age. These trips had a mean of 48.7 km (SD=55.7 km; max=240.8 km) and may coincide with the assumed onset of weaning; they represented 6% of all trips to sea. The most numerous trips (88%) were short-range foraging trips ($\bar{x}$=3.6 km; SD=0.4; max=21.0 km), which happened almost daily (0.9 trips/d, n=426 trips). Transits were movements from one haul-out site to another haul-out site; these trips were characterized as the straight line distance from one haul-out site to another and began as early as 7 months of age but occurred more often after 9 months of age. Transit trips represented 6% of all trips at sea and had a mean distance of 66.6 km (SD=83.7 km; range: 6.5–341.9 km).

Discussion

The differences in diving behavior between young Steller sea lions in Washington and those off Alaska are intriguing. Possible reasons for these differences include variable habitat type, prey resources, or morphological or genetic differences. However, there is no evidence, based on morphology or genetics, to either support or refute differences in the diving behavior that we observed. The evidence of genetic differences between the western and eastern stock of Steller sea lions is based on mtDNA haplotype differences for a segment of the mitochondrial D-loop which does not code for any structural proteins (Bickham et al., 1996; Loughlin, 1997).

One morphological difference between the two stocks is a progressive increase in mass of Steller sea lion pups from east to west (Merrick et al., 1995), but whether this difference in mass continues with increasing age is unknown. Large animals typically dive deeper and longer than smaller (and younger) animals (Schreer and Kovacs, 1997). Larger animals have less drag per unit of mass and generally have more blood than smaller ones and thus are able to store more oxygen. Larger animals also have lower

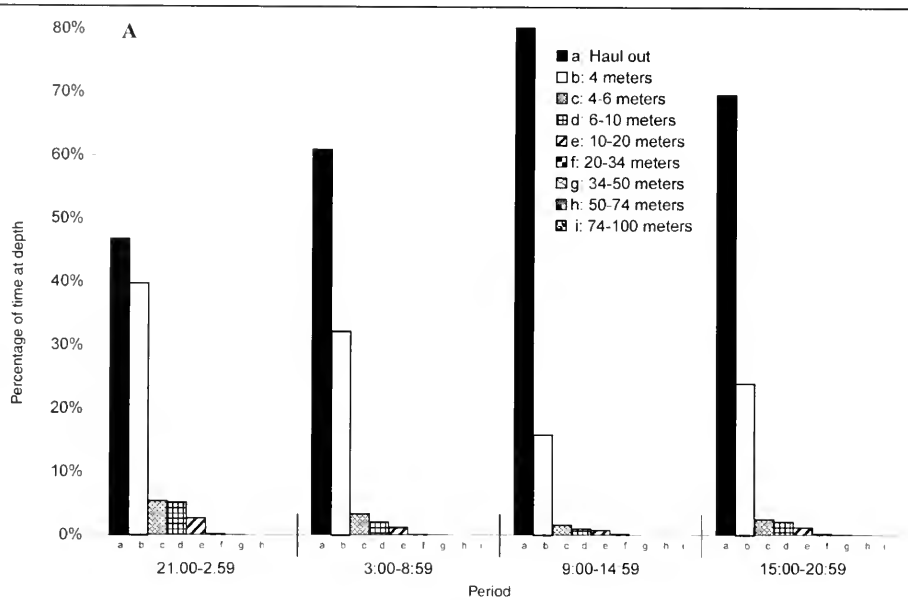

Figure 6

Percentage of time spent at depth for seven young-of-the-year Steller sea lions approximately (**A**) 7–10 months of age in Alaska, and percentage of time spent at depth for three young-of-the-year Steller sea lions approximately (**B**) 11–12 months of age (during May and June) in Alaska. This figure suggests that as young sea lions approach one year of age they tend to spend less time hauled out and that a greater proportion of their dives are deeper.

mass-specific metabolic rates than their smaller counterparts and thus expend less energy and use less oxygen stores (Schreer and Kovacs, 1997). Our sample size of sea lions of comparable age is small; however, we compared the mean mass of three Washington sea lions to the mean mass of three Alaska sea lions of approximately the same age (Table 1) and found that the Alaska animals had less mass than those in Washington (108 kg vs. 145 kg). Whether or not this difference in mass can account for the differences we saw in diving characteristics for animals of similar age (Fig. 3, A and B) is unknown.

The differences in diving characteristics between animals tracked in coastal waters of Puget Sound, Washington, and those tracked in Alaska waters are most likely linked to localized differences in prey habitat. The primary prey of Steller sea lions across their range are fish and cephalopods, both of which have a broad but predictable range in temporal, spatial, and seasonal nearshore availability. Typically, each species makes predictable migrations seasonally from pelagic to nearshore waters where they form large spawning concentrations. The prey are then further concentrated by local transition boundaries such as frontal zones and bathymetric features such as submarine channels (Sinclair et al., 1994). Steller sea lions appear to have the foraging flexibility to take advantage of both the predictable behavioral traits of these prey species, as well as the localized oceanographic conditions that enhance prey concentrations (Sinclair and Zeppelin, 2002).

The primary prey of Steller sea lions in Alaska waters is walleye pollock (*Theragra chalcogramma*), which is consumed year-round (Sinclair and Zeppelin, 2002). Walleye pollock is replaced as a dominant year-round prey item by Pacific whiting (*Merluccius productus*) in Pacific Northwest waters (Gearin et al., 1999). Both species are semidemersal and can be found from near surface waters to depths >1200 m, depending on localized conditions (Hart, 1973; Eschmeyer et al., 1983). The greatest abundances of both species are available to Steller sea lions in nearshore waters over the continental shelf and perhaps as the prey become more available during nighttime diurnal vertical movements.

The physical features of Puget Sound, along with its complex bathymetry and the extensive channels and canyons, provides extensive microhabitat for both predator and prey species to express the full extent of their depth range. In this respect, Puget Sound is comparable to the Gulf of Alaska where Pacific cod (*Gadus macrocephalus*) is the predominant winter prey item for Steller sea lions. Pacific cod is thought to be consumed during spawning when it ap-

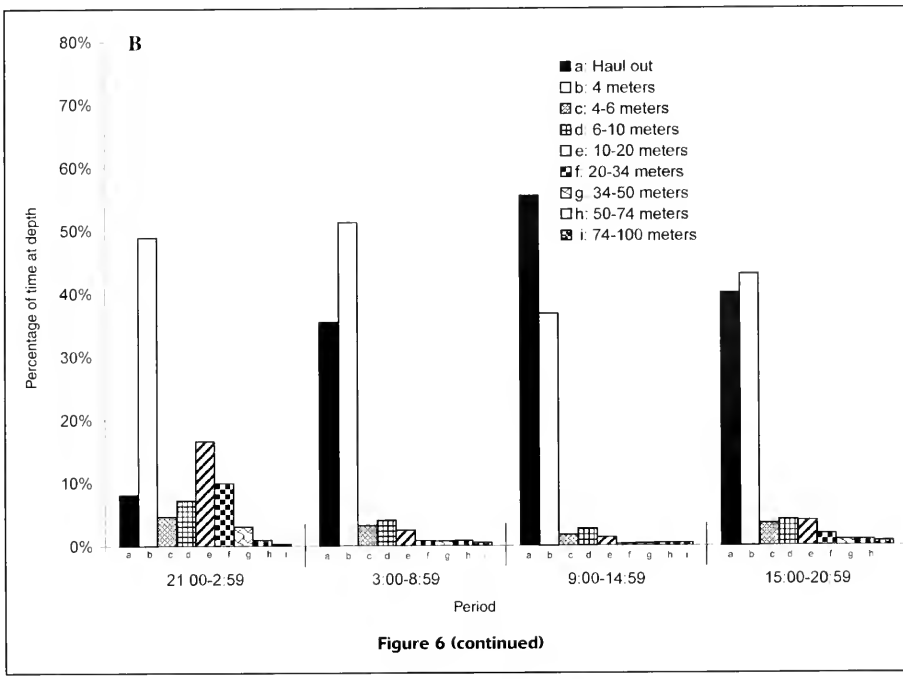

Figure 6 (continued)

pears to concentrate in the deep nearshore channels and gullies of the Gulf of Alaska (Sinclair and Zeppelin, 2002).

The differences in dive depths that we report also could be typical of the variability among individuals. Boveng et al. (1996) analyzed TDR data for six dive-related variables and found that dive duration was the least variable and vertical distance (dive depth) was the most variable among individual Antarctic fur seals (*Arctocephalus gazella*). In our study, there was high individual variability in both dive depth and maximum depth and little variability in dive duration—results similar to those of Boveng et al.'s (1996) study.

A female Steller sea lion nurses her pups during the day, stays with the pup for the first week, then goes to sea on foraging trips. Maternal pup-attendance patterns seem to vary over the sea lion's geographic range; the average range of time for foraging trips during lactation are from about 24 h to 2 d at the southernmost rookery at Año Nuevo Island, California (Higgins et al., 1988; Hood and Ono, 1997; but note that some of this variability may have been the result of El Niño conditions during part of the Higgins et al. study period), about 25 h at Lowrie Island, 19 h at Fish Island, 11 h for Chirikof Island, and 7 h in the Aleutian Islands (Brandon, 2000).

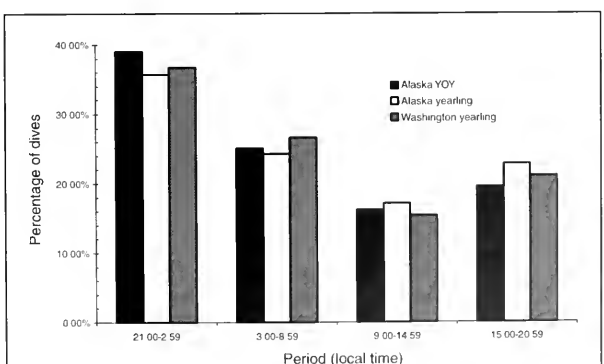

Figure 7

Percentage of dives occurring in each time bin for Alaskan young-of-the-year (YOY), Alaska yearling, and Washington yearling Steller sea lions. Twenty-five animals are represented from 1994 to 2000.

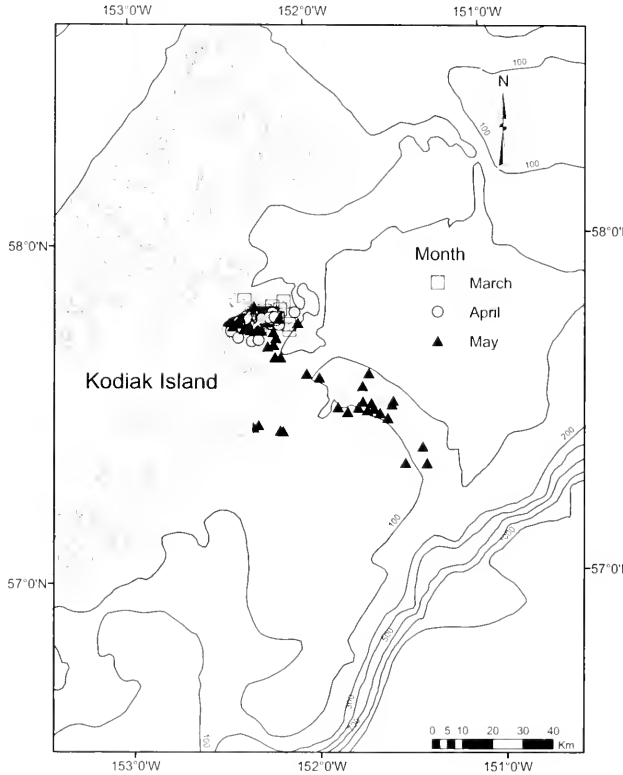

Figure 8

Figure showing the progressive increase in distance of locations from shore for a 9-month-old sea lion over time. This animal (identification number: PTT 21094) was equipped with a satellite transmitter near Kodiak Island in March 2000. Early trips were <15 km from shore in water <50 m in depth near the capture site. Trips became progressively greater as the animal matured through May 2000 when it was venturing over 50 km from shore in water >100 m in depth.

Ontogeny of diving ability has been studied in two other otariids. Baker and Donohue (2000) used data loggers (which they termed "time wet recorders") to measure time spent in the water and diving behavior of northern fur seal (*Callorhinus ursinus*) pups on St. Paul Island, Alaska. These pups began spending substantial time in the water at approximately 40–50 d of age that coincided with growth of the under fur and increases in sea surface temperature. Time spent in the water increased up to about 100 d of age; diving to depth did not occur until they were much older and about to migrate. Horning and Trillmich (1997) conducted an extensive study on the ontogeny of diving behavior in Galapagos fur seals (*Arctocephalus galapagoensis*), a species that weans no sooner than 2 years of age. They found that in young the development of diving behavior was closely linked to dependence on the mother and that substantial diving activity did not occur until one year of age; but even then the young fur seals were still nutritionally dependent on their mothers and did not dive as deep, or for as long, as mature females. The weaning date for Steller sea lions is unknown but is assumed to be between 4 and 12 months, and most pups are weaned just before the next breeding season (11–12 months) (Porter, 1997). The change in diving characteristics that we report is interesting in that it coincides with this period. Prior to weaning these pups forage in the company of their mother and learn to forage on their own; the need to dive deep for long periods to acquire food is compensated by nursing from the mother. Once weaning

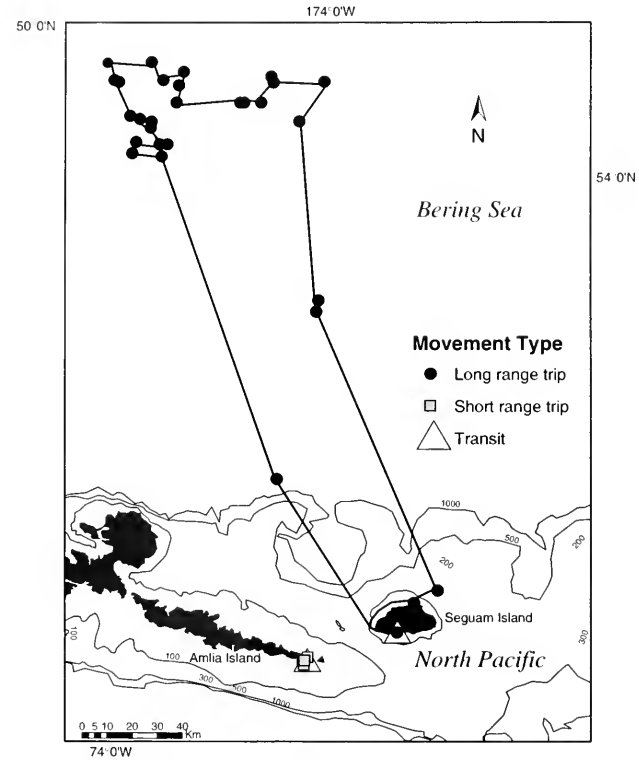

Figure 9

The three types of movement exhibited by two immature Steller sea lions captured at Turf Point, Seguam Island, Alaska, in 2000. A long-range trip (solid circles) >200 km is shown for PTT 14163 as it left and returned to Turf Point. A transit trip (open triangles) for PTT 14111 is shown as it left Turf Point and remained at the east end of Amlia Island where it went on numerous short-range trips (shaded squares).

occurs, the yearlings are forced to explore more areas to acquire food for needed energy. Dives become deeper and longer as these yearlings forage at different depths within the water column. Just before their first birthday, many of these young sea lions are capable of diving to the same depths and for the same duration as those of many adults; they also begin to forage at greater distances and for longer periods. Juveniles that we studied had a mean dive depth of 18.4 m and dive duration of 1.1 min compared to adult females in Alaska that had a mean dive depth of 21 m and dive duration of 1.4 min (Merrick and Loughlin, 1997). Maximum depth in our study was 328 m for a Washington juvenile and 288 m for an Alaska juvenile. Maximum depth information for adult females in Alaska was not provided by the instruments used by Merrick and Loughlin (1997); their maximum depths were characterized by bin data only. They showed that about 5% of dives by adult females in winter were greater than 250 m. In another study, adult females in Alaska were equipped with early-style SLTDRs that had features that recorded time-depth information and these SLTDRs showed that the females frequently dived to 200 m or more (Merrick et al., 1994).

Schreer and Kovacs (1997) summarized maximum dive depth and dive duration for air-breathing vertebrates and developed predictive allometric equations for both parameters based on body mass. We fitted our Steller sea lion body mass data to these equations to estimate maximum dive depth ($27.33M_b^{0.46}$), where M_b represents body mass in kilograms, and maximum dive duration ($6.22M_b^{0.10}$). We found that the maximum dive depth equation provided reasonably close estimates but that dive durations were typically overestimated (Table 3). In some cases measured and

Table 3

The recorded mass, recorded maximum dive depth, and recorded maximum dive duration for individual young Steller sea lions in Alaska and Washington from this study and the estimated maximum dive depth ($27.33M_b^{0.46}$) and estimate maximum dive duration ($6.22\,M_b^{0.1}$) based on allometric equations in Schreer and Kovacs (1997). PTT number is the satellite transmitter identification number. Est.= estimated. n/a = no data obtained.

PTT number	Mass (kg)	Maximum depth (m)	Est. maximum depth (m)	Maximum duration (min)	Est. maximum duration (min)
14073	86.26	168	212.38	>6	9.71
14084	77.18	288	201.79	>6	9.61
14085	154.36	280	277.57	>6	10.30
14087	122.45	256	249.52	>6	10.06
14089	111.11	200	238.61	4–6	9.96
21103	139.23	256	264.70	13	10.19
21106	143.31	328	268.24	>14	10.22
14071	92.00	12	218.77	2–3	9.78
14074	79.80	20	204.91	>6	9.64
14077	n/a	144	n/a	>6	n/a
14078	n/a	288	n/a	>6	n/a
14079	94.90	44	221.91	>6	9.81
14080	106.20	24	233.70	> 6	9.92
14170	Est. 95–105	180	Est. 222.02–232.48	> 14	Est. 9.81–9.91
21094	62.20	152	182.72	>14	9.40
14076	103.70	144	231.15	>6	9.89
14081	n/a	20	n/a	>6	n/a
14072	116.10	100	243.48	>6	10.01
14075	104.00	12	231.46	>6	9.90
14164	79.60	60	204.67	>14	9.64
14167	100.20	60	227.53	3–4	9.86
14111	87.00	40	213.22	8–9	9.72
14114	85.80	16	211.86	7–8	9.71
14116	76.20	40	200.60	5–6	9.59
14163	109.00	252	236.51	>14	9.94

estimated maximum dive depth values differed by large amounts (e.g. sea lion PTT 14071), perhaps because the deployment period was brief, before deep dives occurred. For others (e.g. PTT 14074) the difference may have been due to the young animal's continued dependence on the female for nourishment; deeper dives do not occur until weaning. In addition, we note that our dive duration data were stored in bins of 1-min intervals (from 1 to 6 min in the early instruments and from 1 to 14 min in the recent ones); the exact duration of each dive is unknown.

Movement patterns also suggest that the swimming ability of juvenile sea lions is comparable to that of adults. It is not unusual for young sea lions to travel distances as great as 1784 km from the natal rookery; as they approach adulthood they generally remain within 500 km of their natal rookery (Raum-Suryan et al., 2002). In our study some young sea lions traveled several hundred kilometers between sites while presumably searching for food or venturing from the natal rookery site.

Further analysis of our SDR data is warranted to more fully understand sea lion diving behavior and its relationships with oceanographic parameters, daily and season change, and behavioral features as discussed by Fedak et al. (2001). The time allocation at depth (TAD) index described by them will be a useful method for interpretation of our SDR (and TDR) data. Further analysis of our SDR data is needed to determine if such a study is possible.

Acknowledgments

Field assistance was provided by numerous NMML staff; logistical support was provided by Alaska Helicopters and the captain and crew of the U.S. Fish and Wildlife Service research vessel *Tiglax*. The manuscript was improved by comments from D. DeMaster, G. Duker, T. Gelatt, R. Hobbs, M. Lander, J. Lee, R. Ream, E. Sinclair, and two anonymous reviewers.

Literature cited

Baba, N., H. Nitto, and A. Nitta.
2000. Satellite tracking of young Steller sea lion off the coast of northern Hokkaido. Fisheries Sci. 66:180–181.

Baker, J. D., and M. J. Donohue.
2000. Ontogeny of swimming and diving in northern fur seal (*Callorhinus ursinus*) pups. Can. J. Zool. 78:100–109.
Bickham, J. W., J. C. Patton, and T. R. Loughlin.
1996. High variability for control-region sequences in a marine mammal: implications for conservation and biogeography of Steller sea lions (*Eumetopias jubatus*). J. Mammal. 77:95–108.
Boveng, P. L., B. G. Walker, and J. L. Bengtson.
1996. Variability in Antarctic fur seal dive data: implications for TDR studies. Mar. Mamm. Sci. 12:543–554.
Boyd, I. L.
1993. Selecting sampling frequency for measuring diving behavior. Mar. Mamm. Sci. 9:424–430.
Boyd, I. L., J. P. Y. Arnould, T. Barton, and J. P. Croxall.
1994. Foraging behaviour of Antarctic fur seals during periods of contrasting prey abundance. J. Animal Ecol. 63:703–713.
Brandon, E. A. A.
2000. Maternal investment in Steller sea lions in Alaska. Ph.D. diss., 137 p. Texas A&M University, Galveston, TX.
Calkins, D. G., E. Becker, and K. W. Pitcher.
1998. Reduced body size of female Steller sea lions from a declining population in the Gulf of Alaska. Mar. Mamm. Sci. 14:232–244.
Eschmeyer, W. N., E. S. Herald, and H. Hammann.
1983. A field guide to Pacific coast fishes of North America, 336 p. Boston Houghton Mifflin Company, Boston, MA.
Fancy, S. G., L. F. Pank, D. C. Douglas, C. H. Curby, G. W. Garner, S. C. Amstrup, and W. L. Regelin.
1988. Satellite telemetry: a new tool for wildlife research and management. U.S. Fish and Wildl. Serv. Resour. Publ. 172:154.
Fedak, M. A., P. Lovell, and S. M. Grant.
2001. Two approaches to compressing and interpreting time-depth information as collected by time-depth recorders and satellite-linked data recorders. Mar. Mammal Sci. 17:94–110.
Gearin, P., S. Jeffries, S. Riemer, L. Lehman, K. Hughes, and L. Cooke.
1999. Prey of Steller's sea lions, *Eumetopias jubotus*, in Washington state. *In* Abstracts of the 13th biennial conference on the biology of marine mammals, Wailea, Hawaii November 28 December 3, p. 65. Soc. Marine Mammalogy, Wailea, HI.
Gentry, R. L., and G. L. Kooyman.
1986. Methods and dive analysis. *In* Fur seals, maternal strategies on land and at sea (R. L. Gentry and G. L. Kooyman eds.), p 28–40. Princeton Univ. Press, Princeton, NJ.
Goebel, M. E., J. L. Bengtson, R. L. DeLong, R. L. Gentry, and T. R. Loughlin.
1991. Diving patterns and foraging locations of female northern fur seals. Fish. Bull. 89:171–179.
Hart, J. L.
1973. Pacific fishes of Canada. Bull. Fish. Res. Board Can. 180, 740 p.
Higgins, L. V., D. P. Costa, A. C. Huntley, and B. J. LeBoeuf.
1988. Behavioural and physiological measurements of maternal investment in the Steller sea lion, *Eumetopias jubatus*. Mar. Mamm. Sci. 4:44–58.
Hood, W. R., and K. A. Ono.
1997. Variation in maternal attendance patterns and pup behaviour in a declining population of Steller sea lions (*Eumetopias jubatus*). Can. J. Zool. 75:1241–1246.
Horning, M., and F. Trillmich.
1997. Ontogeny of diving behavior in the Galapagos fur seal. Behaviour 134:1211–1257.
Keating, K. A.
1994. An alternative index of satellite telemetry location error. J. Wildl. Manage. 58:414-421.
Kooyman, G. L., J. O. Billups, and D. W. Farwell.
1983. Two recently developed recorders for monitoring diving activity of marine birds and mammals. *In* Experimental biology at sea (A. G. Macdonald and I. G. Priede, eds.) p. 187–214. Academic Press, New York, NY.
Loughlin, T. R.
1997. Using the phylogeographic method to identify Steller sea lion stocks. *In* Molecular genetics of marine mammals (A. Dizon, S. J. Chivers, and W. F. Perrin, eds.), p. 159–171. Spec. Publ. 3 of the Soc. Mar. Mammal.
Loughlin, T. R, J. L. Bengtson, and R. L. Merrick.
1987. Characteristics of feeding trips of female northern fur seals. Can. J. Zool. 65:2079–2084.
Loughlin, T. R., and R. L. Merrick.
1989. Comparison of commercial harvest of walleye pollock and northern sea lion abundance in the Bering Sea and Gulf of Alaska. *In* Proceedings of the international symposium on the biology and management of walleye pollock, Nov. 14–16, 1988, Anchorage, Alaska, p. 679–700. Alaska Sea Grant Rep. 89-01, Univ. Alaska, Fairbanks.
Loughlin, T. R., A. S. Perlov, J. D. Baker, S. A. Blokhin, and A. G. Makhnyr.
1998. Diving behavior of adult female Steller sea lions in the Kuril Islands, Russia. Biosph. Cons. 1:21–31.
Loughlin, T. R., A. S. Perlov, and V. A. Vladimirov.
1992. Range-wide survey and estimation of total number of Steller sea lions in 1989. Mar. Mamm. Sci. 83:220–239.
Loughlin, T. R., and T. Spraker.
1989. Use of Telazol to immobilize female northern sea lion (*Eumetopias jubatus*) in Alaska. J. Wildl. Dis. 25: 353–358.
Loughlin, T. R., and A. E. York.
2000. An accounting of the sources of Steller sea lion mortality. Mar. Fish. Rev. 62(4):40–45.
McConnell, B. J., C. Chambers, and M. A. Fedak.
1992. Foraging ecology of southern elephant seals in relation to the bathymetry and productivity of the southern ocean. Antarctic Science 4:393–398.
McCullagh, P., and J. A. Nelder.
1989. Generalized linear models, 2nd ed., 261 p. Chapman and Hall, London.
Melin, S. R.
2002. The foraging ecology and reproduction of the California sea lion (*Zalophus californianus californianus*). Ph.D. diss., 150 p. Univ. Minnesota, St. Paul, MN.
Merrick, R. L.
1995. The relationship of the foraging ecology of Steller sea lions (*Eumetopias jubatus*) to their population decline in Alaska. Ph.D. diss., 171 p. Univ. Washington, Seattle, WA.
Merrick, R. L., R. Brown, D. G. Calkins, and T. R. Loughlin.
1995. A comparison of Steller sea lion, *Eumetopias jubatus*, pup masses between rookeries with increasing and decreasing populations. Fish. Bull. 94:753–758.
Merrick, R. L., and T. R. Loughlin.
1997. Foraging behavior of adult female and young-of-the-year Steller sea lions in Alaskan waters. Can. J. Zool. 75: 776–786.
Merrick, R. L., T. R. Loughlin, G. A. Antonelis, and R. Hill.
1994. Use of satellite-linked telemetry to study Steller sea lion and northern fur seal foraging. Polar Res. 13: 105–114.
Merrick, R. L., M. K. Maminov, J. D. Baker, and A. G. Makhnyr.
1990. Results of U.S.-U.S.S.R. joint marine mammal re-

search cruise in the Kuril and Aleutian Islands 6 June–24 July 1989. U.S. Dep. Commer. NOAA Tech. Memo. NMFS F/NWC-177, 63 p.

Pitcher, W., and D. G. Calkins.
1981. Reproductive biology of Steller sea lions in the Gulf of Alaska. J. Mammal. 62:599–605.

Porter, B.
1997. Winter ecology of Steller sea lions (*Eumetopias jubatus*) in Alaska. M.S. thesis, 84 p. Univ. British Columbia, Vancouver, B.C., Canada.

Raum-Suryan, K. L., K. W. Pitcher, D. G. Calkins, J. L. Sease, and T. R. Loughlin.
2002. Dispersal, rookery fidelity, and metapopulation structure of Steller sea lions (*Eumetopias jubatus*) in an increasing and declining population in Alaska. Mar. Mamm. Sci. 18:746–764.

Schreer, J. F., and K. T. Kovacs.
1997. Allometry of diving capacity in air-breathing vertebrates. Can. J. Zool. 75:339–358.

Service-Argos.
1984. Location and data collection system user's guide, 36 p. Service-Argos, Toulouse, France.

Sinclair, E. H., T. R. Loughlin, and W. Pearcy.
1994. Prey selection by northern fur seals (*Callorhinus ursinus*) in the eastern Bering Sea. Fish. Bull. 92:144–156.

Sinclair, E. H., and T. K. Zeppelin.
2002. Seasonal and spatial differences in diet in the western stock of Steller sea lions (*Eumetopias jubatus*). J. Mamm. 83:973–990.

Stewart, B. S., S. L. Leatherwood, P. K. Yochem, and M. P. Heide-Jorgensen.
1989. Harbor seal tracking and telemetry by satellite. Mar. Mamm. Sci. 5:361–375.

Trillmich, F., and K. A. Ono eds.
1991. Pinnipeds and El Niño, responses to environmental stress. Ecological studies 88, 293 p. Springer-Verlag, Berlin.

Vincent, C., B. J. McConnell, V. Ridoux, and M. A. Fedak.
2002. Assessment of Argos location accuracy from satellite tags deployed on captive gray seals. Mar. Mamm. Sci. 18: 156–166.

Werner, R., and C. Campagna.
1995. Diving behaviour of lactating southern sea lions (*Otaria flavescens*) in Patagonia. Can. J. Zool. 73:1975–1982.

Spawning cycles and habitats for ballyhoo (*Hemiramphus brasiliensis*) and balao (*H. balao*) in south Florida

Richard S. McBride
Justin R. Styer
Rob Hudson

Florida Marine Research Institute
Florida Fish and Wildlife Conservation Commission
100 8th Avenue SE
St. Petersburg, Florida 33701-5095
E-mail address (for R. S. McBride): richard.mcbride@fwc.state.fl.us

Abstract—Two halfbeak species, ballyhoo (*Hemiramphus brasiliensis*) and balao (*H. balao*), are harvested as bait in south Florida waters, and recent changes in fishing effort and regulations prompted this investigation of the overlap of halfbeak fishing grounds and spawning grounds. Halfbeaks were sampled aboard commercial fishing vessels, and during fishery-independent trips, to determine spatial and temporal spawning patterns of both species. Cyclic patterns of gonadosomatic indices (GSIs) indicated that both species spawned during spring and summer months. Histological analysis demonstrated that specific stages of oocyte development can be predicted from GSI values; for example, female ballyhoo with GSIs >6.0 had hydrated oocytes that were 2.0–3.5 mm diameter. Diel changes in oocyte diameters and histological criteria demonstrated that final oocyte maturation occurred over a 30- to 36-hour period and that ballyhoo spawned at dusk. Hydration of oocytes began in the morning, and ovulation occurred at sunset of that same day; therefore females with hydrated oocytes were ready to spawn within hours. We compared maps of all locations where fish were collected to maps of locations where spawning females (i.e. females with GSIs >6.0) were collected to determine the degree of overlap of halfbeak fishing and spawning grounds. We also used geographic information system (GIS) data to describe the depth and bottom type of halfbeak spawning grounds. Ballyhoo spawned all along the coral reef tract of the Atlantic Ocean, inshore of the reef tract, and in association with bank habitats within Florida Bay. In the Atlantic Ocean, balao spawned along the reef tract and in deeper, more offshore waters than did ballyhoo; balao were not found inshore of the coral reef tract or in Florida Bay. Both halfbeak species, considered together, spawned throughout the fishing grounds of south Florida.

Manuscript approved for publication 30 January 2003 by Scientific Editor.
Manuscript received 4 April 2003 at NMFS Scientific Publications Office.
Fish. Bull. 101:583–589 (2003).

Combined landings of two halfbeaks species, ballyhoo (*Hemiramphus brasiliensis*) and balao (*H. balao*), constitute a small but valuable bait fishery in south Florida (Berkeley et al., 1975; McBride et al., 1996). Both species occupy coastal pelagic habitat in association with coral reefs (Starck, 1968; Nybakken, 1997). During the 1990s two changes in the halfbeak fishery occurred that caused concerns regarding the exploitation levels in this fishery (McBride, 2001). First, geographic shifts occurred when halfbeak fishing expanded from the Atlantic Ocean into the nearshore waters north of the Florida Keys, an area known as Florida Bay. Second, changes in statewide net fishing regulations[1] created concerns that the net fishermen displaced from other fisheries might preferentially enter the halfbeak fishery, thereby increasing halfbeak fishing effort. These two changes could have specific consequences on halfbeak reproductive output. For example, because some fishermen viewed Florida Bay as a spawning or nursery ground for halfbeaks, it was of interest to learn exactly how concentrated spawning might be in Florida Bay and whether spawning occurred outside Florida Bay. In addition, because halfbeak landings are dominated by a single species, ballyhoo (Berkeley et al., 1975; McBride et al., 1996), it could be argued that these changes in the fishery could disproportionally affect spawning by the less abundant, and potentially more vulnerable target species, balao.

Both ballyhoo and balao are distributed widely in the western and eastern Atlantic Ocean (Collette, 1965), but no study has defined their spawning grounds. Berkeley and Houde (1978) described both species to be small (<32 cm fork length) summer-spawners that rarely live past two years, but in terms of spatial coverage, they collected fish principally from the Miami, Florida, area. We reviewed reports on regional ichthyoplankton collections (e.g. Powell et al., 1989; Limouzy-Paris et al., 1994) and found that the numbers of halfbeak eggs and larvae were too few for characterizing the spawning grounds. Moreover, Berkeley and Houde (1978) suggested that standard ichthyoplankton survey data would underestimate the abundance of halfbeak eggs or larvae for three reasons. First, halfbeak eggs appear to attach to vegetation; therefore oblique tows may not target the appropriate habitats (i.e. benthic or floating vegetation) and halfbeak eggs would be completely lost if pleuston was discarded from ichthyoplankton samples. Second, halfbeak eggs hatch 8–9 days after fertilization and may disperse far away from spawning locations. Third, halfbeak larvae hatch at 5–7 mm and have pigmented eyes; therefore they appear capable of avoiding plankton nets. Various plankton sampling strate-

[1] This referendum (s. 16, Art. X of the Florida Constitution, enacted July 1, 1995) prohibits entangling nets in waters inshore of 3 miles on the Atlantic coast and 9 miles on the Gulf coast of Florida (including Florida Bay). It also prohibits non-entangling nets larger than 500 ft^2 (such as those nets used by commercial halfbeak fishermen), in waters less than 1 mile of Florida's Atlantic coast and 3 miles of the Gulf coast.

gies could be developed to overcome these problems, but we chose an alternative to plankton sampling as a way to define halfbeak spawning grounds.

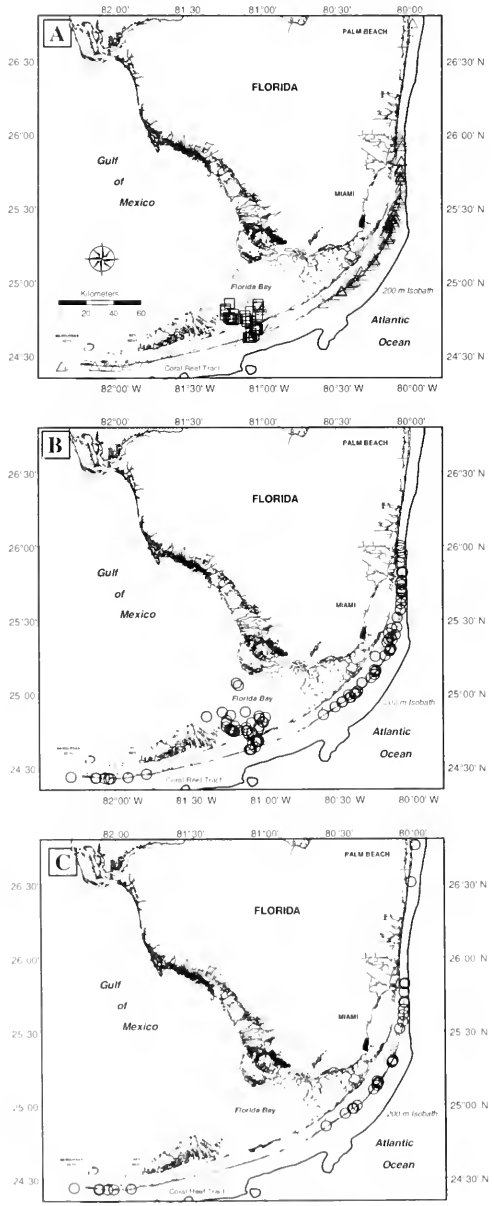

Figure 1

(**A**) Sampling area for halfbeaks (*Hemiramphus* spp.) during 1995–99 in the Atlantic Ocean and in Florida Bay. Each symbol represents an individual sample location where halfbeaks were caught. Fishery-dependent samples (triangles) were taken from commercial lampara net vessels. Fishery-independent samples (squares) were collected in the middle Florida Keys, near Vaca Key (not labeled because of the density of square symbols). Locations of ripe female (**B**) ballyhoo (*Hemiramphus brasiliensis*) and (**C**) balao (*H. balao*) are plotted separately. Ripe females have hydrated eggs, and this condition was determined in B and C by a gonadosomatic index >6.0 (see text for supporting evidence).

In this study, we used collections of adult ballyhoo and balao to define each species' spawning grounds in south Florida. Analyses of gonad histological preparations identified a discrete range of gonadosomatic indices (GSI) for females that were ready to spawn within hours, and the locations of these fishes were plotted by using geographic information system (GIS) software (ArcView, version 3.3., Environmental Systems Research Institute, Inc., Redlands, CA). This synthesis of GIS and GSI data was used to map the spawning grounds of ballyhoo and balao.

Materials and methods

Sampling occurred throughout the south Florida commercial halfbeak fishing grounds, from Palm Beach to the Marquesas Keys (Fig. 1A). The area immediately surrounding Vaca Key was well sampled, but other sections of the middle Florida Keys were not because commercial fishermen used only six fishing ports and their day trips were of limited range. Few samples were obtained from the Palm Beach area because net fishing is no longer allowed in much of this area (McBride, 2001). Halfbeak fishing trips by commercial fishermen were monitored from November 1995 to April 1999 by an onboard biologist during as many as four trips per month. A subsample of fish from the first successful net (a lampara net) set, and occasionally from later sets within a day, was obtained by filling a 5-gallon bucket from the catch as it was transferred from the net to holding boxes. This bucket held 100 to 200 halfbeaks, and these fishes were kept on ice and brought back to the laboratory for processing.

Fishery-independent collections were made by using cast nets and small hooks (sabiki rigs) in the middle Florida Keys. This sampling was specifically designed to include inshore areas where lampara net fishermen could not fish because of regulations associated with Florida's net limitation referendum.[1] The target number of these fishery-independent trips from July 1997 to October 1998 was four per month, and the target sample size for each trip was twelve fish. Additional fishery-independent sampling occurred in the springs of 1997, 1998, and 1999.

In the laboratory, whole body weight was recorded to the nearest 0.1 gram, and the gonads were removed and weighed to the nearest 0.01 g. Sex was identified with the aid of a dissecting binocular microscope (25–50×) when nec-

essary. Weights of fish collected from July 1997 to October 1998 were measured for up to 30 females per species per trip. Fish body and gonad weights were only occasionally recorded for other trips during 1995–99, but these data were included in the mapping of ripe females (i.e. females with hydrated oocytes in ovigerous lamellae) to increase overall sample size. In total, weight data were collected for 2908 halfbeak females from 79 commercial fishing net sets (63 different fishing days) and 59 fishery-independent sampling events (50 different sampling days). Commercial catches contributed 1649 ballyhoo and 757 balao females, and fishery-independent collections added another 497 ballyhoo and 5 balao females. The gonadosomatic index (GSI) was calculated as

$$GSI=(GW/(BW-GW)) \times 100,$$

where GW = gonad weight; and
BW = body weight.

The processes of final oocyte maturation (FOM) were examined by comparing GSIs with changes in whole oocyte size and histological criteria. Oocyte diameters were measured for 39 ballyhoo collected in April 1998 and March–April 1999. Fixed ovary tissue was washed, teased apart, and placed in a solution of 33% glycerin to 67% water. Measurements of at least 300 oocytes per fish were made to the nearest micron with the aid of a video system and image-analysis software (Optimas, vers. 100, Media Cybernetics, Inc., Silver Spring, MD). A minimum-size cut-off of 0.15 mm was used to exclude debris within the petri dish. Initially, oocyte diameters from six ballyhoo were measured from four separate sections of ovaries (left, right, anterior, posterior), but the modal oocyte diameter within each individual was the same for all four sections; therefore tissue from other fish was extracted without regard to location within the ovary. Berkeley and Houde (1978) performed a similar test and came to a similar conclusion. Ovaries from fish (n=930 females) collected during March and May 1997, July 1997–October 1998, and March–April 1999 were prepared for histological examination. Histological methods are presented in McBride and Thurman (2003). Here, the most advanced oocyte stage was recorded (in increasing order of oocyte maturity) as either perinucleolar, cortical alveolar, vitellogenic, or as either of two stages for oocytes in final maturation: nucleus migration and hydration (West, 1990). McBride and Thurman (2003) have reported the size at 50% maturity to be ≥160 mm FL for female balao and ≥198 mm FL for female ballyhoo (approximately 31.5 g and 60.9 g, respectively, using length-weight relationships from Berkeley and Houde [1978; their Fig. 7]). Mean GSIs and 95% confidence limits were determined for fish with regard to their most advanced stage of oocyte development, and a minimum cut-off value was established for GSI values indicating ripe females.

The locations of ripe females were plotted to indicate spawning grounds. Water depth and bottom type of these spawning locations were determined by using the Marine Resources Geographic Information System at the Florida Marine Research Institute (www.floridamarine.org). Point locations were recorded by using a global positioning system hand-held unit. The latitude and longitude of fishery-dependent samples were taken onboard the fishing vessel once the lampara net enclosed the fish. Location data for fishery-independent samples were taken from an anchored position. Depth information was divided into the following categories: area exposed at low tide, 0–1 m, 1–2 m, 2–4 m, 4–6 m, 6–10 m, and 10–20 m; only one of 159 locations was without depth information. Substrate information was divided into one of the following categories: platform margin reefs, patch reefs, other hard bottom, seagrass beds, and bare substrate; 32 of 159 locations did not have substrate information.

Results

Spawning cycles

Ballyhoo and balao had prolonged spawning seasons that peaked in late spring and early summer (Fig. 2). Monthly average GSIs of mature females increased from a low of <0.4 for both species to a high of 6.4 for balao and 6.9 for ballyhoo. The average GSI of individual females with only primary growth oocytes (i.e. their most advanced oocyte stages were perinucleolar or cortical alveolar) fell within a narrow interval of 0.1–0.3 (maximum=0.95, Fig. 3). These females were either small fishes that were immature or they were larger fishes that were regressed (i.e. mature but inactive). Vitellogenesis more than doubled the average GSI values for both species, but all females whose most advanced oocyte stage was vitellogenic had GSIs less than 1.37. Dramatic increases in GSI values also occurred during FOM, and significant differences were evident in the sequential FOM steps of nucleus migration and nucleus breakdown. During nucleus migration, but before hydration, ballyhoo GSIs averaged 3.4 (3.3–3.6; 95% CL) and balao GSIs averaged 5.2 (4.6–5.9). Females with hydrated oocytes had GSIs averaging 7.4 (7.0–7.9; 95% CL) for ballyhoo and 8.7 (6.6–10.8) for balao. Individual female GSIs reached an observed maximum of 13.3 for ballyhoo and 14.2 for balao. By applying these GSI criteria, which indicate that females with a GSI greater than about three had oocytes in FOM, it is evident that the average mature halfbeak female is actively spawning from at least March to August.

Final oocyte maturation also followed a diel cycle. For ballyhoo, FOM began about 30–36 hours before ovulation, hydration of oocytes began about 8–12 hours before ovulation, and ovulation occurred at sunset. Ballyhoo oocytes developed in a group-synchronous pattern, and during FOM, a batch of oocytes increased rapidly in diameter (Fig. 4). Mature female ballyhoo had a bimodal or trimodal distribution of oocyte diameters when spawning. The smallest mode (<1.0 mm oocyte diameter) represented a reservoir of primary growth oocytes and vitellogenic oocytes. Larger modes, between 1 and 3 mm, represented oocytes in FOM. The presence of two larger ooctye modes (~1.0–2.0 and >2.0 mm) in all females sampled during the afternoon period indicated that female ballyhoo typically spawn every day dur-

ing March–April. In total, the trimodal oocyte frequency represents a reservoir of oocytes prior to FOM, one batch of oocytes beginning FOM, and one batch completing FOM. Hydrated oocytes were not observed in balao prior to 1100 h. However, in several ballyhoo collected around dawn (i.e. at approximately 0600–0700 EST), the nucleus in oocytes of the advanced batch was still visible along the chorion but the cytoplasm was lightening in color. This suggested that initiation of hydration at daybreak briefly preceded nucleus breakdown. During the following 12-hour period, oocytes in this maturing clutch advanced from late nucleus migration to nucleus breakdown, and increased in diameter from 1.5–2.0 mm in the morning to 2.0–3.0 mm in the afternoon. Modal egg size for each of three running-ripe ballyhoo (i.e. females with hydrated, ovulated eggs in the ovarian lumen) was 2.35, 2.60, and 2.80 mm diameter. The complete size range of these ovulated eggs was 2.2–3.4 mm diameter. These females were collected at or just before sunset (time: 1810–1855). Most efforts to sample across the full 24-hour cycle failed, apparently because halfbeak do not bite hooks after sundown. A sample of 12 ballyhoo was collected one night, however, by randomly throwing a cast net on dense schools of fish. These fish, collected between 2200 and 2359 hours during March 1997, all appeared to have recently spawned. Histological preparations demonstrated that they had fresh postovulatory follicles, and they contained a distinct clutch of oocytes in early nucleus migration. Whole oocytes from these fish collected at night were not archived in formalin; therefore they were not measured for comparisons to whole oocytes collected at other times during the diel cycle. These patterns of diel reproductive periodicity also appeared to apply to balao, but the available data were not conclusive.

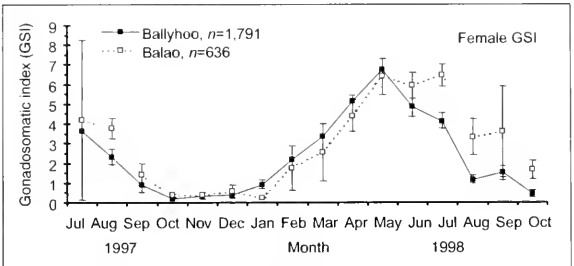

Figure 2

Mean (±95% confidence limits) gonadosomatic indices by month for ballyhoo (*Hemiramphus brasiliensis*) and balao (*H. balao*) females. Values are calculated for fish larger than size at 50% maturity, reported by McBride and Thurman (2003) as ≥198 mm fork length (FL) for ballyhoo and ≥160 mm FL for balao. *n* = number of females.

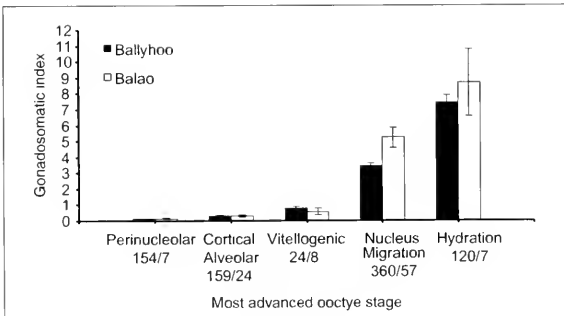

Figure 3

Mean (±95% confidence limits) gonadosomatic indices of female ballyhoo (*Hemiramphus brasiliensis*) and balao (*H. balao*) in various stages of oocyte development. A two-way ANOVA demonstrated a significant effect of both developmental stage and species ($P<0.0001$) on gonadosomatic index. Numbers indicate the number of fish, by stage, for each species. Hydration = nucleus breakdown.

Spawning habitat

In our study it was shown that hydrated oocytes can be inferred from a threshold criterion of GSI >6.0 (Fig. 3), and ripe females (i.e. with a batch of hydrated oocytes) will spawn within hours. Ripe ballyhoo females were distributed throughout the fishing grounds in both the Atlantic Ocean and Florida Bay (Fig. 1B). In the Atlantic, ripe ballyhoo females were caught in water depths from 1 to 20 m (mode: 6–10 m, 36.3% of the sets containing ripe ballyhoo in the Atlantic Ocean). In Florida Bay, ripe ballyhoo females were caught in areas that were exposed at low tide and out to 6-m deep (mode: 2–4 m; 57.9% of the positive sets in Florida Bay). Ripe ballyhoo females were mainly associated with hard bottom or vegetated habitats in both areas. In the Atlantic Ocean, ripe ballyhoo females were collected above platform reefs in 51.7% of the sets, above seagrass beds in 37.9% of the sets, near patch reefs in 5.2% of the sets, and over bare substrate in 5.2% of the sets. In Florida Bay, these fish were also associated with hard bottom substrates, specifically with vegetated bank habitat, in 44.7% of the sets and with seagrass beds in 55.3% of the sets.

Ripe balao females were distributed throughout the Atlantic fishing grounds but not in Florida Bay (Fig. 1C). In the Atlantic, they tended to occur in deeper water than did ripe ballyhoo females (range: 2–20 m; mode: 10–20 m, 51.3% of the sets containing ripe balao). The habitat associations of ripe balao females were similar to those of ripe ballyhoo females in the Atlantic Ocean, but typically reflected areas offshore rather than inshore of the reef. In the Atlantic Ocean, ripe balao females were collected above platform reefs in 58.0% of sets, above seagrass beds

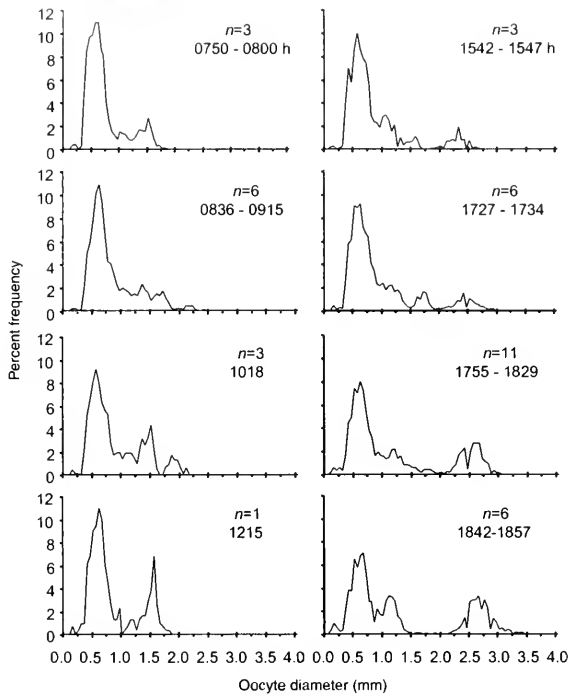

Figure 4

Oocyte diameters for ballyhoo (*Hemiramphus brasiliensis*) collected at different times of the day (EST). At least 300 oocytes were measured per female. Sizes <0.25 mm were not measured representatively because of the minimum size criteria of the image analysis software. Sunset occurred at 1830–1900 EST during this collection period (March–April). *n* = number of females.

in 25.8% of sets, over bare substrate in 9.7% of sets, and above undefined hard bottom in 6.5% of sets.

Discussion

These detailed findings of prolonged summer-spawning seasons, extreme iteroparity, and diel reproductive periodicity are consistent with other studies of halfbeak reproductive biology. Graham (1939), Ling (1958), Talwar (1962, 1967), and Berkeley and Houde (1978) noted a protracted spawning season by hemiramphids during warm months. McBride and Thurman (2003) examined the frequency of postovulatory follicles and reported that both species spawn daily during late spring and early summer, but also that some portion of the ballyhoo population spawns year-round. The present study is the first to follow the diel progression of FOM within the family Hemiramphidae. Lunar periodicity was not evident but it may have been confounded by the highly iteroparous nature of both species.

Spawning halfbeaks were distributed so widely throughout the fishing grounds that no specific areas were identified for the protection of spawning individuals. We noted interspecific differences in spawning areas, but these are not necessarily related to preferences by spawning females *per se*. Instead these differences appeared to be the result of interspecific distribution patterns of adult halfbeaks in general (i.e. adult ballyhoo are a more inshore species compared to adult balao [McBride, pers. obs.]). Because balao were not found in Florida Bay, fishing in Florida Bay does not affect this species. Spawning by ballyhoo was evident in Florida Bay, as predicted by fishing industry participants, but spawning ballyhoo were also widespread along south Florida's coral reef tract. Existing, albeit recent,

regulations[1] should provide some measure of protection for spawning ballyhoo in inshore waters.

Our study design was limited to the presence and absence of spawning females and did not identify concentrations of spawning activity associated with specific habitats. Presumably submerged vegetation is an important microhabitat. Several authors have noted that hemiramphid eggs, including those of ballyhoo, attach by filaments (of the chorion) to vegetation such as *Syringodium filiforme* and *Sargassum* sp. in waters less than approximately 6 m deep (Graham, 1939; Ling, 1958; Talwar, 1962, 1967; Berkeley and Houde, 1978). However, Berkeley and Houde (1978) collected eggs in plankton tows. The specific importance for halfbeak reproductive success of attached versus floating vegetation, or no vegetation, has not been identified.

The methods of this study define the macroscale spawning habitat of halfbeaks based on the distribution of spawning females. We demonstrate here that GSI values, even for highly iteroparous species, can distinguish females with hydrated oocytes from females in a less advanced stage of oocyte development. The GSI value is simple and inexpensive to measure, and by including individual halfbeaks for which we had GSI values but no histological data, we more than tripled our sample size with little additional laboratory cost. We could have instead characterized oocyte development macroscopically and such a modification is well suited when conditions affect weighing devices. But macroscopic characterization of oocyte development usually follows an ordinal scale that may vary between observers.

The distribution of females with hydrated eggs may be a better indication of spawning habitat than the distribution of eggs because hydration occurs for only a few hours (DeMartini and Fountain, 1981; Hunter and Macewicz, 1985; Brown-Peterson et al., 1988; McBride et al., 2002), whereas egg dispersal may occur over several days. In this study we assumed that spawning females move only limited distances within the few hours of the hydration process, and although limited movement has not been documented for either ballyhoo or balao, we believe that our interpretation of the data supports this assumption. The size of the study area was approximately 200 km by 250 km, and it seems reasonable that spawning halfbeaks were not moving extensively within this spatial boundary on an hourly basis. The approach discussed in the present study may meet the needs of other investigators wanting to generate a first approximation of spawning habitats for management purposes, which was the goal of this study. Also, this approach has good potential for use in areas were species identification of halfbeak eggs or larvae is problematic (Noell et al., 2001). Analyses requiring a smaller area or finer spatial resolution will depend on verification of a hydration period that is short in relation to expected fish movements.

The specific example presented in our study was limited because we collected the fish using commercial fishing vessels on routine fishing operations. This was cost-effective, but we were not able to identify spawning habitat preference or to define the complete geographic extent of the spawning grounds within south Florida. Gaps in the distribution of ripe females, which were particularly evident in the middle Florida Keys, were typically related to gaps in sampling coverage. In addition, both species presumably spawn outside the area we sampled. Still, much of the reported geographic range of ballyhoo and balao in the western Atlantic Ocean has been covered in the present study. The remaining shortcomings of this specific example could be resolved by using this approach within a statistically valid sampling design and estimating size-specific batch fecundity to map reproductive rates within a spatial and temporal context. The data resulting from such a comprehensive sampling design would be well-suited for identifying essential spawning habitat, for siting habitat-specific investigations of spawning dynamics, or for validating dispersal models for early life stages of marine fish.

Acknowledgments

We are grateful to many individuals for assistance in this research. First, to the fishermen and processors in the halfbeak fishery, all of whom participated in this survey. T. Brown, J. Hunt, and R. Moretti provided logistical support in Marathon. R. Beaver, K. Krumm, E. Robillard, D. Snodgrass, and J. Whittington assisted in fish collection and processing. G. Gerdeman, P. Nagle, F. Stengard, C. Stevens, and P. Thurman assisted with tissue processing and reproductive staging. C. Anderson assisted in preparing Figure 1 and GIS habitat analyses. B. Mahmoudi, R. Taylor, M. Zimmermann, and two anonymous reviewers provided constructive comments. Editorial assistance was provided by J. Leiby and J. Quinn. This research was funded in part by a grant from the National Oceanic and Atmospheric Administration (NOAA) to the Florida Fish and Wildlife Conservation Commission (Saltonstall-Kennedy Program, NOAA award no. NA77FD0069).

Literature cited

Berkeley, S. A. and E. D. Houde.
1978. Biology of two exploited species of halfbeaks, *Hemiramphus brasiliensis* and *H. balao* from southeast Florida. Bull. Mar. Sci. 28:624–644.

Berkeley, S. A., E. D. Houde, and F. Williams.
1975. Fishery and biology of ballyhoo on the southeast Florida coast. *In* Sea Grant Special Report 4, 1–15 p. Univ. Miami Sea Grant Program, Coral Gables, FL.

Brown-Peterson, N., P. Thomas, and C. R. Arnold.
1988. Reproductive biology of the spotted seatrout, *Cynoscion nebulosus*, in south Texas. Fish. Bull. 86:373–88.

Collette, B. B.
1965. Hemiramphidae (Pisces, Synentognathi) from tropical west Africa. Atlantide Report 8:217–235.

DeMartini, E. E., and R. K. Fountain.
1981. Ovarian cycling frequency and batch fecundity in the queenfish, *Seriphus politus*: attributes representative of serial spawning fish. Fish. Bull. 79:547–60.

Graham, D. H.
1939. Breeding habits of the fishes of Otago Harbour and adjacent seas. Trans. Proc. Royal Soc. New Zealand 69:361–372.

Hunter, J. R. and B. J. Macewicz.
1985. Measurement of spawning frequency in multiple spawning fishes. *In* An egg production method for estimating spawning biomass of pelagic fish: application to the northern anchovy (*Engraulis mordax*) (R. Lasker, ed.), 79–94 p. U.S. Dep. Commer., NOAA Tech. Rep. NMFS 36.

Limouzy-Paris, C. B., M. F. McGowan, W. J. Richards, J. P. Umaran, and S. S. Cha.
1994. Diversity of fish larvae in the Florida Keys: results from SEFCAR. Bull. Mar. Sci. 54:857–870.

Ling, J. K.
1958. The sea garfish, *Reporhamphus melanochir* (Cuvier & Valenciennes) (Hemiramphidae), in South Australia: breeding, age determination, and growth rate. Aust. J. Mar. Fresh. Res. 9:60–110.

McBride, R. S.
2001. Landings, value, and fishing effort for halfbeaks, *Hemiramphus* spp., in the south Florida lampara net fishery. Proc. Gulf Carib. Fish. Inst. 52nd Ann. Meeting, Key West, FL.

McBride, R. S., L. Foushee, and B. Mahmoudi.
1996. Florida's halfbeak, *Hemiramphus* spp., bait fishery. Mar. Fish. Rev. 58:29–38.

McBride, R. S., F. J. Stengard, and B. Mahmoudi.
2002. Maturation and diel reproductive periodicity of round scad (Carangidae: *Decapterus punctatus*). Mar. Biol. 140: 713–722.

McBride, R. S., and P. E. Thurman.
2003. Reproductive biology of *Hemiramphus brasiliensis* and *H. balao* (Hemiramphidae): maturation, spawning frequency, and fecundity. Biol. Bull. 204:57–67.

Noell, C. J., S. Donnellan, R. Foster, and L. Haigh.
2001. Molecular discrimination of garfish *Hyporhomphus* (Beloniformes) larvae in southern Australian waters. Mar. Biotechnol 3: 509–514.

Nybakken, J. W.
1997. Marine biology: an ecological approach, 4th ed., 481 p. Addison Wesley Longman, Inc., Menlo Park, CA.

Powell, A. B., D. E. Hoss, W. F. Hettler, D. S. Peters, and S. Wagner.
1989. Abundance and distribution of ichthyoplankton in Florida Bay and adjacent waters. Bull. Mar. Sci. 44: 35–48.

Starck, W. A., Jr.
1968. A list of fishes of Alligator Reef, Florida, with comments on the nature of the Florida reef fish fauna. Undersea Biol. 1:4–40.

Talwar, P. K.
1962. A contribution to the biology of the halfbeak, *Hyporhamphus georgii* (Cuv. & Val.) (Hemirhamphidae) [*sic*]. Indian J. Fish. 9:168–196.
1967. Studies on the biology of *Hemirhamphus* [*sic*] *marginatus* (Forsskal) (Hemirhamphidae-Pisces). J. Mar. Biol. Assoc. India 9:61–69.

West, G.
1990. Methods of assessing ovarian development in fishes: a review. Aust. J. Mar. Freshwater Res. 41:199–222.

Diets of thornback ray (*Raja clavata*) and tope shark (*Galeorhinus galeus*) in the bottom longline fishery of the Azores, northeastern Atlantic

Telmo Morato
Encarnacion Solà
Maria P. Grós
Gui Menezes

Departamento de Oceanografia e Pescas
Universidade dos Açores
PT-9901-862 Horta, Portugal
E-mail address: telmo@notes.horta.uac.pt

Abstract—Tope shark (*Galeorhinus galeus*) and thornback ray (*Raja clavata*) are the two most captured elasmobranch species by the Azorean bottom longline fishery. In order to better understand the trophic dynamics of these species in the Azores, the diets of thornback ray and tope shark caught in this area during 1996 and 1997 were analyzed to describe feeding patterns and to investigate the effect of sex, size, and depth and area of capture on diet. Thornback rays fed mainly upon fishes and reptants, but also upon polychaetes, mysids, natant crustaceans, isopods, and cephalopods. In the Azores, this species preyed more heavily upon fish compared with the predation patterns described in other areas. Differences in the diet may be due to differences in the environments (e.g. in the Azores, seamounts and oceanic islands are the major topographic features, whereas in all other studies, continental shelves have been the major topographic feature). No differences were observed in the major prey consumed between the sexes or between size classes (49–60, 61–70, 71–80, and 81–93 cm TL). Our study indicates that rays inhabiting different depths and areas (coastal or offshore banks) prey upon different resources. This appears to be related to the relative abundance of prey with habitat. Tope sharks were found to prey almost exclusively upon teleost fish: small shoaling fish, mainly boarfish (*Capros aper*) and snipefish (*Macroramphosus scolopax*), were the most frequent prey. This study illustrates that thornback rays and tope sharks are top predators in waters off the Azores.

Manuscript approved for publication 19 February 2003 by Scientific Editor.
Manuscript received 4 April 2003 at NMFS Scientific Publications Office.
Fish. Bull. 101:590–602 (2003).

The thornback ray (*Raja clavata* L.), is a shallow water bottom-living elasmobranch found in the Atlantic from Iceland and Norway southwards to South Africa, including Madeira and Azores islands. This species is also found in the Mediterranean, western Black Sea, and southwestern Indian Ocean (Stehmann and Bürkel, 1984). The thornback ray is commercially exploited in several countries. In the Azores it is a bycatch of the bottom longline fishery directed toward demersal and deepwater teleost species. Food and feeding habits of the thornback ray have been intensively studied since the end of the 19th century (e.g. Day, 1880–84) and more recently (e.g. Smale and Cowley, 1992; Ellis et al., 1996; Daan et al.[1]). However, only two studies have been conducted on the thornback ray off Portuguese continental waters (Marques and Ré, 1978; Cunha et al., 1986), and none exists for populations inhabiting waters around the oceanic islands or seamounts in the northeastern Atlantic.

The tope shark (*Galeorhinus galeus* (L.)), is a cosmopolitan species that can be found from about 70°N to about 55°S. Distribution of this species includes the Atlantic, Pacific and Indian Oceans (Compagno, 1984). Tope shark is also commercially exploited by several countries around the world, including the Azores, where it is a bycatch of the bottom longline fishery. Compagno (1984) and Olsen (1984) reviewed the biology of this shark; however, there have been relatively few studies on their feeding habits. The diet of tope shark was described by Ford (1921) for individuals landed at Plymouth U.K., by Olsen (1954) in southeastern Australia, and by Ellis et al. (1996) in the northeastern Atlantic Ocean.

Elasmobranchs are among the top predators in marine environments (Ellis et al., 1996); thus they affect the populations of both fish and invertebrates at lower trophic levels. However, feeding studies of elasmobranches in the Azores have been limited to the blue shark (*Prionace glauca*) (Clarke et al., 1996). Tope shark and thornback ray are the two most abundant elasmobranch species landed by the Azorean bottom longline fishery. Information on the feeding habits of these two species contributes to a better understanding of trophic dynamics and food webs—information which is needed as fisheries scientists advance ecosystem principles to fisheries management (Pauly et al., 2000; Pitcher, 2000; Whipple et al., 2000). The purpose of this study was to examine the diet of thornback ray and tope shark, to describe their feeding patterns and the effect of sex, size, depth, and location on their diet.

Materials and methods

Thornback rays and tope sharks were collected between March and May (spring) of 1996 and 1997 during a

[1] Daan, N., B. Johnson, J. R. Larsen and H. Sparholt. 1993. Analysis of the ray (*Raja* spec.) samples collected during the 1991 international stomach sampling project. ICES C.M. 1993/G:15, 17 p.

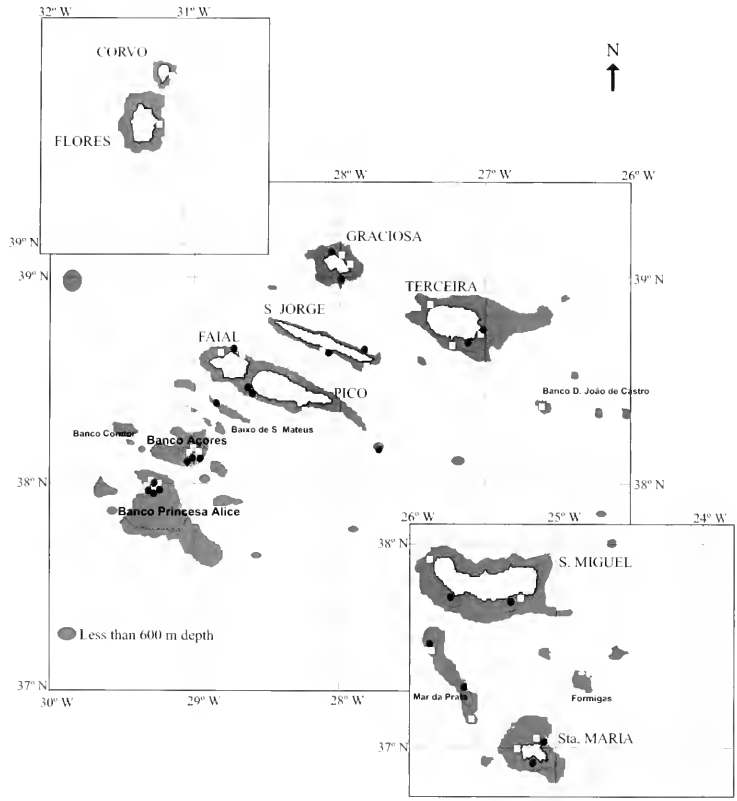

Figure 1

Locations of the longline sets made in the Azores during the spring of 1996 (●) and 1997 (□).

study on demersal fisheries in Azorean waters (Fig. 1). Fishes were caught by longline onboard the RV *Arquipélago*. Line setting began before sunrise (approx. 05:00 h) and hauling started about two hours after setting. From the fish sampled, total length (TL, to the nearest cm) was measured, and sex and maturity were determined by macroscopic examination of gonads and claspers with maturity scales, as proposed by Stehmann (1987). Stomachs were removed and classified as either everted, regurgitated, with bait, empty, or with contents. Individuals falling in any of the first three categories, as well as those that had obviously eaten fish hooked on the longline, were excluded from further analysis. Stomachs with contents were placed in plastic bags and frozen (within about 2 h of capture) for subsequent analysis. Stomach contents, which partly consisted of a turbid suspension, were washed with water in a nylon net of approximately 0.5-mm mesh size to allow easier examination. The items were carefully separated, weighed (after removing the surface water by blotting them in tissue paper), and identified to the lowest possible taxonomic level. Individuals of each identified taxon were counted. Whenever fragments were found, the number of individuals was taken as the smallest possible number of individuals from which fragments could have originated.

Precision estimates in diet studies have been advocated and used by several authors (Ferry and Cailliet, 1996; Morato et al., 1999). We used the cumulative trophic diversity, measured with the Shannon-Wiener index [as $H' = -\sum P_i(\log_e P_i)$, where P_i is the proportion of individuals in the ith species] to measure sample size sufficiency (Hurtubia, 1973). Cumulative numbers of randomly pooled stomachs were plotted against the cumulative trophic diversity. The asymptote of the curve indicates the minimum number of stomachs required. Frequency of occurrence (%O), percentage number (%N), and weight (%W) for each prey type were used to describe the diet of both species (for a review see Hyslop, 1980; Cortés, 1997). Wet weight was used to determine the latter value. The index of relative importance

$IRI=(\%N + \%W) \times \%O$] (Pinkas et al., 1971) and the $\%IRI$ (as $\%IRI_i = 100 \times IRI_i/\sum IRI_i$) were calculated for each prey category and used in diet comparisons. Prey taxa occurring in less than five stomachs were grouped into higher taxonomic categories. Ontogenetic differences in the diet of thornback rays were examined by grouping fish into four size classes (49–60, 61–70, 71–80, and 81–93 cm TL). The diet of thornback rays was also analyzed by sex, depth (0–100, 101–200, 201–350 m), and area of capture (coastal areas and offshore banks). No further analyses were performed for tope shark because their diet was dominated by only one prey category (see "Results" section). To determine if the most important preys were similar for different groups of rays, weighted correlation and concordance analyses were used (Zar, 1999). These methods were preferred to conventional rank correlation methods (e.g. Spearman) because they emphasize the high ranking given to the most important prey categories. Differences in the rankings of IRI values for prey categories between three or more groups (e.g. three size classes) were tested for significance with the top-down concordance method (C_T= top-down concordance coefficient) (Zar, 1999). For paired groups (e.g. males and females) the top-down correlation method (r_T= top-down correlation coefficient) was used (Quade and Salama, 1992; Zar, 1999). Schoener's dietary overlap index (Schoener, 1970) (as $C_{xy}=1-0.5 \sum |P_{xi} - P_{yi}|$, where P_{xi} was the proportion (based on %IRI) of food category i in the diet of x; and P_{yi} was the proportion of food category i in the diet of y) was used to measure the diet overlap between sex, size classes, depth strata, and area of capture.

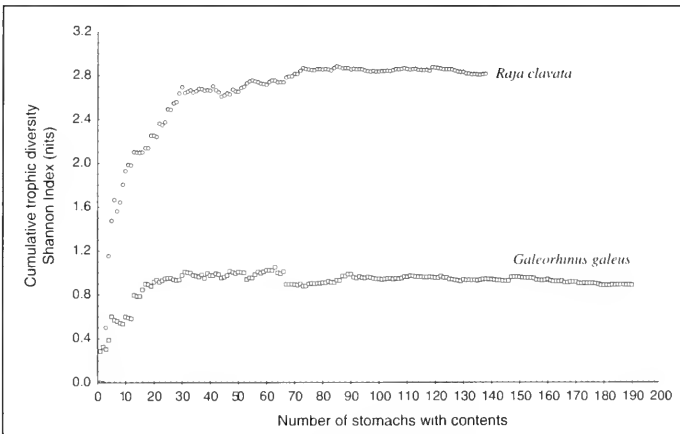

Figure 2

Randomized cumulative trophic diversity curves for thornback ray (*Raja clavata*) and tope shark (*Galeorhinus galeus*).

Cluster analysis was used to describe geographic similarities in the feeding habits of thornback rays. A predator-prey matrix was built from published data. When more than one index was available, the following criteria were used to choose between indexes: IRI or %IRI, %O, %N, %W, %Volume. The number of prey categories included was based on the quality of the description found in the published sources. Eleven different categories were obtained. A distance matrix was then calculated by using Euclidean distance, and the hierarchical form of analysis was applied (Clarke and Warwick, 1994). The grouping of predators was based on the "average linkage method," and a dendrogram was used as a graphic form of representation. Finally, trophic levels (TLv_k) were estimated for each of the samples (k) by using the method proposed by Cortés (1999) [as $TLv_k=1+(\sum P_{ik} \times TLv_i)$, where TLv_i is the trophic level of each prey category as estimated by the author, P_{ik} is the proportion of prey category i in sample k]. Mean trophic levels were also estimated for groups resulting from the cluster analysis, and differences between them were tested by using one-way ANOVA (Zar, 1999).

Results

Thornback rays were caught at depths ranging from 10 to 350 m, but primarily (95%) shallower than 250 m. Out of 237 stomachs examined, the contents of four appeared to have been regurgitated (1.7%), seven contained bait only (2.9%), 88 were empty (37.1%), and 138 contained prey (58.2%). Rays with stomachs containing food measured from 49.0 to 93.0 cm TL. All tope sharks were caught between 10 and 150 m depth, except for one individual taken at 300 m. Out of 365 stomachs examined, 174 (47.7%) were empty, seven (1.9%) contained fish hooked on the longline and 184 stomachs (50.4%) contained prey. Sharks with stomachs containing food ranged from 58.0 to 153.0 cm TL. The cumulative trophic diversity curves of both species appeared to reach an asymptote, suggesting that a sufficient number of stomachs were analyzed for both the thornback ray and tope shark (Fig. 2).

Thornback ray

The main diet components of thornback rays were fish (%IRI=81.6) and crustaceans reptants (%IRI=17.4) (Fig. 3). Fish occurred in 84.1% of stomachs that contained food, and represented 78.0% of total prey weight and 50.2% of total prey number (Table 1). Two benthopelagic species, the snipefish (*Macroramphosus scolopax* [%IRI=34.0]) and the boarfish (*Capros aper* [%IRI=26.8]), were by far the predominant fish prey items. However, some pelagic fish

Table 1

Values for percentage by number (%N), weight (%W), occurrence (%O), and index of relative importance (IRI and %IRI) for prey items observed in stomachs (n=138) of thornback rays (*Raja clavata*) caught off the Azores during the spring of 1996 and 1997. Total values are given in bold font.

Prey items	%N	%W	%O[1]	IRI	%IRI
Algae	0.3	0.0	1.5	0.5	0.0
Bivalvia—*Chlamys* sp.	0.1	0.0	0.7	0.1	0.0
Total Cephalopoda	**1.1**	**1.1**	**5.1**	**11.2**	**0.1**
Octopodoidea unidentified	0.1	0.1	0.7	0.1	0.0
Scaeurgus unicirrhus	0.7	0.8	2.9	4.4	0.1
Cephalopoda unidentified	0.3	0.2	1.5	0.8	0.0
Total Polychaeta	**3.4**	**0.8**	**9.4**	**39.5**	**0.8**
Hirudinea	0.1	0.0	0.7	0.1	0.0
Crustacea					
Stomatopoda	0.1	0.0	0.7	0.1	0.0
Total Natantia	**3.1**	**1.0**	**10.1**	**41.4**	**0.3**
Penaeidea unidentified	1.4	0.3	2.9	4.9	0.1
Solenocera membranacea	0.1	0.1	0.7	0.1	0.0
Solenocera sp.	0.1	0.1	0.7	0.1	0.0
Pandalidae	0.3	0.1	0.7	0.3	0.0
Processa intermedia	0.1	0.0	0.7	0.1	0.0
Processa sp.	0.1	0.0	0.7	0.1	0.0
Caridea unidentified	0.1	0.0	0.7	0.1	0.0
Natantia unidentified	0.9	0.4	2.9	3.8	0.1
Total Reptantia	**31.9**	**17.0**	**47.1**	**2303.2**	**17.4**
Anomura unidentified	0.1	0.1	0.7	0.1	0.0
Scyllaridae *Scyllarus arctus*	4.0	0.8	9.4	45.1	0.9
Diogenidae	1.1	1.7	5.8	16.2	0.3
Paguridea	0.3	0.3	1.5	0.9	0.0
Galatheidae *Galathea* sp.	0.3	0.1	1.5	0.6	0.0
Homolidae *Paromola cuvieri*	0.6	0.1	2.9	2.0	0.0
Calappidae *Calappa granulata*	1.8	1.3	7.3	22.6	0.5
Parthenopidae *Parthenope* sp.	2.8	0.7	0.7	2.5	0.0
Portunidae	0.1	0.0	0.7	0.1	0.0
Total *Liocarcinus* spp.	**14.9**	**8.3**	**16.6**	**385.1**	**5.5**
Liocarcinus marmoreus	9.8	5.1	9.4	140.1	2.8
Liocarcinus corrugatus	3.8	2.7	6.5	42.3	0.8
Liocarcinus spp.	1.3	0.5	2.2	4.0	0.1
Brachyura	4.1	2.4	11.6	75.4	1.5
Reptantia unidentified	0.6	0.4	2.9	2.9	0.1
Decapoda unidentified	0.1	0.0	0.7	0.1	0.0
Total Mysidacea	**6.6**	**0.7**	**3.6**	**26.3**	**0.5**
Isopoda	1.6	0.3	5.1	9.7	0.2
Amphipoda–*Vibilia* sp.	0.1	0.0	0.7	0.1	0.0
Crustacea unidentified	1.1	0.8	4.4	8.4	0.2
Total Pisces	**50.2**	**78.0**	**84.1**	**10811.2**	**81.6**
Myctophidae	0.6	0.3	2.2	2.0	0.0
Moridae *Gadella maraldi*	0.1	0.2	0.7	0.2	0.0
Caproidae *Capros aper*	13.7	24.7	34.8	1336.3	26.8
Macroramphosidae *Macroramphosus scolopax*	16.7	19.3	47.1	1695.6	34.0
Sparidae *Pagellus* spp.	1.0	5.4	4.4	28.2	0.6
Mullidae *Mullus surmuletus*	0.1	3.0	0.7	2.2	0.0
Pomacentridae *Chromis limbota*	0.1	0.2	0.7	0.2	0.0
Carangidae *Trachurus picturatus*	0.9	2.6	3.6	12.6	0.3
Scombridae *Scomber japonicus*	0.4	6.0	2.2	14.1	0.3
Pisces unidentified	16.6	16.3	43.5	1431.2	28.7
Rocks	1.0	0.3	5.1	6.6	0.1
Tissue unidentified	0.4	0.8	2.2	2.6	0.1

[1] Because the %O is a nonadditive index (Cortes, 1997) for grouping fish items into higher taxonomic categories (i.e. Pisces, etc), the %O value was recalculated by considering the number of stomachs with the respective higher taxonomic category. This recalculation affects both the IRI and %IRI values.

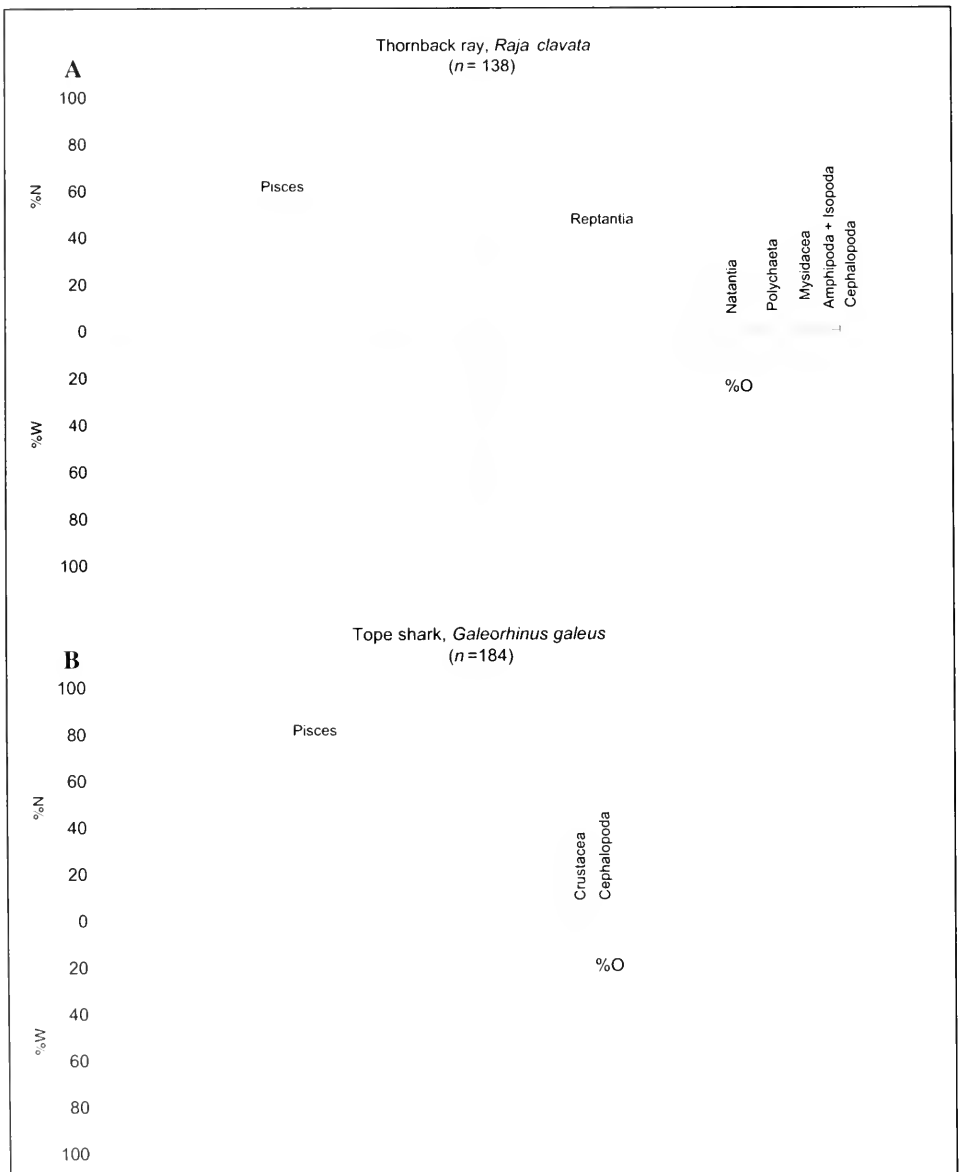

Figure 3

Relative importance of prey categories in the diet of (**A**) thornback ray (*Raja clavata*) and (**B**) tope shark (*Galeorhinus galeus*) ranked from highest IRI values. Where the areas of the boxes are equal to the IRI value [(%N+%W) × %O], %N is the percent number, %W the percent weight, and %O the frequency of occurrence of the prey category. Each tick mark of %O represents 10%.

Table 2

Percentage of relative importance (%IRI) of food categories of *Raja clavata* by sex, total length, depth strata, and areas (coastal and offshore banks). Prey items occurring in less than five stomachs were grouped into higher taxonomic levels. The null hypothesis of not feeding upon the same most important prey categories was tested by using the top-down correlation method (being r_T the top-down correlation coefficient) and the top-down concordance method (being C_T the top-down concordance coefficient). NS = non significant, $^*P<0.01$.

	Sex		Total length (cm)				Depth (m)			Areas	
	F	M	49–60	61–70	71–80	81–93	0–100	101–200	201–350	Banks	Coastal
Cephalopoda	0.52	0.03	1.44	0.00	0.38	0.63	0.03	0.21	5.60	3.48	0.06
Polychaeta	0.62	1.70	0.21	0.43	0.73	6.44	0.54	0.40	15.13	4.23	0.57
Penaeidea	0.34	0.62	0.72	1.32	0.18	0.00	0.19	0.12	14.72	1.41	0.29
Other Natantia	0.10	0.15	0.52	0.11	0.06	0.00	0.48	0.01	0.00	0.08	0.12
Diogenidae	0.07	1.58	1.45	0.00	0.88	0.45	0.69	0.21	0.00	0.00	0.53
Scyllarus arctus	1.54	0.57	1.12	0.25	2.48	0.64	0.76	0.84	4.35	0.91	1.21
Calappa granulata	0.73	0.31	0.45	0.30	0.90	0.36	0.00	1.52	0.00	0.10	0.64
Liocarcinus spp.	8.12	0.60	1.64	3.30	9.49	0.19	10.44	1.43	0.00	0.00	12.30
Other Reptantia	9.20	8.32	1.43	11.88	22.48	0.00	47.44	0.31	0.00	0.52	6.33
Mysidacea	0.68	0.50	0.18	0.62	1.02	0.00	0.00	1.00	2.21	16.79	0.00
Isopoda	0.53	0.00	0.00	0.24	0.30	0.35	0.02	0.47	0.00	0.00	0.31
Capros aper	41.20	24.16	36.26	38.11	23.39	53.34	20.06	38.26	10.63	35.56	32.53
Macroramphosus scolopax	35.15	58.88	53.60	41.65	34.91	37.35	15.81	54.84	36.72	33.50	42.91
Pagellus sp.	0.46	1.07	0.00	1.08	1.24	0.00	0.56	0.19	9.99	2.27	0.43
Myctophidae	0.04	0.12	0.00	0.14	0.09	0.00	0.03	0.04	0.65	1.16	0.01
Trachurus picturatus	0.14	0.57	0.34	0.00	0.87	0.26	1.25	0.01	0.00	0.00	0.40
Other Pisces	0.58	0.82	0.64	0.56	0.61	0.00	1.71	0.15	0.00	0.00	1.36
	r_T=0.70*		C_T=0.74*				C_T=0.51^{NS}			r_T=0.44^{NS}	
Stomachs with contents (n)	89	49	19	47	60	11	47	78	13	24	110

prey were also recorded in the stomachs of thornback rays: the chub mackerel, (*Scomber japonicus* [%IRI=0.3]) and the blue jack mackerel (*Trachurus picturatus* [%IRI=0.3]). Some individuals also fed upon mesopelagic myctophids (%IRI<0.1) and upon shallow water benthic fish such as the red striped mullet (*Mullus surmuletus* [%IRI<0.1]) and the Azorean chromis (*Chromis limbata* [%IRI<0.1]).

Reptants occurred in 47.1% of the stomachs examined and represented 17.0% by weight and 31.9% by number of the total prey found (Fig. 3A). Swimming crabs (*Liocarcinus* spp. [%IRI=5.5]), which include both *L. marmoreus* (%IRI=2.8) and *L. corrugatus* (%IRI=0.8), were the most important reptant prey item in the diet of thornback ray (Table 1). Other important reptants included the lesser locust lobster (*Scyllarus arctus* [%IRI=0.9]), the shame-faced crab (*Calappa granulata* [%IRI=0.5]), as well as some unidentified Diogenidae (%IRI=0.3) and brachyura (%IRI=1.5).

Polychaetes (%IRI=0.8) were the third most important prey category and occurred in 9.4% of the stomachs with food (Fig. 3A). Mysids (%IRI=0.5), natants (%IRI=0.3), isopods (%IRI=0.2), and cephalopods (%IRI=0.1) also occurred in stomachs of thornback rays sampled in the Azores (Table 1).

A comparison of thornback ray's diet in relation to sex, length, depth and area of capture (Table 2) suggests that *C. aper* and *M. scolopax* were by far the most important prey for all subgroups examined. The diets of both sexes were significantly correlated (r_T=0.70, $P<0.01$), indicating a high degree of similarity in the diets of males and females. Both sexes fed primarily upon two benthopelagic fish species (*M. scolopax* and *C. aper*) and reptants (Table 2). Schoener's diet overlap index between males and females was 0.72, also indicating a high level of similarity between diets.

Significant concordance (C_T=0.74, $P<0.01$) was displayed among thornback rays of different size classes (49–60, 61–70, 71–80 and 81–93 cm TL). Prey categories had similar %IRI values for the different size classes (Table 2), with the exception of reptants (both *Liocarcinus* spp. and "other reptants"), which were more important in the diet of the two middle size classes. Schoener's index also suggested a high degree of overlap (>0.60) among all size classes (Table 3).

Examination of depth-related differences was limited by the small sample size of rays from deeper waters ($n_{201-350m}$=13). However, the top-down concordance coefficient suggested that individuals captured at different depths (0–100, 101–200, and 201–350 m) do not feed upon the same most important prey categories (C_T=0.52, $P>0.05$). Reptants (both *Liocarcinus* spp. and "other reptants") and the fish species *T. picturatus* were more important in the diet of rays captured in shallow waters (0–100 m); whereas

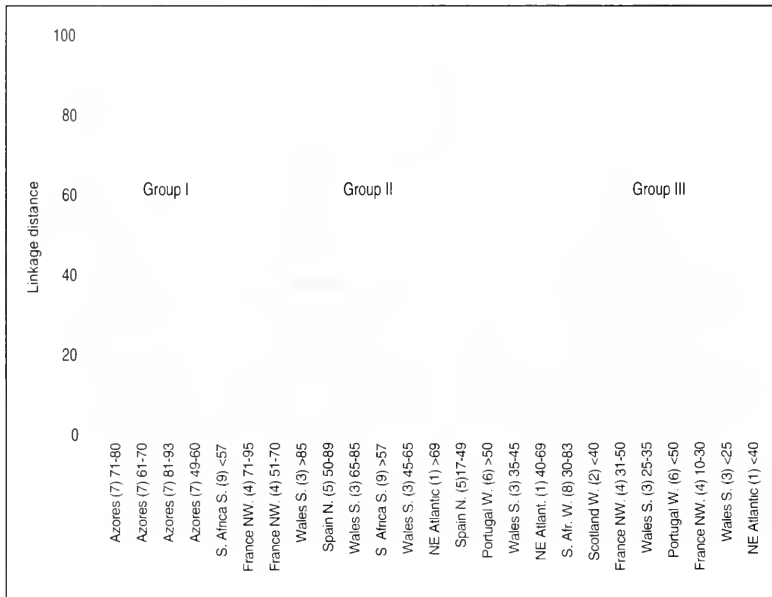

Figure 4

Dendrogram of the cluster analysis (Euclidean distance, average linkage method) for geographic patterns of feeding habits of *Raja clavata*. In parentheses is given the authorship of the studies: 1 = Ellis et al. (1996); 2 = Gibson and Ezzi (1987); 3 = Ajayi (1982); 4 = Quiniou and Andriamirado (1979); 5 = Olaso and Rodriguez-Marin (1995); 6 = Cunha et al. (1986); 7 = the present study; 8 = Ebert et al. (1991); 9 = Smale and Cowley (1992).

polychaetes, cephalopods, penaeids, mysids, seabreams (*Pagellus* sp.), and myctophids were consumed more by rays caught in deeper waters (Table 2). Schoener's overlap index for individuals captured at different depth intervals (Table 3) indicated low overlap (=0.50), supporting the results of the top-down concordance coefficient analysis.

Finally, the diet of rays caught in coastal areas and offshore banks were not significantly correlated (C_T=0.44, P>0.05), indicating that thornback rays feed upon different prey depending on the environment. The Diogenidae, *Liocarcinus* spp., "other reptants," and "other Pisces" were more important prey for rays in coastal areas, whereas polychaetes, penaeids, cephalopods, mysids, seabreams (*Pagellus* sp.), and myctophids were more important for rays caught at offshore banks (Table 2). However, Schoener's index showed a high level of overlap (0.69) between the diets of rays caught in the different locations—most likely due to the high dominance of two benthopelagic fishes in their diets (75.4% and 69.1% for coastal areas and offshore banks, respectively).

Published information on the diet of thornback rays is summarized in Table 4. Estimations of mean trophic levels vary from 3.1, for the smallest size class (South Wales: <25 cm TL), to 4.2 for the Azorean thornback ray (this study; size classes 49–60 and 81–93 cm TL). The arbitrarily chosen cutoff in the cluster analysis was set at 60% dissimilarity, which divided the dendrogram into three groups with similar feeding patterns (Fig. 4). Cluster group I grouped the Azorean populations (all size classes) and had an estimated trophic level of 4.14 (±0.09 SD). Cluster group II contained all other medium and large size classes (i.e. >40 cm TL), with the exception of small rays from the Cantabrian Sea, North Spain (17–49 cm TL), and one small- to

Table 3

Schoener's diet overlap index for thornback rays (*Raja clavata*) size classes and for different depth strata.

	Depth (m)		Total length (cm)			
	101–200	201–350		61–70	71–80	81–93
0–100	0.40	0.29	49–60	0.83	0.66	0.76
201–350		0.50	61–70		0.77	0.77
			71–80			0.62

Table 4

Categorized diets of thornback ray in different geographic locations. Estimation of trophic level (TL) following Cortés (1999) is also presented. Abbrevations of prey categories: POL= Polychaeta; BIV= Bivalvia; ECH = Echinodermata; CEP = Cephalopoda; ISO = Isopoda; AMP = Amphipoda; MYS = Mysidacea; STO = Stomatopoda; NAT= Natantia; REP = Reptantia; PIS = Pisces. PM is the point method (Hyslop, 1980). Numbers in the reference (Ref.) list represent the following studies: 1 = Ellis et al. (1996); 2 = Gibson and Ezzi (1987); 3 = Ajayi (1982); 4 = Quiniou and Andriamirado (1979); 5 = Olaso and Rodríguez-Marín (1995); 6 = Cunha et al. (1986); 7 = present study; 8 = Ebert et al. (1991); 9 = Smale and Cowley (1992). TLv = trophic level.

Location		Size class (cm TL)	Index	Prey categories											Ref.	TLv
				POL	BIV	ECH	CEP	ISO	AMP	MYS	STO	NAT	REP	PIS		
NE Atlantic		<40	PM	5.20	0.50	0.00	4.50	0.20	2.70	2.90	0.00	52.40	16.30	2.60	1	3.2
NE Atlantic		40–69	PM	4.70	3.50	0.00	1.60	0.70	3.70	0.80	0.00	17.00	60.90	5.70	1	3.5
NE Atlantic		>69	PM	3.00	2.90	0.30	0.60	0.00	0.00	0.00	0.00	7.10	73.60	11.30	1	3.6
Scotland	West Coast	<40	%IRI	2.40	0.00	3.60	0.00	0.00	32.90	10.50	0.00	27.90	16.10	0.00	2	3.2
Wales	South Coast	<25	%W	0.00	0.00	0.00	0.00	0.00	0.00	0.00	0.00	63.65	16.15	2.88	3	3.1
Wales	South Coast	25–34.9	%W	3.04	0.00	0.00	0.00	0.00	0.00	0.00	0.00	42.12	38.30	8.68	3	3.4
Wales	South Coast	35–44.9	%W	3.80	0.00	0.00	0.00	0.00	0.00	0.00	0.00	22.23	64.21	3.98	3	3.4
Wales	South Coast	45–64.9	%W	3.90	0.00	0.00	0.00	0.00	0.00	0.00	0.00	1.68	72.88	13.76	3	3.4
Wales	South Coast	65–84.9	%W	1.40	0.00	0.00	0.00	0.00	0.00	0.00	0.00	2.22	85.41	1.33	3	3.3
Wales	South Coast	>85	%W	1.73	0.00	0.00	0.00	0.00	0.00	0.00	0.00	0.00	67.12	25.08	3	3.5
France	NW Coast	10–30	%CN	0.00	2.34	0.00	0.00	0.00	12.50	22.46	0.00	55.97	2.42	0.00	4	3.3
France	NW Coast	31–50	%CN	0.00	3.75	0.00	0.00	0.00	19.35	0.81	0.00	27.02	42.94	0.00	4	3.3
France	NW Coast	51–70	%CN	0.00	16.53	0.00	0.00	0.00	2.02	0.00	0.00	9.27	70.56	0.00	4	3.4
France	NW Coast	71–95	%CN	0.00	21.45	0.00	0.00	0.00	0.00	0.00	0.00	0.32	75.16	0.00	4	3.4
Spain	N Coast	17–49	%V	2.26	0.00	0.00	0.00	0.00	0.00	2.26	0.00	33.87	58.39	0.00	5	3.4
Spain	N Coast	50–89	%V	0.00	0.00	0.00	4.70	0.00	0.00	0.00	0.00	4.41	84.64	6.52	5	3.6
Portugal	West Coast	<50 [1]	%Q	0.01	0.00	0.00	0.01	0.17	0.09	1.83	0.00	86.38	3.36	7.63	6	3.6
Portugal	West Coast	>50 [1]	%Q	0.03	0.00	0.00	0.52	0.00	0.00	0.00	0.00	24.66	73.23	1.52	6	3.5
Portugal	Azores	49–60	%IRI	0.21	0.00	0.00	1.44	0.00	0.00	0.18	0.00	1.24	6.09	90.84	7	4.2
Portugal	Azores	61–70	%IRI	0.43	0.00	0.00	0.00	0.24	0.00	0.62	0.00	1.43	15.73	81.54	7	4.1
Portugal	Azores	71–80	%IRI	0.73	0.00	0.00	0.38	0.30	0.00	1.02	0.00	0.24	36.23	61.11	7	4.0
Portugal	Azores	81–93	%IRI	6.44	0.00	0.00	0.63	0.35	0.00	0.00	0.00	0.00	1.64	90.95	7	4.2
South Africa	West coast	30–86	%IRI	0.00	0.00	0.00	0.00	0.00	0.00	1.13	20.75	41.01	3.01	34.10	8	3.7
South Africa	Cape South	<57	%IRI	0.00	0.00	0.00	0.08	0.00	0.00	20.86	12.39	10.59	47.84	8.23	9	3.5
South Africa	Cape South	>57	%IRI	0.21	0.00	0.00	0.31	0.00	3.21	1.33	5.71	10.72	72.80	5.71	9	3.5

[1] TL was estimated from disk width (DW) and by using the length-length relationship for the Azores; DW=0.1087+0.7002TL (unpuhl. data).

Table 5

Values for percentage by number (%N), weight (%W), occurrence (%O), and index of relative importance (IRI and %IRI) for prey items observed in stomachs of tope shark (n= 184), *Galeorhinus galeus*, caught off the Azores during the spring of 1996 and 1997. Number (No.) and percent occurrence (%O) of fish lenses, fish remains, and otoliths found in stomach, are also presented. Total values are given in bold font.

Prey items	%N	%W	%O[1]	IRI	%IRI
Total Crustacea	**1.0**	**1.0**	**3.3**	**6.5**	**0.03**
Isopoda	3.6	1.1	2.7	12.8	0.3
Crustacea unidentified	1.2	0.0	1.1	1.3	0.0
Total Cephalopoda	**0.8**	**0.2**	**3.3**	**3.2**	**0.02**
Octopodidae	0.6	0.3	0.5	0.5	0.0
Cephalopoda unidentified	3.0	0.0	2.7	8.1	0.2
Total Pisces[2]	**98.2**	**98.8**	**100.0**	**19,700.4**	**99.95**
Sternoptychidae unidentified	0.6	0.2	0.5	0.4	0.0
Synodontidae *Synodus* sp.	0.6	11.5	0.5	6.5	0.2
Trichiuridae *Lepidopus caudatus*	0.6	0.0	0.5	0.4	0.0
Macrouridae unidentified	0.6	0.0	0.5	0.3	0.0
Phycidae *Phycis phycis*	1.2	0.0	1.1	1.4	0.0
Caproidae *Capros aper*	65.0	25.6	38.6	3494.6	93.2
Macroramphosidae *Macroramphosus scolopax*	11.2	2.7	8.2	113.5	3.0
Carangidae *Trachurus picturatus*	2.4	7.6	2.2	21.6	0.6
Total Sparidae	**6.5**	**32.0**	**4.4**	**169.7**	**4.5**
Pagellus acarne	2.4	5.8	1.6	13.3	0.4
Pagellus bogaraveo	2.4	14.4	1.6	27.3	0.7
Pagellus spp.	1.2	11.7	1.1	14.1	0.4
Pagrus pagrus	0.6	0.1	0.5	0.4	0.0
Sparidae unidentified	0.6	0.5	0.5	0.6	0.0
Scombridae *Scomber japonicus*	2.4	18.4	1.6	33.8	0.9
	No. of	%O			
Pairs of fish lenses	493	103			
Otoliths unidentified	118	75			
Fish remains	3	2			

[1] Because the %O is a nonadditive index (Cortes, 1997), when grouping fish items into higher taxonomic categories (i.e. Pisces, etc) the %O value was recalculated considering the number of stomachs with the respective higher taxonomic category. This recalculation will affect both the IRI and %IRI values.

[2] Including unidentified fish, pairs of lenses, otoliths, and fish remains.

medium-size class of South Wales (35–45 cm TL). Cluster group III grouped small rays from several geographic regions, from South Africa (which also includes some large individuals) to NE Atlantic. Estimates of trophic levels were 3.46 (±0.84 SD) for the rays of the cluster group II (i.e. medium and large), and 3.35 (±0.21 SD) for the rays composing cluster group III (i.e. small). The estimated trophic levels for the three cluster groups were significantly different (P<0.001).

Tope shark

The diet of tope shark consisted almost exclusively of fish (%IRI=99.95), along with a few crustaceans (%IRI=0.03) and cephalopods (%IRI=0.02) (Fig. 3B). Recognizable prey from 14 different taxa were identified (Table 5). The boarfish (*C. aper*) was the most important prey item (%IRI=93.2), accounting for 65.0% of food by number (%N), 25.6% by weight (%W), and occurred in 38.6% of stomachs that contained food (%O). The second most important prey item was the snipefish (*M. scolopax* [%IRI=3.0]), which represented 11.2% of food by number and 2.7% by weight. Some commercially important fish species were also found in the stomachs of tope shark; sparids (%IRI=4.5, which included *Pagellus acarne*, *P. bogaraveo*, and *Pagrus pagrus*), the chub mackerel (*S. japonicus* [%IRI=0.9]), and the blue jack mackerel (*T. picturatus* [%IRI=0.6]). These species were more important by weight than by number or occurrence. The stomachs of tope sharks also contained 493 pairs of eye lens and fish that were heavily digested, as well as unidentifiable otoliths.

Discussion

In general, the percentage of empty stomachs for thornback rays and tope sharks was relatively high compared to the percentage from literature reports. The percentage of empty

stomachs for tope shark was 47.7%—much higher than the 4.3% observed by Ellis et al. (1996). The percentage of empty thornback ray stomachs was high (37.1%) when compared to values reported for the North Sea (9%, Daan et al.[1]; and 3.7%, Ellis et al., 1996), Carmarthen Bay, South Wales (4.5%, Ajayi, 1982), west coast of Southern Africa (4.5%, Ebert et al., 1991; and 2.6%, Smale and Cowley, 1992) and the Portuguese mainland coast (2.5%, Cunha et al., 1986). We attribute the high percentage of empty stomachs found in our study to the use of longlines to catch the fish in the Azores (trawls were used in the other studies). Longlining is a passive fishing method, which suggests that fish that feed to satiation have a reduced response to bait odor (Løkkeborg et al., 1995), meaning that fish with full stomachs tend not to eat the bait and be caught. Thus, only those fish with empty stomachs or partial stomach fullness were caught.

Thornback rays captured by longline in the Azores during the spring of 1996 and 1997 fed upon a wide variety of organisms. Fishes (81.6 %IRI) and reptants (17.4 %IRI) dominated the diet, which also consisted of polychaetes, mysids, natants, isopods, and cephalopods. In general, thornback rays in the Azores preyed more heavily upon fish in comparison with the predation patterns described in other studies. Ajayi et al. (1982) reported a predominance of crustaceans (83%W) for all size classes and a low importance of fish (11.6%W) in the diet of thornback rays in Carmarthen Bay, Bristol Channel. They also reported amphipods, polychaetes, and some natants as food items. Using the points method of Hyslop (1980), Ellis et al. (1996) reported that thornback rays from the North Sea fed primarily on crustaceans (78.9%) compared to mollusks (10.2%) and fish (7.3%). Several others have also reported a dominance of crustaceans and low importance of fish in the diet of thornback ray (Fitzmaurice, 1974; Marques and Ré, 1978; Quiniou and Andriamirado, 1979; Cunha et al., 1986; Gibson and Ezzi, 1987; Smale and Cowley, 1992; Olaso and Rodríguez-Marín, 1995; Daan et al.[1]; Ebeling[2]). Polychaetes (Holden and Tucker, 1974; Marques and Ré, 1978), bivalves (Quiniou and Andriamirado, 1979), holothurians (Ebeling[2]), and cephalopods (Holden and Tucker, 1974; Marques and Ré, 1978; Smale and Cowley, 1992; Olaso and Rodríguez-Marín, 1995) that were considered important prey items in the other studies mentioned were not recorded or were insignificant in our samples.

Differences in diet composition of several predators may reflect the geographic peculiarities in fauna composition (e.g. Smale and Cowley 1992), but when comparing diets based on higher taxonomic levels (such as fish, reptants, and natants categories), such geographic differences should not be so obvious. Our geographic analysis (see Fig. 4) distinguished three major groups: I) the Azorean individuals; II) other large individuals; and III) other small individuals. Further, the estimated mean trophic levels for these three major groups were significantly different: 4.14 (±0.09 SD) for the Azores; 3.46 (±0.84 SD) for other large rays; and 3.35 (±0.21 SD) for smaller rays. The higher trophic level for the Azores is a result of a higher degree of piscivory in this region and an increased consumption of decapods and fish by larger rays, compared with small rays. Notwithstanding the difference in sampling methods (longline *vs.* trawl caught), it appears that the Azores can be considered a separate group. In other studies, predator size played the major role in controlling feeding patterns.

The diet of the thornback ray in the Azores consists of a greater proportion of fish than in any other area and may reveal differences in the function of different environments, because seamounts and oceanic islands are the major topographic feature of the Azores region and the other studies were conducted on continental shelves. The general function of oceanic seamount environments is still not completely understood but they are characterized by substantial enhancement of primary production due to topographic effects on local hydrographic conditions (Genin and Boehlert, 1985). However, evidence for enhanced primary production leading to concentrations of fish over seamounts is sparse (Rogers, 1994). Additionally, the availability and relative abundance of the two most important fish prey items found in our work (the benthopelagic species *C. aper* and *M. scolopax*) vary considerably both seasonally (Granadeiro et al., 1998) and annually. Therefore, the high degree of piscivory in the Azores may result from environmental features and exceptional fish prey availability during the sampled years or seasons.

Thornback rays also fed on pelagic fish, as indicated by the presence of chub mackerel and jack mackerel in stomachs—a finding that confirms previous suggestions (see Daan et al.[1]; Ebeling[2]) that thornback rays are active predators and able to feed semipelagically. The most important reptants in the diet, *Liocarcinus* spp., were also reported as the main prey item for thornback rays by Ellis et al. (1996). The level of importance of isopods and amphipods, mysids, cephalopods, and polychaetes in the diet of thornback rays in the Azores was similar to values reported by other authors (Ellis et al., 1996; Daan et al.[1]; Ebeling[2]).

Differences in the dentition of females and males were reported by Quiniou and Andriamirado (1979) but we and Smale and Cowley (1992) observed no differences in the major prey consumed between sexes. Therefore, sexual dimorphism in dentition does not appear to be manifested in dietary preferences between sexes, as was initially expected.

Several studies have demonstrated differences in predation patterns for rays of different size classes—primarily a decrease in importance of crustaceans and an increase of fish with size (e.g. Smale and Cowley, 1992; Ellis et al., 1996; Daan et al.[1]; Ebeling[2]). Some authors attribute these differences to the ability of large predators to prey upon larger prey (Smale and Cowley, 1992); others suggest the difference is due to a pronounced shift from a benthic to a benthopelagic feeding behavior (Skjæraasen and Bergstad, 2000; Ebeling[2]) or the reverse (Quiniou and Andriamirado, 1979). We found no significant size-related differences in diet. Quiniou and Andriamirado (1979) reported shifts in diet at a size of 30 to 40 cm TL but we could not verify these conclusions because our sample included only rays larger than 49 cm.

[2] Ebeling, E. 1988. A brief survey of the feeding preferences of *Raja clavata* in Red Wharf Bay in the Irish Sea. ICES C.M. 1988/G:58, 5 p.

There have been few data indicating dietary differences between thornback rays collected at different depths. Smale and Cowley (1992) reported that bottom type used by rays varies with depth and predicted that the prey spectrum would thus also vary, but no depth-related analyses of diet composition were preformed in their study. Despite similarities in size (i.e. no differences in the mean size by depth strata; Menezes[3]), we found that rays inhabiting different depths prey upon different resources. The decreasing consumption of *Liocarcinus* spp., "other reptants," and *T. picturatus*, and the increasing consumption of penaeids, seabreams, and myctophids with depth of capture of rays, appears to be in general agreement with the relative abundance of prey with depth. Therefore, such depth-related variations in diet may simply reflect differences in prey availability. It is not clear, however, why *Scyllarus arctus*, a species with a known depth distribution of 4 to 50 meters (e.g. Alvarez, 1968; Castellón and Abelló, 1983), appears in stomachs of thornback rays caught between 201 and 350 meters (see Table 2). There is no evidence of vertical migrations of thornback ray associated with feeding activity; therefore this prey was likely eaten at deep water. Thus, the depth distribution range of *S. arctus* in the Azores may be significantly greater than what was previously known. The only study that could corroborate this hypothesis (Fransen, 1991) reported one *S. arctus* caught between 420 and 700 meters depth in the Canary Islands.

Our comparisons between areas (coastal and offshore banks) were unable to clearly separate the influence of depth because nearly all coastal samples were obtained from shallow waters, and offshore bank samples were collected from much deeper waters. Hence, we were incapable of determining whether the high level of polychaetes, penaeids, cephalopods, mysids, seabreams, and myctophids in the diet of rays caught at offshore banks reflects the availability of these prey in these areas, or in deeper waters, or both. Nevertheless, our findings indicate that coastal rays have different diets from rays taken in offshore banks.

Tope sharks preyed almost exclusively upon teleosts, along with very few crustaceans and cephalopods. Previous observations on the feeding behavior of this species suggested that fish and cephalopods are the main prey categories (Ellis et al., 1996; Olsen, 1954). The diet of tope shark in the Azores consists of fewer species (mainly small shoaling fish, mainly boarfish and snipefish) compared to the diet of tope shark documented in previous studies. These two fish were also important diet components of other piscivorous species around the Azores between 1993 and 1997, namely cephalopods (Pierce et al., 1994), elasmobranchs (Clarke et al., 1996), fishes (Clarke et al., 1995; Morato et al., 1999, 2000, 2001) and seabirds (Granadeiro et al., 1998; Ramos et al., 1998a, 1998b). The role of these two small shoaling fish in the marine food web of the Azores is not yet fully understood. The fact that these prey may exhibit strong variation in abundance, raises the question of how well predators can adapt to extensive changes in their availability.

Stomach-content data offer a good snapshot of the feeding habits of fish species, but diets may vary substantially with food availability, depth, location, and season. Caution is, therefore, required when drawing conclusions about the trophic ecology of marine predators. The trophic role of thornback rays and tope sharks in the Azores could be further clarified by year round sampling and by an analysis of stable isotopes (Gu et al., 1996; Jennings et al., 1997; Pinnegar and Polunin, 2000), which could provide a less biased average estimate of predator trophic level.

[3] Menezes, G. 1995–97. Unpubl. data. Department of Oceanography and Fisheries, University of the Azores. Cais de Santa Cruz, PT9901-862 Horta, Portugal.

Acknowledgments

This work is part of a more comprehensive study supported by the European Union (Design optimization and implementation of demersal cruise survey in the Macaronesian Archipelagos (study contract DG XIV/94/034 and DG XIV/95/095). We thank João Gonçalves, Ricardo Serrão Santos, Filipe Porteiro for help with identification of stomach contents, and Helena Krug for help with the identification of otoliths. Special thanks are due to the scientific staff and to the crew of the RV *Arquipélago* for working overtime at sea. We are also grateful to Malcolm J. Smale, Pedro Afonso, Joel Carlin, and Natacha Carvalho for reviewing the manuscript. Comments and suggestions of anonymous reviewers greatly improved the quality of the manuscript.

Literature cited

Ajayi, T. O.
1982. Food and feeding habits of *Raja* species (Batoidei) in Carmarthen Bay, Bristol Channel. J. Mar. Biol. Assoc. U.K. 62:215–223.

Alvarez, R. Z.
1968. Crustáceos decápodos Ibéricos. Investigacion Pesquera, tomo 32, 510 p. Imprenta Juvenil, Barcelona.

Castellón, A., and P. Abelló.
1983. Bathymetric distribution of some Reptantia Decapoda in the Catalan area (Spain). Rapp. Comm. Int. Mer Médit. 28(3):291–294.

Clarke, M. R., D. C. Clarke, H. R. Martins, and H. M. Silva.
1995. The diet of swordfish (*Xiphias gladius*) in Azorian waters. Arquipélago (Life Mar. Sci.) 13A:53–69.
1996. The diet of blue shark (*Prionace glauca*, L.) in Azorean waters. Arquipélago (Life Mar. Sci.) 14A:41–56.

Clarke, K. R., and R. M. Warwick.
1994. Change in marine communities: an approach to statistical analysis and interpretation, 144 p. Natural Environment Research Council, UK.

Compagno, L. J. V.
1984. FAO Species catalogue. Vol. 4, Sharks of the world: an annotated and illustrated catalogue of sharks species known to date. Part 2 Carcharhiniformes. FAO (Food and Agriculture Organization) Fish. Synop. 125(4) Part 2: 251–655.

Cortés, E.
1997. A critical review of methods of studying fish feeding based on analysis of stomach contents: application to elasmobranch fishes. Can. J. Fish. Aquat. Sci. 54:726–738.

1999. Standardized diet compositions and trophic levels of sharks. ICES (International Council for the Exploration of the Sea.) J. Mar. Sci. 56:707–717.

Cunha, P., J. Calvário, J. C. Marques, and P. Re.
1986. Estudo comparativo dos regimes alimentares de *Rajo brachyura* Lafont, 1873, *Raja clavata* Linné, 1758, *Raja montagui* Fowler, 1910 e *Raja naevus* Muller and Henlen, 1841 (Pisces: Rajidae) da costa Portuguesa. Arquivos do Museu Bocage Série A III(8):137–154.

Day, F.
1880–84. The fishes of Great Britain and Ireland, vol. 1, 336 p., and vol. 2, 388 p. William and Norgate, London.

Ebert, D. A., P. D. Cowley, and L. J. V. Compagno.
1991. A preliminary investigation of the feeding ecology of skates (Batoidea: Rajidae) off the west coast of Southern Africa. S. Afr. J. Mar. Sci. 10:71–81.

Ellis, J. R., M. G. Pawson, and S. E. Shackley.
1996. The comparative feeding ecology of six species of shark and four species of ray (Elasmobranchii) in the North-East Atlantic. J. Mar. Biol. Assoc. U.K. 76:89–106.

Ferry, L. A., and G. M. Cailliet.
1996. Sample size and data analysis: are we characterizing and comparing diet properly? *In* GUTSHOP '96. Feeding ecology and nutrition in fish: symposium proceedings (D. MacKinley and K. Shearer, eds), p. 71–80. Am. Fish. Soc., San Francisco, CA.

Fitzmaurice, P.
1974. Size distribution and the food of thornback rays (*Raja clavata* L.) caught on rod and line on the Mayo Coast. Irish Fish. Invest. (ser. B) 11.

Ford, E.
1921. A contribution to our knowledge of the life-histories of the dogfish landed at Plymouth. J. Mar. Biol. Assoc. U.K. 12:468–505.

Fransen, C. H. J. M.
1991. Preliminary report on Crustacea collected in the eastern part of the North Atlantic during the CANCAP and MAURITANIA expeditions of the former Rijksmuseum van Natuurlijke Historie, Leiden, 200 p. Nationaal Natuurhistorisch Museum, Leiden.

Genin, A., and G. W. Boehlert.
1985. Dynamics of temperature and chlorophyll structures above a seamount: an oceanic experiment. J. Mar. Res. 43: 907–924.

Gibson, R. N., and I. A. Ezzi.
1987. Feeding relationships of a demersal fish assemblage on the west coast of Scotland. J. Fish Biol. 31:55–69.

Granadeiro, J. P., L. R. Monteiro, and R. W. Furness.
1998. Diet and feeding ecology of Cory's shearwater *Calonectris diomedea* in the Azores, north-east Atlantic. Mar. Ecol. Prog. Ser. 166:267–276.

Gu, B., S. L. Schelske, and M. V. Hoyer.
1996. Stable isotopes of carbon and nitrogen as indicators of diet and trophic structure of the fish community in a shallow hypereutrophic lake. J. Fish Biol. 49:1233–1243.

Holden, M. J., and R. N. Tucker.
1974. The food of *Raja clavata* Linnaeus 1758, *Raja montagui* Fowler 1910, *Raja naevus* Muller and Henel 1841, and *Raja brachyura* Lafont 1873 in British waters. J. Cons. Int. Explor. Mer 35(2):189–193.

Hurtubia, J.
1973. Trophic diversity measurement in sympatric predatory species. Ecology 19:36–58.

Hyslop, E. J.
1980. Stomach contents analysis—a review of methods and their applications. J. Fish Biol. 17:411–429.

Jennings, S., O. Reñones, B. Morales-Nin, N. V. C. Polunin, J. Moranta, and J. Coll.
1997. Spatial variation in the ^{15}N and ^{13}C stable isotope composition of plants, invertebrates and fishes on Mediterranean reefs: Implications for the study of trophic pathways. Mar. Ecol. Prog. Ser. 146:109–116.

Løkkeborg, S., B. L. Olla, W. H. Pearson, and M. W. Davis.
1995. Behavioural response in sablefish *Anoplopoma fimbria*, to bait odour. J. Fish Biol. 46:142–155.

Marques, V. M., and P. Ré.
1978. Régime alimentaire de quelques Rajidae des côtes Portugaises. Arquivos do Museu Bocage. 20 série VI(34), 8 p.

Morato, T., E. Solà, M. P. Grós, and G. Menezes.
1999. Diets of forkbeard (*Phycis phycis*) and conger eel (*Conger conger*) off the Azores during spring of 1996 and 1997. Arquipélago (Life Mar. Sci.) 17A:51–64.
2001. Feeding habits of two congener species of seabreams, *Pagellus bogaraveo* and *Pagellus acarne*, off the Azores (northeastern Atlantic) during spring of 1996 and 1997. Bull. Mar. Sci. 69(3):1073–1087.

Morato, T., R. S. Santos, and P. Andrade.
2000. Feeding habits, seasonal and ontogenetic diet shift of blacktail comber, *Serranus atricauda* (Pisces: Serranidae), from the Azores, Northeastern Atlantic. Fish. Res. 49(1):51–60.

Olaso, I., and E. Rodriguez-Marin.
1995. Alimentación de veinte especies de peces demersales pertenecientes a la división VIIIc del ICES. Otoño 1991. Inf. Tec. Inst. Esp. Oceanogr. 157, 56 p.

Olsen, A. M.
1954. The biology, migration and growth rate of the school shark, *Galeorhinus australis* (Macleay) (Carcharhinidae) in south-eastern Australian waters. Aust. J. Mar. Freshwat. Res. 5:353–410.
1984. Synopsis of biological data on the school shark, *Galeorhinus australis* (Mcleay 1881). FAO Fish. Synop. 139, 42 p.

Pauly, D., V. Christensen, and C. Walters.
2000. Ecopath, Ecosim, and Ecospace as tools for evaluating ecosystem impact of fisheries. ICES J. Mar. Sci. 57: 697–706.

Pierce, G. J., P. R. Boyle, L. C. Hastie, and M. B. Santos.
1994. Diets of squid *Loligo forbesi* and *Loligo vulgaris* in the northeast Atlantic. Fish. Res. 21:149–163.

Pinkas, L., M. S. Oliphant, and I. L. K. Iverson.
1971. Food habits of albacore, bluefin tuna and bonito in California waters. Calif. Fish Game 152:1–105.

Pinnegar, J. K., and N. V. C. Polunin.
2000. Contribution of stable-isotope data to elucidating food webs of Mediterranean rocky littoral fishes. Oecologia 122: 399–409.

Pitcher, T. J.
2000. Ecosystems goals can reinvigorate fisheries management, help dispute resolution and encourage public support. Fish Fish. 1:99–103.

Quade, D., and I. Salama.
1992. A survey of weighted rank correlation. *In* Order statistics and nonparametrics: theory and applications (P. K. Sen, and I. Salama, eds.), p. 213–224. Elsevier, New York.

Quiniou, L., and G. R. Andriamirado.
1979. Variations du régime alimentaire de trois espèces de raies de la baie de Douarnenez (*Raja montogui* Fowler, 1919; *Raja brachyura* Lafont, 1873; *Raja clavata* L., 1758). Cybium 7:27–39.

Ramos, J. R., E. Solà , L. R. Monteiro, and N. Ratcliffe.
1998a. Prey delivered to roseate tern chicks in the Azores. J. Field Ornithol. 69:419–429.

Ramos, J. R., E. Solà, F. M. Porteiro, and L. R. Monteiro.
1998b. Prey of yellow-legged gull, roseate tern and common tern in the Azores. Seabird 20:31–40.
Rogers, A. D.
1994. The biology of seamounts. Adv. Mar. Biol. 30: 306–350.
Schoener, T. W.
1970. Non-synchronous spatial overlap of lizards in patchy habitats. Ecology 51:408–418.
Skjæraasen, J. E., and O. A Bergstad.
2000. Distribution and feeding ecology of *Raja radiata* in the northeastern North Sea and Skagerrak (Norwegian Deep). ICES J. Mar. Sci. 57:1249–1260.
Smale, M. J., and P. D. Cowley.
1992. The feeding ecology of skates (Batoidea: Rajidae) off the Cape south coast, South Africa. S. Afr. J. Mar. Sci. 12: 823–834.
Stehmann, M.
1987. Quick and dirty tabulation of stomach contents and maturity stages for skates (Rajidae), squaloid and other ovoviviparous and viviparous species of sharks. Am. Elasmobranch Soc. Newsletter 1987(3):5–9.
Stehmann, M., and D. L. Burkel.
1984. Rajidae. *In* Fishes of the North-eastern Atlantic and the Mediterranean (P. J. P. Whitehead, M. BL. Bauchot, J. BC. Hureau, J. Nielse, and E. Tortonese, eds.), vol. 1, p. 163–196. UNESCO (United Nations Educational, Scientific, and Cultural Organization), Paris.
Whipple, S. J., J. S. Link, L. P. Garrison, and M. J. Fogarty.
2000. Models of predation and fishing mortality in aquatic ecosystems. Fish Fish. 1:22–40.
Zar, J. H.
1999. Biostatistical analysis, 4th ed., 663 p. Prentice Hall International Editions, Upper Saddle River, NJ.

Abundance of cetaceans in the southern U.S. North Atlantic Ocean during summer 1998

Keith D. Mullin
Gregory L. Fulling

Southeast Fisheries Science Center
National Marine Fisheries Service, NOAA
3209 Frederic Street
Pascagoula, Mississippi 39567
E-mail (for K. D. Mullin): Keith.D.Mullin@noaa.gov

Abstract—The U.S. Marine Mammal Protection Act requires that the abundance of marine mammals in U.S. waters be assessed. Because this requirement had not been met for a large portion of the North Atlantic Ocean (U.S. waters south of Maryland), a ship-based, line-transect survey was conducted with a 68 m research ship between Maryland (38.00°N) and central Florida (28.00°N) from the 10-m isobath to the boundary of the U.S. Exclusive Economic Zone. The study area (573,000 km^2) was surveyed between 8 July and 17 August 1998. Minimum abundance estimates were based on 4163 km of effort and 217 sightings of at least 13 cetacean species and other taxonomic categories. The most commonly sighted species (number of groups) were bottlenose dolphins, *Tursiops truncatus* (38); sperm whales, *Physeter macrocephalus* (29); Atlantic spotted dolphins, *Stenella frontalis* (28); and Risso's dolphins, *Grampus griseus* (22). The most abundant species (abundance; coefficient of variation) were Atlantic spotted dolphins (14,438; 0.63); bottlenose dolphins (13,085; 0.40); pantropical spotted dolphins, *S. attenuata* (12,747; 0.56); striped dolphins, *S. coeruleoalba* (10,225; 0.91); and Risso's dolphins (9533; 0.50). The abundance estimate for the Clymene dolphin, *S. clymene* (6086; 0.93), is the first for the U.S. Atlantic Ocean. Sperm whales were the most abundant large whale (1181; 0.51). Abundances for other species or taxonomic categories ranged from 20 to 5109. There were an estimated 77,139 (0.23) cetaceans in the study area. Bottlenose dolphins and Atlantic spotted dolphins were encountered primarily in continental shelf (<200 m) and continental slope waters (200–2000 m). All other species were generally sighted in oceanic waters (>200 m). The distribution of some species varied north to south. Striped dolphins, Clymene dolphins, and sperm whales were sighted primarily in the northern part of the study area; whereas pantropical spotted dolphins were sighted primarily in the southern portion.

Manuscript approved for publication 11 February 2003 by Scientific Editor.
Manuscript received 4 April 2003 at NMFS Scientific Publications Office.
Fish Bull. 101:603–613 (2003).

The U.S. Marine Mammal Protection Act (MMPA) requires that stocks of marine mammal species in U.S. waters be maintained at or above their optimum sustainable population (OSP) level, defined as the number of animals that will result in maximum productivity. The MMPA, as amended in 1994, requires that the U.S. National Marine Fisheries Service (NMFS) determine the potential biological removal (PBR) of each stock for management purposes. PBR is an estimate of the maximum number of animals that may be removed from a stock due to human activities (e.g. fisheries bycatch) while allowing the stock to reach or maintain its OSP. The PBR is calculated by using the estimated minimum abundance of a stock, half its maximum net productivity rate (theoretical; or estimated), and a recovery factor (Barlow et al., 1995).

For the U.S. Exclusive Economic Zone (EEZ) adjacent to the Atlantic coast of the continental U.S., the NMFS currently defines 27 taxa of cetaceans as stocks (Waring et al., 2001). These stocks include 24 one-stock species, bottlenose dolphins (*Tursiops truncatus*) that are divided into two stocks, and one mesoplodont beaked whale stock. Abundance estimates are available for most of these stocks from U.S. waters north of the Virginia-Maryland border (38.00°N). In 1998, except for three stocks, abundance estimates were not available for Atlantic cetacean stocks from U.S. waters south of Maryland (Waring et al., 1997). Abundance estimates for these three stocks were based on a small amount of effort from a 1992 winter ship survey south of Cape Hatteras (Mullin and Ford[1]). Other cetacean abundance estimates from U.S. waters south of Maryland are for portions of the continental shelf or continental slope (Blaylock and Hoggard, 1994; Blaylock, 1995; CeTAP[2]; Fritts et al.[3]).

To estimate the abundance of cetaceans in U.S. Atlantic waters south of Maryland, a ship survey was conducted during summer 1998 and the results are reported in this study. Abundance estimates from this area are combined with abundance estimates from surveys of U.S. waters north of the Virginia-Maryland border conducted by the NMFS Northeast Fisheries Science Center to obtain overall abundance estimates for western North Atlantic cetacean stocks (e.g. Waring et al., 2001).

[1] Mullin, K. D., and R. Ford. 1992. Report of NOAA ship *Oregon II* cruise 92-01 (198) (a cetacean survey of U.S. Atlantic waters south of Cape Hatteras, winter 1992). Southeast Fisheries Science Center, P.O. Drawer 1207, Pascagoula, Mississippi 39568.

[2] CeTAP (Cetacean and Turtle Assessment Program). 1982. A characterization of marine mammals and turtles in the mid- and north-Atlantic areas of the U.S. outer continental shelf. Final Report of the Cetacean and Turtle Assessment Program Bureau of Land Management, contract no. AA551-CT8-48, 450 p. U.S. Dep. Interior, Washington D.C.

[3] Fritts, T. H., A. B. Irvine, R. D. Jennings, L. A. Collum, W. Hoffman, and M. A. McGehee. 1983. Turtles, birds, and mammals in the northern Gulf of Mexico and nearby Atlantic waters. Rep. FWS/OBS-82/65, 455 p. U.S. Fish and Wildlife Service, Office of Biological Services, Washington, D.C.

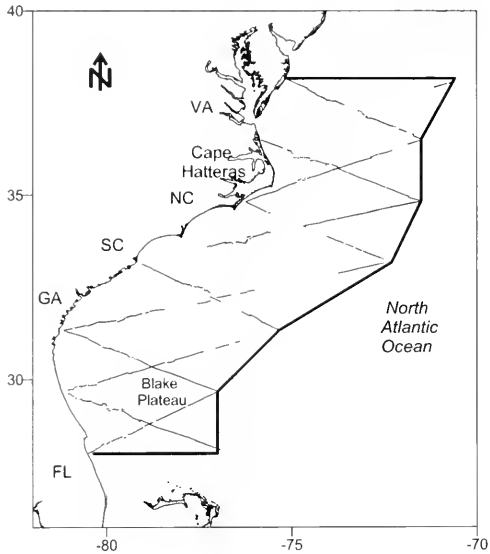

Figure 1

Survey effort (4163 km; thin lines) in Beaufort sea state ≤4 in the southern U.S. Atlantic study area (outlined by thick line) during summer 1998. Blank areas indicate Beaufort sea states >4 that were not included in the survey effort. The 200-, 500-, 1000-, 2000-, and 3000-m isobaths are shown.

Methods

Study area and survey design

The study area (573,000 km^2) was North Atlantic Ocean waters between central Florida (28.00°N) and Maryland (38.00°N) from the 10-m isobath to the boundary of the U.S. EEZ, generally 371 km (200 nmi) from the nearest U.S. point of land (Fig. 1). The study area has a diverse bottom topography and includes a very narrow continental shelf (<200 m) at Cape Hatteras which broadens to form the mid-Atlantic Bight to the north and the Florida-Hatteras Shelf to the south. Beyond the shelf, south of Cape Hatteras are found the following features: the Florida-Hatteras Slope, the Blake Plateau (700–1000 m deep), and the Blake Escarpment. North of the Blake Plateau, the continental slope from 200–2000 m deep is steep and most of the study area has water depths >2000 m. The Gulf Stream is the dominant oceanographic feature in the study area. From the south, the Gulf Stream Front generally follows the upper continental slope northward to Cape Hatteras, where it flows to the northeast. Seaward of the Gulf Stream are Sargasso Sea waters. North of Cape Hatteras and the Gulf Stream Front, cooler waters, which largely originate in the Labrador Sea, drift into the study area from the north and northeast.

Transects covered the study area uniformly in a saw-tooth pattern from a random start at the southernmost inshore point and were surveyed from the 68-m NOAA ship *Relentless* (renamed *Gordon Gunter* in 1999) between 8 July and 17 August 1998 from south to north, and from north to south. Transects were placed to cross the bathymetry gradient. The narrow band of U.S. waters between central Florida and Key West, Florida, were partially surveyed but were not included in the present report.

Data collection

Data were collected by two teams of three observers from the ship's flying bridge, located 14.5 m above the surface of the water, during daylight hours, weather permitting (i.e. no rain, Beaufort sea state <6). Observers used standard line-transect survey methods for cetaceans that were similar to those used from ships in the Pacific Ocean and Gulf of Mexico (e.g., Barlow, 1995; Hansen et al.[4]). Each team had at least two members experienced in shipboard line-transect methods and in the identification of tropical and temperate cetaceans. Two observers searched for cetaceans using 25× binoculars and another observer searched using unaided eye or 7× hand-held binoculars and recorded data. These three observers constituted the "primary team." From 18 July to 17 August, a fourth observer was added to one team to act as a conditionally independent observer (CIO, see below). The area from 90° left and right of the ship's bow to the horizon was searched by the primary team. Observers changed position (including the CIO position) every 30–40 minutes, and each team alternated two-hour watches throughout daylight hours. The survey speed was usually 18 km/h but varied with sea conditions.

Data were recorded on a computer interfaced with a global positioning system (GPS) by a data acquisition program. Data collected for each cetacean sighting included time, position, bearing, and reticle (a measure of radial distance) of the sighting, species, group-size, behavior, bottom depth, sea surface temperature, and associated animals (e.g. seabirds, fish). The bearing and radial distance for sightings that were close to the ship were estimated. Survey effort data were automatically recorded every two minutes and included position, heading, effort status, observer position, and environmental conditions that could affect the observers' ability to sight animals (e.g. Beaufort sea state, position of the sun).

Typically, if a sighting was within a 5.5-km strip on either side of the ship, the ship was diverted from the transect line and approached the group so that observers could identify species and obtain group-size estimates. For each sighting, the final group-size was estimated by a consensus

[4] Hansen, L. J., K. D. Mullin, T. A. Jefferson, and G. P. Scott. 1996. Visual surveys aboard ships and aircraft. *In* Distribution and abundance of marine mammals in the north-central and western Gulf of Mexico: final report; vol. II: technical report (R.W. Davis and G. S. Fargion, eds.), p. 55–132. Outer Continental Shelf (OCS) Study MMS 96-0027. U.S. Dep. Interior, Minerals Mgmt. Service, Gulf of Mexico OCS Region, New Orleans, LA.

Table 1

Number of on-effort cetacean group sightings of each species or other taxonomic category during 4163 km of survey effort in the southern U.S. Atlantic study area during summer 1998. Species are listed in categories pooled to estimate $f(0)$ (see Table 2). The number of sightings used for line-transect and strip-transect abundance estimates are indicated for each species.

$f(0)$ groupings and species	Line-transect	Strip-transect
Large whales		
Fin whale (*Balaenoptera physalus*)	1	0
Minke whale (*B. acutorostrata*)	1	0
Sperm whale (*Physeter macrocephalus*)	29	0
Unidentified large whale	6	0
Cryptic whales		
Dwarf and pygmy sperm whale (*Kogia* spp.)	9	0
Mesoplodon spp.	4	0
Unidentified Ziphiidae	3	0
Unidentified small whale	4	0
Unidentified odontocete	12	0
Small whales and large dolphins		
Pilot whale (*Globicephala* spp.)	10	0
Bottlenose dolphin (*Tursiops truncatus*)	35	3
Risso's dolphin (*Grampus griseus*)	22	0
"Coastal" Atlantic spotted dolphin (*Stenello frontalis*)	24	3
Unidentified *T. truncatus* or *S. frontalis*	7	1
Rough-toothed dolphin (*Steno bredanensis*)	1	0
Small dolphins		
Pantropical spotted dolphin (*Stenella attenuata*)	6	0
Striped dolphin (*Stenella coeruleoalba*)	5	0
Clymene dolphin (*Stenella clymene*)	2	1
"Offshore" Atlantic spotted dolphin (*Stenella frontalis*)	1	0
Unidentified dolphins		
Unidentified dolphins	26	0
Stenella spp.	1	0
Total	209	8

of the primary team. Mixed-species groups were uncommon (five of 217 sightings) and group-size estimates were made separately for each species.

Species identification

Cetaceans were identified to the lowest taxonomic level possible from descriptions in field guides and scientific literature (e.g. Leatherwood and Reeves, 1983; Jefferson et al., 1993; Carwardine, 1995) (Table 1). An observer's ability to make identifications depended on weather and animal behavior. The study area was potentially inhabited by short-finned pilot whales (*Globicephala macrorhynchus*), which are thought to occur within the study area from about Virginia south, and long-finned pilot whales (*G. melas*), thought to occur from near Cape Hatteras north (Payne and Heinemann, 1993). Because the two species cannot be reliably distinguished at sea, they were recorded simply as pilot whales. Two forms of the Atlantic spotted dolphin (*Stenella frontalis*) were tentatively identified: the larger, more coastal form, and the smaller offshore form (Perrin et al., 1994). Abundances were estimated for each form and for all Atlantic spotted dolphins combined because only one stock is currently designated for U.S. Atlantic waters. Coastal and offshore forms of bottlenose dolphins (Hersh and Duffield, 1990), which constitute the two stocks, were recorded, but most sightings could not be clearly categorized; therefore, all bottlenose dolphin sightings were pooled for one overall abundance estimate. Bottlenose and Atlantic spotted dolphins could not always be distinguished at large distances and a separate estimate was made for animals that could not be approached and were identified as "*Tursiops* or *S. frontalis*." Overall abundances for the genus *Kogia* and the genus *Mesoplodon* were estimated. Dwarf sperm whales (*K. sima*) and pygmy sperm whales (*K. breviceps*) were difficult to distinguish and stranding records of both species are numerous from U.S. Atlantic shores (Schmidly[5]). Based on

[5] Schmidly, D. J. 1981. Marine mammals of the southeastern United States and the Gulf of Mexico. U.S. Dep. Interior, U.S. Fish and Wildlife Service Biological Services Program FWS/OBS-80/41, 165 p.

Table 2

Estimate of $f(0)$ for each species group (see Table 1). n = number of sightings used for the estimate of $f(0)$ before truncation (included in n is the number of sightings in parentheses that occurred while the ship was in transit in or near the study area). Truncation = the perpendicular distance, y, at which groups with a greater y were excluded from the analysis. ESW = effective strip width.

Species group	n	$f(0)$ (/km)	CV [$f(0)$]	Truncation (m)	ESW (m)
Large whales	38 (1)	0.300	0.12	5500	6666
Cryptic whales	33 (1)	0.561	0.13	3000	3565
Small whales and large dolphins	121 (22)	0.498	0.10	4000	4016
Small dolphins	20 (6)	0.398	0.11	4500	5025
Unidentified dolphin	27 (0)	0.496	0.10	4000	4032
Total	239 (30)				

stranding records of mesoplodont whales from U.S. Atlantic shores, sightings of *Mesoplodon* were probably True's (*M. mirus*), Gervais's (*M. europaeus*) or Blainville's (*M. densirostris*) beaked whales (Mead, 1989). In some cases cetaceans could only be identified as large whales (>7 m long), small whales (nondolphin, <7 m), dolphins, or odontocetes.

Analytical techniques

For each species or taxonomic category, abundance estimates (N) were made with line-transect methods by using the software program DISTANCE (Colorado Coop. Fish and Wildlife Research Unit, Colorado State Univ., Fort Collins, CO) (Buckland et al., 1993) with the equation

$$N = \frac{A\, n\, S\, f(0)}{2\, L\, g(0)},$$

where A = size of the study area;
n = number of on-effort group sightings;
S = mean group-size estimate;
$f(0)$ = sighting probability density function at perpendicular distance zero;
L = total length of transect line; and
$g(0)$ = probability of seeing a group on the transect line.

The log-normal 95% confidence interval was computed for each abundance estimate because it was a product of estimates and tends to have a skewed distribution. The variance of N was estimated as

$$\mathrm{var}(N) = N^2\left[\frac{\mathrm{var}(n)}{n^2} + \frac{\mathrm{var}(S)}{S^2} + \frac{\mathrm{var}[f(0)]}{f(0)^2} + \frac{\mathrm{var}[g(0)]}{f(0)^2}\right]$$

and the coefficient of variation (CV) was estimated as

$$CV(N) = \frac{\sqrt{\mathrm{var}(N)}}{N}.$$

The sampling unit was the length of the transect completed on-effort each day when the Beaufort sea state was <5. The formula used to estimate each component of the variance is given in Buckland et al. (1993). Var(n) was length-weighted and based on the variation in the number of on-effort group sightings between sampling units that ranged in length from 39 to 229 km/day.

Estimation of $f(0)$

The perpendicular distance, y, was estimated by using bearing and reticle measurements. The reticle readings were converted to radial sighting distances (R) by the method of Lerczak and Hobbs (1998), and the formula $y = R \sin(b)$, where b = angle between the sighting and the transect line. Estimates of $f(0)$ were made by using a hazard-rate, uniform, or half-normal model with exact perpendicular sighting distances. For each species group, outlying values of y were truncated to improve the fit of the model (Table 2). Model selection was determined by using Akaike's information criterion (AIC; Buckland et al., 1993).

The number of groups sighted of most species was insufficient to obtain an estimate of $f(0)$. Therefore, sightings of species with similar sighting characteristics (i.e. body size, group-size, surface behavior, blow visibility) were pooled to estimate $f(0)$ for five categories (Table 1). The abundance for each species was estimated by using the pooled $f(0)$ and var[$f(0)$] for its category. The var[$f(0)$] was assumed to be zero for the strip-transect estimates explained below. If the individual detection functions of all species within a category are indeed very similar, by pooling, the variance, CV, and confidence interval of each abundance estimate was probably underestimated because the variance of $f(0)$ was based on an artificially high sample size. On the other hand, if the true detection functions of the species within a category are highly variable, the variance of $f(0)$ for an individual species may be overestimated.

During the study, effort was sometimes maintained while in transit to and from ports or along the border of the study area, but it usually occurred in a small range of water depths (e.g. parallel to shore) and was excluded because it could have biased abundance estimates. However, due to the small number of sightings for the survey, y from the "transit" sightings were pooled with the on-effort sightings for estimates of $f(0)$ (Table 2).

Estimation of mean group-size

The group-sizes for most species tended to be related to y, because in many cases larger groups are easier to see than small groups with increasing y. In general, the arithmetic mean of group-size may be an overestimate of the true mean group-size and could lead to positively biased abundance estimates. Therefore, a regression of group-size by y was used to estimate an "expected mean group-size" (program DISTANCE). The expected mean group-size was used in the abundance estimate if it was smaller than the arithmetic mean group-size. For estimates based on a small number of sightings, the expected mean group-size was sometimes greater than the arithmetic mean. Because group-size estimates were usually made after the ship approached the group, this was assumed to be an artifact of the small sample size, and the arithmetic mean was used in these cases. Var(S) was the analytical variance for mean group-sizes based on arithmetic means or was estimated as in Buckland et al. (1993:79) for expected mean group-sizes.

Strip-transect estimates

One requirement for unbiased line-transect estimates of abundance is that the cetacean group should not move in response to the ship before it is sighted (Buckland et al., 1993). If cetaceans are not sighted before they respond to the ship, in cases of attraction to the ship, $f(0)$ and abundance will be overestimated. In the Gulf of Mexico, five species appear to be consistently attracted to ships to ride the bow waves (i.e. bottlenose, Atlantic spotted, spinner [*S. longirostris*], Clymene [*S. clymene*], and pantropical spotted dolphins [*S. attenuata*]) (Würsig et al., 1998). All sightings made with 25× binoculars had radial distances >665 m and were assumed to be made before these species were attracted to the ship. If sightings of these species were made at radial distances <665 m, because of the possibility of attraction, they were not included in the line-transect abundance estimate, and a separate strip-transect abundance estimate was made with these sightings. For each species, the width of the strip for strip-transect estimates was set at the line-transect strip width ($1/2f(0)$) for that species (Tables 1 and 2). This procedure yields the same result as the formula given above with $f(0)$ for the species-group category. However, $f(0)$ for small dolphins and for small whales and large dolphins combined was not positively biased by including sightings of groups that were probably attracted to the transect line. For each species, the line- and strip-transect estimates were summed for one overall abundance estimate.

Conditionally independent observer

The central assumption for estimating abundance with line-transect methods is that cetacean groups on the transect line are detected with certainty (i.e. $g(0) = 1$; Buckland et al., 1993). However, this assumption is usually not met during cetacean surveys because of availability and perception bias (i.e. $g(0) < 1$) (Marsh and Sinclair, 1989). Some groups on the transect line are missed because they may not be at the surface during the time the ship is in the area and are not available to be seen, whereas other groups at the surface are missed by observers (i.e. not perceived) because of factors such as observer experience, sea state, and animal behavior, among others.

An attempt was made to estimate $g(0)$ due to perception bias with a conditionally independent observer (CIO) by using methods based on Barlow (1995). The CIO was used when the 4-observer team was on duty and was stationed at 25× binoculars located on a bridge-wing 2.7 m below the primary team. One individual switched teams each day; therefore all seven observers on the ship acted as the CIO at different times. The CIO searched for cetaceans near the transect line (from 30° left to 30° right of the bow) when the primary observers were on-effort. The CIO and the primary team could not see or hear each other. Whenever the primary team made a sighting, the data recorder relayed its bearing and reticle to the CIO. When the CIO made a sighting, the time, bearing and reticle were noted by the CIO, and the sighting was monitored until it was sighted by the primary team or, theoretically, passed abeam, at which time the CIO was to notify the primary team to divert the ship to identify the species and estimate group-size.

Results

Abundance estimates were based on 4163 km of effort in Beaufort sea states ≤4 and 217 on-effort sightings of cetacean species or other taxonomic categories (Fig. 1 and Table 1). At least 13 cetacean species were sighted. The most commonly sighted species (number of sightings) were bottlenose dolphins (38), sperm whales (*Physeter macrocephalus*) (29), Atlantic spotted dolphins (28), and Risso's dolphins (*Grampus griseus*) (22). Thirty sightings occurred during transit in Beaufort sea states ≤4 (861 km) and were used to estimate $f(0)$. Estimates of $f(0)$ ranged from 0.300/km for large whales to 0.561/km for cryptic whales (Table 2).

Conditionally independent observer

The CIO achieved 1775 km of effort (35% of effort, including transit, with Beaufort sea state ≤4) and sighted 21 cetacean groups. Of these, six groups ranging in size from 1 to 10 animals were missed by the primary team and included three unidentified dolphin groups, two unidentified odontocete groups, and one *Mesoplodon* sp. Each of these sightings was observed briefly by the CIO but could not be tracked until they passed the beam of the ship; however, in each of the six cases no sightings were made by the primary team during the time frame it would have been possible to sight them. To estimate $g(0)$ following the analytical methods described by Barlow (1995), a separate estimate of $f(0)$ is therefore required for CIO sightings missed by the primary team. Because there were only six of these, $g(0)$ could not be estimated for any $f(0)$ category, and $g(0) = 1$ and $\text{var}[g(0)] = 0$ was used in each abundance estimate.

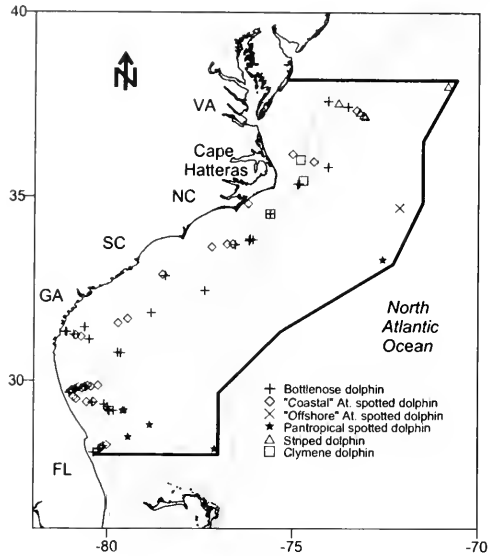

Figure 2

Locations of on-effort sightings of bottlenose dolphins (n=38), "coastal" (n=27) and "offshore" (n=1) Atlantic spotted dolphins, pantropical spotted dolphins (n=6), striped dolphins (n=5), and Clymene dolphins (n=2). The 200-, 500-, 1000-, 2000-, and 3000-m isobaths are shown.

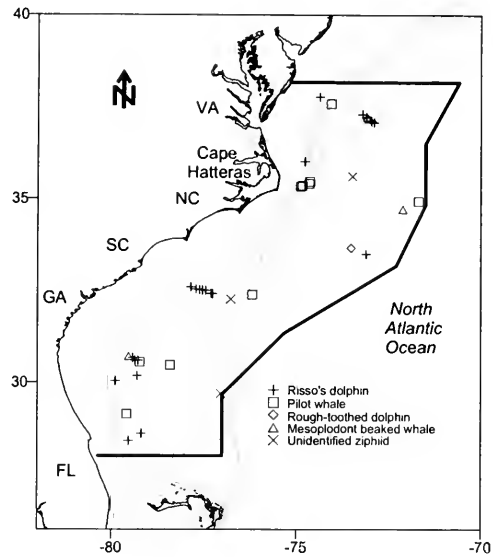

Figure 3

Locations of on-effort sightings of Risso's dolphins (n=22), pilot whales (n=10), rough-toothed dolphins (n=1), *Mesoplodon* spp.(n=4), and unidentified beaked whales (n=3). The 200-, 500-, 1000-, 2000-, and 3000-m isobaths are shown.

Abundance

The following were the most abundant species (abundance; coefficient of variation) observed in our study: Atlantic spotted dolphins (14,438; 0.63); bottlenose dolphins (13,085; 0.40); pantropical spotted dolphins (12,747; 0.56); and striped dolphins (*S. coeruleoalba*) (10,225; 0.91); and Risso's dolphins (9533; 0.50). Sperm whales were the most abundant large whale (1181; 0.51). Abundances for other species or taxonomic categories ranged from 20 to 6086. There were an estimated 77,139 (0.23) cetaceans in the study area.

Group sizes

Mean group sizes for balaenopterids, physeterids, and ziphiids were less than three animals per group. Bottlenose dolphins, pilot whales, Risso's dolphins, and "coastal" Atlantic spotted dolphins were in groups that averaged 12–18 animals. The average group sizes of pantropical spotted, Clymene, and striped dolphins ranged from 75 to 110 individuals (Table 3).

Distribution

Cetaceans were distributed throughout the study area, but few sightings occurred on the eastern Blake Plateau (Fig. 1). The distribution of species varied regionally and by water depth (Fig. 2–4, Table 4). Bottlenose dolphins and "coastal" Atlantic spotted dolphins were sighted throughout the study area but primarily in or near continental shelf waters. Pilot whales and Risso's dolphins were widely distributed seaward of the continental shelf. Sperm whales, unidentified large whales, "offshore" Atlantic spotted dolphins, striped dolphins, and Clymene dolphins occurred almost exclusively in oceanic waters (>200 m) from Cape Hatteras northward. Most pantropical spotted dolphin sightings were in the southern part of the study area.

Discussion

Abundance

Cetacean abundances for the entire study area have not been estimated previously. Based on stranding records and previous surveys within or near the study area, all the species encountered were expected to be sighted. Previous abundance estimates for the western North Atlantic stocks of short-finned pilot whales and of dwarf and pygmy sperm whales, 749 (0.64) and 420 (0.60), respectively, were based on a winter 1992 ship survey in U.S. oceanic waters (>200 m) south of Cape Hatteras (Waring et al., 1997). The 1992 dwarf and pygmy sperm whale estimate is similar to our estimate (580; 0.57); although the 1998 study area was

Table 3

Group size, density and abundance estimates of cetaceans in the southern U.S. Atlantic Ocean during summer 1998 (n = number of on-effort group sightings after truncation, S = mean group-size estimate, D = animals/100 km^2, N = abundance estimate, CV = coefficient of variation, LCI and UCI = lower and upper limits of a log-normal 95% confidence interval).

Species	n	S	CV(S)	D	N	CV(N)	LCI	UCI
Fin whale	1	2.0	—	0.007	41	1.15	6	270
Minke whale	1	1.0	—	0.004	20	1.29	3	156
Sperm whale	28	2.1	0.12	0.206	1181	0.51	445	3136
Dwarf/pygmy sperm whale	8	1.9	0.16	0.101	580	0.57	197	1708
Mesoplodon spp.	4	2.3	0.28	0.061	348	0.76	88	1376
Unidentified Ziphiidae	3	1.7	0.40	0.034	193	0.71	49	755
Pilot whale	9	16.6	0.19	0.892	5109	0.41	2302	11,341
Bottlenose dolphin								
line-transect	31	11.8	0.29	2.194	12,571	0.42	5600	28,222
strip-transect	3	5.0	0.12	0.090	514	0.82	118	2249
sum				2.284	13,085	0.40	6098	28,077
Risso's dolphin	18	15.4	0.26	1.664	9533	0.50	3684	24,671
Atlantic spotted dolphin								
"coastal"								
line-transect	21	17.6	0.25	2.211	12,670	0.71	3471	46,244
strip-transect	3	7.3	0.39	0.132	754	0.64	211	2696
sum				2.343				
"offshore"								
line-transect	1	37.0	—	0.177	1014	0.85	223	4618
strip-transect	0							
sum (coastal and offshore)				2.520	14,438	0.63	4672	44,618
Unid. *T. truncatus* or *S. frontalis*								
line-transect	7	3.9	0.27	0.162	926	0.73	246	3480
strip-transect	1	1.0	—	0.006	34	0.99	6	189
sum				0.168	960	0.71	276	3334
Rough-toothed dolphin	1	8.0	—	0.048	274	1.03	47	1584
Pantropical spotted dolphin	6	77.5	0.25	2.225	12,747	0.56	4420	36,763
Striped dolphin	5	74.6	0.21	1.785	10,225	0.91	2072	50,449
Clymene dolphin								
line-transect	2	110.0	0.37	1.053	6031	0.94	1138	31,963
strip-transect	1	2.0	—	0.010	55	1.15	8	361
sum				1.063	6086	0.93	1293	28,652
Stenella spp.	1	15.0	—	0.089	512	1.15	77	3392
Unidentified large whale	6	1.2	0.14	0.025	143	0.58	48	426
Unidentified small whale	3	2.7	0.63	0.054	309	0.86	53	1796
Unidentified odontocete	11	1.4	0.14	0.101	580	0.36	284	1181
Unidentified dolphin	20	1.2	0.13	0.113	775	0.51	291	2066
Sum (all cetaceans)				13.462	77,139	0.23	49,649	119,850

much larger and many sightings occurred north of Cape Hatteras (Fig.4).

Abundances have also been estimated for small portions of the study area, but direct comparisons to our estimates are difficult. Seasonal abundances were estimated for about 26 cetacean species or genera encountered in U.S. continental shelf and slope waters between Cape Hatteras and Canada during aerial surveys conducted from 1978 to 1982 (CeTAP[2]), including at least 11 species or genera sighted during our survey. Fritts et al.[3] sighted 12 cetacean species during seasonal aerial surveys of the continental shelf and southern Blake Plateau off central

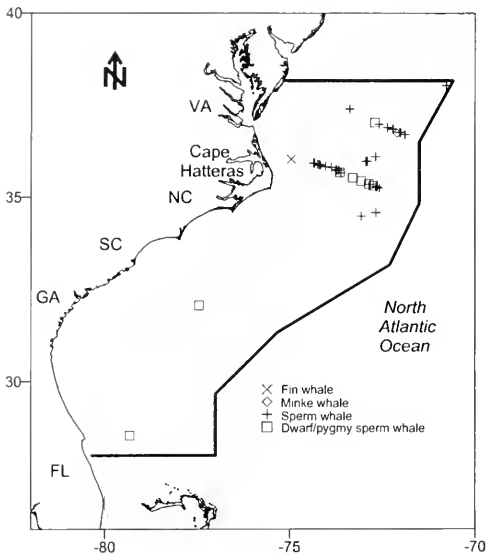

Figure 4

Locations of on-effort sightings of sperm whales (n=29), minke whales (n=1), fin whales (n=1), and dwarf and pygmy sperm whales (n=9). The 200-, 500-, 1000-, 2000-, and 3000-m isobaths are shown.

Florida from 1980 to 1981; eight of these were sighted during our survey.

The abundance estimate reported in the present study for the Clymene dolphin represents the first for this species in any portion of the U.S. Atlantic EEZ. However, the estimate was based on only three sightings and has a large 95% confidence interval (1293–28,652 dolphins). The Clymene dolphin was recognized as a valid species in 1981 and is sympatric with the spinner dolphin in the tropical Atlantic (Perrin et al., 1981). The two species have similar color patterns, and in previous studies both were possibly recognized as *S. longirostris* and were not distinguished (CeTAP[2]; Fritts et al.[3]). The identifications of Clymene dolphins were made by observers with experience from the Gulf of Mexico where both species are relatively common (Hansen et al.[4]; Hansen et al.[6]). There is currently no stock designation for the Clymene dolphin in U.S. Atlantic waters (Waring et al., 2001).

Our estimate of bottlenose dolphins is for waters >10 m in depth; however, this estimate does not include their entire water depth range in U.S. Atlantic waters south of Maryland. Bottlenose dolphins occur year-round in coastal waters <10 m in depth (the inshore boundary of the study area) and in some bays and estuaries from Cape Hatteras south. North of the Cape they have been found close to shore in waters <25 m in depth only during warm months

[6] Hansen, L. J., K. D. Mullin, and C. L. Roden. 1995. Estimates of cetacean abundance in the northern Gulf of Mexico from vessel surveys, 9 p. Southeast Fisheries Science Center, P.O. Drawer 1207, Pascagoula, Mississippi 39568.

Table 4

Mean water depth and sea surface temperature of cetacean species sighted in the southern U.S. Atlantic Ocean during summer 1998 (n=number of groups sighted on-effort; SE=standard error).

		Water depth (m)			Sea surface temperature (°C)		
Species	n	Mean	SE	Range	Mean	SE	Range
Fin whale	1	48	—	—	25.1	—	—
Minke whale	1	3475	—	—	29.5	—	—
Sperm whale	29	3252	122	2195–4389	29.0	0.28	22.8–29.9
Dwarf and pygmy sperm whale	9	2586	493	766–4079	29.6	0.37	26.9–30.9
Mesoplodon spp.	4	2699	735	774–4353	27.2	1.65	24.0–31.1
Unidentified Ziphiidae	3	1817	832	878–3475	29.8	0.15	29.6–30.1
Pilot whale	10	1527	387	251–4280	28.5	0.73	23.2–31.5
Bottlenose dolphin	38	371	89	12–2561	29.3	0.27	23.2–31.3
Risso's dolphin	22	1300	285	44–4755	28.4	0.62	22.9–31.3
"coastal" Atlantic spotted dolphin	27	216	117	13–2524	29.1	0.26	25.1–31.3
"offshore" Atlantic spotted dolphin	1	4298	—	—	27.9	—	—
Rough-toothed dolphin	1	4353	—	—	27.3	—	—
Pantropical spotted dolphin	6	1498	708	598–5030	30.5	0.61	27.6–31.6
Striped dolphin	5	2736	237	2012–3475	23.9	0.37	22.9–25.1
Clymene dolphin	3	756	538	139–1829	27.9	0.59	26.8–28.8

and are assumed to have migrated along-shore from the south (Mead, 1975; Kenney, 1990). Aerial surveys of bottlenose dolphins conducted in the past along the U.S. Atlantic included waters from the shore to 10 m in depth. For waters typically <75 m deep south of Cape Hatteras, the winter 1992 abundance from an aerial survey was 12,435 (0.18) (Blaylock and Hoggard, 1994). For waters <25 m deep from Cape Hatteras to northern New Jersey, the abundance from a summer 1994 aerial survey was 26,809 (0.40) (Blaylock, 1995). The frequency of bottlenose dolphin sightings during these surveys increased substantially inshore of the 10-m isobath boundary of the ship study area and, compared with the estimate from the ship, may account for the generally larger aerial survey estimates even though they are for smaller study areas.

There are currently two genetically distinguishable bottlenose dolphin stocks designated in the U.S. Atlantic: the coastal stock and the offshore stock (LeDuc and Curry, 1998; Waring et al., 2001). Using mitochondrial DNA from skin biopsy samples obtained during the summer 1998 study and other sampling efforts, Torres et al. (in press) reported no offshore form was sampled within 6 km of shore and no coastal from was sampled beyond 39 km from shore or in waters >34 m deep. Therefore an area of overlap of the two forms occurs within the 1998 study area but the fraction of each stock in our estimate (13,085; 0.40) is unknown because the number of biopsy samples between the two boundaries was very small in the Torres et al. (in press) study. However, 20 of the 38 bottlenose groups we used to estimate abundance were found in waters >50 m deep.

Abundances were estimated for ten species and three other genera of cetaceans, but other species are known or expected to occur in the study area. Three of these species, right whales (*Eubalaena glacialis*), humpback whales (*Megaptera novaeangliae*), and harbor porpoises (*Phocoena phocoena*), occur in the study area seasonally, primarily in months other than summer months, and abundances have been estimated from studies of their primary summer ranges north of the study area (e.g. Knowlton et al., 1994; Palka, 1995; Smith et al., 1999).

Additional species expected in at least part of the study area include Bryde's whale (*B. edeni*), Cuvier's beaked whale (*Ziphius cavirostris*), pygmy killer whale (*Feresa attenuata*), false killer whale (*Pseudorca crassidens*), melon-headed whale (*Peponocephala electra*), killer whale (*Orcinus orca*), common dolphin (*Delphinus delphis*), spinner dolphin, and Fraser's dolphin (*Lagenodelphis hosei*). Each of these species is thought to have a tropical to subtropical or broader distribution worldwide (Jefferson et al., 1993), and except for the common dolphin, an abundance estimate for each species is available for the adjacent northern Gulf of Mexico (Hansen et al.[6]). However, except for the spinner dolphin, each of these species is relatively uncommon in the northern Gulf of Mexico and was not encountered every year during four annual spring surveys with effort similar to that in our survey (Hansen et al.[6]). Therefore, many of these species may also be uncommon in the Atlantic study area and were simply not encountered during the 1998 survey. During a late summer 1999 ship survey of the inner half of the southern Atlantic study area that targeted bottlenose dolphins, a group of Fraser's dolphins and melon-headed whales was sighted in water 3000 m deep east of Cape Hatteras (Roden[7]).

Some species may also inhabit the study area seasonally. During the 1992 winter ship survey south of Cape Hatteras (Mullin and Ford[1]), five groups of balaenopterid whales were recorded, three of which were classified as unidentified Bryde's or sei whales. Also during the winter 1992 survey, groups of false killer whales and Cuvier's beaked whales were sighted twice, and pygmy killer whales once. Common dolphins were sighted between Cape Hatteras and Maryland in all seasons, except summer, during the CeTAP[2] study but were sighted once in this area during the late summer 1999 survey (Roden[7]). Common dolphins are expected to occur throughout the area surveyed in 1998 but they may not. Although there are stranding records south of Cape Hatteras (Schmidly[5]), there are no valid stranding or sighting records of common dolphins in the adjacent Gulf of Mexico despite extensive seasonal surveys of the northern Gulf (Jefferson, 1995; Hansen et al.[4]).

Precision

The precision of the abundance estimates was generally poor. For species or genera abundances, only the estimate for bottlenose dolphins (the most commonly sighted species), Risso's dolphins, and pilot whales had a CV ≤ 0.50 (Table 3). The abundance estimate for the Atlantic spotted dolphin, the most abundant species, had a CV = 0.63. In cases where there is human-caused mortality in a cetacean stock, abundance estimates with a CV < 0.50 are generally required to avoid incorrectly classifying a cetacean stock as "strategic" under the U.S. MMPA (i.e. annual human-caused mortality > annual PBR) less than 10% of the time (Wade and DeMaster, 1999). For most species, the variance in the encounter rate, var(n), accounted for more than 70% of the var(N). The distribution of most species was not uniform in the study area and precision might be improved by stratifying estimates by water depth (e.g. shelf and nonshelf) and by area (e.g. north and south of Cape Hatteras).

Biases in abundance estimates

The survey was designed to meet the assumptions of line-transect theory (Buckland et al., 1993). However, the abundance estimates are negatively biased to varying degrees because the central assumption, that cetacean groups on the transect line are detected with certainty (i.e. $g(0)=1$), was not met, and data were not available to correct estimates for perception and availability bias. By using the CIO methods described by Barlow (1995), we attempted to estimate the fraction of groups missed on the transect line by the primary observers due to perception bias. How-

[7] Roden, C. L. 1999. Report of NOAA ship *Oregon II* cruise 99-05 (236) (a cetacean survey of U.S. Atlantic continental shelf and slope waters between New Jersey and central Florida, August–September 1999), 32 p. Southeast Fisheries Science Center, P.O. Drawer 1207, Pascagoula, Mississippi 39568.

ever, there were too few sightings to make $g(0)$ estimates because the overall group encounter rate was lower than anticipated and the CIO was only used for 35% of the total survey effort. In the future, a CIO should be used whenever the primary team is on-effort and the CIO should search an area larger than 30° left and right of the bow. Although the data in proximity of the transect line are most critical for estimating $g(0)$, it is also necessary to have enough data to estimate $f(0)$ for groups missed by the primary team.

More work is needed to develop methods for estimating $g(0)$ in relation to perception bias in the southern U.S. Atlantic. Completely independent observers cannot be used because the ship has to be diverted from the transect line to identify species and make group-size estimates. Because many groups can easily be lost once sighted, the ship must be diverted well before the group passes abeam. Barlow (1995) used a CIO that searched the same area as the primary team with unaided eye or 7× binoculars. The 25× binoculars were used in our study to increase the number of CIO sightings and avoid attraction bias in $f(0)$. Previous experience in the Gulf of Mexico has indicated that many unaided-eye sightings would be of small groups of species that are attracted to the ship to ride the bow waves. Conversely, small groups are the most difficult for an independent observer to track with 25× binoculars because the ship is not diverted and the bearing to the group is constantly changing.

Similar to Barlow's (1995) findings on perception bias, the majority of groups missed by the primary team were apparently small groups, although the group-sizes were not estimated at close range. Barlow (1995) estimated $g(0)$ ranging from 0.73 and 0.79 for small groups of delphinids (<21) and cryptic species (which usually occur in small groups), and $g(0) = 1$ for groups of >20 delphinids. In addition to group-size, the magnitude of perception bias is dependent on behavior, weather (e.g. Beaufort sea state), and the observer: active groups are less likely to be missed than resting groups or species whose behavior does not produce pronounced cues (e.g. blows, splashes).

Availability bias varies by species because of differences in individual dive cycles, group diving behavior, and group-sizes. Long-diving sperm whales and beaked whales will be at the surface for much less time than will many small delphinids, which have much shorter dive cycles. Diving synchrony among members of a group also affects availability bias; if dives are asynchronous, the probability that at least one animal will be at the surface increases with group size.

Barlow (1999) estimated both availability and perception bias for long-diving whales during ship surveys using 25× binoculars in a simulation study and estimated that for dwarf and pygmy sperm whales, Cuvier's beaked whales, and *Mesoplodon* spp., abundance estimates need to be increased 2 to 4 times (i.e. $g(0)$=0.50 to $g(0)$=0.25) to account for these biases. Barlow's (1999) estimates of $g(0)$ for perception or availability bias (or both) are probably representative of the bias in the southern Atlantic survey because similar ship survey methods were used. However, it may not be valid to apply them directly to our abundance estimates because cetacean diving behavior and group sizes may be temporally and geographically specific, and survey conditions and observers may vary among surveys.

For the strip-transect estimates (Table 2), use of the line-transect strip width [$2\times 1/f(0)$] from the 25× binocular sightings as the strip width was assumed to be conservative and somewhat negatively biased. The distance from which animals will come to the ship to ride the bow is unknown, and variable, depending on factors such as the animals' previous behavior, number of opportunities for riding bow waves, and the type of ship. If the strip width was too narrow, the strip-transect estimates would overestimate abundance.

The geographical bathymetric range of the bottlenose dolphin was not covered during the survey. Because bottlenose dolphins undertake seasonal movements in the study area, in order to estimate the entire population size, ship survey estimates need to be combined with same-season abundance estimates from coastal waters <10 m and inshore waters (bays, sounds, and estuaries).

Distribution

Water-depth distributions of cetacean species were for the most part similar to those in the Gulf of Mexico (Mullin et al., 1994; Davis et al., 1998). Bottlenose dolphins and Atlantic spotted dolphins inhabit the continental shelf and shelf-edge region, whereas most other species have primarily oceanic distributions. The offshore form of the Atlantic spotted dolphin has not been identified in the northern Gulf of Mexico. The sightings of some species were highly regional (e.g. sperm whales, striped dolphins, Clymene dolphins, pantropical spotted dolphins) were probably heavily influenced by oceanographic features such as the Gulf Stream. Much more survey effort is needed in summer and other seasons before conclusions can be drawn about each species' distribution.

Acknowledgments

Many people made significant contributions to the success of this survey including the officers and crew of NOAA ship *Relentless* and C. Roden, the Field Party Chief. The *Relentless* was configured for marine mammal surveys through the dedicated efforts of W. Hoggard. The marine mammal observers were C. Brown, C. Burks, C. Cates, W. Hoggard, C. Hubard, T. Martinez, K. Maze-Foley, M. Newcomer, S. Swartz, J. Tobias, and K. Touhey. Environmental and ichthyoplankton data were collected by L. Bero, P. Brown, W. Fambrough, D. Fertl, A. Hamilton, A. Hohn, R. Holmes, E. Keith, E. LaBrecque, J. Litz, and J. Taylor. W. Irvin and T. Pusser were seabird observers. The survey was designed with the help of S. Swartz and the late R. Blaylock. Comments by C. Hubard, K. Maze-Foley, and three anonymous reviewers were very helpful in completing the manuscript.

Literature cited

Barlow, J.
1995. The abundance of cetaceans in California waters. Part I: Ship surveys in summer and fall of 1991. Fish. Bull. 93: 1–14.

1999. Trackline detection probability for long-diving whales. *In* Marine mammal survey and assessment methods (G. W. Garner et al., eds.), p. 209–221. A.A. Balkema, Rotterdam.

Barlow, J., S. L. Swartz, T. C. Eagle, and P. R. Wade.
1995. U.S. marine mammal stock assessments: guidelines for preparation, background, and a summary of the 1995 assessments. U.S. Dep. Commer., NOAA Tech. Memo. NMFS-OPR-6, 73 p.

Blaylock, R. A.
1995. A pilot study to estimate abundance of the U.S. Atlantic coastal migratory bottlenose dolphin. U.S. Dep. Commer., NOAA Tech. Memo. NMFS-SEFSC-362, 9 p.

Blaylock, R. A., and W. Hoggard.
1994. Preliminary estimates of bottlenose dolphin abundance in the southern U.S. Atlantic and Gulf of Mexico continental shelf waters. U.S. Dep. Commer., NOAA Tech. Memo. NMFS-SEFSC-356, 10 p.

Buckland, S. T., D. R. Anderson, K. P. Burnham, and J. L. Laake.
1993. Distance sampling: estimating abundance of biological populations, 446 p. Chapman and Hall, London.

Carwardine, M.
1995. Whales, dolphins and porpoises, 256 p. Dorling Kindersley, New York. NY.

Davis, R. W., G. S. Fargion, N. May, T. D. Leming,
M. Baumgartner, W. E. Evans, L. J. Hansen, and K. D. Mullin.
1998. Physical habitat of cetaceans along the continental slope in the north-central and western Gulf of Mexico. Mar. Mamm. Sci. 14:490–507.

Hersh, S. L., and D. A. Duffield.
1990. Distinction between northwest Atlantic offshore and coastal bottlenose dolphins based on hemoglobin profile and morphometry. *In* The bottlenose dolphin (S. Leatherwood and R. R. Reeves (eds.), p. 129–142. Academic Press, San Diego, CA.

Jefferson, T.A.
1995. Distribution, abundance, and some aspects of the biology of cetaceans in the offshore Gulf of Mexico. Ph.D. diss., 232 p. Texas A&M University, College Station, TX.

Jefferson, T. A., S. Leatherwood, and M. A. Webber.
1993. Marine mammals of the world—FAO species identification guide, 320 p. FAO, Rome.

Kenney, R. D.
1990. Bottlenose dolphins off the northeastern United States. *In* The bottlenose dolphin (S. Leatherwood and R. R. Reeves, eds.) p. 369–386. Academic Press, San Diego, CA.

Knowlton, A. R., S. D. Kraus, and R. D. Kenney.
1994. Reproduction in North Atlantic right whales (*Eubalaena glacialis*). Can. J. Zoo.72:1297–1305.

Leatherwood, S., and R. R. Reeves.
1983. The Sierra Club handbook of whales and dolphins, 302 p. Sierra Club Books, San Francisco, CA

LeDuc, R. G., and B. E. Curry.
1998. Mitochondrial DNA sequence analysis indicates need for revision of the genus *Tursiops*. Rep. Int. Whaling Comm. 47:393.

Lerczak, J. A., and R. C. Hobbs.
1998. Calculating sighting distances from angular readings during shipboard, aerial, and shore-based marine mammal surveys. Mar. Mamm. Sci. 14:590–599.

Marsh, H., and D. F. Sinclair.
1989. Correcting for visibility bias in strip transect aerial surveys of aquatic fauna. J. Wildl. Manage. 53:1017–1024.

Mead, J. G.
1975. A preliminary report on the former net fishery for *Tursiops truncatus* in the western North Atlantic. J. Fish. Res. Board Can. 32:1155–1162
1989. Beaked whale of the genus *Mesoplodon*. *In* Handbook of marine mammals. Volume 4: River dolphins and the larger toothed whales (S. H. Ridgway and R. Harrison (eds.), p. 349–430. Academic Press, San Diego, CA.

Mullin, K. D., W. Hoggard, C. L. Roden, R. R. Lohoefener,
C. M. Rogers, and B. Taggart.
1994. Cetaceans on the upper continental slope in the north-central Gulf of Mexico. Fish. Bull. 92:773–786.

Palka, D.
1995. Abundance estimate of the Gulf of Maine harbor porpoise. *In* Biology of the phocoenids (A. Bjørge and G.P. Donovan, eds.), p. 27–50. Rep. Int. Whaling Comm. (special issue 16).

Payne, P. M., and D. W. Heinemann.
1993. The distribution of pilot whales (*Globicephala* spp.) in the shelf/shelf-edge and slope waters of the northeastern United States, 1978–1988. *In* Biology of northern hemisphere pilot whales (G. P. Donovan, C. H. Lockyer and A. R. Martin, eds.), p. 51–68. Rep. Int. Whaling Comm. (special issue 14).

Perrin, W. F., D. K. Caldwell, and M. C. Caldwell.
1994. Atlantic spotted dolphin—*Stenella frontalis*. *In* Handbook of marine mammals. Volume 5: The first book of dolphins (S.H. Ridgway and R. Harrison, eds.) p. 173–190. Academic Press, San Diego, CA.

Perrin, W. F., E. D. Mitchell, J. G. Mead, D. K. Caldwell and
P. J. H. van Bree.
1981. *Stenella clymene*, a rediscovered tropical dolphin of the Atlantic. J. Mamm. 62:583–598.

Smith, T. D., J. Allen, P. J. Clapman, P. S. Hammond, S. Katona,
F. Larsen, J. Lien, D. Mattila, P. J. Palsbøll, J. Sigurjónsson,
P. T. Stevick, and N. Øien.
1999. An ocean-basin-wide mark-recapture study of the North Atlantic humpback whale (*Megaptera novaeangliae*). Mar. Mamm. Sci. 15:1–32.

Torres, L. G., P. E. Rosel, C. D'Agrosa, and A. J. Read.
In press. Improving management of overlapping bottlenose dolphin ecotypes through spatial analysis and genetics. Mar. Mamm. Sci.

Wade, P. R., and D. P. DeMaster.
1999. Determining the optimum interval for abundance surveys. *In* Marine mammal survey and assessment methods (G. W. Garner, S. C. Amstrup, J. L. Laake, B. F. J. Manly, L. L. McDonald, and D. G. Robertson, eds.), p. 53–66. A.A. Balkema, Rotterdam.

Waring, G. T., D. L. Palka, K. D. Mullin, J. W. Hain, L. J. Hansen,
and K. D. Bisack.
1997. U.S. Atlantic and Gulf of Mexico marine mammal stock assessments—1996. U.S. Dep. Commer., NOAA Tech. Memo. NMFS-NE-114, 245 p.

Waring, G. T., J. M. Quintal, and S. L. Swartz (eds).
2001. U.S. Atlantic and Gulf of Mexico marine mammal stock assessments—2001. U.S. Dep. Commer., NOAA Tech. Memo. NMFS-NE-168, 310 p.

Würsig, B., S. K. Lynn, T. A. Jefferson, and K. D. Mullin.
1998. Behavior of cetaceans in the northern Gulf of Mexico relative to survey ships and aircraft. Aquat. Mamm. 24: 41–50.

Modeling red sea urchin (*Strongylocentrotus franciscanus*) growth using six growth functions*

Laura Rogers-Bennett
California Department of Fish and Game and
University of California, Davis
Bodega Marine Laboratory
2099 Westside Rd.
Bodega Bay, California 94923-0247
E-mail address: rogersbennett@ucdavis.edu

Donald W. Rogers
Chemistry Department
Long Island University
Brooklyn, New York 11201

William A. Bennett
John Muir Institute of the Environment
University of California, Davis
Davis, California 95616

Thomas A. Ebert
Biology Department
San Diego State University
San Diego, California 92182

Abstract—The growth of red sea urchins (*Strongylocentrotus franciscanus*) was modeled by using tag-recapture data from northern California. Red sea urchins (n=211) ranging in test diameter from 7 to 131 mm were examined for changes in size over one year. We used the function $J_{t+1} = J_t + f(J_t)$ to model growth, in which J_t is the jaw size (mm) at tagging, and J_{t+1} is the jaw size one year later. The function $f(J_t)$, represents one of six deterministic models: logistic dose response, Gaussian, Tanaka, Ricker, Richards, and von Bertalanffy with 3, 3, 3, 2, 3, and 2 minimization parameters, respectively. We found that three measures of goodness of fit ranked the models similarly, in the order given. The results from these six models indicate that red sea urchins are slow growing animals (mean of 7.2 ±1.3 years to enter the fishery). We show that poor model selection or data from a limited range of urchin sizes (or both) produces erroneous growth-parameter estimates and years-to-fishery estimates. Individual variation in growth dominated spatial variation at shallow and deep sites (F=0.246, n=199, P=0.62). We summarize the six models using a composite growth curve of jaw size, J, as a function of time, t: $J = A(B - e^{-Ct}) + Dt$, in which each model is distinguished by the constants A, B, C, and D. We suggest that this composite model has the flexibility of the other six models and could be broadly applied. Given the robustness of our results regarding the number of years to enter the fishery, this information could be incorporated into future fishery management plans for red sea urchins in northern California.

Manuscript approved for publication 5 February 2003 by Scientific Editor.
Manuscript received 4 April 2003 at NMFS Scientific Publications Office.
Fish Bull. 101:614–626

Marine invertebrates are being fished at an increasing pace worldwide (Keesing and Hall, 1998). In California, invertebrates have a greater exvessel (wholesale) value than do fin-fish (Rogers-Bennett, 2001). Invertebrate fisheries are now experiencing serious declines as have fin-fish fisheries (Dugan and Davis, 1993; Safina, 1998; Jackson et al., 2001). The once prosperous commercial abalone fishery in California which landed in excess of 2000 metric tons per year in the 1950s and 1960s was closed in 1997 (CDFG Code 5521) following the serial depletion of stocks over time (Karpov et al., 2000). Commercial divers now target red sea urchins and other invertebrates. Red sea urchin landings in California have also declined dramatically from a high of 24 metric tons (t) in 1988 to 6 t in 2002, despite management efforts (Kalvass and Hendrix, 1997). These declines have generated interest in exploring the use of alternative fishery management policies, such as spatially explicit strategies that would protect large old sea urchins (Rogers-Bennett et al., 1995).

Sea urchin growth models are critical in the development of innovative management strategies to sustain the fishery because, among other things, models can be used to predict the time required for sea urchins to enter the fishery (referred to as "years to fishery") and the age of the broodstock. Despite the interest in examining sea urchin growth, modeling efforts have been hampered by several factors including model selection and a lack of data from a sufficiently wide range of urchin sizes. Perhaps as a consequence, estimates of red sea urchin growth have varied widely, ranging from 3 to 12 years for urchins to grow into the fishery (Kato and Schroeter, 1985; Tegner, 1989; Ebert and Russell, 1992; Smith et al., 1998). Because of the wide variation in growth estimates, the number of models and methods being used, and the difficulties that these present

* Contribution 2176 from the Bodega Marine Laboratory, University of Davis, Davis, CA 94923-0247.

for management, there is a need to evaluate a number of growth models with a single data set that encompasses a large range of urchin sizes.

In our study we report the results from six individual growth models applied to data from a one-year tag and recapture study of red sea urchins (*Strongylocentrotus franciscanus*) in northern California. We supplemented the number of juveniles in the field by stocking tagged juveniles. Estimates of the number of years required for urchins to grow to minimum legal size in northern California are generated by the models. We examine the robustness of these results to changes in the parameters and the impact of a limited data set from a small range of urchin sizes on our results. We determine if there are spatial differences in growth between shallow and deep sites. Finally, we rank the models according to quality of fit, present a generic growth curve that combines the six models, and discuss the implications of our results for fishery management.

Materials and methods

Study sites

Growth rates were determined for red sea urchins in the Salt Point (38°33'06"N, 123°19'45"W) and Caspar (39°21'49"N, 123°49'47"W) urchin harvest reserves in northern California. Commercial urchin harvesting is prohibited in these reserves. We examined spatial variation within Salt Point by tagging red sea urchins at one shallow site (5 m) south of the southern border of the Gerstle Cove Reserve and at one deep site (17 m) on the leward side of a large wash-rock. In addition, laboratory-reared juvenile red sea urchins were stocked at the two sites in Salt Point. Both of these sites are relatively isolated, surrounded by sand and seasonally dense kelp (*Nereocystis*). At the Caspar Reserve, sea urchins were tagged outside a small cove with seasonally dense kelp (*Nereocystis*) at a single depth (7 m).

Tagging

Sea urchins at the study sites were tagged internally and recaptured after one year. At Salt Point, wild sea urchins were tagged with tetracycline injections *in situ* by using 0.5–1.2 mL of 1 g tetracycline/100 mL of seawater (cf. Ebert, 1982; Ebert and Russell, 1992). Six hundred and nine red urchins were measured with vernier calipers (±1–2 mm) and tagged at Salt Point on 19 August 1992. Urchins were recaptured from the Salt Point sites on 18 September 1993 (n=374 shallow; n=352 deep). This data set was normalized to one year by using the factor 12/13. Our study was not a longitudinal study examining growth over many years, but rather for one year only.

Juvenile urchins reared in the laboratory for one year (mean test diameter=17.6 mm) were tagged and stocked into the shallow and deep Salt Point sites. Juveniles were tagged by immersion for 24 hours in a calcein solution 125 mg/L seawater, pH adjusted to 8.0 (Wilson et al., 1987). After tagging, juveniles were transported to the Salt Point sites and released. Juveniles were stocked (120 at each of the two depths) on 31 August 1992 and harvested on 18 September 1993 with the adults (see Rogers-Bennett, 2001).

Urchins at the Caspar Reserve were tagged internally with personal individual transponder (PIT) tags on 28 August 1996 and recovered 20 August 1997 (Kalvass[1]). PIT tags are glass coated mini-transponders with unique individual codes that can be read noninvasively by using a Destron® tag reader. Tags were implanted into the body cavity of the sea urchins through the peristomial membrane. PIT tags are too large for tagging small urchins (<40 mm).

Estimates of urchin density were made within a circle (12 m in radius) at each of the two Salt Point sites at the time of harvest. Drift algae collections were made along a 2 × 10 m transect (20 m^2) at each site. Gut contents were collected from a subsample of 20 urchins from each site. Gut contents were fixed in alcohol, sorted on a petri dish, and the most abundant items were recorded from 5 out of 25 10-mm^2 grids (Harrold and Reed, 1985). We used a conservative definition of optimal foods, defining them as fleshy red or brown algae (Harrold and Reed, 1985). Suboptimal foods included green algae, upright and encrusting coralline algae, detritus (animal, plant, and inorganic), plants (*Phyllospadix*), mud, and sand.

Growth measurements

Sea urchins can not be reliably aged by using rings on test ossicles (Pearse and Pearse, 1975; Ebert 1988; Gage, 1992), therefore growth increments after one year must be measured directly. For the urchins tagged with fluorescent dyes (tetracycline and calcein), growth was measured as the change in urchin jaw length ($\Delta J = J_{t+1} - J_t$) after one year (Ebert and Russell, 1993). Urchin jaws were dissected from Aristotle's lantern, excess tissue was removed with 10% sodium hypochlorite, and the jaws were measured to the nearest 0.1 mm. Growth was measured by determining the width of the calcium deposit one year after tagging. Tags on jaws are more accurate than tags on test ossicles because ossicles move toward the oral surface during growth (Duetler, 1926), requiring matching ossicles at the time of tagging with ambitus ossicles at the time of collection (Ebert, 1988).

Fluorescence tagged urchins were identified when exposed to an ultraviolet epi-illuminator (Lite-Mite) on a dissecting scope. Growth increments were determined by using the Confocal Microscope (BioRad MRC-600, BioRad Industries, Hercules, CA) with a BHS fluorescence filter (blue wavelength) and the COMOS software package (BioRad Industries, Hercules, CA). Growth was measured from the fluorescent band (indicating size at tagging) to the esophageal edge of the jaw (final size). Growth was also recorded from a second growth zone at the labial tip of the jaw, represented by a glowing arc when present. Initial jaw size (J_t) equals jaw size after one year (J_{t+1}) minus the

[1] Kalvass, P. 1997. Personal commun. Calif. Dep. Fish and Game, 19160 S. Harbor Dr., Fort Bragg, CA. 95437.

Table 1

Tests for homogeneity of slopes for ln (*diameter*) compared with ln (*jaw*) for shallow and deep samples of red sea urchins from Salt Point, California: SS: sum of squares; df: degrees of freedom; MS: mean square. Treatment (depth) is significant P=0.017 when adjusted for covariate (test diameter).

	SS	df	MS	F-ratio	P
Homogeneity of slopes					
Sample	0.013	1	0.013	3.643	0.058
ln (*jaw*)	21.216	1	21.216	5760.0	0.000
Sample × ln(*jaw*)	0.010	1	0.010	0.723	0.101
Error	0.718	195		0.004	
Adjusted means					
Sample	0.021	1	0.021	5.747	0.017
ln (*jaw*)	29.333	1	29.333	7894.0	0.000
Error	0.728	196			0.004

sum of the esophageal and labial growth. Urchin jaws do not wear or erode as teeth do. Calculating test growth from changes in jaw size may yield a conservative estimate for sublegal red sea urchins (Kalvass et al., 1998).

In the PIT-tagged urchins, growth was measured as the change in test diameter after one year. Juvenile urchins less than 30 mm are too small to survive PIT tag implantation. Large adults (>100 mm) may grow too little in one year to allow growth in test diameter to be measured. Standard errors in measures of test diameter with calipers range from 1–2 mm which may be greater than the growth increment in adults.

Jaw size versus test size

The relationship between jaw length and test diameter was determined from a large sample (n=384) of red sea urchins (sample independent of this study) ranging in size from newly settled individuals to large adults. From this sample we obtained an allometric equation relating jaw and test size. Using this equation we converted all the measures of growth (from fluorescent and PIT tagged urchins) into initial and final jaw size (one year later).

Jaw size is a plastic trait that can vary spatially (Ebert, 1980b; Rogers-Bennett et al., 1995). Food availability has been correlated with the size of Aristotle's lantern (composed of ten jaws and five teeth) such that lanterns are large when food is scarce. Therefore, we examined the relationship between jaw size and test size, segregating the data from the shallow and deep Salt Point sites. To do this we used an ANCOVA (Table 1) with the natural log of test diameter as the covariate. Measurements of the jaw size at tagging from the fluorescent marks allowed for estimates of the test size at tagging using the allometric relationship (Eq. 1). As a control to test for bias in the conversion of jaw size to test diameter with Equation 1, we compared the measured test size at the time of recapture to the predicted test size at the time of recapture using the allometric relationship (Eq. 1). Results indicated that, although there was error in the predicted test size from jaw size, there was no bias.

Results

Red urchin growth

We present growth data from a total of 211 red sea urchins that were tagged internally and recaptured after one year in northern California. Recaptured urchins ranged in test diameter from 7 to 131 mm at the time of tagging. We recovered 161 out of 609 (26.4%) tetracycline-tagged wild urchins from the two sites at Salt Point. In addition, 38 of the 240 (15.8%) stocked juvenile urchins tagged with calcien were also recovered. It is unknown whether untagged urchins included tagged adults which were not growing and therefore not taking up the tetracycline stain. In the Caspar Reserve 12 of 53 (22.6%) PIT-tagged wild urchins were recovered.

We examined spatial variation in growth and found that the change in size (ΔJ) was not significantly different for urchins in the shallow, as compared to the deep Salt Point sites (ANCOVA F=0.246, n=199, P=0.62) with initial jaw size (J_i) as the covariate (independent variable). Similarly, growth rates were not significantly different between juveniles recovered in shallow and deep sites (ANCOVA F=0.387, n=38, P=0.54). Richards function parameter estimates (J_∞, K, n) generated from the shallow site were statistically identical to those for the deep site. Size-frequency distributions of urchins recovered from the shallow site were not significantly different than those at the deep site (K-S mean difference=0.162, P=0.67). Therefore, growth data from the shallow and deep sites were pooled.

Urchin density at the shallow site (4.2 urchins/m^2) was greater than at the deep site (0.75 urchins/m^2). In addition, drift algae abundance was twice as great in the shallow (2.7 g/m^2) as in the deep site (1.4 g/m^2) at the time of urchin harvest (18 September 1993). This resulted in less algae per urchin in the shallow site compared with the deep site (0.63 g/urchin and 1.85 g/urchin respectively) for that sampling date. Guts of urchins from the deep habitats contained more optimal food (fleshy red and brown algae) than guts of urchins in the shallow sites (t=2.79, df=19, P=0.012). Gut fullness was generally uniform, roughly 50 mL/urchin.

Jaw size versus test size

ANCOVA analysis indicated that the slopes of the natural log of test diameter as a function of the natural log of the jaw size are homogenous (P=0.101), but that the adjusted means are significantly different (P=0.017)—urchins in the deeper habitat having larger jaws (Table 1). Therefore, we constructed two allometric equations, one for urchins from the shallow Salt Point site and a second for urchins from the deep Salt Point site. However, the two equations were so similar that they generated identical test diameters for a given jaw size; therefore we pooled our data from the shallow and the deep sites.

We used a larger independent data set of n=384 from wild and cultured urchins to generate the allometric equation relating jaw size to test size. There is a strong relationship (r^2=0.989, df=382) between test diameter (D) and jaw length (J) described by

$$D = 3.31\, J^{1.15} \qquad (1)$$

where D = test diameter (mm); and
J = jaw length (mm).

Equation 1 predicts that urchins of legal size in northern California (test diameters ≥89 mm) have jaw lengths ≥17.5 mm.

A comparison (using the allometric relationship [Eq. 1]) of the measured test size at the time of recapture with the predicted test size revealed no bias in the conversion. Although individual values of measured and predicted test diameters are not identical, the sum of the differences between the two reveals no strong *directional* bias. The sum of the differences between the measured and predicted values equals 41 mm for 139 urchins, resulting in an average discrepancy of 0.30 mm per urchin. This discrepancy is smaller than the initial error in the measurement of test size (see "Materials and methods" section).

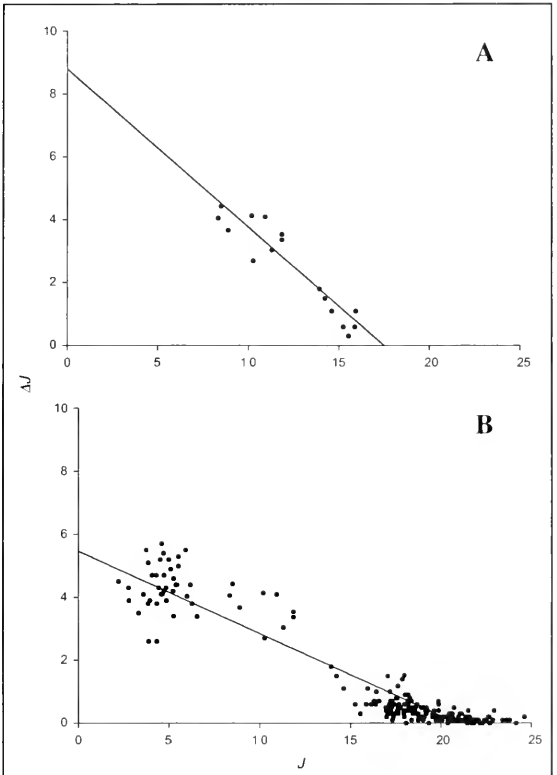

Figure 1

(**A**) Linear function fitted to the middle portion of the urchin growth data set. (**B**) Linear von Bertalanffy function superimposed on the entire data set. J=jaw length (mm); ΔJ=change in jaw length (mm).

The von Bertalanffy model

For many organisms, annual growth rate decreases as size (age) increases. This process is frequently modeled by using the von Bertalanffy equation (von Bertalanffy, 1938)

$$J_{t+1} = J_t + J_\infty(1 - e^{-K}) - J_t(1 - e^{-K}) \qquad (2)$$

or

$$J = J_\infty(1 - e^{-Kt}), \qquad (2a)$$

which leads to a linear decrease in growth rate as a function of size. We make the point here, that J_{t+1} and J_t refer to a discrete data set, whereas J is a smooth, continuous function of t.

Our data and, quite possibly, much of the data collected in similar studies, are not well represented by the von Bertalanffy equation. How is it then that the deficiencies of this well used equation have not come to light? The answer, not surprisingly, lies in the cancellation of errors within data sets that only incompletely cover the critical growth period.

Our data (Figs. 1B and 2) show three features of sea urchin growth that are inconsistent with the von Bertalanffy model: 1) annual growth, $\Delta J = J_{t+1} - J_t$, for juveniles that is lower than anticipated from the model; 2) a maximum or plateau in the growth function, $\Delta J = f(J_t)$, for urchins near jaw size J_t = 5 mm (test diameter 20 mm); and 3) an asymptotic approach of ΔJ to zero (Figs. 1B and 2), which may be ascribed to indeterminate growth for adults of all sizes or to dispersion of final adult urchin sizes (Sainsbury, 1980).

There is a good deal of individual variation in growth rate as a function of J_t, which prevents unequivocal selec-

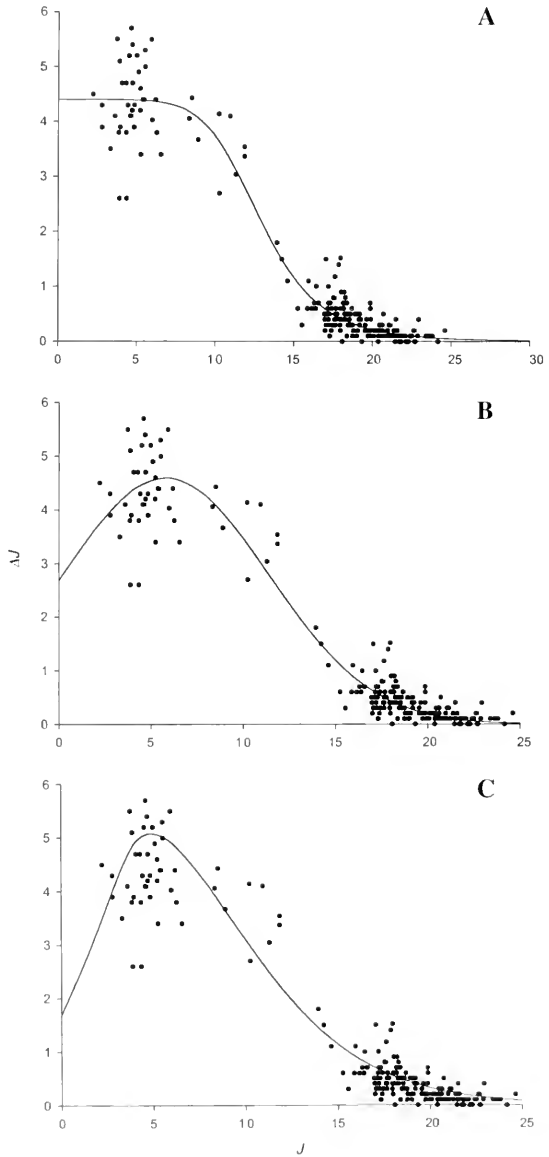

Figure 2

Annual growth as a function of jaw size for six models: logistic dose-response, Gaussian, Tanaka, Ricker, Richards, and von Bertalanffy models. J = jaw length (mm); ΔJ = change in jaw length (mm).

tion of one model. Nevertheless, it is clear that the von Bertalanffy model does not represent the data well over the full range of urchin sizes (J_t). To investigate this point further, we divided our data set into three groups over the range of of J_t . The groups are

1 Juveniles ($J_t < 8$ mm) that do not fall on the linear descent of ΔJ versus J_t characteristic of von Bertalanffy growth.
2 Sublegal, actively growing adults (8 mm< J_t<16 mm) that do follow von Bertalanffy kinetics.
3 Adults (16 mm< J_t < 24 mm) that appear to grow to large J_t but only very slowly, and do not conform to the von Bertalanffy model.

If the data were fitted to the von Bertalanffy equation, all three groups should give the same slope $\Delta J / J_t$ because three segments of the same straight line all have the same slope. Instead, group 1 gives a small positive slope, group 2 gives a negative slope that leads to unrealistic conclusions for early growth rate and time-to-fishery estimates shown in (Fig. 1A), and group 3, excluding growth information from sublegal urchins, yields a plausible mean final jaw size of 22.6 mm but gives a growth rate constant that indicates very slow growth for adults and many decades for time-to-fishery.

In the present study we fitted a decreasing, linear von Bertalanffy function only to the sublegal (group 2) urchins (Fig. 1A) which did conform to von Bertalanffy growth. The von Bertalanffy function for the partial data set of actively growing urchins in (Fig. 1) has a slope of −0.504/yr, a ΔJ intercept of 8.7 mm/yr, and a J_t intercept of 17.3 mm. These results lead one to predict that final grow to 90% of their final size in 3.5 years and that mean final size will be less than the legal size (89 mm test diameter), which is obviously false. We also show the same function superimposed on the entire data set (Fig. 1B) where discrepancies between the von Bertalanffy function and data groups 1 and 3 above are evident. For our data set (Fig. 1) and, we suggest, for urchin growth in general, the von Bertalanffy curve does not represent early growth, and a transition curve or a peaked function reflects actual growth better. For our data set, the von Bertalanffy model gives an overestimate of the rate of urchin growth and an underestimate of the time to enter the fishery.

The slopes of these three line segments give an indication how the von Bertalanffy model, despite its implausible fit to the complete data set, can give plausible growth parameters. Errors in fitting a von Bertalanffy curve to a data set resembling ours lie in opposite directions

for groups 1 and 3 of the growth; consequently they cancel, in whole or in part. In fact, all reported data sets have many more observations falling into group 3 than into group 1, which is either swamped out by group 3 or does not appear at all. This leaves groups 2 and most or all of group 3 to determine the slope of the von Bertalanffy linear function. The average of these two erroneous slopes may or may not be a realistic approximation for urchin growth, depending on the number of measurements in each group.

Alternative growth models

Curves that rise to a maximum and then decay asymptotically are very common in the physical sciences and have been successfully modeled for more than a century (e.g. Wien, 1896). Any rising function multiplied into an exponential decay, e.g. $(x)\ \exp(-x)$, models such a curve more or less well. The problem is not in finding a model but in selecting from among many possibilities. We compared several models in our study and included a Gaussian model for this data set because it has a small sum of squared residuals and because it has well-defined parameters in the arithmetic mean and standard deviation. Here the arithmetic mean merely serves to fix the position of the maximum on the J_t axis and the standard deviation from μ gives the range, in units of J_t, of actively growing animals. The model is descriptive only; it does not imply a mechanism of growth.

We present results from six growth models, the logistic dose-response, Gaussian, Ricker, Tanaka, Richards, and von Bertalanffy models, in order of quality of fit (Fig. 2). Each model is characterized by a different $\Delta J = f(J_t)$, where $f(J_t)$ is a function of annual growth ΔJ versus size at tagging, J_t. Equations 3–8 were input as user-defined functions into a curve-fitting program (TableCurve, Jandel Scientific, now SPSS, Chicago, IL), either as $f(J_t)$ or the equivalent $J_{t+1} - J_t$. In certain cases, additive parameters that make a negligible contribution to the final fit were dropped. This curve-fitting program uses the Levenburg-Marquardt procedure for finding the minimum of the squared sum of deviations. During the least-squares minimization, local minima are occasionally found and must be discarded in favor of the global minimum. Matrix inversion is performed by the Gauss-Jordan method (Carnahan et al., 1969).

We present these models ranked by the fitting criterion of the sum of squared residuals, called "Error Sum of Squares" in the output from the TableCurve fitting program, which we have given the abbreviation RSS. Several

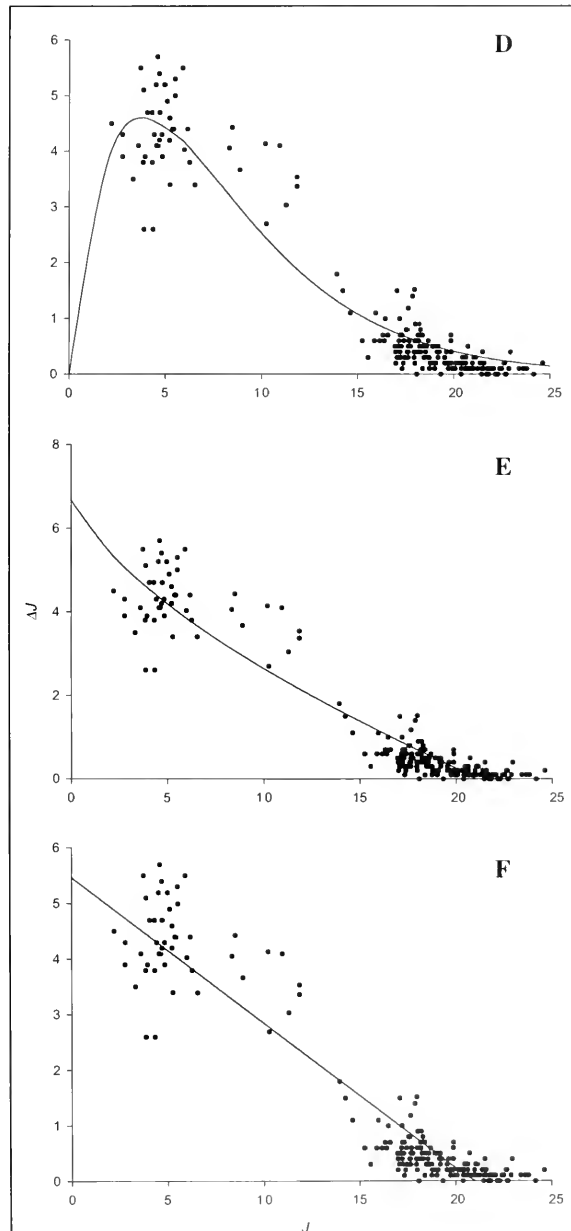

Figure 2 (continued)

Table 2

A comparison of the fitting criteria for six red sea urchin growth functions. r^2 = the coefficient of determination; RSS = the error sum of squares; AIC = Akaike's information criterion; SBC = Schwartz-Bayesian criterion.

	r^2	SE	RSS	AIC	SBC	No. of parameters
Logistic	0.946	0.392	31.9	–393	–383	3
Gaussian	0.945	0.397	32.8	–387	–377	3
Tanaka	0.933	0.436	39.6	–347	–337	3
Ricker	0.918	0.483	48.7	–305	–299	2
Richards	0.900	0.534	59.4	–262	–251	3
von Bertalanffy	0.895	0.545	62.1	–254	–247	2

other fitting criteria are also given in Table 2. We used both the AIC information criterion, $AIC = K\ln(RSS) - K\ln K + 2m$, and the Schwartz-Bayesian criterion $BIC = K\ln(RSS) - (K-m)\ln(K)$, where K is the number of data points, and m is the number of parameters in the fitting equation (Akaike, 1979). These tests of curve-fitting quality were used to bring out any substantive difference between the 2-parameter and 3-parameter equations. The results show that differences between the 2- and 3-parameter cases are swamped out by the data, as might have been anticipated from the disparity between the number of points (K=211) and the number of parameters. For the present data set, in applying either of these criteria, one is essentially seeking the smallest RSS.

Individual models

Logistic dose-response The logistic dose-response curve (time-to-fishery estimate: 6.6 yr)

$$f(J_t) = a/(1+(J_t/b)^c) \tag{3}$$

(Hastings, 1997) fits our data the best of all the models examined here. The curve fit (a=4.4, b=12.9, c=6.8) with RSS = 31.9, is a sigmoidal transition function (TableCurve Windows, vers. 1.0, Jandel Scientific Corp., SPSS, Chicago, IL). There is a transition between a fast-growing group of sea urchins, which maintain a constant growth rate ($f(J_t)$=annual $\Delta J \cong 4.4$ mm/yr up to about J_t=8 mm), to sea urchins growing slowly at a rate that diminishes as J_t increases beyond 16 mm. The inflection point is at $J_t \cong$ 13 mm. There is considerable individual variation in both data groups, but more in the fast-growing group than in the larger slow-growing group.

Gaussian The Gaussian function (time-to-fishery estimate: 6.9 yr), although rarely if ever used in this context,

$$f(J_t) = Ae^{-(J_t-\mu)^2/2\sigma^2} \tag{4}$$

fits the data about as well (RSS=32.8) as the logistic dose-response model. It is a three-parameter model (Rogers, 1983) for which the parameters are maximum growth (A=4.6 mm/yr), size at maximum growth (μ=5.8 mm), and standard deviation (σ=5.6mm) of the distribution of maximum growth versus size. Applied to the present data set, the Gaussian function yields an initial annual growth rate ΔJ=2.8 mm/yr, and a time of entry into the fishery of about 7.0 yr. A strength of the Gaussian model aside from its good fit is that it provides a plausible growth model with maximum ΔJ, not at settlement, but at a jaw size about one third that of adults, and that the parameters are well defined. In this model, annual growth is randomly distributed, according to jaw size, about the maximum in ΔJ.

Tanaka The Tanaka equation (time-to-fishery estimate: 8.2 yr)

$$f(J_t) = \frac{1}{\sqrt{f}} \ln\left|2G + 2\sqrt{G^2 + fa}\right| + d - J_t, \tag{5}$$

where

$$G = \frac{E}{4} - \frac{fa}{E} + f \text{ and } E = \exp\left(\sqrt{f}(J_t - d)\right),$$

can be obtained from its differential form (Tanaka, 1982; Ebert, 1999)

$$\frac{dJ}{dt} = \frac{1}{\sqrt{f(t-c)^2 + a}} \tag{5a}$$

by using a standard integral (Barrante, 1998). The parameters are a=0.0330, d=15.7, and f=0.0773.

The Tanaka model shows an asymptotic approach to zero growth at large J_t, allows for an early lag in growth, and does not force a maximum growth rate on juvenile urchins. The fit to our data set (RSS=39.6) requires three parameters (the parameter c in Eq. 5a drops out). This function has been used to model red sea urchin growth (Ebert and Russell, 1993).

Ricker The Ricker function (time-to-fishery estimate: 9.2 yr) for population growth (Hastings, 1997) translated into terms of urchin growth is

$$f(J) = BJ_t e^{-KJ_t} \tag{6}$$

(Ricker, 1954). This model yields a maximum in the growth function and an asymptotic approach to zero that characterize the data set (Fig. 2D). The empirical fitting parameters are maximum growth rate constant (B=3.15/yr) and K = 0.252 /mm, a constant that controls decrease in growth rate as the animal matures. Fitted to the present data set, it gives RSS = 48.7. Initially, J_t is small and $\Delta J = BJ_t$. At larger J_t, annual ΔJ passes through a maximum as the negative exponential becomes important. Growth, though never zero, will eventually be too small to measure over a one-year period. This model requires an arbitrary specification of the jaw size at settlement which is not well known and to which the resulting $f(J_t)$ curve is quite sensitive.

Richards The Richards function (time-to-fishery estimate: 6.1 yr) incorporates the von Bertalanffy and logistic (as distinct from the "logistic dose-response") models

$$f(J_t) = \left[J_\infty^{-1/n}(1-e^{-K}) + J_t^{-1/n}e^{-K}\right]^{-n} \tag{7}$$

and has an additional "shape parameter" n allowing for an inflection in the curve of J versus t (Richards, 1959; Ebert, 1980a)

$$J = J_\infty(1 - be^{-Kt})^{-n}. \tag{7a}$$

When $n = -1$, this equation is the von Bertalanffy model, and when $n = 1$, it is the logistic model. Minimization of the fitting parameters leads to J_∞ = 21.2 mm, K = 0.239/yr, and n = −0.747 (unitless) with RSS = 59.4. In general, there is another parameter, b, to be determined:

$$b = \frac{(J_\infty - J_{settle})}{J_\infty},$$

where J_{settle} is the jaw size at settlement. In the present case, J_{settle} is very small in relation to J_∞; therefore b is essentially 1.

Minimization can be difficult owing to the singularity at $n = 0$. Minimization of the Richards function from small negative values of n and reasonable guesses as to J_∞ and K leads to a pseudo von Bertalanffy curve with diminishing slope as J_t increases (Fig. 2E). The SSE is better than it is for the true von Bertalanffy model (Fig. 2F) because there is one more fitting parameter. Approaching the $n = 0$ singularity from positive values of n does not produce the desired logistic curve. Rather the fitted n value becomes very large, leading to the Gompertz case (see also Ebert, 1999, chapter 11). The equation with n tending to ∞ does not appear to represent any real case and will not been considered further.

Von Bertalanffy Currently, the most widely used growth model is the von Bertalanffy or Brody-Bertalanffy model (time-to-fishery estimate: 5.9 yr)

$$f(J_t) = J_\infty(1 - e^{-K}) - J_t(1 - e^{-K}) \tag{8}$$

(Brody, 1927; von Bertalanffy, 1938), which produces a decreasing linear function of ΔJ vs. J_t (Walford, 1946) with a slope of $-(1 - e^{-K})$ and

$$J(t) = J_\infty(1 - e^{-Kt}), \tag{8a}$$

where J_∞ = the limiting jaw size at long time t.

The model predicts that the smallest individuals have the fastest growth and yields the shortest time-to-fishery (however, see "Discussion" section). Fitting parameters (ΔJ=5.45 − 0.261 J_t) for the present data set yield J_∞ = 20.9 mm and K = 0.303/yr, and an RSS = 62.14 mm.

Growth curves $\Delta J = f(t)$

Having $\Delta J = f(J_t)$, one can assume a small (essentially zero) initial size at settlement and determine the size 1, 2, 3, . . . years after settlement by a recursive calculation. Six growth curves $J = f(t)$ can be generated from our six models from different functions for $\Delta J = f(J_t)$. We provide a single function

$$J = A(B - e^{-Ct}) + Dt \tag{9}$$

encompassing the entire group of six models, which differs only in the fitting constants A, B, C, and D given in Table 3. Parameters A and C, with B = 1.0, lead to a first-order growth curve familiar from chemical kinetics (Atkins, 1994). When $B \neq 1.0$, the curve is no longer first order but shows deviation near $t = 0$, typically a short delay or induction time. Parameter D indicates growth after "final" growth is achieved (indeterminate growth); in our study it is approximated by a small increase of constant slope. This is used to add growth during the indeterminate growth phase.

Sensitivity to changes in the parameters

We examined the robustness of each of the parameters in the six models by changing them ±10%, then noting the behavior of the model. Results are given in the last two columns of Table 3. In the first two models, ±10 % variation in the parameters yields a change in the estimate of years to fishery of less than 1 year. Other models gave estimated time-to-enter-the-fishery variations over the range shown. See Schnute (1981) and Ebert et al. (1999) for discussions of parameter sensitivity.

Discussion

Our results show that red sea urchins in northern California are slow growing animals. The six models we used to generate growth predictions yielded estimates of the time to enter the fishery (89 mm test diameter) averaging 7.2 ±1.3 years and a range of estimates from 5.9 to 9.2 years. The robustness of this result is important for its use in fishery management. These six growth models, applied to the same data set, give similar growth curves, J versus. t (Eq. 9, Fig. 3) differing mainly at small J. Ranking these diverse models according to goodness of fit with our large data set shows that three models represent the data well, but that the von Bertalanffy model, the most widely used model, describes the data least well (Table 2).

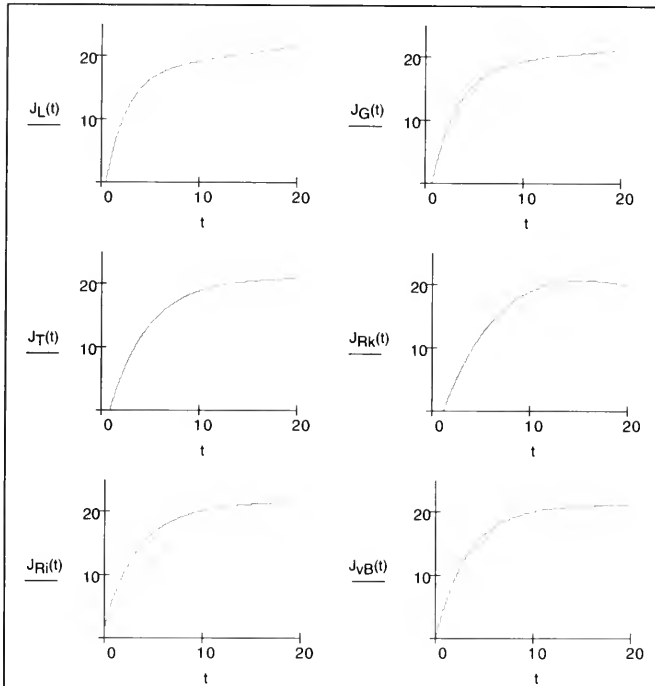

Figure 3

Jaw size (mm) versus time (y) obtained with J_{t+1} $J_t = J = f(J_t)$ onto $J = f(t)$. J_L = logistic dose response, J_G = Gaussian, J_T = Tanaka, J_{Rk} = Ricker, J_{Ri} = Richards, J_{vB} = von Bertalanffy. Note: *A, B, C,* and *D* in Equation 9 characterizing these curves are constants of the model and are not equal in number to the fitting parameters of the curves in Figure 2.

Our results suggest another important caveat: gaps in the data influence parameter estimates and time-to enter-the-fishery estimates. Many studies of sea urchin growth are based on a limited range of urchin sizes, primarily those of slow growing adults. Growth information from juveniles is difficult to obtain because recapturing tagged juveniles is problematic owing to high movement or mortality rates (or both). If growth information from adult urchins is used exclusively, inappropriate models can be fitted to the data ΔJ vs. J_t ($J_t \geq 16$ mm, Figs. 1 and 2) because there is no information at smaller J_t. In our example, lack of growth information from juveniles produced an overestimate of early growth and, as a consequence, an underestimate of the time to enter the fishery (Fig. 1A). Bias toward faster growth rates could lead to more liberal fishing policies and less precautionary management compared with bias toward slower growth rates. This problem has been noted by other researchers (Yamaguchi, 1975; Rowley, 1990; Troynikov and Gorfine, 1998).

Model selection

Model selection has always been an important aspect in applying growth modeling. In our case, with a data set from a broad range of size classes, we find that the six models yield similar growth curves, J versus t, indicating that our results of time to enter the fishery are robust to model selection. The unique features of the models show why the estimates are either longer or shorter than the mean we derive from all six models. Our composite model (Eq. 9) allows for the prediction of the most probable growth trajectory. The error terms (Table 2) describe dispersion about the most probable trajectory.

Both the logistic dose-response and the Gaussian functions qualitatively fit our sea urchin growth data better than the von Bertalanffy or Richards functions (Fig. 2). A comparison of the sum of the squared residuals (RSS) confirms this observation, ranking these models first and second, respectively. We use RSS as our primary criterion

Table 3

Parameters *A*, *B*, *C*, and *D* for the size versus time curves. Models are ordered according to goodness of fit. "Sensitivity" is the sensitivity to a parameter in estimated years to fishery.

Model	*A*	*B*	*C*	*D*	Years to fishery	Sensitivity	Parameters that varied
Logistic	21.3	0.80	0.48	0.22	6.6	<1	*a*, *b*, *c*
Gaussian	23.8	0.78	0.38	0.12	6.9	<1	A, μ, σ
Tanaka	25.6	0.80	0.26	0.02	8.2	1.5	*b*
Ricker	41.1	0.87	0.14	−0.68	9.2	−2.4, 3.5	J_∞, K
Richards	18.5	1.1	0.30	0.06	6.1	1.3, 2.7	J_∞, K
Bertalanffy	21.0	1.01[1]	0.30	0.01[1]	5.9	0.7, 0.6	J_∞, K

[1] These values are forced by the model.

for model selection; however both the AIC information criterion (Akaike, 1979) and the Schwartz-Bayesian criterion confirm the ranking of the models (Table 2). Model selection is discussed in detail elsewhere (Burnham and Anderson, 1998; Quinn and Deriso, 1999).

The Gaussian, Tanaka, and Ricker models yield both ΔJ vs. J_t and J_{t+1} vs. J_t curves that are concave downward and that visually conform with the data. These models are preferred over the Richards curve, which is concave upward, and the von Bertalanffy function, which is linear. The logistic and Gaussian models fit our data better (Table 2) than the other models examined. It is not surprising that the logistic and Gaussian models fit our data well, given the maximum or plateau visible in the data set for ΔJ vs. J_t. The Gaussian mean at $J_t = 4.6$ mm, with a standard deviation of 5.7 mm shows that a data set with $J_t > 4.6 + 5.7 = 10.3$ mm represents urchins that are one standard deviation (σ) above the mean of the growth curve, i. e., 16% of the growing population. Urchins with $J_t > 17.0$ mm, are greater than 2σ above maximal growth, i. e. 2.5% of the growing population. Therefore, a growth curve fit only to adult urchins with $J_t > 17.0$ mm represents only small subset of the total growing population and is not representative of the total population. This demonstrates that data from a limited size range can generate erroneous growth parameters and shorten estimates of time to enter the fishery.

Variation in growth

The plateau in growth rate implied by the logistic dose-response curve or the maximum in growth rate for juvenile urchins well after settlement implied by the Gaussian curve suggests that urchin growth is not at its maximum when sea urchins first settle. It is realistic to imagine that a sea urchin will be at its maximum growth rate sometime after the first year or two.

In this study we found high individual variation in sea urchin growth. Growth in juveniles was especially variable, despite the fact that the juvenile urchins that were stocked were full siblings. We found no evidence for an increase in dispersion as sea urchins grow larger. Data from many sources suggest individual variation in juvenile growth is high. Full sibling red urchins (n=200) reared in the laboratory under identical food, temperature, and light regimes varied in test diameter from 4 to 44 mm at one year (Rogers-Bennett, unpubl. data). Similarly, cultured purple urchins (*S. purpuratus*), varied from 10 to 30 mm at one year (Pearse and Cameron, 1991)—a trend observed in other commercially cultured marine invertebrates (Beaumont, 1994) and fishes (Allendorf et al. 1987).

Our data contain broad distribution in the region of the small size classes, which is consistent with high individual variation in growth (K). Varying the growth constant, K, e.g. in the Ricker model (cf. Sainsbury, 1980), produces dispersion at the smaller size classes. Our urchin growth data also show a wide array of large sizes as well. Models have been used to examine the impact of this type of individual growth variation. In the von Bertalanffy model, if final size, J_∞, is varied 10%, this results in a broad distribution of the largest size classes (Botsford et al., 1994). We see a broad distribution in the largest size classes in our data, with animals larger and smaller than the estimated final size J_∞. Many of the animals smaller than J_∞ could be at their final size. The biological interpretation of this broad distribution at the largest sizes is an open question. There may be a wide array of final sizes because of independent values of K and J_∞ (cf. Sainsbury, 1980) and each individual hits its own final size abruptly or at an asymptotic approach to final size (cf. Beverton, 1992) also known as indeterminate growth (cf. Sebens, 1987).

We suggest that the composite model presented in the present study (Eq. 9) may be useful for a wide array of invertebrates and fishes especially those with a broad array of final sizes.

Spatial patterns in growth

In our study, we found no evidence for spatial patterns in growth. To observe spatial patterns this would have to be detectable above the background of individual variation. Sea urchins from the shallow and deep sites at Salt Point had measurable differences in gut contents, food availability, and oceanographic conditions; however these did not translate into significant differences in growth between

the depths over the year examined. Similarly, no latitudinal differences in red sea urchin growth were found in a large-scale growth study at 18 sites ranging from Alaska to southern California where growth varied between neighboring sites as between much as distant sites (Ebert et al., 1999).

Future studies could be longitudinal and examine temporal patterns in sea urchin growth, for example during and after warm water El Niño years, as has been examined for abalone in southern California (Haaker et al., 1998); however these temporal patterns too would have to be greater than individual variation to be detectable.

Implications for fishery management

Large old sea urchins (>125 mm test diameter) are fished in California despite fishermen receiving lower prices for these sea urchins compared with mid-size animals (Rudie[2]). Many of the large, old urchins have high gonadal weights (>100 g) (Carney, 1991; Rogers-Bennett et al., 1995), thereby potentially contributing more to reproduction than smaller urchins (Tegner and Levin, 1983; Tegner, 1989; Kalvass and Hendrix, 1997). Similarly, large coral-reef fish also have the potential to contribute more to reproduction than smaller fish (Bohnsack, 1993).

In fished areas, size-frequency distributions are heavily skewed to smaller urchins indicating that the larger size classes are absent (Kalvass and Hendrix, 1997). If the abundance and density of red sea urchins is decreased during fishing, this will decrease the chances of fertilization success significantly (Levitan et al., 1992). Sufficient numbers of large broodstock are critical because recruitment does not appear to be successful every year (Ebert, 1983; Pearse and Hines, 1987; Sloan et al., 1987). In addition, fishing can impact recruitment success because the spines of large urchins provide canopy shelter for juveniles; therefore an Allee effect may be present (Tegner and Dayton, 1977; Sloan et al., 1987; Rogers-Bennett et al., 1995). Size-structured red sea urchin models that include variable recruitment or an Allee effect (positive density dependence) resulted in a >50% decrease in estimated population size even at low fishing mortality levels (Pfister and Bradbury, 1996).

Harvest experiments conducted in northern California have shown that management strategies that protect large urchins (upper size limits and harvest reserves) improve recovery and recruitment after six years compared with strategies in which large urchins are harvested (lower size limits only) (Rogers-Bennett et al., 1998). Upper size limits and reserves have been used in the management of the sea urchin fishery in Washington state (Bradbury, 2000) and are currently being considered for California's red sea urchin fishery (Taniguchi[3]).

In conclusion, our work and that of others (Ebert and Russell, 1992, 1993; Ebert et. al., 1999) suggest that red sea urchins are slow growing, long-lived animals. Intense harvest rates may have serious consequences because red sea urchins require seven years to reach harvestable size in northern California. Declines in red sea urchin landings in northern California of more than 80% from the peak of 13,800 t in 1988 (Kalvass, 2000) demonstrate that harvest rates are high. Our growth results suggest that proposed alternative management strategies that would protect large, slow growing broodstock inside reserves or upper size limits for the fishery could be beneficial, in addition to existing regulations, for sustaining the fishery.

Acknowledgments

Special thanks to H. C. Fastenau, D. Canestro and the U. C. Santa Cruz research dive class (1992) for help tagging and measuring red sea urchins. D. Cornelius and the "Down Under" helped harvest urchins. P. Kalvass shared his growth data from PIT tagged sea urchins. F. McLafferty discussed models and "the most probable sea urchin." W. Clark, S. Wang, and F. Griffin gave access to and instruction on the confocal microscope. C. Dewees, H. Blethrow, S. Bennett, and K. Rogers all contributed. This research was funded in part by the California Department Fish and Game, the PADI Foundation, U.C. Davis Natural Reserve System, and the Bodega Marine Laboratory. Comments from M. Lamare and M. Mangel improved the manuscript.

Literature cited

Akaike, H.
1979. A Bayesian extension of the minimum AIC procedure of autoregressive model fitting. Biometrika 66:237–242.

Allendorf, F. W., N. Ryman, N., and F. M. Utter.
1987. Genetics and fishery management: past, present and future. *In* Population genetics and fishery management, p. 1–19. Washington Sea Grant, Seattle, WA.

Atkins, P. W.
1994. Physical chemistry, 5th ed., 1031 p. W.H. Freeman, New York, NY.

Barrante, J. R.
1998. Applied mathematics for physical chemistry, 2nd ed., 227 p. Prentice Hall, Upper Saddle River, NJ.

Beverton, R. J. H.
1992. Patterns of reproductive strategy parameters in some marine teleost fishes. J. Fish Biol. 41:137–160.

Beaumont, A. R.
1994. Genetics and aquaculture. *In* Genetics and evolution of marine organisms, p. 467–486. Cambridge Univ. Press, Cambridge, England.

Bohnsack J.A.
1993. Marine reserves: they enhance fisheries, reduce conflicts and protect resources. Oceanus 36:63–71.

Botsford, L. W., B. D. Smith, and J. F. Quinn.
1994. Bimodality in size distributions: the red sea urchin (*Strongylocentrotus franciscanus*) as an example. Ecol. Appl. 4:42–50.

[2] Rudie, D. 1994. Personal commun. Catalina Offshore Products Inc., 5202 Lovelock St., San Diego, CA 92110.

[3] Taniguchi, I. 2002. Personal commun. Calif. Dep. Fish and Game, 4665 Lampson Ave., Los Alamitos, CA. 90720.

Bradbury, A.
2000. Stock assessment and management of red sea urchins (*Strongylocentrotus franciscanus*) in Washington. J. Shellfish Res. 19:618–619.
Brody, S.
1927. Growth rates. Univ. Missouri Agri. Exp. Sta. Bull. 97.
Burham, K. P., and D. R. Anderson
1998. Model selection and inference: a practical information theoretic approach, 353 p. Springer Verlag. New York, NY.
Carnahan, B., H. A. Luthier, and J. O. Wilkes.
1969. Applied numerical methods, 604 p. Wiley Press, New York, NY.
Carney, D.
1991. A comparison of densities, size distribution, gonad and total-gut indices and the relative movements of red sea urchins *Strongylocentrotus franciscanus* in two depth regimes. M.S. thesis, 43 p. Univ. California, Santa Cruz, CA.
Dugan, J. E., and G. E. Davis.
1993. Applications of marine refugia to coastal fisheries management. Can J. Fish. Aquat. Sci. 50:2029–2042.
Duetler, F.
1926. Uber das Wachstum des Seeigelskeletts. Zool. Jb. (Abt. Anat. Ontag. Tiere) 48:119–200.
Ebert, T. A.
1980a. Estimating parameters in a flexible growth equation, the Richards function Can. J. Fish. Aquat. Sci. 37: 687–692.
1980b. Relative growth of sea urchin jaws: an example of plastic resource allocation Bull. Mar. Sci. 30:467–474.
1982. Longevity, life history, and relative body wall size in sea urchins. Ecol. Monogr. 52:353–394.
1983. Recruitment in echinoderms. Echinoderm Studies 1:169–203.
1988. Calibration of natural growth lines in ossicles of two sea urchins *Strongylocentrotus purpurtaus* and *Echinometra mathaei*, using tetracycline. *In* Echinoderm biology (R. D. Burke, P. V. Mladenov, P. Lambert, and R. L. Parsley, eds.); proceedings of the sixth international echinoderm conference, p. 435–443. A.A. Balkema, Rotterdam.
1999. Plant and animal populations: methods in demography, 312 p. Academic Press, San Diego, CA.
Ebert, T. A., and M. P. Russell.
1992. Growth and mortality estimates for red sea urchins *Strongylocentrotus franciscanus* from San Nicolas Island, California. Mar. Ecol. Prog. Ser. 81:31–41.
1993. Growth and mortality of subtidal red sea urchins *Strongylocentrotus franciscanus* at San Nicolas Island, California, USA: problems with models. Mar. Biol. 117: 79–89.
Ebert, T. A., Dixon, J. D., Schroeter, S. C. Kalvass, P. E. Richmond, N. T. Bradbury, W. A. and D. A. Woodby.
1999. Growth and mortality of red sea urchin *Strongylocentrotus franciscanus* across a latitudinal gradient. Mar. Ecol. Prog. Ser. 190:189–209.
Gage, J. D.
1992. Natural growth bands and growth variability in the sea urchin *Echinus esculentus*: results from tetracycline tagging. Mar. Biol. 114:607–616.
Haaker, P. L., D. O. Parker, K. C. Barsky, and C. Chun.
1998. Growth of red abalone, *Haliotis rufescens* (Swainson), at Johnson's Lee Santa Rosa Island, California. J. Shell. Res. 17:747–753.
Harrold, C., and D. C. Reed.
1985. Food availability, sea urchin grazing, and kelp forest community structure. Ecol. 66:1160–1169.
Hastings, A.
1997. Population biology concepts and models, 227 p. Springer-Verlag, New York, NY.
Jackson, J. B. C., M. X. Kirby, W. H. Berger, K. A. Bjorndal, L. W. Botsford, B. J. Bourque, R. H. Bradbury, R. Cooke, J. Erlandson, J. A. Estes, T. P. Hughes, S. Kidwell, C. B. Lange, H. S. Lenihan, J. M. Pandolfi, C. H. Peterson, R. S. Steneck, M. J. Tegner, and R. R. Warner.
2001. Historical overfishing and the recent collapse of coastal ecosystems. Sci. 293:629–638.
Kalvass, P. E.
2000. Riding the rollercoaster: Boom and decline in the California red sea urchin fishery. J. Shellfish Res. 19: 621–622.
Kalvass, P. E., and J. M. Hendrix.
1997. The California red sea urchin, *Stronglyocentrotus fransiscanus*, fishery: catch, effort, and management trends. Mar. Fish. Rev. 59:1–17.
Kalvass, P. E.; J. M. Hendrix, and P. M. Law.
1998. Experimental analysis of 3 internal marking methods for red sea urchins. Calif. Fish Game 84:88–99.
Karpov, K.A., P. L. Haaker, I. K. Taniguchi, and L. Rogers-Bennett.
2000. Serial depletion and the collapse of the California abalone (Haliotis spp.) fishery. Can. Spec. Publ. Fish. Aquat. Sci. 130:11–24.
Kato, S., and S.C. Schroeter.
1985. Biology of the red sea urchin *Strongylocentrotus franciscanus*, and its fishery in California. Mar. Fish. Rev. 47: 1–19.
Keesing, J. K., and K. C. Hall.
1998. Review of harvests and status of world's sea urchin fisheries points to opportunities for aquaculture. J. Shellfish Res. 17:1597–1604.
Levitan, D. R. M. A. Sewell, and F.-S. Chia.
1992. How distribution and abundance influence fertilization success in the sea urchin, *Strongylocentrotus franciscanus*. Ecol. 73:248–254.
Pearse, J. S., and R. A. Cameron.
1991. Echinodermata: echinoidea. *In* Reproduction of marine invertebrates, vol VI (A. C. Giese, J. S. Pearse and V. B. Pearse, eds.), p. 513–662. Academic Press, New York, NY.
Pearse, J. S., and A. H. Hines.
1987. Long-term population dynamics of sea urchins in a central California kelp forest: rare recruitment and rapid decline. Mar. Ecol. Prog. Ser. 39:275–283.
Pearse, J. S., and V. B. Pearse.
1975. Growth zones in the echinoid skeleton. Am. Zool. 15: 731–753.
Pfister, C. A., and A. Bradbury.
1996. Harvesting red sea urchins: Recent effects and future predictions. Ecol. Appl. 6:29–310.
Quinn, T. J., and R. B. Deriso.
1999. Quantitative fish dynamics, 542 p. Oxford Univ. Press, Oxford, England.
Richards, F. J.
1959. A flexible growth curve for empirical use. J. Exp. Bot. 10:290–300.
Ricker, W. E.
1954. Stock and recruitment. J. Fish Res. Board Can. 11: 559–623.
Rogers, D. W.
1983. BASIC microcomputing and biostatistics, 274 p. The Humana Press Inc., Clifton, NJ.
Rogers-Bennett, L.
2001. Evaluating stocking as an enhancement strategy for the red sea urchin, *Strongylocentrotus franciscanus*: depth-

specific recoveries. *In* Proceedings of the 10th international echinoderm conference; Dunedin, New Zealand, p. 527–531. A.A. Balkema, Rotterdam.

2001. Review of some California fisheries for 2000: Market squid, sea urchin, prawn, white abalone, groundfishes, ocean salmon, Pacific sardine, Pacific herring, Pacific mackerel, nearshore live-fishes, halibut, yellowfin tuna, white seabass, and kelp. Calif. Coop. Oceanic Fish. Invest. Rep. 42:12–28

Rogers-Bennett, L., H. C. Fastenau, and C. M. Dewees.

1998. Recovery of red sea urchin beds following experimental harvest. *In* Proceedings of the 9th internation echinoderm conference, San Francisco, CA, p. 805–809. A.A. Balkema, Rotterdam.

Rogers-Bennett, L., W. A. Bennett, H. C. Fastenau, and C. M. Dewees.

1995. Spatial variation in red sea urchin reproduction and morphology: implications for harvest refugia. Ecological Applications 5:1171–1180.

Rowley, R. J.

1990. Newly settled sea urchins in a kelp bed and urchin barren ground: a comparison of growth and mortality. Mar. Ecol. Prog. Ser. 62:229–240.

Safina, C.

1998. Song for the blue ocean, 458 p. Henry Holt, New York, NY.

Sainsbury, K. J.

1980. Effect of individual variability on the von Bertalanffy growth equation. Can. J. Fish. Aquat. Sci. 37:241–247.

Schnute, J.

1981. A versatile growth model with statistically stable parameters. Can. J. Fish. Aquat. Sci. 38:1128–1140

Sebens, K. P.

1987. The ecology of indeterminate growth in animals. Ann. Rev. Ecol. Syst. 18:371–407.

Sloan, N. A., C. P. Lauridsen, and R. M. Harbo.

1987. Recruitment characteristics of the commercially harvested red sea urchin *Strongylocentrotus franciscanus* in southern British Columbia, Canada. Fish. Res. 5:55–69.

Smith, B. D., L. W. Botsford, and S. R. Wing.

1998. Estimation of growth and mortality parameters from size frequency distributions lacking age patterns: the red sea urchins (*Strongylocentrotus franciscanus*) as an example. Can J. Fish. Aquatic Sci. 55:1236–1247.

Tanaka, M.

1982. A new growth curve which expresses infinite increase. Publ. Amakusa Mar. Biol. Lab. 6:167–177.

Tegner, M. J.

1989. The feasibility of enhancing red sea urchin, *Strongylocentrotus franciscanus*, stocks in California: an analysis of the options. Fish. Bull. 51:1–22.

Tegner, M. J.,and P. K. Dayton.

1977. Sea urchin recruitment patterns and implications of commercial fishing. Science 196:324–326.

Tegner, M. J. and L. A. Levin.

1983. Spiny lobsters and sea urchins: analysis of a predator-prey interaction. J. Exp. Mar. Biol. Ecol. 73:125–150.

Troynikov, V. S., and H. K. Gorfine

1998. Alternative approach for establishing legal minimum lengths for abalone based on stochastic growth models for length increment data. J. Shellfish Res. 17:827–831.

von Bertalanffy, L.

1938. A quantitative theory of organic growth (inquires on growth laws II). Human Biol. 10:181–213.

Walford, L. A.

1946. A new graphic method of describing the growth of animals. Biol. Bull. 90:141–147.

Wien, W.

1896. Uber die Energieverteilung im Emissionspectrum eines Schwarzen Korpers. Annalen der Physik 1896: 662–669. *In* The conceptual development of quantum mechanics (M. Jammer, author), 2nd ed. 1989, p 8–10. Tomask Publishers, American Institute of Physics, Woodby, New York, NY.

Wilson, C. W., D. W. Beckman, J. D. Dean, and J. Mark.

1987. Calcein as a florescent marker of otoliths of larval and juvenile fish. Trans. Am. Fish. Soc. 116:668–670.

Yamaguchi, G.

1975. Estimating growth parameters from growth rate data. Problems with marine sedentary invertebrates. Oecologia 20:321–332.

Age and growth of the blue shark (*Prionace glauca*) in the North Atlantic Ocean*

Gregory B. Skomal
Massachusetts Division of Marine Fisheries
Martha's Vineyard Research Station
P.O. Box 68
Vineyard Haven, Massachusetts 02568
E-mail address: Gregory.Skomal@state.ma.us

Lisa J. Natanson
National Marine Fisheries Service, NOAA
28 Tarzwell Dr.
Narragansett, Rhode Island 02882

Abstract—Age and growth estimates for the blue shark (*Prionace glauca*) were derived from 411 vertebral centra and 43 tag-recaptured blue sharks collected in the North Atlantic, ranging in length from 49 to 312 cm fork length (FL). The vertebrae of two oxytetracycline-injected recaptured blue sharks support an annual spring deposition of growth bands in the vertebrae in sharks up to 192 cm FL. Males and females were aged to 16 and 15 years, respectively, and full maturity is attained by 5 years of age in both sexes. Both sexes grew similarly to age seven, when growth rates decreased in males and remained constant in females. Growth rates from tag-recaptured individuals agreed with those derived from vertebral annuli for smaller sharks but appeared overestimated for larger sharks. Von Bertalanffy growth parameters derived from vertebral length-at-age data are $L_\infty = 282$ cm FL, $K = 0.18$, and $t_0 = -1.35$ for males, and $L_\infty = 310$ cm FL, $K = 0.13$, and $t_0 = -1.77$ for females. The species grows faster and has a shorter life span than previously reported for these waters.

Manuscript approved for publication 5 March 2003 by Scientific Editor.
Manuscript received 4 April 2003 at NMFS Scientific Publications Office.
Fish Bull. 101:627–639 (2003).

The blue shark (*Prionace glauca*) is a large pelagic carcharhinid that is widely distributed in the world's oceans. Throughout its range, it is considered the most abundant species of large shark (McKenzie and Tibbo, 1964; Casey, 1982). In the Atlantic, the blue shark is distributed from Newfoundland to Argentina in the west and Norway to South Africa, including the Mediterranean, in the east (Compagno, 1984). There is strong evidence from tagging data and catch records that blue sharks in the North Atlantic constitute a single stock (Kohler et al., 2002). Moreover, mitochondrial DNA d-loop sequence and nuclear microsatellite analyses indicate no differences between blue sharks from the eastern and western North Atlantic (Shivji[1]).

Distribution and movements of the blue shark are strongly influenced by seasonal variations in water temperature, reproductive condition, and availability of prey (Kohler et al., 2002). Blue sharks make frequent trans-Atlantic movements between the western and eastern regions, utilizing the major North Atlantic current systems (Stevens, 1976, 1990; Casey, 1982, 1985; Kohler et al., 2002). Temporal and geographic patterns of size and sexual segregation have been described for this species, and mating areas and pupping areas are reported to be in the western and eastern regions of the North Atlantic, respectively (Casey, 1982; Kohler et al., 2002). Pregnant females are rare in the western North Atlantic, which is dominated by juveniles of both sexes, adult males, and subadult females (Pratt, 1979; Casey, 1982; Kohler et al., 2002). Catch records from the eastern North Atlantic largely comprised neonates and juveniles of both sexes and adult females (Aasen, 1966; Stevens, 1975, 1976; Connett, 1987; Silva et al., 1996; Kohler et al., 2002).

Although subjected to a number of fisheries, the blue shark is primarily taken as bycatch in longline fisheries throughout the North Atlantic (ICCAT, 2002). Most blue sharks are discarded or only their fins are harvested because of the low palatability of their flesh (Castro et al., 1999). Although incomplete, blue shark landings estimates in the North Atlantic reported to the International Commission for the Conservation of Atlantic Tunas were 25.1 and 24.2 thousand metric tons (t) in 1998 and 1999, respectively (ICCAT, 2002). Domestic longline fisheries in the western North Atlantic rarely land blue sharks, but it was estimated that annual dead discards ranged from 2.8 to 29.3 thousand blue sharks (99.0–1136.3 t) during the period 1987–2000 (Cortés, 2002). The major source of landings in the U.S. has been the recreational fishery, which landed 6.8 thousand blue sharks in 2000 (Cortés, 2002).

* Contribution 8 of the Massachusetts Division of Marine Fisheries, P.O. Box 68, Vineyard Haven, MA 02568.

[1] Shivji, M. 2002. Personal commun. Nova Southeastern University, 8000 North Ocean Dr., Dania Beach, FL 33004.

Ecologically, the blue shark is an apex predator of important teleosts and cephalopods (Stevens, 1973; Tricas, 1978; Kohler, 1987). Historical fisheries have shown that sharks are intrinsically sensitive to sustained exploitation (see review by Castro et al., 1999). Slow growth, late ages at maturity, and low fecundities reflect the life history strategies of *K*-selected species; stock size is closely linked to recruitment (Hoenig and Gruber, 1990). Although the current Fishery Management Plan for Atlantic Tunas, Swordfish, and Sharks has established limits on the U.S. commercial and recreational fisheries that impact blue sharks (NMFS, 1999), no international management is currently in place. Given a single North Atlantic stock for this species, any fisheries exploitation, regardless of its coastal origin, may impact the population. Accurate age determinations are necessary for both the assessment and management of the blue shark because they form the basis for calculations of growth and mortality rates, age at maturity, age at recruitment, and estimates of longevity.

Age and growth of the blue shark have been described by a number of studies to varying degrees. In the North Pacific, Cailliet et al. (1983) and Tanaka et al. (1990) used vertebral growth rings and Nakano (1994) used both vertebrae and length-frequency modes to establish growth curves for the blue shark. In the North Atlantic, Aasen (1966) aged the species by assigning ages to length-frequency modes. Later, Stevens (1975), Silva et al. (1996), and Henderson et al. (2001) established growth curves from vertebral growth rings of juvenile blue sharks sampled in the eastern North Atlantic. Low sample sizes, inadequate size ranges, and the lack of age validation limit the utility of these studies for the North Atlantic blue shark population. Skomal (1990) generated growth curves for the blue shark from vertebral growth rings, tag-recaptures, and length-frequency data. In that study, vertebrae from oxytetracycline (OTC) injected recaptured blue sharks were used to validate age estimates. The purpose of the current study is to augment the work of Skomal (1990) with additional tag-recapture data, with corroborative vertebral readings of a different vertebral processing technique, and with more rigorous growth analyses.

Materials and methods

Interpretation of vertebrae

Vertebrae were obtained from blue sharks caught on research cruises, commercial, and recreational fishing vessels, and at sport fishing tournaments between 1966 and 2001. Primary sampling took place between Cape Hatteras, NC, and the Gulf of Maine (NE coast of the United States). To adequately represent the entire size range of the species, small sharks were obtained from the eastern Atlantic from cooperative fishermen and research scientists. When possible, the 15th through 20th vertebrae were excised for the study. When such precision was not possible, this section of backbone was approximated by cutting at the branchial region adjacent to the fifth gill arch. Excess muscle and connective tissue were removed from the vertebrae with a knife. Vertebrae were stored either frozen or preserved in 10% buffered formalin or 70% ethanol.

Only samples that had measured fork length (FL—tip of the snout to the fork in the tail, over the body curvature), total length (TL—tip of the snout to a point on the horizontal axis intersecting a perpendicular line extending downward from the tip of the upper caudal lobe to form a right angle), or precaudal length (PCL—tip of the snout to the precaudal pit, over the body curvature) were used (Kohler et al., 1995). All lengths reported are in FL unless otherwise noted. TL can be converted to FL by using the regression (Kohler et al., 1995):

$$FL = 0.8313\,(TL) + 1.39 \qquad [n=572\ r^2=0.99].$$

PCL can be converted to FL using the regression (NMFS[2])

$$PCL = 0.9075\,(FL) - 0.3956 \qquad [n=106\ r^2=0.99].$$

One vertebra from each sample was removed for processing. The centrum was sectioned by using a Ray Tech Gem Saw with two diamond blades separated by a 0.6-mm spacer. Each centrum was cut through the middle along the sagittal plane; the resulting bow-tie sections were stored in individual capsules in 70% ethanol. Each section was digitally photographed with a MTI CCD 72 video camera attached to a SZX9 Olympus stereo microscope by using reflected light. All samples were photographed at a magnification of 4×. Band pairs (consisting of one opaque and one translucent band) were counted and measured from the images by using Image Pro 4 software (Media Cybernetics, Silver Spring, MD). Measurements were made from the midpoint of the notochordal remnant of the full bow-tie to the opaque growth bands at points along the internal corpus calcareum. The radius of each vertebral centrum (VR) was measured from the midpoint of the notochordal remnant to the distal margin of the intermedialia along the same diagonal as the band measurements. Specimens previously processed histologically (Skomal, 1990) were used for counts when whole samples for those specimens were not available for reprocessing. Because of the different processing method, histological sections were not used for measurements.

The criterion for what constitutes a band pair (annulus) was based on the contouring of the corpus calcareum in relation to the strength of the band. A clear indentation of the corpus calcareum at the position of an opaque band constituted the consummation of a growth layer within the vertebra and was considered the annulus (Fig. 1). Each layer was considered a temporal growth zone. The first opaque band distal to the focus was defined as the birth mark (BR) and a slight angle change in the corpus calcareum coincided with this mark. In addition, identification of the birth band was confirmed with back-calculation and by comparison of the radius of this band with the radius of vertebrae from young of the year (YOY) and full-term embryos.

[2] NMFS (National Marine Fisheries Service). 2001. Unpubl. data. Apex Predators Program, 28 Tarzwell Dr., Narragansett, RI 02882.

The relationship between VR and FL was calculated to determine the best method for back-calculation of size-at-age data and to confirm the interpretation of the birth band. Age was calculated for each fish based on a birth date of June 1 (Pratt, 1979), corrected for date of capture. Regressions were fitted to the male and female size-at-age data and an ANCOVA was used to test for difference between the two relationships. The relationship between FL and VR was best described by a polynomial equation; therefore the data were ln-transformed before linear regression. The Fraser-Lee equation of the ln-transformed data was derived for back calculation:

$$ln(FL_a) = b + (ln[FL_c]+b)\ (lnradius_a)\ (lnradius_c)^{-1},$$

where a = age;
b = intercept from the regression; and
c = capture.

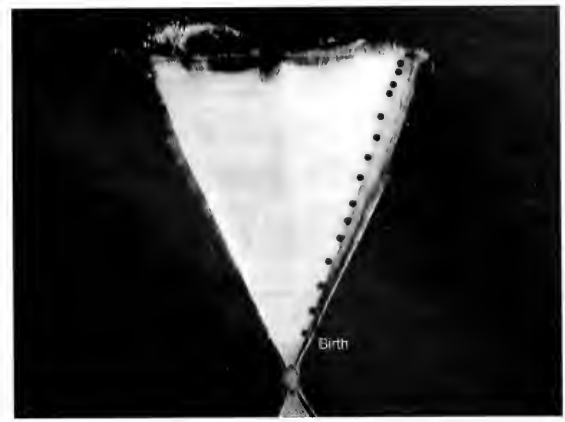

Figure 1
Photograph of a vertebral section from a male blue shark (*Prionace glauca*) estimated to be 14 years old.

Validation

To evaluate the periodicity of band pair formation, vertebrae from OTC-injected and measured tag-recaptured sharks were examined. Over 350 blue sharks of various sizes were measured, tagged, and injected with a 25 mg/kg body weight dose of OTC by scientific personnel aboard research and commercial vessels in the North Atlantic. Upon recapture, vertebrae were removed from injected specimens and stored in 70% ethanol or were frozen. Vertebrae from these sharks were processed, digitally photographed as previously described, and examined for the OTC mark with reflected UV light. The number of band pairs distal to the OTC mark was then compared with the number of years at liberty and expressed as the proportion of the previous complete growth zone.

Data analysis

Aging bias and precision of bands counts were examined by using age-bias plots and the coefficient of variation (Campana et al., 1995). Reader 2 counted 98 sections previously counted by reader 1 (Skomal, 1990). Pairwise comparisons were generated from these data.

Von Bertalanffy growth functions (VBGF) were fitted to length-at-age data by using the following equation (von Bertalanffy, 1938):

$$L_t = L_\infty(1-e^{-K(t-t_0)}),$$

where L_t = predicted length at time t;
L_∞ = mean asymptotic length;
K = a growth rate parameter (yr^{-1}); and
t_0 = the theoretical age at which the fish would have been zero length.

The VBGF was calculated by using the nonlinear regression function in Statgraphics (Manugistics, Inc., Rockville, MD).

Tagging data

From 1963 through 1999, members of the NMFS Cooperative Shark Tagging Program tagged 88,899 and recaptured 4967 blue sharks. Only those sharks reliably measured by biologists or fishermen at both tagging and recapture were used in the analyses. All measurements were converted to FL by using the relationships of Kohler et al. (1995).

The Gulland and Holt (1959) and Francis (1988a) models were used to generate VBGFs from the tag-recapture data. The Gulland and Holt (1959) method uses graphical interpretation of the recapture data to produce estimates of L_∞ and K. Specifically, annualized growth rate (cm/yr) was plotted against average FL (cm) between tagging and recapture to calculate linear regression coefficients. The slope of the line is equal to $-K$ and the x-axis intercept is equal to L_∞.

The Francis (1988a) method (GROTAG) uses maximum likelihood techniques to estimate growth parameters and variability from tagging data. A coefficient of variation of growth variability (v), measurement errors (m and s) and outlier contamination (p) are estimated, as well as growth rates at two user selected lengths (α and β). The reference lengths, α and β, were chosen to lie within the range of tagged individuals. The form of the von Bertalanffy equation becomes

$$\Delta L = \left[\frac{\beta g_\alpha - \alpha g_\beta}{g_\alpha - g_\beta} - L_1\right]\left[1-\left(1+\frac{g_\alpha - g_\beta}{\alpha-\beta}\right)^{\Delta T}\right].$$

The simplest model, a linear fit with minimal parameters (α and s) was used initially and additional parameters

were added to successively increase the model complexity. Significant improvement in the model results were determined by using log likelihood ratio tests in accordance with Francis (1988a). Bootstrapping was used to calculate the 95% confidence intervals for the final parameter estimates. The modeling and bootstrapping were carried out by using a Solver based spreadsheet in MS Excel (Microsoft Corp., Redmond, WA) (Simpfendorfer[3]). The value of t_0 cannot be estimated from tagging data alone, it requires an estimate of absolute size at age, such as size at birth, and was calculated with the VBGF by solving for t_0 such that

$$t_0 = t + (1/K)\left[\ln\{L_\infty - L_t / L_\infty\}\right]$$

where L_t = known length at age (size at birth);
K = the von Bertalanffy growth constant; and
L_∞ = the theoretical maximum attainable length from the VBGF.

The t_0 values were calculated based on an average size at birth of 45 cm FL (Pratt, 1979) with $t = 0$.

Longevity

The oldest fish aged from the vertebral method provides an initial estimate of longevity. However, this value is likely to be underestimated in a fished population. Using a teleost species, Taylor (1958) defined life span (A) as the time required to attain 95% of the L_∞ with the following equation:

$$A_{95} = t_0 + \frac{\log_e(1-0.95)}{k}.$$

This equation can be used to determine life span based on 99% of L_∞ by substituting 0.99 for 0.95 in the equation (Taylor, 1958). Fabens (1965) calculated time of >99% of L_∞ using the equation

$$>99\% = 5\frac{(\ln 2)}{k}.$$

Results

Interpretation of vertebrae

Vertebral samples from 411 blue sharks were used in our study: 287 males, 119 females, and five of unknown sex. These samples comprised free-living sharks ranging from 49 cm to 312 cm FL. In addition, vertebrae from seven late-term embryos ranging from 36 cm to 43 cm FL were examined. Blue shark vertebrae did not have consistent prebirth marks; thus, the first distinct opaque band was generally considered the birth mark. The location of the birth band coincided with a slight angle change (Fig. 1).

The FL-VR relationship was slightly curvilinear and the ln-transformed data provided a better linear fit (Fig. 2). Therefore, we calculated the regressions based on the ln(FL)-ln(VR) relationship

$$\ln(\mathrm{FL}) = 0.89^{*}\ln(\mathrm{VR}) + 3.10 \qquad [n=392\ r^2=0.97].$$

There was no significant difference between the sexes (ANCOVA, $P>0.10$).

Confirmation of the birth band was made by comparison of the BR of all individuals to the VR of YOY and late-term embryos (Fig 2). The VR of seven late-term embryos (mean VR ±95% CI=2.04 ±0.25) was slightly less than the BR value of the total sample (mean BR ±95% CI=2.70 ±0.03; n=351); the mean VR of 11 early YOY was slightly higher than the BR of the entire sample (49–58 cm FL; mean VR ±95% CI =2.97 ±0.18) (Fig. 2). The location of the birth ring between the VR of both the late-term embryos and the YOY indicated that the birth ring was identified correctly.

Validation

OTC-injected recaptured blue sharks provided evidence for the use of vertebral band pairs as age indicators. Vertebrae from two OTC-injected sharks were returned after 0.7 and 1.5 years at liberty (Table 1). OTC injection produced strong fluorescent marks in the vertebral centra of both these sharks (Fig. 3) and the number of annuli past the OTC mark coincided with the number predicted from time at liberty (Table 1). In OTC-injected recaptured shark (B536), an opaque growth band was deposited just after tagging in May (Fig. 3). In recaptured shark B116452, an opaque growth band was deposited just prior to tagging in June (Fig. 3). These results suggest an annual spring deposition of growth zones within the vertebrae. Thus, vertebral annuli were validated in these two sharks, which were up to 4+ years of age; the older of these fish (B536) corresponded to this age. Beyond this age, bands were assumed to be annual on the basis of the similar nature of band deposition.

Comparison of counts between two readers indicated no appreciable bias (Fig. 4). The coefficient of variation fluctuated around 15%. This level of precision was considered acceptable; thus, counts generated by both readers and preparation methods were combined for the analyses. The reader maintained quality control by periodically recounting earlier samples and by cross-checking the readings.

Length-at-age data indicated that males and females grow at roughly the same rate. The overlap in observed size-at-age data, as well as the graphical representation of the VBGF curves, indicated that there is little difference in growth for the sexes (Fig. 5). However, the LOWESS (locally weighted regression smoothing) derived curves as well as the VBGF parameters indicated that, theoretically, females grow slower and to a larger overall size than males (Table 2, Fig. 6). The LOWESS curves clearly showed minor differences in growth beginning at approximately seven years of age (Fig. 6), but this was likely an artifact of low female sample size at older ages. Subsequent analyses are presented for each sex and for sexes combined for ease of comparison with previously published studies.

[3] Simpfendorfer, C. 2000. Personal commun. Mote Marine Laboratory, 1600 City Island Park, Sarasota, FL 33577.

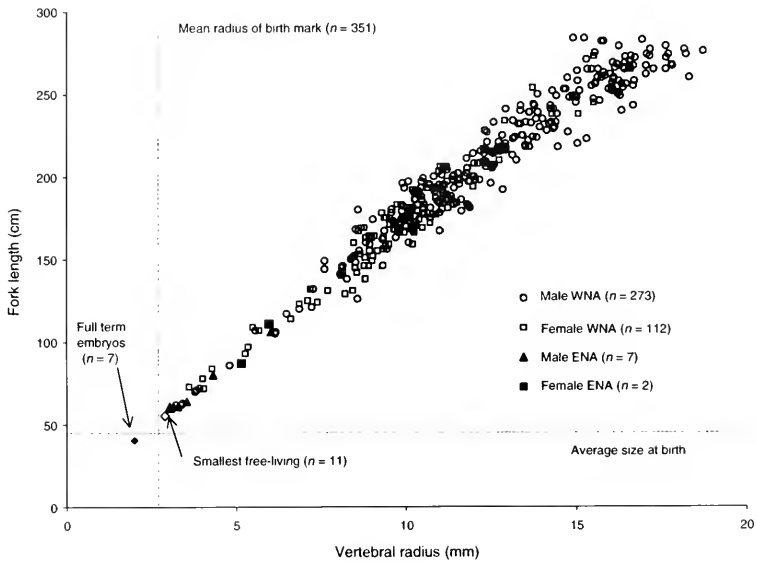

Figure 2

Relationship between vertebral radius and fork length in the blue shark (*Prionace glauca*).

Table 1

Tag-recapture data for OTC-injected recaptured blue shark (*Prionace glauca*). TFL = fork length at tagging, RFL = fork length at recapture.

Sample number	Sex	TFL (cm)	RFL (cm)	Date tagged	Date recaptured	Years at liberty	Growth (cm)	No. of bands after OTC mark
B116452	F	116	162[1]	18 Jun 1987	21 Dec 1988	1.5	33	1.20
B536	M	172	192	9 May 1985	16 Jan 1986	0.7	29	0.68

[1] Calculated from precaudel length.

Tagging data

A total of 43 blue sharks was recaptured with sufficient information for tag-recapture analysis. Data from 18 sharks at liberty >0.9 years were used for Gulland and Holt's (1959) method and all the recaptured sharks were used for the Francis (1988a) method (GROTAG).

The results of the likelihood ratio tests with GROTAG (Francis, 1988a) showed that the more complex nonlinear model with all six parameters was the best fit for these data (Table 3, model 3). The mean annual growth rates are g_{90} = 44.2 cm/yr and g_{180} = 25.5 cm/yr, corresponding to growth rates at a FL= 90 cm and 180 cm, respectively (Fig. 7). Von Bertalanffy estimates from the Gulland and Holt (1959) and GROTAG (Francis, 1988a) methods produced similar von Bertalanffy curves (Table 4, Fig. 8A).

Longevity

The maximum age determined from vertebral band pair counts was 16 and 15 years for males and females, respectively. These ages are likely to be an underestimate of longevity, given the history of fisheries exploitation of this species. Using Taylor's (1958) method, we determined that the age at which 95% and 99% of the L_∞ is reached was 16.5 and 26.1 years, respectively. Fabens (1965) method for >99% longevity produced an estimate of 20.7 years.

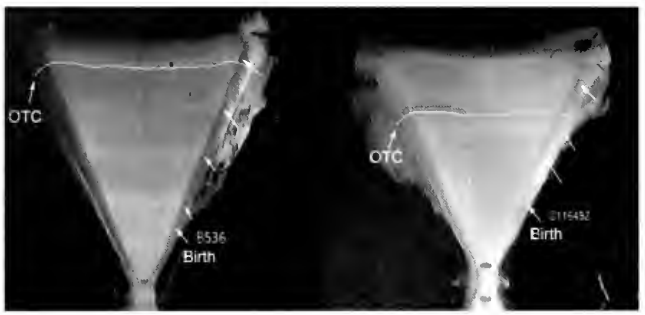

Figure 3

Vertebral sections from two OTC-injected blue sharks (*Prionace glauca*). Annuli and birth marks are indicated.

Discussion

Several methods have been employed to validate or verify (or both) age estimates derived from vertebral banding patterns (Cailliet, 1990). Although corroborative verification often comes from the interpretation of length-frequency data, laboratory and field growth studies, and centrum edge analyses, direct age validation for sharks is limited to the interpretation of vertebral banding patterns in OTC-injected fish.

In his review of elasmobranch age and growth studies, Cailliet (1990) found validated growth curves for only six species, which included three carcharhinids: the lemon (*Negaprion brevirostris*); the sandbar (*Carcharhinus plumbeus*); and the Atlantic sharpnose (*Rhizoprionodon terraenovae*) sharks. Although more than ten years have transpired since this review, validated growth curves for sharks are still lacking. In lamnids, direct validation of annual band deposition with the use of OTC has been reported in a single species, the porbeagle shark, *Lamna nasus* (Natanson et al., 2002). Although age estimates from vertebral banding patterns have been reported for several carcharhinids, including the oceanic whitetip shark, *Carcharhinus longimanus* (Seki et al., 1998; Lessa et al., 1999), the dusky shark, *C. obscurus* (Natanson et al., 1995; Natanson and Kohler, 1996; Simpfendorfer, 2000), the blacktip shark, *C. limbatus* (Wintner and Cliff, 1995), and the bronze whaler, *C. brachyurus* (Walter and Ebert, 1991), age interpretations were not validated and vertebral bands were assumed to be annual. More recently, Simpfendorfer et al. (2002) validated the annual formation of vertebral banding patterns in *C. obscurus* from Western Australian waters.

In the current study, we have validated annual band pair deposition in *Prionace glauca* up to 4+ years in age using vertebrae from two OTC-injected fish. These data indicate that annulus formation occurs in the spring. This seasonal formation is further supported by the marginal increment analysis of Skomal (1990), which shows that one band pair is formed annually. However, the low sample size and the lack of OTC-injected recaptured fish over the entire size range of the species do not allow for full age and growth validation. Clearly, the study requires OTC-injected recaptured blue sharks over a broader size range and greater time at liberty—a requirement that is not atypical of age and growth

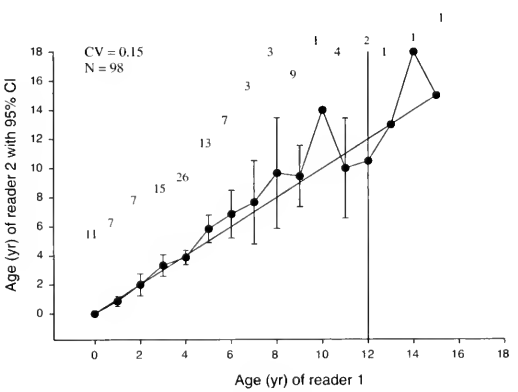

Figure 4

Age bias graph for pair-wise comparison of 98 blue shark (*Prionace glauca*) vertebral counts from two independent readers. Each error bar represents the 95% confidence interval for the mean age assigned by reader 2 to all fish assigned a given age by reader 1. The one-to-one equivalence line is also presented.

studies on large highly migratory elasmobranchs. Wintner and Dudley (2000) used two OTC-injected recaptured individuals to conclude that growth band deposition is annual in the tiger shark (*Galeocerdo cuvier*). Moreover, Natanson et al. (2002) validated annuli in the porbeagle shark up to 11 years of age by using only two OTC-injected and six YOY recaptured individuals, although the species was aged to 25 years.

The processes that govern vertebral growth have yet to be described in elasmobranchs. The pattern varies from one ring per year in most carcharhinids (Cailliet, 1990), and two rings per year in some lamnids (Parker and Stott, 1965; Pratt and Casey, 1983) to the complete absence of periodicity (Natanson, 1984). Some researchers feel that temperature plays a major role in this process (Stevens, 1975; Ferreira and Vooren, 1991). The blue shark, however, remains within a discrete temperature range year-round (Stevens, 1975; Sciarrota and Nelson, 1977; Casey, 1982). Moreover, acoustic tracking has shown that blue sharks experience large changes in body temperature (up to 7°C) as they routinely pass through the thermocline in their daily periodic dives from the surface to depths of 200–600 m (Carey and Scharold, 1990).

The ecology of this species may provide a more likely explanation of annulus formation. Kohler (1987) found a seasonal cycle for energy storage that correlated with the migratory patterns of the blue shark. In general, blue shark condition was found to be at an annual low in the winter and spring. Blue sharks use energy stores during this time for extensive north-south and trans-Atlantic migrations (Casey, 1985; Kohler, 1987) and periodic deep dives (Carey and Scharold, 1990). It is logical that growth may be depressed during these months, thereby causing a check or annulus in the vertebrae.

Tag-recapture data provide verification of the growth curves derived from vertebral banding. Francis (1988b) suggested that growth curves generated from age-length and length-increment (tagging) data are not directly comparable and that the comparison of growth rates at length was more appropriate. Although VBGF parameters derived from tagging data are noticeably higher, growth rates were similar for both methods (Fig. 7). The higher L_∞ and K can be attributed to the different derivation of the VBGF parameters and the absence of older recaptured sharks in the sample.

Pratt (1979) proposed that maturity in the male blue shark occurs at 183 cm FL and this would coincide with an age of 4–5 years based on the results of the present study. Females enter a distinct subadult phase (Pratt, 1979) at 145 cm FL and 2^+ years of age. Full maturity in females is attained at 185 cm FL (Pratt, 1979), which corresponds to about 5 years of age.

Previous estimates of age and growth of the blue shark in the Atlantic have been determined from vertebral banding patterns, and verification has been made from the interpretation of length-frequency and tagging data (Stevens, 1975; Silva et al., 1996; Henderson et al., 2001) (Table 5, Fig. 8). The eastern Atlantic vertebral sample of Stevens (1975) comprised largely females (89%), ranging from 34 cm to 227 cm FL. The resulting growth curve, therefore, largely reflects female growth (Fig. 8C). His use of whole silver-stained centra coupled with the lack of maximum-size fish allowed for the interpretation of only six annuli. From only mean back-calculated lengths at ages two through five, Stevens extrapolated growth of the species with a VBGF to an age of 20 years. Similarly, Silva et al. (1996) and Henderson et al. (2001) investigated age and growth in this species with whole vertebrae from sharks sampled in the eastern North Atlantic. In the former study, vertebral samples from

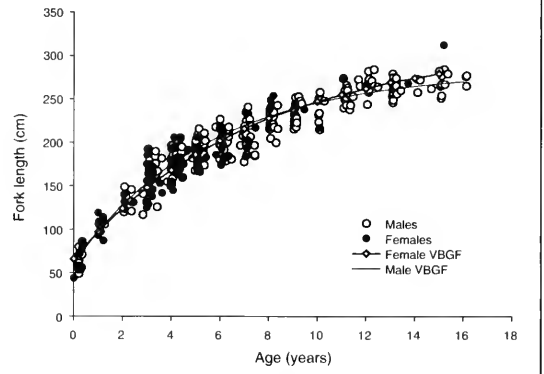

Figure 5

Prionace glauca growth curves and size-at-age data based on vertebral band counts. Von Bertalanffy growth function curves have been fitted to the data by sex.

Table 2

Von Bertalanffy growth function parameters and 95% confidence intervals calculated by using vertebral and tag-recapture methods for the blue shark (*Prionace glauca*). n = number of sharks in sample.

Method		L_∞	K	t_0	n
Vertebral	Combined	286.8	0.17	−1.43	411
	CI	±7.32	0.01	0.20	
	Male	282.3	0.18	−1.35	287
	CI	±7.15	0.02	0.23	
	Female	310.8	0.13	−1.77	119
	CI	±34.8	0.03	0.50	
Tag-recapture					
GROTAG	Combined	302.4	0.23	−0.69	43
Gulland and Holt (1959)	Combined	331.7	0.19	−0.77	18
	CI	±80.0	0.12		

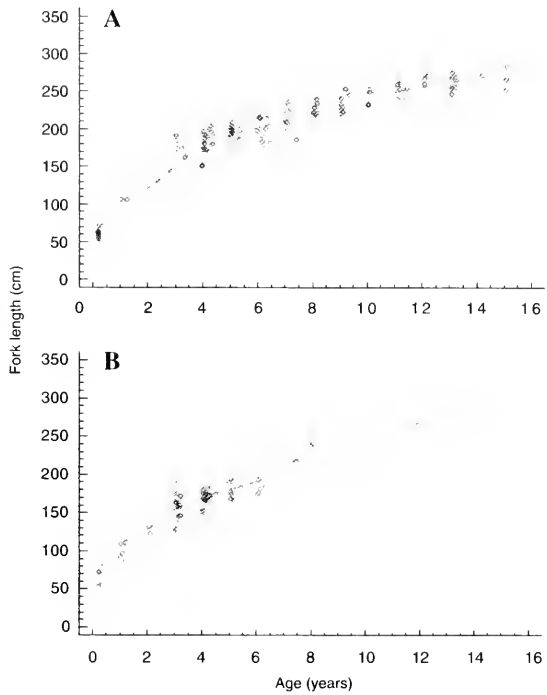

Figure 6

Prionace glauca growth curves and size-at-age data based on vertebral band counts. LOWESS (locally weighted regression smoothing) curves have been fitted to the data by sex: (**A**) males and (**B**) females.

308 juvenile blue sharks collected in the Azores were used to model early growth in this species. Silva et al. (1996) calculated an annual growth rate of 30 cm/yr for the first five years of life and aged the samples to seven years. More recently, Henderson et al. (2001) used 159 vertebrae sampled from blue sharks taken from oceanic waters off Ireland. Like the previous two studies, the size range of samples was limited to juvenile fish less than 191 cm FL and the estimated ages ranged from 1 to 6 years.

Stevens (1975), Silva et al. (1996), and Henderson et al. (2001) modeled blue shark growth with the VBGF. These curves are similar to each other (Silva et al., 1996, Henderson et al., 2001), yet show slower growth than the current study (Fig. 8) despite the fact that we used criteria similar to those of Stevens (1975) for vertebral interpretation. This result is not surprising in light of the fact that these three studies share common methods and sample biases. All three of the previous studies were performed on juvenile sharks from the eastern North Atlantic, the vast majority of which were between 100 and 184 cm FL. Because of the lack of samples from very small fish, one study (Silva et al., 1996) included vertebral readings from full-term embryos in the growth curve. It is well documented that embryonic growth is not comparable to postnatal growth (Casey et al., 1985; Pratt and Casey, 1990) and, therefore, embryos should not be included in a postnatal growth curve. The lack of large and small specimens in the calculations of these growth curves is particularly problematic because validation of the first growth increment is essential as it forms the basis of further counts. Moreover, the smallest and largest of the specimens are the most influential in the estimation of growth (Campana, 2001).

All three of the previous studies used similar whole centrum vertebral processing techniques and band count criteria, which would lead to corroborating counts, yet not necessarily to accurate counts (Campana, 2001). Whole vertebrae simply do not allow for high band resolution in older slower growing fish. Therefore, counts from whole

Table 3

Log-likelihood function values and parameter estimates for three growth models fitted to *Prionace glauca* tagging data using GROTAG (Francis 1988a). For a significant ($P<0.05$) improvement in fit, the introduction of one extra parameter must increase λ by at least 1.92 (Francis 1988a). * indicates fixed parameters. Model 3 shows 95% confidence intervals.

		Model		
Parameter	Symbol (unit)	1	2	3
Log likelihood		−197.29	−176.91	−174.61
Mean growth rates	g90 (cm/yr)	21.53	39.04	44.18 (35.37–54.33)
	g180 (cm/yr)	10.92	21.90	25.46 (19.29–33.41)
Growth variability	v	0*	0.46	0.27 (0.06–0.44)
Measurement error	s (cm)	1.06	1.37	5.39 (2.25–7.40)
	m (cm)	0*	0*	−2.03 (−5.37–2.10)
Outliers	p	0.83	0.28	0.18

vertebrae generally underestimate ages in larger individuals. The counts obtained in the three eastern Atlantic studies may be accurate because they are from juvenile sharks where vertebral bands are not compressed. In fact, juvenile growth from our size-at-age data overlaps the growth curves from these studies. However, the VBGF growth curves and resulting estimates of growth rate and age at maturity from the eastern Atlantic studies are suspect because of the lack of fish at the lower and upper end of the curve. The general lack of maximum-size fish in these studies resulted in the estimation of an artificially inflated L_∞ and, therefore, a lower growth rate (K) for this species (Table 5). Vertebral band deposition was assumed to be annual in these studies, but low sample sizes, sample bias, and lack of validation limits the utility of this previous work. In the current study, the use of sections and the adequate representation of the entire size range for both sexes yielded more accurate age estimates of 16 and 15 years for males and females, respectively.

Age and growth estimates of the blue shark in the North Pacific have been determined by using vertebral bands and length-frequency data (Cailliet et al., 1983; Tanaka et al., 1990; Nakano, 1994). Although the VBGF was used to model growth based on vertebral interpretation, the resulting parameters differed greatly among studies (Table 5). In general, Cailliet et al. (1983) reported a male growth rate similar to that in our present study, but a much smaller L_∞ (Table 5). For females, the latter holds true, but the growth coefficient is much higher (0.25) than reported in our study. Tanaka et al. (1990) found a similar growth trend in the western North Pacific with females growing faster than males, but the VBGF parameters were very different with higher L_∞ and lower K values. When compared to our study, the VBGF parameters of Tanaka et al. (1990) yield slower growth and a greater maximum size for males and a similar growth rate and smaller maximum size for females. Tanaka et al. (1990) attributed these intra- and inter-oceanic differences to the different methods used. More recently, Nakano (1994) sampled blue sharks across the North Pacific and derived VBGF growth parameters that were similar to those of Tanaka et al. (1990), but estimated growth rate to be slower than that of our present study. It is difficult to ascertain whether interoceanic differences in growth are real or are an artifact of method. Although Tanaka et al. (1990) presented data to support the latter within the North Pacific, the much larger maximum size attained by this species in the North Atlantic (Strasburg, 1958; Tanaka, 1984) cannot be overlooked in relation to interoceanic growth differences.

Table 4

Size at age (cm) for the blue shark (*Prionace glauca*) calculated from von Bertalanffy equations based on tag-recapture and vertebral methods.

	Vertebral method			Tag-recapture GROTAG
Age (yr)	combined	male	female	method
0	61.0	60.9	66.1	45
1	95.8	97.4	97.0	99
2	125.2	127.8	124.0	141
3	150.1	153.3	147.6	175
4	171.2	174.5	168.2	201
5	189.0	192.3	186.2	222
6	204.1	207.1	201.9	239
7	216.8	219.5	215.7	252
8	227.6	229.8	227.7	263
9	236.7	238.5	238.2	
10	244.4	245.7	247.4	
11	251.0	251.7	255.4	
12	256.5	256.8	262.4	
13	261.1	261.0	268.5	
14	265.1	264.5	273.9	
15	268.4	267.4	278.5	
16	271.3	269.9		

Longevity estimates for the blue shark indicate that they may live for 26 years when Taylor's (1958) method is employed. On the other hand, Fabens' (1965) method for >99% longevity produced an estimate of 20.7 years, which may be more realistic. The maximum age determined from vertebral band-pair counts was 16 and 15 years for males and females, respectively. An analysis of maximum times at liberty for tagged blue sharks supports the notion that this species does not live as long as previously reported for the North Atlantic. Of the 4967 blue sharks recaptured to date, 99% were at liberty for less than five years. The maximum times at liberty are 9.1 and 8.5 years, despite the 39-year history of the tagging program. The shark at liberty for 9.1 years was a male tagged at an estimated 122 cm FL; size at recapture was not reported. According to our growth curve, the shark was tagged at 1^+ years of age, which would correspond to a maximum age of 10^+ years at recapture. The shark at liberty for 8.5 years, also a male, was estimated to be 198 cm FL at tagging, which would correspond to 5^+ years of age. Therefore, at recapture, this fish would be a maximum age of 13.5 years, although its measured FL at recapture actually corresponds to 11 years on our growth curve. The largest long-term recapture was a male, 244 cm FL at tagging and 266 cm FL at recapture 6 years later. This would correspond to an estimated age of 10 years at tagging and 16 years at recapture, which falls well within the values of directly aged vertebrae (Fig. 5).

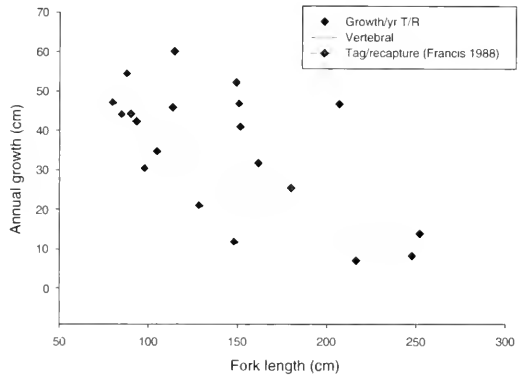

Figure 7

Comparison of the annual growth rates of the blue shark (*Prionace glauca*) derived from multiple aging methods.

The occurrence of sexual differences in growth is well documented in elasmobranchs; females usually grow larger than males (Cortés, 2000). Although the largest blue shark in our study was a 312-cm-FL female, there is little evidence that large females are highly abundant in the North Atlantic. Maximum size male and female specimens in our study, 284 cm FL and 312 cm FL, respectively, represented the largest reliably measured blue sharks from the North Atlantic, with the exception of a 320-cm-FL specimen (sex unspecified) examined by Bigelow and Schroeder (1953). Indeed, a thorough review of the literature reveals that although 288-cm-FL and 279-cm-FL females were reported by Gubanov and Grigor'yev (1975) from the Indian Ocean, males are consistently cited as being very much larger than females in the world's

Table 5

Van Bertalanffy growth function parameters and maximum age derived from vertebral bands in the blue shark (*Prionace glauca*) separated by location and sex.

Sex	Ocean	Region	n	L_∞	K	T_0	Max. age	Authors
Male	North Atlantic	All	287	282.3	0.18	−1.35	16	Current study
		East	112	309.0	0.12	−1.07	5	Silva et al. (1996)
	North Pacific	East	38	246.7	0.18	−1.11	9	Cailliet et al. (1983)
		West	43	308.1	0.10	−1.38	7	Tanaka et al. (1990)
		All	148	319.5	0.13	−0.76	10	Nakano (1994)
Female	North Atlantic	All	119	286.8	0.16	−1.56	15	Current study
		East	82	353.0	0.11	−1.04	6	Stevens (1975)
		East	170	382.0	0.09	−1.19	5	Silva et al. (1996)
	North Pacific	East	88	202.6	0.25	−0.80	9	Cailliet et al. (1983)
		West	152	254.1	0.16	−1.01	8	Tanaka et al. (1990)
		All	123	268.9	0.14	−0.85	10	Nakano (1994)
Combined	North Atlantic	All	411	285.4	0.17	−1.41	16	Current study
		East	336	284.0	0.14	−1.08	5	Silva et al. (1996)
		East	159	314.4	0.12	−1.33	6	Henderson et al. (2001)
	North Pacific	East	130	222.1	0.22	−0.80	9	Cailliet et al. (1983)

oceans (Suda, 1953; Tucker and Newnham, 1957; Aasen, 1966; McKenzie and Tibbo, 1964; Dragonik and Pelzarski, 1983; Stevens, 1984; Francis et al., 2001). Although the largest blue shark reported from the North Pacific was only 254 cm FL (Strasburg, 1958; Cailliet et al., 1983), individuals up to 331 cm FL have been reported from the South Pacific and the largest sharks were all males (Francis et al., 2001). The paucity of females exceeding 225 cm FL in the current study and the complete lack of these specimens in the Stevens (1975), Silva et al. (1996), and Henderson et al. (2001) samples indicate that these fish are rare, inhabit unknown or unfished areas of the Atlantic, or possibly avoid fishing gear. In our study, the VBGF parameters (Table 5) show that females theoretically attain larger sizes than males. However, the low number of large females in this and previous studies may indicate that natural mortality prevents them from attaining these lengths. The occurrence of severe lacerations on female blue sharks incurred during courtship is well documented (Stevens, 1974; Pratt, 1979). Although highly speculative, the long-term cumulative effects of such behavior may act as a source of increased mortality in females of the species, shortening their life-span and limiting the number that reach the larger sizes.

Through an integrated approach incorporating vertebral banding, OTC injection, and tagging data, it has been shown that the blue shark grows faster and lives a shorter life than previously thought in the North Atlantic. We believe that the validated vertebral interpretations generated during this study for the first four years of growth, combined with the vertebral counts and longevity estimates from tag-recapture data, provide vigorous estimates of age and growth for a large pelagic carcharhinid, the blue shark.

Acknowledgments

We thank the many people who contributed to the success of this study on research vessels, at recreational fishing tournaments, and on board private, chartered, and commercial fishing vessels. This study would not have been possible without the staff of the NMFS Apex Predators Program (Narragansett, RI) including Nancy Kohler, Pat Turner, and Ruth Briggs. We especially thank retired NMFS researchers Jack Casey and H. Wes Pratt for giving the senior author the tools necessary to initiate and complete this work. We are grateful to shark-aging pioneer Gregor Cailliet for his moral support and relentless pursuit of this publication. We are indebted to the thousands of fishermen who voluntarily tagged and returned sharks for the NMFS Cooperative Shark Tagging Program. This study was partially funded with support from the Sportfish Restoration Act.

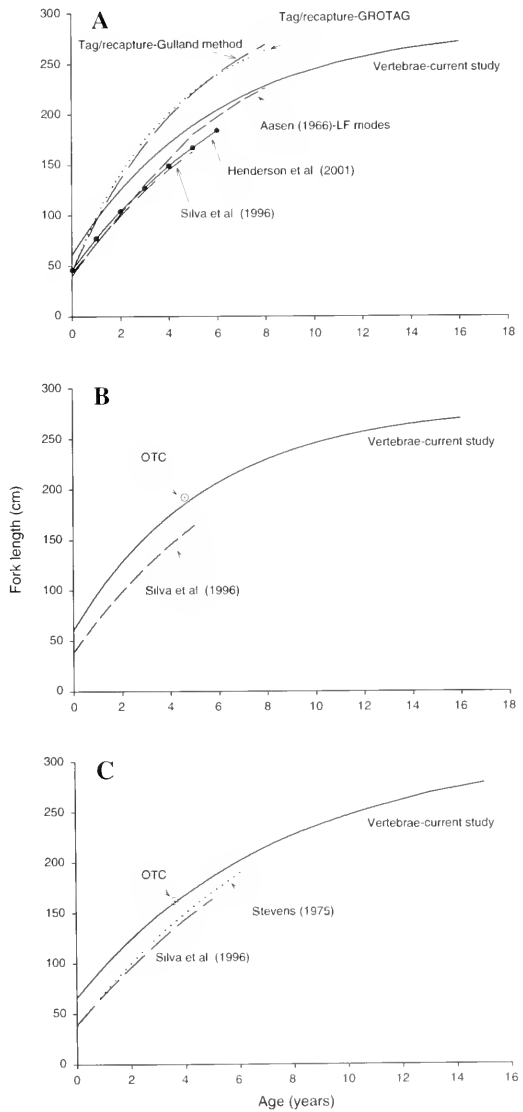

Figure 8

Von Bertalanffy growth curves generated from vertebral and recapture data for (**A**) sexes combined, (**B**) male, and (**C**) female *Prionace glauca*, as compared to OTC-injected recaptured blue sharks; included for comparison are the von Bertalanffy growth curves of other North Atlantic studies.

Literature cited

Aasen, O.
1966. Blahaien, *Prionace glauca* (Linnaeus, 1758). Fisken og Havet 1:1–15.

Bigelow, H.. B., and W. C. Schroeder.
1953. Fishes of the Gulf of Maine, 577 p. U.S. Dep. Int., Fish and Wildl. Serv., Fish. Bull. 53.

Cailliet, G. M.
1990. Elasmobranch age determination and verification: an updated review. *In* Elasmobranchs as living resources: advances in the biology, ecology, systematics, and status of the fisheries (H. L. Pratt Jr., S. H. Gruber, and T. Taniuchi, eds.), p. 157–165. U.S. Dep. Commer., NOAA Tech. Rep. 90.

Cailliet, G. M., L. K. Martin, J. T. Harvey, D. Kusher, and B. A. Welden.
1983. Preliminary studies on the age and growth of blue, *Prionace glauca*, common thresher, *Alopias vulpinus*, and shortfin mako, *Isurus oxyrinchus*, sharks from California waters. *In* Proceedings of the international workshop on age determination of oceanic pelagic fishes: tunas, billfishes, and sharks (E. D. Prince and L. M. Pulos, eds.), p. 179–188. U.S. Dep. Commer., NOAA Tech. Rep. NMFS 8.

Campana, S. E.
2001. Accuracy, precision and quality control in age determination, including a review of the use and abuse of age validation methods. J. Fish. Biol. 59:197–242.

Campana, S. E., M. C. Annand, and J. I. McMillan.
1995. Graphical and statistical methods for determining the consistency of age determinations. Trans. Amer. Fish. Soc. 124:131–138.

Carey, F. G., and J. Scharold.
1990. Movements of blue sharks (*Prionace glauca*) in depth and course. Mar. Biol. 106:329–342.

Casey, J. G.
1982. Blue shark, *Prionace glauca*. Species synopsis. *In* Ecology of the Middle Atlantic Bight fish and shellfish—Monograph 15—fish distribution (M.D. Grosslein and T. Azarovitz, eds.), p. 45–48. MESA New York Bight Atlas, NY Sea Grant, Albany, NY.
1985. Trans-Atlantic migrations of the blue shark: a case history of cooperative shark tagging. *In* World angling resources and challenges; proceedings of the first world angling conference (R. H. Stroud, ed.), p. 253–267. Int. Game Fish Assoc., Ft. Lauderdale, FL.

Casey, J. G., H. L. Pratt Jr., and C. E. Stillwell.
1985. Age and growth of the sandbar shark (*Carcharhinus plumbeus*) from the western North Atlantic. Can. J. Fish. Aquat. Sci. 42(5):963–975.

Castro, J. I., C. M. Woodley, and R. L. Brudek.
1999. A preliminary evaluation of the status of shark species. FAO Fisheries Technical Paper 380, 72 p. FAO, Rome.

Compagno, L. J. V.
1984. FAO species catalogue. Sharks of the world. An annotated and illustrated catalogue of shark species known to date. Part 1. Hexanchiformes to Lamniformes. FAO Fish Synop. 125, vol. 4, 250 p. FAO, Rome.

Connett, S.
1987. Blue sharks studied in the eastern Atlantic. *In* The shark tagger: 1987 summary (J. Casey, H. L. Pratt Jr., N. E. Kohler, and C. E. Stillwell, eds.), p. 8–10. Newsletter of the Cooperative Shark Tagging Program. U.S. Dep. Commer., NOAA, NMFS, Narragansett, RI.

Cortés, E.
2000. Life history patterns and correlations in sharks. Rev. Fish. Sci. 8(4):299–344.
2002. Catches and catch rates of pelagic sharks from the northwestern Atlantic, Gulf of Mexico, and Caribbean. Col. Vol. Sci. Pap. ICCAT 54(4):1164–1181.

Dragonik, B, and W. Pelzarski.
1983. The occurrence of the blue shark, *Prionace glauca* (L.), in the North Atlantic. Rep. Sea Fish. Inst. 19:63–77.

Fabens, A. J.
1965. Properties and fitting of the von Bertalanffy growth curve. Growth 29:265–289.

Ferreira, B. P., and C. M. Vooren.
1988a. Age, growth, and structure of the vertebrae in the school shark *Galeorhinus galeus* (Linnaeus, 1758) from southern Brazil. Fish. Bull. 89:19–31.

Francis, R. I. C. C.
1988a. Maximum likelihood estimation of growth and growth variability from tagging data. NZ J. Mar. Freshwater Res. 22:43–51.
1988b. Are growth parameters estimated from tagging and age-length data comparable? Can. J. Fish. Aquat. Sci. 45: 936–942.

Francis, M. P., L. H. Griggs, and S. J. Baird.
2001. Pelagic shark bycatch in the New Zealand tuna longline fishery. Mar. Freshwater Res. 52(2):165–178.

Gubanov, Ye. P., and V. N. Grigor'yev.
1975. Observations on the distribution and biology of the blue shark *Prionace glauca* (Carcharhinidae) of the Indian Ocean. J. Ichthyol. 15:37–43.

Gulland, J. A., and S. J. Holt.
1959. Estimation of growth parameters for data at unequal time intervals. J. Cons. Int. Explor. Mer 25:47–49.

Henderson, A. C., K. Flannery, and J. Dunne.
2001. Observations on the biology and ecology of the blue shark in the North-east Atlantic. J. Fish. Biol. 58: 1347–1358.

Hoenig, J. M., and S. H. Gruber.
1990. Life history patterns in the elasmobranchs: implications for fisheries management. *In* Elasmobranchs as living resources: advances in the biology, ecology, systematics, and status of the fisheries (H. L. Pratt Jr., S. H. Gruber, and T. Taniuchi, eds), p. 1–16. U.S. Dep. Commer., NOAA Tech. Rep. 90.

ICCAT (International Commission for the Conservation of Atlantic Tunas).
2002. ICCAT data preparatory meeting for Atlantic shark stock assessment. Col. Vol. Sci. Pap. ICCAT, 54(4): 1064–1106.

Kohler, N. E.
1987. Aspects of the feeding ecology of the blue shark in the western North Atlantic. Ph.D. diss., 163 p. Univ. Rhode Island, Kingston, RI.

Kohler, N. E., J. G. Casey, and P. A. Turner.
1987. Length-weight relationships for 13 species of sharks from the western North Atlantic. Fish. Bull. 93:412–418.

Kohler, N. E., P. A. Turner, J. J. Hoey, L. J. Natanson, and R. Briggs.
2002. Tag and recapture data for three pelagic shark species: blue shark (*Prionace glauca*), shortfin mako (*Isurus oxyrinchus*), and porbeagle (*Lamna nasus*) in the North Atlantic Ocean. Col. Vol. Sci. Pap. ICCAT 54(4):1231–1260.

Lessa, R., F. M. Santana, and R. Paglerani.
1999. Age, growth and stock structure of the oceanic whitetip shark, *Carcharhinus longimanus*, from the southwestern equatorial Atlantic. Fish. Res. 42:21–30.

McKenzie, R. A., and S. N. Tibbo.
1964. A morphometric description of the blue shark (*Prionace glauca*) from the Canadian Atlantic waters. J. Fish. Res. Board Can. 21:865–866.
Nakano, H.
1994. Age, reproduction and migration of blue shark in the North Pacific. Bull. Nat. Res. Inst. Far Seas Fish. 31:141–256.
Natanson, L. J.
1984. Aspects of age, growth, and reproduction of the Pacific angel shark, *Squatina californica*, off Santa Barbara, California. M.A. thesis, 71 p. San Jose State Univ., San Jose, CA.
Natanson, L. J., J. G. Casey, and N. E. Kohler.
1995. Age and growth of the dusky shark, *Carcharhinus obscurus*, in the western North Atlantic. Fish. Bull. 93: 116–126.
Natanson, L. J., and N. E. Kohler.
1996. A preliminary estimate of age and growth of the dusky shark *Carcharhinus obscurus* from the south-west Indian Ocean, with comparisons to the western North Atlantic. S. Afr. J. Mar. Sci. 17:217–224.
Natanson, L. J., J. J. Mello, and S. E. Campana.
2002. Validated age and growth of the porbeagle shark, *Lamna nasus*, in the western North Atlantic. Fish. Bull. 100:266–278.
NMFS (National Marine Fisheries Service).
1999. Final fishery management plan for Atlantic tunas, swordfish, and sharks., 1162 p. Highly Migratory Species Management Division, Silver Spring, MD.
Parker, H. W., and F. C. Stott.
1965. Age, size and vertebral calcification in the basking shark, *Cetorhinus maximus* (Gunnerus). Zool. Meded. 40(34):305–319.
Pratt, H. L., Jr.
1979. Reproduction in the blue shark, *Prionace glauca*. Fish. Bull. 77:445–470.
Pratt, H. L., Jr., and J. G. Casey.
1983. Age and growth of the shortfin mako, *Isurus oxyrinchus*, using four methods. Can. J. Fish. Aquat. Sci. 40(11): 1944–1957.
1990. Shark reproductive strategies as limiting factors in directed fisheries, with a review of Holden's method of estimating growth parameters. *In* Elasmobranchs as living resources: advances in the biology, ecology, systematics, and status of the fisheries (H. L. Pratt Jr., S. H. Gruber, and T. Taniuchi, eds), p. 97–110. NOAA Tech. Rep. 90.
Sciarrotta, T. C., and D. Nelson.
1977. Diel behavior of the blue shark, *Prionace glauca*, near Santa Catalina Island, California. Fish. Bull 73:519–528.
Seki, T., T. Taniuchi, H. Nakano, and M. Shimizu.
1998. Age, growth and reproduction of the oceanic whitetip shark from the Pacific Ocean. Fish. Sci. 64(1):14–20.
Silva, A. A., H. M. Silva, and K. Erzini.
1996. Some results on the biology of the blue shark, *Prionace glauca*, in the North Atlantic based on data from a research cruise of the R/V *Arquipelago* in Azorean waters: a summary paper, 9 p. Universidade dos Acores, Horta, Acores, Portugal.
Simpfendorfer, C. A.
2000. Growth rates of juvenile dusky sharks, *Carcharhinus obscurus* (Lesueur, 1818), from southwestern Australia estimated from tag-recapture data. Fish. Bull. 98:811–822.
Simpfendorfer, C. A., R. B. McAuley, J. Chidlow, and P. Unsworth.
2002. Validated age and growth of the dusky shark, *Carcharhinus obscurus*, from Western Australian waters. Mar. Freshwater Res. 53:567–573.
Skomal, G. B.
1990. Age and growth of the blue shark, *Prionace glauca*, in the North Atlantic. M.S. thesis, 82 p. Univ. Rhode Island, Kingston, RI.
Stevens, J. D.
1973. Stomach contents of the blue shark (*Prionace glauca* L.) of southwest England. J. Mar Biol. Assoc. U.K. 53: 357–361.
1974. The occurrence and significance of tooth cuts on the blue shark (*Prionace glauca* L.). J. Mar. Biol. Assoc. U.K. 54:373–378.
1975. Vertebral rings as a means of age determination in the blue shark (*Prionace glauca* L.). J. Mar. Biol. Assoc. U.K. 55:657–665.
1976. First results of shark tagging in the northeast Atlantic, 1972–1975. J. Mar. Biol. Assoc. U.K. 56: 929–937.
1984. Biological observations on sharks caught by sport-fishermen off New South Wales. Aust. J. Mar. Freshwater Res. 35:573–590.
1990. Further results from a tagging study of pelagic sharks in the Northeast Atlantic. J. Mar. Biol. Assoc. U.K. 70: 707–720.
Strasburg, D. W.
1958. Distribution, abundance, and habits of pelagic sharks in the central Pacific Ocean. Fish. Bull. 58:335–361.
Suda, A.
1953. Ecological study of the blue shark (*Prionace glauca* Linne'). South Sea Area Fish Res. Lab. Rep. 26:1–11.
Tanaka, S.
1984. Present status of fisheries biology. *In* Elasmobranchs as fishery resources (T. Taniuchi and M. Suyama, eds.), p. 46–59. Jpn. Soc. Sci. Fish., Fish. Ser. 49.
Tanaka, S., G. M. Cailliet, and K. G. Yudin.
1990. Differences in growth of the blue shark, *Prionace glauca*: technique or population? *In* Elasmobranchs as living resources: advances in the biology, ecology, systematics, and status of the fisheries (H. L. Pratt Jr., S. H. Gruber, and T. Taniuchi, eds.), p. 177–187. U.S. Dep. Commer., NOAA Tech. Rep. 90.
Taylor, C. C.
1958. Cod growth and temperature. J. Cons. Int. Explor. Mer 23:366–370.
Tricas, T.
1978. Relationships of the blue shark, *Prionace glauca*, and its prey species near Santa Catalina Island, California. Fish. Bull. 77:175–182.
Tucker, D. W., and C. T. Newnham.
1957. The blue shark *Prionace glauca* breeds in British seas. Ann. Mag. Nat. Hist., Series 12, 10:673–688.
von Bertalanffy, L.
1938. A quantitative theory of organic growth (inquiries on growth laws II). Hum. Biol. 10:181–213.
Walter, J. P., and D. A. Ebert.
1991. Preliminary estimates of age of the bronze whaler *Corcharhinus brachyurus* (Chondrichthyes: Carcharhinidae) from southern Africa, with a review of some life history parameters. S. Afr. J. Mar. Sci 10:37–44.
Wintner, S. P., and G. Cliff.
1995. Age and growth determination of the blacktip shark, *Carcharhinus limbatus*, from the east coast of South Africa. Fish. Bull. 94:135–144.
Wintner, S. P., and S. F. J. Dudley.
2000. Age and growth estimates for the tiger shark, *Galeocerdo cuvier*, from the east coast of Africa. Mar. Freshwater Res. 51:43–53.

Genetic analysis of juvenile coho salmon (*Oncorhynchus kisutch*) off Oregon and Washington reveals few Columbia River wild fish*

David J. Teel
Donald M. Van Doornik
David R. Kuligowski

Conservation Biology Division
Northwest Fisheries Science Center
2725 Montlake Boulevard East
Seattle, Washington 98112-2097
Present address (for D. J. Teel): Manchester Research Laboratory
7305 Beach Drive E.
Port Orchard, Washington 98366
Email address (for D. J. Teel): David.Teel@NOAA.gov

W. Stewart Grant

P.O. Box 240104
Anchorage, Alaska 99524-0104

Abstract—Little is known about the ocean distributions of wild juvenile coho salmon off the Oregon-Washington coast. In this study we report tag recoveries and genetic mixed-stock estimates of juvenile fish caught in coastal waters near the Columbia River plume. To support the genetic estimates, we report an allozyme-frequency baseline for 89 wild and hatchery-reared coho salmon spawning populations, extending from northern California to southern British Columbia. The products of 59 allozyme-encoding loci were examined with starch-gel electrophoresis. Of these, 56 loci were polymorphic, and 29 loci had $P_{0.95}$ levels of polymorphism. Average heterozygosities within populations ranged from 0.021 to 0.046 and averaged 0.033. Multidimensional scaling of chord genetic distances between samples resolved nine regional groups that were sufficiently distinct for genetic mixed-stock analysis. About 2.9% of the total gene diversity was due to differences among populations within these regions, and 2.6% was due to differences among the nine regions. This allele-frequency data base was used to estimate the stock proportions of 730 juvenile coho salmon in offshore samples collected from central Oregon to northern Washington in June and September-October 1998–2000. Genetic mixed-stock analysis, together with recoveries of tagged or fin-clipped fish, indicates that about one half of the juveniles came from Columbia River hatcheries. Only 22% of the ocean-caught juveniles were wild fish, originating largely from coastal Oregon and Washington rivers (about 20%). Unlike previous studies of tagged juveniles, both tag recoveries and genetic estimates indicate the presence of fish from British Columbia and Puget Sound in southern waters. The most salient feature of genetic mixed stock estimates was the paucity of wild juveniles from natural populations in the Columbia River Basin. This result reflects the large decrease in the abundances of these populations in the last few decades.

Manuscript approved for publication 15 January 2003 by Scientific Editor.
Manuscript received 4 April 2003 at NMFS Scientific Publications Office.
Fish. Bull. 101:640–652 (2003).

Nearshore and riverine distributions of maturing Pacific salmon (*Oncorhynchus* spp.) are well known, largely because of the prevalence of salmon fisheries and the tremendous amount of information gathered to manage these fisheries. Out-migration timings and abundances of smolts in streams as they migrate to the sea are also well known, but information on the distributions and stock origins of wild juveniles in marine waters has been limited by two factors. The first is that a large amount of effort is needed to sample marine-phase juveniles, which generally occur at low densities (Godfrey, 1965; Hartt and Dell, 1986; Orsi et al., 2000). The second factor is that stock origins have been determined only for coded-wire–tagged (CWT) hatchery fish (e.g. Pearcy and Fisher, 1988; Orsi et al., 2000). Because only small proportions of hatchery juveniles are tagged, samples of ocean-caught salmon are largely a mixture of hatchery and wild fish of unknown stock origins. Genetic mixed-stock analysis, although used routinely to estimate the stock compositions of mature returning salmon (e.g. Milner et al., 1985; Shaklee et al., 1999; Beacham et al., 2001), has not been fully exploited to estimate stock origins of immature salmon (but see Guthrie et al., 2000). The study we describe here is the first to use genetic data to estimate the stock origins of ocean mixtures of juvenile coho salmon (*O. kisutch*).

One goal of our study was to create a baseline of allelic frequencies in spawning populations of coho salmon throughout the Pacific Northwest and California. These data were previously used by the National Marine Fisheries Service (NMFS) to define evolutionarily significant units (ESUs) for evaluation under the Endangered Species Act (Johnson et al., 1991; Weitkamp et al., 1995). In the present study, we examine levels of variability among populations and use mixed-stock simulations to assess the usefulness of such a data set as a baseline for genetic mixed-stock analysis. A second goal was to use this baseline of population data to estimate the stock compositions of juvenile coho salmon collected in the early and late summers of 1998, 1999, and 2000 off the Oregon and Washington coasts by the NMFS (Emmett and Brodeur, 2000). We use a standard approach to genetic mixed-stock analysis that yields proportional estimates of stock origin of fish in a mixed-stock sample (e.g., Pella and Milner, 1987). We compare early and

* Contribution 388 to the U.S. GLOBEC program, Woods Hole Oceanographic Institute, Woods Hole, MA 02543.

late summer samples to detect seasonal shifts in stock compositions along the coast and make comparisons with earlier tag-recovery studies to search for decadal shifts in the marine distributions of particular stocks. Recent efforts at Pacific Northwest hatcheries to mark the majority of their releases of coho salmon with a fin clip provide new opportunities to estimate proportions of hatchery and wild coho salmon in ocean samples (Beamish et al., 2000; Lawson and Comstock, 2000). We therefore report genetic estimates for hatchery-marked and unmarked fish in ocean samples and use these estimates to identify hatchery and wild population origins of ocean juvenile coho salmon.

Materials and methods

To establish an allele-frequency baseline, populations of coho salmon were sampled from 89 hatcheries, streams, and rivers between 1984 and 1999 (Fig. 1, Table 1). Samples of skeletal muscle, eye, liver, and heart tissues were collected from adults during spawning operations in hatcheries or from whole juvenile fish in hatchery rearing ponds. All hatchery broods sampled were the progeny of al least 50 adult fish. Wild juveniles were sampled in natal streams and rivers by electroshocking. Wild adult fish were sampled in spawning areas by gaffing and dip-netting.

Samples of juvenile coho salmon in marine waters were collected during NMFS coastal pelagic trawl surveys (Emmett and Brodeur, 2000). Trawls consisted of one-half-hour long surface tows with a 264 Nordic rope trawl along nine transects perpendicular to shore ranging from La Push, Washington (47°55′N) to Cape Perpetua, Oregon (44°15′N) (Fig. 1). Sampling stations began 1–5 nautical miles offshore and continued, in about 5 nautical-mile (nmi) increments, to about 30 nmi offshore. Marine juveniles were sampled 16–24 June and 21–30 September 1998, 16–24 June and 21 September–1 October 1999, and 17–25 June and 19–24 September 2000. Fish were measured and examined for the presence of fin clips and coded wire tags (CWTs). Juveniles in their first ocean summer were separated from older coho salmon by length by using a modification of the criteria of Pearcy and Fisher (1990). Fish with fork lengths less than 330 mm (June) and 450 mm (September–October) were considered to be juveniles in their first year in the ocean. Fish with CWTs, and therefore of known brood year, provided supporting evidence for these criteria with the assumption that growth of hatchery and wild fish was similar.

Tissue samples or whole juvenile fish were frozen on dry ice or in liquid nitrogen and stored at −80°C prior to electrophoretic analysis. We used the methods of Aebersold et al. (1987) for sample preparation and horizontal starch-gel protein electrophoresis. Electrophoretic conditions for 30 enzymes, for which we obtained reliable and interpretable data for 59 loci, are reported in an appendix that can be retrieved at the Northwest Fisheries Science Center website [http://www.nwfsc.noaa.gov]. Guidelines by Utter et al. (1987) were used to infer genotypes from banding patterns. Locus and allelic nomenclature follows Shaklee et al. (1990).

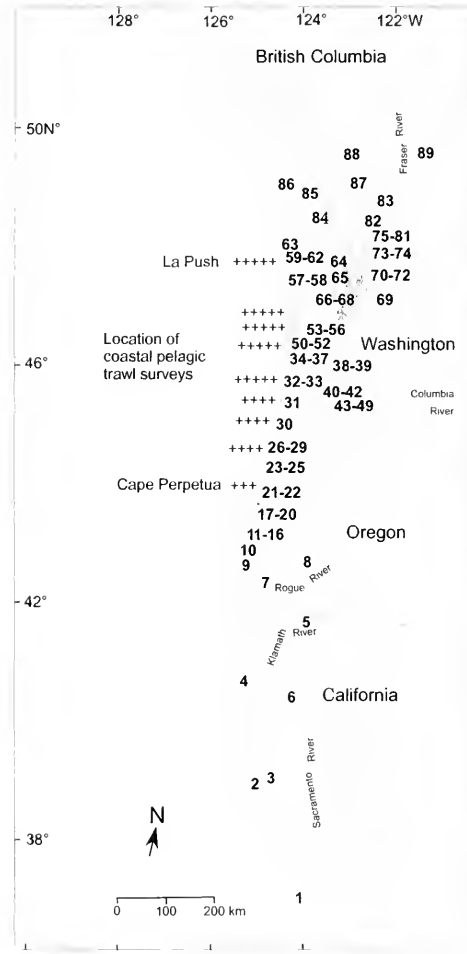

Figure 1

Locations of ocean sampling transect lines (+) and 89 coho salmon populations in California, Oregon, Washington, and British Columbia. Numbers correspond to population names in Table 1.

Genotypic frequencies of polymorphic loci for each baseline sample were examined for departures from expected Hardy-Weinberg proportions with a Fisher's exact test (Guo and Thompson, 1992) by using GENEPOP version 3.1 (Raymond and Rousset, 1995). Hardy-Weinberg tests were performed on isoloci (comigrating protein products of duplicated loci) following Waples (1988).

We estimated allelic frequencies for each sample. Allelic frequencies for isoloci were calculated as mean frequen-

Table 1

Sample information and indices of genetic variability for coho salmon from the Pacific Northwest and California. Map codes refer to Figure 1. Indices of genetic variability are $\%P_{0.95}$ = percentage of $P_{0.95}$ loci and H = heterozygosity.

Source Region and map code	Year sampled	Number of fish	$\%P_{0.95}$	H
California coast				
1 Scott Creek	1994	21	12.5	0.039
2 Little River	1994	27	14.3	0.040
3 Warm Springs Hatchery	1994, 1994	160	16.1	0.041
4 Mad River Hatchery	1994	120	17.9	0.040
Klamath River to Cape Blanco				
5 Iron Gate Hatchery	1994	120	9.0	0.021
6 Trinity Hatchery	1984, 1994	218	9.0	0.028
7 Rogue River (Illinois River, Greyback Creek)	1993	40	7.2	0.022
8 Cole Rivers Hatchery, stock no. 52 (Rogue River)	1993	100	9.0	0.030
9 North Fork Elk and Elk Rivers	1993	32	7.2	0.021
Oregon coast				
10 Sixes River (Crystal and Edson Creeks)	1993	44	7.2	0.026
11 New River (Bether and Morton Creeks)	1993	62	10.7	0.034
12 Butte Falls Hatchery, stock no. 44 (Coquille River)	1993	100	9.0	0.036
13 Cole Rivers Hatchery, stock no. 37 (South Fork Coos River)	1993	129	10.7	0.034
14 Coos River (Millicoma River and Marlow Creek)	1993, 1997	50	12.5	0.033
15 Butte Falls Hatchery, Eel River stock no. 63	1993	100	7.2	0.032
16 Ten Mile Lake	1992	56	7.2	0.030
17 Rock Creek Hatchery, stock no. 55 (Umpqua River)	1993	100	7.2	0.029
18 North Umpqua River (Williams Creek)	1993, 1997	67	7.2	0.025
19 Butte Falls Hatchery, stock no. 18 (Umpqua River)	1993	100	7.2	0.027
20 Smith River (Halfway Creek)	1993	40	10.7	0.034
21 Fall Creek Hatchery, stock no. 113 (Tahkenitch River)	1993	100	7.2	0.030
22 Siuslaw River	1996	51	9.0	0.029
23 Fall Creek Hatchery, stock no. 31 (Alsea River)	1993	100	14.3	0.040
24 Fall Creek Hatchery, stock no. 43 (Alsea River)	1993	95	9.0	0.037
25 Alsea River	1996	62	10.7	0.031
26 Beaver Creek	1993	62	9.0	0.035
27 Yaquina River	1996	54	12.5	0.043
28 Salmon River Hatchery, stock no. 33 (Siletz River)	1993	100	12.5	0.041
29 Siletz River (Forth of July, Sunshine, and Buck Creeks)	1993	50	10.7	0.033
30 Salmon River Hatchery, stock no. 36 (Salmon River)	1993	100	10.7	0.037
31 Trask River Hatchery, stock no. 34 (Trask River)	1992, 1993	220	16.1	0.039
32 Nehalem River Hatchery, stock no. 99 (Nehalem River)	1992	80	12.5	0.045
33 Nehalem River Hatchery, stock no. 32 (Nehalem River)	1993	100	14.3	0.044
Columbia River				
34 Lewis and Clark River	1991, 1993	36	12.5	0.038
35 Big Creek Hatchery	1991	80	12.5	0.040
36 Grays River Hatchery	1987, 1991	200	7.2	0.033
37 Clatskanie River (Carcus Creek)	1991, 1992, 1996	113	10.7	0.033
38 Cowlitz Hatchery early-run	1991	80	9.0	0.027
39 Cowlitz Hatchery late-run	1991, 1992	180	7.2	0.031
40 Scappoose River (Siercks, Raymond, and Milton Creeks)	1991	44	14.3	0.041
41 Lewis River Hatchery early-run	1991	80	5.4	0.027
42 Lewis River Hatchery late-run	1991	80	12.5	0.032
43 North Fork Clackamas River early-run	1998[a]	48	16.1	0.036
44 North Fork Clackamas River late-run	1999[a]	45	14.3	0.028
45 Eagle Creek Hatchery	1991, 1992	180	7.2	0.037

continued

Table 1 (continued)

Source Region and map code	Year sampled	Number of fish	$\%P_{0.95}$	H
46 Sandy River Hatchery	1991, 1992	180	10.7	0.046
47 Sandy River	1991, 1992, 1996	124	10.7	0.043
48 Bonneville Hatchery	1991, 1992	180	10.7	0.043
49 Willard Hatchery	1991	80	7.2	0.032
South Washington coast				
50 Naselle River Hatchery	1991	100	9.0	0.029
51 Nemah River Hatchery	1991	100	10.7	0.029
52 Willapa River Hatchery	1991	100	9.0	0.031
53 Chehalis River (Stillman Creek)	1995	71	9.0	0.026
54 Chehalis River (Satsop River, Bingham Creek)	1995	98	10.7	0.028
55 Bingham Creek Hatchery	1991,[1] 1992,[1] 1995	180	9.0	0.027
56 Chehalis River (Hope Creek)	1994, 1995, 1996	171	9.0	0.030
North Washington coast				
57 Queets River	1995	99	9.0	0.028
58 Clearwater River	1995	100	7.2	0.029
59 Bogachiel River	1987	80	10.7	0.030
60 Sol Duc Hatchery Summer Run	1994[1]	80	7.2	0.030
61 Sol Duc River Summer Run	1995	120	10.7	0.030
62 Sol Duc Hatchery Fall Run	1995[1]	80	9.0	0.032
63 Hoko River	1987	96	9.0	0.033
Puget Sound and Hood Canal				
64 Dungeness Hatchery	1987	80	12.5	0.037
65 Quilcene Hatchery	1994[1]	100	9.0	0.025
66 North Fork Skokomish River	1994,[1] 1995[1]	126	7.2	0.030
67 Dewatto River	1994,[1]1995,[1] 1996[1]	169	9.0	0.028
68 Minter Creek Hatchery	1992,[1] 1995[1]	80	9.0	0.035
69 Soos Creek Hatchery	1994,[1] 1995, 1996	680	9.0	0.034
70 Snoqualmie River (Harris Creek)	1987	120	7.2	0.034
71 Snoqualmie River (Grizzly Creek)	1994,[1] 1995,[1] 1996[1]	215	7.2	0.030
72 North Fork Skykomish River (Lewis Creek)	1995[1]	102	9.0	0.032
73 North Fork Stillaguamish River (Fortson Creek)	1987, 1989 [1]	200	9.0	0.031
74 North Fork Stillaguamish River (Mcgovern Creek)	1987	40	10.7	0.032
75 Upper Skagit River	1993	127	9.0	0.033
76 Skagit River (Carpenter Creek)	1993	139	9.0	0.032
77 Skagit River (West Fork Nookachamps Creek)	1987, 1993	220	9.0	0.035
78 Skagit River (Baker River)	1992 [1]	303	10.7	0.036
79 Skagit River (Suiattle River, All Creek)	1987, 1993	200	10.7	0.032
80 Skagit River (Upper Sauk River)	1992, 1993	200	9.0	0.034
81 Skagit River (Upper Cascade River)	1992, 1993	224	9.0	0.031
82 Samish River (Ennis Creek)	1994,[1] 1995,[1] 1996 [1]	167	9.0	0.035
British Columbia				
83 Chilliwack River Hatchery	1984	100	10.7	0.034
84 Cowichan River Hatchery	1984	80	9.0	0.036
85 Big Qualicum Hatchery	1989,[1] 1991	180	10.7	0.037
86 Robertson Creek Hatchery	1984	100	9.0	0.030
87 Capilano Hatchery	1989,[1] 1991	200	12.5	0.038
88 Squamish River Hatchery	1988[1]	98	7.2	0.035
Upper Fraser River				
89 Spius River Hatchery	1987	200	10.7	0.035
Mean			10.0	0.033

[1] Sample taken from adult fish. All other samples were from juvenile fish.

Table 2

Enzymes and study results for 59 loci in samples of 89 coho salmon populations from the Pacific Northwest and California.

Enzyme or protein name	Enzyme commission number	Locus abbrev.	Number of populations polymorphic	Range of common allele frequency
Aspartate aminotransferase	2.6.1.1	sAAT-1,2*	36	1.000–0.966
		sAAT-3*	1	1.000–0.956
		sAAT-4*	71	1.000–0.839
Adenosine deaminase	3.5.4.4	ADA-1*	34	1.000–0.924
		ADA-2*	15	1.000–0.929
Aconitate hydratase	4.2.1.3	mAH-1*	2	1.000–0.992
		mAH-2*	22	1.000–0.919
		mAH-3*	3	1.000–0.944
		sAH*	60	1.000–0.849
Adenylate kinase	2.7.4.3	AK*	4	1.000–0.993
Alanine aminotransferase	2.6.1.2	ALAT*	12	1.000–0.958
Creatine kinase	2.7.3.2	CK-A1*	8	1.000–0.971
		CK-A2*	22	1.000–0.919
		CK-C1*	4	1.000–0.983
		CK-C2*	9	1.000–0.972
		CK-B*	1	1.000–0.999
Esterase	3.1.-.-	EST-1*	85	1.000–0.652
Fructose-bisphosphate aldolase	4.2.1.13	FBALD-3*	1	1.000–0.996
		FBALD-4*	14	1.000–0.962
Formaldehyde dehydrogenase (glutathione)	1.2.1.1	FDHG*	33	1.000–0.954
Fumarate hydratase	4.2.1.2	FH*	43	1.000–0.835
b-N-Acetylgalactosaminidase	3.2.1.53	bGALA*	89	0.889–0.357
Glyceraldehyde-3-phosphate dehydrogenase	1.2.1.12	GAPDH-2*	64	1.000–0.713
		GAPDH-3*	26	1.000–0.867
		GAPDH-4*	9	1.000–0.975
		GAPDH-5*	0	1.000–1.000
Glucose-6-phosphate isomerase	5.3.1.9	GPI-A*	17	1.000–0.906
		GPI-B1*	1	1.000–0.962
		GPI-B2*	47	1.000-0.815
Glutathione reductase	1.6.4.2	GR*	6	1.000–0.988

continued

cies over both loci and treated as a single tetrasomic locus. Following the recommendations of Waples (1990), allelic frequencies of samples taken in different years from the same location were combined. In general, little temporal allele-frequency variation was detected in coho salmon populations sampled over years (Van Doornik et al., 2002; present study). Levels and patterns of genetic variation within and between populations were estimated with 56 polymorphic loci (Table 2). Average expected heterozygosity per locus (isoloci excluded) for each population was calculated by using an unbiased estimator (Nei, 1978). The proportion of $P_{0.95}$ loci was computed for each population, in which a locus was considered to be polymorphic if the frequency of the most common allele was ≤0.95. Chord distances (Cavalli-Sforza and Edwards, 1967) were computed between all pairs of populations with BIOSYS (Swofford and Selander, 1981), and relationships among populations were depicted with multidimensional scaling (MDS, NTSYS-PC, Exeter Software, NY). Allele-frequency variation among baseline populations was partitioned (Chakraborty et al., 1982) into two geographic levels: 1) populations within regions; and 2) among regions (Table 1). These regions were delimited by geography and by genetic groupings in the MDS analyses.

We used the maximum likelihood procedures of Pella and Milner (1987) and the Statistical Package for Analyzing Mixtures (SPAM; Debevec et al., 2000) to estimate stock contributions to simulated and actual mixtures of coho salmon. Estimates were made by using 56 polymorphic loci (Table 2) and 89 baseline populations, except for analysis of marked (hatchery) fish where only hatchery populations were used (Table 1). Allocations to individual baseline populations were then summed to estimate contributions of regional stock groups (Pella and Milner, 1987). Average mix-

Table 2 (continued)

Enzyme or protein name	Enzyme commission number	Locus abbrev.	Number of populations polymorphic	Range of common allele frequency
Isocitrate dehydrogenase	1.1.1.42	mIDHP-1*	4	1.000–0.964
		mIDHP-2*	11	1.000–0.799
		sIDHP-1*	11	1.000–0.948
		sIDHP-2*	29	1.000–0.851
Lactate dehydrogenase	1.1.1.27	LDH-A1*	7	1.000–0.700
		LDH-A2*	2	1.000–0.995
		LDH-B1*	18	1.000–0.942
		LDH-B2*	20	1.000–0.956
		LDH-C*	0	1.000–1.000
Malate dehydrogenase	1.1.1.37	sMDH-A1,2*	35	1.000–0.976
		sMDH-B1,2*	21	1.000–0.947
Mannose-6-phosphate isomerase	5.3.1.8	MPI*	41	1.000–0.897
α-Mannosidase	3.2.1.24	MAN*	5	1.000–0.981
Dipeptidase	3.4.-.-	PEPA*	63	1.000–0.895
Tripeptide amino peptidase	3.4.-.-	PEPB-1*	10	1.000–0.979
Peptidase-C	3.4.-.-	PEPC*	89	0.903–0.391
Proline dipeptidase	3.4.-.-	PEPD-2*	56	1.000–0.798
Leucyl-L-tyrosine peptidase	3.4.-.-	PEPLT*	19	1.000–0.953
Phosphogluconate dehydrogenase	1.1.1.44	PGDH*	7	1.000–0.967
Phosphoglycerate kinase	2.7.2.3	PGK-1*	14	1.000–0.930
		PGK-2*	13	1.000–0.975
Phosphoglucomutase	5.4.2.2	PGM-1*	72	1.000–0.600
		PGM-2*	32	1.000–0.958
Purine-nucleoside phosphorylase	2.4.2.1	PNP-1*	87	1.000–0.614
Pyruvate kinase	2.7.1.40	PK-2*	14	1.000–0.980
Triose-phosphate isomerase	5.3.1.1	TPI-1*	5	1.000–0.986
		TPI-2*	0	1.000–1.000
		TPI-3*	27	1.000–0.930
		TPI-4*	2	1.000–0.994

ture estimates derived from 100 simulated mixtures were used to evaluate the accuracy of estimated contributions to each region with mixture sizes of 100, 300, and 500 fish. We analyzed mixtures composed of fish entirely from each region and also mixtures that excluded fish from regions south and north of our marine sampling area. Precisions of the stock composition estimates for the actual mixtures were estimated by bootstrapping baseline and mixture genetic data 100 times as described in Pella and Milner (1987).

Stock compositions were estimated for June and September–October. We also combined samples over surveys and made separate estimates from samples of marked (fin-clipped and tagged hatchery fish) and unmarked fish to examine hatchery and wild stock compositions. However, because not all hatchery fish are marked, unmarked fish are a mixture of wild and hatchery fish. We therefore estimated the proportion of hatchery fish for a region in the sample of unmarked fish (P_{UH}) by

$$P_{UH} = (P_{MH}(R_U/R_M))/(S_U/S_M), \quad (1)$$

where P_{MH} = the proportion of hatchery fish from a particular region in the sample of marked fish;
R_U/R_M = the ratio of unmarked to marked releases in a region; and
S_U/S_M = the ratio of unmarked to marked fish in our ocean samples.

The R_U/R_M for 1997 and 1998 brood years varied considerably among regions: California coast 1.0, Klamath River to Cape Blanco 0.01, Oregon coast 0.12, Columbia River 0.12, southern Washington coast 0.03, northern Washington coast 0.69, Puget Sound 0.43, southern British Columbia 0.09, and Upper Fraser River 0.80 (Lavoy[1]; PSMFC[2]). We

[1] Lavoy, L. 2001. Personal commun. Washington Department of Fish and Wildlife, Olympia, WA. 98501.

[2] PSMFC (Pacific States Marine Fisheries Commission). 2001. Regional Mark Information System (RMIS) coded-wire tag on-line database. [Available from Pacific States Marine Fisheries Commission, 45 SE 82nd Dr., Suite 100, Gladstone, OR 97027-2522.]

then subtracted P_{UH} for each region from the genetic estimate of the region's contribution to the sample of unmarked fish. The sum of the remaining values estimated the proportion of wild fish in the sample of unmarked fish. When P_{UH} for a region was greater than the genetic estimate of the region's contribution to the sample of unmarked fish, the percentage of wild fish from that region was considered to be zero.

We estimated regional proportions of hatchery and wild coho salmon in the all-fish marine sample that included both marked and unmarked coho salmon. Regional hatchery contributions to the all-fish sample were made by summing each region's estimated contribution to the sampled marked and unmarked fish, weighted by the proportion of each of these sample types in the total sample. Regional proportions of wild coho salmon in the all-fish sample were made by multiplying a region's estimated proportion of wild coho salmon in the unmarked sample by the proportion of unmarked fish in the total sample.

Results

Baseline genetic data and population structure

Although coho salmon generally have low levels of genetic variability in relation to other Pacific salmon, a sufficient number of polymorphic loci were detected to distinguish many populations and regional population groups. Of 59 loci screened in all 89 populations, 56 were polymorphic, and 29 of these were at the $P_{0.95}$ level of polymorphism in at least one population (Table 2). Allelic frequencies are reported in an appendix that can be retrieved at the Northwest Fisheries Science Center website [http://www.nwfsc.noaa.gov]. Twenty of the 56 polymorphic loci had two alleles per locus, 24 had three alleles per locus, nine had four alleles, two had five alleles, and one had six alleles. Two loci (*BGALA** and PEPC*) varied in all populations studied. Three loci (GAPDH-5*, LDH-C*, and TPI-2*) were monomorphic in all populations. Observed genotypic proportions for polymorphic loci in 128 samples departed significantly ($P<0.05$) from expected Hardy-Weinberg proportions in 75 of 1476 tests (5.1%). There were no consistent trends by population or locus. Because the number of significant tests is close to the number expected by chance for this rejection level, we did not attach any biological significance to these departures.

The percentages of $P_{0.95}$ loci and average heterozygosities over 56 loci for each population appear in Table 1. The percentage of $P_{0.95}$ loci ranged from only 5.4% in Lewis River hatchery early run (population 41) to 17.9% in the Mad River hatchery (4). Average heterozygosities ranged from 0.021 in Iron Gate hatchery (5) and Elk River (9) to 0.046 in Sandy River hatchery (46). Gene diversity analysis of the 89 populations resulted in a total gene diversity (H_T) of 0.035 and an average sample diversity (H_S) of 0.033. Thus, 94.5% of the total genetic diversity was attributable to within-sample variability and 5.5% was attributable to variability among samples. About 2.9% of the total gene diversity was due to variability among populations within regions, and 2.6% was due to variability among the nine regions.

Genetic relationships among populations of coho salmon as revealed by two-dimensional MDS analysis showed that genetic differences among populations were geographically structured (Fig. 2). The first axis in the plot separated populations in coastal Oregon and California from northern populations. Several populations, including two from the Rogue River in southern Oregon (numbers 7 and 8) and Big Qualicum hatchery (85) on Vancouver Island, were positioned near the convergence of the southern and northern population groups. The Iron Gate hatchery sample (5) from the Klamath River, California, clustered with the northern population group. Several genetically discrete groups appeared on smaller geographical scales. However, samples from Iron Gate hatchery (5), Yaquina River (27), Nehalem hatchery (33), Willapa Bay area (50, 51, and 52), Dungeness hatchery (64), McGovern Creek (74), upper Cascade River (81), and Ennis Creek (82) did not cluster with nearby populations. The single population in our study from the upper Fraser River region—Spius hatchery (89) of the Thompson River—was the most genetically distinct in the MDS analysis ($x=-2.3, y=-0.9$) and was positioned beyond the scaling shown in Figure 2. The Little River (2) population also fell outside the area of the plot ($x=5.1, y=2.0$), but was genetically most similar to other California coastal populations (1, 3, and 4).

Genetic estimates of simulated stock mixtures

One demonstration of discreteness among regional groups is the correct allocation in a mixed-stock analysis of simulated samples from baseline populations to their stock of origin. We used simulated sample sizes of 100, 300, and 500 taken from one region at a time; therefore the results represent the accuracy of reallocation back to the region of origin. Table 3 presents the average values of 100 bootstrap resamplings of both the baseline and the mixture samples. For simulated sample sizes of 100, reallocation accuracy ranged from 81% (coastal northern Washington) to 98% (upper Fraser River population) and averaged 88.7% over the nine regions. Average accuracy increased to 92.9% with an increase in the size of the simulated sample to 300. Only marginal improvement (93.6% accuracy) was achieved by increasing the simulated sample size to 500.

We also used mixed-stock analysis of simulated samples to examine the accuracy of composition estimates for California, Puget Sound, and British Columbia regions when fish from these areas were not present in mixtures. Average values for sample sizes of 100 ranged from 0% (California coast, upper Fraser River) to 4% (Oregon coast) and averaged 1.8% over the five regions (Table 4). Increased sample sizes of 300 and 500 resulted in small improvements in average accuracy (1.4% and 1.0 %).

Stock compositions of ocean-caught coho salmon

Genotypes for 56 loci were scored for 730 juvenile coho salmon captured in ocean trawls in 1998–2000 (Table 5). About 65% of the 455 fish in June trawls were sampled

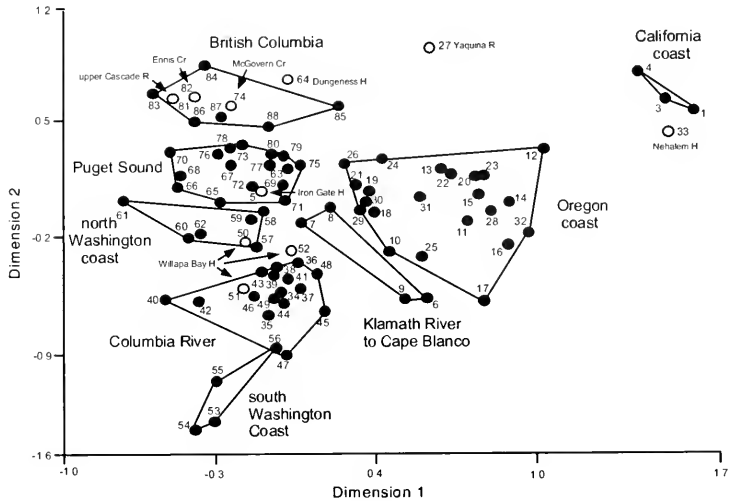

Figure 2

Multidimensional scaling (MDS) of Cavalli-Sforza and Edwards (1967) chord distances based on 56 allozyme loci between samples of 89 populations of coho salmon extending from northern California to southern British Columbia. Location numbers are given in Table 1 and Figure 1. Populations within regions are identified with polygons where possible. Open circles indicate populations that did not cluster closely with nearby populations. Populations 2 from the California coast and 89 from the upper Fraser River fall beyond the scale of the plot.

Table 3

Mean estimated percentage contributions (± standard deviations) of 100 bootstrap resamplings of mixtures composed of fish from only one region. Population numbers are explained in Table 1.

Region (populations)	n=100 Estimate	n=300 Estimate	n=500 Estimate	Region of largest misallocation
California coast (1–4)	95 ±4	97 ±3	97 ±3	Oregon coast
Klamath River to Cape Blanco (5–9)	94 ±5	96 ±3	96 ±3	Columbia River
Oregon coast (10–33)	86 ±7	91 ±4	92 ±3	Klamath River to Cape Blanco
Columbia River (34–49)	84 ±8	92 ±3	93 ±3	Oregon coast
South Washington coast (50–56)	88 ±8	95 ±3	95 ±3	North Washington coast
North Washington coast (57–63)	81 ±10	88 ±5	90 ±4	Puget Sound
Puget Sound (64–82)	85 ±7	90 ±5	90 ±4	British Columbia
British Columbia (83–88)	83 ±9	88 ±6	90 ±5	Puget Sound
Upper Fraser River (89)	98 ±2	99 ±1	99 ±1	Columbia River

in the two northern most transects along the Washington coast, 24% in three transects closest to the Columbia River, and 10% in the four most southern transects along the Oregon coast. Samples from these three areas comprised 43%, 23%, and 33%, respectively, of the 275 fish caught in September trawls. The numbers of offshore juveniles caught in 1998 were too small to provide accurate mixed-stock estimates; therefore the ocean samples collected in 1999 and 2000, and a sample pooled over 1998–2000, were analyzed separately. In the 1998–2000 pooled sample, Columbia River populations were estimated to be the major contributing regional group in June (47%, SD=6%)

Table 4

Actual percentage composition and mean estimated percentage contributions (± standard deviations) of 100 bootstrap resamplings of mixtures composed of 100, 300, and 500 fish. Population numbers are explained in Table 1.

Region (populations)	Actual	n=100 Estimate	n=300 Estimate	n=500 Estimate
California coast (1–4)	0	0 ±1	0 ±0	0 ±0
Klamath River to Cape Blanco (5–9)	0	3 ±4	2 ±2	1 ±2
Oregon coast (10–33)	20	21 ±8	20 ±5	20 ±4
Columbia River (34–49)	50	44 ±11	46 ±6	48 ±5
South Washington coast (50–56)	15	14 ±8	14 ±4	14 ±3
North Washington coast (57–63)	15	10 ±7	12 ±5	12 ±4
Puget Sound (64–82)	0	4 ±5	4 ±3	3 ±2
British Columbia (83–88)	0	2 ±3	1 ±2	1 ±1
Upper Fraser River (89)	0	0 ±1	0 ±1	0 ±0

and September (32%, SD=9%). The Oregon coastal region contributed about 18% (SD=5%) to the June mixture and 21% (SD=7%) to the September sample. The estimated contribution of Puget Sound fish to the pooled ocean samples was much greater in September (17%, SD=7%) than it was in June (3%, SD=2%).

Genetic mixed-stock analysis of ocean-caught hatchery fish with CWTs provided a direct comparison of genetic estimates and a mixed-stock sample of known origins (Brodziak et al. 1992). Only 41 fish had CWTs (Table 6). No fish with CWTs appeared in the 1998 sample. Most of the fish with CWTs in 1999 and 2000 originated from Columbia River (68%, n=28) and Oregon coastal (12%, n=5) hatcheries. In the genetic analysis of the 41 fish, Columbia River hatcheries were estimated to contribute about 22 fish (53%, SD=21%). Approximately 7 fish (16%, SD=17%) were estimated to originate from Oregon coastal hatcheries.

Of the 730 juveniles sampled during the study, 501 (69%) bore hatchery marks (clipped adipose fins). The percentage of unmarked fish in the September sample (35%) was greater than that in June (29%). Genetic mixed-stock estimates for hatchery-marked fish alone indicated that 69% (SD=6%) originated from the Columbia River and 14% (SD=4%) from Oregon coastal hatcheries (Table 7). The sample of unmarked fish, which contained a mixture of wild and unmarked hatchery fish, was estimated to have a much smaller proportion of Columbia River fish (20%, SD=8%) but a larger proportion of coastal Oregon (36%, SD=9%) and northern Washington (25%, SD=7%) fish (Table 7). About 30% of unmarked fish in the pooled ocean sample originated from hatcheries (Eq. 1) and 70% from wild populations. Estimated contributions from hatchery and wild populations of all ocean juveniles sampled (marked and unmarked) were 78% and 22%, respectively. Coho salmon originating in the Columbia River were estimated to comprise 54% of the total sample, but only 1% consisted of wild fish. Oregon coastal rivers contributed 21% to the total ocean sample, and nearly equal proportions were contributed from hatcheries and wild populations.

Discussion

Usefulness of coho salmon allozyme data for mixed-stock analysis

Although the gene diversity analysis indicated that the level of allele-frequency differentiation among populations within regions was similar to that between regions, further analyses showed that the magnitude of regional differentiation in the baseline was sufficient to provide accurate mixed-stock estimates. First, we found several genetically discrete population groups of coho salmon over an area extending from California to southern British Columbia. Most of the samples in the MDS plot clustered with nearby samples, and the north-south arrangement of neighboring population groups indicated that isolation by distance is an important component of genetic population structure on this geographic scale. As with other species of Pacific salmon, natal homing to spawning areas is an important isolating mechanism between populations of coho salmon.

Second, the analysis of simulated stock mixtures also demonstrated that regional differences were sufficient to provide reliable estimates of coho salmon stock compositions. Accurate estimates were obtained from simulated sample sets composed of 100% contributions from each region (Table 3). Third, a more rigorous test of the adequacy of the baseline was made by comparing genetic estimates with direct determinations based on CWTs. These estimates were reasonably accurate, especially for the largest contributing regions (Table 6), given the small sample of only 41 fish bearing CWTs. Both the simulation and CWT mixture results are consistent with the findings of Wood et al. (1987) that estimation accuracy decreases substantially when mixture sample sizes are small and when genetic separation among stocks is limited. Lastly, the analyses of ocean-caught mixture samples themselves appeared to provide reasonable composition estimates (Table 5). Additionally, estimates for samples pooled over years tended to be intermediate between the two annual estimates, as would be expected from pooling.

Table 5

Estimated percentage stock compositions (standard deviations), sample sizes (n), and recoveries of coded wire tags (CWT) for coho salmon sampled in trawl surveys along the Oregon and Washington coasts in June and September 1998, 1999, and 2000. Stock compositions were not estimated for June (n=43) and September (n=18) 1998 because of small sample sizes. None of the 1998 samples contained coded wire tags.

	June		September	
Region	Est.	CWT	Est.	CWT
1999				
n	278		152	
California coast	0 ±1	0	0 ±0	0
Klamath River to Cape Blanco	6 ±6	0	0 ±0	0
Oregon coast	25 ±7	5	25 ±8	0
Columbia River	46 ±9	8	20 ±14	4
South Washington coast	11 ±4	2	9 ±5	0
North Washington coast	10 ±5	2	18 ±15	0
Puget Sound	3 ±4	0	25 ±9	1
British Columbia	0 ±1	0	3 ±3	0
Upper Fraser River	0 ±0	0	0 ±0	0
2000				
n	134		105	
California coast	0 ±0	0	1 ±3	0
Klamath River to Cape Blanco	1 ±7	0	0 ±0	0
Oregon coast	11 ±7	0	17 ±8	0
Columbia River	40 ±11	11	48 ±16	5
South Washington coast	17 ±7	0	6 ±9	0
North Washington coast	21 ±11	0	10 ±16	0
Puget Sound	11 ±8	0	14 ±7	1
British Columbia	0 ±0	0	3 ±8	2
Upper Fraser River	0 ±0	0	0 ±0	0
1998, 1999, and 2000 combined				
n	455		275	
California coast	0 ±0	0	0 ±0	0
Klamath River to Cape Blanco	7 ±4	0	0 ±0	0
Oregon coast	18 ±5	5	21 ±7	0
Columbia River	47 ±6	19	32 ±9	9
South Washington coast	11 ±3	2	9 ±4	0
North Washington coast	13 ±4	2	19 ±11	0
Puget Sound	3 ±2	0	17 ±7	2
British Columbia	0 ±0	0	2 ±2	2
Upper Fraser River	0 ±0	0	0 ±0	0

Nonetheless, the usefulness of the allozyme baseline that we compiled for coho salmon is limited by two factors. First, few samples in the baseline are from California and British Columbia populations. Although the baseline appears to be adequate to analyze stock mixtures of juvenile coho salmon off Oregon and Washington, mixed stock analyses of samples from other marine areas, particularly to the north, requires the sampling of additional populations. Second, our study demonstrated that estimates of stock compositions are not sufficiently accurate to effectively identify stock groups that are absent from mixtures or present in small proportions (Tables 4 and 6). Estimation accuracy can be improved by using additional gene markers. These markers will likely be based on DNA variability because coho salmon minisatellite (Miller et al., 1996; Beacham et al., 1996) and microsatellite (Small et al., 1998a; 1998b; Beacham et al., 2001) loci show much higher levels of polymorphism than do allozyme loci. Recently, variation at eight microsatellite DNA loci and one Mhc locus in coho salmon populations in British Columbia and Washington was used to estimate the stock compositions of fisheries off the west coast of Vancouver Island (Shaklee et al., 1999; Beacham et al., 2001). However, the use of highly polymorphic microsatellite loci may not provide increased discrimination among populations on large geographical scales because of allelic convergence from multiple mutations (Nauta and Weiss-

ing, 1996). Nonetheless, the extension of a DNA baseline to include populations in Oregon and California, may resolve fine-scale (geographic and temporal) differences between coho salmon populations in southern coastal areas.

Stock compositions of ocean-caught juvenile coho salmon

Studies using large purse seines conducted in 1981–85 revealed that juvenile coho salmon were the most abundant of the *Oncorhynchus* species in the nearshore areas along the Oregon and Washington coasts (Pearcy and Fisher, 1988; 1990). Pearcy and Fisher (1988; 1990) captured hatchery-tagged juvenile coho salmon and concluded they were not highly migratory, often remaining close to their point of sea entry for several months. Our genetic results corroborate that finding. Genetic estimates indicate that about 89% of ocean juveniles caught in June and 81% in September originated from the Columbia River and adjacent coastal rivers. Recoveries of hatchery-tagged fish (n=41) also indicate that juveniles remain near river mouths in their first few months after ocean entry; only three of these CWT-marked fish came from hatcheries in other regions.

However, our genetic results indicate that a change has occurred in the distribution of Washington coastal and Puget Sound juvenile coho salmon. In the 1980s, juvenile coho salmon from Washington coastal hatcheries were not recovered along the Washington and Oregon coasts after mid summer, apparently having migrated northward (Pearcy and Fisher, 1988). Pearcy and Fisher (1990) also found that Puget Sound coho salmon did not migrate along the Washington and Oregon coast until sometime between their first and second summer at sea. However, our genetic results showed that in 1998–2000 fish from Washington coastal streams and hatcheries comprised substantial proportions of the juveniles in nearshore areas along the Washington and Oregon coast in both early and late summer (24% and 28%). We also found that juvenile coho salmon from Puget Sound are present in late summer. Our finding that coho salmon from northern stocks move south along the coast during their first summer was substantiated by the catch of CWT-marked fish originating from Puget Sound (n=2) and southern British Columbia (n=2).

Recent reductions in the number of coho salmon smolts released from the region's hatcheries have not resulted in a decrease in the proportion of hatchery juveniles along the Oregon and Washington coasts. Annual releases of hatch-

Table 6

Actual composition and estimated contributions (± standard deviations) of a mixture of 41-CWT fish.

	Actual		Genetic estimate	
Region	Number	%	Number	%
California coast	0	0	1	3 ±4
Klamath River to Cape Blanco	0	0	0	0 ±0
Oregon coast	5	12	7	16 ±17
Columbia River	28	68	22	53 ±21
South Washington coast	2	5	0	0 ±0
North Washington coast	3	7	5	11 ±9
Puget Sound	1	2	5	11 ±18
British Columbia	2	5	2	6 ±11
Upper Fraser River	0	0	0	0 ±0

Table 7

Estimated percentage stock compositions and sample sizes for populations of marked (fish with clipped adipose fins) and unmarked coho salmon sampled in trawl surveys along the Oregon and Washington coasts in 1998, 1999, and 2000. Samples from June and September were combined. Separate estimates for the contributions of hatchery and wild stocks were made by using estimates of hatchery marking rates for each region.

	Marked fish (hatchery fish)	Unmarked fish (hatchery and Wild fish)					
					All fish		
Region	Genetic estimate (n=501) (%)	Genetic estimate (n=229) (%)	Hatchery (%)	Wild (%)	Hatchery (%)	Wild (%)	Total (%)
California coast	0 ±0	1 ±2	0	1	0	0	0
Klamath River to Cape Blanco	1 ±2	1 ±7	0	1	1	0	1
Oregon coast	14 ±4	36 ±9	4	32	11	10	21
Columbia River	69 ±6	20 ±8	18	2	53	1	54
South Washington coast	4 ±4	9 ±5	0	9	3	3	6
North Washington coast	1 ±7	25 ±7	2	23	1	7	8
Puget Sound	6 ±5	8 ±5	6	2	6	1	7
British Columbia	5 ±2	0 ±0	0	0	3	0	3
Upper Fraser River	0 ±0	0 ±0	0	0	0	0	0
Total	100	100	30	70	78	22	100

ery smolts exceeded 64 million fish during the early 1980s but have decreased to about 39 million in recent years, a 40% reduction (PSMFC[2]; NRC[3]). Nonetheless, the proportion of hatchery coho salmon in nearshore marine waters has remained high, averaging 74% in 1981–85 (Pearcy and Fisher, 1990) and 78% in 1998–2000 (present study). This result, therefore, leads to the conclusion that the number of naturally produced juveniles in Oregon and Washington coastal waters has also decreased proportionately during this period. If so, wild populations of coho salmon may also have experienced a decline in abundance on the order of 40%.

Steep declines in Columbia River wild populations are particularly evident. At the beginning of the 20th century, populations in the Columbia River are thought to have been the largest producers of coho salmon in the region (Chapman, 1986; Lichatowich, 1989) and likely contributed a substantial proportion to the nearshore population of juvenile salmon. At present, Columbia River juveniles predominate along the coast. However, these fish are almost entirely releases from hatchery facilities and Columbia River wild coho salmon are conspicuously absent.

Acknowledgments

We are grateful to George Milner and Paul Aebersold who developed much of the allozyme baseline for coho salmon. Sewall Young, Laurie Weitkamp, Kathleen Neely, Bill Waknitz, Kathryn Kostow, Orlay Johnson, Ken Currens, Eric Beamer, Scott Chitwood, Doug Cramer, Marc Miller, and Jennifer Nielsen provided baseline samples. We thank Ed Casillas, Ric Brodeur, Bob Emmett, Cindy Bucher, Susan Hinton, Cheryl Morgan, Paul Bentley, and Joe Fisher for providing coho salmon samples and data from their coastal salmon surveys. This study was supported in part by funds from the Bonneville Power Administration and the U.S. GLOBEC program as part of an initiative to understand the effects of ocean dynamics on salmon populations.

Literature cited

Aebersold, P. B., G. A. Winans, D. J. Teel, G. B. Milner, and F. M. Utter.
1987. Manual for starch gel electrophoresis: a method for the detection of genetic variation. U.S. Dep. Commer., NOAA Tech. Report NMFS 61, 19 p.

Beacham, T. D., J. R. Candy, K. J. Supernault, T. Ming, B. Deale, A. Schulze, D. Tuck, K. H. Kaukauna, J. R. Irvine, K. M. Miller, and R. E. Wither.
2001. Evaluation and application of microsatellite and major histocompatibility complex variation for stock identification of coho salmon in British Columbia. Trans. Am. Fish. Soc. 130:1116–1149.

Beacham, T. D., K. M. Miller, and R. E. Withler.
1996. Minisatellite DNA variation and stock identification of coho salmon. J. Fish Biol. 49:411–429.

Beamish, R. J., D. McCaughran, J. R. King, R. M. Sweeting, and G. A. McFarlane.
2000. Estimating the abundance of juvenile coho salmon in the Strait of Georgia by means of surface trawls. North Am. J. Fish. Manage. 20:369–375.

Brodziak, J., B. Bentley, D. Bartley, G.A.E. Gall, R. Gomulkiewicz, and M. Mangel.
1992. Tests of genetic stock identification using coded wire tagged fish. Can. J. Fish. Aquat. Sci. 49:1507–1517.

Cavalli-Sforza, L. L., and A. W. F. Edwards.
1967. Phylogenetic analysis: models and estimation procedures. Evolution 21:550–570.

Chakraborty, R., M. Hagg, N. Ryman, and G. Stahl.
1982. Hierarchical gene diversity analysis and its application to brown trout population data. Hereditas 97:17–21.

Chapman, D. W.
1986. Salmon and steelhead abundance in the Columbia River in the nineteenth century. Trans. Am. Fish. Soc. 115:662–670.

Debevec, E. M., R. B. Gates, M. Masuda, J. Pella, J. Reynolds, and L. W. Seeb.
2000. SPAM (version 3.2): statistics program for analyzing mixtures. J. Hered. 91:509–511.

Emmett, R. L., and R. D. Brodeur.
2000. Recent changes in the pelagic nekton community off Oregon and Washington in relation to some physical oceanographic conditions. North Pacific Anadr. Fish Comm. Bull. 2:11–20.

Godfrey, H.
1965. Coho salmon in offshore waters. *In* Salmon of the North Pacific Ocean. Part IX. Coho, chinook, and masu salmon in offshore waters, p. 1–39. Int. North Pacific Fish. Comm. Bull. 16.

Guo, S. W., and E. A. Thompson.
1992. Performing the exact test of Hardy-Weinberg proportions for multiple alleles. Biometrics 48:361–372.

Guthrie, C. M., E. V. Farley Jr., N. M. L. Weemes, and E. C. Martinson.
2000. Genetic stock identification of sockeye salmon captured in the coastal waters of Unalaska island during April/May and August 1998. North Pacific Anadr. Fish Comm. Bull. 2:309–315.

Hartt, A. C., and M. B. Dell.
1986. Early oceanic migrations and growth of juvenile Pacific salmon and steelhead trout. Int. N. Pac. Fish. Comm. Rep. 46, 105 p.

Johnson, O. W., T. A. Flagg, D. J. Maynard, G. B. Milner, and F. W. Waknitz.
1991. Status review for lower Columbia River coho salmon. U.S. Dep. Commerce, NOAA Tech. Memo. NMFS F/NWC-202, 94 p.

Lawson, P. W., and R. M. Comstock.
2000. The proportional migration selective fishery model. *In* Sustainable fisheries management: Pacific salmon (E. E. Knudsen, C. R. Steward, D. D. MacDonald, J. E. Williams, and D. W. Reiser, eds.), p. 423–433. Lewis Publishers, Boca Raton, FL.

Lichatowich, J. A.
1989. Habitat alteration and changes in abundance of coho (*Oncorhynchus kisutch*) and chinook (*Oncorhynchus tshawytscha*) salmon in Oregon's coastal streams. *In* Proceedings of the national workshop on effects of habitat alteration on salmonid stocks, May 6–8, 1987, Nanaimo, B.C. (C. D.

[3] NRC (Natural Resource Consultants, Inc.). 1995. Database of artificially propagated anadromous salmon (database). [Available from Environmental and Technical Services Division, NMFS, 525 N.E., Oregon Street, Portland, OR 97232.]

Levings, L. B. Holtby, and M. A. Henderson, eds.), p. 92–99. Can. Spec. Publ. Fish. Aquat. Sci. 105.

Miller, K. M., R. E. Withler, and T. D. Beacham.
1996. Stock identification of coho salmon (*Oncorhynchus kisutch*) using minisatellite DNA variation. Can. J. Fish. Aquat. Sci. 53:181–195.

Milner, G. B., D. J. Teel, F. M. Utter, and G. A. Winans.
1985. A genetic method of stock identification in mixed populations of Pacific salmon, *Oncorhynchus* spp. Mar. Fish. Rev. 47:1–8.

Nauta, M. J., and F. J. Weissing.
1996. Constraints on allele size at microsatellite loci: implications for genetic differentiation. Genetics. 143:1021–1032.

Nei, M.
1978. Estimation of average heterozygosity and genetic distance from a small number of individuals. Genetics 89:583–590.

Orsi, J. A., M. V. Sturdevant, J. M. Murphy, D. G. Mortensen, and B. L. Wing.
2000. Seasonal habitat use and early marine ecology of juvenile Pacific salmon in southeastern Alaska. North Pacific Anadr. Fish Comm. Bull. 2:111–122.

Pearcy, W. G., and J. P. Fisher.
1988. Migrations of coho salmon, *Oncorhynchus kisutch*, during their first summer in the ocean. Fish. Bull. 86: 173–195.
1990. Distribution and abundance of juvenile salmonids off Oregon and Washington, 1981–1985. U.S. Dep. Commerce, NOAA Tech. Report NMFS 93, 83 p.

Pella, J., and G. B. Milner.
1987. Use of genetic marks in stock composition analyses. *In* Population genetics and fishery management (N. Ryman and F. Utter, eds.), p. 247–276. Washington Sea Grant, Univ. Washington Press, Seattle, WA.

Raymond, M., and F. Rousset.
1995. GENEPOP (versions 1.2 and 3.1): population genetics software for exact tests and ecumenism. Heredity 86: 248–249.

Shaklee, J. B., F. W. Allendorf, D. C. Morizot, and G. S. Whitt.
1990. Gene nomenclature for protein-coding loci in fish. Trans. Am. Fish. Soc. 119:2–15.

Shaklee, J. B., T. D. Beacham, L. Seeb, and B. A. White.
1999. Managing fisheries using genetic data: case studies from four species of Pacific Salmon. Fish. Res. 43:45–78.

Small, M. P., R. E. Withler, and T. D. Beacham.
1998a. Population structure and stock identification of British Columbia coho salmon (*Oncorhynchus kisutch*) based on microsatellite DNA variation. Fish. Bull. 96:843–858.

Small, M. P., T. D. Beacham, R. E. Withler, and R. J. Nelson.
1998b. Discriminating coho salmon (*Oncorhynchus kisutch*) populations within the Fraser River, British Columbia, using microsatellite DNA markers. Mol. Ecol. 7:141–155.

Swofford, D. L., and R. B. Selander.
1981. BIOSYS-1: a FORTRAN program for the comprehensive analysis of electrophoretic data in population genetics and systematics. J. Hered. 72:281–283.

Utter, F., P. Aebersold, and G. Winans.
1987. Interpreting genetic variation detected by electrophoresis. *In* Population genetics and fishery management (N. Ryman and F. Utter, eds.), p. 21–45. Washington Sea Grant, Univ. Washington Press, Seattle, WA.

Van Doornik, D. M., M. J. Ford, and D. J. Teel.
2002. Patterns of temporal genetic variation in coho salmon: estimates of the effective proportion of 2-year-olds in natural and hatchery populations. Trans. Am. Fish. Soc. 131:1007–1019.

Waples, R. S.
1988. Estimation of allele frequencies at isoloci. Genetics 118:371–384.
1990. Temporal changes of allele frequencies in Pacific salmon: implications for mixed-stock fishery analysis. Can. J. Fish. Aquat. Sci. 47:968–976.

Weitkamp, L. A., T. C. Wainright, G. J. Bryant, G. B. Milner, D. J. Teel, T. G. Kope, and R. S. Waples.
1995. Status review of coho salmon from Washington, Oregon, and California. U.S. Dep. Commer., NOAA Tech. Memo. NMFS-NWFSC-24, 258 p.

Wood, C. C., S. McKinnell, T. J. Mulligan, and D. A. Fournier.
1987. Stock Identification with the maximum likelihood mixture model: sensitivity analysis and application to complex problems. Can. J. Fish. Aquat. Sci. 44:866–881.

The statistical properties of recreational catch rate data for some fish stocks off the northeast U.S. coast

Mark Terceiro

Northeast Fisheries Science Center
National Marine Fisheries Service, NOAA
166 Water Street
Woods Hole, Massachusetts 02543
E-mail address: mtercer@whsun1.wh.whoi.edu

Abstract—Recreational fisheries in the waters off the northeast U.S. target a variety of pelagic and demersal fish species, and catch and effort data sampled from recreational fisheries are a critical component of the information used in resource evaluation and management. Standardized indices of stock abundance developed from recreational fishery catch rates are routinely used in stock assessments. The statistical properties of both simulated and empirical recreational fishery catch-rate data such as those collected by the National Marine Fisheries Service (NMFS) Marine Recreational Fishery Statistics Survey (MRFSS) are examined, and the potential effects of different assumptions about the error structure of the catch-rate frequency distributions in computing indices of stock abundance are evaluated. Recreational fishery catch distributions sampled by the MRFSS are highly contagious and overdispersed in relation to the normal distribution and are generally best characterized by the Poisson or negative binomial distributions. The modeling of both the simulated and empirical MRFSS catch rates indicates that one may draw erroneous conclusions about stock trends by assuming the wrong error distribution in procedures used to developed standardized indices of stock abundance. The results demonstrate the importance of considering not only the overall model fit and significance of classification effects, but also the possible effects of model misspecification, when determining the most appropriate model construction.

Manuscript approved for publication 30 January 2003 by Scientific Editor.

Manuscript received 4 April 2003 at NMFS Scientific Publications Office.

Fish Bull. 101:653–672 (2003).

Major recreational fisheries in the waters off the northeast U.S. coast target a wide variety of pelagic and demersal fish species (NMFS, 1995, 1996). Fishery data collected in the National Marine Fishery Service (NMFS) Marine Recreational Fishery Statistics Survey (MRFSS) are the basis of fishery catch and effort estimates for most of these recreational fisheries and for indices of population abundance used in stock assessments (USDOC, 1992, 2001). For some stocks, reliable fishery-independent data such as research trawl survey indices are not available, and therefore the recreational fishery data are essential for tracking stock abundance. The intercept (creel sampling) portion of the MRFSS is an interview-type survey of recreational fishing trips and is conducted at public fishing sites such as marinas, launching ramps, fishing piers, and beaches. MRFSS catch estimates are made by expanding intercept survey sample catch rates in numbers, calculated on a per trip basis, by the estimated total number of recreational fishing trips. The estimated total number of fishing trips is calculated from data collected in a MRFSS telephone survey of households located in coastal counties. The U.S. Department of Commerce (USDOC, 1992, 2001) has provided overviews of the MRFSS intercept and telephone survey methods and catch estimation procedures.

In many cases recreational and commercial catch rates used as abundance indices are standardized by using general linear models that assume a lognormal error distribution (Gulland, 1956; Robson, 1966; Gavaris, 1980; Kimura, 1981). Commercial fishery catch-rate data generally meet tests of normality when log-transformed (Gulland, 1956; O'Brien and Mayo, 1988). Because of the efficiency and "integrating" property of commercial fishing gear (including trawls, fixed nets, and longlines), even catch rates on a per tow or per set basis are usually lognormally distributed (Taylor, 1953). An important characteristic of commercial data is that catch rates of zero (tows or sets with no catch of the target species) are rare.

With the assumption that there is an underlying lognormal error distribution, general linear models have often been used to standardize recreational fishery catch rates and compute indices of abundance. This approach has been used in the assessments of bluefin tuna (Brown and Browder, 1994), summer flounder (Terceiro[1]), black sea bass (NEFSC[2]), tautog (NEFSC[2]), winter flounder (NEFSC[3]), and bluefish

[1] Terceiro, M. (ed.). 1993. Assessment of summer flounder (*Paralichthys dentatus*), 1993: report of the stock assessment workshop summer flounder working group. Northeast Fisheries Science Center reference document 93-14, 72 p. Northeast Fisheries Science Center, Woods Hole, MA 02543.

[2] NEFSC (Northeast Fisheries Science Center). 1996a. Report of the 20th northeast regional stock assessment workshop (20th SAW): Stock Assessment Review Committee (SARC) consensus summary of assessments. Northeast Fisheries Science Center reference document 95-18, 210 p. Northeast Fisheries Science Center, Woods Hole, MA 02542.

[3] NEFSC. 1996b. Report of the 21st northeast regional stock assessment workshop (21st SAW): Stock Assessment Review Committee (SARC) consensus summary of assessments. Northeast Fisheries Science Center reference document 96-05d, 200 p. Northeast Fisheries Science Center, Woods Hole, MA 02543.

(NEFSC[4]; Gibson and Lazar[5]). However, Bannerot and Austin (1983) noted that the sampling distribution of recreational catch data is often highly skewed with a longer right-hand tail than might be expected even from a lognormal distribution. Furthermore, depending on the way the catch rate is defined (i.e. catch per trip, day, or hour), recreational fishery catch-rate distributions may contain a high proportion of zero catches.

Hilborn (1985) presented a frequency distribution of numbers of salmon caught per trip in the British Columbia sport fishery that appears to be best characterized by the negative binomial distribution, with a catch per hour frequency best characterized by the Poisson distribution. Jones et al. (1995) investigated the statistical properties of recreational fishery sampling data collected in angler surveys in Virginia and noted that the non-normality of recreational fishery data may violate assumptions of lognormality in methods used to develop indices of abundance, and especially the validity of confidence intervals. Power and Moser (1999) expressed similar concerns about sampled distributions of fish and plankton collected by research trawl nets, noting that the assumption of an underlying normal or lognormal distribution for these types of data is commonplace, and perhaps in error, and that distributions such as the Poisson or negative binomial may be more appropriate. Smith (1990, 1996) recommended various nonparametric resampling methods (e.g. bootstrap confidence intervals) for characterizing the dispersion of highly skewed research trawl survey catch distributions having a large proportion of zero catches. Smith (1999) modeled angling success for salmon, expressed as the catch after the first hour of angling, using a negative binomial distribution model.

In addition to the Poisson and negative binomial, alternatives to the lognormal error model for recreational fishery catch rates also include the delta-lognormal and delta-Poisson error models. These models are combinations of the delta distribution (Pennington, 1983) and lognormal or Poisson model approaches. The delta distribution has been used in modeling fish and plankton abundance indices from research trawl survey data, which are characterized by highly skewed distributions with a relatively high proportion of zero catches (Pennington, 1983). In the combined delta-lognormal and delta-Poisson approaches, indices of abundance are modeled as a product of binomially distributed probabilities of a positive catch and lognormal or Poisson distributed positive catch rates. The delta-lognormal model has been used in modeling fish-spotter data (Lo et al., 1992) and in the standardization of recreational fishery catch rates for bluefin tuna (Brown and Porch, 1997; Turner et al., 1997; Brown, 1999; Ortiz et al., 1999), both characterized by a highly contagious spatial distribution and a large proportion of zeroes. Bluefin and yellowfin tuna catch rates in the commercial and recreational fisheries have also been standardized by using Poisson (Brown and Porch, 1997), negative binomial (Turner et al., 1997), and delta-Poisson error distributions (Brown, 2001; Brown and Turner, 2001) to address these distributional characteristics.

In this study I first examine the statistical properties of recreational fishery catch-rate data as sampled by the MRFSS. Next, I examine the goodness of fit to different statistical distributions of empirical MRFSS catch rates, on both per trip and per hour bases. I then explore the effects of five different assumptions about the error structure of the catch-rate frequency distributions (lognormal, delta-lognormal, Poisson, delta-Poisson, and negative binomial) in deriving standardized indices of abundance with general linear models, using simulated recreational fishery and empirical MRFSS catch per trip (zero catches included) data.

Materials and methods

Overview of statistical methods

This work focuses on catch number per trip sampled in the MRFSS as the index of abundance. The distributional properties of MRFSS catch-per-hour rates are also examined, in order to explore whether the general conclusions reached for catch-per-trip rates are likely to be similar to catch-per-hour rates. Directed trips are defined as those for which interviewed anglers indicated that they were intending to catch a particular species as a primary or secondary target, whether successful or not (zero catches included). In analyses of trips for all species, all trips were used regardless of target or success (zero catches included). Catch rates were expressed as integer (natural) numbers of fish per trip or per hour.

A value of 1 was added to all observations when applying a lognormal transformation to allow inclusion of the zero catch rate observations (this constant was subtracted upon retransformation to the original scale). Expected sample values for the lognormal distribution were calculated by using the normal distribution and log-transformed catch rates (Sokol and Rohlf, 1981). Previous work on MRFSS catch-per-trip data has shown that the value of 1 is the appropriate constant to be added (Terceiro[1]; NEFSC[3]) because it tends to minimize the sum of the absolute value of skew and kurtosis for these distributions (Berry, 1987). The standard logarithmic transform bias correction was applied to express results in the original arithmetic scale (Finney, 1951; Bradu and Mundlak, 1970). No constant was added when data were analyzed under the assumption of binomial, Poisson, or negative binomial error distributions.

The binomial distribution is a discrete frequency (probability) distribution of the number of times an event occurs in a sample in which some proportion of the members possess some variable attribute (Snedecor and Cochran, 1967). Each event is assumed independent of other prior

[4] NEFSC. 1997. Report of the 23rd northeast regional stock assessment workshop (23rd SAW): Stock Assessment Review Committee (SARC) consensus summary of assessments. Northeast Fisheries Science Center reference document 97-05, 191 p. Northeast Fisheries Science Center, Woods Hole, MA 03543.

[5] Gibson, M. R., and N. Lazar. 1998. Assessment and projection of the Atlantic coast bluefish using a biomass dynamic model. A report to the Atlantic States Marine Fisheries Commission Bluefish Technical Committee and Mid-Atlantic Fishery Management Council Scientific and Statistics Committee, 29 p. Rhode Island Division of Fish and Wildlife, Jamestown, RI 02835

Table 1

Descriptive statistics for MRFSS (Marine Recreational Fishery Statistics Survey) 1981, 1988, and 1996 northeast U.S. coast catch per trip, including zero catches. Catch is given in numbers of fish. CV is the coefficient of variation (%). *D* is the Kolmogorov test statistic for normality. Test statistics significant at the 1% level ($P<0.01$) are shown by **, indicating rejection of the null hypothesis that catch rates follow a normal distribution.

Species	No. of trips	Mean	Median	Variance	CV	Skew	*D*
1981							
Bluefish	4615	3.80	0.00	155.09	328	27.78	0.380**
Summer Flounder	3135	1.88	0.00	14.69	204	4.71	0.312**
Atlantic cod	509	2.55	1.00	13.49	144	2.48	0.244**
Scup	269	8.44	2.00	275.10	196	4.08	0.305**
All species	20,280	3.45	0.00	355.94	547	65.48	0.427**
1988							
Bluefish	7294	1.60	0.00	18.65	270	6.42	0.355**
Summer Flounder	4779	2.26	0.00	18.48	190	3.70	0.300**
Atlantic cod	1558	4.56	2.00	21.55	154	3.68	0.258**
Scup	960	9.28	3.00	312.65	190	4.48	0.300**
All species	48,423	2.29	0.00	43.66	289	8.94	0.365**
1996							
Bluefish	5457	1.20	0.00	13.12	301	8.40	0.370**
Summer Flounder	7047	2.33	1.00	13.49	157	3.40	0.263**
Atlantic cod	1099	3.97	1.00	43.34	166	3.29	0.273**
Scup	643	13.83	4.00	524.60	165	3.44	0.273**
All species	81,057	2.57	0.00	47.32	268	10.45	0.354**

events in the same sample (Sokal and Rohlf, 1981). In the present study, the binomial distribution was used only to model the probabilities of a positive catch (as opposed to a zero catch; thus the variable attribute of the observation is either catch or no catch) in the combined delta-lognormal and delta-Poisson models.

The Poisson distribution is also a discrete frequency distribution of the number of times an event (such as catching a fish during a trip) occurs in a sample and is characterized by a small mean value in relation to the observed maximum number of events within the sample (Sokal and Rohlf, 1981). For a Poisson distribution, the expected variance is equal to its mean, and Poisson frequency distributions are more highly skewed than normal or lognormal distributions (Bliss and Fisher, 1953).

The negative binomial is a discrete frequency distribution with a higher degree of dispersion than the Poisson distribution, such that the variance is significantly larger than the mean. A negative binomial distribution will converge to a Poisson as the variance approaches the mean (Bliss and Fisher, 1953). Although not as widely applied as the Poisson in the analysis of count data, there is a growing literature describing the properties of negative binomial regression methods to be used when analyzing "over-dispersed Poisson" frequency distributions (Manton et al., 1981; Lawless, 1987). The dispersion parameter of the negative binomial distribution, k, is a positive exponent relating the mean and variance of the distribution such that as the variance of a distribution exceeds the mean, the value of k decreases and the "over-dispersion" of the distribution in relation to a Poisson distribution increases. The most efficient estimate of the sample parameter, k', is estimated by maximum likelihood (Bliss and Fisher, 1953).

Descriptive statistics and frequency distributions of MRFSS catch per trip and catch per hour observations were compiled by using the SAS FREQ and UNIVARIATE procedures (SAS, 2000). Tests of normality were made with the Kolmolgorov-Smirnov *D*-statistic for normality (test significance expressed as probability < *D*; SAS, 2000). Evaluation of the most appropriate distributional fit to the data was based on inspection of the frequency distribution plots, the parametric chi-square (χ^2) and *G*-statistic goodness-of-fit tests, and the nonparametric Kolmogorov-Smirnov (*D*-statistic) goodness-of-fit test for an intrinsic hypothesis (because the expected distributions were calculated from the observed sample moments; Sokol and Rohlf, 1981). For the chi-square and *G*-tests, when intervals (classes) of catch per trip with fewer than 3 expected instances occurred, expected and observed frequencies for these intervals were pooled with the adjacent intervals to obtain a joint class with an expected frequency of occurrence of 3 or more (Sokol and Rohlf, 1981). Because of the large sample sizes involved (>>100), the *G*-test correction suggested by Williams (1976) proved to be very small in a few test calculations and therefore was not routinely applied. Unrealistic (for recreational fishery catch-rate data) negative expected values computed for the lognormal distributions were excluded, and the remaining positive distribution was raised to the observed sample total, so that the expected proportions at each interval summed to 1.0.

Standardized annual indices of abundance derived from the simulated recreational and empirical MRFSS data were calculated by using maximum likelihood estimation to fit generalized linear models with the SAS GENMOD procedure (SAS, 2000). The SAS (2000) defaults for model specification were generally followed. An identity link function was used under the lognormal distribution assumption (catch rates were ln-transformed prior to analysis). A logistic link function was used under the binomial distribution assumption applied for the probability of positive catch component in the delta-lognormal and delta-Poisson model approaches. A logarithmic link function was used under the Poisson and negative binomial assumptions (SAS, 2000). Type-3 general linear models were fitted in all cases because the results of this type of analysis do not depend on the order in which the terms of the model are specified. The significance of the individual classification effects (factors) in the models was judged by the chi-square statistic (Searle, 1987; SAS, 2000).

The overall goodness of fit of the standardization models was evaluated by using the deviance and log-likelihood statistics. The deviance is defined to be twice the difference between the maximum achievable log likelihood and the log likelihood at the maximum likelihood estimates of the model parameters (McCullagh and Nelder, 1989). The deviance has a limiting chi-square distribution, and so significance is judged by comparison to critical values of the chi-square distribution. The scale parameter (i.e. for normal distributions) was held fixed at 1 for all models to facilitate evaluation of goodness of fit and the degree of overdispersion for models with different error distribution assumptions. Holding the scale parameter fixed has no effect on the estimated intercept or model regression coefficients (e.g. in the study, the year coefficients that serve as the annual indices of abundance), but allows equivalent calculation among models of a "dispersion estimate" (SAS, 2000). This "dispersion estimate," measured after model fitting as the deviance divided by the degrees of freedom (deviance/df), is used to judge whether the data are overdispersed or underdispersed with respect to the error distribution used in model fitting and is therefore useful in evaluating whether the correct error distribution assumption has been used in the model (McCullagh and Nelder, 1989; SAS, 2000).

Descriptive statistics for MRFSS catch rates

The descriptive statistics (mean, median, variance, skewness, and Kolmolgorov-Smirnov (D) normality test statistic) and frequency distributions of MRFSS sample catch rates for 1981, 1988, and 1996 were examined for four species from U.S. Atlantic coast waters (Maine to the east coast of Florida), and in aggregate for all species sampled along the U.S. Atlantic coast. The following individual species were considered: bluefish (*Pomatomus saltatrix*, an example of a Atlantic coast predatory "gamefish"); summer flounder (*Paralichthys dentatus*, a Mid Atlantic Bight demersal flatfish); Atlantic cod (*Gadus morhua*, a New England demersal roundfish); and scup (*Stenotomus*

Table 2

Descriptive statistics for MRFSS (Marine Recreational Fishery Statistics Survey) 1981, 1988, and 1996 northeast U.S. coast catch per trip, positive catches only. Catch is given in numbers of fish. CV is the coefficient of variation (%). D is the Kolmogorov test statistic for normality. Test statistics significant at the 1% level ($P<0.01$) shown by **, indicating rejection of the null hypothesis that catch rates follow a normal distribution.

Species	No. of trips	Mean	Median	Variance	CV	Skew	D
1981							
Bluefish	2288	7.66	4.00	283.32	220	22.02	0.340**
Summer Flounder	1380	4.26	2.67	23.21	113	3.87	0.222**
Atlantic cod	298	4.36	3.00	15.19	89	2.26	0.188**
Scup	165	13.76	7.33	375.88	141	3.39	0.262**
All species	9484	7.33	3.00	732.27	368	47.02	0.395**
1988							
Bluefish	2445	4.75	2.33	40.35	133	4.40	0.254**
Summer Flounder	2326	4.64	3.00	26.92	112	2.94	0.209**
Atlantic cod	1065	6.67	4.00	58.02	114	3.46	0.219**
Scup	614	14.52	7.67	413.03	140	3.88	0.245**
All species	19,094	5.76	3.00	90.39	165	6.49	0.278**
1996							
Bluefish	1666	3.93	2.00	32.26	144	5.61	0.258**
Summer Flounder	4196	3.91	2.66	16.46	104	3.13	0.203**
Atlantic cod	679	6.43	4.00	54.39	115	2.85	0.210**
Scup	438	20.31	12.50	638.90	124	3.05	0.220**
All species	39,094	5.30	2.67	83.43	172	8.35	0.286**

Table 3

Descriptive statistics for MRFSS (Marine Recreational Fishery Statistics Survey) 1981, 1988, and 1996 northeast U.S. coast catch per hour, including zero catches. Catch is given in numbers of fish. CV is the coefficient of variation (%). D is the Kolmogorov test statistic for normality. Test statistics significant at the 1% level ($P<0.01$) shown by (**), indicating rejection of the null hypothesis that catch rates follow a normal distribution.

Species	No. of trips	Mean	Median	Variance	CV	Skew	D
1981							
Bluefish	4615	0.77	0.00	5.57	305	12.21	0.371**
Summer Flounder	3135	0.36	0.00	0.64	221	6.43	0.325**
Atlantic cod	509	0.38	0.17	0.43	172	4.04	0.280**
Scup	269	1.59	0.44	7.96	178	2.79	0.287**
All species	20,280	0.74	0.00	13.23	491	40.11	0.419**
1988							
Bluefish	7294	0.39	0.00	1.26	287	7.26	0.363**
Summer Flounder	4779	0.45	0.00	0.82	200	6.11	0.309**
Atlantic cod	1558	0.96	0.50	1.99	147	3.32	0.249**
Scup	960	2.12	0.67	14.03	177	3.60	0.286**
All species	48,423	0.54	0.00	3.07	325	15.18	0.379**
1996							
Bluefish	5457	0.34	0.00	1.23	322	7.73	0.378**
Summer Flounder	7047	0.52	0.22	0.729	164	4.17	0.271**
Atlantic cod	1099	0.86	0.28	1.99	165	3.12	0.272**
Scup	643	3.06	1.17	27.78	172	3.79	0.281**
All species	81,057	0.62	0.00	4.51	341	35.84	0.385**

Table 4

Descriptive statistics for MRFSS (Marine Recreational Fishery Statistics Survey) 1981, 1988, and 1996 northeast U.S. coast catch per hour, positive catches only. Catch is given in numbers of fish. CV is the coefficient of variation (%). D is the Kolmogorov test statistic for normality. Test statistics significant at the 1% level ($P<0.01$) shown by (**), indicating rejection of the null hypothesis that catch rates follow a normal distribution.

Species	No. of trips	Mean	Median	Variance	CV	Skew	D
1981							
Bluefish	2288	1.56	0.75	10.00	203	9.48	0.317**
Summer Flounder	1380	0.82	0.50	1.07	126	5.35	0.229**
Atlantic cod	298	0.65	0.45	0.56	115	3.64	0.220**
Scup	165	2.56	1.67	10.41	125	2.16	0.242**
All species	9484	1.58	0.67	26.96	328	29.00	0.381**
1988							
Bluefish	2445	1.16	0.63	2.85	145	4.91	0.253**
Summer Flounder	2326	0.93	0.60	1.24	120	5.45	0.212**
Atlantic cod	1065	1.40	1.00	2.29	108	3.14	0.196**
Scup	614	3.31	1.71	17.98	128	3.09	0.223**
All species	19,094	1.37	0.67	6.67	188	11.08	0.301**
1996							
Bluefish	1666	1.13	0.55	3.15	157	4.80	0.270**
Summer Flounder	4196	0.87	0.58	0.90	109	3.93	0.198**
Atlantic cod	679	1.39	0.80	2.49	114	2.68	0.205**
Scup	438	4.49	2.73	34.38	131	3.38	0.228**
All species	39,094	1.29	0.63	8.49	226	28.09	0.331**

Table 5

Summary of goodness of fit tests for 1996 MRFSS (Marine Recreational Fishery Statistics Survey) catch per trip distributions, including zero catches, for bluefish, summer flounder, Atlantic cod, scup, and all species.

Species	Expected number of intervals	Degrees of freedom	χ^2 statistic	G statistic	$\chi^2_{0.01}$	D statistic	$D_{0.01}$
Bluefish							
Mean = 1.20							
Variance = 13.12							
n = 5457							
Lognormal	9	6	7314	5722	17	0.462	0.014
Poisson	7	5	5315	4251	15	0.394	0.014
Negative binomial	23	20	68	27	38	0.007	0.014
Summer flounder							
Mean = 2.33							
Variance = 13.49							
n = 7047							
Lognormal	11	8	8654	4714	20	0.281	0.012
Poisson	10	8	10,902	5772	20	0.307	0.012
Negative binomial	22	19	139	101	36	0.011	0.012
Atlantic cod							
Mean = 3.97							
Variance = 43.34							
n = 1099							
Lognormal	12	9	2138	1068	22	0.360	0.031
Poisson	12	10	8284	2212	23	0.425	0.031
Negative binomial	25	22	48	22	40	0.015	0.031
Scup							
Mean = 13.83							
Variance = 524.60							
n = 643							
Lognormal	28	25	389,173	3850	44	0.541	0.041
Poisson	25	23	6.67e+07	6391	42	0.544	0.041
Negative bionomial	51	48	305	235	74	0.053	0.041
All species							
Mean = 2.57							
Variance = 47.32							
n = 81,057							
Lognormal	14	11	180,754	83,230	25	0.382	0.004
Poisson	13	11	306,000	129,928	25	0.440	0.004
Negative binomial	51	48	1577	1146	74	0.020	0.004

chrysops, a Mid-Atlantic demersal schooling roundfish, likely to yield a relatively high catch per trip). These species were selected as examples because they occur over a broad range along the northeast U.S. coast, are among the most frequently caught by recreational fishermen, and their catch-rate distributions are representative of most species caught by recreational fishermen in the northeast U.S (USDOC, 1992). Four configurations of catch rate distributions were examined: 1) catch per trip distributions including zero catches, 2) catch per trip distributions with positive catches only, 3) catch per hour distributions including zero catches, and 4) catch per hour distributions with positive catches only.

Goodness-of-fit statistics for the lognormal, Poisson, and negative binomial distributions were calculated for the four individual species and for all species to help judge which error structure best characterized the MRFSS catch-rate data. A single year (1996) is presented because of the similarity of the catch distributions across species and time. Given the results of the Kolmogorov-Smirnov D tests from the descriptive statistics work, which indicated that none of the catch rates were normally distributed (see "Results" section), that error structure was not examined further. As with the descriptive statistics analysis, both catch-per-trip and catch-per-hour rates were examined in the goodness-of-fit exercise, both for

Table 6

Summary of goodness-of-fit tests for 1996 MRFSS (Marine Recreational Fishery Statistics Survey) catch per trip distributions, positive catches only, for bluefish, summer flounder, Atlantic cod, scup, and all species.

Species	Expected number of intervals	Degrees of freedom	χ^2 statistic	G statistic	$\chi^2_{0.01}$	D statistic	$D_{0.01}$
Bluefish							
Mean = 3.93							
Variance = 32.26							
n = 1666							
Lognormal	9	6	1803	1026	17	0.312	0.025
Poisson	11	9	2091	1211	22	0.312	0.025
Negative binomial	21	18	425	347	35	0.196	0.025
Summer flounder							
Mean = 3.91							
Variance = 16.46							
n = 4196							
Lognormal	10	7	6068	2863	18	0.270	0.016
Poisson	12	10	3821	2234	23	0.240	0.016
Negative binomial	20	17	699	587	33	0.143	0.016
Atlantic cod							
Mean = 6.43							
Variance = 54.39							
n = 679							
Lognormal	12	9	3376	962	22	0.379	0.040
Poisson	14	12	3419	925	26	0.365	0.040
Negative binomial	27	24	121	88	43	0.147	0.040
Scup							
Mean = 20.31							
Variance = 638.90							
n = 438							
Lognormal	30	27	3.74e+11	6565	47	0.543	0.049
Poisson	32	30	8.09e+07	3477	51	0.475	0.049
Negative binomial	50	47	204	147	72	0.089	0.049
All species							
Mean = 5.30							
Variance = 83.43							
n = 39,094							
Lognormal	11	8	70,234	24,957	20	0.254	0.001
Poisson	16	14	169,662	59,516	29	0.391	0.001
Negative binomial	50	47	12,293	10,217	72	0.201	0.001

all directed trips including zero catches and for positive catches only.

Simulated recreational fishery catch rates

To isolate the consequences of possible model misspecification in deriving standardized indices of abundance, negative binomial distributions with characteristics like those of MRFSS recreational catch-per-trip distributions were simulated by using the SAS RANTBL function (SAS, 2000). The simulated distributions were arranged to provide continuously decreasing, continuously increasing, and peaked (increasing to a peak and then decreasing) trends in an 11-year time series of catch per trip. For the decreasing trend, the simulation procedure began with year 1 set at a mean catch per trip = 3.0, maximum catch per trip of 50 fish per trip, and variance = 81.0, which are characteristic of the MRFSS catch-per-trip distributions for all species (Table 1). For year 1, this combination of mean and variance provided a maximum likelihood estimate of the negative binomial dispersion parameter, k, of 0.23.

The vector of expected probabilities of catch per trip for these initial moments, assuming a negative binomial distribution, was then used to randomly generate 1000

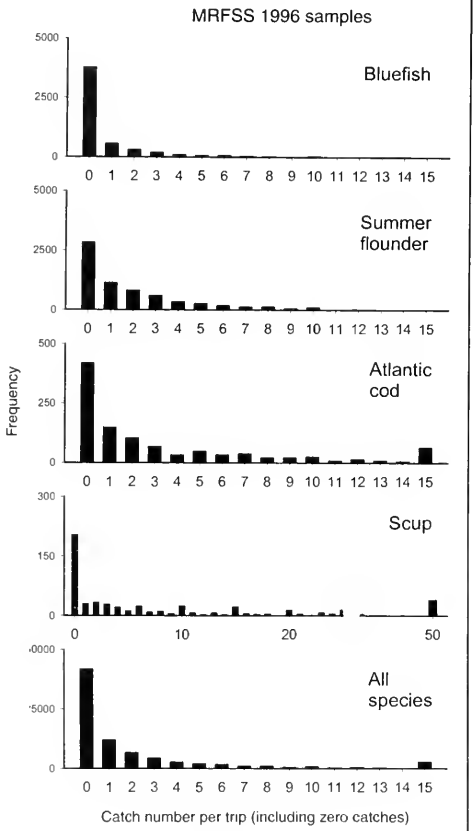

Figure 1

Marine Recreational Fishery Statistics Survey (MRFSS) 1996 sample data for bluefish, summer flounder, Atlantic cod, scup, and all species, Maine to the Florida east coast: catch number per trip (including zero catches). The 15 and 50 fish intervals are "plus groups" because they include totals for larger intervals.

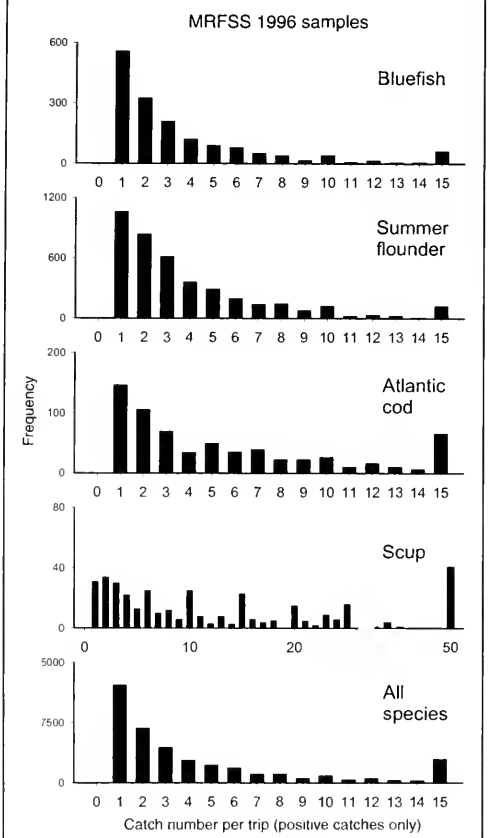

Figure 2

Marine Recreational Fishery Statistics Survey (MRFSS) 1996 sample data for bluefish, summer flounder, Atlantic cod, scup, and all species, Maine to the Florida east coast: catch number per trip (positive catches only). The 15 and 50 fish intervals are "plus groups" because they include totals for larger intervals.

observations of catch per trip (including zeroes) for year 1 (n=1000). The initial mean for year 2 was then set at 10 percent less than year 1 (i.e. 2.7) and the year 2 set of 1000 observations generated under the negative binomial assumption. The dispersion parameter, k, was held constant at the year 1 maximum likelihood estimate of 0.23, resulting in a decrease in variance, a relatively stable coefficient of variation (CV), and less frequent occurrence of large catch-per-trip values, as the mean decreased. These conditions were felt to best reflect the true changes in angler catch per trip as stock abundance declines. The exercise was repeated for years 3 to 11, providing a time series of decreasing simulated recreational fishery catch per trip. The simulated annual distributions, scaled (normalized) to the 11-year time series mean of 1.75, were re-ordered to create the increasing and peaked time series.

Standardized indices of abundance were then calculated from the simulated, trended series by using lognormal, Poisson, negative binomial, delta-lognormal, and delta-Poisson models, with year serving as the single classification vari-

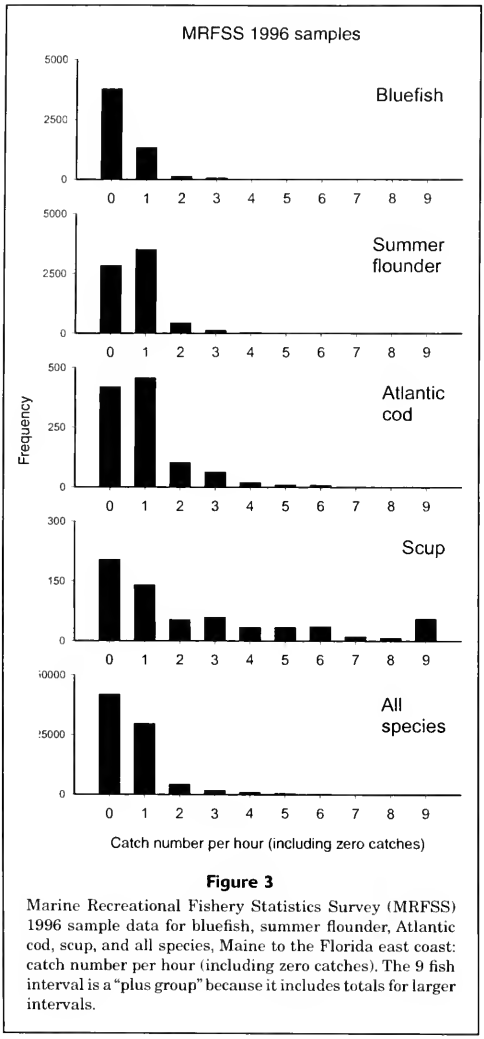

Figure 3

Marine Recreational Fishery Statistics Survey (MRFSS) 1996 sample data for bluefish, summer flounder, Atlantic cod, scup, and all species, Maine to the Florida east coast: catch number per hour (including zero catches). The 9 fish interval is a "plus group" because it includes totals for larger intervals.

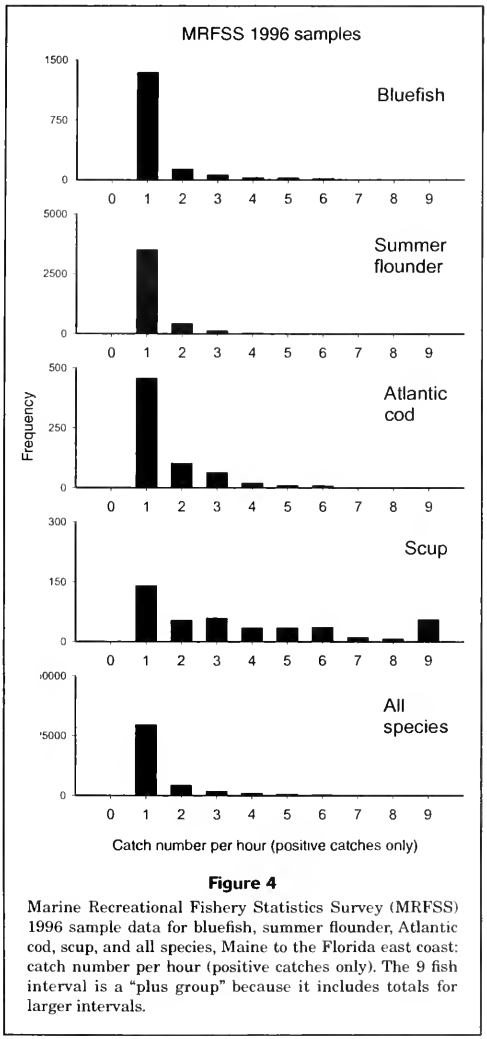

Figure 4

Marine Recreational Fishery Statistics Survey (MRFSS) 1996 sample data for bluefish, summer flounder, Atlantic cod, scup, and all species, Maine to the Florida east coast: catch number per hour (positive catches only). The 9 fish interval is a "plus group" because it includes totals for larger intervals.

able and index of abundance. Modeled in this way, the negative binomial model is expected to provide year-effect coefficients very close in absolute value to the unstandardized, mean simulated catch per trip of the true underlying negative binomial distribution because no other classification effects are present to account for variance from the unstandardized mean. The deviance of the year coefficients provided by the models, assuming the other error distributions, then provides an indication of the degree of model misspecification because virtually all the estimated variance in this particular exercise is due to model (process) error, except for the small amount generated by the random draw from the starting probability distributions.

MRFSS standardized indices of abundance, 1981–98

The potential effect of the assumed error structure on the calculation of standardized indices of abundance was further explored with empirical examples using the 1981–98 MRFSS time series of catch-per-trip rates (zero catches

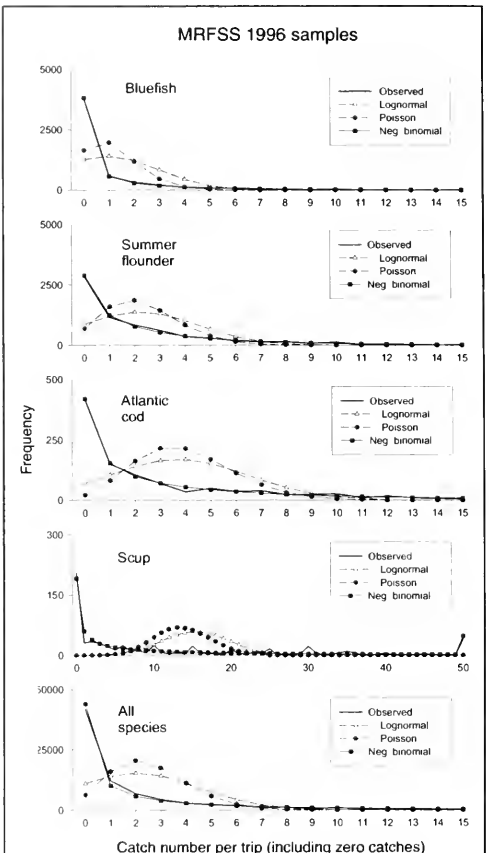

Figure 5

Observed and expected catch number per trip (including zero catches) frequency distributions for bluefish, summer flounder, Atlantic cod, scup, and all species, Maine to the Florida east coast. The 15 and 50 fish intervals are "plus groups" because they include totals for larger intervals.

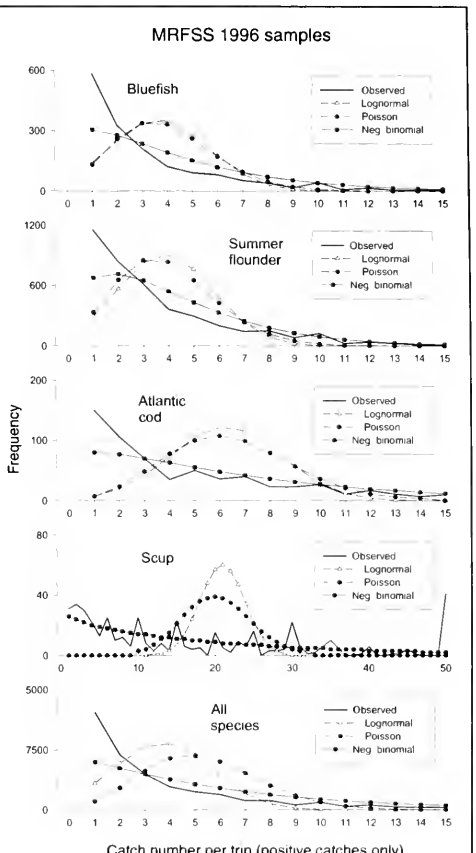

Figure 6

Observed and expected catch number per trip (positive catches only) frequency distributions for bluefish, summer flounder, Atlantic cod, scup, and all species, Maine to the Florida east coast. The 15 and 50 fish intervals are "plus groups" because they include totals for larger intervals.

included) for bluefish, summer flounder, Atlantic cod, scup, and for all species. Annual indices of stock abundance were developed from these MRFSS catch rate data following procedures in previous Atlantic coast bluefish and summer flounder stock assessments (Terceiro[1]; NEFSC[3]; Gibson and Lazar[5]). Standardized indices were calculated by applying lognormal, Poisson, negative binomial, delta-lognormal, and delta-Poisson models, using the main effects classification variables determined in these stock assessments to be statistically significant factors: year, fishing mode (shore, private or rental boat, party or charter boat), state of landing (Maine to Florida), fishing wave (two-month sampling period, e.g. Jan–Feb), fishing area (>3 miles from shore, ≤ 3 miles from shore), and days12, the angler-reported days of saltwater fishing during the previous 12 months (a proxy for angler avidity, experience, or skill, or a proxy for all three characteristics). The retransformed, bias-corrected (when necessary) year coefficients serve as the annual indices of stock abundance. Calculation and evaluation of the MRFSS standardized indices followed the general procedures described in the "Overview of statistical methods" in the "Materials and methods" section.

Table 7

Summary of goodness-of-fit tests for 1996 MRFSS (Marine Recreational Fishery Statistics Survey) catch per hour distributions, including zero catches, for bluefish, summer flounder, Atlantic cod, scup, and all species.

Species	Expected number of intervals	Degrees of freedom	χ^2 statistic	G statistic	$\chi^2_{0.01}$	D statistic	$D_{0.01}$
Bluefish							
Mean = 0.35							
Variance = 1.23							
n = 5457							
Lognormal	6	3	2806	3047	11	0.323	0.014
Poisson	5	3	514	41	11	0.028	0.014
Negative binomial	5	2	514	41	9	0.028	0.014
Summer flounder							
Mean = 0.52							
Variance = 0.72							
n = 7047							
Lognormal	7	4	2022	2430	13	0.245	0.012
Poisson	5	3	1408	1209	11	0.193	0.012
Negative binomial	5	2	1408	1209	9	0.193	0.012
Atlantic cod							
Mean = 0.86							
Variance = 2.00							
n = 1099							
Lognormal	7	4	289	300	13	0.243	0.031
Poisson	5	3	51	11	11	0.051	0.031
Negative binomial	5	2	51	11	9	0.051	0.031
Scup							
Mean = 3.06							
Variance = 27.78							
n = 643							
Lognormal	11	8	546	346	20	0.312	0.041
Poisson	10	8	1209	583	20	0.347	0.041
Negative binomial	19	16	54	39	32	0.032	0.041
All species							
Mean = 0.62							
Variance = 4.51							
n = 81,057							
Lognormal	13	10	144,556	126,529	23	0.575	0.004
Poisson	7	5	54,675	72,657	15	0.036	0.004
Negative binomial	7	4	54,675	72,657	13	0.036	0.004

Results

Descriptive statistics for MRFSS catch rates

Descriptive statistics of MRFSS catch rates for the four catch rate configurations, four individual species, and for all species are presented for the years 1981, 1988, and 1996 (Tables 1–4). These three years are characteristic of the 1981–2002 time series of MRFSS data. Given the similarity among these years, frequency distributions are plotted only for 1996 (Figs. 1–4). Catch rate means, both with and without zero catches, are generally much higher than medians, variances are much larger than the means, skewness is always much larger than zero, and there is a high proportion of zero catch and one-fish catch-rate observations. In all cases, the Kolmogorov-Smirnov D test statistics were significant at the 1% level. All of these factors indicate that MRFSS catch-rate distributions are highly contagious and overdispersed in relation to the normal distribution (Sokol and Rohlf, 1981). Scup has highest frequency of high catch rates (Figs. 1–4). The scup and Atlantic cod samples exhibit modes at regular intervals of high catch-per trip rates (e.g. 10, 15, 20, 25, and 30 fish per trip) that may indicate some degree of digit bias in the sampling.

Table 8

Summary of goodness of fit tests for 1996 MRFSS (Marine Recreational Fishery Statistics Survey) catch per hour distributions, positive catches only, for bluefish, summer flounder, Atlantic cod, scup, and all species.

Species	Expected number of intervals	Degrees of freedom	χ^2 statistic	G statistic	$\chi^2_{0.01}$	D statistic	$D_{0.01}$
Bluefish							
Mean = 1.13							
Variance = 3.15							
n = 1666							
Lognormal	6	3	1508	1462	11	0.446	0.025
Poisson	5	3	590	590	11	0.269	0.025
Negative binomial	5	2	590	590	9	0.269	0.025
Summer flounder							
Mean = 0.87							
Variance = 0.90							
n = 4196							
Lognormal	6	3	3005	3146	11	0.416	0.016
Poisson	5	3	838	921	11	0.210	0.016
Negative binomial	5	2	838	921	9	0.210	0.016
Atlantic cod							
Mean = 1.39							
Variance = 2.49							
n = 679							
Lognormal	6	3	414	368	11	0.356	0.040
Poisson	5	3	145	113	11	0.213	0.040
Negative binomial	5	2	145	113	9	0.213	0.040
Scup							
Mean = 4.49							
Variance = 34.38							
n = 438							
Lognormal	10	7	601	292	18	0.270	0.049
Poisson	11	9	725	324	22	0.280	0.049
Negative binomial	17	14	127	99	29	0.166	0.049
All species							
Mean = 1.29							
Variance = 8.49							
n = 39,094							
Lognormal	7	4	38,171	33,641	13	0.434	0.001
Poisson	8	6	31,475	16,429	17	0.270	0.001
Negative binomial	8	5	31,475	16,429	15	0.270	0.001

For the catch-per-trip configurations, catch rates were best characterized by the negative binomial distribution (Tables 5–6, Figs. 5–6). Note that the calculated chi-square, G-, and D-test statistics were generally significant at the 1% level, so that based on strict interpretation of these results, the null hypothesis that the observed distributions come from one of the theoretical distributions was rejected in all cases. However, the calculated test statistics for the negative binomial distributions were at least an order of magnitude smaller than those for the Poisson and lognormal distributions, suggesting that an underlying negative binomial distribution was much more likely. The distributions of the catch-per-hour rates generally had a truncated range compared to the catch-per-trip rate configurations (Figs. 1–4). For most of the catch-per-hour distributions, the maximum likelihood solution for the negative binomial k parameter occurred at very large values (>1000). The expected frequencies for the negative binomial distribution therefore converged to those expected for a Poisson distribution, resulting in identical test statistic values and indicating that the catch-per-hour rates are best characterized by the Poisson distribution (Tables 7–8, Figs. 7–8).

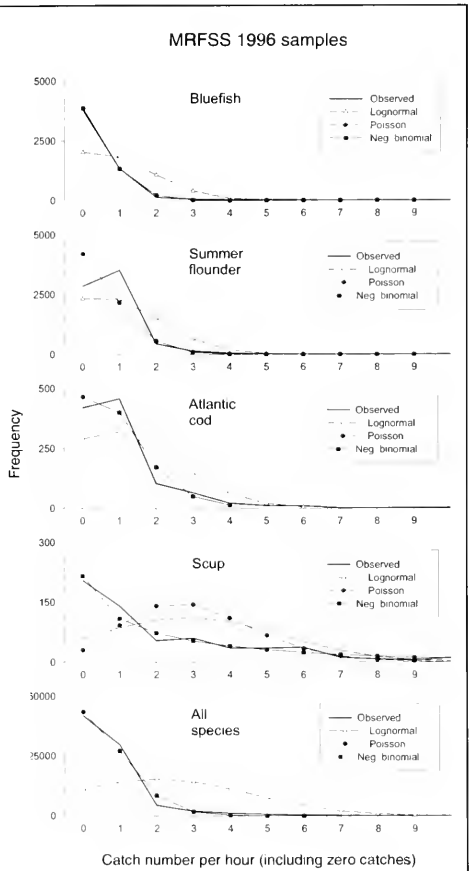

Figure 7

Observed and expected catch number per hour (including zero catches) frequency distributions for bluefish, summer flounder, Atlantic cod, scup, and all species, Maine to the Florida east coast. The 9 fish intervals is a "plus group" because it includes totals for larger intervals.

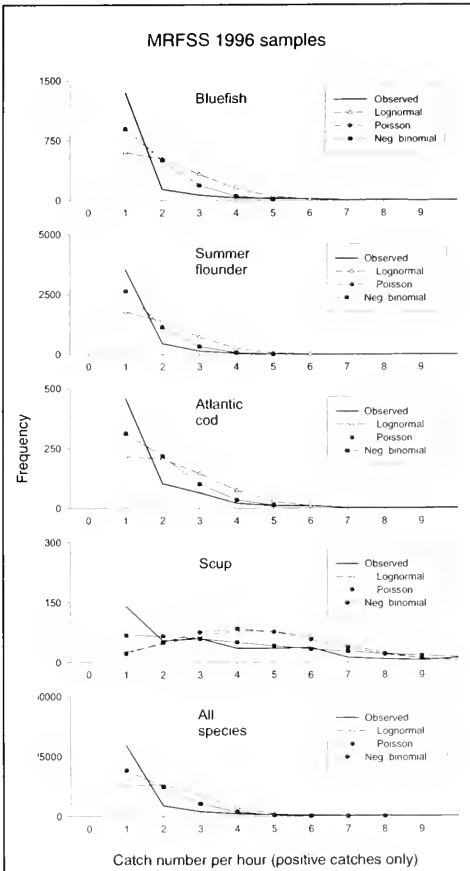

Figure 8

Observed and expected catch number per hour (positive catches only) frequency distributions for bluefish, summer flounder, Atlantic cod, scup, and all species, Maine to the Florida east coast. The 9 fish intervals is a "plus group" because it includes totals for larger intervals.

Simulated recreational fishery catch rates

The eleven simulated distributions of catch per trip had means ranging from 2.80 to 0.98 fish per trip, variances ranging from 31.81 to 4.39, and CVs of about 200%. Simulated variance decreased as the simulated mean decreased because the negative binomial dispersion parameter, k, was held constant at 0.23. The resulting unstandardized, simulated index of abundance declined by 65% over the 11 year series (Table 9).

All standardization model fits were highly significant ($P<0.001$), as characterized by the chi-square statistics for the year effect (Table 10). The three different time series trends had no effect on the results, and therefore only the results for the decreasing series are reported. The Poisson and negative binomial models generated year coefficients as standardized indices of abundance that were very similar to each other and, as expected, virtually identical to the unstandardized annual means, indicating a 65% decline over the time series (Fig. 9). Interestingly, the diagnostic

Table 9

Summary statistics for the simulated recreational fishery catch per trip assuming a negative binomial distribution, configured to decline by 10% in successive time periods (years). For year 1, starting maximum catch per trip was 50 fish per trip, mean was 3.0, variance was 81.00, coefficient of variation (CV) of 300%, and the dispersion parameter of the negative binomial distribution, k, was 0.23. In years 2–11, k was held constant at the year-1 value of 0.23, allowing the variance to decrease as the mean catch declined. Annual simulated means were scaled to the 11 year time series mean (1.75) for comparability with standardized indices calculated for decreasing, increasing, and peaked time series trends.

Year	Simulated mean catch per trip	Simulated maximum catch per trip	Simulated variance	Simulated CV (%)	Scaled simulated catch per trip
1	2.80	47	31.81	201	1.60
2	2.49	39	24.75	200	1.42
3	2.27	37	20.97	202	1.30
4	2.05	34	17.23	203	1.17
5	1.85	31	14.24	204	1.06
6	1.67	29	11.84	206	0.95
7	1.49	26	9.65	209	0.85
8	1.32	21	7.36	206	0.75
9	1.21	21	6.47	211	0.69
10	1.09	19	5.38	213	0.62
11	0.98	17	4.39	215	0.56

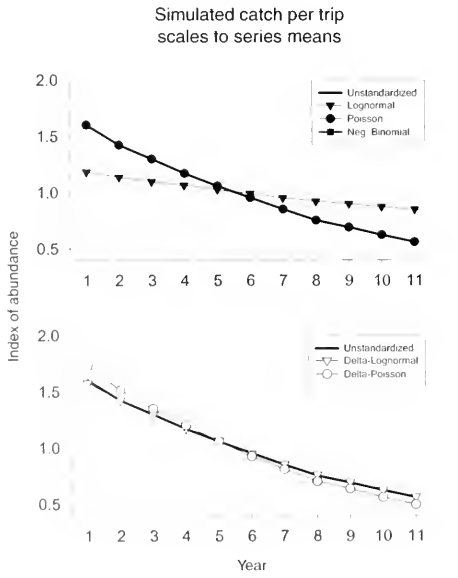

Figure 9

Simulated recreational fishery indices of abundance modeled under different error distribution assumptions.

statistics indicated a better determined year effect (more precise year coefficients) for the Poisson than for the negative binomial. However, the dispersion estimate (deviance/df) for the Poisson model was much greater than 1.0, indicating that the input data were overdispersed with respect to the Poisson distribution (Table 10). The latter was the expected result, given that the variance of the annual simulated data sets was much larger than the mean. The results indicated that the negative binomial was a more appropriate model, with a dispersion estimate closer to 1.0, which was also the expected result given the true negative binomial distribution of the simulated data (SAS, 2000).

The consequence of assuming a lognormal model for the true underlying negative binomial distribution was a more extreme smoothing of the true time series trends than with the other model assumptions, with a decline of only 28% over the time series (Fig. 9). The diagnostic statistics for the lognormal model indicated a significant model fit, but the dispersion estimate was much less than 1.0, indicating that the input data were underdispersed with respect to the lognormal distribution (Table 10). This finding is reflective of the large number of 0 and 1 catch-per-trip observations, and a lack of observations near the mean of the input probability distribution (SAS, 2000). In this simulation exercise, therefore, the lognormal model dispersion estimate of much less than 1.0 is indicative of model misspecification.

As noted in the "Materials and methods" section, the indices of abundance from the delta models are calculated as the product of the year-effect coefficients from the two component models. The interaction of the year coefficients from the binomial proportion positive catches and lognormal or Poisson positive catches components of the delta models

Table 10

Summary of model fits for simulated recreational fishery catch per trip (including zero catches) with a decreasing time series trend. Total model degrees of freedom were 10,989; for the positive catches component of the delta models, degrees of freedom were 4,184. Year-model-effect degrees of freedom were 10, and the year-model effect was highly significant ($P<0.0001$) in all five models.

Criterion	Value	Dispersion estimate (value/df)
Lognormal model		
Deviance	7330	0.6670
Log-likelihood	−13,773	
Year chi-square	183	
Poisson model		
Deviance	51,719	4.7064
Log-likelihood	−7483	
Year chi-square	2049	
Negative binomial model		
Deviance	10,699	0.9736
Log-likelihood	7524	
Year chi-square	239	
Delta models: binomial proportion positive catch		
Deviance	14,546	1.3237
Log-likelihood	−7273	
Year chi-square	78	
Delta-lognormal model: lognormal positive catches		
Deviance	3474	0.8303
Log-likelihood	−5557	
Year chi-square	119	
Delta-Poisson model: Poisson positive catches		
Deviance	15,822	3.7815
Log-likelihood	10,466	
Year chi-square	936	

Table 11

Summary of model fits for estimating indices of abundance from empirical MRFSS (Marine Recreational Fishery Statistics Survey) bluefish catch per trip (including zero catches), 1981–98. Total model degrees of freedom (df) were 130,300; for the positive catches component of the delta models, degrees of freedom were 48,447. All model fits and classification effects were highly significant ($P<0.001$).

Criterion	Value	Dispersion estimate (value/df)
Lognormal model		
Deviance	84,150	0.6458
Log-likelihood	−156,444	
Year chi-square	1835	
Poisson model		
Deviance	675,791	5.1864
Log-likelihood	−19,680	
Year chi-square	20,604	
Negative binomial model		
Deviance	99,393	0.7628
Log-likelihood	190,140	
Year chi-square	2104	
Delta models: binomial proportion positive catch		
Deviance	157,674	1.2101
Log-likelihood	−78,837	
Year chi-square	854	
Delta-lognormal model: lognormal positive catches		
Deviance	39,963	0.8249
Log-likelihood	−64,129	
Yera chi-square	1240	
Delta-Poisson model: Poisson positive catches		
Deviance	249,112	5.1419
Log-likelihood	193,660	
Year chi-square	10,501	

provided some interesting results in this simulation exercise. The binomial model component, common to both delta models, provided a highly significant year effect and indicated a 41% decline in abundance over the time series. The dispersion estimate indicated some overdispersion of the data with respect to the binomial distribution (Table 10).

The lognormal positive catches component of the delta-lognormal model also provided a highly significant year effect and indicated a 39% decline in abundance over the time series, producing a smoothing effect similar to that observed for the lognormal model of catch per trip including zeroes. The dispersion estimate indicated some underdispersion of the data with respect to the lognormal distribution (Table 10). The product of the annual year coefficients from the two delta-lognormal model components, which individually indicated less decline than the unstandardized indices, provided final indices of abundance that declined 64% over the time series (due to the product of two positive fractional values <1 providing a even smaller value <1)—nearly identical to the unstandardized, Poisson, and negative binomial series (Fig. 9).

The Poisson positive catches component of the delta-Poisson model provided a highly significant year effect and indicated a 51% decline in abundance over the time series. The dispersion estimate was much greater than 1.0, indicating overdispersion of the data with respect to the Poisson model (Table 10). The product of the annual year coefficients from the two delta-Poisson model components provided indices of abundance that declined 71% over the time series, a slightly greater decrease than for the other models (Fig. 9). Note again that the delta-lognormal and delta-Poisson models share the same binomial proportion positive catch model components, and therefore annual year coefficients for this component. The decrease estimated by the delta-Poisson model was greater than that for the delta-lognormal because the year coefficients from the Poisson positive catch model were all smaller, and more closely matching the unstandardized positive catch series, than the comparable

Table 12

Summary of model fits for estimating indices of abundance from empirical MRFSS (Marine Recreational Fishery Statistics Survey) summer flounder catch per trip (including zero catches), 1981–98. Total model degrees of freedom (df) were 102,162; for the positive catches component of the delta models, degrees of freedom were 52,507. All model fits and classification effects were highly significant ($P<0.001$).

Criterion	Value	Dispersion estimate (value/df)
Lognormal model		
Deviance	66,452	0.6505
Log-likelihood	−122,989	
Year chi-square	2663	
Poisson model		
Deviance	444,657	4.3525
Log-likelihood	−14,827	
Year chi-square	14,053	
Negative binomial model		
Deviance	96,698	0.9465
Log-likelihood	97,777	
Year chi-square	2560	
Delta models: binomial proportion positive catch		
Deviance	130,341	1.2758
Log-likelihood	−65,171	
Year chi-square	2498	
Delta-lognormal model: lognormal positive catches		
Deviance	36,780	0.7005
Log-likelihood	−65,202	
Year chi-square	1203	
Delta-Poisson model: Poisson positive catches		
Deviance	183,019	3.4856
Log-likelihood	115,991	
Year chi-square	5675	

Table 13

Summary of model fits for estimating indices of abundance from empirical MRFSS (Marine Recreational Fishery Statistics Survey) Atlantic cod catch per trip (including zero catches), 1981–98. Total model degrees of freedom (df) were 20,629; for the positive catches component of the delta models, degrees of freedom were 13,160. All model fits and classification effects were highly significant ($P<0.001$).

Criterion	Value	Dispersion estimate (value/df)
Lognormal model		
Deviance	19,425	0.9416
Log-likelihood	−28,697	
Year chi-square	380	
Poisson model		
Deviance	142,834	6.9239
Log-likelihood	54,501	
Year chi-square	4090	
Negative binomial model		
Deviance	21,824	1.0579
Log-likelihood	98,335	
Year chi-square	323	
Delta models: binomial proportion positive catch		
Deviance	24,997	1.2117
Log-likelihood	−78,837	
Year chi-square	191	
Delta-lognormal model: lognormal positive catches		
Deviance	11,657	0.8858
Log-likelihood	−17,920	
Year chi-square	353	
Delta-Poisson model: Poisson positive catches		
Deviance	75,359	5.7264
Log-likelihood	88,239	
Year chi-square	2805	

lognormal positive catch year coefficients over the course of the time series. For example, the year-11 coefficient from the binomial proportion positive catches model was 0.59; the year-11 lognormal positive catches coefficient was 0.61, providing a product for the year-11 index of 0.36. In contrast, the year-11 Poisson positive catches coefficient was 0.49, providing a product for the year-11 index of 0.29. When these and the other annual coefficients were scaled to the respective series means, the delta-Poisson model indicated a slightly greater decline over the time series.

MRFSS standardized indices of abundance, 1981–98

All standardization models of the MRFSS catch per trip (including zero catches), for the four individual species and for all species, fitted well. In part because of the large number of observations, the overall model fits and the individual classification effects (year, mode, state, wave, and days12) were all highly significant. Only the year effect chi-square statistics are tabulated because the year effect coefficients serve as the annual indices of abundance (Tables 11–15). The year effect was generally the second or third most important effect in the models, after mode and state. The dispersion estimates (deviance/df) for the lognormal models indicated the data were generally underdispersed with respect to the lognormal; the dispersion estimates for the Poisson models indicated overdispersion with respect to that distribution. The dispersion estimates for the negative binomial models and binomial components of the delta models were generally close to 1.0, indicating appropriate model specification (Tables 11–15).

As in the simulated catch-rate exercise, the lognormal standardized abundance indices generally show lower

Table 14

Summary of model fits for estimating indices of abundance from empirical MRFSS (Marine Recreational Fishery Statistics Survey) scup catch per trip (including zero catches), 1981–98. Total model degrees of freedom (df) were 17,604; for the positive catches component of the delta models, degrees of freedom were 11,124. All model fits and classification effects were highly significant ($P<0.001$).

Criterion	Value	Dispersion estimate (value/df)
Lognormal model		
Deviance	32,270	1.8331
Log-likelihood	−30,346	
Year chi-square	332	
Poisson model		
Deviance	375,924	21.3545
Log-likelihood	309,490	
Year chi-square	12,094	
Negative binomial model		
Deviance	18,668	1.0604
Log-likelihood	466,529	
Year chi-square	369	
Delta models: binomial proportion positive catch		
Deviance	22,027	1.2512
Log-likelihood	−11,013	
Year chi-square	174	
Delta-lognormal model: lognormal positive catches		
Deviance	14,340	1.2891
Log-likelihood	−17,225	
Year chi-square	350	
Delta-Poisson model: Poisson positive catches		
Deviance	212,250	19.0804
Log-likelihood	391,327	
Year chi-square	8793	

Table 15

Summary of model fits for estimating indices of abundance from empirical MRFSS (Marine Recreational Fishery Statistics Survey catch per trip for all species (including zero catches), 1981–98. Total model degrees of freedom (df) were 1,033,367; for the positive catches component of the delta models, degrees of freedom were 457,598. All model fits and classification effects were highly significant ($P<0.001$).

Criterion	Value	Dispersion estimate (value/df)
Lognormal model		
Deviance	861,881	0.8341
Log-likelihood	−1,372,576	
Year chi-square	7246	
Poisson model		
Deviance	8,048,246	7.7884
Log-likelihood	277,042	
Year chi-square	28,734	
Negative binomial model		
Deviance	870,357	0.8422
Log-likelihood	3,118,822	
Year chi-square	2243	
Delta models: binomial proportion positive catch		
Deviance	1,351,532	1.3079
Log-likelihood	−675,766	
Year chi-square	11,867	
Delta-lognormal model: lognormal positive catches		
Deviance	466,644	1.0198
Log-likelihood	653,838	
Year chi-square	655	
Delta-Poisson model: Poisson positive catches		
Deviance	3,773,909	8.2472
Log-likelihood	2,414,210	
Year chi-square	10,785	

rates of change in abundance than do the unstandardized, Poisson, or negative binomial indices, with the CV of the lognormal series about 25–50% of the CV of the unstandardized indices (Figs. 10–14). In effect, the lognormal standardization of MRFSS per trip catch rates had an unintended (and undesirable) smoothing effect on the independent annual indices abundance. The Poisson and negative binomial models generally provided interpretations of the trend and annual changes in abundance very similar to those of the unstandardized indices.

For bluefish, the delta-lognormal, and delta-Poisson models provided time series of indices with about the same variability and trend, but slightly different annual changes, as those from the unstandardized, Poisson, and negative binomial models. For summer flounder, Atlantic cod, scup, and all species, the delta-lognormal and delta-Poisson models provided time series of abundance indices that were more variable, with slightly different trends and annual changes, than the unstandardized, Poisson, and negative binomial series. This last result is comparable to that observed for the delta models used with the simulated data and is therefore likely due in part to model misspecification of the positive catch-per-trip component (recall that catch per trip for these examples is best characterized by the negative binomial distribution) and a comparable interaction of the binomial, lognormal, and Poisson model year coefficients.

Discussion

The frequency distributions of recreational fishery catch-rate data as sampled by the MRFSS are highly skewed, often with a significant proportion of zero catch observations. The present study indicates that MRFSS catch rates generally are not normally or lognormally distributed

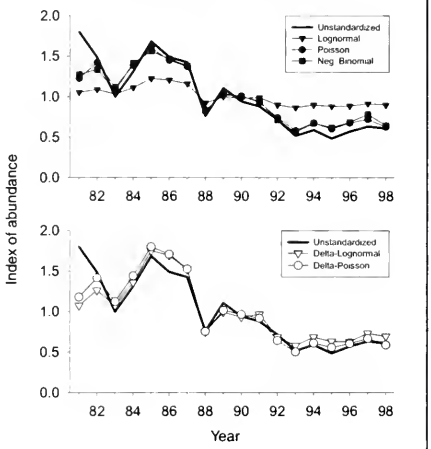

Figure 10

Indices of bluefish abundance (catch number per trip including zero catches) modeled under different error distribution assumptions, 1981–98.

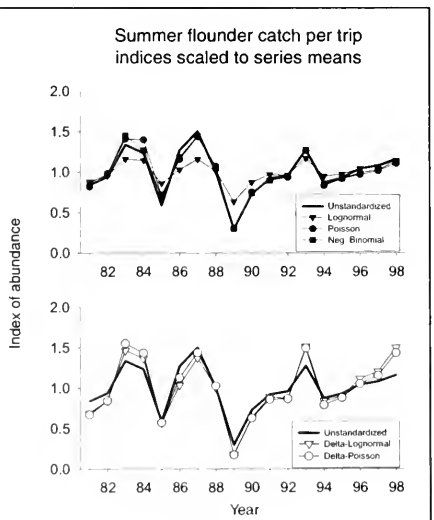

Figure 11

Indices of summer flounder abundance (catch number per trip including zero catches) modeled under different error distribution assumptions, 1981–98.

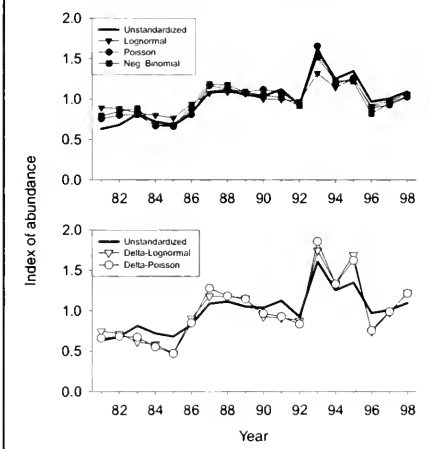

Figure 12

Indices of Atlantic cod abundance (catch number per trip including zero catches) modeled under different error distribution assumptions, 1981–98.

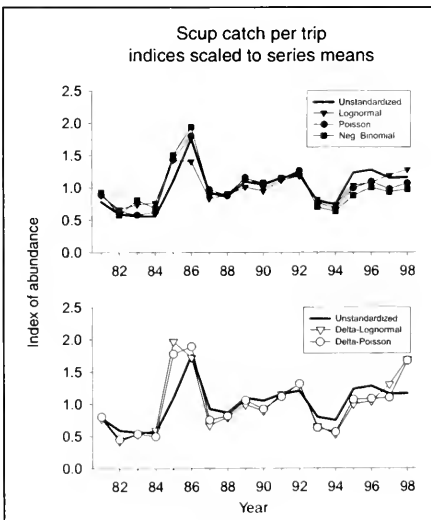

Figure 13

Indices of scup abundance (catch number per trip including zero catches) modeled under different error distribution assumptions, 1981–98.

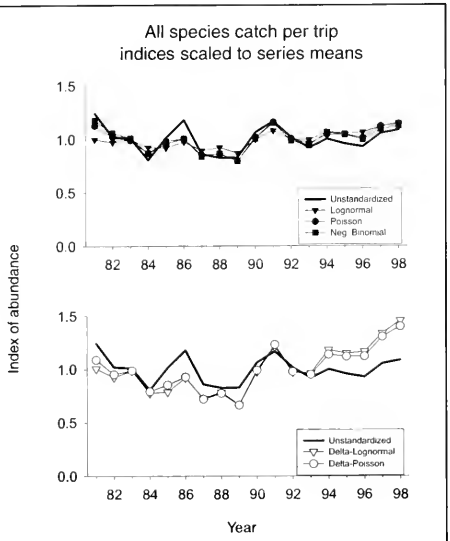

Figure 14

Indices of all species abundance (catch number per trip including zero catches) modeled under different error distribution assumptions, 1981–98.

but usually best characterized by the Poisson or negative binomial distribution, depending on the manner in which the catch rate is configured. This finding suggests that standardization methods for MRFSS catch-rate data where Poisson (in the case of per hour rates) or negative binomial (for per trip rates) error structures are assumed would usually be more appropriate than methods where normal or lognormal error structures are assumed.

The modeling of both the simulated and empirical MRFSS catch rates indicates that one may draw erroneous conclusions about stock trends by assuming the wrong error distribution in procedures used to developed standardized indices of abundance. The results demonstrate the importance of considering not only the overall model fit and significance of classification effects, but also the possible effects of model misspecification, when determining the most appropriate model construction. In particular, the simulation exercise indicates that assuming a lognormal model in the calculation of indices of abundance from recreational fishery catch-per-trip data with a true underlying negative binomial distribution will provide indices that will strongly underemphasize the true trends in the indices, and therefore in stock abundance. This underestimation applies equally to populations that may be declining or increasing faster than the lognormally standardized indices might indicate.

The MRFSS catch-per-trip indices standardized with the negative binomial model, which the descriptive statistics and goodness-of-fit results suggest should be the appropriate model, differ relatively little from the unstandardized indices, indicating that the model effects accounted for a low percentage of the variation in mean catch rate. The classification categories recorded in the general MRFSS sampling are broad, and even measures of angling avidity such as "angler-reported days of saltwater fishing during the previous 12 months" may not be adequate proxies for the real factors (besides stock abundance) that account for variation in recreational fishery mean catch rates. To make standardization analysis of MRFSS catch rate data potentially more useful, by accounting for a significantly larger part of the unexplained variance and thus providing more accurate indices of abundance, more information on the characteristics of individual fishing trips may be needed. Such information might include details on the type of equipment used, the skills, experience, avidity, and identity of the individual fishermen, and detailed temporal and spatial information about fishing trips. In the future, collection of detailed trip data for general recreational fisheries may be best accomplished by the identification and sampling of "test fleets" of known, individual fishermen.

Acknowledgments

I thank Vic Crecco of the Connecticut Department of Environmental Protection, for raising questions about the best way to calculate indices of abundance from recreational fishery catch rate data during debates over the bluefish assessments; Paul Rago of the Northeast Fisheries Science Center, for numerous discussions about statistical distributions and tests; and two anonymous *Fishery Bulletin* referees, whose comments helped improve the quality of the analyses and therefore the usefulness of the results.

Literature cited

Bannerot, S. P., and C. B. Austin.
1983. Using frequency distributions of catch per unit effort to measure fish-stock abundance. Trans. Am. Fish. Soc. 112:608–617.

Berry, D. A.
1987. Logarithmic transformations in ANOVA. Biometrics 43:439–456.

Bliss, C. I., and R. A. Fisher.
1953. Fitting the negative binomial distribution to biological data. Biometrics 9:177–200.

Bradu, D., and Y. Mundlak.
1970. Estimation in lognormal linear models. J. Am. Stat. Assoc. 65:198–211.

Brown, C. A.
1999. Standardized catch rates for yellowfin tuna (*Thunnus albacares*) and bigeye tuna (*Thunnus obesus*) in the Virginia-Massachusetts (US) rod and reel fishery. ICCAT (International Commission for the Conservation of Tunas) Col. Vol. Sci. Pap. Vol. 49(3):357–369.
2001. Standardized catch rates for yellowfin tuna (*Thunnus albacares*) in the Virginia-Massachusetts (U.S.) Rod and reel fishery during 1986–1999. ICCAT (International Commission for the Conservation of Tunas) Col. Vol. Sci. Pap. Vol. 52:190–201.

Brown, C. A., and J. A. Browder.
1994. Standardized catch rates of small bluefin tuna in the Virginia–Rhode Island (U.S.) rod and reel fishery. ICCAT (International Commission for the Conservation of Tunas) Col. Vol. Sci. Pap. Vol. 32(2):248–254.

Brown, C. A., and C. E. Porch.
1997. A numerical evaluation of lognormal, delta-lognormal and Poisson models for standardizing indices of abundance from west Atlantic bluefin tuna catch per unit effort data (preliminary results). ICCAT (International Commission for the Conservation of Tunas) Col. Vol. Sci. Pap. Vol. 46(2):233–236.

Brown, C. A., and S. C. Turner.
2001. Updated standardized catch rates of bluefin tuna, *Thunnus thynnus*, from the rod and reel/handline fishery off the northeast United States during 1980–1999. ICCAT (International Commission for the Conservation of Tunas) Col. Vol. Sci. Pap. Vol. 52:984–1006.

Finney, D. J.
1951. On the distribution of a variate whose logarithm is normally distributed. Suppl. J. Stat. Soc. 7:155–161.

Gavaris, S.
1980. Use of a multiplicative model to estimate catch rate and effort from commercial data. Can. J. Fish. Aquat. Sci. 37:2272–2275.

Gulland, J. A.
1956. On the fishing effort in English demersal fisheries. Fish. Investig. Ser. II Mar. Fish. G. B. Minist. Agric. Fish. Food 20(5), 41 p.

Hilborn, R.
1985. Fleet dynamics and individual variation: why some people catch more fish than others. Can. J. Fish. Aquat. Sci. 42:2–13.

Jones, C. M., D. S. Robson, H. D. Lakkis, and J. Kressel.
1995. Properties of catch rates used in analysis of angler surveys. Trans. Am. Fish. Soc. 124:911–928.

Kimura, D. K.
1981. Standardized measures of relative abundance based on modeling log (c.p.u.e.), and their application to Pacific ocean perch (*Sebastes alutus*). J. Cons. Int. Explor. Mer 39:211–218.

Lawless, J. F.
1987. Negative binomial and mixed Poisson regression. Can. J. Stat. 15(3):209–225.

Lo, N. C., L. D. Jacobson, and J. L. Squire.
1992. Indices of relative abundance from fish spotter data based on delta-lognormal models. Can. J. Fish. Aquat. Sci. 49:2515–2526.

Manton, K. G., Woodbury, M. A., and E. Stallard.
1981. A variance components approach to categorical data models with heterogenous cell populations: analysis of spatial gradients in lung cancer mortality rates in North Carolina counties. Biometrics 37:259–269.

McCullagh, P., and J. A. Nelder.
1989. Generalized linear models, 511 p. Chapman and Hall, London.

NMFS (National Marine Fisheries Service).
1995. Status of the fishery resources off the northeastern United States for 1994. U.S. Dep. Commer., NOAA Tech. Memo. NMFS-NE-108, 140 p.
1996. Our living oceans. Report on the status of U.S. living marine resources, 1995. U.S. Dep. Commer., NOAA Tech. Memo. NMFS-F/SPO-19, 160 p.

O'Brien, L. S., and R. K. Mayo.
1988. Sources of variation in catch per unit effort of yellowtail flounder, *Limanda ferruginea* (Storer), harvested off the coast of New England. Fish. Bull. 86(1):91–108.

Ortiz, M., S. C. Turner, and C. A. Brown.
1999. Standardized catch rates for bluefin tuna, *Thunnus thynnus*, from the rod and reel fishery off the northeast United States from 1980–1997. ICCAT (International Commission for the Conservation of Tunas) Col. Vol. Sci. Pap. Vol. 49(2):254–269.

Pennington, M.
1983. Efficient estimators of abundance, for fish and plankton surveys. Biometrics 39:281–286.

Power, J. H., and E. B. Moser.
1999. Linear model analysis of net catch data using the negative binomial distribution. Can. J. Fish. Aquat. Sci. 56:191–200.

Robson, D. S.
1966. Estimation of the relative fishing power of individual ships. Comm. N.W. Atl. Fish. Res. Bull. 3:5–14.

SAS Institute.
2000. SAS OnlineDoc, version 8. SAS Institute Inc., Cary NC. http://www.sas.com/ts.

Searle, S. R.
1987. Linear models for unbalanced data, 536 p. John Wiley and Sons, Inc., New York, NY.

Smith, B. D.
1999. A probabilistic analysis of decision-making about trip duration by Strait of Georgia sport anglers. Can. J. Fish. Aquat. Sci. 56:960–972.

Smith, S. J.
1990. Use of statistical models for the estimation of abundance from groundfish trawl survey data. Can. J. Fish. Aquat. Sci. 47:894–903.
1996. Analysis of data from bottom trawl surveys. NAFO Scientific Council Studies 28:25–53.

Snedecor, G. W., and W. G. Cochran.
1967. Statistical methods, 593 p. Iowa State Univ. Press, Ames, IA.

Sokal, R. R., and F. J. Rohlf.
1981. Biometry, 859 p. W. H. Freeman and Co., New York, NY.

Taylor, C. C.
1953. Nature of the variability in trawl catches. Fish. Bull. 54:145–166.

Turner, S. C., C. A. Brown, and H. Huang.
1997. Standardized catch rates of small bluefin tuna, *Thunnus thynnus*, from the U.S. rod and reel fishery off Virginia–Rhode Island in 1980–1995. ICCAT (International Commission for the Conservation of Atlantic Tunas) Col. Vol. Sci. Pap. Vol. 46(2):295–310.

USDOC (U.S. Department of Commerce).
1992. Marine recreational fishery statistics survey, Atlantic and Gulf coasts, 1990–1991, 275 p. Current Fisheries Statistics 9204.
2001. Marine recreational fishery statistics survey. U.S. Dep. Commer., Washington, DC. http://www.st.nmfs.gov/st1/recreational/index. [Accessed 30 January 2001.]

Williams, D. A.
1976. Improved likelihood ratio tests for complete contingency tables. Biometrika. 63:33–37.

Scales of spatial variation in demography of a large coral-reef fish—an exception to the typical model?

Ashley J. Williams
School of Marine Biology and Aquaculture
and
CRC Reef Research Centre
James Cook University
Townsville, Queensland, 4811, Australia
E-mail address: ashley.williams@jcu.edu.au

Campbell R. Davies
Bruce D. Mapstone
CRC Reef Research Centre
James Cook University
Townsville, Queensland 4811, Australia

Garry R. Russ
School of Marine Biology and Aquaculture
James Cook University
Townsville, Queensland, 4811, Australia

Abstract—Spatial variation in demographic parameters of the red throat emperor (*Lethrinus miniatus*) was examined among 12 coral reefs in three geographic regions (Townsville, Mackay, and Storm Cay) spanning over 3° of latitude of the Great Barrier Reef, Australia. Estimates of demographic parameters were based on age estimates from counts of annuli in whole otoliths because there was no significant difference in age estimates between whole and sectioned otoliths. There were significant regional differences in age structures, rates of somatic and otolith growth, and total mortality. The Townsville region was characterized by the greatest proportion of older fish, the smallest maximum size, and the lowest rates of otolith growth and total mortality. In contrast the Mackay region was characterized by the highest proportion of younger fish, the largest maximum size, and the highest rates of otolith growth and total mortality. Demographic parameters for the Storm Cay region were intermediate between the other two regions. Historic differences in fishing pressure and regional differences in productivity are two alternative hypotheses given to explain the regional patterns in demographic parameters. All demographic parameters were similar among the four reefs within each region. Thus, subpopulations with relatively homogeneous demographic parameters occurred on scales of reef clusters. Previous studies, by contrast, have found substantial between-reef variation in demographic parameters within regions. Thus spatial variation in demographic parameters for *L. miniatus* may differ from what is assumed typical for a coral-reef fish metapopulation.

Manuscript approved for publication 17 December 2002 by Scientific Editor.
Manuscript received 4 April 2003 at NMFS Scientific Publications Office.
Fish Bull. 101:673–683 (2003).

Estimates of demographic parameters, such as growth and mortality rates, are fundamental to the understanding of a species population dynamics and for predicting responses of populations to exploitation. Processes affecting population dynamics operate at a number of spatial and temporal scales (Levin, 1992) and can result in subpopulations with distinct demographics. Differences in demography between populations may suggest geographic or reproductive isolation (or both) and as such have been used in stock identification for fisheries assessment and management purposes (e.g. Begg et al., 1999).

Identifying the "unit stock" has been the primary focus of studies of spatial structure of harvested populations in most fisheries. Knowledge of spatial structure within a unit stock is important for both fisheries management, because potential yields may vary spatially within a population (Caddy, 1975), and for conservation, in order to maintain intraspecific diversity (Nielson, 1998). Hence, it is important to estimate demographic parameters over a range of temporal and spatial scales to determine the scale(s) at which the parameters vary significantly (Caley et al., 1996) and, therefore, to infer which scales are of greatest importance for assessment and management purposes (Sale, 1998).

Most coral-reef fish exist as metapopulations of sedentary adult populations linked by pelagic larval dispersal (Sale, 1998). Consequently, adult populations of reef fish are commonly spatially segregated and may be exposed to different environmental, biological, and ecological processes, resulting in spatial differences in demographic parameters at a range of spatial scales. Relatively few studies, however, have focussed on spatial variation in demographic parameters of harvested species of coral-reef fish. Those that have, have generally focussed on spatial scales within individual reefs or among reefs within a single region (e.g. Ferreira and Russ, 1995; Hart and Russ, 1996; Newman et al., 1996). Comprehensive multiscale approaches are rare (but see Adams et al., 2000; Meekan et al., 2001).

The spatial structure of coral-reef populations has generated considerable interest in terms of the use of spatial closures, or marine protected areas (MPAs), as an effective tool for their management (Roberts and Polunin,

1991). However, the lack of information about the stock structure of, and connectivity among, adult populations has hindered MPA design (Walters and Bonfil, 1999). Conservation management of the Great Barrier Reef (GBR) has included the use of spatial closures of areas to activities, including fishing, for more than 15 years. The majority of spatial closures to line fishing are of individual coral reefs or groups of reefs. This spatial management strategy is underpinned by the assumption of the metapopulation model of coral-reef fish described above. That is, closing individual reefs to fishing will protect the adult populations on those reefs, and potentially provide a source of larvae to areas open to fishing. Management of line fishing on the GBR currently includes bag limits for recreational fishermen and minimum-size restrictions that are uniform for all fishermen and across the entire area of the fishery. Such management regulations are based on the assumption that the demography of target species does not vary substantially over the species range and on the assumption that that populations on the GBR represent a single, homogeneous stock.

The red throat emperor (*Lethrinus miniatus*) (also known as the trumpet emperor) is a relatively long-lived (>20 years) (Loubens, 1980; Brown and Sumpton, 1998) member of the Lethrinidae and has a restricted distribution in the western Pacific and eastern Indian Oceans (Carpenter and Allen, 1989). On the GBR it is the second most important demersal species in a multispecies line fishery, contributing up to 1000 metric tons annually to the combined commercial and recreational catch (Mapstone et al.[1]; Higgs[2]). As with many tropical lethrinids, information on the biology and ecology of *L. miniatus* is scarce. The limited data available indicate that *L. miniatus* is usually associated with coral reefs, but that it is also commonly caught in deeper water, in sand, and rubble areas between reefs (Carpenter and Allen, 1989; Newman and Williams, 1996; Williams and Russ[3]). The habitat of juvenile *L. miniatus* is unknown, but Williams and Russ[3] have suggested that juveniles may occupy the deeper rubble areas adjacent to reefs. Like some other coral-reef fish, *L. miniatus* is thought to form large aggregations associated with spawning (Russell[4]). These available data suggest that *L. miniatus* adults have the capacity to move among individual reefs on the GBR. This movement pattern contrasts with information on movement patterns of other large coral-reef species such as the coral trout (*Plectropomus leopardus*) (also known as the leopard coral grouper, Heemstra and Randall, 1993) where adults show limited movement within a single reef and very restricted movements between reefs (Davies, 1995). It also contrasts with movement patterns of the majority of coral-reef fish, where adults are known to have very restricted home ranges and display little, if any, movement between reefs (Lewis 1997; Sale, 1998). Therefore the relevant spatial scale affecting demographic parameters of *L. miniatus* may be larger than an individual reef and thus is different from that for most "typical" coral-reef fish.

The central objective of this study was to determine how the spatial patterns in demography of large, more mobile reef fish differ from smaller site-attached reef-fish species. To achieve this we used validated age estimates to examine spatial variation in demographic parameters of populations of *L. miniatus* across two spatial scales most relevant to assessing and managing the species on the GBR: 1) among individual reefs within regions and, 2) among geographic regions. Specifically, we estimated age structures, growth, mortality, and otolith growth rates for among four reefs (all closed to fishing) within each of three geographic regions spanning over 500 km (over 3° of latitude) of the GBR.

Materials and methods

Collection methods

Samples of *L. miniatus* were collected from three geographic regions of the GBR as part of a large-scale manipulative experiment to examine the effects of line fishing on the GBR (Davies et al.[5]; Mapstone et al.[6]). The three regions cover most of the distribution of *L. miniatus* on the GBR (Fig. 1), which is restricted to the southern 50% of the GBR. Within each region *L. miniatus* were collected from six individual reefs. Four of these reefs were zoned "Marine National Park B" and were closed to all forms of fishing (referred to as "closed reefs" in this article) whereas the other two reefs were zoned "General Use B" and were

[1] Mapstone, B. D., J. P. McKinlay, and C. R. Davies. 1996. A description of commercial reef line fishery logbook data held by the Queensland Fisheries Management Authority. Report to the Queensland Fisheries Management Authority from the Cooperative Research Centre for the Ecologically Sustainable Development of the Great Barrier Reef, and the Department of Tropical Environmental Studies and Geography, James Cook University, Queensland, Australia, 480 p. [Available from the Queensland Fisheries Service, G.P.O. Box 46, Brisbane, Queensland, Australia 4001.]

[2] Higgs, J. 2001. Experimental recreational catch estimates for Queensland residents. Results from the 1999 diary round. RFISH technical report no. 3. Queensland Fisheries Service, Australia, 62 p. [Available from the Queensland Fisheries Service, G.P.O. Box 46, Brisbane, Queensland, Australia 4001.]

[3] Williams, D. McB., and G. R. Russ. 1994. Review of data on fishes of commercial and recreational fishing interest on the Great Barrier Reef. Report to the Great Barrier Reef Marine Park Authority, 103 p. [Available from the Great Barrier Reef Marine Park Authority, P.O. Box 1379, Townsville, Queensland, Australia, 4810.]

[4] Russell, M. 2001. Spawning aggregations of reef fishes on the Great Barrier Reef: implications for management. Report from the Great Barrier Reef Marine Park Authority, 37 p. [Available from the Great Barrier Reef Marine Park Authority, P.O. Box 1379, Townsville, Queensland, Australia, 4810].

[5] Davies, C. R., B. D. Mapstone, A. Ayling, D. C. Lou, A. Punt, G. R. Russ, M. A. Samoilys, A. D. M. Smith, D. J. Welch, and D. McB. Williams. 1998. Effects of line fishing experiment 1995–1997: project structure and operations. Supplementary to progress report. CRC Reef Research Centre, Townsville, Australia, 28 p. [Available from the CRC Reef Research Centre, P.O. Box 772, Townsville, Queensland, Australia 4810).

[6] Mapstone, B. D., C. R. Davies, D. C. Lou, A. E. Punt, G. R. Russ, D. A. J. Ryan, A. D. M. Smith, and D. McB. Williams. 1998. Effects of line fishing experiment 1995-1997: progress report. CRC Reef Research Centre, 86 p. [Available from the CRC Reef Research Centre, P.O. Box 772, Townsville, Queensland, Australia 4810].

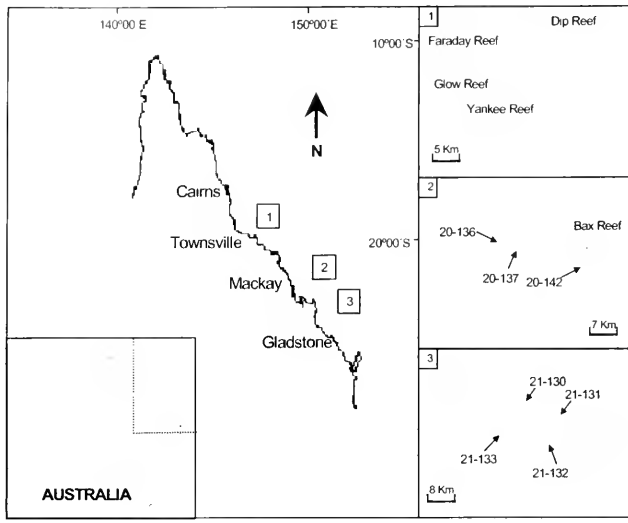

Figure 1

Location of reefs sampled for *L. miniatus* from October 1995 to January 1996 in the 1) Townsville, 2) Mackay, and 3) Storm Cay regions of the Great Barrier Reef, Australia. Reefs maps indicate the relative position of the four reefs closed to fishing that were sampled in regions 1, 2, and 3.

open to line and spear fishing (referred to as "open reefs"). Fishing had been prohibited from the closed reefs for at least seven years prior to sampling. Each reef was sampled for two days by the same four commercial line fishermen using gear and sampling designs standardized across all reefs (Davies et al.[5]). Fork length (FL) was measured to the nearest millimetre immediately upon capture. Sagittal otoliths were removed from frozen frames in the laboratory, cleaned of any residual material, dried, and weighed to the nearest 0.1 mg.

A total of 1015 *L. miniatus* were collected from the four closed reefs in each region between October 1995 and January 1996. Sample sizes from the open reefs were small and mortality and growth estimates from these reefs were unreliable. Therefore, these samples were used only to increase the sample size of older fish for a comparison of the two methods for reading otoliths (whole and sectioned).

Comparison of otolith reading methods

The annual periodicity of opaque increment formation in *L. miniatus* otoliths has been validated (Brown and Sumpton 1998). A subsample of 355 *L. miniatus* otoliths from both open and closed reefs was used to assess whether readings of whole otoliths provided age estimates similar to those from sectioned otoliths, but at substantially lower cost (in time). Otolith weight was used to select a broad range of age classes for this assessment on the assumption that otolith weight was a coarse indicator of age, thus avoiding the need to preread otoliths to obtain a sample covering all age classes. Each otolith in the subsample was read, both whole and sectioned, on three separate occasions in random order with no prior knowledge of collection date, location, or fish size. For consistency, the right otolith was chosen to estimate the age of all fish unless it was missing or damaged, in which case the left one was used. Otoliths to be read whole were placed in a small black dish of immersion oil and examined under reflected light with a stereo dissecting microscope. Counts of opaque increments were made from the nucleus to the dorsoposterior edge on the convex face of the otolith. For otoliths from older fish it was necessary to rotate the otolith approximately 45° to clearly observe increments on the otolith margin.

Otoliths to be sectioned were embedded in epoxy resin and cut transversely, adjacent to the anterior side of the nucleus with a Buehler Isomet low-speed saw. The posterior portion of the otolith was retained and mounted on a glass microscope slide with Crystalbond adhesive. A second transverse cut adjacent to the posterior side of the nucleus resulted in a thin section, incorporating the otolith nucleus, remaining on the slide. Otolith sections were then ground on 800- and 1200-grade sandpaper to remove saw marks and a single drop of immersion oil was placed on sections to fill surface irregularities. Otolith sections were examined under a stereo dissecting microscope with reflected light and a black background. Counts of opaque increments were

made from the nucleus to the proximal surface, along the dorsal margin of the sulcus acousticus.

The precision of age estimates from whole and sectioned otoliths was calculated by using the index of average percent error (Beamish and Fournier 1981). The estimates of age from whole and sectioned otoliths were compared by a paired t-test. Difference in bias between the two reading methods was observed by plotting the difference between the two readings (sectioned age minus whole age) against sectioned age, based on the assumption that sectioned age provided the best estimate of true age (Beamish 1979). The results from this comparison indicated no significant difference between whole and sectioned otolith readings and there was no discernible difference in bias in the plot. As a result, all remaining otoliths were read whole for greater efficiency. Age estimates from whole otoliths were accepted and used in subsequent analyses when counts from the first two readings agreed. If the counts differed, otoliths were read a third time. The otolith was excluded from subsequent analyses if no two counts agreed, but included if any two counts agreed.

Comparison of demographic parameters

The central objective of this study was to estimate the variation in demographic parameters of *L. miniatus*, specifically otolith and somatic growth rates, age structure, and mortality, at different spatial scales. In the first instance, parameters were compared among the four reefs within each region to estimate the magnitude of variation at the inter-reef scale. Data were then pooled from individual reefs within each region to generate regional parameter estimates, which were used to estimate the magnitude of variation at the regional spatial scale.

The relationship between otolith weight and age (representing otolith growth) was examined for each reef by least-squares regression analysis, with otolith weight as the dependent variable. The relationship was compared among reefs within each region and among regions by using analysis of covariance (ANCOVA).

Reef-specific age-frequency distributions were constructed for all reefs. Multidimensional contingency tables were used to compare age frequencies among reefs within regions and among regions. Age classes 4 years and younger and age classes 10 years and older were pooled into 4 and 10$^+$ age classes, respectively, because of low frequencies in the tails of the age distributions. As a result, the analyses included a total of seven age classes.

Age-based catch curves (Ricker, 1975) were used to estimate the instantaneous rate of total mortality (Z) at each reef expressed on an annual basis. The number of fish in each age class was regressed against the corresponding age, and the descending slope provided an estimate of Z. Regressions were fitted from the first age class that was fully selected by the sampling gear through to the oldest age class that was preceded by no more than two consecutive zero frequencies. As a result, the age range used to estimate mortality varied slightly among reefs. Mortality rates were compared among reefs within regions and among regions by using ANCOVA.

The von Bertalanffy growth function (VBGF) provided the best fit to length-at-age data for most reefs according to the parameter estimates of the Schnute (1981) growth function. For consistency, and to enable spatial comparisons of growth, the VBGF was used to estimate growth parameters for each reef and region:

$$L_t = L_\infty\,[1-e^{-K(t-t_0)}],$$

where L_t = the fork length at age t;
L_∞ = the mean asymptotic fork length;
K = the rate at which L_∞ is approached; and
t_0 = the age at which fish have a theoretical length of zero.

It was difficult to obtain a reliable estimate of initial growth because the youngest fish collected was 2 years old. There are also no published size-at-age data for larval or juvenile *L. miniatus*, or any other lethrinid. We constrained the VBGF parameter t_0 to zero to provide a better description of the likely early growth of *L. miniatus*. This procedure also allowed growth curves to be compared among reefs within regions and among regions by using 95% confidence regions of the VBGF parameters L_∞ and K described by Kimura (1980).

Results

Comparison of otolith reading methods

Age estimates from whole and sectioned otoliths did not vary significantly over the range of ages between 2 and 21 years ($t_{0.05,\,2,\,354}$=0.46, P=0.73). That is, for each age class estimated from sectioned otoliths, the average difference between whole and sectioned otolith readings did not differ significantly from zero (Fig. 2). The index of average percent error was very low for whole (1.6%) and sectioned (1.4%) otolith readings, indicating that otolith readings for both methods were highly repeatable. This low index was reflected in the agreement of at least two age estimates for all whole otoliths, and hence no otoliths were excluded from analyses.

Otolith growth

There was a significant positive linear relationship between otolith weight and age for all reefs, with regression coefficients ranging from 0.64 to 0.90. ANCOVA revealed that the slope of this relationship was not significantly different among reefs within each region (Townsville: $F_{3,328}$=1.91, P=0.13; Mackay: $F_{3,341}$=1.02, P 0.38; Storm Cay: $F_{3,267}$=1.55, P=0.20). Thus, otolith weight and age data were pooled for each region to compare the region-specific relationships between otolith weight and age (Fig. 3). The slopes of the region-specific relationships differed significantly among all regions ($F_{2,946}$=28.9, P<0.001). The average growth in otolith weight was greater in the Mackay region (26.91 mg/yr) than in the Storm Cay region (24.48 mg/yr), and was least in the Townsville region (19.50 mg/yr).

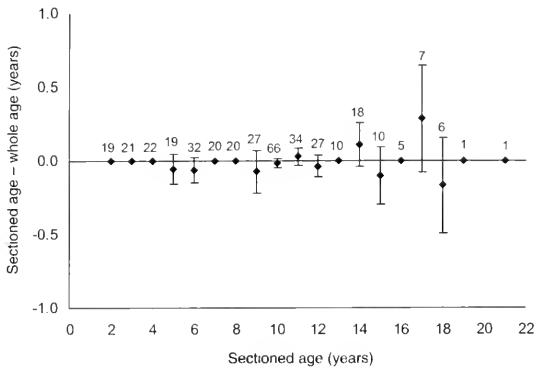

Figure 2

Mean difference in age estimates between whole and sectioned otoliths plotted against estimates of age from counts of annuli in sectioned otoliths of *L. miniatus*. Horizontal line represents no difference between whole and sectioned readings. Sample sizes are shown for each age class. Error bars are 95% confidence intervals.

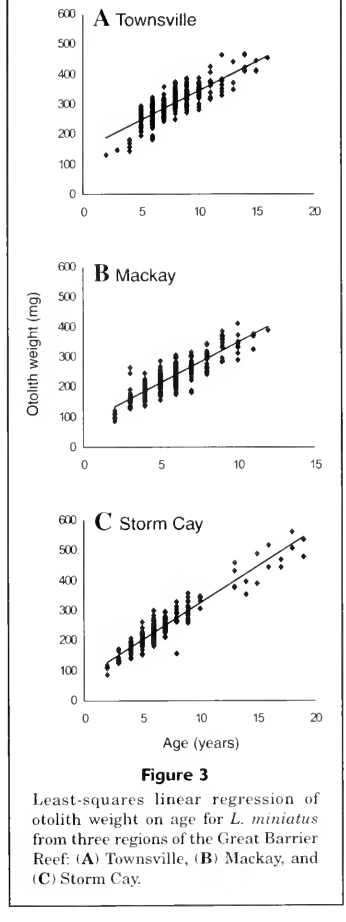

Figure 3

Least-squares linear regression of otolith weight on age for *L. miniatus* from three regions of the Great Barrier Reef: (**A**) Townsville, (**B**) Mackay, and (**C**) Storm Cay.

Age structure

The youngest fish sampled from any reef was two years of age, suggesting that *L. miniatus* becomes vulnerable to standard line fishing gear at this age. All age-frequency distributions for individual reefs were unimodal and the most common mode was 6 years of age. This age is thus assumed to represent the age at which *L. miniatus* is fully recruited to the sampling gear. The relative frequencies of the seven age classes 4 to 10+ were not significantly different among reefs within each region (Townsville: χ^2= 23.59, P=0.17; Mackay: χ^2=27.97, P=0.06; Storm Cay: χ^2=20.29, P=0.32). As a result, age structures from individual reefs were pooled for each region (Fig. 4) and multidimensional contingency tables were used to test for regional differences in age structures. The relative frequencies of the seven age classes were significantly different among all three regions (all regions: χ^2=193.31, P<0.0001, Townsville vs. Mackay: χ^2=172.70, P<0.0001; Townsville vs. Storm Cay: χ^2=91.88, P<0.0001; Mackay vs. Storm Cay: χ^2=22.27, P=0.001). The most obvious difference among regions was the greater relative abundance of older fish (>6 years) in the Townsville region than in the Mackay and Storm Cay regions (Fig. 4). However the oldest fish were from the Storm Cay region, where a small number of fish persisted in the older age-classes up to 19 years of age. The relative abundances of age classes 4 and 5 were greater in the Mackay region than in the Townsville and Storm Cay regions (Fig. 4).

Mortality

Estimates of annual total mortality rates (Z) for individual reefs were generally similar among reefs within each region, with the exception of the Storm Cay region where the estimated Z appeared much lower for reef 21-131 than for other reefs in that region (Table 1). ANCOVA indicated no significant difference in mortality among reefs in any region (Townsville: $F_{3,30}$=0.80, P=0.50; Mackay: $F_{3,20}$=0.08, P=0.97; Storm Cay: $F_{3,15}$=1.14, P=0.37). Therefore mortality rates were estimated for each region from the pooled age structures for all reefs within each region (Fig. 5). A comparison among regions of the regression slopes from the pooled age structures indicated significant differences among regions ($F_{2,18}$=7.11, P=0.005). Tukey's multiple comparison tests revealed that the estimated Z for the Townsville (Z=0.42) and Mackay (Z=0.71) regions differed significantly, whereas the estimate from the Storm Cay region (Z=0.60) did not differ significantly from either Townsville or Mackay.

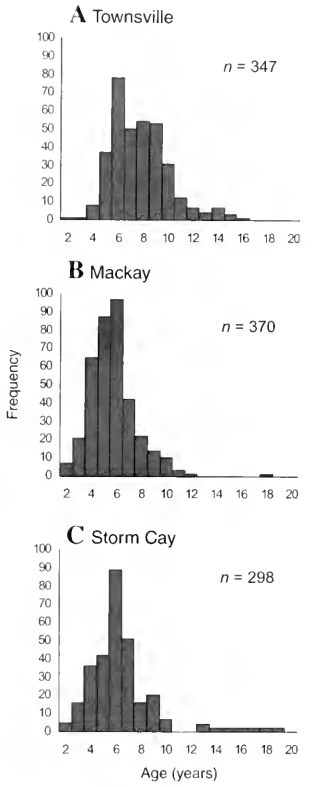

Figure 4

Age structures for *L. miniatus* from three regions of the Great Barrier Reef: (**A**) Townsville, (**B**) Mackay, and (**C**) Storm Cay. Age structures were pooled from four closed reefs within each region.

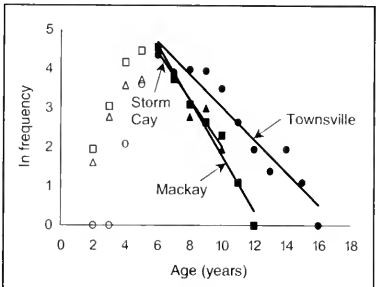

Figure 5

Age-based catch curves for *L. miniatus* from three regions of the Great Barrier Reef: ● = Townsville; ■, Mackay; ▲ = Storm Cay. Catch curves were derived from pooled age structures from four closed reefs within each region. Open data points were not used in the regressions.

Somatic growth

Estimates of VBGF parameters varied considerably among reefs within the Townsville and Mackay regions but in the Storm Cay region, estimates of L_∞ and particularly K were very similar (Table 1). Examination of 95% confidence regions for VBGF parameters for individual reefs (Fig. 6) indicated considerable uncertainty in the estimates of both K and L_∞ and no clear differentiation among reefs within regions. The similarity in VBGF parameters for individual reefs within the Storm Cay region was particularly evident from the 95% confidence regions. In both the Townsville and Mackay regions, three reefs showed overlap in 95% confidence regions, whereas only a single reef in each region appeared to have significantly different VBGF parameters from the others (Fig. 6).

Given the lack of differentiation in growth among reefs, the data from individual reefs were pooled for each region to examine regional patterns in growth. VBGF parameters varied significantly among regions (Table 1) with no overlap in the 95% confidence regions (Fig. 7). It appeared that *L. miniatus* in the Mackay region attained a larger average asymptotic size (L_∞=472.21 mm FL) than in the Storm Cay region (L_∞=462.83 mm FL), where in turn these fish grew larger than fish in the Townsville region (L_∞=453.36 mm FL). It should be noted that the constrained fitting of the VBGF (t_0 set to zero) provided a conservative estimate of regional variation in growth, and regional differences were considerably larger when the VBGF parameter t_0 was not constrained to zero.

Discussion

The scale of spatial variation in demography of a large, potentially more mobile reef fish was found to be larger than that reported for smaller site-attached reef-fish species on the GBR. Estimates of otolith and somatic growth, age structure, and mortality of *L. miniatus* all varied more among regions than among reefs within regions. Furthermore, with the exception of mortality estimates, which differed only between the Townsville and Mackay regions, all estimated parameters were significantly different among all three regions. Despite their relative proximity, the Townsville and Mackay regions consistently showed the greatest difference for each demographic parameter. This indicates that the observed differences did not relate simply to a linear latitudinal gradient among the regions.

Table 1

Total mortality (Z) and von Bertalanffy growth parameters for *L. miniatus* collected from four reefs within three regions of the Great Barrier Reef. The von Bertalanffy growth parameter t_0 was constrained to zero for all reefs.

			Mortality			Growth	
Region	Reef	n	Age range (years)	Z	r^2	L_∞ (mm)	K
Townsville	Glow	110	6-14	0.30	0.74	456.21	0.48
	Dip	90	6-15	0.40	0.89	445.77	0.60
	Yankee	96	6-16	0.31	0.86	462.44	0.40
	Faraday	51	6-11	0.29	0.90	442.26	0.59
	Pooled	347	**6-16**	**0.42**	**0.92**	**453.36**	**0.48**
Mackay	20-136	92	6-11	0.47	0.93	488.87	0.41
	20-137	93	5-11	0.52	0.97	481.68	0.42
	20-142	92	5-10	0.54	0.67	446.28	0.47
	Bax	93	6-12	0.55	0.85	450.78	0.55
	Pooled	370	**6-12**	**0.71**	**0.97**	**472.21**	**0.43**
Storm Cay	21-130	70	6-10	0.76	0.93	466.76	0.38
	21-131	78	6-10	0.43	0.92	463.03	0.39
	21-132	81	6-10	0.66	0.69	453.44	0.38
	21-133	69	6-10	0.77	0.99	467.44	0.38
	Pooled	298	**6-10**	**0.60**	**0.91**	**462.83**	**0.38**

The homogeneity of demographic parameters among reefs within regions presented here is not consistent with a number of studies of other reef fish species on the GBR (e.g. Doherty and Fowler, 1994; Hart and Russ, 1996; Newman et al., 1996). These other studies demonstrated significant differences in age structures, somatic growth, mortality, and otolith growth among individual reefs within a single geographic region for several smaller reef-associated lutjanid, acanthurid and pomacentrid species. The consistency of demographic parameters among reefs within regions found in the present study is consistent with an hypothesis that *L. miniatus* may move over larger distances than "typical" coral-reef fish, including being capable of movements among reefs within a region. There are limited direct data on the movement of *L. miniatus*, and lethrinids in general, or about the range of habitats they occupy. However, *L. miniatus* is frequently found on shoal grounds between reefs and to depths of at least 128 m (Newman and Williams, 1996), suggesting a strong potential for *L. miniatus* to move among reefs. Movements of adults among coral reefs would suggest that *L. miniatus* does not fit the typical metapopulation model for coral-reef fish, in which adults are confined to a single coral reef, and the pelagic larval stage is the only means of dispersal among reefs. Accordingly, differences in conditions among neighboring reefs would be less likely to be manifest in demographic parameters of *L. miniatus* than in the demographic parameters of more sedentary species that inhabit only a single reef for their postsettlement life.

Using microsattelite markers, van Herwerden et al. (in press) examined the genetic structure of *L. miniatus* populations on the GBR. They sampled from two reefs within the Townsville (Dip and Glow) and Mackay (Bax and 20-137) regions in addition to two other reefs in the far southern GBR (Sweetlip and Sandshoe). They found no evidence of stock structure for *L. miniatus* populations on the GBR indicating that the regional patterns in demographic parameters of *L. miniatus* are not a result of distinct genetic stocks. This is consistent with other genetic studies that have demonstrated a lack of genetic structuring of coral-reef fishes over large spatial scales of hundreds to thousands of kilometers (Doherty et al., 1995; Shulman and Bermingham, 1995; Dudgeon et al., 2000).

The observed regional variation in demography may be the result of regional differences in postsettlement processes, such as competition (Jones, 1987), food and habitat availability (Hart and Russ, 1996), population density (Doherty, 1983), and water temperature (Conover, 1992). Alternatively, the regional variation in demography may have resulted from regional variation in recruitment, coupled with density dependent processes (Doherty and Fowler, 1994), or the factors that influence larval survival and settlement. Unfortunately data for these processes for *L. miniatus* are at best limited, restricting any conclusion on the causative factor(s) driving the observed regional patterns. However, because demographic parameters for *L. miniatus* do not show a linear trend with latitude, factors such as water temperature, which have strong latitudinal gradients on the GBR (Lough, 1994), are unlikely to independently explain the observed differences. Meekan et al. (2001) also found that temperature did not appear to be a causal factor driving spatial differences in demography of damselfishes in the tropical eastern Pacific Ocean.

Estimates of numerical density of *L. miniatus* on the GBR are greater in the southern regions (Mackay and Storm Cay) than on reefs in the Townsville region (Wil-

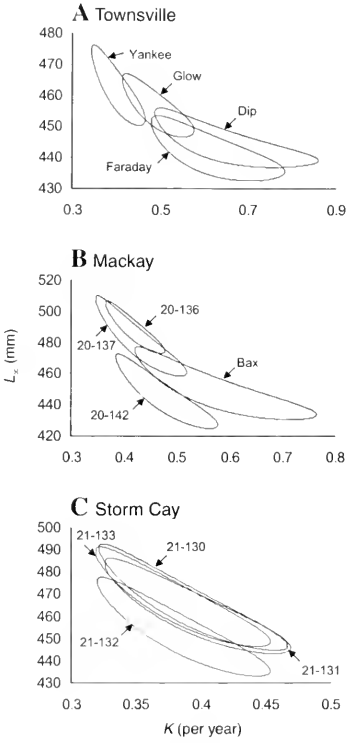

Figure 6

95% confidence regions for *L. miniatus* for the von Bertalanffy growth function (VBGF) parameters K and L_∞ for four individual reefs within each of three regions of the Great Barrier Reef: (**A**) Townsville, (**B**) Mackay, and (**C**) Storm Cay. The VBGF parameter t_0 was constrained to zero in all cases.

liams and Russ[3]). Under the assumptions that demographic parameters are density dependent, and densities are high enough for density-dependent effects to operate, the spatial pattern in densities is consistent with the observed patterns in age structures and mortality. However, the observed patterns in growth are inconsistent with the expected pattern, if density dependence was the dominant influencing mechanism. We would not expect *L. miniatus* to reach a larger size in the southern regions, where densities are higher, compared with the Townsville region, where densities are lower, unless conditions were more favourable in the southern regions. It would be necessary to invoke another mechanism, such as regional differences in food availability, acting in combination with density dependence, to explain the overall pattern of growth, mortality, and age structure.

The likelihood that the observed regional variation is due to a response to regional differences in historic (1960s–1980s) fishing pressure bears consideration. *L. miniatus* are vulnerable to standard line fishing gear from approximately two years of age and are fully recruited to the line fishing gear by six years of age. The reefs in this study had been closed to fishing for seven years prior to sampling. Consequently, all cohorts older than 9 years of age could have been fished prior to the reef closures in 1988, and before the availability of spatially referenced catch and effort data for the commercial fishery. Anecdotal evidence on the development of the fishery and its operation suggests that it developed from the southern ports of Gladstone and Mackay (Fig. 1), which have remained the dominant commercial line fishing ports in the fishery (Mapstone et al.[1]). It seems plausible, therefore, that potentially higher historic fishing effort in the southern two regions could have modified the population structure of *L. miniatus* sufficiently to produce significant differences in demography. Given the longevity of the species, it is also plausible that current differences in the populations are the result of lagged recovery following the closure of the reefs to fishing.

Brown and Sumpton (1998) found small differences in growth rates, and significantly different total mortality rates, between populations of *L. miniatus* in the Swain Reefs and those in the Capricorn-Bunker regions of the southern GBR (separated by ~1° latitude). They attributed the difference in growth estimates to the selectivity of the gear used to obtain samples and to the different mortality rates to differences in fishing pressure between the two regions. They dismissed the possibility that these differences were a result of separate populations with different dynamics. However it is difficult to separate the confounding effects of regional differences in fishing pressure and gear selectivity in sampling; thus variation in growth and mortality between the Swain Reefs and Capricorn Bunker region cannot be dismissed.

The consistency in demographic parameters among reefs within each region suggests that populations of *L. miniatus* may be well mixed at the spatial scale of reef clusters and that any influence of environment on demographics is relatively uniform among reefs within regions. This uniformity may be facilitated by movement of adults among reefs, or by recruitment and postsettlement processes that are relatively uniform within regions. With significant movement of adults among reefs, the benefits of protection from individual reef closures may be limited, depending on the rate of exchange between open and closed reefs, and the level of fishing mortality on open reefs (Russ et al., 1992; DeMartini, 1993; Walters and Bonfil, 1999). In such a scenario, any historical effects of differences in fishing effort among regions would be perpetuated, even though individual reefs were closed to fishing.

In this study whole otoliths of *L. miniatus* provided similar age estimates to those from sectioned otoliths and thus offered a much faster alternative for age estimation for this species, without any apparent loss of precision or

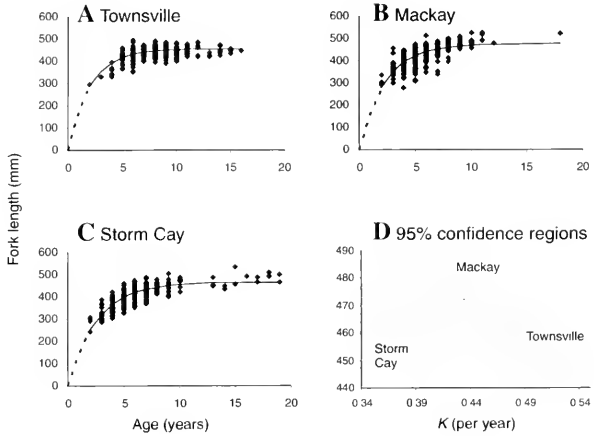

Figure 7

Von Bertalanffy growth function (VBGF) fitted to size-at-age data for *L. miniatus* from three regions of the Great Barrier Reef: (**A**) Townsville, (**B**) Mackay, and (**C**) Storm Cay. The VBGF parameter t_0 is constrained to zero in all cases. Dashed lines represent predicted growth between 0 and 2 years of age. (**D**) 95% confidence regions for the VBGF parameters K and L_∞ for fit to pooled data from four reefs within each of the three regions.

accuracy in relation to those estimated from sectioned otoliths. In contrast, Brown and Sumpton (1998) concluded that whole otoliths from larger and presumably older *L. miniatus* underestimated age by up to 40% with respect to sectioned otoliths. The discrepancy between studies may be due to differences in the techniques used to count increments in whole otoliths. It was noted early in the present study that otoliths from older fish needed to be rotated to reveal a number of increments close to the otolith margin. By not using this technique Brown and Sumpton (1998) may have underestimated ages from whole otoliths of older fish. Readings from whole otoliths have been shown to consistently underestimate the age of a number of reef fish species (e.g. Ferreira and Russ, 1994; Newman et al., 2000) resulting in biased estimates of mortality and subsequent yield estimates (Newman et al., 2000). The results from this study suggest that whole otoliths are adequate for estimating the age of *L. miniatus* and that estimates of demographic parameters presented in the present study were not biased by underestimates of age.

The spatial patterns in the demography of *L. miniatus* described in the present study are based on data collected from a single survey in one year, thus leaving the temporal stability of the patterns open to question. Continued monitoring of the populations will be required to determine the stability of the patterns, and focussed stock structure studies are required to determine the most likely causal mechanism(s) of the patterns. Notwithstanding the need for this work, the significant regional differences in demographic parameters found in the present study suggest different levels of productivity of *L. miniatus* populations in each region. Consequently, there is the potential for less productive populations to be overfished, even where the fishing effort for the stock as a whole is managed at sustainable levels (Caddy, 1975; Sheperd and Brown, 1993). This argues for assessments and management of *L. miniatus* stocks to explicitly consider the regional structure in demography in order to meet both sustainable use and conservation objectives for the Great Barrier Reef World Heritage Area overall and on a regional basis. Furthermore, this study highlights a more general need for the use of multiscale sampling and analyses of fish populations to understand the relative importance of the processes affecting demographic parameters, and the scales at which these processes operate.

Acknowledgments

We acknowledge financial support from the Cooperative Research Centre for the Great Barrier Reef World Heritage Area, the Fisheries Research and Development Corporation, the Great Barrier Reef Marine Park Authority, and the CRC Reef Research Augmentative Grant Scheme. The VBGF ConfRegion program developed by J. Kritzer, CRC Reef Research Centre, was used to estimate the VBGF 95% confidence regions. We would like to thank Robin Stewart, Mary Petersen, and the ELF field team for assistance in the collection and processing of the fish from which this

work arose. We would also like to thank three anonymous reviewers for comments that improved the quality of this manuscript. This manuscript is a contribution from the CRC Reef Effects of Line Fishing Project, CRC Reef Research Centre, Townsville, Australia.

Literature cited

Adams, S., B. D. Mapstone, G. R. Russ, and C. R. Davies.
2000. Geographic variation in the sex ratio, sex specific size, and age structure of *Plectropomus leopardus* (Serranidae) between reefs open and closed to fishing on the Great Barrier Reef. Can. J. Fish. Aquat. Sci. 57:1448–1458.

Beamish, R. J.
1979. Differences in age of Pacific hake (*Merluccius productus*) using whole otoliths and sections of otoliths. J. Fish. Res. Board Can. 36:141–151.

Beamish, R. J., and D. A. Fournier.
1981. A method for comparing the precision of a set of age determinations. Can. J. Fish. Aquat. Sci. 38:982–983.

Begg, G. A., J. A. Hare, and D. D. Sheehan.
1999. The role of life history parameters as indicators of stock structure. Fish. Res. (Amst.) 43:141–163.

Brown, I. W., and W. D. Sumpton.
1998. Age, growth and mortality of redthroat emperor *Lethrinus miniatus* (Pisces: Lethrinidae) from the southern Great Barrier Reef, Queensland, Australia. Bull. Mar. Sci. 62:905–917.

Caddy, J. F.
1975. Spatial model for an exploited shellfish population, and its application to the Georges Bank scallop fishery. J. Fish. Res. Board Can. 32:1305–1328.

Caley, M. J., M. H. Carr, M. A. Hixon, T. P. Hughes, G. P. Jones, and B. A. Menge.
1996. Recruitment and the local dynamics of open marine population. Annu. Rev. Ecol. Syst. 27:477–500.

Carpenter, K. E., and G. R. Allen.
1989. FAO species catalogue. Emperor fishes and large-eyed breams of the world (family Lethrinidae). An annotated and illustrated catalogue of lethrinid species known to date. FAO Fish. Synop. 125, 118 p. FAO, Rome.

Conover, D. O.
1992. Seasonality and the scheduling of life history at different latitudes. J. Fish Biol. 1(suppl. B):161–178.

Davies, C. R.
1995. Patterns of movement of three species of coral reef fish on the Great Barrier Reef. Ph.D diss., 203 p. Dep. Marine Biology, James Cook Univ., Townsville, Queensland, Australia.

DeMartini, E. E.
1993. Modelling the potential of fishery reserves for managing Pacific coral reef fishes. Fish. Bull. 91:414–427.

Doherty, P. J.
1983. Tropical territorial damselfishes: is density limited by aggregation or recruitment? Ecology 64:176–190.

Doherty, P. J., and A. Fowler.
1994. Demographic consequences of variable recruitment to coral reef fish populations: a congeneric comparison of two damselfishes. Bull. Mar. Sci. 54:297–313.

Doherty, P. J., S. Planes, and P. Mather.
1995. Gene flow and larval duration in seven species of fish from the Great Barrier Reef. Ecology 76:2373–2391.

Dudgeon, C. L., N. Gust, and D. Blair.
2000. No apparent genetic basis to demographic differences in scarid fishes across continental shelf of the Great Barrier Reef. Mar. Biol. 137:1059–1066.

Ferreira, B. P., and G. R. Russ.
1994. Age validation and estimation of growth rate of the coral trout, *Plectropomus leopardus*, (Lacepede, 1802) from Lizard Island, Northern Great Barrier Reef. Fish. Bull. 92:46–57.
1995. Population structure of the coral trout, *Plectropomus leopardus* (Lacepede 1802), on fished and unfished reefs off Townsville, Central Great Barrier Reef. Aust. Fish. Bull. 93:629–642.

Hart, A. M., and G. R. Russ.
1996. Response of herbivorous fishes to crown-of-thorns starfish *Acanthaster planci* outbreaks. III. Age, growth, mortality and maturity indices of *Acanthurus nigrofuscus*. Mar. Ecol. Prog. Ser. 136:25–35.

Heemstra, P. C., and J. E. Randall.
1993. FAO species catalogue. vol. 16. Groupers of the world (family Serranidae, subfamily Epinephelinae). An annotated and illustrated catalogue of the grouper, rockcod, hind, coral grouper, and lyretail species known to date. FAO Fish Synop. 125, 292 p. FAO, Rome.

Jones, G. P.
1987. Competitive interactions among adults and juveniles in a coral reef fish. Ecology 68:1534–1547.

Kimura, D. K.
1980. Likelihood methods for the von Bertalanffy growth curve. Fish. Bull. 77:765–776.

Levin, S. A.
1992. The problem of pattern and scale in ecology. Ecology 73:1943–1967.

Lewis, A. R.
1997. Recruitment and post-recruit immigration affect the local population size of coral reef fishes. Coral Reefs 16: 139–149.

Loubens, G.
1980. Biologie de quelques espèces de poissons du lagon Néo-Calédonien. III. Croissance Cah. l'Indo-Pac. 2:101–153.

Lough, J.M.
1994. Climate variation and El Niño–Southern Oscillation events on the Great Barrier Reef: 1958 to 1987. Coral Reefs 13:181–195.

Meekan, M. G., J. L. Ackerman, and G. M. Wellington.
2001. Demography and age structures of coral reef damselfishes in the tropical eastern Pacific Ocean. Mar. Ecol. Prog. Ser. 212:223–232.

Newman, S. J., M. Cappo, and D. McB. Williams.
2000. Age, growth, mortality rates and corresponding yield estimates using otoliths of the tropical red snappers, *Lutjanus erythropterus*, *L. malabaricus* and *L. sebae*, from the central Great Barrier Reef. Fish. Res. 48:1–14.

Newman, S. J., D. McB. Williams.
1996. Variation in reef associated assemblages of the Lutjanidae and Lethrinidae at different distances offshore in the central Great Barrier Reef. Environ. Biol. Fishes 46: 123–138.

Newman, S. J., D. McB. Williams, and G. R. Russ.
1996. Variability in the population structure of *Lutjanus adetii* (Castelnau, 1873) and *L. quinquelineatus* (Bloch, 1790) among reefs in the central Great Barrier Reef. Aust. Fish. Bull. 94:313–329.

Nielson, J. L.
1998. Population genetics and the conservation and management of Atlantic salmon (*Salmo salar*). Can. J. Fish. Aquat. Sci. 55(suppl. 1):145–152.

Ricker, W. E.
1975. Computation and interpretation of biological statis-

tics of fish populations. Bull. Fish. Res. Board Can. 191, 382 p.

Roberts, C. M., and N. V. C. Polunin.
1991. Are marine reserves effective in management of reef fisheries? Rev. Fish Biol. Fish. 1:65–91

Russ, G. R., A. C. Alcala, and A. S. Cabanban.
1992. Marine reserves and fisheries management on coral reefs with preliminary modeling of the effects of yield per recruit. Proc. of the 7th int. coral reef symp. 2, p. 988–995. Univ. Guam, Marine Lab., Mangilao, Guam.

Sale, P. F.
1998. Appropriate spatial scales for studies of reef-fish ecology. Aust. J. Ecol. 23:202–208.

Schnute, J.
1981. A versatile growth model with statistically stable parameters. Can. J. Fish. Aquat. Sci. 38:1128–1140.

Sheperd, S. A., and L. D. Brown.
1993. What is an abalone stock: implications for the role of refugia in conservation. Can. J. Fish. Aquat. Sci. 50:2001–2009.

Shulman, M. J., and E. Bermingham.
1995. Early life histories, ocean currents, and the population genetics of Caribbean reef fishes. Evolution 49:897–910.

van Herwerden, L., J. Benzie, and C. R. Davies.
In press. Microsatellite variation and population genetic structure of red throat emperor (*Lethrinus miniatus*) in the Great Barrier Reef, Australia. J. Fish Biol.

Walters, C. J., and R. Bonfil.
1999. Multispecies spatial assessment models for the British Colombia groundfish trawl fishery. Can. J. Fish. Aquat. Sci. 56:601–628.

The occurrence of yellowfin tuna (*Thunnus albacares*) at Espiritu Santo Seamount in the Gulf of California

A. Peter Klimley
Salvador J. Jorgensen
Bodega Marine Laboratory
University of California, Davis
Westside Road
Bodega Bay, California 94923
Present address (for A. P. Klimley): Department of Wildlife, Fish, and Conservation Biology
University of California Davis
Davis, California 95616
E-mail address (for A. P. Klimley): apklimley@ucdavis.edu.

Arturo Muhlia-Melo
Centro de Investigaciones Biologicas del Baja Norte
Apartado Postal 128
La Paz, Mexico

Sallie C. Beavers
Bodega Marine Laboratory
University of California, Davis
Westside Road
Bodega Bay, California 94923

Pelagic fishes are not evenly dispersed in the oceans, but aggregate at distinct locations in this vast and open environment. Nomadic species such as mackerels, tunas, and sharks form assemblages at seamounts (Klimley and Butler, 1988; Fontenau, 1991). Fishermen have recognized this behavior and have placed moorings with surface buoys in deep waters to provide artificial landmarks, around which fish concentrate and are more easily captured. These fish aggregating devices (termed FADs) are common in the tropical oceans (see review, Holland, 1996). In a sense, it may only be the larger size that separates a seamount from a man-made FAD.

Fish may aggregate at seamounts for very different reasons. The opportunity to feed is greater because biomass at all trophic levels, from primary producer to apex consumer, is greater than in the open ocean (Boehlert and Genin, 1987). The disturbance of flow by the seamount creates eddies downstream that retain nutrients critical to the growth of phytoplankton, and this enrichment supports a greater abundance of consumers from zooplankton to apex predators. The dipole nature of seamount magnetic fields and the outward radiating valleys and ridges of magnetic minimums and maximums might provide landmarks in oceanic landscape that fish use as a reference to guide migration (see discussion of magnetic "topotaxis" in Klimley, 1993). Yellowfin (*Thunnus albacares*) and bigeye (*Thunnus obesus*) tunas do not reside long at the Cross Seamount near Hawaii, an observation inconsistent with the theory that tunas feed on prey that remain aggregated at the site; rather their rapid passage suggests that the site is a landmark used to guide migrations (Holland et al., 1999). Adult yellowfin tuna also stay briefly (<5 min) at FADs off Kaena Point, Oahu (Klimley and Holloway, 1999).

Describing the degree of residency of pelagic fishes at different geographic locations helps ascertain whether the affinity to seamounts and FADs is common throughout the oceans. Holland et al. (1999) determined the rates of dispersion of tuna by attaching unique tags to individuals, releasing them, and later identifying them from these tags. This method results in the removal of individuals from the population and yields a percentage of individuals that have either left the area or have been captured (Holland et al., 1999). Detecting coded ultrasonic tags by an automated monitor provides additional information because marked individuals can be detected repeatedly over a period of time. However, fewer tags can be deployed because of their greater cost. We used this method to reveal synchronicity among visits of yellowfin tuna, time of visits, and duration of visits at the Espiritu Santo Seamount in the Gulf of California.

Methods

We tagged 23 yellowfin tunas with coded ultrasonic beacons during a five-month period between 11 April and 12 September 1998. They were tagged <150 m from two monitoring stations: Espiritu Santo North (ESN) and South (ESS), separated by 500 m at the Espiritu Santo Seamount (24°42'N; 110°18'W) in the southern Gulf of California (Fig. 1). The seamount rose to within 18 m of the surface and extended 700 m along a northwesterly–southwesterly axis. Monitoring station ESN was situated at the northwest end of the seamount ridge at a depth of 47 m; station ESS was at 37 m on the southwest end.

The monitors were deployed for 30 months, during which they recorded when the tagged tuna swam within the 150-m range of reception of the monitors. Using SCUBA, we removed the monitors from the moorings at four-month intervals, downloaded the records of tuna presence near the seamounts to a laptop computer, and replaced the monitors during the same day. We located a station by the rosette of buoys, which floated at a depth of <10 m and which was visible from the surface, by towing a diver at the surface near the GPS coordinates for the mooring.

Manuscript approved for publication 30 January 2003 by Scientific Editor.
Manuscript received 4 April, 2003 at NMFS Scientific Publications Office.
Fish. Bull. 101:684–692 (2003).

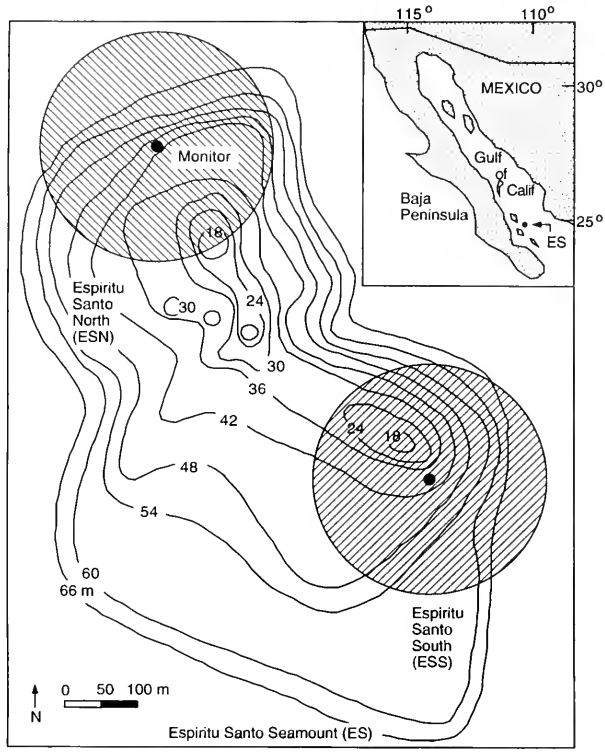

Figure 1

Bathymetric contour map of seamount Espiritu Santo (ES). The circles with cross-hatching indicate the range of the tag-detecting monitor from the seamount. The insert shows the geographic location of the seamount (ES) in the Gulf of California.

We determined the maximum range of signal-detection of one monitor by lowering a transmitter to 10 m under a small boat and lowering the monitor to a similar depth under a larger support vessel. We recorded the separation distance between the two boats using radar because the small boat and transmitter drifted away from the support vessel that was anchored in place at the highest point on the seamount. The VR01 monitor (Vemco Ltd., Shad Bay, Nova Scotia, Canada) detected tags at a distance of 150 m in seas with waves <0.5 m high (see circles, Fig. 1). Later models (Vemco Ltd., VR02) used in the study have a published reception range of ≥500 m in calm seas (see http://www.vemco.com). The range of tag detection by the monitors decreases with rising sea state because of the increase in wave-generated ambient noise.

The tuna were caught by rod and reel and lifted aboard 1–30 minutes after being hooked. Smaller individuals (≤15 kg) were weighed with a scale with a hook that fit into the operculum; intermediate sized fish (>15 and ≤25 kg) were weighed in the net and the net's mass subtracted from the cumulative value; and the masses of largest tuna (>25 kg) were estimated on the basis of their length by using the regression equation, $y=0.216x + 2.981$ given in Moore (1951). The tags were inserted into the peritoneum of the tuna while salt water was flushed over their gills by using the technique described in Klimley and Holloway (1999). The tuna were retained on board for tag implantation less than a minute.

The transmitters (Vemco Ltd., V16-6L) were cylindrical and had a diameter of 16 mm, length of 106 mm, and net mass in water of 16 g. They emitted individually coded tone bursts of 70 kHz separated by 60–90 s intervals. The amplitude of the pulses was 147 dB (re: 1 μP) at a distance of 1 m. The theoretical operating life of a transmitter was 476 days. Each tag was distinguished on the basis of a unique pulse burst by an automated tag-detecting monitor attached to the ESS and ESN detection stations. Water

Table 1

Length and mass of the 23 yellowfin tuna (*Thunnus albacares*) tagged in the present study and the date and time of tagging. "N" indicates tagging near northern monitor; "S" denotes tagging near southern monitor. An asterisk in front of a measurement indicates that the value is derived from the mathematical relationship between mass and length given in Moore (1951); "TL" denotes total length.

Tuna no.	Date	Time (h)	TL (cm)	Mass (kg)	Site (N/S)
1	11 Apr 1998	13:04	80.0	7.3	S
2	11 Apr 1998	13:21	96.0	10.8	S
3	12 Apr 1998	08:46	91.0	10.3	S
4	12 Apr 1998	08:51	106.0	13.8	S
5	12 Apr 1998	09:54	104.0	15.5	S
6	17 Jun 1998	09:54	91.5	17.0	S
7	24 Jun 1998	10:38	86.5	11.3	S
8	26 Aug 1998	10:05	138.0	*51.7	N
9	26 Aug 1998	10:45	58.0	4.5	N
10	26 Aug 1998	11:43	66.0	5.5	N
11	26 Aug 1998	12:16	76.0	7.0	N
12	26 Aug 1998	10:14	155.0	*73.1	N
13	28 Aug 1998	10:50	71.0	7.2	N
14	28 Aug 1998	11:25	155.0	*73.1	N
15	10 Sep 1998	17:44	149.9	*66.2	S
16	10 Sep 1998	18:32	91.5	18.50	S
17	10 Sep 1998	18:44	*75.0	8.50	S
18	10 Sep 1998	19:07	111.8	*27.6	S
19	11 Sep 1998	17:25	114.5	20.5	N
20	11 Sep 1998	17:51	71.0	7.00	N
21	11 Sep 1998	18:25	106.5	20.5	N
22	12 Sep 1998	6:41	104.5	23.0	N
23	12 Sep 1998	7:30	141.0	*55.1	N

temperature was recorded every half hour at the seamount by a Stoaway Tidbit temperature logger (Onset Computers Corp., Pocassett, MA) attached to the mooring line adjacent to the tag-detecting monitor. We calculated a daily temperature by averaging the half-hourly temperatures.

We used log-survivorship analysis (Fager and Young, 1978) to ascertain whether the tunas returned to the monitoring stations after favored time periods. A frequency histogram of the time intervals between randomly occurring point events in a Poisson process is described by a negative exponential distribution. A log-survivor plot of these intervals generates a straight line with a slope proportional to the probability of an event occurring at a given time after the preceding event. This analysis is used to identify intervals between events that occur more frequently than expected by chance because inflections in the resulting curve are more easily distinguished from a straight line than the shape of the distribution on a frequency histogram with a negative exponential distribution. An inflection in the log-survivor curve indicates a change in the probability of an event occurring at a given time after the last event—in our case the time between successive arrivals of tunas within the ranges of the two monitors.

Results

Twenty-three yellowfin tunas were tagged from 11 April 1998 to 12 September 1998 (Table 1). Individuals were tagged during daylight hours from 6:41 to 19:07 hours. The tunas ranged in length from 71.0 to 155.0 cm TL. They ranged in mass from 7.25 to 73.1 kg. There appeared to be two discrete size classes, small individuals varying from 7.25 to 23.0 kg and large ones from 51.7 to 73.1 kg. The masses of the larger individuals were determined from their lengths by using a regression equation (Moore, 1951).

The yellowfin tunas stayed at seamount Espiritu Santo over varying time periods (Fig. 2). Nine of the 23 tunas left the seamount on the same day that they were tagged (Fig. 2A). Two of the nine returned to the seamount once for a single day, one within a week of tagging and the other after two and one-half months. Six tunas stayed intermediate periods of time after tagging, ranging from two to six weeks. One of these tunas (no. 9) was eventually caught at the seamount. Another tuna (no.10) visited for a single day after an absence of five weeks and returned again after a similar period to stay for 15 months. Four

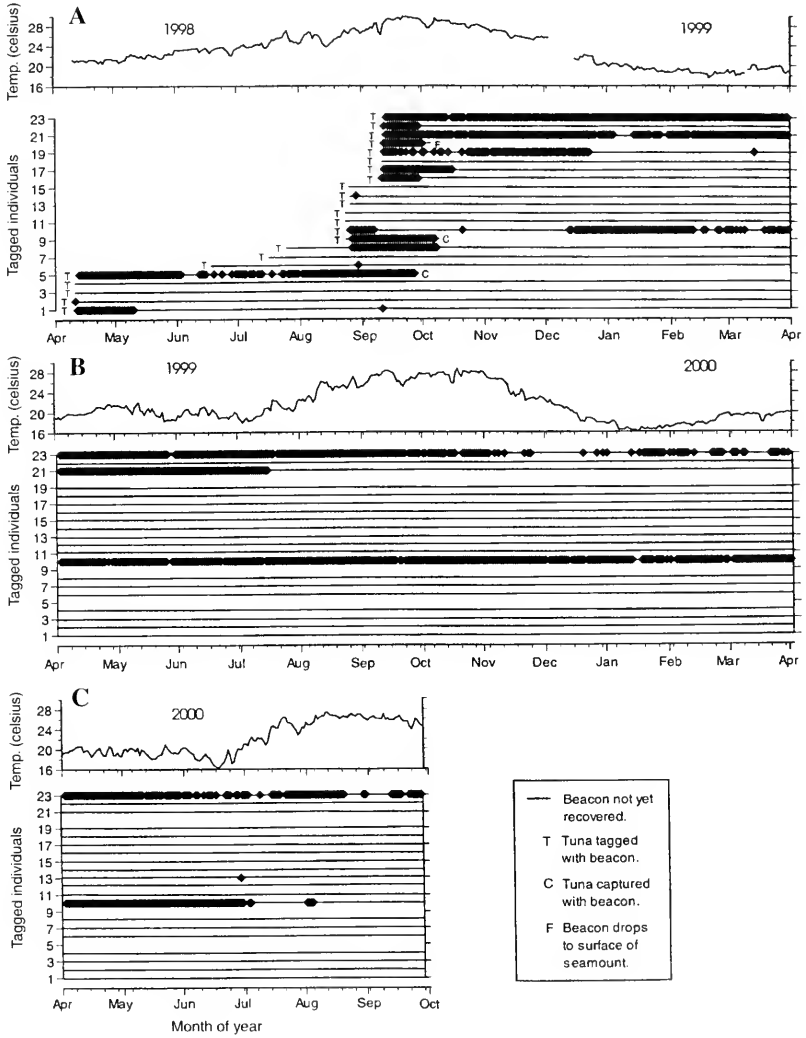

Figure 2

Chronology of daily visits by 23 tagged yellowfin tuna to the seamount and temperature record over a 30-month period beginning April 1998 and ending October 2000. Each visit, indicated by a solid diamond, is based on the detection of a tag during a 24-h period by either the north (ESN) or south (ESS) monitoring stations. The lines in the graphs show that the ultrasonic tag had yet to be recovered from a yellowfin tuna. T = day of tagging, C = day of capture, and F = date of shedding of tag.

individuals (nos. 5, 19, 21, and 23) stayed for longer periods of time, ranging from six to 18 months. One of these tunas (no. 5) was also caught by a fisherman. It is likely that some tunas are nomadic and stay only a single day, whereas others are resident, remaining at the seamount throughout the year.

It is unlikely that the tags on the two tunas (nos. 10 and 23), which stayed at the seamount longest, were shed and lay on the bottom. The reasons supporting their being attached to living tunas are as follows. First, the two tags were not recorded with equal frequency during all times of the day as might be expected of a tag lying at one location within the range of the monitors. The tags were usually detected for a few hours and then absent for a similar period. This pattern of detection is consistent with the tunas moving within the range of the monitor and later outside its range. Second, the two tags were jointly detected after long periods of absence or ceased being detected simultaneously after long periods of presence. This reception pattern is consistent with the two tunas moving in and out of the detection range of the monitors within the same school. Third, one tuna (no. 23) was detected by the monitor on the south side of the seamount, but not on the north side during one day; the same tuna was detected by the northern monitor, but not the southern monitor on the next day. This pattern of detection was consistent with the tuna swimming over the northern region of the seamount on the first day and over the southern region on the second day.

The yellowfin tunas were present at the seamount at all seasons of the year. Five of the tunas tagged during August and September 1998 (nos. 7, 8, 9, 16, and 17) emigrated during early fall as the water temperature began to decrease (Fig. 2A). However, three individuals (nos. 10, 21, and 23) remained at the seamount from January 1999 to April 1999 when the temperature dropped to 18°C. Two (nos. 10 and 23) remained present when the subsurface water temperature descended to 16°C during the following winter of 2000 (Fig. 2B).

The yellowfin tunas remained at the seamount at all times of the day. This is evident from a 24-h record of the arrivals of 10 tunas during a 15-d period from 16 to 30 September 1998 (Fig. 3). The tunas were present more often during daytime, from 06:00 to 18:00 hours, during the first 12 days. Notice the clustering of the different symbols in Figure 3, each indicating a specific tuna, in separate columns during the period from 06:00 to 18:00 hours. However, the amount of time spent at the seamount became more evenly distributed between daytime and nighttime by 28 September. Note the even dispersion of the symbols over the 24-h period during the last three days of the 15-day period. There was little variation evident in the frequency of arrivals at different times of the day when the arrivals were summed over the entire study (Fig. 4). The percentage of arrivals during each hour of the day (see crosshatched polygon) differed little from an even distribution of arrivals (4.2%/h) throughout the day (see dashed circle).

We determined the frequency of various lengths of stays at the north (Fig. 5A) and south sites (Fig. 5B) at the Espiritu Santo Seamount. A stay for a particular tuna was defined as the period of detections with no separation intervals greater than 15 min. Let us say that tuna 1 was detected at 08:00, 08:14, 08:28, and 09:00 hours. The duration of the stay of tuna 1 would be 28 min. The second detection followed the first by 14 min (<15 min), and the third followed the second also by 14 min (also <15 min). However, the fourth detection followed the third by 32 min (>15 min) and was therefore not pooled into a single duration. This stay would then be placed in the 15:00–29:59 min time class in Figure 5. Twenty-seven percent of the detections at ESN and 33% of those at ESS were separated by greater than 15 min and were thus considered single detections and included in the 00:00-h class. Fifty-three percent of the visits to ESN and 37% of the visits to ESS were between 00:01 and 14:59 min. Twenty-one percent of the visits to ESN and 20% of the visits to ESS were between 15:00 and 59:59 min. The majority of visits were less than 1 hour in duration and only a few exceeded an hour.

The intervals spent away from the seamount were similarly short. Sixty percent of all absences at ESN were less than 1 h (Fig. 6) as were 65% of the absences from ESS. Ninety percent of the absences from both sites were less than 5 hours. Only 0.1% of the visits exceeded 23 hours. There appeared to be no favored period of absence as indicated by the smooth slope of both curves in the log-survivor plot. Only 72 periods of absence at ESN and 114 periods at ESS exceeded a day. Of these longer periods, 42% of the absences from ESN (Fig. 7A) and 46% of the absences from ESS (Fig. 7B) were for two days. Only 7 % of the absences from ESN and 4% of the absences from ESS were between 10 and 19 days. Only 2% of periods of absence from ESN exceeding a day were greater than 100 days (Fig. 7A).

Discussion

We found that yellowfin tuna remained at the seamount for periods ranging from a few days to greater than a year. Fifty percent of 458 yellowfin tuna tagged with dart tags at the Cross Seamount off Hawaii were recaptured at that seamount within 15 days of tag application (Holland et al., 1999). This "half-life" of tuna residence was short, suggesting that the seamount served as a landmark to guide migration and not as a destination for feeding.

Thirty-eight yellowfin tuna were tagged with ultrasonic beacons at two buoys off the western coast of Oahu and monitored over a 13-month period by automated "listening" monitors (Klimley and Holloway, 1999). These monitors (VR20) possessed a more sensitive receiver than our monitors (VR01 and VR02). The former had a maximum range of 1.1 km. The maximum published range of our monitors was 0.5 km. Twenty-seven of the tuna returned to the buoys a mean of 4.2 visits per tuna. The mean duration of each visit was only 40.1 min and the mean period of absence was 17.2 days. Seventy-three percent of the tuna tagged on the same day returned together. The tunas often arrived at the same time of the day and returned only to the buoy at which they were tagged. This allegiance of tunas to one school, their predilection for returning to the site of tagging, and the precise timing of their visits are consistent with the theory that the species has migratory pathways consisting of way-points that are visited with regularity. That the tuna spent little time at the FAD suggests that the buoys are not feeding destinations, but rather landmarks used in migration.

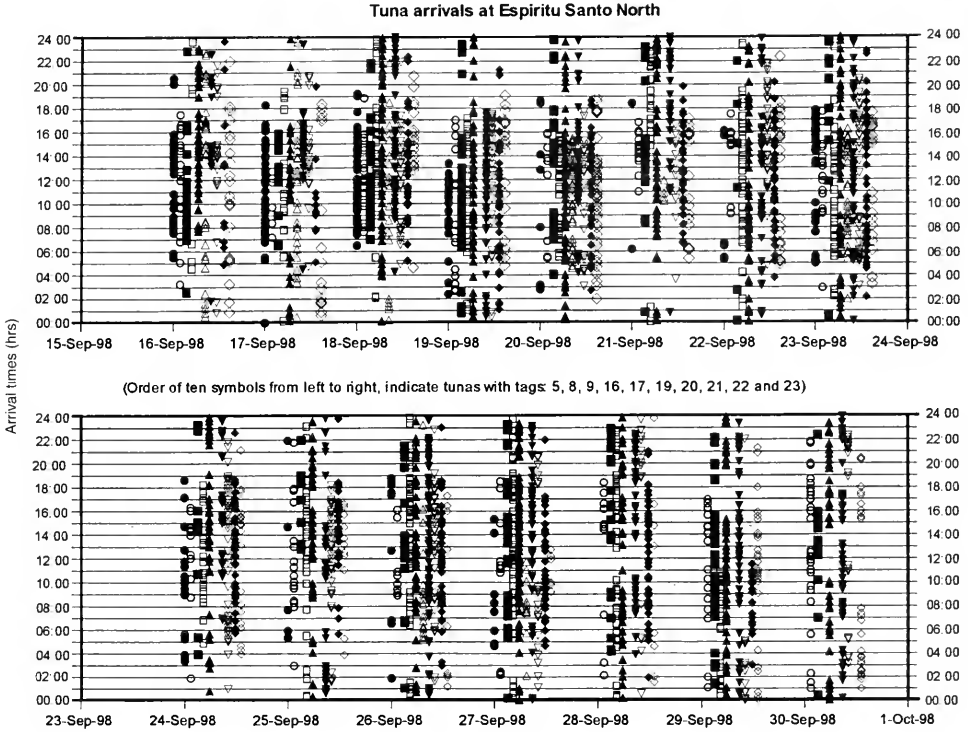

Figure 3

Twenty-four hour chronology of visits by 10 tagged tuna to the monitoring station ESN during 15 days from 16 to 30 September 1998. A unique symbol indicates the presence of a particular individual within the range of the monitor during a 15-min position. Note the predominance of daytime visits during the first nine 24-h periods and then a progressive shift to an equal number of visits during daytime and nighttime (see 28–30 Sept. 1998).

Tuna repeatedly moved in and out of the monitor range over many days or left for the duration of the study. Sixty percent of all absences at ESN and 65 % of the absences from ESS were for less than 1 hour. If these tunas were to swim at a sustained rate of 0.5 m/s (see Magnuson, 1978), they would not move more than 900 m out the reception range of the monitors (60 min × 60 s × 0.5 m/s /2). This close attachment to the seamount contrasts with the behavior of tuna at FADs offshore of Hawaii. Tunas visited the FADs there rarely and spent little time within the range of the monitor before departing for a period of several weeks (Klimley and Holloway, 1999). The present study suggests that the Espiritu Santo Seamount is a substantial feeding ground that can support a year-round resident population of yellowfin tunas. However, other tunas may stay only briefly at the seamount, using it as a landmark, before continuing on their nomadic migrations.

Seamounts have dipole magnetic fields associated with them because of the antiparallel polarity of magnetite within volcanic magma extruded during periods when the earth's polarity was reversed (Parker et al., 1987). Furthermore, maxima (ridges) and minima (valleys) in the magnetic field often lead outward from seamounts due to the extrusion of magma. Klimley (1993) proposed that hammerhead sharks use these for guidance during their nocturnal migrations into the surrounding water to forage. This physical property of the sea floor, originating far below where the fishes swim, could provide a fixed reference (or waypoint) for yellowfin during their migrations. This species of tuna has been shown to sense distinct patterns in a magnetic field (Walker, 1984).

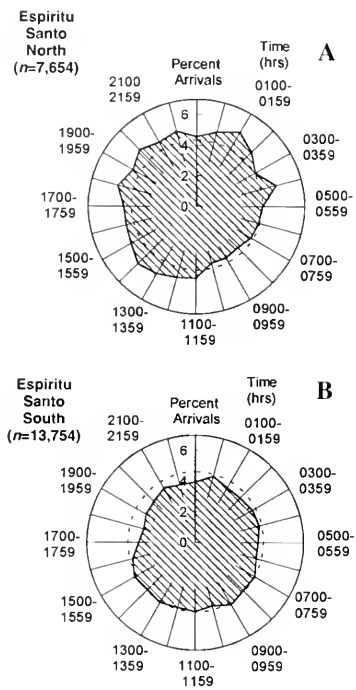

Figure 4

Percentage of visits by 23 yellowfin tuna at different times of day at monitoring stations ESN (**A**) and ESS (**B**). Circle with dashed line indicates an equal percentage of returns occurring every hour of the day.

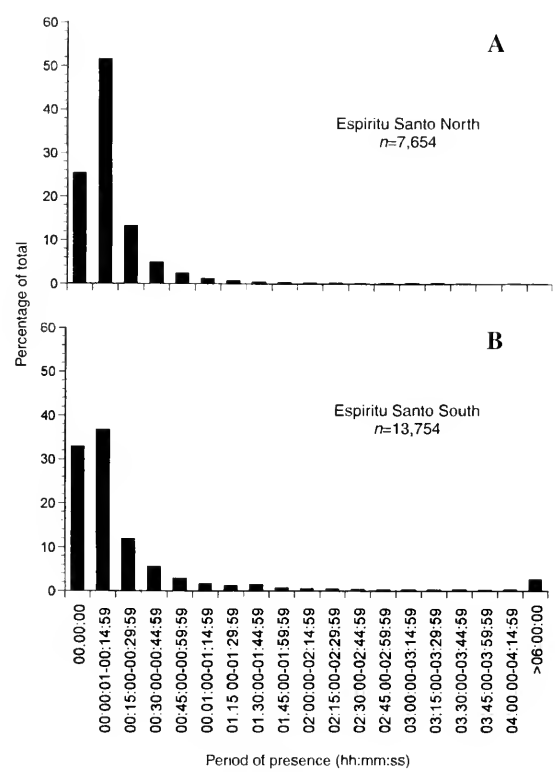

Figure 5

Percentage of visits of increasing duration recorded for 23 yellowfin tuna at monitoring stations ESN (**A**) and ESS (**B**). A single detection of a tagged fish would be placed in the 00:00-min time category.

Conclusions

Twenty-three yellowfin tuna were tagged with coded ultrasonic beacons during a five-month period between 11 April and 12 September 1998. These tunas were captured, tagged, and released <150 m from two monitoring stations: Espiritu Santo North (ESN) and Espiritu Santo South (ESS), which were separated by 500 m, at the Espiritu Santo Seamount in the southern Gulf of California (24°42'N; 110°18'W). The monitors were deployed for a period of 30 months, ranging from April 1998 to October 2000, during which they recorded tagged tunas swimming within their 150 m range of reception. The tunas ranged in length between 71.0 and 155.0 cm TL and in mass from 7.2 to 73.1 kg. The tunas stayed at the Espiritu Santo Seamount for varying time periods. Nine of the 23 tunas left the seamount on the same day that they were tagged. Two of the nine returned to the seamount twice for a single day, one within a week of tagging and another after 2.5 months. Five additional tunas stayed at the seamount for intermediate periods, ranging from two to six weeks. Four individuals stayed for longer periods of time, ranging from 6 to18 months. Tunas were present at the seamount at all times of the day. They moved in and out of the range of the monitors, most often staying for periods <14:59 min. Fifty-three percent of the visits to ESN and 37% of the visits to ESS were of this duration. Smaller percentages of the visits, 21% and 20%, lasted 15:00 to 59:59 min, respectively. The majority of visits were <1 hour in duration and only a few exceeded an hour. The intervals spent away from the seamount were also brief. Sixty percent of all absences at ESN and 65% of the absences from ESS were <1 hour. Ninety percent of the visits to both sites were <5 hours. Only 0.1% of the visits exceeded 23 hours. Tuna individuals

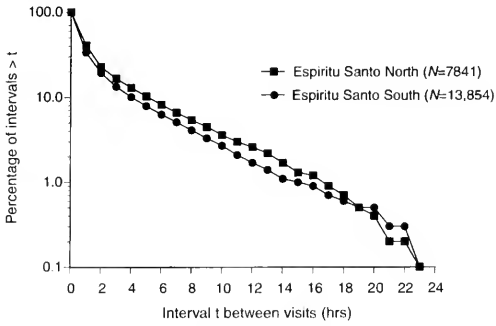

Figure 6

Log-survivor plots of percentages of intervals between successive tuna arrivals greater than time t over 24-h periods at monitoring stations ESN (**A**) and ESS (**B**).

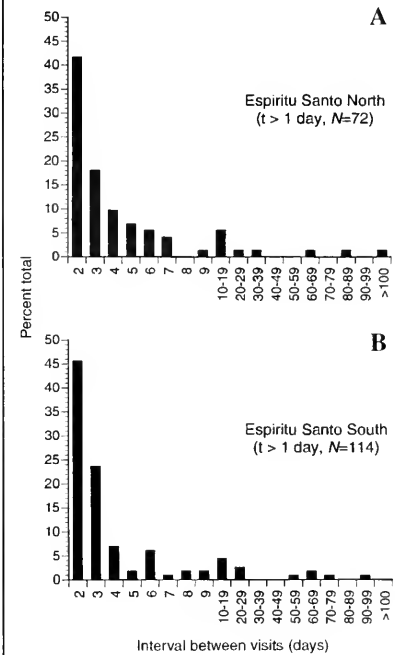

Figure 7

Percentages of visits of greater than one day made by tuna to two monitoring stations with single day intervals ranging from 2–9 days and 10-day intervals ranging from 10–19 to 90–99 days.

may use the site either as a landmark during their migratory transit or as a feeding destination as suggested by the short and long periods of time spent at the seamount.

Acknowledgments

We would like to thank those on the staff of Centro de Investigaciones Biologicas del Baja Norte of La Paz, Mexico, who helped us tag yellowfin tuna at seamount Espiritu Santo. This work was funded by the Biological Oceanography Program of the National Science Foundation (grant: OCE-9802058) and CONACYT of Mexico (grant: PN-9509-1995 and PN-1297-1998).

Literature cited

Boehlert, G. W., and A. Genin.
1987. A review of the effects of seamounts on biological processes. *In* Seamounts, islands, and atolls (B. H. Keating, P. Fryer, R. Batiza, and G. W. Boehlert, eds.), p. 319–334. Geophys. Monogr. Ser. 43.

Fagan, R. M., and D. Y. Young.
1978. Temporal patterns of behavior: durations, intervals, latencies, and sequences. *In* Quantitative ethology (P. W. Colgan, ed), p.78–114. John Wiley & Sons, New York, NY.

Fonteneau, A.
1991. Seamounts and tuna in the tropical Atlantic. Aquat. Living Resour. 4:13–25.

Holland, K. N.
1996. Biological aspects of the association of tunas with FADs. SPC Fish Aggregating Device Information Bull. 2:2–7.

Holland, K. N., P. Kleiber, S. M. Kajiura.
1999. Different residence times of yellowfin tuna, *Thunnus albacares*, and bigeye tuna, *T. obsesus*, found in mixed aggregations over a seamount. Fish. Bull., 97:392–395.

Klimley, A. P.
1993. Highly directional swimming by scalloped hammerhead sharks, *Sphyrna lewini*, and subsurface irradiance, temperature, bathymetry, and geomagnetic field. Mar. Biol. 117:1–22.
1985. Schooling in the large predator, *Sphyrna lewini*, a species with low risk of predation: a non-egalitarian state. Ethology, 70:297–319.

Klimley, A. P., and S. B. Butler.
1988. Immigration and emigration of a pelagic fish assemblage to seamounts in the Gulf of California related to water mass movements using satellite imagery. Mar. Ecol. Progr. Ser. 49:11–20.

Klimley, A. P., and C. Holloway.
1999. Homing synchronicity and schooling fidelity by yellowfin tuna. Mar. Biol. 133: 307–317.

Magnuson, J. J.
1978. Locomotion by scombrid fishes: hydrodynamics, morphology, and behavior. Fish Physiol. 239–313.

Parker, R. L., L. Shure, and J. A. Hildebrand.
1987. The application of inverse theory to seamount magnetism. Rev. Geophys. 25:1–65.

Moore, H. L.
1951. Estimation of age and growth of yellowfin tuna (*Neothunnus macropterus*) in Hawaiian waters by size frequencies. Fish. Bull. 52:131–149.

Walker, M. M.
1984. Learned magnetic field discrimination in yellowfin tuna, *Thunnus albacares*. J. Comp. Physiol 155:673–679.

Larvae of *Dactylopsaron dimorphicum* (Perciformes: Percophidae) from oceanic islands in the southeast Pacific

Mauricio F. Landaeta
Laboratorio de Oceanografía Pesquera y Ecología Larval
Departamento de Oceanografía
Universidad de Concepción
Casilla 160-C
Concepción, Chile

Francisco J. Neira
Faculty of Fisheries and Marine Environment
Australian Maritime College
PO Box 21
Beaconsfield, Tasmania 7270, Australia

Leonardo R. Castro
Laboratorio de Oceanografía Pesquera y Ecología Larval
Departamento de Oceanografía, Universidad de Concepción
Casilla 160-C
Concepción, Chile
E-mail addres (for L. R. Castro, contact author): lecastro@udec.cl

Percophids are a family of small marine benthic fishes common over soft bottoms from inshore to the outer slopes in tropical to temperate regions of the Atlantic and in the Indo-West and southeast Pacific (Reader and Neira, 1998; Okiyama, 2000). Five species belonging to four genera have been recorded around the Salas y Gómez Ridge in the southeast Pacific, all of which are endemic to the area except for *Chrionema chryseres*, a species which also occurs off the Hawaiian Islands and Japan (Parin, 1985, 1990; Parin et al., 1997). Of these five species, larval stages have been described only for *Osopsaron karlik* and *Chrionema pallidum* (Belyanina 1989, 1990).

Dactylopsaron dimorphicum (Parin and Belyanina, 1990) is a dwarf percophid (29 mm maximum body length) previously recorded only at the Cupole (26°S; 86°W) and Baral (25°S; 96°W) seamounts located to the west of the Salas y Gómez Ridge and at the junction of this and the Nazca Ridge, respectively, at depths of 240–345 m (Parin, 1990; Parin et al., 1997). Adults of this monotypic genus differ from other percophids in that the first dorsal fin is positioned at the back of the head and is in line with the mid-operculum, 8–10 digitiform processes are present on the posterior upper opercular margin, and expanded lobes are present at the distal end of the medial branchiostegal rays (Parin, 1990). This species is sexually dimorphic, males have a thicker and much longer first dorsal-fin spine than females (Parin, 1990). There is no information on their reproductive biology and eggs are unknown (Watson et al., 1984).

We describe the postflexion larvae of *D. dimorphicum* using material collected around Salas and Gómez and Easter Islands in the southeast Pacific. We also provide information on the spatial distribution of this species around both islands, and on how to distinguish the larvae from those of teleosts with similar larvae in the area. This note constitutes the first record of *D. dimorphicum* off Easter Island, as well as the first record of the larvae in nearshore waters of both Pacific islands.

Methods

Field work

Larvae were obtained during an oceanographic expedition (CIMAR-5) to Easter Island (27°10′S; 109°20′W) and Salas y Gómez Island (26°30′S; 105°20′W), approximately 3750 km west of Chile, in November 1999. Samples were collected onboard the Chilean navy research vessel *AGOR Vidal Gormaz* by using a bongo sampler equipped with two conical nets (0.6-m diameter mouth openings, 3 m long, 350-µm mesh size). The mouth of each net was fitted with an OSK flowmeter to estimate volume of water filtered. Tows were carried out for 10 min obliquely to the surface from either the maximum permissible depth in shallow (<200 m) stations or from 400 m in deeper stations. Samples around Easter Island were obtained at 10 stations located approximately one nautical mile (nmi) from the coast both during day and night, and along four transects (NW–SE and NE–SW) each containing four stations located at 3, 7, 12, and 20 nmi offshore (Fig. 1). Samples around Salas y Gomez Island were obtained along four transects (N–S and E–W), each containing four stations at 1, 3, 6, and 10 nmi offshore (Fig. 2). Additionally eight deep stations (>1500 m) were also sampled between Easter and Salas y Gómez islands. All samples were fixed in 5% formalin and later preserved in 70% ethanol. Water volume sampled per tow ranged between 112.6 and 517.7 m^3. Larval abundances were standardized to 1000 m^3 and mapped by using SURFER® (Golden Software, Golden, CO). Statistical analyses were performed using STATISTICA (StarSoft, Inc., Tulsa, OK).

Larval identification and processing

Postflexion larvae were identified as those of *Dactylopsaron dimorphicum* by a combination of dorsal and anal-fin meristics (D. IV [III–V] + 22 [20–22]

Manuscript approved for publication 15 January 2003 by Scientific Editor.
Manuscript received 4 April 2003 at NMFS Scientific Publications Office.
Fish Bull. 101:693–697 (2003).

and A. 24 [23–25]; Table 1), and by the presence of the unique digitiform opercular processes (Parin, 1990; Okiyama, 2000). Identification was verified by using fin meristics from cleared and stained specimens (Potthoff, 1984).

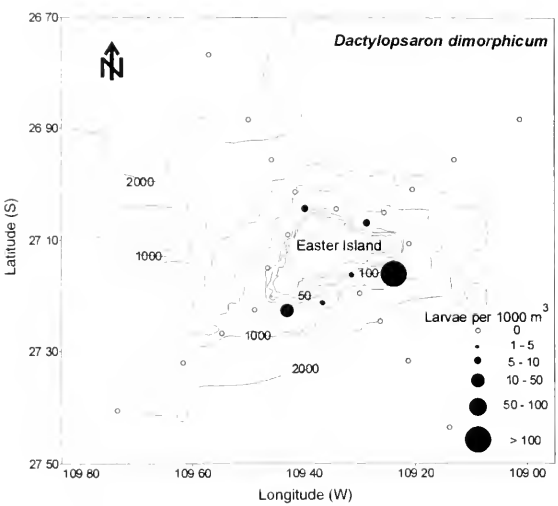

Figure 1

Spatial distribution of postflexion larvae of *Dactylopsaron dimorphicum* (numbers/1000 m^3) around Easter Island in November 1999.

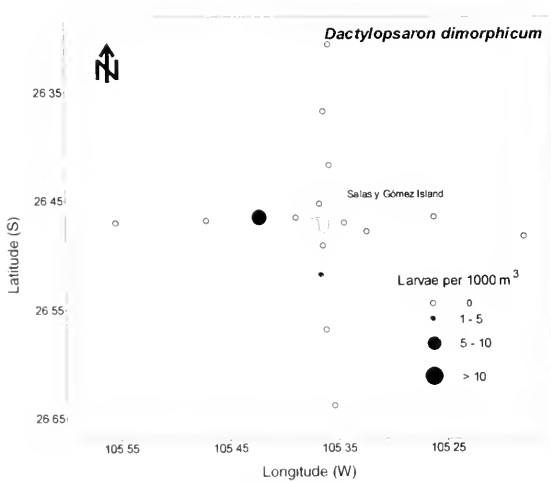

Figure 2

Spatial distribution of postflexion larvae of *Dactylopsaron dimorphicum* (numbers/1000 m^3) around Salas y Gómez Island in November 1999.

A total of 55 postflexion larvae of *D. dimorphicum* (8.2–15.3 mm standard length) were examined to describe morphometrics, meristics, and pigmentation. Three larvae (9.1, 13.1 and 13.4 mm SL) were cleared and stained following the method of Potthoff (1984). Terminology and morphometric measurements follow Neira et al. (1998). Measurements were made to the nearest 0.01 mm by using a dissecting microscope fitted with an eyepiece micrometer. Body length (BL, Neira et al., 1998) in postflexion larvae corresponds to standard length (SL), i.e. tip of snout to posterior margin of hypurals. Measurements of body depth (BD), head length (HL), and preanal length (PAL) were converted to a percentage (%) of SL (Table 2). Eye diameter (ED) and snout length (SnL) were converted to a percentage (%) of HL. Pigment described refers solely to melanin. Illustrations were made with the aid of a camera lucida.

Results

Description of larvae

Postflexion larvae of *Dactylopsaron dimorphicum* are elongate (BD 13.1–18.3%; Table 2), and have a moderate to large head (HL 28.6–36.7%) and an elongate snout (Fig. 3). Eyes are round and pigmented by 8.2 mm SL. The mouth is large, protrusible, and has a long ascending premaxillary process giving a characteristic "duckbill" appearance. Small villiform teeth are present along the premaxilla and dentary. There are no head spines. The digitiform processes on the upper opercular margin are present in larvae >13.2 mm SL; the lower, rearward-directed process that reaches the end of the pectoral-fin base in adults was still forming in the largest larva examined (15.3 mm SL). The branchiostegal membranes are free from the ithsmus. The short first dorsal fin is located at the nape and lies in line with the mid-operculum; pterygiophores of the five first-dorsal fin spines in two of the cleared and stained larvae (13.1 and 13.4 mm SL) were located between the neural spines of the second and third trunk vertebrae. The 9.1-mm-SL cleared and stained larva possessed only 15 of the 17–20 pectoral-fin rays, and first dorsal-fin spines were developing. The elongate pelvic fins are thoracic, i.e. inserted in front of the pectoral-fin bases. Lateral line scales begin to form at >13 mm SL. Larvae are unpigmented, although a few had a small melanophore at the base of the 17 or 18th dorsal-fin ray. There are 31–35 myomeres. The number of vertebrae in the cleared and stained larvae is 34–35 (11–12 + 22–24).

Larval distribution

Postflexion *D. dimorphicum* larvae were collected within 6 nmi off both Easter and Salas and Gómez

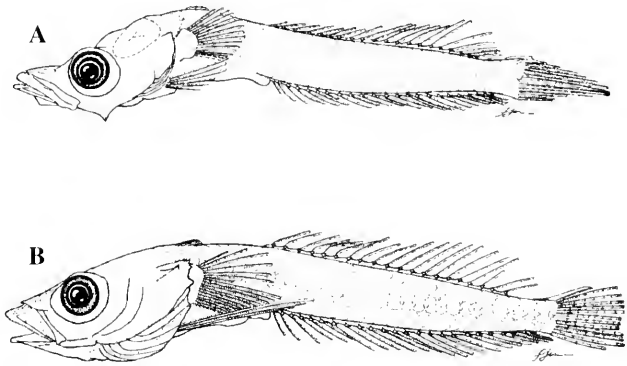

Figure 3

Postflexion larvae of *Dactylopsaron dimorphicum* collected around Easter Island in November 1999. (**A**) 8.5 mm SL; (**B**) 14.8 mm SL. Illustrated by F. J. Neira.

Table 1

Meristic counts of percophid species recorded in submarine ridges of Salas y Gómez Island in the southeastern Pacific (from Parin [1985, 1990] and Okiyama [2000]).

	Dorsal	Anal	Pectoral	Pelvic	Caudal (branched)	Vertebrae
Chrionema chryseres	VI +16	26	23	I, 5	15 (11)	27–28
Chrionema pallidum	VI +14–15	18	20–22	I, 5	15 (11)	27–28
Dactylopsaron dimorphicum	IV [III-V] + 22 [20–22]	24 [23–25]	18 [17–20]	I, 5	14 (8)	34–35[1]
Enigmapercis acutirostris	II +21	25	21	I, 5	15 (8–9)	—
Osopsaron karlik	V-VI +19–20	22–23	19–20	I, 5	14	32

[1] This study.

Table 2

Standard length range (mm), and mean values (±1 SD) of selected body proportions (given as a percentage of body length) of postflexion larvae of *Dactylopsaron dimorphicum* from Easter and Salas y Gomez islands in the southeastern Pacific Ocean (n=55).

Standard length (mm)	8.2–15.3
Head length (%SL)	28.6–36.7 (32.3 ±3.3)
Eye diameter (%HL)	18.2–24.7 (22.0 ±3.1)
Snout length (%HL)	25.6–36.2 (31.0 ±5.5)
Body depth (%SL)	13.1–18.3 (15.3 ±2.2)
Preanal length (%SL)	45.4–56.9 (49.5 ±4.0)

Islands (Figs 1 and 2). Around Easter Island, larvae were caught only in nearshore stations (<2 nmi) over the narrow shelf and were more abundant along the southern edge.

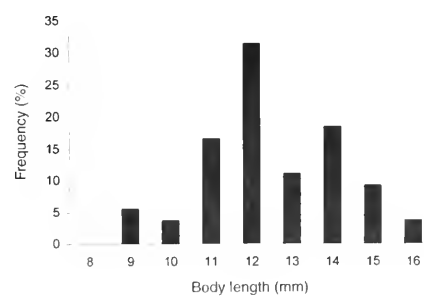

Figure 4

Combined body length (SL, mm) frequency distribution of postflexion larvae of *Dactylopsaron dimorphicum* around Easter Island and Salas y Gómez Island in November 1999.

The highest larval concentrations (>100 larvae/1000 m^3) occurred at the southeastern tip of the island and averaged 27 ±46 larvae/1000 m^3 (Fig. 1). No significant differences were found between day and night larval concentrations (Kruskal-Wallis test=0.047; $P>0.05$). Around Salas and Gómez Island, larvae were caught only at two stations 6 nmi west and south of the island, and in mean concentrations <10 larvae 1000/m^3 (Fig. 2). No larvae were caught in any of the eight stations sampled between the two islands. Body lengths of larvae caught in both islands ranged from 8 to 16 mm SL, and over 30% of the larvae were around 12 mm SL (Fig. 4).

Discussion

Postflexion larvae of *D. dimorphicum* are likely to be confused with those of four other co-occurring percophid species (see Table 1), and those of the creediid *Crystallodytes pauciradiatus* that occur in the same region (Castro and Landaeta, 2002) and have similar bodies with little or no pigment. In the case of the percophids, the digitiform opercular processes exclusive to *D. dimorphicum*, together with dorsal and anal-fin meristics, should be sufficient to distinguish between postflexion larvae of all species. Larval *C. pauciradiatus* can be identified by using myomere counts (56–58 vs. 31–35 in *D. dimorphicum*) and their small, early forming posterior preopercular spines (Reader et al., 2000).

Our collection of *D. dimorphicum* larvae at Easter Island, some 453 km to the southwest of Salas y Gomez Island where it was first described (Parin, 1990), constitutes the first record for Easter Island, thereby extending the known range of this species over the South Pacific plate. Despite numerous past fish surveys around Easter Island (i.e. Randall and Cea-Egaña, 1984; Mujica, 1993), adults of this dwarf percophid had not been reported there, a fact that could be attributed to factors such as collection methods, depth of surveys, and the very small size of these larvae. However, the presence and abundance of larval *D. dimorphicum* reported in this study, and the fact that they were among the five most abundant larval taxa caught around Easter Island (Castro and Landaeta, 2002), implies the existence of a well-established breeding population. Biogeographically, this finding also suggests that larval drift could play an important role in the expansion of this and other fish species that have pelagic larvae in this region of the southeast Pacific. In this context, it is perhaps relevant that expansions of fish ranges are not uncommon in this region, even though both Easter and Salas y Gomez Islands lie in different biogeographic provinces (Parin et al., 1997). A good example is the pentacerotid *Pentaceros decacanthus*, which was regarded as endemic of the Nazca and Salas y Gómez Ridges until it was recorded in Easter Island (Parin and Kotlyar, 1988).

Acknowledgments

We would like to thank Paula Rosenberg and all the crew from the *AGOR Vidal Gormaz* for their help with sampling. We also thank Muneo Okiyama for his comments on identification of percophid larvae. This research was funded by the Comité Oceanográfico Nacional (CONA), Chile, and forms part of a study on distribution patterns and larval accumulation around oceanic islands headed by Leonardo Castro.

Literature cited

Belyanina, T. P.
1989. Ichthyoplankton in the regions of the Nazca and Salas y Gomez submarine ridges. J. Ichthyol. 29(5):84–90.
1990. Larvae and fingerlings of little-known benthic and benthopelagic fishes from the Nazca and Salas y Gomez ridges. J. Ichthyol. 30(6):1–11.

Castro, L. R., and M. F. Landaeta.
2002. Patrones de distribución y acumulación larval en torno a islas oceánicas: Isla de Pascua y Salas y Gómez. Cienc. Tecnol. Mar. CONA 25(1):131–145.

Mujica, A.
1993. Zooplancton de las aguas circundantes a la Isla de Pascua (27°08'S–109°26'W). Cienc. Tecnol. Mar. CONA 16:55–61.

Neira, F. J., A. G. Miskiewicz, and T. Trnski.
1998. Larvae of temperate Australian fishes. Laboratory guide for larval fish identification, 474 p. Univ. Western Australia Press, Nedlands, Australia.

Okiyama, M.
2000. Percophidae (sandfishes, duckbills). *In* The larvae of Indo-Pacific coastal fishes: an identification guide to marine fish larvae (J. M. Leis and B. M. Carson-Ewart, eds.), p. 554–560. Brill, Leiden, The Netherlands.

Parin, N. V.
1985. A new hemerocoetine fish, *Osopsaron karlik* (Percophidae, Trachinoidei) from the Nazca submarine ridge. Jpn. J. Ichthyol. 31(4):358–361.
1990. Percophid fishes (Percophidae) from the Salas y Gomez ridge (Southeast Pacific). J. Ichthyol. 30(1):68–79.

Parin, N. V., and A. N. Kotlyar.
1988. A new boarfish, *Pentaceros quinquespinis* (Pentacerotidae), from the Southeast Pacific. Vopr. Ikhtyol. 28(3): 355–360.

Parin, N. V., A. N. Mironov, and K. N. Nesis.
1997. Biology of the Nazca and Sala y Gómez submarine ridges, an outpost of the Indo–West Pacific fauna in the Eastern Pacific Ocean: composition and distribution of the fauna, its communities and history. Adv. Mar. Biol. 32: 147–242.

Potthoff, T.
1984. Clearing and staining techniques. *In* Ontogeny and systematics of fishes (H. G. Moser, W. J. Richards, D. M. Cohen, M. P. Fahay, A. W. Kendall, and S. L. Richardson, eds.), p. 35–37. Am. Soc. Ichthyol. Herpetol. Special Publication 1.

Randall, J. E., and A. Cea-Egaña.
1984. Native names of Easter Island fishes, with comments on the origin of the Rapanui people. Occas. Pap. Bernice P. Bishop Mus. 25(12):1–16.

Reader, S. E., and F. J. Neira.
1998. Percophidae: sandfishes, duckbills. *In* Larvae of temperate Australian fishes. Laboratory guide for larval fish identification (F. J. Neira, A. G. Miskiewicz, and T. Trnski, eds.), p. 358–361. Univ. Western Australia Press: Nedlands, Australia.

Reader, S. E., J. M. Leis, and D. S. Rennis.
2000. Creediidae (tommyfishes). *In* The larvae of Indo-Pacific coastal fishes. An identification guide to marine fish larvae (J. M. Leis and M. Carson-Ewart (eds.), p. 575–578. Brill, Leiden, The Netherlands.

Watson, W., A. C. Matarese, and E. G. Stevens.
1984. Trachinoidea: development and relationships. *In* Ontogeny and systematics of fishes (H. G. Moser, W. J. Richards, D. M. Cohen, M. P. Fahay, A. W. Kendall Jr., and S. L. Richardson, eds.), p. 554–561. Am. Soc. Ichthyol. Herpetol. Special Publication 1.

Assessment of sampling methods to estimate horseshoe crab (*Limulus polyphemus* L.) egg density in Delaware Bay

Penelope S. Pooler
David R. Smith
U.S. Geological Survey
Leetown Science Center
11700 Leetown Road
Kearneysville, West Virginia 25430
E-mail address (for D. R. Smith, contact author): david_r_smith@usgs.gov

Robert E. Loveland
Department of Ecology and Evolution
Cook College
Rutgers University
New Brunswick, New Jersey 08901

Mark L. Botton
Fordham University
113 West 60th Street
New York, New York 10023

Stewart F. Michels
Delaware Division of Fish and Wildlife
P.O. Box 330
Little Creek, Delaware 19961

Each spring horseshoe crabs (*Limulus polyphemus* L.) emerge from Delaware Bay to spawn and deposit their eggs on the foreshore of sandy beaches (Shuster and Botton, 1985; Smith et al., 2002a). From mid-May to early June, migratory shorebirds stopover in Delaware Bay and forage heavily on horseshoe crab eggs that have been transported up onto the beach (Botton et al., 1994; Burger et al., 1997; Tsipoura and Burger, 1999). Thus, estimating the quantity of horseshoe crab eggs in Delaware Bay beaches can be useful for monitoring spawning activity and assessing the amount of forage available to migratory shorebirds.

We evaluated procedures to estimate horseshoe crab egg density by asking three questions that address sampling at a different spatial scale. 1) How many samples of sediment are needed for precise estimation of egg density within a segment of beach? 2) Does egg density within a segment of beach adequately represent egg density across a larger stretch of beach? 3) How many beach segments should be sampled to monitor bay-wide egg density? We chose these three questions because the objective of egg studies might focus on any of these scales. We ask the first question to determine the sampling effort necessary to detect changes in egg density over time within a specific beach segment. The second question allows us to examine the reliability of using egg density in a beach segment to infer egg density over a larger stretch of beach. The third question deals with the level of precision in estimates of bay-wide egg density and how many beaches must be sampled to detect bay-wide declines in density over time. Understanding the reliability of egg density estimates at multiple scales will help develop effective monitoring programs.

We addressed all three questions with respect to eggs found in both shallow (0–5 cm) and deep (0–20 cm) sediments. Horseshoe crabs are generally thought to lay most of their eggs at a depth of 15–20 cm (Brockmann, 1990; Botton et al., 1994). Through processes of bioturbation and wave-generated sediment activation, horseshoe crab eggs are brought onto the beach and made available to foraging shorebirds (Botton et al., 1994; Kraeuter and Fegley, 1994; Jackson et al., 2002).

Materials and methods

During May and June 1999, we collected sediment on 16 beaches in Delaware Bay (Fig. 1), eight along the eastern shore (New Jersey) and eight along the western shore (Delaware), to estimate egg density. Methods used to collect sediment and extract horseshoe crab eggs are summarized in the present study, but are presented in detail in Smith et al. (2002b). Beach sediment was collected in cores (5 cm diameter) within a 3-m wide strip along a 100-m segment of beach. Each 3-m wide strip was centered on the mid-beach elevation where a majority of horseshoe crab nests occur (Botton et al., 1988). The mid-beach elevation is halfway between the spring high water level and the beach break at the low tide terrace. Within each egg-sampling strip, 40 locations were selected randomly for sediment collection. At each location, a pair of core samples was taken: one to a depth of 5 cm and the other to a depth of 20 cm. We sampled eggs on 25–26 May and 14–15 June 1999, which followed the heaviest spawning activity in Delaware Bay that year (Smith et al., 2002a). We mixed the entire core contents thoroughly and then removed 80-mL aliquots. We ran the aliquots

Manuscript approved for publication
12 February 2003 by Scientific Editor.
Manuscript received 4 April 2003 at NMFS Scientific Publications Office.
Fish Bull. 101:698–703 (2003).

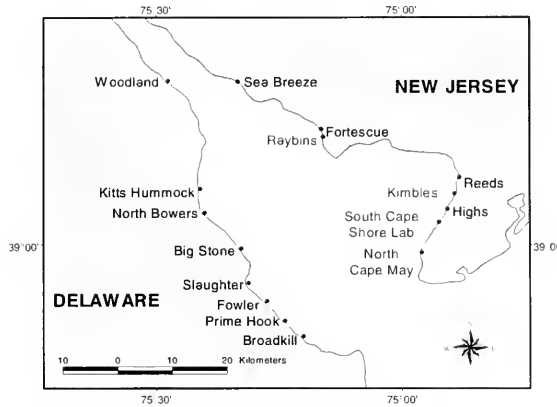

Figure 1

Delaware Bay beaches (•) where horseshoe crab eggs were sampled in May and June 1999.

through a 1-mm sieve to separate eggs and larvae from ambient sediments and then counted eggs (dead or live) and larvae in each aliquot. Depth of aerobic sand varied; thus we measured core volume prior to extrapolating egg counts to totals per core and then estimated the total density of eggs and larvae. The larvae comprised a small fraction of total eggs and larvae, and for the purposes of this paper we evaluated the sampling of eggs only.

Question 1: How many sediment cores should be sampled per beach segment?

We addressed this question in two steps. First, we determined the precision of egg-density estimates as a function of egg density and sample size. Second, we translated the precision of the estimates into statistical power to detect change in egg density over time. For simplicity, variance of the egg-density estimate was calculated from a random sample from an infinite population. Coefficient of variation (CV) was calculated as

$$CV = \sqrt{\mathrm{var}(y)/n}\,/\,\bar{y},$$

where var(y) = variance of eggs among cores; and
$\bar{y}$ = egg density.

We modeled the relationship between egg density and variance among cores (i.e. var[y]=$f[\bar{y}]$ to predict coefficient of variation (CV) for different sample sizes and across the observed range of egg densities (i.e. $CV = \sqrt{f[\bar{y}]/n}\,/\,\bar{y}$). Using predicted CVs, we estimated the probability of detecting a change in egg density over time. The probability of detecting decline (i.e. statistical power) was calculated by using a one-tailed t-test with a type-I error rate of 0.2 and a constant rate of annual change for CVs = {0.1, 0.2, 0.3, 0.4} with the software program TRENDS (Gerrodette, 1993).

Question 2: Is egg density within a beach segment representative of egg densities along a larger stretch of beach?

Smith et al. (2002b) modeled the relationship between counts of spawning females and egg densities within beach segments. Spawning females are counted annually as part of a bay-wide survey of spawning activity (Smith et al., 2002a), and in 1999, egg sampling was conducted on some of the same beaches as the spawning survey (Smith et al., 2002b). For eggs that were sampled in May 1999 on six New Jersey beaches, the relationship was fairly strong, linear, and predictive (r^2=0.62; Smith et al., 2002b). Although we sampled for eggs on only one 100-m segment of beach, we used the above relationship to predict egg densities for all 100-m segments along the beach where spawning females were counted. We limited the predictions to the six New Jersey beaches where we felt the relationship between spawning females and egg densities was sufficiently strong (Smith et al., 2002b). We compared egg density in the observed 100-m segment to the distribution of densities predicted in all 100-m segments on the beach. If the observed density was within the interquartile range of the distribution of predicted densities, we concluded that the 100-m segment was representative of the larger stretch of beach.

Question 3: How many beaches should be sampled?

Using the observed variation in egg density among the 16 beaches sampled in 1999, we predicted the CV for bay-wide egg density estimates as a function of the number of beaches sampled and under a stratified sampling design where the two strata were New Jersey and Delaware. We could not evaluate CV across a range of bay-wide densities because the 1999 results provided only one datum point, and we expected variation among beaches to be a function of egg

Table 1

Mean eggs per core and standard errors (SE) for horseshoe crabs (*Limulus polyphemus*) at 16 beaches sampled in Delaware Bay that were sampled in May and June 1999. Cores were 5 cm in diameter. At 40 random locations on each beach, a pair of sediment cores were sampled: one core at 5 cm depth (shallow sediment) and another at 20 cm depth (deep sediment).

		No. of eggs per core on 25–26 May 1999				No. of eggs per core on 14–15 June 1999			
State	Beach	Shallow sediment	SE	Deep sediment	SE	Shallow sediment	SE	Deep sediment	SE
Delaware	Broadkill	0.0	0.00	1.5	1.47	1.2	0.36	101.7	60.42
	Prime Hook	0.2	0.08	81.9	76.17	7.4	2.06	223.9	112.14
	Fowler	0.1	0.05	1.8	0.65	2.7	1.22	211.3	116.56
	Slaughter	11.7	2.69	814.8	186.04	41.7	5.35	664.5	97.81
	Big Stone	0.1	0.05	11.3	5.09	0.7	0.53	24.2	14.27
	North Bowers	23.0	6.49	950.3	234.18	105.1	23.54	400.4	70.81
	Kitts Hummock	26.4	8.23	325.1	78.63	15.2	5.49	124.8	43.94
	Woodland	0.5	0.17	0.1	0.06	7.0	3.68	60.9	29.75
New Jersey	North Cape May	0.3	0.25	0.0	0.00	0.5	0.33	0.7	0.37
	South Cape Shore Lab.	25.5	0.86	1085.4	140.29	4.5	0.81	1399.2	144.03
	Highs	2.1	0.71	1128.6	96.99	4.4	0.94	1456.8	173.80
	Kimbles	9.7	4.80	1561.3	286.32	1.7	0.55	1008.0	105.63
	Reeds	2.0	0.52	540.4	79.90	18.2	2.52	468.0	62.67
	Raybins	3.5	1.91	65.8	43.88	0.1	0.06	6.7	4.57
	Fortescue	2.0	0.43	645.9	108.71	20.6	3.85	465.7	193.64
	Sea Breeze	27.5	7.95	347.3	94.70	0.2	0.09	3.1	2.01

density. However, we examined the probability of detecting a percentage change in bay-wide egg density over time as a function of the number of beaches sampled by using the 1999 bay-wide egg density as the initial value in the time series.

Results

When the objective is to monitor egg density within a segment of beach, a sample size of 40 sediment cores is sufficient for detecting substantial changes in egg density in the top 20 cm of sediment, but >40 cores would be needed to monitor egg density in the top 5 cm of sediment. Distributions of egg densities were skewed right with median densities of 3 and 275 eggs per core for shallow and deep cores, respectively (Table 1). A sample size of 40 cores resulted in a CV of 0.26 for a median density of eggs 0–20 cm deep (Fig. 2B). In contrast, about 100 cores would need to be sampled to bring the CV down to 0.3 when sampling shallow sediment and when egg density was at the median (Fig. 2A). A CV of 0.3 corresponds to a 75% chance of detecting a 50% decline in egg density over 5 years (Fig. 3A) and an 80% chance of detecting a 40% decline over 10 years (Fig. 3B). A sample size of 60 shallow cores would result in CV of 0.4 for median egg density (Fig. 2A), which would be sufficient for monitoring over 10 years, but not over 5 years. A CV of 0.4 would lead to a better than 85% chance of detecting a 50% decline in density over 10 years (Fig. 3B). Precision and power would improve when sampling higher densities of eggs (Fig. 2).

At most beaches, observed egg densities within a 100-m segment of beach were not representative of egg densities throughout a larger beach. On only two of the six New Jersey beaches examined (South Cape Shore Lab and Reeds) did the observed egg density fall within the interquartile range of beach-wide densities (Fig. 4). On three beaches the observed egg density was greater than all predicted densities, and on one beach observed egg density was less than all predicted densities.

With egg density at the 1999 level and sampling at 16 beaches (i.e. eight beaches per state) distributed throughout the bay, the CV for densities of eggs in 0–20 cm of sediment was 0.26 in May and 0.29 in June (Fig. 5). For densities of shallow eggs, the CV was 0.33 for egg densities in May and 0.43 in June. Variability in egg densities among beaches was greater for sampling in June 1999 than in May 1999.

Discussion

Eggs in shallow sediment (0–5 cm) consistently yielded lower densities and higher variability than eggs in deep sediment (0–20 cm). A sample size of 40 sediment cores was sufficient for estimating and monitoring density of eggs 0–20 cm deep within a 100-m beach segment. However, a larger sample size (≥60 sediment cores) would be needed for estimating and monitoring density of eggs 0–5 cm deep within a segment of beach.

Because egg density in a 100-m segment of beach is not necessarily representative of the larger surrounding beach,

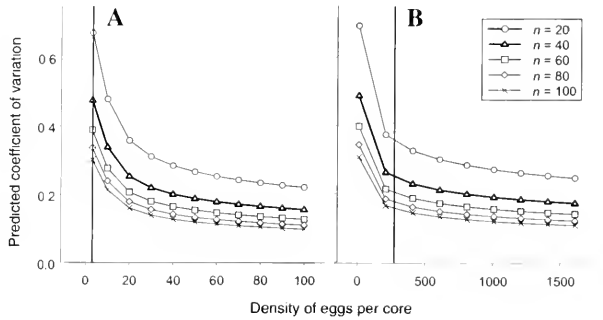

Figure 2

The relationship between density and coefficient of variation (CV) for (**A**) shallow sediment (0–5 cm) and (**B**) deep sediment (0–20 cm). Curves in each figure depend on sample size: circle is n = 20, triangle is n = 40, square is n = 60, diamond is n = 80, and × is n = 100. Vertical lines represent median egg densities that we observed in 1999.

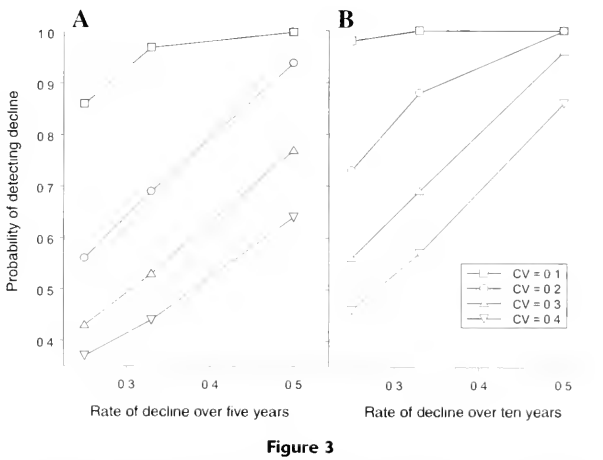

Figure 3

Probability of detecting a decline (i.e. statistical power) for various magnitudes of decline and for annual surveys over five (**A**) and 10 (**B**) years. Statistical power was calculated for a one-tailed t-test with a type-I error rate of 0.2, and a constant annual rate of change.

it is important to realize that if sampling is restricted to a short segment of beach, then the scope of inference is strictly limited to that segment. If a reliable estimate of egg density along a beach is required, then it will be necessary to take samples along the entire beach. Because of the logistics of sampling sediment it would be difficult to sample throughout a long stretch of beach in one stage of sampling. However, a two-stage sampling design could be considered in which beach segments are selected at the 1st stage and sediment cores within segments are selected at the 2nd stage.

Consistent with our findings on sampling within a beach, bay-wide egg density can be more precisely estimated for eggs 0–20 cm deep than for eggs 0–5 cm deep. A stratified

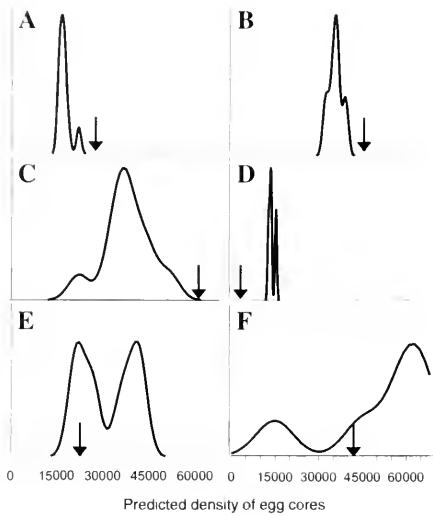

Figure 4

Density curves of predicted egg densities on 100-m beach segments at six New Jersey beaches. An arrow represents the egg density in the observed 100-m segment. These density curves were generated by dividing the area surveyed for spawning females into 100-m segments and using the observed relationship between egg densities and spawning females to predict egg density for each segment. The beaches shown are (**A**) Fortescue, (**B**) Highs, (**C**) Kimbles, (**D**) North Cape May, (**E**) Reeds, and (**F**) South Cape Shore Laboratory.

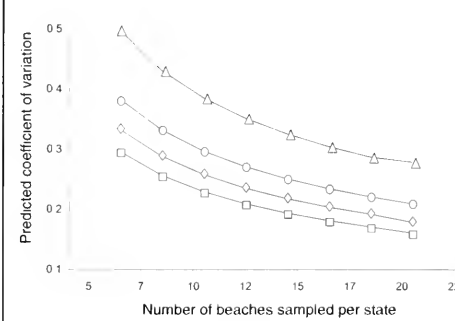

Figure 5

Predicted coefficient of variation (CV) shown for the possible range of number of beaches sampled per state. This figure is based on the observed levels of bay-wide density during the two sampling periods in 1999. Curves are based on egg densities found at different depths and time periods: triangle is shallow sediment in June, circle is shallow sediment in May, diamond is deep sediment in June, and square is deep sediment in May. Shallow sediment is 0 to 5 cm deep, and deep sediment is 0 to 20 cm deep.

random sample of eight beach segments per state would result in CV ≤0.3 for estimates of egg densities 0–20 cm deep. If this level of effort were maintained, it would be sufficient to detect biologically significant declines in egg density over a 5- or 10-year period. However, greater effort would be required to monitor change in egg densities 0–5 cm deep. According to results from the May samples, to estimate egg densities in shallow sediment with CV ≤0.3, a stratified random sample of 10 segments per state would be required.

Sampling eggs is a costly process; therefore sampling efficiency and reducing sample size are important considerations. Although sediment can be collected quickly, the process of extracting and enumerating eggs from the sediment can be time consuming. Quantifying the eggs in surface sediments to assess shorebird forage biomass is likely to be the main objective of many egg sampling studies because horseshoe crab spawning activity can be assessed by other methods, such as through counts of spawning horseshoe crabs (Smith et al., 2002a). However, a primary finding in the present study is that estimating eggs in 0–5 cm of sediment will be more costly than estimating eggs in 0–20 cm of sediment. In the future, alternatives in survey design, such as stratification of the beach foreshore, should be considered to reduce the amount of sediment that needs to be collected for precise estimates of horseshoe crab egg density.

Acknowledgments

This work was funded through the USGS/State Partnership Project (no. 99HQAG0050). Additional funding was provided through the New Jersey Endangered & Nongame Species Program.

Literature cited

Botton, M. L., R. E. Loveland, and T. R. Jacobsen.
1988. Beach erosion and geochemical factors: influence on spawning success of horseshoe crabs (*Limulus polyphemus*) in Delaware Bay. Mar. Biol. 99:325–332.
1994. Site selection by migratory shorebirds in Delaware Bay, and its relationship to beach characteristics and abundance of horseshoe crab (*Limulus polyphemus*) eggs. Auk 111:605–616.

Brockmann, H. J.
1990. Mating behavior of horseshoe crabs, *Limulus polyphemus*. Behaviour 114:206–220.

Burger, J., L. Niles, and K. E. Clark.
1997. Importance of beach, mudflats and marsh habitats to migrant shorebirds on Delaware Bay. Biol. Conserv. 79: 283–292.

Gerrodette, T.
1993. TRENDS: software for a power analysis of linear regression. Wildl. Soc. Bull. 21:515–516.
Jackson, N. L., K. F. Nordstrom, and D. R. Smith.
2002. Geomorphic-biotic interactions on beach foreshores in estuaries. J. Coast. Res. 36:414–424.
Kraeuter, J. N., and S. R. Fegley.
1994. Vertical disturbance of sediment by horseshoe crabs (*Limulus polyphemus*) during their spawning season. Estuaries 17:288–294.
Shuster, C. N., Jr., and M. L. Botton.
1985. A contribution to the population biology of horseshoe crabs, *Limulus polyphemus* (L.), in Delaware Bay. Estuaries 4:363–372.
Smith, D. R., P. S. Pooler, B. L. Swan, S. F. Michels, W. R. Hall, P. J. Himchak, and M. J. Millard.
2002a. Spatial and temporal distribution of horseshoe crab (*Limulus polyphemus*) spawning in Delaware Bay: implications for monitoring. Estuaries 25:115–125.
Smith, D. R., P. S. Pooler, R. E. Loveland, M. L. Botton, S. F. Michels, R. G. Weber, and D. B. Carter.
2002b. Horseshoe crab (*Limulus polyphemus*) reproductive activity on Delaware Bay beaches: interactions with beach characteristics. J. Coast. Res. 18:730–740.
Tsipoura, N., and J. Burger.
1999. Shorebird diet during spring migration stopover on Delaware Bay. Condor 101:635–644.

Larval abundance, distribution, and spawning habits of spotted seatrout (*Cynoscion nebulosus*) in Florida Bay, Everglades National Park, Florida

Allyn B. Powell

Center for Coastal Fisheries and Habitat Research
National Ocean Service
National Oceanic and Atmospheric Administration
101 Pivers Island Road
Beaufort, North Carolina 28516
E-mail address: allyn.powell@noaa.gov

The spotted seatrout (*Cynoscion nebulosus*) is one of the most sought after recreational fish in Florida Bay, and it spends its entire life history within the bay (Rutherford et al., 1989b). The biology of adult spotted seatrout in Florida Bay is well known (Rutherford et al., 1982, 1989b) as is the distribution and abundance of juveniles within the bay. The habitats and diets of juveniles are well documented (Hettler, 1989; Chester and Thayer, 1990; Thayer et al., 1999; Florida Department of Environmental Protection[1]). Nevertheless, the spatial and temporal spawning habits of spotted seatrout and the distribution of larvae have only been partially described (Powell et al., 1989; Rutherford et al., 1989a).

An excellent description of the ecological history of Florida Bay is given by Fourqurean and Robblee (1999). Briefly, Florida Bay is subtropical and is generally oligotrophic. The bay is a network of shallow basins, mud banks, and mangrove islands (keys). Tides are influenced by the Gulf of Mexico and Atlantic Ocean, but mud banks, which are connected to basins by channels, restrict circulation in the bay and attenuate tidal energy very quickly. As a result there is essentially no lunar tide over most of the central and northeastern portion of the bay.

This impediment to circulation could have a negative effect on the recruitment of early-stage planktonic larvae into these portions of the bay. Within the next few decades, plans to restore the Everglades include increasing freshwater flows to Florida Bay. Prerestoration information on larval distribution and spawning patterns of spotted seatrout is a high priority because increased freshwater flows can have potential positive and negative impacts. At low salinities, the planktonic eggs of spotted seatrout could sink to the bottom and would not be viable (Holt and Holt, 2002; Alshuth and Gilmore[2]). On the other hand, increased freshwater flows can alleviate hypersaline conditions that could result in an expansion of the distribution of the early life stages of spotted seatrout (Thayer et al., 1999; Florida Department of Environmental Protection[1]). The objective of the present study is to document the distribution and abundance of spotted seatrout larvae to determine their early life history habitats and spawning habits in Florida Bay.

Methods and materials

To describe the distribution and abundance of spotted seatrout larvae in Florida Bay, I devised a series of ichthyoplankton surveys between 1994 and 1999. The initial survey was conducted during nine nonconsecutive months between September 1994 and August 1995. A total of 14 fixed stations were selected in basins of Florida Bay (Fig. 1). In accordance with recommendations by the South Florida Ecosystem Restoration Prediction and Modeling (SFERPM), Program Management Committee (PMC), Florida Bay was divided into six zones for ease of reporting results (Table 1, Fig. 1). These zones are based on the benthic molluscan and benthic plant communities (Fourqurean and Robblee, 1999). Paired bongo nets, 60 cm wide, were fitted with 0.333-mm mesh and fished from the port side of a 5.4-m boat. Nets were towed during daylight, approximately 1 m below the surface for 5 minutes and volume estimates were obtained from flowmeter readings.

In 1996, sampling was conducted monthly from April through September at stations where recently hatched spotted seatrout occurred during 1994–95 (stations 5, 6, 9–13). In 1996, I used a paired 60-cm bow-mounted push nets with 0.333-mm mesh similar to that described by Hettler and Chester (1990). Nets were fished approximately 1 m below the surface for 3 minutes. The volume of water sampled with the push net was slightly greater than that sampled with the bongo nets (60 m^3 vs. 50 m^3). To test the efficiency of the two gears, both were fished simultaneously at 23 stations during 1996. A Kruskal-Wallis nonparametric test was used to evaluate differences (Sokal and Rohlf, 1981). No significant differences in densities of fish larvae were found between gear types (P=0.50).

During and after September 1997 sampling for spotted seatrout was limited to four stations in four zones (Table 1; stations 6, 15, 16, 17) where paired bow-mounted push nets were employed. Sampling occurred during July and September 1997; March, May, June, July, and September 1998; and May, July, and November 1999.

[1] Florida Department of Environmental Protection. 1995. Fisheries-independent monitoring program, annual report. Florida Department of Environmental Protection, Florida Marine Research Institute, 100 8th Avenue SE, St. Petersburg, FL 33701.

[2] Alshuth, S., and R. G. Gilmore Jr. 1994. Salinity and temperature tolerance limits for larval spotted seatrout, *Cynoscion nebulosus* C. (Pisces: Sciaenidae). Int. Coun. Explor. Sea, Coun. Meet. Pap., ICES-CM-1994/L: 17, 19 p.

Manuscript accepted for publication 19 February 2003 by Scientific Editor.

Manuscript received 4 April 2003 at NMFS Scientific Publications Office.

Fish Bull. 101:704–711 (2003).

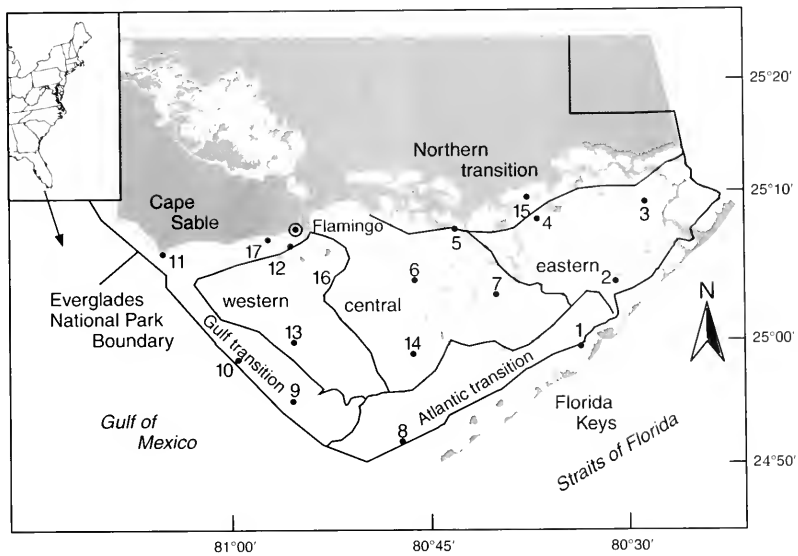

Figure 1

Location of stations in Florida Bay sampled in 1994–99. See Table 1 for station latitudes and longitudes.

Table 1

Florida Bay sampling stations including zone locations as defined by the South Florida Ecosystem Restoration Prediction and Modeling Program, Program Management Committee. Stations 1–14 were sampled in 1994–95; stations 5 ,6, 9–13 in 1996; and stations 6, 15–17 in 1997–99.

Station	Latitude (degrees and minutes)	Longitude (degrees and minutes)	Florida Bay zones	Location
1	24 59.42	80 34.06	Atlantic transition	Cowpens Cut
2	25 04.42	80 31.24	eastern	Butternut Key
3	25 10.54	80 29.12	eastern	Duck Key
4	25 009.24	80 37.12	eastern	between Eagle Key and Madeira Point
5	25 08.30	80 43.19	central	Big Key
6	25 04.57	80 46.32	central	Whipray Basin
7	25 03.54	80 40.12	central	between Calussa and Russel Keys
8	24 52.46	80 47.31	Atlantic transition	between Old Dan and Peterson Key banks
9	24 55.60	80 55.40	Gulf transition	Sprigger Bank
10	24 58.48	80 59.48	Gulf transition	between Oxfoot and Sprigger Banks
11	25 06.49	81 05.16	Gulf transition	Cape Sable
12	25 07.22	80 55.62	Gulf transition	Dave Foy Bank
13	24 59.98	80 55.46	western	between Blue and Ninemile Banks
14	24 59.06	80 46.54	central	between Rabbit and Gopher Keys
15	25 10.80	80 37.80	northern	Little Madeira Bay entrance
16	25 06.00	80 52.50	western	Palm Key Basin
17	25 07.67	80 57.32	Gulf transition	Bradley Key

At stations where replicate tows were taken, densities were averaged. Ichthyoplankton samples were preserved in 95% ethanol. Temperature was measured at all stations with a hand-held thermometer and salinity was measured with a refractometer. Size at age of larvae was estimated from the equation L_n standard length = −1.31 + 1.2162 (L_n age in days) (Powell et al.[3]).

Because of the high coefficient of variation associated with ichthyoplankton samples (Cyr et al., 1992), my sampling design was probably inadequate for multiway statistical comparisons. Therefore, I used nonparametric Kruskal-Wallis tests with $\alpha = 0.10$ (Sokal and Rohlf, 1981) and relied on patterns and trends to infer differences in densities of spotted seatrout between stations and time periods. In the period 1994–95 we tested densities among nine months and 14 stations to determine trends in spatial and temporal spawning habits. We also tested differences between the period 1994–95 and the period 1996 to determine interannual spatial and temporal differences or similarities. Only those months (April through August) that were sampled during the two periods were included. During the period from 1997 through 1999 it was only appropriate to determine spatial differences because we sampled irregularly during this period.

A general description of the diverse habitats in relation to stations in the present study is described by Holmquist et al. (1989, decapod and stomatopod communities); Thayer and Chester (1989, fish distribution, seagrass distribution and abundance, sediment depth, and organic content); Zieman et al. (1989, macrophyte distribution); and Fourqurean and Robblee (1999, general description of the Florida Bay ecosystem).

Results

In 1994–95, salinities were lowest and most variable at stations 1–5 and 7 in the eastern part of Florida Bay (Figs. 1 and 2). Hyperhaline conditions were never observed during this period. Salinities in 1996, which were recorded monthly from April through September at stations where recently hatched spotted seatrout were collected in 1994–95, were generally euhaline and, as in 1994–95, hyperhaline conditions were never observed. From July 1997 through November 1999 at four trout monitoring stations, mean salinities were similar at stations 6, 16, and 17 but were most variable at station 6. Station 15 had the lowest mean salinity and the greatest variation. At this station salinities ranged from 10.0 (March 1998) to 33.0 psu (May 1999). Highest salinities for all four stations were observed in May 1999. Hyperhaline conditions were observed only at station 6 in June 1998 and May 1999 and at station 16 in May 1999 (Fig. 2).

In general, spawning in Florida Bay occurred between March and October and peaked in June, August, and September (Table 2). Densities of spotted seatrout were significantly different among months in 1994–95 ($P<0.01$) and 1996 ($P=0.01$). Spotted seatrout larvae were absent during December, February, and April in 1994–96 (Table 2), and in November 1997–99 (Table 3). Most spawning, based on larval collections, occurred between 26° and 34°C (Fig. 3). The coldest temperature at which larval spotted seatrout were collected was 20°C in March 1998 at station 6. Spotted seatrout larvae were collected mainly at salinities between 25 and 40 psu (Fig. 3), although larvae were collected in salinities as low as 12 psu at station 15.

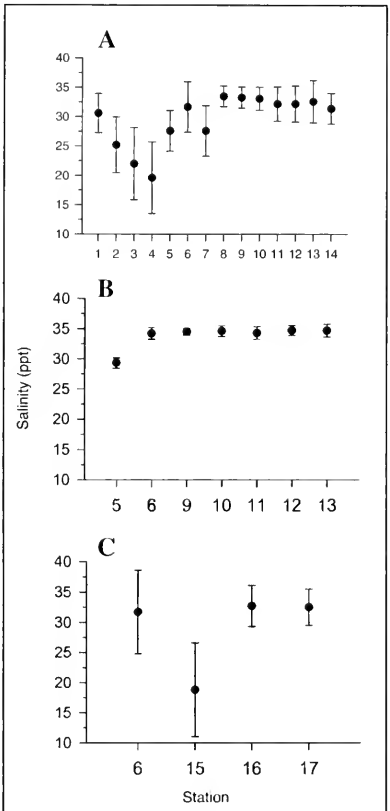

Figure 2

Mean salinities SD for (**A**) 14 stations sampled from September 1994 through August 1995, (**B**) 7 stations sampled monthly from April through September 1996, and (**C**) 4 stations sampled from July 1997 through November 1999. For months that samples were taken, refer to Tables 2 and 3.

[3] Powell, A. B., R. Cheshire, E. H. Laban, J. Colvocoresses, P. O'Donnell, and M. Davidian. In review. Growth, mortality and hatchdate distributions of larval and juvenile spotted seatrout, *Cynoscion nebulosus*, in Florida Bay, 26 p.

Spatially, there were significant differences in densities of spotted seatrout among 14 stations from 1994 through 1995 (P=0.01), and densities were highly variable (Table 2). In addition, a considerable number of zero catches occurred at stations where spotted seatrout were collected at least one time. This high variability indicated that the sampling design was inadequate to properly evaluate the spatial and temporal abundance of spotted seatrout larvae. However, some patterns could be discerned. Generally, larval spotted seatrout were absent or rarely collected in the eastern (stations 2, 3, and 4), Atlantic transition (stations 1 and 14), northern transition (station 15) zones and in a portion of the central zone (station 15) (Tables 2 and 3). They were consistently collected at station 6 in the central zone (Tables 2 and 3).

There were no significant differences (P=0.14) in densities of spotted seatrout among stations in 1996; stations where trout occurred on more than one occasion in 1994–95 (Table 2). As in 1994–95, high mean densities of spotted seatrout occurred at station 6 (Table 2).

Significant differences in spotted seatrout densities at certain stations were observed between the periods 1994–95 and 1996. Differences were observed at stations 9 (P=0.02), station 10 (P=0.02), and station 13 (P=0.02). At these three stations in 1996 spotted seatrout were collected only in one month (August). They were never collected at station 5 in 1996 (Table 2).

Size of larvae was indicative of spawning locations. Recently hatched spotted seatrout larvae (1.0–1.9 mm notochord length; ≤5 d old) were collected mainly in central (stations 5 and 6), Gulf transition (stations 9, 10, 11, 12, 17) and western (stations 13 and 16) zones. Recently hatched larvae were rare at station 4 (eastern zone), station 14 (central zone) and station 15 (northern transition zone). They were absent at station 8 (Atlantic transition zone) (Figs. 4 and 5).

Discussion

Evidence from previous studies (Powell et al., 1989; Rutherford et al., 1989a) and the present study establishes the spatial and temporal spawning habits of spotted seatrout in Florida Bay. Length-frequency distributions of spotted seatrout larvae collected in 1984–85 (Powell et al., 1989) and data from the present study indicate that spotted seatrout spawn mainly in the Gulf transition, central, and western zones of Florida Bay and that there is limited spawning in the northern transition and eastern zones (Figs. 4 and 5). Spawning also occurs in the far northeastern portion of Florida Bay in Little Blackwater and Blackwater Sounds (Rutherford et al., 1989a). However, there is no evidence for spawning in the Atlantic transition zone. The distribution of planktonic larvae is not necessarily a good indicator of postsettlement habitat requirements because abiotic factors related to transport could influence their distribution. However, in Florida Bay larvae are not distributed homogeneously throughout the bay, and mudbanks impede circulation (Fourqurean and Robblee, 1999). The adults are generally nonmigratory and inhabit shallow seagrass-rich environments (Chester and Thayer, 1990). Hence, the dis-

Table 2

Densities (numbers/100 m^3) of larval spotted seatrout in 1994–96. Larvae were not collected in December 1994, February and April 1995, and April 1996. Larvae were absent at stations 1, 2, 3, and 7. Mean densities do not include those months or stations where spotted seatrout were never collected. NS=not sampled.

	1994		1995					1996				
Station	Sep	Nov	May	Jun	Jul	Aug	Mean ±SD	May	Jun	Jul	Aug	Sep	Mean ±SD
4	0	0	0	9.4	0	0	1.6 ±3.8	NS	NS	NS	NS	NS	
5	3.4	0	0	113.2	0	NS	23.3 ±50.3	0	0	0	0	0	0
6	114.9	4.6	0	5.6	14.0	NS	27.8 ±48.9	2.4	82.1	0	31.3	7.5	24.7 ±34.4
8	0	0	0	0	0	3.2	0.5 ±1.3	NS	NS	NS	NS	NS	
9	20.0	2.9	1.9	5.4	11.1	NS	8.3 ±7.5	0	0	0	31.8	0	6.4 ±14.2
10	21.7	0	2.1	9.6	13.7	NS	9.4 ±8.8	0	0	0	16.2	0	3.2 ±7.2
11	13.0	0	1.8	9.3	0	NS	4.8 ±6.0	0	0	1.9	3.4	0	1.1 ±1.5
12	0	0	0	0	1.0	6.7	1.3 ±2.7	0	0	4.7	1.6	50.0	11.3 ±21.7
13	26.3	0	2.0	87.5	8.5	26.0	25.1 ±32.7	0	0	0	3.3	0	0.7 ±1.5
14	14.8	0	0	0	0	3.6	3.1 ±5.9	NS	NS	NS	NS	NS	
Mean ±SD	21.4 ±34.2	0.8 ±1.6	0.8 ±1.0	24.0 ±40.9	4.8 ±6.2	7.9 ±10.4		0.3 ±0.9	11.7 ±31.0	0.9 ±1.8	12.5 ±14.0	8.2 ±18.	

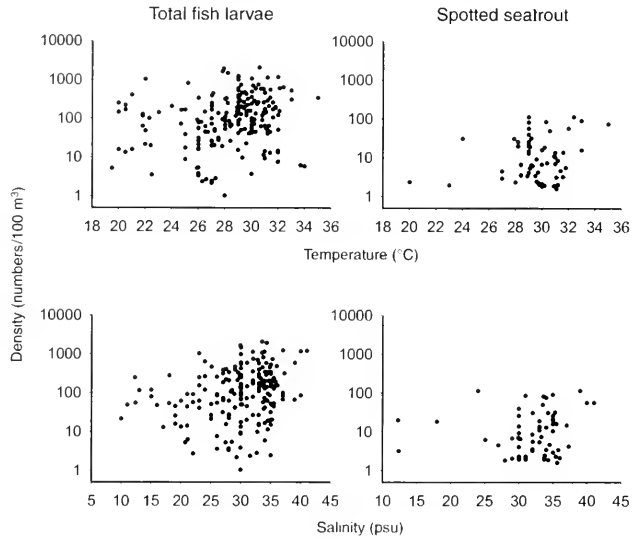

Figure 3

Density of total fish larvae and spotted seatrout versus temperature and salinity. "Total fish larvae" indicates the complete range of temperature and salinity where all collections were made and is provided for visual comparison with spotted seatrout collections.

Table 3

Densities (numbers/100 m^3) of spotted seatrout collected at monitoring stations with a bow-mounted push net with 0.333-mm mesh.

	1997		1998					1999			
Station	Jul	Sep	Mar	May	Jun	Jul	Sep	May	Jul	Nov	Mean ±SD
6	0	6.2	1.2	40.2	57.0	16.0	93.1	56.8	1.1	0	30.2 ±33.2
15	3.2	20.1	0	0	0	0	0	0	0	0	2.6 ±6.7
16	7.1	1.1	1.0	1.2	75.6	0	5.2	0	0	0	9.1 ±23.5
17	6.6	1.0	30.8	0	0	0	0	0	6.9	0	5.0 ±10.1
Mean ±SD	4.2 ±3.3	7.1 ±9.0	8.2 ±15.0	10.3 ±10.4	33.1 ±39.0	4.0 ±8.0	24.6 ±45.7	14.2 ±28.4	2.0 ±3.3	0	

tribution of larvae presented in the present study is most likely a good indication of adult spawning areas.

As indicated by the larval collections in this study, spotted seatrout have a protracted spawning period from March through October, which is similar to that observed in Tampa Bay, Florida (McMichael and Peters, 1989). To the contrary, Stewart (1961) reported that spotted seatrout in Florida Bay spawn throughout the year, and Rutherford et al. (1989a) indicated that some spawning occurred as early as February and continued into December. Powell et al.,[3] studying hatchdate distributions of juveniles, reported peak spawning in early May, late June, and late August.

Seagrass meadows appear to be critical habitats for juvenile spotted seatrout (Chester and Thayer, 1990; Tolan et al., 1997; Rooker et al., 1998; Thayer et al., 1999). Rooker et al. (1998) reported that juvenile spotted seatrout in a Texas estuary prefer *H. wrightii* over *T. testudinum*. In another Texas estuary, Tolan et al. (1997) reported that

juvenile spotted seatrout prefer *H. wrightii* over *Syringodium filiforme*. In Florida Bay juveniles are collected at highest densities in western Florida Bay basins near the Gulf of Mexico in habitats with deeper and more organic sediments and with greater density and biomass of *S. filiforme*. In areas where spotted seatrout juveniles are rare or absent, which generally reflects the distribution of their larvae, organic matter and sediment depth are minimal, water depth is generally deeper, and seagrass standing crop, short shoot densities, and diversity are lower (Thayer and Chester, 1989; Chester and Thayer, 1990).

Spotted seatrout larvae were collected consistently at relatively high densities in Whipray Basin (station 6; central zone) and length-frequency distributions indicate spawning most probably occurs in this area. The majority of larvae collected in this area were 2.0–2.4 mm SL (5 to 6 d old), and it is possible that larvae could have been transported into this area from western Florida Bay. Nevertheless, Whipray Basin is a nursery area for juvenile spotted seatrout (Florida Department of Environmental Protection[1]). However, Whipray Basin has a relatively sparse standing crop of the seagrass *Thalassia testudinum* (12 g/m^2) compared to Palm Key (station 16; western zone) which has a higher standing crop of *T. testudinum* (28 g/m^2) and *Halodule wrightii* (14 g/m^2), and has been demonstrated to be an important nursery area for spotted seatrout juveniles (Florida Department of Environmental Protection[1]).

Spotted seatrout eggs have been collected in other waters ranging from 15 to 50 psu (Holt and Holt, 2002). Presumably, larval spotted seatrout eggs sink to the bottom at salinities <15 psu and are not viable (Alshuth and Gilmore[2]). Therefore, it is surprising that recently hatched (<5-d old) larval spotted seatrout were collected, although infrequently, at Little Madeira Bay (station 15; northern transition zone) and only at 12 psu. Whether these low salinities, which occurred in July and September 1997, were a result of drastic changes in salinities caused by weather events that occurred after hatching is unknown. Still, it is highly unlikely that a significant number of viable eggs can be produced at those low salinities.

The qualitative description of spotted seatrout spawning habits provides necessary baseline data in relation to restoration activities, specifically freshwater inflow. Restoration activities could have both a negative and positive effect because salinity can have significant effects on spotted seatrout reproduction and early life history stage processes (Holt and Holt, 2002). For example, low salinities (as discussed above) could be detrimental to egg viability; whereas, alleviating hypersaline areas could expand the spawning area, particularly in the central zone where hypersalinity conditions are persistent (Orlando et al., 1997; Thayer et al., 1999). At high and low salinities, growth and development rates of larval spotted seatrout have been reported to be reduced because these processes are constrained by undeveloped osmoregulatory functions (Holt and Banks, 1989). On the other hand, there is evidence that spotted seatrout populations have adapted to reproduce in extreme-salinity environments where spawning salinities influence egg buoyancy and the salinity tolerance of early

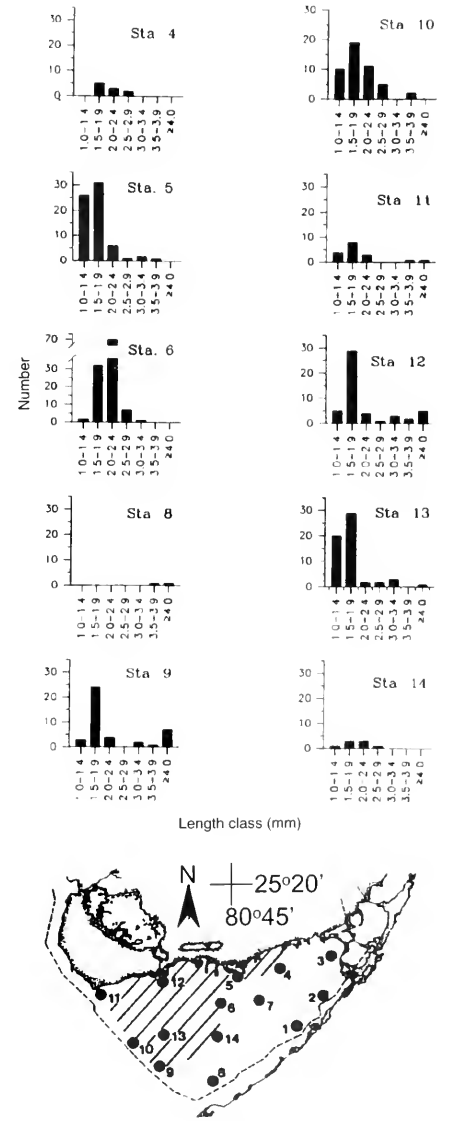

Figure 4

Length-frequency distributions of spotted seatrout by station from 1994–95 collections depicting the spatial spawning habitat. Larvae <2.0 mm were used as criteria to indicate spawning sites. Diagonal lines indicate spawning area. See Table 1 for station locations.

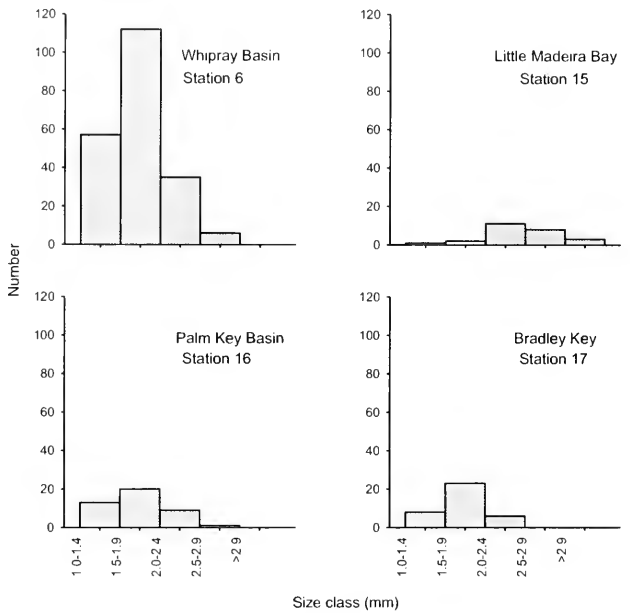

Figure 5

Length-frequency distributions of spotted seatrout from four stations where a bow-mounted push net was used to sample fish from July 1997 through November 1999. See Table 1 for station locations.

larval stages. This adaptation would allow spotted seatrout to spawn over a wide range of salinities.

Future monitoring of spotted seatrout larval abundances to evaluate restoration activities would probably require numerous samples per station because of the high degree of variability as shown by the present study. Therefore, it would seem prudent to continue monitoring spatial spawning habits from larval collections, but to develop a juvenile abundance index to monitor the success of restoration in the Everglades, as well.

Acknowledgments

Sincere appreciation is extended to Al Crosby who was field party chief and processed numerous samples. I am also indebted to other Beaufort Laboratory staff members, notably Robin Cheshire, Peter Crumley, Mike Greene, Donald Hoss, Michael Johnson, and Michael Lacroix for their able assistance in the field; Robin Cheshire, Curtis Lewis, and Harvey Walsh for graphics; James Waters for computer programming; and Dean Ahrenholz, Patti Marraro Joe Smith and an anonymous reviewer for valuable comments in their review of the manuscript. The staff of the Polish Sorting and Identification Center processed many of the ichthyoplankton samples. This study was supported through joint funding from the National Oceanic and Atmospheric Administration Coastal Ocean Program and National Marine Fisheries Service base funds to the Beaufort Laboratory.

Literature cited

Chester, A. J., and G. W. Thayer.
1990. Distribution of spotted seatrout (*Cynoscion nebulosus*) and gray snapper (*Lutjanus griseus*) juveniles in seagrass habitats of western Florida Bay. Bull. Mar. Sci. 46:345–357.

Cyr, H., J. A. Downing, S. Lalonde, S. B. Baines, and M. L. Price.
1992. Sampling larval fish: choice of sample number and size. Trans. Am. Fish. Soc. 121:356–368.

Fourqurean, J. W., and M. B. Robblee.
1999. Florida Bay: a history of recent ecological changes. Estuaries 22:345–357.

Hettler, W. F., Jr.
1989. Food habits of juveniles of spotted seatrout and gray snapper in western Florida Bay. Bull. Mar. Sci. 44: 152–165.

Hettler, W. F., and A. J. Chester.
1990. Temporal distribution of ichthyoplankton near Beaufort Inlet, North Carolina. Mar. Ecol. Prog. Ser. 68:157–168.

Holmquist, J. G., G. V. N. Powell, and S. M. Sogard
1989. Decapod and stomatopod communities of seagrass-covered mud banks in Florida Bay: inter-and intra-bank heterogeneity with special reference to isolated subenvironments. Bull. Mar. Sci. 44:251–262.

Holt, G. J., and M. A. Banks.
1989. Salinity tolerance and development of osmoregulation in larval sciaenids. *In* The early life history of fish (J. H. S. Blaxter, J. C. Gamble, and H. von Westernhagen, eds.); the third ICES symposium, Bergen, Norway 35 October 1988, p. 4–89. Rapp. P.-V. Reun. 191.

Holt, G. J., and S. A. Holt.
2002. Effects of variable salinity on reproduction and early life stages of spotted seatrout. *In* Biology of the spotted seatrout (S. Bortone, ed.), p. 135–145. CRC Press, Washington, DC.

McMichael, R. H., Jr., and K. M. Peters.
1989. Early life history of spotted seatrout, *Cynoscion nebulosus* (Pisces: Sciaenidae), in Tampa Bay, Florida. Estuaries 12:98–110.

Orlando, S. P., Jr., M. B. Robblee, and C. J. Klein.
1997. Salinity characteristics of Florida Bay: a review of the archived data set (1955–95), 89 p. Office of Ocean Resources Conservation and Assessments, National Oceanic and Atmospheric Administration, Silver Spring, Maryland.

Powell, A. B., D. E. Hoss, W. F. Hettler, D. S. Peters, and S. Wagner.
1989. Abundance and distribution of ichthyoplankton in Florida Bay and adjacent waters. Bull. Mar. Sci. 44:35–48.

Rooker, J. R., S. A. Holt, M. A. Soto, and G. J. Holt.
1998. Postsettlement patterns of habitat use by sciaenid fishes in subtropical seagrass meadows. Estuaries 21: 318–327.

Rutherford, E. S., E. S. Thue, and D. G. Buker.
1982. Population characteristics, food habits and spawning activity of spotted seatrout, *Cynoscion nebulosus*, in Everglades National Park. Rep. T-668, 48 p. South Florida Research Center, U. S. National Park Service, Homestead, Florida.

Rutherford, E. S., T. W. Schmidt, and J. T. Tilmant.
1989a. Early life history of spotted seatrout (*Cynoscion nebulosus*) and gray snapper (*Lutjanus griseus*) in Florida Bay, Everglades National Park, Florida. Bull. Mar. Sci. 44:49–64.

Rutherford, E. S., J. T. Tilmant, E. B. Thue, and T. W. Schmidt.
1989b. Fishery harvest and population dynamics of spotted seatrout, *Cynoscion nebulosus*, in Florida Bay and adjacent waters. Bull. Mar. Sci. 44:108–125.

Sokal, R. R., and F. J. Rohlf.
1981. Biometry, 2nd ed., 859 p. W. H. Freeman and Co., San Francisco, CA.

Stewart, K. W.
1961. Contributions to the biology of the spotted seatrout (*Cynoscion nebulosus*) in the Everglades National Park, Florida. M.S. thesis, 103 p. Univ. Miami, Coral Gables, FL.

Tolan, J. M., S. A. Holt, and C. P. Onuf.
1997. Distributoin and community structure of ichthyoplankton in Laguna Madre seagrass meadows: potential impact of seagrass species change. Estuaries 20:450–464.

Thayer, G. W., and A. J. Chester.
1989. Distribution and abundance of fishes among basin and channel habitats in Florida Bay. Bull. Mar. Sci. 44: 200–219.

Thayer, G. W., A. B. Powell, and D. E. Hoss.
1999. Composition of larval, juvenile and small adult fishes relative to changes in environmental conditions in Florida Bay. Estuaries 22:518–533.

Zieman, J. C., J. W. Fourqurean, and R. L. Iverson.
1989. Distribution, abundance and productivity of seagrass and macroalgae in Florida Bay. Bull. Mar. Sci. 44: 292–311.

Effect of analytical conditions in wavelength dispersive electron microprobe analysis on the measurement of strontium-to-calcium (Sr/Ca) ratios in otoliths of anadromous salmonids

Christian E. Zimmerman

Oregon State University
Department of Fisheries and Wildlife
Corvallis, Oregon 97331
Present address: U.S. Geological Survey
Alaska Science Center
1011 E. Tudor Road
Anchorage, Alaska 99503

E-mail address: czimmerman@usgs.gov

Roger L. Nielsen

College of Oceanic and Atmospheric Sciences
104 Ocean Administration
Oregon State University
Corvallis, Oregon 97331

The use of strontium-to-calcium (Sr/Ca) ratios in otoliths is becoming a standard method to describe life history type and the chronology of migrations between freshwater and seawater habitats in teleosts (e.g. Kalish, 1990; Radtke et al., 1990; Secor, 1992; Rieman et al., 1994; Radtke, 1995; Limburg, 1995; Tzeng et al. 1997; Volk et al., 2000; Zimmerman, 2000; Zimmerman and Reeves, 2000, 2002). This method provides critical information concerning the relationship and ecology of species exhibiting phenotypic variation in migratory behavior (Kalish, 1990; Secor, 1999). Methods and procedures, however, vary among laboratories because a standard method or protocol for measurement of Sr in otoliths does not exist. In this note, we examine the variations in analytical conditions in an effort to increase precision of Sr/Ca measurements. From these findings we argue that precision can be maximized with higher beam current (although there is specimen damage) than previously recommended by Gunn et al. (1992).

Wavelength dispersive electron microprobe analysis (WD-EM) has been used by most researchers, although other methods such as proton-induced *x*-ray emission (PIXE)(Babaluk et al., 1997; Markowitz et al., 2000) have been used. WD-EM remains a common and relatively inexpensive method. The conceptual approach among researchers using WD-EM is similar but the methodological approach or analytical (operating) conditions vary. In a comparison of laboratories using common otoliths, Campana et al. (1997) found among-laboratory variation in mean Sr concentrations that could not be described by otolith variability. Although the laboratories were internally consistent in applying their methods, comparisons between laboratories differed. Campana et al. suggested that the sensitivity of WD-EM to operating conditions might have led to this variation between laboratories.

Development of analytical techniques for measuring Sr/Ca ratios has been reviewed to validate techniques in specific studies (Kalish, 1990; Secor, 1992; Toole and Nielsen, 1992; Limburg, 1995). Gunn et al. (1992) analyzed effects of counting times, beam current, accelerating voltage, and beam diameter on measures of Sr and other elements and they warned that beam powers required for WD-EM were sufficient to cause specimen damage including pitting and chemical change. As a result, Gunn et al. (1992) recommended limiting beam power densities to $< 3\mu W/\mu m^2$. This recommendation has been followed in most studies using Sr/Ca ratios to reconstruct the chronology of migrations between the freshwater and marine environments (Table 1). Toole and Nielsen (1992), however, concluded that Sr/Ca precision could be increased, with no loss of accuracy, by using analytic conditions that lead to a beam power density of just over $15\mu W/\mu m^2$ (5-µm beam diameter; accelerating voltage=15 nA; beam current=25 kV). The inherent beam damage was not critical because of the similar behavior of Sr and Ca during progressive beam damage.

In published studies using WD-EM to measure Sr/Ca ratios in otoliths, the operating conditions, including beam power densities, have varied greatly (Table 1). Establishing a microprobe protocol for measurement of Sr/Ca ratios in otoliths involves a balancing act of counting times, beam current, and beam diameter. The selection of optimum conditions is constrained by financial resources, allocation of time for use of instruments, and the required resolution of Sr/Ca ratios for any specific application. Each researcher must weigh the benefits and costs to best answer the question at hand. Generally, these parameters are manipulated to optimize precision and accuracy of analyses in relation to variability within the otolith and implications of the results.

For Sr/Ca ratios to remain an accepted and accurate means of describing migration histories and other life history events, continued analytic and technical refinement and validation are required. We examined the effects of crystal choice, beam diameter, beam current, and beam power densities on Sr/Ca measurements (expressed as atomic ratios) in salmonid otoliths: 1) we measured Sr using both the TAP and PET crystals in regions with high Sr/Ca (>0.003) and low Sr/Ca (<0.001)

Manuscript approved for publication
12 February 2003 by Scientific Editor.

Manuscript received 4 April 2003 at NMFS Scientific Publications Office.

Fish Bull. 101:712–718 (2003).

Table 1

Analytic conditions reported by researchers using wavelength-dispersive (WD) electron spectroscopy to measure Sr/Ca ratios in otoliths. Beam power density was calculated for this study and minimum limit of detection is either directly reported from the work cited or from personal communications.

Source	Beam diameter (μm)	Accelerating voltage (kV)	Beam current (nA)	Beam power density (μW/μm²)	Minimum limit of detection (Sr ppm)
Brown and Severin (1999)	6	15	20	10.61	—
Campana et al. (1997) WD-1	10	25	5	1.59	175
Campana et al. (1997) WD-2	9	15	4	4.25	480
Kafemann et al. (2000)	5×8	15	10	3.75	490
Kalish (1990)	10×10	15	10	1.5	—
Kawakami et al (1998)	1	15	50	954	—
Limburg (1995)	20	20	25	1.59	290
Radtke (1995)	5	15	10	7.63	—
Rieman et al. (1994)	5	15	50	38.14	—
Secor (1992)	5×5	25	20	20.00	580
Thresher et al. (1994)	14	15	25	2.44	311
Toole et al. (1993)	5	15	20	15.27	—
Volk et al. (2000)	10	15	15	2.86	237
Zimmerman and Reeves (2000)	7	15	50	19.50	43

levels; 2) we then compared the results of repeated Sr/Ca measurements collected at the same spots using various beam diameters, while holding accelerating voltage and beam current constant to determine the effect of beam damage on Sr/Ca measurements; and 3) we compared the results of repeated Sr/Ca measurements collected at the same spots using various beam currents, while holding accelerating voltage and beam diameter constant. We argue that increased precision of Sr measurements afforded by higher beam current (and hence, higher beam power densities) is preferable for studies where only measurements of Sr/Ca ratios are required.

Materials and methods

Otolith preparation

Sagittal otoliths from an adult sockeye salmon (*Oncorhynchus nerka*) collected in the Deschutes River, Oregon, and a juvenile chinook salmon (*O. tshawytscha*) collected in the Umatilla River, Oregon, were used to represent high (>0.003) Sr/Ca and low (<0.001) Sr/Ca ratios, respectively (Zimmerman, unpubl. data). High Sr/Ca ratios characterized the saltwater growth region in the sockeye salmon otolith and low Sr/Ca ratios characterized the freshwater growth region of the chinook salmon otolith. Each otolith was mounted sulcus side down with thermo-setting plastic resin on a microscope cover slip attached at one end with super-glue to a standard microscope slide. The otolith was then ground with 1200-grit sandpaper in the sagittal plane to the level of the nucleus. The mounting medium was heated and the otolith turned sulcus side-up. The otolith was then ground with 1200-grit and 2000-grit sandpaper in the sagittal plane to the level of the primordia and polished with 0.05-μm alumina paste. The cover slip was then cut with a scribe and mounted with other prepared otoliths (those used in other studies) on a petrographic slide for microprobe analysis. The slide containing several otoliths was rinsed with deionized water, air dried, and carbon coated (400 Å). Elemental analysis was conducted with a Cameca SX-50 wavelength dispersive microprobe. Strontiantite ($SrCO_3$, USNM R10065) and calcite ($CaCO_3$, USNM 136321) were used as standards for Sr and Ca, respectively. Standards were calibrated with a 30-μm-diameter beam and 10-s counts resulting in minimal effects of beam damage.

Effect of spectrometer (crystal) choice

To evaluate differences in diffracting crystals, we conducted a series of tests where Sr was measured by using both the PET and TAP crystals. A 15 kV, 50 nA beam was used for these comparisons. With a 7-μm-diameter beam, Sr was measured by using the TAP crystal (Sr Lα) and Ca was measured by using the PET crystal (Ca Kα). Two transects of 10 points each were sampled so that the points on adjacent transects covered the same temporal location on the otolith. Sr and Ca were analyzed simultaneously; counting times for the Sr and Ca peaks were 40 s, and background counts were 40 s. A second set of transects covering the same temporal locations in the otolith was sampled, but Sr was measured with the PET crystal (Sr Lα). Because our microprobe has only one PET crystal, simultaneous measurement of elements was not possible. Transects were conducted on both high and low Sr/Ca regions. Sr/Ca ratios

were calculated from normalized mole fractions of Sr and Ca. Limit of detection (3σ; Potts, 1987) was calculated for all points in both high and low Sr/Ca regions.

Effect of beam diameter and beam current

We conducted five repeat measurements at each of five points within the high and low Sr/Ca regions using a 1-, 7-, 15-, 20-, and 25-μm-diameter beam at 15 kV and 50 nA. This resulted in beam power densities of 961, 19.5, 4.2, 2.39, and 1.52μW/μm^2, respectively. We conducted five repeated measurements at each of four locations within the high and low Sr/Ca regions using beam currents of 5, 10, 20, and 30 nA with a 10-m-diameter beam and accelerating voltage of 15 kV, with resulting beam power densities of 1.0, 1.9, 3.8, and 5.7μW/μm^2, respectively. The coefficient of variation (CV) of Sr/Ca ratios was calculated as the $SD_{Sr/Ca}$ × Mean Sr/Ca^{-1} for each beam power density. If beam damage affects precision and accuracy of Sr/Ca ratios, subsequent measurements at the same spot should be increasingly divergent from the first and such divergence should be evident in high coefficients of variation. The limit of detection was used as a measure of precision. Limit of detection (3σ; Potts, 1987) for Sr was calculated for the first measurement taken at each beam power density in each region.

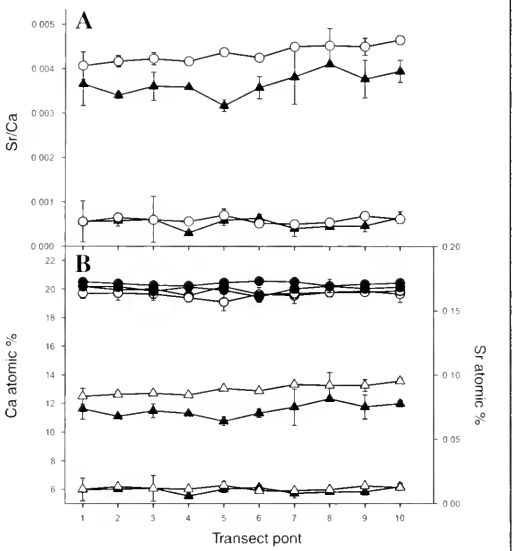

Figure 1

Transects of (**A**) Sr/Ca atomic ratio and (**B**) Ca (circles) and Sr (triangles) as atomic percentage when Sr is measured on the PET crystal (solid symbols) and on the TAP crystal (open symbols). Error bars represent 95% confidence intervals.

Results

Effect of spectrometer (crystal) choice

Spectrometer (crystal) choice for the measurement of Sr had an apparent systematic effect on Sr/Ca ratios at high Sr/Ca levels but no effect at low Sr/Ca levels (Fig. 1A). The mean Sr/Ca level in the high Sr/Ca region was significantly lower (~15%) when Sr was measured on the PET crystal (t=7.189; P<0.001; df=38). Crystal choice had an effect on measurement of both Ca and Sr in the high Sr/Ca region. Ca did not differ significantly between the high and low Sr/Ca regions (P>0.05) but was approximately 2% lower when Sr was measured with the PET crystal (Fig. 1B). This difference was attributable to beam damage, which occurred as Sr was measured. The mean Ca was 197,400 ppm when Sr was measured on the PET crystal and 202,100 ppm when Sr was measured on the TAP crystal.

In the high Sr/Ca region, mean Sr was significantly lower when Sr was measured on the PET crystal (t=11.58; P<0.001; df=38) (Fig. 1B). The mean (±SD) was 7270 ±4 ppm when Sr was measured with the PET crystal and 8870 ±3 ppm when Sr was measured with the TAP crystal. This difference is also reflected in the higher minimum limit of determination for Sr for PET in both the high Sr/Ca (695 ppm) and low Sr/Ca regions (126 ppm). Using the TAP crystal to measure Sr, we found that the minimum limit of determination for Sr was 103 ppm and 65 ppm in the high Sr/Ca and low Sr/Ca regions, respectively. To achieve similar counting statistics for Sr with the PET crystal, count times would need to be increased to 200 seconds on both the peak and background.

Effect of beam diameter and beam current

In repeated measurements with different beam diameters (same beam current) at the same locations, Sr/Ca ratios did not vary greatly with the exception of measurements made with the 1-μm beam (Fig. 2A). The CV of the Sr/Ca ratios for the 1-m beam was high and led to significant variation of Sr/Ca ratios in subsequent measurements at the same point (Table 2). The Sr/Ca ratio was least variable for the 7-μm beam in the high Sr/Ca region (Table 2). Limit of detection (3σ) for Sr ranged from 80 ppm to 172 ppm in the low Sr/Ca region and from 299 ppm to 315 ppm in the high Sr/Ca region under the various beam diameters (Fig. 3A).

Beam current had a significant effect on variation of Sr/Ca and limit of detection for Sr. The greatest variation in Sr/Ca ratios was observed at beam currents 5nA and 10 nA (Fig. 2B). The CV of Sr/Ca ratios was negatively related to beam current (r=−0.93; P>0.05) (Table 3). The CV of Sr was high in all treatments, ranging from 0.23 to 1.17 in the high Sr/Ca region and from 0.11 to 0.46 in the low Sr/Ca region. The CV of Ca was 0.04 for all beam configurations. The limit of detection of Sr as measured at the first sample

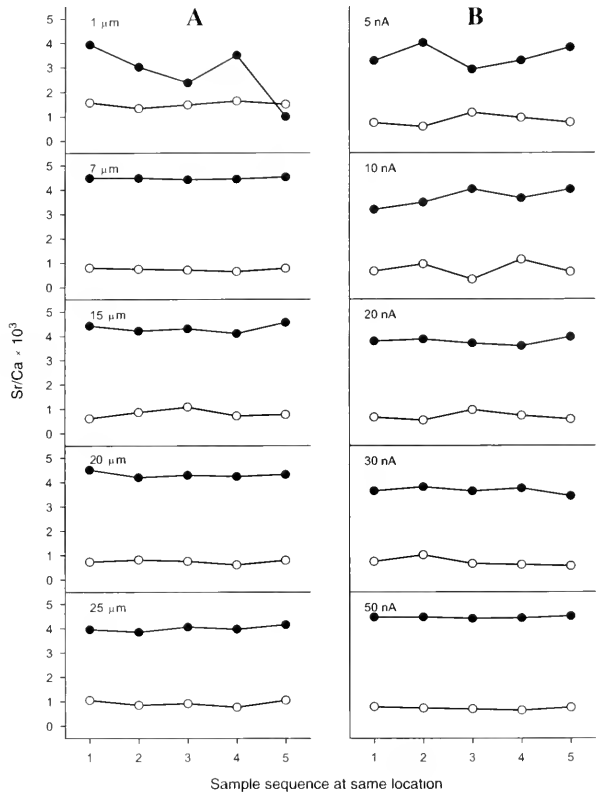

Figure 2

Repeat measures of atomic Sr/Ca with (**A**) varying beam diameters, common beam current (50 nA), and (**B**) varying beam currents, common beam diameter (10 µm). Open circles represent low Sr/Ca regions and solid circles represent high Sr/Ca regions.

for each beam-current configuration ranged from 99 ppm to 290 ppm in the low Sr/Ca region and from 312 ppm to 844 ppm in the high Sr/Ca region (Fig. 3B).

Discussion

In our experiment, for measuring Sr/Ca ratios in otoliths with WD-EM analysis, the TAP crystal was the best choice for the measurement of Sr because it provided the advantage of higher count rates and higher resolution of Sr. Use of the PET crystal to measure Sr has not been reported in the literature. In fact, crystal choice is frequently not reported, making it difficult to know whether TAP or PET crystals have been used to measure Sr. Personal communication with several researchers confirmed that the TAP crystal is commonly used to measure Sr and has been cited as the crystal used (Kalish, 1990; Thresher et al., 1994). Given the different results possible with the use of different crystals to measure Sr, reporting the crystals used should be included in papers reporting Sr/Ca ratios measured on WD-EMs. Note that even though measurements of Sr with the TAP crystal appeared to be the best method for otoliths, the TAP crystal should not be used to measure Sr in materials containing Si because of analytical interference from Si.

Variation of beam diameter has very little effect on the limit of detection of Sr, even at extremely high beam current densities. Rather, variation in beam current had

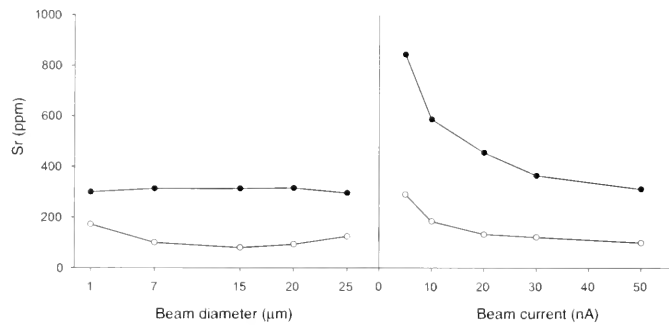

Figure 3

Detection limit of Sr with (**A**) varying beam diameter and (**B**) varying beam current. Open circles represent low Sr/Ca regions and solid circles represent high Sr/Ca regions.

Table 2

Coefficient of variation of Sr/Ca ratios and Sr (in parentheses) in high and low Sr/Ca regions of otoliths.

Beam diameter (μm)	CV Sr/Ca and Sr in low region	CV Sr/Ca and Sr in high region
1	0.076 (0.02)	0.416 (0.41)
7	0.082 (0.07)	0.009 (0.04)
15	0.218 (0.23)	0.041 (0.05)
20	0.107 (0.03)	0.028 (0.02)
25	0.133 (0.13)	0.030 (0.04)

Table 3

Coefficient of variation of Sr/Ca ratios and Sr (in parentheses) in high and low Sr/Ca regions of otoliths under varying beam current.

Beam current (nA)	CV Sr/Ca and Sr in low region	CV Sr/Ca and Sr in high region
5	0.354 (0.94)	0.099 (0.11)
10	0.429 (1.11)	0.098 (0.41)
20	0.239 (1.12)	0.039 (0.45)
30	0.248 (0.23)	0.039 (0.46)
50	0.082 (1.17)	0.009 (0.11)

significant effects on the limit of detection of Sr. As a result, higher beam currents (>20 nA) were appropriate for measuring Sr/Ca ratios in spite of beam damage observed at higher beam power densities. Beam diameters between 7 and 10m provide the best temporal resolution (i.e. covering fewer daily increments). The lower CV of Sr/Ca ratios observed with the 7-m beam diameter was likely due to the lower temporal variation afforded to smaller beam diameters (compared to larger beam diameters) and lower error related to specimen damage (compared to the 1-m beam). The lower CV of Sr/Ca ratios at the 7-μm beam diameter suggested that in spite of beam damage, the Sr/Ca ratio was not dramatically affected by beam damage. However, the increase in CV for the smaller diameters suggested that there are limits to usable beam densities.

Greater precision of Sr/Ca measurements is critical to understanding life history of some species (Markowitz et al., 2000) or in situations where differences in environmental Sr/Ca ratios are less than those observed between ocean water and freshwaters (Rieman et al., 1994; Volk et al., 2000). Volk et al. (2000) found that timing of freshwater entry and length of freshwater residence by summer steelhead (*O. mykiss*) and spring chinook salmon had effects on otolith core or primordia Sr/Ca levels. Summer steelhead and spring chinook enter freshwater and stay for up to several months before spawning. Volk et al. (2000) suggested that

significant egg development during this extended prespawning freshwater residence led to a dilution of the Sr signature in these anadromous fish. Zimmerman and Reeves (2000, 2002) were able to distinguish between resident rainbow trout and summer steelhead in the Deschutes River, Oregon, by comparing the Sr/Ca ratios in primordia and the first summer of juvenile growth (freshwater growth region). In essence the freshwater growth region acts as a proxy for the freshwater environment and significantly higher Sr/Ca ratios in the primordia suggest an anadromous maternal origin. The greater precision of Sr measures afforded by higher beam currents may be important in distinguishing differences in seasonal ecotypes, such as summer steelhead and spring chinook salmon, or in distinuishing estuary habitats from freshwater and ocean environments.

These results are applicable only to otolith calcium carbonate in the mineral form of aragonite. Like Brown and Severin (1999), we have found that crystalline structure affects the distribution of Sr. Vateritic regions should be avoided when measuring Sr/Ca ratios in otoliths. In vateritic portions of otoliths from chinook salmon and steelhead, Sr is often below our minimum detection limit of 43 ppm, yet the concentration of Ca does not differ from that found in aragonitic otolith regions (Zimmerman, unpubl. data).

Studies of fish migration between marine and freshwater environments are based on the general difference between Sr in marine and freshwater environments. Sr concentrations in seawater are generally an order of magnitude greater than in freshwaters (Bagenal et al., 1973; Kalish, 1990). Sr is substituted for Ca in the calcium carbonate matrix of the otolith at levels that correspond to those in the environment (Kalish, 1989; Farrell and Campana, 1996). Given this relationship, it has become a convention to report Sr as a fraction of Ca (Secor and Rooker, 2000). However, Secor and Rooker (2000) pointed out that Ca is relatively invariant in aragonitic otoliths and rarely varies more than 5% within an individual fish. At 8074 points sampled in the primordia, freshwater growth regions, and saltwater growth regions of several species of salmonids the Sr/Ca ratio was entirely driven by differences in Sr (Zimmerman, unpubl. data). At these 8074 points, Sr was highly correlated with the Sr/Ca ratio (r^2=99.45%) and Ca was not correlated with the Sr/Ca ratio (r^2<0.01%). Given this relationship, increasing precision of Sr is desirable to increase precision of the Sr/Ca ratio.

Our results suggest that tests of hypotheses related to Sr/Ca ratios can be conducted at higher beam power densities than suggested by Gunn et al. (1992). High beam power densities resulting from higher beam current and beam diameter of 7 to 10-μm provide greater precision (spatial on the otolith and temporal in the life of the fish) of Sr. This is not true for studies of stock discrimination, such as those described by Thresher (1999), that rely on absolute values of multiple elements, including Sr.

Acknowledgments

Several people provided unpublished information concerning analytic conditions and detection limits. Gordon Reeves, of the U.S. Forest Service Pacific Northwest Research Station, kindly provided office and laboratory space to CEZ. We thank Eric Volk, Ken Severin, and two anonymous reviewers for comments that improved this manuscript.

Literature cited

Babaluk, J. A., N. M. Halden, J. D. Reist, A. H. Kristofferson, J. L. Campbell, and W. J. Teesdale.
1997. Evidence for non-anadromous behaviour of Arctic charr (*Salvelinus alpinus*) from Lake Hazen, Ellesmere Island, Northwest Territories, Canada, based on scanning proton microprobe analysis of otolith strontium distribution. Arctic 50:224–233.

Bagenal, T. B., F. J. H. MacKereth, and J. Heron.
1973. The distinction between brown trout and sea-trout by the strontium content of their scales. J. Fish Biol. 5: 555–557.

Brown, R., and K. P. Severin.
1999. Elemental distribution within polymorphic inconnu (*Stenodus leucichthys*) otoliths is affected by crystal structure. Can. J. Fish. Aquat. Sci. 56:1898–1903.

Campana, S. E., S. R. Thorrold, C. M. Jones, D. Günther, M. Tubrett., H Longerich, S. Jackson, N. M. Halden, J. M. Kalish, P. Piccoli, H. de Pontual, H. Troadec, J. Panfili, D. H. Secor, K. P. Severin, S. H. Sie, R. Thresher, W. J. Teesdale, and J. L. Campbell.
1997. Comparison of accuracy, precision, and sensitivity in elemental assays of fish otoliths using the electron microprobe, proton-induced x-ray emission, and laser ablation inductively coupled plasma mass spectrometry. Can. J. Fish. Aquat. Sci. 54:2068–2079.

Farrell, J., and S. E. Campana.
1996. Regulation of calcium and strontium deposition on the otoliths of juvenile tilapia, *Oreochromis niloticus*. Comp. Biochem. Physiol. 115A:103–109.

Gunn, J. S., I. R. Harrowfield, C. H. Proctor, and R. E. Thresher.
1992. Electron probe microanalysis of fish otoliths—evaluation of techniques for studying age and stock discrimination. J. Exp. Mar. Biol. Ecol. 158:1–36.

Kafemann, R., S. Alderstein, and R. Neukamm.
2000. Variation in otolith strontium and calcium ratios as an indicator of life-history strategies of freshwater fish species within a brackish water system. Fish. Res. 46:313–325.

Kalish, J. M.
1989. Otolith microchemistry: validation of the effects of physiology, age and environment on otolith composition. J. Exp. Mar. Biol. Ecol. 132:151–178.
1990. Use of otolith microchemistry to distinguish the progeny of sympatric anadromous and non-anadromous salmonids. Fish. Bull. 88:657–666.

Kawakami, Y., N. Mochioka, K. Morishita, T. Tajima, H. Nakagawa, H. Toh, and A. Nakazono.
1998. Factors influencing otolith strontium/calcium ratios in *Anquilla japonica* elvers. Env. Biol. Fishes 52:299–303.

Limburg, K. E.
1995. Otolith strontium traces environmental history of subyearling American shad *Alosa sapidissima*. Mar. Ecol. Prog. Ser. 119:25–35.

Markowitz, A., D. Grambole, F. Herrmann, W. J. Trompetter, T. Dioses, and R. W. Gauldie.
2000. Reliable micro-measurement of strontium is the key to cracking the life-history code in the fish otolith. Nucl. Instr. and Meth. B. 168:109–116.

Potts, P. J.
1987. A handbook of silicate rock analysis. Chapman and Hall, New York, NY.
Radtke, R. L.
1995. Otolith microchemistry of charr—use in life history studies. Nordic J. Freshwater. Res. 71:392–395.
Radtke, R. L., D. W. Townsend, S. D. Folsom, and M. A. Morrison.
1990. Strontium:calcium concentration ratios in otoliths of herring larvae as indicators of environmental conditions. Env. Biol. Fish. 27:51–61.
Rieman, B. E., Myers, D. L, and Nielsen, R. L.
1994. Use of otolith microchemistry to discriminate *Oncorhynchus nerka* of resident and anadromous origin. Can. J. Fish. Aquat. Sci. 51:68–77.
Secor, D. H.
1992. Application of otolith microchemistry analysis to investigate anadromy in Chesapeake Bay striped bass Morone saxatilis. Fish. Bull. 90:798–806.
1999. Specifying divergent migration patterns in the concept of stock: the contingent hypothesis. Fish. Res. 43:13–34.
Secor, D. H., and J. R. Rooker.
2000. Is otolith strontium a useful scalar of life cycles in estuarine fishes? Fish. Res. 46:359–371.
Thresher, R. E.
1999. Elemental composition of otoliths as a stock delineator in fishes. Fish. Res. 43:165–204.
Thresher, R. E., C. H. Proctor, J. S. Gunn, and I. R. Harrowfield.
1994. An evaluation of electron-probe microanalysis of otoliths for stock delineation and identification of nursery areas in a southern temperate groundfish, *Nemadactylus macropterus* (Cheilodactylidae). Fish. Bull. 92:817–840.
Toole, C. L., D. F. Markle, and P. H. Harris.
1993. Relationships between otolith microstructure, microchemistry, and early life history events in Dover sole, *Microstomus pacificus*. Fish. Bull. 91:732–753.
Toole, C. L., and R. L. Nielsen.
1992. Effects of microprobe precision on hypotheses related to otolith Sr:Ca ratios. Fish. Bull. 90:421–427.
Tzeng, W. N., K. P. Severin, and H. Wikström.
1997. Use of otolith microchemistry to investigate the environmental history of European eel, *Anquilla anquilla*. Mar. Ecol. Prog. Ser. 149:73–81.
Volk, E. C., A. Blakley, S. L. Schroder, and S. M. Kuehner.
2000. Otolith microchemistry reflects migratory characteristics of Pacific salmonids: using otolith core chemistry to distinguish maternal associations with sea and freshwaters. Fish. Res. 46:251–266.
Zimmerman, C. E.
2000. Ecological relation of sympatric steelhead and resident rainbow trout in the Deschutes River, Oregon. Ph.D. diss., 116 p. Oregon State Univ., Corvallis, OR.
Zimmerman, C. E., and G. H. Reeves.
2000. Population structure of sympatric anadromous and non-anadromous *Oncorhynchus mykiss*: evidence from spawning surveys and otolith microchemistry. Can. J. Fish. Aquat. Sci. 57:2152–2162.
2002. Identification of steelhead and resident rainbow trout progeny in the Deschutes River, Oregon, revealed with otolith microchemistry. Trans. Am. Fish. Soc. 131:986–993.

Fishery Bulletin

Guidelines for contributors

Content of papers

Articles

Articles are reports of 10 to 30 pages (double spaced) that describe original research in one or a combination of the following fields of marine science: taxonomy, biology, genetics, mathematics (including modeling), statistics, engineering, economics, and ecology.

Notes

Notes are reports of 5 to 10 pages without an abstract that describe methods and results not supported by a large body of data. Although all contributions are subject to peer review, responsibility for the contents of articles and notes rests upon the authors and not upon the editor or the publisher. It is therefore important that authors consider the contents of their manuscripts carefully. Submission of an article is un-derstood to imply that the article is original and is not being considered for publication elsewhere. Manuscripts must be written in English. Authors whose native language is not English are strongly advised to have their manuscripts checked for fluency by English-speaking colleagues prior to submission.

Preparation of papers

Text

Title page should include authors' full names and mailing addresses (street address required) and the senior author's telephone, fax number, e-mail address, as well as a list of key words to describe the contents of the manuscript. **Abstract** must be less than one typed page (double spaced) and must not contain any citations. It should state the main scope of the research but emphasize the author's conclusions and relevant findings. Because abstracts are circulated by abstracting agencies, it is important that they represent the research clearly and concisely. **General text** must be typed in double-spaced format. A brief introduction should state the broad significance of the paper; the remainder of the paper should be divided into the following sections: Materials and methods, Results, Discussion (or Conclusions), and Acknowledgments. Headings within each section must be short, reflect a logical sequence, and follow the rules of multiple subdivision (i.e. there can be no subdivision without at least two subheadings). The entire text should be intelligible to interdisciplinary readers; therefore, all acronyms and abbreviations should be written out and all lesser-known technical terms should be defined the first time they are mentioned. The scientific names of species must be written out the first time they are mentioned; subsequent mention of scientific names may be abbreviated. Follow *Scientific style and format: CBE manual for authors, editors, and publishers* (6th ed.) for editorial style and the most current issue of the *American Fisheries Society's common and scientific names of fishes from the United States and Canada* for fish nomenclature. Dates should be written as follows: 11 November 1991. Measurements should be expressed in metric units, e.g. metric tons (t). The numeral one (1) should be typed as a one, not as a lower-case el (l).

Footnotes

Use footnotes to add editorial comments regarding claims made in the text and to document unpublished works or works with local circulation. Footnotes should be numbered with Arabic numerals and inserted in 10-point font at the bottom of the first page on which they are cited. Footnotes should be formatted in the same manner as citations. If a manuscript is unpublished, in the process of review, or if the information provided in the footnote has been conveyed verbally, please state this information as "unpubl. data," "manuscript in review," and "personal commun.," respectively. Authors are advised wherever possible to avoid references to nonstandard literature (unpublished literature that is difficult to obtain, such as internal reports, processed reports, administrative reports, ICES council minutes, IWC minutes or working papers, any "research" or "working" documents, laboratory reports, contract reports, and manuscripts in review). If these references are used, please indicate whether they are available from NTIS (National Technical Information Service) or from some other public depository. Footnote format: author (last name, followed by first-name initials); year; title of report or manuscript; type of report and its administrative or serial number; name and address of agency or institution where the report is filed.

Literature cited

The literature cited section comprises works that have been published and those accepted for publication (works in press) in peer-reviewed journals and books. Follow the name and year system for citation format. In the text, write "Smith and Jones (1977) reported" but if the citation takes the form of parenthetical matter, write "(Smith and Jones, 1977)." In the literature cited section, list citations alphabetically by last name of senior author: For example, Alston, 1952; Mannly, 1988; Smith, 1932; Smith, 1947; Stalinsky and Jones, 1985. Abbreviations of journals should conform to the abbreviations given in the *Serial sources for the BIOSIS previews database*. Authors are responsible for the accuracy and completeness of all citations. Literature citation format: author (last name, followed by first-name initials); year; title of report or article; abbreviated title of the journal in which the article was published, volume number, page numbers. For books, please provide publisher, city, and state.

Tables

Tables should not be excessive in size and must be cited in numerical order in the text. Headings in tables should be short but ample enough to allow the table to be intelligible on its own. All unusual symbols must be explained in the table legend. Other incidental comments may be footnoted (use italic arabic numerals for footnote markers). Use asterisks only to indicate probability in statistical data. Place table legends on the same page as the table data. We accept tables saved in most spreadsheet software programs (e.g. Microsoft Excel). Please note the following:

- Use a comma in numbers of five digits or more (e.g. 13,000 but 3000).
- Use zeros before all decimal points for values less than one (e.g. 0.31).

Figures

Figures include line illustrations, computer-generated line graphs, and photographs (or slides). They must be cited in numerical order in the text. Line illustrations are best submitted as original drawings. Computer-generated line graphs should be printed on laser-quality paper. Photographs should be submitted on glossy paper with good contrast. All figures are to be labeled with senior author's name and the number of the figure (e.g. Smith, Fig. 4). Use Helvetica or Arial font to label anatomical parts (line drawings) or variables (graphs) within figures; use Times Roman bold font to label the different sections of a figure (e.g. **A, B, C**). Figure legends should explain all symbols and abbreviations seen within the figure and should be typed in double-spaced format on a separate page at the end of the manuscript. We advise authors to peruse a recent issue of *Fishery Bulletin* for standard formats. Please note the following:

- Capitalize the first letter of the first word of axis labels.
- Do not use overly large font sizes to label axes or parts within figures.
- Do not use boldface fonts within figures.
- Do not create outline rules around graphs.
- Do not use horizontal lines through graphs.
- Do not use large font sizes to label degrees of longitude and latitude on maps.
- Indicate direction of degrees longitude and latitude on maps (e.g. 170°E).
- Avoid placing labels on a vertical plane (except on *y* axis).
- Avoid odd (nonstandard) patterns to mark sections of bar graphs and pie charts.

Copyright law

Fishery Bulletin, a U.S. government publication, is not subject to copyright law. If an author wishes to reproduce any part of *Fishery Bulletin* in his or her work, he or she is obliged, however, to acknowledge the source of the extracted literature.

Submission of papers

Send four printed copies (one original plus three copies)—clipped, *not stapled*—to the Scientific Editor, at the address shown below. Send photocopies of figures with initial submission of manuscript. Original figures will be requested later when the manuscript has been accepted for publication. Do not send your manuscript on diskette until requested to do so.

Dr. Norman Bartoo
National Marine Fisheries Service, NOAA
8604 La Jolla Shores Drive
La Jolla, CA 92037

Once the manuscript has been accepted for publication, you will be asked to submit a software copy of your manuscript. The software copy should be submitted in WordPerfect or Word format (in Word, save as Rich Text Format). Please note that we do not accept ASCII text files.

Reprints

Copies of published articles and notes are available free of charge to the senior author (50 copies) and to his or her laboratory (50 copies). Additional copies may be purchased in lots of 100 when the author receives page proofs.

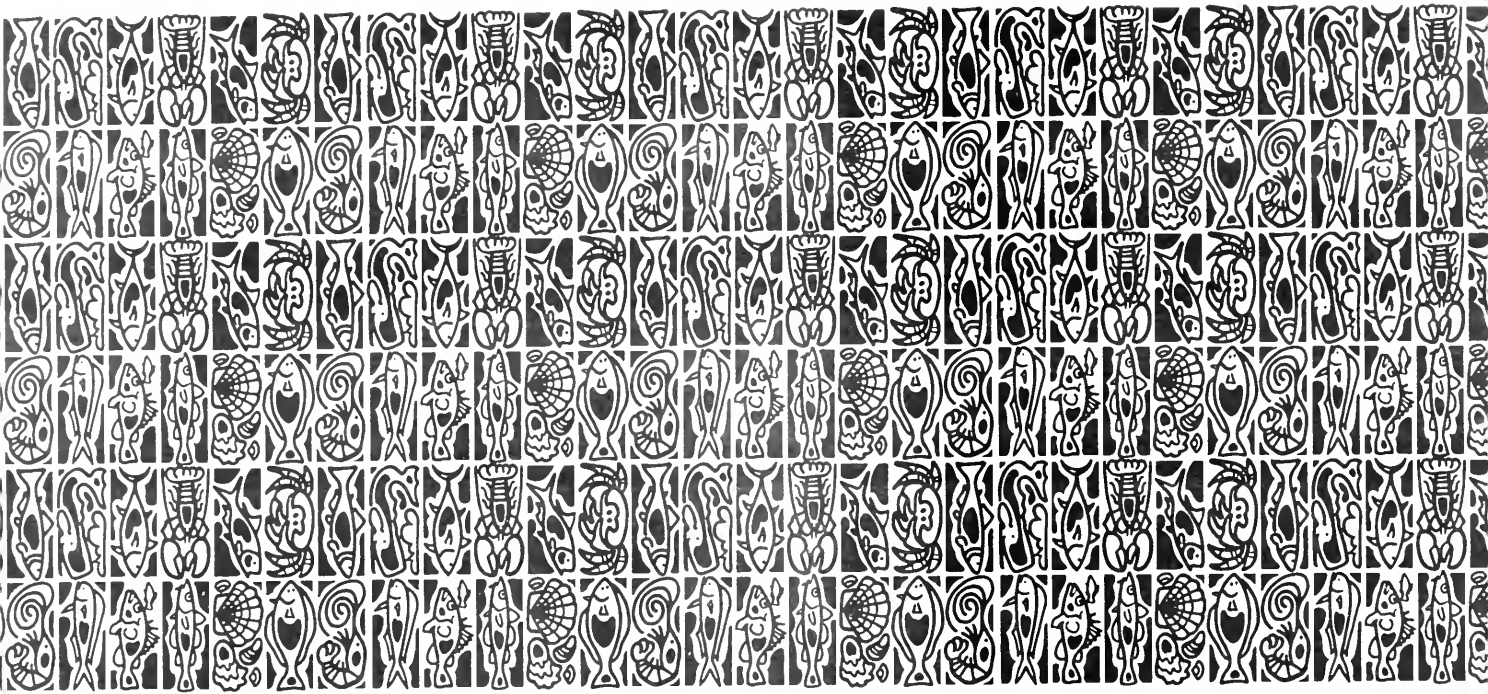

U.S. Department
of Commerce

Volume 101
Number 4
October 2003

Fishery Bulletin

The *Fishery Bulletin* (ISSN 0090-0656) is published quarterly by the Scientific Publications Office, National Marine Fisheries Service, NOAA, 7600 Sand Point Way NE, BIN C15700, Seattle, WA 98115-0070. Periodicals postage is paid at Seattle, WA, and at additional mailing offices. POSTMASTER: Send address changes for subscriptions to Fishery Bulletin, Superintendent of Documents, Attn.: Chief, Mail List Branch, Mail Stop SSOM, Washington, DC 20402-9373

For sale by the Superintendent of Documents, U.S. Government Printing Office, Washington, DC 20402. Subscription price per year: $55.00 domestic and $68.75 foreign. Cost per single issue: $28.00 domestic and $35.00 foreign. **See back for order form.**

Fishery Bulletin

***Fishery Bulletin* web site: fishbull.noaa.gov**

The *Fishery Bulletin* carries original research reports and technical notes on investigations in fishery science, engineering, and economics. It began as the Bulletin of the United States Fish Commission in 1881, it became the Bulletin of the Bureau of Fisheries in 1904 and the *Fishery Bulletin* of the Fish and Wildlife Service in 1941. Separates were issued as documents through volume 46; the last document was No. 1103. Beginning with volume 47 in 1931 and continuing through volume 62 in 1963, each separate appeared as a numbered bulletin. A new system began in 1963 with volume 63 in which papers are bound together in a single issue of the bulletin. Beginning with volume 70, number 1, January 1972, the *Fishery Bulletin* became a periodical, issued quarterly. In this form, it is available by subscription from the Superintendent of Documents, U.S. Government Printing Office, Washington, DC 20402. It is also available free in limited numbers to libraries, research institutions, State and Federal agencies, and in exchange for other scientific publications.

U.S. Department of Commerce
Seattle, Washington

Volume 101
Number 4
October 2003

Fishery Bulletin

Contents

Articles

Notes

Bycatch of lined seahorses (*Hippocampus erectus*) in a Gulf of Mexico shrimp trawl fishery

Julia K. Baum
Jessica J. Meeuwig
Amanda C. J. Vincent

Project Seahorse
Department of Biology
McGill University,
1205 Dr. Penfield Ave.
Montreal, Quebec, H3A 1B1, Canada
Present address (for J. K. Baum): Department of Biology
Dalhousie University
1355 Oxford St.
Halifax, Nova Scotia, B3H 4J1, Canada
E-mail address (for J. K. Baum): baum@mathstat.dal.ca

Abstract—Bycatch studies have largely ignored population level effects on fish species of little commercial interest. Here we analyze bycatch of the lined seahorse (*Hippocampus erectus*) in the bait-shrimp trawl fishery in Hernando Beach, Florida, providing the first fisheries data for this species. Based on catch per unit of effort (CPUE), size, sex, and reproductive status of trawled *H. erectus*, 1) approximately 72,000 seahorses were caught annually by this fleet, from a population of unknown size, 2) trawling affected population cohorts differentially because of temporal and spatial variation in CPUE and population size, and 3) a greater proportion of females than males was removed in trawling. Our findings suggest that trawling may affect seahorse populations through direct mortality, social disruption, and habitat damage. However, the lack of specific abundance or catchability estimates for *H. erectus* means that the precise impact of trawling on this fish remains uncertain. This paper focuses attention on the need for research and monitoring of small fishes that are caught incidentally in nonselective gear.

Manuscript approved for publication 2 June 2003 by Scientific Editor.
Manuscript received 26 June 2003 at NMFS Scientific Publications Office.
Fish. Bull. 101:721–731 (2003).

The incidental capture of marine organisms is now recognized as a serious problem in fisheries management and marine conservation (Alverson et al., 1994; IUCN, 1996; Alverson, 1997; Jennings and Kaiser, 1998; FAO, 1999). Shrimp trawl fisheries are the single greatest source of bycatch, accounting for 35% of the world's total bycatch (Alverson et al., 1994). Bycatch research has focused on marine megafauna, seabirds, and commercially important fish species (see as examples Polacheck, 1989; Graham, 1995; Weimerskirch et al., 1997; Julian and Beeson, 1998; Pikitch et al., 1998; Galloway and Cole, 1999; Diamond et al., 2000). The conservation impacts of bycatch for noncommercial fishes and invertebrate species remain largely unstudied (but see Chan and Liew, 1986; Pettovello, 1999; Milton, 2001). The few studies that have evaluated incidental capture of these species have focused on survival rates of individuals (Hill and Wassenberg, 1990, 2000; Kaiser and Spencer, 1995; Probert et al., 1997; Mensink et al., 2000) without addressing population level effects of bycatch. However, even species that comprise only a small portion of the bycatch in a fishery may experience significant impacts of incidental harvest on their population size and structure.

Seahorses are among those species inferred to be greatly affected by nonselective fishing gear, both because intense trawling often covers seahorse habitat and because their life history traits likely render these fishes vulnerable to overexploitation (Vincent, 1996). Most studied seahorse species are strictly monogamous (i.e. sexually and socially), meaning that removal can disrupt pairs and may reduce reproductive output (e.g. Vincent, 1995; Vincent and Sadler, 1995; Kvarnemo et al., 2000; Perante et al., 2002). Obligatory parental care by males, combined with relatively low fecundity, may reduce the potential for population recovery from overexploitation, although potentially high survival of young may also offset this apparent cost. In addition, sparse distributions and low mobility suggest that seahorses will be slow to recolonize depleted areas (Perante et al., 2002; Vincent et al.[1]).

Seahorses derived from bycatch appear to be contributing greatly to the large and growing international trade in these fishes (Vincent, 1996; Vincent and Perry[2]). Consumer demand for seahorses—both dried for traditional medicine and curiosity trades, and, less frequently, live for the aquarium trade—is very high (Vincent, 1996). Global demand for seahorses has surpassed supply and therefore trade has increased and expanded geographically

[1] Vincent, A. C. J., K. L. Evans, and A. D. Marsden. 2003. Home range behaviour of the monogamous Australian seahorse, *Hippocampus whitei*. Manuscript in review.

(Vincent, 1996; Vincent and Perry[2]), placing populations around the world under greater pressure. Much of this market demand is met from retention of incidental landings in shrimp trawls. Where no market has yet developed, incidentally caught seahorses are discarded and the survival rate for these discarded seahorses is unknown.

Trade records and anecdotal evidence from other countries indicate that the United States has imported and exported considerable numbers of both live and dried seahorses in recent years (Vincent, 1996; Vincent and Perry[2]). In Florida, the primary source of live seahorses in the United States (Larkin and Degner, 2001), these fishes ranked as the seventh most economically important ornamental fish group from 1990 to 1998, and seahorse landings rose 184% during this period, whereas landings of each of the more valuable fish groups declined (Adams et al., 2001). Many seahorses in the United States are probably obtained from bycatch of the shrimp trawl fisheries that operate in known seahorse habitats along the Atlantic coast of the United States.

Our objective was to document bycatch of the lined seahorse (*Hippocampus erectus*) in a live-bait shrimp trawl fishery. This fish is often retained for the aquarium trade. We quantify number, sex, size, and reproductive status of trawl-caught seahorses and examine how these parameters vary temporally and spatially. We also comment on potential conservation concerns resulting from this fishery.

Materials and methods

We focused our study on the lined seahorse (*Hippocampus erectus*) because it was caught much more often than its sympatric congenerics in the Gulf of Mexico—the longsnout seahorse (*H. reidi*) and the dwarf seahorse (*H. zosterae*). *Hippocampus erectus* is a large, deep-bodied seahorse (adult height 5.5 to 18.5 cm: Lourie et al., 1999) and has a geographic range that extends from southern Canada to Argentina. Most species of seahorse have short lifespans and low fecundity: *Hippocampus erectus* lives for about four years (Lourie et al., 1999) and has broods of about 100–1500 young (Teixeira and Musick, 2000). *Hippocampus erectus* is found in shallow waters and offshore to depths of over 70 m, primarily in mangroves and seagrass beds (Vari, 1982). Like many other seahorse species, *H. erectus* is listed as Vulnerable (A2cd) by the International Union for Conservation of Nature and Natural Resources (IUCN, 2002), based on suspected declines resulting from habitat degradation and exploitation. However, as is the case for many small fishes, there is little information known about the biology of *H. erectus*, and no fishery data exist for it.

Seahorse bycatch was assessed in the live-bait shrimp trawl fishery operating from Hernando Beach, Florida (Fig. 1). The fishery, using roller beam trawls, targets pink shrimp (*Penaeus duorarum*) at night in seagrass beds and relocates seasonally in Florida. Hernando Beach was chosen as our study site because it is a moderate-size fishing port with 31 licensed trawlers and is active during the summer sampling period. Boats were equipped with trawls that had a slotted roller along the bottom of the frame, and stainless steel finger bars attached vertically, 5 cm apart along the length of the frame, to limit collection of benthic substratum and other debris (Berkeley et al., 1985). Trawls were towed from each side of the vessel in four configurations: 1) one trawl per side, each measuring either 3.66 m, 4.27 m, or 4.88 m in length, or 2) two trawls per side, each measuring 3.66 m in length. Net mesh sizes were 3.18–3.81 cm and the tail bag stretched mesh size was 2.54–3.18 cm. Trawls usually lasted between 30 and 60 minutes, and fishermen made multiple successive trawls in a night. Shrimp were culled from the catch and held live onboard in aerated holding tanks. Most bycatch was discarded overboard, although some fishermen retained certain species, including seahorses, for sale as aquarium fishes.

Bycatch sampling and data set description

Data on seahorse bycatch in the live-bait shrimp fishery were collected on 95 fishing nights, from June to August 1998 and from June to July 1999, using three methods: 1) we sampled bycatch onboard on 50 nights; 2) we recorded seahorse bycatch data onshore on 14 nights from fishers who retained seahorses to sell; and 3) we received data from fishermen on their seahorse catches (including location, time, number of trawls, and number of seahorses per trawl) on a total of 31 nights. Onboard sampling was semistratified in that we targeted our sampling to cover all lunar and tidal phases and a variety of areas. However, we were dependent on fishersmen's decisions about the time and location of tows. We also collected anecdotal information from 14 experienced fishermen about seahorse catches over time.

During onboard sampling, we recorded the number of seahorses caught, start and end time of trawl, depth and location (Loran co-ordinates) of trawl, tidal and lunar phases, and presence or absence of all bycatch species, including biogenic habitat species. *Hippocampus erectus* found in the catch were placed in a container of surface water while measurements were made. They were then released, except when fishermen chose to retain them for sale. We measured, weighed, determined the sex, and recorded the life history stage, reproductive status, and any injury for each seahorse. Measurements were taken according to Lourie et al. (1999) and included standard length, defined as the length from the tip of the snout to the opercular ridge and from the opercular ridge to straightened tail tip. Seahorses that had lost tail rings were not included in the length analysis. Unless precluded by logistic constraints, wet weights were obtained onboard by using a 60-g Pesola spring scale and onshore by using a 200-g Ohaus electronic balance. Adult males were distinguished from females and juveniles by the presence of a brood pouch. The standard length of the smallest seahorse with a brood pouch (105.3 mm) was used as the division between adults and juveniles with the assumption that males and females matured at the same size. Such an assumption may overestimate the

[2] Vincent, A. C. J., and A. Perry (eds.). 2003. Global trade in seahorses. Manuscript in prep.

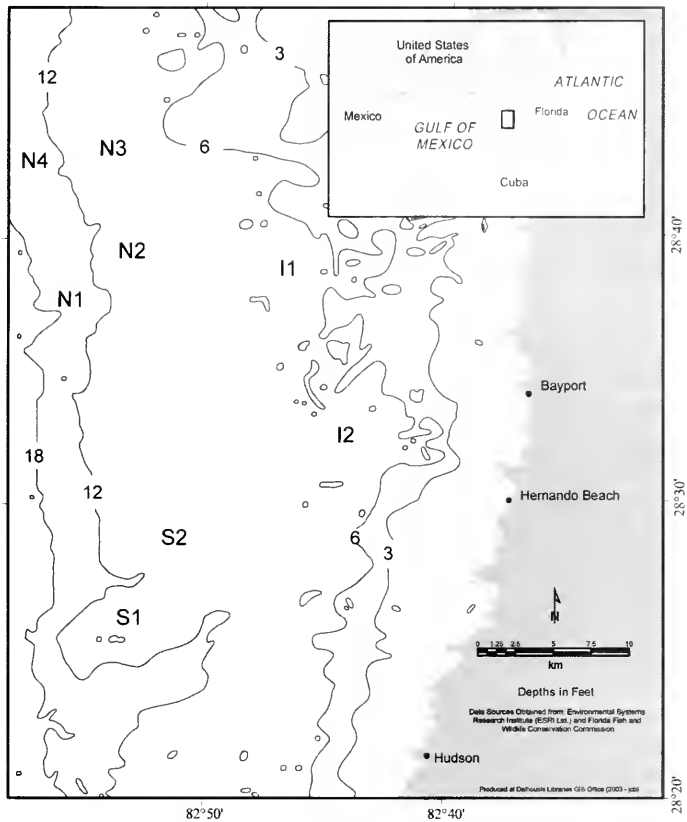

Figure 1

Map of the eastern Gulf of Mexico, showing the study site of Hernando Beach on the western coast of Florida. The shore is shaded; additional solid lines indicate depth contours in feet. Letter and number combinations (e.g. N3) represent fishing areas along the coast.

number of adult females because males that matured after that size would have been included in our analysis as females. We defined males as reproductively active if they were pregnant or had recently released young (as indicated by a loose pouch). Female reproductive state was not included in this analysis because it is difficult to determine reliably. We defined mortality to include seahorses already dead when the net was hauled and those that died onboard.

We evaluated temporal and spatial patterns in catch per unit of effort (CPUE), standard length, population structure, and reproductive status of the seahorse bycatch. Specifically, we tested 1) temporal effects of year, lunar and tidal phase, and 2) spatial effects of area and depth. In our estimates of seahorse CPUE, we used standard length instead of biomass because female weight changes with egg hydration and male weight increases greatly when carrying embryos. Calculating CPUE per length (m) of roller beam trawl controlled for variation in gear size. The sampling unit was thus defined as the total or cumulative standard length of seahorses caught during each tow (per hour), per meter of trawl (per meter). Lunar phases were defined as continuous variables by converting lunar day to its angle, θ, based on a cycle of 29.5 days (=360°), with new moon defined as $\theta = 0°$. These angles were then converted to their cosine and sine functions for inclusion in linear regression (deBruyn and Meeuwig, 2001). Tides were semidiurnal in the Gulf of Mexico, ranging 1.3 m in tidal level in the study area. High and low tides were defined as each lasting two hours, with the remaining time classified as ebb or flood accordingly. Spatial effects were analyzed by dividing the total fishing ground into eight subareas ac-

cording to their position with respect to the depth contour and by identifying discrete geographical clusters of trawls (Fig. 1). We then compared variation among fishing areas within years for those areas with at least five observations (areas I1, I2, N1, N2, S1, S2 in 1998, and areas N1, N3 and N4 in 1999). Interannual spatial comparisons were not possible because there was little overlap in sampled areas between the two years.

Statistical analysis

We based CPUE estimates on all trawls (n=445). Statistical analyses evaluating temporal and spatial variation in seahorse bycatch included only those trawls with nonzero seahorse observations (n=205). The analysis required the data or their residuals to be normal; this was achieved by inverse hyperbolic sine transformations following exclusion of zeros (Zar, 1996). It should be noted that by excluding zeros we overestimated seahorse CPUE and we lost information about areas where seahorses were absent or rare. Our analyses should be interpreted as applying to locations where and times when seahorses were found in sufficient numbers as to be caught.

We examined the data using ANOVA, ANCOVA, linear regression and chi-square analyses (Zar, 1996; SYSTAT, version 7.0, SPSS Inc., Chicago, IL). All two-way and three-way ANOVAs included tests for interactions. We used a general linear model because the data were unbalanced. Interactions were removed from the model if they were found to be nonsignificant. Models were then rerun, followed by pairwise Tukey tests to indicate where significant differences occurred (Zar, 1996; SYSTAT, version 7). We report results for the final ANOVA only. The Yates correction was applied to 2×2 chi-squares (Zar, 1996). All significance levels were set to reject H_0 at P<0.05 and all means are reported with standard errors.

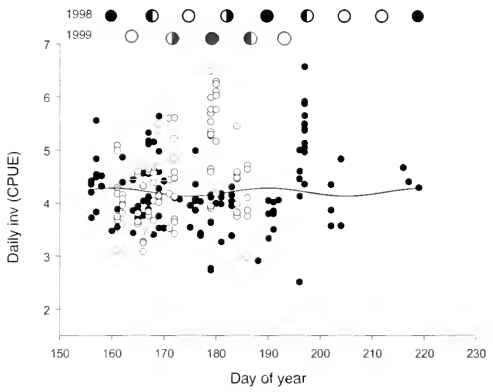

Figure 2

Variation in mean CPUE estimates by lunar phase transformed to inverse hyperbolic sine. The curve represents the predicted values as a function of the cosine (1998) and sine (1999) of day. The lunar phases for both years are indicated. Filled circles and black line are for 1998; open circles and gray line are for 1999.

Results

Bait shrimp fishermen trawled from 11 to 24 km offshore, between 1.8 and 6.4 m deep water (mean=3.76 ±0.87 m). Fishermen typically left port between 17:00 and 19:00 and spent 5.8 ±0.23 h actively trawling per night (n=50 nights). Trawls lasted 40.2 ±11.4 min (n=445) on average, and fishermen usually set 8 to 9 trawls per night. Distance trawled could not be estimated because we were unable to track trawler trajectories continuously and because they changed direction during the tows. The benthic habitat was composed primarily of seagrass (*Thalassia testudinum*) but also included algae, coral, and sponge. Bycatch included at least 118 species of fishes, invertebrates, and marine flora.

Catch per unit of effort

Hippocampus erectus was the only seahorse species commonly caught in this fishery. Almost half of the trawls (46%) caught *H. erectus*, and the number per trawl ranged from 0 to 16, whereas no *H. reidi* and only two of the much smaller species, *H. zosterae*, were caught. In total, 916 *H. erectus* were caught during the 95 documented fishing boat nights of the two fishing seasons, resulting in an overall mean of 9.64 seahorses per fishing boat night. Mean CPUE for *H. erectus* was 24.25 ±2.15 mm/(h×m), about one and a half seahorses per hour per boat. If only trawls with seahorses were included, CPUE was 52.52 ±3.80 mm/(h×m), or about three seahorses per hour per boat (n=205). Very high CPUE was recorded on three nights: 16 July 1998 (mean CPUE=122.0 ±22.5 mm/(h×m), n=12 trawls), 28 June 1999 (mean CPUE=118.1 ±24. mm/(h×m), n=12 trawls) and 30 June 1999 (mean CPUE=154.9 ±36.6 mm/(h×m), n=8 trawls). Bycatch is characterized by a high number of low catches and infrequent large catches. Because the large catches more likely reflect the spatial-temporal distribution characteristics of fish stocks rather than outliers of the data (Ortiz et al. 2000), we analyzed the entire dataset and then tested the robustness of our models by excluding these three nights in order to assess their influence on the CPUE patterns.

CPUE of nonzero trawls varied between years and with lunar phase (Table 1), but not with tidal phase (P=0.15). Trawls captured significantly more seahorses in 1999 than in 1998 (P<0.0005). The effect of lunar phase varied between years: CPUE was highest on the lunar third quarter in 1998, but only weakly significant and had slightly higher CPUE on the full moon in 1999 (Fig. 2). The temporal variation in CPUE was largely driven by the three high CPUE nights, but the effect persisted when these were excluded (Table 1).

Table 1

General linear model of effects of year, lunar phase, and area on the CPUE (mm/(h×m) for nonzero *H. erectus* bycatch trawls in the Hernando Beach bait-shrimp trawl fishery.

	CPUE by trawl			CPUE by trawl (excluding CPUE of three highest nights)		
Source	*n*	*F*	*P*	*n*	*F*	*P*
Year	205	15.2	<0.0005	173	3.9	0.049
Lunar phase	205			173		
$\cos(\theta)$		19.1	<0.0005		4.1	0.045
$\sin(\theta)$		8.9	0.003			
1998 areas (I1, I2, N1, N2, S1, S2)	116	7.4	<0.0005	105	2.3	0.037
1999 areas (N1, N2, N3, N4)	87	8.3	<0.0005	68	0.3	0.85

In both years, there were significant differences in nonzero CPUE trawls among sites. In 1998, CPUE was significantly higher in S2 than in I2, N1, N2 and S1 (Fig. 3A, Table 1). In 1999, CPUE was significantly higher in area N1 than in areas N3 and N4 (Fig. 3B, Table 1). However, both of these spatial patterns, like the lunar patterns, were driven primarily by the high CPUE nights. Removing the three outliers left a significant difference in CPUE by area in 1998 only (Table 1). CPUE did not vary with depth of the fishing ground (P=0.67).

Size of seahorses

Mean standard length of adults (standard length ≥105.3 mm) was 139.5 ±21.7 mm (n=465, range 105.3–202 mm) and mean weight was 11.6 ±5.5 g (n=232, range 3–31 g). *Hippocampus erectus* was sexually dimorphic: males had a brood pouch and were significantly longer than females (n=465, P<0.0005, Table 2), and had a greater weight to standard length ratio, although this latter difference was relatively weak (P=0.04). Juveniles (standard length <105.3 mm) had a mean standard length of 83.3 ±16.7 mm (n=65, range 41.4–105 mm) and a mean weight of 2.4 ±1.0 g (n=38, range 0.9–4.0 g).

In adults, standard length varied by year (n=425, F=7.1, P=0.008) and by lunar phase (n=425, $\cos(\theta)$:F=5.4, P=0.02, $\sin(\theta)$:F=7.7, P=0.006). Mean standard length was greater in 1998 than in 1999 and highest on the new moon. In 1998 significantly larger adult seahorses were caught in areas I2 and S2 than in I1 and S1 (n=229, F=13.7, P<0.0005; Fig. 4). There was no effect of area in 1999 (n=212, F=1.9, P=0.14). Standard length was not related to depth or tide.

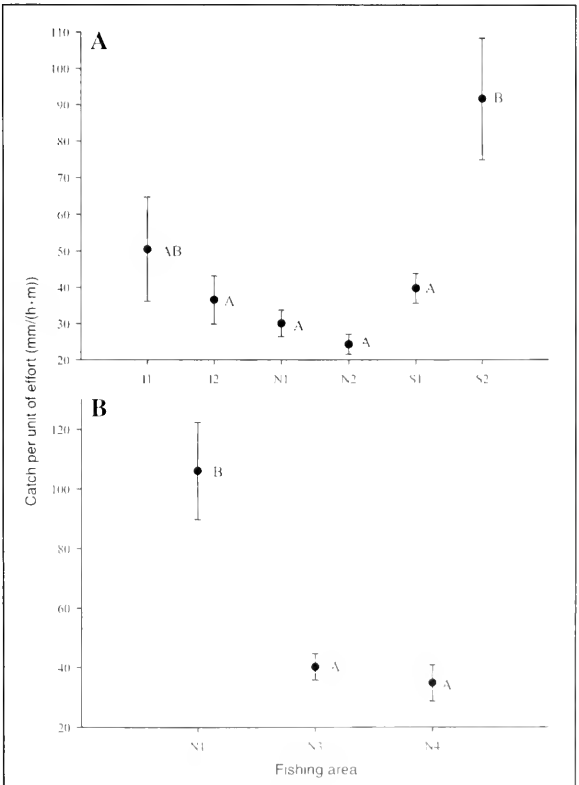

Figure 3

Catch per unit of effort (±standard error) as a function of fishing area in (**A**) 1998 and (**B**) 1999. Letters indicate where significant differences lie at P<0.05.

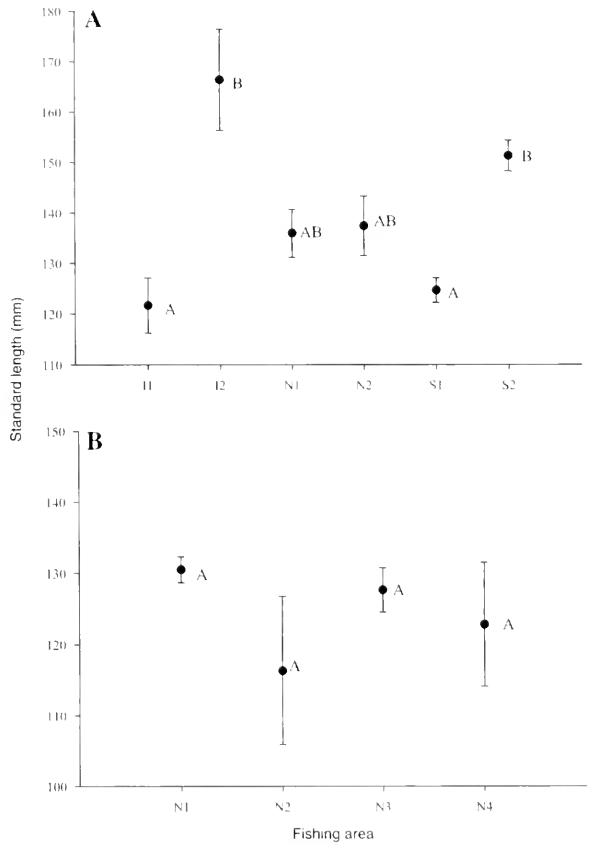

Figure 4

Standard length ±standard error as a function of fishing area in (**A**) 1998 and (**B**)1999. Letters indicate where significant differences lie at $P<0.05$.

Population structure

We assessed population structure in terms of size cohorts, life history stages, sex ratio (males/total) and reproductive status. Standard-length frequency histograms suggested that the 1998 bycatch was composed of three year classes but the largest of these was not evident in 1999 (Fig. 5). Of 530 seahorses measured, 87.7% were considered to be adults. The ratio of juveniles to adults did not differ by year ($P>0.10$) or tidal phase ($P>0.90$). However, significantly more juveniles were caught during the first quarter than during other lunar phases (Table 3). Fishing area had a significant effect on size class, with the highest numbers of juveniles caught in N2 and N3 (Table 3).

The sex ratio (males as fraction of total) of 0.42 differed significantly from a 1:1 ratio ($\chi_c^2=19.56$, df=1, $P<0.001$). The sex ratio did not vary temporally or spatially (Table 3), but it did vary as a function of size class. There were proportionally more males in the larger size class (≥150 mm, 0.61) than in the smaller size class (<150 mm, 0.30) ($\chi_c^2=14.95$, df=1, $P<0.005$).

About 25% of the male seahorses captured in 1998 were considered to be reproductively active, whereas fewer than 1% were reproductively active in 1999. Indeed, male reproductive activity was higher in 1998 than 1999 even after controlling for smaller male size in 1999 (Table 3). The proportion of reproductively active males did not vary with lunar or tidal phase but did vary significantly with area

Table 2

Descriptive statistics (sample size [*n*], mean, standard deviation [SD], minimum [min] and maximum [max]) for standard length and weight of female (F) and male (M) seahorses. *P* values and sample sizes (*n*) indicate results of *t*-tests evaluating sexual dimorphism in SL and weight.

	Sex	*n*	mean	SD	min	max
Standard length (mm)	M	201	146.1	21.9	105.3	200.5
$P<0.0005$, $n=465$	F	264	134.4	20.1	105.3	202.0
Weight (g)	M	105	12.5	5.0	6.0	27.0
$P<0.002$, $n=232$	F	140	11.0	5.8	3.0	31.0

Table 3

Contingency tables on effects of year, lunar phase, and area on population structure of seahorses in the bycatch of the Hernando Beach bait shrimp trawl fishery. Yates corrections were applied to 2×2 contingency tables.

	Juveniles:Adults			Sex ratio			Reproductive state		
Source	df	χ^2	*P*	df	χ^2	*P*	df	χ^2	P
Year	1	2.46	>0.10	1	0.15	>0.50	1	27.89	<0.001
Lunar phase	3	11.00	<0.025	3	3.69	>0.25	3	7.80	>0.05
Area	3	8.84	<0.05	7	13.3	>0.05	2	21.64	<0.001

(Table 3); almost half of the reproductively active males were found in one area (S2), and 83% of them were caught on one of the three nights with very high CPUE (16 July 1998).

Mortality and injury

Fewer than 1% of seahorses died during tows or sorting, but 4.7% ($n=28$ of 588 seahorses) lost tail rings. The mean loss was 22 of the usual 36 tail rings (Lourie et al., 1999), or 61% of the tail (range=8–31 rings lost). Approximately 14% of the losses ($n=4$ of 588 seahorses) appeared to be the result of new wounds, probably caused by the focal trawl. There was no effect of year ($P=0.25$), sex ($P=0.75$), or reproductive status ($P=0.75$) on incidence of seahorse injury. Postrelease mortality is unknown.

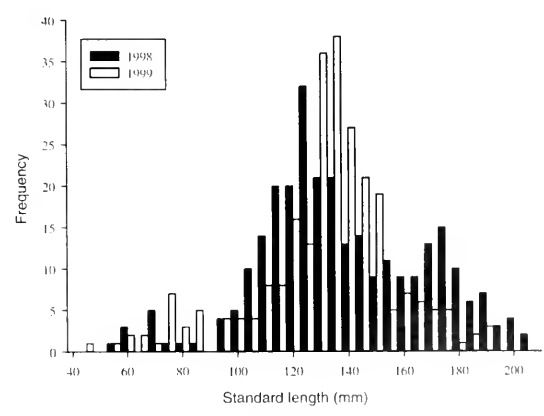

Figure 5

Length-frequency histogram for seahorse bycatch in 1998 and 1999.

Discussion

Direct effects of the trawl fishery on seahorse mortality

We estimate that this fleet catches almost 72,000 seahorses incidentally per annum, based on the mean CPUE and given that 31 boats fished approximately 240 nights per year. Most seahorses were returned to the wild in the Hernando Beach fishery, but this may not be the case in other live-bait shrimp trawl fleets in Florida (Vincent, pers. obs.). We could not determine the potential fishing-induced mortality for the Hernandez Beach *H. erectus* population, even when all trawled seahorses were retained, because seahorse catchability in roller beam trawl gear is unknown and no studies have estimated *H. erectus* density in the wild. Focal behavioral studies on congenerics similar in

size to *H. erectus* have found varied densities: *H. comes*, an exploited species associated with coral reefs in the tropics, had localized densities of 0.019/m^2 in a marine protected area, and much less elsewhere (Perante et al., 2002), and an unexploited species, *H. whitei*, had localized densities of 0.088–0.215/m^2 in a study area, and no seahorses were found over large adjacent areas (Vincent et al.[1]). Our study also suggests very patchy distributions of *H. erectus* (54% of the trawls had no seahorses at all and the number of seahorses per trawl set ranged from 0 to 16).

Although variation in CPUE may reflect differential catchability by habitat, we suggest that in areas where seahorses were caught, temporal rather than spatial effects drove CPUE. It is difficult to make conclusions about variation in CPUE because data were unbalanced, in that the areas trawled differed between years and among lunar phases. However, analysis of variance on a subset of data for three sites (N1, N2, N3) on three lunar phases (1st quarter, full moon, 3rd quarter) for which we had data in both years (n=149 trawls), indicated that there was a strong effect of year, a weaker effect of lunar phase, and no effect of site. These results suggest that CPUE was mainly affected by temporal variation. Lunar patterns in CPUE as a result of fish behavior and ecology are common (e.g. Parrish, 1999). This would be consistent with observations for other species of seahorses: *H. comes* in the Philippines (Vincent et al.[3]) and *H. spinosissimus* and *H. trimaculatus* in Vietnam (Meeuwig et al.[4]) exhibited patterns in CPUE with respect to lunar phase, although these species were also distributed in patches in space.

Data from this study suggest that the *H. erectus* population was spatially structured. In 1999, the mean size of incidentally caught adult seahorses decreased, reflecting the absence of the largest size class of males and an increase in smaller females that year (Fig. 5). We attribute this difference to spatial structuring: the shallower areas (I2, S2) where the largest male and female seahorses were caught in 1998 were not fished during the 1999 sampling season. Most of the seahorse bycatch were adult *H. erectus;* the dearth of juvenile *H. erectus* (and dwarf seahorses, *H. zosterae*) in the trawls reflects low catchability or retention due to mesh size. Similar proportions of juvenile seahorses were caught over the two sampling seasons. The ratio of juveniles to adults appears to be temporally influenced (proportionally more juveniles were caught on new moons), but this variation probably also reflects spatial structuring because these trawls occurred primarily in deeper offshore areas (N2, N3) that were fished almost exclusively during this lunar phase. Perhaps *H. erectus* undergoes ontogenetic movement, between juvenile and adult life history stages, and adults maintain site fidelity. Spatial size structuring probably also occurs in other seahorse species, for the entire population and for adults alone (*H. comes*, Meeuwig[5]; *H. guttulatus*, Curtis[6]). A better understanding of the spatial structuring of populations could allow for spatial control of fishing effort to minimize bycatch.

We found a consistent, female-biased sex ratio in the catch across the two years of our study, with only 42% males. This bias may reflect the sex ratio of the *H. erectus* population: a similar sex ratio (40% males) was found in a population of *H. erectus* in Chesapeake Bay, Virginia (Teixeira and Musick, 2000). Female-biased sex ratios have also been found in *H. zosterae* (33% males) when sampled by pushnet (Strawn, 1958), and in *H. abdominalis* studied underwater in Australia (Martin-Smith[7]). Many other wild populations of seahorses studied underwater, however, have documented equal numbers of males and females (*H. breviceps*: *H. comes*: Moreau and Vincent[8]; Perante et al., 1998; *H. reidi*: Dauwe, 1993; *H. whitei*: Vincent and Sadler, 1995). Sexual dimorphism in *H. erectus* was too slight to explain different catchability of the two sexes and would, in any case, have favored the capture of males. The disproportionate catch of females could have arisen from spatial segregation by sex; the greater catches of reproductively active males in shallower areas suggests that males may spend most of their time inshore of the trawled area. We also cannot discount the possibility that some seahorses classified as females may have been immature males, and the sex ratio in the population could in fact be 1:1.

The proportion of reproductively active seahorses in the bycatch was lower than expected, particularly in 1999. Our study occurred during summer, within the breeding season for the congeneric and sympatric *H. zosterae* in Florida (February to October; Strawn, 1958), and for *H. erectus* in Chesapeake Bay (May to October; Teixeira and Musick, 2000; Vincent, personal obs.). Males of all studied seahorse species were reproductively active almost continuously throughout the breeding season (Dauwe, 1993; Nijhoff, 1993; Vincent and Sadler, 1995; Perante et al., 2002), often remating the same day that they release their young (Vincent and Sadler, 1995). In our study, trawling may have occurred outside the primary breeding areas for male *H. erectus*, but catches of reproductively nonactive adult males during the breeding season also suggest that repeated trawling may have disrupted breeding in the population. A further indication of possible spatial structuring in the population (by reproductive status and size) is that almost half of the reproductively active males caught in 1998 were found in S2, the shallowest area; this area was not sampled in 1999 when few reproductively active males were found. Such spatial structuring offers the possibility of trawling outside the breeding area.

[3] Vincent, A. C. J., J. J. Meeuwig, M. G. Pajaro, and N. C. Perante. Seahorse catches in the central Philippines: characteristics and conservation implications. Manuscript in prep.

[4] Meeuwig, J. J., D. H. Hoang, T. S. Ky, S. D. Job, and A. C. J. Vincent. Bycatch landings of seahorses in central Vietnam. Manuscript in prep.

[5] Meeuwig, J. J. Life history parameters of the exploited seahorse *Hippocampus comes*: a length based analysis. Manuscript in prep.

[6] Curtis, J. 2002. Unpubl. data. Project Seahorse, Fisheries Center, The University of British Columbia, 2204 Main Mall, Vancouver, BC, V6T 1Z4, Canada.

[7] Martin-Smith, K. 2002. Unpubl. data. Project Seahorse, Fisheries Center, The University of British Columbia, 2204 Main Mall, Vancouver, BC, V6T 1Z4, Canada.

[8] Moreau, M-A., and A. C. J. Vincent. 2000. Unpubl. data. Project Seahorse, Fisheries Center, The University of British Columbia, 2204 Main Mall, Vancouver, BC, V6T 1Z4, Canada.

Indirect effects of the trawl fishery on mortality

Direct immediate mortality from trawling and culling was rather low, probably in part because trawl sets were of very short duration in this live-bait fishery. More importantly, most *H. erectus* caught in the Hernando Beach fishery were returned to sea, rather than retained as in some other Florida trawl fisheries (Vincent, pers. obs.). Indirect impacts of the fishery may, however, be considerable.

Seahorses caught in trawls may experience high postrelease mortality. A study in the live-bait shrimp trawl fishery in Tampa Bay, Florida (Meyer et al., 1999), found that only one of four of the congeneric dwarf seahorse (*H. zosterae*) caught as bycatch were alive in the holding tank of seawater 36 hours after collection (Meyer[9]). Such tows lasted only 5 minutes (Meyer et al., 1999); therefore trawl-induced mortality could be greater in the Hernando Beach fishery (with trawls of 30–50 minutes), although *H. erectus* are larger and perhaps more robust than *H. zosterae*. Like other discarded bycatch, seahorses may also be subject to intense predation upon release. Predation on discarded fish has been observed on prawn trawlers in Australia (Hill and Wassenberg, 1990) and within the bait shrimp fishery of Tampa Bay (Meyer et al., 1999). Captains of bait-shrimp boats concurred that this is commonplace in the Hernando Beach fishery, and we frequently observed bottlenosed dolphins (*Tursiops truncatus*) and schools of ladyfish (*Elops saurus*) swimming alongside the boats, feeding on discarded bycatch.

Trawling may significantly disrupt seahorse populations, particularly if they are spatially structured, as the present study suggests. The disproportionate removal of females could reduce mating opportunities, especially if *H. erectus* is monogamous, as are most studied seahorse species (e.g. Vincent, 1995; Vincent and Sadler, 1995; Kvarnemo et al., 2000; Perante et al., 2002). Trawling, on account of repeated intrusion onto breeding grounds, could also disrupt courtship and negatively affect reproduction, In heavily exploited areas of the fishery where fishermen repeatedly trawl productive areas, seahorses may face cumulative stress. For example, tail injuries are likely a serious wound for seahorses, given that their tails are essential to grasp holdfasts and may play a key role in mating competition, as they do with *Hippocampus fuscus* (Vincent, 1994).

Benthic habitat degradation is another potential indirect effect of live-bait shrimp trawling on seahorses. Bottom-fishing gear can reduce habitat complexity by removing emergent epifauna, smoothing sedimentary bedforms and by removing structure-forming species such as corals and sponges (Hutchings, 1990; Auster et al., 1996; Auster and Langton, 1999; Thrush and Dayton, 2002). Roller beam trawls also affect habitat complexity by redistributing macroalgae and seagrass (Meyer et al., 1999). We estimated that seagrasses comprised between 50% and 80% of the volume of the catch for each trawling operation. Although roller beam trawls are assumed to have low impact on seagrass habitat (Tabb and Kenny, 1969; Meyer et al., 1999), the effects of long-term repetitive trawling have not been tested, and it is possible that species composition and abundance, including that of *H. erectus*, have been adversely affected (Watling and Norse, 1998).

[9] Meyer, D. 1999. Personal commun. NOAA Center for Coastal Fisheries and Habitat Research, Beaufort Laboratory, 101 Pivers Island Road, Beaufort, NC 28516.

Summary

Despite the relatively low direct mortality of seahorse per boat, the live-bait trawl fishery has the potential to affect seahorse populations, both directly and indirectly. The key question is whether the level of exploitation, and subsequent impacts, represents a conservation concern. Our evidence is inconclusive. Perhaps only the skewed sex ratio and low proportion of reproductively active males suggest a potential problem. However, fishermen have consistently reported that seahorse catch per boat has declined greatly over the past two decades in this area. Effects of trawling are also almost certainly greater in food shrimp trawl fisheries, which trawl with much larger gear for longer periods, and obtain substantially more bycatch, with higher mortality. Our analysis should thus be seen as a first step in identifying areas for which more information is needed, specifically estimating abundance and fishing mortality, and understanding spatial structuring in *H. erectus*.

This paper focuses attention on the need for research on and monitoring of small fishes that may be affected by nonselective fishing gear. Management responses to minimize bycatch have focused primarily on seabirds, sea turtles, and commercially important finfishes, but trawl fisheries may also have significant impacts on the many small marine organisms obtained as bycatch, even if they comprise only a small proportion of the bycatch. Bycatch excluder devices are unlikely to be effective in reducing incidental catches of these species. Temporal variation in CPUE and spatial population structuring, as observed in our present study for *H. erectus*, suggest that time-area closures may be a pragmatic solution for reducing incidental catch.

Acknowledgments

This paper is a contribution from Project Seahorse. We thank Jana Schulz for her assistance with fieldwork, Daniel and Patricia Mohr for their support during fieldwork, James Boxall for preparing the map, A. DeBruyn, L. Crowder, M. Kaiser, and an anonymous reviewer for providing helpful comments on an earlier draft of this manuscript. This study would not have been possible without the cooperation and support of many of the shrimp boat captains and crew in Hernando Beach. This research was funded through an NSERC summer undergraduate award to JKB, support from the Community Fund (UK) and Guylian Chocolates Belgium for JJM, and an NSERC operating grant to ACJV.

Literature cited

Adams, C., S. Larkin, and D. Lee.
2001. Volume and value of marine ornamentals collected in Florida, 1990–98. Aquar Sci Conserv. 3(1–3):25–36.

Alverson, D. L.
1997 Global assessment of fisheries bycatch and discards: a summary overview. *In* Global trends: fisheries management (E. K. Pikitch, D. D. Huppert, and M. P. Sissenwine, eds.), 115–125 p. Am. Fish. Soc. Symp., Vol. 20.

Alverson, D. L., M. H. Freeberg, S. A. Murawski, and J. G. Pope.
1994 A global assessment of fisheries bycatch and discards, 233 p. FAO Fish. Biol. Tech. Pap. 339. FAO, Rome.

Auster, P. J., and R. W. Langton.
1999. The effects of fishing on fish habitat. *In* Fish habitat: essential fish habitat (EFH) and rehabilitation (L. Benaka, ed.), p. 150–187. Am. Fish. Soc. Rep. 22.

Auster, P. J., R. J. Malatesta, R. W. Langton, L. Watling, P. C. Valentine, C. L. S. Donaldson, E. W. Langton, A. N. Shepard, and I. G. Babb.
1996. The impacts of mobile fishing gear on seafloor habitats in the Gulf of Maine (Northwest Atlantic): implications for conservation of fish populations. Rev. Fish. Sci. 4:185–202.

Berkeley, S. A., D. W. Pybas, and W. L. Campos.
1985. Bait shrimp fishery of Biscayne Bay, 16 p. Fla. Sea Grant Ext. Prog. Tech. Pap. 40. Florida Sea Grant, Gainesville, FL.

Chan, E. H., and H. C. Liew.
1986. Characteristics of an exploited tropical shallow-water demersal fish community in Malaysia. *In* Proceedings of the first Asian fisheries forum (J. L. Maclean, L. B. Dizon, and L. V. Hosillows, eds.), p. 349–352. Asian Fisheries Society, Manila, Philippines.

Dauwe, B.
1993. Ecology of the seahorse *Hippocampus reidi* on the Bonaire coral reef (N.A.): habitat, reproduction and community interaction. M.S. thesis, 65 p. Rijksuniversiteit, Groningen, Netherlands.

deBruyn, A. M. H., and J. J. Meeuwig.
2001. Detecting lunar cycles in marine ecology: periodic regression versus categorical ANOVA. Mar. Ecol. Prog. Ser. 214:307–310.

Diamond, S. L., L. G. Cowell, and L. B. Crowder.
2000. Population effects of shrimp trawl bycatch on Atlantic croaker. Can. J. Fish. Aquat. Sci. 57(10):2010–2021.

FAO (Food and Agriculture Organization of the United Nations).
1999. The state of world fisheries and aquaculture 1998, 112 p. FAO, Rome.

Galloway, B. J., and J. G. Cole.
1999. Reduction of juvenile red snapper bycatch in the Gulf of Mexico shrimp trawl fishery. N. Am. J. Fish. Manag. 19(2):342–355.

Graham, G. L.
1995. Finfish bycatch from the Southeastern shrimp fishery. *In* Solving bycatch: considerations for today and tomorrow, p. 115–119. Univ. Alaska Sea Grant College Program Report 96-03, Fairbanks, AK.

Hill, B. J., and T. J. Wassenberg.
1990. Fate of discards from prawn trawlers in Torres Strait. Aust. J. Mar. Freshw. Res. 41:53–64.
2000. The probable fate of discards from prawn trawlers fishing near coral reefs. A study in the northern Great Barrier Reef, Australia. Fish. Res. 48(3):277–286.

Hutchings, P.
1990. Review of the effects of trawling on macrobenthic epifaunal communities. Aust. J. Mar. Freshw. Res. 41: 111–120.

IUCN (International Union for Conservation of Nature and Natural Resources).
1996. World Conservation Congress, 1st session. Resolutions and recommendations. 1.16 Fisheries by-catch; Montreal, Canada, 14–23 October 1996. IUCN, Gland, Switzerland.
2002. 2002 IUCN red list of threatened species. IUCN, Gland, Switzerland and Cambridge, UK. http://www.redlist.org/ [Accessed 21 January 2003].

Jennings, S., and M. J. Kaiser.
1998. The effects of fishing on marine ecosystems. Adv. Mar. Biol. 34:201–352.

Julian, F., and M. Beeson.
1998. Estimates of marine mammal, turtle and seabird mortality for two California gillnet fisheries: 1990–1995. Fish. Bull. 96:271–284.

Kaiser, M. J., and B. E. Spencer.
1995. Survival of by-catch from a beam trawl. Mar. Ecol. Prog. Ser. 126:31–38.

Kvarnemo, C., G. I. Moore, A. G. Jones, W. S. Nelson, and J. C. Avise.
2000. Monogamous pair bonds and mate switching in the Western Australian seahorse *Hippocampus subelongatus*. J. Evol. Biol. 13:882–888.

Larkin, S. L., and R. L. Degner.
2001. The U.S. wholesale market for marine ornamentals. Aquar. Sci. Conserv. 3(1):13–24.

Lourie, S. A., A. C. J. Vincent, and H. J. Hall.
1999. Seahorses: an identification guide to the world's species and their conservation, 214 p. Project Seahorse, London, UK.

Mensink, B. P., C. V. Fischer, G. C. Cadee, M. Fonds, C. C. Ten Hallers-Tjabbes, and J. P. Boon.
2000. Shell damage and mortality in the common whelk *Buccinum undatum* caused by beam trawl fishery. J. Sea Res. 43(1):53–64.

Meyer, D. L., M. S. Fonseca, P. L. Murphey, R. H. McMichael, Jr., M. M. Byerly, M. W. LaCroix, P. E. Witfield, and G. W. Thayer.
1999. Effects of live-bait shrimp trawling on seagrass beds and fish bycatch in Tampa Bay, Florida. Fish. Bull. 97:193–199.

Milton, D.
2001. Assessing the susceptibility to fishing of populations of rare trawl bycatch: sea snakes caught by Australia's northern prawn fishery. Biol. Conserv. 101:281–290.

Nijhoff, M.
1993. Reproductive cycle of the seahorse *Hippocampus reidi* on the Bonaire coral reef. M.S. thesis, 49 p. Rijksuniversiteit, Groningen, Netherlands.

Ortiz, M., C. M. Legault, and N. M. Ehrhardt.
2000. An alternative method for estimating bycatch from the U.S. shrimp trawl fishery in the Gulf of Mexico, 1972–1995. Fish. Bull. 98:583–599.

Parrish, J. K.
1999. Using behavior and ecology to exploit schooling fishes. Environ. Biol. Fishes 55:157–181.

Perante, N. C., M. G. Pajaro, J. J. Meeuwig, and A. C. J. Vincent.
2002. Biology of *Hippocampus comes* in the central Philippines. J. Fish Biol. 60(4):821–837.

Perante, N. C., A. C. J. Vincent, and M. G. Pajaro.
1998. Demographics of *Hippocampus comes* seahorses in Bohol, central Philippines. *In* Proceedings of the third international conference on the Marine Biology of the South China Sea; Hong Kong 1996, p. 439–448. Hong Kong Univ. Press, Hong Kong.

Pettovello, A. D.
1999. By-catch in the Patagonian red shrimp (*Pleoticus muelleri*) fishery. Mar. Freshw. Res. 50:123–127.

Pikitch, E. K., J. R. Wallace, E. A. Babcock, D. L. Erickson, M. Saelens, and G. Oddsson.
1998. Pacific halibut bycatch in the Washington, Oregon, and

California groundfish and shrimp trawl fisheries. N Am. J. Fish Manag. 18:569–586.

Polacheck, T.
1989. Harbour porpoises and the gillnet fishery: Incidental takes spur population studies. Oceanus 32:63–70.

Probert, P. K., D. G. McKnight, and S. L. Grove.
1997. Benthic invertebrate bycatch from a deep-water trawl fishery, Chatham Rise, New Zealand. Aquatic conservation: marine and freshwater ecosystems 7(1):27–40.

Strawn, K
1958. Life history of the pygmy seahorse, *Hippocampus zosterae* Jordan and Gilbert, at Cedar Key, Florida. Copeia 1958:16–22.

Tabb, D. C., and N. Kenny.
1969. A brief history of Florida's live bait shrimp fishery with description of fishing gear and methods. FAO Fish. Rep. 57:1119–1134.

Teixeira, R. L., and J. A. Musick.
2000. Reproduction and food habits of the lined seahorse, *Hippocampus erectus* (Teleeostei: Syngnathidae) of Chesapeake Bay, Virginia. Rev. Bras. Biol. 61(1):79–90.

Thrush, S., and P. K. Dayton.
2002. Disturbance to marine benthic habitats by trawling and dredging: implications for marine benthic biodiversity. Ann. Rev. Ecol. Syst. 33:449–473.

Vari, R. P.
1982. Fishes of the western North Atlantic, subfamily Hippocampinae. The seahorses, p. 173–189. Sears Foundation for Marine Research Memoir, vol. 1, Yale Univ., New Haven, CT.

Vincent, A. C. J.
1994. Operational sex ratios in seahorses. Behaviour 128: 153–167.
1995. A role for daily greetings in maintaining seahorse pair bonds. Anim. Behav. 49:258–260.
1996. The international trade in seahorses, vii + 163 p. TRAFFIC International, Cambridge, UK.

Vincent, A. C. J., and L. M. Sadler.
1995. Faithful pair bonds in wild seahorses, *Hippocampus whitei*. Anim. Behav. 50:1557–1569.

Watling, L., and E. A. Norse.
1998. Disturbance of the seabed by mobile fishing gear: a comparison to forest clear cutting. Conserv. Biol. 12(6): 1180–1197.

Weimerskirch, H., N. Brothers, and P. Jouventin.
1997. Population dynamics of wandering albatross *Diomedea exulans* and Amsterdam albatross *D. amsterdamensis* in the Indian Ocean and their relationships with long-line fisheries; conservation implications. Biol. Conserv. 79:257–270.

Zar, J. H.
1996. Biostatistical analysis, 3rd ed., 662 p. Prentice Hall, Upper Saddle River, NJ.

Estimates of survival probabilities for oceanic-stage loggerhead sea turtles (*Caretta caretta*) in the North Atlantic

Karen A. Bjorndal

Alan B. Bolten

Archie Carr Center for Sea Turtle Research and Department of Zoology
University of Florida
P.O. Box 118525
Gainesville, Florida 32611
E-mail address (for K. A. Bjorndal): kab@zoology.ufl.edu

Helen R. Martins

Departamento de Oceanografia e Pescas
Universidade dos Açores
PT-9901-862 Horta
Açores, Portugal

Abstract—Estimates of instantaneous mortality rates (Z) and annual apparent survival probabilities (Φ) were generated from catch-curve analyses for oceanic-stage juvenile loggerheads (*Caretta caretta*) in the waters of the Azores. Two age distributions were analyzed: the "total sample" of 1600 loggerheads primarily captured by sighting and dipnetting from a variety of vessels in the Azores between 1984 and 1995 and the "tuna sample" of 733 loggerheads (a subset of the total sample) captured by sighting and dipnetting from vessels in the commercial tuna fleet in the Azores between 1990 and 1992. Because loggerhead sea turtles begin to emigrate from oceanic to neritic habitats at age 7, the best estimates of instantaneous mortality rate (0.094) and annual survival probability (0.911) not confounded with permanent emigration were generated for age classes 2 through 6. These estimates must be interpreted with caution because of the assumptions upon which catch-curve analyses are based. However, these are the first directly derived estimates of mortality and survival probabilities for oceanic-stage sea turtles. Estimation of survival probabilities was identified as "an immediate and critical requirement" in 2000 by the Turtle Expert Working Group of the U.S. National Marine Fisheries Service.

Manuscript approved for publication 21 April 2003 by Scientific Editor.
Manuscript received 26 June 2003 at NMFS Scientific Publications Office.
Fish. Bull. 101:732–736 (2003).

A major gap in our understanding of sea turtle demography is the level of mortality—both natural and human-induced—experienced by wild populations. Lack of directly derived estimates of mortality (or survival) probabilities for the juvenile oceanic-stage in sea turtle populations is a critical source of uncertainty in development of population models and evaluation of management plans. In current population models, survival estimates for juvenile, oceanic-stage sea turtles are fitted parameters, not directly derived estimates, of survival (Chaloupka, in press; Heppell et al., in press). The Turtle Expert Working Group (2000) identified the estimation of survival probabilities as "an immediate and critical requirement." Population models indicate that survival probability of juvenile oceanic-stage loggerhead sea turtles (*Caretta caretta*) has a substantial effect on overall population growth (Chaloupka, in press; Heppell et al., in press).

Catch-curve analyses have been used for many years to estimate survival probabilities for species harvested in commercial fisheries and, less frequently, for other species (Seber, 1982). Estimates of survival probabilities have been generated from catch-curve analyses for subadult neritic-stage populations of loggerhead sea turtles (Frazer, 1987; Epperly et al., 2001) and Kemp's ridley sea turtles (*Lepidochelys kempi*) (Turtle Expert Working Group, 2000) based on stranding data. Catch-curve analyses confound mortality and permanent emigration, and thus generate estimates of apparent survival probability (Φ),

$$\Phi = S\,(1 - \textit{emigration}),$$

where S = true survival probability; and
emigration = the probability of permanent emigration.

We estimated survival probabilities (both Φ and S) for juvenile oceanic-stage loggerhead sea turtles in the waters around the Azores, a developmental habitat for the population of loggerhead sea turtles that nest on beaches in the southeastern United States (Bolten et al., 1998). We applied catch-curve analyses to two age distributions of loggerhead sea turtles.

Methods

Two size distributions were compiled for this study. The first ("total sample") comprised 1600 oceanic-stage loggerhead sea turtles that were captured from 1984 through 1995 in the waters of the Azores. Except for a few of the smallest of these sea turtles found as stranded carcasses, they were collected in dipnets after being sighted at the surface of the ocean from the decks of a

variety of vessels. Loggerhead sea turtles captured on longline hooks were excluded from this sample to meet the requirement of equal probability of capture across the age range (see "Results" section). The turtles were measured, tagged, and released soon after capture. The juvenile loggerhead sea turtles ranged in size from 8.5 to 82.0 cm curved carapace length (mean=33.1 cm, SD=11.6) measured from the anterior point at midline to the posterior notch at midline between the supracaudals (Bolten, 1999). For 248 turtles, straight-line carapace measurements were converted to curved carapace length, as described in Bjorndal et al. (2000).

The second age distribution ("tuna sample") was a subset of the total sample and comprised 733 loggerhead sea turtles captured by crews of commercial tuna vessels in the Azores between 1990 and 1992. We analyzed the tuna sample in addition to the total sample because the tuna sample was collected over a shorter interval (1990–92) than was the total sample (1984–95). In addition, sizes of vessels from which turtles were captured were more consistent for the tuna sample. This collaborative project with the tuna fleet is described in Bolten et al. (1993); sea turtles are not bycatch in the tuna fishery. Sea turtles were sighted at the surface while the crews were scanning for indications of tuna feeding activity. The turtles were then captured in dipnets, tagged and measured by a crew member, and released at sea. The juvenile loggerhead sea turtles ranged from 11.0 to 82.0 cm curved carapace length (mean=33.5, SD=11.2). No conversion from straight to curved measurements was required.

The size distributions were converted to age distributions by using a size-at-age function developed for this population based on a skeletochronological study (Table 1; Bjorndal et al., 2003). Catch curves were generated for each age distribution by plotting the natural log of N_x against x, where N_x is the number of turtles of age x. The catch curves were truncated by excluding age classes with fewer than five individuals, as recommended by Seber (1982). The age at which the population fully recruited to the capture method (threshold age) was identified as the age with the highest $\ln(N_x)$. Linear regression analyses of the values on the right-hand or declining slope of the distribution were used to generate estimates of total instantaneous mortality rate (Z), which is expressed on an annual basis and is the absolute value of the slope of the regression line. Annual apparent survival probability (Φ) was estimated as e^{-Z}. The statistical software S-PLUS (Guide to statistics, vol. 1, MathSoft, Seattle, WA) was used for regression analyses.

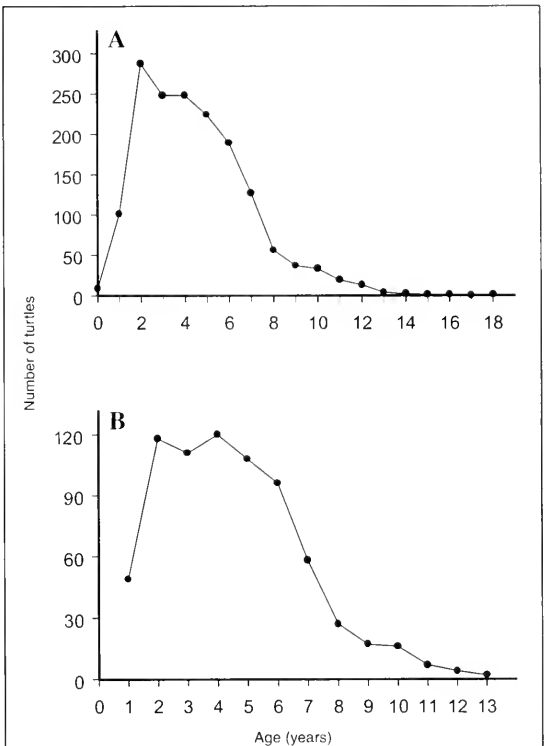

Figure 1

Age distributions of (**A**) total sample (n=1600) and (**B**) tuna sample (n=733).

Results

The age distributions for the two samples are shown in Figure 1 and the catch curves in Figure 2. For catch-curve analyses, the age distributions were truncated to the 12-year age class for the total sample and to the 11-year age class for the tuna sample because older age classes contained fewer than 5 individuals (Seber, 1982). The selection of the appropriate threshold age—the first fully recruited age class to the capture method—can be difficult but is critical for the analyses (Seber, 1982; Isaac, 1990). We designated 2 years as the threshold age for the total sample and 4 years for the tuna sample; in the tuna sample, the 4-year age class was slightly larger than the 2-year age class (120 vs. 118 turtles, Table 1).

We believe that turtles between ages 2 and 12 in the total sample and between 4 and 11 in the tuna sample meet the assumption of equal capture probability. With increase in turtle size, capture probability is a compromise; greater visibility of larger turtles is countered by greater difficulty in capturing larger turtles. Loggerhead sea turtles captured incidentally by longline vessels were excluded from our sample because there is a capture bias toward the largest size classes. The mean size of the turtles in the total sample

(33.1 cm) was significantly different (Kolmogorov-Smirnov test, ks=0.6966, P<0.001) from the mean size of loggerhead sea turtles caught in longline fisheries in the Azores during an experiment conducted in 2000 (49.8 cm; n=224; Bolten, in press).

The catch curves for both samples (Fig. 2) reveal a change in slope at age 6. The 7-year age class includes loggerhead sea turtles with curved carapace lengths >46 cm—the size at which they begin to leave oceanic habitats and recruit to neritic habitats (Bjorndal et al., 2000). Thus, the sharper decline beginning with age 7 reflects the migration of turtles out of the sampling area. Estimates of total instantaneous mortality rate (Z) and annual apparent survival probability (Φ) were generated for three age ranges for each sample: from threshold age to final age, from threshold age to pre-emigration age (6 years), and from pre-emigration age to final age. For the total sample, the age ranges were 2 to 12 years, 2 to 6 years, and 6 to 12 years, respectively; for the tuna sample, the ages were 4 to 11, 4 to 6, and 6 to 11 years (Fig. 2, Table 2).

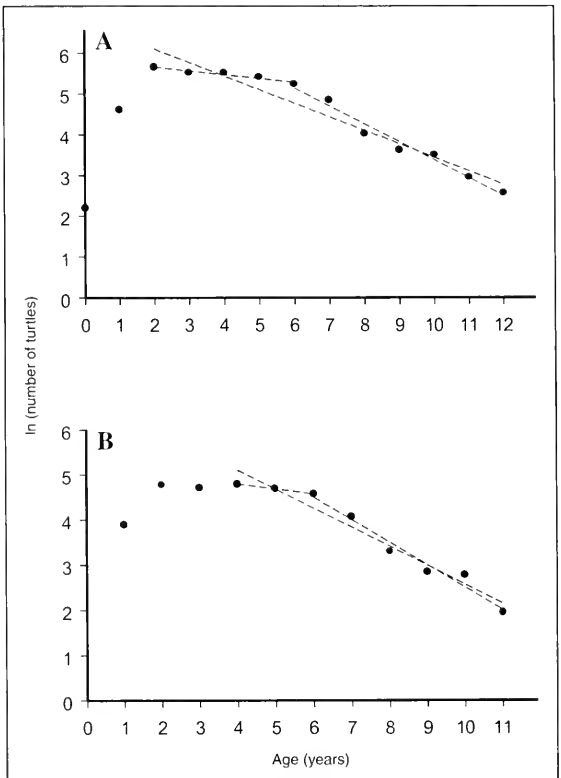

Figure 2

Catch curves for (**A**) total sample and (**B**) tuna sample. Dashed lines are linear regressions for entire sample, threshold age to age 6, and age 6 to final age (see Table 2 for regression statistics).

Discussion

Estimates of mortality and survival generated from catch curves should be interpreted with caution for several reasons. First, the analysis assumes a stable age distribution, which we cannot confirm for North Atlantic loggerhead sea turtles. Second, the analysis assumes that mortality rates were consistent over the years of the study. The similarity of the mortality and survival estimates between the total sample (1984–95) and the tuna sample (1990–92) suggests that the estimates for the total sample are not greatly affected by heterogeneity among years. Third, converting size distributions to age distributions based on a size-at-age function introduces some level of error. We believe the error from our size-at-age function is small, as discussed in Bjorndal et al. (in press).

Fourth, the analysis assumes no size or age effect on mortality rates. The catch curves for both the total sample and tuna sample reveal a size or age effect with a pivot point at age 6. This size or age effect reflects the beginning of emigration out of our study area. Loggerhead sea turtles begin to leave oceanic habitats around the Azores and recruit to neritic habitats at 7 years of age, at ~46 cm curved carapace length (Bjorndal et al., 2000, 2003). This change in slope demonstrates the fifth difficulty in interpreting catch-curve estimates: permanent emigration and mortality are confounded in the estimates. That is, declines in numbers with age, whether they are due to emigration or mortality, are included in the estimate of mortality. The confounding of emigration and mortality can introduce a major error in estimates of mortality in populations—such as sea turtle populations in oceanic and neritic habitats—that undergo developmental migrations.

Because little permanent emigration apparently occurs before the age of 7, the survival estimates for the ages prior to 7 years are our best estimates of true survival (S). As can be seen in Table 2, the estimates of total instantaneous mortality and annual survival are similar for the two samples. We believe that the estimate of S (0.911 and 0.894, respectively, for the total sample and tuna sample) would apply to the entire life stage over the size range from 20 to 65 cm CCL for most sources of mortality other than fisheries biased to large sizes, such as longline fisheries. For predation, as sea turtles increase in size, they outgrow the prey size of some fish predators, but they also grow into the prey size of the largest predators, such as killer whales and humans (although the latter source is now very low in the Azores as a result of legislation and education [senior author, personal obs.]). Death from ingestion of or entanglement in marine debris would probably not vary substantially over this size range. However, mortality from inciden-

Table 1

Size ranges of age classes and age distributions for total sample and tuna sample. CCL is curved carapace length, N_x is the number of turtles in each age class x, and YOY is young of year.

Size range (cm CCL)	Age	Total sample		Tuna sample	
		N_x	$\ln(N_x)$	N_x	$\ln(N_x)$
< 15.0	YOY	9	2.197	—	—
15.0–20.5	1	101	4.615	49	3.892
20.5–26.1	2	287	5.659	118	4.771
26.1–31.7	3	248	5.513	111	4.710
31.7–36.9	4	248	5.513	120	4.787
36.9–41.7	5	224	5.412	108	4.682
41.7–46.5	6	189	5.242	96	4.564
46.5–49.9	7	127	4.844	58	4.060
49.9–52.3	8	56	4.025	27	3.296
52.3–55.0	9	37	3.611	17	2.833
55.0–58.2	10	33	3.497	16	2.773
58.2–61.6	11	19	2.944	7	1.946
61.6–65.0	12	13	2.565	—	—

tal capture in longline fisheries in the Azores does increase with size, with the 2 to 6 year age classes experiencing very little mortality (Bolten, in press). Thus, if our estimate of S (calculated for the age classes between threshold age and age 6) were applied to the entire oceanic stage, the effect of mortality in longline fisheries, or other fisheries biased to large size classes, would be underestimated.

The estimate of 0.911 for annual survival probabilities for oceanic-stage loggerhead sea turtles in the waters of the Azores indicates high survival in this lifestage without mortality from longline fisheries. Species characterized by long life and late sexual maturity, such as loggerhead sea turtles, require very high survival throughout immature stages to maintain populations (Congdon et al., 1993; Crouse, 1999). This high probability of survival is also consistent with the theory that lower predation in oceanic habitats compared to neritic habitats is the selective pressure that maintains oceanic juvenile stages in most species of sea turtles (Bolten, 2003).

In two updated matrix models for North Atlantic loggerhead sea turtles (that differed in stage lengths), Heppell et al. (in press) derived fitted estimates of 0.745 and 0.875 for annual survival probabilities of the oceanic stage, which they defined as spanning 5 to 45 cm carapace length. Chaloupka (in press) derived an estimate of annual survival probability for oceanic-stage loggerhead sea turtles in Australia of 0.67 sampled from a logistic probability density function that ranged from 0.60 to 0.76 and had a mode at 0.67. The tuned estimate of 0.67 was derived from a stochastic simulation model that incorporated empirically based survival probability estimates for all age classes in the model except the oceanic phase (Chaloupka and Limpus, 2002; Chaloupka, in press). The estimate of 0.67 was generated for a size range from posthatchlings that have left the waters directly adjacent to the nesting beach to subadults that begin to leave the oceanic habitats at a size of 69 cm curved carapace length (Chaloupka and Limpus, 2002).

Table 2

Estimates of instantaneous mortality rates (Z) and annual apparent survival probabilities (Φ, estimated as e^{-Z}) for oceanic-stage loggerheads in the waters of the Azores generated from catch-curve analyses. r^2 (coefficient of determination) and P values are from linear regression analyses (see Fig. 2).

Age range (years)	Z	Φ	r^2	P
Total sample				
2 to 12	0.333	0.720	0.935	< 0.001
2 to 6	0.094	0.911	0.923	= 0.009
6 to 12	0.441	0.643	0.974	< 0.001
Tuna sample				
4 to 11	0.421	0.656	0.954	< 0.001
4 to 6	0.112	0.894	0.999	= 0.021
6 to 11	0.498	0.608	0.966	< 0.001

The fitted estimates for annual survival from the Heppell et al. (in press) models and the Chaloupka (in press) model are lower than the estimates in our study, but the size ranges are different. In the Heppell et al. (in press) models and the Chaloupka (in press) model, the oceanic stage includes the posthatchling phase during which loggerhead sea turtles migrate from nesting beaches to their oceanic habitats. We could not include this early posthatchling phase in our estimates of survival of oceanic-stage loggerhead sea turtles in the waters of the Azores because many turtles in this phase

have not reached the Azores and they are younger than our threshold ages. We believe that mortality in this early transitional stage when loggerhead sea turtles first cross the Atlantic may be high. In addition to high rates of predation, winds and currents can overwhelm the swimming and orientation abilities of the posthatchling sea turtles, transporting the turtles to habitats, such as waters off the British Isles, that cannot sustain them (Carr, 1986; Hays and Marsh, 1997). Generating directly derived estimates of survival probabilities of loggerhead sea turtles younger than 2 years of age should be a high priority.

Acknowledgments

This study would not have been possible without the support of our colleagues in the Azores: "Equipa Tartaruga" at the Department of Oceanography and Fisheries (DOP), University of the Azores; the captains and crews of the commercial tuna fleet based in Horta and Pico; and J. and G. Franck of the MY *Shanghai*. We thank M. Chaloupka for encouragement to pursue catch-curve analysis. We thank M. Chaloupka and J. Seminoff for comments on earlier drafts of the manuscript and P. Eliazar for technical assistance. This project was funded by the U.S. National Marine Fisheries Service and the Disney Wildlife Conservation Fund. All work was conducted in compliance with the Institutional Animal Care and Use Committee, University of Florida.

Literature cited

Bjorndal, K. A., A. B. Bolten, T. Dellinger, C. Delgado, and H. R. Martins.
2003. Compensatory growth in oceanic loggerhead sea turtles: response to a stochastic environment. Ecology 84:1237–1249.

Bjorndal, K. A., A. B. Bolten, and H. R. Martins.
2000. Somatic growth model of juvenile loggerhead sea turtles *Caretta caretta*: duration of pelagic stage. Mar. Ecol. Prog. Ser. 202:265–272.

Bolten, A. B.
1999. Techniques for measuring sea turtles. *In* Research and management techniques for the conservation of sea turtles (K. L. Eckert, K. A. Bjorndal, F. A. Abreu-Grobois, and M. Donnelly, eds.), p. 110–114. IUCN/SSC Marine Turtle Specialist Group Publication 4, Washington, DC.
2003. Variation in sea turtle life history patterns: neritic versus oceanic developmental stages. *In* Biology of sea turtles, vol. 2 (P. L. Lutz, J. A. Musick, and J. Wyneken, eds.), p. 243–257. CRC Press, Boca Raton, FL.
In press. Active swimmers—passive drifters: the oceanic juvenile stage of loggerheads in the Atlantic system. *In* Loggerhead sea turtles (A. B. Bolten and B. E. Witherington, eds.). Smithsonian Institution Press, Washington, DC.

Bolten, A. B., K. A. Bjorndal, H. R. Martins, T. Dellinger, M. J. Biscoito, S. E. Encalada, and B. W. Bowen.
1998. Transatlantic developmental migrations of loggerhead sea turtles demonstrated by mtDNA sequence analysis. Ecol. Appl. 8:1–7.

Bolten, A. B., H. R. Martins, K. A. Bjorndal, and J. Gordon.
1993. Size distribution of pelagic-stage loggerhead sea turtles (*Caretta caretta*) in the waters around the Azores and Madeira. Arquipelago 11A:49–54.

Carr, A.
1986. Rips, FADS, and little loggerheads. BioScience 36: 92–100.

Chaloupka, M.
In press. Simulation modeling of population viability for loggerhead sea turtles exposed to competing mortality risks in the western south Pacific region. *In* Loggerhead sea turtles (A. B. Bolten and B. E. Witherington, eds.). Smithsonian Institution Press, Washington, DC.

Chaloupka, M. Y., and C. J. Limpus.
2002. Survival probability estimates for the endangered loggerhead sea turtle resident in southern Great Barrier Reef waters. Mar. Biol. 140:267–277.

Congdon, J. D., A. E. Dunham, and R. C. van Loben Sels.
1993. Delayed sexual maturity and demographics of Blanding's turtle (*Emydoidea blandingii*): implications for conservation and management of long-lived organisms. Conserv. Biol. 7:826–833.

Crouse, D. T.
1999. The consequences of delayed maturity in a human-dominated world. Am. Fish. Soc. Symp. 23:195–202.

Epperly, S. P., M. L. Snover, J. Braun-McNeill, W. N. Witzell, C. A. Brown, L. A. Csuzdi, W. G. Teas, L. B. Crowder, and R. A. Myers.
2001. Stock assessment of loggerhead sea turtles of the western North Atlantic. *In* Stock assessments of loggerhead and leatherback sea turtles and an assessment of the impact of the pelagic longline fishery on the loggerhead and leatherback sea turtles of the western North Atlantic, p. 3–66. NOAA Tech. Memo. NMFS-SEFSC-455.

Frazer, N. B.
1987. Preliminary estimates of survivorship for wild juvenile loggerhead sea turtles (*Caretta caretta*). J. Herpetol. 21:232–235.

Hays, G. C., and R. Marsh.
1997. Estimating the age of juvenile loggerhead sea turtles in the North Atlantic. Can. J. Zool. 75:40–46.

Heppell, S. S., L. B. Crowder, D. T. Crouse, S. P. Epperly, and N. B. Frazer.
In press. Population models for Atlantic loggerheads: past, present and future. *In* Loggerhead sea turtles (A. B. Bolten and B. E. Witherington, eds.). Smithsonian Institution Press, Washington, DC.

Isaac, V. J.
1990. The accuracy of some length-based methods for fish population studies, 81 p. International Center for Living Aquatic Resources Management, Manila, Philippines.

Seber, G. A. F.
1982. The estimation of animal abundance and related parameters, 654 p. Macmillan Publishing Co., New York, NY.

Turtle Expert Working Group.
2000. Assessment update for the Kemp's ridley and loggerhead sea turtle populations in the western North Atlantic. U.S. Dep. Commer., NOAA Tech. Memo. NMFS-SEFSC-444, 115 p.

Developing a growth-transition matrix for the stock assessment of the green sea urchin (*Strongylocentrotus droebachiensis*) off Maine

Yong Chen
School of Marine Sciences
218 Libby Hall
University of Maine
Orono, Maine 04469
E-mail address: ychen@maine.edu

Margaret Hunter
Maine Department of Marine Resources
P.O. Box 8
West Boothbay Harbor, Maine 04575

Robert Vadas
Department of Biological Sciences
University of Maine
Orono, Maine 04469

Brian Beal
Division of Environmental and Biological Sciences
University of Maine
Machias, Maine 04654

Abstract—The green sea urchin (*Strongylocentrotus droebachiensis*) is important to the economy of Maine. It is the state's fourth largest fishery by value. The fishery has experienced a continuous decline in landings since 1992 because of decreasing stock abundance. Because determining the age of sea urchins is often difficult, a formal stock assessment demands the development of a size-structured population dynamic model. One of the most important components in a size-structured model is a growth-transition matrix. We developed an approach for estimating the growth-transition matrix using von Bertalanffy growth parameters estimated in previous studies of the green sea urchin off Maine. This approach explicitly considers size-specific variations associated with yearly growth increments for these urchins. The proposed growth-transition matrix can be updated readily with new information on growth, which is important because changes in stock abundance and the ecosystem will likely result in changes in sea urchin key life history parameters including growth. This growth-transition matrix can be readily incorporated into the size-structured stock assessment model that has been developed for assessing the green sea urchin stock off Maine.

Manuscript approved for publication 17 April 2003 by Scientific Editor.
Manuscript received 26 June 2003 at NMFS Scientific Publications Office.
Fish Bull. 101:737–744 (2003).

The green sea urchin (*Strongylocentrotus droebachiensis*) fishery is the state's fourth largest fishery by value, worth $20.3 million to harvesters in 1999. The fishery is managed by limited entry, a limited number of opportunity dates that are established each year by recommendation of the sea urchin zone council (SUZC), and minimum and maximum size limits. The fishery is further regulated seasonally by two zones that correspond to variation in spawning time along the coast (Vadas et al., 1997).

The Maine sea urchin fishery began in the late 1980s and reached its peak in landings in 1992. It has since experienced a continuous decline in landings, mainly resulting from large decreases in sea urchin stock abundance (Fig. 1). Although the large decrease in abundance is evident in many studies (Steneck and Vadas[1]; Harris[2]) and apparent to the sea urchin fishing industry, the catch-per-unit-of-effort (CPUE) data derived from the fishery have shown no significant decreases over the last 10 years (Fig. 1). We need to perform a formal stock assessment to better understand the population dynamics of the sea urchin stock and to develop an optimal management strategy.

A population dynamics model for the sea urchin stock should provide reliable estimates of model parameters with suitable statistical methods (Hilborn and Walters, 1992; Chen and Paloheimo, 1998; Walters, 1998). A size-structured population dynamics model is needed for the sea urchin fishery because sea urchins are difficult to age and growth varies widely among individuals (Quinn and Deriso, 1999).

One of the key components of a size-structured population dynamics model is a growth-transition matrix, which describes the probability of an organ-

[1] Steneck, R., and R. L. Vadas. 2002. Personal commun. School of Marine Sciences, University of Maine, Orono, ME 04469.
[2] Harris, L. 2002. Personal commun. Department of Zoology, University of New Hampshire, Durham, NH 03824.

size growing from one size class to another size class in a given unit of time (Sullivan et al., 1990; Sullivan, 1992). In practice, two approaches can be used to incorporate a growth-transition matrix into a stock assessment: one is to incorporate the growth-transition matrix and simultaneously estimate matrix parameters with parameters that describe other biological processes in the fishery (Sullivan et al., 1990), and the other approach is to estimate the growth-transition matrix independent of other stock assessment models (Chen et al., 2000). The former considers covariance among different processes by estimating all parameters simultaneously, but makes the analysis more complicated. The latter approach reduces the complexity of modeling but does not consider the covariance of growth and other biological processes. Because size-structured models are often complicated and have many parameters to be estimated, the estimation of a growth-transition matrix outside the main modeling process may be preferable (Chen et al., 2000). In either case, the quality of the growth-transition matrix can greatly influence the quality of the stock assessment. It is thus essential to develop a growth-transition matrix for the Maine sea urchin stock that can capture the variations in growth increments among individuals.

The information required in estimating a growth-transition matrix includes the mean growth increment in a given unit of time and its associated variation for sea urchins of different sizes. Because growth rates of sea urchins vary with size, growth increments also vary with size, and this variation in growth with size is rarely constant. This has been implicit in the statements of model assumptions in many papers (e.g. Sullivan et al., 1990; Sullivan, 1992, Quinn and Deriso, 1999). However, because the variance for growth increments is difficult to estimate, it is often assumed to be constant for organisms of different sizes (Quinn and Deriso, 1999). Such an assumption of constant variation in growth increment is rather unrealistic and may introduce biases in estimating a growth-transition matrix. Thus, for the Maine sea urchin we need to develop an approach that can explicitly consider nonconstant variances for growth increments of sea urchins of different sizes.

Growth of the sea urchin along the Maine coast has not been studied extensively and the data are limited. The data we used for this study were from Vadas et al. (2002) who collected size-at-age data on sea urchins in two habitats (barren and kelp) from three areas along the coast of Maine.

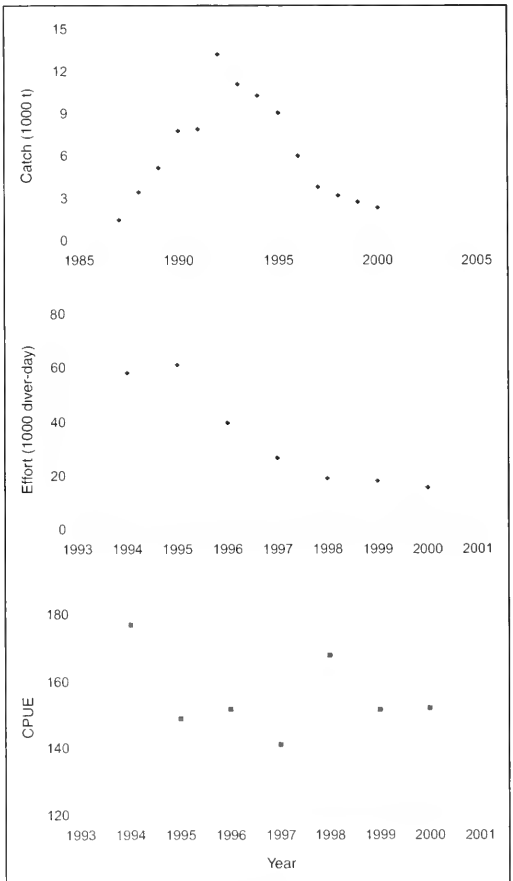

Figure 1

Observed catch measured in metric tons, effort measured in diver-hours, and catch per unit of effort measured in pounds per diver-hour for the sea urchin fishery in management zone 2 in Maine. Zone 1 has a similar temporal pattern.

Methods and materials

Previous studies have indicated that many environmental variables might influence the growth of the sea urchin (Meidel and Scheibling, 1998; Russell, 1998). Sea urchins in favorable habitats, feeding on preferred seaweeds, grow faster than those feeding on less favorable algae and mussels, and sea urchins on barren grounds grow slower. Even in the same habitat, different rates of growth were identified (Vadas, 1977). Previous studies divided the coast of Maine into three regions, northeast, center, and southwest (Vadas et al., 1997). For each region, sea urchin samples were randomly taken from two habitats, barren and kelp. Size-at-age data were collected in 1997–98 for sea urchins in each habitat and area (Vadas and Beal[3]). Detailed descriptions about the derivation of size and age

[3] Vadas, R. L., and B. F. Beal. 1999. Temporal and special variability in the relationships between adult size, maturity and fecundity in green sea urchins: the potential use of a roe-yield standard as a conservation tool. Report to the Maine Department of Marine Resources, Augusta, Maine 04333.

information, justification for dividing the Maine coast, and selection of the habitats can be found in Vadas et al. (1997) and Vadas et al. (2002).

Vadas et al. (1997) modeled the size-at-age data using the von Bertalanffy growth function (VBGF) described as

$$L_t = L_\infty(1 - e^{-K(t-t_0)}), \quad (1)$$

where L_t = size at age t;
L_∞ = defined as the mean asymptotic length that the sea urchin may attain;
K = the Brody growth parameter; and
t_0 = the hypothetical age of size 0 (Ricker, 1975).

For each area and habitat, a VBGF was used to fit the size-at-age data. Three parameters in the VBGF (i.e. L_∞, K, and t_0) and their standard errors were estimated by using the nonlinear least squares method. These estimates were presented in Vadas and Beal[3] and Vadas et al. (2002), and were made available to the authors of the present study (Table 1). Clearly there were large differences in the estimates of L_∞ and K and their associated variations among different areas and habitats (Table 1).

The L_∞'s estimated for different areas and habitats ranged from 63.1 (northeast region with barren habitat) to 95.2 mm (southeast region with kelp habitat) (Table 1) and tended to be smaller than some large individuals observed in the fishery (about 100 mm, Vadas, 1977; Hunter, unpubl. data). This likely resulted from relatively small sample sizes that covered relatively small areas, in a relatively short period, compared with the fishery catch, which targeted larger-size individuals. The exclusion of individuals in the fishery catch that were larger than the L_∞'s estimated in Vadas and Beal[3] and Vadas et al. (2002) from the calculation of the growth-transition matrix may underestimate the variability in sea urchin growth, thus introducing errors in stock assessment. Based on the data collected in the Maine sea urchin fishery (Hunter, unpubl. data) and previous studies (Vadas, 1977), 100 mm was considered a reasonable value for the average asymptotic size (L_∞) for sea urchins on the coast of Maine. However, more extensive sampling needs to be done in the future to verify this estimate.

We might be able to derive an estimate of L_∞ for the Maine sea urchin stock based on the examination of the data collected from the fishery and other studies (Ricker, 1975; Moreau, 1987; Chen et al., 1992). An estimate of K for the whole Maine urchin stock is, however, more difficult because K is an abstract rate describing how fast organisms approach the L_∞ and there are no observations or background information with which to compare estimates (Ricker, 1975; Moreau, 1987). We thus need to develop an approach to estimate K for the Maine sea urchin stock which corresponds to the value we assumed for the L_∞. Many studies have indicated that estimates of K and L_∞ tend to be highly and negatively correlated (e.g. Moreau, 1987; Chen and Harvey, 1994). Thus, a fish population or species with a large L_∞ tends to have a low K value, and *vice versa* (Gallucci and Quinn, 1979; Chen et al., 1992). This suggests a strong relationship between L_∞ and K estimates

Table 1

The average asymptotic size (L_∞) and Broady growth coefficient (K) estimated for different areas and habitats along the coast of Maine in the study done by Vadas et al. (1997, 2002). Coefficient of variation (CV) was calculated by using Equation 2.

		Parameter		Coefficient of variation (CV)	
Area	Habitat	L_∞	K	CV(L_∞)	CV(K)
Northeast	Barren	63.1	0.1404	0.242	1.209
Northeast	Kelp	88.5	0.1263	0.224	0.543
Center	Barren	67.0	0.2315	0.084	0.354
Center	Kelp	63.4	0.3268	0.065	0.248
Southeast	Barren	80.1	0.1776	0.099	0.397
Southeast	Kelp	95.2	0.1181	0.128	0.338

(Pauly, 1980; Stergiou, 1993). Such a relationship may be used to estimate K for a given L_∞ or to estimate L_∞ for a given K. In this study we developed and used the following empirical approach to derive K for a given value of L_∞ and its associated uncertainties in the development of a growth-transition matrix: 1) conduct a regression analysis for K and L_∞ estimated for different areas and habitats along the coast of Maine (Table 1); 2) calculate coefficients of variation (CV) for each K and L_∞ (Table 1) as

$$\mathrm{CV}(K) = \frac{\text{standard error for } K}{K}, \text{ and}$$
$$\mathrm{CV}(L_\infty) = \frac{\text{standard error for } L_\infty}{L_\infty}, \quad (2)$$

and conduct a regression analysis of CV(K) and CV(L_∞) estimates of different areas and habitats (data in Table 1); 3) use 100 mm to approximate L_∞ and use this L_∞ to estimate K from the regression analysis between K and L_∞; and 4) calculate the average CV for L_∞'s of different areas and habitats and then use the average CV(L_∞) to estimate CV(K) from the CV(K)–CV(L_∞) regression equation.

Because K and L_∞ were estimated for different areas and habitats and had different precisions, outliers might arise in the regression analyses. To avoid possible bias introduced by outliers, we used a reweighted least squares (RLS) method for the regression analyses (Chen et al., 1994). This method involves conducting a robust least median of squares (LMS) analysis to identify outliers (Rousseeuw and Leroy, 1987) and justifying the identified outliers by using background information, followed by a weighted LS analysis where justified outliers are weighted by 0 and other data have a weight of 1 (Chen et al., 1994). In the two regression analyses (i.e. steps 1 and 2), L_∞ and CV(L_∞) were used as the independent variables and K and CV(K) were used as the dependent variables. The reason for this choice (instead of the other way around) is that L_∞ is often estimated more reliably and with much smaller

variations (Chen et al., 1992; also see Table 1), whereas K is often less reliably estimated (Moreau, 1987). One of the basic assumptions for a regression analysis is that the independent variable is error free. In practice, this assumption is often relaxed when the independent variable has a much smaller error than the dependent variable (McArdle, 1988). The violation of the normal distribution assumption for the errors in the regression analyses may bias the test for the significance of the regression model and its parameters using common parametric tests (F- or t-tests), but does not necessarily result in biases in the regression analysis (Sen and Srivastava, 1990)."

Given K and L_∞, the growth increment during a unit of time (i.e. year) can be calculated as

$$\Delta L_n = (L_\infty - L_n)(1 - e^{-K}), \tag{3}$$

where K and L_∞ are the true values without errors; n indexes size class; and L_n is the middle point of the n^{th} size class. With Equation 3, we can develop two approaches to estimate the growth-transition matrix. One approach is a Monte Carlo simulation. We can randomly sample H sets of K and L_∞ values from their joint distributions (thus consider their covariance) and then use them in Equation 3 to calculate H sets of ΔL for each size group. We can then derive the probability distribution for ΔL from these H sets of ΔL values for each size group. The Monte Carlo simulation approach is straightforward but requires extensive calculations, in particular when there are a large number of size groups. It is also inconvenient to update the growth-transition matrix when there are new growth data or large changes in growth due to changes in the environment. The second approach is analytic and not so straightforward, but it is easy to update with new information and is less computationally intensive. It is likely that the growth-transition matrix for the Maine sea urchin fishery will need to be updated because of possible changes in growth caused by changes in the sea urchin population size and its ecosystem. Thus we used the second approach, which is described as follows.

Assuming the uncertainties associated with the VBGF parameters L_∞ and K are ΔL_∞ and ΔK respectively, where, $\Delta L_\infty \in N(0, \sigma^2_{L_\infty})$ and $\Delta K \in N(0, \sigma^2_K)$, we have

$$L_\infty = \overline{L}_\infty + \Delta L_\infty \text{ and } K = \overline{K} + \Delta K, \tag{4}$$

where $\overline{L}_\infty$ and $\overline{K}_\infty$ are the estimated parameters. Replacing the true values of L_∞ and K in Equation 3 with Equation 4 and using the approximation $e^{\Delta X} \approx 1 + \Delta X$ for small ΔX, we have

$$\Delta L_n \approx (\overline{L}_\infty - L_n)(1 - e^{-K}) + \left[\Delta L_\infty (1 - e^{-K}) - (\overline{L}_\infty - L_n)\Delta K e^{-K} - \Delta L_\infty \Delta K e^{-K}\right] = \overline{\Delta L}_n + \varepsilon_n, \tag{5}$$

where

$$\overline{\Delta L}_n = (\overline{L}_\infty - L_n)(1 - e^{-\overline{K}}) \tag{6}$$

$$\varepsilon_n = \Delta L_\infty (1 - e^{-\overline{K}}) - (\overline{L}_\infty - L_n)\Delta K e^{-\overline{K}} - \Delta L_\infty \Delta K e^{-\overline{K}}. \tag{7}$$

Thus, the expected (mean) value of ΔL_n is $\overline{\Delta L}_n$ and variance of ΔL_n can be estimated from Equation 7 as

$$\mathrm{Var}(\overline{\Delta L}_n) = \sigma^2_{L_\infty}(1 - e^{-\overline{K}})^2 + (\overline{L}_\infty - L_n)^2 \sigma^2_K e^{-2\overline{K}} - 2\mathrm{Cov}(L_\infty, K)(1 - e^{-\overline{K}})(\overline{L}_\infty - L_n)e^{-\overline{K}}. \tag{8}$$

Items with the order of three and above for ΔL_n and ΔK are omitted in deriving Equation 8 from Equation 7. From Equation 8, it is clear that the variance of the growth increment varies among different size classes.

From $\overline{\Delta L}_n$ estimated in Equation 6, an expected average yearly growth increment was calculated for each size class. The variability for the average yearly growth increment was assumed to follow a normal distribution with a mean of $\overline{\Delta L}_n$ and variance of $\mathrm{Var}(\overline{\Delta L}_n)$ estimated from Equation 8. This distribution was used to determine the vector of probabilities of growing from size class k to other size classes. If d_{low} and d_{up} are the lower and upper ends of size class d, the probability of a sea urchin growing from size class n to size class d can be computed as

$$P_{n \to d} = \int_{d_{low}}^{d_{up}} f(x \mid \overline{\Delta L}_n, \mathrm{Var}(\Delta L_n))dx, \tag{9}$$

where x is a random variable having a density probability distribution defined by $f(x \mid \overline{\Delta L}_n, \mathrm{Var}(\Delta L_n))$ with its expected value of $\overline{\Delta L}_k$ and variance of $\mathrm{Var}(\overline{\Delta L}_k)$ (Quinn and Deriso, 1999). In the present study we assumed that the x variable was a normal density distribution function with a mean of $\overline{\Delta L}_k$ defined by Equation 6 and with a variance of $\mathrm{Var}(\overline{\Delta L}_k)$ defined by Equation 8. The probability of a sea urchin growing from one size to another was estimated for all size classes to form the matrix. Negative growth increments were not permitted. The largest size class acts as a plus group; therefore sea urchins in this group have a probability of 1 of remaining in the group. The model contains 61 size classes, each with 1-mm interval width, ranging from 40 mm in size (midpoint value for size class from 39.5–40.5 mm) to 100 mm.

Because no negative growth was allowed, the summation of the probabilities of a sea urchin of size class k growing into all other size classes was smaller than 1 (because the normal distribution is symmetric). This problem was avoided by standardization which involved dividing the probability of an urchin in a given size class n growing into each size class by the summation of the probabilities of growing from a given size n to all the size classes. All calculations were done in MS-Excel© (Microsoft Office 2000, Microsoft Corporation, Redmond, WA). A worksheet for estimating a growth-transition matrix as described above is available upon request.

Results

The LMS analysis suggested that the logarithmic K and L_∞ data for the barren habitat in the Southwest area was an outlier in the K and L_∞ regression analysis (Fig. 2). The estimated K and L_∞ values for the barren habitat in the Southwest had CVs over 120% and 24%, respectively, much

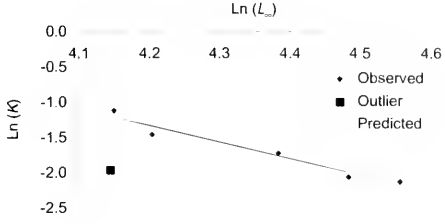

Figure 2

The regression analysis of logarithmic K and L_∞ for different locations and habitats of Maine sea urchins.

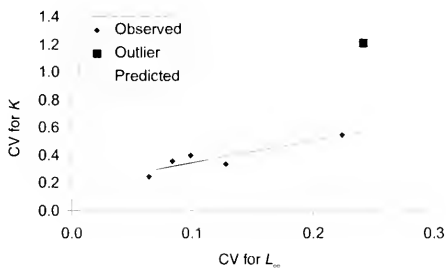

Figure 3

The regression analysis of CVs for K and L_∞ for different locations and habitats of Maine sea urchins.

larger than the estimates for other locations and habitats (Table 1). This was the only site where the K estimate was not significantly different from 0 (thus the VBGF was not significant). We thus concluded that this data point was an outlier because of the poor fit of the VBGF, and subsequently it was given a zero weight in the RLS analysis. The RLS regression equation for K and L_∞ was estimated by

$$Ln(K) = 8.653 - 2.3777\ Ln(L_\infty),$$
$$P=0.0038, \text{adj. } r^2=0.94. \quad (10)$$

The standard deviations for the intercept and slope were 1.2605 and 0.28923, respectively. The P value for Equation 10 indicates that the regression model is significant. The adj. r^2 is the coefficient of determination adjusted for the sample size, suggesting 94% of the variance in ln(K) could be explain by the model.

The LMS analysis of the CVs of parameters K and L_∞ also suggested that the barren habitat in the southwest area was an outlier because it had an exceptionally large CV for K (Fig. 3). We thus concluded that this data point was an outlier and should be given a weight of zero in the RLS analysis. The RLS regression equation for the CVs of parameters K and L_∞ was estimated by

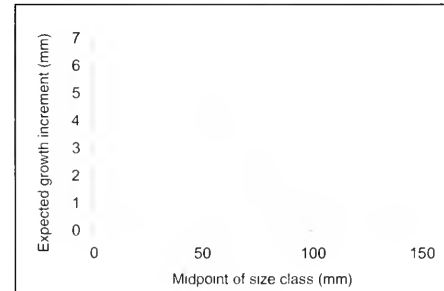

Figure 4

The expected annual growth increment for Maine sea urchins of different size classes.

$$CV(K) = 0.189 + 1.5602\ CV\ (L_\infty),$$
$$P=0.034, \text{adj. } r^2 = 0.76. \quad (11)$$

The standard deviations for the intercept and slope were 0.0561 and 0.42319, respectively. The P value suggested the regression model was significant ($P<0.05$). The value of r^2 suggests 76% of the variance in CV(K) could be explained by the model.

The average CV for L_∞'s of different areas and habitats was 15%. The L_∞ was assumed to have a value of 100 mm in this study as discussed previously. This gave the L_∞ a standard error estimate of 15.0 mm, making its 95% confidence intervals 70 mm to 130 mm. The K value was estimated to be 0.1006 using Equation 10 and L_∞ of 100 mm. Using Equation 11 and the CV for L_∞, the CV for K was estimated to be 42.3%, which yielded the value of 0.0426 for the standard error for K.

The annual expected growth increment decreased quickly with sea urchin size (Fig. 4). The largest expected annual increment was 6 mm for the smallest size class (39.5–40.5 mm) included in the study. The variance for annual growth increments calculated by using Equation 8 was large for small sea urchins. It decreased initially with size, reaching the smallest value at the 59 mm size class (58.5–59.5 mm), followed by a progressive increase with size (Fig. 5). The expected annual growth increment for the largest size class included in this study had the highest variance, which was over eight times as high as the smallest variance (Fig. 5).

The probability distribution of annual growth increment varied among size classes (Fig. 6), reflecting the differences in variances associated with different size classes. The last size class was a plus class, with the probability of staying in the same size class being 1. Figure 6 clearly indicated that no negative growth was allowed.

Discussion

Great variation in growth was observed in the Maine sea urchin stock (Vadas et al., 2002). Such a pattern of variation was reflected in estimating the VBGF parameters for dif-

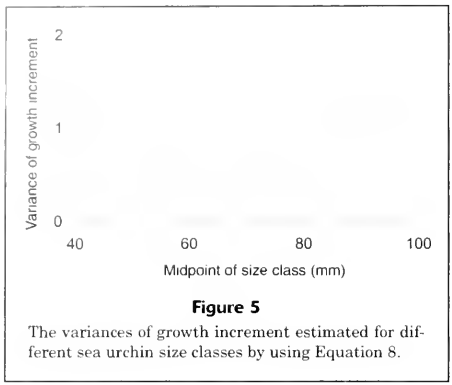

Figure 5

The variances of growth increment estimated for different sea urchin size classes by using Equation 8.

ferent areas and habitats (Table 1). Large standard errors were estimated for the VBGF parameters for sea urchins of the same area and habitat, and large differences occurred in the estimated VBGF parameters between different areas and habitats (Table 1). The approach developed in the present study considered observations made in both the fishery and scientific studies and provided a systematic way to incorporate the large variation in growth into the estimation of a growth-transition matrix, and subsequently into the sea urchin stock assessment.

It should be noted that the algorithm developed for estimating the variance of growth increments is approximate, and violations of the assumptions used in deriving the algorithm may introduce errors in estimating a growth-transition matrix. For example, large errors in estimating K and L_∞ will introduce errors in Equation 5, which was derived by assuming small errors for the two growth parameters. Nonnormal distribution of ΔL with its mean defined by Equation 6 and variance defined by Equation 8 will also result in errors in developing a growth-transition matrix. Other factors that may influence the quality of the estimated growth transition matrix include errors in estimating CVs for K, L_∞ estimated from Equations 10 and 11, and omitting high order items in deriving Equation 8.

Unlike most studies in which the variance for the annual growth increment was assumed to be the same for all size classes (Quinn and Deriso, 1999), our study explicitly suggested that the variance for the annual growth increment changed with size (Fig. 4). The differences in the variance were large between size classes, and changed nonlinearly with size. If a constant variance were used for all size classes, the variance in growth increment would be severely underestimated for large and small fish. This could introduce large biases in a stock assessment.

Size-dependent variation might better describe the variation in annual growth increment. Fish in small size classes tend to grow fast, but their growth tends to be more susceptible to environmental variation than adult growth, often resulting in large variation among individuals (Summerfelt and Hall, 1987). Fish in large size classes (older fish) have to divert some energy to reproduction but tend to have considerable variation in energy allocation strategies among individuals. Differences among adults in the ability to grow can also be considerable because of genetics, specific growth patterns during juvenile stages, and differences in energy allocation between growth and maturation during younger ages (Nikolskii, 1969). This difference may cause large variations in growth for large and old fish (Summerfelt and Hall, 1987; Chen et al., 1988). Compared with old and young ages, growth rates for medium-size and medium-age fish may be less varied (Nikolskii, 1969). This pattern can be reflected realistically in the estimated variation by using the approach derived in our study.

Although the choice of L_∞ was a bit arbitrary in our study, it reflects observations from both the fishery and scientific studies. The largest sea urchins observed in the different scientific studies tend to be smaller than 100 mm, as indicated by the estimated L_∞ values for different areas and habitats (Fig. 1). The inability to observe larger sea urchins in scientific studies may result from relatively small sample sizes, the focus of research (small areas), and the large growth variations even in small spatial scales. The data collected from the fishery were more extensive and covered more areas. This, together with the tendency for taking large individuals in the fishery, may suggest that large individuals are more likely to appear in the fishery, rather than in scientific studies. Thus, it may be reasonable to set the expected value of L_∞ at 100 mm. Also, this higher value corresponds more closely to the upper growth estimates for green sea urchins from the northeast Pacific (Vadas, 1977). The CV was assumed to be 15% for L_∞, resulting in the 95% confidence interval of L_∞ ranging from 70 mm to 130 mm. This range was believed to be a reasonable estimate for the maximum attainable length for green sea urchins on the coast of Maine (Vadas, 1977).

The approach developed in our study can be readily used to incorporate the VBGF parameters estimated from different studies. This can be accomplished by rerunning the regression analyses between K and L_∞ and between CVs for K and L_∞. As more information about the growth of sea urchins on the coast of Maine becomes available, the growth transition matrix can be easily updated to reflect the variation identified in newer studies. The flexibility and ability to easily update and incorporate new information makes this approach desirable to the Maine sea urchin fishery, which is currently undergoing large changes in its population size and has only limited growth data.

The value of 100 mm chosen for L_∞ was rather arbitrary. However, because we considered the negative correlation between K and L_∞ in deriving the growth transition matrix, a small error in the L_∞ estimate would not change the growth-transition matrix greatly. In the future, however, we can conduct a systematic sampling of the stock across its geographical range and derive some forms of weighted average size with a composite variance that captures the range of sizes exhibited by the species. Such an approach would provide us with a better estimate of L_∞.

The growth-transition matrix developed in our study summarizes the growth patterns of sea urchins along the coast of Maine. It can be updated whenever new growth data become available. It can be readily incorporated into

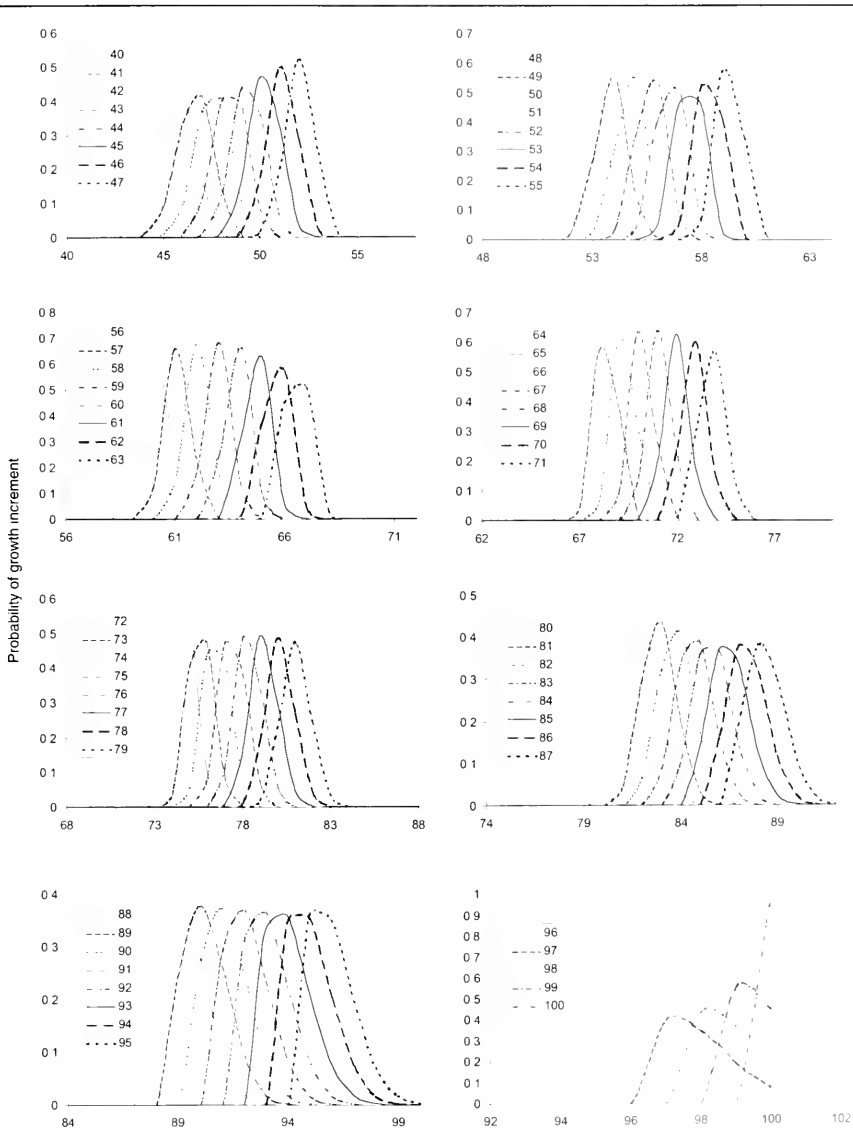

Figure 6

Probabilities of sea urchins growing from one size class to others. Each probability distribution was labeled with the midpoint value of the current size class of the sea urchin.

a size-structured stock assessment model to evaluate the status of sea urchin stock and to evaluate alternative management strategies for the Maine sea urchin fishery (Chen and Hunter, 2003).

Acknowledgments

We would like to thank the Maine Department of Marine Resources, the Northeast Consortium, and the Maine Sea Urchin Zone Council for supporting this study. Constructive and detailed comments from two anonymous reviewers and the scientific editor greatly improved an early version of the manuscript, for which we are grateful.

Literature cited

Chen, S., S. Watanabe, and K. Takagi.
1988. Growth analysis on fish population in the senescence with special reference to an estimation of age at end of reproductive span and life span. Bull. Jpn. Soc. Sci. Fish. 54:1567–1572.

Chen, Y., P. Breen, and N. Andrew.
2000. Impacts of outliers and mis-specification of priors on Bayesian fisheries stock assessment. Can. J. Fish. Aquat. Sci. 57:2293–2305.

Chen, Y., and H. H. Harvey.
1994. Maturation of white sucker, *Catostomus commersoni*, populations in Ontario. Can. J. Fish. Aquat. Sci. 51: 2066–2076.

Chen, Y., and M. Hunter.
2003. Assessing the green sea urchin (*Strongylocentrotus drobachiensis*) stock in Maine, USA. Fish. Res. (Amst.) 60:527–537.

Chen, Y., D. A. Jackson, and H. H. Harvey.
1992. A comparison for von Bertalanffy and polynomial functions in modeling fish growth data. Can. J. Fish. Aquat. Sci. 49:1228–1235.

Chen, Y., D. A. Jackson, and J. E. Paloheimo.
1994. Robust regression approach to analyzing fisheries data. Can. J. Fish. Aquat. Sci. 51:1420–1429.

Chen, Y., and J. E. Paloheimo.
1998. Can a more realistic model error structure improve parameter estimation in modelling the dynamics of fish populations? Fish. Res. (Amst.) 38: 9–19.

Gallucci, V. F., and T. J. Quinn II.
1979. Reparameterizing, fitting, and testing a simple growth model. Trans. Am. Fish. Soc. 108:14–25.

Hilborn, R., and C. Walters.
1992. Quantitative fisheries stock assessment: choice, dynamics, and uncertainty, 570 p. Chapman and Hall, New York, NY.

McArdle, B. H.
1988. The structural relationship: regression in biology. Can. J. Zool. 66:2329–2339.

Meidel, S. K., and R. E. Scheibling.
1998. Size and age structure of the sea urchin *Strongylocentrotus droebachiensis* in different habitats. *In* Echinoderms (R. Mooi, M. Telford, eds.), p 737–742. Proceedings of the 9th international echinoderm conference; San Francisco, 5–9 August 1996. A. A. Balkema, Rotterdam, Netherlands.

Moreau, J.
1987. Mathematical and biological expression of growth in fishes: recent trends and further developments. *In* The age and growth of fish (R. C. Summerfelt and G. E. Hall (eds.), p 81–113. Iowa State Univ. Press, Ames, IA.

Nikolskii, G. V.
1969. Theory of fish population dynamics, 323 p. Oliver & Boyd, Edinburgh, UK.

Pauly, D.
1980. On the interrelationships between natural mortality, growth parameters and mean environmental temperature in 175 fish stocks. J. Cons. Int. Explor. Mer 39:175–192.

Quinn, T. J., II, and R. B. Deriso.
1999. Quantitative fish dynamics, 542 p. Oxford Univ. Press, New York, NY.

Ricker, W. E.
1975. Computation and interpretation of biological statistics of fish populations, 382 p. Bull. Fish. Res. Board Can., vol. 191.

Rousseeuw, P. J., and A. M. Leroy.
1987. Robust regression and outlier detection, 352 p. John Wiley & Sons, New York, NY.

Russell, M. P.
1998. Resource allocation plasticity in sea urchin: rapid diet induced, phenotypic changes in the green sea urchin, *Strongylocentrotus droebachiensis* (Muller). J. Exp. Mar. Biol. Ecol. 220:1–14.

Sen, A. K., and M. S. Srivastava.
1990. Regression analysis: theory, methods and applications, 350 p. Springer-Verlag, New York, NY.

Stergiou, K. I.
1993. Nutrient-dependent variation in growth and longevity of the red bandfish, *Cepola macrophthalma* (L.), in the Aegean Sea. J. Fish Biol. 42:633–644.

Sullivan, P. J.
1992. A Kalman filter approach to catch-at-length analysis. Biometrics 48:237–257.

Sullivan, P. J., H. L. Lai, and V. F. Gallucci.
1990. A catch-at-length analysis that incorporates a stochastic model of growth. Can. J. Fish. Aquat. Sci. 47:184–198.

Summerfelt, R. C., and G. E. Hall.
1987. The age and growth of fish, 530 p. Iowa State Univ. Press, Ames, IA.

Vadas, R. L.
1977. Preferential feeding: an optimization strategy in sea urchins. Ecol. Monogr. 47:337–371.

Vadas, R. L., B. Beal, S. Dudgeon, and W. Wright.
1997. Reproductive biology of green sea urchins along the coast of Maine: final report, 59 p. Maine Cooperative Extension Service and Maine Sea Grant Program, Orono, ME.

Vadas, R. L., B. Smith, B. Beal, and T. Dowling.
2002. Sympatric growth morphs and size bimodality in the green sea urchin (*Strongylocentrotus droebachiensis*). Ecol. Monogr. 72:113–132.

Walters, C. J.
1998. Evaluation of quota management policies for developing fisheries. Can. J. Fish. Aquat. Sci. 55:2691–2705.

Reproductive biology of the blue swimmer crab (*Portunus pelagicus*, Decapoda: Portunidae) in five bodies of water on the west coast of Australia

Simon de Lestang
Norman G. Hall
Ian C. Potter

Centre for Fish and Fisheries Research
Division of Science and Engineering
Murdoch University
South Street
Murdoch, Western Australia 6150
E-mail: (for S. de Lestang): simond@murdoch.edu.au

Abstract—*Portunus pelagicus* was collected at regular intervals from two marine embayments and two estuaries on the lower west coast of Australia and from a large embayment located approximately 800 km farther north. The samples were used to obtain data on the reproductive biology of this species in three very different environments. Unlike females, the males show a loosening of the attachment of the abdominal flap to the cephalothorax at a prepubertal rather than a pubertal molt. Males become gonadally mature (spermatophores and seminal fluid present in the medial region of the vas deferentia) at a very similar carapace width (CW) to that at which they achieve morphometric maturity, as reflected by a change in the relative size of the largest cheliped. Logistic curves, derived from the prevalence of mature male *P. pelagicus*, generally had wider confidence limits with morphometric than with gonadal data. This presumably reflects the fact that the morphometric (allometric) method of classifying a male *P. pelagicus* as mature employs probabilities and is thus indirect, whereas gonadal structure allows a mature male to be readily identified. However, the very close correspondence between the CW_{50}'s derived for *P. pelagicus* by the two methods implies that either method can be used for management purposes. *Portunus pelagicus* attained maturity at a significantly greater size in the large embayment than in the four more southern bodies of water, where water temperatures were lower and the densities of crabs and fishing pressure were greater. As a result of the emigration of mature female *P. pelagicus* from estuaries, the CW_{50}'s derived by using the prevalence of mature females in estuaries represent overestimates for those populations as a whole. Estimates of the number of egg batches produced in a spawning season ranged from one in small crabs to three in large crabs. These data, together with the batch fecundities of different size crabs, indicate that the estimated number of eggs produced by *P. pelagicus* during the spawning season ranges from about 78,000 in small crabs (CW=80 mm) to about 1,000,000 in large crabs (CW=180 mm).

Manuscript approved for publication 19 June 2003 by Scientific Editor.
Manuscript received 26 June 2003 at NMFS Scientific Publications Office.
Fish. Bull. 101:745–757 (2003).

Portunid crabs, such as *Portunus pelagicus*, *Scylla serrata*, and *Callinectes sapidus*, form the basis of important commercial and recreational fisheries. The blue swimmer crab (*P. pelagicus*) is found in sheltered nearshore marine waters and estuaries throughout the Indo-West Pacific (Stephenson, 1962; Kailola et al., 1993). In Australia, the commercial catches of this portunid have increased greatly during the last 20 years, and annual catches in 1998 reached 4377 metric tons (t) (Anonymous, 2000). The commercial fishery for *P. pelagicus* in Western Australia is the largest in Australia; the catch in the 1999–2000 financial year weighed 673 t and fetched a wholesale price of approximately $A3 million (CAES[1]).

Large numbers of portunids frequently enter estuaries as juveniles and remain there for an extended period (Hill, 1975; Potter et al., 1983; Perkins-Visser et al., 1996; Potter and de Lestang, 2000). Although female portunids sometimes become ovigerous in estuaries, such individuals emigrate into coastal marine waters, where they release their eggs (Van Engel, 1958; Metcalf et al., 1995; Potter and de Lestang, 2000). In contrast, the individuals of those assemblages of portunids that occupy marine embayments often do not leave these marine environments to spawn and, in cases where there is a salinity gradient, they spawn in the high salinity regions of those systems (e.g. Campbell, 1984; Sumpton et al., 1994; Prager, 1996; Potter and de Lestang, 2000).

The most common method for determining the size at which male crabs attain maturity is to estimate the size at which the pattern of growth of one of its appendages changes from that which characterizes juvenile crabs to that which characterizes adult crabs (e.g. Hartnoll, 1974; Somerton, 1980; Reeby et al., 1990; Muiño et al., 1999). However, this indirect approach is not precise and requires careful measurements of a considerable number of individuals covering a wide size range. Despite the fact that macroscopic characters can be used to distinguish sequential stages in the development of the vas deferentia of portunids (Ryan, 1967a; Meagher, 1971), few studies have attempted to use such staging to determine the body size at which the gonads of male crabs attain maturity (e.g. Reeby et al., 1990). Sumpton et al. (1994) considered that, as in female *P. pelagicus*, a marked loosening of the attachment of the abdominal flap to the cephalothorax signaled the attainment of maturity in male *P. pelagicus*. However, this criterion has yet to be shown to be valid for the males of this species. Although variations in the size at which crustaceans reach maturity among bodies of water and geographical regions may reflect,

[1] CAES (Department of Fisheries, Catch and Effort Statistics). 2002. Unpubl. data. Western Australian Department of Fisheries, Catch and Effort Statistics. Fisheries Western Australia, WA Marine Research Laboratories, West Coast Drive, Waterman, 6020, Perth, Australia.

in part, differences in such features as genetic composition and density, there is a strong overall tendency for the size at maturity of this crustacean to be inversely related to water temperature (Pillai and Nair, 1971; Jones and Simons, 1983; Polovina, 1989; Dugan et al., 1991; Miliou, 1996; Somerton and Donaldson, 1996; Fisher, 1999).

Estimates of the fecundity of crabs have typically been based on the number of eggs in a single batch of eggs (e.g. Potter et al., 1983; Melville-Smith, 1987; Ingles and Braum, 1989). However, such an approach does not take into account the fact that female crabs often produce more than one batch of eggs during a spawning season (Van Engel, 1958; Pillai and Nair, 1971; Campbell, 1984).

The aims of this study were as follows. 1) Compare the results of three methods directed at determining whether male *P. pelagicus* have attained maturity and elucidate whether each method produces reliable results. 2) Compare aspects of the reproductive biology of *P. pelagicus* in two estuaries and two marine embayments in temperate Australia with those of this species in a large marine embayment in a much warmer and more northern subtropical environment. Particular emphasis will be placed on comparing the size at maturity of both sexes and the periods during which ovigerous females are present, and on proposing reasons for the significance of any differences between the assemblages in these five bodies of water. 3) Use the data collected for one of the marine embayments to determine the age and time of year at which *P. pelagicus* becomes mature and develop a method for deriving the annual fecundity that takes into account the fact that the larger individuals of this species are believed to produce more than one batch of eggs in a spawning season.

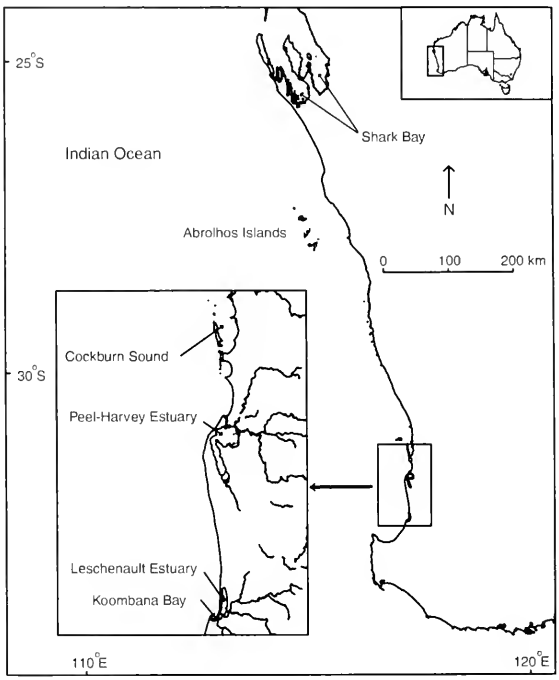

Figure 1

Map showing locations of the five bodies of water in which *Portunus pelagicus* was sampled on the west coast of Australia. The map of Australia (insert top right) shows the location (box) of the five bodies of water, and the map of the lower west of Australia (insert bottom left) shows the location of the four bodies of water sampled in this region.

Materials and methods

Sampling regimes

Up to 100 *Portunus pelagicus* were collected monthly for two years from the Leschenault Estuary (May 1997–April 1999), Koombana Bay, and Cockburn Sound (June 1998–May 2000), for three years from the Peel-Harvey Estuary (May 1995–April 1998), and bimonthly for two years from Shark Bay (July 1998–May 2000). The first four bodies of water are located on the lower west coast of Australia, approximately 800 km to the south of Shark Bay (Fig. 1). The nearshore, shallow waters in each of these bodies of water (water depth <1.5 m) were sampled for *P. pelagicus* by using a 21.5-m seine net with a bunt of 3-mm mesh; whereas offshore deeper waters were sampled by employing a small otter trawl net with a codend of 25-mm mesh and crab traps consisting of either 12- or 76-mm mesh (see Potter and de Lestang, 2000 for further details of the nets and traps). The mean water depths at the deeper offshore sites of the above five bodies of water were 3, 9, 19, 3, and 10 m, respectively. The water temperature at the bottom of the water column at each site was recorded on each sampling occasion.

Measurements and changes at puberty

The carapace width (CW) of each crab, i.e. the distance between the tips of the two lateral spines of the carapace, was measured to the nearest 1 mm. The length and height of the propodus of the largest cheliped, the length of the merus of the second walking leg, and the length of the primary pleopod of each male crab in Cockburn Sound and Shark Bay were measured to the nearest 0.1 mm. Because the relationship between the length of the dorsal propodus of the largest cheliped and the width of the carapace showed the greatest change over the size range of male crabs, that structure was chosen for allometric analysis to determine the size at which males become morphometrically mature.

Sex of small crabs, i.e. with a CW < about 30 mm, was determined with a dissecting microscope to ascertain whether their pleopods bore setae and thus the crabs were females. At CWs > about 30 mm, the female crabs could readily be distinguished from male crabs by their possession of a far wider abdominal flap (Van Engel, 1958; Warner 1977). During the pubertal molt of female portunids, the abdominal flap changes from a triangular to oval shape and from being tightly to loosely fixed to the cephalothorax (Ryan, 1967b; Fielder and Eales, 1972; Ingles and Braum, 1980; Fisher, 1999).

The size and time of occurrence of all ovigerous females were recorded. The ovary of each crab was assigned to one of four stages by using macroscopic characters similar to those described for the development of the ovaries of *P. pelagicus* and other portunids (Ryan, 1967b; Meagher, 1971; Krol et al., 1992; Kumar et al.[2]). The assignment of these stages was augmented by examining the characteristics of a subset of 200 of these ovaries in 6-μm histological sections that had been stained with Mallory's trichrome. For 5–10 ovaries of each macroscopic stage, the diameters of 30 randomly selected oocytes that had been sectioned through the nucleus were measured to the nearest 5 μm. Two measurements (the longest diameter and shortest diameter) for each oocyte were then averaged to provide an estimate of each oocyte diameter.

Male crabs were designated as either morphometrically immature or mature by using differences in the regression equations for the relationships between the natural logarithms of the length of the dorsal propodus of their largest cheliped and carapace width in what were clearly either juvenile (small and gonadally immature) or adult crabs (large and gonadally mature). For full description of the method see Somerton (1980).

On the basis of their macroscopic appearance, the vas deferentia of each male crab were assigned to one of three stages by using criteria derived from the description of gonadal development for *P. pelagicus* by Meagher (1971) and for *P. sanguinolentus* by Ryan (1967a). Aquarium studies by Meagher (1971) showed that male crabs with gonads at stages I and II did not copulate and are thus considered immature, whereas those with gonads at stage III copulated successfully with females and thus have mature gonads.

Ovaries and vas deferentia from a wide size range of at least 20 females and 20 males, respectively, from each sampling occasion in each of the five bodies of water were weighed to the nearest 0.01 g. The mean gonad weight at a constant carapace width for each sex in each month in each water body was determined by using analysis of covariance (ANCOVA) of the natural logarithm of the gonad weight as the dependent variable, month as a fixed factor, and the natural logarithm of the carapace width as a covariate. The common constant carapace width of crabs in all bodies of water was a default value calculated by the ANCOVA.

Size frequency and reproductive data for the corresponding months in the different years in each water body were pooled for describing intra-annual trends in these variables.

Size at maturity

The percentages of female crabs of different carapace widths which, in each water body, had undergone a pubertal molt, were subjected to logistic regression to determine the size at which 50% of the female crabs would have become mature *sensu* Hartnoll (1974). Data for each assemblage were randomly resampled and analyzed to create 1000 sets of bootstrap estimates of the parameters of the logistic regression and estimates of the probability of maturity within the range of recorded carapace widths. The 95% confidence intervals of the CW_{50}'s were derived by using this resampling technique, which produced slightly more conservative estimates than those obtained from the Hessian matrix of the logistic regression and thus reflected better the uncertainty of the parameter that was associated with the data. The 95% confidence intervals of the probability of maturity at each specified carapace width were taken as the 2.5 and 97.5 percentiles of the corresponding predicted values resulting from this resampling analysis. The point estimate of each parameter and of each probability of maturity at the specified carapace width were taken as the medians of the bootstrap estimates.

The percentages of mature male crabs at different carapace widths in each of the five bodies of water, with maturity being assigned by using firstly morphometric and then gonadal criteria (see earlier), were subjected to logistic regressions to determine the CW_{50}'s for these variables. The percentages of male crabs in Cockburn Sound and Shark Bay, which possessed an abdomen that was loosely fixed to the cephalothorax, were likewise subjected to logistic regression analysis. The logistic regressions relating maturity and carapace width for both the females and males in the different assemblages were compared by using a likelihood ratio test, as described by Cerrato (1990) and employing a Bonferroni correction.

Fecundity

The total wet weight of eggs in each batch of eggs of 40 early-stage ovigerous females, i.e. with yellow eggs, from Cockburn Sound and which covered a wide size range, was weighed to the nearest 0.001 g. The number of eggs in each of four replicate subsamples from each batch were recorded, after which each of those subsamples was weighed to the nearest 0.001 g. These data were then used to estimate the total number of eggs in each batch of eggs of each female. The relationship between batch fecundity (BF) and carapace width (CW) was described by using the equation $\ln BF_i = m \ln CW_i + b$.

The number of batches of eggs produced by a full size range of mature females during the spawning period was estimated by determining the spawning period (SP),

[2] Kumar, M., Y. Xiao, H. Williams, G. Ferguson, G. Hooper, and S. Venema. 1999. Blue crab fishery. South Australian Fisheries Assessment Series, 99/02, 64 p. South Australian Research Development Institute, Grenfell Centre Level 14, 25 Grenfell Street Adelaide 5000, Australia.

defined as the time (days) when > 5% of all mature females were ovigerous, and the proportions of ovigerous females among all mature females in sequential 10-mm CW intervals during the spawning period. The proportion of ovigerous females (O_j) in the jth size class during this period also represents the average time a mature female in this size class is ovigerous during that period and takes into account the fact that an ovigerous female spawns at least once during a spawning period and that the brood period (BP) of an ovigerous female is about 18 days at 20°C (Meagher, 1971). Thus, the mean number of batches (NB_j) produced by the mature female crabs in the jth size class during a spawning period (average water temperature 20.4°C) can be estimated with the equation $NB_j=O_jSP/BP$.

The relationship between number of broods and carapace width was described empirically by fitting a modified logistic curve, $NB=1+Nb_{max}/\{1+\exp[-\ln(19)(CW-a)/(b-a)]\}$, ranging upwards from a minimum of one batch to a maximum of $1+NB_{max}$ batches, where a and b are parameters. The total fecundity of crabs at different carapace widths was calculated as the product of batch fecundity, BF, and the number of broods, NB, by using the relationships between BF and CW and NB and CW, as described above.

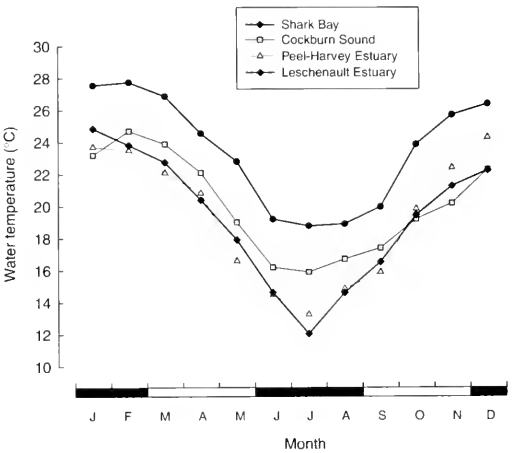

Figure 2

Mean monthly water temperatures for sampling sites in Shark Bay, Cockburn Sound, Peel-Harvey Estuary, and Leschenault Estuary (water temperatures in Koombana Bay were essentially the same as those in Leschenault Estuary). Mean monthly water temperatures in each water body were derived from data pooled for at least two years. The black rectangles on the x axis refer to summer and winter months and open rectangles to autumn and spring months.

Results

Water temperature

Mean monthly water temperatures at the bottom of the water column in the Leschenault Estuary, Peel-Harvey Estuary, Cockburn Sound, and Shark Bay followed the same trends, with values rising to a maximum in mid to late summer and declining to a minimum in mid-winter (Fig. 2). Water temperatures in Koombana Bay were essentially the same as those in Leschenault Estuary. Although the mean monthly water temperatures in the Leschenault and Peel-Harvey estuaries and Koombana Bay in corresponding months were similar, they were lower in these bodies of water than in Cockburn Sound in eight of the twelve months of the year (Fig. 2). However, the mean water temperatures in each month in Shark Bay were greater than those in the corresponding months in each of the above four more southern bodies of water. Thus, for example, although the maximum mean monthly water temperature was 28°C in Shark Bay, it never reached 25°C in any of the other bodies of water (Fig. 2). Likewise, the minimum monthly water temperature was greater in Shark Bay (19°C) than in either Cockburn Sound (16°C) or the Leschenault and Peel-Harvey estuaries (12–13°C).

Macroscopic and histological gonad staging

Macroscopic examination of the gonads of a large number of females and males of *P. pelagicus*, covering a wide size range, and, in the case of females, an histological examination of the ovaries of a subset of these crabs, showed that the ovaries and vas deferentia could be classified into four and three developmental stages, respectively (Tables 1 and 2).

Size at sexual maturity

The minimum carapace widths of female crabs that had undergone their pubertal molt ranged from 61 mm in both the Peel-Harvey Estuary and Shark Bay to 84 mm in the Leschenault Estuary. Although the CW_{50}'s derived for females at maturity in Cockburn Sound (86.4 mm) and Koombana Bay (86.9 mm) were not significantly different ($P>0.05$), both of these values were significantly less ($P<0.05$) than the 92.0 mm for females in Shark Bay (Fig. 3). The high CW_{50}'s for female crabs in the Peel-Harvey (97.5 mm) and Leschenault estuaries (98.0 mm) were not representative of females in their populations as a whole (see "Discussion" section).

The relationships between the dorsal length of the largest cheliped and carapace width of male *P. pelagicus* in each of the five bodies of water were described better by using two log-log lines (Fig. 4A) rather than a single log-log line. The CW_{50}'s of male crabs at morphometric maturity in the four bodies of water on the lower west coast, estimated with data obtained from an allometric approach and employing the above log-log regressions, ranged only from 86.2 mm in the Peel-Harvey Estuary and Cockburn

Table 1

Morphological characteristics of macroscopic stages in the development of the ovaries of *Portunus pelagicus* and the types of oocytes found in each of those stages. Mean diameters of oocytes at different stages in development are shown in parentheses.

Maturity stage	Macroscopic appearance of ovary	Types of oocytes
I Immature	Relatively small, flattened and off white to ivory in color. Anterior region is small, and does not displace the hepatopancreas. The central "H" shaped region, located in the gastric region, is loosely joined to the dorsal surface of the spermathecae. The posterior section, located in the cardiac and intestinal regions, forms two parallel lobes.	Loosely packed oocytes, comprising oogonia (5 μm) and, to a lesser extent, chromatin nucleolar oocytes (10 μm) and perinucleolar oocytes (30 μm). These three types of oocytes are found in each of the next three ovarian stages.
II Early development	Conspicuously larger than stage-I ovaries, pale yellow, oval in cross section and slightly nodulated. The anterior region marginally displaces the hepatopancreas and the central region envelops the dorsal surface of the spermathecae, and the two lobes of the posterior region are starting to become convoluted.	Yolk-vesicle oocytes (90 μm) are present for the first time.
III Late development	Large, yellow, and nodulated. Anterior region displaces the hepatopancreas, and the central and posterior regions occupy almost all of the space in the gastric, posterior and intestinal cavities. Most of the spermathecae are enveloped by ovarian tissue.	Early yolk-granule oocytes (130 μm) surround small areas of early stage oocytes, and some late yolk vesicle oocytes are present.
IV Fully mature	Very large, deep yellow to orange, and highly nodulated. Hepatopancreas is now completely displaced from its former position by the enlargement of the anterior region of the ovary. The gastric, posterior, and intestinal cavities are completely filled with the enlarged central and posterior sections of the ovary. The spermathecae are totally enveloped by the ovary.	Advanced oocytes all at the late yolk-granule stage (250 μm).

Table 2

Morphological characteristics of stages in the development of the vas deferens of *Portunus pelagicus* and the location of spermatophores in those stages.

Maturity stage	External appearance of vas deferentia	Histological appearance of the vas deferentia
I Immature I	Vas deferentia not detectable macroscopically.	NA
II Immature II	Anterior vas deferentia (AVD) becoming enlarged, middle and posterior vas deferentia (MVD and PVD, respectively) straight and opaque.	Spermatophores present in AVD. MVD and PVD contain no spermatophores.
III Mature I	AVD and MVD enlarged and white and PVD enlarged and convoluted but still opaque.	Spermatophores present in AVD and MVD. PVD contains no spermatophores.

Sound to 87.2 mm in the Leschenault Estuary (Fig. 4B). The CW_{50}'s for each of these bodies of water, which were not significantly different ($P>0.05$) from each other, were significantly less at $P < 0.05$ or 0.001 than the 96.0 mm determined for male crabs in Shark Bay.

The CW_{50}'s for males at gonadal maturity in each water body, derived from the prevalence of males with mature gonads, i.e. stage III (Fig. 4C), differed by only 0.3 to 2.2 mm from those derived for males in each corresponding water body by using the prevalence of morphometrically mature males (Fig. 4B). The CW_{50}'s derived for male crabs from gonadal data in the four southern bodies of water, which ranged only from 86.5 to 88.4 mm, did not differ significantly ($P>0.05$). However, on the basis of gonadal data, each of these CW_{50}'s differed significantly at $P<0.05$, 0.01, or 0.001 from the 97.0 mm estimated for male crabs in Shark Bay (Fig. 4C). These trends were parallel to those derived from morphometric data (Fig. 4B).

The logistic curves derived from gonadal data in each of the four southern bodies of water were significantly differ-

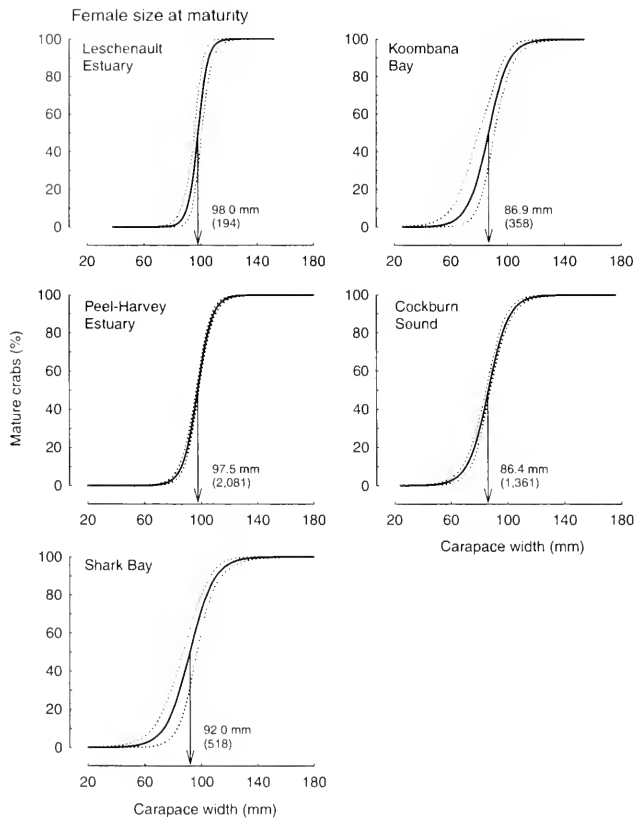

Figure 3

Logistic regressions and their 95% confidence limits fitted to percentage contributions of those adult females which, at each size, had undergone their pubertal molt in each of the five bodies of water sampled in Western Australia. Arrows and measurements denote CW_{50}'s and the numbers in parentheses refer to the number of crabs used to create the regressions.

ent ($P>0.05$) and had steeper slopes than those determined by using morphometric data (Fig. 4). The confidence limits for the logistic curves constructed from gonadal data were also usually tighter than those constructed from morphometric data.

The CW_{50} for male crabs with a loose abdominal flap in Cockburn Sound, i.e. 72.1 mm, differed significantly ($P<0.05$) from that in Shark Bay, i.e. 76.2 mm (data not shown). However, all of the male crabs in Cockburn Sound with carapace widths of 70 to 75 mm and loosely attached abdominal flaps contained gonads at stage I or II and were thus immature.

Trends exhibited by gonad weights and proportions of ovigerous females

The mean monthly gonad weight of mature female crabs with a standard carapace width (104 mm), as determined by ANCOVA (see "Material and methods" section), rose to a sharp peak of about 5 g in October in Koombana Bay and in September in Cockburn Sound (Fig. 5). In contrast, the mean monthly gonad weights of mature female crabs in the Leschenault and Peel-Harvey estuaries remained at <1.5 g and did not tend to peak sharply at any time of the year. The mean monthly gonad weights of mature female

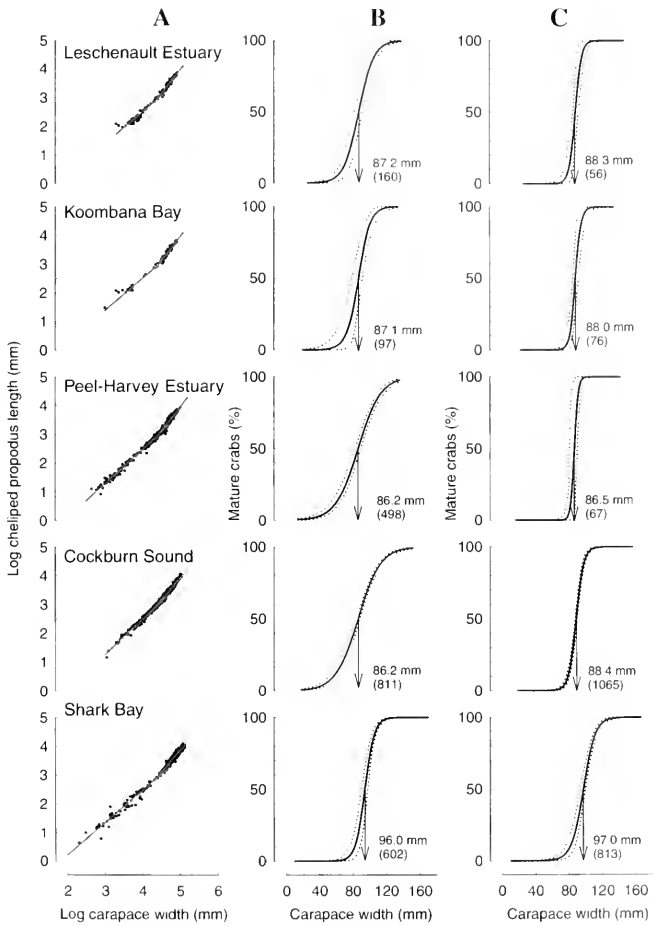

Figure 4

Maturity data for male *Portunus pelagicus* in the five bodies of water sampled in Western Australia. (**A**) Relationship between the natural log of length of the dorsal propodus of the largest cheliped and the natural log of carapace width. Logistic regressions and their 95% confidence limits were fitted to percentage contributions of those adult males, which, at each size, were (**B**) morphometrically mature and (**C**) possessed mature gonads. Arrows and measurements denote CW_{50}'s and the numbers in parentheses refer to the number of crabs used to create the regressions.

crabs in Shark Bay did not peak sharply at any time and were > 1 g in all but two of the ten months in which this embayment was sampled (Fig. 5).

The mean monthly gonad weights of male crabs with a standard carapace width of 118.4 mm, as determined by ANCOVA, varied little and never exceeded 1 g in any of the five bodies of water (data not shown). However, they did reach their maxima at a similar time of the year, i.e. late summer (February) or early autumn (March), in the four bodies of water on the lower west coast of Australia.

The monthly percentage contributions made by ovigerous female crabs from all mature female crabs in Koom-

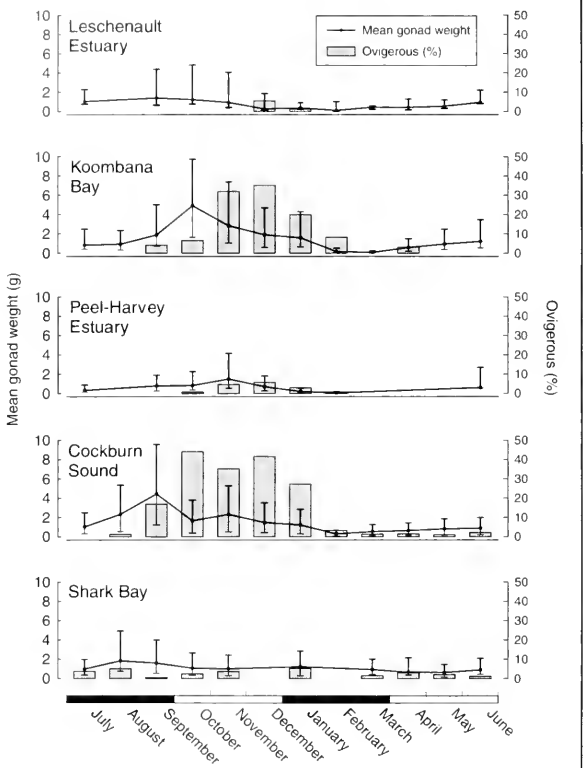

Figure 5

Mean monthly gonad weights ±95% confidence intervals for female *Portunus pelagicus* and the percentage of ovigerous females among all adult female *P. pelagicus* in the five bodies of water sampled. The black rectangles on the *x* axis refer to summer and winter months and open rectangles to autumn and spring months.

bana Bay and Cockburn Sound peaked at 32–36% in November and December in Koombana Bay and at 35–45% in October to December in Cockburn Sound. Although the corresponding percentage contributions of ovigerous female crabs were far lower in the Leschenault and Peel-Harvey estuaries than in the above two embayments, they still reached their maxima at the same time of the year (Fig. 5). Few or no ovigerous female crabs were caught in either of those estuaries or embayments between March and August. Ovigerous females were found in Shark Bay in each of the ten months in which that embayment was sampled and, unlike the situation in the two more southern marine embayments, their monthly contributions to the overall number of adult female crabs did not vary markedly throughout the year (Fig. 5).

Trends exhibited by oocyte development

The maximum diameter of the oocytes increased progressively from 95 μm in stage-I gonads to 315 μm in stage-IV gonads (data not shown). The modal oocyte diameter of the distinct and largest cohort of oocytes in stage IV (240–259 μm) was only slightly less than that of the fertilized yellow external eggs found under the abdominal flap of ovigerous females (300–319 μm). The most advanced oocytes in ovaries at stages III and IV were at the early and late yolk-granule stage, respectively. The presence of two distinct size cohorts of oocytes in the ovaries of large females with grey eggs under their abdomen (i.e. eggs that had been fertilized for several days) is consistent with the view that large female *P. pelagicus* are multiple spawners.

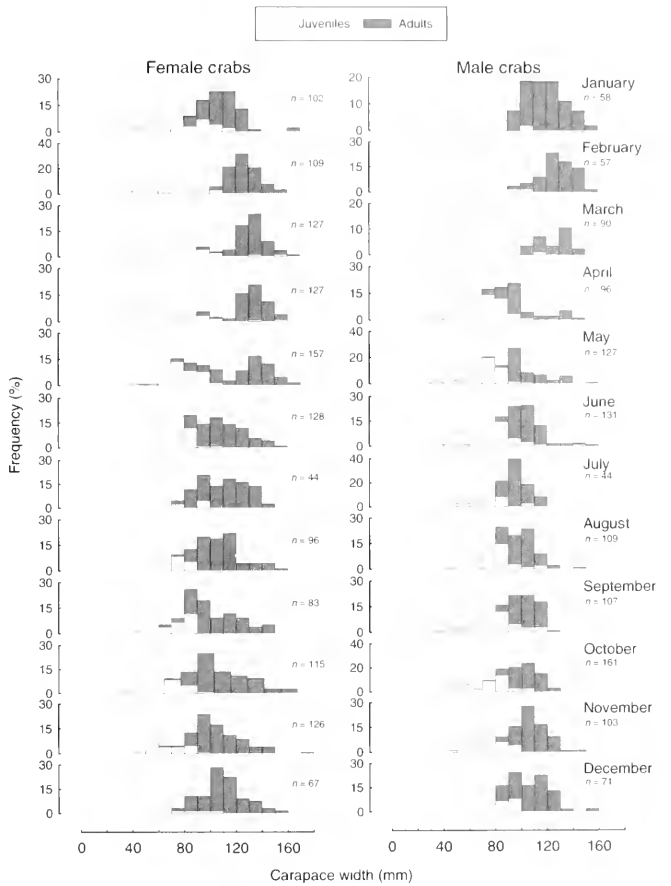

Figure 6

Frequency histograms for the carapace widths of juvenile and adult females and males of *Portunus pelagicus* in Cockburn Sound. *n* = number of crabs measured. Designation of males as mature was based on gonadal criteria described in the text.

Age and time of sexual maturation of *Portunus pelagicus*

The carapace-width frequency data for *P. pelagicus* in inshore and offshore waters in Cockburn Sound demonstrated that, in this marine embayment, males are represented by two main size cohorts in January and February (Fig. 6). The first size cohort represents the 0+ age class that resulted from the spawning period that commenced in the previous August–September, whereas the second cohort corresponds to 1+ crabs, which start to decline markedly in numbers after February and are rarely represented after June (Fig. 6). Although similar trends are exhibited by the data for females, the numbers of 1+ individuals of this sex remained higher for a longer period, i.e. until May. The above trends are entirely consistent with those reported in detailed studies of the age composition and growth of *P. pelagicus* in the Peel-Harvey Estuary (Potter et al., 1983) and Leschenault Estuary (Potter and de Lestang, 2000).

None or very few of the female and male 0+ crabs caught in Cockburn Sound in January, February, and March were mature. However, some of the larger 0+ crabs had become mature by May, i.e. when they would mostly have been

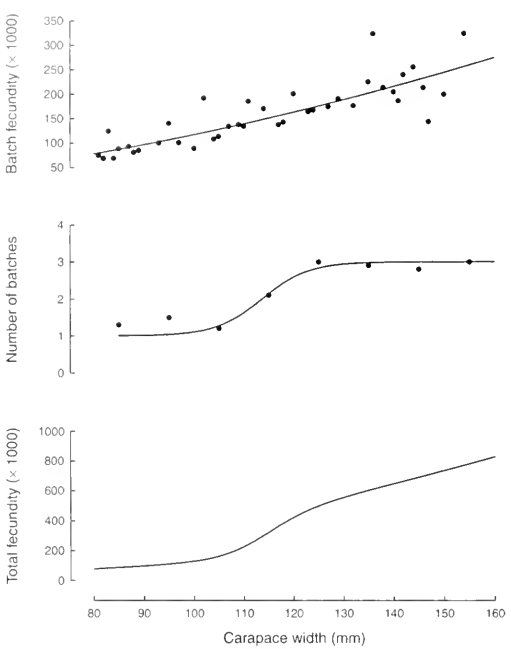

Figure 7

Batch fecundity, mean number of batches, and total fecundity of *Portunus pelagicus* in Cockburn Sound.

between four and eight months old (Fig. 6). The prevalence of mature crabs subsequently increased, with the result that the vast majority of crabs in the following January, i.e when they had just entered their second year of life, were mature (Fig. 6). Thus, all crabs have typically become mature when they are just over one year old.

Fecundity

In Cockburn Sound, the number of eggs recorded for a single batch of eggs under the abdomen of a female, ranged from 68,450 in a crab with a CW of 84 mm to 324,440 in a crab with a CW of 154 mm (Fig. 7). The relationship between batch fecundity (*BF*) and carapace width (*CW*) is described by the following equation: $\ln BF = 1.8208 \ln CW + 3.2862$.

The estimated mean number of egg batches, produced by female crabs in the different size classes over the spawning period, ranged from about one in crabs of 100–109 mm CW to about three in crabs of 150–159 mm CW (Fig. 7). A range of one to three batches per instar corresponds to that recorded by Campbell (1984) for *P. pelagicus* in aquaria experiments. The empirical relationship between the number of batches (NB) and carapace width (CW) is described by $NB_j = 1 + 2/\{1 + \exp[-\ln(19)(CW_j - 113.7)/13.8]\}$.

A combination of the equations for the relationships between batch fecundity and CW and the number of egg batches and CW was then used to determine the relationship shown between total fecundity (TF) and carapace width (CW) and which is shown in Figure 7.

Discussion

Designation of maturity in male crabs

Aquaria studies by Meagher (1971) demonstrated that male crabs with gonads at stage III, i.e. with spermatophores and seminal fluid in the medial vas deferentia, can copulate successfully with females. Because this parallels the situation recorded by Comeau and Conan (1992) for the snow crab (*Chionoecetes opilio*), we likewise regard such gonads as mature. Our study also showed that, because male *P. pelagicus* still possess immature gonads (stage II) when their abdominal flap becomes loosely attached to the cephalothorax, the latter change occurs at a prepubertal

molt and thus, unlike the supposition of Sumpton et al. (1994), does not coincide with the attainment of maturity. The situation in males thus contrasts with that in female *P. pelagicus*, in which the abdominal flap becomes loose as an outcome of the pubertal molt (Fielder and Eales, 1972; Campbell, 1984; Potter and de Lestang, 2000; Smith[3]).

The very close similarity between the corresponding CW_{50}'s derived for male *P. pelagicus* in each of the five bodies of water by using morphometric and gonadal data demonstrates that morphological and gonadal maturity are attained by this species at essentially the same carapace width. However, the question of whether a male crab of about the size of maturity has become morphometrically mature depends on determining whether the relative length of one of its appendages is closer to the regression line which relates the length of that appendage to the carapace width in either juvenile or adult crabs. Because the overall relationship between cheliped length and carapace width of *P. pelagicus* does not undergo a marked shift at around the attainment of maturity, the use of the allometric method never enabled us to determine with absolute certainty whether, in the region of size overlap, a male was morphometrically immature or mature. The lack of precision, when determining maturity with morphometric data, could account for the slopes of the logistic curves for the prevalence of "mature" individuals of *P. pelagicus* derived from these morphometric data in the four southern bodies of water being shallower than those obtained from gonadal data.

From the above, it follows that there would be an advantage in determining the CW_{50}'s for male *P. pelagicus* at maturity by using data on gonadal state obtained by the simple and direct procedure of examining the vas deferentia, rather than relying on data obtained by an allometric method that is indirect and relies on a careful measurement of the appendage lengths and carapace dimensions of a considerable number of individuals. However, the remarkable similarities between the CW_{50}'s derived by using morphometric and gonadal data show that, if it is desirable to avoid damaging the crabs, the data obtained from allometric analysis does yield a close approximation of this important measure for *P. pelagicus*. Thus, the CW_{50} derived from either gonadal or morphometric data for male *P. pelagicus* can be used for developing management plans for this species.

The very close correspondence between the size at which gonadal and morphometric maturity are attained by the males of *P. pelagicus* contrasts with the situation recorded by Comeau and Conan (1992) and Sainte-Marie et al. (1997) for the males of the snow crab *Chionoecetes opilio*. In this latter species, the males attain gonadal maturity at a smaller body size than that at which morphometric maturity is attained following the terminal molt. The males of *C. opilio* with large cheliped and large body size are at a competitive advantage over smaller males when courting (Comeau and Conan, 1992; Sainte-Marie et al., 1997). Because the aquaria studies of Campbell (1984) have shown that the large males of *P. pelagicus* also have a similar competitive advantage during courting, a male of this species with mature gonads and differentiated chelipeds may not be able to compete for females successfully if larger males are present.

Influence of migration on estimates of CW_{50} for female crabs

The mean monthly gonad weights recorded for post-pubertal individuals were less for females in estuaries than in marine embayments, strongly indicating that females often tend to emigrate from the estuaries to their spawning grounds before their gonads are fully developed (Van Engel, 1958; Potter and de Lestang, 2000). Such an emigration from estuaries by mature female *P. pelagicus* reduces the proportion of mature individuals within each carapace width interval, thereby increasing the proportion of immature females in these class intervals. This shifts the logistic curve to the right and consequently increases the CW_{50}, which accounts for the significantly greater CW_{50}'s derived for females in estuaries than in marine environments on the lower west coast of Australia. For this reason, subsequent comparisons of the CW_{50}'s for female crabs in the different bodies of water will focus on those derived for assemblages in the three marine embayments.

In contrast to the CW_{50}'s for females, the CW_{50}'s for males at maturity in the two estuaries and the two marine embayments on the lower west coast of Australia were not significantly different. This presumably reflects the fact that, unlike mature females, the large males of *P. pelagicus* tend to remain in estuaries during the spawning period (Potter and de Lestang, 2000).

Influence of temperature on reproductive biology

The CW_{50}'s derived for males at "maturity" in each of the five bodies of water never differed by more than 2.2 mm, irrespective of whether gonadal or morphometric data were used. However, the maximum CW_{50}'s determined for males in the two estuaries and two embayments by using gonadal and morphometric data, i.e. 88.4 mm for Cockburn Sound and 87.2 mm for the Leschenault Estuary, respectively, were 8.6 and 8.8 mm less than the corresponding CW_{50}'s determined for males in Shark Bay. Furthermore, the CW_{50}'s for female *P. pelagicus* in Koombana Bay and Cockburn Sound were 5.6 and 5.1 mm, respectively, less than that of females in Shark Bay.

The greater CW_{50}'s for *P. pelagicus* in Shark Bay than in the other four bodies of water, which are located approximately 800 km farther south, runs counter to the generalization that the CW_{50}'s for decapods tend to be inversely related to water temperature (e.g. Campbell and Robinson, 1983; Jones and Simons, 1983; Dugan et al., 1991). However, the opposite situation has sometimes been recorded and, in those cases, has been attributed to differences among populations of one or more of the following: density, predation pressure, and food availability (Hines, 1989; Polovina, 1989; Pollock, 1995; McGarvey et al., 1999). It thus appears relevant that the mean density of *P. pelagicus* was far lower

[3] Smith, H. 1982. Blue crabs in South Australia—their status, potential and biology. Report 6, p. 33–51. South Australian Fisheries Industry Council Grenfell Centre Level 14, 25 Grenfell Street Adelaide 5000, Adelaide, Australia.

in the sampling sites in Shark Bay, 0.6 crabs/100 m^2, than those in Cockburn Sound and Koombana Bay, 2.80 and 2.94 crabs/100 m^2, respectively. The mean density in Shark Bay was also far lower than those recorded in the Leschenault and Peel-Harvey estuaries between the middle of spring and middle of autumn, when *P. pelagicus* colonizes estuaries (Potter et al., 1983; Potter and de Lestang, 2000). Furthermore, commercial or recreational fishing pressure (or both), which leads to a reduction in CW_{50}'s at maturity in the spiny lobster (Polovina, 1989), is far greater for *P. pelagicus* in the southern bodies of water than in Shark Bay (Bellchambers[4]). Recent work with microsatellite DNA has also shown that the assemblages of *P. pelagicus* in Shark Bay are genetically distinct from those in more southern bodies of water, such as Cockburn Sound and the Peel-Harvey Estuary (Chaplin et al.[5]).

The marked differences between the CW_{50}'s at maturity for *P. pelagicus* in Shark Bay and bodies of water farther south emphasize the need for managers to take into account this type of variation when determining a minimum legal carapace width (MLCW) for capture. However, the current MLCW for *P. pelagicus* in Western Australia, 127 mm, is well above even the CW_{50} for this species at maturity in Shark Bay.

The prevalence of ovigerous females did not peak sharply at any time of the year in Shark Bay, whereas ovigerous females were found predominantly during spring and summer in Cockburn Sound and Koombana Bay. Moreover, the mean monthly gonad weights of a female *P. pelagicus* of standard carapace width lay within a relatively narrow range of 0.9 to 1.8 g in Shark Bay, whereas they rose to a sharp peak of about 5 g in spring and fell below 1 g in some months in Cockburn Sound and Koombana Bay. The trends exhibited by the reproductive variables of female *P. pelagicus* thus provided strong evidence that reproductive activity extends over much or all of the year in Shark Bay, whereas it occurs predominantly in spring and summer in the two southern embayments. The more protracted spawning period in Shark Bay presumably reflects the presence of higher water temperatures throughout the year and in particular during winter and early spring. Such a conclusion is consistent with the results of other studies, which have shown that water temperature influences ovulation and egg development in *P. pelagicus* and other decapods (Rahaman, 1980; Campbell, 1984; Pollock, 1995; Kumar et al.[2]).

Fecundity

The vast majority of previous estimates of the fecundity of crustaceans have been based on the number of eggs borne by females at a particular time which, in the case of multiple spawners, does not take into account the fact that larger crabs can produce two or more batches of eggs within a spawning period. The few previous attempts to obtain the total fecundity of crustaceans have involved tracking the number of batches of eggs borne by particular individuals at different times (e.g. Chubb et al.[6]). The advantage of the approach developed during the current study is that it uses a combination of batch fecundity and an estimate of the number of batches produced during the spawning period by female *P. pelagicus* of different carapace widths to determine the relationship between the total fecundity and body size of this species in a given population. Because the older crabs have a far longer intermolt period between copulation and egg extrusion than younger crabs, i.e. eight versus four months, they have a far greater amount of time to accumulate the energy reserves required to produce eggs. This difference accounts for the greater number of egg batches produced by larger than small crabs.

[4] Bellchambers, L. 2002. Personal commun. Fisheries Western Australia, WA Marine Research Laboratories, West Coast Drive, Waterman, 6020, Perth, Australia.

[5] Chaplin, J., E. S. Yap, E. Sezmis, and I. C. Potter. 2001. Genetic (microsatellite) determination of the stock structure of the blue swimmer crab in Australia. FRDC project 98/118, 84 p. Murdoch University, South Street, Murdoch, 6150, Perth, Australia.

[6] Chubb, C., C. Dibden, and K. Ellard. 1984. Studies on the breeding stock of the western rock lobster, *Panulirus cygnus*, in relation to stock and recruitment. FIRTA project 85/87, 37 p. Fisheries Western Australia, WA Marine Research Laboratories, West Coast Drive, Waterman, 6020, Perth, Australia.

Acknowledgments

Thanks are expressed to many colleagues and friends, and particularly R. Melville-Smith, D. Fairclough, M. Pember, T. Linke, M. Travers, and W. White, who assisted with sampling. Our thanks are also expressed to the three anonymous referees for their constructive criticisms. Funding was provided by the Australian Fisheries Research and Development Corporation and Murdoch University.

Literature cited

Anonymous.
2000. FAO yearbook. Fisheries statistics. Capture production, 86/1, 713 p. FAO, Rome, Italy.

Campbell, G. R.
1984. A comparative study of adult sexual behaviour and larval ecology of three commercially important portunid crabs from the Moreton Bay region of Queensland, Australia. Ph.D. diss. 253 p. Univ. Queensland, Brisbane, Queensland, Australia.

Campbell, A., and D. G. Robinson.
1983. Reproductive potential of three American lobster (*Homarus americanus*) stocks in the Canadian Maritimes. Can. J. Fish. Aquat. Sci. 40:1958–1967.

Cerrato, R. M.
1990. Interpretable statistical tests for growth comparisons using parameters in the von Bertalanffy equation. Can. J. Fish. Aquat. Sci. 47:1416–1426.

Comeau, M., and G. Y. Conan.
1992. Morphometry and gonad maturity of male snow crab, *Chionoecetes opilio*. Can. J. Fish. Aquat. Sci. 49: 2460–2468.

Dugan, J. E., A. M. Wenner, and D. M. Hubbard.
1991. Geographic variation in the reproductive biology of the sand crab *Emerita analoga* (Stimpson) on the California coast. J. Exp. Mar. Biol. Ecol. 150:63–81.

Fielder, D. R., and A. J. Eales.
1972. Observations on courtship, mating and sexual maturity in *Portunus pelagicus* (L., 1766). J. Nat. Hist. 6: 273–277.
Fisher, M. R.
1999. Effect of temperature and salinity on size at maturity of female blue crabs. Trans. Am. Fish. Soc. 128:499–506.
Hartnoll, R. G.
1974. Variation in growth pattern between some secondary sexual characters in crabs (Decapoda, Brachyura). Crustaceana 27:131–136.
Hill, B. J.
1975. Abundance, breeding and growth of the crab *Scylla serrata* in two South African estuaries. Mar. Biol. 32: 119–126.
Hines, A. H.
1989. Geographic variation in size at maturity in brachyuran crabs. Bull. Mar. Sci. 45:356–368.
Ingles, J., and E. Braum.
1989. Reproduction and larval ecology of the blue swimming crab *Portunus pelagicus* in Ragay Gulf, Philippines. Int. Rev. Hydrobiol. 74:471–490.
Jones, M. B., and M. J. Simons.
1983. Latitudinal variation in reproductive characteristics of a mud crab, *Helice crassa* (Grapsidae). Bull. Mar. Sci. 33:656–670.
Kailola, P. J., M. J. Williams, P. C. Stewart, R. E. Riechelt, A. McNee, and C. Grieve (eds.).
1993. Australian fisheries resources, 422 p. Bureau of Resource Sciences, Canberra, Australia.
Krol, R. M., W. E. Hawkins, and R. M. Overstreet.
1992. Reproductive components. *In* Microscopic anatomy of invertebrates (F. W. Harrison and A. G. Humes, eds.), p. 295–343. Wiley-Liss, New York, NY.
McGarvey, R., G. J. Ferguson, and J. H. Prescott.
1999. Spatial variation in mean growth rates at size of southern rock lobster, *Jasus edwardsii*, in South Australian waters. Mar. Freshw. Res. 50:333–342.
Meagher, T. D.
1971. Ecology of the crab *Portunus pelagicus* (Crustacea: Portunidae) in south Western Australia. Ph.D. diss, 227 p. Univ Western Australia, Perth, Australia.
Melville-Smith, R.
1987. The reproductive biology of *Geryon maritae* (Decapoda, Brachyura) off south west Africa/Namibia. Crustaceana 53:259–275.
Metcalf, K. S., J. van Montfrans, R. N. Lipcius, and R. J. Orth.
1995. Settlement indices for blue crab megalopae in the York River, Virginia: temporal relationships and statistical efficiency. Bull. Mar. Sci. 57:781–792.
Miliou, H.
1996. The effect of temperature, salinity and diet on final size of female *Tisbe holothuriae* (Copepoda, Harpacticoida). Crustaceana 69:742–754.
Muiño, R., L. Fernandez, E. Gonzalez-Gurriaran, J. Freire, and J. A. Vilar.
1999. Size at maturity of *Liocarcinus depurator* (Brachyura: Portunidae): a reproductive and morphometric study. J. Mar. Biol. Assoc. U.K. 79:295–303.
Perkins-Visser, E., T. G. Wolcott, and D. L. Wolcott.
1996. Nursery role of seagrass beds: enhanced growth of juvenile blue crabs (*Callinectes sapidus* Rathburn). J. Exp. Mar. Biol. Ecol. 198:155–171.
Pillai, K. K., and N. B. Nair.
1971. The annual reproductive cycles of *Uca annulipes*, *Portunus pelagicus* and *Metapenaeus affinis* (Decapoda: Crustacea) from the south-west coast of India. Mar. Biol. 11:152–166.
Pollock, D. E.
1995. Changes in maturation ages and sizes in crustacean and fish populations. S. Afr. J. Mar. Sci. 15:99–103.
Polovina, J. J.
1989. Density dependence in spiny lobster, *Panulirus marginatus*, in the northwestern Hawaiian Islands. Can. J. Fish. Aquat. Sci. 46:660–665.
Potter, I. C., P. J. Chrystal, and N. R. Loneragan.
1983. The biology of the blue manna crab *Portunus pelagicus* in an Australian estuary. Mar. Biol. 78:75–85.
Potter, I. C., and S. de Lestang.
2000. Blue swimmer crab *Portunus pelagicus* in Leschenault Estuary and Koombana Bay, south-western Australia. J. R. Soc. West. Aust. 83:221–236.
Prager, M. H.
1996. A simple model of the blue crab, *Callinectes sapidus*, spawning migration in Chesapeake Bay. Bull. Mar. Sci. 58:421–428.
Rahaman, A. A.
1980. Ecological observations on spawning of a few invertebrates of the Madras coast. J. Madurai Kamaraj Univ. 9:71–77.
Reeby, J., P. N. Prasad, and M. S. Kusuma.
1990. Size at sexual maturity in the male crabs of *Portunus sanguinolentus* and *P. pelagicus*. Fish. Technol. 27: 115–119.
Ryan, E. P.
1967a. Structure and function of the reproductive system of the crab *Portunus sanguinolentus* (Herbst) (Brachyura: Portunidae). I. The male system. Mar. Biol. Assoc. India Symp. Ser. 2:506–521.
1967b. Structure and function of the reproductive system of the crab *Portunus sanguinolentus* (Herbst) (Brachyura: Portunidae). II. The female system. Mar. Biol. Assoc. India Symp. Ser. 2:522–544.
Sainte-Marie, B., J. M. Sévigny, and Y. Gauthier.
1997. Laboratory behaviour of adolescent and adult males of the snow crab (*Chionoecetes opilio*) (Brachyura: Majidae) mated noncompetitively and competitively with primiparous females. Can. J. Fish. Aquat. Sci. 54:239–248.
Somerton, D. A.
1980. A computer technique for estimating the size of sexual maturity in crabs. Can. J. Fish. Aquat. Sci. 37: 1488–1494.
Somerton, D. A., and W. Donaldson.
1996. Contribution to the biology of the grooved and triangle tanner crabs, *Chionoecetes tanneri* and *C. angulatus*, in the eastern Bering Sea. Fish. Bull. 94:348–357.
Stephenson, W.
1962. The evolution and ecology of portunid crabs, with especial reference to Australian species. *In* The evolution of living organisms (G. W. Leeper, ed.), p. 34–67. Melbourne Univ. Press, Melbourne, Australia.
Sumpton, W. D., M. A. Potter, and G. S. Smith.
1994. Reproduction and growth of the commercial sand crab, *Portunus pelagicus* (L.) in Moreton Bay, Queensland. Asian Fish. Sci. 7:103–113.
Van Engel, W. A.
1958. The blue crab and its fishery in Chesapeake Bay Part 1. Reproduction, early development, growth and migration. Commer. Fish. Rev. 20:6–17.
Warner, G. F.
1977. The biology of crabs, 202 p. Paul Elek (Scientific Books), London.

Abstract—Culture of a non-native species, such as the Suminoe oyster (*Crossostrea ariakensis*), could offset the harvest of the declining native eastern oyster (*Crassostrea virginica*) fishery in Chesapeake Bay. Because of possible ecological impacts from introducing a fertile non-native species, introduction of sterile triploid oysters has been proposed. However, recent data show that a small percentage of triploid individuals progressively revert toward diploidy, introducing the possibility that Suminoe oysters might establish self-sustaining populations. To assess the risk of Suminoe oyster populations becoming established in Chesapeake Bay, a demographic population model was developed. Parameters modeled were salinity, stocking density, reversion rate, reproductive potential, natural and harvest-induced mortality, growth rates, and effects of various management strategies, including harvest strategies. The probability of a Suminoe oyster population becoming self-sustaining decreased in the model when oysters are grown at low salinity sites, certainty of harvest is high, minimum shell length-at-harvest is small, and stocking density is low. From the results of the model, we suggest adopting the proposed management strategies shown by the model to decrease the probability of a Suminoe oyster population becoming self-sustaining. Policy makers and fishery managers can use the model to predict potential outcomes of policy decisions, supporting the ability to make science-based policy decisions about the proposed introduction of triploid Suminoe oysters into the Chesapeake Bay.

Manuscript approved for publication 16 June 2003 by Scientific Editor.

Manuscript received 26 June 2003 at NMFS Scientific Publications Office.

Fish. Bull. 101:758–768 (2003).

A model for assessing the likelihood of self-sustaining populations resulting from commercial production of triploid Suminoe oysters (*Crassostrea ariakensis*) in Chesapeake Bay

Jodi R. Dew

Jim Berkson

Eric M. Hallerman

Department of Fisheries and Wildlife Sciences
106 Cheatham Hall
Virginia Polytechnic Institute and State University
Blacksburg, Virginia 24061-0321
E-mail address (for J. Berkson, contact author): jberkson@vt.edu

Standish K. Allen Jr.

School of Marine Science
Virginia Institute of Marine Sciences
Gloucester Point, Virginia 23062

The native eastern oyster (*Crassostrea virginica*) population in Chesapeake Bay has declined because of habitat degradation, over-harvest, and disease- and parasite-mediated mortality. Efforts to restore the eastern oyster population in Maryland and Virginia have been hindered by persistent diseases and habitat degradation (Mann et al., 1991; Gottlieb and Schweighofer, 1996). Recent restoration efforts have included intensified reef building programs. In addition to restoring the native oyster, discussions about introducing non-native disease- and parasite-resistant oyster species into the Chesapeake Bay have gone forward since the early 1990s (Mann et al., 1991; Lipton et al., 1992; Gottlieb and Schweighofer, 1996; Hallerman et al., 2002).

In 1997, in-water testing of non-native oyster species (sterile triploids) began in Virginia, first with the Pacific oyster (*Crassostrea gigas*), then with the Suminoe oyster (*Crassostrea ariakensis*) (Calvo et al., 1999; Calvo et al., 2001). Field studies with Pacific oysters showed poor performance under Chesapeake Bay conditions (Calvo et al., 1999). However, field studies with Suminoe oysters demonstrated disease resistance and rapid growth, and individuals reached minimum harvest shell length of about 77 mm in approximately one year (Calvo et al., 2001). These results, and subsequent small-scale trials by industry, evoked strong interest in the commercial culture of Suminoe oysters to supplement the eastern oyster fishery.

Ideally, aquaculture with 100% triploid oysters would pose no risk of establishment of a self-sustaining oyster population (Guo and Allen, 1994a). However, a number of factors make the use of triploids imperfect. For example, recent data have shown that a small percentage of triploid oysters progressively revert toward diploidy with age (Calvo et al., 2001; Zhou, 2002). Reversion of triploids leads to mosaicism in which individuals comprise both diploid and triploid cells. Mosaics themselves are innocuous unless the re-establishment of diploid cells leads to recovered reproductive capability, which could in turn lead to the establishment of a self-sustaining Suminoe oyster population. We define this hazard, "reproductively effective reversion," as the process of yielding mosaics with recovered reproductive capability. Reproductively effective reversion introduces the possibility that triploid Suminoe

oysters planted for aquaculture could become a self-sustaining population of diploid Suminoe oysters and introduce numerous unknown ecological consequences.

Another hazard associated with deployment of triploid Suminoe oysters is the possibility that nontriploids might be stocked inadvertently because of failure to detect them in a mixed batch of triploid and diploid individuals. Although technology to produce "100%" triploids is now available, as practiced on Pacific oyster (Guo and Allen, 1994b; Guo et al., 1996), the reliability of the approach for producing "100%" triploids in Suminoe oyster is yet undetermined. Diploids may enter the population from several sources: chromosomal nondisjunction in tetraploid males producing haploid gametes, low level hermaphrodism in diploid females yielding self-fertilized embryos, and cross-contamination between diploid and triploid cultures (cf. Guo and Allen, 1997). Typically, flow cytometry has been used to determine the presence or absence of diploid cells (Allen, 1983). Flow cytometry has the sensitivity to detect one diploid among a thousand triploid oysters (Allen and Bushek, 1992); thus, the detection threshold is 0.001 with current technology. Should the (nonzero) frequency of diploids be greater than zero but less than one in a thousand, then the batch would be certified 100% triploid. This failure to detect diploid individuals in a mixed batch poses a hazard for stocking other fertile diploid oysters in that batch into culture systems.

Before substantial commercial introduction of triploid Suminoe oysters into the Chesapeake Bay, any environmental hazards of reproduction associated with a range of management scenarios should be assessed. Hazards are defined as undesirable outcomes from an activity (Hallerman and Kapuscinski, 1995). Stocking triploid Suminoe oysters produces two hazards in this model: the inadvertent stocking of diploids and the reproductively effective reversion of triploids. These two hazards may lead to the establishment of a self-sustained Suminoe oyster population and the probability of this occurring is defined as a risk. Risk assessment is the process of 1) identifying hazards posed by management actions, such as deployment of triploid Suminoe oysters, 2) quantifying the associated risks of hazards being realized (Hallerman and Kapuscinski, 1995), such as the population becoming self-sustaining, and 3) evaluating the consequences of the hazards. Quantitative models often are used to assess risk (Lackey, 1994). Building upon data collected on growth, mortality, and reproductively effective reversion for Suminoe oysters, we have developed a quantitative model to estimate the risk associated with large-scale deployment of triploid Suminoe oysters under a range of management scenarios. The model predicts the likelihood of out-planted triploid Suminoe oysters giving rise to a self-sustaining population at a given site in the Chesapeake Bay given user-specified stocking, reproductively effective reversion, reproduction, growth, and mortality rates (both natural and harvest), as well as user-specified management options.

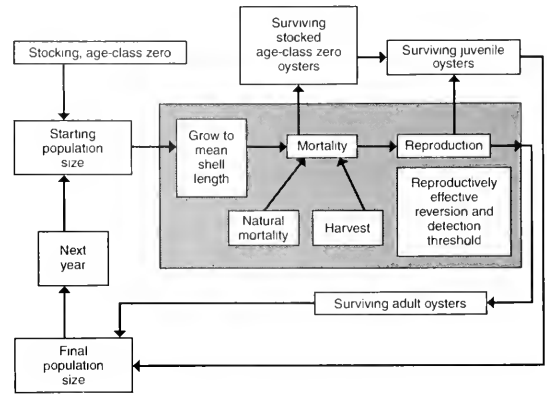

Figure 1

Flow chart depiction of the annual time step in the model for estimating likelihood of establishing self-sustaining reproduction in triploid Suminoe oysters (*C. ariakensis*).

Methods

Overview of model

A quantitative population model of the Suminoe oyster was developed to evaluate the consequences of hazards associated with introducing triploid Suminoe oysters under a range of environmental conditions and management strategies. The model includes set demographic parameters (length-fecundity, oyster density-fertilization efficiency, and salinity-fecundity relationships) and user-specified variables (reproduction, growth, and natural and harvest mortality rates). It includes options for varying stocking rates, harvest rates, and other management actions. Because little is known about Suminoe oyster reproduction, we assumed that Suminoe oysters would behave like the congeneric eastern oysters in Chesapeake Bay; hence, an eastern oyster fecundity model (Mann and Evans, 1998) was used to estimate fecundity of Suminoe oysters. The model assumes that the Suminoe oyster population is closed, i.e. that natural immigration and emigration do not occur. The model is age-structured, and a yearly time step is used. The state variable tracked through time is population size. Intrinsic population growth rate is exponential and without density dependence. The final output of the model is the predicted population size of Suminoe oyster assuming specified demographic parameters and environmental and management variables. The model was programmed in Visual Basic (Microsoft Corp., Redmond, WA).

Modeling approach

In each annual time step for age classes one through six, growth occurs to the mean shell length of the age class, then natural mortality and harvest are imposed, and then reproduction occurs (Fig. 1). Because Suminoe oysters grow quickly in autumn (Cahn, 1950), the annual time step begins in September. Harvest occurs from October to April. Natural mortality occurs at the greatest rates during the summer months. Because an annual time step is being used, the model is designed so that natural mortality and harvest are imposed simultaneously. Reproduction occurs during the summer months. The model simulates reproduction for fertile individuals in all mature age classes. The final population size for a particular age class after natural mortality and harvest becomes the starting value for population size for the next age class in the next time step. All individuals stocked each year are age-class zero individuals. The starting population size for age-class one in the next time step is equal to the sum of all individuals less than one-year old produced by all age classes, plus the number of individuals stocked.

Model variables, parameters, and equations

The initial conditions for the model are determined by the user's choice of specific values for several variables (Tables 1 and 2). The key abiotic variable driving population growth is salinity, because fecundity is highly dependent upon salinity (Mann and Evans, 1998). Biotic variables of the model include mean shell length for each age class, mortality (natural and harvest) for each age class, disease prevalence, total mortality of oysters less than one year old, oyster population density, sex ratio for each age class, and reproductively effective reversion rate for each age class (Table 1). Other variable inputs are stocking rates, harvest regulations, and management strategies.

Stochasticity is programed into the model to incorporate both the uncertainty involved in estimating variable values and environmental variation. Some variables are regarded as stochastic variables because they vary around some mean value from year to year, whereas other variables (such as salinity and sex ratio of the population for each age class) are deterministic in the model because they fluctuate over a longer period of time in the absence of a catastrophe (Kennedy et al., 1996). Stochasticity affects shell length, natural mortality, and reproductively effective reversion rates at each age, and the degree of variance is set by the user as a constant for each year. At each time step, a mean shell length, mortality rate, and reproductively effective reversion rate for each age class is randomly drawn from a log normal distribution around a mean with an associated variance.

We assume that the mean shell length of each age class at the current time step does not affect the mean length of the age class at a subsequent time step, because of large, highly variable growth rates per year (Calvo et al., 2001). Default mean shell length for each age-class values were obtained from Cahn (1950). The user may, of course, specify other mean shell lengths. Growth affects the potential for recruitment through the effect of shell length on fecundity in Equation 1 below.

Table 1
Definitions of model parameters and variables.

Symbol	Parameter and variable definition
A	Area (square meters)
C	Certainty in obtaining the desired harvest rate ($0 \le C \le 1$)
$D_{t,i}$	Oyster density (number of oysters per m^2) at time t for age-class i
$F_{t,i}$	Total fecundity (number of eggs) at time t for age-class i
Fd	Effect of disease on fecundity ($0 \le Fd \le 1$)
$Ff_{t,i}$	Fertilization efficiency at time t for age-class i ($0 \le Ff_{t,i} \le 1$)
Fq_i	Effect of sex ratio on fecundity for age-class i ($0 \le Fq_i \le 1$)
$Frevert_{t,i}$	Total fecundity (number of eggs) of reverted triploid oysters at time t for age-class i
Fs	Effect of salinity on fecundity ($0 \le Fs \le 1$)
$Ftotal_t$	Modified total number of offspring produced at time t for all age classes
H_i	Harvest mortality for age-class i
i	Age class
K_t	Number of stocked oysters at time t
$L_{t,i}$	Mean shell length (mm) at time t for age-class i
$Lmort$	Daily larval mortality rate until settlement
$M_{t,i}$	Natural mortality at time t for age-class i
$N_{t,i}$	Population size (number of oysters) at time t for age-class i
$Ntotal_t$	Total population size (number of oysters) for all age classes at time t
P_{met}	Probability of successful metamorphis ($0 \le P_{met} \le 1$)
$R_{t,i}$	Reproductively effective reversion rate at time t for age-class i ($0 \le R_{t,i} \le 1$)
$T_{t,i}$	Detection threshold at time t for age-class i ($0 \le T_{t,i} \le 1$)
S	Salinity (ppt)
t	Time (years)

An equation for individual size-specific fecundity presented by Mann and Evans (1998) was multiplied by the numbers and mean sizes of females in each mature age class in order to estimate total fecundity for a diploid population:

$$F_{t,i} = 39.06 \times [0.000423 \times L_{t,i}^{1.17475}]^{2.36} \times N_{t,i}, \quad (1)$$

where $F_{t,i}$ = total fecundity (number of eggs produced) at time t for age-class i greater than one;

Table 2
Default values and age-class default values set in the model.

Variable	Default value
A (square meters)	220
C	0.9
Extra timesteps without stocking (years)	20
Fd	1.0
H_t	1.0
Iterations	350
K_t	10000
Minimum shell length-at-harvest (mm)	76.6
S (ppt)	15
t (years)	50

	Age-class default values						
Variable	$i = 0$	$i = 1$	$i = 2$	$i = 3$	$i = 4$	$i = 5$	$i = 6$
Fq_i [1]		0.28	0.66	0.8	0.9	0.95	0.95
$L_{t,i}$ (mm) [2]		54.5	96.9	124.2	151.5	178.7	196.9
$M_{t,i}$ [3]	0.98	0.2	0.2	0.2	0.2	0.2	0.2
$R_{t,i}$ [3]		0	0	0.049	0.009	0.014	0.019
$T_{t,i}$ [3]		0.001	0.001	0.001	0.001	0.001	0.001
Variance of $L_{t,i}$ (mm) [3]		5	10	10	10	10	10
Variance of $M_{t,i}$ [3]		0.05	0.05	0.05	0.05	0.05	0.05
Variance of $R_{t,i}$ [3]		0.0005	0.0005	0.0005	0.005	0.005	0.005

[1] (Yingya et al., 1992).
[2] (Cahn, 1950).
[3] (Calvo et al., 2001).

$L_{t,i}$ = mean shell length (mm) at time t for age-class i greater than one; and
$N_{t,i}$ = population size (number of diploid oysters) at time t for age-class i greater than one.

We recognize that growth forms in oysters are fluid, and that fecundity may be more closely related to weight than to length. However, available growth data for *C. ariakensis* described length-at-age, and therefore we modified Mann and Evans' (1998) fecundity equation to use length as the independent variable.

Equation 1 is used when determining the number of eggs produced by diploid oysters that survived from the previous year. Equation 1 must be modified to determine the number of eggs produced by triploid oysters undergoing reproductively effective reversion. The reproductively effective reversion rate comprises two reproduction-related processes, nondetection of diploids ($T_{t,i}$) and reproductively effective reversion ($R_{t,i}$) of triploids. First, diploid individuals may enter the population through a failure to detect them at frequencies lower than 0.001 in mixed batches with triploids. We make the ecologically conservative assumption that diploid individuals will enter the first age class at the detection threshold of 0.001. After age-class 2, reproductively effective reversion is the percentage of the population that reverts from triploidy to mosaicism (i.e. contains both triploid and diploid gamete cells) and therefore has the potential to reproduce. We conservatively assume that reverted triploids will have full reproductive capabilities, even though this has not yet been observed (Allen, unpubl. data). Default values for reproductively effective reversion were obtained from Calvo et al. (2001). The Mann and Evans (1998) fecundity model was modified to include reproductively effective reversion in the following way:

$$Frevert_{t,i} = 39.06 \times [0.000423 \times L_{t,i}^{1.17475}]^{2.36} \times N_{t,i} \times (R_{t,i} + T_{t,i}), \quad (2)$$

where $Frevert_{t,i}$ = total fecundity (number of eggs produced) for reverted triploid oysters at time t for age-class i greater than one;
$R_{t,i}$ = reproductively effective reversion rate at time t for age-class i greater than one; and
$T_{t,i}$ = diploid detection threshold at time t for age-class i greater than one.

The variable Fs is the effect of salinity on fecundity obtained by using the mean salinity value for the area in Chesapeake Bay where a particular population of Suminoe

oysters is located. The value of Fs ranges from zero (meaning zero fecundity) to one (meaning no effect of salinity on fecundity). For the eastern oyster, when salinity is below 8.0 ppt, Fs is equal to zero, thereby making fecundity zero (Mann and Evans, 1998). When salinity is between 8.0 ppt and 13.5 ppt, there is a positive relationship between salinity and fecundity as described below:

$$Fs = \frac{(S-8)}{5.5}, \quad (3)$$

where Fs = the effect of salinity on fecundity; and
S = salinity (ppt) between 8 ppt and 13.5 ppt.

When salinity is greater than 13.5 ppt, Fs is equal to one denoting no effect of salinity on fecundity. When salinity is greater than 35 ppt, Fs is equal to zero, making fecundity equal to zero (Mann and Evans, 1998). Low or no fertility at high salinity is apparently the case for *C. ariakensis* as well (Langdon and Robinson, 1996).

The variable for disease prevalence, F_d, has a value between 1.0 (no mortality from disease) and 0.0 (all oyster spat die from disease). Recent field studies have suggested that the Suminoe oyster is resistant to diseases on the east coast of North America (Calvo et al., 2001); therefore, the default value of Fd was set at one. Nevertheless, we retained this variable in the model to account for future data sets or other diseases so that the user can select F_d based on the prevalence of disease in the area to be modeled.

Oyster density is determined from the area over which the population occurs. Density affects gamete fertilization efficiency such that more dense oyster deployments (farms, reefs, etc.) exhibit an increased fertilization rate. Levitan (1991) reported the influence of body size and population density on fertilization success and reproductive output, and his equation was rewritten by Mann and Evans (1998) as

$$Ff_{t,i} = 0.0049 \times D_{t,i}^{0.72}, \quad (4)$$

where $Ff_{t,i}$ = fertilization efficiency at time t for age-class i greater than one ranging from zero (meaning zero fertilization) to one (meaning all gametes become fertilized); and
$D_{t,i}$ = oyster density (number of oysters per square meter) at time t for age-class i greater than one.

For diploid oysters, oyster density is equal to the number of oysters in the population divided by the area (m^2). However, the density value for Equation 4 will differ with triploid populations because not all oysters may be able to reproduce; thus we modified the density equation to reflect the density of only undetected diploids and reverted triploids:

$$D_{t,i} = \frac{N_{t,i} \times (R_{t,i} + T_{t,i})}{A}, \quad (5)$$

where A = area (square meters).

The variable for sex ratio, Fq_i, of females to males in the population per age class is a value from 0.0 to 1.0 (Mann and Evans, 1998). Fq_i modifies fecundity so that population size in Equations 1 and 2 comprised females only. The ratios of female-to-male Suminoe oysters at ages 1, 2, 3, and 4 are 0.28, 0.66, 1.00, and 1.00, respectively (Yingya et al., 1992).

Hence, total number of offspring produced per each age class at each time step modified with the previous variables (Mann and Evans, 1998) is as follows:

$$Ftotal_t = \sum (Frevert_{t,i} \times Fs \times Fq_i \times Fd \times Ff_{t,i}), \quad (6)$$

where $Ftotal_t$ = modified total number of offspring produced at time t summed across all age classes.

The number of recruits obtained from the model that survive to the next time step, thereby becoming age class one, depends on the total number of offspring produced from reverted oysters in older age classes, daily mortality rate (ranging from 0.07 to 0.1) until settlement (21 days after fertilization) (Mann and Evans, 1998), the probability of successful completion of metamorphosis (0.25) (Mann and Evans, 1998), and total mortality for settled oysters less than one year old (Thorson, 1966). Hence, the number of individuals that will survive to enter age-class one at the next time step is given by the equation below:

$$N_{t,0} = K_t + \left(Ftotal_t \times \left(Pmet \times (1 - Lmort)^{21} \times (1 - M_0)\right)\right), \quad (7)$$

where K_t = the number of oyster spat stocked at time t;
$Pmet$ = probability of successful completion of metamorphosis;
$Lmort$ = daily larval mortality rate until settlement at 21 days; and
M_0 = total mortality rate for settled oysters less then one year old.

The mortality variables in the model for adult oysters are natural mortality and harvest mortality. Natural mortality determines the proportion of oysters in each age class of the population from nonharvest causes each year. Default natural mortality rates were taken from Calvo et al. (2001) (Table 2). Stochastic values of these variables are chosen from a log normal distribution of the variance around the mean mortality rate for each age class of the population. Harvest-mediated mortality in the population was imposed by randomly selecting individuals for harvest in the age classes whose mean shell length is greater than the set minimum shell length-at-harvest. The harvest rate was a percentage of the population removed from the total population each year.

Certainty of harvest is defined as how certain we are that harvest occurs at a desired harvest rate. This variable in the model captures the effects of different harvest strategies. For example, if oysters are contained in wire cages, the certainty of obtaining a given harvest rate could be 100%. However, for oysters planted on the bottom, the

certainty in obtaining a 100% harvest rate would be lower.

Population size for the current year is determined from the previous year's population size, harvest rate, natural mortality, and certainty in obtaining the desired harvest rate. Thus, the next year's starting population for the next age class greater than one is

$$N_{t+1,i+1} = N_{t,i} \times e^{-((H_i \times C) + M_{t,i})}, \quad (8)$$

where H_i = harvest rate for age-class i greater than one;
C = certainty in obtaining the desired harvest rate; and
$M_{t,i}$ = natural mortality rate at time t for age-class i greater than one.

Total population size is determined by the summation of all individuals across all age classes:

$$Ntotal_t = \sum N_{t,i}, \quad (9)$$

where $Ntotal_t$ = the total population size at time t for all age classes.

Model simulations and output

The model provides two options for output to the user. The first option shows results of one run of the simulation model. The output is a graph showing population size over time. The other output option shows the distribution of outcomes resulting from running the same scenario (i.e. the same input parameter and variable values) a set number of times. This output option shows the probability of the population becoming self-sustaining given the specified set of input conditions and yields probability profiles for risk assessment (Rosenburg and Restrepo, 1994). Probabilities range from 0%, meaning there is a zero probability of a population becoming self-sustaining given a set of input conditions, to 100%, meaning that this outcome will occur every time under the given set of input conditions.

Self-sustainability of a population is tested by running the simulation for a specified number of years with stocking, and then continuing to calculate population size for a specified number of additional years without stocking. Should the population size become zero, then the population is supported solely by stocking. However, should population size prove greater than the number stocked in earlier years, then the population is self-sustaining. The default setting for the simulation is to continue running the simulation twenty years without stocking, reflecting a maximum longevity of 20 years for Suminoe oyster (Cahn, 1950).

To understand the effects of changes in key variables on model predictions, we performed a sensitivity analysis.

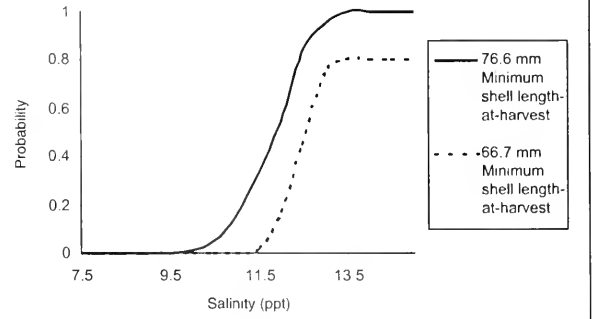

Figure 2

Relationship between salinity at deployment site and probability of a *C. ariakensis* population becoming self-sustaining, when area is set at 100 m^2, stocking size is set at 20,000 oyster, and when all other variables are set at default values. The solid line represents the relationship when the minimum shell length-at-harvest is 77.6 mm. The dashed line represents the relationship when the minimum shell length-at-harvest is 66.7 mm.

A first set of model runs changed the value of only one variable at a time, while keeping all other variables constant at default values. The variables that were changed were salinity, certainty of obtaining the desired harvest rate, minimum shell length-at-harvest, and stocking density. The second set of model runs was similar to the first, except changes were made to the values of two variables at a time while all other variables remained constant at default values. Salinity was varied from 8.5 ppt to 13.5 ppt. Certainty of obtaining the desired harvest rate was varied from 0.5 to 1.0. Minimum shell length-at-harvest was varied from 60 mm to 100 mm. To determine stocking density, the number of oysters stocked was varied from 100 to 1,000,000 oysters, but the area was set at 300 m^2.

All simulation results reported below were obtained by using default values for all variables (Table 2), unless noted otherwise.

Results

Effects of four major variables on the probability of a Suminoe oyster population becoming self-sustaining were examined by using the simulation model. These variables were salinity, certainty of obtaining the desired harvest rate, minimum shell length-at-harvest, and stocking density.

Salinity

Salinity between 8 ppt and 13.5 ppt affected the likelihood of developing self-sustaining populations because when salinity decreases, fecundity decreases (Fig. 2). However, this trend can be altered or masked by the effects of other variables on the probability of a population becoming self-

sustaining. For example, when minimum shell length-at-harvest was lowered from 76.7 mm to 66.7 mm, oysters could be grown in higher salinity areas without increasing the probability of the population becoming self-sustaining (Fig. 2). By harvesting the oysters sooner, there is decreased likelihood of reproductively effective reversion.

Certainty in harvest rate

As the certainty of obtaining the desired harvest rate increased, the probability of the population becoming self-sustaining decreased (Fig. 3). For example, if oysters were grown on the bottom, inability to reliably recapture all individuals is such that the certainty of obtaining the desired harvest rate would be lower than if cages were used. Lower certainty of harvest would increase the likelihood of reproductively effective reversion among older individuals remaining on site, thereby increasing probabilities of both reproduction and the development of a self-sustaining population. In contrast, if oysters were kept in confinements such as wire cages, the certainty in obtaining the desired harvest rate would be high. As a result, this would decrease the likelihood of reproductively competent individuals remaining on site and giving rise to a self-sustaining population.

We also examined the relationship between certainty in obtaining the desired harvest rate and probability of a population becoming self-sustaining when the diploid detection threshold was zero, meaning 100% triploids were stocked (Fig. 3). This procedure distinguished between the effects of the technical problem of detection from the biological problem of reversion. It modeled the ideal scenario where flow cytometry detected any and all diploids in a batch but still allowed reproductively effective reversion to occur in age classes greater than two. When the detection threshold was set at zero and as certainty in obtaining the desired harvest rate increased, the probability of a population of triploid oysters becoming self-sustaining was decreased in relation to a detection threshold of 0.001. For example, when the detection threshold is 0.001 and certainty of harvest is set at 0.75, the probability of the population becoming self-sustaining is 0.082. In contrast, when the detection threshold is 0.000 and certainty of harvest is set at 0.75, the probability of the population becoming self-sustaining is 0.006.

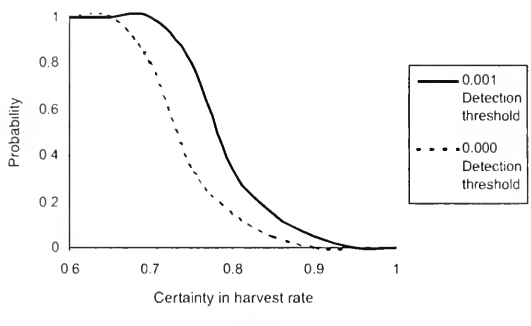

Figure 3

Relationship between the certainty in obtaining a specified harvest rate and probability of a *C. ariakensis* population becoming self-sustaining, when area is 300 m^2 and all other variables are set at default values. The solid line represents the relationship when the detection threshold for diploids is 0.001. The dashed line represents the relationship when the detection threshold for diploids is 0.000.

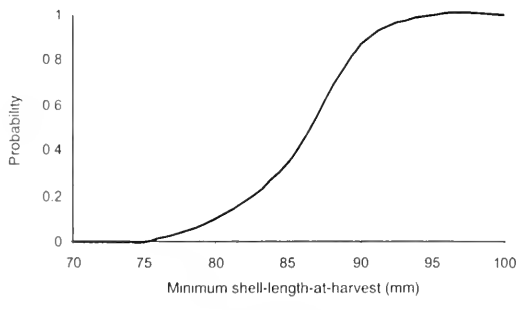

Figure 4

Relationship between minimum shell length-at-harvest (mm) and probability of a *C. ariakensis* population becoming self-sustaining, keeping all other variables at default values.

Minimum shell-length-at-harvest

As the minimum shell-length-at-harvest was increased, the probability of the population becoming self-sustaining increased (Fig. 4). Increased probability of self-sustainability is due to the probability of reproductively effective reversion increasing the longer oysters are in the water, and the number of offspring produced by undetected diploids becoming higher.

Stocking density

With a 0.001 threshold for detecting diploids in triploid batches, and certainty of harvest of 0.9, the probability of the population becoming self-sustaining increased with increased stocking density (Fig. 5). Increased probability of self-sustainability is due to an increase in gamete fertilization efficiency as density increases (Mann and Evans, 1998). In contrast, when the diploid detection threshold was decreased to 0.000, meaning that all oyster spat stocked were indeed triploid, and certainty of harvest

was maintained at the default value of 0.9, higher stocking densities barely increased the probability of the population becoming self-sustaining (Fig. 5). Absence of reproduction from undetected diploids, and the lack of reproduction in mosaic (reverted triploid) oysters until age 3, well past harvest size, were the principal determinants of lowered reproductive risk.

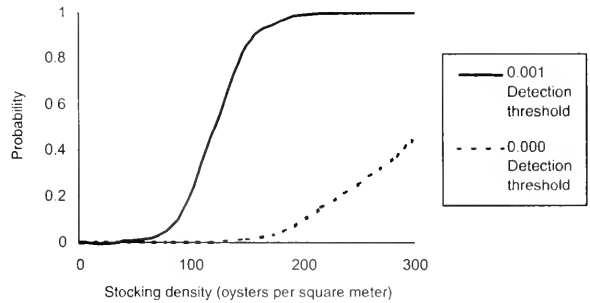

Figure 5

Relationship between stocking density and probability of a *C. ariakensis* population becoming self-sustaining, keeping all other variables at default values. The solid line represents the relationship when the detection threshold for diploids is 0.001. The dashed line represents the relationship when the detection threshold for diploids is 0.000.

Interaction of stocking density and salinity

At lower salinity sites, changes in stocking density had less of an effect on the likelihood of developing a self-sustaining population than at higher salinities when all other variables were set at default values (Fig. 6). Lower salinity decreases fecundity, which counteracts the increased fertilization efficiency at higher population densities.

Interaction of stocking density and certainty of harvest

Stocking density could be increased without increasing the risk of a self-sustaining population by increasing certainty of harvest, and keeping all other variables set at the default values (Fig. 7). Increased certainty of harvest decreased the number of oysters remaining in culture that were able to revert and reproduce, countering the increase in fertilization efficiency from increased density.

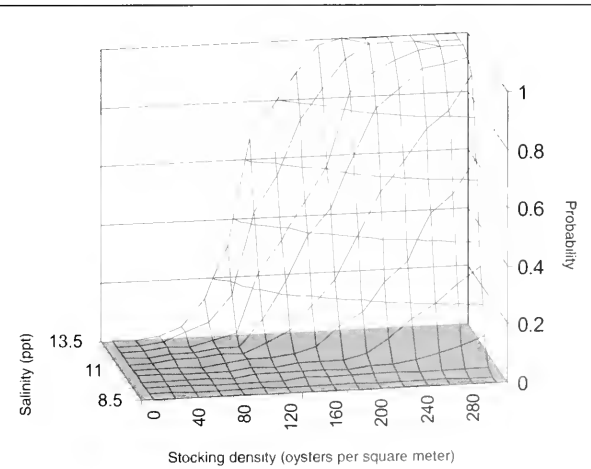

Figure 6

Relationship between stocking density, salinity at deployment site, and the probability of a *C. ariakensis* population becoming self-sustaining, keeping all other variables constant at default values and stocking area set at 300 square meters.

Discussion

The introduction of any non-native species into a new environment poses a number of potential ecological hazards. In general, these are related to two root causes: 1) the associated introduction of epibionts, pathogens, or other infectious agents, and 2) ecological disruption from the persistence of the introduced species (i.e. through reproduction, competition, etc.). To a large degree, associated introductions (with the possible exception of viruses) can be eliminated by adherence to codes of practice for proper quarantine and propagation, such as those set by the International Council for the Exploration of the Seas (ICES, 1994). The second risk of ecological disruption is caused by reproduction and subsequent naturalization. To address this hazard, sterile triploids have been proposed as a means to introduce the Suminoe oyster for commercial aquaculture. This model addresses those elements of risk associated with reproduction. Risk assessment modeling will enable managers to anticipate which management actions can have the greatest impact on decreasing the likelihood of a self-sustaining population. According to our results, risk reduction strategies include stocking Suminoe oysters in relatively low salinity, growing oysters in

confinements (i.e. floating cages, lantern nets, bags, etc.) to maximize the certainty of achieving harvest, harvesting at the earliest possible (and presumably, economically feasible) opportunity, and maintaining a low population density of stocked oysters.

There are several key factors that affect the model's overall predictive value. First, few of the biological parameters that determine reproductive potential of Suminoe oyster are well known. All key parameters in the reproduction equations of the model were based on eastern oyster data (Mann and Evans, 1998) because of a lack of corresponding information about Suminoe oyster. For example, the parameter values in the equation for the relationship of oyster density and fertilization efficiency are not known for Suminoe oysters; therefore those for eastern oysters were used. It is important to determine these parameter values for Suminoe oyster so that the model may more accurately predict the relationship between density and the probability of the population becoming self-sustaining. Also, parameter values relating salinity and fecundity are unknown for Suminoe oyster; therefore eastern oyster parameter values were used. For most oyster species, gametogenesis is decreased or even nonexistent at lower salinities; however, the exact salinity value at which gametogenesis is decreased or absent may vary among species (Amemiya, 1929; Calabrese and Davis, 1970; Kennedy et al., 1996). The Suminoe oyster seems to thrive in estuarine conditions (Huang, 1962; Calvo et al., 2001) and there may be biological parallels to the eastern oyster. However, details about lower reproductive potential in lower salinity waters may be different for Suminoe oysters. In the wild, some populations of Suminoe oyster spawn in early spring in salinity as low as 10 ppt (Zhang and Lou 1956; Huang, 1962); therefore the model may slightly underestimate fecundity of Suminoe oyster in low salinity environments.

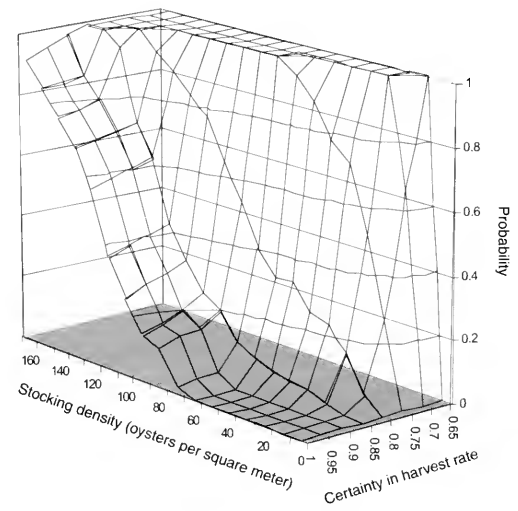

Figure 7

Relationship between stocking density, certainty in obtaining the desired harvest rate, and the probability of a *C. ariakensis* population becoming self-sustaining, keeping all other variables constant at default values and stocking area set at 300 square meters.

In this model, we also assumed that any oyster whose gamete cells reverted from triploid to "reproductive" mosaic or diploid recovered full fecundity. However, studies have yet to quantify recovered reproductive function in reverted triploids (Chandler et al., 1999). It is likely that reverted oysters would exhibit lower fecundity than diploid oysters because revertant oysters are mosaic; i.e. they comprise both triploid gamete-producing cells that are unable to produce viable gametes, and also diploid gamete-producing cells that are able to produce viable gametes. Continuing research with triploid Suminoe oyster should help us fill this gap in knowledge; however, until then, we decided that the model should err on the ecologically conservative side with the assumption that all reverted triploids exhibit full reproductive potential.

Despite its limitations, the model clearly points out key areas of concern, as well as highlights areas where more information or improvements in technology could prove critical. For example, advances in techniques for detecting very low proportions of diploids could reduce risk of a triploid Suminoe oyster population becoming self-sustaining under high stocking rates. Currently, flow cytometry is used for certifying triploid batches in subsampling larval populations (Allen and Bushek, 1992). Up to hundreds of thousands of larvae can be subsampled from a hatchery-scale larval culture. Cells disaggregated from triploid (and intermingled diploid) larvae then can be assayed. The difficulty lies in detecting extremely low levels of diploid cells within the mix. Improved detection by flow cytometry through repeated sampling techniques could help decrease the probability of stocking diploid individuals, thereby decreasing the subsequent chance for reproduction. Improved detection would also allow watermen to stock more Suminoe oysters in a smaller area.

We developed our own demographic model instead of using existing oyster models, such as the time-dependent, energy flow eastern oyster model (Hofmann et al., 1992; Dekshenieks et al., 1993; Hofmann et al., 1994; Powell et al., 1994; Powell et al., 1995; Dekshenieks et al., 1996; Powell et al., 1996; Ford et al., 1999) for various reasons. First, there were only two years of growth, mortality, and reversion rate data available for Suminoe oysters in the Chesapeake Bay (Calvo et al., 2001) and very little information in the literature about the Suminoe oyster in general. Hence, we decided that a demographics-based population dynamics model that tracked population size over time would be the most defensible method for achieving the objective of estimating the probability of a population becoming self-sustaining. Although the time-dependent energy flow model also tracks population size over time, all calcula-

tions are done in terms of energy, which then is converted into population size. Because the available Suminoe oyster data were demographic instead of bioenergetic, we felt a demographic population dynamics model made defensible use of available information. Additionally, the equations of the time-dependent energy flow model included parameters such as filtration rates, respiration, assimilation, and reproduction efficiency. These parameters have yet to be determined for the Suminoe oyster.

The scope of our model could be easily expanded to investigate more detailed scenarios and outputs. Economic aspects could be modeled to examine cost and profit and loss relationships for commercial production of triploid Suminoe oyster under various assumptions. In addition, the model could be adapted to a monthly instead of yearly time step, allowing managers to examine effects of stocking at different times of the year. The model could be made more spatially explicit, allowing managers to examine the probability of a population becoming self-sustaining over a larger area encompassing multiple deployment sites. Physical processes of water flow may have important effects on oyster recruitment. In our model, we assumed that water flow mimicked that in the James River, Virginia, as described in Mann and Evans (1998). Hence, our model is most appropriate for ecosystems where, as in the James River, larvae remain in the approximate area of their production. Clearly, this would not be the case at all sites. In sites where advection of larvae into or out of the area is at issue, one or more terms would have to be added to the model to account for such movement. Additional work is needed to assess a wider range of management options and potential risks.

Acknowledgments

This work was supported by the Virginia Sea Grant College Consortium. We are also grateful for support and help given by Gustavo Calvo, Patricia Flebbe, Rodger Mann, and Alison Williams.

Literature cited

Allen, S. K., Jr.
1983. Flow cytometry: assaying polyploidy fish and shellfish. Aquaculture 33:317–328.

Allen, S. K., Jr., and D. Bushek.
1992. Large scale production of triploid oysters *Crassostrea virginica* using "stripped" gametes. Aquaculture 103:241–251.

Amemiya, I.
1929. Notes on experiments on the early development stages of the Portuguese, American, and English native oysters, with special reference to the effect of varying salinity. J. Mar. Biol. Assoc. U.K. 14:161–175.

Cahn, A. R.
1950. Oyster culture in Japan, 80 p. Office of Technical Services report 134. U.S. Dep. Commer., Washington, DC.

Calabrese, A., and H. C. Davis.
1970. Tolerances and requirements of embryos and larvae of bivalve mollusks. Helgol. Wiss. Meeresunters. 20: 553–564.

Calvo, G. W., M. W. Luckenbach, S. K. Allen, and E. M. Burreson.
1999. Comparative field study of *Crassostrea gigas* and *Crassostrea virginica* in relation to salinity in Virginia. J. Shellfish Res. 18:465–473.
2001. Comparative field study of *Crassostrea ariakensis* and *Crassostrea virginica* in relation to salinity in Virginia. J. Shellfish Res. 20:221–229.

Chandler, W., A. Howe, and S. K. Allen Jr.
1999. Mosaicism of somatic and gametic tissues in *Crassostrea gigas* and *Crassostrea ariakensis*. J. Shellfish Res. 18:293.

Dekshenieks, M. M., E. E. Hofmann, and E. N. Powell.
1993. Environmental effects on the growth and development of eastern oyster, *Crassostrea virginica*, larvae: a modeling study. J. Shellfish Res. 12:241–254.

Dekshenieks, M. M., E. E. Hofmann, J. M. Klinck, and E. N. Powell.
1996. Modeling the vertical distribution of oyster larvae in response to environmental conditions. Mar. Ecol. Prog. Ser. 137:97–110.

Ford, S. E., E. Powell, J. Klinck, and E. Hofmann.
1999. Modeling the MSX parasite in eastern oysters (*Crassostrea virginica*) populations. I. Model development, implementation, and verification. J. Shellfish Res. 18: 475–500.

Gottlieb, S. J., and M. E. Schweighofer.
1996. Oysters and the Chesapeake Bay ecosystems: a case for exotic species introduction to improve environmental quality? Estuaries 19:639–650.

Guo, X., and S. K. Allen Jr.
1994a. Reproductive potential and genetics of triploid *Crassostrea gigas*. Biol. Bull. 187:309–318.
1994b. Viable tetraploids in the Pacific oyster (*Crassostrea gigas* Thunberg) produced by inhibiting polar body I in eggs from triploids. Mol. Mar. Biol. Biotechnol. 3:42–50.
1997. Sex and meiosis in autotetraploid Pacific oyster, *Crassostrea gigas* (Thunberg). Genome 40:397–405.

Guo, X., G. A. DeBrosse, and S. K. Allen Jr.
1996. All-triploid Pacific oysters (*Crassostrea gigas* Thunberg) produced by mating tetraploids and diploids. Aquaculture 142:149–161.

Hallerman, E. M., and A. R. Kapuscinski.
1995. Incorporating risk assessment and risk management into public policies on genetically modified finfish and shellfish. Aquaculture 137:9–17.

Hallerman, E. M., M. Leffler, S. Mills, and S. K. Allen Jr.
2002. Aquaculture of triploid *Crassostrea ariakensis* in Chesapeake Bay: a symposium report. Maryland Sea Grant, Univ. Maryland, College Park, MD. http://www.mdsg.umd.edu/oysters/exotic/workshops.html.

Hofmann, E. E., E. N. Powell, J. M. Klinck, and E. A. Wilson.
1992. Modeling oyster populations III. Critical feeding periods, growth, and reproduction. J. Shellfish Res. 11: 399–416.

Hofmann, E. E., J. M. Klinck, E. N. Powell, S. Boyles, and M. Ellis.
1994. Modeling oyster populations II. Adult size and reproductive effort. J. Shellfish Res. 13:165–182.

Huang, J.
1962. Study on the major cultivated species of oyster in Guangdong province. p. 41–52. *In* Transactions of the annual meeting of Oceanology and Limnology Society of Guangdong, Guangzhou, China. ICES International Council for the Exploration of the Seas, Palægade 2-4, DK-1261, Copenhagen K, Denmark.

1994. Codes of practice on the introduction and transfer of marine organisms, 17 p. Cooperative Research Report 204. ICES, Palgade 2-4 DK-1261, Copenhagen K. Denmark.

Kennedy, V. S., R. I. Newell, and A. F. Eble.
1996. The eastern oyster: *Crassostrea virginica*, 734 p. Maryland Sea Grant, Univ. Maryland, College Park, MD.

Lackey, R. T.
1994. Ecological risk assessment. Fisheries 19:14–18.

Langdon, C. J., and A. M. Robinson.
1996. Aquaculture potential of the Suminoe oyster (*Crassostrea ariakensis*). Aquaculture 144:321–338.

Levitan, D. R.
1991. Influences of body size and population density on fertilization success and reproductive output in a free-spawning invertebrate. Biol. Bull. 181:261–268.

Lipton, D. W., E. F. Lavan, and I. E. Strand.
1992. Economics of molluscan introductions and transfers: the Chesapeake Bay dilemma. J. Shellfish Res. 11:511–519.

Mann, R., E. M. Burreson, and P. K. Baker.
1991. The decline of the Virginia oyster fishery in Chesapeake Bay: considerations for the introduction of a nonendemic species, *Crassostrea gigas*. J. Shellfish Res. 10: 379–388.

Mann, R., and D. A. Evans.
1998. Estimation of oyster, *Crassostrea virginica*, standing stock, larval production, and advective loss in relation to observed recruitment in the James River, Virginia. J. Shellfish Res. 17:239–253.

Powell, E. N., J. M. Klinck, and E. E. Hofmann.
1996. Modeling diseased oyster populations. II. Triggering mechanisms for *Perkinsus marinus* epizootics. J. Shellfish Res. 15:141–165.

Powell, E. N., J. M. Klinck, E. E. Hofmann, and S. M. Ray.
1994. Modeling oyster populations. IV: Rates of mortality, population crashes, and management. Fish. Bull. 92: 347–373.

Powell, E. N., J. M. Klinck, E. E. Hofmann, E. A. Wilson-Ormond, and M. S. Ellis.
1995. Modeling oyster populations. V. Declining phytoplankton stocks and the population dynamics of American oyster (*Crassostrea virginica*) populations. Fish. Res. 24: 199–222.

Rosenberg, A. A., and V. R. Restrepo.
1994. Uncertainty and risk evaluation in stock assessment advice for U.S. marine fisheries. Can. J. Fish. Aquat. Sci. 51:2715–2720.

Thorson, G.
1966. Some factors influencing the recruitment and establishment of marine benthic communities. Neth. J. Sea Res. 3:267–293.

Yingya, C., D. Chenmao, and L. Zhigang.
1992. Studies on the ecology of *Crassostrea rivularis* in Zhanjiang Bay. Tropic. Oceanogr. 11:38–44.

Zhang, X., and Z. Lou.
1956. The oyster. Bull. Biol. 2:27–32. [In Chinese.]

Zhou, M.-F.
2002. Chromosome set instability in 1–2 year old triploid *Crassostrea ariakensis* in multiple environments. M.S. thesis, 72 p. Virginia Institute of Marine Science, Gloucester Point, VA.

Allozyme and RAPD variation in the eastern Pacific yellowfin tuna (*Thunnus albacares*)

Pindaro Díaz-Jaimes

Instituto de Ciencias del Mar y Limnología
Universidad Nacional Autónoma de México
Circuito exterior de Ciudad Universitaria
Apdo. Postal 70-305
México, D.F. 04510
E-mail address: pindaro@mar.icmyl.unam.mx

Manuel Uribe-Alcocer

Instituto de Ciencias del Mar y Limnología
Universidad Nacional Autónoma de México
Circuito exterior de Ciudad Universitaria
Apdo. Postal 70-305
México, D.F. 04510

Abstract—Stock structure of eastern Pacific yellowfin tuna was investigated by analyzing allozymes and random amplified polymorphic DNAs (RAPDs) from 10 samples of 20–30 individuals each, collected between 1994 and 1996 from fishing vessels operating in the Inter-American Tropical Tuna Commission (IATTC) yellowfin regulatory area (CYRA). Allozyme analysis resolved 28 loci, eight of which were polymorphic under the 0.95 criterion: *Aat-S**, *Glud*, *Gpi-F**, *Gpi-S**, *La*, *Lgg*, *Pap-F**, and *6-Pgd*, resulting in a mean heterozygosity over all allozyme loci of $H = 0.052$. Four polymorphic RAPD loci were selected for analysis, resulting in a mean heterozygosity of $H = 0.43$. Eight of 45 pairwise comparisons of allozyme allele frequencies among the ten samples showed significant differences after correction for multiple testing ($P<0.0001$), all of which involved comparisons with the Gulf of California sample. Confirmation of this signal of population structure would have management implications. No significant divergence in RAPD allele frequencies was observed among samples. Weir and Cockerham θ estimated for allozyme loci ($\theta=0.048$; $P<0.05$) and RAPD loci ($\theta=0.030$; $P>0.05$) revealed little population structure among samples. Mantel tests demonstrated that the genetic relationships among samples did not correspond to an isolation-by-distance model for either class of marker. Four of eight comparisons of coastal and offshore samples revealed differences of allele frequencies at the *Gpi-F** locus ($P<0.05$), although none of these differences was significant after correction for multiple testing ($P>0.001$). Results are consistent with the hypothesis that the CYRA yellowfin tuna samples comprise a single genetic stock, although gene flow appears to be greater among coastal samples than between coastal and offshore samples.

Manuscript approved for publication 19 June 2003 by Scientific Editor.

Manuscript received 26 June 2003 at NMFS Scientific Publications Office.

Fish. Bull. 101:769–777.

Yellowfin tuna (*Thunnus albacares*) is a cosmopolitan species inhabiting tropical and subtropical waters in the Atlantic, Pacific, and Indian oceans. This species has accounted for more than a third of the world's tuna production since 1970. The eastern Pacific has contributed from 21% to 26% of the global catch from 1993 through 1997, representing 273,329 metric tons (t) in 1990 to 264,426 t in 1998 (IATTC, 1999).

Yellowfin tuna is a large pelagic fish with a common size of 150 cm (Collette and Nauen, 1983). Spawning occurs throughout the year in the tropical oceans, preferably near islands and coasts (Leis et al., 1991). Growth is rapid and individuals reach maturity by the end of the second year (Suzuki et al., 1978). Schooling of individuals of similar size is observed near surface waters and is often associated with floating objects (Wild, 1994).

Yellowfin tuna is currently considered to comprise a single species (Gibbs and Collete, 1967), although significant morphometric and meristic differences, limited fish movements, and differences among catch data, have been reported for the different regions of the Pacific Ocean (Godsil and Greenhood, 1951; Schaefer, 1955; Joseph et al., 1964; Suzuki et al., 1978; Schaefer, 1991). Population structure in yellowfin tuna has been addressed in the Pacific Ocean by using several independent methods. Morphometric and meristic based studies have shown significant differences (Godsil and Greenhood, 1951; Schaefer, 1955; Kurogane and Hiyama, 1957), and at least three stocks or discrete units (western, central, and eastern Pacific) have been proposed. More recent studies using morphometric multivariate analysis suggest the presence of different stocks between north and south regions in the eastern Pacific (Schaefer, 1991), as well as across the Pacific Ocean (Schaefer, 1991). Additionally, differences in larval distribution, catch rates, and size composition data of yellowfin tuna caught along the equatorial Pacific by longline and purse-seine have been used by Suzuki et al. (1978) to distinguish between western, central, and eastern Pacific groups.

Tagging experiments have shown limited movement of yellowfin tuna between western and eastern Pacific waters (Joseph et al., 1964; Fink and Bayliff, 1970). In the eastern Pacific, the presence of two groups has been suggested: a northern group off Baja California coast and the Revillagigedo Islands and a southern group from the Maria Islands through Chile. Some mixing occurs between them (Fink and Bayliff, 1970). There seem to be marked movements between north and south groups along the coast with limited westward movements (Joseph et al., 1964).

Some studies of population structure using genetic analyses have not revealed the presence of discrete stocks along the Pacific Ocean. Barret and Tsuyuki (1967) used transferrin analysis and did not find differences in allele frequencies between samples from Hawaii and eastern Pacific samples, although heterogeneity was detected within the eastern Pacific samples (IATTC, 1975). Allozyme variation studies in the esterase locus (Fujino, 1970) did not show enough evidence of genetic differentiation between eastern Pacific and Hawaii samples. Furthermore, Scoles and Graves (1993) used restriction fragments length polymorphisms (RFLP) and analysis of mitochondrial (mt) DNA to examine five samples collected across the Pacific Ocean and one from the Atlantic Ocean. Although they detected 34 haplotypes and considerable genetic variation, no evidence of genetic differentiation among samples was found.

However, more recent genetic studies have provided limited evidence of genetic heterogeneity. Ward et al. (1994) analyzed four polymorphic allozyme loci and 18 mtDNA haplotypes in yellowfin tuna from the Pacific Ocean. Although no unique haplotypes were found in the analyzed populations through RFLP analysis, the eastern Pacific samples were found to be different from the central and western Pacific samples in frequency differences at a single locus *GPI-F**, suggesting that the signal of population structure exhibited is due to selective factors contributing to the divergence. Eastern Pacific samples (n=41) were collected in the northeast Pacific off California and at an unspecified site off Mexico (n=40). Comparisons of *GPI-F** allele frequencies from eastern Pacific also included two samples previously analyzed by Sharp (1978) from Roca Partida (Central America) and Ecuador. Their results showed population homogeneity at the *GPI-F** locus for this region.

To date, the methods and logistics used to study divergence in the Pacific yellowfin tuna have been focused on a global rather than a local scale, and sampling has been focused on the wide areas of the west and central Pacific. Local structure in the eastern Pacific yellowfin tuna has not been addressed through a more intense sampling strategy to examine genetic homogeneity in this region. Because tagging studies have shown restricted longitudinal movements by yellowfin tuna, population structure and isolation by distance hypotheses can be tested. To evaluate the stock structure of yellowfin tuna in eastern Pacific, we employed analyses of allozymes and of randomly amplified polymorphic DNA (RAPDs).

RAPDs have proven to be useful genetic markers because of their high levels of polymorphisms (Williams et al., 1990; Welsh et. al., 1991). They have been used to estimate population structure in fishes, including the cod (Kenji, 1998), red mullet (Mamuris et al., 1998), and striped bass (Bielawski and Pumo, 1997). The use of RAPDs, considered as neutral markers, and the simultaneous use of allozyme analyses with intense sampling in a more local area, might provide evidence about the relationship between gene flow and spatial distribution of the eastern Pacific yellowfin tuna, as well as evidence of the presence of local selective factors responsible for the divergence suggested by Ward et al. (1994).

Materials and methods

Sampling

A total of 327 tissue samples from specimens of ten locations were obtained from commercial tuna boats fishing in the tropical eastern Pacific from 1994 to 1996 (Fig. 1). Muscle tissue samples were dissected from specimens at the time of landing and were transported in liquid nitrogen or on dry ice to the Laboratorio de Genética de Organismos Acuáticos of the Instituto de Ciencias del Mar y Limnología in Mexico City. Samples were maintained at −70°C until processing.

Allozyme analysis

For allozyme analysis, 1 cm^3 (about one gram) of tissue sample was ground with a manual homogenizer in 1.5 mL of extraction buffer (0.01M Tris-0.001M EDTA, pH 6.8, and 1% NADP) and centrifuged at 2500 g at 4°C. Electrophoretic runs were performed in 12% (w/v) starch gels (Sigma Chemicals, St. Louis, MO). Four buffer systems were used to analyze nineteen enzymes that resolved 28 loci, eight of which showed polymorphism: *Aat-S** (aspartate aminotransferase), *Glud* (glutamate dehydrogenase), *Gpi-F** and *Gpi-S** (glucose phosphate isomerase), *La* (leucil-L-alanine), *Lgg* (L-leucil-glycil-glycine), *Pap-F** (L-leucil-L-proline) and *6-Pgd* (phosphogluconate dehydrogenase). Enzymes AK (adenilate kinase), CK (creatinine kinase), GAPDH (glyceraldehyde-3-phosphate dehydrogenase), LDH (lactate dehydrogenase), MDH (mMalate dehydrogenase), ME (malic enzyme) and SOD (superoxide dismutase), displayed twenty more loci that were presumably monomorphic. Buffer systems for enzyme analysis were 1) amino-citrate: 0.04M citric acid, 15mL/L of N-3-aminopropyl-morpholine, pH 6.5 (AAT, GPI, and LA); 2) 0.008M Tris, 0.003 M citric acid, pH 6.7 (GLUD and 6-PGD); 3) 0.025 M Tris, 0.192 glycine, pH 8.5 (GPI and LGG); 4) 0.0.076 M Tris, 0.005 M citric acid, pH 8.7 (PAP). Enzyme assays were performed following Harris and Hopkinson (1976). Enzymes showing polymorphism were analyzed for all samples and subjected to population genetic analysis.

RAPD analysis

For RAPD analyses, genomic DNA was extracted from muscle tissue by using standard phenol-chloroform protocols (Sambrook et al., 1989), resuspended in TE buffer (10mM Tris-0.1mM EDTA pH 8.0), and quantified with a Hoefer DyNA quant 200 fluorometer. DNA was amplified with primer F-10 (Operon® Alameda, CA; 5′-GGAAGCTTGG-3′). Amplifying reactions were performed in a final volume of 22 μL consisting of 0.7 to 1 ng/μL of DNA in amplification buffer, 10 mM Tris-HCl, 50 mM KCl, 1.5 mM $MgCl_2$, 33 ng of primer, 10 mM dNTPs, and 1 U of Taq polymerase. Amplification of genomic DNA was performed in a Perkin Elmer®, Foster City, CA (mod. 480), thermal cycler. The program was set for 1 cycle of 1 min. at 36°C, followed by 44 cycles of 1 min. at 36°C; 1 min. at 94°C; 2 min. at 72°C, and

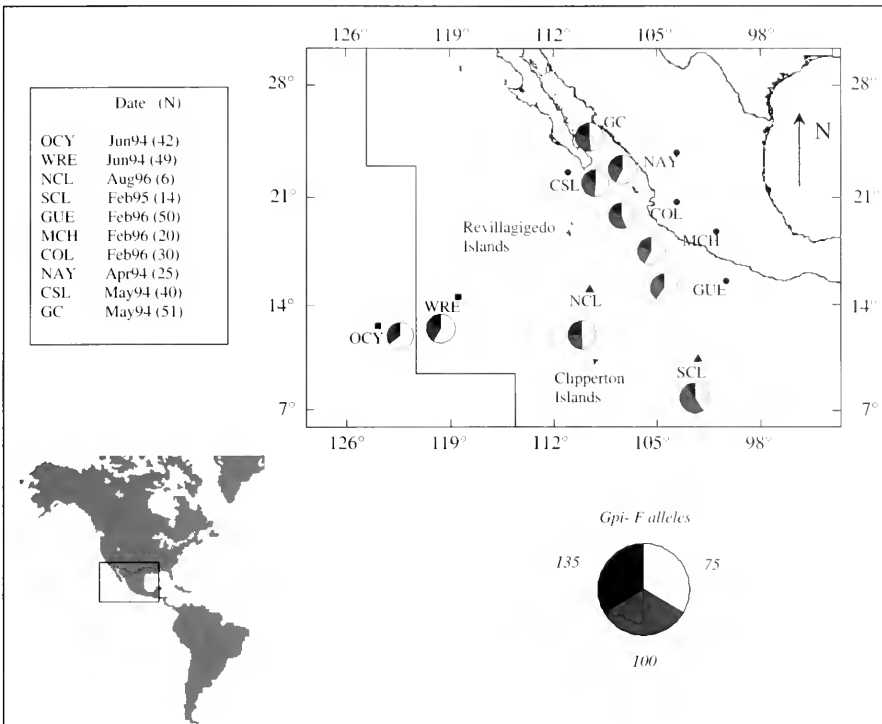

Figure 1

Thunnus albacares. Location of sampling sites, dates, and sample sizes, and *Gpi-F** gene frequencies of eastern Pacific yellowfin tuna. The sites are as follows: OCY = out of CYRA area; WRE = west of the Revillagigedo Islands; NCL = North Clipperton islands; SCL = South Clipperton Islands; MCH = Michoacan; GUE = Guerrero; COL = Colima; CSL = Cape San Lucas; NAY = Nayarit; GC = Gulf of California. Symbols are ● coastal, ▲ intermediate, ■ offshore.

a final cycle of 15 min. at 72°C. Optimal DNA concentrations for amplification were determined by testing several dilutions, one of which was taken as the standard for every subsequent amplification.

Amplified fragments were resolved by electrophoresis in 1.5% agarose gels (Sigma Chemicals) for 3 to 4 h. at 90 mA (100 V). A 100bp DNA Ladder (GibcoBRL, Gaithersburg, MD, 15628-019) was used as size standard. After electrophoresis, gels were stained with ethidium bromide and photographed in a UV light transilluminator.

Data analysis

Allelic frequencies, test of conformity of genotype distributions with Hardy-Weinberg, and heterozygous deficit were determined by using Genepop version 3.3 (Raymond and Rousset[1]). Homogeneity of allozyme and RAPD allele frequencies was evaluated by using the exact probability test (Raymond and Rousset, 1995) consisting of a contingency analysis for every polymorphic locus and an estimation of their probability values by the combined probability of Fisher (Sokal and Rohlf, 1995) as implemented in the TFPGA program (Miller[2]). Pairwise comparisons were conducted to determine allele frequency differences among samples in order to define sources of variation. Based on the longitudinal differentiation pattern observed by Ward et al. (1994) and the morphological latitudinal differences within eastern Pacific samples reported by Schaefer (1991)

[1] Raymond, M. L., and F. Rousset 1995a GENEPOP (version 1.2): population genetics software for exact tests and ecumenicist. J Heredity 86:248–249

[2] Miller, M. P. 1997. Tools for genetic populations analyses (TFPGA) 1.3: a windows program for the analysis of allozyme and molecular population genetic data, 29 p. Computer software distributed by the author at http://bioweb.usu.edu/mpmbio.

at north-south of the 15–20°N range, spatial homogeneity was tested at the following levels: overall samples (O), among longitudinal regions (L; coastal, intermediate, and offshore localities), and latitudinal regions (N; north-south of the 15–20° range). The Gulf of California sample was excluded from this analysis because the large variation found in this sample (reflected in the significant differences shown in allele frequency homogeneity from pairwise comparisons) would not allow an accurate assessment of whether longitudinal or latitudinal differentiation exists or not. Significance levels were adjusted for multiple testing through the Bonferroni sequential method (Rice, 1989).

Population subdivision was estimated by using the Weir and Cockerham (1984) method through the TFPGA program. Standard error and confidence intervals were obtained through jackknife and bootstrapping procedures, respectively, with F_{ST} Pro 1.0 (Weir, 1990). Estimates of population subdivision were partitioned into the following levels: O, over all the samples; L, longitudinal regions (coastal, intermediate and offshore); and N, latitudinal regions.

We used the θ statistic to estimate gene values between sample pairs (Slatkin, 1993) that are defined as M_θ. An "isolation by distance" model was evaluated from the correlation between the distance between localities measured as geographic separation in nautical miles (nmi), and the M_θ values by means of the Mantel test (Hellberg, 1994) in both allozymes and RAPDs.

The patterns of the amplification products resulting from the RAPD analysis were subjected to the same analyses as allozymes with the procedures described in Lynch and Milligan (1994). RAPD fragments were interpreted under the following assumptions: 1) fragments were considered to behave as dominant genes (Williams et al., 1990); 2) every polymorphic fragment was considered derived from a two-allele locus; 3) the equilibrium of Hardy-Weinberg was assumed for all genotypes, and 4) each fragment was considered to be an independent locus.

Only those fragments clearly defined and having consistent intensity were recorded. Because of this, the Michoacan sample, with poor consistency in the banding patterns, was excluded from the RAPD analysis. The allele frequency of every fragment was calculated on the basis of the inferred homozygous recessive genotypes. Because of the dominant nature of the alleles, and in order to correct the bias originated by calculating the recessive allelic frequencies, we chose the estimation based on the Taylor expansion (Kendall and Stuart, 1977, cited in Le Corre et al., 1997) as implemented in TFPGA program. This reduction on the bias is based on the equation resulting from the second order expansion of Taylor (see details in Lynch and Milligan, 1994).

Results

Allozymes

Of the 28 analyzed allozyme loci, eight (28.5%) showed polymorphism under the 0.95 criterion. The observed heterozygosities per sample over all allozyme loci ranged from 0.027 to 0.083 (mean 0.052). Allozyme frequencies for the eight polymorphic loci detected are shown in Table 1. After adjusting levels of significance by the Bonferroni procedure, significant deviation of genotypic frequencies from those expected under Hardy-Weinberg was found in the loci *Lgg* and *Pap-F** for the Gulf of California sample and in the *Aat-S** locus for two localities—west of Revillagigedo Islands, and the Gulf of California (P<0.0006, Table 1). Deviations displayed for both locations corresponded to a heterozygous deficit (P<0.0006, after Bonferroni correction).

Comparison of allozyme allele frequencies among all collections (overall) by the exact probability test revealed significant heterogeneity at loci *Glud*, *La*, and *Lgg*, after Bonferroni adjustment (P<0.006). Pairwise comparisons among samples to test allele homogeneity gave significant differences for nine of 45 comparisons after correction for multiple tests (P<0.001), seven of which involved comparisons with the Gulf of California (GC) sample. The remaining significant differences were between Guerrero-Nayarit, and Cape San Lucas-Nayarit comparisons (Table 2), resulting from significant heterogeneity at *Glud*, *La*, and *Lgg* loci.

In general, allozyme analysis displayed low levels of differentiation. The θ value over all loci was different from zero (P<0.05) and showed that 4.8% of the variance was attributable to differences among samples (Table 3).

Individual loci showed θ values ranging between 0.0037 and 0.27. Highly significant values at loci *La* (θ=0.13 ±0.089) and *Lgg* (θ=0.27 ±0.253) evidently resulted from their weak polymorphism in some samples (Table 3).

Allele frequency homogeneity was tested among coastal, intermediate, and offshore regions (Table 4). Significant heterogeneity was found by exact test between coastal and offshore comparisons (P=0.0043) but was found to be not significant between coastal and intermediate regions (P=0.0632). Subdivision as measured by θ among coastal, intermediate, and offshore localities was not different from zero. However, for the *Gpi-F** locus the population subdivision among regions (0.0058) was twice as large as that noted among samples (θ=0.003), but neither value was significant (Table 3). No latitudinal differentiation by the exact test or population subdivision estimated by the θ index was found between north and south regions (data not shown).

The gene flow values (M_θ) were high (mean 24.8 migrants per generation). A lack of correlation between gene flow estimations and geographic distance by means of the Mantel test was observed (r^2=–0.144; P=0.22), resulting in a rejection of the isolation by distance model.

For the *Gpi-F** locus, paired tests of significance (data not shown) showed discrepancies in the *Gpi-F*/75* allele frequencies among localities from the coast with those located at the CYRA limits (Fig. 1, Table 5). Four of eight comparisons of coastal and offshore samples revealed differences of allele frequencies at this locus (P<0.05), although none of these differences was significant after correction for multiple testing (P>0.001).

RAPDs

The primer OPF-10 produced 11 amplified fragments, with sizes from 200 to 600 bp (base pairs). Four of the fragments

Table 1

Allele frequencies for allozymes and RAPDs, samples size (n) and agreement to the Hardy-Weinberg equilibrium (HW) for every loci and sample of *Thunnus albacares*. Significance values for HW tests were adjusted for multiple comparisons with an initial α level of 0.0006 [(0.05/(8 loci × 10 samples)]. P = probability of significance for allele frequency heterogeneity per locus, * = significant at $\alpha = 0.006$. — = no data. OCY = out of CYRA area; WRE = west of the Revillagigedo Islands; NCL = North Clipperton islands; SCL = South Clipperton Islands; MCH = Michoacan; GUE = Guerrero; COL = Colima; CSL = Cape San Lucas; NAY = Nayarit; GC = Gulf of California.

		Collection										
Locus	Allele	OCY	WRE	NCL	SCL	GUE	MCH	COL	CSL	NAY	GC	P
*Aat-S**	–90	0.171	0.266	0.250	0.231	0.154	0.275	0.077	0.092	0.0	0.234	
	–100	0.829	0.734	0.750	0.769	0.846	0.725	0.923	0.908	1.0	0.766	
	n	41	32	6	13	39	20	26	38	25	47	0.011
	HW	yes	no	yes	yes	yes	yes	yes	yes	—	no	
Glud	100	0.700	0.634	0.667	0.857	0.663	0.775	0.914	0.788	0.680	0.395	
	85	0.300	0.366	0.333	0.143	0.337	0.225	0.086	0.212	0.320	0.605	*
	n	40	41	6	14	49	20	29	40	25	43	
	HW	yes	yes	yes	yes	yes	yes	yes	yes	yes	yes	
*Gpi-F**	135	0.071	0.134	0.250	0.091	0.190	0.079	0.185	0.125	0.160	0.200	
	100	0.262	0.280	0.250	0.500	0.230	0.316	0.370	0.363	0.260	0.314	
	75	0.667	0.586	0.500	0.409	0.580	0.605	0.444	0.512	0.580	0.486	0.526
	n	42	41	6	11	50	19	27	40	25	35	
	HW	yes	yes	yes	yes	yes	no	yes	yes	yes	yes	
*Gpi-S**	–60	0.402	0.536	0.417	0.571	0.360	0.425	0.414	0.449	0.479	0.338	
	–100	0.598	0.464	0.583	0.429	0.640	0.575	0.586	0.551	0.521	0.663	0.015
	n	41	42	6	14	50	20	29	39	24	40	
	HW	yes	yes	yes	yes	yes	yes	yes	yes	yes	yes	
La	120	0.0	0.024	0.0	0.0	0.0	0.0	0.0	0.0	0.1	0.2	
	100	1.0	0.976	1.0	1.0	1.0	1.0	1.0	1.0	0.9	0.8	*
	n	42	42	6	14	50	20	24	40	20	50	
	HW	yes	—	—	—	—	—	—	—	yes	yes	
Lgg	115	0.0	0.024	0.0	0.0	0.0	0.0	0.0	0.0	0.0	0.349	
	100	1.0	0.976	1.0	1.0	1.0	1.0	1.0	1.0	1.0	0.651	*
	n	42	42	6	14	50	20	24	24	24	43	
	HW	yes	—	—	—	—	—	—	—	—	no	
*Pap-F**	110	0.0	0.0	0.0	0.0	0.02	0.05	0.0	0.0	0.0	0.083	
	100	1.0	1.0	1.0	1.0	0.98	0.95	1.0	1.0	1.0	0.917	0.055
	n	42	42	6	14	50	20	29	40	25	48	
	HW	—	—	—	—	yes	yes	—	—	—	no	
6-Pgd	100	0.902	0.903	0.667	0.821	0.939	1.0	0.966	1.0	0.840	0.938	
	90	0.098	0.097	0.333	0.179	0.061	0.0	0.034	0.0	0.160	0.062	0.007
	n	41	31	6	14	49	20	29	40	25	48	
	HW	yes	yes	yes	yes	yes	—	yes	—	yes	yes	
F10-1	*a*	0.406	0.282	0.234	0.322	—	0.083	0.505	0.355	0.282	0.246	
	b	0.594	0.718	0.766	0.678	—	0.917	0.495	0.645	0.718	0.754	0.572
	n	9	8	7	9	—	6	9	10	8	9	
	HW	—	—	—	—	—	—	—	—	—	—	
F10-2	*a*	0.406	0.603	0.441	0.322	—	0.278	0.322	0.355	1.0	0.322	
	b	0.594	0.397	0.559	0.678	—	0.722	0.678	0.645	0.0	0.678	0.369
	n	9	8	7	9	—	6	9	10	8	9	
	HW	—	—	—	—	—	—	—	—	—	—	
F10-3	*a*	0.406	0.475	0.329	0.625	—	0.397	0.406	0.529	0.371	0.406	
	b	0.594	0.525	0.671	0.375	—	0.603	0.594	0.471	0.629	0.594	0.912
	n	9	8	7	9	—	6	9	10	8	9	
	HW	—	—	—	—	—	—	—	—	—	—	
F10-4	*a*	0.115	0.282	0.234	0.178	—	0.083	0.246	0.219	0.138	0.246	
	b	0.885	0.718	0.766	0.822	—	0.917	0.754	0.781	0.862	0.754	0.929
	n	9	8	7	9	—	6	9	10	8	9	
	HW	—	—	—	—	—	—	—	—	—	—	

Table 2

Pairwise-sample comparisons of allele frequency homogeneity for *Thunnus albacares*. Probability values in allozymes are above the diagonal (—) and RAPDs are below the diagonal (—). * = significant values after Bonferroni correction for multiple tests (initial α was 0.05). na = data not available. OCY = out of CYRA area; WRE = west of the Revillagigedo Islands; NCL = North Clipperton islands; SCL = South Clipperton Islands; MCH = Michoacan; GUE = Guerrero; COL = Colima; CSL = Cape San Lucas; NAY = Nayarit; GC = Gulf of California.

Sample	OCY	WRE	NCL	SCL	GUE	MCH	COL	CSL	NAY	GC
OCY	—	0.5807	0.7391	0.3414	0.4386	0.8254	0.0295	0.1525	0.0194	*<0.001
WRE	0.9316	—	0.9482	0.6047	0.4330	0.1180	0.0012	0.0084	0.0192	*<0.001
NCL	0.9797	0.9770	—	0.9232	0.3494	0.7307	0.1567	0.0859	0.4779	0.0174
SCL	0.9798	0.8088	0.8915	—	0.3989	0.0717	0.3414	0.1093	0.0287	*<0.001
GUE	0.5935	0.4732	0.9095	0.7757	—	0.4137	0.1723	0.5932	*<0.001	*<0.001
MCH	na	na	na	na	na	—	0.0500	0 1532	0.0096	*<0.001
COL	0.9385	0.7864	0.9155	0.9794	0.4569	na	—	0.8237	0.0082	*<0.001
CSL	0.9475	0.9703	0.9824	1.000	0.6576	na	0.9849	—	0.0012	*<0.001
NAY	0.9656	0.9984	0.8418	0.4965	0.4101	na	0.4206	0.5707	—	*<0.001
GC	0.9458	0.9637	0.9987	0.9977	0.9743	na	0.9715	0.9874	0.6518	—

Table 3

Estimates of population subdivision θ (Weir and Cockerham, 1984) for allozymes of *Thunnus albacares* partitioned into longitudinal regions θ_L (regions) (i.e. coastal-intermediate-offshore) and samples θ_0 (overall). n.v. = negative values. P = probability of significance of subdivision estimations. Significance of single-locus values was corrected with an initial level of 0.006 (0.05/8 loci). Means and standard error were obtained by the jackknife method. Confidence intervals obtained by 1000 resamplings through bootstrapping are also shown. * = signifcant values after Bonferroni correction.

Locus	$\theta_{L\,(regions)}$	P	$\theta_{0(overall)}$	P
*Aat-2**	0.0152	0.072	0.029	0.007
Glud	0.0009	0.227	0.086	>0.006*
*Gpi-1**	0.0058	0.086	0.003	0.210
*Gpi-2**	0.0014	0.780	0.0037	0.007
La	n.v.	0.012	0.13	>0.006*
Lgg	0.0073	0.004	0.27	>0.006
*Pap-1**	n.v.	0.068	0.024	0.001
6-Pgd	0.044	>0.006*	0.02	>0.006*
Mean	0.0067 ±0.0042		0.048 ±0.022	
CI 95%	0.0003–0.0199		0.019–0.101	

Table 4

Pairwise-regions comparison of allele frequencies for *Thunnus albacares*. Probabilities of nonheterogeneity for allozymes (based on exact tests) are above the diagonal (—) and RAPDs are below the diagonal (—). * = significant after corrected for multiple tests (Rice, 1989).

Region	Coastal	Intermediate	Offshore
Coastal	—	0.0632	0.0043*
Intermediate	0.9998	—	0.5384
Offshore	0.9039	0.9126	—

were polymorphic for all samples (Table 1). No significant heterogeneity of RAPD allele frequencies was found for any locus between any paired sample comparison, among all collections, nor among latitudinal or longitudinal regions (P=0.4806).

The mean θ value for all fragments and samples (overall), as well as regional estimations derived from RAPDs (0.0302), were not significantly different from zero and displayed some negative values. Estimations of gene flow between sample pairs (M_θ) from RAPD data averaged 29.2 migrants per generation. The evaluation of the relationships between geographic distances and the gene flow estimations in pairwise collections (M_θ), through the Mantel test, showed a nonsignificant correlation (r^2=0.413, P=0.984).

Discussion

The test of conformance to the Hardy-Weinberg frequencies showed significant differences in *Lgg* and *Pap-F** loci only in the Gulf of California sample, where polymorphism at those loci was also consistently found. Similar results were obtained, with smaller differences in locus *Aat-S** from the west of the Revillagigedo Islands and the Gulf of California samples. Considering the fact that our samples were provided by the commercial fleet, they could have included representatives of different schools with differences in genotypic distributions originated by differences in age classes or sexual ratios (or for both) among schools because recruitment of individuals into new schools has been reported to be mainly by aggregating individuals of

Table 5

Comparison of *Gpi-F** allele frequencies for *Thunnus albacares* among data from the present study and those reported in Ward et al. (1994). — = data absent.

Locus Allele	Western/Central[1]	Eastern[1]	Eastern (present data)			
			Offshore	Intermediate	Coastal	Pooled
*Gpi-F**						
135	0.026	0.100	0.103	0.147	0.163	0.145
100	0.640	0.269	0.301	0.412	0.301	0.307
75	0.332	0.631	0.596	0.441	0.566	0.548
40	0.002	—	—	—	—	—
n	346	178	83	17	196	296

[1] Allele frequencies for *Gpi-F** reported in Ward et al. (1994).

similar sizes (Collette and Nauen, 1983). Because recruitment to the original tuna schools has been reported as well (Kimley and Holloway, 1999), random processes could also induce differences in genotypic frequencies that favor aggregation of some genotypes, while segregating some others, causing a kind of Wahlund effect that is reflected by a heterozygous deficit as shown by the homozygous excess for loci and locations having HW deviations, especially as shown in the Gulf of California sample.

The estimations of population structure based on allozymes showed a small but significant value different from zero (θ=0.048; P<0.01). The Gulf of California sample contributed to the significant subdivision value as shown when that collection was excluded from the regional subdivision analysis, as well as to significant heterogeneity of its allele frequencies when paired comparisons were made.

The small value of θ for overall estimations on RAPD data is probably due to the small sample size. The negative values of θ from overall and regional estimations resulted from subtracting the large value of the correction derived from the variation expected of the sample sizes from the small value of variation due to fluctuations in allele frequencies. The fact that RAPD data are considered dominant could reduce information about the true allele distributions by subestimation of null allele frequencies notwithstanding the correction applied to recessive genotypes, which is dependent on the sample sizes (Lynch and Milligan, 1994). Other assumptions for RAPD data limit the value of this marker, especially when estimations are derived from a small number of loci and sample sizes. Additional constraints are related to the limited number of alleles (two) to estimate dominant markers, which tend to subestimate the polymorphism and thus reduce the significance of relatively small discrepancies in allele distributions.

No differentiation between coastal and offshore samples was found in our study because of the slight, nonsignificant differences in the estimation of the subdivision by regions. Although the overall estimation was not different from zero, the allele homogeneity analysis showed allele-frequency heterogeneity between coastal and offshore samples, and nonheterogeneity between coastal and intermediate samples.

These results are consistent with the migration reports through tagging studies; evidence exists for the presence of two main yellowfin tuna groups in the eastern Pacific that mix to some extent (Fink and Bayliff, 1970) and that migrate longshore from around the 20°N to the mouth of the Gulf of California and to the zone between the Revillagigedo and the Clipperton islands, and back again (Joseph et al., 1964; Fink and Bayliff, 1970), although longitudinal movements are restricted to the limits of yellowfin regulatory area (CYRA). Similarly, important northward movements along the coasts to the mouth of the Gulf of California, and subsequently to the western coasts of Baja California, have been reported. Although the estimation of θ for allozymes showed a significant value, it was notably influenced by the heterogeneity found between the Gulf of California sample and all other samples.

Discarding the variation displayed by loci *La*, *Lgg*, and *Pap-F**, originating mainly from Gulf of California sample, the estimation of subdivision was still marginally significant after Bonferroni correction, which should be considered as evidence that the Gulf of California sample may represent a partially isolated population with different allele frequencies. Oceanographic conditions inside the Gulf are somewhat different from those of the Pacific Ocean where there are warmer waters at the end of the year, especially during yellowfin tuna spawning seasons. There is also high productivity characterized by the presence of significant biomass abundance of sardine or anchovy schools (Cisneros-Mata et al., 1995), which represents opportunities to establish the feeding and consequently the spawning grounds for eastern Pacific yellowfin tuna. Likewise, there is a trend of migratory movements through the Gulf of California by different groups of yellowfin tunas (Fink and Bayliff, 1970). These movements promote stock mixing and help to explain the wide polymorphism displayed in this sample, in contrast to the weak variation found in other samples from the coast and offshore regions. Further genetic research, including sequential temporal sampling of young fishes in order to ensure the presence of individu-

als that originated in discrete spawning grounds, should be undertaken to prove the presence of an independent unit inside the Gulf of California, which, if confirmed, might necessitate new stock management strategies.

Allele frequencies for *Gpi-F** locus found in the present study, apparently, correspond to those reported by Ward et al. (1994 and 1997). These authors reported a higher proportion of the allele *Gpi-F*75* (0.571) in the eastern Pacific region and a gradual decrement of the same allele toward the central (0.423) and western Pacific regions (0.330), where allele *Gpi-F*100* (0.650) had the higher proportion. In the present study, the highest frequencies for the allele *Gpi-F*75* corresponded to the region of the eastern Pacific, situated in the limits of the yellowfin tuna regulatory area (offshore region), and there was a slight decrease in frequencies towards the coastal area (Table 5). Furthermore, allele frequencies for the *Gpi-F*75* allele from the coastal locality, Colima (0.444), and the intermediate locality southeast, Clipperton Islands (0.409), have coincidences with those reported by Ward et al. (1994) for the collection Hawaii 92 (0.423) in the central Pacific region.

The similarities in the *Gpi-F** allelic frequencies between eastern (Colima and Clipperton) and central Pacific samples (Hawaii 92) might possibly be attributed to the extended migrations of yellowfin tuna in the eastern Pacific brought about by the strong influence of warm waters on tuna movements because of the increased depth of the thermocline layer in that area, which was reflected by a decrease in catches (Joseph and Miller, 1988; Wild, 1994) and which possibly led to the mixing of the eastern and central Pacific stocks.

The low number of RAPD loci analyzed and the uncertainty of fulfilling some assumptions, such as the genetic identity of each band needed for qualitative and quantitative interpretation of data in terms of allelic frequencies, do not allow us to consider our estimations of subdivision reliable with the RAPD method. Additionally, the lack of reliability of estimations associated with high sampling variances by using randomly collected fishery samples highlights the need to design more efficient spatial and temporal sampling strategies in local and wide areas, as well as the need for alternative hypervariable markers to assess the divergence patterns observed in highly migratory species.

Acknowledgments

We are grateful to Ernesto Escobar from Pescados Industrializados S. A. PINSA for allowing the sampling, and Robert Olson from IATTC for providing the Gulf of California samples. We thank Monica Domínguez-Lopez, Yolanda Hornelas-Orozco, Evangelina Castillo, and Alma Hernández-Pérez, for collection and processing of samples, Luis Eguiarte and Valeria Souza for the facilities provided in their laboratory and three anonymous reviewers for their valuable comments. This manuscript benefited from the critical reading of John Graves, Jan McDowell, and Barbara Rutan. Funding for this project was provided by the Programa de Apoyo a Estudiantes de Posgrado (PADEP) and by the project 1N20598 of the Programa de Apoyo a Proyectos de Investigación e Innovación Tecnológica. Dirección General de Asuntos del Personal Académico, Universidad Nacional Autónoma de México.

Literature cited

Barret, I., and H. Tsuyuki.
1967. Serum transferrin polymorphism in some scombroid fishes. Copeia 1967:551–557.

Bielawski, J. P. and D. E. Pumo.
1997. Randomly amplified polymorphic DNA (RAPD) analysis of Atlantic coast striped bass. Heredity 78:32–40.

Cisneros-Mata, M. A., Nevarez-Martinez, M. O., and Hammann, M. G
1995. The rise and fall of the Pacific sardine, *Sardinops sagax caeruleus* Girard, in the Gulf of California, Mexico. CALCOFI Rep. 36:136–143.

Collette, B. B., and C. E. Nauen.
1983. Scombrids of the world: an annotated and illustrated catalogue of tunas, mackerels, bonitos and related species known to date. *In* FAO species catalogue, vol. 2, 137 p. FAO Fish. Synop. 1325. FAO, Rome.

Fink, B. D., and W. H. Bayliff.
1970. Migrations of yellowfin and skipjack tuna in the eastern Pacific Ocean as determined by tagging experiments, 1952–1964. Inter-Am. Trop. Tuna Comm. Bull. 15:1–227.

Fujino, K.
1970. Immunological and biochemical genetics of tunas. Trans. Am. Fish. Soc. 99:152–178.

Gibbs, R. H., and B. B. Collette.
1967. Comparative anatomy and systematics of the tunas, genus *Thunnus*. Fish. Bull. 86:835–838.

Godsil, H. C., and E. C. Greenhood.
1951. A comparison of the populations of yellowfin tuna (*Neothunnus macropterus*) from the eastern and central Pacific, 33 p. Calif. Dep. Fish Game Fish. Bull. 82.

Harris, H., and D. A. Hopkinson.
1976. Handbook of enzyme electrophoresis in human genetics, 273 p. Am. Elsevier Publishing Co., New York, NY.

Hellberg, M. E.
1994. Relationships between inferred levels of gene flow and geographic distance in a philopatric coral, *Ballanophyllia elegans*. Evolution 48:1829–1854.

IATTC (Inter-American Tropical Tuna Commission).
1975. Annual report of the Inter-American Tropical Tuna Commission, 169 p. IATTC, LaJolla, CA.
1999. Annual report of the Inter-American Tropical Tuna Commission, 357 p. IATTC, LaJolla, CA.

Joseph, J., F. G. Alverson, B. D. Fink, and E. B. Davidoff.
1964. A review of the population structure of yellowfin tuna, *Thunnus albacares*, in the eastern Pacific Ocean. Inter-Am. Trop. Tuna Comm. Bull. 9(2):53–112.

Joseph, J., and F. R. Miller.
1988. El Niño and the surface fishery for tunas in the eastern Pacific. Proceedings of the Tuna Fisheries Research Conference, Japan Fish. Far Seas Fish. Res. Lab. Maguro Gyogyo Kyogikai Gijiroku, Suisancho-Enyo Suisan Kenkyusho:199–207

Kenji, S.
1998. Genetic variation and local differentiation in the Pacific cod *Gadus macrocephalus* around Japan revealed by mtDNA and RAPD markers. Fish. Sci. 64(5):673–679.

Kimley, A. P., and C. F. Holloway.
1999. School fidelity and homing synchronicity of yellowfin tuna, *Thunnus albacares*. Mar. Biol. 133:307–317.
Kurogane, K., and Y. Hiyama.
1957. Morphometric comparison of the yellowfin tuna taken from the Equatorial Pacific. Jpn. Soc. Sci. Fish. Bull. 23: 388–293.
Leis, J. M., T. Trnski, M. Harmelin-Vivien, J.-P. Renon, V Dufour, M. K. El Moundi, and R. Galzin.
1991. High concentrations of tuna larvae (Pisces: Scombridae) in near-reef waters of french polynesia (Society and Taumotu islands). Bull. Mar. Sci. 48(1):150–158.
Le Corre, S., S. Dumolin-Lapegue, and A. Kremer.
1997. Genetic variation at allozyme and RAPD loci in sessile oak *Quercus petraea* (Matt.) Liebl.: the role of history and geography. Mol. Ecol. 6:519–529.
Lynch, M., and B. G. Milligan.
1994 Analysis of population genetic structure with RAPD markers. Mol. Ecol. 3:91–99.
Mamuris, Z., A. P. Apostodilis, A. J. Theodoru, and C. Triantaphyllidis.
1998. Application of random amplified polymorphic DNA (RAPD) markers to evaluate intraspecific genetic variation in red mullet (*Mullus barbatus*). Mar. Biol. 132: 171–178.
Raymond, M. L., and F. Rousset.
1995. An exact test for population differentiation. Evolution 49:1280–1283.
Rice, W. R.
1989. Analyzing tables of statistical tests. Evolution 43: 223–225.
Sambrook, J., E. F. Fritsch, and T. Maniatis.
1989. Molecular cloning: a laboratory manual, 2nd ed., 999 p. Cold Spring Harbor Laboratory, Cold Spring Harbor, NY.
Scoles, D. R., and J. E. Graves.
1993. Genetic analysis of the population structure of yellowfin tuna, *Thunnus albacares*, from the Pacific Ocean. Fish. Bull. 91:690–698.
Schaefer, K. M.
1991. Geographical variation in morphometric characters and gill-raker counts of yellowfin tuna *Thunnus albacares*, from the Pacific Ocean. Fish. Bull. 9:690–698.
Schaefer, M. B.
1955. Morphometric comparison of yellowfin tuna from southeast Polynesia, Central America, and Hawaii. Inter-Am. Trop. Tuna Comm. Bull. 1:89–136.
Sharp, G. D.
1978. Behavioral and physiological properties of tunas and their effects on vulnerability to fishing gear. *In* The physiological ecology of tunas (G. D. Sharp and A. E. Dizon, eds.), p. 397–449. Academic Press, New York, NY.
Slatkin, M.
1993. Isolation by distance in equilibrium and non-equilibrium populations. Evolution 47:264–279.
Sokal, R., and F. J. Rohlf.
1995. Biometry, 3rd ed., 776 p. W. H. Freeman and Co., New York, NY.
Suzuki, Z., P. K. Tomlinson, and M. Honwa.
1978. Population structure of Pacific yellowfin tuna. Inter-Am. Trop. Tuna Comm. Bull. 17:273–441.
Ward, R. D., N. G. Elliott, P. M Grewe, and A. Smolenski.
1994. Allozyme and mitochondrial DNA variation in yellowfin tuna (*Thunnus albacares*) from the Pacific Ocean. Mar. Biol. 118:531–539.
Ward, R. D., N. G. Elliott, B. H. Innes, A. J. Smolenski, and P. M. Grewe.
1997. Global population structure of yellowfin tuna, *Thunnus albacares*, inferred from allozyme and mitochondrial DNA variation. Fish. Bull. 95:566–575.
Weir, B. S.
1990. Genetic data analysis, 377 p. Sinauer, Sunderland, MA.
Weir, B. S., and C. C. Cockerham.
1984. Estimating *F* statistics for the analysis of population structure. Evolution 38:1358–1370.
Welsh, J., C. Petersen, and M. McCelland.
1991. Polymorphisms generated by arbitrary primed PCR in the mouse: application to strain identification and genetic mapping. Nucl. Acids Res. 19:303–306.
Wild, A.
1994. A review of the biology and fisheries for yellowfin tuna, *T. albacares*, in the eastern Pacific Ocean. FAO Fish. Tech. Pap. 336(2):52–107.
Williams, J. G, A. R. Kubelik, J. Livak, J. A. Rafalaski, and S. V. Tingey.
1990. DNA polymorphisms amplified by arbitrary primers are useful as genetic markers. Nucl. Acids Res. 18: 6531–6535.

The early life history of swordfish (*Xiphias gladius*) in the western North Atlantic

John Jeffrey Govoni
Elisabeth H. Laban
Jonathan A. Hare

Center for Coastal Fisheries and Habitat Research
National Oceanic and Atmospheric Administration
101 Pivers Island Road
Beaufort, North Carolina 28516-9722
E-mail address (for J. J. Govoni): Jeff.Govoni@noaa.gov

Abstract—Lengths and ages of swordfish (*Xiphias gladius*) estimated from increments on otoliths of larvae collected in the Caribbean Sea, Florida Straits, and off the southeastern United States, indicated two growth phases. Larvae complete yolk and oil globule absorption 5 to 6 days after hatching (DAH). Larvae <13 mm preserved standard length (PSL) grow slowly (~0.3 mm/d); larvae from 13 to 115 mm PSL grow rapidly (~6 mm/d). The acceleration in growth rate at 13 days follows an abrupt (within 3 days) change in diet, and in jaw and alimentary canal structure. The diet of swordfish larvae is limited. Larvae <8 mm PSL from the Caribbean, Gulf of Mexico, and off the southeastern United States eat exclusively copepods, primarily of one genus, *Corycaeus*. Larvae 9 to 11 mm eat copepods and chaetognaths; larvae >11 mm eat exclusively neustonic fish larvae. This diet indicates that young larvae <11 mm occupy the near-surface pelagia, whereas, older and longer larvae are neustonic. Spawning dates for larvae collected in various regions of the western North Atlantic, along with the abundance and spatial distribution of the youngest larvae, indicate that spawning peaks in three seasons and in five regions. Swordfish spawn in the Caribbean Sea, or possibly to the east, in winter, and in the western Gulf of Mexico in spring. Elsewhere swordfish spawn year-round, but spawning peaks in the spring in the north-central Gulf of Mexico, in the summer off southern Florida, and in the spring and early summer off the southeastern United States. The western Gulf Stream frontal zone is the focus of spawning off the southeastern coast of the United States, whereas spawning in the Gulf of Mexico seems to be focused in the vicinity of the Gulf Loop Current. Larvae may use the Gulf of Mexico and the outer continental shelf off the east coast of the United States as nursery areas. Some larvae may be transported northward, but trans-Atlantic transport of larvae is unlikely.

Manuscript approved for publication 17 April 2003 by Scientific Editor.
Manuscript received 26 June 2003 at NMFS Scientific Publications Office.
Fish. Bull. 101:778–789 (2003).

Swordfish (*Xiphias gladius*) live in warm waters of the world's oceans, as well as in large enclosed basins such as the Caribbean and Mediterranean seas, and the Gulf of Mexico (Berkeley, 1983). Swordfish are highly migratory throughout their global range. The worldwide population structure, as currently understood, has at least three breeding units: Mediterranean, northwestern Atlantic to the tropical South Atlantic, and Indo-Pacific (Kotoulas et al., 1995; Chow and Takeyama, 2000; Reeb et al., 2000). For the purpose of fishery management, the International Commission for the Conservation of Atlantic Tunas (ICCAT) recognizes only North Atlantic and South Atlantic stocks. Possible genetic exchange between eastern and western North Atlantic populations is incompletely documented.

Swordfish reportedly spawn yearround in the western North Atlantic in different seasons and regions. Spawning season and location has been inferred from the abundance of small larvae (Gorbunova, 1969; Richards and Potthoff, 1980; Potthoff and Kelley, 1982; Grall et al., 1983; Govoni et al., 2000), gonad maturation (LaMonte, 1944; Beckett, 1975), or oocyte cytology (Taylor and Murphy, 1992; Arocha, 1997; Arocha, 2002). The observation of live females with running eggs, hooked on long-lines, and followed to the fishing vessel by several smaller males (Lee[1]; Berkeley[2]) corroborates spawning in some seasons and locations. Although gonad condition and oocyte status can indicate spawning season, the resolution of spawning location can be ambiguous with these methods because mature gonads and hydrated oocytes can be found in several seasons within the range of these highly migratory fishes. The determination of age and the distribution of young larvae, along with realistic estimates of water velocity and trajectory, help to resolve this ambiguity.

Beyond spawning, the early life history of swordfish in any ocean is incompletely described (Palko et al., 1981). Larvae undergo a stark change in physical appearance between ~8 and 13 mm preserved standard length (PSL), from a typical scombroid larval form to a juvenile istiophorid one (Collette et al., 1984). At this juncture in development, larvae develop characteristic preorbital, supraorbital, posttemporal, and preopercular spines; enlarged and spinous dorsal, ventral, and lateral scale anlagen; and a continuous long dorsal fin that extends along most of the dorsal aspect. Swordfish retain these larval characters until they are at least 188 mm PSL (Arata, 1954; Potthoff and Kelley, 1982), a size at which most fishes are considered juveniles. By using the ages and lengths of larvae hatched in the laboratory and reared through yolk and oil globule absorption (Sanzo, 1910; Yasuda et al., 1978), along with length frequencies of larvae caught in the western North Atlantic,

[1] Lee, D. J. 1995. Personal commun. Southeast Fisheries Science Center, NMFS, 75 Virginia Beach Drive, Miami, FL 33149.

[2] Berkeley, S. A. 1998. Personal commun. Long Marine Laboratory, Univ. California, Santa Cruz, 100 Shaffer Road, Santa Cruz, CA 95060.

Arata (1954) inferred the age and growth of larvae from 6 to 192 mm preserved total length (PTT). Aside from this effort, the age of larval swordfish has been undetermined and growth has not been described. Diets of larvae have been reported (Gorbunova, 1969), but the apparent transition in diet has neither been detailed nor reconciled with changes in physical features and growth. Similarly, the vertical distribution of larvae has not been reconciled with their diet or growth. Most larvae are collected near the surface of the ocean, typically in neuston nets, but some larvae are collected in nets that sample below the surface (Govoni et al., 2000).

In the present study, we resolve and summarize the early life history of swordfish in the western North Atlantic. We report estimated age, describe growth, relate growth to feeding, morphological features, and vertical distribution, and infer spawning time and location and the sources and fates of swordfish larvae. This study supplements that of Govoni et al. (2000) by providing the dimension of time, i.e. age of larvae, to the spatial distribution and possible transport of these larvae.

Methods

Collections of larvae

Ichthyoplankton collections from cruises in 1989 (in the northeastern Caribbean about the Lesser Antilles), 1991 and 1997 (off the southeastern United States), and 2000 (in the Straits of Florida and off the southeastern United States), produced 63 larvae that were preserved in 95% ethanol (for examination of otolith microstructure). Samples were collected either from the neuston (i.e. taken with a 1.0×0.5 m neuston net) or from depth intervals (i.e. taken with a 1-m MOCNESS [multiple opening and closing net and environmental sampling system] [Wiebe et al., 1976]). Larvae were measured for preserved standard length (PSL), the conventional length measure for larval fishes (Kendall et al., 1984), and lower-jaw-fork-length (LJFL), the measure in common use for juvenile and adult swordfish (Megalofonou et al., 1995).

Otolith excision and examination

Of the 63 larvae collected, sagittae were found and successfully excised from 37 larvae, lapilli from 32, and asterisci from six. Otoliths were mounted on glass slides and dried before examination. Broken sagittae and lapilli, and some large sagittae, were embedded in plastic, sectioned with a saw, and polished (Secor et al., 1991).

Otolith growth increments were counted along the longest axis of each sagitta and lapillus by using a compound light-transmission microscope; increments in asterisci were fewer and less defined and were not counted. Three blind counts were made by the same observer. Although increments were consistently visible on both sagittae and lapilli, counts from individual larvae were greater on sagittae (Student's t-test; $P<0.001$). Standardized counts (the standard deviate of each repeated count) on the right and left sagittae were not significantly different (nested ANOVA; $P<0.05$). Increment counts from either the left or right sagitta, decided by coin toss, were used for age and growth rate determination. The mean of three replicate counts was rounded to a whole number.

Increment counts from sagittae were used to estimate larval age. Increments were assumed to form daily (Campana, 2001). The core increment was assumed to form at hatching (Jones, 1986). The first increment outside of the core increment was counted as one. Age from hatching (AFH) was the number of increments counted from the core increment on sagittae. This definition differs from that of Prince et al. (1991) who counted the core increment as increment one for the istiophorid blue marlin (*Makaira nigricans*) and for a single larval swordfish that was 8.5 PSL. The radius of each otolith was measured by image analysis.

Growth model

The best empirical fit among a suite of regressions of estimated age (AFH) and length (PSL)—linear, polynomial, and piece-wise, and moving—was chosen to describe somatic growth (Forbes and Lopez, 1989; Hare and Cowen, 1995; Rogers et al., 2001). Criteria for best fit were the following: the interpretation of fit from graphical display; regression coefficients (r^2), and dispersion or convergence of regression residuals. The model of best fit was also applied to the estimated age and lower jaw fork length (LJFL) to allow comparison with published accounts of juvenile swordfish growth.

Diet

Sixty-eight specimens from the present collections and from Govoni et al. (2000), all with undamaged alimentary canals, were examined for gut contents. These specimens were taken in the northeastern Caribbean (3 specimens), Gulf of Mexico (5), and off the southeastern coast of the United States (60). Food was identified to the lowest taxon possible following Govoni et al. (1983).

Physical features of larvae

Histological sections of three larvae, 21.5, 30.0, and 52.0 mm PSL, were cut as a preliminary aid to the location of otoliths within the cranium and to determine the histological constitution of the larval alimentary canal.

Time and location of spawning

Spawning dates were estimated from the ages of larvae (estimated from the growth model (AFH)), plus 3 days (the incubation period at 25°C for swordfish eggs given by Yasuda et al. [1978]). Spawning dates are thus days from fertilization (DFF). Spawning location was inferred by applying DFF to larval swordfish lengths reported in the present study, as well as lengths given in Govoni et al. (2000), taking into consideration the time that eggs and larvae were at large and adrift (DFF) and the location where

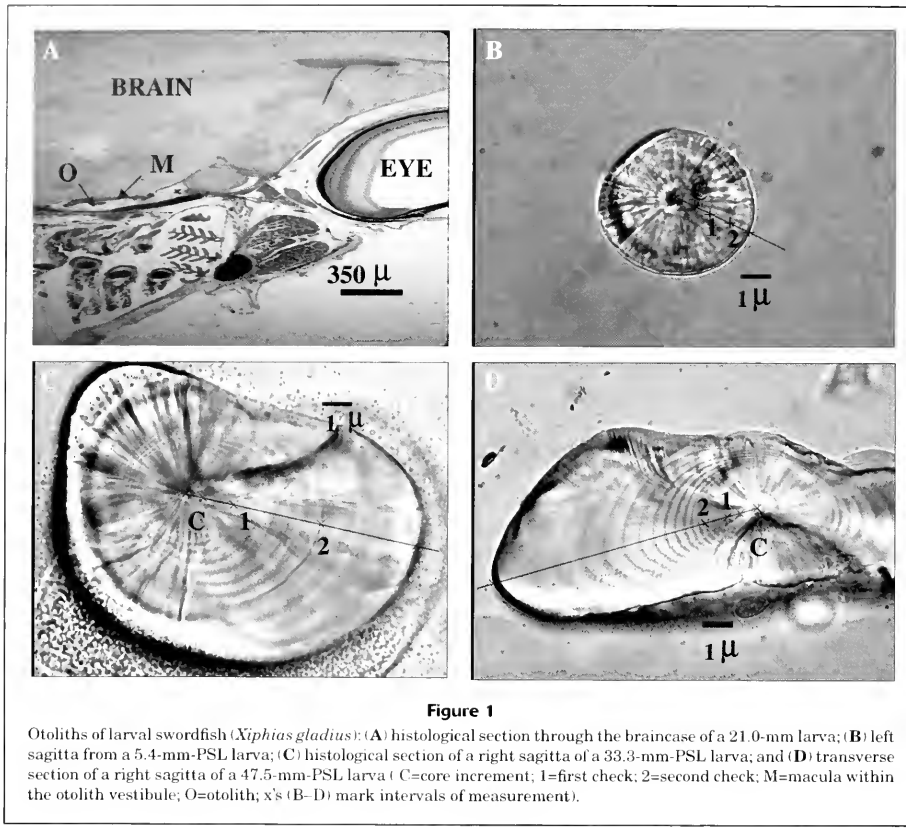

Figure 1

Otoliths of larval swordfish (*Xiphias gladius*): (**A**) histological section through the braincase of a 21.0-mm larva; (**B**) left sagitta from a 5.4-mm-PSL larva; (**C**) histological section of a right sagitta of a 33.3-mm-PSL larva; and (**D**) transverse section of a right sagitta of a 47.5-mm-PSL larva (C=core increment; 1=first check; 2=second check; M=macula within the otolith vestibule; O=otolith; x's (B–D) mark intervals of measurement).

larvae were collected, and back-calculating the geographic origin of eggs with mean axial trajectories and velocities of water currents for the Yucatan, Gulf Loop, Florida Currents, and the Gulf Stream (~1.5 m/s [Maul and Vukovich, 1993; Olson et al., 1994; Boicourt et al., 1998]) and the Caribbean Sea (~0.2 m/s [Mooers and Maul, 1998]).

Results

Otolith structure and increment counts

Sagittae and lapilli were round, extremely small, and lacked rostra or sulci in larvae <5 mm PSL (Fig. 1, A and B). A rostrum developed on sagittae at ~5.5 mm PSL (Fig. 1C). Lapilli did not develop rostra, and remained symmetrical with growth.

Two checks, distinct zones of irregular increment spacing and opacity, were evident on most sagittae (Fig. 1, B–D). The first check was evident at the third increment on all sagittae examined. The second check was found on sagittae from larvae >3.8 PSL but varied from the seventh to tenth increment.

Growth model

A piece-wise regression (Table 1; Equations 5–7) with two linear segments provided the best fit with biologically realistic parameters. An assigned intercept of 3.2 mm PSL was used for the first segment; this value was obtained by adjusting the length at hatching with the scale given by Yasuda et al. (1978) and by accounting for shrinkage due to preservation. Growth rate for the first segment was 0.3 mm/d and 5.9 mm/d PSL for the second segment (Fig. 2A). The intersection of the two linear segments was at an estimated age of 13.3 d AFH., 3 to 6 d after the observed second check. The PSL of larvae at the intersection was 11.0 mm.

Growth rate in LJFL, also modeled with a piecewise regression, was 0.2 mm/d for the first segment (the upper and lower jaws of larvae <11 mm PSL are of equal length,

Table 1

Summary of models evaluated for describing growth of larval swordfish. Models 1–6 were preserved standard length (PSL) as a function of estimated age from hatching (AFH); model 7 was lower jaw fork length (LJFL) as a function of AFH. There were three model types: linear regression (models 1 and 2), 2nd order polynomial (models 3 and 4), and piecewise regression (models 5–7). *Y*-intercepts (model parameter *a*) were estimated by the regression in Equations 1, 3, and 5 but were fixed at an observed length at hatching of 3.2 mm from Yasuda et al. (1978) in Equations 2, 4, 6, and 7 ("ns" denotes that *a* was not significantly different from an assigned *a* of 3.2 at α=0.05; * = *y*-intercept significantly different from 3.2 at α=0.05; na = not applicable; *b* and *c* are slopes; and *d* is the inflection point).

	Model parameters				Model fit	
Model	*a*	*b*	*c*	*d*	r^2	Residuals
1. $PSL = a + b\text{AFH}$	−39.11*	4.15	na	na	0.81	not normal
2. $PSL = 3.2 + b\text{AFH}$	3.20 na	1.47	na	na	0.81	not normal
3. $PSL = a + b\text{AFH} + c\text{AFH}^2$	11.31 ns	−2.77	0.22	na	0.92	normal
4. $PSL = 3.2 + b\text{AFH} + c\text{AFH}^2$	3.20 na	−1.75	0.19	na	0.91	normal
5. $PSL = a + b\text{AFH} + c(\text{AFH} - d) \times (\text{AFH } d)$	−2.22*	0.76	5.10	13.53	0.89	normal
6. $PSL = 3.2 + b\text{AFH} + c\ (\text{AFH}-d) \times (\text{AFH} \geq d)$	3.20 na	0.26	5.60	13.29	0.89	normal
7. $LJFL = 3.2 + b\text{AFH} + c\ (\text{AFH} - d) \times (\text{AFH} \geq d)$	3.20 na	0.16	3.28	11.24	0.77	ns

Table 2

Diet composition of 68 larval swordfish (*Xiphias gladius*) in the western North Atlantic.

Diet item	% Frequency of occurrence (among larvae with food)	% total number (among all food items)
Copepodites and adult copepods (unidentifiable)	5	2
calanoids		
Eucalanus	2	1
cyclopoids		
Corycaeus spp.	59	74
Oithona spp.	4	2
Chaetognaths	2	1
Larval and juvenile fishes	33	16
Invertebrate eggs	2	2
Chyme	5	2

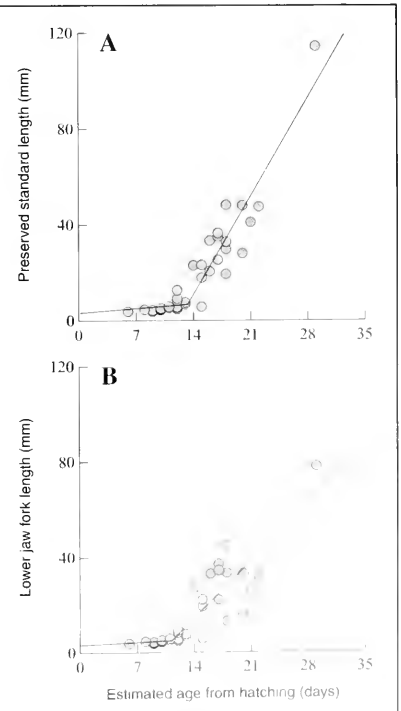

Figure 2

Growth of larval swordfish from the western North Atlantic: (A) estimated age and PSL; (B) estimated age and LJFL.

hence PSL=LJFL) and 3.4 mm/d for the second segment (Fig. 2B).

The fit of the piecewise regression for PSL and LJFL was unchanged by inclusion or exclusion of the estimated age of the largest larva.

Diet

The diet of larvae is limited and transitional. Larvae <8.3 mm PSL ate copepods exclusively, primarily a single cyclopoid genus, *Corycaeus* spp., but also another cyclopoid, *Oithona* spp., and the calanoid *Eucalanus* (Table 2). Larvae 9.0 to 11.0 mm PSL ate copepods (Fig. 3A) and chaeto-

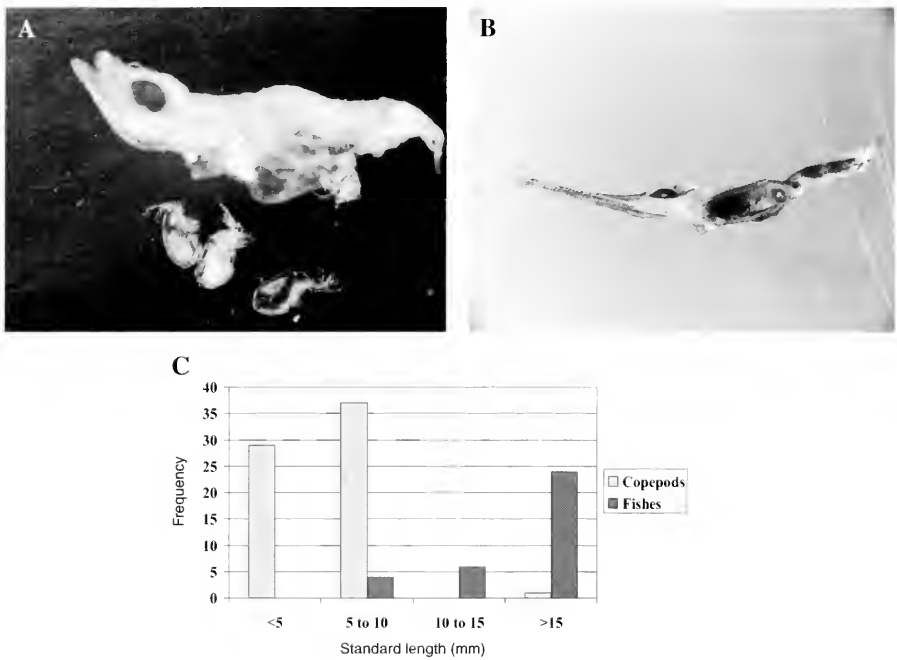

Figure 3

Diet composition of larval swordfish from the western North Atlantic: (**A**) a 3.9-mm-PSL larva and cyclopoid copepods (genus *Corycaeus*) that were removed from the gut; (**B**) a 12.7-mm larva with a larval fish in its gut; and (**C**) the frequency of occurrence of copepods and larval fishes in the guts of larval swordfish.

gnaths. Larvae >11.0 mm PSL ate almost exclusively larval and juvenile fishes (Fig. 3, B and C). Remnant jaws and heavy pigmentation of many of the fishes eaten, indicated that most were neustonic. One exocoetid was identified by intact pectoral fins and counts of vertebrae.

Jaw and alimentary canal structure

The structure of the alimentary canal and jaws changed concomitantly. The alimentary canal began to change from three segments (foregut, midgut and hindgut), typical of larval fishes (Govoni et al., 1986a), to four segments (esophagus, stomach, anterior intestine, and posterior intestine) between 9.0 and 12.0 mm PSL. Jaws change during this period from the beak-like jaws to the elongate rostral bill of the istiophorids (Fig. 3, A and B). Gastric glands were evident in the fundic region of the stomach (ventricili-gastric cecum), close to the junction with the esophagus in the 30.0-mm-PSL larva (Fig. 4, A and B). The pyloric region of the stomach (pars pylorica) was evident in the 21.5-mm-PSL larva and the 30.0-mm larva.

Time and location of spawning

Back-calculated spawning dates demonstrated year-round spawning and peaks in three seasons and five regions (Fig. 5, A–C). Larvae collected in the eastern Caribbean were spawned in the winter (northern hemisphere) only. Larvae collected in the western Gulf of Mexico were spawned in spring. In the north-central Gulf of Mexico, larvae were spawned in all seasons, but spawning peaked in spring. Off south Florida, larvae were spawned in all seasons, and spawning peaked peaked in spring. Larvae collected off the southeastern United States were spawned throughout the year whereas larvae collected in the north-central Gulf of Mexico and in southern Florida waters were spawned mostly in spring and early summer.

Modes of the number of larvae collected and their estimated DFF advanced slightly in day of the year from the north-central Gulf of Mexico to off the southeastern United States. Larvae <10 DFF were collected both in the north-central Gulf of Mexico and off the southeastern United States (Fig. 5D), but not off South Florida.

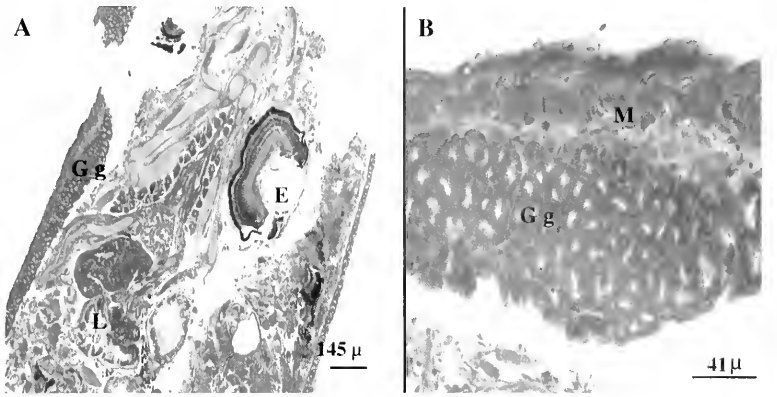

Figure 4

Photomicrographs of a 30.0-mm-PSL swordfish larva: (**A**) fundic stomach; (**B**) gastric glands in stomach mucosa (Gg=gastric glands; M=mucosa; L=stomach lumen with larval fish remains; E=eye of eaten larval fish).

Discussion

The first check on sagittae apparently corresponds with the completion of yolk and oil globule absorption and the beginning of feeding. Sanzo (1910) and Yasuda et al. (1978) reported hatching 3 days after fertilization when larvae were ~4 mm live total length (LTL), or 3.8 mm live standard length (scaled from their drawings), and complete yolk and oil globule absorption 8 d after fertilization (or 5 DAH) when larvae were ~5 mm LTL, or 4.3 mm live standard length. Larvae from the present material had completed yolk and oil absorption between 3.8 and 3.9 mm PSL and had the first check 3 increments after the core increment. Temperature and feeding influence the growth rate of fish larvae and their otoliths, but larvae are typically collected in water 25 ±1°C (Arata, 1954; Tåning, 1955; Tibbo and Lauzier, 1969; Markle, 1975; Govoni et al., 2000), as were the larvae collected for age determination. This temperature is common to the Gulf Stream and its progenitor currents (Schmitz et al., 1993; Hitchcock et al., 1994), and is similar to the temperature used to rear larvae (Sanzo, 1910; Yasuda et al., 1978). The difference in length at complete yolk and oil absorption between Sanzo (1910) and Yasuda et al. (1978) and the present collections probably owes to shrinkage of larvae with death and preservation (e.g. Theilacker, 1980).

The second check follows concomitant changes in diet and morphological features that take place between 8 and 13 mm PSL or from 7 to 11 DFH. An acceleration in somatic growth follows the second check within a day or so. Young swordfish larvae eat copepods; older larvae other larval fishes. The most striking morphological change of larval swordfish is in the jaws. Swordfish larvae <13 mm SL have beak-like jaws that are typical of the larval scombroid fishes (Collette et al., 1984), particularly those of the wahoo (*Acanthocybium solandri*) and scaleless tuna (*Gymnosarda unicolor*); older larvae develop bill-like jaws with elongate rostral cartilages anterior of the premaxillaries and equally elongate mandibles (McGowan, 1988). The constitution of the alimentary canal changes as well. The development of a functional stomach with gastric glands in larval swordfish, which typically arises during the metamorphosis of fishes (Govoni et al., 1986a), is evident in the larvae of other scombroid fishes where it is accompanied similarly by a change in diet from zooplankton to fish (Kaji et al., 1999; Shoji et al., 1999). A switch from zooplankton to fish is common among istiophorid larvae, but it is neither as exclusive nor abrupt (Voss, 1953; Lipskaya and Gorbunova, 1977) as it is with swordfish. Accelerated growth after such a dietary shift is also a common trait of scombroid larvae (Shoji et al., 1999).

Swordfish larvae grow rapidly, faster than other larval fishes with reportedly rapid growth. Growth rates reported in the present study are for larvae that have survived predation and possibly variable feeding success; these rates do not necessarily represent average larval growth of the overall population. Growth rates of larvae >11 mm PSL (13 DAH), 5.6 mm/d, are nonetheless faster than the larval growth rates of other fast-growing larvae that survive in the sea, e.g. sablefish (*Anoplopoma fimbria*) (Boehlert and Yoklavich, 1985), and the oceanic-pelagic common dolphinfish (*Coryphaena hippurus*) reared in the laboratory at high food densities without predation (Hassler and Hogarth, 1977; Kraul, 1991). The growth rate of larval swordfish <13 mm LJFL, 3 mm/d, is slower than the maximum (16 mm LJFL/d) and sustained (10 mm LJFL/d) growth

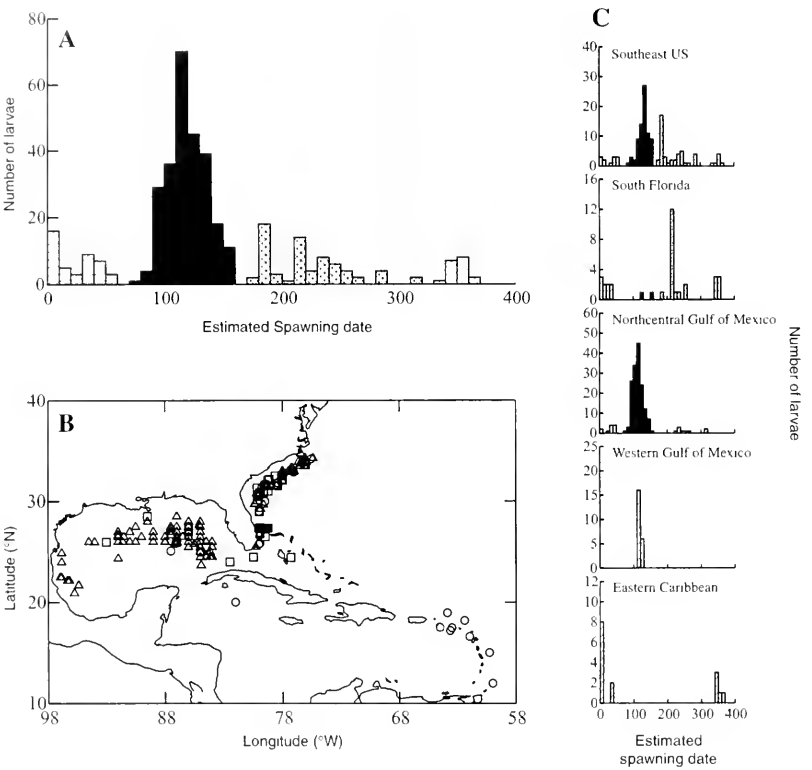

Figure 5

Estimated spawning dates (day of the year) for swordfish larvae collected from the Caribbean Sea, the Gulf of Mexico, and off the southeast coast of the United States (hatched bars and circles depict winter in the northern hemisphere, filled bars and triangles spring-summer, and cross-hatched bars and squares summer-fall): (**A**) number of larvae and estimated spawning dates; (**B**) geographical distribution of larval collections; (**C**) number of larvae and estimated spawning date by region; (**D**) number of larvae by region and season.

rate of larval blue marlin over the first 100 days or <1000 mm LJFL (Prince et al., 1991).

Larval and juvenile swordfish from the western North Atlantic and Mediterranean exhibit four growth phases. Growth is linear for larvae <11 mm PSL, for larvae 11 to 115 PSL, and for juveniles 510 to 740 mm LJFL (Megalofonou et al., 1995). Growth becomes allometric for larger juveniles (Ehrhardt, 1992). Larvae <11 mm grow ~0.1 mm LJFL/d. After the acceleration of growth, larvae in the western North Atlantic grow at ~3 mm LJFL/d, whereas young juveniles in the Mediterranean grow at 23 mm LJFL/d (Megalofonou et al., 1995). Growth slows in older juveniles <250 mm LJFL to ~2.5 mm LJFL/d (Ehrhardt, 1992). Adult growth (Berkeley and Houde, 1983; Tserpes and Tsimenides, 1989) may constitute a fifth phase, as recognized by Yabe et al. (1959) for Pacific swordfish.

The limited diet of larval swordfish is unusual; few larval fishes prey almost exclusively upon either copepods or larval fishes. Swordfish larvae 12.0 mm total length (TL) eat zooplankton, and larger larvae >12.0 mm TL eat other fish larvae (Gorbunova and Lipskaya, 1975), including conspecifics (Arata, 1954). Larval fishes as a whole are selective feeders; *Corycaeus* is selected by larval percoids in the Gulf of Mexico (Govoni et al., 1986b). Young larval istiophorids from the Florida Current eat primarily cyclopoid copepods of the genera *Corycaeus*, *Farranula*, and *Oithona* (Post et al., 1997), before they become piscivorous (Gorbunova and Lipskaya, 1975). Closely related genera of fishes exhibit

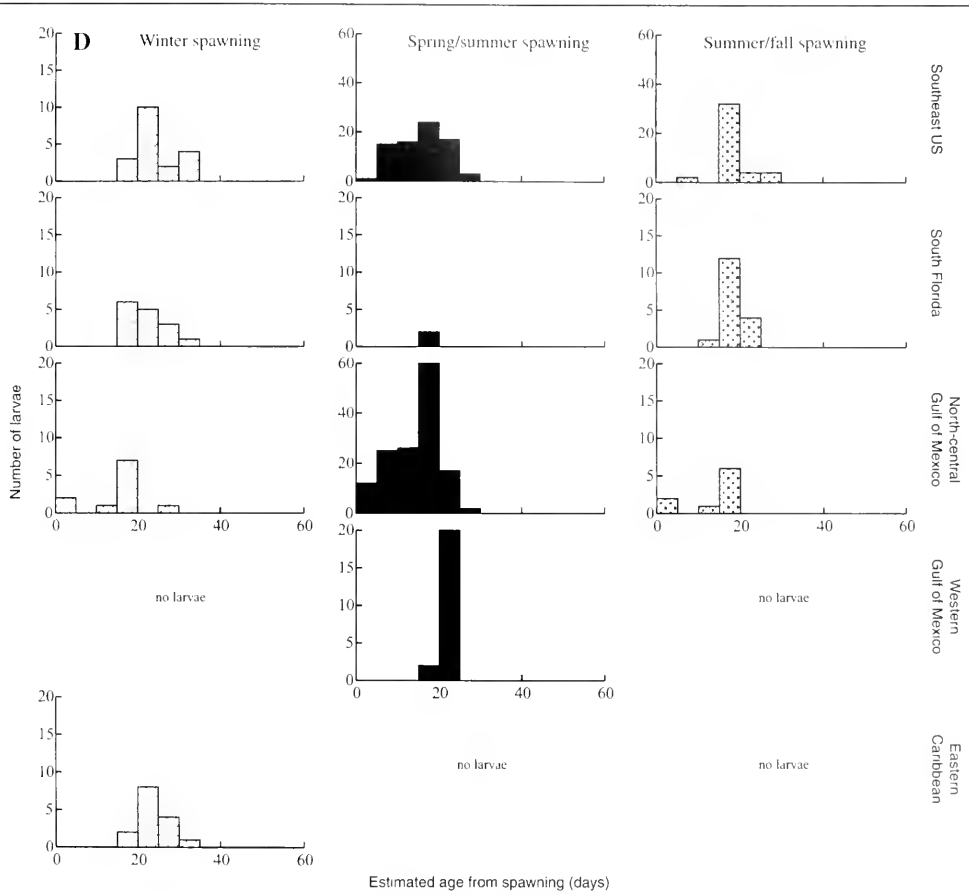

Figure 5 (continued)

different diets, even when occupying the same space (e.g. Govoni et al., 1983; 1986b). Larvae of the related istiophorids have limited diets, but these are not as exclusive or abruptly changing as that of swordfish. Diets of larvae examined in our study showed no evidence of cannibalism.

The diet of larval swordfish helps to resolve their vertical distribution. Most larvae have been collected at the surface in neuston or dip nets (Tåning, 1955; Yabe et al., 1959; Gorbunova, 1969; Nishikawa and Ueyanagi, 1975), although some have been collected in plankton nets that fished principally below the surface (Grall et al., 1983; Govoni et al., 2000). The diet of swordfish larvae indicates that larvae <11 mm PSL may live in the near surface water, whereas larvae >11 mm are neustonic. *Corycaeus* is a common neritic copepod of the Caribbean, the Florida Current, and the continental shelf off the southeast coast of the United States; *Corycaeus* is not neustonic (Owre and Foyo, 1967; 1972; Paffenhöfer, 1983; 1985). That *Corycaeus* is eaten almost exclusively by young swordfish larvae implies that these larvae occupy the near-surface pelagia. Istiophorid larvae undertake dietary shifts (Voss, 1953; Gorbunova and Lipskaya, 1975; Lipskaya and Gorbunova, 1977) and changes in vertical distribution (Bartlett and Haedrich, 1968; Leis et al., 1987) that are similar to those of swordfish larvae, but conflicting evidence exists for vertical distribution of larval istiophorids. Gorbunova and Lipskaya (1975) implied that istiophorid larvae accumulate in surface waters during the day and disperse below the surface

at night, but Bartlett and Haedrich (1968) indicated the reverse. Large swordfish larvae are caught during the day and night in the neuston. The restricted diets of both large and small larvae implies little vertical movement.

The overall modal increase in larval age from the Gulf of Mexico to the north indicates that spawning takes place in the north-central Gulf of Mexico and off the southeast coast of the United States and that there is possible northward transport. Estimated ages, along with velocities and trajectories of currents, indicate that larvae could be transported from considerable distances, but only if they remain within the axes of major currents. The smallest larva collected off the Carolinas was 3.9 mm PSL and had an estimated age of 7 d AFH (this specimen was previously reported as being approximately 4 days old in Govoni et al. [2000]). With 3 days incubation at 25°C added to this estimated age, a swordfish egg and larva would be planktonic for 10 days. With a mean axial trajectory and velocity of the Florida Current and Gulf Stream of 1.5 m/s (Olson et al., 1994), a larva 3.9 mm PSL could be transported from as far away as 910 km, which could place the origin of this larva in the Straits of Florida, if its northward progress had not been checked by eddies so typical of the Gulf Loop Current (Maul and Vukovich, 1993) and Gulf Stream, particularly after the Gulf Stream exits the Straits of Florida (e.g. Lee et al., 1991; Govoni and Hare, 2001). Off the southeast coast of the United States, swordfish larvae aggregate in the western Gulf Stream frontal zone (Govoni et al., 2000), where northward current velocities are considerably slower than 1.5 m/s (Marmorino et al., 1999). Because larvae reside primarily in the western Gulf Stream frontal zone where northward velocities are slower and where the front itself is so frequently distorted by meanders and eddies, it is unlikely, but not impossible, that a larva as young as 7 d AFH collected off the Carolinas of the United States could have been transported from the Straits of Florida.

The largest and oldest larva examined, one collected off South Carolina (Govoni and Hare, 2001), was 115 mm PSL and had an estimated age of 30 d AFH; with 3 days incubation this fish could have been at large for 33 days and would have traveled 4290 km, given the mean axial trajectories and velocities of the Caribbean Sea (~0.2 m/s) and the Yucatan, Gulf Loop, and Florida Currents (~1.5 m/s). This calculation might place the spawning origin of this larva in the eastern Caribbean Sea or south of the Sargasso Sea if a direct, unchecked passage is assumed.

Inference of the seasonality and geography of spawning is limited and biased by the unsystematic temporal and spatial distribution of the present collections of larval swordfish and by uncertainties about the rate and trajectory of transport of eggs and larvae. Yet, taken as a whole, spawning dates, back-calculated from larvae collected in various regions of the western North Atlantic, and the abundance and spatial distribution of the youngest larvae indicate a spawning distribution with modes in three seasons and five regions. The western Gulf Stream frontal zone is the focus of spawning off the southeastern coast of the United States. Spawning in the Gulf of Mexico seems to be focused in the vicinity of the northern most arc of the Gulf Loop Current.

Estimated spawning dates and the spatial distribution of young larvae offer an alternative to gonad condition and oocyte status as a means of resolving spawning season and location. Spawning season and location resolved in the present study corroborate the scenario recently proposed by Arocha (1997). Rather than the single breeding unit currently recognized for the western North Atlantic by ICCAT, Chow and Takeyama (2000) and Arata (1997) proposed two spawning groups: one south of the Sargasso Sea and east of the Lesser Antilles, and the other in the Windward Passage of the Antilles, the Yucatan Channel, and the Straits of Florida up to 35°N latitude. Accordingly, spawning begins in December south of the Sargasso Sea. Larvae from this spawning group transit into the Caribbean, are retained there by its anticyclonic circulation, and use the southeastern Caribbean as a nursery area. Arocha (1997) implied that the second group spawns progressively later in the year and that larvae are transported with the Gulf Loop and Florida Currents, and the Gulf Stream. Arocha (1997) speculated that larvae and juveniles use the Gulf of Mexico and waters inshore of the Gulf Stream as a nursery area. Spawning dates and abundances of young larvae corroborate Arocha's (1997) proposed scenario for the seasonality and location of spawning and confirm spawning off the southeastern United States in the late spring and summer in the northern hemisphere. Spawning dates and abundance of young larvae also indicate the Gulf of Mexico as a nursery area. Further, large numbers of juveniles discarded from the longline fishery prosecuted in the vicinity of the Charleston Gyre (Cramer, 2001) and the collection of larvae there (Govoni and Hare, 2001) indicate that the waters off the southeastern coast of the United States serve as a nursery area.

Swordfish larvae are collected elsewhere in the western North Atlantic, although they are rarely caught north of Cape Hatteras, North Carolina (Tibbo and Lauzier, 1969). The trajectory of the Gulf Stream north of Cape Hatteras is convoluted and its velocity is slower, ~1 m/s (e.g. Bowers and Rossby, 1989; Flierl and Davis, 1993; Hare et al., 2002); the transit period of plankton from Cape Hatteras to the Azores is 120–300 days (Scheltema, 1971). Swordfish spawned in the western North Atlantic would be juvenile fish by the time they reached the eastern North Atlantic. North of Cape Hatteras, the Gulf Stream sheds eddies into the Sargasso Sea (McGuillicuddy et al., 1998); thus, the general location for juvenile swordfish that are spawned and not retained in the western North Atlantic may well be the central Atlantic and Sargasso Sea.

Swordfish are multiple spawners (Arocha, 2002) and adults may move and spawn among regions of the western North Atlantic. Movement of spawning adults, along with transport of larvae, may result in the genetically well-mixed population of the western North Atlantic (Alvarado Bremer et al., 1995a).There is apparently no genetic exchange between northwestern Atlantic and Mediterranean reproductive populations (Alvarado Bremmer et al., 1995b; Chow and Takeyama, 2000). Transoceanic migration of adult fish is possible, but cross-Atlantic transfer of swordfish larvae is not likely. Swordfish larvae, collected principally in water ≥25°C (Govoni et al., 2000), probably perish as Gulf Stream water cools when it traverses the northern western North

Atlantic (Scheltema, 1971; Cowen et al., 2000; Gaylord and Gaines, 2000). Larvae that are not retained by eddies of the Gulf Loop Current and the Gulf Stream may be diverted to the central Atlantic (McGuillicuddy et al., 1998) and probably do not transit to the eastern North Atlantic.

Acknowledgments

We thank L. R. Settle [NOAA - NOS, Center for Fisheries and Habitat Research (CCFHR)] for the collection of some of the swordfish specimens reported in our study. M. M. Leiby (Florida Department of Natural Resources) loaned SEAMAP collections. F. Arocha (Universidad de Oriente, Venezuela), S. A. Berkeley (Oregon State University), and D. L. Lee and J. L. Cramer (NOAA-Fisheries, Southeast Fisheries Science Center) provided invaluable counsel on swordfish biology. D. W. Ahrenholz and M. H. Prager (CCFHR, National Marine Fisheries Service, NOAA), W. J. Richards (Fisheries, Southeast Fisheries Science Center, NOAA), and F. Arocha provided reviews of the manuscript.

Literature cited

Alvarado Bremer, J. R., A. J. Baker, and J. Mejuto.
1995a. Mitochondrial DNA control region sequences indicate extensive mixing of swordfish (*Xiphias gladius*) in the Atlantic Ocean. Can. J. Fish. Aquat. Sci. 52:1720–1732.

Alvarado Bremer, J. R., J. Mejuto, T. W. Greig, and B. Ely.
1995b. Global population structure of the swordfish (*Xiphias gladius*) as revealed by analysis of the mitochondrial DNA control region. J. Exp. Mar. Biol. Ecol. 197:295–310.

Arata, G. F.
1954. A contribution to the life history of the swordfish, *Xiphias gladius* Linnaeus, from the south Atlantic coast of the United States and the Gulf of Mexico. Bull. Mar. Sci. Gulf Caribb. 4:183–243.

Arocha, F.
1997. The reproductive dynamics of swordfish *Xiphias gladius* L. and management implications in the northwestern Atlantic. Ph.D. diss., 350 p. Univ. Miami, Miami, FL.
2002. Oocyte development and maturity classification of swordfish from the north-western Atlantic. J. Fish Biol. 60:13–27.

Bartlett, M. R., and R. L. Haedrich.
1968. Neuston nets and South Atlantic larval blue marlin (*Makaira nigricans*). Copeia 1968:469–474.

Beckett, J. S.
1975. Biology of swordfish, *Xiphias gladius* L., in the northwest Atlantic ocean. *In* Proceedings of the international billfish symposium Kailua-Kona, Hawaii, 9–12 August 1972, part 1: Report of the symposium (R. S. Shomura and F. Williams, eds.), p. 103–106. NOAA Tech. Rep. NMFS-SSRF-675.

Berkeley, S. A.
1983. Atlantic swordfish stock structure data and suggestions for its interpretation. Int. Comm. Conserv. Atl. Tuna, Collect. Vol. Sci. Pap. 18:839–845.

Berkeley, S. A., and E. D. Houde.
1983. Age determination of broadbill swordfish, *Xiphias gladius*, from the Straits of Florida, using anal fin spine sections. *In* Proceedings of the international workshop on age determination of oceanic pelagic fishes: tunas, billfishes, and sharks (E. D. Prince and L. M. Pulos, eds.), p. 137–143. NOAA Tech. Rep. NMFS-SSRF-8.

Boehlert, G. W., and M. M. Yoklavich.
1985. Larval and juvenile growth of sablefish, *Anoplopoma fimbria*, as determined from otolith increments. Fish. Bull. 83:475–481.

Boicourt, W. C., W. J. Wiseman Jr., A. Valle-Levinson, and L. P. Atkinson.
1998. Continental shelf of the southeastern United States and the Gulf of Mexico: in the shadow of the western boundary current. *In* The sea (A. R. Robinson and K. H. Brink, eds.), vol. 11, p. 135–183. John Wiley & Sons, New York, NY.

Bowers, A. S., and T. Rossby.
1989. Evidence of cross-frontal exchange processes in the Gulf Stream based on isopycnal RAFOS float data. J. Phys. Oceanogr. 19:1177–1190.

Campana, S. E.
2001. Accuracy, precision and quality control in age determination, including a review of the use and abuse of age validation methods. J. Fish Biol. 59:197–242.

Chow, S., and H. Takeyama.
2000. Nuclear and mitochondrial DNA analyses reveal four genetically separated breeding units of the swordfish. J. Fish Biol. 56:1087–1098.

Collette, B. B., T. Potthoff, W. J. Richards, S. Ueyanagi, J. L. Russo, and Y. Nishikawa.
1984. Scombroidei: development and relationships. *In* Ontogeny and systematics of fishes (H. G. Moser, W. J. Richards, D. M. Cohen, M. P. Fahay, A. W. Kendall, and S. L. Richardson, eds.), p. 591–620. Am. Soc. Ichthyol. Herpetol. Spec. Publ. 1.

Cowen, R. K., K. M. M. Lwiza, S. Sponaugle, C. B. Paris, and D. B. Olson.
2000. Connectivity of marine populations: open or closed? Science 287:857–859.

Cramer, J.
2001. Geographic distribution of longline effort and swordfish discard rates in the Straits of Florida and oceanic waters of the continental shelf, slope, and Blake Plateau off Georgia and the Carolinas from 1991 to 1995. *In* Island in the stream: the ecology and fisheries of the Charleston Bump (G. R. Sedberry, ed.), p. 97–103. Am. Fish. Soc. Symp. 25.

Ehrhardt, N. M.
1992. Age and growth of swordfish, *Xiphias gladius*, in the northwestern Atlantic. Bull. Mar. Sci. 50:292–301.

Flierl, G. R., and C. S. Davis.
1993. Biological effects of Gulf Stream meandering. J. Mar. Res. 51:529–560.

Forbes, T. L., and G. R. Lopez.
1989. Determination of critical periods in ontogenetic trajectories. Funct. Ecol. 3:525–632.

Gaylord, B., and S. D. Gaines.
2000. Temperature or transport? Range limits in marine species mediated solely by flow. Am. Nat. 155:769–789.

Gorbunova, N. N.
1969. Breeding grounds and food of the larvae of the swordfish *Xiphias gladius* Linneus (Pisces, Xiphiidae). Probl Ichthyol. 9:375–387.

Gorbunova, N. N., and N. Ya. Lipskaya.
1975. Feeding of larvae of the blue marlin, *Makaira nigricans* (Pisces, Istiophoridae). J. Ichthyol. 15:95–101.

Govoni, J. J., G. W. Boehlert, and Y. Watanabe.
1986a. The physiology of digestion in fish larvae. Environ Biol. Fishes 16:59–77.

Govoni, J. J., and J. A. Hare.
2001. The Charleston Gyre as spawning and larval nursery habitat for fishes. *In* Island in the stream: the ecology and fisheries of the Charleston Bump (G. R. Sedberry, ed.), p. 123–136. Am. Fish. Soc. Symp. 25.

Govoni, J. J., D. E. Hoss, and A. J. Chester.
1983. Comparative feeding of three species of larval fishes in the northern Gulf of Mexico: *Brevoortia patronus*, *Leiostomus xanthurus*, and *Micropogonias undulatus*. Mar. Ecol. Prog. Ser. 13:189–199.

Govoni, J. J., P. B. Ortner, F. Al-Yamani, and L. Hill.
1986b. Selective feeding of spot, *Leiostomus xanturus*, and Atlantic croaker, *Micropogonias undulatus*, larvae in the northern Gulf of Mexico. Mar. Ecol. Prog. Ser. 28: 175–183.

Govoni, J. J., B. W. Stender, and O. Pashuk.
2000. Distribution of larval swordfish, *Xiphias gladius*, and probable spawning off the southeastern United States. Fish. Bull. 98:64–74.

Grall, C., D. P. de Sylva, and E. D. Houde.
1983. Distribution, relative abundance, and seasonality of swordfish larvae. Trans. Am. Fish. Soc. 112:235–246.

Hare, J. A., J. H. Churchill, R. K. Cowen, T. J. Berger, P. C. Cornillon, P. Dragos, S. M. Glenn, J. J. Govoni, and T. N. Lee.
2002. Routes and rates of larval fish transport from the southeast to the northeast United States continental shelf. Limnol. Oceangr. 47: 1774–1789.

Hare, J. A., and R. K. Cowen.
1995. Effects of age, growth rate, and ontogeny on the otolith size-fish size relationship in bluefish, *Pomatomus saltatrix*, and the implications for back-calculation of size in fish early life history stages. Can. J. Fish. Aquat. Sci. 52:1909–1922.

Hassler, W. W., and W. T. Hogarth.
1977. The growth and culture of dolphin, *Coryphaena hippurus*, in North Carolina. Aquaculture 12:115–122.

Hitchcock, G. L., T. Rossby, J. L. Lillhridge, E. J. Lessard, E. R. Levine, D. N. Connors, K. Y. Borsheim, and M. Mork.
1994. Signatures of stirring and mixing near the Gulf Stream front. J. Mar. Res. 52:797–836.

Jones, C.
1986. Determining age of larval fish with the otolith increment technique. Fish. Bull. 84.91–104.

Kaji, T., M. Tanaka, M. Oka, H. Takeuchi, S. Ohsumi, K. Teruya, and J. Hirokawa.
1999. Growth and morphological development of laboratory-reared yellowfin tuna *Thunnus albacares* larvae and early juveniles, with special emphasis on the digestive system. Fish. Sci. 65:700–707.

Kendall, A. W., Jr., E. H. Ahlstrom, and H. G. Moser.
1984. Early life stages of fishes and their characters. *In* Ontogeny and systematics of fishes (H. G. Moser, W. J. Richards, D. M. Cohen, M. P. Fahay, A. W. Kendall, and S. L. Richardson, eds.), p. 11–22. Am. Soc. Ichthyol. Herpetol., Spec. Publ. 1.

Kotoulas, G., A. Magoulas, N. Tsimenides, and E. Zouros.
1995. Marked mitochondril DNA differences between Mediterranean and Atlantic populations of the swordfish, *Xiphias gladius*. Mol. Ecol. 4:473–481.

Kraul, S.
1991. Larviculture of the mahimahi, *Coryphaena hippurus*, in Hawaii, USA. J. World Aquacult. Soc. 24:410–421.

LaMonte, F.
1944. Note on breeding grounds of blue marlin and swordfish off Cuba. Copeia 4:258.

Lee, T. N., J. A. Yoder, and L. P. Atkinson.
1991. Gulf Stream frontal eddy influence on productivity of the southeast U.S. continental shelf. J. Geophys. Res. 96: 22,191–22,205.

Leis, J. M., B. Goldman, and S. Ueyanagi.
1987. Distribution and abundance of billfish larvae (Pisces: Istiophoridae) in the Great Barrier Reef lagoon and Coral Sea near Lizard Island, Australia. Fish Bull. 85:757–766.

Lipskaya, N. Ya., and N. N. Gorbunova.
1977. Feeding of sailfish larvae. Oceanology 17:340–344.

Markle, G. E.
1975. Distribution of larval swordfish in the Northwest Atlantic Ocean. *In* Proceedings of the international billfish symposium Kailua-Kona, Hawaii, 9–12 August 1972, part 1: Report of the symposium (R. S. Shomura and F. Williams, eds.), p. 252–260. NOAA Tech. Rept. NMFS-SSRF-675.

Marmorino, G. O., D. R. Lyzenga, and J. A. C. Kaiser.
1999. Comparison of airborne synthetic aperture radar imagery with in situ surface-slope measurements across Gulf Stream slicks and a convergent front. J. Geophys. Res. 104:1405–1422.

Maul, G. A., and F. M. Vukovich.
1993. The relationship between variations in the Gulf of Mexico Loop Current and Straits of Florida volume transport. J. Phys. Oceanogr. 23:785–796.

McGowan, C.
1988. Differential development of the rostrum and mandible of the swordfish (*Xiphias gladius*) during ontogeny and its possible functional significance. Can. J. Zool. 66:496–503.

McGuillicuddy, D. J., A. R. Robinson, D. A. Siegel, H. J. Jannasch, R. Johnson, T. D. Dickey, J. McNiel, A. F. Michaels, and A. H. Knap.
1998. Influence of mesoscale eddies on new production in the Sargasso Sea. Nature 395:263–266.

Megalofonou, P., J. M. Dean, G. DeMetrio, C. Wilson, and S. Berkeley.
1995. Age and growth of juvenile swordfish, *Xiphias gladius* Linnaeus, from the Mediterranean Sea. J. Exp. Mar. Biol. Ecol. 188:79–88.

Mooers, C. N. K., and G. A. Maul.
1998. Intra-Americas sea circulation: coastal segment (3,W). *In* The sea (A. R. Robinson and K. H. Brink, eds.), vol. 11, p. 183–208. John Wiley & Sons, New York, NY.

Nishikawa, Y., and S. Ueyanagi.
1975. The distribution of the larvae of swordfish, *Xiphias gladius*, in the Indian and Pacific oceans. *In* Proceedings of the international billfish symposium Kailua-Kona, Hawaii, 9–12 August 1972, part 1: Report of the symposium (R. S. Shomura and F. Williams, eds.), p. 261–264. NOAA Tech. Rep. NMFS-SSRF-675.

Olson, D. B., G. L. Hitchcock, A. J. Mariano, C. J. Ashjian, G. Peng, R. W. Nero, and G. P. Podestá.
1994. Life on the edge: marine life and fronts. Oceanography 7:52–60.

Owre, H. B., and M. Foyo.
1967. Copepods of the Florida Current. Fauna Caribaea I, Crustacea, part 1: Copepoda, 137 p. Inst. Mar. Sci., Univ. of Miami, Miami, FL.
1972. Studies on Caribbean zooplankton. Description of the program and results of the first cruise. Bull. Mar. Sci. 22: 483–521.

Paffenhofer, G.-A.
1983. Vertical zooplankton distribution on the northeastern Florida shelf and its relation to temperature and food abundance. J. Plankton Res. 5:15–33.

1985. The abundance and distribution of zooplankton on the southeastern shelf of the United States. *In* Oceanography of the southeastern U.S. continental shelf (L. P. Atkinson, D. W. Menzel, and K. A. Bush, eds.), p. 104–117. Am. Geophysical Union, Washington, DC.

Palko, B. J., G. L. Beardsley, and W. J. Richards.
1981. Synopsis of the biology of the swordfish, *Xiphias gladius* Linnaeus, 21 p. NOAA Tech. Rep. NMFS Circ. 441.

Post, J. T., J. E. Serafy, J. S. Ault, T. R. Capo, and D. P. de Sylva
1997. Field and laboratory observations on larval Atlantic sailfish (*Istiophorus platypterus*) and swordfish (*Xiphias gladius*). Bull. Mar. Sci. 60:1026–1034

Potthoff, T., and S. Kelley.
1982. Development and structure of the vertebral column, fins and fin supports, branchiostegal rays and squamation in the swordfish *Xiphias gladius*. Fish. Bull. 80:161–186.

Prince, E. D., D. W. Lee, J. R. Zweifel, and E. B. Brothers.
1991. Estimating age and growth of young Atlantic blue marlin *Makaira nigricans* from otolith microstructure. Fish. Bull. 89:441–459.

Reeb, C. A., L. Arcangeli, and B. A. Block.
2000. Structure and migration corridors in Pacific populations of the swordfish *Xiphius gladius*, as inferred through analyses of mitochondrial DNA. Mar. Biol. 136: 1123–1131.

Richards, W. J., and T. Potthoff.
1980. Larval distributions of scombrids (other than bluefin tuna) and swordfish in the Gulf of Mexico in the spring of 1977 and 1978. Int. Comm. Conserv. Atl. Tuna, Coll. Vol. Sci. Pap. 9:680–694.

Rogers, J. S., J. A. Hare, and D. G. Lindquist.
2001. Otolith record of age, growth, and ontogeny in larval and pelagic juvenile *Stephanolepis hispidus* (Pisces: Monacanthidae). Mar. Biol. 138:945–953.

Sanzo, L.
1910. Uovo e larva di Pesce-spada (*Xiphias gladius* L.). Riv. Mens. Pesca Idrobiol. 12:206–209.

Scheltema, R. S.
1971. The dispersal of the larvae of shoal-water benthic invertebrate species over long distances by ocean currents. *In* Fourth European marine biology symposium (D. J. Crisp, ed.), p. 7–28. Cambridge Univ. Press, Cambridge, UK.

Schmitz, W. J., J. R. Luyten, and R. W. Schmitt.
1993. On the Florida Current T/S envelope. Bull. Mar. Sci. 53:1048–1065.

Secor, D. H., J. M. Dean, and E. H. Laban.
1991. Manual for otolith removal and preparation for microstructural examination, 85 p. Electric Power Research Institute and the Belle W. Baruch Institute for Marine Biology and Coastal Research, Univ. South Carolina, Columbia, SC.

Shoji, J., T. Maehara, and M. Tanaka.
1999. Short-term occurrence and rapid growth of Spanish mackerel larvae in the central waters of the Seto Inland Sea, Japan. Fish. Sci. 65:68–72.

Täning, Å.
1955. On the breeding areas of the swordfish (*Xiphias*). Deep-Sea Res. 3(suppl.):438–450.

Taylor, R. G., and M. D. Murphy.
1992. Reproductive biology of the swordfish *Xiphias gladius* in the Straits of Florida and adjacent waters. Fish. Bull. 90:809–816.

Theilacker, G. H.
1980. Changes in body measurements of larval northern anchovy, *Engraulis mordax*, and other fishes due to handling and preservation. Fish. Bull 78:685–692.

Tibbo, S. N., and L. M. Lauzier.
1969. Larval swordfish (*Xiphias gladius*) from three localities in the western Atlantic. J. Fish. Res. Board Can. 26: 3248–3251.

Tserpes, G., and N. Tsimenides.
1989. Age determination and growth of swordfish *Xiphias gladius* L., 1958 in the Aegean Sea. Fish Res. 8:159–168.

Voss, G. L.
1953. A contribution to the life history and biology of the sailfish, *Istiophorus americanus* Cuv. and Val., in Florida waters. Bull. Mar. Sci. Gulf Caribb. 3:206–240.

Wiebe, P. H., K. H. Burt, S. H. Boyd, and A. W. Morton.
1976. A multiple opening/closing net and environmental sensing system for sampling zooplankton. J. Mar. Sci. 34 313–326.

Yabe, H., S. Ueyanagi, S. Kikawa, and H. Watanabe.
1959. Study on the life-history of the sword-fish, *Xiphias gladius* Linnaeus. Rep. Nankai Reg. Fish. Res. Lab. 10: 107–150.

Yasuda, F., H. Kohno, A. Yatsu, H. Ida, P. Arena, F. L. Greci, and Y. Taki.
1978. Embryonic and early larval stages of the swordfish, *Xiphias gladius*, from the Mediterranean. J. Tokyo Univ. Fish. 65:91–97.

Does the size of subsamples taken from multispecies trawl catches affect estimates of catch composition and abundance?

Donald S. Heales
David T. Brewer
CSIRO Marine Research
233 Middle St.
Cleveland, Queensland 4163, Australia
E-mail address (for D. S. Heales): don.heales@marine.csiro.au

You-Gan Wang
Dept. of Biostatistics
Harvard University
Boston, Massachusetts 02115

Peter N. Jones
CSIRO Mathematical and Information Sciences
233 Middle St.,
Cleveland, Queensland 4163, Australia

Abstract—Although subsampling is a common method for describing the composition of large and diverse trawl catches, the accuracy of these techniques is often unknown. We determined the sampling errors generated from estimating the percentage of the total number of species recorded in catches, as well as the abundance of each species, at each increase in the proportion of the sorted catch. We completely partitioned twenty prawn trawl catches from tropical northern Australia into subsamples of about 10 kg each. All subsamples were then sorted, and species numbers recorded. Catch weights ranged from 71 to 445 kg, and the number of fish species in trawls ranged from 60 to 138, and invertebrate species from 18 to 63. Almost 70% of the species recorded in catches were "rare" in subsamples (less than one individual per 10 kg subsample or less than one in every 389 individuals).

A matrix was used to show the increase in the total number of species that were recorded in each catch as the percentage of the sorted catch increased. Simulation modelling showed that sorting small subsamples (about 10% of catch weights) identified about 50% of the total number of species caught in a trawl. Larger subsamples (50% of catch weight on average) identified about 80% of the total species caught in a trawl.

The accuracy of estimating the abundance of each species also increased with increasing subsample size. For the "rare" species, sampling error was around 80% after sorting 10% of catch weight and was just less than 50% after 40% of catch weight had been sorted. For the "abundant" species (five or more individuals per 10 kg subsample or five or more in every 389 individuals), sampling error was around 25% after sorting 10% of catch weight, but was reduced to around 10% after 40% of catch weight had been sorted.

Manuscript approved for publication 9 March 2003 by Scientific Editor.
Manuscript received 26 June 2003 at NMFS Scientific Publications Office.
Fish Bull. 101:790–799 (2003).

Concerns are held worldwide regarding the sustainability of bycatch species taken in trawls, particularly prawn trawls. Under the voluntary FAO Code for Responsible Fisheries, managers are required to "take measures to conserve target species, associated or dependent species and nontarget species and their environment" (FAO, 1995). An essential part of this process is the accurate monitoring of population sizes and structures.

With large trawl catches, subsampling is often the only cost-effective or feasible way to describe the bycatch composition. How well these subsamples represent the total catch depends on how diverse the catch is, how well the catch is mixed before the subsamples are taken, and what proportion of the catch is taken as a subsample.

There is a large literature on subsampling theory for terrestial insect studies (Van Ark and Meiswinkel, 1992), aquatic macroinvertebrate studies (Vinson, 1996; Walsh, 1997), and marine ecological studies (Andrew and Mapstone, 1987). However, in most of these studies, samples of very small animals collected in the field can be resuspended in fluid and mixed evenly in the laboratory before the subsamples are taken. In fisheries, in direct contrast, large catches are extremely difficult to manipulate and redistribute evenly before subsampling. A few fisheries studies have examined the impact of subsampling on estimates of the abundance and different size ranges of one or a few dominant species. For example, in the *Crangon* trawl fisheries in Belgian waters, sampling strategy had only a minor effect on the reliability of estimates of size selectivity for the targeted shrimp (Polet and Redant, 1999). In UK waters, subsampling trawled fish (both target species and discards) from either the sorting conveyor or the pound made no difference to catch composition estimates (Tamsett et al., 1999).

However, in tropical trawl fisheries, over one hundred species can be recorded in a single catch. Under ESD (ecological sustainable development) guidelines, all these species (both target and bycatch) are equally important but there has been very little research on subsampling techniques applicable to such diverse catches. A recent study in Australia's Northern Prawn Fishery (NPF) examined the accuracy of subsampling from large, diverse catches of fish and invertebrates (Heales et al., 2000). For most of the "abundant"

species, their position on trawler sorting trays from which the bycatch subsamples were collected, had little effect on the accuracy in representing the catches.

Although the accuracy of subsampling is a general problem for all multispecies fisheries, few other studies have been published on the topic. Reliable techniques for subsampling are needed, however, especially with the demands that bycatch species, as well as the target species, should be ecologically sustainable. We describe here research done in Australia's NPF but the results and methods are applicable to many sampling problems in fisheries.

The NPF is a large tropical trawl fishery that extends from Cape York in Queensland to Cape Londonderry in Western Australia. In addition to catching penaeid prawns (e.g. 8531 metric tons (t) in 1997–98, Taylor and Die, 1999), its bycatch component is estimated at over 38,000 t a year (Pender et al., 1992) or more than 80% of the total catch in the tiger prawn fishery (Brewer et al., 1998). The neighboring Torres Straits Prawn Fishery (TSPF) also has an estimated annual bycatch of 4800 t (Williams, 1985).

The NPF has a management requirement to assess the impact of trawling on nontarget species. The bycatch of both these prawn trawl fisheries (NPF and TSPF) is very diverse. Ramm et al. (1990) recorded 115 fish taxa in their study of NPF waters, and Brewer et al. (1998) recorded over 250 species from one area of the NPF. At least 390 fish species, 234 invertebrate taxa, and 43 elasmobranch species have been recorded in a current bycatch project in the NPF (Stobutzki et al., 2000).

Despite the lack of knowledge on the ability of subsamples to accurately represent such diverse catches, many studies of trawl communities in Northern Australia have used subsampling techniques to estimate catch rates. In two bycatch studies of the NPF, the smaller catches were entirely sorted and the larger catches subsampled (Poiner and Harris, 1986; Harris and Poiner, 1991). Trawl catches in another bycatch study were spread evenly over the sorting tray and a visually estimated fraction of the catch was subsampled (Ramm et al., 1990). Other workers simply subsampled without confirming the accuracy of their subsampling techniques (Blaber et al., 1990 and 1994; Martin et al., 1995; Brewer et al., 1998; Wassenberg et al., 1998).

A lack of knowledge of trawl impacts on nontarget species has led to the present CSIRO study that describes the bycatch from the NPF and provides a framework for any future bycatch monitoring program. As part of that study, we made the first assessment of the accuracy of subsampling over a range of subsample sizes as a tool for estimating the total catch composition of a large multispecies fishery.

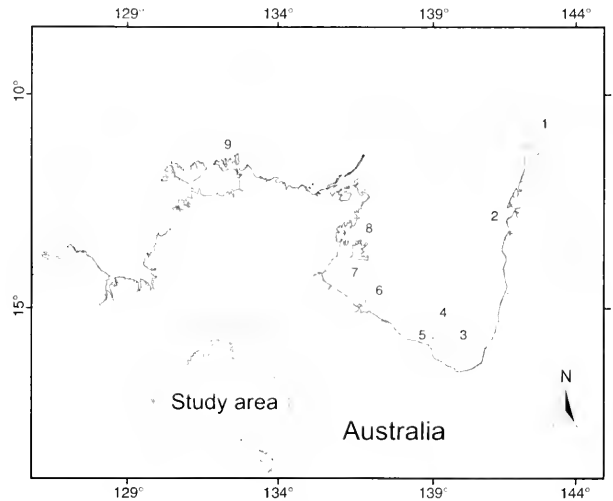

Figure 1

Map of the Torres Straits Fishery (area 1—broken line) and Northern Prawn Fishery (unbroken line), Australia, showing the managed area of the fisheries and the regions where samples were collected. Regional codes are 1 = Torres Straits, 2 = Weipa, 3 = east of Mornington Island, 4 = north of Mornington Island, 5 = west of Mornington Island, 6 = east of Vanderlin Islands, 7 = south of Groote Eylandt, 8 = north of Groote Eylandt, 9 = Melville Island.

Materials and methods

Data were collected from a series of 14 trawl samples taken during two research cruises of the RV *Southern Surveyor*. These samples were collected from one region of the Torres Straits Prawn Fishery (TSPF), and from eight of the major tiger prawn (*Penaeus esculentus* and *P. semisulcatus*) fishing regions of the Northern Prawn Fishery (NPF), (namely Weipa, east of Mornington Island, north of Mornington Island, west of Mornington Island, north of Vanderlin Islands, south of Groote Eylandt, north of Groote Eylandt, and Melville Island) (Fig. 1). All trawls were undertaken in either late summer 1997 (February–March, the end of the wet season) or in mid-spring 1997 (September–October, the dry season). We used a single 14-fathom Florida-Flyer prawn trawl net so that the data would be comparable with data from either of the two nets used by the twin-rigged commercial NPF vessels in the tiger prawn fishery. All trawls were done at night, again to be comparable with the fishery. Duration of trawls ranged from 1 to 3 hours (Table 1), and depths ranged from 23 to 42.3 m.

A further six trawl catches were sampled by a scientific observer on board commercial NPF vessels fishing for tiger prawns north of Mornington Island in late May 1997, and north of Groote Eylandt in late September 1997. Each trawl sample consisted of the entire catch from one of the two 14-fathom Florida-Flyer prawn trawl nets used by these vessels. All trawls were done at night. Their duration

Table 1

Summary of catch data for 20 entirely sorted trawls from the Northern Prawn Fishery and Torres Straits Prawn Fishery. "Bycatch individuals" refers to the total number of bycatch animals (fish and invertebrates) in each trawl. "Fish species" refers to the total number of fish species recorded in the bycatch of each trawl. (*n*) is the total number.

Region	Duration of trawl (h)	Start time of trawls	Catch weight (kg)	Subsamples (*n*)	Bycatch individuals (*n*)	Fish species (*n*)	Invertebrate species (*n*)	All species (*n*)
Torres Straits	1.2	0400	94	9	4151	74	21	95
Weipa	2.7	0220	166	16	4911	92	36	128
East of Mornington Island	1.0	0415	274	24	7313	90	18	108
East of Mornington Island	2.9	0250	87	8	2019	77	45	122
North of Mornington Island	3.3	1845	182	16	9762	101	36	137
North of Mornington Island	3.0	2215	194	17	11015	94	42	136
North of Mornington Island	3.2	1840	445	36	13,826	114	52	166
North of Mornington Island	2.0	0350	71	7	1771	60	30	90
North of Mornington Island	2.2	0330	100	10	5067	77	34	111
West of Mornington Island	1.6	0415	174	16	5976	100	21	121
West of Mornington Island	1.7	0400	269	26	6967	87	24	111
North of Vanderlin Islands	2.7	0310	156	15	7182	71	19	90
South of Groote Eylandt	2.0	0345	315	27	23,751	105	25	130
South of Groote Eylandt	2.7	0250	165	17	3856	64	25	89
North of Groote Eylandt	2.5	2230	147	12	5558	68	28	96
North of Groote Eylandt	3.0	0215	85	9	2792	60	34	94
North of Groote Eylandt	3.5	1830	158	13	5664	89	43	132
North of Groote Eylandt	3.5	2215	169	15	8289	96	63	159
North of Groote Eylandt	3.5	2215	189	16	5748	96	43	139
Melville Island	3.0	0130	170	14	4635	60	30	90
Total			3610	323	140,253			

ranged from 3 to 3.5 hours (Table 1), and depths ranged from 29 to 41 m.

Sample collection

On the research vessel, catches were spilled from the codend onto the flat deck (equivalent to the sorting tray on commercial vessels). The entire catch of each trawl was progressively partitioned by shovelling the catch into consecutively numbered boxes (subsample replicates), each of about 10 kg (according to the methods described by Heales et al., 2000). Partitioning of the catch began at the outer edges and continued in a clockwise direction, and subsamples were taken from each of four major compass directions: north, east, south, and west until the entire catch had been collected in successively numbered boxes. The direction of the ship's bow was always designated as north.

Samples on the research vessel were sorted immediately. Fish and invertebrates were identified to the lowest taxonomic level possible (mostly species). Where this was not possible, the data were grouped to genus and in a few cases to family. Total numbers and weights were recorded for each species in each subsample and entered directly into a relational database.

On the commercial vessels, the catches were spilled onto the sorting tray and the commercial-size prawns were removed. The bycatch would then normally move down a trash chute and spill overboard. However, to sample a catch, the trash chute was diverted so that all the bycatch was collected in consecutively numbered boxes (subsample replicates) each of approximately 10 kg.

All samples collected from commercial vessels were frozen on board and transported to the laboratory for subsequent sorting, identification, and data entry according to the methods described above.

Although most bycatch species were identified to species level, some could only be identified to genus and in a few cases to family. In order to be consistent in terms used throughout this study, we use the term species (plural form) even when referring to multispecies groups.

The methods used to collect subsamples on both the research and commercial vessels differed only in the position from which subsamples were taken (see earlier "Material and methods" section). However, a previously published study (Heales et al., 2000) showed that the majority of the "abundant" bycatch species were evenly distributed throughout the catch. Consequently, for all analyses we combined the 14 catches collected from the research vessel with the six catches from commercial vessels.

Data analysis

Abundance groupings Within each catch, there was a large range of species (both fish and invertebrates) and they

occurred at many different levels of relative abundance. To obtain an overview of how rarely, or how frequently, different species occurred in catches, we reduced each occurrence of a species in a catch to an index of relative abundance. We concentrated solely on determining the accuracy of taking different size subsamples in representing the range of relative abundances (from very low to very high) of the species in these catches.

The relative abundance indices were based on the average number of individuals of a given species that were recorded in a standardized 10-kg subsample taken from that catch. To generate this index, we used the following equation:

$$n = 10 \times (TotNum / Weight), \quad (1)$$

where n = the mean number of individuals of a given species per 10-kg subsample;
TotNum = the total number of individuals of that species in the whole catch; and
Weight = the total weight of the catch in kg.

We derived a separate index of abundance for each species in every catch where it was recorded. Thus, a species that occurred in all 20 catches would have 20 different abundance indices in the analysis.

To highlight the differences in distribution between the two extremes of the "rare" species and the "abundant" species when estimating catch composition, we grouped the indices of abundance into 11 categories, ranging from less than one individual per 10-kg subsample, up to 10 or more individuals per subsample. Species with abundance indices of less than one individual per 10-kg subsample were classed as "rare"; those with one to less than five individuals were classed as "common"; and those with five or more individuals per 10-kg subsample were classed as "abundant."

For example, the common ponyfish (*Leiognathus moretoniensi*), was classed as "abundant" in 11 of the 20 catches, as "common" in eight catches, and "rare" in one catch. Because a species could have different abundance indices in each catch, individual species are not referred to by name in the results. Instead, we refer to the occurrence of each species in a catch, as one *case* of some relative abundance index that was recorded in that catch (i.e. one "case" of species by trawl abundance). The relative frequency of all the cases (i.e. abundance indices) in each of the three abundance categories (throughout the combined 20 catches) was then calculated.

To calculate the average number of bycatch individuals per 10-kg subsample (over all the catches), the following equation was used:

$$X = 10 \times (Total\ number / Total\ weight) \quad (2)$$

where X = the mean number of bycatch individuals (per 10-kg subsample);
Total number = the total number of all bycatch individuals (summed over all 20 catches); and
Total weight = the total weight (kg) of all bycatch individuals (summed over all 20 catches).

We then examined the average occurrence ratios within 10-kg subsamples for the "rare," "common," and "abundant" species.

Catch composition To examine the relationship between the number of recorded species and the weight of sorted catch, the subsamples were first analyzed in the order that they were collected. The cumulative number of species (both fish and invertebrates) was plotted against the cumulative weight of sorted catch, for each of the 20 catches. Each catch was also summarized in terms of the percentage of species recorded for each 10% increment of weight of sorted catch.

The order (position on the sorting tray) where the subsamples were collected on both the research and commercial vessels was just one of the many possible ways that a catch can be divided into 10-kg subsamples. To determine the level of accuracy in recording the number of species in a catch, we examined 200 combinations of subsample selection (with no replacement), by randomly reordering the subsamples using Monte Carlo simulations for each catch. We also calculated the cumulative number and percentage of species recorded, as well as the cumulative weight and percentage of the sorted catch, for each catch. The proportion of species recorded was fitted as a power function of the proportion of the weight of sorted catch, as described by the following asymptotic equation (Snedecor and Cochran, 1980):

$$y = p^k + \varepsilon, \quad (3)$$

where y = the proportion of species recorded;
p = the proportion of the weight of catch sorted;
k = the mean exponential parameter; and
ε = the random normal error term, with unequal variance.

The variance of ε is assumed to be $p\,(1-p)\,\sigma^2$ to ensure that the variance of y is fixed at zero when $p = 0$ and 1. This formulation has the property that, when none of the catch has been sorted, no species will have been recorded. It also ensures that $y = 1$ when $p = 1$, i.e. when all the catch has been sorted, all of the species have been recorded. The estimate of σ^2 was obtained by fitting the following model according to the SAS procedure NLIN (version 7, SAS Inst., Cary NC):

$$y^* = p^k / \sqrt{(p(1-p)) + \varepsilon^*}, \quad (4)$$

where $y^* = y / \sqrt{(p(1-p))}$ and $\varepsilon^* = \varepsilon / \sqrt{(p(1-p))}$; and
ε^* now has homogeneous variance structure.

Different k values were estimated for each catch to reflect the variation in the relationship. The mean k_i value for a given catch (i=1–20) was obtained from 200 analyses for that catch. The predicted y values i.e. $\bar{y}_p$ (at p=0.1, 0.2 etc. to 1.0) were obtained by averaging p^k values across the 20 catches (note that this is different from $p^{\bar{k}}$ where $\bar{k}$ is the mean k value for the 20 catches). We defined the $\bar{y}_p$ values as the predicted expected proportion of species recorded after p proportion of catches had been sorted.

The corresponding 95% confidence interval for the predicted mean values ($\bar{y}_p$) was evaluated by using the width 1.96 σ_m, where σ_m^2 is the variance of $\bar{y}_p$ given by

$$\sigma_m^2 = V(p^k) + V(\varepsilon) = \left(\log(p)\bar{y}_p\sigma_k\right)^2 + p(1-p)\sigma^2, \quad (5)$$

where $\bar{y}_p$ = the predicted mean proportion;
σ^2 = obtained from the mean squared residuals across 20 catches by 200 analyses; and
σ_k^2 = the estimated variance of k across 20 catches by 200 analyses.

All p and y values are presented as percentages in results.

Abundance estimates The effect of taking different size subsamples, on estimating the total number of a given species in a catch, was determined by using a running mean (of the estimate of abundance) calculated from the equation

$$s = \left|(n / p - TotNum) / TotNum\right|, \quad (6)$$

where s = the absolute proportion of sampling error;
n = the observed number of that species after p proportion (by weight) of the catch has been sorted; and
$TotNum$ = the total number of individuals of that species in the whole catch.

The values for s are truncated at 1 for ease of presenting results.

We used the following statistical model in which s is subtracted from 1 in order to correspond to the equation used for species composition:

$$1 - s = p^k + \varepsilon, \quad (7)$$

where $1-s$ is fixed at 1 when $p = 1$, and the $\text{var}(\varepsilon) = (1-p)\sigma^2$ to ensure that there is no sampling error when the entire catch has been sorted.

To obtain estimates of σ^2, we fitted the following model:

$$(1-s)/\sqrt{(1-p)} = p^k / \sqrt{(1-p)} + \varepsilon / \sqrt{(1-p)}, \quad (8)$$

where the errors for this model have homogeneous variance structure. The variance of a predicted $(1-s)$ is given by an equation similar to Equation 5 (for species composition):

$$\sigma_m^2 = \left(\log(p)(1-s)\sigma_k\right)^2 + (1-p)\sigma^2. \quad (9)$$

To examine the accuracy in recording the abundance of all the species in a catch, we modeled the order (200 times) in which subsamples were taken (as described above for catch composition estimates). For each (species by trawl) case, i.e. where a species was recorded at any level of abundance, we calculated the sampling error s for ranges of p from 0.1 to 0.9. We grouped all the (species by trawl) cases of different levels of abundance into eight categories for these analyses. They were <1; 1 to <2; 2 to <3; 3 to <4; 4 to <5; 5 to <10; 10 to <50 and 50 or more per 10-kg subsample respectively.

The SAS procedure NLIN was used to fit the power curve for catch composition, as well as the separate power curves for sampling error for the different abundance classes.

Results

General results

Catches ranged in size from 71 to 445 kg, with an average of 117 species per trawl (84 fish and 33 invertebrate species). A total of 140,253 fish and invertebrates were recorded from 323 subsamples taken from the 20 prawn trawl catches that were sorted entirely (Table 1). Subsamples weighed, on average, 11.2 kg and contained 434 individuals (or 389 individuals per standardized (std) 10-kg subsample). We identified a total of 276 fish and 141 invertebrate species.

A total of 69.3% (1617 out of 2333) of the (species × trawl) cases of relative abundance were recorded at ratios of less than one individual per std 10-kg subsample (or less than one in every 389 individuals), when averaged over all 20 catches; they were classed as "rare" (Fig 2). A further 19% (442 out of 2333) of the (species × trawl) cases of relative abundance were recorded at ratios that fell between one individual per std 10-kg subsample and less than five individuals per 10-kg subsample (or between one in 389 and less than five in 389 individuals), when averaged over all 20 catches; they were classed as "common." The remaining 11.7% (274 out of 2333) of the (species × trawl) cases of relative abundance were recorded at ratios of five or more individuals per std 10-kg subsample (or five or more in every 389 individuals), when averaged over all 20 catches); they were classed as "abundant" (Fig 2).

Catch composition

The number of species recorded increased as the weight of sorted catch increased in 19 of the 20 catches. This relationship appeared to reach an asymptote in the remaining large catch of 445 kg (Fig 3, A and B).

After 10% of all 20 catches were sorted, the cumulative percentage of species recorded ranged from 31% (in the 315 kg catch) to 78% (in the 182 kg catch) (Table 2). To detect 80% of the species present in a single catch, from 20% to 70% of the catch had to be sorted.

Simulation modelling showed that sorting 10% of catch weight detects (on average) 50% of the species present, with the confidence interval ranging from 44% to 57% (Fig 4). Sorting 50% of the catch was necessary to detect 80% of the species present.

Abundance estimates The simulation model showed that the mean sampling error curves (for the eight abundance categories) decreased as increasing percentages of the catch had been sorted (Fig 5). After 10% of the weight of

Table 2

The percentage of species recorded as more of the catch is sorted (10% increments). Percentages were calculated separately for 20 trawl catches that were completely sorted. The demarcation line denotes where 80% or more of the species in each catch were recorded.

Region	Catch weight (kg)	Number of species	Cumulative % of species recorded (in 10% Wt increments)								
			10%	20%	30%	40%	50%	60%	70%	80%	90%
North of Mornington Island	71	90	51	62	70	76	81	86	90	94	97
North of Groote Eylandt	85	94	49	60	69	75	81	85	89	93	97
East of Mornington Island	87	122	56	66	74	79	84	88	91	95	97
Torres Straits	94	95	60	70	76	81	86	89	92	95	98
North of Mornington Island	100	111	56	66	74	79	84	88	91	95	97
North of Groote Eylandt	147	96	50	61	69	76	81	86	90	93	97
East of Vanderlin Islands	156	90	39	52	61	69	75	81	86	91	96
North of Groote Eylandt	158	132	65	74	80	84	88	91	94	96	98
South of Groote Eylandt	165	89	51	63	71	77	82	86	90	94	97
Weipa	166	128	54	65	73	78	83	87	91	94	97
North of Groote Eylandt	169	159	57	68	75	80	85	88	92	95	98
Melville	170	90	46	58	67	73	79	84	89	93	97
West of Mornington Island	174	121	52	63	71	77	82	86	90	94	97
North of Mornington Island	182	137	78	84	88	91	93	95	96	98	99
North of Groote Eylandt	189	139	61	71	77	82	86	90	93	95	98
North of Mornington Island	194	136	67	76	81	85	89	92	94	96	98
West of Mornington Island	269	111	52	63	70	77	82	86	90	94	97
East of Mornington Island	274	108	40	53	62	69	76	82	87	92	96
South of Groote Eylandt	315	130	31	44	54	63	70	77	84	89	95
North of Mornington Island	445	166	61	71	77	82	86	90	93	95	98

catches had been sorted, only two abundance categories (from ≥10 to <50, and ≥50 per subsample) had mean sampling error rates below 25%.

For the "rare" species (<one per subsample), the gradient of the mean sampling error curve was close to constant (Fig 6). The 95% upper confidence interval was over 100% until more than 40% of the catches had been sorted. Even when 90% of the catches had been sorted, the mean sampling error was just below 10%, and the 95% upper confidence interval remained above 25%.

For the "abundant" species (five or more per subsample), the mean sampling error curve started just below 25% after 10% of catches had been sorted, and fell below 10% when more than 40% of the catches had been sorted (Fig 6). The 95% confidence interval did not fall below 25% until 50% of catches had been sorted.

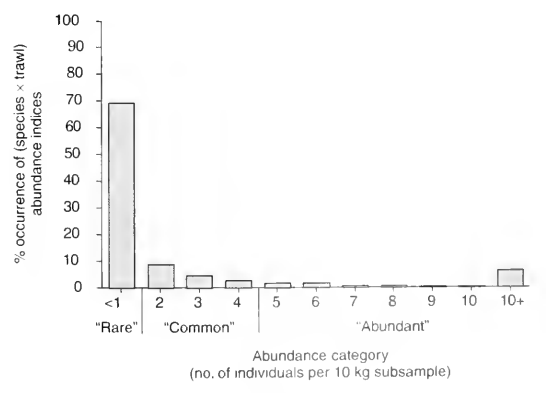

Figure 2

The percentage frequency of occurrence of 2333 cases of (species × trawl) relative abundance for bycatch species recorded from 20 trawl catches. The cases are grouped into 11 categories of abundance indices based on the average number of a species recorded per 10-kg subsample of catch.

Discussion

This study shows that a large subsample is required to accurately represent the species composition of a large multispecies catch from

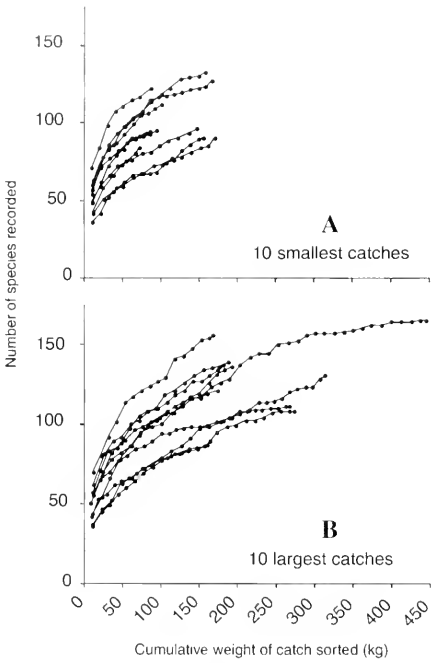

Figure 3

The cumulative numbers of bycatch species recorded as the weight of catch analysed increased for (**A**) the 10 smallest and (**B**) the 10 largest catches that were entirely sorted.

the Northern Prawn Fishery (NPF). As more of the catch is sorted, more new species are encountered. On average, 50% of the catch weight needs to be sorted to record 80% of the species in a single catch. Our data suggest that taking subsamples of between 10% and 30% of catch weight can result in highly variable percentages (from 31% to 88%) of the total species in the catch. When estimating the relative abundance of individual species within a catch, subsampling small percentages of catch weight (around 10%) results in a sampling error around 80% for "rare" species, and around 25% for "abundant" species.

The sampling error (when estimating the relative abundance of a species in a trawl) is a function of the total number of bycatch individuals caught in that trawl. For example, 10 individuals of species "*X*" may occur in one trawl, at a ratio of one in every 100 bycatch individuals. In the very next trawl, 10 individuals of species "*X*" may occur at a ratio of only one in every 1000 bycatch individuals because other "abundant" species have swamped its occurrence ratio. As a consequence, the sampling error for the same number of individuals of species "*X*" varies greatly between trawls.

There are two sources of within-trawl variation to take into account when calculating catch rates for individual species. The first is due to changes in catchability at the trawl-species interface (either on the sea floor or in the water column). The second is due to on-deck subsampling techniques. This study has been able to allocate percentages of sampling error based on the occurrence rate of a species of interest within individual catches. To do this, we calculated the average occurrence ratios for the different categories of relative abundance used in this study. For example, "rare" species occurred at a rate of less than one individual in every 389 bycatch individuals; "abundant" species occurred at a rate of five or more individuals in every 389 bycatch individuals. These ratios can now be applied to species of interest recorded in other trawl catches and the average sampling errors can be calculated.

Monitoring catch rates of a suite of "indicator" bycatch species is a possible future option for measuring the health of nontarget species in trawl fisheries such as the NPF. Stobutzki et al. (2001) identified a suite of small NPF fish species that are more likely to be impacted by trawling.

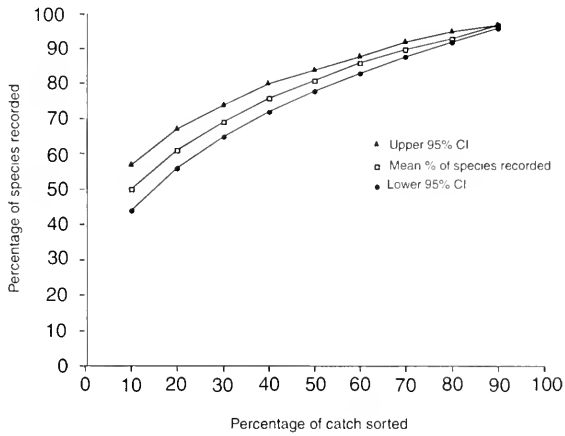

Figure 4

The mean percentage (and 95% CI) of species recorded as increasing percentages of catch weight were sorted. Curves were generated from 200 random selections of the numbered order in which subsamples were collected from each catch.

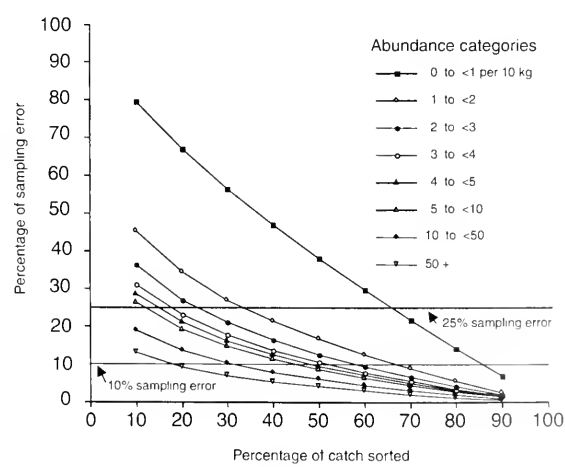

Figure 5

The mean percentage of sampling error calculated when estimating the relative abundance of bycatch species grouped into eight categories of relative abundance. Curves were generated from 200 random selections of the numbered order in which subsamples were collected from each catch.

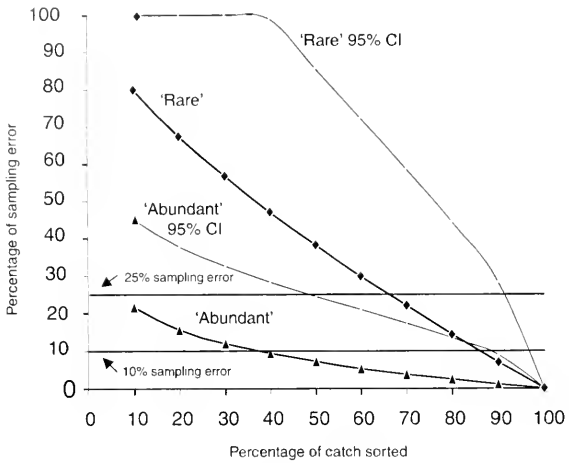

Figure 6

The mean percentage of sampling error calculated when estimating the relative abundance of the "rare" (<1 individual per 10-kg subsample) and the "abundant" bycatch species (5 or more individuals per 10-kg subsample). Curves were generated from 200 random selections of the numbered order in which subsamples were collected from each catch.

The catch rates of many of these most-at-risk species are extremely low. Our data suggest that extremely high sampling errors will be incurred if monitoring catch rates of species on this list is undertaken. These errors must be incorporated into any models that assess the impact of trawling on populations of these species.

The range of data in the present study includes many of the sources of variation likely to be encountered in setting up a wide-ranging bycatch monitoring program. The results we present are a valuable guide to the accuracy of subsampling. In particular, this study emphasizes the value of collecting large subsamples, especially when one is restricted to representing the bycatch of an area by only one or a few trawls. This problem is common for research cruises when many regions need to be sampled in a short time (e.g. Blaber et al., 1994), and is also a common problem for observers on commercial fishing vessels where catch sampling is often restricted by the nature of commercial practices. Because there is a high level of sampling error when estimating the abundances for "rare" species, reliable estimates will require either taking large subsamples or sorting entire catches.

The size of some catches in our study may be larger than those of many other tropical prawn trawl fisheries in Australia and overseas. However, the data in the matrix on the range of cumulative species (per proportion of catch sorted, Table 2) will allow managers of other trawl fisheries to better understand the implications and likely accuracy of bycatch sampling programs.

Acknowledgments

We thank S. Cook, M. Farmer, C. Liron, D. Milton, J. Salini, I. Stobutzki, T. Wassenberg, G. Fry, and others for their valued help in sorting the catches both on board the RV *Southern Surveyor* and in the Cleveland laboratory. We also thank D. McKay, the skipper of FV *Apolloair*, and P. Hoschke, the skipper of FV *Ventura*, and their respective crews, for their help in collecting commercial trawl samples. We also thank J. Bishop, S. Blaber, B. Hill, D. Milton, and V. Mawson for their valuable comments on the manuscript. This work was undertaken with the support of FRDC grant no 96/257

Literature citations

Andrew, N. L., and B. D. Mapstone.
1987. Sampling and the description of spatial patterns in marine ecology. Oceanogr. Mar. Biol. Annu. Rev. 25:39–90.

Blaber, S. J. M., D. T. Brewer, and A. N. Harris.
1994. Distribution, biomass and community structure of demersal fishes of the Gulf of Carpentaria, Australia. Aust. J. Mar. Freshw. Res. 45:375–396.

Blaber, S. J. M , D. T. Brewer, J. P. Salini, and J. Kerr.
1990. Biomasses, catch rates and abundances of demersal fishes, particularly predators of prawns, in a tropical bay in the Gulf of Carpentaria, Australia. Mar. Biol. 107: 397–408.

Brewer, D., N. Rawlinson, S. Eayrs, and C. Burridge.
1998. An assessment of bycatch reduction devices in a tropical Australian prawn trawl fishery. Fish. Res. 720:1–21.

FAO (Food and Agriculture Organization of the United Nations).
1995. Code of conduct for responsible fisheries, 41 p. FAO, Rome, Italy.

Harris, A. N., and I. R. Poiner
1991. Changes in species composition of demersal fish fauna of the Southeast Gulf of Carpentaria, Australia, after 20 years of fishing. Mar. Biol. 111:503–519.

Heales, D. S., D. T. Brewer, and Y.-G. Wang.
2000. Subsampling multi-species trawl catches from tropical northern Australia: does it matter which part of the catch is sampled? Fish. Res. 48:117–126.

Martin, T. J., D. T. Brewer, and S. J. M. Blaber.
1995. Factors affecting distribution and abundance of small demersal fishes in the Gulf of Carpentaria. Mar. Freshw. Res. 46:909–920.

Pender, P. J., R. S. Willing, and B. Cann.
1992. NPF bycatch a valuable resource? Aust. Fish. 51(2): 30–31.

Poiner, I. R., and A. N. M. Harris.
1986. The effect of commercial prawn trawling on the demersal fish communities of the south-eastern Gulf of Carpentaria. *In* Torres Strait fisheries seminar, Port Moresby, 11–14 February 1985 (A. K. Haines, G. C. Williams, and D. Coates, eds.), p. 239–261. Australian Government Publishing Service, Canberra, Australia.

Polet, H., and F. Redant.
1999. Effect of population structure, sampling strategy and sample size on the estimates of selection parameters for shrimp (*Crangon crangon*) trawls. Fish. Res. 40:213–225.

Ramm, D. C., P. J. Pender, R. S. Willing, and R. C. Buckworth.
1990. Large scale spatial patterns of abundance within the assemblage of fish caught by prawn trawlers from Northern Australian waters. Aust. J. Mar. Freshw. Res. 41:79–95.

Snedecor, G. W., and W. G. Cochran.
1980. Statistical methods, 7th ed., 593 p. Iowa State Univ. Press, Ames, IA.

Stobutzki, I., S. Blaber, D. Brewer, G. Fry, D. Heales, M. Miller, D. Milton, J. Salini, T. Van der Velde, T. Wassenberg, P. Jones, Y-G. Wang, M. Dredge, T. Courtney, K. Chilcott, and S. Eayrs.
2000. Ecological sustainability of bycatch and biodiversity in prawn trawl fisheries. Rep. 96/257, 512 p. Fisheries Research Development Corp., Deakin West, Australia.

Stobutzki, I., M. Miller, and D. Brewer.
2001. Sustainability of fishery bycatch: a process for assessing highly diverse and numerous bycatch. Environ. Conserv. 28(2):167–181.

Tamsett, D., G. Janacek, and M. Emberton.
1999. A comparison of methods for onboard sampling of discards in commercial fishing. Fish. Res. 42:127–135.

Taylor, B., and D. Die, eds.
1999. Northern prawn fishery assessment report, 1997 and 1998. AFMA (Australian Fisheries Management Authority), Canberra, Australia.

Van Ark, H., and R. Meiswinkel.
1992. Subsampling of large light trap catches of *Culcoides* (Diptera: Ceratopogonidae). Onderstepoort J. Vet. Res. 59: 183–189.

Vinson, M. R.
1996. Effects of sampling area and subsampling procedure on comparisons of taxa richness among streams. J. North Am. Benthol. Soc. 15(3):392–399.

Walsh, C. J.
1997. A multivariate method for determining optimal subsample size in the analysis of macroinvertebrate samples. Mar. Freshw. Res. 48:241–248.

Wassenberg, T. J., C. Y. Burridge, M. Connell, and N. Gribble.
1998. A validation of short-duration scientific tows as a representation of long commercial-length tows: comparing the catch rates, size composition and species composition of prawn trawler bycatch in the far northern Great Barrier Reef, Australia. Fish. Res. 36:35–46.

Williams, G. C.
1985. The Torres Straits prawn fishery. *In* Torres Strait fisheries seminar, Port Moresby, 11–14 February 1985 (A. K. Haines, G. C. Williams, D. Coates, eds.), p. 233–238. Australian Government Publishing Service, Canberra, Australia.

Age and growth of blue rockfish (*Sebastes mystinus*) from central and northern California

Thomas E. Laidig
Donald E. Pearson
Southwest Fisheries Science Center
National Marine Fisheries Service
110 Shaffer Rd
Santa Cruz, California 95060
E-mail: tom.laidig@noaa.gov

Lorraine L. Sinclair
Pacific States Marine Fisheries Commission
411 Burgess Drive
Menlo Park, California 94025

Abstract—Otoliths from blue rockfish (*Sebastes mystinus*), were aged by using a combination of surface and break-and-burn methods. The samples were collected between 1978 and 1998 off central and northern California. Annual growth increments in the otoliths were validated by using edge analysis for females up to age 23 and for males to age 25. The first annual growth increment was identified by comparing the diameter of the otolith from fish known to be one year old collected in May (when translucent zone formation was completed) to the mean diameter of the first translucent zone in the otoliths from older fish. Our estimated maximum ages of 44 years for males and 41 years for females were much older than those reported in previous studies. Von Bertalanffy growth models were developed for each sex. Females grew faster and reached larger maximum length than males. The growth models were similar to those generated in other studies of this species in southern and central California. Fish from northern and central California had similar maximum sizes, maximum ages, and growth model parameters.

Manuscript approved for publication 17 April 2003 by Scientific Editor.
Manuscript received 26 June 2003 at NMFS Scientific Publications Office.
Fish. Bull. 101:800–808.

Accurate information on age and growth is critical for reliable assessments and effective management of fish stocks. Most assessments of west coast groundfish stocks use age-based models (PFMC, 2001). It is important to obtain reliable ages for maturity schedules, age-specific fecundity, and age-specific selectivity, as well as estimates of aging accuracy, in order to correctly estimate biomass and acceptable biological catch numbers for these assessments. Inaccurate age estimates can lead to over-harvesting or denial of fishing opportunities.

In the present study, we examine age and growth of blue rockfish (*Sebastes mystinus*). The blue rockfish is a schooling species that occurs from Sitka Strait (southeast Alaska) to northern Baja California (Love et al., 2002). They reach a maximum size of 508 mm fork length (FL). Blue rockfish are frequent inhabitants of nearshore rocky reefs, and are commonly found from the surface to about 90 m water depth. Blue rockfish comprise a major fraction of the recreational fishery off California (Miller and Geibel, 1973; Karpov et al., 1995) but are less common in the commercial fishery. In 1994, blue rockfish landings off California totaled 172 metric tons (t) from recreational fisheries and only 68 t from commercial fisheries (Rogers et al., 1996).

Age structure of blue rockfish has been determined previously by using length-frequency analyses, tag-and-recapture studies, scales, and whole otoliths (Wales, 1952; Miller and Geibel, 1973; McClure, 1982; MacGregor, 1983; Karpov et al., 1995). We estimated age by examining the surface of whole otoliths and broken-and-burnt cross sections of otoliths. Aging the surface of whole otoliths is only effective for young rockfish (Six and Horton, 1977; Kimura et al., 1979; Chilton and Beamish, 1982). The break-and-burn technique (Chilton and Beamish, 1982) is used widely for age determinations of west coast groundfish (including Dover sole [*Microstomus pacificus*], sablefish [*Anoplopoma fimbria*], and numerous species of rockfishes).

We used edge analysis to verify the annual periodicity of growth increments in the otoliths of blue rockfish. Edge analysis and marginal increment analysis have been used to validate annual growth increments in numerous species. In recent studies, Crabtree and Bullock (1998) validated the first seven annual growth increments in black grouper, and Brown and Sumpton (1998) validated the ages of the redthroat emperor off Australia. The procedure has been used to validate annual growth increments in many rockfish species, including redfish, (Mayo et al., 1981), yellowtail (Kimura et al., 1979), shortbelly (Pearson et al., 1991), widow (Pearson, 1996), gopher, and kelp rockfish (Lea et al., 1999).

Methods

Rockfish sampling

Otoliths of blue rockfish were obtained from 1) the recreational catch of commercial passenger fishing vessels (CPFV); 2) the catches of midwater trawls deployed from a research vessel; and 3) specimens speared by researchers equipped with SCUBA (Table 1). CPFV landings were available from Monterey to Bodega Bay, California, from 1978 to 1998. All fish were caught at depths deeper than 20 m; total length (TL) and sex were recorded for each specimen, and otoliths were removed. Pelagic young-of-the-year blue rockfish were caught in a 13 × 13 m midwater trawl deployed periodically from the RV *David Starr Jordan* off the central California coast from Monterey to Marin counties during 1988–93 at depths of 5–30 m. In the laboratory, each specimen was measured (standard length [SL]) and otoliths were removed and attached to microscope slides for later examination. Specimens were taken with spears from 1988 to 1998 in water depths of 1–20 m off Sonoma and Mendocino counties (Table 1). Some cohorts were sampled throughout their first year after first settlement, thus providing specimens of known age. We measured each specimen, determined sex, and removed otoliths. All fish lengths (either TL or SL) were standardized to FL for comparisons (by using equations from Echeverria and Lenarz, 1984).

Table 1

Number of specimens collected by year for blue rockfish (*Sebastes mystinus*) from three different sampling methods.

Year	Recreational catch	Diver spears	Midwater trawls
1978	12		
1980	64		
1981	214		
1982	215		
1985	31		
1986	77		
1988		109	35
1989		217	11
1990		206	38
1991		157	34
1992		122	7
1993		190	8
1994		138	
1995		18	
1997	15	43	
1998	27	45	

Otolith examination

Ages were estimated by counting the number of translucent zones from the surface of whole otoliths for young blue rockfish (less than 5 years of age) and by using the break-and-burn method (Chilton and Beamish, 1982) for fish greater than 5 years old. Whole otoliths were viewed through a dissecting microscope at 20–40× magnification with reflected light. For the break-and-burn method, whole otoliths were broken in half through the core, and one broken section was burned and viewed through a dissecting microscope at 20–40× magnification. Two readers determined ages independently by counting the number of translucent zones observed in both whole and broken-and-burnt otoliths. The precision of age estimates was compared by using the average percent error (APE; Beamish and Fournier, 1981). Otolith diameter was measured from the dorsal to the ventral edge through the core of the otolith. The diameter of the otolith at each presumed annual growth increment was measured from a video image of the cross section of a broken section of the otolith from the dorsal edge to the ventral edge of the translucent zone along a transverse axis through the core.

Validation of growth increments

Validation of growth increments as being produced annually was conducted in four parts. First, we conducted an edge analysis (Pearson, 1996) to determine if only one translucent zone formed along the edge of the otolith during a year. We identified the leading growth edge as either "opaque" or "translucent" on otoliths collected throughout the year to determine when the translucent zone was formed. An examination of edge analysis data was conducted on each age class from 1 to 44 years to determine if only one opaque and one translucent zone formed annually, and if they had formed, then these ages were considered validated.

Second, to identify the first annual growth increment, the average diameter of otoliths from known age one-year-old fish was compared to the average diameter of the first translucent zone from older fish. We determined the length of one-year-old fish at the time of translucent zone completion (as determined by the edge analysis) by plotting fish length against Julian date of capture and then determined the best model that described this relationship.

Third, we determined the predicted otolith diameter of a fish at the time of translucent zone completion. For this analysis, we used fish lengths from young-of-the-year (YOY; both pelagic and settled) and one-year-old blue rockfish for which ages were known by following a cohort through time. Fish length was plotted against total otolith diameter, and the best model for this relationship was determined. Using this relationship and the size of a one-year-old fish (established from the previous model), we calculated otolith diameter for one-year-old fish.

Fourth, mean diameters of the first, second, and third translucent zone of all otoliths from older fishes were measured. The diameters of these three translucent zones were compared to each other by using a Student's t test. If the first translucent zone corresponded to the diameter of an otolith at the time of completion of the first translucent zone and the first translucent zone was significantly different from the second and third zones, then the assumption that the first translucent zone was equivalent to the first annual growth increment was considered validated.

Growth

A von Bertalanffy growth curve was fitted to the fish length and age data. The form of the equation was

$$L_t = L_\infty (1 - e^{-k(t - t_0)}),$$

where L_t = fish length (mm FL) at age t;
L_∞ = maximum fish length (mm FL),
k = growth completion rate (per year);
t = age (years); and
t_0 = theoretical age (years) when the fish was length zero.

Parameters for the growth curve were calculated iteratively by using the method described by Schnute (1981). Growth models were developed separately for males and females to account for possible sex-specific growth rates (Echeverria, 1986). Growth curves were fitted for the entire sampling area and separately for the northern and southern areas to examine potential latitudinal trends in growth and by mode of collection. Growth curves were compared by using the extra sum of squares principle (Draper and Smith, 1981; Ratkowsky, 1983; Pearson and Hightower, 1991).

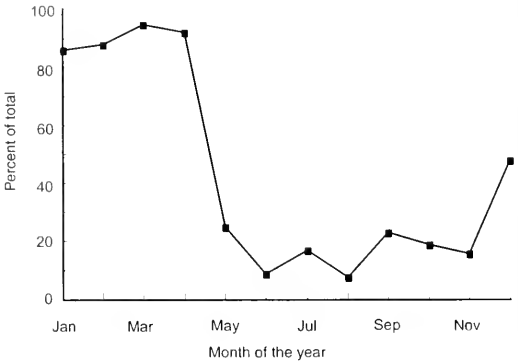

Figure 1

Percentage of blue rockfish (*Sebastes mystinus*) having a translucent zone along the otolith edge in each month (n=927).

Results

A total of 1980 blue rockfish were examined; 655 of these fish were caught by hook-and-line from CPFV, 133 pelagic juveniles were collected in midwater trawls offshore, and 1245 fish were speared. Maximum size of fish from the CPFVs was 365 mm FL for males and 444 mm FL for females. Maximum size of speared fishes was 360 mm FL for males and 412 mm FL for females. The oldest fish from the CPFVs were a 44-year-old male and a 40-year-old female, and the oldest speared fish were a 39-year-old male and a 41-year-old female. There was a 5.6% APE between readers. When ages were not in agreement, the readers would discuss the differences and if no consensus could be reached, the suspect otoliths were discarded.

Validation of growth increments

A subset (out of 1900 otoliths used for aging) of 927 (603 from CPFV and 324 from spearing) otoliths ranging from 1 to 44 growth increments was examined for edge analysis. Formation of the translucent zone followed a seasonal pattern for all otoliths combined (Fig. 1). A translucent zone developed from December through April, followed by an opaque zone that developed from May to November. Translucent zones in over 70% of the otoliths were completely formed by 1 May (or 120 Julian days), and formation of the opaque zone was complete by January in over 80% of the otoliths. From these results, we concluded that only one translucent and one opaque zone formed during a calendar year. Because only one translucent zone was shown to form each year, the annual periodicity of these zones was established. To complete the validation at each age, an edge analysis should be conducted for each age class individually (Campana, 2001). There were enough samples to conduct an edge analysis for females up to age 23 and males to age 25, and, in all instances, only one opaque and one translucent zone formed annually. Therefore, female blue rockfish were validated up to 23 years and males up to 25 years.

The length of a fish at the conclusion of translucent zone formation (determined from the edge analysis) was calculated. The first translucent zone was calculated to be complete on 1 May, one year after the assumed parturition on 1 January, or 365 Julian days + 120 Julian days = 485 days from parturition. The relationship between date of capture and FL was described with the linear equation: FL=0.16 × (date of capture) + 30.9 (n=99, r^2=0.91; Fig. 2). From this equation, a fish would be 108.5 mm FL at the time of completion of the first translucent zone (1 May, one year after parturition).

The relationship between fish length and otolith diameter (Fig. 3) was best described by the linear equation *otolith diameter* (mm) = 0.02 × (mm FL) − 0.02 (n=198, r^2=0.95). From this equation and a fish length of 108.5 mm FL at the time of the first translucent zone completion, an otolith diameter of 2.19 mm was the estimated size of the predicted translucent zone.

Diameters of the first and second translucent zones (n=509, df=508, P<0.001) and the second and third translucent zones (n=151, df=150, P<0.05) differed significantly. From a comparison of first, second, and third translucent zone diameters in the otoliths of all blue rockfish against fish length, the average observed diameter for the first translucent zone was 2.17 mm (Fig. 4), compared to the estimated diameter of 2.19 mm (from the above equation), the average observed diameter of the second zone was

3.00 mm, and the average observed diameter of the third zone was 3.67 mm (Fig. 4).

Growth

Growth between the sexes was significantly different ($P<0.05$); females grew faster and reached a larger maximum size than did males (Fig. 5). The von Bertalanffy growth model parameters for females were $t_0 = -1.34$ years, $k = 0.149$/year, and $L_\infty = 400.16$ mm FL and for males were $t_0 = -0.95$ years, $k = 0.195$/year, and $L_\infty = 329.41$ mm FL.

Growth models for both sexes were not significantly different ($P>0.05$) between the southern CPFV and northern speared samples (Fig. 6). The models representing males were virtually identical, with parameters for the CPFV model of $t_0 = -0.94$ years, $k = 0.195$/year, and $L_\infty = 331.66$ mm FL, and for the speared model of $t_0 = -0.99$ years, $k = 0.194$/year, and $L_\infty = 323.14$ mm FL. There was no significant difference between females; $t_0 = -1.94$ years, $k = 0.107$/year, and $L_\infty = 430.74$ mm FL for the CPFV samples and $t_0 = -1.14$ years, $k = 0.166$/year and $L_\infty = 393.34$ mm FL for the speared. Females from CPFV were larger at ages after 15 years than those that had been speared.

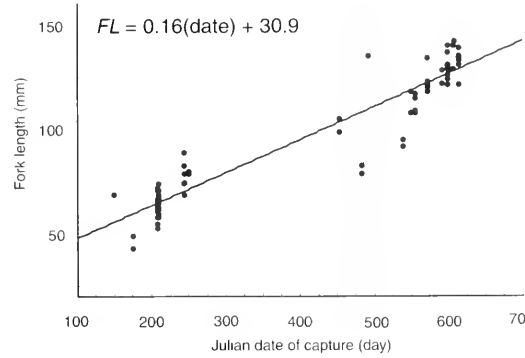

Figure 2

Growth of blue rockfish (*Sebastes mystinus*) collected nearshore during their first 1.5 years. Solid line is the fitted linear growth model (n=99; r^2=0.91). Vertical line represents 1 May, one year after the parturition date of 1 January (i.e. 365 +120=485 days).

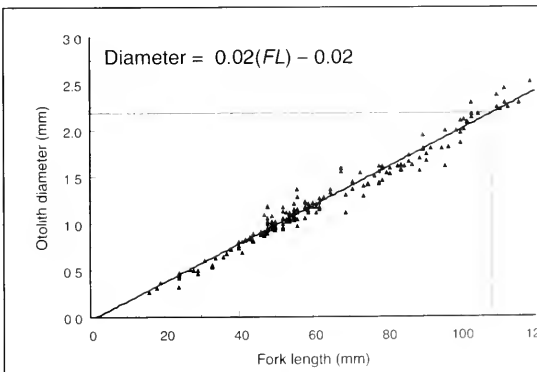

Figure 3

Change in otolith diameter with fish length for young-of-the-year and one-year-old blue rockfish (*Sebastes mystinus*). Solid line is the fitted linear model (n=198; r^2=0.95). Dashed line represents an estimated total otolith diameter of 2.19 mm for a fish of 108.5 mm FL (i.e. fish length at time of translucent zone completion).

Discussion

We estimated the age (using the break-and-burn technique) of blue rockfish to be greater than that reported in earlier studies. Aging the scales of blue rockfish, Miller and Geibel (1973) reported maximum ages of 24 and 17 years for females and males, respectively, whereas the oldest of either sex reported by MacGregor (1983) was only 13 years. Based on modal progression of length distributions, the estimate of the oldest individuals of either sex calculated by Karpov et al. (1995) was 17 years. In a study of blue rockfish off Newport, Oregon, McClure (1982) examined otolith surfaces and determined that the oldest female was 16 years, and the oldest male was only 12 years. In aging males to 44 years and females to 41 years, our study more than doubled the recorded maximum ages for blue rockfish, demonstrating the value of the break-and-burn section method for accurate age determination.

Age data were validated by using an edge analysis and the first translucent zone was validated as corresponding to the first annual growth increment. Campana (2001) pointed out that there are problems in using edge analysis as a validation tool. Specifically the extension of younger, validated ages to older, nonvalidated ages. In our study, we validated ages up to 23 years for females and up to 25 years for males; ages of older fish could not be positively validated. Therefore, caution must be taken when using the older ages.

The growth rates of blue rockfish in our study were similar to those estimated by others in California, but slower than conspecifics off Oregon (Fig. 7). MacGregor (1983) examined blue rockfish from southern California and determined the combined male and female growth

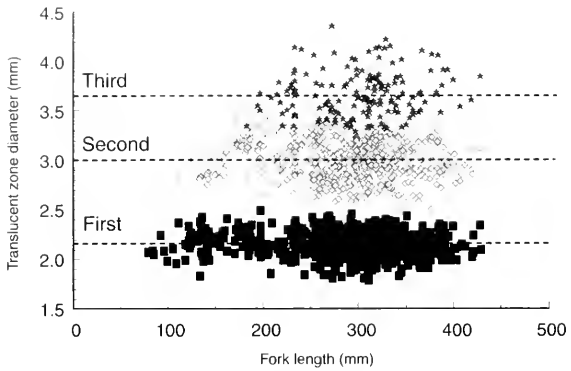

Figure 4

Diameter of the first, second, and third translucent zones in otoliths from blue rockfish (*Sebastes mystinus*) at various lengths. Dashed lines represent the mean diameters.

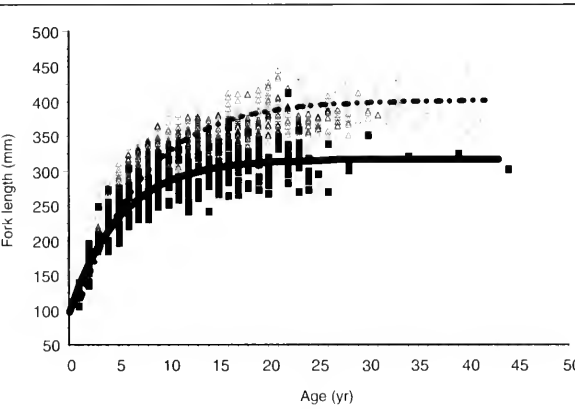

Figure 5

Von Bertalanffy growth models for all male (solid line) and female (dashed line) blue rockfish (*Sebastes mystinus*). (n=348 for males and n=1348 for females.)

rate and calculated k (instantaneous growth rate) to range from 0.13–0.16/years, which was comparable to k in our study (0.2/year for males and 0.15/years for females; mean k=0.17/year). Karpov et al. (1995) calculated k for the combined male and female growth rate from modal progressions studies to be 0.12/year. This also was similar but less than the k from our present study. On the other hand, McClure (1982) estimated a much faster growth rate for blue rockfish off Oregon, with a k for males of 0.23/years and for females of 0.31/year. Although the Oregon fish were larger at age (Fig. 7), maximum sizes from Oregon and California were similar; the largest specimen from Oregon was 460 mm FL (McClure, 1982) and the largest individual from our study was 444 mm FL.

The difference in growth between studies may be attributed to a temporal difference in the collection of fish. Two thermal regime shifts have occurred in the Pacific Ocean over the past 25 years; one in 1977 and the other in 1989 (Hare and Mantua, 2000). The samples from our study came from two different thermal regimes, but the growth

curves were not statistically different (Table 1). Therefore, these regimes did not appear to effect the growth of adult fish. Out of the four other surveys mentioned above, three came from one of these two regimes, and the fourth, Miller and Geibel (1973), came from an earlier regime. If there were any effects from the three different thermal regimes, it would seem clear that these differences would show up between samples from such varied regimes. However, the only study with different measures of growth was that from Oregon (McClure, 1982), with samples that were collected during the same regime as two of the other studies (MacGregor, 1983; and the present study). Therefore, thermal regime alone does not seem to have a major impact on the growth of blue rockfish, although further analysis is needed to confirm this point.

These differences in growth parameters between fish from California and Oregon may be attributed to differences in aging methods. Wilson and Boehlert (1990) found that estimates of growth based on aging of otolith surfaces were higher for *Sebastes pinniger*, but were similar to growth rates estimated from otolith sections for *S. diploproa*. The ages of *S. alutus* determined from otolith surfaces had poor correlation with ages from otolith cross-sections for fish older than 17 years, but there was close agreement for younger fish (Stanley and Melteff, 1987). Reading ages from the surface of an otolith may underestimate the age of a rockfish (Munk, 2001) and thus result in greater size-at-age and growth rate estimates. However, aging methods may not be the only factor influencing the growth discrepancies. Miller and Geibel (1973) and MacGregor (1983) both used scales to age blue rockfish (which also can underestimate the age of fish [Beamish and MacFarlane, 1987]), and, yet, their growth models more closely approximated the model produced by our study.

Faster growth estimated for blue rockfish off Oregon may reflect a latitudinal difference in growth. Fraidenburg (1980) examined length and age composition of *Sebastes flavidus* and reported evidence of a north-to-south cline of decreasing size-at-age. Pearson and Hightower (1991) studied *S. entomelas* and noted smaller k values and larger average maximum lengths with increasing latitude. Boehlert and Kappenman (1980) reported faster growth in the north for *S. diploproa* and no difference in growth with latitude for *S. pinniger*. They postulated that because the fish live demersally on the continental shelf, latitudinal variation in environmental factors may be insufficient to explain the difference in growth rates and that differential exploitation by the fishery may be a possible influence on growth. Blue rockfish live at relatively shallow depths where environmental and biological factors may have a greater influence on their populations.

Although blue rockfish display a possible latitudinal trend in growth rate between California and Oregon, within California no latitudinal trend in growth rates was observed. Specimens from both the southern CPFV sample and the northern speared sample areas had translucent zone completion by 1 May, which was consistent with the findings of Miller and Geibel (1973) using ages from scales. Individual fish in our study also had similar maximum ages and maximum fish lengths in the north and south areas.

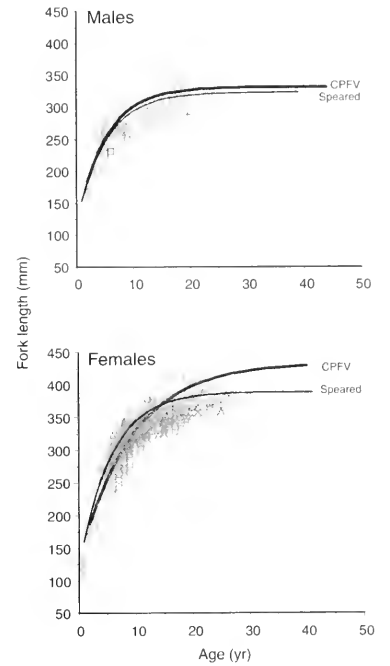

Figure 6

Von Bertalanffy growth models for male and female blue rockfish (*Sebastes mystinus*) from the CPFV (thick line) and speared samples (narrow line). Individual data points are plotted for blue rockfish from CPFV (open circle) and speared samples (open triangles).

No latitudinal trend in growth rates was observed over the 280 km between the centers of the two sampling areas. Although growth rates varied throughout their study area from Half Moon Bay in the north to Morro Bay in the south, Miller and Geibel (1973) likewise observed no latitudinal trend in growth for blue rockfish.

Blue rockfish have average maximum ages and growth rates when compared to other rockfish species. Maximum ages for rockfishes (*Sebastes* spp.) range from 12 years for the relatively small calico rockfish to 205 years for rougheye rockfish, one of the largest species (Cailliet et al., 2002; Love et al., 2002). According to Love and Johnson (1998), of the 38 species most accurately aged, most lived to more than 40 years. Love et al. (1990) found growth rates for three species that share the blue rockfish habitat (black, k=0.12–0.21/year; yellowtail, k=0.16–0.20/year; and widow rockfish, k=0.14–0.22/year) to be similar to that for blue rockfish (k=0.17 years). Mean k values for rockfish varied

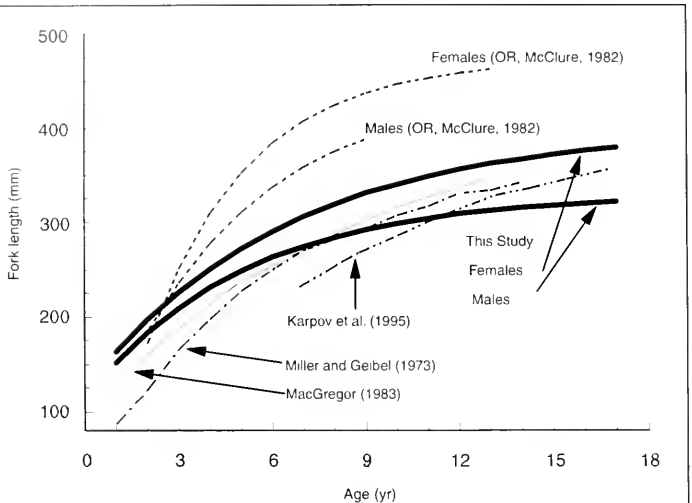

Figure 7

Growth models from five published studies of blue rockfish (*Sebastes mystinus*).

from 0.04/year for female silvergrey rockfish to 0.62/year for the shorter-lived dwarf Puget Sound rockfish, with the average range of k values occurring from 0.1 to 0.3/years (Love et al., 1990; Beckman et al., 1998). This considerable longevity and relatively slow growth rate have significant effects on the ability of many rockfish stocks to withstand exploitation.

The age and growth relationships described in this study indicate that both recruitment of blue rockfish to the fishery and their maturity occur at younger ages than previously reported. Blue rockfish enter the fishery at a size of approximately 200 mm (Miller et al., 1967; Miller and Geibel, 1973). This length equates to ages of 2–4 years as determined in our study compared to 3–5 years as estimated by Miller et al. (1967). The new estimates for age at which 50% of individuals are mature (using fish lengths from Miller and Geibel, 1973) are even more striking: our estimated age at 50% maturity is 5–6 years for males and 5 years for females, whereas estimates from Miller and Geibel (1973) and Echeverria (1986) were 7 years for males and 7–8 years for females. Similarly, the youngest mature males and females in these early studies were 4–5 years, whereas we estimated the age to be 3 years.

The changes observed in our study in age-at-length, maximum age, recruitment age, and age at 50% maturity have important implications for stock assessments. Accurate information on age composition, weight-at-age, age specific availability to the fishery, and maturity-at-age is crucial to the proper functioning of the stock synthesis model (Methot, 1990), which is used for Pacific coast groundfish. If incorrect age data are used, it could lead to erroneous estimates of population size, and subsequently to either overfishing or an unnecessary reduction in allowable catch.

Acknowledgments

We would like to thank all the port samplers who collected the CPFV catch data. We also thank the crew and scientific personnel aboard the RV *David Starr Jordan* for collecting samples. We thank James Chess, Edmund Hobson, Dan Howard, and Kelly Silberberg for braving the cold waters of the Pacific Ocean to collect the nearshore specimens. We also thank Churchill Grimes and Mary Yoklavich for their many constructive comments and the reviewers of this manuscript.

Literature cited

Beamish, R. J., and D. A. Fournier.
1981. A method of comparing the precision of a set of age determinations. Can. J. Fish. Aquat. Sci. 38:982–983.

Beamish, R. J., and G. A. MacFarlane.
1987. Current trends in age determination methodology. *In* Age and growth of fish (R. C. Summerfelt and G. E. Hall, eds), p. 15–42. Iowa State Univ. Press, Ames, IA.

Beckmann, A. T., D. R. Gunderson, B. S. Miller, R. M. Buckley, and B. Goetz.
1998. Reproductive biology, growth, and natural mortality of Puget Sound rockfish, *Sebastes emphaeus* (Starks, 1911). Fish. Bull. 96:352–356.

Boehlert, G. W., and R. F. Kappenman.
1980. Variation of growth with latitude in two species of rockfish (*Sebastes pinniger* and *S. diploproa*) from the northeast Pacific Ocean. Mar. Ecol. Prog. Ser. 3:1–10.

Brown, I. W., and W. D. Sumpton.
1998. Age, growth and mortality of redthroat emperor *Lethrinus miniatus* (Pisces: Lethrinidae) from the southern Great Barrier Reef, Queensland, Australia. Bull. Mar. Sci. 62:905–917.

Cailliet, G. M., A. H. Andrews, E. J. Burton, D. L. Watters, D. E. Kline, and L. A. Ferry-Graham.
2002. Age determination and validation studies of marine fishes: do deep-dwellers live longer? Exp. Gerontology 36: 739–764.

Campana, S. E.
2001. Accuracy, precision and quality control in age determination, including a review of the use and abuse of age validation methods. J. Fish. Biol. 59:197–242.

Chilton, D. E., and R. J. Beamish.
1982. Age determination methods for fishes studied by the groundfish program at the Pacific Biological Station, 102 p. Can. Spec. Publ. Fish. Aquat. Sci. 60.

Crabtree, R. E., and L. H. Bullock.
1998. Age, growth, and reproduction of black grouper, *Mycteroperca bonaci*, in Florida waters. Fish. Bull. 96:735–753.

Draper, N., and H. Smith.
1981. Applied regression analysis, 2d ed., 709 p. John Wiley and Sons, New York, NY.

Echeverria, T.
1986. Sexual dimorphism in four species of rockfish genus *Sebastes* (Scorpaenidae). Environ. Biol. Fishes 15: 181–190.

Echeverria, T., and W. H. Lenarz.
1984. Conversions between total, fork, and standard lengths in 35 species of *Sebastes* from California. Fish. Bull. 82: 249–251.

Fraidenburg, M. E.
1980. Yellowtail rockfish, *Sebastes flavidus*, length and age composition off California, Oregon, and Washington in 1977. Mar. Fish. Rev. 42:54–56.

Hare, S. R., and N. J. Mantua.
2000. Empirical evidence for North Pacific regime shifts in 1977 and 1989. Prog. Oceanogr. 47:103–145

Karpov, K. A., D. P. Albin, and W. H. Van Buskirk.
1995. The marine recreational fishery in northern and central California, 192 p. Calif. Dep. Fish Game Fish Bull. 176.

Kimura, D. K., R. R. Mandapat, and S. L. Oxford.
1979. Method, validity, and variability in the age determination of the yellowtail rockfish (*Sebastes flavidus*) using otoliths. J. Fish. Res. Board Can. 36:377–383.

Lea, R. N., R. D. McAllister, and D. A. VenTresca.
1999 Biological aspects of nearshore rockfishes of the genus *Sebastes* from central California, 109 p. Calif. Dep. Fish Game Fish Bull. 177.

Love, M. S., and K. Johnson.
1998. Aspects of the life histories of grass rockfish, *Sebastes rastrelliger*, and brown rockfish, *S. auriculatus*, from southern California. Fish. Bull. 87:100–109.

Love, M. S., P. Morris, M. McCrae, and R. Collins.
1990. Life history aspects of 19 rockfish species (Scorpaenidae: *Sebastes*) from the Southern California Bight, 38 p. NOAA Tech. Rep. NMFS 87

Love, M. S., M. Yoklavich, and L. Thorsteinson.
2002. The rockfishes of the northeast Pacific, 405 p. Univ. California Press, Berkeley, CA.

MacGregor, J. S.
1983. Growth of the blue rockfish (*Sebastes mystinus*). CALCOFI (Calif. Coop. Ocean. Fish. Investig.) Rep. XXIV: 216–225.

Mayo, R. K., V. M. Gifford, and A. Jearld Jr.
1981. Age validation of redfish, *Sebastes marinus* (L.), from the Gulf of Maine–Georges Bank region. J. Northwest Atl. Fish. Sci. 2:13–19

McClure, R. E.
1982. Neritic reef fishes off central Oregon: aspects of life histories and recreational fishery. M.S. thesis, 94 p. Oregon State Univ., Corvallis, OR.

Methot, R. D.
1990. Synthesis model: an adaptable framework for analysis of diverse stock assessment data. Bull. Int. North Pac. Fish. Comm. 50:259–277.

Miller, D. J., and J. J. Geibel.
1973. Summary of blue rockfish and lingcod life histories; a reef ecology study; and giant kelp, *Macrocystis pyrifera*, experiments in Monterey Bay, California, 137 p. Calif. Dep. Fish Game Fish Bull. 158.

Miller, D. J., M. W. Odemar, and D. W. Gotshall.
1967. Life history and catch analysis of the blue rockfish (*Sebastodes mystinus*) off central California, 1961–1965. Calif. Dep. Fish Game Mar. Res. Operations Ref. 67-14: 1–130.

Munk, K. M.
2001. Maximum ages of groundfish in waters off Alaska and British Columbia and considerations of age determination. Alaska Fish. Res. Bull. 8:12–21.

Pearson, D. E.
1996. Timing of hyaline-zone formation as related to sex, location, and year of capture in otoliths of the widow rockfish, *Sebastes entomelas*. Fish. Bull. 94:190–197.

Pearson, D. E., and J. E. Hightower.
1991. Spatial and temporal variability in growth of widow rockfish (*Sebastes entomelas*), 47 p. NOAA Tech. Memo., NOAA-TM-NMFS-SWFSC 167.

Pearson, D. E., J. E. Hightower, and J. T. H. Chan.
1991. Age, growth, and potential yield for shortbelly rockfish, *Sebastes jordani*. Fish. Bull. 89:403–409

PFMC (Pacific Fishery Management Council).
2001. Status of the Pacific coast groundfish fishery through 2001 and recommended acceptable biological catches for 2002. Pacific Fishery Management Council, Portland, OR.

Ratkowsky, D. A.
1983. Nonlinear regression modeling, 276 p. Marcel Dekker, New York, NY.

Rogers, J. B., M. Wilkins, D. Kamikawa, F. Wallace, T. Builder, M. Zimmerman, M. Kander, and B. Culver.
1996. Status of the remaining rockfish in the *Sebastes* complex in 1996 and recommendations for management in 1997. Appendix E: Status of the Pacific coast groundfish fishery through 1996 and recommended biological catches for 1997: stock assessment and fishery evaluation, 59 p. Pacific Fishery Management Council, Portland, OR.

Schnute, J.
1981. A versatile growth model with statistically stable parameters. Can. J. Fish. Aquat. Sci. 38:1128–1140.

Six, L. D., and H. F. Horton.
1977. Analysis of age determination methods for yellowtail rockfish, canary rockfish, and black rockfish off Oregon. Fish. Bull. 75:405–414.

Stanley, R. D., and B. R. Melteff
1987. A comparison of age estimates derived from the surface and cross-section method of otolith reading for Pacific ocean perch (*Sebastes alutus*). Lowell Wakefield fisheries symposium: proceedings of the international rockfish symposium, Anchorage, Alaska, USA, Oct. 20–22, 1986. Alaska Sea Grant Rep. 87-2, p. 187–196. Univ. Alaska, Anchorage, AK.

Wales, J. H.
1952. Life history of the blue rockfish, *Sebastodes mystinus*. Calif. Fish Game 38(4):485–498.

Wilson, C. D., and G. W. Boehlert.
1990. The effects of different otolith ageing techniques on estimates of growth and mortality for the splitnose rockfish, *Sebastes diploproa*, and canary rockfish, *S. Pinniger*. Calif. Fish Game 76:146–160.

Abstract—The reproductive activity and recruitment of white mullet (*Mugil curema*) was determined by observations of gonad development and coastal juvenile abundance from March 1992 to July 1993. Adults were collected from commercial catches at three sites in northeastern Venezuelan waters. Spawning time was determined from the observation of macroscopic gonadal stages. Coastal recruitment was determined from fish samples collected biweekly by seining in La Restinga Lagoon, Margarita Island, Venezuela. The examination of daily growth rings on the otoliths of coastal recruits was used to determine their birth date and estimate the period of successful spawning. Fish with mature gonads were present throughout the year but were less frequent between September and January when spawning individuals migrated offshore. In both years, juvenile recruitment to the lagoon was highest between March and June when high densities of 25–35 mm juveniles were observed. Back-calculated hatching-date frequency distributions revealed maximum levels of successful spawning in December–January that were significantly correlated with periods of enhanced upwelling. The relation between the timing of successful spawning and the intensity of coastal recruitment in white mullet was likely due to variations in food availability for first-feeding larvae as well as to variations in the duration of the transport of larvae shoreward as a result of varying current conditions associated with upwelling.

Manuscript approved for publication 10 June 2003 by Scientific Editor.

Manuscript received 26 June 2003 at NMFS Scientific Publications Office.

Fish. Bull. 101:809–821

Reproduction and recruitment of white mullet (*Mugil curema*) to a tropical lagoon (Margarita Island, Venezuela) as revealed by otolith microstructure*

Baumar J. Marin E.

Antonio Quintero

Instituto Oceanográfico de Venezuela
Universidad de Oriente
Cumaná 6101
Edado Sucre, Venezuela
E-mail address (for B. J. Marin E.): bmann@sucre.udo.edu.ve

Dany Bussière

Julian J. Dodson

Département de biologie
Université Laval,
Ste-Foy
Québec, Canada G1K 7P4

White mullet (*Mugil curema*) is a widespread coastal pelagic fish occurring from Massachussetts to southern Brazil. Considered to be catadromous, the juvenile fish recruit to lagoons and estuaries following a period of offshore spawning (Blaber, 1987; Ibañez-Aguirre, 1993; Ditty and Shaw, 1996). White mullet is an important economic resource supporting many small communities through both fishing and aquaculture (Alvarez-Lajonchere, 1982; Gómez and Cervigón, 1987). Small schools of mullet are captured with gill and "atarraya" nets near the coast and in neritic waters and between 300 and 400 metric tons are sold annually on Margarita Island, Venezuela.

Reproductive periodicity in white mullet varies over its geographic distribution. Several authors have reported protracted or continuous reproduction in tropical waters and generally two spawning peaks per year (Jacot, 1920; Anderson, 1957; Angell, 1973; Moore, 1974; Alvarez-Lajonchere, 1976, 1980; Yañez-Arancibia, 1976; Rodriguez and Nascimento, 1980; Garcia and Bustamente, 1981; Franco, 1986; Ibanez-Aguirre, 1993). Figure 1 summarizes previous work describing the spawning periods of *M. curema* based on gonad development and estimated according to the arrival of juveniles in the coastal zones. The spawning period is quite variable. Angell (1973) suggested that schooling occurs in coastal areas just prior to the offshore spawning migration and that the departure of individuals for the spawning grounds causes a reduction of the gonadosomatic index in the nearshore populations. Moore (1974) also reported that during the spawning period fully ripe fish are rare in coastal collections. Despite these studies, little is known of the factors influencing reproductive patterns of the white mullet. Ibanez-Aguirre (1993) suggested that the timing of reproduction in *M. curema* in Tamiahua Lagoon, Mexico, is an adaptation to avoid competition with juveniles of the conspecific *Mugil cephalus*. In areas of favorable thermal regimes, *M. curema* may penetrate a wider range of salinities and competitively exclude *M. cephalus* (Moore, 1974).

The periodicity of white mullet reproduction may be related to environmental variability that signals periods of optimal early growth and survival. Stability of the water column and suit-

* Contribution of Québec-Océan, Pavillon Alexandre-Vachon, Local 2078, Université Laval, Québec, Qc. G1K 7P4.

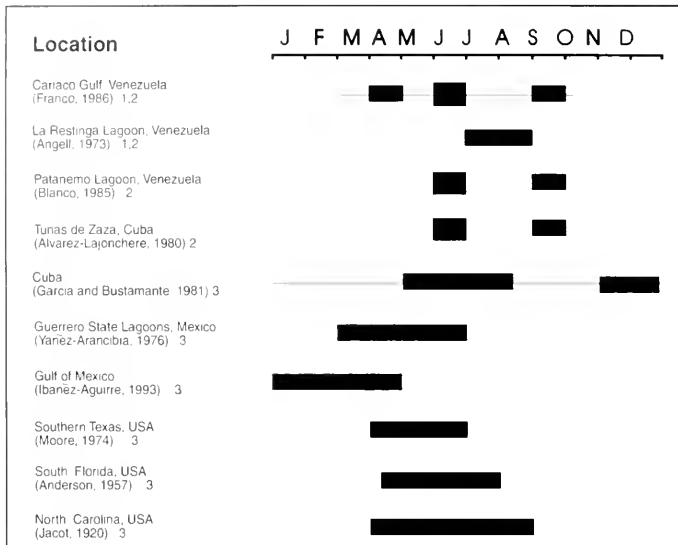

Figure 1

Spawning periods for white mullet (*Mugil curema*) in tropical waters, based on the histological observations of gonads (1), macroscopic observations of gonads (2), and estimated from the arrival of juveniles in coastal areas (3). Thin horizontal lines indicate periods of continuous but minor spawning between periods of peak spawning.

able food in coastal lagoons, river deltas, and estuarine mangrove areas have been identified as important factors influencing the recruitment of juvenile Mugilidae (Yañez-Arancibia, 1976; Blaber and Blaber, 1980; Blaber, 1987; Vieira, 1991). Based on macroscopic gonad observations of schools of white mullet captured offshore, Etchevers (1974) proposed that the spawning of white mullet recruiting along the southern coast of Margarita Island, Venezuela, occurs between La Tortuga Island and Margarita Island in the vicinity of the 1000-m deep Cariaco trench (Fig. 2). Seasonal environmental variability in this area is mainly generated by the alternation between upwelling during the dry season and freshwater discharge during the wet season (Gómez, 1983; Müller-Karger et al., 1989). The rainy season strongly influences the eastern Caribbean as freshwater plumes from the Amazon and Orinoco Rivers lower salinities throughout the region. Both upwelling and freshwater runoff produce intense peaks in coastal primary production (Gines 1972; Ferraz-Reyes et al., 1987; Müller-Karger et al., 1989), which could influence spawning periodicity and recruitment success. The purpose of this study was to document the periodicity of reproduction and recruitment of *M. curema* along the southern coast of Margarita Island and to examine their relationship with environmental signals, particularly those associated with upwelling.

Methodological advances in counting daily growth increments in otoliths of marine fishes (Pannella, 1971; Campana and Nielsen, 1985) have greatly aided studies of the age, growth, and recruitment of larval and juvenile fishes (Wilson and Larkin, 1980; McBride and Conover, 1991; Jenkins and May, 1994; Sirois and Dodson, 2000). For the striped mullet (*M. cephalus*), a close relative of the white mullet, Radtke (1984) showed that the first increment is formed one day after hatching and that additional increments are formed daily thereafter. Daily growth rings have also been demonstrated in laboratory studies for *M. so-iuy* by Li et al. (1993). In the present study, we examined the microstructure of the otoliths of juveniles recruiting to a coastal lagoon in order to back-calculate the date of hatching and hence the time of successful spawning. We first validated that otolith growth increments of juvenile *M. curema* were formed daily.

Material and methods

Reproductive periodicity was documented from samples of adult fish taken monthly from commercial catches in three fishery zones in Venezuela: 1) the Chacopata zone, located between Chacopata lagoon and Coche and Cubagua Islands; 2) the Cariaco Gulf zone; and 3) the Margarita zone located along the southern coast of Margarita Island and the northern coast of Cubagua Island (Fig. 2). Measurements of water temperature, salinity, and rainfall were

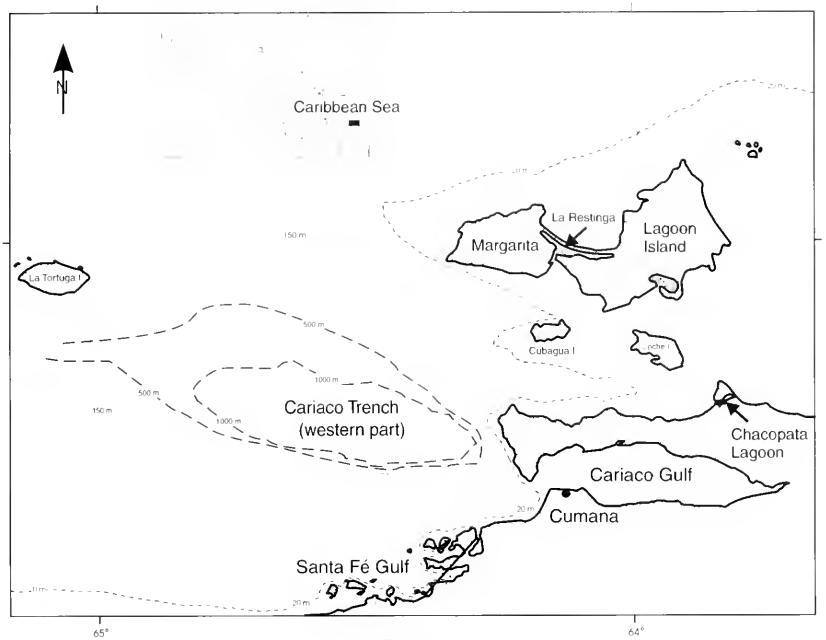

Figure 2

Map of the northeastern coast of Venezuela showing locations mentioned in the text.

collected periodically throughout the entire study period at the La Salle meteorological station, next to La Restinga Lagoon on Margarita Island.

Total (TL) and standard (SL) lengths of adult mullet were measured to the nearest 0.5 cm and total and gutted body mass were recorded to the nearest 0.1 g. Sexual maturity was determined by observation of the gonads and gonadal stages were classified as follows:

Stage I Ovaries transparent and inconspicuous, whitish-yellow in color and rounded with a small diameter. Testes longer than ovaries and ribbonlike in form.

Stage II Ovaries rounder and wider than in stage I, and yellow in color. Testes thinner, and wider than stage I, but still with thin edges and a ribbonlike form; white in color.

Stage III Ovaries large, pale yellow, smooth in appearance, turgid, and round. Ovocytes easily distinguished macroscopically (as granular). Testes milky-white in color (bright), turgid, and wider in appearance and having thicker edges than in stage II.

Stage IV Spawned (spent) ovaries purple and wrinkled in appearance. Testes whitish, or transparent with white patches, and wrinkled in appearance.

Recruitment periodicity was documented from samples of juveniles seined at semimonthly intervals at the mouth of La Restinga Lagoon (Fig. 2). The 2-cm mesh beach seine measured 1.5 m deep and 50 m long. Juvenile white mullet were distinguished from other juvenile mullets according to the descriptions of Alvarez-Lajonchere et al. (1976). White mullet juveniles were characterized by a scaly gray appearance as opposed to the shiny metallic gray appearance of a sympatric mullet species (*Mugil incilis*). For white mullet, recruitment is defined as the appearance of juveniles in coastal areas (Vieira, 1991). We calculated catch per unit of effort (CPUE) as the number of juveniles per seine haul. For all samples, standard length of fish was measured to the nearest 1 mm. Otolith analysis was restricted to one sampling period per month. After examining size-frequency distributions of juveniles captured in the lagoon, the otoliths of approximately 20 individuals representing all cohorts collected on a given sampling date were analyzed. The otoliths (sagittae) were removed with needles, rinsed in water, and then attached to strips of masking tape. The otolith was then sanded to obtain a transversal section (Fig. 3) with a thickness of approximately 20 μm by using the technique described by Secor et al. (1992) and a metallurgic jig adapted from Neilson and Geen (1986). Readings of the number of increments were made along the curvilinear surface running from the nucleus to the edge of the otolith (Fig. 3). Because daily growth increments were

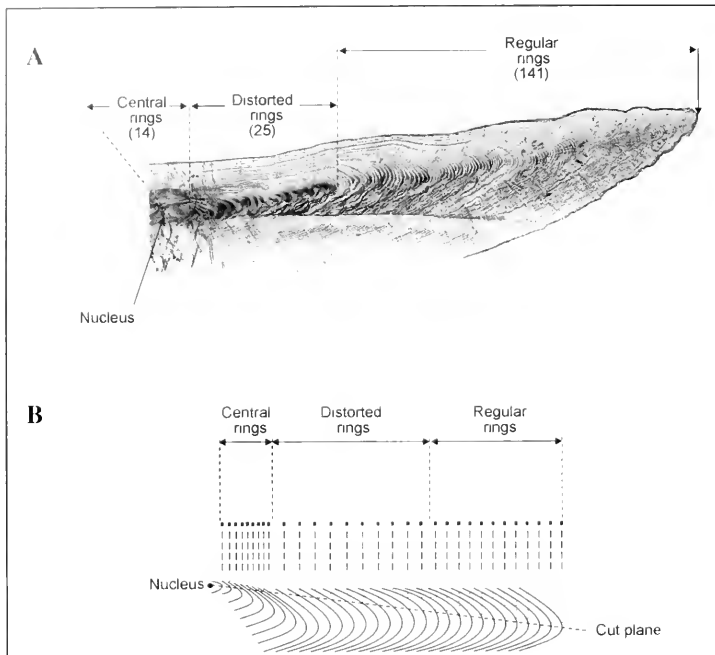

Figure 3

(**A**) Photomicrograph in optical microscopy of the posterior radius of a polished otolith from a 180-day-old juvenile white mullet (*Mugil curema*). Different sequences of rings are indicated which result from a horizontal plane not aligned with the changing growth plane of the otolith. Numbers of rings in each sequence are shown in parentheses. (**B**) Schematic presentation of the changing growth plane of the otolith, the cut plane, and the resultant increment distortion (black rectangles represent the distance between adjacent rings).

less consistent in the anterior field, otolith counts were always made along the posterior radius of the sagittae. We also measured the area of the nucleus, which represents the prehatch zone. All measurements were made under a microscope which was connected to an image analyzer and computer.

To evaluate the error in counting growth increments on otoliths, one reader made 7 independent counts of the number of growth increments on otoliths obtained from 11 juveniles representing the size-range of sampled fish. The number of growth increments ranged from 63 to 289 (mean=147) and the mean coefficient of variation was 8.71% (SD=2.13%) (Fig.4). We therefore considered an error of approximately 10% for the counts of growth increments. In applying the technique to the subsamples of the different cohorts sampled in the lagoon, at least two counts were made for each otolith. All counts were made by the same person.

To evaluate if otolith growth increments were formed daily, we read the otoliths of juveniles sampled on successive sampling dates and compared the average increase in the number of otolith increments to the number of days between samplings (Struhsaker and Uchiyama, 1976; Jordan, 1993; Jenkins and May, 1994). Birthdate was obtained by subtracting the number of daily growth rings on otoliths from the date of capture. We used the hatching mark as defined for *M. cephalus* (Radtke, 1984) and *M. iso-iuy* (Li et al., 1993) to locate the hatching mark on the otoliths of the white mullet.

Knowing that white mullet embryos hatch from 24 to 40 hours after fertilization (Anderson, 1957; Houde et al., 1976), we back-calculated hatching dates of recruits to estimate when successful spawning occurred. We examined the relationship between the spawning dates of recruits and an index of the intensity of upwelling. In calculating this index, we determined wind stress based on data from Fundación La Salle, Margarita Island, and Cumaná Airport meteorological stations. The upwelling index (UI) was based on Bowden's (1983) theoretical calculations as follows:

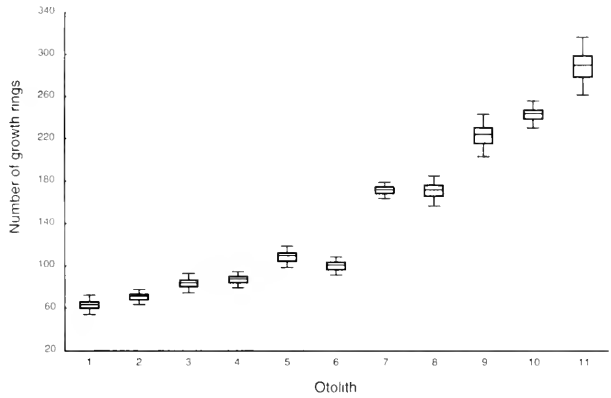

Figure 4

Number of growth increments (counted on seven independent occasions) on otoliths from 11 juvenile white mullet of varying size. Means, standard errors, and standard deviations are illustrated.

$$UI = \frac{\tau_{sx} \cdot 100}{\rho_w \cdot f},$$

where f = Coriolis parameter;
τ_{sx} = surface wind stress; and
ρ_w = average density of the water (1025 kg/m^3).

The term f was calculated as

$$f = 2\,\omega \sin(f_i),$$

where ω = angular velocity of rotation of the earth (7.29×10^{-5} s [seconds]); and
f_i = latitudinal position at the place i.

The term τ_{sx} represents surface wind stress measured in the x-axis perpendicular to the coast (Bowden, 1983), often considered in terms of the empirical equation

$$\tau_{sx} = k \times \rho_a \times W^2,$$

where k = empirical drag coefficient (1.11 to 3.25, as a function of wind velocity; Bowden 1983);
ρ_a = mean density of the air (1.25 kg/m^3); and
W = wind velocity.

The drag coefficient, k, changes as a function of wind velocity and gives values equivalent to those of Bakun et al. (1974).

The relationship between upwelling and the birth dates of successful recruits (captured in La Restinga Lagoon) was determined in two steps. First, we calculated the birth dates of juveniles captured during one monthly sampling period during each of the 18 months of the study by applying the frequency distribution of birth dates of aged juveniles to the total catch for that date. A total of 398 juveniles were aged by otolith analysis. If x% of aged fish captured on a given date were hatched on Julian Day y, this percentage was applied to the total catch of juveniles for that sampling date. Secondly, all fish hatched on a given day were summed across the 18 monthly sampling dates. This frequency distribution was then correlated with the distribution of UI estimates over the same period of time as that of the birth dates.

Before proceeding with correlation, trends in birth date and UI data series were described by using a smoothing spline. The spline fit uses a set of smoothly spliced 3rd degree polynomial segments (Simonoff, 1996; JMP® software, version 3.2.1, SAS Institute, Cary, North Carolina). Predicted values were correlated with the raw data points in order to optimize the value of lambda used to fit the smoothing spline. Increasing the value of lambda increases the degree of smoothing but weakens the correlation between predicted and raw data. Pearson correlation and cross-correlation functions were used to describe the temporal relationship between upwelling and the date of hatching of fish recruited to the coastal lagoon.

Results

The white mullet surveyed in the commercial catches measured from 4 to 36 cm SL. The largest fish were from the Chacopata zone where the most abundant sizes classes were those from 22 to 30 cm. The most abundant sizes in the Cariaco Gulf and Margarita Island zones were 20 to

26 cm and 18 to 26 cm, respectively. The mullet from the Margarita zone were mainly juveniles and small adults (Fig. 5).

Maturity and reproductive periodicity

An examination of gonad maturity revealed that 90% of the male and female mullet in the Margarita zone were immature or at developing stages (I and II) and only 10% in developed and spawning stages (III and IV). In contrast, 53.8% of females and 42.8% of males of the population of generally larger mullet sampled at Chacopata were in developed and spawning stages. Finally in the Cariaco Gulf zone, where the fish were of intermediate size, compared to fish at Margarita and Chacopata, 41.2% of females and 32.7% of males were in developed and spawning stages.

Throughout our study, sexually mature (stage-III) fish were present in the samples from the Chacopata fishery (Fig. 6), and their abundance showed a marked seasonal pattern. Mature and spent fish were least abundant (<25% of the population) between September and January and most abundant from April to August 1992 and May to June 1993. In contrast, in the Margarita fishery, immature (stage-I) fish dominated the samples and mature fish only occurred sporadically (Fig. 6). Finally, in the Cariaco Gulf zone, immature and maturing fish (stage-I, and stage-II) generally dominated the population, except in July when mature fish became abundant.

Otolith microstructure

The otolith of *M. curema* had a round nucleus with a mean radius of 9.26 μm (95% confidence interval (CI)=0.54, n=8), and the dark area in the center had a mean diameter of 4.97 μm (CI=0.82, n=8). The otolith was round during the larval period and became ovoid when mullet reached 10–12 mm (SL). In the early juvenile stage (18–20 mm SL), the otolith was strongly elongated and the anterior end was arrow-like. In juveniles (>20 mm SL), the otolith was always thin, concave, and umbrella shaped in form (Fig. 3).

Validation of otolith increment lines

The otolith increments counted for the first strong cohort present in the lagoon during March and April 1992 demonstrated that the average number of increments added during the 14-day interval between sampling collections was close to 14 days (Table 1). This indicated that otolith increments were formed daily, as observed in other species of mullet.

Juvenile recruitment

The catch-per-unit-of-effort measurements for juveniles captured in La Restinga Lagoon demonstrated a seasonal pattern and high recruitment from March to early July 1992 and from late March to May 1993, and low recruitment during the remaining months (Fig. 7). The recruitment peak in 1992 was more than twice that in 1993. The periods of strong recruitment were associated with the rainy season in northeastern Venezuela (Fig. 7), as previously reported by Okuda et al. (1978), Gómez (1983), and Ferraz-Reyes (1989).

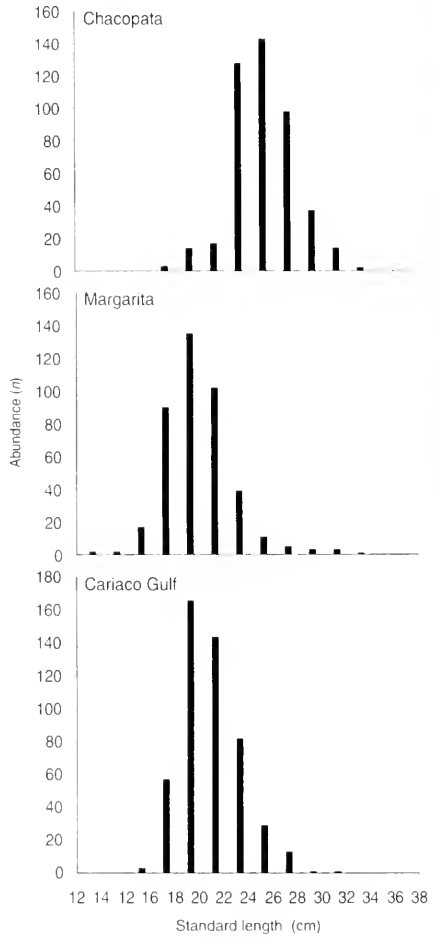

Figure 5

Length-frequency distributions of white mullet surveyed in the commercial catches from the three fishery zones of northeast Venezuela.

The discontinuous length-frequency distributions of juveniles sampled biweekly suggested the presence of four cohorts in the lagoon during the study period (Fig. 8). Two cohorts were present on 5 March 1992, the first sampling date. The cohort of smaller juveniles, referred to as the first cohort, had a mean length of 29.8 mm (range of 18 to

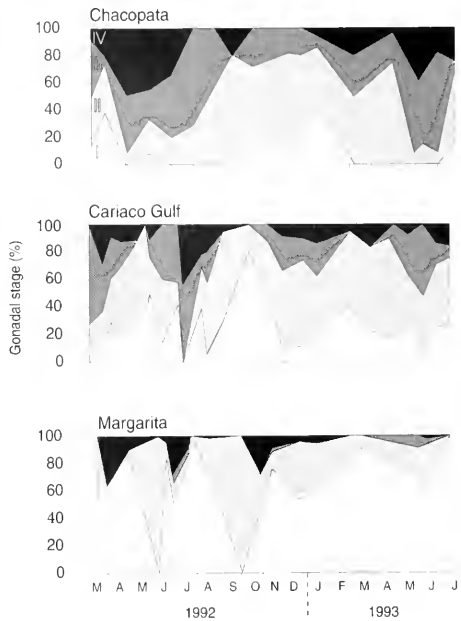

Figure 6

Percent composition of four maturity stages (I to IV, see text for definitions) of *Mugil curema* (males and females combined) captured from Margarita, the Cariaco Gulf, and the Chacopata fishery zones of northeast Venezuela.

36 mm) and varied in age from 50 to 70 days (Fig. 9). The cohort of larger juveniles, referred to as the second cohort, had a mean length of 105 mm (range of 90 to 130 mm), and otolith analysis indicated an age of 160 to 240 days (Fig. 8). This cohort was present until May 1992 and was largely absent thereafter (Fig. 7). A third cohort was first observed in mid October 1992. It measured from 50 to 100 mm in length, overlapping the length distribution of cohort 1. As such, no clear distinction could be made between these two cohorts on these dates. The third cohort became more distinct in December 1992 and January 1993 as individuals from the first cohort left the lagoon. These individuals were aged from 95 to 200 days old in December. This cohort was present until approximately April 1993 and disappeared thereafter (Fig. 9). Finally, a fourth cohort first appeared in March 1993 and consisted of fish of similar size and age as the first cohort observed in March of the previous year.

The back-calculated hatching dates showed that the second, older cohort observed in the lagoon in March 1992 was composed of mullet that had hatched between August and October 1991 (Fig. 10). The younger cohort in the March 1992 sample originated from continuous hatching from late December 1991 to late March 1992. The back-calculated hatching dates indicated that larval production of successful recruits was almost absent during April and May 1992 but small increases were observed in June and July 1992. The third cohort, which first appeared in September 1992, was

Table 1

Validation of daily increment formation in the otoliths of juvenile white mullet (*Mugil curema*) sampled at 14-day intervals in March and April 1992. *n* = number of otoliths in sample, mean age (standard deviation) is given in days on date of capture, and "difference" is the difference in mean age between successive sampling dates.

Sampling dates	5 March 1992	19 March 1992	2 April 2 1992
n	15	20	19
Mean age (SD)	56.46 (4.81)	70.85 (9.88)	84.3 (11 24)
Difference		14.39	13.45

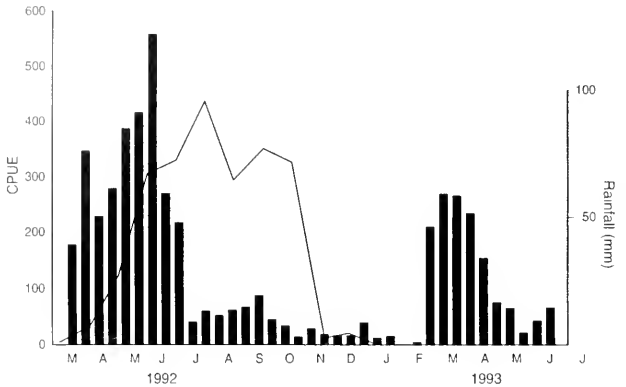

Figure 7

Histogram of monthly abundance of juvenile white mullet as indicated by catch per unit of effort (CPUE) from semimonthly sampling in La Restinga lagoon from March 1992 to July 1993. The continuous black line presented in the first annual cycle represents the mean monthly rainfall averaged over the period 1985–93.

Table 2

Correlation analyses of hatching date and upwelling index data series. Increasing lambda values used to fit the smoothing spline weakens the r^2 values between observed and predicted values of birth date and upwelling index over time (columns 2 and 3). In contrast, increasing lambda values strengthen the correlation (Pearson's correlation) between the two data series (column 4). BD = birth date, UI = upwelling index

Data series	Hatching dates (r^2, P)	Upwelling index (r^2, P)	BD versus UI (r, P)
Raw data	—	—	0.28, <0.05
Smoothing spline λ = 1	0.82, <0.000	0.86, <0.000	0.36, <0.000
Smoothing spline λ = 10	0.73, <0.000	0.74, <0.000	0.41, <0.000
Smoothing spline λ = 100	0.67, <0.000	0.63, <0.000	0.45, <0.000
Smoothing spline λ = 1000	0.64, <0.000	0.54, <0.000	0.52, <0.000
Smoothing spline λ = 10,000	0.56, <0.000	0.45, <0.000	0.57, <0.000
Smoothing spline λ = 100,000	0.48, <0.000	0.40, <0.000	0.64, <0.000

composed of individuals that had hatched between June and August 1992. Finally, individuals in the fourth cohort, which first appeared in the lagoon in March 1993, were fish that had hatched in January and February 1993.

The hatching dates of recruits coincided with periods of increasing upwelling, particularly during January and February of 1992 and 1993 (Fig. 10). The use of increasing levels of lambda to fit the smoothing spline increasingly weakened the correlations between predicted and observed values of birth dates and UI index and strengthened the correlations between birth dates and the upwelling index (Table 2). Choosing a lambda value of 10 resulted in r^2 values greater than 0.70 (P<0.000) between the raw and predicted data series and in an r value of 0.41 (P<0.000) between birth date and the upwelling index. Cross-correlation analysis between these two series revealed that the strongest correlation (r=0.52, P<0.000) occurred when the upwelling index lagged behind birth dates by 8 days and by 46 days. These lag periods reflect the coincidence of the major peak of upwelling with the two peaks of birth dates that are separated by approximately 35 days. Given the estimated 10-day error associated with aging otoliths, the 8-day lag cannot be interpreted.

Discussion

Our sampling of white mullet in the coastal waters of northeastern Venezuela revealed the presence of mature fish throughout the year, but abundance was lowest

between August and January. Mullet from the Margarita zone were small (4 to 36 cm in SL) and mostly immature (>80%). Because size at maturity of white mullet is 24 cm (Marin and Dodson, unpubl. data), most of the adults in the lagoon were probably in their first spawning cycle. Similarly, mullet from the Cariaco Gulf zone also appeared to be young adults in their first spawning cycle. In contrast, mullet from the Chacopata zone were larger and generally in more advanced stages of gonadal development. This finding suggests that the Chacopata mullet were part of a prespawning aggregation, and the location of the aggregation agrees with the more offshore location of the Chacopata fishery.

Because white mullet spawn offshore (Jacot, 1920; Anderson, 1957; Ditty and Shaw, 1996), the small proportion of mature fish in the coastal fisheries from July to April is likely explained by the migration of adults to the offshore spawning grounds. If this is so, reproduction is not indicated by an increase in the frequency of fish in advanced stages, but rather is associated with the disappearance of maturing and mature fish from coastal areas. The disappearance of fish in advanced stages from coastal areas as the spawning season approaches was also reported by Angell (1973) and Moore (1974). The analysis of birth dates of juveniles sampled in the La Restinga Lagoon indicates that successful spawnings are concentrated in the periods of increased upwelling and also coincide with the end of the rainy season. The spawning season may or may not be concentrated at these times but larvae that hatch during upwelling events are most likely to successfully recruit to the lagoon.

Although reproduction in tropical fishes is often protracted, peaks in successful spawning may nevertheless be initiated by environmental cues (Redding and Patiño, 1993). The white mullet possibly uses temperature or other signals associated with upwelling to synchronize its spawning with upwelling events. The variations in the timing of recruitment of white mullet in different geographical regions may be the result of variation in the timing of favorable conditions that enhance survival. Such conditions may include increased primary production (Ferraz-Reyes, 1983; Müller-Karger et al., 1989) or hydrographic mechanisms likely to facilitate transport of larvae to coastal nursery areas (Blaber, 1987), so that survival is increased. Populations likely have adequate time to adapt to environmental conditions in particular areas because local hydrographic patterns develop over geological time scales (Bakun, 1986; Sinclair, 1988; Heath, 1992).

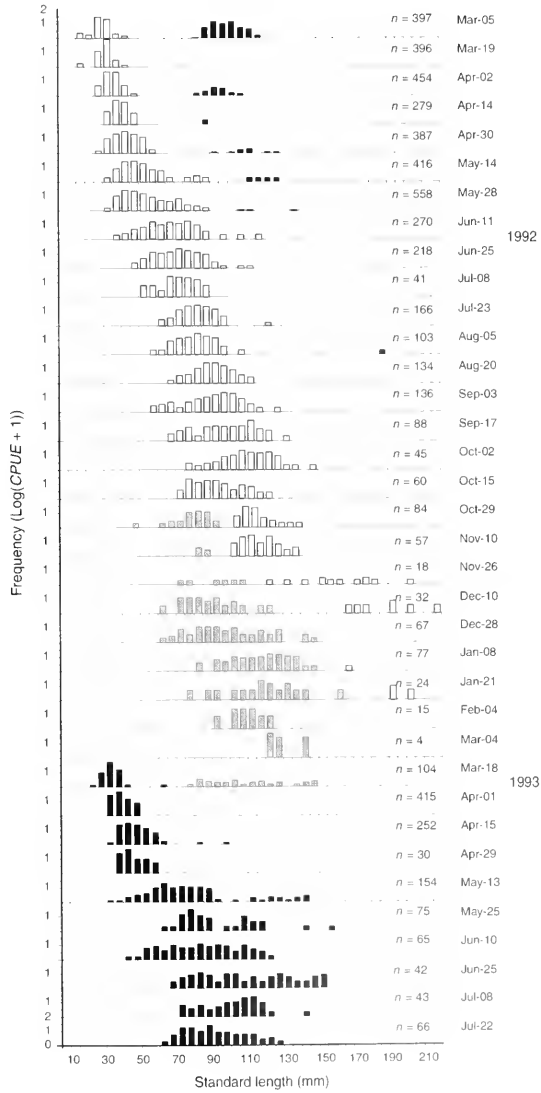

Figure 8

Semimonthly size distributions of juvenile white mullet from March 1992 to July 1993 in La Restinga Lagoon. The abundance for each size class is presented as the Log CPUE + 1. From top to bottom, open bars represent cohort 1, black bars represent cohort 2, gray bars represent cohort 3, and black bars represent cohort 4. Cohorts were identified by discontinuities in size distributions of juveniles. n = number of fish sampled.

Strong offshore transport of surface waters occurs during upwelling events, so that a rapid metamorphosis to the demersal stage may be critical for the coastal recruitment of white mullet. This rapid metamorphosis is suggested for several offshore spawning fishes with pelagic larvae that subsequently recruit to estuaries (Creutzberg et al., 1978; Heath, 1992) or that remain near the bottom during ebb flow, once close to the coast, thereby reducing offshore transport (Bartsch and Knust, 1994). White mullet undergo metamorphosis to the demersal stage 14 days after hatching (Houde et al., 1976) at which time they would be entrained in the inshore transported water that occurs at depths greater than 50 m in the coastal zone of northeastern Venezuela (Quintero, unpubl. data). Several studies suggest that increased mortality is caused by increased predation associated with the change to bottom habitat (Johannes, 1978; Bakun, 1986). Heath (1992) suggested that mortality from predation is particularly high during migration to nursery areas. Given the time to metamorphosis (14 days) and the age of white mullet when they enter the lagoon (50 to 70 days for the first cohort), metamorphosis to the demersal stage most probably occurs at least one month before entry into the lagoon (Anderson, 1957; Caldwell and Anderson, 1959; Yañez-Arancibia, 1976; Vieira, 1991).

During the demersal period at sea, white mullet may be exposed to considerable mortality due to benthic predators. Variation in the abundance of recruitment pulses into La Restinga Lagoon may reflect the interplay between spawning time and the mortality during transport to the coastal area. At some point between metamorphosis and lagoon entry, juvenile mullet also develop active swimming behavior to facilitate passive transport. We observed intensive recruitment of small mullet into the lagoon between March and June by individuals that had hatched the previous December to February. The timing of their hatching means that their return to the lagoon was likely facilitated by prevailing currents. In contrast, recruitment of mullet to the lagoon over the remainder of the year was weak and sporadic, and fish were much larger and older. At its first appearance in the lagoon, the third cohort was twice the age of the first cohort. These fish were not produced during a period when currents would likely have facilitated larval transport to the lagoon (little upwelling) and their lower densities may partially reflect increased mortality during the more prolonged return to the lagoon. We propose that spawning during periods of weak upwelling causes a delay in transport to coastal nursery areas and consequently decreased survival.

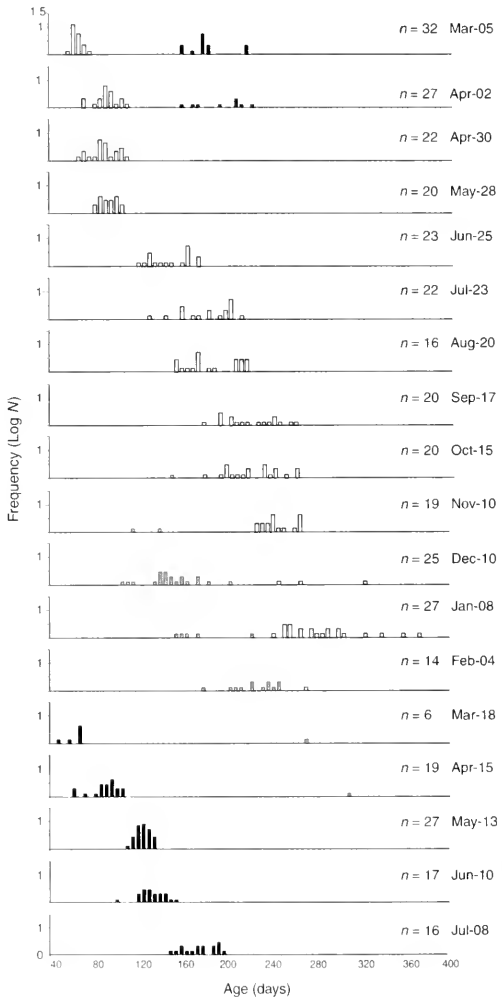

Figure 9

Monthly age distributions of juvenile white mullet from March 1992 to July 1993. Age was calculated by counting daily growth rings starting with the hatch mark. From top to bottom, open bars represent cohort 1, black bars represent cohort 2, gray bars represent cohort 3 and black bars represent cohort 4. n = number of otoliths examined.

Periods of hatching leading to successful recruitment, from late December to March, coincided with moderate peaks in the upwelling index. This successful recruitment may be the result of moderate levels of wind speed (<6 m/s^2), that promote moderate upwelling and yield optimal trophic conditions for fish larvae (Cury and Roy, 1989). Coastal upwellings in northeast Venezuelan waters are caused by

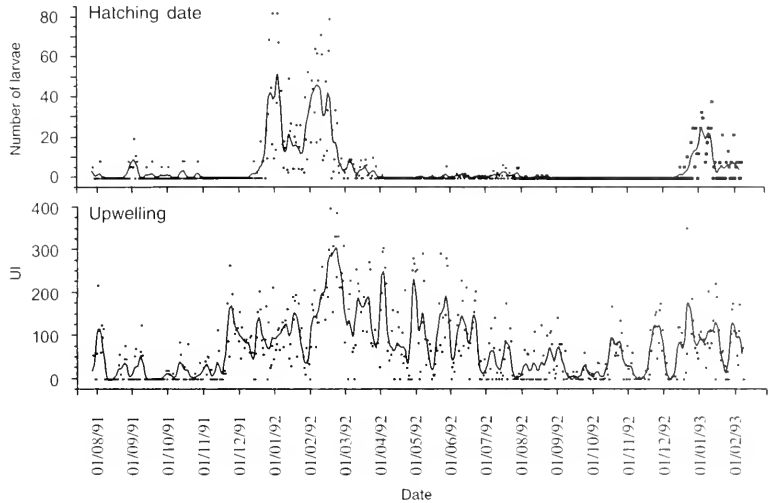

Figure 10

(**Upper panel**) Frequency distribution of hatching dates for juvenile white mullet recruits caught in 1992 and 1993 in La Restinga lagoon. Points represent raw data. Continuous black line represents the trend line generated after application of a smoothing spline (lambda=10). (**Lower panel**) Upwelling index (UI) for northeastern Venezuela calculated from August 1991 to March 1993. See text for description of calculation. Points represent raw data. Continuous black line represents the trend line generated following application of a smoothing spline (lambda=10).

moderate levels of wind stress and this differs from the strong upwellings observed in such places as Peru and Senegal. The relation between the timing of successful spawning and the intensity of coastal recruitment in white mullet is likely due to variations in the duration of the transport of larvae and juveniles to the shore as a result of varying current conditions as well as variations in food availability for first-feeding larvae.

Acknowledgments

This work is part of a Ph.D. thesis submitted to Laval University by the senior author who was financially supported by the Fundayacucho Program of Scholarships. We thank the technical and analytical assistance of the zooplankton staff of IOV-UDO (Instituto Oceanográfico de Venezuela, Universidad de Oriente), Domingo Figueroa and Rafael Briceño, and Caroline Berger for her work in the field survey, figure preparation and the processing of otoliths with Julie Paquet. Martin LLano, of the Metereological Station of Fundacion La Salle, kindly supplied the enviromental data. We thank Luis Trocolis, Jose Luis Fuentes, and Alfredo Gómez from de Edimar-UDO, Nueva Esparta, for laboratory support, Jose Bechara, Casimiro Quiñones, and Jean Paul Boulianne for advice and statistical support and Idelfonso Liñeros and Jesus Marcano for support and complementary information. This work was funded by grants from NSERC (Natural Sciences and Engineering Research Council of Canada) and FCAR (Fonds pour la Formation des Chercheurs et L'Aide à la Recherche, Québec, Canada) to Julian J. Dodson and GIROQ (Groupe Interuniversitaire de Recherches en Oceanographie du Québec) and by the Consejo de Investigación-Universidad de Oriente, proyecto LISA-92 (CI-5-019-00554/92).

Literature cited

Alvarez-Lajonchere, L.
1976. Contribución al estudio del ciclo de vida de *Mugil curema* Valenciennes (Pisces: Mugilidae). Cien. Ser. 8 Investig. Mar. (Havana) 28:3–130.
1980. Composición por especies y distribución de las postlarvas y juveniles de Lisas (Pisces, Mugilidae) en tunas de Zaza, Cuba. Rev. Investig. Mar. Cuba 1(2–3):28–60.
1982. The fecundity of mullet (Pisces, Mugilidae) from Cuban waters. J. Fish. Biol. 21:607–613.
Anderson, W. W.
1957. Early development, spawning, growth and occurrence of the white mullet (*Mugil curema*) along the south Atlantic

Coast of the United States. Fish. Bull. Wildl. Serv. 57(120): 415–425.

Angell, C.
1973. Algunos aspectos de la biologia de la lisa, *Mugil curema* Valenciennes, en aguas hipersalinas del nororiente de Venezuela. Contrib. Fund. La Salle. Cienc. Nat. 51: 223–238.

Bakun, A.
1986. Local retention of planktonic early life stages in tropical reef bank demersal systems: the role of vertically-structured hydrodynamic processes. *In* IOC/FAO workshop on recruitment in tropical coastal demersal communities, Ciudad del Carmen, Campeche, México. Workshop Rep. 44(suppl), p. 16–32.

Bakun, A., D. R. McLain, and F. V. Mayo.
1974. The mean annual cycle of coastal upwelling off western North America as observed from surface measurements. Fish. Bull. 72:843–844.

Bartsch, J., and R. Knust.
1994. Simulating the dispersion of vertically migrating sprat larvae (*Sprattus sprattus*) in the German Basin with a circulation and transport model system. Fish. Oceanogr. 3:92–105.

Blaber, S. J. M.
1987. Factor influencing recruitment and survival of mugilids in estuaries and coastal waters of Southeastern Africa. *In* Common strategies of anadromous and catadromous fishes (M. Dadswell, R. Klauda, C. Saunders, R. Rulifson, and J. Cooper, eds.), p. 507–518. Am. Fish. Soc.Symp. 1?

Blaber, S. J. M., and T. G. Blaber.
1980. Factors affecting the distribution of juvenile estuarine and inshore fish. J. Fish. Biol. 17:143–162.

Bowden, K. F.
1983. Physical oceanography of coastal waters, 302 p. Ellis Horwood Ltd., Chichester, UK.

Caldwell, D. K., and W. W. Anderson.
1959. Offshore occurrence of larval white mullet, *Mugil curema*, in the western Gulf of Mexico. Copeia 1959:252.

Campana, S. E., and J. D. Nielsen.
1985. Microstructure of fish otoliths. Can. J. Fish. Aquat. Sci. 42:1014–1032.

Creutzberg, F., A. T. G. W. Eltink, and G. J. van Noort.
1978. The migration of plaice larvae *Pleuronectes platessa* in the western Wadden sea. *In* Physiology and behaviour of marine organisms (D. S. Lunsky and A. J. Berry, eds.), p. 243–251. Pergamon Press, New York, NY.

Cury, P., and C. Roy.
1989. Optimal environmental window and pelagic fish recruitment success in upwelling areas. Can. J. Fish. Aquat. Sci. 46:670–680,

Ditty, J. G., and R. F. Shaw.
1996. Spatial and temporal distribution of larval striped mullet (*Mugil cephalus*) and white mullet (*M. curema*, family: Mugilidae) in the northern Gulf of Mexico, with notes on mountain mullet, *Agonostomus monticola*. Bull. Mar. Sci. 59:271–288.

Etchevers, S. L.
1974. Fecundidad de la lisa (*Mugil curema* Valenciennes) en el Oriente de Venezuela. Bol. Cientif. Téc. Ser. Recur. Mar. CIC UDO (Centro de Ingeniería y Computación, Universidad de Oriente) 1(1), 19 p.

Ferraz-Reyes, E.
1983. Estudio del fitoplancton de la Cuenca Tuy–Cariaco, Venezuela. Bol.Inst.Oceanogr.Venez.Univ.Oriente.22(1/2): 111–124.
1989. Influencia de los factores físicos en la distribucion vertical de la biomasa fitoplanctónica en el Golfo de Cariaco (Venezuela). Bol. Inst. Oceanogr. Venez. Univ. Oriente. 28(1/2):47–56.

Ferraz-Reyes, E., E. Mandelli, and G. Reyes-Vasquez.
1987. Fitoplancton de la Laguna Grande del Obispo, Venezuela. Bol. Inst. Oceanogr. Venez. Univ. Oriente. 26(1/2): 111–124.

Franco, L.
1986. Biología y reproducción de la lisa, *Mugil curema* Valenciennes (Pisces: Mugilidae) en el Golfo de Cariaco, Venezuela. M.S. thesis, 103 p. Instituto Oceanografico de Venezuela, Univ. Oriente, Cumana, Venezuela.

Garcia, A., and G. Bustamante.
1981. Resultados preliminares del desove inducido de lisa (*Mugil curema* Valenciennes) en Cuba. Acad. Cienc. Cuba Inf. Cient.-Téc. 158:7–26.

Gines, H.
1972. Cartas pesqueras de Venezuela. Caracas, 328 p. Fundación La Salle de Ciencias Naturales. M.E.L.S.A., Madrid, Venezuela.

Gómez, A.
1983. Pigmentos clorofílicos, producción primaria y abundancia plantónica en el canal de entrada de la Laguna de la Restinga, Venezuela. Bol. Inst. Oceanogr. Univ. Oriente 22:43–64.

Gómez, A., and F. Cervigón.
1987. Perspectivas del cultivo de peces marinos en el Caribe Sur y noreste de Suramérica. Rev. Latinoam. Acuicult. 34 40–50.

Heath, M. R.
1992. Field investigations of the early life stages of marine fish. Adv. Mar. Biol. 28:1–173.

Houde, E. D., S. A. Berkley, J. J. Klinovsky, and R. C. Schekter.
1976. Culture of larvae of the white mullet, *Mugil curema* Valenciennes. Aquaculture 8:365–370.

Ibañez-Aguirre, A. L.
1993. Coexistence de *Mugil cephalus* and *M. curema* in a coastal lagoon in the Gulf of Mexico. Mar. Biol. 42:959–961.

Jacot, A. P.
1920. Age, growth and scale characters of the mullets, *Mugil cephalus* and *Mugil curema*. Trans. Am. Microsc. Soc. 39: 199–229.

Jenkins, G. P., and H. M. A. May.
1994. Variation in settlement and larval duration of King George whiting, *Sillaginodes punctata* (Sillaginidae), in Swan Bay, Victoria, Australia. Bull. Mar. Sci. 54(1): 281–296.

Johannes, R. E.
1978. Reproductive strategies of coastal marine fishes in the tropics. Environ. Biol. Fishes 3:65–84.

Jordan, A. R.
1993. Age, growth and back-calculated birthdate distribution of larval jack mackerel, *Trachurus declives* (Pisces: Carangidae) from eastern Tasmanian coastal waters. Aust. J. Mar. Freshw. Res. 45:19–33.

Li, C., S. Xueshen, Y. Feng, Y. Chunwu, and H. Ruidong.
1993. Daily growth increments in otoliths of mullet larva, *Mugil so-iuy* Basilewsky, and determination from field-collected ones. Oceanol. Limnol. Sin. 24(4):345–349.

McBride, R. S., and D. O. Conover.
1991. Recruitment of young-of-the-year bluefish *Pomatus saltatrix* to the New York Bight: variation in abundance and growth of spring- and summer-spawned cohorts. Mar. Ecol. Prog. Ser. 78:205–216.

Moore, R. H.
1974. General ecology, distribution and relative abundance

of *Mugil cephalus* and *Mugil curema* on the south Texas coast. Contr. Mar. Sci. 18:241–255.

Muller-Karger, F. E., C. R. McClain, T. R. Fisher, W. E. Esaias, and R. Varela.
1989. Pigment distribution in the Caribbean Sea: observations from space. Prog. Oceanogr. 23:23–64

Neilson, J. D., and G. H. Geen.
1986. First-year growth rate of Sixes R. chinook salmon as infered from otoliths: effects on mortality and age at maturity. Trans. Am. Fish. Soc. 115:28–33.

Okuda, T., J. Benitez, and G. Cedeno.
1978. Caracteristicas hidrograficas del Golfo de Cariaco, Venezuela. Bol. Inst. Oceanogr. Venez. Univ. Oriente 17: 69–87.

Panella, G.
1971. Fish otoliths: daily growths layers and periodic patterns. Science. 173:1124–1127.

Radtke, R. L.
1984. Formation and structural composition of larval striped mullet otoliths. Trans. Am. Fish. Soc. 113:186–191.

Redding, M., and R. Patiño.
1993. Reproductive physiology. *In* Fish physiology (E. Evans, ed.), p. 503–534. CRC Press, Boca Raton, FL.

Rodriguez, C. L., and I. V. do Nacimiento.
1980. Estudio microscópico dos ovarios de *Mugil curema* Valenciennes, Brasil. *In* I simposio Brasileiro de aquacultura, Recife, 1978, p. 213–219. Academia Brasileira de Ciencias, Rio de Janeiro, Brazil.

Secor, D. H., J. M. Dean, and E. H. Laban.
1992. Otolith removal and preparation for microstructural examination. *In* Otolith microstructure examination and analysis (D. K. Stevenson and S. E. Campana, eds.), p. 9–57. Can. Spec. Publ. Fish. Aquat. Sci. 117.

Simonoff, J. S.
1996. Smoothing methods in statistics. Springer-Verlag, New York, NY.

Sinclair, M.
1988. Marine populations: an essay on population regulation and speciation, p. 252. Univ. Washington Press, Seattle, WA.

Sirois, P., and J. J. Dodson.
2000. Critical periods and growth-dependant survival of larvae of an estuarine fish, the rainbow smelt *Osmerus mordax*. Mar. Ecol. Prog. Ser. 203:233–245.

Struhsaker, P., and J. H. Uchiyama.
1976. Age and growth of the nehu, *Stolephorus purpureus* (Engraulidae), from the Hawaiian islands as indicated by daily growth increments in sagittae. Fish. Bull. 74:9–17.

Vieira, J. P.
1991. Juvenile mullets (Pisces: Mugilidae) in the estuary Lagoa dos Patos, RS, Brazil. Copeia 1991:409–418.

Wilson, K. H., and P. A. Larkin.
1980. Daily growth rings in the otoliths of juvenile sockeye salmon *Oncorhynchus nerka*. Can. J. Fish. Aquat. Sci. 37: 1495–1498.

Yañez-Arancibia, L. A.
1976. Observaciones sobre *Mugil curema* Valenciennes, en areas naturales de crianza, crianza, maduración, crecimiento, madurez y relaciones ecológicas. Ann. Cent. Cienc. Mar Limnol Univ. Nac. Autón. México 2:211–243.

Fecundity and spawning season of striped mullet (*Mugil cephalus* L.) in South Carolina estuaries*

Christopher J. McDonough
William A. Roumillat
Charles A. Wenner
Marine Resources Research Institute
South Carolina Department of Natural Resources
217 Fort Johnson Road
Charleston, South Carolina 29422-2559
E-mail address (for C. J. McDonough): mcdonoughc@mrd.dnr.state.sc.us

Abstract—Fecundity in striped mullet (*Mugil cephalus*) from South Carolina correlated highly with length and weight, but not with age. Oocyte counts ranged from 4.47×10^5 to 2.52×10^6 in 1998 for fish ranging in size from 331 mm to 600 mm total length, 2.13×10^5 to 3.89×10^6 in 1999 for fish ranging in size from 332 mm to 588 mm total length, and 3.89×10^5 to 3.01×10^6 in 2000 for fish ranging in size from 325 mm to 592 mm total length. The striped mullet in this study had a high degree of variability in the size-at-age relationship; this variability was indicative of varied growth rates and compounded the errors in estimating fecundity at age. The stronger relationship of fecundity to fish size allowed a much better predictive model for potential fecundity in striped mullet. By comparing fecundity with other measures of reproductive activity, such as the gonadosomatic index, histological examination, and the measurement of mean oocyte diameters, we determined that none of these methods by themselves were adequate to determine the extent of reproductive development. Histological examinations and oocyte diameter measurements revealed that fecundity counts could be made once developing oocytes reached 0.400 μm or larger. Striped mullet are isochronal spawners; therefore fecundity estimates for this species are easier to determine because oocytes develop at approximately the same rate upon reaching 400 μm. This uniform development made oocytes that were to be spawned easier to count. When fecundity counts were used in conjunction with histological examination, oocyte diameter measurements, and gonadosomatic index, a more complete measure of reproductive potential and the timing of the spawning season was possible. In addition, it was determined that striped mullet that recruit into South Carolina estuaries spawn from October through April.

Manuscript approved for publication 19 June 2003 by Scientific Editor.
Manuscript received 26 June 2003 at NMFS Scientific Publications Office.
Fish. Bull. 101:822–834

The striped mullet (*Mugil cephalus* L.) is distributed circumglobally in tropical and semitropical waters between latitudes 42°N and 42°S (Thompson, 1963; Rossi et al., 1998). Even though considered a marine species, striped mullet are euryhaline and can be found year round throughout the full range of estuarine salinities in the southeastern United States (Jacot, 1920; Anderson, 1958). Striped mullet are a commercially important fish throughout the world sustaining both fisheries and aquaculture industries. In the southeastern United States (North Carolina and Florida) there are significant commercial fisheries for striped mullet, whereas in South Carolina and Georgia landings are more limited (NMFS[1]).

The primary fishery in most of these states is for "roe" mullet during the fall spawning migration. Throughout the rest of the year mullet are fished commercially for bait, if they are fished at all (Anderson, 1958). Striped mullet have a significant economic impact in the areas where they are more heavily fished by the commercial fisheries and the landings of this species from 1994 to 1998 yielded a landings (wholesale) value of 38.2 million dollars. Striped mullet are also one of the most important forage fishes that are found in the estuaries of the southeastern United States and represent a significant food source for upper-level piscivores (Wenner et al.[2]).

The biological features of striped mullet has been well documented (Jacot, 1920; Anderson, 1958; Thomson, 1963, 1966; Chubb et al., 1981), but much less information is available on the biological aspects of reproduction in the wild (Anderson, 1958; Stenger, 1959; Greeley et al., 1987; Render et al., 1995). There is a large body of work concerning striped mullet reproduction in aquaculture but many of these studies have used artificial manipulation of the reproductive cycle. Although the maturation process of oocytes may have been the same as that in wild striped mullet, the environment and conditions under which maturation occurs were artificial (Shehadeh et al., 1973a; Kuo et al., 1974; Pien and Liao, 1975, Kelly, 1990; Tamaru et al., 1994; Kuo, 1995). In addtion, despite the demonstrated ability to initiate reproduction (both in and out of season) for striped mullet, the majority of aquaculture studies have had to rely on wild fish for broodstock (Kuo et al., 1974; Pien and Liao, 1975; Kuo, 1995).

* Contribution 522 of the Marine Resources Institute, South Carolina Dept. of Natural Resources, Charleston, SC 29422-2559

[1] National Marine Fisheries Service. 2001. Personal commun. Statistics and Economic Division, 1315 East-West Highway, Silver Spring, Md. 20910. http://www.st.nmfs.gov/st1/index.html.

[2] Wenner, C. A., W. A. Roumillat, J. E. Moran, M. B. Maddox, L. B. Daniel, and J. W. Smith. 1990. Investigations on the life history and population dynamics of marine recreational fishes in South Carolina, part 1. Completion report, project F-37, p. 3–13 and project F-31, p. 6–35. South Carolina Marine Resources Research Institute, P.O. Box 12559, Charleston, SC 29422

In the southeastern United States the spawning season lasts from two to five months depending on the coastal area involved (Jacot, 1920; Broadhead, 1956; Anderson, 1958; Arnold and Thompson, 1958; Stenger, 1959; Dindo and MacGregor, 1981; Greeley et al., 1987; Render et al., 1995; Hettler et al., 1997). Striped mullet are considered isochronal spawning fishes (Greeley et al., 1987; Render et al., 1995), i.e. they have synchronous gamete development and individuals spawn all their reproductive material at once or in batches over a very short time period (days, as opposed to weeks). There have been limited observations of offshore spawning activity (Arnold and Thompson, 1958), and few examples of eggs and larvae collected offshore (Anderson, 1958; Finucane et al., 1978; Collins and Stender, 1989). Collins and Stender (1989) concluded that striped mullet spawn in and around the edge of the continental shelf off the coasts of North Carolina, South Carolina, Georgia, and the east coast of Florida (an area often referred to as the South Atlantic Bight) and have a protracted spawning season from October to April. This spawning season contrasts with that estimated by most other studies (Jacot, 1920; Broadhead,1956; Anderson, 1958; Arnold and Thompson, 1958; Stenger, 1959; Dindo and MacGregor, 1981; Greeley et al., 1987; Render et al., 1995; Hettler et al., 1997). These studies based their estimates on the reproductive condition of migrating adults and the subsequent recruitment of juvenile fish back into coastal estuaries—not on actual data on the offshore presence of striped mullet larvae. Female mullet have been shown to mature at two to three years of age at a size range from 230 mm to 350 mm standard length (Thomson, 1951, 1963; Greeley et al., 1987). Determination of spawning activity in mullet has been estimated by using gonadosomatic indices (Dindo and MacGregor, 1981; Render et al., 1995), examination of oocyte size and maturity stage (Stenger, 1959; Greeley et al., 1987), and by the presence of enlarged, developing ovaries in migrating fish (Jacot, 1920; Anderson, 1958).

The purpose of the present study was to develop size- or age-related estimates of fecundity in striped mullet from South Carolina estuaries. These fecundity estimates were determined in order to develop models for estimating potential fecundity from catch data, such as length and weight data. In addition, other indicators of reproductive activity such as gonadosomatic indices and oocyte size were examined to provide information on the duration of the spawning season. Potential fecundity estimates can give a barometer of reproductive potential based on morphological information from catch curve data and size-frequency distributions.

Materials and methods

Striped mullet were collected monthly from January 1998 through December 2000 by using a randomly stratified sampling regime within three different estuarine systems along the South Carolina coast: (Ashepoo-Combahee-Edisto (ACE) Basin, Charleston Harbor, and the Cape Romain estuary, Fig. 1). The female striped mullet used for fecundity estimates were collected from October through February each year because these were the only months when fecund females were present. Fecund female striped mullet were defined as specimens in the tertiary stage of vitellogenesis with oocyte diameters greater than 400 μm and that had gonadosomatic indices greater than 5.0. The vitellogenic stage for each specimen used in the fecundity estimates was confirmed histologically. Fish were captured during daylight ebbing tides with water levels ranging from 0.3 to 2.0 meters, and the majority (67.8%) were caught during late ebb. The fish were primarily caught with a 184-m trammel net with an outside stretch mesh of 350 mm and an inside stretch mesh of 63.5 mm, although a few of the 1999 samples (5) and the 2000 samples (3) were obtained by using a cast net 1.8 m in diameter and equipped with 10-mm mesh. Eight fecund females were also captured by using an electroshock boat in the freshwater and low-salinity areas of the Cooper River (one of the three rivers that make up the Charleston Harbor Estuary) in October 2000. The areas included in the present study have been sampled on a monthly basis since 1991 with trammel nets by the Inshore Fisheries Group of the South Carolina Department of Natural Resources as part of a gamefish monitoring program. During this period reproductively developing striped mullet of both sexes were generally observed from October through February and were presumably heading offshore to spawn (Jacot, 1920; Anderson, 1958; Arnold and Thompson, 1958). Male striped mullet that were reproductively developed were easy to discern because they were usually leaking milt and were not analyzed further. All other fish were brought back to the laboratory and eviscerated in order to determine sex and to collect ovaries for reproductive analysis. All of the samples were kept on ice and were generally examined within twenty-four hours of capture.

Standard morphometric measurements included total length (TL) in mm, fork length in mm (FL), and standard length in mm (SL), total weight (TW) in grams, ovary weight (OW) in grams, sex, and maturity. Body weight (BW) was calculated as total weight minus ovary weight ($BW=TW-OW$). Saggital otoliths were removed for aging. A small section of the posterior end of the ovaries, at the junction of the two lobes, was also removed for histological examination. The whole ovaries were fixed in 10% seawater-buffered formalin and the histological sample was fixed in 10% neutral-buffered formalin. Histological samples were processed by using standard procedures for paraffin embedding and sectioning (Humason, 1967). The sections were dried on slides and stained by using standard haematoxylin and eosin-Y staining techniques (Humason, 1967). Examination of the histological sections for maturity stage was done by using a compound microscope at 100× magnification. Each histological section was evaluated by two separate readers to determine agreement on maturity stage. If there was a discrepancy in maturity staging for any specimen, the discrepancy was either resolved by the two readers or that specimen was not used in the analysis. There were no discrepancies between readers on any of the reproductively developing females. Maturity was assessed according to a modified version of the schedule used by Wenner et al. (1986) adapted to work with isochronal

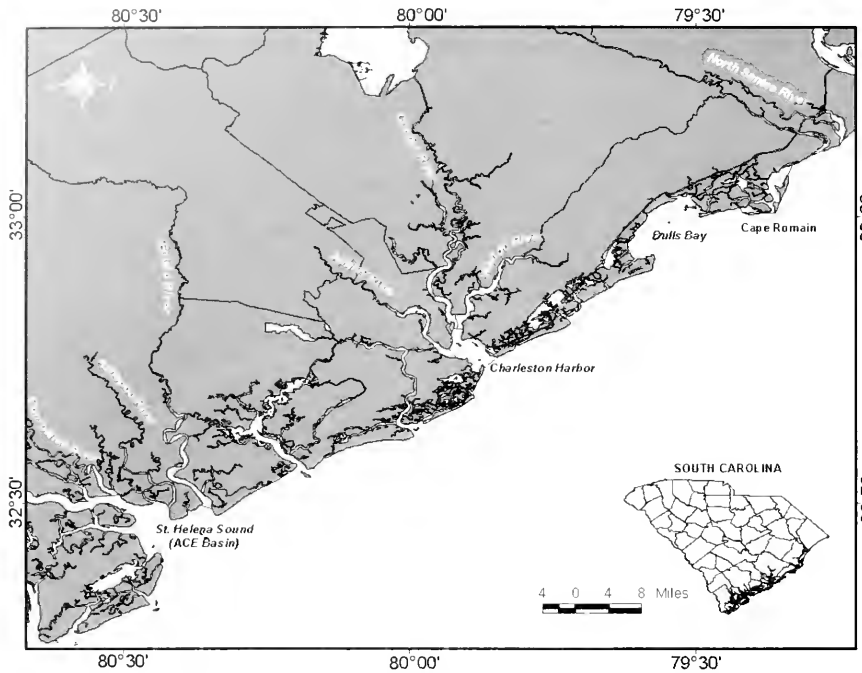

Figure 1

The South Carolina coast with the locations of estuaries and major river basins where striped mullet were collected from 1998 to 2000.

spawning fish, as well as previous models of reproductive development (Stenger, 1959; Wallace and Selman, 1981) (Table 1). This evaluation method was based on identification of morphological characteristics evident in histological sections. Each specimen was evaluated by two (in some cases three) readers and discrepancies between readers were either resolved or the specimen was excluded from the analysis.

A gonadosomatic index (GSI) was calculated for each specimen following the method of Render et al. (1995) where GSI was expressed as gonad weight (GW) divided by body weight (BW) such that

$$GSI = (GW/BW) \times 100.$$

The GSI values of the fecundity specimens were compared among the three sampling years, as well as with GSI values for female striped mullet collected during the rest of the year that were mature but not reproductively active.

Fecundity determinations were made from a total of 129 advanced-stage developing ovaries: 50 from 1998, 37 from 1999, and 42 from 2000. All of the ovaries were determined by histological examinations and criteria outlined in Table 1 to be actively vitellogenic, having tertiary yolk-stage oocytes. All oocytes counted for fecundity were 400 μm or larger and in the tertiary yolk stage (Pien and Liao, 1975) (Fig. 2). This 400-μm threshold has also been used in other studies of oocyte development in striped mullet for determining the point at which the oocytes that would be spawned during that year were identifiable (Shehadeh et al., 1973a). Unlike other species (particularly batch spawners), where fecundity counts should ideally be conducted by using hydrated oocytes only, the striped mullet oocytes used for fecundity counts were still presumably several weeks from hydration and spawning. However, because mullet are synchronous spawners, it is relatively easy to distinguish the developing oocytes from the undeveloped ones because of the drastic difference in size between the two, as well as by the uniformity in size of the developing oocytes once they reach 400 μm.

Fecundity was estimated by using a modified gravimetric method. The fixed whole ovary was patted dry and reweighed. The ovarian lobes were divided into four discrete regions along each lobe's longitudinal axis and three subsamples (chosen at random) were taken between the two lobes and preserved in 50% isopropyl until oocyte counts could be conducted. The subsamples ranged in weight from 0.025 g to 0.033 g. The subsamples from each specimen

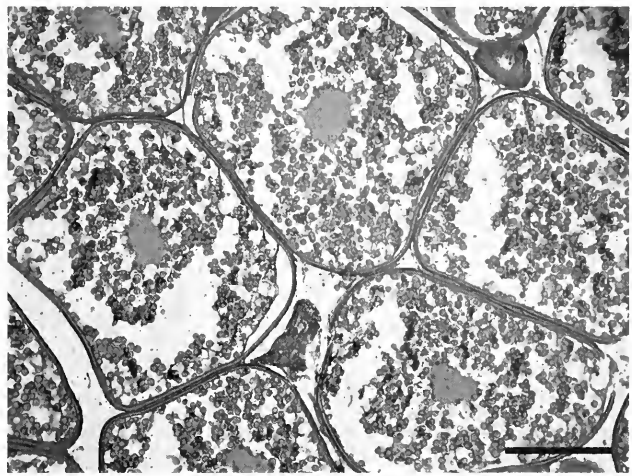

Figure 2
A striped mullet oocyte in the tertiary yolk stage of vitellogenesis. Scale bar = 250 μm.

Table 1
Histological criteria used to determine reproductive stage in female striped mullet (*Mugil cephalus*) once sexual differentiation has occurred (Wenner et al.: see footnote 2 in the general text).

Reproductive stage	Description
1. Immature	Inactive ovary with previtellogenic oocytes and no evidence of atresia. Oocytes are < 80 μm, lamellae still contain somatic and connective tissue bundles. Ovary wall is very thin (one or two cell layers).
2. Developing	Developing ovary have enlarged oocytes generally greater than 120 μm in size. Cortical alveoli are present and actual vitellogenesis occurs after oocytes reach 180 μm in size and continue to increase in size. Abundant yolk globules with oocytes reaching a size of >600 μm.
3. Running ripe	Completion of yolk coalescence and hydration in most oocytes.
4 Atretic or Spent	More than 30% of developed oocytes undergoing the atretic process.
5 Inactive or Resting	Previtellogenic oocytes only but traces of atresia possible. In comparison to immature females, most oocytes are >80 μm, lamellae have some muscle and connective tissue bundles. Lamellae are larger, have moore oocytes, and are elongated. A thicker ovarian wall with blood vessels, muscle, and nerve tissue.

were then teased apart. After separation, the oocytes were spread out on a Bogorov tray and counts of oocytes, greater than 400 μm, were made by using a dissecting microscope at 12× magnification. Each subsample was counted twice and counts were averaged. A third count was performed if the first two counts differed by more than 10%. Oocyte density was calculated by dividing the mean number of oocytes by the mean weight of all three subsamples for each specimen. The oocyte density was then used to calculate the total oocyte number for each ovary, or individual fecundity, by multiplying mean oocyte density by whole ovary weight.

In order to determine mean oocyte diameter for each specimen, 20–30 oocytes were removed from each counted subsample and grouped together in a petri dish. Each oocyte was then measured along the longest axis by using Optimas™ Image Analysis software (version 6, Media Cybernetics, Bothell,WA). Mean oocyte diameter was calculated as the average of all measurements for each

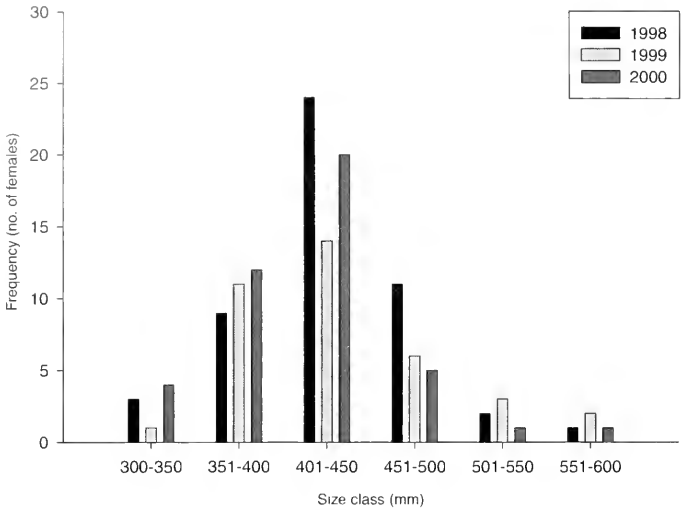

Figure 3

Size-frequency distribution of female striped mullet used in fecundity determinations from South Carolina estuaries from 1998 to 2000. n (number of fish in sample) = 50 fish for 1998, n = 37 for 1999, and n = 42 for 2000.

subsample. The overall mean oocyte diameter for each specimen resulted from the calculated average of the means of the three subsamples. Measurements were not made on fresh oocytes but shrinkage was estimated from the amount of whole ovary shrinkage because fresh ovary weight and preserved (in 10% formalin) ovary weight were known. The estimated unpreserved oocyte diameter was determined by multiplying the preserved oocyte diameter by 1 and adding the percentage of ovary shrinkage. The difference in the preserved oocyte diameter and the estimated fresh oocyte diameter was then compared by using a paired t-test to determine if there was a significant difference between preserved and unpreserved oocyte diameters.

Age was determined by using the left sagittal otolith, which was embedded in epoxy resin. A 0.5-mm transverse section encompassing the otolith core was cut with an Isomet low-speed saw with diamond wafering blades. The thin section of the otolith was embedded in epoxy and observed with a dissection microscope at the magnification appropriate for the otolith's size. Age was recorded as the number of rings (annular bands) present. The otoliths were initially aged by one reader. A second reader then evaluated a subsample of specimens from 1998 and 2000 and all the otoliths from 1999. Ages were validated by the percentage of agreement between the two age determinations, an analysis of variance (ANOVA) between the two groups of ages, and a paired t-test comparing the means and variances of the two groups (Campana et al., 1995).

Results

Fecund female striped mullet (again, defined as those females with ovaries containing oocytes >400 μm in the tertiary stage of vitellogenesis) were collected from late October through February; most of the specimens were caught in November and December for all three years. Size-frequency distributions did not vary over the three years of the study (Fig. 3). Fewer fish (n=37) were taken in 1999 versus 1998 (n=50) and 2000 (n=42). The most abundant size class for each year was that from 401 to 450 mm. In the overall size-frequency distributions, fecund females made up greater than 44% of those fish larger than 400 mm in 1998 and comprised all of the specimens over 500 mm. In 1999 the fecund females made up 12.5% of fish in the 401–450 mm size range, 39% of the fish in the 451–500 mm size range, and 100% of the fish in the size classes over 500 mm. In 2000, fecund females made up 17.7% of the 401–450 mm size class, 35.7% in the 451–500 mm size range and, like 1998 and 1999, all of the specimens over 500 mm.

The majority of females used in our fecundity study were 3 or 4 years old (Fig. 4), accounting for 80.0% of the specimens in 1998 and 73.3% in 1999. However, the age distribution in 2000 showed that the frequency of 2-, 3-, and 4-year-olds was the same and that these three ages made up 82.0% of the fecund fish sampled that year. Three-year-old fish made up the largest single group in 1998 and 1999. The age determined from the otoliths was validated as part

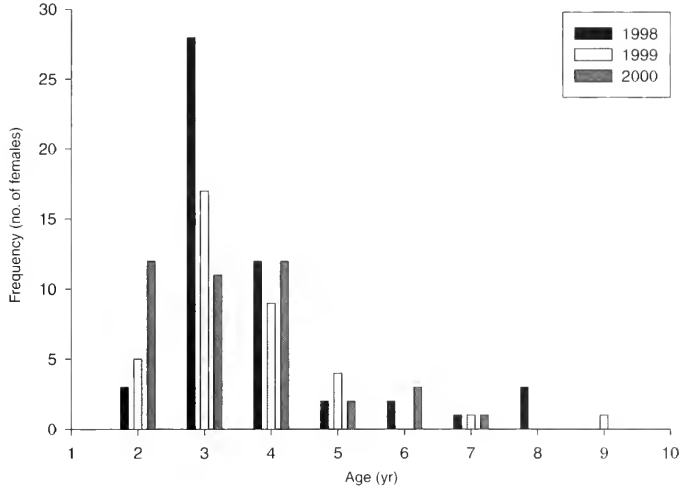

Figure 4

Age-frequency distribution of fecund striped mullet in South Carolina estuaries from 1998 to 2000. n (number of fish in sample) = 50 fish for 1998, n = 37 for 1999, and n = 42 for 2000.

of another study where size and age structure of striped mullet in South Carolina was examined (Wenner and McDonough, unpubl. data[3]). A comparison of multiple readings of the same group of otoliths assessed aging precision. One year (1999) was chosen at random and all of the otoliths (n=1234) from that year were aged by a second reader. The ages of the two independent determinations were then compared by using a one-way ANOVA and a t-test. The variance statistic was 2.78 for the original ages and 2.81 for the second age reads, which were not significantly different (P=0.001) and both had almost identical normalized residuals. Overall, there was an 83.4% agreement on ages between readers. The results from the ANOVA (F=1555.0, df=10, P=0.000) and the t-test (t=2.898, df=1233, significance [2-tailed]=0.004) both confirmed that there was no significant difference between the separate age determinations. Therefore, the age recorded by the first reader for all specimens was used in the analysis.

The length-weight relationship for fecund female striped mullet was compared by using a linear regression of (natural) log-transformed body weight against total length to see if there were any differences between years. The regression coefficients from each year were compared by using a test of significance between more than two slopes (Zar, 1984). The weight measurement used was total body weight minus gonad weight (TW-OW=BW) because ovary weight had a considerable influence on total body weight in the fecund specimens (GSI values of 7.7 to 27.7). There was no significant difference in the total length to Ln body weight regressions between different years (F=9.22, P=0.001, df=129). Because there was little difference in the regressions between years and in order to increase sample size, data from all three years were combined to obtain the overall total-length to Ln-body-weight relationship of Ln $BW = -11.1 + 2.92\,(TL)$ (Fig. 5). In contrast, the length and body-weight-at-age relationships were highly variable; a wide range of sizes occurred in the 2-, 3-, and 4-year age classes (Fig. 6). The high degree of variability was also exacerbated by the smaller number of fish age 5 or older.

The gonadosomatic index (GSI) for fecund mullet ranged from 7.7 to 27.5 in 1998, 9.3 to 27.7 in 1999, and 9.5 to 26.6 in 2000. In contrast, the GSI for mature females that were not undergoing any reproductive development ranged from almost zero to 4 for all three years of the study. The relationship of GSI to size (TL or BW) was not very strong in any year. However, GSI was positively correlated (P=0.01) with oocyte diameter and negatively correlated with oocyte density (Table 2) because of the inverse relationship of oocyte density and oocyte diameter. The correlation coefficient for GSI and age were very close to zero and slightly negative (Table 2).

Mean GSI by month for males and females (Fig. 7) increased from October through April, peaking in November–

[3] Wenner, C. A., and C. J McDonough. 2001. Cooperative research on the biology and assessment of nearshore and estuarine fishes along the southeast coast of the U.S. Part IV: Striped mullet, *Mugil cephalus*. Final rep, Grant no. NA77FF0550, 82 p. Marine Resources Research Institute, South Carolina Dept of Natural Resources, P.O. Box 12559 Charleston, S.C. 29422-2559

December. The duration of the reproductive season, as evidenced by advanced reproductive condition determined by the GSI, was also confirmed from histological assessments of maturity stages for all gonads collected during this time period (not just those used for the fecundity study) which indicated that reproductively developing males were present August through February, whereas reproductively developing females were present August through April (Fig. 8).

There was no significant difference in oocyte density among subsamples taken from different areas of the ovary lobe. This result was obtained by using an ANOVA of oocyte densities between the four divided areas of the ovary lobes where subsamples were taken (F=0.421, df=3). This analysis allowed us to accept the assumption that oocytes were equally distributed throughout the ovary lobes, which provided validation for the random sampling of oocytes from different areas of the lobe in order to determine individual fecundity.

The regression of individual fecundity with total length (TL) was not a linear relationship, whereas the regression of fecundity on body weight (BW) was linear. Therefore, the comparisons of individual fecundity to total length (TL) and body weight (BW) were made by using both the raw data and the data with natural log transformations. The range of specimen total lengths was 291 to 600 mm in 1998, 332 to 588 mm in 1999, and 325 to 592 mm in 2000 and for body weight 242 to 2149 g in 1998, 335 to 2008 g in 1999, and 284 to 2144 g in 2000. Mean fecundity, compared between years with a two sample t-test, was significantly different between 1999 and 2000 (t=0.019, df=78, P=0.985) but was not significantly different between 1998 and 1999 (t=0.974, df=86, P=0.336)

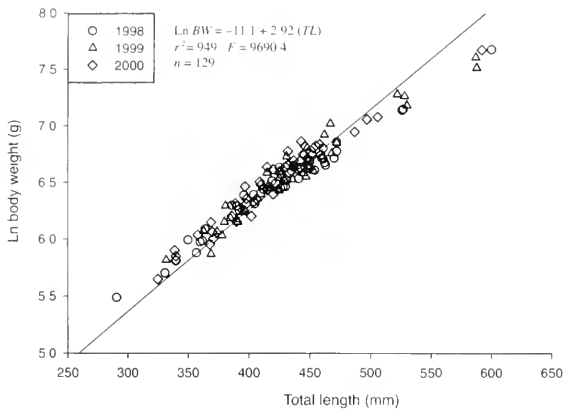

Figure 5

Regression analysis of log-transformed (Ln) body weight on total length for fecund striped mullet in South Carolina estuaries from 1998 to 2000. n (number of fish in sample) = 129.

Table 2

Pearson correlation coefficients, with significance values, for the morphological variables and fecundity of striped mullet in South Carolina estuaries from 1998 to 2000. n (number of fish in sample) = 129. TL = total length, BW = body weight, ODM = oocyte diameter, ODN = oocyte density, GSI = gonadosomatic index, FEC = fecundity.

		Age	TL	BW	ODM	ODN	GSI	FEC
Age	Pearson correlation	1.000						
	significance (2-tailed)							
TL	Pearson correlation	0.117	1.000					
	significance (2-tailed)	0.186						
BW	Pearson correlation	0.164	0.951**	1.000				
	significance (2-tailed)	0.062	0.000					
ODM	Pearson correlation	0.004	0.101	0.029	1.000			
	significance (2-tailed)	0.964	0.254	0.741				
ODN	Pearson correlation		−0.050	−0.008	0.095	−0.628**	1.000	
	significance (2-tailed)	0.575	0.927	0.282	0.000			
GSI	Pearson correlation	−0.029	0.128	−0.006	0.543**	−0.645**	1.000	
	significance (2-tailed)	0.746	0.147	0.947	0.000	0.000		
FEC	Pearson correlation	0.113	0.892**	0.888**	0.059	0.142	0.260**	1.000
	significance (2-tailed)	0.200	0.000	0.000	0.504	0.105	0.003	

** Correlation is significant at the 0.01 level (2-tailed).

and between 1998 and 2000 (t=1.368, df=92, P=0.179). However, given that the mean fecundity was 1.18 million oocytes in 1998, 1.16 million oocytes in 1999, and 1.09 million oocytes in 2000, the difference in mean fecundity between 1999 and 2000 was probably not biologically significant. It was determined that data could be pooled across years for several reasons. The coefficients of determination for each year indicated that there was a similarly strong relationship of fecundity to total length and body weight in all three years and the coefficients of variation for each year (0.408 for 1998, 0.594 for 1999, and 0.457 for 2000 at P=0.001) were not significantly different. By pooling the data from all three years we were able to determine two models of potential fecundity based on total length (TL) and body weight (BW) (Fig. 9):

Ln *Fecundity* = −6.86 + 3.42(Ln *Total Length*)
[r^2=0.803, F=527.2, df=129]

Ln *Fecundity* = 6.95 + 1.05(Ln *Body Weight*)
[r^2=0.804, F=530.6, df=129].

The r^2 values for untransformed data were very close to the values obtained with transformed data (r^2=0.795, F=502.9 for fecundity on total length [TL] and r^2=0.787, F=479.4 for fecundity on body weight [BW]). The high r^2 values, as well as the high correlation coefficients between fecundity and total length and body weight (Table 2) indicated that potential fecundity was size dependent.

Unlike fecundity, oocyte density did not change with size (TL or BW) in 1998 and 1999 and increased with size in 2000. The increase in density in 2000 was due to a group of fish captured in freshwater in October having relatively low GSIs and high densities of oocytes that also happened to be some of the largest fish captured that year. Oocyte density was negatively correlated with GSI (Table 2), and thus indicated that increasing GSI resulted in lower oocyte densities.

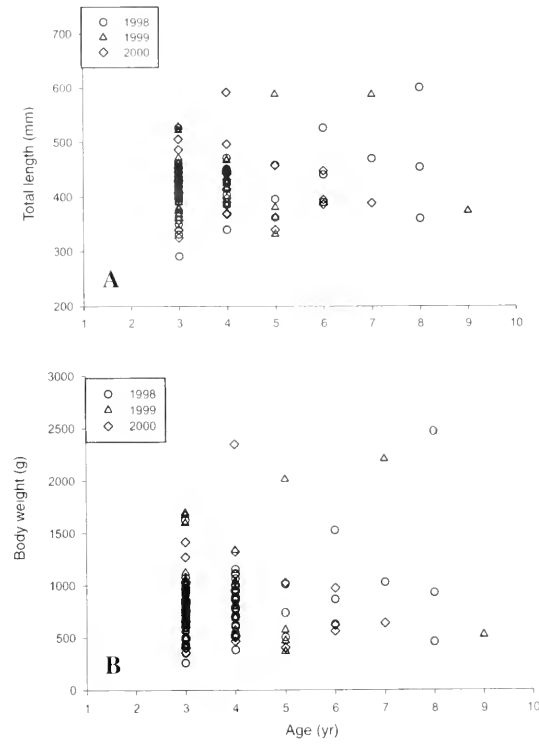

Figure 6

Relationship of total length (**A**) and body weight (**B**) to age for fecund striped mullet in South Carolina estuaries from 1998 to 2000. n (number of fish in sample) = 129.

There was not a high degree of variability in oocyte diameter over the entire size range for the three years of the study. Oocyte diameter did appear to increase with age in 2000 and remained stable for 1998 and 1999. However, the increase in oocyte diameter in 2000 was not statistically significant.

In a comparison of mean oocyte diameter in each size class (total length) by month of capture, the data for all three years were pooled in order to obtain adequate representation in each month. Oocyte size ranged from 463 to 682 μm and the mean size was 596 μm. The largest mean oocyte diameters were found in specimens captured in January and February. Specimens were captured during the months of November and December for all size classes and there was an increase in oocyte diameter with each progressive month. In particular, females in the 400–500 mm size range (which represented the largest number of specimens) were examined and there was a progression of increasing oocyte diameter with month of capture through the reproductive season.

The increase in oocyte size, as the reproductive season progressed, was more apparent when mean oocyte diameter by month for each year separately was examined. Specimens were collected from October through February in 1998, November through January in 1999, and October through December in 2000. Equal effort was made during all of these months of each year to capture specimens, but they were not always available for capture. There was an increase in mean oocyte size per month as the spawning season progressed in all three years (Fig. 10). Even though the largest oocyte size measured was 682 μm, this measurement was that of a preserved oocyte. If we factor in a mean shrinkage of 4%, maximum oocyte size becomes 709 μm.

The paired t-test showed no significant difference between the preserved oocytes and the predicted size of fresh oocytes (t=–26.2, df=128, P=0.000).

Discussion

Fecundity in striped mullet from South Carolina correlated highly with length and weight, but not with age. Oocyte counts ranged from 4.47×10^5 to 2.52×10^6 in 1998 for fish ranging in total length from 331 mm to 600 mm, 2.13×10^5 to 3.89×10^6 in 1999 for fish ranging in total length from 332 mm to 588 mm, and 3.89×10^5 to 3.01×10^6 in 2000 for fish ranging in total length from 325 mm to 592 mm. These fecundity levels correspond with general fecundity levels (2.0×10^5 to 14.0×10^6) found in striped mullet in northeast Florida (Greeley et al., 1987), the Gulf Coast (Render et al., 1995) as well as studies in Europe and Asia (review by Alvarez-Lajonchere, 1982). One marked difference in fecundity between the present study and some in the literature was the difference in oocyte density. Render et al. (1995) found densities ranging from 798 to 2616 oocytes/g ovary weight, whereas densities in the present study ranged from 1710 to 14,817 oocytes/g ovary weight. However, although fecundity increased with both total length and body weight in 1998 and 1999, densities did not. The lower oocyte densities in the larger fish were most likely indicative of larger oocytes. This feature is common in both synchronous and asynchronous spawning fishes (Greeley et al., 1987; Render et al., 1995; Fox and Crivelli, 1998; DeMartini and Lau, 1999). Because total length and body weight were more highly correlated with increased fecundity, the larger specimens would have made a greater individual reproductive contribution during any given spawning season (Korhola et al., 1996; Kaunda-Arara and Ntiba, 1997; DeMartini and Lau, 1999). Making estimates of potential fecundity from age alone was difficult because of the variability in the size-at-age relationship; however, fecundity estimates from total length or body weight appeared more reliable and reflected values closer to the fecundity levels observed in the present study.

Previous studies have reported that female mullet become reproductively mature at three years of age (Thomson, 1951; 1963; Stenger, 1959; Chubb et al., 1981; Render et al., 1995). Greely et al. (1987) suggested that fecundity specimens collected in northeastern Florida were as young as two years at maturity. But, Greely et al. (1987) did not age the striped mullet used in their study and inferred age from a size-at-age growth schedule (Thomson, 1966). In the present study, two-year-olds made up only a small percentage of the fecund fish in 1998 and 1999. However, the results were different for the 2000 specimens in that there was an almost equal distribution in the age frequency of two-, three-, and four-year- olds. However, three- and four-year-olds made up the greatest percentage of females with advanced ovaries. Maturing fish were those undergoing active vitellogenic development and were generally captured in and around inlets or estuaries. Our study would suggest that female striped mullet reach 50% maturity at age 2 and 100% maturity at age 3. Three- and four-year-olds made up the majority of reproductively advanced fish in all years, whereas less abundant older fish made less of a contribution towards total reproductive effort.

There are several possible explanations accounting for the wide age distribution in maturity stages; the most likely is that fecundity is size related despite the highly variable growth rates and the widely ranging size at age in adult striped mullet. Size at maturity has been found to range widely from 230 mm standard length (Thomson, 1963; Greeley et al., 1987; Tamaru et al., 1994) up to 410 mm standard length (Thomson, 1963; 1966; Chubb et al., 1981) for two- and three-year-old fish. The lower end of this size range agrees quite readily with the lower size range (291 mm TL=239 mm SL) found in our study. In a concurrent study of maturity schedules related to size and age in South Carolina striped mullet (McDonough, unpubl. data), male striped mullet were found to mature at two years of age and as small as 250 mm total length (190 mm standard length). Other species of mullet have been shown to mature over a wide range of sizes. The Pacific mullet (Mugil so-iuy) becomes mature upon reaching approximately 430 mm total length (Okumus and Bascinar, 1997).

Monthly GSI levels clearly showed that the time period of reproductive activity is from October through April. Female striped mullet in all reproductive developmental stages were observed during the course of our sampling, with the exception of stage-3 (hydrated oocytes) females and females with

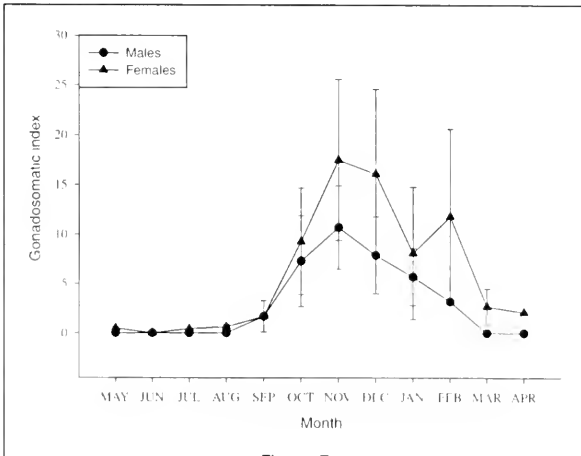

Figure 7

Mean gonadosomatic index value by month for male and female striped mullet from South Carolina estuaries from 1998 to 2000. n (number of fish in sample) = 455.

recently spawned ovaries (characterized by the presence of postovulatory follicles). Atretic ovaries were observed from December through May. There were no postovulatory follicles observed, indicating that any atretic ovaries were not from recently spawned fish. The fish with atretic ovaries were characteristically emaciated for their size (TL and BW) and were most common from January through March. The presence of females with atretic ovaries starting in December is strong evidence that spawning occurred in November, if not earlier, and females with atretic ovaries caught as late as May demonstrate that spawning may still occur as late as April. Additional evidence for the October through April spawning period has also been shown in backcalculated birth dates for juvenile striped mullet by daily growth increments (McDonough and Wenner, 2003). This evidence supports the concept of offshore spawning in striped mullet and a yet undetermined time period required for moving from the estuaries to the spawning areas and for returning again to the estuaries. Other authors have come to the same conclusion from similar evidence in estuaries throughout the southeast (Jacot, 1920; Broadhead, 1956; Anderson, 1958; Stenger, 1959; Shireman, 1975; Dindo and MacGregor, 1981; Greeley et al., 1987; Render et al., 1995; Hettler et al., 1997). All of the fecundity specimens were caught from October through February when the mean monthly GSI was highest. Pien and Liao (1975) found that mullet oocytes reached a hydrated size of 900 to 1000 μm. The size of oocytes used for fecundity counts in the present study ranged from 463 to 682 μm. The maximum size of oocytes in the tertiary stage of vitellogenesis from our study was 600 μm or greater. This result agrees with those of previous studies where the maximum size of oocytes prior to either hydration or atresia (if spawning did not occur) ranged from 600 to 700 μm (Shehadeh et al., 1973b; Kuo et al., 1974). There was no evidence of prespawning atresia in any of the specimens used for fecundity estimates.

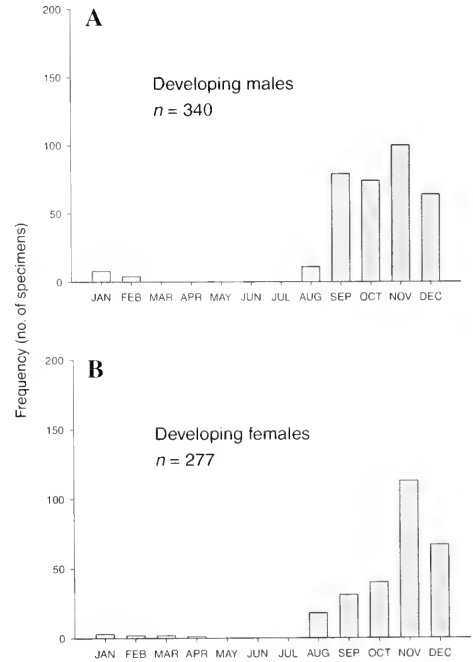

Figure 8

Frequency distribution of reproductively developing male (**A**) and female (**B**) striped mullet by month in South Carolina estuaries from 1998 to 2000.

The appropriateness of using a GSI alone to determine the level of reproductive development has been questioned, particularly for serial or asynchronous spawning fishes (De Vlaming et al., 1980; Hunter and Macewicz, 1985). Striped mullet can have a wide range of GSI values that range from practically zero to over thirty (Render et al., 1995). The GSI range for females in our study ranged from almost zero to 27.7. Because of the high variability in GSI with size, it does not appear appropriate to use GSI alone in order to assess reproductive development in striped mullet. When used in conjunction with histological analysis and mean oocyte diameter of tertiary-stage oocytes, GSI does provide excellent supporting evidence of reproductive schedules and spawning season duration. GSI is probably more appropriately used for isochronal spawning fishes than for serial spawning fishes because of the uniform development of oocytes in the former. However, it is still difficult to meet all the basic assumptions of the GSI index as given by De Vlaming et al. (1980) because of the high variability of GSI with size. Another technique that has been used in aquaculture situations to assess maturity and sex involves the use of a cannula to remove oocytes from the ovaries of live fish which are then evaluated (Shehadeh, et al., 1973a; Kuo et al., 1974). This technique, although useful for determining sex and the extent or stage of reproductive development, would be inappropriate for estimating potential fecundity.

Historically, reproductively developing mullet have been found in southeast United States waters from November through December (Jacot, 1920; Anderson, 1958; Stenger, 1959). During our study, reproductively developing mullet were caught in the Charleston Harbor Estuary from October through February. Gonad development of these fish was discernible through gross morphological observation, and histological sections showed that vitellogenesis was well underway. Other studies have shown that previtellogenic oocytes were usually less than 160 μm and that the onset of vitellogenesis began when the oocytes reached a size of 180 μm (Dindo and MacGregor, 1981; Greeley et al., 1987; Tamaru et al., 1994; Render et al., 1995). Developing individuals caught during our study that were not used for fecundity counts had less-developed ovaries, GSI values less than 7, and mean oocyte diameters less than

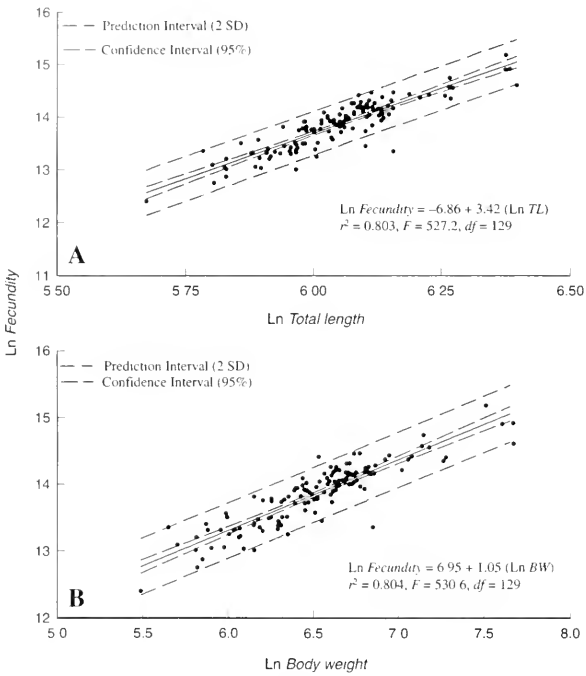

Figure 9

Regression of the natural log (Ln) transformation of individual fecundity on total length (**A**) and body weight (**B**) for striped mullet combined data, 1998 to 2000, from South Carolina estuaries. *n* (number of fish in sample) = 129.

350 μm. The vitellogenic activity in these ovaries was still in the primary and secondary stages. These specimens could not be used for fecundity counts because not all of the oocytes destined for that year's spawning batch had developed enough to be separable from the smaller oocytes that would not develop. Once the developing oocytes reached a size of 400 μm or larger, they became more uniform in size and in appearance and it was obvious which oocytes would constitute that year's spawn. At that point, fecundity could be determined more accurately because all the oocytes to be counted were significantly and equally larger. This point in particular is important in that it makes fecundity estimates from nonhydrated oocytes more accurate for isochronal spawning fishes, such as striped mullet. Fecundity estimates made in fishes that are batch-spawners should only be made from hydrated oocytes because of the presence of multiple developmental stages (Hunter and Macewicz, 1985). The presence of different vitellogenic stages in the ovary of a repeat-spawning fish makes it necessary to determine individual batch fecundity and spawning frequency before any estimate of annual fecundity can be made. In isochronal spawning fishes, such as striped mullet, this process is made simpler by the fact that oocytes mature at a similar rate (Greeley et al., 1987). During early vitellogenesis (180 μm to 350 μm), there is a higher degree of variability in the rate of development and a range of developmental stages would be present from the presence of precortical alveoli through secondary and tertiary vitellogenesis (Render et al., 1995). Estimating numbers of oocytes (uniform in an individual but varying in size because of season) during this stage would naturally make oocyte density and oocyte-size relationships inconsistent. This could possibly be corrected by using some timing factor such as month during the spawning season. The present study did demonstrate an inverse relationship between oocyte density and oocyte diameter. When month of capture was taken into consideration, oocyte density decreased with increasing oocyte size as the spawning season progressed.

In conclusion there were several biological aspects of striped mullet reproduction demonstrated in this study. Fecundity levels in striped mullet increased with total

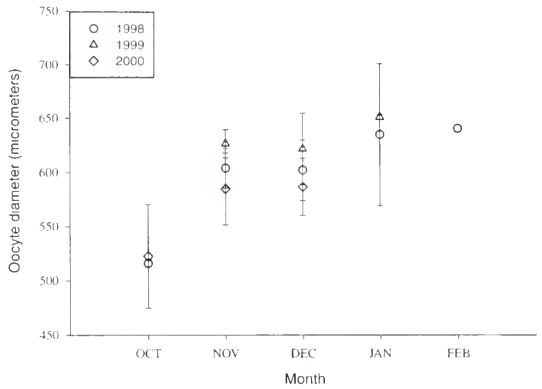

Figure 10

Mean oocyte diameter per month during the spawning season for striped mullet in South Carolina estuaries 1998 to 2000. Error bars represent standard deviation.

length (TL) and body weight (*BW=TW–OW*). Oocyte density remained relatively stable with size in the fecund fish and this allowed reasonable estimates of potential fecundity based on total length and body weight. Age-specific fecundity was highly variable and there appeared to be no consistent relationship. The reproductive season for striped mullet in South Carolina extends from October through April as determined by mean monthly GSI levels and histological confirmation of reproductive state. Potential spawning periods would also occur within this period as evidenced by the elevated GSI levels and the presence of atretic (or possible postspawning) ovaries from December through May. The gonadosomatic index itself is more useful to evaluate reproductive potential when used in conjunction with other techniques, such as histological analysis and oocyte diameter. The models of potential fecundity as they relate to size (total length and body weight) could be useful when applied to catch statistics of length and weight in populations with known size- and age- frequency distributions. This application would allow reasonable estimates of potential fecundity for these populations.

Acknowledgments

This study would not have been possible without the assistance of everyone in the Inshore Fisheries group at the Marine Resources Research Institute of the South Carolina Department of Natural Resources, which includes Myra Brouwer, John Archambault, Hayne Von Kolnitz, Will Hegler, Erin Levesque, Alice Palmer, Chad Johnson, Richie Evitt, Larry Goss, and Travis Waits. We especially thank Chad Altman of the South Carolina Department of Health and Environmental Control for the freshwater specimens. We also thank Myra Brouwer for assistance with map figures and the anonymous referees for careful review and suggestions for this manuscript. This research was made possible by National Marine Fisheries Service MARFIN, grant no. NA77FF0550.

Literature citations

Anderson, W. W.
1958. Larval development, growth, and spawning of striped mullet (*Mugil cephalus*) along the south Atlantic coast of the United States. Fish. Bull. 58:501–519.

Alvarez-LaJonchere, L.
1982. The fecundity of mullet (Pisces, Mugilidae) from Cuban waters. J. Fish Biol. 21:607–613.

Arnold, E. L., and J. R. Thompson.
1958. Offshore spawning of the striped mullet, *Mugil cephalus*, in the Gulf of Mexico. Copeia 1958.130–132.

Broadhead, G. C.
1956. Growth of the black mullet, *Mugil cephalus*, in west and northwest Florida. Mar. Lab. Tech. Ser. 25:1–29.

Campana, S. E., M. C. Annand, and J. I. McMillan.
1995. Graphical and statistical methods for determining the consistency of age determinations. Trans. Am. Fish. Soc. 124:131–138.

Chubb, C. F., I. C. Potter, C. J. Grant, R. C. J. Lenanton, and J. Wallace.
1981. Age, structure, growth rates, and movements of sea mullet, *Mugil cephalus* L., and yellow eye mullet, *Aldrichetta forsteri* (Valenciennes), in the Swan-Avon river system, Western Australia. Aust. J. Mar. Freshw. Res. 32:605–628.

Collins, M. R., and B. W. Stender.
1989. Larval striped mullet (*Mugil cephalus*) and white mullet (*Mugil curema*) off the southeastern United States. Bull. Mar. Sci. 45(3):580–589.

DeMartini, E. E., and B. B. Lau
1999. Morphometric criteria for estimating sexual maturity in two snappers, *Etelis carbunculus* and *Pristipomoides setholdti*. Fish. Bull. 97:449–458.

De Vlaming, V. L., H. S. Wiley, G. Delahunty, and R. Wallace.
1980. Goldfish (*Carassius auratus*) vitellogenin: induction, isolation, properties and relationship to yolk proteins. Comp. Biochem. Physiol. B 67B:613–623

Dindo, J. J., and R. MacGregor.
1981. Annual cycle of serum gonadal steroids and serum lipids in striped mullet. Trans. Am. Fish. Soc. 110:403–409.

Finucane, J. H., L. A. Collins, and L. E. Barger.
1978. Spawning of the striped mullet, *Mugil cephalus*, in the northwestern Gulf of Mexico. Northeast Gulf Sci. 2: 148–150.

Fox, M. G., and A. J. Crivelli.
1998. Body size and reproductive allocation in a multiple spawning centrarchid. Can. J. Fish. Aquat. Sci. 55(3): 737–748.

Greeley, M. S., D. R. Calder, and R. A. Wallace.
1987. Oocyte growth and development in the striped mullet, *Mugil cephalus*, during sesonal ovarian recrudescence: relationship to fecundity and size at maturity. Fish. Bull. 85: 187–200.

Hettler, W. F., D. S. Peters, D. R. Colby, and E. H. Laban.
1997. Daily variability in abundance of larval fishes inside Beaufort Inlet. Fish. Bull. 95:477–493.

Humason, G. L.
1967. Animal tissue techniques, 426 p. W.H. Freeman and Co., San Francisco, CA.

Hunter, J. R., and B. J. Macewicz.
1985. Measurement of spawning frequency in multiple spawning fishes. *In* An egg production method for estimating spawning biomass of pelagic fish: application to the northern anchovy, *Engraulis mordax*. NOAA Tech. Rep. NMFS 36:79–94.

Jacot, A. P.
1920. Age, growth, and scale characters of the mullets, *Mugil cephalus* and *Mugil curema*. Trans. Am. Fish. Soc. 39(3): 199–229.

Kaunda-Arara, B., and M. J. Ntiba.
1997. The reproductive biology of *Lutjanus fulviflamma* (Forsskål, 1775) (Pisces: Lutjanidae) in Kenyan inshore marine waters. Hydrobiologia 353(1/3):153–160.

Kelly, C. D.
1990. Effects of photoperiod and temperature on ovarian maturation in the striped mullet, *Mugil cephalus*. Pac. Sci. 44(2):187–188

Korhola, A., P. Solemdal, P. Bratland, and M. Fonn.
1996. Variation in annual egg production in individual captive Atlantic cod (*Gadhus morhua*). Can. J. Fish. Aquat. Sci. 53(3):610–620

Kuo, C. M.
1995. Manipulation of ovarian development and spawning in grey mullet, *Mugil cephalus* L. Israel J. Aquacult. Bamidgeh 47(2):43–58.

Kuo, C. M., C. E. Nash, and Z. H. Shehadeh.
1974. A procedural guide to induce spawning in grey mullet (*Mugil cephalus* L.). Aquaculture 3(1974):1–14

McDonough, C. J., and C. A. Wenner.
2003. Growth, recruitment, and abundance of juvenile *Mugil cephalus* in South Carolina estuaries. Fish. Bull. 101:343–357.

Okumus, I., and N. Bascinar.
1997. Population structure, growth, and reproduction of introduced mullet, *Mugil so-iuy*, in the Black Sea. Fish. Res. 33:131–137.

Pien, P. C., and J. C. Liao.
1975. Preliminary report of histological studies on the grey mullet gonad related to hormone treatment. Aquaculture 5:31–39.

Render, J. H., B. A. Thompson, and R. L. Allen.
1995. Reproductive development of striped mullet in Louisiana estuarine waters with notes on the applicability of reproductive assessment methods for isochronal species. Trans. Am. Fish. Soc. 124(1):26–36.

Rossi, A. R., M. Capula, D. Crosetti, D. E. Campton, and L. Sola
1998. Genetic divergence and phylogenetic inferences in five species of Mugilidae (Pisces: Perciformes). Mar. Biol. 131: 213–218.

Shehadeh, Z. H., C. M. Kuo, and K. K. Milisen.
1973a. Validation of an *in vivo* method for monitoring ovarian development in the grey mullet (*Mugil cephalus* L.). J. Fish Biol. 1973(5):489–496.

Shehadeh, Z. H., W. D. Madden, and T. P. Dohl.
1973b. The effect of exogenous hormone treatment on spermiation and vitellogenesis in the grey mullet, *Mugil cephalus* L. J. Fish Biol. 1973(5):479–487.

Shireman, J. V.
1975. Gonadal development of striped mullet (*Mugil cephalus*) in freshwater. Prog. Fish Cult. 37(4):205–208.

Stenger, A. H.
1959. A study of the structure and development of certain reproductive tissues of *Mugil cephalus* Linnaeus. Zoologica 44(2):53–70.

Tamaru, C. S., C. S. Lee, C. D. Kelley, G. Miyamoto, and A. Moriwake.
1994. Oocyte growth in the Striped mullet, *Mugil cephalus* L., at different salinities. J. World Aquacult. Soc. 25: 109–115.

Thomson, J. M.
1951. Growth and habits of the sea mullet, *Mugil dobula* Gunther, in Western Australia. Aust. J. Mar. Freshw. Res. 2:193–225.
1963. Mullet life history strategies. Aust. J. Sci. 25:414–416. The grey mullets. Oceanogr. Mar. Biol. Annu. Rev. 4: 301–335.

Wallace, R. A., and K. Selman.
1981. Cellular and dynamic aspects of oocyte growth in teleosts. Am. Zool. 21:325–343.

Wenner, C. A., B. A. Roumillat, and C. W. Waltz.
1986. Contributions to the life history of black seabass, *Centropristis striata*, off the southeastern United States. Fish. Bull. 84.723–741.

Zar, J. H.
1984. Biostatistical analysis, 2nd ed., p. 292–305. Prentice Hall Inc., Englewood Cliffs, NJ.

Marine fish assemblages associated with fish aggregating devices (FADs): effects of fish removal, FAD size, fouling communities, and prior recruits

Peter A. Nelson

Department of Biological Sciences
Northern Arizona University
Flagstaff, Arizona 86011-5640
Present address: Center for Marine and Biodiversity & Conservation
Scripps Institution of Oceanography
University of California, San Diego
La Jolla, California 92093-0202

E-mail address: pnelson@ucsd.edu

Abstract—Fishes are widely known to aggregate around floating objects, including flotsam and fish aggregating devices (FADs). The numbers and diversity of juvenile fishes that associated with floating objects in the nearshore waters of the eastern tropical Pacific were recording by using FADs as an experimental tool. The effects of fish removal, FAD size, and the presence or absence of a fouling community at the FAD over a period of days, and the presence of prior recruits over a period of hours were evaluated by using a series of experiments. The removal of FAD-associated fish assemblages had a significant effect on the number of the dominant species (*Abudefduf troschelii*) in the following day's assemblage compared to FADs where the previous day's assemblage was undisturbed; there was no experimental effect on combined species totals. Fishes do, however, discriminate among floating objects, forming larger, more species-rich assemblages around large FADs compared to small ones. Fishes also formed larger assemblages around FADs possessing a fouling biota versus FADs without a fouling biota, although this effect was also closely tied to temporal factors. FADs enriched with fish accumulated additional recruits more quickly than FADs that were not enriched with fish and therefore the presence of prior recruits had a strong, positive effect on subsequent recruitment. These results suggest that fish recruitment to floating objects is deliberate rather than haphazard or accidental and they support the hypothesis that flotsam plays a role in the interrelationship between environment and some juvenile fishes. These results are relevant to the use of FADs for fisheries, but emphasize that further research is necessary for applied interests.

Manuscript approved for publication 13 June 2003 by Scientific Editor.

Manuscript received 26 June 2003 at NMFS Scientific Publications Office.

Fish. Bull. 101:835–850

Fishes associate with floating objects in nearly all oceans of the world (Gooding and Magnuson, 1967; Hunter and Mitchell, 1967; Klima and Wickham, 1971; Crawford and Jorgenson, 1993; Kingsford, 1993; Druce and Kingsford, 1995; Massuti et al., 1998; Hampton and Bailey, 1999; Parin and Fedoryako, 1999). Fishes also gather around fish aggregating devices (FADs), floating objects deployed to concentrate target species or bait fishes and improve the catch for artisanal, sport, or commercial fisheries. The physical attributes of a floating object, such as a FAD, may affect the ability of potential fish recruits to locate the floating object or may affect the adaptive advantages of associating with that object (or both)—a topic that has been addressed in numerous prior studies (e.g. Hunter and Mitchell, 1968; Wickham et al., 1973; Wickham and Russell, 1974; Fedoryako, 1989; Rountree, 1989; Safran, 1990; Safran and Omori, 1990; Friedlander et al., 1994; Hall et al., 1999b). However, the present study is apparently the first to address empirically the effects of disturbance, fouling communities, and prior recruits by examining both the number and the diversity of fishes that aggregate around FADs. In addition, this study addresses the effect of FAD size, a factor well represented in prior studies but frequently confounded by temporal or design issues. FADs are widely used to enhance sport and commercial fisheries, but are expensive to build, deploy, and maintain; therefore better information about the effects of FAD size and fouling could aid design efforts. Given the bycatch associated with the FAD fishery for tuna in the eastern tropical Pacific (Hall et al., 2000), for example, we need a better understanding of how fishes use FADs in order to manage fisheries for FAD-associated species (Lennert-Cody and Hall, 2000). Finally, careful study of how differing characteristics of floating objects affect fish recruitment may provide important clues regarding the adaptive significance of fish associations with flotsam and drift algae—a phenomenon widely noted but poorly understood.

Prior research has suggested that rates of immigration and fish removal from FADs similar to those seen in the present study were high from one day to the next (Nelson, 1999), and Wickham and Russell (1974) reported that mid-water FADs, which were fished daily, produced a larger cumulative catch than mid-water FADs, which were undisturbed during the same period and then fished once at the end of the conclusion of the study. I tested the hypothesis that, over time, the size and diversity of FAD-associated fish assemblages are reduced by the repeated removal of these fishes compared with undisturbed assemblages. Effective management or use of FADs deployed for fisheries purposes and an understanding of the ecological relationship between flotsam and fishes associated with flotsam will depend in part on patterns of immigration and loss to fish assemblages.

There have been numerous attempts to equate flotsam structure (size, complexity, orientation, etc.) with the number of associated fishes (e.g. Hunter and Mitchell, 1968; Dooley, 1972; Wickham et al., 1973; Wickham and Russell, 1974; Rountree, 1989; Druce and Kingsford, 1995), but the results have been equivocal, except when the analysis was restricted to a single species (e.g. *Histrio histrio*, Dooley, 1972; *Decapterus punctatus*, Rountree, 1989). Huge aggregations have been associated with very small objects—IATTC (Inter-American Tropical Tuna Commission) records include a report of 55 metric tons of mostly yellowfin tuna (*Thunnus albacares*) fished from beneath a 1-m length of floating polypropylene rope (Hall et al., 1999b); therefore, despite the intuitive appeal, there is no clear reason to expect that size of FAD *per se* is an important factor in determining the size of associated assemblages. Thus, object size remains an unresolved problem in understanding flotsam-associated communities. If there are optimal FAD sizes, these may be species specific, and economical FAD design depends upon controlled experiments in the field.

Fouling organisms (sessile invertebrates and algae that colonize flotsam) are believed to have a strong, positive effect on the subsequent recruitment and retention of fishes by commercial fishermen (Gaertmer and Medina-Gaertner, 1999; Hall et al., 1999a; Hallier and Parajua, 1999; Suzuki, 1999). However, prior to the results presented here, there appear to have been no controlled tests of the hypothesis that the presence of fouling organisms enhances fish recruitment to a floating object. I also compared the numbers and diversity of fishes associated with FADs that are equipped with artificial (lead weight) fish versus FADs without these artificial fish. The latter experiment was intended to determine the importance of prior recruits to subsequent patterns of recruitment. To test a similar hypothesis over the short term (hours versus days) and using living fish instead of painted models, I also compared recruitment to FADs enriched with real fish (juvenile *Abudefduf troschelii*) to unenriched FADs.

I tested the hypothesis that each of these factors would affect the number of fishes associated with FADs (combined and individual species), as well as the species diversity of FAD-associated fish assemblages. Both the size of these FAD-associated fish assemblages and their species diversity provide insight on recruitment processes and the use of floating objects by fishes. Although the association of fishes with floating objects has been well documented, very little is known regarding the behavioral and ecological processes behind these assemblages. The results reported in the present study provide new information on the role of flotsam and FAD characteristics in determining the number and diversity of these assemblages, and some clues towards understanding why and how fishes aggregate beneath floating objects.

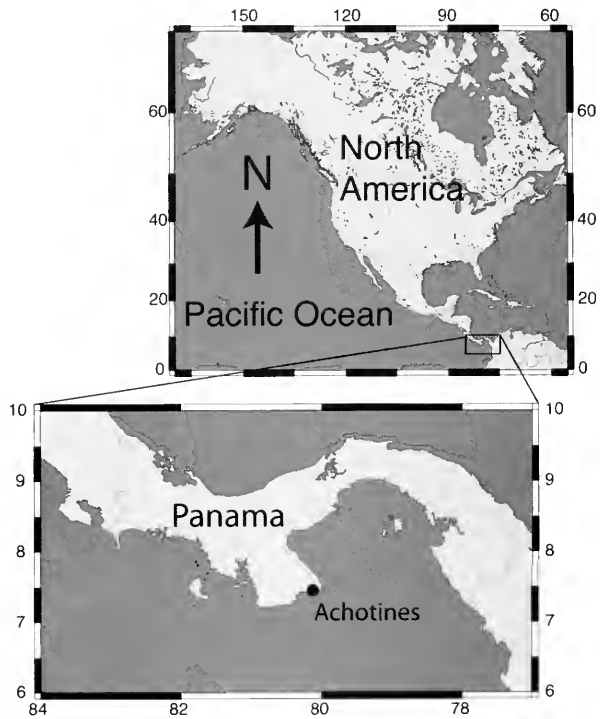

Figure 1
Location of the study site at Achotines, Panama, Central America.

Materials and methods

Study site and FAD construction

All research was conducted between July and October 1997 on the Pacific coast of Panama, Central America, from the Inter-American Tropical Tuna Commission laboratory at Achotines, near the tip of the Azuero Peninsula (Fig. 1). Experimental FADs were constructed of three tuna purse-seine buoys lashed together and anchored to the substrate with a 25-kg cast concrete block unless otherwise noted (Fig. 2). The length of the anchor lines allowed the FADs to rest at the surface at all tidal heights. Each buoy was roughly 25 cm in cross sectional diameter, and approximately 35 cm in length. The FADs were detachable from their moorings by detaching a large (2 m diameter) loop on the anchor line that held a 2-kg line weight (Fig. 2). This design allowed me to change FADs for another treatment. The FAD arrays were deployed nearshore (within 1.5 km;

Fig. 3) and in shallow water (14–25 m). The FAD treatments were not assigned randomly to FAD positions; instead, I assigned treatments uniformly across the FAD array because the total number of FADs was relatively low (8–10) and, given the small number of experimental units, in order to reduce the possibility that the results be confounded by positional effects.

The anchored FADs were spaced approximately 100 m apart. The maximum horizontal underwater visibility measured was 27 m, and typically averaged much less. Assuming that vision was the principal means by which fishes located these objects, it is therefore highly unlikely that fishes treated the FAD array as a single "object" or moved from FAD to FAD within the array. I believe that it was unlikely that any fish transferred from one FAD to another for the following reasons. 1) The horizontal underwater visibility was always much less than the distance between FADs. 2) Observations suggest that short-term, daytime fidelity was high; once a fish associated with a floating object, it was unlikely to leave that object during the day (Nelson, 1999). 3) Crossing an open stretch of water for another floating object (presumably within detection range) entails a potential risk for a fish. Moser et al. (1998) did note that the larger juveniles and adult fishes associated with floating *Sargassum* showed little apparent fidelity to this habitat and would move between their research boats, floating observation equipment, and the *Sargassum* habitat. However, the fishes that were observed to move between these floating objects were juvenile carangids between 10 and 20 cm in length (Moser et al., 1998), whereas the fishes in the present study were generally much smaller and presumably less vagile.

Longshore currents ran roughly west to east through the experimental area, and rarely in the reverse (Fig. 3). I recorded an estimate of current direction using an underwater compass and the angle of the FAD anchor lines. This estimate represented the sum of the forces due to windage on the FAD buoys and currents.

Censusing FADS

FAD-associated fish assemblages were censused by direct visual observation by divers using mask and snorkel. Most other studies of fish assemblages associated with floating material have employed nets or quantitative fishing methods for sampling purposes (e.g. Kojima, 1960; Dooley, 1972; Kingsford, 1992, 1995), but Hunter and Mitchell (1968) compared data from net captures, automated photography and direct visual observations and found that the visual observations agreed well with the other methods, and provided behavioral information not available with the other methods. In my study, a FAD was approached by swimming

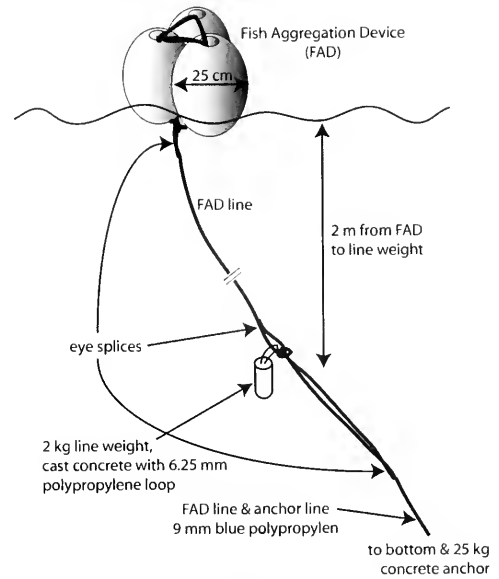

Figure 2

Design of detachable fish aggregating devices (FADs) used in the present study.

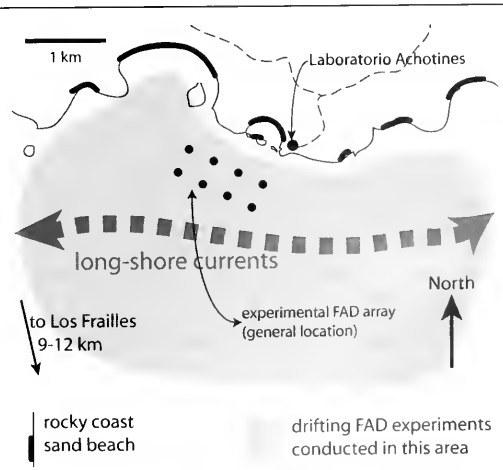

Figure 3

Coastline and general location of experiments and observations. The laboratory (Laboratorio Achotines) is located at approximately 7°5′N lat, 80°10′W long.

slowly and quietly at the surface from a distance of at least 12 m. All fishes associated (defined below) with the floating object were counted and identified; therefore the statistical unit in all of the experiments described below was a single FAD-associated assemblage of fishes at a given date and time. Horizontal underwater visibility, measured with a Secchi disk, was always sufficient to allow the identification of species and to count individual fishes from a minimum distance of 2 meters.

Any fish observed within 2 m of a FAD was considered to be "FAD-associated." Very few fishes were observed outside of this range, and with rare exceptions, fishes responded to the approach of an observer first by swimming towards the observer and then by moving closer to the FAD, rather than away from it. Different species of fishes used the space around and below the FAD differently, as both Gooding and Magnuson (1967) and Hunter and Mitchell (1967) described, but the juvenile fishes that predominated in the present study were unambiguous regarding their relationship to the FADs. After fishes resumed their prior positions in relation to a FAD, continued observations of these fishes revealed that there was no inclination to abandon that FAD. The appearance of potential predators invariably resulted in a tightening of the spatial distribution around the FAD.

When the experiment required the capture of FAD-associated fishes, I used a smaller (1.1×1.3 m) version of the diver-operated liftnet described by McCleneghan and Houk (1978). Captured fishes were preserved for further studies, held in grow-out facilities in the laboratory to verify species identification, or released 1.5 km down-current over rocky reef habitat to ensure that they had effectively been removed from the FAD array.

Diversity calculations

Measurements of species diversity provided a means of monitoring treatment effects on the composition of FAD-associated assemblages. I measured species diversity using species richness (S, the raw number of species observed), and the Brillouin index (HB). S is simple and widely used, but increases with sample size, and, where sample sizes are unequal, HB provides a less biased measure of diversity (Magurran, 1988). In addition, HB was chosen over one of the more commonly used information theory indices (e.g. the Shannon-Wiener index) because 1) FAD-associated assemblages are not a random sample of potential recruits (different species vary in their attraction to floating objects) and 2) each of these assemblages was completely censused—not sampled (Magurran, 1988, and references therein).

HB is calculated as

$$HB = \frac{\ln N! - \sum \ln n_i!}{N},$$

where N = the total number of fishes of all species observed; and

n_i = the number of individuals within the ith species (Magurran, 1988).

Statistical analyses

I used a two-way repeated measures ANOVA (α=0.05) to test for treatment differences, differences among observation dates and evidence of treatment-by-sample interaction for assemblage sizes (no. of fish(es)), species richness (S) and species diversity (HB). Because individual species differed in their relative abundance and had different ecological requirements, there was the potential for the dominant species to bias comparisons of experimental treatments where assemblage size (a combinination of all species) was used. For all experiments except for the recruit-enriched experiment, I repeated the statistical analyses twice: once using the number of sergeant major damselfish (*Abudefduf troschelii*) only and again using all fishes combined but with *A. troschelii* removed. For the artificial fish experiment where rainbow runner (*Elagatis bipinnulata*) were particularly abundant, I ran separate analyses for *A. troschelii* alone, *E. bipinnulata* alone, and for all species minus the numbers of *A. troschelii*. When no fishes were present at a FAD, HB was undefined; the "missing" data were replaced according to the procedures of Zar (1996) and the degrees of freedom were reduced accordingly.

Fish-removal experiments

Observations on similar FADs during a previous field season at the same location suggested that the turnover rate of fish associated with anchored FADs is high, especially when the initial assemblage is large, but that some recognizable individuals did persist from day-to-day (Nelson, 1999). If immigration and emigration rates were as high as suspected, FADs cleared of fish on a daily basis should not differ significantly from undisturbed FADs in their mean assemblage size or in the average number of species associated with these FADs. Wickham and Russell (1974) compared the catches of bait fishes associated with FADs subject to daily purse-seine sets versus those allowed to "soak" undisturbed for three days prior to a single purse-seine set and concluded that sufficient emigration and immigration occurred on a daily basis to remove any appreciable effect of daily removals. I sought to address similar questions, but by using a different system (juvenile reef fishes versus bait fishes).

To test these hypotheses, I deployed eight identical FADs on 30 June 1997 in two lines of four FADs each, oriented roughly parallel to shore (Figs. 2 and 3). Fishes associated with all eight FADs were counted and identified on a daily basis, beginning 3 July 1997. Alternate FADs were cleared of all fish, following the daily counts; the remaining FADs were left undisturbed in such a way as to distribute the treatments evenly among the FAD array. After three consecutive days of these observations (series 1), the treatments were reversed, and previously undisturbed FADs were cleared, and those that had been cleared regularly were left undisturbed (series 2). The treatments were reversed in an attempt to control for possible positional effects of the FADs. However, the two series were necessarily run consecutively, not concurrently; therefore treatment position was confounded by sample date. I used a 2 (cleared vs.

undisturbed) by 2 (first series vs. second series) by 6 (sample date) model and I used a repeated measures ANOVA (repeated on sample date) on the following dependent variables: assemblage size (total no. of fishes), species richness (S), and HB. I repeated analyses of assemblage-size effects looking at the number of *A. troschelii* only, and the total number of fishes minus the number of *A. troschelii*.

FAD size

To determine the effect of FAD size on the associated assemblage size and diversity, I compared FAD-associated fish assemblages between triple-size FADs and single FADs. An existing anchored array of eight FADs (two lines parallel to the coast of four FADs each, Fig. 3) was cleared of fishes on 24 July 1997. As the fish were removed from the FADs, each FAD was replaced with a fresh (i.e. clean and unfouled) single or triple-size FAD, placed at alternating positions. The single FADs were constructed as described above and in Figure 2; the triple-size FADs were identical to the single FADs, except that they consisted of nine, rather than three, purse-seine buoys lashed together and had the effect of nearly tripling the wetted surface area (although inner buoys are less exposed than outer ones) and the volume of the FAD, and of increasing the maximum linear dimension of the FAD by a factor of two. Treatments were not reversed for this or subsequent experiments because sample date appeared to be the major factor determining assemblage size for any species, based on the previous experiment. Note that in each of these experiments, except for the recruit-enrichment experiment that used drifting FADs, treatments were assigned uniformly throughout the FAD arrays so that onshore, offshore, or longshore biases in recruitment due to oceanographic processes would not confound the results. Fishes at all FADs were counted and identified on three dates (26, 28, and 30 July 1997), each observation separated from the next by 48 hours. No fish were collected, with the exception of one balistid, taken from the array on 26 July because it was the first of that species to be observed associated with a FAD. Data were analyzed for experimental effects on total assemblage size, species diversity (S and HB), the number of *A. troschelii*, and total number of fishes minus the number of *A. troschelii*.

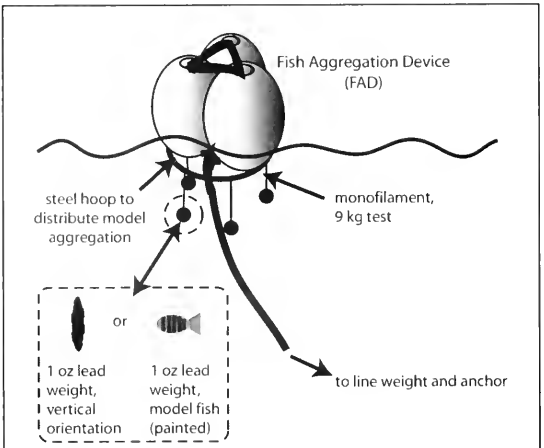

Figure 4

Treatments for the artificial fish experiment involved suspending artificial fish, lead weights of an equivalent mass and volume, or nothing (control) from a steel hoop lashed beneath the FAD.

Presence of absence of a fouling community

To determine whether the presence of a fouling community on a floating object affected the associated fish assemblage, I compared FAD-associated assemblage sizes and species richness between fouled and unfouled (control) FADs. Control FADs were scrubbed of all fouling organisms. Fouled FADs had been deployed for a minimum of 14 days (range: 14–22 days) in the study area, and had accumulated fouling that completely covered the wetted surface of the FAD with gooseneck barnacles (*Lepas* sp.), hydroids, and bryozoans. Grapsid crabs and polychaete worms (*Amphimone vagans*) were also intermittent associates of fouled FADs. Control and fouled FADs were deployed on 8 September 1997 in an alternating array of eight buoys, with four FADs per treatment (layout and spatial distribution of treatments follow that of the FAD size experiment). All fishes were cleared from FAD positions prior to deploying the FADs, and data collection commenced 24 hours later. Data were collected on four consecutive days (9, 10, 11, and 12 September 1997) and analyzed for experimental effects on total assemblage size, species diversity (S and HB), the number of *A. troschelii*, the number of *E. bipinnulata*, and total number of fishes minus the number of *A. troschelii*.

Artificial fish experiment

I tested the hypothesis that potential recruits would distinguish between FADs with an "assemblage" of artificial fish suspended beneath them, FADs with an "assemblage" of suspended material equal to the artificial fish in size but not resembling fish in appearance, and control FADs without anything suspended beneath them (Fig. 4). I constructed artificial fish from 31.25-g lead fishing weights. These weights were flattened, tear-drop–shaped objects, painted a dull yellow with black bars to resemble juvenile *Abudefduf troschelii* and suspended, by using monofilament (20 lb. test) and a steel hoop, beneath the "artificial fish FADs" (Fig. 4). I suspended oblong 31.25-g lead fishing weights beneath "weighted FADs," and the control FADs had only a steel hoop beneath each (Fig. 4). These FADs were deployed in an anchored array, and the various treatments were distributed in an alternating pattern throughout the array. FAD positions were cleared of fishes,

Table 1

Fish species and life history stages observed at all experimental FADs (combined data) with relative importance by frequency and abundance. 1 = coastal pelagic species; 2 = substrate-associated species; and 3 = possible flotsam specialists. J = juvenile; A = adult.

No.	Species	Family	Stage	Frequency (%)	Abundance (%)
1	*Abudefduf troschelii*[2]	Pomacentridae	J	34.1	81.4
2	*Elagatis bipinnulata*[1]	Carangidae	J	16.9	8.1
3	*Polydactylus approximans*[2]	Polynemidae	J	6.4	1.8
4	*Mugil* sp.[2]	Mugilidae	J	6.4	1.3
5	*Lutjanus argentiventris*[2]	Lutjanidae	J	6.4	1.1
6	*Epinephelus panamensis*[2]	Serranidae	J	3.4	0.5
7	*Hoplopagrus guntheri*[2]	Lutjanidae	J	3.2	0.5
8	*Canthidermis maculatus*[1]	Balistidae	J	2.8	0.4
9	*Gnathanodon speciosus*[2]	Carangidae	J	1.5	0.2
10	*Alectis ciliaris*[1]	Carangidae	J		
11	*Caranx caninus*[1]	Carangidae	J		
12	*Caranx caballus*[1]	Carangidae	J	14.7	3.9
13	*Caranx vinctus*[1]	Carangidae	J	(nos. 10–14)	
14	*Seriola peruana*[1]	Carangidae	J		
15	*Tylosaurus acus pacificus*[1]	Belonidae	A		
16	*T. crocodilus fodiator*[1]	Belonidae	A		
17	*Fistularia commersonii*[2]	Fistulariidae	J		
18	*Syngnathus auliscus*[2]	Syngnathidae	J		
19	*Lobotes pacificus*[3]	Lobotidae	J and A		
20	*Mulloidichthys dentatus*[2]	Mullidae	J	4.1	0.7
21	*Sectator ocyurus*[3]	Kyphosidae	A	(nos. 15–26)	
22	*Parapsettus panamensis*[2]	Ephippidae	J		
23	*Hypsoblennius brevieeps*[2]	Blenniidae	?		
24	goby (unidentified)[2]	Gobiidae	?		
25	*Aluterus scriptus*[2,3]	Balistidae	J and A		
26	*Balistes polylepis*[2]	Balistidae	J		
	26 species	16 families		100	100

and treatment FADs were deployed on 24 September 1997. FADs were monitored daily as described above, from 25 September through 3 October 1997 (sampling days=9). Data were analyzed for experimental effects on total assemblage size, species diversity (*S* and *HB*), number of *A. troschelii*, number of *E. bipinnulata*, and total number of fishes minus the number of *A. troschelii*.

Recruit-enriched vs. nonenriched FADs

I tested the hypothesis that the presence of prior recruits (juvenile sergeant major damselfish, *Abudefduf troschelii*) would have a positive effect on subsequent recruitment to a FAD. I used *A. troschelii* because these were the most important species associated with FADs by frequency and abundance (Table 1). It is possible that the selection of a particular species as the prior recruit might affect the subsequent recruitment of the same or different species (via intra- or interspecific competition for example), but I had no basis for predicting the direction of such effects.

Given the strong day-to-day changes in assemblage sizes, this test required frequent, short-interval observations of the experimental FADs. I used drifting, rather than anchored, FADs to provide a more realistic (and conservative) test of the effect. (Drifting objects should result in fewer chance encounters by potential fish recruits carried by currents through a fixed FAD array, but anchored FADs are much easier to track for longer experiments.) I deployed four drifting FADs (constructed from 3 buoys—the "single" size) in the stippled area indicated in Figure 3. Two of these FADs were enriched with nine *A. troschelii* per FAD, previously collected from anchored FADs and released in close proximity to drifting FADs immediately after deployment. The two control FADs received no sergeant majors to start. Both groups were checked immediately following deployment to verify that the fish had associated with the experimental FADs and to check against quick recruitment to the control FADs. To minimize the potential transfer of fish with the boat, I accelerated sharply when leaving a FAD enriched with sergeant majors and when checking

the FADs, entered the water from the boat a minimum of 10 m from each FAD.

The FADs were deployed from an inflatable boat at 50-m intervals in a roughly linear array, and checked at hourly intervals. The FADs did not maintain their initial spatial arrangement, but I did not move any FAD once the drift began unless FAD-to-FAD distance had been reduced to less than 10 m. In this instance, I moved one or more FADs to a minimum FAD-to-FAD distance of 50 m after checking for any FAD-associated fishes. In none of these instances were any FAD-associated fishes observed. I monitored the drift for four hours; deteriorating weather and fading light, however, did not permit additional observations.

I used linear regression to test the hypothesis that the number of FAD-associated fishes changed over time for the enriched FADs and for the nonenriched FADs. I used a *t*-test to compare the slopes of the two regression models and to test the hypothesis that the treatments accumulated fish at different rates.

Results

Twenty-six species of fishes from 16 families were recorded, including species associated with reef, soft bottom, and coastal pelagic habitats as adults (Table 1). Only juvenile specimens were observed clearly associated with FADs, with the exception of *Aluterus scriptus* and *Lobotes pacificus*, of which both juvenile and adult forms were observed in close, continuous proximity to the FADs. Two needlefish species (*Tylosaurus acus pacificus* and *T. crocodilus fodiator*) appeared occasionally in close proximity to the FADs, but they were not clearly associated with the FADs. An adult *Lobotes pacificus* (tripletail) was observed once and a single adult *Aluterus scriptus* (scrawled filefish) were observed on three separate instances. Horizontal underwater visibility averaged 13.4 m (±1.7 SE) for all sampling days combined.

Juvenile sergeant major damselfish (*Abudefduf troschelii*) were the dominant species by frequency of occurrence and numerical abundance (Table 1) for all experiments. The damselfish was followed in rank overall by juvenile rainbow runner (*Elagatis bipinnulata*), although this species was observed with the FADs only during the fouling and model fish experiments. Juvenile threadfin (*Polydactylus approximans*), mullet (*Mugil* sp.), and yellow snapper (*Lutjanus argentiventris*) were equally frequent but differed slightly in abundance (*P. approximans*>*Mugil* sp.>*L. argentiventris*; Table 1). The latter pattern was consistent across all experiments. Specimens from a suite of juvenile carangids (excluding *E. bipinnulata*) were also observed frequently.

Fish-removal experiments

Sample date, series, and treatment combined to have a significant effect on *A. troschelii* abundance (three way interaction, P=0.03), but there was no clear pattern; the remaining species (combined species less numbers of *A. troschelii*) were influenced by sample date (date by series interaction, P<0.01) but not by treatment (P=0.73, Table 2, Fig. 5). Measures of diversity varied between series (series: S, P<0.01; HB, P=0.01) but were unaffected by treatment. Thus, fish removal or fish disturbance may contribute to assemblage sizes for individual species (e.g. *A. troschelii*), but, in the present study, the total number of combined species was unaffected.

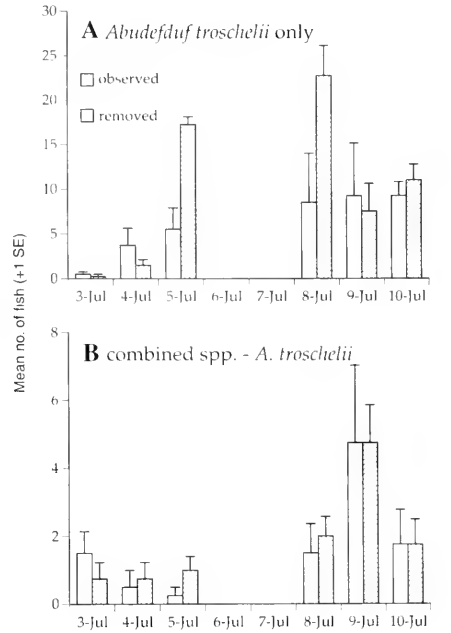

Figure 5

Repeated fish-removal effects (disturbed vs. undisturbed [observed only]) on aggregation size (mean no. of fishes) for *Abudefduf troschelii* alone (**A**) and for all species combined less *A. troschelii* (**B**). See Tables 3–5 for sample sizes and ANOVA results for assemblage size and diversity measures.

FAD size

Abudefduf troschelii was strongly affected by a combination of treatment and sample date (date by treatment interaction, P=0.03, Table 3, Fig. 6). Results from the remaining species combined were comparable with larger total numbers at the larger FADs, although not statistically significant (treatment, P=0.07). Although both measures of diversity (S and HB) suggested that the treatment may have had a positive effect on diversity (S, treatment, P=0.02), species richness was positively correlated with sample size. HB, a diversity measure comparatively unaf-

Table 2

Repeated measures ANOVA results (cleared FADs vs. undisturbed FADs, $n_1=n_2=12$) in fish-removal experiment.

Dependent variable	Factor(s)	F	df	P	$1-\beta$
Number of fishes	treatment	0.12	1, 12	0.73	0.06
(all species combined)	series	35.3	1, 12	<0.01	>0.99
	treatment × series	0.64	1, 12	0.44	0.11
	date	5.53	2, 24	0.01	0.81
	date × series	48.5	2, 24	<0.01	>0.99
	date × treatment	3.22	2, 24	0.06	0.55
	3-way interaction	0.06	2, 24	0.94	0.06
Number of fish	treatment	16.7	1, 12	<0.01	0.97
(*A. troschelii* only)	series	5.92	1, 12	0.03	0.61
	treatment × series	0.27	1, 12	0.61	0.08
	date	3.10	2, 24	0.06	0.53
	date × series	7.71	2, 24	<0.01	0.93
	date × treatment	2.95	2, 24	0.07	0.51
	3-way interaction	4.24	2, 24	0.03	0.69
Number of fishes	treatment	0.05	1, 12	0.82	0.06
(all spp. minus *A. troschelii*)	series	13.3	1, 12	<0.01	0.93
	treatment × series	0.01	1, 12	0.94	0.05
	date	2.93	2, 24	0.07	0.51
	date × series	4.06	2, 24	0.03	0.66
	date × treatment	0.07	2, 24	0.93	0.06
	3-way interaction	0.31	2, 24	0.74	0.09
Species richness (S)	treatment	0.63	1, 12	0.44	0.11
	series	11.8	1, 12	<0.01	0.90
	treatment × series	0.63	1, 12	0.44	0.11
	date	0.43	2, 24	0.66	0.11
	date × series	0.63	2, 24	0.54	0.14
	date × treatment	0.69	2, 24	0.51	0.15
	3-way interaction	2.08	2, 24	0.37	0.37
Species diversity (HB)[1]	treatment	1.05	1, 10	0.33	0.15
	series	8.79	1, 10	0.01	0.79
	treatment × series	0.54	1, 10	0.48	0.10
	date	1.43	2, 22	0.26	0.27
	date × series	2.80	2, 22	0.08	0.49
	date × treatment	0.12	2, 22	0.12	0.07
	3-way interaction	0.61	2, 22	0.55	0.14

[1] Missing data were replaced according to the directions in Zar (1996), and the degrees of freedom were reduced accordingly. "3-way interaction" refers to interactions between treatment, series, and dates.

fected by sample size (Magurran, 1988), was marginally nonsignificant (HB, treatment, P=0.07, Table 3).

Presence or absence of a fouling community

Treatment and sample date combined to have a significant effect on the number of *A. troschelii* (date by treatment interaction, $P<0.01$)—an effect contributing to the similar significant interaction effect for all species combined (Fig. 7, Table 4). Although the mean numbers of fish(es) were consistently higher at fouled FADs for *E. bipinnulata* alone and for all species minus *A. troschelii*, the only significant main effects were due to sample date (Table 4, Fig. 7). Species diversity (HB), though not richness (S), was significantly affected by sample date ($P=0.02$).

Artificial fish experiment

Experimental treatments (FADs with model fish, with lead weights or with nothing, Fig. 4) had no effect on any measured parameter—combined species, *A. troschelii* alone, *E. bipinnulata* alone, combined species less *A. troschelii*, species richness and diversity (Fig. 8, Table 5). All measures were significantly affected ($P<0.01$) by sample date except for *E. bipinnulata* alone (date, $P=0.48$). Although individual FADs varied in the number of associated *E. bipinnulata*,

Table 3

FAD-size effects and repeated measures ANOVA results (single FADs vs. triple-size FADs, $n_1=n_2=12$).

Dependent variable	Factor(s)	F	df	P	$1-\beta$
Number of of fishes	treatment	24.1	1, 6	<0.01	0.99
(all species combined)	date	10.7	2, 12	<0.01	0.97
	date × treatment	2.56	2, 12	0.12	0.41
Number of fish	treatment	10.9	1, 6	0.02	0.79
(*A. troschelii* only)	date	18.2	2, 12	<0.01	>0.99
	date × treatment	4.55	2, 12	0.03	0.66
Number of fishes	treatment	4.84	1, 6	0.07	0.45
(all spp–*A. troschelii*)	date	0.42	2, 12	0.67	0.10
	date × treatment	0.29	2, 12	0.75	0.09
Species richness (*S*)	treatment	11.3	1, 6	0.02	0.81
	date	0.38	2, 12	0.69	0.10
	date × treatment	0.38	2, 12	0.69	0.10
Species diversity (HB)	treatment	5.00	1, 6	0.07	0.46
	date	3.39	2, 12	0.07	0.52
	date × treatment	0.40	2, 12	0.68	0.10

these numbers were strikingly constant across sample date and, to a lesser extent, across treatments (Fig. 8).

Recruit-enriched vs. nonenriched FADs

Enriched FADs showed significantly higher rates of recruitment than nonenriched FADs: the regression line for the enriched FADs had a significant slope ($F_{(1,8)}$=20.76, P<0.01), but the regression line for the nonenriched FADs did not ($F_{(1,8)}$=2.29, P=0.17; Fig. 6). All additional fish were juvenile sergeant major damselfish, *Abudefduf troschelii*. These slopes are significantly different (t=3.05, 2 tailed test, v=6, P=0.02; Fig. 9); enriched FADs accumulated fish at a significantly higher rate (2.5 fish per hour) than did nonenriched FADs that accumulated fish at a rate of 0.1 fish per hour. Horizontal underwater visibility was 15 m at the beginning of the experiment.

Discussion

FAD size, the presence of a fouling community, and the presence of prior recruits all had positive effects on the size of FAD-associated assemblages, although the latter factor was assessed over a period of hours, whereas the former were assessed over days. The repeated removal of an existing assemblage also had significant effects due at least partially to treatment, but in all of these analyses sample date appeared to play the largest role in determining the numbers of fish(es) at these FADs. The presence of artificial fish or comparable-size weights did not significantly affect assemblage sizes. There was little support for the hypothesis that any of these factors might affect the species diversity of these assemblages; only species richness was significantly increased along with an increase in FAD size and this result may be an effect of assemblage size rather than object characteristics. Where treatment effects did significantly affect the numbers of fishes, their effects

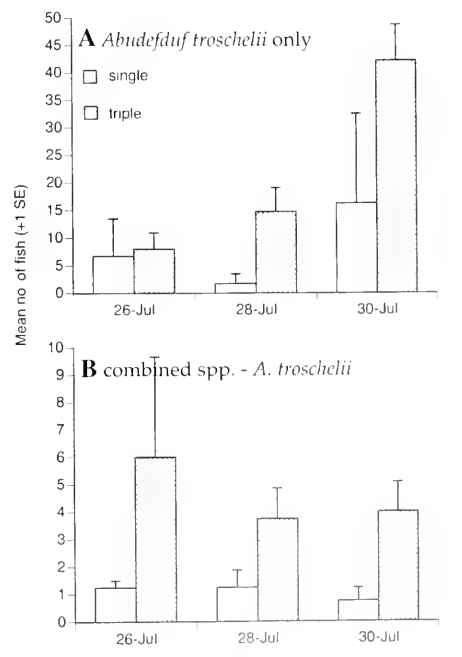

Figure 6

FAD-size effects (single FADs vs. triple-size FADs) on aggregation size (mean no. of fishes) for *Abudefduf troschelii* alone (**A**) and for all species combined less *A. troschelii* (**B**). See Tables 3–5 for sample sizes and ANOVA results for assemblage size and diversity measures.

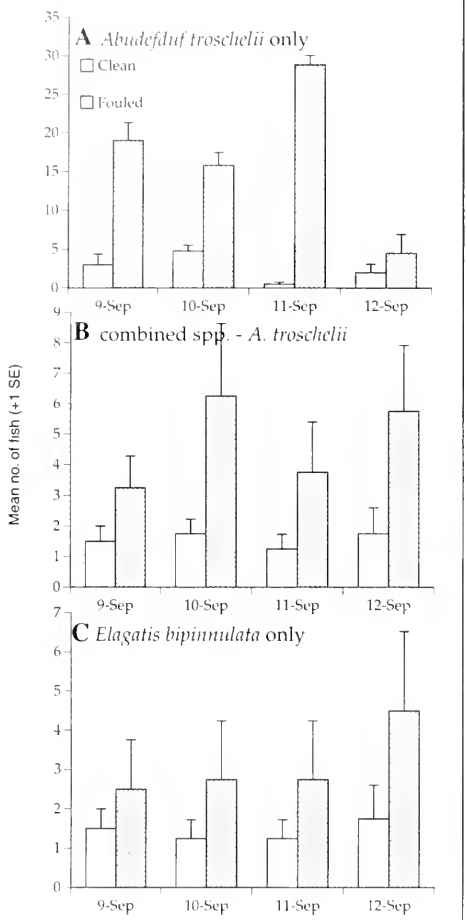

Figure 7

Effects of fouling community (fouled vs. unfouled [control]) on aggregation size (mean no. of fishes) for *Abudefduf troschelii* alone (**A**), for all species combined less *A. troschelii* (**B**), and for *Elagatis bipinnulata* alone (**C**). See Tables 3–5 for sample sizes and ANOVA results for assemblage size and diversity measures.

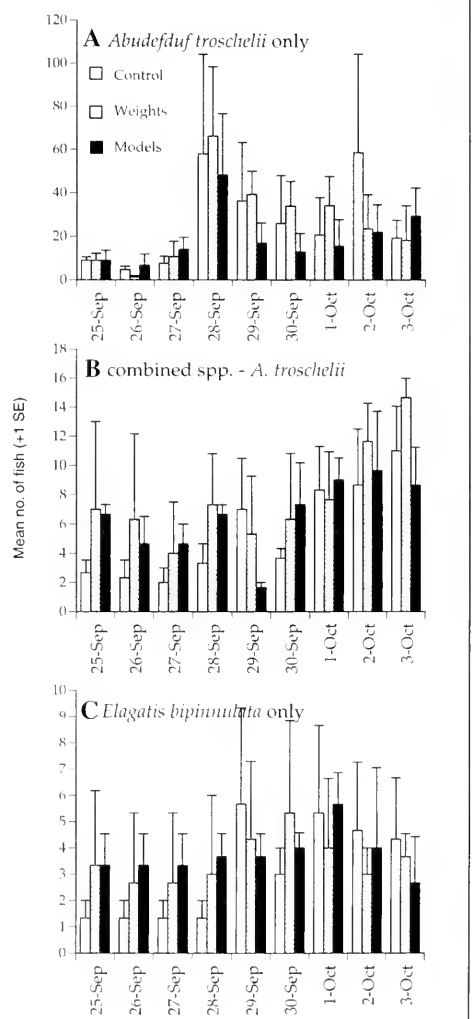

Figure 8

Artificial-fish effects (empty [control] FADs, FADs with weights, versus FADs with artificial fish) on aggregation size (mean no. of fishes) for *Abudefduf troschelii* alone (**A**), for all species combined less *A. troschelii* (**B**), and for *Elagatis bipinnulata* alone (**C**). See Tables 3–5 for sample sizes and ANOVA results for assemblage size and diversity measures.

on *Abudefduf troschelii* were generally the strongest. It is not clear whether this is a species-specific effect or if these results are due to the fact that *A. troschelii* was the most numerically important species.

The absence of a significant treatment main effect in the fish-removal experiments suggests that recruitment and loss from these anchored FADs is sufficiently rapid so that the complete removal of all fishes on a daily basis has no effect on the next day's assemblage size or diversity. These

Table 4

Repeated measures ANOVA results (absence of fouling community vs. presence of a fouling community, $n_1=n_2=16$) in fouling community experiment.

Dependent variable	Factor(s)	F	df	P	$1-\beta$
Number of fishes	treatment	39.8	1, 6	<0.01	0.99
(all species combined)	date	24.4	3, 18	<0.01	0.97
	date × treatment	33.5	3, 18	<0.01	0.41
Number of fish	treatment	165	1, 6	<0.01	>0.99
(*A. troschelii* only)	sate	19.7	3, 18	<0.01	>0.99
	date × treatment	25.2	3, 18	<0.01	>0.99
Number of fish	treatment	1.06	1, 6	0.34	0.14
(*E. bipinnulata* only)	date	4.89	3, 18	0.01	0.84
	date × treatment	2.15	3,18	0.13	0.45
Number of fishes	treatment	3.01	1, 6	0.13	0.30
(all spp.–minus *A. troschelii*)	date	3.88	3, 18	0.03	0.73
	date × treatment	2.27	3, 18	0.12	0.47
Species richness (S)	treatment	2.49	1, 6	0.17	0.26
	date	3.00	3, 18	0.06	0.60
	date × treatment	0.60	3, 18	0.62	0.15
Species diversity (HB)	treatment	1.74	1, 6	0.23	0.19
	date	4.35	3, 18	0.02	0.79
	date × treatment	1.91	3, 18	0.16	0.40

Table 5

Repeated measures ANOVA results (control [no weights and no artificial fish] vs. weights and vs. artificial fish, $n_1=n_2=n_3=27$) in the artificial fish experiment.

Dependent variable	Factor(s)	F	df	P	$1-\beta$
Number of fishes	treatment	0.13	2, 6	0.88	0.06
(all species combined)	date	3.52	8, 48	<0.01	0.97
	date × treatment	0.37	8, 48	0.98	0.20
Number of fish	treatment	0.12	2, 6	0.89	0.06
(*A. troschelii* only)	date	3.34	8, 48	<0.01	0.95
	date × treatment	0.41	8, 48	0.97	0.22
Number of fishes	treatment	0.29	2, 6	0.76	0.08
(all spp. minus *A. troschelii*)	date	4.82	8, 48	<0.01	>0.99
	date × treatment	0.73	8, 48	0.75	0.41
Number of fish	treatment	0.05	2, 6	0.95	0.06
(*E. bipinnulata* only)	date	0.95	8, 48	0.48	0.38
	date × treatment	0.36	8, 48	0.94	0.20
Species richness (S)	treatment	0.41	2, 6	0.68	0.10
	date	9.87	8, 48	<0.01	>0.99
	date × treatment	0.90	8, 48	0.58	0.50
Species diversity (HB)[1]	treatment	0.13	2, 5	0.88	0.06
	date	4.44	8, 47	<0.01	0.99
	date × treatment	1.00	8, 47	0.45	0.56

[1] Missing data were replaced according to the directions in Zar (1996), and the degrees of freedom were reduced accordingly.

results are consistent with those obtained by Wickham and Russell (1974). A similar result would occur if these FADs had a predictable carrying capacity and recruitment was sufficiently rapid that removal of the assemblage was followed by its replacement before the next observation. However, assemblage sizes within treatments varied widely from one day's observations to the next; therefore recruitment, rather than carrying capacity, seems to determine assemblage size.

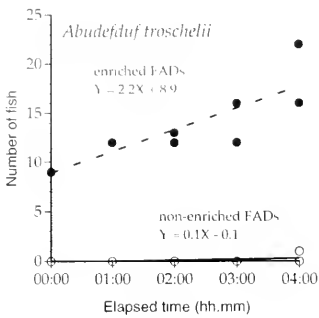

Figure 9

Changes in the number of fish associated with enriched (solid circles) and nonenriched (open circles) drifting FADs over time. Enriched FADs showed significantly higher rates of recruitment than did nonenriched FADs; the slopes of the regression lines are significantly different (t=3.05, 2-tailed test, v=6, P=0.02).

There appears to be insufficient time or stability for such factors as competition or predation to influence the size or diversity of these FAD-associated fish assemblages. Despite these results, individual fish do remain with a specific FAD for days: On at least five separate occasions associated with some of the other experiments described in this paper, individuals recognizable by scars and bite marks were sighted repeatedly as many as six days after the initial observation (Nelson, unpubl. data). Although the FADs and the associated fishes described in the present study are not directly comparable to FADs and fishes targeted in fisheries-scale operations, these experiments are among the first controlled efforts at understanding the effects of disturbance or fishing for FAD-associated assemblages.

The average assemblage size for all experiments and treatments varied considerably, often significantly, over time (Tables 2–5). Significant interaction effects between sample date and FAD treatments may be indicative of day-to-day recruitment fluctuations, dependent upon recruitment variability. A significant interaction may result when these effects are large and are in evidence regardless of the experimental treatment (i.e. occur in concert across treatments). Significant sample date effects (and series effects in the fish-removal experiment, Table 2) are likely a result of temporal fluctuations in the numbers of fishes available to recruit to the FADs.

Note that the two series in the fish-removal experiment differed not only in which FADs were given a particular treatment (positional effects), but also in time—the two series were necessarily run consecutively, not concurrently. I believe, however, it to be unlikely that positional effects influenced any of the results reported in the present study: treatments were assigned to FADs within the arrays in such a way as to ensure that inshore, offshore, or longshore positions were equally weighted among treatments. Significant series main effects, independent of additional factors, were found only for species richness and diversity (HB)—a result I attribute to changes in the availability of potential recruit species. Temporal patterns of juvenile reef fish recruitment are often variable and may be affected by such factors as spawning periodicity (Love et al., 1990), variable predation (Nelson, 2001), or changing physical oceanographic processes (Doherty, 1991; Levin, 1994; Kingsford and Finn, 1997). Rountree (1989), also, found that the mean numbers of the most abundant species observed around a FAD array off South Carolina varied widely during FAD deployment, albeit over a much longer time period (nearly 200 days). Thus, differences in assemblage size and diversity over time are not unexpected.

FAD size had significant, positive effects on assemblage size and species richness. Although tripling the FAD size resulted in a nearly threefold increase in the number of associated fishes (combined species), the response may not be linear. (Note, however, that Rountree (1989) demonstrated that the number of *Decapterus punctatus* associated with midwater FADs exhibited a significant, positive linear response to FAD size.) Further research will be necessary to resolve the effect of FAD size on numbers of aggregating fishes. Also of interest is the significant increase in species richness attributable to increased FAD size. Bortone et al. (1977) suggested that species diversity may be a function of "clump size" for *Sargassum*-associated fish assemblages, and Moser et al. (1998) found greater numbers of fish species under large (10–20 m diameter) mats of floating *Sargassum* than they did under smaller clumps (<1 m diameter) or in open water. However, the changes in species richness from this experiment could well be an effect of assemblage size; treatment effects on species diversity measured using the Brillouin index (HB) were marginally nonsignificant (Table 3, P=0.07). Significant sample date differences in treatment and evenness are due to large fluctuations in the abundance of the dominant species, *Abudefduf troschelii*, ranging at the triple-size FADs from 1 to 55 individuals over the course of 11 days.

Fishes were five times more numerous on average at fouled FADs than they were at comparable FADs lacking fouling organisms, but measures of diversity showed no significant treatment effect (Table 4). There was a significant interaction between treatment and sample date for the present experiment (Table 4) that may have been due to fluctuations in assemblage sizes among sample dates across both FAD treatments. The species composition of these assemblages was similar to that of other experiments, except that *Elagatis bipinnulata* were regularly observed: *Abudefduf troschelii* were the dominant species by abundance, followed by *E. bipinnulata*, and *Mugil* sp. All were small, young-of-the-year fishes (the largest *E. bipinnulata* individuals reached approximately 80 mm SL) and seemed not to be feeding on the larger invertebrates forming much of the colonizing community. During casual observations of FAD-associated fishes, I observed fish feeding on plankton carried past the FADs, but no physical contact with the FAD or fouling organisms. Ibrahim et al.

(1996) reported that none of the gut contents from FAD-associated fishes included sessile organisms found on their FADs (fish size ranges included specimens 8–14, 15–99, and ≥100 mm SL—the first two size categories are comparable to the fishes in the present study). Larger, piscivorous fishes do feed at least occassionally on smaller fishes associated with floating objects (Gooding and Magnuson, 1967), but published gut content studies are conflicting. Some suggest that piscivorous species that associate with flotsam rely on other sources of food (e.g. Gooding and Magnuson, 1967; Hunter and Mitchell, 1967; Brock, 1985), while others suggest that flotsam- (or algae-) associated fishes form an important food resource for these larger piscivorous fishes (Dooley, 1972; Manooch et al., 1984; Coston-Clements et al., 1991). Morgan et al. (1985) noted the occurrence of at least two members of the *Sargassum*-associated invertebrate fauna among the stomach contents of several species of pelagic fishes. From the perspective of flotsam- or FAD-associated fishes, opportunistic predation by piscivores that do not associate with FADs may be more important than predation by other members of the assemblage. Additional gut content data from juvenile and nonpiscivorous fishes are sorely lacking. I address possible explanations for the results of the present study below.

I recorded no significant treatment effect attributable to differences between FADs with artificial fish, FADs deployed with artificial-fish–sized weights, or control FADs. I attribute significant sample date effects to day-to-day changes in constituent individuals and the fluctuating availability of potential recruits. Numbers of *E. bipinnulata* were strikingly constant across treatments and sample dates in this experiment (Table 5, Fig. 8) and in the fouling experiment (Fig. 7) and seemed to indicate an apparently unusual characteristic of this species—individuals remaining associated with a given FAD for multiple days. Although the experiment was intended to distinguish between FADs with prior recruits versus FADs without prior recruits, the lack of a significant treatment effect does not negate the possibility that potential recruits would distinguish between occupied and unoccupied FADs. The painted artificial fish and lead weights clearly lacked many attributes of living fish. However, comparable numbers of recruits found at all treatments suggest that a change in the structural complexity of the FADs did not affect assemblage size or diversity. Although the addition of four small lead weights (artificial fish were painted and oriented differently but were still lead weights) did not appear to increase appreciably the visible surface area of those FADs, the subsequent experiment with live fishes instead of artificial fish had a dramatic effect on recruitment; therefore sizeable changes in the physical size of a FAD may be necessary to yield a response in fish recruitment. The potential roles of structural complexity and orientation of FADs will be informative areas for future research. Past investigations in these areas (e.g. Hunter and Mitchell, 1968; Klima and Wickham, 1971; Wickham et al., 1973) have provided a useful beginning, but more work is needed.

Although sample sizes were small, the presence of prior *Abudefduf troschelii* "recruits" (enriched FADs) had a significant effect on patterns of subsequent recruitment; this effect contrasted sharply with FADs lacking fish at the start of this experiment (nonenriched FADs). For this species, these results point to a social aspect to these aggregations, and sociality may also be involved in the recruitment of other species, particularly the schooling fishes *Caranx* spp., *Polydactylus approximans*, and *Mugil* spp., as suggested for some scombrids (e.g. Dagorn and Fréon, 1999). The addition of fishes below a FAD may increase recruitment rates by rendering the object more visible, although the artificial fish experiment indicated that simply adding fish-size objects beneath a FAD does not affect recruitment. Comparisons between these two experiments are tenuous, however, because the artificial fish experiment employed anchored FADs observed over a period of days, whereas the enriched FAD experiment used drifting FADs observed over a course of hours.

Why do FAD size, the presence of a fouling community, and the actual presence of prior recruits at a FAD each have the effect of increasing the size and, possibly, the diversity of FAD-associated assemblages of juvenile fishes? The simplest explanation is that these factors contribute to the target strength of the object, increasing the visual, olfactory, or auditory stimulus (or some combination) of the floating object. Larger objects should be easier to find, especially if potential recruits rely on vision to explore their environment. Kellison and Sedberry (1998) found that the fishes associated with mid-water floating structures that were tethered to an artificial reef decreased in abundance over time (193 days), and suggested that the loss in buoyancy associated with the development of a fouling community may have reduced the effective size of these floating objects, accounting for fewer associated fishes (see also Hunter and Mitchell, 1968; Rountree, 1989). To account for the positive effects of a fouling community observed in the present study, it seems reasonable to suppose that fouling organisms may be detected by olfactory means; Sweatman (1988) has shown that some larval fishes use olfactory cues for settlement on reefs. Further experiments, for example experiments controlling for FAD size, odor cues, and visibility of the FADs, are needed to determine why some of these factors exhibit these effects.

Future research on the role of flotsam as shelter from predators and as a conveyance to suitable habitat could yield evolutionary explanations for the attraction to floating objects. For these small fishes, such objects likely represent a shelter from predators (Mitchell and Hunter, 1970). Some species do respond to the approach of an observer by positioning themselves so that the FAD is between them and the observer. Particularly during daylight and crepuscular hours when visually-oriented predators are most active, flotsam may offer refuge in a habitat where there is little alternative refuge. During the day, when onshore winds drive drifting objects towards shallow water, flotsam and drift algae, unlike anchored FADs, may also offer a comparatively safe conveyance to more suitable habitat. Thus, there may be adaptive advantages for juvenile reef fishes in associating with floating objects.

Although the juvenile fishes associated with the FADs used in the present study are not of interest to any fishery, the patterns observed from them may be relevant to FADs

deployed commercially to aggregate fish species at various life history stages. FAD size is clearly relevant to those interested in studying potential improvements to FAD design. Carefully controlled studies on the importance of surface area versus volume and the orientation of FAD structures are needed. The role of a fouling community, too, deserves further investigations. Although a fouling community may weigh down streamers (trailing pieces of buoyant material intended to increase the subsurface of area of a FAD), such a community may also improve recruitment and possibly retention of recruits around a FAD. Finally, the importance of the initial recruits to a floating object should be studied further. Enriching a FAD may increase the speed at which additional fishes are recruited. Improved artificial fish may prove more effective than the items used in the present research. FADs are an important tool in a number of artisanal (small-scale fishery based on traditional methods), sport, and commercial fisheries, especially in tropical waters where FAD fisheries particularly target tunas (Scombridae), jacks (Carangidae), and *Coryphaena* spp. (Galea, 1961; Klima and Wickham, 1971; Beets, 1989; Hilborn and Medley, 1989; Friedlander et al., 1994; Higashi, 1994; Hall et al., 1999b). Due largely to the potential for fisheries enhancement, considerable research has been focused on the importance of floating-object characteristics and the numbers of fishes attracted to such objects; however, the results have been difficult to interpret and are often conflicting (Rountree, 1989; Kingsford, 1993; Druce and Kingsford, 1995). Because log sets in tuna purse-seine fisheries (where fishermen target fish associated with drifting logs or FADs) are associated with high levels of bycatch (Hall, 1998; Lennert-Cody and Hall, 2000), the behavior and ecology of flotsam-associated species is in urgent need of study so that a means of reducing bycatch may be devised.

This study made use of FADs floating at the surface; studies by other researchers have employed similar tools or they have used FADs tethered in mid-water. No one has examined the effects of FAD position in relation to the surface, and the implicit assumption appears to be that there is no biologically significant difference. This assumption has not been tested, although comparisons between data from floating structures, whether at the surface, mid-water, or tethered close to the bottom, are common in the literature. I have made comparisons between my data from surface FADs and results from mid-water FADs (e.g. Wickham and Russell, 1974; Rountree, 1990); such comparisons may be misleading and should be interpreted with caution.

The results from the present study indicate that turnover rates at nearshore anchored FADs are high and that undisturbed FAD assemblages may show little difference in these rates from disturbed FADs. Fishes recruiting to these FADs discriminate among potential floating objects, forming larger, more species-rich assemblages around triple-size FADs than around single FADs. FADs possessing a fouling biota also attract larger (though no more diverse) assemblages than do clean FADs. The latter effect was complicated by temporal fluctuations that overlay these treatment effects, resulting in day-to-day changes in the total numbers of fishes in both treatments (Table 4, Fig. 7). Further, the presence of prior recruits in the enrichment experiment had a strong effect on subsequent recruitment. Thus, the association of juvenile fishes with floating objects is not a haphazard process, and floating-object characteristics play potentially important roles in fish recruitment to these objects. These results suggest that associating with flotsam may be adaptive, rather than an accidental behavior and support Kingsford's hypothesis (Kingsford, 1993) that floating material is an important environmental component in the relationship between environment and some juvenile fishes.

Acknowledgments

For help in the field, I am grateful to I. Nelson and D. Mansue. W. L. Montgomery, S. Shuster, and to two anonymous reviewers who provided helpful criticism. Funding was provided by the American Museum of Natural History (Lerner-Gray Fund), American Society of Ichthyologists and Herpetologists (Raney Award), Animal Behavior Society, International Women's Fishing Association (Max Coan Memorial Scholarship), Seaspace/Houston Underwater Club, Smithsonian Tropical Research Institute (STRI), and Sigma Xi. D. R. Robertson of STRI and D. Margulise, R. Olson, and V. Scholey of the Inter-American Tropical Tuna Commission provided invaluable advice and logistical support.

Literature cited

Beets, J.
1989. Experimental evaluation of fish recruitment to combinations of fish aggregating devices and benthic artificial reefs. Bull. Mar. Sci. 44:973–983.

Bortone, S., P. A. Hastings, and S. B. Collard.
1977. The pelagic-*Sargassum* ichthyofauna of the eastern Gulf of Mexico. Northeast Gulf Sci. 1:60–67.

Brock, R. E.
1985. Preliminary study of the feeding habits of pelagic fish around Hawaiian fish aggregation devices or can fish aggregation devices enhance local fisheries productivity? Bull. Mar. Sci. 37:40–49.

Coston-Clements, L., L. R. Settle, D. E. Hoss, and F. A. Cross.
1991. Utilization of the *Sargassum* habitat by marine invertebrates and vertebrates—a review. NOAA Tech. Memo. NMFS-SEFSC-296:32.

Crawford, R. E., and J. K. Jorgenson.
1993. Schooling behaviour of arctic cod, *Boreogadus saida*, in relation to drifting pack ice. Environ. Biol. Fish. 36: 345–357.

Dagorn, L., and P. Fréon.
1999. Tropical tuna associated with floating objects: a simulation study of the meeting point hypothesis. Can. J. Fish. Aquat. Sci. 56:984–993.

Doherty, P. J.
1991. Spatial and temporal patterns in recruitment. *In* The ecology of fishes on coral reefs (P. F. Sale, ed.), p. 261–294. Academic Press, San Diego, CA.

Dooley, J.
1972. Fishes associated with the pelagic *Sargassum* complex, with a discussion of the *Sargassum* community. Contrib. Mar. Sci. 16:1–32.

Druce, B. E., and M. J. Kingsford.
1995. An experimental investigation on the fishes associated with drifting objects in coastal waters of temperate Australia. Bull. Mar. Sci. 57:378–392.
Fedoryako, B. I.
1989. A comparative characteristic of oceanic fish assemblages associated with floating debris. J. Ichthyol. 29: 128–137.
Friedlander, A., J. Beets, and W. Tobias.
1994. Effects of fish aggregating device design and location on the fishing success in the U.S. Virgin Islands. Bull. Mar. Sci. 55:592–601.
Gaertmer, D., and M. Medina-Gaertner.
1999. An overview of the relationship between tunas and floating objects in the south of Caribbean Sea. IATTC (Inter-American Tropical Tuna Commission), Spec. Rep. 11:66–86.
Galea, J. A.
1961. The "Kannizzati" fishery. Gen. Fish. Counc. Mediterr. Sess. Rep. 6:85–91.
Gooding, R. M., and J. J. Magnuson.
1967. Ecological significance of a drifting object to pelagic fishes. Pac. Sci. 21:486–497.
Hall, M. A.
1998. An ecological view of the tuna-dolphin problem: impacts and trade-offs. Rev. Fish Biol. Fish. 8:1–34.
Hall, M. A., D. L. Alverson, and K. I. Metuzals.
2000. By-catch: problems and solutions. Mar. Pollut. Bull. 41:204–219.
Hall, M. A., M. Garcia, C. Lennert-Cody, P. Arenas, and F. Miller.
1999a. The association of tunas with floating objects and dolphins in the eastern Pacific Ocean: a review of the current purse-seine fishery. IATTC, Spec. Rep. 11:87–194
Hall, M. A., C. Lennert-Cody, M. Garcia, and P. Arenas.
1999b. Characteristics of floating objects and their attractiveness for tunas. IATTC, Spec. Rep. 11:396–446.
Hallier, J. P., and J. I. Parajua.
1999. Review of tuna fisheries on floating objects in the Indian Ocean. IATTC, Spec. Rep. 11:195–221.
Hampton, J., and K. Bailey.
1999. Fishing for tunas associated with floating objects: review of the western Pacific fishery. IATTC, Spec. Rep. 11:222–284.
Higashi, G. R.
1994. Ten years of fish aggregating device (FAD) design development in Hawaii. Bull. Mar. Sci. 55:651–666.
Hilborn, R., and P. Medley.
1989. Tuna purse-seine fishing with fish-aggregating devices (FAD): models of tuna FAD interactions. Can. J. Fish. Aquat. Sci. 46:28–32.
Hunter, J. R., and C. T. Mitchell.
1967. Association of fishes with flotsam in the offshore waters of Central America. Fish. Bull. 66:13–29.
1968. Field experiments on the attraction of pelagic fish to floating objects. J. Cons. Int. Explor. Mer 31:427–434.
Ibrahim, S., M. A. Ambak, L. Shamsudin, and M. Z. Samsudin.
1996. Importance of fish aggregating devices (FADs) as substrates for food organisms of fish. Fish. Res. 27:265–273.
Kellison, G. T., and G. R. Sedberry.
1998. The effects of artificial reef vertical profile and hole diameter on fishes off South Carolina. Bull. Mar. Sci. 62: 763–780.
Kingsford, M. J.
1992. Drift algae and small fish in coastal waters of northeastern New Zealand. Mar. Ecol. Progr. Ser. 80:41–55.
1993. Biotic and abiotic structure in the pelagic environment: importance to small fishes. Bull. Mar. Sci. 53:393–415.
1995. Drift algae: a contribution to near-shore habitat complexity in the pelagic environment and an attractant for fish. Mar. Ecol. Progr. Ser. 116:297–301.
Kingsford, M. J., and M. Finn.
1997. The influence of phase of the moon and physical processes on the input of presettlement fishes to coral reefs. J. Fish Biol. 51:176–205.
Klima, E. F., and D. A. Wickham.
1971. Attraction of coastal pelagic fishes with artificial structures. Trans. Am. Fish. Soc 1:86–99.
Kojima, S.
1960. Fishing for dolphins in the western part of the Japan Sea. V. Species of fishes attracted to bamboo rafts. Bull. Jpn. Soc. Sci. Fish. 26:379–382.
Lennert-Cody, C. E., and M. A. Hall.
2000. The development of the purse seine fishery on drifting fish aggregating devices in the eastern Pacific Ocean: 1992–1998. *In* Pêche thonière et dispositifs de concentration de poissons: colloque DCP, Martinique, Octobre 1999, p. 78–107. Institut Français de Recherche pour l'Exploitation de la Mer, Issy-les-Moulineaux, France.
Levin, P. S.
1994. Fine-scale temporal variation in recruitment of a temperate demersal fish: the importance of settlement versus post-settlement loss. Oecologia 97:124–133.
Love, M. S., M. H. Carr, and L. J. Haldorson.
1990. The ecology of substrate-associated juveniles of the genus *Sebastes*. Environ. Biol. Fish. 30:225–243.
Magurran, A. E.
1988. Ecological diversity and its measurement, 179 p. Princeton Univ. Press, Princeton, NJ.
Manooch, C. S., III, D. L. Mason, and R. S. Nelson.
1984. Food and gastrointestinal parasites of dolphin *Coryphaena hippurus* collected along the southeastern and Gulf coasts of the United States. Bull. Jpn. Soc. Sci. Fish. 50: 1511–1525.
Massuti, E., S. Deudero, P. Sanchez, and B. Morales-Nin.
1998. Diet and feeding of dolphin (*Coryphaena hippurus*) in western Mediterranean waters. Bull. Mar. Sci 63. 329–341.
McCleneghan, K., and J. L. Houk.
1978. A diver-operated net for catching large numbers of juvenile marine fishes. Calif. Fish Game 64:305–307.
Mitchell, C. T., and J. R. Hunter.
1970. Fishes associated with drifting kelp, Macrocystis pyrifera, off the coast of southern California and northern Baja California. Calif. Fish Game 56:288–297.
Morgan, S. G., C. S. Manooch III, D. L. Mason, and J. W. Goy.
1985. Pelagic fish predation on *Cerataspis*, a rare larval genus of oceanic penaeoids. Bull. Mar. Sci. 36:249–259.
Moser, M. L., P. J. Auster, and J. B. Bichy.
1998. Effects of mat morphology on large *Sargossum*-associated fishes: observations from a remotely operated vehicle (ROV) and free-floating video camcorders. Environ. Biol. Fish. 51:391–398
Nelson, P. A.
1999. The ecology and behavior of flotsam-associated marine fish aggregations. Ph.D. diss., 137 p. Northern Arizona Univ., Flagstaff, AZ.
2001. Behavioral ecology of young-of-the-year kelp rockfish, *Sebastes atrovirens* Jordan and Gilbert (Pisces: Scorpaenidae). J. Exp. Mar. Biol. Ecol. 256:33–50.

Parin, N. V., and B. I. Fedoryako.
1999. Pelagic fish communities around floating objects in the open ocean. IATTC, Spec. Rep. 11:447–458.
Rountree, R. A.
1989. Association of fishes with fish aggregation devices: effects of structure size on fish abundance. Bull. Mar. Sci. 44:960–972.
1990. Community structure of fishes attracted to shallow water fish aggregation devices off South Carolina, U.S.A. Environ. Biol. Fish. 29:241–262.
Safran, P.
1990. Drifting seaweed and associated ichthyofauna: floating nursery in Tohoku waters. Mer 28:225–239.
Safran, P., and M. Omori.
1990. Some ecological observations on fishes associated with drifting seaweed off Tohoku coast, Japan. Mar. Biol. 105:395–402.
Suzuki, Z.
1999. Distribution of floating logs in the Pacific and purse seine sets on tunas associated with logs by Japanese boats in the tropical western and central Pacific. IATTC, Spec. Rep. 11:459–479.
Sweatman, H. P. A.
1988. Field evidence that settling coral reef fish larvae detect resident fishes using disolved chemical cues. J. Exp. Mar. Biol. Ecol. 124:163–174.
Wickham, D. A., and G. M. Russell.
1974. An evaluation of mid-water artificial structures for attracting coastal pelagic fishes. Fish. Bull. 72:181–191.
Wickham, D. A., J. W. Watson Jr., and L. H. Ogren.
1973. The efficacy of midwater artificial structures for attracting pelagic sport fish. Trans. Am. Fish. Soc. 3:563–572.
Zar, J. H.
1996. Biostatistical analysis, 3rd ed., 662 p. Prentice Hall, Upper Saddle River, NJ.

Age and growth of the bastard grunt (*Pomadasys incisus*: Haemulidae) inhabiting the Canarian archipelago, Northwest Africa

José G. Pajuelo
José M. Lorenzo
Departament of Biology
University of Las Palmas de Gran Canaria
Campus Universitario de Tafira
35017 Las Palmas de Gran Canaria, Spain
E-mail address (for J. G. Pajuelo): jpaguelo@dbio.ulpgc.es

Muriel Gregoire
Faculty of Biology
University of Liége
Liége, Belgium
Present address: Departament of Biology
University of Las Palmas de Gran Canaria
Campus Universitario de Tafira
35017 Las Palmas de Gran Canaria, Spain

Abstract—The bastard grunt (*Pomadasys incisus*) is one of the most abundant coastal demersal fishes inhabiting the Canary Islands. Age and growth were studied from samples collected between October 2000 and September 2001. Growth analysis revealed that this species is a fast growing and moderately short-lived species (ages up to seven years recorded). Length-at-age was described by the von Bertalanffy growth model (L_∞=309.58 mm; k=0.220/year; t_0=−1.865 year), the Schnute growth model (y_1=126.66 mm; y_2=293.50 mm; a=−0.426; b= 5.963), and the seasonalized von Bertalanffy growth model (L_∞=309.93 mm; k=0.218/year; t_0=−1.896 year; C=0.555; t_s=0.652). Individuals grow quickly in their first year, attaining approximately 60% of their maximum length; after the first year, their growth rate drops rapidly as energy is probably diverted to reproduction. The parameters of the von Bertalanffy weight growth curve were W_∞=788.22 mm; k=0.1567/year; t_0=−1.984 year. Fish total length and otolith radius were closely correlated, r^2=0.912. A power relationship was estimated between the total length and the otolith radius (a=49.93; v=0.851). A year's growth was represented by an opaque and hyaline (translucent) zone—an annulus. Backcalculated lengths were similar to those predicted by the growth models. Growth parameters estimated from the backcalculated sizes at age were L_∞=315.23 mm; k=0.217/year; and t_0=−1.73 year.

Manuscript approved for publication 19 June 2003 by Scientific Editor.
Manuscript received 26 June 2003 at NMFS Scientific Publications Office.
Fish. Bull. 101:851–859 (2003).

The family Haemulidae consists of 16 genera (126 species), including the genus *Pomadasys*. This genus is represented by 37 species distributed around the world. Members of this family are commonly referred to as grunt (Bauchot and Huraeu, 1990). Only the bastard grunt (*Pomadasys incisus* (Bowdich, 1825)) is found off the Canary Islands. The bastard grunt is a coastal demersal fish species inhabiting marine and brackish waters along the eastern central Atlantic coasts from the Strait of Gibraltar to Angola, and also in the Canaries, Azores, and Cape Verde Islands (Bauchot and Hureau, 1990). In the Canary Islands, where the bastard grunt is one of the most abundant species, it has been observed in high densities in schools along coastal waters.

Information on the biology of the bastard grunt is not available anywhere in the world. Despite its widespread occurrence, the bastard grunt has no commercial value for its low quality meat and it is discarded in the Canarian archipelago. The need for a biologically based discard management strategy and the paucity of data available on the biology of this species have prompted an investigation into aspects of its life history. We report aspects of age and growth, which are important parameters in models for managing the population of the bastard grunt off the Canary Islands.

Materials and methods

A total of 878 individuals of *P. incisus* were collected at weekly intervals from discarded commercial catches taken between October 2000 and September 2001 off Gran Canaria (Canary Islands, central-east Atlantic, 27°57′24″N–15°35′23″W).

Each fish was measured to the nearest mm for total length (L_t) and weighed to the near 0.1 g for total body weight (W_t). Sex was assessed visually and sagittal otoliths were removed, cleaned, and stored dry for later age determination.

Age estimation was made by identifying and counting annuli following Williams and Bedford (1974). An annulus was defined as a hyaline zone formed annually in the winter season when there is low growth and an opaque zone formed annually in the summer season when there is increased growth. The whole otoliths were placed in a blackened bottom watch glass containing water and examined under a compound microscope (10×) with reflected light. Counts of the growth bands were made

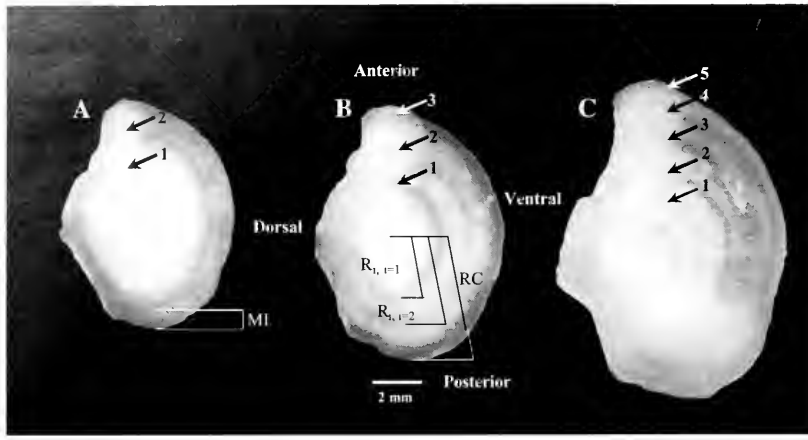

Figure 1

Saggital otoliths of *P. incisus* collected off the Canary Islands: (**A**) from a two-year-old (182 mm); (**B**) from a three-year-old (202 mm); and (**C**) from a five-year-old (265 mm) fish. *Ri* is the radius of the i^{th} band (distance from the centre of the otolith to the outer margin of the annulus), *Rc* is the radius of the otolith at capture, and MI is the marginal increment measured.

by two readers without knowledge of the size and sex of the specimens, or previous counts of the other reader. Counts were made for otoliths of each individual on two separate occasions, and only coincident readings were accepted. The same approach was used to determine the final number of bands in each specimen, and a consensus was reached between readers on the final counts. Reproducibility of the resultant age estimates was evaluated with the coefficient of variation (CV) (Chang, 1982) and the index of average percent error (IAPE) (Beamish and Fournier, 1981).

To validate that rings were formed annually in the bastard grunt, we analyzed the monthly mean marginal increment (Hyndes and Potter, 1997). Marginal increment, estimated as the distance between the outer edge of the outermost annual ring and the periphery of each otolith, was measured (to the nearest 0.01 mm) with an ocular micrometer (Fig. 1). Measurements were always made along the longest axis of the otolith. The pattern expected in the marginal increment would be a minimal value at the start of the growth period, increasing with time until the measurement fell to a minimum again at the formation of the next period of growth (Pilling et al., 2000). The size of the marginal increment varies both with the age of the fish and the time of sampling during the year. Because older fish grow slower than younger fish, a smaller marginal increment is expected. For this reason, to assess the possibility of false annulus formation among either younger or older bastard grunt, quantitative marginal increment analyses should be standardized for age. Therefore, we used age class to standardize our analyses. Owing to the wide range of ages encountered, however, there were insufficient samples to fully accomplish this standardization. It was necessary to combine the ages in two or more age groups representing fast, moderate, and slow-growing individuals (Pilling et al., 2000). Mean marginal increments were plotted against month of capture, and the minimum was used to indicate the month of annulus formation.

Once the periodicity and timing of ring formation were verified, the age of each fish was determined from the number of annuli, the assumed birthdate, and the sampling date. It was assumed that annulus formation began 1 January, corresponding to the peak of spawning in the species (Gregoire[1]). The difference between the date of capture and the birthdate was used to estimate a fractional age (Gordoa and Molí, 1997). This fraction was added to the number of annuli read in the otoliths to avoid any potential bias in growth estimates due to differences in sampling date (Gordoa and Molí, 1997).

Length-at-age was described by the three-parameter specialized von Bertalanffy growth model (Ricker, 1973):

$$L_t = L_\infty(1 - e^{-k(t-t_0)}),$$

the four-parameter Schnute growth model (Schnute, 1981):

[1] Gregoire, M. 2001. Edad y crecimiento del roncador *Pomadasys incisus* (Bowdich, 1825) de Gran Canaria (Islas Canarias). Unpubl. data. ULPGC Socrates/Erasmus Research Report, 34 p. Departament of Biology, University of Las Palmas de Gran Canaria. 35017 Las Palmas de Gran Canaria. Spain.

$$L_t = \left[y_1^b + (y_2^b - y_1^b)\left(\frac{1 - e^{a(t-A_1)}}{1 - e^{-a(A_2-A_1)}} \right) \right]^{\frac{1}{b}},$$

and the seasonalized von Bertalanffy growth model (Pitcher and Macdonald, 1973)

$$L_t = L_\infty \left(1 - e^{-k(t-t_0)+\left(\frac{Ck}{2\pi}\sin(2\pi(t-t_s))\right)} \right),$$

where A_1 = the smallest age in the sample;
A_2 = the largest age in the sample;
T_0 = the age at zero length;
L_t = the length-at-age;
L_∞ = the predicted asymptotic length;
y_1 = the estimated mean length of A_1-year-old fish;
y_2 = the estimated mean length of A_2-year-old fish;
C = the amplitude of the fluctuation in seasonal growth;
t_s = the point of the minumum growth (t_s=WP+0.5); and
k = the Brody growth constant (Schnute, 1981; Sparre and Venema, 1995).

The models were fitted to data with the Marquardt's algorithm for nonlinear least squares parameter estimation (Gayanilo et al., 1996). A nonparametric, one-sample test was applied to test for residual randomness and a Bartlett's test was used to test for their homoscedasticity. Von Bertalanffy growth model parameters were also estimated for observed W_t as a function of age by substituting weights in place of lengths in the growth equation and incorporating b derived by the weight-length regression (Sparre and Venema, 1995):

$$W_t = W_\infty (1 - e^{-k(t-t_0)})^b,$$

where W_t = the weight at age; and
W_∞ = the predicted asymptotic weight.

Backcalculated size of each fish at the time of formation of each annulus was determined by a backcalculation formula consistent with the body proportional hypothesis (Campana, 1990; Francis, 1990). The measurements were the following: the radius of the i^{th} band (Ri, 0.01 mm, distance from the center of the otolith to the outer margin of the annulus) and the radius of the otolith at capture (Rc, 0.01 mm, distance from the center of the otolith to the periphery). These measurements were always made along the longest axis of the otolith (Fig. 1). The relationship between the radius of the otolith at capture (Rc) and the total length was estimated as a power function (nonlinear relationship). It is estimated by fitting the data by a regression of $\log(L_t)$ on $\log(Rc)$ consistent with the body proportional hypothesis (BPH). The length of an individual when the i^{th} band was laid down (Li, mm) was calculated as

$$Li = (Ri/Rc)^v Lc,$$

where Lc = the length-at-capture; and
v = a constant derived from the relationship of total length to otolith radius (Francis, 1990).

The von Bertalanffy growth curve was fitted to the backcalculated length-at-age by means of Marquardt's algorithm for nonlinear least squares parameter estimation (Gayanilo et al., 1996).

Results

Of the 878 fish examined, 377 (42.9%) were males and 412 (46.9%) females. The remaining 89 (10.1%) individuals were immature and could not be identified macroscopically. Fish varied in size from 103 to 304 mm L_t, and weighed between 8.7 and 137.1 g W_t. Males varied from 143 to 298 mm L_t, and total mass was from 9.3 to 114.7 g W_t. Female total length varied between 134 and 304 mm and total mass was from 13.2 to 137.1 g. Immature fish varied from 103 to 186 mm L_t and from 8.7 to 29.6 g W_t. No significant differences were found between males and females in mean size (Student's t-test, t=1.03<$t_{0.05,787}$=1.65) or weight (Student's t-test, t=1.57<$t_{0.05,787}$=1.65).

Sagittae of bastard grunt are ovate and laterally compressed. Annuli were clearly differentiated under reflected light on a black background: the opaque zones are milky in appearance and the hyaline zones relatively transparent (Fig. 1). The number of annuli counted for each individual were similar for the two readers. Of the 878 otoliths examined, 22 (2.5%) were rejected as unreadable, three were completely translucent, eight were broken, and 11 had poorly defined growth zones. Of the remaining 856 otoliths, consensus was reached for 812 (94.8%). The index of average percent error (IAPE) of band counts for each reader did not differ greatly, and was slighly lower for the first author (2.47) than for the second (2.69). The precision of the age estimates was also expressed as the CV as recommended by Campana (2001). The level of precision was approximately 5% for both readers.

Marginal increments were measured for 812 individuals. In the otoliths with one and two annuli (fast-growing young individuals), the lowest monthly mean marginal increments were recorded in January and increased throughout the year (Fig. 2). The marginal increments in the otoliths with three and more than three annuli (moderate and slow-growing individuals) also followed a similar trend. Thus, irrespective of the age of the fish, the marginal increments declined markedly and then rose progressively only once during a 12-month period. Therefore, only one annulus is formed in December–February.

Alternating opaque and hyaline zones were clearly visible on the otoliths. Up to seven marks, assumed to be annuli, were visible in the otoliths sampled. Two- and three-year-old fish were the dominant age classes and over 80% of fish were three years old or less (Table 1). Over 45% of the growth was achieved by the end of the first year. By the end of the second year, fish had attained 60% of the mean observed length.

The three growth models provided a good fit to the data (Table 2, Fig.3). Length-at-age was adequately described

by the three models with the statistically suitable absolute error structure because it provided both residual randomness and homoscedasticity. The computed value of 0.15 for the winter point of the seasonalized von Bertalanffy growth model indicated that the lowest growth rate occurred at about two months after the birth date, meaning that the growth rate was reduced in winter.

No significant difference was found between the von Bertalanffy growth models with a likelihood ratio test (F=0.15<$F_{0.05,2,1560}$), and a significant difference was found between the von Bertalanffy growth models and the Schnute growth model with the same test (F>$F_{0.05;2,1560}$); therefore, the specialized von Bertalanffy growth model was chosen because it has fewer parameters making it statistically more robust, its parameters are commonly used in mortality estimates and per recruit modelling, and because it allows for comparison between growth studies conducted on other species (Booth, 1997). No significant differences were found between mean lengths-at-age of males and females with a Student's t-test (t=0.52<$t_{0.05,787}$=1.65) or between the von Bertalanffy growth curves for separate sexes with a Hotelling's T^2 test (T^2=4.73<$T_0{}^2{}_{0.05,3,784}$=7.89). The data were pooled as a single growth model. In fitting the growth curve to the age-length data, age 0 was disregarded because this age group was not well represented. The von Bertalanffy growth curve derived from the observed weight at age for males and females was not significantly different (Hotelling's T^2-test, T^2=6.91<$T_0{}^2{}_{0.05,3,784}$=7.89; Fig. 4).

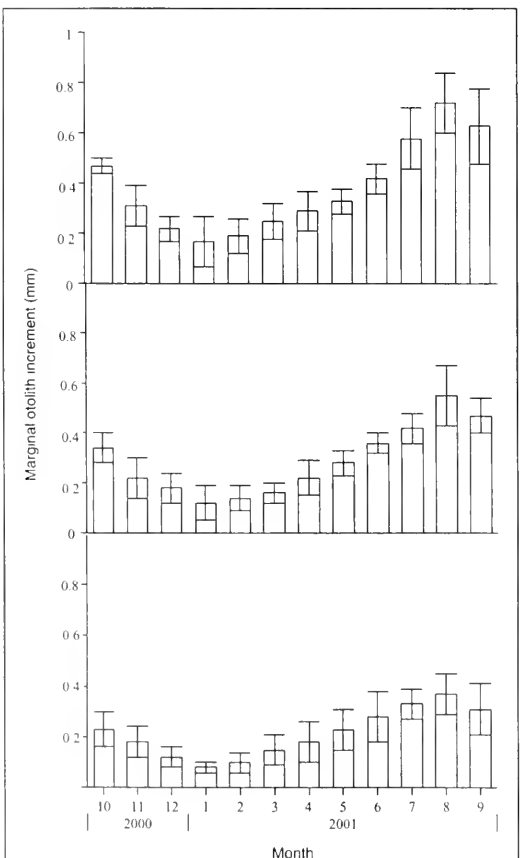

Figure 2

Mean monthly marginal increment from otoliths with one and two, three, and more than three annuli, representing fast, moderate, and slow-growing individuals of *P. incisus* off the Canary Islands. Standard errors are identified by the bars.

Fish total length and otolith radius were closely correlated (Fig. 5). The value of the derived constant (v=0.851) was different from one (Student t-test; t=14.61 > $t_{0.05,810}$=1.65). Backcalculated size at time of annulus formation was used to provide length-at-age data unbiased by differences in sampling date and to estimate the von Bertalanffy equation (Table 3). Backcalculated lengths were similar to those predicted by the growth models. Growth parameters estimated from the backcalculated sizes at age were L_∞=315.23 mm; k=0.217/year; and t_0=−1.733 year. The data was pooled as a single growth model because no significant differences in the growth parameters were found between males and females (Hotelling's T^2-test, T^2=48.3>$T_0{}^2{}_{0.05,3,784}$=7.89).

Discussion

Age estimation in fishes is complicated by the phenomenon of "stacking" of growth zones towards the otolith margin, particularly in older fish (Buxton and Clarke, 1991). In many cases age determination is difficult because whole otoliths are so thick that light does not pass through (Buxton and Clarke 1991); however, in the bastard grunt off the Canary Islands the translucency of the otoliths allows aging with relative ease. The values of the IAPE and the CV suggested that the precision levels obtained are according to the reference point values indicated by Campana (2001). The oldest age estimate obtained in the present study was seven years and the phenomenon of stacking was not evident.

The otoliths of the bastard grunt have a ring pattern common to teleost fishes. Marginal increment analysis demonstrated that one annulus, consisting of one opaque zone and one hyaline zone, is formed annually. These rings are believed to be deposited during periods of fast and slow growth, respectively (Williams and Bedford, 1974). Seasonal growth cycles might be related to physiological changes produced by the influence of temperature, feeding regime, and reproductive cycle (Morales-Nin and Ralston, 1990). The seasonalized von Bertalanffy growth model reveals the reduc-

Table 1

Sample size per age group (age-length key) and percentage (in parentheses) within each age group for all fish of *P. incisus* collected off the Canary Islands. *n* is the number fish by age class and SD is the standar deviation. Total length classes are given in 10-mm intervals.

	Age groups (year)							
Size (mm)	0	I	II	III	IV	V	VI	VII
100	2 (40.0)	3 (60.0)						
110	1 (8.1)	10 (90.9)						
120	1 (5.6)	17 (94.4)						
130		19 (100.0)						
140		15 (71.4)	6 (28.6)					
150		4 (17.4)	19 (82.6)					
160			33 (100.0)					
170			47 (95.9)	2 (4.1)				
180			69 (70.4)	29 (29.6)				
190			52 (46.6)	61 (53.4)				
200			25 (20.5)	96 (78.6)	1 (0.9)			
210			14 (12.8)	89 (81.6)	6 (5.5)			
220			5 (5.9)	57 (67.0)	23 (27.1)			
230				14 (27.0)	38 (73.0)			
240				2 (10.0)	17 (85.0)	1 (5)		
250				1 (6.6)	9 (60.0)	4 (26.8)	1 (6.6)	
260					2 (20.0)	6 (60.0)	2 (20.0)	
270					1 (25.0)	1 (25.0)	2 (50.0)	
280						1 (33.3)	1 (33.3)	1 (33.3)
290							1 (100)	
300								1 (100.0)
Mean	107	125	176	212	236	261	275	295
n	4	68	270	351	97	13	7	2
SD	5.77	12.64	17.28	18.06	12.36	11.43	11.40	14.14

Table 2

Parameters estimates, standard errors, and 95% cofidence intervals for the specialized von Bertalanffy, Schnute, and seasonalized von Bertalanffy growth models for all *P. incisus* collected off the Canary Islands. All models were pooled without the age-0 class.

		95% confidence intervals		
Parameter	Estimate	Standard error	Lower	Upper
Specialized von Bertalanffy growth model (r^2=0.91)				
L_∞ (mm)	309.58	8.06	294.07	325.08
k (/year)	0.220	0.031	0.157	0.283
t_0 (year)	−1.865	0.055	−2.007	−1.723
Schnute growth model (r^2=0.87)				
y_1 (mm)	126.66	1.51	124.54	128.78
y_2 (mm)	293.50	9.50	286 68	300.32
A	−0.426	0.077	−0.578	−0.274
B	5.963	0 664	4.659	7.267
Seasonalized von Bertalanffy growth model (r^2=0.91)				
L_∞ (mm)	309.93	7.68	295.21	324.65
K (/year)	0.218	0.032	0.153	0.282
t_0 (year)	−1.896	0.049	−2.067	−1.725
C	0.555	0.212	0.138	0.971
t_s	0.652	0.061	0.532	0.773

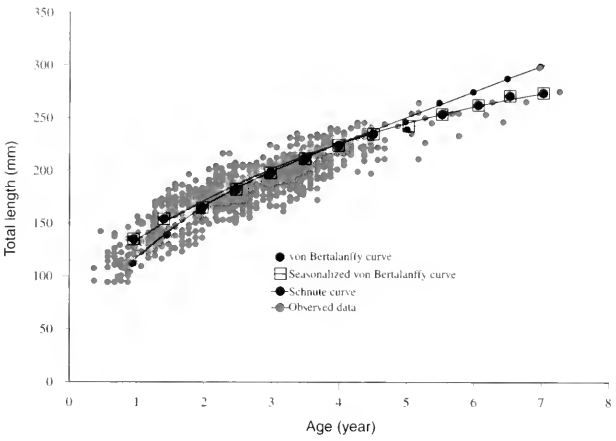

Figure 3

Von Bertalanffy specialized and seasonalized growth curves and the Schnute growth curve for all individuals of *P. incisus* collected off the Canary Islands.

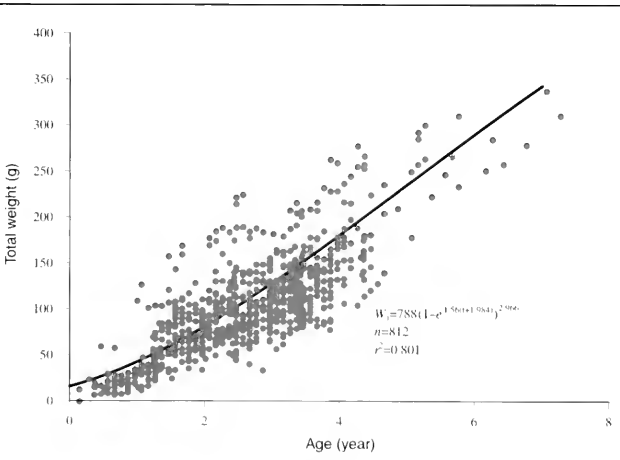

Figure 4

Von Bertalanffy growth curve derived from observed weight at age for all *P. incisus* collected off the Canary Islands.

tion of somatic growth and the formation of the hyaline zone during the winter months. The high correlation found between L_t and otolith radius indicates that otoliths are a useful structure for estimating the age and for indicating the past growth history of bastard grunt.

The coefficients of determination for each fitted curve show that the three models explain more than 88% of the growth pattern. The use of the von Bertalanffy model to describe growth has been criticized for several reasons (Booth, 1997). These include the use of parameters that

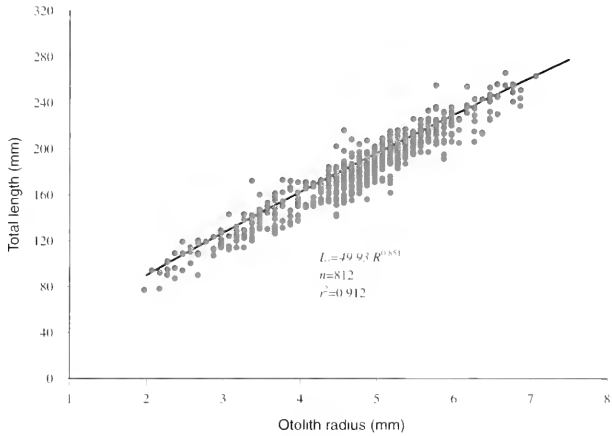

Figure 5

The relation of otolith length to total length for *P. incisus* collected off the Canary Islands.

Table 3

Backcalculated length-at-age for all *P. incisus* collected off the Canary Islands.

Age (year)	Number of fish	Annulus number						
		I	II	III	IV	V	VI	VII
1	68	119						
2	270	123	179					
3	351	127	172	219				
4	97	132	168	212	235			
5	13	129	178	205	245	26		
6	7	122	170	221	233	257	275	
7	2	128	174	214	239	260	279	293
Mean		126	173	214	238	259	277	293
Number of backcalculated lengths at age		808	740	470	119	22	9	2
Annual growth increment (mm)		126	47	41	24	21	18	16
Annual growth increment (%)		43.0	16.1	13.9	8.2	7.2	6.1	5.4

have little biological meaning (Schnute, 1981) and the absence of parameters that take into account seasonal changes in growth rate (Pauly, 1980; Moreau, 1987). Nevertheless, the von Bertalanffy growth model has been used extensively to describe the growth of grunts. The growth model provides a simple description of growth which can be compared between species and species groups (Booth, 1997). The special and the seasonal forms of the von Bertalanffy growth model were chosen for the present study because they contain fewer parameters than the Schnute growth model.

Backcalculated lengths-at-age are in close agreement with the length estimated from otoliths readings. The results obtained with the backcalculation method are very satisfactory because they show the consistency in the interpretation of the sequence of growth increments of the bastard grunt off the Canary Islands and reduce the effect of size-selective sampling bias on the length estimates for youngest fish in the sample (Campana, 2001).

The growth parameters obtained are reasonable because the theoretical maximal length value is higher than the size of the largest fish sampled and the growth coefficient

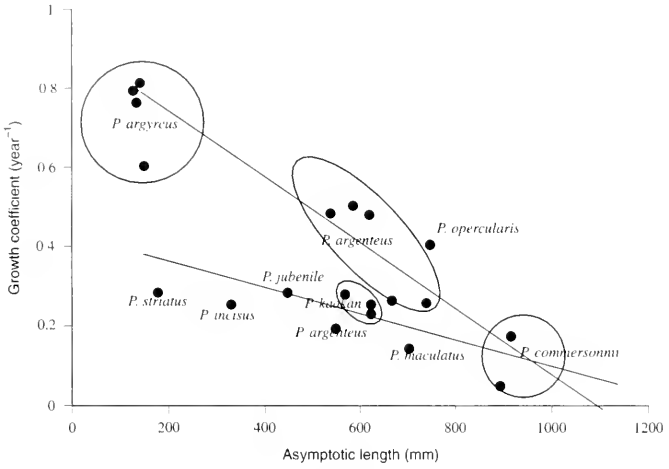

Figure 6

The relation of asymptotic length to the growth coefficient for different species of the *Pomadasys* genus.

value indicates a relatively fast attainment of maximum size, characteristic of the moderately short life cycle for this species. However, the estimations of t_0 tend to be negative and different from zero for values affected by the small sample size of smaller fish. These estimations suggest that the von Bertalanffy growth model does not accurately describe growth in the early stages. *Pomadasys incisus* grows quickly in its first year, attaining approximately 60% of its maximum length. After the first year, the annual growth rate drops rapidly. This change in growth rate is attributable to the utilization of available energy for reproduction instead of somatic growth; in the study area the maturation process begins in the second year of life (Gregoire[1]).

Two different patterns of growth rate in relation to asymptotic length are observed for *Pomadasys* species (Fig. 6). The pattern of *P. incisus* is similar to that observed for *P. striatus, P. jubeline, P. kaakan, P. maculates,* and *P. commersonnii*—species characterized by a high or moderate asymptotic length and low or moderate growth coefficient (Latif and Shenouda, 1972; Wallace and Schleyer, 1979; Edwards et al., 1985; Iqbal, 1989; Al-Husaini et al., 2001; Pauly[2]). However, it differs substantially from that observed for *P. argyreus*, a species with a very low asymptotic length (<151 mm) and a very high growth coefficient (0.62–0.83/year), and for *P. opercularis* and *P. argenteus*, species characterized by a high asymptotic length and a high growth coefficient (550–741 mm; 0.28–0.52/years) (Deshmukh, 1973; Nzioka, 1982; Brothers and Mathews, 1987; Majid and Imad, 1991; Ingles and Pauly[3]).

Results of models used in fisheries management, e.g. analytical yield-per-recruit models (Beverton and Holt, 1957), are sensitive to uncertainty in the estimates of input parameters such as the von Bertalanffy growth parameters. Several estimations of growth in *Pomadasys* species have been derived through length-based methods, which for slow growing species are uncertain. The growth parameters from this study are the first otoliths-based estimates of growth for *P. incisus*. Similar estimates obtained from different growth models and methods suggest that the current estimation could be considered a good estimation of the growth pattern for the species and adequate for use as an input parameter in models for the management of the species.

Acknowledgments

The authors are grateful to the three anonymous reviewers for their constructive, critical, and useful comments on the manuscript.

[2] Pauly, D. 1978. A preliminary compilation of fish length growth parameters. Ber. Inst. Meereskunden, Universitat an der Kiel 55, 200 p. Institut fur Meereskunde, Dusternbrooker Weg 20, 24105 Kiel, Germany.

[3] Ingles, J., and D. Pauly. 1984. An atlas of the growth, mortality and recruitment of Philippine fishes. ICLARM Technical Report 13, 127 p. World Fish Center (ICLARM) Jalan Batu Maung, Batu Maung, 11960 Bayan Lepas, Penang, Malaysia.

Literature cited

Al-Husaini, M., S. Al-Ayoub, and J. Dashti.
2001. Age validation of nagroor, *Pomadasys kaakan* (Cuvier, 1830) (family: Haemulidae) in Kuwaiti waters. Fish. Res. 53:71–81.

Bauchot, M. L., and J. C. Hureau.
1990. Haemulidae. *In* Check-list of the fishes of the eastern tropical Atlantic (J. C. Quero, J. C. Hureau, C. Karrer, A. Post, and L. Saldanha, eds.), p. 786–787. UNESCO, Paris, France.

Beamish, R. J., and D. A. Fournier.
1981. A method for comparing the precision of a set of age determinations. Can. J. Fish Aquat. Sci. 38:982–983.

Beverton, R. J. H., and S. J. Holt.
1957. On the dynamics of exploited fish populations. Fisheries Investigations Series II, XIX, 533 p. Her Majesty's Stationery Office, London, UK.

Booth, A. J.
1997. On the life history of the lesser gurnard (Scorpaeniformes: Triglidae) inhabiting the Agulhas Bank, South Africa. J. Fish. Biol. 51:1155–1173.

Brothers, E. B., and C. P. Mathews.
1987. Application of otolith microstructural studies to age determinations of some commercially valuable fish of the Arabia Gulf. Kuwait Bull. Mar. Sci. 9:127–157.

Buxton, C. D., and J. R. Clarke.
1991. The biology of the white musselcracker *Sparadon durbanensis* (Pisces: Sparidae) on the Eastern Cape Coast, South Africa. S. Afr. J. Mar. Sci. 10:285–296.

Campana, S. E.
1990. How reliable are growth back-calculations based on otoliths? Can. J. Fish. Aquat. Sci. 47:2219–2227.
2001 Accuracy, precision and quality control in age determination, including a review of the use and abuse of age validation methods. J. Fish. Biol. 59:197–242.

Chang, W. B.
1982. A statistical method for evaluating the reproducibility of age determinations. Can. J. Fish. Aquat. Sci. 39: 1208–1210.

Deshmukh, V. M.
1973. Fishery and biology of *Pomadasys hasta* (Bloch). Indian J. Fish. 20:497–522.

Edwards, R. R. C., A. Bakhader, and S. Shaher.
1985. Growth, mortality, age composition and fishery yields of fish from the Gulf of Aden. J. Fish. Biol. 27:13–21.

Francis, R. I. C. C.
1990. Back-calculation of fish length: a critical review. J. Fish Biol. 36:883–902.

Gayanilo, F. C., P. Sparre, and D. Pauly.
1996. FAO-ICLARM stock assessment tools (FiSAT) user's guide, 126 p. FAO (Food Agric. Organ. U. N.) Comp. Inf. Ser. (Fish.) 8.

Gordoa, A., and B. Molí.
1997. Age and growth of the sparids *Diplodus vulgaris*, *D. sargus* and *D. annularis* in adult populations and the differences in their juvenile growth patterns in the north-west Mediterranean Sea. Fish. Res. 33:123–129.

Hyndes, G. A, and I. C. Potter.
1997. Age, growth and reproduction of *Sillago schomburgkii* in south-western Australin, nearshore waters and comparisions of life history styles of a suite of *Sillago* species. Environ. Biol. Fish. 49 435–447.

Iqbal, M.
1989. A note on the population dynamics of *Pomadasys kaakan* (Haemulidae) from Pakistan. Fishbyte 7:4–5.

Latif, A., and S. Shenouda.
1972. Biological studies on *Rhonciscus striatus* (family Pomadasidae) from the Gulf of Suez. Bull. Inst. Ocean. Fish. 2:103–134.

Majid, A., and A Imad
1991. Growth of *Pomadasys kaakan* (Haemulidae) off the coast of Pakistan. Fishbyte 9:30–33.

Morales-Nin, B., and S. Ralston.
1990. Age and growth of *Lutjanus kasmira* (Forskal) [*sic*] in Hawaiian waters. J. Fish Biol. 36:191–203.

Moreau, J.
1987. Mathematical and biological expression of growth in fishes: recent trends and further developments. *In* Age and growth of fish (R. C. Summerfelt and G. E. Hall, eds.), p. 81–113. Iowa State Univ. Press, Ames, IA.

Nzioka, R. M.
1982. Biology of the small spotted grunt *Pomadasys opercularis* (Playfair 1866) (Pisces: Pomadasyidae) around Malindi in Kenya. Kenya J. Sci. Tech. 3:69–81.

Pilling, G. M., R. S. Millner, M. W. Easey, C. C. Mees, S. Rathachasen, and R. Azemia.
2000. Validation of annual growth increments in the otoliths of the lethrinid *Lethrinus mahsena* and the lutjanid *Aprion virescens* from sites in the tropical Indian Ocean, with notes on the nature of growth increments in *Pristipomoides filamentosus*. Fish. Bull. 98:600–611.

Pauly, D.
1980. On the interrelationships between natural mortality, growth parameters, and mean enviromental temperature in 175 fish stocks. J. Cons. Int. Explor. Mer 39:175–195.

Pitcher, T. J., and P. D. M. Macdonald.
1973. Two models for seasonal growth in fishes. J. Appl. Ecol. 10:597–606.

Ricker, W. E.
1973. Linear regressions in fishery research. J. Fish. Res. Board Can. 30:409–434.

Schnute, J.
1981. A versalite growth model with statistically stable parameters. Can. J. Fish. Aquat. Sci. 38:1128–1140.

Sparre, P., and S. C. Venema.
1995. Introducción a la evaluación de recursos pesqueros tropicales, parte 1, manual, 420 p. FAO (Food Agric. Organ. U. N.) Doc. Téc. Pesca 306(1).

Wallace, J. H., and M. H. Schleyer.
1979. Age determination in two important species of South Africa angling fishes, the knob (*Argyrosomus hololepidotus* Lacep) and the spotted grunter (*Pomadasys commersonnii* Lacep). Trans. R. Soc. S. Afr. 44:15–26.

Williams, T., and B C. Bedford.
1974. The use of otoliths for age determination. *In* The ageing of fish (T. B Bagenal, ed.), p. 114–123 Unwin Brothers, Old Woking, Surrey, UK.

Evaluating the efficacy of managing West Coast groundfish resources through simulations

André E. Punt

School of Aquatic and Fishery Sciences
University of Washington
1122 NE Boat Street
Seattle, Washington 98195-5020
E-mail address: aepunt@u.washington.edu

Abstract—Management of West Coast groundfish resources by the Pacific Fishery Management Council involves Federal government and academic scientists conducting stock assessments, generally using the stock synthesis framework, applying the 40-10 rule to determine harvest guidelines for resources that are not overfished and conducting rebuilding analyses to determine harvest guidelines for resources that have been designated as overfished. However, this management system has not been evaluated in terms of its ability to satisfy the National Standard 1 goals of the Sustainable Fisheries Act. A Monte Carlo simulation framework is therefore outlined that can be used to make such evaluations. Based on simulations tailored to a situation similar to that of managing the widow rockfish (*Sebastes entomelas*) resource, it is shown that catches during recovery and thereafter are likely to be highly variable (up to ±30% from one year to the next). Such variability is far greater than has been presented to the decision makers to date. Reductions in interannual variability in catches through additional data collection are, however, unlikely. Rather, improved performance will probably arise from better methods for predicting future recruitment. Rebuilding analyses include quantities such as the year to which the desired probability of recovery applies. The estimates of such quantities are, however, very poorly determined.

Manuscript approved for publication 24 April 2003 by Scientific Editor.
Manuscript received 26 June 2003 at NMFS Scientific Publications Office.
Fish. Bull. 101:860–873 (2003).

National Standard 1 of the Sustainable Fisheries Act (SFA) of 1996 states that "Conservation and management measures shall prevent overfishing while achieving, on a continuing basis, the optimum yield from each fishery for the United States industry." The need to satisfy this National Standard has led *inter alia* to the requirement for the eight Regional Fishery Management Councils to develop control rules that are used to assess whether overfishing is occurring[1] or a stock is in an overfished state (e.g. Restrepo and Powers, 1999). In addition, the SFA specifies that a rebuilding plan has to be developed for any fish stocks that are designated as overfished. This plan needs to include the time period by which the stock will be rebuilt to B_{MSY} (the average biomass associated with maximum sustainable yield, MSY), and the strategy by which the stock is to be rebuilt.

The Pacific Fishery Management Council (PFMC) has adopted the "40-10" rule to manage groundfish stocks that are not designated as being overfished. This rule determines the harvest guideline for each groundfish stock by computing the catch corresponding to an F_{MSY} proxy ($F_{40\%}$[2] for flatfish, $F_{50\%}$ for rockfish in the *Sebastes* complex, and $F_{45\%}$ for other species) and reducing it if the spawning output is estimated to be less than 40% of the estimated B_0. This reduction in catch is linear with spawning output, being 0 at $0.4B_0$ and 100% at $0.1B_0$. For stocks that are designated as being in an overfished state (defined for West Coast groundfish as being that the spawning output is less than $0.25B_0$) a rebuilding plan is developed.[3] The main features of the technical aspects of a rebuilding plan (referred to as a rebuilding analysis) identified by the Scientific and Statistical Committee of the PFMC are outlined in Appendix 1. In brief, the rebuilding analysis used by the PFMC involves projecting the best estimates of the current age-structure of the overfished population forward under a range of alternative fishing mortality rates and selecting the fishing mortality rate that has a Council-selected probability that the population recovers to the proxy for B_{MSY} of $0.4B_0$ within a time frame consistent with the specifications of the SFA.

Detailed stock assessments are available for only a small subset of the 81 species included in the PFMC Groundfish Management Plan. Of these species, nine (bocaccio [*Sebastes paucispinis*], canary rockfish [*Sebastes pinniger*], cowcod [*Sebastes levis*], darkblotched rockfish [*Sebastes crameri*], lingcod [*Ophiodon elongates*], Pacific ocean perch [*Sebastes alutus*], Pacific whiting [*Merluccius productus*], widow rockfish [*Sebastes entomelas*], and yelloweye rockfish [*Sebastes ruberrimus*]) have been designated overfished and rebuilding plans have been or are being developed for them. The direct consequences

[1] In the present study, and consistent with usage by the Pacific Fishery Management Council, "overfishing" means that the level of fishing mortality exceeds that associated with MSY and "being in an overfished state" means that the current spawning output is less than 25% of the pre-exploitation equilibrium spawning output, B_0 (spawning output is the product of egg production-at-age and numbers-at-age).

[2] $F_{x\%}$ is the fishing mortality rate at which the spawning output-per-recruit is reduced to $x\%$ of its unfished level.

[3] One implication of this is that the 40-10 rule is not actually used if the stock is assessed to be below $0.25B_0$.

for industry of the implementation of a rebuilding plan can be substantial (e.g. a reduction in the catch of canary rockfish from 883 metric tons (t) in 1999 to only 90 t in 2001), although there are also indirect consequences in the form of reductions in the harvest of nonoverfished species to prevent overharvesting of overfished species through technical interactions.

The performance of the method commonly used for assessments of West Coast species has been evaluated to some extent (e.g. Sampson and Yin, 1998; Ianelli, 2002). However, the performance of this assessment method in combination with the rules used to determine harvest guidelines has not been evaluated.

Management procedures[4] are combinations of stock assessment methods and catch control laws that have been evaluated by means of Monte Carlo simulation to assess the extent to which they are able to satisfy the management objectives for a fishery. Evaluation of management procedures by means of Monte Carlo simulation has been argued to be essential because "if a management procedure is unable to perform adequately in the ideal world represented on a computer, what basis is there to assume that it will perform adequately in the real world?" (Sainsbury[5]). One caveat to this argument is that it is only possible to evaluate a management procedure if it is fully specified and if it will be followed for several years in reality.

Management procedures have been adopted by the International Whaling Commission for managing commercial and aboriginal whaling (e.g. IWC, 1992, 2001) and by southern African nations for managing a variety of pelagic and demersal resources (Butterworth and Bergh, 1993; Cochrane et al., 1998; Geromont et al., 1999). Management procedures are under consideration in Australia (Punt et al., 2001) and New Zealand (Starr et al., 1997). If it can be assumed that the same rules will be applied to modify rebuilding plans each time new information on abundance and year-class strength becomes available, it is possible to consider the combination of the assessment method, the default 40-10 rule, and rebuilding plans as a "management procedure" and evaluate it by means of Monte Carlo simulation. This study therefore involves determining from past practice the "management procedure" being applied by the PFMC. However, this "management procedure" has not been formally adopted in any way and the approach to managing West Coast groundfish could change in time.

This paper first outlines a simulation framework (a management procedure evaluation, MPE, framework) within which the expected performance of the approach used by the PFMC to determine harvest guidelines can be evaluated. It then evaluates variants of this approach for scenarios similar to that of managing the fishery for widow rockfish.

[4] Also referred to as "harvest strategies" (Punt et al., 2001), "management decision rules" (Starr et al., 1997), "fisheries control systems" (Hilborn, 1979), and "operational management procedures" (Barnes, 1999).

[5] Sainsbury, K. G. 2001. Personal commun. CSIRO Marine Research, Castray Esplanade, Hobart, TAS 7000, Australia.

Materials and methods

The steps in evaluating management procedures are as follows:

1 Identification of the management objectives and representation of these by using a set of quantitative performance statistics.
2 Identification of a range of alternative management procedures.
3 Development and parameterization of a set of alternative structural models (called operating models) of the system.
4 Simulation of the future use of each management procedure to manage the system (as represented by each operating model). For each year of the projection period, the simulations involve the following steps:
   a Generation of the data available for assessment purposes.
   b Application of a method of stock assessment to the generated data to determine key assessment-related quantities (e.g. current age-structure, spawning output in relation to target and limit levels, historical trends in recruitment) and any inputs to the catch control law.
   c Application of the catch control law element of the management procedure to determine a harvest guideline.
   d Determination of the biological implications of this harvest guideline by setting the catch for the "true" population represented in the operating model based on it. The step can potentially include "implementation uncertainty" (Rosenberg and Brault, 1993).

The harvest guideline is not updated every year in the simulations described in this article, but rather every third year (co-incident with the results from each new survey) and thus reflects the intended frequency with which assessments for West Coast groundfish species are conducted. Each simulation trial (i.e. each combination of an operating model variant and candidate management procedure) involves 100 simulations of an 80-year management period. The four steps listed above are discussed in detail below.

Note that for the application considered in this paper then, there are three "models": 1) the operating model that represents "reality" for the simulations, 2) an assessment model (a stock synthesis-like approach), and 3) a model to calculate the harvest guidelines. The data available to the last two models are generated from the first model.

The operating model

The operating model has been taken to be virtually identical to that on which the population assessments and rebuilding analysis calculations are based (Appendix 1), with two exceptions: 1) the approach used to generate recruitment and 2) the allowance for variability over time in commercial selectivity. Commercial selectivity is given

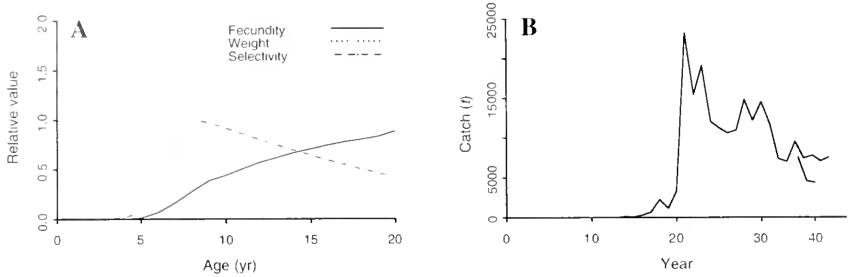

Figure 1

Biological parameters (**A**) and catch history (**B**) for widow rockfish (*Sebastes entomelas*).

by the following double-logistic equation:

$$S_{y,a} = S'_{y,a} / \max_{a'} S'_{y,a'}$$
$$S'_{y,a} = \frac{1}{1+e^{-\delta_1(a-a^1_{50}+\gamma_y)}} \frac{1}{1+e^{-\delta(a^2_{50}-a)}}, \quad (1)$$

where $S_{y,a}$ = the selectivity on fish of age a during year y;

$a^1_{50}, a^2_{50}, \delta_1, \delta_2$ = the parameters of the double-logistic equation;

γ_y = the deviation from the average selectivity pattern in year y:

$$\gamma_y = \rho_S \gamma_{y-1} + \varepsilon^S_y \qquad \varepsilon^S_y \sim N(0;\sigma^2_S),$$

ρ_S = the interannual correlation in the deviation from average selectivity; and

σ_S = a measure of the standard deviation of the interannual deviations from average selectivity.

Recruitment is assumed to be governed by a Beverton-Holt stock-recruitment relationship:

$$R_y = \frac{R_0 4h(\tilde{B}_y / B_0)}{4h+(5h-1)(\tilde{B}_y / B_0 - 1)} e^{\varepsilon^R_y - \sigma^2_R/2} \qquad \varepsilon^R_y \sim N(0;\sigma^2_R), \quad (2)$$

where R_0 = the "virgin recruitment" (the number of zero-year-olds at the pre-exploitation equilibrium level);

$\tilde{B}_y$ = the spawning output at the start of year y;

h = the "steepness" of the stock-recruitment relationship (the fraction of virgin recruitment expected at $0.2B_0$); and

σ_R = the standard deviation of the logarithms of the random fluctuations in recruitment about its expected value.

The biological parameters of the operating model are set to those for widow rockfish (Fig. 1A), and the catches for the 40 years prior to the year in which the management procedure is first applied (referred to as "projection year 1") are set to the actual catches for widow rockfish (Fig. 1B). The baseline values for the parameters h, σ_R, ρ_S, and σ_S (Table 1) are educated guesses. The baseline choice for steepness, h, is lower than the posterior mean for this quantity (0.65) obtained by Dorn (2002) because, increasingly, West Coast rockfish are being found to be less productive than initially anticipated (e.g. Ianelli, 2002). The value assumed for the extent of variation in recruitment, σ_R, although based on the collection of estimates of this parameter by Beddington and Cooke (1983), is nevertheless also largely an educated guess. Sensitivity to the values for both h and σ_R is explored.

Table 1

The baseline parameters of the operating model and the values used in the tests of sensitivity. N/A = not available.

Parameter	Baseline value	Sensitivity values
ρ_S	0.707	N/A
σ_S	0.4	N/A
h	0.4	0.25; 0.7
σ_R	0.6	0.4; 1
M	0.15/yr	N/A
Spawning output in year 41	$0.2B_0$	$0.1B_0$; $0.4B_0$

The biomass at the start of year 1 is assumed equal to B_0, which is defined as the mean of the distribution for the unfished biomass which would arise given variability in recruitment about its expected value. However, this specification has little impact on the results. For example, the alternative that is defined to be the median of the distribution for the unfished biomass would only change B_0 by about 5%.

The value for B_0 for each simulation is selected so that the spawning output at start of year 41 (projection year 1) equals a prespecified fraction of B_0 (baseline fraction

Table 2

The parameters on which the generation of future data is based. n^e is the sample size for the multinomial distribution.

Data source	First year collected	Frequency	Precision
Catch rates	14	Every year	$\sigma^c = 0.4$
Fishery age-composition	21	Every year	n^e=200
Survey indices	13	Every third year	σ^s=0.5
Survey age-composition	13	Every third year	n^e=200

0.2—i.e. just below the level that defines an overfished stock). Sensitivity to alternative values for the ratio of the spawning output at the start of year 41 to B_0 is explored (Table 1).

Generating future data

The data available for assessment purposes are survey indices of relative abundance, age-composition data from surveys, catch-rate–based indices of relative abundance, and age-composition data from the commercial catches. Table 2 lists the baseline specifications regarding the frequency at which the various data sources are collected and the parameters that determine the sampling variability associated with each data source.

The survey and catch-rate indices are generated by using the equations

$$B_y^{s,obs} = B_y^s e^{\varepsilon_y^s - (\sigma^s)^2/2}, \qquad \varepsilon_y^S \sim N\left(0;(\sigma^s)^2\right); \quad (3a)$$

$$I_y = B_y^e e^{\varepsilon_y^c - (\sigma^c)^2/2}, \qquad \varepsilon_y^c \sim N\left(0;(\sigma^c)^2\right); \quad (3b)$$

where $B_y^{s,obs}$ = the survey index for year y;

B_y^s = the survey selected-biomass during year y:

$$B_y^s = \sum_{a=0}^{a_{max}} w_a S_a^s N_{y,a} e^{-Z_{y,a}/2}; \quad (4a)$$

w_a = the mass of an animal of age a;

S_a^s = the selectivity of the survey gear on animals of age a (assumed to be governed by a logistic function and to be independent of time);

$N_{y,a}$ = the number of animals of age a at the start of year y;

$Z_{y,a}$ = the total mortality on animals of age a during year y;

σ_s = the standard deviation of the random fluctuations in survey catchability;

a_{max} = the oldest age considered in the operating model;

I_y = the catch-rate index for year y;

B_y^e = is the exploitable biomass during year y;

$$B_y^e = \sum_{a=0}^{a_{max}} w_a \frac{S_{y,a}F_y}{Z_{y,a}} N_{y,a}(1 - e^{-Z_{y,a}}); \quad (4b)$$

F_y = the fully selected fishing mortality during year y; and

σ^c = the standard deviation of the random fluctuations in fishery catchability.

Note that Equations 3a and 3b assume that the survey and fishery catchability coefficients are unity. This assumption can be made without loss of generality because the stock assessment method is not provided with this information and instead estimates these catchability coefficients. Note also that the key difference between the survey index and the catch-rate index is that selectivity for the latter changes over time (see Eq. 1), whereas selectivity for the former is time-invariant.

The age-composition data are generated by selecting a sample multinomially from the age-composition of the survey catch and of the fishery catch (see Eqs. 5a and 5b for the relative survey and fishery catches-at-age):

$$S_a^s n_{y,a} e^{-Z_{y,a}/2}; \quad (5a)$$

$$\frac{S_{y,a}}{Z_{y,a}} n_{y,a}(1 - e^{-Z_{y,a}}). \quad (5b)$$

The PFMC management procedure

The "PFMC management procedure" (see Fig. 2 for an overview) involves first conducting a stock assessment by fitting an age-structured population dynamics model to the available data by maximizing a likelihood function. This approach mimics the common use of the stock synthesis framework (Methot, 2000) when conducting assessments of West Coast groundfish resources. The likelihood function is determined by assuming that the age-composition data are multinomially distributed (in the simulations with effective sample sizes given by the actual effective sample sizes) and by assuming that the survey and catch-rate series are log-normally distributed about the appropriate model quantities. The estimable parameters of the model are the annual recruitments, the annual fishing mortalities, the catchability coefficients, and the parameters that determine selectivity (the survey and fishery selectivity are [correctly] assumed to be governed by logistic and double-logistic equations). The values for the remaining parameters (weight-at-age, fecundity-at-age, and natural mortality) are assumed to be known without error. The key outputs from the assessment are time-series of recruitments and spawning out-

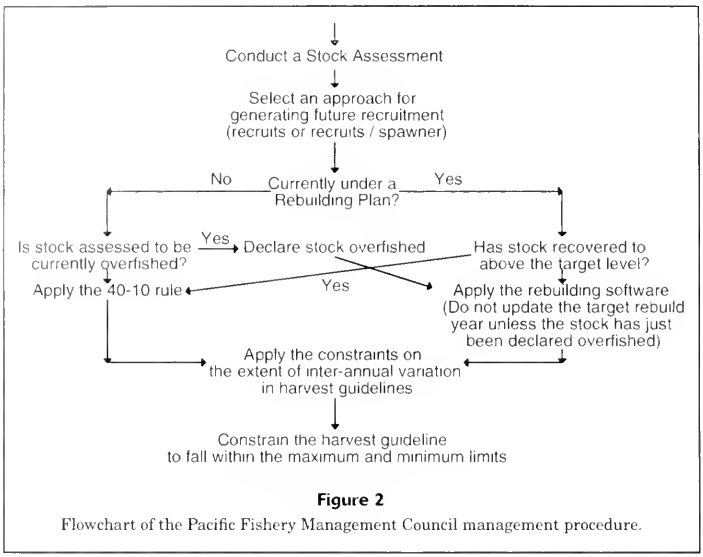

Figure 2

Flowchart of the Pacific Fishery Management Council management procedure.

puts, and the age structure at the start of the last year of the assessment.

An estimate of the pre-exploitation equilibrium spawning output (i.e. $\hat{B}_0$) is obtained by multiplying the average recruitment for the first ten years of the assessment period by the spawning output-per-recruit in the absence of fishing. This approach to estimating $\hat{B}_0$ has been used for several rebuilding analyses for West Coast groundfish species. If the estimate of the current spawning output exceeds $0.4\hat{B}_0$ or if it exceeds $0.25\ \hat{B}_0$ and the resource is not currently under rebuilding (i.e. has not yet been declared to be in an overfished state), a raw harvest guideline is computed using the 40-10 rule. On the other hand, if the estimate of the current spawning output is less than $0.25\ \hat{B}_0$ or the stock is currently under a rebuilding plan and the spawning output has not yet recovered to $0.4\ \hat{B}_0$, the raw harvest guideline is based on the application of the rebuilding analysis (see Appendix 1 for further details).

It is necessary to know the maximum possible rebuilding period, T_{max}, when using a rebuilding analysis to calculate a harvest guideline. If the stock is declared overfished in the present year, T_{max} is computed as described in Appendix 1. On the other hand, if the stock is currently under a rebuilding plan, T_{max} is taken to be the value computed when the stock was first declared overfished. Therefore, the implementations of the rebuilding plans considered in this paper are based on the assumption that the T_{max} and the probability of recovery by T_{max} are set when the first rebuilding analysis is conducted and not changed thereafter. The probability of recovery by T_{max} is taken to be 0.6 in this paper because this is the probability on which management of widow rockfish is currently based. This probability ranges between 0.55 and 0.92 among the seven overfished groundfish resources for which it has been selected by the PFMC.

Calculation of a harvest guideline using the 40-10 rule and application of the rebuilding analysis requires the ability to generate future recruitment. For the purposes of the present study (and consistent with current practice), future recruitment is either generated from the estimates of recruitment from the assessment or by multiplying the spawning output by a generated value for the recruits-per-spawning output ratio. The pool of recruitment to recruits-per-spawning output is taken to be those for the last 23 years of the assessment period less those for the last three years. The last three years are excluded because of their known poor precision. The approach used to generate recruitment therefore leads to the set of recruitments used to conduct projections changing with time. Allowing the set of recruitments to change with time is needed to avoid an inconsistency between the recruitments used for projections and the recruitments on which the estimate of B_0 is based.

Allowance is made for the raw harvest guideline to be constrained so as not to change by more than a prespecified percentage from that for the previous year and not to fall outside of specified limits, although this option is not part of the baseline simulations.

One aspect of the actual management process that is ignored in the simulation of the PFMC management procedure is the time-lag between the collection of data and their use in assessments (for example, catch-at-age information from surveys conducted in one year would usually not be available for use in the assessments conducted in the following year) and that between assessments

Table 3

The performance statistics used in the present study. For consistency with the definition of recovery used by the Pacific Fishery Management Council, "recovery by year x" is defined as the spawning output being larger than $0.4B_0$ at or before year x. Some of the statistics are based on the "actual" (i.e. operating model) spawning output and others are based on the "assessed" (i.e. assessment model) spawning output.

Abbreviation	Description
F_{rec}	The fraction of the simulations in which the stock is assessed to be overfished at the start of the first projection year that actually recover by the maximum possible recovery year determined from the rebuilding analysis conducted in projection year 1.
Y_{rec}	The median year in which the actual spawning output first reaches $0.4B_0$.
P_{decl}	The proportion of simulations in which the spawning output is assessed to be below $0.25B_0$ (i.e. overfished) at the start of projection year 1
$5\%D/50\%D$	The lower 5th and median of the distribution of the actual spawning output in projection years 20 and 60 expressed in relation to the actual pre-exploitation spawning output, B_0.
AAV	Average annual absolute change in catch evaluated after 20 and 60 years, i.e. $AAV = \sum_{y}\lvert C_y - C_{y-1}\rvert / \sum_{y} C_y$, where C_y is the catch during year y.
$\overline{C}$	Average annual catch over projection years 1–20 and 1–60.
P_{rec}	The fraction of simulations in which actual spawning output reached $0.4B_0$ sometime between projections years 1 and 20 and between projection years 1 and 60 (but may have dropped below $0.4B_0$ again).

being conducted and their being used for management purposes.

The performance statistics

A variety of performance statistics are considered (Table 3). These consider both the performance of the management procedure in terms of the behavior of the rules used for management (statistics F_{rec}, Y_{rec}, and P_{decl}) and of satisfying the goals established by the SFA in relation to the status of the population and the fishery (statistics $5\%D$, $50\%D$, $\overline{C}$, AAV, and P_{rec}). The choice of years 20 and 60 in the definitions of the latter five statistics is meant to capture "short"-term and medium-term considerations. For instance, recovery should have occurred by year 60 in most cases and the population should be well above $0.25B_0$ after 20 years. The catch and catch variability statistics for the first 20 years provide an indication of the likely impacts of recovery on the industry.

The need to examine aspects of the behavior of the management rules can be understood from Figure 3, which shows results for four simulations for the combination of a PFMC management procedure and an operating model variant. The solid lines are the "true" time-trajectories of spawning output (expressed in relation to the pre-exploitation level) and the dotted lines reflect the estimates of this ratio each time an assessment is conducted (every third year for the analyses shown in Fig. 3). The up arrows indicate when the assessment first indicates that the population is overfished (based on the model estimates of spawning output)—note that a population may be identified to be overfished more than once during a given simulation. The down arrows indicate the years in which recovery is predicted by the rebuilding analysis software (with the estimates from the assessment) to occur with 60% probability. The solid bar parallel to the x-axis indicates the years in which management is based on the rebuilding plan (rather than the 40-10 rule). The bar will stretch from the up arrow to the down arrow unless the population is assessed to have recovered to $0.4B_0$ (when management reverts to being based on the 40-10 rule).

There are several possible impacts of the difference between the perceived and true state of the system. For example, the population can erroneously be assessed not to be overfished in the first projection year (e.g. simulation 1 in Fig. 3). The statistic P_{decl} is designed to capture the frequency of this possibility. Even if the population is assessed to be overfished, there is no guarantee that it will recover with the expected probability and in the "correct" year. For example, for simulation 1, the stock assessment indicates that recovery occurs in year 71 (the solid bar consequently stops in year 71) even though the true population size is less than 30% of B_0 at that time. The statistic F_{rec} attempts to capture whether the rebuilding analysis performs as expected given that the population is assessed to be overfished at the start of the first projection year.

There are other aspects to evaluating the behavior of the management rules in relation to the perceived and true state of the system (e.g. the difference between the true and estimated biomasses and recruitments). Although it is straightforward to evaluate these aspects (e.g. Patterson and Kirkwood, 1995; Punt et al., 2002), they are not considered in detail in this paper to reduce the volume of results presented.

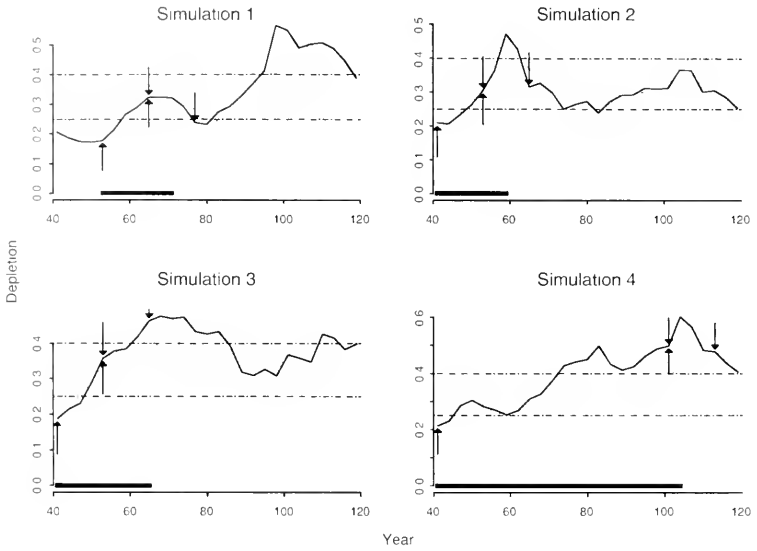

Figure 3

Time-trajectories of the "true" and the assessment model-estimated ratio of the spawning output to B_0 (depletion) for four simulations. The up arrows indicate the years in which the stock was declared to be in need of rebuilding and the down arrows show the values of T_{max}. The horizontal bars indicate the years during which the stock is under a rebuilding plan. Year 41 is the first "projection year," i.e. the first year in which the management procedure is used to determine the catches (the catches for the years prior to year 41 are set equal to the historical catches—see Fig. 1A)

Results and discussion

Detailed results for a single operating model variant and management procedure

Figures 4 and 5 and Table 4 summarize aspects of a simulation trial in which the operating model has its baseline parameterization (Tables 1 and 2) and in which the management procedure used to set harvest guidelines is the PFMC management procedure with no constraints on interannual variation in harvest guidelines other than an upper limit of 10,000 t. The lack of any constraints on changes in harvest guidelines has been imposed because the PFMC has not adopted any such constraints. The harvest guideline is updated every third year.

Figure 4 shows the time-trajectories of catch, spawning output in relation to the pre-exploitation equilibrium level ("true" and estimated), and the perceived fishing mortality on which the harvest guideline is based for three of the 100 simulations that constitute a simulation trial. The horizontal bars on the x–axis again reflect the year during which the stock is managed by using the results from the rebuilding analysis rather than the 40-10 rule. The most notable feature of Figure 4 is the high variability in annual catches. This variability arises for several reasons: 1) the additional information on population biomass obtained each time a survey occurs changes the perceived status of the resource and hence how far the spawning output is from the target level of $0.4B_0$; 2) an extension of the assessment period changes the set of recruitments on which generation of future recruitment is based; and 3) a change from being under a rebuilding plan to being managed by means of the 40-10 rule can lead to marked changes in catch. The latter is evident by the change in fishing mortality and catch when the spawning output is estimated to reach $0.4B_0$ (i.e. the end of the horizontal bar). A marked impact due to the addition of data for a single 3-year period may appear surprising. However, effects of this nature have already been observed for West Coast species (see, for example, the 2002 update to the sablefish [*Anoplopoma fimbria*] stock assessment [Schirripa and Methot[6]]).

[6] Schirripa, M. J., and R. Methot. 2002. Status of the sablefish resource off the continental U.S. Pacific Coast in 2001. *In* Stock assessment and fishery evaluation: appendix to the status of the Pacific Coast groundfish fishery through 2001 and acceptable biological catches for 2002, x + 122 p. Pacific Fishery Management Council, 7700 NE Ambassador Place, Portland, OR 97220.

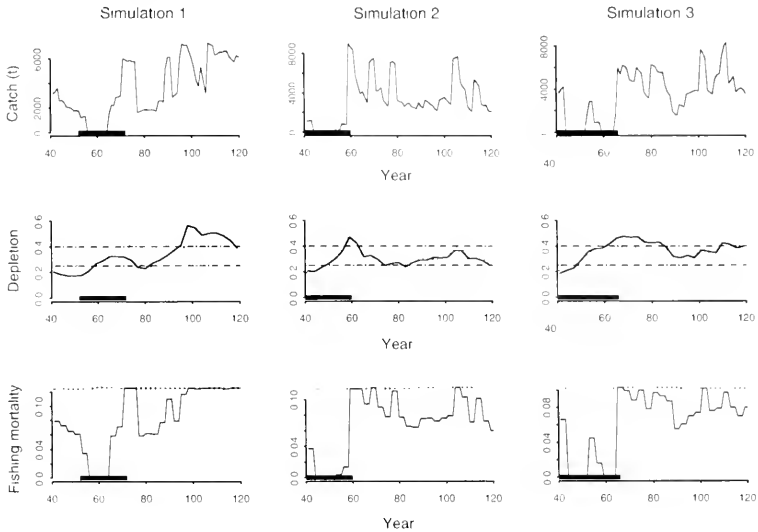

Figure 4

Time-trajectories of catch (**upper panels**), spawning output in relation to the pre-exploitation level (solid line is "true"; dotted line is estimated) (**center panels**), and perceived fishing mortality (used to set the harvest guideline [solid line]; dotted line=F_{MSY} proxy) (**lower panels**) for three individual simulations. The results in this figure pertain to the baseline operating model and baseline Pacific Fishery Management Council management procedure.

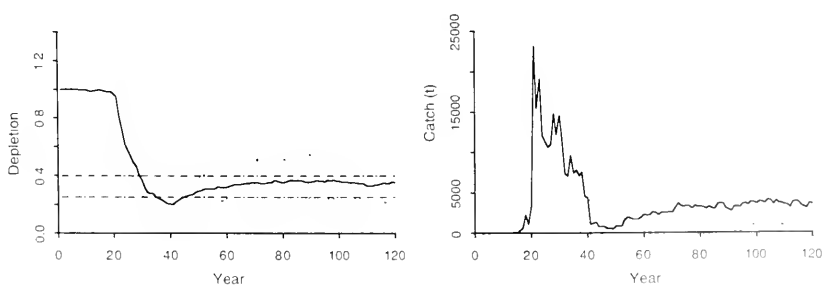

Figure 5

Piecewise medians (solid lines) and 90% intervals (dotted lines) for spawning output in relation to the pre-exploitation equilibrium level (left panel) and catch (right panel). The results in this figure pertain to the baseline operating model and baseline Pacific Fishery Management Council management procedure.

The extent of variability in catch in Figure 4 differs markedly from the way advice on expected catches during the rebuilding period is presented to the decision makers (e.g. Fig. 6). One way to improve the presentation of information on expected catches would be to include some individual catch trajectories from those on which the rebuilding analysis is based. However, even these would severely underestimate the actual extent of uncertainty

Table 4

Performance statistics (see Table 3 for definitions) for six alternative management procedure variants. All of the calculations in this table relate to the baseline operating model. PFMC = Pacific Fishery Management Council. N/A = not applicable.

				Results after 20 years					Results after 60 years				
Management procedure	F_{rec}	Y_{rec}	P_{decl}	5%D	50%D	AAV	$\overline{C}$	P_{rec}	5%D	50%D	AAV	$\overline{C}$	P_{rec}
Baseline	0.22	72	0.82	0.22	0.33	0.33	1759	0.32	0.23	0.36	0.25	2847	0.80
With constraints	0.27	61	0.82	0.24	0.40	0.38	591	0.54	0.24	0.41	0.17	2440	0.89
No 10 years and estimated F_{MSY}	0.42	68	0.82	0.24	0.34	0.30	1652	0.27	0.25	0.41	0.24	2649	0.84
Preferred	0.59	62	0.82	0.25	0.39	0.31	950	0.49	0.28	0.54	0.21	1961	0.96
PFMC (baseline)	N/A	95	N/A	0.19	0.29	0.23	2273	0.07	0.24	0.33	0.20	2851	0.55
PFMC (preferred)	N/A	64	N/A	0.23	0.36	0.30	1239	0.45	0.30	0.48	0.20	2265	0.93

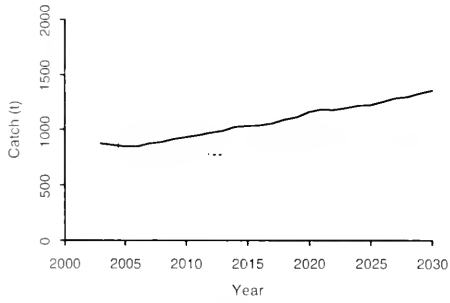

Figure 6

Time-trajectories of catch (median and 95% intervals) for the annual catch for widow rockfish based on a rebuilding analysis conducted in 2002.

because they are conditioned on knowing the age-structure of the population at the start of the projection period and are based on fixed levels of fishing mortality during the rebuilding period.

The impact of estimation uncertainty is also evident in Figure 4. The following are three examples of this: 1) management based on the rebuilding plan only starts in year 53 in simulation 1 because, prior to this year, the stock assessment indicates (erroneously) that the stock is above rather than below $0.25B_0$; 2) the resource is predicted to have recovered to $0.4B_0$ in year 71 in simulation 1 (and hence management is based on the 40-10 rule thereafter)—however, the spawning output is really only slightly larger than $0.3B_0$ at this time; and 3) in simulation 3 the assessment model indicates that the spawning output has recovered to above $0.4B_0$ in year 65 when, in fact, it recovered to $0.4B_0$ three years earlier.

The results of all 100 simulations are summarized by the time-trajectories in Figure 5. The trajectories of catch in Figure 5 are notably less variable that the individual trajectories in Figure 4 because, for instance, the 5th, median, and 95th intervals for the catch in year 80 are obtained by sorting all 100 year-80 catches and taking the appropriate percentiles. Unlike the individual trajectories, the median trajectories of catch and spawning output show quite smooth changes over time. This result highlights the importance of the AAV statistic that captures interannual variation in catches within individual simulations.

Overall, there is a high probability (0.82) that the assessment model identifies that the spawning output is less than $0.25B_0$ at the start of the projection period (Table 4). However, the probability that recovery occurs at or before the T_{max} year predicted from the rebuilding analysis conducted in projection year 1 is rather low (0.22) and 50% of simulations exceed $0.4B_0$ only in year 72 (i.e. after 30 years). The probability of being below the overfished level of $0.25B_0$ still exceeds 5% after 60 years of management with this management procedure although there is an 80% probability that the spawning output recovers to $0.4B_0$ sometime during the first 60 years of management with the management procedure.

It should be noted that the impact of recruitment variability and assessment errors following recovery to $0.4B_0$ can be consequential. For example, the probability of having reached $0.4B_0$ after 60 years of management by using the management procedure exceeds 0.8 but the median value of the ratio of the spawning output in year 60 to B_0 is nevertheless still less than 0.4 (Table 4, Fig. 5). One reason for the spawning output not stabilizing at $0.4\,B_0$ is a discrepancy between the fishing mortality rate that stabilizes the population at B_0 (deterministically) and $F_{50\%}$. For the baseline steepness of 0.4, the fishing mortality required to stabilize the spawning output at $0.4\,B_0$ actually corresponds to a lower fishing mortality than $F_{50\%}$ (closer to $F_{63\%}$).

Sensitivity to alternative management procedures

Table 4 includes results for a range of variants of the baseline management procedure designed to improve its performance. The following are areas where improved performance is desirable: 1) the extent of interannual variability in catches; 2) the similarity between the year

in which the rebuilding analysis indicates recovery will occur and the year at or before which it actually occurs; and 3) the probability of being below the overfished level after 20 and 60 years.

The first variant of the baseline management procedure ("with constraints" in Table 4) involves imposing maximum and minimum catch limits of 30 and 8000 t and constraining changes in harvest guideline not to exceed 25% from one year to the next, except in the first year when reductions of up to 99% are allowed. This variant leads to much lower interannual variation in catches when a 60-year period is considered (17% compared with 25%) but the AAV is actually higher for the first 20 years. This variant also leads to higher probabilities of recovery. However, there is still a large discrepancy between the actual year of recovery to $0.4B_0$ and the year that underlies the management procedure (the value of F_{rec} in Table 4 is only 0.27 for the "with constraints" variant).

The second variant considered ("no 10 year and estimated F_{MSY}" see Table 4) drops the requirement that T_{max} be defined as 10 years if the resource can be recovered in 10 years and instead always sets T_{max} to T_{min} plus one mean generation. It also allows the F_{MSY} proxy used when applying the 40-10 rule to differ from the default value of $F_{50\%}$ by setting it to F_{rep} (Jakobsen, 1993) if F_{rep} is lower than F_{MSY}. Estimating (rather than fixing) F_{MSY} is consistent with the recommendation of Brodziak (2002). The major performance difference between this variant and the baseline management procedure is the increased value of F_{rec}.

The "preferred" variant in Table 4 combines the features of the "with constraints" and "no 10 years and estimated F_{MSY}" variants. Compared with the baseline management procedure, it leads to a markedly increased value for F_{rec} (remarkably close, in fact, to the desired value of 0.6), slightly lower catch variability, a less than 5% chance of being overfished after 20 years, and higher probabilities of being recovered to $0.4B_0$ after 20 and 60 years of management. The major disadvantage of this variant is the lower catches and that it leaves the spawning output well above 40% of B_0 after 60 years (see row "preferred" in Table 4).

Prior to the adoption of Amendment 11 of its Groundfish Management Plan, the PFMC set harvest guidelines using only the 40-10 rule.[7] Table 4 therefore also lists results for management procedures based on the 40-10 rule. When the 40-10 rule is applied without any constraints ("PFMC (baseline)" in Table 4), the probability of recovery and the values for the "50%D" statistic are lower (particularly the former) than for the "preferred" variant. In contrast, application of the 40-10 rule with constraints ("PFMC (preferred)" in Table 4) leads, arguably, to no more than a slight difference in catch (the 40-10 rule achieves higher catches) and probability of recovery (the "preferred" variant achieves a higher probability of recovery). The remaining analyses of this paper focus on the "preferred" variant. Future consideration of management procedures for West Coast groundfish resources should consider a management procedure that is based simply on the 40-10 rule and has no associated rebuilding analysis component, at least for comparative purposes. At present, however, such a management procedure would be inconsistent with the SFA because it would not specify the time to recover to the proxy for B_{MSY} (even if the results of this paper suggest that there is considerable uncertainty associated with the estimation of this particular quantity).

[7] Albeit with different target fishing mortality levels.

Sensitivity to alternative operating model specifications

The values assumed for h and σ_R in the baseline operating model are somewhat arbitrary. Table 5 therefore examines the sensitivity of the results for the "preferred" management procedure to varying the values assumed for these parameters, as well as that of the size of spawning output at the start of the first projection year to B_0.

The results are, as expected, sensitive to all three of the factors considered. Increasing σ_R from 0.4 through 0.6 to 1 leads to lower and more variable catches, a slightly higher probability of recovery in the first 20 years and a markedly higher value of 50%D after 60 years (0.74 for σ_R=1 compared to 0.46 for σ_R=0.4). The ability to detect an overfished stock declines slightly as the extent of variation in recruitment increases. The management procedure behaves as expected as steepness is increased from 0.25 through 0.4 to 0.7; the probability of recovery is markedly higher for high values of steepness even though the management procedure does identify cases with low steepness, and accordingly sets very low harvest guidelines in such cases. However, it is perhaps noteworthy that the probability of correctly identifying that the resource is overfished is lowest for the least productive scenario. The catches for the scenario in which the spawning output is 10% of B_0 at the start of the first projection year are much lower than for the baseline scenario, particularly over the first 20 years. However, these lower catches are necessary to achieve recovery (the median value of the statistic 50%D after 60 years is 0.52 and there is a 0.93 probability of the spawning output having recovered to $0.4B_0$ after 60 years for this scenario).

The behavior of the management procedure can be evaluated in terms of whether it eventually allows the stock to recover to $0.4B_0$ and whether it keeps the stock away from the overfished level of $0.25B_0$. The "preferred" management procedure can be argued to satisfy this criterion, except possibly for the scenario with the lowest steepness but, even in this case, the probability of recovery is 0.6 after 60 years.

The value for the F_{rec} statistic varies markedly depending on steepness and the ratio of the spawning output at the start of the first projection year to B_0. Although the "preferred" management procedure performs well for the baseline scenario in terms of recovering the resource by the predicted value for T_{max}, this good performance is clearly a fortunate anomaly. However, it does help to highlight that predictions of the year-to-recovery from rebuilding analyses should be interpreted with considerable caution.

Sensitivity to data quality

The data-related specifications for the baseline trial (Table 2) could be considered to be data-rich. It is therefore

Table 5

Performance statistics (see Table 3 for definitions) for 10 variants of the baseline operating model. All of the calculations in this table relate to the preferred management procedure. N/A = not applicable.

				Results after 20 years					Results after 60 years				
Operating model scenario	F_{rec}	Y_{rec}	P_{decl}	5%D	50%D	AAV	$\bar{C}$	P_{rec}	5%D	50%D	AAV	$\bar{C}$	P_{rec}
Baseline	0.59	62	0.82	0.25	0.39	0.31	950	0.49	0.28	0.54	0.21	1961	0.96
Structural changes													
σ_R=0.4	0.59	63	0.86	0.24	0.38	0.26	1242	0.44	0.25	0.46	0.18	2379	0.87
σ_R=1	0.59	61	0.72	0.23	0.41	0.43	417	0.54	0.32	0.74	0.32	592	0.96
h=0.25	0.15	94	0.76	0.20	0.28	0.76	86	0.02	0.23	0.38	0.50	126	0.60
h=0.7	0.84	53	0.87	0.31	0.46	0.16	3427	0.93	0.40	0.61	0.14	3951	1.00
Initial spawning out = 0.1 B_0	0.42	72	1.00	0.19	0.29	0.43	417	0.05	0.27	0.52	0.23	1375	0.93
Initial spawning out = 0.4 B_0	N/A	N/A	N/A	0.31	0.50	0.21	2881	0.92	0.30	0.66	0.19	2849	0.97
Data-related changes													
Deterministic data	0.68	61	0.84	0.29	0.38	0.30	957	0.51	0.31	0.55	0.20	2050	0.98
n^e=50	0.68	60	0.82	0.26	0.39	0.32	785	0.56	0.29	0.55	0.22	1938	0.97
σ^e=1	0.56	62	0.79	0.20	0.39	0.31	987	0.48	0.31	0.57	0.22	1962	0.97
5-yr update frequency	0.55	62	0.80	0.21	0.38	0.27	1160	0.49	0.27	0.53	0.19	1980	0.95

important to assess the sensitivity of the results to the quality of the data. The row "deterministic data" in Table 5 provides results for a trial in which the survey biomass index, the catch-rate index, and the age-composition data are known without error. The results from this trial provide an upper bound on the impact of improved data quality on the assessment results.[8] Somewhat surprisingly, the results for this trial are not notably better than for the baseline trial—the most notable difference between the baseline trial and the "deterministic data" trial being the higher values for the "5%D" statistics for the latter trial. The lack of major improvement in performance arises because, even with perfect information on spawning output and recruitment, it is still not possible to estimate B_0 exactly by multiplying average recruitment for the first 10 years of the assessment period by spawning output-per-recruit in the absence of fishing (hence the value of 0.84 for P_{decl}). Furthermore, the rebuilding analyses are still based on generating future recruitment by using spawning output and recruitment data for only 20 years, which is clearly a major source of variability in the predictions from the rebuilding analysis.

Decreasing the catch-at-age sample size from 200 to 50 has relatively little impact on the values for the performance statistics (the AAV statistic is marginally higher and the average catch, particularly for the 20-year projection horizon, is lower). Decreasing the precision of the catch-rate data has a rather larger impact. This is most evident in the value for the "5%D" statistic which is 0.2 rather than 0.25, as is the case for the baseline trial. The "5-yr update frequency" scenario in Table 5 examines the implications conducting assessments every fifth rather than every third year. The results are not markedly sensitive to the interassessment period although the lower values for the "5%D" statistics are perhaps noteworthy.

[8] The assessment still ignores interannual changes in selectivity; therefore the assessment results will not be exactly the same as the true values

General remarks

The framework developed in this paper provides an objective basis for contrasting different management procedures and evaluating their sensitivity to uncertainty. Given such a framework, it becomes possible to compare variants of one class of management procedure (e.g. Table 4) and to compare variants among different classes of management procedure.

The management procedure options presented in this paper are but a small subset of those possible. In particular, it should be possible to improve performance by modifying the approach used to generate future recruitment when conducting rebuilding analyses to make use of some form of stock-recruitment relationship. One reason for expected improved performance is that it may then be feasible to estimate the fishing mortality rate corresponding to $0.4B_0$ rather than having to set it to the default value of $F_{50\%}$ or basing it on F_{rep}. Other possible management procedure options include 1) not increasing the rebuilding fishing mortality rate selected when the rebuilding analysis was first conducted if a stock is recovering faster than initially anticipated; 2) not decreasing the rebuilding fishing mortality rate as long of the probability of recovery by T_{max} is at least 0.5; and 3) smoothing the discontinuity that arises when a stock changes status from being under a rebuilding plan to being managed with the 40-10 rule when the

stock has recovered to $0.4B_0$. In terms of the last option, one of the issues considered an early rebuilding analysis for widow rockfish involved fishing mortality increasing to its target level as the stock approaches $0.4B_0$ (MacCall[9]).

The values for the F_{rec} statistic highlight that the predictions of the time to recovery (even in a probabilistic sense) from rebuilding analyses are highly uncertain. The uncertainty of this estimate of the time to recovery is due to the uncertainty about current stock size and that associated with making long-term predictions based on a short time-series of spawning output and recruitment data.

Although the performance of the management procedures is less than ideal, the results are almost certainly optimistic because the operating model is extremely simple and considers no major structural uncertainties (except for variability in selectivity over time). In contrast, Punt et al. (2002) found that including spatial structure in an operating model and assessing the stock by using a spatially aggregated assessment approach led to assessments that were markedly in error. However, the simulations conducted by Punt et al. (2002) were developed for a far more data-poor situation than that for West Coast groundfish, although there is also clearly spatial structure in the West Coast groundfish fishery. Another source of uncertainty not considered in this paper but that may be of critical importance to the management of West Coast groundfish species is the impact of environmental regime shifts, which have been argued to impact long-term trends in recruitment (e.g. Francis et al., 1998).

An important aspect of this study is the ability to focus on the relationship between the overall performance of a management procedure and the performance of its constituent parts. For example, the results for the "deterministic data" scenario in Table 4 show that given the approach used to conduct the future projections, even perfect information from surveys and very large age-composition samples are unlikely to lead to marked improvements over the current situation if that situation is adequately modeled by the baseline operating model. Identification of the key sources of uncertainty could be used to focus future management-related research activities.

The computational requirements of the calculations outlined above are substantial. In particular, the need to apply a fairly complicated method of stock assessment once every three years means that rapid evaluation of management procedures is (currently) computationally not feasible. It is possible, in principle, to simplify the management procedure considerably by assuming that the results from a stock assessment can be mimicked by generating a biomass estimate based on the "true" biomass but with some random error (e.g. Hilborn et al., 2002). However, although such an approach may be satisfactory for some management procedures (e.g. those that set the harvest guideline equal to some fraction of the current biomass), this is not the case for PFMC-type management procedures that depend on the (assessed) age-structure of the population.

[9] MacCall, A. D. 2002. Personal commun. NMFS Santa Cruz Laboratory, 110 Shaffer Rd, Santa Cruz, CA 95060.

It needs to be recognized that any simulation study is by design case-specific. However, the conclusions of this study may be relevant to a fairly broad set of West Coast rockfish species owing to their similar biology and exploitation history—the two factors most likely to impact the relative performance of different management procedures.

Acknowledgments

Discussions with Alec MacCall, John DeVore, and Richard Methot are gratefully acknowledged as are the comments on an earlier version of this paper by Pamela Mace and two anonymous reviewers. This work was funded through NMFS grant NA07FE0473.

Literature cited

Barnes, W. R.
1999. Viewpoint: an industry view of the application of operational management procedures to setting total allowable catches for the South African pelagic fishery. ICES. J. Mar. Sci. 56:1067–1069.

Beddington, J. R., and J. G. Cooke.
1983. The potential yield of fish stocks. FAO Fish. Tech. Pap. 242:1–47.

Brodiak, J.
2002. In search of optimal harvest rates of west coast groundfish. N. Am. Fish. Manage. 22:258–271

Butterworth, D. S., and M. O. Bergh.
1993. The development of a management procedure for the South African anchovy resource. *In* Risk evaluation and biological reference points for fisheries management (S. J. Smith, J. J. Hunt, and D. Rivard, eds.), p. 83–89. Can. Spec. Publ. J. Fish. Aquat. Sci. 120.

Cochrane, K. L., D. S. Butterworth, J. A. A. De Oliveira, and B. A. Roel.
1998. Management procedures in a fishery based on highly variable stocks and with conflicting objectives: experiences in the South African pelagic fishery. Rev. Fish. Biol. Fish. 8:177–214.

Dorn, M. W.
2002. Advice on west coast rockfish harvest rates from Bayesian meta-analysis of stock-recruit relationships. N Am. Fish. Manage. 22:280–300.

Francis, R. I. C. C.
1992. Use of risk analysis to assess fishery management strategies: a case study using orange roughy (*Hoplostethus atlanticus*) on the Chatham Rise, New Zealand. Can. J. Fish. Aquat. Sci. 49:922–930.

Francis, R. S., A. Hare, A. Hollowed, and W. Wooster.
1998. Effects of interdecadal variability on the oceanic ecosystems of the NE Pacific. Fish. Oceanogr. 7:1–21.

Geromont, H. F., J. A. A. De Oliveira, S. J. Johnston, and C. L. Cunningham.
1999. Development and application of management procedures for fisheries in southern Africa. ICES J. Mar. Sci. 56:953–966.

Hilborn, R.
1979. Comparison of fisheries control systems that utilize catch and effort data. J. Fish. Res. Board Can. 36: 1477–1489.

Hilborn, R., A. Parma, and M. Maunder.
2002. Exploitation rate reference points for west coast rockfish: are they robust and are there better alternatives? N. Am. Fish. Manage. 22:365–375.
Ianelli, J. N.
2002. Simulation analyses testing the robustness of productivity determinations from West-Coast Pacific ocean perch stock assessment data. N. Am. Fish. Manage. 22: 301–310.
IWC (International Whaling Commission).
1992. Report of the Fourth Comprehensive Assessment Workshop on Management Procedures. Rep. Int. Whal. Comm. 42:305–321.
2001. Report of the standing working group on the development of an Aboriginal subsistence whaling management procedure. J. Cetacean Res. Manag. 4(suppl.):148–177.
Jakobsen, T.
1993. The behaviour of F_{low}, F_{med} and F_{high} in response to variation in parameters used for their estimation. *In* Risk evaluation and biological reference points for fisheries management (S. J. Smith, J. J. Hunt, and D. Rivard, eds.), p. 119–125. Can. Spec. Publ. J. Fish. Aquat. Sci. 120.
Methot, R. D.
2000. Technical description of the stock synthesis assessment program, 56 p. NOAA Tech. Memo., NMFS-NWFSC-43.
Patterson, K. R., and G. P. Kirkwood.
1995. Comparative performance of ADAPT and Laurec-Shepherd methods for estimating fish population parameters and in stock management. ICES J. Mar. Sci. 52: 183–196.
Punt, A. E., A. D. M. Smith, and G. Cui.
2001. Review of progress in the introduction of management strategy evaluation (MSE) approaches in Australia's South East Fishery. Mar. Freshw. Res. 52:719–726.
2002. Evaluation of management tools for Australia's South East Fishery. 2. How well do commonly-used stock assessment methods perform? Mar. Freshw. Res. 53:631–644.
Restrepo, V. R., and J. E. Powers.
1999. Precautionary control rules in US fisheries management: specification and performance. ICES. J. Mar. Sci. 56:846–852.
Rosenberg, A. A., and S. Brault.
1993. Choosing a management strategy for stock rebuilding when control is uncertain. *In* Risk evaluation and biological reference points for fisheries management (S. J. Smith, J. J. Hunt, and D. Rivard, eds.), 243–249. Can. Spec. Publ. J. Fish. Aquat. Sci. 120.
Sampson, D. B., and Y. Yin.
1998. A Monte Carlo evaluation of the stock synthesis assessment program. *In* Fishery stock assessment models (F. Funk, T. J. Quinn II, J. Heifetz, J. N. Ianelli, J. E. Powers, J. F. Schweigert, P. J. Sullivan, and C. I. Zhang, eds.), p. 315–338. Alaska Sea Grant, Fairbanks, AK.
Starr, P. J., P. A. Breen, R. H. Hilborn, and T. H. Kendrick.
1997. Evaluation of a management decision rule for a New Zealand rock lobster substock. Mar. Freshw. Res. 48: 1093–1101.

Appendix 1 : An overview of the technical aspects of the PFMC's rebuilding analysis

The key steps of the PFMC's rebuilding analysis are 1) to select the maximum allowable rebuilding time (T_{max}), 2) to develop specifications for projecting the population size at the start of the current year-to-year T_{max}, and 3) to calculate the target fishing mortality rate so that the probability of the spawning output rebuilding to $0.4B_0$ at or before T_{max} equals a prespecified value, p_{rec} (taken to be 0.6 for purposes of the present study).

Projecting the population forward and defining B_0

The population projections are based on the equation

$$N_{y,a} = \begin{cases} R_y & \text{if } a = a_{min} \\ N_{y-1,a-1} e^{-(M+S_{a-1}F)} & \text{if } a_{min} < a < a_{max} \\ N_{y-1,a_{max}-1} e^{-(M+S_{a_{max}-1}F)} + N_{y-1,a_{max}} e^{-(M+S_{a_{max}}F)} & \text{if } a = a_{max}, \end{cases} \quad \text{(A.1)}$$

where $N_{y,a}$ = the number of animals of age a at the start of year y;
M = the instantaneous rate of natural mortality (assumed to be independent of age);
S_a = the selectivity for animals of age a;
F = the fully selected (i.e. $S_a \rightarrow 1$) fishing mortality;
R_y = the recruitment (both sexes) during year y;
a_{min} = the lowest age class considered in the model; and
a_{max} = the oldest age class considered in the model (treated as a plus-group).

The age structure of the population at the start of the first year of the projection period is taken to be that from the most recent assessment. A variety of approaches are available to generate future recruitment (PFMC[10]). However, for consistency with the approach used in the bulk of the rebuilding analyses conducted to date, future recruitment is either based on randomly sampling recruitments (with replacement) from a prespecified historical period or based on randomly sampling the ratio of the recruitment to the spawning output that spawned that recruitment (with replacement) and then multiplying by current spawning output. The choice between basing the projections on sampling recruitments or sampling recruits-per-spawning output is determined by regressing each of these on time and selecting whichever has the lesser slope. The reason for doing this is that the lack of a trend in recruits-per-spawning output is indicative of a stock-recruitment relationship with low "steepness" (Francis, 1992), whereas the lack of a trend in recruitment is indicative of a stock-recruitment relationship with high "steepness."

The pre-exploitation equilibrium spawning output used to determine the rebuilding target is computed by multiplying the unfished spawning output-per-recruit by the average recruitment over a prespecified number of historical years. Note that the range of years on which to base the estimate of B_0 will usually differ from that on which generation of future recruitment is based.

[10] PFMC (Pacific Fishery Management Council). 2001. SSC terms of reference for groundfish rebuilding analysis, 9 p. Pacific Fishery Management Council, 7700 NE Ambassador Place, Portland, OR 97220.

It should also be noted that no account is taken of uncertainty regarding the current age structure, natural mortality, selectivity, etc., although the projections do account for uncertainty about future recruitment

Selecting the maximum allowable rebuilding period

The maximum allowable rebuilding time, T_{max}, is defined as the maximum of 10 years and the sum of the mean generation time and the minimum possible rebuilding time. This specification implements the requirement of the SFA to "take into account the status and biology of any overfished stocks of fish, [and] the needs of fishing communities." The minimum possible rebuilding period for a given future projection is computed by projecting the population forward with zero fishing mortality and by identifying the year in which the spawning output first reaches $0.4B_0$. T_{min} is the median of the distribution for this year constructed by conducting projections for many different (random) realizations of future recruitment.

Calculating the target fishing mortality rate

The target fishing mortality rate and hence the harvest guideline are determined by projecting the population forwards many times (100 times for the purposes of this paper), each time with a different sequence of future recruitment and for a variety of alternative Fs and then identifying the level of F that corresponds to the spawning output having reached $0.4B_0$ by T_{max} with the prespecified probability p_{rec}.

Distribution, demography, and discard mortality of crabs caught as bycatch in an experimental pot fishery for toothfish (*Dissostichus eleginoides*) in the South Atlantic

Martin G. Purves
Marine and Coastal Management
P.O. Box X2, Roggebaai 8012
Cape Town, South Africa
Present address: Resources Assessment Group
47 Prince's Gate
London SW7 7QA, United Kingdom
E-mail address: m.purves@imperial.ac.uk

David J. Agnew
Renewable Resources Assessment Group
Imperial College
Royal School of Mines
Prince Consort Road
London, SW7 2BP, United Kingdom

Guillermo Moreno

Tim Daw
MRAG Ltd
47 Princes Gate
London, SW7 2QA, United Kingdom

Cynthia Yau
Zoology Department
University of Aberdeen
Aberdeen, AB24 2TZ, United Kingdom

Graham Pilling
Centre for Environment, Fisheries and Aquaculture Science (CEFAS)
Pakefield Road
Lowestoft, NR33 OHT, United Kingdom

Abstract—Between March 2000 and April 2001 two commercial fishing vessels fished for toothfish (*Dissostichus eleginoides*) off South Georgia using pots. A significant number of lithodid crabs (three species of *Paralomis* spp.) were caught as bycatch. *Paralomis spinosissima* occurred in shallow water, generally shallower than 700 m. *Paralomis anamerae*, not previously reported from this area and therefore representing a considerable southerly extension in the reported geographic range of this species, had an intermediate depth distribution from 400 to 800 m. *Paralomis formosa* was present in shallow waters but reached much higher catch levels (and, presumably, densities) between 800 and 1400 m. Differences were also noted in depth distribution of the sexes and size of crabs. Depth, soak time, and area were found to significantly influence crab catch rates. Few crabs (3% of *P. spinosissima* and 7% of *P. formosa*) were males above the legal size limit and could therefore be retained. All other crabs were discarded. Most crabs (>99% of *P. formosa*, >97% of *P. spinosissima*, and >90% of *P. anamerae*) were lively on arrival on deck and at subsequent discard. Mortality rates estimated from re-immersion experiments indicated that on the vessel where pots were emptied directly onto the factory conveyor belt 78–89% of crabs would survive discarding, whereas on the vessel where crabs were emptied down a vertical chute prior to being sorted, survivorship was 38–58%. Of the three, *P. anamerae* was the most vulnerable to handling onboard and subsequent discarding. *Paralomis spinosissima* seemed more vulnerable than *P. formosa*.

Manuscript approved for publication 17 April 2003 by Scientific Editor.
Manuscript received 26 June 2003 at NMFS Scientific Publications Office.
Fish Bull. 101:874–888 (2003).

The Commission for the Conservation of Antarctic Marine Living Resources (CCAMLR) and its Scientific Committee were pioneers in the development of the "ecosystem approach" for the management of fisheries. Using this approach the Commission is bound to consider the impact of any fishery on both the target, dependent, and related species. Currently, the most important fishery in CCAMLR waters is the longline fishery for Patagonian toothfish (*Dissostichus eleginoides*) and fishing grounds near South Georgia Island and Shag Rocks in CCAMLR subarea 48.3 (South Atlantic sector) are among the most important. Mitigation measures, including requirements for setting at night, in the winter, and with specialized gear, have been introduced to reduce incidental mortality of birds being hooked by longlines. However, these measures impose severe

operational restrictions on the fishery, and low levels of bird mortality still occur (CCAMLR[1]).

Pot fishing for toothfish has recently been tried around South Georgia (Agnew et al., 2001), and although pots do not catch birds, they do take lithodid crabs as bycatch. Crabs are largely a "nuisance" catch when fishing for toothfish, but this bycatch is clearly of concern in relation to crab populations, and must be considered within the CCAMLR's ecosystem approach. A small amount of exploratory crab fishing has already taken place around South Georgia Island and Shag Rocks. Only 798 metric tons (t) of crabs have been taken in directed crab fisheries since 1992; by the FV *Pro Surveyor* (July–August 1992; 299 t; CCAMLR[2]), the FV *American Champion* (September 1995–January 1996; 497 t; CCAMLR[3]), and the FV *Argos Helena* (August 1999; 2 t) (CCAMLR[4]). A pot fishery for toothfish is likely to take place in deep water where current longline fishing concentrates (around the 1000 m contour: Agnew et al., 1999) rather than in shallower waters (<400 m) where crab fishing has taken place (Otto and Macintosh, 1996; Watters, 1997). Toothfish pot fishing may therefore impact different crab population components from those impacted by the crab fishery.

We investigated the likely effects of toothfish pot fishing on crabs caught as bycatch on board two commercial fishing vessels. These vessels conducted three separate trials fishing for toothfish around South Georgia between March 2000 and April 2001. This paper reports on the species of crab taken during these trials, as well as the distribution of crabs and their biological characteristics. In common with many other crab fisheries (Hoggarth, 1991; Schmidt and Pengilly, 1993) retention size limits are set for the fishery around South Georgia. Only males greater than 102 mm carapace width for *Paralomis spinosissima* and 90 mm for *P. formosa* may be retained. All undersize and female crabs from both the toothfish pot fishery and the crab fishery must be discarded. We also report results of experiments on survival of such discards.

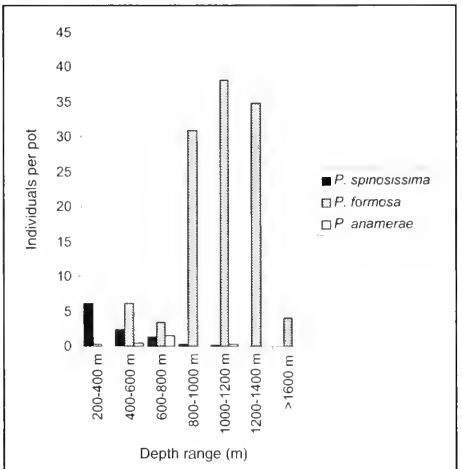

Figure 1

Catch in numbers per pot of the three dominant crab species by depth range as found during fishing operations of the *Argos Georgia* from May to April 2000. Pots were set between 211 m and 1651 m depth.

Methods

During the first cruise (March to May 2000), two observers were deployed on board the FV *Argos Georgia* (cruise G1). Detailed information was collected on the number of toothfish and the numbers and species composition of crabs caught in the pots. Information was also collected on fishing results, such as catch rates, fish bycatch, and the commercial viability of this fishing method (Agnew et al., 2001), and the diet of toothfish (Pilling et al., 2001). In the second and third toothfish pot cruises single observers were deployed on the *Argos Georgia* (cruise G2) and another vessel, the FV *Argos Helena* (cruise H), which fished simultaneously from January to April 2001. Fishing gear and the configuration of gear was similar for all three cruises. The semiconical pots of approximately 80 cm height were constructed of steel frames and covered with 80-mm polysteel (Movline) mesh. A collapsible funnel entrance was situated on the side of the pot, orientated horizontally, and tapering to the pot's interior. A drawstring held the bottom mesh together in the middle. This configuration allowed the pots to be emptied easily when hauled aboard and to be stacked on top of each other when not in use. A panel was sewn into the pots by using biodegradable sisal twine to ensure that crabs could eventually escape from lost pots and to prevent "ghost fishing." However, catch handling methods were different on the two vessels; the pots were emptied directly onto the factory conveyor belt on the *Argos Georgia* and emptied down a chute to the factory level on the *Argos Helena*.

During the first cruise (March to May 2000) depth of fishing, determined as water depth by onboard echo sounders, was related to the species of crab caught. *Paralomis spinosissima* were generally caught in relatively shallow waters, whereas *P. formosa* tended to be caught in much greater numbers in deeper waters (Fig. 1). *Paralomis anamerae*

[1] CCAMLR (Commission for the Conservation of Antarctic Marine Living Resources). 1999. Report of the Working Group for Fish Stock Assessment, 110 p. Annex 5 in the report of the eighteenth meeting of the Scientific Committee. CCAMLR, P.O. Box 213, North Hobart, Tasmania 7002, Australia.

[2] CCAMLR. 1992. Report of the working group for fish stock assessment, 164 p. Annex 5 in the Report of the eleventh meeting of the Scientific Committee. CCAMLR, P.O. Box 213, North Hobart, Tasmania 7002, Australia.

[3] CCAMLR. 1997. Report of the working group for fish stock assessment, 169 p. Annex 5 in the Report of the sixteenth meeting of the Scientific Committee. CCAMLR, P.O. Box 213, North Hobart, Tasmania 7002, Australia.

[4] CCAMLR. 2000. CCAMLR statistical bulletin, 153 p. CCAMLR, P.O. Box 213, North Hobart, Tasmania 7002, Australia.

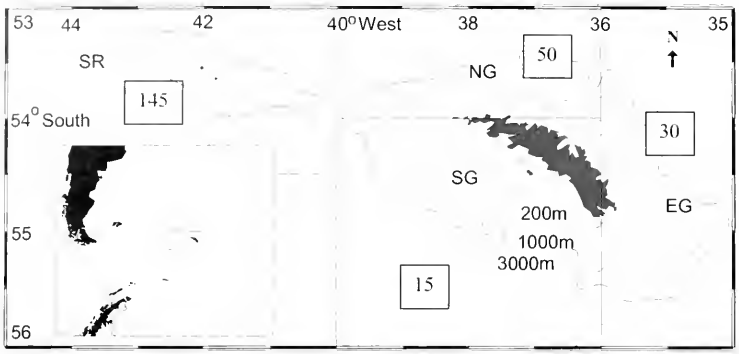

Figure 2

Map of areas used in the study. SR=Shag Rocks, NG=North South Georgia, EG=East South Georgia, SG=South South Georgia, and the 200-m, 1000-m and 3000-m bathymetric contours are shown. The total number of hauls in each of these areas were as follow: SR=145, NG=50, EG=30, and SG=15. Inset shows the position of the study area in relation to the South Atlantic.

(Macpherson, 1988) were caught at intermediate depths. Other influences on crab catch rates were investigated by using two cruises in 2001, which covered the study area more evenly (most hauls in cruise G1 were concentrated in a small area around southeast Shag Rocks; see Fig. 2). For each species two generalized linear models were constructed with Splus statistical software (version 2000, Mathsoft Engineering & Education, Inc., Cambridge, UK): a binomial link model for the probability of encountering a crab of that species (pe) and a Gaussian link model for the natural logarithm of CPUE (catch in numbers per pot) for all nonzero catches. Both models were of the form $\lambda = p_1 \times \text{depth} + p_2 \times \text{area} + p_3 \times \text{vessel} + p_4 \times \text{soak time}$, where for the binomial models, λ was set to 1 if crabs had been caught and 0 if they had not, and for the Gaussian models, λ was set to ln(numbers per pot) for all sets catching crabs. Area and vessel parameters were factors. Depth and soak time were modeled as linear continuous variables, except in the case of the Gaussian model for *P. formosa*, where a third-order polynomial best described the relationship between CPUE and depth. Predictions from the two models were combined to predict crab catch rates per pot,

$$\hat{U} = p(e) \times \exp[\hat{u} \pm 1.96 \times SE],$$

where $\hat{u}$ = the predicted ln(CPUE) from the Gaussian model; and

SE = the standard error from the Gaussian model.

Biological data were collected from all crabs in randomly selected pots. Carapace widths, carapace lengths, chela height, and chela length were measured to the nearest millimeter below by using calipers. Weights were measured to the nearest 5 g below with spring-balanced scales. Sex, maturity stage, condition of the carapace, and an index of vitality (Table 1) were recorded for a subsample of crabs, selected as a random portion across species from the contents of selected pots. Identification of the uncommon species, *Paralomis anamerae*, *Neolithodes diomedeae,* and *Lithodes murrayi*, was confirmed by using dried specimens in London (at Imperial College and the British Museum of Natural History).

Male size at maturity was determined from the allometric relationship between carapace length (L) and right (dominant) chela size (height, CH, or length, CL). The slope of the L-CH or L-CL relationship is assumed to change when crabs reach maturity. Around South Georgia, Otto and Macintosh (1996) used L and CH to determine the size at maturity of male *P. spinosissima,* and around the Falkland Islands Hoggarth (1991) used L and CL. For both *P. spinosissima* and *P. formosa* we found that the intersection of the two lines corresponding to the onset of maturity was not easy to identify from the relationship between CL and L. We therefore used CH in our relationships. Following the methods of Somerton and Otto (1986), two linear regression lines were fitted to natural logarithms of L and CH or CL. These lines represent juvenile and adult phases in the L-CH or CL relationship and intersected at a point taken as the L at which males became mature. The regression lines of best fit were determined by minimizing the combined residual sums of squares, and standard errors were estimated by using 500 bootstraps (sampling with replacement).

Females were classified into two categories, "eggs absent" and "eggs present." The vast majority of "eggs absent" females were small immature animals, but some large animals were also encountered in this category. Consequently, for estimating size at maturity, females in the "eggs present" category were defined as "mature" and those in the "eggs absent" category were classified as "immature" up to the size at which the proportion of females with eggs (i.e. mature) reached 90%, after which they were classified as "mature without eggs." Female size at maturity was deter-

Table 1
Relative index used for assessing vitality in *Paralomis* spp.

Vitality index	Description	Characteristics
1	Lively	Limbs supported and held out. Limbs resist manipulation. Crabs actively pinch objects. Can hang on smooth end of forceps by 1 claw (weakest on large crabs).
2	Lively but limp	Legs hang when picked up. Claws weak and can be opened—not capable of supporting own weight on forceps. Mouthparts move, indicating life when submerged in seawater.
3	Dead	No signs of life. Mouthparts do not move when submerged.
4	Dead and eaten	Only shell or carapace remaining.

mined by plotting the proportion of mature females against size (carapace width) and determining the point of 50% maturity (Sm_{50}). Logistic curves of the form [*proportion mature* = $1/(1 + \exp(-r(carapace\ width - Sm_{50})))$] were used to estimate 50% maturity (Sm_{50}) and its standard error by using the nonlinear fitting function in Splus.

Three different experiments were conducted between March 2000 and April 2001 to assess crab discard survival rates. During cruise G1 a number of alive and active crabs from one haul were tagged through one of the lateral plates of the abdomen with Hallprint plastic T-bar tags and maintained in running seawater before they were placed in pots prior to the next setting. Once these pots were rehauled, the vitality of the tagged crabs was assessed by using the four point relative scale shown in Table 1. A control group of crabs were similarly tagged and kept onboard in running seawater to monitor any effect that tagging might have had on survival. Survival experiments conducted on cruises G2 and H differed in that crabs were selected at random and included individuals that were already "limp" prior to re-immersion. Crabs were tagged with thin strips of masking tape around their legs prior to re-immersion. To ensure that the same crabs were assessed for vitality after rehauling, pots were marked and sealed off to prevent any new captures.

Estimates of the total survival that can be expected after discarding were made in the following manner. By observing crabs on arrival on deck we determined the proportion of animals that arrived on deck as lively ($lively_0$), or limp ($limp_0$), or dead. Using the data from the survival experiments we set $p(lively,lively)$ as the probability that a lively animal that is discarded will recover to a lively condition (this was estimated by calculating the proportion of experimentally re-immersed lively animals that were recovered as lively). We defined $p(limp,lively)$ similarly. The proportion of discarded animals that were lively and would continue to be lively is $lively_0 \times p(lively,lively)$ and the proportion of discarded animals that were limp but would recover to a lively condition is $limp_0 \times p(limp,lively)$. The overall survivorship, S, is then

$$S = lively_0 \times p(lively,lively) + limp_0 \times p(limp,lively).$$

In our experiments, some of the damage may have occurred on rehauling the pots after re-immersion, a situation that would not normally occur once crabs have been discarded. $p(lively,lively)$ can be corrected for this by adding to it the proportion of animals that were not lively when first hauled (i.e. $1-lively_0$), termed the rehaul correction. For instance, suppose that 1% of the crabs were not lively on the first hauling, and in the experiment 4% of the re-immersed lively crabs were not lively on recovery. The rehaul correction would indicate that 1% of the re-immersed crabs would have been damaged anyway simply by the hauling process, and that therefore the correct damage rate attributed simply to the initial capture and discarding would be 3%.

Results

Crab catch

The majority of the bycatch comprised two species of lithodid crabs (Anomura: Lithodidae), *Paralomis spinosissima* and *P. formosa*. Both species have been previously reported in catches around Shag Rocks and South Georgia (Otto and Macintosh, 1996) and have formed a large proportion of the total catch of crab (Table 2). Crab species formed 69.5% of the total weight of all species caught, including toothfish, and 98.2% of the total numbers of individuals caught.

Three other species of crab were also identified during the pot trials. The most abundant of these was *Paralomis anamerae* (Macpherson, 1988), which like the other *Paralomis* species, was subject to detailed biological sampling. 12,370 individuals of this species (1 721 kg) were caught. All individuals were discarded because they were smaller than the minimum size limit for the smaller of the two regulated species, *P. formosa*. Two other species, *Neolithodes diomedeae* and *Lithodes murrayi*, were also caught in small numbers.

Distribution

Crab distribution was investigated for the areas as defined in Figure 2. There were too few data from South of South Georgia; therefore the analysis was restricted to data from Shag Rocks, North South Georgia, and East South Georgia. A few pot strings had been left for several days because

Table 2

Species proportion (no. of crabs and percentage) and discard rates for crabs caught during the pot trials around South Georgia during the period March 2000 to April 2001.

	Number kept	Number discarded	% total crab catch by number	% total crab catch by weight	Discard rate
Paralomis formosa	22,803	300,660	70.1%	63.1%	93%
Paralomis spinosissima	3576	121,580	27.1%	35.4%	97%
Paralomis anamerae	0	12,370	2.7%	1.4%	100%
Neolithodes diomedeae	0		<0.1%	<0.1%	
Lithodes murrayi	0		<0.1%	<0.1%	

Table 3

The results of fitting generalized linear models on the probability of encountering crabs, and the catch rate of crabs (numbers per pot) for nonzero catches. ANOVA results: the significance of adding each parameter to the general linear model is presented. For the binomial model of the probability of encounter, a chi-squared significance test was used; for the Gaussian model of ln(CPUE) an F test was used. Coefficients p_1..p_4 are given with standard error in parentheses. For those models including "area" the standard case was for East South Georgia (EG), and the parameters for North South Georgia and Shag Rocks (NG, SR) are given. Analyses were performed with Splus statistical software. Final models were constructed by using only the significant parameters (italicized in this table). n = number of crabs in sample. Poly (1), Poly (2), and Poly (3) are the coefficients of each of the three orders in a 3rd order polynomial.

Parameter	Probability of encountering *P. formosa*	Ln(CPUE) for nonzero catches of *P. formosa*	Probability of encountering *P. spinosissima*	Ln(CPUE) for nonzero catches of *P. spinosissima*
ANOVA results				
n	101	91	101	82
Depth (m)	*<0.001*	*<0.001*	*<0.001*	*<0.001*
Area	>0.05	>0.05	>0.05	*<0.01*
Vessel	>0.05	>0.05	>0.05	>0.05
Soak time (h)	>0.05	*<0.05*	>0.05	*<0.01*
Coefficients p_1 p_4				
n	101	91	101	82
Intercept	−2.2358 (1.4373)	1.7229 (0.4301)	8.5065 (1.5822)	3.217 (0.4877)
Depth (m)	0.0098 (0.0035)	Poly(1): 4.6387 (5.3605) Poly(2): −8.4647 (6.2257) Poly(3): −1.3614 (4.4808)	−0.0106 (0.0022)	−0.0055 (0.0008)
Area				NG: 1.1304 (0.3241) SR: 1.2771 (0.2875)
Soak time (h)		0.0447 (0.0221)		0.0638 (0.0191)

of bad weather, and to eliminate these the maximum soak time was limited to 39 hours. The mid-depth of the set (average of the depth at the start and end of the set) was used to indicate setting depth, and the analysis was restricted to sets whose depth range was less than 200 m. The data from 45 sets (19% of total) were omitted from analyses because they did not meet these criteria for area, depth, or soak time.

For the binomial encounter models, the only significant factor was depth (Table 3). For the Gaussian catch per pot model, depth, and soak time were significant for both species and area was significant for *P. spinosissima*. However, the depth effects were opposite for the two species, so that *P. spinosissima* decreased in abundance with depth and *P. formosa* increased in abundance with depth, at least up to about 1000 m depth (Fig. 3). There were insufficient data from the cruises in 2001 to establish the effect of depths shallower than 300 m and deeper than 1100 m, although the limited sampling at depths greater than 1200 m in year 2000 (Fig. 1) suggests that catch rates of *P. formosa* would continue to decline at these depths, as suggested by the generalized linear models in Figure 3.

The sex ratio of *P. formosa* was skewed towards males in shallow water (<800 m) and females in deep water (Fig. 4). The mean size of *P. formosa* of both sexes also decreased significantly with an increase in depth (Fig. 5). Although catch rates in numbers were usually much higher in deeper water, smaller crabs of no commercial

value often dominated catches. Only about 38% of *P. spinosissima* sampled between 200 and 400 m were males, whereas this proportion increased to about 76% in depths of 600 to 800 m (Fig. 4). The mean carapace width of males remained relatively constant between 200 to 800 m, but female *P. spinosissima* decreased in size with an increase in depth (Fig. 5).

Size frequencies

Males achieved larger sizes than females in all three species (Fig. 6). Only 5.7% of the sampled *P. spinosissima* individuals were of legal size (carapace width greater than 102 mm), of which only 6% were females. A difference was also noted in the percentage of legal-size *P. spinosissima* for the different areas: 10% at South Georgia and only 3.8% at Shag Rocks. For *P. formosa* only 11.6% (n=1012) were larger than the minimum legal size of 90 mm. Of these legal crabs only 6% (n=63) were females, indicating that few females would be processed if carapace width was the only criterion used to select crabs that could be taken legally. No obvious difference was noted in the percentage of legal-size crabs caught in the two main fishing areas.

Although a legal-size limit is not specified for *P. anamerae* (sizes ranged from 39 to 96 mm), only two crabs (0.2% of sample) were larger than the legal limit for *P. formosa* (90 mm). A peak in the length distribution of this species occurred between 55 and 57 mm, and few crabs were larger than 77 mm.

Differences in the size-frequency distribution of the sexes was more pronounced for *P. formosa* than for the other two species; females peaked at 65–72 mm and males peaked at between 85 and 90 mm carapace width (Fig. 6). For *P. spinosissima* female size distribution peaked between 78 and 82 mm and males peaked at 87 to 92 mm carapace width (Fig. 6). Males and females of *P. anamerae* had a relatively even size distribution up to carapace widths of 65 mm. Most of the larger crabs were males; only 6.8% of individuals larger than 65 mm were females. Maximum widths recorded were 121 mm (*P. spinosissima*), 120 mm (*P. formosa*), and 91 mm (*P. anamerae*).

Size at maturity

There was no significant difference between female size at maturity at Shag Rocks and South Georgia for either species (t-tests on Sm_{50} estimated by fitting logistic models to the proportion mature at size, P>0.05). The close allometric relationship found between carapace width and length (Table 4) made it possible to alter between these two types of measurements (Table 5). Combining the two areas, female size at maturity was 55.1 mm carapace length (57.1 mm carapace width) for *P. formosa* and 61.2 mm carapace length (67.7 mm carapace width) for *P. spinosissima* (Fig. 7). These sizes are very similar to the 61.7 mm

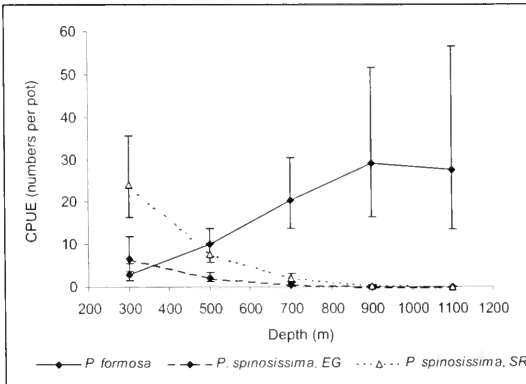

Figure 3

General-linear-model–predicted CPUE (numbers per pot) for the two species (*Paralomis formosa* and *P. anamerae*) at different depths standardized for a soak time of 18 h (the average used in the study). For *P. spinosissima* predictions at East South Georgia and Shag Rocks are presented separately (EG, SR, respectively).

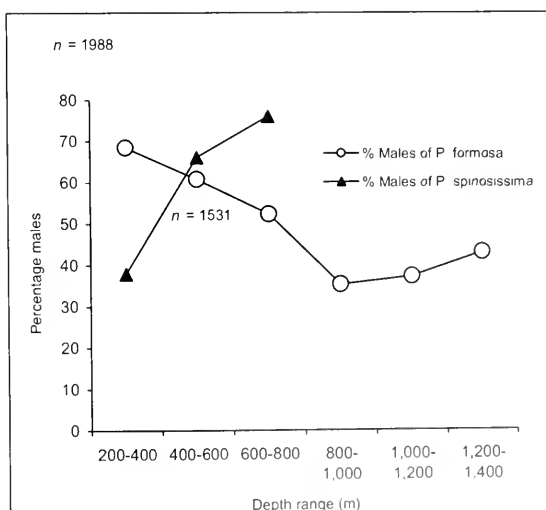

Figure 4

The percentage of males of *Paralomis formosa* and *P. spinosissima* found at different depth ranges during random sampling of the crab bycatch; all data from cruises G1 (*Argos Georgia* cruise 1), G2 (*Argos Georgia* cruise 2), and H (*Argos Helena* cruise) were used.

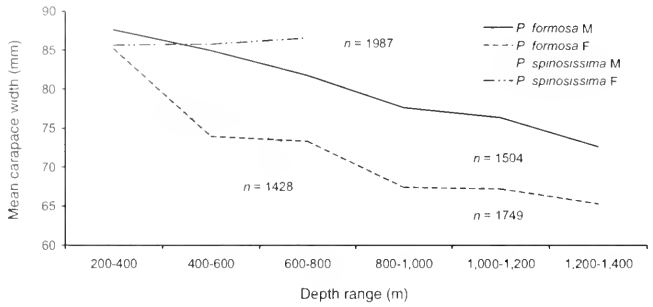

Figure 5

Mean carapace width of the males (M) and females (F) of *P. formosa* and *P. spinosissima* found at different depth distributions.

Table 4

Parameters of the regression *carapace width* = *carapace length* × slope + intercept (all ages and sexes combined). *n* = number of crabs in sample.

Species	Intercept	Slope	Correlation coefficient	*n*
P. spinosissima	6.457	0.994	0.977	367
P. formosa	1.976	1.032	0.969	351
P. anamerae	5.700	0.917	0.979	28

Table 5

The size at maturity (Sm_{50}) for males and females of both *Paralomis* species. The standard errors (SE) for male carapace lengths are shown in parentheses.

	P. spinosissima		*P. formosa*	
	Carapace length (mm)	Carapace width (mm)	Carapace length (mm)	Carapace width (mm)
Males	67.3 (0.10)	73.4	64.0 (0.16)	68.0
Females	61.2	67.7	55.1	57.1

carapace length reported by Otto and MacIntosh (1996) for *P. spinosissima* from Shag Rocks and South Georgia.

Unfortunately, owing to limited sampling of male crabs around South Georgia, estimates of male sexual maturity were only available for Shag Rocks. Too few samples of *P. anamerae* were available for determination of the onset of female or male maturity in either area. Male size at maturity (Sm_{50}) was determined at a carapace length of 67.3 mm (SD=2.3 mm derived from bootstrap resampling with replacement) for *P. spinosissima* and at 64.0 mm (SD= 3.6 mm) for *P. formosa* (Fig. 8).

Crab survival rate

Approximately 5000 crabs were examined for carapace damage on the cruises in 2001. The results (Table 6) indicated that the level of visible damage to these crabs prior to discarding was very low (2% of crabs of all species). The vitality of these crabs was also assessed (according to the index in Table 1). Most crabs were lively on arrival on deck and prior to discard (Table 6). Differences were, however, noted in both carapace condition and the vitality of crabs between the two fishing vessels. Pairwise χ^2 comparisons

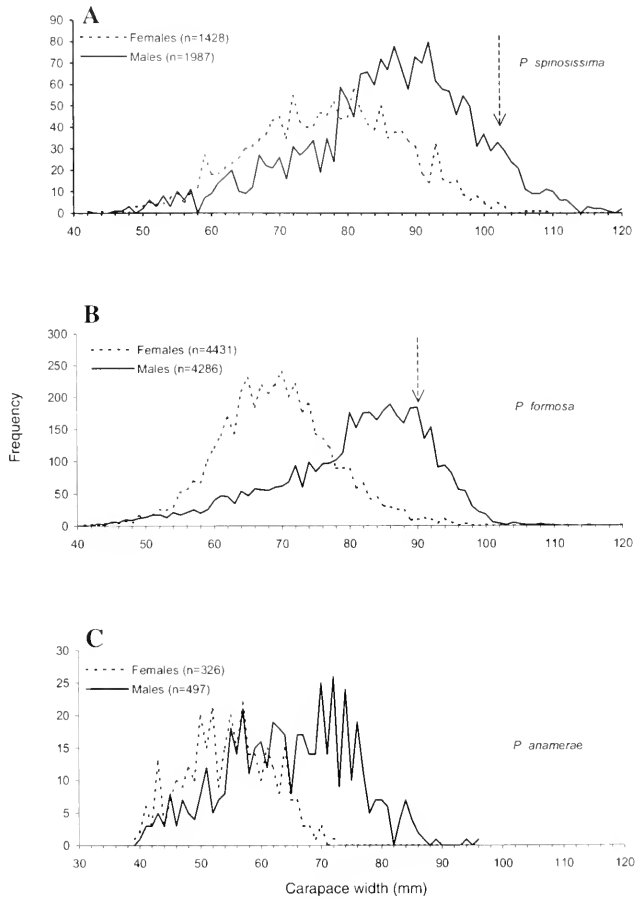

Figure 6

Carapace-width frequency distribution for the three *Paralomis* species (mm). (**A**) *P. spinosissima*, (**B**) *P. formosa*, (**C**) *P. anamerae*. The minimum legal size (102 mm for *P. spinosissima* and 90 mm for *P. formosa*) is indicated with a vertical line and arrow.

between the vitality indices of *P. formosa* and *P. spinosissima* clearly showed that both species displayed significantly lower vitality on the *Argos Helena* than on the *Argos Georgia* (Table 7).

The processing environment of the two vessels may explain these differences. On the *Argos Helena* crabs were likely to sustain more damage as pots were emptied down a vertical chute before entering the processing area below deck. On the *Argos Georgia* pots were emptied on a horizontal conveyer belt leading to the factory. Interestingly, there was no significant difference between the vitality displayed by *P. anamerae* between the two vessels, although this may be a result of the smaller sample size for this species. For the *Argos Georgia*, the vitality of *P. anamerae* was significantly lower than for either *P. formosa* or *P. spinosissima*.

The results of the three survival experiments are shown in Table 8. Experiment 1 re-immersed only lively crabs and included a control set of animals retained on deck in a large tank for the same length of time as the re-im-

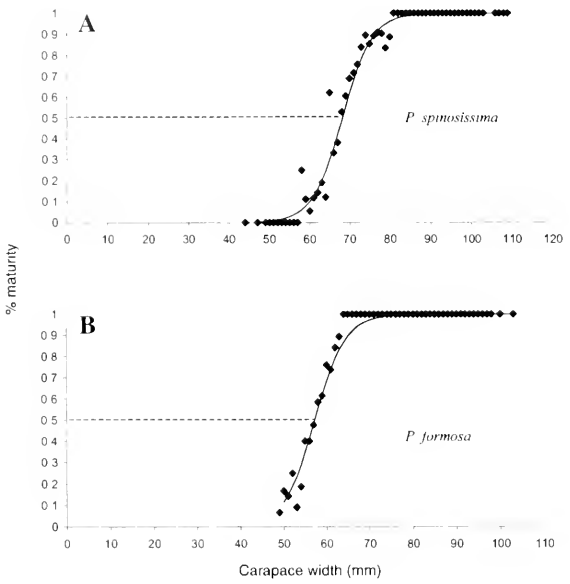

Figure 7

Size at female maturity for (**A**) *P. spinosissima* and (**B**) *P. formosa*. The size at maturity $L_{(50)}$ carapace width was 67.7 mm and 57.1 mm for the two species, respectively.

Table 6

The number and percentages of crabs of the different species assessed for carapace condition and vitality prior to being discarded during 2001 (G2=*Argos Georgia* cruise no. 2, H=*Argos Helena*).

	Carapace condition					Vitality index						
	Damaged		Undamaged			Lively		Limp		Dead		
Species and cruise	No.	%	No.	%	Total	No.	%	No.	%	No.	%	Total
Paralomis formosa												
G2	48	1.9	2431	98.1	2479	2294	98.9	26	1.1	0	0.0	2320
H	23	2.7	814	97.3	837	745	97.4	19	2.5	1	0.1	765
Total	71	2%	3245	98%	3316	3039	98%	45	1%	1	0%	3085
Paralomis spinosissima												
G2	17	1.5	1143	98.5	1160	1122	98.4	17	1.5	1	0.1	1140
H	18	2.0	874	98.0	892	767	94.8	39	4.8	3	0.4	809
Total	35	2%	2017	98%	2052	1889	97%	56	3%	4	0.2%	1949
Paralomis anamerae												
G2	0	0.0	45	100.0	45	31	86.1	5	13.9	0	0	36
H	2	2.7	72	97.3	74	62	92.5	5	7.5	0	0	67
Total	2	2%	117	98%	119	93	90%	10	10%	0	0%	103

Table 7

Results of pairwise χ^2 comparisons of the vitality of crabs on first being caught by different cruises (from Table 6). G2 = *Argos Georgia* cruise no. 2 and H = *Argos Helena*, F = *P. formosa*, S = *P. spinosissima*, A = *P. anamerae*. χ^2 values are given, together with significance, df = 2 for all except italicized results, when df was 1 because of the absence of any dead crabs in the comparisons. NS = not significant.

	G2-F	H-F	G2-S	H-S	G2-A
G2-F					
H-F	10.49, $P<0.01$				
G2-S	2.9, NS	—			
H-S	—	6.99, $P<.05$	20.7, $P<0.001$		
G2-A	*35.2, P<0.001*	—	29.2, $P<0.001$	—	
H-A	—	5.5, NS	—	1.14, NS	*0.49, NS*

mersion process. Out of the 35 lively control animals a similar proportion died during the experiment as in the re-immersed group (8%), but a lower proportion of the control group were lively following the experiment (63%). The lower proportion of lively animals in the control group may have been a result of interruptions in the supply of oxygenated water and the continual disturbance on deck due to the ship's motion. Consequently, controls were not performed in experiments 2 and 3.

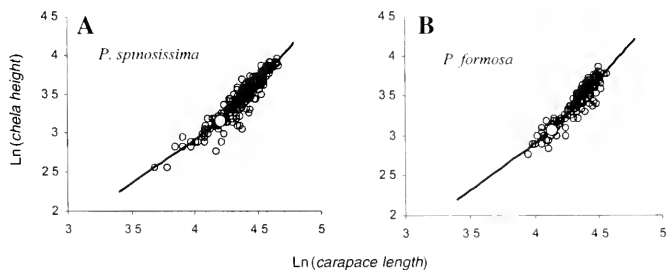

Figure 8

Chela allometry in male (**A**) *P. spinosissima* and (**B**) *P. formosa* sampled at Shag Rocks in 2001. The intersections of fitted curves were used to determine size at maturity.

Experiments 2 and 3 took a random sample of lively and limp crabs and subjected them to re-immersion. The proportions of lively crabs at the beginning of the re-immersion experiments were lower than the proportions estimated for the population as a whole in Table 6, with the exception of *P. spinosissima* in experiment 2. However, sample sizes were much smaller in the experiments and the crabs were subject to greater handling times than those assessed in Table 6; therefore the results presented in Table 6 are more likely to be representative of the condition of discarded crabs than results presented in Table 8.

In experiment 1 on cruise G1, no limp animals were subjected to re-immersion. In comparing the results of immersing lively animals, there was no significant difference between the results for experiment 1 and 2 (cruises G1 and G2 on the *Argos Georgia*) for either *P. formosa* or *P. spinosissima*. Combining the results of the experiments for G1 and G2, there was a significantly lower vitality after re-immersion for both species on the *Argos Helena* compared with the *Argos Georgia* (Table 7). On the *Argos Georgia* there was no significant difference in vitality after re-immersion between *P. formosa* and *P. spinosissima*, whereas on the *Argos Helena* vitality for *P. spinosissima* was significantly lower than vitality for *P. formosa*. These results are similar to the initial assessment of vitality prior to re-immersion (Table 6), where significantly fewer *P. spinosissima* were lively in comparison with *P. formosa* on the *Argos Helena*, but there was no difference between the two species on the *Argos Georgia*.

A single re-immersion experiment performed on 15 *P. anamerae* crabs (11 were "lively" and 4 were "limp"), on the *Argos Helena* in April 2001, resulted in a mortality rate of 73%. Only 27% of the crabs that were "lively" before re-immersion were still "lively" after the rehaul. Although more data need to be collected on the survival rate of this species, this high mortality rate, together with the higher incidence of individuals of *P. anamerae* found to be "limp" during vitality assessments (Table 8; 10% compared to 3% of *P. spinosissima* and 1% of *P. formosa*), seems to indicate that this bycatch species might be particularly vulnerable to onboard handling and discarding.

Crabs that were physically damaged (i.e. had missing legs or cracked carapaces) before being subjected to re-immersion were less likely to survive than undamaged crabs. Of the 19 damaged *P. spinosissima* (13 of these were "lively" and 6 were "limp"), 58% did not survive re-immersion and only 32% of these were still "lively." The effect of damage

Table 8

Results of survival-rate experiments. For each experiment the number of re-immersions is given, together with the total number of crabs in lively and limp condition that were re-immersed and their condition on rehauling the crab pots after re-immersion.

	Number of re-immersions	Number of crabs	Initial condition	Condition after re-immersion		
P. formosa						
Experiment 1				Lively	Limp	Dead
(cruise G1)	2	30	Lively	20	6	4
		0	Limp	0	0	0
Experiment 2				Lively	Limp	Dead
(cruise G2)	6	98 (93%)	Lively	81	11	6
		7	Limp	4	1	2
Experiment 3				Lively	Limp	Dead
(cruise H)	3	49 (91%)	Lively	27	21	1
		5	Limp	0	2	3
P. spinosissima						
Experiment 1				Lively	Limp	Dead
(cruise G1)	2	42	Lively	35	3	4
		0	Limp	0	0	0
Experiment 2				Lively	Limp	Dead
(cruise G2)	6	60 (100%)	Lively	55	5	0
			0Limp	0	0	0
Experiment 3				Lively	Limp	Dead
(cruise H)	10	167 (88%)	Lively	71	67	29
		23	Limp	1	6	16

Table 9

Estimation of total survival rate for *P. formosa* and *P. spinosissima* based on results from re-immersion experiments. Because there was no significant difference between the responses of lively animals between experiments 1 and 2, these data were pooled to give a single estimate for the *Argos Georgia*. On the *Argos Georgia* no limp *P. spinosissima* were encountered during the re-immersion experiments; therefore *p(limp,lively)* was set equal to *p(limp,lively)* from experiment 3. Three calculations are presented: the first according to the text description without the rehaul correction, the second including this rehaul, and the third where the original proportions of lively animals $p(lively_o)$ were used from the experimental data in Table 8 rather than the data from the larger sample in Table 6.

	$p(lively_o)$ from Table 6, without rehaul correction	$p(lively_o)$ from Table 6, with rehaul correction	$p(lively_o)$ from Table 8, without rehaul correction	$p(lively_o)$ from Table 8, with rehaul correction
P. formosa				
Argos Georgia	78.7%	79.8%	77.5%	83.7%
Argos Helena	53.7%	56.2%	50.0%	58.4%
P. spinosissima				
Argos Georgia	86.9%	88.5%	88.2%	88.2%
Argos Helena	40.5%	45.4%	37.9%	48.5%

was not so pronounced for *P. formosa*, although of the 12 crabs that were damaged prior to re-immersion (10 were "lively" and 2 were "limp"), only 58% were "lively" upon recovery. The mortality rate of 17% for damaged specimens was more than double the 8% overall mortality found during re-immersion experiments for this species. Most of the dead crabs examined after re-immersion had been attacked by isopods and amphipods and only the shell remained. It is possible that these organisms were in fact responsible for killing the crabs, particularly where damage to the shell allowed access to the softer tissues of the crab.

Calculations of survival rate are given in Table 9 both with and without the re-haul correction. As discussed above, the more accurate estimate of $lively_o$ is probably from Table 6 because of the additional handling stress associated with the experiment. However, Table 9 also presents results obtained from data in Table 8 to estimate this probability. The results suggest that the survival rate

of discarded crabs would be high on the *Argos Georgia*, between 77% and 88% for both *P. formosa* and *P. spinosissima* (77–84% for the former, 87–88% for the latter). On the *Argos Helena* discard survival rate was much lower, 50–58% for *P. formosa* and 38–49% for *P. spinosissima*.

Discussion

Crab species

Three previously unreported or rarely reported crab species, *Paralomis anamerae*, *Neolithodes diomedeae* (Benedict, 1894), and *Lithodes murrayi* (Henderson, 1888), were found in our study. The most abundant of these was *P. anamerae*, found at mid-range depths. The only other record of *P. anamerae* is the original description of the species based on four specimens obtained from the continental shelf of Argentina at depths of 132–135 m (Macpherson, 1988). The specimens obtained from South Georgia, at depths of 530–1210 m, therefore represent a considerable southerly extension in the reported geographic distribution of this species, as well as a notable increase in its bathymetric range. López Abellán and Balguerias (1994) reported both *P. spinosissima* and *P. formosa* from a 1986–87 trawl survey on the shelf, but no other species of crabs.

A certain amount of confusion surrounds the identification of *Paralomis* species around South Georgia. *Paralomis aculeata* is found in the CCAMLR database, but almost certainly because of its inclusion in the FAO species identification guide for the Southern Ocean (Arnaud 1985, in Fischer and Hureau, 1985), attributed to Henderson (1888). This species is not mentioned in Macpherson (1988), even as a junior synonym. Conversely, none of the *Paralomis* species identified in the present paper appear in Fischer and Hureau (1985). It is not clear, therefore, which species of *Paralomis* CCAMLR scientific observers have been identifying as *P. aculeata*. Twenty-two specimens of *N. diomedeae* were collected at depths ranging from 420 to 1294 m. This species has previously been recorded from South Georgia (Macpherson, 1988).

Sixteen *L. murrayi* specimens were found on southeast Shag Rocks and west South Georgia, approximately 60 nmi apart, at depths of between 450 m and 605 m. *Lithodes murrayi* is mainly reported from the southern Indian Ocean around Prince Edward, Crozet, and Possession Islands, as well as Macquarie Islands, Mozambique Channel, and southern New Zealand at depths of 35–200 m (Hale, 1941; Yaldwyn and Dawson, 1970; Arnauld, 1976; Arnauld and Do-Chi, 1977; Kensley, 1977). However, it has been reported in small numbers in CCAMLR statistical catch records from 1993–94, 1997–98 and 1998–99 and by CCAMLR observers (CCAMLR[1]). We have confirmed the identification and the extension of the range of this species to South Georgia. Klages et al. (1995) reported on the distribution of *L. murrayi* off Peter Island, close to the Antarctic continent between 180 and 260 m depth, and a circum-Antarctic distribution has been claimed for the species (Macpherson, 1988). The present study therefore represents the greatest depth recorded for it.

Distribution

Catch rates of *P. spinosissima* encountered in our study were lower than experienced in the September 1995–January 1996 crab fishery by the FV *American Champion*. Watters (1997) reported that average catch rates of legal-size male *P. spinosissima* were between 14.2 and 28.4 males per pot in the Shag Rocks and northwest South Georgia areas (53.5–54°S, 37–40°W). Although the toothfish pots operated by the *Argos Georgia* from March and May 2000 produced catch rates between 0.5 and 4 crabs/pot, the proportion of legal-size males was very low (3%), resulting in legal (retained) crab catch rates of less than 1/pot (note that the retention rates given in Table 2 are lower than those calculated from the length-frequency sampling, Fig. 6). Retention rates for the 1992 FV *Pro Surveyor* cruise (July–August 1992) were 36% (Otto and MacIntosh[5]). The retention rates on the Argos Helena's experimental crab fishery in 1999 were much lower than this (8% and 14% for *P. spinosissima* and *P. formosa* respectively) (Purves[6]). The low retention rate is most likely to be a consequence of the pot design used on vessels G and H, where the collapsible funnel entrances might have restricted the catch to smaller size crabs.

A further feature of the *American Champion* crab fishery was the restriction of fising effort to depths of less than 500 m. The present trials were targeted at toothfish rather than crabs and were conducted according to an experimental plan that distributed fishing effort over time, area, and the full depth range of longlines used in the main toothfish fishery. Accordingly, fishing occurred over a much wider depth range than was used by the previous crab fisheries. Our very high catch rates of *P. formosa* in deep water were therefore not reported by Watters (1997). However, even our catch rates did not result in high numbers of retained legal-size crabs on the *Argos Georgia* because the proportion legally permitted was only 10.5%. Interestingly, even in shallow water (400–800 m) *P. formosa* appeared to be more common than *P. spinosissima*. Only in waters less than 400 m deep did *P. spinosissima* become the dominant species. This finding confirms the results of Watters (1997) who found that *P. spinosissima* catch rates declined at depths deeper than 300 m. Catch rates of *P. spinosissima* were low even in these depths (5 crabs/pot). Only 9 of the total of 110 sets of the Argos Georgia were conducted in depths shallower than 400 m because the main target of the fishery was toothfish.

The differences found in our study in the distribution by depth of the different sexes and sizes of crabs might

[5] Otto, R. S., and R. A. MacIntosh. 1992. A preliminary report on research conducted during experimental crab fishing in the Antarctic during 1992 (CCAMLR Area 48). Document WG-FSA-92/29, 20 p. CCAMLR, P.O. Box 213, North Hobart, Tasmania, Australia

[6] Purves, M. G. 1999. Report of the South African designated CCAMLR observer on board the British registered longliner "Argos Helena" in Statistical Subarea 48.3, 31 August to 23 September 1999, 13 p. CCAMLR, P.O. Box 213, North Hobart, Tasmania, Australia

indicate that recruitment of *P. formosa* takes place in deeper water. This conclusion is based on a decrease in size with increasing depths, the higher proportion of females encountered in deeper water, and increasing crab densities at depth. For *P. spinosissima* this trend was not so pronounced, although crabs of this species were also generally of a smaller size in deeper water. However, contrary to the case with *P. formosa*, females were more prevalent in shallower water. Very few females of *P. spinosissima* were encountered in deep water. These rather unusual findings might suggest ecological partitioning of the benthic habitat, and warrant further investigation.

Another unexpected result of our work was the discovery of a third species of *Paralomis, P. anamerae*, at intermediate depths. This species was apparently not present in the *American Champion* or *Pro Surveyor* catches, presumably again because of the depth restriction in these cruises.

Maturity

For *P. spinosissima* our estimate of 67.3 mm carapace length at 50% male maturity is similar to the 66.4 mm carapace length found by Otto and MacIntosh (1996) at Shag Rocks for this species. Unfortunately, as can be seen from Figure 8, relatively few small *P. formosa* males were encountered and size at maturity for this species (64.0 mm carapace length) is likely to have been poorly estimated in our analysis. However, if it is assumed that male *P. formosa* mature at the same size in relation to female *P. formosa*, as in the case of *P. spinosissima*, the female maturity data presented in Table 5 would suggest that male *P. formosa* would mature at 60.4 mm carapace length (64.3 mm carapace width) rather than the 64.0 mm shown in Figure 8.

Watters and Hobday (1998) have also examined size at maturity for *P. spinosissima* and *P. formosa*, although their samples were taken from South Georgia rather than Shag Rocks. Using a method based on finding the maximum of the second derivative of smoothing spline fits to chela height and carapace width data, they found that size at morphometric maturity for *P. spinosissima* was 73 mm carapace length. This size is similar to that which Otto and Macintosh (1996) obtained for *P. spinosissima* at South Georgia using the same technique as we did. Watters and Hobday's (1998) results for *P. formosa* are, however, for a higher size at maturity (80 mm carapace length) than that for *P. spinosissima*, which would seem to be at variance with our results and the apparent relative sizes of the two species (see Fig. 6 and CCAMLR[2]).

The minimum size limits for crabs at South Georgia were set by CCAMLR in 1992 but, in common with many crab stocks (Schmidt and Pengilly, 1993), these measures were not accompanied by rigorous analysis of the effectiveness of these measures in meeting management objectives. For *P. spinosissima*, Otto and Macintosh's[5] male maturity results for *P. spinosissima* were used, and allowing males at least one opportunity to breed and an assumed growth per moult of 15%, minimum size limits were calculated as 94 mm and 84 mm carapace width at South Georgia and Shag Rocks, respectively (CCAMLR[2]). These results are very similar to our own, but the CCAMLR limit of 102 mm width was based on the then-existing processing requirements rather than on these calculations. Our results suggest, allowing at least one opportunity to breed, that the limit should be 83 mm for *P. spinosissima*. For *P. formosa*, taking our more conservative figure of 64.0 mm carapace length at 50% maturity, the catch size limit should be set at 78 mm carapace width (the less conservative figure, 60.4 mm carapace length, would suggest a size limit of 74 mm carapace width).

Hoggarth (1991) reviewed minimum size limits for a number of stocks of lithodid crabs and found that minimum legal sizes were about 70% of the maximum size for males, which would suggest 85 mm and 84 mm carapace width for *P. spinosissima* and *P. formosa*, respectively. It should, however, also be taken into account that these estimates were probably biased because of the greater sampling effort made at Shag Rocks. Note that the length-frequency distribution for *P. formosa* in Figure 6B appears to indicate a lower maximum size for males of this species than for males of *P. spinosissima*. However, the largest *P. formosa* actually encountered was 120 mm carapace width. Furthermore, Figure 6B seems to be truncated at the larger sizes, suggesting perhaps that a proportion of the large adult population was not encountered during fishing.

Discard mortality

Our results demonstrate that, although a high proportion of crabs is likely to survive the physical strain of being hauled to the surface from potentially great depths, some undersize individuals and nontarget females can be expected to die following discarding. The most significant factor affecting discard survivorship was handling on board the vessel. On the *Argos Georgia*, where crabs were unloaded from pots and sorted on a conveyor belt, survivorships were high, up to 88%, and *P. spinosissima* survived better than *P. formosa*. By contrast, on the *Argos Helena*, where crabs went down a chute prior to processing, survival rate was between 38% and 58% and *P. formosa* survived considerably better than *P. spinosissima*. In general, *P. anamerae* was the most vulnerable species, followed by *P. spinosissima*, and the least vulnerable—*P. formosa*.

Studies of the discard mortality of lithodid crabs in North Pacific fisheries have produced a variety of results. Stevens (1990) found that crabs discarded from commercial sole trawls suffered high mortalities (47.3%), but Byersdorfer and Watson[7] and Zhou and Shirley (1995) both reported relatively low mortalities (<2%) resulting from handling when fishing with pots. Our results support these previous studies and extend them to the Antarctic, clearly indicating that where handling on a pot vessel is reduced, mortalities are relatively low (<15% mortality). When crabs are

[7] Byersdorfer, S., and L. J. Watson. 1992. A summary of biological data collected during the 1991 Bristol Bay red king crab tagging study. Technical Fishery Report 92-14, 30 p. Alaska Department of Fish and Game, Division of Commercial Fisheries, P.O. Box 25526, Juneau, AK 99802-5526.

handled on a pot vessel, as they would be on a trawl vessel, mortalities are higher.

Other factors, which could not be tested in the re-immersion experiment, may also affect the rate of crab survival. We re-immersed crabs in pots, whereas normally they would be simply dropped into the sea and would be subject to predation from birds and fish before they reached the bottom. The effect of discarding crabs away from their original habitat is unknown, but our results demonstrate a clear depth separation between the two species; therefore one would expect at least an energetic cost if crabs have to relocate. The crabs subjected to re-immersion experiments were sampled immediately before being discarded. They might suffer further damage through the actual discard process; for instance Stevens (1990) speculated that, while traveling through offal chutes, they could become entangled in machinery or suffer further damage upon impact with the surface of the water. Ideally crabs should have been sampled after being through the full discarding procedure, but this was not practical. Finally, eggs often became dislodged during handling and this loss possibly impacted reproductive success.

Zhou and Shirley (1995) presented results that indicate that there are no long-term effects of handling on crab survival, feeding rate, or crab condition; therefore we might reasonably expect that the survival rates seen in our experiments would also be the relevant long-term survival rates. However, even with relatively low discard mortality, the impacts of repeated catching and discarding of individuals will have a cumulative effect on crab populations. Both retained and discarded bycatch should therefore continue to be reported and be incorporated into crab population models. The presence of such a large discarded bycatch might provide the opportunity for the retention (and removal from the population) of parasitized crabs, as suggested by Basson (1994).

Crabs are an inconvenience in a fishery targeting toothfish. *In situ* observations made during the AUDOS experiments on the UK's January 2000 survey confirm that toothfish seek to avoid direct contact with crabs (Yau et al., 2002), although crabs do form a component of their food (Pilling et al., 2001). An inverse relationship was found in the present study between toothfish numbers in pots and crab numbers in pots, suggesting toothfish avoid pots with large crab populations (Fig. 9). Therefore, conducting the toothfish pot fishery in an area of low crab abundance is sensible, and our data do suggest that, at intermediate depths, the crab catch should be low and composed primarily of large *P. formosa*. Avoidance of areas of high crab bycatch will also reduce the mortality associated with discarding female and undersize male crabs. These discard levels are very high (>93%)—considerably higher than those in the Bering Sea (85%: Stevens, 1996). Such high discard levels could be reduced further by developing new pot designs to limit crab catches to larger, legal-size animals—for instance designs with excluder panels (Stevens, 1996)—or perhaps by reducing the minimum size limit.

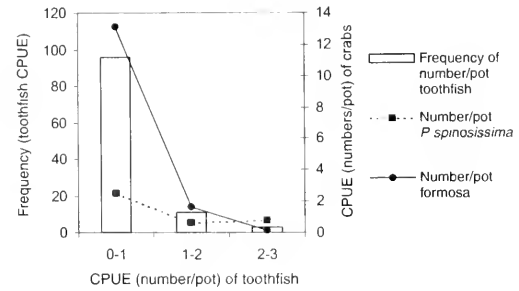

Figure 9

The frequency distribution of the number of toothfish caught per pot compared with the CPUE's of *Paralomis spinosissima* and *P. formoso* (numbers/pot) and of toothfish (*Dissostichus eleginoides*) catches (numbers/pot), as found during the first cruise of the *Argos Georgia* during March to May 2000.

Acknowledgments

We wish to acknowledge the assistance of Argos Ltd. and the excellent cooperation of the captains of the two vessels, Captain Joaquín Abraldes Gonzalez and Captain Jose Andres Sampedro and their crew. Permission to publish these data was kindly granted by Argos Ltd. The Government of South Georgia and the South Sandwich Islands funded the research by MRAG Ltd. on South Georgia fisheries.

Literature citations

Agnew, D. J., T. M. Daw, M. G. Purves, and G. M. Pilling.
2001. Fishing for toothfish using pots: results of trials undertaken around South Georgia, March–May 2000. CCAMLR (Commission for the Conservation of Antartic Marine Living Resources) Sci. 8:93–105.

Agnew, D. J., L. Heaps, C. Jones, A. Watson, K. Berkieta, and J. Pearce.
1999. Depth distribution and spawning pattern of *Dissostichus eleginoides* at South Georgia. CCAMLR Sci. 6:19–36.

Arnauld, P. M.
1976. Peches experimentales de *Lithodes murrayi* Henderson, 1888 (Crustacea, Anomura) aux îles Crozet (SW de l'Océan Indien). Thetys 3:167–172.

Arnauld, P. M., and T. Do-Chi.
1977. Données biologiques et biometriques sur les lithodes *Lithodes murrayi* (Crustacea: Decapoda: Anomura) des Îles Crozet (SW de l'Océan Indien). Mar. Biol. 39:147–159.

Basson, M.
1994. A preliminary investigation of the possible effects of rhizocephalan parasitism on the management of the crab fishery around South Georgia. CCAMLR Sci. 1:175–192.

Benedict, J. E.
1894. Descriptions of new genera and species of crabs of the family Lithodidae, with notes on the young of *Lithodes*

camtschaticus and *Lithodes brevipes*. Proc. U.S. Natl. Mus. 17:479–488.

Fischer, W., and J. C. Hureau (eds.)
1985. FAO species identification sheets for fishery purposes, Southern Ocean, vol. 1., p. 232. FAO (Food and Agriculture Organization of the United Nations), Rome, Italy.

Hale, H. M.
1941. Decapod crustacea. Br. Aust. N.Z. Antarct. Res. Exped. 1929–1931. 48:257–285.

Henderson, J. R.
1888. Report on the Anomura collected by H.M.S. Challenger during the years 1873–76. Rep. Sci. Res. Voy. H.M.S. Challenger, Zool. 27(I-vii):1–221, plates 1–21.

Hoggarth, D. D.
1991. An ecological and economic assessment of the Falkland Islands inshore crab, *Paralomis granulosa*. Ph.D. diss., 312 p. Imperial College, Univ. London, London, UK.

Kensley, B.
1977. The South African Museum's Meiring Naude cruises. Part 2. Crustacea, Decapoda, Anomura and Brachyura. Ann. S. Afr. Mus. 72:161–188.

Klages, M., J. Gutt, A. Starmans, and T. Bruns.
1995. Stone crabs close to the Antarctic continent: *Lithodes murrayi* Henderson, 1888 (Crustacea; Decapoda; Anomura) off Peter I Island (68°51–S, 90°51–W). Polar Biol. 15:73–75.

López-Abellán, L. J., and E. Balguerias.
1994. On the presence of *Paralomis spinosissima* and *Paralomis formosa* in catches taken during the Spanish survey Antartida 8611. CCAMLR Sci. 1:165–173.

Macpherson, E.
1988. Revision of the family Lithodidae Samouelle, 1819 (Crustacea, Decapoda, Anomura) in the Atlantic Ocean. Mongr. Zool. Mar. 2:9–153.

Otto, R. S., and R. A. MacIntosh.
1996. Observations on the biology of the Lithodid crab *Paralomis spinosissima* from the Southern Ocean near South Georgia. *In* Proceedings of the international symposium on biology, management and economics of crabs from high latitude waters, Anchorage, Alaska, October 1995, p. 627–647. Alaska Sea Grant, Fairbanks, AK.

Pilling, G. M., M. G. Purves, T. M. Daw, D. J. Agnew, and J. C. Xavier.
2001. The stomach contents of Patagonian toothfish around South Georgia (South Atlantic). J. Fish Biol. 59: 1370–1384.

Stevens, B. G.
1990. Survival of king and tanner crabs captured by commercial sole trawls. Fish. Bull. 88:731–744.
1996. Crab bycatch in pot fisheries: causes and solutions. *In* Proceedings of the solving bycatch workshop, September 25–27, 1995, Seattle, Washington (T. Wray, ed.), p. 151–158. Alaska Sea Grant, Fairbanks, AK.

Schmidt, D. C., and D. Pengilly.
1993. Review of harvest strategies used in the management of lithodid crab in Alaska. *In* Proceedings of the international symposium on management strategies for exploited fish populations: October 21–24, 1992, Anchorage, Alaska (G. Kruse, D. M. Eggers, R. J. Marasco, C. Pautzke, and T. J. Quinn, eds.), p. 385–407. Alaska Sea Grant, Fairbanks, AK.

Somerton, D. A., and R. S. Otto.
1986. Distribution and reproductive biology of the golden king crab, *Lithodes aequispina*, in the eastern Bering Sea. Fish. Bull. 84:571–584.

Watters, G.
1997. Preliminary analyses of data collected during experimental phases of the 1994/95 and 1995/96 antarctic crab fishing seasons. CCAMLR Sci. 4:141–159.

Watters, G., and A. J. Hobday.
1998. A new method for estimating the morphometric size at maturity of crabs. Can. J. Fish. Aquat. Sci. 55:704–714.

Yaldwyn, J. C., and E. W. Dawson.
1970. The stone crab *Lithodes murrayi* Henderson: the first New Zealand record. Rec. Dom. Mus. (Wellingt.) 6: 275–284.

Yau, C., M. A. Collins, P. M. Bagley, I. Everson, and I. G. Priede.
2002. Scavenging by megabenthos and demersal fish on the South Georgia slope. Antarct. Sci. 14:16–24.

Zhou, S., and T. C. Shirley.
1995. Effects of handling on feeding, activity and survival of red king crabs *Paralithodes camtschaticus* (Tilesius, 1815). J. Shellfish Res. 14:173–177.

The physiological effects of multiple forced submergences in loggerhead sea turtles (*Caretta caretta*)

Erich K. Stabenau

Kimberly R. N. Vietti

Department of Biology
Bradley University
1501 W Bradley Ave.
Peoria, Illinois 61625

E-mail address (for E. K. Stabenau): eks@bradley.edu

Abstract—Sea turtles are subjected to involuntary submergence and potential mortality due to incidental capture by the commercial shrimp fishing industry. Despite implementation of turtle excluder devices (TEDs) to reduce at-sea mortality, dead stranded turtles continue to be found in near-record numbers along the coasts of the western Atlantic Ocean and northern Gulf of Mexico. Although this mortality may be due to an increase in the number of turtles available to strand, one alternative explanation is that sea turtles are repetitively submerged (as one fishing vessel follows the path of another) in legal TEDs. In the present study, laboratory and field investigations were undertaken to examine the physiological effects of multiple submergence of loggerhead sea turtles (*Caretta caretta*). Turtles in the laboratory study were confined during the submersion episodes, whereas under field conditions, turtles were released directly into TED-equipped commercial fishing nets. Under laboratory and field conditions, pre- and postsubmergence blood samples were collected from turtles submerged three times at 7.5 min per episode with an in-water rest interval of 10, 42, or 180 min between submergences. Analyses of pre- and postsubmergence blood samples revealed that the initial submergence produced a severe and pronounced metabolic and respiratory acidosis in all turtles. Successive submergences produced significant changes in blood pH, Pco_2, and lactate, although the magnitude of the acid-base imbalance was substantially reduced as the number of submergences increased. In addition, increasing the interval between successive submergences permitted greater recovery of blood homeostasis. No turtles died during these studies. Taken together, these data suggest that repetitive submergence of sea turtles in TEDs would not significantly affect their survival potential provided that the animal has an adequate rest interval at the surface between successive submergences.

Manuscript approved for publication 25 March 2003 by Scientific Editor.

Manuscript received 26 June 2003 at NMFS Scientific Publications Office.

Fish. Bull. 101:889–899 (2003).

The five sea turtle species inhabiting the waters of the U.S. Gulf of Mexico and Atlantic Ocean are considered to be threatened or endangered. One contributing factor to sea turtle mortality is incidental capture in the nets of commercial shrimping vessels. The National Research Council's Committee on Sea Turtle Conservation (1990) suggested that as many as 5500 to 55,000 loggerhead (*Caretta caretta*) and Kemp's ridley (*Lepidochelys kempi*) sea turtles were killed annually during shrimping-related activities. More recently, two independent studies statistically confirmed the relationship between shrimping activity and the appearance of stranded sea turtles in the U.S. Gulf of Mexico and the Atlantic Ocean (Caillouet et al., 1991; Crowder et al., 1995). Because of the impact of trawl-related mortality on sea turtle populations, the U.S. government passed regulations in 1987 requiring that commercial shrimping vessels pull nets equipped with certified turtle excluder devices (TEDs). TEDs are designed to exclude any turtle that may enter into shrimping nets, while not affecting the catch of the target species. Crowder et al. (1995) reported that the sea turtle population off the coast of South Carolina continued to decline when TED regulations were implemented; however, the rate of decline decreased significantly after full-time TED use.

In spite of the TED regulations, near-record numbers of dead stranded sea turtles have been found on U.S. Gulf of Mexico and Atlantic Ocean beaches (Shaver-Miller[1]). Although there may be other man-related or natural causes for this continued sea turtle mortality, there are two plausible reasons for the increased mortality during shrimping activities. First, commercial shrimp fishermen generally do not carry legally certified TEDs in their trawl nets and the TEDs that are used are often installed incorrectly or purposely sewn shut. Second, the shrimp fishermen may pull legal TEDs; however, the turtles are repetitively submerged as they are caught in the TEDs of vessels that follow each other. These successive submergences may exacerbate the physiological effects experienced by sea turtles during a forced submersion, and thus, may limit their survival potential.

Sea turtles spend approximately 99% of their time under the surface of the water. During the brief period at the surface, the turtle will exhale and inhale a solitary breath and then dive under the surface (Jackson, 1985). In fact, multiple breaths by sea turtles are generally seen only after prolonged dives. Minimal information is available on the physiological effects of forced submergences of sea turtles. It has been suggested that voluntary dives by sea turtles are aerobic in nature (Wood et al., 1984), whereby oxygen availability minimizes the metabolic production of lactic acid. The turtles may accumulate carbon dioxide, resulting in a respira-

[1] Shaver-Miller, D. 2002. Personal commun. Texas coordinator, Sea Turtle Stranding and Salvage Network, USGS, Corpus Christi, Texas 78406.

tory acidosis that is ameliorated by hyperventilation at the surface. Therefore, voluntary diving in the absence of any other external stressor does not limit sea turtle survival potential.

In contrast, forced submergence of Kemp's ridley and loggerhead sea turtles produces significant blood respiratory and metabolic derangements. Stabenau et al. (1991) reported that forced submergence of Kemp's ridley sea turtles for less than 7.5 min in shrimp nets equipped with TEDs resulted in significant increases in blood lactic acid and Pco_2, and decreases in blood pH. Moreover, several hours were required for these turtles to fully recover blood homeostasis (National Marine Fisheries Service, unpubl. data[2]). However, the study by Stabenau et al. (1991) did not address the physiological effects of multiple forced submergences of sea turtles. It is plausible that repeated submergence induces progressive, significant blood acid-base disturbances, and limits sea turtle survival potential. Therefore, the present study examined the physiological effects of multiple forced submergences on loggerhead sea turtles.

This investigation was divided into two phases. First, a laboratory component was conducted to examine the feasibility of a multiple submergence study. This phase of the research permitted characterization of the magnitude of the acid-base disturbance under controlled conditions. Second, a field investigation was conducted to expose turtles to TED-equipped commercial fishing nets. Data from these studies may offer greater insight into potential sea turtle mortality caused by multiple capture in commercial shrimping nets carrying legal TEDs.

Materials and methods

Laboratory study

Thirty-nine headstarted 2-year-old loggerhead sea turtles reared in captivity at the National Marine Fisheries Service (NMFS) Galveston Laboratory were used in this phase of the study. Each turtle was randomly placed into experimental (submerged, 37.0 ±0.2 cm, 6.51 ±0.06 kg, n=21) or control (nonsubmerged, 36.9 ±0.2 cm, 6.45 ±0.10 kg, n=18) treatments. All turtles were of comparable size and weight and therefore any alterations in blood parameters between experimental and control turtles represented treatment effects rather than size effects. It should be noted that the turtles used in our study were representative of the average size of dead stranded turtles and those animals used in annual TED certification tests.

The study was initiated by collecting presubmergence blood samples from the experimental turtles immediately prior to their individual confinement in a weighted canvas bag. Each turtle was then submerged for 7.5 min in seawater filled tanks. Postsubmergence blood samples were collected within 30 s of bringing the turtle out of the water to minimize blood acid-base changes. Following an in-water rest interval of 10 (treatment 1), 42 (treatment 2), or 180 (treatment 3) min, a presubmergence blood sample was collected and the turtle was submerged a second time. A postsubmergence blood sample was then collected immediately upon surfacing. The turtle was then submerged a third time, following the same rest interval between the first and second submergence episodes, and pre- and postsubmergence blood samples were collected as described above. The seventh serial blood sample was collected 180 min after the final submergence in all turtles. Blood samples were also collected from control turtles over the same time intervals to ensure that repetitive handling and blood sampling did not alter blood homeostasis. All blood samples were collected into heparinized vacutainers from the dorsal cervical sinus as described by Owens and Ruiz (1980). No more than 4–6% of blood volume was collected during the serial sampling to minimize potential physiological effects associated with blood volume depletion.

Field study

Thirty-six headstarted 2-year-old loggerhead sea turtles reared in captivity from the NMFS Galveston Laboratory were used in this phase of the study. The turtles were transported from Galveston, TX, to Panama City, FL, where they were placed into large pens in St. Andrews Bay. The submergence study was initiated after a minimum of 21 days of natural conditioning in the in-water pens. Each turtle was randomly placed into experimental (submerged, 35.9 ±0.2 cm, 6.77 ±0.09 kg, n=24) or control (nonsubmerged, 35.4 ±0.3 cm, 6.46 ±0.12 kg, n=12) treatments. As in the laboratory study, all experimental and control turtles were of comparable size and weight.

The study was initiated by collecting presubmergence blood samples from the experimental turtles immediately prior to their individual confinement in a weighted mesh bag. Each turtle was then submerged using the standard protocol for TED certification tests. Briefly, the mesh bag containing a turtle was placed onto a line connecting the trawl vessel to the headrope on the shrimp net. Divers then released the turtle (without handling the animal) into the mouth of the trawl. Often, turtles were observed vigorously swimming in the trawl until being overcome by the net. Although the shrimp net was equipped with a TED, divers held the escape door closed for 5 min. The turtle was then permitted to leave the trawl and surface. Thus, the total submergence time was approximately 7.5 min, including the time for the weighted mesh bag containing the turtle to reach the headrope for release into the trawl, the 5 min within the trawl, and the time for the turtle to surface. Turtles were immediately captured at the surface and returned to the trawl vessel for postsubmergence blood sampling. Typically, postsubmergence blood samples were collected within 1–2 min of the turtle surfacing. Following a rest interval of 10 (treatment 4), 42 (treatment 5), or 180 (treatment 6) min in water-filled containers on the trawl vessel, a presubmergence blood sample was collected and the turtle was submerged a second time. A postsubmergence blood sample was then collected immediately upon surfacing. The turtle was then submerged a third time,

[2] National Marine Fisheries Service. 1994. Unpubl. data. [Available from E. K. Stabenau, Bradley University, 1501 W. Bradley Ave., Peoria, IL 61625.]

following the same rest interval between the first and second submergence episodes, and pre- and postsubmergence blood samples were collected as described above. A seventh serial blood sample was collected 180 min after the final submergence in all turtles. Blood samples were also collected from nonsubmerged control turtles over the same time intervals to ensure that repetitive handling and blood sampling did not alter blood homeostasis. The blood sampling technique and volume collected was identical to that described for the laboratory component of the study.

Blood and plasma analyses

In the laboratory study, blood Pco_2 and pH were analyzed immediately following collection by using a clinical blood gas analyzer with electrodes thermostatted at 37°C. Both variables were corrected to turtle cloacal temperature using requisite correction factors for sea turtle blood and plasma (Stabenau and Heming, 1994). In the field study, blood gases (Po_2 and Pco_2) and pH were analyzed on the trawl vessel immediately following collection using a blood gas analyzer with electrodes thermostatted to turtle body temperature (27–28.5°C). The remaining analyses were comparable for both the laboratory and field components of the submergence study. Packed red cell volume (hematocrit) was determined by following centrifugation of heparinized microcapillary tubes. Two hundred microliters of whole blood were then added to 10% trichloroacetic acid for lactate analysis. The deproteinized samples were centrifuged, and the supernatant removed and stored at −70°C. Lactate was determined spectrophotometrically by using standard enzymatic techniques (Sigma, kit 826-B, Saint Louis, MO). The remaining whole blood was then centrifuged, the plasma removed and stored at −70°C. Plasma Na^+ and K^+ were measured with flame photometry (Jenway, model PFP7, Essex, England), and plasma Cl^- was determined with electrometric titration (Haake-Bucher, model 4425000, Saddle Brook, NJ). Plasma glucose was measured spectrophotometrically (Sigma, kit 16-20), and plasma osmolality was determined with a vapor pressure osmometer (Wescor, model 5500, Logan, UT). For the laboratory study, plasma norepinephrine was analyzed with HPLC (BAS, model LC-300, West Lafayette, IN).

All data are expressed as means ±SE. Where appropriate, the data was analyzed with one-way ANOVA. *Post-hoc* comparisons between means were analyzed with Tukey's multiple comparison test. A fiduciary level of $P \leq 0.05$ was regarded as significant.

Results

Blood pH, Pco_2, and lactate

The initial submergence of loggerhead sea turtles under laboratory and field conditions produced a dramatic and severe acidosis in all experimental turtles. Blood pH fell an average of 0.54 ±0.03 (range 0.49 to 0.59 pH units) and 0.63 ±0.06 (range 0.53 to 0.73 pH units) in laboratory turtles and field turtles, respectively, following initial submergence (Figs. 1A and 2A). The blood acidosis was derived from respiratory and metabolic components as evident from a positive proton-lactate deficit (Buffer capacity×ΔpH−Δ[lactate]), and from significant increases in blood Pco_2 and lactate (Figs. 1 and 2). The initial submergence also produced significant decreases in blood Po_2 and increases in plasma norepinephine ($P \leq 0.05$, $n=24$ for Po_2 and $n=11$ for norepinephrine). In contrast, minimal changes in blood pH, Pco_2, and lactate were observed following collection of the first two blood samples in nonsubmerged control turtles (Figs. 1 and 2).

Recovery of the respiratory and metabolic derangements in submerged turtles was dependent on the interval between successive submergences. A 10-min in-water rest interval between the first and second submergence (treatment-1 and -4 turtles) permitted partial recovery of blood pH (Figs. 1A and 2A) and Pco_2 (Figs. 1B and 2B), but blood pH remained significantly different from presubmergence values. Washout of additional lactate was also detected in these animals, whereby blood lactate concentration increased higher than the postsubmergence value (Figs. 1C and 2C). Turtles with a 42-min surface interval (treatment-2 and -5 turtles) between the first and second submergence had partial to complete recovery of blood pH (Figs. 1A and 2A), complete recovery of blood Pco_2 (Figs. 1B and 2B), and slight recovery of blood lactate (Figs. 1C and 2C). Only the blood lactate remained significantly different from the initial presubmergence value after the 42-min rest interval. Turtles with a 180-min in-water recovery interval (treatment-3 and -6 turtles) showed complete recovery of blood pH and Pco_2, although the lactate concentration was slightly higher than baseline levels (Figs. 1 and 2). Blood Po_2 and plasma norepinephrine recovered completely regardless of the surface interval ($P>0.05$, $n=24$ and $n=11$ for Po_2 and norepinephrine, respectively). Nonsubmerged control turtles in the laboratory and the field exhibited few significant changes in blood pH, Pco_2, or lactate, whether the interval between the second and third serial blood sample was 10, 42, or 180 min (Figs. 1 and 2).

The second 7.5-min submergence produced a drop in blood pH and an increase in Pco_2 (Figs. 1 and 2) in all of the experimental animals, and significant differences occurred in treatment 2–6 turtles. It is noteworthy, however, that the severity of the acid-base imbalance was not as drastic as the acidosis measured following the first submergence. The mean pH difference (ΔpH) between the second pre- and postsubmergence ranged from 0.11 and 0.16 in treatment-1 and -4 turtles (animals with a 10-min interval between submergences), respectively, to 0.50 in treatment-3 turtles and 0.66 in treatment-6 turtles (animals with a 180-min interval between submergences). The acidosis in treatment-1 and -4 turtles resulted, in part, from the continual elevation in blood lactate. In contrast, the longer surface interval between the two submergence episodes resulted in enhanced recovery of acid-base variables. Therefore, the turtles with a surface interval of 42 or 180 min had increased production of CO_2 and lactate in relation to turtles with a brief surface interval (Figs. 1 and 2). Comparable changes in blood Po_2 and norepinephrine were measured following the second submergence ($P \leq 0.05$, $n=24$ and $n=9$

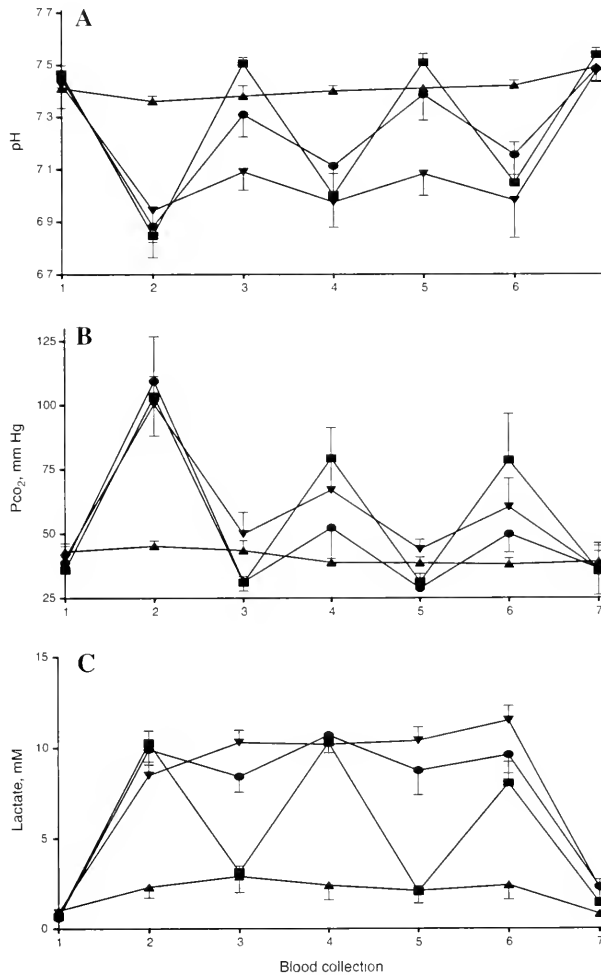

Figure 1

Blood pH (**A**), Pco_2 (**B**), and lactate (**C**) measured prior to and after three successive forced submergence episodes in loggerhead sea turtles in the laboratory. Blood collection 1, 3, and 5 are presubmergence samples, whereas blood collection 2, 4, and 6 are postsubmergence samples. Blood collection 7 was taken 180 min after the final submergence. The surface interval between the submergences was 10 min (▼), 42 min (●), or 180 min (■). Data from control sea turtles (▲) are shown for comparison.

for Po_2 and norepinephrine, respectively). Collection of the fourth sample from nonsubmerged control turtles revealed no significant changes in blood pH, Pco_2, or lactate when compared to the third sample (Figs. 1 and 2).

The remaining serial blood samples revealed comparable patterns in the blood pH, Pco_2, Po_2, lactate, and norepinephrine. Turtles given a longer rest interval at the surface (after the second submergence) had enhanced recovery of

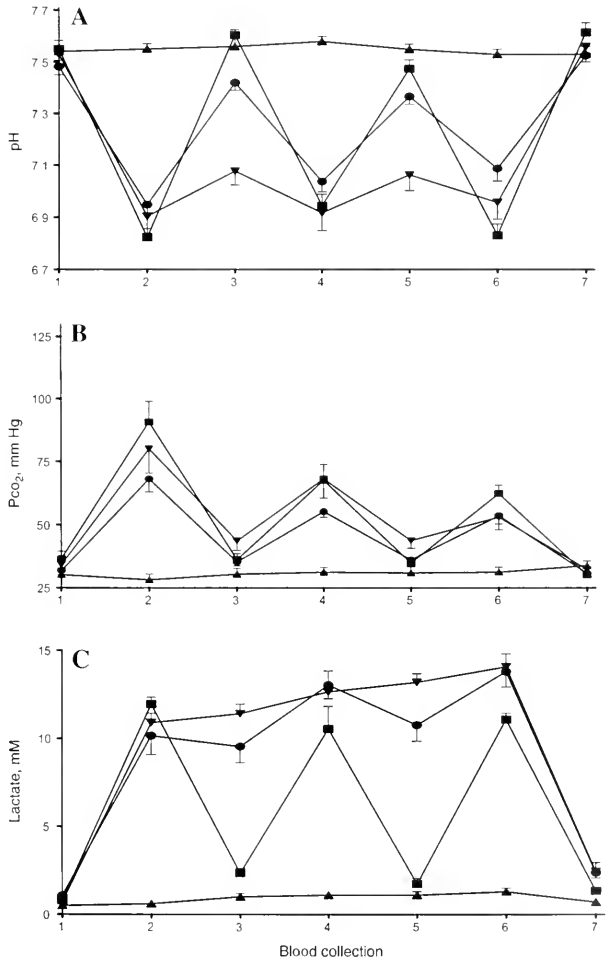

Figure 2

Blood pH (**A**), Pco_2 (**B**), and lactate (**C**) measured prior to and after three successive forced submergence episodes in loggerhead sea turtles in TED-equipped nets. Blood collection 1, 3, and 5 are presubmergence samples, whereas blood collection 2, 4, and 6 are postsubmergence samples. Blood collection 7 was taken 180 min after the final submergence. The surface interval between the submergences was 10 min (▼), 42 min (●), or 180 min (■). Data from control turtles (▲) are shown for comparison.

blood acid-base variables, whereas a brief surface interval permitted minimal recovery of blood homeostasis (Figs. 1 and 2). Submersion of experimental turtles a third time resulted in similar changes in blood pH, Pco_2, and lactate to that measured following the second submersion, and the length of the at-surface rest interval affected the magnitude of recovery of blood acid-base status. The seventh serial sample collected 180 min after the final postsubmer-

Table 1

Mean (±SE) plasma Na^+, K^+, and plasma osmotic pressure (OP) prior to and following laboratory multiple forced submergences of sea turtles with a 10-min, 42-min, or 180-min rest interval. Serial blood sampling regime is described in the "Materials and methods" section. Significant differences between samples 1 and 2, 3 and 4, and 5 and 6 are indicated by an asterisk (*), whereas significant differences of samples from the initial blood sample (serial sample 1) are denoted by a pound sign (#).

	10 min			42 min			180 min		
Treatment	Na^+ (mM)	K^+ (mM)	OP (mosm/kg)	Na^+ (mM)	K^+ (mM)	OP (mosm/kg)	Na^+ (mM)	K^+ (mM)	OP (mosm/kg)
Control	153 ±3	4.0 ±0.2	319 ±3	152 ±4	3.9 ±0.3	305 ±2	158 ±4	4.3 ±0.4	322 ±4
Serial sample									
1	144 ±5	4.5 ±0.3	319 ±6	158 ±6	3.9 ±0.2	314 ±11	162 ±2	4.1 ±0.1	296 ±3
2	159 ±6	5.9 ±0.6	341 ±4	163 ±3	6.1 ±0.6*#	364 ±10*#	187 ±2*#	6.9 ±0.3*#	342 ±5*#
3	145 ±3	4.9 ±0.2	330 ±5	156 ±2	4.1 ±0.3	336 ±8	160 ±4	4.4 ±0.1	308 ±4
4	166 ±7#	6.2 ±0.3#	351 ±14#	160 ±6	5.5 ±0.2#	342 ±15	179 ±4	6.7 ±0.5*#	339 ±4*#
5	158 ±6	5.1 ±0.1	335 ±11	147 ±6	4.1 ±0.3	334 ±12	158 ±6	3.9 ±0.2	305 ±5
6	154 ±5	6.1 ±0.3#	340 ±12	157 ±9	4.8 ±0.3	345 ±12#	181 ±2	5.7 ±0.5*	323 ±8#
7	139 ±3	4.8 ±0.4	323 ±8	149 ±6	4.4 ±0.3	331 ±7	158 ±10	4.4 ±0.5	305 ±3

gence sample revealed that blood pH, Pco_2, and lactate recovered completely for all experimental turtles (Figs. 1 and 2). Minimal changes in blood pH, Pco_2 and lactate were detected in laboratory and field control turtles during collection of the 5–7 serial blood samples (Figs. 1 and 2).

Ions, glucose, and osmotic pressure

Postsubmergence blood samples from laboratory turtles revealed elevations in plasma Na^+, K^+, and osmotic pressure when compared to the corresponding presubmergence values (Table 1). Significant increases in the plasma Na^+, K^+, and osmotic pressure were observed more frequently in turtles with a longer in-water rest interval between successive submergences (Table 1). In contrast, the plasma ion concentrations and osmotic pressure of control turtles did not substantially change ($P>0.05$, $n=9$) during serial blood sample collection. In addition, no significant differences in plasma glucose and Cl^- ($P>0.05$, $n=10$) were measured in any of the experimental turtles. Although most of the postsubmergence changes in the blood parameters in experimental turtles were not significant (Table 1), and minimal alterations in blood chemistry were observed in control turtles, the results suggested that there was a relationship between blood acid-base status and plasma osmolality and ion concentration. Therefore, correlation analyses were used to determine the interdependence of these variables.

Figure 3 shows the results of the correlation analyses, where pH is plotted versus ion concentration (i.e. Na^+, K^+, and Cl^- concentration), osmolality, or hematocrit. Nonsubmerged control turtles had a significant correlation between blood pH and plasma chloride, and pH and hematocrit (Fig. 3). As pH declined, there were slight, yet significant, increases in the $[Cl^-]$ and hematocrit. However, no correlation was detected between pH and plasma $[Na^+]$, $[K^+]$, or osmolality in these animals. In contrast, a significant correlation was detected between blood pH and plasma $[Na^+]$, $[K^+]$, $[Cl^-]$, osmolality, and hematocrit in experimentally submerged turtles (Fig. 3). In each case, a decrease in blood pH led to an increase in the correlated variable. These data are consistent with significant water movement into and out of the red blood cells during and after forced submersion.

Brief forced submergence of loggerhead turtles in trawl-equipped fishing nets had a profound effect on the plasma ionic status (Table 2). Plasma $[K^+]$ increased significantly immediately following submergence in all experimental turtles. Significant increases were also observed in the plasma $[Na^+]$ and osmotic pressure, although these changes did not occur in turtles from all of the experimental treatments (Table 2). Turtles partially to completely recovered from the ionic imbalances, although subsequent submergences caused significant increases in plasma K^+ and nonsignificant increases in plasma Na^+ and osmolality in most experimental turtles (Table 2). Ionic homeostasis in forcibly submerged turtles was achieved within 180 min of the final submergence, whereby plasma ion concentrations were comparable to the initial presubmergence values (Table 2). The plasma ion concentrations and osmotic pressure in nonsubmerged control turtles were unaffected by serial blood sampling. Thus, ionic changes in experimental turtles resulted from the forced submergence and not from handling and repetitive blood sampling.

Discussion

Acid-Base status

Multiple submergences of 2-year-old loggerhead sea turtles under laboratory and field conditions produced sig-

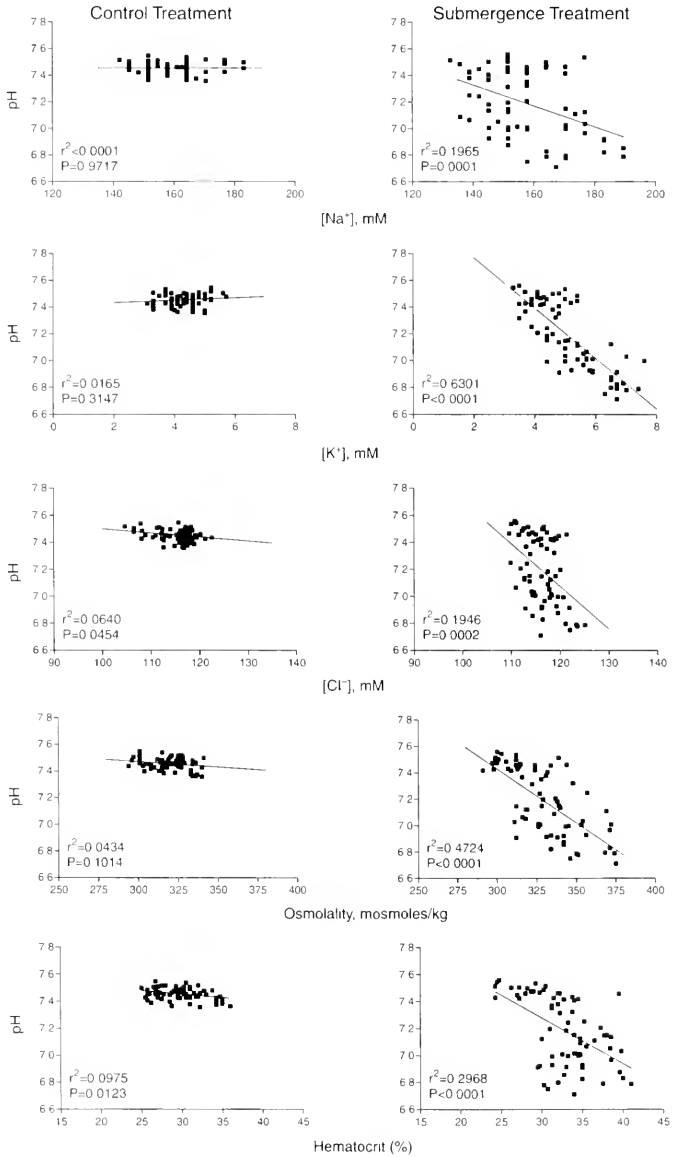

Figure 3

Relationship between blood pH and plasma [Na+], [K+], [Cl−], osmolality, and hematocrit in control (left column) and submerged (right column) loggerhead sea turtles. The lines are best fits to the data. Significance of the correlated variables is noted on each figure.

Table 2

Mean (±SE) plasma Na^+, K^+, and plasma osmotic pressure (OP) prior to and following multiple forced submergences of sea turtles in TED-equipped nets with a 10-min, 42-min, or 180-min rest interval. Serial blood sampling regime is described in the "Materials and methods" section. Significant differences between samples 1 and 2, 3 and 4, and 5 and 6 are indicated by an asterisk (*), whereas significant differences of samples from the initial blood sample (serial sample 1) are denoted by a pound sign (#).

	10 min			42 min			180 min		
Treatment	Na^+ (mM)	K^+ (mM)	OP (mosm/kg)	Na^+ (mM)	K^+ (mM)	OP (mosm/kg)	Na^+ (mM)	K^+ (mM)	OP (mosm/kg)
Control	150 ±3	3.0 ±0.2	313 ±8	139 ±6	3.4 ±0.2	321 ±7	151 ±1	3.1 ±0.1	310 ±5
Serial sample									
1	153 ±2	3.3 ±0.3	318 ±4	160 ±4	3.1 ±0.2	331 ±12	164 ±2	4.5 ±0.7	325 ±9
2	171 ±8	5.5 ±0.3*#	345 ±4*#	186 ±8*#	5.0 ±0.4*#	368 ±10	188 ±4	7.0 ±0.6*#	355 ±3*#
3	156 ±6	4.3 ±0.0#	332 ±4	163 ±3	2.8 ±0.1	338 ±11	163 ±10	3.6 ±0.3	314 ±3
4	171 ±8	5.3 ±0.1*#	349 ±1#	181 ±3	4.9 ±0.3*#	361 ±13	176 ±10	6.2 ±0.3*#	352 ±9*
5	166 ±4	4.3 ±0.1#	334 ±2	160 ±8	2.9 ±0.2	332 ±9	173 ±10	4.0 ±0.2	323 ±3
6	166 ±12	5.1 ±0.1#	335 ±11	185 ±4*#	4.5 ±0.4*#	343 ±14	175 ±18	5.3 ±0.0	333 ±11
7	157 ±4	3.7 ±0.1	325 ±2	161 ±6	2.6 ±0.2	326 ±9	159 ±11	3.6 ±0.6	320 ±4

nificant blood metabolic and respiratory disturbances. The most dramatic changes in blood pH, Pco_2, and lactate occurred following the first of the three forced submergences in all of the experimental turtles (Table 3). Under laboratory conditions, the turtles exhibited an average pH change of 0.54 U following the first submergence, whereas initial submergence of 2-year-old loggerhead sea turtles in TED-equipped commercial fishing nets induced a pH decrease of 0.63 U. The initial acid-base disturbances measured in our study were comparable in magnitude to those measured in Kemp's ridley and loggerhead sea turtles in standard TED certification trials (Table 3).

The second and third submergences of 2-year-old loggerheads sea turtles did not result in similar changes in blood pH, Pco_2, and lactate, as was measured following the initial submergence (Table 3). To our knowledge, no information is available in the literature on the physiological effects of multiple submergences in sea turtles for comparison. Obviously, the interval between the submergence episodes directly influenced the magnitude of the blood acid-base imbalance during successive submergences. A longer time interval at the surface led to enhanced recovery of blood pH, Pco_2, and lactate. Lutz and Dunbar-Cooper (1987) reported that loggerhead sea turtles captured during trawling at Cape Canaveral, Florida, exhibited a 16.8% decline in lactate 180 min following submergence. Those authors proposed that the rate of lactate decline was dependent on the magnitude of the lactate concentration, so that 10 mM of lactate would decline at a rate of 1.25 mM lactate/h. However, in the present study, the rate of lactate decline was considerably higher than that suggested by Lutz and Dunbar-Cooper (1987). Lactate declined 70.0% and 79.6% within 180 min of the submergence episodes in treatment 3 turtles, whereas no decline was measured in treatment 1 turtles (10 min interval) between submergences. In fact, it was apparent that lactate continued to washout into the bloodstream during the 10-min recovery phases in these turtles (Fig. 1, Table 3). Thus, turtles with a brief period between the submergence episodes would have a limited ability to release the CO_2 retained during submersion or to break down lactic acid produced during the course of the forced dive. Lactate declined 15.2% and 18.7% during the 42-min interval between submergences in treatment-2 turtles. Blood lactate declined 80.9%, 76.0%, and 82.5% in treatment-1, -2, and -3 turtles, respectively, during the final 180-min recovery period. Thus, the overall rate of lactate decline in the final 180 minutes of the laboratory study was 2.6 ±0.2 mM/h. Finally, the elevated lactate concentration in sea turtles during the 180-min postsubmergence recovery time interval suggests that the samples were collected too soon to permit complete recovery of blood lactate.

Comparable rates of lactate clearance measured in the laboratory submergence study were detected following forced submergences of loggerhead sea turtles in TED-equipped fishing nets. Substantial retention of CO_2 and additional washout of lactate occurred during the 10-min postsubmergence recovery interval in treatment-4 turtles. Treatment-5 turtles exhibited a 6% drop in the blood lactate concentration during the first 42-min postsubmergence recovery interval and a 17.5% decrease in the blood lactate during the second recovery interval. Thus, the 42-min postsubmersion recovery interval permitted recovery of blood gases, but was inadequate to clear the blood lactate (Fig. 2, Table 3). Lactate declined 80.4% and 83.8%, respectively, during the first two 180-min postsubmergence recovery intervals in treatment-6 turtles. As was the case for laboratory submerged sea turtles, a longer surface interval ultimately resulted in an increased ability to recover from the submersion episodes. In fact, lactate declined 82.7%, 82.8%, and 87.9%, respectively, in treatment-4, -5, and -6 turtles 180 minutes after the final submersion episode (Fig. 2, Table 3).

Table 3

Effects of forced submergence on blood pH, Pco_2, and lactate in Kemp's ridley (LK) and loggerhead (CC) sea turtles. Data are expressed as the mean difference (Δ) between post- and presubmergence values. Data from this study are provided from the three submergence episodes of treatment 1–3 turtles under the laboratory protocol and treatment 4–6 turtles in the field protocol. ND = not determined

Species	Turtle size (kg)	Submergence duration (min)		ΔpH	ΔPco$_2$ (mm Hg)	Δlactate (mM)	Reference
LK	5–16.5	≤7.3		0.37	12.8	8.5	Stabenau et al. (1991)
	5–6	≤7.3		0.31	24.5	15.1	TED certification tests[1]
CC	5–6	4.3		0.33	ND	13.4	TED certification tests[1]
	5–6	12.5		0.52	ND	17.2	
CC	6.5–7.0	7.5	treatment 1	1) 0.49	61.1	7.6	Laboratory study
				2) 0.11	16.3	−0.1	
				3) 0.10	15.3	1.1	
			treatment 2	1) 0.57	70.8	9.3	
				2) 0.20	20.9	2.3	
				3) 0.23	21.1	1.1	
			treatment 3	1) 0.59	98.7	9.6	
				2) 0.50	68.6	7.2	
				3) 0.46	67.3	5.9	
			treatment 4	1) 0.63	45.8	10.2	Field study
				2) 0.16	24.5	1.9	
				3) 0.11	9.3	0.9	
			treatment 5	1) 0.53	36.3	9.1	
				2) 0.38	19.9	3.5	
				3) 0.28	17.5	3.0	
			treatment 6	1) 0.73	54.2	11.2	
				2) 0.66	31.3	9.2	
				3) 0.65	27.5	9.3	

[1] Data were collected by one of the authors (EKS) during standard TED certification tests in 1993–94. Samples were collected from the cervical sinus of Kemp's ridley and loggerhead sea turtles prior to and following forced submergences in a commercial shrimp net equipped with a TED. Turtles in these studies were permitted to exit the TED-equipped net.

It must be noted that any discussion on lactate production and recovery following submersion is applicable to environmental conditions comparable to those reported in this study. For example, lactate formation and recovery rates of lactate build-up would be significantly influenced by water temperature. Longer recovery rates may take place in cold water, whereas warmer waters may lead to additional lactate production thereby influencing the rate of lactate elimination. In addition, the blood lactate concentrations measured in this study may underestimate the true lactate burden. Lactate has been shown to partition into other tissues, including the shell, following submersion of freshwater turtles (Jackson et al., 1999). Finally, sea turtle size could potentially alter lactate production and elimination. Results from submersion experiments conducted in our laboratory indicate that smaller animals exhibit a significant acidosis and lactate build-up in comparison to larger sea turtles. Whether less acidosis and lactate build-up is due to additional lactate buffering by the larger sea turtles warrants further investigation.

Ions, osmolality, and hematocrit

There are three primary mechanisms for recovery of blood pH following an acid-base disturbance: cellular buffering, and respiratory and renal compensation. Cellular responses occur immediately following the disturbance, whereas respiratory and renal adjustments occur within minutes to hours, respectively. Previously, Stabenau et al. (1991) reported that Kemp's ridley sea turtles exhibited a significant increase in plasma $[K^+]$ following trawl submergences. However, those authors reported that trawl stress had no effect on plasma $[Cl^-]$, $[Na^+]$, or hematocrit. In the present study, a cellular response to the severe acid-base disturbance caused by the multiple forced submergences was suggested by alterations in plasma ion concentrations, osmolality, and hematocrit during the blood acidosis. As shown in Figure 3, decreases in blood pH were correlated with increases in $[K^+]$, $[Na^+]$, $[Cl^-]$, osmolality, and hematocrit.

Hematocrit (percent packed red blood cells) changes may result from washout of additional red blood cells into the bloodstream, from areas such as the spleen, in order to provide more red blood cells during the hypoxic phases of the forced submergence. This explanation, however, is unlikely given that substantial fluctuations in hematocrit were observed during the course of the submergence experiments and that a normal hematocrit was measured in the final serial blood sample. A more plausible explanation is that there was an osmotically obliged influx of water into the red blood

cells, swelling the cells, and leading to increases in hematocrit, and in plasma ion concentration and osmotic pressure. Red cell volume is regulated in animals through transport of intracellular and extracellular solutes. Although there is minimal information available in the literature concerning regulatory volume transport in reptiles, the mechanisms of regulatory volume increase (RVI) and regulatory volume decrease (RVD) are known in other lower vertebrates. For example, Cala (1983) reported that in *Amphiuma* (amphiuma [common name]) red cells, the mechanism of RVD is K^+_{out}/H^+_{in} counter-transport coupled with $Cl^-_{out}/HCO_3^-_{in}$ exchange (where the subscripts in and out represent transport into and out of the cell, respectively), whereas RVI is accomplished by Na^+_{in}/H^+_{out} transport coupled with $Cl^-_{in}/HCO_3^-_{out}$ exchange (Cala, 1983). Other studies have suggested that red cell RVD occurs because of electroneutral KCl cotransport out of the cell and RVI occurs because of electroneutral NaK2Cl or NaCl cotransport into the cell (Haussinger and Lang, 1991). It is impossible to determine which of these mechanisms, if any, were involved in regulating red cell volume in sea turtles during and following forced submergence. These transporters, however, have been shown to be sensitive to cellular hypoxia (i.e. low Po_2) and low blood pH (Cossins and Gibson, 1997)—conditions present in the experimental turtles following submergence. In addition, hypoxic and acidotic conditions were absent in nonsubmerged control turtles which did not experience substantial shifts in plasma ion concentrations, osmotic pressure, or hematocrit.

Effects of handling

Significant changes in blood pH, Pco_2, and lactate were occasionally detected in nonsubmerged control turtles. However, it is impossible to determine if these changes resulted from repetitive handling during blood sampling or from increased activity while free-swimming in a large circular tank following blood collection. Nevertheless, control turtle blood lactate concentration was substantially less than the lactate measured following forced submergence in experimental turtles (Figs. 1 and 2). In addition, the blood pH remained fairly constant in the control turtles during collection of the seven serial samples.

Laboratory versus field experimentation

It should be noted that conducting the study under laboratory and field conditions provided unique benefits for analyzing the physiological effects of submersion. For example, the laboratory conditions permitted collection of blood samples immediately upon termination of the submersion period, whereas in the field, sea turtles had to be transported back to the trawl vessel for postsubmersion blood sampling. Turtles forcibly submerged under laboratory or field conditions hyperventilated upon surfacing. Stabenau et al. (1991) reported a 9- to 10-fold increase in the breathing frequency of trawled Kemp's ridley sea turtles. Comparable breathing rates were observed in the present study after submersion and, thus, it is plausible that the blood Pco_2 measured in turtles under field conditions underestimated the actual buildup in blood CO_2 (see Table 3 for a comparison of the blood Pco_2 under laboratory and field conditions). In contrast, the field experiment permitted examining the physiological stress of semiwild turtles in TED-equipped commercial fishing nets following a minimum of 21 days of in-water conditioning. The greater acidosis measured in forcibly submerged turtles resulted from increased swimming activity during the forced submergence. This is confirmed by a postsubmergence increase in blood lactate of 10.1 mM under trawling conditions versus 8.8 mM following laboratory submergence. Under laboratory and field conditions, the behavior of the turtles following submergence was monitored up to their release. It is unclear, however, if the acid-base and ionic imbalance caused by forced submersions would alter long-term normal physiology and behavior. It is plausible that repetitive alteration of blood pH by the magnitude measured in the present study may have pathological consequences. For example, no information is available on whether turtles resume normal diving and feeding behavior following prolonged or multiple forced submersions, or whether turtles become more susceptible to repeated submersions in TED-equipped nets.

Use of turtles reared in captivity

Two-year-old loggerhead sea turtles reared in captivity were used for all of the submergence experiments. It was assumed that these animals were adequate surrogates for wild sea turtles. In fact, similar-size animals from the NMFS Galveston Laboratory are used in annual TED certification trials. Nevertheless, there may be differences in the physiology of captive and wild turtles subjected to forced submergences. For example, it is possible that wild sea turtles would be exposed to forced submergences following lengthy, voluntary dives. No information is available in the literature on the acid-base and ionic status of wild sea turtles following prolonged voluntary dives or forced multiple submergences. If dives are anaerobic, then subjecting wild sea turtles to multiple forced submergences may adversely affect survival potential.

Conclusions

The data suggest that forced submergences of 2-year-old loggerhead sea turtles reared in captivity produce significant blood metabolic and respiratory acidosis. Repetitive submergences did not augment the acidosis, rather subsequent submergences resulted in less severe acid-base disturbances. Under trawl conditions, the turtle must recover from any physiological acid-base disturbance when it is freed from a TED-equipped net. Recovery is accomplished, in part, by the turtle immediately surfacing and hyperventilating (Jackson, 1985; Stabenau et al., 1991). This behavior was observed following each submergence episode. Turtles would then resume normal voluntary diving behavior, presumably after partial-to-complete recovery from the acid-base disturbance. These data suggest that repetitive submergences of sea turtles in TED-equipped

nets would not significantly affect their survival potential, provided that the turtles have a recovery interval between successive submergences. However, it should be noted that the latter statement is based on comparable-size turtles that may be submerged in shrimp nets equipped with legally certified and installed turtle excluder devices. Poor installation or lack of use of legal TEDs would result in augmenting the acid-base imbalance in the turtles. Increasing the magnitude of the blood acid-base and ionic disturbance during each submersion would increase the length of time necessary to achieve partial or complete recovery.

Acknowledgments

Grateful appreciation is expressed to personnel from the National Marine Fisheries Service Galveston and Pascagoula Laboratories for their assistance in turtle husbandry and in conducting the submersion protocol under laboratory and very difficult field conditions. These studies were conducted under appropriate threatened and endangered species permits issued by the U.S. Fish and Wildlife Service, Texas Park and Wildlife Department, and the Florida Department of Natural Resources.

Literature cited

Caillouet, C. W., M. J. Duronslet, A. M. Landry, D. B. Revera, D. J. Shaver, K. M. Stanley, R. W. Heinly, and E. K. Stabenau.
1991. Sea turtle strandings and shrimp fishing effort in the Northwestern Gulf of Mexico, 1986–89. Fish. Bull. 89:712–718.

Cala, P. M.
1983. Volume regulation by red blood cells: mechanisms of ion transport. Mol. Physiol. 4:33–52.

Cossins, A., and J. Gibson.
1997. Volume-sensitive transport systems and volume homeostasis in vertebrate red blood cells. J. Exp. Biol. 200:343–352.

Crowder, L. B., S. R. Hopkins-Murphy, and J. A. Royle.
1995. Effects of turtle excluder devices (TEDs) on loggerhead sea turtle strandings with implications for conservation. Copeia 1995:773–779.

Haussinger, D., and F. Lang.
1991. The mutual interaction between cell volume and cell function: a new principle of metabolic regulation. Biochem. Cell Biol. 69:1–4.

Jackson, D. C.
1985. Respiration and respiratory control in the green turtle, *Chelonia mydas*. Copeia 1985:664–671.

Jackson, D. C., Z. Goldberger, S. Visuri, and R. N. Armstrong.
1999. Ionic exchanges of turtle shell *in vitro* and their relevance to shell function in the anoxic turtle. J. Exp. Biol. 202(part 5):513–520.

Lutz, P. L., and A. Dunbar-Cooper.
1987. Variations in blood chemistry of the loggerhead sea turtle *Caretta caretta*. Fish. Bull. 85:37–44.

National Research Council.
1990. Decline of sea turtles: causes and prevention, 259 p. National Academy Press, Washington, DC.

Owens D. W., and G. J. Ruiz.
1980. New methods of obtaining blood and cerebrospinal fluid from marine turtles. Herpetologica 36:17–20.

Stabenau, E. K., and T. A. Heming.
1994. The *in vitro* respiratory and acid-base properties of blood and tissue from the Kemp's ridley sea turtle, *Lepidochelys kempi*. Can. J. Zool. 72:1403–1408.

Stabenau, E. K., T. A. Heming, and J. A. Mitchell.
1991. Respiratory, acid-base and ionic status of Kemp's ridley sea turtles (*Lepidochelys kempi*) subjected to trawling. Comp. Biochem. Physiol. 99A:107–111.

Wood, S. C., R. N. Gatz, and M L. Glass.
1984. Oxygen transport in the green sea turtle. J. Comp. Physiol. B. 154:275–280.

Quantitative determination of the timing of otolith ring formation from marginal increments in four marine teleost species from northwestern Australia

Peter C. Stephenson

Western Australian Marine Research Laboratories
West Coast Drive (off Elvire St)
Waterman, Western Australia, 6020, Australia
E-mail address: pstephenson@fish.wa.gov.au

Norm G. Hall

School of Biological and Environmental Sciences
Murdoch University
Murdoch, Western Australia, 6150, Australia

Abstract—The sectioned otoliths of four fish species from a tropical demersal trawl fishery in Western Australia revealed a series of alternating translucent and opaque zones in reflected light. The translucent zones, referred to as growth rings, were counted to determine fish ages. The width of the opaque zone on the periphery of the otolith section as a proportion of the width of the previous opaque zone (index of completion) was used to determine the periodicity of growth-ring formation.

This article describes a method for modeling changes in the index of ring completion over time, from which a parameter for the most probable time of growth-ring formation (with confidence intervals) can be determined. The parameter estimate for the timing of new growth-ring formation for *Lethrinus* sp. 3 was from mid July to mid September, for *Lutjanus vitto* from early July to the end of August, for *Nemipterus furcosus* from mid July to late September, and for *Lutjanus sebae* from mid July to mid November. The confidence intervals for the timing of formation of growth rings was variable between species, being smallest for *L. vitta*, and variable between fish of the same species with different numbers of growth rings.

The stock assessments of these commercially important species relies on aging information for all the age classes used in the assessment. This study demonstrated that growth rings on sectioned otoliths were laid down annually, irrespective of the number of growth rings, and also demonstrated that the timing of ring formation for these tropical species can be determined quantitatively (with confidence intervals).

Manuscript approved for publication 3 June 2003 by Scientific Editor.

Manuscript received 26 June 2003 at NMFS Scientific Publications Office.

Fish. Bull 101:900–909 (2003).

The Pilbara fish trawl fishery, operating on the North West Shelf of Western Australia, has developed rapidly in the last ten years and is now the most valuable commercial scalefish fishery in Western Australia. Catch from this fishery was valued at $7 million (wholesale value) in 2001. In this multispecies fishery, *Lutjanus vitta* (Quoy and Gaimard, 1824) (brownstripe red snapper), *Nemipterus furcosus* (Valenciennes, 1830) (fork-tailed threadfin bream, also known as rosy threadfin bream), *Lethrinus* sp. 3 (Carpenter and Niem, 2001) (lesser spangled emperor, known locally as blue-spot emperor) made up 8%, 10%, and 20% respectively of the total scalefish trawl catch in 2000. The highly prized species, *Lutjanus sebae* (Cuvier, 1828) (red emperor), although comprising only 4% of the catch, is important because of its high market value.

In 1993 a research project was commenced to determine the fishing effort required for optimal level of catches in the Pilbara trawl fishery (Stephenson and Dunk[1]). The project relied on validated age composition data for *L.vitta*, *L.* sp. 3, *N. furcosus*, and *L. sebae*. The growth rings on otoliths have been shown to be formed annually for only one to three growth rings for *N. furcosus* (Sainsbury and Whitelaw, 1984), and for two to three growth rings for *L. sebae* (McPherson and Squire, 1992). After pooling of all age classes, Davis and West (1992) showed that growth rings of *L. vitta* were formed annually.

Determining age composition involves counting growth rings on hard parts of fish (otoliths, scales, spines, bones) and determining the timing of growth-ring formation. Sagittal otoliths are commonly used for aging teleost fishes and recent studies (Hyndes et al., 1992; Milton et al., 1995; Newman et al., 1996) have indicated that for some species sectioned otoliths give more reliable age estimates than whole, or broken-and-burnt otoliths. The periodicity of ring formation is commonly determined by the mark-recapture method in which fish are injected with chemical markers and the number of rings created between injection and recapture are compared (Ferreira and Russ, 1992; Francis et al., 1992; Newman et al., 1996).

An alternative to mark-recapture is marginal increment analysis in which the distance from the growth ring to the edge of the otolith, for a sample of fish, is tracked over time (Campana, 2001) and a sharp drop in this marginal increment, once a year, is taken as an indication of annual ring formation. The analysis is often performed on

[1] Stephenson, P. C., and I. Dunk. 1996. Relating fishing mortality to fish trawl effort on the North West Slope of Western Australia. Final report of project 93/25 to the Fisheries Research and Development Corporation, 1995, 44 p. Western Australia Marine Research Laboratories, PO Box 20, North Beach, Western Australia 6092, Australia.

pooled age classes (Barger, 1985; Manickchand-Heileman and Kenny, 1990; Murphy and Taylor, 1990; Ross et al., 1995; Pearson, 1996; Morales-Nin and Moranta, 1997; Van der Walt and Beckley, 1997) or on a restricted number of age classes (Sainsbury and Whitelaw, 1984; McPherson and Squire, 1992).

Analysis with pooled data has limited value because there may be different patterns of growth-ring formation at different life stages (e.g. at sexual maturity) and pooled data may have interage differences masked by dominant age groups (Beamish and McFarlane, 1983; Hyndes et al., 1992). Studies in which data were pooled only for young and old fish, due to low fish numbers, reduced these problems and improved the credibility of the results (Hyndes et al., 1992; Fletcher and Blight, 1996; Hesp et al., 2002).

Accounts of statistical analysis of the marginal increment data are rare. Davis and West (1992) used ANOVA to show that there were differences in the marginal increment of urohyal bones of *L. vitta* with time of year. As this seasonal pattern was the same for age classes 1 to 6, Davis and West (1992) pooled the data and used a graphical representation to show the time of formation of the annual rings.

This article describes a method for modeling changes in the index of completion of an otolith growth increment over time. This method enables quantitative determination of the most probable time of growth-ring formation (with confidence intervals) and is illustrated for the species *L. vitta*, *L.* sp. 3, *N. furcosus*, and *L. sebae*, from the Pilbara fish trawl fishery.

Materials and methods

Between October and November 1993 and between October and November 1994, samples of 30 fish of each species were randomly selected each month from fishery-independent trawl surveys. For the other months between January 1994 and March 1995, samples of 30 fish of each species were randomly selected each month from commercial catches. The samples came from an area between 115°30′E longitude and 120°E longitude; between the 50 meter and 100 meter depth isobaths.

The sagittal otoliths were extracted from each sampled fish and the right otolith was embedded in epoxy resin and then sectioned transversely through the otolith core to a thickness of 0.4 mm. A Gemmaster high speed saw with a 100 mm by 0.1 mm diamond tipped saw blade was used for sectioning. The otolith sections were set on 76 mm by 50 mm glass slides with casting resin and covered with cover slips. The sections were viewed with a dissecting microscope with an attached color video camera connected to a personal computer and a color monitor. Transmitted light revealed alternating wide opaque and narrow translucent zones. The translucent zones, referred to in the present study as growth rings, were counted to determine fish ages.

The distance from the outer extremity of the last wide, dark band to the otolith edge, w_t, is referred to as the marginal increment and the distance between the outer edges of the second to last and the last dark band is denoted by w_{t-1}. The distances w_t and w_{t-1} on the portion of the otolith ventral to the sulcus towards the proximal margin were measured on the computer screen. The index of completion, c_t, was determined by using the formula of Tanaka et al. (1981)

$$c_t = \frac{w_t}{w_t - 1} \qquad (1)$$

and written to a file by using a computer program written in the programming language "HiSoft Basic" (version 2.0. MichTron, Auburn Hills, MI).

The index of completion, c_t, we expect to increase over time, and then decrease abruptly when a new growth ring is formed. The timing of formation of a new ring would occur at the same time for a fish species with the same number of rings, but there would be considerable variability in timing and detection between species and individuals (Fig. 1).

The increase in the index of completion over time, t, is modeled as a strictly increasing function $f(t, a, b, d)$ with the following parameters: maximum value, a, rate of increase, b, and horizontal translation, d.

For our study, data were collected over a period of 18 months (October 1993 to March 1995) and the relation between the index of completion and time was expressed as two functions, denoted F_1 and F_2

$$F_1 : \hat{c}_1 = f(t, a, b, d_1) \text{ and } F_2 : \hat{c}_2 = f(t, a, b, d_2), \qquad (2)$$

where $\hat{c}_1$ and $\hat{c}_2$ = the estimates of the index of completion;
t = the time in months from $t = 0$ (1 October 1993) to $t = 18$ (31 March 1995); and
d_1, d_2 = the translation parameters for functions F_1 and F_2 respectively.

If the point (c_i, t) is associated with function F_1, the value of the normal probability density function of the observed deviation from F_1, evaluated at observation, i, is given by

$$\lambda_{1,i} = \frac{1}{\sigma\sqrt{2\pi}} \exp\left(\frac{(c_i - \hat{c}_1)^2}{2\sigma^2} \right),$$

and similarly the value of the normal probability density function of the observed deviation from F_2, evaluated at observation, i, is given by

$$\lambda_{2,i} = \frac{1}{\sigma\sqrt{2\pi}} \exp\left(\frac{(c_i - \hat{c}_2)^2}{2\sigma^2} \right),$$

where σ^2 is the variance of the residuals when F_1 is fitted to the data and where it is assumed to be equal to the variance of the residuals when the function F_2 is fitted.

To ensure the tractability of the subsequent analysis, we assume that the probability, P_t, of a point with index of completion c_t, at time t, being represented by F_1, is given by the logistic function

$$P_t = \frac{1}{1 + \exp\left[\ln(19) \frac{(R - t)}{(S - R)} \right]}, \qquad (3)$$

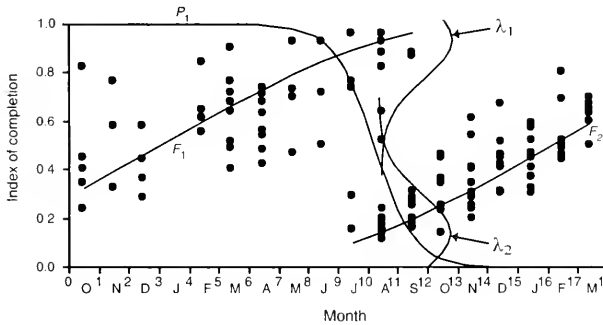

Figure 1

Values of index of completion at time t, (c_i, t) for *L. vitta* with five growth rings during the monthly time intervals from 1 October 1993 (t=0) to 31 March 1995 (t=18). Also illustrated are the functions F_1 and F_2 fitted to (C_i, t) and the function P_t representing the probability that (C_i, t) is most likely represented by function F_1. The likelihood functions, λ_1 and λ_2 are shown for the values of index of completion when t = 10.4.

where R, S, and R–(S–R) are the values of t corresponding to the 50th, 95th, and 5th percentiles of the logistic function. The probability that the index of completion is associated with F_2, rather than F_1, is calculated as 1–P_t.

Figure 1 illustrates typical values of the index of completion at time t and the functions F_1 and F_2 representing these points before and after new growth-ring detection. The most likely time at which a new growth ring is detected is given by the value of t when P_t=0.5. The likelihood functions λ_1 and λ_2 are illustrated for t = 10.4 months. When $\lambda_{1,i}$ is high, (c_i, t) is likely to lie closest to F_1 and when $\lambda_{2,i}$ is high, (c_i, t) is likely to lie closest to F_2.

As a point (c_i, t) will be associated with either F_1 or F_2 (but not both), it follows that the likelihood function K is given by

the probability of the observed deviation from F_1, given that the point is associated with F_1	×	probability that the point is represented by F_1	+	the probability of the observed deviation from F_2, given that the point is associated with F_2.	×	probability that the point is represented by F_2.

That is, $$K_{t,i} = \lambda_{1,i}P_t + \lambda_{2,i}(1 - P_t).$$

The overall log-likelihood associated with all the observed points (c_i, t), , for i = 1 to n in a particular age class is given by

$$\sum_{i=1}^{n} \ln(K_{t,i}) = \sum_{i=1}^{n} \ln\left[\lambda_{1,i}P_t + \lambda_{2,i}(1 - P_t)\right].$$

The parameters of the functions F_1 and F_2 (i.e. a, b, d_1, and d_2, as well as σ, R, and S) were estimated separately for each value of the number of rings by maximizing the log-likelihood.

The value of $t = R$ corresponds to the month where a value of the index of completion is equally likely to be on either F_1 or F_2; that is, the point where the drop in the index of completion occurs. The value of S and R–(S–R) correspond to the 95th and the 5th percentiles for the time at which a new growth ring is likely to be detected, indicating reliability of the estimate of the time of ring formation $t = R$.

Results

The plots of index of completion versus time reflected this growth pattern in the four species we studied, with the growth rate decreasing as the time of new growth-ring detection approached.

The temporal pattern of growth of the otolith suggests the index of completion could be modeled with a logistic function

$$F(t,a,b,d) = \frac{a}{1+\exp\left[\ln 19\frac{(d-t)}{b}\right]},$$

with the maximum value a = 1, phase shift d, and rate of increase b.

A characteristic of otolith growth is that the distance between growth rings decreases each year, thus, the rate of increase in the marginal increments will be greater for fish with few rings and less for fish with many rings. On the other hand, the index of completion, being the ratio of

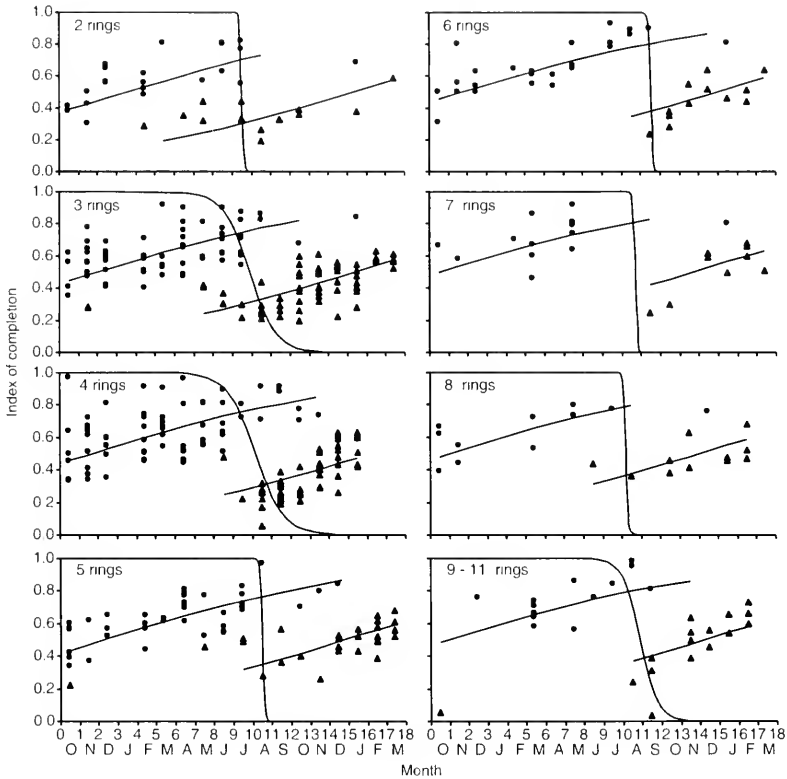

Figure 2

Index of completion at time t, (c_i, t), for *L.* sp. 3 for growth-ring categories 2, 3, 4, 5, 6, 7, 8, and 9–11 sampled between the months 1 October 1993 (t=0) to 31 March 1995 (t=18). The solid circles (●) represent those (c_i, t) most likely represented by $\hat{c}_1$ and lying closest to the function F_1 and the solid triangles (▲) are those most likely represented by $\hat{c}_2$ and lying closest to the function F_2. The logistic function, P_t, indicates the probability that points (c_i, t) are most likely represented by function F_1.

the marginal increment to the width of the previous band, would be expected to be constant at the same time of year for a particular species, regardless of the ring count.

Thus, during the maximization of the objective function

$$\sum_{i=1}^{n} \ln(K_{i,j}),$$

the rate of increase parameter b is assumed constant for all ring counts for a species, but the other parameters (d_1, d_2, R, and S) are estimated for each number of rings for each species.

Figure 2 shows the pattern of changes in the index of completion for *L.* sp. 3 for otoliths with two to eleven growth rings from 1 October 1993 (t=0) to 31 March 1995 (t=18). The data were pooled for the older age classes (nine or more growth rings) because of the small numbers of old fish in the samples. The points indicating the values of index of completion, c_i, are represented with different symbols according to whether they are most likely to be represented by $\hat{c}_1$ (lying closest to the function F_1) or most likely to be represented by $\hat{c}_2$ (lying closest to the lower line F_2). The function P_t represents the probability of points being represented by line F_1. The time where P_t=0.5 is the most likely time of detection of the formation of a new growth ring.

In the other three species, *L. vitta*, *N. furcosus*, and *L. sebae*, the points representing index of completion, (c_i, t) and functions, F_1, F_2, and P_t are illustrated in Figures 3, 4,

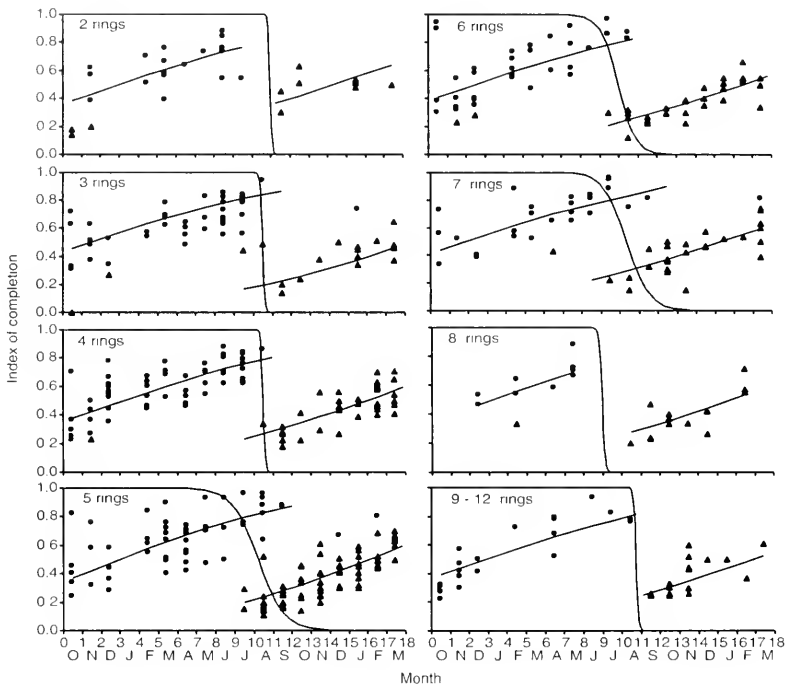

Figure 3

Index of completion at time t, (c_i, t), for *L. vitta* for growth-ring categories 2 ,3, 4, 5, 6, 7, 8, and 9–12 sampled between the months 1 October 1993 (t=0) to 31 March 1995 (t=18). The solid circles (●) represent those (c_i, t) most likely represented by $\hat{c}_1$ and lying closest to the function F_1 and the solid triangles (▲) are those most likely represented by $\hat{c}_2$ and lying closest to the function F_2. The logistic function, P_t, indicates the probability that points (c_i, t) are most likely represented by function F_1.

and 5. Because of the smaller numbers of fish, the data was pooled for *L. vitta* with 9–12 growth rings, for *N. furcosus* with 7–9 growth rings, and for *L. sebae* with 13–14 and 15–19 growth rings.

The estimates of the parameters b, d_1, d_2 (the rate of increase and phase shift of F_1 and F_2), R, the time of formation of a new growth ring, with the range $\pm(S–R)$, and the standard deviation (σ) for the four species are listed in Table 1.

The estimated time of formation of a new ring varied between age classes and occurred for *L.* sp. 3 from mid July to mid September, for *L. vitta* from early July to early September, for *N. furcosus* from mid July to late September, and for *L. sebae* from mid July to mid November.

The confidence intervals are small for *L.* sp. 3 and *L. vitta* and generally larger for *N. furcosus* and *L. sebae* where reading increments was more difficult. The confidence interval was smaller for *L. sebae* with 12–19 growth rings because the clarity of the rings generally improved for older fish.

The difference between the phase shift for functions F_1 and F_2, that is d_2–d_1, was between 11 to 13 months. This difference indicated an annual cycle of growth-ring formation. The standard deviation, σ, of the values of index of completion was lowest for for *L. vitta* (0.1–0.14) and highest for *L. sebae* (0.11–0.21) and *L.* sp. 3 (0.11–0.24).

Discussion

With different starting values for the parameters, the method we described found that the time of detection of growth-ring formation for the four species was consistent. Although the timing varied considerably for different numbers of growth rings, the estimate was generally similar for each species.

Other marginal increment studies on these species produced estimates of the times for growth-ring formation

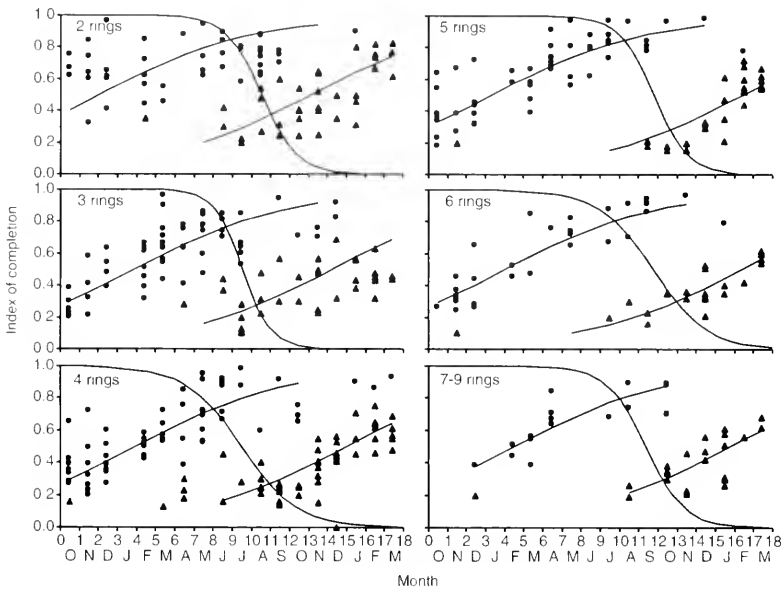

Figure 4

Index of completion at time t, (c_t, t), for *N. furcosus* for growth-ring categories 2 ,3, 4, 5, 6, and 7–9 sampled between the months 1 October 1993 (t=0) to 31 March 1995 (t=18). The solid circles (●) represent those (c_t, t), most likely represented by $\hat{c}_1$ and lying closest to the function F_1 and the solid triangles (▲) are those most likely represented by $\hat{c}_2$ and lying closest to the function F_2. The logistic function, P_t, indicates the probability that (c_t, t) are most likely represented by function F_1.

that are consistent with those determined in the present study (Table 2). Davis and West (1992) found that the time of formation of a new translucent growth-ring on urohyal bones for *L. vitta* was October, later than the timing found in our study. Sainsbury and Whitelaw (1984) found the marginal increment values on whole otoliths from *N. furcosus* had low values in July 1979 and in May 1980 (earlier than observed in the present study for sectioned otoliths) but the sampling reported by Sainsbury and Whitelaw (1984) was very sparse: four sampling times in 1979 and two in 1980. McPherson and Squire (1992) reported that the mean monthly marginal increment of the first two age classes for *L. sebae* appeared to have a minimum between July and September that is consistent with the present study.

In our study, the growth zones on *L. vitta* were generally clearly defined; the opaque zone was easily distinguished from the translucent zone, and there were few discontinuities (areas of dissimilar structure or optical density within the growth zone). This clear definition was especially noticeable for the outer growth zones of the otolith for older fish which often had very clear dark zones. This finding is consistent with the small confidence intervals for this species, especially in the fish with a greater number of growth rings in their otoliths. The growth rings on *L.* sp. 3 and *N. furcosus* had poor contrast and had many discontinuities which made the analysis difficult. For young *L. sebae*, there were many discontinuities within the growth zones which made locating the translucent zone difficult. For fish with two to four growth rings, low values of the index of completion occurred when t = 7 and also when t = 12 (Fig. 5). For the older *L. sebae* (where the number of rings is greater than or equal to 12) the wide zone was very dark and by increasing the magnification, the marginal increment could be measured relatively easily. The narrow confidence limits for the timing of growth-ring formation for *L. sebae* are consistent with this explanation but the small number of data points results in less reliable measures in the timing of new ring formation.

The time of formation of the new growth ring was slightly earlier for *L. vitta* than for *L.* sp.3, *N. furcosus*, or *L. sebae*. The calculation of an earlier growth-ring formation may be attributed to the more clearly defined translucent zone in *L. vitta* which may be detectable earlier in

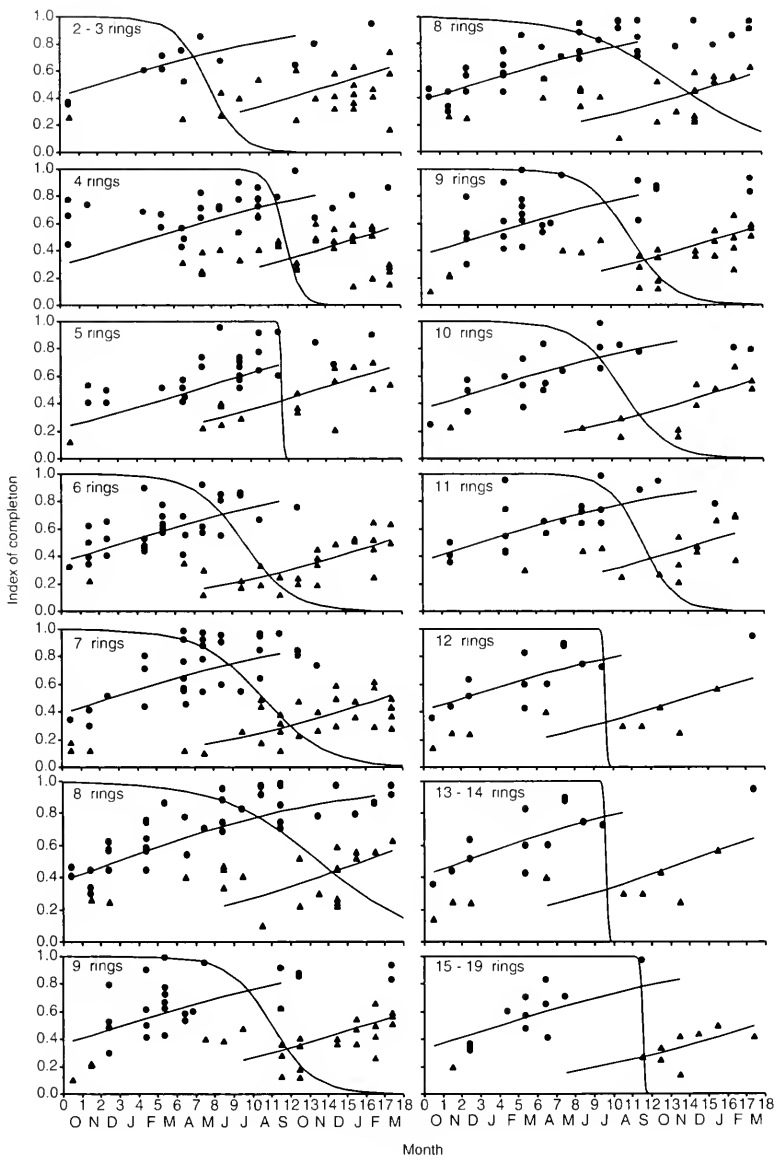

Figure 5

Index of completion at time t, (c_i, t), for *L. sebae* for growth-ring categories 2–3, 3, 4, 5, 6, 7, 9, 10, 11, 12, 13–14, and 15–19 sampled between the months 1 October 1993 (t=0) to 31 March 1995 (t=18). The solid circles (●) represent those (c_i, t) most likely represented by $\hat{c}_1$ and lying closest to the function F_1 and the solid triangles (▲) are those most likely represented by $\hat{c}_2$ and lying closest to the function F_2. The logistic function, P_t, indicates the probability that (c_i, t) are most likely represented by function F_1.

Table 1

Parameter estimates for the fit of two functions to the index of completion data. The parameters are the rate of increase, b, the phase shifts d_1 and d_2, the time of new growth-ring detection $t = R$ with the confidence interval (5th and 95th percentiles), and the standard deviation, σ, of the observed values of index of completion for points fitted to function F_1 and F_2.

	rings	n	b	d_1	d_2	R	Month	σ
Lutjanus sp. 3	2	36	20.3	3.6	15.3	9.5 ±0.1	Jul	0.14
	3	134	20.3	2.0	15.4	9.9 ±2.0	Jul	0.13
	4	146	20.3	1.7	16.2	10.2 ±2.1	Aug	0.13
	5	72	20.3	2.3	14.8	10.5 ±0.1	Aug	0.24
	6	38	20.3	1.7	14.9	11.5 ±0.2	Sep	0.11
	7	22	20.3	0.6	13.7	10.7 ±0.1	Aug	0.12
	8	22	20.3	1.1	14.0	10.2 ±0.1	Aug	0.12
	9–11	29	20.3	0.9	14.2	10.9 ±1.3	Aug	0.15
Lutjanus vitta	2	31	15.8	3.0	14.3	10.9 ±0.1	Aug	0.13
	3	62	15.8	1.5	18.3	10.5 ±0.2	Aug	0.14
	4	96	15.8	3.4	15.9	10.5 ±0.2	Aug	0.10
	5	127	15.8	2.7	16.3	10.2 ±2.0	Aug	0.12
	6	66	15.8	2.5	16.5	10.0 ±1.3	Aug	0.12
	7	56	15.8	2.0	15.4	10.3 ±1.7	Aug	0.11
	8	24	15.8	3.3	15.8	9.0 ±0.2	Jul	0.10
	9–12	39	15.8	3.1	16.2	11.1 ±0.2	Sep	0.10
Nemipterus furcosus	2	85	11.9	2.0	13.1	10.6 ±2.7	Aug	0.18
	3	95	11.9	3.9	14.2	9.5 ±2.2	Jul	0.17
	4	116	11.9	4.0	15.0	9.5 ±4.3	Jul	0.14
	5	82	11.9	3.3	16.4	11.8 ±2.6	Sep	0.11
	6	53	11.9	4.0	16.4	11.8 ±4.2	Sep	0.10
	7–9	39	11.9	4.5	15.8	11.4 ±3.0	Sep	0.10
Lutjanus sebae	2–3	34	17.4	1.9	14.4	7.8 ±2.5	May	0.17
	4	62	17.4	5.0	15.9	11.9 ±1.2	Sep	0.21
	5	43	17.4	5.1	13.4	11.6 ±6.7	Sep	0.14
	6	60	17.4	3.3	17.0	9.6 ±3.7	Jul	0.13
	7	63	17.4	2.6	17.0	10.6 ±4.9	Aug	0.16
	8	60	17.4	2.8	15.8	13.5 ±7.6	Nov	0.15
	9	52	17.4	3.2	15.9	11.0 ±3.3	Sep	0.19
	10	32	17.4	3.3	15.9	10.6 ±3.4	Aug	0.15
	11	34	17.4	3.1	14.9	11.6 ±2.6	Sep	0.17
	12	22	17.4	2.1	13.9	9.6 ±0.1	Jul	0.12
	13–14	23	17.4	4.7	14.6	13.3 ±0.4	Nov	0.21
	15–19	21	17.4	4.0	17.6	11.5 ±0.2	Sep	0.11

Table 2

The timing of growth-ring formation for the four species in the present study and for comparative studies

	Lutjanus sp.3	*L. vitta*	*Nemipterus furcosus*	*L. sebae*
Present study	July–September	July–September	July–September	July–November
Davis and West (1992)		October		
Sainsbury and Whitelaw (1984)			May–July	
McPherson and Squire (1992)				July–September

the year than it is in the other three species. Similarly, the apparent earlier timing of new ring creation in our study, compared to the findings of Davis and West (1992) may have been due to the fact that the translucent zone can probably be detected closer to the time of formation in sectioned otoliths than in urohyals (Reshetnikov and Claro, 1976).

In summary, modeling the change in index of completion over time enabled estimates to be made of the time of the formation of a new growth ring (with confidence intervals) for four tropical species. Although the index of completion was modeled with a logistic function in the present study, alternative functions (e.g. sine or linear), gave very similar results. The technique is a useful addition to marginal increment analysis because it can be used in place of previous subjective methods to determine quantitatively the timing of new ring formation.

Acknowledgments

This project was financed by the Fisheries Research and Development Corporation (FRDC) (project 94/25) and the Department of Fisheries, Western Australia where the main author was employed for the duration of the project. The authors thank Mike Moran (Department of Fisheries, Western Australia) for obtaining FRDC funding and providing critical advice and encouragement. The senior author also thanks Robert Black (University of Western Australia) for his valued suggestions and encouragement. Stephen Newman (Department of Fisheries, Western Australia) provided advice on reading and interpretation of otolith bands, Iain Dunk (Department of Fisheries, Western Australia) collected samples, sectioned otoliths, and acted as the second reader for fish aging and marginal increment analysis. Tony Paust, Ken Bryers, Justin Chidlow, Daryn Payne (Department of Fisheries, Western Australia) assisted in sample collection. I also acknowledge the assistance of M. G. Kailis, Kraus Fishing Company, and Westmore Seafoods whose vessels were used for sample collection, and two anonymous referees for their constructive comments.

Literature cited

Beamish, R. J., and G. A. McFarlane.
1983. The forgotten requirement for age validation in fisheries biology. Trans. Am. Fish. Soc. 112:735–743.

Barger, L. E.
1985. Age and growth of Atlantic Croakers in the Northern Gulf of Mexico based on sectioned otoliths. Trans. Am. Fish. Soc. 114:847–850.

Campana, S. E.
2001. Accuracy, precision and quality control in age determination, including a review of the use and abuse of age validation methods. J. Fish Biol. 59:197–242.

Carpenter, K. E., and V. H. Niem.
2001. FAO species identification guide for fishery purposes. The living marine resources of the Western Central Pacific, vol. 5. Bony fishes, part 3 (Menidae to Pomacentridae), p. 2791–3380. FAO (Food and Agriculture Organization of the United Nations), Rome, Italy.

Davis, T. L. O., and G. J. West.
1992. Growth and mortality of *Lutjanus vittus* (Quoy and Giamard) from the North West Shelf of Australia. Fish. Bull. 90:395–404.

Ferreira, B. P., and G. R. Russ.
1992. Age, growth and mortality of the inshore coral trout *Plectropomus maculatus* (Pisces: Serranidae) from the Central Great Barrier Reef, Australia. Aust. J. Mar. Freshw. Res. 43:1301–1312.

Fletcher, W. J., and S. J. Blight.
1996. Validity of using translucent zones of otoliths to age the pilchard *Sardinops sagax neopilchardus* from Albany, Western Australia. Mar. Freshw. Res. 47:617–624.

Francis, R. I. C. C., L. J. Paul, and K. P. Mulligan.
1992. Ageing of adult snapper (*Pagrus Auratus*), from otolith annual ring counts: validation by tagging and oxytetracycline injection. Aust. J. Mar. Freshw. Res. 43:1069–1089.

Hesp, S. A., I. A. Potter, and N. G. Hall.
2002. Age and size composition, growth rate, reproductive biology, and habitats of the West Australian dhufish, *Glaucosoma hebraicum*, and their relevance to management of this species. Fish. Bull. 100:214–227.

Hyndes, G. A., N. R. Loneragan, and I. C. Potter.
1992. Influence of sectioned otoliths on marginal increment trends and age and growth estimates for the flathead *Platycephalus speculator*. Fish. Bull. 90:276–284.

Manickchand-Heileman, S. C., and J. S. Kenny.
1990. Reproduction, age, and growth of the whitemouth croaker *Micropogonias furnieri* (Desmarest 1823) in Trinidad waters. Fish. Bull. 88:523–529.

McPherson, G. R., and L. Squire.
1992. Age and growth of three dominant Lutjanus species of the Great Barrier Reef inter-reef fishery. Asian Fish. Sci. 5:25–36.

Milton, D. A., S. A. Short, M. F. O'Neill, and S. J. Blaber.
1995. Ageing of three species of tropical snapper (Lutjanidae) from the Gulf of Carpentaria, Australia, using radiometry and otolith counts. Fish. Bull. 93:103–115.

Morales-Nin, B., and J. Moranta.
1997. Life history and fishery of the common dentex (*Dentex dentex*) in Mallorca (Balearic Islands, western Mediterranean). Fish. Res. 30:67–76.

Murphy, M. D., and R. G. Taylor.
1990. Reproduction, growth and mortality of red drum *Sciaenops ocellatus* in Florida waters. Fish. Bull. 88: 531–542.

Newman, S. J., D. M. Williams, and G. R. Russ.
1996. Age validation, growth and mortality rates of the tropical snappers (Pisces: Lutjanidae) *Lutjonus adetii* (Castelnau, 1973) and *L. quinquelineatus* (Bloch, 1790) from the Central Great Barrier Reef. Aust. J. Mar. Freshw. Res. 47:575–584

Pearson, D. E.
1996. Timing of hyline-zone formation as related to sex, location, and year of capture in otoliths of the widow rockfish, *Sebastes entomelas*. Fish. Bull. 94:190–197.

Reshetnikov, Y. S., and R. M. Claro.
1976. Cycles of biological processes in tropical fishes with reference to *Lutjanus synagris*. J. Ichthyol. 16:711–733.

Ross, L. J., T. M. Stevens, and D. S. Vaughan.
1995. Age, growth, mortality, and reproductive biology of red drums in North Carolina waters. Trans. Am. Fish. Soc. 124:37–54.

Sainsbury, K. J., and A. W. Whitelaw.
1984. Biology of Peron's threadfin bream *Nemipterus peronii* (Valenciennes), from the North West Shelf of Australia. Aust. J. Mar. Freshw. Res. 35:167–185.

Tanaka, K., Y. Mugiya, and J. Yamada.
1981. Effects of photoperiod and feeding on daily growth patterns in otoliths of juvenile *Tilapia nilotica*. Fish. Bull. 79:459–465

Van der Walt, B.A., and L. E. Beckley.
1997. Age and growth of *Sarpa salpa* (Pisces: Sparidae) off the coast of South Africa. Fish. Res. 31:241–248.

Application of DNA-based techniques for the identification of whaler sharks (*Carcharhinus* spp.) caught in protective beach meshing and by recreational fisheries off the coast of New South Wales

Ricky W. K. Chan

School of Biological, Earth and Environmental Sciences
The University of New South Wales, UNSW
Sydney, New South Wales 2052, Australia
Present address: Educational Testing Centre
The University of New South Wales
ULD 3 East Parcel Centre
Rosebery, New South Wales 2018, Australia
E-mail address: sharkman@etc.unsw.edu.au

Patricia I. Dixon

Centre for Marine and Coastal Studies
The University of New South Wales, UNSW
Sydney, New South Wales 2052, Australia

Julian G. Pepperell

Pepperell Research and Consulting
PO Box 1475
Noosaville D.C., Queensland 4566, Australia

Dennis D. Reid

New South Wales Fisheries
PO Box 21
Cronulla, New South Wales 2230, Australia

The International Union for the Conservation of Nature's (IUCN) development of the Shark Specialist Group is indicative of the increasing environmental awareness of sharks' crucial ecological role as apex predators and that they are being threatened by human activities. Although the conservation status of certain carcharhinid species (*Carcharhinus limbatus, C. obscurus,* and *C. plumbeus*) are presently considered at low risk or near threatened according to the IUCN's threatened species categories,[1] species from the genus *Carcharhinus* are known to inhabit the waters of New South Wales (NSW), Australia (Stevens, 1984; Last and Stevens, 1994); however their conservation status has not been determined. Known as whaler or "requiem" sharks, they are also commonly caught off the coast of New South Wales in commercial fisheries (Stevens and Wayte[2]; Tanner and Liggins[3]), recreational fisheries (Pepperell, 1992; Gartside et al., 1999; Steffe et al.[4]) and by protective beach meshing (Reid and Krogh, 1992; Dudley, 1997).

Because of morphological similarities between a number of shark species in the genus *Carcharhinus* (Last and Stevens, 1994; Naylor and Marcus, 1994), taxonomic identification to species level has been difficult or inaccurate (or both)(Stevens and Wayte[2]). Historical catches of certain species of sharks in NSW commercial fisheries, recreational fisheries, and protective beach meshing have been recorded to genus level only (Pepperell, 1992; Reid and Krogh, 1992; Tanner and Liggins[3]). Formally trained Australian Fisheries Management Authority (AFMA) observers aboard commercial longlining vessels may experience difficulties in identification if distinguishing parts of a shark are discarded prior to confirmation of species (Stevens and Wayte[2]). Similarly, observers of protective beach meshing may find species identification difficult on severely decomposed sharks. Without proper identification, the exact number of individual species inhabiting NSW waters and the number of each species being landed cannot be determined (Chan, 2001).

The rise of molecular biological techniques in marine forensic science has facilitated the development of accurate taxonomic identification of shark species by sampling biological tissue (Martin, 1991; Lavery, 1992; Heist and Gold, 1999). DNA techniques require only muscle tissue, allowing biopsy tissue to be taken from specimens that can be released, rather than having to sacrifice the shark to obtain liver and heart tissue for allozyme analysis (Godfrey, 1997). Methods of taxonomic identification include PCR-based restriction fragment length poly-

[1] Musick, J., and S. Fowler. 2000. *Carcharhinus limbatus, C. obscurus* and *C. plumbeus* *In* IUCN 2002. 2002 IUCN red list of threatened species. http://www.iucn.org/redlist/2000index.html. [Accessed 1 October 2002.]

[2] Stevens, J. D., and S. E. Wayte. 1998. A review of Australia's pelagic sharks resources. Fisheries Research and Development Corporation project 98/107, 64 p. CSIRO Marine Research, GPO Box 1538, Hobart, Tasmania 7001 Australia.

[3] Tanner, M., and G. W. Liggins. 2000. New South Wales commercial fisheries statistics 1993/94 to 1996/98, 82 p. New South Wales Fisheries, PO Box 21, Cronulla, NSW 2230 Australia.

[4] Steffe, A. S., J. J. Murphy, D. J. Chapman, B. E. Tarlinton, G. N. G. Gordon, and A. Grinberg. 1996. An assessment of the impact of offshore recreational fishing in New South Wales waters on the management of commercial fisheries. Fisheries Research and Development Corporation Project 94/053, 139 p. New South Wales Fisheries, PO Box 21, Cronulla, NSW 2230 Australia.

Manuscript approved for publication 24 June 2003 by Scientific Editor.
Manuscript received 13 July at NMFS Scientific Publications Office.
Fish. Bull. 101:910–914 (2003).

morphism (PCR-RFLP; Martin, 1991), DNA sequencing techniques (Heist and Gold, 1999), isoelectric focusing of muscle proteins (Renon et al., 2001; Smith and Benson, 2001) and direct multiplex PCR amplification (Shivji et al., 2002). These techniques use the differences in the sequences of nucleotide bases within a DNA strand among species. DNA techniques have high sensitivity, are easily reproduced, and allow the development of a unique "DNA fingerprint" for each species (Martin, 1991; Innes et al., 1998; Pepperell and Grewe, 1999). It was the aim of this project to initiate a shark DNA database for species identification of pelagic sharks (beginning with species from the genus *Carcharhinus*) in New South Wales by using PCR-RFLP techniques.

Materials and methods

Sharks of the genus *Carcharhinus* landed by recreational fisheries and caught in NSW beach meshing were identified to species level by using morphometric taxonomic guides and dentition identification (Cliff and Wilson, 1994; Last and Stevens, 1994; Naylor and Marcus, 1994). Positively identified sharks were retained as voucher specimens (see "Acknowledgments" section). A tissue biopsy (5–10 g) from the dorsal region on either side of all voucher specimens and unidentified sharks was taken and stored in 75% ethanol prior to DNA extraction. Mitochondrial DNA (mtDNA) of specimens from six species of the genus *Carcharhinus* (*C. brachyurus*, *C. brevipinna*, *C. falciformis*, *C. leucas*, *C. limbatus*, and *C. obscurus*; see Table 1 for sample sizes) was extracted by using a Fastprep DNA Extraction kit (BIO101, Integrated Sciences, Sydney, New South Wales) following the manufacturer's instructions. Approximately 200–300 mg of tissue was placed in a sterilized 1.5-mL eppendorf tube and after the addition of 1 mL Fastprep lysis buffer, incubated at 56°C for three hours prior to the extraction stage (Chan, 2001). Following the extraction procedure of the Fastprep protocol, quality and quantity of DNA was measured by using a GeneQuant DNA/RNA calculator (Amersham Biosciences, Sydney, New South Wales).

The polymerase chain reaction (PCR) was used to amplify the 1146 nucleotide base-pair (bp) cytochrome *b* (cyt *b*) region of the mtDNA (Martin and Palumbi, 1993; Kitamura et al., 1996). For each 50 µL PCR reaction, 100–200 ng of template mtDNA was used, 1.5 mM $MgCl_2$, 1X PCR buffer, 2 mM of dNTP, 5 mM of each external primer (5′–TGACTTGAARAACCAYCGTTG–3′ and 3′–CTCCAG-TCTTCGRCTTACAAG–5′) and two units of DyNAzyme EXT DNA polymerase (Finnzymes, GeneWorks, Adelaide, South Australia) were added to a sterilized 200 µL PCR tube. The PCR was undertaken in a MJR MiniCycler (MJR, GeneWorks) with a heated bonnet on a cycle of 94°C for three minutes, followed by 35 cycles of 94°C denaturing for 45 seconds, 48°C annealing for 30 seconds, 72°C extension for 90 seconds, and a final 10-minute extension time at 72°C (Chan, 2001).

To determine if the cyt *b* region was successfully amplified, 10 µL of PCR product was added to 2 µL loading dye (25% bromophenol blue, 40% sucrose in distilled water) and loaded into wells of a 1.5% w/v agarose gel submerged in 0.5X TBE (Tris-borate-EDTA, pH 8) buffer, with 1 µg of a 100-bp DNA ladder (Sigma-Aldrich, Sydney, New South Wales) added to 5 µL distilled water added to each side-end well. The gel was subject to electrophoresis at 125 V for 45–60 minutes and then stained in ethidium bromide for 10 minutes, de-stained in fresh distilled water for 20 minutes prior to illumination under ultraviolet (UV) light to determine the success and yield of the amplification.

To obtain species-specific profiles, restriction fragment length polymorphism (RFLP) was used on the entire 1146 bp cyt *b* fragment (Martin, 1991; Chan, 2001). The successful amplified reaction products had the primers, taq polymerase, and buffer chemicals removed by using a BRESAspin PCR purification kit (GeneWorks). For each RFLP reaction, 30 µL of purified PCR-amplified cyt *b* mtDNA (300–1000 ng; 30 µL of distilled water was used for control reactions), 5 µL of 10X buffer, one unit of a restriction enzyme (*Alu* I, *Hae* III, *Pst* I, *Taq* I, and *Xho* I) and distilled water up to 50 µL volume was added to a sterilized 200 µL PCR reaction tube and incubated at 37°C for 2 hours in the MJR minicycler (with heated bonnet), with the exception of *Taq* I (incubated at 65°C for two hours in a water bath). After the allotted digestion time, 10 µL of loading dye was added to each tube prior to loading into a 1.5% w/v agarose gel submerged in 0.5X TBE buffer. In both end wells, 5 µL of distilled water + 1 µg of a 100 bp DNA ladder was added. The gel was subject to electrophoresis at 125 V for 60–90 minutes, stained in ethidium bromide for 10 minutes, and destained in fresh distilled water for 20 minutes prior to illumination under UV light. Enzyme-digested DNA fragments >100 bp were then "scored" to the nearest 25 bp based upon migration of the DNA fragment (the smaller the fragment, the faster the migration) and recorded for each enzyme and sample (Martin, 1991) by using the 100-bp DNA ladder as a standard measuring guide for size estimation.

Results and discussion

PCR-RFLP profiles were successfully developed for six species of the genus *Carcharhinus*; distinct and discrete patterns were observed for each species with five restriction enzymes (Table 1, and Chan, 2001). The only intraspecific polymorphism observed was for two specimens of *C. brevipinna* with the *Xho* I restriction enzyme. Increasing the sample size of all species may identify more intraspecific polymorphisms. Because of the relatively small sample sizes, no statistical analyses were undertaken. Other restriction enzymes were tested (Chan, 2001), and with the possible inclusion of other species from the genus *Carcharhinus* into this database in the future, these restriction enzymes may be required in order to discern the additional species. Because some of the fragment sizes were rounded to the nearest 25 bp, the sum of the fragments for a restriction enzyme of a species may be more than 1146 bp, the size of the cyt *b* uncleaved region for sharks (Martin and Palumbi, 1993). Fragments <100 bp were not recorded because the DNA ladder had a lower limit of 100 bp.

Table 1

Summary of PCR-RFLP banding patterns for the cytochrome *b* (cyt *b*) region in *Carcharhinus* spp. Fragment sizes are given in number of base pairs (bp) and have been rounded to the nearest 25 bp. Where the enzyme appeared not to have cleaved the cyt *b* region, it was scored "1146." *n* = denotes sample size. ✓ = denotes fragment size present.

		Carcharhinus species						
Enzyme	Fragment size	*C. limbatus* (*n*=9)	*C. brachyurus* (*n*=12)	*C. leucas* (*n*=3)	*C. obscurus* (*n*=29)	*C. falciformis* (*n*=12)	*C. brevipinna* Haplotype 1 (*n*=6)	*C. brevipinna* Haplotype 2 (*n*=2)
Alu I	1000				✓			
	700		✓					
	600						✓	✓
	500					✓		
	450	✓						
	350	✓		✓			✓	✓
	300		✓			✓		
	200				✓			
Hae III	1100	✓		✓				
	975		✓			✓	✓	✓
	750				✓			
	225				✓			
	175		✓		✓	✓	✓	✓
Pst I	1146		✓		✓	✓	✓	✓
	975	✓		✓				
	175	✓						
Taq I	1146	✓					✓	✓
	1100			✓	✓			
	850		✓					
	650					✓		
	325		✓					
	300					✓		
Xho I	1146	✓		✓	✓		✓	
	850		✓			✓		✓
	325		✓			✓		

These techniques can be used to complement morphometric identification (Cliff and Wilson, 1994; Last and Stevens, 1994; Naylor and Marcus, 1994) or can be used to identify "cryptic" species when morphological identification cannot be done. Other "cryptic" species caught in beach meshing and by recreational fisheries can be added to the DNA database, such as hammerhead sharks (*Sphyrna* spp.) which are commonly caught and are recorded in catch records to genus level only (Pepperell, 1992; Reid and Krogh, 1992; Chan, 2001). Although this project positively identified six species from the genus *Carcharhinus*, other species of this genus are known to inhabit the NSW coastline (Stevens, 1984; Last and Stevens, 1994). During the warmer months, when the northern currents extend farther south to the Sydney region, transient tropical *Carcharhinus* spp. may appear off the coast. In the northern regions of NSW, there have been recorded catches of the blacktip reef shark (*C. melanopterus*) by shore-based anglers (Gartside et al., 1999). Although transient tropical whaler sharks may not have permanent stocks in NSW waters, it is important to discern them from resident *Carcharhinus* spp. prior to any species-specific stock assessment. Given the number of shark species and difference in life histories (Last and Stevens, 1994; Smith et al., 1998), identification to species level is crucial.

The use of genetic techniques allows, for the first time, accurate identification of species of whaler sharks that were landed by recreational fisheries and caught in protective beach meshing in NSW and that have been historically recorded to genus level. Continual sampling and formal identification are required for comparison of catches between species of *Carcharhinus*. Genetic techniques have the potential to be used for all other shark species and fisheries within the Australian Fishing Zone (AFZ). The use of genetic techniques has been employed in the field of law enforcement to prevent the selling of protected fish species at local fish markets where the majority of the carcass is not retained (Ward et al., 1999). This use could

be extended to ensure that protected shark species such as the grey nurse shark (*Carcharias taurus*), white shark (*Carcharodon carcharias*), and the smalltooth sand tiger shark (*Odontaspis ferox*) are not sold.

This project is the first time that *Carcharhinus* spp. have been formally identified to species level in the 60-year history of NSW protective beach meshing and only the second time in NSW recreational fisheries after Stevens (1984). The depositing of voucher specimens and all DNA biopsies at the Australian Museum ensures that these valuable and irreplaceable biological samples can be used in future research. It is evident that DNA techniques can be used to taxonomically identify "cryptic" specimens, especially *Carcharhinus* spp., and *Sphyrna* spp. to species level that were once recorded to genus level only in many fisheries based in NSW (Pepperell, 1992; Reid and Krogh, 1992; Chan, 2001; Tanner and Liggins[3]). It is important that sharks that are caught be recorded to the lowest taxonomic level for management and conservation strategies. Long-term routine sampling and recording to species level will provide useful data on which conservation management strategies can be developed as part of the Australian national plan of action for the conservation and management of sharks.

Acknowledgments

The authors would like to acknowledge the assistance of the NSW Game Fishing Association and all NSW recreational gamefishing clubs, their officials and their anglers who cooperated with the research, NSW protective beach meshing contractors and observers, NSW Fisheries staff, and the numerous volunteers (Joanne Bennett, Tanya Compton, Rikkè Dano, Paul Godfrey, Gary Henry, Andrew Hodges, Alex Irwin, Jeff Murphy, Julie Needham, Milena Rantala, and Clint Wilson) who helped collect samples. We thank Ed Heist and Andrew Martin for their comments on the manuscript and specially thank Bill Sherwin (UNSW) and Marie Roseline Yardin for their assistance in this project. This project was funded by NSW Fisheries and the National Heritage Trust Coast and Clean Seas' Marine Species Protection Program (CCS Project no. 9856). Voucher shark specimens were retained at the Australian Museum, Sydney, NSW, Australia (Collection Manager, Fish Section) and NSW Fisheries, NSW, Australia (Dennis Reid).

Literature cited

Chan, R.W. K.
2001. Biological studies on sharks caught off New South Wales. Ph.D. diss., 314 p. School of Biological Science, Univ. New South Wales, Sydney, Australia.

Cliff, G., and R. B. Wilson.
1994. Natal Sharks Board's field guide to sharks and other marine animals, 57 p. Group Editors, Durban, South Africa.

Dudley, S. F. J.
1997. A comparison of the shark control programs of New South Wales and Queensland (Australia) and KwaZulu-Natal (South Africa). Ocean Coast. Manag. 34:1–27.

Gartside, D. F., B. Harrison, and B. L. Ryan.
1999. An evaluation of the use of fishing club records in the management of marine recreational fisheries. Fish. Res. 41:47–61.

Godfrey, P.
1997. Identification of sharks caught in NSW waters using allozyme electrophoresis. B.S. (Hons.) thesis, 54 p. Centre for Marine and Coastal Studies, Univ. New South Wales, Sydney, Australia.

Heist, E. J., and J. R. Gold.
1999. Genetic identification of sharks in the U.S. Atlantic large coastal shark fishery. Fish. Bull. 97:53–61.

Innes, B. H., P. M. Grewe, and R. D. Ward.
1998. PCR-based genetic identification of marlin and other billfish. Mar. Freshw. Res. 49:383–388.

Kitamura, T., A. Takemura, S. Watabe, T. Taniuchi, and M. Shimizu.
1996. Mitochondrial DNA analysis for the cytochrome *b* gene and D-loop region from the bull shark *Carcharhinus leucas*. Fish. Sci. 62:22–27.

Last, P. R., and J. D. Stevens.
1994. Sharks and rays of Australia, 513 p. CSIRO (Commonwealth Scientific and Industrial Research Organisation) Publishing, Melbourne, Australia.

Lavery, S.
1992. Electrophoretic analysis of phylogenetic relationships among Australian carcharhinid sharks. *In* Sharks: biology and fisheries (J. G. Pepperell, ed.), p. 97–108. Aust. J. Mar. Freshw. Res. 43.

Martin, A. P.
1991. Application of mitochondrial DNA sequence analysis to the problem of species identification of sharks. *In* Conservation biology of elasmobranchs (S. Branstetter, ed.), p. 53–59. NOAA Tech. Rep. NMFS 115.

Martin, A. P., and S. R. Palumbi.
1993. Protein evolution in different cellular environments: cytochrome *b* in sharks and mammals. Mol. Biol. Evol. 10: 873–891.

Naylor, G. J. P., and L. F. Marcus.
1994. Identifying isolated shark teeth of the genus *Carcharhinus* to species: relevance for tracking phyletic change through the fossil record. Am. Mus. Novit. 94:1–53.

Pepperell, J. G.
1992. Trends in the distribution, species composition and size of sharks caught by gamefish anglers off South-eastern Australia, 1961–90. *In* Sharks: biology and fisheries (J. G. Pepperell, ed.), p. 213–225. Aust. J. Mar. Freshw. Res. 43.

Pepperell, J. G., and P. M. Grewe.
1999. A field guide to Indo-Pacific billfishes, 16 p. CSIRO Publishing, Melbourne, Australia.

Reid, D. D., and M. Krogh.
1992. Assessment of catches from protective shark meshing off New South Wales beaches between 1950 and 1990. *In* Sharks: biology and fisheries (J. G. Pepperell, ed.), p. 283–296. Aust. J. Mar. Freshw. Res. 43.

Renon, P., M. M. Colombo, F. Colombo, R. Malandra, and P. A. Biondi.
2001. Computer-assisted evaluation of isoelectric focusing patterns in electrophoretic gels: identification of smoothhounds (*Mustelus mustelus*, *Mustelus asterias*) and comparison with lower value shark species. Electrophoresis 22:1534–1538.

Shivji, M., S. Clarke, M. Pank, L. Natanson, N. Kohler, and M. Stanhope.
2002. Genetic identification of pelagic shark body parts for

conservation and trade monitoring. Conserv. Biol. 16: 1036–1047

Smith, P. J., and P. G. Benson.
2001. Biochemical identification of shark fins and fillets from the coastal fisheries in New Zealand. Fish. Bull. 99: 351–355.

Smith, S. E., D. W. Au, and C. Show.
1998. Intrinsic rebound potentials of 26 species of Pacific sharks. Mar. Freshw. Res. 49:663–678.

Stevens, J. D.
1984. Biological observations on sharks caught by sport fishermen off New South Wales. Aust. J. Mar. Freshw. Res. 35:573–590.

Ward, R. D., R. K. Daley, J. Andrew, and G. K. Yearsley.
1999. Protein fingerprinting. *In* Australian seafood handbook: an identification guide to domestic species (G. K. Yearsley, P. R. Last, and R. D. Ward, eds.), chap. 9, p. 358–392. CSIRO Marine Research, Hobart, Australia.

Red sea urchins (*Strongylocentrotus franciscanus*) can live over 100 years: confirmation with A-bomb ^{14}carbon

Thomas A. Ebert
Department of Zoology
Oregon State University
Corvallis, Oregon 97331-2914
E-mail address: ebertt@sciences.oregonstate.edu

John R. Southon
Center for Accelerator Mass Spectrometry
Lawrence Livermore National Laboratory
Livermore, California 94551-9900

Red sea urchins (*Strongylocentrotus franciscanus*) along the west coast of North America, like most large sea urchins in temperate waters worldwide, are the focus of a commercially important fishery. In a review of biological data for purposes of fishery management, the life span of red sea urchins was suggested to be 7–10 years (Sloan, 1986) and they have been included with much shorter-lived species for illustrating complex population dynamics (Hastings and Higgins, 1994). Recent work with tetracycline and calcein tagging (Ebert, 1998; Ebert et al., 1999), however, has shown that individuals continue to grow throughout life, although at a very slow rate, and large individuals are estimated to be in excess of 100 years old. A potential problem with the studies using tetracycline and calcein is that one-year time intervals were used between tagging and recapture and therefore it is possible that occasionally there may have been very good years for growth that were missed. If occasional growth spurts occurred, largest sizes would have been attained in much less than 100 years. The potential problem of missed good years for growth could be resolved with a marker that captures a longer period of time. The accuracy of age estimates has consequences for resource management where size limits may need adjustment in order to protect older individuals (Hilborn and Walters, 1992; Congdon et al., 1994; Ebert, 1998). There is also the need to understand the evolution of life histories of species where long life tends to be an indicator of uncertainty in individual reproductive success (Murphy, 1968; Roff, 1992; Stearns, 1992).

Enhanced radiocarbon in the oceans due to atmospheric testing of nuclear weapons that began in the 1950s (Nydal and Lovseth, 1983; Broecker et al., 1985, Duffy et al., 1995) provides a permanent marker in carbonate-based skeletal elements that are not reworked by resorption and deposition during growth and hence has a long time period between mark and recovery. The enhanced radiocarbon marker has been used in various studies to validate the periodic (usually annual) nature of growth zones in fish (Kalish, 1993, 1995; Campana, 1997; Campana et al., 2002) and invertebrates (Turekian et al., 1982; Witbaard et al., 1994; Peck and Brey, 1996) where validation by chemical tags such as tetracycline has been impractical. Red sea urchins lack interpretable growth zones (Breen and Adkins, 1976) and therefore there is no natural feature to serve as a cross check for studies using chemical tags. In the present study we present a test and confirmation of age in red sea urchins estimated from tetracycline tagging using an enhanced ^{14}C signal in the ocean from nuclear weapons testing.

Materials and methods

Red sea urchins were tagged with tetracycline from 1989 to 1992 in northern California, Oregon, and Washington and collected after time intervals of approximately one year (details presented in Ebert et al., 1999). It is not possible to determine whether a live sea urchin has a tetracycline mark and therefore large collections had to be made. Skeletal elements were cleaned with sodium hypochlorite bleach to remove all organic material not bound in the calcite of the skeleton, and then skeletal ossicles were examined by using UV illumination to detect the tetracycline marks, which fluoresce yellow. Growth increments were measured in jaws of Aristotle's lantern of 1582 tagged-recovered red sea urchins and used to estimate growth parameters. Jaw ossicles, the demipyramids of Aristotle's lantern, are internal skeletal elements that grow around all surfaces but not equally in all directions so that a change in jaw length, ΔJ, is mostly at the end closest to the esophagus and there is little growth closest to the mouth, the labial end, where the teeth extend from the jaw.

The Tanaka function (Eq. 1) was used to describe growth (Tanaka, 1982, 1988) because it can model data that show an initial lag, an exponential phase with a maximum, and can include continuing growth throughout life. This function is described in greater detail elsewhere (Tanaka, 1982, 1988; Ebert et al., 1999). The usual formulation of the Tanaka model is Δsize as a function of size at time t and Δt is assumed to be fixed for all individuals in the sample, usually at Δt = 1 year (Tanaka, 1982, 1988; Ebert, 1998; Ebert et al., 1999) and not included explicitly in the equation. In the present study we estimated the amount of jaw that would have to be removed to represent the time span from the time of collection in the 1990s with relatively high ^{14}C levels to the time before atmospheric testing of atomic bombs (relatively low ^{14}C) and

Manuscript approved for publication 10 July 2003 by Scientific Editor.
Manuscript received 13 July 2003 at NMFS Scientific Publications Office.
Fish. Bull. 101(4):915–922 (2003).

therefore the Tanaka model was modified from previous uses to make ΔJ a function of $J_{t+\Delta t}$, the size on the date of recapture rather the date of marking, which is the usual way of estimating growth parameters. Also, Δt was explicitly included as a variable (Eq. 2),

$$\Delta J = J_{t+\Delta_t} - \frac{1}{\sqrt{f}} \ln\left[2G + 2\sqrt{G^2 + fa}\right] - d \quad (1)$$

where

$$G = E/4 - fa/E - f\Delta t \quad (2)$$

and

$$E = \exp\left(\sqrt{f}\,(J_{t+\Delta t} - d)\right). \quad (3)$$

The three parameters of the Tanaka function, a, d, and f, have biological meaning: "a" is related to maximum growth rate, which is approximately $1\sqrt{a}$; "d" shifts the size at which growth is maximum; and "f" is a measure of the rate of change of the growth rate. A graphical presentation of how changes in these parameters change the growth curve is given in Ebert et al. (1999).

Explicit use of Δt and making ΔJ a function of $J_{t+\Delta t}$ required a modification of the usual presentation of the Tanaka function. In Ebert et al. (1999) Equation 2 was written as

$$G = E/4 - fa/E + f \quad (4)$$

with no Δt and with "+ f". Equation 3 was written as

$$E = \exp\left(\sqrt{f}\,(J_t - d)\right). \quad (5)$$

with J_t, rather than $J_{t+\Delta t}$. Tetracycline tagging for a period of one year, $\Delta t = 1$, provides the Tanaka parameter estimates and these parameters were used to estimate a *Δjaw* size that would cover the time from the date of collection to a time, Δt, before A-bomb testing; Δt is time run backwards from the date of collection, which is the reason for the sign change from Equation 4 to Equation 2.

The samples of red sea urchins that were selected for radiocarbon analysis were part of the tagging study at Halftide Rocks off San Juan Island, Washington (Ebert et al., 1999). Individuals were tagged with tetracycline on 26 October 1991 and collected again on 21 October 1992. The recaptured tagged individuals (n=365) are part of the 1582 tagged sea urchins from northern California, Oregon, and Washington that were used to estimate Tanaka parameters. For ^{14}C analysis, specimens were selected from the Halftide Rocks collection that did not show fluorescence in the skeleton and therefore probably had not been handled in 1991. The use of untagged individuals for radiocarbon analyses avoids any possible contamination from handling and tagging in 1991.

Cleaned jaws for ^{14}C analysis were cemented to aluminum blocks with a two-part epoxy cement and aligned so that the esophageal margin was approximately parallel with the block base. The block was held on the stage of a small milling machine and the stage tilted so that the jaw was as parallel as possible with the milling bit. Approximately 0.5 mm of the jaw surface was removed and sides were milled to remove recently deposited calcite and to expose the underlying older skeleton. The jaw was measured and successive samples were milled from the esophageal edge to a depth of 0.5 mm, which produced samples larger than 1 mg of carbonate in most cases. Samples were placed in individual reaction chambers, evacuated, acidified with orthophosphoric acid, and heated. The evolved CO_2 was converted to graphite by reduction with an excess of hydrogen in individual reactors with iron powder as a catalyst (Vogel et al., 1987). Analysis of ^{14}C in the graphite targets was done at the Center for Accelerator Mass Spectrometry, Lawrence Livermore National Laboratory, and reported as $\Delta^{14}C‰$ (Stuiver and Polach, 1977), which includes a correction for a $\delta^{13}C$ of –3 based on stable isotope analyses. Mean precision (1 standard deviation) of radiocarbon measurements was 4.2‰ (range: 3.0–7.9).

Results

Of the 1582 tag recoveries from all sites, 739 jaws showed a growth increment, ΔJ, of ≤0.02 cm and of these only 13 had a labial measurement >0, which is at the end of the jaw at the mouth opening. The smallest nonzero measurements were 0.001 cm and therefore growth less that this was recorded as 0; 54 sea urchins in the sample had clear tetracycline marks but 0 measurable growth. For large jaws, the measured labial component was too small to be measured and therefore all of the calculated ΔJ since the late 1950s was milled from the esophageal end of the jaw only.

Tetracycline tagging indicated that annual jaw growth (Fig. 1) was very slow for large sea urchins and many individuals showed annual increments of less than 0.01 cm. The resulting growth curve of jaw length as a function of age (Fig. 2A) showed that at least some large individuals would be expected to have ages in excess of 100 years. If this age estimate is correct, a drop in ^{14}C should be found in successive small slices removed from large jaws, which would first show current ^{14}C levels and then drop to prebomb levels. Because the Halftide Rocks samples were collected in 1992 we used Δt = 35 years, which would go back to 1957. Using Equations 1–3, growth parameters given in Fig. 1, and Δt = 35 years, we estimated the increment to be between 1 and 2 mm for jaws between 2.5 and 2.6 cm (Fig. 2B).

Successive milled samples from the esophageal ends of large jaws (Fig. 3, A–D) showed a precipitous drop in radiocarbon to prebomb levels over 1–2 millimeters, in agreement with predictions. Variations across replicates and samples probably are the result of differences in the width of milled samples and an inability to remove all recently deposited calcite or to follow the exact growing edge of the jaw with the milling machine. Smaller jaws (Fig. 3, E–G) were not expected to show a prebomb signature, and indeed they did not. They do, however, indicate the ^{14}C level to be expected in recent skeletal material and emphasize the rapid change in radiocarbon shown in large jaws. Changes in ^{14}C in successive milled samples in jaws

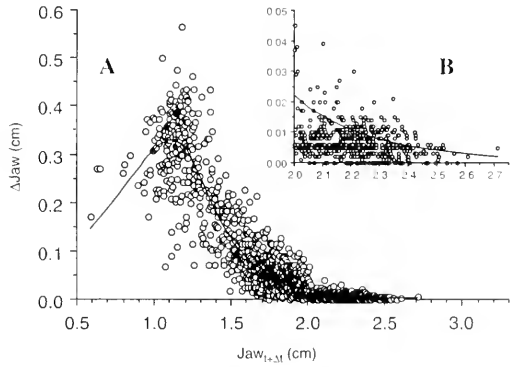

Figure 1

Jaw growth increments, ΔJ, for tagged red sea urchins (*Strongylocentrotus franciscanus*) from northern California, Oregon, and Washington; fitted line is the Tanaka function (Tanaka, 1982, 1988; Ebert et al., 1999) with f = 10.95650 ±0.35064 SE(standard error), d = 0.04937 ±0.01664, and α = 8.63029 ±0.16659; Δt is approximately 1 year for all samples; (**A**) entire data set; n = 1582; (**B**) restricted scale to show just jaws larger than 2.0 cm and degree of scatter; n = 336; conversion to body diameter, D, from jaw length, J, is $D = 4.8951 J^{1.2817}$; therefore jaw lengths of 2.0 and 2.7 cm would have expected test diameters of 11.9 and 17.9 cm, respectively.

E–G are similar to changes shown in coral samples from the Galápagos (Guilderson and Schrag, 1998) and may indicate that ^{14}C levels in surface waters in regions of strong upwelling were still rising when sea urchin were collected in 1992. The conclusion is that ^{14}C analysis supports the age estimates based on tetracycline tagging and use of the Tanaka function: large red sea urchins are old and may have ages of 100 years or more

Discussion

The largest reported red sea urchins, with body diameters over 19 cm, are from British Columbia, Canada, (Bureau, 1996) and with estimated jaw lengths of about 2.8 cm would be expected to be around 200 years old (Fig. 2A). Age estimates of 100+ years far exceed estimates of life span for other sea urchins (Table 1) based on growth lines in ossicles. Natural growth lines, however, tend to underestimate ages of old individuals because very small increments will have alternations of dark and light areas that are difficult or impossible to resolve and hence counts underestimate age (Ebert, 1988). For example, the maximum age estimate for *Strongylocentrotus droebachiensis*, the commercial species of the U.S. east coast, is 25 years by counts of growth lines (Robinson and MacIntyre, 1997) but at least twice this if tagging and size structure (Russell et al., 1998) are used. Similarly, tagging and size structure of *Evechinus chloroticus* (Lamare and Mladenov, 2000) have indicated survival rates similar to *S. franciscanus* but the maximum number of growth lines reported was only 10 (Dix, 1972). Survival rate, however, is not a fixed parameter for a species and there is local variation, as well as geographic patterns, evident in the survival rate for *S. franciscanus* (Ebert et al. 1999).

Estimates of annual survival rates based on growth parameters and mean size for red sea urchins from southern California to Alaska (Ebert et al., 1999) indicate that very old individuals would not be expected in southern California where few individuals attain ages of 50 years. At more northern locations, the probability of long life increases (Fig. 4) and ages of 100+ are expected, particularly in Washington and Alaska. The mechanism causing the latitudinal pattern are unclear. Latitudinal differences in survival may be due to increased disease outbreaks associated with higher temperatures in the south (Ebert et al. 1999) or the presence of more predator species in the south (Tegner, 2001). Physiological senescence related to temperature is unlikely because there is no pattern to growth differences associated with latitude (Ebert et al., 1999) and no evidence for physiological decline in relative gonad size in the south (Tegner and Levin, 1983) or north (Kramer and Nordin, 1975). The largest individuals continue to develop gonad masses in accord with the same allometric relationships as smaller individuals. It is reasonable to conclude that senescence does not occur in red sea urchins.

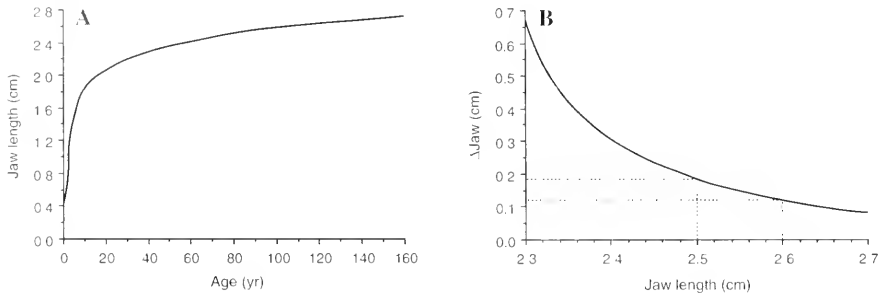

Figure 2

(**A**) Growth curve for jaws of red sea urchins from northern California, Oregon, and Washington using Tanaka parameters and an initial jaw size of 0.44 cm, the approximate jaw size for a 1-year-old red sea urchin; (**B**) change in jaw size, Δjaw, with $\Delta time$ = 35 years starting with a final jaw length; Δjaw is the estimate of how much of the jaw would have to be removed to expose prebomb calcite for sea urchins collected in 1992.

Table 1

Maximum age estimates for sea urchins based on growth zones in skeletal ossicles.

Species	Years	Reference
Lytechinus variegatus	4	Beddingfield and McClintock (2000)
Strongylocentrotus nudus	6	Kawamura (1966)
Psammechinus miliaris	7	Jensen (1969)
Paracentrotus lividus	8	Crapp and Willis (1975)
Sphaerechinus granularis	9	Lumingas and Guillou (1994)
Evechinus chloroticus	10	Dix (1972)
Psammechinus miliaris	10	Gage (1991)
Strongylocentrotus intermedius	10	Agatsuma (2001)
Echinus acutus var. *norvegicus*	11	Gage et al. (1986)
Loxechinus albus	11	Gebauer and Moreno (1995)
Echinus esculentus	12	Nichols et al. (1985)
Allocentrotus fragilis	15	Sumich and McCauley (1973)
Echinus elegans	21	Gage et al. (1986)
Strongylocentrotus droebachiensis	24	Robinson and MacIntyre (1997)
Echinus affinis	28	Gage and Tyler (1985)
Sterechinus neumayeri	40	Brey et al. (1995)
Sterechinus antarcticus	75	Brey (1991)

Red sea urchins larvae spend at least two months in the plankton (Strathmann, 1978) during which time they can be carried far along the coast or out to sea. There is year-to-year variation in settlement and recruitment and years of zero success and greater variation at northern sites (Bernard and Miller, 1973, Low, 1975, Tegner and Dayton, 1981, Duggins, 1983, Pearse and Hines, 1987, Sloan et al., 1987, Ebert et al., 1994). An important point, however, is that these authors reported some recruitment at study sites and so extreme longevity would at first seem unnecessary for species survival. The important issue for evolution of life histories, however, is not whether some individuals recruit to the population but how successful an individual is each year in leaving offspring. The long life of adult red sea urchins emphasizes the difficulties individuals have in successfully having offspring that settle in suitable habitat and survive to reproductive age. Many annual reproductive episodes appear to be required to succeed and therefore red sea urchins are classic bet hedgers that use resources to promote annual survival of adults as well as to reproduce (Stearns, 1992).

Attributes of a long life span have consequences for resource management. The implications for management of the red sea urchin resource have been explored by us-

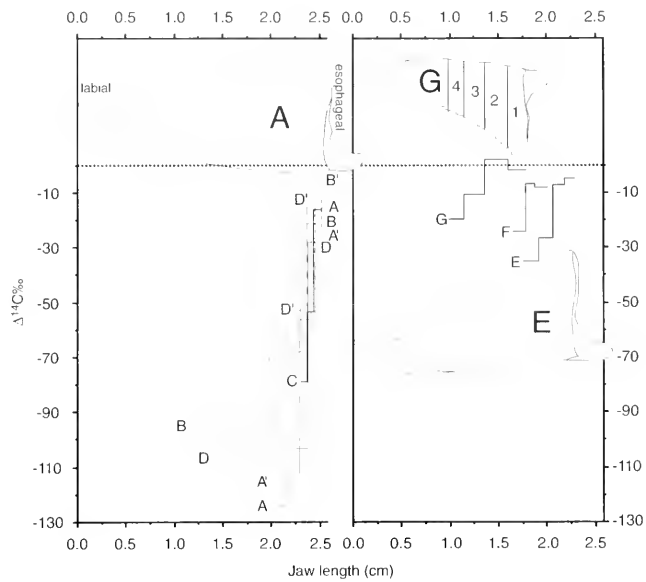

Figure 3

Change in $\Delta^{14}C$ ‰ with successive milled samples from the esophageal end of red sea urchin jaws collected at Halftide Rocks, Washington (48°28.8'N, 1220°59.8'W), 21 Oct. 1992. Step width in lines is the width of a milled sample. Jaws of three sea urchins are drawn but a total of 7 were sampled; jaw lengths are A = 2.58 cm, B = 2.54, C = 2.53, D = 2.51, E = 2.29, F = 2.01, G = 1.80 cm; primes represent replicate jaws from the same sea urchin; jaw C is labeled just at the final milled sample (initial sample is just below the initial sample for jaw A); bands labeled 1 through 4 on jaw G show how samples were milled from the jaw after the surface layer had been removed by approximately 0.5 mm. Shaded areas of the jaw, which were not sampled, indicate an area below the top surface where a shelf exists for articulation with the epiphysis, another ossicle of Aristotle's lantern.

ing elasticity analysis (de Kroon et al., 1986) of a matrix model and have shown that small changes in survival of individuals larger than 9 cm would have a greater effect on population maintenance than survival of smaller sea urchins (Ebert, 1998). The conclusion from matrix analysis, which is supported by the ^{14}C test of growth and age of *Strongylocentrotus franciscanus* we present in our study, is that the preservation of large individuals must be included in long-term management plans for this species as well as for other long-lived sea urchins in developing fisheries such as that for *Evechinus chloroticus* (Barker, 2001). Finally, our work strongly suggests that life spans of other exploited sea urchin species should be explored in greater detail in developing management plans because preservation of large and old individuals may be very important for the long-term viability of these fisheries.

Acknowledgments

Tagging and processing sea urchins were done in collaboration with S. Schroeter and J. Dixon, with support from the Pacific States Fishery Commission, a self-imposed landing tax of sea urchin fishermen administered by the Calif. Dept. Fish & Game, Oregon Sea Urchin Community Commission, and Ore. State Univ. Sea Grant; field work was facilitated by resource managers in California, Oregon, and Washington (P. Kalvass, N. Richmond, A. Bradbury). Stable isotope analysis was done at the University of California at Davis and radiocarbon analysis was funded by a Center for Accelerator Mass Spectrometry minigrant at Lawrence Livermore National Laboratory and was carried out under the auspices of the US DOE. The manuscript benefited from a critical reading by G. Fox.

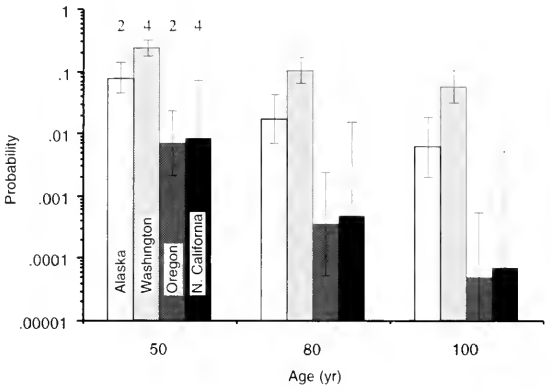

Figure 4

Probabilities of attaining ages of 50, 80, and 100 years for red sea urchins (*Strongylocentrotus franciscanus*) at sites from Alaska to northern California; estimates were based on Tanaka growth parameters and size-frequency distributions (Ebert et al., 1999); numbers of sites are shown at the tops of bars and there are two samples at each site; error bars are 2 SEs.

Literature cited

Agatsuma, Y.
2001. Ecology of *Strongylocentrotus intermedius*. *In* Edible sea urchins: biology and ecology (J. M. Lawrence, ed.), p. 333–346. Developments in aquaculture and fisheries science, no. 32. Elsevier Science B. V., Amsterdam, Netherlands.

Barker, M. F.
2001. The ecology of *Evechinus chloroticus*. *In* Edible sea urchins: biology and ecology (J. M. Lawrence, ed.), p. 245–260. Developments in aquaculture and fisheries science, no. 32. Elsevier Science B. V., Amsterdam, Netherlands.

Beddingfield, S. D., and J. B. McClintock.
2000. Demographic characteristics of *Lytechinus variegatus* (Echinoidea: Echinodermata) from three habitats in a north Florida bay, Gulf of Mexico. Mar. Ecol. 21:17–40.

Bernard, F. R., and D. C. Miller.
1973. Preliminary investigation on the red sea urchin resources of British Columbia [*Strongylocentrotus franciscanus* (Agassiz)]. Fish. Res. Board Can. Tech. Rep. 400: 1–37.

Breen, P. A., and B. E. Adkins.
1976. Growth rings and age in the red sea urchin, *Strongylocentrotus franciscanus*. Fish. Res. Board Can. Manuscr. Rep. Ser. 1413.

Brey, T.
1991. Population dynamics of *Sterechinus antarcticus* (Echinodermata: Echinoidea) on the Weddell Sea shelf and slope, Antarct. Antarctic Sci. 3:251–256.

Brey, T., J. Pearse, L. Basch, J. McClintock, and M. Slattery.
1995. Growth and production of *Sterechinus neumayeri* (Echinoidea: Echinodermata) in McMurdo Sound, Antarct. Mar. Biol. 124:279–292.

Broecker, W. S., T.-H. Peng, G. Ostlund, and M. Stuiver.
1985. The distribution of bomb radiocarbon in the ocean. J. Geophys. Res. 90:6953–6970.

Bureau, D.
1996. Relationship between feeding, reproductive condition, jaw size and density in the red sea urchin, *Strongylocentrotus franciscanus*. M.S. thesis, 90 p. Simon Fraser Univ., Burnaby, Canada.

Campana, S. E.
1997. Use of radiocarbon from nuclear fallout as a dated marker in the otoliths of haddock *Melanogrammus aeglifinus*. Mar. Ecol. Prog. Ser. 150:49–56.

Campana, S. E., L. J. Natanson, and S. Myklevoll.
2002. Bomb dating and age determination of large pelagic sharks. Can. J. Fish. Aquat. Sci. 59:450–455.

Congdon, J. D., A. E. Dunham, and R. C. van Loben Sels.
1994. Demographics of common snapping turtles (*Chelydra serpentiana*): implications for conservation and management of long-lived organisms. Am. Zool. 34:397–408.

Crapp, G. B., and M. E. Willis.
1975. Age determination in the sea urchin *Paracentrotus lividus* (Lamarck), with notes on the reproductive cycle. J. Exp. Mar. Biol. Ecol. 20:157–178.

de Kroon, H., A. Plaisier, J. van Groenendael, and H. Caswell.
1986. Elasticity: the relative contribution of demographic parameters to population growth rate. Ecology 67: 1427–1431.

Dix, T. G.
1972. Biology of *Evechinus chloroticus* (Echinoidea: Echinometridae) from different localities. 4. Age, growth, and size. N. Z. J. Mar. Freshw. Res. 6:48–68.

Duffy, P. B., D. E. Eliason, A. J. Bourgeois, and C. C. Covey.
1995. Simulation of bomb radiocarbon in two global ocean general circulation models. J. Geophys. Res. 100:22545–22563.

Duggins, D. O.
1983. Starfish predation and the creation of mosaic patterns in a kelp-dominated community. Ecology 64:1610–1619.
Ebert, T. A.
1988. Calibration of natural growth lines in ossicles of two sea urchins, *Strongylocentrotus purpuratus* and *Echinometra mathaei*, using tetracycline. *In* Echinoderm biology: proceedings of the sixth international echinoderm conference (R. D. Burke, P. V. Mladenov, P. Lambert, and R. L. Parsley, eds.), p. 435–443. A. A. Balkema, Rotterdam, Netherlands.
1998. An analysis of the importance of Allee effects in management of the red sea urchin *Strongylocentrotus franciscanus*. *In* Echinoderms: San Francisco. Proceedings, 9th international echinoderm conference (R. Mooi and M. Telford, eds.), p. 619–627. A. A. Balkema, Rotterdam, Netherlands.
Ebert, T. A., J. D. Dixon, S. C. Schroeter, P. E. Kalvass, N. T. Richmond, W. A. Bradbury, and D. A. Woodby.
1999. Growth and mortality of red sea urchins *Strongylocentrotus franciscanus* across a latitudinal gradient. Mar. Ecol. Prog. Ser. 190:189–209.
Ebert, T. A., S. C. Schroeter, J. D. Dixon, and P. E. Kalvass.
1994. Settlement patterns of red and purple sea urchins (*Strongylocentrotus franciscanus* and *S. purpuratus*) in California, USA. Mar. Ecol. Prog. Ser. 111:41–52.
Gage, J. D.
1991. Skeletal growth zones as age-markers in the sea urchin *Psammechinus miliaris*. Mar. Biol. 110:217–228.
Gage, J. D., and P. A. Tyler.
1985. Growth and recruitment of the deep-sea urchin *Echinus affinis*. Mar. Biol. 90:41–53.
Gage, J. D., P. A. Tyler, and D. Nichols.
1986. Reproduction and growth of *Echinus acutus* var. *norvegicus* Duben & Kören and *E. elegans* Duben & Kören on the continental slope off Scotland. J. Exp. Mar. Biol. Ecol. 101:61–83.
Gebauer, P., and C. A. Moreno.
1995. Experimental validation of the growth rings of *Loxechinus albus* (Molina, 1782) in southern Chile (Echinodermata: Echinoidea). Fish. Res. 21:423–435.
Guilderson, T. P., and D. P. Schrag.
1998. Abrupt shift in subsurface temperatures in the tropical Pacific associated with changes in El Niño. Science 281:240–243.
Hastings, A., and K. Higgins.
1994. Persistence of transients in spatially structured ecological models. Science 263:1133–1136.
Hilborn, R., and C. J. Walters.
1992. Quantitative fisheries stock assessment: choice, dynamics, and uncertainty, 570 p. Chapman & Hall, New York, NY.
Jensen, M.
1969. Breeding and growth of *Psammechinus miliaris* (Gmelin). Ophelia 7:65–78.
Kalish, J. M.
1993. Pre- and post-bomb radiocarbon in fish otoliths. Earth Planet. Sci. Lett. 114:549–554.
1995. Radiocarbon and fish biology. *In* Recent developments in fish otolith research (D. H. Secor, J. M. Dean, and S. E. Campana, eds.), p. 637–653. Univ. South Carolina Press, Columbia, SC.
Kawamura, K.
1966. On the age determining character and growth of a sea urchin, *Strongylocentrotus nudus*. Sci. Rep. Hokkaido Fish. Exp. Station 6:56–61.
Kramer, D. E., and D. M. A. Nordin.
1975. Physical data from a study of size, weight and gonad quality for the red sea urchin (*Strongylocentrotus franciscanus* (Agassiz)) over a one-year period. Fish. Res. Board Can. Manuscr. Rep. Ser. 1372:68.
Lamare, M. D., and P. V. Mladenov.
2000. Modelling somatic growth in the sea urchin *Evechins chloroticus* (Echinoidea: Echinometridae). J. Exp. Mar. Biol. Ecol. 243:17–43.
Low, C. J.
1975. The effect of grouping of *Strongylocentrotus franciscanus*, the giant red sea urchin, on its population biology. Ph.D. diss., 157 p. Univ. British Columbia, Vancouver, Canada.
Lumingas, L. J. L., and M. Guillou.
1994. Growth zones and back-calculation for the sea urchin, *Sphaerechinus granularis*, from the Bay of Brest, France. J. Mar. Biol. Assoc. U. K. 74:671–686.
Murphy, G. I.
1968. Pattern in life history and the environment. Am. Nat. 102:391–411.
Nichols, D., A. A. T. Sime, and G. M. Bishop.
1985. Growth in populations of the sea-urchin *Echinus esculentus* L. (Echinodermata: Echinoidea) from the English Channel and Firth of Clyde. J. Exp. Mar. Biol. Ecol. 86:219–228.
Nydal, R., and K. Lovseth.
1983. Tracing bomb ^{14}C in the atmosphere 1962–1980. J. Geophys. Res. 88:3621–3621.
Pearse, J. S., and A. H. Hines.
1987. Long-term population dynamics of sea urchins in a central California kelp forest: rare recruitment and rapid decline. Mar. Ecol. Prog. Ser. 39:275–283.
Peck, L. S., and T. Brey.
1996. Bomb signals in old Antarctic brachiopods. Nature 380:207–208.
Robinson, S. M. C., and A. D. MacIntyre.
1997. Aging and growth of the green sea urchin Bull. Aquacul. Assoc. Can. 91:56–60.
Roff, D. A.
1992. The evolution of life histories, 535 p. Chapman & Hall, New York, NY.
Russell, M. P., T. A. Ebert, and P. S. Petraitis.
1998. Field estimates of growth and mortality of the green sea urchin, *Strongylocentrotus droebachiensis*. Ophelia 48:137–153.
Sloan, N. A.
1986. Red sea urchin. Underwater world. DFO/2322 UW/53, 4 p. Fisheries and Oceans Canada, Ottawa, Canada.
Sloan, N. A., C. P. Lauridsen, and R. M. Harbo.
1987. Recruitment characteristics of the commercially harvested red sea urchin *Strongylocentrotus franciscanus* in southern British Columbia, Canada. Fish. Res. 5:55–69.
Stearns, S. C.
1992. The evolution of life histories, 249 p. Oxford Univ. Press, New York, NY.
Strathmann, R.
1978. Length of pelagic period in echinoderms with feeding larvae from the northwest Pacific. J. Exp. Mar. Biol. Ecol. 34:23–27.
Stuiver, M., and H. A. Polach
1977. Discussion: reporting of ^{14}C data. Radiocarbon 19: 355–363.
Sumich, J. L., and J. E. McCauley
1973. Growth of a sea urchin, *Allocentrotus fragilis*, off the Oregon Coast. Pac. Sci. 27:156–167.

Tanaka, M
1982. A new growth curve which expresses infinite increase. Publ. Amakusa Mar. Biol. Lab. 6:167–177.
1988. Eco-physiological meaning of parameters of ALOG growth curve. Publ. Amakusa Mar. Biol. Lab. 9:103–106.

Tegner, M. J.
2001. The ecology of *Strongylocentrotus franciscanus* and *Strongylocentrotus purpuratus*. *In* Edible sea urchins: biology and ecology (J. M. Lawrence, ed.), p. 307–332. Developments in aquaculture and fisheries science, no. 32. Elsevier Science B. V., Amsterdam, Netherlands.

Tegner, M. J., and P. K. Dayton.
1981 Population structure, recruitment and mortality of two sea urchins (*Strongylocentrotus franciscanus* and *S. purpuratus*) in a kelp forest. Mar. Ecol. Prog. Ser. 5: 255–268.

Tegner, M. J., and L. A. Levin.
1983. Spiny lobsters and sea urchins: analysis of a predator-prey interaction. J. Exp. Mar. Biol. Ecol. 73:125–150.

Turekian, K. K., J. K. Cochran,. Y. Nozaki, I. Thompson, and D. S. Jones.
1982. Determination of shell deposition rates of *Arctica islandica* from the New York Bight using natural ^{228}Ra and ^{228}Th and bomb produced ^{14}C. Limnol. Oceanogr. 27: 737–741.

Vogel, J. S., J. R. Southon, and D. E. Nelson.
1987. Catalyst and binder effects in the use of filamentous graphite for AMS. Nucl. Instru. Methods Phys. Res. Sec. B 29:50–56.

Witbaard, R., M. I. Jenness, K. van der Borg, and G. Ganssen.
1994. Verification of annual growth increments in *Arctica islandica* L. from the North Sea by means of oxygen and carbon isotopes. Neth. J. Sea. Res. 33:91–101.

Abundance and distribution of cetaceans in outer continental shelf waters of the U.S. Gulf of Mexico

Gregory L. Fulling
Keith D. Mullin
Carrie W. Hubard

Southeast Fisheries Science Center
National Marine Fisheries Service, NOAA
3209 Frederic Street
Pascagoula, Mississippi 39567
E-mail address (for G. L. Fulling): Greg.Fulling@noaa.gov

The U.S. Marine Mammal Protection Act (MMPA) requires that stocks of marine mammal species in U.S. waters be maintained at or above their optimum sustainable population (OSP) level, defined as the number of animals that results in the maximum net productivity. To meet this requirement for each stock, the U.S. National Marine Fisheries Service (NMFS) estimates annual human-caused mortality and potential biological removal (PBR), the maximum number of animals that may be removed from a stock due to human activities (e.g. fisheries bycatch) while allowing the stock to reach or maintain its OSP. PBR is calculated by following specific criteria and using the estimated abundance of the stock, its maximum net productivity rate (theoretical or estimated), and a recovery factor (Barlow et al., 1995; Wade and Angliss, 1997). The NMFS is required to prepare an annual stock assessment report (SAR) for each stock to update abundance, stock structure, maximum net productivity, human-caused mortality, PBR, and status (e.g. Waring et al., 2001).

Cetaceans in the U.S. Gulf of Mexico (U.S. GOM) occur in two species assemblages that overlap in upper continental slope waters (~200–1000 m). The oceanic waters (>200 m) are routinely inhabited by 20 species that, in most cases, inhabit deep warm-temperate to tropical waters throughout the world. Bottlenose dolphins (*Tursiops truncatus*) and Atlantic spotted dolphins (*Stenella frontalis*) are the only two species commonly found in continental shelf waters (<200 m) (Mullin and Hansen, 1999).

In the U.S. GOM the distribution of *T. truncatus* ranges from inshore waters to deep waters of the continental slope (Blaylock and Hoggard, 1994; Hansen et al.[1]; Mullin and Hoggard[2]). In the U.S. GOM, the NMFS divides *T. truncatus* into 38 stocks: 33 inshore stocks (bays, sounds, and estuaries); 3 coastal stocks (western, northern, and eastern) from shore to 9 km seaward of the 18-m (10-fm) isobath; 1 outer continental shelf (OCS) stock from the coastal boundary to 9 km seaward of the 183-m (100-fm) isobath; and 1 continental shelf edge and slope stock from the OCS boundary out to the U.S. Exclusive Economic Zone (EEZ) (Waring et al., 2001). The abundance estimate for the OCS *T. truncatus* stock is 50,247 dolphins (CV=0.18) and is based on aerial surveys conducted during fall which covered all the U.S. GOM shelf waters over 3 years in sections, west, central, and east, in 1992, 1993, and 1994, respectively (Blaylock and Hoggard, 1994; Waring et al., 2001).

One U.S. GOM *S. frontalis* stock is recognized, and the abundance, 3213 dolphins (CV=0.44), is estimated from ship surveys of shelf edge and oceanic waters >100 m deep conducted from 1991–94 (Hansen et al.[1]). Abundance estimates for *S. frontalis* for the U.S. GOM OCS were not made from the 1992–94 aerial surveys although *S. frontalis* groups were sighted (Waring et al., 2001). The majority of *S. frontalis* are thought to inhabit the shelf-edge region. However, data from opportunistic sightings (e.g. Mills and Rademacher, 1996) and a summer 1994 ship survey of the eastern GOM (Hofstetter, 2002) have indicated that they are common throughout eastern GOM shelf waters >10 m deep, and in oceanic waters <500 m.

The NMFS Southeast Fisheries Science Center (SEFSC) conducts annual spring and fall ichthyoplankton surveys in the U.S. GOM. The spring survey targets the entire oceanic portion of the U.S. GOM, and the fall survey focuses on shelf waters from the U.S.-Mexico border to southern Florida. Since 1991, abundance estimates of oceanic cetacean species in the U.S. GOM have been based primarily on data collected during annual spring surveys (Hansen et al.[1]; Mullin and Hoggard[2]; Mullin and Fulling[3]). Because of the lack of current assessment information on and the uncertainty of abundance estimates for *T. truncatus* and *S. frontalis* in OCS waters, cetacean surveys were conducted during the fall ichthyoplankton surveys from 1998 to 2001. From these surveys, we report the abundance and distribution of cetaceans in OCS waters (20–200 m deep) of the U.S. GOM.

[1] Hansen, L. J., K. D. Mullin, and C. L. Roden. 1995. Unpublished report. Estimates of cetacean abundance in the northern Gulf of Mexico from vessel surveys, 20 p. Southeast Fisheries Science Center, 3209 Frederic St., Pascagoula, MS 39567.

[2] Mullin, K. D., and W. Hoggard. 2000. Visual surveys of cetaceans and sea turtles from aircraft and ships. *In* Cetaceans, sea turtles and seabirds in the northern Gulf of Mexico: Distribution, abundance and habitat associations. Volume II: Technical report (R.W. Davis, W. E. Evans, and D. Würsig, eds.), p. 111–172. OCS Study MMS 96-0027. Minerals Management Service, Gulf of Mexico OCS Region, New Orleans, LA. 70123.

[3] Mullin, K. D., and G. L. Fulling. 2003. Unpublished report. Abundance of cetaceans in the oceanic northern Gulf of Mexico, 1996–2001, 35 p. Southeast Fisheries Science Center, 3209 Frederic Street, Pascagoula, MS 39567.

Manuscript approved for publication 10 July 2003 by Scientific Editor.
Manuscript received 20 July 2003 at NMFS Scientific Publications Office.
Fish. Bull. 101:923–932 (2003).

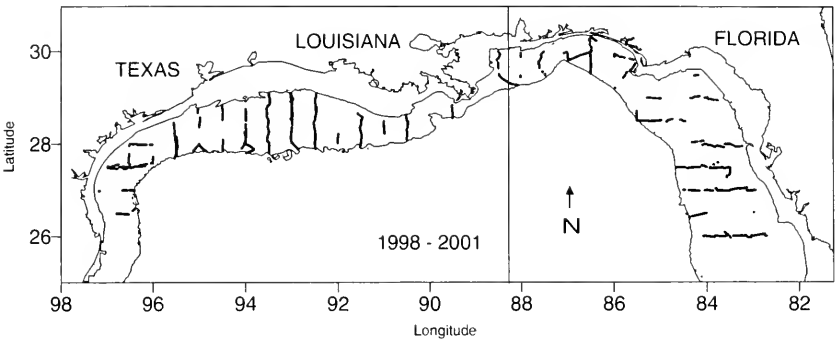

Figure 1

Survey effort in Beaufort sea state of ≤3 (dark lines), east (1342 km) and west (2202 km) of Mobile Bay, Alabama (bold vertical line), in the northern U.S. Gulf of Mexico outer continental shelf (20–200 m) during fall 1998–2001. The 20- and 200-m isobaths (thin lines) are shown.

Methods

Study area

The study area (245,800 km^2) included continental shelf waters of the U.S. GOM between the U.S-Mexico border and Key West, Florida, between the 20- and 200-m isobaths (Fig. 1). However, survey effort did not extend south of 26.0°N in the southeastern GOM and therefore abundance estimates were extrapolated for this region. The shelf is wide (up to 200 km) off the Florida peninsula and off northern Texas and Louisiana, and narrower off the Florida Panhandle near DeSoto Canyon, the Mississippi River Delta, and southern Texas. The continental slope is a steep escarpment from 1000 to 2000 m in the eastern GOM.

Survey design and data collection

Surveys were conducted from the 68-m NOAA Ship *Gordon Gunter* (1998, 1999, and 2001) and the 52-m NOAA Ship *Oregon II* (2000). The four surveys ranged from 28 to 32 days between 28 August and 2 October and were divided into two legs of 12 to 19 days. Standard ship-based, line-transect survey methods for cetaceans, similar to those used in the Pacific Ocean and U.S. GOM, were used (e.g. Barlow, 1995; Hansen et al.[4]). Surveys were conducted 24 hours a day along a predetermined trackline between plankton stations uniformly spaced 30 nmi apart. The trackline uniformly covered the shelf waters roughly 10–200 m deep in 1998–2001 (Fig. 1).

Data were collected by two teams of three observer—one team positioned on the flying bridge 14.5 m above the waterline (*Gunter*) and the other team positioned 9.2 m above the waterline (*Oregon II*) during daylight hours while the vessels moved between plankton stations, weather permitting (i.e. no rain, Beaufort sea state <6). Each team had at least two members experienced in ship-based, line-transect methods and in identification of tropical cetaceans. The left- and right-side observers searched to the horizon in the arc from 10° right and left of the ship's bow to the left and right beams (90°), respectively, using 25× binoculars. The third observer searched, using unaided eye or 7× hand-held binoculars, and recorded data. Observers changed position every 30–40 minutes, and the two teams alternated 2-h watches throughout daylight hours. Survey speed was usually 18 km/h (~10 knots) but varied with sea conditions.

Data were recorded on a computer interfaced with a global positioning system (GPS) by an in-house BASIC data acquisition program (Southeast Fisheries Science Center, NMFS, Pascagoula, MS). For each cetacean sighting, time, position, bearing and reticle (a measure of radial distance) of the sighting, species, group-size, behavior, bottom depth, sea surface temperature, and associated animals (e.g. seabirds, fish) were recorded. The bearing and radial distance for groups sighted without 25× binoculars and close to the ship were estimated. Survey effort data were automatically recorded every 2 minutes and included the ship's position and direction, effort status, observer positions, and environmental conditions that could affect the observers' ability to sight animals (e.g. Beaufort sea state, sun position). Typically, if a sighting was within a 5.5-km strip on either side of the ship, the ship was diverted from the trackline to approach the group to allow the observers to identify species and estimate group-size by consensus.

Cetaceans were identified to the lowest taxonomic level possible. Observers' ability to make identifications depended on weather and animal behavior. Differences between *T. truncatus* and *S. frontalis* could not always be

[4] Hansen, L. J., K. D. Mullin, T. A. Jefferson, and G. P. Scott. 1996. Visual surveys aboard ships and aircraft. *In* Distribution and abundance of marine mammals in the north-central and western Gulf of Mexico: Final report. Volume II: Technical report (R.W. Davis and G.S. Fargion, eds.), p. 55–132. OCS Study MMS 96-0027. Minerals Management Service, Gulf of Mexico OCS Region, New Orleans, LA. 70123.

distinguished at long distances and were therefore sometimes recorded as "*T. truncatus* + *S. frontalis*."

Analytical techniques

Survey effort that was parallel to the bathymetry gradients, occurred in waters outside the OCS study area, or occurred in a Beaufort sea state ≥4 was excluded from analyses (Fig. 1). Survey effort used in analyses is summarized in Table 1. Survey effort was not uniformly distributed throughout the study area due to poor survey conditions, particularly in the eastern GOM, during two of the four years. Because *S. frontalis* sightings were clearly more numerous in the east, we delineated the study area into west (106,186 km^2) and east (139,614 km^2) regions at 88°15.0'W (ca. Mobile Bay, Alabama) and estimated abundances separately for each region. A combination of line-transect and strip-transect methods were used to make abundance estimates. Line-transect methods were used for sightings detected with 25(binoculars, which constituted the majority of sightings (129/140). Strip-transect methods were used for the 11 sightings that were made without the 25× binoculars (naked-eye sightings) and that were observed by the primary team.

Line-transect estimates

For each species or species group (i) [i.e. *T. truncatus*, *S. frontalis*, rough-toothed dolphins (*Steno bredanensis*) and *T. truncatus*+*S. frontalis*] detected by 25× binoculars, and for each region (j) (east and west), abundance estimates were made with line-transect methods ($N_{Li,j}$) by using the software program DISTANCE (Colorado Coop. Fish and Wildlife Research Unit, Colorado State Univ., Fort Collins, CO) (Laake et al., 1993; Buckland et al., 2001) and by incorporating data into the following equation:

$$N_{Li,j} = \frac{A_j \cdot n_{Li,j} \cdot S_{Li,j} \cdot f_i(0)}{2 \cdot L_j \cdot g(0)}, \qquad (1)$$

where A_j = area of region j;
$n_{Li,j}$ = number of group sightings of species i in region j;
$S_{Li,j}$ = mean group size of species i in region j;
$f_i(0)$ = sighting probability density function at perpendicular distance zero for species i;
L_j = total length of transect line in region j; and
$g(0)$ = probability of seeing a group on the transect line.

The parameter $g(0)$ was not estimated; $g(0) = 1$ was used for each abundance estimate. Abundances were negatively biased because observers usually miss some groups at the surface on the transect line, and some groups were under the surface while in the observation area, therefore $g(0) < 1$ (see "Discussion" section). The log-normal 95% confidence interval was computed (Buckland et al., 2001) for each abundance estimate because it was a product of estimates and tended to have a skewed distribution. The variance of $N_{Li,j}$ was estimated by using

Table 1

Total survey effort (km) during 1998–2001 in waters 20–200 m and under Beaufort sea state conditions ≤3.

Year	West	East	Total
1998	174	67	241
1999	477	120	597
2000	281	0	281
2001	448	629	1077
Total	1380	816	2196

$$\mathrm{var}(N_{Li,j}) = N_{Li,j}^2 \left(\frac{\mathrm{var}(n_{Li,j})}{n_{Li,j}^2} + \frac{\mathrm{var}(S_{Li,j})}{S_{Li,j}^2} + \frac{\mathrm{var}[f_i(0)]}{f_i(0)^2} \right). \qquad (2)$$

The sampling unit was the length of the transect completed on-effort each day with Beaufort sea state ≤3 in a region. The formula used to estimate each component of the variance is given in Buckland et al. (2001). Var($n_{Li,j}$) was length-weighted and based on the variation in the number of on-effort group sightings between sampling units that ranged up to 191 km/d.

Estimation of $f(0)$

The perpendicular distance (y) was estimated by using bearing and reticle measurements. The reticle readings were converted to radial sighting distances (R) by the method of Lerczak and Hobbs (1998; $y = R \sin(b)$, where b=angle between the sighting and the transect line). Because of the difference in observer height (5.3 m) between the *Oregon II* and *Gunter*, each ship could potentially yield a different sighting function, $g(x)$. However, only seven sightings were made in sea states ≤3 from the *Oregon II* during the one year it was used; therefore data from both ships were pooled. Estimates of $f_i(0)$ were made by using a hazard-rate, uniform, or half-normal model with exact perpendicular sighting distances and no adjustments. Model selection was determined by using Akaike's Information Criterion (AIC; Buckland et al., 2001).

The number of *S. bredanensis* groups and the number of *T. truncatus*+*S. frontalis* groups sighted was insufficient to estimate $f(0)$ for each. Because the *S. bredanensis* group and *T. truncatus*+*S. frontalis* group had similar sighting characteristics (e.g. body size, group-size, surface behavior), we pooled them with sightings of *T. truncatus* to estimate $f_i(0)$. Total number of sightings for both *T. truncatus* and *S. frontalis* was sufficient to estimate $f_i(0)$ for each without pooling with other species. Truncation for *T. truncatus*, *S. bredanensis*, and *T. truncatus* + *S. frontalis* was 3300 m, and was 5000 m for *S. frontalis*. Each estimate of $f_i(0)$ was based on pooled sightings from the east and west regions.

Estimation of mean group-size

Group-sizes tend to be related to y, because in many cases larger groups are easier to see than small groups with

increasing y. In general, the arithmetic mean of group-size may be an overestimate of the true mean group-size and could lead to positively-biased abundance estimates. Therefore, a regression of group-size by y was used to estimate an "expected mean group-size" (program DISTANCE) and it was used if the regression was significant ($P<0.15$). $\text{Var}(S_L)$ was the analytical variance for mean group-sizes based on arithmetic means or was estimated as in Buckland et al. (2001:74) for expected mean group-sizes.

Strip-transect estimates

One requirement for unbiased line-transect estimates of abundance is that the cetacean group should not move in response to the ship before it is sighted (Buckland et al., 2001). If cetaceans are not sighted before they respond to the ship, in cases of attraction to the ship, $f(0)$ and abundance will be overestimated. During previous U.S. GOM surveys, groups of *T. truncatus* or *S. frontalis* were consistently attracted to ride the bow waves as the ship approached (Würsig et al., 1998). Therefore, the abundance and variance of groups sighted by naked eye (N_S) were estimated by

$$N_{S_{i,j}} = \frac{A_j \cdot n_{S_{i,j}} \cdot S_{S_{i,j}}}{2 \cdot L_j \cdot w_i} \quad (3)$$

and

$$\text{var}(N_{S_{i,j}}) = N_{S_{i,j}}^2 \left(\frac{\text{var}(n_{S_{i,j}})}{n_{S_{i,j}}^2} + \frac{\text{var}(S_{S_{i,j}})}{S_{S_{i,j}}^2} \right), \quad (4)$$

where $w_i = 1/f_i(0)$ which was treated as a constant, i.e. strip width, w_i, was equal to the line-transect effective strip half-width $[1/f_i(0)]$ with $\text{var}(w_i) = 0$.

For each region, species total abundance ($N_{T_{i,j}}$) was the line-transect and strip-transect estimates added, $N_{T_{i,j}} = N_{L_{i,j}} + N_{S_{i,j}}$. Total U.S. GOM OCS abundance for each species was $N_{T_i} = \Sigma N_{T_{i,j}}$. The coefficient of variation (CV) for each abundance was estimated as $\text{CV}(N) = [\text{var}(N)]^{1/2}/N$ and the CV for each summed abundance as

$$CV(N_{sum}) = \left(\sum CV^2(N) \cdot N^2 \right)^{1/2} \Big/ \sum N. \quad (5)$$

Results

Abundance estimates were based on 2196 km of effort and 140 sightings (Figs. 1 and 2). For east and west regions, there was 816 km of effort and 73 sightings, and 1380 km of effort and 67 sightings, respectively (Tables 1 and 2). Only three cetacean species were encountered. Groups of *T. truncatus* (30 east region, 45 west region) and *S. frontalis* (34 east, 12 west) were the most frequently encountered (Fig. 2, Table 2) and *S. bredanensis* groups (1 east, 2 west) were also sighted. *Tursiops truncatus* and *S. frontalis* were estimated to have $f(0)$ of 0.6238/km (CV=0.12) and 0.4101/km (CV=0.11), and an effective strip half-width of 1603 and 2438 m, respectively (Figs. 3 and 4). *Steno bredanensis* and *T. truncatus*+*S. frontalis* abundances were based on an $f(0)$ = 0.6059/km (CV=0.11) and an effective strip half-width of 1650 m.

Mean group-sizes (from 25× binocular sightings) of *T. truncatus* for east (9.8, 0.25) and west (10.0, 0.18) regions were similar (Table 2), and had an overall range of 1–68 animals. The mean group size of *S. frontalis* was larger in the east (24.3, 0.19) than the west (15.6, 0.21) with an overall range of 1–267 animals. Group-sizes of *S. bredanensis* were 8, 11, and 20 animals. The east mean group-size for both *T. truncatus* and *S. frontalis* is the size-biased or expected mean group-size because the expected mean was significantly smaller that the arithmetic mean, 10.9 (P=0.14) and 31.9 (P=0.08), respectively.

The most abundant species (number of individuals; CV) found in U.S. GOM OCS waters was *S. frontalis* (30,772; 0.27); the vast majority (91%) occurring in the east (27,997; 0.29). The density of *S. frontalis* was about eight times greater in the east compared to the west (20.1 and 2.6 dolphins/100 km^2, respectively). The abundance of *T. truncatus* was 25,320 (0.26); there was greater abundance in the east (15,198; 0.34) than in the west (10,122; 0.29) but with similar densities (10.9 and 9.5 dolphins/100 km^2, respectively). The total OCS abundance of *S. bredanensis* was 1238 (0.65), and that of *T. truncatus*+*S. frontalis*, 1868 (0.37).

Discussion

Both *T. truncatus* and *S. frontalis* occur in northern GOM waters outside the OCS (i.e. waters <20 m or >200 m). About 23,000 *T. truncatus* inhabit inshore and coastal waters (≤20 m) (Waring et al., 2001) and nearly 3000 occur in oceanic waters (Mullin and Fulling[2]). Both the "coastal" and "offshore" ecotypes of *T. truncatus* (Hersh and Duffield, 1990) occur in the northern GOM (LeDuc and Curry, 1998). How these ecotypes are distributed in the northern GOM and western North Atlantic is being investigated from skin biopsy samples collected, in part, during the 1998–2001 OCS surveys. Using mitochondrial DNA, obtained from biopsy samples collected during a U.S. Atlantic ship survey, Torres et al. (2003) reported no offshore form was sampled within 6 km of shore and no coastal from was sampled beyond 39 km from shore or in waters >34 m deep. Forty-seven percent (35/75) of the GOM OCS *T. truncatus* groups were in waters >34 m deep.

Ship surveys of northern GOM waters indicate that very few *S. frontalis* (<500 animals) occur in oceanic waters, and those that do are usually found close to the shelf edge in waters <500 m deep (Davis et al., 1998; Mullin and Fulling[2]). The smaller "offshore" or "Gulfstream" *S. frontalis* that occurs in parts of the oceanic Atlantic (Perrin, 2002) has not been recorded for the northern GOM. During the 1998–2001 surveys, *S. frontalis* was sighted in waters <20 m deep. However, because sampling was not perpendicular to bathymetry, abundance estimates were not calculated. This species is not known to occur in U.S. GOM inshore waters (Mullin and Hansen, 1999).

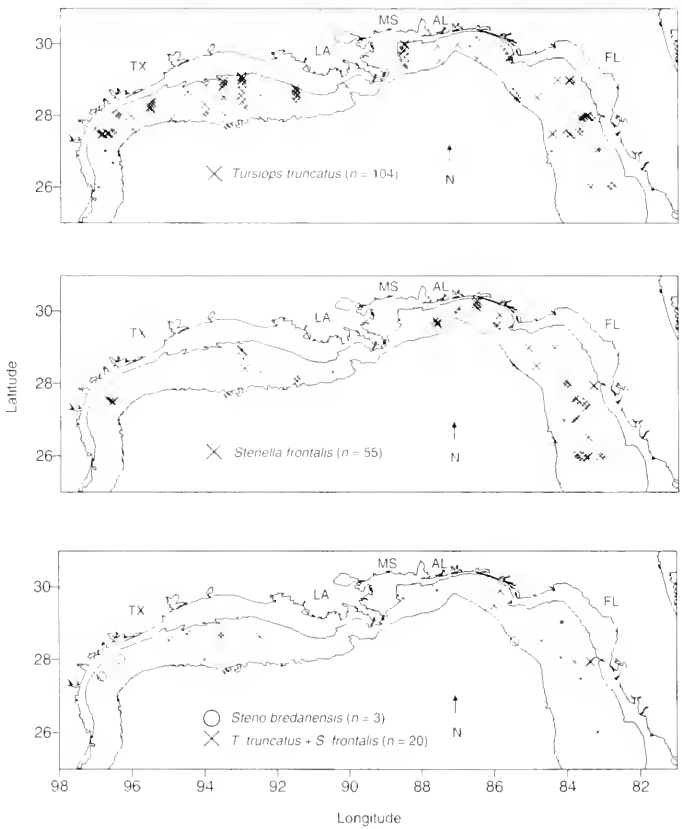

Figure 2

Locations of all on-effort sightings of *Tursiops truncatus* (top), *Stenella frontalis* (center), *Steno bredanensis*, and *T. truncatus*+*S. frontalis* (bottom) in the northern U.S. Gulf of Mexico outer continental shelf (20–200 m) during fall 1998–2001. Numbers of sightings shown are prior to truncation. The 20- and 200-m isobaths (thin lines) are shown (AL=Alabama, FL=Florida, LA=Louisiana, MS=Mississippi, TX=Texas).

Abundance

The abundance estimates for cetaceans reported in the present study are the first ship-based estimates for the U.S. GOM OCS. Abundance estimates for *T. truncatus* on the OCS (25,320; 0.26) are half the estimate in the pre-2002 SARs (50,247; 0.18) (e.g. Waring et al., 2001), that were based on aerial surveys conducted during fall 1992–94 (Blaylock et al., 1994; Waring et al., 2001). The abundance estimate for *S. frontalis* for the entire U.S. GOM in SARs prior to 2002 (3,213; 0.44) was based on data from ship surveys of OCS and oceanic waters >100 m deep (Waring et al., 2001; Hansen et al.[1]). Our current abundance estimate of *S. frontalis* (30,772; 0.27) for the OCS is almost an order of magnitude larger.

During the 1991–94 aerial surveys, there were 13 sightings of *S. frontalis* groups and 10 sightings that were identified as *T. truncatus*+*S. frontalis* in OCS waters (SEFSC, NMFS, Pascagoula, MS, unpubl. data). Using these sightings and 139 *T. truncatus* sightings to estimate $f(0)$, we estimated the abundance of *S. frontalis* from the aerial survey data to be 14,866 (0.37) for the U.S. GOM OCS [west, 3,526 (0.86); east, 11,340 (0.40)].

There are several potential reasons for the differences in abundances of the two species from ship and aerial surveys. The U.S. GOM OCS east of 85.5°W makes up about 44% of the U.S. GOM OCS. Aerial survey abundance estimates in this area were based on a small number of transect lines grouped in two places and most of the area was not

Table 2

Group-size, density and abundance estimates of cetaceans in the northern U.S. Gulf of Mexico outer continental shelf (waters 20–200 m deep) during fall 1998–2001 (n=number of group sightings, S=mean group-size, D=animals/100 km^2, N=abundance estimate, CV=coefficient of variation, R=reticle sightings, and K=naked eye sightings).

Species and stratum	n	S	CV(S)	D	N	CV(N)	95% CI
Tursiops truncatus							
East-R	27	9.8	0.25	10.1	14,132	0.40	6426–31,082
East-K	3	6.7	0.70	0.8	1066	0.85	139–8182
East total	30			10.9	15,198	0.38	7442–31,035
West-R	41	10.0	0.18	9.2	9786	0.30	5502–17,406
West-K	4	3.5	0.34	0.3	336	0.67	94–1201
West total	45			9.5	10,122	0.29	5790–17,696
OCS total	75			10.3	25,320	0.26	15,457–41,478
Stenella frontalis							
East-R	32	24.3	0.19	19.5	27,226	0.30	15,093–49,113
East-K	2	11.0	0.09	0.6	771	0.55	252–2358
East total	34			20.1	27,997	0.29	15,978–49,057
West-R	11	15.6	0.21	2.6	2712	0.42	1192–6169
West-K	1	4	—	0.6	63	1.17	9–433
West total	12			2.6	2775	0.41	1279–6023
OCS total	46			12.5	30,772	0.27	18,418–51,412
Steno bredanensis							
East-R	0	—	—	—	0	—	—
East-K	1	11	—	0.4	586	0.85	118–2902
East total	1			0.4	586		
West-R	2	14	0.43	0.6	652	0.98	115–3715
West-K	0	—	—	—	0	—	—
West total	2			0.6	652		
OCS total	3			0.5	1238	0.65	384–3990
T. truncatus+*S. frontalis*							
East-R	8	2.4	0.22	0.7	983	0.57	324–2983
East-K	0	—	—	—	0	—	—
East total	8			0.7	983		
West-R	8	4.8	0.28	0.8	885	0.47	355–2207
West-K	0	—	—	—	0	—	—
West total	8			0.8	885		
OCS Total	16			0.8	1868	0.37	920–3793

surveyed (see Fig.1 in Baumgartner [1997]). Complete coverage would have certainly led to more *S. frontalis* sightings and it is possible the lines that were surveyed were in areas with more *T. truncatus*. Blaylock and Hoggard (1994) estimated from aerial surveys that about 31% of the *T. truncatus* in OCS waters west of Mobile Bay were in rather a small area from the Mississippi River Delta west to about 90.5°W. Our ship survey effort in this area was small and resulted in only one sighting of *T. truncatus* (Fig. 2). Therefore, our ship-based estimates may have underestimated the abundance of *T. truncatus* in the western OCS. Aerial abundances were based on survey lines that extended from 9.3 km past the 18 m (10 fm) curve to 9.3 km past 183 m (100 fm) curve; therefore the area surveyed was somewhat different than our 20–200 m OCS study area for ship surveys. Aerial survey effort in waters >200 m may have resulted in more sightings of *T. truncatus* than *S. frontalis* because the deeper waters are not the common habitat of *S. frontalis* (Mullin and Fulling[2]) and sightings in waters <20 m would have also been biased toward *T. truncatus*.

Stenella frontalis and *T. truncatus* are similar in length and shape. *Stenella frontalis* are born without spots and become progressively more spotted with age, but young animals look very similar to *T. truncatus* (see Herzing, 1997). Therefore, depending on the composition of the group, from a distance *S. frontalis* are not always easily distinguished from *T. truncatus*; therefore it is possible that some groups were misidentified as *T. truncatus* during aerial surveys, leading to bias in the relative abundance of each species.

The annual PBR for the OCS stock of *T. truncatus* was 432 dolphins, and for the U.S. GOM stock of *S. frontalis*,

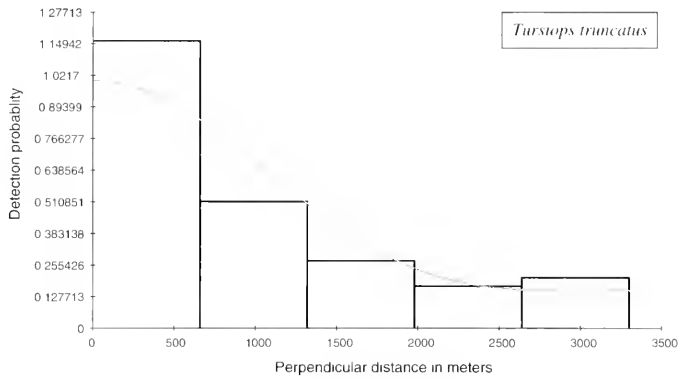

Figure 3

Plot of the detection function of pooled sightings of *Tursiops truncatus* in the northern U.S. Gulf of Mexico.

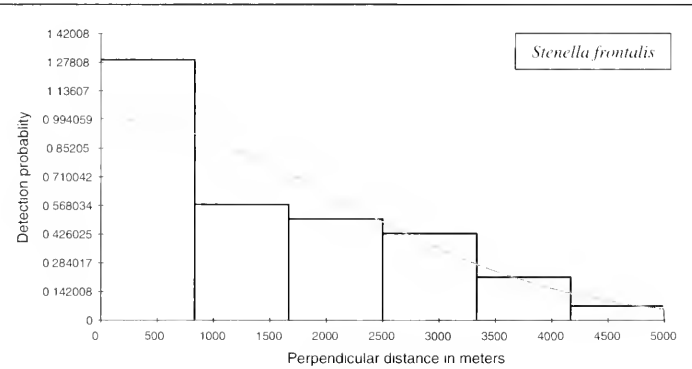

Figure 4

Plot of the detection function of pooled sightings of *Stenella frontalis* in the northern U.S. Gulf of Mexico.

23 dolphins (Waring et al., 2001). Using the abundances, we estimated that the annual PBR would be 204 dolphins for *T. truncatus* and 246 dolphins for *S. frontalis* (Table 2). Although these changes in both PBRs are large, the annual fishery-related mortality and serious injury for each species is estimated to be <3 dolphins in the U.S. GOM OCS (Waring et al., 2001).

Precision

The precision of the abundance estimates for *T. truncatus* (CV=0.26) and *S. frontalis* (CV=0.27) was good, although they were achieved after four years of effort. In cases where there is human-caused mortality in a cetacean stock, abundance estimates with a CV < 0.50 are generally required to avoid incorrectly classifying a cetacean stock as "strategic" under the U.S. MMPA (i.e. annual human-caused mortality>annual PBR) less than 10% of the time (Wade and DeMaster, 1999).

Bias

The surveys were designed to meet the assumptions of line-transect theory (Buckland et al., 2001). However, the abun-

dance estimates were negatively biased because the central assumption that all cetacean groups on the transect line are detected (i.e. $g(0)=1$), certainly was not met, and data were not collected to correct estimates for perception and availability bias (Marsh and Sinclair, 1989). Barlow (1995) estimated perception bias in a ship survey in the Pacific Ocean, and although the group-sizes were not estimated at close range, the majority of groups missed by the primary team were apparently small groups. From this, Barlow (1995) estimated $g(0)$ to range from 0.73 and 0.79 for small groups of delphinids (<21 animals). Delphinids have relatively short dive-cycles but diving synchrony among members of a group can affect availability bias; if dives are asynchronous, the probability that at least one animal will be at the surface increases with group-size. Because availability bias varies by species due to differences in individual dive cycles, group diving behavior, and group-sizes, we were not able to address this potential bias based on Barlow's (1995) results.

The use of the effective strip half-width $[1/f_i(0)]$ from the 25× binocular sightings for the strip width for the strip-transect estimates (Table 2) was assumed to be conservative and somewhat negatively biased. The distance from which animals will come to the ship to ride the bow is unknown and variable, depending on factors such as the animals' previous behavior, number of bowriding opportunities, and the type of ship. If the strip width was too narrow, the strip-transect estimates of abundance would be positively biased.

Our abundance estimates were for the entire U.S. OCS, but the surveys did not extend south of 26.0°N in the eastern Gulf. Sightings from a 1994 survey of the eastern Gulf (Hoffstetter, 2002) indicated that the distribution of *T. truncatus* and *S. frontalis* does not change dramatically between 26.0°N and Key West; therefore we believe this potential bias is minimal.

Because our estimates are from four combined years, another source of bias would occur if there were annual shifts in cetacean distribution, that is, if the majority of animals of any species occurred in a different part of the OCS in one year during fall compared to others years. However, there was no indication that this variation in distribution occurred and therefore potential bias is probably minimal. Potential bias due to the seasonality of the survey is also possible but cannot currently be addressed.

Additionally, survey effort from the 2001 cruise was the most complete effort of all years and may have carried more weight than all the other cruises. However, the 2001 survey provided adequate eastern GOM coverage. Variable survey effort in the fall is common because tropical weather can create rough sea conditions. Additionally, fall surveys always began in the west and terminated in the east. Because the same cruise track was always followed, we rarely had the opportunity to survey those areas not surveyed previously during nighttime transit, and thus may have created both a spatial and temporal bias.

Distribution

The observed distributions of both *T. truncatus* and *S. frontalis* were not surprising given previous descriptions of their distributions. The greater number of *S. frontalis* in the U.S. GOM off Florida compared to the western GOM was suggested by Schmidley and Melcher (1974), and the distribution of sightings reported by Mills and Rademacher (1996) supported this finding. The density of *S. frontalis* was much greater in the eastern GOM OCS than the western GOM OCS but the density of *T. truncatus* was similar in the two regions (Table 2).

The West Florida Shelf and Texas-Louisiana Shelf are very different marine environments, but how habitat differences specifically affect cetacean density patterns is not clear. The oceanography of the U.S. GOM continental shelf is complex, variable both spatially and temporally, and difficult to characterize briefly. Nevertheless, there are some clear distinctions between eastern and western OCS. First, there are 3415 active oil and gas platforms in the U.S. GOM OCS (0–200 m); the vast majority of these platforms (with their attendant boat and helicopter traffic) occur in waters west of Mobile Bay (MMS[5]). Also, ~95% of the U.S. GOM fisheries landings by weight occur west of Mobile Bay (10 years of NMFS[6] data). Additionally, sediment- and nutrient-laden fresh water from the Mississippi River and its distributary, the Atchafalaya River, usually moves west and predominately affects the Texas-Louisiana and Mississippi-Alabama shelves. The bottom of the Texas-Louisiana Shelf is primarily clay-slit mud and sand, and that of the West Florida Shelf is a mosaic of sand, gravel, shell, and coral (Rabalais et al., 1999). Primary production associated with the Mississippi River outflow is the highest measured in the GOM (Lohrenz et al., 1999). However, productivity on the West Florida Shelf can be enhanced by a variety processes (e.g. Gilbes et al., 1996). The deep eastern GOM is subject to the quasi-annual incursion of the Loop Current, which can extend to the Mississippi-Alabama Shelf (Wiseman and Sturges, 1999). This incursion can lead to upwelling episodes along the Loop Current front that may increase productivity along the shelf edge and on the West Florida Shelf (Paluszkiewicz et al., 1983; Gilbes et al., 1996). Baumgartner et al. (2001) reported greater sighting rates of cetaceans in the eastern GOM shelf-edge and oceanic waters and suggested that greater feeding opportunities may occur because of the influence of the Loop Current. Griffin and Griffin (2003), whose study included coastal waters (<20 m), reported that *S. frontalis* on the West Florida Shelf was found in deeper, more saline, and less turbid water than those where *T. truncatus* was found.

Demersal fish (e.g. sciaenids) are abundant and diverse on the western GOM OCS, but less abundant on the eastern OCS (Darnell et al.[7]; Darnell et al.[8]). The known prey of

[5] Mineral Management Service, Gulf of Mexico Region website: http://www.gomr.mms.gove/homepg/fastfacts/WaterDepth/WaterDepth.html. [Accessed on 7/8/2003.]

[6] National Marine Fisheries Service web site: http://www.st.nmfs.gov/st1/commercial/. [Accessed on 8 July 2003.]

[7] Darnell, R. M., R. E. Defenbaugh, and D. Moore. 1983. Northwestern Gulf shelf bio-atlas; a study of the distribution of demersal fishes and penaeid shrimp of the soft bottoms of the continental shelf from the Rio Grande to the Mississippi River Delta. Open File Report No. 82-04, 438 p. Minerals Management Service, Gulf of Mexico OCS Region, New Orleans, LA 70123.

T. truncatus from the GOM consist primarily of demersals, at least close to shore, but they also prey on pelagic species (Barros and Odell, 1990). The prey of *S. frontalis* are not well characterized but descriptions include epipelagic and mesopelagic fish and squid, and benthic invertebrates (Perrin, 2002). Richard and Barbeau (1994) observed "spotted dolphins" feeding on flyingfish (Exocoetidae) in waters 28–35 m deep on the West Florida Shelf. This is not uncommon because *S. frontalis* have been routinely observed feeding on flyingfish at night during haulback of longline gear during NMFS fisheries assessment surveys (Grace[9]). Fertl and Würsig (1995) describe *S. frontalis* feeding on a school of small clupeid fish at the surface south of the Florida Panhandle. A *S. frontalis* satellite-tracked for 24 days off Texas stayed in waters 12–63 m deep (mean, 32.6 m) and 58.1% of its dives were <10 m (Davis et al., 1996). These shallow dives observed by Davis et al. may indicate feeding on epipelagic species.

The occurrence of *S. bredanensis* in continental shelf waters of the U.S. GOM is interesting because this species is usually described as inhabiting oceanic waters (e.g. Jefferson, 2002). In the northern GOM, the estimated density of *S. bredanensis* was larger in OCS waters during fall (0.50 dolphins/100 km^2; Table 2) than that estimated for oceanic waters during spring (0.32 dolphins/100 km^2) (Mullin and Fulling[2]). In fact, if there is no OCS-oceanic shift in distribution between spring and fall, there may be similar numbers of *S. bredanensis* in northern GOM shelf waters (1238; 0.65) as in oceanic waters (1231; 0.45). One of the groups sighted in OCS waters was near the shelf-edge (183 m) but the other two sightings were at depths of 31 m and 33 m off Texas (Fig. 2). The use of shelf waters in the U.S. GOM by this species may not be atypical; two sightings of *S. bredanensis* were made on the West Florida Shelf in waters <55 m deep during August 1994 (Hofstetter, 2002). Pitman and Stinchomb (2002) provide evidence that *S. bredanensis* may be specialized predators of dolphinfish (*Coryphaena hippurus*) in the Pacific Ocean. Dolphinfishes have a circumtropical distribution but occur in oceanic and shelf waters in the northern GOM commonly associated with *Sargassum* and other drifting materials (Hoese and Moore, 1998). *Steno bredanensis* in the northern GOM are commonly found near flotsam, as they are in the Pacific—a place where dolphinfish tend to aggregate.

The abundance estimates presented in this study are the first ship-based estimates of *T. tursiops* and *S. frontalis* from Gulf of Mexico OCS waters. Although probably negatively biased, these estimates provide reliable data for the management of these species. Our results suggest that the diverse U.S. GOM environments provide an excellent natural experiment and opportunity to further understand the ecology of these sympatric cetacean species in OCS pelagic waters.

[8] Darnell, R. M., J. A. Kleypas, and R. E. Defenbaugh. 1987. Eastern Gulf shelf bio-atlas; a study of the distribution of demersal fishes and penaeid shrimp of the soft bottoms of the continental shelf from the Mississippi River Delta to the Florida Keys. OCS Study 86-0041, 548 p. Minerals Management Service, Gulf of Mexico OCS Region, New Orleans, LA 70123.

[9] Grace, M. A. 2003. Personal commun. NOAA, 3209 Frederic Street, Pascagoula, MS 39567.

Acknowledgments

Many people made significant contributions to the success of the surveys including the officers and crews of NOAA ships *Gordon Gunter* and *Oregon II* and the field party chiefs. The marine mammal observers were H. Adams, N. Baertlein, C. Brown, J. Brusher, C. Burks, C. Cates, J. Contillo, L. Csuzdi, A. Debose, A. Beier-Engelhaupt, K. Maze-Foley, J. Henne, W. Hoggard, K. Hough, J. Litz, T. Martinez, M. Newcomer, C. Palmer, K. Rademacher, C. Roden, C. Sinclair, S. Stienessen, J. Tobias, CWH, KDM, and GLF. The comments of two anonymous reviewers improved the manuscript significantly. This work was conducted under Marine Mammal Research permit 779-1339 issued to the SEFSC and supported by Interagency Agreement 15958 between the NMFS, SEFSC and the Minerals Management Service, Gulf of Mexico Region.

Literature cited

Barlow, J.
1995. The abundance of cetaceans in California waters. Part I: Ship surveys in summer and fall of 1991. Fish. Bull. 93: 1–14

Barlow, J., S. L. Swartz, T. C. Eagle, and P. R. Wade.
1995. U.S. marine mammal stock assessments: guidelines for preparation, background, and a summary of the 1995 assessments. NOAA Tech. Memo. NMFS-OPR-6:73.

Barros, N. B., and D. K. Odell.
1990. Food habits of bottlenose dolphins in the southeastern United States. *In* The bottlenose dolphin (S. Leatherwood and R. R. Reeves, eds.), p. 309–328. Academic Press, San Diego, CA.

Baumgartner, M. F.
1997. The distribution of Risso's dolphin (*Grampus griseus*) with respect to the physiography of the northern Gulf of Mexico. Mar. Mamm. Sci. 13:614–638

Baumgartner, M. F., K. D. Mullin, L. N. May, and T. D. Leming.
2001. Cetacean habitats in the northern Gulf of Mexico Fish. Bull. 99:219–239

Blaylock, R. A., and W. Hoggard
1994. Preliminary estimates of bottlenose dolphin abundance in the southern U.S. Atlantic and Gulf of Mexico continental shelf waters, 10 p. NOAA Tech. Memo. NMFS-SEFSC-356.

Buckland, S. T., D. R. Anderson, K. P. Burnham, J. L. Laake, D. L. Borchers, and L. Thomas.
2001. Introduction to distance sampling: estimating abundance of biological populations, 432 p. Oxford University Press, New York, NY.

Davis, R. W., G. S. Fargion, N. May, T. D. Leming, M. Baumgartner, W. E. Evans, L. J. Hansen, and K. D. Mullin.
1998. Physical habitat of cetaceans along the continental slope in the north-central and western Gulf of Mexico Mar. Mamm. Sci. 14:490–507.

Davis, R. W., G. A. J. Worthy, B. Würsig, S. K. Lynn, and F. I. Townsend.
1996. Diving behavior and at-sea movements of an Atlantic spotted dolphin in the Gulf of Mexico. Mar. Mamm. Sci. 12:569–581.

Fertl, D., and B. Würsig.
1995. Coordinated feeding by Atlantic spotted dolphins (*Stenella frontalis*) in the Gulf of Mexico. Aquat. Mamm. 21(1):3–5.

Gilbes, F., C. Tomas, J. J. Walsh, and F. E. Müller-Karger.
1996. An episodic chlorophyll plume on the West Florida Shelf. Cont. Shelf Res. 16:1201–1224.

Griffin, R. B., and N. J. Griffin.
2003. Distribution, habitat partitioning and abundance of Atlantic spotted dolphins, bottlenose dolphins, and loggerhead sea turtles on the eastern Gulf of Mexico continental shelf. Gulf Mex. Sci. 21:23–34.

Hersh, S. L., and D. A. Duffield.
1990. Distinction between northwest Atlantic offshore and coastal bottlenose dolphins based on hemoglobin profile and morphometry. *In* The bottlenose dolphin (S. Leatherwood and R. R. Reeves, eds.), p. 129–142. Academic Press, San Diego, CA.

Herzing, D. L.
1997. The life history of free-ranging Atlantic spotted dolphins (*Stenella frontalis*): age classes, color phases and female reproduction. Mar. Mamm. Sci. 13:576–595.

Hoese, H. D., and R. H. Moore.
1998. Fishes of the Gulf of Mexico, Texas, Louisiana, and adjacent waters, 422 p. Texas A&M Univ. Press, College Station, TX.

Hoffstetter, T. C.
2002. Distribution and abundance of marine mammals in the northeastern Gulf of Mexico relative to sea surface temperature and depth. M.Sc. thesis, 74 p. Univ. Southern Mississippi, Hattiesburg, MS.

Jefferson, T. A.
2002. Rough-toothed dolphin, *Steno bredanensis*. *In* Encyclopedia of marine mammals (W. F. Perrin, B. Würsig, and J. G. M. Thewissen, eds.), p. 1055–1059. Academic Press, San Diego, CA.

LeDuc, R. G., and B. E. Curry.
1998. Mitochondrial DNA sequence analysis indicates need for revision of the genus *Tursiops*. Rep. Int. Whal. Comm. 47:393.

Lerczak, J. A., and R. C. Hobbs.
1998. Calculating sighting distances from angular readings during shipboard, aerial, and shore-based marine mammal surveys. Mar. Mamm. Sci. 14:590–599.

Lohrenz, S. E., D. A. Wiesenburg, R. A. Arnone, and X. Chen.
1999. What controls primary production in the Gulf of Mexico? *In* The Gulf of Mexico large marine ecosystem (H. Kumpf, K. Steidinger, and K. Sherman, eds.), p. 151–170. Blackwell Science, Malden, MA.

Marsh, H., and D. F. Sinclair.
1989. Correcting for visibility bias in strip transect aerial surveys of aquatic fauna. J. Wildl. Manag. 53:1017–1024.

Mills, L. R., and K. R. Rademacher.
1996. Atlantic spotted dolphins (*Stenella frontalis*) in the Gulf of Mexico. Gulf Mex. Sci. 14:114–120.

Mullin, K. D., and L. J. Hansen.
1999. Marine mammals of the northern Gulf of Mexico. *In* The Gulf of Mexico large marine ecosystem (H. Kumpf, K. Steidinger, and K. Sherman, eds.), p. 269–277. Blackwell Science, Malden, MA.

Paluszkiewicz, T., L. P. Atkinson, E. S. Posmentier, and C. R. McClain.
1983. Observations of a Loop Current frontal eddy intrusion onto the West Florida Shelf. J. Geophys. Res. 88: 9639–9651.

Pitman, R. L., and C. Stinchcomb.
2002. Rough-toothed dolphins (*Steno bredanensis*) as predators of mahimahi (*Coryphaena hippurus*). Pac. Sci. 56: 447–450.

Perrin, W. F.
2002. *Stenella frontalis*. Mamm. Species 702:1–6.

Rabalais, N. N., R. S. Carney, and E. G. Escobar-Briones.
1999. Overview of continental shelf benthic communities of the Gulf of Mexico. *In* The Gulf of Mexico large marine ecosystem (H. Kumpf, K. Steidinger, and K. Sherman, eds.), p. 171–195. Blackwell Science, Malden, MA.

Richard, K. R., and M. A. Barbeau.
1994. Observations on spotted dolphins feeding nocturnally on flying fish. Mar. Mamm. Sci. 10:473–477.

Schmidley, D. J., and B. A. Melcher.
1974. Annotated checklist and key to the cetaceans of Texas waters. Southwest. Nat. 18:453–464.

Torres, L. G., P. E. Rosel, C. D'Agrosa, and A. J. Read.
2003. Improving management of overlapping bottlenose dolphin ecotypes through spatial analysis and genetics. Mar. Mamm. Sci. 19:502–514.

Wade, P. R., and R. P. Angliss.
1997. Guidelines for assessing marine mammal stocks: report of the GAMMS workshop April 3–5, 1996, Seattle, WA, 93 p. NOAA Tech. Memo. NMFS-OPR-12.

Wade, P. R., and D. P. DeMaster.
1999. Determining the optimum interval for abundance surveys. *In* Marine mammal survey and assessment methods (G. W. Garner, S. C. Amstrup, J. L. Laake, B. F. J. Manly, L. L. McDonald, and D. G. Robertson, eds.), p 53–66. A. A. Balkema, Rotterdam, Netherlands.

Waring, G. T., J. M. Quintal, and S. L. Swartz (eds.).
2001. U.S. Atlantic and Gulf of Mexico marine mammal stock assessments—2001, 310 p. NOAA Tech. Memo. NMFS-NE-168.

Wiseman, W. J., Jr., and W. Sturges.
1999. Physical oceanography of the Gulf of Mexico: processes that regulate its biology. *In* The Gulf of Mexico large marine ecosystem (H. Kumpf, K. Steidinger, and K. Sherman (eds.), p 77–92. Blackwell Science, Malden, MA.

Würsig, B., S. K. Lynn, T. A. Jefferson, and K. D. Mullin.
1998. Behavior of cetaceans in the northern Gulf of Mexico relative to survey ships and aircraft. Aquat. Mamm. 24: 41–50.

Abundance of horseshoe crabs (*Limulus polyphemus*) in the Delaware Bay area

David Hata

Jim Berkson

Department of Fisheries and Wildlife Sciences
Virginia Polytechnic Institute and State University
Blacksburg, Virginia 24061-0321
E-mail address (for J. Berkson, contact author): jberkson@vt.edu

In recent years, increasing commercial landings of horseshoe crabs (*Limulus polyphemus*) along the Atlantic coast of the United States have raised concerns that the present resource is in decline and insufficient to support the needs of its user groups. These concerns have led the Atlantic States Marine Fisheries Commission (ASMFC) to implement a fishery management plan to regulate the harvest (ASMFC[1]). In order to properly manage any species, specific management goals and objectives must be established, and these goals depend on the resource users involved (Quinn and Deriso, 1999). Horseshoe crabs present a distinct resource management challenge because they are important to a diverse set of users (Berkson and Shuster, 1999).

Horseshoe crabs lay their eggs on sandy beaches in spring and summer, and migrating shorebirds rely heavily on the eggs to supply the energy required to complete their migration (Rudloe, 1980; Shuster and Botton, 1985; Castro and Myers, 1993; Botton et al., 1994; Myers, 1996; Thompson, 1998; Tsipoura and Burger, 1999). Biomedical companies catch horseshoe crabs for their blood, from which they produce Limulus Amebocyte Lysate (LAL) (Novitsky, 1984; ASMFC[1]). LAL is used to detect contamination of injectable drugs and implantable devices by Gram-negative bacteria and is the most sensitive means available for detecting endotoxins (Novitsky, 1984). Finally, horseshoe crabs are harvested commercially for bait in the American eel (*Anguilla rostrata*), catfish (*Ictalurus* spp.), and whelk (*Busycon* spp.) fisheries (ASMFC[1]).

The goal of the ASMFC fishery management plan is to ensure a sustainable population level that will support the continued use by these diverse ecological, biomedical, and fishing interests (ASMFC[1]). Proper management of the resource requires information on the status and dynamics of the horseshoe crab population (Berkson and Shuster, 1999). However, the status of the population is poorly understood, and there is currently no reliable information on which to base any management scheme. Available fishery-independent surveys were not designed for horseshoe crabs, and are of little or no value in assessing their status (ASMFC[2]). Towards this end, the states of New Jersey, Delaware, and Maryland in conjunction with the ASMFC and the National Fish and Wildlife Foundation, funded a pilot benthic trawl survey for the fall of 2001. Data collected during this pilot trawl survey were used to estimate the horseshoe crab population size in the Delaware Bay area.

Methods

This study was conducted in the vicinity of Delaware Bay, which is the center of abundance for horseshoe crabs on the Atlantic coast (Shuster, 1982). The study area extended from north of Cape May, New Jersey, to south of Ocean City, Maryland (39°10′N to 38°10′N), and from shore out to 22.2 km (Fig. 1). The area was divided into four strata based on distance from shore and topography, both of which influence crab distribution. Distance from shore was considered important because horseshoe crab abundance decreases with depth (Botton and Ropes, 1987a). Therefore, the area was split into an inshore zone from 0 to 5.6 km (0 to 3 nautical miles [nmi]) from shore and an offshore zone from 5.6 to 22.2 km (3 to 12 nmi) from shore. Topography was also considered important because commercial fishermen stated that crabs are more abundant in troughs (Burke[3]; Eutsler[4]; Munson[5]). For this study, troughs were defined as at least 2.4 m deep, no more than 1.8 km wide, and more than 1.8 km long. These dimensions are common for troughs identified as important by the fishermen. The inshore and offshore zones were both further divided into trough and nontrough areas. The resulting strata were inshore trough, inshore nontrough, offshore trough, and offshore nontrough.

The study area was divided into grids of one-minute latitude by one-minute longitude. A grid was considered inshore if the majority of its area was in water and inshore of the 5.6-km dividing line. A grid was considered offshore if the majority of its area was offshore of the 5.6-km dividing line and inshore of the 22.2-km boundary. A grid was also considered a trough if the long axis of a trough passed through the grid.

[1] ASMFC (Atlantic States Marine Fisheries Commission). 1998. Interstate fishery management plan for horseshoe crab. Fishery management report no. 32, 58 p. Atlantic States Marine Fisheries Commission. 1444 Eye Street, NW, Sixth Floor, Washington, DC 20005.

[2] ASMFC. 1999. Horsehoe crab stock assessment report for peer review. Stock assessment report No. 98-01 (supplement), 47 p. Atlantic States Marine Fisheries Commission, 1444 Eye Street, NW, Sixth Floor, Washington, DC 20005.

[3] Burke, C. 2001. Personal commun. 25 Cove Drive, North Cape May, NJ 08204

[4] Eutsler, J. 2001. Personal commun. 11933 Gray's Corner Road, Berlin, MD 21811.

[5] Munson, R. 2001. Personal commun. Box 358, Newport, NJ 08345.

Manuscript approved for publication 6 March 2003 by Scientific Editor.

Manuscript received 22 July 2003 at NMFS Scientific Publications Office.

Fish Bull. 101:933–938 (2003).

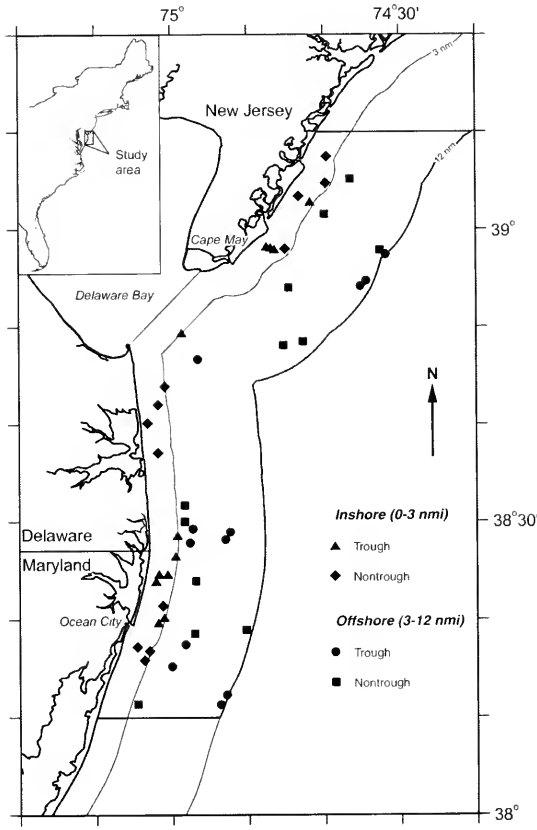

Figure 1

Study area and sampling locations. Symbols indicate type and location of strata. Day and night tows were made at each location.

A grid was considered nontrough if no trough long axis passed through it. Each grid was therefore assigned to one of the four strata. Twelve grids were randomly selected in each stratum, for a total of 48 unique sampling locations. The fishermen also stated that time of day influenced horseshoe crab catchability (Burke[3]; Eutsler[4]; Munson[5]). Therefore, grids were sampled both in daylight and at night. The second tow in a grid (day or night) was made near the location of the first to reduce location variability, but slightly offset to avoid possible influence of the first tow on the catch of the second. The second tow was also made more than 24 hours after the first to avoid interactions, but no more than four days later, to avoid introducing other unknown variability. Abundance estimates from the daytime and nighttime samples were calculated separately for comparison.

Our study was conducted in the fall, between 10 September and 16 October 2001. The stock assessment model adopted by the ASMFC requires abundance information on newly mature crabs, and identification requires that crabs have undergone a terminal molt. Crabs reportedly molt in the late summer and fall in the Delaware Bay area (Burke[3]; Eutsler[4]; Munson[5]).

Sampling was conducted from a chartered 16.8-meter commercial fishing vessel. For capturing horseshoe crabs, commercial fishermen typically use a flounder trawl equipped with a Texas sweep (Burke[3]; Eutsler[4]; Munson[5]; Michels[6]). This modified sweep consists of a chain line in-

[6] Michels, S. 2001. Personal commun. Delaware Department of Natural Resources and Environmental Control, Division of Fish and Wildlife, 89 Kings Hwy., P.O. Box 1401, Dover, DE 19901.

stead of rope, which runs from wing to wing of the net (Fig. 2).The net ropeline is attached behind the sweep chain. In addition, usually three rows of weight chain are attached behind the sweep chain. The chain sweep is considered more effective in digging crabs out of the bottom than the typical ground gear of most research trawls. We used a standard two-seam flounder trawl with an 18.3-m headrope and 24.4-m footrope. The net consisted of 14-cm stretched mesh polypropylene throughout and was equipped with chafing gear on the bag. The net was attached to the trawl doors by 91-m ground cables wrapped in rubber cookies. Tow duration was usually 15 minutes (bottom time), except for one tow in the Delaware Bay shipping channel, which was reduced to 7.5 minutes. We assumed that density was not affected by tow duration (e.g. gear saturation was not a factor).

All horseshoe crabs were culled from the catch, and either all or a subsample were examined. For subsamples of a large catch, 50 crabs greater than 150 mm prosomal width were examined, as well as all small, soft, and shedding crabs. Horseshoe crabs that were not examined were counted separately by sex. Examined crabs were measured for prosomal width and identified to sex and maturity. Maturity classifications were as follows: immature; primiparous (mature horseshoe crabs that had not spawned yet); and multiparous (crabs that had spawned at least once [Table 1]). When catches were subsampled, characteristics of examined crabs were extrapolated to all crabs in that tow. Abundance was estimated for each demographic group as well as for the total.

Tow distances were determined for most tows from beginning and ending positions and recorded by using Loran C. These are minima because they do not consider any deviations from a straight path. Distances were not recorded for three tows; therefore they were estimated as the mean distance of all other tows. Net width was estimated as half of the mean of the headrope and footline lengths (Fridman, 1986). The tow distance and net width were used to calculate the swept area to determine the density of horseshoe crabs. We assumed that the ground cables and trawl doors were not effective in catching crabs; therefore all fishing was done only by the net. No information is available on the efficiency of the ground cables or doors for horseshoe crabs, but we do not believe horseshoe crabs are mobile enough, nor swim fast enough, to be effectively herded by them.

The mean density (crabs/km^2) and variance in each stratum were calculated by assuming a Δ-distribution (Aitchison and Brown, 1957; Pennington, 1983), and these estimates were combined by using formulas for a stratified random design (Cochran, 1977). The Δ-distribution model is applicable to skewed data that consist of a portion of zero catches when the frequency of nonzero catches follows a lognormal distribution (Pennington 1983; Pennington 1996). With such skewed data, the estimator of the mean as defined for the Δ-distribution model is more efficient than the sample mean estimator derived from the normal distribution (Smith, 1988). Areas by stratum and total area were substituted for the numbers of grids per stratum and total number of grids for determining stratum weights (Table 2). Latitudinal and longitudinal distances, and therefore grid areas, differed by latitude; therefore grid areas were calculated separately for each minute of latitude. The total number of grids in each stratum was determined for each latitude to calculate the area by stratum and the total area. Ninety-five percent confidence intervals of the stratified mean density and population total were calculated by using the effective degrees of freedom (Cochran, 1977). Mean densities, totals, and confidence limits for demographic groups did not sum to the values calculated by using all horseshoe crabs combined because the stratum mean calculated by the Δ-distribution is a function of the stratum variance, which varies by demographic group.

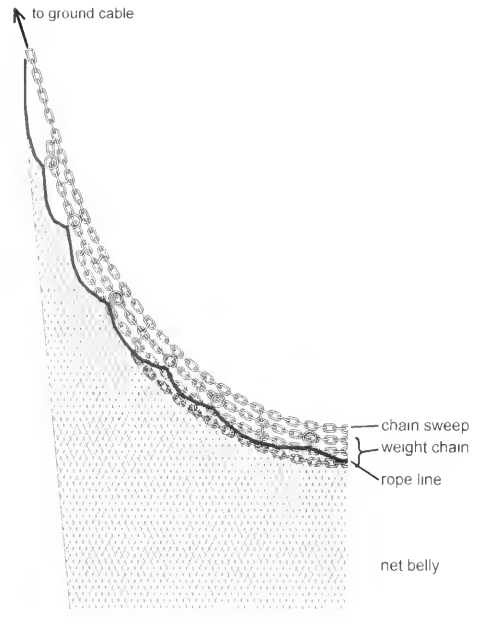

Figure 2

Diagrammatic representation of the Texas sweep used on the flounder trawl.

Results

The mean abundance estimate for all crabs within the study area based on day sampling was 6.81 million crabs within the 2912-km^2 study area (Table 3). The mean abundance estimate for all crabs based on night sampling was 11.40 million crabs in the study area (Table 3).

Table 1

Criteria used in this study for classifying horseshoe crab maturity stage.

	Female	Male
Immature	Gonopores not hard and elevated, no modified pedipalps, soft, membranous area of ventral prosoma (doublure) pale colored.	Hard, elevated gonopores discernible on genital operculum, no modified pedipalps.
Primiparous	Soft, membranous area of ventral prosoma dark colored (indicating presence of eggs), no rub marks on upper opisthosoma.	Gonopores as above, modified pedipalps, both pedipalp digits intact on both sides.
Multiparous	Soft, membranous area of ventral prosoma dark colored, rub marks present on opisthosoma indicating previous amplexus.	Gonopores as above, modified pedipalps, smaller pedipalp digit broken off from at least one side.

Abundance estimates by stage class provided additional information. Multiparous males were estimated at 2.40 million for day sampling and 4.23 million for night sampling. Multiparous females were the next most abundant group, estimated at 1.63 million for day sampling and 2.25 million for night sampling (Table 3).

Primiparous males were uncommon during daylight sampling, estimated at only 84,000 during the day, as compared to 307,000 at night. In contrast, primiparous females were estimated at 338,000 and 361,000 for day and night sampling, respectively.

The estimated abundance of mature males (primiparous and multiparous combined) exceeded that of mature females: 2.48 million to 1.97 million for sampling during the day and 4.54 million to 2.61 million for night sampling. Estimates of immature horseshoe crabs showed that the opposite trend with greater numbers of females than males, 1.34 million to 0.38 million, respectively, for day sampling and 2.31 million to 1.19 million, respectively, for night sampling. With both mature and immature horseshoe crabs, estimates derived from night sampling were higher than those derived from day sampling (Table 3).

Confidence intervals for the estimates were wide, but informative. Confidence limits for total horseshoe crab abundance were 2.29 million to 11.33 million for day sampling and 5.95 million to 16.85 million for night sampling. The lower confidence limits provide useful reference points for conservative, risk-averse management schemes.

Table 2

Horseshoe crab survey stratum sizes. Sampling grids were one minute longitude by one minute latitude. The area of grids sampled in each stratum is denoted by a, the total area (km^2) of the stratum is A, n is the number of grids sampled, and N is the total number of grids in that stratum. Strata are the following: I NT = inshore nontrough, I TR = inshore trough, O NT = offshore nontrough, and O TR = offshore trough.

	Stratum				
	I NT	I TR	O NT	O TR	All
a	32.48	32.51	32.50	32.55	130.04
A	560.07	165.18	1964.87	222.06	2912.17
n	12	12	12	12	48
N	207	61	726	82	1076

Discussion

The study does not estimate actual population size, but rather the total number of horseshoe crabs available to the survey gear. Horseshoe crabs remain at the beaches where they were spawned for the first one to two years of life and gradually disperse offshore as they grow (Rudloe, 1981; Shuster, 1982). Crabs of these early age classes were undoubtedly in shallow shelf waters and coastal embayments beyond the reach of the vessel. Even if they were present, crabs of early age classes may have been too small to be caught in the gear. The study also excluded adults that may have been in shallow waters and embayments. It is also unlikely that 100% of the horseshoe crabs under the gear were in fact captured because some may have been buried too deep in the substrate to have been dug out by the gear. For all of these reasons, abundance estimates can legitimately be considered minimum population estimates. Results can be used as abundance indices for comparison between years, if the study is continued in the future.

The differences between day and night estimates may be the result of horseshoe crabs burying themselves during the day. Alternatively, the horseshoe crabs may be able to detect and avoid the trawl during the day. Night and day collections at individual locations were correlated (r=0.71) suggesting that both were a true reflection of horseshoe crab abundance at that site, although at different levels of efficiency. If the catches were uncorrelated, it would not be possible to determine which, if either, sample accurately represented true abundance. The larger catches and lower

Table 3

Stratified mean density (crabs/km^2), standard deviation (SD), and coefficient of variation of the mean (CV) for horseshoe crab demographic groups and for all crabs combined. Estimated population totals by demographic group and for all crabs combined are given in thousands. UCL and LCL denote upper and lower 95% confidence limits, respectively. Estimates were determined separately for day and night sampling. Because the Δ-distribution was used to calculate stratum means, demographic group values do not sum to those calculated by using all crabs.

	Density (crabs/km^2)			Population total (1000s)		
Demographic group	Mean	SD	CV	Total	UCL	LCL
Day						
Immature females	461	167	0.36	1341	2395	288
Primiparous females	116	40	0.34	338	588	88
Multiparous females	561	126	0.23	1634	2428	839
Immature males	129	45	0.35	377	659	95
Primiparous males	29	7	0.24	84	129	40
Multiparous males	823	207	0.25	2396	3699	1093
All horseshoe crabs	2338	718	0.31	6809	11,326	2291
Night						
Immature females	792	216	0.27	2308	3656	960
Primiparous females	124	26	0.21	361	522	199
Multiparous females	773	145	0.19	2250	3157	1343
Immature males	410	119	0.29	1193	1939	447
Primiparous males	106	40	0.38	307	555	60
Multiparous males	1453	353	0.24	4231	6434	2029
All horseshoe crabs	3915	873	0.22	11,400	16,853	5947

coefficients of variation from the night estimates suggest that the night estimates are more efficient and are probably better estimates of true abundance.

The results of the present study are intermediate between previous estimates of ocean abundance. Botton and Ropes (1987a) estimated that between 2.3 and 4.5 million adults occurred on the continental shelf between New Jersey and Virginia from National Marine Fisheries Service (NMFS) trawl surveys, in contrast to a mean of 7.1 million adults (primiparous and multiparous combined) estimated in the present study area. However, the trawl gear used in the NMFS surveys was inefficient for capturing horseshoe crabs, and the inshore extent was limited by the survey vessel size (Botton and Ropes, 1987a; ASMFC[2]). Botton and Haskin (1984) sampled within 5.6 km of the New Jersey coast using hydraulic clam dredges and obtained horseshoe crab densities of 14,600 to 23,000 per km^2. These densities are much higher than our nighttime estimate of 7900 horseshoe crabs per km^2 (weighted by stratum area) within 5.6 km. The gear we used was probably more efficient in capturing horseshoe crabs than that employed by the NMFS survey but may have been less efficient than the hydraulic dredge. Differing methods between the studies do not allow for a comparison over time.

It is interesting to note that in both the night-based and day-based estimates, females made up the majority of the immature animals, whereas males made up the majority of the mature animals. This could be due to the commercial fishery's preference for harvesting gravid females (Botton and Ropes, 1987b). The continual focused harvest of mature females may reduce their population enough to cause this change in sex ratios. Alternatively, mature females or immature males may have been more abundant outside the study area.

Conclusion

The continuation of annual trawl surveys could allow a full stock assessment to be conducted. The Horseshoe Crab Stock Assessment Subcommittee of the Atlantic States Marine Fisheries Commission has developed a stock assessment plan (HCSAS[7]) based on the catch-survey method derived by Collie and Sissenwine (1983). Unlike age-based stock assessment models, the catch-survey method requires only abundance of primiparous and multiparous horseshoe crabs (HCSAS[7]). The commercial fishery is selective for gravid females (Botton and Ropes, 1987b), and effort is biased toward areas of high abundance (Burke[3]; Eutsler[4]; Munson[5]); therefore commercial data are of limited use for stock assessment. A fishery-independent

[7] HCSAS (Horseshoe Crab Stock Assessment Subcommittee). 2000. Stock assessment of Atlantic coast horseshoe crabs: a proposed framework, 19 p. A report to the Horseshoe Crab Technical Committee, Atlantic States Marine Fisheries Commission, 1444 Eye Street, NW, Sixth Floor, Washington, DC 20005.

trawl survey is the best way to provide estimates of abundance while controlling catchability (Hilborn and Walters, 1992; Gunderson, 1993). This study demonstrates the utility of annual trawl surveys to obtain that information.

Acknowledgments

This research was funded by the states of New Jersey, Delaware and Maryland through the Atlantic States Marine Fisheries Commission, and by the National Fish and Wildlife Foundation. We are indebted to M. Millard, P. Pooler, D. Smith, and E. Smith for providing statistical advice. We thank J. Brust, P. Himchak, S. Michels, M. Millard, T. O'Connell, and D. Smith of the Horseshoe Crab Stock Assessment and Technical Committees of the ASMFC, and B. Walls and C. N. Shuster Jr. for their input, support, and encouragement in this study. We are grateful to C. Burke, J. Eutsler, and R. Munson for their valuable input regarding horseshoe crab fishing. J. Eutsler and T. Canham provided invaluable assistance in the field. This manuscript was improved by the comments and suggestions of B. Murphy and E. Smith, M. Davis, J. Dew, W. Grogan, L. Hurton, J. McGhee, and A. Williams, and three anonymous reviewers. We greatly appreciate the time and effort of all involved.

Literature cited

Aitchison, J., and J. A. C. Brown.
1957. The log-normal distribution, 176 p. Cambridge Univ. Press, Cambridge, UK.

Berkson, J., and C. N. Shuster Jr.
1999. The horseshoe crab: the battle for a true multiple-use resource. Fisheries 24(11):6–10.

Botton, M. L., and H. H. Haskin.
1984 Distribution and feeding of the horseshoe crab, *Limulus polyphemus*, on the continental shelf off New Jersey. Fish. Bull. 82:383–389.

Botton, M. L., and J. W. Ropes.
1987a. Populations of horseshoe crabs, *Limulus polyphemus*, on the northwestern Atlantic continental shelf. Fish. Bull. 85:805–812.
1987b. The horseshoe crab, *Limulus polyphemus*, fishery and resource in the United States. Mar. Fish. Rev. 49(3): 57–61.

Botton, M. L., R. E. Loveland, and T. R. Jacobsen.
1994. Site selection by migratory shorebirds in Delaware Bay, and its relationship to beach characteristics and abundance of horseshoe crab (*Limulus polyphemus*) eggs. Auk 111:605–616.

Castro, G., and J. P. Myers.
1993. Shorebird predation on eggs of horseshoe crabs during spring stopover on Delaware Bay. Auk 110:927–930.

Cochran, W. G.
1977. Sampling techniques, 3rd ed., 428 p. John Wiley and Sons, Inc., New York, NY.

Collie, J. S., and M. P. Sissenwine.
1983. Estimating population size from relative abundance data measured with error. Can. J. Fish. Aquat. Sci. 40: 1871–1879.

Fridman, A. L.
1986. Calculations for fishing gear designs, 241 p. Fishing News Books, Ltd., Farnham, UK.

Gunderson, D. R.
1993. Surveys of fisheries resources, 248 p. John Wiley and Sons, Inc., New York, NY.

Hilborn, R., and C. J. Walters.
1992. Quantitative fisheries stock assessment: choice, dynamics and uncertainty, 570 p. Chapman and Hall, New York, NY.

Myers, J. P.
1996 Sex and gluttony on Delaware Bay. Nat. Hist. 95: 68–77.

Novitsky, T. J.
1984 Discovery to commercialization: the blood of the horseshoe crab. Oceanus 27:13–18.

Pennington, M.
1983. Efficient estimators of abundance, for fish and plankton surveys. Biometrics 39:281–286.
1996. Estimating the mean and variance from highly skewed marine data. Fish. Bull. 94:495–505.

Quinn, T. J., II, and R. B. Deriso.
1999. Quantitative fish dynamics, 542 p. Oxford Univ. Press, New York, NY.

Rudloe, A.
1980. The breeding behavior and patterns of movement of horseshoe crabs, *Limulus polyphemus*, in the vicinity of breeding beaches in Apalachee Bay, Florida. Estuaries 3:177–183.
1981. Aspects of the biology of juvenile horseshoe crabs, *Limulus polyphemus*. Bull. Mar. Sci. 31:125–133.

Shuster, C. N., Jr.
1982. A pictorial review of the natural history and ecology of the horseshoe crab, *Limulus polyphemus*, with reference to other Limulidae. *In* Physiology and biology of horseshoe crabs (J. Bonaventura, C. Bonaventura, and S. Tesh, eds.), p. I–52. Alan R. Liss, Inc., New York, NY.

Shuster, C. N., Jr., and M. L. Botton.
1985. A contribution to the population biology of horseshoe crabs, *Limulus polyphemus* (L.), in Delaware bay. Estuaries 8:363–372.

Smith, S. J.
1988. Evaluating the efficiency of the Δ-distribution mean estimator. Biometrics 44:485–493.

Thompson, M.
1998. Assessments of the population biology and critical habitat for the horseshoe crab, *Limulus polyphemus*, in the South Atlantic Bight. M.S. thesis, 136 p. Medical Univ. South Carolina, Charleston, SC.

Tsipoura, N., and J. Burger.
1999. Shorebird diet during spring migration stopover on Delaware Bay. Condor 101:635–644.

Use of pop-up satellite archival tags to demonstrate survival of blue marlin (*Makaira nigricans*) released from pelagic longline gear

David W. Kerstetter
Virginia Institute of Marine Science
The College of William & Mary
Rt 1208 Greate Road
Gloucester Point, Virginia 23062
E mail address: bailey@vims.edu

Brian E. Luckhurst
Division of Fisheries
Department of Agriculture and Fisheries
P.O. Box CR 52
Crawl CRBX, Bermuda

Eric D. Prince
National Marine Fisheries Service
75 Virginia Beach Drive
Miami, Florida 33146

John E. Graves
Virginia Institute of Marine Science
The College of William & Mary
Rt 1208 Greate Road
Gloucester Point, Virginia 23062

Blue marlin (*Makaira nigricans*) support commercial and recreational fisheries throughout the tropical and subtropical waters of the Atlantic Ocean. The species is taken in directed recreational and artisanal fisheries in several areas and constitutes an incidental catch of the widespread commercial pelagic longline fishery. Although blue marlin comprise only a small fraction of the catch of the pelagic longline fishery that targets tunas and swordfish, this fishery accounts for the majority of fishing mortality on Atlantic blue marlin (ICCAT, 1997; 2001).

Atlantic blue marlin were last assessed in 2000 by the Standing Committee for Research and Statistics (SCRS) of the International Commission for the Conservation of Atlantic Tunas (ICCAT). The assessment indicated that the total biomass of Atlantic blue marlin is only about 40% of that necessary to produce maximum sustainable yield (MSY) and that current harvests are more than twice the replacement yield, further contributing to the decline of the stock (ICCAT, 2001). A reduction in fishing mortality of approximately 60% is needed simply to halt the decline in stock abundance (Goodyear, 2000).

One means of reducing fishing mortality on blue marlin, without severely impacting catches of target species of the pelagic longline fishery, is to release those blue marlin that are alive at the time longline gear is retrieved (hauled back). Jackson and Farber (1998) reported that 48% of blue marlin caught in the Venezuelan longline fishery are alive at the time of haulback. Data from the U.S. observer program between 1992 and 1996 indicate that 66% of blue marlin were released alive from the domestic longline fishery (Lee and Brown, 1998) and U.S. National Marine Fisheries Service (NMFS) data and mandatory pelagic longline logbook submissions between 1987 and 1991 indicate that 59.8% of blue marlin are released alive from commercial pelagic longline gear (Cramer, 1998).

ICCAT has been encouraging the release of live blue marlin for several years, and in 2000 the Commission mandated that all live blue marlin and white marlin be released from commercial longline and purse seine vessels. However, for such a management measure to significantly reduce fishing mortality, released animals must have a reasonably high postrelease survival rate.

Little information exists about postrelease survival of blue marlin, especially of animals taken on pelagic longline gear. In general, recovery rates of billfish tagged with conventional (streamer) tags have been quite low (<2%; Jones and Prince, 1998; Ortiz et al., 1998). This observation is consistent with high postrelease mortality, although low recovery rates could also result from tag shedding and a lack of reporting recovered tags (Bayley and Prince, 1994; Jones and Prince, 1998). Results of acoustic tracking studies of blue marlin captured on recreational gear suggest that postrelease survival over periods of a few hours to a few days is relatively high, although mortalities have been noted (reviewed in Pepperell and Davis, 1999). More recently, pop-up satellite archival tags (PSATs) have been used to study postrelease survival of blue marlin taken in a recreational fishery. Graves et al. (2002) attached nine PSATs to blue marlin caught on recreational gear off Bermuda. Eight of the tags detached from the animals and reported as expected after five days; net displacement and direction, tag inclination, and temperature data for all eight individuals were consistent with postrelease survival for five days.

In this note, we present the results of a study evaluating the postrelease survival of blue marlin from pelagic longline fishing gear in the western North Atlantic. We include analyses of the movement and behavior of these animals for tagging periods of both five days and thirty days.

Manuscript approved for publication
9 March 2003 by Scientific Editor.
Manuscript received 12 July 2003
at NMFS Scientific Publications Office.
Fish.Bull. 101:939–948 (2003).

Materials and methods

Pop-up satellite tags

There has been rapid development in PSAT technology over the past few years, and there are currently several PSAT models commercially available from different vendors. PSATs vary in many features: in the number of functions (temperature, pressure, tag inclination, light level) they measure; in the parameters and release time for which they can be programed; in the onboard data that they can manipulate and store, in the data they transmit, in their emergency release mechanisms or emergency programming (or both), and in their cost. PSATs have been used on several large pelagic teleosts, including North Atlantic bluefin tuna (e.g. Block et al., 1998; Lutcavage et al., 1999), swordfish (Sedberry and Loefer, 2001), and blue marlin (Graves et al., 2002).

The two tag models used to evaluate postrelease survival of blue marlin in this study—the Microwave Telemetry Inc. (Columbia, MD) PTT-100 (5-day tag) and the Wildlife Computers (Redmond, WA) PAT (30-day tag), are similar in external appearance. Both are slightly buoyant, measure approximately 38 cm by 4 cm diameter (including antenna) and weigh between 65 and 75 g (air weight minus attachment leader and tag head). The size of these tags is sufficiently small as to not appear to impose a major drag on a large marine teleost such as a blue marlin (Block et al., 1998). The greatest exterior differences between the two tag types are their color (the 5-day tags are black and the 30-day tags are grey and white) and the presence of a small metal emergency release mechanism on the attachment leader of the 30-day tag. Both tag models can withstand a minimum pressure equivalent to a depth of about 1000 meters, which is well below the maximum observed depth of previous acoustic tracking analyses of blue marlin movements (Holland et al., 1990; Block et al., 1992).

The 5-day tags (n=7; described in this paper as 5D-1 through 5D-7) were programmed by the manufacturer to detach from the fish 122 hours after activation. A release time of five days was chosen for this PSAT because several blue marlin tagged with conventional tags have been recaptured within five days, demonstrating a return to feeding behavior (E. Prince, unpubl. data). Moreover, mortalities of released blue marlin that have been observed with acoustic telemetry have occurred within 48 hours of release (Pepperell and Davis, 1999). The 5-day tags measured water temperature once an hour and stored the average of two hourly values, for a total of 61 temperature means (from 122 measurements).

The 5-day tags also reported two average inclinometer values, one before the tag released from the fish and one after. These values can be used to infer active forward movement by the fish. This instrument measures the percentage of deployment time that the tag was at an attitude of less than 30° above horizontal by taking a reading every two minutes and either adding or subtracting this percentage from the running total value. Because this value is bracketed with maximum (255) and minimum (0) boundaries, and measurements are taken at short-duration intervals, a mortality or tag shedding event displaying a lack of forward movement will show clearly as an almost vertical reading, even if the fish was initially quite active.

The 30-day tags (n=2; described within this paper as 30D-1 and 30D-2) were programmed by the user to release 32 days following deployment, allowing for a full 30 days of data collection. The release time for the 30-day tags was chosen, in part, to test the assumption that five days was a sufficient duration to capture the rate of postrelease mortality resulting from interaction with longline gear, and to obtain more detailed behavioral data over a longer time interval. It should be noted, however, that a longer release time may bias estimates of postrelease survival because there is an increased period for tag malfunction, physical damage to the tag, or other sources of mortality to occur (Goodyear, 2002). Using the manufacturer's software (PatHost programming software, version 2.06, Wildlife Computers) the 30-day tag was programmed to record temperature values (sensitivity=0.05°C) every minute, and the data were collated for transmission as the fraction of time during each hour-long period that the tag was within each of 12 user-defined bins between the following temperatures (°C): ≤5, 7.5, 10, 12.5, 15, 17.5, 20, 22.5, 25, 27.5, 30, and 60 (for 30D-1) and ≤7.5, 10, 12.5, 15, 17.5, 20, 22.5, 25, 27.5, 30, 32.5, and 60 (for 30D-2). Similarly, direct pressure measurements (measured sensitivity=0.5 m) were taken every minute and collated for transmission as the percentage of time during each hour that the tag was within each of 12 user-defined categories between the following depths (m): <0, 2.5, 5, 10, 15, 25, 50, 100, 250, 500, 750, and 1000 (30D-1 and 30D-2). These two tags also recorded minimum and maximum depths and temperatures for each hour during deployment. Finally, the tags recorded light level measurements every minute, and these data were used to calculate a local time of midnight and duration of daylight, thereby allowing a later estimate of daily position.

Analyses

The slightly buoyant tags detached from the fish after the specified intervals, floated to the surface, and transmitted archived data to satellites in the Argos satellite system. Position information and sections of stored data were captured with each satellite pass (Arnold and Dewar, 2001), transmitted to a ground station, and ultimately to the authors by means of the Internet. Location data were analyzed by using the computer program PROGRAM INVERSE (version 2.0, National Geological Survey, 1975; modified by M. Ortiz, NMFS Southeast Fisheries Science Center, Miami, FL) to determine net direction and minimum net displacement from the point at which the blue marlin was tagged and released to the position of the tag at the time of the first precise position (location code 1, 2, or 3) determined by the Argos satellite system. Temperature data from the 5-day tags deployed off Florida were categorized by time of collection as daylight, nighttime, or a composite dawn and dusk period (one hour before and after sunrise and one hour before and after sunset), for analysis of temperature by light level using a one-way ANOVA (Zar, 1999).

Tag deployment

Four commercial longline vessels (48–70 feet LOA [length overall]) in the western North Atlantic Ocean were used for the present study. All carried approximately 20 miles of longline on one large spool, centrally mounted amidships. Gear was set off the stern and retrieved from a hauling station located on one side, approximately amidships—a standard vessel configuration for the U.S. Gulf of Mexico and east coast swordfish fleet. Fishing gear was also typical for vessels in this fleet. A mainline of single-strand monofilament was used and a variety of terminal gear configurations. Different lengths of dropper lines or numbers of hooks between floats (or both) were used in attempts by captains to increase billfish catch rates, although all modifications to the gear were within the range of terminal gear configurations used in this pelagic longline fishery. Leader lengths ranged from 5 to 20 fathoms (9.2–36.6 m), and the buoy drops generally were 10 to 15 fathoms (18.3–27.5 m). Vessels in this study used a combination of "J" hooks (8/0–9/0 sizes) and circle hooks (16/0 size). Bait was either mackerel (Scomber sp.) or squid (*Illex* sp.), and almost every set used chemical lightsticks of varying colors attached to the leader approximately 2 meters above the hook.

PSATs were prepared for attachment to blue marlin prior to departure of the vessels. A large, hydroscopic, surgical-grade nylon tag head was attached to the PSAT with an approximately 20 cm length of 300-pound-test Momoi® brand (Momoi Fishing Co., Ako City, Japan) monofilament line. Metal crimps, covered with black heat-shrink tubing to minimize potential abrasion along the fish's body, were used to attach the monofilament line to the PSAT and the tag head. Individual PSATs were activated and tested at the start of each fishing day prior to the morning haulback. The white flotation bulbs of the 30-day tags were colored black with a permanent marker prior to deployment to decrease their visibility while attached to the fish.

PSATs were attached to all blue marlin that were caught on commercial pelagic longline gear, weighed more than approximately 100 pounds (45.0 kg), and were observed to be in relatively good physical condition, e.g. no large wounds to the viscera. Of the ten blue marlin caught during this study, all but one passed this minimum standard (the one fish that was rejected arrived at the side of the vessel missing the posterior half of its body due to several large bites). Fish were brought alongside the vessels just aft of the hauling station along the rail prior to tagging. Several fish required up to two minutes to become calm enough to be tagged accurately. Many longline captains attempt to save as much leader material as possible from bycatch fishes, and bringing a fish close to the vessel prior to cutting the line is a common practice. The FV *Ark Angel* had a removable section of rail that facilitated tag attachment; on the other three vessels one was forced to lean out over a rail to attach a tag. The average distance between the top of the rail and the fish (freeboard) was approximately one meter. The PSAT tag head was carefully inserted about 5–10 cm below (ventral) the midpoint of the anterior dorsal fin. Tag heads were implanted to a depth of about 8 cm by using a modified tagging applicator approximately 2 meters in length. A conventional streamer tag was attached well posterior of the PSAT by using a standard tagging applicator. Total tagging time, from identification of the fish on the leader as a blue marlin to release following tagging, was less than 5 minutes per fish.

Blue marlin were released by the standard commercial release protocol of cutting the leader near the hook and allowing the hook to remain in the fish. Approximate weights were estimated, and physical location of the hook noted for each blue marlin. An "ACESS" condition scale, analogous to the human neo-natal APGAR test (Apgar, 1953), was developed to quickly evaluate the condition of each fish on a scale of 0–10 by examining five characteristics and assigning each a score of 0–2 (poor to good). These characteristics included overall activity, color, condition of the eyes, stomach eversion, and the general state of the body musculature (presence of bites or lacerations). The time of day, vessel location, and surface water temperature were recorded immediately after tagging. The location of a hooked fish on the longline was also noted in order to estimate the "soak time" of that hook, i.e. the maximum time the fish could have been hooked.

Results and discussion

Seven 5-day PSATs were deployed on blue marlin off Bermuda (n=1) and Florida (n=6) during 2000, and two 30-day PSATs were deployed on blue marlin off North Carolina and Virginia during the summer of 2001 (Tables 1 and 2). Tags were attached onboard four vessels during six trips, ranging from one to eleven fishing days each. The captains all later indicated that the PSAT tagging procedures had minimal interference with normal longlining operations.

Although the captains attempted to target blue marlin by fishing in different areas and with slightly different gear than usual for swordfish trips, the catch rates for this species were not notably different from the catch rates in NMFS data; the catch rate for the trips in 2000 was slightly above average for both season and location, whereas the catch rate in 2001 was below the norm. Of the four trips in 2000, the average CPUE for blue marlin was approximately 0.08 per 100 hooks (7 blue marlin/8650 estimated total hooks), which is comparable to the reported blue marlin CPUE of 0.05 per 100 hooks for the NMFS southeast statistical region for the third quarter of 1998 (Cramer, 2000). For all billfish, excluding swordfish, the CPUE was 0.15 per 100 hooks (12 billfish/8650 estimated total hooks). This value is also comparable to the reported billfish CPUE of 0.12 per 100 hooks for the NMFS southeast statistical region for the third quarter of 1998 (Cramer, 2000). For the three trips in 2001, the blue marlin and billfish CPUEs were lower: 0.04 blue marlin per 100 hooks (3 blue marlin/7780 estimated total hooks) and 0.12 billfish per 100 hooks (9 billfish/7,780 estimated total hooks). These similar catch rates, even when targeting billfish, could be the result of decreased abundance, an inability of the gear to effectively target billfish, or unfavorable water conditions in the study areas.

Of the ten blue marlin caught on the trips, nine were alive and in relatively good physical condition. Based on

Table 1

Summary of pop-up satellite archival tag information for blue marlin (*Makaira nigricans*) released from pelagic longline gear in the western North Atlantic Ocean. Soak time is the maximum time that the blue marlin could have been hooked at that position on the longline. See text for a description of ACESS scores. .

Tag type	Tag number	Soak time (h)	Estimated weight (lb)	ACESS Score	Did tag report?
PTT-100	5D-1	11	200	10	yes
PTT-100	5D-2	12	325	10	yes
PTT-100	5D-3	13	250	10	no
PTT-100	5D-4	14	180	8	yes
PTT-100	5D-5	16	150	9	yes
PTT-100	5D-6	19	275	8	no
PTT-100	5D-7	9	120	10	yes
PAT	30D-1	6	400	10	yes
PAT	30D-2	35	350	9	yes

Table 2

Net movement of blue marlin released from pelagic longline gear in the western North Atlantic Ocean and equipped with pop-up satellite archival tags. Compass direction indicates the bearing from point of release to point of first transmission. Compass direction and straight-line distances between release and first transmission (net movement) were calculated with PROGRAM INVERSE (version 2.0, National Geological Survey, modified by M. Ortiz, NMFS Southeast Fisheries Science Center, Miami, FL). Distances are given in nautical miles (nmi), and kilometers (km). Note that the 30-day tags (30D-1 and 30D-2) did not have inclometers.

Tag number	Location of release	Location of first transmission	Compass direction	Net movement nmi (km)	Net movement per day (km)	Percentage of time less than 30 degrees above horizontal
5D-1	64.99°W, 31.99°N	64.10°W, 30.35°N	155°	107.8 (199.7)	21.2 (39.3)	46.77
5D-2	79.16°W, 28.64°N	79.48°W, 30.81°N	353°	130.8 (242.2)	25.7 (47.6)	47.74
5D-4	79.48°W, 28.59°N	78.37°W, 29.45°N	48°	77.0 (142.6)	15.1 (28.0)	46.77
5D-5	79.41°W, 28.58°N	77.48°W, 28.91°N	79°	103.7 (192.0)	20.4 (37.8)	47.72
5D-7	79.54°W, 28.69°N	78.09°W, 29.77°N	49°	100.0 (185.2)	19.7 (36.4)	47.29
30D-1	74.62°W, 36.79°N	62.10°W, 35.96°N	91°	608.3 (1,126.4)	19.6 (36.3)	—
30D-2	74.61°W, 34.67°N	50.08°W, 40.30°N	67°	1,214.7 (2,249.4)	39.2 (72.6)	—

a 10-point maximum, the ACESS score of the tagged blue marlin ranged from 8 to 10 (Table 1). Of the fish that received a score of less than 10, the primary reason was a loss of color, and minor body musculature lacerations. All blue marlin were hooked in the jaw, whether caught on a "J" hook (n=9) or a circle hook (n=1).

Soak time, the maximum period that the hooked fish could have been on the hook, did not appear to have an effect on either the reporting of the PSAT tags or the ACESS-scored physical condition of the blue marlin (Table 1). The two tags that did not report (5D-3 and 5D-6) were attached to fish with calculated soak times of 13 and 19 hours, respectively, both well under the maximum soak time of 35 hours. The one particularly long soak time (tag 30D-2) resulted from a parting of the mainline during an offshore storm and a subsequent two-day haulback. Boggs (1992) noted that substantial numbers of striped marlin were caught while gear was rising during haulback. Assuming similar behavior among other istiophorid species, this observation may explain the good to excellent condition noted for the blue marlin in our study even after extended soak times. Developing hook-timer technology may allow further description of the relationship, if any, between soak time and the actual length of time that a fish is hooked on the gear.

PSAT performance

The two PSAT models used for our study reflect the rapidly developing technology in this field. The difference in types and amounts of data recorded presented an apparent trade-off between the parameters measured (the resolu-

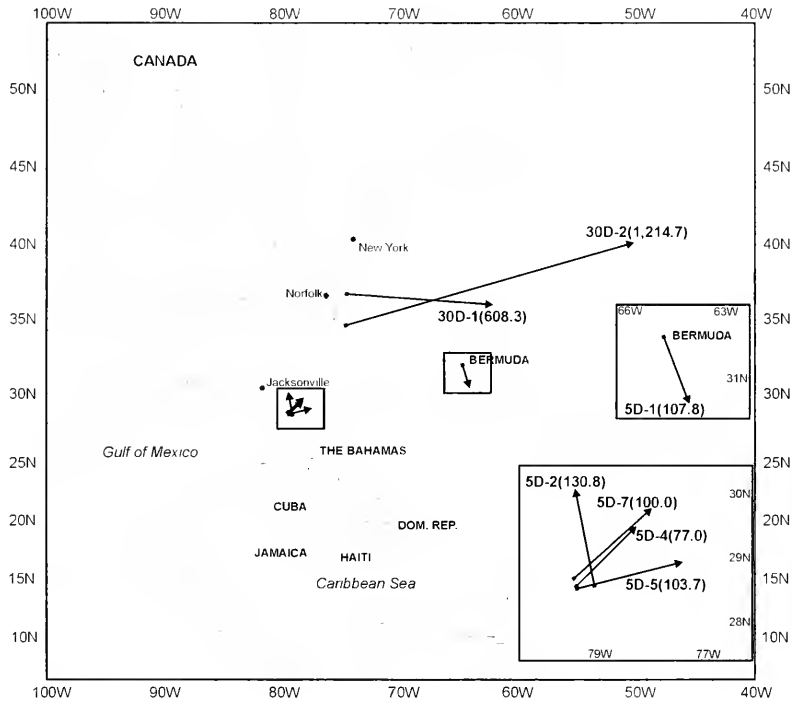

Figure 1

Map showing points of release (squares) and points of pop-up (arrow tips at end of straight lines) for seven of nine blue marlin released from pelagic longline gear in the western North Atlantic Ocean and equipped with pop-up satellite archival tags in 2000 and 2001. The tag identifier for each fish and straight-line distance in nautical miles between point of release and location where tag transmitted data to the Argos satellite are provided in parentheses.

tion of the data), and the probability of recovering (i.e. receiving) all the data recorded, as well as cost. The older, less-expensive 5-day tags stored far fewer data points but transmitted all of them. In contrast, the newer 30-day tags captured far more detailed data, yet only transmitted a fraction of them because of technological constraints, such as a short battery life, file corruption, and occasional problems with satellite uplink. Less than half of the 744 possible hourly histograms were recovered after final processing (46.5% for 30D-1 and 47.6% for 30D-2). However, of the reported histograms that were not corrupted, there was fairly consistent reporting across hours of the day, with an average of 14.75 records (range: 6–23) per hour of day for 30D-1 and 14.42 (range: 8–21) for 30D-2.

The small data storage capacity of the 5-day tag provided information regarding the thermal histories of blue marlin. However, the frequency of temperature recording, and subsequent averaging, limited the utility of the temperature data alone to infer survival. In contrast, the 30-day tags provided higher resolution data on temperature and depth, despite some significant gaps in the time series. In comparing the two tag models used in this study, the less expensive 5-day tags may be sufficient for the specific purpose of evaluating survival, although the greater detail provided by the 30-day tags may be desirable for additional behavioral analyses. Several models of archival satellite tags are currently available—all with differing data collection and storage capabilities. The high costs of tagging-related research, both for equipment and personnel time, therefore require choosing the tag model that is best matched to data needs to answer the specific scientific question of a study.

Net movement

All blue marlin tagged in this study undertook significant movements (Table 2, Fig. 1). The blue marlin released off Bermuda moved away from the islands 199.7 km (107.8 nmi) in a southeast direction over five days. Graves et al. (2002) noted similar movements away from the tagging locations for blue marlin released from the recre-

ational fishery off Bermuda. The four blue marlin tagged off Florida during 2000 moved northeast to east in direction, which is inconsistent with the generally northward flow of the Gulf Stream as it exits the Florida Straits. Both the direction and distance moved by these five fish are evidence of their survival; had these fish been dead and floating, the expected path of movement would have been northward at a velocity of 1.5–3 knots in the Gulf Stream. Of the two fish tagged in 2001, one (30D-1) moved 1126.4 km (608.3 nmi) northeast toward the central north Atlantic, and the other (30D-2) moved 2249.4 km (1214.7 nmi) north toward the Grand Banks.

According to the minimum straight-line distances, blue marlin in this study moved an average of 0.95 nmi/hour (22.9 nmi/day average; range: 15.1–39.2 nmi), which is slightly faster than the average speed of 0.73 nmi/hour (17.6 nmi/day average; range: 10.9–26.4 nmi) reported by Graves et al. (2002). The results of both PSAT studies are consistent with the swimming velocities of 1–2 nmi/hour reported in the acoustic tracking of Pacific blue marlin by Holland et al. (1990), but at the lower end of the range of directly measured swimming speeds of 0.29–4.37 nmi/hour for blue marlin with an acoustic tag reported by Block et al. (1992). However, both measurements from acoustic studies were of short duration deployments. As noted in Block et al. (1992), high initial movement rates would be consistent with actions likely taken by ram-ventilating fish under oxygen debt; slower average speeds over the duration of the deployment could result from the averaging of high initial speed with later slower movements upon the return to normal behavioral patterns.

Forward movement and inclinometer data

The inclinometer values for each of the seven reporting 5-day tags indicated that the PSAT was depressed below 30° above horizontal for an average of 47.25% (range: 46.77–47.74%) of the measurements. These values indicate continual forward movement through the end of the 5-day sampling period and are similar to the observations of Graves et al. (2002), who reported substantial forward movement for more than 40% of their inclinometer measurements. They are also consistent with the observed net displacements of the blue marlin in the present study. Inclinometer values following release for all PSATs indicated that the tags were floating in a vertical position.

Depth and temperature

The temperature data of the 5-day tags indicated numerous vertical movements into cooler water for each fish (Fig. 2, A–E). The maximum temperature recorded by each tag was equivalent to, or slightly greater than, the sea surface temperature (SST) recorded by available SeaWIFS satellite data for that area and date. The slightly higher temperature is possibly an artifact of the 5-day tag; its black coloration may have absorbed heat from direct sunlight while at the surface. Each fish demonstrated movement into slightly cooler waters immediately following release, a behavior also noted in acoustic tracking studies (e.g. Holland et al., 1990; Holts and Bedford, 1993), although it is likely that this movement to cooler waters was still within the upper strata of the water column.

Differences in vertical behavior were noted among individuals. The vast majority (98.6%) of values reported by the 5-day tag on the Bermuda-released fish fell within a range of 2°C (28.6°–30.6°C) (Fig. 2A). This range is smaller than those reported by Graves et al. (2002) for blue marlin in the same general area (range: 26–31°C) but of a much smaller sample size (n=1 vs. n=8 recovered tag datasets). The four blue marlin tagged with 5-day tags off Florida exhibited greater variation in thermal habitat, but their temperature values remained within a range of 6.5°C (Fig. 2, B–E). These four fish also displayed greater vertical movements during the morning hours, especially 5D-3 and 5D-7 (Fig. 2, B and E). For the four blue marlin tagged with 5-day PSATs off Florida in 2000, there was a significant difference between the average temperature during the night, day, and a composite dawn and dusk period (one-way ANOVA; P=0.0003, 2 df).

The 30-day PSATs provided much more detailed temperature information than the 5-day tags, as well as depth data, allowing for a higher resolution of blue marlin vertical movements over the course of a day. The two fish with the 30-day tags spent the vast majority of their total time within the upper five meters of the water column (65.4% for tag 30D-1 and 81.5% for 30D-2, Fig. 3). The higher temperatures recorded by tag 30D-1 are likely due to the warmer surface waters encountered by that fish as it moved toward the central Atlantic, whereas the blue marlin with tag 30D-2 moved northeast into cooler waters near the Grand Banks (Fig. 1). Examination of the temperature histograms generated the by tags for each hour-long period also indicates that these two fish spent all of the first two (30D-1) and six (30D-2) days following release at or near the surface (depth ≤5 m). Only after this initial period did the fish resume the repetitive deep diving behavior seen later during the deployments.

The two 30-day tags deployed in 2001 recorded a broader range of temperatures (30D-1: 29.6–17.8°C and 30D-2: 30.6–16.6°C) than the 5-day tags attached to the blue marlin in 2000. This apparent difference may relate to the measurement protocol of each type of tag. The 5-day tags recorded temperature once an hour and stored the average of two hourly values. In contrast, the 30-day tags recorded temperature values every minute and stored them in the form of an hourly histogram. Inspection of the 30-day tag data revealed that excursions into cooler water were typically of short duration. It is therefore likely that such an excursion could have been missed with a once-an-hour temperature measurement by the 5-day tag. Alternatively, if a lower temperature were encountered at one measurement, it would probably be increased by being averaged with another (likely warmer) measurement from the previous or next hour before being archived. It can be shown mathematically that if the two observations in each pair are independent (which would occur if they are sufficiently separated in time), then the effect of averaging them would be to reduce the variance by one-half. However, cases can be constructed where the observations in each pair would not

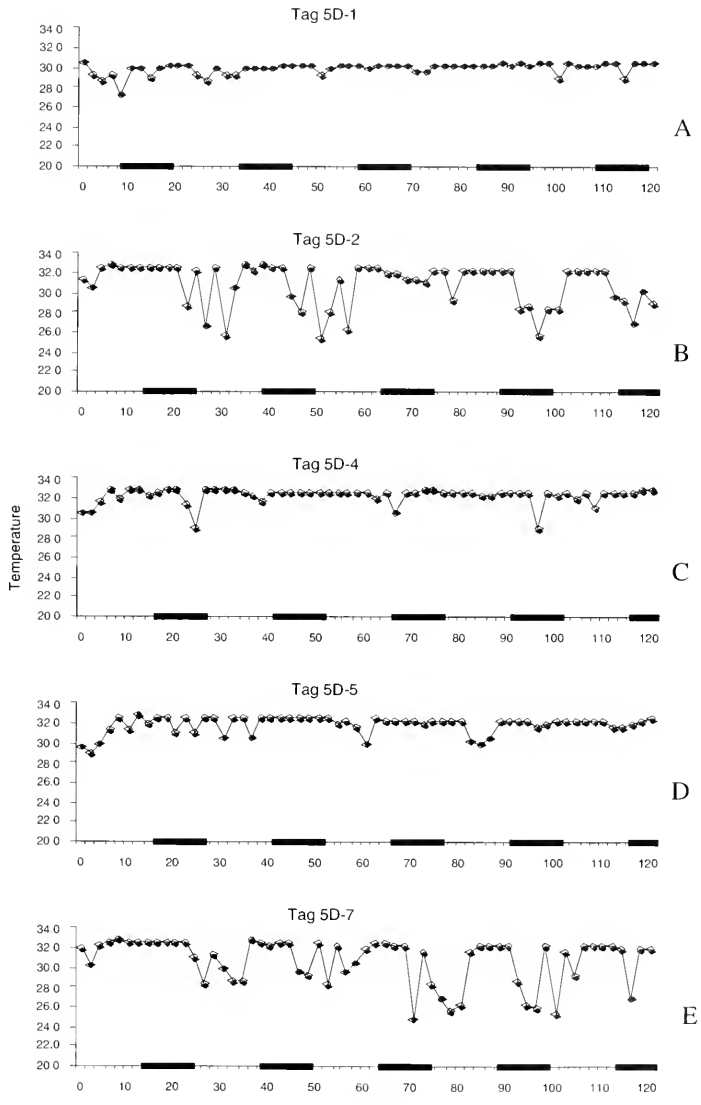

Figure 2

Temperature records for blue marlin released from pelagic longline gear in the western North Atlantic Ocean and equipped with PTT-100 (5-day) pop-up satellite archival tags. Temperature readings were taken once an hour and the average value of two consecutive hours was stored. Temperatures are in degrees centigrade, and the black bars indicate approximate hours of darkness.

be independent. It is therefore not possible to accurately describe the effects (i.e. to reconstruct the actual data or data ranges) of the averaging process of the 5-day tags. Although we feel that any direct comparison of inferred 5-day tag data with the observed data from the 30-day tags would be inappropriate because of the inability to describe this averaging effect, we note that the reported 5-day tag data are not inconsistent with those data from the 30-day tags.

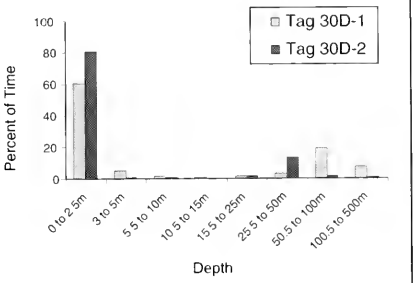

Figure 3

Percentage of total time at depth for blue marlin released from pelagic longline gear in the western North Atlantic Ocean and equipped with PAT (30 day) pop-up satellite archival tags.

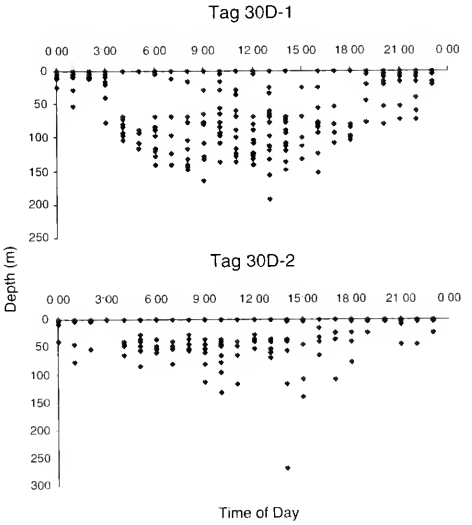

Figure 4

Maximum depths as a function of time of day for blue marlin released from pelagic longline gear in the western North Atlantic Ocean and equipped with PAT (30-day) pop-up satellite archival tags. Both individuals demonstrated a tendency to have greater maximum depths during daylight hours.

The 30-day tags provided considerable information on blue marlin movements at depth. Each hour-long histogram included both the maximum and minimum depths for the hour interval, as well as the percentage of time spent within each predetermined depth bin. For example, during the hour between 10:00 and 11:00 a.m. on 25 July, 30D-1 reported a maximum depth of 28 m and a minimum depth of 0 m, During this hour the fish spent 42 minutes between 0 and 2.5 m, only 72 seconds between 3 and 15 m, and almost 17 minutes between 15.5 and 28 m.

Examination of the maximum and minimum depth values by hour suggests a relationship between movement to depth and daylight hours (Fig. 4). Both blue marlin with 30-day tags made deeper dives during the day than at night. This pattern is similar to diurnal vertical migrations observed in bigeye tuna (*Thunnus obesus*) (Holland et al., 1990; Dagorn et al., 2000), and swordfish (Sedberry and Loefer, 2001) and may relate to feeding within the deep scattering layer.

Billfish survival

Seven of the nine deployed tags successfully reported data. Three independent lines of data transmitted by these tags suggest that seven of the blue marlin carrying these tags and released from pelagic longline gear survived for periods of five or thirty days. First, changes in temperature (5-day tags) or temperature and depth (30-day tags) were consistent with vertical excursions within the water column. Secondly, the direction and magnitude of net displacement cannot be explained by local current patterns and thus imply active movement. Finally, the inclinometer readings (5-day tags only) are consistent with sufficient forward propulsion to depress tags below 30° above horizontal for almost one-half of the measurement periods.

The thermal histories of three fish tagged with 5-day tags (5D-1 off Bermuda and 5D-4 and 5D-5 off Florida) showed little variation (Fig. 2, A, C, and D). Because of the infrequent sampling of temperature by these tags (once an hour, and two hourly values were averaged), it is possible that short-duration dives to cooler waters were not sampled, or that detailed information was lost in the averaging of the two hourly measurements. Alternatively, the thermal histories for these tags could be interpreted as those of fish that died and remained floating at the surface. However, given the preference of individuals for shallow depths recorded by the 30-day tags, even the minimal variations in temperature observed by the 5-day tags may be consistent with movement to depths and postrelease survival. Additionally, the net displacements cannot be attributed solely to local currents (Fig. 1), and inclinometer values indicate continued forward movement throughout the five-day period. We maintain, therefore, that these fish were alive for the whole five-day post-release period.

The reason that two tags did not report data could have been result of mortality (the blue marlin died and sank to a depth at which the tag was crushed or lost positive buoyancy) or of other factors, such as tag malfunction or mechanical damage to the tag. Neither tag contained prerelease software or an emergency release device. There did not appear to be a relationship between the weight of the fish and a nonreporting tag. Both fish with nonreporting tags were hooked in the jaw with "J" hooks. The blue marlin with tag 5D-3 was in excellent condition and actively swam away from the vessel, whereas the fish that received tag 5D-6 was in good condition and actively swam away from the vessel, albeit more slowly than several of the others. It is worth noting that this fish also had an orange streamer tag attached to it from a previous capture, but it was not possible to retrieve this tag without compromising the release protocol.

The results of the present study can be used to generate rough estimates of postrelease survival rate for blue marlin released from the western North Atlantic pelagic longline fishery. This project observed that seven of nine deployed PSATs reported data as programmed (if the two nonreporting tags were indeed mortalities); this results in a 77.8% postrelease survival rate. Combining postrelease mortalities with estimates of mortality at the time of haulback, the compounded mortality for blue marlin conservatively ranges from 65.4% (Jackson and Farber, 1998) to 53.5% (Cramer, 1998). However, the relatively small number of tags deployed in this study clearly limits the general applicability of the these results, as did the prior limitation that only live fish greater than 100 pounds, without clearly mortal wounds, would be tagged. Fortunately, all of the fish encountered alive (one was dead on haulback) met these two requirements. The 77.8% estimate of postrelease survival is nevertheless comparable with the 89% survival rate (8 of 9 reporting PSAT tags) reported by Graves et al. (2002) for blue marlin caught in the recreational fishery off Bermuda—a fishery in which many blue marlin are resuscitated prior to release.

The sample size required for an Atlantic-wide estimate of postrelease mortality would be large given the need to account for different gear configurations, as well as variables such as environmental conditions, season, and geographic area (Goodyear, 2002). Such a project would be extremely expensive with current technology. However, evolving PSAT technology presents the opportunity for additional work describing the interactions between pelagic longline gear and catch species, such as the billfishes. New high-resolution PSATs provide fine-scale data on habitat preferences and behavior, allowing the eventual refinement of models that standardize historical catch-per-unit-of-effort data for pelagic longline gear (e.g. Hinton and Nakano, 1996; Hinton, 2001). Such standardization efforts, if correctly applied, may permit more accurate blue marlin stock assessments (Venizelos et al., 2001).

This study demonstrates that PSAT technology is well suited to estimate postrelease survival rates for blue marlin from the pelagic longline fishery, with minimal interference to normal commercial fishing operations. The relatively high rate of survival of blue marlin inferred from these data for five and thirty days following release from pelagic longline gear demonstrates that management measures requiring live release, such as those recently adopted by ICCAT, can significantly reduce fishing mortality on Atlantic blue marlin.

Acknowledgments

The authors would like to thank Captains Bobby Lamb (FV *Ark Angel*), Keith Garner (FV *Deliverance*), David Kolesar (FV *Triple Threat*), Greg O'Neil (FV *Carol Ann*), and Baker Dunn (FV *Triple Threat*), as well as their crews, for providing assistance in deploying the pop-up tags. We would also like to thank vessel owners Willie Etheridge and Vince Pyle for their assistance in coordinating available vessels. Paul Howey, Roger Hill, and Melinda Braun provided technical assistance with the tags, and Heidi Dewar kindly assisted with the interpretation of the tag data. John Hoenig helpfully assisted with some of the statistical methods. Support for this project was provided by the Bermuda Department of Agriculture and Fisheries, the U.S. National Marine Fisheries Service, and the Hewit Family Foundation.

Literature cited

Apgar, V.
1953. A proposal for a new method of evaluation of the newborn infant. Curr. Res. Anesth. Analg. July–August: 260–265.

Arnold, G., and H. Dewar.
2001. Electronic tags in marine fisheries research: a 30-year perspective. *In* Electronic tagging and tracking in marine fisheries (J. R. Sibert and J. L. Nielsen, eds.), p. 7–34. Kluwer Academic Publishers, Dordrecht, Netherlands.

Bayley, R. E., and E. D. Prince.
1994. A review of tag release and recapture files for *Istiophoridae* from the Southeast Fisheries Science Center's Cooperative Gamefish Tagging Program, 1954 to present. ICCAT (Int. Comm. Conserv. Atl. Tunas) Coll. Vol. Sci. Pap. 41:527–548.

Block, B. A., D. T. Booth, and F. G. Carey.
1998. Depth and temperature of the blue marlin, *Makaira nigricans*, observed by acoustic telemetry. Mar. Biol. 114: 175–183.

Block, B. A., H. Dewar, C. Farwell, and E. D. Prince.
1998. A new satellite technology for tracking the movements of Atlantic bluefin tuna. Proc. Natl. Acad. Sci. U. S. A. 95: 9384–9389.

Boggs, C. H.
1992. Depth, capture time, and hooked longevity of longline-caught pelagic fish: timing bites of fish with chips. Fish. Bull. 90:642–658.

Cramer, J.
1998. Pelagic longline billfish by-catch. ICCAT (Int. Comm. Conserv. Atl. Tunas) Coll. Vol. Sci. Pap. 47:143–154.
2000. Species reported caught in the U.S. commercial pelagic longline and gillnet fisheries from 1996 to 1998. NMFS Sustainable Fisheries Division SFD-99/00-78:1–33.

Dagorn, L., P. Bach, and E. Josse.
2000. Movement patterns of large bigeye tuna (*Thunnus*

obesus) in the open ocean, determined using ultrasonic telemetry. Mar. Biol. (Berlin) 136(2):361–371.

Goodyear, C. P.
2000. Biomass projections for Atlantic blue marlin: potential benefits of fishing mortality reductions. ICCAT (Int. Comm. Conserv. Atl. Tunas) Coll. Vol. Sci. Pap. 52: 1502–1506.
2002. Factors affecting robust estimates of the catch and release mortality using pop-up tag technology. *In* Symposium on catch and release in marine recreational fisheries (A. Studholme, E. D. Prince, and J. Lucy, eds.), p. 172–179. Spec. Pub. Am. Fish. Soc.

Graves, J. E., B. E. Luckhurst, and E. D. Prince.
2002. An evaluation of pop-up satellite tags for estimating post-release survival of blue marlin (*Makaira nigricans*). Fish. Bull. 100:134–142.

Hinton, M.G.
2001. Status of the blue marlin in the Pacific Ocean. Status of the tuna and billfish stocks in 1999. IATTC Stock Assess. Rep. 1:284–318.

Hinton, M G., and H. Nakano.
1996. Standardizing catch and effort statistics using physiological, ecological, or behavioral constraints and environmental data, with an application to blue marlin (*Makaira nigricans*) catch and effort data from the Japanese longline fisheries in the Pacific. Inter.-Am. Trop. Tuna Comm. Bull. 21(4):171–200.

Holland, K., R. Brill, and R. K. C. Chang.
1990. Horizontal and vertical movements of Pacific blue marlin captured and released using sportfishing gear. Fish. Bull. 88:397–402.

Holts, D. B., and D. W. Bedford.
1993. Horizontal and vertical movements of the shortfin mako shark, *Isurus oxyrinchus*, in the southern California bight. Aust. J. Mar. Freshw. Res. 44(6):901–909.

ICCAT (International Commission for the Conservation of Atlantic Tunas).
1997. Report for the biennial period, 1996–97. Part 1 (1996), vol. 2, 204 p. ICCAT, Madrid, Spain.
2001. Report of the fourth ICCAT billfish workshop. ICCAT Coll. Vol. Sci. Pap. 53:1–22.

Jackson, T. L., and M. I. Farber.
1998. Summary of at-sea sampling of the western Atlantic Ocean, 1987–1995, by industrial longline vessels fishing out of the port of Cumaná, Venezuela: ICCAT enhanced research Program for billfish 1987–1995. ICCAT Coll. Vol. Sci. Pap. 47:203–228.

Jones, C. D., and E. D. Prince.
1998. The cooperative tagging center mark-recapture database for Istiophoridae (1954–1995) with an analysis of the west Atlantic ICCAT billfish tagging program. ICCAT Coll. Vol. Sci. Pap. 47:311–322.

Lee, D. W., and C. J. Brown.
1998. SEFSC pelagic observer program data summary for 1992–1996. NOAA Tech. Memo. NMFS-SEFSC-408:1–21.

Lutcavage, M. E., R. W. Brill, G. B. Skomal, B. C. Chase, and P. W. Howey.
1999. Results of pop-up satellite tagging of spawning size class fish in the Gulf of Maine: do North Atlantic bluefin tuna spawn in the mid-Atlantic? Can. J. Fish. Aquat. Sci. 56(2):173–177.

Ortiz, M., D. S. Rosenthal, A. Venizelos, M. I. Farber, and E. D. Prince.
1998. Cooperative Tagging Center annual newsletter: 1998. NOAA Tech. Memo. NMFS-SEFSC-423:1–23.

Pepperell, J. G., and T. L. O. Davis.
1999. Post-release behavior of black marlin *Makaira indica* caught and released using sportfishing gear off the Great Barrier Reef (Australia). Mar. Biol. 135:369–380.

Sedberry, G. R., and J. K. Loefer.
2001. Satellite telemetry tracking of swordfish, *Xiphias gladius*, off the eastern United States. Mar. Biol. 139: 355–360.

Venizelos, A., M. I. Farber, and D. D. Benetti.
2001. An evaluation of assumptions associated with blue marlin depth distribution towards the possible incorporation to the standardization of catch and effort statistics for use in stock assessment. ICCAT Coll. Vol. Sci. Pap. 53: 258–262.

Zar, J. H.
1999. Biostatistical analysis, 4th ed., 663 p. Prentice-Hall, Inc., Upper Saddle River, NJ.

Acknowledgment of reviewers

The editorial staff of *Fishery Bulletin* would like to thank the following referees for their time and efforts in providing reviews of the manuscripts published in 2002–2003. Their contributions have helped ensure the publication of quality science.

Dr. Kenneth W. Able
Dr. Peter B. Adams
Dr. Dennis M. Allen
Dr. Allen H. Andrews
Dr. Sharon A. Appleyard
Dr. Freddy Arocha
Dr. Francisco Arreguin-Sanchez
Dr. David W. Au

Mr. John Babaluk
Dr. M. Banks
Dr. Luiz R. Barbieri
Dr. William H. Bayliff
Dr. Terry D. Beachman
Dr. Daniel W. Beckman
Dr. Steven J.M. Blaber
Dr. H.L. Blankenship
Dr. Barbara Block
Dr. James A. Bohnsack
Dr. Jesper Boje
Dr. Steven Branstetter
Dr. Craig Brown
Dr. Barry D. Bruce
Dr. Lewis H. Bullock
Mr. Michael Burton
Dr. Morgan S. Busby
Dr. Mark J. Butler

Dr. Steven X. Cadrin
Dr. Gregor M. Cailliet
Dr. James Carretta
Dr. Patrice Cayre
Dr. Meng-Hsien Chen
Dr. Milani Y. Chaloupka
Dr. Mary Christman
Dr. Mark R. Collins
Dr. Richard E. Condrey
Dr. David O. Conover
Dr. P.D. Cowley
Dr. Paul Crone
Dr. Larry B. Crowder
Dr. D.P. Cyrus

Dr. John M. Dean
Dr. Heidi Dewar
Dr. James G. Ditty
Dr. W.D. Dupaul

Dr. Anne-Marie Eklund
Dr. John M. Emlen
Dr. Charles E. Epifanio
Dr. James A. Estes
Dr. Bruce T. Estrella

Dr. Beatrice Padovani Ferreira
Dr. Richard C. Ferrero
Dr. Clark T. Fontaine
Dr. Alain Fonteneau
Dr. Michael G. Frisk
Dr. Lee A. Fuiman

Dr. Francisco J. Garcia-Rodriguez
Dr. Tony Gharrett
Dr. Vincent F. Gallucci
Mr. Bert Geary
Dr. James Gelsleichter
Dr. Kenneth J. Goldman
Dr. Charles M. Guthrie

Dr. Malcolm Haddon
Dr. Philip S. Hammond
Dr. John Hampton
Dr. Matthew Hare
Ms. Kristen Hart
Dr. Graeme Hays
Dr. Edward J. Heist
Dr. Aaron C. Henderson
Dr. Tyrrell A. Henwood
Dr. Ray Hilborn
Dr. Peter Himchak
Dr. Michael G. Hinton
Dr. John J. Hoey
Dr. Wayne Hoggard
Dr. Kim N. Holland
Dr. John R. Hunter

Dr. James N. Ianelli
Dr. Ana L. Ibanez Aguirre
Dr. Baban S. Ingole

Dr. Larry D. Jacobson
Dr. G. Janacek

Dr. Desmond M. Kahn
Dr. Michel J. Kaiser

Dr. Steven Kalinowski
Dr. Gregory Todd Kellison
Dr. S. Kelly
Dr. Mariano Koen-Alonso
Dr. Christopher C. Koenig
Dr. Nancy E. Kohler

Dr. Han-Lin Lai
Dr. M.D. Lamare
Dr. T.E. Lankford
Dr. Bruce M. Leaman
Dr. Kenneth M. Leber
Dr. W.C. Leggett
Dr. Christopher M. Legault
Dr. Patrick Lehodey
Dr. Jeffrey M. Leis
Dr. R.J.G. Lester
Dr. Karen E. Limburg
Dr. Jason S. Link
Dr. Nancy C.H. Lo
Ms. Linda Lombardi-Carlson
Dr. Peter L. Lutz
Dr. Joanne Lyczkowski-Shultz

Dr. Pamela M. Mace
Ms. Beverly J. Macewicz
Dr. Gary L. Maillet
Ms. Nancy E. Maloney
Dr. Mark Mangel
Ms. Jan Mason
Dr. Bernard J. McConnell
Dr. John McDonald
Mr. Lawrence W. McEachron
Dr. M.G. Meekan
Dr. Richard L. Merrick
Dr. Julian D. Metcalfe
Dr. David L. Meyer
Dr. David A. Milton
Dr. R. Mohan
Dr. Robert K. Mohn
Dr. H. Geoffrey Moser
Dr. Robert G. Muller
Ms. Kristen Munk
Mr. Michael D. Murphy

Dr. Lisa J. Natanson
Mr. David Nemerson
Dr. Nathaniel Newlands
Dr. Stephen J. Newman
Dr. Scott Nichols
Dr. David L. Nieland

Dr. Marcelo E. Oliva
Dr. Jeff Olsen
Dr. Mauricio Ortiz
Dr. Robert S. Otto

Dr. Debra Palka
Dr. Glenn R. Parsons
Dr. Donald E. Pearson

Dr. Michael Pennington
Dr. Pierre Pepin
Dr. James H. Petersen
Dr. Mark S. Peterson
Dr. Daryl J. Pierce
Dr. Eric N. Powell
Dr. Michael H. Prager
Dr. André E. Punt

Dr. Stephen Ralston
Dr. Renata M.A. Ramos
Dr. Carol Reeb
Dr. Carlos Robles
Dr. Jay R. Rooker
Dr. Steven W. Ross
Dr. Sherylynn Rowe

Dr. Susan E. Safford
Dr. Bernard Sainte-Marie
Dr. R.A. Santos

Dr. Kurt M. Schaefer
Dr. Michael Schirripa
Dr. D.C. Schneider
Dr. Kenneth Severin
Dr. Jean-Marie Sevigny
Dr. Richard Shaw
Dr. Kyle Shertzer
Dr. Colin Simpfendorfer
Dr. G.B. Skomal
Dr. Thomas R. Sminkey
Mr. Joseph W. Smith
Dr. Sean Y. Sol
Dr. David A. Somerton
Dr. Patrick J. Sullivan

Dr. C.S. Tamaru
Dr. Mark Terceiro
Ms. Vicky Thayer
Dr. Stephen C. Turner
Dr. W-N Tzeng

Dr. Wolfgang Vogelbein
Dr. Eric Volk

Dr. You-Gan Wang
Dr. Robert D. Ward
Mr. William Watson
Mr. Grant West
Dr. Bradley M. Wetherbee
Dr. Erik Williams
Dr. Sabine Petra Wintner
Dr. David M. Wyanski

Dr. Yongshun Xiao

Mr. Mark Zimmermann

Fishery Bulletin Index

Volume 101(1–4), 2003

List ot titles

101(1)

101(2)

Fishery Bulletin Index

Volume 101(1–4), 2003

List ot authors

Fishery Bulletin Index

Volume 101(1–4), 2003

List ot subjects

This statement is required by the Act of August 12, 1970, Section 3685, Title 39, U.S. Code, showing ownership, management, and circulation of the *Fishery Bulletin*, publication number 366-370, and was filed on 30 September, 2003. The *Bulletin* is published quarterly (four issues annually) with an annual subscription price of $55.00 (sold by the Superintendent of Documents, U.S. Government Printing Office, Washington, DC 20402). The complete mailing address of the office of publication is NMFS Scientific Publications Office, NOAA, 7600 Sand Point Way NE, BIN C15700, Seattle, WA 98115. The complete mailing address of the headquarters of the publishing agency is National Marine Fisheries Service, NOAA, Department of Commerce, 1335 East-West Highway, Silver Spring, MD 20910. The name of the publisher is Willis Hobart and the managing editor is Sharyn Matriotti, their mailing address is NMFS Scientific Publications Office, 7600 Sand Point Way NE, BIN 15700, Seattle, WA 98115. The owner is the U.S. Department of Commerce, 14th St. N.W., Washington, DC 20230; there are no bondholders, mortgages, or other security holders. The purpose, function, and nonprofit status of the organization (agency) and the exempt status for Federal income tax purposes has not changed during the preceding 12 months. The extent and nature of circulation is as follows: total number of copies (A) (average number of copies of each issue during the preceding 12 months) was 1490 and the actual number of copies of the single issue published nearest to the filing dates was 1278. Paid circulation (B) is handled by the U.S. Government Printing Office, Washington, DC 20402, and the total number printed for sales (mail subscriptions and individual sales) was 525 for the average number of copies each issue during the preceding 12 months and 475 the actual number of copies of the single issue published nearest to the filing date (C). Free distribution (D) by mail; samples, complimentary and other free copies (average number of copies each issue during the preceding 12 months) was 845 and the actual number of copies of the single issue published nearest to the filing date was 782. Free distribution outside the mail (E) by carriers or other means was 0 for both average number of copies and actual number of copies. Total free distribution (F) was 0 for both average number of copies and actual number of copies of the single issue published nearest the filing date. The total distribution (G; sum of D and B) (average number of copies each issue during the preceding 12 months) was 1370 and the actual number of copies of the single issue published nearest to the filing date was 1257. There were 95 copies (avg annual) not distributed (H). The total (I sum of G and H) is equal to the net press run figures shown in Item A: 1490 and 1278 copies, respectively. I certify that the statements made by me above are correct and complete: (Signed) Willis Hobart, Publisher

Fishery Bulletin

Guidelines for contributors

Content of papers

Articles

Articles are reports of 10 to 30 pages (double spaced) that describe original research in one or a combination of the following fields of marine science: taxonomy, biology, genetics, mathematics (including modeling), statistics, engineering, economics, and ecology.

Notes

Notes are reports of 5 to 10 pages without an abstract that describe methods and results not supported by a large body of data. Although all contributions are subject to peer review, responsibility for the contents of articles and notes rests upon the authors and not upon the editor or the publisher. It is therefore important that authors consider the contents of their manuscripts carefully. Submission of an article is understood to imply that the article is original and is not being considered for publication elsewhere. Manuscripts must be written in English. Authors whose native language is not English are strongly advised to have their manuscripts checked for fluency by English-speaking colleagues prior to submission.

Preparation of papers

Text

Title page should include authors' full names and mailing addresses (street address required) and the senior author's telephone, fax number, e-mail address, as well as a list of key words to describe the contents of the manuscript. **Abstract** must be less than one typed page (double spaced) and must not contain any citations. It should state the main scope of the research but emphasize the author's conclusions and relevant findings. Because abstracts are circulated by abstracting agencies, it is important that they represent the research clearly and concisely. **General text** must be typed in double-spaced format. A brief introduction should state the broad significance of the paper; the remainder of the paper should be divided into the following sections: Materials and methods, Results, Discussion (or Conclusions), and Acknowledgments. Headings within each section must be short, reflect a logical sequence, and follow the rules of multiple subdivision (i.e. there can be no subdivision without at least two subheadings). The entire text should be intelligible to interdisciplinary readers, therefore, all acronyms and abbreviations should be written out and all lesser-known technical terms should be defined the first time they are mentioned. The scientific names of species must be written out the first time they are mentioned; subsequent mention of scientific names may be abbreviated. Follow *Scientific style and format. CBE manual for authors, editors, and publishers* (6th ed.) for editorial style and the most current issue of the *American Fisheries Society's common and scientific names of fishes from the United States and Canada* for fish nomenclature. Dates should be written as follows: 11 November 1991. Measurements should be expressed in metric units, e.g. metric tons (t). The numeral one (1) should be typed as a one, not as a lower-case el (l).

Footnotes

Use footnotes to add editorial comments regarding claims made in the text and to document unpublished works or works with local circulation. Footnotes should be numbered with Arabic numerals and inserted in 10-point font at the bottom of the first page on which they are cited. Footnotes should be formatted in the same manner as citations. If a manuscript is unpublished, in the process of review, or if the information provided in the footnote has been conveyed verbally, please state this information as "unpubl. data," "manuscript in review," and "personal commun.," respectively. Authors are advised wherever possible to avoid references to nonstandard literature (unpublished literature that is difficult to obtain, such as internal reports, processed reports, administrative reports, ICES council minutes, IWC minutes or working papers, any "research" or "working" documents, laboratory reports, contract reports, and manuscripts in review). If these references are used, please indicate whether they are available from NTIS (National Technical Information Service) or from some other public depository. Footnote format: author (last name, followed by first-name initials); year; title of report or manuscript; type of report and its administrative or serial number; name and address of agency or institution where the report is filed.

Literature cited

The literature cited section comprises works that have been published and those accepted for publication (works in press) in peer-reviewed journals and books. Follow the name and year system for citation format. In the text, write "Smith and Jones (1977) reported" but if the citation takes the form of parenthetical matter, write "(Smith and Jones, 1977)." In the literature cited section, list citations alphabetically by last name of senior author. For example, Alston, 1952; Mannly, 1988; Smith, 1932; Smith, 1947; Stalinsky and Jones, 1985. Abbreviations of journals should conform to the abbreviations given in the *Serial sources for the BIOSIS previews database*. Authors are responsible for the accuracy and completeness of all citations. Literature citation format: author (last name, followed by first-name initials); year; title of report or article; abbreviated title of the journal in which the article was published; volume number, page numbers. For books, please provide publisher, city, and state.

Tables

Tables should not be excessive in size and must be cited in numerical order in the text. Headings in tables should be short but ample enough to allow the table to be intelligible on its own. All unusual symbols must be explained in the table legend. Other incidental comments may be footnoted (use italic arabic numerals for footnote markers). Use asterisks only to indicate probability in statistical data. Place table legends on the same page as the table data. We accept tables saved in most spreadsheet software programs (e.g. Microsoft Excel). Please note the following:

- Use a comma in numbers of five digits or more (e.g. 13,000 but 3000).
- Use zeros before all decimal points for values less than one (e.g. 0.31).

Figures

Figures include line illustrations, computer-generated line graphs, and photographs (or slides). They must be cited in numerical order in the text. Line illustrations are best submitted as original drawings. Computer-generated line graphs should be printed on laser-quality paper. Photographs should be submitted on glossy paper with good contrast. All figures are to be labeled with senior author's name and the number of the figure (e.g. Smith, Fig. 4). Use Helvetica or Arial font to label anatomical parts (line drawings) or variables (graphs) within figures; use Times Roman bold font to label the different sections of a figure (e.g. **A**, **B**, **C**). Figure legends should explain all symbols and abbreviations seen within the figure and should be typed in double-spaced format on a separate page at the end of the manuscript. We advise authors to peruse a recent issue of *Fishery Bulletin* for standard formats. Please note the following:

- Capitalize the first letter of the first word of axis labels.
- Do not use overly large font sizes to label axes or parts within figures.
- Do not use boldface fonts within figures.
- Do not create outline rules around graphs.
- Do not use horizontal lines through graphs.
- Do not use large font sizes to label degrees of longitude and latitude on maps.
- Indicate direction of degrees longitude and latitude on maps (e.g. 170°E).
- Avoid placing labels on a vertical plane (except on y axis).
- Avoid odd (nonstandard) patterns to mark sections of bar graphs and pie charts.

Copyright law

Fishery Bulletin, a U.S. government publication, is not subject to copyright law. If an author wishes to reproduce any part of *Fishery Bulletin* in his or her work, he or she is obliged, however, to acknowledge the source of the extracted literature.

Submission of papers

Send four printed copies (one original plus three copies)—clipped, *not stapled*—to the Scientific Editor, at the address shown below. Send photocopies of figures with initial submission of manuscript. Original figures will be requested later when the manuscript has been accepted for publication. Do not send your manuscript on diskette until requested to do so.

Dr. Norman Bartoo
National Marine Fisheries Service, NOAA
8604 La Jolla Shores Drive
La Jolla, CA 92037

Once the manuscript has been accepted for publication, you will be asked to submit a software copy of your manuscript. The software copy should be submitted in WordPerfect or Word format (in Word, save as Rich Text Format). Please note that we do not accept ASCII text files.

Reprints

Copies of published articles and notes are available free of charge to the senior author (50 copies) and to his or her laboratory (50 copies). Additional copies may be purchased in lots of 100 when the author receives page proofs.